



सत्यमेव जयते

INDIAN AGRICULTURAL  
RESEARCH INSTITUTE, NEW DELHI.

**I. A. R. I. 6.**

MGIPC—SI —6 AR/54--7-7-54—10,000.







# THE JOURNAL OF PHYSICAL & COLLOID CHEMISTRY

(Founded by Wilder D. Bancroft)



*Editor*

S. C. LIND

*Editor for Colloid Chemistry*

HARRY B. WEISER

*Associate Editors*

E. J. BOWEN

B. L. CRAWFORD, Jr.

K. FAJANS

J. H. HILDEBRAND

C. N. HINSHELWOOD

J. R. PARTINGTON

J. W. WILLIAMS

*Assistant Editor*

LOUISE KELLEY

*Volume 52*

25000



IARI

BALTIMORE

1948



# CONTENTS

## NUMBER 1, JANUARY, 1948

The Potentials of Falling Drops. A. Frumkin and J. Bagotskaja . . . . .	1
Solubilization of Water-Insoluble Dye by Colloidal Electrolytes and Non-Ionizing Detergents. James W. McBain, Arthur G. Wilder, and R. C. Merrill, Jr. . . . .	12
Laurate-Ion Activity in Solutions of Potassium Laurate in the Absence and Presence of Neutral Salts. I. M. Kolthoff and Warren F. Johnson . . . . .	22
The Effect of Temperature and Molecular-Weight Distribution on the Morphology of Natural and Synthetic High Polymers. Ernst A. Hauser and D. S. le Beau . . . . .	27
Calculation of the Surface Energy of Liquid Argon and Mercury. George Jura . . . . .	40
A Dual-Surface B.E.T. Adsorption Theory. William C. Walker and Albert C. Zettlemoyer . . . . .	47
Active Magnesia. IV. Application of Dual-Surface Theory. Albert C. Zettlemoyer and William C. Walker . . . . .	58
Monodisperse Colloids and Higher-Order Tyndall Spectra. Victor K. La Mer . . . . .	65
Electrophoretic Mobilities and Conductometric Activities of Potassium, Sodium, and Lithium Salts of Gum Arabic. D. R. Briggs . . . . .	76
Some Correlating Principles of Detergent Action. Walter C. Preston . . . . .	84
Colloidal Structures in Binary Soap Systems. Todd M. Doscher and Robert D. Vold . . . . .	97
Aqueous Systems of Non-Ionic Detergents as Studied by X-Ray Diffraction. Sullivan S. Marsden, Jr., and James W. McBain . . . . .	110
Critical Micelle Concentrations as Determined by Refraction. H. B. Klevens . . . . .	130
Electrical Conductivity of Crystalline and Liquid-Crystalline Soap-Water Systems. R. D. Vold and M. J. Heldman . . . . .	148
Phase Study of Rosin Soap-Sodium Chloride-Water and Rosin Soap-Sodium Silicate-Water Systems. R. C. Merrill and Raymond Getty . . . . .	167
Stability of Synthetic Keratin Fibers in Alcohol-Water Mixtures. Theoretical Basis for a New Method for Solubilizing Feather Keratin. Harold P. Lundgren, Andrew M. Stein, Virginia M. Koorn, and Richard A. O'Connell . . . . .	180
Electrophoretic and Ultracentrifugal Investigations of Rabbit Liver Nucleoprotein. Q. Van Winkle and Wesley G. France . . . . .	207
Homogeneity and the Electrophoretic Behavior of Some Proteins. Robert A. Alberty, Elmer A. Anderson, and J. W. Williams . . . . .	217
X-Ray Diffraction Studies in the System $\text{NiO-Cr}_2\text{O}_3\text{-ZrO}_2$ . W. O. Milligan and L. Merten Watt . . . . .	230
Sedimentation Equilibria of Polydisperse Non-Ideal Solutes. I. Theory. Michael Wales . . . . .	235
The Effect of Size, Shape, and Flexibility of the Solute Molecules on the Properties of Colloidal Solutions. Maurice L. Huggins . . . . .	248
The Dependence of the Scattering of Light on Angle and Concentration in Linear Polymer Solutions. Bruno H. Zimm . . . . .	260
Some Physical and Chemical Properties of Weight-Fractionated Lignosulfonic Acid, including the Dissociation of Lignosulfonates. F. M. Emsberger and Wesley G. France . . . . .	267

## NUMBER 2, FEBRUARY, 1948

Viscosity of Solutions and Suspensions. I. Theory. Vladimir Vand . . . . .	277
Viscosity of Solutions and Suspensions. II. Experimental Determination of the Viscosity-Concentration Function of Spherical Suspensions. Vladimir Vand . . . . .	300
Viscosity of Solutions and Suspensions. III. Theoretical Interpretation of Viscosity of Sucrose Solutions. Vladimir Vand . . . . .	314

Affinity and Reaction Rate Close to Equilibrium. I. Prigogine, P. Outer, and Cl. Herbo	321
The Cryoscopic Behavior of Carbon Tetrachloride. Arthur W. Davidson, W. J. Argersinger, Jr., and Carl I. Michaelis	332
The Use of Ion Exchangers for the Determination of Physical-Chemical Properties of Substances, Particularly Radiotracers, in Solution. I. Theoretical. Jack Schubert	340
The Use of Ion Exchangers for the Determination of Physical-Chemical Properties of Substances, Particularly Radiotracers, in Solution. II. The Dissociation Constants of Strontium Citrate and Strontium Tartrate. Jack Schubert and J. W. Richter	350
The Thermal Decomposition of Tertiary Butyl Acetate. Charles E. Rudy, Jr., and Paul Fugassi	357
The Effect of Surface-Active Agents upon Dispersions of Lead Monoxide in Xylene. V. R. Damerell and M. J. Vogt	363
The Maximum Possible Rate of Evaporation of Liquids. S. S. Penner	367
Thermodynamics of Adsorption from Solutions I. The Molality and Activity Coefficient of Adsorbed Layers. Ying Fu, Robert S. Hansen, and F. E. Bartell	374
Gaps in Physical Constants Data for Hydrocarbons. Nancy Corbin, Mary Alexander, and Gustav Egloff	387
Physical Chemistry of Flotation. XI. Kinetics of the Flotation Process. K. L. Sutherland	394
Vapor Pressure-Temperature Relationships Among the Branched Paraffin Hydrocarbons. Harry Wiener	425
<b>New Books:</b>	
Organic Analytical Reagents. Vol. II. By Frank J. Welcher. Reviewed by I. M. Kolthoff	431
Symposium on Plasticizers. Reviewed by E. J. Meehan	431
Physical Chemistry. By E. D. Eastman and G. K. Rollefson. Reviewed by William N. Lipscomb	431
Richter-Anschutz: The Chemistry of the Carbon Compounds. Vol. IV. The Heterocyclic Compounds and Organic Free Radicals. Translated by M. F. Darken and A. J. Mee. Reviewed by Lee Irvin Smith	432
Advances in Enzymology. Vol. 7. Edited by F. F. Nord. Reviewed by W. M. Sandstrom	433
Colloids. Their Properties and Applications. By A. G. Ward. Reviewed by L. H. Reyerson	433
The Chemistry of Portland Cement. By Robert Herman Bogue. Reviewed by William N. Lipscomb	434
Tables of the Bessel Functions $J_0(z)$ and $J_1(g)$ for Complex Arguments. Reviewed by S. C. Lind	434
Organic Analytical Reagents. Vol. III. By Frank J. Welcher. Reviewed by I. M. Kolthoff	435
Monograph on the Progress of Research in Holland during the War. Technological and Physical Investigations on Natural and Synthetic Rubbers. By A. J. Wilshut. Reviewed by R. F. Dunbrook	435

## NUMBER 3, MARCH, 1948

Introduction to Symposium on Radiation Chemistry and Photochemistry. S. C. Lind	437
The Relation of Radiation Chemistry to Photochemistry. E. W. R. Steacie	441
Chemical Reactions Produced by Ionization Processes. Joseph O. Hirschfelder	447

Controlled-Electron Reactions. George Gloekler	451
Spontaneous Dissociation of Ions. J. A. Hipple	456
The Mass-Spectrometric Detection of Free Radicals. G. C. Eltenton	463
Electron Microscopy of Radiation Polymerization Products. John H. L. Watson	470
Benzene Formation in the Radiochemical Polymerization of Acetylene. Charles Rosenblum	474
Radiation Chemistry of Aqueous Solutions. A. O. Allen	479
On the Existence of Free Atoms and Radicals in Water and Aqueous Solutions Subjected to Ionizing Radiation. F. S. Dainton	490
Quenching of Fluorescence in Solution. G. K. Rollefson and H. Boaz	518
The Reversible Photobleaching of Dyes and Pigments. Robert Livingston	527
The Photochemistry of the Aldehydes. F. E. Blacet	534
Some Aspects of the Photochemistry of Ketones. W. Albert Noyes, Jr.	546
Transformation of Organic Substances by Alpha Particles and Deuterons. Irving A. Breger	551
Radiation Chemistry. IV. An Interpretation of the Effect of State on the Behavior of Some Organic Compounds and Solutions. Milton Burton	564
Radiation Chemistry of the Geiger-Mueller Counter Discharge. Paul B. Weisz	578
Reactions of Carbon Tetrachloride with Bromine Activated by Isomeric Nuclear Transition and by the Neutron-Gamma Reactions. John E. Willard	585
Chemical Effects in Nuclear Electron Emission. T. H. Davies	595
The Szilard-Chalmers Reaction in the Chain-Reacting Pile. R. R. Williams	603

## NUMBER 4, APRIL, 1948

Polymer Fractionation of Heat-Polymerized Non-Conjugated Vegetable Oils. I. M. Bernstein	613
Reversible Photobleaching of Chlorophyll. John J. McBrady and Robert Livingston	662
The Diffusion and Sedimentation of Sodium Thymonucleate. Herbert Kahler	676
Polyamide Antifoams. I. Relation Between Chemical Constitution and Effectiveness. Arthur L. Jacoby	689
Filtration of Aerosols by Granular Charcoal. Sidney H. Katz and Duncan Macrae	695
Analytical Treatment of Multicomponent Systems. Louis A. Dahl	698
Binary Systems of Some Carboxylic Acids. I. Systems Containing Benzoic Acid or a Substituted Benzoic Acid as One of the Components. Kurt Mislow	729
Binary Systems of Some Carboxylic Acids. II. Systems Containing Heterocyclic Acids as the Components. Kurt Mislow	740
Liquidus-Solidus Points of the Manganese-Nickel System. Jack M. Paul and G. V. Beard	750
The Viscosity of Solutions of Primary Alcohols and Fatty Acids in Benzene and in Carbon Tetrachloride. W. J. Jones, S. T. Bowden, W. W. Yarnold, and W. H. Jones	753
Communication to the Editor: Temperature Control for a Constant-Temperature Water Bath. H. S. Schwenk	761
New Books:	
Organic Chemistry. By Paul Karrer. Translated by A. J. Mee. Reviewed by Lee Irvin Smith	762
Encyclopedia of Chemical Technology. Edited by Raymond E. Kirk and Donald F. Othmer. Reviewed by S. C. Lind	762
Psychrometric Tables and Charts. By O. T. Zimmerman and Irvin Lavine. Reviewed by S. C. Lind	762
Tables of Spherical Bessel Functions. Vol. II. Reviewed by S. C. Lind	762

## NUMBER 5, MAY, 1948

Foaming of Mixtures of Hydrocarbons. J. V. Robinson and W. W. Woods . . . . .	763
Heredity and Environment. Wilder D. Bancroft. . . . .	767
The Effect of Alkaline Electrolytes on Micelle Formation in Soap Solutions. Reynold C. Merrill and Raymond Getty. . . . .	774
Coagulation of Hydrous Ferric Oxide Sols by Electrolytes. Elizabeth F. Tuller and E. I. Fulmer. . . . .	787
The Fixing of Molecular Orientation. John F. Dreyer . . . . .	808
Radiation Chemistry. V. Effect of Molecular Size. Milton Burton . . . . .	810
Beryllium Fluoride in Water and Ethanol Solutions. Robert H. Linnell and Helmut M. Haendler . . . . .	819
The Effect of Temperature and Impurities on Certain Photochemical Reactions in Solids. C. F. Goodeve and M. R. Taylor . . . . .	828
Studies on the Aging of Precipitates and Coprecipitation. XI. The Solubility of Lead Chromate as a Function of the Particle Size. D. R. May and I. M. Kolthoff. . . . .	836
Beaker-Type Centrifugal Sedimentation of Subsieve Solid-Liquid Dispersions. I. Theory. Henry E. Robison and S. W. Martin . . . . .	854
The Osmotic Behavior of Some Colloidal Electrolytes as Determined by Means of the Hill-Baldes Vapor-Tension Apparatus. Manuel N. Fineman and James W. McBain. . . . .	881
Diffusion across Oil-Water Interfaces. Eric Hutchinson . . . . .	897
On the Experimental Bases for the Calculation of the Sulfuric Acid Vapor Pressure above the Sulfuric Acid-Water System. E. Abel. . . . .	908

## NUMBER 6, JUNE, 1948

Solubilization of Dimethylaminoazobenzene in Solutions of Detergents. I. The Effect of Temperature on the Solubilization and upon the Critical Concentra- tion. I. M. Kolthoff and W. Stricks . . . . .	915
Zones of Mutual Protection against Crystallization in Dual-Oxide Systems. Harry B. Weiser, W. O. Milligan, and G. A. Mills . . . . .	942
Melting and Evaporation as Rate Processes. S. S. Penner . . . . .	949
A New and Easily Constructed Precision Coulometer. Elliott L. Abers and Roy F. Newton . . . . .	955
X-Ray Diffraction Analysis of Indium Hydroxide and "Indium Chromate." Ann Palm . . . . .	959
Infrared Absorption Spectra of Some Amino Acids and their Complexes. Irving M. Klotz and Dieter M. Gruen . . . . .	961
Surface Tension of Solids and Methods of Measuring the Same. George Antonoff . . . . .	969
The Application of Flow Birefringence Measurements to High-Polymer Solutions. Michael Wales . . . . .	976
Sedimentation Equilibria of Polydisperse Non-Ideal Solutes. Experiment. Michael Wales, J. W. Williams, J. O. Thompson, and R. H. Ewart . . . . .	983
The Densities of Magnesium-Cadmium Solid Solutions. J. M. Singer and W. E. Wallace. . . . .	999
The Distribution of Thorium Nitrate between Water and Certain Alcohols and Ketones. B. F. Rothschild, C. C. Templeton, and Norris F. Hall. . . . .	1006
Studies on Aging of Precipitates and Coprecipitation. XLI. The Bulkiness and Porosity of Silica Powder. I. Shapiro and I. M. Kolthoff. . . . .	1020
Determination of Sedimentation Constants in the Sharples Supercentrifuge. H. K. Schachman. . . . .	1034
Metal Electrons and Alloy Catalysis. The System Gold-Cadmium. George-Maria Schwab and Soteria Pesmatjoglou . . . . .	1046
The Catalytic Action of Salt Pairs. George-Maria Schwab and Alexander Karatzas . . . . .	1053



Critical Densities and Related Properties of Liquids. Sidney W. Benson . . . . .	1060
Molecular-Weight Determinations of Non-Volatile Substances Based on the Evaporation Velocities of their Solutions. Alexander Schönberg and Mohamed Zaki Barakat. . . . .	1074
Relation of the Physical Properties of the Isomeric Alkanes to Molecular Structure. Surface Tension, Specific Dispersion, and Critical Solution Temperature in Aniline. Harry Wiener . . . . .	1082
Desensitization by Sensitizing Dyes. John Spence and B. H. Carroll . . . . .	1090
Communications to the Editor:	
The Oxidation of Ferrous Sulfite in Air. James R. Pound . . . . .	1103
Anodic Behavior of Aluminum in a Magnetic Field. George Antonoff and Anne Rowley . . . . .	1105
New Books:	
Small Wonder: The Story of Colloids. By Gessner G. Hawley. Reviewed by L. H. Reyerson . . . . .	1108
Physikalische Chemie. By Werner Kuhn. Reviewed by Robert Livingston. . . . .	1109
Organic Syntheses. Volume 27. Edited by R. L. Shriner. Reviewed by R. M. Dodson . . . . .	1109
Colloid Science. A Symposium. Reviewed by J. W. Williams . . . . .	1109
Conversion Factors and Tables. By O. T. Zimmerman and Irvin Lavine. Reviewed by S. C. Lind . . . . .	1110
Research. A Journal of Science and its Applications. Reviewed by S. C. Lind. . . . .	1110

## NUMBER 7, OCTOBER, 1948

Heats of Adsorption. I. Conway Pierce and R. Nelson Smith . . . . .	1111
Heats of Adsorption. II. R. Nelson Smith and Conway Pierce . . . . .	1115
Temperature Lag and Chemical Kinetics. William S. Horton. . . . .	1129
The Vapor Pressure of Benzotrifluoride Measured by the Rodebush Manometer. G. W. Sears and E. R. Hopke . . . . .	1137
Solubility Study of an Aqueous Potassium Laurate-Potassium Silicate System. Reynold C. Merrill . . . . .	1143
Absolute Reaction Kinetics of Tobacco Mosaic Virus and a Proposed Theory of Denaturation. George A. Boyd and James J. Eberl . . . . .	1146
A Note on the Mathematics of Adsorption in Beds. Neal R. Amundson . . . . .	1153
Interfacial Tension at Elevated Pressures and Temperatures. I. A New and Improved Apparatus for Boundary-Tension Measurements by the Pendent-Drop Method. E. A. Hauser and A. S. Michaels . . . . .	1157
Silicic Chemistry. A New Branch of Colloid Science. Ernst A. Hauser. . . . .	1165
Emulsion Polymerization of Styrene. Ernst A. Hauser and Eli Perry. . . . .	1175
An Electron Diffraction Study of Oxide Films Formed on Hastelloy Alloys A, B, C, and D. J. W. Hickman and E. A. Gulbransen . . . . .	1186
Moisture Relationships of Cellulose. I. The Heat of Wetting in Water and in Certain Organic Liquids. Maurice Wahba . . . . .	1197
The Adsorption of Water Vapor on Glass Surfaces. Rashad I. Razouk and Ahmed S. Salem . . . . .	1208
The Surface Tension and Viscosity of Solutions of Uranyl Salts. W. E. Grant, W. J. Darch, S. T. Bowden, and W. J. Jones . . . . .	1227
Weathering Sequence of Clay-Size Minerals in Soils and Sediments. I. Fundamental Generalizations. M. L. Jackson, S. A. Tyler, A. L. Willis, G. A. Bourbeau, and R. P. Pennington . . . . .	1237
Communications to the Editor:	
A Comparison of the Sensitivity of Spectrographic and Radiotracer Methods. Stuart H. Wilson . . . . .	1260

Additions to the Article "Melting and Evaporation as Rate Processes." S. S. Penner . . . . .	1262
Phase Equilibrium Description. V. C. Williams . . . . .	1263
New Books:	
Chemical Process Principles. Part II. Thermodynamics. Part III. Kinetics and Catalysis. By O. A. Hougen and K. M. Watson. Reviewed by N. H. Ceaglske. . . . .	1264
Colorimetric Methods of Analysis. By F. D. Snell and C. T. Snell. Reviewed by I. M. Kolthoff and E. B. Sandell . . . . .	1265
The Water Soluble Gums. By C. L. Mantell. Reviewed by Fred Smith . . . . .	1266
The Systematic Identification of Organic Compounds. By Ralph L. Shriner and Reynold C. Fuson. Reviewed by Scott MacKenzie . . . . .	1266
Surface Chemistry for Industrial Research. By J. J. Bikerman. Reviewed by F. E. Bartell . . . . .	1266
Research in Industry. Its Organization and Management. C. C. Furnas, <i>Editor</i> . Reviewed by Edgar L. Piret . . . . .	1267
Proteins and Amino Acids in Nutrition. Melville Sahyun, <i>Editor</i> Reviewed by Ancel Keys . . . . .	1268
Newer Methods of Preparative Organic Chemistry. Reviewed by Lee Irvin Smith . . . . .	1268
Volmetric Analysis. Vol. II. Titration Methods. By I. M. Kolthoff and V. A. Stenger. Reviewed by Harvey Diehl . . . . .	1269
Monograph on the Progress of Research in Holland during the War. Chemical and Physical Investigations on Dairy Products. By H. Eilers, R. N. J. Saal, and M. van der Waarden. Reviewed by Robert Jenness . . . . .	1271
Organic Analytical Reagents. Vol. IV. By Frank J. Welcher. Reviewed by R. M. Dodson . . . . .	1272
Mechanical Behavior of High Polymers. Vol. VI of High Polymers. By Turner Alfrey, Jr. Reviewed by E. J. Meehan . . . . .	1272
Fatty Acids and their Derivatives. By A. W. Ralston. Reviewed by Donald H. Wheeler . . . . .	1273
Synthetic Methods of Organic Chemistry, A Thesaurus. Vol. I, 1942-1944. By W. Theilheimer. Translated by Hans Wynberg. Reviewed by Lee Irvin Smith . . . . .	1273
Encyclopedia of Chemical Reactions. Vol. II Cadmium, Calcium, Carbon, Cerium, Cesium, Chlorine, Chromium. Compiled and edited by C. A. Jacobson. Reviewed by I. M. Kolthoff . . . . .	1274
The Development of Theoretical Electrochemistry By R. M. Fuoss. Reviewed by I. M. Kolthoff . . . . .	1274
Nuclear Forces. I. By L. Rosenfeld. Reviewed by Edward L. Hill . . . . .	1274
The Chemical Constitution of Natural Fats. By T. P. Hilditch. Reviewed by W. O. Lundberg . . . . .	1275
Isomerism and Isomerization of Organic Compounds. By Ernst David Bergmann Reviewed by R. M. Dodson . . . . .	1276

## NUMBER 8, NOVEMBER, 1948

The Thermodynamic Properties of Sodium Silicate. N. W. McCready . . . . .	1277
The Electrochemical Properties of Mineral Membranes. VIII. The Theory of Selective Membrane Behavior. C. E. Marshall . . . . .	1284
The Pore Size-Surface Area Distribution of a Cracking Catalyst. T. D. Oulton. . . . .	1296
The Kinetics of the Thermal Decomposition of Tertiary Butyl Propionate. Earl Warrick and Paul Fugassi . . . . .	1314
Studies on Aging of Precipitates and Coprecipitation. XLII. Aging of Silver Bromide in the Dry State. I. Shapiro and I. M. Kolthoff. . . . .	1319
Effusion of Gases at Critical Velocities. A Micromethod for Molecular Weights of Gases and Vapors. S. W. Benson and R. Coswell . . . . .	1332

Homogeneity and the Electrophoretic Behavior of Some Proteins. II. Reversible Spreading and Steady-State Boundary Criteria. E. A. Anderson and R. A. Alberty . . . . .	1345
A Contribution to the Knowledge of Sodium Contamination on Cracking Catalysts. M. O. Baker, S. D. Chesnutt, and T. P. Wier, Jr. . . . .	1364
Colloid Properties of Some Western Clays. E. R. Harrington . . . . .	1373
Thixotropic Qualities of Soap-Hydrocarbon Systems. C. J. Boner . . . . .	1383
A Semimicro Diffusion Method for the Characterization of High-Polymer Fractions M. C. Brooks and R. M. Badger . . . . .	1390
Colloid Properties of Layer Silicates. W. F. Bradley and R. E. Grim . . . . .	1404

## NUMBER 9, DECEMBER, 1948

The Effect of Water and Other Additives on the Fiber Structure of Calcium Soap Greases D. H. Birdsall and B. B. Farrington . . . . .	1415
Properties of Systems of Calcium Stearate and Cetane as Deduced from X-Ray Diffraction Patterns. R. D. Vold and Marjorie J. Vold . . . . .	1424
Use of Aluminum Soaps and Other Fuel Thickeners in Gelling Gasolines. W. H. C' Rueggeberg . . . . .	1444
Rheological Properties of Incendiary Gels. Leo Finkelstein . . . . .	1460
Variability and Inhomogeneity of Aluminum Dilaurate. K. J. Mysels and James W. McBain . . . . .	1471
The Effect of Additives on the Physical-Chemical Properties of Soap Gels in Organic Solvents. G. S. Hattiangdi, S. P. Adarkar, J. P. Jassawalla, and M. Prasad . . . . .	1481
The Electrical Behavior of Dodecylammonium Chloride in Water-Organic Solvent Systems. A. W. Ralston and D. M. Eggenberger . . . . .	1494
Soap-in-Oil Systems. A. S. C. Lawrence . . . . .	1504
New Books:	
Weiss Magnetons as Components of Nuclear and Subnuclear Structures. By Theodore van Schelven Reviewed by S. Sugden . . . . .	1511
Inorganic Process Industries. By Kenneth A. Kobe. Reviewed by Charles A. Mann . . . . .	1511
Molybdenum Steels, Irons, Alloys. By R. S. Archer, J. Z. Briggs, and C. M. Loeb, Jr. Reviewed by R. L. Dowdell . . . . .	1512



## ERRATA

*Volume 52, Number 1, January, 1948*

*Page 242:* Equation 28 should read

$$M_{0z} = \frac{c_x}{\int_{c_a}^{c_x} \frac{dc_x}{M_{1z}} + K_a}$$

*Volume 50, Number 4, July, 1946*

*Page 348:* In the description of the standard taper ground joint below figure 1 substitute "19/22" for "11/22".



## ERRATA

*Volume 53, Number 9, December, 1949*

*Page 1460:* Correction to the paper entitled "The Theory of Absolute Reaction Rates Applied to the Study of Polarographic Waves," by Henry Eyring, Leon Marker, and Ting-Chang Kwoh:

The advantage of the method of plotting the first derivative of the polarographic wave to reveal the liberation of more than one product was called to our attention by Dr. Karl Zimmerman, who presented it at the January 1947 meeting of the Oregon Academy of Sciences and later in amplified form at the 115th Meeting of the American Chemical Society in San Francisco, April, 1949. This was practically contemporaneous with Heyrovsky's similar treatment (*Analyst* **72**, 229 (1947)). Through an oversight this information was omitted from the authors' paper.

*Volume 54, Number 2, February, 1950*

In the table of contents the page reference for the sixth article should be 239.

*Pages 237-8:* In the paragraph beginning "Table 1 summarizes" delete from "The most striking feature" to the end of the paragraph, the last word to be deleted being "chemisorption."





# THE POTENTIALS OF FALLING DROPS<sup>1</sup>

A. FRUMKIN AND J. BAGOTSKAJA

*Institute of Physical Chemistry, Academy of Sciences, University of Moscow,  
Moscow, U.S.S.R.*

*Received August 25, 1947*

According to the theory developed by Frumkin and Levich (3, 4), the velocity of fall of a mercury drop of radius  $a$  in a viscous medium is related to the electrical conductivity of the medium and the charge of the drop by the following expression:

$$U = \frac{2}{9} \frac{(\rho - \rho')ga^2}{\mu} \frac{3\mu + 3\mu' + \epsilon^2\kappa^{-1}}{2\mu + 3\mu' + \epsilon^2\kappa^{-1}} \quad (1)$$

where  $\mu$  and  $\mu'$  are the viscosities of the medium and the mercury, respectively,  $\epsilon$  is the charge per unit surface of the mercury,  $\kappa$  is the electrical conductivity of the medium,  $\rho'$  and  $\rho$  are the densities of the medium and the mercury, and  $g$  is the acceleration of gravity. This relationship derives from the effect of the charge on the tangential motion of the surface. The tangential motion drags along the charges of the double layer, reducing their density in the front (lower) part of the drop and increasing it in the rear (upper); as a result, a potential difference is set up between the two ends of the drop which retards the tangential motion. This potential difference is continually evened out, owing to the electrical conductivity of the medium. The relation between the velocity of the tangential motion of the surface at the equator of the drop,  $V$ , and the velocity of fall,  $U$ , is given by the formula:

$$V = \frac{1}{3} \frac{(\rho - \rho')ga^2}{2\mu + 3\mu' + \epsilon^2\kappa^{-1}} = \frac{3U\mu}{2(3\mu + 3\mu' + \epsilon^2\kappa^{-1})} \quad (2)$$

The term  $\epsilon^2\kappa^{-1}$  in the denominator results from the above retardation effect due to the electric field. At  $\frac{\epsilon^2}{3\kappa} \gg \mu + \mu'$ ,  $V \sim 0$  and  $U \sim U_s$ , where  $U_s$  is the velocity of fall according to Stokes's formula, i.e., the drop falls like a solid sphere. At  $\epsilon = 0$ ,  $V$  takes on its maximal value equal to  $\frac{U\mu}{2(\mu + \mu')}$  and

$$U = U_s \frac{3\mu + 3\mu'}{2\mu + 3\mu'}$$

It is assumed in the theory that the drop can be considered ideally polarizable, i.e., that ions can neither be formed nor discharged on its surface, and that the changes in the charge distribution due to the motion are relatively small. The

<sup>1</sup> Presented at the Twenty-first National Colloid Symposium, which was held under the auspices of the Division of Colloid Chemistry of the American Chemical Society at Palo Alto, California, June 18-20, 1947.

dependence of  $U/U_*$  on  $\epsilon$  and  $\kappa$  derived from this theory has been experimentally confirmed (2). It is also possible to determine by this theory the magnitude of the field that is set up during the fall of a drop from the values of  $U$ ,  $\epsilon$ , and  $\kappa$ . The respective mathematical expressions are given in the papers of Frumkin and Levich (3, 4). We shall present them here in a slightly different form, which more clearly reveals their physical significance. The potential distribution in a medium in which a drop of radius  $a$  is falling is given by the formula (3)

$$\varphi = \frac{\epsilon(\rho - \rho')ga^4}{3\kappa(2\mu + 3\mu' + \epsilon^2\kappa^{-1})} \frac{\cos \theta}{r^2} \quad (3)$$

where  $r$  is the distance from the center of the drop and  $\theta$  the angle between the radius-vector and the direction of fall; the potential  $\varphi$  is taken equal to zero at a great distance from the drop. Inside the drop  $\varphi_*$  = constant due to metallic conductivity. According to equations 1 and 2, equation 3 can be written in the following form:

$$\varphi = \frac{\epsilon Va^2}{\kappa} \frac{\cos \theta}{r^2} \quad (4)$$

At the surface of the drop

$$\varphi_a = \frac{\epsilon V}{\kappa} \cos \theta \quad (5)$$

Equation 4 describes the field of a dipole situated in the center of the drop whose moment,  $M$ , equals

$$M = \frac{\epsilon Va^2 K}{\kappa} \quad (6)$$

where  $K$  is the dielectric constant of the medium; the positive end of the dipole is directed downward.<sup>2</sup> It follows from equation 5 that there exists a potential difference

$$\Delta\Phi = \frac{2\epsilon V}{\kappa} = \frac{2M}{Ka^2} = \frac{2}{3} \frac{\epsilon(\rho - \rho')ga^2}{\kappa(2\mu + 3\mu' + \epsilon^2\kappa^{-1})} \quad (14)$$

<sup>2</sup> The magnitude of the dipole moment is determined by the distribution of charge density in the double layer and of free charges on the surface of the drop. Each surface element,  $ds$ , of the double layer contributes a vertical component of the dipole moment equal to

$$\frac{K}{4\pi} (\varphi_i - \varphi_a) \cos \theta \, ds = -\frac{K}{4\pi} \left( \varphi_i - \frac{\epsilon V}{\kappa} \cos \theta \right) \cos \theta \, ds \quad (7)$$

Furthermore, the surface of the drop carries free charges whose density, according to equation 4, is equal to:

$$-\frac{K}{4\pi} \left( \frac{\partial \varphi}{\partial r} \right)_{r=a} = \frac{K}{4\pi} \times \frac{2\epsilon V}{\kappa a} \cos \theta \quad (8)$$

The free charge contributes a component of the dipole moment on a surface element  $ds$  equal to:

$$\frac{K}{4\pi} \times \frac{2\epsilon V}{\kappa a} \cos \theta \times a \cos \theta \, ds = \frac{K}{4\pi} \times \frac{2\epsilon V}{\kappa} \cos^2 \theta \, ds \quad (9)$$

between the front and rear of the drop. Experimentally we can measure the potential difference between various points of a tube in which drops are falling (potential of falling drops). Let us denote by  $E$  the change in potential per unit length of the tube and assume, furthermore, that the drops fall one after another along a single vertical line. Let the number of drops simultaneously present in unit length of the tube be  $N$ , and the cross-sections of the tube and the drop be  $S$  and  $s$ , respectively. Then, obviously:

$$E = \frac{4\pi}{K} \frac{NM}{S} = \frac{4\pi a^2 \epsilon V}{\kappa S} N = 2N\Delta\Phi \frac{s}{S} \quad (15)$$

$4\pi a^2 \epsilon$  gives the total charge of the inner sheet of the drop  $\epsilon$ . Finally, from equation 15 we obtain for the current flowing in the external circuit when the column of liquid is short-circuited:

$$I_0 = E\kappa S = 4\pi a^2 \epsilon VN = \epsilon VN \quad (16)$$

Adding expressions 7 and 9 and integrating over the surface of the sphere we obtain:

$$M = -\frac{K}{4\pi} \int_0^\pi \varphi_1 a^2 \cos \theta \sin \theta d\theta + \frac{K}{4\pi} \int_0^\pi \frac{6\pi \epsilon V a^2}{\kappa} \cos^2 \theta \sin \theta d\theta = \frac{Ka^2 \epsilon V}{\kappa}$$

i.e., equation 6

The appearance of a dipole moment of the drop of stationary value  $M$  can be pictured as follows: If the potential differences arising from the motion were not evened out by the electrical conductivity of the medium, the dipole moment of the drop would increase continuously, owing to convective transfer of the double-layer charges. It can easily be shown that its increment in unit time would be

$$\frac{2aV\epsilon K}{C} \quad (10)$$

where  $C$  is the capacity of the double layer.

The radial current on unit surface of the drop is evidently equal to

$$j = \kappa \left( \frac{\partial \varphi}{\partial r} \right)_{r=a} = -\frac{2\epsilon V}{a} \cos \theta = -\frac{2M\kappa}{Ka^3} \cos \theta \quad (11)$$

where the current flowing to the drop is considered positive. The charge density on the outer sheet of the double layer differs from its equilibrium value

$$\epsilon = -C\varphi_1$$

by a magnitude

$$\Delta\epsilon = C\varphi_a = \frac{C\epsilon V}{\pi} \cos \theta = \frac{CM}{Ka^2} \cos \theta \quad (12)$$

It follows from a comparison of equations 11 and 12 that the inhomogeneity of the charge distribution arising from the motion of the surface should decrease by a factor of  $1/\epsilon$  in time

$$\tau = -\frac{\Delta\epsilon}{j} = \frac{1}{2} \frac{Ca}{\kappa} \quad (13)$$

The quantity  $\tau$  thus expresses the relaxation time of the electrical field of the drop. Multiplying equation 10 by equation 13 we actually obtain:

$$\frac{2aV_0\epsilon K}{C} \times \frac{1}{2} \frac{Ca}{\kappa} = \frac{\epsilon Va^2 K}{\kappa}$$

Expression 16 can be obtained, in order of magnitude, by the following elementary considerations. The motion of the surface transfers in unit time through the equatorial cross-section of the drop a quantity of electricity equal to  $2\pi a\epsilon V$  across a distance of the order of  $2a$ ; this is equivalent to a current of  $4\pi a^2\epsilon V = \epsilon V$ , or  $\epsilon VN$  for  $N$  drops. Such considerations cannot, of course, give the value of the numerical coefficient, which can be found only from more complicated computations.

Equation 15 can also be written down in another form, more convenient for experimental verification. Denote by  $E_{12}$  the potential difference between two points of the column a distance  $l$  apart. Then, referring to equation 2 we have:

$$E_{12} = \frac{4\pi a^2 \epsilon V}{\kappa S} Nl = \frac{6\pi a^2 U\mu\epsilon Nl}{\kappa S(3\mu + 3\mu' + \epsilon^2\kappa^{-1})} \quad (17)$$

Let the drops fall one after another and let the time between the formation of two successive drops (the dropping time) be  $t_0$ . Then  $UN = 1/t_0$ ; hence

$$E_{12} = \frac{6\pi a^2 \mu\epsilon l}{\kappa S t_0 (3\mu + 3\mu' + \epsilon^2\kappa^{-1})} = \frac{6a^2 \mu\epsilon l}{\kappa R^2 t_0 (3\mu + 3\mu' + \epsilon^2\kappa^{-1})} \quad (18)$$

where  $R$  is the radius of the tube in which the drops are falling.

Frumkin and Levich (3) attempted to verify these relations on Bach's measurements (1) of the currents arising when mercury drops fall in aqueous solutions. However, in the conditions of Bach's experiments the quantity  $\epsilon$  could not even approximately be considered constant, neither was it determined experimentally. Therefore, despite the approximate agreement between the computed and observed values of  $I_0$ , this verification cannot be considered sufficiently convincing.

In the present investigation the relations derived were verified under conditions approaching as closely as possible the assumptions lying at the basis of the theory. The hydrodynamical theory was worked out on the assumption that the Reynolds number for the fall of the drops was less than unity; therefore, in this investigation, as in that of Bagotskaja and Frumkin (2), solutions of electrolytes in glycerol were chosen for the medium. Since the viscosity of mercury is small compared to that of glycerol, we can in this case neglect  $\mu'$  in comparison with  $\mu$  and write equation 18 in the following form:

$$E_{12} = \frac{6a^2 \mu\epsilon l}{\kappa R^2 t_0 (3\mu + \epsilon^2\kappa^{-1})} \quad (18a)$$

The measurements were carried out with the apparatus depicted in figure 1. Under a pressure of about 25 cm. of mercury, drops of mercury 0.60–0.65 mm. in radius were forced out of a capillary into a solution of potassium bromide in glycerol with a small water content (1–2 per cent). The dropping time was approximately 0.4 sec., the viscosity of the solutions at 20°C. 8–14 poises, and the velocity of fall of the drops about 1.0–1.2 cm./sec. Prior to the measurements the solution heated to 50–60°C. (to reduce the viscosity) was saturated for 6 hr. in a side vessel (B) with electrolytic hydrogen purified from oxygen over palladium and dried over calcium chloride. In addition, hydrogen was passed

through the solution at room temperature for about 24 hr. The solution must be scrupulously purified from oxygen in order that the initial charge of the drop should not change during its fall. The oxygen-free solution was forced by hydrogen pressure into the measuring vessel A, a vertical tube of radius 0.76 cm. preliminarily flushed with hydrogen. The solutions were prepared from chemically pure glycerol which was not purified any further. Potassium bromide was

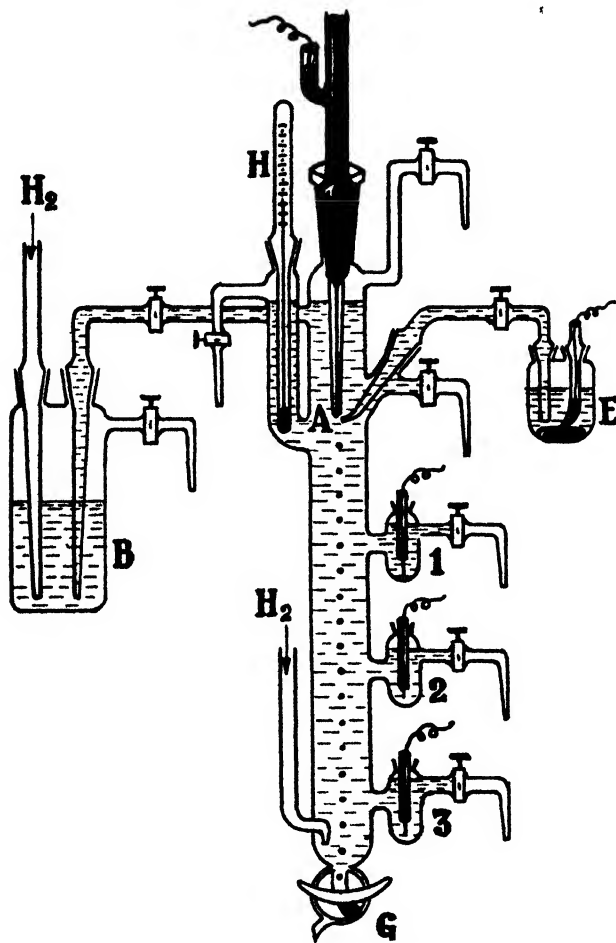


FIG. 1. The apparatus

twice recrystallized and heated to 400°C. before use. The solutions were prepared directly in the vessel B. The potential arising from the fall of the drops was measured by means of silver-silver bromide electrodes 1, 2, and 3, prepared by the electrolytic deposition of silver on platinum followed by anodic polarization in a potassium bromide solution. The distance between electrodes 1 and 2 was 4.0 cm.; that between electrodes 2 and 3 was 5.7 cm. The drops were given a definite charge by means of an E.M.F. in the circuit consisting of the auxiliary

electrode E, the solution, and the growing drop. The auxiliary electrode consisted usually of a mercury surface in the same solution;  $\epsilon$  was computed from the equation  $i = \epsilon A$ , where  $i$  is the mean charging current measured by a sensitive galvanometer, and  $A$  is the surface area of the drops formed in unit time. The latter was calculated from the radius of the drops and the dropping period. The radius of the drops under the given conditions of dropping was determined from their weight. To this end the drops were collected in the lower part of the tube A and evacuated therefrom by way of the stopcock g. The radius of the drops varied slightly during one series of measurements, depending on the value of the charge, and the potentials of the falling drops were calculated using the value of the radius determined experimentally under the given conditions. The temperature was measured by a thermometer (H) immersed in the solution. Since the temperature varied slightly during a series of measurements (within  $0.5^\circ\text{C}.$ ), the viscosity and electrical conductivity of the medium were determined for several close temperatures by the usual methods and the values corresponding to the experimental conditions were found by interpolation. The potential difference between the silver-silver bromide electrodes was measured by a d.c. cathode voltmeter of sensitivity approximately 1 mv. per scale division. Since the internal resistance of the entire system was very great, the apparatus was carefully insulated by paraffin supports and shielded from external electrical influences by a grounded Faraday cage. Since the potentials of the silver-silver bromide electrodes differed and, in addition, varied slightly with time, the quantities  $E_{12}$  and  $E_{23}$  were determined from the shift of the potential difference between electrodes 2 and 1 or 1 and 2 during the dropping of the mercury relative to the value observed after the dropping was stopped.

Figures 2, 3, and 4 show curves representing the observed dependence of  $E_{12}$  and  $E_{23}$  on the charge density on the drop (full-line curves) and curves computed by equation 18a at various values of  $\kappa$  (dotted lines). The quantity  $\epsilon$  was varied from  $30\text{--}40 \times 10^{-6}$  to  $-16 \times 10^{-6}$  coulombs/cm.<sup>2</sup> At more negative values of  $\epsilon$  the dropping became irregular. The agreement between the experimental and theoretical values of  $E$  can be considered quite satisfactory, especially if it is borne in mind that the theoretical formula contains no arbitrary constants. The discrepancy is somewhat greater for the smallest values of  $\kappa$ ; we shall return to this circumstance later on. In accordance with equation 17a  $|E_{23}|$  was always greater than  $|E_{12}|$ , since the distance between the electrodes 3 and 2 exceeded that between 2 and 1 by a factor of 1.42. As equation 18a demands, the quantity  $E$  increases with decreasing  $\kappa$ ; as  $\epsilon$  increases in absolute value,  $E$  increases, passes through a maximum, and then drops off. If  $t_0$  and  $a$  are considered independent of  $\epsilon$ , then according to equation 18a, the maximal value of  $E$  corresponds to  $\epsilon = (3\mu\kappa)^{\frac{1}{2}}$ . The maximum is clearly pronounced on the experimental  $E, \epsilon$  curves when the electrical conductivity of the solution is small enough.

There are, however, some differences between the experimental and the theoretical curves. In the first place, the experimental values in all cases pass through zero not at  $\epsilon = 0$ , as the theory demands, but at somewhat more negative values of  $\epsilon$ , so that the observed  $E, \epsilon$  curves are slightly displaced towards more negative

$\epsilon$  relative to the theoretical curves. A similar shift was observed in measurements of the velocity of fall of drops as a function of their charge (2). It was

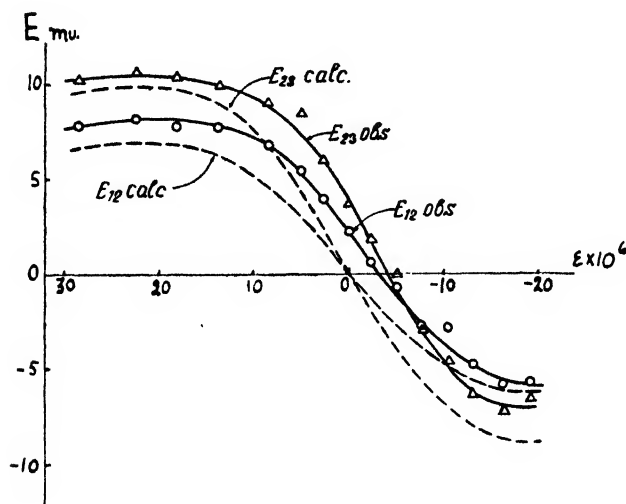


FIG. 2. Relation between the potentials of falling drops  $E_{12}$  and  $E_{23}$  and charge density  $\epsilon$  in glycerol.  $\sim 1$   $N$  potassium bromide;  $\mu = 7.8$ ;  $\kappa = 2.1 \times 10^{-4}$ . ---, theoretical curves; O, experimental values of  $E_{12}$ ;  $\Delta$ , experimental values of  $E_{23}$ .

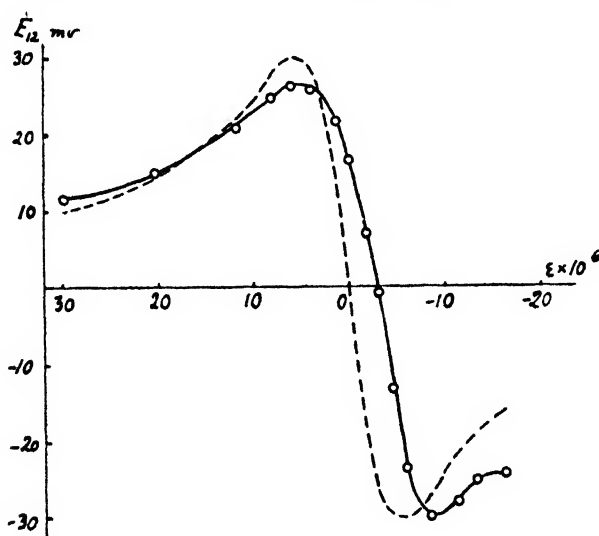


FIG. 3. Relation between the potential of falling drops  $E_{12}$  and charge density  $\epsilon$ . 0.03  $N$  potassium bromide;  $\mu = 9.0$ ;  $\kappa = 1.1 \times 10^{-5}$ . ---, theoretical curve; O, experimental values.

suggested in that paper that the displacement was due to traces of oxygen or other depolarizers (e.g., mercury ions) in the solution, which during the fall of the drop slightly shift its charge in the positive direction. Hence, in order to

obtain the zero value of  $\epsilon$  midway between the electrodes, which should evidently correspond to the measured zero value of  $E$ , we must give the drop an initial negative charge. This explanation is corroborated by the circumstance that the displacement of the experimental curve relative to the theoretical is greater for the  $E_{23}$  curves than for the  $E_{12}$  curves (figure 2). Since the path of the drops is longer in the first case than in the second, the increase of the initial charge due to diffusion of the depolarizer from the solution to the surface of the drop should be greater.<sup>3</sup> The effect of variation of the charge during the growth and fall of the

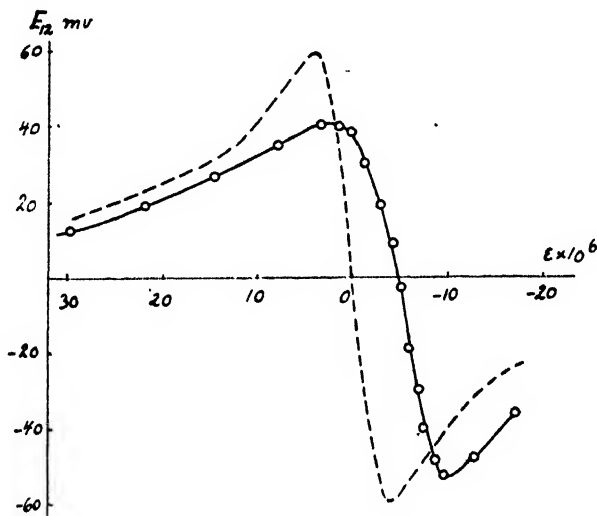


FIG. 4. Relation between the potential of falling drops  $E_{12}$  and charge density  $\epsilon$ . 0.015 *N* potassium bromide;  $\mu = 13.5$ ;  $\kappa = 4.1 \times 10^{-6}$ . ---, theoretical curve; O, experimental values.

drops on the potentials  $E_{21}$  and  $E_{32}$  is much stronger when purification of the solution from oxygen has been less thorough. Figure 5 shows curves obtained after a purification which was limited to bubbling hydrogen through the glycerol for  $1\frac{1}{2}$  hr. at room temperature. As appears from the figure, in this case the variation of the initial value of  $\epsilon$  hardly affects the values of  $E$  and only with very large initial negative  $\epsilon$  does  $E$  slightly decrease. Evidently, under the action of the dissolved oxygen, the charge of the drop approaches a definite

<sup>3</sup> In this case, however, the quantitative relations are not quite clear. Indeed, the distance from the tip of the capillary to the midpoint between electrodes 3 and 2 was 8.8 cm. and to the midpoint between electrodes 1 and 2, 4 cm. The ratio of the displacements of the zero values of  $E_{23}$  and  $E_{12}$  compared with the point  $\epsilon = 0$  should therefore have been 2.2. Actually, the mean value of this ratio from four series of measurements was 1.4. This discrepancy can only be explained by assuming that the change in the charge occurs to a considerable extent during the growth of the drop. Computations show that if the concentration of the depolarizer were the same throughout the system, the variation of the charge during the growth of the drop could be neglected. It is, however, possible that the concentration of the depolarizer was higher near the tip of the capillary than on the remaining path of the drop, owing to the proximity of the electrode F.



positive value, practically independent of its initial value. A comparison of the experimental and the theoretical curves shows another source of divergence between theory and experiment which is more strongly felt in more dilute solutions. As appears from figure 4, at sufficiently small values of  $\kappa$  the maximum observed values of  $E$  are definitely lower than the theoretical, which especially affects the positive branch of the curve. The cause of this divergence becomes apparent if, using equation 15, we compute the potential differences between the

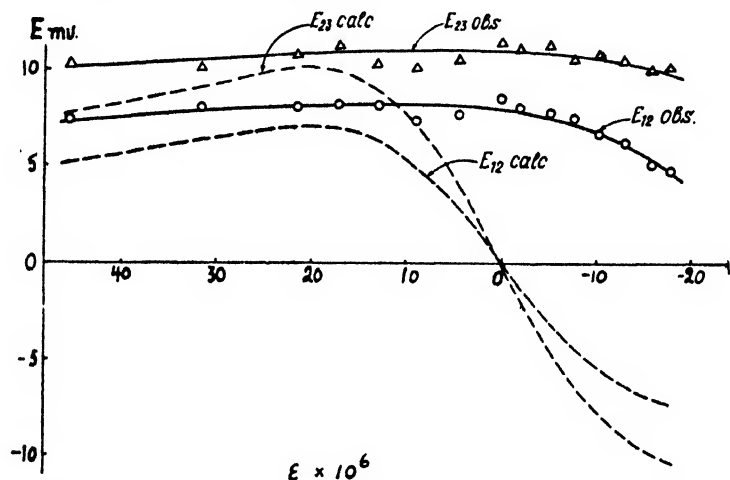


FIG. 5. Relation between the potentials of falling drops  $E_{12}$  and charge density  $\epsilon$  in glycerol after incomplete removal of oxygen.  $\sim 1 N$  potassium bromide;  $\mu = 8.3$ ;  $\kappa = 1.9 \times 10^{-4}$ . ---, theoretical curves; O, experimental values of  $E_{12}$ ;  $\Delta$ , experimental values of  $E_{23}$ .

TABLE 1  
Maximum values of  $\Delta\Phi$  in solutions of different conductivity

$\kappa$	$\mu$	$E_{12}$ (OBSERVED) MAXIMUM POSITIVE VALUE	$Nl$	$\Delta\Phi$
		volts		volts
$1.99 \times 10^{-4}$	7.9	0.003	6.4	0.10
$1.06 \times 10^{-5}$	9.3	0.025	7.5	0.27
$4.15 \times 10^{-6}$	13.1	0.040	8.0	0.36

front and rear ends of the drop  $\Delta\Phi$  which correspond to the maximum observed values of  $E$  in solutions of different conductivity.

As appears from table 1, the values of  $\Delta\Phi$  are very large and in dilute solutions at any rate are comparable to the potential difference in the double layer of the drop corresponding to an even distribution of charge. The latter as a rule was not measured in our experiments but can be estimated from the values of  $\epsilon$  and the capacity of the double layer. For example, in a solution with  $\kappa = 4.2 \times 10^{-6}$  the experimental maximum value of  $E_{12}$  corresponded to a positive  $\epsilon$  equal to

$7.5 \times 10^{-6}$  (if the variation of  $\epsilon$  during the fall of the drop is taken into consideration, i.e., assuming that  $\epsilon = 0$  at  $E_{12} = 0$ ); whence, putting the capacity of the double layer equal to  $30 \times 10^{-6}$ , we find  $\varphi_i - \varphi_a = 0.25$ . Thus in dilute solutions the variation of the potential distribution due to the tangential motion of the surface is so great that it completely distorts the initial charge distribution. Under these conditions the charge density at the front end of the drop should approach zero independently of its initial value, whereas at the opposite end it can grow to values at which (in the case of positive  $\epsilon$ ) ionization of the mercury begins. Under these conditions a further dilution of the solution cannot therefore cause a marked increase in  $\Delta\Phi$  or  $E$ .

If we proceed from the theoretical rather than the experimental values of  $\Delta\Phi$ , the limits of quantitative application of the theory can be established as follows: It has already been pointed out that for the theory to be strictly applicable the variation of the potential difference between mercury and solution must be small compared with its initial value, i.e.

$$\frac{1}{2}\Delta\Phi < \frac{\epsilon}{C}$$

whence,

$$\frac{\epsilon V}{\kappa} < \frac{\epsilon}{C}$$

and

$$\kappa > VC$$

The most interesting case is that when  $\Delta\Phi$  reaches its maximum value. It follows from equation 14 that the maximum value of  $\Delta\Phi$  corresponds to  $\epsilon = (2\mu C)^{\frac{1}{2}}$  and  $V = \frac{2}{3} U_s$ . If we put  $U_s \sim 1$  and  $C \sim 30 \times 10^{-6}$ , then from condition 19 we obtain:

$$\kappa > 10^{-5}$$

Our measurements were thus carried out up to values which already lie outside the lower limit of the strict applicability of the theory for drops of the given dimensions.

The agreement between the theory developed and the results of measurements of the potentials of falling drops leads to the following interesting conclusion. The mathematical relations were derived on the assumption that extension or compression affect the potential difference in the double layer only insofar as they change the charge density  $\epsilon$ .

This assumption remains valid only if the relaxation time of the double layer itself is small compared with the computed relaxation time of the electrical field of the drop as a whole (equation 13):

$$\tau = \frac{1}{2} \frac{Ca}{\kappa}$$

At  $C \sim 3 \times 10^{-5}$ ,  $a \sim 6 \times 10^{-2}$ , and  $\kappa \sim 4 \times 10^{-4}$ ,  $\tau \sim 2 \times 10^{-3}$ . It thus follows from our experiments that the relaxation time of the double layer for glycerol solutions is less than  $2 \times 10^{-3}$ . In the case of aqueous solutions, for which however equally trustworthy measurements are not yet available, similar calculations show that the upper limit for the relaxation time of the double layer is of the order of  $10^{-5}$  or even less.

It is of interest to compare the observed values of the potentials of fall of drops with the values of the potentials which should arise under similar conditions of fall of solid particles (Dorn effect). The mathematical expression for this case was deduced by Smoluchowski (5). In our notation it has the form:

$$E = \frac{K(\varphi_i - \varphi_a)}{3\mu\kappa S} (\rho - \rho')ga^3N \quad (20)$$

The quantity  $\varphi_i - \varphi_a$  here expresses the ordinary  $\zeta$ -potential of colloid chemistry. Putting  $\varphi_i - \varphi_a = 0.1$  and  $\kappa = 4 \times 10^{-6} \text{ ohm}^{-1} \text{ cm.}^{-1}$  under the conditions of our experiments, we obtain by Smoluchowski's formula:

$$E \sim 10^{-7} \text{ volts/cm.}$$

whereas the observed values of  $E$  were  $10^{-2}$  volts/cm., i.e., they exceeded the calculated values for solid spheres by a factor of  $10^5$ . In solutions of higher electrical conductivity the difference will be even greater.

#### SUMMARY

It is shown that when mercury drops fall in a viscous medium the tangential motion of the surface displaces the charges of the double layer from the lower to the upper end of the drop, giving rise to a potential difference between the two ends. For drops of radius 0.6 mm., viscosity of the solution 13, and electrical conductivity  $4 \times 10^{-6}$  the potential difference between the lower and upper ends of the drop reaches 0.4 volt. Measurements of the potential differences between various points of a liquid column in which drops are falling bear out the correctness of the expressions for the potentials of falling drops derived by Frumkin and Levich. In accordance with the theory, with increase in the charge density the absolute value of the potential of falling drops first increases, reaches a maximum, and then drops off. It also follows from these measurements that the relaxation time of the electrical double layer at the mercury-solution interface in glycerol is less than  $2 \times 10^{-3}$  sec.

#### REFERENCES

- (1) BACH: *Acta Physicochim. U.R.S.S.* **1**, 27 (1934).
- (2) BAGOTSKAJA AND FRUMKIN: *Compt. rend. acad. sci. U.R.S.S.* **55**, 135 (1947).
- (3) FRUMKIN AND LEVICH: *Acta Physicochim. U.R.S.S.* **21**, 193 (1946).  
FRUMKIN: *J. Colloid Sci.* **1**, 277 (1946).
- (4) LEVICH: *Acta Physicochim. U.R.S.S.*, in press.
- (5) SMOLUCHOWSKI: In Graetz's *Handbuch der Elektrizität und des Magnetismus*, Vol. 2, p. 385 (1914).

# SOLUBILIZATION OF WATER-INSOLUBLE DYE BY COLLOIDAL ELECTROLYTES AND NON-IONIZING DETERGENTS<sup>1</sup>

JAMES W. MCBAIN, ARTHUR G. WILDER,<sup>2</sup> AND R. C. MERRILL, JR.<sup>3</sup>

*Department of Chemistry, Stanford University, California*

*Received August 25, 1947*

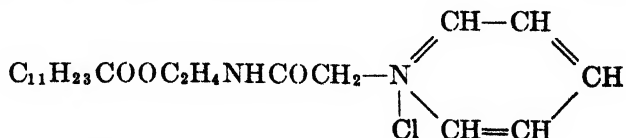
Solubilization (4) consists in the spontaneous passage of an insoluble substance into a dilute solution of a detergent to form a thermodynamically stable colloidal solution. Recent studies from the Stanford laboratory are those of Merrill (6, 8), Sister Agnes Ann Green (3, 5), and Richards (7). An extensive survey of the relevant literature has been given by Sister Agnes Ann Green (2).

The present work describes the solubilization of water-insoluble dye over a complete range of concentration from 0 to 100 per cent detergent, using hexanolamine oleate and two non-ionic detergents. These and other results are contrasted with ordinary solution in mixed solvents. In each case strong solubilization appears as soon as colloid is present. Other results refer to solubilization by bile salts and the enhancing effect of added sodium salts thereon. Some comparisons are made with the osmotic behavior of the respective detergents.

## MATERIALS AND METHOD

The experimental method has been described previously (5). Well-crystallized dye was used, measurements being made after the first week of mild agitation on successive samples until constancy indicated that equilibrium was attained. Each sample was centrifuged for 30 min. and allowed to stand for 24 hr. before taking clear supernatant liquid for analysis.

The hexanolamine oleate was prepared by mixing equivalent weights of oleic acid (Kahlbaum) and hexanolamine, kindly supplied by the Shell Development Company. Nonaethylene glycol monolaurate was obtained from the Glyco Products Co., Inc. The pure bile acids were supplied by Riedel de Haen and neutralized with carbon dioxide-free sodium hydroxide. Detergent "X" is a condensation product of isoöctylphenol<sup>4</sup> and ethylene oxide. Triton NE (polyalkylene ethyl alcohol) was supplied by Rohm and Haas. The Catol 607 was especially purified by the Emulsol Corporation; it has the following formula:



<sup>1</sup> Presented at the Twenty-first National Colloid Symposium, which was held under the auspices of the Division of Colloid Chemistry of the American Chemical Society at Palo Alto, California, June 18–20, 1947.

<sup>2</sup> Present address: Permanente Metals Corporation, Permanente, California.

<sup>3</sup> Present address: Philadelphia Quartz Company, Philadelphia, Pennsylvania.

<sup>4</sup> (2-Methylheptyl)phenol.

The purified Oronite sulfonate was supplied by the Oronite Chemical Company. It is a sodium sulfonate of a trisubstituted benzene having a total of eighteen carbon atoms in the three substituting alkyl groups. It contained 67.57 per cent active material, 32 per cent water, and 0.40 per cent sodium sulfate.

The dyes were supplied by the Calco Company, and were Orange OT (F.D. and C. Orange No. 2; 1-*o*-tolylazo-2-naphthol) and Yellow AB (F.D. and C. Yellow No. 3; phenolazonaphthalamine).

#### RESULTS WITH HEXANOLAMINE OLEATE

The colloidal electrolytic detergent hexanolamine oleate was selected for study because it offered an opportunity to compare solubilization in an isotropic solution with that in an anisotropic solution at moderate temperature, and also because it is miscible with water in all proportions. An equilibrium temperature

TABLE 1

*Solubilization of Orange OT (mol. wt. 262.3) in aqueous solutions of hexanolamine oleate (mol. wt. 400.0) at 70°C.*

DETERGENT	DYE PER MOLE OF DETERGENT	MOLAR RATIO $\times 10^2$ DYE/SOAP
<i>weight per cent</i>	<i>grams</i>	
0.5	7.56	2.86*
1.0	8.32	3.18*
5.0	8.20	3.12*
10.0	5.30	2.02
16.66	5.38	2.05
20.0	5.50	2.10
25.0	5.44	2.07
50.0	7.12	2.72
90.0	12.90	4.92
100.0	16.20	6.18

\* Indicates suspending action.

of 70°C. was chosen for most of the studies with this detergent, since solutions above approximately 10 per cent are viscous solutions, or even jellies, at room temperatures. The data obtained are summarized in table 1. The solubilization decreases smoothly from 100 per cent detergent down to 10 per cent; that is, from an isotropic phase through two liquid-crystalline phases, and the ordinary isotropic soap solution. Below 5 per cent the values appear erratic, owing to suspending action on small particles or fragments of dye.

The phase diagram of Gonick and McBain (1) had to be partially revised, in that it was found that at 70°C. the heterogeneous region between isotropic solution and the first liquid-crystalline phase extended from 15 per cent to 30 per cent instead of from 28 per cent to 34 per cent. The revised phase diagram is given in figure 1. The circles represent the points originally established by Gonick and McBain, and the crosses the values which were obtained by sealing samples of various concentrations in evacuated tubes and observing them be-

tween crossed polaroids while gradually raising the temperature and keeping the contents stirred.

At 25°C., solutions of hexanolamine oleate were studied over a concentration range from about 5 per cent down to 0.025 per cent. To avoid suspension in the

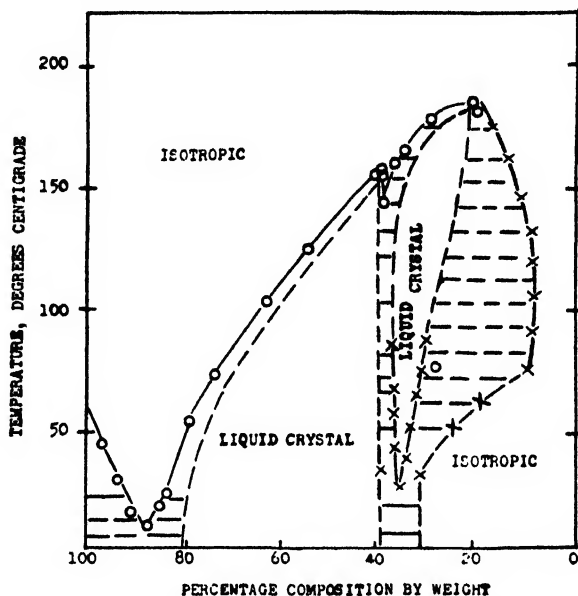


FIG. 1. Phase diagram for hexanolamine oleate

TABLE 2

*Solubilization of Orange OT by solutions of hexanolamine oleate at 25°C*

DETERGENT	DYE PER 100 CC. OF SOLUTION	DYE PER GRAM OF DETERGENT	MOLAR RATIO $\times 10^2$ DYE/SOAP
<i>weight per cent</i>	<i>mg.</i>	<i>mg.</i>	
0.025	0.04	1.53	0.23
0.053	0.09	1.67	0.26
0.126	0.64	5.10	0.78
0.25	1.41	5.72	0.87
0.48	2.82	5.93	0.91
0.84	5.14	6.09	0.93
1.00	6.22	6.21	0.95
2.83	20.70	7.31	1.12
4.78	36.88	7.71	1.18

dilute solutions the method developed by Sister Agnes Ann Green (5) was used, in which the dye was dissolved in *n*-hexadecane. The *n*-hexadecane itself is not solubilized (7). Results are set forth in table 2 and plotted in figure 2. The milligrams of dye solubilized and the molar ratio of dye to soap both show an increase over this range. The increase is rapid at first, trebling between 0.0255

and 0.1265, and then it slopes into a nearly linear increase with concentration up to 5 per cent detergent. Solubilization appears to follow the usual course of beginning distinctly below the so-called critical concentration for micelles, owing to promotion of formation of micelle through interaction of detergent with the solubilized material. For hexanolamine oleate the critical concentration is approximately 0.12 per cent. The solubilization curves and the osmotic coefficients for hexanolamine oleate appear to be very similar to those for potassium oleate.

For 5 per cent hexanolamine oleate the solubilization at 70°C. is twice that at 25°C. No adequate explanation has yet been given of this usual temperature coefficient of solubilization.

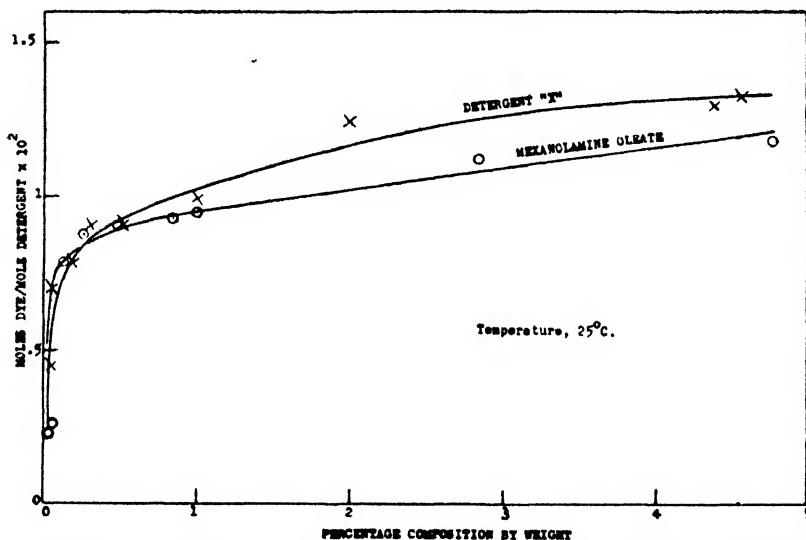


FIG. 2. Solubilization of Orange OT by dilute aqueous solutions of hexanolamine oleate and the non-ionic Detergent "X", at 25°C.

When 10 equivalents per cent excess of the amine is added to a 1 per cent solution of hexanolamine oleate, the solubilization is scarcely affected; it falls from a molar ratio of 0.65 to  $0.63 \times 10^2$ .

#### RESULTS WITH CATOL 607

The cation-active detergent Catol 607 (mol. wt. 394.9) solubilizes Orange OT at 0°C., as shown in table 3. Table 4 shows the solubilization at 25°C. and also shows how greatly it is enhanced by the addition of progressive amounts of potassium chloride. All these results are compared in figure 3.

#### RESULTS WITH NON-IONIZING DETERGENTS

Nonaethylene glycol monolaurate (mol. wt. 600), Triton NE (mol. wt. not measured), and Detergent "X" (mol. wt. 636) are non-ionizing detergents miscible with water in all proportions. Unlike hexanolamine oleate, which is also miscible

TABLE 3

*Solubilization of Orange OT in aqueous solutions of Catol 607 at 0°C.*

NORMALITY	DYE PER 100 CC. OF SOLUTION	DYE PER GRAM OF DETERGENT	MOLAR RATIO $\times 10^4$ DYE/CATOL
	mg.	mg.	
0.0002	0	0	0
0.0005	0.008	0.40	6
0.0010	0.02	0.46	7
0.0025	0.04	0.40	6
0.0050	0.13	0.66	10
0.0075	0.30	0.99	15
0.0090	0.51	1.4	21
0.0120	0.75	1.6	24
0.0150	1.12	1.8	28
0.0180	1.36	1.9	29
0.0220	1.77	2.0	30
0.0325	3.10	2.4	36
0.0600	5.72	2.4	36.4
0.0900	8.71	2.5	36.9

TABLE 4

*Solubilization of Orange OT in moles dye  $\times 10^3$  per mole of Catol 607 solutions at 25°C., as influenced by potassium chloride*

NORMALITY OF CATOL	WITHOUT SALT	POTASSIUM CHLORIDE				
		0.010 N	0.030 N	0.0668 N	0.1468 N	0.6468 N
0.0002	0	1.9	2.3	1.9	2.8	
0.0005	2.4			5.3		
0.0010	1.9	2.6	5.7	4.9	5.3	7.5
0.0025	1.6	2.3				8.2
0.0050	2.7	4.7	5.7	6.6		
0.0075	2.8	4.5				
0.0090	3.6	4.9	6.0	6.6		8.1
0.0120	4.6					
0.0150	5.1	6.4	6.7	7.2	7.5	9.0
0.0180	5.3					
0.0220	5.9	6.1	6.9	7.0	7.4	9.2
0.0280	6.1	6.3	6.6	7.1	7.4	8.9
0.0325	5.7	5.9				9.0
0.060	5.6	6.2			7.1	9.0
0.090	5.7	6.0			7.6	9.4

with water but passes through two ranges of liquid-crystalline phases, all these solutions are free-flowing isotropic liquids over the whole concentration range at 25°C.

Solubilization by nonaethylene glycol monolaurate at 25°C. is much greater



than by hexanolamine oleate at 25°C. but is very similar to that of hexanolamine oleate at 70°C. The results are shown in table 5. Nonaethylene glycol monolaurate is a better solubilizer than potassium laurate, solubilizing twice as much

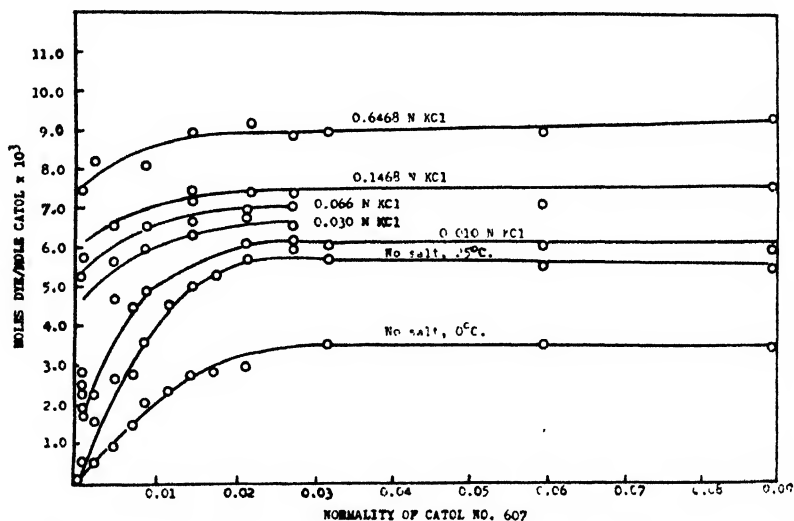


FIG. 3. Solubilization of Orange OT by solutions of a cation-active detergent with and without added potassium chloride.

TABLE 5

*Solubilization of Orange OT by nonaethylene glycol monolaurate at 25°C.*

DETERGENT	DYE PER 100 CC. OF SOLUTION	DYE PER GRAM OF DETERGENT	MOLAR RATIO $\times 10^2$ DYE/SOAP
<i>weight per cent</i>	<i>mg.</i>	<i>mg.</i>	
0.06	0.34	5.52	1.26
0.12	0.81	6.60	1.51
0.21	1.81	8.41	1.93
0.25	2.11	8.51	1.95
0.49	4.19	8.55	1.96
1.32	11.45	8.68	1.99
5.0	42.5	8.49	1.94
7.95	70.6	8.88	2.03
11.0	97.5	8.77	2.01
15.46	130	8.41	1.93
20.98	180	8.57	1.97
28.10	245	8.71	2.00
37.49	365	9.72	2.23
89.95	2055	22.74	5.24
100.00	3075	30.75	7.04

on a weight basis and five times the amount on the basis of mole ratio. Its critical concentration is also lower than that of potassium laurate.

The results for Detergent "X" are given in table 6 and in figures 2 and 4. Its

TABLE 6  
*Solubilization of Orange OT by Detergent "X" (mol. wt. 636) at 25°C.*

COMPOSITION BY WEIGHT	DYE PER 100 CC. OF SOLUTION	DYE PER GRAM OF DETERGENT	MOLAR RATIO $\times 10^3$ DYE/SOAP
<i>per cent</i>	<i>mg.</i>	<i>mg.</i>	
0.0169	0.032	1.89	0.46
0.0292	0.085	2.91	0.71
0.0562	0.177	3.15	0.76
0.1401	0.510	3.66	0.89
0.2566	0.961	3.75	0.91
0.509	1.93	3.83	0.93
1.003	3.66	3.99	0.99
2.011	10.38	5.17	1.25
4.392	23.45	5.30	1.30
4.550	25.00	5.49	1.33
7.262	41.80	5.73	1.40
14.489	78.75	5.47	1.32
26.047	148	5.68	1.38
49.367	337	6.83	1.66
74.785	850	11.36	2.76
100.0	3250	32.49	7.89

TABLE 7  
*Solubilization of Orange OT in aqueous solutions of Triton NE (assumed mol. wt. 600) at 25°C.*

TRITON NE PER 100 CC. OF SOLUTION	DYE PER 100 CC. OF SOLUTION	DYE PER GRAM OF TRITON NE	MOLAR RATIO $\times 10^3$ DYE/TRITON
<i>grams</i>	<i>mg.</i>	<i>mg.</i>	
0.008	0.06	7.5*	1.72
0.010	0.1	10.0*	2.29
0.050	0.3	6.0*	1.37
0.10	0.62	6.2*	1.42
0.50	2.5	5.0*	1.15
1.00	5.4	5.4*	1.24
2.07	8.7	4.7	1.08
3.00	11.3	4.7	1.08
4.15	18.0	4.8	1.10
5.0	25.7	5.1	1.17
6.0	30.5	5.0	1.15
8.3	36.5	4.9	1.12
10.0	50.4	5.0	1.15
11.07	52.	5.1	1.17
14.76	77.	5.2	1.19
19.68	99.	5.0	1.17
19.69	99.	5.0	1.17
26.25	129.	5.1	1.17
35.00	173.	4.9	1.12

\* Results high, owing to suspending of fine particles of dye.

critical concentration is about the same as that for the other two non-ionizing detergents studied. The results with Triton NE are given in table 7.

## SOLUBILIZATION OF ORANGE OT AND YELLOW AB BY BILE SALTS

Yellow AB is about 3.5 times more soluble than Orange OT in solutions of bile salts. Sodium cholate is not as effective as sodium deoxycholate but sodium dehydrocholate is of a lower order of magnitude altogether, solubilizing only 1/85th as much as the deoxycholate. Conductivity and osmotic coefficient show that sodium dehydrocholate contains very little colloid. The results are given in tables 8 and 9, where it is also shown that in every case the solubilization is enhanced by the presence of 0.025 *N* sodium salt. This corrects the opposite indication given in reference 6.

TABLE 8

*Solubilization of Orange OT and Yellow AB at 25°C. by 0.1 N sodium deoxycholate*

	WITHOUT SALT		WITH 0.025 <i>N</i> NaCl		WITH 0.025 <i>N</i> Na <sub>2</sub> SO <sub>4</sub>	
	Orange OT	Yellow AB	Orange OT	Yellow AB	Orange OT	Yellow AB
Milligrams of dye per 100 cc. ....	14.87	47.50	17.15	51.50	16.75	50.50
Grams of dye per mole . . . . .	1.487	4.750	1.715	5.150	1.675	5.05
Mole ratio $\times 10^3$ dye/detergent ..	5.66	1.92	6.52	2.08	6.38	2.04

TABLE 9

*Solubilization of Orange OT at 25°C. by 0.1 N sodium cholate and sodium dehydrocholate*

	WITHOUT SALT	WITH 0.025 <i>N</i> NaCl
Sodium cholate		
Milligrams of dye per 100 cc. . . . .	10.45	11.53
Grams of dye per mole . . . . .	1.045	1.153
Mole ratio $\times 10^3$ dye/detergent . . . . .	3.98	4.90
Sodium dehydrocholate		
Milligrams of dye per 100 cc. ....	0.174	0.226
Grams of dye per mole . . . . .	0.0174	0.0226
Mole ratio $\times 10^3$ dye/detergent . . . . .	0.0664	0.0860

## PURIFIED ORONITE SULFONATE

Solubilization of Orange OT by 1 per cent solutions of purified Oronite sulfonate (mol. wt. 432.6) at 25°C. is as follows, where the milligrams per gram and the molar ratio have been calculated on the basis of the active constituent in this commercial sample:

Milligrams of dye per 100 cc. of solution . . . . .	8.40
Milligrams of dye per gram. ....	12.4
Mole ratio dye/soap . . . . .	$2.04 \times 10^{-2}$
Grams of dye per mole.	5.36

## DISCUSSION

It is of interest to compare and contrast ordinary molecular solutions of dye by mixed solvent with solubilization by aqueous colloidal electrolytes. This is done in figure 4. The solubility of Orange OT at 25°C. in aqueous acetone is excessively small until there is a preponderance of acetone:

Per cent acetone...	8.1	16.5	34.6	54.3	76.1	100
Grams of dye per mole	0.0029	0.0071	0.0066	0.055	0.37	13.6

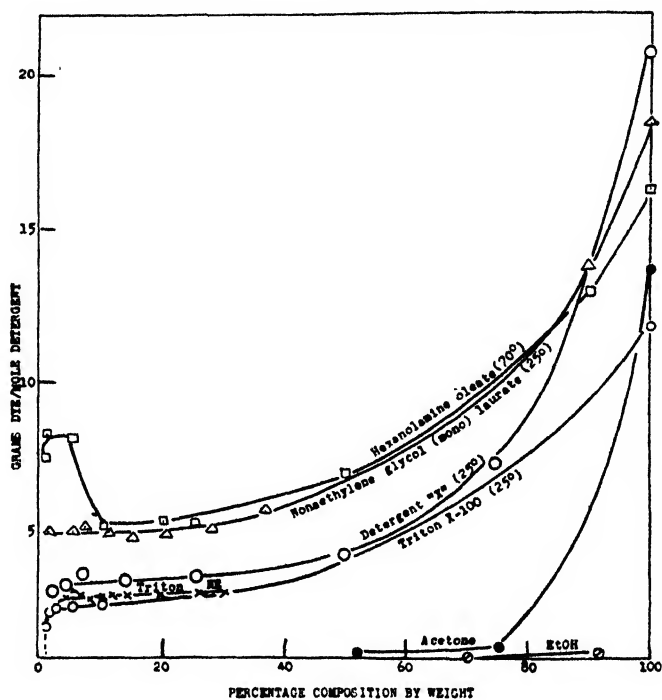


FIG. 4. Solubilization of Orange OT by one anion-active detergent and three non-ionic detergents over the whole range from 0 to 100 per cent, as compared with mere solubility in mixtures of water with acetone or ethyl alcohol.

Similarly in ethyl alcohol, which is a much poorer solvent, the values are:

Per cent ethyl alcohol . . . . .	7.6	15.5	32.3	50.8	71.0	93.7
Grams of dye per mole . . . . .	0	0.0015	0.0022	0.013	0.055	0.17

For 7.35 per cent butyl alcohol the solubility is 0.0011 g. per mole, since butyl alcohol is a better solvent than acetone. All such data show that a very large proportion of good solvent is required to make the dye soluble in the aqueous mixture and, conversely, a very small amount of water seriously cuts down the solubility in the organic solvent.

In complete contrast, a very low percentage of colloidal electrolyte produces a high relative solubilization by the detergent in water. However, the solvent power of the 100 per cent pure liquid detergents is several times greater than the solubilizing power of the same weight of detergent in aqueous solution.

It is also of interest to compare solubilization with the osmotic coefficient, because the osmotic coefficient clearly shows the onset of micelle formation. An example of this is given in figure 5. The osmotic coefficient of the ratio of the observed lowering of freezing point to that of fully dissociated ideal electrolyte is  $g = \theta/3.716 m$ . The curves in figure 5 are antibatic. However, as in all cases on record, it is seen that the so-called critical concentration for micelle formation is distinctly anticipated in a lower concentration by a small amount of solubilization. This is significant because it shows that the colloidal complex between

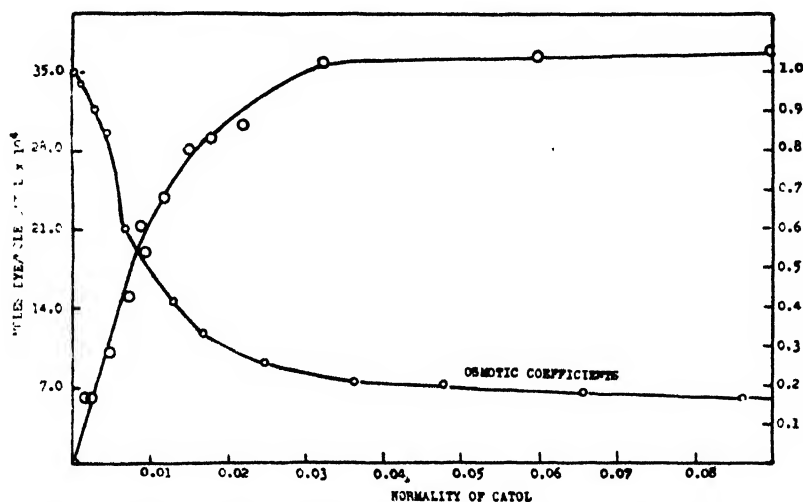


FIG. 5. Solubilization of Orange OT by the cation-active detergent Catol as compared with the amount of colloid, indicated by the departure of the osmotic coefficient from the value of unity.

detergent and solubilized material is formed with positive affinity, and therefore the presence of even this small amount of dye promotes the formation of micelles in a solution otherwise too dilute for the presence of colloid. It clearly follows that the method of determining critical concentration for the formation of micelle by titration with dyes such as pinacyanol, etc., must lead to concentrations slightly but definitely lower than the true values.

#### SUMMARY

The solubilization of water-insoluble dye in aqueous systems by four non-ionizing detergents and one ionizing colloidal electrolyte, hexanolamine oleate, has been determined over the whole range of concentration from 0 to 100 per cent detergent, and contrasted with the behavior of solutions in mixed solvents.

Added salts strongly promote solubilization by bile salts and the cationic

detergent Catol 607, but sodium dehydrocholate is a far poorer solubilizer than the cholate or deoxycholate.

A few results with other solutions are recorded.

The solubilization of dye per gram of detergent is far from being equal to the solubility of the dye in that pure anhydrous detergent.

#### REFERENCES

- (1) GONICK, E., AND MCBAIN, J. W.: J. Am. Chem. Soc. **68**, 683 (1946).
- (2) GREEN, SISTER AGNES ANN: Ph.D. Dissertation, Stanford University, 1946.
- (3) GREEN, SISTER AGNES ANN, AND MCBAIN, J. W.: J. Phys. Chem. **51**, 286 (1947).
- (4) MCBAIN, J. W.: *Advances in Colloid Science*, Vol. I. pp. 99-142. Interscience Publishers, Inc., New York (1942).
- (5) MCBAIN, J. W., AND GREEN, SISTER AGNES ANN: J. Am. Chem. Soc. **68**, 1731 (1946).
- (6) MCBAIN, J. W., AND MERRILL, R. C., JR.: Ind. Eng. Chem. **34**, 915 (1942).
- (7) MCBAIN, J. W., AND RICHARDS, P. H.: Ind. Eng. Chem. **38**, 642 (1946).
- (8) MERRILL, R. C., JR., AND MCBAIN, J. W.: J. Phys. Chem. **46**, 10 (1942).

### LAURATE-ION ACTIVITY IN SOLUTIONS OF POTASSIUM LAURATE IN THE ABSENCE AND PRESENCE OF NEUTRAL SALTS<sup>1,2</sup>

I. M. KOLTHOFF AND WARREN F. JOHNSON

*School of Chemistry, University of Minnesota, Minneapolis, Minnesota*

*Received August 25, 1947*

In a recent publication (4) results of the measurement of the sodium-ion activity in aqueous solutions of various anionic detergents have been reported. Use has been made of negatively charged collodion membranes, the potential difference between the inside and the outside of the membrane being determined by the ratio of the cation activities of the solutions inside and outside of the membrane (1, 2, 3, 5). The method gives excellent results as long as we are dealing with one kind of cation only and not with a mixture of cations. It was found that the sodium-ion activity in solutions of sodium salts of detergents decreases slightly with increasing detergent concentration in a way similar to the decrease of the sodium-ion activity in solutions of sodium salts of strong electrolytes. However, at the critical concentration of the detergent, where marked micellization occurs, the sodium-ion activity was found to decrease abruptly. In the micelle the detergent anions are associated and are closely packed together. The net negative charge of the micelle is equal to the sum of the charges of the sodium

<sup>1</sup> Presented at the Twenty-first National Colloid Symposium, which was held under the auspices of the Division of Colloid Chemistry of the American Chemical Society at Palo Alto, California, June 18-20, 1947.

<sup>2</sup> This investigation was carried out under the sponsorship of the Office of Rubber Reserve, Reconstruction Finance Corporation, in connection with the synthetic rubber program of the United States Government.

ions which are held by electrostatic forces as "counter ions" close to the surface of the negatively charged micelle. The small activity coefficient of the sodium ions in solutions of micellized sodium salts of detergents is not caused by the formation of 'undissociated' detergent salt, but by the facts that the negative charges in the micelle are very close together and that these charges are in fixed positions.

An attempt was made (4) to measure the anion activity in solutions of anionic detergents using positively charged collodion membranes. Further studies are necessary to interpret the preliminary results which have been obtained.

In the present work it was decided to measure the anion activity of a solution of a fatty acid soap by a classical method. The silver salts of fatty acid soaps are slightly soluble in water. By measuring the E.M.F. of a cell composed of a half-cell consisting of a silver electrode in a suspension of the silver salt of the fatty acid in a solution of the potassium salt of the fatty acid and another half-cell serving as a reference electrode, the activity of the anion of the soap can be found under varying conditions. The E.M.F. of the above type of cell involves a liquid-junction potential which we have tried to reduce to very small values by a suitable salt bridge. The measurement of individual ion activity is always made uncertain by the occurrence of an unavoidable liquid-junction potential. In the present study we have measured the laurate-ion activity in aqueous solutions of potassium laurate of varying concentrations in the absence and presence of varying amounts of potassium nitrate. The following cell was used

Ag; Ag laurate (s), K laurate ( $C_1$ ),  $\text{KNO}_3$  ( $C_2$ ) || (KCl (satd.),  $\text{Hg}_2\text{Cl}_2$ (s); Hg

The experimental results reported below indicate clearly that the conclusions drawn from the measurements are not obscured by the liquid-junction potential.

#### EXPERIMENTAL

The lauric acid used was obtained from the Eastman Kodak Company. The neutralization equivalent weight of the sample was 200.3. The acid was dissolved in alcohol and neutralized with alcoholic potassium hydroxide. The potassium laurate was twice recrystallized from alcohol.

Silver laurate was prepared by dissolving lauric acid in alcohol, neutralizing with alcoholic sodium hydroxide to 95 per cent, and then adding an alcoholic solution of silver perchlorate dropwise to the solution of sodium laurate, which was kept at approximately  $50^\circ\text{C}$ . During the preparation all of the silver solutions and the precipitated silver laurate were protected from light. The silver laurate was filtered hot, using a sintered-glass filter, and washed repeatedly with warm alcohol. The product was dried in a vacuum oven at  $35^\circ\text{C}$ .

#### *Preparation of electrodes*

Two methods of preparing the silver electrodes were used. The first method was the electrodeposition of silver on platinum wires, sealed into soft-glass tubing, from a solution of potassium argentocyanide. After the silver had been put onto the electrodes a thin film of silver iodide was put on electrolytically, the cur-

rent and time being controlled so that the thickness of the film could be controlled. Coatings of various thickness were tried to obtain optimum conditions. A coating approximately 0.1 micron thick was found to give entirely satisfactory results. Films of silver iodide of greater thickness gave the same potential but were slow in reaching their equilibrium value.

The second procedure used to prepare the silver electrodes gave more satisfactory results, since the electrodes attained their equilibrium potential as soon as the cells had reached temperature equilibrium. The platinum wire was smeared with a silver oxide paste and then dried in an air oven at 80°C. When dry the electrodes were heated in an atmosphere of nitrogen at 400°C. for a period of 6 hr. to decompose the silver oxide to silver. After the electrodes had cooled they were reduced electrolytically in 0.02 *N* perchloric acid solution for 6 hr. at a current density of 0.015 amp. per square centimeter. Before use they were washed repeatedly with conductivity water and twice with the same solution as in the cell.

Solutions of potassium laurate were prepared by volume at 25°C. These solutions were transferred to 4-oz. screw-cap bottles which were painted black, an excess of silver laurate was added, and the bottles were capped with caps having a silver liner. The bottles were placed in a 30°C. ( $\pm 0.1^\circ$ ) thermostat which provided end-over-end agitation. After the solutions were saturated with silver laurate they were transferred to half-cells which were painted black, each half-cell being provided with two silver electrodes. The half-cells were rinsed twice before filling. A saturated calomel half-cell was attached through a saturated potassium nitrate salt bridge and the cell placed in a 30°C. ( $\pm 0.1^\circ$ ) thermostat. Some solid silver laurate was always transferred into the half-cells when they were filled to make certain the solution was always saturated with respect to silver laurate.

In some cases two cells were prepared for each concentration, each cell having two silver electrodes. The electrodes agreed to  $\pm 1$  mv., the values reported being the average of these readings. Most of the results are for a single cell which had two electrodes, the results agreeing to  $\pm 1$  mv.

The range of laurate concentrations investigated was from 0.001 *M* to 0.100 *M*, between which concentrations the critical concentration of potassium laurate (0.023 *M*) occurs. The effect of added electrolyte was studied at two concentrations of potassium nitrate. The E.M.F.'s of the cells as a function of the concentration of potassium laurate without potassium nitrate, with 0.1 *M* potassium nitrate, and with 0.5 *M* potassium nitrate are given in table 1. These values include the junction E.M.F.'s. A plot of the data given in table 1 is shown in figure 1.

Though the E.M.F. data given here are not corrected for the junction potentials, the sudden breaks in the curves are significant. These breaks correspond to the critical concentrations obtained from solubilization data. It can be seen from figure 1 that we have two linear branches for the branch of the curve from  $C_{\text{laurate}} = 0.001$  *M* to the critical concentration, the slope being 0.0637 volt.

It may be concluded that in the concentration range between 0.001 *M* to the



TABLE 1

*E.M.F. of the cell as a function of the concentration of potassium laurate at 30°C.  $\pm 0.1^\circ$  with and without added potassium nitrate*

CONCENTRATION OF POTASSIUM LAURATE	CONCENTRATION OF KNO <sub>3</sub>	E.M.F. OF CELL	LOG C <sub>LAURATE</sub>
<i>moles per liter</i>	<i>moles per liter</i>	<i>volts</i>	
0.0010	0	-0.2028	-3.000
0.0050	0	-0.1599	-2.301
0.0100	0	-0.1400	-2.000
0.0200	0	-0.1200	-1.699
0.0250	0	-0.1165	-1.602
0.0500	0	-0.1208	-1.301
0.0750	0	-0.1186	-1.125
0.1000	0	-0.1205	-1.000
0.00395	0.1	-0.1658	-2.403
0.0198	0.1	-0.1331	-1.703
0.0500	0.1	-0.1345	-1.301
0.1000	0.1	-0.1315	-1.000
0.001	0.5	-0.1989	-3.000
0.005	0.5	-0.1549	-2.301
0.010	0.5	-(0.1418)	-2.000
0.020	0.5	-0.1530	-1.699
0.050	0.5	-0.1536	-1.301
0.100	0.5	-0.1548	-1.000

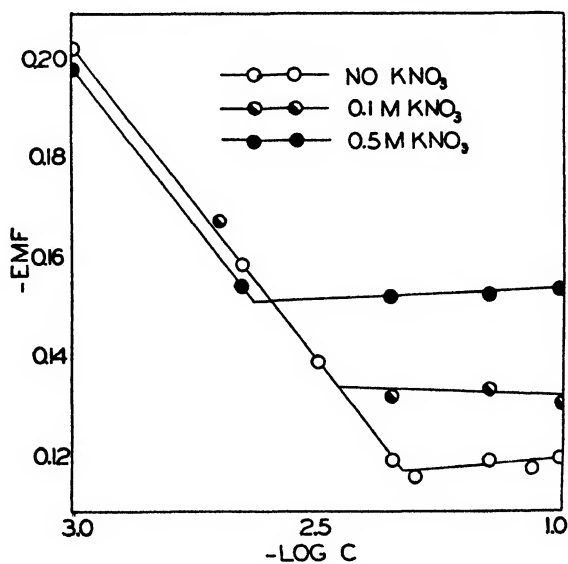


FIG. 1. E.M.F. vs. log  $C$  at 30°C. for the cell  
 Ag; Ag laurate, K laurate ( $C$ ), KNO<sub>3</sub> (0 or 0.1  $M$ ) : KNO<sub>3</sub> (satd.) · KCl (satd.), Hg<sub>2</sub>Cl<sub>2</sub>;Hg

critical concentration the laurate-ion activity in potassium laurate solutions changes with the soap concentration as does that of the anion of a strong univalent salt. When the concentration is greater than the critical concentration, the E.M.F. remains essentially constant to concentrations as high as 0.1 *M* potassium laurate. This implies that the activity of the laurate ion remains constant in this range (critical concentration to 0.1 *M*).

These results do not agree with the measurements of laurate-ion activity as found using positively charged collodion membranes (1). In the latter work it was found that the laurate-ion activity went through an apparent maximum at a concentration of about 0.006 *M* sodium laurate and declined rapidly thereafter. The reliability of the positively charged membranes in solutions of colloidal electrolytes is questionable.

The critical concentrations found from the E.M.F. measurements are compared with those found by the solubilization of dimethylaminoazobenzene in table 2. The agreement between these values is very good and may be taken as evidence that we are in fact measuring the activity of laurate ion in the solutions.

TABLE 2

*Critical concentration of potassium laurate in the absence and presence of added electrolyte (KNO<sub>3</sub>) at 30°C.*

CONCENTRATION OF KNO <sub>3</sub>	CRITICAL CONCENTRATION	
	E. M. F. (silver electrode)	Solubilization
	moles per liter	moles per liter
0.0	0.022	0.023
0.10	0.012	0.012
0.50	0.0055	0.005

The most interesting result of this study is that the activity of the laurate ion remains practically constant after reaching the critical concentrations up to 0.1 *M*. No measurements have been made at potassium laurate concentrations greater than this. The results obtained in 0.5 *M* potassium nitrate are particularly interesting, because at this constant high concentration of indifferent electrolyte the liquid-junction potentials at various potassium laurate concentrations should be identical. It is seen then that in 0.5 *M* potassium nitrate the laurate-ion activity at potassium laurate concentrations between 0.005 *M* and 0.1 *M* remains constant. The results indicate that no further micellization of unmicellized laurate occurs at concentrations above the critical concentration, at least up to 0.1 *M* laurate, the highest concentration measured.

#### SUMMARY

The E.M.F. of cells consisting of silver, silver laurate, and potassium laurate solutions in the presence and absence of potassium nitrate *vs.* a saturated calomel half-cell has been measured, using a saturated potassium nitrate salt bridge.

Plotting E.M.F. *vs.*  $\log C$ , both in the absence and in the presence of potassium nitrate, gave curves consisting of two straight lines. The point of intersection of the two straight lines corresponds exactly to the critical concentration of potassium laurate in the particular medium. The activity of the laurate ion changes with the concentration of potassium laurate in a way similar to that of the anion in a uni-univalent strong electrolyte. Above the critical concentration the activity of the laurate ion remains constant up to a concentration of 0.1 *M* potassium laurate, the highest concentration measured. This result indicates that no micellization of unmicellized laurate occurs at concentrations above the critical one.

## REFERENCES

- (1) CARR, C. W., GREGOR, H. P., AND SOLLNER, K.: *J. Gen. Physiol.* **28**, 179 (1945).
- (2) CARR, C. W., AND SOLLNER, K.: *J. Gen. Physiol.* **28**, 119 (1944).
- (3) GREGOR, H. P., AND SOLLNER, K.: *J. Phys. Chem.* **50**, 53, 88 (1946).
- (4) KOLTHOFF, I. M., CARR, C. W., AND JOHNSON, W. F.: *J. Phys. Colloid Chem.* **51**, 636-44 (1947).
- (5) SOLLNER, K.: *J. Am. Chem. Soc.* **65**, 2260 (1943).

THE EFFECT OF TEMPERATURE AND MOLECULAR-WEIGHT DISTRIBUTION ON THE MORPHOLOGY OF NATURAL AND SYNTHETIC HIGH POLYMERS<sup>1</sup>

ERNST A. HAUSER

*Massachusetts Institute of Technology, Cambridge, Massachusetts*

AND

D. S. LE BEAU

*Midwest Rubber Reclaiming Company, East St. Louis, Illinois**Received August 25, 1947*

## NATURAL RUBBER

Fractionation studies of the molecular-weight distribution of *Cryptostegia grandiflora* rubber have shown that it is predominantly composed of polyisoprene chains of both quite low and rather high molecular weights (2). Previous work based on electron microscopy (1) and ultramicroscopy with incident light (3) has indicated that differences in the morphology of polymers of high and low molecular weights can be observed.

Of all natural rubbers, *Cryptostegia* rubber has proved most suitable for such studies because of its peculiar molecular-weight distribution. Hevea

<sup>1</sup> Presented at the Twenty-first National Colloid Symposium, which was held under the auspices of the Division of Colloid Chemistry of the American Chemical Society at Palo Alto, California, June 18-20, 1947.

rubber shows a rather uniform distribution of molecular weights over a wide range, whereas guayule rubber is characterized by the predominance of low-molecular-weight fractions. Specimens made from carefully prepared fractions revealed that the low molecular weights (sol) are characterized either by films which, when deposited from solutions on the wire screen, collapse completely after evaporation of the solvent, or show a preponderance of globules held together by very fine threads. In contrast thereto, preparations made from high-molecular-weight fractions (gel) are characterized by threads or bands and no globules or only a very few. Inasmuch as it is impossible to obtain an absolutely perfect fractionation, the presence of some globules can be expected even in the gel fraction. It has been assumed that the formation of the globules is the result of syneresis, the fraction of lower molecular weight showing less

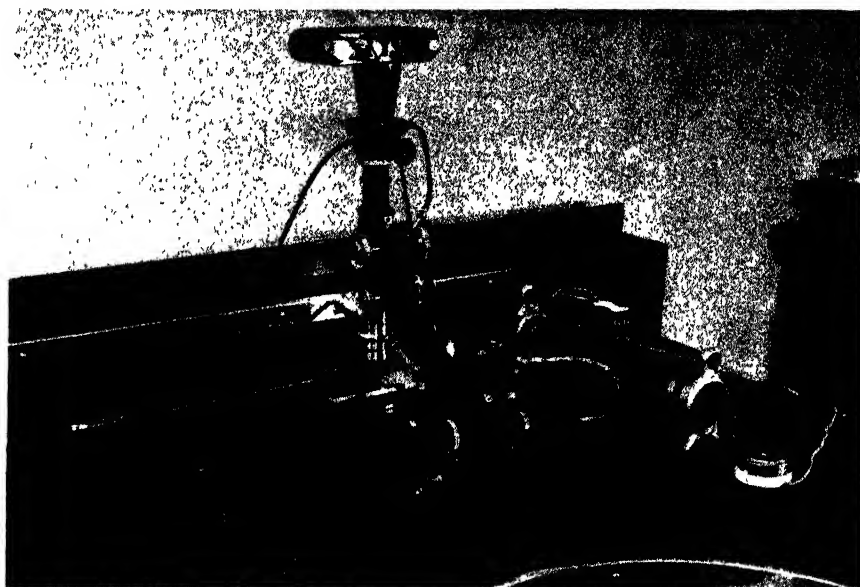


FIG. 1. Ultropak microscope equipped with heatable substage, micro Iiso attachment, and Leica camera.

resistance toward flow and being squeezed out of the more or less aligned long chains, which upon evaporation of the solvent are under considerable tension.

Previously reported studies of the morphological changes which *Cryptostegia* rubber undergoes with time have indicated that this separation of the low from the high molecular-weight fraction is not instantaneous (4), as had been the assumption based on the results obtained with the electron microscope (1), but occurs at room temperature over a period of hours. A logical deduction from these observations seemed to be that these changes could be accelerated by increasing the temperature at which the samples are studied. To test this assumption an electrically heatable substage was built for the ultramicroscope, which made it possible to study any changes in the morphology of the preparation at different temperatures and for different lengths of time (figure 1).

Whereas the formation of globules from a *Cryptostegia* sample required 20 hr. (4) at room temperature, an identical effect could be observed already after 3 hr. if the temperature was raised to 38°C. and kept there during observation (figure 2). If the temperature was raised to 45°C. and again kept constant, the globule formation appeared fully developed within 10 min. (figure 3). Indeed, globule formation proceeded so quickly that indications of it developed during the time necessary for the first exposure of the film (figure 3a). Unfortunately, it is impossible to reproduce preparations of identical polymer thread diameters every time. It can be expected, however, that the size of the polymer

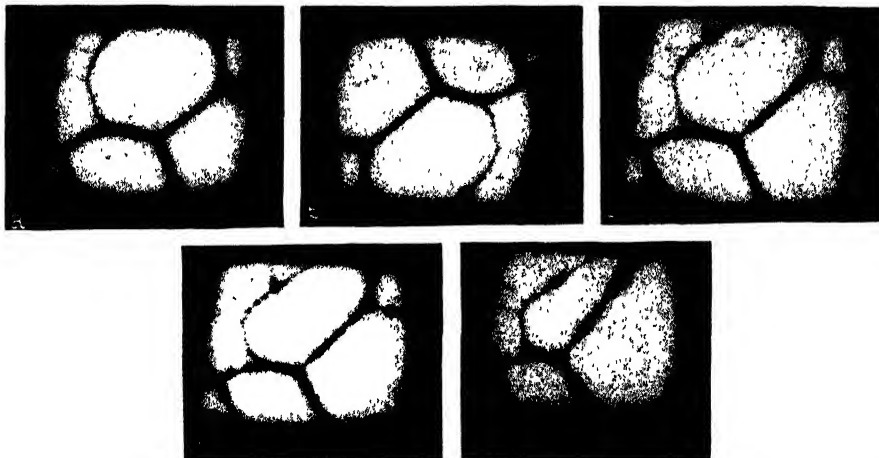


FIG 2 *Cryptostegia* rubber heated to 38°C.: (a) 2 min., (b) 60 min., (c) 90 min., (d) 120 min., (e) 180 min

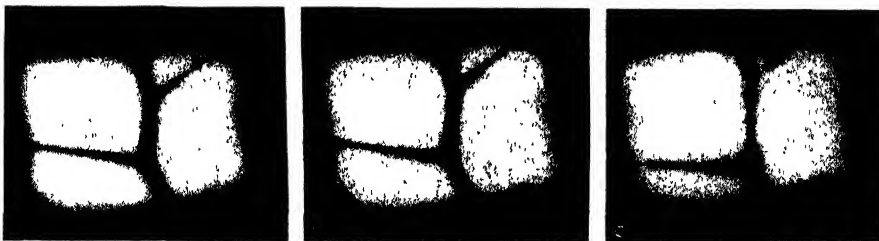


FIG 3 *Cryptostegia* rubber heated to 45°C.: (a) 2 min., (b) 5 min., (c) 15 min

thread under observation will have some bearing on the speed of globule formation. Therefore it is impossible to correlate the time of globule formation accurately with the temperature at which it occurred. Undoubtedly the ease and speed with which these globules are formed will depend on the configuration of the polymer chain.

The electron bombardment of the polymer, such as would occur during the time needed for the study of the preparation in the electron microscope, will raise the temperature of the samples well above those referred to in these experiments. This makes the apparently instantaneous globule formation, recorded in the first investigations with the electron microscope (1), understandable.

## BALATA

That balata does not show the formation of globules at room temperatures and presents a very distinct morphological picture of extremely ragged films has already been reported (3). Even threads are rarely observed. If, however, the film deposited on the water surface was immediately, and while still in the solvated state, deposited on the screen support, single threads could be obtained. As the solvent evaporated these threads became rigid. The stiffness of the thread can be easily seen in figure 4. If, however, the polymer film was deposited from its solution on the surface of water of 70°C., the resultant film lost its original raggedness to some extent and formed threads and even some blobs (3). This change in the morphology is a function of time and temperature. Increasing temperatures will result in considerable flow and the formation of globules (figure 5). If the preparations are then rapidly cooled to room temperature and left to rest for 12 hr., the balata threads become stiff again. If the preparation is heated longer, flow becomes more pronounced and the threads break. Upon rapid cooling they remain and the globules do not disappear (figure 6). Inasmuch as balata is known to be of a comparatively low average molecular weight, the size of the molecular chains alone cannot be considered the predominant factor hindering flow. Thus the theoretical concept that higher temperatures are needed to permit polyisoprene chains of *trans*-configuration to vibrate sufficiently to permit flow seems to be substantiated by these photomicrographs. The fact that balata exhibits elasticity above this temperature now finds its explanation. It is the temperature needed to permit the low-molecular-weight fractions to exercise fully their lubricating effect which is essential for the property of elasticity. (One other observation deserves attention. The samples which have not been heated or have been heated only for a short time are opaque. Upon heating their index of refraction changes and the threads and globules become translucent and retain this property after cooling (cf. figure 5 with figure 6). This might find its explanation in the known fact that balata changes at this temperature from the  $\alpha$ - to the  $\beta$ -modification and does not revert to the  $\alpha$ -modification even when cooled (5).

## POLYISOBUTYLENE (VISTANEX)

The results obtained so far, therefore, seemed to justify the application of this technique to a more detailed study of the influence of molecular size on the flow and the general morphological aspects of a polymer. For this purpose various molecular-weight fractions ranging from 40,000 to 300,000 of polyisobutylene were studied separately and also in mixtures with one another. To anyone familiar with molecular-weight determinations it is known that the figures represent average molecular weights only and that we therefore are not dealing with strictly monodisperse systems. The molecular weights mentioned here were calculated according to the method of Staudinger.

It was also considered of importance to study the effect that different solvents might have on the morphology of the polymer. Therefore the polyisobutylene samples were prepared from solutions in benzene as well as in xylene.

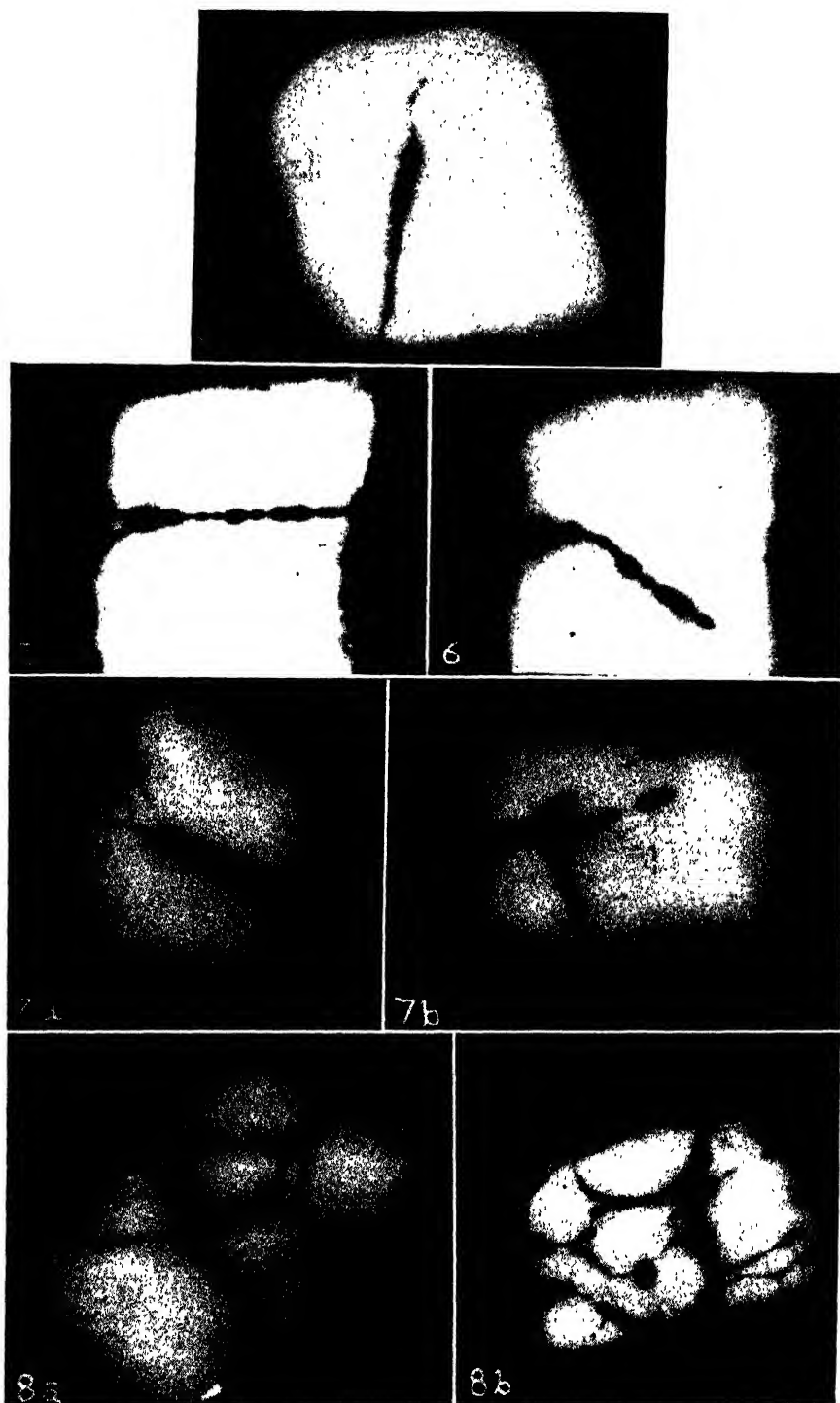


FIG. 4. Balata

FIG. 5. Balata heated to 65°C.

FIG. 6. Balata heated to 70°C. and cooled

FIG. 7. Vistanex (MW 41,330): (a) in benzene; (b) in xylene

FIG. 8. Vistanex (MW 64,200): (a) in benzene; (b) in xylene

Polyisobutylene was chosen for this study because it is chemically highly stable and changes in morphology due to oxidation, which could be very pronounced because of the great development of surfaces, can therefore be discounted.

All pictures were taken instantaneously and at room temperature.

Polyisobutylene having an average molecular weight of 41,330 gives films of little strength which show great flow and break very easily. Threads, if formed, are coarse and heavy and their flow can be readily followed. Very little, if any, difference can be found between films prepared from benzene or xylene solutions (figure 7).

Vistanex having an average molecular weight of 64,200 still shows great flow. However, networks can also be noticed; the films become stronger and do not collapse as easily. Again no difference could be found between films prepared from benzene or xylene solutions (figure 8).

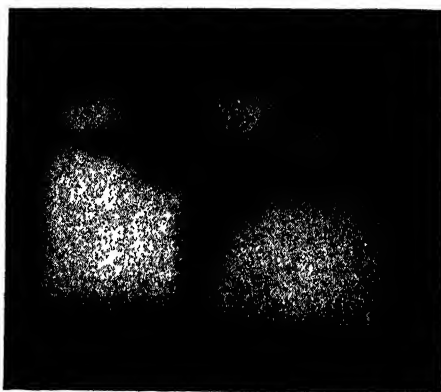


FIG. 9. Vistanex (MW 84,200) in benzene

Vistanex of an average molecular weight of 82,400 yields considerably stronger films, although flow is still predominant. The threads, however, are becoming finer (figure 9).

Vistanex having an average molecular weight of 91,080 yields considerably more netted films of fine threads. The blobs are becoming smaller and better defined. The films are strong and will support themselves over a period of weeks (figure 10).

Polyisobutylene of an average molecular weight of 100,000 to 130,620 shows very fine but very strongly netted films. Flow is evidenced, although the blobs are very small. The preparation technique had to be changed slightly. The film had to be picked up from the water surface before solvent evaporation had taken place. The solvent was permitted to evaporate after the preparation had been placed on the support so that coherent films, which would cover the screen completely, could be avoided (figure 11).

Polyisobutylene having an average molecular weight of about 300,000 shows very fine netting with very fine globules (figure 12).



The changes occurring with increasing molecular weight of a polymer are clearly visible over the range of molecular sizes investigated. Again, high molecular weights result in netting, very fine threads, and very small globules if such are present at all. Low-molecular-weight polymer was again found to

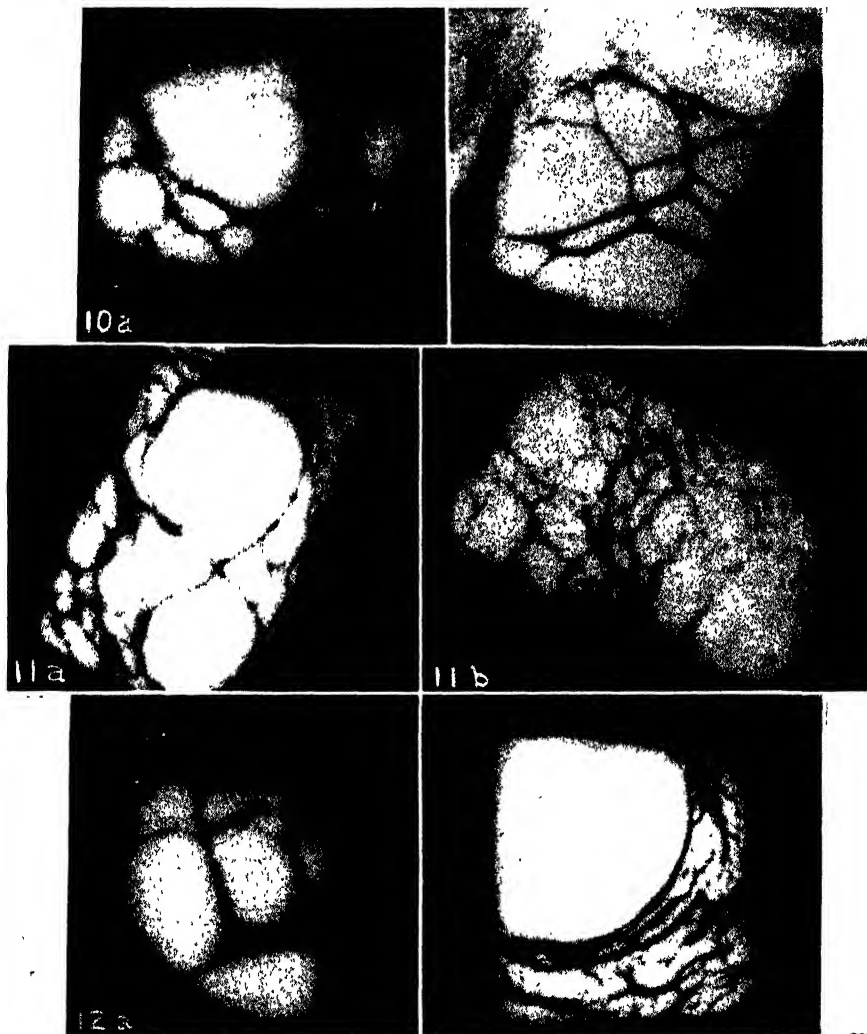


FIG. 10 Vistanex (MW 91,080): (a) in benzene; (b) in xylene

FIG. 11. Vistanex: (a) MW 110,000 in benzene; (b) MW 140,000 in xylene

FIG. 12. Vistanex (MW 300,000): (a) in benzene; (b) in xylene

give large globules and little or no netting. However, in the fractions of lowest molecular weight the globules almost lose their identity and the original threads appear to flow in sections. This flow occurs with such rapidity that it is often impossible to record it on a photographic film.

If, however, a high-molecular-weight fraction of polyisobutylene was heated to 45°C. for more than 1 hr., no changes could be observed in its morphology. No flow occurred at that temperature.

It was also of interest to study the morphology of predetermined mixtures of very high as well as of very low molecular weights. For this purpose mixtures of the xylene solutions of 41,330 and 300,000 molecular-weight fractions of polyisobutylene were prepared in the following proportions: 90 parts MW 300,000/10 parts MW 41,330; 75 parts MW 300,000/25 parts MW 41,330; 50 parts MW 300,000/50 parts MW 41,330; 10 parts MW 300,000/90 parts MW 41,330. Figure 13 shows the progressive changes with increasing amounts of the low-molecular-weight fraction. Figure 13a proves that the morphology of a mixture containing predominantly polymer of MW 300,000 nevertheless has changed considerably from figure 12. The nets are of a much coarser character than those obtained from the pure 300,000 molecular-weight fraction. As the amount of low-molecular-weight fraction is increased (figure 13 b, c), the network disappears and the threads are either fine or quite coarse. When the mixture is made up of 90 parts of low molecular weight (41,330), networks have disappeared completely and only very fine threads studded with bead-like globules can be observed (figure 13 d, e). Even though these globules indicate strong flow, the films formed from this mixture are much stronger and the indiscriminate flow in sections so characteristic for the pure 41,330 molecular-weight fraction has disappeared.

Identical results, although not as distinct, have been obtained from a similar series of experiments using mixtures of the molecular-weight fractions 41,330 and 130,620.

#### BUTYL RUBBER

A series of five different polymers, prepared from feed stocks containing 0.5, 2.5, 3.5, 4.5, and 8 per cent of diolefin, were studied for their morphological differences. Inasmuch as the rate of polymerization of isobutylene is greater than that of the diolefin, the polymer samples actually contained less diolefin than originally present in the feed stock. The 0.5 per cent diolefin polymer contained 0.4 per cent unsaturation, the 2.5 per cent polymer 2 per cent unsaturation, the 3.5 per cent polymer 2.8 per cent unsaturation, the 4.5 per cent polymer 3.7 per cent unsaturation, and the polymer made with 8 per cent diolefin in its feed stock contained 6 per cent unsaturation. The Wijs method at 0°C. was used for the determination of the unsaturation. It is well known that increasing amounts of diolefin decrease the rate of polymerization as well as the molecular weight of the polymer. It has also been found that samples containing greater amounts of diolefins lose their rubber-like characteristics and become more and more resinous (7).

The present samples were prepared to a conversion of between 50 and 70 per cent, the lower conversion limits being obtained for high diolefin content. The molecular weight of the sample marked 2.5 per cent corresponds to that generally found for commercially produced Butyl rubber.

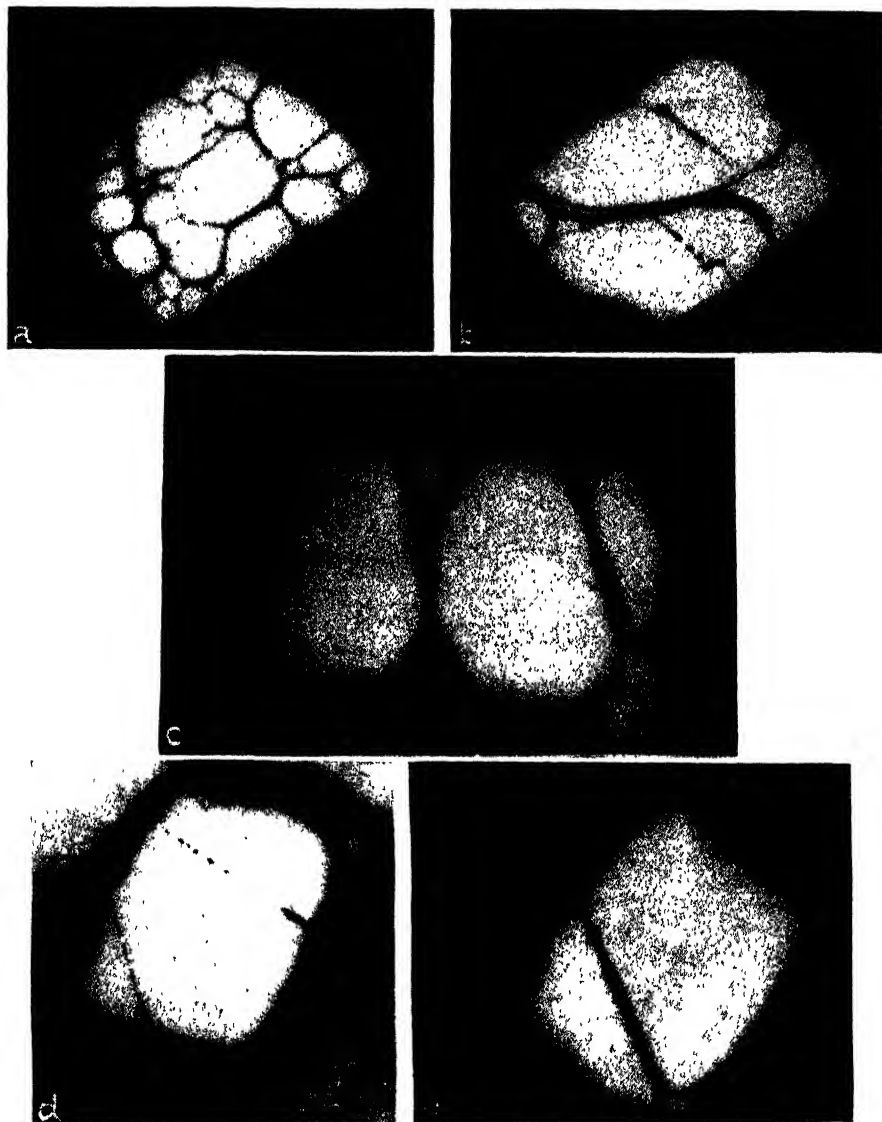


FIG. 13. Vistanex: mixtures of different molecular weights

	MW 40,000	MW 300,000
(a) .. . . .	10 parts	90 parts
(b) .	25 parts	75 parts
(c) ...	50 parts	50 parts
(d), (e)....	90 parts	10 parts

Figures 14 and 15 show the effects of the amount of diolerins copolymerized with the isobutylene. Figures 14a and 14b represent Butyl rubber pre-

pared from feed stock containing 0.5 per cent of diolefin. These copolymers resemble the lower-molecular-weight Vistanex samples in their morphology. Netting of not too fine fibers with a considerable amount of fair-sized globules can be noticed.

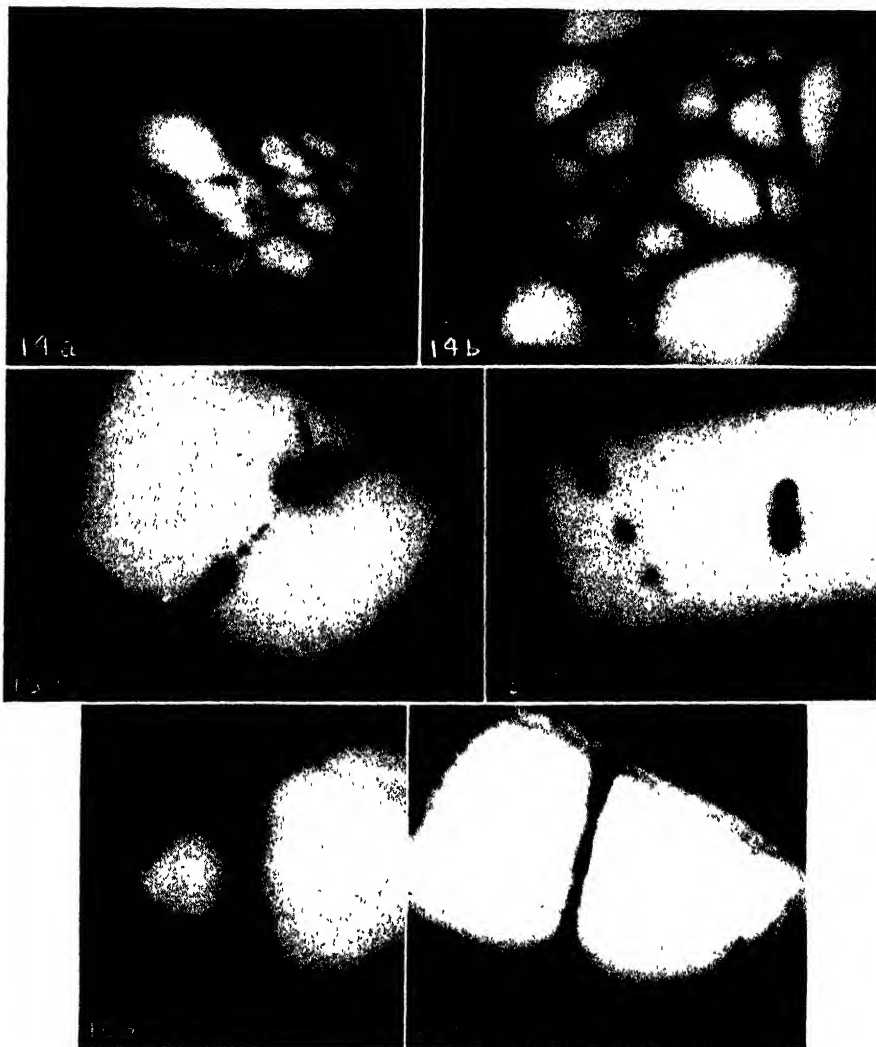


FIG. 14. Butyl rubber (0.5 per cent diolefin): (a) in benzene; (b) in xylene

FIG. 15. Butyl rubber (2.5 per cent diolefin): (a) in benzene; (b) in xylene

FIG. 16. Butyl rubber (3.5 per cent diolefin): (a) in benzene; (b) in xylene

Figure 15 shows the corresponding copolymer containing 2.5 per cent diolefin in the feed stock. This sample shows considerable flow and can in general be compared to Vistanex 41,330 in its morphology.

Figures 16 and 17 represent the general morphology obtainable from Butyl

rubber containing 3.5 per cent and 4.5 per cent of diolefin in the feed stock. The flow was so great that the threads broke and disappeared before any photomicrograph could be made. This condition is predominant for any Butyl rubber studied and containing more than 3.5 per cent of diolefin in the feed stock. The apparent raggedness of threads is a consequence of the tremendous flow. Each of the protuberances visible on the threads is the remnant of an original thread which broke and contracted during the observation of the sample. Figure 18 represents Butyl rubber containing 8 per cent of diolefin in the feed

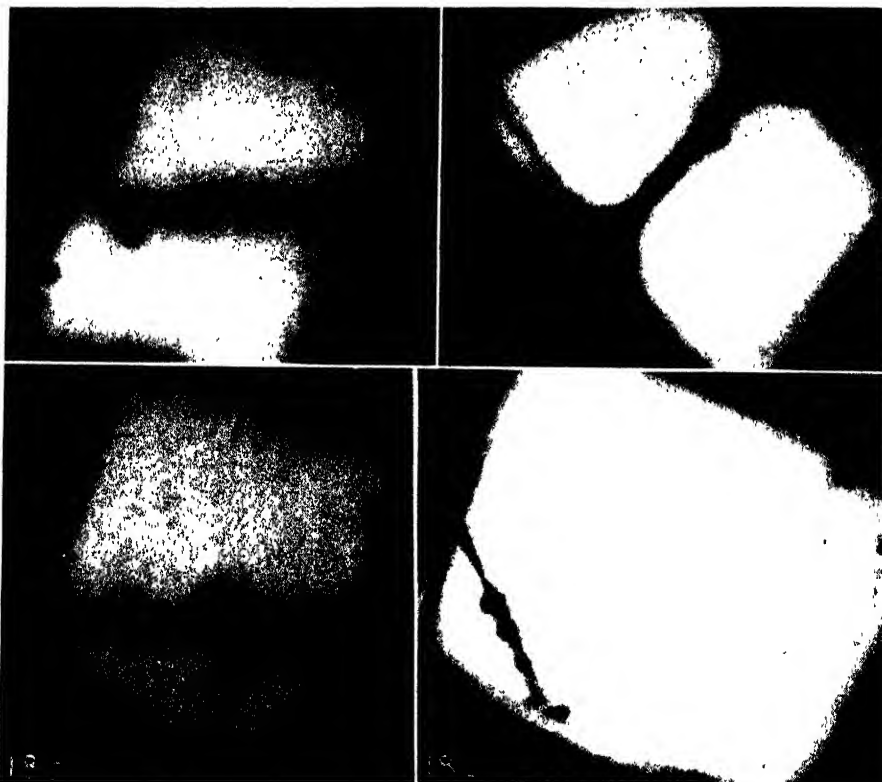


FIG. 17. Butyl rubber (4.5 per cent diolefin): (a) in benzene; (b) in xylene  
FIG. 18. Butyl rubber (8 per cent diolefin): (a) in benzene; (b) in xylene

stock. The films are very weak and even the few ragged threads to be seen are extremely rare. Mostly the whole preparation collapsed before any photomicrograph could be taken.

Results of experiments carried out with Butyl rubber in an industrial laboratory seem to substantiate our contention that molecular-weight distribution of an elastomer is of primary importance for the properties of the product (8).

This series of experiments also proved that the influence of the solvent on the morphology of the polymers is small if present at all. Polymeric substances of high molecular weight have a tendency to form continuous films if the solvent

evaporates too quickly when the polymer film is spread. Therefore, slowly evaporating solvents are preferred in such cases. However, the possible effect of the chemical and physical characteristics of a solvent has as yet not been investigated in detail. Some preliminary studies carried out with six different solvents on pale crepe sol did not reveal any startling differences in its morphology as long as good solutions were obtained.

#### POLYSTYRENE

A series of molecular-weight fractions of polystyrene were prepared by emulsion polymerization (6). Sodium stearate was used throughout as emulsifier. In the preparation of the 8,000 MW polymer benzoyl peroxide was used as catalyst. Polymerization was carried out for 5 hr. at 60°C. The 40,000 and 250,000 MW polymers were obtained by polymerizing the monomer for 4 hr. at 70°C. with the same catalyst. The polymers of 400,000 and 1,000,000 MW were obtained by polymerization for 5 hr. at 60°C. with potassium persulfate as catalyst.

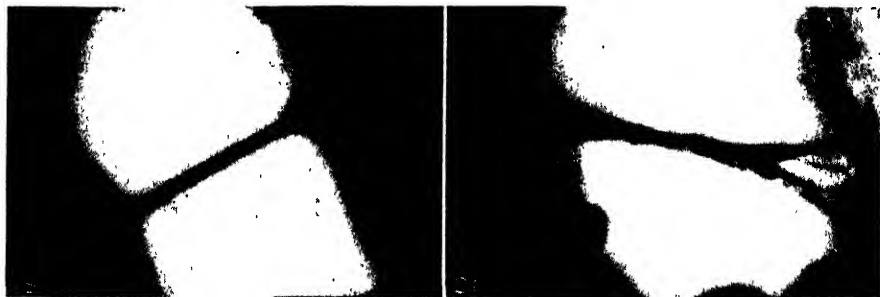


FIG. 19. Polystyrene (MW 8000)

FIG. 20. Polystyrene (MW 40,000)

Preparation of adequate specimens was rather difficult because of the tendency of the polymer to form films which did not break. As with the high-molecular-weight polyisobutylene fractions the preparation of the samples had to be carried out in such a way that evaporation of the solvent occurred after deposition of the film on the wire support. The threads are very stiff and the contours of the broken films are often ragged. Mostly only single threads can be observed, although the higher-molecular-weight fractions indicate a tendency for netting.

Figure 19 represents polystyrene with a molecular weight of 8000; figure 20 polystyrene of 40,000 MW.

If these preparations are subjected to high temperatures, up to 95°C., no changes at all are visible or only some indication of flow at the places where the threads are connected with the wire grid. If a mixture is prepared containing 75 per cent of the 8000 MW fraction and 25 per cent of the 250,000 MW fraction and a film deposited therefrom, and such a preparation is heated to a temperature of 90°C., the formation of globules becomes evident. This clearly demonstrates that globule formation is the result of a polydisperse system, besides the fact that

the facility of globule formation also depends on the molecular configuration and the temperature to which the preparation is subjected.

All of the above experiments show that morphological characteristics which have been observed for lyogels in the electron microscope do not represent the original morphological characteristics of these substances. Electron bombardment and the subsequent rise in temperature will cause changes occurring so quickly that the final observations as recorded do not represent the original sample. Therefore, we do not consider it possible to study such phenomena as flow or the influence of temperature, both of which are of great importance for technological applications of a polymer as well as of scientific interest for the evaluation of its structure.

It is of interest to mention here that in all studies of flow and molecular configuration a very sharp and distinct break occurred at a very definite temperature. The preparations could be heated for a considerable period of time at a certain temperature without inducing flow. If this temperature was raised to the point where enough energy had been introduced, a point which was particular for each polymer system, flow occurred almost instantaneously. Thus if a system would show flow at 70°C., no changes whatsoever could be observed at 68°C., even if the system were kept at that temperature for more than 1 hr.

#### SUMMARY

The influence of temperature on the morphology of preparations of natural and synthetic rubbers, polyisobutylene, and polystyrene has been studied by equipping the incident-light ultramicroscope with a heatable substage. The influence of molecular configuration, molecular-weight distribution, and type of solvent on the morphology is discussed. Experimental and visual proof is offered that the formation of globules, as well as the speed of their occurrence, depends on the molecular configuration, molecular-weight distribution, and temperature.

The authors are greatly indebted to the Esso Laboratories of Standard Oil Development Company for supplying them with the samples of Butyl rubber and of polyisobutylene (Vistanex) and the molecular-weight description of the latter. They also want to express their thanks to Mr. Eli Perry for the polystyrene samples and to Mr. Alan Michaels for the construction of the heatable microscope substage.

#### REFERENCES

- (1) HALL, C. E., HAUSER, E. A., *et al.*: Ind. Eng. Chem. **36**, 634 (1944).
- (2) HAUSER, E. A., AND LE BEAU, D. S.: India-Rubber J. **90**, 601 (1946).
- (3) HAUSER, E. A., AND LE BEAU, D. S.: Ind. Eng. Chem. **37**, 786 (1945); **38**, 335 (1946); India-Rubber J. **91**, 453 (1946).
- (4) HAUSER, E. A., AND LE BEAU, D. S.: J. Phys. Colloid Chem. **51**, 278 (1947).
- (5) HAUSER, E. A., AND SUSICH, G. VON: Kautschuk **7**, 120 (1931).
- (6) PERRY, E.: M. S. Thesis, Department of Chemical Engineering, Massachusetts Institute of Technology, June, 1947.
- (7) REHNER, J.: Lecture at Godfrey L. Cabot Seminar, Boston, Massachusetts, November 16, 1945.
- (8) Private communication.

CALCULATION OF THE SURFACE ENERGY OF  
LIQUID ARGON AND MERCURY<sup>1</sup>

GEORGE JURA

*Department of Chemistry, University of California, Berkeley, California**Received August 25, 1947*

## I. INTRODUCTION

Only a few calculations have been made of the total surface energy of either liquids or solids, and most of the available calculations are for the surfaces of ionic crystals at 0°K. The calculations for the solid are of particular importance, since direct measurements are exceedingly difficult. At present, there are no measurements with which this writer is familiar of the surface energy of solids that may be considered reliable. Perhaps the best work in this field is that of Johnson, Lipsett, and Maass (11, 12), who determined the surface energy of sodium chloride as 400 ergs cm.<sup>-2</sup> Their result can be considered only as an upper bound since there is some doubt in regard to the method of area measurement used by these workers. This figure, 400 ergs cm.<sup>-2</sup>, is much higher than that calculated by Born (1), 147 ergs cm.<sup>-2</sup> for the 100 plane, and than that calculated by Dent (3) from the Born theory of the lattice energy of ionic solids. Dent, using the most refined form of the theory, obtained a value for sodium chloride of 76 ergs cm.<sup>-2</sup> This value is also lower than that measured by Jaeger (10), 180 ergs cm.<sup>-2</sup> for molten sodium chloride.

The general success of the Born theory is such that normally a great deal of credence would be placed in any results obtained from the theory. However, the disparity between the calculated and observed results—the fact that the calculated value for the solid is lower than the measured value for the liquid at much higher temperature—has led some investigators to reserve judgment concerning the validity of the calculations of the surface energy.

It is evident that the ability to calculate the surface energy of a liquid would be a great advantage in the elucidation of the properties of the surfaces of both liquids and solids. One of the results of such a calculation for liquids would be an increased confidence in the results obtained for solids.

In this paper some calculations are made for liquid argon and mercury. Although the equations appear completely different from those used for solids, they are in reality the same. The apparent difference in the calculation is due to the manner in which the number of molecules at a given distance is determined. For a solid the totality of interactions with a given molecule is obtained by a summation over the lattice positions. For liquids, the number of interactions at a distance  $r$  is obtained from the distribution function, and the totality of the interactions is obtained by integration. Because of certain techniques which are peculiar to solids, the discussion of solids is deferred to a later time.

<sup>1</sup> Presented at the Twenty-first National Colloid Symposium, which was held under the auspices of the Division of Colloid Chemistry of the American Chemical Society at Palo Alto, California, June 18–20, 1947.



Because of the difficulties of enumeration of the positions of the atoms or molecules, very few calculations for liquids are extant. The best known is that of Stephan (16), who purported to show that the energy of surface formation was one-half the energy of vaporization. This treatment has been shown by Harkins (6) to be incorrect.

Rayleigh (15) set up a general mathematical scheme whereby the surface energy of a liquid could be calculated. His results have been put in better form by Fowler and Guggenheim (4). These equations, however, have not been applied to any liquid. The treatment in this paper is a modification of the above.

## II. THEORY

The most usual definition of the surface energy of a solid or liquid is the energy required to form 1 sq. cm. of surface. For theoretical calculations this definition leaves much to be desired. A useful definition is obtained as follows: When the surface is increased, molecules are moved from the interior into the surface region. If there are  $n$  molecules per square centimeter of surface region, then the surface energy is the difference in energy between the  $n$  molecules in the surface region and  $n$  molecules in the interior of the solid or liquid. The calculation of the surface energy thus involves the calculation of the energy of a molecule in the bulk phase and of all of the molecules in the surface region.

Hildebrand (7) has shown that the energy,  $E_{\text{vap.}}$ , required to remove a molecule from a liquid to zero pressure in the gas phase is

$$E_{\text{vap.}} = -\frac{2\pi N_0}{V} \int_0^\infty W_0(r)\varphi(r)r^2 dr \quad (1)$$

where  $N_0$  is Avogadro's number,  $V$  the molal volume of the liquid,  $W_0(r)$  the distribution function of the molecules in the liquid,  $\varphi(r)$  the potential function between two molecules; and  $r$  the distance between two molecules. In a like manner the energy of a molecule in the surface region can be written

$$E_i = -\frac{2\pi N_0}{V} \int_0^\infty W_i(r)\varphi(r)r^2 dr \quad (2)$$

where  $W_i(r)$  is the distribution function about this molecule. For all  $n$  of the molecules in the surface region the energy is

$$E_s = -\frac{2\pi N_0}{V} \int_0^\infty \varphi(r)r^2 \left\{ \sum_{i=1}^{i=u} W_i(r) \right\} dr \quad (3)$$

The expression for the surface energy then becomes

$$E_s = \frac{2\pi N_0}{V} \int_0^\infty \varphi(r)r^2 \left\{ \sum_{i=1}^{i=u} (W_0(r) - W_i(r)) \right\} dr \quad (4)$$

In equations 2, 3, and 4 a tacit assumption has been made that the molar volume in the bulk is equal to that in the surface region. This assumption, how-

ever, is only slightly erroneous. The change in molal volume in surface formation is related to the free surface energy by the relationship (14)

$$\frac{(\partial\gamma)}{(\partial P)_T} = \Delta V \quad (5)$$

where  $\gamma$  is the free surface energy and  $P$  the external pressure. Unfortunately the quantity  $\left(\frac{\partial\gamma}{\partial P}\right)_T$  cannot be experimentally determined. Unpublished calculations for solid argon show that there is an expansion of the intermolecular distance in the first layer of the solid of the order of 1 per cent. This expansion introduces an exceedingly small change in the molal volume. Thus, it does not appear that this assumption can lead to an appreciable error.

In theory, all of the functions appearing under the integral sign can be evaluated from first principles. The enormous mathematical difficulties encountered, however, are so great that only approximate values for the functions can be obtained. The approximate nature of the theoretical functions makes it advisable to use the values of the functions as determined by experiment. Of the three functions,  $W_0(r)$ ,  $\varphi(r)$ , and  $W_i(r)$ , only  $W_0(r)$  can be experimentally determined in detail. The potential function  $\varphi(r)$  can be determined in a number of ways, and in at least two forms from experimental data. Although no two of the proposed potential functions agree in detail for all values of  $r$ , the differences are small so that no serious error is introduced by using any of the proposed equations. For the distribution of the molecules in the surface region,  $W_i(r)$ , no experimental data are available. The validity of the calculations presented in this paper is based on the approximation of the form of  $W_i(r)$ .

The distribution about a given molecule in the surface region is made up of two parts: (1) the molecules in the liquid phase, and (2) the molecules in the vapor phase. If the concentration of molecules in the vapor phase is low, i.e., the temperature is such that the vapor pressure is low, the concentration is so low that the magnitude of the interactions with the molecules in the gas phase will be small compared to the interactions in the liquid. Thus, at these low temperatures, only the contribution of the molecules in the liquid need be considered.

Previously, it has been pointed out that the change in the interatomic distance in the surfaces of solids and liquids of the rare gases is small, on the order of 1 per cent. Since there is no appreciable change in the interatomic distance, any change in the distribution function must be due to the asymmetry found in the surface. For van der Waals molecules, it has been shown by Lennard-Jones (13) that 80 per cent of the total interaction is due to the nearest neighbors. These two facts indicate that the distribution function in the surface region on the liquid side of the interface is substantially the same as in the interior. In the numerical evaluation of the surface energy, it is assumed that the distribution function is the same regardless of the position of the molecule.

Figure 1a exhibits a two-dimensional lattice. The molecule marked A is in the interior and if a line is drawn through the center of this molecule, one-half of the molecular centers will be on each side of this line. The horizontal line through the center of molecule A is such a line. Figure 1b exhibits the same lat-

tice when the molecules above A have been removed so that A is in the surface. The important fact is that in surface formation one-half of the neighbors of a molecule in the top layer are not removed. Those atoms whose centers lie in the same plane remain as neighbors, next nearest neighbors, etc. For the two-dimensional lattice shown in figure 1a only one of the four nearest neighbors is removed in surface formation. Thus if the assumption is made that only the nearest neighbors need be considered, then for the two-dimensional lattice the surface energy is one-fourth of the energy of vaporization. By making the same assumptions as above for the three-dimensional lattices involving cubic and hexagonal close packing, the ratio of the surface energy to the energy of vaporization would still be one-fourth.

If a liquid is considered instead of a solid it is reasonable that again one-half of the molecules will not be removed from the vicinity of a molecule in the surface region. Many of the surrounding molecules will remain in the surface. Since a liquid does not have a lattice structure, it is not possible to enumerate the position of the surrounding molecules as simply as for the lattice of a solid,

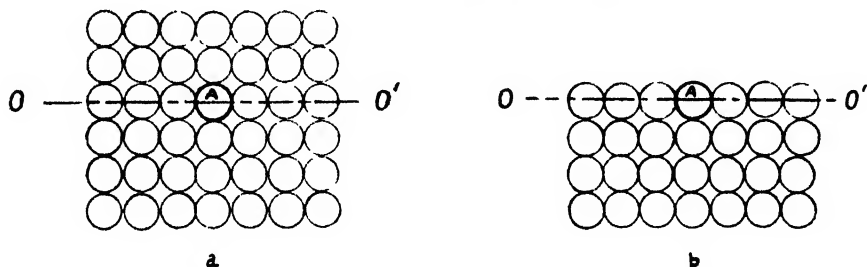


FIG. 1. (a) A two-dimensional square lattice; (b) the same as figure 1 (a) except that a surface (1.0) has been formed through molecule A. Note that only one of the four nearest neighbors has been removed in surface formation.

and an adjustment must be made in the limits of integration of the distributive function.

The assumption made in this paper is that any atom whose center is a distance of  $r_0/2$ , where  $r_0/2$  is the closest distance of the nearest neighbors, remains in the surface. Figure 2 illustrates the necessary calculations under the assumptions that have been made. The circle composed of the solid and dotted lines at some distance  $r$  represents some value of the distribution function  $W_0(r)$ . If the molecule were in the interior the total contribution to the energy would be obtained by integrating completely through  $2\pi$  radians. The energy of a molecule in the surface would be obtained by integrating along the dotted section of the line  $OO'$  which has been placed a distance of  $r_0/2$  above the center of the atom. The surface energy is then integral around the solid arc above the line  $OO'$ .

It is evident that the calculated results will depend upon the exact position of the line  $OO'$  and that some justification for the chosen placement is necessary. First, the position of  $OO'$  through the center can be ruled out on the basis that this position appears unreasonable from the discussion on the simple lattice model. Also, the calculated results are much too high to agree with the experimental

results. These latter calculations have not been carried to completion, but those made show that the ratio of surface formations to that of vaporization is over 0.67. This is much higher than the observed values. The ratio of surface formation to the energy of vaporization is used here in the sense defined by Harkins (6), that the surface may be considered to be monomolecular. Later it will be shown that only about 78 per cent of the surface energy is contributed by the molecules in the first layer.

The limit of integration cannot be placed much higher than  $r_0/2$ , since to do so would actually place many molecules in the "second" rather than the first layer. That is, as many molecules as possible are placed in the top layer of the surface.

Finally, if the nearest-neighbor approximation is made and the integration carried through for the most probable distance, it is found that the ratio of surface energy to the energy of vaporization is one-fourth, which is in agreement with the result obtained for a lattice. Thus it appears that the placing of the limit of integration at  $r_0/2$  is reasonable.

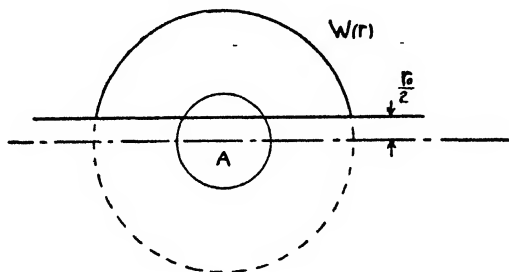


FIG. 2. A graphical illustration of the method of calculation. The center of molecule O is placed on a hypothetical geometrical surface  $OO'$ . The larger circle, composed of solid and dotted lines, represents the value of the distribution function  $W(r)$ . The surface energy is the integral of  $W(r)$  along the solid line.

The equation for the contribution to the energy of a molecule in the surface region to the surface energy in terms of the approximations made can now be written. The area of a spherical cap of height  $h$  of a sphere whose radius is  $r$  is

$$A = 2\pi rh$$

If the atom is a distance  $\alpha$  below the surface, the height  $h$  of the cap is  $r - \alpha - \frac{r_0}{2}$ .

Thus the contribution to the surface energy may be written

$$E = \frac{\pi N_0}{V} \left( r - \alpha - \frac{r_0}{2} \right) W(r) \varphi(r) r^2 dr \quad (6)$$

If an arbitrary molecule is chosen in the surface, then the total surface energy is the difference in energy between a column whose area is that of the molecule and extending theoretically, to an infinite depth, and a similar column in the interior of the liquid. The number of molecules at a distance  $\alpha$  below the center of the chosen molecule is

$$\frac{\pi r_0^2 N_0 W(\alpha)}{V}$$

Thus, the contribution of this column to the surface energy can be written:

$$E_{\text{col.}} = \frac{\pi^2 r_0^2 N_0^2}{V^2} \int_0^\infty W(\alpha) d\alpha \int_{\alpha+(r_0/2)}^\infty \left( r - \alpha - \frac{r_0}{2} \right) W(r) \varphi(r) r^2 dr \quad (7)$$

The equation is written in the above form to indicate clearly how the two necessary numerical integrations are performed to obtain the final results. The integral of equation 6 is first evaluated for various values of  $\alpha$ , and these results are then multiplied by  $W(\alpha)$  and integrated with respect to  $\alpha$ . The number of such columns per square centimeter may be estimated on the assumption of close packing. Thus the surface energy may be evaluated by two numerical integrations and the assumption of the packing of the molecules in the surface region.

The calculations have been made for mercury at 20°C. and argon at -185.7°C., and are given in table 1 with the experimentally determined values. For argon

TABLE 1  
*Observed and calculated surface energies of liquid argon and mercury*

	<i>E</i> (CALCULATED)	<i>E</i> (OBSERVED)
	<i>ergs cm.<sup>-2</sup></i>	<i>ergs cm.<sup>-2</sup></i>
Argon . . . . .	32	35
Mercury . . . . .	500	525

the distribution function used was that of Gingrich (5) and the potential function that of Buckingham (2), using the tenth power as the exponent of the distance in the repulsive potential. For mercury the distribution function of Wakeham and Boyd (17) was used and the potential function was that proposed by Hildebrand (8). The values in table 1 for the observed values were calculated from the surface tension-temperature data presented in the *International Critical Tables* (9).

An examination of the values in table 1 shows that the agreement between the calculated and observed values is excellent. The agreement indicates that the surface energy of a liquid can be properly calculated by the use of a distribution function rather than the assumption of a lattice.

It is true that equally good agreement between observed and calculated values for the surface energy can be obtained if it is assumed that the liquid has the same lattice as that of the solid. For example, if it is assumed that liquid argon has a face-centered cubic structure, and the interatomic distance is adjusted to give the proper density of the liquid, then the calculated surface energy is also 32 *ergs cm.<sup>-2</sup>* the same as that obtained by the use of the distribution function. Even though equally good results can be obtained by considering the liquid as a lattice, the treatment is one that cannot be condoned. Liquids are known not to possess a lattice structure, and any essentially correct treatment cannot be based upon the lattice concept even though in a numerical computation it gives the correct or same answer as a method not based on a lattice structure.

The calculated values for both argon and mercury are lower than the observed values. This, however, is not believed to be significant. The difference is

certainly less than that which might be expected solely from the estimation of the limits of integration, that is, the number of molecules that are neighbors of a molecule in the surface region.

Apart from the actual agreement between observed and calculated surface energies of the liquids, two other facts of considerable importance are obtained. The first of these is the thickness of the surface region. These calculations show that 99 per cent of the effect of the surface for this class of molecule is to be found within 15 Å. or roughly four molecular diameters of the surface. Of this quantity, approximately 78 per cent is concentrated in the first layer. These results indicate that the assumption that the surface of this class of liquids is monomolecular is energetically justifiable as a first approximation, but that in any refined treatment at least four layers must be considered.

Since van der Waals forces are the shortest-range molecular forces known, it appears reasonable to assume that to within 1 per cent, the surface region is at least four layers thick. Dent has calculated for ionic solids that the surface region to an approximation of 1 per cent is thirty layers deep. Since the coulomb forces are the longest-range molecular forces, it is reasonable that this would be the maximum thickness of the surface region. Thus, these two computations place an upper and a lower bound on the thickness of the surface region. One other result appears to be inherent in this treatment. The energy of vaporization of most liquids when their vapor pressures are low is only slightly dependent upon the temperature. For most calculations no great error is made if it is assumed that  $\left(\frac{\partial E}{\partial T}\right) = 0$ . Since the expression for the surface energy is of the same form as that for the energy of vaporization, it would be predicted that when the vapor pressure is low the derivative of the surface energy with respect to the temperature would be small. That is, as a first approximation the surface energy should be independent of the temperature. Within the experimental error of the determination of the surface energies of most liquids, it is found that the surface energy is independent of temperature. The above statement is equivalent to stating that the surface tension is a linear function of the temperature. At those temperatures where the vapor pressure is low, this is true within experimental error for nearly all "normal" liquids.

### III. SUMMARY

1. An equation for the surface energy of a liquid is set up in terms of the potential function, distribution function, and molal volume. By an appropriate approximation of the limits of the bulk distribution function, it is possible to use the distribution function determined in the interior of the liquid.
2. The above expressions are applied to liquid argon and mercury. The calculated values for the surface energy are 32 and 500 ergs cm.<sup>-2</sup>, respectively. These are comparable to the observed values of 35 and 525 ergs cm.<sup>-2</sup>
3. From the above calculations it is found that 99 per cent of the surface energy is to be found within four molecular diameters of the surface and that approximately 78 per cent of the effect is in the first layer.

4. The expression for the surface energy indicates that at low temperatures the surface energy should vary with temperature in approximately the same manner as energy of vaporization. This means that when the vapor pressure is low, for most liquids the derivative of the surface tension with respect to the temperature should be approximately zero. This is in accord with most measurements.

## REFERENCES

- (1) BORN, M.: *Encyclopedie der mathematischen Wissenschaft* **5**, 743 (1943).
- (2) BUCKINGHAM, R. A.: *Proc. Roy. Soc. (London)* **A168**, 264 (1938).
- (3) DENT, B. M.: *Phil. Mag.* [7] **8**, 530 (1929).
- (4) FOWLER, R. H., AND GUGGENHEIM, E. A.: *Statistical Thermodynamics*, p. 445. University Press, Cambridge (1939).
- (5) EISENSTEIN, A., AND GINGRICH, N. S.: *Phys. Rev.* **58**, 307 (1942); **62**, 261 (1942).
- (6) HARKINS, W. D.: *J. Am. Chem. Soc.* **44**, 653 (1922).
- (7) HILDEBRAND, J. H., AND WOOD, S. E.: *J. Chem. Phys.* **1**, 817 (1933).
- (8) HILDEBRAND, J. H., WAKEHAM, H. R., AND BOYD, R. N.: *J. Chem. Phys.* **7**, 1094 (1939).
- (9) *International Critical Tables*, Vol. IV, p. 423. McGraw-Hill Book Company, Inc., New York (1928).
- (10) JAEGER, F. M.: Reference 9, p. 443.
- (11) LIPSETT, S. G., JOHNSON, F. M. G., AND MAASS, O.: *J. Am. Chem. Soc.* **49**, 925, 1940 (1927).
- (12) LIPSETT, S. G., JOHNSON, F. M. G., AND MAASS, O.: *J. Am. Chem. Soc.* **50**, 2701 (1928).
- (13) LENNARD-JONES, J. E., AND INGRAM, A. E.: *Proc. Roy. Soc. (London)* **A107**, 636 (1925).
- (14) LEWIS, G. N., AND RANDALL, M.: *Thermodynamics and the Free Energy of Chemical Substances*, p. 248. McGraw-Hill Book Company, Inc., New York (1923).
- (15) RAYLEIGH, LORD: As quoted by Fowler and Guggenheim in reference 4.
- (16) STEFAN, J.: *Wied. Ann.* **29**, 655 (1896).
- (17) WAKEHAM, H. R., AND BOYD, R. N.: *J. Chem. Phys.* **7**, 958 (1939).

A DUAL-SURFACE B.E.T. ADSORPTION THEORY<sup>1</sup>

WILLIAM C. WALKER<sup>2</sup> AND ALBERT C. ZETTMLOYER

*William H. Chandler Laboratory of Chemistry, Lehigh University, Bethlehem, Pennsylvania*

*Received August 25, 1947*

In recent years the multimolecular adsorption theory of Brunauer, Emmett, and Teller (5) has become one of the most important and useful tools in the field of gas adsorption. In its linear form the simple basic equation ( $n = \infty$ ),

$$\frac{x}{v(1-x)} = \frac{1}{v_m C} + \frac{(c-1)x}{v_m c} \quad (1)$$

<sup>1</sup> Presented at the Twenty-first National Colloid Symposium, which was held under the auspices of the Division of Colloid Chemistry of the American Chemical Society at Palo Alto, California, June 18-20, 1947.

<sup>2</sup> Post-Doctoral Fellow in the Lehigh Institute of Research.

where  $x$  = relative pressure, i.e., measured pressure divided by condensation pressure of the adsorbate,

$v$  = measured volume of gas adsorbed,

$c$  = constant related to heat of adsorption, and

$v_m$  = constant, the volume required to complete a unimolecular layer,

has been widely used for the determination of surface areas. Usually, measurements of the adsorption of nitrogen on the adsorptive or catalytic solid at the temperature of liquid nitrogen have been employed in the calculation.

Most data for nitrogen, as well as for other gases, give linear plots of  $x/v(1 - x)$  versus  $x$  between 0.05 and 0.35 relative pressure. The deviations from linearity generally occur outside of this range and can be conveniently divided into two groups: the cases where the data show too little adsorption, and those where the data show too much adsorption. Too little adsorption at higher relative pressures is usually interpreted as being due to the pores, i.e., the "n" effect (3, 4, 10) or to the heat of adsorption in the second and succeeding layers being less than the heat of liquefaction (1). Modifications of the simple B.E.T. equation based on these concepts increase the range of linearity to 0.7 relative pressure and sometimes beyond.

Too large adsorption below 0.05 relative pressure is characteristic of most adsorption data (3). For this deviation, which is generally attributed to adsorption on the more active portions of the surface, no modifications of the basic theory have been proposed. Too large adsorption at higher pressures has been attributed to a heat of adsorption in the second layer greater than the heat of liquefaction (3). A modified B.E.T. equation is available to handle this case (5), but there are no instances in the literature of its application to data. It may be shown, however, that for very low net heats in the second layer this equation predicts a slight deviation in this direction. As the net heat is increased, the deviation changes to decidedly too little adsorption at high relative pressures. This equation also predicts excessive adsorption at lower pressures. Details will be presented in a future communication.

In a few cases there has apparently been too much adsorption at both high and low pressures, and these effects encroach upon the usually linear region so as to make the plot of  $x/v(1 - x)$  versus  $x$  concave to the pressure axis over practically all of this region (9, 16). The magnitude of the concavity in these instances cannot be accounted for by too high a heat of adsorption in the second layer.

In the present paper an attempt is made to show that some cases where too much adsorption is observed can be explained by non-homogeneity of the surface.

#### SURFACE NON-HOMOGENEITY

The B.E.T. theory assumes that a single value for the heat of adsorption in the first layer, that is, a single value of  $c$ , applies to the entire surface of the adsorbent. In many adsorbents different portions of the surface differ widely in chemical nature, as in the case of mixed, promoted, or supported catalysts. Associated with these various portions of the surface there may be expected to be



different heats of adsorption and consequently different  $c$  values. Furthermore, even when the solid is chemically uniform, the heat of adsorption may be expected to vary considerably over different portions of the surface. Taylor (15) suggested this idea in his theory of active spots, and others (7, 12, 13, 14) have made quantitative calculations of the differences to be expected at edges and corners and on different faces of the same crystal.

Langmuir (11) expanded his adsorption equation to take care of this inhomogeneity of the adsorbing surface in the following manner:

$$v = \frac{v_{mA} b_A p}{1 + b_A p} + \frac{v_{mB} b_B p}{1 + b_B p} + \dots + \frac{v_{mi} b_i p}{1 + b_i p} \quad (2)$$

where the total  $v_m$  is the sum of the  $v_{mi}$ 's and where the  $b_i$ 's depend upon the corresponding heats of adsorption on the different surface elements. Qualitatively, Langmuir could account for the different  $v_m$ 's obtained with different adsorbates on the same adsorbent with this equation, but quantitatively the large number of constants prevents an adequate test.

The Langmuir equation, of course, deals only with unimolecular adsorption. For multimolecular adsorption, the B.E.T. equation can also be rearranged and expanded to express the volume adsorbed as the sum of the volumes adsorbed on the different surface elements:

$$v = \frac{x}{1-x} \left[ 1 + \frac{v_{mA} c_A}{(c_A - 1)x} + 1 + \frac{v_{mB} c_B}{(c_B - 1)x} + \dots + \frac{v_{mi} c_i}{(c_i - 1)x} \right] \quad (3)$$

Here each  $c_i$  is related to that particular heat of adsorption effective over the surface element  $v_{mi}$ . In general, a large number of parameters will be needed to represent completely the adsorptive properties of a surface, but important conclusions can be reached if two terms, rather than the customary single term represented in equation 1, are employed:

$$v = \frac{x}{1-x} \left[ 1 + \frac{v_{mA} c_A}{(c_A - 1)x} + 1 + \frac{v_{mB} c_B}{(c_B - 1)x} \right] \quad (4)$$

This equation, then, involves the assumption that the surface is of a dual nature.

#### CHARACTERISTICS OF DUAL SURFACES

Equation 4 is to be applied to data which are not adequately handled by the B.E.T.  $n = \infty$  equation. Therefore, a comparison of the two equations is instructive. The most significant comparison can be made by applying the B.E.T. equation 1 to isotherms obeying the dual-surface equation. It is desirable to study the relationships in the 0.05 to 0.35 relative pressure region, which is usually plotted, and in the region below 0.05 relative pressure. The effect of the pores may obviate any comparison for actual data above 0.35.

#### *Region between 0.05 and 0.35 relative pressure*

Suppose a hypothetical surface is made up of two parts. With the four parameters of equation 4 assigned, the isotherm can be calculated. And from the

known values of  $v$  at various intervals of  $x$ , the B.E.T. functions can be calculated and the B.E.T. plot constructed.

Figure 1 shows this plot when both  $v_{m_A}$  and  $v_{m_B}$  are assigned values of 10, so that the total  $v_m$  is 20, but  $c_A$  is taken as 100 and  $c_B$  as 2. There is a pronounced concavity toward the relative pressure axis. Line I represents the best straight line through the points as calculated by the method of least squares. The  $v_m$  calculated from the slope and intercept of this line is 15.98, which is 20.1 per cent lower than the correct value of 20; the  $c$  value is 20.4, intermediate between the values assumed for  $c_A$  and  $c_B$ .

The highest reasonable value of  $v_m$  that can be obtained from figure 1 corresponds to line II, the line of lowest reasonable slope. From line II,  $v_m$  is 17.9, which is 10.5 per cent low, and  $c$  is 9.6. Thus, when surface non-homogeneity

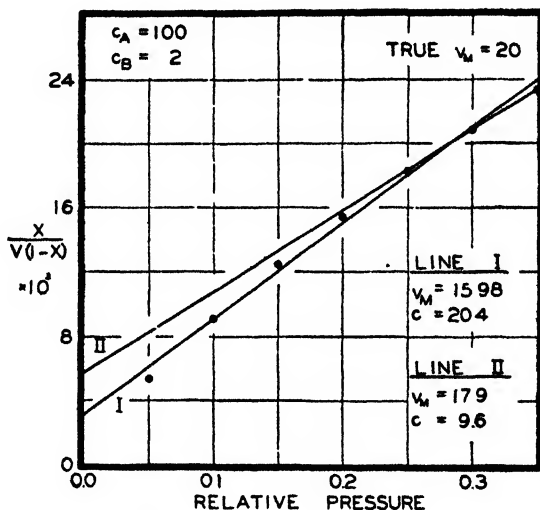


Fig. 1. Typical deviation of usual B.E.T. plot when one  $c$  is very low

causes the B.E.T. plot to be curved in this manner, the correct  $v_m$  cannot be determined from a usual B.E.T. plot.

If three of the four parameters are kept fixed, the effect of varying the fourth can be studied. In figure 2, the per cent error in  $v_m$  from the best straight line is plotted against the logarithm of  $c_B$  for equal values of  $v_{m_A}$  and  $v_{m_B}$ . A family of curves is given, each for a different fixed value of  $c_A$ : 1, 2, 5, 10, 50, and 10,000. When the  $c$ 's are different and one of them falls unusually low (less than 30), the error in  $v_m$  becomes large. At high values of  $c_B$  these curves approach asymptotes as  $c_B$  approaches infinity. If these curves were extended below  $c_B = 1$ , they would asymptotically approach 50 per cent error since, with  $c_B$  equal to zero, there would be no adsorption on half of the surface.

The  $c$  value obtained from the best straight line is always intermediate between  $c_A$  and  $c_B$ , as indicated in figure 3, but generally reaches a minimum at a low value of  $c_B$ . As  $c_B$  becomes very large, the average  $c$  approaches an asymptote which is the value when  $c_B$  is infinite. If the curves in figure 3 were extended to  $c_B =$

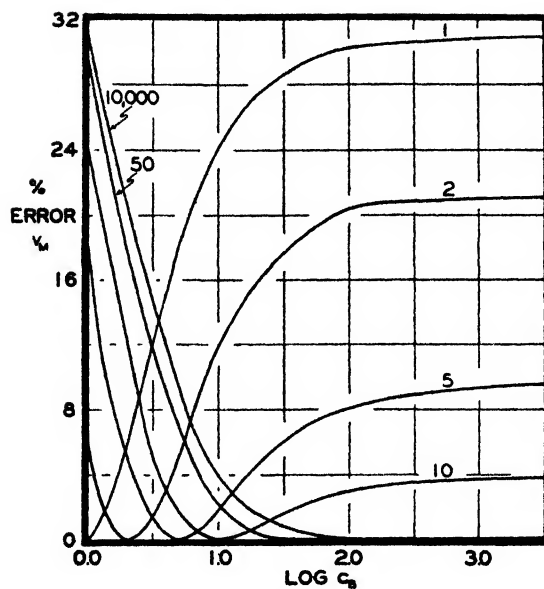


FIG. 2. Error in  $v_m$  as a function of  $c_A$  and  $c_B$  for a 1:1 ratio of surfaces

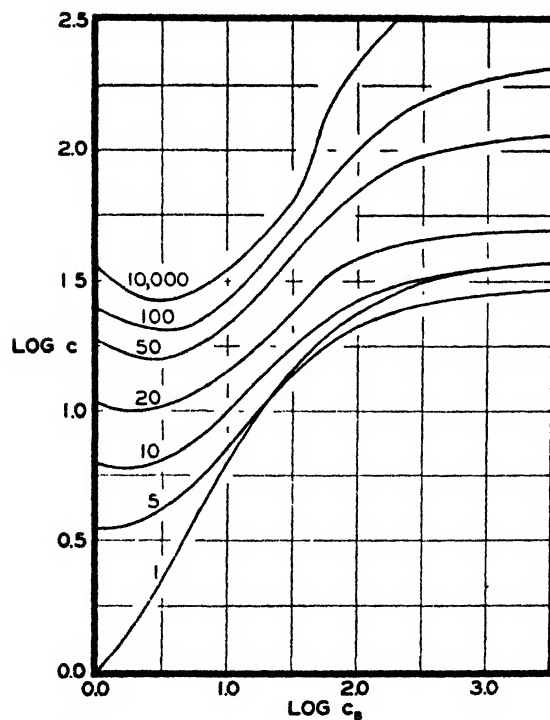


FIG. 3. Over-all  $c$  as a function of  $c_A$  and  $c_B$  for a 1:1 ratio of surfaces

0, then the  $c$  from the B.E.T. plot would approach  $c_A$ . It is evident that the  $c$  obtained from a linear-appearing B.E.T. plot is not necessarily an acting value.

Although the calculated over-all  $v_m$  is only precisely equal to  $v_{mA}$  plus  $v_{mB}$  when  $c_A$  is equal to  $c_B$ , the value is not much in error when both  $c_A$  and  $c_B$  are large (say, above 30). Fortunately,  $c$  has usually been found to lie between 50 and 500 for the adsorption of nitrogen at the temperature of liquid nitrogen (8). Several exceptionally low values of  $c$ , however, have been reported recently (16, 18).

In the above considerations of the variations of  $v_m$  and  $c$  with  $c_A$  and  $c_B$ , the ratio of  $v_{mA}$  to  $v_{mB}$  was kept constant, but the  $v_m$  and  $c$  obtained are also dependent upon this ratio. This dependency is illustrated in figure 4 for  $c_A$  equal to 100 and  $c_B$  equal to 2. The error in the  $v_m$  obtained from the best straight line reaches a maximum of about 27 per cent when the second portion of the surface is 80 per cent of the total. The  $c$  value falls gradually as the per cent of the  $c_B$  surface increases. For a system in which both  $c$ 's are known, it is evident that the  $c$  value

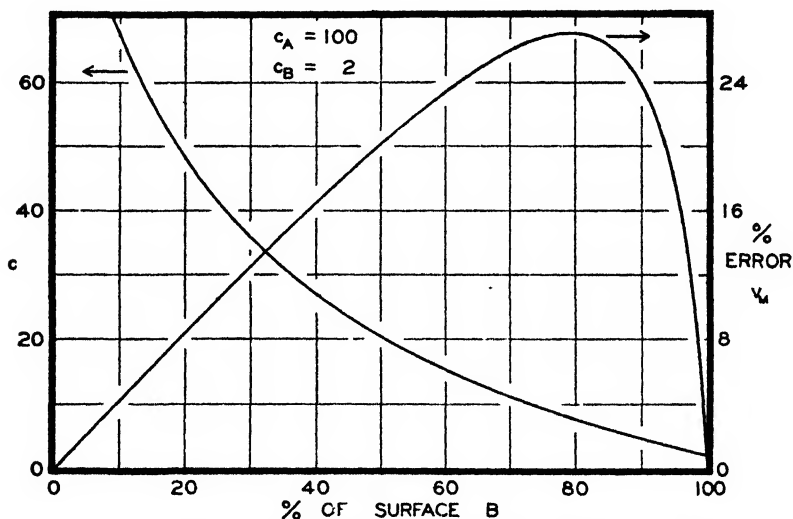


FIG. 4. Influence of ratio of extents of two surfaces present

determined from the best straight line may be employed as a measure of the relative amounts of the two surfaces present.

#### *Region below 0.05 relative pressure*

From figure 5 it is learned that the dual-surface theory leads to curvature of the B.E.T. plot if the  $c$  values differ, even though both  $c$  values are large. The curvature, however, sets in only at low relative pressures. The straight line in figure 5 was calculated by the method of least squares from points in the region of 0.05 to 0.35 relative pressure where the plot is essentially linear. As straight lines are drawn through points at lower relative pressures,  $v_m$  and  $c$  change so as to approach asymptotically the values for the portion of the surface having the higher heat of adsorption.

B.E.T. plots typically "tail off" below 0.05 relative pressure (4), and the con-

cept of active spots has generally been given as a qualitative explanation. The dual-surface concept provides a quantitative approach to this phenomenon.

#### TREATMENT OF DATA

If an adsorbent possesses the properties of a dual surface, the solution of equation 4 will give a more precise value of  $v_m$ , the proper  $c$  values for the two surfaces and the amounts of each surface present.

#### *Simultaneous equations*

The four parameters of equation 4 can be obtained from four simultaneous equations set up with four sets of data for  $v$  and  $x$ . There is only one real solution

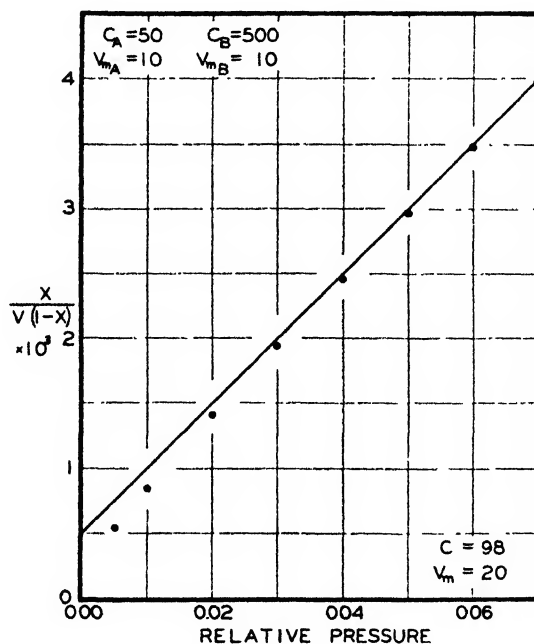


FIG. 5 Typical deviation at low relative pressures

to the set of four equations. The solution, however, is tedious and sensitive to which four adsorption points are chosen. If one of the parameters, such as one of the  $c$ 's, is known independently, then only three simultaneous equations are needed. In either case, however, a graphical solution is more desirable.

#### *Graphical solutions*

One  $c$  may be known; it may, for example, have been determined from adsorption measurements made on one of the pure substances of which the composite material is composed. In the data of figure 1 then,  $c_A$  may be known to be 100.

If  $c_A$  is known, the following graphical approximation method which makes use of all the measured points can be used: A value of  $v_{mA}$  is chosen at random. The

isotherm for the first portion of the surface is then calculated from the B.E.T.  $n = \infty$  equation 1 and subtracted from the total isotherm. The resulting isotherm is then tested for linearity on a B.E.T. plot. If the B.E.T. plot for this second portion of the surface is concave to the pressure axis, the value chosen for  $v_{mA}$  is too low, and if convex, the value is too high. On the basis of these observations, new approximations are made until a straight line is obtained. Small variations in the choice of  $v_{mA}$  markedly affect the linearity. Finally, from the linear plot  $v_{mB}$  and  $c_B$  are calculated.

Both  $c$ 's may be known; they may, for example, have been determined from measurements on the first of a series of similar samples. In this case the dual-surface equation (equation 4) can be arranged in a linear form

$$\frac{v(1-x)[1+(c_A-1)]}{c_A x} = v_{mA} + v_{mB} \frac{c_B}{c_A} \frac{1+(c_A-1)x}{1+(c_B-1)x} \quad (5)$$

The intercept and slope of the plot of equation 5 are directly  $v_{mA}$  and  $v_{mB}$ , respectively.

Another procedure if both  $c$ 's are known is to use a graph such as figure 4 as a calibration curve. The  $c$  from the best straight line of the B.E.T. plot will give the ratio of the extents of the two portions of the surface as well as the error in the  $v_m$  from this line. This information will establish the extents of the two portions of the surface.

### *Adaptability*

Application of the dual-surface theory provides a method for measuring the extents of various portions of a composite surface through physical adsorption. The only necessary requirement is that the adsorbate be chosen to give a low  $c$  (below about 30) for one portion of the surface. The remainder of the surface may consist of a multitude of different surfaces so long as their  $c$  values are all relatively high. Analysis of the adsorption data will then give the extent of each portion of the surface.

### HEATS OF ADSORPTION

In the B.E.T. theory

$$c = \frac{a_1 b_2}{b_1 a_2} e^{(E_1 - E_L)/RT} \quad (6)$$

where the coefficient of the exponential is usually taken as unity. The value of the average net differential heat ( $E_1 - E_L$ ) for adsorption in the first layer can then be readily calculated from the  $c$  value determined from the B.E.T. plot. The values of  $E_1 - E_L$  determined in this manner, the so-called B.E.T. heats of adsorption, have generally been found to be much lower than calorimetric or isosteric heats (2). According to the statistical calculations of Cassie (6), the ratio of the constants should be much lower than unity. Alteration in this direction would give rise to better agreement between B.E.T. and other heats of adsorp-

tion. For purposes of discussion here, however, the ratio will still be taken as unity; the conclusions arrived at will be independent of this choice.

A linear-appearing B.E.T. plot, it should be borne in mind, does not necessarily mean that the surface is predominantly uniform in nature with respect to heat of adsorption.

### Single surface

From the nature of the B.E.T. assumptions, it might be at first supposed that with one over-all  $c$  value the plot of B.E.T. heat of adsorption *versus* volume ad-

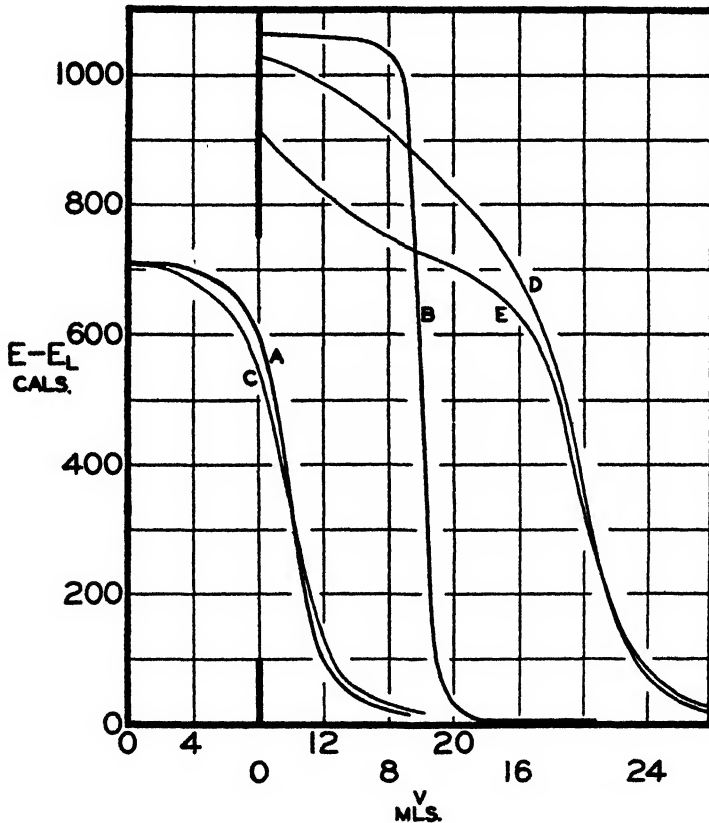


FIG. 6. Theoretical net differential heats of adsorption as a function of the volume adsorbed

sorbed would display a first-order break where  $v$  equals  $v_m$ . Further consideration indicates that this cannot be so, since for the first portions of gas going on the surface, the B.E.T. theory considers that some of the gas is adsorbed in the second and higher layers. The first layer is theoretically not completed until  $p_0$  is reached. As a consequence of the B.E.T. theory, it may be shown that

$$v_1 = (1 - x)v \quad (7)$$

where  $v_1$  is the volume adsorbed into the first layer. This is a surprisingly simple relationship.<sup>3</sup> Equation 7 was obtained in another way by Cassie (6).

The net differential heat of adsorption may be shown to fall off gradually according to the equation:

$$E - E_L = RT \ln c \frac{dv_1}{dv} = \frac{RTc \ln c}{2(c-1)} \left[ 1 - \frac{V-1+2/c}{\sqrt{(V-1)^2 + 4V/c}} \right] \quad (8)$$

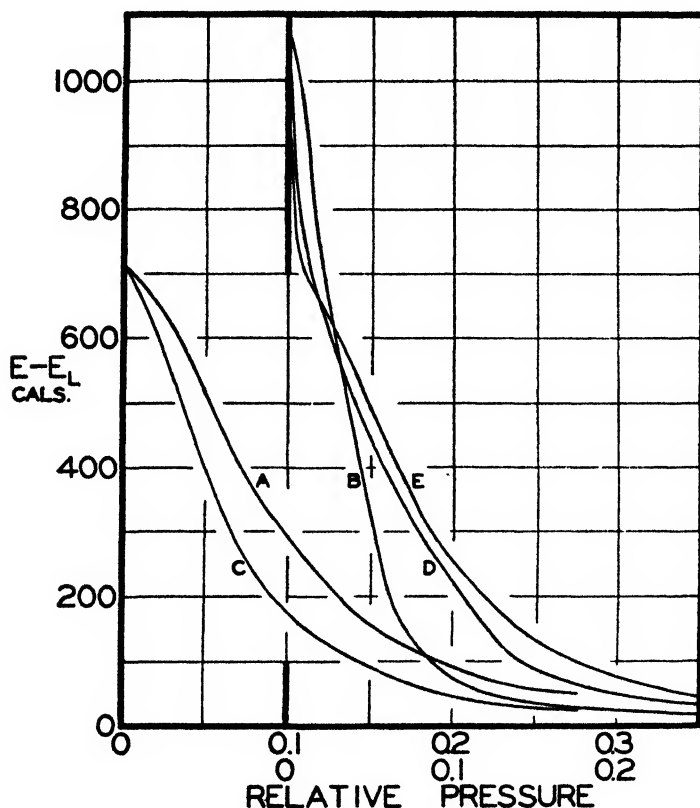


FIG. 7. Theoretical net differential heats of adsorption as a function of relative pressure

where  $V = v/v_m$ . For equation 8, the usual assumption of no net heat of adsorption in the second and succeeding layers has been used.

Plots of equation 8 for  $c$  equal to 100 (curve A) and 1000 (curve B) with  $v_m$  equal to 10 are given in figure 6; the breaks in the curve would be even less abrupt at lower  $c$  values. In figure 7, the plots of the net heats of adsorption *versus* the relative pressure (curves A and B) fall off more gradually.

<sup>3</sup> The asymptote of the plot of  $v_1$  against  $x$  may be determined to estimate  $v_m$ , but this method does not seem to offer any advantage over the older Point B method of Emmett and Brunauer.



### Dual surface

If the  $c$  value for one portion of the surface is low, it has been shown previously that the estimated  $v_m$  from the best straight line of the B.E.T. plot may be much too low. The heat-of-adsorption plot, on the other hand, may be expected to be affected only slightly, because relatively little adsorption will take place on the area of low  $c$  value at low relative pressure. This is demonstrated in figure 6, where with  $c_A$  and  $c_B$  assigned values of 100 and 1, respectively, and  $v_{m_A}$  and  $v_{m_B}$  both 10, the shape and position of the curve (curve C) is only slightly altered from that for the single surface with  $c$  equal to 100 and  $v_m$  equal to 10. The net heat for the dual surface is also plotted against the relative pressure in figure 7 (curve C).

When the dual surface is composed of a portion with a  $c_A$  of 100 and  $v_{m_A}$  of 10, and a portion with a  $c_B$  of 1000 and a  $v_{m_B}$  of 10, the gradual decrease (curves D) of figures 6 and 7 is obtained. Even for the first amount of gas adsorbed the calculated (or measured) heat of adsorption does not represent the maximum that is operating. When only 20 per cent of the surface is the B portion with the relatively high heat of adsorption (active spots), then the curve shows two breaks (curves E); for this plot  $v_{m_A}$  is 16 and  $c_A$  is 100, whereas  $v_{m_B}$  is 4 and  $c_B$  is 1000.

It is evident from these curves that for an actual surface where there is a distribution of heats of adsorption with a small part of the surface having a very high heat, the plot of differential heat of adsorption *versus* volume adsorbed will be very steep at low volumes with an increasing slope. This curve can be fairly regular or it may have points of inflection, depending upon the relative extents of the portions of the surface with various heats of adsorption.

### SUMMARY

A dual-surface theory of adsorption based on the multimolecular adsorption theory of Brunauer, Emmett, and Teller is presented. This theory involves the concept of an adsorbing surface made up of two portions differing in their  $c$ 's or heats of adsorption.

Adsorption data for such a surface show the following characteristics when plotted according to the usual linear form of the B.E.T. equation: (1) Both  $c$ 's large: linear from 0.05 to 0.35 relative pressure with points falling below the straight line at lower pressures. (2) One  $c$  small: concave to the pressure axis.

When the B.E.T. plot is concave to the pressure axis from 0.05 to 0.35, the  $v_m$  obtained from the best straight line in this region is too small. The value of  $c$  and the error in  $v_m$  are given for a wide range of  $c$ 's for the two portions of the surface.

The dual-surface equation presents a method for measuring the extent of a portion of a solid surface by physical adsorption.

Methods are presented for analyzing appropriate data for the "true" total  $v_m$  and the relative amounts of the two surfaces present.

The authors acknowledge the assistance of James A. Long in carrying out some of the calculations. This work was partially supported by the Westvaco Chlorine Products Corporation.

## REFERENCES

- (1) ANDERSON, R. B.: J. Am. Chem. Soc. **68**, 686 (1946).
- (2) BEEBE, R. A., BISCOE, J., SMITH, W. R., AND WENDELL, C. B.: J. Am. Chem. Soc. **69**, 95 (1947).
- (3) BRUNAUER, S.: *The Adsorption of Gases and Vapors*, Vol. I, pp. 158-9. Princeton University Press, Princeton (1943).
- (4) BRUNAUER, S., DEMING, L. S., DEMING, W. E., AND TELLER, E.: J. Am. Chem. Soc. **60**, 309 (1938).
- (5) BRUNAUER, S., EMMETT, P. H., AND TELLER, E.: J. Am. Chem. Soc. **60**, 309 (1938).
- (6) CASSIE, A. B. D.: Trans. Faraday Soc. **41**, 450 (1945).
- (7) DE BOER, J. H., AND CUSTERS, J. F. H.: Z. physik. Chem. **B25**, 225 (1934).
- (8) EMMETT, P. H.: J. Am. Chem. Soc. **68**, 1784 (1946).
- (9) JOYNER, L. G., AND EMMETT, P. H.: 110th Meeting of the American Chemical Society, Division of Colloid Chemistry, Paper No. 45 (1946).
- (10) JOYNER, L. G., WEINBERGER, E. B., AND MONTGOMERY, C. W.: J. Am. Chem. Soc. **67**, 2182 (1945).
- (11) LANGMUIR, I.: J. Am. Chem. Soc. **40**, 1361 (1918).
- (12) LENEL, F. V.: Z. physik. Chem. **B23**, 379 (1933).
- (13) ORR, W. C. J.: Trans. Faraday Soc. **35**, 1247 (1939).
- (14) STRANSKI, I. N.: Z. Elektrochem. **36**, 25 (1930).
- (15) TAYLOR, H. S.: Proc. Roy. Soc. (London) **A108**, 105 (1925); J. Chem. Phys. **1**, 68 (1933).
- (16) ZETTLEMOYER, A. C., SCHWEITZER, E. D., AND WALKER, W. C.: J. Am. Leather Chem. Assoc. **41**, 253 (1946).
- (17) ZETTLEMOYER, A. C., AND WALKER, W. C.: Ind. Eng. Chem. **39**, 69 (1947).
- (18) ZETTLEMOYER, A. C., AND WALKER, W. C.: J. Phys. Colloid Chem. **52**, 58 (1948).

ACTIVE MAGNESIA. IV<sup>1</sup>

## APPLICATION OF DUAL-SURFACE THEORY

ALBERT C. ZETTLEMOYER AND WILLIAM C. WALKER<sup>2</sup>*William H. Chandler Laboratory of Chemistry, Lehigh University, Bethlehem, Pennsylvania**Received August 25, 1947*

In a previous paper (4) the unusual results of the adsorption of nitrogen on commercial active magnesia were presented. For these data the plots of the linear form of the multimolecular adsorption equation of Brunauer, Emmett, and Teller (2) showed a distinct curvature in the usually linear region. This curvature introduced an uncertainty in the position of the proper straight line for area determination by this method. It was suspected that the value of  $v_m$  obtained from the least-squares line might not be of significance, because the phenomenon that caused the curvature might erase the validity of a  $v_m$  obtained

<sup>1</sup> Presented at the Twenty-first National Colloid Symposium, which was held under the auspices of the Division of Colloid Chemistry of the American Chemical Society at Palo Alto, California, June 18-20, 1947.

<sup>2</sup> Post-Doctoral Fellow at the Lehigh Institute of Research.

from this plot. Accordingly the modifications of the B.E.T. theory in the literature were examined in an attempt to explain these data and more definitely establish  $v_m$ .

A concept was required which would account for excessive adsorption at a relative pressure of about 0.35. Of the modifications in the literature only two fulfill this requirement. Both of these take into account net heats of adsorption beyond the first layer. Brunauer, Emmett, and Teller (2) have presented an equation to handle net heat in the second layer, and Anderson's modification (1) will handle excessive heat in the second and through about the ninth layer. These modifications did not give satisfactory fit to the data. A new approach was devised, however, which showed very satisfactory agreement. This modification is presented in the preceding paper (3), where it has been referred to as the dual-surface theory.

Concepts involving pores have not been treated, since they predict less rather than more adsorption at pressures just beyond the usually linear region. In the following discussions  $n$  will be kept infinite for simplicity and only relative pressures below 0.35 will be considered, so that the presence of pores can be fairly safely ignored.

#### HEAT IN SECOND LAYER

Brunauer, Emmett, and Teller (2) have given the following equation, which does not include the usual assumption that the heat of adsorption in the second layer is equal to the normal heat of liquefaction:

$$v = \frac{v_m cx}{(1-x)} \frac{1 + (b-1)(2x-x^2)}{1 + (c-1)x + (b-1)cx^2} \quad (1)$$

where all symbols have their usual significance and  $b = e^{(E_2 - E_L)/RT}$ .

For convenience in calculation this equation may be expressed in the following manner:

$$v = v_m \left( \frac{cx + bcF}{1 + cx + bcF} \right) \quad (2)$$

where

$$F = \frac{x^2}{1-x} \quad (3)$$

and

$$G = \frac{x^2(2-x)}{(1-x^2)} \quad (4)$$

Equation 2 can be put into two linear forms for testing its applicability to data but in each case the value for one of the constants must be estimated before the plot is made, and the other two are evaluated from the resulting plot. The best estimate for the first constant is taken to be the one which makes the plot most nearly linear.

In the first linear form,

$$\frac{1}{v} (x + bG) = \frac{1}{v_m c} + \frac{1}{v_m} (x + bF) \quad (5)$$

the value of  $b$  is estimated, and  $(x + bG)/v$  is plotted against  $(x + bF)$ . When this equation was applied to data for the adsorption of nitrogen on commercial active magnesia, it was found that the plots were concave to the  $(x + bF)$  axis regardless of the value selected for  $b$ . Although the degree of curvature is almost independent of  $b$ , the values of  $v_m$  and  $c$  vary greatly, as may be seen in table 1.

Since the curvature of this plot was so insensitive to  $b$ , equation 2 was put into another linear form,

$$x \left( \frac{v_m}{v} - 1 \right) = \frac{1}{c} + b \left( F - \frac{v_m G}{v} \right) \quad (6)$$

where the value of  $v_m$  can be estimated and  $x \left( \frac{v_m}{v} - 1 \right)$  plotted against  $\left( F - \frac{v_m G}{v} \right)$ .

TABLE 1  
*Dependence of  $v_m$  and  $c$  on the estimate of  $b$*

$b$	$v_m$	$c$	$b$	$v_m$	$c$
1.0	39.5	44	2.0	32.8	109
1.3	36.0	68	2.5	31.2	160
1.5	35.3	74	5	27.6	56
1.7	34.4	85	10	25.9	13

Using this equation the shape of the plot varied considerably with the choice of  $v_m$ , but in no case was it linear over an appreciable pressure range. In spite of the non-applicability of this equation to the data, one of the best isotherms calculated from it was compared with the data for a typical run (run No. 42, grade 2642) and the deviation is plotted in figure 1 for comparison with the other theories.

#### HEAT IN SECOND AND SUCCEEDING LAYERS

Anderson (1) has devised a modification of the B.E.T. theory in which the heat of adsorption in the second and succeeding layers is assumed to be different from the heat of liquefaction:

$$\frac{x}{v(1 - kx)} = \frac{1}{kv_m c} + \frac{(c - 1)x}{v_m c} \quad (7)$$

This equation is applied by finding by trial and error the value of  $k$  for which the plot of  $x/v(1 - kx)$  vs.  $x$  is a straight line. In a large number of cases Anderson has been able to fit the equation to the data up to relative pressures of 0.7 to 0.9. In the case of nitrogen adsorption on active magnesia (run No. 42, grade 2642)  $k$  was found to equal 1.20. This value gave a plot that was most nearly linear over

the greatest range, but this range was very short and extended up to a relative pressure of only about 0.35. At higher pressures the points deviate drastically in the direction of too little adsorption. Thus the equation is found to apply well at low pressures but not at the higher pressures for which it was designed.

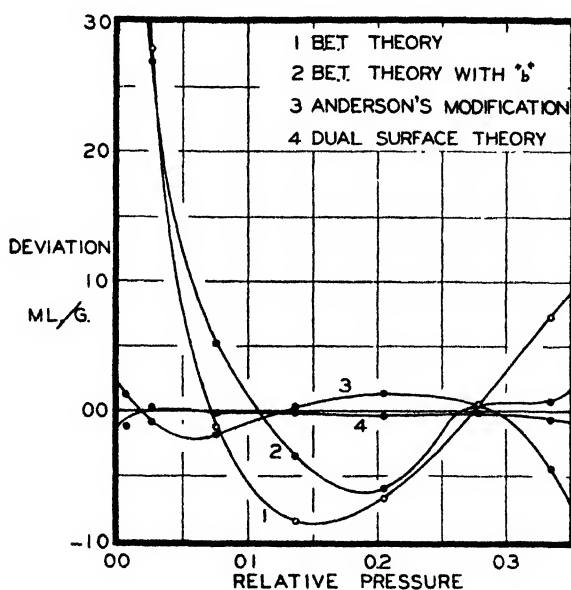


Fig. 1. Deviation of nitrogen adsorption isotherm from isotherms calculated by various theories.

TABLE 2

*Results of application of various methods to run No. 42*

METHOD	SPECIAL CONSTANT	$v_m$	$c$
B.E.T. .		38.6	60.3
B.E.T. (with second layer)	$b = 1.5$ to $1.7$	36-34	70-90
Anderson . .	$k = 1.20$	34.82	99
Dual surface		45.1	1 35, 130
Graphical.		(11.3 + 33.8)	
Algebraic . .		46.9	
		(13.3 + 33.6)	1.21, 134

When  $k$  is greater than 1.0, the heat of adsorption in the second and succeeding layers is greater than the heat of liquefaction. The values of the constants obtained from the linear portion of the plot of equation 7 for  $k = 1.20$  are given in table 2, and the agreement of the experimental data with the isotherm calculated from these values is shown in figure 1.

## DUAL-SURFACE THEORY

While seeking for an explanation for the curvature of the B.E.T. plots for nitrogen adsorption on commercial active magnesias, the authors examined the effect of surface duality on the linearity of the usual B.E.T. plot (3). It was found that if one portion of the surface has a very low heat of adsorption, the B.E.T. plot is concave to the pressure axis. Since these theoretical plots are very similar to the experimental ones, the dual-surface equation:

$$v = \frac{x}{1-x} \left[ \frac{v_{mA} c_A}{1 + (c_A - 1)x} + \frac{V_{mB} C_B}{1 + (C_B - 1)x} \right]$$

was applied to these data.

The only direct method of evaluating the four constants of this equation is by the solution of four simultaneous equations obtained from four points on the isotherm. Since this method is very cumbersome and is based on only four of the measured points, it was very desirable to get an independent value for one of the constants.

In contrast to the curvature obtained with the commercial active magnesias from sea water, the adsorption of nitrogen on c.p. magnesia gave a perfectly linear B.E.T. plot. This observation indicated that the surface duality in commercial active magnesia is probably due to impurities which cover part of the surface. If this notion is correct, then one portion of the dual surface should be magnesium oxide, and the  $c$  for this portion should be obtainable by adsorption on the c.p. material. Several runs with c.p. magnesia showed the  $c$  to be 130 ( $\pm 4$ ). With this independent value for one of the  $c$ 's, it is possible to use either the solution of three simultaneous equations or a graphical method to evaluate the remaining constants.

The use of simultaneous equations is much less satisfactory than a graphical solution, since a slight error in one of the chosen points may introduce considerable error into the results. The graphical solution was carried out as previously described (3). Values for  $v_{mA}$  for the clean part of the surface were estimated. For each estimate the isotherm for adsorption on the clean part of the surface was calculated, using the B.E.T. equation for  $n = \infty$ . This isotherm was subtracted from the experimental data to give the isotherm for adsorption on the other portion of the surface. This isotherm was then plotted according to the linear form of the B.E.T. equation. The estimate for  $v_{mA}$  which made this plot most linear was considered to be the correct one, and  $v_{mA}$  and  $c_B$  were obtained from the slope and intercept of this straight line. Plots for four estimates of  $v_{mA}$  for active magnesia 2642 are shown in figure 2. It will be noted that the shape of the plot changes radically with a small change in  $v_{mA}$ . The figure indicates that a  $v_{mA}$  of 33.8 produces a very satisfactory straight line from 0.05 to 0.35 relative pressure which gives values of  $v_{mB}$  and  $c_B$  of 11.3 and 1.35, respectively. This combination of a normal and a very low  $c$  should produce the observed curved B.E.T. plot according to the dual-surface theory. The total isotherm calculated using these constants is in very close agreement with the experimental data. In figure 1 the

deviation of the experimental data from the calculated isotherm of the dual-surface equation is compared with the deviations from the isotherms calculated from the other concepts discussed above. This graph clearly shows that surface duality affords a much more adequate explanation of nitrogen adsorption on active magnesia than any of the other modifications of the B.E.T. theory.

It is of interest to note that this analysis of magnesia 2642 attributes to it a total  $v_m$  of 45.1 ml. per gram, a value which is considerably in excess of that obtained by any other method. These results are compared in table 2. Where

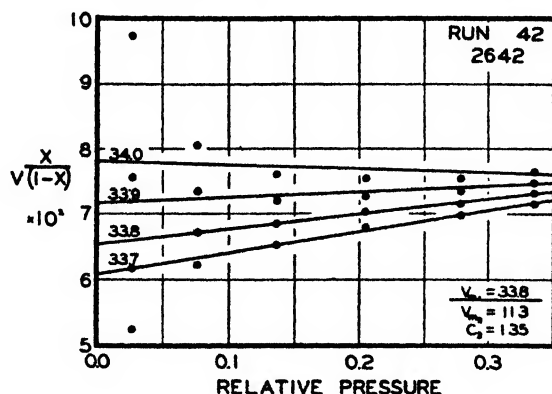


FIG. 2. Graphical application of dual-surface theory to run No. 42 on magnesia 2642

TABLE 3

*Application of dual-surface equation to commercial active magnesias*

GRADE	RUN	$c_A : c_B$	$v_{m_A} + v_{m_B} = v_m$	B.E.T. $v_m$
XP.....	44	130; 1.03	48.5 + 17.0 = 65.5	54.9
2642 .....	42	130; 1.35	33.8 + 11.3 = 45.1	38.6
2642 .....	49	130; 2.38	32.8 + 8.7 = 41.5	34.0
2642* .....	P	130; 3.47	37.5 + 9.5 = 47.0	44.0

\* Degassed for 20 hr. at 490°C. instead of 1 hr. at 250°C.

dual-surface analysis applies, total  $v_m$  will always be higher than that obtained from any form of the B.E.T. equation.

It should be pointed out that while the dual-surface equation contains four constants, only three were varied to fit the equation to the data. Thus, in this application the dual-surface equation contains only three adjustable constants, as do the other modifications with which it has been compared here.

In order to confirm the uniqueness of the evaluation of the dual-surface constants discussed above, four points on the isotherm were selected and used to set up four simultaneous equations which could be solved for the constants. Solution of these equations gave results in very close agreement with the graphical results as indicated in table 2. This calculation also demonstrated that this solution is the only real one.

The above discussion is centered about run No. 42 on active magnesia 2642. The results of the application of the dual-surface equation to several other measurements on different batches of magnesia 2642 as well as magnesia XP are shown in table 3.

The data in table 3 indicate that the total  $v_m$ 's obtained from the dual-surface equation are approximately 20 per cent greater than those from the B.E.T. equation. These increases in area place the nitrogen adsorption areas in much better agreement with the areas obtained from x-ray diffraction measurements (5). These data also show that the surface usually contains about 25 per cent of surface with low heat of adsorption.

#### SUMMARY

The non-conformity of the data for nitrogen adsorption on commercial active magnesias to the B.E.T. equation could not be explained by any modification of the B.E.T. theory already in the literature.

The dual-surface equation was found to be in very excellent agreement with the data, however. Application of this equation to typical data showed 75 per cent of the surface to have a  $c$  of 130, while the remainder had a  $c$  of 1.35. The total area was found to be greater than that found by other methods. Solution of simultaneous equations showed this result to be unique.

As in the previous papers of this series, this work has been supported by the Westvaco Chlorine Products Corporation.

#### REFERENCES

- (1) ANDERSON, R. B.: J. Am. Chem. Soc. **68**, 686 (1946).
- (2) BRUNAUER, S., EMMETT, P. H., AND TELLER, F.: J. Am. Chem. Soc. **60**, 309 (1938).
- (3) WALKER, W. C., AND ZETTLEMOYER, A. C.: J. Phys. Colloid Chem. **52**, 47 (1948).
- (4) ZETTLEMOYER, A. C., AND WALKER, W. C.: Ind. Eng. Chem. **39**, 69 (1947).
- (5) ZETTLEMOYER, A. C., AND WALKER, W. C.: J. Phys. Colloid Chem. **51**, 763 (1947).



MONODISPERSE COLLOIDS AND HIGHER-ORDER TYNDALL SPECTRA<sup>1</sup>

VICTOR K. LA MER

*Department of Chemistry, Columbia University, New York, New York**Received August 25, 1947*

## INTRODUCTION

The recent discovery of methods for preparing aerosols (12) and more particularly sulfur hydrosols (7), whereby stabilized sols of any desired strictly monodisperse size in the colloidal range can be prepared at will, furnishes a new tool for reinvestigating many problems of colloid science. The use of such monodisperse preparations greatly simplifies the interpretation of data which are dependent upon particle size.

When a polydisperse preparation is employed, it becomes necessary to know not only the average size but also the parameters which specify the particular size distribution. The particular distribution is often very difficult of reproduction, but more important still, the existence of a distribution of particle size will often obscure any simple relations that actually exist between particle size and the property being investigated. The net result has been that with polydisperse preparations only uncertain or ambiguous relations are finally discovered, in spite of much tedious and painstaking investigation. The purpose of this paper is to assemble some of the results of recent investigations, as yet not published in detail, wherein clear-cut unambiguous interpretations of the effect of particle size have been attained by the use of these new methods of preparation.

Optical properties in general, and in particular the angular scattering of incident light and its transmission through turbid media, are most sensitive to variation in particle size. These properties will accordingly be treated in detail, since they have furnished the criteria necessary for specifying the droplet radius and the monodisperse character of the preparations employed in testing other relations dependent upon size.

Monodisperse colloids exhibit a beautiful optical effect, which has until recently (7, 12) escaped experimental detection and verification, despite much careful investigation in the field of colloid optics, because the sols employed previously have not been sufficiently monodisperse. The designation "higher-order Tyndall scattering spectra" specifies the character of the effect.

Although first demonstrated by Sinclair and the writer (12) in 1941 while engaged in a search for a method of preparing monodisperse aerosols, the effect can be demonstrated and reproduced most simply and conveniently with sulfur hydrosols (7).

<sup>1</sup> Presented at the Twenty-first National Colloid Symposium, which was held under the auspices of the Division of Colloid Chemistry of the American Chemical Society at Palo Alto, California, June 18-20, 1947.

## PREPARATION AND OPTICAL PROPERTIES OF MONODISPERSE SULFUR SOLS

When the conditions of proper concentration, temperature, and the absence of interfering nuclei are controlled,—for example, when optically clear solutions of 0.001 *M* sodium thiosulfate and 0.003 *M* hydrochloric acid are mixed thoroughly and instantaneously in *clean* glass flasks and observed with a beam of parallel natural white light passed through the flasks,—the resulting solution remains crystal clear (11) for about  $68 \pm 1$  min. at 25°C. During this time molecularly dispersed sulfur is being produced by the homogeneous chemical reaction until a degree of supersaturation is reached which can no longer be tolerated by the system.

This reproducible time limit is signaled by the appearance of the well-known Rayleigh type of Tyndall beam, and corresponds to a phase transition wherein droplets of lambda sulfur existing as a supercooled liquid having radii of the order of  $10^{-6}$  cm. (0.01 micron) are formed from the molecularly dispersed sulfur.

The beam of scattered light is at first of very low intensity. It is characterized by a pure blue color, the intensity of which is distributed symmetrically in respect to the scattering angle  $\theta$  as  $(1 + \cos^2 \theta)$ . This blue light, as is well known, is completely polarized at  $\theta = 90^\circ$ . The intensity,  $I$ , of the scattered light increases exceedingly rapidly at first, as a result of the relatively rapid growth of the droplets and the strong dependence of intensity upon the particle radii.

Thus, in this initial range of size designated as region 1 in figure 1, where  $r/\lambda$  is  $< 1/10$  the simple limiting law of Rayleigh is valid: namely,

$$I = k'r^6/\lambda^4 \quad (1)$$

Here  $k'$  is a constant independent of the radius  $r$  and the wave length. Accordingly, in this region the scattered intensity increases  $(5)^6 = 15,625$ -fold when  $0.01 \mu$  particles grow to  $0.05 \mu$ . This great increase in intensity occurs over a period of a few minutes and represents a kinetic process meriting further investigation.

As an empirical law of scattering valid for any value of  $r/\lambda$  we may employ equation 2, where the exponent  $y$  is variable.

$$I = kr^2 (r/\lambda)^y \quad (2)$$

In region 1,  $y$  is a constant equal to 4 and equation 2 reduces to equation 1. For increasing values of  $r/y$ ,  $y$  decreases, reaching a negative value of about 2.2 before finally approaching zero as required by geometrical optics (see figure 1).

During the first hour of growth of the droplets, i.e., during the second hour after mixing the reagents corresponding to region II, the purity of the blue color diminishes to a pastel or almost grey shade; the angle of complete polarization shifts from  $\theta = 90^\circ$  to larger, i.e., backward, angles; the degree of polarization at  $\theta = 90^\circ$  decreases from the initial value of 100 per cent, and the symmetrical  $(1 + \cos^2 \theta)$  distribution of the intensity of the scattered light passes over to a pattern which corresponds to greater scattering in the forward than in the reverse directions to the incident beam.

The optical effects appearing in region II are now also well understood. The droplets of sulfur have exceeded the limit  $r = \lambda/10$  corresponding for green light to  $r > 0.05 \mu$ , with the result that the Rayleigh limiting law is no longer valid and must be replaced by the more general solution first obtained by Mie.

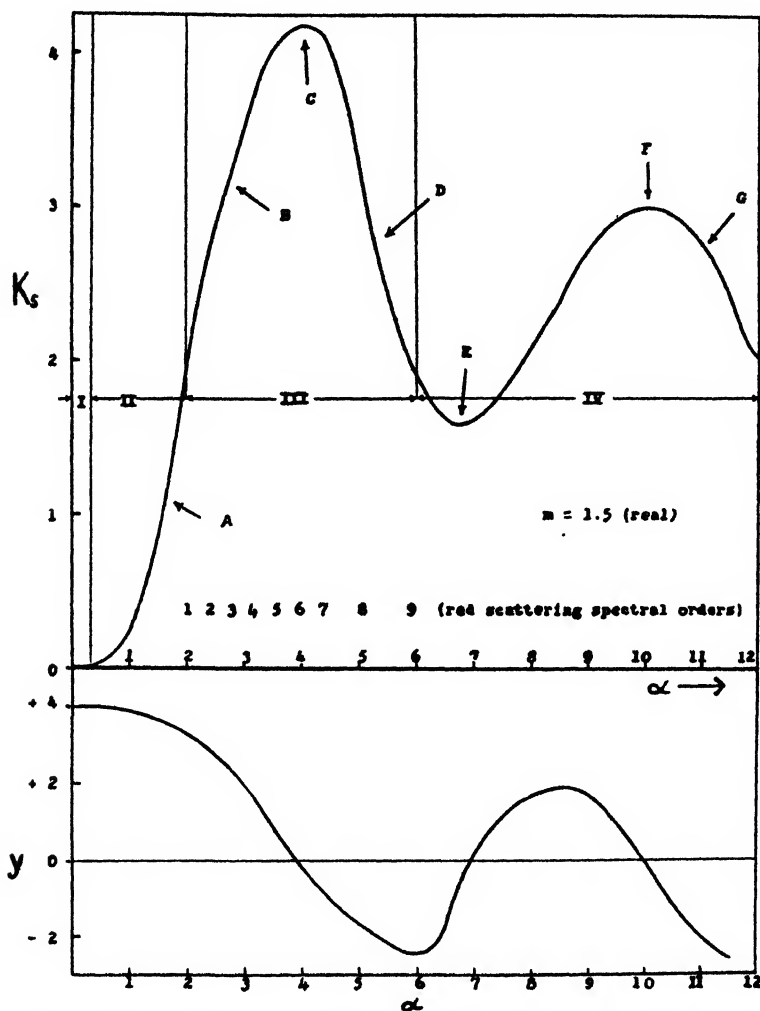


FIG. 1. Monodisperse colloids. A, yellow transmission; B, red transmission; C, magenta transmission; D, blue transmission; E, green transmission; F, magenta transmission; G, blue transmission.

The properties of degree of polarization and angle of maximum polarization of white light have been utilized by us as a quantitative measure of the growth of the particle radius. These criteria, however, suffer from the restriction that they are useful only for the range  $r \simeq 0.05$  to  $0.2 \mu$  in the most favorable cases of relative refractive index and spherical character of the particles. The changes

in the above properties can also be correlated with the decrease in the value of  $y$ , the exponent of  $r/\lambda$  in the empirical scattering law. In the region just described  $y$  decreases from 4 to about 3. As will be developed in more detail later, the value of the exponent  $y$  can be used as a convenient measure of particle size by determining its value from transmission measurements.

#### HIGHER-ORDER TYNDALL SPECTRA

Fortunately, when some of the above properties lose their size-sensitive or monotonic character, a new factor enters which furnished an even better measure of particle size. The higher-order Tyndall spectra first make their appearance for the given concentration of acid and thiosulfate after a lapse of about 2 hr. following mixing, at which time the droplet radius is approximately  $0.2 \mu$ , corresponding to a value of  $\alpha = 2\pi r/\lambda \simeq 2.5$  (region III).

At this point a red band appears in the scattered light which becomes more sharply distributed in angle and more distinctive in color with the progress of time. The angle  $\theta$  characterizing the maximum intensity of the red band also changes with time in a highly reproducible manner, as described previously (5, 10).

Soon after the appearance of the first band a second band appears; thereafter alternating green and red bands make their respective appearances in a surprisingly reproducible manner, in respect to angle, color quality, and time, until at least nine such superimposed spectral orders can be detected by the naked eye.<sup>2</sup> The growth of the droplets may be stopped at any arbitrary time or size by adding 60–70 per cent of the stoichiometric amount of iodine (plus potassium iodide), based upon the initial concentration of thiosulfate. The sol is then stabilized.

The most important feature is that the investigator can now mix stabilized sols of different but uniform sizes in arbitrary proportions, thereby preparing at will a polydisperse system of any desired mean size and arbitrary distribution about the mean.

The purity of the spectral colors to the naked eye furnishes a trained observer with a ready qualitative estimate of the degree of monodispersity, while the number of spectral orders gives a ready rough measure of the size. In the size

<sup>2</sup> The visual counting of spectral orders can be made easier if the transversely scattered beam is observed through a polaroid oriented to pass the component whose electric vector is vertical to the plane defining the direction of incident and observed light. In the notation of Krishnan we observe the angular position and intensity of the component  $V_u$ , the subscript indicating that the incident light is unpolarized. The angle of maximum red intensity can be determined to  $\pm 1^\circ$  if red and green filters are employed and the intensity ratio  $I_{\text{red}}/I_{\text{green}}$  (5) for  $V_u$  is plotted against the angle  $\theta$ .

Polarized monochromatic incident light extending into the ultraviolet can of course be used in connection with photoelectric receptors (A. S. Kenyon and V. K. La Mer, in press). However, the contrast between the alternating red and green intensities to which the eye is most sensitive and which is obtained with white incident light makes this simpler method quite satisfactory for many purposes and eliminates the need for more elaborate equipment.

range in which the orders occur, brilliant colors imply a strictly monodisperse character, while pastel shades indicate less monodisperse distributions. Opalescence is a mark of polydispersity.

These impressions of size and distribution can be made less subjective and more quantitative by measuring with color filters,  $I_{\text{red}}/I_{\text{green}}$ , the ratio of the intensities of the red to green scattered light, and plotting the results as a function of angle (5). By studying the depolarization of incident polarized light in the manner developed by Krishnan (6, 16) further information regarding shape and optical anisotropy of the particles and their distribution can be gained. Such studies are now in progress in the Columbia University Laboratories.

The angular positions of these spectra have been calibrated (5) in terms of their radii, from computations based upon the extensive tables now available for the complex functions that appear in the equations of the Mie theory. The Mie equations (5, equation 2) give a general and rigorous solution of the problem of the scattering of light by isotropic spheres of any size and of any index of refraction (real or complex). This calibration has been made in terms of (a) depolarization at  $90^\circ$ ; (b) the angle (5) of the maximum red intensity of the higher-order Tyndall spectra; (c) the transmitted light as a function of wave length (1, 2, 8); and (d) rate of sedimentation and Stokes' law (5) as an independent check, in the case of larger particles.

#### QUANTITATIVE MEASURE OF MONODISPERSITY

Although many investigators claim that the colloids which they have prepared are monodisperse, an application of the criterion of higher-order Tyndall spectra shows that their preparations are in reality somewhat polydisperse. The following experiment (5) will show the discriminating character of the higher-order Tyndall spectra.

A very dilute mixture of hydrochloric acid and thiosulfate was divided into aliquot portions A and B. When the particles in A had reached a size  $r = 0.467 \mu$  the sol was stabilized by addition of iodine; 20 min. later sol B was stabilized. The calibration curve indicated that for B  $r = 0.476 \mu$ , an increase of 2 per cent. Sol A exhibited six red orders with an order of maximum intensity at  $\theta = 136^\circ$ . Sol B exhibited six and one-half orders with a distinct green band of maximum intensity at  $\theta = 134^\circ$ . The addition of 10 per cent of A to 90 per cent of B reduced the intensity of the red band. When equal parts of A and B were mixed the red and green bands were annulled and an essentially white color prevailed, as indicated by the ratio  $I_{\text{red}}/I_{\text{green}} \simeq 1$ . In other words, by mixing two sols whose particles differed only 2 per cent in radius, our new criterion of monodispersity was obliterated. No wonder these higher-order scattering spectra have not been previously observed.

#### TRANSMISSION AS FUNCTION OF WAVE LENGTH

An alternate optical method of determining particle radius  $r$  consists in measuring the transmission as a function of wave length through a column of the sol

of given length  $l$  and number of particles  $n$ . The transmission  $T$ ,  $I$  being transmitted intensity and  $I_0$  incident intensity, is given by the expression (1, 8):

$$T = \frac{I}{I_0} = e^{Snl} = e^{-K_s \pi r^2 n l} \quad (3)$$

Here  $K_s$  is a function of  $r/\lambda$ , and  $m$  is calculable from the Mie theory for a given value of the relative refractive index  $m$ .  $S$  is the scattering cross section.  $K$  was introduced by Stratton and Houghton (18) for the purpose of calculating the transmission of light through fogs. Their artificial fogs and mists, however, were so non-uniform in particle size that only a very rough indication of the size could be obtained with equation 3, a restriction which has since been surmounted by the use of monodisperse aerosols<sup>3</sup> or monodisperse sulfur hydrosols (1).

In our practice, the function  $K_s$  is plotted as ordinate against  $\alpha = 2\pi r/\lambda$  as abscissa, both on a logarithmic scale. The measured  $\ln I/I_0$  curve for a sol of given radius  $r$  is then plotted on the same graph, using  $\log 1/\lambda$  as ordinate. The value of  $r$  can then be calculated from the transposition along the abscissa which is necessary to fit the characteristic maxima or minima of the measured curve with the theoretical  $K_s$  curve, equation 4.

$$\log K_s + \log \ln I/I_0 = \log r^2 + \log n + \log \pi l \quad (4)$$

The transmission method of determining  $r$  has the important practical advantage over the angles of the higher-order Tyndall spectra that it is not restricted to strictly monodisperse sols. Transmission will work quite satisfactorily for moderately polydisperse sols when the angle method is no longer applicable. With a moderately polydisperse sol the characteristic maxima and minima of transmission are of course less pronounced, but nevertheless a comparison can generally be made. This  $r$  so obtained is a mean value weighted optically and dependent upon the form of the distribution of particle size and the scattering law for the particular range of particle size.

Table 1 gives a summary of some recent results (1) of angle scattering and transmission performed upon aliquots of the same sol. Column 1 gives the elapsed time after mixing. Column 2 gives the number of orders, observed visually, with their respective angles,  $\theta_1, \theta_2, \dots, \theta_s$  in column 3, again observed visually without the aid of color filters. Column 4 gives the radius as computed from a calibration curve based upon the Mie theory and sedimentation, and column 5 gives the radius as computed from the observed minimum in the transmission curve as outlined above.

The radii are not always exactly proportional to the elapsed time after mixing. This is not surprising, since the data are assembled from the results of different observers, who used solutions of different origin and history as well as slightly different initial concentrations of reactants and temperatures.<sup>4</sup>

<sup>3</sup> La Mer, V. K., Sinclair, D., and Hochberg, S.: Unpublished OSRD reports, 1941 and 1942.

<sup>4</sup> The time of appearance of the Tyndall beam is very sensitive to the concentration of thiosulfate and less sensitive to the concentration of acid. Time of appearance inversely

A reproducible dependence of size upon elapsed time after mixing is predicated upon the assumption that the phase change from a homogeneous to a heterogeneous reaction is brought about by the appearance of exactly the same number of nuclei of the same size. The available evidence indicates that the kinetics of this phase transition is one of self-nucleation, produced by spontaneous local

TABLE 1

*Determination of radius from angular position of orders ( $\theta_1, \theta_2 \dots$  etc.) and from the wavelength minimum of transmission curve*

ELAPSED TIME AFTER MIXING	ORDERS	ANGLES	$r$ (ANGLES)	$r$ (TRANSMIS- SION)
		$\theta_1, \theta_2, \theta_3, \theta_4$		
<i>minutes</i>				
180	4	51, 81, 110, 146	0.323	0.307
180	4	51, 78, 112, 147	0.323	0.310
208	4	45, 82, 120, 151	0.352	0.35
208	4	47, 76, 110, 152	0.345	0.34
322	5	51, 71, 119, 149, 176	0.33	0.35
322	5	43, 73, 97, 121, 155	0.38	0.39
328	6	37, 57, 76, 106, 132, 160	0.41	0.38
502	6	41, 56, 81, 100, 130, 159	0.39	0.39
502	6	36, 55, 80, 105, 131, 161	0.43	0.41
510	7	36, 50, 70, 92, 115, 140, 165	0.45	0.45
722	8	30, 47, 56, 72, 87, 103, 126, 147	0.49	0.51
840	8	28, 43, 55, 77, 96, 110, 131, 150	0.51	0.53
849	7	32, 46, 60, 78, 100, 119, 146	0.49	0.52
904	8	31, 47, 62, 81, 96, 120, 145, 168	0.49	0.49

fluctuations of molecularly dispersed sulfur from the average conditions of uniform density. The transition occurs at a critical degree of supersaturation which is again surprisingly reproducible for a given set of conditions. It cor-

proportional to  $(S_2O_8)^{3/2}(H^+)^{1/2}$  is a good working formula in the range 0.0005-0.0015  $M$  of reactants. The speed of the homogeneous reaction is also approximately doubled for each  $15^\circ$  rise in temperature. The nucleation process and the subsequent growth of the particles are sensitive to the viscosity and the ionic strength of the medium. The rate of the homogeneous reaction as measured by the time of appearance of the Tyndall beam exhibits a positive Brønsted primary kinetic salt effect, indicating a kinetic reaction between ions of the same sign (experiments of Miss Ethel Zaiser). Exact agreement between elapsed time and radii can therefore be expected only for identical solutions under identical conditions. The surprising fact is that the data in table 1 show reproducibility with respect to elapsed time in the hands of different investigators.

responds to a constant value of  $\ln I/I_0$  equivalent to a concentration of molecularly dispersed sulfur of approximately  $5 \times 10^{-6}$  moles per liter. The number of particles  $n$  present may also be computed from equation 4 by shifting the ordinates of the experimental  $\ln I/I_0$  curve to make the absolute values of characteristic points on the  $K$  curve coincide.

The results of these calculations show that although reasonably constant, the character of the process does actually vary somewhat, but the number of particles involved is always nearly  $10^6$  per cubic centimeter. Apparently there are other factors, such as the presence of foreign disturbing nuclei, which we have not as yet been able to eliminate completely in our techniques. The agreement between the values of columns 4 and 5 is an over-all measure of the accuracy with which an observer can determine the minimum in the transmission curve, and the calibration of the angular scattering in terms of Mie's theory and sedimentation (5).

#### DEPENDENCE OF EXPONENT UPON $r$

In figure 1 we have sketched the behavior of  $K_s$  for transparent spheres of relative index of refraction (real) equal to 1.5, plotted against  $\alpha = 6.28r/\lambda$ , the dimensionless variable occurring in all forms of the theory. The course of  $K_s$ , calculated for single spheres is not as smooth as is indicated in figure 1 (compare figure 1 in reference 2). The mathematically computed curve shows some waviness and several secondary maxima in the first principal maxima in the neighborhood of  $\alpha = 4$ . Since all preparations usually encountered in the laboratory will exhibit some slight distribution of particle size about the mean, these oscillating minor effects will be smoothed out in practice. The lower curve gives the smoothed approximate course of  $y$ , the exponent of  $r/\lambda$  in equation 2, as a function of  $\alpha$ . Here particularly no attempt has been made to reproduce the oscillatory character of  $y$ , which would be obtained by taking finite difference coefficients for the computed points of  $K_s$ . The computed points are not sufficiently close together to make such differential coefficients reliable. They would have no significance in comparison with experimental data.

If the scattered light is orange ( $\lambda = 0.628 \mu$ ), the scale for the radius becomes exactly  $\alpha/10$ . For other wave lengths  $\lambda$  it is related by the factor  $(0.628/\lambda)$ . The  $\alpha$  values corresponding to the spectral orders which appear in region III are indicated on the graph. In region IV ( $\alpha > 6$ ), the investigator must rely upon the form of the transmission curve for the measure of  $r$ . It is interesting to point out that the maximum occurs at  $\alpha \simeq 4$  and  $K_s \simeq 4.2$ . This means that a spherical droplet of radius  $0.33 \mu$  will scatter 4.2 times as much green light, to which the eye is most sensitive, as one would expect from an elementary application of geometric optics using the geometric area  $\pi r^2$  of the droplet as the intercepting area. However, since a disc of area  $\pi r^2$  also diffracts from its edge an amount of light, within a very small angle, which is again proportional to  $\pi r^2$ , the actual amount of light by which a large intercepting sphere or disc reduces the transmission, as ordinarily measured, is equal to  $2\pi r^2$  and not  $\pi r^2$ . The limiting value of  $K_s$  as  $r \rightarrow \infty$  is consequently 2 and not 1. This unexpected finding was



encountered experimentally early in the work on aerosols. The total amount of light scattered, obtained by integrating the measured angular values over the surface of a sphere, was actually one-half the value obtained from transmission on the same preparation (13, 14). This paradox (15, 18) was clarified by the investigations of Brillouin (4) and Sinclair (13, 17). Unaware of Brillouin's work, van de Hulst (19) has since reached substantially the same conclusions.

Along the  $K$ , curve of figure 1 the quality of the color of the light transmitted by a monodisperse colloid of the size indicated when  $m = 1.5$  has been shown. From equation 2 we see that  $(\partial \ln K / \partial \ln \lambda)_r = -y$  and  $(\partial \ln K / \partial \ln r) = (y + 2)$ . Rough values of  $y$  as a function of  $\alpha$  are sketched in the lower curve. When blue light is transmitted, equation 2 takes the form

$$I = kr^2 (\lambda/r)^{2.2}$$

i.e., the usual relation between  $\lambda$  and  $r$  is inverted.

A maximum in the  $K$  curve corresponds to a magenta-colored transmission arising from the greater scattering of green as compared to red and blue light. Since the eye is most sensitive to green, a particle radius corresponding to this maximum gives the maximum visual obscuration.

These optical findings were employed in controlling and improving the quality of the smoke emitted by the vapor condensation type of screening smoke generators invented by Irving Langmuir and Vincent Schaefer of the General Electric Company. These generators were manufactured by the Standard Oil, Servel, and Besler companies for the Army and Navy. A combustion-type generator developed by Mr. John Hession, Jr., of the Columbia University group and manufactured by York-Shipley for the Navy was controlled by the same principles (3, 13).

#### TOXICITY OF AEROSOLS AND PARTICLE SIZE

In the fall of 1943 the Central Aerosol Laboratory at Columbia University was asked to investigate, in coöperation with Mr. Randall Latta of the U. S. Department of Agriculture, the effect of particle size upon the toxicity of DDT aerosols to malaria-bearing mosquitoes. Previous attempts to determine the relation by using aerosols produced by the Freon insecticide bomb were not decisive, since the aerosols produced by that device not only exhibited a wide distribution of particle sizes, but the distribution and its mean value varied with the elapsed time following the opening of the valve. It was also thought that the screening smoke generators then being developed by the Columbia University group might be used for the large-scale dispersal of DDT.

An investigation (9) of the effect of particle size upon toxicity of DDT aerosols to mosquitoes using the La Mer-Sinclair laboratory-type generator for the preparation of monodisperse aerosols showed that none of the screening smoke generators were suitable without fundamental modifications in their principles of operation.

DDT is a contact poison, and the effectiveness of such aerosols is determined by the extent of their deposition upon the insect. In the case of a static atmo-

sphere (9) the toxicity (deposition) depended upon the rate of fall of the droplets upon the resting drosophila or mosquitoes. Thus, when the toxicity product (i.e., the product of  $c$ , the amount of DDT in the aerosol, times the median time of exposure,  $t_{50}$ , necessary to kill 50 per cent of the population of female *Aedes aegypti* mosquitoes resting in cages) was plotted against the radii of the homogeneous aerosol particles, whose size was determined and controlled by the optical methods given above, the data fell, for a logarithmic plot, upon a line with a slope of  $-2$ ; i.e.,

$$\begin{aligned}\log Ct_{50} &= -2 \log r + \text{const.} \\ Ct_{50} &= \text{constant}/r^2\end{aligned}$$

In other words, the toxicity was controlled by Stokes's law of fall for droplets between  $r = 0.3$  to 5 (possibly 8) microns. The deposition at  $r = 5$  microns was  $(5/0.3)^2 = 25/0.09 = 270$ -fold greater than for 0.3 micron, the particle size produced by the screening smoke generators available at that time. There was evidence that above a radius of 8 microns the toxicity no longer increased with increasing radius.

These experiments were extended (14) to include a study of the effect of wind velocity. DDT aerosols, again of very uniform particle radius, were generated at the entrance to a wind tunnel 1 sq. ft. in area and 30 ft. long. The aerosols impinged upon mosquitoes, located in cages in the tunnel, at calibrated wind velocities of 2, 4, 8, and 16 miles per hour. The law of deposition, as judged by the toxicity to populations of mosquitoes, proved to be

$$\log M = k \log (D^2V) + \text{const.} \quad (9)$$

Here  $M$  = mg. of aerosol (or DDT) per square foot necessary to kill 50 per cent of the females,  $D$  = diameter of oil aerosol particles, and  $V$  = wind velocity in miles per hour. In the range of  $D^2V = 2$  to 200 microns<sup>2</sup> miles hour<sup>-1</sup>, which corresponds to 300 to 1 mg. of DDT per square foot, the data conform to equation 9 with a slope of  $k = -1$  (exactly).

As  $D^2V$  is increased,  $M$  continues to decrease but at a less rapid rate,  $k$  now decreasing continuously from  $-1$  to zero. For the range  $D^2V = 800$  to 7000,  $k$  is zero, indicating complete independence of  $M$  upon  $D^2V$ . This behavior was interpreted as indicating that a saturation of deposition in respect to size and wind velocity has been achieved and that the  $M$  value necessary for 50 per cent kill is constant at 8 mg. DDT per square foot. These wind tunnel results furnish a confirmation of the earlier experiments performed on an almost static atmosphere. Thus for a wind velocity of 4 mi./hr. the minimum value of the diameter for 50 per cent kill is given by the critical value of  $D^2V = 800$ , i.e.

$$D^2 = \frac{800 \text{ microns}^2 \text{ miles hour}^{-1}}{4 \text{ miles hour}^{-1}} = 200 \text{ microns}$$

or  $D = 14$ , corresponding to a radius of 7 microns. If the wind velocity is 2 mi./hr., a 10-micron radius is needed. For an 8 mi./hr. wind (a maximum practical value) a 3.5-micron radius will suffice to give the same percentage kill.

Since the particle size produced by the then existing screening smoke generators, operating under the Langmuir-Schaefer principle (Esso, Servel, and Besler) or under the Hession combustion-type principle (Hession-York and Todd Shipyard), could not easily be increased over 1 micron, and since the temperatures at which these generators operated were sufficient to decompose DDT, a new type of insecticidal aerosol generator was developed in the Columbia University Laboratories by Dr. Seymore Hochberg and the writer. This generator produces aerosols of fairly uniform and controllable particle size of mass median diameter of 2-40 microns or even larger, at low temperatures (350-500°F.). Significant thermal destruction of DDT or other more thermally sensitive insecticides or plant hormones is thus prevented.

In the Langmuir-Schaefer type of screening smoke generator all of the high-boiling oil is evaporated at approximately 900°F. and low pressure. The vapor is then chilled by passage through tubes to produce an aerosol of 0.2-0.5 microns radius. On the other hand, in Hochberg's insecticidal aerosol generator the rapid expansion and the grinding action of superheated steam disperses entrained droplets of oil, insecticidal liquids, or dispersed solid particles by passing the mixture through a capillary, annulus, or slit passage whose length need only be several times or more that of the diameter of the capillary, i.e., of the distances between the facing walls of the annulus or slit. Insecticidal generators operating upon this principle were used by the Armed Forces during World War II for insect control in the United States and overseas.

#### SUMMARY

It is shown that the laws relating to the optical properties of scattering and transmission and the insecticidal (deposition) properties of aerosols and hydrosols may be determined in an unambiguous fashion by employing strictly monodisperse preparations of controllable particle size.

#### REFERENCES

- (1) BARNES, M. D., KENYON, A. S., ZAISER, E., AND LA MER, V. K.: *J. Colloid Sci.* **2**, 349 (1947).
- (2) BARNES, M. D., AND LA MER, V. K.: *J. Colloid Sci.* **1**, 79 (1946).
- (3) BAXTER, JAMES PHINNEY, 3RD: *Scientists Against Time*, Chap. XIX, pp. 282-8. Little, Brown and Company, Boston (1946).
- (4) BRILLOUIN, L.: Applied Mathematics Panel, NDRC, Reports No. 87.1 (December, 1943) and 87.2 (April, 1944).
- (5) JOHNSON, I., AND LA MER, V. K.: *J. Am. Chem. Soc.* **69**, 1184 (1947).
- (6) KRISHNAN, R. S.: *Proc. Indian Acad. Sci.*, a series of papers in Volumes **1A** to **10A** (1934-39).
- (7) LA MER, V. K., AND BARNES, M. D.: *J. Colloid Sci.* **1**, 71 (1946).
- (8) LA MER, V. K., AND BARNES, M. D.: *J. Colloid Sci.* **2**, 361 (1947).
- (9) LA MER, V. K., HOCHBERG, S., HODGES, K., AND WILSON, I.: OSRD Report No. 4447 (1944); in press, *J. Colloid Sci.*
- (10) LA MER, V. K., AND JOHNSON, I.: *J. Am. Chem. Soc.* **67**, 2055 (1945).
- (11) LA MER, V. K., AND KENYON, A. S.: *J. Colloid Sci.* **2**, 257 (1947); also reference 7.
- (12) LA MER, V. K., AND SINCLAIR, DAVID: OSRD Report No. 119, or NDRC Division B, Report No. 57 (1941); OSRD Report No. 1668 (1943).

- (13) LA MER, V. K., AND SINCLAIR, D.: OSRD Report No. 1857 (1943); available through the U. S. Department of Commerce, Office of Publications, as No. 944.
- (14) LATTI, RANDALL, *et al.*, AND LA MER, V. K., HOCHBERG, S., *et al.*: OSRD Report No. 5566 (1945); National Research Council Insect Control Committee Report No. 119; in press, Academy of Sciences, Washington, D. C.
- (15) MIDDLETON, A. H.: *Visibility in Meteorology*, p. 18. Toronto Press, Toronto (1941).
- (16) PERRIN, F.: *J. Chem. Phys.* **10**, 415 (1942).
- (17) SINCLAIR, DAVID: *J. Optical Soc. Am.* **37**, 475 (1947).
- (18) STRATTON, J. A., AND HOUGHTON, H. G.: *Phys. Rev.* **38**, 159 (1931).
- (19) VAN DE HULST, H. C.: "Optics of Spherical Particles," Dissertation, Utrecht, 1946.

## ELECTROPHORETIC MOBILITIES AND CONDUCTOMETRIC ACTIVITIES OF POTASSIUM, SODIUM, AND LITHIUM SALTS OF GUM ARABIC<sup>1,2</sup>

D. R. BRIGGS

*Division of Agricultural Biochemistry, University of Minnesota,  
St. Paul 1, Minnesota*

*Received August 25, 1947*

Certain deviations from the equivalent conductivity-concentration relationships which are characteristic of ordinary electrolytes in solution have been observed in the case of soaps (4) and dyestuffs (5), in that, as the concentration of such an electrolyte is increased, the equivalent conductivity passes through a minimum value followed by a sometimes sharp rise and finally by a slow decrease again. An electrolyte which shows this phenomenon is characterized by a tendency to form aggregates in solution at some fairly definite minimum concentration, below which it exists in a state of ordinary ionic solution but above which it exhibits to an increasing extent the properties of a colloid. This concentration is designated as its critical concentration, and appears to coincide closely with the concentration of the initial minimum in the equivalent conductivity curve. The increase in equivalent conductivity which accompanies the aggregation of the micelle-forming ion, as was pointed out by McBain many years ago, is due to an increased mobility of the micelle over that of the unaggregated ion and results from the decreased viscous resistance encountered, per unit of charge, by the aggregate. Mobility measurements on the micellar ions have confirmed this hypothesis. The final decrease in equivalent conductivity occurs as the effects of increasing ionic strength ultimately overshadow the effects of the aggregation process. Substances which exhibit this property are heteropolar in composition, containing one residue in the molecule which has a

<sup>1</sup> Presented at the Twenty-first National Colloid Symposium, which was held under the auspices of the Division of Colloid Chemistry of the American Chemical Society at Palo Alto, California, June 18-20, 1947.

<sup>2</sup> Paper No. 2352, Scientific Journal Series, Minnesota Agricultural Experiment Station.

low affinity for water and which is responsible for the tendency of the molecules (or the ions containing the non-polar residues) to aggregate. These substances act as *colloid* electrolytes only by virtue of their tendency to form aggregates from simpler ions in solution, and it may well be that their conductivity properties, as colloid electrolytes, are overshadowed by the changes which accompany the process of aggregation through which they become colloid electrolytes. In order to study the conductivity properties of colloid electrolytes, as such, it would appear to be desirable to investigate materials which are colloid electrolytes, not by virtue of an aggregation in solution, but which exist as colloid electrolytes even at the lowest possible concentrations to be employed and which do not have any obvious tendency to change in their degree of dispersion or aggregation with change in concentration.

The potassium, sodium, and lithium salts of purified and electro-dialyzed gum arabic (1) appear to be examples of such colloid electrolytes. While the molecules of the gum are not entirely homogeneous as to size or composition, they are nevertheless of colloidal dimensions, having a molecular weight of about  $300,000 \pm 50,000$  (6) and an equivalent weight of about  $1200 \pm 30$  (1). The gum appears to be predominantly hydrophilic in character, being soluble in all proportions in water; it is not surface active at a water-air interface (although it collects at a quartz-water interface). Its solutions in water show true viscous flow up to high concentrations, and it exhibits no tendency to form gels. On the basis of these evidences of a strong over-all affinity for water, it would seem probable that gum arabic in water is molecular and that any tendency for it to aggregate in water solution would be negligible.

This paper reports studies on the conductivity and mobility properties of these salts of gum arabic.

Figure 1 shows the equivalent conductivities (corrected for the conductivity of the water) of the potassium, sodium, and lithium salts of gum arabic in water at 25°C. plotted against the equivalent concentration of the solutions. The conductometric data shown in graph form in this figure were obtained with the usual Wheatstone bridge arrangement, using a 1000-cycle A.C. source. The data are a repetition of conductometric data previously reported (1) for these colloid electrolytes, but correction has been made in the present instance for the conductivity due to the solvent. It will be noted that, through the concentration range studied (0.00053 *N* to 0.042 *N*, corresponding to a weight concentration range of 0.625 g. to 50.0 g. per 1000 g. of water), no minimum in the curve is detected but there is an *increase* in the equivalent conductivity to a maximum followed by a slow decrease as the concentration increases.

That the observed course of the equivalent conductivity-concentration curve cannot be explained by an increase in the mobility of the arabate ion is indicated by direct determinations of the mobility of the colloid. Table 1 gives mobility data at 25°C. obtained on sodium arabate at pH 7.0 at various concentrations of the colloid electrolyte without and with the addition of various amounts of sodium chloride. These data were obtained by the microelectrophoresis tech-

nique (2), using quartz particles upon which the arabate was adsorbed. Figure 2 shows a graph of these data in which the mobility is plotted against the logarithm of ionic strength. Five additional points are included in figure 2 which were obtained with the Tiselius macroelectrophoresis method at 0.5°C. in acetate

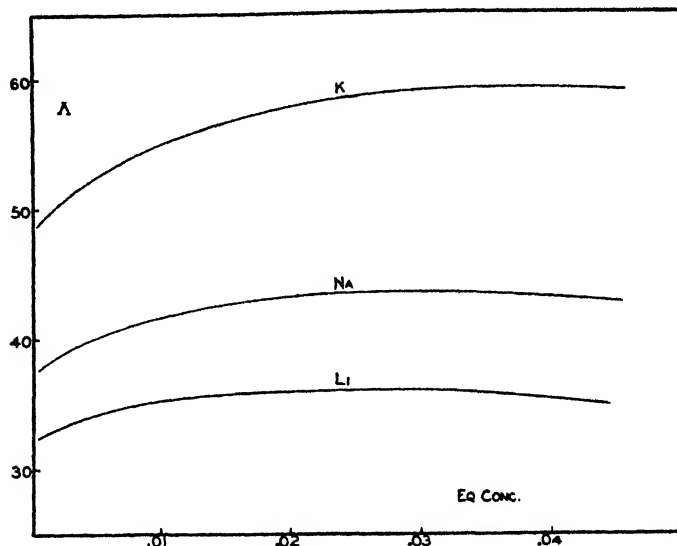


FIG. 1. Equivalent conductivities at varying equivalent concentrations of the lithium, sodium, and potassium arabates.

TABLE 1

*Mobilities of arabate ion in solutions of sodium arabate alone and in presence of added sodium chloride (determined by microelectrophoresis method)*

ARABATE ALONE			WITH 0.0005 N NaCl ADDED		WITH 0.001 N NaCl ADDED		WITH 0.002 N NaCl ADDED		WITH 0.005 N NaCl ADDED		WITH 0.010 N NaCl ADDED		WITH 0.020 N NaCl ADDED	
Concentration		m	Total concentration	m	Total concentration	m	Total concentration	m	Total concentration	m	Total concentration	m	Total concentration	m
grams per cent	equiv./liter	cm. <sup>2</sup> /volt sec. × 10 <sup>4</sup>	equiv./liter	cm. <sup>2</sup> /volt sec. × 10 <sup>4</sup>	equiv./liter	cm. <sup>2</sup> /volt sec. × 10 <sup>4</sup>	equiv./liter	cm. <sup>2</sup> /volt sec. × 10 <sup>4</sup>	equiv./liter	cm. <sup>2</sup> /volt sec. × 10 <sup>4</sup>	equiv./liter	cm. <sup>2</sup> /volt sec. × 10 <sup>4</sup>	equiv./liter	cm. <sup>2</sup> /volt sec. × 10 <sup>4</sup>
0.25	0.002	4.07			0.003	3.67	0.004	3.41	0.007	2.92	0.012	2.42	0.022	2.16
0.375	0.003	3.78			0.004	3.37	0.005	3.14	0.008	2.85	0.013	2.26		
0.50	0.004	3.54	0.0045	3.38	0.005	3.24	0.006	3.09					0.024	2.00
0.75	0.006	3.30			0.007	3.08	0.008	2.94	0.011	2.60	0.016	2.25		
1.00	0.008	3.10	0.0085	3.00	0.009	2.90	0.010	2.77	0.013	2.45	0.018	2.15	0.028	1.90

buffer at pH 6.2 and at higher ionic strengths than those for most of the microelectrophoresis data. (The values for these mobilities as shown in figure 2 have been recalculated to 25°C. upon the assumption that the mobility difference at these two temperatures would be a function only of the temperature differences

in the viscosity of the solvent.) These data show a smooth continuation of the data obtained by the microelectrophoresis method and serve to confirm the correctness of the latter, even though in this case the gum was adsorbed on quartz particles. It is of interest to recognize that the effect of the ionic strength upon the mobility of sodium arabate is, within experimental error, the same whether it derives from added sodium chloride or from the sodium arabate itself, where it is assumed that the arabate ion, even though carrying a number of charges (200 or so per molecule), acts as a corresponding number of monovalent ions insofar as the contribution to the ionic strength is concerned. Apparently the point charges are so remote from each other in this colloid that they can act as monovalent charges in this respect. This is probably not the case with all

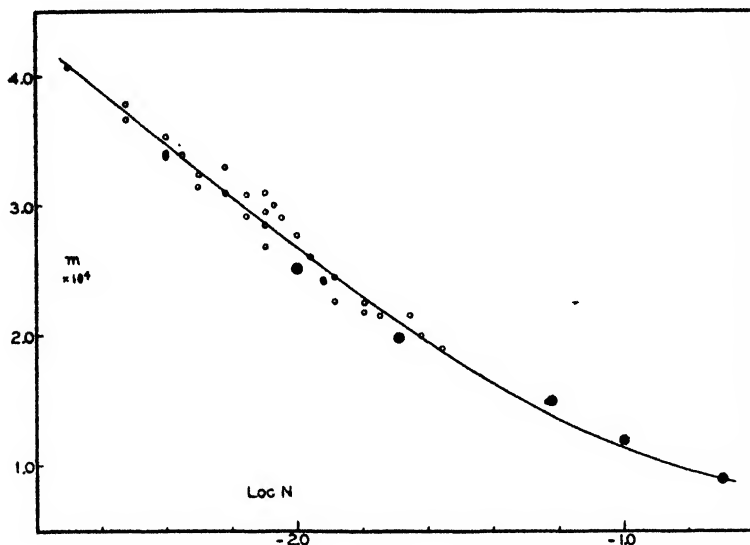


FIG. 2. Mobility (cm.<sup>2</sup>/volt sec.) of sodium arabate at various ionic strengths ( $N$ ). Small circles refer to data obtained by microelectrophoresis method at pH 7.0 on solutions of sodium arabate without and with added sodium chloride. Double circles refer to data obtained by Tiselius electrophoresis method on solutions of sodium arabate in acetate buffers of pH 6.2.

colloid electrolytes. Such a situation, however, is quite fortunate in the present instance, since it makes it more easily possible to observe relationships which are uncomplicated by the strong ionic strength effects of polyvalent ions.

While these mobility observations have been made on the sodium salt, it has been found that there exist only insignificant differences between these values and those of the potassium or lithium salts at equivalent concentrations of colloid electrolyte. In the calculation which follows, it is assumed that the mobilities of the colloid ion are independent of the cation for these three cations.

It is evident from the data in figure 2 that the mobility of the colloid ion decreases continuously with increase in concentration of the colloid electrolyte and that the rise in equivalent conductivity illustrated in figure 1 cannot be explained on this basis.

The observed equivalent conductivity of the arabate salt in solution,  $\Lambda_{\text{obsd.}} = \alpha(\lambda_{\text{Ar}} + \lambda_c)$ , where  $\alpha$  is the conductometric activity of the arabate salt,  $\lambda_{\text{Ar}}$  is the equivalent conductance of the arabate ion, and  $\lambda_c$  is the equivalent conductance of the cation (lithium, potassium, or sodium in these experiments). Values for  $\lambda_{\text{Ar}}$  can be calculated from the measured mobility of the colloid, i.e.,  $\lambda_{\text{Ar}} = mF$ , where  $m$  is the mobility in  $\text{cm}^2/\text{volt sec.}$  and  $F = 96,500$  coulombs. Values for  $\lambda_c$  are not obtainable by direct measurement on the arabate salt but, since the contribution to the ionic strength of the cation of these salts is demonstrated to be so near to that contributed by any added chloride salt of the cation, it may be reasonably assumed that  $\lambda_c$  is equal to that of the cation in the corresponding chloride solution of an equivalent concentration. Such values of  $\lambda_c$  have been calculated from the equivalent conductivities, at  $25^\circ\text{C.}$ , of potassium

TABLE 2

*Mobility of arabate ion, equivalent conductivities of component ions and of the potassium, sodium, and lithium arabates, and the conductometric activities of these salts in aqueous solution at various concentrations at  $25^\circ\text{C.}$*

CONCENTRATION OF ARABATE		MOBILITY OF ARABATE ION $\text{cm}^2/\text{volt sec} \times 10^4$	$\lambda_{\text{Ar}}$	$\lambda_{\text{K}}$	$\lambda_{\text{Na}}$	$\lambda_{\text{Li}}$	$\lambda_{\text{Ar}} + \lambda_{\text{K}}$	$\lambda_{\text{Ar}} + \lambda_{\text{Na}}$	$\lambda_{\text{Ar}} + \lambda_{\text{Li}}$	$\Delta_{\text{KAr}}$	$\Delta_{\text{NaAr}}$	$\Delta_{\text{LiAr}}$	$\alpha_{\text{KAr}}$	$\alpha_{\text{NaAr}}$	$\alpha_{\text{LiAr}}$
grams/1000 g. water	equiv./liter		$\text{ohm}^{-1}$	$\text{ohm}^{-1}$	$\text{ohm}^{-1}$	$\text{ohm}^{-1}$	$\text{ohm}^{-1}$	$\text{ohm}^{-1}$	$\text{ohm}^{-1}$	$\text{ohm}^{-1}$	$\text{ohm}^{-1}$	$\text{ohm}^{-1}$	per cent	per cent	per cent
0.625	0.00053	5.18	50.0	73.4	49.9	38.4	123.4	99.9	88.4	48.8	37.5	32.6	39.6	37.5	36.9
1.25	0.00106	4.63	44.7	73.1	49.5	38.1	117.8	94.2	82.8	49.6	38.4	32.7	42.1	40.8	39.5
2.5	0.0021	4.04	39.0	72.1	49.1	37.7	111.1	88.1	76.7	50.4	38.7	32.8	45.4	43.9	42.8
5.0	0.0042	3.44	33.2	71.2	48.4	37.2	104.4	81.6	70.4	51.9	39.6	34.0	49.7	48.5	48.3
10.0	0.0085	2.85	27.5	70.0	47.6	36.5	97.5	75.1	64.0	54.5	41.2	34.9	55.9	54.8	54.5
20.0	0.0169	2.26	21.8	68.4	46.5	35.6	90.2	68.3	57.4	57.2	42.9	35.9	63.4	62.8	62.3
25.0	0.0212	2.07	19.9	67.4	46.2	35.2	87.3	66.1	55.1	58.2	43.2	36.0	66.6	65.4	65.3
40.0	0.034	1.70	16.4	66.6	45.5	34.5	83.0	61.9	50.9	58.5	43.3	35.9	70.5	70.0	70.6
50.0	0.042	1.65	15.9	66.2	44.7	34.1	82.1	60.6	50.0	58.9	43.0	35.1	71.6	71.0	70.2

chloride, sodium chloride, and lithium chloride as given in the *International Critical Tables* (3), using the relationship, for potassium chloride for example,

$$\lambda_{\text{K}^+} = \frac{\lambda_{\text{K}^+}^\infty}{\Lambda_{\text{KCl}}} \times \Lambda_{\text{KCl}}$$

where  $\lambda_{\text{K}^+}$  and  $\Lambda_{\text{KCl}}$  = the equivalent conductivities of potassium ion and of potassium chloride at the observed ionic strength,  $\lambda_{\text{K}^+}^\infty$  and  $\Lambda_{\text{KCl}}^\infty$  = the equivalent conductivities of potassium ion and potassium chloride at infinite dilution.

Table 2 gives the values of the weight concentration of arabic salts (per 1000 g. of water), the equivalent concentration of arabic salts, the mobilities of the arabate ion at these equivalent concentrations, the observed values of  $\Delta_{\text{KAr}}$ ,  $\Delta_{\text{NaAr}}$ , and  $\Delta_{\text{LiAr}}$ , the values of  $\lambda_{\text{Ar}}$ ,  $\lambda_{\text{K}}$ ,  $\lambda_{\text{Na}}$ , and  $\lambda_{\text{Li}}$ , together with values of  $(\lambda_{\text{Ar}} + \lambda_c)$  and the values of

$$\alpha = \frac{\Lambda_{\text{obsd.}}}{\lambda_{\text{Ar}} + \lambda_c}$$

for each salt at each concentration of the colloid electrolyte.



Figure 3 illustrates the manner in which  $\alpha$  changes with the equivalent concentration of the colloid salts. The conductometric activities of the arabates are seen to increase with concentration and approach a limiting value of about 75 per cent of theoretical at the higher colloid concentrations. The relationship is nearly independent of the identity of the cation (a slight lyotropic effect is evident). (There are included also in figure 3 several points calculated for  $\alpha$  from conductivity measurements on sodium arabate in the presence of varying amounts of added sodium chloride. These solutions are those given in table 1. The equivalent concentrations plotted in this case are those of the sodium arabate alone. It is evident from these points, while they do not fall exactly on the curve for the other data, that the observed effect is a function of colloid

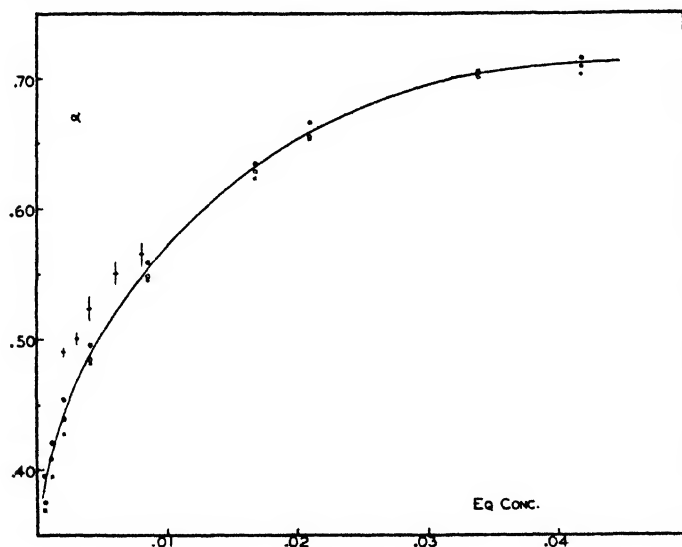


FIG. 3. Variation in conductometric activity of arabate salts in solution with change in their equivalent concentrations.

concentration alone and is independent of the total ionic concentration in the solution.)

The relationships existing between the observed values of the equivalent conductivity of sodium arabate,  $\Lambda_{\text{NaAr}}$ , the calculated values of  $\lambda_{\text{Na}}$  (in sodium chloride), the values of  $\lambda_{\text{Ar}}$  (calculated from mobility of the colloid ion), of  $\alpha\lambda_{\text{Na}}$  and of  $\alpha\lambda_{\text{Ar}}$  are shown in figure 4, where these values are plotted against the equivalent concentration of the colloid electrolyte. It is seen that  $\Lambda_{\text{NaAr}}$ , which is equal to  $\alpha(\lambda_{\text{Ar}} + \lambda_{\text{Na}})$ , increases with increase in concentration of the colloid electrolyte entirely because of the increase in the current-carrying capacity of the sodium gegenion as the concentration of colloid increases. After a concentration of about 30 g. of arabate per liter is reached, the gegenion reaches a limit in its capacity to carry current and the value of  $\Lambda_{\text{NaAr}}$  then begins a slow decrease, due to the continued decrease in mobility of the colloid ion of the electrolyte.

This increase in the current-carrying capacity of the gegenions with increased

concentration of the colloid may be pictured as due to a decrease in the energy barrier which they must encounter as they leave the region of the colloid particle

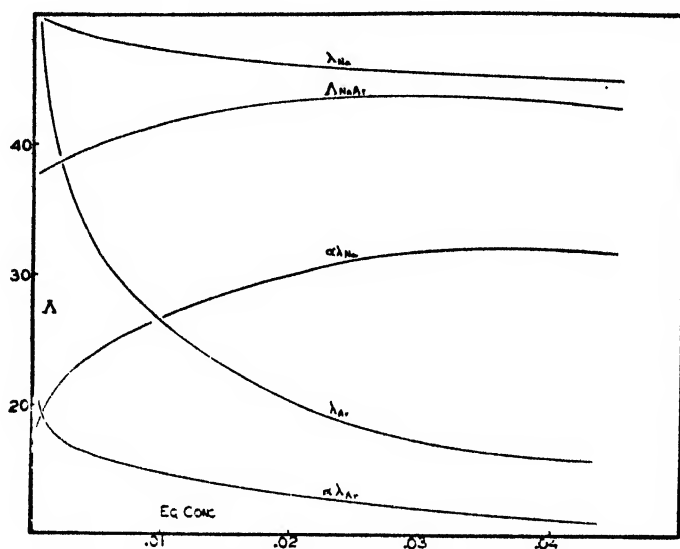


FIG. 4. Illustrating the manner in which the equivalent conductivities of sodium arabate ( $\Lambda_{NaAr}$ ), of the arabate ion ( $\lambda_{Ar}$ ), of sodium ion ( $\lambda_{Na}$  in sodium chloride), and the values of  $\alpha\lambda_{Na}$  and  $\alpha\lambda_{Ar}$  change with the equivalent concentration of sodium arabate solutions.

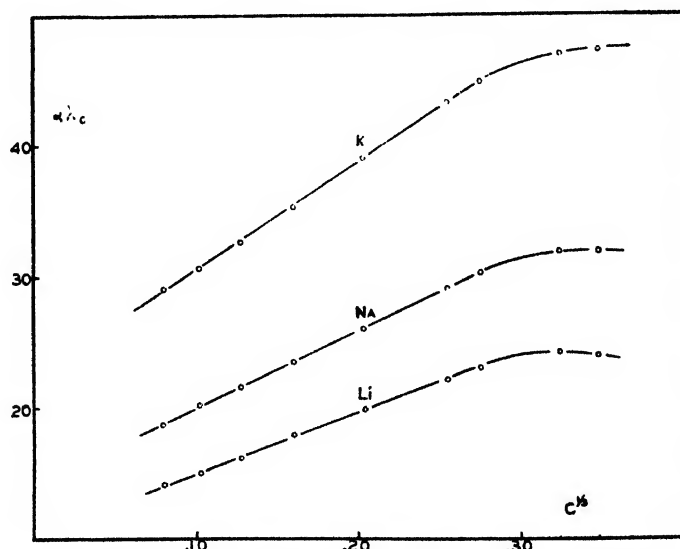


FIG. 5. Illustrating the manner in which the values of  $\alpha\lambda_0$  for the lithium, sodium, and potassium arabates change with the cube root of their equivalent concentrations in solution.

and move into the intermicellar regions of the liquid under the influence of the applied electric field. An adequate explanation of the effect has not yet been

arrived at. That it is not a simple volume effect (i.e., proportional to the volume of disperse phase) is indicated by the curvilinear relationship which the factor,  $\alpha\lambda_c$ , shows against concentration, as illustrated in figure 4. A good linear relationship is shown against the cube root of concentration, as is illustrated in figure 5, where the values of  $\alpha\lambda_c$  for the potassium, sodium, and lithium gegenions are plotted against  $\sqrt[3]{\text{Conc.}}$ . This would appear to indicate that the current-carrying capacity of the gegenions increases directly with one dimension of the volume of the colloid phase, i.e., is proportional to the average linear distance spanned in the solution by the colloid micelles. This relationship holds, in the case of these colloid electrolytes, up to a total colloid concentration of approximately 30 g. per liter, above which there apparently exists no further possibility of reducing the resistance to their movement in the electric field. The equivalent conductivity of the gegenions at this concentration has reached only about 75 per cent of that of the same ions when present as chlorides in solution at the same ionic strengths. This may mean that only about 75 per cent of the potential gegenions exist in that region of the micelle where they are free to move independently of the motion of the colloid ion, i.e., in the region of the solvent in the double layer which is not carried along by the colloid ion.

In any case, it must be recognized that the equivalent conductivity-concentration relationships which exist for these colloid electrolytes, while somewhat similar in appearance to those which have been observed for agglomerating colloid electrolytes such as the dyes and soaps, require a different explanation than that based upon an increased mobility, due to agglomeration, of the ions giving rise to the colloid component.

#### REFERENCES

- (1) BRIGGS, D. R.: J. Phys. Chem. **38**, 867 (1934).
- (2) BRIGGS, D. R.: Ind. Eng. Chem., Anal. Ed. **12**, 703 (1940).
- (3) *International Critical Tables*, Vol. VI. McGraw-Hill Book Company, Inc., New York (1929).
- (4) MCBAIN, J. W.: Trans. Faraday Soc. **9**, 99 (1913).
- (5) MOILLIET, J. L., COLLE, B., ROBINSON, C., AND HARTLEY, G. S.: Trans. Faraday Soc. **31**, 120 (1935).
- (6) OAKLEY, H. B.: Trans. Faraday Soc. **31**, 136 (1935).

SOME CORRELATING PRINCIPLES OF DETERGENT ACTION<sup>1</sup>

WALTER C. PRESTON

*The Procter & Gamble Company, Ivorydale, Ohio**Received August 26, 1947*

Detergent solutions exhibit a striking characteristic when quantitative data on their physical properties are plotted against concentration. Figure 1 illustrates this for sodium dodecyl sulfate, the data for conductivity (8), surface and interfacial tension (15), osmotic pressure (7), density (6), and high-frequency conductivity (17) being taken from the literature and the detergency curve from our own work, to be discussed later. Each curve shows a break, an inflection, occurring within a narrow concentration band lying between 0.18 per cent and 0.25 per cent (0.063–0.083 *M*). The dodecyl sulfate is not unique with respect to these inflections. Extensive data show that each detergent is characterized by a concentration band within which some far-reaching alteration must be taking place, and there are ample grounds for believing that the critical phenomenon here occurring is the beginning of large-scale colloid formation. Recognition of this fact is fundamental to an understanding of detergency phenomena.

Washing a bundle of soiled clothes is a complex operation in which many factors are involved. Low surface tension, low interfacial tension, low contact angles, and high wetting, spreading, dispersing, suspending, and emulsifying power have all been recognized as factors. So, also, is the actual solubilization of certain soils by detergents. But what unifying element is there in the whole picture?

The unifying element is the architecture of the detergent molecule or ion, which is in all cases characterized both by great length and by a dual hydrophilic-hydrophobic nature. The typical pattern is that of soap, consisting of a long hydrocarbon chain, at the end of which is a water-soluble, polar group. When particles such as this are inserted in water, water molecules are pushed apart, an interface between water and hydrocarbon chain is created, and free energy is therefore stored up in the interface. The free energy of the system can be reduced by expelling the detergent particle in either of two ways.

First, the particles may be expelled to the surface and concentrate there in an oriented layer, polar groups directed downward into water and non-polar hydrocarbon chains sticking upward into the air. Such an adsorbed surface layer means lowered surface tension, in accordance with the Gibbs law. The stronger the hydrophilic character of the polar end and the hydrophobic character of the non-polar end, the stronger will be the thermodynamic compulsion to surface activity. Going a step farther we may use the concepts of a "center of polarity," a "center of non-polarity," and a "polar-non-polar moment." A

<sup>1</sup> Presented at the Twenty-first National Colloid Symposium, which was held under the auspices of the Division of Colloid Chemistry of the American Chemical Society at Palo Alto, California, June 18–20, 1947.

certain distance separates the centers of polarity and non-polarity, and the farther apart these centers are the greater the moment which orients the particles in the surface and therefore the more complete the orientation.

Secondly, the thermodynamic urge toward a reduction of free surface energy may also be satisfied by a partial expulsion of the detergent particles from the water system by coalescence of the crystalloidally dissolved particles into col-

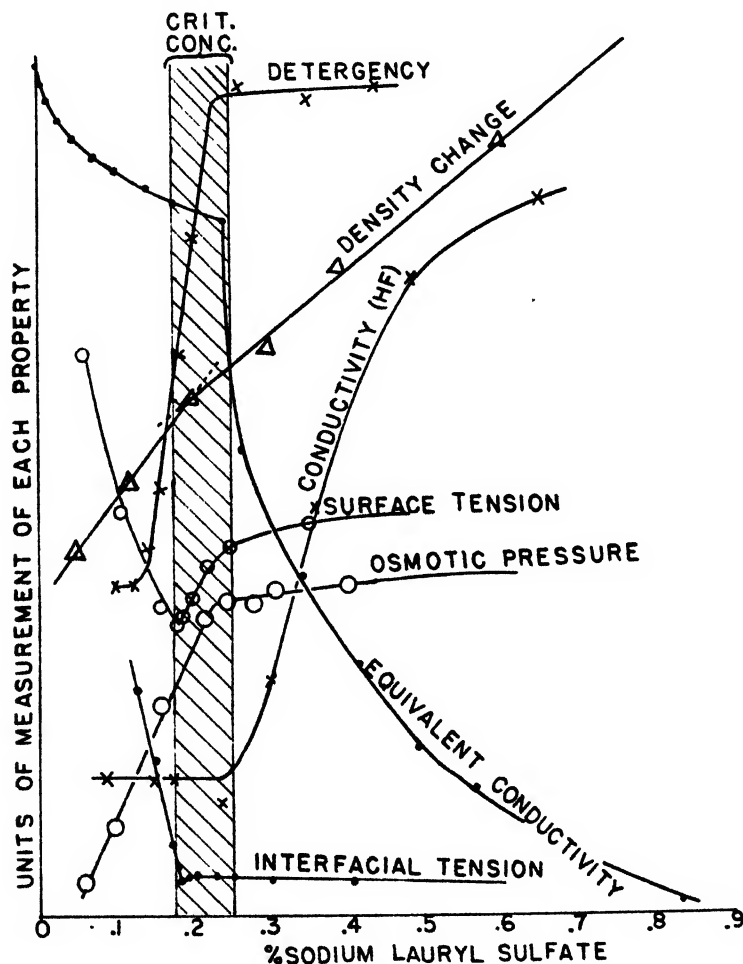


FIG. 1. Physical property curves for sodium dodecyl sulfate. Temperature = 25–38°C.

loidal aggregates. One such crystalloidal particle inserted into water creates an interface of area  $A$  and of surface tension  $\gamma$ , possessing a definite amount of free surface energy,  $\gamma A$ . Two such particles independently would create twice as much interface and twice as much free surface energy. But if these two particles were to coalesce, hydrocarbon tails intertwined or dissolved in one another, the interfacial area would be less than  $2A$  and the free surface energy

would be less than  $2\gamma A$ . If fifty such crystalloidal particles were to coalesce into one large micelle, the reduction in surface energy would be large.

Surface activity and tendency to form colloidal micelles are thus two different manifestations of the same fundamental character possessed by all detergents because of their chemical and spatial constitution.

It is unlikely that the adsorbed surface layers or the colloidal aggregates (at least in dilute solutions) are made up of molecules in the case of either the anionic or the cationic detergents, since such detergents are ionized like other strong electrolytes. The ions are the surface-active, micelle-forming constituents at low concentrations, the micelles being formed only when the reduction in free energy resulting from coalescence outweighs the electrostatic repulsion which ions of like charge have for one another.

In addition to ionizing and forming colloid, soaps hydrolyze to form free fatty acid or acid soap, but we can for good reasons, if perhaps hastily, dismiss these hydrolysis products from consideration as active washing constituents. On the one hand, adding acid to soap produces free fatty acid or acid soap but does not increase washing power, and on the other hand, adding alkali to soap represses hydrolysis without destroying washing power. Furthermore, synthetic detergents such as the alkyl sulfates and sulfonates cleanse well and yet do not hydrolyze at all under normal laundry conditions. The theory that soap solutions cleanse because of their hydrolysis alkalinity was discredited long ago.

The role of colloidal aggregates in the washing process cannot be treated so casually, for it is obvious that tendency to form colloid is common to all good detergents. All workers in this field now agree that the first sharp downward inflection in the equivalent conductivity curve (figure 1) marks the beginning of colloid formation on a large scale, and the concentration at which this occurs is commonly called the "critical concentration of micelle formation."

There has been much controversy as to the nature of the colloidal particles. Hartley (5), for example, postulates the simplest possible micelle (figure 2) in dilute solution, roughly spherical in shape, two ion-lengths in diameter, made up of long-chain ions arranged with their polar heads turned outward, in contact with water, and their long chains constituting the hydrocarbon interior, and surrounded by a Coulomb cloud of gegenions in variable number. McBain (9), on the other hand, insists upon the existence of two distinct kinds of micelle, the (small) ionic and the (large) neutral or lamellar type (figure 2).

The existence of lamellar micelles at *high soap concentrations* (5 per cent or higher) is indicated by x-ray data,<sup>2</sup> but there is no direct evidence as to the shape and structure of the micelles in dilute solutions of laundry strength, i.e., of the order of a few tenths of 1 per cent concentration. For present purposes, however, the important point is that no micellar structure has yet been postulated which has a long polar-non-polar configuration with centers of polarity and non-polarity separated by great distances, and this configuration being lacking, one

<sup>2</sup> X-ray work on soap solutions is becoming extensive. See references cited by McBain (9) and more recent work by McBain *et al.* (10) and by Harkins *et al.* (4).

would not, *a priori*, expect the micelles to be surface active or to contribute to the washing process by virtue of surface activity.

This last statement requires further comment, for the micelles do solubilize many forms of dirt by solution in their interior; furthermore, they may act as a reservoir to restore the equilibrium when soap in true solution is destroyed or exhausted, as by acids or by heavy loads of dirty clothes. On these grounds probably rests whatever justification there was for the assertion which was popular some years ago that soaps wash "because of their colloidal properties," despite the fact that innumerable other substances possess colloidal properties but are valueless in washing.

Figure 3 illustrates qualitatively what occurs (exclusive of the results of hydrolysis) on the basis of Hartley's concept as the concentration of an anionic

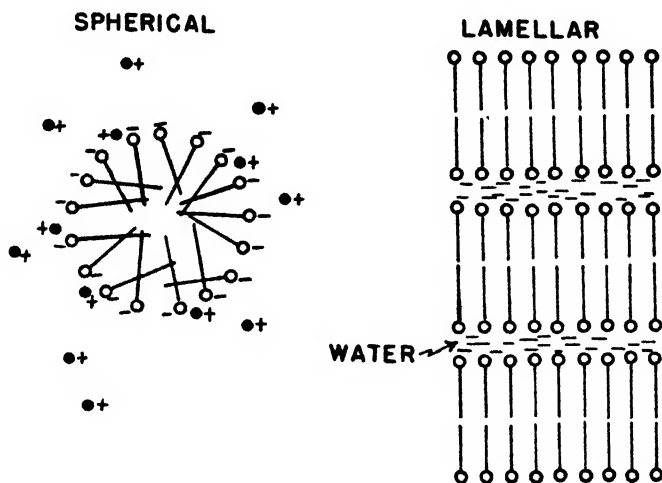


FIG. 2. Two proposed structures of soap micelles

detergent in water is increased (14). At first only ions are present and these increase in direct proportion to the increase in total concentration. But soon micelles begin to appear,<sup>3</sup> first in small amounts, then in rapidly increasing amounts, and as they do so the rate of increase of the anions decreases to zero. The greater the number of ions which aggregate to form each unit micelle, the narrower the concentration band would be within which aggregation would occur and the larger the fraction of the detergent which would exist in aggregated form. Since some positively charged sodium ions attach themselves to or are constituent parts of the negatively charged micelle, the rise of the curve for sodium-ion concentration also becomes more gradual. The adherence of a considerable number of sodium ions to the micelle would necessitate mathematically,

<sup>3</sup> McBain (9) believes that some few ionic micelles exist even at great dilutions and that the critical concentration of (lamellar) micelle formation is not so sharply defined as indicated in the drawing.

according to the law of mass action, that eventually the anion curve should actually fall (5). Support for this conclusion has recently been found in the work with pinacyanol, which has led Harkins and his associates (2) to suggest that when the critical concentration is reached, some of the previously existing crystalloid transforms into micellar form. The existence of a maximum in the curve for the long-chain ion also affords the most satisfying explanation of the minimum in the surface-tension curve, as has been pointed out by both Alexander (1) and Powney and Addison (15), if the long-chain ion is in reality the surface-active species in the solution.

For present purposes, the chief significance of figure 3 is that the concentration of long-chain ions reaches its maximum at about the same concentration as

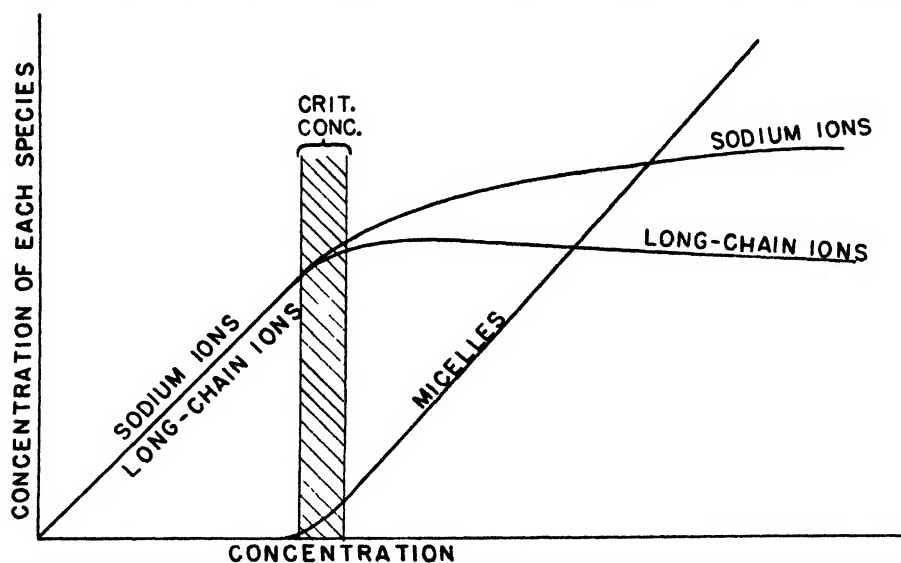


FIG. 3. Effect of change in total concentration upon the concentration of ions and micelles

that at which micelle formation becomes extensive. Possible correlation of this fact with detergency phenomena is interesting and is possible if we consider some results of washing artificially soiled cloth, the load of cloth being small so as not to affect greatly the concentration of free detergent in solution. Plotting whiteness of washed cloth against concentration of detergent, the typical curve (after an initial uncertain flat, due at least partially to adsorption on the cloth and the soil) rises to a maximum and then flattens out; washing efficiency increases up to a certain point, a critical washing concentration, beyond which further additions of detergent have little effect. If we were to find experimentally that the break in the washing curve and the break in the curve for paraffin-chain ion *vs.* total concentration (figure 3) occur at the same concentration, we might postulate that the amount of washing increases as the amount of fatty ion increases, that when the one ceases to increase the other ceases to increase or that *washing is proportional to the concentration of fatty anion*. This



is of course but a short step from saying that *washing is caused by the fatty anions*, —that they are the active constituents of the solution with respect to washing just as they are with respect to surface activity and colloid formation.

Figure 1 shows for one detergent at one temperature the band known as the critical concentration of micelle formation. For other detergents and at other temperatures the concentrations at which these inflections occur will be different, but from such curves these concentrations may be read off and then plotted as has been done in figure 4 for a homologous series of sodium alkyl sulfates. From such charts for the alkyl sulfates, the alkyl sulfonates, the soaps, etc., we can conclude that while in general the critical concentrations increase a little as the temperature is increased, yet this temperature effect is minor compared with the

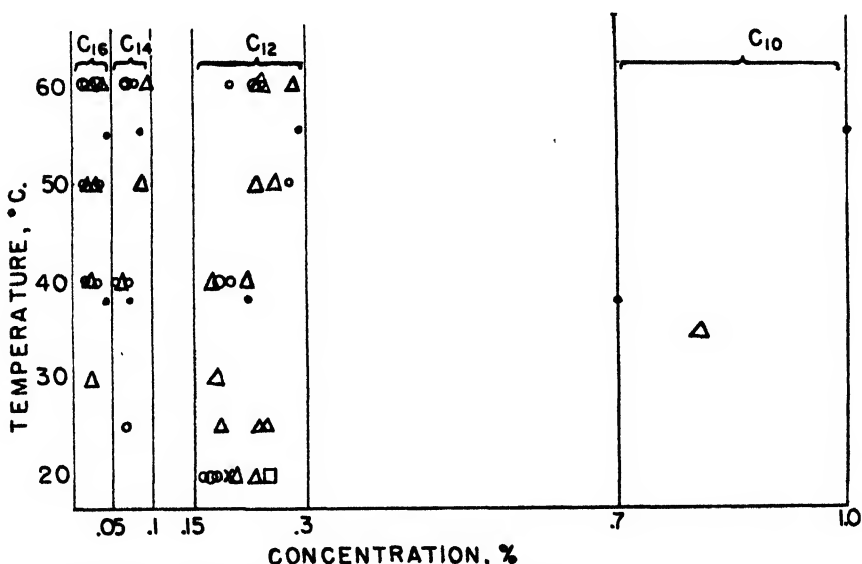


FIG. 4. Breaks in physical property curves of alkyl sulfates.  $\Delta$ , equivalent conductivity;  $\square$ , viscosity;  $\times$ , density;  $\circ$ , interfacial tension;  $\circ$ , surface tension;  $\bullet$ , detergency.

effect of chain length. The longer the hydrocarbon chain, the lower the critical concentration.

Figure 5 shows detergency results at 55°C. for the series of sodium alkyl sulfates which were pictured in figure 4. White cotton muslin soiled with a lamp-black-vaseline mixture was washed in a launderometer with various concentrations of alkyl sulfate, and the whiteness of the resulting washed cloths was determined photometrically. The curves rise steeply and then break off at rather well-defined critical concentrations. The longer the chain, the lower the concentration required to wash. When these critical washing concentrations are inserted in figure 4 they fall, for each chain length, in the same concentration region within which the breaks in the other physical properties occur. This is true also of the detergency points obtained similarly for alkyl sulfates at 38°C.

Figures 6, 7, 8, and 9 show a similar set of detergency curves at 71°, 55°, 38°, and 25°.

and 21°C. for the sodium soaps from laurate to stearate. The whiteness grades here recorded have been corrected for the cleaning action of water and mechan-

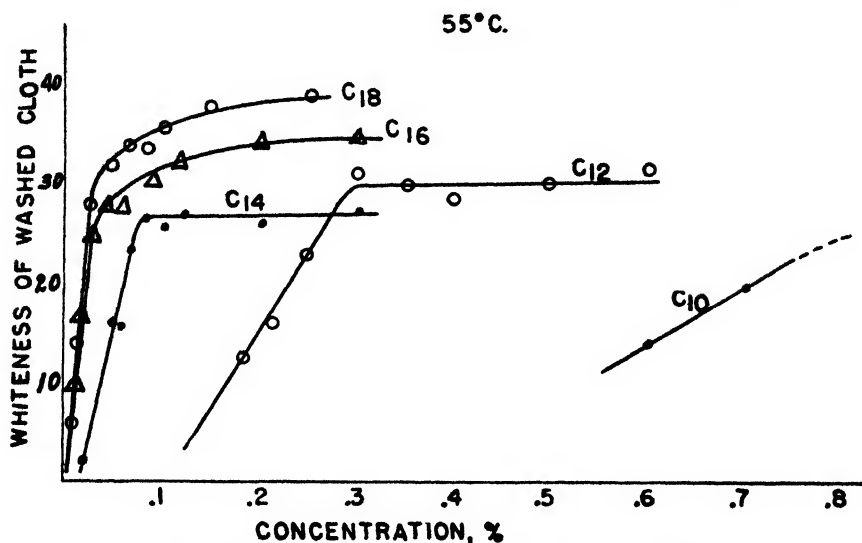


Fig. 5. Detergency curves for alkyl sulfates at 55°C.

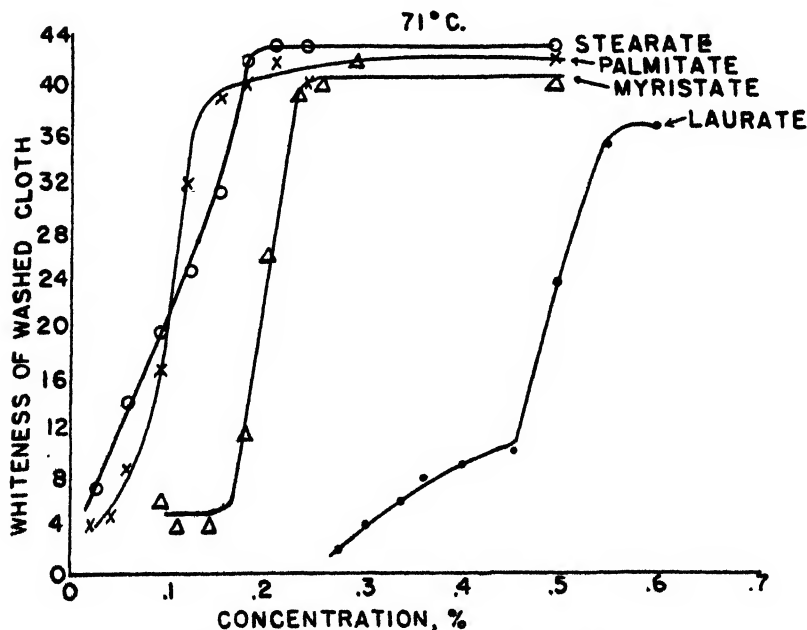


Fig. 6. Detergency curves for sodium soaps at 71°C.

ical agitation alone, at the temperatures in question; i.e., zero on the whiteness scale represents the whiteness to which the cloth is washed in the absence of

soap. In figure 6 there is an anomaly in that the stearate ( $C_{18}$ ) curve lies slightly to the right of that for palmitate ( $C_{16}$ ). This anomaly occurs again at  $55^{\circ}\text{C}$ .

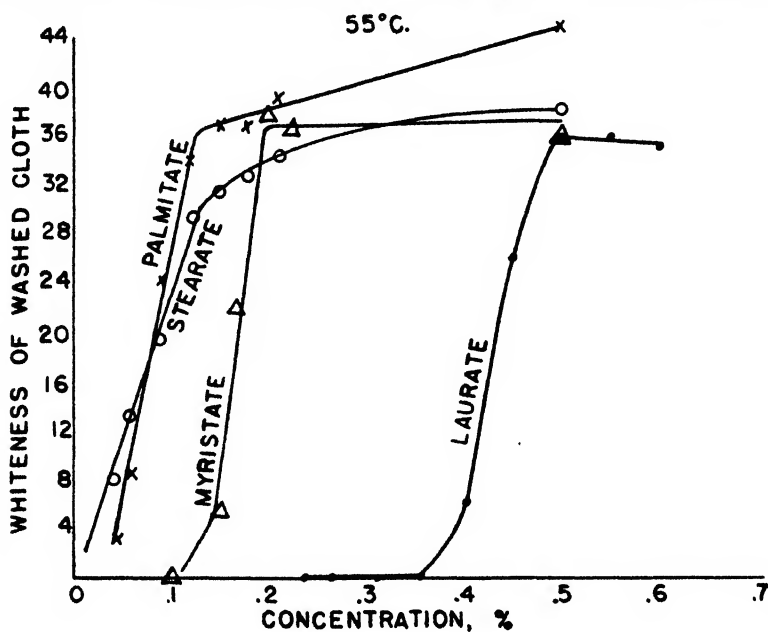


Fig. 7. Detergency curves for sodium soaps at  $55^{\circ}\text{C}$ .

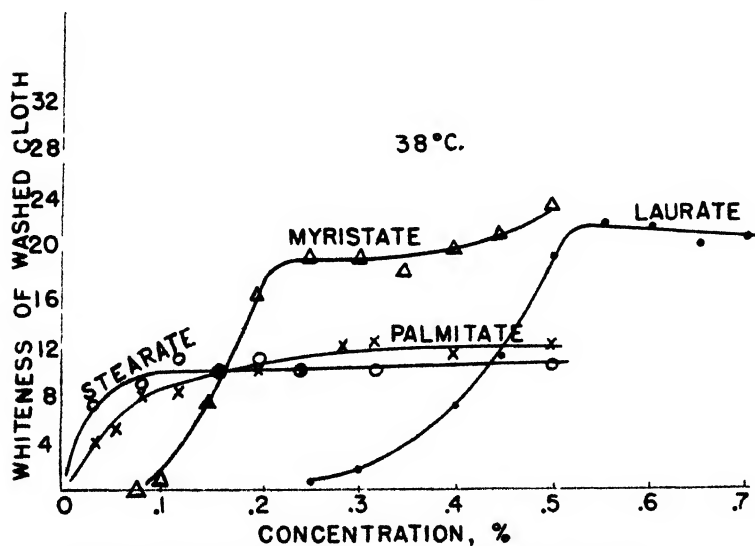


Fig. 8. Detergency curves for sodium soaps at  $38^{\circ}\text{C}$ .

as shown in figure 7. The break in the stearate curve is here less sharp, but the positions of the other curves are relatively unchanged.

The temperature effect is more marked when the temperature falls to  $38^{\circ}\text{C}$ .

as in figure 8. None of the soaps wash as white as at 55° or 71°C., but both palmitate and stearate are obviously too poor for practical usefulness at 38°C.

Stearate was so poor as to be excluded from the set at 21°C. (figure 9). Even myristate is now below par. Only laurate remains good at this temperature.

For present purposes, however, we are not so much concerned with the effect of temperature on maximum whiteness as with the critical phenomena which are apparent in these curves. For any one of these soaps,<sup>4</sup> the break in the detergency curve and the inflections in conductivity, pH, density, interfacial tension, etc., all occur at roughly the same point, and if the one set of breaks is to be attributed to colloid formation it is reasonable to attribute the other set to the same cause.

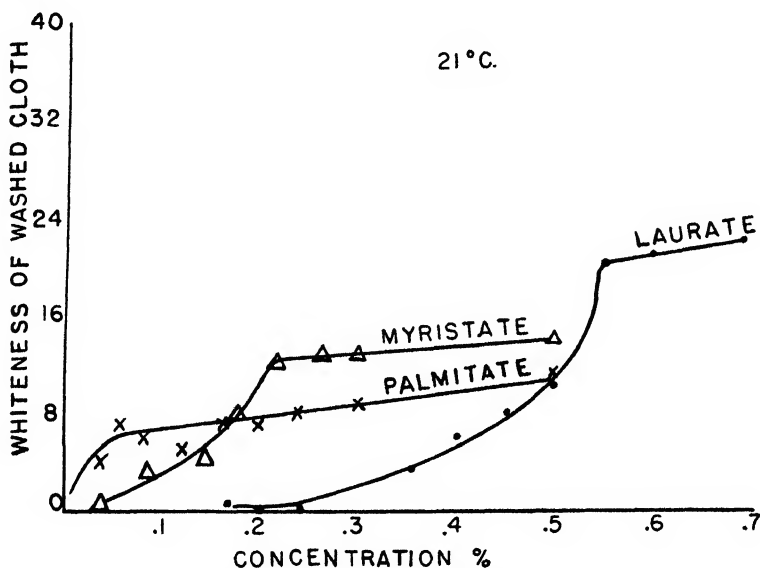


FIG. 9. Detergency curves for sodium soaps at 21°C.

Curves of this kind for sodium and potassium soaps and for sodium alkyl sulfates and sulfonates all show that if we consider only the length of the hydrocarbon chain (thus excluding the  $\text{—COONa}$  group of soap) we can plot critical washing concentration against the number of carbon atoms (as in figure 10) with the interesting result that the points for all four detergents fall close to a smooth curve, as if differences in the polar heads ( $\text{—COO}^-$ ,  $\text{—SO}_4^-$ , and  $\text{—SO}_3^-$ ) have slight effect, compared with chain length. The apparent deviation of the points for palmitate and stearate from the curve may be attributed to destruction of soap by the extensive hydrolysis which occurs at these great dilutions, the degree of hydrolysis being greater for the palmitate and stearate than for the laurate and myristate.

A comparison of the curves in figures 6 to 9 shows that as the temperature

<sup>4</sup> The oleate is intentionally omitted, since its critical concentration of micelle formation is not well established.

falls there is not much change in the critical concentration. In this connection it is interesting to look at the solubility curves for the soaps, as shown in figure

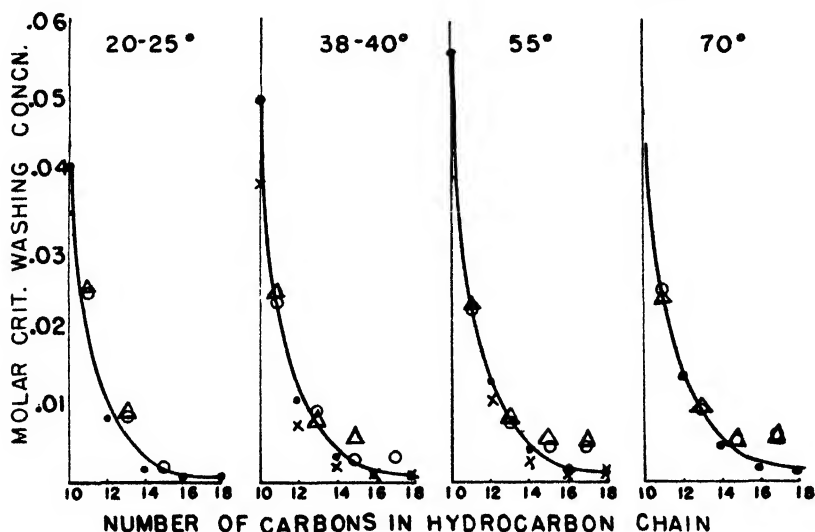


FIG. 10. Correlation between critical washing concentration and length of hydrocarbon chain. X, sodium alkyl sulfates; ●, sodium alkyl sulfonates; ○, sodium soaps; △, potassium soaps.

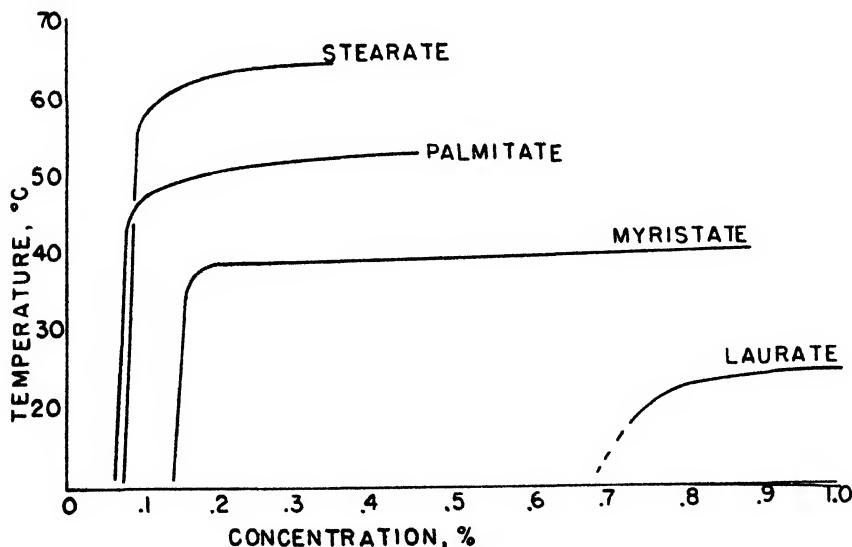


FIG. 11. Solubility curves for sodium soaps, exclusive of hydrolysis products

11. These curves, obtained in our own laboratory, are in fair agreement with those of Ekwall (3) and Stauff (18) except in the case of the laurate. After an initial break at a critical temperature,  $T_K$ , the curves appear to be nearly flat, but this is only because the abscissa scale is so expanded. In reality, all the

curves continue to rise. That for sodium palmitate, for example, rises to 70°C. at 25 per cent concentration before a second liquid phase (middle soap) begins to appear (16).

While acid soap or free fatty acid from hydrolysis may precipitate to a small extent to the left of the steep portion of the solubility curve, it is not until we pass this curve going to the right that neutral soap crystals form. To the left of this line we have predominantly an ionic solution; to the right of it we have an ionic solution containing in addition macroscopically visible neutral soap crystals.

If, at a temperature below  $T_K$ , the concentration of fatty anions were plotted against total concentration of soap, we should expect to obtain, at least as a first approximation, a straight line rising at a 45° angle at first, and then breaking to a horizontal line at a concentration corresponding to the solubility limit of the soap. Having once reached the solubility limit, further additions of soap would not dissolve and therefore could not increase the concentration of anions. Similarly if, for example, a hot 1 per cent solution of sodium myristate were cooled to 30°C., only some 0.15 per cent would remain in solution; the remaining 0.85 per cent would precipitate. Thus the solubility of the soap should set a practical limit on washing, and as a result we should expect the critical washing concentration to fall on the steep slope of the solubility curve. Experimentally, the agreement with this expectation is considered good on the whole, although the critical washing concentration of sodium laurate falls a little to the left of the solubility curve of figure 11, while those for the other soaps lie somewhat to the right of their solubility curves. In the case of the sulfonates, there is better agreement between washing concentrations and the solubility results obtained both by Tartar (19) and by ourselves.

If we work at temperatures above  $T_K$ , with increasing soap concentration we soon come to the invisible changes in the solution resulting from colloid formation, as previously discussed. Beyond this critical concentration of colloid formation, further additions of soap increase the amount of colloid but not appreciably that of the long-chain ions; hence the detergency curve should, and does, level off. The critical washing concentration and the critical concentration of colloid formation should, according to our theory, coincide. Within reasonable limits of experimental error they do so, and they seem to fall not far from an upward extension of the steep slope of the solubility curve. The critical washing concentration is thus independent of whether the second phase which separates from the solution is made up of colloidal aggregates or of macroscopic solid crystals.

The theory predicts that the critical washing concentrations should fall along *ABC* of figure 12 for sodium soaps and sodium alkyl sulfonates. Potassium soaps and sodium alkyl sulfates are so extremely soluble that normal washing temperatures for them are always above  $T_K$ , so that in their case only the *BC* part of the curve is involved. The shaded band *BC* is so drawn in order to indicate that it is a band with ill-defined edges, and not a sharp line. The formation of colloid is only *relatively* sudden.

Experimentally, we find that the molar critical washing concentration is essentially the same for the sodium as for the potassium soaps, and that the detergency curves for sodium, ammonium, magnesium, copper, and triethanolamine alkyl sulfates all show breaks at about the same molar concentrations. The identity of the hydrocarbon chain is seemingly more important than the difference between sodium and the other cations. This would be surprising if the active washing constituent were either the molecule or a colloidal particle containing much cation, but it is not surprising on the basis of the concept here proposed, the concept of the importance of the long-chain ion which would of course be the same whether derived from a sodium salt or from any other salt.

The hypothesis that the long-chain ion is the active constituent of detergent solutions is applicable to both anionic and cationic detergents. In the case of

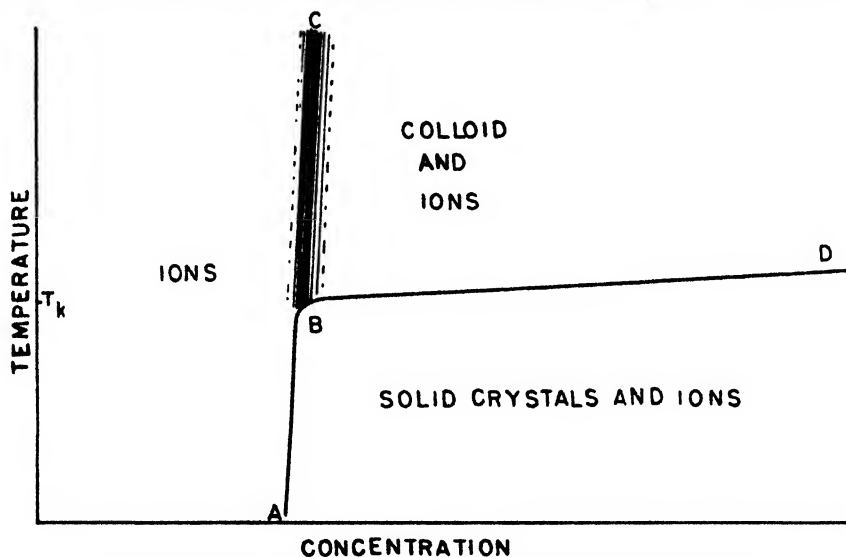


FIG. 12. Qualitative phase diagram for colloidal electrolytes

the non-ionized type, the molecule itself would be the active constituent. The importance of the concept should perhaps be stressed as a counterbalance to the emphasis which we are placing in this Symposium on the extremely interesting phenomenon of solubilization of hydrocarbons, dyes, etc., by the colloidal micelle. The two types of cleaning action should be considered as supplementary to one another. Solubilization, however, appears to *begin* at the critical concentration of colloid formation (11, 12, 13) and to be indicative of it. On the other hand, at this critical concentration washing power has practically attained its maximum. With further increments of detergent, the total solubilization increases, often almost linearly, whereas the detergency curve rises little, if at all. In fact, in many cases we have observed it to fall. This would seem to relegate solubilization to a minor rôle in the usual laundering processes.

Supporting the concept here proposed are many washing tests and observations which we have not time to present. On the other hand, there are some facts

which do not as yet seem to fit into the picture. Examples are the effect of alkaline salts in shifting the steep slope of the detergency curve of soap to the left, without affecting the horizontal portion of the curve appreciably, and the effect of fatty acid amides (20) and higher alcohols (21) in shifting the steep slope of the alkyl sulfate curves to the left, while at the same time increasing markedly the whiteness to which soiled cloths can be washed at high concentrations. Correlation of critical washing phenomena with other critical phenomena has been poor with sodium oleate, perhaps because of the ill-defined breadth of the concentration band over which it transforms into micellar form. But despite isolated pieces which have not yet been fitted into the mosaic, so many pieces do fit that we may say that the mass of the evidence now available is favorable to the hypothesis.

#### SUMMARY

Detergency curves are given showing the existence of a critical washing concentration which is characteristic of each detergent and which coincides with its critical concentration of colloid formation. Detergent action, colloid formation, and surface activity are different manifestations of the same characteristic of the detergent. The long-chain ion is the active constituent in each manifestation. Colloid formation begins, and washing power and surface activity reach their maximum, at the concentration at which further additions of detergent either (a) do not dissolve (at low temperature) or (b) dissolve to form colloid (at higher temperature), and thus in neither case is further increase in the number of long-chain ions in the solution possible. The critical washing concentration is essentially a function of the length of the non-polar "tail" of the detergent. Solubilization of foreign matter is a function of the colloidal micelle and plays a secondary rôle in the usual washing process.

#### REFERENCES

- (1) ALEXANDER, A. E.: *Trans. Faraday Soc.* **38**, 248 (1942).
- (2) CORRIN, M. L., KLEVEN, H. B., AND HARKINS, W. D.: *J. Chem. Phys.* **14**, 486 (1946).
- (3) EKWALL, P.: *Kolloid-Z.* **85**, 16 (1938).
- (4) HARKINS, W. D., *et al.*: *J. Chem. Phys.* **13**, 534 (1945); *J. Colloid Sci.* **1**, 105 (1946); *J. Am. Chem. Soc.* **68**, 220 (1946).
- (5) HARTLEY, G. S.: *Aqueous Solutions of Paraffin Chain Salts*. Hermann et Cie, Paris (1936).
- (6) HESS, K., PHILIPPOFF, W., AND KIESSIG, H.: *Kolloid-Z.* **88**, 40 (1939).
- (7) HESS, K., AND SURANYI, L. A.: *Z. physik. Chem.* **A184**, 321 (1939).
- (8) HOWELL, O. R., AND ROBINSON, H. G. B.: *Proc. Roy. Soc. (London)* **A155**, 386 (1936).
- (9) MCBAIN, J. W.: In *Colloid Chemistry, Theoretical and Applied*, edited by Jerome Alexander, Vol. 5, pp. 102-20. Reinhold Publishing Corporation, New York (1944).
- (10) MCBAIN, J. W., *et al.*: *J. Am. Chem. Soc.* **68**, 296, 547 (1946).
- (11) MCBAIN, J. W., AND GREEN, A. A.: *J. Am. Chem. Soc.* **68**, 1731 (1946).
- (12) MCBAIN, J. W., AND JOHNSON, K. E.: *J. Am. Chem. Soc.* **66**, 9 (1944).
- (13) MCBAIN, J. W., AND MERRILL, R. C., JR.: *J. Phys. Chem.* **46**, 10 (1942).
- (14) MURRAY, R. C.: *Trans. Faraday Soc.* **31**, 206 (1935).
- (15) POWNEY, J., AND ADDISON, C. C.: *Trans. Faraday Soc.* **33**, 1243 (1937).



- (16) ROSEVEAR, F. B.: Unpublished data.
- (17) SCHMID, G., AND LARSEN, E. C.: *Z. Elektrochem.* **44**, 651 (1938).
- (18) STAUFF, J.: *Z. physik. Chem.* **A185**, 45 (1939); **A187**, 119 (1940); *Kolloid-Z.* **89**, 224 (1939).
- (19) TARTAR, H. V., AND WRIGHT, K. A.: *J. Am. Chem. Soc.* **61**, 539 (1939).
- (20) U. S. patents 2,383,525; 2,383,737; 2,383,738; 2,383,739; 2,383,740.
- (21) U. S. patents 2,166,314 and 2,166,315.

## COLLOIDAL STRUCTURES IN BINARY SOAP SYSTEMS<sup>1</sup>

TODD M. DOSCHER AND ROBERT D. VOLD

*Department of Chemistry, University of Southern California, Los Angeles 7, California*

*Received August 25, 1947*

As a result of numerous investigations, the phase rule has been found to be applicable to binary systems of soap and water (21) and of soap and a hydrocarbon (sodium stearate-cetane) (4), and to a ternary system of sodium stearate-cetane-water (5). Numerous separate and distinct phases have been identified in these systems, and interest in them has been aroused owing to their importance in the technology of toilet and laundry soaps, lubricating greases, and cosmetic creams. No detailed attempts, however, have been made to elucidate the molecular structures of these phases nor to relate the physical properties to the constitution of the phases. If such information were available, it would be possible to predict and specify the performance of systems which have not yet been completely investigated, and the technology of these materials would then be placed on a more scientific basis.

It is true that the determination of the colloidal structure of these soap systems—ranging as they do from crystalline solids to isotropic solutions, from transparent elastic gels to hard wax-like solids, from emulsions to soft liquid-crystalline phases—is a difficult task. Experiments toward this end are under way in these laboratories. However, there have already been presented in the literature sufficient experimental data on the diverse properties of these systems—viscosity, optical behavior, conductivity, vapor pressure, heats of transition, and specific volume—to make it possible to advance plausible structures for some of the observed phases which are in accord with all the experimental evidence now available.

It is hoped that the following discussion will permit deduction of the basic modes of interaction of soap molecules in systems containing other molecules, either polar or non-polar.

<sup>1</sup> Presented at the Twenty-first National Colloid Symposium, which was held under the auspices of the Division of Colloid Chemistry of the American Chemical Society at Palo Alto, California, June 18-20, 1947.

## I. DESCRIPTION OF THE PHASES

Before proceeding with the analysis of the colloidal structures, it would be well to summarize the chief characteristics of the various phases encountered in these systems.

*Anhydrous soap phases*

(1) *Soap fibers or crystalline soap*: The curd fiber phase is a hard, opaque, white solid which, if previously melted in a container, forms a cake impenetrable to a stirring rod. Between crossed polaroids this phase is dark. This is the common crystalline form of soaps and gives a three-dimensional x-ray spacing. Although fibers are usually present, in which the soap molecules are aligned perpendicular to the fiber axis (28), these fibers may often be submicroscopic. Recent work has shown that this so-called curd phase may consist of a number of different crystalline species. The usual curd phase of sodium stearate is transformed into the supercurd at 89°C. with a heat of transition of 945 cal. per mole.

(2) *Wax-type phases*: The waxy phases can be readily distinguished from the curd fiber phases. Waxy soap, stable between 132° and 167°C., is considerably more translucent than the curd phase and individual structural units, fibers or crystals, are no longer visible in the microscope. Waxy soap is stiff, but sufficiently softer than the curd phase so that a glass rod may be pushed through a cake of it. Between crossed nicols in the polarizing microscope, waxy soap has a characteristic somewhat grainy, predominantly golden, slightly iridescent structure. Subwaxy soap, 117–132°C. is not readily distinguished from waxy soap by visual inspection at the transition temperature. It is a somewhat darker, duller yellow between crossed nicols. Superwaxy soap is another wax-type phase, stable between 167° and 198°C., which is difficult to distinguish from waxy soap by visual inspection at the transition temperature. It is appreciably softer than the waxy phase, but does not flow readily in an inverted tube. Between crossed nicols it has a coarser, through brighter and whiter-golden color. It is highly transparent and is predominantly the color of the transmitted light when viewed through the mikropolychromar.

Calorimetric measurements have shown the heats of transition between these phases of sodium stearate to be as follows: supercurd–waxy, 5180 cal. per mole; subwaxy–waxy, 4030 cal. per mole; and waxy–superwaxy less than 200 cal. per mole. Dilatometric measurements have also shown that the largest increase in specific volume below 200°C. occurs at the supercurd–subwaxy transition.

(3) *Neat-type phases*: At 205°C. superwaxy soap is transformed into subneat soap with a heat of transition of 1600 cal. per mole and a relatively large increase in specific volume. At a still higher temperature, the subneat phase is transformed into neat soap with an absorption of 1560 cal. per mole and a small increase in specific volume. The transition between superwaxy soap and subneat soap is readily obtained from microscopic examination because of the marked increase in iridescence and translucence and decrease in rigidity.

Both neat and subneat soaps are definitely liquid crystalline, and typical,

multicolored, focal conic structures may be observed between crossed nicols. The neat soap is distinguished from subneat by the greater delineation of structural units in the former. Conductivity measurements indicate that neat soap behaves like a typical electrolyte shortly below its melting point, whereas subneat soap does not. Neat soap flows readily in large tubes and looks like a very soft, turbid gel.

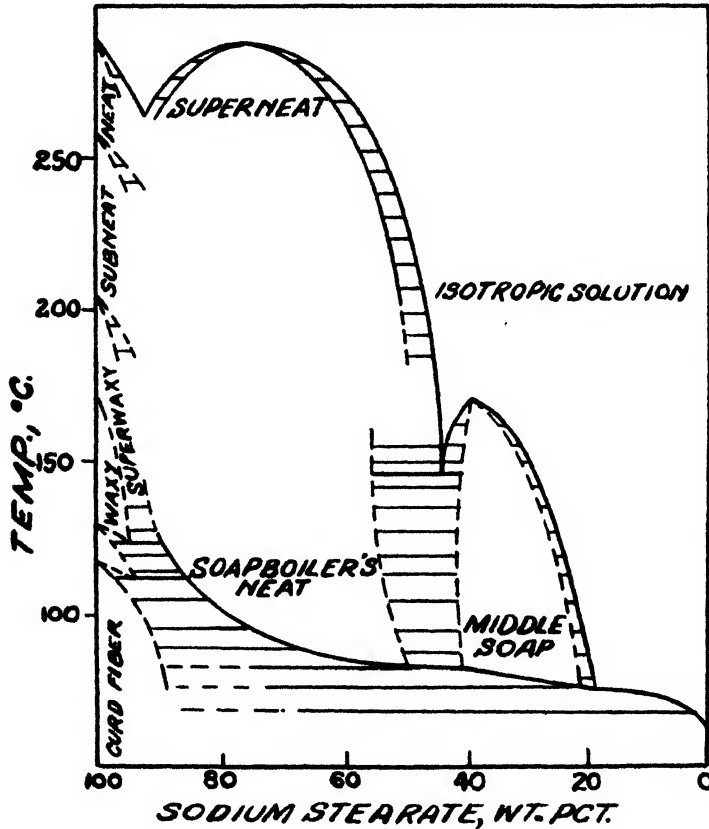


FIG. 1. Sodium stearate-water system

#### *Aqueous soap phases*

The phase diagram for the sodium stearate-water system is reproduced in figure 1 (21). All the phases observed in anhydrous sodium stearate are shown to extend into the binary system to some extent. The boundaries of these phases have been further delineated in a recent investigation of the electrical conductivity of the sodium stearate-water system by Vold and Heldman (33). In addition, at least two and possibly three new phases are observed in the sodium stearate-water system at temperatures above 100°C. and below 90 per cent soap.

(1) *Aqueous middle soap*: This phase is nearly transparent. It is highly doubly refracting, and large velvety focal conic sections may be observed between crossed nicols if the system is permitted to age for a sufficient length of time.

Middle soap is surprisingly stiff and does not flow in an inverted tube despite vigorous pounding.

(2) *Soapboiler's neat soap*: This phase is also doubly refracting and flows much more readily than aqueous middle soap in an inverted tube. Soapboiler's neat soap is not as translucent as middle soap, and the focal conics and polarization colors of this phase between crossed polaroids are considerably less pronounced than those of middle soap. Soapboiler's neat soap coarsens on heating, and liquid-crystalline structures develop slowly displacing the predominantly coarse, golden structure observed at lower temperatures. It has been assumed that at sufficiently high temperatures, the soapboiler's neat phase is transformed into superneat soap before melting to isotropic liquid (see phase diagram).

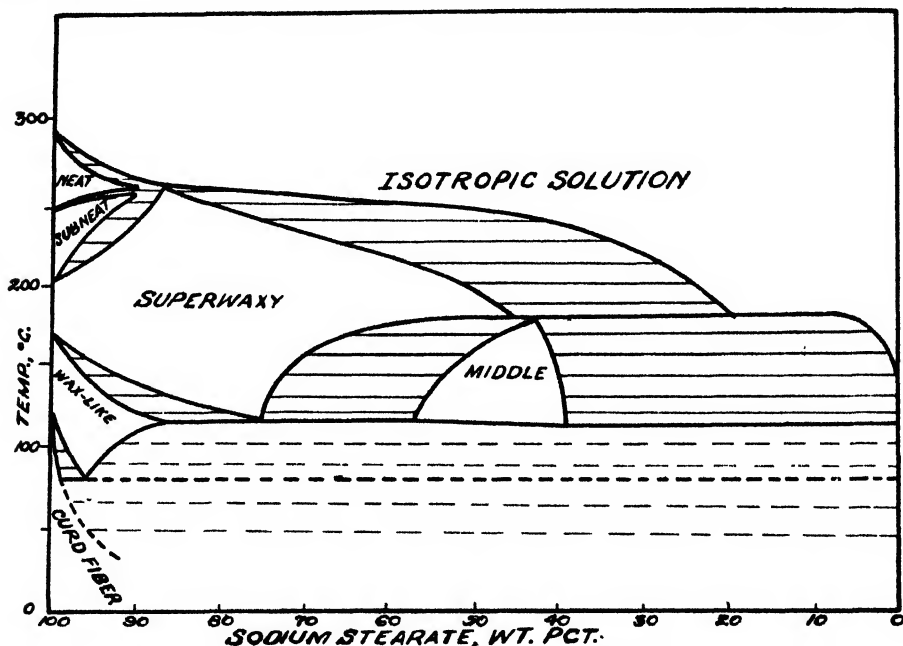


FIG. 2. Sodium stearate-cetane system

However, no confirmatory evidence has yet been brought to bear on this point and there is a possibility that superneat soap is the same phase as soapboiler's neat but with a different texture.

#### *Cetane system phases*

The phase diagram for the sodium stearate-cetane system is presented in figure 2.

(1) *Non-aqueous middle soap*: Only one phase, not already identified, was observed in the cetane system, non-aqueous middle soap. This phase is liquid crystalline and displays marked polarization colors between crossed nicols. Although on long standing at a constant temperature smectic structures were observed, the microscopic appearance of this phase usually consists of iridescent,

coarse-grained, multihued patches. In lieu of sharp contours, the oriented or optically structured areas were distinguished by changes in the orientation of colored bands which transversed each area. This phase is comparatively soft and though it does not flow in an inverted tube, it will flow readily under the application of a small shearing force.

(2) *Superwaxy soap*: The most prominent phase in the cetane system has been identified as superwaxy soap. At low temperatures in the polarizing microscope it has the typical golden translucence of anhydrous superwaxy soap. However, on raising the temperature, the texture of the phase appears to coarsen and it assumes a granular appearance. Although the over-all color is still golden, extinction occurs over small regions and dark and light areas are perceived. At higher temperatures, slightly below the melting point, the structure is still coarser—marble-like (4). Focal conic sections and other optical structures are absent in superwaxy soap, although there is a slight development of polarization colors, particularly when thin sections of the system are being viewed.

## II. STRUCTURE OF THE PHASES IN THE CETANE SYSTEM

Examination of the two binary diagrams shows that in both systems the anhydrous phases can incorporate only small amounts by weight of the second component before transforming into new phases. At soap concentrations less than 90–95 per cent, only two phases in addition to isotropic solution can exist at temperatures above 100°C., viz., soapboiler's neat soap (and possibly superneat) and aqueous middle soap in the aqueous system, and superwaxy soap and non-aqueous middle soap in the cetane system. The curd fiber equilibria are still present at lower temperatures in both systems. That this same type of behavior should be found on addition of cetane or water seems rather surprising, in view of the great difference in polarity of the two liquids. It has been possible to correlate the observed phase behavior in each case with postulated structures for the phases concerned.

### *Curd fiber phases*

At low temperatures the cohesive forces between the sodium stearate molecules in the crystalline curd are relatively unaffected by cetane and therefore it is only slightly soluble in this phase (4). As the temperature of the systems containing more than 60 per cent soap is raised further, a new phase, superwaxy soap, is formed which is capable of incorporating within itself all the cetane that is present in the system.

### *Superwaxy soap*

The formation of the various waxy phases has been attributed to progressive thermal disgregation along the length of the hydrocarbon tails of the soap molecules (30). This may indeed be considered to be a partial liquefaction of the soap molecules. Direct evidence for this hypothesis is shown by the much larger heat effects associated with the transitions to the waxy phases and the correspondence between chain length and the magnitude of the thermal effect at

these transitions. It is interesting to observe that the temperatures at which large amounts of cetane are incorporated into the soap lattice correspond to the temperature range over which the interchain forces are overcome in sharply defined steps in the anhydrous system. This correspondence leads directly to the concept that in superwaxy soap the cetane is held between the hydrocarbon tails of the soap molecules.

Some additional insight into the structure of superwaxy soap may be obtained by considering McBain and de Bretteville's x-ray investigations of this phase of anhydrous sodium stearate (17). The subwaxy and waxy phases were found to yield diffraction patterns which were similar to the pattern for the curd phase, whereas superwaxy soap, in which the long " $c \sin \beta$ " spacing decreased markedly and in which only one distinct short spacing is revealed, resembles the higher-temperature, liquid-crystalline phases. However, the increase in specific volume (29) at the waxy-superwaxy transition is very small, which requires that the molecules remain closely packed in superwaxy soap. On the assumption that the waxy phase is monoclinic and that in superwaxy soap the molecules are hexagonally packed, calculations based on McBain and de Bretteville's data show the specific volumes of the two phases to be equal within experimental error. It is logical therefore to conclude that superwaxy soap, in the anhydrous system, consists of clusters of hexagonally packed rows of double molecules in which the chains are rotating around their axes which are inclined at an angle to the basal planes.

The hydrocarbon tails in superwaxy soap therefore do have liquid-like character, and accordingly may be expected to be miscible with non-polar liquids. There are several ways in which this miscibility may occur. First of all, the cetane may be solubilized, *viz.*, enter between the non-polar terminals of the soap molecules (16). Secondly, the cetane may form sheets about the clusters of the hexagonally packed soap molecules in superwaxy soap. Finally, a cetane molecule may replace a sodium stearate molecule in the hexagonally packed lattice.

The second possibility may be ruled out immediately because of the large quantity of cetane, between 40 and 50 per cent at 170°C., which may be incorporated into the superwaxy phase. If the cetane did form sheets about the clusters, a much smaller percentage of cetane would give rise to a colloidal suspension rather than a homogeneous phase. Solubilization of the cetane between the ends of the non-polar tails of the soap molecule must also be ruled out, since in aqueous solutions a molecule as big as cetane is only slightly solubilized (19). Further, in a non-aqueous system, the major energy change which effects solubilization, *viz.*, the free-energy decrease accompanying the disappearance of the polar-non-polar interface, is absent, and therefore solubilization would be expected to be even less. Further, it has been shown that in aluminum dilaurate-benzene systems (15) and in cetane-sodium stearate systems (31) which have been heated above 150°C. and then cooled, there is little or no change in the long spacings compared to those of the anhydrous systems.

It therefore seems likely that the cetane replaces sodium stearate molecules in

the superwaxy lattice. In order for a cetane molecule to do this, a certain amount of energy is required to overcome the forces of attraction between the polar heads. When a cetane molecule is transferred from the liquid state to the superwaxy lattice, it will assume the orientation, vibration, and rotation of the hydrocarbon tails of the soap molecules, which although partially liquefied are semirigidly constrained by the interaction of the polar heads of the molecules. This pseudocrystallization of the solid would be expected to liberate the energy required for the separation of the polar groups.

There is reason to believe that the replacement of sodium stearate molecules by cetane does not occur completely at random. Since superwaxy soap, even upon the inclusion of 20–25 per cent cetane at 150°C., is still a fairly rigid system, and threads are not readily pulled out of a mass of the system, a significant number of the dipole interactions between the terminal polar groups must still persist despite this partial solution process. This observation would

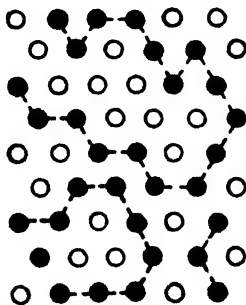


FIG. 3. Schematic representation of cross section through cluster of molecules in superwaxy soap, showing the formation of chains of soap molecules by lateral association of polar groups. ●, sodium stearate; ○, cetane.

indicate that a high degree of contiguity of soap molecules is maintained within the clusters of hexagonally packed soap and cetane molecules, as suggested by figure 3. Such an arrangement is also in accord with the greater solubility of cetane in the superwaxy phase than in the curd phase, since the abnormal entropy of mixing associated with the solution of small molecules in a system of kinked chains (12, 24) will facilitate the solution of cetane in the chains in superwaxy soap.

Although the lattice-like arrangement of the soap and cetane molecules within clusters precludes the existence of a true smectic structure (2), the liquid-crystalline state is itself not prohibited, since the orientation of one cluster need not be common to adjacent ones. The pronounced yellow color of this liquid-crystalline phase between crossed polaroids is evidence that the molecules are tilted (1). This liquid-crystalline structure would resemble one of C. Herrmann's intermediate liquid-crystalline arrangements, PoPoR (10), which was attributed by K. Herrmann to several low-temperature liquid-crystalline phases (11). This structure for superwaxy soap therefore accounts for the optical behavior and capacity for dissolving cetane which has been observed in the system under consideration.

A structure identical to the one postulated above is not necessarily common to all soap-hydrocarbon systems. The deviation from this structure will be primarily a function of the nature of the hydrocarbon. For example, aromatic hydrocarbons may be more readily oriented by the constrained rotating tails of the soap molecules and indeed may even interact somewhat with the dipoles at the polar terminals. Also, a large "spherical" or globular molecule could not readily replace a soap molecule in the superwaxy lattice without causing a marked expansion of the lattice. For this reason superwaxy soap or its counterpart would not extend to as high concentrations of hydrocarbon in such systems.

### *Non-aqueous middle soap*

At temperatures above 115°C. on increasing the cetane concentration to 50 per cent, a new phase, non-aqueous middle soap, is formed which is a smectic, liquid-crystalline phase. The transition from superwaxy soap to middle soap may be accounted for on the basis of the increased amount of cetane in the system.

With an increasing quantity of cetane, a point is reached at which molecules of cetane become sufficiently contiguous to separate the clusters of commonly oriented soap and cetane molecules, and, further, to cause the subdivision of the previously existing aggregates into smaller ones. The subdivision of the aggregates by the penetration of cetane would lead to the formation of sheets of commonly oriented soap and cetane molecules. It would also be expected that these would attain a greater degree of freedom with respect to one another, each layer being comparable to a liquid-type surface film. The increased mobility of the sheets of molecules is itself sufficient to account for the smectic properties of the phase. Under these conditions sheets of commonly oriented molecules could be continuously joined by the deformation of these fluid aggregates, as shown in figure 1 of reference 2.

Since non-aqueous middle soap may be filtered, e.g., forced through a mat of filter papers under a pressure of about 10 lb. per square inch (5), the aggregates in this phase cannot be much larger than of colloidal dimensions. It should be pointed out that the existence of such aggregates in non-aqueous middle soap is not incompatible with its being a single homogeneous phase (13). It therefore seems plausible that non-aqueous middle soap consists of aggregates of parallel oriented soap and cetane molecules. These aggregates have at least one dimension comparable to the wave length of the visible spectrum and are separated from each other by dimensions comparable to their own in which the soap and cetane molecules are more randomly arranged.

There are a number of other observations in the literature which indicate that the formation of non-aqueous middle soap may be of rather wide occurrence. Gallay *et al.* (7) have noted the fact that fibers may be formed from dilute soap-paraffin oil systems at about 125°C., but that these break up as the temperature is lowered below this transition. Mead and McCoy (23) have similarly observed a system of aluminum oleate in mineral oil which showed the normal elasticity of a gel, but which flowed under the application of a small shearing



stress. McBain and Smith (20) have also shown the existence of a similar phase in a sodium stearate-aromatic hydrocarbon system, although the melting point of the phase in their system is considerably higher than in the cetane system. Finally, Marsden, Mysels, and Smith (15) have concluded on the basis of x-ray investigations of several soap-hydrocarbon systems that micellar aggregates of soap molecules exist in dilute soap systems above 125°C.

### III. STRUCTURE OF THE AQUEOUS PHASES

Since there is still no general experimental agreement on the nature of the curd phases (3, 6, 18, 32), no attempt will be made to discuss them in this paper.

#### *Soapboiler's neat soap*

At temperatures above 100°C. after approximately 5 per cent of water is added to sodium stearate, a new phase is formed, soapboiler's neat soap, which does not exist in the anhydrous system. Soapboiler's neat soap occupies the same conspicuous position in the aqueous system as does superwaxy soap in the cetane system.

There can be little doubt that the water is disposed around the polar terminals of the soap molecules, and it might be expected that the only effect of water would be to reduce the attractive forces between the dipolar heads. If this were the only effect of the added water, however, the melting point of the system would be expected to drop rapidly. Furthermore, under these conditions soapboiler's neat soap should exhibit enhanced liquid-crystalline structures above 125°C., since the association of the hydrocarbon chains would also be significantly reduced at this temperature. This is not the case. Soapboiler's neat soap, although it is double refracting and liquid crystalline, does not develop intense polarization colors nor typical smectic optical figures unless it is in equilibrium with isotropic liquid or at temperatures in the neighborhood of 200°C., or higher. Furthermore, the melting point of soapboiler's neat soap, containing about 15 per cent of water, is somewhat higher than that of anhydrous soap. The addition of water thus restrains thermal dissociation, with the result that in soapboiler's neat soap the internal forces of association are of comparable strength to those in the neat phase of anhydrous sodium stearate.

In order to discuss the structure of soapboiler's neat soap most effectively, it seems advisable first to consider that of neat soap itself. Conductivity measurements (33) of subneat and neat soap have shown that in neat soap the system appears to be salt-like, since the temperature dependence of its conductivity can be represented by an equation similar to those for ionic crystals just below their melting point. On the other hand, in subneat soap the energy of activation for conductance is much higher. X-ray investigations (17) have shown that no significant change in the type of packing occurs at the subneat-to-neat transition, although there is an increase in the angle of tilt of the hydrocarbon chains and in the lateral spacings. These observations may be correlated by a transition in the nature of the packing of the polar groups, as shown in figure 4.

The molecular configuration of subneat soap shown above permits the sodium

ions of any molecule pair to be coordinated by oxygen atoms of adjoining soap molecules. It is also found by the use of Hirschfelder models that such coordination, as indicated by the diagram, prohibits the oxygen atoms from lying in a single plane. This arrangement is seen to place the sodium ions in potential wells, so that their mobility is impeded and the energy of activation for conductance will accordingly be high.

As the temperature is raised, the coulombic binding energy is overcome by kinetic energy and the ions will separate from each other. It is an accepted fact that resonance will occur between the two oxygen atoms of a carboxylate ion and also that under such conditions the resonating group is planar. It can be shown with the use of accurate atomic models, excluding excessive deformation of normal bond angles, that the occurrence of resonance requires a greater angle of tilt of the hydrocarbon chains with respect to the planes of the polar heads, as shown in figure 4B. X-ray investigations have actually shown such an increase

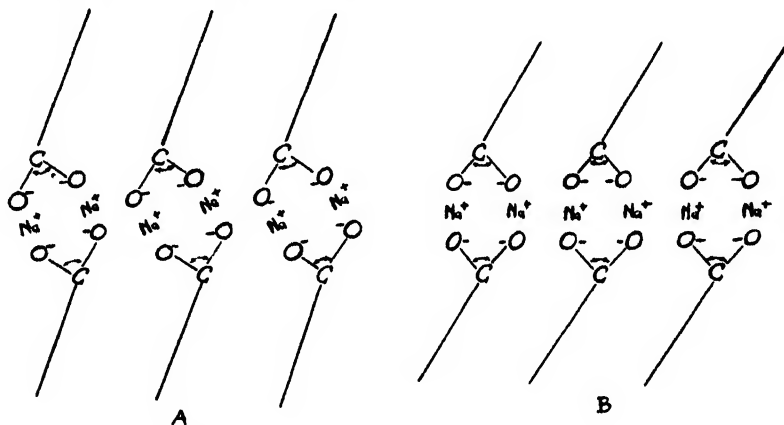


FIG. 4A. Possible configuration of molecules in subneat soap

FIG. 4B. Possible configuration of molecules in neat soap

to occur at the subneat-to-neat transition (17). The configuration of neat soap shown in figure 4B takes into account the necessity of coplanarity of the resonating group and also places the sodium ions in an equipotential force field. This will facilitate migration of the sodium ions under an applied electromotive force and therefore the energy of activation for conductance will be lowered, as confirmed by the experimental data. It should also be noted that the configuration shown for neat soap permits the hydrogen atoms on the alpha carbon atoms to be close enough to the oxygen atoms of adjacent anions to permit coordination and thus increase the rigidity of the configuration.

Starting with the facts that soapboiler's neat soap is stable up to temperatures which are slightly higher than those at which neat soap melts to isotropic liquid and that the conductivity of soapboiler's neat is very high, it is at once apparent that the water molecules must be effective in stabilizing an ionic lattice which may perhaps be similar to that suggested for neat soap. A possible structure is shown in figure 5, in which the molecules of water act to bind the soap ions.

The positions of the sodium ions, which are distributed in the interstices of the lattice, are not shown. This is not an unusual structure, since an arrangement which resembles this has been verified by x-ray diffraction for oxalic acid dihydrate (27). The hydration of the anion terminals would also tend to decrease the coordination of the hydrogen atoms on the alpha carbon atoms with the oxygen atoms of adjacent anions; hence, at high temperature, the internal mobility of soapboiler's neat soap would be increased. This would account for the increased development of polarization colors and focal conic structures in superneat soap.

The apex of the superneat hump in the various soap-water systems studied to date occurs at varying ratios of two to six molecules of water to one of soap (21), indicating that a definite stoichiometric hydrate is not formed. The excess of water beyond that shown in figure 5 which may be incorporated without loss of

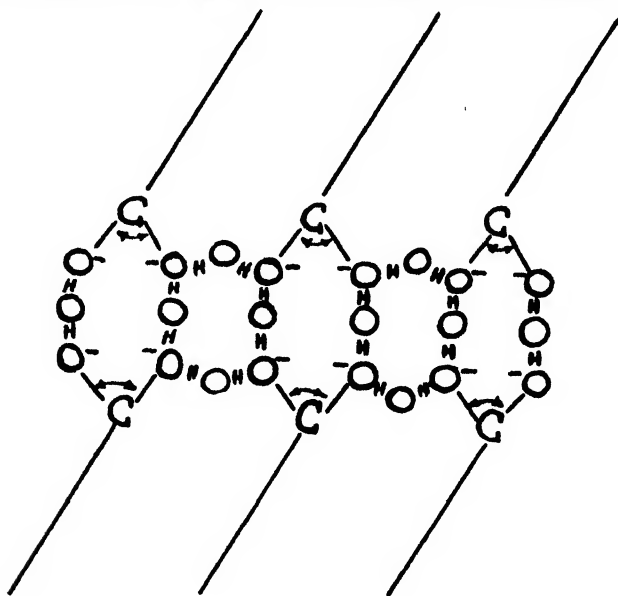


FIG. 5. Possible configuration of molecules in soapboiler's neat soap

stability may be assumed to be bound by the sodium ions. Further addition of water beyond the amounts required for this structure quickly results in a loosening of the packing, due to preferential polarization of the small water molecules in the vicinity of the polar heads. Accordingly, the stability is greatly decreased, as shown by the rapid drop in melting point.

#### *Aqueous middle soap*

At higher concentrations of water another factor is necessarily introduced since a new phase is again formed, *viz.*, aqueous middle soap. This phase is revealed by a sudden rise in the melting point of the system as the soap concentration is reduced below 40 per cent. X-ray examination of supercooled middle soap gels in these laboratories (25) indicates that there are present long spacings of the order of magnitude (*ca.* 75 Å.) similar to those found in concentrated

solutions of soap. This result indicates that the micellar structure of the soap and water molecules is maintained in aqueous middle soap. It is therefore quite plausible to believe that the occurrence of the smectic state in aqueous middle soap is due to the existence of micelles in which the orientation is continuous over a dimension comparable to that of the wave length of visible light and that these micelles are interpenetrated by a dilute solution of soap in water. The essential difference between the isotropic solution of micelles and aqueous middle soap would then be the extent of micellar formation.

The formation of the micelles in dilute solutions is chiefly a result of the decrease in free energy which accompanies the transfer of a dispersed soap molecule to the aggregate with the accompanying decrease in the polar-non-polar interface (9). In aqueous middle soap there will of course exist a large interface between the micelles and the free liquid, but nevertheless the configuration must represent a minimum potential energy. Such a disperse structure will be expected to resist a small shearing stress, since an appreciable fraction of the applied force will be used in the deformation of the micelles, or, in general, in changing the interfacial relations between the micelles and the free liquid which constitute the equilibrium condition. This phenomenon is comparable to the anomalous viscosity of dispersions of hexane in nitrobenzene or phenol in water (26). The structural viscosity of these liquid-liquid dispersions is, of course, of much smaller magnitude than the structural viscosity of colloidal rubber sols or clay suspensions. The rheological behavior of aqueous middle soap appears to be similar to the type of behavior exhibited by such liquid-liquid dispersions. The consistency is high, as judged by finger tests, and the yield value appears high since it does not flow in a 15-mm. glass tube which is inverted and jarred. The true yield value, however, as determined with a cutting-wire plastometer (14) or falling-ball viscometer (22), is very small. Thus the proposed micellar structure for aqueous middle soap is in accord with its rheological as well as optical properties. Hughes has also come to the conclusion that middle soap is of a micellar nature, on the basis of x-ray investigations (8).

#### IV. SUMMARY

A detailed examination of the binary systems of sodium stearate-water and sodium stearate-cetane has revealed a similarity in the phase relations in both systems. Both soapboiler's neat soap, which exists at high soap concentrations in the water system, and superwaxy soap existing at high soap concentrations in the cetane system appear to be fairly close-packed molecular structures which resemble the structures deduced for the anhydrous soaps. Both these phases may be considered to be a type of solid solution in which the water or cetane is dissolved in the soap and forms a part of the soap lattice. Aqueous and non-aqueous middle soaps which occur at lower soap concentrations appear to be micellar phases; that is, they may be regarded as being composed of fluid-like micellar aggregates of soap and the solvent component of the binary system.

#### REFERENCES

- (1) BERNAL, J.: *Trans. Faraday Soc.* **29**, 1032 (1933).
- (2) BRAGG, W.: *Trans. Faraday Soc.* **29**, 1056 (1933).

- (3) BUEGER, M. J., SMITH, L. B., RYER, F. V., AND SPIKE, J.: *Proc. Natl. Acad. Sci. U. S.* **31**, 226 (1945).
- (4) DOSCHER, T. M., AND VOLD, R. D.: *J. Colloid Sci.* **1**, 291 (1946).
- (5) DOSCHER, T. M.: Doctoral Dissertation, University of Southern California, February, 1947.
- (6) FERGUSON, R. H., ROSEVEAR, F. B., AND NORDSIECK, H.: *J. Am. Chem. Soc.* **69**, 141 (1947).
- (7) GALLAY, W., PUDDINGTON, I. E., AND TAPP, J.: *Can. J. Research* **22B**, 66 (1944).
- (8) HUGHES, EDWARD: Lecture at California Institute of Technology, March, 1946.
- (9) HARKINS, W. D., MATTOON, R. W., AND CORRIN, M. L.: *J. Am. Chem. Soc.* **68**, 220 (1946).
- (10) HERRMANN, C.: *Z. Krist.* **79**, 186 (1931).
- (11) HERRMANN, K.: *Z. Krist.* **81**, 317 (1932).
- (12) HUGGINS, M. L.: *J. Phys. Colloid Chem.* **52**, 248 (1948).
- (13) KAST, W., AND ORNSTEIN, L. S.: *Trans. Faraday Soc.* **29**, 931 (1933).
- (14) KONECNY, C.: Master's Thesis, University of Southern California, September, 1945.
- (15) MARSDEN, S., MYSELS, K., AND SMITH, G. H.: *J. Colloid Sci.* **2**, 265 (1947).
- (16) MCBAIN, J. W.: *Advances in Colloid Sci.* **1**, 123 ff. (1942).
- (17) MCBAIN, J. W., AND DE BRETTEVILLE, A.: *J. Chem. Phys.* **11**, 426 (1943).
- (18) MCBAIN, J. W., DE BRETTEVILLE, A., AND ROSS, S.: *J. Chem. Phys.* **11**, 179 (1943).
- (19) MCBAIN, J. W., AND RICHARDS, P. H.: *Ind. Eng. Chem.* **38**, 642 (1946).
- (20) MCBAIN, J. W., AND SMITH, G. H.: *J. Phys. Colloid Chem.* **51**, 1189 (1947).
- (21) MCBAIN, J. W., VOLD, R. D., AND FRICK, M.: *J. Phys. Chem.* **44**, 1013 (1940).
- (22) MCBAIN, J. W., AND WATTS, O. O.: *J. Rheol.* **3**, 437 (1932).
- (23) MEAD, B., AND MCCOY, J.: *Colloid Symposium Monograph* **4**, 44 (1925).
- (24) MEYER, K. H.: *Z. physik. Chem.* **B44**, 383 (1939).
- (25) MONTGOMERY, R.: Research Report, University of Southern California, February, 1947.
- (26) OSTWALD, W.: *Australian J. Exptl. Biol. Med. Sci.* **9**, 83 (1932).
- (27) ROBERTSON, M. J., AND WOODWARD, J.: *J. Chem. Soc.* **1936**, 1817.
- (28) THIESSEN, P. A., AND EHRLICH, E.: *Z. physik. Chem.* **A165**, 453 (1933).
- (29) VOLD, M. J.: *J. Am. Chem. Soc.* **63**, 1427, (1941).
- VOLD, R. D., AND VOLD, M. J.: *J. Am. Chem. Soc.* **61**, 808 (1939).
- (30) VOLD, R. D.: *J. Am. Chem. Soc.* **63**, 2915 (1941).
- (31) VOLD, R. D.: Unpublished experiments in these laboratories.
- (32) VOLD, R. D.: *J. Phys. Chem.* **49**, 315 (1945).
- (33) VOLD, R. D., AND HELDMAN, M.: *J. Phys. Colloid Chem.* **52**, 148 (1948).

AQUEOUS SYSTEMS OF NON-IONIC DETERGENTS AS STUDIED BY X-RAY DIFFRACTION<sup>1</sup>SULLIVAN S. MARSDEN, JR.,<sup>2</sup> AND JAMES W. MCBAIN*Department of Chemistry, Stanford University, California**Received August 25, 1947*

During the past decade a number of papers have been published, first in Germany (5-9, 11-13, 19, 21, 22) and then in this country (3, 4, 10, 17, 20), on the diffraction of x-rays by aqueous solutions of anionic and cationic detergents. The experimental results described in these papers have established the presence of lamellar micelles in these solutions. Supplementary work on the diffraction of x-rays by detergent solutions containing solubilized hydrocarbons has indicated that these hydrocarbons are incorporated within the micelle.

In recent years a number of non-ionic detergents and other surface-active agents have become commercially available. Instead of having an ionizing hydrophilic group at one end of a long hydrocarbon chain, as do the usual detergents, these non-ionic materials have either a glyceryl group or a polyethylene oxide chain ending in a hydroxyl group. It was of interest to know the fine structure of both aqueous systems of these materials and aqueous systems containing solubilized hydrocarbons.

## APPARATUS

The source of x-radiation was a General Electric XRD-1 unit having a tube with copper target and beryllium windows. The radiation was filtered through nickel foil and collimated through guarded pinholes placed 7.5 cm. apart. The pinholes used for the Detergent "X" solutions were about 0.025 in. in diameter; those used for the other systems were 0.010 in. in diameter. For the side spacings, a sample-to-film distance of 50 mm. was used, but for the long spacings this distance was increased to 163 or 200 mm.

## MATERIALS

Detergent "X", a non-ionic detergent, is the product of condensation of iso-octylphenol and ethylene oxide. It is a yellow, slightly viscous liquid whose molecular weight, as measured by Dr. E. Gonick in this laboratory, is about 636. On the basis of this molecular weight, it is estimated that the average ethylene oxide chain in this preparation is ten units long.

The samples of diglycol monolaurate, polyethylene glycol (400) monolaurate,

<sup>1</sup> Presented at the Twenty-first National Colloid Symposium, which was held under the auspices of the Division of Colloid Chemistry of the American Chemical Society at Palo Alto, California, June 18-20, 1947.

This paper is based upon a dissertation submitted by Sullivan S. Marsden, Jr., to the Department of Chemistry and the Graduate School of Stanford University in partial fulfillment of the requirements for the degree of Doctor of Philosophy, August, 1947.

<sup>2</sup> Lever Brothers Company Fellow in Chemistry.

and glyceryl monolaurate were kindly supplied by Glyco Products, Inc. The former two are slightly viscous yellow liquids whose properties, as well as those of the latter, are described in the catalog of the donor. These materials, since they are merely commercial products, are not chemically pure.

The Emulphor O, a white wax-like solid, was supplied by General Dyestuff Co. and was described as the condensation product of oleyl alcohol and ethylene oxide.

Triton X-100, supplied by Rohm and Haas, is the condensation product of diisobutylphenol and ethylene oxide. From its molecular weight of about 600, it is estimated that there is an average of nine or ten ethylene oxide groups per molecule. This material has a chemical formula somewhat similar to that of the Igepals, the German non-ionic detergents developed by I. G. Farbenindustrie.

The  $\alpha$ -*n*-decyl glyceryl ether is a white crystalline solid whose melting point is 38°C.

The benzene was c.p., thiophene free, and was dried over sodium and distilled.

The dimethyl phthalate was supplied by the Eastman Kodak Company and was used without further purification.

#### METHODS

The two-component systems were prepared by weighing the detergent and water into 2-dram glass vials having screw tops lined with pure tin foil. They were mixed for 8–24 hr., the length of time being greater for the more viscous samples. For the multiphase systems, the vials were then centrifuged in order to separate the phases and determine their properties and relative proportions.

The three-component systems (Triton X-100–water–benzene) were prepared by making a stock solution of the detergent in either benzene or water and then adding the third component to portions of this stock solution. Thus the ratio of the two components could be kept constant while the third was varied.

Samples of the systems were then sucked up into Pyrex-glass capillaries having a wall thickness of 0.03–0.04 mm., a diameter of about 0.8 mm., and a length of about 2 in. The "wet" end of the capillary was sealed first and then the "dry" end sealed and warmed until a small glass bubble formed, which was used as an indication that the capillary was completely sealed. At all times the liquid was kept more than  $\frac{1}{2}$  in. from the flame, a procedure which decreased thermal decomposition and vaporization to a negligible amount. After preparation, the capillaries were again centrifuged to ensure phase separation, except in the cases where patterns of mixed phases were desired.

The capillaries were then mounted in front of the pinhole by means of a small piece of moulding clay, by a method previously described (16). Exposures of 10 or 12 hr. were used for the long spacings of the more concentrated systems, whereas exposures of 20–24 hr. were necessary for the more dilute. Exposures of 10 or 12 hr. were used for all short spacings.

Measurements of the long spacings were made directly from the films by use of drafting dividers; it is believed that greater accuracy could be obtained by

this method than by measurement of the peaks of the microphotometer tracings, particularly for patterns of the more dilute samples.

Since most of the surface-active materials used in this work were liquids and gave no long spacing, it was decided to try to cool them below their melting points and obtain pictures of the solids. It has been reported (14) that liquids could be x-rayed below their melting points by playing a stream of liquid nitrogen on a glass capillary containing the liquid. This was successfully modified by using a stream of cold carbon dioxide gas from subliming dry ice.

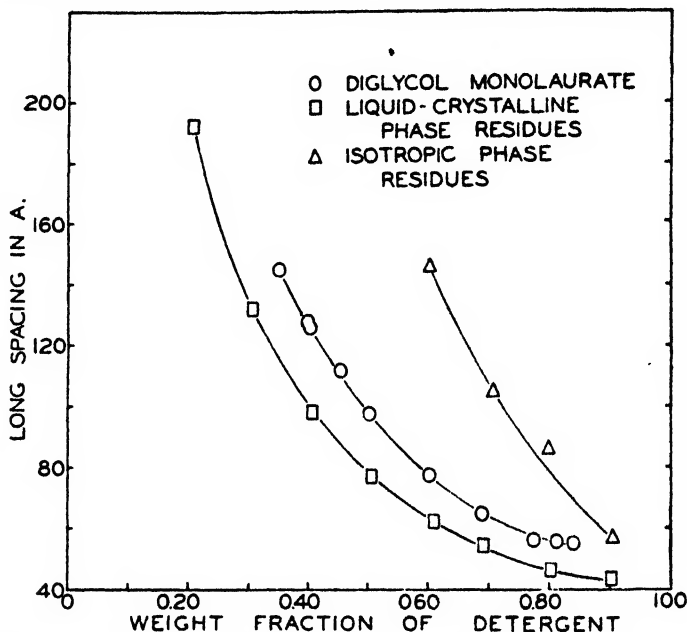


FIG. 1. Diethylene glycol monolaurate: plot of long spacing *versus* the weight fraction of detergent.

All preparations and photographs were made at room temperature, which was  $29^{\circ}\text{C.} \pm 3^{\circ}$ . All concentrations are expressed on the basis of weight units, i.e., either weight per cent or weight fraction.

#### RESULTS AND DISCUSSION

Aqueous systems of diglycol monolaurate at concentrations from about 45 per cent to 85 per cent consist of two distinct phases: one is isotropic and gives no long spacings; the other is liquid-crystalline and gives a long spacing which is *not* a linear function of the concentration as expressed in per cent by weight (figure 1, middle curve). However, when long spacing is plotted *versus* the reciprocal of the concentration in per cent by weight, a straight line results (figure 2).

The ratio of liquid-crystalline phase to isotropic phase decreases rapidly with increasing concentration. Above 85 per cent the systems are single phase and isotropic and give no long spacings; from 25 per cent to 45 per cent the systems



are extremely viscous pastes or emulsions which show weak birefringence and give long spacings down to about 35 per cent. Below 25 per cent the systems are thin emulsions. The transition from isotropic liquid to the two-phase system at 85 per cent is quite sharp, whereas the change from two distinct phases to emulsified phases is gradual.

The variation of long spacing with the reciprocal of the concentration is decidedly in contrast to that of ionic detergents, where the relation is almost linear with concentration. It is similar to that found by Palmer and Schmitt (18) in their study of aqueous emulsions of nerve lipids. As an aid to understanding these systems, one may set up a model of an ideal, two-component, one-phase, smectic, liquid-crystalline system. One component is a long-chain

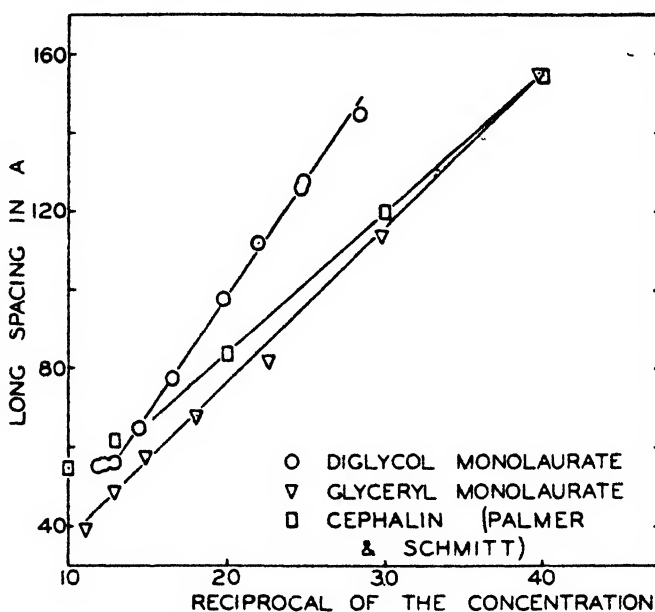


FIG. 2. Diethylene glycol monolaurate: plot of long spacing *versus* the reciprocal of the concentration in per cent by weight.

hydrocarbon compound which has a hydrophilic group at one end, such as a detergent or similar surface-active substance. The other component is water.

Consider first the pure anhydrous detergent in the smectic liquid-crystalline state (figure 3). It will have a liquid or average orientation in the  $xz$ -plane and "crystalline" or definite orientation in the  $y$  or vertical direction. It will give a long x-ray diffraction spacing equal to  $L_s \cdot \sin \beta$ , where  $L_s$  is the double length of the detergent molecule and  $\beta$  is the angle of tilt of the detergent molecule to the basal plane.

Consider the addition of water to this liquid-crystalline detergent, making the simplifying assumptions that (1) the density of the detergent equals that of water, that is, weight per cent equals volume per cent; and (2) all of the water that enters the system forms uniform layers between the hydrophilic ends of the

detergent molecules. Then these aqueous systems will give a new long spacing  $L_s$ , which is the sum of the detergent layer,  $L_s \sin \beta$ , and the water layer,  $L_w$  (figure 4).

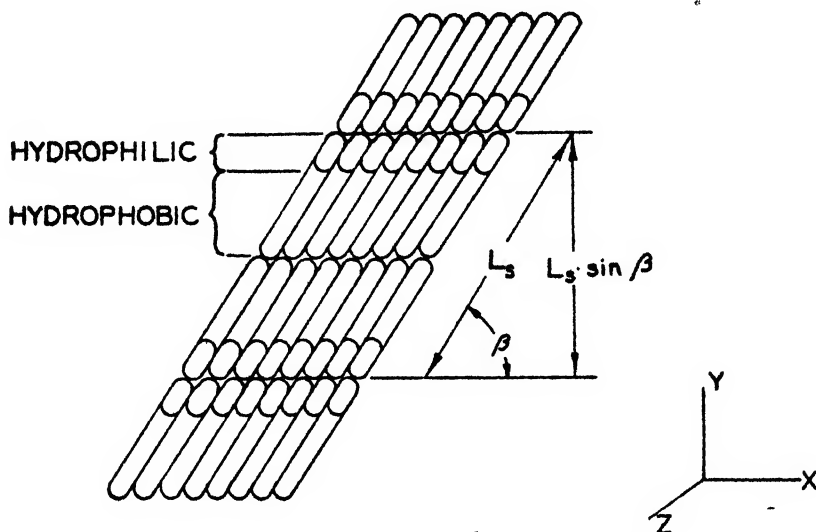


FIG. 3. Anhydrous smectic liquid crystal

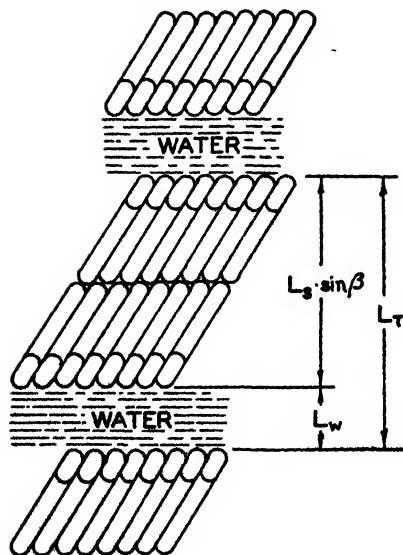


FIG. 4. Hydrous smectic liquid crystal

$$L_T = L_s \sin \beta + L_w \quad (1)$$

$$\frac{L_w}{1-C} = \frac{L_s \sin \beta}{C}$$

$$L_w = \frac{1-C}{C} \cdot L_s \sin \beta \quad (2)$$

$$L_T = \frac{L_s \sin \beta}{C} \quad (3)$$

$$\log L_T = \log(L_s \sin \beta) - \log C \quad (4)$$

ASSUME  $L_s \sin \beta$  CONSTANT

$$\frac{d(\log L_T)}{d(\log C)} = -1 \quad (5)$$

Thus, for the ideal system, the total long spacing varies as the reciprocal of the concentration times a constant, which is the product of the double length of the molecule and  $\sin \beta$ .

The relation between total long spacing and concentration for this ideal system

corresponds to that actually found for the aqueous systems of diglycol monolaurate.

Consider again the ideal system. Take the logarithms of both sides of equation 3. For a given substance,  $L_c$  is constant. Also assume that  $\beta$  is constant. Then equation 4 is a straight line and for the ideal system, a log-log plot of  $L_c$  and  $c$  is a straight line of slope  $-1$  and intercept equal to  $L_c \cdot \sin \beta$ .

The experimental results for diglycol monolaurate were plotted on these coordinates (figure 5, middle curve). The slope was numerically slightly greater than  $-1$ . The chemical purity of this material was doubtful, so it was decided to check the properties of the two phases. An 80.0 per cent system was prepared, the two phases separated, and the water removed in a vacuum desiccator

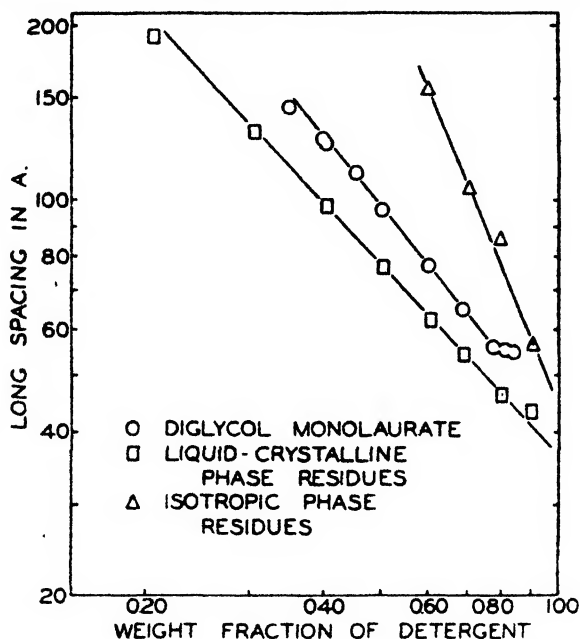


FIG. 5. Log-log plot of experimental results for diglycol monolaurate

over phosphorus pentoxide. The isotropic phase lost less than 10 per cent by weight, whereas the liquid-crystalline phase lost more than 30 per cent. From these residues, additional aqueous systems were prepared and photographed. These new systems differed from the original systems both in long spacing (figure 1) and in physical appearance, i.e., the amount and type of phase present at a given concentration. This shows that the original diglycol monolaurate was not chemically homogeneous, and that there is an unequal distribution of the components between the two phases in the original aqueous system.

The residues from the isotropic phase were somewhat hydrophobic, and its aqueous systems contained a greater proportion of isotropic phase than did systems of the original material. The residues from the liquid-crystalline phase readily mixed with water to form new systems which were more strongly birefringent and more highly colored than aqueous systems of the original material.

It can be seen that the long spacings of the systems from the isotropic phase residues increase considerably more rapidly than do those from the liquid-crystalline phase residues. When these are plotted on log-log coordinates (figure 5) the slope of the line for the liquid-crystalline phase residues is  $-1$ , whereas that for the isotropic phase residues is considerably greater. As was shown in equation 5, the rate of decrease of the log of the total long spacing with respect to the log of the concentration equals unity when only water is entering the structure. But if this rate is numerically greater than unity, something else must be happening.

Work by other investigators with aqueous solutions of ionic detergents has shown that the addition of hydrocarbon results in an increase of long spacing of the solution. This has been explained as due to the hydrocarbon forming layers between the hydrophobic ends of the molecules similar to the water layers between the hydrophilic ends.

Therefore, it is here postulated that the greater rate of increase of long spacing than can be attributed to the addition of water alone is actually due to hydrocarbon entering the lamellar structure in layers between the hydrophobic ends of the molecules. This hydrocarbon is assumed to be present in the original material as an impurity, and evidently collects in the isotropic phase, which serves as a reservoir from which it is progressively abstracted. Since the isotropic phase residues give aqueous systems which have a long spacing, they must evidently also contain some of the surface-active material.

Returning to the aqueous systems of the original material, in the isotropic region between 85 per cent and 100 per cent water is taken up by the surface-active material without the formation of a liquid-crystalline phase. Evidently this water penetrates between the sides of the detergent molecules, possibly with hydrogen bonding to the oxygen atoms of the carboxylate group or the ether oxygen of the diethylene glycol. There is no change in the numerical value of the side spacing halo of 4.6 Å. when going from 100 to 85 per cent, but there is an increase in the relative intensity of a halo corresponding to a Bragg spacing of 7-8 Å.

Considering the other extreme of the concentration range, there is the possibility that structure may persist below that found in this investigation, but it becomes increasingly more difficult to detect it because of both the decreasing intensity with dilution and the approach of the diffraction pattern to the main x-ray beam. At any rate, no diffraction was observed for aqueous systems of the original material below 35 per cent and for the liquid-crystalline phase residues below 21.5 per cent, although a number of systems below these concentrations were photographed.

Since both the original diglycol monolaurate and the isotropic phase residues probably contained hydrocarbon, not too much can be learned from the intercepts of the log-log long spacing-concentration curve (figure 5). However, the liquid-crystalline phase residues apparently have very little, if any, of this impurity, and so their intercept at  $c = 1.00$ , namely, 36.8 Å., should be equal to  $L_s \cdot \sin \beta$ .

The long spacing of this material when cooled to below its melting point is 49

$\text{\AA}$ ., a value which agrees well with the calculated extended double length of the molecule, i.e., about  $50 \text{ \AA}$ . This would indicate that in the frozen material the molecules are practically perpendicular to the basal planes. Since the intercept of the log-log plot is  $36.8 \text{ \AA}$ ., this would indicate an angle of about  $48^\circ$  for the diglycol monolaurate molecules in the hydrous liquid-crystalline structure of this material. Because of the various assumptions this value is only approximate.

It will be noted that the long spacings for the cooled samples of original diglycol monolaurate and the isotropic phase residues are very close to their respective intercepts, a fact which would indicate that the molecules are still tilted, when cooled, if there is hydrocarbon present to allow freer arrangement of the hydrophobic ends of the detergent molecule.

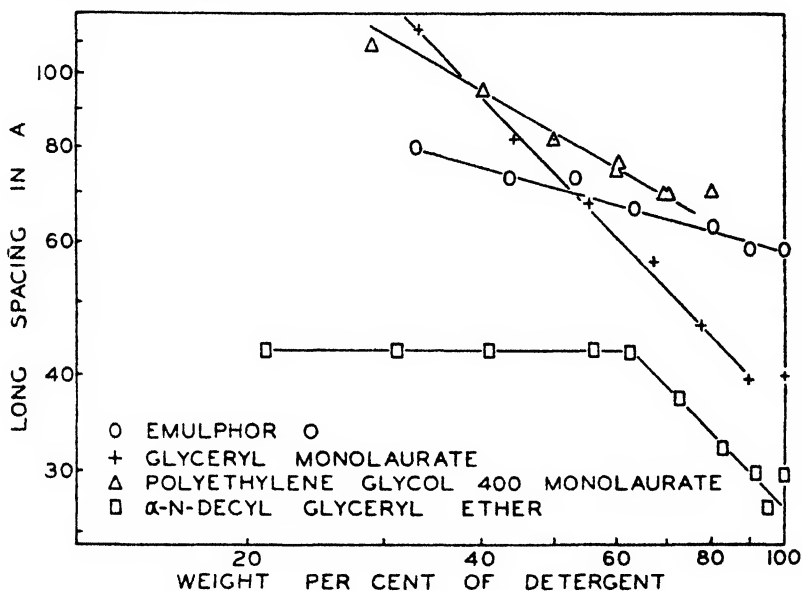


Fig. 6. Log-log plot of long spacing versus weight per cent of detergent for Emulphor O, glyceryl monolaurate, polyethylene glycol 400 monolaurate, and  $\alpha$ -n-decyl glyceryl ether.

#### *Polyethylene glycol 400 monolaurate*

This material is the monoester of "lauric" acid with polyethylene glycol, having an average molecular weight of 400 (i.e., about nine ethylene oxide units; commercial "lauric" acid consists usually of the acid obtained from coconut oil). Its aqueous systems consist of either one or two phases, depending on the concentration. One phase is clear, isotropic, and gives no long spacing; the other is liquid-crystalline and gives a long spacing which increases with dilution. When the long spacing is plotted versus concentration on log-log coordinates (figure 6), the points approximate a straight line which has a slope numerically less than  $-1$  (actually about  $-0.6$ ). Because of the variation of the relative amounts of each phase with concentration, not much information can be obtained from the curve other than to say that all of the water does not go into the lamellar layers.

*Glyceryl monolaurate*

The aqueous systems of glyceryl monolaurate are either homogeneous or consist of two layers, depending on the concentration. Both layers are birefringent and both give the same long spacing, which also varies as the reciprocal of the concentration (figure 2).

When the results for glyceryl monolaurate are plotted on log-log coordinates (figure 6), the resulting line has a slope very close to  $-1$ , indicating that there is probably little or no hydrophobic material present. The intercept is  $35.5 \text{ \AA}$ . The long spacing of the solid material is  $39.5 \text{ \AA}$ , which is  $2.2 \text{ \AA}$  longer than the value reported (15) for pure glyceryl monolaurate in the stable  $\beta$  form (tilted at an angle of  $59^\circ$  to the basal plane). Assuming that this  $2.2 \text{ \AA}$  is due to a longer average hydrocarbon chain of the glyceryl mono "laurate", the calculated length of the molecule is  $45.4 \text{ \AA}$ . This gives a value of  $51^\circ$  for the angle  $\beta$ , for the detergent molecules in the hydrous, smectic, liquid-crystalline state. This is only approximate because of the doubtful chemical homogeneity of the original material.

The fact that the aqueous systems of this material separate into two layers might be attributed to impurities. Among other things the manufacturer states that a small amount of soap has been added to make it self-emulsifying. This soap, in a finely dispersed condition, could be the reason for the appearance of two layers.

 *$\alpha$ -n-Decyl glyceryl ether*

The aqueous systems of this material are one-phase and liquid-crystalline between 62 per cent and 100 per cent. In this region they give a long spacing which increases with decreasing concentration. Below 62 per cent they consist of an emulsion which settles into two layers. The less dense layer is birefringent and gives a long spacing which is constant for all concentrations. The relative amount of this layer, which probably contains most of the glyceryl ether, decreases regularly with decrease of concentration. The denser layer is clear, isotropic, and gives no long spacing; it probably consists mostly of water. During the preparation of these systems there was a marked cooling effect when the components were mixed.

The observed long spacing of the solid glyceryl ether is  $29.7 \text{ \AA}$ ; a calculated length of the double molecule is  $37.4 \text{ \AA}$ , which would indicate an angle of tilt of  $52\text{--}53^\circ$  for the molecules in the solid material.

When the long spacings are plotted *versus* concentration on log-log coordinates (figure 6), they fall close to two straight lines, one being for the liquid-crystalline systems and the other for the emulsions.

Consider first the line for the liquid-crystalline systems. The slope is  $-1$ , indicating that all of the water is going into the lamellar layers. The intercept of about  $27 \text{ \AA}$  indicates that the molecules are tilted at an angle of about  $49^\circ$  in the liquid-crystalline condition.

The reason for the abrupt formation of an emulsion at 62 per cent glyceryl ether is not known. The long spacing of this emulsion is constant at  $43.2 \text{ \AA}$ ;

if the molecules are still tilted at an angle of  $\beta = 49^\circ$ , as they are in the liquid-crystalline condition, then there is a constant water layer about 16 Å. thick between the glyceryl groups. Even if  $\beta$  has changed to  $90^\circ$ , there must be a constant water layer 6 Å. thick between the glyceryl groups.

### *Emulphor O*

Below about 90 per cent these aqueous systems are clear isotropic solutions, except in the region of about 53 per cent where they are clear, stiff jellies. The viscosity of the solutions increases with concentration. From 90 per cent to 100 per cent the systems are white, wax-like, and solid. Aqueous systems from 100 per cent to about 30 per cent give a long spacing which increases with dilution.

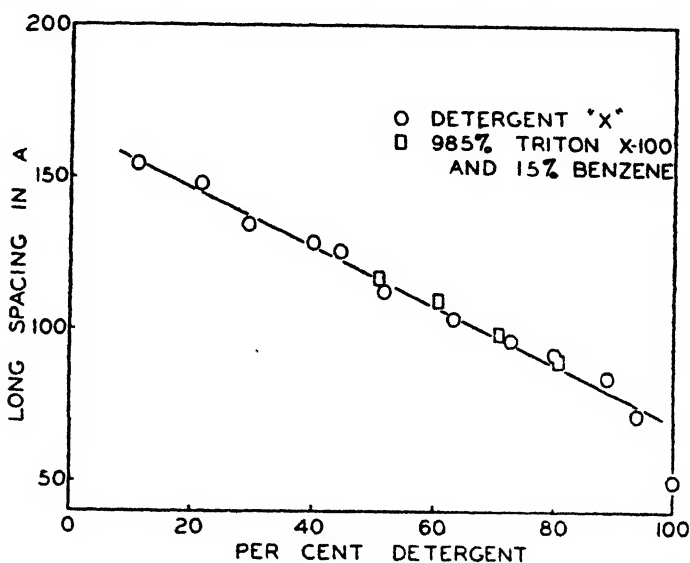


Fig. 7. Plot of long spacing *versus* per cent of detergent for Detergent "X" and 98.5 per cent Triton X-100:1.5 per cent benzene solutions.

When these long spacings are plotted *versus* concentration on log-log coördinates, they approximate a straight line which has a slope numerically less than  $-1$  (figure 6). This would indicate that not all of the water being added to the system is going into the lamellar layers; it is either going between the ethylene oxide portions of the chains or else between the lamellar micelles that probably exist in these solutions.

### *Detergent "X"*

Aqueous systems of this material are all isotropic solutions which have anomalous viscosities such as were previously observed by Boedeker (2). Although detergent "X" itself does not give a long spacing, its aqueous systems from 11 per cent to 94 per cent give long spacings which increase linearly with dilution (figure 7). The relative intensity and sharpness of the long spacing are

greatest at about 70 per cent; both qualities decrease with increasing or decreasing concentration from this region.

This type of variation of long spacing with concentration is the same as has been found by other investigators for solutions of ionic detergents. It is believed that these aqueous solutions of detergent "X" contain lamellar micelles similar to those that exist in solutions of ionic detergents.

When detergent "X" is frozen and photographed, it gives a long spacing of about 50 Å.; this agrees well with the calculated single length of the average extended molecule (51 Å.). If the molecules are arranged in both the solid material and lamellar micelles with the hydrocarbon ends together and the hydrophilic ends together, as they are in the case of the ionic detergents, then one would expect a first order of twice 50 Å. (times  $\sin \beta$ ) for the solid material, and also spacings of more than this for the first order of the solutions. However, these were

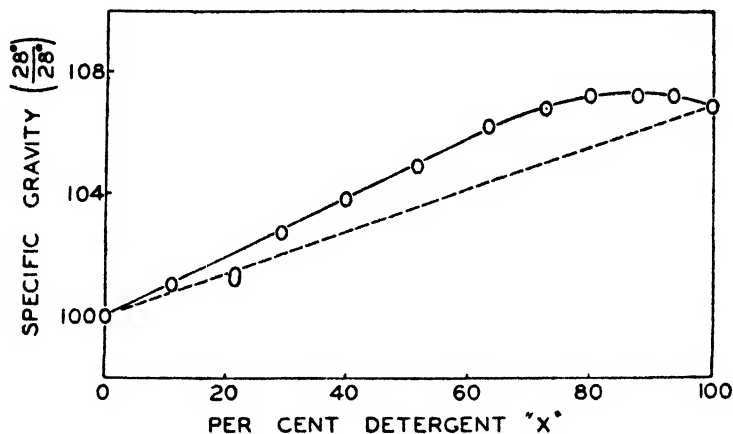


FIG. 8. Variation of specific gravity of aqueous Detergent "X" solutions with concentration.

not found. On the basis of this system and the very thorough study of the ternary system Triton X-100-water-benzene (see below), it is believed that the observed values are actually the second (and fourth) order and that the first (and third) order is either missing or very weak. The values of long spacing on the graphs are the observed ones multiplied by a factor of two, giving what is believed to be the true repeating pattern of the systems. This same peculiarity, i.e., strong second order of diffraction but no first, has previously been observed by Ross and McBain (20) for aqueous systems of hexanolamine oleate.

An alternative explanation to the above would be an angle of tilt of 30° or less, which is considerably less than has been reported for any other substances. It is believed that the first explanation is the more probable.

In the course of this investigation it was desired to know the variation of specific gravity of aqueous detergent "X" solutions with concentration. These were determined with a small pycnometer and are plotted in figure 8. It can be seen that in the region between 75 per cent and 100 per cent, the solutions of detergent "X" have a specific gravity greater than that of pure detergent "X";



this indicates the strong association of the water and detergent molecules through hydrogen bonding with the ether oxygen atoms and hydroxyl group. The greatest deviation of the observed values from the expected straight line, i.e., the greatest difference between the full and broken line, is in the region of 70 per cent, which coincides with the concentrations giving the strongest and sharpest x-ray patterns.

Short spacings of detergent "X" and its aqueous solutions consist of a halo whose maximum intensity corresponds to a Bragg spacing of  $4.5 \text{ \AA}$ . This value remains constant but the intensity decreases with dilution. In dilute solutions the water halo becomes relatively stronger and this causes an apparent shift in the side spacing. This shift becomes noticeable at about 30 per cent.

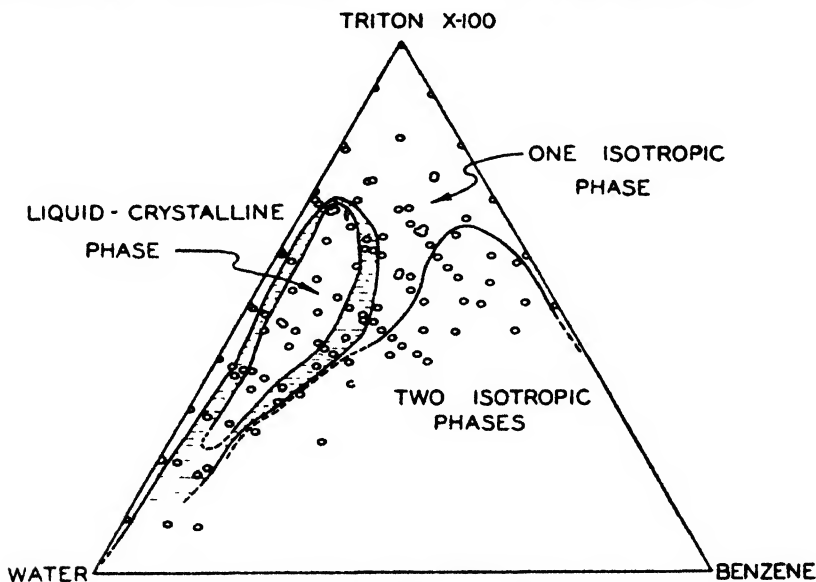


FIG. 9. Phase diagram for the Triton X-100-water-benzene system

The side spacing halo,  $4.5 \text{ \AA}$ , is believed to be due to the average or liquid arrangement of the chain-like molecules within the micelle, similar to that postulated by other investigators for ionic detergents.

#### *Triton X-100-water-benzene*

In order to study the solubilization of hydrocarbons in aqueous systems of a non-ionic detergent, it was decided to treat the problem as the phase study of a three-component system, the components being detergent, water, and a hydrocarbon. The detergent used was Triton X-100; the hydrocarbon was benzene. Single systems were made by first preparing a stock solution of Triton X-100 in either water or benzene and then diluting portions of this stock solution with the third component. Thus the ratio of two components was kept constant while the third was varied.

On the basis of more than one hundred points examined, the phase diagram looks something like figure 9. The individual points studied are included with

the phase boundaries as far as they have been determined (dashed lines indicate tentative phase boundaries). It is to be emphasized that this phase diagram is not complete; in particular, the region in the lower left-hand corner needs clarification. It is primarily used as a convenient method of presenting the physical appearance of the particular systems studied.

It will be noted that Triton X-100 is miscible with water in all proportions. With benzene, it is probably miscible in all proportions except for a very slight precipitate, which is probably an impurity.

The x-ray results can be described by several general statements. Neither of the two-component systems, i.e., Triton X-100 in water or Triton X-100 in benzene, gives long spacings, indicating that two components are not enough to form a lamellar structure for this system. The addition of about 1 per cent of benzene to aqueous systems of Triton X-100 is sufficient to form enough of a structure to diffract x-rays, but the addition of about 10 per cent of water to benzene solutions of Triton X-100 is necessary to give this minimum amount of structure.

Triton X-100 itself, which is a liquid, does not give a long spacing, but when cooled below its melting point, it gives a long spacing of 46.5 Å. This is very close to the calculated single length of the average extended molecule, i.e., about 47 Å. It is believed that this is a second order of diffraction, although no first order is visible.

Samples in the liquid-crystalline region are generally quite viscous, highly birefringent, and very beautifully colored in the polarizing microscope. They give long spacings which are very highly oriented, the diffraction being perpendicular to the axis of the capillary in which the sample is mounted. This indicates that the lamellar structure is oriented parallel to the axis of the capillary when it is filled. The short spacings of the liquid-crystalline samples, which consist of two broad halos, are not oriented.

Of the systems in the region where two isotropic phases exist, only the less dense (more concentrated or benzene) phase gives a long spacing. These long spacings are not oriented, and none are so sharply defined as those in the region of the liquid-crystalline samples. The long spacings of the samples in the region where one isotropic phase exists are also non-oriented and of about the same sharpness as those in the two isotropic phase regions.

In the heterogeneous regions which contain both liquid-crystalline and isotropic phases (dashed area on figure 9), the two phases have different long spacings. In every case, the long spacing of the isotropic phase is either equal to or greater than that of the coexisting liquid-crystalline phase.

For the change of long spacing with concentration, consider first the aqueous systems to which benzene has been added in various amounts, i.e., solubilization of benzene by the aqueous solution of the detergent. When the total long spacing is plotted against per cent Triton X-100, the curves in figure 10 result. The curves are identified by the original concentration of the aqueous stock solution of Triton X-100. For example, the curve consisting of circled points and labeled "80.4%" is for the long spacing of a series of three-component systems made by adding various amounts of benzene to portions of a stock solution of 80.4 per cent

Triton X-100 in water. Then, as more benzene is added, the total concentration of Triton X-100 decreases; it is these latter concentrations, at different dilutions, which are plotted as abscissae of figure 10.

It will be noted that in general the long spacing increases very rapidly with the addition of benzene, much more rapidly than can be accounted for by having only benzene go into the lamellar layers. Evidently, both benzene and water go into the lamellar structure to form layers similar to those in the aqueous systems of diglycol monolaurate. The breaks in the curves in the heterogeneous region are quite evident; the long spacings of the coexisting phases are connected by the four vertical dashed lines.

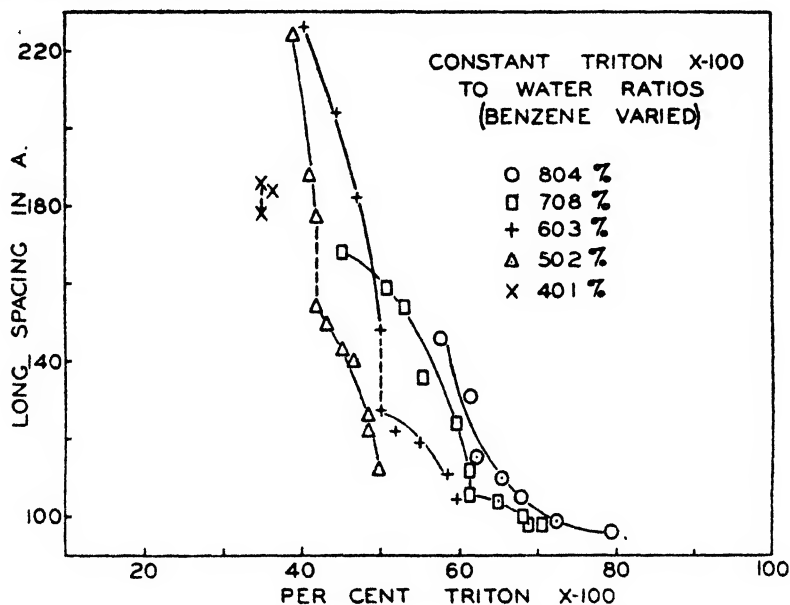


FIG. 10. Plot of long spacing versus weight per cent Triton X-100 for constant Triton X-100 to water ratios (benzene varied).

Now consider the Triton X-100-benzene systems to which water has been similarly added in various amounts (figure 11). Again the total long spacing is plotted against final per cent Triton X-100, with the points being identified by the concentration of X-100 in the original stock solution. It will be noted that the long spacings for the isotropic systems are very close to one line, while those for the liquid-crystalline systems fall very close to another.

From a consideration of the curves of figures 10 and 11, it can be shown, as follows, that all of both the benzene and water does not go into lamellar layers between layers of Triton X-100 molecules. If it did, we would get for both of these graphs the same curved line (concave upward), intersecting the axis at 100 per cent Triton X-100 and  $L \cdot \sin \beta$ , and fulfilling the other conditions previously derived for the hydrous, smectic, liquid-crystalline condition.

Since different curves are obtained for both the liquid-crystalline systems and

the isotropic systems, there is something distinctly different between the two; if this difference were constant for all concentrations one might attribute it to a change in the angle of tilt,  $\beta$ , but, since the difference varies with concentration, it must be something else. (This is, of course, on the assumption that  $\beta$  is not a gradual function of concentration.)

No long spacings were observed below concentrations of about 30 per cent; since the rate of increase of the long spacing with respect to decreasing concentration is very high in this region, and since the difficulty of observing these very long spacings becomes extremely great just below this concentration, it is hard to say whether the lamellar structure has disappeared or whether it just could not be observed. For some systems (such as the dilutions of 80.4 per cent and

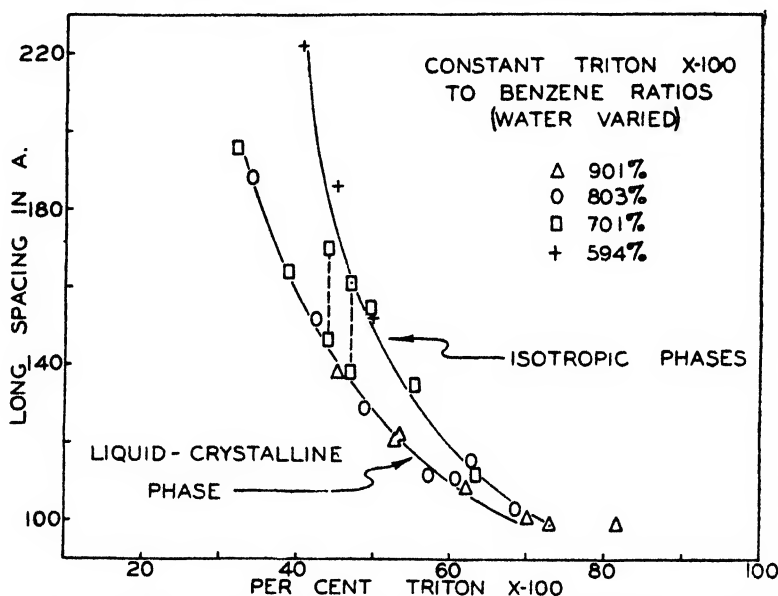


Fig. 11. Plot of long spacing *versus* weight per cent of Triton X-100 for constant Triton X-100 to benzene ratios (water varied).

70.8 per cent on figure 10 and those of 90.1 per cent on figure 11) the lack of an observed long spacing in the more dilute region must be attributed to something other than the above two reasons. It is believed that this other factor is an insufficient amount of either water or benzene to form the lamellar structure. As was previously mentioned, at least 10 per cent of benzene is necessary and 1 per cent of water is necessary to form a lamellar structure (this latter figure applies only to concentrations of Triton X-100 of over 50 per cent).

If the points for the liquid-crystalline systems from figure 10 are superimposed on figure 11, they fall fairly close to the line, with a couple of exceptions. If all of the points for the liquid-crystalline systems from both figure 10 and figure 11 are replotted on log-log coordinates (figure 12), they lie approximately on a straight line of slope equal to  $-1$ . On the basis of the model of the hydrous, smectic,

liquid crystal previously set up, this would indicate that in the region of the straight line all of the water and benzene added is going into the lamellar layers. On this same basis, one would expect an intercept at 100 per cent Triton X-100 of  $L_c \cdot \sin \beta$ ; however, as can be seen from the phase diagram (figure 9), the upper boundary of the liquid-crystalline region is at about 70 per cent Triton X-100. Above 82 per cent Triton X-100 no long spacings were observed for the isotropic solutions; the water and benzene evidently are going between the detergent molecules *prior* to any formation of lamellar structure becoming apparent to x-ray examination. As was mentioned previously, the observed long spacing of the frozen Triton X-100 was 46.5 Å., a value which agreed well with the calculated average length of the molecule. Since no long spacings less than this value were

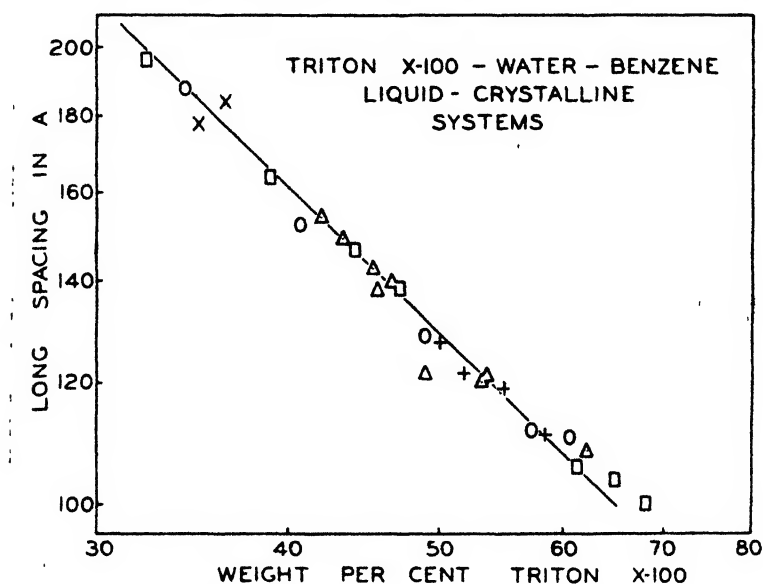


FIG. 12. Log-log plot of long spacing *versus* weight per cent of Triton X-100 for liquid-crystalline systems.

observed for any of the three-component systems, it is believed that the molecules of the Triton X-100 are perpendicular to the basal planes, i.e.,  $\beta = 90^\circ$ .

The above interpretation has a few weak points and exceptions, but a major part of the experimental evidence supports it well.

The relation of long spacing to concentration for the isotropic solutions is not so clear cut as that for the liquid-crystalline systems. Although the points for the isotropic solutions with constant ratios of Triton X-100 to benzene (figure 11) fall on a continuous line, those for solutions with constant ratios of Triton X-100 to water (figure 10) fall on different lines which are dependent upon the original ratio of detergent to water. Even when all are plotted on log-log coordinates (figure 13), they give only a rather incoherent mass. However, as with the liquid-crystalline systems it can be said that part of the water and benzene goes

between the chains prior to the formation of the lamellar layers, as evidenced by the lack of long spacings in concentrations of above 82 per cent Triton X-100. Also, most but not all of the remaining water and benzene goes into the lamellar layers; this reservation must be made because of the complexity introduced by the formation of the second, isotropic, non-lamellar phase.

A part of this investigation which needs to be discussed separately is the thin isotropic region that exists on the phase diagram between the liquid-crystalline region and the Triton X-100-water coordinate. This was studied by preparing a stock solution of 98.5 per cent Triton X-100 + 1.5 per cent benzene and then diluting portions of it with water; the results are plotted on figure 7 with those of Detergent "X"; the variation of long spacing with concentration is practically the

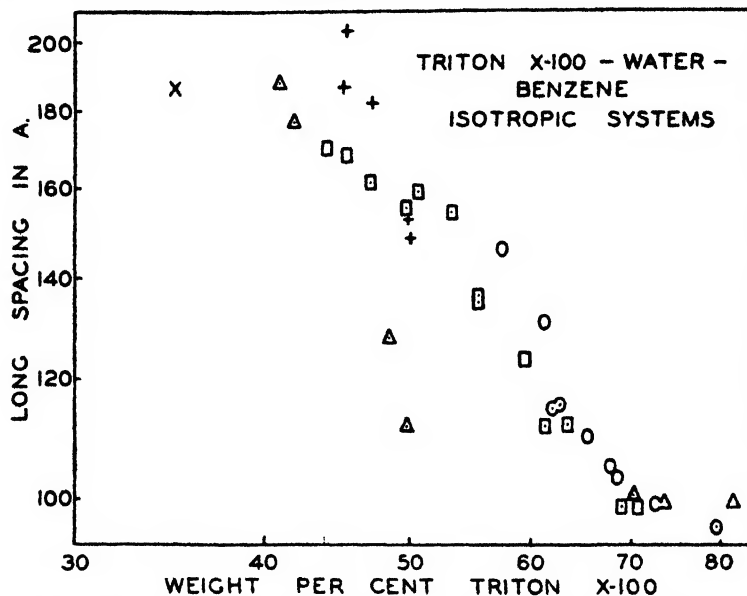


FIG. 13. Log-log plot of long spacing versus weight per cent of Triton X-100 for isotropic systems.

same as that for Detergent "X", although the diffraction is not as strong and the results do not cover as great a range of concentration. Now the only difference between the structural formula for these two detergents is the configuration of the octyl group attached to the phenoxy ring. Detergent "X" has a 6-methyl-*n*-heptyl group and Triton X-100 has diisobutyl substitution (a 1,1,3,3-tetra-methylbutyl group). The length of the average polyethylene oxide chain differs by less than one unit, which should make little difference in the chemical properties. Yet the aqueous systems of Detergent "X" have a lamellar structure, while those of Triton X-100 do not (until benzene is added). There are at least two plausible explanations of this. One is that the configuration of the octyl group is vital for the formation of the lamellar structure. Another is that there is a small amount of an impurity of a hydrophobic nature in the original Detergent "X" which favors the formation of this lamellar structure by going into

layers between the hydrocarbon ends of the molecules. The results with the aqueous systems of Triton X-100 containing 1.5 per cent of benzene tend to support this latter explanation strongly.

#### *Triton X-100-water-dimethyl phthalate*

Dimethyl phthalate has the unique property of being insoluble in both water and paraffin hydrocarbons. Recent work in this laboratory by Miss McHan has shown that this material is solubilized by aqueous detergent solutions and that the solubilization is greater (on the basis of moles of phthalate per mole of detergent) in the decinormal solutions than in stronger solutions. This has led to the explanation that the phthalate is solubilized more by a type of micelle that exists in dilute solutions than by the lamellar micelle which exists in more concentrated solutions.

It was of interest to compare the solubilization of this substance with that of benzene by an aqueous solution of Triton X-100. Accordingly, dimethyl phthalate was added in portions to a 50.2 per cent Triton X-100 solution in water and x-ray photographs were taken of samples of this ternary system. From zero to 12.6 per cent phthalate (which was the range of concentration studied) the systems were clear and isotropic; the viscosity became less upon gradual addition of the phthalate. None of these systems gave a long spacing, indicating that there was no regular lamellar structure. The striking difference between this ternary system and the ternary system Triton X-100-water-benzene in the same concentration range, which produced a long spacing, indicates that dimethyl phthalate is not solubilized like benzene by incorporation within a regular lamellar structure, but is evidently solubilized by some other mechanism.

#### *The effect of time*

Five to seven months after some of the foregoing systems were studied, it was decided to rephotograph a number of the same capillaries to see if they had changed with time.

The aqueous systems of  $\alpha$ -*n*-decyl glyceryl ether and Emulphor O gave patterns which were identical with the original ones.

The aqueous systems of diglycol monolaurate (along with those made from the isotropic and liquid-crystalline phase residues), glyceryl monolaurate, and polyethylene glycol 400 monolaurate gave spacings which were longer than those of the original photographs. This increased length was only a matter of a couple of Ångström units for the more concentrated systems, but came to 10 or 12 Å. for the more dilute. The very dilute systems gave no pattern upon rephotographing, whereas they had previously given patterns. The above experimental facts can be explained on the basis of hydrolysis of these detergents, which are merely esters, with some of the resulting decomposition products going into the lamellar layers to increase the long spacing. The very dilute systems would be expected to hydrolyze to a greater extent, with the resulting destruction of the lamellar structure.

The aqueous systems of Detergent "X" gave no pattern a year after preparation. No explanation is offered here.

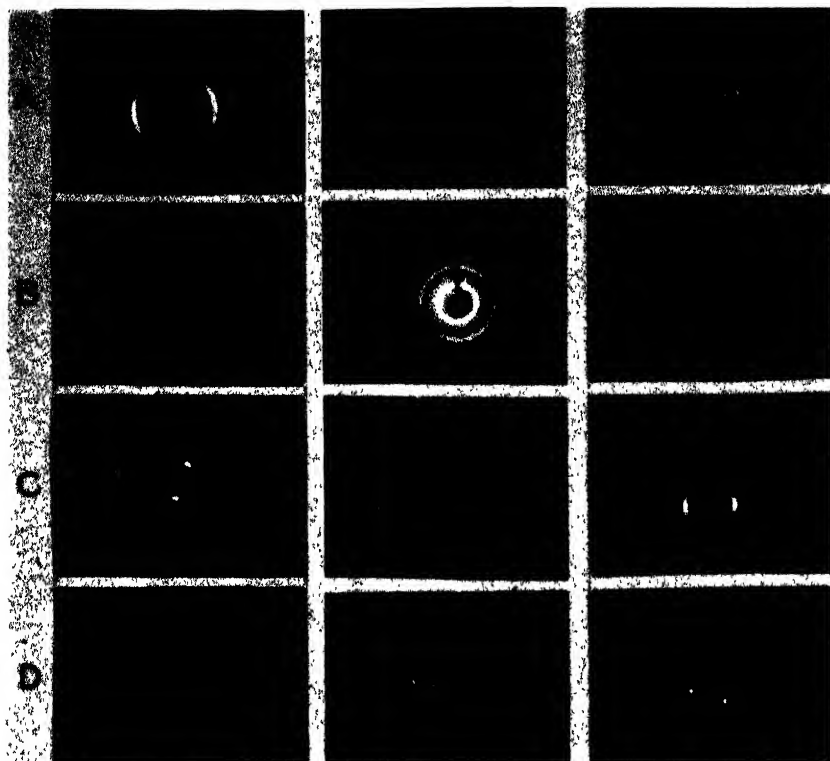


FIG. 14

FIG. 15

FIG. 16

FIG. 14. Typical x-ray diffraction patterns of aqueous systems of non-ionic detergents. A, 72.5 per cent  $\alpha$ -*n*-decyl glyceryl ether (liquid crystal). B, 41.0 per cent  $\alpha$ -*n*-decyl glyceryl ether (liquid-crystalline phase). C, 60.3 per cent diglycol monolaurate (liquid crystalline phase). D, 69.1 per cent liquid-crystalline phase residues of diglycol monolaurate.

FIG. 15. Typical x-ray diffraction patterns of aqueous systems of non-ionic detergents. A, 63.5 per cent Emulphor O (isotropic solution). B, 44.1 per cent glyceryl monolaurate (liquid-crystalline phase). C, 62.5 per cent Triton X-100, 24.5 per cent water, 13.0 per cent benzene (isotropic phase). D, 50.2 per cent Triton X-100, 33.0 per cent water, 16.8 per cent benzene (liquid-crystalline phase).

FIG. 16. Typical x-ray diffraction patterns of aqueous systems of non-ionic detergents. A, 43.1 per cent Triton X-100, 42.8 per cent water, 14.1 per cent benzene (liquid crystal). B, 59.8 per cent Triton X-100, 39.3 per cent water, 0.9 per cent benzene (isotropic solution). C, 65.0 per cent Triton X-100, 25.5 per cent water, 9.5 per cent benzene (liquid crystal). D, 44.2 per cent Triton X-100, 37.0 per cent water, 18.8 per cent benzene (mixed isotropic and liquid-crystalline); the faint inner circle is the diffraction from the isotropic phase; the four spots are diffraction from the liquid-crystalline phase.

Figures 14, 15, and 16 are reproductions of some typical x-ray diffraction patterns of aqueous systems of non-ionic detergents. These were all 12-hr. exposures with Cu  $K_{\alpha}$  radiation, and a sample-to-film distance of 200 mm. They have been reproduced actual size.



## GENERAL CONCLUSIONS AND SUMMARY

From the information obtained in this investigation, one can see that, beyond a doubt, aqueous systems of some non-ionic detergents have a definite repeating structure that will diffract x-rays. By analogy with the lamellar structure found for aqueous systems of ionic detergents, together with supporting x-ray evidence (oriented diffraction, the ratio of the various orders of diffraction to each other, i.e., 1:2:3, and the variation of long spacing with concentration), it is evident that this repeating structure is of a lamellar type, rather than a hexagonal type as found by Bernal and Fankuchen (1) for aqueous systems of tobacco mosaic virus.

However, not all aqueous systems of non-ionic detergents or surface-active materials give a lamellar structure (e.g., Triton X-100), and not all aqueous systems give the same type of lamellar structure. Some (Detergent "X", Emulphor O, and some concentrations of the system Triton X-100-water-benzene) are isotropic solutions which probably contain lamellar micelles similar to those found in solutions of ionic detergents. The rest (diglycol monolaurate, glyceryl monolaurate, polyethylene glycol 400 monolaurate,  $\alpha$ -n-decyl glyceryl ether, and some concentrations of the system Triton X-100-water-benzene) give liquid-crystalline systems which consist of regular alternating layers of detergent molecules and water molecules; some of these systems also contain layers of hydrophobic material. Whether or not the aqueous systems of one of these detergents will have a lamellar structure and what sort of lamellar structure depends on the type of hydrophilic group and the length of this group relative to the length of hydrocarbon chain. The presence of a hydrocarbon or other hydrophobic material in the system has a strong influence toward the formation of a lamellar structure of either type.

A good deal of evidence has been presented to show that some detergent molecules are tilted in these lamellar layers or micelles at an angle to the basal plane (diglycol monolaurate, glyceryl monolaurate,  $\alpha$ -n-decyl glyceryl ether), whereas others are perpendicular to the basal plane (Triton X-100-water-benzene systems). This angle of tilt could not be determined accurately, but it is in the neighborhood of  $50^\circ$  and may vary for different substances. This existence of an angle of tilt of other than  $90^\circ$  is contrary to what has always been assumed (for simplicity's sake) to be the case for aqueous systems of ionic detergents.

It has been shown that some of the water in these lamellar structures is between the detergent chains, besides that existing in the lamellar layers or between the micelles. It is probable that this water goes between the chains by hydrogen bonding to the ether oxygen atoms prior to the formation of the lamellar layers.

A new model of an ideal, hydrous, smectic, liquid-crystalline system has been set up and analyzed. It has been extremely useful in the interpretation of the experimental results of this investigation, and should be useful in the study of other hydrous liquid-crystalline systems, a number of which are known in the biological sciences.

Grateful thanks are extended to Lever Brothers Company, whose generous fellowship has made possible this study.

## REFERENCES

- (1) BERNAL, J. D., AND FANKUCHEN, F.: *J. Gen. Physiol.* **25**, 111 (1941).
- (2) BOEDEKER, K.: *Kolloid-Z.* **94**, 161 (1941).
- (3) HARKINS, W. D., MATTOON, R. W., AND CORBIN, M. L.: *J. Am. Chem. Soc.* **68**, 220 (1946).
- (4) HARKINS, W. D., MATTOON, R. W., AND CORBIN, M. L.: *J. Colloid Sci.* **1**, 105 (1946).
- (5) HESS, K.: *Fette u. Seifen* **49**, 81 (1942).
- (6) HESS, K., AND GUNDERMANN, J.: *Ber.* **70B**, 1800 (1937).
- (7) HESS, K., KIESSIG, H., AND PHILIPPOFF, W.: *Naturwissenschaften* **26**, 184 (1938).
- (8) HESS, K., KIESSIG, H., AND PHILIPPOFF, W.: *Kolloid-Z.* **83**, 40 (1939).
- (9) HESS, K., KIESSIG, H., AND PHILIPPOFF, W.: *Fette u. Seifen* **48**, 377 (1941).
- (10) HUGHES, E. W., SAWYER, W. M., AND VINOGRAD, J. V.: *J. Chem. Phys.* **13**, 131 (1945).
- (11) KIESSIG, H.: *Kolloid-Z.* **96**, 252 (1941).
- (12) KIESSIG, H.: *Kolloid-Z.* **96**, 213 (1942).
- (13) KIESSIG, H., AND PHILIPPOFF, W.: *Naturwissenschaften* **27**, 593 (1939).
- (14) LONSDALE, K., AND SMITH, H.: *J. Sci. Instruments* **18**, 133 (1941).
- (15) MALKIN, T., AND EL SHURBAGY, M. R.: *J. Chem. Soc.* **1936**, 1628.
- (16) MARSDEN, S. S.: *Rev. Sci. Instruments* **16**, 192 (1945).
- (17) MATTOON, R. W., STEARNS, R. S., AND HARKINS, W. D.: *J. Chem. Phys.* **15**, 209 (1947).
- (18) PALMER, K. J., AND SCHMITT, F. O.: *J. Cellular Comp. Physiol.* **17**, 385 (1941).
- (19) PHILIPPOFF, W.: *Kolloid-Z.* **96**, 255 (1941).
- (20) ROSS, S., AND MCBAIN, J. W.: *J. Am. Chem. Soc.* **68**, 296 (1946).
- (21) STAUFF, J.: *Kolloid-Z.* **89**, 224 (1939).
- (22) STAUFF, J.: *Kolloid-Z.* **96**, 244 (1941) (abstracted).

CRITICAL MICELLE CONCENTRATIONS AS DETERMINED  
BY REFRACTION<sup>1</sup>H. B. KLEVENS<sup>2</sup>*George Herbert Jones Chemical Laboratory, University of Chicago, Chicago, Illinois**Received August 25, 1947*

There are a number of methods which have been applied to the determination of the critical micelle concentration (C.M.C.) of soaps and detergents, but most of them have involved some extraneous influence. For example, conductivity and transport-number determinations require the application of external electric forces (24, 30); the spectral dye method requires the use of dyes (3, 13); solubilization studies require the use of dyes or hydrocarbons (10, 19, 21); and viscosity involves the application of a shearing force (29). No evidence has been advanced to show that the application of electric forces as in conductivity measurements has any effect on the C.M.C. value, but this possibility must not be precluded.

<sup>1</sup> Presented at the Twenty-first National Colloid Symposium, which was held under the auspices of the Division of Colloid Chemistry of the American Chemical Society at Palo Alto, California, June 18-20, 1947.

<sup>2</sup> Present address: Chemical & Physical Research Laboratories, Firestone Tire & Rubber Company, Akron, Ohio.

It has been shown (16) that the C.M.C. values determined by use of the spectral dye method were at all times smaller than those determined by conductivity and by solubility-temperature measurements. In addition, those C.M.C. values which were determined by solubilization were also lower than those obtained from other measurements. This is in agreement with the reported lowering of C.M.C. which occurs upon the addition of a hydrocarbon to a soap solution (17).

The use of refraction to show changes in aggregation has been applied to many colloid systems, and its direct application to the determination of C.M.C. in the case of sodium lauryl sulfate has been demonstrated by Hess, Philippoff, and Kiessig (11). Further preliminary studies on various fatty acid soaps and on a series of sodium alkyl sulfonates have substantiated the validity of this method (12, 15). No changes can occur in the equilibrium composition of soap solutions during measurement of refraction, for this method does not involve the addition of an extraneous substance or the application of some external field of force.

The instrument used for these measurements was a Rayleigh-Haber-Löwe type of interferometer. The portable model used contains a mirror system which allows the light beam to pass twice through the sample. Thus the effective length of the cell is doubled, increasing the range and accuracy considerably. The effective layer thickness used for most measurements, especially those of dilute solutions, was 160.290 mm. The entire instrument, except for the operating and recording portion, was placed in a thermostat and the temperature was controlled by water circulation. Temperatures did not vary by more than  $\pm 0.003^\circ\text{C}$ . For a large number of organic compounds the refractive index changes by 1-2 in the fourth place upon a change in temperature of  $1^\circ\text{C}$ . However, extreme care did not have to be taken as to temperature control in these measurements, for the interferometer is a differential-type instrument, i.e., the optics permit the determination of the difference in refractive indices of solvent and solution simultaneously. Although the temperature at which the measurements were made did not have to be carefully controlled, it was necessary to determine accurately the temperature of solvent and solution at the time the readings were made. To insure equilibrium between solvent and solution and the small separate water bath in which the interferometer cell was suspended, dial readings were made at intervals of 5 min. until constant values were obtained. The water bath was stirred to hasten this equilibrium. Temperature readings were made with a calibrated Beckmann thermometer.

At higher temperatures, use of the standard cover slips supplied with the interferometer cells was not sufficient to prevent evaporation, as was seen by the schlieren effect of the interference bands which are used to measure  $\Delta n$ , the difference in refractive index between solution and solvent. A set of cell covers which could be sealed to the glass and metal portion of the interferometer cell by waxes which were not solubilized by soap solutions was used at higher temperatures. Wax seals were made semipermanent, and the cells were filled through a hole in the cover slip to which a tube with a standard taper at its end was attached. By means of this assembly,  $\Delta n$  values could be determined at temperatures as high as  $70^\circ\text{C}$ . without any error due to the instability of the inter-

ference bands. A similar assembly proved very satisfactory in previous work with volatile solvents. All dial readings were made in triplicate and the average value used for the determination of  $\Delta n$ . The instrument was calibrated by the use of standard sodium chloride solutions. The usual accuracy in  $\Delta n$  in these measurements was  $2 \times 10^{-7}$ . Kruis and Geffcken (5) have described precautions and refinements which would allow an accuracy in  $\Delta n$  of  $1 \times 10^{-8}$ , but this degree of accuracy was not necessary in these determinations.

The fatty acid soaps were prepared by multiple fractionation of the corresponding esters, followed by saponification and repeated recrystallizations first

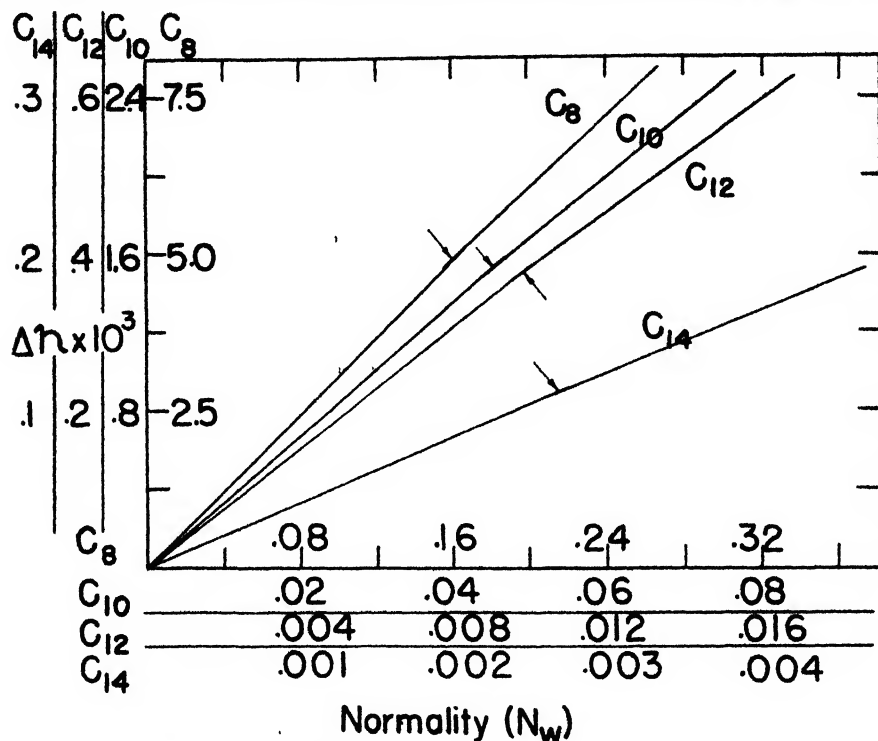


FIG. 1. Variation in refractive indices of sodium alkyl sulfonates with concentration. Arrow denotes break in curve which is the critical micelle concentration.

from ethanol and finally from acetone. The sodium alkyl sulfonates, kindly supplied by Professor H. V. Tartar, are samples similar to those used by him and his coworkers as reported in their publications (28, 29, 30). The amine hydrochlorides, supplied by the Research Laboratories of Armour and Company, were subsequently recrystallized five times. Various properties of these cationic detergents have been described by Ralston, Hoerr, and others in various papers (24).

The change in degree of aggregation of soap molecules as the C.M.C. is passed is shown by a change in slope of two lines which represent the measured refractive-index difference between that of the total system and that of water

( $\Delta n$ ) as a function of concentration. The curves in figure 1 show the changes in refractive index with concentration for the sodium alkyl sulfonate series. The value of the slope,  $\Delta(\Delta n)/\Delta c$ , where  $\Delta(\Delta n)$  is the difference in refractive-index increments of two solutions whose concentration difference is  $\Delta c$ , for these detergents as well as those obtained for the fatty acid soaps and the cationic amine hydrochlorides are collected in table 1. The difference in the slopes in

TABLE 1  
Values of slope,  $\Delta(\Delta n)/\Delta c$ , for various soaps

SOAP	SLOPE ( $\times 10^4$ )		CHANGE IN SLOPE BETWEEN NEIGHBORING MEMBERS IN THE SERIES ( $\times 10^4$ )		PER CENT INCREASE IN SLOPE
	Below C.M.C.	Above C.M.C.	Below C.M.C.	Above C.M.C.	
Potassium fatty acid soaps					
C <sub>10</sub> ....	312	292			
C <sub>12</sub> ....	369	345	57	53	17.0
C <sub>14</sub> ....	403	381	34	36	9.5
Sodium alkyl sulfonates					
C <sub>8</sub> .	303	284			
C <sub>10</sub> .	343	327	40	43	13.5
C <sub>12</sub> ....	379	367	34	40	15.0
C <sub>14</sub> .	424	397	45	30	10.0
C <sub>16</sub> .	461	438	37	41	8.5
Alkylamine hydrochlorides					
C <sub>12</sub> ....	407	376			
C <sub>14</sub> ..	437	408	30	32	7.5
C <sub>16</sub> .....	466	438	29	30	6.5

a homologous series seems, within experimental error, to be fairly uniform and is probably a function of additivity due to the stepwise increase in chain length. These increments are included in table 1 and, although their numerical increase is not uniform per unit increase in chain length, the percentage rise in slope values is numerically similar to the corresponding changes in C.M.C. These data are shown in table 2. The regularity of the per cent decrease in the fatty acid soaps and in the alkyl sulfonates was indicative of a relationship which has been developed below. Measurements at different temperatures as seen in the results in table 2 probably account for some of the irregularity noted.

The data for typical systems, where the changes in refractive index at 25°C. of potassium laurate and sodium dodecyl sulfonate at 35°C. with concentration are shown, are collected in tables 3 and 4. The reliability of the data is illustrated in figure 2, where chord plots of the values in table 3 are drawn. These plots are

TABLE 2  
*Critical micelle concentrations as determined by refraction*

SOAP	TEMPERATURE	C.M.C.	DECREASE IN C.M.C.
Fatty acid soaps			
	°C.	moles per liter	per cent
KC <sub>8</sub> . . . . .	25	0.39	75
KC <sub>10</sub> . . . . .	25	0.098	74
KC <sub>12</sub> . . . . .	25	0.0255	74
KC <sub>14</sub> . . . . .	25	0.0066	73
KC <sub>16</sub> . . . . .	35	0.0018	
Sodium alkyl sulfonates			
C <sub>8</sub> . . . . .	25	0.155	74
C <sub>10</sub> . . . . .	25	0.041	76
C <sub>12</sub> . . . . .	35	0.010	71
C <sub>14</sub> . . . . .	45	0.0029	69
C <sub>16</sub> . . . . .	52	0.0009	
Alkylamine hydrochlorides			
C <sub>10</sub> . . . . .	25	0.04	67
C <sub>12</sub> . . . . .	30	0.013	76
C <sub>14</sub> . . . . .	40	0.0031	74
C <sub>16</sub> . . . . .	50	0.008	69
C <sub>18</sub> . . . . .	60	0.00025	

measures of the change in  $\Delta n$  with concentration, i.e.,  $\Delta(\Delta n)/\Delta c$ , as functions of concentration. This manner of plotting these data shows more strikingly the break in  $\Delta n$  with concentration at the C.M.C. The averages of the chord plot values are those which would correspond to the values of the slopes of the lines in the plots of  $\Delta n$  as a function of concentration.

## TEMPERATURE EFFECTS

Various results have been reported regarding the effect of temperature on the C.M.C. From conductivity measurements of sodium alkyl sulfonate solutions by Wright, Abbott, Sivertz, and Tartar (30), of alkylamine hydrochlorides by

TABLE 3  
*Refractive indices of potassium laurate (25°C.)*

$N_w (\times 10^2)$	$\Delta N_w = \Delta c (\times 10^2)$	$\Delta n (\times 10^3)$	$\Delta(\Delta n) (\times 10^4)$	$\frac{\Delta(\Delta n)}{\Delta c} (\times 10^2)$
0.432		0.1633		
	1.083		4.100	3.78
1.515		0.5733		
	0.274		1.027	3.76
1.789		0.6760		
	0.300		1.120	3.73
2.089		0.7880		
	0.259		0.979	3.77
2.348		0.8859		
	0.132		0.498	3.77
2.480		0.9357		
	0.066		0.247	3.75
2.546		0.9604		
	0.057		0.202	3.54
2.603		0.9806		
	0.052		0.191	3.60
2.655		0.9997		
	0.148		0.502	3.39
2.803		1.0499		
	0.116		0.401	3.45
2.919		1.0900		
	0.410		1.440	3.51
3.329		1.2340		
	0.436		1.522	3.49
3.765		1.3862		
	1.490		5.219	3.50
5.255		1.9081		
	1.089		3.793	3.48
6.344		2.2874		
	0.973		2.391	3.46
7.317		2.6265		
	1.083		3.755	3.45
8.400		3.0020		

Ralston and Hoerr (24), and of other soap solutions by various workers it has been shown that the C.M.C. increases with increasing temperature. Bury and Parry, from density measurements of potassium laurate solutions, have shown that the C.M.C. decreases with increasing temperature (1). Ekwall has stated that the C.M.C. is temperature independent, on the basis of conductivity measurements on sodium fatty acid soap solutions (4). The application of the spectral dye method to temperature effects indicated that the C.M.C. decreased

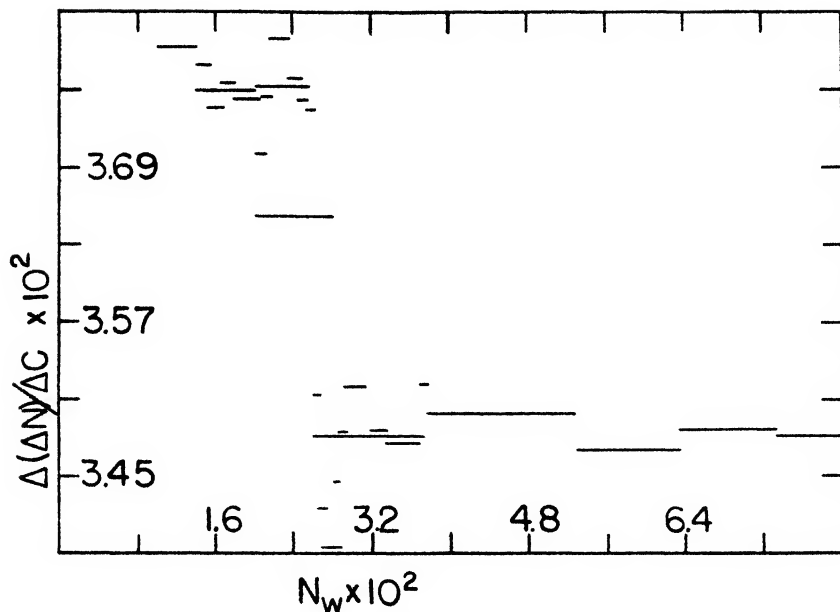
with increasing temperature, but these results were shown to be a property of this particular method (16). These observations are due to changes in the spectra of the dyes which shift with changes in temperature. The decreases noted are caused by changes in the aggregation of the dye, and it is this factor rather than the formation of micelles which brings about this reported decrease in C.M.C.

TABLE 4  
*Refractive indices of sodium dodecyl sulfonate (55°C.)*

$N_w (\times 10^3)$	$\Delta N_w = \Delta c (\times 10^3)$	$\Delta n (\times 10^4)$	$\Delta(\Delta n) (\times 10^4)$	$\frac{\Delta(\Delta n)}{\Delta c} (\times 10^3)$
0.662		2.537		
	0.094		3.56	3.79
0.756		2.893		
	0.077		2.92	3.79
0.833		3.185		
	0.070		2.67	3.80
0.906		3.452		
	0.029		1.10	3.78
0.935		3.562		
	0.028		1.06	3.77
0.963		3.668		
	0.027		1.02	3.79
0.990		3.770		
	0.058		2.20	3.80
1.048		3.990		
	0.068		2.48	3.65
1.116		4.238		
	0.092		3.35	3.64
1.208		4.573		
	0.137		2.98	3.64
1.345		5.071		
	0.183		6.71	3.67
1.528		5.742		
	0.226		8.27	3.66
1.754		6.569		
	0.190		6.99	3.68
1.944		7.268		
	0.216		7.95	3.68
2.160		8.063		
	0.160		5.87	3.67
2.320		8.650		

The data in table 5 indicate that the C.M.C. of various soaps and detergents increases with increase in temperature as determined by refraction. This is true not only of anionic but also of cationic detergents. A plot of a portion of these data as seen in figure 3 indicates that the C.M.C. does not change much in the region between 20–40°C. but that the increase is much larger above 40°C. This suggests that this temperature dependence of micelle formation might yield some information as to forces of attraction between molecules in a micelle.





[FIG. 2. Chord area plot of change in refractive-index increment with potassium laurate concentration (25°C.), showing break at critical micelle concentration.

TABLE 5  
*Change in critical micelle concentrations with temperature*

TEMPERATURE	C.M.C.	TEMPERATURE	C.M.C.
Sodium decyl sulfonate		Potassium laurate	
°C.	<i>moles per liter</i>	°C.	<i>moles per liter</i>
25	0.041	25	0.0255
		30	0.0260
35	0.042	35	0.0270
45	0.045	45	0.0305
55	0.049	55	0.0350
65	0.055	65	0.0420
Sodium dodecyl sulfonate		Potassium myristate	
35	0.010	25	0.0066
45	0.011	35	0.0070
55	0.012	45	0.0074
65	0.014	55	0.0079
		65	0.0086

The results in table 5 indicate that the C.M.C. as measured by refraction increases with increasing temperature, is symbatic with corresponding changes observed from conductivity and density measurements (24, 29, 30), and is anti-

batic with the C.M.C values as determined by the spectral dye method. These refraction data seem to agree with the conception that most colloidal aggregations are temperature dependent and that they will have less tendency to aggregate at elevated temperatures, owing to increased thermal agitation of the coalescing units.

A presentation of the data showing the change in C.M.C. with increase in chain length at a definite temperature as seen in table 6 indicates that there is a definite correlation between C.M.C. and chain length. The data are satisfied approximately by the following equation:

$$\text{C.M.C.} = a(2n)^{\frac{b-c}{n}}$$

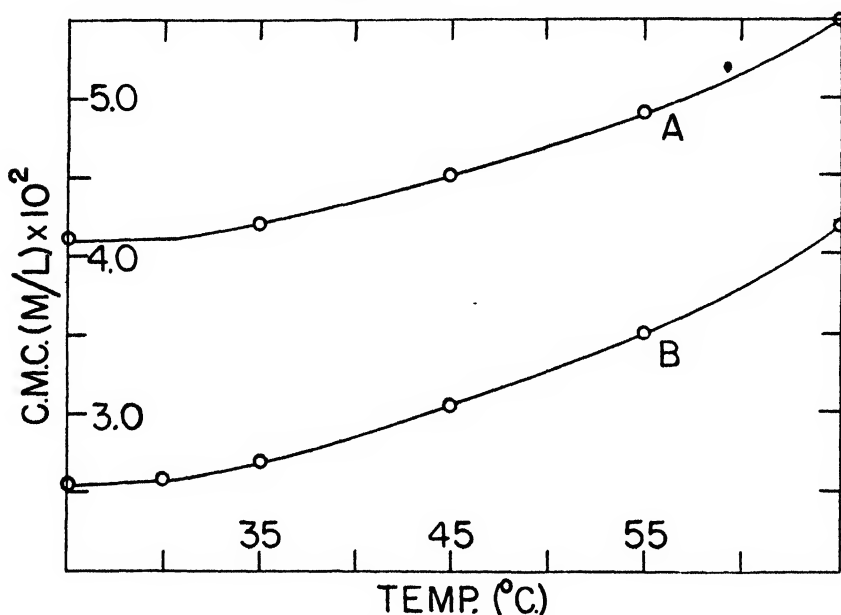


FIG. 3. Effect of temperature upon critical micelle concentration of (A) sodium decyl sulfonate and (B) potassium laurate.

in which  $b = f(a, T)$ . In the above  $a$  = a constant characteristic of the most insoluble member of the particular homologous series at the temperature at which the measurements are made;  $b$  = a constant equal to the maximum number of carbon atoms in the least soluble member of the particular homologous series at a definite temperature ( $b$  thus is dependent on  $a$  and the temperature,  $T$ );  $c$  = the number of carbon atoms in the hydrocarbon chain; and  $n = 2$  for an even number of carbon atoms and 1 for an odd number of carbon atoms.

The values of the constant,  $a$ , at various temperatures are presented in table 7. These data are used to calculate the C.M.C. of various soaps at definite temperatures. A comparison of the experimental with the calculated values, as well as predicted values for the various soaps containing odd numbers of carbon atoms, is included in table 6. There are at the present time no data available

on these soaps with an odd number of carbon atoms except those of Hess, Philippoff, and Kiessig (11). Since their data do not agree with the present results nor with those of Ekwall (4) or Stauff (27) in the case of the soaps with

**TABLE 6**  
*Effect of change in chain length on the critical micelle concentration*

[illegible]

\* Bury and Parry (1).

an even number of carbon atoms, no comparison with their results has been attempted.

Figure 4 shows a plot of the logarithm of C.M.C. as a function of the number of carbon atoms in the straight-chain hydrocarbon portion of the soap molecule. The data of Ekwall and of Stauff on the sodium fatty acid soaps are included with the data on potassium soaps. It has been shown that the sodium and potassium

TABLE 7  
Values of constant  $a$  at various temperatures

SOAP SERIES	TEMPERATURE	$b$	$a$
	°C.		
Potassium fatty acid.....	25	14	0.0066
	35	14	0.0070
	45	16	0.0019
Sodium alkyl sulfonates . . .	35	12	0.010
	40	14	0.0025
	50	16	0.0007
Alkyltrimethylammonium bromides.	25	12	0.0151
	40	12	0.0164
	60	16	0.0010

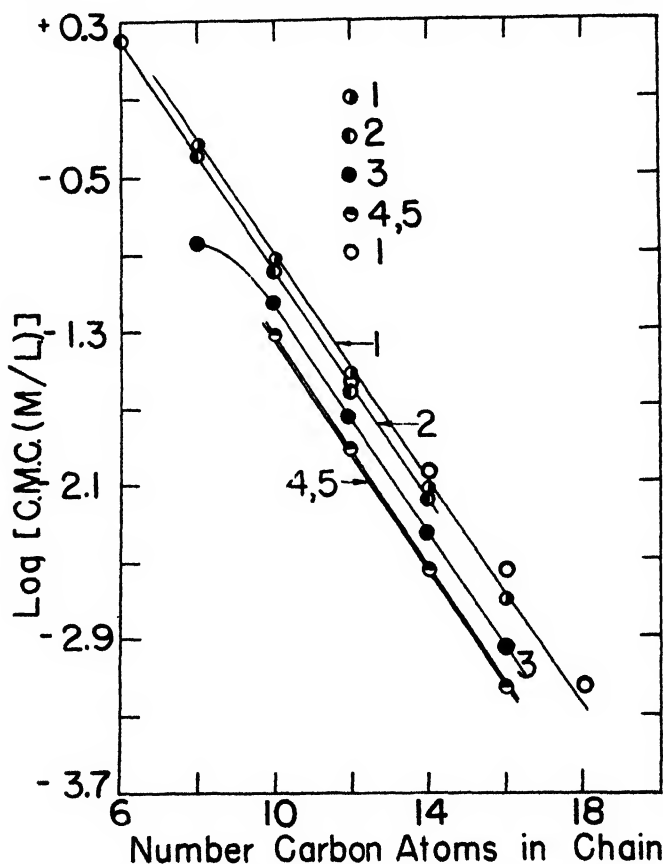


FIG. 4. Change in critical micelle concentration with increase in chain length as determined by various methods. Curve 1, potassium fatty acid soaps (45°C., refraction); clear circles are data on sodium fatty acid soaps (17–80°C., conductivity (4)); curve 2, potassium fatty acid soaps (25°C., refraction); curve 3, alkyltrimethylammonium bromides (25°C., conductivity (25)); curve 4, sodium alkyl sulfonates (55°C., refraction); curve 5, sodium alkyl sulfonates (60°C., conductivity (3)).

salts of various fatty acids, although quite different as to solubility, have identical values of C.M.C. The values obtained by these two authors scatter somewhat from the data obtained in the present measurements. Ekwall's measurements were made at various temperatures between 17° and 80°C., and he reported no change in C.M.C. with temperature which does not agree with other results. The effect of temperature on the C.M.C. can be noted by a comparison of curves 1 and 2 in figure 4. Curve 1 includes the data of the fatty acid soaps at 25°C.; curve 2 those at 45°C.

The values of C.M.C. at 60°C. for the sodium alkyl sulfonates (30) as determined by conductivity are compared with values as determined by refraction at 50°C. in curves 4 and 5. The refraction data are obtained from interpolation of the curves of C.M.C. *vs.* temperature. It can be seen that there is again good agreement between these two methods of C.M.C. determination.

One important series of cationic detergents, the alkylamine hydrochlorides, was found not to fit this general relationship. These values were taken from the conductivity data of Ralston and Hoerr (24). It was thought that perhaps only the anionic soaps followed the proposed equation, but the data on the alkyltrimethylammonium bromides (25) (curve 3, figure 4) indicate that the cationics also can be equated similarly. The data in curves 1-5 are for soaps which were prepared from highly purified alcohols and esters previous to saponification. The amine hydrochlorides may contain a small amount of the next higher homolog and the system would act like a soap mixture having a lower C.M.C. than the pure soap (13). The addition of a small amount of an impurity,—another soap, an electrolyte, a hydrocarbon or oil, or the fatty acid of the soap,—will cause a decrease in the C.M.C. of the pure soap.

#### EFFECT OF ADDED ELECTROLYTES

As has been stated above, the addition of an electrolyte will at all times cause some decrease in the C.M.C. of a soap. Murray (22) indicated that the Krafft point (temperature above which a substance is exceedingly soluble) of potassium cetyl sulfonate is raised by the addition of potassium chloride. Hartley and Runnicles (9) noted that in sodium chloride solutions there was a decrease in the amount of paraffin-chain salts necessary to obtain the same diffusion coefficient obtained with a salt-free system. Hartley (6, 8) reported a decrease in the C.M.C. of cetylpyridinium chloride from 0.0009 *N* to less than 0.0001 *N* in the presence of 0.032 *N* sodium chloride. Tartar and Cadle (28) have shown that the breaks in the solubility curves of sodium alkyl sulfonates shift toward higher temperatures and lower concentrations as the concentration of sodium chloride increases. On the basis of the above results, it was stated that the solubility of the detergents, at temperatures which are below those required for micelle formation, can be described by an activity product relationship. Using the Debye-Hückel theory for the activity coefficient of an electrolyte in solutions of different ionic strengths, they show that the mass action law is valid in the case of the transition from ionic to micellar soap as well as in the transition from ionic to crystalline solid soap. Wright and Tartar (29) stated that a decrease in the

degree of ionization would increase the stability of the micelle, owing to a lowering of the electrical charge. Since this would be affected by cation concentration in the case of anionic soaps, a decrease in C.M.C. would be expected in the case of the addition of sodium chloride. Wright, Abbott, Sivertz, and Tartar (30) have shown that in solutions which were equimolal with respect to sodium chloride and to sodium lauryl sulfonate the C.M.C. decreased by 26 per cent.

If an addition of a number of positive ions is made to a solution of an anionic soap, the concentration of gegenions in the vicinity of the soap molecules will increase considerably. This would bring about a decrease in the degree of ionization and should enhance the stability of the micelle. It would follow then that this addition of an electrolyte would be coupled with a lower value of the C.M.C.

Tartar and his coworkers (28, 30) had previously stated that, on the basis of their preliminary conductivity and solubility studies, the addition of electrolytes indicates that the behavior of micellization in soap solutions follows the principle of ionic strength or the Debye-Hückel relationships. Corrin and Harkins (2), in their more extensive work in which they used various dyes to follow micelle formation, state that these relationships do not explain the behavior of micelle formation. The use of the dye technique (3), based on the earlier reported work of Hartley (7) and Sheppard and Geddes (26), has been shown to yield values which were at all times smaller than those determined by conductivity, by solubility, or by refraction (15, 16). This may be due to one of a number of factors: (1) the dye could act as a salt and, as has been shown by reference to previous work, would cause a decrease in the C.M.C.; (2) the dye could act like a hydrocarbon and in this way would also cause a decrease in the C.M.C. (17, 20, 23); and (3) from previous reported data on the increase in fluorescence of dyes at the C.M.C. (14, 17) due to adsorption and orientation of the dye in or on the micelle, it can be deduced that the dye forms a complex or a mixed micelle with the soap. It has been shown recently that the C.M.C. of a soap is decreased by the addition of another soap with a lower C.M.C. (13). Also, some unreported work of the author indicates that the addition of long-chain alcohols and fatty acids to soaps depresses the C.M.C., and there is some suggestion that as in the case of the dye-soap and the soap-soap mixtures, a mixed micelle is formed.

It was of interest to determine whether the results reported as to the non-applicability of the mass action law could be obtained by refraction studies. Since it had been shown that hydrolysis played no part in these results, for similar results had been found in the case of alkyl sulfonates, alkyl sulfates, and fatty acid soaps (2, 30), the following study was made with potassium laurate.

The procedure used involved the addition of potassium laurate to salt solutions, followed by the determination of the refractive indices of these solutions. For each series, two straight lines were obtained which were similar to those shown in figure 1. The intersection of each pair of lines is the C.M.C., and the values obtained for these are collected in table 8. It can be seen from these data that the C.M.C. is reduced to a fairly constant value, which is not affected by further increase in salt concentration. This would indicate a high degree of saturation of gegenions which form an ionic cloud in the region of the micelles. Further in-

crease in salt concentration to about 0.5 *N* would then have little effect on the degree of ionization, for the added ions would not on the average approach the micelle through the ionic cloud of the gegenions. At higher salt concentrations

TABLE 8

*Effect of added electrolytes upon critical micelle concentration of potassium laurate*

MOLARITY OF SALT	C.M.C. ( $\times 10^3$ )	$\frac{\text{C.M.C. (PURE SOAP)}}{\text{C.M.C. (WITH SALT)}}$	ACTIVITY PRODUCT ( $\times 10^3$ )
Potassium chloride			
	<i>moles per liter</i>		
0	2.55		
0.0252	1.59	1.60	0.40
0.0670	1.19	2.14	0.79
0.1005	1.02	2.50	1.02
0.2124	0.71	3.60	1.51
0.3825	0.48	5.32	1.83
0.5014	0.41	6.22	2.02
Potassium bromide			
0.0265	1.55	1.64	0.25
0.1735	0.79	4.04	1.37
Potassium iodide			
0.0166	1.81	1.41	0.30
0.2615	0.63	4.04	2.54
Potassium nitrate			
0.0306	1.54	1.65	0.47
0.1380	0.88	2.90	1.21
0.3331	0.53	4.81	1.70
Potassium sulfate			
0.0188	1.41	1.81	0.53
0.0525	1.03	2.47	1.13
0.1375	0.59	4.33	1.62
Potassium pyrophosphate			
0.0187	0.88	2.36	0.66
0.0507	0.69	3.70	1.39
0.0742	0.53	4.80	1.66

the typical salting-out effect would occur, with crystallization of the soap taking place. This would probably involve a fairly definite and somewhat orderly aggregation of micelles.

When the above data are plotted as in figure 5, it can be seen that the decrease in C.M.C. of potassium laurate, an anionic soap, is affected only by the equivalent

concentration of the added electrolyte. The use of  $\text{Br}^-$ ,  $\text{I}^-$ , or  $\text{NO}_3^-$  in place of  $\text{Cl}^-$  has little or no measurable effect on the change in C.M.C. These results, although the actual values are different from those determined by dye titration, are in agreement with previous findings (2). The data showing the effect of the addition of potassium sulfate and potassium pyrophosphate are included in table 8 and these C.M.C. values are shown to fall on the curve in figure 5.

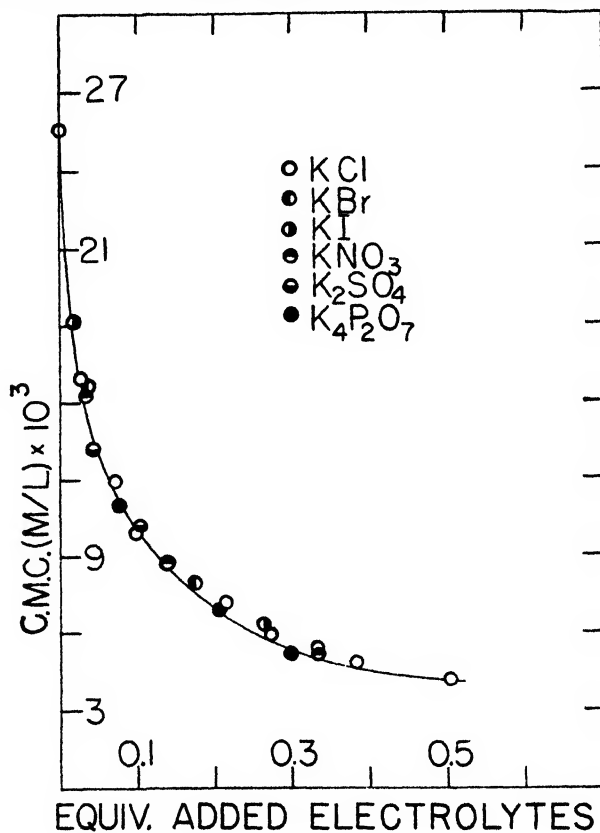


FIG. 5. Change in critical micelle concentration of potassium laurate in the presence of added electrolytes (25°C.).

It is evident from the above that the activity product concept cannot fit the data, and that the concept advanced by Corrin and Harkins is probably correct. Data in table 8 indicate that the activity product increases with increasing equivalent concentration of additive.

#### SOAP MIXTURES

Recently a preliminary report has shown the change in C.M.C. in the case of soap mixtures, as determined by spectral changes in dye solutions (13). These preliminary results indicated that over a certain mole fraction range the soap with the higher C.M.C. acted like a salt, depressing the C.M.C. of the other soap.



Corresponding changes in refraction could be used to determine additional properties of these mixed micelles.

It was necessary, in order to obtain C.M.C. from the intersection of two lines of refractive index *vs.* concentration, to have a constant mole ratio (moles of one soap/total moles of soap in mixture) for each series. Dilutions were made then, by weight, from stock solutions having definite mole ratios. The data in table 9 and figure 6 are the C.M.C. values obtained by the above method for various soap mixtures. The curves obtained are similar to those obtained by the spectral dye method, except for a vertical displacement of the

TABLE 9  
*Critical micelle concentrations of soap mixtures*

MOLE FRACTION $\text{KC}_{14}$	C.M.C. OF MIXTURE	$\frac{\text{C.M.C. (MIXTURE)}}{\text{C.M.C. (KC}_{14})}$
Potassium myristate + potassium laurate		
0	0.0255	3.86
0.152	0.014	2.12
0.301	0.011	1.67
0.452	0.010	1.52
0.645	0.0078	1.18
1.0	0.0066	1.0
Potassium myristate + potassium caprate		
0	0.099	15.63
0.110	0.052	7.88
0.305	0.015	2.27
0.450	0.012	1.82
1.0	0.0066	1.0
Potassium myristate + sodium lauryl sulfate		
0	0.0058	0.88
0.380	0.0064	0.97
0.645	0.0062	0.94
1.0	0.0066	1.0

curves, which can be explained by the differences found in the C.M.C. of the pure soaps due to the method used. The spectral dye values were found in all cases to be smaller than those determined by refraction or by conductivity as has been shown previously (16).

The data in figure 6 indicate that the largest change in C.M.C. occurs when there is the largest difference in the C.M.C. of the pure soaps. At all times the C.M.C. of the mixture lies between those of the pure soaps. This is further exemplified in the case of mixtures of potassium myristate and sodium dodecyl sulfate, which have about the same initial C.M.C. There is, as can be seen in figure 6, practically no change in C.M.C. upon the mixing of these two soaps.

The difference in the tendency of pure soaps to form micelles will control the micelle formation of their mixtures. The rate of decrease in C.M.C. of the mixture will be largest at low mole fractions of the soap with the lower C.M.C.; the greater the difference in the C.M.C. of the pure soaps, the greater will be the effect on the more soluble (higher C.M.C.) soap.

The C.M.C. of these mixtures would correspond to the C.M.C. of the mixture of sodium dodecyl sulfonate and calcium dodecyl sulfonate. The latter C.M.C.

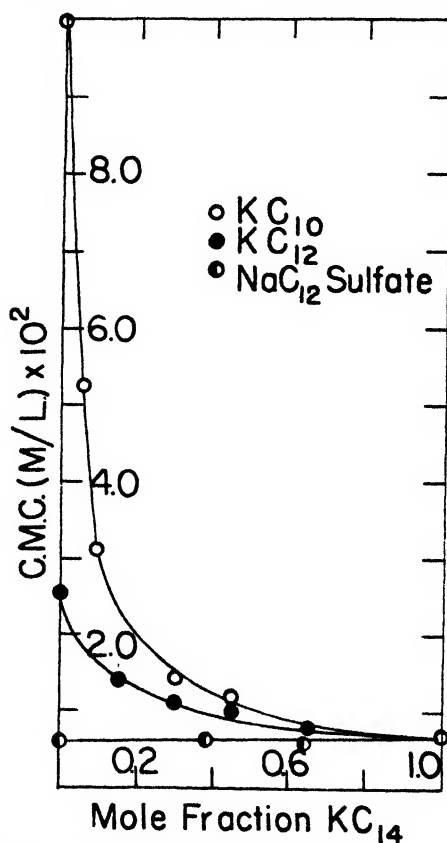


FIG. 6. Critical micelle concentrations of mixtures of potassium myristate and other soaps (25°C.).

value could be obtained, as has been shown in the case of soap-hydrocarbon mixtures (10), from the minimum of the solubility curve of the calcium soap in sodium dodecyl sulfonate. This latter effect has been shown to be one of a number of solubilization types in which solubilization involves the formation of mixed aggregates (18). From this point of view, it is obvious that at concentrations above the C. M.C. solubilization is occurring in which the less soluble soap is being solubilized by the more soluble one.

#### SUMMARY

1. Refractive indices of dilute soap solutions are characterized by two straight lines which intersect at the critical micelle concentration (C.M.C.).

2. The critical micelle concentration of soap solutions is seen to increase with temperature. There was little increase over the range 20–40°C., but a marked increase occurred above 40°C.

3. A relationship is presented which shows that the critical micelle concentration of a member of a series can be determined if the values of other members of the same series are known. The critical micelle concentration is a logarithmic function of the number of carbon atoms in the hydrocarbon chain.

4. The addition of electrolytes to soap solutions decreases the critical micelle concentration but this decrease does not follow the mass action law. The addition of potassium chloride to potassium laurate decreases the critical micelle concentration to less than 15 per cent of the original value.

5. Soap mixtures have critical micelle concentration values which are intermediate between the original values. Small mole ratios of the less soluble soap will show the largest changes in critical micelle concentration of the mixtures. In considering soap mixtures, the difference in the tendency of different soaps to form micelles controls the micelle formation of their mixtures.

#### REFERENCES

- (1) BURY, C. R., AND PARRY, G. A.: *J. Chem. Soc.* **1935**, 626.
- (2) CORBIN, M. L., AND HARKINS, W. D.: *J. Am. Chem. Soc.* **69**, 683 (1947).
- (3) CORBIN, M. L., KLEVENS, H. B., AND HARKINS, W. D.: *J. Chem. Phys.* **14**, 480 (1946).
- (4) EK WALL, P.: *Z. physik. Chem.* **A161**, 195 (1932); *Kolloid-Z.* **101**, 135 (1942).
- (5) GEFFCKEN, W., AND KRUIS, A.: *Z. physik. Chem.* **B23**, 175 (1933).
- (6) HARTLEY, G. S.: *Trans. Faraday Soc.* **30**, 444 (1934).
- (7) HARTLEY, G. S.: *Aqueous Solutions of Paraffin-chain Salts*. Hermann et Cie, Paris (1936).
- (8) HARTLEY, G. S.: *J. Chem. Soc.* **1938**, 1968.
- (9) HARTLEY, G. S., AND RUNNICLES, D. F.: *Proc. Roy. Soc. (London)* **A168**, 420 (1938).
- (10) HELLER, W., AND KLEVENS, H. B.: *J. Chem. Phys.* **14**, 567 (1946).
- (11) HESS, K., PHILIPPOFF, W., AND KIESSIG, H.: *Kolloid-Z.* **88**, 40 (1939).
- (12) KLEVENS, H. B.: *J. Chem. Phys.* **14**, 567 (1946).
- (13) KLEVENS, H. B.: *J. Chem. Phys.* **14**, 742 (1946).
- (14) KLEVENS, H. B.: Paper presented before the Division of Colloid Chemistry at the 110th Meeting of the American Chemical Society, which was held in Chicago, Illinois, September 9–13, 1946.
- (15) KLEVENS, H. B.: *J. Colloid Sci.* **2**, 301 (1947).
- (16) KLEVENS, H. B.: *J. Phys. Colloid Chem.* **51**, 1143 (1947).
- (17) KLEVENS, H. B.: *J. Am. Chem. Soc.* **70** (1948).
- (18) KLEVENS, H. B.: Paper presented before the Division of Colloid Chemistry at the 112th Meeting of the American Chemical Society, which was held in New York City, September 15–19, 1947.
- (19) KOLTHOFF, I. M., AND JOHNSON, W. F.: *J. Phys. Chem.* **50**, 440 (1946).
- (20) LINGAFELTER, E. C., WHEELER, O. L., AND TARTAR, H. V.: *J. Am. Chem. Soc.* **68**, 1490 (1946).
- (21) MCBAIN, J. W.: *Advances in Colloid Science*. Interscience Publishers, Inc., New York (1942).
- (22) MURRAY, R. C.: *Trans. Faraday Soc.* **31**, 199 (1935).
- (23) POWNEY, J., AND ADDISON, C. C.: *Trans. Faraday Soc.* **33**, 1243 (1937); **34**, 372, 625 (1938).
- (24) RALSTON, A. W., AND HOERR, C. W.: *J. Am. Chem. Soc.* **64**, 772 (1942).
- (25) SCOTT, A. B., AND TARTAR, H. V.: *J. Am. Chem. Soc.* **65**, 692 (1943).

- (26) SHEPPARD, S. E., AND GEDDES, A. L.: *J. Chem. Phys.* **13**, 63 (1945).
- (27) STAUFF, J.: *Z. physik. Chem.* **A183**, 55 (1938).
- (28) TARTAR, H. V., AND CADLE, R. D.: *J. Phys. Chem.* **43**, 1173 (1939).
- (29) WRIGHT, K. A., AND TARTAR, H. V.: *J. Am. Chem. Soc.* **61**, 544 (1939).
- (30) WRIGHT, K. A., ABBOTT, A. D., SIVERTZ, V., AND TARTAR, H. V.: *J. Am. Chem. Soc.* **61**, 549 (1939).

## ELECTRICAL CONDUCTIVITY OF CRYSTALLINE AND LIQUID-CRYSTALLINE SOAP-WATER SYSTEMS<sup>1</sup>

R. D. VOLD AND M. J. HELDMAN<sup>2</sup>

*Department of Chemistry, University of Southern California, Los Angeles 7, California*

*Received August 25, 1947*

The present study was undertaken with a twofold objective: first, to determine phase boundaries in soap systems in regions of composition and temperature where other methods have failed, and second, to learn more about the nature of the various phases and the changes occurring at the observed transitions. Phase changes can be deduced from changes in slope of the resistance-temperature curves, while the absolute values of the conductance, both A.C. and D.C., and their dependence on temperature and frequency help to distinguish between dipole oscillation, surface conductivity, and ionic or micellar migration as the mechanism of the process. In some instances these data can also be used to deduce possible internal structures of the different phases.

Preliminary experiments were carried out with anhydrous sodium palmitate. Systems of anhydrous and hydrous sodium stearate up to 12.8 weight per cent water were then investigated with varying thermal and pressure treatment before and during measurement. Specific conductances of two of the liquid-crystalline phases—soapboiler's neat and middle soap—were also determined.

Previous attempts to study the electrical properties of solid and semisolid soap systems have been few and relatively unsuccessful. Fischer and Hooker (9) determined the change in conductivity resulting from what we now know to be the separation of solid soap from solution, although they believed that it was due to inversion of an emulsion or solution. Bhatnagar and Prasad (2) studied the conductivity of "molten" alkali metal soaps at 182–207°C., but did not establish sufficiently the purity and moisture content of their samples, nor were the questions of adequate electrode contact and possible chemical decomposition carefully considered. In the present investigation great pains were taken to

<sup>1</sup> Presented at the Twenty-first National Colloid Symposium, which was held under the auspices of the Division of Colloid Chemistry of the American Chemical Society at Palo Alto, California, June 18–20, 1947.

<sup>2</sup> Present address: Department of Chemistry, East Los Angeles Junior College, Los Angeles, California.

establish a valid experimental technique, and it was shown by comparison with previous literature that sharp changes in the slope of the resistance-temperature curves could be attributed to phase changes in the system.

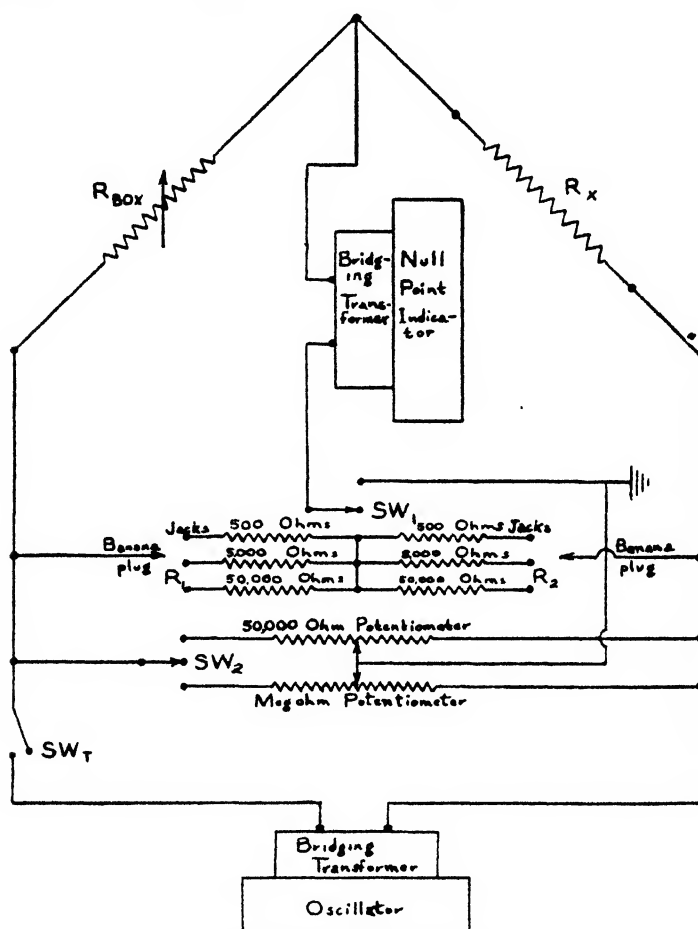


FIG. 1. Schematic diagram of the bridge circuit; the symbols are described in the text

#### APPARATUS AND MATERIALS

##### *Conductivity bridge*

Conductivities were determined with a Wheatstone bridge which was constructed largely from ordinary radio parts<sup>3</sup> and is shown schematically in figure 1. The potential source for the bridge was an audio-frequency oscillator with a range of 20-20,000 cycles, giving a pure wave form and having no frequency

<sup>3</sup> Full details of circuit diagram and component parts can be found in the doctoral dissertation of M. J. Heldman, which is on file in the Library of the University of Southern California. The oscillator constructed was similar to model 200B of the Hewlett Packard Co., Palo Alto, California, an instrument now commercially available, but not purchasable at the time when this investigation was commenced.

drift after a half-hour of operation. An electronic null-point indicator using a "magic eye" tube was constructed, somewhat modified from a previously described instrument (11, 13). A modified Wagner shield (12), made of radio volume controls, was incorporated as shown in figure 1.

Resistance arms  $R_1$  and  $R_2$  were made of carbon resistors and values of the ratio, needed in calculations, determined independently of the absolute values at frequent intervals so as to eliminate error due to change in resistance with time. The observed drift was only a few per cent per year.  $R_{\text{box}}$  consisted of a combination of a 9999-ohm 4-decade Leeds & Northrup box and a 2-decade 990,000-ohm box made partly of non-inductive resistors and partly of inductive 10-watt 50,000-ohm resistors. These were calibrated against known resistances on a d.c. bridge.

Within the range of 100–100,000 ohms and 100–5000 cycles the precision of measurement was a few tenths of a per cent. Below 100 ohms the reproducibility was within a few ohms, and was also poorer above 100,000 ohms, although still within a few per cent even at a megohm.

### *Conductivity cells*

Most of the measurements were made in cells constructed of 7-mm. Corning glass tubing 705AJ or 772, into which were sealed respectively Kovar or tungsten wires of 0.05 cm. diameter. The electrodes were sealed parallel to each other through the bottom of the tube, about 3–6 mm. apart, and protruding into the tube from 3 to 9 mm. Since the tubes were originally about 15 cm. long, they could be opened and resealed repeatedly without difficulty. The wires were carefully cleaned (22) before use, and no visible indication of electrode corrosion or sample decomposition was ever detected. Cell constants were calculated from measured resistances at 25°C. of solutions of acetic acid of known concentration, using standard values (15) for the equivalent conductivity.

During measurement several cells were suspended vertically in a small air oven, wired with one common electrode with the additional lead attached to a terminal strip, thus permitting easy substitution of any cell as the unknown resistance in the bridge. Temperature was determined by a calibrated thermometer placed in the midst of the group of cells, previous tests having shown no thermal gradients in the oven greater than one or two degrees over the range from 20° to 300°C.

For work at temperatures below 100°C. and with drier samples it was necessary to use a different cell in order to maintain electrode contact and reduce the resistance to measurable values. The cell used is shown in figure 2, and consisted essentially of a hollow cylinder serving as one electrode, the other electrode being a plunger which was maintained in contact with the sample by means of pressure from a Carver press. The samples used were generally under 3 mm. in thickness, and the soap from which they were formed was not placed in the cell until the metal surfaces had been thoroughly cleaned, rinsed with alcohol and ether, and dried at 105°C. The cell was mounted in a stainless-steel can between the jaws of a Carver press, and maintained at temperature by means of dibutyl

phthalate circulated by a small centrifugal pump from a 2-gallon thermostat. Temperature control within  $0.5^{\circ}$  was achieved at temperatures from  $20^{\circ}$  to  $100^{\circ}\text{C.}$ , although supplementary cooling by tap water circulating through a copper coil was necessary at the lower temperatures.

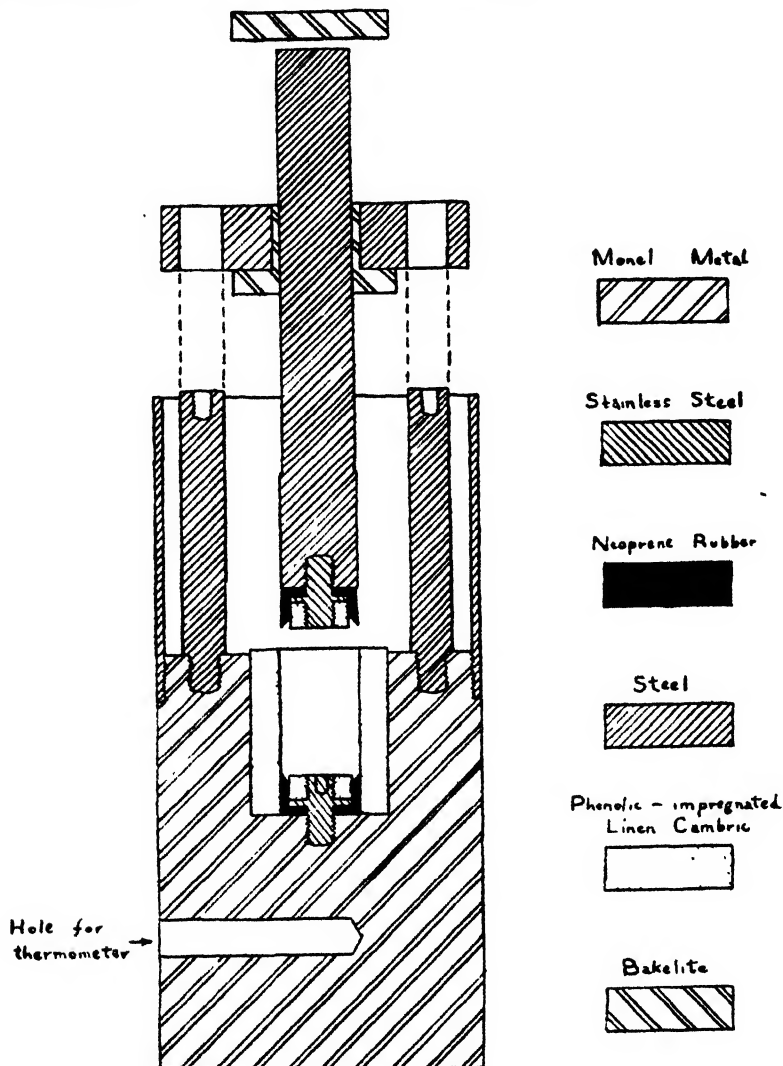


FIG. 2. The plunger cell. The diameter of the stainless-steel cylinder is 2.5 in.; the rest of the cell is drawn to scale.

### Materials

The sodium palmitate used was the identical preparation employed in an earlier investigation (29). The sodium stearate was made by neutralization of an alcoholic solution of an unusually pure stearic acid (20) with carbonate-free, alcoholic sodium hydroxide with exclusion of carbon dioxide, special care being

taken to avoid any excess of alkali which would have resulted in an electrolytic impurity. Great care was taken during the drying of the wet gel to avoid scorching and decomposition (19). The best-quality soap made in this way, given the laboratory designation "sodium stearate A," was used throughout this investigation.

#### TECHNIQUE OF MEASUREMENT AND EXPERIMENTAL RESULTS

Anhydrous sodium palmitate, sodium stearate systems with 0–12.8 per cent water, and two much more dilute samples were studied in the glass cells. Powdered soap, previously dried at 105°C., was weighed into the cell together with the requisite amount of water with not more than 2 min. exposure to air. Homogenization was achieved by heating in the oven to about 300°C. and inverting fifteen or twenty times. After cooling, the tube was opened at the top and a glass rod inserted which filled most of the vapor space, thus minimizing change in sample composition at elevated temperatures. The cell was then resealed, reheated to 300°C., and cooled in the oven to about 50 to 60°C. over the course of an hour.

With sodium palmitate, cell resistances were measured after enough time at each temperature to reach a constant value, only a few minutes being required. Values for sodium stearate were determined on continuous heating at about 1° per 3–4 min. That this procedure gives valid results was shown by the good agreement in transition temperatures obtained from curves determined at different rates of heating, although high results were found if the rate exceeded 1° per 2 min. At least duplicate runs were made over the temperature region where transitions were expected on the basis of an initial preliminary run.

The data obtained are shown in figures 3–15, the vertical arrows marking the points of phase transitions. Runs beginning at elevated temperatures were usually started after the sample had been held at the temperature in question overnight. Where two numbers are given on the graphs, the first is the transition temperature and the second is the identification number under which the given transition appears in the summary of table 2.

It is evident that the specific resistance of a given sample at a given temperature often varied considerably from run to run, but that the lack of absolute reproducibility does not change the temperatures at which breaks appear in the resistance-temperature curves. The lack of absolute reproducibility is not surprising in view of the possibility of variable electrode contact, of the presence of submicroscopic cracks in the more solid phases, of lack of equilibrium due to the constantly changing temperature, or of slight corrosion of the electrodes (although none was observed). This irreproducibility causes no serious difficulty in the present work, where the main emphasis is on the temperatures of changes in slope, and in cases where the temperature coefficient of conductivity is calculated, the variations in absolute value are negligible contrasted with the change resulting from a change in temperature.

That the changes in slope of the resistance-temperature curves may be attributed to phase changes occurring in the sample is shown by the good agreement



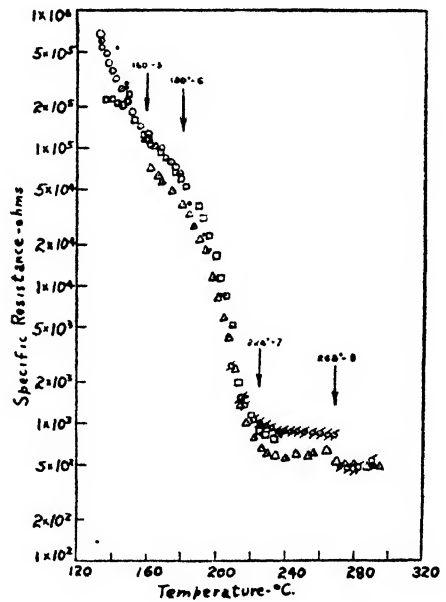
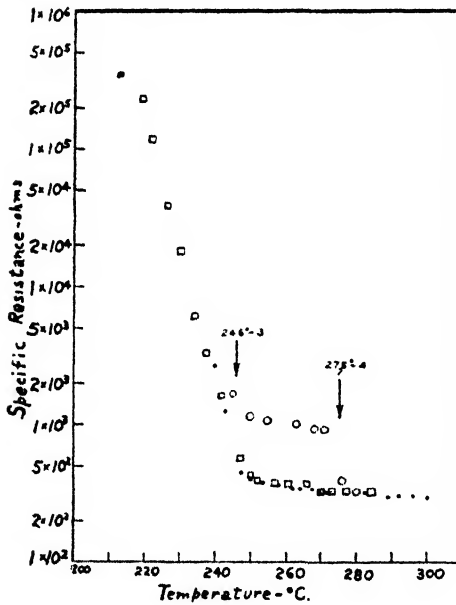
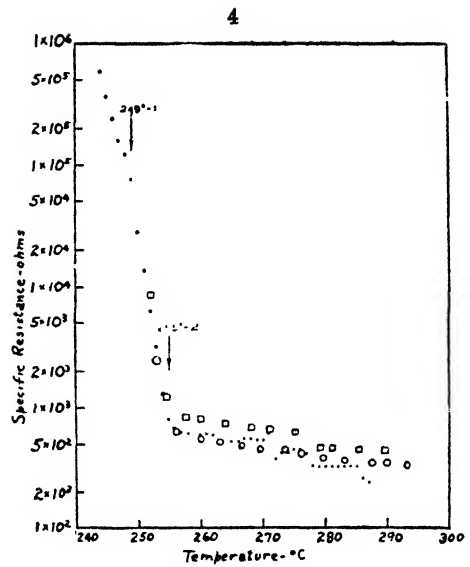
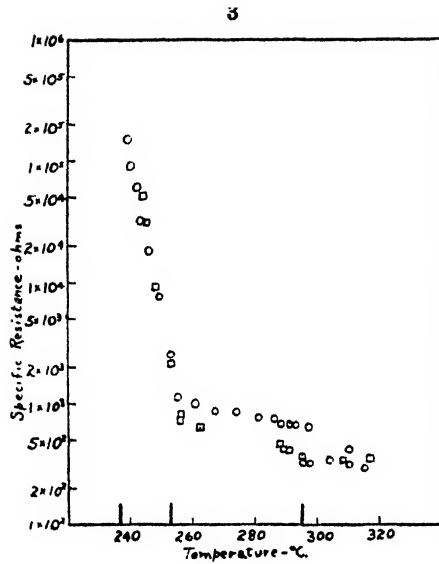


FIG. 3. Resistance-temperature curve for sodium palmitate containing 0.0 per cent water, determined at about 1000 cycles.  $\circ$ , measurements obtained when heated;  $\square$ , measurements obtained when cooled. The vertical bars along the abscissa are temperatures of previously reported phase transitions (25).

FIG. 4. Specific resistances of sodium stearate containing 0.0 per cent water, determined at 960 cycles.  $\square$ , first run;  $\circ$ , second run;  $\bullet$ , third run.

FIG. 5. Specific resistances of sodium stearate containing 0.5 per cent water, determined at 420 cycles.  $\square$ , first run (cooling);  $\circ$ , second run;  $\bullet$ , third run (cooling). Some tabulated points were omitted for the sake of clarity in graphing.

FIG. 6. Specific resistances of sodium stearate containing 1.0 per cent water, determined at 960 cycles.  $\odot$ , first run;  $\triangle$ , second run;  $\square$ , third run;  $\circ$ , fourth run;  $\bullet$ , fifth run. Some tabulated points were omitted for the sake of clarity in graphing.

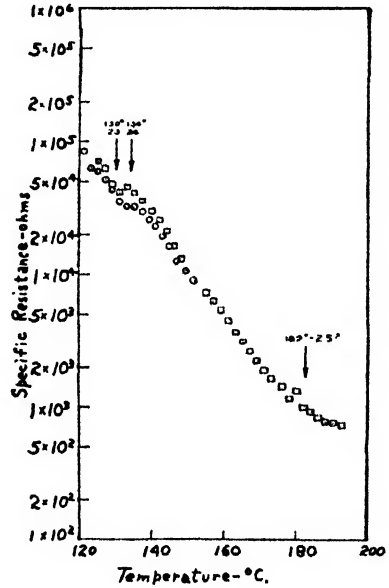
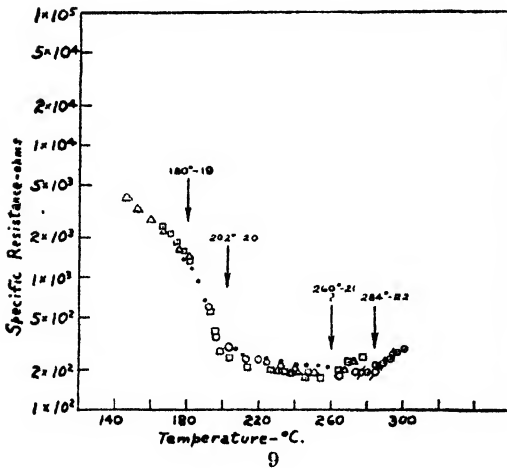
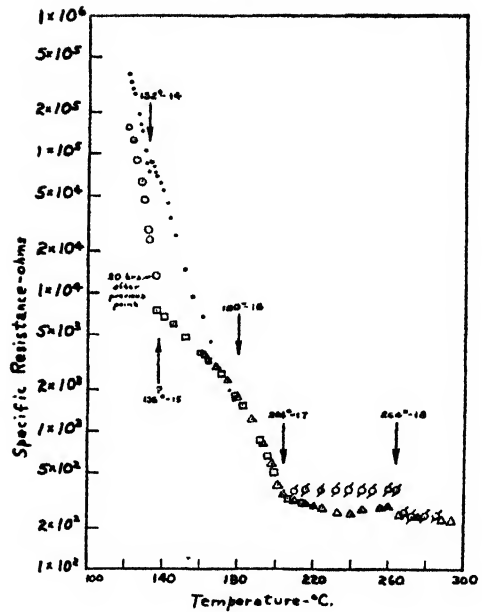
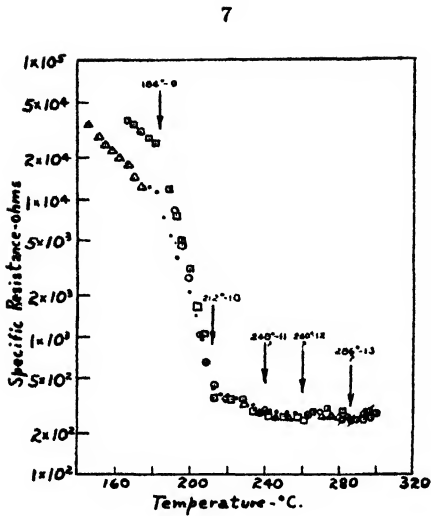


FIG. 7. Specific resistances of sodium stearate containing 2.0 per cent water, determined at 420 cycles.  $\square$ , first run (cooling);  $\triangle$ , second run;  $\odot$ , third run (cooling);  $\bullet$ , fourth run;  $\oslash$ , fifth run. Some tabulated points were omitted for the sake of clarity in graphing.

FIG. 8. Specific resistances of sodium stearate containing 2.4 per cent water, determined at 420 cycles.  $\oslash$ , first run;  $\triangle$ , second run;  $\square$ , third run;  $\odot$ , fourth run;  $\bullet$ , fifth run. Some tabulated points were omitted for the sake of clarity in graphing.

FIG. 9. Specific resistances of sodium stearate containing 2.5 per cent water, determined at 420 cycles.  $\square$ , first run (cooling);  $\triangle$ , second run;  $\odot$ , third run (cooling);  $\bullet$ , fourth run;  $\oslash$ , fifth run. Some tabulated points were omitted for the sake of clarity in graphing.

FIG. 10. Specific resistances of sodium stearate containing 3.3 per cent water, determined at 960 cycles.  $\square$ , first run;  $\odot$ , second run.

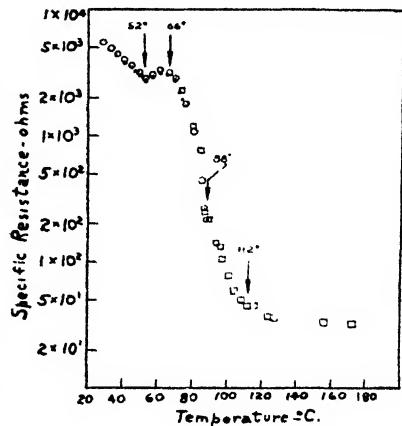
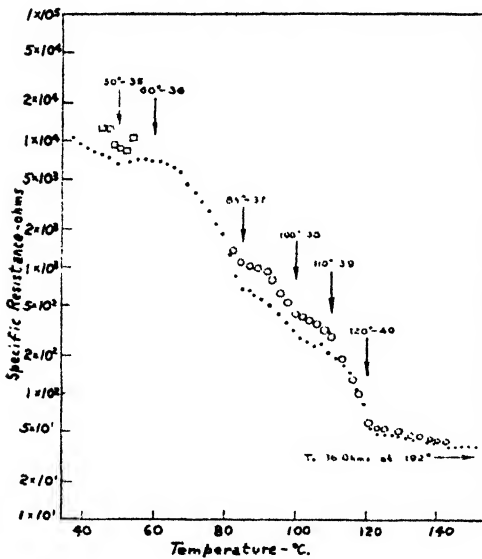
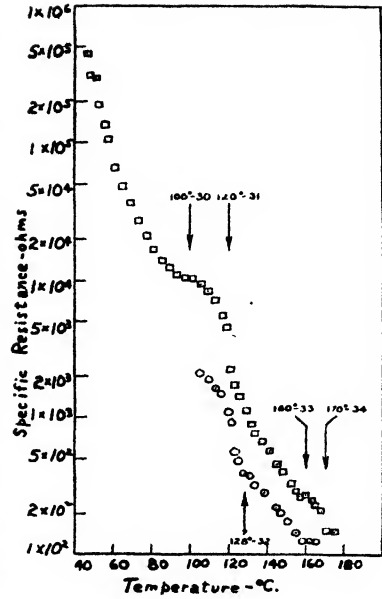
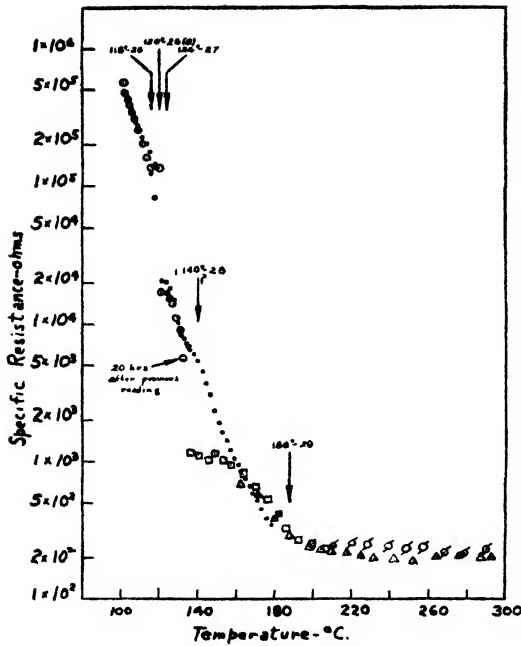


FIG. 11. Specific resistances of sodium stearate containing 4.4 per cent water, determined at 960 cycles.  $\square$ , first run;  $\triangle$ , second run;  $\square$ , third run;  $\circ$ , fourth run;  $\bullet$ , fifth run. Some tabulated points were omitted for the sake of clarity in graphing.

FIG. 12. Specific resistances of sodium stearate containing 6.5 per cent water, determined at 960 cycles.  $\square$ , first run;  $\circ$ , second run. Some tabulated points were omitted for the sake of clarity in graphing.

FIG. 13. Specific resistances of sodium stearate containing 12.8 per cent water, determined at 960 cycles.  $\square$ , first run;  $\circ$ , second run;  $\bullet$ , third run. Some tabulated points were omitted for the sake of clarity in graphing.

FIG. 14. Specific resistances of sodium stearate containing 28.7 per cent water, determined at 960 cycles.  $\square$ , first run;  $\circ$ , second run;  $\bullet$ , third run. Some tabulated points were omitted for the sake of clarity in graphing.

between the temperature of these breaks and the established transition temperatures of known systems. Thus the curve for anhydrous sodium palmitate shows marked changes at 256° and 295°C., compared with literature values of 253° and 295°C. (29).

The data obtained with the plunger cell are summarized in table 1, which gives the temperatures of changes of slope in the resistance-temperature curves on samples prepared in the same way as those used in the glass cells. Great difficulties were encountered experimentally because of lack of attainment of constant value for the resistance as the pressure was varied, and because of changes of over-all composition of samples, not only during heating but also on application of pressure. Resistances usually but not always decreased on increasing the pressure, and sometimes increased and sometimes decreased when the

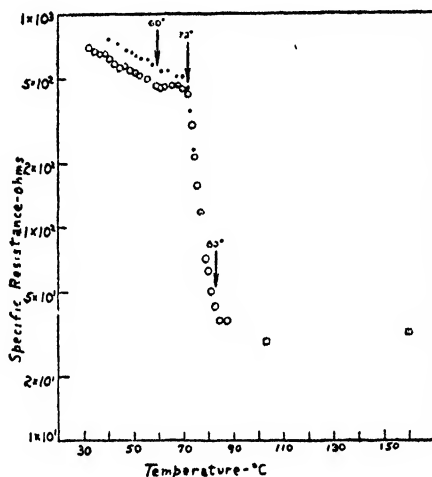


Fig. 15. Specific resistances of sodium stearate containing 69.3 per cent water, determined at 960 cycles. ○, first run; ●, second run; □, observations made with good contact at higher temperatures.

system was allowed to stand at constant pressure. Moreover, when the pressure was released and then reapplied, a lower resistance was usually obtained than the initial value. During a run drier samples often absorbed water to a final value around 1 weight per cent, while wetter samples usually lost water to a final composition around 3.5 per cent. Merely keeping a sample at a pressure of 5000 lb./in.<sup>2</sup> for 1 hr. at room temperature lowered the water content from 9.4 to 4.8 per cent.

In order to obtain comparable data in a single run the following procedure was always followed. The sample was placed in the press at the lowest temperature at which the resistance was measurable and at a pressure (usually a few thousand pounds per square inch) at which a constant resistance measurement was obtained. Thereafter no adjustment of pressure was made, even though it

decreased somewhat owing to deformation of gaskets, etc. The temperature was then raised as rapidly as possible in 2° steps and the resistance measured after 20 min. standing at each temperature. Samples were analyzed for water content before and after each run by drying to constant weight at 105°C. In this way fairly reproducible temperatures of slope changes were obtained, although duplicate curves differed considerably in absolute value and occasionally in details of slope.

TABLE 1

*Summary of conductimetric results with sodium stearate-water systems in plunger cells*

WATER CONTENT		TEMPERATURES OF "BREAKS" IN THE "LRT" CURVES	ADDITIONAL OBSERVATIONS
Before run	After run		
<i>per cent</i>	<i>per cent</i>	°C.	
0.44	0.74	77, 83, 89	Definite flattening off of the curve at 95°C.
0.48	1.06	52	The "break" noted is doubtful
0.98	1.10	56, 66, 72	The "break" at 56°C. is a discontinuous† one
—	0.93	51, 73	
3.47	3.40	52	The "break" noted is discontinuous†
3.60	3.73	52	The "break" noted is discontinuous†
3.50	3.31	48, 52	The two temperatures noted represent the beginning and end of a "hump" in the curve
13.2	4.0	51, 69	These samples had long and varied, but different, pressure histories before the runs
13.2	3.6	50, 71	

† That is, there are discontinuities in the LRT curves at these temperatures.

\* Logarithm of resistance vs. temperature.

## DISCUSSION

### *Phase boundaries*

Combination of the new conductivity data with existing information in the literature (18, 24, 26) has made possible rather definitive location of the boundaries of the high-temperature phases of sodium stearate in the binary system, as shown in figure 16. A brief résumé will suffice to show how the curves were drawn from the existing data.

The eutectoid between subneat, superwaxy, and soapboiler's neat soap is determined by points 6, 9, 16, 19, 25, and 29, which occur at constant temperature

TABLE 2

*Conductimetric changes occurring in sodium stearate systems of low water content*  
(The numbers in parentheses refer to points on the LRT curves of figures 4 to 13)

COMPOSITION OF SAMPLE AND FREQUENCY OF MEASUREMENT TYPE OF CHANGE OF SLOPE OF LRT CURVE	SAMPLE A, 0.0% WATER, 960 CYCLES	SAMPLE B, 0.5% WATER, 420 CYCLES	SAMPLE C, 1.0% WATER, 960 CYCLES	SAMPLE D, 2.0% WATER, 960 CYCLES	SAMPLE E, 2.4% WATER, 960 CYCLES	SAMPLE F, 2.5% WATER, 420 CYCLES	SAMPLE H, 3.9% WATER, 960 CYCLES	SAMPLE I, 4.4% WATER, 960 CYCLES	SAMPLE J, 6.5% WATER, 960 CYCLES	SAMPLE K, 12.8% WATER, 960 CYCLES	IDENTIFICATION ON FIGURE 16
Most marked change: change in LRT curve from large slope to almost flat	255° (2)	246° (3)	224° (7)	212° (10)	204° (17)	202° (20)	187° (25?)	188° (29)	(160° (33)) (170° (34))	120° (40)	■
Changes occurring at temperatures higher than the most marked change above	278° (2-a)	275° (4?)	268° (8)	240° (11?) 260° (12?) 286° (13?)	264° (18)	260° (21?) 284° (22)					●
Inflection of LRT curve previous to most marked change above	249° (1?)		180° (6)	184° (9)	180° (16)	180° (19?)		140° (28?)			▲
Discontinuous changes or apparent anomalies such as increases of slope or "flats"					132° (14) 136° (15)		130° (23) 134° (24)	116° (26) 120° (26-a) 124° (27)	120° (31)	50° (35) 60° (36)	○
Other changes			160° (5)						128° (32?) 100° (30)	85° (37) 100° (38) 110° (39)	⊖

Literature values: references 18, 24, 26.

independent of composition. The composition of the eutectoid at about 3.5 per cent water is deduced by extrapolation of the right-hand boundary of the subneat field to the eutectoid temperature, confirmed by a difference in the nature of the change in the resistance-temperature curves at higher and lower compositions (*cf.* figures 9 and 10).

The upper boundary of the subneat field is marked by points 2, 3, 7, 10, 17, and 20, at all of which there is evidence for decrease in amount of a phase having a very large temperature coefficient of conductivity. The uppermost point on this boundary, 2, is in good agreement with the known transition temperature of subneat to neat soap.

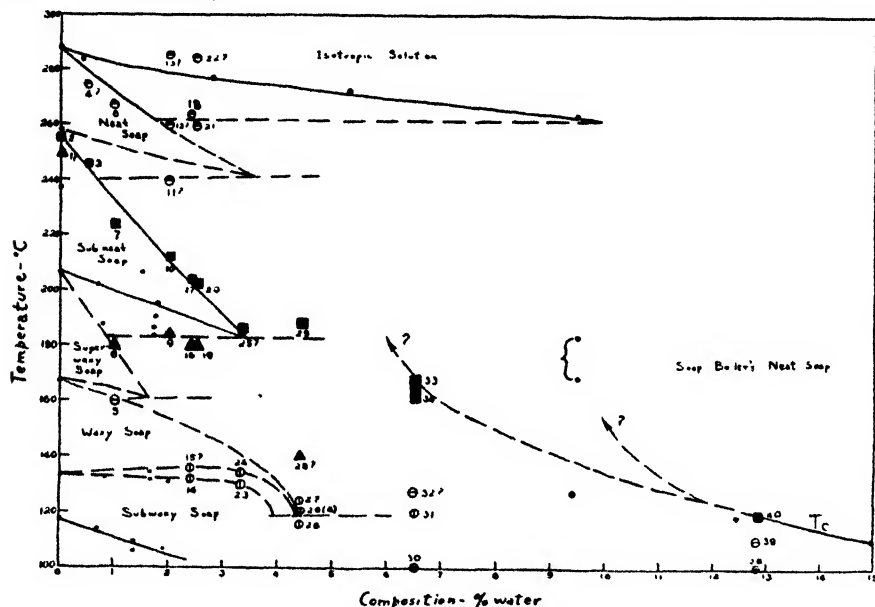


FIG. 16. Phase diagram of sodium stearate-water. ●, previously reported phase transitions (18, 24, 26). A full explanation of the meaning of other symbols is given in table 2.

The upper boundary of the neat field is established by points 4, 8, and 12, which define a curve which extrapolates to a composition containing about 3.7 per cent water at the somewhat less certain eutectoid temperature of about 240°C.

Points 13 and 22 agree reasonably well with the  $T_i$  curve determined visually (18). An eutectoid flat just above 260°C. is indicated by points 12, 18, and 21, in good agreement with the value of 262°C. postulated earlier (18) on the basis of the observed minimum in the  $T_i$  curve.

No direct conductimetric evidence was obtained for the eutectoid between superwaxy, waxy, and soapboiler's neat soap. However, consideration of the right-hand boundaries of the superwaxy and waxy phases shows that it must occur close to 160°C. Points 33 and 34, although at about this temperature, are marked by the same type of change in the resistance-temperature curve as is point 40, which was known to be on the boundary of the soapboiler's neat phase.

The high resistance of samples with less than 2 per cent water made measurement of resistance impossible for such systems in the region of the subwaxy-waxy transition. However, points 14, 15, 23, 24, 26, and 27 are in good agreement with calorimetric data (26), indicating little change in this transition temperature on addition of water, and establish the course of the waxy and subwaxy boundaries in the slightly more hydrous region. The eutectoid between waxy, subwaxy, and soapboiler's neat soap is set at about 116°C. by points 26 and 31.

The chief importance of these results is the demonstration that many of the anhydrous phases of sodium stearate can incorporate only very small amounts of water before undergoing structural rearrangement, as postulated elsewhere in this Journal (7), which results in the formation of a different phase. Thus, the conductimetric data, in agreement with calorimetric evidence (26), show that neat and subneat soap can incorporate only 4 and 3 per cent water, respectively, before breaking down to soapboiler's neat soap, whereas previously it had been supposed that 10 per cent water could be incorporated in the homogeneous phase. Similarly, the conductimetric data indicate that waxy soap cannot contain more than 4.5 per cent water nor exist as the equilibrium phase below 116°C., as contrasted with literature results, based on very meager vapor-pressure work (17), which show a tongue of waxy soap extending down to 100°C. at 15 per cent water.

In the case of the more dilute systems (figures 14 and 15) the resistance-temperature curve of the system containing 69.3 per cent water shows an abrupt change of slope at 83°C., agreeing within 3° with the literature value (18) for the completion of formation of middle soap. The corresponding temperature in the 28.7 per cent system for formation of soapboiler's neat soap was not accurately determined because of some difficulty with that sample at higher temperatures. In both these systems the curves showed changes indicative of phase changes occurring below  $T_c$ .

#### *Nature of the phase diagram*

The systems containing 12.8, 28.7, and 69.3 per cent water all show a similar feature in the resistance-temperature curve—a fairly steep fall of resistance with temperature, broken by a slight increase with the temperature, followed by a very rapid decrease of resistance with temperature—which certainly suggests that a similar series of phase changes occurs in all three systems. The temperatures of these changes in the three systems are respectively 50°, 52°, 60°C. and 60°, 66°, and 72°C. At first thought these changes might be thought to be related to the temperatures of initial formation of middle soap and soapboiler's neat soap. However, the eutectoids due to the coexistence of isotropic solution-curd-middle soap and isotropic solution-soapboiler's neat-curd phase occur at 76°C. and 82°C., respectively (18). Since there is no break in the resistance curves at these temperatures it can be concluded, in accord with other evidence (26, 28), that these eutectoids do not extend into the concentrated region. This certainly suggests the existence of homogeneous phases containing substantial amounts of water, as contrasted with the classical picture of a heterogeneous region with some one "curd" phase, containing only very little water, in equilibrium with isotropic solution.



The present data permit some choice to be made between the conflicting views of Buerger, Smith, *et al.* (4, 5) and Ferguson and coworkers (8) as to the nature of solid soap. From x-ray work on quenched samples Buerger and coworkers have shown that a given sample may exist at room temperature in a variety of crystalline forms, depending on the minimum temperature at which mechanical agitation occurred prior to undisturbed cooling. Even though the critical temperatures determined in this way for the formation of each phase do not necessarily correspond to equilibrium transition temperatures, it may well be that such samples will undergo transitions at these temperatures on reheating. Although detailed data have not been published for sodium stearate, it is stated that such a phase map shows two different crystalline forms, delta or alpha, which may be realized below  $T_c$ , the temperatures of agitation required to produce these forms being essentially independent of composition. The conductimetric data, although obtained on unagitated systems formed by spontaneous cooling and presumably giving the equilibrium temperatures of phase transitions, are in accord with the concept of two phase boundaries occurring between room temperature and the  $T_c$  curve, and at temperatures only slightly dependent on composition. A somewhat similar situation exists in the case of sodium oleate (27), where calorimetric evidence showed the existence of a transition occurring at constant temperature independent of composition from 15 to 75 per cent water in sodium oleate systems, formed by spontaneous cooling from whatever phase existed at higher temperatures.

This behavior differs from that which would be anticipated on the basis of Ferguson's concept (8), also based on x-ray examination of samples at room temperature, that a single phase—in this instance,  $\beta$ -sodium palmitate—itself containing very little water, exists over the whole composition range at room temperature in equilibrium with isotropic liquid. Ferguson also presents very persuasive evidence that some of the separate phases adduced by Buerger, which he believes to be stoichiometric hydrates, are in reality merely different members of a single solid-solution phase. Nevertheless, some such multiplicity of phases as proposed by Buerger, whether they be hydrates or solid solutions, seems to be necessary to explain the conductimetric, calorimetric, and rheological (14, 16) behavior of soap systems.

The results obtained with the plunger cell, although limited to temperatures usually below 80°C. and systems containing less than 4 per cent water, provide further insight into the reversibility of the genotypic (23) and alpha-beta (3, 26) transitions. Calorimetric work (26) in closed cells had shown that  $\alpha$ -sodium stearate, prepared by crystallization at room temperature, underwent a transition at 52°C. which was apparently irreversible on cooling, since duplicate runs on samples which had been heated above this temperature failed to show the transition. X-ray investigation (3) showed that this transition was due to decomposition of the hemihydrate (alpha) to a less hydrous form called beta, although there is no agreement as to whether beta is a stoichiometric hydrate or a solid-solution phase (3, 8). On heating the beta form in a sealed tube at 47°C. in the presence of a drop of water and cooling, it was found (3) that conversion to alpha had taken place. Despite the fact that the conductimetric samples had been

cooled from the melt above 300°C., all except that with 0.7 per cent water had an inflection in the resistance-temperature curve at 48–52°C., indicative of the presence of at least some alpha phase in the initial sample at room temperature.

This raises the interesting question as to whether alpha may not occur as a stable phase at room temperature in systems containing more water, and prepared by spontaneous cooling from soapboiler's neat or middle soap without agitation. Possibly the conductimetric transition at 50°, 52°, and 60°C. in the systems containing respectively 12.8, 28.7, and 69.3 per cent water is related to this phase change. According to the phase map (5)  $\alpha$ -sodium stearate should occur over most of the composition range at room temperature, provided the system has been formed on cooling the high-temperature phase with agitation below some temperature below  $T_c$ , followed by undisturbed cooling. Such an interpretation would again approach the classical view of the nature of the system at room temperature.

Although most of the present systems failed to show the genotypic transition at 69–73°C. on reheating after having been cooled from the isotropic melt, it did occur in those containing 0.9, 3.6, and 4.0 per cent water. Previous calorimetric work (26) had shown that beta formed by heating alpha underwent further transition to lambda at about 70°C. (the genotypic transition), but that this transition was generally missing once the sample had been heated into the subwaxy phase, this effect being attributed to difficulty of reversibility of the lambda-supercurd transition. In view of the conductimetric results it must be concluded that under some circumstances lambda can be formed on cooling supercurd even though gamma, which does not give the genotypic transition, usually results from such treatment.

Obviously not only the maximum temperature to which a sample has been heated, but also the rate of cooling, the relative humidity during cooling, and the extent and temperature of any mechanical agitation during cooling, will be important determinants of which of several possible phases is actually present at room temperature.

#### *Structural implications*

If the conductivity is due to dipole rotation or oscillation rather than to migration of ions, it is possible (10) to calculate a "relaxation time" for re-orientation of the particles from the frequency range in which the conductivity falls off markedly, and thus sometimes to determine the size and shape of the particle. Table 3 shows the conductivity of certain of the soap phases as a function of frequency. No systematic variation of resistance with frequency was found in the case of mixtures of superwaxy and soapboiler's neat soap, nor with subneat soap nor the isotropic solution.

Unfortunately, the range of frequencies available (420–7800 cycles) is presumably too low to detect any such effect, particularly since it is known (6) that frequencies of 0.8–4.0 megacycles are required to show anomalous dispersion in the case of proteins of molecular weight around 70,000. Since the aggregates in the liquid-crystalline soap phases are of the order of the wave length of visible

light in size, they would have similar particle weights and might be expected to have relaxation times of similar magnitude. However, it seems unlikely that dipole rotation can account for the conductivities observed in the present work, since the values obtained (specific conductance *ca.*  $10^{-6}$  ohms $^{-1}$ ) are much greater than those usually observed (*ca.*  $10^{-10}$  ohms $^{-1}$ ) in cases of dipole rotation (1). Moreover, a few exploratory measurements of D.C. resistance gave results substantially the same as the A.C. values.

Since the conductivity is sufficiently high to suggest ionic migration as the probable mechanism, it becomes of interest to speculate as to whether either the

TABLE 3  
*Frequency dependence of conductivity of sodium stearate-water samples*

TEMPERATURE	COMPOSITION, PER CENT WATER	SPECIFIC RESISTANCE	FREQUENCY
°C.		ohms	cycles
168.5	2.0	14,000	420
168.5	2.0	13,800	3500
168.5	2.0	13,500	7800
168.5	2.5	2,050	420
168.5	2.5	2,100	3500
168.5	2.5	2,050	7800
214.0	2.0	325	420
214.0	2.0	325	3500
214.0	2.0	325	7800
214.0	2.0	250	420
214.0	2.0	255	3500
214.0	2.0	250	7800
240.5	0.5	78,000	420
240.5	0.5	78,000	3500
300.0	0.5	310	420
300.0	0.5	315	3500
300.0	0.5	315	7800

negative ion and negative aggregates or the positive ion or both contribute appreciably to the observed conductivity, and as to whether the medium in which they move is lattice-like or essentially liquid in nature. Presumably the main contribution is made by the sodium ion, since the strong van der Waals attraction along the length of the hydrocarbon chains tends to keep each negative ion parallel to its neighbors. That the sodium ion alone is responsible for the conductivity is assumed in the following discussion.

Examination of the values obtained shows that the conductivity of subneat soap, both anhydrous and containing small amounts of water, increases extremely rapidly with the temperature, while for neat soap the conductivities, though high,

increase much less rapidly. Interpretation of these results according to the theory of absolute reaction rates leads to some remarkable conclusions.

For the movement of ions on a lattice, the equation developed (1) by Eyring and Wynne-Jones can be used:

$$\kappa = \frac{N(Ze)^2 d^2}{h} e^{\Delta S^*} R e^{-\Delta H^*/RT}$$

Here  $\kappa$  is the specific conductance in absolute units,  $N$  is the number of ions per cubic centimeter,  $Ze$  is the charge on the ion,  $h$  is Planck's constant,  $d$  is the sepa-

TABLE 4  
*Energies and entropies of activation for conductivity in subneat and neat soap*

WATER	$\kappa$	$T$	$E$	$A$	$\Delta S^*$
Subneat soap					
<i>per cent</i>	<i>abs. ohms<sup>-1</sup> cm.<sup>-1</sup></i>	<i>°K.</i>	<i>cal. per mole</i>	<i>abs. ohms<sup>-1</sup> cm.<sup>-1</sup></i>	<i>cal./deg./mole</i>
0.0	7.7 × 10 <sup>-13</sup> 3.2 × 10 <sup>-14</sup> 1.67 × 10 <sup>-16</sup>	527 523 517	3.3 × 10 <sup>6</sup>	4 × 10 <sup>12.6</sup>	615
0.5	1.67 × 10 <sup>-12</sup> 5 × 10 <sup>-14</sup>	519 503	1.2 × 10 <sup>6</sup>	8 × 10 <sup>17</sup>	211
1.0	7.7 × 10 <sup>-13</sup> 1 × 10 <sup>-13</sup>	489 473	7.1 × 10 <sup>4</sup>	4 × 10 <sup>19</sup>	127
2.0	1.67 × 10 <sup>-12</sup> 1.4 × 10 <sup>-13</sup>	483 465	6.2 × 10 <sup>4</sup>	1 × 10 <sup>16</sup>	110
2.5	2.5 × 10 <sup>-12</sup> 9 × 10 <sup>-13</sup>	468 457	3.7 × 10 <sup>4</sup>	4 × 10 <sup>6</sup>	62
Neat soap					
0.0	1.85 × 10 <sup>-13</sup> 1.54 × 10 <sup>-13</sup>	538 528	1.1 × 10 <sup>4</sup>	3.6 × 10 <sup>-8</sup>	2.1
0.5	2.78 × 10 <sup>-13</sup> 2.63 × 10 <sup>-13</sup>	533 523	2.8 × 10 <sup>3</sup>	3.6 × 10 <sup>-11</sup>	Negative

ration of potential minima in the direction of motion (lattice points),  $\Delta S^*$  is the entropy increase in passing from the normal to the activated state, and  $\Delta H^*$  is the heat of activation, identified with the activation energy of the Arrhenius equation,  $K = Ae^{-E/RT}$ . Calculations of  $A$ ,  $E$ , and  $\Delta S^*$  for subneat and neat soap, based on this equation, are given in table 4. The number of ions per cubic centimeter is taken as  $2 \times 10^{21}$ , while  $d$  is assumed to be 4 Å., neither of these values being very critical for the conclusion to be drawn from the enormous values of  $\Delta S^*$  which result.

For subneat soap, the rapid variation in conductivity with temperature gives

rise to a very large calculated activation energy. Since, however, the conductivity itself is high, the temperature-independent factor  $A$ , containing the term  $e^{\Delta S^*/R}$ , is very large. The values are too large to render the basic picture—that of a semi-rigid lattice at all temperatures within the range of existence of the phase—at all reasonable. Qualitatively, the results may be interpreted by supposing that within the subneat soap phase, the structure is changing from lattice-like at lower temperatures to a condition of lesser regularity at higher temperatures, in which aggregates, still composed of an extensive array of parallel molecules, move freely in a matrix of less ordered structures. This would be the kind of transformation here occurring over a range 30–40°C. which ordinarily accompanies the melting of an ionic crystal at a single temperature, except that the residual order in neat soap extends over a larger number of molecules. Such a postulate might also account for the large discrepancy between the calorimetric and dilatometric values for the transition temperature between subneat and neat soap (25), since energy would be absorbed as soon as degradation of the lattice began while the structural rearrangement giving rise to the change in volume might not occur until the transformation was complete.

For neat soap, the calculated activation energy is smaller, and the  $A$  value correspondingly smaller. In consequence the value of  $\Delta S^*$  becomes much more sensitive to the assumptions made as to the distance between potential minima (lattice sites). Doscher and Vold (7) have suggested that the conductivity in this phase is essentially salt-like. This is based on the observation that, instead of the enormous values of  $\Delta S^*$  for subneat soap, one has values of the order of a few calories per degree, suggesting that the activated state is one in which the positive ions are “in transit” between lattice points and more or less randomly distributed, so that  $\Delta S^*$  is of the order of that associated with the order-disorder transition ( $2R \ln 2$ ) (21). In view of the picture now presented for subneat soap, the degree and extent of regularity to be associated with the “lattice” itself in neat soap are uncertain, in so far as deductions from the conductivity data are concerned.

Examination of figures 14 and 15 shows that middle soap and soapboiler's neat soap have nearly identical values of specific resistance, which results in the equivalent conductivity of middle soap being much larger than that of soapboiler's neat soap. This result is in accord with the hypothesis (7) that soapboiler's neat soap has a lattice-like structure, whereas middle soap is predominantly micellar in nature.

#### SUMMARY

A technique has been developed for determination of the electrical conductivity of solid and semi-solid soap systems. Resistances were determined as a function of temperature for sodium stearate systems containing from 0 to 69 per cent water from room temperature to as high as 300°C. The results obtained permit derivation of details of the phase diagram in the region of high concentration, and show that none of the anhydrous phases studied can incorporate more than 3 or 4 weight per cent water without transformation to another phase.

It is concluded that a multiplicity of solid phases, rather than equilibrium between a single curd phase and isotropic solution, is required to explain the observed properties of the system below  $T_c$ .

Interpretation of the temperature coefficient of conductivity of subneat sodium stearate according to the theory of absolute reaction rates gives so abnormally large a value for the entropy of formation of the activated state as to suggest progressive destruction of the "lattice" with rising temperature over the whole range of existence of this phase. Values obtained similarly for neat soap resemble more closely those for the conductivity of ordinary salts.

#### REFERENCES

- (1) BARRER, R. M.: *Diffusion in and through Solids*, pp. 264, 294, 303. The Macmillan Company, New York (1941).
- (2) BHATNAGAR, S. S., AND PRASAD, M.: *Kolloid-Z.* **34**, 193 (1924).
- (3) BUEGER, M. J., SMITH, L. B., DE BRETTEVILLE, A., AND RYER, F. V.: *Proc. Natl. Acad. Sci. U. S.* **28**, 526 (1942).
- (4) BUEGER, M. J., SMITH, L. B., AND RYER, F. V.: *J. Am. Oil Chem. Soc.* **24**, 193 (1947).
- (5) BUEGER, M. J., SMITH, L. B., RYER, F. V., AND SPIKE, J. E., JR.: *Proc. Natl. Acad. Sci. U. S.* **31**, 226 (1945).
- (6) COHN, E. J.: *Chem. Rev.* **24**, 217 (1939).
- (7) DOSCHER, T. M., AND VOLD, R. D.: *J. Phys. Colloid Chem.* **52**, 98 (1948).
- (8) FERGUSON, R. H., ROSEVEAR, F. B., AND NORDSIECK, H.: *J. Am. Chem. Soc.* **69**, 141 (1947).
- (9) FISCHER, M. H., AND HOOKER, M. O.: *The Lyophilic Colloids*, Chap. V. C. C. Thomas, Springfield, Illinois (1933).
- (10) FUOSS, R.: *J. Chem. Education* **19**, 231 (1942).
- (11) HAGUE, B.: *Alternating Current Bridge Methods*, p. 238. Pitman and Sons, New York (1938).
- (12) Reference 11, pp. 542-551.
- (13) HOVORKA, F., AND MENDENHALL, E. E.: *J. Chem. Education* **16**, 239 (1939).
- (14) KONECNY, C. C.: "The Rheological Properties of Mixed Soap Systems," M. S. Thesis, University of Southern California, 1945.
- (15) LANGE, N. A.: *Handbook of Chemistry*, p. 1384. Handbook Publishers, Inc., Sandusky, Ohio (1946).
- (16) LYON, L. L.: "The Rheological Properties of Solid Soap Systems," Ph. D. Dissertation, University of Southern California, 1944.
- (17) MCBAIN, J. W., AND LEE, W. W.: *Oil & Soap* **20**, 17 (1943).
- (18) MCBAIN, J. W., VOLD, R. D., AND FRICK, M.: *J. Phys. Chem.* **44**, 1013 (1940).
- (19) PHILIPSON, J. M.: "The Preparation of Pure Sodium Stearate" (unpublished), Research Report, University of Southern California Library, 1945.
- (20) PHILIPSON, J. M., HELDMAN, M. J., LYON, L. L., AND VOLD, R. D.: *Oil & Soap* **21**, 315 (1944).
- (21) SEITZ, F.: *The Modern Theory of Solids*, p. 504. McGraw-Hill Book Company, Inc., New York (1940).
- (22) STUPAKOFF LABORATORIES: Sheet 1, *Catalog of Technical Data, Series KA*, Pittsburgh, Pennsylvania (1944).
- (23) THIESSEN, P. A., AND EHRLICH, E.: *Z. physik. Chem.* **B19**, 299 (1932).
- (24) VOLD, M. J., MACOMBER, M., AND VOLD, R. D.: *J. Am. Chem. Soc.* **63**, 168 (1941).
- (25) VOLD, R. D.: *J. Am. Chem. Soc.* **63**, 2920 (1941).
- (26) VOLD, R. D.: *J. Phys. Chem.* **49**, 315 (1945).
- (27) VOLD, R. D.: *J. Phys. Colloid Chem.* **51**, 797 (1947).
- (28) VOLD, R. D., AND LYON, L. L.: *Ind. Eng. Chem.* **37**, 497 (1945).
- (29) VOLD, R. D., AND VOLD, M. J.: *J. Am. Chem. Soc.* **61**, 808 (1939).

PHASE STUDY OF ROSIN SOAP-SODIUM CHLORIDE-WATER  
AND ROSIN SOAP-SODIUM SILICATE-WATER SYSTEMS<sup>1</sup>

R. C. MERRILL AND RAYMOND GETTY

*Philadelphia Quartz Company, Philadelphia, Pennsylvania**Received August 25, 1947*

Rosin and silicates have been used in soaps for many years. The detergent action of silicates and of mixtures of silicates with fatty acid soaps is well established (for references see 10). Recent studies have been made of the detergent action of rosin, both alone and mixed with fatty acid soaps (2, 13, 14, 15). In order to overcome the tendency of soaps from ordinary wood or gum rosin to darken on aging, the rosin has been refined and made more resistant to oxidation by hydrogenation, dehydrogenation, and polymerization (1, 15). Soaps from dehydrogenated or disproportionated rosin have proved satisfactory as emulsifying agents for GR-S rubber (3). Mixed fatty acid-rosin soaps usually contain sodium silicates, both to improve detergency and to harden the soap.

The addition of rosin to a tallow soap stock makes it easier to add the large amount of sodium silicates justified on the basis of detergency. Possible explanations are that the rosin increases the miscibility of the soap with silicate solutions or the range of temperatures over which the hot soap-silicate mixtures in the crutcher solidify on cooling. The purposes of the present investigation of the phase behavior of rosin soap-sodium chloride-water and rosin soap-sodium silicate-water systems were to provide data of value to the manufacturers and users of rosin soap mixtures and to attempt to determine the method by which the addition of rosin makes concentrated soap-silicate mixtures more readily prepared. The data are also of interest in studying the behavior of high-polymer latex emulsions stabilized by rosin soaps (6). No previous systematic study has apparently been published on these systems, although McBain has referred to preliminary unpublished data on sodium abietate (7). Livingston has presented a hypothetical diagram for rosin soap-sodium hydroxide-water systems based on a few experimental points, but primarily by analogy with the diagrams of McBain and collaborators for fatty acid soaps (6).

## EXPERIMENTAL

The two types of rosin used in this work were a wood rosin of N Color grade representing a typical refined wood rosin commonly used in yellow laundry soaps and a hydrogenated rosin sold under the trade name Staybelite. Both were supplied through the courtesy of the Hercules Powder Co. The N wood rosin had an acid number of 162, and a saponification number of 184 corresponding to an average molecular weight of 349 for the sodium soap. The saponification number of sample A of the hydrogenated rosin was 175, giving the cor-

<sup>1</sup> Presented at the Twenty-first National Colloid Symposium, which was held under the auspices of the Division of Colloid Chemistry of the American Chemical Society at Palo Alto, California, June 18-20, 1947.

responding sodium soap an average molecular weight of 343. Sample B of the hydrogenated rosin had a saponification number of 159. Its sodium soap was less soluble in water and more readily salted out by electrolytes. Other characteristics of regular wood and hydrogenated rosin soaps have been published (1, 15). The soaps were made by saponification with sodium ethoxide in alcohol, and dried at 105°C.

The sodium silicate was a regular commercial product of the Philadelphia Quartz Co. It was the same as that used in previous phase studies on a typical commercial mixed soap, and on sodium palmitate. A complete analysis has been given (10, 11). The stock silicate solution contained 45.5 per cent solids with a silica-to-alkali ratio by weight of 2.46. The sodium chloride was c.p. and the water freshly distilled. All data were obtained by the synthetic method used in previous investigations (7, 9, 10, 11). Mixtures of soap, water, and sodium chloride, or silicate (if included), in 13 x 50 mm. sealed Pyrex tubes were heated in an oil bath until the contents were completely isotropic and homogeneous. The mixture was then allowed to cool slowly, and the temperature ( $T_i$ ) recorded at which the first trace of liquid crystal, or turbidity due to a second immiscible isotropic liquid, appeared. The use of crossed polaroids facilitated the first determination. After standing at room temperature or below for several days the temperature,  $T_c$ , was determined at which all traces of solid disappeared on slow heating with frequent shaking. In all cases these two temperatures on calibrated thermometers agreed within 2° or 3°. Concentrated rosin soap systems containing large amounts of salt or silicate did appear to form some white opaque solid, quite similar in appearance to the "curd fiber" phase of fatty acid soap systems. However, the transition from curd fiber to liquid crystal was not observed. As a matter of convenience the solution temperatures on the concentrated systems forming liquid crystals were observed on cooling, whereas those of the more dilute solutions forming crystalline or amorphous solid were determined on heating. Equilibrium measurements can be made more rapidly in this manner. Systems forming liquid crystals showed little, if any, tendency to supercool.

Solution temperatures for the dark brown N wood rosin soap systems were determined on relatively thin films before a bright light.

## RESULTS

The solubilities of wood rosin and hydrogenated rosin soaps in water and, for the latter, in 0.025 *N* sodium hydroxide solution, at various temperatures are given in table 1 and shown in figure 1. At temperatures above the solubility curves the systems were homogeneous isotropic solutions. Below temperatures given by the curves the amorphous or crystalline solid at low and medium concentrations was not completely soluble. Above a soap concentration of about 40 per cent for both the hydrogenated and the wood rosin soap, liquid crystals were formed at the solution temperature. At room temperature the wood rosin soap systems remained liquid crystalline, whereas those of the hydrogenated rosin consisted of an insoluble solid or "curd" in contact with dilute



soap solution. Curve A of figure 1 gives the solubilities of the wood rosin soap and curve C that of the hydrogenated rosin soap in distilled water. Curve B represents the solubility of the hydrogenated rosin soap in 0.025 N sodium hydroxide solution.

TABLE 1

*Solution temperatures for systems of rosin soap-water and rosin soap-dilute alkali solutions*

N WOOD ROSIN SOAP	SOLUTION TEMPERATURE	HYDROGENATED ROSIN SOAP	SOLUTION TEMPERATURE	HYDROGENATED ROSIN SOAP IN 0.025 N NaOH	SOLUTION TEMPERATURE
<i>per cent</i>	<i>°C.</i>	<i>per cent</i>	<i>°C.</i>	<i>per cent</i>	<i>°C.</i>
4.97	<1	1.12	<1	5.03	<1
10.1	<1	5.25	<1	7.03	37
20.2	7	7.12	<1	10.1	40
25.3	11	9.23	65	27.4	70
29.1	14	10.2	69	30.0	72
34.8	20	15.1	63	34.9	77
40.1	26	15.9	68	50.2	106
44.9	32	20.0	66	54.9	112
49.1	35	20.2	81	60.0	119
51.1	39	25.0	85	67.1	122
52.2	38	28.2	88	75.4	108
52.5	42	34.8	98	77.6	105
54.5	45	43.9	118		
59.5	48	46.5	125		
65.2	51	47.6	127		
67.5	44	50.2	132		
69.3	43	52.4	136		
69.5	42	52.8	137		
71.0	38	54.0	139		
71.7	41	65.5	142		
74.0	40	57.6	145		
74.2	30	59.9	147		
80.0	62	62.5	151		
84.7	120 (?)	65.0	154		
88.1	115 (?)	65.2	154		
90.6	116 (?)	68.3	157		
		75.1	146		
		80.0	117		
		81.8	86		
		82.1	78		
		83.2	123		
		84.0	112		
		84.8	130		
		86.6	>190		

The number of moles of sodium hydroxide in the systems shown in curve B varied from 7.8 per cent of the moles of soap at 10 per cent soap to 1 per cent at 45 per cent soap.

Rosin soap-water systems form liquid crystals which, like those of aqueous

fatty acid soap systems, have a pronounced maximum solution temperature or minimum solubility (8). They appear to differ however, in forming only one liquid-crystalline phase showing a maximum stability. The hydrogenated rosin soap resembles the fatty acid soaps and many other detergents such as the long-chain sulfonates, sulfates, and amine salts in showing the very sharp change in solubility at a fairly definite concentration known as the Krafft point. This change in solubility occurs at a lower soap concentration in the sodium hydroxide solution. Rosin soaps show no abrupt change in solubility when the system becomes sufficiently concentrated to form liquid crystals, as do fatty acid soaps.

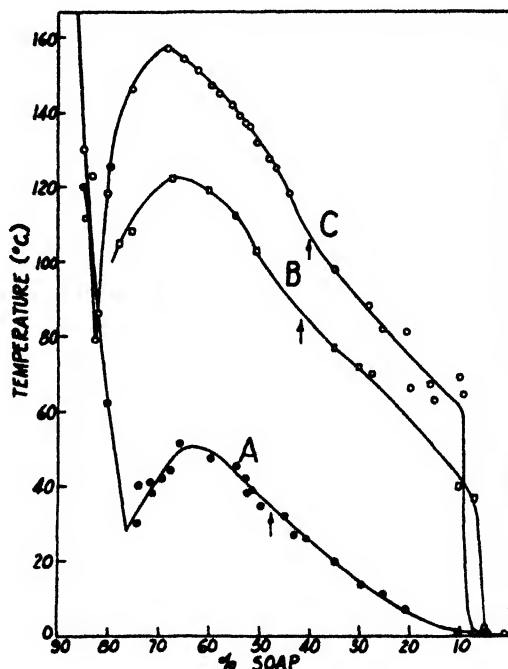


FIG. 1. Solubility curves for rosin soaps. Curve A, N wood rosin soap in distilled water; curve B, hydrogenated rosin soap A in 0.025 N sodium hydroxide solution; curve C, hydrogenated rosin soap in distilled water. Arrows indicate concentrations above which liquid crystal forms on cooling from isotropic solution.

Both liquid-crystalline and crystalline or amorphous hydrogenated rosin soaps are, in general, more soluble in 0.025 N sodium hydroxide than in pure water. The solubility of crystalline fatty acid soap is generally reduced by sodium hydroxide and salts; that of the liquid-crystalline phase, middle soap, is increased, whereas that of the liquid-crystalline phase, neat soap, is again reduced by sodium hydroxide and salts. The hydrogenated soap is much less soluble than the ordinary wood rosin soap. This reduction in solubility, due mostly to conversion of the unsaturated double bonds of the abietic and pimaric acids and other unsaturated molecules in the rosin to saturated derivatives, is considerably greater than that between sodium oleate and sodium stearate (8).

The more pertinent comparison with sodium linoleate cannot be made, because no phase studies have been made of that soap.

The effect of sodium hydroxide on the solution temperatures of 10, 20, 30, and 40 per cent rosin soap systems is given in table 2.

The addition of sodium hydroxide to a hydrogenated rosin soap system first increases, and then decreases its solubility.

The influence of sodium chloride on the solubility of the hydrogenated rosin soap in water is given in table 3 and shown in figure 2. The curves represent the solubility at definite temperatures (i.e., are isotherms) as deduced by linear

TABLE 2

*Effect of alkali on solution temperatures of hydrogenated rosin soap systems*

ROSIN SOAP	SOLUTION TEMPERATURE IN				MOLE PER CENT EXCESS NaOH IN*		
	H <sub>2</sub> O	0.001 N NaOH	0.025 N NaOH	0.25 N NaOH	0.001 N NaOH	0.025 N NaOH	0.25 N NaOH
<i>per cent</i>							
10	61†		72‡	58	0.31	7.8	78
20	75†		58‡	61	0.13	3.4	34
30	90†	74	72‡	72	0.081	1.9	20
40	107†	82	82‡		0.053	1.2	

\* Based on moles of soap in system.

† Data from curve C in figure 1.

‡ Data from curve B in figure 1.

TABLE 3

*Solution and transition temperatures for hydrogenated rosin soap-sodium chloride-water systems*

*A. Liquid-crystal forms*

ROSIN SOAP	NaCl	SOLUTION TEMPERATURE
<i>per cent</i>	<i>per cent</i>	°C.
59.8	1.01	138
60.3	3.13	118
49.1	1.17	135
51.0	2.07	126
49.1	3.16	>165
56.9	2.26	125
47.8	2.01	116
53.8	2.50	115
64.2	2.53	97
68.5	0.95	120
66.1	1.66	112
66.7	0.52	127
68.2	2.00	100
70.5	1.11	111
71.5	2.14	77
59.6	3.80	117
60.1	3.39	>175

TABLE 3—continued

*B. An isotropic, amorphous, or crystalline phase separates first on cooling*

HYDROGENATED ROSIN SOAP	NaCl	$T_c$ OR $T_i$	$T_h^*$	$T_l^*$
<i>per cent</i>	<i>per cent</i>	$^{\circ}\text{C.}$	$^{\circ}\text{C.}$	$^{\circ}\text{C.}$
46.1	1.15	119		
40.4	1.09	112		
45.2	2.55	117		
35.1	3.94	>180		
45.4	1.04	115		
36.6	1.99	105		
30.0	0.98	88		
29.6	2.61	99		
20.0	1.03	82		
20.1	2.34	85		
3.88	2.93	>165		
15.6	0.85	76		
3.28	1.61	<20		
4.00	0.47	<1		
16.9	2.48	83		
7.41	0.83	<20		
7.06	1.61	92		
21.0	0.33	78		
39.1	0.38	90		
6.93	2.49	131	117	105
13.3	2.21	90	—	86
7.03	2.33	119	105	99
13.0	3.68	149	—	—
24.8	3.57	166	102	98
42.2	3.56	>180		
16.4	2.91	135	102	95
9.82	2.91	143	110	99
7.31	3.44	163	117	85
42.1	3.18	163	90	82
36.8	2.79	142	95	83
24.8	2.88	133	95	83
11.3	2.72	118	102	92

At the temperature  $T_i$  these systems became turbid on cooling from homogenous isotropic solution, owing to separation of a second immiscible isotropic solution.  $T_h$  is the temperature at which on further cooling the system again became homogenous.  $T_l$  is the temperature at which on still further cooling a birefringent phase, apparently liquid crystal or a fluid suspension of crystals, appeared. Compositions for which a  $T_h$  or  $T_l$  is given are  $T_i$ ; all others are  $T_c$ .

interpolation from the solution temperatures of systems of known composition (circles). The intercepts on the 0 per cent salt axis representing the solubility in pure water were obtained from curve C of figure 1. The intercepts on the 0 per cent soap axis correspond to the solubility of sodium chloride in pure water, which is 27 per cent at 60°C.

Above about 40 per cent soap where a liquid crystal is the saturating phase,

the addition of sodium chloride decreases the solubility of the soap. The liquid-crystalline phase of the rosin soap behaves like the neat-soap phase of the fatty acid soaps in being "salted out" by sodium chloride rather than being "salted in", as is the other liquid-crystalline phase middle soap. Below approximately 40 per cent, where amorphous or crystalline soap is the saturating phase, the first addition of sodium chloride appears to increase, but in general its effect is to decrease, solubility. At low soap concentrations the addition of salt results in the formation of two immiscible isotropic solutions in the characteristic indentation or "bay region" shown also by systems of the fatty acid soaps.

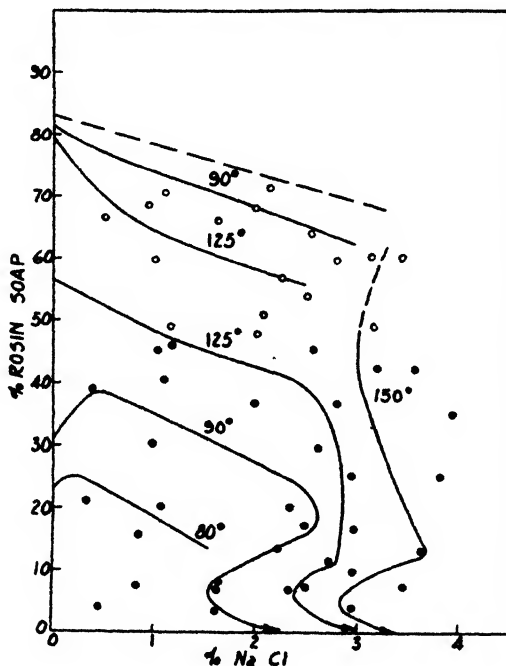


FIG. 2. Solubility curves for hydrogenated rosin soap A-sodium chloride-water systems. Isotherms at 80°, 90°, 125°, and 150°C. Open circles represent compositions forming liquid crystal first on cooling from isotropic solution; filled circles those forming a second immiscible isotropic liquid or amorphous or crystalline solid.

Systems of composition between the upper 125°C. and 90°C. isotherms and approximately the dotted line are homogeneous isotropic solutions at the temperatures indicated. For compositions above the dotted line the temperature required to form a homogeneous isotropic system increases rapidly with concentration.

Systems of low rosin soap and high salt concentration corresponding to compositions in the bay region first showed separation of a second immiscible isotropic liquid on cooling from homogeneous isotropic solution, as do the corresponding fatty acid soap systems. However, rosin soap systems differ by again becoming homogeneous and isotropic on further cooling. On still further

cooling they become birefringent, owing to separation of liquid crystal or a colloidal suspension of finely divided crystalline material.

TABLE 4

*Solution and transition temperatures for hydrogenated rosin soap-sodium chloride-0.025 N sodium hydroxide systems*

ROSIN	NaCl	$T_c$ OR $T_i$	$T_h$	$T_l$
<i>per cent</i>	<i>per cent</i>			
24.8	2.64	159	—	85
7.07	2.38	—	—	92
11.0	2.68	—	—	85
10.0	1.98	—	—	85
4.98	1.83	—	—	89
10.0	1.30	93	80	76
4.22	1.60	105	—	91
34.8	2.40	150	99	—
26.1	2.34	130	102	89
15.0	2.15	—	—	88
5.15	2.15	114	—	94
29.4	2.96	170	97	92
20.0	2.97	157	97	96
5.05	3.21	140	112	94
15.1	3.62	168	110	89
5.04	3.75	168	105	—
39.9	2.10	133	100	81
11.7	3.23	141	—	—
29.9	2.08	126	100	83
4.88	2.73	119	105	96
19.8	2.14	—	—	81
18.0	2.58	124	97	90
4.05	0.73	<20		
4.11	2.33	116		
40.2	0.49	86		
27.1	1.81	122		
30.1	0.46	81		
17.4	1.87	116		
40.0	1.31	88		
14.2	2.45	119		
30.0	1.31	87		
20.1	1.31	84		
48.1	1.21	106		
11.9	0.62	66		
24.6	0.27	70		
32.1	0.57	80		
3.00	1.11	82		
7.14	1.08	87		
10.8	1.71	112		

Isotropic systems whose composition lies in regions where systems are ordinarily anisotropic have been reported previously (e.g., 4, 16), although it is not

known with certainty whether these systems are anomalous or represent isotropic phase fields. The existence of homogeneous isotropic phases which form two immiscible isotropic phases on heating and a birefringent phase on cooling has not previously been reported for colloidal electrolyte systems.

Several systems in this region were isotropic when stationary but became definitely birefringent when flowed back and forth in the tube. The ease with which flow birefringence is observed shows the presence of readily oriented anisometric particles or micelles in such systems.

The temperatures plotted in the "bay region" of figure 2 are those at which the homogeneous isotropic solution existing at high temperatures formed two immiscible isotropic solutions on cooling. Homogeneous isotropic phases exist over a specific range at temperatures below those indicated only in this region. Isotherms showing the temperatures at which these systems again become

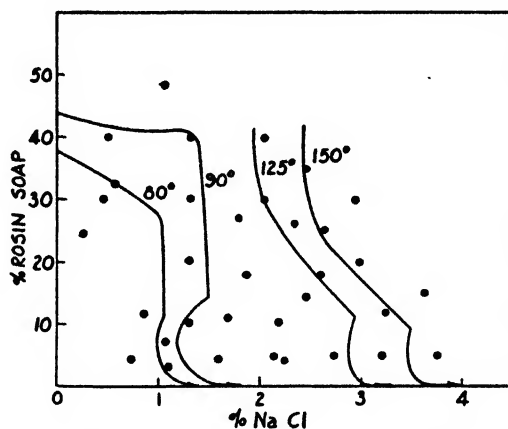


FIG. 3. Solubility curves for hydrogenated rosin soap-sodium chloride-0.025 *N* sodium hydroxide systems. Isotherms at 80°, 90°, 125°, and 150°C.

homogeneous and isotropic, and at which a birefringent phase is formed on still further cooling, are of the same general shape as those indicated.

In order to see whether the alkalinity of the silicates might be in part responsible for their behavior with soap systems, a portion of the ternary phase diagram for rosin soap-sodium chloride-water was determined in 0.025 *N* sodium hydroxide solution instead of pure water. The data are given in table 4 and figure 3. The excess sodium hydroxide based upon the weight of soap varied up to around 7.8 mole per cent for 10 per cent soap. The per cent excess was greatest in dilute solution where the degree of hydrolysis is proportionately greater. Figure 3 shows that the added sodium hydroxide contributes to the salting out of the soaps. The difference in the miscibility of sodium chloride and silicates with soap systems is not due to the difference in alkalinity or pH.

Figure 4 shows the solubility of hydrogenated rosin soap B in solutions of a sodium silicate with a silica-to-alkali ratio of 2.46. The data are given in table 5.

The diagram is qualitatively similar to those with sodium chloride, although

TABLE 5

*Solution and transition temperatures for systems containing hydrogenated rosin soap B,  
1:2.48 ratio sodium silicate, and water*

ROSIN SOAP	SILICATE	$T_s$ OR $T_i$
A. Remains isotropic		
<i>per cent</i>	<i>per cent</i>	
23.0	4.75	108
10.9	4.85	103
13.5	5.70	107
9.74	8.23	108
28.1	9.88	>160
28.3	14.9	>160
5.00	3.22	81
6.00	11.9	135
12.9	3.30	87
4.11	5.87	98
20.2	10.4	>150
24.1	2.14	90
25.0	12.7	>150
13.9	12.3	>165
18.9	7.28	120
20.0	1.36	86
10.3	2.26	82
4.03	2.25	72
3.79	8.10	106
3.76	15.0	136
11.8	15.0	149
32.1	11.7	130
B. Liquid-crystal forms		
33.3	2.45	112
69.4	6.28	157
44.2	6.56	144
79.8	4.88	>165, <190
39.7	19.8	160
32.7	14.9	139
58.5	18.8	143
76.0	9.73	>165
59.7	5.07	>165
60.3	12.8	162
49.4	9.06	158
42.3	2.80	130
45.6	14.0	162
40.3	16.3	156
33.7	8.49	122
75.4	3.34	144

the data are not sufficiently numerous to show any increased soap solubility in low concentrations of silicate. (Note that the scale of the horizontal axis of



figure 4 is more than four times that of figures 2 and 3.) The slopes of the isotherms above about 32 per cent soap, where liquid crystal is in equilibrium with isotropic solution, are less than those below this concentration, where amorphous soap is the saturating phase. Figure 4 shows that the "bay region" where two isotropic immiscible liquids are in equilibrium is just as pronounced in systems with silicate as in those with sodium chloride. Complete separation of these two phases was considerably more difficult in the silicate systems, however, probably owing to their higher viscosity. For this reason the isotropic

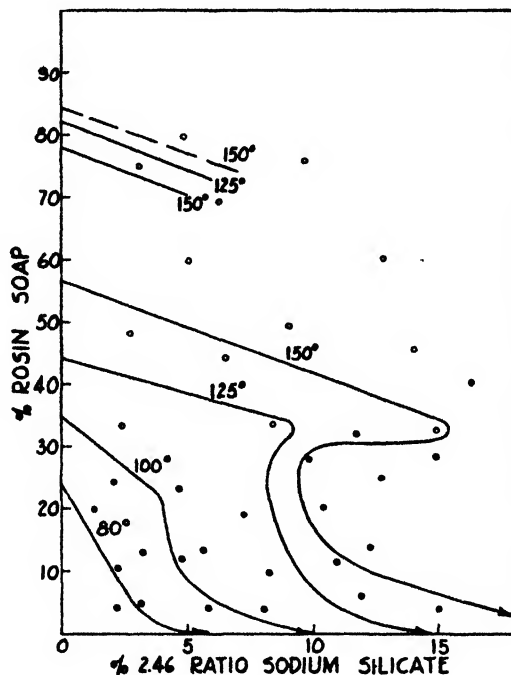


Fig. 4. Solubility curves for hydrogenated rosin soap B-1:2.46 ratio sodium silicate-water systems. The per cent of the 1:2.46 ratio silicate is on an anhydrous basis. Open circles represent compositions forming liquid crystal first on cooling from isotropic solution; filled circles those forming a second immiscible isotropic liquid or amorphous or crystalline solid. Compositions between the two dotted 150°C. isotherms are homogenous and isotropic at that temperature.

solutions which, in this range of concentrations, probably exist at temperatures below a region of two immiscible isotropic phases and above a temperature where a birefringent phase separates, were not completely studied.

Since sample B of the hydrogenated rosin soap was used in obtaining the data in table 5, they are not strictly comparable with those in the previous tables and figures. Data on the silicate system obtained with sample A of the hydrogenated rosin soap, although not sufficiently complete for a phase diagram, do show definitely that it is much more miscible than sample B with silicate. For example, about 10 per cent of anhydrous silicate is required to raise the

solution temperature of a 40 per cent system of hydrogenated rosin soap A to 125° C., whereas only 5 per cent is needed to raise that of the same concentration of sample B. The miscibility of these two commercial samples of hydrogenated rosin soap with electrolytes varied considerably. The much greater miscibility of silicates as compared with chloride is even larger than that indicated by comparison of figures 2-4 inclusive.

#### DISCUSSION

Although the present data cover systems only up to 88 per cent soap, it appears that the addition of water to an anhydrous rosin soap markedly reduces to a minimum the temperature at which a homogeneous isotropic liquid forms. Further addition of water stabilizes the crystal lattice of the soap, presumably by forming a liquid-crystalline phase, and the system shows a maximum solution or melting temperature. The minimum occurs for the hydrogenated rosin soap at around 82 per cent and the maximum at 67 per cent, corresponding, on the average, to approximately 3 and 10 moles of water per mole of soap, respectively. For the wood rosin soap the minimum is at around 76 per cent and the maximum at 63 per cent, corresponding to about 6 and 11 moles of water per mole of soap. The maximum for the hydrogenated rosin soap system is at least 80° above the minimum, that of the wood rosin soap at least 20°.

The maximum probably does not represent a stoichiometric hydrate. The flatness of the maximum and the fairly large radius of curvature (figure 1) indicate that the hydrate, whether stoichiometric or not, is considerably dissociated in solution. The change in slope of the solubility curve at the transition from amorphous or crystalline to liquid-crystalline is not so marked as in the case of the fatty acid soaps. This indicates that the structure of the liquid-crystalline technical rosin soap which consists largely of three-ring compounds is less abruptly stabilized than that of the long straight-chain fatty acid soaps.

The solubility curve in water of colloidal electrolytes which show a fairly sharp change indicative of micelle formation in freezing point, conductivity, and other physicochemical properties at a particular concentration also shows a marked change in slope at about this same concentration (Krafft point). The existence of this marked change of slope in colloidal electrolyte systems might be regarded as indicating a "critical concentration" for micelle formation. Our data would then suggest that micelle formation in solutions of ordinary wood rosin soaps occurs very gradually over a range of concentrations, whereas solutions of the hydrogenated rosin would show a "critical concentration". Kolthoff and Johnson (5) have shown by the dye solubilization technique that a rosin soap differs from fatty acid soaps by not showing a critical concentration. It would be interesting to see if hydrogenated rosin soaps show a "critical concentration" by the dye solubilization, electrical conductivity, or osmotic coefficient methods for studying micelle formation. A positive result would not be entirely unexpected, since changing the three hydroxyl groups of the three-ring compound sodium cholate to the ketone groups of sodium dehydrocholate

converts a typical solubilizing colloidal electrolyte to one which has no solubilizing action (12).

One of the practical implications of this work is that the effect of rosin in making it easier to incorporate large amounts of silicate in a soap system may be attributed both to the increased miscibility of the soap with silicate and to providing a range of solidification points for the system.

#### SUMMARY

Solubility curves for the very soluble wood rosin and the less soluble hydrogenated rosin soap in water and, for the latter, in 0.025 *N* sodium hydroxide, show both similarities to and differences from those of long-chain fatty acid soaps. Ternary diagrams of the hydrogenated rosin soap with sodium chloride in water and in 0.025 *N* sodium hydroxide solution are qualitatively similar to those with fatty acid soaps but at low soap concentrations exhibit hitherto unreported behavior. Large amounts of a sodium silicate with an  $\text{SiO}_2/\text{Na}_2\text{O}$  ratio by weight of 2.46 are incorporated into concentrated hydrogenated rosin soap systems without changing very much the phase behavior.

Rosin makes it easier to incorporate large amounts of silicates in fatty acid soap systems by increasing miscibility and by providing a range of solidification temperatures for the system.

#### REFERENCES

- (1) BORGLIN, J. N., ELLIOTT, H. A., AND MOSHER, P. R.: *Ind. Eng. Chem.* **36**, 752 (1944).
- (2) BORGLIN, J. N., MOSHER, P. R., NOBLE, BARBARA, AND PUNSHON, T.: *Oil & Soap* **20**, 77 (1943).
- (3) CUTHBERTSON, G. R., COE, W. S., AND BRADY, J. L.: *Ind. Eng. Chem.* **38**, 975 (1946).
- (4) GONICK, E., AND MCBAIN, J. W.: *J. Am. Chem. Soc.* **68**, 683 (1946).
- (5) KOLTHOFF, I. M., AND JOHNSON, W. F.: *J. Phys. Chem.* **50**, 440 (1946).
- (6) LIVINGSTON, H. K.: *J. Phys. Colloid Chem.* **51**, 443 (1947).
- (7) MCBAIN, J. W.: In *Colloid Chemistry*, edited by J. Alexander, Vol. 1, p. 132. Chemical Catalog Company, Inc., New York (1926).
- (8) MCBAIN, J. W., AND LEE, W. W.: *Oil & Soap* **21**, 227 (1944).
- (9) MCBAIN, J. W., VOLD, R. D., AND GARDINER, K. W.: *Oil & Soap* **20**, 221 (1943).
- (10) MERRILL, R. C.: *Ind. Eng. Chem.* **39**, 158 (1947).
- (11) MERRILL, R. C., AND GETTY, R.: *J. Am. Chem. Soc.* **69**, 1875 (1947).
- (12) MERRILL, R. C., AND MCBAIN, J. W.: *J. Phys. Chem.* **46**, 10 (1942).
- (13) POHLE, W. D.: *Oil & Soap* **17**, 150 (1940); **18**, 244, 247 (1941); *Soap* **18**, 29, 69 (1942).
- (14) POHLE, W. D., AND SPEH, C. F.: *Oil & Soap* **17**, 100, 214 (1940).
- (15) VAN ZILE, B. S., AND BORGLIN, J. N.: *Oil & Soap* **21**, 164 (1944); **22**, 331 (1945).
- (16) VOLD, M. J.: *J. Am. Chem. Soc.* **63**, 1429 (1941).

# STABILITY OF SYNTHETIC KERATIN FIBERS IN ALCOHOL-WATER MIXTURES

## THEORETICAL BASIS FOR A NEW METHOD FOR SOLUBILIZING FEATHER KERATIN<sup>1</sup>

HAROLD P. LUNDGREN, ANDREW M. STEIN, VIRGINIA M. KOORN, AND  
RICHARD A. O'CONNELL

*Western Regional Research Laboratory,<sup>2</sup> Albany, California*

*Received August 25, 1947*

### CONTENTS

I. General consideration of protein stability and the stability of synthetic protein fibers.....	180
II. Force-temperature behavior of synthetic feather keratin fibers in alcohol-water solutions.....	183
A. Introduction.....	183
B. Apparatus.....	186
C. Force-temperature behavior of feather keratin fibers in water.....	187
D. Influence of alcohols on force-temperature behavior.....	189
E. Interpretation of effects of alcohols on the fiber system.....	190
F. Influence of inorganic ions on force-temperature relations.....	192
G. Nature of the non-electrostatic interactions in feather keratin fibers.....	195
H. Evidence for disulfide cross-links in feather keratin fibers.....	197
I. Conclusions relative to force-temperature studies.....	198
III. Application of alcohol-water systems to the solubilization of feathers.....	199
IV. Possible application of the solvent system alcohol-water-salt to the solubilization of other proteins.....	204
V. Summary.....	205
VI. References.....	206

### I. GENERAL CONSIDERATIONS OF PROTEIN STABILITY AND THE STABILITY OF SYNTHETIC PROTEIN FIBERS

Significant progress has been made during the past decade in the development of synthetic protein fibers, and we can expect further progress as our knowledge of the molecular size and interactions in protein systems is enlarged. We have seen casein fibers develop from a laboratory curiosity to a product of commercial interest, and we have seen various other proteins transformed into synthetic fibers. We have come to recognize that proteins in general are fiber-forming materials, yet we have also learned that proteins differ among themselves in the fiber-forming characteristics and in the ease with which they can be stabilized in the fibrous state.

<sup>1</sup> Presented at the Twenty-first National Colloid Symposium, which was held under the auspices of the Division of Colloid Chemistry of the American Chemical Society at Palo Alto, California, June 18-20, 1947; also at a meeting of the American Association for the Advancement of Science, Colby Junior College Conference on Textiles, New London, New Hampshire, July 9, 1947.

<sup>2</sup> Bureau of Agricultural and Industrial Chemistry, Agricultural Research Administration, United States Department of Agriculture.

Hardly more than two decades ago proteins were regarded as colloids of indefinite size, the properties of which were determined by the state of dispersion and by the materials adsorbed on the surface produced by the dispersion. Proteins are now recognized as natural high polymers, many of which have been shown to possess definite molecular weights and definite compositions and to obey the phase rule in solubility; furthermore, proteins have been shown to react stoichiometrically with acids and bases, with anionic and cationic detergents, and with acidic and basic dyes. Protein molecules are also now recognized as flexible chains. These chains are stabilized in network structure as in wool, feathers, hides, and silk, or they are curled-up and stabilized in corpuscular configuration as in casein, soybean proteins, peanut proteins, zein from corn, and a host of others.

But there is much yet to be learned about proteins, particularly in regard to the forces which determine their stability, including their ease of denaturation, of solubilization, of transformation into the fibrous state, and of stabilization of the fibrous configuration. For instance, interchain forces such as the disulfide cross-links in wool, as Harris (6) has shown, determine the ability of a fiber to withstand the effects of solvents such as water.

The significance of molecular interaction can be stated in a general way: The sum total of physical properties of any substance is determined by the degree of mutual interaction between constituent structural units; that is, solubility or insolubility, hardness, flexibility, and tensile strength are directly related to the number, kind, and distribution of the bonds that hold the molecules together.

Proteins vary widely in solubility depending on the degree of mutual interaction of their chains. Some proteins, such as silk, collagen, and keratin, are insoluble in the common neutral solvents. This property is desirable if the materials are to be used directly as articles of commerce, but it presents difficulties when we seek to disperse them in order to utilize them for such purposes as synthetic fibers. Even among the corpuscular proteins we find striking differences in solubility; some are soluble in water at neutral pH; others dissolve in neutral salt solutions, yet many others, including various seed and nut proteins, are relatively soluble in water or neutral salt solutions, but are much more soluble when their solutions are made alkaline. A certain few corpuscular native proteins classified as prolamines, including zein and gliadin, are recognized by their solubility in aqueous alcohol solutions.

To be suitable as a raw material for synthetic fibers a protein must have an appropriate chain length. A protein consisting only of short chains cannot be expected to give fibers of desirable quality. For instance, the protein salmine of molecular weight 5000 does not form fibers, whereas egg albumin of molecular weight 45,000 can be transformed into oriented fibers having dry strengths over 2 g. per denier. The next consideration in the handling of a protein is the fact that the solvent must not degrade the protein chain, and this is where the use of alkali has limitations. For instance, in the dispersion of feather keratin in alkali at pH 13-14 rapid hydrolysis of the protein chain occurs, with the result that fibers prepared from such dispersions show progressively poorer quality as

the aging is continued. It is for these reasons that new and milder methods for the dispersion of industrially interesting and difficultly soluble proteins such as feather keratin are being sought.

Chemical utilization of feather keratin is one of the problems assigned to the Western Regional Laboratory for investigation. Poultry feathers are practically pure protein, are cheap, and are available in this country in quantities estimated at over 100,000,000 pounds annually.

The attractive forces that stabilize the protein chains in feathers are presumably similar to those in other proteins with the exception that in feathers, as in wool, because of the large proportion of cystine, there is extensive disulfide cross-linking between neighboring chains. But even when these bonds are broken by reducing agents the protein is insoluble in the common non-alkaline solvents. The attractive forces which remain are presumed to be (a) hydrogen bonds such as could occur between the backbone of neighboring chains or between side chains, (b) electrostatic bonds between acidic and basic residues on the side chains, and possibly (c) van der Waals forces between polarizable portions of neighboring chains.

The energy required to dissociate these bonds and separate the protein chains, whether to rearrange them by denaturation, to dissolve them, or to separate them mechanically, will depend on the number, kind, and distribution of the bonds; this energy will vary with the environment surrounding the protein. Just as the energy required to separate the ions of a crystal of an inorganic salt in the dry condition is high compared with that in water, so is the thermal energy required to denature a native corpuscular protein lowered when the protein is placed in water. For example, in the dry condition egg albumin is stable to temperatures well above 100°C., whereas in water it denatures rapidly at 60°C. When ethyl alcohol is added to the water the rate of denaturation is increased as a function of the amount of alcohol added. As Eyring (5) has pointed out, the solvents water and alcohol act as catalysts in lowering the thermal energy required to denature the protein chains. Similar effects of environment would be expected in the solubilization of proteins.

The problem, then, of finding a suitable means for solubilizing feather keratin consists essentially in finding the appropriate solvent catalyst which favors the dissociation of protein chains without degrading them.

One approach is through the application of synthetic detergents (10) in aqueous solution at neutral pH. After the disulfide bonds are reduced, the feather keratin is solubilized with anionic or cationic detergents through the formation of complexes of protein and detergent. The keratin in these complexes, as determined from measurements in the ultracentrifuge, by diffusion, and by osmotic pressure, has a molecular weight comparable in size to that of egg albumin (14). Concentrated solutions are highly viscous and exhibit birefringence of flow, indicating that the protein is unfolded. The solutions have desirable spinning properties; upon extrusion and coagulation the fibers which form can be extracted free of detergent with 70 per cent aqueous acetone; with sufficient stretch the fibers show a relatively high degree of crystalline orientation.

The detergent method is applicable to various proteins, the principal re-

quirement being that they have a sufficient number of acidic and basic groups necessary for the primary interaction between the protein and the detergent. Collagen is an exception: it cannot be handled by the detergent method. The detergent method is further limited by the relatively large amounts of detergent required, necessitating extractions which are slow and inconvenient particularly for fibers having large diameter.

Feathers, after reduction with bisulfite or monothioglycol, can be dissolved at pH values close to neutrality in a number of solvents which are recognized as hydrogen-bond dissociating agents. Thus, for example, reduced feathers will dissolve in 40 per cent urea solutions, 48 per cent guanidine solutions, and 64 per cent sodium salicylate solutions, all of which are protein denaturants. Jones and Mecham (8) in this Laboratory have compared the effects of detergents with several of these agents and in general found them to be equally effective and to disperse a maximum of about 80 per cent of the feather material. Furthermore, chemically reduced feathers can also be dispersed in agents which dissolve silk, such as anhydrous formic acid and saturated aqueous lithium bromide. The principal disadvantage of these methods from practical considerations is the relatively high cost of the agents required.

This paper describes the theoretical basis of a new method for solubilizing feathers in neutral solutions which do not require high concentrations of expensive special agents. The new method is not specifically limited to feather keratin; for example, isinglass collagen can be solubilized, plasticized, and transformed into fibers. The new procedure involves the use of aqueous alcohol mixtures.

## II. FORCE-TEMPERATURE BEHAVIOR OF SYNTHETIC FEATHER KERATIN FIBERS IN ALCOHOL-WATER MIXTURES

### *A. Introduction*

An effective method for studying protein-solvent interaction involves the measurement of the thermoelastic properties of fibers in the selected solvent. The mechanical behavior of the fibers is highly sensitive to variations in the solvent environment; furthermore, the effects of temperature on the system are reversible, thus making the results amenable to thermodynamic considerations.

We have already referred to the pronounced influence of water alone in favoring the separation of protein chains by the difference in stability of wet and dry egg albumin towards heat; and similarly this stability difference is apparent in the wetting of the synthetic protein fibers. For instance, uncured feather keratin fibers which give dry strengths of 1 g. per denier have a wet strength, in the relaxed condition, of 0.1 to 0.3 g. per denier.

The first effect of wetting the fiber at low temperatures is a shortening, probably the result of attraction of water by the polar groups with the simultaneous fission of weak secondary interchain attractions. The curling entropy favors a shortening of the water-plasticized network chains to a somewhat less extended state.

Application of heat to the fiber in this state causes a slight expansion provided

the temperature is below the critical region, which is approximately at 45°C. for a feather keratin fiber near the isoelectric point. The expansion is typical of a normal solid material. Beyond 45°C. a rather sudden change of state takes place; the fiber contracts to a relaxed state in which it now exhibits the thermo-elastic behavior of a typical rubber-like material. We shall discuss the nature of the forces that stabilize the network chains in this rubber-like state. Just as the presence of alcohol in water lowers the thermal energy necessary for denaturation of egg albumin, as we pointed out earlier, alcohol-water mixtures containing inorganic electrolytes lower the thermal and mechanical energy required to maintain constant length in the fibers. This effect of the solvent mixture is through dissociation of the stabilizing attractions.

It is more convenient to measure changes in the equilibrium force required to maintain the fiber at constant length with changes in solvent environment than it is to measure changes in length. Furthermore, the experimental arrangement for equilibrium force-temperature studies permits the study of stress relaxation in the fiber following rapid elongation. The measurement of stress relaxation when carried out in the same environments as the equilibrium force-temperature measurements also gives information regarding the nature of interactions in the fiber affected by the solvent environment.

The equilibrium force on a network system is a function not only of the temperature, but also of the internal attractions of the system analogous to the pressure of a real gas. The comparison between the force-temperature of chain systems with the pressure-temperature relation among ordinary molecules is given in figure 1. When rubber, for example, is stretched more than 10 per cent the force increases with temperature as indicated; normal solid materials exhibit a negative temperature coefficient of force. The slope of the force-temperature curve is a measure of the entropy of chain curling, and the intercept is a measure of interchain attractions.

Figure 2 summarizes the various forces acting on a fiber network surrounded by a solvent. Tending to disperse the network chains in this case is the osmotic swelling force in addition to the mechanical deforming force, and the thermal kinetic force. Opposing these forces are the attractive forces holding the network together. In addition, there is the small contribution of the hydrostatic force of the solvent acting on the fiber. The corresponding changes in energy in the fiber-solvent system may be represented as follows:

$$\Delta F_s + f\Delta L + T\Delta S = \Delta E + P\Delta V \\ = \Delta H$$

where  $f\Delta L$  is the mechanical work of deformation,  $f$  being the applied force and  $\Delta L$  the resulting elongation;  $\Delta F_s$  is the free energy of solvation, that is, the free-energy decrease involved in the interaction of the protein with the solvent medium;  $T\Delta S$  is the change in kinetic energy of the system,  $T$  being the absolute temperature and  $\Delta S$  the change in entropy;  $\Delta E$  is the change in the fiber network energy;  $P\Delta V$  is the hydrostatic work done, where  $P$  is the hydrostatic pressure



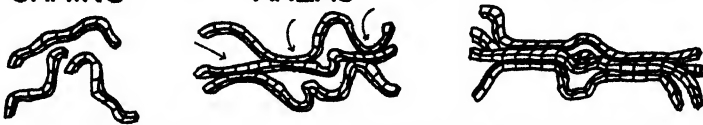
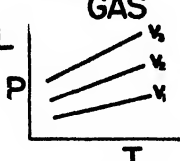
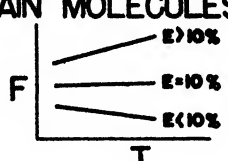
GAS $\rightleftharpoons$ LIQUID $\rightleftharpoons$ SOLID	
FREE CHAINS $\rightleftharpoons$ MESOMORPHIC AREAS $\rightleftharpoons$ CRYSTALLITES 	
<b>IDEAL</b>  $PV = RT$ $P = \frac{RT}{V} = B(V)T$	<b>CHAIN MOLECULES</b>  $F = -A(E) + B(E)T$
<b>REAL</b> $P = -\frac{a}{V^2} + \frac{RT}{V-b}$ $= -A(V) + B(V)T$	

FIG. 1. Comparison of states of interaction in chain systems with ordinary molecules. Rubber, for example, at greater than 10 per cent elongation exhibits a positive temperature coefficient of force which characterizes the rubber-like state.

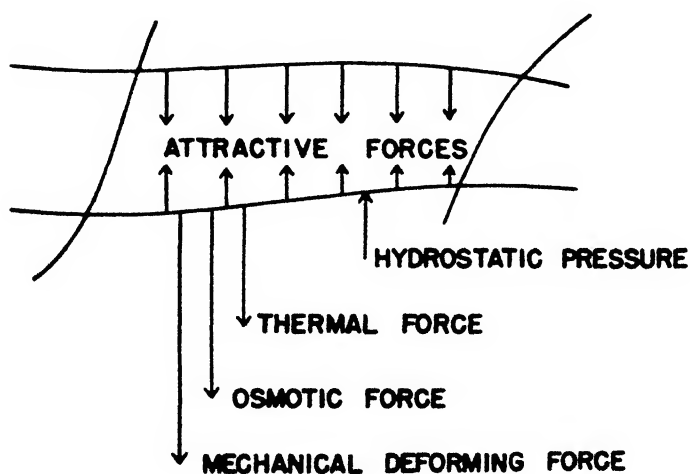


FIG. 2. Dispersive and cohesive forces in fiber network and solvent system

and  $\Delta V$  the change in volume of the fiber system associated with a change of state. From these considerations the relation between the equilibrium force and temperature for the fiber-solvent system is derived as follows:

$$\begin{aligned} f &= \left[ \frac{\partial H}{\partial L} \right]_T - T \left[ \frac{\partial S}{\partial L} \right]_T - \left[ \frac{\partial F_s}{\partial L} \right]_T \\ &= \left[ \frac{\partial H - \partial H_s}{\partial L} \right]_T - T \left[ \frac{\partial S - \partial S_s}{\partial L} \right]_T \end{aligned}$$

but

$$- \left[ \frac{\partial S - \partial S_s}{\partial L} \right]_T = + \left[ \frac{\partial f}{\partial T} \right]_L$$

and therefore at constant elongation,

$$f = A + BT$$

### B. Apparatus

The apparatus illustrated in figure 3 was used to measure the equilibrium force-temperature and the rate of stress relaxation in the fiber. It consists of a thermostated chamber,  $\Lambda$ , in which the fiber and the solvent are placed. One end of the fiber is attached to a hook at the bottom of the chamber and the other to a stiff wire communicating the tension on the fiber to a torsion wire above the chamber. The torsion wire, made of tempered beryllium-copper alloy, is reversible to small displacements. The small displacements of the torsion wire are magnified by an optical lever arrangement illustrated in the diagram. A mirror on the torsion wire reflects the focused image of a slit or cross hair over a uniform scale placed on the wall opposite the mirror. By this arrangement, for example, a 0.1-mm. displacement of a 10-cm. fiber is magnified to a 4-cm. displacement on the scale; accordingly a 10-cm. fiber undergoing a total displacement of 0.1 mm. can be considered as behaving essentially at constant length.

Temperatures from 5° to 80°C. are maintained in the thermostat chamber by circulating mixtures of water from two baths, one at 80°C. and the other of ice water.

A motion-picture camera is used to record the variation in force; this arrangement is particularly useful when the measurement of the rate of stress relaxation is desired. Taking into account the period of oscillation of the torsion wire, it is possible, in this manner, to record the force on the fiber at 0.1-sec. intervals. Besides the known speed of the camera, a secondary record of the time is kept by photographing the sweep of a 10-sec. stopwatch during the experiment.

The desired elongation on the fiber is obtained by adjustment of the height of the platform on which the fiber chamber rests. This adjustment is made by shift of a lever which operates, between adjustable stops, a cam arrangement on which the platform is placed.

When the decay of stress is to be followed, the desired elongation is applied to the fiber and the motion-picture camera is started simultaneously. The initial rapid decay of stress is recorded at consecutive 0.1-sec. interval exposures; later on, when force-temperature measurements are carried out, single exposures are made from time to time as required. At the end of the experiment the film is developed; the scale readings are measured with a microcomparator; the readings are converted to force with the calibration values for the system and finally, the force or stress is plotted as ordinate against the recorded time as abscissa.

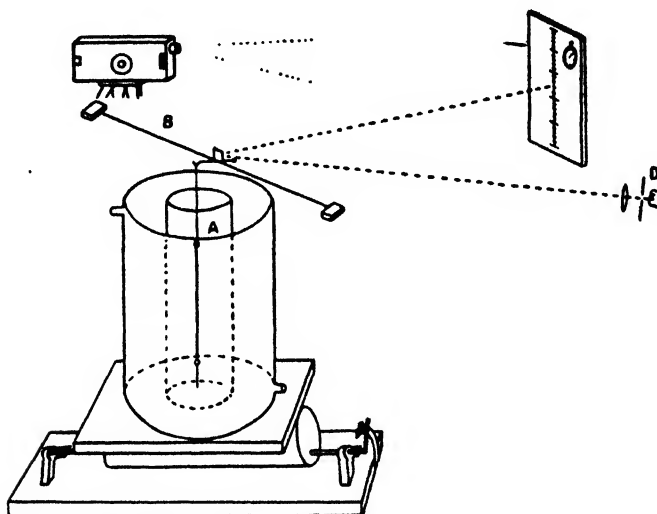


FIG. 3. Diagram of apparatus for measurement of equilibrium force-temperature behavior and stress relaxation of single fibers. The effect of temperature and solvent on the force on the fiber thermostated in chamber A is communicated by a stiff wire to the torsion wire B; the displacement of the torsion wire, enlarged by the optical lever system, is recorded by the motion-picture camera. A secondary record of time is kept by photographing the sweep of a 10-sec. stop watch. Desired elongation of the fiber is obtained by lowering the platform with a lever-cam system operating between adjustable stops.

#### *C. Force-temperature behavior of feather keratin fibers in water*

Figure 4 illustrates a typical relaxation curve for the keratin fibers in water in the isoelectric region at approximately pH 5. The upper curve is a record of the change in tension on the fiber with time, showing the initial rapid fall and the subsequent approach to a state where the force changes so slowly that it can be considered essentially constant. In this constant region the force at equilibrium on the fiber network system at constant elongation is a measure of energy required to displace the network chains in the solvent and at the temperature studied. The variation of the force with temperature is reversible. Characteristic of a rubber-like material, the force decreases when the temperature is decreased. Because the system is reversible with temperature, thermodynamic

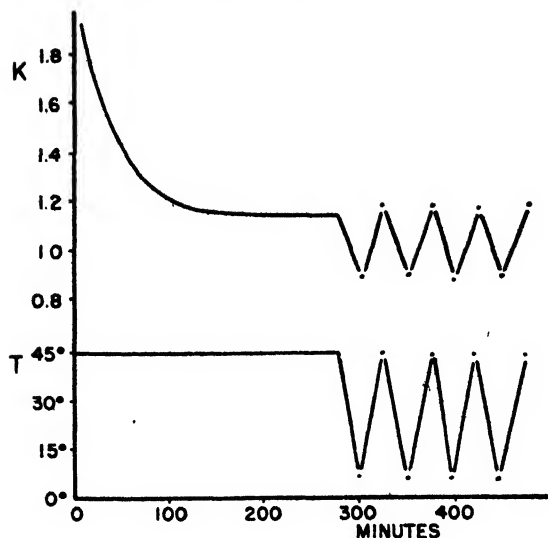


FIG. 4. Relaxation of stress in a synthetic feather keratin fiber following rapid elongation, and the effect of temperature on the equilibrium force at constant length. Following the initial rapid relaxation the stress changes slowly with time and can be considered essentially as constant. The positive temperature coefficient of force indicates the rubber-like state of the relaxed fiber.

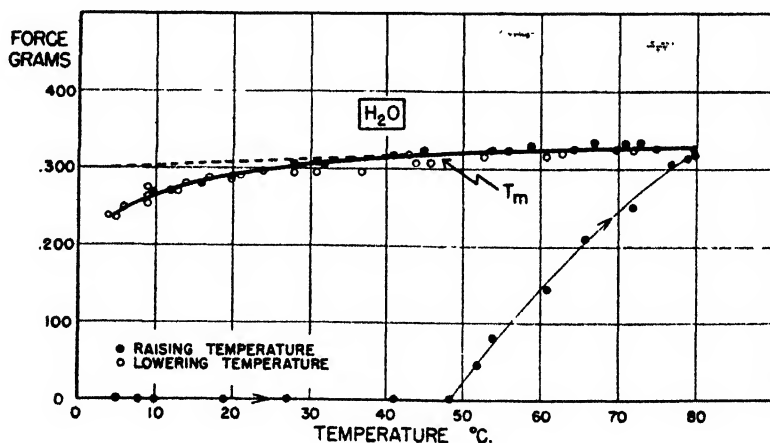


FIG. 5. Equilibrium force-temperature behavior of a relaxed synthetic keratin fiber in water in the isoelectric region. Above a critical temperature region,  $T_m$ , the force varies linearly with a positive temperature coefficient. Below the critical region the force deviates from linear behavior. The approach to the equilibrium rubber-like state during the heating of a previously unrelaxed fiber is illustrated.

generalizations can be applied. For the present discussion we shall be concerned only with the effect of solvents on the equilibrium force-temperature behavior. Figure 5 shows the reversible equilibrium force-temperature behavior of a re-

laxed feather keratin fiber in water in the isoelectric region over the temperature range 5°C. to 80°C. The average diameter of the dry fibers used for this investigation was 0.013 cm.; the average wet diameter (relaxed) was 0.024 cm.

The course of relaxation of the fiber to this rubber-like state can be followed in the same apparatus in another manner. The wet unrelaxed fiber is attached in the chamber in the solvent below the critical temperature region at, for example, room temperature, and the force is adjusted to zero or to a low value.

Figure 5 also illustrates the transition in state of the fiber on relaxation. As the temperature is raised, the first effect is a slight elongation of the fiber, typical of thermoelastic behavior of "normal" solid materials, but then as the temperature approaches the critical region around 45°C., the force on the fiber suddenly increases as the constrained fiber tends to contract as shown in the figure. The equilibrium value of the force is reached as the fiber becomes rubber-like. It is apparent from the figure that the fiber shows a marked hysteresis on cooling; only a slight deviation from the straight-line behavior is apparent below the transition temperature, which is interpreted as due to recombination of the aligned chains. Presumably on long standing in the cold, further chain interaction would take place to give the state similar to that of the original unrelaxed fiber.

For the experiments which follow we have adopted as a standard state the fiber relaxed in boiling water. We shall compare the effects on the system of added alcohols, inorganic electrolyte, and finally reducing agent.

#### *D. Influence of alcohols on force-temperature behavior*

The equilibrium force is markedly affected by the addition of alcohols and electrolytes to the system. Figure 6 illustrates the influence of added ethyl alcohol on the fiber-water system. As previously, the fibers are in the isoelectric region; the elongation is 75 per cent over the boil-relaxed length.<sup>3</sup>

At constant elongation of 75 per cent the influence of the alcohol on the equilibrium force is fourfold; first, at *low* temperatures and in all concentrations of added alcohol, the equilibrium force is *higher* than the corresponding values in water alone. The significant feature is the *negative* temperature coefficient of force. Second, at temperatures *above* an apparent critical temperature region, which is around 40° to 50°C., and in concentrations of alcohol *below* 80–90 per cent concentration by weight, the equilibrium force is *lower* than the corresponding values in water. Furthermore, the values *decrease* progressively as the concentration of the alcohol *increases* to about 50 per cent. The principal effect of the several alcohol concentrations under these conditions is on the intercept values of the force-temperature curves; the slopes are practically the same and similar to the value for water alone. Third, at alcohol concentrations *above* 50 per cent the equilibrium force increases and becomes greater than the value in water as the concentration of alcohol approaches 100 per cent. The fourth

<sup>3</sup> Change in the elongation of the fibers will change the slopes of the curves, but the relative difference for different alcohol mixtures is not significantly altered. For all of the studies reported in this discussion the fibers were compared at similar elongation.

characteristic effect of alcohol on the fiber system is illustrated in figure 7. The variation of alcohol type from methyl to ethyl to *n*-propyl causes a progressive decrease in the equilibrium force. The comparison is made at 50 per cent concentration by weight for each of the alcohols; this concentration gives close to the minimum value of the force for each alcohol.<sup>4</sup>

An apparent critical temperature region is seen for each solution; this region shifts progressively to lower temperatures in changing from methyl to ethyl to *n*-propyl alcohol. In each alcohol solution the fiber below the critical temperature exhibits the characteristic negative temperature coefficient of force;

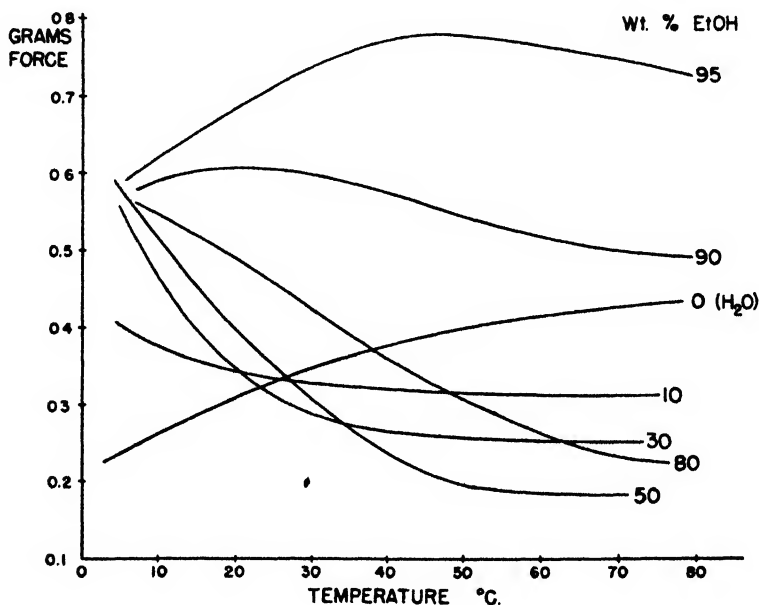


FIG. 6. Influence of aqueous ethyl alcohol on the force-temperature behavior of a relaxed synthetic feather keratin fiber. At low temperatures and in concentrations of ethyl alcohol below 80-90 per cent concentration by weight, the fiber exhibits a negative temperature coefficient of force. Above an apparent critical region, which shifts with alcohol concentration, the equilibrium force decreases with increase of alcohol concentration and reaches a minimum value in the neighborhood of 50 per cent concentration by weight. At higher concentrations the force increases continuously as the concentration of alcohol approaches 100 per cent.

the slopes of the curves and the intercept values vary progressively with change in alcohol from methyl to ethyl to propyl. Above the critical temperature range these alcohols influence principally the intercept values, the slopes being similar and also similar to the slope of the water curve.

<sup>4</sup> Actually, there is a small shift in the maximum effect for the alcohols; the methyl alcohol mixtures have greatest effect on the fiber around 50 per cent concentration, whereas for propyl alcohol the maximum is closer to 40 per cent. The specific effects of the alcohols are also observed when compared on a mole per cent basis of alcohol concentration.

### *E. Interpretation of the effects of alcohols on keratin fibers*

In the light of thermodynamic considerations the negative temperature coefficient of force exhibited by the fiber system below the critical temperature in solutions of the three alcohols indicates normal solid thermoelastic behavior. It is apparent that the network chains have undergone extensive aggregation. The higher force required to maintain constant length in the fiber in the new state indicates that the new condition favors curling of the chains. The contribution to the force is from both a change in the internal energy and a change in the en-

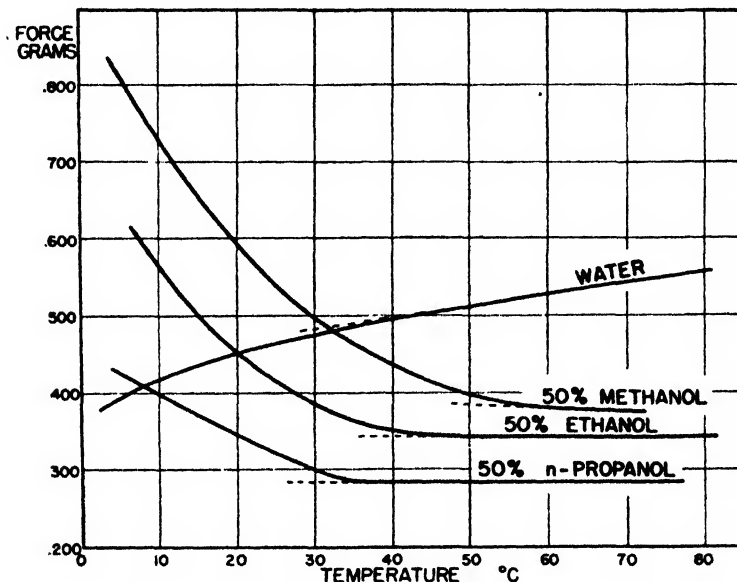


FIG. 7. Influence of aqueous methyl, ethyl, and *n*-propyl alcohols on the force-temperature behavior of a relaxed synthetic feather keratin fiber. A critical region is apparent in the alcohol-water mixtures which shifts progressively with change of solvent from methyl to ethyl to propyl alcohol. Below the critical region the fiber exhibits a negative temperature coefficient of force. The slopes as well as the intercepts of the curves vary progressively with change of solvent. Above the critical temperature region the alcohols progressively lower the equilibrium force, the principal effect being on the intercept of the force-temperature curve.

trophy of the system. The interactions stabilizing the aggregated chains decrease progressively in changing from methyl to ethyl to *n*-propyl alcohol.

The new state of interaction in the fiber is comparable to gel formation in solution. As we shall see later in this discussion, gel formation does occur in solutions of feather keratin in alcohol-water mixtures below a similar critical temperature region.

Further similarity in the behavior of the fibers and the solutions of feather keratin is evident from the influence of added urea. In both cases added urea reduces the extent of interactions until the fibers remain rubber-like over the entire temperature range within which they can be studied and the keratin solutions similarly remain liquid.

Above the critical temperature region the fibers have rubber-like properties in water as well as in solutions of all three alcohols below 80 per cent concentration by weight. The main effect of the alcohols is on the intercept values of the force-temperature curve. This indicates that change in the internal energy of the fiber system is the principal effect of the solvents at these temperatures. This change is accounted for by interaction of the alcohols with the protein, with resulting dissociation of the attractions which stabilize the fiber network. Because progressively lower temperatures are required to maintain constant length in the fibers when the solvent is changed from methyl to ethyl to *n*-propyl alcohol, we conclude that these alcohols, in this order, are progressively more effective in dissociation of internetwork attractions.

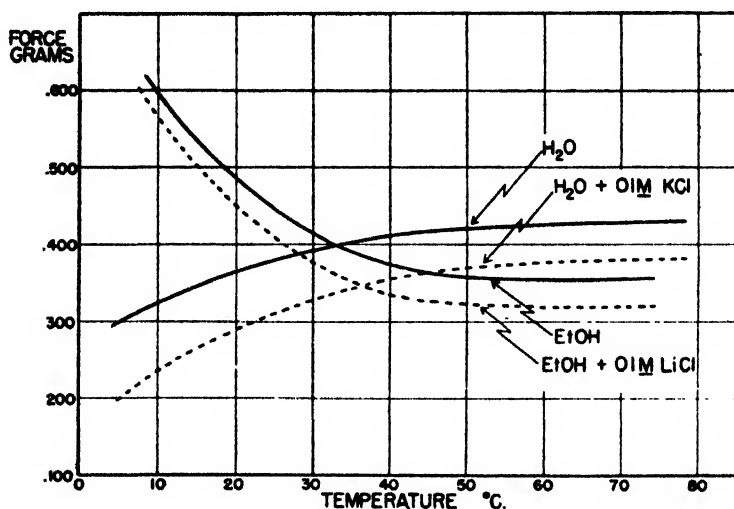


FIG. 8. Influence of added salt on the force-temperature behavior of relaxed synthetic feather keratin fibers in water and in 30 per cent aqueous ethyl alcohol. Added salt lowers the equilibrium force in water and the aqueous alcohol mixtures over the range of temperature indicated.

#### *F'. Influence of inorganic ions on force-temperature relations*

The equilibrium force on the fiber both in water and in the several alcohols is markedly affected by added electrolytes. In the presence of salt in low concentration the equilibrium force, in either case, is lowered. For example, figure 8 illustrates the influence of lithium chloride and potassium chloride of ionic strength = 0.1 on the equilibrium force in water and in 30 per cent concentration by weight of ethyl alcohol. In both water and aqueous alcohol decrease in force occurs above, as well as below, the critical temperature region. The effects of the alcohols and electrolytes are reversible; upon their removal by washing with water, the force-temperature behavior reverts to the characteristic behavior in water.

The effect of salt in altering the equilibrium force in the isoelectric fiber suggests that we are dealing here with the stability of interchain salt linkages,



subject to similar variation in activity coefficient as are soluble dipolar ions, amino acids, and native proteins in the presence of electrolyte ions (4).

The interaction between ions and dipolar ions is known from both theory and experiment to vary with the ionic strength and dielectric constant of the solution. This behavior is accounted for by the theory of Scatchard and Kirkwood (12) and Kirkwood (9). According to the theory the change in free energy due to electrostatic interaction between dipolar ions and inorganic ions should vary directly with the ionic strength and inversely with the square of the dielectric constant. For example, the following expression was derived for the free energy of interaction of glycine with inorganic ions:

$$\Delta F_D = -RT \log \gamma = RT \log S/S_0 = \frac{RT(68.4 \times 10^6) R^2 \Gamma}{D^2 T^2} \frac{1}{a} \frac{1}{2}$$

in which  $\gamma$  is the activity coefficient of the dipolar ion,  $S$  its solubility in salt solution, and  $S_0$  its solubility in pure water.  $D$  is the dielectric constant of the solution and  $T$  is the absolute temperature.  $R$  is the average dipole distance, and  $a$  is the "collision radius," that is, the sum of the radii of the dipolar ion and the inorganic ions.  $\Gamma/2$  is the ionic strength in moles per liter.

When the free-energy change is measured from the solubility ratio at higher ionic strengths a second effect enters in, which must be taken into account, so that the solubility behavior represents only those changes due to electrostatic forces. This secondary effect is the salting out of the dipolar ion by the inorganic ions. Accordingly, a salting-out term must be added to the logarithm of the solubility ratio.

Now to come back again to the behavior of the fibers as a function of ionic strength and dielectric constant, where if the foregoing considerations apply, the equilibrium force, which is decreased in the solvent mixture, should vary similarly with the ionic strength and with the inverse square of the dielectric constant, but with a negative slope. This behavior is observed under limiting conditions as shown in figure 9. This figure is a three-dimensional plot of the variation of the equilibrium force ratio with the ionic strength on one axis and the dielectric constant ratio on the other.  $D_0$  is the dielectric constant of pure water, and  $D$  is the dielectric constant of the solvent under consideration. The equilibrium force ratio,  $f/f_0$ , is the ratio of the force,  $f$ , measured in the solvent under consideration to  $f_0$ , the force in water selected as the standard condition. Starting at the upper left of the figure we see that at low ionic strength the force decreases linearly as a limiting condition with the inverse square of the dielectric constant of the solvent. Significantly, the force varies independently of the alcohol type. Similarly with increase in the ionic strength the equilibrium force falls; the deviation from linearity is probably due to the salting-out effect of the ions on the protein. When the variation of the force with alcohol is compared at ionic strength 0.1, it is seen that although the limiting behavior appears to be linear, the behavior differs from that in low ionic strengths by an apparent specific effect for each alcohol. It is concluded from these considerations that electrostatic interactions are involved in both low and higher salt concentrations; in the higher salt concentration an additional

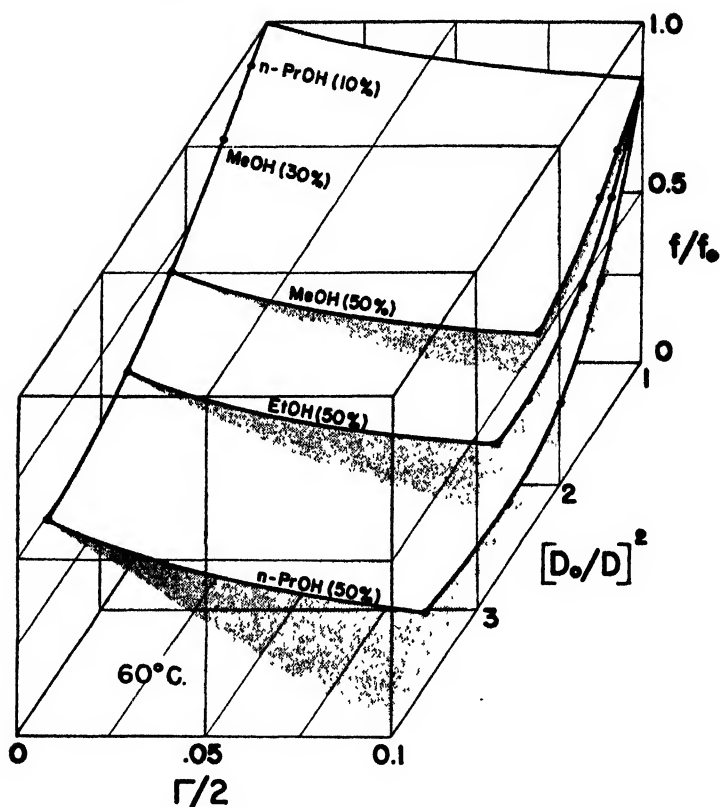
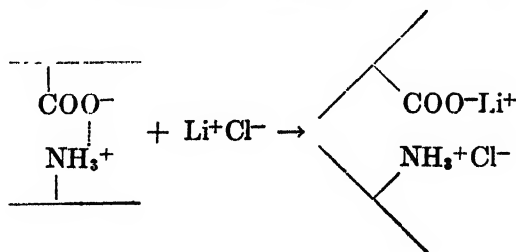


FIG. 9. Equilibrium force on fiber in alcohol-water-lithium chloride mixtures. Three-dimensional plot of the variation in the equilibrium force ratio for a keratin fiber as a function of the ionic strength and the square of the dielectric constant ratio of the solvent. The equilibrium force ratio is the ratio of the force in the solvent under consideration to the force in pure water;  $D_0$  is the dielectric constant of pure water and  $D$  is the dielectric constant of the alcohol-water mixture. At low ionic strength the equilibrium force varies with the inverse squares of the dielectric constant of the solution independent of the type of alcohol. At higher salt concentration the three alcohols exhibit apparent specific behavior.

non-electrostatic interaction is involved. The electrostatic interaction involves presumably the salt linkage connecting neighboring chains. The severance of salt linkages by the interaction with inorganic ions can be considered as follows:



*G. Nature of the non-electrostatic interactions in feather keratin fibers*

## (1) van der Waals attractions

Feather keratin contains a relatively high proportion of leucine compared with many proteins; it is possible that non-electrostatic attractions of the van der Waals type between the hydrocarbon residues are affected by the alcohols. As we shall see, however, the influence of the alcohols is not specific for feather keratin alone; other proteins with smaller proportion of hydrocarbon residues are similarly affected by the alcohols. On this consideration it appears doubtful that the principal effect of the alcohols in the fibers involves the van der Waals attractions.

## (2) Hydrogen bonds

In view of the similarity in the effect of the alcohol-water mixture on the fibers and the influence of urea, it is inferred that hydrogen bonds in the fiber are involved, urea being recognized as an agent which attacks hydrogen bonds. In considering hydrogen bonds as principally affected by the alcohol-water system, we are confronted with differences in the effect of methyl, ethyl, and propyl alcohols. The energy of hydrogen bonding involving the various alcohols would not be expected to differ significantly; furthermore, on purely geometrical considerations the small differences in size of methyl, ethyl, and propyl alcohols would not seem to account for the specific effects observed.

It is possible, however, to account satisfactorily for the specific effects of the alcohols on the basis of the influence of salts on the activity of alcohols in water solutions. It is known that added electrolytes increase the activity of alcohols in water as a result of selective interaction between the ions and the solvent (2, 3, 13). Because the water molecules are more polarizable than alcohol molecules, the water tends to move into these regions where the electric field is greatest. This tendency of the water molecules to cluster around ions results in a displacement, i.e., a salting out of the alcohol with the result that the activity of the alcohol in the solution is increased.

That the increase in the activity of alcohol favors its interaction with the protein is evident from the following experiment. When washed feather keratin fibers or feathers are dried to constant weight at 105°C. and then placed in absolute methyl, ethyl, or *n*-propyl alcohol a non-specific interaction between the protein and alcohol takes place. The combination is stable to heating at 105°C.; the keratin binds in each case approximately 0.5 per cent by weight of each alcohol by relatively strong attraction. If the protein-alcohol material is placed in water, the water displaces the alcohol so that when the keratin is again dried at 105°C. the weight comes back again to the original value. Other proteins combine with absolute alcohol, including silk and wool as well as the carbohydrates, cotton, viscose, and pectin (7, 11). The interaction of the alcohols with the carbohydrates, in particular, gives further evidence that alcohols interact through hydrogen bonding.

The apparent specific effects of the force at equilibrium on the fiber system

of methyl, ethyl, and *n*-propyl alcohols in water solution is accounted for on the basis of the necessarily increasing tendency for these alcohols to be salted out, in this order, from solution. It is well known that increase in the size of a hydrocarbon residue of a substance causes a pronounced increase in the tendency of the material to be salted out from solution.

Accordingly we interpret the influence of the alcohols in water mixtures as dependent on their activity. The non-electrostatic interaction which takes place probably involves hydrogen bonds. As a result of the interaction the equilib-

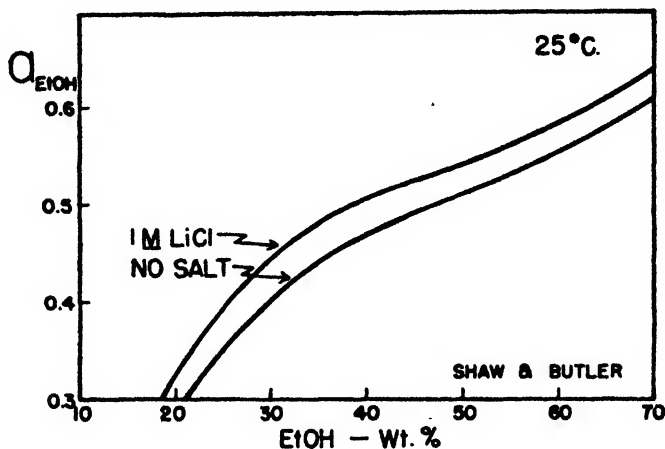
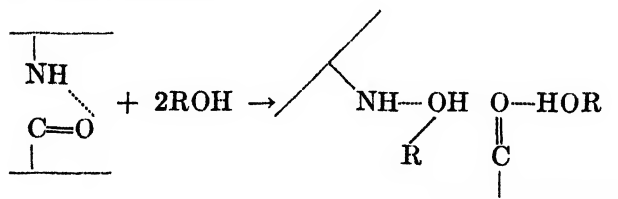


FIG. 10. Variation in activity of ethyl alcohol with increasing alcohol concentration. Addition of salt to ethyl alcohol solution raises the activity of the alcohol, owing to the salting-out effect. The data are from Shaw and Butler.

rium force necessary to maintain constant length in the fiber is lowered. The reaction can be written as follows:



Similar reaction of alcohols with hydrogen-bonded serine residues can occur also. The addition of salt to the alcohol-water mixtures favors this reaction through its tendency to salt out the alcohol. The influence of lithium chloride on the activity of ethyl alcohol in water is illustrated in figure 10. The data are from Shaw and Butler (13).

We conclude therefore that feather keratin combines with alcohols, presumably through hydrogen bonding, and that this interaction in water-alcohol mixtures is favored by salt, which increases the activity of the alcohol through the salt-

ing-out effect on the alcohol. The increase in effectiveness of methyl, ethyl, and *n*-propyl alcohols in this order in the interaction with feather keratin is attributed to their increasing tendency to be salted out from solution. We further conclude that the interaction of alcohols in the fiber severs interchain attractions, with the result that lower force is required to maintain constant length in the fiber. Experiments indicate that feather keratin also reacts with the salt. The resulting severance of the salt linkages similarly lowers the equilibrium force on the fiber.

#### H. Evidence for disulfide cross-links in feather keratin fibers

So far in this discussion we have considered the effects of alcohols and electrolytes on the fiber system. It is apparent that there are attractions still

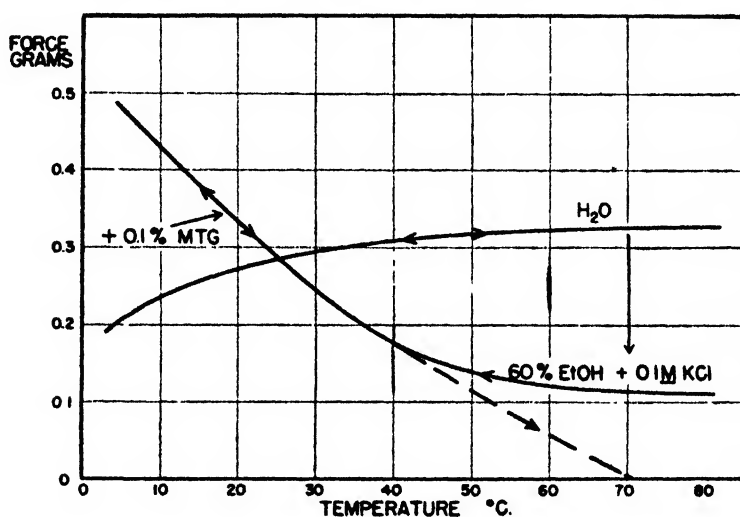


FIG. 11. Effect of added reducing agent on the keratin fiber-solvent system. At temperatures above the critical region the added reducing agent, in this case 0.1 per cent monothioglycol, rapidly lowers the force on the fiber and the fiber dissolves in the alcohol water-salt mixture.

present in the fiber; otherwise it would dissolve in the solvent mixture above the critical temperature region. The 50 per cent propyl alcohol solution containing 0.1 *N* lithium chloride does not dissolve the fiber even on heating the solution to the boiling point. Neither does the fiber dissolve when urea is added. On the other hand, when a reducing agent such as monothioglycol or bisulfite is added, the fiber dissolves rapidly in the alcohol-water-salt mixture at temperatures above the critical region. Figure 11 illustrates the effect of the added reducing agent, in this case 0.1 *M* monothioglycol to an ethyl alcohol-water-salt mixture. This agent was added below the critical region and the temperature was raised. As seen, the force falls rapidly to zero and the fiber dissolves soon afterwards. On cooling of the solution, the protein precipitates in amorphous form.

It is apparent from the behavior of the fiber that reducible bonds are present which assist in maintaining fiber structure. Considering the high proportion of cystine in the keratin, it is inferred that these bonds are disulfide cross-links. This belief is confirmed by the following analysis: Before reduction there is no evidence for free sulfhydryl groups in the fibers according to the nitroprusside reaction, whereas following treatment with cyanide a strongly positive reaction for free sulfhydryl groups in the fibers is obtained. We conclude, therefore, that disulfide cross-links are present in the fiber which help to maintain the fiber network structure.<sup>5</sup>

### *I. Conclusions relative to force-temperature studies*

In the foregoing discussion of the force-temperature behavior of uncured synthetic feather keratin fibers in the isoelectric region, we have shown that at least three types of interchain attractions stabilize the fiber network structure.

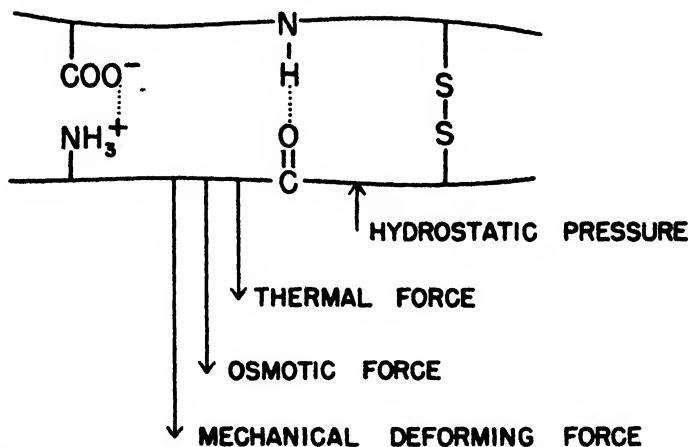


FIG. 12. Summary of effect of forces on synthetic feather keratin fiber

These interactions as illustrated in figure 12 include (1) electrostatic interactions, presumably between acidic and basic groups on the protein side chains, (2) non-electrostatic interactions, apparently hydrogen bonds which probably involve the backbone as well as the side-chain interactions, and (3) disulfide cross-links between cysteine residues. Complete separation of the keratin fiber network is possible when a reducing agent is present.

Figure 13 gives a qualitative description of the influence of the solvent system alcohol-water-salt-reducing agent, on the mechanical work,  $f\Delta L$ , required to

<sup>5</sup> In this connection it is significant that although apparently all of the sulfhydryl groups are oxidized in the fibers, the contributions of disulfide cross-linkages to the fiber wet strength is small. It appears that only a relatively small proportion of the disulfide bonds present are effective in cross-linking the network chains; the remainder probably connect segments along the same chain and are not effective in stabilizing the network structure. Further investigation of these reactions may lead to means of increasing the proportion of effective disulfide cross-links.

overcome the total network energy of the dry fiber. The conditions which favor complete and simultaneous separation of the network chains form the basis for a new method for solubilizing the keratin directly from feathers at neutral pH, to be described briefly in the following section.

### III. APPLICATION OF ALCOHOL-WATER SYSTEMS TO THE SOLUBILIZATION OF FEATHERS

In the previous section we described how synthetic feather keratin fibers dissolve in the solvent system water-alcohol-salt-reducing agent when the temperature is above a critical region, and how the protein precipitates from the dilute solution on cooling. Feathers will also dissolve in the solvent system

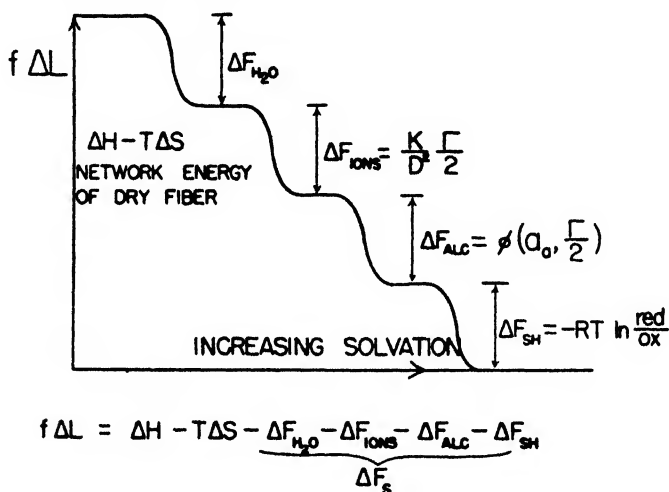


FIG. 13 Qualitative description of the influence of the solvent system alcohol-water-salt-reducing agent on the mechanical work,  $f\Delta L$ , required to overcome the network energy of the fibrous keratin,  $\Delta H - T\Delta S$ , as decreased through increasing solvation involving the interaction with water and alcohol presumably through hydrogen bonds, with inorganic salt involving the salt linkages, and with reducing agents involving the disulfide bonds.

at elevated temperatures and the solutions, similarly to the behavior of the fibers, gel when cooled below a critical temperature range. For example, when 100 g. of washed dry feathers is treated with a liter of the solvent (for example, 50 per cent by weight methyl alcohol containing 0.1 *N* sodium bisulfite) for  $\frac{1}{2}$  hr. at 80°C., about 80 g. of the feather material dissolves.<sup>6</sup> This 80 per cent limit is characteristic for feathers, the same limit being obtained when feathers are dispersed with detergents or with 40 per cent aqueous urea together with a reducing agent.

The gels which form on cooling the warm filtered solutions of feather keratin are thermoreversible; their transition temperature, similar to the behavior of

<sup>6</sup> Other reducing agents such as 0.2 *N* monothioioglycol may be used. Added electrolyte increases the rate of dispersion as well as the solubility of feather keratin.

the fibers, is progressively lowered with change of the solvent from methyl to ethyl to *n*-propyl alcohol. A comparison of the "gel temperature" of the keratin in solutions of these alcohols and with several other alcohols is given in table 1. As seen, two of the other alcohols listed give lower gel temperatures than *n*-propyl alcohol. Significantly, glycerol and glycols give high values for the gel temperature. This behavior is taken as evidence for tendency of the difunctional alcohols to cross-link through hydrogen bonding.

TABLE 1  
*Comparison of gel temperatures of feather keratin dispersed in various aqueous alcohol-water mixtures\**

ALCOHOL	GEL TEMPERATURE (APPROXIMATE)
	°C.
Glycerol . . . . .	70
Ethylene glycol . . . . .	55
Methyl alcohol . . . . .	49
Ethyl alcohol . . . . .	37
<i>n</i> -Propyl alcohol . . . . .	28
Tetrahydrofurfuryl alcohol . . . . .	22

\* The concentration of each alcohol was 45 per cent by weight, the concentration of keratin (reduced) was 10 per cent, and the pH of the solutions was 7.5.

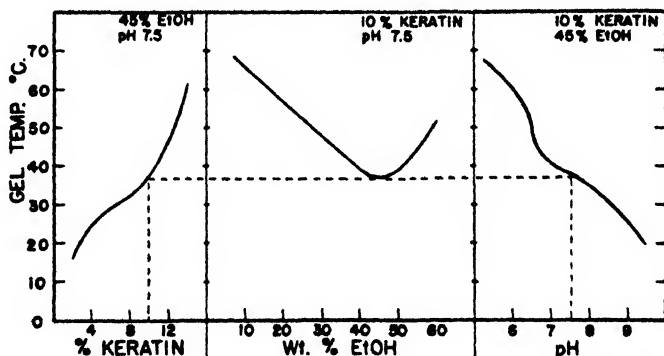


FIG. 14. Variation of gel temperature of solubilized feather keratin with change in pH, ethyl alcohol concentration, and concentration of dissolved protein.

The gel temperature also varies with the concentration of the dissolved protein as well as with the pH of the solution. These effects are illustrated in figure 14. The pH dependency indicates that the mechanism of gel formation is related to the net charge of the protein, that is, to the degree in which salt linkages are severed by shift in the pH. Further discussion of the gel properties of dispersed feather keratin will be postponed for later report.

Feather keratin protein can be recovered from the solvent either by pouring the solution into an excess of water, in which case the protein precipitates, or else by pressing out excess solvent from the gel and drying the residue in a vacuum or in a current of air.



The recovered protein is again soluble in the alcohol-water mixtures, but only when sufficient reducing agent is present. The apparent rapid oxidation of the sulfhydryl groups in the protein is characteristic for this protein. In the reduced form the solubility of the keratin reaches a maximum in the alcohol-water mixtures in the neighborhood of 50 per cent concentration by weight of alcohol, and also increases, within a limit, with increase in salt concentration. At higher salt concentration the characteristic salting out of the protein from solution takes place. The maximum value of the solubility is difficult to determine because of the tendency for gelation in higher concentration of dissolved protein. The gel temperature approaches the boiling point of the solvent around 12 per cent total dissolved protein.

The recovered protein is of high molecular weight, as determined by osmotic pressure and diffusion; the average is at least as high as measured for the keratin dispersed by the detergent method (14). Discussion of the physical-chemical characteristics of the alcohol-water dispersed keratin will also be presented in a later discussion.

Further insight into the mechanism of the interaction of alcohols with feather keratin is provided from comparison of the rates of solubilization of the recovered protein in methyl, ethyl, and propyl alcohols. For these experiments 0.2-g. samples of the protein were added to 10-cc. quantities of the solvent. The alcohol concentrations were 50 per cent by weight and each contained 0.1 *N* lithium chloride and 0.2 *N* monothioglycol. The protein dissolves most rapidly in the propyl alcohol mixture. On comparing the temperature at which the protein dissolves with equal rates in the three solutions we find that for propyl alcohol at 45°C. the rate is similar to that in ethyl alcohol at 60°C. and in methyl alcohol at 70°C. Accordingly, the free energy of activation for solubilization decreases progressively in the methyl, ethyl, and propyl alcohol mixtures in the ratio

$$\Delta_{Me}F' : \Delta_{Et}F' : \Delta_{n-Pr}F' = 1:0.97:0.93$$

The rates of stress relaxation of the keratin fibers are similarly influenced by these solvent mixtures. The rate measurements, in accord with the equilibrium force-temperature and solubility measurements, confirm the view that the alcohol-water-salt-solvent system is a catalyst for the solubilization of keratin in the same sense that alcohol-water mixtures, as mentioned earlier, are catalysts for the denaturation of native corpuscular proteins.

So far we have discussed the comparative effects of methyl, ethyl, and *n*-propyl alcohols on the keratin. Certain other alcohols are apparently more effective in their interaction with feather keratin. A particularly interesting alcohol, in this regard, is 1,3-glycerol dichlorohydrin, compared, for example, with isopropyl alcohol:



Glycerol dichlorohydrin combines firmly with the keratin, as is apparent from the experiments which follow. Isopropyl alcohol, on the other hand, is less firmly bound; it behaves similarly to *n*-propyl alcohol with feather keratin. Glycerol dichlorohydrin is not completely miscible with water; it forms two phases, the water phase containing about 11 per cent of the alcohol. When the alcohol is added to a solution of feather keratin at pH 7, the protein is extracted into the alcohol layer. This transfer is favored by the addition of salt in accord with the effect of salt on the activity of alcohols discussed earlier. Other proteins,

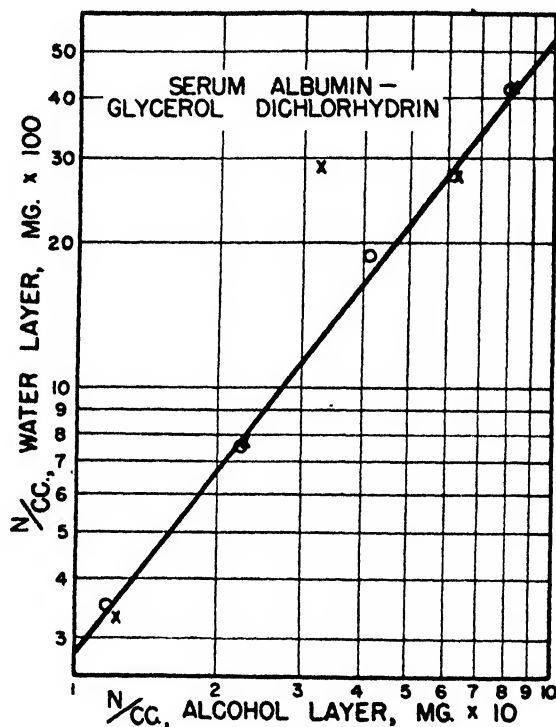


FIG. 15. Logarithmic plot of the partition of bovine serum albumin between water and glycerol dichlorohydrin. The higher concentration of serum albumin in the alcohol phase (saturated with water) than in the water (saturated with alcohol) is attributed to interaction in solution between the alcohol and the protein. The partition is of the form  $y = cx^n$ , for which  $c$ , the partition constant, is 0.55 and  $n = 1.3$ .

for example, serum albumin, are similarly extracted from the aqueous phase by this alcohol. The partition of serum albumin by the water-glycerol dichlorohydrin system is illustrated in figure 15.

That glycerol dichlorohydrin is rather firmly bound to the proteins is shown from the fact that complexes are precipitated on the addition of sufficient salt to the solution. These complexes, similarly to the protein-detergent complexes, are highly plasticized and can be pulled into fibers. Also similar to the protein-detergent behavior is the apparent limiting stoichiometric interaction. But

where the ratio of detergent to protein varies in proportion to the number of acidic or basic groups, the proportion of the alcohol bound is several times these values. Thus, for feather keratin the ratio approximates one molecule of the alcohol for each five amino acid residues, whereas for serum albumin the proportion is one alcohol for every three residues. The range over which this limiting combination takes place is evident from figure 16, in which the percentage nitrogen in the dried precipitated complex is plotted against the amount of glycerol dichlorohydrin added to the solution. The behavior of egg albumin is also shown for comparison. The mole ratio in this case is 1:2. The molecular weight of the keratin was considered as 40,000, equivalent to the value estimated earlier in studies on the protein-detergent complexes (14). The pure proteins, feather keratin and serum albumin, have similar nitrogen content, namely 16.1 per cent.

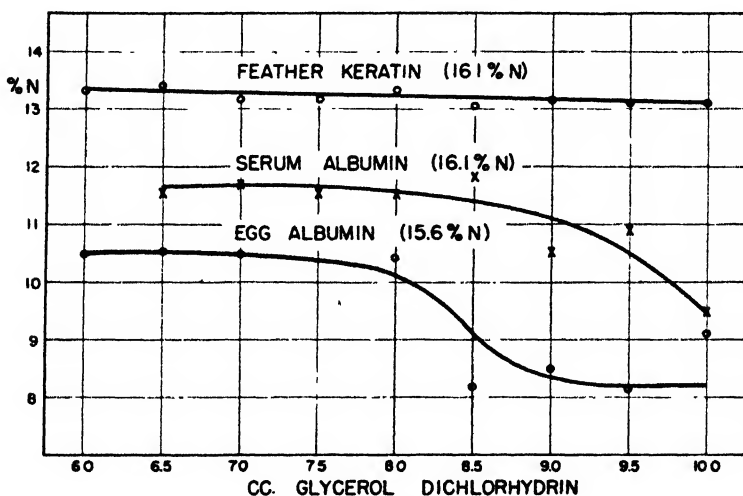


FIG. 16. Apparent stoichiometric interaction of feather keratin, serum albumin, and egg albumin with glycerol dichlorohydrin. Nitrogen content of precipitated complexes from solutions of the three proteins treated with increments of glycerol dichlorohydrin. The bound alcohol is in apparent stoichiometric proportion.

The value for egg albumin is 15.6 per cent nitrogen. The average amino acid residue weight for all proteins was taken as 115. The dichlorohydrin used was freshly distilled and the protein solutions were pH 7. The complexes were precipitated by the addition of excess lithium chloride, or also by shift in pH toward the isoelectric region. Examination of solutions of mixtures of serum albumin and glycerol dichlorohydrin by electrophoretic analyses, however, did not disclose combination between the protein and alcohol. It appears, then, that the interaction occurs under precipitation conditions.

That combination of glycerol dichlorohydrin with the proteins involves secondary interaction is inferred from the fact that no chloride is liberated and the pH of the solutions does not change. Furthermore, the complexes decompose on continued washing with fresh water or with ethyl alcohol. The solvents

apparently replace the dichlorohydrin through mass-action effect. Glycerol dichlorohydrin probably interacts with the protein through hydrogen bonds. Significantly, glycerol dichlorohydrin was found to dissolve nylon; the interaction in this case can only involve hydrogen bonds.

The greater attraction of the dichlorohydrin for the proteins is probably related to the presence of the electron-attracting chlorine atoms which tend to render the hydrogen of the alcohol hydroxyl more electropositive. Further research along these lines may lead to the development of desired water-insoluble plasticizers for proteins. The difficulty with the dichlorohydrin in this connection is its tendency to decompose with time, giving free hydrochloric acid.

#### IV. POSSIBLE APPLICATION OF THE SOLVENT SYSTEM ALCOHOL-WATER-SALT TO THE SOLUBILIZATION OF OTHER PROTEINS

We have already indicated that the solvent system alcohol-water-salt is not necessarily specific for reduced feather keratin. As a matter of fact, mixtures of alcohol and water are recognized solvents for the following prolamines: hordein from barley, secalin from rye, zein from corn, and gliadin from wheat. These proteins readily dissolve in alcohol-water mixtures and are apparently not denatured until heat is applied. Other proteins, the blood proteins for example, are soluble to a limited extent in their native form in alcohol-water mixtures provided the temperature is in the neighborhood of 0°C. On the other hand, the alcohol-water-salt solvent mixture at elevated temperatures will dissolve other proteins to a greater or lesser extent.<sup>7</sup> With several proteins examined in this isoelectric region, the denatured protein coagulates or forms gels when the solutions are cooled below the respective critical temperature regions or when the amount of dissolved protein is greater than 10 to 12 per cent (see figure 17). These gels, similar to the feather keratin gels, are thermoreversible. The dissolved denatured protein in each case appears to be of high molecular weight and accordingly should be suitable for synthetic fibers. The three proteins, feather keratin, isinglass collagen, and peanut protein, compared in the figure were measured in 50 per cent ethyl alcohol solutions in their isoelectric region and at 60°C. The solubility is plotted as a function of the ionic strength of the solution.

All three of the proteins dissolve in the solvent mixture. The solubility in each case increases abruptly with increase in ionic strength of lithium chloride, owing to the salting in of the protein. In the intermediate zone of salt concentration shown, the amount of dissolved protein is greater than 11 to 12 per cent and the solutions are gelled at this temperature and pH and with the alcohol mixture. At higher salt concentration the amount of dissolved protein decreases to less than 11 to 12 per cent, owing to the salting-out effect on the protein.

The possibilities of general application of the solvent system alcohol-water-salt for the recovery of difficultly soluble proteins for industrial uses are being

<sup>7</sup> Jirgensons (J. Colloid Sci. 1, 539 (1946)) has observed a peptizing effect of mixtures of alcohol, water, and salts on potato globulin, casein, and hemoglobin.

investigated. It is expected that the method will be more effective in certain cases than in others; numerous factors are involved that determine the solubility of the proteins, among which are those indicated in this discussion: namely, the activity of the alcohol, as influenced by salt, the relative magnitudes of the salting-in and salting-out effects on the protein, and the activity coefficient of the salt. Nevertheless, it is foreseen that the solvent system will be applicable to certain protein systems such as feather keratin and perhaps to certain collagens for which other methods are less practicable.

These experiments, together with experiments on the fiber-spinning properties of alcohol-solubilized proteins, also in progress, will be presented in a later discussion.

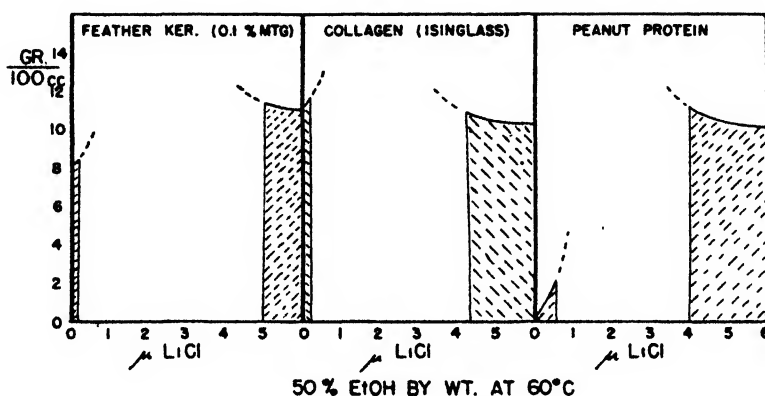


FIG. 17. Maximum solubility of reduced feather keratin, isinglass collagen, and peanut protein in 50 per cent by weight ethyl alcohol-water with increasing salt concentration. All three proteins dissolve in the solvent mixture. The solubility in each case increases abruptly with increase in ionic strength, owing to the salting-in of the protein. In the intermediate zone of salt concentration shown, the amount of dissolved protein is greater than 11 to 12 per cent, and the solutions are gelled at this temperature and pH and with this alcohol mixture. At higher salt concentrations, the amount of dissolved protein decreases to less than 11 to 12 per cent as a result of the salting-out effect on the protein.

#### SUMMARY

General consideration has been given to the stability of proteins and synthetic fibers; the limitations of several methods for solubilizing proteins were mentioned.

A method for the measurement of the equilibrium force-temperature behavior of single fibers has been described. The method was applied to the study of synthetic feather keratin fibers in alcohol-water-salt mixtures.

Evidence was given for the following three types of interactions which stabilize the fiber network structure: (1) salt linkages, which interact with inorganic ions in conformity with the theory of dipolar ion-ion interaction; (2) non-electrostatic interactions, presumably hydrogen bonds, which interact with the alcohols, methyl, ethyl, and *n*-propyl (favored by increase in activity of the al-

cohol by the addition of salt); and (3) disulfide cross-links, which interact with reducing agents.

The increasing specific interaction observed with methyl, ethyl, and *n*-propyl alcohols is accounted for on the basis of their increasing tendency to be salted out from solution.

When reducing agent is added to the keratin fiber in the alcohol-water-salt mixture, the equilibrium force falls to zero above the critical temperature for the mixture and the fiber rapidly dissolves. Application of this solvent system to the solubilization of feathers at neutral pH has been given.

Similarly to the behavior of the fibers, the solubilized protein exhibits a critical temperature region below which the solution sets to thermoreversible gel.

The recovered protein is of high molecular weight and as such is suitable as a raw material for synthetic fibers.

Illustration of the solubilization of isinglass collagen and peanut protein by alcohol-water-salt mixtures has been given.

Discussion has been given of the formation, isolation, and composition of complexes between feather keratin, serum albumin, egg albumin, and glycerol 1,3-dichlorohydrin.

#### VI. REFERENCES

- (1) ÅKERLÖF, G.: J. Am. Chem. Soc. **52**, 2353 (1930); **54**, 4130 (1932).
- (2) BUTLER, J. A. V., AND THOMSON, D. W.: Proc. Roy. Soc. (London) **A141**, 86 (1933).
- (3) BUTLER, J. A. V., THOMSON, D. W., AND MACLENNAN, W. H.: J. Chem. Soc. **1933**, 674.
- (4) COHN, E. J., AND EDSALL, J. T.: *Proteins, Amino Acids and Peptides*. Reinhold Publishing Corporation, New York (1943).
- (5) EYRING, H., AND STEARN, A. E.: Chem. Rev. **24**, 253 (1939).
- (6) HARRIS, M., MIZELL, L. R., AND FOURT, L.: Ind. Eng. Chem. **34**, 833 (1942).
- (7) JANSSEN, E. F., WAISBROT, S. W., AND RIETZ, E.: Ind. Eng. Chem., Anal. Ed. **16**, 523 (1944).
- (8) JONES, C. B., AND MECHAM, D. K.: Arch. Biochem. **3**, 193 (1943).
- (9) KIRKWOOD, J. G.: J. Chem. Phys. **2**, 351 (1934).
- (10) LUNDGREN, H. P.: Textile Research J. **15**, 335 (1945).
- (11) MEASE, R. T.: Ind. Eng. Chem., Anal. Ed. **5**, 317 (1933).
- (12) SCATCHARD, G., AND KIRKWOOD, J. G.: Physik. Z. **33**, 207 (1932).
- (13) SHAW, R., AND BUTLER, J. A. V.: Proc. Roy. Soc. (London) **A129**, 519 (1930).
- (14) WARD, W. H., HIGH, L., AND LUNDGREN, H. P.: J. Polymer Research **1**, 22 (1946).

ELECTROPHORETIC AND ULTRACENTRIFUGAL INVESTIGATION  
OF RABBIT LIVER NUCLEOPROTEIN<sup>1</sup>

Q. VAN WINKLE AND WESLEY G. FRANCE

*Department of Chemistry, The Ohio State University, Columbus, Ohio**Received August 25, 1947*

## INTRODUCTION

Nucleoproteins are known to be intimately associated with such biologically important entities as the chromosomes, genes, and viruses and have received a considerable amount of study in connection with virus diseases and cancer. The naturally occurring tissue nucleoproteins which are found in the nuclei (chromosomes and genes) and cytoplasm of normal plant and animal cells have not been as intensively studied, however. Only calf thymus nucleohistone has been characterized with regard to its molecular weight, particle shape, and electrophoretic behavior (2, 3, 5, 6, 7). This leaves a large and important field open for further investigation.

For this investigation, it was decided to prepare rabbit liver nucleoprotein by a mild method, determine the homogeneity of the preparation by means of electrophoresis, sedimentation velocity, and diffusion studies, and obtain information concerning the molecular weight, particle shape, and electrophoretic mobility of the liver nucleoprotein.

## EXPERIMENTAL PROCEDURES

*Electrophoresis measurements*

Electrophoretic studies were made by the moving-boundary method, using a Tiselius electrophoresis apparatus and standardized techniques which have been described by Longworth and MacInnes (11, 13).

*Sedimentation-velocity measurements*

An air-driven, vacuum ultracentrifuge of the Beams type was used for sedimentation-velocity measurements on rabbit liver nucleoprotein. This ultracentrifuge has been described elsewhere (10). The sedimenting boundaries were followed by means of the schlieren bands which were formed in conjunction with a long-focal-length schlieren lens and a knife edge. For a few of the ultracentrifuge runs, the Lamm scale method (9) was used to record the concentration gradients in the sedimenting boundaries. Scale photographs were taken through 6 mm. of solution with a scale distance of approximately 6 cm. All measurements were made at a speed of 30,000 R.P.M., corresponding to a centrifugal force in the center of the cell of approximately 60,000 times gravity.

Sedimentation constants were calculated from the equation,

$$s = \frac{\Delta x}{\Delta t} \cdot \frac{1}{\omega^2 x_m} \quad (1)$$

<sup>1</sup> Presented at the Twenty-first National Colloid Symposium, which was held under the auspices of the Division of Colloid Chemistry of the American Chemical Society at Palo Alto, California, June 18-20, 1947.

and were reduced to sedimentation in water at 20°C. by means of the following relationship:

$$s_{20} = s \left( \frac{\eta_t}{\eta_{20}} \right)_{\text{H}_2\text{O}} \cdot \left( \frac{\eta_{\text{soln.}}}{\eta_{\text{H}_2\text{O}}} \right)_t \cdot \frac{(1 - v\rho)_{\text{H}_2\text{O}}}{(1 - v\rho)_{\text{soln.}}} \quad (2)$$

The symbols used in equations 1 and 2 have been standardized by Svedberg and Pedersen (21). A partial specific volume of 0.658 was assumed for rabbit liver nucleoprotein. It is the value which has been reported for calf thymus nucleohistone by Carter and Hall (3).

### *Diffusion measurements*

Measurements of diffusion coefficients were made in the Tiselius electrophoresis apparatus, using a standard 11-ml. cell in which the limbs were divided into two sections by a central parting plane. This cell was mounted in a special rack which could be moved out of the optical path without disturbing the diffusing boundaries. Such an arrangement made it possible to perform electrophoresis experiments during the intervals between diffusion photographs. The use of the electrophoresis apparatus for diffusion measurements has been described by Longworth (12).

The diffusion experiments were performed at 1.0°C. and the diffusion constants were calculated by two different methods: (1) the maximum ordinate-area method, and (2) the method of moments. The following relationship was used in calculating diffusion constants by the maximum ordinate-area method:

$$D = \left( \frac{A}{H} \right)^2 \cdot \frac{1}{4\pi t} \quad (3)$$

where  $A$  is the area under the diffusion curve ( $\text{cm}^2$ ),  $H$  is the maximum height of the curve ( $\text{cm}.$ ), and  $t$  is the time of diffusion ( $\text{sec}.$ ). The procedure used in calculating diffusion constants by the method of moments has been described by Neurath (17). The diffusion constants calculated for a temperature of 1.0°C. were corrected to water at 20°C. by the following equation:

$$D_{20} = D_T \frac{\eta_T}{\eta_{20}} \cdot \frac{293}{T} \quad (4)$$

where  $D_T$  is the measured diffusion constant,  $T$  is the absolute temperature of the experiment,  $\eta_T$  is the viscosity of the solvent at temperature  $T$ , and  $\eta_{20}$  is the viscosity of water at 20°C.

## PREPARATION AND CHARACTERIZATION OF NUCLEOPROTEIN

### *Method of preparation*

Three preparations of rabbit liver nucleoprotein were made, using the procedure given by Mirsky and Pollister (16). The rabbits were killed by decapitation and the livers were removed immediately and homogenized in a Waring blender in the presence of four times their weight of ice-cold saline solution (0.14  $M$  sodium chloride) buffered to pH 6.8 to remove albumin and globulins.



The nucleoprotein, which is insoluble in 0.14 *M* sodium chloride solution, remained in the residue. It was subsequently dissolved by treating the residue with 1 *M* sodium chloride solution. Purification of the dissolved nucleoprotein was obtained by precipitating it in 0.14 *M* sodium chloride solution and redissolving the precipitate in the 1 *M* solution. All solutions were buffered to pH 6.8. The nucleoprotein was precipitated and dissolved three times, with all operations being carried out in a cold room at 0°C. The dry weight of nucleoprotein obtained amounted to 0.1 per cent of the weight of the wet livers taken.

### Analyses

Nitrogen and phosphorus analyses were made on dried preparations of the liver nucleoprotein, using a standard micro-Kjeldahl method for nitrogen and a

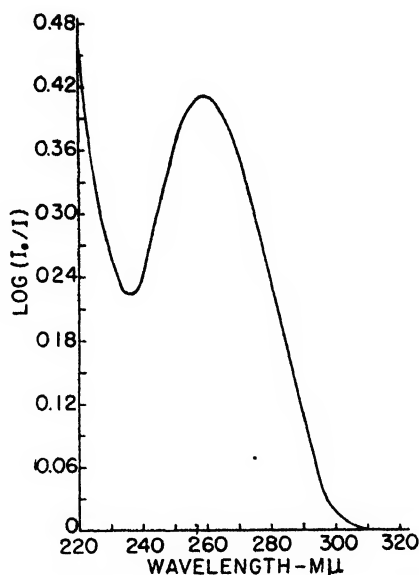


FIG. 1. Ultraviolet absorption curve for rabbit liver nucleoprotein dissolved in water

colorimetric method for phosphorus (1). The averages of three determinations were: per cent N = 16.83; per cent P = 4.97.

Assuming that the nucleoprotein derives its phosphorus content solely from its nucleic acid component and using 9.91 per cent as the phosphorus content of the nucleic acid component, the percentage of nucleic acid in the nucleoprotein is estimated to be approximately 50 per cent.

The Dische diphenylamine reaction described by Schneider (18) and Seibert (19) was used in a qualitative manner to identify desoxyribose nucleic acid in the nucleoprotein. A strong positive test was obtained. Also, an ultraviolet absorption curve was obtained on a sample of liver nucleoprotein which had been dialyzed against distilled water. The curve, shown in figure 1, exhibits the characteristic nucleic acid absorption maximum at 2600 Å. (8).

## EXPERIMENTAL RESULTS

*Electrophoretic measurements*

Electrophoretic experiments with rabbit liver nucleoprotein were performed at various pH's in buffer solutions of two different ionic strengths: namely, 0.02 and 1.02. Nucleoprotein which had been precipitated three times and phosphate buffers at pH's 8.0, 7.1, and 6.2 were used for the experiments at ionic strength 0.02. Examples of the type of electrophoretic patterns which were obtained with the dilute phosphate buffers are shown in figures 2 and 3. From the patterns it is evident that the nucleoprotein is relatively free of slow-

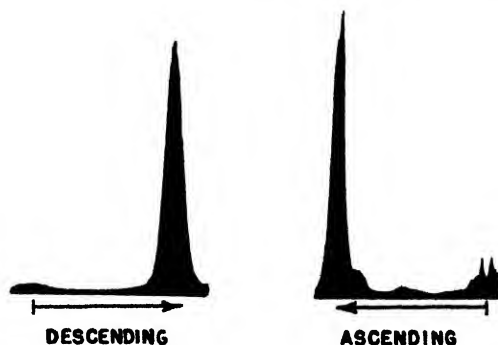


FIG. 2. Electrophoretic patterns for rabbit liver nucleoprotein dissolved in 0.02  $\mu$  phosphate buffer, pH 6.2. Electrolysis time, 43 min. Field strength, 8.55 volts/cm.

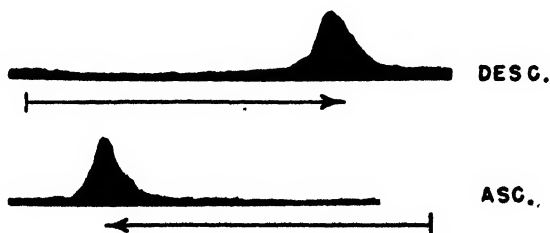


FIG. 3. Electrophoretic patterns for rabbit liver nucleoprotein dissolved in 0.02  $\mu$  phosphate buffer, pH 8.0. Electrolysis time, 66.7 min. Field strength, 8.62 volts/cm.

moving impurities. However, the nucleoprotein peak itself exhibited an appreciable amount of spreading during the electrolysis, which is indicative of electrophoretic heterogeneity. The mobilities obtained at 0°C. are given in table 1 for both the rising and the descending boundaries. Mobilities calculated from the velocity of the rising boundary were corrected for the  $\delta$  effect according to the method of Longworth and MacInnes (14). The average mobilities of the rising and descending boundaries are plotted *versus* pH in figure 6. A comparison of the results obtained by Hall (7) for calf thymus nucleohistone with those for rabbit liver nucleoprotein indicates that the nucleohistone exhibits mobilities which are greater by 10 per cent, over the pH range investigated. The liver nucleoprotein is insoluble in 0.02 ionic strength acetate buffer at pH 4.

The electrophoresis experiments at ionic strength 1.02 were conducted on a nucleoprotein sample which had been precipitated once, several which had been precipitated twice, and one which was an aliquot of the first crude solution of nucleoprotein obtained in the preparation procedure described above. One molar sodium chloride solutions were used, which were buffered with 0.02 ionic strength phosphate or acetate. All the solutions were opalescent and it was often necessary to use infrared-sensitive film in conjunction with a Wratten 25 filter and a 300-watt tungsten projection lamp in order to obtain uniformly exposed electrophoretic patterns. The electrophoretic patterns obtained for the crude extract of nucleoprotein in 1 *M* sodium chloride, 0.02 ionic strength phosphate, pH 7.1, are shown in figure 4. The nucleoprotein is the leading component or group of components in these patterns. In figure 5 are shown

TABLE 1  
*Electrophoretic mobilities of rabbit liver nucleoprotein at 0°C.*

SAMPLE NUMBER OF TIMES PRECIPITATED	BUFFER SOLUTION	pH	$\Delta n \times 10^4$	MOBILITY $\times 10^4$		
				Descend- ing	Ascend- ing	Average
3	0.02 $\mu$ phosphate	8.0	2.58	1.46	1.40	1.43
3	0.02 $\mu$ phosphate	7.1	4.85	1.26	1.26	1.26
3	0.02 $\mu$ phosphate	6.2	5.65	1.15	1.18	1.17
None	1 <i>M</i> NaCl, 0.02 $\mu$ phosphate	7.1	0.73	1.02	1.05	1.04
				0.94		
1	1 <i>M</i> NaCl, 0.02 $\mu$ phosphate	7.2	1.64	1.08*	1.08*	1.08
2	1 <i>M</i> NaCl, 0.02 $\mu$ phosphate	7.2	1.46	0.81*	0.95*	0.82
					0.83*	
2	1 <i>M</i> NaCl, 0.02 $\mu$ phosphate	5.4	--	0.84*	0.89*	0.87
				0.78*	0.84*	0.81
				0.59	0.69	0.64
2	1 <i>M</i> NaCl, 0.02 $\mu$ acetate	3.9		--	0.98	--
				--	0.65	--
				--	0.50*	--
				--	0.41	--

patterns obtained for nucleoprotein which received two precipitations, and which was dissolved in 1 *M* sodium chloride, 0.02 ionic strength phosphate, pH 7.2. The leading components in the ascending and descending patterns are nucleoprotein. However, on the ascending side the nucleoprotein fraction is split into two separate peaks. At pH 6.4 no splitting of the nucleoprotein peak on the ascending side was observed. However, at pH 5.4 both the ascending and the descending peaks split into two components. The patterns obtained for nucleoprotein which received two precipitations showed an appreciable amount of heterogeneous, slow-moving material to be present at all pH's studied. At pH 3.9, in 1 *M* sodium chloride, 0.02 ionic strength acetate buffer, the nucleoprotein peak split into a number of components, and, in this instance, the fastest component moved with a mobility of thymus nucleic acid (see Stenhagen and

Teorell (20)). This suggests the possibility that nucleic acid has been split away from protein and is migrating as a separate component. In view of what is already known concerning the salt-like character of the bond between nucleic acid and protein in nucleoproteins (4, 6, 15), the tendency of nucleic acid to split away from protein in 1 *M* sodium chloride solutions is to be expected.

The mobilities obtained for nucleoprotein in 1 *M* sodium chloride solutions are listed in table 1 and plotted as a function of pH, in figure 6. In table 1, the column  $\Delta n \times 10^4$  represents the refractive-index difference between nucleoprotein solution and buffer solution as obtained from the area under the nucleo-

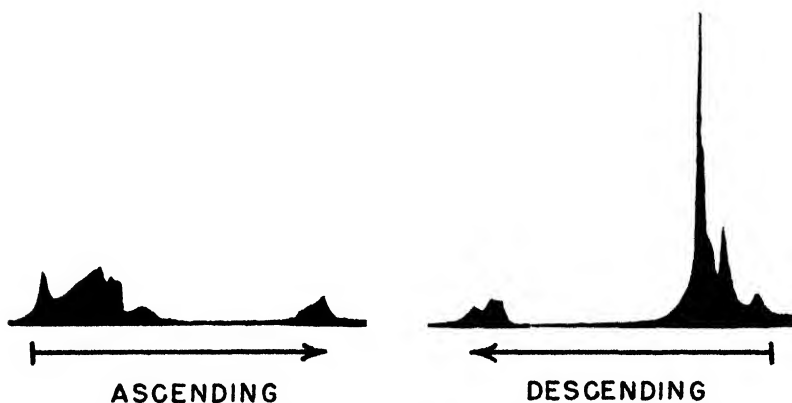


FIG. 4. Crude solution: 1 *M* sodium chloride, 0.02  $\mu$  phosphate, pH 7.1. Electrolysis time, 610 min. Field strength, 1.34 volts/cm.



FIG. 5. Rabbit liver nucleoprotein precipitated two times. Dissolved in 1 *M* sodium chloride, 0.02  $\mu$  phosphate, pH 7.2. Electrolysis time, 299 min. Field strength, 1.61 volts/cm.

protein peak of the descending pattern. In all cases, the mobilities listed in table 1 represent anionic migration. For some of the runs in 1 *M* sodium chloride solutions a number of mobilities have been listed, corresponding to the number of relatively fast moving peaks which were observed in the electrophoretic patterns, and, in addition, the components which were accompanied by turbidity have been starred.

#### *Sedimentation-velocity measurements*

Sedimentation-velocity measurements were made on rabbit liver nucleoprotein which had been precipitated three times and which was dissolved in 1 *M* sodium

chloride, 0.02 ionic strength phosphate, pH 6.4. Three different nucleoprotein concentrations were studied in order to determine the effect of concentration on the sedimentation constant. By means of the scale method, the sedimenting boundary was found to contain possibly three closely spaced peaks or components. The sedimentation data recorded in table 2 are average values for

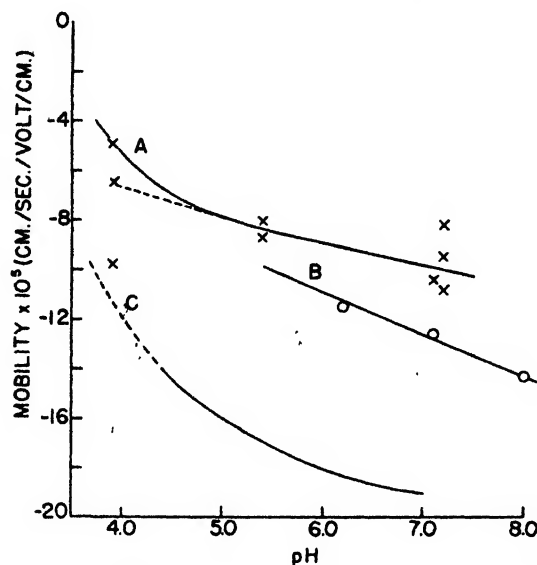


FIG. 6. Electrophoretic mobility *versus* pH. Curve A, rabbit liver nucleoprotein in 1 *M* sodium chloride buffer solutions; curve B, rabbit liver nucleoprotein in 0.02  $\mu$  phosphate buffer solutions; curve C, thymus nucleic acid in 0.1  $\mu$  buffer solutions (from Stenhagen and Teorell (20)).

TABLE 2  
*Sedimentation-velocity determinations on rabbit liver nucleoprotein*  
Centrifugal force: 60,000  $\times$  gravity

CONCENTRATION OF PROTEIN	<i>S</i> <sub>20</sub>
<i>g./100 ml.</i>	<i>Svedbergs</i>
0.22	10.4
0.11	15.4
0.09	16.8
0.00	26.3*

\* Extrapolated value.

the group of peaks. The extrapolation to zero concentration was made by plotting  $1/s_{20}$  *versus* concentration.

#### *Diffusion measurements*

Diffusion measurements were made in dilute phosphate buffers and in 1 *M* sodium chloride solutions, using rabbit liver nucleoprotein which had been precipitated three times. These measurements also showed the existence of

a molecular inhomogeneity and the inhomogeneity was greater in 1 *M* sodium chloride solutions than in the dilute phosphate buffers. The average values of two determinations in 1 *M* sodium chloride, 0.02  $\mu$  phosphate solution, pH 6.4 are:  $D_A = 0.78 \times 10^{-7}$  cm.<sup>2</sup>/sec. and  $D_M = 1.08 \times 10^{-7}$  cm.<sup>2</sup>/sec. for water at 20°C.  $D_M$  is the diffusion constant calculated by the method of moments. The diffusion curves obtained in 0.02  $\mu$  phosphate buffer, pH 7.10, were found to more nearly approach the ideal Gaussian distribution law, and are shown in figure 7. The values,  $D_A = 1.52 \times 10^{-7}$  and  $D_M = 1.78 \times 10^{-7}$  (water at 20°C.), which were obtained from these curves are too high, however, because there

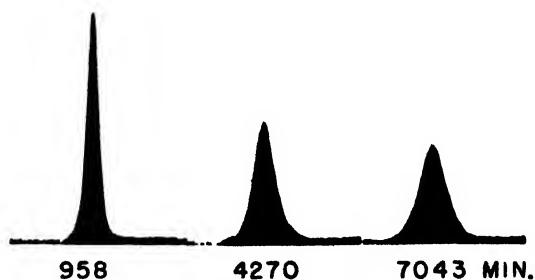


FIG. 7. Diffusion photographs for rabbit liver nucleoprotein in 0.02  $\mu$  phosphate buffer, pH 7.1.

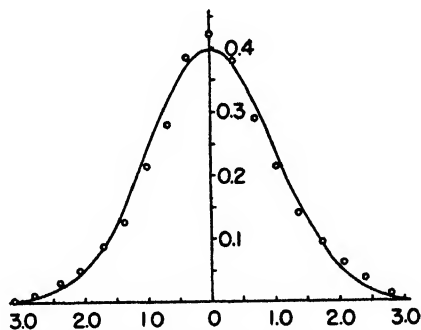


FIG. 8. Comparison of experimental diffusion curve (circles) with normal Gaussian distribution curve (solid line). Rabbit liver nucleoprotein in 0.02  $\mu$  phosphate buffer, pH 7.1. Diffusion time, 7064 min.

was insufficient buffer present to repress the diffusion potential set up by the rapidly diffusing gegenions of the nucleoprotein molecules.

#### CALCULATIONS

Two quantities can be calculated from the sedimentation and diffusion constants reported above. They are (1) the molecular weight of the unhydrated molecule, and (2) the relative degree of asymmetry of the molecule. The molecular weight is obtained from the formula,

$$M = \frac{RTs}{D(1 - V\rho)} \quad (5)$$

where  $s = 26.3 \times 10^{-13}$  cm./sec./dyne/g.  
 $V = 0.658$  cc./g.  
 $\rho = 0.9982$  g./cc.  
 $D = 0.78-1.0 \times 10^{-7}$  cm.<sup>2</sup>/sec.  
 $R = 8.313 \times 10^7$  dyne cm./degree  
 $T = 293^\circ\text{A}.$

The result is:

$$M = 1,600,000-2,300,000$$

The frictional ratio,  $f/f_0$ , can be calculated by means of the equation:

$$f/f_0 = 10^{-8} \left( \frac{1 - V\rho}{D_{20}^2 s_{20} V} \right)^{\frac{1}{2}} \quad (6)$$

using the same constants as were used in equation 5. The result is:

$$f/f_0 = 2.6-3.3$$

By assuming that the nucleoprotein molecule has the shape of an elongated ellipsoid, the Perrin equation can be applied:

$$f/f_0 = \frac{(1 - \rho^2)^{\frac{1}{2}}}{\rho^{\frac{2}{3}} \log \frac{1 + (1 - \rho^2)^{\frac{1}{2}}}{\rho}}$$

where  $\rho = b/a$  (axial ratio),  
 $b$  = equatorial radius, and  
 $a = \frac{1}{2}$  length of the axis of rotation.

The axial ratio calculated for rabbit nucleoprotein is then within the range of 1/40 to 1/60.

#### SUMMARY

1. The method of Mirsky and Pollister has been used to isolate nucleoprotein from rabbit liver.

2. The presence and approximate percentage of nucleic acid in rabbit liver nucleoprotein were determined by means of its ultraviolet absorption spectrum and its phosphorus content. Per cent nucleic acid = 50.

3. The Dische diphenylamine color reaction was used to demonstrate the presence of desoxyribose nucleic acid in the rabbit liver nucleoprotein.

4. Electrophoretic mobility determinations on rabbit liver nucleoprotein in dilute aqueous phosphate buffers show that its mobilities approximate those obtained by Hall for calf thymus nucleohistone.

5. Mobilities of rabbit liver nucleoprotein in 1 *M* sodium chloride solution were found to be 20-30 per cent lower than in dilute aqueous phosphate buffers. Also, the nucleoprotein exhibited a tendency to dissociate into protein and nucleic acid in 1 *M* sodium chloride solutions.

6. Sedimentation, diffusion, and electrophoretic measurements indicate that rabbit liver nucleoprotein, as prepared by the method of Mirsky and Pollister, is inhomogeneous with respect to its molecular kinetic and electrokinetic properties.

7. Combined measurements of sedimentation and diffusion constants yield a molecular weight which ranges between 1,600,000 and 2,300,000 and an axial ratio for the nucleoprotein molecule which lies between 40:1 and 60:1.

Acknowledgment is made for the generous Grant-in-Aid provided by the Graduate School and the Research Foundation of the Ohio State University which made this work possible.

#### REFERENCES

- (1) BODANSKY, A.: *J. Biol. Chem.* **99**, 197-206 (1932-33).
- (2) CARTER, R. O.: *J. Am. Chem. Soc.* **63**, 1960-4 (1941).
- (3) CARTER, R. O., AND HALL, J. L.: *J. Am. Chem. Soc.* **62**, 1194-6 (1940).
- (4) COHEN, S. S.: *J. Biol. Chem.* **158**, 255 (1945).
- (5) EULER, H. V., AND HAHN, L.: *Arkiv Kemi, Mineral. Geol.* **22A**, Nr. 17 (1946).
- (6) EULER, H. V., AND HAHN, L.: *Arkiv Kemi, Mineral. Geol.* **23A**, Nr. 5 (1946).
- (7) HALL, J. L.: *J. Am. Chem. Soc.* **63**, 794-8 (1941).
- (8) HEYROTH, F. F., AND LOOFBOUROW, J. R.: *J. Am. Chem. Soc.* **53**, 3441 (1931).
- (9) LAMM, O.: In T. Svedberg and K. O. Pedersen's *The Ultracentrifuge*. pp. 253-64. Oxford University Press, London (1940).
- (10) LANG, E. R., VAN WINKLE, Q., AND FRANCE, W. G.: *J. Colloid Sci.* **2**, 315 (1947).
- (11) LONGSWORTH, L. G.: *Chem. Rev.* **30**, 323-40 (1942).
- (12) LONGSWORTH, L. G.: *Ann. N. Y. Acad. Sci.* **41**, 267 (1941).
- (13) LONGSWORTH, L. G., AND MACINNES, D. A.: *Chem. Rev.* **24**, 271-87 (1939).
- (14) LONGSWORTH, L. G., AND MACINNES, D. A.: *J. Am. Chem. Soc.* **62**, 705 (1940).
- (15) LONGSWORTH, L. G., AND MACINNES, D. A.: *J. Gen. Physiol.* **25**, 507-16 (1942).
- (16) MIRSKY, A. E., AND POLLISTER, A. W.: *Proc. Natl. Acad. Sci. U. S.* **28**, 344-52 (1942).
- (17) NEURATH, H.: *Chem. Rev.* **30**, 357-94 (1942).
- (18) SCHNEIDER, W. C.: *J. Biol. Chem.* **161**, 293-303 (1945).
- (19) SEIBERT, F. B.: *J. Biol. Chem.* **133**, 593-9 (1940).
- (20) STENHAGEN, E., AND TEORELL, T.: *Trans. Faraday Soc.* **35**, 743 (1939).
- (21) SVEDBERG, T., AND PEDERSEN, K. O.: *The Ultracentrifuge*, pp. 17-38. Oxford University Press, London (1940).



HOMOGENEITY AND THE ELECTROPHORETIC BEHAVIOR OF SOME PROTEINS<sup>1</sup>

ROBERT A. ALBERTY, ELMER A. ANDERSON, AND J. W. WILLIAMS

*Department of Chemistry, University of Wisconsin, Madison, Wisconsin**Received August 25, 1947*

## INTRODUCTION

Electrophoresis is a sensitive test of the homogeneity of a protein, because two molecules which are identical except for several ionizable amino acid residues will in general have sufficiently different mobilities to be observed. Before a protein is considered to be electrophoretically homogeneous, it should satisfy both of the following tests: (1) The protein should migrate as a single boundary in an electric field in buffers of various hydrogen-ion concentrations and ionic strengths. The existence of proteins, such as human and horse albumins, which form only one boundary in electrophoresis in a certain pH range but form two boundaries in another pH range (6, 17), emphasizes the need for testing each apparently homogeneous protein in this way. (2) The rate of spreading of the protein boundary under conditions such that convection and anomalous electrical effects are avoided should be no greater than that due to diffusion alone. Descending protein boundaries in general spread faster than expected for diffusion and sharpen upon reversal of the current, but this is due to the variation in electric field strength through the boundary and does not necessarily indicate heterogeneity. The electrical spreading factors are in general reversed in the ascending boundary, which is sharpened because it is moving into a region of lower field strength. Longworth (10) has shown that the spreading may be greater on the ascending side if the mobility of the protein ion is greater than that of the buffer ion of the same sign and that these spreading effects may be compensated or enhanced by the pH effect. However, if the electrophoresis experiment is carried out at the average isoelectric point of the protein and at a low protein concentration so that the electric field and pH are essentially constant through the protein boundary, the same rate of spreading is observed in both limbs of the U-tube. In this case there is no spreading caused by conductivity or pH differences, and reversible spreading indicates heterogeneity. Convection caused by the temperature gradient set up by electrical heating in the electrophoresis cell must be kept negligible by operating near the temperature of maximum density of the buffer and using sufficiently low power dissipations. Spreading of a protein gradient caused by convection would not be expected to be reversed by reversing the field, while spreading caused by electrical inhomogeneity of the protein is reversed upon reversing the field.

The diagrams of refractive-index gradient for such an electrophoresis experiment are shown in figure 1. Electrophoresis of a 0.7 per cent solution of human

<sup>1</sup> Presented at the Twenty-first National Colloid Symposium, which was held under the auspices of the Division of Colloid Chemistry of the American Chemical Society at Palo Alto, California, June 18-20, 1947.

$\gamma_2$ -globulin at pH 7.2,  $\Gamma/2 = 0.10$ , was carried out at a potential gradient of 2.40 volts/cm. After 240 min. the field was reversed for an equal period of time, and the sharpening of the gradient is evident. The fact that the correct diffusion constant was obtained from the final curve is evidence that irreversible spreading effects are negligible.

In the case of an inhomogeneous protein the protein gradient is spread simultaneously by diffusion and by the differences in the rates and direction of migration of the differently charged protein ions. Sharp *et al.* (14, 15, 16) have shown that when diffusion during an electrophoresis spreading experiment is negligible compared to the electrical spreading, the mobility distribution may be obtained from the refractive-index gradient curves, and a heterogeneity constant ( $H$ ) may

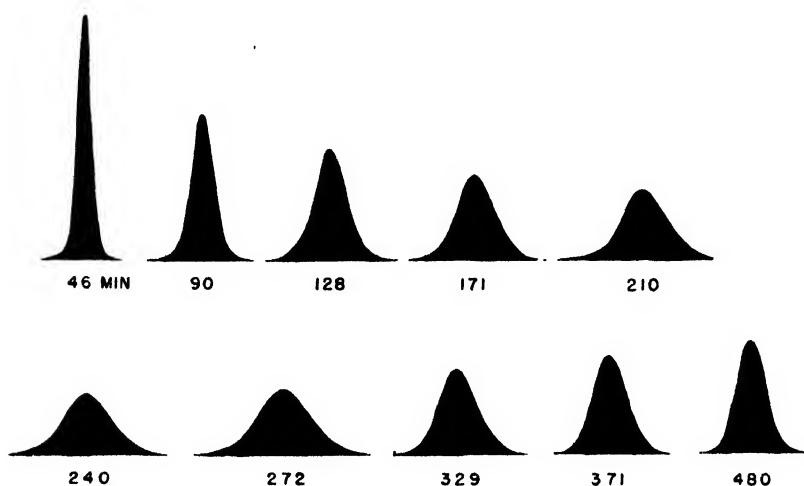


FIG. 1. Refractive-index gradient curves for human  $\gamma_2$ -globulin at pH 7.2 during electrophoresis.  $E = 2.40$  volts/cm. Current reversed at 240 min.

be calculated from the time rate of change of the standard deviation of the gradient,  $\Delta\sigma/\Delta t$ .

$$H = \frac{\Delta\sigma}{\Delta t E} \quad (1)$$

$E$  is the electric field strength.

In the case in which diffusion of the protein during the experiment is not negligible and the mobility distribution may be represented by the Gaussian probability function, Alberty (1) has shown that the experimental refractive-index gradient will have Gaussian form, and a heterogeneity constant,  $h$ , may be calculated by using equation 2.

$$D^* = \frac{\sigma^2 - \sigma_0^2}{2t_E} = D + \frac{E^2 h^2}{2} t_E \quad (2)$$

In this equation  $\sigma_0$  is the standard deviation of the gradient curve at the moment the field is applied, and  $\sigma$  is the standard deviation after electrophoresis for

$t_E$  seconds. According to this equation, the "apparent" diffusion constant,  $D^*$ , should plot as a straight line against time of electrophoresis and extrapolate back to the normal diffusion constant,  $D$ , at zero time. In order to apply this method it is necessary that all the protein molecules in the sample have the same diffusion constant, and this is fulfilled within the experimental error in measuring the diffusion constant for the proteins studied here. The heterogeneity constant,  $h$ , is actually the standard deviation for the mobility distribution  $g(u)$ .

$$g(u) = \frac{1}{h\sqrt{2\pi}} e^{-u^2/2h^2} \quad (3)$$

The mobility distribution for the protein may therefore be plotted by using the value of  $h$  determined from the slope of the graph of  $D^*$  vs.  $t_E$  and tabulated values for the Gaussian probability function.

As a check on the elimination of convection, the field should be reversed for an equal period of time to bring the boundary back to its initial state except for diffusion. If the field is reversed at time  $t_1$ , the apparent diffusion constant during the reversal period is given by equation 4.

$$D^* = D + \frac{E^2 h^2 (2t_1 - t_E)^2}{2 t_E} \quad (4)$$

According to this equation the apparent diffusion constant becomes equal to the true diffusion constant at  $t_E = 2t_1$ . Equation 4 may also be used to calculate the heterogeneity constant from data obtained during the reversal period.

A protein which shows reversible spreading in electrophoresis at the average isoelectric point must contain molecules with isoelectric points higher than the average and molecules with isoelectric points lower than the average. The isoelectric point distribution may be determined electrophoretically by studying the reversible spreading at several pH's in the isoelectric range. If the rate of change of the average mobility of the protein with pH,  $du/dpH$ , is constant in this range and the heterogeneity constant is independent of pH, the mobility distribution may be used directly to calculate the isoelectric point distribution. These conditions appear to apply in the case of human  $\gamma_2$ -globulin (see experimental section) and horse pseudoglobulin (11). The isoelectric point,  $pI$ , of molecules with a mobility  $u$  at the average isoelectric point of the protein,  $pI_{av}$ , is given by equation 5.

$$pI = pI_{av} - \frac{u}{\frac{du}{dpH}} \quad (5)$$

It is the purpose of this paper to test the electrophoretic homogeneity of several purified proteins and to show how the mobility and isoelectric point distributions may be determined for those which show reversible spreading.

#### EXPERIMENTAL

In order to avoid possible electrical spreading effects the electrophoresis spreading experiments were carried out as close to the average isoelectric point of the

protein as possible. Such a procedure has already been suggested by Longworth, Cannan, and MacInnes (8). The protein solutions were made up at a concentration of 0.7 g. per 100 cc. and dialyzed in Visking bags for at least 48 hr. Some of the protein solutions had to be centrifuged lightly to remove insoluble material before electrophoresis.

More care is required in the performance of electrophoresis spreading experiments than in the usual analytical experiments, because the initial boundaries must be sharp and lower current densities must be used to avoid convection in the prolonged experiments. In the experiments to be described the boundaries were formed in the usual Tiselius electrophoresis cell and compensated into the optical system at a rate of about 1 cm. per hour, using a mechanically driven syringe. The schlieren optical system was constructed with two schlieren lenses, so that the light passed through the cell in a parallel beam. This made it unnecessary to compensate the boundaries to the central portion of the cell in order to avoid convergence errors. After 1-1½ hr. compensation the mechanically driven syringe was stopped and the boundaries were allowed to diffuse until the maximum gradient could be recorded by the optical system. Several pictures were taken before the electric field was applied in order to calculate the standard deviation of the diffusion curve at the moment the field was applied, or in other cases a picture was taken just as the field was applied. The photographs were taken on Eastman C.T.C. plates, using the cylindrical-lens schlieren system for the photography, and these photographs were enlarged 6.40 times and traced. A diagonal slit 0.5 mm. wide was used in the optical path rather than a diagonal knife edge. Using a diagonal knife edge it was found that different values for the diffusion constant were calculated from photographs obtained when the diagonal knife edge was brought in from below the optical axis and from photographs obtained when the diagonal knife edge was brought in from above. Since there is no reason for using one arrangement in preference to the other, the diagonal slit method was used and the band of light forming the gradient curve was bisected. The bisection was accomplished by averaging the ordinates of the two edges of the band of light and constructing the corresponding mean curve. The diffusion constants determined by using a diagonal knife edge also depended upon the exposure time, because the broad edge of the diffraction band between the light and dark areas in the photograph moved into the light area as the exposure was increased. However, using the diagonal slit, it was found that the diffusion constant obtained was independent of the exposure time.

In order to keep thermal convection to a negligible amount, the generation of heat in the electrophoresis cell was kept below approximately 0.02 watt/cc. Although higher heat dissipations than this are practical in analytical electrophoresis experiments of shorter duration and with higher protein concentrations, it was found that in experiments lasting from 10 to 15 hr. and with low protein concentrations (0.5-0.7 per cent), higher heat dissipations often caused convection. The maximum current density which could be used with this limitation on the power was calculated from the conductivity of the buffer against which the protein was dialyzed. Thus, the maximum potential gradient which may

be used depends upon the specific conductivity of the buffer, and higher potential gradients are permissible with buffers of lower conductivity.

#### IMMUNE LACTOGLOBULIN (PSEUDO)<sup>2</sup>

This protein, the one responsible for the immune properties of bovine milk (18), moved as a single peak in electrophoresis at pH 8.6,  $\Gamma/2 = 0.10$ , with less than 5 per cent of proteins of sufficiently different mobility to be resolved. The globulin was prepared by salt fractionation methods to be described in a future publication by Hansen.<sup>2</sup> The data for a typical experiment with immune lactoglobulin are shown in table 1. The apparent diffusion constants,  $D^*$ , were calculated from the half-widths ( $x_i$ ) of the experimental gradient curves measured on the tracing at the point of inflection.

$$D^* = \frac{(x_i)^2 - (x_i)_0^2}{2t_\pi G^2} \quad (5)$$

The magnification factor from cell to enlarged tracing,  $G$ , is 6.68 in this case. The apparent diffusion constants are plotted against time of electrophoresis in figure 2. Note that the rate of spreading was slightly greater in the left limb of the U-tube, while the heterogeneity constants of  $0.67 \times 10^{-5}$  on the left and  $0.64 \times 10^{-5}$  on the right agree reasonably well. The fact that the apparent diffusion constant extrapolates back to the known diffusion constant for this protein at zero time ( $1.9 \times 10^{-7}$  cm.<sup>2</sup> sec.<sup>-1</sup> at 0°C. (18)) and returns to this value after reversal of the current for an equal period of time is good evidence that thermal convection and irreversible electroosmosis spreading are negligible. The curved lines representing the change in apparent diffusion constant during the reversal period have been calculated from equation 4, using the value of  $h$  determined from the initial straight-line portion. The agreement between the theory and the experimental points is evidence that the mobility distribution may be represented by the Gaussian function. The mobility distribution for  $h = 0.65 \times 10^{-5}$  has been plotted in figure 3, using a table of values for the Gaussian distribution function. In order to represent the percentage of protein molecules having mobilities less than the values given on the abscissa, without drawing the S-shaped Gaussian integral curve, these percentages have been indicated at the corresponding positions on the probability curve.

In the case of the following proteins only the heterogeneity constants and the conditions of the experiment will be given, because the data and calculations are similar to those in the above example. All the spreading experiments are summarized in table 3.

#### HUMAN $\gamma_2$ -GLOBULIN

The human  $\gamma_2$ -globulin was prepared from normal human plasma by methods developed at the University of Wisconsin (3) and contained less than 2 per cent of  $\gamma_1$ - and  $\beta$ -globulins and albumin, as judged by electrophoresis in veronal

<sup>2</sup> The authors are indebted to Mr. R. G. Hansen for the sample of this protein.



buffer at pH 8.6,  $\Gamma/2 = 0.10$ . The heterogeneity constant for this protein was determined at its average isoelectric point, pH 7.2–7.3 at  $\Gamma/2 = 0.10$ , and about 0.5 pH unit on either side. As shown by table 2 the heterogeneity constant

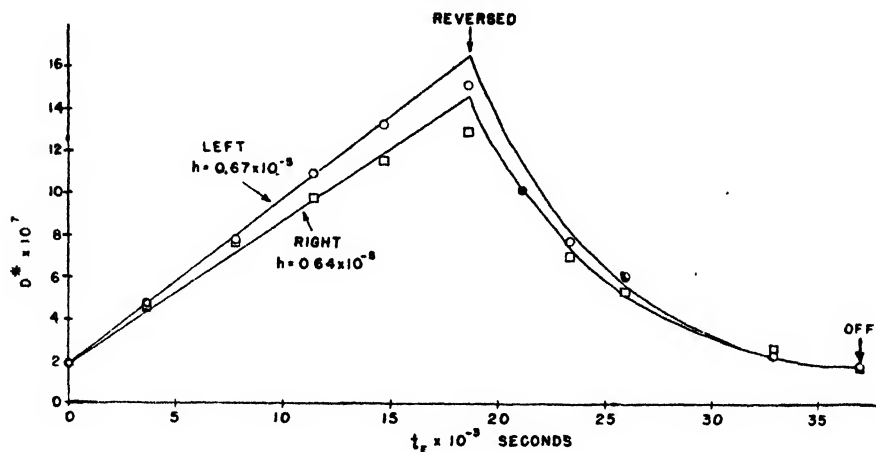


FIG. 2. Determination of the electrophoretic heterogeneity constant of immune lactoglobulin (pseudo). pH = 5.81; ionic strength = 0.10;  $E = 1.85$  volts/cm.

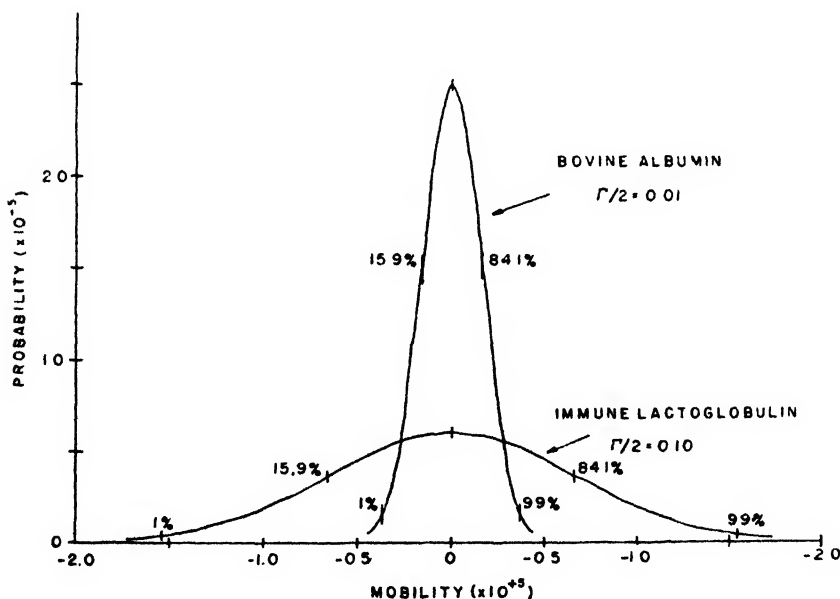


FIG. 3. Mobility distributions for bovine albumin and immune lactoglobulin (pseudo)

was essentially independent of pH in the neighborhood of the isoelectric point.

The fact that the heterogeneity constants determined from the ascending and descending boundaries agree within the experimental error shows that electrical

sharpening on the ascending side and electrical spreading on the descending side caused by the small  $\delta$  and  $\epsilon$  boundaries was not appreciable. This independence of the heterogeneity constant of pH in the isoelectric range has been also observed by Sharp, Cooper, and Neurath (15) in the case of horse pseudoglobulin GI. Since the spread in mobilities is essentially independent of pH, the mobility-pH curves for the various charged species must have approximately the same slope. In other words, it appears that the molecules with the greatest positive charge at pH 6.66 are the same molecules as those with the most positive charge at pH 7.83.

The data from table 2 are plotted in figure 4 except for the spreading experiment at pH 7.21, for which the mobility would fall very close to the straight line through the other two points and would not change the conclusions drawn from the simpler graph with straight lines. Gaussian probability curves for the mobility distributions which were determined at pH 6.66 and 7.83 have been plotted at the corresponding pH. These plots show, for example, that at pH 6.66, although the average mobility is  $+0.6 \times 10^{-5}$ , some of the molecules have negative mobilities and hence have isoelectric points below pH 6.66. Likewise,

TABLE 2  
*Heterogeneity constants for human  $\gamma_2$ -globulin at  $\Gamma/2 = 0.10$*

pH	*	HETEROGENEITY CONSTANT = $h$	
	(Descending)	Ascending	Descending
6.66	$+0.8 \times 10^{-5} \text{ cm}^2\text{volt}^{-1}\text{sec}^{-1}$	$0.52 \times 10^{-5}$	$0.51 \times 10^{-5} \text{ cm}^2\text{volt}^{-1}\text{sec}^{-1}$
7.21	—	$0.55 \times 10^{-5}$	
7.83	$-0.6 \times 10^{-5}$	$0.50 \times 10^{-5}$	$0.47 \times 10^{-5}$

a fraction of the molecules have positive mobilities at pH 7.83 and therefore have isoelectric points above this pH. Dotted lines connecting the standard deviations of the two distribution curves intersect the zero mobility axis at pH 6.90 and 7.74, so that the standard deviation in the isoelectric points is  $7.74 - 7.32 = 0.42$  pH unit. Using this value for the standard deviation of the isoelectric point distribution, the probability curve for the isoelectric points has been drawn in the lower part of figure 4. The percentages of molecules having isoelectric points less than the values given on the abscissa have been indicated at the corresponding positions on the probability curve. According to this calculation 98 per cent of the protein molecules have isoelectric points within a range of two pH units and 60 per cent of the molecules have isoelectric points within a range of 0.42 pH unit.

#### BOVINE ALBUMIN<sup>3</sup>

Although this preparation showed a small amount of  $\alpha$ -globulin in electrophoresis at pH 4.52,  $\Gamma/2 = 0.10$ , the boundary did not show reversible spread-

<sup>3</sup> The crystallized bovine plasma albumin prepared by the Armour Laboratories was used for these experiments.



ing much greater than the experimental error. The apparent diffusion constant obtained was only slightly greater than that determined by Stern, Singer, and Davis (20) at pH 7.0 ( $D_{20w} = 6.1 \times 10^{-7}$ , or  $D_{0.01 \text{ } N \text{ NaAc}} = 3.2 \times 10^{-7}$ ). During electrophoresis in 0.01 ionic strength buffer at pH 5.01 a larger amount (about 15 per cent) of a rather heterogeneous component with a more positive mobility

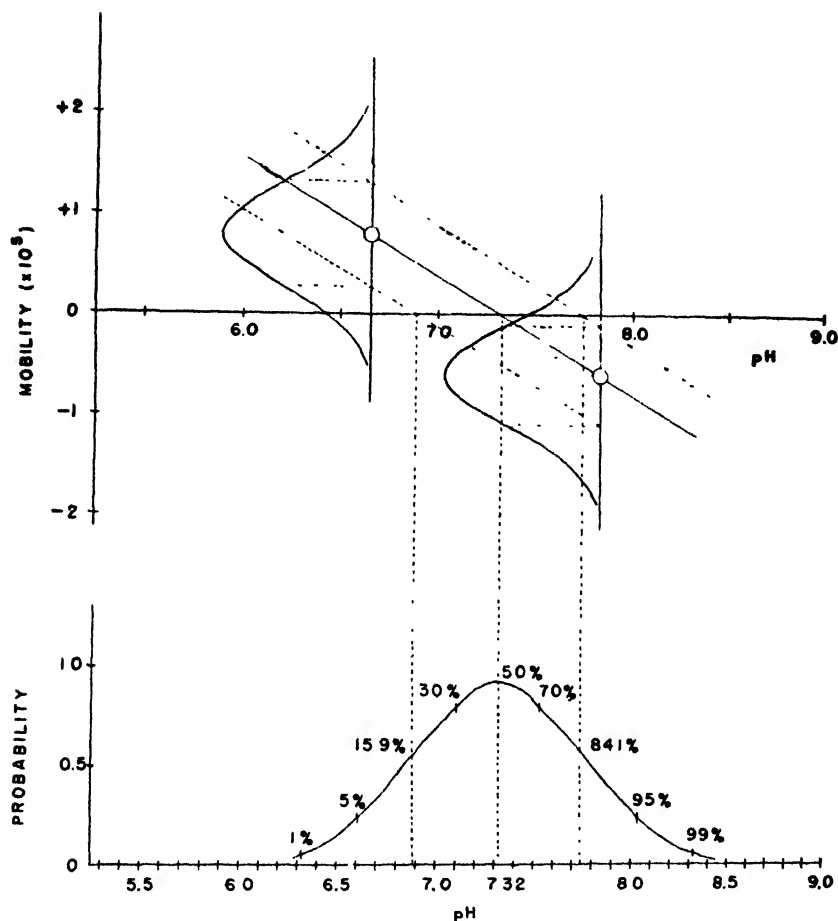


FIG. 4. Determination of the isoelectric point distribution for human  $\gamma_2$ -globulin at 0.10 ionic strength.

appeared. In addition, at this ionic strength the albumin boundary showed reversible spreading, leading to a heterogeneity constant of  $0.16 \times 10^{-5}$ . The mobility distribution is plotted in figure 3 for comparison with immune lactoglobulin. Reversible spreading caused by this small heterogeneity could not easily be observed in the spreading experiment at 0.10 ionic strength with a potential gradient of 1.95 volts/cm.

TABLE 3  
Electrophoresis spreading experiments

PROTEIN	$\Gamma/2$	pH*	BUFFER SALTS†	$\kappa \times 10^3$	$E$ volts $\text{cm}^{-1}$	HEATING‡ watts $\text{cc}^{-1}$	$D_0^\circ, 0.1 N \text{ NaCl}$ $\times 10^7$ $\text{cm}^2 \text{ sec}^{-1}$	%average $\times 10^4$ $\text{cm}^2 \text{ sec}^{-1} \text{ vol} \text{ l}^{-1}$	$k \times 10^4$ $\text{cm}^2 \text{ sec}^{-1} \text{ vol} \text{ l}^{-1}$
Human $\gamma$ -globulin . . . . .	0.10	6.66	0.08 N NaCl	5.55	1.92	0.0196	2.0 (19)	+0.8	0.52
			0.02 N NaCac						
	0.10	7.21	0.08 N NaCl	5.50	1.90	0.0197			0.55
			0.02 N NaCac						
Immune lactoglobulin . . . . .	0.10	7.83	0.08 N NaCl	5.26	1.50	0.0141		-0.6	0.48
			0.02 N NaV						
	0.10	5.81	0.1 N NaOAc	3.90	1.85	0.0131	1.9 (18)		0.66
Bovine albumin . . . . .	0.10	4.52	0.1 N NaOAc	5.42	1.95	0.0191	3.2 (20)	+0.2	Negligible 0.16
	0.01	5.01	0.01 N NaOAc	0.479	5.47	0.0140		A (85%) -0.3 B (15%) +1.1	
	0.10	5.22	0.04 N NaOAc	5.18	1.66	0.0136	3.8 (12)		0.2
$\beta$ -Lactoglobulin . . . . .			0.06 N NaCl						
	0.01	5.31	0.01 N NaOAc	0.456	5.75	0.0148		A (70%) 0.0 B (30%) +1.4	
	0.10	4.58	0.1 N NaOAc	3.84	1.89	0.0133	4.0 (9)	0.0	0.2
Ovalbumin . . . . .	0.01	4.72	0.01 N NaOAc	0.475	5.52	0.0142		A (75%) -0.2 B (15%) +0.5 C (10%) +1.7	
Ribonuclease . . . . .	0.055	7.82	0.0208 M total phosphate	1.73	2.65	0.0119	5.3 (2) 6.6 (13)	+0.2	Negligible

\* Measured with a glass electrode at 25°C.

† V = diethyl barbiturate; Cac = cacodylate; OAc = acetate.

‡ Heat dissipation in the electrophoresis cell =  $i^2/q^2\kappa$ , where  $q$  is the cross-sectional area of the electrophoresis cell.

§ Measured on descending boundary.

¶ Average of ascending and descending boundaries.

$\beta$ -LACTOGLOBULIN<sup>4</sup>

This protein has been studied electrophoretically by Pedersen (11), who found the isoelectric point to be pH 5.20 at  $\Gamma/2 = 0.02$ , and by Li (7), who observed three components in his preparation at pH 4.8 and 6.5 but only one in the isoelectric region. Li gives pH 5.1 as the isoelectric point of the main component at 0.10 ionic strength. In electrophoresis spreading experiments carried out at pH 5.22 and 0.1 ionic strength, the gradient curves for  $\beta$ -lactoglobulin were symmetrical and very nearly of Gaussian form. A small amount of reversible spreading was observed, leading to a heterogeneity constant of  $0.2 \times 10^{-5}$ . Upon reversal of the current for an equal period of time, a diffusion constant of  $3.8\text{--}4.0 \times 10^{-7}$  ( $D_{20w} = 7.3\text{--}7.7 \times 10^{-7}$ ) was observed, which is in agreement with  $D_{20w} = 7.3 \times 10^{-7}$  obtained by Polson (12).

In order to determine the heterogeneity constant more accurately, an experiment was carried out at 0.01 ionic strength (pH 5.31) so that a higher potential gradient could be used. In this experiment, the protein was resolved into two components. The minor component, which made up about 30 per cent, had a mobility of  $+1.4 \times 10^{-5}$ , while the major component did not migrate appreciably. Although there was asymmetry between the ascending and descending boundaries, the major component showed reversible spreading in both limbs of the U-tube, indicating that in addition to the resolution of two components, the major component is perhaps not an electrophoretically homogeneous protein.

OVALBUMIN<sup>5</sup>

Ovalbumin has been studied electrophoretically by Tiselius and Svensson (21) and by Longworth (9). Longworth gives the average isoelectric point of the two electrically separable constituents as pH 4.58 at  $\Gamma/2 = 0.10$ , and so a spreading experiment was carried out under these conditions. There was no indication of the separation of a second component as the boundary was quite symmetrical, but the boundary did show reversible spreading leading to a heterogeneity constant of  $0.2 \times 10^{-5}$ . Upon reversal of the current for an equal period of time the apparent diffusion constant returned to  $3.8\text{--}4.0 \times 10^{-7}$ , in agreement with the diffusion constant determined by Longworth (9).

In electrophoresis at 0.01 ionic strength at the isoelectric point determined by Tiselius and Svensson (21), pH 4.72, three electrically separable components were resolved. The mobilities and relative amounts of these components are given in table 3.

<sup>4</sup> The authors are indebted to Dr. J. A. Bain for the sample of this protein. The globulin was prepared by alcohol fractionation methods to be described in a future publication, and as judged by electrophoresis in veronal buffer at pH 8.6,  $\Gamma/2 = 0.10$ , it contained less than 7 per cent of proteins with sufficiently different mobilities to be resolved.

<sup>5</sup> The authors are indebted to Dr. A. Polson for this sample of ovalbumin, which had been recrystallized six times and dried by ice sublimation.

RIBONUCLEASE<sup>6</sup>

This protein was studied at the isoelectric point determined by Rothen (13), pH 7.8, at an ionic strength of approximately 0.055. The boundaries in both limbs of the U-tube became slightly asymmetrical during electrophoresis, but they became symmetrical again after the current had been reversed for an equal time period. Any reversible spreading was small, and the skewness of the boundaries might have been caused by a conductivity difference across the boundary or some inhomogeneity. The diffusion constant obtained after reversal of the current was  $6.2 \times 10^{-7}$  (2, 13a).

## DISCUSSION

It has been the purpose of this paper to emphasize that a symmetrical moving boundary for a protein is not sufficient evidence for electrophoretic homogeneity. Some proteins, such as the antibody globulins, apparently contain molecules of different average net charge, although all the molecules have the same diffusion constant within the errors of the present methods. In the case of heterogeneous proteins of this type, the mobility determined by measuring the velocity of the center of area of the gradient curve is the *average* mobility for the protein, and the intersection of the curve representing average mobilities at various hydrogen-ion concentrations with the zero mobility axis is the *average* isoelectric point. A method has been presented here for estimating the width of the isoelectric range, assuming that the *u*-pH curves are linear in this range and have the same slope for all the charged forms of the protein. In the case of human  $\gamma_2$ -globulin the mobility distribution may be represented by the Gaussian probability function, and this leads to a Gaussian distribution of the isoelectric points. If the *u*-pH curves are not linear and the heterogeneity constant is a function of pH in the isoelectric range, a non-Gaussian distribution of isoelectric points would be obtained, but to study such distributions refinements will have to be made in existing methods.

It is possible to draw definite conclusions from electrophoresis spreading experiments only under certain restricted conditions. The theory leading to equations 2 and 4 assumes a Gaussian distribution of mobilities, the absence of extraneous spreading effects, and the same diffusion constant for all the protein molecules present. It is not necessary for all the molecules to have the same diffusion constant if the spreading resulting from diffusion is negligible compared to that caused by electrophoretic inhomogeneity, and in this particular case the actual distribution in mobilities may be obtained directly from the gradient curves. In order to reduce spreading caused by conductivity and pH effects, it is necessary to carry out spreading experiments at the average isoelectric point of the protein, because at present little is known about the conductivity and pH gradients which cause spreading and sharpening effects in moving protein boundaries. Thus, spreading experiments yield information concerning

<sup>6</sup> The authors are indebted to Dr. M. Kunitz for the crystalline sample of this protein.

homogeneity only in the isoelectric range, and it is possible that a protein may appear to be homogeneous near its isoelectric point but not be homogeneous in another pH range. Another important consideration for electrophoresis spreading experiments is that in order to avoid convection the field strength must remain below a maximum determined by the conductivity of the buffer and the allowable power dissipation. Using the schlieren optical system, the minimum increase in the apparent diffusion constant which we consider significant is about  $1 \times 10^{-7}$  cm.<sup>2</sup> sec.<sup>-1</sup> after an electrophoresis of 5 hr. duration. Accepting this minimum increase in  $D^*$ , the *minimum* heterogeneity constant which may be determined in a 10-hr. experiment (5 hr. in each direction) is  $0.17 \times 10^{-5}$  at a potential gradient of 2 volts/cm.,  $0.084 \times 10^{-5}$  at 4 volts/cm.,  $0.056 \times 10^{-5}$  at 6 volts/cm., and  $0.033 \times 10^{-5}$  at 10 volts/cm. These figures show that spreading experiments at higher potential gradients (lower ionic strengths) will be a more sensitive test of electrophoretic homogeneity. However, under these conditions there is more danger from anomalous spreading effects because of the lower ratio of salt to protein.

With the possible exception of ribonuclease, none of the proteins studied have been found to be completely homogeneous by the electrophoretic criteria. It is not surprising that the antibody proteins, human  $\gamma_2$ -globulin and immune lactoglobulin, show reversible spreading in view of the fact that they contain many different antibodies. It might be expected that proteins with simpler biological functions would be more likely to be homogeneous by all criteria. The same procedures should be applicable to the study of the homogeneity of other colloidal electrolytes, such as the bacterial polysaccharides, viruses, and gelatin.

#### REFERENCES

- (1) ALBERTY, R. A.: Paper presented before the Division of Physical and Inorganic Chemistry at the 111th Meeting of the American Chemical Society, Atlantic City, New Jersey, April 18, 1947.
- (2) BRIDGMAN, W. B., AND WILLIAMS, J. W.: *Ann. N. Y. Acad. Sci.* **43**, 1945 (1942).
- (3) DEUTSCH, H. F., GOSTING, L. J., ALBERTY, R. A., AND WILLIAMS, J. W.: *J. Biol. Chem.* **164**, 109 (1946).
- (4) HOCH, H., AND MORRIS, C. J. O. R.: *Nature* **156**, 234 (1945).
- (5) LEUTSCHER, J. A., JR.: *J. Am. Chem. Soc.* **61**, 2888 (1939).
- (6) LI, C. H.: *J. Am. Chem. Soc.* **68**, 2746 (1946).
- (7) LONGSWORTH, L. G., CANNAN, R. K., AND MACINNES, D. A.: *J. Am. Chem. Soc.* **62**, 2580 (1940).
- (8) LONGSWORTH, L. G.: *Ann. N. Y. Acad. Sci.* **41**, 267 (1941).
- (9) LONGSWORTH, L. G.: *J. Phys. Chem.* **51**, 171 (1947).
- (10) PEDERSEN, K. O.: *Biochem. J.* **30**, 961 (1936).
- (11) POLSON, A.: *Kolloid-Z.* **87**, 149 (1939).
- (12) ROTHEN, A.: *J. Gen. Physiol.* **24**, 203 (1940).
- (13a) ROTHEN, A.: *Ann. N. Y. Acad. Sci.* **43**, 229 (1942).
- (14) SHARP, D. G., TAYLOR, A. R., BEARD, D., AND BEARD, J. W.: *J. Biol. Chem.* **142**, 193 (1942).
- (15) SHARP, D. G., COOPER, G. R., AND NEURATH, H.: *J. Biol. Chem.* **142**, 203 (1942).
- (16) SHARP, D. G., HEBB, M. H., TAYLOR, A. R., AND BEARD, J. W.: *J. Biol. Chem.* **142**, 217 (1942).

- (17) SHARP, D. G., COOPER, G. R., ERICKSON, J. O., AND NEURATH, H.: J. Biol. Chem. **144**, 139 (1942).
- (18) SMITH, E. L.: J. Biol. Chem. **164**, 356 (1946).
- (19) STENHAGEN, E.: Biochem. J. **32**, 714 (1938).
- (20) STERN, K. G., SINGER, S., AND DAVIS, S.: J. Biol. Chem. **167**, 321 (1947).
- (21) TISELIUS, A., AND SVENSSON, H.: Trans. Faraday Soc. **36**, 16 (1940).

## X-RAY DIFFRACTION STUDIES IN THE SYSTEM $\text{NiO-Cr}_2\text{O}_3\text{-ZrO}_2$ <sup>1</sup>

W. O. MILLIGAN AND L. MERTEN WATT

*Department of Chemistry, The Rice Institute, Houston, Texas*

*Received August 25, 1947*

Mutual protective action has been previously observed in several dual oxide systems such as:  $\text{CuO-Fe}_2\text{O}_3$  (1),  $\text{NiO-Al}_2\text{O}_3$  (2),  $\text{Fe}_2\text{O}_3\text{-Cr}_2\text{O}_3$  (3), and  $\text{Cr}_2\text{O}_3\text{-ZrO}_2$  (4). In these dual systems of hydrous oxide gels heated at various temperatures, the presence of one oxide prevents or retards the crystallization of the other. In this paper the phenomenon of mutual protective action has been extended to the ternary oxide system  $\text{NiO-Cr}_2\text{O}_3\text{-ZrO}_2$ . The entire range of compositions at a constant temperature level has been systematically studied, using methods previously used in two-component systems.

### EXPERIMENTAL

#### *Preparation of samples*

Sixty-six gels corresponding to compositions of every 10 mole per cent in the ternary system  $\text{NiO-Cr}_2\text{O}_3\text{-ZrO}_2$  were selected for preparation and study as indicated in table 1. The gels were prepared at room temperature by the addition of a slight excess of ammonium hydroxide to mixtures of solutions of nickelous nitrate (0.5 *M* with respect to  $\text{NiO}$ ), chromic nitrate (0.5 *M* with respect to  $\text{Cr}_2\text{O}_3$ ), and zirconium nitrate (0.5 *M* with respect to  $\text{ZrO}_2$ ), using a rapid-mixing device described elsewhere (5). The amounts of ammonium hydroxide solution required were determined by preliminary titrations using a glass electrode for determination of pH values. In one set of experiments the resulting gels were thrown down in a centrifuge and transferred without further washing into evaporating dishes, in which they were allowed to dry in air at room temperature. In a second set of experiments duplicates were prepared of all gels (table 1) rich in nickel or chromium. These samples were washed in a centrifuge

<sup>1</sup> Presented at the Twenty-first National Colloid Symposium, which was held under the auspices of the Division of Colloid Chemistry of the American Chemical Society at Palo Alto, California, June 18-20, 1947.

until the supernatant liquid no longer gave a test for nitrate ions, and were air-dried as described above.

Separate portions of each of the samples were heated for 2-hr. periods at  $500^\circ\text{C}$ . in a thermostatically controlled electric furnace.

TABLE 1  
*Composition of gels in the system  $\text{NiO-Cr}_2\text{O}_3\text{-ZrO}_2$*

SAMPLE NUMBER	COMPOSITION, MOLE PER CENT			SAMPLE NUMBER	COMPOSITION, MOLE PER CENT		
	NiO	$\text{Cr}_2\text{O}_3$	$\text{ZrO}_2$		NiO	$\text{Cr}_2\text{O}_3$	$\text{ZrO}_2$
1	100	0	0	34	50	10	40
2	90	0	10	35	40	10	50
3	80	0	20	36	30	10	60
4	70	0	30	37	20	10	70
5	60	0	40	38	10	10	80
6	50	0	50	39	10	20	70
7	40	0	60	40	10	30	60
8	30	0	70	41	10	40	50
9	20	0	80	42	10	50	40
10	10	0	90	43	10	60	30
11	0	0	100	44	10	70	20
12	0	10	90	45	10	80	10
13	0	20	80	46	20	70	10
14	0	30	70	47	30	60	10
15	0	40	60	48	40	50	10
16	0	50	50	49	50	40	10
17	0	60	40	50	60	30	10
18	0	70	30	51	70	20	10
19	0	80	20	52	60	20	20
20	0	90	10	53	50	20	30
21	0	100	0	54	40	20	40
22	10	90	0	55	30	20	50
23	20	80	0	56	20	20	60
24	30	70	0	57	20	30	50
25	40	60	0	58	20	40	40
26	50	50	0	59	20	50	30
27	60	40	0	60	20	60	20
28	70	30	0	61	30	50	20
29	80	20	0	62	40	40	20
30	90	10	0	63	50	30	20
31	80	10	10	64	40	30	30
32	70	10	20	65	30	30	40
33	60	10	30	66	30	40	30

#### *X-ray diffraction analysis*

X-ray diffraction patterns were obtained for all of the samples which were heated to  $500^\circ\text{C}$ . Chromium  $K_\alpha$  x-radiation was employed, using a vanadium pentoxide filter to remove the  $K_\beta$  x-radiation. The results of the x-ray examination are given in figures 1 and 2.

## DISCUSSION

*Impure samples*

Samples rich in nickel oxide and chromic oxide which were not washed free of ammonium nitrate were found to be brownish rather than green in color and to yield some weak x-ray diffraction lines distinct from those of nickel oxide and chromic oxide. These weak diffraction lines and the brown color vanished when the samples were heat-treated to a temperature of 600°C. or higher. These results suggested that (a) the ammonium nitrate oxidized the chromic oxide during its decomposition which occurred when the unwashed gels were heated

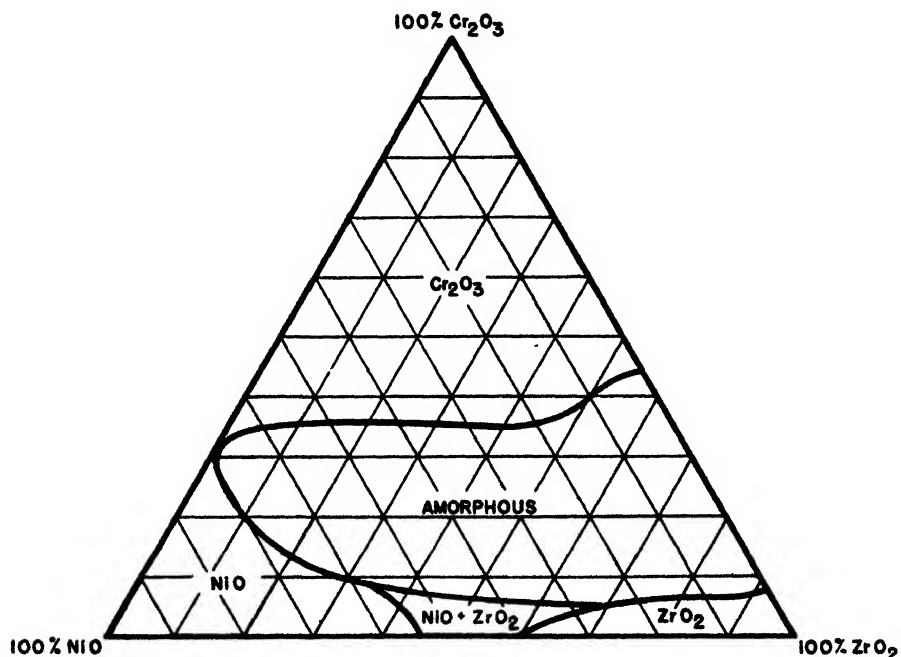


FIG. 1. X-ray diffraction patterns of NiO-Cr<sub>2</sub>O<sub>3</sub> gels heated to 500°C.

to 500°C., and (b) the new chromium oxide (probably protected or stabilized by the nickel oxide) was stable to 500°C. but not to 600°C.

Washed NiO-Cr<sub>2</sub>O<sub>3</sub> gels heated to 500°C. do not yield these extra diffraction lines, but these mixed oxides heated in the presence of added ammonium nitrate become brown in color and show the new lines. It is believed that these extra diffraction lines correspond to a chromium oxide intermediate between Cr<sub>2</sub>O<sub>3</sub> and CrO<sub>3</sub>. Further studies are being carried out in this laboratory.

*Pure samples*

The results in figures 1 and 2 refer only to samples free of the "intermediate chromium oxide" discussed above. It will be noted in figure 1 that the system NiO-Cr<sub>2</sub>O<sub>3</sub> exhibits marked mutual protection, and that as little as 30 mole per



cent of chromic oxide renders the nickel oxide essentially amorphous. There is little indication of solid solution. On the original negatives it is apparent that wide bands of nickel oxide occur superimposed on the pattern of chromic oxide

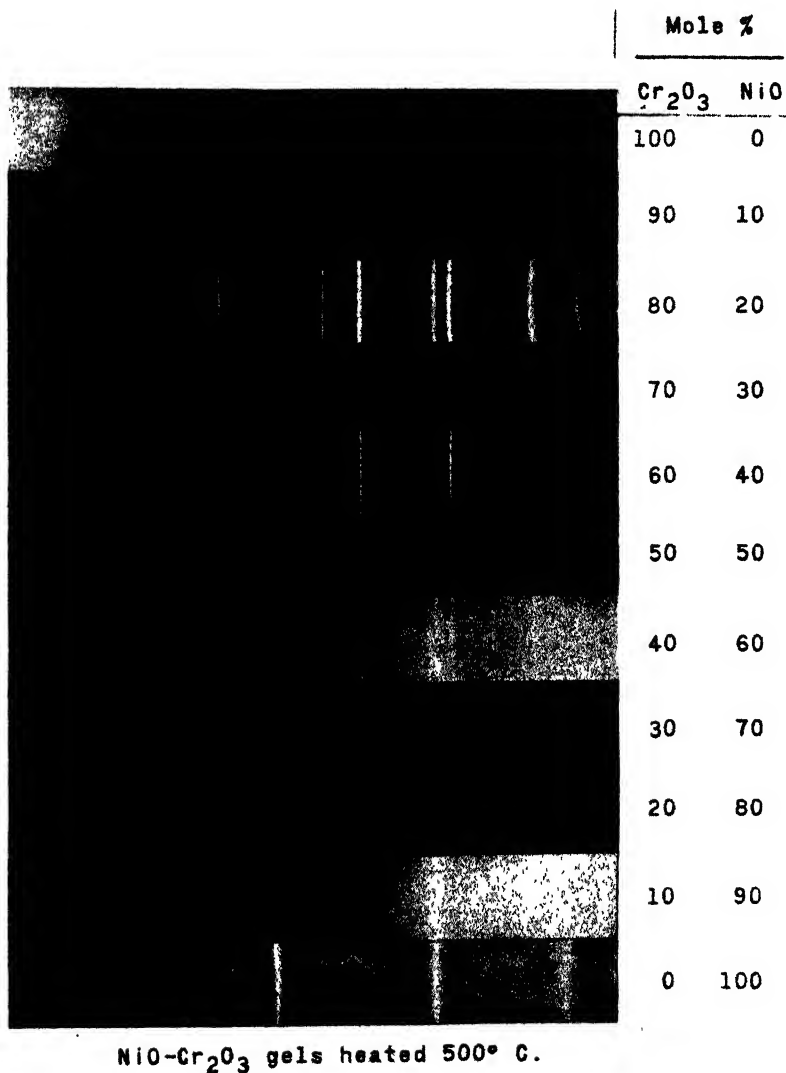


FIG. 2. X-ray diffraction examination of gels in the system  $\text{NiO-Cr}_2\text{O}_3\text{-ZrO}_2$  after heating to  $500^\circ \text{C}$ .

in the range of 60-40 mole per cent nickel oxide. The mixed gels appear to consist in part of mixtures of very small crystals of chromic oxide (relatively larger) and nickel oxide (relatively smaller). The occurrence of mixtures of crystals in this two-component portion of the three-component system is especially

evident at higher temperature levels (600–700°C.); these unfinished studies at higher temperatures will be reported in a subsequent paper.

The results of the extensive x-ray diffraction study of the entire three-component system are given in figure 2. It is inherent in this method of presenting a large amount of data in summarized form, that the degree of crystallinity cannot be represented concurrently with the other results shown. Figure 2 is extended simply to summarize the composition regions wherein amorphous and crystalline phases are found. It should be noted that since samples were only prepared every 10 mole per cent, the boundaries between the various amorphous and crystalline regions may not be as sharp as the figure suggests.

An extremely large composition region exists wherein all samples are essentially amorphous to x-rays. It is evident that each oxide is mutually preventing the crystallization of the others. It would be expected that the amorphous zone would diminish in area if the samples were heat-treated to a higher temperature level.

A slight amount of shift in the interplanar spacings of the chromic oxide pattern was observed in the two-component system  $\text{Cr}_2\text{O}_3$ – $\text{ZrO}_2$ , in confirmation of previous results (4). In the system  $\text{NiO}$ – $\text{ZrO}_2$  it will be noted that there exists a small composition region in which the gels consist of mixtures of crystals of nickel oxide and zirconium oxide. This zone would probably widen at higher temperatures in analogy to the behavior of the system  $\text{Cr}_2\text{O}_3$ – $\text{ZrO}_2$  (4).

#### SUMMARY

The following is a brief summary of the results of this investigation:

1. Mutual protective action against crystallization, previously observed in several two-component systems, has been extended to the three-component system  $\text{NiO}$ – $\text{Cr}_2\text{O}_3$ – $\text{ZrO}_2$ .

2. An extensive amorphous zone of composition has been observed in this system at a temperature level of 500°C. In this amorphous region each oxide exerts a mutual protective action by preventing the crystallization of the others.

3. In samples rich in chromic oxide and nickel oxide, which were not washed free of ammonium nitrate, it has been found that during heat-treatment at 500°C. the decomposing ammonium nitrate may partially oxidize the chromic oxide to form a new crystalline phase exhibiting new diffraction lines.

4. This new crystalline phase is believed to consist of an oxide of chromium intermediate between  $\text{Cr}_2\text{O}_3$  and  $\text{CrO}_3$  and is being studied further.

The authors are grateful to Gordon L. Bushey and Harry B. Whitehurst for their assistance in preparing and examining some of the samples employed in this work.

#### REFERENCES

- (1) MILLIGAN AND HOLMES: *J. Am. Chem. Soc.* **63**, 149 (1941).
- (2) MILLIGAN AND MERTEN: *J. Phys. Chem.* **50**, 465 (1946).

- (3) MILLIGAN AND MERTEN: *J. Phys. Colloid Chem.* **51**, 521 (1947).
- (4) MILLIGAN AND WATT: Results presented before the Division of Colloid Chemistry at the 111th meeting of the American Chemical Society, which was held in Atlantic City, New Jersey, April 14-18, 1947.
- (5) WEISER AND MILLIGAN: *J. Phys. Chem.* **40**, 1071 (1936).

## SEDIMENTATION EQUILIBRIA OF POLYDISPERSE NON-IDEAL SOLUTES

### I. THEORY<sup>1,2</sup>

MICHAEL WALES

*Department of Chemistry, University of Wisconsin, Madison, Wisconsin*

*Received August 25, 1947*

#### INTRODUCTION

The usefulness of sedimentation methods in physical chemistry has been amply demonstrated. There are two distinct methods of approach, one based on the sedimentation-equilibrium and the other on sedimentation-velocity observations. The possibility of making a molecular-weight analysis of a mixture is one of the great advantages of the ultracentrifugal techniques. Much progress in this direction has been made in the case of the globular protein and polysaccharide systems, but the interpretation of the data in the case of solutions containing long-chain solute molecules has had its difficulties.

In an article by Svedberg (10), having to do with the cellulose molecule, detailed consideration is given to the application of the combined sedimentation-velocity and diffusion data to the study of solute size and size distribution in solutions containing cellulose and its derivatives. However, there are here some serious experimental problems to be overcome before success can be complete. We shall prefer at this time to investigate the possibility of the application of the sedimentation-equilibrium method to systems containing long-chain molecules.

The interpretation of equilibrium ultracentrifuge data for systems of this kind has been rendered difficult by pronounced deviations from Henry's law at very low concentrations. However, progress can be made by taking account of the deviations from ideality, if we can assume that at a given temperature these deviations are the same as in the other thermodynamic properties, such as osmotic pressure (12).

<sup>1</sup> Presented at the Twenty-first National Colloid Symposium, which was held under the auspices of the Division of Colloid Chemistry of the American Chemical Society at Palo Alto, California, June 18-20, 1947. This paper is based on a thesis submitted by Michael Wales to the Faculty of the University of Wisconsin in partial fulfillment of the requirements for the degree of Doctor of Philosophy, October, 1947.

<sup>2</sup> This work was supported in part by a grant from the Wisconsin Alumni Research Foundation.

## THEORETICAL

Consider a column of solution of unit cross-section and length,  $dx$ , in a centrifugal field. At equilibrium, the change in potential energy in moving  $c_x$  grams of materials through the distance  $dx$  to a point where the concentration is  $c_x + dc_x$  will be balanced by the work done against the osmotic-pressure difference  $\left(\frac{\partial p}{\partial x}\right)dx$ .

Let the osmotic pressure be given by

$$p = \frac{RT}{M_{nx}} c_x + b' c_x^2 \quad (1)$$

at any point at a distance  $x$  from the center of rotation in the column of solution of unit cross-section.

Then the condition for equilibrium in the column is

$$c_x(1 - \bar{V}\rho)\omega^2 x dx = \left(\frac{\partial p}{\partial x}\right) dx \quad (2)$$

where  $\omega$  is the angular velocity and  $\bar{V}$  the partial specific volume of solute. This is equivalent to stating that the partial molal free energy of the solute is the same at all points, at equilibrium. Differentiating equation 1 and remembering that

$$M_{nx} \equiv M_{0x} = \frac{\sum_i c_{ix}}{\sum_i \frac{c_{ix}}{M_i}} \quad (3)$$

where the subscript refers to species  $i$ , we obtain

$$\sum_i c_i \omega^2 x (1 - \bar{V}\rho) = RT \sum_i \frac{dc_i}{dx} \frac{1}{M_i} + 2b' \frac{dc_x}{dx} \sum_i c_i \quad (4)$$

If this equation is broken up into  $i$  equations, using the separation functions  $b_i$ ,

$$c_i \omega^2 x (1 - \bar{V}\rho) = \frac{RT}{M_i} \frac{dc_i}{dx} + b_i \frac{dc_x}{dx} c_i \quad (5)$$

where

$$b' = \frac{1}{2} \frac{\sum_i b_i c_i}{\sum_i c_i} \quad (6)$$

No assumption is made as yet as to the behavior of the separation functions  $b_i$ . Suppose, however, that for the system under consideration

$$\frac{\partial b'}{\partial c} = 0 \quad (7)$$

(from experimental measurements of osmotic pressure)

$$\frac{\partial b'}{\partial M} = 0 \quad (8)$$

(for measurements on successive fractions). Furthermore, suppose that  $b'$  does not vary with molecular-weight distribution for polydisperse material.<sup>3</sup> It must be also emphasized that equation 8 and the last condition would not be expected to hold for material containing molecules of different composition and/or very different degrees of branching. Employing equation 6 and reformulating the conditions

$$0 = \frac{\partial b'}{\partial c} = \frac{1}{2} \frac{\partial}{\partial c} \sum_i b_i \gamma_i; \quad \sum_i \frac{\partial b'}{\partial c} \gamma_i = 0 \quad (9)$$

where  $\gamma_i$  is the weight fraction of species  $i$  in the mixture.

Since  $\partial b'/\partial c$  is zero for any distribution of  $\gamma_i$ 's,

$$\frac{\partial b_i}{\partial c} = 0 \quad (10)$$

and from equation 8

$$\left. \frac{\partial b_i}{\partial M_i} \right|_{\gamma_i=1} = 0 \quad (11)$$

then it follows that

$$b_i = f(\gamma_1, \dots, \gamma_n), \quad b_i = 2b' \text{ when } \gamma_i = 1, \quad (12)$$

$$\gamma_j = \gamma_k = \dots = \gamma_n = 0$$

Formulating equation 6 in terms of the  $\gamma_i$  and performing an arbitrary variation in the  $\gamma_i$  we have

$$\sum_i \{\gamma_i \delta b_i + b_i \delta \gamma_i\} = 0 = 2\delta b', \quad \sum_i \delta \gamma_i = 0 \quad (13)$$

where

$$\delta b_i = \sum_j \frac{\partial b_i}{\partial \gamma_j} \delta \gamma_j \quad (14)$$

Using the method of undetermined multipliers and combining the terms of equations 13 and 14 we obtain

$$\sum_i \left\{ \sum_j \gamma_j \frac{\partial b_i}{\partial \gamma_j} + b_i - a \right\} \delta \gamma_i = 0 \quad (15)$$

and since the  $\delta \gamma_i$  are arbitrary

$$-\sum_j \gamma_j \frac{\partial b_i}{\partial \gamma_j} = b_i - a \quad (16)$$

where  $a$  is an arbitrary constant.

An obvious solution to this set of equations is found by applying the boundary conditions of equation 12.

<sup>3</sup> The system polystyrene-butanone is believed to exhibit this behavior, on the basis of a large number of osmotic measurements on solutions of 0.1-2 per cent by weight. (R. H. Ewart and H. C. Tingey: Paper presented at the 111th Meeting of the American Chemical Society, which was held at Atlantic City, New Jersey, April 14-18, 1947.)

$$a = b_i = b_j = b_k = \dots b_n = 2b' \quad (17)$$

While there is some doubt as to whether this is the only solution of equation 16, it is certainly the simplest solution and hence to be preferred on physical grounds, in the absence of any other information.

Now returning to equation 5:

$$M_{wz} \equiv M_{1z} = \frac{\sum_i M_i c_i}{\sum_i c_i} = \sum_i M_i \gamma_i$$

$$M_{1z} = \frac{RT \frac{dc_z}{dx}}{xc_z(1 - \bar{V}_\rho)\omega^2} \left\{ 1 + c_z \sum_i \frac{M_i b_i \gamma_i}{RT} \right\} = M_{1z}^{\text{ideal}} \left\{ 1 + c_z \sum_i \frac{M_i b_i \gamma_i}{RT} \right\} \quad (18)$$

It can be seen from this equation that the more non-ideal the  $p/c$  vs.  $c$  curve i.e., the larger the  $b_i$ 's, the greater will be the deviation from ideality. The higher the concentration of the solution and the higher the molecular weight of the solute, the greater will be the deviation from ideality. For very low molecular weights the deviation becomes negligible (in practice, below about  $M_w = 60,000$  for 0.1 per cent solutions in carbon tetrachloride, and for somewhat higher molecular weights in methyl ethyl ketone). It is also obvious that if  $b_i$  is some involved function of the  $M_i$ 's or the  $\gamma_i$ 's or both, a theoretically exact calculation of a true  $M_w$  from the  $dc/dx$  and  $c_z$  obtained experimentally would be extremely difficult, to say the least. If the  $b_i$ 's are all the same function of total concentration, the calculations are simple. However, assuming that all the  $b_i$ 's are equal and constant, as previously justified, in the case of a suitable solvent

$$M_{1z} = \frac{\frac{dc_z}{dx}}{c_z \left( 2Ax - B \frac{dc_z}{dx} \right)} \quad (19)$$

\* An alternative and more compact formulation, proposed by Dr. R. H. Ewart, General Laboratories, U. S. Rubber Company, Passaic, New Jersey, is here reproduced.

Making use of equation 1 it follows by the application of the Duhem equation that

$$\frac{RT}{M} \frac{d \ln c_z}{dx} + 2b' dc_z = (1 - \bar{V}_\rho)\omega^2 x dx, \quad B = \frac{2b'}{RT}$$

or if

$$2A = \frac{(1 - \bar{V}_\rho)\omega^2}{RT}$$

$$\frac{dc_z}{dx} = \left( 2Ax - B \frac{dc_z}{dx} \right) M c_z$$

This represents the important correction for non-ideal solutions in a monodisperse system.

With polydisperse systems it is not possible to solve the Duhem equation in order to get

where

$$B = \frac{20gb'}{RT}$$

$$A = \frac{(1 - \bar{V}_\rho)\omega^2}{2RT}$$

$$b' = \frac{\text{mm. solvent}}{\left(\frac{\text{grams polymer}}{100 \text{ g. solution}}\right)^2}$$

In any event the maximum uncertainty in an experimental determination of  $B$  is about 10 per cent. Variations with molecular weight of this order of magnitude could not be readily detected. The error in  $M_{1z}$  resulting from an uncertainty in  $B$  is:

$$\frac{\Delta M_{1z}}{M_{1z}} = c_z M_{1z} \Delta B \quad (20)$$

For polystyrene-butanone, an especially favorable case, this amounts to an error of about 1 per cent for a molecular weight of 100,000 at 0.3 per cent by weight, assuming 10 per cent error in  $B$ . This indicates an error of 5 per cent due to this cause at  $M_w = 500,000$ . This error could, of course, be decreased by going to lower concentrations. A concentration of 0.2 per cent by weight is still high enough to obtain fair results. A considerable improvement would result from the use of the osmotic balance in determining  $B$  (4).

In an actual ultracentrifugal experiment an excess pressure of 1/2 to 18 atm. may be developed in the sedimentation cell by the centrifugal field. The constant  $B$  is evaluated from measurements at atmospheric pressure. An expression for its rate of change with pressure should prove useful.<sup>5</sup> It is estimated that

---

the above for each solute component. However, since for such systems it has been found that

$$p = RT \sum_i \frac{c_i}{M_i} + b' c^2$$

it is consistent with the Duhem equation if

$$\frac{dc_{1z}}{dx} = \left( 2Ax - B \frac{dc_z}{dx} \right) M_i c_{1z}$$

In these equations  $B$  is a constant. However, it should be emphasized that this is merely an assumption which happens to be consistent with the Duhem equation. This is the important equation for treating polydisperse non-ideal solutions of polymers, and equation 19 follows directly from it by summation. It can also be shown that equation 25 can be obtained from it with complete generality, provided  $B$  is a constant.

<sup>5</sup> In general, and using Lewis and Randall's notation

$$\frac{\partial F_1}{\partial c_2} = \frac{RT}{M_2} \left\{ \frac{\partial \ln a_2}{\partial c_2} \right\}$$

and

this effect is negligible compared with the uncertainty in  $B$ , on the basis of the data of Gee and Treloar (3) on the partial specific volume of rubber in benzene. In any event the extremely high speeds are used only for samples of very low molecular weight, where the non-ideality correction is unimportant anyway. For cases where this is appreciable,  $P < 2$  atm. over atmospheric.

Now  $M_1$  has been obtained. If it is calculated correctly,  $M_2, M_3, M_4, M_5 \dots$  etc. may be obtained from it and its change with height in the sedimenting column in principle. This is demonstrated in the following way:

$$\frac{dM_1}{dx} = \frac{\sum_i M_i \frac{dc_i}{dx}}{c_x} - \frac{1}{c_x^2} \frac{dc_x}{dx} \sum_i c_i M_i \quad (21)$$

Then from equation 19

$$\begin{aligned} \sum_i M_i \frac{dc_i}{dx} &= \left\{ 2Ax - B \frac{dc_x}{dx} \right\} \sum_i M_i^2 c_i \\ &= \left\{ \frac{dc_x}{dx} / c_x M_{1x} \right\} \sum_i M_i^2 c_i \end{aligned} \quad (22)$$

Substituting in equation 5 and remembering that

$$M_2 \equiv M_x = \frac{\sum_i M_i^2 c_i}{\sum_i M_i c_i} \quad (23)$$

we obtain

$$M_{2x} = M_{1x} + M_{1x} \left( \frac{d \ln M_{1x}}{d \ln c_x} \right) \quad (24)$$

$$\frac{\partial}{\partial p} \left( \frac{\partial F_2}{\partial c_2} \right) = \frac{RT}{M_2} \frac{\partial}{\partial p} \left\{ \frac{\partial \ln a_2}{\partial c_2} \right\} = \frac{RT}{M_2} \frac{\partial}{\partial c_2} \left\{ \frac{\partial \ln a_2}{\partial p} \right\}$$

$$\frac{\partial \ln a_2}{\partial p} = \frac{M_2}{RT} \{ \bar{V}_2 - V_2 \}$$

where the volumes are partial specific and specific volumes, respectively. So that

$$\frac{\partial}{\partial p} \frac{\partial F_2}{\partial c_2} = \frac{\partial}{\partial c_2} (\bar{V}_2 - V_2)$$

It can be shown that

$$\frac{\partial F_2}{\partial c_2} = \frac{RT}{M_2 c_2} + 20gb'$$

Hence

$$\left( \frac{\partial B}{\partial p} \right)_T = \frac{20g}{RT} \frac{\partial b'}{\partial p} = \frac{1}{RT} \frac{\partial}{\partial c_2} (\bar{V}_2 - V_2)$$

which is very small, since  $\bar{V}_2 \cong V_2$ .



It can be shown in a similar manner that

$$M_{qx} = M_{(q-1)x} + M_{1x} \left( \frac{d \ln M_{(q-1)x}}{d \ln c_x} \right) \quad (25)$$

for all values of  $q$ , positive or negative, where  $M_q$  is defined as:

$$M_q = \frac{\sum_i M_i^q c_i}{\sum_i M_i^{q-1} c_i} \quad (26)$$

It is thus possible to obtain "point" values of any moment (molecular weight) by knowing the moment below it as a function of concentration. In theory, the initial moment may be any moment and need not have been calculated from the change in concentration with distance. However, it can be seen that to do the reverse calculation involves an arbitrary constant of integration. Nevertheless in certain cases where at some region of the sedimentation cell  $M_1$  and  $M_2$  are close together, the integration constant for  $M_0$  may be evaluated with a fair degree of precision.<sup>6</sup>

For  $M_{0x} = M_{nx}$  we have, from equation 24:

$$M_{1x} = M_{0x} + M_{1x} \left( \frac{d \ln M_{0x}}{d \ln c_x} \right) \quad (27)$$

<sup>6</sup> It can be proven that there is no point in the cell, except for the monodisperse case, at which the material has the same average molecular weights as the whole polymer. For the concentrations at which the zeroth, first, and second moments have the same values as the over-all values for the whole polymer, we have:

$$\begin{aligned} c_0^* &= \frac{\int_a^b \frac{x c_x dx}{M_{1x}}}{\int_a^b \frac{x dx}{M_{1x}}} \\ c_1^* &= \frac{\int_a^b x c_x \{M_{2x} - M_{1x}\} dx}{\int_a^b x \{M_{2x} - M_{1x}\} dx} = \frac{\int_a^b c_x^2 x \frac{dM_{1x}}{dc_x} dx}{\int_a^b c_x x \frac{dM_{1x}}{dc_x} dx} \\ c_2^* &= \frac{\int_a^b x c_x \{M_{3x} M_{2x} - M_{2x}^2\} dx}{\int_a^b x \{M_{3x} M_{2x} - M_{2x}^2\} dx} \end{aligned}$$

Here

$$\begin{aligned} c_0^* &= \text{the concentration where } M_{0x} = M_0 = M_n \\ c_1^* &= \text{the concentration where } M_{1x} = M_1 = M_w \\ c_2^* &= \text{the concentration where } M_{2x} = M_2 = M_z \end{aligned}$$

and  $x$  is the distance from the center of rotation to any point. It can be seen that all concentrations are unequal, except when  $M_{1x} = M_{2x} = M_{3x}$  etc., the monodisperse case.

The solution of this equation is

$$M_{0z} = \frac{c_z}{\int_{c_a}^{c_z} \frac{dc_z}{M_{1z}}} + K_a \quad (28)$$

where  $K_a$  is a constant of integration. This form was used by Lansing and Kraemer (6). Criteria for estimating  $K_a$  can be developed. By combining two moment recursion formulae:

$$M_{0z} = M_{1z} \left\{ 2 + \left( \frac{d \ln \frac{M_{1z}}{M_{0z}}}{d \ln c_z} \right) \right\} - M_{2z} \quad (29)$$

It is now possible to make two approximations. The derivative in the brackets may be taken as zero or as equal to

$$\frac{d \ln \frac{M_{2z}}{M_{1z}}}{d \ln c_z}$$

Then one obtains a value for  $M_{0z}$  at some point which can be used to evaluate the integration constant in equation 28. This should be done at a point in the sedimentation cell where all moments are as close together as possible, excluding the ends of the column. For positively skewed molecular-weight distributions the derivative in equation 29 should be positive. Hence if it is taken to be zero, the result will be too low. Conversely, if it is taken to be equal to

$$\frac{d \ln \frac{M_{2z}}{M_{1z}}}{d \ln c_z}$$

the result will be too high. For fractionated material this choice is frequently immaterial, since there is a region in the cell where

$$\frac{d \ln \frac{M_{2z}}{M_{1z}}}{d \ln c_z}$$

is very close to zero. However, in other cases this procedure may not be very satisfactory. The best that can be done is to take the mean of the two approximations.

Having derived relationships for calculating "point values" of various average molecular weights, or moments, it remains to convert them into the corresponding values for the whole polymer. This may be readily done by means of the following expressions:

$$M_0 \equiv M_n = \frac{\int_a^b dw}{\int_a^b \frac{dw}{M_{0x}}} \quad (30)$$

$$M_1 \equiv M_w = \frac{\int_a^b M_{wx} dw}{\int_a^b dw} \quad (31)$$

$$M_q = \frac{\int_a^b dw \prod_{p=1}^{p=q} M_{px}}{\int_a^b dw \prod_{p=1}^{p=q-1} M_{px}} \quad (32)$$

$q = 2, 3, 4 \dots$

$$\left. \begin{aligned} dw &= xc_x dx && \text{for a sector-shaped cell} \\ dw &= c_x dx && \text{for a linear cell} \end{aligned} \right\} \quad (33)$$

Sometimes in the sector-shaped cell a factor  $(x \pm \delta)$  must be substituted for  $x$  in case the point of the sector does not coincide with the center of rotation.

Now the problem of obtaining information about the molecular-weight distribution of the polymer presents itself. We may proceed in two different ways: first, to calculate as many moments of the distribution as possible and try to fit them by some empirical distribution curve; or second, to solve an integral equation.

(1) Since the  $q^{\text{th}}$  moment depends essentially on the derivatives of the concentration up to and including  $d^q c_x / dx^q$ , the uncertainty in the moments will be the larger, the higher the moment. This is due to the fact that  $dc_x / dx$  is obtained experimentally using the Lamm scale method (6, 11), and as one goes to higher and higher derivatives the uncertainty in the derivatives becomes larger and larger. Also, the portion of solution very near the high-concentration end of the cell becomes the decisive factor in determining the value of the moments, as higher moments are calculated.

It has been found possible in practice to go only as high as  $M_3 \equiv M_{s+1}$  with any degree of reliability. The foregoing recursion formulae are used, slopes being computed graphically with a tangent meter. The criteria for reliability are admittedly meager. Values of  $M_{3x}$  which increase regularly with concentration without too much irregular variation are taken as being reliable. At that,  $M_3$  may be in error by as much as  $\pm 20$  per cent, judging from experiments on mixtures of polymers (13). The recursion formula is also used in calculating  $M_s$  in preference to the older methods which gave average values of  $M_s$  over an interval instead of point values (6, 12).

In practice, four moments are usually available. Thus, these moments may be used to estimate the constants in the following distribution functions (2, 6, 9):

$$dW = \frac{1}{M_n \beta \sqrt{\pi}} e^{-(1/\beta^2 \ln^2(M/m))} \quad (34)$$

where

$$m = M_p e^{0.5\beta^2}, M_n \equiv M_0 = M_p e^{0.45\beta^2}, \text{ and } M_q = M_p e^{\beta^2(0.45 + \frac{1}{2}q)} \\ W(p) dp = \frac{(1-\alpha)^{b+2}}{\Gamma(b+2)} p^{b+1} \alpha^p dp \quad (35)$$

where  $p_q = q^{\text{th}}$  moment expressed as a degree of polymerization  $= \frac{b+q+1}{1-\alpha}$  and functions of the type

$$M^n e^{-\alpha M^2} \quad (36)$$

What we have here, then, is a curve which can be considered to approach the true distribution on a basis of agreement with four moments. It must be also remembered that there is an added uncertainty in  $M_n$  due to the approximation procedure we have described.

Unfortunately, equations 34, 35, and 36 frequently cannot be made to fit the behavior exhibited by imperfectly fractionated polystyrenes at all (13). In this event the total distribution curve (or moments) may be resolved into two superimposable distributions by splitting the  $\ln c_x$  vs.  $M_{wx}$  curve into two parts and proceeding with each part as before. This leads to a rough visualization of the shape of the true distribution curve. This method was applied to data for some polystyrene fractions, and the results will be discussed with other experimental data (13).

(2) If one attempts to fit a generalized curve, such as a sum of terms of the form of equation 34, 35, or 36, to a set of moments, the labor is so great that it is just as easy to solve the integral equation of sedimentation equilibrium, which will now be developed. This gives the distribution function directly<sup>7</sup> and the solution offers no theoretical mathematical difficulties for a continuous distribution of molecular weights. This procedure is similar in principle to that of Rinde (8).

From equation 5 it follows that

$$c_s = c_p \exp M G(x) \quad (37)$$

where

$$G(x) = A(x^2 - x_p^2) - B(c_x - c_p) \quad (38)$$

<sup>7</sup> It has been shown that, in theory, an infinite number of moments of any distribution may be determined from a sedimentation equilibrium experiment. This means that one and only one real positive function, the differential molecular-weight distribution curve, is defined by the experiment and in principle the solution of equation 41 is unique. The restriction of continuity of  $f(M)$  is not necessary for this conclusion. The only source of trouble is that an inordinately large number of terms may be required in equation 44 to represent  $\gamma(M)$ . This is to be expected, of course, with discontinuous distributions. It may also occur with a distribution with two widely separated peaks, as in associated polyvinyl chloride (1). This difficulty may be removed in some cases by use of equation 45. A Fourier integral representation of  $f(M)$  or  $\gamma(M)$  has been tried but has proven impracticable.

using some reference point  $x_p$ ,  $c_p$ . Let the initial over-all concentration of species  $i$  be  $c_{0i}$ . Then

$$c_{ip} = \frac{c_{0i} \left\{ \frac{b^2 - a^2}{2} + \delta(b - a) \right\}}{\int_a^b (x + \delta) \exp M_i G(x) dx} \quad (39)$$

from a material balance on species  $i$ . Here  $\delta$  is a correction for non-coincidence of the center of the cell sector with the center of rotation and is included since it was found necessary for the cell used in this investigation. The distances of the ends of the column of solution from the center of rotation are denoted by  $a$  and  $b$ . Hence

$$c_i = \frac{c_{0i} \left\{ \frac{b^2 - a^2}{2} + \delta(b - a) \right\} \exp M_i G(x)}{\int_a^b (x + \delta) \exp M_i G(x) dx} \quad (40)$$

Passing to a "continuous" distribution of molecular weights,

$$\frac{c_x}{c_0} = \left\{ \frac{b^2 - a^2}{2} + \delta(b - a) \right\} \frac{\int_0^\infty \frac{f(M) \exp MG(x) dM}{\int_a^b (x + \delta) \exp MG(x) dx}}{\quad} \quad (41)$$

Here  $f(M)$  is the differential weight-distribution function of the polymer;  $c_x/c_0$ , the ratio of the concentration at distance  $x$  to the initial concentration, and  $G(x)$  are known functions of  $x$ . All constants are known experimentally. The arbitrary constant in  $G(x)$  may now be set equal to zero, since it cancels out in equation 41. This equation may be solved by letting

$$\frac{c_x}{c_0} = \int_0^\infty \gamma(M) \exp MG(x) dM \quad (42)$$

where

$$\gamma(M) = \left\{ \frac{b^2 - a^2}{2} + \delta(b - a) \right\} \frac{f(M)}{\int_a^b (x + \delta) \exp MG(x) dx} \quad (43)$$

Assuming that  $\gamma(M)$  may be represented by a finite number of terms of the form  $M'^\kappa e^{-\kappa M}$

$$\gamma(M) = \theta^\kappa e^{-\kappa M} \sum_{j=1}^n \theta_j M^j \quad (44)$$

This is justified in general, since  $\gamma(M)$  is zero at  $M = 0$  and at  $M \rightarrow \infty$ .

The expression

$$\gamma(M) = M^m \sum_{j=1}^n \theta_j e^{-\kappa_j M} \quad (45)$$

could also be used, although equation 44 is more general. Here, the exponent  $m$  is selected from a consideration of the moment ratios, a narrow distribution requiring higher values of  $m$  than a broad distribution (10). This solution requires a great deal more numerical labor than equation 44. Substituting equation 44 into equation 42 and integrating,

$$\frac{c_x}{c_0} = \sum_{j=1}^n \frac{\theta_j j!}{q^{j+1}} \quad (46)$$

where

$$q = K - G(x) \quad (47)$$

The constant  $K$  is arbitrary but must be taken so that  $q$  is always positive.

Let

$$p = \frac{1}{q} \quad (48)$$

then

$$\sum_{j=1}^n \theta_j j! p^{j-1} \equiv \sum_{j=1}^n r_j p^{j-1} = \frac{1}{p^2} \left( \frac{c_x}{c_0} \right) = \psi(p) \quad (49)$$

The function  $\frac{1}{p^2} \left( \frac{c_x}{c_0} \right)$  is known from the experimental data and equations 46 and 47. This is then fitted by a polynomial in  $p$  of the form

$$\psi(p) = g_0 + g_1 p + g_2 p^2 + \dots \quad (50)$$

Then, equating coefficients:

$$r_i \equiv g_{i-1}, \quad \theta_i = \frac{g_{i-1}}{j!} \quad (51)$$

The use of equation 45 in the same manner gives:

$$\frac{c_x}{c_0} = \Gamma(m+1) \sum_{j=1}^n \frac{\theta_j}{\{K_j - G(x)\}^{m+1}} \quad (52)$$

Here one selects experimental points  $(c_n, x)$  to determine as many constants  $K_j$  and  $\theta_j$  as required. It can be easily seen that the solution of equation 52 is extremely tedious. The criteria for a fit are (1) that the final  $f(M)$  obtained shall be everywhere positive, or at least if negative in places the contribution from these areas be negligible compared to the rest; (2) that equation 46 represent  $c_x/c_0$  well over the whole range.

Now the function  $\gamma(M)$  has been evaluated.

The integral  $\int_a^b (x + \delta) \exp MG(x) dx$  is then evaluated, numerically or otherwise (depending on  $G(x)$ ), and from equation 43 the function  $f(M)$  may be obtained. At worst, the integral in the denominator of equation 43 may be evaluated numerically for a set of values of  $M$ , and  $f(M)$  may be obtained as a set of numerical values. Needless to say, this whole calculation is very time-consuming. There is also the question of the correctness of the final result.

A particular advantage of this method is a determination of  $M_n$  free from approximation.

This seems to be the best, if not the easiest, way to interpret sedimentation-equilibrium data. Even if no great reliance is to be placed on the function  $f(M)$  as such, the value of  $M_0 \equiv M_n$  calculated from it by integration is subject to no approximation, and is as reliable as values of  $M_w$  calculated from the data by methods outlined here. The ideal characterization of a polymer sample from equilibrium ultracentrifuge data would consist of specifying  $f(M)$  as a solution of equation 41 and then giving values of  $M_n$  and  $M_w$  calculated from it. Such data are fully as reliable as osmotic-pressure and light-scattering evaluations of the same quantities, provided the solvent-polymer system is of the type treated here and the molecular weight of the polymer is not excessively high. For samples of extremely low molecular weight where it is difficult to find a suitable membrane for osmotic-pressure work, this approach offers a very precise and reliable method for the determination of  $M_n$ . It should be also pointed out that in this molecular-weight range the correction for non-ideal behavior is negligible, thus simplifying the solution of equation 41 and permitting a wide choice of solvents.

So, with such advances in theory as are here described, and with the development of potentially more precise experimental techniques (5), it is felt that we can be more optimistic than Mosimann (7), who has remarked that the sedimentation-equilibrium method cannot be used for cellulose derivatives of molecular weight higher than 80,000. And in extending the range of the instrument, there are important problems which now may be studied.

For instance, on the basis of data recently obtained (13), it is believed that reliable information about the molecular size distribution of high polymers may result from sedimentation-equilibrium studies. This method could be also extended to association colloids.

#### SUMMARY

Equations have been developed to permit the calculation of molecular weights and molecular-weight distributions in non-ideal systems from sedimentation-equilibrium experiments. A general method for the computation of any moment of the molecular-weight distribution has been developed. The range of usefulness of this relationship is limited by the accuracy of the experimental data available.

All derivations in this paper rest upon the assumption that

$$b' \equiv \frac{\partial(p/c)}{\partial c} = \frac{1}{2} \sum_i b_i \gamma_i$$

where the  $b_i$ 's are independent of molecular weight and concentration. Here  $b$  is the osmotic pressure,  $c$  is the concentration, and  $\gamma_i$  is the fraction of species  $i$  in the polymer mixture.

It is believed that, in principle, the best method of characterizing a polymer by sedimentation equilibrium is to calculate the weight-distribution curve

from the measurements. By using this curve one may obtain  $M_0 \equiv M_n$  and  $M_1 \equiv M_w$ .

This method of evaluation of  $M_n$  does not require a membrane and can be used for polymers of very low molecular weight.

The writer wishes to express his gratitude to Dr. J. W. Williams, under whose direction this work was carried out. Further, he desires to thank Dr. R. H. Ewart of the General Laboratories, United States Rubber Company, Passaic, New Jersey, and Dr. Gerson Kegeles of this Laboratory for their unfailing interest and coöperation.

#### REFERENCES

- (1) DOTY, P., WAGNER, H., AND SINGER, S.: *J. Phys. Colloid Chem.* **51**, 32 (1947).
- (2) FLORY, P. J.: *Chem. Rev.* **39**, 137 (1946).
- (3) GEE, G., AND TRELOAR, L. R. G.: *Trans. Faraday Soc.* **38**, 147 (1942).
- (4) JULLANDER, I.: *Arkiv. Kemi, Mineral. Geol.* **21**, 1 (1945)
- (5) KEGELES, G.: *J. Am. Chem. Soc.* **69**, 1302 (1947).
- (6) LANSING, W. D., AND KRAEMER, E. O.: *J. Am. Chem. Soc.* **54**, 1369 (1935).
- (7) MOSIMANN, H.: *Helv. Chim. Acta* **26**, 369 (1942)
- (8) RINDE, H.: *Dissertation*, Upsala, 1928.
- (9) SCHULZ, G. V.: *Z. physik. Chem.* **B43**, 25 (1939); for discussion see BOYER, R. F.: *Ind. Eng. Chem., Anal. Ed.* **18**, 342 (1942).
- (10) SVEDBERG, T.: *J. Phys. Colloid Chem.* **51**, 1 (1947).
- (11) SVEDBERG, T., AND PEDERSEN, K. O.: *The Ultracentrifuge*. Oxford University Press, London (1940).
- (12) WALES, M., BENDER, M. M., WILLIAMS, J. W., AND EWART, R. H.: *J. Chem. Phys.* **14**, 353 (1946)
- (13) WALES, M., THOMPSON, J. O., WILLIAMS, J. W., AND EWART, R. H.: Part II of this series, in preparation.

### THE EFFECT OF SIZE, SHAPE, AND FLEXIBILITY OF THE SOLUTE MOLECULES ON THE PROPERTIES OF COLLOIDAL SOLUTIONS<sup>1,2</sup>

MAURICE L. HUGGINS

*Kodak Research Laboratories, Rochester, New York*

*Received August 25, 1947*

#### INTRODUCTION

An equation has been deduced by the writer (6-11) for the entropy of mixing of solutions of large flexible chain molecules, on the basis of which it has been possible to explain the large deviations from the ideal solution "laws" which are

<sup>1</sup> Presented at the Twenty-first National Colloid Symposium, which was held under the auspices of the Division of Colloid Chemistry of the American Chemical Society at Palo Alto, California, June 18-20, 1947.

<sup>2</sup> Communication No. 1159 from the Kodak Research Laboratories.



observed, even when the heat of mixing is negligible. Several others (1-5, 13-16), using different procedures, have arrived at essentially equivalent results. It is now generally agreed that this theory and the equations deduced thereby are fundamentally correct, though requiring some extension to make them quantitatively applicable to high concentrations or to actual solutions which do not conform closely to the model chosen for the theoretical development.

It is not at first apparent whether the large deviations from the ideal solution laws, obtained theoretically and experimentally, result primarily from the large size of the solute molecules, their *shape*, or their *flexibility*. To settle this question, in part, equations for the entropy of mixing and related quantities have been derived by methods not differing greatly from those used for solutions of chain molecules, for solutions of large spherical and large rodlike molecules.<sup>3</sup>

In the present paper equations are derived for the general case of rigid solute particles of any assumed shape. These reduce, for the special cases previously dealt with, to the equations then obtained. In this treatment, the hypothetical lattice assumption is avoided, since it is both artificial and unnecessary (*cf.* 5).

#### DERIVATION OF GENERAL EQUATIONS

We consider a solution of  $N$  solvent and  $N$  solute molecules, occupying a volume  $V$ . We wish to calculate the dependence on concentration of the entropy of mixing, i.e., the difference between the entropy of the solution and the sum of the entropy of  $N$  solvent molecules in pure liquid solvent and the entropy of  $N$  solute molecules in pure liquid solute.

The entropy of the solution consists, in part, of the entropy associated with internal randomness of the molecules, and with their vibration, rotation, and orientation. For the solvent molecules we may reasonably assume, as a close approximation, that the entropy (per molecule) of these types is the same whether the molecules are in the (dilute) solution or in the pure solvent liquid. For the solute molecules, we can likewise assume that the entropy (per molecule) of these types is independent of the concentration in the low concentration range in which we are interested, differing from that in the pure liquid solute by a constant amount.

With these assumptions, we may limit our consideration to the distributional entropy associated with the irregular placement of the two kinds of molecules in the solution. For the present, we assume the distribution to be perfectly random, realizing that our results will have to be modified when applying them to solutions in which intermolecular forces tend to produce departures from perfect randomness.

To compute the distributional entropy of the solution, we imagine the volume,  $V$ , to be at first unoccupied by molecules; we then (hypothetically) add the

<sup>3</sup> These results were presented at the Colloquium on High Polymers at Strasbourg, France, November 25-30, 1946. (The printed report (11) includes only the treatment of the spherical case.) Some of the equations and constants presented there and in this paper are equivalent to some previously derived by a different procedure by Zimm (16), as will be shown.

$N$  solute molecules, one at a time, and deduce the entropy contribution of each such addition. Assuming additivity of volumes, the volume remaining after all the solute molecules have been added is equal to the volume which  $N$  solvent molecules would occupy in the pure solvent. We may, with negligible error, assume the entropy associated with filling this volume of the solution with solvent molecules to be the same as that associated with filling the same volume of pure solvent. The contribution of the solvent molecules to the entropy of mixing is thus (practically) zero. (In effect, we assume that the distributional entropy of the pure liquid solvent within a region of given volume is independent of the shape of that region. This assumption is certainly inaccurate for very high concentrations, i.e., when the volume filled by solvent is not large relative to the molecular volume,  $v_1$ .)

With the foregoing assumptions and approximations we can write for the entropy of mixing of the solution:

$$\Delta S_m = S - S_1^0 - S_2^0 = \sum_{i=1}^{N_2} S_i + k \ln N_2! \quad (1)$$

$S_i$  is the contribution of the  $i^{\text{th}}$  solute molecule, added as indicated above, to the total distributional entropy of the solution, and  $k$  is the Maxwell-Boltzmann constant. The last term takes account of the fact that all the solute molecules are alike. The partial molal entropy of mixing of the solvent, which is required for substitution into the thermodynamic equations for the equilibrium properties of the solution, is

$$\bar{S}_1 = \frac{R}{k} \left( \frac{\partial \Delta S_m}{\partial N_1} \right)_{N_2} \quad (2)$$

$$= \frac{R}{k} \sum_{i=1}^{N_2} \left( \frac{\partial S_i}{\partial N_1} \right)_{N_2} \quad (3)$$

According to well-known principles of statistical mechanics,

$$S_i = k \ln (V_i / av_2) \quad (4)$$

where  $V_i$  is the volume available for the center of the  $i^{\text{th}}$  molecule,  $v_2$  is the volume of that (or any other solute) molecule, and  $a$  is a constant, which, for our present purpose, does not need to be evaluated. (If the requirement is made that the molecule centers must be placed at lattice points, as in the previous derivations,  $a = 1$ .)

For  $i = 1$ , obviously,

$$V_1 = V_1 = V \quad (5)$$

The center of the second solute molecule ( $i = 2$ ) can be placed in the solution anywhere within the volume,  $V$ , except where overlapping of the first and second molecules would result. This limitation is obviously a function of the shapes and relative orientations of the two molecules. In general, for any shape of molecule,

$$V_2 = V - k_2 v_2 \quad (6)$$

where  $k_2 v_2$  is the volume ruled out because it would produce overlapping, averaged over all relative orientations and integrated over all distances between the atomic centers. Since the volume of a spherical shell of thickness  $ds$  is  $4\pi s^2 ds$ ,

$$k_2 v_2 = 4\pi \int_{s=0}^{\infty} s^2 p_s ds \quad (7)$$

$p_s$  being the average probability of overlapping when the molecule centers are a distance  $s$  apart.

The volume ruled out for the center of the third solute molecule, as a result of the presence of the first two, is approximately  $2k_2 v_2$ . A small correction term must be included to take account of the chance that the first two molecules are so close together that certain regions are doubly ruled out, being too close to both the first and the second molecules. This term must be proportional to the square of the volume of a simple solute molecule and inversely proportional to the volume available for the center of the second molecule. Hence:

$$V_3 = V - 2k_2 v_2 + \frac{k_3 v_2^2}{V - k_2 v_2} \quad (8)$$

The volume available for the center of the fourth solute molecule is the total volume, minus three times the volume ruled out by each of the three already-placed molecules independently, plus the volume doubly ruled out (by molecule pairs 1 and 2, 1 and 3, and 2 and 3), minus the volume triply ruled out. The equation is:

$$V_4 = V - 3k_2 v_2 + k_3 v_2^2 \left[ \frac{1}{V - k_2 v_2} + \frac{2}{V - 2k_2 v_2 + k_3 v_2^2 (V - k_2 v_2)^{-1}} \right] - \frac{k_4 v_2^3}{(V - k_2 v_2)[V - 2k_2 v_2 + k_3 v_2^2 (V - k_2 v_2)^{-1}]} \quad (9)$$

Similar considerations lead to the following relationship for the volume available for the center of the  $i^{\text{th}}$  molecule:

$$V_i = V d_i \quad (10)$$

where

$$d_i = \sum_{j=1}^i (-1)^{j+1} c_{ij} \mathbf{V}_2^{j-1} / N_2^{j-1} \quad (11)$$

and

$$c_{ij} = k_j \sum_{h_1=1}^{h_2-1} \sum_{h_2=2}^{h_3-1} \sum_{h_3=3}^{h_4-1} \cdots \sum_{h_{j-2}=j-2}^{i-2} \frac{h_1}{d_{h_1+1} d_{h_2+1} d_{h_3+1} \cdots d_{h_{j-2}+1}} \quad (12)$$

Here  $h_1, h_2$ , etc.,  $i$  and  $j$  are integers; the  $k_j$  are constants which depend on the shape of the molecules; and  $\mathbf{V}_2$  is the volume fraction of solute, defined by the equation

$$\mathbf{V}_2 = v_2 N_2 / V \quad (13)$$

$V$ , the total volume of the solution, is given by the equation

$$V = v_1 N_1 + v_2 N_2 \quad (14)$$

Defining  $n$  as the ratio of the average volume per solute molecule to that per solvent molecule (including intermolecular space),

$$n = v_2/v_1 \quad (15)$$

Hence

$$\mathbf{V}_2 = \frac{nN_2}{N_1 + nN_2} \quad (16)$$

$$\left( \frac{\partial \mathbf{V}_2}{\partial N_1} \right)_{N_2} = - \frac{nN_2}{(N_1 + nN_2)^2} = - \frac{\mathbf{V}_2^2}{nN_2} \quad (17)$$

From equations 3, 4, and 10 we obtain:

$$\bar{S}_1 = R \left[ N_2 \left( \frac{\partial \ln V}{\partial N_1} \right)_{N_2} + \sum_{i=1}^{N_2} \left( \frac{\partial \ln d_i}{\partial N_1} \right)_{N_2} \right] \quad (18)$$

From equations 14, 13, and 15:

$$N_2 \left( \frac{\partial \ln V}{\partial N_1} \right)_{N_2} = \frac{v_1 N_2}{V} = \frac{\mathbf{V}_2}{n} \quad (19)$$

For the other term in equation 18 we can write:

$$\sum_{i=1}^{N_2} \left( \frac{\partial \ln d_i}{\partial N_1} \right)_{N_2} = \left( \frac{\partial \mathbf{V}_2}{\partial N_1} \right)_{N_2} \sum_{i=1}^{N_2} \left( \frac{\partial \ln d_i}{\partial \mathbf{V}_2} \right)_{N_2} \quad (20)$$

$$= - \frac{\mathbf{V}_2^2}{nN_2} \sum_{i=1}^{N_2} \left( \frac{\partial \ln d_i}{\partial \mathbf{V}_2} \right)_{N_2} \quad (21)$$

For a small value of  $i$ ,  $\left( \frac{\partial \ln d_i}{\partial \mathbf{V}_2} \right)_{N_2}$  can be computed as a power series in  $\mathbf{V}_2$ , from equations 11 and 12. As  $i$  increases, the computations rapidly become laborious; they are, however, perfectly straightforward. The coefficients can be expressed as simple functions of  $i$ ; from these one can then deduce the following general expression:

$$- \left( \frac{\partial \ln d_i}{\partial \mathbf{V}_2} \right)_{N_2} = \frac{Ai}{N_2} + \frac{Bi^2}{N_2^2} \mathbf{V}_2 + \frac{Ci^3}{N_2^3} \mathbf{V}_2^2 + \frac{Di^4}{N_2^4} \mathbf{V}_2^3 + \dots \quad (22)$$

$$\text{where } A = k_2, \quad (23)$$

$$B = k_2^2 - k_3, \quad (24)$$

$$C = k_2^3 - \frac{5}{2} k_2 k_3 + \frac{k_4}{2}, \quad \text{and} \quad (25)$$

$$D = k_2^4 - \frac{13}{3} k_2^2 k_3 + \frac{3}{2} k_2 k_4 + k_3^2 - \frac{k_5}{6} \quad (26)$$

Performing the summation indicated in equation 21, and substituting into equation 18 yields

$$\bar{S}_1 = \frac{R}{n} (\mathbf{V}_2 + K_2 \mathbf{V}_2^2 + K_3 \mathbf{V}_2^3 + K_4 \mathbf{V}_2^4 + K_5 \mathbf{V}_2^5 + \cdots) \quad (27)$$

$$\text{where } K_2 = \frac{1}{2} (k_2), \quad (28)$$

$$K_3 = \frac{1}{3} (k_2^2 - k_3), \quad (29)$$

$$K_4 = \frac{1}{4} \left( k_2^3 - \frac{5}{2} k_2 k_3 + \frac{k_4}{2} \right), \quad \text{and} \quad (30)$$

$$K_5 = \frac{1}{5} \left( k_2^4 - \frac{13}{2} k_2^2 k_3 + \frac{3}{2} k_2 k_4 + k_3^2 - \frac{k_5}{6} \right) \quad (31)$$

This is the relationship we have been seeking. Substitution of the appropriate  $k_i$  constants for a particular molecular shape gives the desired dependence of the partial molal entropy on concentration (assuming perfect randomness of mixing).

If the heat of mixing of the solution is zero,

$$\ln a_1 = -\bar{S}_1/R \quad (32)$$

With this relationship and the appropriate thermodynamic equations, one may obtain theoretical equations for the osmotic pressure and other equilibrium properties of such solutions.

#### LARGE SPHERICAL SOLUTE MOLECULES

For the case of spherical solute molecules which are large compared with the solvent molecules,

$$k_2 = 8 \quad (33)$$

since the center of the second solute molecule cannot be anywhere within a sphere which has twice the radius, or eight times the volume, of the first solute molecule (figure 1). This result can be obtained from equation 7, putting  $p_s$  equal to unity for  $s$  between zero and  $r_2$  (twice the molecular radius) and equal to zero otherwise.

The constant  $k_3$  may be computed in the following way: The volume of overlapping of two spheres, each of radius  $2r_2$ , is

$$v_s = v_2 \left( 8 - \frac{3s}{r_2} + \frac{s^3}{16r_2^3} \right) \quad (34)$$

for  $s$  between  $2r_2$  and  $4r_2$  and zero for  $s$  greater than  $4r_2$  (figure 2). The probability that the center of molecule 2 is at a distance between  $s$  and  $s + ds$  from the center of molecule 1 is zero for  $s < 2r_2$ ; for larger values of  $s$ ,

$$dp_s = \frac{4\pi s^2 ds}{V - 8v_2} \quad (35)$$

The average volume doubly ruled out is

$$\bar{v} = \int_{s=2r_2}^{4r_2} v_s dp_s = \frac{34v_2^2}{V - 8v_2} \quad (36)$$

This is the last term of equation 8; hence

$$k_3 = 34 \quad (37)$$

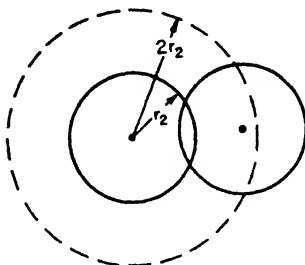


FIG. 1. The center of the second sphere cannot come within a distance  $2r_2$  from the center of the first sphere.

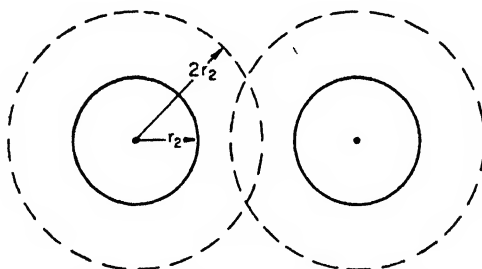


FIG. 2. If the distance between sphere centers is less than  $4r_2$  the two large spheres, each of radius  $2r_2$ , overlap.

An approximate value for  $k_4$ , the constant concerned with the mutual overlapping of three spheres of radius  $2r_2$ , is readily computed. The probability that sphere 2 overlaps sphere 1 (to any extent) is

$$p_{12} = \int_{s=2r_2}^{4r_2} \frac{4\pi s^2 ds}{V - k_2 v_2} = \frac{56v_2}{V - k_2 v_2} \quad (38)$$

The value of  $s$  which would give the correct average volume of overlapping of the first and second spheres (equation 36) is

$$\bar{s}_{12} = 3.07r_2 \quad (39)$$

The probability that (with spheres 2 and 1 mutually overlapping) sphere 3 overlaps sphere 1 is

$$p_{13} = \frac{56v_2(1 - 0.04)}{V - 2k_2 v_2 + k_3 v_2(V - k_2 v_2)^{-1}} \quad (40)$$

The factor  $(1 - 0.04)$  takes account of the fact that the centers of spheres 2 and 3 cannot be closer together than  $2r_2$ . Its approximate magnitude is computed on the assumption that both  $s_{12}$  and  $s_{13}$  have the average value given by equation 39.

The probability that  $s_{23}$  is between  $2r_2$  and  $4r_2$ , when both 1 and 2 and 1 and 3 overlap, is approximately the area of the zone on the surface of a sphere of radius  $\bar{s}_{12}$ , which includes all points between  $2r_2$  and  $4r_2$  from a point on that sphere, divided by the surface area of the whole sphere. This is

$$p_{23} = \frac{3}{2(3.07)^2} = 0.16 \quad (41)$$

Multiplying  $p_{12}$ ,  $p_{13}$ , and  $p_{23}$  together gives the probability,  $p_{123}$ , that there is mutual overlapping of all three spheres. We may compute a rough value for the average volume of mutual overlapping on the assumption that it is the same as if, in all cases, all three distances between sphere centers were equal to  $3.07r_2$ , as given by equation 39. An exact value for this volume has not been computed. It should, however, be somewhat larger (perhaps 10–15 per cent) than twice the value of a cone having a base equal in area to the area of mutual overlapping in the plane of the sphere centers and an altitude equal to the distance from that plane of either peak of the mutual overlap region. In this way the average value of mutual overlap (for those spheres showing 123 overlap) has been calculated to be:

$$\bar{v}'_{123} > 0.134 r_2^3 \quad (42)$$

The average volume of 123 overlap, for all of the third molecules added to the solution volume, is approximately

$$\bar{v}_{123} = p_{12}p_{13}\bar{v}'_{123} \quad (43)$$

Hence

$$\bar{v}_{123} > \frac{15.3r_2^3}{(V - k_2r_2)[V - 2k_2r_2 + k_3r_2(V - k_2r_2)^{-1}]} \quad (44)$$

Comparison with equation 9 leads to the result:

$$k_4 > 15.3 \quad (45)$$

Adding 10–15 per cent, for the reason just mentioned, we conclude that, approximately,

$$k_4 = 18 \quad (46)$$

Substituting equations 33, 37, and 46 into equations 27–31 gives:<sup>4</sup>

<sup>4</sup> In equations 54 and 55 of reference 11, the coefficient of  $\nabla^2$  should be  $\frac{\gamma}{8} - 42$  and  $-\left(\frac{\gamma}{8} - 42\right)$ , respectively.

$$\bar{S}_1 = R \left[ \frac{\mathbf{V}_2}{n} + \frac{4}{n} \mathbf{V}_2^2 + \frac{10}{n} \mathbf{V}_2^3 - \frac{40}{n} \mathbf{V}_2^4 - \left( \frac{792 + \frac{k_5}{30}}{n} \right) \mathbf{V}_2^5 \dots \right] \quad (47)$$

This may be compared with Raoult's law, which may be put in the form

$$\bar{S}_1 = R \left[ \frac{\mathbf{V}_2}{n} + \left( \frac{1}{n} - \frac{1}{2n^2} \right) \mathbf{V}_2^2 + \left( \frac{1}{n} - \frac{1}{n^2} + \frac{1}{3n^3} \right) \mathbf{V}_2^3 + \dots \right] \quad (48)$$

or, for large  $n$ ,

$$\bar{S}_1 = R \left[ \frac{\mathbf{V}_2}{n} + \frac{\mathbf{V}_2^2}{n} + \frac{\mathbf{V}_2^3}{n} + \dots \right] \quad (49)$$

The coefficients of the square and higher powers of  $\mathbf{V}_2$  are different, but in both cases they all approach zero as  $n$  increases. Dilute solutions of spherical molecules should (if the heat of mixing is negligible) behave as nearly "ideal" solutions, obeying Raoult's law quite closely.

#### LARGE ROD-LIKE MOLECULES

We next consider solutions of rod-like (cylindrical) solute molecules which are large, both in length and in cross section, compared with the solvent molecules. Let the length and cross-sectional radius of each rod be  $l_2$  and  $r_2$ , respectively.

For a given angle,  $\theta$ , between the axes of the first and second rods, the volume ruled out for the center of the second rod as a result of the presence of the first is that outlined by dashed lines in figure 3. Calculation of the magnitude of this volume, averaged over all values of  $\theta$ , leads to

$$k_2 = \frac{l_2}{r_2} \quad (50)$$

The volume of the cylindrical solute molecule is

$$v_2 = \pi r_2^2 l_2 \quad (51)$$

The volume per solvent molecule, if spherical, is

$$v_1 = \alpha_1 r_1^3 \quad (52)$$

the constant  $\alpha_1$  depending on their closeness of packing. If "close-packed"

$$\alpha_1 = 2^{\frac{1}{2}} = \sqrt{32} \quad (53)$$

For "simple cubic packing",

$$\alpha_1 = 8 \quad (54)$$

We may thus write

$$k_2 = \frac{\alpha_1}{\pi} \left( \frac{r_1}{r_2} \right)^3 n \quad (55)$$



and so

$$K_2 = \frac{\alpha_1}{2\pi} \left( \frac{r_1}{r_2} \right)^3 n \quad (56)$$

and

$$\bar{S}_1 = R \left[ \frac{\mathbf{V}_2}{n} + \frac{\alpha_1}{2\pi} \left( \frac{r_1}{r_2} \right)^3 \mathbf{V}_2^2 + \dots \right] \quad (57)$$

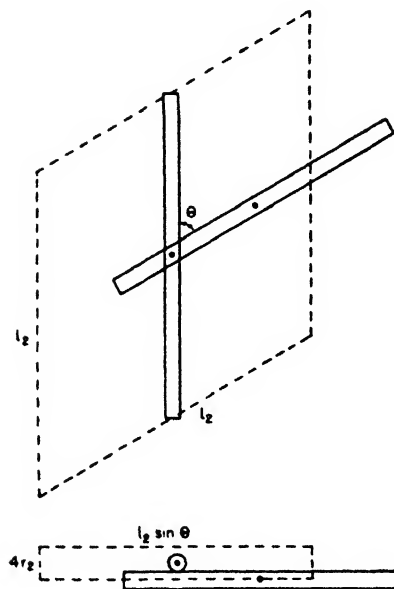


FIG. 3. Two rods in contact, as seen in plan and elevation. The region ruled out for the center of the second rod, as a result of the presence of the first rod, is that bounded by the dashed lines.

(As Dr. Zimm has emphasized, in discussing the subject with the writer, the coefficients in these equations are not correct when  $r_2$  is not large relative to  $r_1$ .)

The important thing to note here (as already pointed out by Zimm) is that, for a constant cross-sectional radius of the solute molecule, the magnitude of the coefficient of  $\mathbf{V}_2^2$  is independent of the length of that molecule, a result similar to that which has been obtained for randomly kinked chain molecules, but different from that (see equation 47) for large spherical solute molecules and different from Raoult's law (equations 48-49).

#### DISCUSSION AND CORRELATION WITH PREVIOUS RESULTS

For comparison with equations 47, 48, 49, and 57, the corresponding equation for solutions of randomly kinked chain molecules, composed of segments equal

in size to the solvent molecules (with zero heat of mixing), may be put in the form

$$\bar{S}_1 = R \left[ \frac{\mathbf{V}_2}{n} + \left( \frac{1}{2} - \mu_s \right) \mathbf{V}_2^2 + \cdots \right] \quad (58)$$

where  $\mu_s$  is about equal to the reciprocal of the coördination number. ( $\mu_s$  is a function of the relative sizes of the chain segments and solvent molecules, but is practically independent of  $n$ .)

Equations 57 and 58 are alike in showing a dependence of the coefficient of  $\mathbf{V}_2^2$  on the relative dimensions of the solvent molecules and the solute molecule cross sections, with no dependence on the length of the solute molecule.

McMillan and Mayer (12) have derived a series expansion for the osmotic pressure, Zimm (16) writing their result in the form

$$\pi = RT \left( \frac{1}{M_2} c + A_2 c^2 + A_3 c^3 + \cdots \right) \quad (59)$$

where  $c$  is the concentration of solute in mass per unit volume of solution,  $M_2$  is the molecular weight of the solute, and  $A_2, A_3, \dots$  are constants. Comparison with the equations previously deduced by the writer (e.g., equation 9 of reference 9) shows that Zimm's  $A_2$  and the writer's  $\mu$  are related by means of the equation

$$A_2 = \frac{d_1}{M_1 d_2^2} \left( \frac{1}{2} - \mu \right) \quad (60)$$

Here  $d_1$  and  $d_2$  are the densities of the pure components.

For solutions with no heat of mixing,

$$\mu = \mu_s \quad (61)$$

Comparing equations 27, 28, and 58 of this paper, it is seen that

$$K_2 = \frac{k_2}{2} = n \left( \frac{1}{2} - \mu_s \right) \quad (62)$$

Therefore,

$$K_2 = \frac{n M_1 d_2^2}{d_1} A_2 = \frac{v_2 M_1 d_2^2}{v_1 d_1} A_2 \quad (63)$$

For solutions of large rigid spheres, Zimm has deduced

$$A_2 = \frac{16\pi r_2^3 N_0}{3M_2^2} \quad (64)$$

where  $N_0$  is Avogadro's number. Substituting into equation 63, it is readily shown that

$$K_2 = \frac{k_2}{2} = 4 \quad (65)$$

in agreement with this paper.

For long rigid rods, Zimm has deduced

$$A_2 = \frac{\pi N_0 r_2 l_2^2}{2M_2^2} \quad (66)$$

Substituting into equation 63 leads to

$$K_2 = \frac{k_2}{2} = \frac{l_2}{2r_2} \quad (67)$$

conforming to the result obtained here.

In view of Zimm's discussion of the significance of his results and their application to actual solutions, it seems unnecessary at this time to go into these matters further.

A few words may be added, however, concerning the effect of flexibility in the molecules. Flexibility obviously gives more randomness and so more entropy. If, though, the molecular flexibility, and so the related intramolecular entropy, do not change with concentration in the concentration range of interest (i.e., in dilute solutions), this flexibility has no effect on the partial molal entropies or derived quantities, *provided* the distribution of shape and of relative orientations of neighboring molecules remains the same. This is likely to be the case if the heat of mixing of the solution is zero, but not otherwise. If the solute molecules attract each other (more than each attracts solvent molecules), flexibility increases the possibility of close approach of their centers and changes the magnitudes of the shape constants,  $k_2$ ,  $k_3$ , etc.

#### SUMMARY

Using a non-lattice treatment, equations have been deduced for the concentration dependence of the partial molal entropy of the solvent in a dilute solution containing large solute molecules, as a function of their size and shape. Some of the shape constants, for spherical and rod-like solutes, have been evaluated. Insofar as there is overlapping, the results are in agreement with those obtained by Zimm, extending the theoretical work of McMillan and Mayer. Flexibility of the solute molecules should have little effect on the results, unless the heat of mixing is not negligible.

#### REFERENCES

- (1) ALFREY, T., AND DOTY, P.: J. Chem. Phys. **13**, 77 (1945).
- (2) FLORY, P. J.: J. Chem. Phys. **9**, 660 (1941).
- (3) FLORY, P. J.: J. Chem. Phys. **10**, 51 (1942).
- (4) GUGGENHEIM, E. A.: Proc. Roy. Soc. (London) **A183**, 203, 213 (1944).
- (5) HILDEBRAND, J. H.: J. Chem. Phys. **15**, 225 (1947).
- (6) HUGGINS, M. L.: J. Chem. Phys. **9**, 440 (1941).
- (7) HUGGINS, M. L.: J. Phys. Chem. **46**, 151 (1942).
- (8) HUGGINS, M. L.: Ann. N. Y. Acad. Sci. **43**, 1 (1942).
- (9) HUGGINS, M. L.: J. Am. Chem. Soc. **64**, 1712 (1942).
- (10) HUGGINS, M. L.: Polymer Bull. **1**, 25 (1945).
- (11) HUGGINS, M. L.: J. chim. phys. **44**, 9 (1947).
- (12) McMILLAN, W. G., AND MAYER, J. E.: J. Chem. Phys. **13**, 276 (1945).
- (13) MILLER, A. R.: Proc. Cambridge Phil. Soc. **39**, 54, 131 (1943).
- (14) ORR, W. J. C.: Trans. Faraday Soc. **43**, 12 (1947).
- (15) SCOTT, R. L., AND MAGAT, M.: J. Chem. Phys. **13**, 172 (1945).
- (16) ZIMM, B. H.: J. Chem. Phys. **14**, 164 (1946).

THE DEPENDENCE OF THE SCATTERING OF LIGHT ON ANGLE AND CONCENTRATION IN LINEAR POLYMER SOLUTIONS<sup>1</sup>

BRUNO H. ZIMM

*Department of Chemistry, University of California, Berkeley, California**Received August 25, 1947*

## I. INTRODUCTION

In this paper some additions to the theory of the scattering of light from solutions of linear polymers will be described, and some recent data will be analyzed with their aid.

Since the proposal by Debye (2; see also 1, 3, 6, 7, 9) to use the light scattered from solutions of high polymers and other similar particles to study the size and shape of the particles, progress has been made in two divergent directions. First, the scattering as a function of angle has been worked out for several different particle shapes, but only where the particles are isolated in space. Secondly, the scattering as a function of concentration of particles is well understood, but only for particles which are small compared to the wave length. Our present problem is to fill this gap by obtaining the scattering as a function of both angle and concentration for particles comparable in size to the wave length.

A partial solution of this problem for molecules of thread-like or rod-like shapes will be discussed below.

## II. DESCRIPTION OF THE THEORY

In this section the theoretical considerations that lead to the final formulas will be outlined. More complete discussion will be reserved for later work.

The calculation of the intensity of the light scattered from an assemblage of particles is simple in principle and may be described as follows: The particles are subdivided into "segments," all of which are small compared to the wave length and have the same optical properties. Each of these segments scatters light as an electric dipole set in motion by the incident light independently of the others. The law of scattering from such a particle is well understood, and the scattering which it gives is known as Rayleigh scattering.

The next step is to add up the scattered amplitudes from each of the constituent segments, taking due account of the phase of the scattered light. This phase will vary, depending on the distance the ray must traverse in getting to the particular segment and from there to the observer. As a result, interference effects arise, which vary with the angle of scattering. A study of these interference effects permits conclusions to be drawn about the distribution of the scattering segments with respect to one another.

The distribution of the segments with respect to one another is controlled by

<sup>1</sup> Presented at the Twenty-first National Colloid Symposium, which was held under the auspices of the Division of Colloid Chemistry of the American Chemical Society at Palo Alto, California, June 18-20, 1947.

two things: the shape of the individual molecules, and the distribution of the molecules with respect to each other. The former has already been studied in connection with the scattering from single particles. The latter has also been studied by this author (8) in its application to the thermodynamics of polymer solutions, but its application to light scattering from such solutions is new and leads to the formulas that will be discussed in this paper.

The details of the development are too lengthy to be presented here. The results, however, are rather simple. The formula for the intensity of the scattered light,  $I$ , as a function of the angle between the directions of propagation of the incident and scattered rays,  $\vartheta$ , and the concentration of scattering particles in weight per unit volume,  $c$ , is the following:

$$I(\vartheta, c) = H \{ M_2 P(\vartheta) c - 2A_2 M_2^2 P^2(\vartheta) c^2 + [4A_2^2 M_2^2 P^4(\vartheta) + 3A_3 M_2^2 P^2 Q(\vartheta)] c^3 + \dots \} \quad (1)$$

In this formula  $M_2$  is the molecular weight of the solute particles,  $A_2$ ,  $A_3$ , and  $H$  are constants depending only on temperature but characteristic of the particular solvent and solute, and  $P(\vartheta)$  and  $Q(\vartheta)$  are functions characterized by the shape and size of the solute particles. For rod-like particles whose thickness is negligible compared to their length, the function  $P(\vartheta)$  is:

$$P(\vartheta) = \frac{1}{x} \int_0^{2x} \frac{\sin \omega}{\omega} d\omega - \left( \frac{\sin x}{x} \right)^2 \quad (2)$$

The dimensionless variable

$$x = \frac{2\pi L \sin \vartheta/2}{\lambda}$$

has been introduced here, where  $L$  is the length of the rod. For coiling thread-like particles, in the sense of Kuhn (5), the function  $P(\vartheta)$  is

$$P(\vartheta) = \frac{2}{\mu^2} (e^{-\mu} - 1 + \mu) \quad (3)$$

where again the dimensionless variable

$$\mu = \frac{8}{3} \pi^2 \frac{R^2 \sin^2 \vartheta/2}{\lambda^2}$$

has been introduced with  $R$  the root-mean-square distance between the ends of the coiling chain.

The function  $Q(\vartheta)$  has not been worked out, since it represents only a small correction in dilute solutions and its evaluation, though certainly practicable, would be very tedious.

Equation 1 can be put into a simpler form by taking the reciprocal of  $I$  and multiplying by the concentration. When this is done the following results:

$$\frac{Hc}{I} = \frac{1}{M_2 P(\vartheta)} + 2A_2 c + [3A_3 Q(\vartheta) - 4A_2^2 P(1 - P)] c^2 + \dots \quad (4)$$

Both  $P(\vartheta)$  and  $Q(\vartheta)$  become unity when either  $\sin \vartheta/2$  or  $R/\lambda$  or  $L/\lambda$  is small compared to unity, so that in these limiting cases equation 4 becomes merely:

$$H \frac{c}{I} = \frac{1}{M_2} + 2A_2c + 3A_3c^2 \quad (5)$$

This limiting equation has been derived previously (3). The same constants that appear in equation 5 appear in a closely related form for the osmotic pressure,  $\pi$ , equation 6:

$$\frac{\pi}{RT} = \frac{1}{M_2} c + A_2c^2 + A_3c^3 + \dots \quad (6)$$

where  $R$  and  $T$  have their usual meanings.

TABLE 1  
*Corrected\* dissymmetry coefficients and root-mean-square chain lengths for polystyrene fractions*

FRACTION	SOLVENT	CONCENTRATION, GRAMS PER 100 ML.							
		1 000	0.500	0 250	0.125	0.0625	0.0313	$c = 0^\dagger$	$R(\text{\AA.})$
RT-H.	Toluene		0.47	0.50	0.78	1.00	1.28	1.59	2370
	Ethylene dichloride	0.21	0.25	0.45	0.79	0.98	1.25	1.64	2390
	Butanone	0.43	0.46	0.72	1.00	1.15	1.24	1.39	2100
	Butanone-isopropanol	1.00	1.00	1.13	1.17	1.14	1.15	1.19	1900
BZO-4.	Ethylene dichloride		0.11	0.17	0.22	0.34		0.45	1100
	Butanone		0.16	0.29	0.35	0.43	0.52	0.53	1230
	Butanone-isopropanol		0.28	0.27	0.31	0.38		0.35	990
JNZ-7	Butanone		0.23	0.33	0.44	0.54	0.59	0.64	1350
JNZ-4	Butanone			0.56	0.80	1.03	1.15	1.41	2100
JNZ-1	Butanone			0.67	1.04	1.39	1.59	2.00	2770

\* Corrected for the scattering from the solvent.

† Extrapolated values.

### III. COMPARISON WITH EXPERIMENT

The comparison of the theory just described with experiment will now be undertaken. The data are taken from an earlier work (4) which was not designed to test this theory, and they are therefore not in the most convenient form; however, they are the best available.

The data from reference 4 are given in tables 1 and 2. The materials were five fractions of high-molecular-weight polystyrene. The absolute intensity of scattering at right angles to the incident beam was measured along with the ratio (dissymmetry ratio) of the intensities scattered at two other angles, one an acute and the other an obtuse angle. These latter angles varied somewhat with the

refractive index of the solvent used; they are tabulated in table 3. No measurements were made of the relation between the intensities at right angles and at either of the dissymmetry angles; the only way of relating these is by a process of interpolation.

One method of plotting the data is shown in figure 1. From equation 4, considering only the first two terms on the right, it is evident that plots of  $c/I$  at different concentrations against  $\sin \vartheta/2$  should form a family of parallel curves, displaced up or down according to the different values of  $2A_2c$ . Such plots are

TABLE 2

*Intensity of transversely scattered light in arbitrary units for solutions of polystyrene fractions*

FRACTION	SOLVENT	SOLVENT SCAT- TERING	CONCENTRATION, GRAMS PER 100 ML.					
			1.000	0.500	0.250	0.125	0.0625	0.0313
RT-II	Toluene	2.8	33.6	31.3	32.7	25.2	18.0	13.1
	Ethylene dichloride	1.5	46.2	53.4	48.0	38.2	26.1	14.0
	Butanone	1.2	358	315	236	158	93.6	48.4
	Butanone-isopropanol	1.5	3231	1411	678	336	161	80.9
BZO-4	Ethylene dichloride	1.3	70.5	60.8	44.1	27.4		
	Butanone	1.1	304	195	130.5	67.5	40.0	
	Butanone-isopropanol	1.6	675	327	165	87		
JNZ-7	Butanone	1.5		207	149	95.9	53.5	30.1
JNZ-4	Butanone	0.6			202	152	84.6	45.5
JNZ-1	Butanone	0.6			234	172	105	54.6

TABLE 3

*Angles of observation in different solvents*

SOLVENT	$\vartheta_1$	$\vartheta_2$
Toluene	54.7°	125.3°
Ethylene dichloride	53.0°	127.0°
Butanone	51.2°	128.8°
Butanone-isopropanol	51.2°	128.8°

shown in figure 1 for the two fractions JNZ-1 and JN-7. The parameters were adjusted so that the curves pass through all the points at zero concentration, and then parallel curves were drawn through the values of  $c/I_{90^\circ}$  at the other concentrations. The fact that the points corresponding to the other two angles then generally fall on the curves may be taken as evidence of the agreement of experiment and theory. (Actually, since only the ratio and not the absolute values of the two points at the acute and obtuse angles was measured there was some room for adjustment. This was not sufficient to invalidate the above conclusion, however.)

The above method of treating the data is obviously cumbersome and other methods were therefore developed. The treatment of the dissymmetry data will first be discussed. Let us define a dissymmetry coefficient,  $q$ , as one less than the ratio of the intensities,  $I_1$  and  $I_2$ , scattered at angles  $\vartheta_1$  and  $\vartheta_2$ ,  $\vartheta_1$  being less than  $\vartheta_2$ , i.e.,  $q = (I_1/I_2) - 1$ . It was observed empirically at the time when the data in reference 4 were obtained that when the reciprocal of the dissymmetry coefficient was plotted against concentration, a very good straight line resulted. We shall now show that this linear relationship can be derived from equation 4.

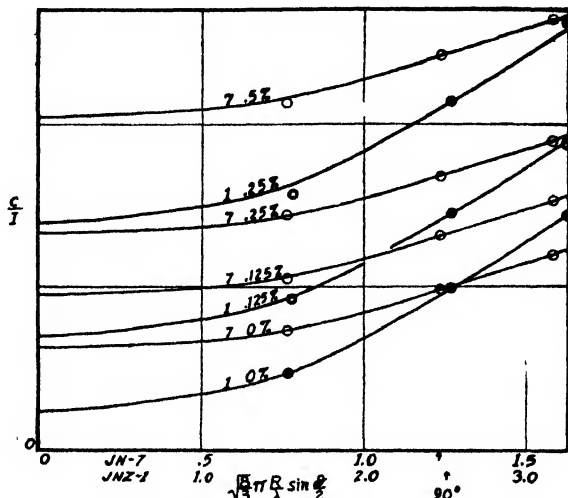


FIG. 1. Concentration over intensity as a function of angle of scattering for polystyrene fractions JN-7 and JNZ-1.

Substituting equation 4 for  $I(\vartheta)$  into the definition of  $q$ , and neglecting the term involving  $A_3$ , we can immediately show that

$$q = \frac{\frac{1}{M_2 P(\vartheta_2)} - \frac{1}{M_2 P(\vartheta_1)}}{\frac{1}{M_2 P(\vartheta_1)} + 2A_2 c} = \frac{\frac{P(\vartheta_1)}{P(\vartheta_2)} - 1}{1 + 2A_2 M_2 P(\vartheta_1) c} \quad (7)$$

Inverting both sides of this equation yields the desired linear relation:

$$\frac{1}{q} = \frac{1}{[q]} + \frac{2A_2 M_2 P(\vartheta_1)}{[q]} c \quad (8)$$

where  $[q] = \frac{P(1)}{P(2)} - 1$  is the limiting dissymmetry coefficient at infinite dilution.

From  $[q]$  the characteristic dimensions of the particle,  $R$  or  $L$ , may be computed, as was actually done in reference 8. Here, however, we are particularly interested in the slope of the  $1/q$  plot, from which the product of the constants  $A_2$  and  $M_2$  may be found, since  $P(\vartheta_1)$  is known from equation 3.



From a plot of the reciprocal dissymmetry coefficients from reference 4 the product,  $A_2M_2$ , is found and is given in the third column of table 4.

The product,  $A_2M_2$ , may also be obtained from the data for  $I_{90^\circ}$  as a function of concentration, which were measured independently of the dissymmetry ratios. From equation 4, we see that the slope over the intercept of a plot of the quantity  $c/I_{90^\circ}$  against  $c$  gives the quantity  $A_2M_2P_{90^\circ}$ . Since  $P_{90^\circ}$  is known,  $A_2M_2$  may be found.

From a plot of the data from reference 4 the values of  $A_2M_2$  are found and are given in the fourth column of table 4.

We should note that both these methods of obtaining  $A_2M_2$  are independent of

TABLE 4  
*Interaction constants,  $A_2$ , for polystyrene fractions*

FRACTION	SOLVENT	$A_2M_2$		$M_2$	$A_2$
		From $\eta$	From $I_{90^\circ}$		
RT-II	Toluene	890	2440*		
	Ethylene dichloride	1160	1240		
	Butanone	310	410		
	Butanone-isopropanol	20	0		
BZO-4	Ethylene dichloride	350	200*		
	Butanone	225	120*		
	Butanone-isopropanol	60	0		
JN-7	Butanone	220	220	$2.0 \times 10^6$	$11.0 \times 10^{-6}$
JNZ-4	Butanone	470	580	$5.8 \times 10^6$	$9.2 \times 10^{-6}$
JNZ-1	Butanone	760	820	$10.4 \times 10^6$	$7.6 \times 10^{-6}$

the absolute intensity of scattering, which is more difficult to determine experimentally and subject to more uncertainty than the relative intensity.

The agreement between the values of  $A_2M_2$  determined in the two different ways is satisfactory, considering the evident scatter of the experimental results, with the exception of three cases that are marked with an asterisk in the table. It is quite possible that the lack of agreement here is also experimental error, since these samples were just the ones that scattered the least light. It is also possible, however, that they represent a real deviation from the theory caused by some unexpected complication in the molecular structure or purity of these samples.

From the intercept of the plot of  $c/I_{90^\circ}$  against  $c$  the molecular weight,  $M_2$ , of the solute can be found if the constants occurring in the parameter  $H$  have been determined. The reader is referred to the original paper for the latter. This has been done for the three samples which were most carefully measured and the results are given in the fifth column of table 4. The values of  $A_2$  from the average of the third and fourth columns and the molecular weights are given in column

six. (Owing to the different method of plotting the data, these figures differ somewhat from those of the original paper. The data there were treated in a way which the author feels is superseded by the present method.)

The values of  $A_2$  for the three JN fractions, which are comparable because they were all prepared from the same material, show a marked decrease as the molecular weight increases. This behavior has been theoretically predicted in a previous paper (8). The molecular weights are too high, however, for the approximate formula theoretically derived for the molecular-weight dependence of  $A_2$  to be valid.

The osmotic pressures of solutions of fractions JNZ-1 and JN-7 in butanone were also measured. These may be compared with the theoretical values from equation 6 and the constants  $M_2$  and  $A_2$  as determined above. The results are shown in figure 2, where the circles are the experimental points and the solid line

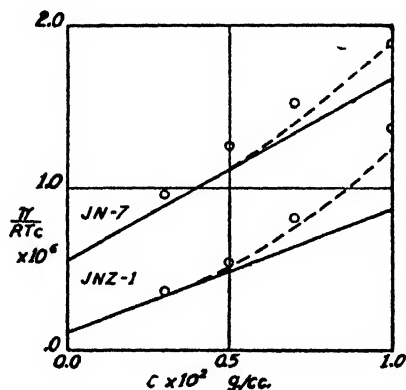


FIG. 2. Comparison of observed values of the osmotic pressure of fractions JN-7 and JNZ-1 with values calculated from light-scattering data with the aid of the theory.

is calculated from the light-scattering data and equation 6. It has been assumed that the osmotic (number-average) molecular weights are 10 per cent less than the light-scattering (weight-average) values. The dotted line is the presumed extrapolation of the theoretical line to higher concentrations. It is seen that the agreement is not unsatisfactory if it is assumed that the constant,  $H$ , is about 10 per cent too large and a liberal allowance is made for terms in  $c^3$  and  $c^4$ . Unfortunately, light-scattering data were not taken at concentrations high enough to show the presence of these higher terms.

#### IV. CONCLUSION

The agreement of the theory with the experimental data available at the time of writing seems quite satisfactory in view of the incomplete nature of both. It is hoped that the theory will be of use in the better interpretation of data to be obtained in the future. It has not been possible in this brief report to enlarge on the assumptions involved or the extensions which will probably be necessary. It certainly seems, however, that useful understanding can be achieved from

measurements of the intensity of light scattered as a function of angle and concentration in dilute polymer solutions.

## REFERENCES

- (1) BORN, M.: *Optik*. Edwards Bros., Ann Arbor, Michigan.
- (2) DEBYE, P.: *J. Applied Phys.* **15**, 338 (1944).
- (3) DEBYE, P.: *J. Applied Phys.* **17**, 392 (1946).
- (4) DOTY, P., AFFENS, W., AND ZIMM, B. H.: *Trans. Faraday Soc.*, in press.
- (5) KUHN, W.: *Kolloid-Z.* **68**, 2 (1934).
- (6) OSTER, G., DOTY, P. M., AND ZIMM, B. H.: *J. Am. Chem. Soc.* **69**, 1193 (1947).
- (7) STRATTON, J. A.: *Electromagnetic Theory*. McGraw-Hill Book Company, Inc., New York (1941).
- (8) ZIMM, B. H.: *J. Chem. Phys.* **14**, 164 (1946).
- (9) ZIMM, B. H., STEIN, R. S., AND DOTY, P. M.: *Polymer Bull.* **1**, 90 (1945).

SOME PHYSICAL AND CHEMICAL PROPERTIES OF WEIGHT-FRACTIONATED LIGNOSULFONIC ACID, INCLUDING THE DISSOCIATION OF LIGNOSULFONATES<sup>1</sup>

F. M. ERNSBERGER<sup>2</sup> AND WESLEY G. FRANCE

*Department of Chemistry, The Ohio State University, Columbus, Ohio*

*Received August 25, 1947*

The development of high-efficiency synthetic resin ion exchangers has made it possible to remove inorganic acids and salts from sulfite pulp process waste liquor. The absence of conducting impurities makes possible the subsequent determination of neutral impurities by an electrophoretic method. Using these techniques to prepare solutions of lignosulfonates with known gravimetric content of lignosulfonate ion, a number of measurements can be made which were previously hindered by the heterogeneous composition of waste sulfite liquor. In the first section of this paper is reported the effect of the molecular weight variable on the surface activity and other properties of the lignosulfonate ion.

The second section deals with a property not primarily a function of molecular weight: namely, the dissociation of lignosulfonates. It has been observed by several investigators (9) that prolonged dialysis of waste liquor leaves a residual solution which is neutral in pH and contains 10–20 per cent ash (dry basis). According to the familiar concepts of lignin chemistry, this residue is a metallic salt of high-molecular-weight lignosulfonic acid. Yet the Donnan theory of

<sup>1</sup> Presented at the Twenty-first National Colloid Symposium, which was held under the auspices of the Division of Colloid Chemistry of the American Chemical Society at Palo Alto, California, June 18–20, 1947.

This paper is a contribution from The Ohio State University, Research Foundation, Master Builders Company Fellowship.

<sup>2</sup> Present address: U. S. Naval Ordnance Test Station, Inyokern, California.

membrane processes involving colloidal electrolytes requires that the metallic salt of a non-diffusible anion be hydrolyzed to the acid by dialysis. The fact that membrane hydrolysis does not occur suggested that the dissociation of lignosulfonates is abnormal.

#### WEIGHT-FRACTIONATED LIGNOSULFONIC ACID

##### *Preparation of fractions*

One liter of commercial waste liquor (122 g. total solids) was dialyzed in 160 cm. of 5 cm. diameter Visking cellulose sausage casing against 5 liters of distilled water. Both inner (dialysate) and outer (diffusate) solutions were vigorously agitated by bubbling air in this and subsequent dialysis treatments. After 1 hr. the diffusate was discarded. It contained 13.1 g. of solids, predominantly sugars and salts. A second and a third diffusate, obtained after 5- and 16-hr. dialysis periods, constituted the crude low-weight fraction.

The dialysate at this point contained 48.5 g. of solids. It was evaporated to 600 ml. and passed over a column of the hydrogen-cycle cation-exchanger Amberlite IR-100-H (analytical grade). Conversion of the lignosulfonates to lignosulfonic acid was necessary at this point to hasten their diffusion. Dialysis was recommenced, and four more diffusates were recovered over a period of 36 hr. These were combined to form the crude medium-weight fraction. The undiffused residue constituted the high-weight fraction.

In evaporating the solutions of the three fractions to convenient volumes, it was necessary to take special precautions to avoid chemical changes. Neutral lignosulfonates are more stable than the free acid, so each solution was neutralized with barium hydroxide before evaporation. The volumes were reduced slowly in a current of warm air to a solids concentration of about 1 per cent.

To insure the absence of all inorganic acids and salts, the crude fractions were treated first with the cation-exchange resin, then with the acid-adsorbent resin Amberlite IR-4B. The acid-adsorbent resin adsorbs very little lignosulfonic acid, owing to the large size of the anion, so the effluent contained only lignosulfonic acid and neutral substances, referred to hereafter as sugars.

The concentration of solids in each fraction was determined by neutralizing a portion of the solution with sodium hydroxide and evaporating to dryness in a vacuum oven at 80°C.

The sugar content of each fraction was determined by electrolyzing a 25-ml. sample of the ammonium salt in such a way that a falling lignosulfonate-ion boundary was formed, and then drying a 5.00-ml. sample of the clear catholyte.

##### *Molecular weight*

Average molecular weights were determined by a diffusion method, similar in principle to that used for lignosulfonates by Schwabe and Hasner (8, 10).<sup>3</sup> The

<sup>3</sup> While this manuscript was in preparation Pennington and Ritter (8) reported a diffusion study of waste liquor, using sintered-glass membranes. Their results were not referred to known gravimetric concentrations of lignosulfonate ion.

design of the diffusion cell (figure 1) departs considerably from that used by these investigators, and includes original features of design, as well as adaptations from the work of McBain and Liu (7) and of Hartley and Runnicles (4). The dimensions of the cell were dictated by the desire to make photometric measurements of relative concentration at any time during a diffusion run by placing the cell in the chamber of a Coleman Model 10 Spectrophotometer. It was necessary to provide stops for the photometer to limit the light beam to a size accommodated by the 10 x 12 mm. window in the cell. The internal volume of the cell was made as small as possible to increase the time rate of change of concentration. Selasporous porcelain was found to be much superior to Pyrex sintered glass for dif-

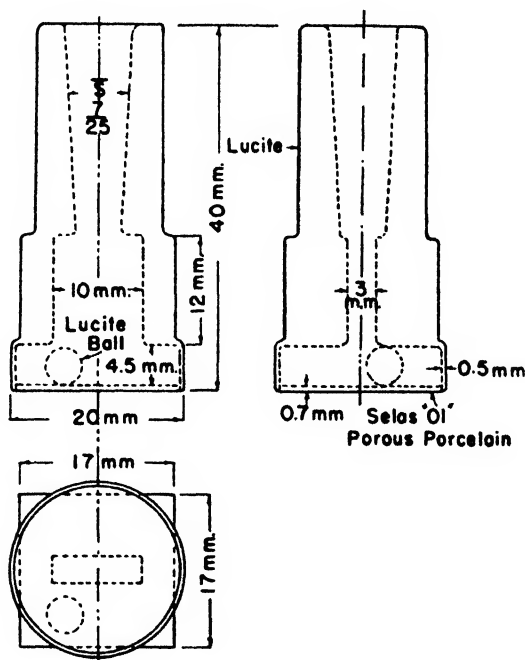


FIG. 1. Diffusion cell

fusion membranes because of its great mechanical strength, high porosity, and fine average capillary radius.

The cell was filled by sucking through the porcelain disc a 0.005–0.015 *N* solution of sodium lignosulfonate in 0.05 *N* potassium chloride, at pH 4.5. The cell was then closed with a standard-taper ground-glass stopper (not illustrated) and immersed in a thermostated (25°C.) bath consisting of 11 liters of 0.04 *N* potassium chloride at pH 4.5. The potassium chloride served to minimize the membrane potential which would otherwise be established by the diffusion of the sodium lignosulfonate. Continuous mixing of the cell contents was secured by inclining the long axis of the cell at an angle of 15° to the vertical and rotating the cell continuously about that axis at 6 R.P.M. This mechanical mixing was sup-

plemented by gravitational mixing provided by the 25 per cent higher concentration of potassium chloride inside the cell. The solvent bath was kept homogeneous by motor stirring. The large volume of this bath maintained essentially zero concentration on the solvent side of the diffusion membrane. After a period of  $\frac{1}{2}$ –1 hr., allowed for establishment of a stable concentration gradient in the membrane, the first photometric reading was taken. Readings were taken at 3- or 4-hr. intervals thereafter, to 12 hr. The data were plotted in accordance with the equation

$$\log (c_t/c_0) = (K/\sqrt[3]{M})t$$

where  $c_0$  and  $c_t$  are concentrations at times 0 and  $t$  hr.,  $M$  is the molecular weight, and  $K$  is an empirical constant. The value of  $K$  was determined by calibration runs with two non-associated (11) dyes, Orange II (Rowe Color Index 151) and Azogrenadine S (C. I. 54).

TABLE 1  
*Physical and chemical constants of lignosulfonic acid fractions*

FRACTION	AVERAGE MOLECULAR WEIGHT	SUGARS, PER CENT OF TOTAL SOLIDS	EQUIVALENT WEIGHT OF SODIUM SALT	H <sup>+</sup> /S	E <sub>1</sub> <sup>1%</sup> 1 cm. (λ 420)
High.....	9500	0.00	519	1.01	12.0
Medium... ..	2140	2.62	316	1.37	7.6
Low.....	250 920	31.0	249	1.84	2.7

Molecular-weight values calculated from the diffusion data are given in table 1. The spread between the highest and lowest values emphasizes the polydispersity of lignin preparations. In terms of the Freudenberg hypothetical lignin unit (2), it appears that lignosulfonate particles containing from one to more than fifty such units are present in waste liquor.

No constant molecular-weight value could be obtained for the low-weight fraction, owing to slow polymerization of the acid. The first value in table 1 was obtained immediately after preparation, the second after 13 days. Intermediate values were found at intermediate ages.

#### *Equivalent weight*

The equivalent weight of the sodium salt was determined by potentiometric titration of each sample of lignosulfonic acid with sodium hydroxide. The maximum slope of the titration curve is in each case at pH 7. The determination of the equivalent weight of lignosulfonates by this method was reported earlier by Freudenberg (3), but the determination of both equivalent weight and molecular weight on the same fractions constitutes unambiguous evidence that the lignin in waste liquor is polysulfonated.

The equivalent weights show a well-marked trend toward lower values with lower molecular weight, indicating that the lower-weight fractions of waste liquor lignin are more highly sulfonated, as might be expected.

### *Hydrogen ion-sulfur ratio*

In the work of Freudenberg and Lautsch cited above, it was reported that equivalent weights calculated from sulfur analysis of a pure lignosulfonate do not agree with those calculated from potentiometric titration of the free acid; values of the ratio of hydrogen ion to sulfur atoms ranging from 1.07 to 1.21 were discovered for samples of waste liquor from eight stages of the cook. This anomaly was ascribed to the presence of carboxyl groups. The anomalous values of the  $H^+/S$  ratio appearing in table 1 confirm Freudenberg's observation, but establish two important additional facts: (1) the magnitude of the departure from the normal ratio of unity is a function of molecular weight, and (2) the departure from the normal ratio approaches zero with increasing molecular weight.

### *Color intensity*

The specific extinction coefficients in table 1 were determined with the Beckman Ultraviolet Spectrophotometer. The same order of increasing extinctions is observed at all wave lengths where measurements have been made,—from 250 to 800 millimicrons. No explanation of the variation in color intensity with molecular weight can yet be offered.

### *Adsorption on Portland cement*

As a measure of the surface activity of the three fractions, adsorption isotherms were determined, using a sample of normal Portland cement as adsorbent in each case. The technique of measurement was similar to that used in an earlier paper (1). The isotherms (figure 2) show pronounced increase in surface activity with molecular weight. Assuming that the sulfonate groups are the points of adsorptive attachment, it is to be expected that the large lignosulfonate molecules will have the greater probability of adsorption.

## DISSOCIATION OF LIGNOSULFONATES

### *Preparation of pure lignosulfonates*

A dried waste sulfite liquor was dissolved in water and dialyzed in Visking regenerated cellulose sausage casing against a continuous flow of distilled water until all diffusible substances were removed. The material discarded in the diffusate, consisting mainly of carbohydrates, inorganic salts, and low-molecular-weight lignosulfonates, made up approximately half the weight of the starting material.

The dialyzed solution of calcium lignosulfonate was passed through a column of the cation-exchange resin Amberlite IR-100-H. The resulting acid gave a potentiometric titration curve characteristic of a strong acid. The equivalent weight derived from the titer was 502 g. The ash content was 0.2 per cent (dry basis).

Solutions of ammonium, sodium, and barium lignosulfonates were prepared by titrating portions of the lignosulfonic acid preparation to pH 7 with dilute solutions of the corresponding bases. The sodium hydroxide solution was prepared

carbonate-free by diluting a filtered 50 per cent solution of reagent sodium hydroxide pellets. A solution of calcium lignosulfonate was prepared by titrating the lignosulfonic acid with calcium amalgam.

### *Conductance measurements*

Dilutions of the lignosulfonic acid and its salts were made with triple-distilled water, and the conductivities measured with a conductivity bridge of the Jones-

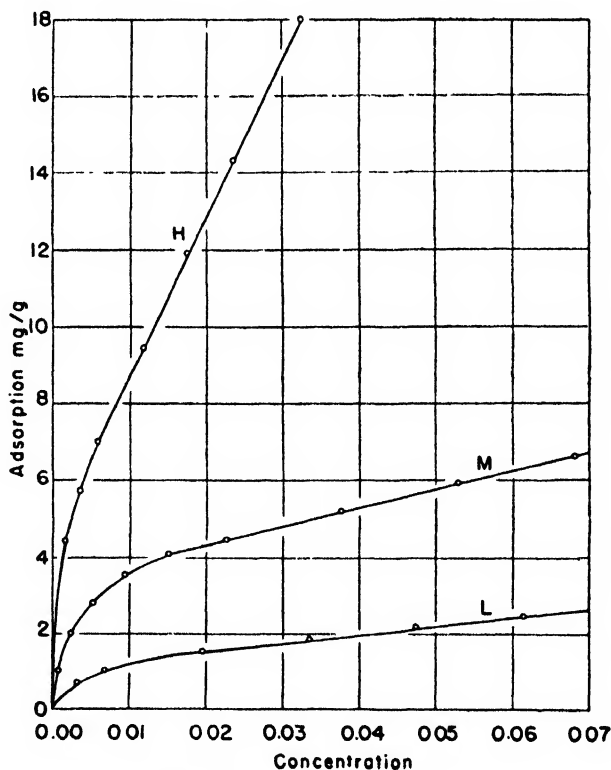


FIG. 2. Adsorption isotherms

Josephs type (Leeds & Northrup). The equivalent conductances of the free acid are given in table 2, and of the salts in table 3.

Inspection of the conductivity data revealed that neither the salts nor the acid are sufficiently dissociated to permit the evaluation of the complete-dissociation equivalent conductance of lignosulfonate ion by the usual extrapolation of the plot of equivalent conductance *versus*  $\sqrt{N}$ . Attention was therefore turned to the measurement of transference numbers as a means of evaluating this quantity.

### *Transference numbers of ammonium lignosulfonate*

The moving-boundary method, developed by MacInnes and Longworth (6), appeared to be admirably suited to the purpose, owing to the ease of observing



boundaries formed by the colored lignosulfonate ion. The necessary choice of conditions leading to stable boundaries was complicated by the relatively undissociated character of lignosulfonates, but in the case of the ammonium salt a simple system of "autogenic" boundaries could be used. The cation-following boundary was made to rise from a silver anode, and the anion-following boundary was made to fall from a platinum cathode. The thermostated tube in which the motion of the boundaries was observed was 0.055 cm. (2) in cross section and contained 1 ml. of sample. The tube was volume-calibrated by delivery of mercury. The source of potential was a 400-volt battery. The value and constancy of the electrolysis current were determined by a potentiometer connected across a stand-

TABLE 2  
*Equivalent conductance of lignosulfonic acid*

NORMALITY $\times 10^4$	EQUIVALENT CONDUCTANCE (25°C.)
14.84	268
8.90	276
4.46	288
2.96	297
1.48	309
1.11	312
0.66	323
0.44	326
0.22	333

TABLE 3  
*Equivalent conductances of lignosulfonates*

NORMALITY $\times 10^4$	EQUIVALENT CONDUCTANCE (25°C.)			
	Ammonium	Sodium	Calcium	Barium
37.2			36.0	34.9
14.8		73.7	41.1	39.8
7.40	96.5	80.4	45.8	45.8
3.70	105	88.7	51.5	50.3
1.86	114		59.5	57.7

ard resistor. The current was kept constant by manual regulation. The motion of both boundaries was recorded, though the falling boundary was observed to be more stable.

Experimental data are given in table 4. The values of  $t_{LS}$  (transference number of lignosulfonate ion) give a linear plot against  $\sqrt{N}$  in agreement with theory; those of  $t_{NH_4}$  give a curve. For this reason, as well as the greater stability of the falling boundary, it was assumed that the anion-boundary measurements were more accurate, and  $1 - t_{LS}$  was tabulated as the value of the ammonium-ion transference number. Measurements at lower concentrations were unusable, because the boundaries were nearly invisible and were too fragile to withstand the increased disturbing effect of electroosmosis.

*Calculation of degree of dissociation*

The transference data in table 4 may be used to calculate lignosulfonate-ion conductance with the aid of three assumptions: (1) Assume that the linear relationship between  $t_{LS}$  and  $\sqrt{N}$  is accurate between  $N = 0.0000$  and  $N = 0.0588$ ;

TABLE 4  
*Transference numbers of ammonium lignosulfonate*

$N$	$t_{LS}$	$t_{NH_4}$	$1 - t_{LS}$
0.0588	0.450	0.535	0.550
0.0352	0.491	0.497	0.509
0.0234	0.520	0.463	0.480
0.0117	0.555	0.404	0.445
(0.0000)	(0.640)		(0.360)

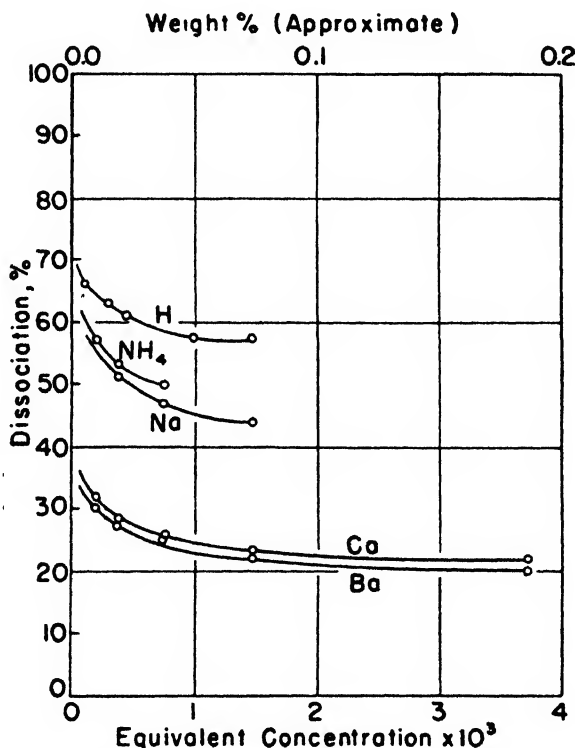


FIG. 3. Dissociation of lignosulfonates

this relationship may then be used to estimate transference numbers in solutions too dilute for direct measurement. (2) Assume that the conductance of ammonium ion in ammonium lignosulfonate is constant between  $N = 0.0000$  and  $N = 0.0037$  and equal to its literature value, 74.5. This is equivalent to assuming that the lignosulfonate ion alone changes in mobility, accounting for the change

in transference numbers. This assumption enables the calculation of lignosulfonate-ion conductances as a function of concentration from the equation  $\lambda_{LS} = 74.5 (t_{LS}/1 - t_{LS})$ . (3) Assume that the conductance of lignosulfonate ion is independent of the identity of the cation associated with it. This permits transfer of lignosulfonate-ion conductances estimated for ammonium lignosulfonate to the sodium, calcium, and barium salts, and to the acid itself.

The degree of dissociation was calculated as the ratio of the observed equivalent conductance to the complete-dissociation equivalent conductance. The latter was calculated by adding the equivalent conductance of the appropriate cation (*Smithsonian Physical Tables*) to the equivalent conductance of lignosulfonate ion. The results are reproduced in figure 3.

It is evident from the nature of the above calculations that dissociations cannot be measured in this way at concentrations appreciably removed from zero.

### *Significance of dissociation data*

The exceptionally small ionization of lignosulfonates in contrast to ordinary organic sulfonates explains some of the observed properties of sulfonated lignin. As already suggested, it explains the negligible membrane hydrolysis of lignosulfonates. As a corollary, it explains why a solution of lignosulfonic acid behaves like a cation-exchange resin, a phenomenon which is readily observed by confining the lignosulfonic acid in a dialysis sack and dipping the sack into a salt solution. The parallel between lignosulfonic acid and commercial cation-exchange resins can be extended further: the order of decreasing dissociation evident in figure 3 is the same as the order of increasing cation affinity for commercial resins. The mechanism of commercial resins has not been explained, but it seems safe to suggest that synthetic cation-exchange resins of the sulfonate type act in a similar manner to lignosulfonic acid. Indeed, W. Lautsch (5) has successfully prepared cation-exchange resins by condensing lignosulfonates with formaldehyde.

The positive adsorption of lignosulfonate ion by Portland cement can likewise be explained as due to the affinity of lignosulfonate ions for the cations on the surface of insoluble crystalline salts. The negligible adsorption of lignosulfonate ions by such adsorbents as silica confirms this view.

### SUMMARY

Pure lignosulfonic acid, prepared from a commercial sulfite pulp process waste liquor by ion exchange, was separated into three molecular-weight groups by fractional diffusion. The average molecular weights were estimated from the diffusion constants. The surface activity and certain other properties were measured for each fraction. The dissociations of a sample of lignosulfonic acid and of four of its salts were determined at low concentrations by a conductimetric method. In contrast to the complete dissociation characteristic of low-molecular-weight sulfonates, the lignosulfonates show dissociations from 20 to 60 per cent.

## REFERENCES

- (1) ERNSBERGER, F. M., AND FRANCE, W. G.: *Ind. Eng. Chem.* **37**, 598 (1945).
- (2) FREUDENBERG, K.: *Chem.-Ztg.* **68**, 39 (1944).
- (3) FREUDENBERG, K., AND LAUTSCH, E.: *Cellulosechem.* **22**, 97 (1944).
- (4) HARTLEY, G. S., AND RUNNICLES, D. E.: *Proc. Roy. Soc. (London)* **A168**, 401 (1938).
- (5) LAUTSCH, W.: *Die Chemie* **57**, 149 (1944).
- (6) MACINNES, D. A., AND LONGSWORTH, L. G.: *Chem. Rev.* **11**, 172 (1932).
- (7) MCBAIN, J. W., AND LIU, T. H.: *J. Am. Chem. Soc.* **53**, 59 (1931).
- (8) PENNINGTON, D., AND RITTER, D. M.: *J. Am. Chem. Soc.* **69**, 665 (1947).
- (9) SCHENCK, W. A.: *Paper Trade J.* **117**, No. 14, 97 (1943).
- (10) SCHWABE, K., AND HASNER, L.: *Cellulosechem.* **20**, 61 (1942).
- (11) VALKO, E.: *Trans. Faraday Soc.* **31**, 230-45 (1935).

# VISCOSITY OF SOLUTIONS AND SUSPENSIONS. I

## THEORY<sup>1</sup>

VLADIMIR VAND

*Research Laboratories, Lever Brothers and Unilever Limited, Port Sunlight, Cheshire, England*

*Received June 24, 1947*

### 1. INTRODUCTION

Viscosity is one of the physical properties which is comparatively easily measured. On the other hand, the theoretical interpretation of the measurements presents considerable difficulties but is of great fundamental importance, as the viscosity data should be able, if properly interpreted, to supply or to supplement information on the amount of hydration or solvation, on the shape of the suspended or dissolved particles, their rigidity and state of aggregation, and on the forces acting between the particles, which are properties of great interest to colloidal chemistry as well as to industry.

There are generally two ways of attack open to deal with the problem. For solutions of small molecules, laws can be derived on the same lines as for liquids in general, depending on their internal structure and molecular forces. The whole subject of the internal structure of liquids, in spite of remarkable progress, is still far from completely satisfactory quantitative understanding. Another line of attack can be based on the application of the equations of hydrodynamics to the streaming of the liquid around each suspended particle.

It can be demonstrated from the relation between viscosity and electrical conductivity (Jaeger (12)) that Stokes's resistance law fully holds for the small

<sup>1</sup> The symbols used in this paper are the following:

- $a$  = radius of a rigid sphere
- $a_{ik}$  = components of the velocities of deformation
- $A^0 = c_i c_k a_{ik}^0$ , summation convention being used
- $c$  = concentration by volume
- $c_i = x_i/r$ , direction cosines
- $D$  = thickness of a layer of low viscosity along walls
- $k$  = shape factor;  $k = 2.5$  for rigid spheres
- $K$  = interaction constant in wall effect
- $N$  = number of particles per unit volume
- $Q$  = interaction constant in mutual interaction
- $r$  = radial coördinate
- $t$  = time
- $V$  = total volume of suspension
- $u_i = u, v, w$ , components of velocity
- $x_i = x, y, z$ , rectangular coördinates
- $\alpha = a/r$
- $\kappa$  = rate of shear
- $\eta$  = viscosity;  $\eta/\eta_0 = \eta_r$ , relative viscosity
- $\tau$  = shearing stress

ions in spite of their diameter being hardly greater than that of water molecules. This fact shows that the equations of hydrodynamics can be applied with sufficient approximation even for molecular dimensions.

The simplest theoretical case is that of a suspension of rigid spheres. The solution of the problem for elongated or soft particles represents additional complications, so that the problem of spherical suspensions must be understood before embarking on more general solutions. We shall limit ourselves mostly to the discussion of the suspensions of rigid spherical particles, as the methods for generalization of the problem have been fully treated by several investigators (see, for example, Burgers (4), Peterlin (14), etc.).

The first attempt to treat mathematically the viscosity of suspensions is due to Einstein (6), who derived for the relative viscosity of suspensions of rigid spheres the equation:

$$\eta_r = \eta/\eta_0 = 1 + kc \quad (1.1)$$

where  $\eta$  is the viscosity of the suspension,  $\eta_0$  is the viscosity of the pure liquid,  $k = 2.5$  for rigid spheres, and  $c$  is the concentration by volume. The derivation introduces certain simplifications which are valid only for infinitely dilute suspensions. The values of  $k$  were calculated by several workers for different shapes, rigidities, and Brownian movement of particles. In general, for elongated particles, it is found that  $k > 2.5$ , but for soft or liquid spherical particles the value of  $k$  can drop below 2.5.

A way of approach to the problem of higher concentrations which includes the interaction of the particles was used by Guth, Gold, and Simha (10) (see also Eirich and Simha (9)). They extended the Einstein equation by a method of "successive reflections" assuming that the disturbance of flow around a first sphere is compensated by an additional flow around the second sphere in order to fulfil the conditions of continuity of velocity at its surface.

By using a single reflection, they obtained

$$\eta_r = (1 + 0.5c - 0.5c^2)/(1 - 2c - 9.6c^2) \quad (1.2)$$

According to Eirich, the formula agrees with measurements about up to concentrations of the order of 8 per cent.

Other theoretical and empirical viscosity formulae were derived by Baker (1), de Bruijn (3), Eilers (5), Hess (11), Vand (15), and others.

## 2. DEFINITION OF THE VISCOSITY OF A SUSPENSION

Before embarking on the problem of the derivation of viscosity formulae, it is necessary to make quite clear what is meant by the viscosity of a suspension. For isotropic incompressible Newtonian liquids, if the terms of inertia are neglected, one obtains the following equation for the amount of kinetic energy,  $W$ , transformed into heat in unit time as a result of internal friction (Eirich (9)):

$$\frac{dW}{dt} = 2\eta \iiint_V a_{ik} a_{ik} dV \quad (2.1)$$

where  $\eta$  is the viscosity of the liquid,

$$a_{ik} = \frac{1}{2} \left( \frac{\partial u_i}{\partial x_k} + \frac{\partial u_k}{\partial x_i} \right) \quad i, k = 1, 2, 3 \quad (2.2)$$

are the velocities of deformation,  $u_i$  the three components of velocities expressed in rectangular coördinates,  $a_{ik}$  is summed tensorially over twice-occurring indices from 1 to 3, and the integral is taken over the whole volume of the liquid.

The quantities  $dW/dt$  and  $a_{ik}$  can be determined experimentally in a given measuring apparatus, and equation 2.1 can thus serve for determining the viscosity for a true liquid.

There are several possible ways of extending the definition of viscosity (equation 2.1) for a heterogeneous suspension. One way is to define the viscosity by the formula 2.1 unchanged, where  $a_{ik}$  are the *instantaneous* velocities of deformation. This definition has the disadvantage that these are such complicated factors that it is practically impossible to calculate or to measure them in any apparatus. Since  $a_{ik}$  are not practically observable quantities,  $\eta$  defined as above is not experimentally determinable.

There is another possibility of defining the viscosity of a suspension, which is also identical with the current experimental practice:

$$\eta = \frac{d\bar{W}/dt}{2 \iiint_V \bar{a}_{ik} \bar{a}_{ik} dV} \quad (2.3)$$

where quantities with a bar are time averages over a sufficiently long period of time  $T$ . Thus

$$\bar{a}_{ik} = \frac{1}{2} \left( \frac{\partial \bar{u}_i}{\partial x_k} + \frac{\partial \bar{u}_k}{\partial x_i} \right) \quad (2.4)$$

where

$$\bar{u}_i = \lim_{T \rightarrow \infty} \frac{1}{T} \int_T u_i dt \quad (2.5)$$

This definition has the advantage that the viscosity defined by equation 2.3 does not fluctuate with time. In the region of concentrations where there are no complications due to thixotropy, etc.,  $\eta$  is a unique and characteristic constant of a given suspension, if the flow is slow, the conditions in the apparatus are approximately stationary, and if the volume of the apparatus is sufficiently large for the disturbing effects at the walls to be neglected. This is experimentally feasible if proper precautions in the construction of the apparatus are taken. Since  $\bar{a}_{ik}$  and  $d\bar{W}/dt$  can be determined from the layout of the apparatus by the same methods as those for pure liquids,  $\eta$  is a measurable quantity.

Let us consider an idealized Couette apparatus, consisting of concentric cylinders so large that their curvature can be neglected compared to their distance apart, and the streaming can therefore be considered as occurring between two plane parallel plates. Streaming of such a type will be called an idealized

"Couette streaming". It will be further assumed that the driving force of one of the cylinders is constant. It is a matter of experience that if such an apparatus is filled with an inhomogeneous suspension (of a concentration below that of the region of anomalous behavior), and if the wall effects are neglected, a streaming will develop which will have the mean components of velocities similarly distributed to those of a homogeneous liquid. If the fluid is incompressible the conditions of continuity inside of the liquid as well as on the walls must be fulfilled, whether homogeneous or not, and the detailed deviations from the steady streaming due to inhomogeneities, or fluctuations, due to the symmetry of the arrangement, are as likely to be positive as negative and will cancel out on averaging.

For Couette streaming there will thus be no component of average velocity perpendicular to the walls, and no component perpendicular to the direction of relative motion of the walls. The mean velocity of streaming will be a linear function of the distance from the wall. The origin of the coördinate system will be set moving with the fluid at the origin, and the axis of the coördinate system  $x, y, z$  so that the components of mean velocities are given by

$$u = \kappa y, \quad v = 0, \quad w = 0 \quad (2.6)$$

where  $\kappa$  is the mean rate of shear. (Since time averages only are to be considered, the bar over the symbols, meaning the time average, will be omitted.) Then

$$a_{ik} a_{ik} = \frac{\kappa^2}{2} \quad (2.7)$$

and equation 2.3 defining the viscosity can be written

$$dW/dt = \eta \kappa^2 V \quad (2.8)$$

where  $V$  is the total volume of the liquid in which the heat is liberated. Since in our case

$$1/V \cdot dW/dt = \kappa \tau \quad (2.9)$$

where  $\tau$  is the shearing stress, we obtain

$$\tau = \eta \kappa \quad (2.10)$$

Let us keep  $\tau$  constant and introduce into the suspension of viscosity  $\eta$  a further particle, small compared with the volume of the viscometer. This would cause a further disturbance of streaming, which would change the original value  $\kappa$  of the rate of shear to  $\kappa + d\kappa$ . From equation 2.10 it immediately follows that, since  $\tau$  is constant,

$$\eta \kappa = (\eta + d\eta)(\kappa + d\kappa) \quad (2.11)$$

which can be written as

$$d\eta/\eta = -d\kappa/\kappa \quad (2.12)$$

as the increase of viscosity  $d\eta$  is small. Equation 2.12 is a fundamental differential equation connecting the dynamic quantity  $d\eta$  with the kinematic quantity



$dk$ . It should be noted that this equation follows from the definition 2.3, and that it is valid for idealized Couette streaming for any kind of suspension whatever and for any kind or shape of the introduced particle. It reduces the essentially dynamic problem of finding the increase of viscosity to a kinematic problem of finding  $dk$ , which is easier to handle, as the concept of forces is eliminated from the discussion.

This is also the reason why it is preferable to regard the Couette cylinder as driven with a constant *force* per unit area, and not at a constant *speed*, although in practice the latter arrangement might be preferred for the actual measurements. The final deductions, of course, are equally valid for either arrangement.

### 3. HYDRODYNAMIC EQUATIONS OF STREAMING OF AN INCOMPRESSIBLE FLUID AROUND A SPHERE

Let us turn our attention to suspensions of rigid spherical particles. In order to calculate their viscosities, the change of rate of shear due to the introduction of an additional sphere into the suspension must be known. Let us consider first in more detail the hydrodynamic equations of general streaming of an incompressible homogeneous fluid under a system of shears, which will develop round a rigid sphere. The system of shears in the fluid before addition of the sphere is given by the velocities of deformation  $a_{ki}^0$ , which in general can vary from point to point, but which must satisfy the equations of continuity in the fluid and at the walls. In considering the original streaming near the origin of the coördinate system, the origin being assumed to move with the fluid, it is assumed that the  $a_{ki}^0$  vary so slowly that at the distances from the origin of the order of the radius  $a$  of the sphere, the velocities of the liquid are given with sufficient accuracy by,

$$u_i^0 = \left( \frac{\partial u_i^0}{\partial x_l} \right)_0 x_l \quad (3.1)$$

i.e., the higher terms of velocity are neglected.

The addition of one rigid sphere of radius  $a$  at the origin would not satisfy the conditions of continuity of the original streaming at its surface and a new field of motion must be found which, when superimposed additively over the original field, would restore the conditions of continuity. This new field is given by the additional velocities  $u_i'$  throughout the liquid, which in the most condensed form can be expressed as

$$u_i' = -\frac{1}{2} e^{-(5r^2/2a^2)} \cdot a_{ki}^0 \frac{\partial l_{kl}}{\partial x_l} \quad (3.2)$$

where the tensor

$$l_{kl} = \left( \frac{a}{r} \right)^5 \cdot e^{(5r^2/2a^2)} \cdot x_k x_l \quad (3.3)$$

and

$$r^2 = x_1^2 + x_2^2 + x_3^2$$

The velocities  $u'_i$  thus cannot be expressed by a potential, so that the additional motion is rotational.

After carrying out the differentiation, we obtain

$$u'_i = -\frac{5}{2} \frac{a^3}{r^5} \left(1 - \frac{a^2}{r^2}\right) a_{ki}^0 x_k x_l - \frac{a^5}{r^5} a_{il}^0 x_l \quad (3.4)$$

In order to prove that the above equations represent the streaming induced by the presence of the sphere, it is necessary to show that they restore the conditions of continuity of the original streaming.

At the surface of the sphere,  $r = a$  and equation 3.4 reduces to

$$u'_i = -a_{il}^0 x_l = -\frac{1}{2} \left( \frac{\partial u_i^0}{\partial x_l} + \frac{\partial u_l^0}{\partial x_i} \right) x_l \quad (3.5)$$

This equation, combined with the velocities of the original motion, given by equation 3.1 gives

$$u_i^0 + u'_i = \frac{1}{2} \left( \frac{\partial u_i^0}{\partial x_l} - \frac{\partial u_l^0}{\partial x_i} \right) x_l \quad (3.6)$$

This, however, represents a rigid rotation of the sphere, and equation 3.6 thus fulfills the condition of continuity at the surface of the sphere. To demonstrate this on a special case, let us consider Couette streaming:

$$u_1^0 = \kappa x_2, \quad u_2^0 = 0, \quad u_3^0 = 0 \quad (3.7)$$

Then equation 3.6 reduces to

$$u_1 = \frac{1}{2} \kappa x_2, \quad u_2 = -\frac{1}{2} \kappa x_1, \quad u_3 = 0 \quad (3.8)$$

which represents a rigid rotational motion of the sphere with an angular velocity  $\kappa/2$  around the third axis.

It remains to prove that the condition of continuity of the additional streaming is also fulfilled throughout the liquid. The derivatives of velocities, after carrying out the necessary differentiations, are:

$$\frac{\partial u'_i}{\partial x_m} = \frac{5}{2} \alpha^3 [(5 - 7\alpha^2) c_i c_m A^0 - (1 - \alpha^2) \delta_{im} A^0 - 2A_{im}^0 + 2\alpha^2 (A_{im}^0 + A_{mi}^0)] - \alpha^5 a_{im}^0 \quad (3.9)$$

where, in order to bring the formula into a more manageable form, the following symbols are used:

$\alpha = \frac{a}{r}$  is a dimensionless quantity

$c_i = \frac{x_i}{r}$  are the direction cosines

$$A^0 = \frac{x_k x_l}{r^2} a_{kl}^0 = c_k c_l a_{kl}^0 \quad (3.10)$$

$$A_{im}^0 = c_i c_l a_{mi}^0$$

$$\delta_{im} = 1 \text{ for } i = m, \quad \delta_{im} = 0 \text{ for } i \neq m$$

The condition of continuity for an incompressible fluid is

$$\partial u_1 / \partial x_1 + \partial u_2 / \partial x_2 + \partial u_3 / \partial x_3 = 0 \quad (3.11)$$

After substituting equation 3.9 in equation 3.11, we obtain

$$\Sigma \partial u'_i / \partial x_i = -\alpha^5 \Sigma a_{i,i}^0 \quad (3.12)$$

But as the original streaming fulfilled the condition of continuity, i.e.,

$$\Sigma a_{i,i}^0 = 0 \quad (3.13)$$

it follows that

$$\Sigma \partial u'_i / \partial x_i = 0 \quad (3.14)$$

and the validity of equation 3.2 is proved.

It is of interest for further calculations to know the velocities of deformation  $a'_{im}$  of the additional field due to the presence of a sphere. They are obtained easily from equation 3.9:

$$a'_{im} = \frac{5}{2} \alpha^3 [(5 - 7\alpha^2) c_i c_m A^0 - (1 - \alpha^2) \delta_{im} A^0 - (1 - 2\alpha^2) (A_{im}^0 + A_{mi}^0)] - \alpha^5 a_{im}^0 \quad (3.15)$$

For the special case of Couette streaming, equation 3.4 can be written, using for  $x_1 = x, x_2 = y, x_3 = z$ :

$$\begin{aligned} u' &= -\frac{5}{2} \kappa \left[ \frac{a^3 x^2 y}{r^5} \left( 1 - \frac{a^2}{r^2} \right) - \frac{1}{2} \frac{a^5 y}{r^5} \right] \\ v' &= -\frac{5}{2} \kappa \left[ \frac{a^3 x y^2}{r^5} \left( 1 - \frac{a^2}{r^2} \right) - \frac{1}{2} \frac{a^5 x}{r^5} \right] \\ w' &= -\frac{5}{2} \kappa \left[ \frac{a^3 x y z}{r^5} \left( 1 - \frac{a^2}{r^2} \right) \right]. \end{aligned} \quad (3.16)$$

These equations can also be obtained directly from Oseen's formulae (Burgers (4); Oseen (13)). At points far away from the sphere

$$\begin{aligned} u' &= -\frac{5}{2} \kappa a^3 x^2 y / r^5 \\ v' &= -\frac{5}{2} \kappa a^3 x y^2 / r^5 \\ w' &= -\frac{5}{2} \kappa a^3 x y z / r^5 \end{aligned} \quad (3.17)$$

These equations can be generalized for a sphere which is not at the origin of the coordinate system.

If the coordinates of the center of the sphere  $S$  are  $x_s, y_s, z_s$ , then by a simple transformation of coordinates, the velocities at a point  $A$  having coordinates  $x_A, y_A, z_A$  are found to be:

$$\begin{aligned} u'_{A(s)} &= -\frac{5}{2} \kappa a^3 (x_A - x_s)^2 (y_A - y_s) / r_{As}^5 \\ v'_{A(s)} &= -\frac{5}{2} \kappa a^3 (x_A - x_s) (y_A - y_s)^2 / r_{As}^5 \\ w'_{A(s)} &= -\frac{5}{2} \kappa a^3 (x_A - x_s) (y_A - y_s) (z_A - z_s) / r_{As}^5 \end{aligned} \quad (3.18)$$

where

$$r_{As}^2 = (x_A - x_s)^2 + (y_A - y_s)^2 + (z_A - z_s)^2$$

The full equations 3.4 can also be expressed in a similar form,  $x_i, x_k, x_l$  being replaced by the differences of coördinates of the point  $A$  and of the center  $s$  of the sphere.

The simplified equations 3.17 can be easily visualized.

Figure 1 represents the additional streaming in the plane  $z = 0$ . The streaming at great distances is radial, with a maximum at  $45^\circ$  and  $225^\circ$  towards the sphere and at  $135^\circ$  and  $315^\circ$  away from the sphere. The stream tubes are cones, the velocity falling off with the square of the distance from the sphere.

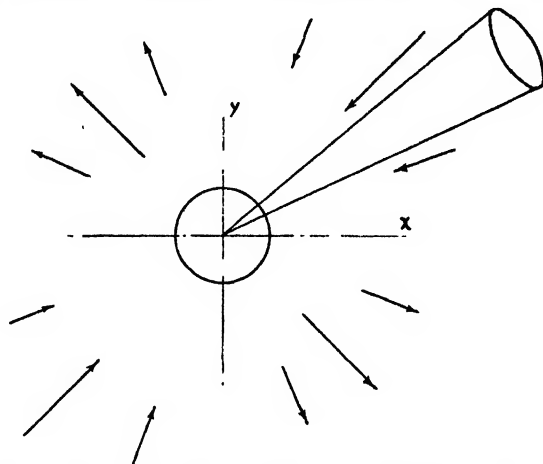


FIG. 1. Schematic section of the additional streaming through plane  $z = 0$ . At great distances, the streaming is radial and the stream tubes are cones.

In order to complete the hydrodynamic treatment, the Stokes-Navier differential equations

$$\frac{\partial u_i}{\partial t} + u_k \frac{\partial u_i}{\partial x_k} = \frac{\eta}{\rho} \Delta u_i - \frac{1}{\rho} \frac{\partial p}{\partial x_i} + \frac{1}{\rho} F_i \quad (3.19)$$

should be fulfilled throughout the liquid;  $\rho$  is the density of the liquid,

$$\Delta u_i = \sum_k \frac{\partial^2 u_i}{\partial x_k^2}$$

$F_i$  are the components of forces acting on unit volume of the liquid, and  $p$  is the pressure.

These equations are non-linear, as they contain the "inertia" terms  $u_k \frac{\partial u_i}{\partial x_k}$ . As only a slow motion is considered, the inertia terms can be neglected. When the streaming is stationary and the outside forces can be neglected, the Stokes-Navier equations are simplified into

$$\partial p / \partial x_i = \eta \Delta u_i \quad (3.20)$$

This is justified when the "Reynolds number"  $R = \rho ua/\eta$  is small compared with unity ( $\rho$  = density,  $u$  = velocity,  $a$  = characteristic length in the instrument).

Couette streaming (equation 3.7) obviously fulfills equations 3.20 by a solution  $\partial p/\partial x_i = 0$ , or  $p = \text{const.}$

In order to show that the additional streaming shown in equation 3.2 or 3.16 fulfils the Navier-Stokes equations (equations 3.20), let us differentiate equation 3.16 twice and add the second derivatives:

$$\begin{aligned}\Delta u &= -5\kappa a^3 y r^{-5} (1 - 5x^2 r^{-2}) \\ \Delta v &= -5\kappa a^3 x r^{-5} (1 - 5y^2 r^{-2}) \\ \Delta w &= 25\kappa a^3 x y z r^{-7}\end{aligned}\tag{3.21}$$

The Navier-Stokes equations are again fulfilled by a solution

$$p = p_0 - 5\eta\kappa a^2 x y r^{-5}\tag{3.22}$$

which reduces to a constant value  $p_0$  at infinity, is everywhere continuous and single-valued in the whole region of space  $r \geq a$ , and represents thus a physically possible pressure distribution in the surrounding liquid.

At the surface of the sphere,  $r = a$  and the pressure is not uniform. However, forces on the sphere resulting from this non-uniformity of pressure at different points of its surface cancel out on integration over the surface of the sphere, so that the resultant force is zero

This shows that a translational motion of the sphere relative to the liquid need not be considered and the so-called Stokes terms vanish. The sphere itself, however, is strained, and if not rigid, it is liable to undergo deformation. Equations 3.22 might serve as a starting point for calculations on non-rigid particles, such as droplets of an emulsion, where the inequalities of pressure should be balanced, for example, by surface-tension forces.

Limiting the dimension to rigid particles only, it remains to show how equations 3.20 behave for higher concentrations.

The particle density  $N$  will be assumed constant throughout the space. Then the pressure in any fixed point in suspension would be given by summing up all the contributions of individual particles:

$$p = p_0 - 5\eta N \kappa a^3 \iiint x y r^{-5} dV\tag{3.23}$$

The interaction of particles, as will be seen later, can be expressed by increasing  $\kappa$  to a certain higher value, but as the integral owing to its symmetry properties vanishes, the same solution as for Couette streaming of a pure liquid is obtained:

$$p = p_0$$

If the particle density  $N$  is not considered constant, but statistically fluctuating, or if there is rapid motion, then the solution begins to be complicated, and Stokes terms of resistance would appear in the solution.

## 4. DERIVATION OF A VISCOSITY FORMULA WITHOUT INTERACTIONS

In the preceding part the influence of a single sphere on the motion of a fluid subjected to shear has been discussed. Attention will now be turned to the suspension of spheres, assuming, for simplicity, that the spheres are uniformly distributed throughout the liquid, that the majority of them are so far from the walls that the simplified equations 3.17 can be used throughout to express the additional streaming due to each sphere with sufficient accuracy, and that the distances between the individual spheres are sufficiently large so that the direct interactions between the spheres can be neglected.

Starting with a suspension already containing  $N$  spheres per unit volume, so that the volume occupied by the spheres per unit volume of the suspension is  $\frac{4}{3}\pi a^3 N$ , the effect on the streaming of a further addition of  $dN$  spheres per unit volume will be investigated.

In the case of idealized Couette streaming given by average velocities

$$u = \kappa y, \quad v = 0, \quad w = 0 \quad (4.1)$$

one wall  $y = y_A$  has a velocity  $u_A = \kappa y_A$ , and the other wall  $y = y_B$  has a velocity  $u_B = \kappa y_B$ . By taking a slab of suspension of a thickness  $dy$  parallel to the walls, one can calculate the resulting additional velocity  $d^2 u_A$  at a point of the wall  $x = 0, y = y_A, z = 0$ , due to the combination of the velocity fields of all the additional spheres in the slab. By taking one sphere, the coördinates of which are  $x_s, y_s, z_s$ , it is found that for  $y_A > y_s > y_B$ , the velocity  $u'_{A(s)}$  at the point of the wall  $0, y_A, 0$ , due to this sphere is, according to equations 3.18:

$$u'_{A(s)} = -\frac{5}{2}\kappa a^3 x_s^2 (y_A - y_s) r_{As}^{-5} \quad (4.2)$$

The total additional velocity  $d^2 u_A$  will be given by integrating over the whole slab:

$$d^2 u_A = -\frac{5}{2}\kappa a^3 dN dy (y_A - y_s) \int_{-\infty}^{\infty} \int_{-\infty}^{\infty} x_s^2 r_{As}^{-5} dx_s dz_s \quad (4.3)$$

As

$$\int_{-\infty}^{\infty} \int_{-\infty}^{\infty} x_s^2 r_{As}^{-5} dx_s dz_s = \frac{2}{3}\pi (y_A - y_s)^{-1} \quad (4.4)$$

we obtain:

$$d^2 u_A = -\frac{5}{3}\pi \kappa a^3 dN dy \quad (4.5)$$

It should be noted that the additional velocity  $d^2 u_A$  is independent of the distance  $y_A - y_s$  of the slab from the wall, as this cancels out.

If another point at the wall had been chosen, the same result could be obtained by a simple transformation of the coördinates. The additional velocity is thus also independent of the coördinates of the point chosen on the wall, and the effect of the slab is to change uniformly the velocity of the whole wall  $A$  by

$$d^2 u_A = -\frac{5}{3}\pi \kappa a^3 dN dy \quad (4.6)$$

Similarly the velocity of the wall  $B$  would be changed by

$$d^2u_B = +\frac{5}{8}\pi\kappa a^3 dN dy \quad (4.7)$$

We are interested in the *relative* velocity  $u_r$  of the walls, which is experimentally determined. Before the addition of the sphere this was

$$u_r = u_A - u_B = \kappa(y_A - y_B) \quad (4.8)$$

and the change due to the addition of the slab was

$$d^2u_r = d^2u_A - d^2u_B = -\frac{1}{8}\pi\kappa a^3 dN dy \quad (4.9)$$

The change of the relative motion due to the effect of all the slabs can then be obtained by integrating from  $y_B$  to  $y_A$ :

$$du_r = -\frac{1}{8}\pi\kappa a^3 dN \int_{y_B}^{y_A} dy = -\frac{1}{8}\pi\kappa a^3 dN (y_A - y_B) \quad (4.10)$$

By differentiating equation 4.8,

$$du_r = d\kappa \cdot (y_A - y_B) \quad (4.11)$$

and the addition of  $dN$  spheres per unit volume would change the shear  $\kappa$  by

$$d\kappa = -\frac{1}{8}\pi\kappa a^3 dN \quad (4.12)$$

As  $\frac{4}{3}\pi a^3 N = c$  is the concentration by volume,

$$\frac{4}{3}\pi a^3 dN = dc \quad (4.13)$$

and

$$d\kappa/\kappa = -k dc \quad (4.14)$$

where the constant  $k = 5/2$  for rigid spheres.

Applying now the relation 2.12, we obtain finally

$$d\eta/\eta = k dc \quad (4.15)$$

which on integration gives the well-known Arrhenius formula:

$$\log_e(\eta/\eta_0) = kc \quad (4.16)$$

where the integration constant  $\eta_0$  is the viscosity of the pure liquid.

The Arrhenius formula is thus obtained when it is assumed that there is *no interaction* between the particles.

## 5. INFLUENCE OF PROXIMITY OF A WALL

The preceding discussion dealt with the problem of a suspension of spherical particles under the simplifying assumption that the dimensions of the apparatus are so large compared with the dimensions of the particles that only a negligible proportion of the particles can be regarded as at a small distance from the walls of the apparatus. In principle, it is always possible to build a Couette apparatus of dimensions as large as may be required, but in actual practice there are limita-

tions. For example, there is often not a sufficient quantity of a suspension available to fill up a large instrument, or there is the difficulty of temperature control. Since capillary viscometers of the Ostwald type have many advantages over the Couette apparatus, it is worth while to investigate in more detail the so-called "wall effects", and then to correct the readings of smaller instruments rather than to use excessively large instruments for the measurements.

We shall investigate in more detail and more rigorously the full interaction between a wall and a sphere placed at a point  $x_s, y_s, z_s$  in proximity to an infinite wall  $y = y_A$ , the original streaming of the fluid being again given by

$$u^0 = \kappa y, \quad v^0 = 0, \quad w^0 = 0$$

The second wall  $y = y_B$  would be assumed to be at so great a distance that its effect can be neglected in the proximity of  $y_A$ .

After the addition of the sphere the new streaming described by equation 3.16 will not fulfill the condition of continuity at the wall, as in general for  $y = y_A$  the normal component  $v' \neq 0$ . A further additional field must be sought which would bring the condition of continuity back to fulfillment over the whole wall. The normal components over the wall can be made to vanish by a method of "mirror images". Let us imagine behind the wall a "mirror image" streaming given by  $\partial u^0 / \partial y = -\kappa$ , and place a mirror image  $M$  of the sphere  $s$  at a point

$$x_M = x_s, \quad y_M = 2y_A - y_s, \quad z_M = z_s$$

The normal component of the field of the original sphere  $s$  at the point  $A$  of coördinates  $0, y_A, 0$  at the wall is, according to equation 3.16:

$$v'_{A(s)} = -\frac{5}{2}\kappa_0 \left[ \frac{a^3 x_s (y_A - y_s)^2}{r_{As}^5} \left( 1 - \frac{a^2}{r_{As}^2} \right) - \frac{1}{2} \frac{a^5}{r_{As}^5} x_s \right] \quad (5.1)$$

and of the field of the mirror image  $M$ :

$$v'_{A(M)} = +\frac{5}{2}\kappa_0 \left[ \frac{a^3 x_M (y_A - y_M)^2}{r_{AM}^5} \left( 1 - \frac{a^2}{r_{AM}^2} \right) - \frac{1}{2} \frac{a^5}{r_{AM}^5} x_M \right] \quad (5.2)$$

As

$$x_M = x_s, \quad (y_A - y_M) = -(y_A - y_s), \quad r_{AM} = r_{As} \quad (5.3)$$

the sum of the two components at the wall

$$v'_{A(s)} + v'_{A(M)} = 0 \quad (5.4)$$

and the condition of continuity is satisfied.

However, the introduction of the streaming of the sphere at  $M$  will cause at  $s$  an additional velocity of deformation  $a'_{12}$  proportional to  $a_{12}^0$ ,

$$a'_{12} = K a_{12}^0 \quad (5.5)$$

The constant  $K$ , according to equation 3.15, is

$$K = \frac{5}{2}\alpha^3 - 4\alpha^5, \quad \text{where} \quad \alpha = \frac{a}{2(y_A - y_s)} \quad (5.6)$$



so that the sphere  $s$  will be subject not to  $a_{12}^0$  but to  $a_{12}^0 + a'_{12}$ . To maintain continuity, the mirror image  $M$  must also be subject to an additional velocity of deformation  $-a'_{12}$ . These fields, however, must be again compensated by fields  $a''_{12}$ ,  $a'''_{12}$ , etc. of diminishing strength.

As the presence of the velocities of deformation  $a'_{12}$ ,  $a''_{12}$ , etc. combined with their mirror-image fields would bring their normal components of velocity over the whole wall always to zero, the addition of fields of this type would maintain the condition of continuity over the wall, even if the reflections are repeated an infinite number of times.

Hence we obtain the relations

$$a'_{12} = K a_{12}^0, \quad a''_{12} = K a'_{12}, \text{ etc.} \quad (5.7)$$

and the final field  $a_{12}$  for  $K < 1$  would be obtained by adding an infinite number of the reflections

$$a_{12} = a_{12}^0 + a'_{12} + a''_{12} + \dots \quad (5.8)$$

or

$$a_{12} = a_{12}^0(1 + K + K^2 + \dots) = a_{12}^0/(1 - K) \quad (5.9)$$

If  $K < 1$ , the series is convergent, and a field  $a_{12}$  exists which not only fulfils the condition of continuity over the whole wall, but also restores this condition over the surface of the spheres  $s$  and  $M$ .

Substituting for  $K$  from equation 5.6 we obtain

$$a_{12} = a_{12}^0[1 - \frac{5}{18}a^3/(y_A - y_s)^3 + \frac{1}{8}a^5/(y_A - y_s)^5]^{-1} \quad (5.10)$$

which shows that if the center of the sphere is at a distance  $(y_A - y_s)$  from an infinite wall, the conditions of continuity are restored if a value of  $a_{12}$  is substituted instead of  $a_{12}^0$  in the equations (equations 3.16) of the motion of the fluid round the sphere.

It should be noted that equation 5.10 is still not a rigorous expression, as the following approximations were used in its derivation: (1) The effect of higher derivatives of  $u_i$  was neglected. (2) Tangential components of velocities over the wall were not brought to a constant value, as they should have been for a liquid of non-zero viscosity.

The effect of higher derivatives of  $u_i$  can be assumed to decrease very rapidly with increasing distance from the wall, so that this effect can be regarded as negligible. The calculation of a further compensation field to make the value of the tangential velocity constant over the whole wall represents a difficult problem of solving functional equations. The method of mirror images, which is successful in satisfying the conditions of continuity, is of no further help here.

It is, however, a practice in classical hydrodynamics to neglect fields of the tangential type, assuming that they fall off very rapidly with the distance from the wall. There is still an open field for improvement of the theory, but the mathematical difficulties are a serious obstacle for further investigation.

After combining the final streaming of the sphere  $s$  and of its mirror image  $M$

and dividing by 2 in order to obtain the contribution to streaming at the point  $A$  of the wall due to *one* sphere, we have  $v' = 0$ , i.e., the streaming at  $A$  is tangential to the wall, the velocity components being

$$\begin{aligned} u'_{A(s)} &= -\frac{5}{2}\kappa \left[ \frac{a^3 x_s^2}{r_{As}^5} \left( 1 - \frac{a^2}{r_{As}^2} \right) - \frac{1}{2} \frac{a^5}{r_{As}^5} \right] (y_A - y_s) \\ w'_{A(s)} &= -\frac{5}{2}\kappa \frac{a^3 x_s z_s}{r_{As}^5} \left( 1 - \frac{a^2}{r_{As}^2} \right) (y_A - y_s) \end{aligned} \quad (5.11)$$

where, according to equation 5.10,

$$\kappa = \kappa_0 [1 - \frac{5}{16} a^3 / (y_A - y_s)^3 + \frac{1}{8} a^5 / (y_A - y_s)^5]^{-1} \quad (5.12)$$

We can now proceed further as in Section 4, considering again a slab  $dy$  containing  $dN$  additional spheres per unit volume, and obtaining the total additional velocities  $d^2 u_A$ ,  $d^2 w_A$  at the point  $A$  due to the slab by integrating over the whole slab. Owing to the symmetry of the expression for  $w'_{A(s)}$  in  $x$  and  $z$ , we obtain  $d^2 w_A = 0$ , so that there remains only the solution of the integral

$$d^2 u_A = -\frac{5}{2} \kappa a^3 dN dy (y_A - y_s) \iint_{xz} \left( \frac{x^2}{r^5} - \frac{a^2 x^2}{r^7} - \frac{1}{2} \frac{a^2}{r^5} \right) dx dz \quad (5.13)$$

Putting  $y = y_A - y_s$ , it follows that:

$$d^2 u_A = -\frac{5}{2} \kappa a^3 dN dy (y_A - y_s) \left[ \frac{2}{3} \pi / (y_A - y_s) - \frac{7}{15} a^2 \pi / (y_A - y_s)^3 \right] \quad (5.14)$$

Substituting for  $\kappa$  from equation 5.12, the retardation of the wall  $A$  is found to be

$$\begin{aligned} d^2 u_A &= -\frac{5}{2} \kappa_0 \pi a^3 dN dy \left( 1 - \frac{7}{10} \frac{a^2}{(y_A - y_s)^2} \right) \\ &\quad \cdot \left( 1 - \frac{5}{16} \frac{a^3}{(y_A - y_s)^3} + \frac{1}{8} \frac{a^5}{(y_A - y_s)^5} \right)^{-1} \end{aligned} \quad (5.15)$$

At a great distance from the wall  $A$ ,  $(y_A - y_s) \gg a$ , and this formula reduces to the simplified formula 4.5. On the other hand, as no center of a sphere can approach to the walls  $A$  and  $B$  nearer than its radius  $a$ , equation 5.15 must be replaced by the condition  $d^2 u_A = 0$ , when

$$|y_A - y_s| < a \text{ and } |y_B - y_s| < a \quad (5.16)$$

A similar expression would be obtained for the slabs in the immediate vicinity of the wall  $B$ , the signs being appropriately changed. We are interested only in the change of the relative velocity  $u_r$  of the two walls  $A$  and  $B$ , intending to obtain the effect of all the slabs by integrating from  $y_B$  to  $y_A$ . Instead of writing the expressions in full, and integrating, as in Section 4, the calculation can be simplified by considering the effect of one wall  $A$  only.

Equations 5.15 and 5.16 can be also written as follows, substituting for

$$(y_A - y_s)/a = \xi, \quad (y_B - y_s)/a = \xi_B, \quad dy = a d\xi$$

$$d^2u_A = -\frac{5}{3}\kappa_0\pi a^3 dN dy + \frac{5}{3}\kappa_0\pi a^3 dNaF(\xi) d\xi \quad (5.17)$$

for  $1 \leq \xi < \xi_B - 1$ , where

$$F(\xi) = \frac{\frac{7}{16}\xi^3 - \frac{5}{16}\xi^2 + \frac{1}{8}}{\xi^5 - \frac{5}{16}\xi^2 + \frac{1}{8}}$$

and

$$d^2u_A = -\frac{5}{3}\kappa_0\pi a^3 dN dy + \frac{5}{3}\kappa_0\pi a^3 dNa d\xi$$

for  $0 < \xi < 1$  and for  $\xi_B - 1 < \xi < \xi_B$ .

But the first terms on the right-hand sides are identical with equation 4.5 and thus the "wall effect" alone is represented by the second terms of equation 5.17. Hence the additional change of velocity of the wall  $A$  due to the "wall effect" alone of all the slabs is represented by

$$(du_A)_w = \frac{5}{3}\kappa_0\pi a^4 dN \left[ \int_0^1 d\xi + \int_1^{\xi_B-1} F(\xi) d\xi + \int_{\xi_B-1}^{\xi_B} d\xi \right] \quad (5.18)$$

The middle integral in equation 5.18 can be written as

$$\int_1^{\xi_B-1} F(\xi) d\xi = \int_1^\infty F(\xi) d\xi - \int_{\xi_B-1}^\infty F(\xi) d\xi \quad (5.19)$$

The numerical value of the integral

$$\int_1^\infty F(\xi) d\xi = 0.603$$

was found by development in series and integration.

It should be noted that if the distance of the wall  $B$  from the wall  $A$  is of the order of  $a$ , then the last integral in equation 5.19 is not negligibly small and should be taken into calculation. However, it rapidly decreases to zero with the increasing distance of the walls, so that for all practical purposes, where the distance of the walls is several times that of  $a$ , this integral can be neglected.

It follows that

$$(du_A)_w = \frac{5}{3}\kappa_0\pi a^3 dN \cdot 2.603a \quad (5.20)$$

In a similar manner, for the wall  $B$

$$(du_B)_w = -\frac{5}{3}\kappa_0\pi a^3 dN \cdot 2.603a \quad (5.21)$$

The required change of the relative velocity  $u_r$  of the two walls can be written as

$$\begin{aligned} du_r &= du_A + (du_A)_w - du_B - (du_B)_w \\ &= -\frac{10}{3}\kappa_0\pi a^3 dN(y_A - y_B - 2.603a) \\ &= -\frac{10}{3}\kappa_0\pi a^3 dN(y_A - y_B - 2D) \end{aligned} \quad (5.22)$$

where  $D = 1.3015a$ .

The final result of the discussion is thus that the wall effect is fully accounted for, if in our formulae the distance  $y_A - y_B$  between the walls is diminished by  $2.603a$ . It is as if along each wall there were a layer of a thickness  $D = 1.301a$  which does not contribute to  $du_r$ , i.e., which can be regarded as of *viscosity of a pure liquid*. The measured uncorrected values of viscosity of suspensions will tend to be *smaller* in small instruments than in larger ones.

The above discussion of the wall effect elucidates many apparently anomalous results on suspensions, as the "sigma phenomenon" etc. In the region of high concentrations, considerable slip at the wall might develop due to the layers of low viscosity along the walls which might finally completely overshadow the effects of shear inside of the suspension, making the measurements useless. It should be noted that this slip is quite distinct from the phenomenon called "plug flow" of the Bingham body, as it develops even in the region of concentrations where the suspensions behave in bulk as a true Newtonian liquid.

## 6. INTERACTION OF THE PARTICLES

The formula for the interaction of the particles follows directly from equations 3.15. Around each sphere there develops a field of velocities of deformation  $a'_{im}$  superimposed over the original field  $a^0_{im}$ , and so a second sphere will find itself subjected to a combined field  $a^0_{im} + a'_{im}$ . However, the first sphere would be subject to an additional field  $a'_{im}$  of the second sphere, and in order to satisfy conditions of continuity, it will develop a further field  $a''_{im}$ , and finally a series of fields  $a'_{im}, a''_{im}, a'''_{im} \dots$  etc. of decreasing strength develops for each pair of spheres. The final resulting field is then obtained by a summation of an infinite series, as in the case of the "wall effect", and by an integration over all possible positions of the second sphere with respect to the first sphere. The integration can be performed first for each individual term of the series, and the terms summed afterwards.

However, the odd members of the series will vanish on integration, owing to the symmetry properties of the integral. As there is no first-order interaction between the spheres and the rest of the suspension, we shall start with the discussion of the "second order" field  $a''_{im}$  due to the "reflection" from the first sphere to the second sphere and back.

The field  $a''_{pq}$  can be obtained by substituting equations 3.15 into themselves, which after rather laborious but otherwise straightforward calculation, omitted here owing to its length, gives as a result

$$a''_{na} = \frac{5}{2}\alpha^6(10 - 20\alpha^2 + 9\alpha^4)c_p c_q A^0 - \frac{5}{2}\alpha^6(5 - 12\alpha^2 + 7\alpha^4)\delta_{pq}A^0 + \frac{5}{2}\alpha^6(5 - 16\alpha^2 + 12\alpha^4)(A^0_{pq} + A^0_{qp}) + \alpha^{10}a^0_{pq} \quad (6.1)$$

This represents the second-order field of velocities of deformation  $a''_{pq}$  acting on the first sphere due to the presence of a second sphere at a distance  $r$  under directional cosines  $c_i$ , when itself originally subjected to velocities of deformation,  $a^0_{ia}$ . The field does not cancel out on integration.

In any volume element there are  $N dV$  additional spheres present, and the field

of velocities of deformation due to all of these spheres is given by the integration (in polar coördinates) which will be denoted by a bar over the symbol:

$$\bar{a}_{pq}'' = N \cdot \int_{r=2a}^{\infty} \int_S a_{pq}'' dS dr \quad (6.2)$$

It is convenient to perform the double integration over the surface of the sphere  $S$  first, the variables being the direction cosines, and then to perform the integration over radius  $r$ . As no center of a sphere can approach to a given sphere nearer than  $2a$ , this integration should be carried from  $r = 2a$  to  $\infty$  and not over the whole space.

As we are examining Couette streaming, in which the coördinate system is set so that for  $p = q$ ,  $a_{pq}^0 = 0$ , we can restrict ourselves to a case of  $p \neq q$ .

After carrying the necessary double integrations over the sphere, we obtain

$$\bar{a}_{pq}'' = Na_{pq}^0 \pi \left[ 30a^6 \int_{2a}^{\infty} \frac{dr}{r^4} - 80a^8 \int_{2a}^{\infty} \frac{dr}{r^6} + 56a^{10} \int_{2a}^{\infty} \frac{dr}{r^8} \right] \quad (6.3)$$

or

$$\bar{a}_{pq}'' = Na_{pq}^0 \pi a^3 \left[ \frac{5}{4} - \frac{1}{2} + \frac{1}{16} \right] = \frac{1}{16} \pi a^3 Na_{pq}^0 \quad (6.4)$$

As  $\frac{1}{3} \pi a^3 N = c$  is the concentration by volume, it follows that

$$\bar{a}_{pq}'' = Qca_{pq}^0, \quad Q = \frac{3}{8}Q \quad (6.5)$$

where  $Q = 0.60937$  is the sought interaction constant. The second-order interaction field is thus proportional to the concentration of the suspension and to the original field  $a_{pq}^0$ , as would be expected.

In a similar manner we obtain for even, higher-order, interactions

$$\bar{a}^{(4)} = Qc\bar{a}'', \quad \bar{a}^{(6)} = Qc\bar{a}^{(4)}, \text{ etc.}$$

The final field  $\bar{a}$  is given by a sum of all of the even-order fields concerned:

$$\bar{a} = a^0(1 + Qc + (Qc)^2 + \dots) = \frac{a^0}{1 - Qc} = a^0 \left( 1 + \frac{Qc}{1 - Qc} \right) \quad (6.6)$$

As  $Q < 1$  and  $c < 1$ , it follows that  $Qc < 1$ , and the series is convergent for any  $c$ , i.e., a field  $\bar{a}$  always exists.

The above result means that at a concentration  $c$  every sphere of the suspension develops an additional streaming as if subjected to a field  $\kappa Qc/(1 - Qc)$ , in addition to the actual field  $\kappa$ . Now the formula 4.14 can be corrected for the interactions:

$$\frac{d\kappa}{\kappa} = -k dc - k \frac{Qc}{1 - Qc} dc - kc \frac{d}{dc} \left( \frac{Qc}{1 - Qc} \right) dc \quad (6.7)$$

where the first term on the right-hand side corresponds to the Arrhenius term without interactions and the second is the effect of interactions on the field increase due to the particles *added*, whereas the third is the effect of the change of concentration on the interaction field due to the particles *already present* in the suspension.

By integrating equation 6.7, a viscosity formula corrected for interactions is obtained:

$$\log_e \eta_r = kc/(1 - Qc) \quad (6.8)$$

## 7. COLLISION EFFECT

In the above discussion the hydrodynamic effects of collisions of the particles have been neglected. At high concentrations, there would be also other causes contributing to the increase of viscosity, due for example to the neglect of higher derivatives of  $u_i$  in equation 3.1 at the outset of the calculation. The density  $N$  is also not strictly constant, and a density distribution, such as shown on figure 2, would develop round each sphere. Each sphere would leave two empty channels, from which other spheres had been pushed aside. It is believed, however, that such effects would influence only terms of higher power than the second, so

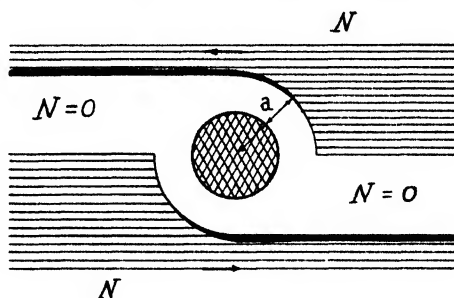


FIG. 2. Distribution of the density  $N$  round a sphere in consideration. The sphere leaves two empty channels, from which the other spheres were pushed aside (regions of high density represented by thick lines).

that our attention will be limited to the collision effect, which affects the second-power term.

The actual collision process would differ for suspensions with strong and with weak Brownian motion. For the latter case, according to Bingham (2), the collision process can be pictured as follows:

In a suspension, spheres in the same stratum have the same velocity and do not change their mutual distances. However, spheres in different strata under the shearing motion of the liquid move with unequal velocity, and collisions occur, depending primarily on the concentration, but also upon any association (attraction) or repulsion forces which may exist between them.

We shall only deal with the simple case of no forces between the spheres and no Brownian movement. These collisions do not resemble collisions in a gas, as the colliding particles roll round each other till they reach such positions that a disengagement through further shear takes place.

There will be some kinetic energy transformed into heat during the collision, the amount of which would depend on the rate of shear. As we are dealing with only slowly moving suspensions, and as the kinetic energy depends on the square

of the velocities, these effects would be negligible under the above conditions, and the only effect would be caused by purely geometrical factors. To calculate this effect, it is necessary to know for each sphere the average fraction of time spent in collisions.

The origin of coördinates will be set in the point of contact, as this would remain stationary with respect to the stratum of liquid passing through it during the collision. Then the velocity of the center of each sphere with regard to this point will be  $u = \kappa y$  before collision.

Introducing polar coördinates  $\omega, \phi$  (see figure 3):

$$y = a \cos \omega \sin \phi \quad (7.1)$$

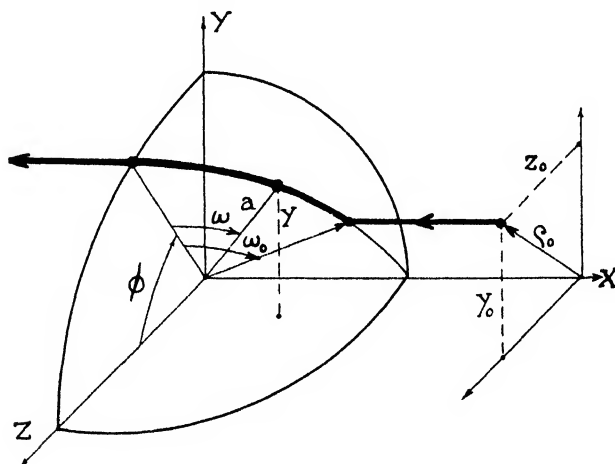


FIG. 3. Geometry of the collision process. Point of contact is at the origin. The path of a center of a sphere before, during, and after a collision is represented by a thick line.

The velocity of rotation  $d\omega/dt$  will be thus

$$a \, d\omega/dt = \kappa y \cos \omega \quad (7.2)$$

and the time  $t$  spent

$$t(\omega_0, \phi) = \int_{\omega_0}^0 dt = \int_{\omega_0}^0 \frac{a \, d\omega}{\kappa y \cos \omega} = \int_{\omega_0}^0 \frac{d\omega}{\kappa \sin \phi \cos^2 \omega} = -\frac{\tan \omega_0}{\kappa \sin \phi} \quad (7.3)$$

The time spent during the collision of a pair of spheres depends thus only on their initial angles of contact,  $\omega_0, \phi$ , of the collision.

In order to calculate the total time  $T$  spent per unit time by *one* sphere in collisions with other spheres, we must transform the origin of the coördinates in its center. Let  $N$  be the number of spheres per unit volume. Then

$$T' = \int_{\phi=0}^{2\pi} \int_{\rho=0}^{2a} t \kappa y_0 N \rho \, d\rho \, d\phi = - \int \int \tan \omega_0 \cdot \rho^2 N \, d\rho \, d\phi \quad (7.4)$$

where  $\rho^2 = y_0^2 + z_0^2$  of the other spheres in the new coördinate system.

As  $\tan \omega_0 = \sqrt{4a^2/\rho^2 - 1}$ ,

$$\frac{4}{3}\pi a^3 N = c \quad (7.5)$$

$$T = -\pi N \int_0^{2a} \sqrt{4a^2 - \rho^2} d(\rho^2) = \frac{16}{3}\pi N a^3 = 4c \quad (7.6)$$

Thus the time  $T$  spent per unit time by each sphere in collision is four times the concentration if there are no attractive or repulsive forces.

The time would be lengthened by attractive and shortened by repulsive forces. It would be also influenced by Brownian movement and to some extent also by forces arising from mutual hydrodynamical interactions. We can thus write generally  $T = r_2 c$ , where  $r_2 = 4$  for the simplified case of spheres without forces and no Brownian movement.

This important result clearly shows that the influence of collisions on viscosity must be large even at moderate concentrations. It signifies that at any time there is present a concentration  $c_2 = r_2 c_1^2$  of "doublets", i.e., of pairs of colliding spheres, where  $c_1$  is the concentration of the "singlets". Similar calculations to those on doublets would give the concentration of "triplets", or triple collisions, to be to a first approximation  $c_3 = r_3 c_1 c_2$ , where the time constant  $r_3$  is to be again determined from geometrical considerations. We have then the following system of equations:

$$\begin{aligned} c &= c_1 + c_2 + c_3 + \dots \\ c_2 &= r_2 c_1^2 \\ c_3 &= r_3 c_1 c_2 = r_2 r_3 c_1^3 \quad \text{etc.} \end{aligned} \quad (7.7)$$

which give an equation for  $c_1$ :

$$c - c_1 - r_2 c_1^2 - r_2 r_3 c_1^3 - \dots = 0$$

This equation can be solved by an infinite series, so that we obtain:

$$\begin{aligned} c_1 &= c - r_2 c^2 - (r_2 r_3 - 2r_2^2) c^3 - \dots \\ c_2 &= r_2 c^2 - 2r_2^2 c^3 - \dots \\ c_3 &= r_2 r_3 c^3 - \dots \quad \text{etc.} \end{aligned} \quad (7.8)$$

It should be noted that equation 7.8 is only an approximation, as there are several ways in which doublets, triplets, etc. can be created (for example, by disruption of a multiplet). Such processes, however, would influence higher-order terms only.

We can now consider that a suspension is composed of a mixture of particles of various shapes, each kind of particle having its own characteristic shape factor  $k$ . There will be a partial concentration  $c_1$  of single spheres having a shape factor  $k_1$ ,  $c_2$  of doublets having a shape factor  $k_2$ ,  $c_3$  of triplets having  $k_3$ , etc. The resulting mean shape factor  $\bar{k}$ , of a mixture, which should enter the calculation



of the viscosity, is then given by a weighted average of the shape factors of all the particles present, i.e.,

$$\bar{k} = \frac{k_1 c_1 + k_2 c_2 + k_3 c_3 + \dots}{c} \quad (7.9)$$

Substituting for the partial concentrations from equations 7.8, we obtain:

$$\bar{k} = k_1 + r_2(k_2 - k_1)c + [r_2 r_3(k_3 - k_1) - 2r_2^2(k_2 - k_1)]c^2 + \dots \quad (7.10)$$

This value of  $\bar{k}$  should be now substituted in the viscosity equation (6.8) so that:

$$\log \eta_r = [k_1 c + r_2(k_2 - k_1)c^2 + \dots]/(1 - Qc) \quad (7.11)$$

For rigid spheres, the value  $r_2 = 4$  has been derived. The numerical values of  $r_3$  and of the shape factors  $k_2$ ,  $k_3$ , etc. are not known. We shall not carry out the

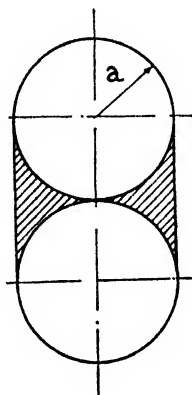


FIG. 4. Schematic representation of the immobilized liquid during a collision of two spheres. The immobilized volume is represented by a shaded area.

calculation for  $r_3$  but attempt only the calculation of the shape factors. The shape factors can in principle be calculated from a rigorous hydrodynamic theory, which should include Stokes terms, but as the mathematical difficulties are considerable we shall limit ourselves only to the substitute of a correct treatment, estimating the values of the shape factors by means of the help of fictitious "immobilized liquid".

Let us start with a pair of rigid spheres in a non-slipping contact, i.e., with a dumbbell-shaped rigid body (figure 4). According to Eirich and Mark (8) the shape factor of a body having slots, crevices, etc. is primarily given by its outer outline, so that the liquid filling the holes can be regarded as "immobilized" by the particle. A colliding pair of spheres can be regarded as immobilizing all the liquid which is situated in a space in the neighborhood of the point of contact. As the volume of the resulting body would be greater than the sum of the volumes of the two separate spheres, increase of the shape factor  $k$  of the colliding pair would result. The "immobilized" liquid, of course, has no sharp boundary, but for convenience it can be regarded as being limited by some fictitious sharp

boundary, drawn so that the viscosity increase of the resulting rigid body is the same as that of a real pair of colliding spheres. The immobilized liquid is, as a consequence of geometrical similarity, proportional to the volume of the spheres.

The immobilized volume can be roughly estimated to be of the order of the volume enclosed inside a cylinder, as shown in figure 4. This volume is for a pair of particles equal to

$$2\pi a^3 - \frac{4}{3}\pi a^3 = \frac{2}{3}\pi a^3$$

The immobilized liquid increases the original volume  $\frac{8}{3}\pi a^3$  to  $\frac{10}{3}\pi a^3$ , i.e., by a factor 5/4. The shape factor is thus approximately increased in the same ratio, i.e.,  $k_2 = 5/4 \cdot k_1 = 25/8$ . As the resulting body is now non-spherical, but approximately an ellipsoid of axial ratio 1:2, the shape factor should be further increased by a factor 2.54/2.50, a value obtained from the data for ellipsoids by Burgers (4) on the assumption of small Brownian motion. Hence a final value of  $k_2 = 3.175$  is obtained. However, this value is known with less certainty than the other constants of the theory.

For triplets we can obtain a value of  $k_3$ , considering that there would be in the first approximation two points of contact, each immobilizing  $\frac{2}{3}\pi a^3$  of liquid. The original volume of  $\frac{4}{3}\pi a^3$  would be increased thus to  $\frac{10}{3}\pi a^3$ , i.e., by a factor 4/3. Neglecting the further influence of the non-spherical shape of the triplet, we obtain for  $k_3$  the value 3.34. The shape factor, however, would not increase much further; for very large clots of particles the ratio would depend only on the kind of packing of the particles, and for example for cubical packing of spheres it would be increased by  $6/\pi = 1.91$  times, and  $k_\infty = 4.78$ . We have seen that as the concentration is further increased, clots of three, four, etc. particles would begin to form in greater quantities and rotate as a whole. When equilibrium is reached these clots will have a certain average size. Finally, there must come a concentration at which the clots come in contact across the entire space occupied by the suspension. Before this region is reached, the clots, which in average have shapes not very far from spherical—since greatly elongated shapes are more quickly disrupted by shear—behave as individual particles, immobilizing an amount of liquid given by the kind of packing of the particles in the clot.

When the clot extends over the whole suspension, it is expected that other laws begin to be valid, as the particles will assume positions determined by their neighbors, and a definite structure begins to be built as the shear progresses. The viscous behavior of the suspension will be replaced by a plastic behavior.

Similar considerations would apply also to non-spherical, to non-rigid, and to solvated particles. The numerical values of the constants, however, should be then modified appropriately.

## 8. SUMMARY

1. Taking into account the mutual interaction of the particles and their collisions, the following theoretical formula (7.11) for the relative viscosity  $\eta_r$  of suspensions of rigid spheres having a volume concentration  $c$  was derived:

$$\log_e \eta_r = \frac{k_1 c + r_2(k_2 - k_1)c^2 + \dots}{1 - Qc}$$

2. This formula is believed to be valid accurately up to second-power terms and, as will be shown in following papers, agrees very well with the observed values of viscosity of artificial suspensions and solutions over a wide range of concentrations.

3. For rigid, non-solvated spheres without mutual forces and without Brownian motion, the following values of the constants were derived from theory:

Einstein shape factor of single spheres	$k_1 = 2.5$
Shape factor of collision doublets	$k_2 = 3.175$
Collision time constant	$\tau_2 = 4$
Hydrodynamic interaction constant	$Q = 0.609$

4. The equation 7.11 can be written as a power series:

$$\eta_r = 1 + k_1 c + \left[ \frac{1}{2!} k_1(k_1 + 2Q) + \tau_2(k_2 - k_1) \right] c^2 + \dots$$

$$= 1 + 2.5c + 7.349c^2 + \dots$$

in which form it is more suitable for comparison with experiments.

5. The wall effect was investigated and it was found that the measured value of the viscosity of a suspension in a given instrument is modified by the presence of walls by the same amount as if along each wall there were a layer of a thickness  $D$  of viscosity of the pure liquid. Its theoretical thickness was found to be  $D = 1.301a$ , where  $a$  is the radius of the spheres.

The author is indebted to the Directors of Lever Brothers and Unilever Limited for their permission to publish this paper, and to Dr. F. Eirich and Mr. T. R. Lomer for valuable help.

#### REFERENCES

- (1) BAKER, F.: J. Chem. Soc. **103**, 1653 (1913).
- (2) BINGHAM, E. C.: *Fluidity and Plasticity*. McGraw-Hill Book Company, Inc., New York (1922).
- (3) BRUIN, H. DE: Rec. trav. chim. **61**, 863 (1942); Chem. Zentr. **1943**, 935.
- (4) BURGERS, J. M.: *Second Report on Viscosity and Plasticity*, p. 128. N. V. Noord-Hollandsche Uitgeversmaatschappij, Amsterdam (1938).
- (5) EILERS, H.: Kolloid-Z. **97**, 313 (1941).
- (6) EINSTEIN, A.: Ann. Physik [4] **19**, 286 (1906); **34**, 591 (1911).
- (7) EIRICH, F.: Reports on Progress in Physics **7**, 329 (1940).
- (8) EIRICH, F., AND MARK, H.: Papier-Fabr. **27**, 251 (1937).
- (9) EIRICH, F., AND SIMHA, R.: Sitzunzsh. d. Mathem. Naturw. Kl. (II b) **146**, 513 (1937).
- (10) GUTH, E., AND SIMHA, R.: Kolloid-Z. **74**, 266 (1936).
- (11) HESS, K.: Kolloid-Z. **27**, 1 (1920); **31**, 338 (1922).
- (12) JAEGER, F. M.: *Second Report on Viscosity and Plasticity*, p. 96. N. V. Noord-Hollandsche Uitgeversmaatschappij, Amsterdam (1938).
- (13) OSEEN, C. W.: *Hydrodynamik*. Leipzig (1927).
- (14) PETERLIN, A.: Z. Physik **111**, 232 (1938).
- (15) VAND, V.: Nature **155**, 364 (1945).

iodide in water is high, being 81.3 per cent by weight at 20°C., and increasing slightly with increasing temperature. The solution contained about 1 part of pure glycerol per 2 parts of water. The approximate composition of the solution was thus zinc iodide 82 per cent, water 12 per cent, and glycerol 6 per cent. The solution was always washed off the spheres by distilled water after a series of measurements was finished, and was reëvaporated back again to saturation. The concentration was then brought to an equilibrium, after cooling to room temperature, by frequent shaking; the supernatant saturated liquid was then separated from the crystals after standing overnight. Owing to the reëvaporation of the solutions, the exact chemical composition of the mixture used was not accurately known, and successive batches proved to have slightly different viscosities. This did not affect the accuracy of the measurements, as the viscosity of each zinc iodide solution remained unchanged throughout each series of measurements. The densities of all batches were practically that of the glass spheres. No sedimentation of the spheres was observed during the periods of time required for carrying on the measurement in Ostwald viscometers. However, as the suspension could be kept under measurement in a Couette apparatus for a long period of time, some changes in concentration due to sedimentation were detected which were allowed for.

After standing overnight, the majority of the spheres sank to the bottom of the viscometer but some spheres floated to the surface. This was a very sensitive test that the density of the liquid was very slightly less than the average density of the spheres. As the concentrations by volume of the suspensions in the viscometer were calculated from the weight of the spheres added into the viscometer, from the average density of the spheres, and from the volume of the viscometers which was accurately determined, the density of the liquid does not enter into the calculation, and does not need to be known accurately.

#### 4. OSTWALD VISCOMETERS

Two standard U-tube Ostwald viscometers No. 3 and No. 4, described by the British Standards Institution (2), were used. To supplement the measurements, a third viscometer of a Couette type was used. Details of the dimensions of the Ostwald viscometers are given below.

*Viscometer No. 3:* Radius of the capillary  $R_3 = 0.115$  cm. Volume  $V = 28.15$  cm.<sup>3</sup> up to the filling mark. Reduction formula, including kinetic-energy correction:  $\nu = 0.482t - 7/t$ , where  $\nu$  is the kinematic viscosity in centistokes and  $t$  is the time of efflux in seconds.

*Viscometer No. 4:* Radius of the capillary  $R_4 = 0.19$  cm. Volume  $V = 44.0$  cm.<sup>3</sup> Reduction formula including kinetic-energy correction:  $\nu = 1.946t - 11.4/t$ .

The viscometers were handled and calibrated as described in the British Standards Institution pamphlet, but the methods of protecting the liquid against moisture, filling the viscometer, driving the suspension in the upper bulb, stirring the suspension, and adjusting the level of the liquid were sufficiently novel to warrant description (see figure 1).

The viscometer, placed in a constant-temperature bath maintained at  $20^{\circ}\text{C} \pm 0.1^{\circ}$  has attached to its shorter tube (A) a mixing vessel (M) to which is attached a drying tube (D) very loosely packed with calcium chloride. The longer tube (H) of the viscometer is connected to the supply of compressed air by means of a drying tube (E) filled also with calcium chloride. Between the tube H and the vessel E is an opening (F), through which the stream of air passing slowly through the drying vessel E normally escapes into the atmosphere. If the opening F is

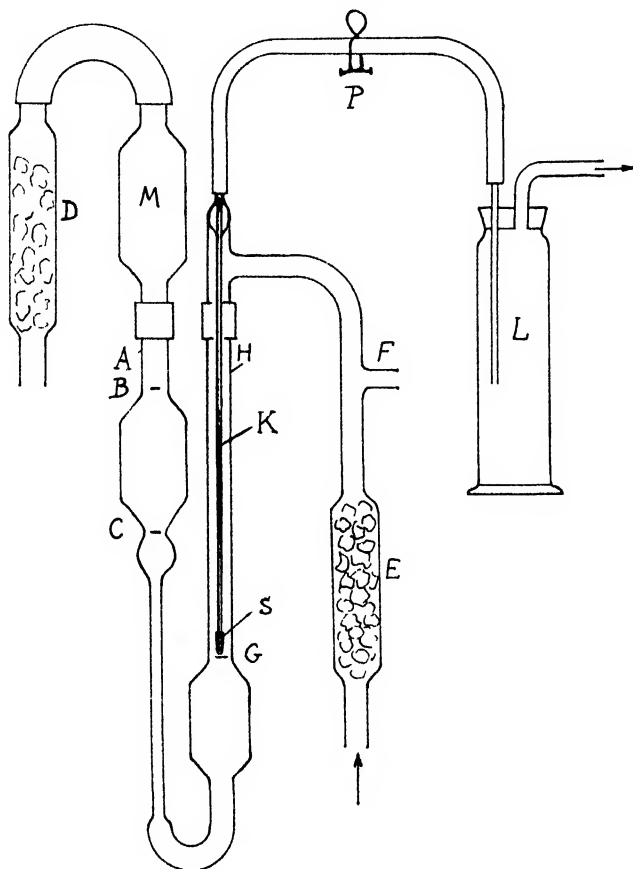


FIG. 1. Arrangement for protecting the liquid against moisture and for filling, stirring, and adjusting the level of the liquid in an Ostwald viscometer (not to scale).

closed by a finger, the air cannot escape and the resulting pressure drives the liquid from the lower bulb into the upper bulb of the viscometer, until the liquid reaches above the mark B. By releasing the finger from the opening F, the pressure is immediately relieved and the liquid streams through the capillary by gravity from the upper bulb of the viscometer past the marks B and C, when the time-measuring stopwatch is released and stopped, till it comes again to rest (level with the filling mark G). If it is desired to stir the content of the viscometer, then the vent F is kept closed as long as stirring is desired. The content of

the viscometer is thus driven into the mixing vessel M, and the air bubbling through the liquid causes a thorough agitation of the contents. The viscometer is then ready for a measurement. If there is an excess of liquid in the viscometer, the level can be brought accurately to the mark G, but not below, by means of a pipetting arrangement, which is permanently built in the apparatus. This consists of a fine capillary (K) reaching down exactly to the mark G. This capillary communicates by a narrow tube with a graduated measuring vessel (L), in which any excess of liquid can be drained off by opening a pinch clamp (P) and applying a vacuum to the vessel L. Over the end of the capillary K was slipped a small sieve (S) rolled out of a very fine copper gauze through which the spheres did not pass, so that only the zinc iodide solution was drained off, the amount of the added glass spheres remaining unaltered. The procedure of measurements was as follows: The viscometer was filled by removing the drying vessel D, inserting a long-stemmed funnel through the mixing vessel M, and pouring zinc iodide solution through the funnel. The drying vessel D was then replaced and the excess of the solution was pipetted off into the vessel L, until level with the mark G. The viscosity of the pure solution was then measured several times. Then a small weighed amount of glass spheres was added through the dry long-stemmed funnel and vessel M, the liquid driven in the vessel M and thoroughly stirred together with the spheres. The resulting suspension increased in volume by the volume of the spheres and the corresponding volume of the pure zinc iodide solution was then pipetted off, so that as a result the glass spheres were added to a constant volume, defined by the mark G. Several (usually twelve) determinations of the time of flow were then made, six determinations with stirring, six without stirring the content by bubbling, and mean values taken. A further small amount of glass spheres was then added, and the procedure repeated. The concentration was so increased from zero by increments of about 2-3 per cent, until a concentration was reached at which measurements of viscosity in a given instrument were no more practicable. In order to avoid cumulative errors on weighing, the spheres were added from a weighing bottle, and the bottle was weighed when full and after each addition of the spheres. The difference of the weight from its initial value when full indicated the amount of the spheres present at any time in the viscometer without any cumulative error of weighing.

##### 5. MEASUREMENTS FROM OSTWALD VISCOMETERS

The results of measurements are presented in the following tables. In tables 1 and 2 are given in the first, second, and third columns the uncorrected concentrations, times of efflux, and apparent viscosities of suspensions corrected only for kinetic energy. In the fourth column is given the corrected concentration in the capillary of the instrument.

In order to obtain this, the following corrections were applied: First the concentration was corrected for unequal drainage of spheres and liquid from the walls of the mixing vessel M and the top part of the viscometer, as some spheres remain clinging on the walls after emptying of the vessel, whereas the liquid tends to run down along the walls in the bulb of the viscometer, thus decreasing the real

TABLE 1

*Viscosity measurement on suspensions of glass spheres in standard Ostwald viscometer No. 3*

UNCORRECTED VOL- UME CONCENTRA- TION	TIME	OBSERVED KINE- MATIC VISCOSITY	CORRECTED CON- CENTRATION IN CAPILLARY	$1 - \eta_0/\eta$	CORRECTED FOR WALL EFFECT, $1 - \eta_0/\eta$
<i>per cent</i>	<i>seconds</i>	<i>centistokes</i>	<i>per cent</i>		
0	55.54	26.66	0	0.000	0
1.742*	57.93	27.82	1.942	0.042	0.0541
4.82	63.01	30.27	5.375	0.120	0.1545
9.00	69.70	33.50	10.035	0.205	0.2640
11.94	75.96	36.53	13.32	0.270	0.3478
16.92	87.48	42.07	18.87	0.366	0.4720
21.00	100.64	48.48	23.42	0.450	0.5790
25.95	118.87	57.29	28.92	0.535	0.6890
31.55	146.20	70.50	35.16	0.622	0.8010
36.30	186.20	89.76	40.45	0.703	0.9050
40.80	240.52	116.07	45.50	0.770	0.9920

\* Stirred and unstirred suspensions gave identical results.

TABLE 2

*Viscosity measurement on suspensions of glass spheres in standard Ostwald viscometer No. 4*

UNCORRECTED VOL- UME CONCENTRA- TION	TIME	OBSERVED KINE- MATIC VISCOSITY	CORRECTED CON- CENTRATION IN CAPILLARY	$1 - \eta_0/\eta$	CORRECTED FOR WALL EFFECT, $1 - \eta_0/\eta$
<i>per cent</i>	<i>seconds</i>	<i>centistokes</i>	<i>per cent</i>		
0	14.705	27.86	0	0.000	0.000
3.055	15.81	30.06	3.260	0.074	0.0861
6.11	17.16	32.74	6.52	0.148	0.1722
9.16	18.64	35.67	9.78	0.218	0.254
12.42	20.40	39.16	13.28	0.288	0.335
15.06	22.24	42.79	16.09	0.349	0.406
18.86	25.92	50.01	20.13	0.443	0.516
22.10	29.45	56.96	23.60	0.511	0.594
26.05	34.84	67.52	27.81	0.587	0.683
29.95	41.83	81.23	31.97	0.657	0.764
32.80	49.78	96.62	35.02	0.712	0.828
35.80 S*	61.01	118.61	38.22	0.7650	0.890
35.80 N	59.74	116.00	38.22	0.7598	0.884
39.08 S	70.22	136.5	41.70	0.7958	0.926
39.08 N	83.08	162.0	41.70	0.8280	0.963
42.75 S	90.4	176.0	45.65	0.8418	0.978
42.75 N	128.2	250.0	45.65	0.8885	1.032
46.80 S	133.5	260.0	50.00	0.8929	1.038
46.80 N	195.0	380.0	50.00	0.9266	1.078

\* Stirred, S; unstirred, N. Where not otherwise stated, stirred and unstirred suspensions gave identical results.

concentration in the bulb. The amount of the spheres left behind is approximately proportional to the concentration, and by direct counting of spheres clinging to selected areas in the mixer it was found that for 1 per cent suspension

there are, on the average, 72.6 spheres clinging per square centimeter of the wall. This was also checked by direct weighing of the spheres washed down from the walls. As the average volume of each sphere is  $1.15 \times 10^{-6}$  cm.<sup>3</sup>, the area of the mixer and viscometer covered by the spheres was 84.3 cm.<sup>2</sup> for viscometer No. 3 and 94.3 cm.<sup>2</sup> for viscometer No. 4, and as the volume of viscometer No. 3 is 28.15 cm.<sup>3</sup> and the volume of viscometer No. 4 is 44.0 cm.<sup>3</sup>, the concentration is to be multiplied by 0.9750 for viscometer No. 3 and by 0.9821 for viscometer No. 4.

The second correction to be applied is that of the general increase of concentration in a vessel filled with spheres due to the absence of sphere centers in a layer along the walls of a thickness equal to the radius of spheres. The concentration is to be multiplied by  $V/(V - Sa)$ , where  $V$  is the average volume of the suspension in the upper bulb of the viscometer,  $S$  is the average surface of the upper bulb, and  $a$  is the radius of the spheres. Both volume and surface occupied by the suspension vary as the viscometer is emptying. By assuming that the average volume and surface is that when the upper bulb is half-filled, we obtain:

$$\text{For viscometer No. 3: } V = 8 \text{ cm.}^3, S = 20.7 \text{ cm.}^2$$

$$\text{For viscometer No. 4: } V = 13 \text{ cm.}^3, S = 28.3 \text{ cm.}^2$$

It is thus necessary to multiply further the concentration by 1.0171 for viscometer No. 3 and by 1.0144 for viscometer No. 4.

The third correction to be applied is that due to further increase of concentration of the suspension entering the capillary, owing to the radius of the spheres being non-negligible compared with the radius of the capillary. The concentration is to be further multiplied by  $1/(1 - a/R)^2$ . As the radius of the capillary of the viscometer No. 3 is  $R_3 = 0.115$  cm., and of the viscometer No. 4 is  $R_4 = 0.19$  cm., we obtain that it is necessary to multiply further the concentration entering the capillary by 1.1234 for viscometer No. 3 and by 1.0721 for viscometer No. 4.

Carrying all the three multiplications we obtain finally that the concentrations obtained by weighing should be multiplied for viscometer No. 3 by 1.1140 and for viscometer No. 4 by 1.0680, in order to obtain the concentration in the capillary on which the viscosity measurements are actually performed. The corrected concentrations are given in the fourth columns of tables 1 and 2. In the fifth columns are given the values of  $1 - \eta_0/\eta_3$  and  $1 - \eta_0/\eta_4$ , where  $\eta_0$  is the viscosity of the pure zinc iodide solution, and  $\eta_3$  and  $\eta_4$  are the viscosities observed in the viscometers No. 3 and No. 4 uncorrected for wall effect. It is permissible to replace ratios of kinematic viscosities by the ratios of dynamic viscosities if the suspension does not change density on increase of concentration.

## 6. COUETTE VISCOMETER

In order to provide an independent check on the results obtained with the capillary instruments it was also decided to make measurements in a Couette apparatus. These measurements, however, require considerably longer time



than the measurements with the Ostwald viscometers, and there is a danger that they might be more influenced by various errors; also, the readings of deflections are not as accurate as the readings of time of flow. On the other hand, the wall effects are much reduced especially at higher concentrations, as the dimensions of the Couette apparatus are considerably larger than the dimensions of the capillary. Details of the dimensions of the Couette viscometer were: radius of inside cylinder  $R_1 = 0.625$  cm.; length of inside cylinder = 2.580 cm.; radius of outside cylinder  $R_2 = 1.800$  cm.; volume  $V = 50$  cm.<sup>3</sup>, approximately. The reduction formula is  $\eta = 0.987\alpha/\omega$  in poises, where  $\alpha$  is the deflection of the cylinder in degrees and  $\omega$  is the velocity of rotation radians per second (calibrated by pure glycerol).

The design of the instrument differed slightly from the conventional instruments. As it was important that the suspensions of spheres be well stirred in order to eliminate errors due to sedimentation, it was decided to build an instrument with a fixed outer cylinder and a rotating inner cylinder, so that the outer cylinder can be connected to a supply of dried compressed air which serves for stirring purposes. Incidentally, it was found that this arrangement is more mechanically stable than if the outer cylinder is rotating, so that the stabilizing bearings centering the inner cylinder are not necessary; this eliminates troublesome friction and so increases the accuracy of measurements. The viscometer arrangement is shown in figure 2. The outer cylinder consisted of a glass vessel (A) to the bottom of which was attached a glass tube (H) connecting it through the drying vessel (E) to a supply of compressed air. This air normally escaped through the opening F, but if this was closed by a finger, the air entered the vessel A and mixed the contents by bubbling. The top of the vessel A was stoppered by a stopper, bearing a long narrow glass tube (G) and a stoppered filling funnel (U), both reaching above the level of the constant-temperature bath maintained at  $20^\circ\text{C} \pm 0.1^\circ$ . The whole vessel A was immersed in the bath, a procedure which ensured more accurate temperature control. The inner cylinder (C') was suspended from a pulley (P) by means of a fine wire suspension (S) which measured the torque exercised on the cylinder by reading the position of a dial (D) against the pointer Q. Both the dial and the pointer rotate, the dial D being rigidly connected by means of a long rod (L) with the inner cylinder (C'), the pointer Q being rigidly connected with the pulley P by means of a hollow shaft (T) which runs in bearings (B). If the speeds of rotation are not excessive, the reading of the pointer Q against the rotating dial D is not inconvenient. The rod L passes down the glass tube G without touching it, so that the cylinder C is suspended on the wire S quite freely. The tube G prevents any moist air entering the apparatus, but it allows the excess air to escape. The pulley P is driven by a fine thread from a variable-speed drive connected to a synchronous motor, so that altogether twenty different speeds are available, ranging from 0.0344 to 8.750 radians per second, as measured on the pulley P by means of a stopwatch.

As there was no accurate mark which could serve as an indication of the volume of the instrument, a different method of preparing the required concentrations

was adopted, i.e., the instrument was filled by a known volume of the zinc iodide solution, and then small amounts of spheres successively added as required, through the filling funnel U. The zinc iodide solution was not withdrawn from the instrument after the addition of the spheres. The concentrations were then calculated on a basis of a constant volume of the liquid phase.

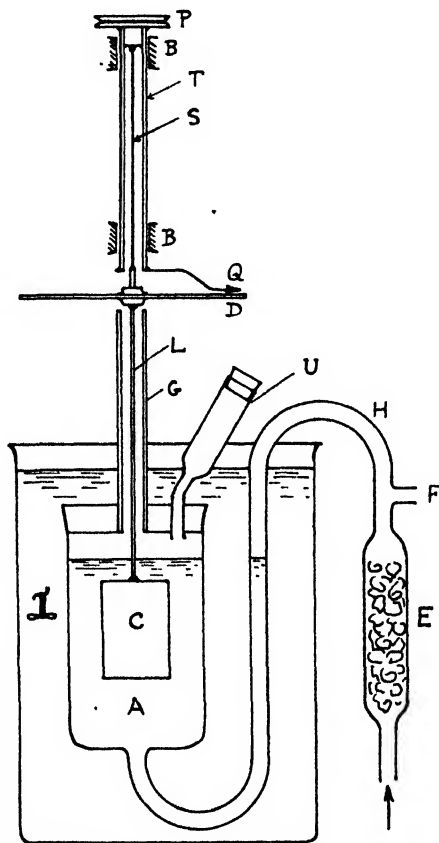


FIG. 2. Couette viscometer with an air stirring arrangement (not to scale)

#### 7. MEASUREMENTS FROM COUETTE VISCOMETER

The results of measurements are presented in table 3. In the first column is given the uncorrected volume concentration obtained by weighing. In the second column is given the observed viscosity in poises. Below 40 per cent the same values were obtained for stirred as for unstirred suspensions. Above 40 per cent two values of viscosity are given: the values of concentration followed by a letter N refer to unstirred suspensions, the values followed by a letter S refer to suspensions immediately after air stirring. It was soon found that the stirring has a profound influence on the viscosity at concentrations above 40 per cent. The influence could be easily studied, as it was not necessary to stop

the rotation of the instrument in order to stir its contents. The viscosity after stirring was greater than normal, the deflection decreasing with time exponentially to its normal value. After reaching the minimum, the deflection started again to increase slowly owing to sedimentation. As this increase was linear with time, the measurements could be corrected for this component. It was usual to plot the logarithm of the deflection corresponding to the unstirred suspension, corrected for sedimentation, against logarithm of the velocity of angular rotation of the cylinder. For a given concentration, a straight line resulted whose slope below concentrations of 47 per cent was unity, but above this concentration the slope appears to increase with increased concentration, i.e., the

TABLE 3

*Viscosity measurement on suspensions of glass spheres in a Couette viscometer*

Zinc iodide solution; viscosity = 69.8 centipoises

UNCORRECTED VOLUME CONCENTRATION	OBSERVED VISCOSITY	CORRECTED CONCENTRATION	$1 - \eta_0/\eta_c$	CORRECTED $1 - \eta_0/\eta$
<i>per cent</i>	<i>poises</i>	<i>per cent</i>		
35.0	3.59	35.5	0.8059	0.827
36.6	4.23	37.1	0.835	0.857
37.8	5.05	38.3	0.862	0.886
39.7 N*	5.78	40.2	0.879	0.904
39.7 S	5.92	40.2	0.882	0.906
44.5 N	8.50	45.1	0.918	0.944
44.5 S	11.00	45.1	0.9365	0.962
47.0 N	8.77	47.6	0.9205	0.946
47.0 S	16.20	47.6	0.956	0.982
49.3 N	13.44	50.0	0.9480	0.974
49.3 S	26.01	50.0	0.972	0.998
51.3 N	24.12	52.0	0.9710	0.997
51.3 S	43.00	52.0	0.984	1.011
53.4 N	25.75	54.1	0.9728	0.998
53.4 S	58.00	54.1	0.988	1.015

\* Stirred, S; unstirred, N. Where not otherwise stated, stirred and unstirred suspensions gave identical results.

suspension starts behaving as a non-Newtonian liquid. Above concentrations of 50 per cent, the increase of deflection with concentration is comparatively small. This was due to slipping of the cylinder in the suspension. The corrections for slipping then appear to be larger than the values to be measured, hence measurements on suspensions having concentrations above 53.4 per cent have been discontinued, and their behavior observed qualitatively only. In order to measure viscosities above this concentration, either a much larger instrument or much smaller glass spheres would be necessary.

On increasing the concentration further, it was observed that the suspensions acquire a definite yield value, i.e., retain the shape to which they have been worked, and the rotating cylinder simply makes a hole in the suspension, in which it freely rotates and the deflection drops to zero. On further increase of concen-

tration the suspension finally draws air into the vacant interstices between the spheres, and the system is now composed of three components: glass spheres, air bubbles, and liquid. The behavior of such a system is, of course, more complicated owing to the surface-tension forces at the air-liquid interfaces which give to the system a considerable rigidity. At the end of the concentration series we have finally dry spheres, which are in reality a two-component system of glass and air. Their behavior is determined by the coefficient of friction of glass on glass in air.

The following corrections were applied: The concentration increase due to the presence of the walls was calculated from the average volume of the viscometer and from the total surface of the walls. Both quantities varied slightly as the concentration was increased, but this change was neglected and it was taken for the average volume  $V = 50 \text{ cm.}^3$  and for the total surfaces  $S = 100 \text{ cm.}^2$ , which gives as a result that in order to obtain the corrected concentration, the concentration obtained by weighing is to be multiplied by 1.013. The corrected concentration is given in the third column of table 3. In the fourth column are given the values of  $1 - \eta_0/\eta_c$ , where  $\eta_0 = 0.698$  poise is the viscosity of the solution used, and  $\eta_c$  is the viscosity of the suspension as observed.

#### 8. EVALUATION OF THE WALL EFFECT

By comparing the results obtained from different instruments, it is evident that the uncorrected values of the relative viscosities do not agree with each other, and that the application of the corrections for the wall effect is necessary.

According to theory, the wall effect can be accounted for by assuming that along each wall of the instrument there is a layer of a thickness  $D$  which has a viscosity of a pure liquid.

Solving the usual equations for a flow of liquid through a capillary and for a Couette apparatus under the assumption of a layer at the wall of lower viscosity, we obtain

$$\eta_0/\eta - 1 = H_x(\eta_0/\eta_x - 1) \quad (3)$$

where  $\eta_0$  is the viscosity of the pure liquid in the layer at the wall,  $\eta_x$  is the "viscosity" observed in the instrument  $x$ ,  $\eta$  is the true viscosity of the suspension, and  $H_x$  is a correction constant for slip in the instrument  $x$ , which for a capillary of a radius  $R_x$  is

$$H_x = (1 - D/R_x)^{-4} \quad (4)$$

and for a Couette apparatus

$$H_x = \frac{(1 + D/R_1)^2(1 - D/R_2)^2}{(1 - 2D)/(R_2 - R_1)} \quad (5)$$

where  $D$  is the thickness of the layer of viscosity  $\eta_0$ ,  $R_1$  is the radius of the inner cylinder, and  $R_2$  is the radius of the outer cylinder of the Couette apparatus.

If  $D$  is known, then for each apparatus it is possible to calculate the slip constant  $H$ , and then the true viscosity  $\eta$  of the suspension can be calculated from

the viscosity observed by means of equation 3. If the thickness of the layer  $D$  of the lower viscosity is not known, it is possible to determine it from measurements in two or more viscometers of different dimensions.

From theoretical consideration it was found that  $D = 1.301a$ . However, it was thought better to calculate the thickness  $D$  of the layer of low viscosity from the measurements, and to compare it with its theoretical value.

The following procedure was adopted: The values of  $1 - \eta_0/\eta_x$  of the three instruments were plotted against the *corrected* concentrations. Smooth curves were drawn through the points, and the values corresponding to concentrations of 5 per cent, 10 per cent, etc. given in the first column of table 4 were read off the curves and tabulated in the second, third, and fourth columns.

TABLE 4  
*Interpolated values of stirred suspensions*

CORRECTED CONCENTRATION	$1 - \eta_0/\eta_1$	$1 - \eta_0/\eta_2$	$1 - \eta_0/\eta_c$	$\Pi_3/\Pi_1$	$\Pi_3/\Pi_c$	$\Pi_4/\Pi_c$
<i>per cent</i>						
5	0 105	0 114		1.085		
10	0 205	0 223		1 088		
15	0 300	0 328		1 092		
20	0 392	0.438		1.118		
25	0 475	0 534		1 122		
30	0 552	0 622		1 126		
35	0 622	0 710	0 794	1.140	1.275	1 118
40	0 700	0 800	0 881	1.142	1 261	1.101
45	0 764	0 875	0 935	1.145	1 223	1 071

For a given concentration it is possible to calculate the ratios  $H_x/H_y$  from the equation, following from equation 3:

$$H_x/H_y = \frac{1 - \eta_0/\eta_y}{1 - \eta_0/\eta_x} \quad (6)$$

The three sets of values of  $H_x/H_y$  are given in the fifth, sixth, and seventh columns of table 4. From these values the thickness  $D$  of the layer can be calculated from the following equations:

For a comparison of two Ostwald viscometers:

$$(H_3/H_4)^{1/4} = (1 - D/R_4)/(1 - D/R_3) \quad (7)$$

obtained from equation 4.

For a comparison of an Ostwald and a Couette viscometer (approximate formula):

$$D = \frac{1 - (H_x/H_c)^{1/4}}{1/2(R_2 - R_1) + (R_2 - R_1)/2R_1R_2 - (H_x/H_c)^{1/4}/R_x} \quad (8)$$

The resulting fifteen values of the thickness of the layer  $D$  are given in table 5.

Taking all these values as having the same weight, their mean value and probable error of the arithmetic mean was found to be  $D = 7.04 \times 10^{-3} \pm 0.27 \times 10^{-3}$  cm. If we compare this with the radius of the spheres  $a = 6.5 \times 10^{-3}$  cm., we obtain  $D = 1.08a$ , which is slightly less than the theoretical value of  $D = 1.301a$ . Remembering all the approximations introduced in the theoretical calculations, the agreement of the theory with the experiment seems to be thus quite satisfactory.

#### 9. DISCUSSION OF THE EXPERIMENTAL RESULTS

Having found the value of  $D$  it is now possible to correct the viscosities for the wall effect. The experimental value of  $D = 7.04 \times 10^{-3}$  cm. was used for the reduction. The values of  $H_x$  were now calculated for the three instruments using equations 4 and 5:  $H_3 = 1.288$ ,  $H_4 = 1.163$ , and  $H_c = 1.027$ . These values were used for calculating the corrected  $1 - \eta_0/\eta$  as given in the last

TABLE 5  
*Calculated values of  $D$  from  $H_x/H_y$*

CORRECTED CONCENTRATION	$D$ FROM $H_3/H_4$	$D$ FROM $H_3/H_c$	$D$ FROM $H_4/H_c$
<i>per cent</i>			
5	$5.69 \times 10^{-3}$		
10	$5.87 \times 10^{-3}$		
15	$6.11 \times 10^{-3}$		
20	$7.69 \times 10^{-3}$		
25	$7.92 \times 10^{-3}$		
30	$8.14 \times 10^{-3}$		
35	$8.94 \times 10^{-3}$	$7.55 \times 10^{-3}$	$6.37 \times 10^{-3}$
40	$9.07 \times 10^{-3}$	$7.20 \times 10^{-3}$	$5.50 \times 10^{-3}$
45	$9.20 \times 10^{-3}$	$5.30 \times 10^{-3}$	$3.92 \times 10^{-3}$
Mean value of $D = 7.04 \times 10^{-3} \pm 0.27 \times 10^{-3}$ cm.			

columns of tables 1, 2, and 3. By plotting  $1 - \eta_0/\eta$  against concentration, it can be demonstrated that all three sets of viscosities closely agree with each other up to concentrations of 45 per cent, i.e., nearly over the whole range of concentrations over which the suspensions behave as true liquids. It is now possible to read off the values of viscosities for various concentrations from the curve, and these for values increasing by 5 per cent are given in table 6, which represents the final result of the measurements in the three instruments. In the first column is given the concentration, in the second column the relative fluidity  $1/\eta_r$  of the suspensions, in the third column its reciprocal, or relative viscosity, and in the fourth column the value of  $(1 - \eta_0/\eta)/c$ , the limit of which towards zero concentrations should be 2.5 according to theory.

Now we are in a position to express the above results as an empirical power series, as in this form we shall be able to compare the theoretical results with the experiment. By analyzing the fourth column of table 6, it is easy to derive that it satisfies the following power series, as can be seen in the last column of table 6:

$$(1 - \eta_0/\eta)/c = 2.5 + 0.92c - 4.0c^2 \quad (9)$$

which can be written as:

$$\eta_r = 1 + 2.5c + 7.17c^2 + 16.2c^3 + \dots \quad (10)$$

The accuracy of the coefficients of the higher-power terms, of course, rapidly decreases as the power is increased, and their numerical values are also influenced by the accuracy of the corrections applied to the measurements.

The experimental results will now be compared with the theory. This can be most conveniently done by comparing the second-power terms of equation 2 with equation 10. The theoretical formula 2, which takes into account the colli-

TABLE 6

*Final values of viscosities and fluidities of suspensions of spherical particles as a function of concentration*

Averaged from the corrected results of the three viscometers

CONCENTRATION <i>c</i>	RELATIVE FLUIDITY $1/\eta_r$	RELATIVE VISCOSITY $\eta_r$	$\frac{1 - \eta_0/\eta}{c}$ (OBSERVED)	$\frac{1 - \eta_0/\eta}{c}$ (CALCULATED FROM EQUATION 9)
<i>per cent</i>				
0	1.000	1.000	(2.50)	2.500
5	0.873	1.145	2.54	2.536
10	0.745	1.342	2.55	2.552
15	0.617	1.621	2.55	2.548
20	0.494	2.024	2.53	2.524
25	0.380	2.632	2.48	2.480
30	0.275	3.636	2.41	2.416
35	0.180	5.556	2.34	2.332
40 N	0.095	10.53	2.26	2.228
40 S	0.085	11.77	2.28	2.228
45 N	0.055	18.18	2.10	2.104
45 S	0.030	33.33	2.16	2.104
50 N	0.030	33.33	1.94	1.960
50 S	0.005	200.00	1.99	1.960

sions, gives a value 7.349, which is only about 2.5 per cent more than the experimental value of 7.17. This is well within experimental error.

We can thus conclude that the agreement of the theory with experiment on rigid spheres is very good up to the second-power terms, i.e., as far as the theory was developed.

#### SUMMARY

The viscosity of suspensions of rigid spheres was measured in a range of concentrations 0-50 per cent. Glass spheres having an average radius of 0.0065 cm. suspended in zinc iodide solution were used, and the measurements were corrected for wall effects. The results were compared with a theoretical formula; the agreement is satisfactory.

The author is indebted to the Directors of Lever Brothers and Unilever Limited for their permission to publish this paper, to Dr. F. Eirich for the loan of the glass spheres, and to Mr. T. R. Lomer for help with the measurements.

## REFERENCES

- (1) BANCELIN, M.: *Compt. rend.* **152**, 1382 (1911).
- (2) British Standards Institution, No. 188 (1937).
- (3) EIRICH, F., BUNZL, M., AND MARGARETHA, H.: *Kolloid-Z.* **74**, 276 (1936).
- (4) ODÉN, S.: *Nova Acta Regiae Soc. Sci. Upsaliensis* [4] **3**, No. 4 (1913).
- (5) VAND, V.: *J. Phys. Colloid Chem.* **52**, 277 (1948).

## VISCOSITY OF SOLUTIONS AND SUSPENSIONS. III

## THEORETICAL INTERPRETATION OF VISCOSITY OF SUCROSE SOLUTIONS

VLADIMIR VAND

*Research Laboratories, Lever Brothers and Unilever Limited, Port Sunlight, Cheshire, England*

*Received June 24, 1947*

## 1. INTRODUCTION

In a previous paper (7) the author derived a theoretical formula for the relative viscosity  $\eta_r$  of a suspension believed to be valid up to second-power terms:

$$\log_e \eta_r = \frac{k_1 c + r_2(k_2 - k_1)c^2 + \cdots}{1 - Qc} \quad (1)$$

where  $c$  is the volume concentration of the particles of the suspension. The following values of the constants were derived from theory for rigid spheres without mutual forces and without Brownian movement:

Shape factor of single spheres	$k_1 = 2.5$
Shape factor of collision doublets.....	$k_2 = 3.175$
Collision time constant.....	$r_2 = 4$
Hydrodynamic interaction constant.....	$Q = 0.609$

The object of this paper is to apply equation 1 after certain modifications to solutions of simpler molecules such as those of sucrose.

According to Jaeger (4), Stokes's resistance law holds for small ions in water, which means that the hydrodynamic laws are still valid with fair approximation for molecular dimensions. It is thus to be expected that for solutions of larger molecules the numerical values of the constants in equation 1 would be approximately the same as for large particles, with the exception of the collision constant  $r_2$ , which probably is modified by the presence of strong Brownian motion. The magnitude of  $r_2$  indicates the proportion of time spent by particles in a collision, and this time will probably be (a) shortened for particles of molecular size due to Brownian motion, (b) shortened for particles with repulsive forces,



and (c) lengthened for particles with attractive forces. If the particles are not spherical, the shape factors would be modified according to the average shape of single molecules, collision doublets, triplets etc. The values of the shape factor  $k_1$  for elliptical and rod-like particles for weak and strong Brownian motion have been calculated (see, for example, Burgers (2)), and the shape factors of higher orders can be estimated. Finally, the solvation of the molecules and the variation of solvation with concentration is to be taken into account, and will be discussed in more detail.

## 2. THEORY OF HYDRATION

In equation 1  $c$  is the volume concentration of the suspended particles, so that if the particles are solvated, the volume of the solvation envelopes is to be included in  $c$ . Thus

$$c = hs \quad (2)$$

where  $s$  is the concentration by volume of the solute without hydration envelopes and  $h$  is the hydration constant, which is unity if there is no hydration. This constant depends in general on concentration and temperature.

It is evident that in order to apply equation 1 to solutions, viscosity must be known as a function of the volume concentration  $c$ . However, the volume concentration is not directly accessible to measurement; the only measurable quantities are the weight concentration ( $W$ ) of the solute, the density ( $D$ ) of the solution, and the density ( $D_0$ ) of the pure solvent. If the density ( $D_H$ ) of the hydration envelope differs from  $D_0$ , there is a change of volume on mixing. From simple considerations of volumes before and after mixing, the following relations are obtained:

$$D_s s = x \quad (3)$$

$$D_0 + (h - 1) \cdot (D_0 - D_H) = D_s y \quad (4)$$

where  $D_s$  is the density of each particle of the solute (hydration envelope excluded), which can be assumed to be independent of  $W$ , and where

$$x = DW \quad (5)$$

$$y = 1 - (D - D_0)/DW \quad (6)$$

are both observable quantities.

The hydration envelope can be regarded as consisting of water molecules held to the molecule of the solute by certain binding forces, as a result of which an activation energy  $E$  is to be overcome by the molecules leaving the envelope. In equilibrium, the average number of molecules entering the envelope must be equal to the number leaving the envelope. The number of molecules entering would be proportional to the following factors: (a) the surface area of the envelope, which is approximately proportional to  $h^{2/3}$  (as  $h$  is proportional to the volume of the hydrated particles); (b) the concentration of the water molecules round the envelope, which is proportional to  $(1 - hs)$  and which also varies

slightly with temperature; (c) the velocity of the incoming molecules, which would depend on the absolute temperature  $T$ . For a perfect gas it would be proportional to  $T^{1/2}$ , but for liquids we must consider also other factors, such as variation of free volume etc., so that we may summarize the influence of temperature in a term  $T^m$ , where  $m = \frac{1}{2}$  for a perfect gas but may have a different value for liquids.

The number of molecules leaving the envelope would be proportional to: (a) the number of water molecules in the hydration envelope, proportional to  $(h - 1)$ ; (b) the relative number of water molecules, the thermal energy of which is greater than the activation energy  $E$ , which is necessary for leaving the envelope. This is proportional to  $\exp(-E/kT)$ . The dependence of  $h$  on  $s$  and  $T$  is thus:

$$h^{2/3}(1 - hs)T^m = K(h - 1) \exp(-E/kT) \quad (7)$$

where  $K$  is a proportionality constant.

If  $T$  is constant,

$$\frac{h^{2/3}(1 - hs)}{h - 1} = \frac{h_0^{2/3}}{h_0 - 1} \quad (8)$$

where  $h_0$  is the hydration at infinite dilution. Developing equation 8 into a power series, we obtain:

$$h = h_0 - \frac{3h_0^2(h_0 - 1)}{h_0 + 2} s + \dots \quad (9)$$

Substituting  $x$  for  $s$  from equation 3 and substituting equation 9 into equation 2, we obtain

$$c = \frac{h_0}{D_s} x - \frac{3h_0^2(h_0 - 1)}{D_s^2(h_0 + 2)} x^2 + \dots \quad (10)$$

which can be substituted into equation 1.

For practical calculations it is better to rearrange equation 1 in the following form:

$$\frac{x}{\log_e \eta_r} = q_0 + q_1 x + q_2 x^2 + \dots \quad (11)$$

as a plot of  $x/\log_e \eta_r$  against  $x$  is usually nearly a straight line, so that determination of terms  $q_0$ ,  $q_1$ , etc. does not present difficulties. The following relations are then valid:

$$q_0 = D_s/h_0 k_1 \quad (12)$$

$$k_1 q_1 = \frac{3(h_0 - 1)}{h_0(h_0 + 2)} - \frac{r_2(k_2 - k_1)}{k_1} - Q \quad (13)$$

etc. The numerical values of these terms can then be compared with theory. For this purpose, the density of the solute particles,  $D_s$ , is to be known. It is to be expected that its value is of the same magnitude as the density of the pure

solute in the solid state. It can be, however, obtained from considering the variation of  $y$  with  $x$ .

Assuming the density  $D_H$  of the hydration envelope to be independent of  $h$  and differentiating equation 4, we obtain:

$$D_s \cdot (dy/dh) = D_0 - D_H \quad (14)$$

As

$$\frac{dy}{dh} = \left( \frac{dy}{dx} \right) \cdot \left( \frac{dx}{ds} \right) \cdot \left( \frac{ds}{dh} \right)$$

and as for  $x = 0$ , using equations 3 and 9,

$$\left( \frac{dy}{dx} \right)_0 = y'_0, \quad \left( \frac{dx}{ds} \right)_0 = D_s, \quad \left( \frac{ds}{dh} \right)_0 = \frac{h_0 + 2}{3h_0^2(1 - h_0)}$$

then, substituting in equation 14, we obtain

$$D_s^2 y'_0 \frac{h_0 + 2}{3h_0^2(1 - h_0)} = D_0 - D_H \quad (15)$$

Substituting equation 15 in equation 4, we obtain

$$D_s^2 \frac{h_0 + 2}{3h_0^2} y'_0 + D_s y_0 - D_0 = 0 \quad (16)$$

where  $y'_0$  and  $y_0$  are values of  $y$  and its first derivative for  $x = 0$ , which can be determined from the experimental measurements of the densities  $D$  at different weight concentrations  $W$ , and which thus can be regarded as known.

By substituting for  $h_0$  from equation 12 we finally obtain an equation for  $D_s$ :

$$D_s = \frac{3D_0 - 2y'_0 k_1^2 q_0^2}{3y_0 + y'_0 k_1 q_0} \quad (17)$$

Once  $D_s$  is calculated from equation 17, it can be used to calculate  $h_0$  from equation 12, provided the value of  $k_1$  can be assumed to be known from theory. It is then valuable to consider the variation of  $h_0$  with temperature, as this gives the value of the activation energy  $E$  from equation 7. The value of  $D_H$  can be calculated from equation 15. Finally,  $r_2$  can be calculated from equation 13, provided  $Q_1$ ,  $k_1$ , and  $k_2$  are assumed to be known from theory.

The viscosity data combined with the density data thus give us an important insight into the mechanism of the hydration.

### 3. DISCUSSION OF THE VISCOSITY OF SUGAR SOLUTIONS

In order to provide a practical example of application of the results obtained in previous paragraphs, aqueous sucrose solutions will be discussed, as they provide a system the viscosity and density of which are very well known.

Sucrose has a formula  $C_{12}H_{22}O_{11}$ , containing one pyranose and one furanose ring (Fleury and Courtois (3)). The space occupied by a molecule can be estimated from x-ray crystal data: the unit cell is monoclinic with  $a = 10.65 \text{ \AA}$ ,

$b = 8.70 \text{ \AA}$ ,  $c = 8.00 \text{ \AA}$ ,  $\beta = 105^\circ 44'$ , containing two molecules per unit cell; the calculated density is 1.57. Assuming that the long axis of the molecule is along the  $a$  edge, the cross-section of the space occupied by one molecule is  $33.6 \text{ \AA}^2$ , whereas the length is  $10.65 \text{ \AA}$ . This can be fitted by a rotation ellipsoid of the axial ratio of  $a/b = 1.84$ . The shape factor of such an ellipsoid is  $k_1 = 2.57$  (Burgers (2)). Its variation on hydration can be neglected.

The calculations are given in tables 1 and 2, together with all the necessary measurements. The temperature is given in the first column of the tables. In the second column of table 1 are given concentrations by weight,  $W$ , at which the viscosities were measured. The viscosities were taken from measurements of Bingham and Jackson (1) (kinetic-energy corrections applied), and are given in the third column. One value for  $W = 0.2$  at  $100^\circ\text{C}$ . was interpolated. In the fourth column are given the densities  $D$  of the solutions, taken from the tables of Landolt-Börnstein (5). As these data are not given for  $80^\circ\text{C}$ . and  $100^\circ\text{C}$ ., the values were extrapolated from the densities at lower temperatures by assuming constant second differences, which is sufficient for our purposes. The results derived from these figures are however, less reliable.

From the densities,  $x$  and  $y$  were calculated and  $x/\log_e \eta_r$  tabulated in the last column. From the graph of  $x$  as a function of  $y$ , the values of  $y_0$  and  $y'_0$  were obtained and tabulated in table 2; the graph proved to be nearly a straight line, indicating thus approximate constancy of  $y'$ . Then the values of  $D_s$  were calculated from equation 17, using  $q_0$  obtained by analyzing the values of  $x/\log_e \eta_r$  as a function of  $x$ . It should be noted that the values of  $D_s$  so obtained are very near to the density of 1.57 of solid sugar, which might be useful to bear in mind for systems the density data of which are insufficiently known.

Assuming now  $k_1 = 2.57$ , the values of  $h_0$  were calculated from equation 12. It should be noted that they decrease rapidly with increasing temperature. By assuming  $Q = 0.6$ ,  $k_2 = 3.175$  to be approximately the same as for rigid spheres for lack of better values, the value of  $r_z$  was calculated from equation 13. Finally,  $D_H$  was calculated from equation 14. It is convenient to express the amount of hydration as an average number  $H$  of water molecules present in a hydration envelope of one molecule of sucrose. It is given by a relation

$$H = (h - 1)M_s D_H / M_H D_s$$

where  $M_s = 342$  is the molecular weight of sucrose and  $M_H = 18$  is the molecular weight of water. Substituting values  $h_0$  at infinite dilution, corresponding values of  $H_0$  were calculated and are given in the last column of table 2.

The next step was to analyze the values of  $h_0$  as a function of temperature, in order to determine the activation energy  $E$  of equation 7. As the value of  $m$  is not known and as this term has very little influence on  $E$ , it was assumed that  $m$  is zero, and the values of  $\log [h_0^{2/3}/(h_0 - 1)]$  were plotted against  $1/T$ . It was found that an approximately linear relation holds, the values obeying an equation:

$$\log_e \left( \frac{h_0^{2/3}}{h_0 - 1} \right) = 5.26 - \frac{1306}{T} \quad (18)$$

TABLE 1

*Application of the theory to aqueous sucrose solutions*

TEMPERATURE	$H'$	$\eta_r$	$D$	$z$	$\frac{z}{\log_e \eta_r}$
°C.					
0	0	1	0.99987	0	
0	0.2	2.127	1.08546	0.2171	0.2877
0	0.4	8.258	1.18349	0.4734	0.2242
0	0.6	133.1	1.29560	0.7774	0.1589
20	0	1	0.99823	0	
20	0.2	1.951	1.08096	0.2162	0.3235
20	0.4	6.171	1.17645	0.4706	0.2586
20	0.6	56.50	1.28646	0.7719	0.1913
40	0	1	0.99232	0	
40	0.2	1.822	1.07366	0.2147	0.3579
40	0.4	4.984	1.16759	0.4670	0.2907
40	0.6	32.57	1.27615	0.7657	0.2198
60	0	1	0.98330	0	
60	0.2	1.718	1.06358	0.2127	0.3929
60	0.4	4.215	1.15693	0.4628	0.3217
60	0.6	20.92	1.26468	0.7588	0.2496
80	0	1	0.97183	0	
80	0.2	1.659	1.0506*	0.2101	0.4152
80	0.4	3.752	1.1445*	0.4578	0.3162
80	0.6	15.19	1.2520*	0.7512	0.2761
100	0	1	0.95838	0	
100	0.2	1.610†	1.0350*	0.2070	0.4349
100	0.4	3.405	1.1302*	0.4521	0.3690
100	0.6	11.83	1.2381*	0.7428	0.3006

\* Extrapolated.

† Interpolated.

TABLE 2

*Calculated constants of aqueous sucrose solutions*

 Assumed:  $k_1 = 2.57$ ,  $Q = 0.6$ ,  $k_2 = 3.175$ 

TEMPERATURE	$y_0$	$v_0'$	$D_s$	$q_0$	$-q_1$	$q_2$	$h_0$	$r_1$	$D_H$	$H_0$
°C.										
0	0.6000	0.0250	1.624	0.347	0.288	0.059	1.818	2.098	1.102	10.54
20	0.6134	0.0175	1.594	0.384	0.295	0.057	1.613	2.007	1.086	7.93
40	0.6174	0.0160	1.572	0.420	0.302	0.052	1.456	1.902	1.092	6.02
60	0.6195	0.0130	1.555	0.461	0.336	0.076	1.312	2.033	1.094	4.17
80	0.622*	0.008*	1.541	0.481	0.327	0.073	1.247	1.803	1.055	3.21
100	0.625*	0.004*	1.522	0.497	0.311	0.063	1.193	1.489	1.009	2.43

\* Extrapolated.

From this it follows that  $E = 1.79 \times 10^{-13}$  ergs = 2.58 kg.-cal. per mole. Pauling (6) gives for the hydrogen bond in ice a value of 4.5 kg.-cal. per mole. The forces in the hydration envelope thus seem to be smaller than those found in a hydrogen bond of ice, but they are of the right order of magnitude for a weaker type of a hydrogen bond.

#### CONCLUSIONS

1. It was assumed that sucrose molecules behave in solution as a suspension of rigid particles resembling ellipsoids of axial ratio 1.84, having shape factors  $k_1 = 2.57$ ,  $k_2 = 3.175$ , and hydrodynamic interaction constant  $Q = 0.6$ , found from the theory of viscosity of suspensions.

2. From these data, the collision time constant  $\tau_2$  was calculated. It decreases from 2.098 at 0°C. to 1.489 at 100°C. It is considerably smaller than the theoretical value  $\tau_2 = 4$  found for rigid spheres without mutual forces and without Brownian motion. This can be qualitatively explained as the decrease of the collision time owing to a strong Brownian motion; the decrease is more marked at higher temperatures, where the Brownian motion is stronger.

3. The density  $D_s$  of the sucrose molecules in solution without hydration envelopes was found to decrease from 1.624 to 1.522 as the temperature is increased, a phenomenon similar to a thermal expansion. These values agree well with the density of solid sucrose, which is 1.57 at 20°C.

4. The density  $D_H$  of the hydration envelopes was found to decrease from 1.102 to 1.009 as the temperature is increased. It is higher than the density of water, so that sucrose solutions show a contraction on mixing.

5. The hydration  $h_0$  of the sucrose molecules at infinite dilution varies greatly with temperature, from 1.818 at 0°C. to 1.193 at 100°C. If it is expressed as the number of molecules of water per molecule of sucrose, it varies from 10.54 molecules at 0°C. to 2.43 molecules at 100°C.

6. From the variation of hydration with temperature, the activation energy  $E$  necessary to be overcome in order to allow escape of water molecules from the hydration envelope can be calculated. It was found to be 2.58 kg.-cal. per mole, which is less than the value for hydrogen bonds in ice, but it is of the expected order for hydrogen bonds in a liquid.

7. As sucrose has eight hydroxyl groups and three other hydrophilic oxygens, and as it is probable that the water molecules associate with those groups and oxygens by means of hydrogen bonds, and as above 0°C. less than eleven molecules of water are associated with one molecule of sucrose, it is probable that each hydrophilic group attaches to itself no more than one water molecule at a time.

#### SUMMARY

The theoretical viscosity formula derived for suspension of rigid particles, combined with the density data, is applied to solutions of sucrose. Information is thus obtained on hydration, collision constants, and densities of the molecules and their hydration envelopes.

The author is indebted to the Directors of Lever Brothers and Unilever Limited for their permission to publish this paper.

## REFERENCES

- (1) BINGHAM, E. C., AND JACKSON, R. F.: Bur. Standards Bull. **14**, Sci. Paper No. **298**, 59 (1917).
- (2) BURGERS, J. M.: *Second Report on Viscosity and Plasticity*, p. 128. N.V. Noord-Hollandsche Uitgeversmaatschappij, Amsterdam (1938).
- (3) FLEURY, P., AND COURTOIS, J.: Compt. rend. **214**, 366 (1942).
- (4) JAEGER, F. M.: *Second Report on Viscosity and Plasticity*, p. 96. N.V. Noord-Hollandsche Uitgeversmaatschappij, Amsterdam (1938).
- (5) LANDOLT-BÖRNSTEIN: *Physikalisch-Chemische Tabellen*, Vol. I, p. 463. J. Springer, Berlin (1923).
- (6) PAULING, L.: *The Nature of the Chemical Bond*, p. 304. Cornell University Press, Ithaca, New York (1942).
- (7) VAND, V.: J. Phys. Colloid Chem. **52**, 277 (1948).

## AFFINITY AND REACTION RATE CLOSE TO EQUILIBRIUM

I. PRIGOGINE, P. OUTER, AND CL. HERBO

*Faculty of Science, University of Brussels, Brussels, Belgium*

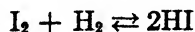
*Received August 12, 1947*

## I

The link between thermodynamic quantities and reaction rates has been discussed by numerous authors ever since the very beginning of modern physical chemistry (12, 18, 20). Yet in classical thermodynamics, limited essentially to the study of equilibrium states, research work has not led to very satisfactory results.

The theory of absolute rates of reaction, which we owe principally to H. Eyring and his school, demonstrates that the value of the kinetic constants of an elementary reaction is determined essentially by such thermodynamic quantities as energy and entropy of activation. On the other hand, these researches did not show whether or not any link exists between thermodynamic concepts and the value of the over-all reaction rate, a function of the kinetic constants and of the concentration.

To illustrate the point, let us consider the synthesis of hydriodic acid:



The reaction rate is

$$v = \vec{v} - \bar{v} = \vec{k}C_{\text{I}_2}C_{\text{H}_2} - \bar{k}C_{\text{HI}}^2 \quad (1)$$

where  $\vec{v}$  and  $\bar{v}$  represent the rates of the two opposite reactions and  $\vec{k}$  and  $\bar{k}$  the corresponding kinetic constants.

The study of the relationship between the over-all rate close to equilibrium and the thermodynamic concepts is the object of the present work.

This problem can be readily studied by employing the methods of the chemical thermodynamics of irreversible phenomena, which we owe principally to Th. De Donder (2, 3, 4) and his school (15, 16, 17) and also to Eckart (5), Onsager (14), Meixner (13), etc. Let us recall briefly some results which we shall need here.

The presence of irreversible phenomena is characterized thermodynamically by a definite positive production of entropy. We can say that irreversible phenomena (diffusion, thermal or electric conduction, chemical reactions) create entropy but cannot destroy it. In systems at uniform temperature, this production of entropy is none other than the non-compensated heat of Clausius divided by the absolute temperature.

Let us limit ourselves to uniform systems (without diffusion) in mechanical and thermal equilibrium. The only irreversible phenomenon which we shall then have to consider is the chemical reaction. It is proved that the production of entropy per unit of time, due to a chemical reaction, is

$$\frac{Av}{T} > 0 \quad (2)$$

where  $v$  is the rate of the reaction,  $T$  the absolute temperature, and  $A$  the chemical affinity. Th. De Donder has shown that this affinity can be easily calculated; for example, from the chemical potentials  $\mu_\gamma$  we have

$$A = - \sum_\gamma \nu_\gamma \mu_\gamma \quad (3)$$

where  $\nu_\gamma$  is the stoichiometric coefficient of the constituent  $\gamma$  in the reaction.

Formula 2 gives us directly the fundamental inequality of De Donder:

$$Av > 0 \quad (4)$$

Affinity and reaction rate have therefore the same sign. At thermodynamic equilibrium we have simultaneously:

$$A = 0, \quad v = 0 \quad (5)$$

Let us note that equations 4 and 3 are quite independent of the particular conditions in which the chemical reaction takes place (e.g.,  $V$  and  $T$  constant or  $P$  and  $T$  constant).

These relations express an intrinsic connection between reaction rates and thermodynamic concepts. Let us examine more closely their kinetic consequences.

## II

A reaction rate is a function of different macroscopic variables such as concentration, temperature, and mass of catalyst. Let us call  $x_1, x_2 \dots x_{\lambda+1}$  these different variables. Thus:

$$v = v(x_1, x_2, \dots x_{\lambda+1}) \quad (6)$$



The affinity  $A$  of the reaction is equally a function of some at least of these variables.

$$A = A(x_1, x_2 \cdots x_{\lambda+1}) \quad (7)$$

Let us eliminate one of the variables,  $x_{\lambda+1}$  for example, between equations 6 and 7, from which we obtain:

$$v = f(x_1 \cdots x_\lambda, A) \quad (8)$$

By virtue of equation 3 the function thus obtained cancels itself out at the same time as the affinity  $A$ . Thus

$$f(x_1, x_2 \cdots x_\lambda; 0) = 0 \quad (9)$$

This holds whatever the values of  $x_1 \cdots x_\lambda$  may be.

Let us develop  $f$  in a power series of the variable  $A$ . By virtue of equation 9 we obtain a linear law between  $v$  and  $A$  close to equilibrium.

$$v = \left( \frac{\delta f}{\delta A} \right)_{x_1 \cdots x_\lambda} A \quad (10)$$

The angular coefficient

$$a \equiv \left( \frac{\delta f}{\delta A} \right)_{x_1 \cdots x_\lambda} \quad (11)$$

is generally a function of  $\lambda$  variables. If, in the course of different experiments, these variables maintain constant values, this angular coefficient will also retain a constant value. Let us also observe that on account of the inequality 4 and of equation 10 the angular coefficient (equation 11) is positive.

Let us first show by a simple example that the linear law (equation 10) is perfectly in accord with the form which the usual laws of kinetics assume close to equilibrium. Let us return again to example 1. By using relation 3 between affinity and the chemical potentials, equation 1 can easily be expressed in the form:

$$v = \vec{k} C_{\text{I}_2} C_{\text{H}_2} (1 - e^{-(A/RT)}) \quad (12)$$

In the case of a perfect gas the chemical potentials are of the form

$$\mu_\gamma = \mu_\gamma^0(T) + RT \log C_\gamma$$

where  $\mu_\gamma^0(T)$  depends only on the temperature. By virtue of equation 3 the affinity of the reaction (1) takes in that case the form:

$$A = RT \log \frac{K(T)}{C_{\text{I}_2}^{-1} C_{\text{H}_2}^{-1} C_{\text{HI}}^2}$$

where  $K(T) = \frac{\vec{k}}{\bar{k}}$  is the constant of Guldberg and Waage. In using this value of affinity, formula 1 immediately takes the form of expression 12.

Close to equilibrium we have:

$$\left| \frac{A}{RT} \right| \ll 1 \quad (13)$$

from which we have

$$v = \vec{k} C_{\mathbf{1}_2} C_{\mathbf{H}_2} \frac{A}{RT} \quad (14)$$

We thus find again the linear law (equation 10).

We observe besides that the angular coefficient (equation 11) has a simple physical significance.

The linear relation (equation 10) has a double aspect. On the one hand, owing to its thermodynamic character, it has an extreme generality. It is independent of all hypotheses as to the mechanism of the reaction. Furthermore, relations of this type are found in all irreversible phenomena. Thus in the case of a system at non-uniform temperature a "thermal affinity" can be introduced, linked to the gradient of temperature. The linear relation between affinity and reaction rate is then reduced to Fourier's classical law. The laws of diffusion, viscosity, or thermodiffusion are obtained in an analogous manner.

On the other hand, formula 10 holds only close to equilibrium. As soon as we move away from equilibrium the relation between affinity and rate becomes more complex.

### III

The relations which we have obtained are easily extended to the case where the system under consideration is the seat of many simultaneous chemical reactions. The fundamental inequality of De Donder (3), expressing the positive production of entropy, becomes

$$\sum_{\rho} A_{\rho} v_{\rho} > 0 \quad (15)$$

where  $v_{\rho}$  is the rate of the  $\rho^{\text{th}}$  reaction and  $A_{\rho}$  its affinity. At thermodynamic equilibrium we have simultaneously

$$A_{\rho} = 0; \quad v_{\rho} = 0 \quad (\rho = 1 \cdots r) \quad (16)$$

while close to equilibrium we shall have the linear and homogeneous laws between affinities and rates:

$$v_{\rho} = \sum_{\lambda} a_{\rho\lambda} A_{\lambda} \quad (17)$$

It can easily be shown that the usual kinetic laws lead, close to equilibrium, to formula 17.

In all the simple cases we have moreover  $a_{\rho\lambda} = 0$  for  $\rho \neq \lambda$  and relations 17 are reduced to:

$$v_{\rho} = a_{\rho\rho} A_{\rho} \quad (18)$$

each rate becoming proportional to its affinity.

These formulae lead us to several interesting conclusions. To illustrate the point let us consider a series of consecutive reactions. For example:



The rate at which the final product F appears is equal to the rate of the  $r^{\text{th}}$  reaction and will be proportional, by virtue of equation 18, to the affinity  $A_r$ . When the intermediate product P is unstable, its concentration is difficult to measure and the affinity  $A_p$  is not generally accessible to calculation. Nevertheless, when a quasi-steady state is established, where all the rates of the consecutive reactions become equal, we have:

$$v = v_1 = v_2 = \cdots = v_r \quad (20)$$

and by virtue of equation 18

$$a_{11}A_1 = a_{22}A_2 = \cdots = a_{rr}A_r \quad (21)$$

from which, representing the total affinity of the reaction by  $A = \sum_p A_p$ ,

$$\frac{A_1}{\frac{1}{a_{11}}} = \frac{A_2}{\frac{1}{a_{22}}} = \cdots = \frac{A_r}{\frac{1}{a_{rr}}} = \frac{A}{\sum_p \frac{1}{a_{pp}}} \quad (22)$$

The rate at which the final product appears becomes thus

$$v = v_r = \frac{A}{\sum_p \frac{1}{a_{pp}}} \quad (23)$$

Thus the rate becomes proportional to the total affinity  $A$ . In particular,  $v$  is cancelled out for  $A = 0$ , while outside of the quasi-steady system  $v$  is cancelled out in conformity with equation 18 for  $A_r = 0$  but can be different from zero for  $A \neq 0$ .

We can call  $1/a_{pp}$  the relative "reaction resistance" to the partial reaction  $p$  and  $\sum_p 1/a_{pp}$  the "total reaction resistance."

When one stage is particularly slow—for example, that which corresponds to the  $j^{\text{th}}$  reaction—we have

$$a_{jj} \ll a_{pp} \text{ for } p \neq j$$

and formula 23 is reduced to

$$v_r = a_{jj}A \quad (24)$$

In other terms, the rate at which the final product appears is governed by the total affinity and by the reactional resistance of the rate-determining  $j^{\text{th}}$  step only.

A formula, analogous to equation 23, valid for the coöperation between dissolution and diffusion, was established by Fischbeck (16).

## IV

In the present work we have verified the validity of linear relations between affinities and reaction rates. We have chosen the antagonistic reactions of hydrogenation of benzene and of dehydrogenation of cyclohexane, because these complex reactions have been the object of detailed kinetic studies in our laboratory (8-11). On the one hand, the experiments consist in the measurement of resulting rates of antagonistic reactions under carefully determined conditions of temperature and partial pressures, and on the other hand in the measurements of constants of equilibrium at different temperatures. A knowledge of the constants of Guldberg and Waage are in fact necessary in the calculations of the affinities of gaseous mixtures.

The apparatus, the preparation of the catalysts, and the experimental technique have been described in previous papers (8). Let us simply recall that the experiments were carried out by the flow method.

The principle of the determination of instantaneous rates of reaction by the dynamic method has been established by Herbo (8). If a gaseous mixture of hydrogen and benzene of invariable composition but of increasing flow is directed towards the chamber of reaction, the yield per hour (that is, the quantity of benzene transformed per unit of time) tends asymptotically towards a maximum. On the contrary, the rate of transformation (that is, the ratio of benzene transformed to the quantity transformable when the reaction is complete) tends asymptotically towards zero (see also on this subject Damköhler (1)). Let  $D_e$  and  $D_s$  denote, respectively, the flow of benzene at the entrance and the exit of the reaction chamber, and  $\theta$  and  $\nu$  the rate of transformation and the yield per hour. By definition we have:

$$\theta = \frac{D_e - D_s}{D_e}$$

$$\nu = D_e - D_s, \quad \text{hence} \quad \nu = \theta D_e$$

For sufficiently large flows the rate of transformation is inversely proportional to the flow  $D_e$ . Under these conditions, the yield per hour is maximum and independent of the flow. Let us show that this yield can be identified with the instantaneous rate of the reaction. Let us divide the reaction chamber in our minds into elementary volumes. The yield per unit of time in each of these volumes increases as the steady concentrations of the reactants come closer to the initial concentrations. If the flow of the gaseous mixture is sufficiently large, the concentrations of the reactants in the last element of volume are indefinitely close to the concentrations in the first element. Under these conditions, the sum of the elementary yields is maximum and cannot increase further with the flow of the gaseous mixture. It is really a question of initial rate of reaction, since the partial pressures of the gaseous constituents are infinitely close to the initial partial pressures in the entirety of the reaction chamber. If a mixture of hydrogen, benzene, and cyclohexane is directed towards the reaction chamber, the maximum yield is a measure of the initial rate resulting from the two antagon-

istic reactions ( $v'$ ). Let us express this resulting rate in grams of benzene transformed per unit of time and let us consider it as positive if there is formation of benzene and as negative in the opposite case. Thus:

$$v' = D_s - D_e$$

The affinity  $A$  of the gaseous mixture under the same conditions of temperature and partial pressures is given by the formula:

$$A = RT(\log K + \log P_e - \log P_b - 3 \log P_h)$$

where  $R$  is the constant of perfect gases in calories mole<sup>-1</sup> degree<sup>-1</sup>,  $T$  is the temperature in degrees Kelvin,  $P_e$ ,  $P_b$ , and  $P_h$  are the partial pressures in atmospheres of the three constituents of the gaseous mixture, and  $K$  is the equilibrium constant of Guldberg and Waage:

$$K = \frac{(P_b)_e (P_h)_e^3}{(P_e)_e} \quad (25)$$

The measurements of  $K$  at different temperatures have been made in two different ways. In the first series of experiments, we have directed gaseous mixtures of hydrogen, benzene, and cyclohexane towards the reaction chamber. From one experiment to another we have modified the temperature of the catalyst and we have measured in each case the corresponding maximum yield. If the antagonistic reactions are indicated by a formation of benzene ( $D_s > D_e$ ), the yield per hour is positive. If, on the contrary, the reaction of hydrogenation outweighs the reaction of dehydrogenation, the hourly yield is negative ( $D_s < D_e$ ). The temperature at which the gaseous mixture passes on to the catalyst without being transformed is determined by graphic interpolation ( $D_s = D_e$ ). It is the temperature at which the initial mixture is in equilibrium.  $K$  is calculated by means of equation 25, by taking:

$$P_h = (P_h)_e, \quad P_b = (P_b)_e, \quad \text{and} \quad P_e = (P_e)_e$$

in another series of experiments we have directed towards the catalyst, which is kept at a constant temperature, gaseous mixtures of well-known composition. From one experiment to another we have systematically modified the proportion of the three constituents, and in each case we have measured the corresponding maximum yield. This time, we obtain by graphic interpolation the composition of the gaseous mixture in equilibrium at the temperature of the catalyst. These two series of determinations have given values for  $K$  in agreement with the formula of Schultze (19) within the range of experimental errors:

$$\log K = \frac{51,500}{4.573 T} - 20.69$$

Tables 1 and 2 and figures 1-6 reproduce some of the results obtained.

These experimental results show that the linear law between reaction rate and affinity is well satisfied in a wide region on both sides of the state of equilibrium of the reaction:



TABLE 1

*Affinity and reaction rate in the system hydrogen-benzene-cyclohexane*Catalyst: 50% Ni, 25% ZnO, 23% Cr<sub>2</sub>O<sub>3</sub> (mole per cent). Weight of catalyst: 200 mg.

PARTIAL PRESSURES			RATIO A/R	v' grams per hour	TEMPERATURES °K.
P <sub>b</sub>	P <sub>c</sub>	P <sub>h</sub>			
atm.	atm.	atm.			
0.0242	0.104 (see figure 1)	0.899	-720	-29	488
			-531	-21.5	498
			-274	-9	509
			+16	+1	523
			+231	+7	533
			+403	+16	546
0.0172	0.252 (see figure 2)	0.771	-188	-9	501
			+73	+1	513
			+293	+10.5	523.5
			+589	+20	535
0.0487	0.0784 (see figure 3)	0.912	-812	-32	497
			-217	-13	522
			-60	-4.5	533
			+172	+4.5	544
			+403	+14.5	555
			-139	-7	529
			-583	-24	510
			-812	-33.5	497
0.0977	0.0262 (see figure 4)	0.925	-1150	-36	500
			-686	-21	524
			-271	-11.5	545
			-85	-3	554
			+84	+1	561
			+323	+8	571
			+526	+13	582

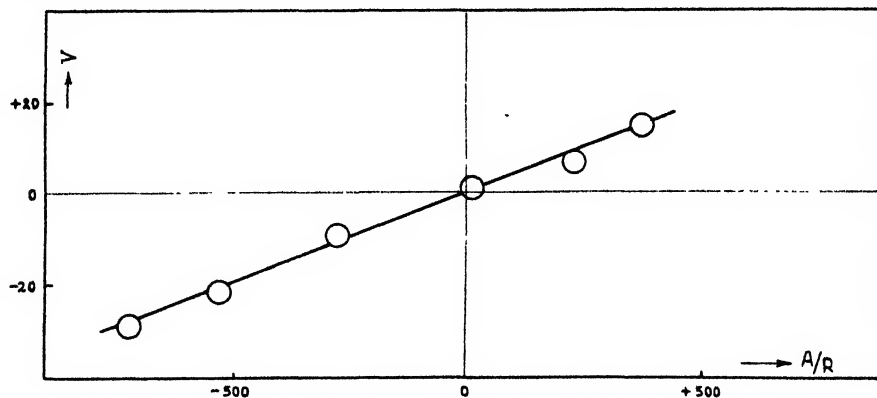


FIG. 1. Rate of formation of benzene in grams per hour plotted against the ratio of affinity to molar gas constant. First set of data of table 1.

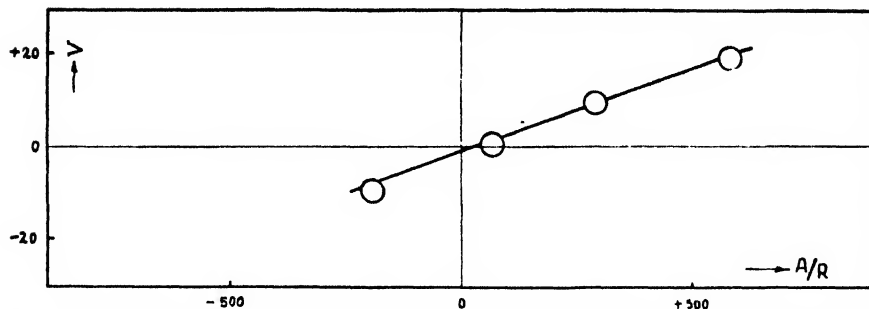


FIG. 2. Rate of formation of benzene in grams per hour plotted against the ratio of affinity to molar gas constant. Second set of data of table 1.

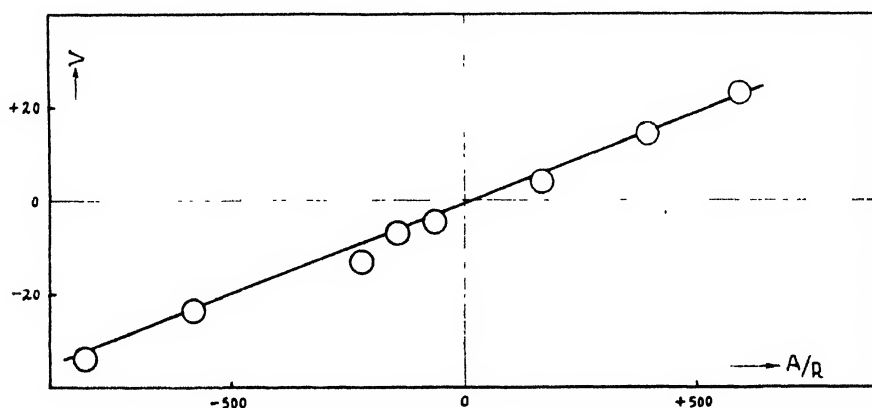


FIG. 3. Rate of formation of benzene in grams per hour plotted against the ratio of affinity to molar gas constant. Third set of data of table 1.

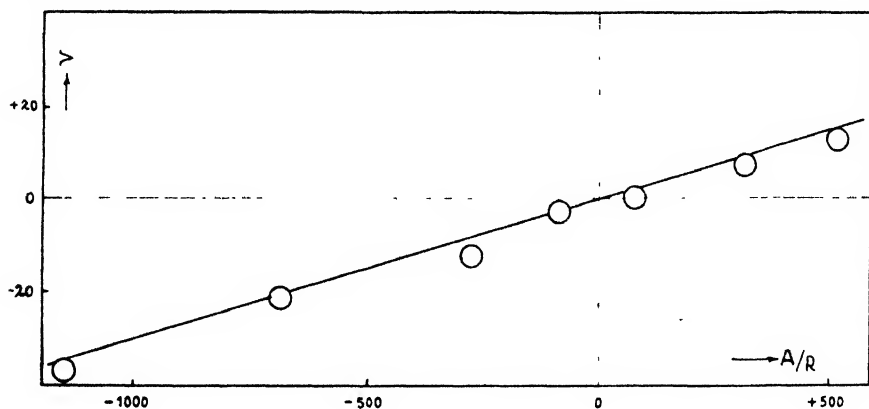


FIG. 4. Rate of formation of benzene in grams per hour plotted against the ratio of affinity to molar gas constant. Fourth set of data of table 1.

Thus in the case of mixtures having a constant composition but studied at different temperatures, the linear law has been verified in an interval of temperature of about 100°C.

TABLE 2

*Affinity and reaction rate in the system hydrogen-benzene-cyclohexane*Catalyst: 50% Ni, 10% ZnO, 40% Cr<sub>2</sub>O<sub>3</sub> (mole per cent)

WEIGHT OF CATALYST  mg.	PARTIAL PRESSURES			RATIO $A/R$	$v'$  grams per hour	TEMPERATURE  °K.
	$P_b$ atm.	$P_o$ atm.	$P_h$ atm.			
175 ..... (see figure 5)	0.179	0.073	0.792	-197	-24	548
	0.204	0.048	0.790	-323	-31	
	0.051	0.195	0.799	+328	+32	
	0.107	0.145	0.796	+86	+9	
	0.154	0.097	0.792	-92	-15	
	0.128	0.121	0.797	0	-1	
	0.077	0.017	0.786	+227	+29	
	0.179	0.073	0.781	-154	-21	
	0.128	0.121	0.782	+1	+1	
50..... (see figure 6)	0.294	0.024	0.714	-690/R	-8	563
	0.225	0.042	0.765	0	-1	
	0.100	0.075	0.859	+996	+11	
	0.146	0.063	0.825	+690	+7	

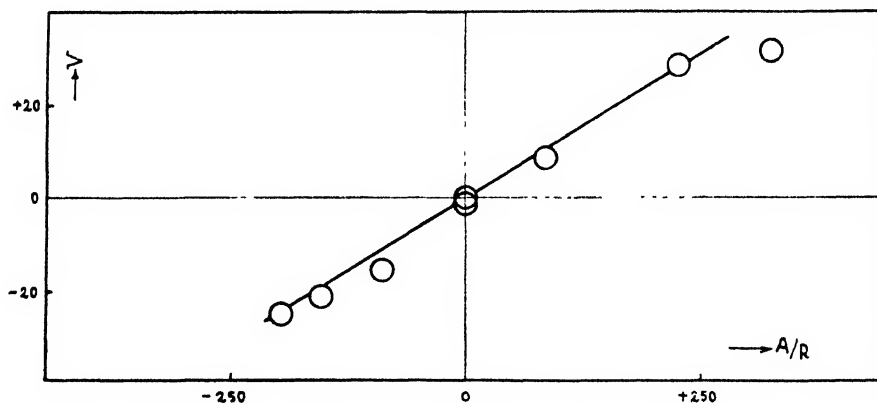


FIG. 5. Rate of formation of benzene in grams per hour plotted against the ratio of affinity to molar gas constant. First set of data of table 2.

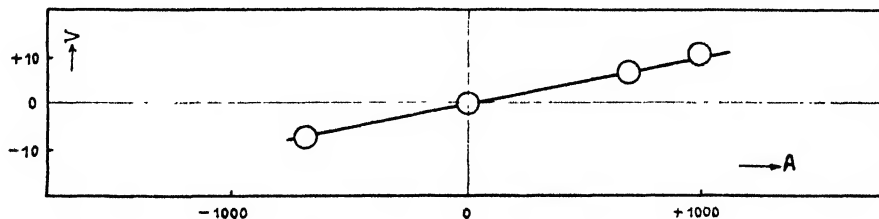


FIG. 6. Rate of formation of benzene in grams per hour plotted against the affinity. Second set of data of table 2.



Let us note that in experiments 5 and 6 the predictions of the theory are exceeded, for the theory requires a linear law if one only of the variables is modified (cf. Section II). On the contrary, in the series of experiments 5 and 6 the values of the three partial pressures  $P_c$ ,  $P_b$ , and  $P_h$  are modified simultaneously. The angular coefficient  $a$  (equation 11) should vary. In fact  $a$  remains constant in a wide interval, which shows that the influence exercised on  $a$  by the composition of the gaseous mixture must be very slight.

Let us again observe that, the reaction rate being proportional to the over-all affinity of the succession of consecutive reactions which lead from benzene to cyclohexane, we can, by virtue of the developments of Section III, see in this an argument in favor of the fact that a quasi-steady regime is obtained on the surface of the catalyst.

## SUMMARY

The thermodynamics of irreversible phenomena, based mainly on the concept of entropy production, leads to linear and homogeneous relations between affinities and reaction rates close to equilibrium. These laws have been verified experimentally in the case of the catalytic reaction of the hydrogenation of benzene and the inverse reaction of the dehydrogenation of cyclohexane. The method used for measuring rates is the dynamic method of high flow rates. The domain of validity of these laws is discussed. In a quasi-steady state, particularly simple relations are established.

## REFERENCES

- (1) DAMKOHLER, G.: In A. Eucken and M. Jakob's *Der Chemie-Ingenieur*, Vol. III, p. 468. Akademische Verlagsgesellschaft m.b.H., Leipzig (1939).
- (2) DE DONDER, TH.: *L'affinité*. Gauthier-Villars, Paris (1927).
- (3) DE DONDER, TH.: Bull. classe sci., Acad. roy. Belg., December 14, 1937.
- (4) DE DONDER, TH., AND VAN RYSSELBERGHE, P.: *Affinity*. Stanford University Press (1936).
- (5) ECKART, C.: Phys. Rev. **58**, 267, 269 (1940).
- (6) FISCHBECK, K.: In A. Eucken and M. Jakob's *Der Chemie-Ingenieur*, Vol. III. Akademische Verlagsgesellschaft m.b.H., Leipzig (1939).
- (7) GLASSTONE, S., LAIDLER, K., AND EYRING, H.: *The Theory of Rate Processes*. McGraw-Hill Book Company, Inc., New York (1941).
- (8) HERBO, CL.: Bull. soc. chim. Belg. **50**, 257 (1941); **51**, 44 (1942).
- (9) HERBO, CL., AND HAUCHARD, V.: Bull. soc. chim. Belg. **52**, 135 (1943).
- (10) HERBO, CL., AND HOU, C.: Bull. soc. chim. Belg. **54**, 203 (1945).
- (11) HERBO, CL., AND OUTER, P.: Bull. soc. chim. Belg. **56**, in press (1947).
- (12) JOUQUET, E.: Ann. phys. **5**, 5 (1926), for bibliography of early work up to 1926.
- (13) MEIXNER, Y.: Z. physik. Chem. **B53**, 235 (1943).
- (14) ONSAGER, L.: Phys. Rev. **37**, 405 (1931); **38**, 2265 (1931).
- (15) PRIGOGINE, I.: *Étude thermodynamique des phénomènes irréversibles*. Desoer, Liège (in press).
- (16) PRIGOGINE, I., AND DEFAY, R.: *Thermodynamique chimique conformément aux méthodes de Gibbs et De Donder*, Vol. I, Vol. II. Desoer, Liège (1944; 1946).
- (17) PRIGOGINE, I., AND HANSEN, R.: Bull. classe sci., acad. roy. Belg., April 11, 1942.
- (18) SCHEFFER, F. E. C., AND BRANDSMA, W. F.: Rec. trav. chim. **45**, 522 (1926), for bibliography of early work up to 1926.
- (19) SCHULTZE, C. R.: Angew. Chem. **49**, 268 (1936).
- (20) VAN'T HOFF, J. H.: *Vorlesungen über theoretische und physikalische Chemie*, p. 181. Vieweg, Braunschweig (1898).

THE CRYOSCOPIC BEHAVIOR OF CARBON TETRACHLORIDE<sup>1</sup>

ARTHUR W. DAVIDSON, W. J. ARGERSINGER, JR., AND CARL I. MICHAELIS

*Department of Chemistry, University of Kansas, Lawrence, Kansas**Received July 24, 1947*

In the course of a series of investigations, now in progress in this laboratory, of phase equilibria in systems consisting of pairs of organic compounds (4, 22), our attention has been attracted to the distinctly unusual course of those portions of the temperature-concentration curves in which the solid phase is crystalline carbon tetrachloride. These are noteworthy not only for their steep slopes and for their complete lack of the downward concavity usually observed in freezing-point curves, but also for the strikingly sharp break, or change in slope, which they exhibit at a temperature in the neighborhood of  $-48^{\circ}\text{C}$ .

Both of these peculiarities have, it is true, been observed previously. Carbon tetrachloride has been conspicuous, among the common solvents, for its unusually high cryoscopic constant, while the break in its freezing-point curves has been commented on especially by Wyatt (23), who has correctly attributed it to a transition between the two crystalline modifications of carbon tetrachloride. Since, however, up to the present scarcely more than qualitative explanations (20) have been offered for these facts, it appeared worth while to attempt a quantitative interpretation of the freezing-point data in terms of the theory of the ideal solution. Such an interpretation is indeed scarcely possible in the case of the system carbon tetrachloride-acetone as described by Wyatt, since his data are presented in graphical form only. But for the systems carbon tetrachloride-chloroform (figure 1) as reported by Kanolt (9) and by Sameshima and Hiramatsu (15), carbon tetrachloride-carbon disulfide as reported by Timmermans (20), and carbon tetrachloride-2,6 lutidine (figure 2) as studied in this laboratory (22), application of solution theory brings out an interesting concordance between the experimental data and the temperature-concentration curve as calculated from the Schröder-LeChatelier equation, as will be shown below.

The existence of two solid modifications of carbon tetrachloride was first suggested by Tammann as early as 1898 (19) and was again pointed out by Goldschmidt (6). McCullough and Phipps (11) characterize the high- and low-temperature forms as cubic and monoclinic, respectively, and even suggest, as do Johnston and Long (8), the possible usefulness of the transition temperature as a fixed point in thermometry. Nevertheless this transition point was overlooked, curiously enough, in both of the studies cited above of the carbon tetrachloride-chloroform system.

## THE HIGH-TEMPERATURE OR CUBIC MODIFICATION, SOLID I

Values previously reported in the literature for the melting point of Solid I (4, 7, 8, 9, 10, 11, 13, 15, 16, 17, 18, 21, 22, 23) have varied from  $-21.8^{\circ}$  to

<sup>1</sup> Presented at the Midwest Regional Meeting of the American Chemical Society, which was held in Kansas City, Missouri, June, 1947.

$-24.2^{\circ}\text{C}$ . Among these the most dependable value, from the standpoint both of purity of material and of accuracy of temperature measurement, appears to be the recent one of Hicks, Hooley, and Stephenson (7),  $-22.9^{\circ}\text{C}$ . or  $250.3^{\circ}\text{K}$ ., which we shall use in this discussion. The results of several other very careful determinations cluster closely about this figure; the slightly higher values obtained in this laboratory (4, 22) are probably to be accounted for in terms of the difficulty of accurate calibration of the temperature scale in this region.

The calorimetric data required for the calculation of the course of the ideal temperature-concentration curve with carbon tetrachloride as solid phase are

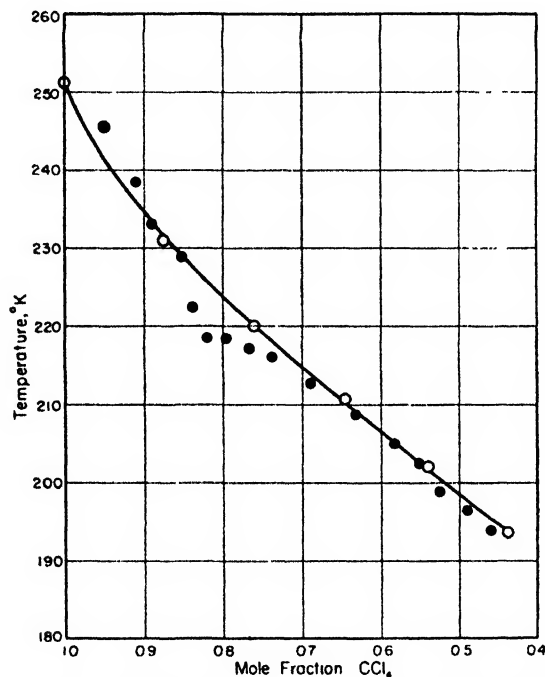


FIG. 1. System carbon tetrachloride-chloroform. O, data of Kanolt; ●, data of Sameshima and Hiramatsu.

available also from several of the researches cited above (7, 8, 10, 18). Again, the most reliable value for the heat of fusion of the cubic form appears to be that of Hicks, Hooley, and Stephenson, who report it as 601 cal. per mole. When this unusually low value is introduced into the familiar equation for the cryoscopic constant

$$K_f = \frac{RT_m^2 M}{1000L_f}$$

where  $T_m$  is the melting point,  $M$  the molecular weight, and  $L_f$  the molal heat of fusion, we obtain, for the limiting ratio of freezing-point depression to molality, the remarkably high figure of 31.8. Thus the extremely high slope of the curve

in the vicinity of the freezing point—seventeen times as great as in the case of water, for example—is readily accounted for.

Furthermore, from the consideration of the integral form of the Schröder-LeChatelier equation

$$\ln x = \frac{L_f}{R} \left( \frac{1}{T_m} - \frac{1}{T} \right) \quad (1)$$

where  $x$  is the mole fraction of a component in the solution which is in equilibrium

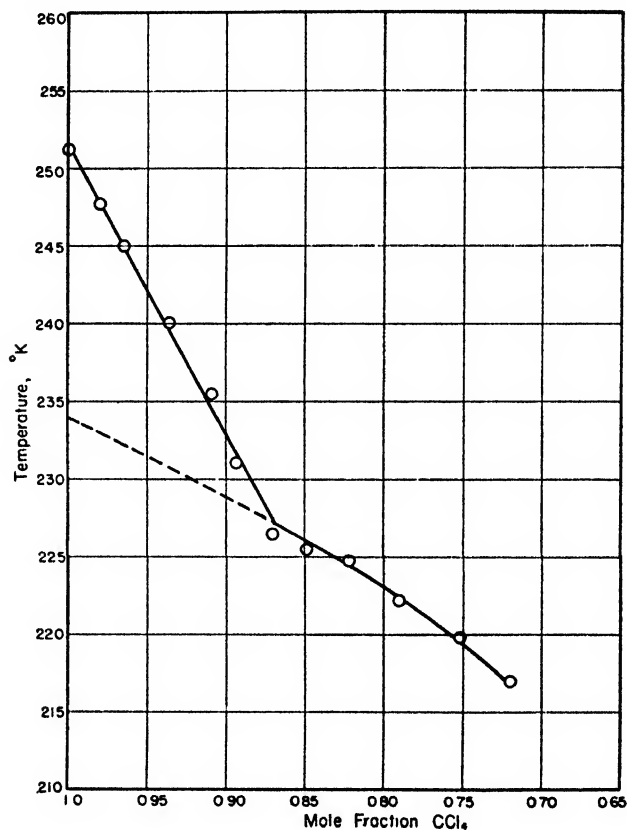


FIG. 2. System carbon tetrachloride-2,6-lutidine

at the temperature  $T$  with the same component in the solid state, it may readily be shown (1, 14) that for any substance for which the molal entropy of fusion,  $L_f/T_m$ , is less than  $2R$  cal. per degree, the conventional freezing-point curve ( $T$  as ordinate against  $x$  as abscissa) must be concave *upward* over part of its length—specifically, from the freezing point down to the temperature at which the value of  $L_f/T$  becomes equal to  $2R$ , where there is a point of inflection. For carbon tetrachloride, the molal entropy of fusion is only 2.40 cal. per degree; hence the theoretical  $T - x$  curve is concave upward between the freezing point

and 151°K. In the experimental curves the concavity is detectable, but the point of inflection cannot be realized because of transition to the low-temperature form at about 225°K. Since the molal entropy of fusion of the monoclinic form, as will be shown presently, is well above  $2R$  cal. per degree, the lower branch of the theoretical curve is convex upward throughout its length.

#### THE LOW-TEMPERATURE OR MONOCLINIC MODIFICATION, SOLID II

Since Solid II becomes metastable above the transition point, no direct determination of its melting point or heat of fusion exists. It is possible, however, to calculate reasonable values for these two quantities from known experimental data. The heat of transition as reported by Hicks, Hooley, and Stephenson is 1095 cal. per mole, in good agreement with the values given by several earlier workers (8, 10, 18). Since in the derivation of the simple Schröder-LeChatelier equation for the freezing-point curve the variation of the heat of fusion with temperature is assumed to be negligible over the range considered, it is consistent to take as the heat of fusion of Solid II the sum of the heat of transition and the heat of fusion of Solid I. Thus the value  $1095 + 601 = 1696$  cal. per mole is obtained as the heat of fusion of Solid II.

The abnormally low entropy of fusion of the cubic form of carbon tetrachloride is very simply accounted for by the existence of the transition between the two forms, and the large heat effect accompanying this change. When a solid melts, a highly ordered arrangement of molecules, atoms, or ions breaks down to a nearly completely random arrangement in the liquid. This change in order alone gives a contribution of about  $R$  cal. per deg.-mole to the entropy of fusion (5). For very simple molecules, e.g., monatomic elements, which have approximately the same rotational, vibrational, and structural entropies in the liquid as in the solid state, this is the major part of the entropy of fusion. All solids exhibit also some volume change on fusion, and this adds a second contribution, usually rather small, to the entropy of fusion. Finally, most crystalline solids are characterized not only by fixed *positions* of their molecules, but also by fixed *orientations*. When such solids melt, the molecules become able to rotate freely, so as to give a random distribution in orientation as well as in position. This change from fixed orientation, or rather from slight libration about a fixed orientation, in the solid state, to completely free rotation in the liquid state, contributes a large term—usually the largest, in fact—to the entropy of fusion of such solids.

In the case of many substances, however, of which carbon tetrachloride is an example, the two enantiotropic forms are believed to differ in the nature and extent of molecular rotation in the crystalline state (12, 21). At very low temperatures, the molecules are held almost rigidly in the lattice, with only slight vibrational and oscillatory rotational motion, or libration, possible. These motions increase with increasing temperature, but not until the transition temperature is reached and the thermal energy becomes equal to the lattice potential energy, does completely free rotation become possible. Then the rotation of each molecule weakens the local molecular forces and thus facilitates

the rotation of its neighbors, so that the onset of free molecular rotation throughout the crystal—marked in many cases by an increased symmetry in crystal structure—occurs quite sharply at a definite transition temperature. When all the molecules in a crystal begin to rotate freely at a definite temperature, the energy that must be supplied appears as the heat of transition, which in the case of the monoclinic-cubic transition of carbon tetrachloride has the relatively large value of 1095 cal. per mole.

Now, although in principle there might be a transition from libration to free rotation in the solid state for any substance, yet for most the transition temperature is not realized below the melting point, and so the transition does not occur. However, in crystals in which the intermolecular forces are relatively weak, and steric relationships favorable to free rotation, the transition is likely to be realized. In such cases the major contribution to the entropy of fusion—that associated with the libration-rotation change—becomes rather an *entropy of transition*, leaving only the smaller order-disorder and volume change terms to be observed at the actual fusion point (2). A moderately high degree of dimensional symmetry in the molecule, and of spherical symmetry in particular, is especially favorable for the occurrence of libration-rotation transitions in the solid state, and consequently of low entropies of fusion. Symmetry alone is not an infallible criterion, however, because certain substances with unsymmetrical and even highly polar molecules, such as hydrogen chloride, also exhibit such a transition, whereas benzene, with its relatively symmetrical molecule, does not. In the case of carbon tetrachloride, the molecules rotate freely in the solid state above the transition point at about  $-48^{\circ}\text{C}.$ , and the entropy of fusion at the melting point, corresponding only to the order-disorder and volume changes, has the low value of 2.40 cal. per deg.-mole.

The melting point of Solid II may be calculated from the heats of fusion and the melting point of Solid I in the following way: If we may assume that the heat capacities of the two solid forms and of the pure liquid are approximately equal over the temperature range from the transition temperature to the melting point of the cubic form—an assumption equivalent to those made in the derivation of the Schröder-LeChatelier equation for the two freezing-point curves—then both the entropies and the heats of fusion and transition are additive, and we may write

$$L_2 = L_1 + L_i \quad (2)$$

and

$$S_2 = S_1 + S_i \quad (3)$$

or

$$\frac{L_2}{T_2^0} = \frac{L_1}{T_1^0} + \frac{L_i}{T_i} \quad (4)$$

In these equations  $L_1$  and  $L_2$  are the molal heats of fusion, and  $T_1^0$  and  $T_2^0$  the melting points, of Solid I and Solid II, respectively;  $L_i$  is the heat of transition,

and  $T_i$  the transition temperature. Equations 2 and 4 may readily be solved for  $T_2^0$ , to give:

$$T_2^0 = \frac{L_1 + L_i}{\frac{L_1}{T_1^0} + \frac{L_i}{T_i}} \quad (5)$$

The values reported for the transition temperature of carbon tetrachloride (3, 6, 7, 10, 11, 13, 17, 18, 21, 23) vary even more widely, from  $-45^\circ\text{C}.$  to  $-48^\circ\text{C}.$ , than do those for the melting point of Solid I, a fact which makes the usefulness of this transition temperature as a fixed thermometric point exceedingly dubious. The value reported by Hicks, Hooley, and Stephenson,  $-47.8^\circ\text{C}.$ , again seems the most reliable. Using this value for  $T_i$  in equation 3, we obtain for  $T_2^0$ , the melting point of Solid II, the value  $234^\circ\text{K}.$ , or  $-39^\circ\text{C}.$  This calculated value is in good agreement with the value obtained by extrapolation to  $x = 1$  of the lower branch of our freezing-point curve for the system carbon tetrachloride-lutidine (figure 2).

The ideal freezing-point curves for Solids I and II may now be calculated entirely from properties of the pure substance. These curves are defined by equation 1, which for the two solid modifications may conveniently be put in the forms

$$\log x = \frac{L_1}{2.303R} \left( \frac{1}{T_1^0} - \frac{1}{T} \right) \quad (1a)$$

and

$$\log x = \frac{L_2}{2.303R} \left( \frac{1}{T_2^0} - \frac{1}{T} \right) \quad (1b)$$

Substitution of the known values for  $L_1$ ,  $L_2$ ,  $T_1^0$ , and  $T_2^0$  gives, respectively,

$$\log x = 0.525 - 131 \frac{1}{T} \quad (6)$$

and

$$\log x = 1.587 - 371 \frac{1}{T} \quad (7)$$

In figure 3, where  $\log x$  is plotted as ordinate against  $1/T$  as abscissa, are shown the straight lines corresponding to equations 6 and 7, together with experimental data for the system carbon tetrachloride-chloroform, as given by Kanolt (9), the system carbon tetrachloride-carbon disulfide, as given by Timmermans (20), and our own data for the system carbon tetrachloride-lutidine (22). Since it appears almost certain that the variations among the melting points of pure carbon tetrachloride reported by the several observers are due principally to differences in temperature scale calibration, each set of data has been corrected by the constant temperature increment necessary to bring the melting points into concordance.

It will be seen that all the experimental points so corrected fall close to the theoretical curve, the deviations, of course, increasing with decreasing concentration of carbon tetrachloride. Such agreement might indeed have been expected for a system consisting of two such similar substances as carbon tetrachloride and chloroform, although perhaps not for the other two systems. Sameshima and Hiramatsu (15), it is true, found evidence for a compound  $\text{CHCl}_3 \cdot 4\text{CCl}_4$  with a congruent melting point at  $-55^\circ\text{C}$ ., but no such compound has been reported by any other observers. Neither Wyatt's curve for carbon tetrachloride-carbon

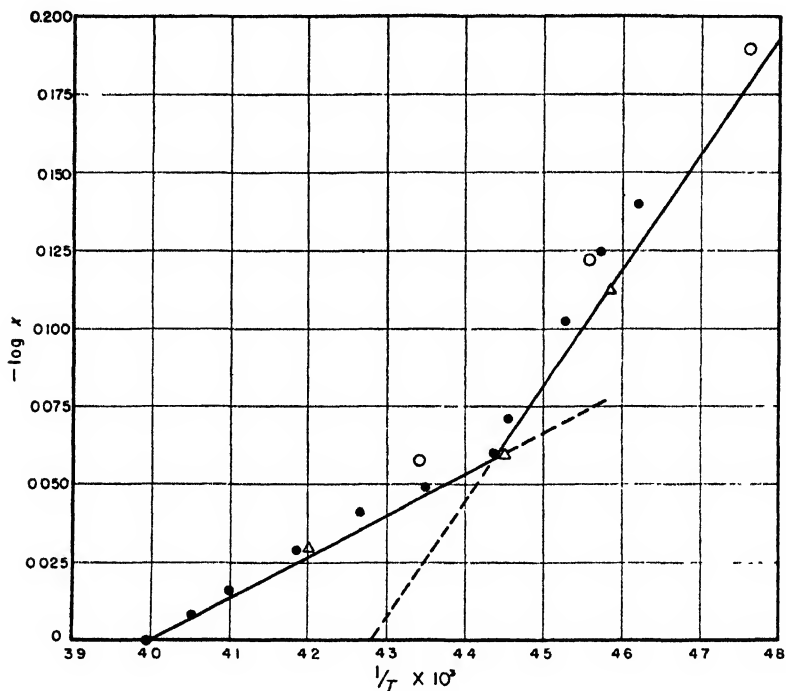


FIG. 3. Theoretical freezing-point curve for carbon tetrachloride.  $\circ$ , experimental data, chloroform as solute.  $\bullet$ , experimental data, lutidine as solute.  $\triangle$ , experimental data, carbon disulfide as solute.

disulfide nor our own for carbon tetrachloride-lutidine revealed the existence of any addition compound stable in the solid state in these systems. In the carbon tetrachloride-pyridine system (4), however, where a solid addition compound of the formula  $\text{C}_5\text{H}_5\text{N} \cdot 2\text{CCl}_4$  is known to exist, the experimental points (not shown in figure 3) are found to deviate widely from the theoretical straight line, even in the neighborhood of the melting point. In view of all these facts the existence of the addition compound reported by Sameshima and Hiramatsu seems highly improbable; we may conclude rather that the three systems for which data are shown in figure 3 conform closely to ideal behavior.



## SUMMARY

The course of the theoretical freezing-point curve for systems in which carbon tetrachloride is the solid phase has been calculated. The reasons for the unusually high heat of transition and low heat of fusion of carbon tetrachloride have been discussed. Experimental data for several systems containing carbon tetrachloride are shown to be in accord with the theoretical freezing-point curve.

## REFERENCES

- (1) ARGERSINGER, W. J., JR.: *Trans. Kansas Acad. Sci.* **49**, 216 (1947).
- (2) BAKER, W. O., AND SMYTH, C. P.: *J. Am. Chem. Soc.* **61**, 1695 (1939).
- (3) BILTZ, W., AND MEINECKE, E.: *Z. anorg. Chem.* **131**, 9 (1923).
- (4) DAVIDSON, A. W., VANDER WERF, C. A., AND BOATRIGHT, L. G.: *J. Am. Chem. Soc.* **69**, 3045 (1947).
- (5) GLASSTONE, S.: *Theoretical Chemistry*, p. 489. D. Van Nostrand Company, Inc., New York (1944).
- (6) GOLDSCHMIDT, V.: *Z. Krist.* **51**, 21 (1912).
- (7) HICKS, J. F. G., HOOLEY, J. G., AND STEPHENSON, C. C.: *J. Am. Chem. Soc.* **66**, 1064 (1944).
- (8) JOHNSTON, H. L., AND LONG, E. A.: *J. Am. Chem. Soc.* **56**, 31 (1934).
- (9) KANOLT, C. W.: *Natl. Bur. Standards (U. S.), Sci. Papers* **20**, No. 520, p. 619 (1926); *International Critical Tables*, Vol. IV, p. 98, McGraw-Hill Book Company, Inc., New York (1928).
- (10) LATIMER, W. M.: *J. Am. Chem. Soc.* **44**, 90 (1922).
- (11) McCULLOUGH, J. C., AND PHIPPS, H. E.: *J. Am. Chem. Soc.* **50**, 2213 (1928).
- (12) PAULING, L.: *Phys. Rev.* **36**, 430 (1930).
- (13) PHIPPS, H. E., AND REEDY, J. H.: *J. Phys. Chem.* **40**, 89 (1936).
- (14) ROOZEBOOM, F. W. B.: *Die heterogenen Gleichgewichte*, Vol. 2, Part 1, p. 276. Friedrich Vieweg und Sohn, Brunswick (1904).
- (15) SAMESHIMA, J., AND HIRAMATSU, T.: *Bull. Chem. Soc. Japan* **9**, 260 (1934).
- (16) SKAU, E. L.: *J. Phys. Chem.* **37**, 609 (1933).
- (17) SKAU, E. L., AND MEIER, H. F.: *J. Am. Chem. Soc.* **51**, 3519 (1929).
- (18) STULL, D. R.: *J. Am. Chem. Soc.* **59**, 2726 (1937).
- (19) TAMMANN, G.: *Wied. Ann. [Neue Folge]* **66**, 490 (1898).
- (20) TIMMERMANS, J.: *Bull. soc. chim. Belg.* **37**, 409 (1928).
- (21) TURKEVICH, A., AND SMYTH, C. P.: *J. Am. Chem. Soc.* **62**, 2468 (1940).
- (22) VANDER WERF, C. A., DAVIDSON, A. W., AND MICHAELIS, C. I.: *J. Am. Chem. Soc.*, in press.
- (23) WYATT, W. F.: *Trans. Faraday Soc.* **25**, 43, 48 (1929).

THE USE OF ION EXCHANGERS FOR THE DETERMINATION OF  
PHYSICAL-CHEMICAL PROPERTIES OF SUBSTANCES,  
PARTICULARLY RADIOTRACERS, IN SOLUTION. I

THEORETICAL<sup>1</sup>

JACK SCHUBERT<sup>2</sup>

*Clinton Laboratories, Oak Ridge, Tennessee and The Argonne National Laboratory, Chicago, Illinois*

*Received August 20, 1947*

INTRODUCTION

Realization of the fact that it is not necessary to have knowledge concerning the exact mass-action law or adsorption equation which fits ion-exchange data has led to the use of ion exchangers for purposes other than the usual recovery, concentration, and purification operations reviewed by Sussman and Mindler (13). One bypasses the necessity for such information in most cases by devising the experiment so as to measure relative effects.

It is the purpose of this paper to present the concepts and methods which enable one to employ ion exchangers, specifically cation exchangers, for the qualitative and quantitative determination of many physical-chemical properties. The experimental results obtained by applying the equations and concepts developed here will be given in subsequent papers. Many of the resulting applications are quite unique, inasmuch as they require only radiochemical concentrations, that is, about  $10^{-10}$  mole of an element. Thus the dissociation constants of complexes such as strontium tartrate have been measured (12) when the concentration of  $\text{Sr}^{++}$  was about  $10^{-11}$  mole per liter.

Briefly, the applications for which we have used ion exchangers include: (a) the determination of the dissociation constants of complex ions, (b) the rapid detection and evaluation of the relative complex-forming properties of organic salts, (c) measurements of the activity coefficient of tracer substances in the presence of large concentrations of a foreign electrolyte, (d) the detection and study of radiocolloids, (e) the qualitative determination of the state of a radioelement in solution, and (f) the determination of the valence and relative basicity of a cationic radioelement.

Because the bulk of the experimental work has been done with the acid-resistant and high-capacity synthetic resin cation exchangers (7), the discussion will be restricted to these types of cation exchangers.

The methods discussed here are uniquely applicable for studying the properties of radiochemical concentrations of substances when large amounts of foreign

<sup>1</sup> The specific material discussed here was derived from part of the studies made and reported by the writer as a member of the Argonne National Laboratory, Chicago, Illinois, and the Clinton Laboratories, Oak Ridge, Tennessee, and is based on work performed under Manhattan District Contract No. W-7405-Eng-39.

<sup>2</sup> Present address: Department of Physiological Chemistry, University of Minnesota, Minneapolis 14, Minnesota.

electrolytes are present. However, the procedures are useful as well in studies involving macroscopic concentrations.

#### GENERAL PROPERTIES OF CATION EXCHANGERS

A cation exchanger may generally be considered to be a porous salt containing an insoluble anion and exchangeable cations. The cations undergo exchange on acid groups such as phenolic, sulfonic, and carboxyl groups (7).

Experimentally, it has been found that with resin particles of 60-100 mesh:

(1) At any given pH the adsorption of a given cation will decrease as the concentration of foreign cations is increased (2).

(2) No significant adsorption of anions or neutral substances in true solution takes place (2, 12).

(3) The adsorptive capacity of the adsorbent for a given cation increases with increasing pH.<sup>8</sup> This phenomenon has been known to occur with carbonaceous exchangers (8) and has been shown to occur with the synthetic amberlite resins as well (12).

(4) The adsorption reaches a reproducibly constant value in about 2 to 4 hr. (2).

(5) The affinity of a cation for the adsorbent increases with increasing valence; thus, the monovalent, divalent, and trivalent cations, for example, form separate groups. Some overlapping may occur, but this rule serves as a good first approximation (2).

Proceeding from the above observations, we can now present the methods for applying ion exchangers to specific problems.

#### MEASUREMENT OF DISSOCIATION CONSTANTS OF COMPLEX IONS HAVING ZERO OR NET NEGATIVE CHARGE

A complex ion is considered to be formed when a chemical bond exists between an ion and an atom or group of atoms or other ions so that the forces acting between them lead to the formation of an aggregate with sufficient stability to make it convenient for the chemist to consider it as an independent species (9). In general, the equilibrium for the complex ion,  $M_xA_y^c$ , may be written (4):



and from the law of mass action:

$$K_a = \frac{[M^{+a}]^x [A^{-b}]^y}{[M_xA_y^c]} = \frac{(M^{+a})^x (A^{-b})^y}{(M_xA_y^c)} \cdot \frac{\gamma_M^{+a} \gamma_A^{-b}}{\gamma_{(M_xA_y^c)}} \quad (2)$$

where  $[ ]$ ,  $[ ]$ , to represent thermodynamic activities, and parentheses represent stoichiometric concentrations. In the latter case we

<sup>8</sup> This is not the case with the synthetic cation-exchange resin, Dowex 50 (W. C. Bauman and J. Eichhorn: *J. Am. Chem. Soc.* **69**, 2830 (1947)), since it contains nuclear sulfonic acid groups as the sole ion-active group.

$$K_c = \frac{(M^{+a})^x(A^{-b})^y}{(M_xA_y^c)} \quad (3)$$

The constant  $K_c$  is the "instability" constant of the complex ion, because it is a measure of its tendency to dissociate into simple ions. We shall refer to  $K_c$  and/or  $K_a$  as the "dissociation constant" of a complex ion.

Two well-known physical methods which have been used for the determination of complex ions are solubility and E.M.F. measurements. Additionally, the "frog's heart" method (5) has been used to measure the dissociation constants of the calcium, strontium, and magnesium citrate complexes, and is based on the observation that the amplitude of contraction of the ventricle of the isolated frog's heart is a function of calcium-ion concentration.

With a given weight and volume of solution, the adsorption isotherm of a tracer cation,  $M^{+a}$ , has been found to be linear over a very wide range of concentrations of the tracer, i.e.,

$$\frac{MR_a}{M^{+a}} = \text{constant} = \lambda_0 = \frac{\text{per cent adsorbed} \times \text{volume of solution}}{(100 - \text{per cent adsorbed}) \times \text{g. exchanger}} \quad (4)$$

where R is the anionic part of the exchanger.

The procedure for the determination of the dissociation constant of a complex ion involves the determination of the per cent adsorption of the cation in a solution of known and constant ionic strength in the absence of a specific complex-forming agent, and in the presence of the same.

Since one measures *relative* adsorptions, no need exists for knowledge concerning the formulation of the base-exchange reaction *per se*. In addition, as shown later, the absolute value of the dissociation constant can be determined when the adsorption is measured at two different concentrations of complex-forming agent, independent of information as to the nature of the adsorption equilibria in the total absence of the specific complex-forming agent.

We shall assume the following conditions to exist in deriving the equation from cation-exchange equilibria for determining the dissociation constant of the complex ion,  $M_xA_y^c$ , where  $c \leq 0$ :

- (1) The complex-forming ions are "swamped" by excess neutral salt; the ionic strength remains nearly constant.
- (2) The concentration of  $M^{+a}$  is negligible as compared to that of the complex-forming anion,  $A^{-b}$ ; actually,  $M^{+a}$  is present in radiochemical concentrations ( $\sim 10^{-9}$  mole per liter).
- (3) All pairs of solutions which are compared have the same pH, volume of solution, and weight of adsorbent.
- (4) The exchanger used has been previously saturated with the cation component of the bulk electrolyte.
- (5) No adsorption of the complex-forming anion or of the complex ion takes place.

The symbols to be employed in the discussion are as follows:

$a$  = per cent of  $M^{+a}$  which has been adsorbed by the exchanger at equilibrium when the complex-forming anion,  $A^{-b}$ , is present

$a_0$  = same as  $a$  when  $A^{-b}$  is absent

$s$  = per cent of  $M^{+a}$  which remains in solution at equilibrium when  $A^{-b}$  is present (actually  $s = 100 - a$ )

$s_0$  = same as  $s$  when  $A^{-b}$  is absent ( $s_0 = 100 - a_0$ )

$\lambda_0$  =  $a_0/s_0$ , i.e., slope of adsorption isotherm

$(A^{-b})$  = concentration of complex-forming anion in moles per liter

$(M^{+a})$  = concentration of the cation which is bound in the complex ion, expressed in  $\alpha$ ,  $\beta$ , or  $\gamma$  counts per minute per milliliter

$(M_x A_y^c)$  = concentration of the complex ion expressed in terms of the counts per minute per milliliter of  $M^{+a}$  which are bound in the complex, or  $(M_x A_y^c) = s - a_0/\lambda_0$ , as will be evident from the subsequent discussion

$(MR_a)$  = concentration of adsorbent for given conditions at equilibrium expressed in counts per minute per milliliter of  $M^{+a}$

From equation 4 we have

$$(M^{+a}) = MR_a/\lambda_0 \quad (5)$$

Substituting the value of  $M^{+a}$  from equation 5 into equation 3 we find

$$K_c = \frac{(MR_a)^x (A^{-b})^y}{\lambda_0^x (M_x A_y^c)} \quad (6)$$

It is seen that  $(M_x A_y^c)$  is equal to the total counts remaining in solution at equilibrium less the counts of  $M^{+a}$ , the value of the latter being simply  $(MR_a)/\lambda_0$ . Hence, equation 6 is conveniently expressed as

$$K_c = \frac{(\text{counts } M^{+a} \text{ adsorbed})^x (A^{-b})^y}{\lambda_0^x \left[ \text{total counts, } M^{+a}, \text{ remaining in solution} - \frac{\text{counts } M^{+a} \text{ adsorbed}}{\lambda_0} \right]} \quad (7)$$

or,

$$K_c = \frac{(a)^x (A^{-b})^y}{\lambda_0^x \left[ s - \frac{a}{\lambda_0} \right]} \quad (8)$$

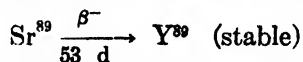
When the experiment is performed in such a manner that an arbitrary, known concentration of  $A^{-b}$  is always present, then one can calculate  $\lambda_0$  from the adsorption results at two concentrations of  $A^{-b}$ , namely,  $A_1^{-b}$  and  $A_2^{-b}$ . From equation 8 we have

$$K_c = \frac{(a_1)^x (A_1^{-b})^y}{\lambda_0^x \left[ s_1 - \frac{a_1}{\lambda_0} \right]} = \frac{(a_2)^x (A_2^{-b})^y}{\lambda_0^x \left[ s_2 - \frac{a_2}{\lambda_0} \right]}$$

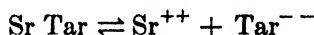
Solving for  $\lambda_0$  we find

$$\lambda_0 = \frac{(a_1)(a_2)^x (A_2^{-b})^y - (a_2)(a_1)^x (A_1^{-b})^y}{(s_1)(s_2)^x (A_2^{-b})^y - (a_2)(a_1)^x (A_1^{-b})^y} \quad (9)$$

An example of the data obtained by ion-exchange methods is furnished by the results (12) of a study of the dissociation constant of strontium tartrate. The experimental set-up consisted of 0.5 g. of air-dried cation-exchange resin converted to its ammonium salt and 50 ml. of a solution containing a known amount of tartaric acid, 0.2 molar in ammonium chloride and about  $10^{-9}$  mole of radiostrontium. The radiostrontium used was  $\text{Sr}^{89}$  decaying as follows:



At two different concentrations of tartaric acid the dissociation constants,  $K_c$ , for the reaction:



were found to be  $1.99 \times 10^{-2}$  and  $2.04 \times 10^{-2}$ , respectively. The average value,  $2.02 \times 10^{-2}$  or  $\text{p}K_c = 1.69$ , is in good agreement with that of Cannan and Kibrick (3), who found  $\text{p}K_c = 1.65$  from a study of hydrogen electrode titration curves of potassium chloride-strontium chloride mixtures at an ionic strength of 0.2. The agreement between the two values is even closer when corrections for activity coefficients are considered.

We may summarize the advantages of the ion-exchange method for the determination of the dissociation constants as follows: (1) Only tracer quantities of elements are necessary. (2) It is workable over wide temperature and pH ranges. From the biochemical point of view this is important because one can measure the stability of a complex under physiologically important conditions. (3) It is both rapid and simple. Additionally, different cations can be worked with simultaneously in the same solution by the use of a tracer mixture followed by radiochemical analysis. (4) It appears to be capable of good accuracy and precision.

The method as such should serve as a valuable tool for the study of the solution thermodynamics of complex ions. For example, detailed studies of the variation of  $K_c$  of strontium citrate with temperature and in, say, dioxane-water mixtures, would yield data of fundamental value. Furthermore, it would be of interest to apply the method to compounds of biological importance, e.g., metal proteinates.

Paper II of this series will report (with J. W. Richter) the results obtained from a study of the dissociation constants of metallic citrates and tartrates of strontium.

#### RAPID DETECTION AND EVALUATION OF RELATIVE COMPLEX-FORMING PROPERTIES

Aside from the quantitative measurements of dissociation constants, ion exchange may be applied for rapidly testing the efficacy of complex-forming agents toward radioclements in a given solution. One can employ such a ratio of weight of adsorbent to volume of a given solution that the adsorption of a cationic radioclement is in the region of 50 per cent. The addition of equimolar concentrations of different reagents to individual solutions will serve as a means then of

detecting complex-forming action and of determining qualitatively the relative strength of the different complexes formed. This procedure is of great use in devising schemes for chromatographic separations of inorganic elements.

#### DETERMINATION OF ACTIVITY COEFFICIENTS

It has been shown (2) that the adsorption of mixtures of monovalent and divalent cations by a synthetic resin like Amberlite IR-1 obeys the law of mass action (*a*) when the activities of the solid-phase components are expressed in terms of their mole fractions, (*b*) when the thermodynamic activities of the ions in the solutions are employed, and (*c*) when the anionic part of the adsorbent is taken to have an apparent charge of unity. These results agree with the equations developed by Vanselow (14) based on experimental work with inorganic zeolites. He was the first to point out the utility of cation exchange as a method for measuring activity coefficients and applied it to the barium-cadmium exchange reaction on bentonite (15).

Consider a system containing a cation exchanger which is saturated with a cation  $M^{+n_1}$  and immersed in a solution containing the cations  $P^{+n_2}$ ,  $Q^{+n_3}$ , etc. Under equilibrium conditions, the reaction is:

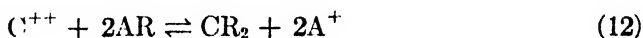


where R designates the insoluble anionic part of the exchanger.

The thermodynamic expression of the equilibrium constant is:

$$K_a = \frac{a^c PR_{n_2} a^d QR_{n_3} \cdots a_{M^{+n_1}}^e}{a_{P^{+n_2}}^c a_{Q^{+n_3}}^d \cdots a_{MR_{n_1}}^r} \quad (11)$$

For the reaction involving the monovalent cation  $A^+$  and the divalent cation  $C^{++}$  we may write:



The exchange constant,  $K_a$ , becomes

$$K_a = \frac{(CR_2)(CR_2 + AR)(A^+)^2 \gamma_{A^+}^2}{(AR)^2 (C^{++}) \gamma_{C^{++}}} \quad (13)$$

where the quantities in parentheses are the concentrations in moles per liter and  $\gamma_{A^+}$  and  $\gamma_{C^{++}}$  are the activity coefficients of cations  $A^+$  and  $C^{++}$ , respectively.

If  $C^{++}$  is present in radiochemical amounts in a solution of  $A^+$ , then equation 13 becomes

$$K_a = \frac{(CR_2)(A^+)^2 \gamma_{A^+}^2}{(AR)(C^{++}) \gamma_{C^{++}}} \quad (14)$$

since  $(AR) \gg (CR_2)$ .

It is convenient to introduce  $K_c$ , namely:

$$K_c = \frac{(CR_2)(A^+)^2}{(AR)(C^{++})} \quad (15)$$

Thus we can now determine  $\gamma_{c^{++}}$  by means of the following relation:

$$\gamma_{c^{++}} = \frac{K_c}{K_a} \times \gamma_{A^+}^2 \quad (16)$$

Since  $C^{++}$  is present in effect at zero concentration, the activity coefficient of  $A^+$  is exactly that of its pure solution. The quantities  $K_c$  and  $K_a$  are easily determined (2), so that by choosing a bulk electrolyte for which the activity coefficients are known we have a simple means of directly measuring the activity coefficient of an electrolyte present in that solution in concentrations of the order of  $10^{-3}M$ . Naturally,  $C^{++}$  and  $A^{++}$  are actually expressed in terms of the Lewis and Randall mean activity coefficients.

The way is clear, then, for a systematic investigation of the thermodynamics of numerous solutions of mixed electrolytes. Utilizing the techniques of radiochemical analysis, one can study the activity coefficients of several electrolytes simultaneously. Measurement of activity coefficients of radiotracers in uranyl nitrate solutions has been made (10).

#### RADIOCOLLOID INVESTIGATIONS

There exist many instances where the adsorption of a radiotracer by a cation exchanger is the result of processes other than cation exchange. It is possible to relate such anomalous behavior to radiocolloid formation and consequently to utilize cation exchangers for the detection and study of this phenomenon.

Several naturally occurring radioelements have been shown to exist in the colloidal state under the proper conditions of pH, etc. Such phenomena as slow diffusion, inability to dialyze through membranes, and inversion of charge are obtained with radiocolloids.

As expected, it is found that colloidal substances are adsorbed by a cation exchanger, not through cation exchange, but because the exchanger offers a favorable site for adsorption by virtue of its surface properties. In such cases, one would anticipate, as is indeed the case, that any finely divided material such as charcoal and inorganic oxides as well as the surfaces of the vessels containing the radiocolloid would serve as adsorption sites. From the known behavior of the cation exchangers as given earlier in this paper, we can establish criteria for detecting and interpreting radiocolloidal behavior by means of cation exchange. It is of interest to add that the conclusion drawn as to the existence and nature of radiocolloids from cation-exchange data has been confirmed (1) from studies of diffusion rates, ultracentrifugation, and dialysis.

##### *1. Effect of increasing bulk electrolyte concentration over wide ranges*

In contradistinction to the adsorption of a cation, the adsorption of a radiocolloid will remain relatively unaffected or even increase with increasing bulk electrolyte concentration. Thus the bulk electrolyte may act as a coagulating agent and enhance the degree of adsorption of the radiocolloid.

There exist conditions under which the concentration and the type of bulk electrolyte and the quantity of adsorbent are so fixed that the adsorption of any



true cation, regardless of valence, is very small or negligible, yet even in these cases the adsorption of radiocolloids will at times exceed 90 per cent. Such behavior allows the conclusion that the proportion of true cation coexisting with the particular element is very small.

### *2. Effect of increasing the concentration of the radiocolloid*

When one has a solution containing a known concentration of a true cationic radioelement, then the adsorption of the cation as its concentration is increased (say from  $10^{-9}$  to  $10^{-1}M$ ) by means of inactive carrier is quite characteristic from the mass-action expression (2). A radiocolloid behaves quite differently under similar conditions and generally the adsorption will not be affected in the same manner.

### *3. Effect of pH*

Generally, a decrease in the pH of a given solution results in a decrease in adsorption of a cation because of (a) reduction in the actual capacity per gram of the exchanger and (b) the mass-action effect of the hydrogen ion. Many radiocolloids, on the other hand, will be increasingly adsorbed as acid is added to the solution. It may be found that a certain acid concentration dissolves the radiocolloid. This condition will often reveal itself by a very striking and sudden change in the degree of adsorption of the element affected.

### *4. Effect of complex-forming agents*

While the adsorption of a radiocolloid is relatively unaffected by many substances, both inorganic and organic, the addition of small amounts of some substances will result in a remarkable decrease in its adsorption. Naturally, this effect will be greater, the stronger is the complex formed. It is possible therefore to determine the relative complex-forming strength of a series of anions toward a colloid by determining, for example, the effect of a given concentration on the adsorption. Naturally all other conditions such as quantity of adsorbent and volume of solution would be kept constant.

When experimenting with colloids, particularly radiocolloids, it is important to take into account factors such as their mode of preparation, conditions, and length of previous storage, and the order of addition of reagents. The criteria given here for the study of radiocolloids can be expanded to include effects such as the rôle of adsorption, reversibility of behavior and the like, but those given above have proved ample. Paper III of this series will give the results of the study of a large number of radiocolloids by the ion-exchange method.

### *5. Eluting characteristics*

Once an element is adsorbed by the exchanger, useful information may be obtained by separating out the exchanger and placing it in fresh solution. Depending on the cation concentration of the new solution, more or less of the adsorbed material will be displaced, assuming the absence of complex-forming action. If the material was adsorbed by cation-exchange properties, then it

will be displaced to an extent dependent on the effective cation concentration in the solution. An adsorbed radiocolloid usually will not be eluted by such a procedure.

In general, one can employ the eluting studies instead of merely studying the adsorption properties above, not only for radiocolloid studies but in the other cases discussed in this paper.

#### QUALITATIVE DETERMINATION OF THE STATE OF A RADIOELEMENT IN SOLUTION

From the information given in the preceding sections, it is apparent that the criteria exist for rapidly determining whether in a given solution a given substance is a cation, an anion, or a colloid. For example, if the substance is not adsorbed under conditions where adsorption of even the more weakly adsorbed cations such as  $\text{Na}^+$  and  $\text{K}^+$  occurs to an appreciable extent, then we can conclude that we are dealing with an anionic or neutral substance.

Experimental conditions, in particular the ratio of solution volume to adsorbent weight, should be chosen so that the extent of adsorption of the more weakly adsorbed and more strongly adsorbed cations is determinable to a significant extent.

#### DETERMINATION OF THE VALENCE AND RELATIVE BASICITY OF A RADIOELEMENT

If an unknown radioelement proves to be a cation, then it is possible to determine its probable valence and even its relative basicity. This is most conveniently done by choosing as a standard some bulk electrolyte in which the relative adsorption under given conditions of known cations of various valence groups is known. The elements will arrange themselves according to valence. It may be found, for example, by a single experiment, that an unknown cation is adsorbed to an extent characteristic of the trivalent cations. This immediately furnishes a valuable clue.

Furthermore, it has been shown by Jenny (6) and others (2) that for a given valence series of cations, the adsorption of cations will in general be greater, the smaller is the hydrated radius in solutions. Thus, we find that the order of increasing adsorption of the alkaline earths, for example, is  $\text{Ba}^{++} > \text{Sr}^{++} > \text{Ca}^{++}$ . The ease of removal is in the reverse order.

Even if the adsorption result is on the borderline between two valence states, we can at least specify which two valence states are indicated. The particular valence state in the adsorbent (see below) can be placed in many cases, by determining the dependence of adsorption of the unknown cation with changes in the concentration of the bulk electrolyte. It follows from the mass-action expression that the variation in adsorption of the radioelement will vary as some definite power of the bulk electrolyte concentration, depending on the valence which the adsorbed radiocation possesses in the adsorbent. In general, the valence which an adsorbed cation possesses in the adsorbent will be its maximum valence, up to and including the tetravalent state.

With experience it is found that ion exchange is a very rapid and simple method for characterizing the nature of radioelements in solution and for classifying qualitatively the chemical nature of unknown radioisotopes.

It should also be mentioned that the relative effects of complex-forming agents on a radioelement also serve as a means of placing the valence and basicity of an element. For example, the Th(IV) citrate complex forms one group, the rare earth citrate complexes fall in another group, etc. Within each group the behavior of each element relative to the other is related to the basicity (11).

#### DISCUSSION

While the organic ion exchangers are very stable toward a great variety of reagents (2), it is important to recognize some of their limitations. In general, they are affected by nitric acid and should not be employed with solutions of nitric acid which are stronger than 0.1 *M*. On the other hand, they are quite stable toward even 6 *M* solutions of hydrochloric or sulfuric acid. They undergo serious changes in solutions more alkaline than  $\text{pH} = 9$ .

Anionic exchangers are, generally, more sensitive to temperature than the cation exchangers, becoming unstable in the regions of 40°C. The organic cation exchangers, depending on the particular solution environment, appear to be stable even at temperatures approaching 100°C.

The inorganic cation exchangers such as the sodium aluminosilicates are not stable in acid solutions and function best in the pH region of  $\sim 4.5$ –7. They have the further disadvantage of sometimes reacting with the heavy metals to form insoluble silicates which cannot be removed by ordinary cation-active reagents. Additionally, their adsorptive capacity is relatively low compared to the organic exchangers and varies with particle size.

The extent to which the principles and methods described here can be applied to the study of the complex-forming action of biological substances such as proteins and amino acids is a problem deserving of attention.

By utilizing other phases of the behavior of ion exchangers it should be possible to extend their uses as a physicochemical tool. The kinetics of the adsorption process can probably be useful, for example, in establishing further criteria by which true ions and colloids can be distinguished from one another.

#### SUMMARY

The exchange of cations by the synthetic resin cation exchangers is made the basis for numerous applications to physical-chemical problems. Many of these applications require only radiochemical concentrations of an element. It is shown how it is possible to measure quantities such as the dissociation constants of complex ions and activity coefficients of electrolytes present in nearly zero concentration in the presence of macroscopic concentrations of another electrolyte. In addition, a knowledge of the behavior of cation-exchange systems is utilized for the detection and study of radiocolloids, the qualitative determination of the state of a radioelement in solution, and the determination of the valence and basicity of cationic radioelements.

## REFERENCES

- (1) BOYD, G. E., BROSI, A. R., CONN, E., LESLIE, W., AND SCHUBERT, J.: Unpublished work.
- (2) BOYD, G. E., SCHUBERT, J., AND ADAMSON, A. W.: *J. Am. Chem. Soc.* **69**, 2818 (1947).
- (3) CANNAN, R. K., AND KIBRICK, A.: *J. Am. Chem. Soc.* **60**, 2314 (1938).
- (4) GLASSTONE, S.: *Physical Chemistry*, p. 955. D. Van Nostrand Company, Inc., New York (1940).
- (5) HASTINGS, A. B., McLEAN, F. C., EICHELBERGER, L., HALL, J. L., AND DaCOSTA, E.: *J. Biol. Chem.* **107**, 351 (1934).
- (6) JENNY, H.: *J. Phys. Chem.* **36**, 2217 (1932).
- (7) MYERS, R. J.: "Synthetic Resin Ion Exchangers," in *Advances in Colloid Science*, Vol. I. Interscience Publishers, Inc., New York (1942).
- (8) NELSON, R., AND WALTON, H. F.: *J. Phys. Chem.* **48**, 406 (1944).
- (9) PAULING, L.: *The Nature of the Chemical Bond*, 2nd edition, p. 3. Cornell University Press, Ithaca, New York (1940).
- (10) SCHUBERT, J.: Unpublished work.
- (11) SCHUBERT, J., AND REVINSON, D.: Unpublished work.
- (12) SCHUBERT, J., AND RICHTER, J. W.: *J. Phys. Colloid Chem.* **52**, 350 (1948).
- (13) SUSSMAN, S., AND MINDLER, A. B.: *Chem. Ind.* **16**, 789 (1945).
- (14) VANSELOW, A. P.: *Soil Sci.* **33**, 95 (1932).
- (15) VANSELOW, A. P.: *J. Am. Chem. Soc.* **54**, 1307 (1932).

THE USE OF ION EXCHANGERS FOR THE DETERMINATION  
OF PHYSICAL-CHEMICAL PROPERTIES OF SUBSTANCES,  
PARTICULARLY RADIOTRACERS, IN SOLUTION. II

THE DISSOCIATION CONSTANTS OF STRONTIUM CITRATE AND STRONTIUM  
TARTRATE<sup>1</sup>

JACK SCHUBERT<sup>2</sup> AND J. W. RICHTER<sup>3</sup>

*Clinton Laboratories, Oak Ridge, Tennessee*

*Received August 20, 1947*

INTRODUCTION

Cations of the alkaline earths readily form complex ions with the anions of carboxylic acids. The most commonly used methods for measuring the dissociation constants of these complex ions are the determination of solubility (7) and electrometric procedures (4, 6). The dissociation constants of the citrate complexes of calcium, strontium, and magnesium have also been studied, using a

<sup>1</sup> The specific material discussed here is derived from part of the studies reported in May 1945 by the authors and is based on work performed under Manhattan District Contract No. W-7405-Eng-39 at the Clinton Laboratories, Oak Ridge, Tennessee.

<sup>2</sup> Present address: Department of Physiological Chemistry, University of Minnesota, Minneapolis 14, Minnesota.

<sup>3</sup> Present address: Department of Chemistry, University of Minnesota, Minneapolis 14, Minnesota.

frog heart preparation (5). These techniques, except the ion-exchange method, require that all of the components of the complex ion be present in macroscopic concentration. Paper I of this series included a discussion of the theory and a development of the equations employed when using a cation exchanger for the determination of the dissociation constants of certain soluble complex ions (9). A unique feature of the ion-exchange method is the fact that the dissociation constant of an organometallic complex ion is measured when the metal component is present in radiochemical concentrations, i.e., about  $10^{-11}$  mole per liter.

In this paper we shall present the experimental procedures and the results obtained from an ion-exchange study of the dissociation constants of the complex ions of strontium citrate and strontium tartrate. The measurements involved the determination of the percentage of radiostrontium which was adsorbed by the cation exchanger in the presence and absence of a known amount of citric acid or tartaric acid and in a solution adjusted to constant ionic strength with ammonium chloride.

## EXPERIMENTAL

### *The adsorbent*

In all cases the adsorbent used was the cation exchanger Amberlite IR-1<sup>4</sup> classified into particles of 40–60 mesh. The resin was converted to the ammonium form,  $\text{NH}_4\text{R}$ , by treating the hydrogen form,  $\text{HR}$ , of the resin with excess ammonium chloride at a pH of 7.5. The resin was washed free of excess salts with distilled water and was air dried. The ammonium resin contained 1.92 millimoles of exchangeable ammonium ion,  $\text{NH}_4^+$ , per gram of the air-dried material. The moisture content of the resin as determined by drying a sample to constant weight at  $110^\circ\text{C}$ . was found to be 18 per cent.

### *Solutions*

All the chemicals used were chemically pure. Stock solutions of citric acid and tartaric acid were made up just before they were used. Spectrographic analyses of the solutions after equilibration with the resin revealed no detectable quantities of foreign cations or of carrier strontium.

### *Radiotracer*

The tracer used was carrier-free  $\text{Sr}^{89}$  which has a half-life of 53 days,  $\text{Sr}^{89} \xrightarrow[53 \text{ d}]{\beta^-} \text{Y}^{89}$  (stable). A stock solution of ammonium chloride was "spiked" with the tracers. This solution was used to prepare all the solutions used in the experiments reported here. On the average the experimental solutions contained about 80 counts of  $\text{Sr}^{89}$  per second at 8 per cent geometry, i.e., a minimum of  $10^{-11}$  mole per liter.

<sup>4</sup> Manufactured by the Rohm and Haas Company, Resinous Products Division, Philadelphia, Pennsylvania.

*Analytical procedures*

Concentrations of ammonium ion in the equilibrium solutions were determined by a micro Kjeldahl procedure (10). The radiations from  $\text{Sr}^{89}$  were measured directly in a Geiger-Müller counter after evaporation of a given aliquot. Factors such as the geometry and the self-absorption characteristics were kept as uniform as possible. Inasmuch as the experiment consisted in measuring relative beta activities, no corrections for decay, self-absorption, and the like were found necessary.

*Equilibrium procedure*

A given weight of  $\text{NH}_4\text{R}$  and a given volume of solution were shaken for 3-hr. periods, after which the mixture was centrifuged and the centrifugant analyzed for the content of radiostrontium. It would have been advisable to determine the radiostrontium in the resin as well, had not conditions been chosen so as to yield results of optimum accuracy without necessitating a direct analysis on the resin.

Rate studies have shown that 3 hr. is sufficient time for the adsorption of the tracer to reach a reproducibly constant value (2).

## RESULTS AND DISCUSSION

The stoichiometric dissociation constant,  $K_c$ , for the complex ions of types like strontium citrate and strontium tartrate is given by the relation (4, 5, 6, 7):

$$K_c = \frac{(\text{SrA})^{2-z}}{(\text{Sr}^{++})(\text{A}^z)} \quad (1)$$

where A = the anionic part of the complex ion  $(\text{SrA})^{2-z}$  and  $z$  = the charge on the anion.

The equation which expresses the value of  $K_c$  in terms of cation-exchange equilibria follows:

$$K_c = \frac{(a)(A)}{\lambda_0 \left[ s - \frac{a}{\lambda_0} \right]} \quad (2)$$

where  $a$  = the per cent of the cation which is adsorbed by the exchanger at equilibrium when the complex-forming anion,  $\text{A}^z$ , is present,

$s$  = the per cent of the cation which remains in solution when  $\text{A}^z$  is present (i.e.,  $s = 100 - a$ ),

$A$  = the molar concentration of the complex-forming anion, and

$\lambda_0$  = the ratio  $a/s$  when A is absent from the solution, i.e., the slope of the adsorption isotherm.

*Effect of pH on adsorption of strontium*

All pairs of solutions must be compared at the same pH because the capacity of an ion exchanger, and hence  $\lambda_0$ , usually increases (8) with increasing pH. Measurements of the effect of pH on the adsorption of radiostrontium were made

at constant ionic strength ( $\mu = 0.2$ ) and are tabulated in table 1. It is seen that as the pH increased from 5 to 8 the variation of  $\lambda_0$  with pH is linear within experimental error (figure 1).

TABLE 1\*

*Adsorption of tracer concentrations of radiostrontium† from solutions of ammonium chloride ( $\mu = 0.20$ ) as a function of pH ( $t = 25^\circ\text{C}.$ )*

pH OF SOLUTION AT EQUILIBRIUM	Sr <sup>++</sup> IN SOLUTION AT EQUILIBRIUM	Sr <sup>++</sup> ADSORBED AT EQUILIBRIUM (CALCULATED)	$\lambda_0$
	<i>per cent</i>		
5.1	24.0	76.0	3.16
5.2	21.2	78.8	3.72
5.4	19.2	80.8	4.21
5.7	16.3	83.7	5.13
6.0	15.3	84.7	5.54
6.6	11.9	88.1	7.40
7.4	9.4	90.6	9.64
8.0	7.8	92.2	11.8

\* 0.5 g. of air-dried  $\text{NH}_4\text{R}$  was shaken with 50 ml. of solution for 3 hr. The pH of the solutions was adjusted with ammonium hydroxide.

† The original solutions contained 4900 counts of  $\text{Sr}^{90}$  per minute at a geometry of 8 per cent.

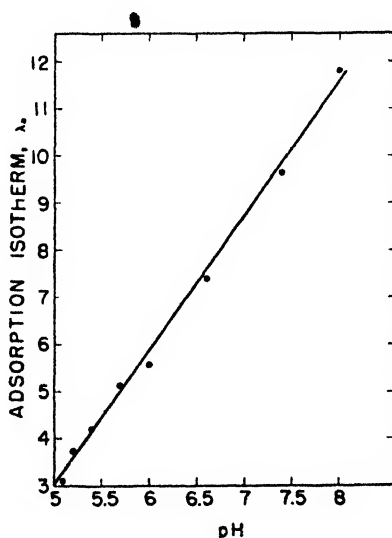


FIG. 1. Effect of pH on the adsorption isotherm,  $\lambda_0$ , of radiotracer  $\text{Sr}^{++}$  from 50 ml. of 0.20 M ammonium chloride by 0.5 g. (0.96 mole) of ammonium resin,  $\text{NH}_4\text{R}$ .  $t = 25^\circ\text{C}.$

#### *Dissociation constant of strontium tartrate*

Measurements were made under conditions similar to those employed in studying the variation of the adsorption of radiostrontium as a function of pH. The ammonium-ion concentration was kept constant at 0.2 mole per liter.

The total ionization of tartaric acid,  $\text{H}_2\text{C}_4\text{H}_2\text{O}_6$ , is practically complete at the pH and ionic strengths employed in our experiments (3). It has been shown that (4) the dissociation constant,  $K_c$ , of strontium tartrate is given by the relation:

$$K_c = \frac{(\text{Sr}^{++})(\text{Tar}^{--})}{(\text{Sr Tar})} \quad (3)$$

where  $\text{Tar}^{--}$  = the ionized anionic part of the tartaric acid molecule.

In table 2 are given the data from which the dissociation constant was calculated. Each point represents the average of at least two runs. The value of  $\lambda_0$  was obtained from figure 1. Equation 2 was used to calculate  $K_c$ . The average value found,  $2.02 \times 10^{-2}$  or,  $\text{p}K_c = 1.69$ , is in good agreement with the value of Cannan and Kibrick (4), who found  $\text{p}K_c = 1.65$  from a study of hydrogen electrode titration curves of potassium chloride-strontium chloride mixtures at a constant ionic strength of 0.2. While the agreement with their

TABLE 2\*

*The dissociation constant of strontium tartrate as calculated from ion-exchange data at  $25^\circ \pm 1^\circ\text{C}$ .*

CONCENTRATION OF TARTARIC ACID	pH OF SOLUTION AT EQUILIBRIUM	TRACER $\text{Sr}^{++}$ ADSORBED AT EQUILIBRIUM (CALCULATED)	TRACER $\text{Sr}^{++}$ IN SOLUTION AT EQUILIBRIUM	$\lambda_0$	$K_c$	$\text{p}K_c$
moles/liter		per cent	per cent			
0.10	5.46	41.1	58.9	4.20	$1.99 \times 10^{-2}$	
0.05	7.11	71.9	28.1	8.84	$2.04 \times 10^{-2}$	
Average.					$2.02 \times 10^{-2}$	1.69

\* 0.5 g. of air-dried ammonium resin was shaken for 3 hr. with 50 ml. of the solution which contained a total of 0.2 mole per liter of ammonium ion.

result is very good, it is possible to ascribe the direction of the deviation to the difference in the bulk electrolytes which were employed. There is evidence to indicate that the activity coefficient of a tracer substance is greatly influenced by the bulk electrolyte (2). The activity coefficient of potassium chloride at an ionic strength of 0.2 is greater than that of ammonium chloride at the same ionic strength. It is expected, therefore, that the activity coefficient,  $\gamma$ , of radiosttrontium would be slightly greater (at least for mixtures of halide salts) in solutions of potassium chloride than in solutions of ammonium chloride. From the relation

$$K_c = K_a \frac{\gamma_{\text{Sr}^{++}} \gamma_{\text{Tar}^{--}}}{\gamma_{\text{Sr Tar}}} \quad (4)$$

where  $K_a$  is the thermodynamic dissociation constant, it is seen that the dissociation constant of strontium tartrate dissolved in ammonium chloride would tend to be less than in potassium chloride solutions.



*Dissociation constant of strontium citrate*

From the known ionization constants of citric acid (1) it can be shown that under the conditions of our experiments, citric acid is completely ionized to the tertiary citrate ion,  $\text{Cit}^{--}$ , where  $\text{Cit}^{--}$  represents the anionic part,  $\text{C}_6\text{H}_5\text{O}_7$ .

TABLE 3  
Dissociation constant of strontium citrate,  $\text{Sr Cit}^-$ , calculated from ion-exchange data at  $25^\circ \pm 1^\circ\text{C}$ .

SAMPLE NO.	WEIGHT OF $\text{NH}_4\text{R}$	VOLUME OF SOLUTION	CONCENTRATION OF CITRIC ACID	pH OF SOLUTION AT EQUILIBRIUM	RADIOSTRONTIUM ADSORBED	TOTAL CONCENTRATION OF $\text{NH}_4$	SLOPF, $\lambda_0$ , FOR GIVEN CONDITIONS*	$K_c$	$\text{p}K_c$
	grams	ml.			per cent	moles/liter			
A	0.50	50.0	0	8.10	94.6	0.165	17.3		
A'	0.5	50	0	8.10	94.5	0.165			
1..	0.5	50	0.02	7.76	54.5	0.165	15.8	$1.63 \times 10^{-3}$	
1'..	0.5	50	0.02	7.76	54.7	0.165	15.8	$1.66 \times 10^{-3}$	
2..	0.5	50	0.01	7.64	67.1	0.165	15.4	$1.53 \times 10^{-3}$	
3..	0.5	50	0.005	7.10	73.4	0.165	13.1	$1.33 \times 10^{-3}$	
							Average	$1.54 \times 10^{-3}$	2.81
4...	5.0	50	0	6.80	67.8	1.05	2.1		
4'...	5.0	50	0.05	6.80	20.6	1.05	2.1	$7.03 \times 10^{-3}$	
5..	10.0	50	0	6.72	80	1.05	4.0		
5'..	10.0	50	0.05	6.70	30.4	1.05	4.0	$6.12 \times 10^{-3}$	
							Average	$6.58 \times 10^{-3}$	2.18

\* The values of  $\lambda_0$  for samples A'-3 were estimated from equation 6 as described in the text.

The dissociation constant for strontium citrate has been shown (5, 6) to be given by the relation:

$$K_c = \frac{(\text{Sr}^{++})(\text{Cit}^{--})}{(\text{Sr Cit}^-)} \quad (5)$$

In the present series of experiments the dissociation constant of strontium citrate was studied at two different concentrations of ammonium ion, 0.16<sub>5</sub> and 1.0<sub>5</sub> moles per liter. The results obtained are tabulated in table 3. Each point represents the average of at least two separate runs.

The  $\text{p}K_c = 2.81$  found for strontium citrate when the total ammonium-ion concentration was 0.16<sub>5</sub> moles is in good agreement with the value  $\text{p}K_c = 2.70$  reported by Hastings *et al.* (5), and the value,  $\text{p}K_c = 2.92$ , reported by Joseph (6). The expected salt effect was manifested when an increase in the total salt concentration to 1.0<sub>5</sub> molar resulted in a more than fourfold increase in the dissociation constant.

In order to calculate the  $K_c$  for strontium citrate when the total  $\text{NH}_4^+ = 0.16_s M$ , it was necessary to make the assumption that the change in  $\lambda_0$  with pH was the same as when the concentration of  $\text{NH}_4^+ = 0.20$ . An indication as to the validity of the assumption that the effect of pH on  $\lambda_0$  is the same over such a short range of salt concentrations is the fact that the values of  $\lambda_0$  which are obtained at any one pH are in perfect agreement with the ones which are calculated from the mass action expressions (2). The latter relation assumes that  $\lambda_0$  varies as the square of the ammonium-ion concentration. For example, at a pH of 8.1 we find that when  $(\text{NH}_4^+)_b = 0.20 M$ ,  $\lambda_0^b = 11.84$ . Then we can calculate  $\lambda_0^a$  when  $(\text{NH}_4^+)_a = 0.16_s M$  by means of the relation

$$\lambda_0^a = \frac{\lambda_0^b \times (\text{NH}_4^+)_b^2}{(\text{NH}_4^+)_a^2} = 1.47\lambda_0^b \quad (6)$$

whence  $\lambda_0^a = 17.4$ , which is in agreement with the experimentally observed value given in table 3.

#### SUMMARY

The ion-exchange method was used to measure the dissociation constants of strontium citrate and strontium tartrate. All the measurements were made at 25°C. and at a pH of about 7. The ionic strength of the solutions was furnished entirely by ammonium salts, since the total concentration of radiostrontium was of the order of  $10^{-11}$  mole per liter. The  $pK_c$  for strontium tartrate was found to be 1.69 when the total ammonium-ion concentration in solution was 0.16<sub>s</sub> mole. Under the same conditions the  $pK_c$  of strontium citrate was equal to 2.81. When the total ammonium-ion concentration was 1.05 moles per liter, the  $pK_c$  of strontium citrate was 2.18. These results are in excellent agreement with the values reported in the literature.

Supplementary studies showed that as the pH increased from 5 to 8 there was a steady and marked increase in the amount of radiostrontium adsorbed by the cation exchanger. This result emphasizes the importance of pH control in cation-exchange reactions.

The authors wish to thank Mr. N. M. Byerly and the Clinton Laboratories Analytical Group for making some of the analyses reported here.

#### REFERENCES

- (1) BJERRUM, N., AND UNMACK, A.: Kgl. Danske Videnskab. Selskab, Math.-fys. Medd. **9**, 153 (1929).
- (2) BOYD, G. E., SCHUBERT, J., AND ADAMSON, A. W.: J. Am. Chem. Soc. **69**, 2818 (1947).
- (3) BRITTON, H. T. S.: *Hydrogen Ions*, Vol. I, p. 194. D. Van Nostrand Company, Inc., New York (1943).
- (4) CANNAN, R. K., AND KIBRICK, A.: J. Am. Chem. Soc. **60**, 2314 (1938).
- (5) HASTINGS, A. B., McLEAN, F. C., EICHELBERGER, L., HALL, J. L., AND DaCOSTA, E.: J. Biol. Chem. **107**, 351 (1934).
- (6) JOSEPH, N. R.: J. Biol. Chem. **164**, 529 (1946).
- (7) MUUS, J., AND LEBEL, H.: Kgl. Danske Videnskab. Selskab, Math.-fys. Medd. **13**, No. 19 (1936).

- (8) NELSON, R., AND WALTON, H. F.: *J. Phys. Chem.* **48**, 406 (1944).  
(9) SCHUBERT, J.: *J. Phys. Colloid Chem.* **52**, 340 (1948).  
(10) TREADWELL, F. P., AND HALL, T. W.: *Analytical Chemistry*, 9th edition, Vol. II, p. 493. John Wiley and Sons, Inc., New York (1942).

## THE THERMAL DECOMPOSITION OF TERTIARY BUTYL ACETATE<sup>1</sup>

CHARLES E. RUDY, JR., AND PAUL FUGASSI

*Department of Chemistry, Carnegie Institute of Technology, Pittsburgh, Pennsylvania*

*Received August 20, 1947*

In a flow experiment carried out at 360°C., Hurd and Blunck (6) showed that *tert*-butyl acetate pyrolyzed into isobutylene and acetic acid. Their distillation analysis indicated the absence of isomeric butylenes, and qualitative tests upon the products showed the absence of acetaldehyde, ketene, and acetic anhydride. As it appeared from the analytical data that the gaseous decomposition of *tert*-butyl acetate might have a simple mechanism, it has been investigated in greater detail because organic decompositions of this type are rare and further information upon the less complex reactions is desirable. In this paper the kinetics of the decomposition of *tert*-butyl acetate will be described.

### PREPARATION OF ESTER

The ester was prepared from *tert*-butyl alcohol and acetic anhydride, using the procedure of Norris and Rigby (8). Eastman's "practical" acetic anhydride was distilled and a fraction separated boiling in the range 132°–137°C. The alcohol was an Eastman product and was purified by crystallization and distillation according to the procedure of Schultz and Kistiakowsky (10). After the ester was stripped from the reacting mixture, the crude product was purified by distillation, using a 5-ft. vacuum-jacketed column with wire-spiral packing. After two distillations the refractive index of the distillate reached a constant value. The purified ester had a standard boiling point of 97.7°C., a specific gravity,  $d_4^{25}$ , of 0.8604, and a refractive index,  $n_D^{25}$ , of 1.3837. The values cited are in close agreement with those given by Norris and Rigby (8) and by Bryant and Smith (2).

### EXPERIMENTAL PROCEDURE

The decomposition of the ester was followed in a constant-volume system by measuring the pressure at definite time intervals. A glass diaphragm gauge with

<sup>1</sup> Presented before the Division of Physical and Inorganic Chemistry at the 104th Meeting of the American Chemical Society, which was held in Buffalo, New York, September, 1942.

This paper is abstracted from the thesis submitted by Charles E. Rudy, Jr., to the Faculty of the Graduate School of the Carnegie Institute of Technology in partial fulfillment of the requirements for the degree of Doctor of Science in Chemistry, April, 1942.

electrical contacts, similar to the one described by Daniels (4), was used for the pressure measurements. The reaction cell had a volume of about 60 cc. and was connected to the vacuum line with the shortest possible length of 2-mm. capillary tubing. The cell could be closed off from the vacuum line with a glass stopcock sealed with Picein cement. The stopcock was equipped with an electrical heater so that the Picein cement could be melted when it was necessary to manipulate the stopcock. It was found that, over periods of some hours, small amounts of the reaction products dissolved in the solid cement, so an arrangement was used by which a short column of mercury could be placed in the capillary tube leading to the reaction cell after the cell had been filled with reactant. The column of mercury effectively shielded the product gases from the lubricant during the course of an experiment. In the vacuum line mercury "cut-offs" were used throughout, so that the ester came in contact only with glass and mercury. The vacuum line and cell could be evacuated with a two-stage mercury diffusion pump backed by a Hyvac oil pump.

A mercury-vapor thermostat was employed for the constant-temperature bath. It was constructed of steel in the form of a Dewar flask. Mercury vapor was confined to the annular space between the inner and outer cylinders. The inner cylinder was filled with a mixture of fused nitrites. Thermocouple readings taken at various distances from the bottom of the inner cylinder indicated that the temperature was constant within  $0.2^\circ$  at  $360^\circ\text{C}$ . over a distance of about 4 in., starting at a point 1 in. above the bottom of the inner cylinder. At the temperatures where experiments were carried out, the temperature gradient would be still smaller. The reaction cell was located in the constant-temperature zone. A calibrated, four-junction, copper-constantan thermocouple was placed alongside the cell and was used for measuring the temperature of the cell. The calibration of the thermocouple checked very closely over a range of  $120^\circ$  with the temperatures predicted from the known vapor pressures of mercury. The vapor thermostat was provided with a modified Coffin barostat (3), in which the mercury in the control manometer was replaced by ethylene glycol, and a separate mercury manometer was provided for reading the gas pressure over the boiling mercury.

#### HOMOGENEITY OF THE REACTION

In clean glass vessels the decomposition of the ester is heterogeneous and not reproducible. However, if the products of the decomposition are allowed to remain in the cell for some time at the temperature of the reaction, the glass surface becomes inert and measurements are reproducible. The period of time necessary to inactivate the surface decreases markedly as the temperature is increased. At  $360^\circ\text{C}$ . the surface is inert after being in contact with the reaction products overnight. At  $300^\circ\text{C}$ . much longer times are required for surface deactivation. The surfaces of all cells used for taking the data given here were deactivated at  $360^\circ\text{C}$ . Similar effects have been reported for the decomposition of other *tert*-butyl compounds (10). The nature of the deactivation process is not known, but it appears probable that isobutylene forms a polymeric film on the surface. Inspection of a deactivated cell gave no evidence of a film, but

some evidence in favor of this assumption was obtained by means of the following experiment: To a reaction cell 3.2 g. of 200-mesh Pyrex powder was added and a series of rate measurements was made at 291°C. In the first experiment the rate of decomposition was immeasurably fast. The reaction products were allowed to remain in the flask overnight, and the experiment was repeated the following day. With successive experiments the rate of decomposition decreased, until at the seventh experiment the rate was approximately ten times faster than the normal rate. When the glass powder was removed from the cell, it was found to be light brown in color indicating that some type of film had been formed. No film was visible on the walls of the cell.

In carrying out the experiments reported here, the surface was deactivated at 360°C. and a series of experiments made at lower temperatures. The surface was treated again at 360°C., and check experiments were made at the lower temperature. This procedure was repeated several times, and excellent checks were obtained. The fact that experimental values could be closely reproduced, together with the fact that a plot of  $\log k$  vs.  $1/T$  is a straight line over a wide temperature range, indicates that the reaction as studied is essentially homogeneous.

#### ORDER OF THE REACTION

Within the accuracy of measurement the final pressure,  $p_\infty$ , is twice the initial pressure,  $p_0$ , as obtained by extrapolating pressure readings back to zero time. The decomposition of the ester is first order, as indicated by the fact that the usual  $\log(p_\infty - p_t)$  vs. time plot gave straight lines out to 95 per cent decomposition. In addition, as tabulated in table 1, the time of half-life is independent of the initial pressure, and the ratio of the time of three-quarters life to the time of half-life is 2, as required by a first-order process.

#### VELOCITY CONSTANTS AND ENERGY OF ACTIVATION

Velocity constants were calculated graphically by preparing plots of  $\log(p_\infty - p_t)$  vs. time and measuring the slope of the best straight line through the experimental points. The values of  $k$  determined in this manner are tabulated in table 2.

If the logarithms of the velocity constants listed in table 2 are plotted against the reciprocal of the absolute temperature, a straight line is obtained whose equation is

$$\log k (\text{sec.}^{-1}) = 13.342 - \frac{40,500}{2.3RT} \quad (1)$$

The energy of activation for the decomposition of *tert*-butyl acetate is accordingly 40,500 cal.

#### LOW-PRESSURE EXPERIMENTS

A series of experiments were made in the vicinity of 290°C. in which low initial pressures of ester were used. The experimental data are shown in table 3. The

TABLE 1  
*Times of fractional life*

TEMPERATURE	$p_0$	$t^{1/2}$	$t^{3/4}$	$t^{5/4}/p^{1/2}$
°C.	mm. Hg	min.	min.	
303.1	127.2	1.18	2.40	2.04
303.3	102.5	1.27	2.42	1.91
303.5	117.7	1.23	2.43	1.98
291.2	23.9	2.32	4.97	2.14
292.1	158.1	2.33	4.83	2.07
279.6	236.8	4.63	9.67	2.09
278.3	79.5	5.72	11.52	2.02
269.0	195.3	11.57	23.60	2.04
256.2	208.3	26.30	54.20	2.06
243.6	274.1	74.50	155.30	2.08

TABLE 2  
*Velocity constants*

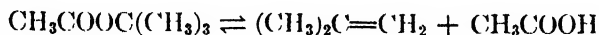
TEMPERATURE	$p_0$	$k \times 10^3$	TEMPERATURE	$p_0$	$k \times 10^3$
°C.	mm. Hg	sec. <sup>-1</sup>	°C.	mm. Hg	sec. <sup>-1</sup>
303.8	132.9	9.33	279.6	236.8	2.054
303.3	102.5	9.40	278.3	160.0	2.042
303.5	117.7	9.60	278.7	51.8	1.935
303.4	13.6	9.56	278.3	79.5	1.918
303.5	111.9	9.76	268.6	143.0	0.980
303.1	202.7	9.31	268.7	113.6	0.968
303.1	59.4	9.44	268.8	263.1	1.000
303.1	127.2	9.43	269.0	195.3	0.975
303.2	84.3	9.34	268.1	88.1	0.962
291.4	116.8	4.40	254.9	205.9	0.357
291.4	128.6	4.39	255.1	65.3	0.371
291.8	130.8	4.61	255.2	126.6	0.386
291.5	176.6	4.47	255.2	163.4	0.392
292.1	122.3	4.40	255.4	140.0	0.391
291.9	167.4	4.69	256.2	208.3	0.413
292.1	71.4	4.80	256.3	126.5	0.415
292.1	158.1	4.59	255.7	101.3	0.412
291.5	136.8	4.59	255.8	224.5	0.412
291.2	23.9	4.44	255.6	50.0	0.383
291.4	51.3	4.50	242.2	181.1	0.145
290.9	28.7	4.43	242.6	150.0	0.138
291.4	55.5	4.70	243.4	146.6	0.148
278.4	141.8	1.960	243.6	274.1	0.147
279.1	107.4	1.953	242.7	172.6	0.151
279.3	189.1	1.989			

velocity constants given in the last column of this table are the values given in the third column corrected to 291°C. The average value of the constants given in the last column is  $4.46 \times 10^{-3}$  compared to the value  $4.38 \times 10^{-3}$  obtained

from the preceding equation. It is apparent that the value of  $k$  is not decreasing with the pressure and that the pressure at which falling off in  $k$  will be obtained is less than 3.8 mm., as would be expected for a molecule as complicated as *tert*-butyl acetate.

## DISCUSSION

The analytical data of Hurd and Blunck (6), together with the fact that the pressure doubles, indicate that the decomposition of *tert*-butyl acetate occurs according to the equation



and that the equilibrium lies far to the right. It is of interest to determine whether thermodynamic data would predict an equilibrium favoring the products and insignificant dimerization of acetic acid at the temperatures and pressures used in our experiments.

TABLE 3  
*Low-pressure experiments*

TEMPERATURE	$p_0$	$k \times 10^3$	$k \times 10^3$
°C	mm.	sec. <sup>-1</sup>	sec. <sup>-1</sup>
291.40	17.0	4.32	4.21
291.45	16.0	4.99	4.86
290.20	12.8	3.80	4.03
290.75	10.4	4.44	4.51
290.80	9.9	4.27	4.33
291.20	6.3	4.80	4.72
290.80	5.8	4.42	4.48
291.25	5.5	3.84	3.77
291.30	3.8	5.35	5.27

Since the decomposition of the ester is an endothermic reaction, the equilibrium constant was calculated at 525°K., which is approximately the lowest temperature at which rate measurements were made. Unfortunately, the free energy of formation of *tert*-butyl acetate is not known, so that approximations must be made. An approximation based on the methods of Parks and Huffman (9) yielded  $\Delta F^0$  at 525°K. = -10,600 cal. for the reaction as written above. Another approximation, based in part on the free-energy equations of Bruins and Czarnecki (1), gives at 525°K.  $\Delta F^0$  = -12,600 cal. As these values yield an equilibrium constant of about  $10^5$ , it is obvious that the reaction is essentially complete as written. For the dimerization of acetic acid there are available the data of MacDougall (7) and Fenton and Garner (5). At 525°K. both sets of data predict approximately an equilibrium constant around  $5 \times 10^4$  for the dissociation of the dimer. Assuming that acetic acid vapor is present at a partial pressure of 300 mm., which is higher than any pressure encountered in our data, the degree of dissociation of the dimer is around 0.98, a value which is sufficiently high to indicate that dimerization would not affect the pressure readings.

It appears that the polymerization or decomposition of isobutylene does not proceed at appreciable velocities under the conditions of our experiments. The thermal polymerization of isobutylene has been investigated by Steacie and Shane (11), and their data indicate that the rate of polymerization would be very small at the temperatures used here. The pyrolysis of isobutylene is known to occur at temperatures higher than the temperature at which polymerization is rapid.

The decomposition of *tert*-butyl acetate is very likely a unimolecular reaction. The simplicity of the products and the low temperatures required for decomposition would indicate that a chain mechanism involving free radicals is not an important part of the reaction mechanism. Assuming that the decomposition process is unimolecular, the conventional picture would visualize the approach of the carbonyl oxygen of the ester to a hydrogen atom on one of the methyl groups, leading to the formation of a cyclic six-membered ring which by electron shift splits into isobutylene and acetic acid. It is assumed that the ring is closed by the formation of a hydrogen bond between carbon and oxygen. This type of hydrogen bond has not been recognized at room temperatures, and it appears unlikely that it would exist at higher temperatures. An equally valid visualization of the decomposition would have the ether oxygen approach a hydrogen atom on the methyl group, forming a cyclic four-membered ring which then decomposes. Because of strain energy the four-membered ring is apparently a less popular concept than the six-membered ring. On the basis of the transition-state theory the formation of a cyclic ring should result in an abnormal frequency factor, but reference to equation 1 shows that the frequency factor is normal for the decomposition of *tert*-butyl acetate. It seems unlikely that a cyclic intermediate is the explanation of the reaction mechanism.

Ethyl acetate is reasonably stable at 290°C., while *tert*-butyl acetate decomposes rapidly at this temperature. At 550°C. Hurd and Blunck (6) found that the main products of the decomposition of ethyl acetate were ethylene and acetic acid, but that small amounts of acetaldehyde, formaldehyde, methane, hydrogen, carbon monoxide, and ketene were present. The complexity of the products suggests that a complicated mechanism is operative in the decomposition of ethyl acetate. The difference in the behavior of ethyl acetate and *tert*-butyl acetate is paralleled by ethyl bromide and *tert*-butyl bromide. Ethyl bromide decomposes, entirely or in part, by a bromine atom chain, while *tert*-butyl bromide decomposes in a unimolecular process. The substitution of two hydrogen atoms for two methyl groups in *tert*-butyl acetate or *tert*-butyl bromide gives a molecule of greater stability. One feels intuitively that the difference in inductive effects between two methyl groups and two hydrogen atoms is not sufficiently great to account for the observed difference in stability. While the lack of a chain mechanism in the decomposition of *tert*-butyl compounds might be explained by the assumption that isobutylene reacts readily with free radicals and inhibits the chain, such an assumption does not explain why the unimolecular process in the decomposition of *tert*-butyl compounds should have a lower energy of activation than the chain process in the decomposition of the corresponding



ethyl compound. It appears that some peculiarity accompanies the *tert*-butyl grouping, but the nature of this peculiarity is not apparent.

## SUMMARY

1. The thermal decomposition of *tert*-butyl acetate into isobutylene and acetic acid has been studied by a static method in the temperature range 243–303°C. and at pressures from 5 to 275 mm.

2. The reaction in treated glass flasks is homogeneous and has an energy of activation of 40,500 cal.

3. The variation of the velocity constant,  $k$ , with absolute temperature,  $T$ , is given by the equation:

$$\log k (\text{sec}^{-1}) = 13.342 - \frac{40,500}{2.3RT}$$

4. It is suggested that the decomposition is a unimolecular process.

## REFERENCES

- (1) BRUINS AND CZARNECKI: *Ind. Eng. Chem.* **33**, 201 (1941).
- (2) BRYANT AND SMITH: *J. Am. Chem. Soc.* **58**, 1014 (1936).
- (3) COFFIN: *J. Am. Chem. Soc.* **55**, 3646 (1933).
- (4) DANIELS: *J. Am. Chem. Soc.* **50**, 1115 (1928).
- (5) FENTON AND GARNER: *J. Am. Chem. Soc.* **60**, 771 (1938).
- (6) HURD AND BLUNCK: *J. Am. Chem. Soc.* **60**, 2419 (1938).
- (7) MACDOUGALL: *J. Am. Chem. Soc.* **58**, 2585 (1936).
- (8) NORRIS AND RIGBY: *J. Am. Chem. Soc.* **54**, 2088 (1932).
- (9) PARKS AND HUFFMAN: *The Free Energies of Some Organic Compounds*. The Chemical Catalog Company, Inc., New York (1932).
- (10) SCHULTZ AND KISTIAKOWSKY: *J. Am. Chem. Soc.* **56**, 395 (1934).
- (11) STEACIE AND SHANE: *Can. J. Research* **16B**, 210 (1938).

## THE EFFECT OF SURFACE-ACTIVE AGENTS UPON DISPERSIONS OF LEAD MONOXIDE IN XYLENE

V. R. DAMERELL AND M. J. VOGT

*Department of Chemistry, Western Reserve University, Cleveland, Ohio*

*Received July 24, 1947*

The work herein described is a continuation of the study of the effect of surface-active agents upon the particle-size distribution of solids dispersed in xylene. In this paper dispersions of finely divided lead monoxide (litharge) have been so investigated.

## CHEMICALS

The xylene was a Merck reagent-quality product which was further purified by a fractional distillation over barium oxide, to remove water. The fraction

used for the work was a mixture of *o*- and *m*-xylenes boiling between 137° and 138.5°C. The lead monoxide was a Harshaw Chemical Co. product with a lead content corresponding to 99.4 per cent PbO. It was a powder of such fineness that 0.2 per cent remained suspended in xylene after 2 hr. with no surface-active agent present. The additives used in connection with the lead oxide and xylene

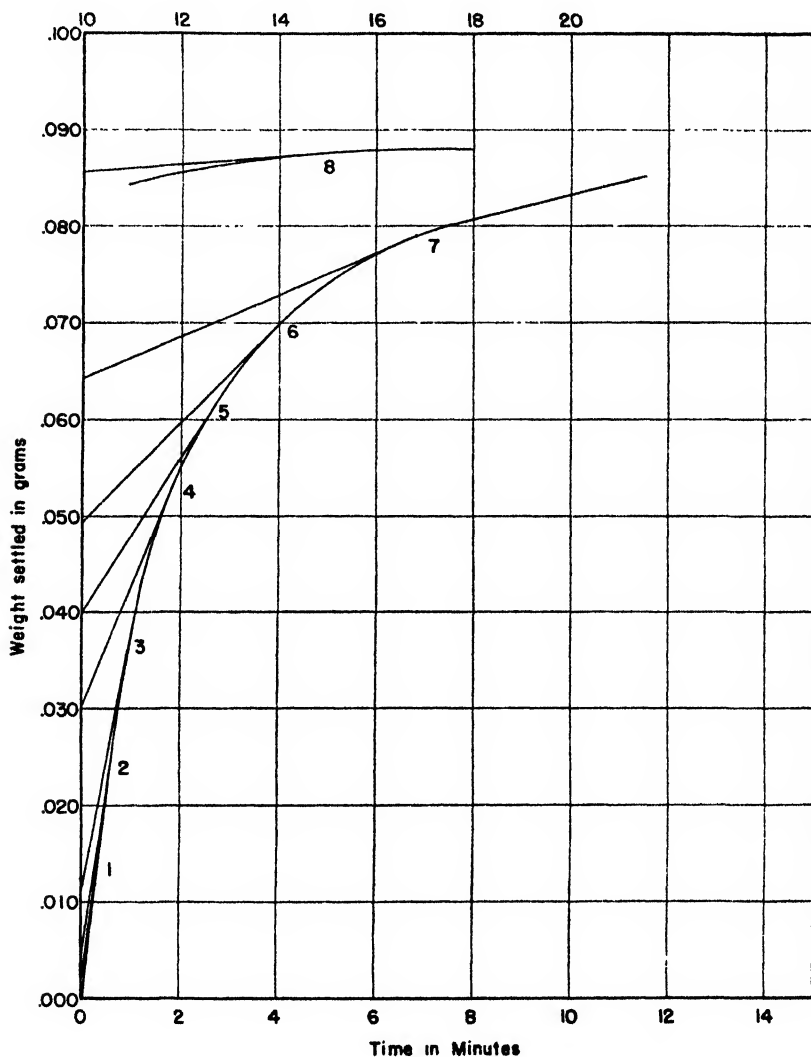


Fig. 1. Sedimentation curve with tangents. Oleic acid used as surface-active agent.

were four: sodium dioctyl sulfosuccinate (Aerosol OT), lecithin, oleic acid, and sulfur. These were all of the purest grade obtainable.

#### PREPARATION OF LEAD MONOXIDE-XYLENE SYSTEMS

Systems for study contained 500 ml. xylene, 0.5000 g. lead monoxide, and 0.001 mole of surface-active agent. These amounts were chosen for the reasons

given in previous papers (1, 2, 3). To avoid the effect of varying amounts of water all systems used for study were prepared at the same time, using the freshly

TABLE 1  
*Data for a typical sedimentation curve—oleic acid*

(1)	(2)	(3)	(4)	(5)	(6)	(7)	(8)	(9)	(10)	(11)
WEIGHT ON RIGHT PAN	CHANGE IN WEIGHT	HEIGHT*	TEMPER- ATURE	VOLUME CORREC- TION	TEMPERA- TURE COR- RECTION	TOTAL CORREC- TION	CORRECT WEIGHT	WEIGHT SETTLED	WEIGHT SETTLED CORRECTED	TIME
grams	grams	°C.	°C.	grams	grams	grams	grams			min.
2.626		-0.3	24.8	-0.0031	-0.0075	-0.011	2.615	0.000	0.000	0.0
2.660	0.034						2.649	0.034	0.035	0.9
2.670	0.010						2.659	0.044	0.045	1.3
2.680	0.010						2.669	0.054	0.055	2.1
2.690	0.010						2.679	0.064	0.065	3.2
2.695	0.005						2.684	0.069	0.070	4.0
2.700	0.005						2.689	0.074	0.075	5.3
2.705	0.005						2.694	0.079	0.080	7.5
2.708	0.003						2.697	0.082	0.083	9.8
2.709	0.001						2.698	0.083	0.084	10.9
2.710	0.001						2.699	0.084	0.085	11.5
2.711	0.001						2.700	0.085	0.086	12.7
2.712	0.001						2.701	0.086	0.087	15.7
2.713	0.001						2.702	0.087	0.088	18.0
2.714	0.001	-0.4	24.7	-0.0037	-0.0073	-0.011	2.703	0.088	0.089	23.2
2.715	0.001						2.704	0.089	0.090	30.5
2.720	0.005	-0.5	24.2	-0.0045	-0.0066	-0.013	2.709	0.094	0.095	300.0

\* The thermometer stem was also used to measure the height of the xylene.

TABLE 2  
*Weight of settled material for different radius intervals—oleic acid*

(1)	(2)	(3)	(4)	(5)		(6)
TANGENT NUMBER	RADIUS	ABSCISSAE TIMES	WEIGHT INTERCEPTS	PARTICLE-SIZE DISTRIBUTION		
				Weight	Weight percentage	
	<i>cm. <math>\times 10^{-4}</math></i>	<i>min.</i>	<i>grams</i>	<i>grams</i>	<i>per cent</i>	
1	12	0.45	0.002	0.002	2	
2	10	0.65	0.005	0.003	3	
3	8	1.02	0.011	0.006	6	
4	6	1.83	0.030	0.019	20	
5	5	2.61	0.040	0.010	11	
6	4	4.08	0.050	0.010	11	
7	3	7.26	0.064	0.014	15	
8	2	16.3	0.086	0.022	23	
	Less than 2	300.	0.095	0.009	9	
			Total	0.095	100	

distilled xylene and carefully dried lead oxide. Each bottle of suspension was then sealed with paraffin until it was used. This procedure did not eliminate traces of water, but it tended to keep the water content constant.

When a system was to be examined the paraffin seal on the bottle was broken

and a little xylene was removed. The surface-active agent was dissolved in this xylene, which was then returned to the bottle.

#### MEASUREMENT OF PARTICLE-SIZE DISTRIBUTION

Sedimentation analysis was used to determine particle-size distribution. The apparatus used for this has been described previously (1, 2, 3). After addition of the surface-active agent as described above, each bottle was shaken 150 times immediately prior to the start of the sedimentation analysis. The contents of the bottle were then poured rapidly into a Dewar flask containing a balance pan. The moment pouring ceased a stop watch was started. The flask and balance pan were quickly put in position in a sedimentation balance and weighing started. After practice, the time required to do the steps just enumerated following

TABLE 3

*Effect of 0.001 mole of surface-active agent upon 0.5000 g. of lead monoxide dispersed in 500 ml. of xylene*

SURFACE-ACTIVE AGENT		PARTICLE-SIZE DISTRIBUTION IN WEIGHT PERCENTAGES							
		Above 12 microns radius	10-12 microns radius	8-10 microns radius	6-8 microns radius	4-6 microns radius	3-4 microns radius	2-3 microns radius	0-2 microns radius
Blank ....	(1)	22	5	9	10	22	14	10	7
	(2)	21	5	8	10	21	16	11	7
Sulfur .	(1)	3	3	5	24	24	13	17	11
	(2)	3	4	4	23	24	13	19	11
Lecithin..	(1)	6	10	7	10	20	16	23	8
	(2)	7	10	8	10	16	16	23	10
Sodium dioctyl sulfo- succinate. . . . .	(1)	4	6	5	15	17	14	23	15
	(2)	4	8	10	14	23	15	16	11
Oleic acid.....	(1)	3	4	6	19	22	15	22	10
	(2)	2	3	6	20	21	15	23	10

shaking was  $0.4 \pm 0.02$  min. Sedimentation analyses were then run as previously described, care being taken to correct for errors due to temperature changes, evaporation, and other factors (1). A typical result from such an experiment is shown in table 1. The corrected sediment weights, shown in column 10 in table 1, were then plotted against time (column 11), as shown in figure 1. Tangents drawn from this curve with a tangentimeter gave the weight of settled material corresponding to stated radius intervals, and results were obtained as in table 2. Column 4 in table 2 gives the weight of particles where the tangents intercept the  $y$ -axis. Column 5 gives the weight of the particles within the indicated size range, and column 6 expresses this weight particle-size distribution in per cent. The calculation of radius corresponding to a given time of settling was made by using the Stokes law equation, as described earlier (1, 2, 3).

The percentage particle-size distribution results for the four systems studied are given in table 3. This distribution applies only to about 20 per cent of the lead monoxide which remained in suspension after pouring. Nevertheless, it was sufficient to indicate the effect of the surface-active agent.

#### SUMMARY

The effect of sulfur, lecithin, sodium dioctyl sulfosuccinate, and oleic acid upon the particle-size distribution of lead monoxide dispersed in xylene has been studied. All of these substances were effective in lowering the average size of the lead monoxide particles.

#### REFERENCES

- (1) DAMERELL, V. R., GAYER, K., AND LAUDENSLAGER, H.: J. Phys. Chem. **49**, 436-42 (1945).
- (2) DAMERELL, V. R., AND MATTSON, R.: J. Phys. Chem. **48**, 134-41 (1944).
- (3) DAMERELL, V. R., AND URBANIC, A.: J. Phys. Chem. **48**, 125-33 (1944).

## THE MAXIMUM POSSIBLE RATE OF EVAPORATION OF LIQUIDS

S. S. PENNER

*Jet Propulsion Laboratory, California Institute of Technology, Pasadena 4, California*

*Received July 24, 1947*

#### I. INTRODUCTION

The maximum possible rate of evaporation of a liquid occurs during vaporization into a vacuum. The actual rate of evaporation observed in experimental tests is always less than this maximum possible rate. Treatments for specific experimental conditions have been reported in the literature (2, 11, 12).

An expression for the maximum possible rate of droplet vaporization may be derived from the kinetic theory of gases. For the evaporation of spherical droplets, the resulting relation may be written as follows (3, 6, 9):

$$-\frac{dr}{dt} = \frac{P_s}{\rho_l} \sqrt{\frac{M}{2\pi RT}} \quad (1)$$

where  $r$  = radius of the spherical droplet at the time  $t$ ,

$P_s$  = vapor pressure of the liquid at the absolute temperature  $T$ ,

$M$  = molecular weight of the evaporating liquid,

$\rho_l$  = density of the liquid, and

$R$  = gas constant per mole.

An alternate expression for the maximum possible rate of decrease of droplet radius with time ( $-dr/dt$ ) may be obtained by considering the behavior of the molecules at the surface of an evaporating liquid.

## II. A THEORY FOR THE RATE OF EVAPORATION OF LIQUIDS

Since vaporization is a surface phenomenon, the rate of loss of molecules from a spherical droplet would be expected to be proportional to the number of molecules exposed at the surface, i.e.,

$$-\frac{dn_v}{dt} = kn_s \quad (2)$$

where  $n_v$  = total number of molecules in a spherical drop,

$n_s$  = number of molecules exposed at the surface, and

$k$  = proportionality constant which depends on temperature.

Only the molecules which are exposed at the droplet surface and also have enough energy to escape are in a position to vaporize at any given time. The rate constant  $k$  may therefore be equated to the frequency of oscillation of energetic molecules multiplied by a factor expressing the probability of the occurrence of activated molecules. The frequency of oscillation, in turn, may be set equal to the frequency of collision of energetic molecules at the droplet surface with other liquid molecules.<sup>1</sup> Collision between an energetic molecule and another liquid molecule may be followed by a redistribution of energy resulting in the escape of one of the molecules from the liquid surface and leaving a liquid molecule of average energy in the droplet.<sup>2</sup>

A Maxwell-Boltzmann velocity distribution for the liquid molecules is assumed throughout the following discussion (5, 8).

If  $\Delta E_{\text{vap}}$  represents the activation energy per mole for evaporation, then

$$n_s e^{-\Delta E_{\text{vap}}/RT} \quad (3)$$

excited molecules, with energies in excess of  $\Delta E_{\text{vap}}$  per mole, are present at the droplet surface at a given time.

The mean collision frequency of energetic molecules at the droplet surface may be equated to the root-mean-square velocity of energetic molecules divided by the mean free path. The root-mean-square velocity of the molecules with energy in excess of  $\Delta E_{\text{vap}}$  is calculated by application of the Maxwell-Boltzmann distribution law in two dimensions. Accordingly, the number of molecules,  $dn_E$ , with energy per mole between  $E$  and  $E + dE$  is given by the relation:

$$dn_E = \frac{n_s}{RT} e^{-E/RT} dE \quad (4)$$

<sup>1</sup> This mechanical model for evaporation should be regarded as a highly approximate description of a complicated phenomenon. A "bubble theory" for evaporation has recently been described by O. K. Rice (J. Chem. Phys. 15, 314 (1947)). The quantitative kinetics of evaporation is discussed by Jellinek (5).

<sup>2</sup> Note added in proof: At the suggestion of Professor J. G. Kirkwood, the kinetics of vaporization have been treated by use of Eyring's theory of reaction rates. Good agreement with Knudsen's equation can be obtained if the activated complex formed during evaporation and sublimation is considered to behave like a gaseous molecule. It is possible to justify the assumption that the frequency factor for evaporation is equal to the collision frequency of energetic molecules by combining the results obtained from the statistical analysis with an empirical equation.

The square of the linear velocity of molecules with energy  $E$  per mole is

$$c^2 = 2E/M \quad (5)$$

Thus

$$\bar{c}^2 = \frac{1}{n_s e^{-\Delta E_{\text{vap}}/RT}} \int_{\Delta E_{\text{vap}}}^{\infty} \frac{n_s}{RT} e^{-E/RT} \cdot \frac{2E}{M} dE$$

or

$$\bar{c}^2 = \frac{2}{M} (\Delta E_{\text{vap}} + RT) \quad (6)$$

The root-mean-square velocity of molecules with energy in excess of  $\Delta E_{\text{vap}}$  per mole is therefore

$$C = \sqrt{\bar{c}^2} = \sqrt{\frac{2}{M} (\Delta E_{\text{vap}} + RT)} = \sqrt{\frac{2}{M} \Delta H_{\text{vap}}} \quad (7)$$

since (4, p. 477)

$$\Delta E_{\text{vap}} + RT = \Delta H_{\text{vap}} \quad (8)$$

It can be seen from equations 6 and 8 that the kinetic energy per mole of molecules with energy in excess of the activation energy for evaporation is equal to the heat of vaporization per mole.

If  $L$  represents the mean free path of the liquid molecules, then the energetic molecules make  $C/L$  collisions per second on the droplet surface. By analogy with chemical reactions the rate constant  $k$  may therefore be expressed as follows:

$$k = \frac{C}{L} e^{-\Delta E_{\text{vap}}/RT} = \frac{c}{L} \sqrt{\frac{2\Delta H_{\text{vap}}}{M}} e^{-\Delta H_{\text{vap}}/RT} \quad (9)$$

where  $C/L$  represents a frequency factor and  $e$  is the base of the natural logarithms.

From equations 2 and 9 it follows that

$$-\frac{dn_v}{dt} = \frac{c}{L} \sqrt{\frac{2\Delta H_{\text{vap}}}{M}} e^{-\Delta H_{\text{vap}}/RT} n_s \quad (10)$$

For a sphere of radius  $r$ :

$$\begin{aligned} n_s &= 4\pi r^2 n^{2/3} \\ n_v &= \frac{4}{3}\pi r^3 n \end{aligned} \quad (11)$$

where  $n$ , the number of molecules per cubic centimeter, is given by the relation

$$n = \rho_l \frac{N}{M} \quad (12)$$

and  $N$  represents the Avogadro number.

The mean free path  $L$  of the molecules in a liquid is approximately given by the following relation (4, p. 480):

$$L = \left( \frac{M}{\rho_l N} \right)^{1/3} \cdot \frac{1}{u} \left( \frac{RT}{M} \right)^{1/2} \quad (13)$$

Here  $u$  represents the velocity of sound in the liquid, and  $\gamma$  is the ratio of the specific heat at constant pressure to the specific heat at constant volume of the evaporating compound.

Combining equations 10 to 13 leads to the desired result:

$$-\frac{dr}{dt} = c \sqrt{\frac{2\Delta H_{\text{vap}}}{RT\gamma}} u e^{-\Delta H_{\text{vap}}/RT} \quad (14)$$

### III. COMPARISON BETWEEN THE THEORETICAL EXPRESSIONS FOR THE MAXIMUM POSSIBLE RATE OF VAPORIZATION

Equations 1 and 14 may be used to calculate the rate of decrease of droplet radius with time, provided experimental data are available for the vapor pressure, heat of vaporization, and sound velocity. Results for a number of different liquids near room temperature are summarized in table 1.

Reference to the data summarized in table 1 indicates that the values of  $-dr/dt$  calculated from equations 1 and 14 are generally of the same order of magnitude. The agreement is relatively poor for associated liquids such as water, methyl alcohol, and ethyl alcohol. Comparison of the data for the straight-chain hydrocarbons,  $n$ -pentane to  $n$ -octane, indicates that the discrepancy between calculated values increases with chain length. Finally, it should be noted that the value of  $-dr/dt$  near room temperature calculated from equation 1 is, in nearly all cases, greater than the value obtained from equation 14. Mercury and carbon disulfide are notable exceptions to this rule. The singular behavior of mercury is not surprising, since liquid metals are known to exhibit peculiarities. For example, liquid metals do not conform to Pitzer's definition of a perfect liquid (10).

Some of the observed discrepancies may probably be ascribed to errors in numerical values of the experimentally determined quantities. The relatively large differences observed for associated liquids and the longer straight-chain paraffins may possibly be explained by the failure of either equation 7 or equation 13. Equation 13 was derived by treating the individual liquid molecules as free spheres (4), an approximation which would be expected to be relatively poor for strongly associated liquids or for straight-chain hydrocarbons.

It may be of interest to note that the disagreement between the calculated values for  $-dr/dt$  can be somewhat reduced for carbon disulfide by replacing equation 13 with the corresponding relation for the mean free path in a liquid obtained from the equation of Eyring and Hirschfelder (1). The free volume of carbon disulfide at 20°C. calculated from the formula of Eyring and Hirschfelder is nearly twice as great as that derived from equation 13. Use of the relation derived by Eyring and Hirschfelder would therefore increase the value of  $R$  given in table 1 for carbon disulfide from 0.46 to 0.56. (See footnote of table 1 for the definition of  $R$ .)

The temperature dependence of  $-dr/dt$  is different in equations 1 and 14. It is therefore of interest to compare calculated values of  $-dr/dt$  for the same liquid at a number of different temperatures. In order to extend the range of



calculation, it proved necessary to extrapolate some of the available experimental data. Although this step introduced an added uncertainty, the order of magnitude of the calculated results should not be changed. Relevant data for water, benzene, carbon tetrachloride, chloroform, and mercury are summarized in table 2.

Reference to the data summarized in table 2 indicates that the values of  $-dr/dt$  calculated from equation 14 increase more rapidly with temperature

TABLE 1

*The maximum possible rate of decrease of droplet radius with time near room temperature for a number of liquids\**

COMPOUND	TEMPERATURE	$-dr/dt$ CALCULATED FROM EQUATION 1	$-dr/dt$ CALCULATED FROM EQUATION 14	$R^\dagger$
	°C.	cm./sec	cm./sec.	
Water	25	0.342	0.0493	7.0
Methyl alcohol	25	3.01	0.467	6.4
Ethyl alcohol	20	1.28	0.0476	27
<i>n</i> -Pentane	25	23.8	29.4	0.81
<i>n</i> -Hexane	25	7.37	4.53	1.6
Cyclohexane	18.4	2.92	1.87	1.6
<i>n</i> -Heptane	25	2.29	0.660	3.5
<i>n</i> -Octane	25	0.750	0.0991	7.6
Acetone	25	7.45	3.70	2.0
Ethyl ether	20	18.2	14.4	1.3
Benzene	20	2.56	1.68	1.5
Pyridine	20	0.475	0.131	3.6
Chloroform	20	3.96	3.31	1.2
Carbon tetrachloride	20	2.41	1.94	1.2
Carbon disulfide	20	7.03	15.3	0.46
Mercury	20	$4.28 \times 10^{-6}$	$16.1 \times 10^{-6}$	0.27

\* Most of the data on vapor pressure, heat of vaporization, and sound velocity were obtained from the Landolt-Börnstein *Tabellen* and the *Handbook of Chemistry and Physics*. Vapor pressures and heats of vaporization for the hydrocarbons were obtained from the results published by the American Petroleum Institute, Research Project 44.

†  $R$  = ratio of  $-dr/dt$  calculated from equation 1 to  $-dr/dt$  calculated from equation 14.

than the values calculated from equation 1. As the result,  $R$  decreases as the temperature increases for all of the liquids considered.

From the numerical values given for benzene, carbon tetrachloride, and chloroform, it can be seen that equations 1 and 14 lead to identical results for these compounds at approximately 40°C.

The value of  $R$  for water is found to decrease rapidly as the temperature is raised but does not reach unity even at the normal boiling point. The results for associated liquids may not be significant because of some of the uncertainties inherent in the derivation of equation 14.

In conclusion, it might be pointed out that the preceding analysis offers the possibility of an independent estimate for the free volume of a liquid. If equa-

TABLE 2  
*The maximum possible rate of decrease of droplet radius with time at different temperatures for a number of liquids*

COMPOUND	TEMPERATURE	$-dr/dt$ CALCULATED FROM EQUATION 1	$-dr/dt$ CALCULATED FROM EQUATION 14	R
	°C.	cm./sec.	cm./sec.	
Water.....	0	0.0537	0.0063	8.5
	5	0.0972	0.0099	9.8
	10	0.136	0.0149	9.1
	15	0.187	0.0225	8.3
	20	0.254	0.0336	7.6
	30	0.455	0.0716	6.4
	40	0.780	0.145	5.4
	100	10.17	4.54	2.2
Benzene.....	10	1.57	0.889	1.8
	20	2.56	1.68	1.5
	30	4.03	3.07	1.3
	40	6.15	5.38	1.1
	50	9.11	9.10	1.0
Carbon tetrachloride.....	0	0.883	0.585	1.5
	10	1.49	1.09	1.4
	20	2.41	1.94	1.2
	30	3.77	3.37	1.1
	40	5.67	5.69	1.0
	50	8.31	9.41	0.88
Chloroform.....	0	1.55	0.994	1.6
	10	2.50	1.85	1.4
	20	3.96	3.37	1.2
	30	6.04	5.81	1.0
	40	8.92	9.73	0.92
	50	12.7	15.5	0.82
Mercury.....	0	$6.80 \times 10^{-7}$	$22.5 \times 10^{-7}$	0.30
	20	$4.28 \times 10^{-8}$	$16.1 \times 10^{-8}$	0.27
	40	$2.10 \times 10^{-8}$	$9.4 \times 10^{-8}$	0.22
	60	$8.50 \times 10^{-8}$	$43.0 \times 10^{-8}$	0.20
	80	$2.91 \times 10^{-4}$	$16.9 \times 10^{-4}$	0.17
	100	$8.74 \times 10^{-4}$	$56.9 \times 10^{-4}$	0.15
	150	$8.52 \times 10^{-3}$	$71.0 \times 10^{-3}$	0.12
	200	$5.01 \times 10^{-3}$	$51.4 \times 10^{-3}$	0.10

tions 1 and 14 are identical, then the cube root of the free volume  $V_f^{1/3} = L$  may be calculated from the relation

$$L = \frac{2e\rho_l}{MP} \sqrt{\pi RT \Delta H_{vap}} e^{-\Delta H_{vap}/RT} \left( \frac{M}{\rho_l N} \right)^{1/3} \quad (15)$$





GAPS IN PHYSICAL CONSTANTS DATA FOR HYDROCARBONS<sup>1</sup>

NANCY CORBIN, MARY ALEXANDER, AND GUSTAV EGLOFF

*Universal Oil Products Company, Chicago, Illinois**Received August 20, 1947*

In the course of studying data from a complete literature survey of the physical constants of hydrocarbons, it became apparent that numerous gaps exist. Many of the possible hydrocarbons are not known, and many known compounds have not been investigated from the standpoint of their physical constants. Our study showed that of the astronomical number of possible hydrocarbons only about fifty-two hundred have been investigated.

The problem of the correlation of physical properties with structure is one which has engaged the attention of an ever-increasing number of scientists. From the time of Kopp, in the middle of the nineteenth century, to the present time numerous correlations have been proposed, varying broadly in scope and accuracy. Many of the early attempts covered a wide field and included both hydrocarbons and compounds with functional groups. In recent years, as more data became available, the tendency has been to narrow the field in the interests of greater accuracy.

The questions may be asked: Why is so much effort expended in developing correlations? What purpose do they serve? On the practical side, correlations make it possible to predict the physical constants of unknown compounds and, in addition, inaccuracies in existing data may be located and corrected. From the more theoretical point of view, correlations play an important rôle in the evaluation of structural effects and provide a basis for the interpretation of chemical and physical phenomena.

It is apparent that an indispensable condition, without which no correlation is possible, is the availability of reliable data on whatever property is under consideration.

Data used in correlations must be for pure compounds of definite and known structure. The importance of purity cannot be overemphasized; many of the older physical constants data are unreliable because of the presence of impurities. Recent developments in hydrocarbon chemistry have improved this situation, and it is now more feasible to prepare and purify a desired compound. A study of the literature will usually reveal whether synthesis or isolation from a natural source will be more satisfactory from the standpoint of ease of purification. Once the compound has been prepared, its purification depends on the amount and nature of the impurities. The time-honored method of fractional distillation is being supplemented by other techniques, such as azeotropic distillation, extraction, fractional crystallization, and the method of percolation through adsorbents. In addition to techniques of purification, new methods are available for testing the purity of the product. These include

<sup>1</sup> Presented before the Division of Petroleum Chemistry at the 112th Meeting of the American Chemical Society, which was held in New York City September 15-19, 1947.

quantitative study of time-freezing curves (12), analysis of ultraviolet and infrared absorption spectra, and use of the mass spectrometer. By employing one or more of these methods the nature of the impurities as well as their amount is revealed, and further purification is facilitated.

When the desired purity has been attained, the determination of the physical constants should be carried out with equal care. Accurately calibrated apparatus and rigid control of conditions are necessary. Preferably, each constant should be determined over a range of conditions,—for example, the boiling point at varying pressures, and the density and refractive index at a number of temperatures.

Among the hydrocarbons, the number and accuracy of the physical constants data vary widely from one class of compounds to another. In order to illustrate these variations, an analysis of the data appearing in the four volumes of *Physical Constants of Hydrocarbons* (7) has been made. Table 1 shows the total number of hydrocarbons in each class, and the percentage of compounds for which each physical constant has been recorded. These figures indicate only the percen-

TABLE 1  
*Compounds for which physical constants have been recorded*

CLASS OF HYDROCARBONS	TOTAL NUMBER OF COMPOUNDS	MELTING POINT	BOILING POINT	DENSITY	REFRACTIVE INDEX
		<i>per cent</i>	<i>per cent</i>	<i>per cent</i>	<i>per cent</i>
Alkane...	196	60.2	88.8	85.2	76.5
Unsaturated aliphatic	601	19.6	96.2	81.5	73.4
Alicyclic	1242	22.3	87.2	79.8	73.9
Mononuclear aromatic....	1400	43.2	68.2	48.9	43.9
Polynuclear aromatic....	1728	82.6	32.8	15.4	13.9

tages of compounds for which at least one value of a physical constant has been recorded. They give no clue as to the quantity and reliability of the data.

Taking the alkanes as a basis for comparison, differences among the classes may be readily analyzed. It should be noted that the state of aggregation at normal temperatures is an important factor influencing the determination of physical constants. For example, data on melting points are more numerous for solid compounds and on boiling points for liquids. For the unsaturated aliphatic hydrocarbons, the proportion of compounds for which melting points have been recorded is far smaller than for the alkanes, that of boiling points somewhat greater, and that of density and refractive index about the same. The alicyclic and mononuclear aromatic compounds have a smaller proportion of all four constants, and the polynuclear aromatics exceed the alkanes only in the percentage of melting points, the other three constants being distinctly fewer. The cause of the distribution of percentages for the polynuclear aromatics is that for a large proportion of these compounds the melting point is the only constant which has been determined.

Evidence of the amount of reliable data may be gained from an analysis of the "best values" appearing in the *Physical Constants* volumes (7). In order to calculate a "best value" it was necessary to have data sufficiently numerous and consistent to form a basis for statistical treatment to find the most probable correct value for a given constant. The figures representing the percentages of "best values" are shown in table 2.

The most striking fact brought out by this table is the paucity of reliable data for the known hydrocarbons. Even among the alkanes, the data for almost 60 per cent of the compounds are insufficient for the calculation of any "best values" whatsoever. About 85 per cent of the unsaturated aliphatics and 95 per cent of each of the other three classes of hydrocarbons have been so superficially studied that no "best values" can be computed.

From table 2 it is apparent that the data for the alkanes are more nearly complete than for any other class of hydrocarbons. The data on the alkanes have been further amplified by the authoritative values recently determined at the National Bureau of Standards (27). This investigation included all the paraf-

TABLE 2  
Compounds for which "best values" have been computed

CLASS OF HYDROCARBONS	TOTAL NUMBER OF COMPOUNDS	MELTING POINT	BOILING POINT	DENSITY	REFRACTIVE INDEX
		per cent	per cent	per cent	per cent
Alkane...	196	28.1	35.7	41.8	32.6
Unsaturated aliphatic.	601	4.0	16.5	15.8	13.0
Alicyclic	1242	0.2	2.7	5.1	3.5
Mononuclear aromatic....	1400	4.9	5.6	6.3	4.3
Polynuclear aromatic....	1728	4.5	0.8	0.3	0.05

fin isomers from the pentanes through the octanes. Among higher alkanes the proportion of isomers which have been investigated decreases sharply, owing in part to the large number of possible compounds.

All of the normal alkanes through pentatetracontane,  $C_{45}H_{92}$ , are known, and at least one physical constant has been determined for each compound. Above this, nine normal alkanes have been investigated, the highest being heptacontane,  $C_{70}H_{142}$ . From propane through normal dodecane "best values" of all four constants have been calculated. For the twenty-four compounds from  $C_{13}$  through  $C^{36}$ , "best values" for all four constants have been determined on only five compounds. Above  $C^{36}$  the data are insufficient to calculate any "best values", and often the only recorded physical constant is a melting point. For the normal alkanes higher than tetracosane,  $C_{24}H_{50}$ , boiling points have been determined only at pressures below atmospheric, if at all.

The completeness of the alkane data relative to other classes of hydrocarbons is reflected in the large number of correlations for these compounds. Relationships covering melting points, boiling points, densities, and refractive indices

have been worked out by Mibashan (23). Boiling points, densities or molecular volumes, and refractive indices or molal refractions have been covered by Egloff and coworkers (8, 10), Francis (11), and Rossini and coworkers (24). Densities and refractive indices have been treated by Huggins (13) and Kurtz and Lipkin (21, 22). Calingaert and Hladky (2) have derived relationships for molecular volume. Boiling-point relations have been worked out by Burnop (1), Kinney (16, 18), Klages (20), and Wiener (25). Ivanovsky and Brancker (15) have treated melting points of alkanes.

The data for the other hydrocarbons present a sharp contrast to those for the alkanes. For the unsaturated aliphatic compounds the percentages of "best values" are far lower than for the alkanes in spite of the fact that the percentage of compounds for which a constant has been recorded (table 1) is nearly the same. In the case of boiling points, even more have been recorded for the unsaturated aliphatics than for the alkanes (96.2 per cent as compared to 88.8 per cent), but the percentage of "best values" is only about half of that for alkanes (16.5 per cent as compared to 35.7 per cent). This relative dearth of "best values" shows that the data for the individual compounds are often scarce and unreliable. In many cases only one or two values for a constant are available in the literature,<sup>9</sup> and in other cases the values recorded by different authors do not agree.

The alkenes or monoölefins have been more extensively studied than the other types of unsaturated aliphatics. Even for these, "best values" are very scarce above  $C_{10}$ . From  $C_{12}$  through  $C^{16}$  the only "best values" are those for the normal olefins with the double bond in the 1-position, and above this only one "best value", the melting point of 1-octadecene, has been calculated.

Correlations for unsaturated aliphatics are less numerous than for alkanes. Rossini and coworkers (24) have presented a method for calculating boiling points, densities, and refractive indices of monoölefins. Molecular volumes and molal refractions of unsaturated aliphatics have been treated by Huggins (14), and boiling points by Burnop (1), Klages (20), Kinney (16), and Egloff, Sherman, and Dull (10).

Alicyclic compounds have been even less thoroughly investigated than the unsaturated aliphatics. Although the percentages of compounds for which constants have been recorded are of the same order of magnitude as for the unsaturated aliphatics, the percentages of "best values" are very much smaller. The greater proportion of compounds for which "best values" have been calculated are the alkyl derivatives of cyclopentane and cyclohexane.

The boiling point and the density or molecular volume are the only alicyclic constants which have been related to structure. Boiling points are used in the correlations of Burnop (1), Klages (20), and Kinney (16, 18), and molecular volumes in those of Kurtz and Lipkin (21) and Egloff and Kuder (9).

Among the mononuclear aromatics, the percentage of compounds for which each constant has been recorded is significantly less than for the alkanes. Often only one or two different properties have been determined for a compound. For example, many compounds are represented only by a melting point or a boil-



ing point, whereas most of the lower alkanes are represented by at least three and often all four constants. The low proportion of "best values" shows that many compounds have been the subject of such a small number of investigations that no evaluations can be made.

For the alkylbenzenes through the  $C_9$  compounds, all possible isomers are known and have been studied extensively enough so that "best values" have been calculated for three or four of the physical constants. In the  $C_{10}$  group twenty-one of the twenty-two possible isomers are known, but only forty-five of a possible total of eighty-eight "best values" can be calculated. The  $C_{11}$  group is represented by only thirty-six out of fifty compounds, with only eighteen out of a possible two hundred "best values". As the number of carbon atoms increases, the proportion of known isomers decreases rapidly. The normal alkylbenzenes have been more widely investigated than any of the other isomers, and all of these are known through normal docosylbenzene ( $C_{23}H_{50}$ ), with the exception of  $C_{16}H_{34}$ ,  $C_{21}H_{42}$ ,  $C_{25}H_{52}$ , and  $C_{27}H_{56}$ . Of the other series of mononuclear aromatics, such as alkenylbenzenes, alkynylbenzenes, and polyphenyl aliphatics, only the first few members are known.

The boiling-point calculations of Burnop (1), Klages (20), and Kinney (17, 19) can be applied to mononuclear aromatics, and correlations of boiling point, molecular volume, and molal refraction have been worked out for several homologous series by Corbin, Alexander, and Egloff (3, 4, 6).

The polynuclear aromatics have been investigated even less than the mononuclears. For many of the polynuclears the only recorded physical constant is the melting point, and frequently only one or two values for this constant are given in the literature. This is shown by a comparison of the figures in table 1 and table 2. Melting points have been recorded for 82.6 per cent of the known polynuclear aromatic hydrocarbons—a greater percentage than for the alkanes—but the data are suitable for calculation of "best values" in only 4.5 per cent of the compounds. The percentages of "best values" for the other constants are so low as to be almost negligible.

The most extensively investigated group of polynuclears is that of naphthalene and its alkyl derivatives. However, the data are scattered and sparse, and even the normal alkyl naphthalenes are completely represented only as high as 1- and 2-butyl derivatives.

The only correlations which include the polynuclears are the boiling-point calculations of Burnop (1), Klages (20), and Kinney (19), and these are very general in nature.

It must be emphasized that the above citations are not intended to be a complete coverage of published correlations, but simply representative examples. Even so, it is apparent that the alkanes have been studied more extensively than the other classes of hydrocarbons. Not only are the alkanes treated in a greater number of studies, but the proportion of compounds to which the relations may be applied is larger. In fact it may be said that the boiling point, density, and refractive index of any alkane may be calculated with a fair degree of accuracy. The method of calculation developed by Taylor, Pignocco, and

Rossini (24) can be applied to all alkanes. Likewise the structural determination of boiling points set forth by Wiener (25) can be applied to unknown alkanes. This method of calculation can also be extended to other physical properties (26). The good agreement of values calculated by these methods with the experimental data among the lower alkanes indicates that extrapolations to higher members should be reliable.

Calculations according to Taylor, Pignocco, and Rossini (24) are applicable to all monoölefins, but the average deviation of the calculated from the experimental values is appreciably greater than for the alkanes; estimations of properties of unknown olefins will therefore be less reliable.

For the alicyclic hydrocarbons the correlations are few, and cover only a small proportion of the possible isomers; extrapolations are possible only for limited types of compounds.

A similar situation exists for the mononuclear aromatics. The work of Kinney (12, 13) on boiling points includes different types of aromatic hydrocarbons, but the average deviation is rather large. Correlations based on homologous series of mononuclear aromatics may be extrapolated to other compounds of a particular series, but the majority of compounds are not included in any series for which relations have been worked out. In addition, these correlations do not represent the experimental data as well as the correlations of aliphatics; the average deviations are appreciably larger. The decrease in accuracy of most aromatic correlations as compared to those for aliphatics is a reflection of the relative quality of the data for these two classes of compounds.

For polynuclear aromatics no predictions of physical constants can be made except for a limited number of boiling points, because of the lack of sufficient data on which to base any conclusions.

The alkanes are the only compounds for which the data permit extensive correlations, and even here authoritative values are lacking for the majority of compounds. In order to correct this situation, more and better data on physical constants are necessary. The constants should be carefully determined on pure compounds. To facilitate the calculation of relationships either of two approaches will be helpful: First, to determine the constants of a number of hydrocarbons in one homologous series, or second, to determine the properties of all possible isomers of a given number of carbon atoms. Investigations of physical constants will be more immediately helpful if they supplement existing data, rather than open up entirely new fields. For example, a study of some higher alkanes and alkenes would provide a means for testing the validity of extrapolations of existing correlations. In the alicyclic group only the hydrocarbons of lower molecular weight have been thoroughly investigated, and studies of higher members, especially cyclopentane and cyclohexane derivatives, would make possible the extension of correlations which have already been proposed. Among aromatic compounds the number of possible isomers of a given molecular weight increases rapidly with the number of carbon atoms, and studies based on homologous series will probably be most useful for correlations. Several series of mononuclear aromatics have been studied, but in most cases they are short, and data on higher members are necessary. In addition, many series have not been

investigated at all. Along another line, the data on dialkylbenzenes are inconsistent, and a comparison of ortho, meta, and para compounds above the xylenes would clarify the effect of position of substitution on the physical constants. An apparent discrepancy in physical constants data has been noted for the pentylbenzenes (5). Both the normal boiling points and the change of boiling points with pressure are greater than would be expected for these compounds. Accurate vapor-pressure data would make it possible to determine whether these compounds really are anomalous, or whether the present experimental data are at fault. The polynuclear aromatics have been so little investigated that almost any reliable data would be welcome. In order to supplement existing data, however, the study of homologous series of alkyl derivatives of naphthalene and indene would be a good starting point.

Many of the compounds of higher molecular weight for which data are inadequate have boiling points too high to be easily determined at a pressure of 760 mm. Also, many of the compounds are solid at 20° or 25°C., and their densities and refractive indices have not been determined at standard conditions. These difficulties may be alleviated by determining the boiling point over a sufficient pressure range and the density and refractive index over a sufficiently large temperature range so that extrapolation to standard conditions is possible. When this procedure is not feasible, correlations may be based on the boiling point at a specified low pressure, or on density or refractive index at some temperature other than 20°C.

Supplementing existing data by the accurate determination of physical constants of pure compounds is necessary in order to serve both practical and theoretical needs, and it is to be hoped that the next few years will produce an increasing amount of research along this line. While excellent results have already been attained, the amount of research so far completed is infinitesimal compared to the whole, despite more than a century of effort.

#### SUMMARY

The importance of correlations between the physical properties and the structure of hydrocarbons is stressed. The quality and quantity of data needed for such correlations is discussed, and the available data analyzed. The analysis shows the percentage of known alkanes, unsaturated aliphatics, alicyclics, mononuclear aromatics and polynuclear aromatics for which each of four physical constants (melting point, boiling point, density, and refractive index) has been recorded. Further analysis shows the percentage of compounds in each class for which the data were adequate to calculate a "best value." A comparison of correlations covering the different classes of hydrocarbons shows that the quality and quantity of data are reflected in correlations. Suggestions are made for further research on physical constants.

#### REFERENCES

- (1) BURNOP, V. C. E.: *J. Chem. Soc.* **1938**, 826.
- (2) CALINGAERT, G., AND HLADKY, J. W.: *J. Am. Chem. Soc.* **58**, 153 (1936).
- (3) CORBIN, N., ALEXANDER, M., AND EGLOFF, G.: *Ind. Eng. Chem.* **36**, 156 (1946).
- (4) CORBIN, N., ALEXANDER, M., AND EGLOFF, G.: *Ind. Eng. Chem.* **38**, 610 (1946).

- (5) CORBIN, N., ALEXANDER, M., AND EGLOFF, G.: J. Phys. Colloid Chem. **51**, 528 (1947).
- (6) CORBIN, N., ALEXANDER, M., AND EGLOFF, G.: Ind. Eng. Chem. **39**, 1147 (1947).
- (7) EGLOFF, G.: *Physical Constants of Hydrocarbons*, Reinhold Publishing Corporation, New York: Vol. I. *Paraffins, Olefins, Acetylenes, and Other Aliphatic Hydrocarbons* (1939); Vol. II. *Cyclanes, Cyclenes, Cyclynes, and Other Alicyclic Hydrocarbons* (1940); Vol. III. *Mononuclear Aromatic Hydrocarbons* (1946); Vol. IV. *Polynuclear Aromatic Hydrocarbons* (1947).
- (8) EGLOFF, G., AND KUDER, R.: J. Phys. Chem. **45**, 836 (1941); **46**, 296 (1942); Ind. Eng. Chem. **34**, 372 (1942).
- (9) EGLOFF, G., AND KUDER, R.: J. Phys. Chem. **46**, 28 (1942).
- (10) EGLOFF, G., SHERMAN, J., AND DULL, R. B.: J. Phys. Chem. **44**, 730 (1940).
- (11) FRANCIS, A. W.: Ind. Eng. Chem. **33**, 554 (1941); **35**, 442 (1943); **36**, 256 (1944).
- (12) GLASGOW, A. R., JR., STREIFF, A. J., AND ROSSINI, F. D.: J. Research Natl. Bur. Standards **35**, 355 (1945).
- (13) HUGGINS, M. L.: J. Am. Chem. Soc. **63**, 116 (1941).
- (14) HUGGINS, M. L.: J. Am. Chem. Soc. **63**, 916 (1941).
- (15) IVANOVSKY, L., AND BRANCKER, A. V.: Petroleum **5**, No. 10, 169 (1942).
- (16) KINNEY, C. R.: Ind. Eng. Chem. **32**, 559 (1940).
- (17) KINNEY, C. R.: Ind. Eng. Chem. **33**, 791 (1941).
- (18) KINNEY, C. R.: J. Am. Chem. Soc. **60**, 3032 (1938).
- (19) KINNEY, C. R.: J. Org. Chem. **6**, 220 (1941).
- (20) KLAGES, F.: Ber. **76**, 788 (1943).
- (21) KURTZ, S. S., JR., AND LIPKIN, M. R.: Ind. Eng. Chem. **33**, 779 (1941).
- (22) KURTZ, S. S., JR., AND LIPKIN, M. R.: J. Am. Chem. Soc. **63**, 2158 (1941).
- (23) MIBASHAN, A.: Trans. Faraday Soc. **41**, 374 (1945).
- (24) TAYLOR, W. J., PIGNOCCO, J. M., AND ROSSINI, F. D.: J. Research Natl. Bur. Standards **34**, 413 (1945).
- (25) WIENER, H.: J. Am. Chem. Soc. **69**, 17 (1947).
- (26) WIENER, H.: Private communication (April 25, 1947).
- (27) WILLINGHAM, C. B., TAYLOR, W. J., PIGNOCCO, J. M., AND ROSSINI, F. D.: J. Research Natl. Bur. Standards **35**, 219 (1945).

## PHYSICAL CHEMISTRY OF FLOTATION. XI

### KINETICS OF THE FLOTATION PROCESS

K. L. SUTHERLAND

*Division of Industrial Chemistry, Commonwealth Council for Scientific and  
Industrial Research, Melbourne, Australia*

*Received August 27, 1947*

#### I. INTRODUCTION

To determine the theoretical rate of flotation of mineral in a cell, it is necessary to make use of a simplified model of the system, which ignores unimportant variables while retaining essential features. Theories of air-mineral adhesion are discussed and the direct encounter hypothesis is chosen for detailed investigation. Any failure of the subsequent theory to describe the kinetics of the process is certainly due to oversimplification of the encounter hypothesis and some attempt is made to assess the importance of the simplifications.

## II. THEORIES OF AIR-MINERAL ADHESION

Taggart (21) observed that gas is deposited on non-polar surfaces from solutions supersaturated with the gas. In the subaeration and agitation machines there are regions of high pressure and low pressure before and after the impeller blade. These pressures produce super- and under-saturation, respectively, of the pulp. The air can then precipitate from the supersaturated liquid on the particles of mineral, and it is postulated that all mineral which floats has been buoyed to the surface by air attached in this way. Taggart also observed that, in one test at least, conditioned particles falling on stationary air bubbles do not adhere, and he therefore declares the encounter process inadequate. Despite Taggart's assertion that "this idea (i.e., the encounter hypothesis) (was) conceived in ignorance and born in litigation, was fostered by selfish interest and, unfortunately, was copied into some textbooks", Bogdanov and Filanovski (3) obtain opposite results in similar tests. They present direct evidence by cinematographic record for the collision theory. Particles with a hydrophobic surface fell on a stationary air bubble. They adhered. Bubbles rising with a speed of  $18 \text{ cm sec}^{-1}$  (about 0.09 cm. radius) collided with and adhered to suspended mineral particles (about 0.0075 cm. radius). The time required for adhesion to the bubble of suitably conditioned mineral was between 2 and 10 millisecc.

Gaudin (6a) and earlier investigators postulated a direct encounter, leading to adhesion between suspended mineral and the rising bubble. Treating this process theoretically Gaudin showed that no encounter was possible between a bubble and a mineral particle in an ideal fluid (compare later). Further, he stated that in some experiments he found that "it is very difficult to cause coursing air bubbles to pick up well-prepared mineral particles" (6, p. 92). Despite these difficulties Gaudin considers that the theory is more plausible than the gas-precipitation hypothesis, which he criticizes on the grounds that (1) vacuum and pressure near the impeller blades follow so rapidly that bubble growth is not possible; (2) it is not possible for one bubble to grow simultaneously on scores of particles, yet heavily armored bubbles are common in suitable systems; (3) the precipitation theory must lead to equal rates of flotation<sup>1</sup> of small and large particles, which is not so. The first objection is not important, since supersaturated pulp could be flung from the impeller and the growth of the bubble could proceed slowly in pulp distant from agitation (see also page 409). The second and third objections are sufficiently important to warrant dismissal of the theory as the major method by which mineral is attached to *bubbles which buoy it to the surface*.

This conclusion is strengthened by the observation of Malozemoff and Ramsey (13), who found that the operating capacity of a mechanical flotation cell is chiefly dependent upon that volume of the cell through which air bubbles are passing. Design of the cell will influence the aerated volume but cannot markedly influence the supersaturation of dissolved air produced by the impeller.

In a pneumatic cell supersaturation is still possible but is smaller than in the

<sup>1</sup> The term "rate of flotation" is used in this paragraph in the sense of the number of particles floating per unit time rather than in the sense of the weight of mineral floating per unit time.

mechanical cell, and the operation might have been expected to provide evidence for the encounter hypothesis. Unfortunately, in the usual operation of a pneumatic cell the large amount of air used obscures the process, since it sweeps much pulp into the froth. The life of bubbles in the froth is five to twenty times that in the pulp, so that the mineral adheres while in the froth. Plante and Sutherland (16) have described a process for separating ergot from rye by pneumatic flotation: the floating particles (grain) were never carried mechanically into the froth. The coursing air bubbles collided and adhered to grain, the most effective part of the cell being immediately above the blanket through which air was introduced. Gaudin (6b) also considers that the probability of encounter in the agitation cell is higher than in the pneumatic cell because the bubbles are small and hence provide a large collision area per unit volume; they have a longer life in the cell and the ratio of mineral size to bubble size is greater than for the pneumatic cell. These intuitive ideas are not entirely correct, but with modification the argument is sound.

Precipitation of gas on a hydrophobic surface may be a great help in flotation. Most flotation operators are familiar with the more rapid flotation of a mineral or concentrate which is being refloat. Hallimond (10) showed that preagitation of xanthate-treated galena with air greatly increased the rate of flotation. Usually the induction period (see page 401) is greatly decreased on a mineral surface if previous contact has been made with an air bubble. This behavior has been ascribed to thin layers of air on the mineral surface, e.g., the observations of de Witt (27) on covellite, and of Harvey *et al.* (11) and of Pease and Blinks (15) on bubble nuclei, which are important in determining the behavior of liquids.

If gas precipitates on mineral particles during flotation in a cell, subsequent flotation may still be ascribed to collision between an air bubble and an aggregate consisting of a mineral particle and a minute air bubble. The aggregate may have a density greater than or even less than that of the pulp. The theoretical approach adopted in this paper will still be valid, but for the smaller sizes of mineral the aggregate will be very much larger than the particle. It then follows from our theory that the chances of an aggregate floating are better than those for the mineral particle by itself, particularly in the smaller size ranges.

### III. ASSUMPTIONS IN THEORETICAL TREATMENT OF FLOTATION RATE, USING THE DIRECT ENCOUNTER HYPOTHESIS

In 1932 Gaudin (6c) considered collision between an air bubble and a mineral particle in a flotation cell, assuming that (1) water is non-viscous and incompressible; (2) water is infinitely divisible (i.e., the mineral particles are large compared with the molecules or their mean free path); (3) bubble and particle are rigid spheres; (4) bubble and particle are the only disturbing factors in the cell; (5) motion of bubble and particle is irrotational (i.e., there is streamline motion of the water past these spheres). He deduced that collision is possible only if the center of the particle lies on the central line of motion of the bubble.

His analysis, however, was based on an implicit, but erroneous, assumption that two bodies move independently in a fluid, that is, there is no interaction of their velocity fields.

The motion of two spheres toward one another has not been successfully analyzed except when the spheres move along their line of centers (17). Mathematical treatment is possible, however, if the mass of one of the spheres is zero, i.e., if the particle is inertia-less; it will then travel along a streamline of the liquid passing around the second sphere. Our treatment of collision in an ideal fluid will embody the assumption that (*G*) inertial effects be neglected for the smaller sphere. The question of the forces of adhesion between the air bubble and mineral being sufficient to prevent the aggregate parting is discussed in Section IX.

Considering these assumptions in detail, we may say with respect to the first, that the results obtained for a non-viscous, incompressible fluid are an excellent approximation to the behavior in a viscous, slightly compressible fluid such as water.

The second assumption will lead to significant errors only if the size of the particle (or air bubble) is less than 0.1 micron. Particles as small as this will not be considered.

Particles are not spherical, but we can define a spherical particle which behaves essentially as the mineral. Calculations based on this assumption for other hydrodynamic problems show a good approximation to actual behavior. Departure from sphericity of the bubble is more serious. The bubbles are deformed (flattened on top) and the motion of bigger bubbles shows instability (oscillation). Hence the velocity of the bubble relative to the particle used in this paper will be determined from an experimental equation describing the motion. There will be an error, however, in deriving the "collision area", which error is difficult to evaluate.

The most serious error appears to be in assumption 4. It is implicitly assumed that (*a*) there is no coalescence of bubbles; (*b*) bubbles do not cluster around one particle (19); (*c*) bubbles do not hinder each other while rising (7). Assumption (*a*) was proved valid by experiments described in Section IX. We have not studied the importance of factor (*b*) and factor (*c*) is shown in Appendix I to be relatively unimportant.

Assumption 5 is not seriously in error, though for the bubble sizes studied the motion is not completely streamline (irrotational). The theory can be applied into the region of turbulent flow, e.g., Stokes's law can be extrapolated well into the region of turbulence without errors exceeding, say, 10 per cent.

Neglect of inertial effects (assumption 6) slightly lowers the calculated collision rate for the small particles common in flotation.

#### IV. SYMBOLS USED IN THE THEORETICAL TREATMENT

- A* = overflow rate of froth from cell per unit of cell volume ( $\text{sec.}^{-1}$ )
- B* = buoyancy force on the bubble
- C* = constant of integration, which is determined by the streamline chosen

- $D$  = maximum distance at which the center of a particle can lie from the line of motion of the bubble (figure 1) for collision to be possible (cm.)  
 $d$  = density of mineral particle to be floated (g. cm.<sup>-3</sup>)  
 $d_w$  = density of pulp (g. cm.<sup>-3</sup>)  
 $E$  = distance of particle from center of line of motion of the bubble (cm.)  
 $F$  = Stokesian resistance to a sphere  
 $f = w'_f/w'_0$   
 $G$  = grade of unfloatable pulp  
 $G_c$  = grade of concentrate  
 $g$  = acceleration due to gravity (980 cm. sec.<sup>-2</sup>)  
 $h$  = height of attached bubble  
 $k, k_1, k_2$  = constants  
 $l$  = distance travelled by bubble in cell (cm.)  
 $L$  = capillary attraction of particle and bubble corrected for hydrostatic forces  
 $N$  = number of particles removed per unit volume of pulp after time  $t$  sec. (cm.<sup>-3</sup>)  
 $N_0$  = number of particles initially present per unit volume of pulp (cm.<sup>-3</sup>)  
 $N'$  = number of bubbles per unit volume of pulp (cm.<sup>-3</sup>)  
 $\Delta N_r$  = number of particles of radius  $r$  per unit volume of pulp (cm.<sup>-3</sup>)  
 $\Delta N_\lambda$  = number of particles with an induction period  $\lambda$  initially present per unit volume (cm.<sup>-3</sup>)  
 $\Delta_r N_0$  = number of particles of radius  $r$  initially present per unit volume (cm.<sup>-3</sup>)  
 $\Delta N'_R$  = number of bubbles of radius  $R$  per unit volume of pulp (cm.<sup>-3</sup>)  
 $n$  = number of collisions per unit time (sec.<sup>-1</sup>)  
 $n_f$  = number of fruitful collisions per unit time (sec.<sup>-1</sup>)  
 $n_{rf}$  = number of fruitful collisions in the cell between bubbles and particles of radius  $r$  cm.  
 $n_{rf}$  = number of fruitful collisions when bubble is loaded  
 $n_L$  = number of particles attached to a bubble  
 $P$  = volume of pulp entering cell per unit time per unit cell volume (sec.<sup>-1</sup>)  
 $Q$  = weight of mineral particle in water  
 $p = 3\pi\theta \operatorname{sech}^2 \left( \frac{3V\lambda}{4R} \right) RrVN'$  (sec.<sup>-1</sup>)  
 $p' = 3\pi RrVN'$  (sec.<sup>-1</sup>)  
 $p_1 = 3\pi\theta \operatorname{sech}^2 \left( \frac{3V\lambda}{4R} \right) RrVN'$  (cm.<sup>-1</sup> sec.<sup>-1</sup>)  
 $R$  = radius of bubble (cm.)  
 $\bar{R}$  = mean radius of bubbles  
 $R_m$  = rate of flotation (g. sec.<sup>-1</sup> cm.<sup>-3</sup>)



- $\Delta_r R_m$  = rate of flotation of particles of radius  $r$  (g. sec.<sup>-1</sup> cm.<sup>-3</sup>)  
 $\Delta_R R_m$  = rate of flotation of particles by bubbles of radius  $R$  (g. sec.<sup>-1</sup> cm.<sup>-3</sup>)  
 $\bar{R}_m$  = average rate of flotation (g. sec.<sup>-1</sup> cm.<sup>-3</sup>)  
 $m R_m$  = rate of flotation of sample containing only particles of mean radius  
 $f R_m$  = rate of flotation from cell in continuous operation (g. sec.<sup>-1</sup> cm.<sup>-3</sup>)  
 $f R'_m$  = rate of flotation from cell in continuous operation when conditions are steady (g. sec.<sup>-1</sup> cm.<sup>-3</sup>)  
 $t R_m$  = rate of removal of ore in tailing (g. sec.<sup>-1</sup> cm.<sup>-3</sup>)  
 $r, r_1, r_2, r_k, r_n$  = radius of particles (cm.)  
 $s$  = distance travelled by particle on bubble surface (cm.)  
 $t_c$  = time of contact between bubble and particle (sec.)  
 $t$  = time variable (sec.)  
 $T'$  = surface tension (dynes cm.<sup>-1</sup>)  
 $V$  = velocity of bubble relative to the particles (cm. sec.<sup>-1</sup>)  
 $\bar{V}$  = velocity of average-sized bubble (cm. sec.<sup>-1</sup>)  
 $V'$  = velocity of particle around bubble surface, arcial velocity (cm. sec.<sup>-1</sup>)  
 $W$  = total weight of gangue in concentrate (g.)  
 $w$  = concentration of mineral removed from pulp after a time  $t$  sec. (g. cm.<sup>-3</sup>)  
 $w_0$  = concentration of mineral in the feed (g. cm.<sup>-3</sup>)  
 $w'_0$  = concentration of gangue in the pulp (g. cm.<sup>-3</sup>)  
 $w'_f$  = concentration of gangue in the overflow liquid (g. cm.<sup>-3</sup>)  
 $w_c$  = concentration of mineral removed from unit volume of pulp into the concentrate at a time  $t$  (g. cm.<sup>-3</sup>)  
 $w'_c$  = concentration of gangue removed from unit volume of pulp into the concentrate at a time  $t$  (g. cm.<sup>-3</sup>)  
 $\Delta r^w$  = concentration of particles of radius  $r$  removed from the pulp after a time  $t$  (g. cm.<sup>-3</sup>)  
 $\Delta_r w_0$  = concentration of particles of radius  $r$  initially in the pulp (g. cm.<sup>-3</sup>)  
 $x$  = polar coördinate  
 $\alpha$  = contact angle measured from mineral through pulp  
 $\rho$  = radius of curvature of bubble in the planes perpendicular to the plane of contact  
 $\rho_0$  = radius of curvature of bubble at its apex  
 $\theta$  = proportion of particles retained in the froth after fruitful collision  
 $\xi$  = velocity potential of the liquid relative to the bubble  
 $\lambda$  = induction period necessary for air-mineral adhesion (sec.)  
 $\eta$  = viscosity of pulp (poises)  
 $\nu$  = kinematic viscosity of the pulp (stokes)

- $\sigma$  = density of air bubble (g. cm.<sup>-3</sup>)  
 $\sigma_g$  = density of gas in air bubble (g. cm.<sup>-3</sup>)  
 $\phi$  = polar coördinate  
 $\psi$  = probability of gangue adhesion  
 $\zeta(r, R, \text{etc.})$  = function of  $r, R, \text{etc.}$

# V. COLLISION BETWEEN BUBBLE AND PARTICLE

Ramsey (17) shows that the equation to the streamlines of a fluid moving past a sphere of radius  $R$  (the bubble) is

$$\sin^2 \phi = \frac{Cx}{x^3 - R^3} \quad (1)$$

where  $(x, \phi)$  is the polar coördinate of the streamline (figure 1). As the inertialess particle will travel along a streamline it will just touch the bubble if it is travelling on the streamline whose closest approach to the bubble is  $r$  cm., the

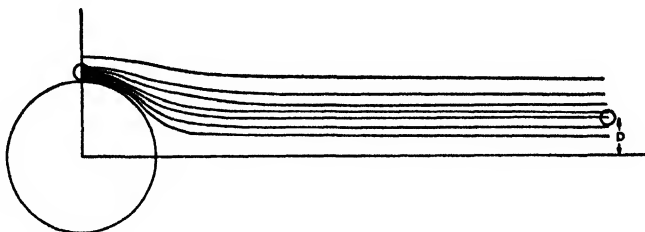


FIG. 1. Path of particle in streamline

radius of the particle (figure 1). This streamline which passes through the point  $\left(x = R + r, \phi = \frac{\pi}{2}\right)$  enables us to determine the constant in equation 1, viz.:

$$C = \frac{(R + r)^3 - R^3}{R + r} \quad (2)$$

When the particle is at an infinite distance above the bubble, then  $\phi = 0$  and we require the value of  $x \sin \phi$  which is equal to  $D$  cm., the maximum distance at which the center of the particle can lie from the center of the line of motion of the bubble in order to just collide with it. Substituting in equation 1, we have

$$x \sin \phi = \sqrt{\frac{(R + r)^3 - R^3}{R + r}} \cdot \frac{x^3}{x^3 - R^3}$$

and taking the limit as  $\phi \rightarrow 0$  (i.e.,  $x \rightarrow \infty$ )

$$D = \sqrt{\frac{r(3R^2 + 3rR + r^2)}{R + r}} \quad (3)$$

If, as is true in flotation,  $r$  is small compared with  $R$ , then terms containing  $r^3$  only will be negligible and hence

$$D = \sqrt{3rR} \quad (4)$$

This quantity,  $D$ , defines the "collision radius" of the bubble for a particle of radius  $r$ . All particles lying within this distance from the line of motion of the

bubble will collide with it. The number of collisions per second ( $n$ ) between the bubble and a suspension of particles ( $N_0$  per cm.<sup>3</sup>) is therefore

$$n = \pi D^2 V N_0 = 3\pi R r V N_0 \quad (5)$$

where  $V$  is the velocity of the bubble relative to the particles. If the bubble is an oblate spheroid (about the axis of motion) the number of collisions is

$$n = 3k\pi R r V N_0$$

where  $k$  is a factor which is less than unity, the amount depending upon the eccentricity of the ellipsoid ( $R$  is here the radius of the ellipsoid perpendicular to the axis of motion).

If  $N'$  bubbles are present per cubic centimeter, the number of collisions is

$$n = 3\pi R r V N_0 N' \quad (6)$$

#### VI. RATE OF FLOTATION

The rate of flotation is assumed to be governed by the rate of collision between mineral and air bubbles in the pulp. It is observed that bubbles sometimes drop their load when they reach the froth, owing to coalescence and subsequent decrease in area of surface holding the mineral. We will suppose that a fraction  $(1 - \theta)$  of the particles is returned at any instant to the pulp by coalescence either at froth-pulp interface or in pulp owing to coalescence of bubbles or to some turbulent condition which will strip the particle from the bubble. Usually  $\theta$  will be close to unity.

If the bubble is practically completely covered with particles before it has risen into the froth, the last part of its journey to the surface is ineffective, for collision cannot lead to adhesion. If the pulp density of floating mineral is large or the grade of feed is high (as it is in cleaning operations) then "crowding" becomes important. Under usual conditions the "collision area" on top of the bubble will be free from particles which slide to the bottom of the bubble (3).

In addition to the above factors, not every collision will be fruitful, since a finite time of contact between bubble and particle is needed to ensure adhesion (the induction period  $\lambda$ ). This period is of the order of magnitude of 0.005–0.1 sec. (5, 20), although in special systems it is considerably longer (25). When a particle is at a distance  $\sqrt{3Rr}$  cm. from the line of motion of the bubble, it is obvious that the bubble will only be touched for an infinitesimally short time before the particle leaves it following the streamline flow of the liquid. As the particle lies nearer to the line of motion of the center of the bubble, it will be in contact for longer and longer periods before it reaches a position where it can leave the bubble. Let the particle be  $E$  cm. distant from the center of line of motion of the bubble. Then the point  $(x = r + R, \phi)$  at which the particle strikes the bubble surface is derived from equation 1.

Since  $\lim_{x \rightarrow \infty} (x \sin \phi)$  is equal to  $E$ , the constant  $C$  is equal to  $E^2$ . Equation 1 becomes

$$\sin^2 \phi = \frac{E^2 x}{x^3 - R^3} \quad (7)$$

and the polar coördinate of the point where the particle strikes the bubble is

$$\left( x = r + R, \phi = \arcsin E \sqrt{\frac{R + r}{(R + r)^3 - R^3}} \right)$$

or neglecting  $r^3$

$$\phi = \arcsin (E/\sqrt{3Rr}) \quad (8)$$

The velocity potential of the liquid relative to the bubble is given by

$$\xi = Vx \cos \phi + \frac{1}{2}VR^3x^{-2} \cos \phi \quad (9)$$

The arcial velocity—

$$V' = -\frac{1}{x} \frac{\partial \xi}{\partial \phi} = V \sin \phi + \frac{1}{2}VR^3x^{-3} \sin \phi \quad (10)$$

Although the center of the particle travels on a circle of radius  $(R + r)$  after touching the bubble, we may consider it as moving on a circle of radius  $R$  without being in error by more than 10 per cent for the size of bubble and particle usual in flotation. This simplification is used in equation 15 and subsequently. From equation 10

$$V' = V \sin \phi + \frac{1}{2}V \frac{R^3}{(R + r)^3} \sin \phi \quad (11)$$

The time to travel from the point  $(R + r, \phi)$  where the particle collides to the point  $(R + r, \pi - \phi)$  where it leaves the bubble is given by

$$t_c = \int_{\phi}^{\pi-\phi} \frac{(R + r) d\phi}{V \sin \phi \left\{ 1 + \frac{1}{2} \left( \frac{R}{r + R} \right)^3 \right\}} \quad (12)$$

since  $dt_c = \frac{ds}{V'}$  and  $ds = (R + r) d\phi$  is the distance travelled on the bubble surface in a time  $dt_c$ .

Hence

$$t_c = \frac{4(R + r)}{V \left\{ 2 + \left( \frac{R}{r + R} \right)^3 \right\}} \log_e \cot \frac{\phi}{2} \quad (13)$$

Substituting for  $\phi$  from equation 8

$$E = \sqrt{3Rr} \operatorname{sech} \frac{Vt_c \left\{ 2 + \left( \frac{R}{r + R} \right)^3 \right\}}{4(R + r)} \quad (14)$$

or approximating

$$E = \sqrt{3Rr} \operatorname{sech} \left( \frac{3Vt_c}{4R} \right)^2 \quad (15)$$

\* A more accurate approximation would be

$$E = \sqrt{3Rr} \operatorname{sech} \left( \frac{3Vt_c}{4(R + 2r)} \right)$$

If the particle is to adhere to the bubble, then the induction period  $\lambda$  must be less than or equal to  $t_c$ .

Equation 15 then defines  $E$  for a given  $\lambda$ :

$$E = \sqrt{3Rr} \operatorname{sech} \left( \frac{3V\lambda}{4R} \right) \quad (16)$$

Figure 2 shows equation 14 plotted for different values of  $R$  and  $\lambda$  and also shows the effective area of contact for each bubble after reducing to unit volume of air.  $V$  is calculated from Allen's equation (see Appendix I).

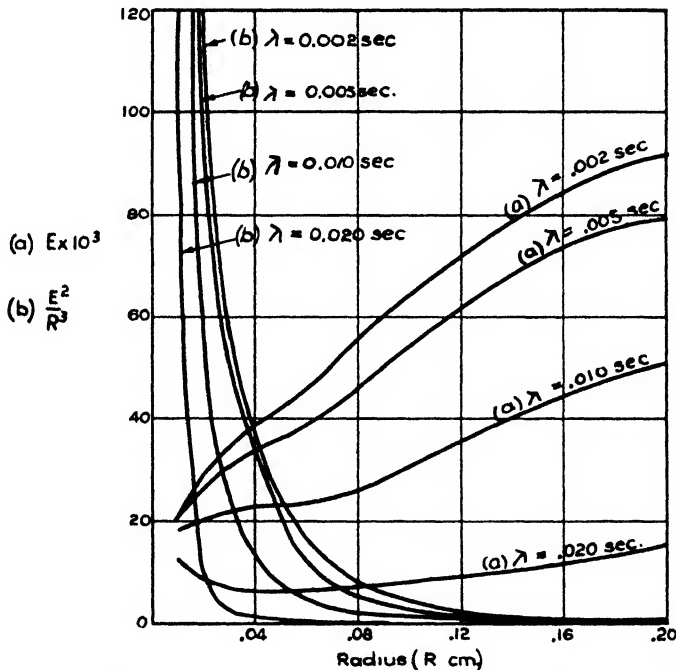


FIG. 2. The relationship between (a) bubble size and the effective contact radius  $E$  and (b) bubble size and the effective area of contact per unit volume of bubble ( $E^2/R^3$ ).

We now replace equation 6 by

$$n_f = 3\pi RrVN_0N' \operatorname{sech}^2 \left( \frac{3V\lambda}{4R} \right) \quad (17)$$

where  $n_f$  is the number of collisions per unit time per unit volume which lead to adhesion.

The rate of flotation ( $\text{g. cm.}^{-3} \text{ sec.}^{-1}$ ) is then

$$R_m = 4\pi^2 \theta \operatorname{sech}^2 \left( \frac{3V\lambda}{4R} \right) Rr^4 N_0 N' Vd \quad (18)$$

where  $\theta$  is introduced to allow for particles removed from the bubble after fruitful collision (page 401) and  $d$  is the density of the particles. Hence  $R_m$  is pro-

portional to the pulp density and the rate of aeration. It is directly proportional to the radius of the mineral but is related in a more complex manner to the bubble size, viz:  $RV \operatorname{sech}^2 \left( \frac{3V\lambda}{4R} \right)$ .

Suppose that in a batch cell the rate of flotation is studied with time. Let  $w_0$  g. cm.<sup>-3</sup> be the initial concentration of the mineral. Then if  $(w_0 - w)$  is the concentration at  $t$  sec.,<sup>3</sup> the rate of flotation is given by

$$R_m = \frac{dw}{dt} = p(w_0 - w) \quad (19)$$

where  $p$  is a constant. Integrating between the limits 0 and  $t$

$$w = w_0(1 - e^{-pt}) \quad (20)$$

But at the concentration  $(w_0 - w)$  g. cm.<sup>-3</sup> we have from equation 18

$$R_m = 4\pi^2 \theta \operatorname{sech}^2 \left( \frac{3V\lambda}{4R} \right) Rr^4 VN' d(N_0 - N) \quad (21)$$

where  $N_0$  and  $N$  are the number of particles per cm.<sup>3</sup> of cell pulp which were present originally and which were removed respectively, i.e.,  $(N_0 - N)$  is the number remaining. Since

$$w_0 = \frac{4}{3}\pi r^3 dN_0 \text{ and } w = \frac{4}{3}\pi r^3 dN \quad (22)$$

we have from equations 21 and 22

$$R_m = 3\pi\theta \operatorname{sech}^2 \left( \frac{3V\lambda}{4R} \right) RrVN'(w_0 - w) \quad (23)$$

Comparison of equations 19 and 23 shows that

$$p = 3\pi\theta \operatorname{sech}^2 \left( \frac{3V\lambda}{4R} \right) RrVN' \quad (24)$$

and hence equation 20 becomes

$$w = w_0 \{ 1 - e^{-3\pi\theta \operatorname{sech}^2 (3V\lambda/4R) RrVN' t} \} \quad (25)$$

and substituting from equation 25 in equation 23 for  $w$ , we can derive the variation of rate with time.

A Denver subaeration flotation cell of depth 25 cm. contains 10<sup>4</sup> cm.<sup>3</sup> of pulp. The following values are typical:

$$\begin{array}{lll} R = 0.03 \text{ cm.} & r = 5 \times 10^{-3} \text{ cm.} & V = 6 \text{ cm. sec.}^{-1} \\ N' = 20 \text{ bubbles cm.}^{-3} & \theta = 1 & w_0 = 0.01 \text{ g. cm.}^{-3} \end{array}$$

<sup>3</sup> No mineral will appear in the froth until a time  $t$  sec. after aeration commences, i.e., until bubbles have risen from bottom of cell to the top.  $t$  is dependent upon bubble size,  $Vt$  being equal to the depth of the cell. The time can be considered as starting after this initial period.

A typical time required for a 90 per cent recovery is 60 sec. (e.g., for sized quartz floated with cetyltrimethylammonium bromide). Then from equation 20 the value of  $\lambda$  is 0.009 sec., a value which is plausible.

It is generally known that the rate of flotation is governed approximately by an exponential law. Thus Beloglazov (2), Züniga (28), and Gründer and Kadur (9) found that the rate of flotation at any time was approximately proportional to the amount of floatable material remaining in the cell.

#### VII. VARIATION IN GRADE OF CONCENTRATE WITH THE TIME WHEN GANGUE IS PRESENT

Let  $w_0$  g. cm.<sup>-3</sup> be the initial concentration of mineral to be floated, and  $w'_0$  g. cm.<sup>-3</sup> the concentration of gangue. Let  $\psi$  be the probability of flotation of gangue after collision ( $\psi$  to include the sech and  $\theta$  terms). Since  $\psi$  will be small and  $w'_0$  is usually large compared with  $w_0$  we can, with good approximation, consider  $w'_0$  constant throughout a batch test.

Mineral and gangue will be carried into the concentrate by the walls of the bubble cells. The extent of draining (proportional to the height of froth) determines the amount of pulp left in the walls. This pulp will not have the same composition as that in the cell, because gangue and mineral settle from it. In the mineral concentrate, the overflow of liquid is  $A$  cm.<sup>3</sup> sec.<sup>-1</sup> per cm.<sup>3</sup> of cell volume carrying  $Aw'_f$  g. sec.<sup>-1</sup> of gangue into the concentrate ( $w'_f$  = concentration of gangue in the overflow liquid). The value of  $w'_f$  may be considered constant throughout the experiment and, judging from Schuhmann's results (18), may have values between 0.5  $w'_0$  and 0.1  $w'_0$  for sizes of particles of less than 7 microns and 35 microns, respectively. The coarser the mineral the more rapidly does the gangue leave a froth.

The grade of the feed is

$$G = \frac{w_0}{w_0 + w'_0} \quad \text{i.e.,} \quad \frac{1 - G}{G} = \frac{w'_0}{w_0} \quad (26)$$

If  $w_c$ ,  $w'_c$  are the weights of mineral and gangue, respectively, in the concentrate (produced from 1 cm.<sup>3</sup> of pulp), then the grade is

$$G_c = \frac{w_c}{w_c + w'_c} \quad \text{i.e.,} \quad \frac{1 - G_c}{G_c} = \frac{w'_c}{w_c} \quad (27)$$

From equation 23 for the gangue

$$\begin{aligned} R_m t &= 3\pi\psi RrVN'w'_0 t \\ &= p'\psi w'_0 t \end{aligned} \quad (28)$$

where  $p' = 3\pi RrN'V$ .

In the same time  $Aw'_f t$  g. is carried over by the froth liquid.

The total weight ( $W$ ) of gangue appearing in the concentrate is

$$\begin{aligned} W &= p'\psi w'_0 t + Aw'_f t \\ &= w'_0 t \{p'\psi + fA\} \end{aligned} \quad (29)$$

where  $f = w'_f/w'_0$  is constant for any size range and has values less than unity and greater than zero.

The amount of mineral floated in the time  $t$  is  $w$ , and from equations 25, 26, 27, 28, and 29 we have:

$$\frac{1 - G_c}{G_c} = \frac{1 - G}{G} \frac{(p'\psi + fA)t}{1 - e^{-pt}} \quad (30)$$

If, in a batch float, the grade of concentrate is studied, then it is apparent from equation 30 that the grade falls steadily as time increases.

#### VIII. RATE OF FLOTATION OF MINERAL WHICH EXHIBITS A SIZE RANGE

Hitherto the mineral floated has been considered to be of uniform size. Since the rate of flotation depends upon  $r$ , the radius of particle floated, the average rate of flotation does not equal the rate of flotation of the average size particles. In the analysis which follows the presence of gangue is neglected.

Let the number of particles  $\Delta N_r$  with a radius between  $r$  and  $r + \Delta r$  be given by

$$\Delta N_r = N_0 \zeta(r) \Delta r \quad (31)$$

where  $\zeta(r)$  is a size-distribution function.

Corresponding to equation 17 we have that the number of fruitful collisions for particles in the size range  $r, r + \Delta r$

$$\begin{aligned} \Delta_r n_f &= 3\pi \operatorname{sech}^2 \left( \frac{3V\lambda}{4R} \right) RrV \Delta N_r N' \\ &= 3\pi \operatorname{sech}^2 \left( \frac{3V\lambda}{4R} \right) RrVN' N_0 \zeta(r) \Delta r \end{aligned} \quad (32)$$

and the weight of mineral floated in time  $\Delta t$  is

$$\frac{4}{3}\pi r^3 d\Delta_r n_f \Delta t = 4\pi^2 \operatorname{sech}^2 \left( \frac{3V\lambda}{4R} \right) R dVN r^4 N_0 \zeta(r) \Delta t \Delta r$$

If  $\Delta_r N_0$  particles of radius between  $r$  and  $r + \Delta r$  are originally present and  $\Delta N_r$  are removed after a time  $t$ , the rate of flotation is

$$\begin{aligned} \Delta_r R_m &= 3\pi\theta \operatorname{sech}^2 \left( \frac{3V\lambda}{4R} \right) RrVN' \left\{ \frac{4}{3}\pi r^3 d\Delta_r N_0 - \frac{4}{3}\pi r^3 d\Delta N_r \right\} \\ &= 3\pi\theta \operatorname{sech}^2 \left( \frac{3V\lambda}{4R} \right) RrVN' (\Delta_r w_0 - \Delta_r w) \end{aligned} \quad (33)$$

and

$$\frac{d\Delta_r w}{dt} = p(\Delta_r w_0 - \Delta_r w) = \Delta_r R_m \quad (34)$$

Hence

$$\Delta_r w = \Delta_r w_0 (1 - e^{-3\pi\theta \operatorname{sech}^2 \left( \frac{3V\lambda}{4R} \right) RrVN' t}) \quad (34)$$



and substituting for  $\Delta_r w$  in equation 33 from equation 35:

$$\Delta_r R_m = 3\pi\theta \operatorname{sech}^2\left(\frac{3V\lambda}{4R}\right) RVN' r \Delta_r w_0 e^{-3\pi\theta \operatorname{sech}^2(3V\lambda/4R) RrVN't}$$

The total flotation rate is the sum of the flotation rates for each size of particle, and

$$\begin{aligned} \Delta_r w_0 &= \frac{4}{3} \pi r^3 N_0 d\zeta(r) \Delta r \\ R_m &= 4\pi^2 \theta \operatorname{sech}^2\left(\frac{3V\lambda}{4R}\right) RVN' dN_0 \int_0^\infty r^4 \zeta(r) e^{-3\pi\theta \operatorname{sech}^2(3V\lambda/4R) RrVN't} dr \end{aligned} \quad (35)$$

The effect of a particle distribution and correlation with experimental results is discussed in Appendix II.

#### IX. RATE OF FLOTATION BY BUBBLES WHICH HAVE A SIZE DISTRIBUTION

Let the number of bubbles with a radius between  $R$  and  $R + \Delta R$  be given by

$$\Delta N'_R = N'\zeta(R) \Delta R \quad (36)$$

We may derive the rate of flotation along lines similar to that employed for the particle-size distribution. The result has a formal resemblance to equation 36. However, the bubble-size distribution, unlike the particle-size distribution, is independent of time. Considering therefore flotation due to bubbles of size between  $R$  and  $R + \Delta R$  cm, equation 23 becomes

$$\Delta_R R_m = 3\pi\theta \operatorname{sech}^2\left(\frac{3V\lambda}{4R}\right) RrV\zeta(R)N'(w_0 - w) \Delta R \quad (37)$$

and therefore

$$\int_0^\infty d_R R_m = R_m = 3\pi\theta r(w_0 - w)N' \int_0^\infty VR \operatorname{sech}^2\left(\frac{3V\lambda}{4R}\right) \zeta(R) dR \quad (38)$$

i.e.,

$$\frac{dw}{dt} = 3\pi\theta \operatorname{sech}^2\left(\frac{3\bar{V}\lambda}{4\bar{R}}\right) \bar{R}r\bar{V}N'(w_0 - w) \quad (39)$$

since

$$\int_0^\infty \zeta(R) dR = 1 \quad (40)$$

and the mean radius of the bubble is defined from

$$\bar{V}\bar{R} \operatorname{sech}^2\left(\frac{3\bar{V}\lambda}{4\bar{R}}\right) = \frac{\int_0^\infty VR \operatorname{sech}^2\left(\frac{3V\lambda}{4R}\right) \zeta(R) dR}{\int_0^\infty \zeta(R) dR} \quad (41)$$

The value of  $V$  as a function of  $R$  is given by equation 62. Equation 39 can be integrated as previously.

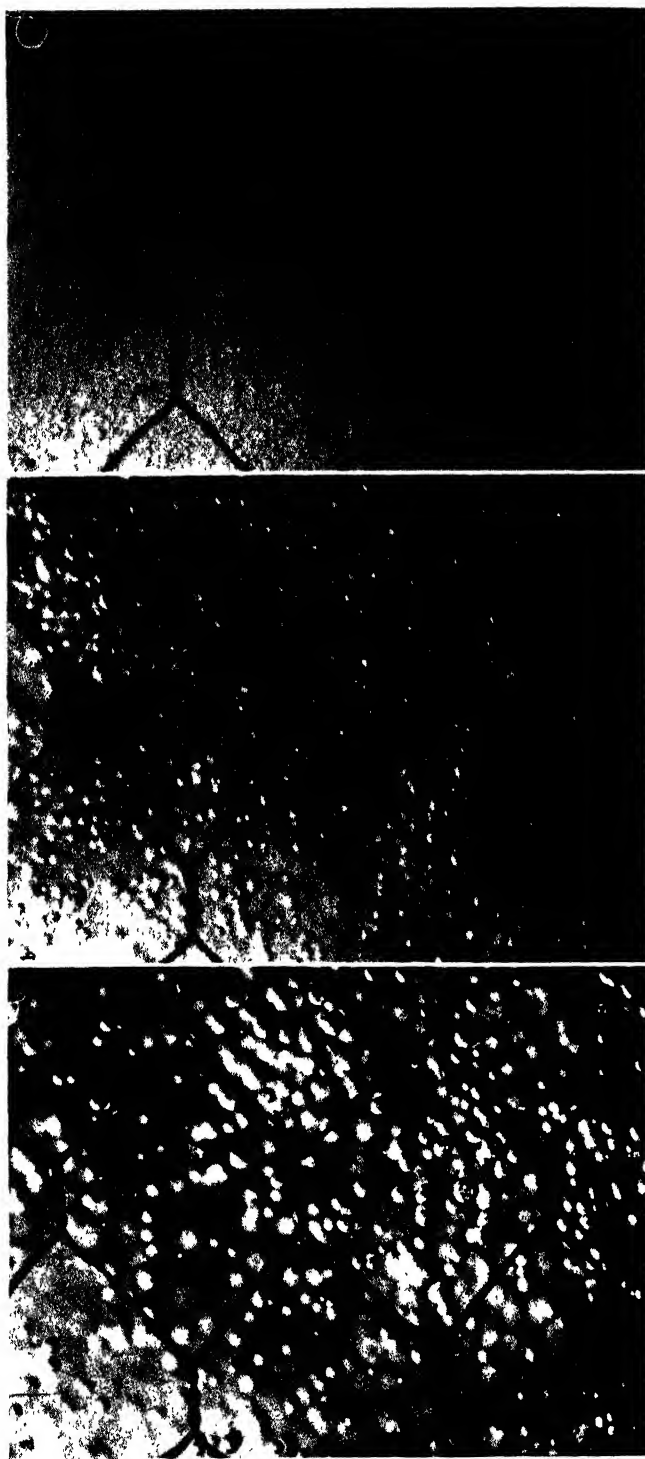


FIG. 3. Photographs of bubble in a flotation cell Frother, (a) 2.5, (b) 5, and (c) 10 mg of pine oil per liter, respectively.

To obtain the distribution in bubble size a 2000-g. Denver subaeration machine with a glass side was photographed. Figures 3a, 3b, 3c show the effect of 2.5, 5, and 10 mg. of pine oil per liter of water, respectively, on bubble size when the impeller was rotated at a low speed to avoid excessive froth. These bubbles were illuminated by a lamp which gave a flash of 10 microsec. All motion of the bubbles was thus "stopped". The distribution in bubble sizes is given in figure 4. It will be noted that nearly all bubbles are spherical. By measuring the depth of focus of the photographs the number of bubbles per cubic centimeter of pulp could be calculated. Thus there were three, seven, and twenty-five bubbles per cubic centimeter of pulp in the photographs reproduced here.

Cinematographic records were made at speeds between 800 and 2000 frames per second, using an arc lamp for illumination. These again showed little or no departure of bubbles from sphericity, no coalescence with one another, and

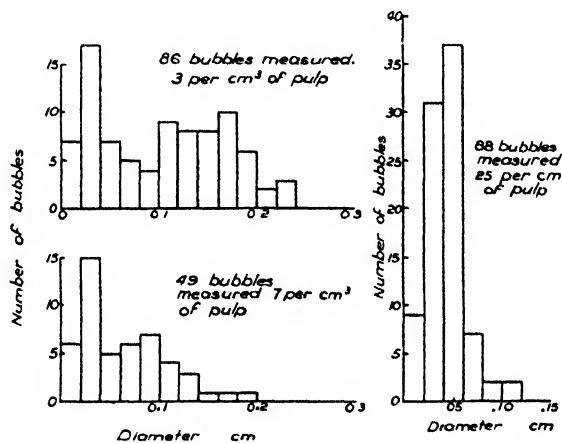


FIG. 4. Distribution of bubble sizes corresponding to aeration and pine oil concentration shown in figure 3.

uniform speeds of ascent. The speed of the fluid flow was measured from suspended spheres of density equal to that of the pulp.

Volkova (22, 23, 24) has calculated the force of adhesion between an air bubble and mineral particle when the latter is small. If the particle is not free to move, then the force separating bubble from mineral is the buoyancy of the bubble. Since the area of adhesion must be small on a small particle, the force of adhesion is also small. Volkova confirmed his theoretical calculations experimentally and then stated that the force parting bubble and mineral when these collide is determined by the buoyancy force on the bubble. This is not correct for movement in a fluid. His subsequent argument leads to the result that for all particles there is a maximum size of bubble which can adhere and that for small particles these bubbles are so small that flotation does not seem possible: firstly, because the rate of ascent of these bubbles is far too small and secondly, such bubbles will normally disappear by dissolution. In the photographs shown in figure 3 bubbles smaller than 0.002 cm. radius have been neglected. In figures

3a and 3b there are about as many bubbles of, say, average radius 0.001 cm. as there are bubbles of radius greater than 0.002 cm. Nevertheless they constitute an insignificant proportion of the air passing through the cell and they have an average terminal ascending velocity of about 0.02 cm. sec.<sup>-1</sup> which will not allow them to escape from the pulp. Now the excess pressure over atmospheric inside a bubble of radius 0.001 cm. is 0.14 atm. Hence these bubbles will dissolve readily and the gas will be precipitated on the mineral (*vide* reference 21) and on larger bubbles.

In a viscous fluid the parting force is not the buoyancy of the bubble but the viscous drag on the particle and its own weight in the fluid. As the particle slides down the bubble it attains much of the velocity of the bubble surface. The radial velocity of the particle is determined from the velocity potential  $\xi$  (equation 9) of the fluid

$$\frac{\partial \xi}{\partial x} = V \cos \phi - V R^3 x^{-3} \cos \phi \quad (42)$$

This is a maximum for  $\phi = \pi$ . Since the particle is attached to the bubble,  $x$  has the value  $(R + r)$  and

$$\left(\frac{\partial \xi}{\partial x}\right)_{\max} = V \left[ \left(\frac{R}{R+r}\right)^3 - 1 \right] \simeq -V \frac{3rR}{(R+r)^2} \quad (42a)$$

The negative sign indicates that the radial velocity is in the direction away from the center of the sphere. The viscous force,  $F$ , on the particle will not exceed the Stokesian resistance, i.e.,

$$F < 6\pi\eta r \frac{3rR}{(R+r)^2} V \quad (43)$$

The only other force attempting to separate bubble and particle is an impulsive force,  $I$ , due to the inertia of bubble and mineral. From the principle of conservation of momentum (considering viscous and gravitational forces absent, as the effect of these are calculated above) the terminal velocity of the aggregate, bubble and particle, may be derived as

$$\frac{R^3 d_w V - r^3(d - d_w)v}{R^3 d_w + r^3(d - d_w)} \quad (43a)$$

where  $V$ ,  $-v$  are the upward velocities of bubble and particle, respectively, before attempting to separate and the remaining terms give the apparent masses of the bodies concerned. Equation 42a gives the velocity of the fluid and hence of the particle, relative to the bubble. When the bubble moves with a velocity  $V$ , then the velocity of the particle immediately prior to the attempt at separation is

$$-v = V \left\{ 1 - \frac{3rR}{(R+r)^2} \right\} \quad (43b)$$

The difference between the initial and final velocities given in equations 43l

and 43a, respectively, divided by the time,  $t$  sec., in which the velocity is changing, enables the impulsive force,  $I$ , to be calculated:

$$I = \frac{\frac{4}{3}\pi R^3 r^3 d_w (d - d_w)}{R^3 d_w + r^3 (d - d_w)} \frac{V}{t} \left\{ \frac{3rR}{(R + r)^2} \right\} \quad (43c)$$

Neglecting the smaller terms, we obtain:

$$I < \frac{12\pi r^4 V}{Rt} \quad (43d)$$

TABLE 1

*Comparison of the adhesional force ( $L$ ), the weight and Stokesian resistance ( $Q + F$ ), and the buoyancy of the bubble ( $B$ )*

Stable adhesion when  $L > Q + F$ .  $\alpha = 45^\circ$ . Velocity of ascent from appropriate Reynolds number and coefficient of resistance. Density of particles = 4 g.cm.<sup>-3</sup>

DIAMETER OF PARTICLE	DIAMETER OF BUBBLE	VELOCITY OF ASCENT	$L$	$Q + F$	$B$
microns	cm.	cm. sec. <sup>-1</sup>	dynes	dynes	dynes
25	0.38	33.5	0.40	$8.1 \times 10^{-4}$	28.2
50			0.78	$3.9 \times 10^{-3}$	
75			1.16	$1.1 \times 10^{-2}$	
100			1.52	$2.1 \times 10^{-2}$	
200			2.89	$1.3 \times 10^{-1}$	
500			6.87	1.7	
25	0.18	18	0.39	$9.9 \times 10^{-4}$	2.99
50			0.75	$4.6 \times 10^{-3}$	
75			1.08	$1.2 \times 10^{-2}$	
100			1.39	$2.3 \times 10^{-2}$	
200			2.35	$1.3 \times 10^{-1}$	
500			3.80	1.7	

Table 1 compares the value of  $F + Q$ , where  $Q$  is the weight of the particle in the fluid, with the buoyancy force of bubbles ( $B = \frac{4}{3}\pi R^3 d_w g$ ) and the adhesional force  $L$  which is given by Wark (26) as

$$L = \pi r T \left( \sin \alpha - \frac{r}{\rho} \right) \quad (44)$$

where  $\alpha$  is the contact angle,  $T$  the surface tension of the pulp,  $r$  the radius of circle of contact, and  $\rho$  the principal radius of curvature at the circle of contact in the plane perpendicular to the solid. To calculate  $\rho$  it is necessary to know the forces acting on bubble and particle. Thus Wark's equation for the bubble contour becomes

$$\frac{2}{\rho} = \frac{2}{\rho_0} - \frac{d_w g h}{T} - \frac{Q + F}{\pi r^2 T} \quad (45)$$

where  $\rho_0$  is the curvature of the bubble at its apex and  $h$  is the distance of the

apex from the plane of contact. Volkova (23) shows that for small areas of adhesion  $h$  may be put equal to  $2R$ , the diameter of the bubble before adhesion, and that  $\rho_0$  is approximately equal to  $R$ . Thus:

$$\frac{1}{\rho} = \frac{1}{R} - \frac{d_w g R}{T} - \frac{Q + F}{2\pi r^2 T} \quad (46)$$

The  $(Q + F)$  term replaces the usual buoyancy force due to the bubble. The impulsive force is probably so small that it can be neglected. It can only be large if  $t$  is small (equation 43d). For the example cited in table 1 the impulsive force does not exceed the adhesional force,  $L$ , except if the particle can be detached from the bubble in less than  $10^{-4}$  sec. This is not feasible and for a period of even so short a time as  $10^{-2}$  sec., the force is from 30 to  $10^6$  times smaller than  $L$ , and is always smaller than the  $(Q + F)$  force.

Calculation from equation 46 shows that the bubble shape involves no re-entrant surface and consequently the aggregate is stable. It is apparent that the adhesional forces are sufficient for flotation however small the particle.

#### X. RATE OF FLOTATION OF A SAMPLE THE PARTICLES OF WHICH DO NOT HAVE A UNIFORM INDUCTION PERIOD

Let the number of particles  $\Delta N_\lambda$  which have an induction period between  $\lambda$  and  $\lambda + \Delta\lambda$  sec. be given by:

$$\Delta N_\lambda = N_0 \zeta(\lambda) \Delta\lambda \quad (47)$$

Then an analysis corresponding to that in the preceding section leads to

$$R_m = p' \theta w_0 \int_0^\infty \zeta(\lambda) \operatorname{sech}^2 \left( \frac{3V\lambda}{4R} \right) e^{-p'\theta t \operatorname{sech}^2 (3V\lambda/4R)} d\lambda \quad (48)$$

where  $p' = 3\pi R r V N'$  and  $w_0 = \frac{4}{3}\pi r^3 N_0 d$ .

Corresponding to equation 25 the weight of mineral floated at a time  $t$  is given by

$$\begin{aligned} w &= w_0 \int_0^\infty \zeta(\lambda) \{1 - e^{-p'\theta t \operatorname{sech}^2 (3V\lambda/4R)}\} d\lambda \\ &= w_0 \int_0^\infty \zeta(\lambda) d\lambda - w_0 \int_0^\infty \zeta(\lambda) e^{-p'\theta t \operatorname{sech}^2 (3V\lambda/4R)} d\lambda \end{aligned} \quad (49)$$

Since the total number of particles originally present in the sample is  $N_0$ , it follows from equation 47 that

$$\int_0^\infty \zeta(\lambda) d\lambda = 1 \quad (50)$$

Hence equation 49 becomes

$$\frac{w_0 - w}{w_0} = \int_0^\infty \zeta(\lambda) e^{-p'\theta t \operatorname{sech}^2 (3V\lambda/4R)} d\lambda \quad (51)$$

If we put  $z = p'\theta \operatorname{sech}^2 \left( \frac{3V\lambda}{4R} \right)$ , then equation 48 becomes

$$\begin{aligned} \frac{w_0 - w}{w_0} &= \frac{2R}{3V} \int_0^{p'\theta} e^{-zt} \frac{\zeta(\lambda)}{z \sqrt{1 - \frac{z}{p'\theta}}} dz \\ &= \frac{2R}{3V} \int_0^\infty e^{-zt} \frac{\zeta(\lambda)}{z \sqrt{1 - \frac{z}{p'\theta}}} dz - \frac{2R}{3V} \int_{p'\theta}^\infty e^{-zt} x \frac{\zeta(\lambda)}{z \sqrt{1 - \frac{z}{p'\theta}}} dz \quad (52) \end{aligned}$$

TABLE 2

*Weight of mineral ( $w$  g.) floated in a Denver cell originally containing  $w_0$  g. (= 469 g.) of spheres after various times  $t$  sec.*

$t$	$w$	$\frac{w_0 - w}{w_0}$
30	182	0.6119
60	335	0.2857
120	385	0.1791
180	408	0.1301
240	420	0.1045
300	427	0.0896

It is shown in Appendix III that the second integral is negligible for certain numerical values of  $p'\theta$ . If it is neglected, then the inverse Laplace transformation can be applied and the integral is

$$\frac{3V}{2R} \frac{\zeta(\lambda)}{z \sqrt{1 - \frac{z}{p'\theta}}} = \frac{1}{2\pi i} \int_{-\infty}^{+\infty} e^{-zt} \left( \frac{w_0 - w}{w_0} \right) dt \quad (53)$$

where  $i = \sqrt{-1}$ .

If therefore a batch test is made in a flotation cell and an analytic function determined empirically for  $(w_0 - w)/w_0$  from the experimental data then, provided this function fulfils the conditions of the Laplace transformation, the function  $\zeta(\lambda)$  can be evaluated.

To evaluate the distribution likely in a flotation pulp, spheres of a calcium glass were prepared. The fraction between 52 and 72 mesh was separated and each particle allowed to roll down an inclined slope. Only those which were completely spherical rolled straight and were collected. A sample was photographed, and more than 98 per cent of the particles were spheres. The average diameter was 0.0252 cm. After cleaning by ignition at 650°C., the spheres were floated in a 2000-g. subaeration Denver cell, using 20 mg. of laurylamine hydrochloride per liter as collector and frother. The pH value was 7.0, the temperature 20°C. The rate of air flow into the cell was constant at 55 cm.<sup>3</sup> per second. The weights of concentrate taken at various times are shown in table 2. The

low rate of air flow was essential to enable easy removal of the concentrate: at the full rate the float was over completely in less than 1 min.

From table 2 an analytic function relating  $(w_0 - w)/w_0$  to the time  $t$  with an accuracy of better than 1 per cent and of the required form is

$$\frac{w_0 - w}{w_0} = \frac{1.614 \times 10^{-6}}{(47.46 + t)^2} - \frac{22.62}{(47.46 + t)^3} + \frac{2.747 \times 10^4}{(47.46 + t)^4} + \frac{2.39 \times 10^8}{(47.46 + t)^5} \quad (54)$$

Integrating equation 53 after substitution from equation 54 we have:

$$\zeta(\lambda) = \frac{3V}{2R} z^2 \sqrt{1 - \frac{z}{p'\theta}} e^{-47.46z} \{1.614 \times 10^{-6} - 11.31z + 4.578 \times 10^3 z^2 + 9.975 \times 10^6 z^3\} \quad (55)$$

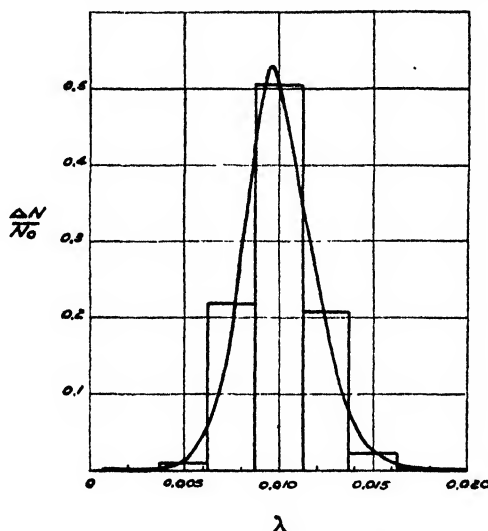


FIG. 5. Distribution in values of the induction period for flotation of spheres

For the sample studied it is assumed that  $\theta$  is unity and the following measured values  $r = 0.0126$  cm.,  $R = 0.064$  cm.,  $V = 12$  cm. sec.<sup>-1</sup>,  $N' = 5$  bubbles cm.<sup>-2</sup> of pulp enable  $p'$  to be calculated. The value of  $z$  is found from  $p' \operatorname{sech}^2 \left( \frac{3V\lambda}{4R} \right)$ . A plot showing  $\Delta N_\lambda / N_0$  is given in figure 5. The curve shows a typical distribution of  $\lambda$  values.

With a sample containing particles with different induction periods the curve relating weight of mineral floated with time will no longer be a simple exponential one. Calculation of the effect of varying induction period on the rate of flotation under continuous operating conditions is difficult, but qualitatively the result resembles that for a distribution of particle sizes (see Appendix II).

#### XI. STATE OF CONTINUOUS OPERATION

In correlating the batch test and a continuously operating cell, factors such as the accumulation of soluble products which may affect adsorption of collector,



rate of adsorption of collector, etc. are neglected. Let the rate of flow of ore into cell be  $Pw_0$  g. sec.<sup>-1</sup>, where  $P$  cm.<sup>3</sup> per cm.<sup>3</sup> of cell volume is the volume of pulp entering the cell per second. At a time  $t$ , the total weight of ore that has been in the unit volume of the cell which originally contained  $w_0$  g. of ore is

$$(1 + Pt)w_0 \text{ g.}$$

The weight of ore floated per unit volume of cell when  $w$  g. cm.<sup>-3</sup> has been removed is

$${}_fR_m = p\{w_0(1 + Pt) - w\} \quad (56)$$

At the same time mineral is removed in the tailing at the rate

$${}_tR_m = (P - A)\{w_0(1 + Pt) - w\} \quad (57)$$

where  $A$  cm.<sup>3</sup> is the volume of liquid removed per second per unit volume of cell with the concentrate.

The total rate ( ${}_fR_m + {}_tR_m$ ) is

$$R_m = \frac{dw}{dt} = (p + P - A)\{w_0(1 + Pt)\} - w \quad (58)$$

For the boundary condition  $t = 0, w = 0$ ,

$$w = w_0 \left\{ Pt + \frac{p - A}{p + P - A} (1 - e^{-(p+P-A)t}) \right\} \quad (59)$$

where  $p$  is as usual. Substituting for  $w$  from equation 59 in equation 56 the rate of flotation is

$${}_fR_m = \frac{Ppw_0}{p + P - A} \left\{ 1 + \frac{P - A}{P} e^{-(p+P-A)t} \right\} \quad (60)$$

When  $t$  is large (steady conditions) equation 60 becomes

$${}_fR'_m = \frac{Ppw_0}{p + P - A} = \frac{3\pi\theta \operatorname{sech}^2\left(\frac{3V\lambda}{4R}\right) RrN'V'Pw_0}{3\pi\theta \operatorname{sech}^2\left(\frac{3V\lambda}{4R}\right) RrN'V' + P - A} \quad (61)$$

This equation is of the form  $\frac{k_2 r}{r + k_3}$  and will be of value in determining the variation of rate of flotation with size in continuous test.  ${}_fR'_m$  can be calculated from batch cell tests, since  $p$  is deducible from these.

If we calculate the ratio of equation 60 to equation 61 then we obtain curves of the type shown in figure 6. Data presented by Schuhmann (18) for the rate of flotation of a copper mineral with time are also plotted in the same figure. The experimental curve cannot be accurately described by an equation of the type given. This is discussed in Appendix II of this paper, where Schuhmann's curve is shown to be compounded probably of a number of exponential curves.

## XII. VARIATION OF FLOTATION RATE WITH PARTICLE SIZE

The variation in flotation rate for particles of different size in continuous flow tests is deduced from equation 61. Figure 7 shows curves for which  $\frac{P - A}{p}$

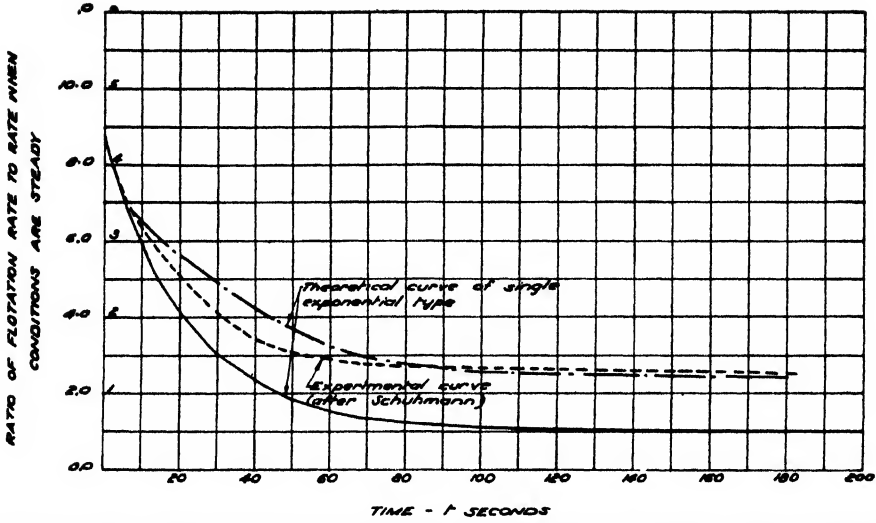


Fig. 6. Ratio of flotation rate to rate under steady conditions during a continuous test

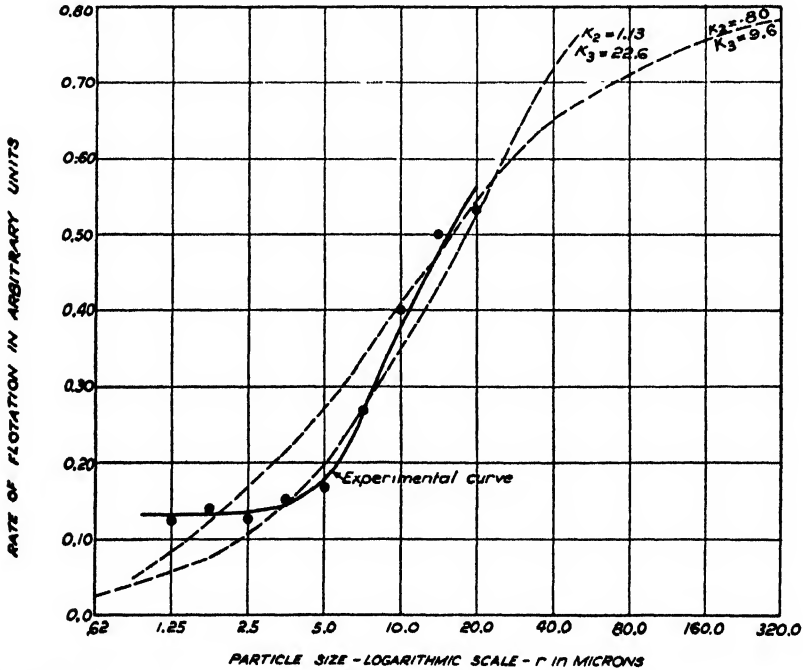


Fig. 7. Relationship between rate of flotation and size of particle floated during continuous tests.

is varied and data obtained by Gaudin, Schuhmann, and Schlechten (8). The curve does not fit the smaller values of  $r$  and unfortunately there are insufficient data to determine whether the flotation rate increases linearly with radius, as

claimed by the author, or whether it is described by the relation above. Gaudin Schuhmann, and Schlechten have suggested that the smaller particles aggregate to non-aerated flocs. If this is true it is difficult to see why they were able to find smaller particles in their method of measurement of particle size. Their method was to follow the rate of sedimentation, which rate depends upon the size of particle or aggregate. If special precautions were taken to disperse these aggregates, then their hypothesis may be proved by conducting the sedimentation experiments without dispersing agents. Because the flotation rate is constant, the number of particles to maintain the size of the flocs constant must increase enormously as the mineral size is decreased.

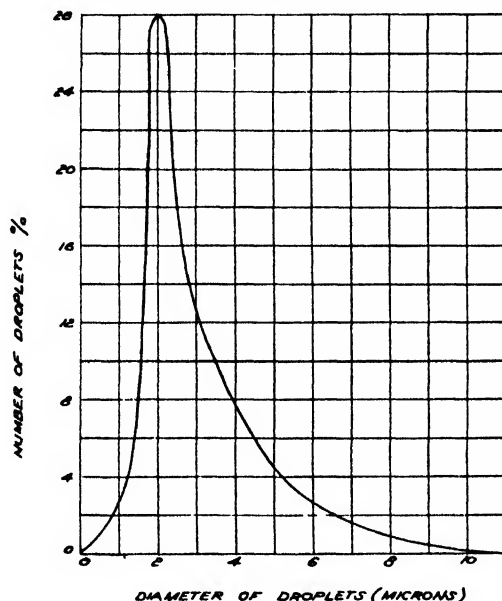


FIG. 8. Curve showing distribution of particle size in an emulsion (after Clayton (3))

"Sliming" is an example of the flocculation of small particles on larger ones, but excellent flotation of mineral is still obtainable when the conditions in the pulp are such that "sliming," and therefore presumably flocculation of small particles, is absent. It is possible that conditions for "sliming" were present in the above experiments.

An analogous system is shown in the distribution of droplet sizes in an emulsion. One would expect, *a priori*, a distribution range from large particles to almost infinitely small particles. Figure 8 shows an actual frequency curve (4). Droplets of less than 2 microns are almost completely absent—this being common to many emulsions (excluding those in which the viscosity is very high) and it is usually postulated that because Brownian movement is so marked for particles of less than 2 micron diameter frequent collisions ensure coalescence, which gives a smaller surface and hence a decrease in free energy for the system. Whilst flocculation presumably leads to only a small decrease in free energy due to

diminution in "free surface," the study of colloids shows that flocculation is frequent and is a stable condition. That the rate of flotation becomes constant when the mineral particles possess a diameter less than 2 microns and that emulsion droplets aggregate to form drops of the same size may be a coincidence, but it provides a useful starting point for discussion. Odén (14) has measured the size of flocs produced by the coagulation of barium sulfate suspensions and found sizes between 1 and 13 microns, according to the concentration of flocculating agent. These flocs contained between 50 and 120,000 particles. The flocs were formed under quiescent conditions, and the larger-sized particles may disintegrate if placed, for example, in a flotation cell. No data are available to show the variation in size of floc when a standard amount of coagulating agent is added to suspensions containing particles of different sizes.

#### APPENDIX I

##### *The effect of bubble loads on rate of flotation*

Allen's equation (1) describes the relationship between bubble size and terminal velocity for the size of bubble common in flotation:

$$V = 0.5 \left[ \frac{(d_w - \sigma)g}{d_w} \right]^{2/3} \frac{R - 0.0034}{\nu^{1/3}} \quad (62)$$

$d_w$  is the density of the pulp,  $\sigma$  that of the bubble, and  $\nu$  the kinematic viscosity. For the experimental values used in this paper

$$V = 229(R - 0.0034) \quad (63)$$

Allen only claims that his equation is accurate to a bubble radius of 0.05 cm., but his data do not extend beyond this value. An assumption made in our use of Allen's equation is that when many bubbles are present the hindered rate of rise will not differ greatly from that of the single bubble. Gaudin (7) discusses the data of Kermack, M'Kendrick, and Ponder (12) for solids and finds corrections to the Stokes equation of the order of 5 per cent for an 0.005 ratio of volume of dispersed solid to volume of liquid. If the same data are typical of a dispersion of gas bubbles in water, the error due to the use of Allen's equation will be less than 5 per cent, since Allen's equation is more accurate than Stokes's equation.

*Effect of load on bubble:* If the bubble carries a load which is sufficiently large, the terminal velocity is considerably decreased. Rewrite Allen's equation

$$V = k_2(d_w - \sigma)^{2/3}(R - 0.0034) \quad (64)$$

where

$$k_2 = \frac{0.5g^{2/3}}{\nu^{1/3}d_w^{2/3}}$$

The density of the bubble, when  $n_L$  particles of radius  $r$  and density  $d$  are attached, is

$$\frac{\frac{4}{3} \pi R^3 \sigma_g + \frac{4}{3} \pi r^3 n_L d}{\frac{4}{3} \pi R^3} \quad (65)$$

where  $\sigma_g$  = density of the gas. Hence

$$\begin{aligned} V &= k \left( d_w - \sigma_g - \frac{r^3}{R^3} n_L d \right)^{2/3} (R - 0.0034) \\ &\simeq k \left( d_w - \frac{r^3}{R^3} n_L d \right)^{2/3} (R - 0.0034) \end{aligned} \quad (66)$$

since

$$\sigma_g \simeq 0.001 \text{ g. cm.}^{-3}$$

Now the number of fruitful collisions in a distance  $\Delta l$  is

$$\begin{aligned} \Delta l n_f &= 3\pi R r N N' k \left( d_w - \frac{r^3}{R^3} n_L d \right)^{2/3} (R - 0.0034) \\ &\times \operatorname{sech}^2 \left\{ \frac{3k \left( d_w - \frac{r^3}{R^3} n_L d \right)^{2/3} (R - 0.0034) \lambda}{4R} \Delta l \right\} \end{aligned} \quad (67)$$

If it is assumed that the bubbles carry the full load the whole distance, then we get an upper limit to the extent to which loading would increase the flotation rate.

Taking the ratio of collision rate for loaded to unloaded bubbles we have from equations 67 and 17:

$$\frac{n_f}{n_f} = \left( 1 - \frac{r^3}{R^3} n_L \frac{d}{d_w} \right)^{2/3} \frac{\operatorname{sech}^2 \left\{ \frac{3k \left( d_w - \frac{r^3}{R^3} n_L d \right)^{2/3} (R - 0.0034) \lambda}{4R} \right\}}{\operatorname{sech}^2 \left\{ \frac{2k d_w^{2/3} (R - 0.0034) \lambda}{4R} \right\}} \quad (68)$$

For  $d = 3 \text{ g. cm.}^{-3}$ ,  $r = 0.005 \text{ cm.}$ ,  $R = 0.1 \text{ cm.}$ ,  $d_w = 1.2 \text{ g. cm.}^{-3}$ , and  $\lambda = 0.0166$  it is calculated that 10, 100, and 1000 particles increase the flotation rate by 0.0, 2.0, and 15 per cent, respectively. The effect is relatively unimportant unless the particles are large and the bubble small.

## APPENDIX II

### *Flotation rate when sample has a distribution of particle sizes*

Equation 35 gives the flotation rate when the distribution of mineral sizes is described by a function  $\zeta(r)$ . It is more usual to determine the size range of a sample by screening and weighing the mineral lying between two screen sizes. The screen openings are generally related by a geometric factor, e.g., each screen opening is  $1/2$  to  $1/\sqrt{2}$  the preceding sizes. We have chosen therefore the geometric mean of each screen size as representing the sample.

It is convenient to replace the integral of equation 35 by the sum,

$$R_m = 3\pi\theta \operatorname{sech}^2\left(\frac{3V\lambda}{4R}\right) RVN' w_0 \sum_{r_k=r_1}^{r_n} r_k f(W_k) e^{-3\pi\theta \operatorname{sech}^2(3V\lambda/4R) RVN' r_k} \quad (69)$$

where  $r_1, r_2 \dots r_n$  are the geometric mean size of each screening and  $w_0 f(W_k)$  is the amount of mineral of radius  $r_k$ .

TABLE 3  
*Mill feed (after Gaudin)*

WEIGHT PER CENT	SIZE RANGE (DIAMETER IN MICRONS)	GEOMETRIC MEAN RADIUS (MICRONS)
0.5	416-295	175.2
3	295-208	123.9
7	208-147	87.4
13	147-104	61.8
17.5	104-74	43.6
14	74-52	31.0
10	52-37	21.93
7	37-26	15.51
9	26-13	9.19
6	13-6.5	4.60
11	6.5-0.5	0.902
2	0.5-0.0	

TABLE 4  
*Rate of flotation of each size and total rate compared with average rate*

Time (seconds) . . . . .	10	50	100	150	200	300	500
$\frac{R_m}{w_0} \times 10^4$ . . . . .	176.1	47.3	16.5	8.10	5.49	2.43	1.11
$\frac{mR_m}{w_0} \times 10^4$ . . . . .	208.5	67.5	20.37	4.02	0.98	0.08	0.00

Gaudin has given an average mill feed which will serve as an example (6, p. 142) (see table 3). The mean radius for the sample excluding the 0.5-0.0 micron size is 35.9 microns. Assuming a value of  $3\pi\theta \operatorname{sech}^2\left(\frac{3V\lambda}{4R}\right) RVN'$  of 7.86, the rate of flotation of particles of the mean radius is

$$mR_m = 0.0276w_0 e^{-0.0282t} \quad (74)$$

If the rate of flotation for each of the size distributions is calculated, then on summing these rates we may compare them with the rate for the average particle (table 4). For this sample the rate of flotation of the sample would be smaller at first than that of a sample consisting of the average-sized particles. A sample could also be chosen such that the initial rate is greater than that consisting of average-sized particles.

The behavior of an ore containing a size range of particles is important when steady flotation conditions are observed in continuous tests. It will be noticed above that the variation of the flotation rate with time is no longer a simple exponential curve but is the sum of a number of exponential terms. If data determined by Schuhmann (18) are examined, the curve showing flotation rate with time is found not to be a simple exponential curve. This may be due to either variation in particle size or induction period or both. The ratio of rates of flotation of initial to steady conditions is given by equations 60 and 61, which have the following form for a distribution of mineral sizes:

$$\frac{\sum_{r_k=r_1}^{r_m} fR_m}{\sum_{r_k=r_1}^{r_m} fR'_m} = 1 + \frac{\sum_{r_k=r_1}^{r_m} \frac{r_k w_0 \zeta(W_k)}{p_1 r_k + P - A} \frac{p_1 r_k - A}{P} e^{-(p_1 r_k + P - A)t}}{\sum_{r_k=r_1}^{r_m} \frac{r_k w_0 \zeta(W_k)}{p_1 r_k + P - A}} \quad (70)$$

where the symbols are as previously and

$$p_1 = 3\pi\theta \operatorname{sech}^2 \left( \frac{3V\lambda}{4R} \right) RVN'$$

Consider a sample containing 50 per cent of particles of 100-micron radius and 50 per cent 20-micron radius. Here

$$\zeta(W_1) = \zeta(W_2) = 0.5$$

$$r_1 = 100 \times 10^{-4} \text{ cm.}, \quad r_2 = 20 \times 10^{-4} \text{ cm.}$$

and let  $p_1 = 5$ ,  $A = 5 \times 10^{-4} \text{ cm.}^3$ , and  $P = 5 \times 10^{-3} \text{ cm.}^3$ . Then

$$\frac{\sum_{k=1}^2 fR_m}{\sum_{k=1}^2 fR'_m} = 1 + 5.65e^{-0.0545t} + 0.815e^{-0.0145t} \quad (71)$$

For this sample the arithmetic mean is 60 microns, the geometric mean 45 microns. Hence the rates of flotation of samples of these sizes are

$$\left( \frac{fR_m}{fR'_m} \right)_{\text{arith.}} = 1 + 5.9e^{-0.0345t} \quad (72)$$

and

$$\left( \frac{fR_m}{fR'_m} \right)_{\text{geom.}} = 1 + 4.4e^{-0.025t} \quad (73)$$

Figure 9 shows the ratio of rate of flotation at different times to the final rate calculated from equations 71, 72, and 73.

The behavior of the sample possessing particles whose size is the geometric mean of the sample above shows an initial rate lower than that given by the simple exponential function. It is then higher and finally is lower again. This is the behavior when a single exponential curve is compared with Schuhmann's data.

## APPENDIX III

*Conditions for neglect of second integral of equation 41*

From equation 55 we can substitute in equation 52 and deduce the value of  $(w_0 - w)/w_0$ , i.e.

$$\frac{w_0 - w}{w_0} = \int_0^\infty ze^{-xz}(A + Bz + Cz^2 + Dz^3)dz - \int_m^\infty ze^{-xz}(A + Bz + Cz^2 + Dz^3)dz \quad (74)$$

where  $A = 1.614 \times 10^{-6}$ ,  $B = -11.31$ ,  $C = 4.578 \times 10^3$ ,  $D = 9.475 \times 10^6$ ,  $p'\theta = z$ , and  $x = t + 47.46$ .

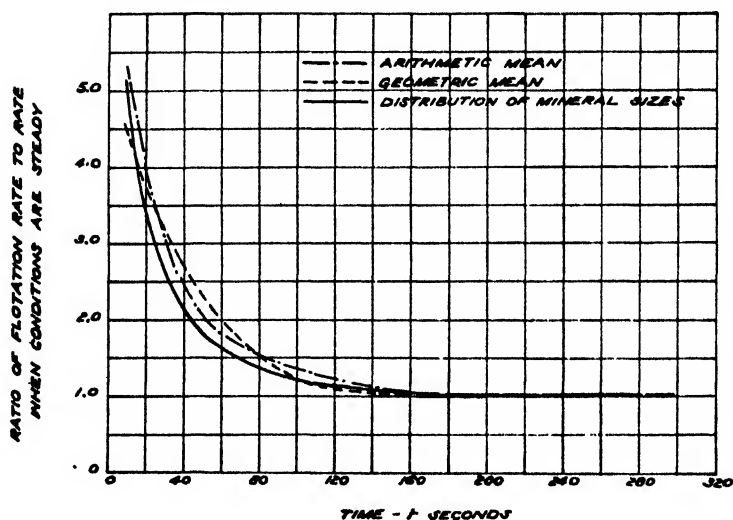


FIG. 9. Comparison of ratio of initial rates of flotation to rate under steady conditions during a continuous test for a sample with a size distribution of particles and a sample with particles with the geometric and arithmetic mean.

Therefore

$$\frac{w_0 - w}{w_0} = \frac{A}{x^2} + \frac{2!B}{x^3} + \frac{3!C}{x^4} + \frac{4!D}{x^5} - \zeta_1(t) \quad (75)$$

where

$$\begin{aligned} \zeta_1(t) = & \frac{A}{x^2} e^{-xm}(xm + 1) \\ & + \frac{B}{x^3} e^{-xm}(x^2 m^2 + 2xm + 2) \\ & + \frac{C}{x^4} e^{-xm}(x^3 m^3 + 3x^2 m^2 + 6xm + 6) \\ & + \frac{D}{x^5} e^{-xm}(x^4 m^4 + 4x^3 m^3 + 12x^2 m^2 + 24xm + 24) \end{aligned} \quad (76)$$



This is smaller than the experimental value of  $\frac{w_0 - w}{w_0}$  by the term  $\xi_1(t)$  (see equation 52). Now  $\xi_1(t)$  will have its largest value when  $t = 0$ , i.e., when  $x = 47.46$ . For an accuracy of 1 per cent in the function  $\frac{w_0 - w}{w_0}$  it is only necessary that the ratios of each of the following terms

$$\frac{A}{x^2} \text{ and } \frac{A}{x^2} - \frac{A}{x^2} e^{-xm}(xm + 1)$$

$$\frac{A}{x^3} \text{ and } \frac{A}{x^3} - \frac{A}{x^2} e^{-xm}(x^2 m^2 + 2xm + 2), \text{ etc.}$$

shall not exceed 1.01. The dominant term for experiments conducted over periods of less than 15 min. is  $D/x^5$  and we can consider that the total error will not exceed twice that in the  $D/x^5$  term. Hence require

$$\frac{D}{x^5} \left/ \left[ \frac{D}{x^5} \{1 - e^{-xm}(x^4 m^4 + 4x^3 m^3 + 12x^2 m^2 + 24xm + 24)\} \right] \right. \leq 1.005 \quad (77)$$

For  $x = 50$  this requires a value of  $z$  greater than 0.25.

Since  $z = 3\pi\theta rRVN' \operatorname{sech}^2 \left( \frac{3V\lambda}{4R} \right)$  and assuming that  $\lambda = 0.002$  sec.,  $R = 0.1$  cm.,  $V = 20$  cm. sec.<sup>-1</sup>,  $N' = 5$  then we estimate that the smallest particle size to which this section of the mathematical treatment will apply is 30 microns provided the constant 47.46 is not altered as particle size is diminished. If  $\lambda$  is larger than 0.002 sec. and particularly if the rate of aeration is increased, this minimum size can be reduced. *It is essential to calculate the error for each set of experimental conditions.*

#### SUMMARY

The direct-encounter hypothesis for adhesion of mineral to bubble in a flotation cell is investigated. It is shown theoretically that:

- (1) the "collision area" of a bubble is proportional to the product of bubble radius ( $R$ ) and mineral particle radius ( $r$ );
- (2) the area over which fruitful collision is possible is given by

$$3rR \operatorname{sech}^2 \left( \frac{3V\lambda}{4R} \right)$$

(The induction period ( $\lambda$ ) almost entirely governs the  $\operatorname{sech}$  term, because the ratio of bubble velocity ( $V$ ) to its radius ( $R$ ) does not alter appreciably.)

- (3) induction periods can be calculated and these are probably as accurate as the experimental values;
- (4) when there is a distribution of particle sizes the rate of flotation is the sum of a number of exponential functions of time;
- (5) when there is a distribution of bubble sizes the mean rate of flotation is equal to the rate of flotation with suitably defined mean size of bubble; experimental methods of determining bubble size and number are described;

- (6) the variation of flotation rate with mineral size, under continuously operating conditions, is given by an equation of the form

$$\text{rate} \propto \frac{r}{r + k_s}$$

This equation fails to predict the uniform flotation rate which has been found by some authors at small sizes. The possibility of flocculation of particles is discussed.

The author wishes to thank Mr. G. K. Batchelor and particularly Mr. A. Pillow of the Aerodynamics Section, Division of Aeronautics, for many helpful discussions on the presentation of this paper. Dr. I. W. Wark very kindly criticized the manuscript.

The work described in this paper was carried out as part of the program of the Division of Industrial Chemistry of the Council for Scientific and Industrial Research, Australia.

#### REFERENCES

- (1) ALLEN, H. S.: *Phil. Mag.* [5] **50**, 323 (1900).
- (2) BELOGLAZOV, K. F.: *Tsvetnye Metal.* **1939**, No. 9, 70; *Chem. Abstracts* **35**, 17\* (1941).
- (3) BOGDANOV, O. S., AND FILANOVSKI, M. SH.: *J. Phys. Chem. (U.S.S.R.)* **14**, 224-7 (1940).
- (4) CLAYTON, W.: *Emulsions and their Technical Treatment*, 4th edition. J. and A. Churchill, Ltd., London (1943).
- (5) EIGELES, M. A.: *Compt. rend. acad. sci. U.R.S.S.* **24**, 340 (1939).
- (6) GAUDIN, A. M.: *Flotation*, McGraw-Hill Book Co., Inc., New York (1932): (a) pp. 88-98, (b) p. 96, (c) p. 88.
- (7) GAUDIN, A. M.: *Principles of Mineral Dressing*, p. 190. McGraw-Hill Book Co., Inc., New York (1939).
- (8) GAUDIN, A. M., SCHUHMAN, R., JR., AND SCHLECHTEN, A. W.: *J. Phys. Chem.* **46**, 902-10 (1942).
- (9) GRÜNDER, W., AND KADUR, E.: *Metall. u. Erz.* **37**, 367 (1940).
- (10) HALLIMOND, A. F.: *Mining Mag.* **74** (April, 1945).
- (11) HARVEY, E. N., *et al.*: *J. Cellular Comp. Physiol.* **24**, 1, 23 (1944); *J. Am. Chem. Soc.* **67**, 156 (1945).
- (12) KERMACK, W. O., M'KENDRICK, A. G., AND PONDER, E.: *Proc. Roy. Soc. Edinburgh* **49**, 170-97 (1929).
- (13) MALOZEMOFF, P., AND RAMSEY, R. H.: *Eng. Mining J.* **142**, 45 (1941).
- (14) ODÉN, S.: *Kolloid-Z.* **26**, 100 (1920).
- (15) PEASE, D. C., AND BLINKS, L. R.: *J. Phys. Chem.* **51**, 556 (1947).
- (16) PLANTE, E. C., AND SUTHERLAND, K. L.: *J. Phys. Chem.* **48**, 203 (1943).
- (17) RAMSEY, A. S.: *A Treatise on Hydromechanics. Part II. Hydrodynamics*, p. 160. G. Bell and Sons, London (1935).
- (18) SCHUHMAN, R., JR.: *J. Phys. Chem.* **46**, 891 (1942).
- (19) SIEDLER, P., MOELLER, A., AND REDDENHASE, T.: *Kolloid-Z.* **60**, 320 (1932).
- (20) SVEN-NILSSON, I.: *Ing. Vetenskaps Akad. Handl. No. 133* (1935).
- (21) TAGGART, A. F.: *Handbook of Ore Dressing*. John Wiley and Sons, Inc., New York. 1927 edition, pp. 797-9, 806-8; 1945 edition, Section 12, pp. 52-4.
- (22) VOLKOVA, Z.: *Acta Physicochim. U.R.S.S.* **20**, 467 (1945).
- (23) VOLKOVA, Z.: *Acta Physicochim. U.R.S.S.* **21**, 171 (1946).

- (24) VOLKOVA, Z.: *Acta Physicochim. U.R.S.S.* **21**, 563 (1946).  
 (25) WARK, I. W.: *J. Phys. Chem.* **40**, 663 (1936).  
 (26) WARK, I. W.: *J. Phys. Chem.* **37**, 639 (1933).  
 (27) DE WITT, C. C.: *J. Am. Chem. Soc.* **57**, 775 (1935).  
 (28) ZŮNIGA, H. G.: *Bol. minero soc. nacl. mineria (Santiago, Chile)* **47**, 83 (1935); *Chem. Abstracts* **30**, 7511<sup>6</sup> (1936).

## VAPOR PRESSURE-TEMPERATURE RELATIONSHIPS AMONG THE BRANCHED PARAFFIN HYDROCARBONS

HARRY WIENER

*Department of Chemistry, Brooklyn College, Brooklyn, New York*

*Received July 24, 1947*

### INTRODUCTION

The difference in normal boiling point between a branched-chain paraffin and its straight-chain isomer can be expressed (4) as a function of two structural variables by the equation<sup>1</sup>

$$\Delta t = \frac{98}{n^2} \Delta w + 5.5 \Delta p \quad (1)$$

In this paper, it is shown that the boiling points of branched-chain paraffins also obey this law at pressures other than 760 mm. of mercury, with only the empirical constants changed.

In any equation relating the vapor pressures and temperatures of paraffins, the constants involved will differ for individual isomers, and are therefore functions of molecular structure. If the boiling points of isomeric paraffins at different pressures are linear functions of the structural parameters  $\Delta w$  and  $\Delta p$ , it is probable that the constants of temperature-pressure equations will be represented by similar functions of these two variables. For the Antoine vapor-pressure equation this rule holds, and the constants can be correlated by such functions.

### BOILING POINTS AT DIFFERENT PRESSURES

The general form of equation 1, at pressures other than 760 mm. of mercury, is

$$\Delta t = \frac{k}{n^2} \Delta w + b \Delta p \quad (2)$$

For a single group of isomers  $n$  is constant, and equation 2 becomes

$$\Delta t = a \Delta w + b \Delta p \quad (3)$$

<sup>1</sup>  $w$  is the sum of the distances, in terms of carbon-carbon bonds, between the members of all pairs of carbon atoms in the molecule;  $p$  is the number of pairs of carbon atoms separated by three bonds;  $\Delta t = t_n - t_{iso}$ ;  $\Delta w = w_n - w_{iso}$ ;  $\Delta p = p_n - p_{iso}$ .

Accurate values for the boiling points of many branched-chain paraffins at pressures other than 760 mm. of mercury are available, as a result of experiments carried out at the National Bureau of Standards, and may be used to determine whether equations 2 and 3 hold at different pressures. In these experiments, Willingham, Taylor, Pignocco, and Rossini (5) determined the temperatures of the liquid-vapor equilibrium for numerous hydrocarbons over a wide range of pressures, including the boiling points of seventeen octanes (all except 2,2,3,3-tetramethylbutane) at twenty fixed pressures ranging from 47.7 to 779.3 mm. of mercury, above about 12°C.

Equation 3 was fitted to the observed boiling points of these seventeen octanes at three pressures,—779.3, 402.4, and 57.5 mm. of mercury,—by the method of least squares. The values of the two constants of equation 3, obtained in this manner, are: at 779.3 mm.,  $a = 1.520$ ,  $b = 5.56$ ; at 402.4 mm.,  $a = 1.485$ ,  $b = 5.31$ ; at 57.5 mm.,  $a = 1.386$ ,  $b = 4.68$ .

The variation of the two constants with pressure is well represented by the equations

$$a = 0.118 \log P + 1.178 \quad (4)$$

$$b = 0.77 \log P + 3.32 \quad (5)$$

As  $k = 64a$  for the octanes, the general equation for the difference in boiling points of two isomers, as a function of their structure and of pressure, becomes

$$\Delta t = (7.55 \log P + 75.39) \frac{\Delta w}{n^2} + (0.77 \log P + 3.32) \Delta p \quad (6)$$

The manner in which this equation reproduces the observed values is shown in table 1. The average deviations for the seventeen octanes are  $\pm 0.59^\circ\text{C}$ . at 779.3 mm.,  $\pm 0.53^\circ\text{C}$ . at 402.4 mm., and  $\pm 0.49^\circ\text{C}$ . at 57.5 mm. of mercury. Equation 6, therefore, appears to be applicable about equally well over the pressure range from 50 to 800 mm. of mercury. Comparison of values calculated from this equation with observed boiling points for some lower paraffins at other pressures supports this conclusion, the average deviations being well below  $0.5^\circ\text{C}$ .

The ratio of the constants  $a$  and  $b$  of equation 3 varies with pressure. The fraction  $b/a$  decreases from 3.66 at 779.3 mm. to 3.58 at 402.4 mm. and to 3.37 at 57.5 mm. of mercury. This indicates that at low temperatures, the relative importance of the structural factor, compactness ( $w$ ), becomes somewhat increased over that of the parameter representing interatomic attraction forces ( $p$ ).

Inspection of table 1 also shows that compounds for which  $\Delta p = -4$  have increasing values of  $\Delta t$  at decreasing pressures, while for compounds which have  $\Delta p = 0$ ,  $\Delta t$  falls rapidly with decreasing pressure.<sup>2</sup> Other factors being equal, the separation by distillation of a branched-chain from a normal paraffin isomer, or of two branched-chain isomers, is therefore best performed at low pressures if the two compounds have widely different values of  $\Delta p$ , while better results are

<sup>2</sup> For values of  $\Delta w$  and  $\Delta p$ , see table 3.

obtained at higher pressures for substances which have the same, or only slightly different, values of  $\Delta p$ .

## CONSTANTS OF THE ANTOINE EQUATION

The Antoine equation (2)

$$t = \frac{B}{A - \log P} - C \quad (7)$$

TABLE 1

*Boiling points of octanes*

COMPOUND*	57.5 mm. Hg			402.4 mm. Hg			779.3 mm. Hg		
	$\Delta t_{\text{calcd}}$	$\Delta t_{\text{obsd}}$	Deviation	$\Delta t_{\text{calcd}}$	$\Delta t_{\text{obsd}}$	deviation	$\Delta t_{\text{calcd}}$	$\Delta t_{\text{obsd}}$	Deviation
8	0.00	0.00	0.00	0.00	0.00	0.00	0.00	0.00	0.00
2M7	6.93	7.26	+0.33	7.43	7.81	+0.38	7.60	8.03	+0.43
3M7	6.42	6.24	-0.18	6.55	6.61	+0.06	6.60	6.76	+0.16
4M7	7.80	7.21	-0.59	8.04	7.75	-0.29	8.12	7.96	-0.16
3E6	7.29	6.71	-0.58	7.16	7.03	-0.13	7.13	7.13	0.00
22M6	18.02	17.12	-0.90	19.31	18.39	-0.92	19.75	18.84	-0.91
23M6	10.06	9.62	-0.44	10.13	9.97	-0.16	10.17	10.06	-0.11
24M6	13.35	14.83	+1.48	13.98	15.87	+1.89	14.20	16.25	+2.05
25M6	13.86	14.91	+1.05	14.85	16.12	+1.27	15.19	16.57	+1.38
33M6	14.22	13.46	-0.76	14.59	13.68	-0.91	14.72	13.69	-1.03
34M6	8.17	7.99	-0.18	7.79	7.98	+0.19	7.65	7.93	+0.28
2M3E5	9.55	9.94	+0.39	9.26	10.03	+0.77	9.17	10.00	+0.83
3M3E5	9.04	8.81	-0.23	8.38	7.86	-0.52	8.18	7.38	-0.80
223M5	15.10	15.66	+0.56	15.20	15.87	+0.67	15.25	15.81	+0.56
224M5	24.95	24.64	-0.31	26.73	26.00	-0.73	27.34	26.44	-0.90
233M5	11.81	12.03	+0.22	11.35	11.30	-0.05	11.22	10.88	-0.34
234M5	12.32	12.27	-0.05	12.23	12.27	+0.04	12.21	12.19	-0.02

\* The Geneva names of the alkanes are conveniently abbreviated as follows, the last number indicates the longest chain; M represents methyl, E ethyl; numbers before capital letters indicate position of groups.

TABLE 2

*Reference values for the normal paraffins*

COMPOUND	A	B	$w_n$	$p_n$
<i>n</i> -Butane . . .	6.830	945.9	10	1
<i>n</i> -Pentane . . .	6.852	1064.6	20	2
<i>n</i> -Hexane . . .	6.878	1171.5	35	3
<i>n</i> -Heptane . . .	6.903	1268.6	56	4
<i>n</i> -Octane . . .	6.924	1355.1	84	5
<i>n</i> -Nonane . . .	6.945	1435.2	120	6
<i>n</i> -Decane . . .	6.954	1501.3	165	7

with  $t$  in °C. and  $P$  in mm. of mercury, is known (3) to give very accurate correlation of boiling point with pressure for organic liquids. In the tables of the American Petroleum Institute (1), complete sets of values of the constants  $A$ ,  $B$ , and  $C$  are given for the paraffins up to  $C_{18}H_{38}$ .

The variation of these constants with changes in isomeric structure can be represented by relations similar to equation 2. Equation 2 was therefore fitted to the data for  $A$  and  $B$ , given in the A.P.I. tables, by the method of least squares, leading to equations 8 and 9. The constant  $C$  is calculated by substituting into

TABLE 3  
*Constants of the Antoine equation*

COMPOUND	$\Delta w$	$\Delta \phi$	$A_{API}$	$B_{API}$	$A_{scaled}$	$B_{scaled}$	$C_{scaled}$	AVERAGE DEVIATION
2M3.....	1	1	6.748	882.8	6.780	893.9	235.81	
2M4.....	2	0	6.804	1027.3	6.816	1032.6	234.56	0.02
22M3.....	4	2	6.738	950.8	6.736	946.6	236.05	
2M5.....	3	0	6.839	1135.4	6.841	1138.2	227.15	0.03
3M5 .....	4	-1	6.849	1152.4	6.850	1154.1	227.50	0.03
22M4.....	7	0	6.755	1081.2	6.791	1093.7	229.98	0.08
23M4.....	6	-1	6.810	1127.2	6.825	1131.8	228.98	0.05
2M6.....	4	0	6.880	1240.	6.866	1236.0	220.11	
3M6... ..	6	-1	6.862	1238.	6.870	1246.6	220.56	
3E5 .....	8	-2	6.873	1249.8	6.874	1257.3	221.41	
22M5.. ..	10	0	6.815	1190.3	6.811	1187.0	222.83	0.03
23M5... ..	10	-2	6.858	1240.	6.855	1241.0	222.49	
24M5 .....	8	0	6.848	1204.	6.830	1203.3	224.20	
33M5 .....	12	-2	6.818	1223.5	6.837	1224.6	223.49	0.26
223M4. ....	14	-2	6.800	1205.0	6.818	1208.3	223.26	
2M7... ..	5	0	6.917	1337.5	6.889	1323.9	212.66	0.11
3M7... ..	8	-1	6.899	1331.5	6.890	1332.1	213.35	0.18
4M7.....	9	-1	6.901	1327.7	6.883	1325.9	213.60	0.24
3E6. ....	12	-2	6.891	1327.9	6.884	1334.1	214.74	0.27
22M6.....	13	0	6.837	1273.6	6.833	1273.9	215.50	0.07
23M6 .....	14	-2	6.870	1315.5	6.870	1321.6	215.70	0.17
24M6.. ....	13	-1	6.853	1287.9	6.855	1300.9	217.92	0.32
25M6 .....	10	0	6.860	1287.3	6.854	1292.6	216.21	0.28
33M6 .....	17	-2	6.851	1307.9	6.848	1302.9	216.46	0.06
34M6 .....	16	-3	6.880	1330.0	6.877	1336.1	216.63	0.20
2M3E5 .....	17	-3	6.864	1318.1	6.870	1320.9	217.74	0.20
3M3E5 .....	20	-4	6.867	1347.2	6.871	1338.1	217.10	0.30
223M5. ....	21	-3	6.825	1294.9	6.842	1304.9	219.60	0.25
224M5 .....	18	0	6.820	1262.5	6.797	1242.6	218.07	0.18
233M5... ..	22	-4	6.843	1328.0	6.857	1325.6	218.64	0.34
234M5 .....	19	-3	6.854	1315.1	6.856	1317.3	217.93	0.04
2233M4 .....	26	-4	6.877	1327.8	6.829	1300.6	223.13	

the Antoine equation the values of  $A$  and  $B$  obtained in this way, together with the normal boiling points, when available. If the normal boiling point is not recorded in the literature,  $C$  may be obtained by using the boiling temperature calculated from equation 1. For table 4, the boiling points of some of the nonanes were estimated, considering both experimental and calculated values.

The equations to be used for the calculation of  $\Delta A$  and  $\Delta B$ , with the least-

TABLE 4  
Predicted values for the nonanes

COMPOUND	$\Delta w$	$\Delta p$	$t_{\text{ubed}}$	$A$	$B$	$C$
2M8	6	0	143.3	6.912	1405.6	205.4
3M8	10	-1	144.2	6.911	1412.8	206.4
4M8	12	-1	142.5	6.900	1402.9	206.6
3E7	16	-2	143.0	6.900	1410.2	207.9
4E7	18	-2	141.2	6.889	1400.3	208.2
22M7..	16	0	130.5	6.856	1356.2	210.7
23M7.	18	-2	140.5	6.889	1400.3	208.9
24M7	18	-1	133.6	6.867	1373.3	210.9
25M7	16	-1	136.5	6.878	1383.2	209.6
26M7	12	0	135.2	6.878	1375.9	209.0
33M7	22	-2	137.3	6.867	1380.6	209.1
34M7	22	-3	140.5	6.889	1407.6	210.7
35M7	20	-2	137.0	6.878	1390.4	210.9
44M7	24	-2	135.0	6.856	1370.7	209.8
2M3E6.	24	-3	138.6	6.878	1397.7	211.1
2M4E6	22	-2	134.4	6.867	1380.6	212.0
3M3E6	28	-4	140.0	6.877	1404.9	211.6
3M4E6	26	-4	141.0	6.889	1414.8	212.0
223M6	28	-3	133.4	6.855	1377.9	213.3
224M6	26	-1	126.5	6.823	1333.8	211.9
225M6	22	0	124.1	6.823	1326.6	212.4
233M6	30	-4	137.2	6.866	1395.1	212.9
234M6	28	-4	139.0	6.877	1404.9	212.6
235M6	24	-2	131.4	6.856	1370.7	213.4
244M6	28	-2	130.0	6.833	1350.9	211.8
334M6	32	-5	139.6	6.877	1412.2	213.8
33E5	32	-6	146.5	6.899	1439.2	211.7
22M3E5.	32	-4	133.8	6.855	1385.2	214.8
23M3E5	34	-6	142.4	6.888	1429.1	214.3
24M3E5	30	-4	136.7	6.866	1395.1	213.4
2233M5	38	-6	140.2	6.866	1409.6	213.5
2234M5	34	-4	133.0	6.844	1375.3	214.1
2244M5	32	0	122.3	6.811*	1316.7*	212.8
2334M5	36	-6	141.5	6.877	1419.4	213.7

\* For 2,2,4,4-tetramethylpentane,  $\frac{1}{2}$  of  $\Delta A_{\text{calcd}}$  and of  $\Delta B_{\text{calcd}}$  were used, in order to give partial correction to a large error characteristic of this compound

squares constants reduced to the minimum number of significant figures, are

$$\Delta A = \frac{0.45}{n^2} \Delta w + 0.022 \Delta p \quad (8)$$

$$\Delta B = \frac{400}{n^2} \Delta w + 27 \Delta p \quad (9)$$

$A$  and  $B$  are obtained by subtracting the calculated values of  $\Delta A$  and  $\Delta B$  from the reference values for the normal paraffins, given in table 2.

The values of  $A$  and  $B$ , as given by the A.P.I. tables and as calculated from equations 8 and 9, are compared in table 3. The average deviations are  $\pm 0.010$  for  $A$  and  $\pm 5.7$  for  $B$ .

An estimate of the error resulting from this method of calculation is best obtained by comparing observed and calculated boiling points at different pressures. For this reason, boiling points were calculated, from the Antoine equation and calculated values of  $A$ ,  $B$ , and  $C$ , for the 466 points at which the vapor pressure-temperature equilibrium of twenty-three branched alkanes was studied by Willingham, Taylor, Pignocco, and Rossini (5). The average deviation between observed and calculated boiling temperatures for each of these paraffins is given in table 3 (last column). For all 466 boiling points, the average deviation, disregarding sign, was  $\pm 0.17^\circ\text{C}$ . This agreement is satisfactory.

The deviation between observed boiling points and values calculated by the method given here is due to three factors: (a) the error due to inadequate representation of the data by the Antoine equation; this error is small, generally below  $0.1^\circ\text{C}$ ., and is randomly distributed; (b) the error due to the use of equations 8 and 9 in calculating  $A$  and  $B$ ; this is the main error for the compounds in table 3, where its average value is seen to vary from 0.1 to  $0.3^\circ\text{C}$ .; for each compound, the error due to this factor is, roughly, inversely proportional to the pressure, so that it becomes quite large below 100 mm. of mercury; (c) the error in the observed boiling point used in the calculation of constant  $C$ ; this error is constant and independent of pressure for each compound; it is the main component of the uncertainty of calculated boiling points for the nonanes. As more accurate boiling-point values for the branched-chain nonanes become available, the values of the constant  $C$  should be changed accordingly, in order to reduce the error inherent in the calculations.

Calculated values of  $A$ ,  $B$ , and  $C$ , together with the boiling-point values used in the calculation of  $C$ , for the thirty-four branched nonanes, are given in table 4.

#### SUMMARY

The boiling points of the branched-chain alkanes at pressures from 57 to 780 mm. of mercury are expressed as functions of two structural variables by equations of the form  $\Delta t = \frac{k}{n^2}\Delta w + b\Delta p$ . The coefficients  $k$  and  $b$  are given by simple logarithmic functions of the pressure.

The constants  $A$  and  $B$  of the Antoine equation, for branched-chain alkanes, are related by equations of similar form. When the constant  $C$  is evaluated from the normal boiling point, the average deviation between observed and calculated boiling points, tested on 466 points at which the vapor pressure-temperature equilibrium of isomeric alkanes is given in the literature, is  $\pm 0.17^\circ\text{C}$ .

#### REFERENCES

- (1) American Petroleum Institute Research Project 44 at the National Bureau of Standards. Selected Values of Physical and Thermodynamical Properties of Hydrocarbons. Tables 1k, 2k, 3k, dated March to June, 1944
- (2) ANTOINE, C.: *Compt. rend.* **107**, 681 (1888).
- (3) THOMSON, G. W.: *Chem. Rev.* **38**, 1 (1946).
- (4) WIENER, H.: *J. Am. Chem. Soc.* **69**, 17 (1947).
- (5) WILLINGHAM, C. B., TAYLOR, W. J., PIGNOCOCCO, J. M., AND ROSSINI, F. D.: *J. Research Natl. Bur. Standards* **35**, 219 (1945).



## NEW BOOKS

*Organic Analytical Reagents. Vol. II.* By FRANK J. WELCHER. 530 pp. New York: D. Van Nostrand Co., Inc., 1947. Price: \$8.00 (series price, \$7.00).

The first volume of this "handbook" was published early in 1947 and was reviewed in this Journal (*J. Phys. Colloid Chem.* **51**, 1035 (1947)). The rapid publication of Volume II of this series will be appreciated by all analytical chemists and other chemists who are interested in the analytical application of organic reagents and solvents. The general nature of the book and the classification of the various compounds have been described in the review of the first volume.

The present volume comprises ten chapters dealing with organic acids, halogen-substituted acids, hydroxy acids, amino acids, miscellaneous acids, acyl halides, acid anhydrides, esters, amines, and quaternary ammonium compounds. As in the first volume an index of names and synonyms of organic reagents and an index of the uses of organic reagents are given at the end of the book.

The application of the reagents is confined to inorganic analysis. As in the first volume the literature is covered thoroughly up to January 1, 1946, and the reviewer did not discover any serious omissions. Under safranin the application of this substance as an adsorption indicator in argentometric titrations might have been mentioned. Also, a brief general discussion of the use of various compounds as oxidation-reduction indicators (e.g., benzdine, diphenylamine, diphenylbenzidine, etc.) with a list of oxidation potentials would be desirable.

This second volume is a welcome addition to the library of analytical chemists.

I. M. KOLTHOFF.

*Symposium on Plasticizers.* 85 pp. New York: Interscience Publishers, Inc., 1947. Price: \$1.75.

This volume consists of five papers which were given at a Symposium on Plasticizers held at the University of Buffalo on June 7 and 8, 1946, together with a brief introduction by E. F. Izard. The papers are reprinted without change from the *Journal of Polymer Science*, Vol. 2, No. 2 (1947).

The papers are: "Survey of Plasticizers for Vinyl Resins" by M. C. Reed; "Application of a Mechanistic Theory of Solvent Action to Plasticizers and Plasticization" by Arthur K. Doolittle; "Internal Plasticization; The Effect of Chemical Structure" by V. L. Simril; "Effect of Plasticizers on Second-order Transition Points of High Polymers" by R. F. Boyer and R. S. Spencer; and "Creep Behaviour of Plasticized Vinylite VYNW" by W. Cuken, T. Alfrey, Jr., A. Janssen, and H. Mark.

Workers in the field of plasticizers will find it convenient to have this collection of articles if they do not have access to the journal in which they appeared. It seems that such a publication as this might be increased in value if the informal discussion held at the Symposium were given in abbreviated form.

E. J. MEEHAN.

*Physical Chemistry.* First edition. By E. D. EASTMAN AND G. K. ROLLEFSON. viii + 504 pp. New York and London: McGraw-Hill Book Company, Inc., 1947. Price: \$4.50.

This excellent introductory text in physical chemistry has been prepared by revision and extension of a syllabus in use at the University of California since 1942. Its publication, delayed by the untimely death of Professor Eastman, will be of interest to those who wish more descriptive material than most such texts provide, particularly with respect to the more recent ideas in chemistry.

The arrangement of subject matter is somewhat unusual in some respects. The chapters are generally short, with numerous exercises and problems at the end of nearly all. The first law of thermodynamics is introduced immediately after the descriptions of the interactions and states of material systems, and is followed by its applications in thermochem-

istry. The chapter on the liquid state follows the chapters relating to the gaseous and solid states, an arrangement which permits discussion from both of the applicable points of view. The chapters on atomic structure, molecular structure, and radioactivity and nuclear reactions are particularly good, as are also the numerous other discussions throughout from the structural point of view. The second law of thermodynamics is introduced after a short chapter on solutions, and is followed by a discussion of phase equilibria in one-component systems. Then, before introducing the student to more complicated phase equilibria in multicomponent systems, the authors make a careful unification and extension of concepts in discussions of escaping tendency and the properties of ideal solutions. The excellent chapters on chemical equilibria and kinetics contain numerous exercises worked out in detail and, subsequently, numerous problems for the student. The chapters on conductance and transference and on electromotive force are well done, as are also the final chapters on interactions of light with matter and on surface phenomena.

As a result of the somewhat more descriptive point of view even some of the simple derivations are not included, but references to standard works where they may be found are given, and they may usually easily be supplied in the lectures. The literature references are somewhat too few, and very often quite troublesome to follow up when only the author and year are given; this tendency detracts somewhat from the book's value as a reference work. The first editions of all technical books contain errors, and a few of the important ones present here may be worth noting. Cerium is not the only rare earth in which the  $4f$  electrons play a chemical rôle (p. 189), as is evidenced by higher valence states of praseodymium and terbium. The authors have confused the meanings of the terms "lattice" and "structure" in the chapter on the crystalline state, and have used them interchangeably. A number of the restrictions on thermodynamic variables in statements and equations in Chapter XV have been omitted. Thus (p. 156)  $\Delta A = 0$  for a reversible process only if  $V$  (as well as  $T$ ) is constant. Equation (4) on p. 257 and the statements regarding  $\Delta F$  in Section 10, below, are, of course, true with the restrictions that both  $p$  and  $T$  are constant. Equation (8) on p. 260 and the first equation on p. 267 need the restriction that  $p$  is constant. The second equation on p. 267 is true only when  $T$  is constant, and is given correctly on p. 259.

The publishers have cooperated in presenting this book extremely well, on excellent paper, and with very few misprints.

Under the guidance of a competent teacher the student will find this an excellent beginning text in physical chemistry, and it is most heartily recommended.

WILLIAM N. LIPSCOMB.

*Richter-Anschutz: The Chemistry of the Carbon Compounds. Vol. IV. The Heterocyclic Compounds and Organic Free Radicals.* Third English edition, based upon the twelfth German edition. Translated by M. F. Darken and A. J. Mee. xv + 498 pp. New York: Elsevier Publishing Company, 1947. Price: \$12.00.

This is the fourth, and final, volume of the literal translation of Richter-Anschutz. The text is that of the twelfth German edition, published in 1935; the material in this translation corresponds to Volume III (heterocyclic compounds) and to a portion of Volume II, part 2 (radicals), of the German edition. The section on the heterocyclic compounds was written by F. Reindel and the translation is by M. F. Darken; the section on radicals was written by Ludwig Anschutz and the translation of this is by A. J. Mee.

The book is the standard "Richter", well known to all chemists. The conventional plan of treatment has been followed. The book-making is good but, all in all, it is difficult to understand the necessity for a translation of a book now twelve years old—a book which can hardly be of much more than historical value, and this reviewer feels that the energy put into the making of this book could well have been expended more profitably on something else. The price (\$12.00) is excessive.

LEE IRVIN SMITH.

*Advances in Enzymology*. Vol. 7. Edited by F. F. NORD. xi + 665 pp. 215 Fourth Avenue, New York: Interscience Publishers, Inc., 1947. Price: \$8.75.

This seventh annual review maintains the high standard set by previous issues. Some two or three years ago the editor, Dr. F. F. Nord, included articles in areas of biochemistry not primarily enzymatic in nature but dealing with various phases of natural phenomena that at some point are involved in enzymatic processes. The same is true of this volume.

A lucid survey of the properties of protoplasm by William Seifriz follows a discussion of the use of enzyme reactions to study cell permeability, the latter article by S. C. Brooks. Optically active syntheses (both biological and chemical) are surveyed by P. D. Ritchie. Professor G. Hevesy has collected the most important work on the use of radioactive phosphorus, sulfur, and iodine in turnover studies, in which field he is preëminent.

Two articles deal with the important field of the porphyrins—the general chemistry of the tetrapyrroles and their metallic derivatives is considered by S. Granick and H. Gilder, while H. Theorell has written an accompanying article on heme-linked groups and the hemoproteins.

Two reviews treat more directly with enzyme systems. Frank H. Johnson describes the work done on luminescent bacteria, a field in which he and E. N. Harvey have contributed much; a major portion of the paper considers the physicochemical principles involved. In a paper entitled "Kidney Enzymes and Essential Hypertension" Schales discusses the enzymatic nature of renin and of hypertensinase as well as the balance between their actions, and concludes with a consideration of the clinical aspects of hypertension.

Attention has recently turned to the need evidenced by microorganisms for vitamins; these bodies yield interesting studies on the rates of reactions involving intermediate metabolism. A chapter dealing particularly with nicotinic and pantothenic acids comes from the pen of Henry McIlwain.

The list of antibacterial substances obtained from fungi and green plants has grown very rapidly since the first observations on penicillin. F. Kavanagh lists thirty-eight compounds which have been definitely characterized; in addition he notes others which have not been as thoroughly studied.

Fromageot has a paper on the oxidation path in the animal body of the major sulfur compounds. The last chapter by F. M. Hildebrandt is a very readable survey of the recent problems and advances in the field of industrial fermentations.

Dr. Nord has again rendered biochemistry a distinct service in securing outstanding workers to write the twelve articles; the international scope is indicated by the fact that five of the surveys were prepared in England, Sweden, and France. Subject and author indexes for this volume are appended, as well as a cumulative index for the first seven volumes.

W. M. SANDSTROM.

*Colloids. Their Properties and Applications*. By A. G. WARD. 133 pp. New York: Interscience Publishers, Inc., 1947. Price: \$1.75.

This little volume on colloids attempts to cover the field of colloid science as completely as possible but in a very elementary way. The author divides the work into three parts: I. The Nature of the Colloidal State. II. The Colloidal Systems. III. Colloids in Industry and in Living Matter.

The discussion of all phases of the subject is reasonably well brought up to date. An elementary description of such research instruments as the ultramicroscope, the surface balance, and the electron microscope is given in order to show their usefulness in experimenting with substances in the colloidal state. In order to emphasize the relative size of substances in the colloidal state the author feels that the average student would better understand these relations if he had a supermicroscope which magnified 100,000,000 times. He could therefore follow each dimension in the book with a parenthetical figure obtained by this multiplication. This may appeal to the student who is just beginning to study the subject.

The volume is written in a pleasing manner and may be considered as a non-mathematical

introduction to the subject. As such it may find a useful place among beginning students. Part III has some well-chosen chapters but seems to be somewhat too brief and too lacking in its attempt to cover a large subject. Less than four pages are devoted to colloids and living matter.

L. H. REYERSON.

*The Chemistry of Portland Cement.* By ROBERT HERMAN BOGUE. xv + 572 pp. New York: Reinhold Publishing Corporation, 1947. Price: \$10.00.

This excellent book is written primarily for the cement chemist, and from the point of view of the research chemist concerned with the chemical problems of the industry. In these respects Dr. Bogue is well qualified, having served since 1924 as Research Director of the very effective group under the Portland Cement Association Fellowship of the National Bureau of Standards.

The book is divided into three parts. Part I, The Chemistry of Clinker Formation, deals with high-temperature reactions in the dry state. Part III, The Chemistry of Cement Utilization, is concerned with the reactions of cement with water or solutions. Part II, The Phase Equilibria of Clinker Components, is an excellent presentation of the principles and techniques of high-temperature phase research, followed by an extensive description of the system  $\text{CaO}-\text{Al}_2\text{O}_3-\text{SiO}_2$  (these three oxides constitute over 90 per cent of commercial Portland cements). Then follow descriptions of other systems involving the additional clinker constituents  $\text{MgO}$ ,  $\text{FeO}$ ,  $\text{TiO}_2$ ,  $\text{Fe}_2\text{O}_3$ ,  $\text{K}_2\text{O}$ ,  $\text{Na}_2\text{O}$ , and  $\text{Li}_2\text{O}$ .

The book has been very carefully prepared, and there appear to be very few errors. The omission of  $b$  and  $c$  unit-cell dimensions for orthorhombic  $\text{Ca}_2\text{Fe}_2\text{O}_5$  on page 141, and the use of the term "octagon" instead of "octahedron" on page 142 may be mentioned. The careful reader may wish that the author had been more critical of some of the results reported, although his completeness in reviewing the literature resolves many of the chronologically earlier errors. Thus the conclusion (page 144) that a structure having the different interatomic distances of  $\text{Fe}-\text{O}$ ,  $\text{Ca}-\text{O}$ ,  $\text{Si}-\text{O}$ , and  $\text{Al}-\text{O}$  could not produce an x-ray powder diffraction pattern of sharp lines is highly questionable. The two-page description of a paper by Flint and Wells (page 285 ff.) leads to the very unlikely values of the second, third, and fourth ionization constants for the species  $\text{H}_4\text{SiO}_4$ , all on the order of  $10^{-12}$ , whereas they may reasonably be expected to differ from one another and from the first ionization constant by a factor of about  $10^{-4}$  or  $10^{-5}$ . The author's choice to be less critical, as well as his decisions to limit his discussion to cements of the Portland class, and to omit descriptions of routine tests have, however, kept the book from becoming unduly lengthy.

The remarkable thoroughness with which the book has been prepared is quite apparent in the (somewhat lengthy) history of cement manufacture, the careful documentation of ideas and results, the excellent list of references at the end of each of the thirty chapters, and the inclusion of many as yet unpublished investigations. This book will probably remain an authoritative text for the cement chemist for many years to come. It should also be of interest to chemists in other fields and to the non-specialist, particularly if he is connected with the cement industry.

The publishers have been especially careful in the presentation of the photomicrographs and electron-microscope photographs in this generously illustrated book, and in the reproduction of the many prelabelled phase diagrams.

WILLIAM N. LIPSCOMB.

*Table of the Bessel Functions  $J_0(z)$  and  $J_1(z)$  for Complex Arguments.* Second edition.

Prepared by the Mathematical Tables Project, National Bureau of Standards. 381 pp. New York: Columbia University Press, 1947. Price: \$7.50.

The tabular material is identical with that in the first edition. Some minor revisions have been made in the introduction, including the relation between the tabulated functions on the  $45^\circ$  ray and the ber and bei functions.

Certain errors in the labeling of the graphs in the first edition have been corrected on pages XV and XVII.

S. C. LIND.

*Organic Analytical Reagents. Vol. III.* By FRANK J. WELCHER. 593 pp. New York: D. Van Nostrand, Co., Inc., 1947. Price: \$8.00 (series price, \$7.00).

The main purpose of this comprehensive work has already been stated in the review of the first volume (*J. Phys. Colloid Chem.* **51**, 1035 (1947)). The present volume is of particular interest to all analytical chemists because it gives all the applications of such important reagents as dipyrldyl and its derivatives, dioximes, monoöximes, nitroso compounds, (including cupferron) carbazides, and diphenylthiocarbazone. The book is divided into three parts. Part I (157 pages) deals with heterocyclic nitrogen compounds and contains five chapters; Part II (258 pages) deals with the oximes (nine chapters); and Part III (164 pages) discusses acidic imino compounds (five chapters). The literature is covered almost completely and few omissions have been found. The use of pyridine in the Karl Fischer reagent for the determination of water might have been mentioned. A list of oxidation potentials of the ferrous-ferrie iron complexes of dipyrldyl and derivatives should have been included, and also their use as indicators certainly deserves a special section.

Analytical chemists are indebted to the author and his coworkers for making this important reference book available. The author also deserves praise for the rapid appearance of the successive volumes.

I. M. KOLTHOFF.

*Monograph on the Progress of Research in Holland During the War. Technological and Physical Investigations on Natural and Synthetic Rubbers.* By A. J. WILSCHUT. 14.5 x 20.5 cm. xi + 173 pp.; 72 fig.; 17 tables. New York: Elsevier Publishing Company, Inc., 1946. Price: \$3.00.

This monograph is one of a series on the progress of research in Holland during World War II. Part I of the monograph deals with technological investigations and Part II with physical investigations on rubbers. In Chapter 1 elastic high-polymeric substances are classified into "real" rubbers and rubber-like materials. The distinction is based on vulcanization, the former being vulcanizable and the latter non-vulcanizable. Compounding formulae for both pure gum and carbon black stocks are given and the mechanical, electrical, chemical, and physical properties, together with aging data of the stocks, are given and discussed.

Chapter 2 includes measurements on the plasticity of unvulcanized rubbers, special aging tests, and a discussion of the mechanism of aging. This is followed by a mathematical interpretation of the stress-strain curve.

Chapter 3 discusses vulcanization with non-sulfur vulcanizing agents. In addition to those known to the authors up to the year 1939, 2,4-toluylene diisocyanate is mentioned as being capable of vulcanizing rubber in benzene solution. The greater part of this chapter is devoted to a discussion (with data) of the vulcanization of rubber with synthetic resins. A discussion of Van der Meer's theory of the vulcanization of rubber by phenolic resins, based on the formation of quinones as intermediates, is given.

Chapter 4 of Part II is devoted to a résumé of the importance of fundamental physical measurements in the determination of the structure of high polymers.

Chapter 5 on "Plasticity and Elasticity" is somewhat of a review and not entirely a report of investigations which were carried out in the Netherlands during the war period, as indicated in the introduction.

The calculation of degree of crystallization of rubber from thermodynamic data, as is done on page 105, is open to question because the points for tension of the partly crystallized rubber are time dependent (see Bekkedahl: *J. Research Natl. Bur. Standards* **13**, 411 (1934)). Several hours may be required for equilibrium to be reached between the amor-

phous and crystalline states, during which time the tension would continue to drop. Thus, the calculated degree of crystallinity would be greater the greater the time taken to obtain measurements of tension at each temperature. In the experiments described by Wildschut the tension was measured after 10 min. at each temperature. At longer times the higher values for the amount of crystallinity in natural rubber would be more in line with the x-ray results of Field (*J. Applied Phys.* **12**, 23 (1941)), and the degree of crystallinity determined from birefringence by Treloar (*Reports on Progress in Physics* **9**, 121 (1942-43)).

In the discussion of internal friction (page 129) reference should have been made to the electrical resonance types of forced vibrators development for the measurement of dynamic modulus and internal friction. The apparatus of Naunton and Waring was described at about the same time (*Proc. Rubber Tech. Conference, London, 1938*, 805) as the Kosten type referred to by the author. Improvements have been made over the Naunton and Waring vibrator in later apparatus developed in this country (Gehman, Woodford, and Stambaugh: *Ind. Eng. Chem.* **33**, 1032 (1941); Dillon, Prettyman, and Hall: *J. Applied Phys.* **15**, 309 (1944)).

Chapter 6 deals with the mechanical properties of rubber and rubber-like substances at very low temperatures and at temperatures up to 100°C. An apparatus for the determination of the tensile strength of rubber at the temperature of liquid hydrogen (-253°C.) is described and illustrated. Data for the experiments are presented. The chapter concludes with data on the tensile strength of rubber as a function of the degree of swelling.

Chapter 7 describes the work of Goppel on the determination of the amount of crystalline material in stretched raw and vulcanized rubber. The crystalline material in raw rubber increases with age, approaching a maximum of about 30 per cent. The amount of crystalline material in stretched vulcanized rubber does not exceed 30 per cent and Goppel therefore pictures stretched vulcanized rubber as an amorphous phase with dispersed oriented crystallites and not as a crystalline phase with some amorphous material around the crystallites.

Several investigations on the electrical properties of rubber are treated briefly in Chapter 8. It is concluded that "the cause of the dielectric losses in natural rubber and analogous substances lies in the electrical asymmetry of the rubber molecules themselves."

The monograph of 173 pages concludes with the chapter "General Conclusions," in which are summarized the important deductions reached from experimental work recorded in previous chapters. Those interested in the research and technology of rubber will find the monograph interesting and stimulating. Certain new approaches to the problem of the structure of rubber are recorded for the first time.

R. F. DUNBROOK.

# INTRODUCTION TO SYMPOSIUM ON RADIATION CHEMISTRY AND PHOTOCHEMISTRY<sup>1</sup>

S. C. LIND

*Institute of Technology, University of Minnesota, Minneapolis, Minnesota*

*Received October 23, 1947*

It is significant that this, the first symposium on radiation chemistry, is held soon after the close of World War II. The reason, I think, is not far to seek. While radiation chemistry is not directly a part of nuclear chemistry, the two are of necessity closely related. The high-energy particles that produce chemical reaction are of nuclear origin, and now that fission produces these particles in great abundance, their chemical effects become the subject of enhanced interest.

But not only has nuclear fission brought renewed emphasis upon radiation chemistry, it also brings new and very active agents. While it is true that alpha particles, which have been the principal activating agents in what we may call classical radiation chemistry, are practically absent in fission, nevertheless new types of high-speed particles may more than compensate for the lack of alpha radiation. Certainly in fission there is no dearth of ionization which, after all, is the first condition for chemical effects.

High-speed neutrons would not be expected to produce ordinary chemical action, since they act on nuclei and not on the electronic system of the elements through which they pass. But in sharing their energy with light nuclei they liberate high-velocity particles such as protons that are capable of producing chemical actions much like those caused by alpha particles. Moreover neutrons, in acting on the nuclei of different elements, bring about reactions of "discomposition" which, as Dr. Burton (2) recently pointed out, have proved to be of great interest. Perhaps we may hear more of the behavior of neutrons in this regard during this present conference.

Another source of chemical activation besides the abundant beta and gamma radiation consists in the fission fragments themselves. They have velocity and energies far beyond those of recoil atoms from alpha particles and would hence be expected to produce ionization and chemical action in enhanced degree.

Quite aside from fission, the chemical reactions accompanying ionization have taken on an increased interest for biochemistry in liquid and solid systems. Biologists, almost from the beginning, have recognized that ionization is the controlling factor in the effects produced in living tissues by x-rays and  $\gamma$ -rays. Some chemical studies have been made of these effects. There is, however, an increasing desire to be able to fix the locus of the effect within the molecular structure of radiated tissues. Especially do we need the answer to the question as to what part or particular radical in the large molecules is effective in absorbing the radiation and bringing about the observed changes.

<sup>1</sup> Presented at the Symposium on Radiation Chemistry and Photochemistry which was held at the University of Notre Dame, Notre Dame, Indiana, June 24-27, 1947

Tentatively this problem may be approached from the standpoint of ionization. We know the stopping power and specific ionization of many simple molecules for alpha particles passing through them in the gaseous state. Indirect evidence from chemical effects indicates ionization to be largely independent of the state of aggregation. In mixtures of the gases (and presumably in liquids and solids) the law of mixtures applies to stopping power and ionization. The kinetics of many reactions in gaseous mixtures have been studied and elucidated on this basis; the rate of reaction is proportional to the total ionization produced in the mixture by the passage of alpha rays.

Suppose then that we have in a single organic molecule groups of different character,—let us say, one or more carboxyl groups and a long hydrocarbon chain. What can we predict about the action of alpha radiation on the different radicals? Will the probability of action on a given group be dependent by chance on its part of the total stopping power as might be expected if it were a free gas molecule, or will some chain effect transfer the activation imparted at one point or to one group to some other part of the molecule? In liquid hydrocarbons bombarded by high-voltage cathode rays Schoepfle and Fellows (6) have shown that abundance of methyl groups replacing hydrogen in the straight-chain hydrocarbons increases the ratio of methane to hydrogen in the gases liberated. This result indicates that, when ionization removes a bonding electron, hydrogen or methane is produced depending on whether the broken bond be one holding a hydrogen atom or one holding a methyl group. We also have strong evidence of similar action in the behavior of aliphatic acids of various chain lengths, as recently reported by the M.I.T. group in work on a project of the American Petroleum Institute (1, 3, 7), particularly in the elimination of carbon dioxide and methane. What happens to the rest of the molecular chain following the removal of carbon dioxide or some other radical is of the greatest interest. Over-all reactions of the type  $\text{RCOOH} \rightarrow \text{CO}_2 + \text{RH}$  have been shown to represent the larger part of the chemical action. It would be surprising, however, if sometimes in the long-chain carboxylic acids the removal of hydrogen or of a methyl group, instead of merely causing condensation within the single molecule, did not cause a molecular doubling, thus producing a dicarboxylic acid of double chain length. Such doubling seems to be the usual thing in the hydrocarbon gases, as shown by Lind and Bardwell (5) and more recently by Honig and Sheppard (3). To determine whether such condensation does take place would require a complete quantitative examination of all the reaction products, including the solid or liquid phase.

If such analysis showed the complete absence of doubled molecules containing carboxyl groups, it would represent a marked difference from the behavior of the saturated hydrocarbons. The influence of the carboxyl group in causing a one-sided reaction resulting exclusively in its own elimination would indicate an interpretation of considerable interest. Admitting that initial ionization should occur at any part of the chain dependent on the stopping power of any given radical in the chain, we are faced with the conclusion that the seat of activation is in some



way transferred to the carboxyl group. The result is the liberation of either carbon dioxide or carbon monoxide molecules. That the amount of carbon monoxide found could not be produced by reduction of carbon dioxide by hydrogen or methane under action of alpha rays is known from direct experiment (4). The mechanism of transfer of activation along the chain might be by electron exchange from group to group. Aside from any theory, if selective action within the molecule can be firmly established, a conclusion of great interest to biochemistry will have been reached.

To go into the general theory of the reaction mechanism of radiation chemistry would not be suitable for this brief introduction. Presumably, theory will frequently form a part of our subsequent discussions and may be postponed in detail for later occasions. However, some general remarks may not be out of place.

The fixing of mechanism in chemical kinetics is always difficult and often uncertain. Radiation chemistry is no exception, but does offer certain advantages. The employment of radon as a source of radiation affords definite conditions much simpler in some respects than in photochemistry. On the other hand, the action of alpha particles is so general and unselective that secondary action frequently introduces serious complications which prevent a complete kinetic study. For example, reactions of the aliphatic hydrocarbons are too complicated to be suitable for kinetic analysis or theory. The stability of gaseous carbon dioxide or water under alpha radiation is a great convenience, but even carbon dioxide is subject to secondary combination with hydrogen or methane.

Generally two ideas have dominated the theory of radiation chemistry: One is that the ions themselves are the direct agents in the reactions. There is a great deal of exact quantitative evidence in favor of this theory but little theoretical support. A second idea that has had great support in recent years is that the chemical effects of radiation are brought about by the action of free radicals or atoms. There is strong theoretical but little experimental evidence of quantitative character supporting this view. We know practically nothing of the way in which the energy of alpha particles is expended except by ionization. Since the average energy expended per ion pair produced is about 35 e.v. and the ionization potential of most gases is about half this quantity, there has been a surprising amount of speculation as to what the other half may do in bringing about action through the intermediation of free radicals, atoms, or excited states.

Last fall at Chicago, Professor Franck called attention to the difference between the energy spent per ion-pair and the ionization potential of eight simple gases, including the five inert gases. The difference varies from 3.2 e.v. for helium to 18.0 e.v. for nitrogen. Presumably this difference would contribute to additional reaction over and above that due to ionization. But what are the experimental facts?<sup>2</sup> Let us take the simple case of acetylene polymerization. If we introduce radon into pure acetylene at any pressure, about twenty molecules

<sup>2</sup> See also the discussion by Dr. Charles Rosenblum later in this Symposium (*J. Phys. Colloid Chem.* **52**, 474 (1948)).

of acetylene polymerize to solid cuprene per ion-pair. The rate of the reaction is proportional to the gas pressure and to the quantity of radon. The kinetics are excellent. But this alone tells nothing about ionization. But now if one adds to the acetylene one of the inert gases helium, neon, nitrogen, argon, krypton, or xenon, the rate of polymerization is increased and good kinetics are obtained only by substituting for the partial pressure of acetylene the sum of its partial pressure and the equivalent (in terms of specific ionization) pressure of the respective inert gas. In other words, the reaction rate is proportional to the total ionization of both gases, not of acetylene alone. This is a severe test, including gases with a large range of specific ionization from helium to xenon. But the kinetics are so perfect that no room is left for the intervention of other types of activation. The same yield is obtained whether from helium with its small difference of 3.2 e.v. or from nitrogen having a difference of 18.0 e.v.

Of course one can say that the activation of whatever nature is only proportional to the ionization. But besides the lack of experimental evidence a new difficulty must be faced. If  $C_2H_2^+$  ions are produced from  $N_2^+$  by collision with  $C_2H_2$  molecules, will the free radical production still be in the same proportion as

in  $C_2H_2 \xrightarrow{\alpha} C_2H_2^+ + e^-$  If this assumption is too violent, then the alternative seems to be clustering about the positive ion, whether  $C_2H_2^+$  or  $N_2^+$ .

It should be emphasized that conclusions cannot be drawn from one reaction. The evidence from all reactions should be considered as a whole. Naturally, exceptions occur and sometimes chain mechanisms are found (e.g.,  $Cl_2 + H_2$  or  $CO + Cl_2$ ). The reaction between hydrogen and bromine is very complicated, hardly suitable for a basic kinetic study under alpha radiation.

The claim that removal of ions from the system reduces the rate of reaction should be reexamined. *A priori*, one would not expect that enough ions could be withdrawn by fields below the threshold for new ionization by shock.

In closing let us recall some of the indirect supports of the cluster theory.

(1) Exclusive oxidation when oxygen is present. Affinity of oxygen for electrons furnishes oxygen upon recombination of positive and negative ions.

(2) Smaller  $M/N$  values in the absence of oxygen.

(3) Occlusion of small amounts of inert gas in solid cuprene polymerized by  $\alpha$ -rays. The inert gas is easily liberated by gently heating the vessel wall, thus restoring the partial pressure of inert gas.

(4) Carbon dioxide alone is not decomposed by  $\alpha$ -rays, but when a suitable acceptor for the  $CO_2^+$  ion is introduced, such as hydrogen or methane, addition reaction ensues with rate proportional to both  $CO_2^+$  and  $CH_4^+$  (or  $H_2^+$ ) ions.

(5) In any mixture of reactants the rate is proportional to the sum of both ions, not to one species alone as might be assumed if a radical of one kind were instrumental.

(6) Reactions such as the polymerization of acetylene show no characteristics of chain mechanism, differentiating them sharply from reactions having a true chain mechanism, such as the reaction of hydrogen with chlorine or of carbon monoxide with chlorine.

## REFERENCES

- (1) BREGER, I., AND BURTON, V. L.: J. Am. Chem. Soc. **68**, 1639 (1946).
- (2) BURTON, M.: J. Phys. Colloid Chem. **51**, 618 (1947).
- (3) HONIG, R. E., AND SHEPPARD, C. W.: J. Phys. Chem. **50**, 119, 144 (1946).
- (4) LIND, S. C., AND BARDWELL, D. C.: J. Am. Chem. Soc. **47**, 2688 (1925).
- (5) LIND, S. C., AND BARDWELL, D. C.: J. Am. Chem. Soc. **48**, 2335 (1926).
- (6) SCHOEPFLE, C. S., AND FELLOWS, C. H.: Ind. Eng. Chem. **23**, 1396 (1931).
- (7) SHEPPARD, C. W., AND BURTON, V. L.: J. Am. Chem. Soc. **68**, 1636 (1946).

THE RELATION OF RADIATION CHEMISTRY TO  
PHOTOCHEMISTRY<sup>1,2</sup>

E. W. R. STEACIE

*Division of Chemistry, National Research Council, Ottawa, Canada**Received October 23, 1947*

## INTRODUCTION

In a broad sense there is, of course, no distinction between radiation chemistry and photochemistry. In practice, however, there are a number of essential differences between the two. The object of the present paper is to raise a number of the more important questions for discussion, rather than to give an over-all picture of radiation chemistry, since this will be done in later papers. The discussion will be confined entirely to the gaseous state for simplicity, and also to avoid duplication of the materials in the papers of Allen, Burton, and others.

A great deal of fundamental work has been done on the physics of the processes which occur when a beam of ionizing radiation is sent through matter. It is found that roughly half the energy of the beam is expended in the production of ions, and the remainder in the production of excited molecules. The quantitative comparison of the number of molecules reacting with the number of ions formed has proved a much more difficult task than the determination of quantum yields. Also, the preoccupation with ionization has delayed until quite recently a recognition of the importance of excited molecules and of secondary reactions involving atoms and radicals. It should be emphasized that it is possible for the ion-pair yield to have no direct significance, and to be nothing but a rough measure of the number of molecules concomitantly excited, and causing reaction.

## THE PRIMARY PROCESS

In photochemical reactions the primary process is, of course, strongly dependent on the wave length, and in fact the reactant may be quite transparent to a

<sup>1</sup> Presented at the Symposium on Radiation Chemistry and Photochemistry which was held at the University of Notre Dame, Notre Dame, Indiana, June 24-27, 1947.

<sup>2</sup> Contribution No. 1557 from the National Research Laboratories, Ottawa, Canada

range of wave lengths. Reactions can therefore be investigated over a range of wave lengths, and in some cases distinctly different primary processes may be found in different spectral regions.

In the case of reactions initiated by penetrating radiation, or by fast particles, the situation is quite different. Since the energy of the particle is merely slowly frittered away in its passage through matter, the results will in general be independent of the energy of the individual particles (or quanta) and dependent merely on the total energy absorbed. Thus for any given fast particle we may get molecules in several different states of excitation, together with several different ion-species. Furthermore, in a mixture of gases all substances present will absorb radiation to a greater or less extent, and the situation may become highly complex.

Spectroscopy is, of course, the foundation on which our knowledge of the photochemical primary process rests. The results of mass spectrometry occupy a similar position in the case of radiation chemistry, and furnish a great deal of information on the ions present, their appearance potentials, whether they are primary or secondary products, etc.

It should be emphasized that essentially photochemistry and radiation chemistry are in the same boat. A complete knowledge of the energy states of a molecule involves also a knowledge of the ionization potentials, and of the appearance potentials of ionized fragments. Both subjects need complete potential-energy surfaces for molecules of moderate complexity, and the indications are that these are not going to be forthcoming in the near future.

In the general case a photochemical reaction may be regarded as consisting of three stages: (1) Absorption of light leading to the formation of an excited molecule. (2) The excited molecule by decomposition or reaction gives rise to products. These may be the final products, or they may be atoms and radicals. (3) Secondary reactions of atoms and radicals. In many cases step 2 follows step 1 so rapidly that the result is kinetically the same as if absorption of radiation led directly to decomposition.

In the case of a radiochemical reaction the primary process unquestionably leads both to ionization and to the formation of excited molecules. The fact that there are thus two distinct and simultaneous primary processes complicates matters considerably.

There has been a great diversity of opinion as to the relative importance of ions or excited molecules in the over-all reaction leading to the final stable products. In the case of discharge reactions, Lunt (8) takes the extreme view that excited molecules are all important. Most workers are inclined to regard excited molecules as only a minor complication in all types of radiochemical reactions. Eyring, Hirschfelder, and Taylor (3) consider ions and excited molecules to be of roughly equal importance. We shall return later to a further consideration of excited molecules.

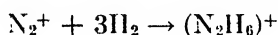
#### SECONDARY PROCESSES—IONS

There has been a great deal of discussion concerning the mechanism by which the ions formed in the primary step lead to the chemical reactions which follow.

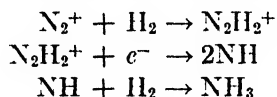
The mobilities of ions are often smaller than might be anticipated on the basis of kinetic theory. This was at one time interpreted on the basis of clustering, neutral molecules being held to a central ion by polarization forces. However, it has since been shown that the effects can be explained on the basis of drag due to such forces, without actual clustering.

In the meantime various attempts were made to explain chemical action on the basis of such clusters. The main difficulty with such mechanisms is that, like the old intermediate-compound theory of catalysis, they explain too much, and it is very difficult to put the cluster theory in a form from which predictions can be made.

In a number of cases clustering reactions have been postulated which involve only one clustered molecule, which is thus in effect a stoichiometrically distinct substance. Thus Brewer and Westhaver (1) propose two alternative mechanisms for the synthesis of ammonia in a discharge. The first, which they favor, is



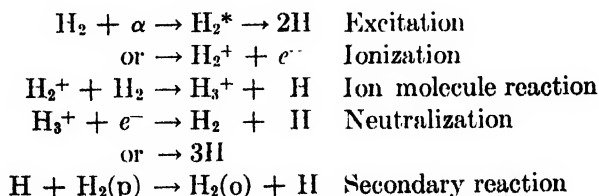
followed by neutralization of the charge on  $\text{N}_2\text{H}_6^+$  and its split into  $2\text{NH}_3$ . This is a typical and distinct cluster mechanism, since a four-body collision is impossible. As an alternative they propose the sequence



These steps really involve normal bimolecular reactions of ions, i.e., the first step in which one molecule is clustered is indistinguishable from a normal association reaction. It is apparent that no hard and fast line can be drawn between mechanisms involving clusters and those involving ionic reactions.

The first clear-cut postulation of ionic reaction mechanisms for non-chain reactions was by Eyring, Hirschfelder, and Taylor (4) about ten years ago. They pointed out that it was possible to account for the facts in some of the best-investigated reactions by assuming that the ions underwent plausible, and to some extent known, reactions leading to the formation of atoms and radicals. These atoms and radicals then entered into normal elementary reactions and behaved exactly as they would have in photochemical systems.

Thus in the conversion of para-hydrogen to ortho-hydrogen under the influence of  $\alpha$ -particles they have shown that the results can be satisfactorily explained on the assumption that the main processes occurring are:



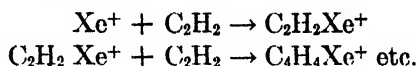
In a similar way they have explained other reactions (4, 7).

It seems probable that at least the majority of radiochemical reactions can be explained in this way. If such a viewpoint is adopted we can treat photochemistry and radiation chemistry as a consistent whole. It therefore seems both logical and desirable to consider the facts from this point of view, at least as a working hypothesis. It is of course possible, and even probable, that clustering may prove to be a complication in certain cases.

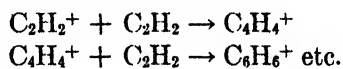
One reaction for which the clustering hypothesis has been most strongly held is the polymerization of acetylene. Approximately twenty molecules of acetylene are polymerized per ion-pair. It has been suggested by Lind that, in the absence of obvious chain characteristics, it is unlikely that stepwise addition takes place, and hence that the only alternative is a cluster of about twenty molecules of acetylene, which react on neutralization. In the first place this appears to strain the cluster idea rather severely. Secondly, it is now known that the polymerization of unsaturated hydrocarbons can be sensitized by free radicals, and hence there is nothing against a mechanism involving stepwise addition as a result of the action of atoms or radicals.

It should also be pointed out that chain-transfer reactions may occur as in other polymerization reactions. There is thus no reason why the size of the polymer unit should bear any relation to the magnitude of the ion-pair yield.

It has also been suggested (2, 5) that since an ion is essentially a free radical, ions might sensitize the polymerization directly, i.e.,



or



#### SECONDARY PROCESSES—EXCITED MOLECULES

In radiochemical reactions in gases, as we have seen above, excitation and ionization occur in about equal amounts. Excited molecules may therefore be expected to be of considerable importance. In the case of hydrogen, such molecules will frequently dissociate into atoms, and their behavior can be adequately predicted, at least qualitatively. With more complex substances we may expect difficulties in the formulation of mechanisms. In the first place the excited molecules are formed in an incidental sort of way along with ions. We have no way of knowing the properties of such excited molecules, and neither spectroscopy nor mass spectrometry can be of assistance. Further, in view of the statistical nature of our knowledge of the dissipation of energy in the gas, we have no way of knowing how many different states of excitation may exist, and in fact we have every reason to expect a considerable number. Also, although roughly equal amounts of energy are dissipated in ionization and excitation we have no way of knowing how many excited molecules are formed per ion.

Excited molecules may therefore be expected to be a source of uncertainty in radiation chemistry, and the more quantitative our knowledge becomes regard-

ing the properties and reactions of ions, the more difficulty we may expect from effects due to excited molecules.

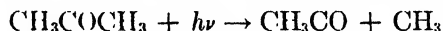
#### THE CARRY-OVER OF INFORMATION FROM ONE REACTION TO ANOTHER

In the past ten or fifteen years tremendous progress has been made in disentangling the elementary reactions involved in photochemical secondary processes, and in correlating this information with other fields of kinetics. We are now in the position where we have a great deal of reasonably accurate information about the rates of the more important elementary reactions. There are still large gaps in our knowledge, and certain questions, for example, the effect of surface, cannot be given satisfactory answers, but much useful information is available.

The same atoms and radicals will be involved in the reactions of radiation chemistry and the most intimate relationship between photochemistry and radiation chemistry will undoubtedly be in the mechanisms of the secondary processes.

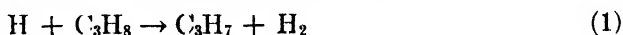
The secondary reactions of photochemistry are, of course, ordinary thermal reactions of the atoms and radicals involved. In applying the results of one investigation to the interpretation of another it is assumed that the behavior of the same species will be *exactly* the same in both cases. The successful correlation of a large body of information in this way indicates that this assumption is, in general, justified. However, there are indications that in certain cases energy may be carried over from the primary step, and that the "hot" radicals or atoms thus formed may react quite differently from similar atoms or radicals whose energy contents correspond to thermal equilibrium.

We may consider here a few typical cases in which hot radicals have been postulated. In the photolysis of acetone, the primary step appears to be



This is followed by secondary reactions in which  $\text{CH}_3\text{CO}$  either decomposes to  $\text{CH}_3$  and  $\text{CO}$ , or dimerizes to form biacetyl. To explain the results in detail Herr and Noyes (6) were obliged to assume that a certain fraction of the acetyl radicals formed in the primary step carry over sufficient energy to enable their virtually instantaneous decomposition. If this is the case the properties of these acetyl radicals may be expected to vary with the energy available, i.e., with the wave length of the light used, and this appears to be confirmed by experiment.

As a second case we may consider the formation of the propyl radical by reactions of hydrogen atoms. There are indications that propyl radicals may be formed from either propane or propene by the reactions (11)



and



Reaction 1 is practically thermoneutral; hence the possibility of  $\text{C}_3\text{H}_7$  being formed with much excess energy does not exist. Reaction 2 is strongly exothermic, and the propyl radical at the moment of its formation will contain the entire heat of reaction.

The most likely reaction of the propyl radical, if left to itself, is



The activation energy of this reaction is not definitely known, but it has been estimated to be between 25 and 40 kg.-cal. Hence propyl formed from reaction 1 may be expected to be stable at room temperature. The excess energy carried by propyl in reaction 2, however, is sufficient to enable reaction 3 to occur, and we may therefore expect propyl radicals to decompose to an appreciable extent at room temperature. These conclusions appear to be substantiated by the experimental results of Rabinowitch, Davis, and Winkler (10).

Ogg and Williams (9) have recently suggested that "fast" hydrogen atoms may react differently from "thermal" ones in the photolysis of hydrogen iodide. In view of the fact that such fast atoms are known to be formed in ionic reactions, the result is especially significant.

In radiation chemistry higher energies are involved, both in ionization and in molecular excitation. It may therefore be anticipated that the carry-over of energy into the secondary reactions may be both more frequent and more important. This may be troublesome in the correlation of the results with those of photochemistry.

#### THERMOCHEMICAL DATA

In building up photochemical mechanisms, data on bond strengths are of great importance in order to decide what reactions are possible. This has been a difficult question, and at one time bond strengths were certainly the scandal of photochemistry. To-day the position is greatly improved, and we may feel that we know the bond strengths in at least simple hydrocarbons and alkyl radicals with some certainty. We are thus beginning to get the thermochemistry of elementary reactions on firm ground.

In radiation chemistry modern mass spectrometry is building up reliable data on ionization and appearance potentials, and the thermochemistry of ionic reactions has advanced enormously in recent years. We are still, however, highly deficient in our knowledge of the states of excitation of complex molecules.

#### REFERENCES

- (1) BREWER, A. K., AND WESTHAVER, J. W.: *J. Phys. Chem.* **34**, 153 (1930).
- (2) EYRING, H.: *J. Chem. Phys.* **7**, 792 (1939).
- (3) EYRING, H., HIRSCHFELDER, J. O., AND TAYLOR, H. S.: *J. Chem. Phys.* **4**, 479 (1936).
- (4) EYRING, H., HIRSCHFELDER, J. O., AND TAYLOR, H. S.: *J. Chem. Phys.* **4**, 570 (1936).
- (5) GARRISON, W. M.: *J. Chem. Phys.* **15**, 78 (1947).
- (6) HERR, D. S., AND NOYES, W. A., JR.: *J. Am. Chem. Soc.* **62**, 2052 (1940).
- (7) HIRSCHFELDER, J. O., AND TAYLOR, H. S.: *J. Chem. Phys.* **6**, 783 (1938).
- (8) LUNT, R. W.: *Trans. Faraday Soc.* **32**, 1691 (1936).
- (9) OGG, R. A., AND WILLIAMS, R. R.: *J. Chem. Phys.* **13**, 586 (1945).
- (10) RABINOWITCH, B. S., DAVIS, S. G., AND WINKLER, C. A.: *Can. J. Research* **B21**, 251 (1943).
- (11) STEACIE, E. W. R.: *Atomic and Free Radical Reactions*. Reinhold Publishing Corporation, New York (1946).



CHEMICAL REACTIONS PRODUCED BY IONIZATION PROCESSES<sup>1</sup>

JOSEPH O. HIRSCHFELDER

*Department of Chemistry, University of Wisconsin, Madison, Wisconsin**Received October 23, 1947*

To understand the chemical reactions produced by radioactivity and other ionizing agents, it is necessary to consider in great detail all of the fundamental processes involved:

1. The primary and secondary ionizations.
2. The excitation without ionization.
3. The electron attachments and negative-ion formation.
4. The simple reactions between ions and neutral molecules.
5. The formation of clusters, if any.
6. The neutralization of the ions to form atoms and free radicals.
7. The subsequent fate of the free radicals and ions.

If the ionization occurs in the liquid or solid phase, additional complications arise due to steric trapping of the various ions and intermediate products. Also, the ionization potentials for the molecules in either the liquid or the solid phase are entirely different from those in the gas. Let us consider just the reactions in the gas phase.

The following presentation is largely a ramification of some work which was carried out ten years ago by Hugh S. Taylor, Henry Eyring, and the author (7, 8, 10).

## I. PRIMARY PROCESSES

We must first consider the following facts:

(1) An alpha particle ionizes everything within 1 Å. of its path. This can be seen from the following calculation:

About 25,000 ion-pairs per centimeter of path are produced by  $\alpha$ -particles in air.

$$\sigma = 4\pi r^2 = 25,000 \times \frac{22,414}{6 \times 10^{23}} = 10^{-15} \text{ cm.}^2 = \text{cross-section for ionization}$$

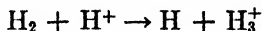
$$r \simeq 10^{-8} \text{ cm.} = \text{radius of ionization}$$

(2) Approximately four-fifths of the total ionization is produced by secondary electrons (2, 12, 13).

(3) Approximately as many molecules are dissociated by excitation without ionization as by ionization. The reasons for this are as follows: (a) Only one-half of the energy given up by an alpha particle, 33 e.v. per ion-pair, can be accounted for by the ions it produces. The rest of the energy must go into excitation without ionization. (b) Bethe (1) and Blackett (3) showed that, when  $\alpha$ -particles pass through hydrogen, there is a 50 per cent greater probability for

<sup>1</sup> Presented at the Symposium on Radiation Chemistry and Photochemistry which was held at the University of Notre Dame, Notre Dame, Indiana, June 24-27, 1947.

excitation of the molecule than for ionization. (c) Smith and Essex (13) have actually separated the chemical reactions due to excitation from those due to ionization. They placed the material to be studied, in their case ammonia, between the plates of an electrostatic condenser. They passed alpha particles through the material and measured the number of molecules reacting per ion-pair as a function of the voltage applied across the condenser. By increasing the potential across the condenser beyond a saturation point, they sucked off all of the ions formed. The remaining chemical reactions were then due either to excitation without ionization or to ionic reactions of the type



which yield free radicals or atoms without neutralization. In any case, they succeeded in making an experimental separation of the reaction number per ion-pair with and without the electrostatic field.

Thus  $\alpha$ -,  $\beta$ -, and  $\gamma$ -rays all have the same chemical action, because they all produce secondary ionization which produces the main body of ion-pairs.

There can be little specificity of the chemical actions of various types of radiation. These effects should be measurable in terms of roentgens of dosage received. In a very few cases the duration as well as the accumulated dosage of the exposure is important, and these cases must be examined separately. This lack of reciprocity (here, reciprocity is used in the same sense as in the exposure of photographic plates) must depend on the density of ion-pairs and interactions of intermediate products. It would be difficult to understand such behavior in the gas phase. Studies of lack of reciprocity should be of great interest, as they would help to reveal the mechanism of the reactions.

## II. MASS-SPECTROGRAPHIC STUDY OF THE PRIMARY PROCESSES

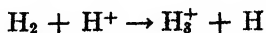
A mass spectrograph is an excellent instrument for study of the primary processes. There are a number of different types of information which can be obtained by using the mass spectrograph in different ways.

### A. Primary formation of positive ions

First, study pure gases (rather than mixtures) at very low pressures and measure the relative abundance of both the positive and the negative ions at potentials of 1000 e.v. or more. This relative abundance of the ions is the same as if these ions were formed by any high-voltage ionizing source, such as the secondary radiation from  $\alpha$ -,  $\beta$ -, or  $\gamma$ -rays. For most gases this information is available in the literature, although often no attempt has been made by the experimenter to study the negative ions.

### B. Reactions between ions and neutral molecules

Ions can easily react with neutral molecules:



Such reactions can be investigated in the older types of mass spectrographs which operate at relatively high pressures. They can be studied by varying the gas

pressure and the gas composition (of a mixture). The tendency to form clusters can also be studied in this manner. This type of information is very useful, but experimenters with the mass spectrograph have regarded the secondary reactions as a nuisance, and instead of studying them, have tried to eliminate them. For such information one searches through the mass-spectrographic literature of the late 1920's.

### *C. Negative-ion formation and electron attachment*

Much additional experimental work needs to be done on negative ions. They have not been studied with the care which they deserve. Some molecules will pick up an electron to form a negative ion; other molecules will not be able to pick up an electron unless the electron has enough kinetic energy first to dissociate the molecule into fragments which have electron affinity. Bradbury (4, 5, 6, 11) found that  $^1\Sigma$  diatomic molecules do not form negative ions. An example of a  $^1\Sigma$  molecule trying unsuccessfully to attach an electron is shown in a potential-energy diagram which I computed quantum mechanically (figure 1).

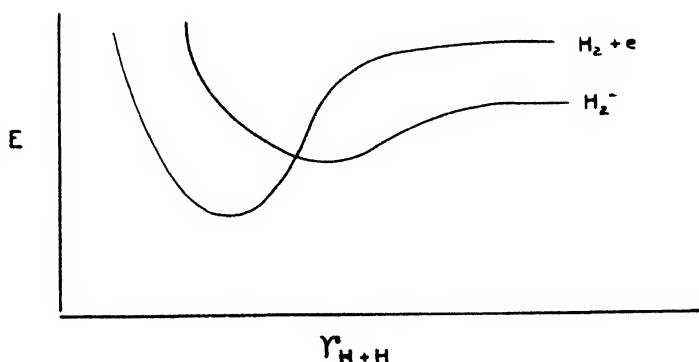


FIG. 1. A potential-energy diagram for hydrogen

Here, it is apparent that the  $H_2^-$  is metastable with respect to  $H_2 + e$  and would have a very short lifetime. Glockler (9) has studied the electron attachment of more complicated molecules. Both water and oxygen will readily attach electrons and even small traces of water vapor or oxygen will suffice to remove all of the slow electrons from a gas.

### III. THE NEUTRALIZATION OF THE IONS

Now at last we are in a position to consider the over-all reaction. From the mass-spectrographic studies we can estimate the numbers of each of the various species of ions which are produced per ion-pair in the gas mixture. When a positive and a negative ion react, they release an energy of the order of 10 e.v., or 230 kg.-cal. per mole. Because of resonance considerations, the resulting products tend to split up into free radicals and atoms in such a way as to use up as much of this energy as possible. I do not know of any direct experimental studies of neutralization reactions. As a result, we must guess what processes take place and we have only the basic quantum-mechanical principles to guide us. How-

ever, the limited amount of energy available restricts the number of chemical bonds which can be broken to three or four. Usually the over-all reaction rate is not affected critically by the exact mechanism of the neutralization reaction.

#### IV. SUBSEQUENT FATE OF THE FREE RADICALS

We are now left with a mess of free radicals and atoms produced in any one of three ways:

1. Products of dissociation of the molecule without ionization.
2. Free radicals formed by reactions between ion and neutral molecule.
3. Products of neutralization reactions.

The subsequent fate of the free radicals and ions is the same as we would expect from a study of photochemical reactions in which these same free radicals are produced in known numbers in the reaction mixture. At this point the ionization reactions become equivalent to photochemical reactions.

#### V. EXAMPLES (SEE REFERENCES 7, 8, 10)

1. Ortho-para hydrogen conversion.
2. Synthesis of hydrogen bromide.
3. Oxidation of carbon monoxide.

#### VI. SUMMARY

Chemical reactions produced by ionizing radiation can be studied and understood in terms of a sequence of steps. The procedure is quite general in its scope and applicability.

#### REFERENCES

- (1) BETHE, H. A.: *Ann. Physik* **5**, 325 (1930).
- (2) BETHE, H. A.: *Ann. Physik* **5**, 400 (1930).
- (3) BLACKETT, P. M. S.: *Proc. Roy. Soc. (London)* **A135**, 132 (1932).
- (4) BLOCH, F., AND BRADBURY, N. E.: *Phys. Rev.* **48**, 689 (1935).
- (5) BRADBURY, N. E.: *Phys. Rev.* **44**, 883 (1933); *J. Chem. Phys.* **2**, 827, 840 (1934).
- (6) BRADBURY, N. E., AND TATEL, H. E.: *J. Chem. Phys.* **2**, 835 (1934).
- (7) EYRING, H., HIRSCHFELDER, J. O., AND TAYLOR, H. S.: *J. Chem. Phys.* **4**, 479 (1936).
- (8) EYRING, H., HIRSCHFELDER, J. O., AND TAYLOR, H. S.: *J. Chem. Phys.* **4**, 570 (1936).
- (9) GLOCKLER, G., AND LIND, S. C.: *The Electrochemistry of Gases and Other Dielectrics*, Chap. VI. John Wiley and Sons, Inc., New York (1939).
- (10) HIRSCHFELDER, J. O., AND TAYLOR, H. S.: *J. Chem. Phys.* **6**, 783 (1938).
- (11) LOEB, L. B.: *Phys. Rev.* **48**, 684 (1935).
- (12) RUTHERFORD, E., CHADWICK, J., AND ELLIS, C. D.: *Radiations from Radioactive Substances*, p. 145. Cambridge University Press, London (1930).
- (13) SMITH, C., AND ESSEX, H.: *J. Chem. Phys.* **6**, 188 (1938).

CONTROLLED-ELECTRON REACTIONS<sup>1</sup>

GEORGE GLOCKLER

*Department of Chemistry and Chemical Engineering, State University of Iowa, Iowa City, Iowa**Received October 23, 1947*

Activation of chemical reactions can be brought about by a variety of external agents such as catalysts, increase in temperature of the reacting system, and the presence of various types of radiation. Radiation which can initiate reaction in a chemically quiescent system is of two kinds: (1) light of varying frequency, such as visible or ultraviolet light, x-rays, and gamma rays on the one hand; and (2) particle rays, such as alpha and beta particles, atoms and radicals, recoil atoms and ions on the other. The ultimate agent which causes chemical reaction to ensue is in many cases the electron. This particle, if given sufficient speed, can force another electron of a neutral molecule to a higher orbit or even remove it, i.e., ionize the molecule. It can produce dissociation accompanying these actions and hence create a new energy-rich species in a system which then can undergo further chemical change.

If an alpha ray or an x-ray passes through a gas there are produced excited molecules, ions, and electrons. These secondary electrons will have varying speed, and they in turn will produce energy-rich molecules, atoms, radicals, and ions. In any form of electrical discharge similar action will take place, electrons having been produced in the electric discharge. In these electrical devices electrons of varying speed are created and the whole reaction picture is one of great complexity.

To arrive at an understanding of the reaction mechanism where high-energy particles are the initiators of the reaction sequence, it is of great interest to know just what minimum of energy or speed an electron must possess in order to produce a certain kind of activation. Hence it is of interest to study chemical reactions in simple systems and determine the minimum energy of electrons starting the reaction. Furthermore, it is also important to find out how the reaction varies in amount as the initiating electrons gain greater speed. It would be expected that a molecule would be brought into a reactive state only when the impacting electron has reached sufficient speed to lift the molecule from its ground state to some higher energy level in accordance with its energy-level diagram, as obtained, for example, from the spectroscopy of the molecule. Were it true that ions of the molecules were the only activating centers for chemical reaction, then it might be expected that reaction should begin only at the ionization potential of the molecule, for the impinging electron would have to have kinetic energy equal to the ionization potential of the molecule before ions could be produced in the system. If ions were the only reactive agents, then resonated states or excited levels of the molecule would not serve as reaction initiators. This proposal is obviously not true, because it is well known that photochemical action is pos-

<sup>1</sup> Presented at the Symposium on Radiation Chemistry and Photochemistry which was held at the University of Notre Dame, Notre Dame, Indiana, June 24-27, 1947.

sible in many cases where the absorbed quantum of light does not have sufficient energy to ionize the molecule. Hence lower energy levels than ionization can lead to reactive states, and it may be expected that electrons with energy less than the ionization potential of the molecule can produce active centers in a reaction system.

The study of chemical reactions started with electrons of known speed or "controlled electrons" will give information concerning the resonance states of molecules which can start these changes. It will be seen that the simple reactions studied so far can be completely understood on the basis of the energy states of the molecules as given by quantum theory and band spectroscopy.

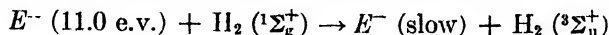
The simplest way of obtaining electron streams of known speed is to use the electrons from a hot filament, as in a radio tube, and to accelerate them by means of an electric field obtained from a battery. In this way electrons of any speed may be produced. The potential of the battery is applied between a filament and a grid. This region is made of small dimension (less than 1 mm.) so that very few collisions happen between filament and grid or before the electrons have obtained their full speed corresponding to the battery potential. Some electrons will not be caught by the grid wires but will pass through the meshes of the grid into the region between the grid and plate. Here they will make impacts with gas molecules, having attained full speed. The region between grid and plate is usually field-free and the electron speed is therefore not further altered. Whenever the potential of the battery is changed and reaches such a value that the electrons attain a critical potential of the molecules under investigation, the latter can be placed into an excited or higher energy level. Depending on the reaction system, arrangements can be made to show that chemical reaction has taken place. The most convenient method is usually to follow pressure changes of the reaction system.

In this manner the following reactions have been studied (4):

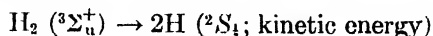
1. The dissociation of hydrogen into atoms.
2. The dissociation of hydrogen into atoms in the presence of mercury.
3. The dissociation of oxygen.
4. The dissociation of nitrogen.
5. The synthesis of ammonia.
6. The reaction between nitrogen and oxygen.
7. The decomposition of sodium azide.
8. The reaction between carbon monoxide and hydrogen.
9. The decomposition of sulfur dioxide.

The simplest type of chemical reaction that has been studied with electrons of controlled speed is the dissociation of diatomic molecules as, for example, the dissociation of hydrogen molecules into two atoms (3). It might be expected that electrons with 4.34 e.v. of energy could dissociate hydrogen molecules, because this amount of energy is equivalent to the heat of dissociation. However, electrons of this speed cannot transfer this amount of energy to the hydrogen molecule, since there exists no electronic energy level in the molecule of this

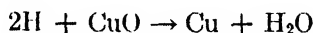
amount of energy. At least the probability of such energy transfer is extremely low and this action has not yet been observed. It was found experimentally that electrons with about 11.0 e.v. can transfer their energy to hydrogen molecules and place them into the antisymmetric ( $^3\Sigma_u^+$ ) state:



But the hydrogen molecules in the antisymmetric state will dissociate into two atoms with kinetic energy:



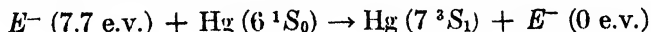
The resulting atoms were detected by their reaction with a copper oxide surface (kept at room temperature):



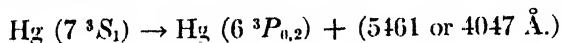
The resulting water vapor was frozen out in a liquid-air trap and later identified by its vapor pressure.

In the same reaction vessel a critical potential of hydrogen was found by the Franck-Hertz method (2) at 11.4 e.v. Hence the demonstration is complete in this case that electrons must bring hydrogen molecules into a quantum-mechanical energy level before they will react chemically. It is then supposed that similar actions will take place in hydrogen gas, whether electrons are produced by alpha particles, x-rays, or any other energetic radiation. To this extent then do these experiments with slow electrons also indicate the possible reaction mechanism in electric discharges. Electrons of greater speed than 11.0 e.v. will carry on this process with varying probability, and of course other quantum jumps will become possible as the electrons are given energies greater than 11.0 e.v.

A variation of the experiment (7) on hydrogen dissociation just described involved the admixture of mercury vapor with hydrogen gas. It may then be expected that mercury atoms can be brought into the resonated state ( $6^3P_1$ ) and that they may then transfer their energy (4.9 e.v.) to the hydrogen molecules by an impact of the second kind, causing their dissociation for which the excitation energy of the mercury atoms is sufficient (4.9 e.v. compared with 4.34 e.v.). However, the first disappearance of hydrogen molecules was noted when the impinging electrons had about 7.7 e.v. of energy, a quantity which is sufficient to transfer a mercury atom to the  $7^3S_1$  state:

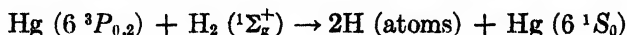


It is likely that the excited mercury atoms drop to the metastable  $6^3P_{0,2}$  states with emission of radiation:

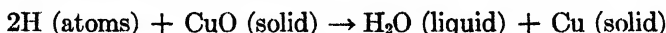


The metastable  $P$  states have a much longer life and hence much greater opportunity to collide with hydrogen molecules. Furthermore, this energy is much nearer to the heat of dissociation of hydrogen molecules, enhancing the possi-

bility of energy transfer, since it is known that impacts of the second kind are more likely if the energy to be dissipated as kinetic energy is a minimum:

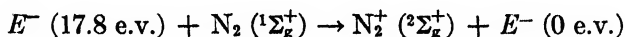


The hydrogen atoms so produced can then react with the copper oxide surface present in the experimental tube. The observed pressure decrease results from the freezing out of the water formed:



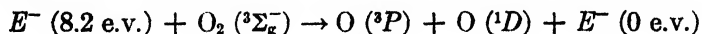
The mercury-sensitized reaction did not occur at 4.9 e.v. as expected, but at 7.7 e.v. This fact may be connected with the relative resonance probability of mercury atoms.

Nitrogen molecules are dissociated by electrons of 17.8 volts of energy (12). Again it is seen that electrons cannot transfer the dissociation energy (about 7 or 9 e.v.) to nitrogen molecules with sufficient frequency to be detected in the experimental set-up used at the time. At the higher voltage mole-ions may be produced, since the ionization potential of nitrogen molecules is 15.7 e.v. These mole-ions may be the species which is frozen out or adsorbed on the walls of the reaction vessel:

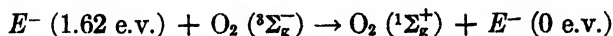


The energy of 17.7 e.v. is not high enough to produce nitrogen atoms and atomic ions (11). However, the act of neutralization of the mole-ion ( $\text{N}_2^+$ ) on the plate of the experimental tube may furnish the energy of dissociation.

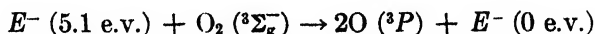
In the case of oxygen gas it was found that 8.0-volt electrons can cause effective impacts which make oxygen molecules adsorbable on glass and mercury surfaces (8, 9),



but some slight reaction is also noted even with electrons of lesser energy (3-5 e.v.),



or



Ozone does not seem to form until the impinging electrons have 25-28 e.v. of energy (9, 17). No particular change in pressure drop is noted at the ionization potential of the oxygen molecule (12.5 e.v.).

Ammonia can be synthesized from a hydrogen-nitrogen gas mixture. The product is formed more readily at 17 e.v. after the ionization potential of the nitrogen molecule (15.7 e.v.) has been reached. The gas mixtures richer in nitrogen give greater yields, indicating that perhaps nitrogen mole-ions are involved in the reaction mechanism (4).

Nitrogen and oxygen react after impact with 19.0-volt electrons with a further increase in reaction rate at 23 e.v. (10, 16). The product is nitrogen dioxide.



Thin films of sodium azide deposited on a plate will decompose when bombarded with electrons of known speed. The first reaction happens at 11.65 e.v. and further reaction rate changes are noticeable at higher impact potentials of electrons (14).

Carbon monoxide is decomposed by controlled-electron impact at 14 and 19 e.v. (1). It will react with hydrogen at 14.0, 20.0, and 27.0 e.v. The chief reaction product is formaldehyde. The ionization potential of the carbon monoxide molecule is 14.0 e.v. Excited molecular ions appear at 16.52 and 19.63 e.v. Hence the experiments carried out to the present would indicate an ion mechanism. However, the experimental arrangements may not have been sensitive enough to detect reaction at lower voltages, where either excited neutral states or dissociation alone may be the responsible reaction mechanism.

Sulfur dioxide is decomposed at 12.2 and 15.7 e.v. by electron impact. In the first case mole-ions ( $\text{SO}_2^+$ ) and at the higher voltage  $\text{SO}^+$  ions and oxygen atoms are produced (15).

One feature of the usual experimental tube used in investigations of reactions activated by controlled electrons is the presence of the hot filament. It can cause reaction by its high temperature, independent of the emitted electrons. In favorable cases such "zero-volt-rates" may be small and can be readily corrected for. In the case of hydrocarbons, pyrolysis on the filament would be serious. In such cases the filament can be placed in another compartment and the electrons can be allowed to enter the reaction chamber proper through a small orifice. Appropriate pumping can be used to remove the thermal decomposition products due to the filament. Acetylene was shown to polymerize (6) in such an apparatus by using 40-volt electrons.

A study on the synthesis of ammonia (5) initiated by alkali ions is of interest to the present discussion of controlled-electron reactions. In this case ions of lithium, sodium, and potassium were shot into mixtures of nitrogen and hydrogen of varying proportions. It was found that ammonia was formed only after these alkali ions had passed through an accelerating field of sufficient magnitude that the respective positive ions could ionize nitrogen molecules. The latter were considered the important agent in the mechanism, because mixtures rich in nitrogen gave better yields. It is seen that positive ions of low velocity do not cause ammonia formation. On the cluster theory (13) reaction might be expected independent of ion velocity.

#### SUMMARY

This review of reactions activated by electrons of controlled speed seems to show that the initial acts of the reaction sequence are to be interpreted on the basis of the quantum states of the interacting molecules, as given by their energy-level diagram. Only very few reactions have been studied. The greatest need is the development of more sensitive detecting agents, so that reaction on-set can be discovered even in cases where the probability of energy transfer is very low and where the means used in the past have not been delicate enough to show the beginning of reaction.

## REFERENCES

- (1) CARESS, A., AND RIDEAL, E. K.: Proc. Roy. Soc. (London) **A120**, 370 (1928).
- (2) FRANCK, J., AND JORDAN, P.: *Anregung von Quantensprüngen durch Stöße*. J. Springer, Berlin (1927).
- (3) GLOCKLER, G., BAXTER, W. P., AND DALTON, R. H.: J. Am. Chem. Soc. **49**, 58 (1927).
- (4) GLOCKLER, G., AND LIND, S. C.: *The Electrochemistry of Gases and Other Dielectrics*. John Wiley and Sons, Inc., New York (1939).
- (5) GLOCKLER, G., AND LOEPPERT, R. H.: Trans. Electrochem. Soc. **80**, 221 (1941).
- (6) GLOCKLER, G., AND MARTIN, F. W.: Trans. Electrochem. Soc. **74**, 67 (1939).
- (7) GLOCKLER, G., AND THOMAS, L. B.: J. Am. Chem. Soc. **57**, 2352 (1935).
- (8) GLOCKLER, G., AND WILSON, J. L.: J. Am. Chem. Soc. **54**, 4544 (1932).
- (9) HENRY, L. A. M.: Bull. soc. chim. Belg. **40**, 339 (1931).
- (10) HENRY, L. A. M.: Bull. soc. chim. Belg. **40**, 371 (1931).
- (11) HERZBERG, G.: *Molecular Spectra and Molecular Structure of Diatomic Molecules*. Prentice-Hall, Inc., New York (1939).
- (12) HUGHES, L. A.: Phil. Mag. **41**, 778 (1921); **48**, 56 (1924).
- (13) LIND, S. C.: *The Chemical Effects of Alpha Particles and Electrons*. The Chemical Catalog Company, Inc., New York (1928).
- (14) MÜLLER, R. H., AND BROUS, G. C.: J. Am. Chem. Soc. **53**, 2428 (1931); J. Chem. Phys. **1**, 482 (1933).
- (15) NEKREASOV, N., AND SCHNEERSON, A.: Acta Physicochim. U.R.S.S. **2**, 711 (1935).
- (16) WANSBROUGH-JONES, O. H.: Proc. Roy. Soc. (London) **A127**, 511 (1930).
- (17) WANSBROUGH-JONES, O. H.: Proc. Roy. Soc. (London) **A127**, 530 (1930).

SPONTANEOUS DISSOCIATION OF IONS<sup>1</sup>

J. A. HIPPLE

*National Bureau of Standards, Washington, D. C.**Received October 23 1947*

## INTRODUCTION

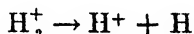
When a molecule is struck by an electron having an energy of 10-20 electron volts or higher, it may simply lose an electron or, in addition, split into various fragments. This fragmentation is a reproducible phenomenon which is a fundamental characteristic of the particular type of molecule being studied—the relative probability of the formation of a fragment having a particular mass being dependent on the temperature of the molecules and the energy of the electrons. The mass spectrometer is the most powerful tool available for the study of some of the primary processes which are of basic interest to those attempting to attain a more complete understanding of the more complicated reactions in the general field of radiation chemistry. In this connection, information is required on the appearance potentials of the various fragments as well as their relative abundance.

<sup>1</sup> Presented at the Symposium on Radiation Chemistry and Photochemistry which was held at the University of Notre Dame, Notre Dame, Indiana, June 24-27, 1947.

From the early days of mass spectroscopy, soon after the turn of the century, processes of ionization and dissociation have been studied by this means. Several reviews of this work have been written (3, 10, 14), but there is none currently up to date. The present discussion will be concerned only with two aspects of this general field which have been of recent interest. The first of these deals with metastable ions,—molecular ions which dissociate spontaneously into smaller fragments with a characteristic decay constant; the second aspect, ions formed with initial kinetic energy, is included because the effect on the mass spectrum (with the conventional instrument) shows some similarity to that observed with the metastable ions, and similar experimental techniques are applicable in both cases.

#### METASTABLE IONS

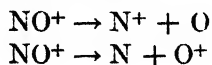
During the war the urgency of obtaining rapid analyses of hydrocarbon mixtures led to the development of the mass spectrometer for this purpose. As a result of this, the spectra of a large number of hydrocarbons were obtained by automatic recording. Almost invariably on these records there appeared rather diffuse peaks at positions which usually did not correspond to integral mass numbers. It is true that peaks of this nature had been noticed previously, but they had been glibly interpreted as ions of high kinetic energy. However, as data were obtained on a large number of hydrocarbons it became evident that this interpretation was not tenable and some other explanation would be necessary. If the ions should dissociate into two or more fragments after leaving the ion gun but before proceeding far in the magnetic analyzer, it was known that peaks of this type could occur. For instance, Smyth (13) reported that in the case of hydrogen the molecular ion would dissociate during transit to give an apparent mass ( $m^*$ ) of  $1/2$ . Thus,



The atomic ion shares the energy acquired in the ion gun with the neutral fragment, giving rise to a peak having an apparent mass of  $1/2$ , since the analyzer consisting simply of a magnetic field alone sorts out ions according to their momentum rather than their mass. The relationship between the apparent mass ( $m^*$ ), the mass ( $m_0$ ) of the parent ion before dissociation, and the mass ( $m$ ) of the fragment ion is given by the expression:

$$m^* = \frac{m^2}{m_0}$$

It was found that this reaction could be detected only at high pressures and was therefore "triggered" by collision with neutral hydrogen molecules in the analyzer. Hence this must be classed as a secondary process. Hogness and Lunn (9) reported a similar effect in nitric oxide:



These they showed to be dissociations induced by collision.

In the precision mass spectrographs in which there is a considerable distance of free flight between the region of electrostatic deflection and the magnetic analyzer, the diffuse peaks due to dissociation in transit may become very pronounced but the center of gravity of the peak agrees with the predicted value to a high degree of accuracy (1). Mattauch and Lichtblau (12) found their apparatus particularly suitable for studies of dissociation during transit and identified twenty-eight different reactions of this type.

In all this earlier work it appeared that the dissociations were induced by collision, since they were relatively greatly enhanced as the pressure in the instrument was increased. This is in contrast to the diffuse peaks in the spectra of hydrocarbons studied in mass spectrometers of recent design. Here the diffuse peaks vary linearly with the pressure, indicating that they must be primary rather than secondary processes. As soon as it was shown that the reaction was of a primary nature, it was logical to conclude that the dissociation was truly spontaneous, i.e., the ions formed by electron impact had an appreciable lifetime of the order of the transit time through the instrument. Consider, for instance, the diffuse peak at  $m^* = 31.9$  observed in *n*-butane. If it is assumed that this is due to the spontaneous loss of a  $\text{CH}_3$  radical from the parent ion  $\text{C}_4\text{H}_{10}^+$ , it is found that all the experimental facts can be explained. In this case the following transition occurs:



The parent mass is here 58 and the product 43. However, if the dissociation occurs after the ion emerges from the ion gun, the propyl ion will have  $43/58$  of the original energy and will apparently have the mass  $43/58 \times 43$ , or 31.9. This accounts for its position on the mass scale. Figure 1 shows a drawing of the electrode arrangement in the ion gun. Between plates 1 and 2 a small potential accelerates the ions formed by the electron impact through the slit in plate 2. The main accelerating potential is then applied between plates 2 and 3, and we are discussing the case of ions which dissociate after passing through plate 3, but before proceeding far into the analyzer region. Let us consider that the ion has acquired a kinetic energy of 1000 e.v. and then dissociates at the entrance to the analyzer. For the aforementioned reaction, this means that the propyl ion, instead of having a kinetic energy of 1000 e.v., will have  $43/58 \times 1000$ , or approximately 740 v. If the analyzer is so adjusted that mass 31.9 is focussed on the exit slit (not shown in figure 1) and the kinetic energy of the ions is then measured, they should have the kinetic energy just predicted. This prediction has been confirmed in this manner for this reaction as well as others (8).

There remains the possibility that the reaction is induced by some agency which does not vary with the pressure (such as the edge of the slit in plate 3). Such conjectures seemed like remote possibilities, but this question can be completely settled by studying the relative peak heights as a function of the transit time. Let us refer once more to figure 1. If the transition is truly metastable, the number of metastable ions will decay exponentially with time. Those which dissociate between plates 2 and 3 will appear on the mass scale between  $m$  and  $m^*$ ,

and those which dissociate in the weak field existing between the region of the electron beam and plate 2 will appear essentially as mass  $m$  (mass 43 in our example). A large number will dissociate before reaching plate 2 because of their relatively slow motion in this region. Now if the voltage difference between plates 1 and 2 is increased, less time will be spent in reaching the slit in plate 2 and in turn the ions will pass through plate 3 earlier in their lifetime. Consequently, the diffuse peaks should increase relative to the rest of the spectrum. By studying the peak heights in relationship to  $E_1$ ,  $E_2$ , and the geometry of the ion source, the actual decay curve may be reconstructed (7). The result of this study for metastable  $C_4H_1^+$  is illustrated in figure 2. A reasonably good straight

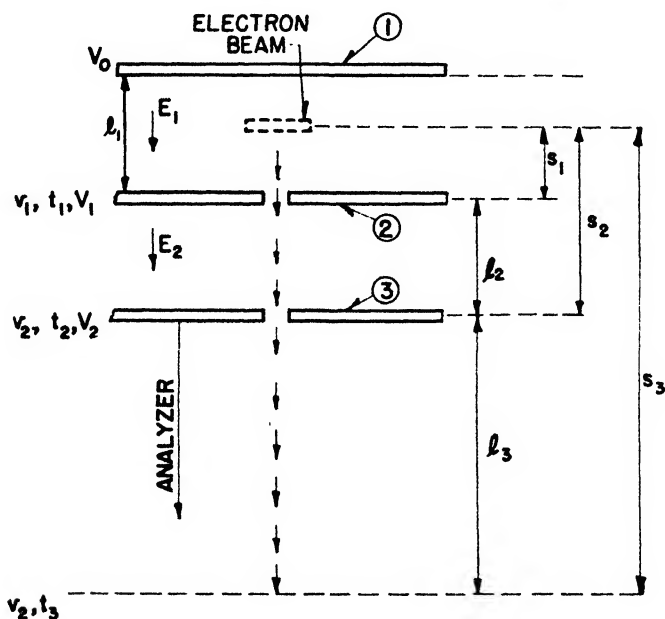


FIG. 1. Essential components of an ion gun to illustrate the method of studying metastable ions.

line is obtained in this semi-log plot. The half-life in this case is approximately  $2 \cdot 10^{-6}$  sec. The voltages indicated refer to various values of  $V_1 - V_0$ .

From figure 2 it is possible to determine the relative number of ions initially in the state responsible for this metastable transition. This is found to be approximately 5 per cent of the number of  $\text{C}_4\text{H}_{10}^+$  ions which traverse the mass spectrometer and reach the ion collector without dissociating.

Unfortunately, this method is limited to the study of states having a half-life of the order of microseconds. It seems reasonable to expect that there are many metastable states outside our narrow range of observation. If the half-life is either longer or shorter than this observable range, the peaks would have the normal sharp appearance and would appear at integral mass numbers (excluding in all this discussion thus far multiply charged peaks).

Attempts have been made to detect an activation energy for the metastable transitions. Within the accuracy of the measurements (0.2 v.) the diffuse peak at 31.9 has the same appearance potential as the ionization potential of the parent ion. In the case of several hydrocarbons, preliminary results indicate some difference in this energy.

It had been thought that there was previously no evidence for purely spontaneous dissociation as distinct from that induced by collision. In a private communication, Professor B. Rosen has pointed out that he felt that there was some evidence for metastable transitions in  $\text{CO}^{++}$  (5). The reaction is

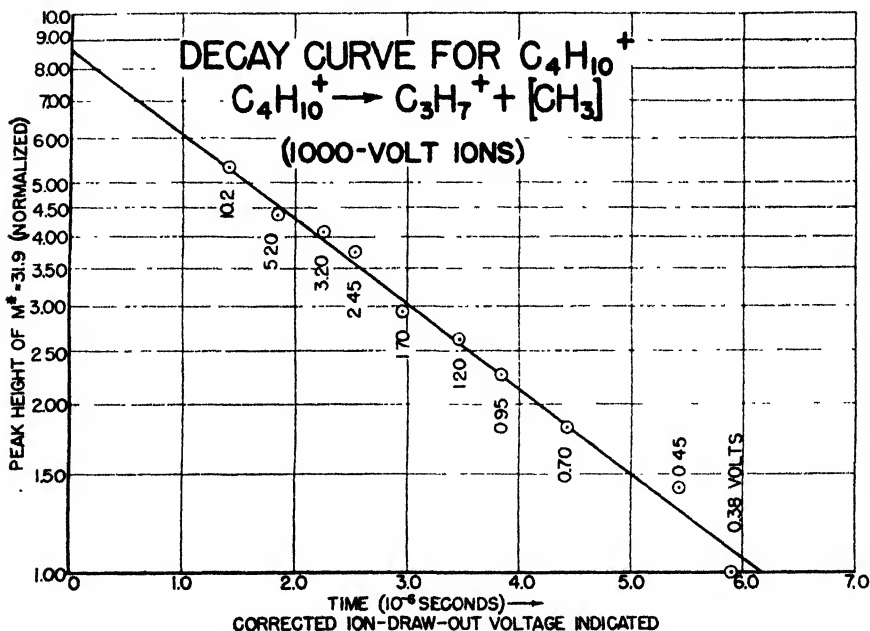
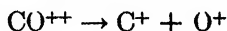


FIG. 2. Decrease with time of the number of ions in the metastable state responsible for the diffuse peak at the apparent mass 31.9 in the mass spectrum of *n*-butane.

giving peaks at 10.3 and 18.3. Briefly, the argument that this is a metastable transition is this: The ions at 10.3 and 18.3 have a much lower appearance potential than that of  $\text{CO}^{++}$ . It is suggested that the electronic state from which they are formed has a maximum in the potential energy curve and that the decay takes place by leakage through this potential barrier. The parent ion  $\text{CO}^{++}$  is absent at the lower energies, because it decays too rapidly to be detected as mass 14. This experiment was performed without many of the important developments in experimental technique which are available to us today and there is one experimental fact that apparently is unexplained. In the spectrum published in this work, the peak at 18.3 is more than ten times larger than that at 10.3, whereas the above explanation would demand that they be of equal height. Apparently no data were obtained on the effect of pressure and transit time.

An attempt was made to study this interesting reaction with the advantage of the availability of improved equipment developed during the intervening fifteen years. It was planned that a study of these peaks would be made as the pressure and transit time was varied and this would be followed by a measure of the appearance potentials. Unfortunately, this program had to be abandoned because the peaks at 18.3 and 10.3 could not be detected, although the instruments used should have been sufficiently sensitive for this purpose. The search was made on the 90° instrument at the Westinghouse Research Laboratory by Dr. R. E. Fox and on the Consolidated mass spectrometer at the Bureau of Standards by Mr. V. H. Dibeler. It will probably be desirable to make a more careful search at even higher sensitivity when this is possible.

#### IONS FORMED WITH KINETIC ENERGY

The technique of measuring the energy of the ions at the exit slit of the mass spectrometer by applying a stopping potential, which was used in studying metastable transitions, suggests its application to the determination of the kinetic energy of the fragment ions in dissociation by electron impact. The kinetic energy of the dissociated ions has been studied in the past with the mass spectrometer and similar equipment, particularly by Tate and his students (2, 6, 11). However, these methods were applicable primarily to diatomic molecules. The use of the stopping potential or energy analyzer at the exit end of the mass spectrometer presents some desirable features in the study of more complicated molecules.

If the stopping potential between the exit slit and the ion collector is carefully adjusted so that ions formed initially with thermal energy (such as  $C_4H_{10}^+$  in butane) only are unable to reach the collector, these ions will form a so-called inverted spectrum; they will be accelerated back against the exit slit, knocking out secondary electrons which are in turn accelerated to the ion collector giving rise to a negative current. Under these conditions, the peaks at mass 58 and 43 in *n*-butane are inverted, whereas the peaks at lower mass are not. Evidently these are formed with considerable initial kinetic energy. As the stopping potential is increased, more and more of the peaks become inverted as their initial kinetic energy is no longer sufficient to surmount the increased stopping potential. It has been found that all of the lower-mass ions in *n*-butane have appreciable kinetic energy (several electron volts). This throws some uncertainty on the correlation of such appearance-potential measurements with thermochemical data—a simultaneous measurement of the kinetic energy as has been performed with diatomic molecules should be a distinct advance. Measurements made in this manner would tend to eliminate the possibility of discrepancy in the interpretation of the data obtained with the mass spectrometer, such as that pointed out by Douglas and Herzberg (4).

A major difficulty in the study of ions of high kinetic energy with the mass spectrometer is the large number which are lost before reaching the ion collector. This is not only bothersome in the measurement of appearance potentials but is also one cause of the variation in mass spectra as obtained on different instruments or on the same instrument at different times. Washburn and Berry (15)

in an interesting note have pointed out that a large number of ions are lost because there is no focussing in the direction of the magnetic field. As the accelerating voltage is increased, less will be lost because there will be less time for them to drift beyond the slit. Peaks corresponding to ions having a large initial energy will increase rapidly with accelerating voltage. By studying this rate of increase, Washburn and Berry made deductions about the initial energies of the ions.

#### SUMMARY

The dissociation of molecular ions during transit through mass spectrometers is discussed. The early work in this field is briefly reviewed and interpreted in relation to recent experiments. It is shown that the same experimental technique should be valuable in the study of ions formed with appreciable kinetic energy. An experiment of this nature is described.

#### REFERENCES

- (1) BAINBRIDGE, K. T., AND JORDAN, E. B.: Phys. Rev. **51**, 595 (1937).
- (2) BLEAKNEY, W.: Phys. Rev. **35**, 1180 (1930).
- (3) DE GROOT, W., AND PENNING, F. M.: *Handbuch der Physik*, 2nd edition, Vol. 23. Julius Springer, Berlin (1933).
- (4) DOUGLAS, A. E., AND HERZBERG, G.: Can. J. Research **20**, 71 (1942).
- (5) FRIEDLANDER, F., KALLMANN, H., LASAREFF, W., AND ROSEN, B.: Z. Physik **76**, 60 (1932).
- (6) HAGSTRUM, H. D., AND TATE, J. T.: Phys. Rev. **59**, 362 (1941).
- (7) HIPPLE, J. A.: Phys. Rev. **71**, 594 (1947).
- (8) HIPPLE, J. A., FOX, R. E., AND CONDON, E. U.: Phys. Rev. **69**, 347 (1946).
- (9) HOGNESS, T. R., AND LUNN, E. G.: Phys. Rev. **30**, 26 (1927).
- (10) KALLMANN, H., AND ROSEN, B.: Physik. Z. **32**, 521 (1931).
- (11) LOZIER, W. W.: Phys. Rev. **36**, 1285 (1930).
- (12) MATTAUCH, J., AND LICHTBLAU, H.: Physik. Z. **40**, 16 (1939).
- (13) SMYTH, H. D.: Phys. Rev. **25**, 452 (1925).
- (14) SMYTH, H. D.: Rev. Modern Phys. **3**, 347 (1931).
- (15) WASHBURN, H. W., AND BERRY, C. E.: Phys. Rev. **70**, 559 (1946).



THE MASS-SPECTROMETRIC DETECTION OF FREE RADICALS<sup>1</sup>

G. C. ELTENTON

*Shell Development Company, Emeryville, California**Received October 23, 1947*

This paper attempts, in very summarized form,<sup>2</sup> to describe the salient features of an apparatus consisting of a closely coupled reactor and mass spectrometer suitable for the identification of certain intermediates occurring in thermal cracking and flame reactions. Only a few representative examples of the results obtained are briefly discussed. It should be emphasized that the object of the research was to investigate the application of the method to a wide range of problems rather than to the detailed study of a particular problem. Many of the results therefore are of a semiquantitative or even qualitative character.

## THE PRINCIPLE OF THE METHOD

If a free radical  $R$  exists in a gas it will have an ionization potential  $I_R$  which will be less than the appearance potential  $A_R$  required to form the same ion  $R^+$  by electron bombardment of the parent molecule. The difference in energy  $A_R - I_R$  will be the sum of the energies required for dissociating, exciting, and giving kinetic energy to the two fragments into which the parent molecule is split by bombardment. Provided therefore electron-impact energies  $E$  lying between the limits  $A_R > E > I_R$  are used, any ion current of mass corresponding to  $R$  may be attributed to a chemical process and not an electron-dissociation process, provided of course there are no other end products or intermediates furnishing  $R^+$  by electron impacts of energy less than  $E$ .

Table 1 will serve as an illustration in the case of the thermal decomposition of ethane to give hydrogen and ethylene. Let us suppose that we are interested in the detection of the ethyl, methyl, and methylene radicals. At first sight it would seem that in the case of ethyl there is a quite large (4.2 v.) difference between the ionization potential of the radical and the appearance potential in ethane. However, since ethylene is a product the concentration of which is vastly greater than that of the ethyl radical, the  $C^{13}$  isotope of ethylene will have a mass coinciding with that of  $C_2H_5$ , so that it becomes necessary to take 10.9 v. instead of 12.9 v. as the upper limit of usable electron energy. Thus, the usable difference of energy is only 2.2 v. In the case of the methyl radical the situation is simpler and the electron energy can be raised to 14.2 v. before any  $CH_3^+$  will appear by electron dissociation. The usable difference then is 4.2 v., and there is no danger of measuring the isotope  $C^{13}H_2^+$ , since this would require 16.2 and 19.2 v., respectively, from ethane and ethylene. For the detection of methylene we have at our disposal an energy difference of  $16.2 - 11.9 = 4.3$  v., so it should be slightly easier to detect, if present, than the methyl radical.

<sup>1</sup> Presented at the Symposium on Radiation Chemistry and Photochemistry which was held at the University of Notre Dame, Notre Dame, Indiana, June 24-27, 1947.

<sup>2</sup> A more detailed description will be found in three connected articles by the author appearing elsewhere (1).

The second problem which has to be solved is that of bleeding out a continuous sample of gas from the reactor at high pressure and injecting it as rapidly as possible into the ionization chamber, where the pressure must be maintained below 0.001 mm. Clearly, it would be useless to maintain the required pressure dif-

TABLE 1  
*Ionization and appearance potentials in ethane and ethylene*

ION	$I_R$ volts	$A_R$ FROM $C_2H_6$ volts	$A_R$ FROM $C_2H_4$ volts
$C_2H_5^+$ .....	8.7	12.9	
$C_2H_4^+$ .....	10.9	12.2	10.9
$CH_3^+$ .....	10.0	14.2	
$CH_2^+$ .....	11.9	16.2	19.2

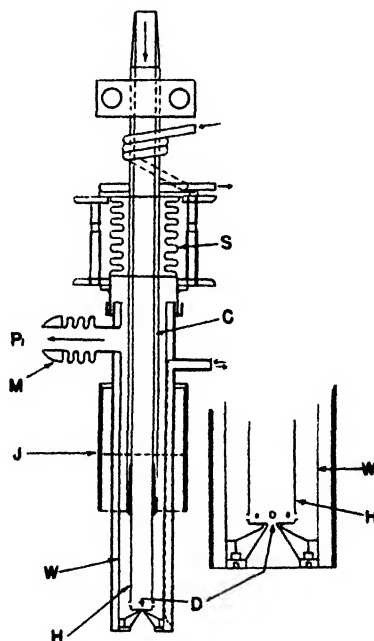


FIG. 1. High-pressure reactor (63). H, stainless-steel furnace; W, water-cooled jacket; J, joints for attachment to mass spectrometer and to exhaust M; C, copper conductor; S, expansion joint; D, diaphragm recess. Enlarged view of furnace bottom is given in the inset on the right.

ferential by means of long capillaries. The only alternative is to use very small holes in thin metal or quartz foil and to expand, by fast pumping, the gas sample bleeding into the ionization chamber. One type of reactor used for high reaction pressures is illustrated in figure 1. This reactor is attached to the mass spectrometer by means of a joint (J) in such a manner that the small diaphragm (D) in the stainless-steel furnace (H) lies in a plane about 1 cm. above the electron

beam (not shown) which is injected perpendicular to the axis of the reactor. The gas enters a heavy copper tube at the top, which also serves to conduct the large A.C. currents required to heat the thin walls of H. After reaction the main bulk of the gas is pumped away *via* a water-cooled annular space leading to a pump ( $P_1$ ). By proper design of the heater H it is possible to maintain a sensibly zero temperature gradient above the diaphragm D without exposing more than a few square millimeters of hot surface to the low-pressure gas in the ionization chamber. Thus the small sample of gas issuing through the diaphragm is in temperature equilibrium with the reactor and constitutes the only source of thermally activated or decomposed molecules.

Two other types of furnace—namely, a heated quartz tube and a grid of short carbon filaments—were also used for studies at low pressures.

#### SUMMARIZED RESULTS ON LIGHT HYDROCARBONS

Hydrocarbons up to and including the butenes were studied in more or less detail. No methylene radicals were detectable even at low pressures (*ca.* 0.01 mm.) of methane heated with carbon filaments. Only when passing diazomethane through the furnace was there any evidence of  $\text{CH}_2$  formation. Methyl radicals, however, were readily detectable in all cases except with pure ethylene, and the concentration was not appreciably decreased in the presence of oxygen or nitric oxide. In a number of instances small amounts ( $< 1$  per cent) of lead tetramethyl were added to the carrier gas so that the reactivity of the latter with the methyl radical could be studied. In figure 2 the results of some such experiments are illustrated for the carrier gases oxygen, ethane, propene at a reaction pressure of 1.1 mm. It will be noticed that the concentration of methyl radicals appears highest in oxygen and lowest in propene. The main cause of this result is probably the variation in the frequency factors of the reactions between the methyl radicals, produced by the lead tetramethyl, and the carrier gases. In the case of oxygen the difference may be enhanced as a result of the poisoning of the lead liberated in the reaction. The curves show clearly that as the reactor temperature is increased beyond that required for the total decomposition of the lead tetramethyl, the concentration of methyl tends to decrease to a minimum and then rise again as the carrier gas (in the case of a hydrocarbon) itself begins to decompose. The decrease is attributable to the fact that as the temperature increases, the lead tetramethyl is decomposed nearer to the entrance to the furnace and further from the sampling diaphragm. Hence the individual methyl radicals make more collisions before reaching the diaphragm and the probability of interaction and removal is increased. This effect illustrates rather clearly the reason for the failure of the mirror method to detect radicals at pressures above a few millimeters of mercury. Owing to the large distance between the furnace and the mirror, and the large number of collisions made in the comparatively hot intervening gas, the radicals have little chance of reaching the mirror. Using a reactor such as that shown in figure 1 no such difficulty is encountered and radicals have been detected up to pressures of 140 mm. in the case of ethane and methane. A little consideration of the dependence of the partial pressure of the

radicals in the ionization chamber, the total pressure in which is about 0.001 mm. and independent of the reaction pressure, will show that radicals will only be detectable at high pressures if the order of their production is equal to or greater than the order of their removal. Since the latter, in the case of ethane, is certainly bimolecular, we must conclude from our results that the production of methyl radicals is also bimolecular. If, therefore, conditions are established in

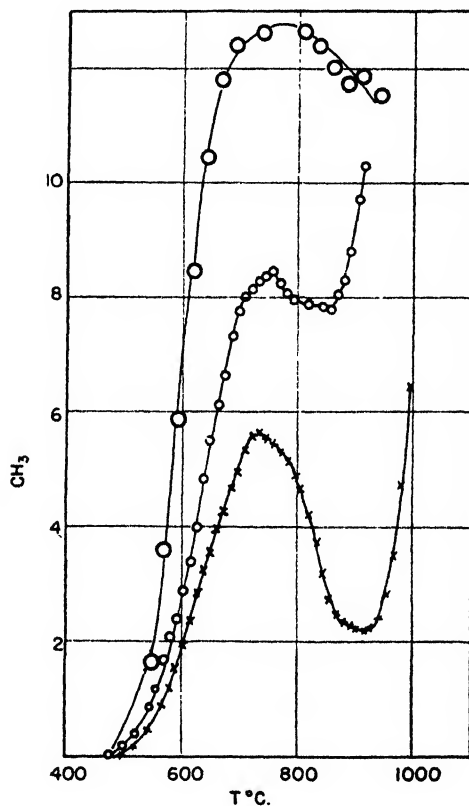


Fig. 2. Production of methyl in mixtures of 0.6 per cent lead tetramethyl in oxygen (O), ethane (e), and propene (X). Quartz reactor R1. Pressure *ca.* 1.1 mm.

which detailed balancing pertains, it follows that the recombination of two methyl radicals occurs in a triple collision, as postulated by Kuchler and Theile (2).

In the interaction of methyl radicals and propene it is not surprising that we found evidence of the allyl radical. At higher temperatures, where propene itself is decomposing into methyl radicals, no evidence was found of the residual vinyl radical, although the electron-energy requirements for detection are quite favorable. Large amounts of ethene were found at temperatures where methyl was abundant, and we may therefore conclude that the concentration of vinyl is lowered as a result of its high reactivity.

## FLAME STUDIES

Since radicals had been detected at relatively high pressures during the decomposition of hydrocarbons, it was natural to attempt an extension of the technique into the field of combustion. One of the main obstacles to a unique interpretation of results stems from the large variety of products and intermediates. Thus, if formaldehyde is created in the flame it may dissociate under electron impact to give an apparent radical ion  $\text{CHO}^+$ . Similarly, acetylene, which was found in abundance in a propane-oxygen flame, may give  $\text{CH}^+$ . In a

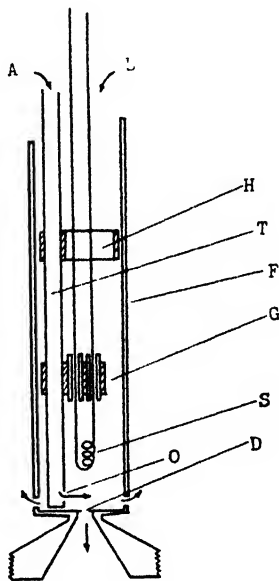


FIG. 3. Internal modifications of steel reactor R3 for flame studies. Gas components A and B enter as shown, and the flame extends from the side hole O across the diaphragm D. The distance OD can be varied by oscillating the tube T in a vertical direction, lateral movement being prevented by the spring guide H. A retractable platinum-iridium coil (S) moving in guides (G) serves to ignite the mixture.

preliminary survey, however, it is possible to overcome some of these ambiguities and to deduce certain facts concerning the chemical sequence by using a flow-pulsating or a mechanically oscillating flame.

Figure 3 shows the internal modifications of the reactor when used for studying the products of a flame burning just above the sampling diaphragm. One of the reactants A enters down the tube T and encounters the other reactant B in the vicinity of a side hole O. The flame spreads across the diaphragm and by small cyclic variations in the flow of A and B the flame can be caused to move further to the right or left. Alternatively in some experiments the tube T was mechanically and cyclically moved up and down, a procedure which induced a certain horizontal movement of the flame zones across the area of the diaphragm. The consequences of such a technique can best be explained by reference to figure 4,

where an idealized flame with reaction zones ABCDE, in which the products ABCDE are a maximum, is represented. If now the diaphragm, represented by X, is moved from X to a new position Y further from the tip of the flame, the concentration of the products ABCDE will tend to vary in the manner shown by the curves in the lower part of the figure as X passes through successive positions on its way to Y and back to X.

We can in this way speak of the phase of the products ABC etc., and it is obvious that if the heights of two mass-spectral peaks corresponding to  $A^+$  and  $B^+$  differ in phase, then  $A^+$  cannot be the electron dissociation product of B or *vice versa*.

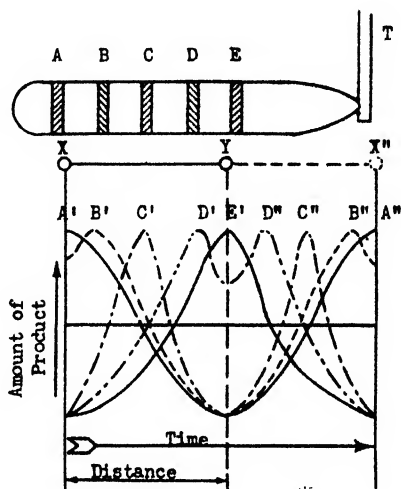


FIG. 4. Schematic representation of reaction zones in a horizontal flame pulsating across the sampling diaphragm. If the latter moves from X to Y, corresponding to an elongation of the flame, the intensities of the zonal products ABCDE entering the ionization chamber will pass through maxima A', B', C', D', and E'. As the flame contracts, the pattern will be repeated, and the maxima on an unfolding time scale will appear at D'', C'', B'', and A''

Figure 5 illustrates the type of results obtained with a pulsating oxygen-in-methane flame. The differences in phase show that since oxygen is richest in the inner cone of this particular flame, the chemical sequence must be  $O_2$ ,  $CH_3O$ ,  $CH_2O$ ,  $CHO$ ,  $CO$ , and  $CH_4$ . Unfortunately it is not possible to say anything concerning the existence of  $CH_4O$ , since this would have a mass equal to that of  $O_2$ . However, it is clear that methyl alcohol cannot be the parent of more than one of the above-mentioned intermediates.

By applying additional heat to the reactor the temperature coefficients of some of the intermediates were briefly studied. In this way it was possible to show the development of methyl radicals in a zone intermediate between the oxygen- and the methane-rich zones. We could find no such development when methane was replaced with propane. The formaldehyde exhibited a negative temperature

coefficient on the other hand, and since some evidence was obtained that the  $\text{HO}_2$  radical was present, these and other related results given in reference 1 tend to support theories advanced by B. Lewis and coworkers.

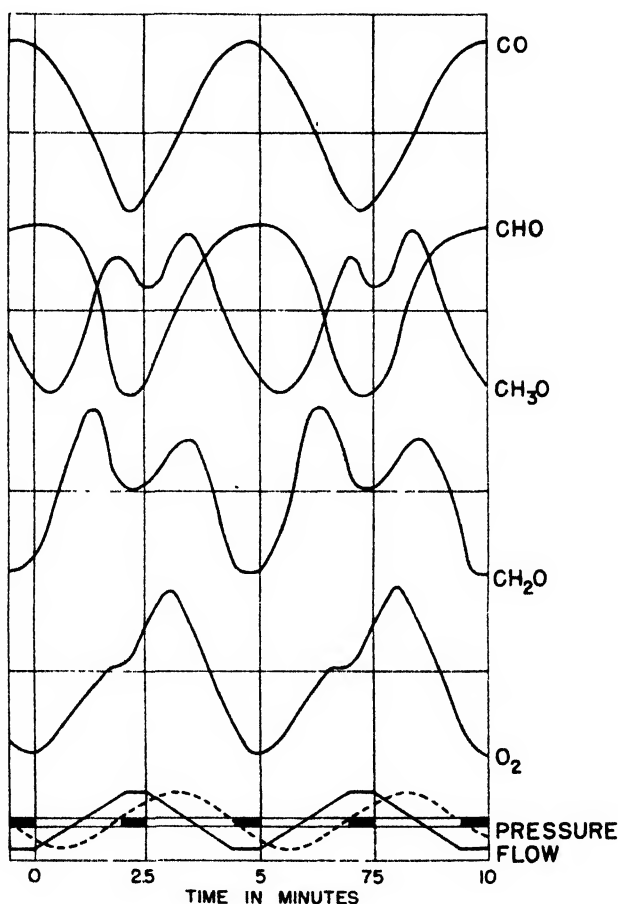


FIG. 5. Summarized phase curves for intermediates measured with a pulsating oxygen-in-methane flame. The amplitudes have been equalized to facilitate recognition of the phase relationships. The solid block marks at the base represent signals transmitted from the flow controller to a solenoid-operated pen giving phase reference points. The flow and pressure lines represent the variation of these parameters during the cycle.

In conclusion emphasis should be laid on the preliminary character of many of the results. Considerable improvements in technique are possible and these should be made before rigid conclusions can be drawn.

#### REFERENCES

- (1) ELTENTON, G. C.: *J. Chem. Phys.* **15**, 455 (1947).
- (2) KÜCHLER, L., AND THEILE, H.: *Z. physik. Chem.* **B42**, 359 (1939).

ELECTRON MICROSCOPY OF RADIATION POLYMERIZATION PRODUCTS<sup>1</sup>

JOHN H. L. WATSON

*Medical Research Institute, The Henry Ford Hospital, Detroit, Michigan**Received October 23, 1947*

The main emphasis in this work is related to the polymerization of acetylene, since this problem was of most importance to the Shawinigan Chemicals Ltd. under whose auspices it was begun. Interest was first directed toward a study of the catalytic polymer known as cuprene, and this led to an investigation of the polymers formed from acetylene under alpha-ray bombardment and corona discharge. This in turn led to preliminary work with polymers of hydrogen cyanide and cyanogen.

References for some of the observations recorded here may be found in previously published papers (1, 4). Prior to the publication of these investigations the acetylene polymer, regardless of the method of production, was always referred to as "cuprene" and was assumed to possess the same structure and to be the same substance. In electron micrographs each polymer type studied is found to be quite different from the others; therefore there seems to be reason for suggesting that for clarity in the discussion each should be referred to by a different name. The names *cuprene*, *alprene*, and *coprene* will be used for the catalytic, alpha-ray, and corona types, respectively. It is to be noted that there are, in addition, various forms of cuprene itself which are recognizably different in electron micrographs, although no attempt has been made as yet to classify them. The particular catalyst appears to be the variable factor which introduces the differences. Likewise there may be recognizably different forms of both alprene and coprene; further investigation of controlled samples will settle this point. The so-called "gunks" which occur in reaction tubes and in ionization or radiation chambers are undoubtedly polymerization products whose microphysical properties would also be worth electron-microscope examination.

Cuprene is formed chemically at about 300°C. and is a brown cork-like mass with all the characteristics of a light, dry solid. Alprene is a soft brown powder formed at normal temperature and pressure by alpha-ray bombardment. Coprene, which was available in the form of solid brittle sheets, is formed when acetylene gas is acted upon by a corona discharge.

In electron micrographs cuprene is seen to be a fibrous material. The polymerization has started upon the catalyst surface and a hollow fiber has grown from it. On the other hand, the polymerization process initiated by alpha-ray bombardment results in round particles joined one to the other in haphazard arrangement by relatively short, thick necks. The action of a corona discharge upon acetylene is to form an almost structureless film which looks the same in electron

<sup>1</sup> Presented at the Symposium on Radiation Chemistry and Photochemistry which was held at the University of Notre Dame, Notre Dame, Indiana, June 24-27, 1947.



micrographs as it appears to the eye, except of course that it is seen on a sub-microscopic scale.

The cuprene fiber has both a longitudinal and a transverse structure and is always a tube. The cross section of this tube is variable and many shapes have been observed, including ribbon-like, square, rectangular, oval, round, and even hexagonal ones. It is theorized that a combination of catalyst active-center properties and molecular dimensions determines the resultant fiber shapes. An interesting experiment, important from the point of view of understanding the catalytic mechanism, involves growing cuprene fibers on microscope specimen screens for a matter of seconds before stopping the action abruptly. In this way small, newly formed cuprene filaments can be examined. Usually each is observed to carry a small piece of heavy material near its tip. Since copper is always found in a cuprene growth even in those areas which are completely removed from the original catalyst, it is suggested that these small bodies are pieces of copper, reduced from the oxide by a hydrogen atmosphere which, carried along by the fiber, continue to catalyze the reaction. Electron-diffraction studies detect a faint presence of copper but no recognizable structure. In a recent private communication from Dr. A. Y. Mottlau of the Esso Laboratories the usual, organic three-halo pattern of grating constants of approximately 1, 3, and 2 Å. is claimed for cuprene.<sup>2</sup>

The alprene particles are rather large. Measured statistical constants are given in table 1 for a number of samples of alprene, along with those for some other polymerization products.

A number of comments are in order respecting the data for the alprene samples in this table. (1) It is seen that there is considerable variety in the data from sample to sample. (2) In all but one case (sample No. 3) very tiny particles (less than 300 m $\mu$ ) are conspicuous by their absence, *and in no case is there a continuous distribution down to the limit of resolution.* (3) The standard deviations are relatively high, averaging about 35.5 per cent of the mean diameter for these five alprene samples. (4) In sample 3 there is definite evidence in the results for the presence of a double distribution, which would account in this case for the much higher value of standard deviation.

In electron micrographs the particles of alprene appear to be perfectly round, but actually from shadow-casting experiments they are found to be flattened somewhat under their own weight as they lie on the supporting surface. In addition, they distort or flow spontaneously around holes in a supporting film and therefore have the properties of a very viscous liquid. The joining necks are 50–100 m $\mu$  in length and are not artifacts nor electron optical illusions. To demonstrate the physical presence of the necks they have been stretched, a

<sup>2</sup> *Added in proof.* Dr. Mottlau finds further that when brown cuprene is calcined in nitrogen at 700°F. the electron-diffraction pattern becomes somewhat sharper and closely approaches that normally given by acetylene black (3). This confirms the earlier claims of the author (4) that when this polymer is heated to above 300°C. a partial disintegration to carbon black occurs. Consequently it appears doubtful to assume that diffraction patterns of this material arise from the polymer alone, for it is equally possible that disintegration products contribute.

process which not only lengthens the necks but distorts the particle shapes permanently in a manner similar to that achieved by stretching tar. In electron micrographs the alprene looks very similar to normal liquid latex except for the presence of the necks, which in stereoscopic pairs give it the appearance of molecular models. This type of alprene throws no x-ray or electron diffraction pattern, a fact accounted for by its quasi-liquid nature.

It is very questionable, of course, that alprene particles can be identified absolutely with Lind's cluster-ions; at any rate many more than nineteen or twenty neutral acetylene molecules are contained in clusters the size of these particles, and from photographic contrast in the micrographs we know that all of these

TABLE I  
*Particle-size data for several radiation polymerization products*

SAMPLE	MEAN DIAMETER	STANDARD DEVIATION	APPROXIMATELY 65 PER CENT OF THE PARTICLES LIE BETWEEN
	m $\mu$	m $\mu$	m $\mu$
Alprene:			
Sample No. 1 (oxidized)	490	130	360-620
Sample No. 2 (oxidized)	740	210	530-950
Sample No. 3 (unoxidized)	380	220	160-600
Sample No. 4 (unoxidized), prepared in the presence of hydrogen	720	180	540-900
Sample No. 5 (unoxidized), prepared in the presence of krypton	500	200	300-700
Hydrogen cyanide polymer (unoxidized)	540	200	340-740
Hydrogen cyanide polymer (unoxidized), prepared in the presence of xenon	760	140	620-900
Cyanogen polymer:			
Decomposed to paracyanogen	85	50	35-135
Prepared in the presence of nitrogen	130	90	40-220
Coprene	Structure in the flakes of less than 30 Å.		

polymer particles have relatively high densities. Either the cluster-ion or the free-radical hypothesis could account for the existence of both the particles and the joining necks by consideration of a combination of polymerization and condensation mechanisms. Both would be consistent with the relatively high values of standard deviation. It is not evident immediately why there is no continuous distribution of particle sizes toward those of extremely small diameters, unless we can assume that some lack of further "seeding" occurs at some abrupt point prior to the end of particle growth.

The coprene flakes appear to have a very fine unresolvable structure such as might exist if the material were deposited originally as a fine-particle mist. From considerations of existing microscope resolution and measurements made on the micrographs, this structure is deemed to be less than 30 Å. This is a

suitable place to refer to a paper (2) which contains a discussion of the contaminating or polarizing layers deposited in electron microscopes due to electron action. It is suggested that hydrocarbon vapors unavoidably present in the instrument are polymerized and deposited under electron bombardment. The deposits in this case are again structureless films which contaminate all surfaces inside the instrument, including those of the specimen itself. It should be noted that the brown stains which always occur on metal surfaces under electron bombardment *in vacuo* are significant only to the extent that they indicate contamination by hydrocarbon polymerization. Electron microscopy of samples of electron and corona radiation polymerization products formed in controlled experiments may throw considerable light not only on some of the problems of radiation chemistry but also on the subject of contamination in electron microscopes.

One fact concerning the contamination phenomenon is particularly worth noting here. The deposition of contaminant is always greatly enhanced at or near a conducting, electrically grounded surface, indicating that the process of polymerization and deposition is electrical and that probably a negative free radical or ion is involved.

Although the polymerization mechanism for the formation of hydrogen cyanide polymer is probably similar to that for alprene, the appearance in micrographs is somewhat different. The shapes of the particles are much more variable, necessitating some choice of the particle shape in order to secure the statistical constants given in the table. Since the major portion of the material is composed of round particles, these alone are measured to give the tabled values. Some are extremely huge and are able to absorb sufficient energy from the electron beam to appear to become less viscous and oscillate like suspended liquid droplets. Often one large particle so bombarded will separate into two or three. All of the sample material is composed of smooth rounded units, a fact which indicates its semiliquid nature. There is some evidence for joining necks between the particles, but these are not as obvious as they are in alprene.

The cyanogen polymers formed under alpha-ray bombardment have a much reduced mean particle size. All of the groups seen in the micrographs appear to be aggregates of small particles of mean diameter about 130 m $\mu$ . These particles are often straight-edged, do not appear to be joined together by necks, and from their appearance are probably solid.

From the samples studied to date we may conclude: (1) that the alpha-ray polymers deposit as fairly large, definite particles whose size and shape are recognizable; (2) that the electron or corona polymers deposit as films possessing extremely fine structure; (3) that catalytically grown polymers are formed as fibers; (4) that the appearance of these fibers varies according to the catalyst used; and (5) that polymers formed from the same source substance, but polymerized in different ways, are different materials and should be notated as such.

These results are necessarily preliminary and qualitative or semiquantitative, but they may serve to increase the growing body of data which will be used to clarify our knowledge of the mechanisms of photochemical and radiation-chemical

phenomena. Possible future applications of electron microscopy in this subject may involve: (1) examination of polymerization products from controlled slow-electron reactions; (2) classification of the microphysical properties of a large number of substances polymerized by a wide variety of types of radiation; and (3) examination of the polymerization products which probably occur to "kill" Geiger-counter tubes.

#### REFERENCES

- (1) WATSON, J. H. L.: *J. Phys. Colloid Chem.* **51**, 654 (1947).
- (2) WATSON, J. H. L.: *J. Applied Phys.* **18**, 153 (1947).
- (3) WATSON, J. H. L.: The Electrochemical Society, Preprint 92-4, Autumn meeting, 1947.
- (4) WATSON, J. H. L., AND KAUFMANN, K.: *J. Applied Phys.* **17**, 996 (1946).

### BENZENE FORMATION IN THE RADIOCHEMICAL POLYMERIZATION OF ACETYLENE<sup>1</sup>

CHARLES ROSENBLUM

*Merck & Co., Inc., Rahway, New Jersey*

*Received October 23, 1947*

Throughout the discussion of the polymerization of acetylene under the influence of alpha particles, the significant fact that considerable formation of benzene occurs has been neglected. This product was first identified (11) by its absorption spectrum, and the kinetics of its formation (13, 14) studied subsequent to its identification. This observation is so important for the proper interpretation of radiochemical reaction mechanisms that the salient experimental results, and conclusions based upon them, will be reviewed. Details will be largely omitted since they have been reported fully elsewhere (11, 13, 14).

#### IDENTIFICATION OF BENZENE

The formation of benzene was demonstrated by connecting a cylindrical vessel (4.9 cm. in diameter and 50 cm. long), filled with an acetylene-radon mixture, through an appropriate arrangement of traps and stopcocks to a cylindrical absorption vessel located between a Leiss hydrogen-discharge tube and the slit of a Hilger E-1 quartz-prism spectrograph. After 7 days the acetylene-radon mixture was introduced into the absorption tube, and the absorption spectrum of the gas mixture taken in the wave-length region 230-270 m $\mu$ . The photographic plate revealed the characteristic multibanded spectrum of benzene. Comparison of this spectrum, as well as two others obtained by additional independent experiments, with that of pure benzene vapor confirmed this conclusion. Obvi-

<sup>1</sup> Presented at the Symposium on Radiation Chemistry and Photochemistry which was held at the University of Notre Dame, Notre Dame, Indiana, June 24-27, 1947.

ously a volatile product containing benzene was formed in addition to the well-known cuprene-like solid.

It was further ascertained that the volatile product consisted almost entirely of benzene. This fraction was separated as a white solid by freezing in a carbon dioxide-acetone mixture and removing the remaining acetylene-radon mixture. The freezing mixture was removed, and the condensate allowed to expand to fixed pressures into a restricted volume which included the absorption tube. Absorption spectra taken at pressures of 2.6 mm., 1.16 cm., and 2.70 cm. of mercury were compared with those produced on the same plate by a range of pressures of pure benzene vapor. Visual comparison indicated the presence of <4.5 mm., <2.5 cm., and 2.5-3.0 cm. of benzene, respectively. Furthermore, the melting point of this product was 5.3-5.7°C., and other samples obtained from later experiments melted over the range 5.3-5.6°C. The vapor pressures of the latter product over a large range of temperatures proved to be very close to that of pure benzene. In view of these observations, it is clear that benzene constitutes by far the major portion of a volatile product formed during the radiochemical polymerization of acetylene; and it was estimated that about 15-20 per cent of the reacted acetylene could be accounted for in this way. The production of benzene appeared, furthermore, to be proportional to the amount of radon decayed, indicating that benzene is formed simultaneously with the high polymer. This was confirmed in the later kinetic study.

It is not excluded that other products are likewise formed, though none was identified. Should such products be isolated, they will probably have a higher molecular weight than benzene; hence they would divert relatively even larger amounts of acetylene from the formation of solid polymer than does benzene. In subsequent kinetic considerations, however, it will be assumed that the volatile product is exclusively benzene.

It is of interest to note that benzene was also found in a glass cylinder filled with pure acetylene placed adjacent to a similar vessel containing radon. One must thus conclude that acetylene polymerizes under the influence of  $\beta$ - $\gamma$  radiation by a mechanism similar to that of the alpha-particle reaction.

#### RATE OF BENZENE FORMATION

Five experiments were performed to ascertain the rate at which benzene was formed. The apparatus consisted of a spherical reaction vessel connected through stopcocks and traps to a vacuum pump and a manometer. After successive introduction of radon and acetylene, the total pressure and amount of benzene were measured periodically. The latter determination was effected by freezing out the benzene in a separate trap adjacent to the manometer, returning the acetylene-radon mixture to the reaction vessel which was closed off, and noting the magnified pressure of the benzene. From a knowledge of the ratio of restricted volume to the total reaction volume, the partial pressure of benzene in the reaction system was calculated. After each measurement, the benzene was returned to the main vessel and the reaction allowed to continue.

One typical set of data is presented in table 1. In this run, 38 millicuries of

radon was mixed with acetylene at a pressure of 627.2 mm. in a vessel having a volume of 573 ml. and a radius of 5.15 cm. Columns 1 and 3 show, respectively, the total gas pressure and the partial pressure of benzene at each interval; and the difference is the partial pressure of acetylene recorded in the fifth column. Column headings  $e_{\text{total}}^{-\lambda T}$  and  $e_{\text{C}_6\text{H}_6}^{-\lambda T}$  represent the fraction of radon remaining at the time that respective pressures were measured; they correspond roughly to time lapses of 1, 2, 3, 5, 8, and 14 days. The fraction of acetylene which reacts to form benzene, computed as  $\frac{3P_{\text{C}_6\text{H}_6}}{-\Delta P_{\text{C}_2\text{H}_2}}$ , is given in column 6.

It is clear from these typical results, and substantiated by other experiments (13, 14), that 20 per cent of the reacting acetylene is converted initially to benzene, and that the extent of this conversion appears to drop gradually as the polymerization progresses. Had this fraction remained constant throughout

TABLE I  
*Data on radon-sensitized reaction in acetylene*

(1)	(2)	(3)	(4)	(5)	(6)	(7)	(8)
$P_{\text{total}}$	$e_{\text{total}}^{-\lambda T}$	$P_{\text{C}_6\text{H}_6}$	$e_{\text{C}_6\text{H}_6}^{-\lambda T}$	$P_{\text{C}_2\text{H}_2}$	FRACTION OF $\text{C}_2\text{H}_2 \rightarrow \text{C}_6\text{H}_6$	$P_{\text{C}_6\text{H}_6}$ (CALCULATED)	Secondary $\text{C}_6\text{H}_6$ reaction
mm. Hg		mm. Hg		mm. Hg		$-\Delta P_{\text{C}_2\text{H}_2}/15$	mm. Hg
627.2	1.000		1.000	627.2			
595.3	0.853	2.29	0.850	593.0	0.201	2.28	2.26
568.2	0.691	3.88	0.688	564.3	0.185	4.19	4.12
545.4	0.555	5.60	0.558	539.8	0.192	5.83	5.58
516.6	0.408	6.92	0.406	509.7	0.176	7.83	6.93
486.5	0.240	7.93	0.239	478.6	0.160	9.91	8.46
457.7	0.0804	9.48	0.080	448.2	0.159	11.93	9.58

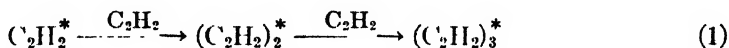
the reported run, the benzene partial pressures would have had the values listed in column 7, which are computed as  $-\Delta P_{\text{C}_2\text{H}_2}/15$  from the decrease in acetylene pressure. The benzene deficiency is attributed to a secondary radiochemical reaction of benzene which is known to occur (9, 13, 14). The velocity of this reaction (13, 14) is insufficient in itself to account completely for the small benzene deficiency. It is necessary to assume a "catalytic effect" of the large excess of acetylene similar to that of inert gases (5, 12). In column 8 are listed the benzene pressures to be expected if the fraction of acetylene reacting to form benzene remains constant at 20 per cent and the secondary benzene reaction proceeds at an enhanced rate. The belief that the small drop in benzene yield is due to a secondary reaction is supported by acetylene polymerization experiments (13, 14) in the presence of added benzene and using 93 millicuries of radon. In both cases, the initial yield is equivalent to less than 20 per cent, indicating an increased velocity of the secondary reaction. In view of the above considerations, it appears safe to assume that the benzene is formed simultaneously with the high-polymeric product and is not an intermediate product. It is probable

that the benzene was missed by earlier workers (4, 12) because of the fifty- to hundred-fold higher radiation intensity employed, which accelerated the secondary polymerization of benzene. A report (10) that the weight in air of the cuprene-like solid produced was equal to the weight of reacted acetylene is vitiated by the known capacity of the polymer to absorb large quantities of oxygen (6).

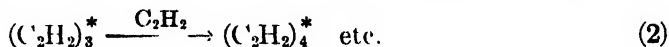
#### DISCUSSION

The over-all  $M/N$  calculated from the data in table 1 is  $21 \pm 2$ . Admitting that one-fifth of the reacting acetylene produces benzene, one must conclude that the interpretation of the ion yield as a cluster of 21 acetylene molecules is untenable. It would be necessary to have not a single cluster type but at least two sizes<sup>2</sup> of clusters, of 3 and  $\approx 18$  acetylene molecules, to account for a net  $M/N = 21$  in which benzene formation is involved. This would require furthermore that about 1.5 trimer clusters be formed for each large cluster, a requirement which is entirely at variance with the cluster mechanism. The picture is still further complicated, to the detriment of the cluster theory, by the likelihood that other products are formed, even if produced in small quantities. Finally, the  $M/N$  for benzene formation, in terms of reacting acetylene molecules, is  $\approx 0.2 \times 21$  or  $\approx 4.2$ , not 3, as anticipated by a cluster explanation. In any case, even the value of 4.2 is an arbitrary yield at best, since only ions are considered as initiating reaction, radicals and molecules being neglected.

The writer prefers to explain the radiochemical polymerization of acetylene without benefit of clusters or ions, because of its striking similarity to the photochemical (2, 3, 7) reaction. The radiochemical reaction is regarded as proceeding by means of successive bimolecular reactions (8) between a normal acetylene molecule and an excited molecule or polymer. The mechanism may be represented by



where  $C_2H_2^*$  is an excited acetylene molecule or radical, and  $(C_2H_2)_2^*$  and  $((C_2H_2)_3)^*$  stand for excited polymers presumed to be linear in character. At the trimer stage two reactions may occur: further polymerization as in the reaction



and cyclization to form benzene



Reaction 3 is possible thermochemically, since the heat of formation of benzene vapor from acetylene is  $\approx 143$  kg.-cal., while the heat of formation of a linear

<sup>2</sup> At the Symposium and in an earlier publication (13) the  $M/N$  was considered as an average yield. This leads to a high polymer cluster of 26 instead of 18, and a frequency ratio of 2:1 instead of 1.5:1. The  $M/N$  more properly represents a sum of yields, and was so treated in the above calculation.

trimer from acetylene is  $\approx 138$  kg.-cal., taking the heat of formation (1) per  $\text{—C}\equiv\text{CH—}$  group as 46 kg.-cal. Accordingly the rearrangement of the trimer is exothermic by but 5 kg.-cal., a value which is probably small compared to the energy of the excited trimer. This total energy may be dissipated as heat; or it may be transferred to a normal acetylene molecule by collision either with an excited benzene molecule after reaction 3 has occurred, or with an excited trimer at the time of cyclization. Such a collision is not indispensable, however, since benzene can absorb about 130 kg.-cal. before undergoing decomposition.

The mechanism by which reaction 2, for formation of high polymer, is terminated cannot be specified. It is possible that here too cyclization occurs, with the ultimate dissipation of excitation energy as heat.

#### SUMMARY

1. Benzene has been identified as a major product in the radiochemical polymerization of acetylene, and appears to be produced simultaneously with the cuprene-like polymer. Approximately one-fifth of the reacting acetylene is utilized for benzene formation.

2. These observations are incompatible with the ion-cluster theory of radiochemical reactions.

3. A mechanism based on a sequence of bimolecular reactions between a normal acetylene molecule and an excited molecule or polymer is proposed. It is suggested that benzene formation results from the cyclization of a linear trimer.

#### REFERENCES

- (1) FLORY, P. J.: *J. Am. Chem. Soc.* **59**, 1149 (1937).
- (2) KATO, S.: *Bull. Inst. Phys.-Chem. Research (Tokyo)* **10**, 343 (1931).
- (3) KEMULA, W., AND MRAZEK, S.: *Z. physik. Chem.* **23B**, 358 (1933).
- (4) LIND, S. C., BARDWELL, D. C., AND PERRY, J. H.: *J. Am. Chem. Soc.* **48**, 1556 (1926).
- (5) LIND, S. C., AND BARDWELL, D. C.: *J. Am. Chem. Soc.* **48**, 1575 (1926).
- (6) LIND, S. C., AND SCHIFFLETT, C. H.: *J. Am. Chem. Soc.* **59**, 411 (1937).
- (7) LIVINGSTON, R., AND SCHIFFLETT, C. H.: *J. Phys. Chem.* **38**, 377 (1934).
- (8) MELVILLE, H. W.: *Trans. Faraday Soc.* **32**, 258 (1936).
- (9) MUND, W., AND BOGAERT, E.: *Bull. soc. chim. Belg.* **34**, 410 (1925).
- (10) MUND, W., AND KOCH, W.: *Bull. soc. chim. Belg.* **34**, 241 (1925).
- (11) MUND, W., AND ROSENBLUM, C.: *J. Phys. Chem.* **41**, 469 (1937).
- (12) ROSENBLUM, C.: *J. Phys. Chem.* **38**, 683 (1934).
- (13) ROSENBLUM, C.: *Bull. soc. chim. Belg.* **46**, 503 (1937).
- (14) ROSENBLUM, C.: *J. Phys. Chem.* **41**, 651 (1937).



RADIATION CHEMISTRY OF AQUEOUS SOLUTIONS<sup>1</sup>

A. O. ALLEN

*Clinton Laboratories, Oak Ridge, Tennessee**Received October 23, 1947*

## I. INTRODUCTION

The decomposition of water by alpha rays was first studied about 1905, and is thus one of the oldest radiation-chemical reactions. Subsequent work by Duane and Scheuer (3), by Nurnberger (8), and by Lanning and Lind (6) established that the water decomposes smoothly under alpha bombardment into hydrogen and oxygen gases, with some of the oxygen, however, remaining combined with the water as hydrogen peroxide. The yield of the decomposition was equal approximately to 2 molecules of hydrogen formed per 100 e.v. of radiation energy absorbed by the solution. The reaction seemed to be a typical example of radiation decomposition of a simple molecule, and to exhibit no particularly complex features.

In 1929, however, Risse (9) announced that under irradiation by x-rays pure water would not decompose at all. He showed that the formation of peroxide in x-ray irradiated water came from combination of dissolved oxygen gas from the air with water and that, if no air or other impurity was present, nothing happened to the water. This observation was confirmed by the careful studies of Hugo Fricke and collaborators (5), who measured the gas produced from the water, as well as the hydrogen peroxide. Small quantities of gas were indeed found, but the gas consisted of hydrogen and carbon dioxide, rather than hydrogen and oxygen, and must have arisen from the decomposition of organic impurities present in the water. By careful purification from organic matter, the gas yield was decreased but never dropped to zero. Fricke concluded that the best way to purify water completely is to irradiate it with x-rays.

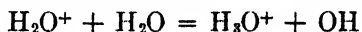
Aqueous solutions, however, are profoundly affected by x-rays; inorganic solutes are oxidized or reduced, and dissolved organic compounds decompose with evolution of hydrogen and sometimes of carbon dioxide. The total amount of solute reacting for any given total quantity of energy absorbed by the solution is of the order expected for the decomposition of pure compounds—i.e., around 1 molecule reacting per 100 e.v. absorbed. Evidently, all or a large part of the chemical activation obtained in the water is transferred in some way to the solute molecules. The radiation activates the water to an energy-rich form which has sufficient lifetime to meet and react with the molecules of a solute before its energy is dissipated, even when the solution is very dilute. The extensive and careful work of Hugo Fricke in this field laid the groundwork for

<sup>1</sup> Presented at the Symposium on Radiation Chemistry and Photochemistry which was held at the University of Notre Dame, Notre Dame, Indiana, June 24-27, 1947

Based on work performed under Contract No. W-35-058-Eng 71 for the Atomic Energy Project at the Clinton laboratories.

our understanding of the radiation chemistry of solutions and of biological systems, and was in every respect a model of penetrating experimental research.

The activated water is now generally believed to consist of free radicals, H and OH, formed by decomposition of the water molecules under irradiation. No other sort of active water species would have sufficient lifetime in a liquid environment to be able to react with highly dispersed solute molecules with high efficiency. Besides, the formation of these radicals appears to follow necessarily the process of simple ionization in liquid water. Free electrons will react with water to produce hydrogen atoms and hydroxide ions, as is well known from the facts of electrolysis. The positive residue,  $\text{H}_2\text{O}^+$ , can react with water to produce OH radicals:



Because of the high solvation energy of the proton, this reaction is several volts exothermic. It would not be expected to possess much, if any, activation energy, and probably occurs almost immediately after the ionization process. The first result of the ionization of water is therefore believed to be the formation of H and OH radicals, located at a distance from one another.

Radiation produces excitation of molecules as well as ionization, and some of the excited molecules in water might be expected to decompose into H and OH before being deactivated by collision. Radicals formed in this way might be expected often to undergo initial recombination as a result of the "cage effect," but some of them may be able to get out of the cage, as Dainton (2) has pointed out. The radicals, therefore, largely arise from ionization of the water molecules with, perhaps, a further contribution of unknown magnitude from electronically excited water.

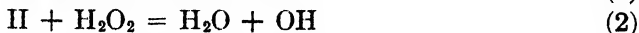
In the following discussion recombination of radicals (in or out of the cage) refers to the union of H and OH radicals to yield water; combination of radicals refers to reactions which do not yield water (e.g.,  $2\text{OH} \rightarrow \text{H}_2\text{O}_2$ ); back-reaction refers to any reaction which causes ultimate conversion of products to water (e.g.,  $\text{OH} + \text{H}_2 \rightarrow \text{H}_2\text{O} + \text{H}$ ).

## II. BACK-REACTION IN THE DECOMPOSITION OF WATER

In the absence of any solute with which they can react, the free radicals formed by the decomposition of water will disappear by reaction with one another. If an OH radical reacts with an H atom one simply gets water molecules back again, but if an H reacts with another H or an OH with another OH, the new molecules  $\text{H}_2$  and  $\text{H}_2\text{O}_2$  will be produced. The question now remains as to why the hydrogen and peroxide are not found in appreciable quantities on irradiation of pure water with x-rays, but are very much in evidence when alpha particles are used.

The answer lies in the existence of a back-reaction between the products of the decomposition to re-form water under the radiation. The products, hydrogen and hydrogen peroxide, insofar as they stay dissolved in the water, will be able to react with the free radicals H and OH formed by the decomposition of

further water molecules. They will behave like any other oxidizable or reducible solutes. The result will be destruction of the products with the formation of water. The most probable equations are:



This mechanism supposes that hydrogen peroxide is the primary decomposition product, with oxygen gas arising as a secondary product from peroxide decomposition. Data obtained on the Atomic Energy Project have shown that, with either fast electrons from a Van de Graaff machine or radiation from a chain-reacting pile, one gets only hydrogen peroxide from water on very short exposures; oxygen appears only on longer exposures, and is clearly a secondary product.

The apparent lack of reactivity of pure water when irradiated by x-rays might then be ascribed to a steady-state concentration of products so low as to be undetectable by the methods used for analysis. This explanation was verified by some experiments by J. A. Ghormley and myself (1). We were able to show that, on irradiation with 1 m.e.v. electrons or x-rays from a Van de Graaff generator, a steady state of hydrogen and peroxide concentration is reached at levels of the order of a few micromoles per liter, corresponding to a few millimeters pressure of hydrogen gas over the water. The steady-state concentrations increased with increasing intensity of radiation. The difference between the alpha-ray and x-ray effect on water is, therefore, to be traced to a difference in the steady-state concentrations of the products characteristic of the two types of radiation.

The steady-state concentration for alpha particles has not been determined, but it is known that the rate of evolution of hydrogen remains undiminished up to pressures of hydrogen of several hundred millimeters. The pressure of hydrogen at the steady state for alpha particles must then lie at pressures well above atmospheric.

In the course of work on the Atomic Energy Project, we have had occasion to irradiate water with various other types of radiation. With deuteron beams from a cyclotron, the initial yield for the decomposition of water was about 0.54 molecule decomposed per 100 e.v. absorbed (E. Shapiro); but when 1 atm. of electrolytic gas was maintained over the water, the yield was less than 0.1 (A. Krueger). Such reduction in rate at a pressure of 1 atm. suggests that with this radiation a steady state would be obtained at pressures not very far above atmospheric.

Mr. Ghormley and I are currently studying the decomposition of water in which much of the hydrogen is replaced by its radioactive isotope tritium. The average energy of the  $\beta$ -ray from tritium is only about 5000 e.v., so that the velocities of the electrons, and therefore their ionizing characteristics, are closer to those of cyclotron deuterons than to those of fast electrons. The experiments are complicated by the disappearance of hydrogen from the water by its decay to helium, with corresponding release of excess oxygen. Results so far are highly preliminary, but appear to indicate steady-state pressures of around 10–20 cm.

of hydrogen gas over the water. This is considerably higher than was found with 1-m.e.v. electrons.

The value of the steady-state pressure appears to be correlated with the density of energy release along the track of the charged particle which is responsible for the decomposition. Fast electrons, such as those generated in the water by the absorption of hard x-rays, have the lowest density of energy loss along their track and give the lowest steady state; the tritium betas and the cyclotron deuterons have a higher density of energy release and give a higher steady state; the alpha particle is still more intensely ionizing and probably gives a still higher steady state.

Results on steady-state hydrogen pressures and initial yields of hydrogen evolution from water by various kinds of radiation are summarized in table 1.

TABLE 1  
*Decomposition of water by various types of radiation*

RADIATION		AVERAGE DENSITY OF ENERGY LOSS, $E/R$	INITIAL DECOM- POSITION YIELD (HYDROGEN PER 100 E.V. ABSORBED)	STEADY-STATE PRESSURE OF HYDROGEN
Type	Energy			
	<i>k.e.v.</i>	<i>k.e.v./cm air</i>	<i>molecules</i>	
Electrons	1000	3	0.2-0.5	1-2 cm.
Electrons (tritium betas)	5	70	0.1-0.4	10-20 cm.
Deuterons	8000	175	0.54	60 cm or more
Alpha rays	5000	1430	2.0	Well over 1 atm
Pile radiation (fast neutrons mixed with gamma rays)			~1	30-100 cm.

A column is included of approximate values of the average density of energy release of each type of radiation, as given by the energy of the radiation divided by its total range in centimeters of air at N.T.P.

### III. EFFECT OF SOLUTES ON THE STEADY STATE

We are currently engaged at the Clinton Laboratories in studying the steady-state levels of decomposition products which can be obtained in water by various types of radiation. One fact which seems to be emerging from our work is that almost anything dissolved in the water has the effect of increasing the amount of decomposition which can be obtained. Some solutes are oxidized or reduced by radiation, but those which are apparently not affected still can increase the steady-state pressure of hydrogen and oxygen over the solution from what it would be if the water were pure. The best-known example is the effect of bromide or iodide ions on the decomposition of water by x-rays or fast electrons. Fricke found that irradiation of dilute solutions of potassium bromide or potassium iodide would not produce iodine or bromine as one might expect, but instead resulted in the formation of hydrogen and hydrogen peroxide. Work by J. A. Ghormley and myself at the Metallurgical Laboratory of the University of Chicago, using fast electrons as a source of radiation, showed (1) that the bromide

effect was due to an increase by the bromide ions of the steady-state concentration of hydrogen and peroxide (or oxygen); a steady pressure of 40 cm. of electrolytic gas was reached over  $4 \times 10^{-6}$  *M* potassium bromide solution. Hydrochloric acid and nitric acid were found to exert similar effects with the fast electrons at concentrations of 0.01 *N*; sulfuric and phosphoric acids at the same concentration did not increase the steady state very much, if at all, beyond the level obtained with pure water. Pure water which had stood in a sealed Pyrex vessel for some time gave a much higher steady state than given in a freshly filled vessel, a result which seems to indicate that dissolved Pyrex glass increases the steady-state level.

At the Clinton Laboratories we have been studying the effect on water of radiation from the chain-reacting pile. This is a mixed radiation consisting of fast neutrons and gamma rays. Steady states seem to be obtained at hydrogen pressures of the order of 30–100 cm., but the results are extremely irreproducible, probably because of the influence of dissolved or colloidal material coming from the walls of the fused silica containers used. Addition of 1 *N* sulfuric acid or 1 *M* potassium chloride to the water gives reproducible results, but the pressure, instead of leveling off at 1 or 2 atm., continues to rise and is still going up at pressures of several dozen atmospheres. In all cases thus far established, the solutes have the effect of increasing the steady-state level of decomposition products, although it is conceivable that some solute might be found which would lower it. The concentration required to produce a given increase of the steady state varies considerably with different solutes. Bromide and iodide ions and dissolved glass are effective at very low concentrations, while sulfuric acid and potassium chloride require considerably higher concentrations. We ascribe these effects to an inhibition of the back-reaction by the dissolved substances.

#### IV. PROBABLE CHAIN CHARACTER OF THE BACK-REACTION

Equations 1 and 2 above imply that the back-reaction is a chain reaction. It is, in fact, analogous in every respect to the well-known chain reaction between hydrogen and chlorine in the gas phase to form hydrogen chloride. Here the place of the Cl atom is taken by the OH radical, which would be expected to have a very similar chemistry, and  $\text{H}_2\text{O}_2$  takes the part of  $\text{Cl}_2$ . The irreproducibility of the results on water decomposition, and the sensitivity to traces of certain types of impurities, are characteristic of chain reactions carried by free radicals or atoms. The impurities act by reacting with the chain-carrying radicals to form bodies which are incapable of carrying on the chain. Thus the dissolved glass probably reacts with OH radicals to form some sort of persilicic acid radical which is incapable of reacting with hydrogen molecules; the back-reaction chain is thereby interrupted by a very small concentration of dissolved glass, and the steady-state level of products in the water is increased.

The reaction mechanism is particularly clear in the case of 0.01 *N* nitric acid solution, irradiated at the Metallurgical Laboratory by high-energy electrons. Here it was found that in very short irradiations hydrogen constituted almost all of the gas produced; after the irradiation was stopped, however, oxygen continued

to come out of the solution by a first-order thermal reaction with a half-life of about 7 min., and when this reaction was complete the gas contained exactly one-third oxygen, so that the net reaction was decomposition of water. Here the oxidizing radicals were evidently tied up with the nitric acid to form some sort of pernitric acid which was thermally unstable, but unlike hydrogen peroxide would not react very readily with hydrogen under irradiation. Hydrogen gas, therefore, continued to come off to much higher pressures than would have been obtained with pure water; the oxygen was evolved later by thermal decomposition of the pernitric acid. For long irradiations a steady state was attained, and this gas probably consisted mostly of hydrogen. The thermal decomposition of the pernitric acid, of course, takes place whether the radiation is present or not; the oxygen evolved from it combines with hydrogen under the action of the radiation, and the steady state is achieved when the rate of oxygen formation by pernitric acid decomposition balances the rate of oxygen consumption by reaction with hydrogen under radiation. The steady-state pressure, therefore, depends both on the radiation intensity and on the volume of gas phase available over the liquid, since both of these factors affect the rate of change of concentration of hydrogen dissolved in the liquid. The pernitric acid molecule is apparently much less susceptible to attack by hydrogen atoms or other reducing free radicals than the oxygen or the hydrogen peroxide molecule. Nitric acid solution thus offers a particularly clear-cut case, because the existence of the complex between the oxidizing free radical and the solute is demonstrated by its thermal decomposition after the irradiation is stopped. With sulfuric acid or dissolved glass the existence of the complex is not so readily demonstrated, but it seems reasonable to assume that similar mechanisms are operating here for inhibition of the back-reaction.

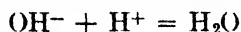
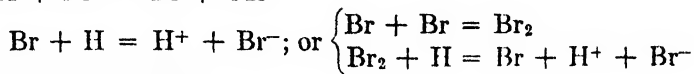
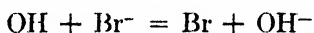
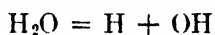
#### V. THE PROPORTION OF RADICALS AVAILABLE FOR REACTION WITH SOLUTES

Before discussing solution phenomena further, it may be well to consider more closely the differences between the effects of different kinds of radiation on pure water. Fast electrons excite or ionize only 1 per cent or less of the molecules which they traverse, so that the distribution of radicals initially formed in water by such radiation is almost uniform. More heavily ionizing radiations, such as slow electrons and alpha or other heavy particles, have a very much greater probability of producing ionization when they traverse a molecule; with such radiation the radicals will, therefore, be formed initially in high concentration within a narrow zone located along the track of the particle. Many of these radicals will recombine with one another before they have a chance to get out into the main body of the solution and react with dissolved substances. Only the fraction of radicals that get out will be available for initiation of back-reaction chains. Those that do not get out will produce a certain yield of hydrogen and hydrogen peroxide. The fraction that gets out cannot be unity even in the case of fast-electron irradiation, because the fast electrons will eventually be slowed down, and as slow electrons at the end of their trajectories they will produce dense ionization similar to that produced by alpha rays. These little regions of dense

ionization (hot spots) will provide a continuing source of hydrogen and hydrogen peroxide, when a solution is irradiated with hard x-rays or fast electrons, regardless of what happens to the majority of the free radicals which are available for reaction with solutes. The steady-state decomposition levels are, of course, directly related to the fraction of radicals which combine within the hot spots. The larger the fraction of radicals which do not get out of the hot spots, the higher the concentration of decomposition products must be for the rate of back-reaction to balance the rate of forward reaction. The steady-state decomposition level of pure water, therefore, provides a measure of the fraction of total radicals which do not get out of the hot spots. In considering the reactions in irradiated aqueous solutions, it is important to remember that this fraction, though small, is not equal to zero, and that a continuing production of water decomposition products is to be expected in any solution irradiated.

#### VI. OXIDATION AND REDUCTION OF SOLUTES AND DECOMPOSITION OF WATER IN SOLUTIONS

The mechanism whereby bromide or iodide ion increases the steady-state concentration of decomposition products in water irradiated by hard x-rays probably typifies the behavior of many oxidizable or reducible solutes. Bromide or iodide ions undoubtedly react with the free OH radicals to give hydroxide ions and free halogen atoms. The free halogen atoms, unlike OH radicals, cannot react with molecular hydrogen, so that the back-reaction is interrupted. The halogen atoms will eventually react with hydrogen atoms (possibly first combining to halogen molecules) and will thus be reduced back to halide ions. Thus the net effect of the whole process is to cause radicals to disappear with the formation of hydrogen ions and hydroxide ions—that is, of water. In the form of chemical equations:



The sum of these processes is zero, indicating no net reaction.

Since hydrogen and hydrogen peroxide continue to be formed at a considerable rate, they must be produced in some other way than by interaction of radicals. As indicated above, the source of these products is probably the small regions of high ionization density (comparable to the ionization density of alpha rays) which lie at the end of each electron track (including, of course, secondary and tertiary electrons). Radicals formed in these little regions will react with one another to produce a certain yield of reaction products before they have a chance to get out into the solution and suffer reaction with the bromide ions or bromine atoms.

Since oxidizing agents in water are reduced by radiation and reducing agents

are oxidized, prolonged irradiation should bring the concentrations of reduced and oxidized forms of any dissolved material to a certain ratio. This ratio should depend upon the redox potential of the couple involved, the type of radiation, the concentration of hydrogen peroxide in the solution, etc. When this steady state is reached with respect to the solutes, however, hydrogen and hydrogen peroxide or oxygen should still be evolved from the solution, since the radicals which would otherwise cause back-reaction will be used up in reaction with the oxidizing and reducing agents in the solution. The gases should continue to come off, unless they are confined and the pressure built up until the concentrations of the dissolved gases become so high that they can effectively compete with the other solutes for reaction with the free radicals. The sensitization of water decomposition by bromide and iodide solutions is on this view simply one example of what is probably a very general effect; it is unusual only in that the steady state for the bromine-bromide couple lies so far toward the bromide side that the oxidized form is present at an undetectably low concentration.

An alternative mechanism for the continuing production of hydrogen peroxide and hydrogen in solutions of potassium bromide was proposed by Dainton (2). He supposed that bromine atoms in solution react not only with the free hydrogen atoms to form bromide ions, but also with hydroxyl radicals to form HOBr. The HOBr could then be supposed to react further with other OH radicals to form hydrogen peroxide. Using up OH radicals in this way would set free an equivalent amount of hydrogen atoms which would have no other course than to recombine with one another to form  $H_2$ . This mechanism is certainly possible, but I believe that its introduction is unnecessary. The conclusion that continuing production of decomposition products of water must be occurring as a result of slow-electron effects appears to be inevitable and, in the existing state of the experimental data, no further hypothesis is needed to explain the bromide effect. The hot-spot hypothesis predicts that hydrogen and peroxide evolution should occur at the same rate in all solutions of active oxidizing or reducing agents, after a constant ratio of the concentrations of the oxidized and reduced forms is obtained. There are no experimental data on this point, and studies on long-time irradiations of various solutions would clearly be highly desirable. In the case of bromide solutions, the two theories proposed give different predictions regarding the kinetics of the reaction as affected by the type of radiation, the bromide concentration, etc., and an extensive kinetic study of the reaction would be of interest.

The continuing production of peroxide and hydrogen in irradiated solutions, regardless of other processes occurring, which is here postulated, must be of considerable importance in the irradiation of solutions of organic compounds. The hydrogen and the peroxide must always compete with other solutes present for reaction with the free radicals. The interpretations given by Lea (7), Weiss (10), and others, in terms of simple free-radical mechanisms, of the kinetics of radiation-induced reactions in complicated organic systems are no doubt too simple. I believe a much more thorough study of the kinetics of radiation effects in simple solutions, such as potassium bromide, sodium nitrite, etc., must be made before



we have a proper background for understanding the behavior of more complicated systems.

#### VII. RATES OF HYDROGEN EVOLUTION, AND EFFECTS OF SIZE OF GAS VOLUME

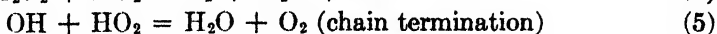
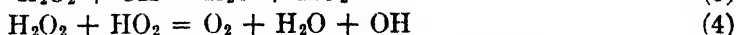
Decomposition studies obviously include not only determinations of the steady-state concentration of hydrogen, but also of the rate at which the hydrogen initially comes off, and the way in which this rate decreases with increasing product concentration before the steady state is finally obtained. Well-established initial yield values have been published for various solutions with x-rays, and for water with alpha rays. Expressed as molecules of hydrogen formed per 100 e.v. absorbed, the yield, according to Fricke, is the same (0.57) for x-ray irradiation of solutions of  $\text{Br}^-$ ,  $\text{I}^-$ ,  $\text{NO}_2^-$ ,  $\text{SeO}_3^{--}$ ,  $\text{AsO}_3^{--}$ , and  $\text{Fe}(\text{CN})_6^{--}$ , but much higher (up to 4) for solutions of  $\text{Fe}^{++}$ . For alpha rays on water, the value is close to 2.0. For cyclotron deuterons on water, the initial yield was 0.54, while the current work on tritium betas appears to indicate a still lower value of about 0.1–0.4. In the decomposition of pure water by fast electrons, the initial curvature of the pressure-dose plot was so great, because of the low steady-state pressure, that no good estimate could be made of the initial yield, although it appeared to be in the range of 0.2–0.5 (see table 1).

A variety of initial yields from pure water exposed to different radiations seems, at first sight, incompatible with the free-radical theory. The energy required to produce a certain amount of ionization is well known to be nearly independent of the type of radiation. The yield of free radicals should, therefore, be nearly the same in all cases. At the beginning of an irradiation, with no dissolved decomposition product or other substance present to react with the radicals, all the radicals must react with one another to give either  $\text{H}_2\text{O}$  back again or  $\text{H}_2$  and  $\text{H}_2\text{O}_2$ . The probability of like or unlike radicals reacting might be the same, whether the radicals react in the zone of high concentration or outside in the main body of the solution. The initial yield of products should then be the same regardless of the type of radiation.

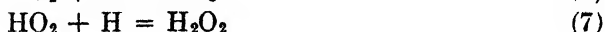
It may be that this is actually so, and that the initial yield is actually 2.0 for all kinds of radiation. With less densely ionizing radiations than alpha particles (deuterons, electrons), the yield may always be reduced so fast by back-reaction of the first portion of product formed that the true initial slope cannot be seen. If this is the case, the great initial curvature of the plot of hydrogen evolution *vs.* dosage must be supposed to decrease rapidly and give way to a curve of relatively constant slope, which curves over toward the steady state much more slowly.

We have observed such behavior at later stages for curves representing as a function of time the decomposition of 1 *N* sulfuric acid solution under pile radiation, and (impure) water under tritium betas; the curve, which initially bends over and appears to be approaching the steady state, stops bending and continues to rise almost linearly. Such behavior could not be obtained if products are disappearing by a simple chain reaction, while the chains are terminated by bimolecular reactions of radicals; such a mechanism leads to a smooth exponential

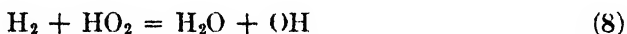
curve. The "breaks" in the slope of the curve must indicate the setting in of another mechanism, with the nature of the radicals being altered. One possible cause of this change is not hard to find; it lies in the reactions which lead to the decomposition of hydrogen peroxide, the primary product, to oxygen. This decomposition is known to have a very high yield with x-rays (4, 9) and is a chain; the chief mechanism probably is:



Oxygen in its turn is known to be reduced to peroxide under radiation; this must occur in two steps:



As soon as the concentration of peroxide in the water has become appreciable, the radical  $\text{HO}_2$  must begin to play a part in the reactions. It will be seen that equations 3 and 7 involve an oxidation-reduction couple, which will lead to the suppression of reactions of H and OH in the same way that the  $\text{Br}-\text{Br}^-$  couple does; in this case,  $\text{H}_2\text{O}_2$  is the reducing agent of the couple,  $\text{HO}_2$  the oxidizing agent. Reactions 5 and 6 constitute another such couple, with  $\text{HO}_2$  in this case being the reducing agent and  $\text{O}_2$  the oxidizing agent. These reactions would stop the back-reaction, as the bromide couple does, if the radical  $\text{HO}_2$  could not carry on the reaction chain. It may be, however, that  $\text{HO}_2$  can react with hydrogen, though perhaps rather sluggishly, to carry on the chain to some extent:



Insofar as reaction 8 occurs, accumulation of  $\text{H}_2\text{O}_2$  and  $\text{O}_2$  will not lead to complete suppression of the back-reaction chain.

In any event, peroxide competes with hydrogen for reaction with the OH radicals, and the net yield of water decomposition at any time must depend on the relative concentrations of  $\text{H}_2$ ,  $\text{H}_2\text{O}_2$ , and  $\text{O}_2$  in solution, as well as on the absolute concentration of  $\text{H}_2$ . It follows that the curve of yield *vs.* concentration of dissolved hydrogen will depend on the relative volumes of gas and liquid present in the system, since a large gas volume will allow most of the hydrogen to escape, while the peroxide will remain behind in solution. The concentration of hydrogen at the steady state, and therefore the pressure of gas over the water, will accordingly depend on the gas-to-liquid volume ratio; the larger the relative gas space, the higher the steady-state pressure, since large gas space favors excess peroxide, which inhibits back-reaction. The steady-state pressure over water by a given radiation should thus not be a characteristic constant, but should vary with the available volume.

Our studies of water decomposition under pile radiation suggest such an effect. Pressures of hydrogen over the water after long irradiations are higher when the gas volume in the sealed exposure tubes is comparable to the volume

of water than when the gas volume is small or zero. (Of course, the opposite is true for short irradiations, since the larger the gas volume the greater the total amount of decomposition needed to obtain any given pressure.) These results are not too convincing because of irreproducibility. There are no data available for other types of radiation to test this effect.

The system containing water, hydrogen peroxide, hydrogen, oxygen, and free radicals is obviously of great kinetic complexity. Studies of yields of water decomposition and formation in systems in which the concentrations of hydrogen, oxygen, and peroxide are independently varied, by various types of radiation at different intensities and temperatures, should, however, prove sufficient to unravel the puzzle. The great difficulty we find is to avoid extraneous contamination of the water.

Returning to the question of the initial yields for water decomposition by different kinds of radiation, there is another explanation which would allow the observed differences in initial rates to be real. It has been suggested that activation energy may be required for the combination of two OH radicals to  $\text{H}_2\text{O}_2$ , because of the dipole repulsion between the radicals when they approach in the proper configuration to combine. No activation energy would be anticipated for the reaction of H with H or with OH. Now it is clear that if the combination of OH's is slow while that of H's is fast, the OH radicals will immediately assume a much higher concentration than the H, and nearly all H formed will, consequently, combine with OH rather than with another H. Thus the main reaction will simply be recombination of unlike radicals to water, and the yield of  $\text{H}_2$  and  $\text{H}_2\text{O}_2$  will be very small. The kinetics are simple, and it is readily calculated that at room temperature an activation energy of 5500 cal. for combination of OH radicals will lead to 98 per cent recombination of H and OH to water. Now in the zones of high radical concentration, the freshly formed OH radicals will be in an excited state, and the local effective temperature of the water and everything else in the hot spots will be high because of the great local energy release. This high temperature will cause the reaction rates of OH with H or with another OH to become more nearly equal, so that in the hot spots formation of peroxide and hydrogen can occur with a relatively good yield. On this view, radicals getting out of the high concentration zone do not contribute to the initial yield, and affect the results only by causing back-reactions. Thus the initial yield should be a direct measure of the amount of continuing decomposition yield found when the back-reaction is completely inhibited by oxidizing or reducing agents such as bromide. At present we do not have enough data to decide between this theory and the alternative propounded above: namely, that the initial yield is always high but is decreased so rapidly by back-reaction that it cannot be measured. By a thorough study of the reaction kinetics in various systems, one should be able to determine indirectly the rate of dimerization of OH, and hence to decide between the theories.

Experimental results reported in this paper as having been obtained on the Atomic Energy Project were performed at the Metallurgical Laboratory of the University of Chicago under contract with the Manhattan District, and at the

Clinton Laboratories operated by the Monsanto Chemical Company under contract with the Atomic Energy Commission. The writer is happy to acknowledge his indebtedness to Professor James Franck and to Professor Milton Burton for many helpful discussions.

#### REFERENCES

- (1) ALLEN, A. O.: Paper presented at the 110th Meeting of the American Chemical Society, which was held at Chicago, Illinois, September, 1946.
- (2) DAINTON, F. S.: National Research Council of Canada, Division of Atomic Energy, Report CRC-304 (1946) (not classified).
- (3) DUANE, W., AND SCHEUER, O.: *Le radium* **10**, 33 (1913).
- (4) FRICKE, H.: *J. Chem. Phys.* **3**, 364 (1935).
- (5) FRICKE, H., HART, E. J., AND SMITH, H. P.: *J. Chem. Phys.* **6**, 229 (1938) and earlier papers.
- (6) LANNING, F. C., AND LIND, S. C.: *J. Phys. Chem.* **42**, 1229 (1938).
- (7) LEA, D. E.: *Actions of Radiations on Living Cells* The Macmillan Co., New York (1947)
- (8) NURNBERGER, C. E.: *J. Phys. Chem.* **38**, 47 (1934).
- (9) RISSE, O.: *Z. physik. Chem.* **140**, 133 (1929)
- (10) WEISS, J.: *Nature* **157**, 184 (1946).

## ON THE EXISTENCE OF FREE ATOMS AND RADICALS IN WATER AND AQUEOUS SOLUTIONS SUBJECTED TO IONIZING RADIATION<sup>1</sup>

F. S. DAINTON

*Laboratory of Physical Chemistry, University of Cambridge, Cambridge, England*

*Received October 23, 1947*

### I. INTRODUCTION

Ionizing radiation is usually taken to mean x- and  $\gamma$ -rays or beams of fast charged particles (protons, deuterons,  $\alpha$ -particles,  $\beta$ -rays, and cathode rays<sup>2</sup>). In the passage of the charged particles through water, water molecules are ionized by impact. Such ion-pairs will be created along the track of a single ionizing particle or along  $\delta$ -rays immediately adjacent to it. X-rays and  $\gamma$ -rays consist of high-energy quanta, and absorption of such a quantum by a water molecule results in the ejection of a photoelectron or Compton recoil electron of high energy. The fast secondary electrons thus produced ionize other water molecules by impact, and the net result of absorption of x-rays and  $\gamma$ -rays is therefore very similar to absorption of fast electron beams, i.e., cathode or  $\beta$ -rays. An important difference between x-,  $\gamma$ -,  $\beta$ -, and cathode rays on the one hand, and

<sup>1</sup> Presented at the Symposium on Radiation Chemistry and Photochemistry which was held at the University of Notre Dame, Notre Dame, Indiana, June 24-27, 1947.

<sup>2</sup> Neutron beams will not be considered in this article.

massive particle beams ( $p, d, \alpha$ ) on the other, is the much greater ion density in the case of the latter. For example, Lea (35) calculates that the number of primary ionizations per micron of path of a 100-kv. electron through water is 4.7, whereas with a 1-m.e.v. particle the corresponding number is 264.

To the chemist studying the chemical changes induced by the absorption of one of these types of radiation by water or aqueous solutions, the most important problem is to discover the link between immediate consequences of the absorption of the radiation (*cf.* the primary act in photochemical processes) and the ultimate change which is observed. There are two approaches to this problem. The first is to consider theoretically the probable fate of the particles formed in the primary radiochemical act, and the possible chemical changes which may result. The second method is to deduce the number and nature of the primary particles<sup>3</sup> from the observed magnitude and character of the chemical reaction. This argument will be the stronger if similar changes can be produced in aqueous solution by well-recognized processes not involving the use of ionizing radiation. It is here that the link with photochemistry occurs.

In the present paper both these methods will be applied. In the second approach particular reference will be made to some preliminary results on the radiation-induced polymerization of certain vinyl compounds in dilute aqueous solutions.

## II. THEORETICAL

In most radiation-induced reactions the rate of energy absorption can be calculated and hence the number of molecules decomposing per erg of absorbed energy evaluated. The latter quantity has always been considered to be of less significance than the ion-pair yield ( $M/N$ ), defined as the number of molecules transformed per ion-pair formed.  $M/N$  can be accurately evaluated in certain gaseous systems where the saturation current can be measured. In liquid water the number of ion-pairs formed ( $N$ ) cannot be measured, and it has been commonly assumed that the average energy to create an ion-pair is the same as that required in air, *viz.*, 32.5 e.v. per ion-pair formed by light particles and 35 e.v. per ion-pair formed by massive particles. The ion-pair yield is then put equal to the product of 32.5 e.v. (or 35 e.v.) and the number of molecules reacted divided by the energy (in electron volts) absorbed during reaction. In several discussions of the variation of  $M/N$ , so determined, with concentration and other variables, it has been pointed out (17, 36) that along the particle track  $\text{H}_2\text{O}^+$  ions are formed which rapidly dissociate into a hydrion and hydroxyl radical ( $\text{H}^+ + \text{OH}$ ), whilst the secondary electron is not slowed down to thermal speeds, and therefore not captured, until it has travelled some distance from the track. The electron attachment process postulated is  $\text{H}^+ + e \rightarrow \text{H}$ ; hence the net effect of the ionization is regarded as the production of a high concentration of hydroxyl radicals along the track and of hydrogen atoms at much lower concentration contained in

<sup>3</sup> Only indirect action will be considered here, i.e., any small changes brought about in dilute aqueous solution by the action of the radiation directly on the solute will be ignored.

a cylinder of very much larger radius than the track, which is the axis of the cylinder. Gray, Dale, and Meredith,<sup>4</sup> applying Lea's modification of Jaffé's formulae to the passage of a 5-m.e.v.  $\alpha$ -particle through water, calculate that the initial hydroxyl-radical concentration is molar and confined to a cylinder  $8 \times 10^{-4} \mu$  radius, whilst the radius of the hydrogen atom column is  $1.5 \times 10^{-2} \mu$  initially, corresponding to a molality of 0.0087. Implicit in all calculations of this kind are three assumptions: (a) that  $\text{H}_2\text{O}^+$  is the only positive ion formed, (b) that any radicals produced by excitation can be omitted from consideration, and (c) that the radicals as formed have only thermal energies and are in ground states. Assumption (b) is explicitly stated by Lea, and is presumably made on the grounds that the radicals formed by direct dissociation of the water molecules may recombine almost as soon as they are formed. It will be useful to reexamine the primary radiochemical act in the light of these assumptions.

The various single ionization energies of water (12.56, 18.5, 18.9 e.v.) are about half the value (32.5 or 35 e.v.) of the mean energy assumed to be dissipated when an ion-pair is created. It is unlikely that the excess energy, which in all cases exceeds 12.56 e.v., is located on the electron, for it is probable that such a fast electron would bring about further ionization of some of the water molecules with which it is bound to collide. We conclude therefore that the ionizing particle ( $\alpha$ ,  $\beta$ , etc.) does not ionize every water molecule which it hits, but that a certain fraction of these collisions result in excitation. Guidance on these problems can be obtained by considering the results of electron impact and discharge experiments on water vapor, and the results of Bethe's calculations for electron impact in atomic hydrogen gas, and then to consider how the conclusions reached for water vapor must be modified when the target water molecules form part of the quasi-structure of liquid water.

#### A. THE EFFECT OF IONIZING RADIATION ON WATER VAPOR

The electronic structure of the normal state of the water molecule, omitting the  $K$  electrons of the oxygen atom, is represented by Mulliken (45) as:

	$(2sa_1)^2$	$[yb_1]^2$	$[xa_1]^2$	$(2xb_1)^2, {}^1A_1$
Approximate location . . . . .	O	HOH	HOH	O
" $I_{\text{vert}}$ " in electron volts . . . . .	32	18	17	12.7

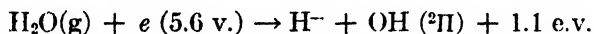
Square brackets enclose bonding electrons which take part in both hydroxyl bonds; and the lone pairs, i.e., non-bonding electrons, of the oxygen atoms are in round brackets. " $I_{\text{vert}}$ " denotes the calculated ionization potentials for removal of one electron, assuming that the configuration of the water molecule is unaltered during the process. Mulliken has also predicted that an excited state of the water molecule exists which lies  $\sim 7$  e.v. above the ground state and in which one of the non-bonding  $2xb_1$  electrons is raised to the  $3sa_1$  orbital. He attributes the continuous absorption of water vapor beginning at  $\lambda$  1780 Å. to excitation to this level, in which state the molecule predissociates, possibly to

<sup>4</sup> Private communication.

molecular hydrogen  $H_2$  ( $^1\Sigma_g^+$ ) and an excited oxygen atom  $O$  ( $^1D$ ). Using a vacuum spectrograph of high dispersion, Price (55; see also 56) confirmed this view and was able to fit the bands at  $\lambda$  1250 Å. into a Rydberg series and hence to obtain the accurate value of 12.56 e.v. for the first ionization potential of water.

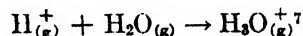
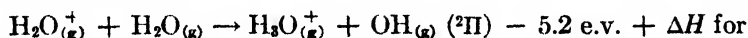
### 1. The number and kind of ions and radicals formed by impact

(a) The ions formed by electron impact on water molecules in the vapor phase have been identified, and their relative abundance determined mass spectrographically in several investigations. The earlier work has been reviewed by Smyth and Mueller (62) and a more recent study using a mass spectrograph of higher resolving power has been made by Mann, Hustrulid, and Tate (41). The lowest potential at which ions are formed is 5.6 v. (41), when a very weak  $H^-$  current appears. The current passes through a maximum at 7.1 v. as the voltage is increased, and the shape of the current voltage curve is typical of a resonance capture process. Presumably the inelastic collision causes excitation to a repulsive ( $HO-II$ ) level at the normal water configuration. Contrary to expectations based on the known values of the electron affinities of  $H$  and  $OH$ ,<sup>5</sup> the electron is retained by the hydrogen atom and we may write



The excess energy,  $\ll 1.1$  e.v., will probably appear as translational energy.

The next ionization occurs at 12.7 v. according to Smyth and at  $13.0 \pm 0.2$  v. according to Mann, Hustrulid, and Tate, and large positive-ion currents of  $H_2O^+$  and  $H_3O^+$  are observed.  $H_2O^+$  is formed by detachment of a  $2x_{b1}$  non-bonding oxygen electron, and since the  $H_3O^+$  yield is proportional to the square of the partial pressure of water vapor, this latter ion is formed by the secondary bimolecular reaction.<sup>6</sup>



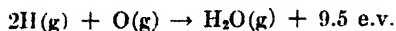
<sup>5</sup>  $E_{OH} = 4.81$  e.v. (Lederle (38)).

$E_H = 0.70$  e.v. (Hylleraas (29)).

$D_{H_2O \rightarrow H+OH} = 5.2$  e.v. (Dwyer and Oldenberg (19)).

<sup>6</sup> There is a real paucity of information about  $\Delta H$  for  $H_2O + H^+ \rightarrow H_3O^+$ . For the process  $H^+(g) \rightarrow H^+(aq)$ , values range around 260 kg.-cal (Gurney (28) estimates 276 kg.-cal.; Latimer (33) gives 258 kg.-cal.), but the proton undoubtedly has more than one water molecule of hydration. Assuming that the bond energy of  $O-H$  is no weaker in  $H_3O^+$  than in  $H_2O$ , then  $\Delta H \ll 110$  kg.-cal. Juzo (30) has estimated this proton affinity of water as 170 kg.-cal. It seems likely that the reaction  $H_2O^+ + H_2O \rightarrow H_3O^+ + OH$  is at least thermoneutral and may be exothermic, and may therefore be a very facile process.

<sup>7</sup> Based on the values



and



See Skinner (59) and Dwyer and Oldenberg (19).

Smyth observed a surge in the  $\text{H}_2\text{O}^+$  ion current at 16.0 v., but since this is less than the next " $I_{\text{vert}}$ " value calculated by Mulliken (45), and since Mann, Hustulid, and Tate were unable to detect this effect, we shall disregard it.<sup>8</sup> Neglecting the small amounts of  $\text{O}^+$  formed at 18.5 or 18.8 v. and 28.1 v., the next ions to be formed in any abundance are  $\text{H}^+$  and  $\text{OH}^+$ , which according to the earlier investigations appear together at 18.5 v.; but according to Mann *et al.* only  $\text{HO}^+$  appears at 18.7 v. and  $\text{H}^+$  does not occur until a potential of  $19.5 \pm 0.2$  v. is reached. These effects may be due to removal of a bonding electron and the existence of two repulsive levels  $\text{H}^+\cdots\text{OH}$  and  $\text{HO}^+\cdots\text{H}$  lying close together. The values of the appearance potentials indicate that the ionization potentials of a hydrogen atom and a hydroxyl radical are approximately equal, *viz.*, 13.6 e.v., and that when  $\text{H}^+ + \text{OH}$  are formed the excess kinetic energy of about a volt is taken up as kinetic energy of these products. Traces of  $\text{H}_2^+$  and  $\text{O}^+$  observed as the potential was raised above 20 v. suggested that reactions such as  $\text{H}_2\text{O} \rightarrow 2\text{H} + \text{O}^+ + e$ ;  $\text{H}_2\text{O} \rightarrow \text{H}_2^+ + \text{O} + e$ ;  $\text{H}_2\text{O} \rightarrow \text{H}_2^+ + \text{O}^+ + 2e$ , could occasionally be brought about with very low efficiency by electron impact. Very small amounts of the negative ions  $\text{OH}^-$ ,  $\text{O}^-$ , and  $\text{H}_2\text{O}^-$  were also produced.

For the elucidation of the radiation chemistry of water vapor it is desirable to know the relative probability of these reactions at all impact energies. Unfortunately, data are available only for energies of 50 e.v. and 100 e.v. and the values relevant to these two energies were carried out by two different investigators (62 and 41). They are given below:

Ion	$\text{H}_2\text{O}^+$	$\text{HO}^+$	$\text{H}^+$	$\text{H}_2\text{O}^+$	$\text{O}^+$	$\text{H}_2^+$
Associated atom or radical.	—	H	OH	OH	$\text{H}_2, 2\text{H}$	$\text{O}^+, \text{O}$
Relative abundance at 50 v. (62)	$10^3$	$2 \times 10^2$	$2 \times 10^2$	$2 \times 10^2$	20	5
Relative abundance at 100 v. (41)	—	$2.3 \times 10^2$	$0.5 \times 10^2$	?	20	0.7
Appearance potential in volts (62)	12.7	18.9	18.9	12.7	18.5	33.5
Appearance potential in volts (41)	13.0	18.7	19.5	13.8	$\begin{Bmatrix} 18.8 \\ 28.1 \end{Bmatrix}$	$23 \pm 2$

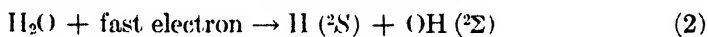
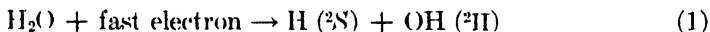
Two important points in connection with this table are: (a) if the electron loses only that amount of energy corresponding to a narrow band, of which the appearance potential is the lower limit, all the atoms and radicals given in the table will be in ground electronic states but may have excess vibrational or translational energy, and (b) the relative yields will alter as the energy of the impact electrons is increased. With regard to the second point the results of electron-impact experiments on monatomic gases are instructive (see 44 and 8). In many cases there is evidence that the cross-section for ionization or electronic excitation by inelastic collision rises rapidly from zero at the resonance potential, passes through a maximum at a value 3 to 4 times the resonance potential, and

<sup>8</sup> Sugden (private communication) has, however, detected this I.P. at 16.0 v.



then falls off according to some inverse power law of the electron energy. Assuming as a working hypothesis that a similar type of relation holds for molecules, we would conclude in the case of water vapor that at 50 v. the  $\text{H}_2\text{O}^+$  yield is in the region of its maximum, but that the maxima for  $\text{HO}^+$  and  $\text{H}^+$  have not been attained. Since a large number of the total ionizations in irradiated material of any kind are due to impact ionization by secondary electrons of energies of the order of 50 to 100 v., it seems likely that in irradiated water vapor, about two-thirds of these secondary ions will be  $\text{H}_2\text{O}^+$  and a third will comprise  $\text{H}^+$  and  $\text{OH}^+$ , the latter probably in excess. Concerning the relative occurrence of the different ions at very high electron speeds corresponding to the impacts involved with the initial ionizing particle ( $\alpha$ -ray,  $\beta$ -ray, etc.) resulting in primary ionization, no comments will be made.

(b) *Uncharged atoms and radicals*: Such uncharged dissociation products of water formed by direct collision with electrons may often be identified by their characteristic ultraviolet absorption or emission spectra. It has been established in many investigations (see, for example, 9, 34, 54) that ground state ( $^2\text{S}$ ) hydrogen atoms and ground state ( $^2\text{H}$ ) and excited ( $^2\Sigma$ ) hydroxyl radicals are formed by the passage of electrical discharge through water vapor.<sup>9</sup> The reactions may be written:



Spectroscopic methods are not restricted to detection of uncharged entities, and it has been suggested by Rodebush and Wahl (58) that the emission bands observed at 3564 and 3328 Å. in discharges through water vapor may be due to the  $\text{OH}^+$  ion.

Little progress can be made towards calculation of the cross-sections of the water molecules corresponding to each of the processes of ionization and dissociation for all ranges of electron speeds until much more is known about the potential-energy curves of the various excited levels of the water molecule and its positive ion. However, since all these processes of ionization and dissociation are essentially electronic excitation by electron impact, the velocity variation will be similar to that for inelastic electron impact with atoms.

We may summarize the primary radiochemical act in water vapor rather crudely as follows: Assume that 35 e.v. is the mean value of the energy required to create one ion-pair and that only a fraction, say 50 per cent, of the ion ultimately produced are formed in primary collisions. A small percentage of the collisions of the ionizing particle will be elastic, but the majority will be inelastic involving either ionization, with formation of  $\text{H}_2\text{O}^+$ ,  $\text{H}^+$  (and  $\text{OH}$ ),  $\text{OH}^+$  (and  $\text{H}$ ), or excitation probably with dissociations to  $\text{H } (^2\text{S})$  and  $\text{OH}$  in either the  $^2\text{H}$  or the  $^2\Sigma$  state. The electron ejected in the primary ionization will, on the average,

<sup>9</sup>  $\text{OH } (^2\Sigma)$  radicals are detected by the water bands at 3064 Å. in emission, and  $\text{OH } (^2\text{H})$  radicals by the same bands in absorption after the discharge has ceased.  $\text{H}$  atoms ( $^2\text{S}$ ) are detected by emission of the Balmer line series after excitation by impact with electrons.

possess at least sufficient energy for one further ionization. If the dissociative ionizations are about as numerous as those in which only  $\text{H}_2\text{O}^+$  is formed, the average energy lost per ionizing collision is about 16 e.v., and 19 e.v. are used to excite water molecules. A small fraction of the 19 e.v. will be lost in elastic collisions. Without knowledge of the potential-energy curves of the various states of the water molecule we cannot be certain about the actual energy requirements of the dissociation reactions 1 and 2; hence there is no certainty as to whether the dissociating fragments have excess translational energy. If the process is one of electronic excitation to purely repulsive levels, some excess translational energy will be most probable. In passing we note that for each initial ionization, the minimal energy requirements for reactions 1 and 2 would allow two dissociations of type 2 and three dissociations of type 1. The net effect is therefore formation of atoms and radicals ( $\text{H}$ ,  $\text{OH}$  ( $^2\Pi$  and  $^2\Sigma$ )), ions ( $\text{H}_2\text{O}^+$ ,  $\text{H}^+$ ,  $\text{OH}^+$ ), and electrons of thermal velocities. The relative efficiencies of all these processes will vary with the energy of the ionizing particle.<sup>10</sup>

## 2. Radicals formed by charge neutralization of ions

The subsequent fates of these diverse substances is fairly certain. The radicals may recombine in pairs by a three-body reaction: e.g.,  $2\text{H} + \text{M} \rightarrow \text{H}_2 + \text{M}$ ;  $\text{H} + \text{OH} + \text{M} \rightarrow \text{H}_2\text{O} + \text{M}$ ;  $2\text{OH} + \text{M} \rightarrow \text{H}_2\text{O}_2 + \text{M}$ . Although there is considerable doubt about the last-named reaction, the over-all effect is of formation of hydrogen, oxygen, and hydrogen peroxide, and it is likely that this type of reaction affords an important means whereby some of the energy of the radiation is degraded to thermal energy. Excited radicals and ions which combine, in the spectroscopic sense, with lower states will either emit radiation (e.g., the water bands) or be deactivated. The positive ions  $\text{H}_2\text{O}^+$ ,  $\text{H}^+$ , and  $\text{HO}^+$  will ultimately be discharged by slow electrons or negative ions, processes which are discussed below. The  $\text{H}_2\text{O}^+$  ion may react bimolecularly with a water molecule to form the  $\text{H}_3\text{O}^+$  ion, and this ion also will ultimately be neutralized. There will be some negative ions present, traces of  $\text{H}^-$ ,  $\text{OH}^-$ , and possibly  $\text{H}_2\text{O}^-$ . Although the electron affinity of water is probably very low, the ion  $\text{H}_2\text{O}^-$  may be formed by direct bimolecular addition of an electron. Electron swarm experiments<sup>11</sup> in water vapor suggest that this ion may readily dissociate to form  $\text{H}$  and  $\text{OH}^-$ .

The discharge of the positive ions  $\text{H}_2\text{O}^+$ ,  $\text{H}_3\text{O}^+$ ,  $\text{H}^+$ , and  $\text{OH}^+$  may be brought about by (i) bimolecular reaction with an electron, (ii) reaction *i* with a third body present, and (iii) electron transfer from a negative ion in a bimolecular collision.<sup>12</sup> The first process is impossible with monatomic ions and will involve the dissociation of the resultant molecule in the other cases. Because of the

<sup>10</sup> See, for example, Bethe's discussion of the passage of electrons through atomic hydrogen gas (8, 44).

<sup>11</sup> For details of the investigation of electron capture by water see Bradbury and Tatel (10), Bailey and Duncanson (4), and Loeb (40).

<sup>12</sup> Radiative capture of electrons is usually a process of very low probability (42) and is therefore omitted from consideration.

large ionization potential of the hydroxyl radical the H and O atoms formed when  $\text{HO}^+$  is neutralized by this process will have great excess energy. The same conclusion will also apply to the fragments ( $\text{H} + \text{OH}$ ) formed by neutralization of  $\text{H}_2\text{O}^+$  and the fragments (presumed to be  $2\text{H} + \text{OH}$ ) formed from  $\text{H}_3\text{O}^+$ . The third body in the ternary processes will most likely be a water molecule and, since the energy liberated is so large, it is not improbable that some dissociation of water may result even in this case. The electron-transfer processes will involve the negative ions  $\text{H}_2\text{O}^-$ ,  $\text{H}^-$ , and  $\text{OH}^-$  and in this case also, transfer of an electron to a positive ion will release so much energy (except, possibly, in the case of  $\text{OH}^-$  as negative ion) that some at least of these processes will result in the production of dissociation products of water. The maximum amount of energy which can be released by this mechanism on the average is 16 e.v. per ion-pair; and with the wastage of energy attendant on charge neutralization processes it is unlikely that more than two water molecules are dissociated in this way.

### 3. *The total number of radicals formed per ion-pair*

The qualitative and empirical nature of the preceding discussion illustrates the pressing need for a careful theoretical investigation of the individual processes. For the present we shall assume as a basis for further discussion that in water vapor subject to ionizing radiation about two water molecules are dissociated to H ( $^3\text{S}$ ) and OH ( $^2\Pi$  or  $^2\Sigma$ ) by direct impact with the ionizing particles for each ion-pair formed, and that neutralization of the positive ions ultimately results in the dissociation of yet another water molecule.

At this point it is convenient to consider what other evidence exists to support the view that the major part of the radiochemical change in gaseous systems is due to direct dissociation by impact rather than due to charge neutralization of ions.

Firstly, there are the theoretical analyses by Eyring, Hirschfelder, and Taylor (20) of the effect of  $\alpha$ -particles on hydrogen gas and hydrogen bromide. These authors concluded that for each ion-pair in hydrogen about six atoms were formed, four *via*  $\text{H}_2^+$  and two by direct dissociation. Slightly larger figures are given for dissociations of hydrogen bromide and bromine. However, it must be pointed out that the number of atoms formed by direct dissociation was taken as the difference between (a) the total number of atoms necessary to account for the experimentally observed rates and  $M/N$  values in these reactions (based on certain reaction mechanisms, velocity constants, diffusion coefficients, etc.) and (b) the number of atoms judged on theoretical grounds to be formed *via* ions. It is conceivable that the number of atoms formed *via* ions was overestimated. A most useful test of this point would be to determine the percentage reduction in rate when all the ions were discharged (as indicated in the following paragraph).

Secondly, if the reaction zone is confined between two plates charged to a sufficiently high potential for the saturation current to be attained, all ion neutralization processes will be prevented and any residual radiochemical change must be attributed to direct excitation. Smith and Essex (61) have carried out experiments of this kind on the decomposition of ammonia by  $\alpha$ -particles

and conclude that only 30 per cent of the reaction is caused by the ions. In this case the ionization potential is 11.3 e.v. and the energy required to create one ion-pair is 37 e.v. Kolumban and Essex (32) have studied the  $\alpha$ -ray-induced decomposition of nitrous oxide and found that  $M/N$  was only slightly reduced by a field giving 50 per cent saturation. Results of this kind are of great interest, but may not be entirely conclusive. When ions enter into rapid reactions with molecules the ions discharged in this way may not be those formed in the primary act. For example, in water vapor the reaction  $\text{H}_2\text{O}^+ + \text{H}_2\text{O} \rightarrow \text{H}_3\text{O}^+ + \text{OH}$  occurs very readily and therefore  $\text{H}_2\text{O}^+$  ions formed initially will not be discharged at the cathode. Instead,  $\text{H}_3\text{O}^+$  ions will be removed and in this case part of the residual chemical change when a saturation field is applied will still be due to ionization.

TABLE 1  
*Some comparative data on reactions of various gases*

REACTION	RADIOCHEMICAL		PHOTOCHEMICAL	
	Ionizing radiation	$M/N$	Wave-length range $\text{\AA}$	Quantum yield
Decomposition of $\text{NH}_3$	$\left\{ \begin{array}{ll} \alpha & (61) \\ \text{electrons} & (1) \end{array} \right\}$	$\left\{ \begin{array}{l} 1.37 \\ 1.20 \end{array} \right\}$	2144	1 (51)
Decomposition of $\text{HI}$	$\left\{ \begin{array}{ll} \alpha & (11) \\ x & (27) \end{array} \right\}$	$\left\{ \begin{array}{l} 6+ \\ 8 \end{array} \right\}$	2000-2800	2 (49)
Decomposition of $\text{N}_2\text{O}$	$\left\{ \begin{array}{ll} \alpha & (32) \\ \text{electrons} & (24) \end{array} \right\}$	$\left\{ \begin{array}{l} 4.4 \\ 3.9 \end{array} \right\}$	1850-2000	1.3 (52)
Decomposition of $\text{H}_2\text{S}$	$\alpha$ (64)	2.7	2080	1.0 (53)
Decomposition of $\text{CO}$	$\alpha$ (14)	$\sim 2$	1295	1.0 (48)
Polymerization of $(\text{CN})_2$	$\alpha$ (39)	7.4	2150	3.0 (50)
Oxidation of $\text{CO}$	$\alpha$ (39)	6.5	1295, 1470	$\sim 0.4$ (47)

Thirdly, if the radicals formed in the radiochemical primary act can be made by other means, the extent of reaction caused by each radical may be measured, and comparison of this result with the  $M/N$  value obtained in the radiochemical reaction will indicate the total number of radicals produced when the mean energy for creation of an ion-pair is absorbed. The most obvious comparison is between  $M/N$  and the quantum yield of the corresponding photochemical reaction. A number of examples are given in table 1 in which the ionic yield is considerably greater than the quantum yield. Unfortunately we still lack any evidence of this kind for water vapor.

#### 4. Possible kinetic consequences

The rate of formation of hydrogen atoms and hydroxyl radicals in water vapor will be given by

$$\frac{d[H]}{dt} = \frac{d[OH]}{dt} = r \frac{\text{rate of energy absorption per cubic centimeter}}{\text{mean energy absorbed per ion-pair}} = krR$$

when  $R$  is the dose rate in roentgens  $\text{sec.}^{-1}$ ,  $k$  is the number of ion-pairs formed per cubic centimeter per roentgen, and  $r$  is the number of hydrogen atoms (and hence hydroxyl radicals also) formed when the mean energy to create an ion-pair is absorbed. From the discussion in the preceding pages,  $r$  may be taken as between 3 and 4, but it must be remembered that the radicals are not uniformly distributed. Initially they will be concentrated along the ionizing particle track and, owing to the distance travelled by the secondary electrons before capture, there will be an excess of hydroxyl radicals along the center of the track of the ionizing particles, and this excess will be larger the greater the ion density, i.e., with heavier particles. The radicals will diffuse from the track and in so doing will undergo collision with water molecules. The four possible reactions which may occur at these collisions are two exchange reactions



and



The latter two reactions, which would lead to formation of the observed products, require too large an activation energy to occur appreciably at room temperature. If  $H$  or  $OH$  were excited, these reactions would occur more easily. However, it is known that no excited hydrogen atoms are formed and hydrogen peroxide is not formed easily in the reaction vessel containing water vapor through which a discharge is passed. We therefore conclude that the only product-forming reactions are between like radicals in the three-body collisions: e.g.,  $2H + M \rightarrow H_2 + M$ . The reaction between unlike radicals,  $H + OH + H_2O \rightarrow 2H_2O$ , will serve only to reduce the ionic yield, and since the measured velocity constant of this reaction is so very high ( $4.9 \times 10^{17} \text{ cc.}^2 \text{ molecule}^{-2} \text{ sec.}^{-1} = 1.2 \times 10^4 \times \text{ternary collision rate (Oldenberg 1939 (54))}$ ), in fact larger by a factor of  $1.5 \times 10^3$  than the rate constant of  $H_2 + 2H \rightarrow 2H_2$ , we should expect the ionic yield to be less than  $r$  in value.

In water vapor at low pressures it is possible that either  $H$  or  $OH$  or both may diffuse to, and be adsorbed by, the wall of the reaction vessel. Whether this is the case could readily be deduced from the relation of the ionic yield to the dose rate. Following well-established methods, it can be shown that if adsorption is negligible, the rate of formation of products  $= krRP$ , where  $P$  is the probability that in radical encounters in pairs, products and not water are formed.  $P$  is less than unity and the ionic yield  $= krP$  and is independent of the dose rate  $R$ . If, on the other hand, most of the radicals are removed by adsorption, the reaction rate is approximately  $= P\left(\frac{krR}{\Delta}\right)^2$ , where  $\Delta$  represents the mean rate constant

of diffusion of the radicals to the wall and will decrease with increasing vessel dimensions. In this case the ionic yield will increase with the dose rate. Since an increase of pressure of the reactants will increase the number of ternary collisions leading to reaction but decrease the diffusion rate, a corollary to the above conclusions is that the ion-pair yield in a given vessel should be independent of the dose rate at high pressures and proportional to dose rate at low pressures. At constant dose rate the ionic yield should increase with pressure. Existing data on the radiation chemistry of water vapor are unfortunately too scanty to permit a decision as to whether adsorption is an important factor or not in this system.

#### B. EFFECT OF IONIZING RADIATIONS ON LIQUID WATER AND AQUEOUS SOLUTIONS

Much has already been written on this subject<sup>13</sup> and what follows is merely intended to draw attention to important matters the investigation of which would appear likely to yield fruitful results.

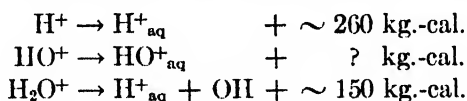
The obvious difference between vapor and liquid water is the close approach of the water molecules and the tendency to a quasi-regular structure based on hydrogen bonding. This difference has several important consequences. In the first place, assuming that the mechanism of energy dissipation of a rapidly moving charged particle is essentially similar to that in the vapor phase, the ion density (number of ions per micron path) will be much greater in the liquid. Secondly, any ions formed may become hydrated and the hydration energy is likely to be higher than the energy released when the same ion becomes attached to one water molecule in the gas phase. This is a factor modifying the stability of any ions formed and their likelihood of being transformed into radicals. Thirdly, the much lower mean intermolecular separation implies a lower diffusion rate away from the ion tracks and a much higher probability of recombination of radicals, owing to the omnipresence of water molecules to act as third bodies, and also the possibility of immediate recombination by the Franck-Rabinowitch mechanism (21) of radicals formed from the same water molecule by impact dissociation. Finally, the lifetime of any excited species would be much shorter than in the vapor. It is convenient to consider these effects in relation to (i) the nature, number, and spatial distribution of the radicals formed and (ii) various possible types of kinetic behavior.

##### 1. *The neutral species formed in liquid water*

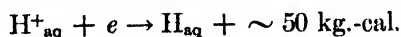
Although there is no direct evidence available, a plausible assumption is that the possible ions and neutral entities formed by absorption of the radiation are those which are formed in the vapor; i.e.,  $\text{H}_2\text{O}^+$ ,  $\text{HO}^+$ , and  $\text{H}^+$  in quantity, and traces of  $\text{O}^+$  and some negative ions and  $\text{H}(^2\text{S})$ ,  $\text{OH}(^2\Pi)$ , and  $\text{OH}(^2\Sigma)$ . We have no knowledge of the relative yields of these substances, or of the energy required to produce them, which may be slightly different from the energy required in

<sup>13</sup> For reviews see Allsopp (2), Lea (37), Burton (12), Dainton and Miller (16), and Weiss (63).

the vapor phase. Most of them will be formed in close proximity to one another along the main track or secondary tracks, whilst the associated electrons will spread a considerable distance from the track before being captured. The first question which arises is whether the H atoms and OH radicals formed by dissociation have an appreciable lifetime. They are formed within the solvent cage and for this reason are sometimes considered as largely recombining, only a small fraction escaping and becoming available for reaction, either with another of its own kind or with the solute. However, the arguments presented in Section II, A,1 (page 493) indicate that some, at least, of the dissociations result in excited atoms and radicals being formed, which as such may escape from the solvent sheath by reaction with it; e.g., see the reactions in Section II, A,4. Such types of reactions are not new, but have been postulated to account for the development of unsaturation in paraffin solvents containing ketones which are decomposing photochemically into radicals (46). It would be particularly interesting to know whether water does enter into exchange reactions with H and OH radicals.<sup>14</sup> As far as we are aware there have been no observations reported of light emission from irradiated water, but also no search for this phenomenon has been made. The results of a direct test for excited ( $^2\Sigma$ ) OH radicals are therefore not available. In default of this information we can only comment that the deactivation probability is likely to be much higher in the liquid state than in the vapor at low pressures. In this connection it is of interest to note that Oldenberg (54 (1938)) has found the radiative lifetime of excited ( $^2\Sigma$ ) OH to be unusually high, viz.,  $4 \times 10^{-6}$  sec. H and OH are also produced in the ionization process in which  $\text{HO}^+$  and  $\text{H}^+$ , respectively, are formed. These radicals will not be formed in the same solvent cage; hence the principles discussed by Franck and Rabinowitch do not apply. The recombination of these species will be governed by whatever laws control collision frequencies in solution, it being remembered that locally their concentrations may be quite high. The positive ions  $\text{H}^+$ ,  $\text{OH}^+$ , and  $\text{H}_2\text{O}^+$ , even if formed "bare", will not remain so and the following hydration processes will probably occur readily



The last of these reactions will augment the hydroxyl-radical concentration in or near the track. The chances of capture of the slow electrons may be considerably higher in water than in vapor, owing to the large number of water molecules present which may form  $\text{H}_2\text{O}^-$  and the appreciable number of hydrons which may serve as acceptors for some of the electrons by



<sup>14</sup> The reaction of hydroxyl with water is being investigated in this laboratory by a study of the photolysis of  $\text{H}_2\text{O}^{18}$  in  $\text{H}_2\text{O}^{18}$ . It can be shown that if the evolved oxygen is enriched in the  $\text{O}^{18}$  isotope the reaction  $\text{HO}^{18} + \text{HO}^{18}\text{H} \rightarrow \text{HO}^{18}\text{H} + \text{O}^{18}\text{H}$  is occurring.

Whether all the electrons can be removed in this way will depend on the concentration of electrons and hence on the ion density of the track. It may be that with light particles all the electrons are so removed, whereas with  $\alpha$ -particles only a small fraction undergoes this reaction. In the latter case some of the electrons may be captured by the positive ions which have diffused from the column, since they will also be in excess over the hydroxide ions which are present in the water and which would neutralize some of the positive ions by charge transfer.

The position may be summarized as follows: Assuming the same kind of primary radiochemical processes to occur in liquid water as in the vapor, hydrogen atoms and hydroxyl radicals are again the ultimate particles formed, but the number of excited and ground-state radicals diffusing freely and separately through the medium is likely to be reduced, owing to the much closer approach of the water molecules which favors deactivation of excited species and recombination of H and OH formed by direct dissociation of the same water molecule. The same dense packing of the water molecules implies much higher local concentrations of radicals than exists in the vapor for the same radiation, and as the ion density along the track increases, so also does the hydroxyl-radical concentration increase along the center of the track, whilst the reverse is true along the periphery.

## 2. Possible kinetic consequences

Several calculations have been made recently (35, 36) of the spatial distribution of the radicals and some results are quoted on page 491. In the opinion of the present writer some of the assumptions on which these are made are unjustified; the available data do not warrant detailed calculations but only permit a qualitative picture of the events, and the prime task at present is to develop some unambiguous experimental method for identifying and counting the radicals which are formed. An attempt to achieve this aim is described in the experimental section. For the present we shall mention briefly the kinetic consequences which are possible in the system outlined in the previous paragraph.

(a) *Pure water*: Destruction of radicals by adsorption at the vessel wall will be quite unimportant and the ionic yield will be independent of the dose rate, for the same reasons which hold in water vapor. If recombination of  $H + OH \rightarrow H_2O$  is occurring to an appreciably greater extent in the liquid, then for a given radiation we would expect  $(M/N)$  gas to exceed  $(M/N)$  liquid. Opposing this effect will be the relatively greater frequency of collision of radicals of the same kind (2H or 2OH) compared with those between dissimilar radicals ( $H + OH$ ) in liquid water, owing to the high local concentrations of radicals in which one or the other is in excess. The experiments of Duane and Scheuer (18) indicate that for  $\alpha$ -rays  $(M/N)$  gas  $< (M/N)$  liquid and we therefore conclude that with  $\alpha$ -rays the latter effect predominates. With x-rays and  $\gamma$ -rays the ion density is much less, the mixing of the H and OH radicals is much more marked, and we should expect  $(M/N)_{x,\beta,\gamma} < (M/N)_{\alpha,p,d}$  for liquid water, and possibly to be less than  $(M/N)_{x,\beta,\gamma}$  for water vapor. From the data in the literature there are some indications that this may be the case; in fact, for a considerable period (22, 57)



it was considered doubtful whether pure water was decomposed by x-rays at all. In those experiments in which decomposition was detected (25, 31), the ionic yield was undoubtedly very low, certainly lower than the value obtained by Günther and Holzapfel (26) using x-rays on water vapor in the presence of excess xenon. The possibility of a radiation-induced back-reaction existing and thus accounting for the low yield must not be overlooked.

(b) *Dilute aqueous solutions*: In dilute aqueous solutions most of the radiation is absorbed by the solvent, and any changes in the solute can be interpreted (26) by assuming that it reacts with either the hydrogen atoms or the hydroxyl radicals or both. Certain aspects of the kinetics of such indirect actions have been frequently discussed, in particular, the change of ionic yield with dilution for  $\alpha$ -particles and x-rays. We are more interested in the relation between ion-pair yields and dose rate, but shall include the other matters for the sake of completeness.

In all cases of indirect action it is sufficient to presume that at a simple bimolecular collision between a solute molecule and H or OH there is a probability of removal of the radical and of changing the solute.<sup>15</sup> Radicals will also be recombining, but kinetically it is of the greatest importance to distinguish three kinds of recombination: (1) The Franck-Rabinowitch type, in which the H and OH units may not escape from their common solvent cell and hence never behave as separate entities or encounter a solute molecule. The result of this type of recombination is merely to reduce the fraction of those radicals which are initially formed which are available for reaction, i.e., capable of separate existence. (2) The second type is recombination in pairs after escape from the solvent "cell", i.e., after a finite period of separate and distinct existence. This may effectively prevent radicals from reacting with the solute, and will occur at a rate proportional to the square of the concentration, and may lead to liberation of hydrogen and oxygen and formation of hydrogen peroxide, or merely to reformation of water. (3) Type 3 is merely a special case of type 2, in which the solute reacts exclusively (or preferentially) with either H or OH. The excess of the other radicals, OH or H, respectively, have then no possible fate but to recombine and liberate hydrogen in the case of a reducing solute and  $O_2 + H_2O_2$  in the case of an oxidizing solute.

We may include all these types of behavior in the simple equation:

$$\frac{dn}{dt} = kr'R - k_1nS - k_2n^2 \quad (1)$$

where  $R$  is the dose rate in roentgens  $\text{sec}^{-1}$ ,  $k$  is the number of ion-pairs created per cubic centimeter when 1 roentgen is absorbed,  $r'$  is the net number of radicals formed per ion-pair and capable of a separate existence (i.e.,  $r'$  = total number of radicals formed, less those which will undergo recombination of type 1),  $k_1$  is the velocity constant for removal of radicals by reaction with the solute and is in

<sup>15</sup> These two probabilities are usually the same but not necessarily so; e.g., in the inactivation of enzymes (Dale *et al.*) it is possible that several encounters, each involving destruction of a radical, are necessary before the enzyme molecule is inactivated.

cc. radical<sup>-1</sup> sec.<sup>-1</sup> units,  $k_2$  is the velocity constant for recombination of type 2, and  $S$  is the solute concentration in molecules per cubic centimeter. Whereas  $S$  is uniform throughout the system,  $n$ , the number of radicals per cubic centimeter, is never so. The kinds and degrees of non-uniformity have been discussed and should be borne in mind, in considering equation 1, which, for this reason and because  $k_1$  and  $k_2$  probably have different values for H and OH, is only useful in qualitative discussions. Suppose  $P$  is the probability that when a radical is removed by reaction with the solute, the solute molecule is chemically changed. The rate of chemical reaction is  $k_1 n S P$  and if this attains a steady value for a given solute concentration, then  $n$ , the "concentration" of radicals, also attains a steady value and the variation of  $n$  with the dose rate  $R$ , solute concentration, and type of radiation (which by determining the spatial variation of  $n$  will profoundly effect  $k_2$ ) will be obtained by putting  $dn/dt = 0$ . We must recognize several  $M/N$  values, according as they refer to change of solute or production of  $H_2$  or  $O_2 + H_2O_2$ , and whether  $M/N$  is defined as the reaction rate divided by the rate of formation of ion pairs at any instant<sup>16</sup> or as the gross change divided by the total number of ion-pairs formed during a considerable period of time.<sup>17</sup> It is now possible to distinguish several different kinetic situations.

1. All the available radicals react with the solute, which is therefore neither a reducing nor an oxidizing agent, and which is either in great excess or  $k_1$  is large, i.e.,  $k_2 n^2 \ll k_1 n S$ . The instantaneous ionic yield with respect to solute =  $k_1 n S P / k R = r' P$  and is independent of dose rate and solute concentration. The reaction rate =  $k r P R$ ; hence the integral ionic yield is also independent of  $S$ . No side products,  $H_2$  or  $O_2$ , are formed; hence the ionic yield of this process is zero.

2. At very low concentrations of solute, particularly of such substances which do not react readily with either H or OH, the situation may arise that  $k_2 n > k_1 S$ , in which case the instantaneous ionic yield with respect to the solute will be given by

$$k_1 n S P / k R \simeq k_1 S P \left( \frac{r'}{k k_2 R} \right)^{\frac{1}{2}}$$

i.e.,  $(M/N)_{\text{instantaneous}}$  will decrease with concentration of solute and with increase of dose rate.

3. When the solute reacts preferentially with either H or OH, side products are formed either by being merely in excess or by reacting with one another at a rate which effectively competes with their removal by reaction with solute. In the former case the  $M/N$  values will be the same as the value with respect to the solute, but in the latter the relation is more complex.

The difference between the effects caused by "light" and "heavy" particle radiation is readily seen. With x-,  $\gamma$ -, and  $\beta$ -rays the concentrations of H and OH within the tracks are lower and more evenly distributed than with  $\alpha$ -,  $p$ -, or  $d$ -rays, where the radicals are in much greater local concentration and where there

<sup>16</sup> We shall refer to this as the instantaneous  $M/N$  value.

<sup>17</sup> We shall refer to this as the integral or gross  $M/N$  value.

are local predominances of one or other radical. In this latter case the fraction of the available radicals which recombine may well be higher than in the former, i.e.,  $k_2$  is larger for heavy-particle beams than for x-,  $\gamma$ -, and  $\beta$ -rays. The expectation is therefore that the concentration at which the ionic yield becomes dependent on solute concentration and dose rate will be smaller for x-rays than for, say,  $\alpha$ -rays. Correspondingly, if  $r'$  is the same for x- and  $\gamma$ -rays there will be a region of concentration for which the ionic yield with respect to the solute will be larger for x-rays than for  $\alpha$ -rays at the same dose rate. The only clear evidence in support of this view seems to be the work of Gray, Dale, and Meredith,<sup>18</sup> who found that in the inactivation of carboxypeptidase, the ionic yield for x-rays, though small, was yet much larger than the value for  $\alpha$ -rays; e.g., at a concentration of  $5 \times 10^{-3} M$ ,  $(M/N)_\alpha = 0.08 \times (M/N)_x$ . These authors also point out that if, with heavy-particle beams, the hydroxyl-radical concentration along the center of the particle track is much higher than the hydrogen-atom concentration spread over the whole of the track, then a reducing solute will show a dependence of  $M/N$  on concentration different from an oxidizing solute even though they react with their respective radicals with equal readiness.

### III. EXPERIMENTAL: DETECTION AND ESTIMATION OF "AVAILABLE" RADICALS BY INDUCED POLYMERIZATION OF WATER-SOLUBLE VINYL COMPOUNDS

#### A. INTRODUCTORY: PROBLEM AND METHOD OF ATTACK

The discussion in the preceding pages indicates that a pressing need in the study of the radiation chemistry of water is knowledge of the number, distribution, and type (suspected to be H atoms and OH radicals) of radicals available for reaction when a given dose of radiation of any kind is applied. The maximum number per cubic centimeter in time  $t$

$$= k\tau' \int_0^t R dt$$

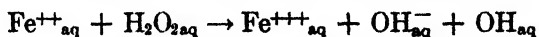
(see page 503), i.e., if none are lost by recombination. To ensure this latter condition it is essential that  $k_{18} \gg k_2 n$  (equation 1, page 503), and in order to minimize direct action on any solute,  $S$  should be as small as possible. It is therefore necessary to choose a solute which reacts very rapidly with either H or OH or both; i.e., keep  $k_1$  large. If these conditions are satisfied the rate of disappearance of solute  $= k\tau' RP$  and  $M/N = r'P$ ; hence if  $P$  is known,  $k\tau'$  can be found. It is also essential that the substrate react with uncharged water fragments only, and not with  $H^+$ ,  $OH^-$ , free electrons, or positive ions such as  $H_2O^+$ , etc. In order to identify these uncharged radicals the nature of their reaction with the selected solute should either be thoroughly known or readily capable of thorough investigation from studies of non-radiochemical systems.

These conditions are most likely to be satisfied by a reaction of solute and radical which does not involve a transfer of charge between the two, and suggests a non-ionic solute capable of adding H or OH. Such an addition reaction

<sup>18</sup> Private communication.

also raises the possibility of identifying the H or OH added to the solute by some modern refined method of analysis. If either H or OH can be so identified, the other fragment must also have been formed by the action of the radiation. A further feature of practical importance in studying the kinetics is that the change shall be readily followed; and to obtain reaction times of reasonable length with the sources of radiation available a reaction is to be preferred for which it would be likely that the ionic yield would be much greater than unity.

It seemed that such numerous and complicated requirements would most nearly be met by using some water-soluble vinyl compound, stable to high acid and alkali concentration, but likely to be polymerized to some insoluble product by the free-radical rather than the ionic mechanism. Such a solute would be likely to contain an electronegative substituent such as  $\text{COOCH}_3$ ,  $\text{COOH}$ ,  $\text{CN}$ , etc. Fortunately the recent work of Evans, Baxendale, and others (5, 6, 7) in which the polymerization in water of a number of these compounds was initiated by hydroxyl radicals generated by the reaction



provides a basis for selection of a suitable monomer. The monomer selected from amongst those studied by these workers was acrylonitrile ( $\text{CH}_2=\text{CHCN}$ ), and was chosen because aqueous solutions of this substance were found not to absorb light of wave lengths greater than  $2300 \text{ \AA}$ ., and it was hoped to initiate the polymerization by the hydroxyl radicals formed in the photolysis of hydrogen peroxide in aqueous solutions, the absorption of which begins at  $3700 \text{ \AA}$ . and extends to shorter wave lengths. This reaction, namely,



is to be preferred to the  $\text{Fe}^{++}\text{-H}_2\text{O}_2$  system as a source of hydroxyl radicals because of its simplicity and much lower temperature coefficient. Acrylonitrile proved to be satisfactory in almost all respects; however, polyacrylonitrile was found to be relatively insoluble in many of the common solvents such as acetone, benzene, chloroform, and carbon tetrachloride and only soluble in specially highly polar solvents such as dimethyl formamide and succinonitrile, which did not have the volatility desired for making thin films of polymer for infrared spectra determinations. Polymethacrylonitrile was readily soluble in acetone, in which its molecular weight could be determined and from solutions in which even films could be fairly easily deposited. Both nitriles were stable in air-free aqueous solutions of high and low pH (0.5 *N* sulfuric acid or sodium hydroxide) for indefinite periods, and both were therefore used in the experiments described below.

## B. EXPERIMENTAL METHODS

### 1. Preparation of materials

The nitriles were supplied by the National Research Council of Canada (acrylonitrile) and I.C.I. (methacrylonitrile) and were distilled *in vacuo* before use. It has not yet been possible to free methacrylonitrile monomers entirely

from water, and the OH infrared absorption band at 2.7 is always present, however slightly, in the monomer and also in the polymer formed by the thermal- or benzoyl peroxide-catalyzed polymerization of such monomer samples. It is hoped finally to remove these traces by distillation of the monomer from dehydrating agents. The boiling points at 760 mm. of the samples used were: acrylonitrile, 78.2°C.; methacrylonitrile, 90°C. The ferrous sulfate used was of the Analar brand. The hydrogen peroxide, ex Laporte and guaranteed free from stabilizer, was dissolved in distilled water and standardized by the usual methods before use. The deaerated pure water for the radiochemical experiments was prepared from distilled water by distillation twice from permanganate, then twice from alkaline manganous sulfate solution in a stream of oxygen-free nitrogen, and was finally run into the nitrogen-filled reaction vessel by means of an apparatus designed to exclude air at all stages.

### 2. Sources

The  $\gamma$ -ray sources used were 600-mc. radium samples and were enclosed in a platinum cylinder. The x-ray source was a G.E.C. Maximar Deep X-ray Therapy Unit, continuous rating 15 ma. at 220 kv., made available in Addenbrooke's hospital by the courtesy of Professor J. S. Mitchell. The mercury-vapor lamp was a vertical hot lamp operated at 150 v. and 2.2 amp.

### 3. Procedure

(a)  *$\gamma$ -Ray reaction:* A glass reaction cell (see figure 1) of 20 ml. capacity and with a central cavity into which the radiation source could be closely fitted was filled with monomer solution of known strength. The radium capsule source was placed in the cavity for allotted time intervals, and the insoluble polymer formed was separated by filtering through close-mesh sintered glass, or by centrifuging. In the quantitative work with acrylonitrile the precipitated polymer was washed with methanol and dried at 70°C. to constant weight. The work with  $\gamma$ -rays has so far been restricted to acrylonitrile.

(b) *X-ray work:* A quartz reaction vessel, normally used for photochemical work, consisting of a flat cylinder 2 cm. deep and having plane ends of diameter 7 cm., contained the monomer solution, and was held horizontally at the predetermined distance (4 cm.) from the aluminum filter of the Maximar set, from which the 1-mm. copper filter had been removed. To avoid overheating, irradiation for longer than 30 min. was intermittent, 30-min. irradiation periods alternating with 5-min. cooling periods. The polymer was separated as described above. When preparing specimens for infrared spectroscopic examination very great pains were taken to remove water. The polymer was always washed several times with a volatile non-hydroxyl-containing solvent, then transferred to a warm (50°C.) watch glass, pressed with a warm agate pestle to a thin layer and successively heated in an oven for 30 min. at 50°C., ground, and placed in a desiccator connected to the vacuum line. Constant weight was achieved after the first series of such operations, but the sequence was repeated three times and the final sample, by then in the form of a fine powder, was left in a high-vacuum desiccator until required, a period never less than several days.

(c) *Photochemical work:* A quartz reaction vessel, of similar dimensions to that described in the preceding paragraph and containing the hydrogen peroxide-monomer solution, was held vertically in a water thermostat made of copper with quartz windows and mounted on the same optical bench as the mercury lamp, a quartz lens, iris diaphragm, and 1.5-mm. thick Pyrex-glass filter which transmitted  $\lambda\lambda > 2900 \text{ \AA}$ . The polymer was separated and dried in the manner already described.



FIG. 1. 0.273 *M* acrylonitrile in deaerated pure water. *Left:* control, unirradiated; photographed after 11 days; no turbidity even after 20 days when central cavity was empty. *Right:* After 20 hr. exposure from 600 mc. radium placed in central cavity; note flocculent suspension of polymer.

(d) *Other measurements:* It had been hoped to measure the unchanged monomer still remaining in the solution after irradiation, as a check on the absence of any processes other than polymerization. No progress has yet been made by chemical means in this direction, largely owing to the fact that acrylonitrile, at any rate, does not appear to add halogens smoothly and is somewhat prone to undergo substitution as well. All measurements except ultraviolet spectra determinations have therefore been confined to the final polymers.

The ultraviolet absorption spectrum of the monomer solutions was obtained in the usual way at concentrations 0.2 to 0.3 *M*, path length 1–50 mm., and exposure times 1–4 min., using a Hilger E315 Spectrometer with a hydrogen lamp source.

Analyses for carbon, hydrogen, and nitrogen were carried out by Weiler and Strauss, Oxford.

Infrared spectra were measured in collaboration with Dr. D. A. Ramsay and

Dr. G. B. B. M. Sutherland in the Department of Colloid Science, using the Hilger D209 infrared double-beam spectrometer with automatic recording. Earlier some thirty runs were made with a single-beam instrument, but in this case, absorption by atmospheric water vapor was a considerable embarrassment. Acrylonitrile polymers were difficult to examine satisfactorily because attempts to prepare a thin film of this material failed; samples of the polymer were therefore ground into a paste in dry nujol and the paste held between rock salt plates. Under these conditions there was a considerable loss of energy due to scattering and no measurements of the concentration and absorption-path lengths were possible. Polymethacrylonitrile films could be made quite readily by deposition from acetone solution onto a clean mercury surface, according to a technique developed by Dr. Ramsay. None of these films was wholly transparent and some energy was lost by scattering.

*Molecular-weight* determinations are still highly undeveloped. Some few measurements were made viscometrically with the usual type of apparatus on unfractionated polymers. In applying the Staudinger equation the basic constant ( $k'$ ) was taken as  $10^{-4}$  for a linear vinyl polymer, using the formula

$$\text{Lt}_{c \rightarrow 0} \left( \frac{\eta_{sp}}{c} \right) = k' x M$$

where  $M$  is the molecular weight,  $x$  is the number of units in the chain of the sub-molecule ( $= 2$ ), and  $c$  is the concentration in sub-molecules per liter.

*Dosage rates* were calculated by the usual methods. The x-ray dose rates were obtained from direct calibrations of the output of the machines used.

*Traces of ferric ion* were estimated colorimetrically with 7-iodo-8-hydroxyquinoline-5-sulfonic acid, according to the methods recommended by the staff of Hopkins and Williams, Ltd.<sup>19</sup>

### C. RESULTS

The principal results obtained to date are summarized in the following paragraphs. It must be remembered that they all refer to preliminary work and are more an indication of the detailed program to be carried out than of work accomplished for which finality is claimed.

#### 1. The hydrogen peroxide-photosensitized polymerization of acrylonitrile and methacrylonitrile

Aqueous solutions of both nitriles do not absorb light of wave lengths greater than 2300 Å. and are quite stable when exposed either to light  $\lambda > 3000$  Å. or to the full light of a mercury arc. If the solution also contains dissolved hydrogen peroxide free from stabilizer, illumination with these wave lengths causes polymerization of the nitrile, which is detected by precipitation of the polymer. The onset of polymerization is marked by the appearance of turbidity in the solution and this turbidity does not become apparent until the reactant mixture

<sup>19</sup> *Organic Reagents for Metals*, p. 79. Hopkins and Williams Ltd. (1938).

has been illuminated for some time. This induction period appears to be increased by a decrease of the incident light intensity or the hydrogen peroxide concentration, but no detailed measurements have been made. The suspensions of the polymer in water seem to show a greenish-yellow fluorescence in ultra-violet light. All the polymers made in this way were of lower molecular weight than the x-ray polymers made from monomer solution of the same strength. The infrared absorption spectra of the polymers prepared photochemically showed clearly the presence of CH, CN, and OH groups. It was also notable that the ratio of the intensities of the OH to CH or CN bands was higher with the "photochemical" polymer than with the "radio" polymers, in keeping with the shorter chain lengths of the former.<sup>20</sup> In all the experiments carried out hitherto the initial monomer concentration exceeded 0.1 *M* and no oxygen evolution was detected. Nevertheless, there was always a slight but measurable decrease in hydrogen peroxide concentration, and it is of interest that, in three experiments in which the change in hydrogen peroxide concentration was carefully determined, the weight of polymer formed divided by the number of hydrogen peroxide molecules destroyed was of the same order as the mean molecular weight. The protocol of a single experiment illustrates most of these points:

*Run G Polymer G<sub>1</sub> (CH<sub>2</sub>=CHCN):*  $\lambda > 3000 \text{ \AA.}$  from mercury arc (150 v., 2.1 amp.); *T* = 25°C.

(H<sub>2</sub>O<sub>2</sub>) initially = 0.1047 *M*      (*m*<sub>1</sub>)<sub>0</sub> = 0.247 *M*

(H<sub>2</sub>O<sub>2</sub>) finally = 0.1042 *M*      (*m*<sub>1</sub>)<sub>f</sub> = not determined

Weight of dry polymer = 0.4270 g. } therefore percentage polymeriza-  
Volume of solution = 80 cc.      } tion = 40.8

Induction period = 50 ± 5 min.

Total irradiation = 4.17 hr.

*Remarks:*

No gas evolution; usual greenish yellow color of suspended polymer; left from February 28 to March 4 in vacuum desiccator.

*Analysis:*

	C <i>per cent</i>	H <i>per cent</i>	N <i>per cent</i>	Total
Calculated for C <sub>3</sub> H <sub>3</sub> N.....	67.9	5.66	26.4	
Found.....	67.4	5.7	26.1	97.2

Note: Deficit due to OH?

*Infrared spectrum:*

Ground into nujol. Detected CN (4.4–4.5  $\mu$ ), unbonded OH (2.7 $\mu$ ), and a little broad diffuse absorption up to 3  $\mu$  due to bonded OH. Nujol CH masked adsorption at 3.4  $\mu$ . Considerable scatter.

*Molecular weight ( $\bar{M}$ ):*

Of the order 5000.

<sup>20</sup> In some cases appreciable hydrogen bonding was detected.



*Calculations:*

Moles  $\text{H}_2\text{O}_2$  destroyed =  $4 \times 10^{-5}$

Number of moles of monomer removed per  $\text{H}_2\text{O}_2$  removed ( $\bar{P}$ ) =

$$\frac{0.4270}{53 \times 4 \times 10^{-5}} = 2.0 \times 10^2 \text{ (cf. } \bar{P} \text{ from } \bar{M} \text{)}$$

*Note:*

For the same irradiation time, pure hydrogen peroxide (0.1047 *M*) illuminated under the same conditions evolved about 10 cc. of oxygen, i.e., equivalent to  $90 \times 10^{-5}$  moles of hydrogen peroxide destroyed. Final concentration of hydrogen peroxide = 0.0950 *M*.

2. *The x- and γ-ray-induced polymerization of acrylonitrile and methacrylonitrile in dilute aqueous solution*

These reactions are remarkably similar to the photochemical reactions described under Section III,C,1. An induction period, which is increased by decrease of dose rate or monomer concentration is observed, no gas appears to be

TABLE 2  
*Polymerization of acrylonitrile induced by gamma rays*

SOURCE STRENGTH	MEAN DOSE RATE	[ <i>m</i> ]	$-\frac{100}{[m]} \cdot \frac{d[m]}{dt}$	SECOND-ORDER CONSTANT $\times 10^4$	INDUCTION PERIOD
<i>millicuries</i>	<i>r/min.</i>	<i>M</i>	<i>hr.</i> <sup>-1</sup>	<i>mole</i> <sup>-1</sup> <i>sec.</i> <sup>-1</sup>	<i>hours</i>
600	40	0.209	4.05	5.4	3.7
600	40	0.1045	1.95	5.2	$8 \pm 0.4$
600	40	0.0522	1.07	5.7	$19 \pm 1$
600	40	0.178	3.49	5.45	3.4
1200	80	0.178	3.7	5.8	1.95

evolved, and the OH group vibration frequency is apparent in the infrared absorption spectra of the dry polymers. The major differences between the radio polymers and the photochemical polymers which have been prepared so far is the higher molecular weight and lower OH/CH absorption intensity ratio of the former. Two other observations of importance are (a) that the ionic yield when measured was found to be considerably smaller than the weight-average degree of polymerization and (b) that an equimolar concentration of ferrous sulfate only slightly retards the polymerization and is itself oxidized in the process.<sup>21</sup>

The kinetics of the γ-ray-induced polymerization of acrylonitrile in dilute aqueous solution have been described (15), and are summarized in table 2 and in figures 2 and 3. The reaction is second order with respect to monomer concentration and the rate appears to be independent of source strength. The ion-pair yield is  $10^4$  for the 600-mc. source at the highest concentration used and

<sup>21</sup> The ratio of rate of oxidation of  $\text{Fe}^{++}$  and initiation of polymerization suggests that  $\text{Fe}^{++}$  is less than a tenth as efficient as monomer in reacting with the radicals produced by the action of x-rays on water.

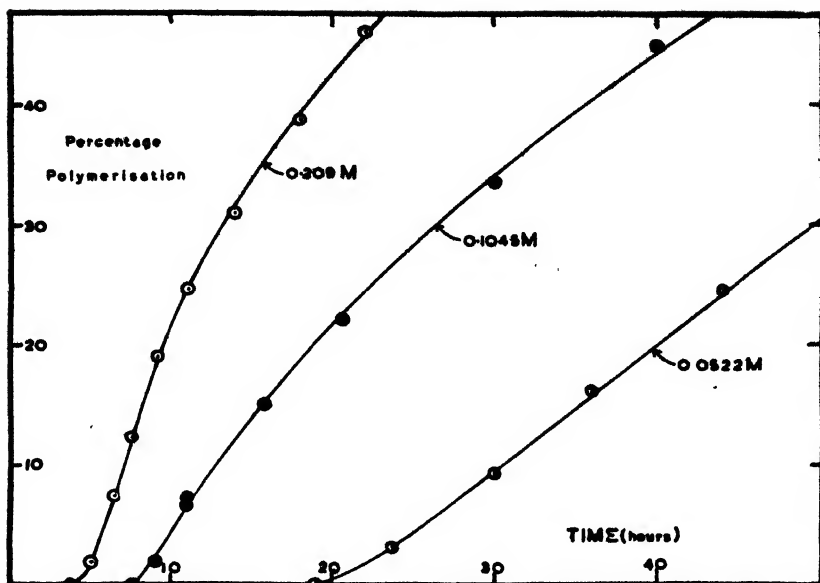


FIG. 2. Polymerization of acrylonitrile in dilute aqueous solution at 20°C. Source: 600 mc. radium in platinum cylinder. Radiation:  $\gamma$ -rays from 0.2406 to 1.761 m.e.v.;  $\sim 3.6 \times 10^8$  quanta  $\text{cm}^{-2} \text{sec}^{-1}$  at 1 cm.

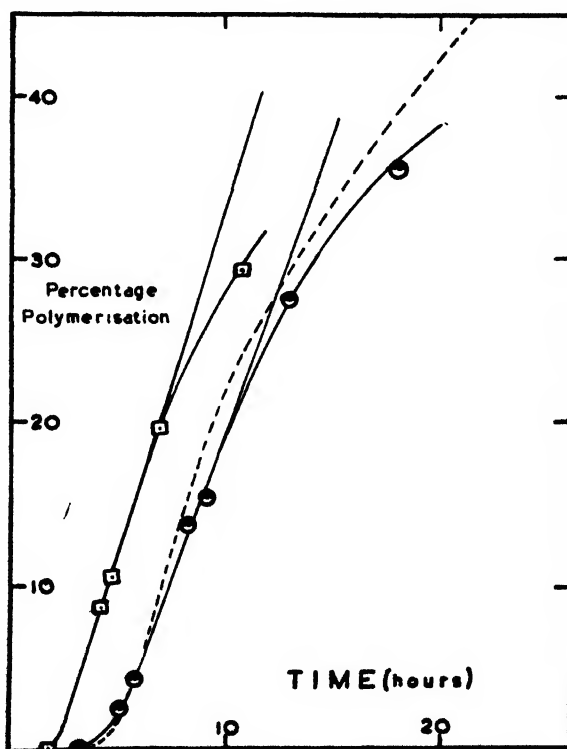


FIG. 3. Polymerization of acrylonitrile in dilute aqueous solution at 20°C. Effect of source strength.

- 0.178 M; 1200 mc. radium;  $k = 5.8 \pm 0.3$  liters  $\text{mole}^{-1} \text{sec}^{-1}$
- 0.178 M; 600 mc. radium;  $k = 5.5 \pm 0.2$  liters  $\text{mole}^{-1} \text{sec}^{-1}$
- - - 0.209 M; 600 mc. radium;  $k = 5.4 \pm 0.15$  liters  $\text{mole}^{-1} \text{sec}^{-1}$

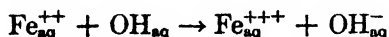
varies inversely with the dose rate. The induction period is shortened by increase of monomer concentration or increase of dose rate.

#### IV. DISCUSSION

The experimental results outlined in the preceding sections permit certain tentative conclusions and indicate how further quantitative work along these lines may lead to an estimate of the kind, number, and spatial distribution of the number of radicals available for reaction, i.e., the value of  $r'$  defined on page 503. The conclusions may be stated.

##### A. NATURE OF THE RADICALS

The presence of OH in the "radio" polymer is strongly supported by the similarity of the hydrogen peroxide photosensitized reaction to the radiochemical reaction. In the photochemical reaction no decomposition of the hydrogen peroxide to oxygen was detected, and it is concluded that under the conditions of the photochemical experiments all the hydroxyl radicals, which are known to be the only products of the primary act (13), are incorporated in the final polymer by virtue of the part they play in initiating, and possibly also in terminating, polymerization chains. In passing we note that measurements of OH/CH infrared absorption intensities on "photo" polymers of known molecular weight containing a number of hydroxyl radicals determined from the fall in hydrogen peroxide concentration during reaction offer the possibility of calibrating the infrared method and hence counting the OH radicals per molecule by this method. This possibility will be explored, since such a method might be applied to give an absolute measure of the OH radicals formed for a given dose in the radiochemical reaction. Less substantial confirmatory evidence is provided by the fact that the presence of ferrous sulfate in amounts equal to the monomer concentration caused a slight retardation of the x-ray-induced polymerization of the methacrylonitrile. Ferrous ions are known to be oxidized by hydroxyl radicals according to the reaction



and hence should be effective competitors of the methacrylonitrile molecules for hydroxyl radicals. In agreement with this expectation, traces ( $\sim 10^{-4}M$ ) of  $\text{Fe}^{+++}$  were found in a solution after irradiation, but the ionic yield of  $\text{Fe}^{+++}$  was of the order of 0.2, which is smaller by a factor of at least 10 than the ionic yield<sup>22</sup> for this reaction in the absence of any other solute. We conclude that ferrous ions are less reactive to hydroxyl radicals than methacrylonitrile.<sup>23</sup>

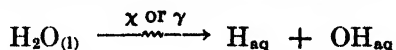
If hydroxyl radicals are formed by the action of radiation on water, then hydrogen atoms must be formed in equal amounts. No gas evolution was detected in any of the experiments, although with doses larger than  $10^5$  roentgens

<sup>22</sup> Fricke and Hart (23) give  $M/N = 3$  for oxidation of ferrous sulfate by x-rays.

<sup>23</sup> See table III in reference 7, where a similar result in the competition between ferrous ions and methyl acrylate for OH radicals is apparent.

on 80 cc. of solution some would have been expected, and it must be presumed that these atoms do not recombine but react with monomer molecules, thereby initiating polymerization. Initiation of the polymerization of vinyl compounds in the gas phase by hydrogen atoms is well established (see, for example, 43).

We conclude that the primary radiochemical act in water can be written



#### B. NUMBER OF RADICALS AVAILABLE FOR REACTION ( $r'$ )

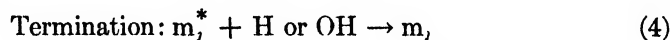
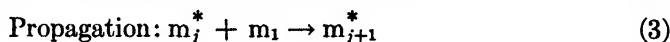
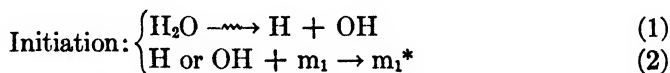
The study of the radiochemically induced polymerization of vinyl compounds may be used to count the number of radicals available for reaction when the mean energy for creation of an ion-pair is absorbed, by several distinct methods. Firstly, irrespective of the mode of termination of the chains, each completed polymer molecule will, in its production, have caused the destruction of two radicals: either 2H, 2OH, or H and OH. Knowledge of the molecular-size distribution curves and total weight of polymer formed for a given radiation dose will permit the calculation of the total number of polymer molecules formed. Hence, if no radicals are lost by recombination (the form of the dependence of  $M/N$  on the dose rate will reveal whether this is true or not), and if there are no side reactions, the total number of radicals formed will be twice the number of polymer molecules formed. Secondly, the rate of polymerization measured as rate of disappearance of monomer will be an experimentally ascertainable function of the rate of production of radicals and the velocity constants for initiation, propagation, and termination processes of the polymerization reaction. The values of these latter constants may be measured by studying non-radiochemical polymerizations of the same monomer, e.g., the polymerization photosensitized by hydrogen peroxide. Hence the rate of production of radicals associated with a given dose rate can be determined and  $r'$  calculated. Thirdly, it may be possible to make the infrared analytical method quantitative for the estimation of OH groups in the final polymer and so provide a useful supplement to the first method.

None of these methods have been applied as yet in the form described above, but it is perhaps not without significance that whereas in the photochemical polymerization of methacrylonitrile in hydrogen peroxide solution in the one case examined the mean kinetic chain length (= monomer molecules used  $\div$  hydrogen peroxide used) was approximately the same as the mean chain length determined viscometrically, in the radiochemical polymerization of the same monomer, the ionic yield was always considerably smaller than the mean chain length. If further work substantiates this observation, we must conclude that the number of radicals available per ion-pair in water is less than unity.

#### C. SPATIAL DISTRIBUTION OF THE RADICALS

In their studies (5, 6, 7) of the polymerization of methyl methacrylate in aqueous solution induced by hydroxyl radicals formed by the  $\text{Fe}^{++}$ - $\text{H}_2\text{O}_2$  reaction, Baxendale, Evans, and coworkers find the mode of chain termination to depend

upon the hydroxyl-radical concentration. At low values of initiator concentration the predominant mode is interaction of growing polymers in pairs, but at high concentrations of initiator termination by interaction of a growing chain with a hydroxyl radical becomes important. Kinetic studies will show whether this is also the case in the polymerization of acrylo- and methacrylo-nitriles by hydroxyl radicals. If the kinetics of the radiochemical polymerization indicate that the termination is by hydroxyl radicals and hydrogen atoms, although the over-all rate corresponds to a radical concentration which if averaged over the whole volume of the solution is inadequate for this type of termination to predominate, it must be concluded that the available radicals are unevenly distributed when produced radiochemically, being present in high local concentrations. There appears to be some evidence for this effect in the  $\gamma$ -ray-induced polymerization of acrylonitrile, where the independence of the reaction rate on dose rate and the second-order kinetics can only be accounted for by the reaction scheme<sup>24</sup>:



where \* denotes growing polymer and  $m_1$  = monomer. The scheme leads to

$$-\frac{d[m_1]}{dt} = \frac{k_2 k_3}{k_4} [m_1]^2$$

In conclusion, it is perhaps not unjustifiable to state the hope that quantitative measurements of the kind described in this paper may lead to further knowledge concerning the radiochemistry of water.

## V. SUMMARY

From a consideration of the molecular structure of water, electron-impact data on water vapor, and the general mechanism of energy loss of fast charged particles passing through matter, it is concluded that the primary radiochemical act in water vapor is in part ionization, with formation of  $\text{H}_2\text{O}^+$ , and  $\text{H}^+$  (and  $\text{OH}$ ), and  $\text{OH}^+$  (and  $\text{H}$ ), and in part excitation, probably with dissociation to  $\text{H}$  ( $^2\text{S}$ ) and  $\text{OH}$  (in either the  $^2\Pi$  or  $^2\Sigma$  states). Charge neutralization and ion-neutral molecule reactions result in more  $\text{H}$  atoms and  $\text{OH}$  radicals being formed. The possible effects of radical recombination and wall adsorption on the magnitude of the ionic yield of water vapor and its dependence on dose rate are next discussed.

In liquid water it is assumed that the mechanism of energy dissipation is substantially the same as in the vapor. The major differences in effect are that in

<sup>24</sup> Chain transfer has been disregarded, because it would not affect the rate of monomer consumption, and conceivable chain-transfer reactions with water are appreciably endothermic.

the liquid there will be: (a) increased ion density, (b) increased energy and probability of hydration of the ions, (c) increased chances of deactivation of excited species, and (d) immediate (i.e., Franck-Rabinowitch) recombination of a portion of the  $H + OH$  radical pairs formed by dissociation of the same water molecules. The kinetics of the radiolysis of pure water and of indirect action on solutes are discussed from this point of view, and it is concluded that in high solute concentrations the ionic yield should be independent of both solute concentration and dose rate. At low solute concentration under conditions where only a fraction of the available radicals react with the solute,  $H_2 + H_2O_2$  are to be expected among the primary products and the ionic yield becomes a function of the dose rate and solute concentration. The independence of the ionic yield on concentration of solute should persist to lower concentrations the lower the track density and hence the lighter the ionizing particle.

Very preliminary results are presented on the x- and  $\gamma$ -ray-induced and the hydrogen peroxide-photosensitized polymerization of acrylonitrile and methacrylonitrile in dilute aqueous solution. In the reaction photosensitized by hydrogen peroxide the primary act is  $H_2O_2 \xrightarrow{h\nu} 2OH$  and under the conditions of experiment, all the OH radicals initiate polymerization chains. The kinetic chain length and degree of polymerization data are not inconsistent, and the OH groups present in the final polymer may be detected by infrared spectroscopic analysis. In the radiochemical reactions similar polymers are formed, the infrared spectra of which also show the OH group to be present. The kinetics of these reactions, insofar as they have been elucidated, combined with other evidence, indicate that H atoms and OH radicals are formed by the action of x- and  $\gamma$ -rays on water and that these species are probably not uniformly distributed but exist in high local concentration.

#### REFERENCES

- (1) ALLIBONE, T. E., AND GEDYE, G. R.: *Proc. Roy. Soc. (London)* **A130**, 346 (1930).
- (2) ALLSOPP, C. B.: *Trans. Faraday Soc.* **40**, 79 (1944).
- (3) AMDUR, I., AND ROBINSON, A. L.: *J. Am. Chem. Soc.* **55**, 1395 (1933).
- (4) BAILEY, V. A., AND DUNCANSON, W. E.: *Phil. Mag.* **10**, 145 (1930); **14**, 1033 (1932).
- (5) BAXENDALE, J. H., BYWATER, S., AND EVANS, M. G.: *Trans. Faraday Soc.* **42**, 675 (1946).
- (6) BAXENDALE, J. H., EVANS, M. G., AND KILHAM, J. K.: *Trans. Faraday Soc.* **42**, 668 (1946).
- (7) BAXENDALE, J. H., EVANS, M. G., AND PARK, G. S.: *Trans. Faraday Soc.* **42**, 155 (1946).
- (8) BETHE, H.: *Handbuch der Physik* **24**, (i), 519 (1933).
- (9) BONHOEFFER, K. F., AND PEARSON, T. G.: *Z. physik. Chem.* **B14**, 1 (1931).
- (10) BRADBURY, N. E., AND TATEL, H. E.: *J. Chem. Phys.* **2**, 835 (1934).
- (11) BRATTAIN, K. G.: *J. Phys. Chem.* **42**, 617 (1938).
- (12) BURTON, M.: *J. Phys. Colloid Chem.* **51**, 611 (1947).
- (13) BURTON, M., AND ROLLEFSON, G. K.: *Photochemistry and the Mechanism of Chemical Reaction*, pp. 175, 379. Prentice-Hall, Inc., New York (1939).
- (14) CAMERON, A. T., AND RAMSAY, WM.: *J. Chem. Soc.* **93**, 965 (1908).
- (15) DAINTON, F. S.: In press.
- (16) DAINTON, F. S., AND MILLER, N.: 11th Intern. Congress, in press.
- (17) DALE, W. M., GRAY, L. H., AND MEREDITH, W. J.: Private communication.

- (18) DUANE, W., AND SCHEUER, O.: *Le Radium* **10**, 33 (1913).
- (19) DWYER, R. J., AND OLDENBERG, O.: *J. Chem. Phys.* **12**, 351 (1944).
- (20) EYRING, H., HIRSCHFELDER, J. O., AND TAYLOR, H. S.: *J. Chem. Phys.* **4**, 479, 570 (1937).
- (21) FRANCK, J., AND RABINOWITCH, E.: *Trans. Faraday Soc.* **30**, 120 (1934).
- (22) FRICKE, H., AND BROWNSCOMBE, E. R.: *Phys. Rev.* **44**, 240 (1933).
- (23) FRICKE, H., AND HART, E. J.: *J. Chem. Phys.* **3**, 60 (1935).
- (24) GEDYE, G. R.: *J. Chem. Soc.* **1931**, 3016.
- (25) GHORMLEY, J. A.: Quoted by Burton in reference 12.
- (26) GÜNTHER, P., AND HOLZAPFEL, L.: *Z. physik. Chem.* **B42**, 346 (1939).
- (27) GÜNTHER, P., AND LEICHTER, H.: *Z. physik. Chem.* **B34**, 443 (1936).
- (28) GURNEY, R. W.: *Ions in Solution*. The Macmillan Company, New York (1936).
- (29) HYLLEBRASS, E. A.: *Z. Physik* **60**, 624 (1930).
- (30) JUZA, R.: *Z. anorg. Chem.* **231**, 121 (1937).
- (31) KERNBAUM, M.: *Le radium* **6**, 225 (1909).
- (32) KOLUMBAN, A. D., AND ESSEX, H.: *J. Chem. Phys.* **8**, 450 (1940).
- (33) LATIMER, W. M.: *Oxidation Potentials*. Prentice-Hall, Inc., New York (1938).
- (34) LAVIN, G. I., AND STEWART, F. B.: *Nature* **123**, 607 (1929).
- (35) LEA, D. F.: *Actions of Radiations on Living Cells*. Cambridge University Press, London (1946).
- (36) Reference 35, p. 47.
- (37) Reference 35, Chap. II.
- (38) LEDERLE, E.: *Z. physik. Chem.* **B17**, 362 (1932).
- (39) LIND, S. C., BARDWELL, D. C., AND PERRY, J. H.: *J. Am. Chem. Soc.* **48**, 1556 (1926).
- (40) LOEB, L. B.: *Phys. Rev.* **48**, 689 (1935).
- (41) MANN, M. M., HUSTRULID, A., AND TATE, J. T.: *Phys. Rev.* **58**, 340 (1940).
- (42) MASSEY, H. S. W.: *Negative Ions*. Cambridge University Press, London (1938).
- (43) MELVILLE, H. W.: *Proc. Roy. Soc. (London)* **A163**, 511 (1937).
- (44) MOTT, N. F., AND MASSEY, H. S. W.: *Theory of Atomic Collisions*. Oxford University Press, London (1933).
- (45) MULLIKEN, R. S.: *J. Chem. Phys.* **3**, 506 (1935).
- (46) NORRISH, R. G. W.: *Trans. Faraday Soc.* **33**, 1521 (1937).
- (47) NOYES, W. A., JR., AND LEIGHTON, P. A.: *Photochemistry of Gases*, p. 253. Reinhold Publishing Corporation, New York (1941).
- (48) Reference 47, p. 254.
- (49) Reference 47, p. 262.
- (50) Reference 47, p. 369.
- (51) Reference 47, pp. 373 *et seq.*
- (52) Reference 47, p. 397.
- (53) Reference 47, p. 408.
- (54) OLDENBERG, O., AND COWORKERS: *J. Chem. Phys.* **2**, 713 (1934); **3**, 266 (1935); **4**, 642, 781 (1936); **6**, 169, 439, 779 (1938); **7**, 485 (1939).
- (55) PRICE, W. C.: *J. Chem. Phys.* **4**, 149 (1936).
- (56) RATHENAU, G.: *Z. Physik* **87**, 32 (1934).
- (57) RISSE, O.: *Z. physik. Chem.* **A140**, 133 (1929).
- (58) RODEBUSH, W. H., AND WAHL, M. H.: *J. Chem. Phys.* **1**, 696 (1933).
- (59) SKINNER, H. A.: *Trans. Faraday Soc.* **41**, 645 (1945).
- (60) SMALLWOOD, H. M.: *J. Am. Chem. Soc.* **56**, 1542 (1934).
- (61) SMITH, C., AND ESSEX, H.: *J. Chem. Phys.* **6**, 188 (1938).
- (62) SMYTH, H. D., AND MUELLER, D. W.: *Phys. Rev.* **43**, 116 (1933).
- (63) WEISS, J.: *Nature* **153**, 748 (1944).
- (64) WOURTZEL, E.: *Le Radium* **11**, 289 (1919).

QUENCHING OF FLUORESCENCE IN SOLUTION<sup>1</sup>

G. K. ROLLEFSON AND H. BOAZ

*Department of Chemistry, University of California, Berkeley, California**Received October 23, 1947*

The study of the quenching of fluorescence is of particular interest to the subject of chemical kinetics because it is concerned with a large number of relatively simple reactions. In all reactions of this kind the rate is studied by observing the decrease in concentration of a reactant; the latter quantity is determined by the intensity of the fluorescence. Furthermore there is no net reaction in systems of this kind, a fact which greatly facilitates the taking of unambiguous quantitative measurements. For the purposes of this discussion we shall apply the term fluorescence to the emission of light by a photoactivated system within a short time interval after the absorption of light has occurred. The length of the time interval elapsing between the absorption and emission processes is not of importance, except in so far as it may influence the relative importance of the different reactions which the activated molecule may undergo.

The intensity of fluorescence which is observed in any solution is determined by the number of light quanta absorbed by unit volume of the solution and the rate of the fluorescence process relative to the rates of the other processes which the activated molecule may undergo. The intensity is also often modified by the absorption of the fluorescence by the unactivated molecules of the fluorescent substance, but this effect is usually small at low concentrations. The competing processes may be divided according to the kinetic point of view into first and second or higher order reactions. The first-order reactions include deactivation by the solvent, all kinds of spontaneous internal conversion processes, and those which may be induced by the presence of the solvent. In addition, any second-order reactions involving the light-absorbing substance will appear to be first order in any given set of quenching experiments.

If  $A^*$  represents the concentration of photoactivated molecules in a given system, the rate of each first-order deactivation process may be expressed by a differential equation of the form  $dA^*/dt = kA^*$ . Let  $k_1, k_2, \dots$  be the rate constants for the various processes of this kind; then the total rate of deactivation of  $A^*$  by first-order reactions is  $dA^*/dt = (k_1 + k_2 + \dots)A^*$ . The fraction reacting by any one path is the constant for that path divided by the sum of the constants for all of the first-order paths. In some systems, such as solutions of fluorescein in water, the principal process is the deactivation by emission of radiation. On the other hand, there are many more systems in which the non-radiative processes are of relatively great importance and the quantum yield of fluorescence is low.

The average life of a photoactivated molecule is defined as the reciprocal of the sum of the rate constants for the first-order reactions, i.e.,  $1/(k_1 + k_2 + \dots)$ .

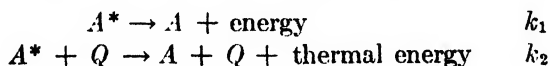
<sup>1</sup> Presented at the Symposium on Radiation Chemistry and Photochemistry which was held at the University of Notre Dame, Notre Dame, Indiana, June 24-27, 1947.



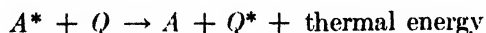
The magnitude of the lifetime thus determined is one of the major factors in determining the importance of second-order processes.

Under the heading of second-order processes are included those cases in which the intensity of fluorescence is reduced by formation of a complex between the fluorescent substance and the substance added. Thus the quenching of the fluorescence of uranyl ion by oxalate is due to the formation of the weak electrolyte uranyl oxalate, in which much of the absorbed energy is used in bringing about the decomposition of the oxalate. Such a possibility for the mechanism of the quenching process must always be considered but it is by no means a universal one. For example, it was shown by Rollefson and Stoughton (3) that the quenching of acridone or the acid form of fluorescein by potassium iodide did not cause any decrease in the activity of the fluorescent molecules in solution. In these cases the constancy of the activity was demonstrated by studying the distribution of the fluorescent substance between the aqueous solution and the benzene as the quencher was added. This technique is applicable only in those cases in which the fluorescent substance exists in the form of neutral molecules in the solution. With ionic solutes the question as to whether or not a complex is formed must be answered from other considerations. Sometimes a change in the absorption spectrum of the solution when the quencher is added will show the presence of a complex. Such is the case in the uranyl oxalate system. There are, however, bound to be some systems for which it will be difficult to make a definite decision concerning the nature of the molecules present in the mixture of solutes. In the discussion which is to follow we shall not be concerned with systems in which definite complexes are formed, but we shall limit ourselves to those cases in which the quenching process can be attributed to a close approach of the quencher molecule to the photoactivated molecule.

The competition of the second-order quenching process with all of the first-order processes mentioned above is represented by the two equations



or



By these we do not propose to limit ourselves with respect to the right-hand members of the equations but merely indicate that we are dealing with processes of these kinetic types. The constant  $k_1$  for the first reaction is the sum of the constants for all of the possible first-order processes. Similarly,  $k_2$  is the sum of the constants for all possible mechanisms for quenching which are kinetically of the first order with respect to both the photoactivated molecules and the quencher. The fraction of the  $A^*$  molecules which react by a first-order process in the presence of a quencher is  $1/(1 + (k_2/k_1)(Q))$ . The ratio of the intensity of the fluorescence in the presence of the quencher to that from the solution without quencher is also given by this fraction. The ratio  $k_2/k_1$  is called the

quenching constant, and will be designated by  $k$ . Hence, the equation for the action of a quencher may be put into the form

$$I_0/I = 1 + k(Q)$$

in which the intensity of fluorescence in the absence of a quencher is designated by  $I_0$ , and that with the quencher present is  $I$ . ( $Q$ ) is the concentration of the quencher. This equation was derived from this point of view by Stern and Volmer (4) in 1920. In 1931 Frank and Vavilov (1) proposed a modification of this equation in which the right-hand member of the equation was multiplied by an exponential factor to allow for the quenching which occurs because a molecule

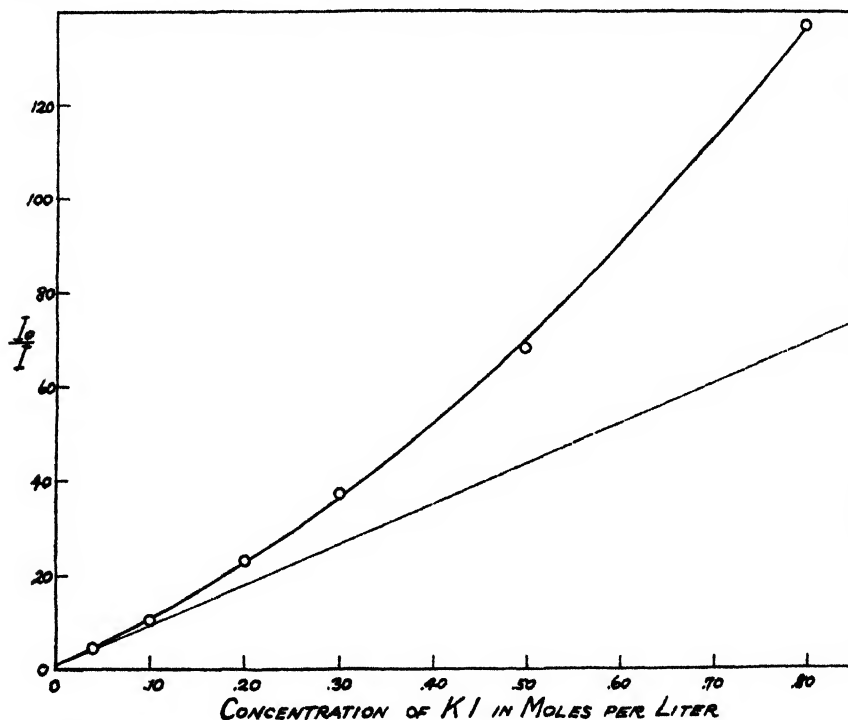


FIG. 1. Intensity of fluorescence as a function of the concentration of quencher

of quencher happens to be within the necessary sphere of action at the time the absorbing molecule is activated. This so-called static quenching has been discussed extensively by W. N. Sveshnikoff (6), who concluded that it is not important.

The equation given above requires that a plot of the values of  $I_0/I$  against the concentrations of the quencher should be a straight line, with a slope equal to  $k$ . Actually,  $k$  is affected to a marked degree by the ionic strength of the solutions if both the reactants are charged molecules. Even if the ionic strength is kept constant by the addition of a non-quenching salt or if we study the quenching of the fluorescence of a neutral molecule, there is a noticeable tendency for the quenching constant to increase at high concentrations of the quencher. This fact is illustrated by the curve shown in figure 1, which represents the

quenching of acridone by potassium iodide. The curvature at high concentrations can be explained in more than one way. It is of course possible that it is due to the static quenching proposed by Frank and Vavilov, since the data shown here go to much higher quenching than was studied by Sveshnikov in the experiments in which he obtained negative results. On the other hand, it may be that the increased quenching is due to a small amount of a third-order

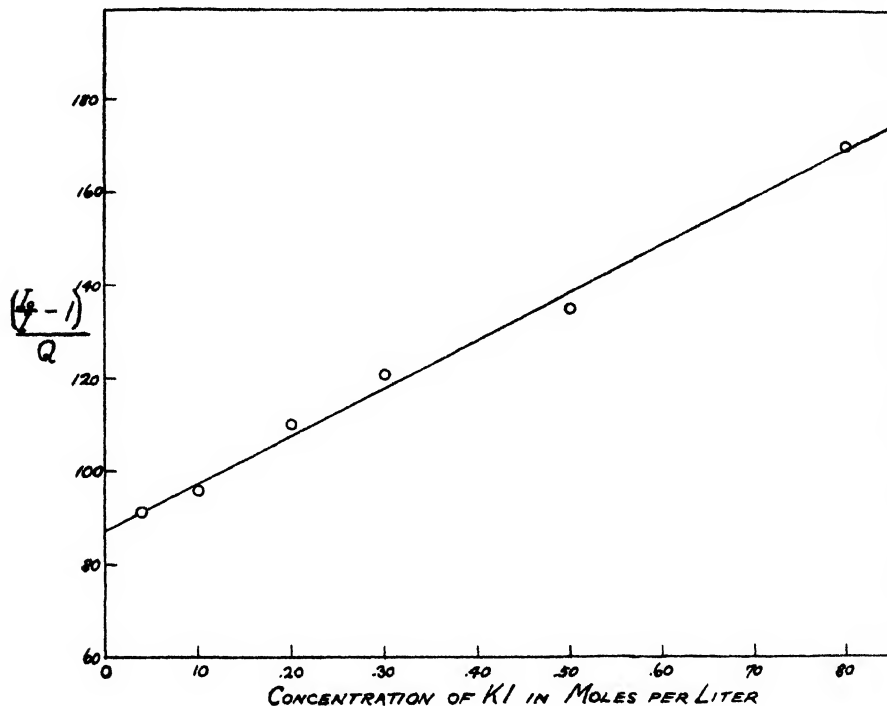


FIG. 2. Quenching constant as a function of the concentration of the quencher

process. The effect of such a process can be shown by writing the quenching equation in the form:

$$I_0/I = 1 + k(Q) + k'(Q)^2$$

It readily follows from this equation that:

$$\left( \frac{I_0}{I} - 1 \right) / (Q) = k + k'(Q)$$

If the values for the left-hand member of this equation are plotted as ordinates with values of  $(Q)$  as abscissas, a straight line should be obtained with an intercept of  $k$  and a slope of  $k'$ . Such a plot is shown in figure 2 and it is apparent that the data fit the above equation quite well. Since the Frank and Vavilov equation can be reduced to the same form as a first approximation, these data do not suffice to decide between third-order processes and the so-called static quenching. For the present it is sufficient to say that the data support the

idea that quenching is primarily a competition of a second-order reaction with the fluorescence process and any other first-order processes which may be occurring.

The quenching constant as defined above is a ratio of a bimolecular rate constant to the sum of some monomolecular rate constants, or it may be looked upon as the product of a bimolecular constant and the lifetime of the photo-activated molecule under the conditions prevailing in the solution. A ratio of the constants for the action of two quenchers on the same fluorescent molecule is therefore the ratio of the two bimolecular rate constants, but if we consider the ratio of the constants for the action of one quencher on two different photo-activated molecules the result is the ratio of the rate constants multiplied by the ratio of the lifetimes. If the only variable condition is the concentration of the quencher, the latter ratio may be considered a constant which it would be necessary to evaluate for the consideration of absolute reaction rates but need not be evaluated if only relative values are to be considered. In the discussion which is to follow we shall be concerned with such relative values.

In the older literature it is said that the substances which may act as quenchers for fluorescence can be arranged in a series such that any given substance is a better quencher than those that follow it but poorer than those which precede it in the series. The non-validity of this idea was pointed out by Rollefson and Stoughton (3) in 1941. They presented evidence that a considerable number of fluorescent substances can be divided roughly into two groups. One of these groups is quenched by substances such as iodide, thiocyanate, bromide, etc. but not by nitrate. The other group is quenched by iodate, bromate, nitrate, etc. but is only slightly affected by iodide. It is apparent therefore that any discussion of the quenching process must be prepared to deal with a significant amount of specificity.

Recently La Mer (7) and his students have published some discussion of quenching viewed as a diffusion-controlled process. That diffusion is an important factor in determining the rate of the quenching process in many cases cannot be denied, since there are many instances in which the magnitude of the quenching constant is definitely dependent on the viscosity of the solution. Such a viscosity dependence is by no means universal, as is shown by the fact that the quenching of the quinine fluorescence by silver ion is independent of the viscosity. Furthermore, the wide variation in the ratios of the quenching constants calculated for various pairs of quenchers on different fluorescers cannot be explained as due to diffusion.

In order to emphasize the specificity of the quenching constants consider the data tabulated in table 1. The data for acridone, acridonesulfonic acid, and anthracenesulfonic acid are taken from the paper of Stoughton and Rollefson (5) and the other values have been obtained recently by the authors. It is apparent that even if we limit ourselves to dyes which belong to one of the two groups set up by Rollefson and Stoughton, the ratios are far from being constants determined solely by the nature of the quenchers. Any theory which pretends to explain the quenching action must be able to account for these specific effects.

In the remainder of this paper various possible mechanisms for the quenching process and possible means of distinguishing between them are to be discussed. It is to be understood that these mechanisms do not exclude diffusion effects but supplement them.

A consideration of the properties of photoactivated molecules leads to the conclusion that the possible mechanisms for quenching can be grouped under three broad headings: (1) The quencher induces internal conversion of the excitation energy into thermal energy. (2) The quencher removes a relatively large quantity of energy by a specific transfer. (3) The activated molecule enters into some chemical reaction with the quencher, and the net effect is reversed by subsequent dark reactions.

TABLE 1  
*Some typical examples of quenching constants*

FLUORESCER	QUENCHER		$\frac{k_I^-}{k_{Ag^+}}$	
	Ag <sup>+</sup>	I <sup>-</sup>		
Acridone	12.2	92.0	7.55	
Anthracenesulfonic acid	70.8	7.25	0.104	
Acridonesulfonic acid	12.6	50.1	3.98	
	QUENCHER			
	IO <sub>3</sub> <sup>-</sup>	NO <sub>2</sub> <sup>-</sup>	I <sup>-</sup>	OH
	73	55	0.1	173
	25	13	0.1	44
	25	18		
1-Naphthol-4-sulfonate	24	9	0.1	0

The induced internal conversion of the excitation energy into thermal energy may be brought about in a number of ways. One which certainly must be given consideration is the possibility that the presence of the quencher causes an effect analogous to the phenomenon referred to as induced predissociation in gaseous systems. In this case it is not necessary for the photoactivated molecule to dissociate but only necessary for it to pass to another electronic state from which it returns to the lowest state by collisional deactivation rather than by the emission of radiation. The probability of such a transfer occurring depends on the specific nature of the selection rule which must break down and the intensity of the field supplied by the quencher. An example of this type of induced transfer is furnished by the magnetic quenching of the fluorescence of iodine. An effect of this sort is not ordinarily linear with the field strength, so it is not to be expected that the ratio of the quenching constants for two quenchers acting on a series of fluorescent molecules will be constant. However, it is to be expected that the order of arrangement of the quenchers would be the same for all molecules if this is the mechanism for the quenching process. Furthermore, it is to be expected that positive ions would be as effective as

negative ions in quenching and doubly charged ions would be even more effective. It is apparent that the data which have been presented are not in accord with such a hypothesis.

An induced internal conversion of the excitation energy need not involve the breakdown of a selection rule. It is perfectly possible that all that a quencher needs to do is perturb the vibrations so that the energy is distributed into more degrees of freedom. The ease with which such an effect may occur may be related to the polarizability of the fluorescent molecule. Whatever the details of the mechanism may be, it is apparent that such effects should depend on the field of force of the quencher molecule whether it is due to a charge on that molecule, van der Waals forces, or other effects such as the polarizability of the molecules. No general effect of this type can account for the specificity manifested by the data.

The second type of quenching mechanism, the removal of a relatively large quantity of energy by a specific transfer, is obviously capable of supplying any degree of specificity needed. Many studies have been made of gaseous systems which show that the maximum quenching efficiency is obtained when the energy to be removed from the photoactivated molecule is just that required to transfer the quencher from its lowest state to a definite excited state. A particular example is furnished by the quenching of the fluorescence of mercury vapor. In that case it has been shown that the molecules which are the best quenchers have an energy difference between two of the lowest vibrational states which is approximately equal to the  $6\ ^3P_1 - 6\ ^3P_0$  difference in the mercury atom. As another example it is known that when Hg ( $6\ ^3P_1$ ) collides with a sodium atom, the mercury atom returns to the lowest state and the sodium takes up the energy, going to the  $9\ ^2S_{1/2}$  state.

In dealing with substances in solution we do not have complete information concerning the energy states for either the fluorescent or the quencher molecules. It was pointed out by Rollefson and Stoughton that there is no correlation between the efficiency of a quencher and its absorption spectrum. It is necessary therefore to find some energy difference which corresponds to a transition between two states for which some selection rule forbids the transition by the absorption or emission of radiation. At the same time, if this transfer is not going to return the fluorescent molecule to its lowest state we must find some evidence for an intermediate energy level in that molecule. One possibility is suggested by the work of the late Professor G. N. Lewis and his students (2). They have demonstrated the existence of metastable states by studies of the phosphorescence of these molecules in rigid media. In some cases proof has been presented that the metastable states thus detected are triplet states. Most of the substances investigated have not had the quenching of their fluorescence studied, but a few such do exist. Fluorescein and rhodamine, which belong to the iodide-quenched group, have differences between the upper singlet and the triplet states of 6-10 kg.-cal. per mole, whereas in  $\alpha$ -naphthylamine, which is in the other group, the difference is near 30.

The nature of the transition in the quencher must be such that its occurrence

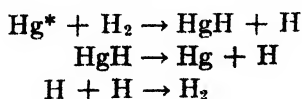
by absorption of radiation is of low probability, i.e., it must be contrary to some selection rule but such rules do not hold in collisions. An unpairing of electrons in both molecules would be expected to be of lower probability than unpairing in only one. The quenching of the fluorescence of many dyes by oxygen may be due to a  $S \rightarrow S$  transition in the dye with a  $T \rightarrow S$  transition in the oxygen. The energy difference between the lowest singlet and triplet states of oxygen is known to be of the right magnitude for this purpose.

Adequate data for a test of this mechanism are not available but can be obtained readily. Obviously it is capable of accounting for extremely specific effects. If this is the mechanism for the majority of the cases of quenching, it should be possible to arrange a list of quenchers in order according to the effective energy difference. Thus, iodide might be towards one end of such a series and iodate towards the other. Substances such as silver ion, which quench both of the classes which we have mentioned, may be in the middle or may have two effective energy differences. It is to be noted that the effectiveness of one quencher may be less than that of another, either because its effective energy-level separation is too large or because it is too small.

Unfortunately, most of the work of Lewis and his associates has been done with non-electrolytes in non-polar solvents, whereas the work on quenching has been done with electrolytes in solution in water or at least a polar solvent. In order to test the singlet-triplet idea adequately, work must be done on non-aqueous systems. Even if no correlation is found between the singlet-triplet separations and the efficiencies of various quenchers in such non-aqueous systems, a study of such systems will permit gradual variations in conditions which are bound to shed light on the mechanism of quenching.

Before leaving the discussion of the mechanism it should be pointed out that although attention has been called to the singlet-triplet differences, there are other transitions which may be the important ones. A positive correlation between the singlet-triplet difference and quenching efficiency would be strong evidence for this mechanism, but a failure to observe such a correlation would not disprove it. The test is actually quite severe, since it requires that if iodide ion quenches fluorescein because of an energy difference in each which is in the range of 5-10 kg.-cal. per mole, then iodide ion cannot effectively quench any substance with a difference of 25-30 kg.-cal. per mole unless we assume a second and larger difference in the iodide.

The third type of quenching mechanism is one in which the photoactivated molecule enters into a reaction which is followed by dark reactions of such a nature that no net reaction occurs. An example of this type is the dissociation of hydrogen by  $\text{Hg}^*$ . This reaction probably involves the sequence:



Electron transfers, such as postulated by Weiss, i.e., oxidation-reduction reactions, may occur in solutions. Although there is no correlation between the

oxidizing (or reducing) strength of a substance and its quenching power, it must be considered that the photoactivated molecule may enter into a reaction with a substance which is such that in the absence of photoactivation the equilibrium is far in favor of the original substances. Another type of reaction which might occur is illustrated by the anthracene-dianthracene photostationary state. Although in that case the reaction product is produced in sufficient quantity to observe, such would not be the case if the back-reaction were faster. It is possible also that in some cases a dye may be reduced by a quencher and re-oxidized by dissolved oxygen. Such cases may be detected by eliminating oxygen from the solution, a procedure not ordinarily followed, or by prolonged illumination. The latter procedure is not desirable, since some side-reaction becomes apparent on long illumination in most systems.

In reviewing these three proposed mechanisms for quenching it is to be noted that specific examples have been cited for each type. Although these examples have been taken from gaseous systems it would be unwise to say that similar examples cannot be found in solutions. Therefore we must admit the possibility that all three types of mechanism play a rôle in solutions. It has been pointed out that for the first type of mechanism the effectiveness of a quencher should depend on some general type of property, such as the field of force around the quencher, and not to any significant extent on the chemical composition of the quencher. The fact that such forces cannot account for the highly specific effects observed does not mean that they may not aid in bringing about a change by some other mechanism. Thus the general electrostatic field of a quenching ion may modify the energy differences in a fluorescent molecule in such a way as to make the quenching action different from that which occurs when an uncharged molecule is used as a quencher. The high degree of specificity apparent in the quenching action is strongly in favor of either the specific energy transfer or the chemical reaction as the mechanism of quenching, with the former preferred.

If the ideas presented in this discussion should be confirmed by later experiments we have in these studies a means of greatly increasing our knowledge concerning the energy states of both the quencher and the fluorescent molecules. Such information may be of great value in seeking correlations between the rates of other reactions involving these substances. Even if such a goal is not achieved, the quenching of fluorescence is still a means of studying the effects of various factors on the rates of reaction.

#### SUMMARY

In this paper the quenching of fluorescence is viewed as a second-order process competing with the various first-order processes which the photoactivated molecule undergoes. An experimental test of the validity of this view is presented.

In discussing the mechanism of quenching three types of processes are offered for consideration. They are: (1) The quencher induces internal conversion of the excitation energy into thermal energy. (2) The quencher removes a relatively large quantity of energy by a specific transfer. (3) The activated



molecule enters into some chemical reaction with the quencher, and the net effect is reversed by subsequent dark reactions.

■ Examples are presented of all three types of action occurring in gaseous systems. Some preliminary data, however, indicate that the specific energy transfer may be of major importance in the quenching of dyes by various ions. It is pointed out that if this view is supported by additional data we have in these studies a means for obtaining data concerning metastable states which cannot now be obtained in any other way.

#### REFERENCES

- (1) FRANK, I. M., AND VAVILOV, S. I.: *Z. Physik* **69**, 100 (1931).
- (2) LEWIS, G. N., AND KASHA, M.: *J. Am. Chem. Soc.* **66**, 2100 (1944).
- (3) ROLLEFSON, G. K., AND STOUGHTON, R. W.: *J. Am. Chem. Soc.* **63**, 1517 (1941).
- (4) STERN, O., AND VOLMER, M.: *Z. wiss. Phot.* **19**, 275 (1920).
- (5) STOUGHTON, R. W., AND ROLLEFSON, G. K.: *J. Am. Chem. Soc.* **61**, 2634 (1939).
- (6) SVESHNIKOFF, W. N.: *Acta Physicochim. U.R.S.S.* **4**, 453 (1936).
- (7) UMBERGER, J., AND LA MER, V. K.: *J. Am. Chem. Soc.* **67**, 1099 (1945); also three papers presented at the 111th Meeting of the American Chemical Society, which was held at Atlantic City, New Jersey, April, 1947.

## THE REVERSIBLE PHOTOBLEACHING OF DYES AND PIGMENTS

ROBERT LIVINGSTON

*School of Chemistry, Institute of Technology, University of Minnesota,  
Minneapolis, Minnesota*

*Received October 23, 1947*

The primary process of a photochemical reaction may be defined as including (12) "the initial act of absorption and those immediately following processes which are determined by the properties of the initially excited electronic state." The photochemist who studies the reactions of simple molecules in the gas phase has the distinct advantage that more or less complete information in regard to the primary process may be obtained directly from spectroscopic data. This advantage does not exist for the photochemistry of complex molecules. Indeed, the study of the primary process in such complicated reactions as dye-sensitized photooxidations in solution is often the most difficult part of the investigation of the reaction. It is doubtful if the detailed nature of the primary process, or as it is sometimes called (15) the "inner or hidden" mechanism, of any photochemical reaction involving dyes or pigments is known with any certainty.

Until fairly recently it was maintained very tenaciously by a group of photochemists that fluorescence and photochemistry were complementary processes.

<sup>1</sup> Presented at the Symposium on Radiation Chemistry and Photochemistry which was held at the University of Notre Dame, Notre Dame, Indiana, June 24-27, 1947.

That is, all of the photochemical action was produced by a direct interaction between a substrate molecule and the sensitizing molecule in the relatively short-lived excited state which leads to fluorescence. This hypothesis is scarcely consistent with the well-known fact (4) that there is no parallelism between the efficiency of dyes as photosensitizers and their maximum fluorescent yields obtained in the absence of the substrate. Indeed, dyes are known which are capable of sensitizing photooxidation with yields approaching unity, but whose maximum fluorescence yields in the absence of the reactants are less than 0.01. More definite evidence against this simple theory was obtained by Gaffron (2) in the study of chlorophyll-sensitized photooxidations and in the photochemical autooxidation of rubrene. Particularly in the latter case, it was demonstrated that the minimum life of the activated state which leads to the chemical reaction must be more than a thousandfold greater than the life of the fluorescent state. Thus, the photochemical evidence seems to demand the existence of a long-lived activated form of the sensitized molecule, which is reached indirectly through the first excited state (1).

Further evidence for the existence of long-lived excited states of complex molecules comes from the studies of Vavilov (18, 20), Kautsky (6), Pringsheim (14), Lewis (9), and others on dyes adsorbed or dissolved in extremely viscous solvents. Under these conditions a phosphorescence is observed which has the same wave-length distribution as the ordinary fluorescence but whose life is temperature dependent. At very low temperatures, when the life of this radiation is relatively long, a new long-lived emission becomes detectable. This long-lived fluorescence<sup>2</sup> has a life which is independent of temperature and a mean wave length which is distinctly longer than that of the ordinary fluorescence. The heat of activation which is associated with the life of the phosphorescence is equal to or greater than the difference in energy between the phosphorescent quanta and the long-lived fluorescent quanta. Jabłoński (5) was the first to interpret these facts in terms of a simple energy diagram involving three electronic levels. The absorption and fluorescence of the molecule are due to transitions between the ground state, *A*, and the first excited state, *B*. Radiative transitions between these states and the third state, *C*, which has an energy level between *A* and *B*, are forbidden. However, a radiationless transition (internal conversion) (19) between states *B* and *C* can occur. Since the molecules are in solution, the (generalized) oscillational energy in excess of the thermal amount is quickly lost by collision with solvent molecules. Phosphorescent emission occurs when a molecule in state *C* acquires sufficient energy of activation to revert to state *B*. Since phosphorescence is not commonly observed in solution at ordinary temperatures, it must be possible for state *C* to go over to a high oscillational level of state *A* and so degrade its energy as heat. This radiationless transition determines the life of state *C* under ordinary conditions. In

<sup>2</sup> The older definitions of fluorescence and phosphorescence (13) are used in this paper. Delayed emission the half-life of which is strongly temperature dependent is called phosphorescence, while delayed emission whose half-life is temperature independent is referred to as long-lived fluorescence. Lewis and his coworkers (9) adopted the opposite convention.

extremely viscous solvents or in the absorbed state, this radiationless transition becomes relatively unimportant and phosphorescence is observed. At low temperatures the life of the phosphorescence exceeds the natural life of the temperature-independent long-lived fluorescence, which then becomes the dominant process.<sup>3</sup>

Additional information regarding the inner mechanism of photosensitization by chlorophyll can be obtained from a study of the reversible photobleaching of chlorophyll solutions. This effect was discovered by Porret and Rabinowitch (16) in 1937; its existence was confirmed and it was further studied by Livingston in 1941 (10). Recently the investigation of this phenomenon has been renewed by McBrady and Livingston (11). Unlike the reversible photobleaching of thiazine dyes (3, 21), the photobleaching of chlorophyll solutions occurs in the absence of added reducing agents. The studies of Holst (3) show that the bleaching of methylene blue in the presence of phenylhydrazine is a typical case of a photostationary state, analogous to the photochemical stationary state involving iodine and ferrous ion (17). In cases of this type there appears to be little probability of obtaining information regarding the nature of the primary process by a study of the reversible bleaching. However, since chlorophyll is photobleached in solutions containing no added reactants, it appears much more probable that the course of the bleaching may be directly related to the primary process of photosensitization.

Figures 1, 2, and 3 illustrate typical cases of photobleaching of chlorophyll solutions. The duration of each experiment in seconds is plotted as abscissa and the decrease in molarity of chlorophyll as ordinate. The interval between measurements is 5 sec. The point at the end of each light interval is indicated by a circle; that following a dark interval, by a solid dot. In the experiments illustrated by the figures the source of actinic light was a 1000-watt projection lamp, equipped with suitable lenses and with filters which transmit the red end of the spectrum and absorb most of the infrared as well as the blue-violet end of the spectrum. The solutions were made up in purified methanol, and were  $2 \times 10^{-6} M$  in respect to chlorophyll *a*. The details of the experimental measurements have been discussed elsewhere (11). In computing the decrease in the molarity of chlorophyll it was assumed (16) that the bleached form of chlorophyll does not absorb at all in the red end of the spectrum.

Figure 1 is typical of the bleaching in air-free methanol solutions. Under these conditions the steady-state bleaching ranged from 0.2 to 0.6 per cent, depending upon the sample of solvent and chlorophyll used. The steady-state bleaching was attained in less than 3 sec. (which was the period of the galvanome-

<sup>3</sup> No discussion of either the cause of the long life of state *C* or the mechanism by which the molecule goes from state *B* to state *C* is included in the preceding statement. These controversial points have been treated extensively elsewhere (1, 7, 8, 9), and it would be beyond the scope of the present paper to present them adequately. In the opinion of the author, the experimental facts obtained for different types of compounds cannot be fitted by any one simple formulation which attempts to specify the exact nature of the electronic states and of the radiationless transitions.

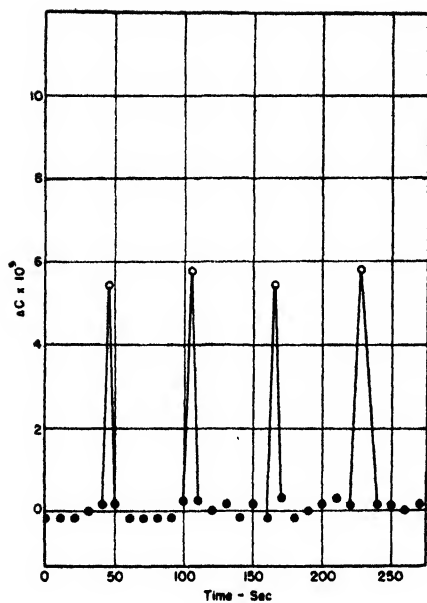


FIG. 1

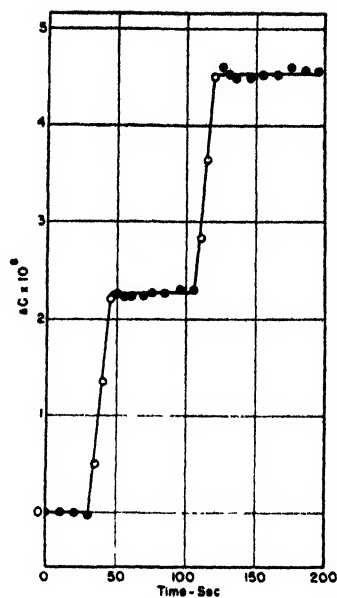


FIG. 2

FIG. 1. Reversible bleaching of chlorophyll in air-free methanol solutions

FIG. 2. Irreversible bleaching of chlorophyll in the presence of air

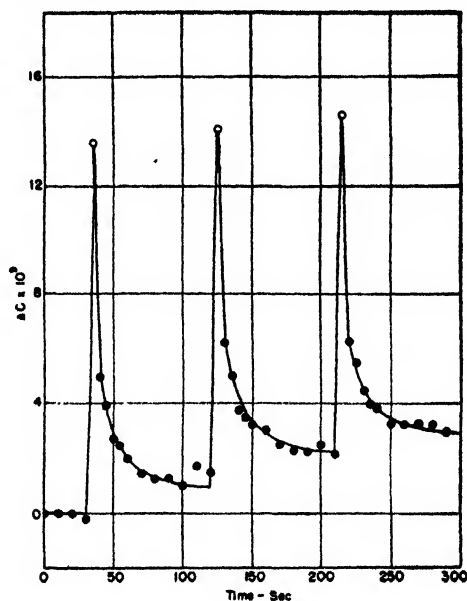


FIG. 3. Reversible bleaching of chlorophyll (prepared with carbon tetrachloride) in air-free methanol solutions.

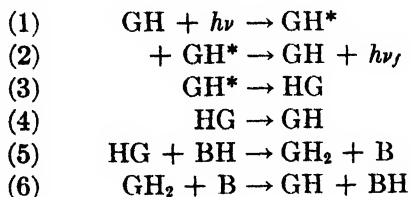
ter used) and the half-life of the bleached material was less than 0.5 sec. Experiments performed with different intensities of the actinic light demonstrated that the steady-state bleaching is directly proportional to the square root of

the intensity of the absorbed light. The initial concentration of chlorophyll appears to have no effect upon the bleaching except indirectly, owing to the change in the intensity of the absorbed light. Both the steady-state bleaching and the rate of the reverse dark reaction appear to be independent of temperature in the range from 5° to 25°C. The reversible bleaching is always accompanied by a relatively slow irreversible bleaching, its rate usually being less than 10 per cent of the reversible effect.

Oxygen completely inhibits the reversible bleaching and somewhat increases the irreversible action. However, even in solutions saturated with air, the rate of the irreversible reaction is never more than 20 per cent of the rate of the reversible process which would be observed in the same solution in the absence of air. Figure 2 illustrates the bleaching of a solution saturated with air.

The reverse reaction, which occurs in the dark, appears to be sensitive to small traces of impurities. For example, the bleaching of solutions of chlorophyll prepared by a slightly modified procedure follows the course illustrated by figure 3 rather than figure 1. The only difference in the two methods of preparation was that in the latter case (figure 3) carbon tetrachloride was substituted for the ether which was used as a solvent in the standard method of purifying chlorophyll. Further experiments showed that this difference was due to impurities present in the carbon tetrachloride used in the experiments. Table 1 summarizes the effects produced by a number of different added substances. It is noteworthy that reactive reducing agents (such as hydroquinone) are practically without effect, while oxalic acid and oxidizing agents (such as methyl red and iodine) have a marked effect. The striking change produced by dilute solutions of iodine is paralleled by the efficiency with which iodine quenches the fluorescence of chlorophyll and changes its absorption spectrum. Iodine apparently forms a compound with chlorophyll and so modifies its photochemical properties.<sup>4</sup>

Although the data presently available are not sufficient to permit a definite decision as to the mechanism of the reversible bleaching, it is possible to set up a series of reaction steps which are consistent with the known facts:



The symbols used have the following significance: GH is normal chlorophyll; GH\* is electronically excited (singlet state) chlorophyll; HG is long-lived activated chlorophyll (probably in a tautomeric, triplet state); GH<sub>2</sub> is the partly reduced, bleached form of chlorophyll; and BH is a reactive, reducing impurity present in the solvent. This mechanism leads to the following expression for the change in chlorophyll concentrations,  $\Delta C$ , at the steady state. In agreement

<sup>4</sup> The evidence for these effects of iodine will be presented elsewhere with Dr. W. Watson.

with the experiments, this equation indicates that the steady-state bleaching is proportional to the square root of the intensity of absorbed light and that it

TABLE 1  
*The effect of added substance upon the reversible bleaching of chlorophyll*

SOLVENT	ADDED SUBSTANCE	M	$\Delta C/\Delta C_0$	$\varphi$	REVERSE REACTION		REFERENCE
					Order	$k(g)$	
CH <sub>3</sub> OH . . . .	None <sup>(a)</sup>		1	$\geq 4 \times 10^{-4}$	2	$\geq 6 \times 10^8$	(11)
CH <sub>3</sub> OH . . .	Oxygen	$< 10^{-4}$	0				(10,11,16)
CH <sub>3</sub> OH . .	Fe <sup>++</sup>		0				(16)
CH <sub>3</sub> OH .	Allylthiourea	0.05	$\sim 1$		2		(10, 11)
CH <sub>3</sub> OH . .	Hydroquinone	0.01	$\sim 1$		2		(10)
CH <sub>3</sub> OH . . .	Isoamylamine	50 per cent	$\sim 1$		2		(10)
CH <sub>3</sub> OH .	Carbon dioxide		$\sim 1$		2		(16)
(CH <sub>3</sub> ) <sub>2</sub> CO .	— (b)	—					(10)
CH <sub>3</sub> OH . . .	Formic acid <sup>(c)</sup>	0.01	30		2		(16)
CH <sub>3</sub> OH . . .	Formic acid	0.01	3		2		(10)
CH <sub>3</sub> OH	Formic acid	0.01	$\sim 1$		2		(11)
CH <sub>3</sub> OH	Impurity in carbon tetrachloride <sup>(d)</sup>	?	2	$1 \times 10^{-4}$	2	$3 \times 10^7$	(11)
CH <sub>3</sub> OH . . .	Methyl red	$10^{-5}$	4				(11)
CH <sub>3</sub> OH . .	Oxalic acid	$10^{-4}$	3	$7 \times 10^{-4}$	1	$2 \times 10^{-1}$	(11)
CH <sub>3</sub> OH .	Iodine <sup>(e)</sup>	$10^{-5}$	150	$1 \times 10^{-3}(?)$	1(?)	$\sim 10^{-2}(?)$	(11)
CCl <sub>4</sub> . . . . .	Impurities <sup>(f)</sup>	?	$< 1$	$4 \times 10^{-4}$	2	$4 \times 10^5$	(11)

<sup>(a)</sup> The data are consistent with reference 16. Reference 10 indicates  $k \approx 6 \times 10^8$ .

<sup>(b)</sup> Qualitatively similar to methanol solutions except that the irreversible reaction is faster.

<sup>(c)</sup> These divergent results suggest that the effect is due to an impurity in the formic acid.

<sup>(d)</sup> The addition of allylthiourea neutralizes the effect of this impurity.

<sup>(e)</sup> A compound between iodine and chlorophyll is apparently formed.

<sup>(f)</sup> The irreversible reaction accounts for about half of the yield. An after-bleaching occurs for about 0.5 sec. after the light is cut off.

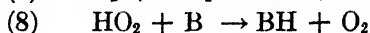
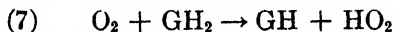
<sup>(g)</sup> Second-order  $k$ 's are expressed in liters/mole  $\times$  sec.; the first-order  $k$ 's in reciprocal seconds.

varies with an uncontrolled factor, the concentration and the chemical nature of an unknown impurity.

$$\Delta C = \left[ \frac{k_2}{k_2 + k_3} \times \frac{k_4 (BH)}{k_4 + k_5 (BH)} \times \frac{I}{k_6} \right]^{\frac{1}{2}}$$

$I$  indicates the intensity of the absorbed light (in appropriate units) and  $k_i$  is the rate constant for the  $i^{\text{th}}$  reaction step.

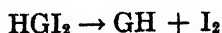
While the assumption that the partly reduced radical,  $\text{GH}_2$ , is the bleached form of chlorophyll is plausible, it is completely arbitrary. In fact, the evidence presented in table 1 suggests that it is more likely that the bleached form is the partly oxidized radical,  $\text{G}$ . The former alternative was chosen in the present mechanism since it is consistent with the following (1) simple explanation for the inhibitory action of oxygen:



These reactions fit in with the  $\text{HO}_2$  mechanism (21) of sensitized autooxidations. In the presence of a relatively high concentration of a reducing agent, as allylthiourea (2), the  $\text{HO}_2$  would be reduced and the radical  $\text{B}$  would react, presumably, with some of the radicals formed in the reaction chain.

Another way in which the inhibition by oxygen could be explained would be to assume that the paramagnetic oxygen molecule catalyzes steps 3 and 4 (increasing their absolute rates at least one hundredfold). Since these steps are radiationless transitions which (presumably) violate the intercombination rule, this assumption appears quite plausible. This explanation has the advantage that it does not require that  $\text{GH}_2$  be the bleached form of chlorophyll. Furthermore, it is consistent with the reported (6) quenching of chlorophyll phosphorescence by oxygen. It is questionable, however, whether it can be reconciled with the experimental data on sensitized autooxidations (2). It is obviously inconsistent with the  $\text{HO}_2$  mechanism (21) for photooxidations. Gaffron's mechanism (2) for these reactions, which postulates that the reaction is initiated by a direct interaction between molecules of the reductant and of activated chlorophyll, may possibly be compatible with this assumption, but would lead to the (untested) prediction that high concentrations of oxygen should retard the autooxidations.

Professor Franck<sup>5</sup> has suggested that the action of iodine in enhancing the bleaching and changing the reverse reaction to first order is due to the addition of an iodine molecule to a double bond of an excited chlorophyll molecule, thereby interrupting the resonating system. This photochemical reaction is preceded by a dark reaction between chlorophyll and iodine.<sup>4</sup> The reverse reaction will be the unimolecular dissociation (or rearrangement) of the bleached compound,  $\text{HGI}_2$ , as follows:



This mechanism leads to the prediction that iodine should increase the quantum yield of bleaching as well as reduce the rate of the reverse reaction. A similar explanation for the effects of methyl red and of oxalic acid seems probable.

#### REFERENCES

- (1) FRANCK, J., AND LIVINGSTON, R.: J. Chem. Phys. **9**, 184 (1941).
- (2) GAFFRON, H.: Ber. **60B**, 755 (1927); Biochem. Z. **264**, 251 (1933).

<sup>5</sup> Private communication.

- (3) HOLST, G.: Z. physik. Chem. **A179**, 172 (1937); **A182**, 321 (1938).
- (4) HURD, F., AND LIVINGSTON, R.: J. Phys. Chem. **44**, 865 (1940).
- (5) JABLOŃSKI, A.: Acta Phys. Polon. **4**, 311 (1935).
- (6) KAUTSKY, H., HIRSCH, A., AND FLESCH, W.: Ber. **65**, 401 (1932); **68**, 152 (1935).
- (7) LEWIS, G., AND CALVIN, M.: J. Am. Chem. Soc. **67**, 1232 (1945).
- (8) LEWIS, G., AND KASHA, M.: J. Am. Chem. Soc. **66**, 2100 (1944).
- (9) LEWIS, G., LIPKIN, D., AND MAGEL, T.: J. Am. Chem. Soc. **63**, 3012, 3005 (1941).
- (10) LIVINGSTON, R.: J. Phys. Chem. **45**, 1312 (1941).
- (11) McBRADY, J., AND LIVINGSTON, R.: J. Phys. Colloid Chem. **52**, No. 4 (1948).
- (12) NOYES, W. A., AND LEIGHTON, P. A.: *The Photochemistry of Gases*, p. 153. Reinhold Publishing Corporation, New York (1941).
- (13) PRINGSHEIM, P.: *Fluorescenz and Phosphorescenz*, p. 160. J. Springer, Berlin (1928).
- (14) PRINGSHEIM, P., AND VOGELS, H.: J. Chem. Phys. **33**, 345 (1936).
- (15) RABINOWITCH, E.: *Photosynthesis*, Vol. I, p. 494 Interscience Press, Inc., New York (1945).
- (16) RABINOWITCH, E., AND PORRET, P.: Nature **140**, 321 (1937).
- (17) RIDEAL, E., AND WILLIAMS, E. G.: J. Chem. Soc. **127**, 258 (1925).
- (18) SCHISCHLOWSKY, A., AND VAVILOV, S.: Z. Physik (U.S.S.R.) **5**, 379 (1934).
- (19) TELLER, E.: J. Phys. Chem. **41**, 109 (1937).
- (20) VAVILOV, S., AND LEVSHIN, W.: Z. Physik **35**, 920 (1926).
- (21) WEISS, J.: Trans. Faraday Soc. **35**, 48 (1939).

## THE PHOTOCHEMISTRY OF THE ALDEHYDES<sup>1</sup>

F. E. BLACET

*Department of Chemistry, University of California, Los Angeles, California*

*Received October 23, 1947*

The absorption spectra and vapor pressures of the aldehydes are such as to invite photochemical studies of them in the gaseous phase. They all have a first region of absorption in the near ultraviolet with a span of approximately 1000 Å. On the long-wave-length side this region is always discontinuous in character, showing some fine structure in the case of the more simple molecules. The fine structure blends into a diffuse or what has been designated a predissociation spectrum, and this in turn changes over to a continuum on the short-wave-length fringe of the region. A second absorption region soon starts in below this and continues perhaps another thousand Ångström units well into the Schumann region. A few investigators have ventured into this second region, but for the most part it remains unexplored, waiting for the development of better equipment and better technique for quantitative studies. We shall return in this discussion, therefore, to the first absorption region, where much work has been done. It is believed that here at least a beginning has been made toward an appreciation of the chemical processes which follow the absorption of radiant energy.

<sup>1</sup> Presented at the Symposium on Radiation Chemistry and Photochemistry which was held at the University of Notre Dame, Notre Dame, Indiana, June 24-27, 1947.



In figure 1 are given microphotometer tracings of acetaldehyde, propionaldehyde, and isobutyraldehyde (21). The spectrum of normal butyraldehyde coincides almost exactly with that of isobutyraldehyde showing, however, slightly more pronounced bands. Similarities and differences in structure are apparent. Detail structure becomes less evident with decreasing wave length and with increasing molecular weight. Attention is called particularly to acetaldehyde. One can see the distinct structure reported by Henri and Schou (16) as extending to 3300 Å. The bands which they reported as becoming more and more diffuse at shorter wave lengths extend well beyond the limit of 2820 Å. set by them. These bands are most intriguing, but they are not of sufficient detail to make possible a mathematical interpretation of the spectrum. However, from th

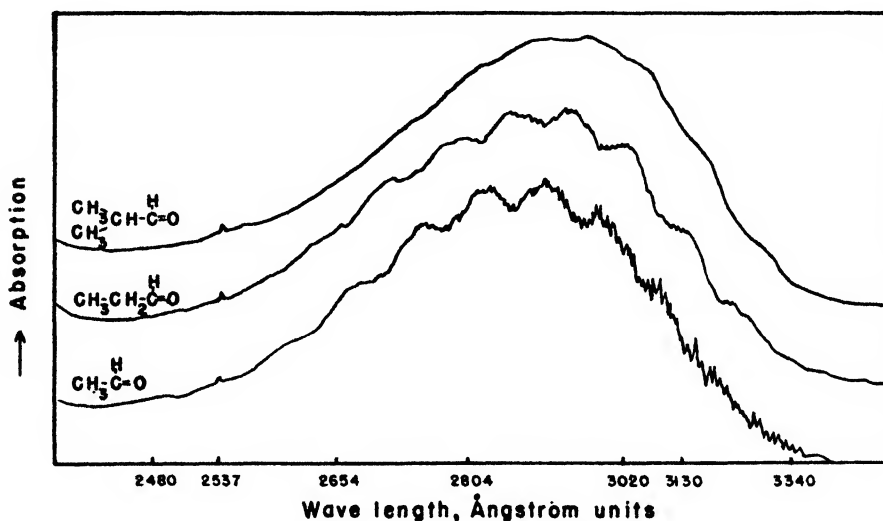


FIG. 1. Microphotometer tracings of the absorption spectra of acetaldehyde, propionaldehyde, and isobutyraldehyde. The positions of the principal lines of the mercury arc are indicated.

interpretation which had been given to somewhat similar spectra of diatomic molecules, a physical concept of such spectra of polyatomic molecules was formulated by Henri (15) and others somewhat as follows: Bands having distinct structure indicate electronic excitation with lives of the order of  $10^{-8}$  sec. With the aldehydes these occur on the long-wave-length side of this region of absorption. The continuum which lies on the short-wave-length side was conceived to represent molecular dissociation, which takes place within the period of one vibrational cycle, i.e., in approximately  $10^{-13}$  sec. The intermediate diffuse bands were designated as predissociation spectra by Henri. Predissociation has been described in various ways, but we can do no better than follow the lead of Burton and Rollefson (13) and consider predissociation as a decomposition process which occurs after a time greater than one vibration period has elapsed following absorption. The mercury arc lines make possible the study

of the aldehydes with monochromatic radiation in each absorption type (see figure 1). Such chemical studies should serve to extend and amplify our general interpretations of the absorption spectra of complex molecules.

For formaldehyde (16), acrolein, and crotonaldehyde (10) the first absorption region is shifted a few hundred Ångström units to longer wave lengths and in general shows more detailed structure. The ketones have absorption spectra similar to the aldehydes in this region. Since the carbonyl group is common to all these compounds, absorption is thought to represent the excitation of an electron associated with this group.

As supporting evidence for the processes attributed to the types of spectra in this region, some of the aldehydes at any rate show pronounced fluorescence at long wave lengths. This fluorescence diminishes in intensity as the bands become less evident and is no longer discernible in the continuum. The absorption and fluorescence spectra, with their interpretation, led to predictions twenty or more years ago that no dissociation of these compounds would take place if they were irradiated with monochromatic light falling in the wavelength range of fine structure bands (15). In the diffuse range some dissociation might occur, while in the continuum all absorption leads to dissociation in a period of time far shorter than that between molecular collisions. These predictions,—namely, that radically different chemical results were to be expected at different wave lengths,—stimulated investigation and early results were reported to be in general agreement with them. However, since most early experiments were little more than qualitative in nature, it would perhaps have been better to say that they were not in disagreement with spectral interpretations.

As indicated in figure 1, the mercury arc is a convenient light source for detailed study of the aldehydes. With proper equipment individual lines of sufficient intensity can be isolated to study the chemical effect of absorption in each region. This has been done with several aldehydes under various other experimental conditions. In general, marked changes in chemical results have not been found as consistently, on going from one type of absorption to another, as one might have supposed. For example, in figure 2 decomposition quantum yields of three aldehydes are shown to vary rather uniformly over most of the spectral region shown in figure 1 (19, 20).

Because of its markedly different types of absorption, crotonaldehyde,  $\text{CH}_3\text{CH}=\text{CHCHO}$ , was thought originally to be a good substance to investigate in the hope of correlating absorption spectra with chemical processes (10). It was soon learned, however, that at room temperature no photolysis occurs even with the full force of the mercury arc (6). At elevated temperatures some decomposition will take place, as shown in figure 3 (5). In a sense it may be said that the early interpretation of spectra is substantiated, since no measurable decomposition was obtained in the region of many bands. However, the fact that the quantum-yield curve extends over two electronic regions of absorption indicates, perhaps, that it is the amount of energy absorbed and not the absorption type that is most important. A study of the photochemical oxidation of crotonaldehyde at room temperature has given results which conform to this

idea (9). In this case the smooth oxidation curve cuts across three types of absorption spectra.

Acrolein,  $\text{CH}_2=\text{CHCHO}$ , like crotonaldehyde, dissociates very little at room temperature (2). Unlike crotonaldehyde, however, it may photopolymerize extensively, as shown in figure 4. A small amount of photodecomposition was found at room temperature. The high polymerization quantum yields found at wave lengths which fall in a region of absorption which appears continuous may be accounted for by assuming that the free radicals produced in photodecomposition serve as nuclei around which polymerization occurs.

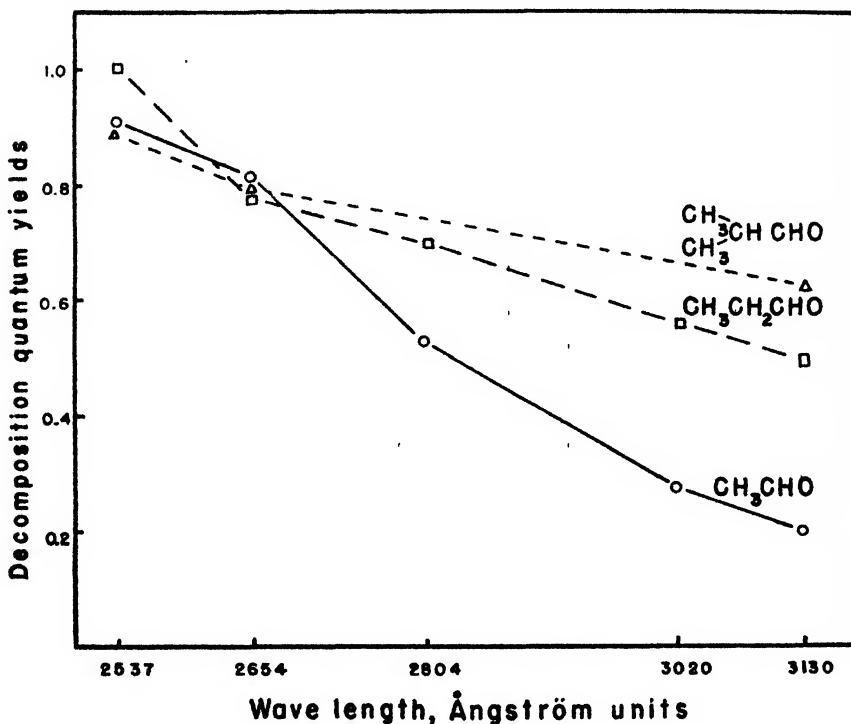


FIG. 2. Decomposition quantum yields of acetaldehyde, propionaldehyde, and isobutyraldehyde at several wave lengths distributed over the absorption region.

Of the saturated members of the aldehyde family acetaldehyde has received more photochemical attention than all the others put together. It is the typical aldehyde of the general formula  $\text{RCHO}$ , and, in a broad sense, information obtained from a study of it may be applied to the other compounds of the series. Exceptions to this statement may be found, of course, but if one is to obtain an over-all concept of the photochemistry of the aldehydes in a short time he must not mire down in details. It is reasonable to suppose that most apparent exceptions will turn into logical variations, as more and better data are obtained. We shall follow the lead, therefore, of Rollefson and Burton (23), Noyes and Leighton (22), and finally, Steacie (25), all of whom have given a prominent

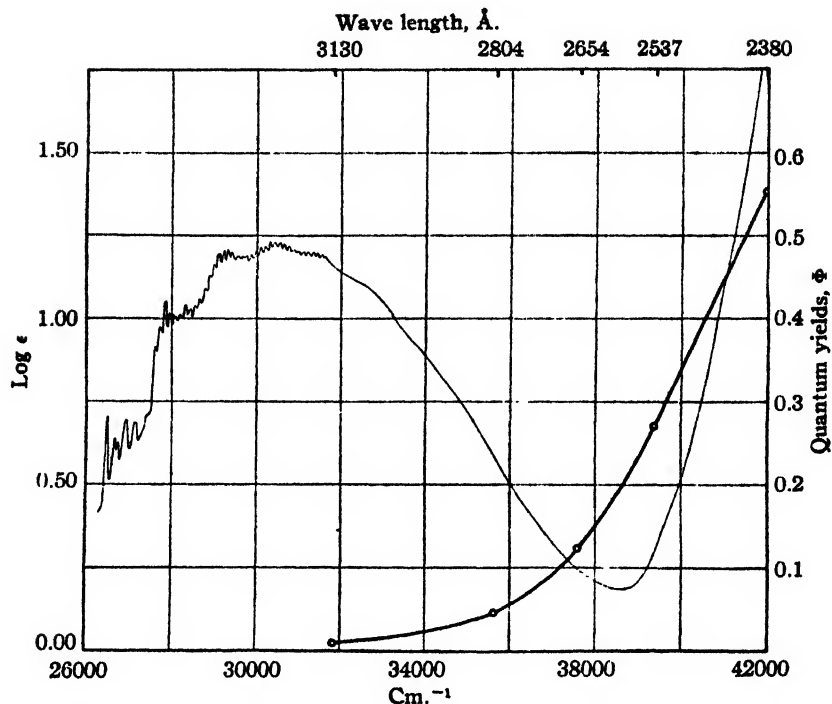


FIG. 3. Showing the variations of the molecular extinction coefficients (irregular curve) of crotonaldehyde and quantum yields of decomposition (smooth curve) with wave length. The quantum yields were obtained at 245°.

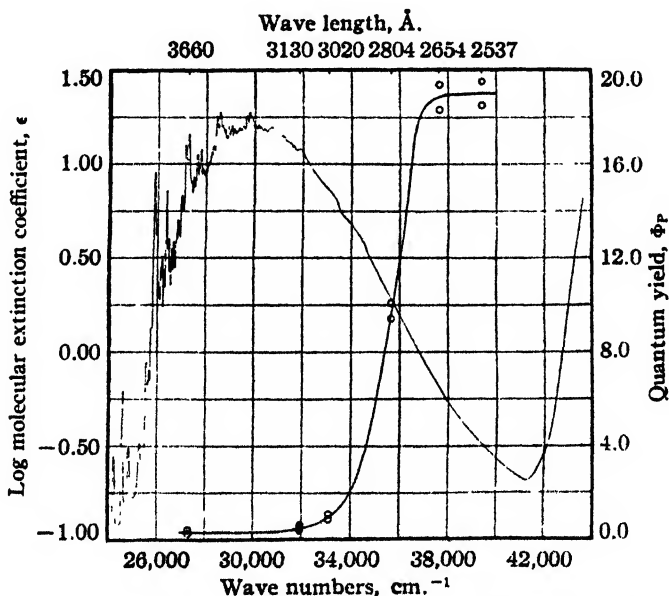
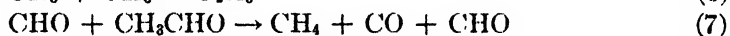
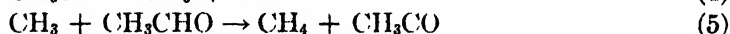


FIG. 4. Showing the relationship between the character of absorption (irregular curve) and quantum yields of polymerization (smooth curve) of acrolein.

place to acetaldehyde in their books on photochemical and free-radical reactions, and focus our attention for the remaining time on this compound.

Two important chemical processes are reported to occur when acetaldehyde is irradiated. One is referred to as decomposition and the other as polymerization. There is a strong tendency among us to treat the polymerization as an unfortunate nuisance, to ignore it as much as possible, therefore, and to confine our attention to the cleaner and more easily handled gaseous products. Only under certain circumstances is such an approach justified.

One of these is high-temperature photolysis. At 310°C., where thermal dissociation may be neglected, Leermakers (17) found that approximately 300 acetaldehyde molecules decompose for each quantum absorbed. This is evidence that a chain mechanism is operating, involving most certainly some free radicals. Leermakers chose to assume that the primary dissociation is into a methyl and a formyl radical, followed by one or more of the chain possibilities which can be formulated from the following equations:



These equations are almost identical with those proposed by Rice and Herzfeld for the thermal dissociation of this compound; as we review the subject it would be surprising if this were not so. High quantum yields, without condensation, are difficult to visualize without a radical mechanism. Once radicals are formed in a primary process there is little reason to suppose that the influence of this photochemical act will be felt very far down the chain. A chain process, in order to go far, must be self sustaining, and it makes little difference whether it was initiated by the absorption of a photon or by an unusually energetic molecular collision.

At elevated temperatures the only decomposition products definitely established are methane and carbon monoxide. Hydrogen was included by Leermakers partly to account for a residual gas volume and partly because it had been found in the room-temperature photolysis of aldehydes (19, 20). At best, only a small percentage of hydrogen can be expected at high temperatures, percentages so small as to be within the probable limit of error of ordinary chemical methods of analysis. Yet a qualitative proof of the presence or absence of traces of hydrogen might throw considerable light on reactions 2 and 3. In the laboratory of the author, such a proof is to be sought with the aid of the mass spectrometer. If hydrogen is found, we can only say that one or more of several reactions, including 2 and 3, are not ruled out. The complete absence of hydrogen gas

would indicate that atomic hydrogen is not formed in the system either as a primary or as a secondary product.

Leermakers' equations include two cyclic processes, equations 4 and 5 constituting one, and equation 7 the other. If hydrogen is found in an amount equivalent to the photons absorbed, the likelihood of equation 7 being important would diminish. In any event there is little evidence to be found in support of number 7.

As chain-breaking reactions, two alternatives are given—equations 6 and 8. It has been shown by chemical analysis that ethane is not a photolysis product at room temperature (8). Mr. R. K. Brinton in our laboratory has confirmed this result in recent weeks by means of the mass spectrometer. It does not follow, however, that reaction 6 is not important at elevated temperatures where reaction 4 doubtless almost always occurs. Nevertheless, after consideration of a number of factors, Leermakers was inclined to favor equation 8 over 6 as a chain-terminating step.

Primary dissociation into other radicals, such as hydrogen atoms and acetyl, would give secondary reactions similar to the ones used above and would explain the experimental facts equally well. Also, as far as over-all products are concerned, some dissociation directly into the stable molecules methane and carbon monoxide would make no difference at elevated temperatures. Such dissociation would, however, have a bearing on the average chain length. For example, if no such process occurred in Leermakers' experiments quoted above, the average chain length was 300. If, on the other hand, 50 per cent of the primary dissociation was by a non-radical mechanism, the chains averaged 600 cycles in length. It is important to know, therefore, more about the initial photochemical steps.

From studies at lower temperatures considerable has been learned about the probable primary processes. Much work has been done in a temperature range of from  $-40^{\circ}\text{C.}$  to  $+150^{\circ}\text{C.}$  Some of the data are conflicting; nevertheless, the over-all picture seems to be developing in a logical manner and there is no sharp demarcation between high-temperature and low-temperature mechanisms. One mechanism blends into the other as the various secondary reactions change in relative importance with temperature.

As the temperature is decreased the photolysis products become more complex, and at room temperature a condensed product must be reckoned with. For the most part this is a polymer of the original aldehyde. Its formation appears to be promoted by free radicals in the manner indicated previously for acrolein. A complete study of this so-called polymer has not been made. However, a partial analysis of the acetaldehyde condensate has revealed the presence in relatively small amounts of biacetyl, glyoxal, and formaldehyde (1). The amounts of these compounds relative to carbon monoxide found at three different temperatures are given in table 1. The variation of products with temperature should be noted. Tests for acetone and methylglyoxal, which can be postulated as other products, were negative. It may be noted that carbon monoxide, methane, and hydrogen were the only non-condensable products

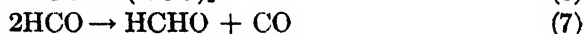
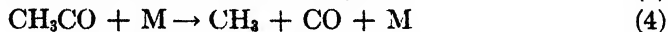
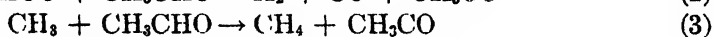
found. An extensive search again revealed no ethane and, as stated before, in a study which is in progress now, the mass spectrometer has substantiated the chemical analyses. No unsaturated hydrocarbons were detected. On the basis of these results and many others involving quantum yields for the most part,

TABLE 1

*Relative number of moles of acetaldehyde photolysis products based on unit carbon monoxide as a standard of comparison*

TEMPERATURE	CARBON MONOXIDE	HYDROGEN	METHANE	BIACETYL	GLYOXAL	FORMALDEHYDE
°C.						
25	1.00	0.063	0.87	0.084	0.014	0.018
60	1.00	0.049	0.92	0.012	0.0076	0.0022
102	1.00	0.033	0.94	0.007	0.000	<0.0015

the following processes have been set forth in an attempt to account for all detected photolysis products except, of course, the polymer:



This is a marked expansion over the original concept of low-temperature acetaldehyde photolysis, in which it was considered that activation followed principally by polymerization occurred in the banded absorption regions and that dissociation by reaction 1a occurred in the continuum (24). The discovery of hydrogen as a product (19, 20) first forced the consideration of free radicals as primary products, which in turn enter the appropriate secondary processes to give the observed final products. As more products were identified, the equations have increased until we have what is shown here. It must be emphasized at once that other mechanisms may be postulated to account for most of the observed products and that the equations given should be regarded simply as postulates for discussion purposes and as aids in planning new experiments. Equations 5, 6, and 7 are given to account for the formation of biacetyl, glyoxal, and formaldehyde, respectively. They involve bi-free-radical processes and occur less frequently as temperature is increased and the radicals are used in other reactions. From the data given in table 1, it is evident that they vanish almost completely from the system at 100°C. and certainly would be of no consequence

in high-temperature photolysis. This is true, of course, because high temperature favors the reaction of these radicals in other ways.

For example, at 300°C. it is reasonable to suppose, as Leermakers did, that the formyl radical will dissociate somewhat readily into carbon monoxide and a hydrogen atom, the hydrogen atom then reacting with the aldehyde to give stable  $H_2$ . Most estimates agree, however, that 20-30 kg.-cal. per mole are required to dissociate the formal radical (25); consequently it should be thermally fairly stable at room temperature. To account for the hydrogen gas, therefore, reaction 2 above is given. This reaction can be recognized as a combination of two of Leermakers' reactions, wherein the postulation of atomic hydrogen is eliminated. It explains the facts but requires much more study. So far no one has devised an unambiguous test for it.

Reactions 3 and 4 constitute one of the chain processes postulated for elevated temperatures. It continues to operate slowly at room temperature with an apparent activation energy of 8 or 9 kg.-cal. for the over-all process. Some evidence for these equations has been obtained by mixing acetaldehyde with azomethane and irradiating the system with a wave length, 3660 Å., which is absorbed by azomethane and not by acetaldehyde (7). When a relatively high ratio of acetaldehyde to azomethane is present in the system, carbon monoxide is found as a photolysis product. This is interpreted as meaning that methyl radicals, which are known to be produced by the irradiation of azomethane (12), initiate the cycle, i.e., equations 3 and 4. Not until the acetaldehyde to azomethane ratio was greater than 8 to 1 was more than a trace of carbon monoxide produced. This means that the rate-determining step of the cycle must have an appreciably higher activation energy than the corresponding reaction of methyl radicals with azomethane.

In reactions such as 2 and 3 it has been somewhat tacitly assumed always that it is the aldehyde hydrogen which is attacked by the radicals. By substituting deuterium for this hydrogen we hope to test this point. If equation 2 goes as indicated,  $D_2$  gas should be obtained. If, on the other hand,  $DH$  gas is found wholly or in part, some revision of the mechanism will be necessary. Likewise in the same experiment, if some  $CH_4$  is obtained instead of  $CH_3D$  we shall have evidence that the methyl radical may attack the hydrocarbon end of the aldehyde molecule.

Reaction 8 is included without evidence, except that it enables us to arrive at a better material balance of the products reported. The question will be raised, why not use equation 1a equally well? That brings us to the last topic to be discussed: namely, the primary processes.

At certain wave lengths, at any rate, a third primary dissociation into acetyl radicals and hydrogen atoms is energetically possible in addition to processes 1a and 1b given above. It has been omitted, partly because there is no experimental evidence which requires that it be a part of the mechanism, and partly because there is some evidence that it does not occur in fact. For example, Burton has reported no detectable atomic hydrogen by the metallic mirror technique (11). Also, no acetyl iodide has been detected when photolysis was



carried out with iodine in the system (3, 4). By analogy with acetone we should expect to find acetyl iodide if such a primary process occurred to any great extent.

Concentrating on the two primary processes given above, therefore, we find that they have been the subject of considerable variation of opinion. At first, reaction 1a was adequate to explain the available facts. With the discovery of hydrogen as a product, reaction 1b was postulated. When it was learned that the hydrogen increased with decreasing wave length, as shown by the ratio of hydrogen to carbon monoxide, it was naturally assumed by some investigators that reaction 1a predominates at long wave lengths and reaction 1b becomes increasingly probable at shorter wave lengths. This idea was supported by some exploratory work with metallic mirrors (18).

However, full credit should be given to Gorin (14) for pointing a way to test the efficiency of both reactions 1a and 1b. He showed that by adding sufficient iodine vapor to the system, both the methyl and formyl radicals are eliminated completely and no secondary reactions can occur. With iodine the methyl radical gives methyl iodide and the formyl radical gives hydrogen iodide and carbon monoxide. From the limited number of experiments which he was able to perform he concluded: (1) that both reactions 1a and 1b occur at wave lengths of 3100 Å. and 2600 Å., but that reaction 1a, and not 1b, becomes more important at shorter wave lengths, and (2) that at both wave lengths the sum of the quantum yields of reactions 1a and 1b approximated unity.

These experiments have been repeated and extended considerably in our laboratory. Our results are not always in agreement with Gorin's; nevertheless our basic conclusions are not greatly different. The effectiveness of iodine in stopping secondary processes is shown in figure 5, in which quantum yields are plotted against temperature at the wave lengths 3130 and 2654 Å. for experiments both with and without iodine. The quantum yield of carbon monoxide is a measure of the sum of the quantum yields of both reactions 1a and 1b. In the presence of sufficient iodine the quantum yield of methane is a measure of the quantum yield of reaction 1a and the quantum yield of methyl iodide is a measure of the quantum yield of reaction 1b. The sum should equal that of carbon monoxide. Within the limits of experimental error, which still are rather large, that relationship has been found to be true, as shown in figure 6. The fact that the quantum yields of methyl iodide are apparently constant at values well below unity for iodine pressures above 1 mm. indicates strongly that *activated* aldehyde molecules do not react with iodine vapor at low temperatures. It may be noted that at 3130 Å. reaction 1b predominated almost if not entirely to the exclusion of reaction 1a. However, at  $\lambda$  2654 reaction 1a occurs almost as frequently as 1b. In fact, at  $\lambda$  2380 it has been found that the two primary reactions do have an equal probability of occurring.

It should be noted also that at no wave length studied does the sum of the quantum yields of reactions 1a and 1b equal 1. At  $\lambda$  3130 only about 20 per cent of the absorbed energy causes decomposition. Fluorescence accounts for a little of the remainder, but the best estimates indicate not more than 3 or 4

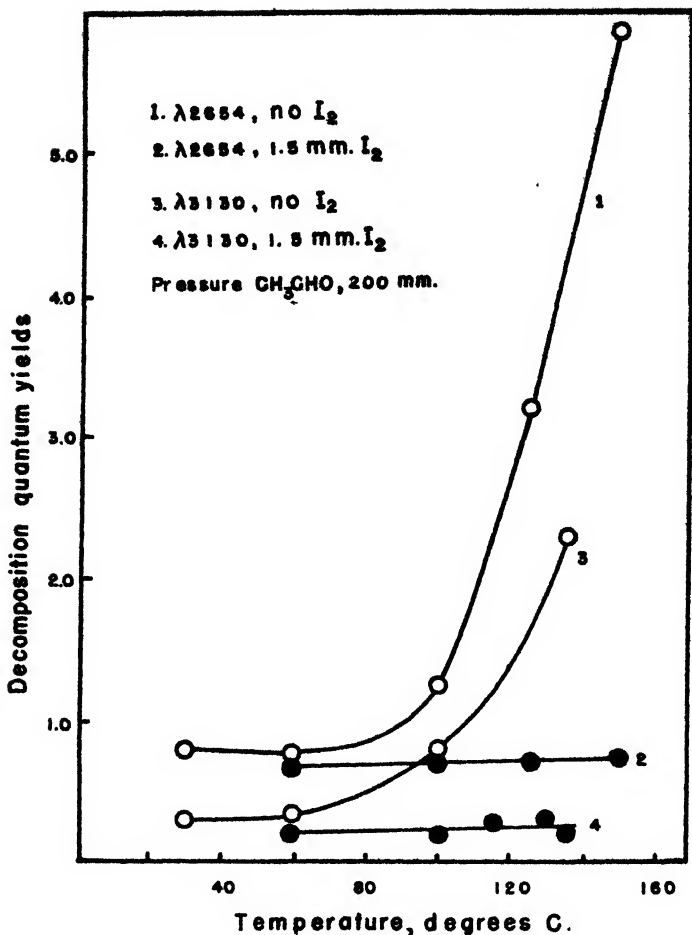


FIG. 5. Quantum yields of carbon monoxide production from acetaldehyde *vs.* temperature, with and without iodine present and at two different wave lengths.

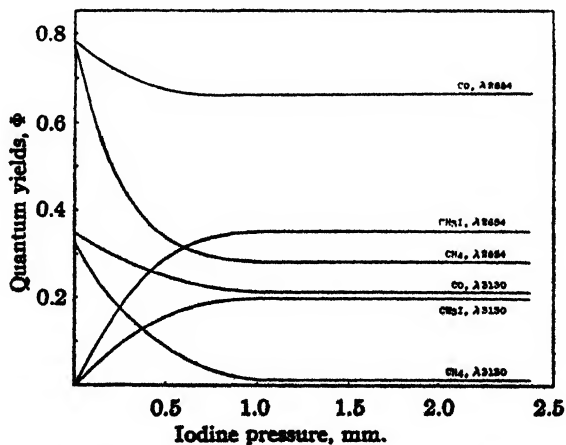


FIG. 6. Quantum yields *vs.* iodine pressure at  $\lambda$  3130 and  $\lambda$  2654; acetaldehyde pressure, 200 mm.; temperature, 60°C.

per cent. The bulk of the energy at this wave length must therefore be dissipated thermally. At shorter wave lengths the amounts lost in this way become diminishingly less.

In conclusion it should be emphasized again that without doubt much remains to be learned about the photochemistry of the aldehydes. However, the establishment of the primary processes with reasonable certainty should give us a better foundation upon which to build than we had before. In the study of other compounds it seems reasonable that much time and unnecessary experiments might be saved by attempting to go more directly to the primary processes than we have been in the habit of doing in the past.

## REFERENCES

- (1) BLACET, F. E., AND BLAEDEL, W. J.: J. Am. Chem. Soc. **62**, 3374 (1940).
- (2) BLACET, F. E., FIELDING, G. H., AND ROOF, J. G.: J. Am. Chem. Soc. **59**, 2375 (1937).
- (3) BLACET, F. E., AND HELDMAN, J. D.: J. Am. Chem. Soc. **64**, 889 (1942).
- (4) BLACET, F. E., AND LOEFFLER, D. E.: J. Am. Chem. Soc. **64**, 893 (1942).
- (5) BLACET, F. E., AND LU VALLE, J. E.: J. Am. Chem. Soc. **61**, 273 (1939).
- (6) BLACET, F. E., AND ROOF, J. G.: J. Am. Chem. Soc. **58**, 73 (1936).
- (7) BLACET, F. E., AND TAUROG, A.: J. Am. Chem. Soc. **61**, 3024 (1939).
- (8) BLACET, F. E., AND VOLMAN, D. H.: J. Am. Chem. Soc. **60**, 1243 (1938).
- (9) BLACET, F. E., AND VOLMAN, D. H.: J. Am. Chem. Soc. **61**, 582 (1939).
- (10) BLACET, F. E., YOUNG, H., AND ROOF, J. G.: J. Am. Chem. Soc. **59**, 608 (1937).
- (11) BURTON, M.: J. Am. Chem. Soc. **58**, 1655 (1936).
- (12) BURTON, M., DAVIS, T. W., AND TAYLOR, H. A.: J. Am. Chem. Soc. **59**, 1038 (1937).
- (13) BURTON, M., AND ROLLEFSON, G. K.: J. Chem. Phys. **6**, 416 (1938).
- (14) GORIN, E.: Acta Physicochim. U.R.S.S. **9**, 681 (1938); J. Chem. Phys. **7**, 256 (1939).
- (15) HENRI, V.: Trans. Faraday Soc. **25**, 765 (1939).
- (16) HENRI, V., AND SCHOU, S. A.: Z. Physik **49**, 774 (1928).
- (17) LEERMAKERS, J. A.: J. Am. Chem. Soc. **56**, 1537 (1934).
- (18) LEIGHTON, P. A.: J. Chem. Phys. **7**, 781 (1939).
- (19) LEIGHTON, P. A., AND BLACET, F. E.: J. Am. Chem. Soc. **54**, 3165 (1932); **55**, 1766 (1933).
- (20) LEIGHTON, P. A., LEVANAS, L. D., BLACET, F. E., AND ROWE, R. D.: J. Am. Chem. Soc. **59**, 1843 (1937).
- (21) LEVANAS, L. D.: Doctorate Thesis, Stanford University, 1936.
- (22) NOYES, W. A., JR., AND LEIGHTON, P. A.: *The Photochemistry of Gases*. Reinhold Publishing Corporation, New York (1941).
- (23) ROLLEFSON, G. K., AND BURTON, M.: *Photochemistry and the Mechanism of Chemical Reactions*. Prentice-Hall, Inc., New York (1939).
- (24) SMITH, J. H. C.: Carnegie Inst. Wash. Reprints **27**, 178 (1928).
- (25) STEACIE, E. W. R.: *Atomic and Free Radical Reactions*. Reinhold Publishing Corporation, New York (1946).

SOME ASPECTS OF THE PHOTOCHEMISTRY OF KETONES<sup>1</sup>

W. ALBERT NOYES, JR.

*Department of Chemistry, University of Rochester, Rochester, New York**Received October 23, 1947*

The ketones have been the subject of numerous photochemical investigations, largely because they absorb in a convenient part of the spectrum and because it seemed, from early work, that the products would be simple and easily identifiable. The simple aliphatic ketones all absorb, in the vapor phase, from about 2300 to about 3200 Å. Other absorption regions are present below 2000 Å., but few studies of the photochemical behaviors of these compounds have been made at these short wave lengths.

The photochemistry of the simple ketones has been reviewed (6) recently, and there is no point in repeating all references to the literature of this subject at the present time. Acetone does show some evidence of banded structure in its spectrum in the region from about 2900 Å. to about 3200 Å. (25, 26, 27). Available information indicates that such a structure is not found in the near-ultraviolet spectra of any other ketones, although discrete bands are found for those investigated in the far ultraviolet (10, 11, 12, 13, 19, 27, 28, 29).

It is impossible from existing data and from the present state of knowledge to draw any precise conclusions from spectroscopy concerning the primary process during optical absorption. Acetone does fluoresce both in the blue and in the green parts of the spectrum, the latter result being due undoubtedly to biacetyl (2, 20, 21), which is a common impurity in acetone and which is synthesized photochemically when acetone is exposed to ultraviolet light. The green fluorescence seems to be excited by all wave lengths between 3130 and 2537 Å. (5, 17), but no corresponding information exists as regards the blue, which is only known definitely to be excited by 3130 Å. radiation. The absence of fluorescence when radiation below 2000 Å. is used (17), the excitation at least of green fluorescence by 2537 Å. radiation where all indications of structure in the absorption spectrum have disappeared, and the existence of weak fluorescences in methyl ethyl ketone (21) and in diethyl ketone (21), neither of which has been shown to have a discrete absorption spectrum, all tend to prove that the appearance of the spectrum of a polyatomic molecule is not a safe guide as to whether the absorption of light leads to excitation, to predissociation, or to immediate dissociation.

The weak blue fluorescence observed in acetone is probably to be ascribed to the acetone molecule itself for the following reasons (18): (a) It is observed in acetone in a flow system which does not permit of accumulation of products of reaction (2); (b) it is observed with oxygen present and thus under conditions which prevent biacetyl synthesis (2, 5); (c) it is observed at temperatures up to 200°C. at which no biacetyl is formed (16). Since the fluorescence efficiency for

<sup>1</sup> Presented at the Symposium on Radiation Chemistry and Photochemistry which was held at the University of Notre Dame, Notre Dame, Indiana, June 24-27, 1947.

the blue is independent of the intensity of the exciting light (18), it seems probable that the radiation is from excited acetone molecules and not from a recombination spectrum of some sort. Part of the radiation absorbed, at least at 3130 Å. and probably also at other wave lengths, must produce excited molecules.

At room temperature the quantum yield of acetone decomposition is low (6), but it has been shown (5) that fluorescence cannot be mainly responsible for this low yield. The fact that there is an appreciable blue fluorescence at 135°C. (18), where the quantum yield of carbon monoxide formation from acetone is well within the experimental error of unity, is further proof either that the yield of excited molecules in the primary process is very small or that the majority of these molecules dissociate under ordinary experimental conditions.

More information is needed concerning the character of the blue fluorescence in acetone. The only photographs have been obtained (2, 5, 18) under conditions which would make detection of any structure most unlikely. Owing to the low intensity, spectrographs of low dispersion have been used, often with wide slits. At present no evidence of structure exists, although there is one slight maximum near 4600 Å. The limits of emission are from about 3850 Å. to about 5000 Å. If the emission is truly continuous (i.e., if the apparent absence of structure is not due to a great deal of overlapping structure) when observed under high dispersion with high resolution, either the upper or the lower state must be repulsive. A repulsive upper state is improbable because blue fluorescence is observed at temperatures where the ( $\text{CH}_3\text{CO}$ ) radical is very unstable (16, 18). A repulsive lower state must separate into ethane and carbon monoxide, since insufficient energy remains after emission of any of the above wave lengths to permit any other mode of dissociation (18).

The effect of pressure on the quenching of the blue fluorescence (18) indicates that at least two upper levels must be involved, one of much longer life than the other. The long-lived state must be insensitive to collisions with acetone, although it must be deactivated or dissociated with greater probability at high temperatures than at low. In view of the photochemical data at high temperatures dissociation is more probable than simple deactivation.

The following conclusions concerning the primary process in acetone are derivable from all of the facts at our disposal: (a) Some excited molecules are formed at 3130 Å. and perhaps at other wave lengths. (b) Either the number of excited molecules formed is very small, or they must dissociate, particularly at high temperatures. (c) A very high efficiency of production of methyl radicals is probable, because at high temperatures about 1.4 molecules of methane are produced per quantum absorbed by acetone (1, 7). (d) Direct dissociation into ethane and carbon monoxide cannot be proved until further efforts have been made to detect structure in the emission bands. (e) A primary dissociation into  $\text{CH}_3$  and  $\text{CH}_3\text{CO}$  at room temperature is indicated by the synthesis of amounts of biacetyl dependent on experimental conditions. (f) The instability of  $\text{CH}_3\text{CO}$  depends both on wave length and on temperature (6, 30). (g) No conclusive evidence for or against a primary dissociation into ethane and carbon monoxide has been found (6).

A great many secondary steps have been suggested to account for the photochemical decomposition of acetone. The general picture is now quite clear, although there are some disagreements as to details. In view of excellent reviews recently published there seems to be no point in discussing these steps in detail. One matter, however, needs further attention. There is evidence from several sources (2, 5, 18) that biacetyl does not accumulate indefinitely in acetone exposed to radiation at room temperature. Since the spectrum of biacetyl is excited to a high intensity when its pressure is quite low (2, 20), it probably receives energy from excited acetone molecules. This may cause it to dissociate part of the time. That this is the case is indicated by two effects: (a) collisions enhance rather than quench the green fluorescence; (b) the green fluorescence of "acetone" grows weaker rapidly as the temperature is raised.

Pure biacetyl excited by the 3660 Å. line of mercury shows an abnormal change of fluorescence efficiency with pressure, i.e., the efficiency increases as the pressure increases (3, 15). This same effect is observed for the green fluorescence in acetone (18). The lifetimes of the green emitter in acetone and of the emitter in biacetyl have been shown to be the same (2). Excited biacetyl molecules produced under these conditions must be able to dissociate (or at least pass into a state incapable of fluorescence) unless they lose some energy by collision. If this is true, collisions involving sufficient energy should be able to raise metastable or excited biacetyl molecules to states capable of dissociation. In this way the absence of green fluorescence at 135°C. in acetone, even when biacetyl is present, can be explained.

From the above discussion it can be concluded that dissociations of excited or metastable molecules must be considered in any complete picture of the photochemistry of acetone and of biacetyl. The distinction between molecules which absorb when they are in higher vibration levels of the ground state and those which acquire energy by collision *after they are activated* is one which cannot be investigated except with diatomic and very simple polyatomic molecules. The temperature effect on fluorescence can be explained qualitatively either way, providing predissociation is more probable in higher than in lower vibration levels of the upper state. The character of the blue fluorescence in acetone is such that the initially formed state is quenched by collisions, whereas the green requires the reverse to be true for the initially formed excited state of biacetyl. These facts are best explained as due to the effect of collisions on transfer between upper levels. Since this explanation is equally effective in dealing with the temperature effect, it is tentatively accepted. The long lifetimes of the upper state of biacetyl ( $1.5 \times 10^{-3}$  sec. (2)) and of acetone ( $>10^{-5}$  sec. (18)) are ample for collisional effects on the upper state to be important.

Brief mention will be made in conclusion of only two other ketones: diethyl ketone and methyl *n*-butyl ketone. While diethyl ketone does show a weak fluorescence (21) (probably due to bipropionyl), the quantum yield of carbon monoxide formation is very close to unity and independent of temperature (8, 14). The primary dissociation must have a yield very close to unity. If the products of the primary dissociation are  $C_2H_5$  and  $COC_2H_5$ , the latter radical

must be sufficiently unstable even at room temperature to give carbon monoxide virtually 100 per cent of the time. The fluorescence, which is probably identical with that of propionaldehyde (21), may be due to bipropionyl and be excited by a very small number of excited diethyl ketone molecules produced in the primary process. No detailed studies of this fluorescence have been made.

The decomposition of methyl *n*-butyl ketone has been studied by Norrish and his coworkers (4, 22, 23, 24), who gave strong evidence that a substantial portion of the primary process yields acetone and propene without there being intermediate free radicals. This point of view is further supported by the invariance of the yields of these compounds with temperature from 25°C. to 300°C. (9). Analogous behavior has been found for other ketones all of which have at least one alkyl group three or more carbon atoms in length. These molecules constitute the best examples of primary dissociation into completed molecules as distinguished from free radicals. For steric reasons, events of this type are more probable with long alkyl groups than with short, particularly since the carbon-carbon bond broken is not the one adjacent to the carbonyl group.

In this brief discussion we have made little or no mention of secondary processes. Even in the case of acetone so many have been suggested that a study of the kinetics becomes hopelessly complex, and definite conclusions concerning the complete mechanism cannot be reached on such a basis alone. Other means of proving or disproving individual steps must be used: mirrors for reaction with radicals; use of iodine, nitric oxide, unsaturated compounds, etc. for reaction with radicals; introduction of radicals from other sources; fluorescence; wall effects; spectroscopy, to mention only a few. Even these aids to reaction kinetic studies do not always furnish proof free from all doubt concerning individual steps. Neither experimental evidence nor theory predicts much about reactions between excited molecules and other molecules.

Data on the photochemical reactions of complex molecules must cover many variables. The precision is often poor because of experimental difficulties. As a result most mechanisms cannot be established in detail beyond a reasonable doubt. However, one can and should avoid as far as possible the postulation of steps which violate common sense and which are so vague and unsupported by evidence that no experimental method can be devised either to prove or to disprove them. Generally speaking, one should start with a simple mechanism and complicating steps should be added only when such steps have been proven absolutely necessary.

#### SUMMARY

1. Acetone is the only ketone which shows positive evidence of structure in its spectrum at wave lengths longer than 2500 Å.
2. The appearance of the spectra of complex molecules (particularly those of a low order of symmetry) is not a safe guide to the nature of the primary process.
3. Studies of the fluorescence of acetone indicate that, at least at 3130 Å. and perhaps at other wave lengths, some activated molecules are produced in the primary process.

4. Both excited acetone and excited biacetyl molecules can dissociate as a result of additional energy acquired by collisions, thus making the yield of the primary dissociation dependent on temperature and, to some extent, on pressure.

5. No positive evidence exists that simple ketones can dissociate directly into completed molecules, but a further study of the fluorescence may provide additional information on this point.

6. Ketones possessing long alkyl groups apparently do dissociate into completed molecules in the primary process.

7. The difficulties of proving all details of the mechanisms of ketone decomposition beyond a reasonable doubt are pointed out.

#### REFERENCES

- (1) ALLEN, A. O.: J. Am. Chem. Soc. **63**, 708 (1941).
- (2) ALMY, G. M., AND ANDERSON, S.: J. Chem. Phys. **8**, 805 (1940).
- (3) ALMY, G. M., AND GILLETTE, P. R.: J. Chem. Phys. **11**, 188 (1943).
- (4) BAMFORD, C. H., AND NORRISH, R. G. W.: J. Chem. Soc. **1933**, 1531.
- (5) DAMON, G. H., AND DANIELS, F.: J. Am. Chem. Soc. **55**, 2363 (1933).
- (6) DAVIS, WALLACE, JR.: Chem. Rev. **40**, 201 (1947).
- (7) DAVIS, WALLACE, JR.: Unpublished results on acetone at elevated temperatures.
- (8) DAVIS, WALLACE, JR.: Unpublished results on diethyl ketone.
- (9) DAVIS, WALLACE, JR., AND NOYES, W. A., JR.: J. Am. Chem. Soc. **69**, 2153 (1947).
- (10) DUNCAN, A. B. F.: J. Chem. Phys. **3**, 131 (1935).
- (11) DUNCAN, A. B. F.: J. Chem. Phys. **8**, 444 (1940).
- (12) DUNCAN, A. B. F., ELLS, V. R., AND NOYES, W. A., JR.: J. Am. Chem. Soc. **58**, 1454 (1936).
- (13) ELLS, V. R.: J. Am. Chem. Soc. **60**, 1864 (1938).
- (14) ELLS, V. R., AND NOYES, W. A., JR.: J. Am. Chem. Soc. **60**, 2031 (1938).
- (15) HENRIQUES, F. C., JR., AND NOYES, W. A., JR.: J. Am. Chem. Soc. **62**, 1038 (1940).
- (16) HERR, D. S., AND NOYES, W. A., JR.: J. Am. Chem. Soc. **62**, 2052 (1940).
- (17) HOWE, J. P., AND NOYES, W. A., JR.: J. Am. Chem. Soc. **58**, 1404 (1936).
- (18) HUNT, R. E., AND NOYES, W. A., JR.: J. Am. Chem. Soc. **70**, (1948).
- (19) LAWSON, MARTHA, AND DUNCAN, A. B. F.: J. Chem. Phys. **12**, 329 (1944).
- (20) MATHESON, M. S., AND NOYES, W. A., JR.: J. Am. Chem. Soc. **60**, 1862 (1938).
- (21) MATHESON, M. S., AND ZABOR, J. W.: J. Chem. Phys. **7**, 536 (1939).
- (22) NORRISH, R. G. W.: Acta Physicochim. U.R.S.S. **3**, 171 (1935).
- (23) NORRISH, R. G. W.: Trans. Faraday Soc. **30**, 103 (1934).
- (24) NORRISH, R. G. W., AND BAMFORD, C. H.: Nature **138**, 1016 (1936).
- (25) NORRISH, R. G. W., CRONE, H. G., AND SALTMARSH, O. D.: J. Chem. Soc. **1934**, 1456.
- (26) NOYES, W. A., JR.: Trans. Faraday Soc. **33**, 1495 (1937).
- (27) NOYES, W. A., JR., DUNCAN, A. B. F., AND MANNING, W. M.: J. Chem. Phys. **2**, 717 (1934).
- (28) SCHEIBE, G., AND LINSTRÖM, C. F.: Z. physik. Chem. **B12**, 387 (1931).
- (29) SCHEIBE, G., POVENZ, F., AND LINSTRÖM, C. F.: Z. physik. Chem. **B20**, 292 (1933).
- (30) STEACIE, E. W. R.: *Atomic and Free Radical Reactions*, Reinhold Publishing Corporation, New York (1946); pp. 200 *et seq.* summarize the work on acetone decomposition.



TRANSFORMATION OF ORGANIC SUBSTANCES BY  
ALPHA PARTICLES AND DEUTERONS<sup>1,2</sup>

IRVING A. BREGER

*Department of Geology, Massachusetts Institute of Technology,  
Cambridge, Massachusetts**Received October 23, 1947*

## INTRODUCTION

A study of the effects of alpha particles and deuterons on organic compounds has been carried on at the Massachusetts Institute of Technology for the past five years as part of a general program of research concerning the possible rôle of radioactivity in petroleum genesis. This work is one phase of a project on the origin of petroleum being sponsored by the American Petroleum Institute. Biochemical and other factors are being studied at the Scripps Institute of Oceanography in California and at the Pennsylvania State College.

High temperatures and pressures have long been considered important sources of energy for the formation of petroleum in nature. Recently, however, Treibs (13, 26, 31, 32, 33) discovered certain porphyrins in crude oils. The ratio between these porphyrins and their decarboxylated analogues indicated that temperatures above 250°C. or 300°C. were precluded. No evidence that high pressure is a factor in petroleum formation has yet been offered.

The suggestion that radiations from the radioactive constituents of sedimentary rocks might be a source of energy for the conversion of gaseous paraffins to petroleum was first made by Lind and Bardwell (19, 20, 21) about twenty years ago. While agreeing that radiation is a potential source of energy for geochemical conversions, Bell, Goodman, and Whitehead (3) stated in 1940 that the formation of petroleum from gaseous hydrocarbons is unlikely from geological considerations. Rather, they suggested that a more reasonable process for petroleum formation by radioactivity would be through the decomposition and conversion of the solid and semi-solid organic compounds in marine sediments.

When it appeared from preliminary considerations that radioactivity may play an important rôle in petroleum genesis, American Petroleum Institute Project 43C was established at the Massachusetts Institute of Technology to investigate the effects of alpha particles, deuterons, and neutrons on pure organic compounds and on complex organic extracts from marine sediments.

In order to evaluate quantitatively the rôle of radioactivity in petroleum genesis, it is first necessary to establish the distribution and content of radioactive elements in sediments bearing organic source materials. Experiments in

<sup>1</sup> Presented at the Symposium on Radiation Chemistry and Photochemistry which was held at the University of Notre Dame, Notre Dame, Indiana, June 24-27, 1947.

<sup>2</sup> Contribution from American Petroleum Institute Research Project 43C, which is located at the Massachusetts Institute of Technology: W. L. Whitehead, *Director*; Clark Goodman, *Physical Director*.

this direction have been carried out for the past few years under the sponsorship of the Geological Society of America, and will be reported in the near future.

#### ALPHA-PARTICLE BOMBARDMENTS

Radon, which is an excellent source of alpha particles, was especially useful in this research, since alpha particles account for more than 75 per cent of the energy liberated by terrestrial radioactive elements (1). Since the half-life of radon is only 3.85 days, chemical work on the bombarded material can be postponed until the dangerous initial activity has decayed to a negligible level. On the other hand, the decay rate is not so rapid as to make measurement of the amount of radon introduced into the bombardment vessel difficult.

The procedure for bombarding organic compounds with the alpha particles from radon was recently reported by Sheppard and Whitehead (28). The

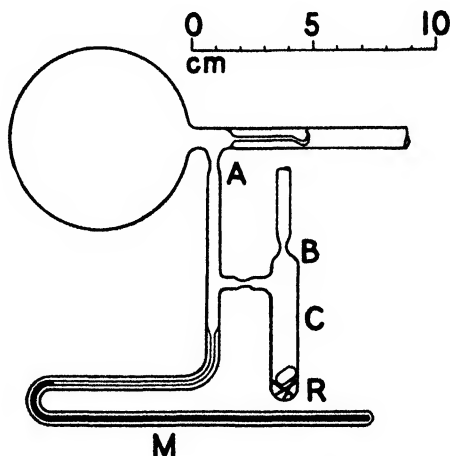


FIG. 1. Apparatus for the bombardment of organic substances by the alpha particles from radon.

material to be bombarded was coated on the inner wall of a 250-ml. Pyrex bulb (figure 1) to which was attached a manometer (M) and a side chamber (C). The stem was provided with a hook seal (A) of thin glass tubing which could be broken by a magnetic plunger at the time of analysis. After the needles were inserted into the side chamber, the system was evacuated through B and then sealed off at that point. By careful shaking, the glass needles (R) were broken under the impact of a glass pellet. The side chamber was next heated to facilitate the transfer of the radon into the larger volume of the main bulb, and was then sealed off and removed. The bulb was next set aside for about 3 hr. to allow the radioactive deposit from the radon to attain equilibrium. Measurements and calculations were then made to determine the quantity of radon originally introduced into the bulb.

Preliminary irradiations were carried out by exposing small quantities of fatty acids to the alpha particles from 100-millicurie sources of radon. Fatty

acids were chosen for these studies, since Wells and Erickson (38) and Trask and Wu (30) had shown the presence of 2-34 parts of fatty acid per 100,000 parts of marine sediment. Clarke and Mazur had, moreover, found the ether-extractable lipids from diatoms to contain from 60 to 80 per cent of free fatty acids (11). Since these straight-chain fatty acids, tentatively identified by the above investigators as ranging from capric ( $C_{10}H_{19}COOH$ ) to mellissic ( $C_{29}H_{59}COOH$ ), are among the simplest organic substances found in petroleum source beds, initial studies were begun on this class of compounds.

Although acetic acid, owing to its water solubility, would be found in source sediments only in interstitial or connate waters, it was, nevertheless, bombarded in an effort to establish the conversion pattern for acids. As shown in table 1, which is taken from a paper by Sheppard and Burton (29), decarboxylation resulting in the hydrocarbon methane was a predominant reaction. Since these results appeared promising, fatty acids of varied chain lengths were irradiated.

TABLE 1  
*Gaseous products from bombardment of fatty acids with alpha particles*

CONSTITUENTS	VOLUME PER CENT			
	Acetic	Caprylic	Lauric	Palmitic
H <sub>2</sub>	18	33	42	48
CO <sub>2</sub>	37	51	41	34
CO	22	10	11	6
H <sub>2</sub> O*		3	4	10
CH <sub>4</sub> *	20	0.7	0.6	0.4
C <sub>2</sub> H <sub>6</sub> *	3 7	1.0	0.5	0.6
C <sub>3</sub> H <sub>8</sub> *		0.4	0.1	0.1
C <sub>4</sub> H <sub>10</sub> *		0.7	0.2	0.8

\* Mass-spectrometric analyses.

The gas from each of these experiments was analyzed (table 1), and in the case of lauric and palmitic acids the hydrocarbon produced was isolated. By means of physical properties the residue from lauric acid was identified as undecane and that from palmitic acid as pentadecane. Data on the two isolated hydrocarbons are shown in tables 2 and 3, which are also taken from the paper by Sheppard and Burton.

Kinetic measurements on capric, caprylic, lauric, and palmitic acids indicated that gas production in the initial stages of the irradiation was proportional to the fraction of radon decayed. This is shown for a typical palmitic acid bombardment in figure 2. As the pressure of the gas increased the relationship became non-linear, owing to partial absorption of the radiation in the gas produced.

During the fatty acid phase of these investigations, which are further discussed by Honig (16), a number of other alpha bombardments were carried out on compounds which warranted study in connection with the genesis of petroleum. Gas analyses for several of these irradiations are shown in table 4.

TABLE 2  
*Liquid product from lauric acid*

PHYSICAL PROPERTIES	LIQUID PRODUCT	n-UNDECANE (12)
$d_4^{20}$ . . . . .	0.730	0.7402
$n_D^{20}$ . . . . .	1.4178	1.4173
$n_F^{20} - n_C^{20}$ . . . . .	0.0072	0.0070
Per cent carbon . . . . .	84.6	84.6
Per cent hydrogen . . . . .	14.9	15.4
Molecular weight . . . . .	152	156.3
Boiling point, °C. . . . .	195.5	195.8
Melting point, °C. . . . .	-26.3	-25.6
Double bonds per molecule . . . . .	0	0

TABLE 3  
*Liquid product from palmitic acid*

PHYSICAL PROPERTIES	LIQUID PRODUCT	n-PENTADECANE (2, 12)
$d_4^{20}$ . . . . .	0.7670	0.7689
$n_D^{20}$ . . . . .	1.4323	1.4326 (2)
$n_F^{20} - n_C^{20}$ . . . . .	0.0081	0.0076
Per cent carbon . . . . .	84.6	84.8
Per cent hydrogen . . . . .	15.4	15.2
Molecular weight . . . . .	209	212.2
Boiling point, °C. . . . .	273.0	272.7
Melting point, °C. . . . .	7-8	10.0
Double bonds per molecule . . . . .	0	0

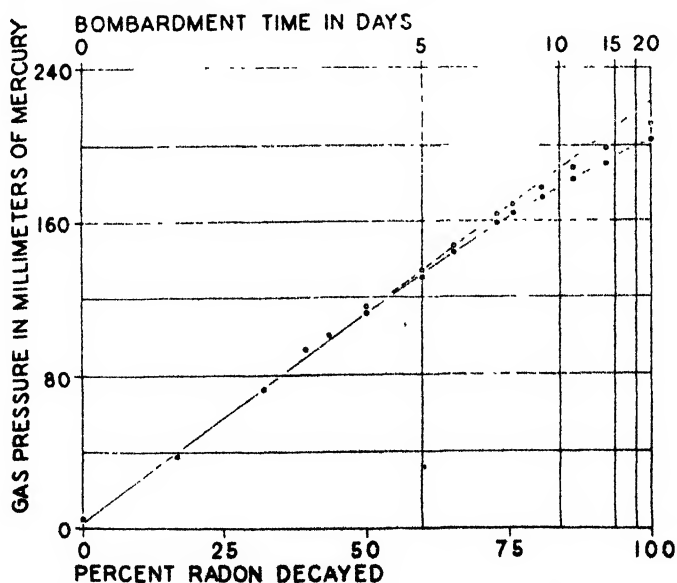


FIG. 2. Bombardment of palmitic acid by alpha particles;  
gas formation curve

Hexadecane and octacosane were bombarded to determine the effect of radiation on the hydrocarbon formed during a fatty acid decarboxylation. In each case the gaseous products were analyzed and were found to consist of approximately 95 per cent of hydrogen and 5 per cent of gaseous hydrocarbons. No liquid hydrocarbons lighter than hexadecane or octacosane could be distilled from the bombarded residue.

Since it is uncertain as to whether acids exist in sediments mostly in the free state or as calcium or sodium salts, calcium palmitate was prepared and irradiated by alpha particles. Gas analysis indicated a lesser degree of decarboxylation than in the case of the free acid; hydrogen, however, was liberated to a much greater extent. Far less gas was formed here than with the free

TABLE 4  
*Gaseous products from alpha-particle bombardments*

	VOLUME PER CENT								
	H <sub>2</sub>	CO <sub>2</sub>	CO	H <sub>2</sub> O	CH <sub>4</sub>	C <sub>2</sub> H <sub>6</sub>	C <sub>3</sub> H <sub>8</sub>	C <sub>4</sub> H <sub>10</sub>	NH <sub>3</sub>
Hexadecane. . .	95.5				0.9	1.0	1.0	1.2	
Octacosane. . .	94.3								
Calcium palmitate . . .	82.5	11.7	1.8		1.5				
Cetyl palmitate	85.0	4.0	3.0	1.8	1.0	1.0	1.0		
Sebacic acid. . . . .	26.3	68.9	2.1		0.6	← 3.0 →			
Glycine . . . . .	19.0	55.8	6.5	2.5	4.8	—	—	—	11.4
Trimethylacetic acid..	31.0	47.0	10.0	2.0	7.0	1.0	3.0	—	
Cholesterol . . .	89.1	1.1	2.1	2.5	4.6	0.2	0.4	—	
Octadecyl alcohol . . . .	90.3	1.3	3.7	3.2	0.6	0.4	0.5	—	
Dodecylamine . . .	69.0								31.0
Hexamethylenediamine.	63.1								33.7
Athabaska tar. . . . .	87.0				6.0	← 7.0 →			
Asphaltenes. . .	93.0	3.0		1.0	2.0	1.0	1.0		
Crude oil . . .	91.0				3.9	← 4.1 →			

acid. Small amounts of gaseous hydrocarbons were produced, but no hydrocarbon could be isolated from the residue.

Cetyl palmitate, which has been reported in marine organisms (5, 18), yielded very little gas, of which 85 per cent was hydrogen and only 4 per cent carbon dioxide. Again, small amounts of gaseous hydrocarbons were produced. From the small amount of carbon dioxide liberated from cetyl palmitate and calcium palmitate, it appears that decarboxylation is dominant in the presence of a free acid. This may be evidence that the resonance of the carboxyl group is significant in the decarboxylation mechanism.

Sebacic acid was bombarded as an example of a dicarboxylic acid and, as might be expected, the gas formed from it contained a higher percentage of carbon dioxide than that from caprylic acid. The usual small quantities of methane and higher hydrocarbons were also produced.

Irradiation of glycine, which was investigated as a simple unit of a protein molecule, led to the formation of a very small amount of gas which contained

56 per cent of carbon dioxide and 11 per cent of ammonia. It is interesting to note that only 5 per cent of methane was formed, indicating that very few molecules were both decarboxylated and deaminated. This might conceivably be an example of hydrogenation. When a small quantity of glycine was irradiated by deuterons, the yellow-brown product had a strong caramel-like odor which suggested that sugar formation might have taken place.

Analysis of gas produced during the irradiation of trimethylacetic acid showed a high percentage of carbon dioxide. Methane and other gaseous hydrocarbons were also formed in appreciable quantities. Unfortunately no analysis was run for isobutane.

The gaseous products from cholesterol and octadecyl alcohol contained about 90 per cent of hydrogen. In neither case, however, was there over several per cent of carbon monoxide and carbon dioxide. As usual, methane, ethane, and propane were found present. It was considered possible that the side chain in cholesterol might be split off, but this has not yet been thoroughly investigated. Octadecyl alcohol and sterols are especially interesting, since they have been identified in corals and sponges (4, 6, 7, 18, 37). From preliminary work it appears that the hydroxyl group in these alcohols is stable, and that the predominant process is dehydrogenation.

Gaseous products from dodecylamine or hexamethylenediamine contained approximately 33 per cent of ammonia and 65 per cent of hydrogen. Deamination, therefore, appears to be a relatively easy reaction to carry out.

Gilsonite, Athabaska tar, asphaltenes, and crude oil evolved fairly large quantities of hydrogen and small amounts of gaseous hydrocarbons, but no other data were obtained for these reactions. Samples of crude oil containing relatively high percentages of porphyrins were chosen for this work, and it was established by ultraviolet studies that the porphyrins are unaffected by the radiation.

#### DEUTERON BOMBARDMENTS

Since natural radioactive sources, such as radon, were frequently of insufficient intensity for practical chemical studies, an investigation was made to determine if the deuteron beam from the M.I.T. cyclotron would serve as a satisfactory substitute. This problem was approached both theoretically and experimentally by Sheppard and Honig (15, 27), the experimental work consisting of parallel bombardments of methane and *n*-butane with alpha particles and deuterons. While it was not possible to prove the complete identity of the chemical effects of these two particles, it was demonstrated that the effects were very similar. The deuteron beam has, consequently, been employed where relatively large quantities of conversion products were required for complete identification. Alpha-particle bombardments, on the other hand, were reserved for pilot runs and kinetic measurements.

Evidence was presented by Sheppard and Honig that the energy absorption is predominantly an electronic process, and that the energy is distributed among the various states of excitation and ionization of the reacting system in a manner

which is independent of the charge and mass of the bombarding particle and only slightly dependent on its velocity.

Equipment for the cyclotron work has now reached a fairly high degree of efficiency and versatility, and the improved liquid bombardment chambers used in this work have been described in a recent article (17).

Most recent bombardments have been run with a gas-collecting system composed of three 3-liter bulbs and one 5-liter bulb. The entire chamber-bulb system is evacuated, and the evolved gas is collected in four fractions over the period of the run. By this means it is possible to determine from the gas analyses if any significant trend has taken place during the course of the bombardment. A recently developed recording manometer will make available a record of the rate of gas formation during each irradiation. Observation of these curves will make it possible to stop bombardments before back-reaction takes place, i.e., before the primary conversion products are present in sufficiently high percentages so that they are affected by the radiation.

Irradiation of solids in the cyclotron has been rather difficult. Since over-exposure results in extensive decomposition and charring, it has been necessary to develop a moving target holder capable of holding a relatively large quantity of powder.

The first solid target holder used in this research was described in a paper by Honig (17). This was capable of holding only 7 g. of solid material in one position, and of that sample only about one-half was actually exposed to the deuteron beam.

After careful consideration of a number of possible designs, the moving target shown in figure 3 was finally built. This consists of a rotating hollow drum about the periphery of which is packed the solid to be irradiated. The material is cooled by water entering the interior of the drum through the hollow shaft, which in turn enters the gas chamber through a Wilson seal. The powder is held in place by means of a strip of 2-mil copper foil. A small 1 r.p.m. motor set beyond the cyclotron magnetic field drives the drum through nearly 360° after which the direction of rotation is reversed, an operation necessary to prevent fouling of the water lines. The rotating chamber, which is capable of holding about 35 g. of powder, is shown in position in the cyclotron in figure 4. Complete details regarding this solid target holder, the gas-collecting bulb system, and the recording manometer will be published in the near future.

To prevent chemical interaction and catalytic effects, all bombardment chamber surfaces or thermocouple junctions in contact with solid or liquid organic compounds were carefully gold-plated.

One of the first large-scale deuteron bombardments was carried out to determine the effects of radiation on a naphthenic acid such as is commonly found in naphthene-base crudes. These acids, several of which are shown in figure 5, are known to occur in many crude oils in the range from 0.06 to 1.6 per cent. Although the majority contain cyclopentane rings, cyclohexanecarboxylic acid, which was used in this work, has been isolated and identified in Baku (25, 34, 35, 36) and California crudes (23, 35). Since the possibility of forming

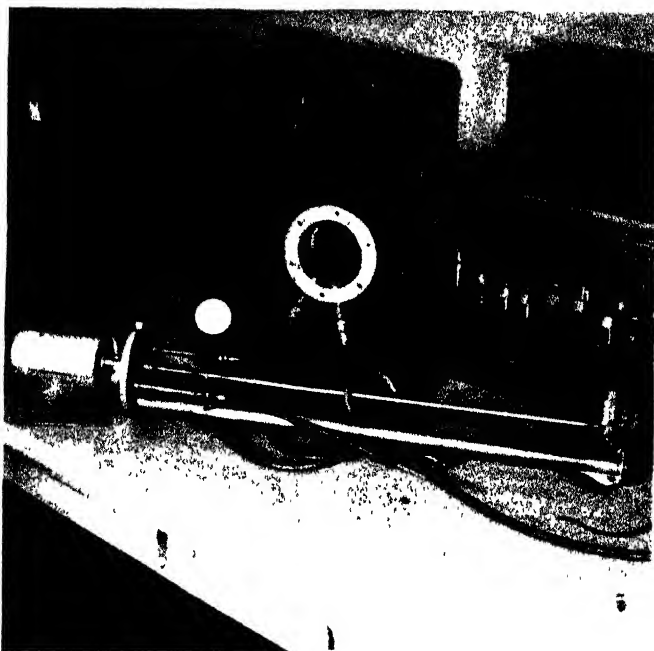


FIG. 3. Revolving target holder for the bombardment of solid organic compounds by deuterons.

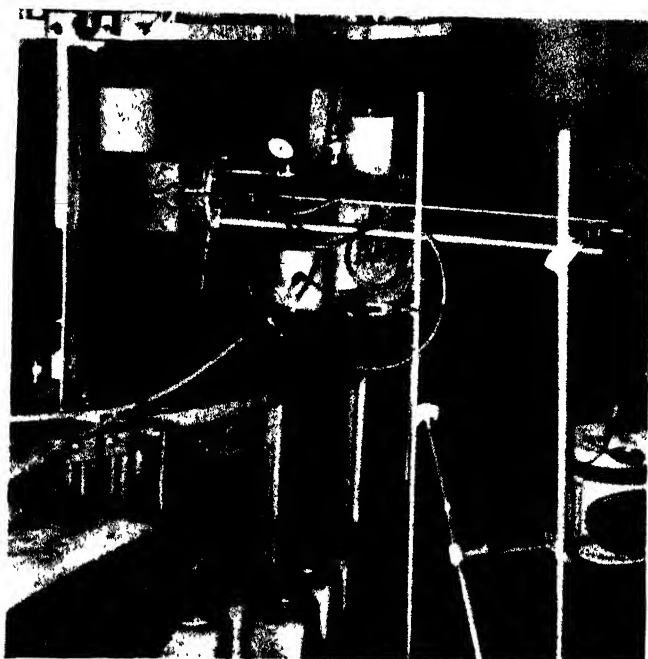


FIG. 4. Revolving target holder shown in position in the cyclotron



cycloparaffins by radioactive decarboxylation of these acids was of particular importance to the radioactivity theory of petroleum genesis, several preliminary alpha bombardments were run as pilot experiments. Identification of the conversion product as a mixture of saturated and unsaturated  $C_6$  hydrocarbons prompted a large-scale deuteron bombardment of the acid. This work, which

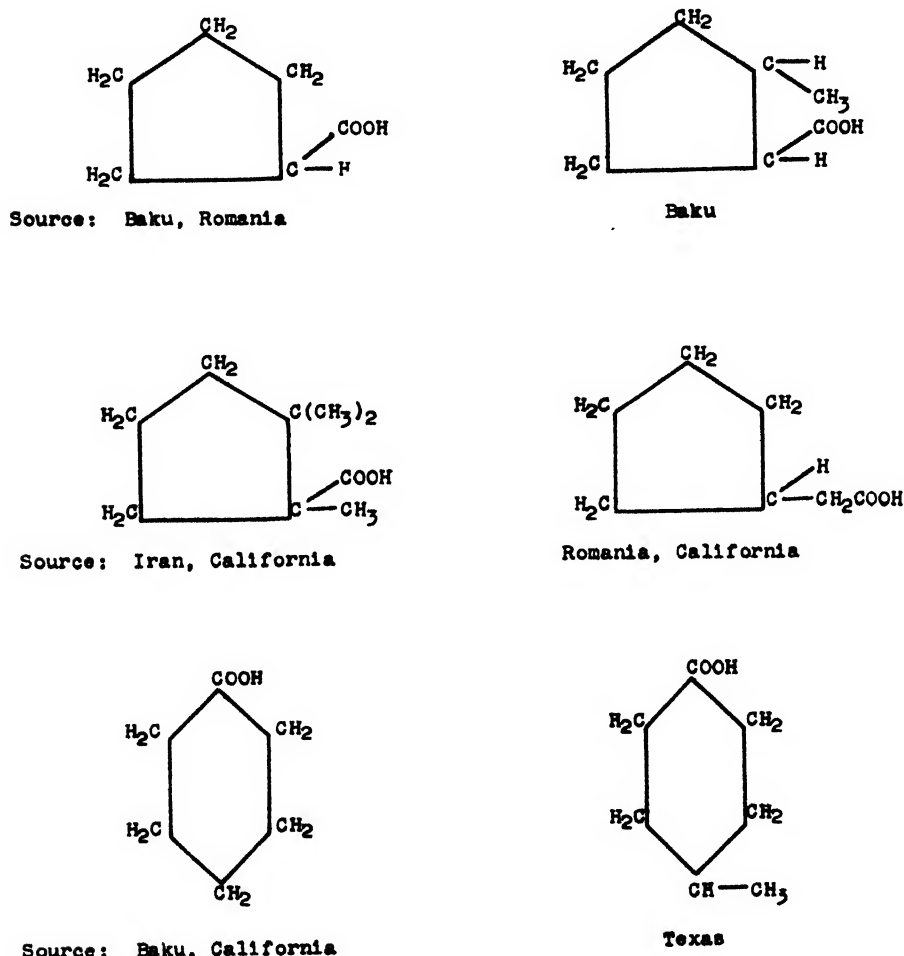


FIG. 5. Selected naphthenic acids and major source

was recently described in detail (8), led to the isolation of 3 g. of cyclohexane containing 12.5 per cent of cyclohexene. The entire yield was approximately 3.5 per cent, based upon the acid irradiated.

Analyses of the conversion products of this and other bombardments have been facilitated by the use of infrared spectra and a mass spectrometer. The course of analysis has occasionally necessitated the development of new types of micro and semimicro fractionating columns and molecular stills, some of

which were quite novel and will be described in the near future. Both orthodox and new uses of chromatography have been important in the purification of materials prior to bombardment and in the isolation of products after bombardment.

Since large-scale work such as that carried out for the naphthenic acid may lead to the formation of minor reaction products in identifiable quantities, about 85 g. of caproic acid was irradiated in the cyclotron with the purpose of obtaining a material balance. This acid was chosen since its decarboxylation products, pentane and carbon dioxide, are easily determined by use of the mass spectrometer. All the gas evolved in the reaction was collected and analyzed, and the liquid residue which remained after recovery of unchanged caproic acid is being subjected to exhaustive chemical analysis. To date, evidence has been obtained that di-*n*-amyl ketone is a minor product of this reaction.

Benzoic acid was irradiated in an effort to determine if the hydrogen usually evolved during the irradiation of organic substances would enter the double bonds of the ring to yield a hydrogenated product. The volume of gas formed was very small, but it is noteworthy that it consisted of 85 per cent of carbon dioxide and only 1.8 per cent of hydrogen. Several attempts have thus far been made to identify the cream-colored, infusible reaction product in an effort to determine the presence of hydrogenated bonds. To date, however, no evidence has been obtained that cyclohexanecarboxylic acid or cyclohexane rings were produced.

Since hydrogen has been a major gaseous product of all reactions except this last one, and since natural gas associated with petroleum normally contains only trace quantities of hydrogen, the radioactive theory of petroleum genesis has here been confronted with a serious problem. Although it has been proposed that hydrogen could disappear by diffusion to the atmosphere, the question arose as to the possibility that hydrogenation of unsaturated substances might take place under the influence of radioactivity. Since the benzoic acid study offered little assistance towards solution of this problem, a fairly large quantity of oleic acid was carefully and laboriously purified (39) to remove all the stearic acid. Impurities probably present in the form of linoleic and linolenic acids in the final product were relatively unimportant to the object of the work. Approximately 55 g. of the purified acid was exposed to a beam of deuterons, and the irradiated liquid was carefully examined for reaction products. All non-acidic material was removed by means of saponification and extraction. This step was then followed by a separation of the acid salts into water-soluble and water-insoluble fractions. The water-soluble portion was then acidified, and the recovered acids were chromatographed on alumina, the effluent being collected in 10-ml. portions in the form of aluminum salts. Recovery of the acids from these salts led to the identification of 3 per cent of stearic acid based on material bombarded. Since the original oleic acid, when submitted to the same analytical procedure, yielded no stearic acid, this was considered to be complete proof that hydrogenation had taken place.

The non-saponifiable fraction from the bombarded oleic acid yielded a colorless hydrocarbon in 3 per cent over-all yield. Present indications are that this

is 8-heptadecene; however, since this hydrocarbon has apparently never previously been prepared in a high state of purity, final identification by means of physical properties has been retarded. Physical properties for the 8-heptadecene obtained in this work will be published in the near future, along with evidence that this is probably the first time the compound has been prepared in pure form. A synthesis of this type suggests the possible use of deuteron bombardments to bring about low-temperature conversions which are not possible by chemical means. A coöperative effort with other M.I.T. laboratories has been made to decarboxylate dimethylenegluconic acid, and although the experiment was of a preliminary and rough nature, the gas produced contained 85 per cent of carbon dioxide, indicating that decarboxylation had probably taken place.

TABLE 5  
*Gaseous products from deuteron bombardment of crotonic acid*

COMPONENT	VOLUME PER CENT*	COMPONENT	VOLUME PER CENT*
H <sub>2</sub> . . . . .	8.2	C <sub>4</sub> H <sub>8</sub> . . . . .	0.2
CO <sub>2</sub> . . . . .	69.8	C <sub>6</sub> H <sub>12</sub> . . . . .	0.1
CO . . . . .	3.6	C <sub>8</sub> H <sub>16</sub> . . . . .	0.1
H <sub>2</sub> O . . . . .	5.1	C <sub>6</sub> H <sub>12</sub> . . . . .	0.1
CH <sub>4</sub> . . . . .	0.4	Acetone . . . . .	0.4
C <sub>2</sub> H <sub>6</sub> . . . . .	0.4	Methylacetylene . . . . .	2.7
C <sub>2</sub> H <sub>2</sub> . . . . .	1.4	Butadiene . . . . .	0.1
C <sub>3</sub> H <sub>8</sub> . . . . .	0.8	Toluene† . . . . .	0.2
C <sub>3</sub> H <sub>6</sub> . . . . .	7.4	Benzene . . . . .	0.2

\* Average of two mass-spectrometric analyses.

† The crotonic acid was purified by recrystallization from toluene.

A preliminary deuteron bombardment was run on crotonic acid to investigate the extent of hydrogenation of the double bond. Although the bombardment was somewhat unsatisfactory, gas analysis (table 5) did indicate that a high degree of decarboxylation had taken place. Crotonic acid was originally chosen because its decarboxylation products are gaseous propene and carbon dioxide, both of which can be easily detected by the mass spectrometer. If propane were the hydrogenated product, then this, too, could be determined with facility. The absence of propene in a quantity equivalent to the carbon dioxide was interesting, and corroborated the conclusions of Lind and others (19) that the unsaturated gaseous hydrocarbons react and polymerize more readily than do the saturated compounds.

#### CONCLUSIONS

The purpose of this work has been to determine the effects of radioactivity on organic substances which are known to exist in marine sediments under petroleum-producing conditions. To date, it has been shown that fatty acids can be radiochemically converted into the aliphatic components of crude oil and that naphthenic acids can be converted into the alicyclic components.

Long-chain alcohols, amines, and acids have been irradiated, and it has been demonstrated that deamination and decarboxylation are relatively easy re-

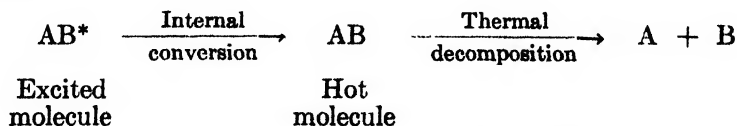
actions to carry out but that dehydroxylation (or dehydration) is very difficult. Considering the energies of the C—N, C—C, and C—O bonds (24), deamination and dehydroxylation (or dehydration) occur in the expected order. The C—H bond, which, however, is stronger than any of the above bonds, breaks quite readily. This cleavage, therefore, cannot be explained solely on the basis of bond energies.

The reactions induced by alpha particles or deuterons are probably combinations of photochemical and ionization effects. The photochemical decarboxylations of gaseous formic, acetic, and propionic acids studied by Burton (9, 10, 14) are significant in this respect. Ionization effects in the liquid or solid state have been more difficult to establish with certainty.

Previous to the work summarized in this paper, photochemical and radiation experiments were carried out for the most part in the gas phase. It has, therefore, been difficult to make comparisons regarding reaction mechanisms. It is important to note, however, that in most instances the reactions induced by alpha particles and deuterons have led in several clear-cut directions and have not yielded the complex mixtures of products which might have been anticipated if the decomposition had been a random process.

Since thermal decarboxylation of fatty acids has been known for many years (22), an effort was made to correlate the manner in which energy is absorbed and distributed in thermal processes and in these radiochemical reactions. In discussing mechanisms in the case of fatty acids, Sheppard and Whitehead (28) pointed out that at relatively low temperatures pyrolysis tends to produce ketones from fatty acids and that decarboxylation becomes predominant only at considerably elevated temperatures. It appeared, therefore, that the molecules under alpha-particle or deuteron bombardment decomposed under conditions of high activation, i. e., they were "very hot". Recently, this idea was reaffirmed separately by James Franck,<sup>3</sup> who pictured these reactions as simulated thermochemical dissociations following internal conversion of the excitation or ionization energy of the decomposing molecules into vibrational energy to produce a "hot molecule".

Once having produced this "hot molecule", then molecular decomposition would be expected at that bond having the least potential energy requirement for cleavage.



The work described in this paper is an excellent example of that which can be done in borderline fields. In this particular instance the geological advice and inspiration of Professor W. L. Whitehead, and the physical approach and counsel of Professor Clark Goodman deserve infinitely more appreciation than these few words may seem to convey.

<sup>3</sup> Discussion at the Symposium on Radiation Chemistry and Photochemistry which was held at the University of Notre Dame, Notre Dame, Indiana, June 24-27, 1947.

Other contributors to this work have been C. W. Sheppard and R. E. Honig, who are no longer associated with the project, and Virginia L. Burton and Earl C. Farmer, who have aided notably in the work here reported.

## REFERENCES

- (1) American Petroleum Institute (50 West 50th Street, New York): *Annual Report of Progress—Fundamental Research on Occurrence and Recovery of Petroleum*, (1943).
- (2) BADIN, E. J.: *J. Am. Chem. Soc.* **65**, 1809–13 (1943).
- (3) BELL, K. C., GOODMAN, C., AND WHITEHEAD, W. L.: *Bull. Am. Assoc. Petroleum Geol.* **24**, 1529–47 (1940).
- (4) BERGMANN, W., AND LESTER, D.: *Science* **92**, 452–3 (1940).
- (5) BERGMANN, W., AND LESTER, D.: *J. Org. Chem.* **6**, 120–2 (1941).
- (6) BERGMANN, W., McLEAN, J. J., AND LESTER, D.: *J. Org. Chem.* **8**, 271–82 (1943).
- (7) BERGMANN, W., AND STANSBURY, H. A., JR.: *J. Org. Chem.* **8**, 283–4 (1943).
- (8) BREGER, I. A., AND BURTON, V. L.: *J. Am. Chem. Soc.* **68**, 1639–42 (1946).
- (9) BURTON, M.: *J. Am. Chem. Soc.* **58**, 1645–54 (1936).
- (10) BURTON, M.: *J. Am. Chem. Soc.* **58**, 1655–7 (1936).
- (11) CLARKE, H. T., AND MAZUR, A.: *J. Biol. Chem.* **141**, 283–9 (1941).
- (12) DOSS, M. P.: *Physical Constants of the Principal Hydrocarbons*, 4th edition. The Texas Company, New York (1943).
- (13) FISCHER, H., AND TREIBS, A.: *Ann.* **466**, 188–242 (1928).
- (14) HENKIN, H., AND BURTON, M.: *J. Am. Chem. Soc.* **60**, 831–6 (1938).
- (15) HONIG, R. E., AND SHEPPARD, C. W.: *J. Phys. Chem.* **50**, 119–43 (1946).
- (16) HONIG, R. E.: *Science* **104**, 27–8 (1946).
- (17) HONIG, R. E.: *Rev. Sci. Instruments* **18**, 389–94 (1947).
- (18) KIND, C. A., AND BERGMANN, W.: *J. Org. Chem.* **7**, 424–7 (1942).
- (19) LIND, S. C.: *The Chemical Effects of Alpha Particles and Electrons*, pp. 150–2. The Chemical Catalog Company, Inc., New York (1928).
- (20) LIND, S. C., AND BARDWELL, D. C.: *Science* **60**, 364–5 (1924).
- (21) LIND, S. C., AND BARDWELL, D. C.: *J. Am. Chem. Soc.* **48**, 2335–51 (1926).
- (22) MARKLEY, K. S.: *Fatty Acids*. Interscience Publishers, Inc., New York (1947).
- (23) NEY, W. O., *et al.*: *J. Am. Chem. Soc.* **65**, 770 (1943).
- (24) PAULING, L.: *The Nature of the Chemical Bond*, 2nd edition. Cornell University Press, Ithaca, New York (1945).
- (25) SACHANEN, A. N.: *The Chemical Constituents of Petroleum*. Reinhold Publishing Corporation, New York (1945).
- (26) SHEPPARD, C. W.: *Bull. Am. Assoc. Petroleum Geol.* **28**, 924–52 (1944).
- (27) SHEPPARD, C. W., AND HONIG, R. E.: *J. Phys. Chem.* **50**, 144–52 (1946).
- (28) SHEPPARD, C. W., AND WHITEHEAD, W. L.: *Bull. Am. Assoc. Petroleum Geol.* **30**, 32–51 (1946).
- (29) SHEPPARD, C. W., AND BURTON, V. L.: *J. Am. Chem. Soc.* **68**, 1636–9 (1946).
- (30) TRASK, P. D., AND WU, C. C.: *Bull. Am. Assoc. Petroleum Geol.* **14**, 1451–63 (1930).
- (31) TREIBS, A.: *Ann.* **410**, 42–62 (1934).
- (32) TREIBS, A.: *Z. angew. Chem.* **49**, 551 (1936).
- (33) TREIBS, A.: *Z. angew. Chem.* **49**, 682–6 (1936).
- (34) TSCHITSCHIBABIN, A. E.: *Compt. rend. acad. sci. U.R.S.S.* **1930A**, 382–4; *Chem. Zentr.* **101**, II, 2854–5 (1930); *Chem. Abstracts* **25**, 2551<sup>9</sup> (1931).
- (35) TSCHITSCHIBABIN, A. E., *et al.*: *Chimie & industrie Special No.*, 306–18 (1932); *Chem. Zentr.* **103**, II, 952 (1932); *Chem. Abstracts* **26**, 3654<sup>8</sup> (1932).
- (36) TSCHITSCHIBABIN, A. E., *et al.*: *Bull. acad. sci. U.R.S.S.* [7] **1932**, 203–24; *Chem. Zentr.* **104**, I, 3389 (1933).
- (37) VALENTINE, F. R., JR., AND BERGMANN, W.: *J. Org. Chem.* **6**, 452–61 (1941).
- (38) WELLS, R. C., AND ERICKSON, E. T.: *U. S. Geol. Survey Professional Paper* **166D** (1940).
- (39) WHEELER, D. H., AND RIEMENSCHNEIDER, R. W.: *Oil & Soap* **16**, 207–9 (1939).

## RADIATION CHEMISTRY. IV

AN INTERPRETATION OF THE EFFECT OF STATE ON THE BEHAVIOR OF SOME ORGANIC COMPOUNDS AND SOLUTIONS<sup>1, 2</sup>

MILTON BURTON

*Department of Chemistry, University of Notre Dame, Notre Dame, Indiana**Received October 23, 1947*

Radiation chemistry embraces a wide array of causes and effects. All the chemistry ensuant on the action of the various high-energy particles and radiations and of the recoils produced in emission of, or by impact with, these particles is included. The mere classification of the primary processes involved produces a rather complicated diagram of interrelated phenomena (3).

It is possible, of course, to examine each of the phenomena separately and to see how each in turn is affected by the class of material in which the event occurs (e.g., its state, nature of bonding, type of compound and nature of substrate, and size, complexity, thermodynamic stability, etc. of the compounds), by the nature of the particle or radiation (e.g., its mass and its energy), and the conditions of temperature, pressure, and radiation density. For over-all understanding such an approach is essential. However, it is a matter of some convenience to examine the phenomena which may occur in a limited class of materials with variable but related characteristics. Organic compounds are particularly convenient for study because they are related in this way, because their bonding is mainly of the covalent type, and because back-reactions (other than the reverse of the primary reaction) usually do not occur.

A significant amount of data on the radiation chemistry of organic compounds has been existent for a long time (9, 13), but they have not been generally interpreted on the basis of the Eyring-Hirschfelder-Taylor theory (5). A beginning of such interpretation and an attempt at correlation have been made (4, 18). The major principles developed are that in radiation chemistry the nature and relative amounts of the products are governed by the nature and relative amounts of the parent groupings and that the liquid state, molecular size, molecular complexity, and thermodynamic stability, particularly as evidenced by resonance, all tend to decrease susceptibility to high-energy radiation. However, these effects have thus far been treated in a very general way. It now seems desirable to consider in detail some of the phenomena that occur, so that inconsistencies can be explained and the underlying important factors can be established.

Limiting ourselves to organic compounds, we wish to see what the primary processes are, how they are affected by the nature of the compound and by its state, what the consequent secondary (i.e., essentially chemical) processes are, and how they are affected by similar considerations. Also, the nature and conditions of irradiation must be examined.

<sup>1</sup> Presented at the Symposium on Radiation Chemistry and Photochemistry which was held at the University of Notre Dame, Notre Dame, Indiana, June 24-27, 1947.

<sup>2</sup> Work on radiation chemistry at the University of Notre Dame is assisted by the Office of Naval Research of the United States Navy Department under Contract N6ori 165 T.O.II.

## THE PRIMARY PROCESS

As in all chemical reactions, the primary process is essentially physical. In most cases, it involves the transfer of energy from a high-energy particle or photon to a relatively quiescent molecule. In some cases the primary process of radiation chemistry is really secondary to a radioactive process (as in recoil phenomena ensuant on gamma emission). However, for the main part, it is possible to consider the primary process as involving the interaction of an energetic charged particle and a molecule.

*Effect of particle size*

The amount of energy transferred per unit of path length increases with the mass of the incident particle. Roughly, highly energetic heavy particles produce one ion every 5–10 molecules of path, whereas electrons of the same velocity produce one ion in every 500 molecules of path. The electrons ( $\delta$ -electrons) emitted in the ionization process by fast heavy particles can themselves cause ionization (slightly less effectively than do the heavy particles). In heavy-particle irradiation the ratio of total ionization (part of which is by  $\delta$ -electrons) to primary ionization is of the order of four.<sup>3</sup> Thus, depending on the energy of the heavy particle, the nearest distance between resultant ions is on the average 15–30 molecules. The distance which  $\delta$ -electrons travel before production of an excitation or ionization process is not a matter of immediate concern. That distance is certainly less than 500 molecules. Obviously, the density of ionization or excitation in the heavy-particle path is not thereby attenuated, although with proper geometry of the  $\delta$ -electrons it might be slightly increased.

The primary process is in part ionization and in part excitation of the molecules by the incident charged particles. Measurements on the gaseous state indicate that the average energy expended in the production of an ion is about twice the ionization potential; i.e., about half the energy produces primary ionization and the remainder primary excitation.<sup>3</sup>

One conclusion from these facts is that the distance between ions or between ions and excited molecules or between excited molecules is already sufficiently great with heavy-particle excitation so that substantially no difference should be observed in the gas phase between the chemical effects of alpha and electron irradiation per unit amount of energy absorbed. This matter has not been systematically investigated. On the other hand, the excited molecules and ions are sufficiently close together in the case of heavy-particle irradiation (on the average the nearest excited neighbor may be 8–15 molecules away) so that some special effect may be detectable in the liquid phase, because of the Rabinowitch-Wood effect (19, 20). According to simple mechanical experiments of those investigators, in the liquid state two molecules collide with each other repeatedly after an initial collision before one of them can escape the surrounding cage of molecules. The result is that reaction between excited molecules or ions initially sufficiently close to each other is particularly favored in the liquid case and that,

<sup>3</sup> A brief résumé of the early theory and experiments on interactions of nuclear radiation with matter is given by Rutherford, Chadwick, and Ellis (22). A detailed review by R. L. Platzman is now in preparation.

in consequence, some essentially different chemical effects should be produced in liquids by heavy particles and by light particles. Preliminary work conducted at the Metallurgical Laboratory indeed showed such an effect, which will be the subject of a later report, but in the interest of both accuracy and certainty of interpretation more extensive data are required.

### *Effect of state*

When a high-velocity charged particle interacts with a molecule, the processes that occur depend in part on the possible levels to which the molecule can be excited and in part on the various ionization potentials. There are two classes of primary processes: excitation and ionization. The former leads to reactions similar to those of photochemistry.<sup>4</sup> The latter may involve a number of phenomena such as secondary ion formation resultant from decomposition of the original ions, simultaneous ionization and decomposition, and multiple ionization. The relative amounts of excitation and of ionization will depend on the number and heights of the various excited and ionization states but usually, as already stated, the ratio does not vary far from unity for large molecules.<sup>8</sup> According to Gibson and Eyring (8) relative molecular ionization runs fairly parallel to relative stopping power for a number of interesting cases. They found that the ratio of the two values varied only from 0.996 to 1.38 for substances as diverse as carbon dioxide and azomethane. For methyl iodide the value was 1.37 and for nitric oxide 1.29. This result means that in these cases the relative amounts of excitation and of ionization are not greatly affected by substantial differences in energy states characteristic of different molecular systems.

The relative stopping power of a substance for energetic particles of a particular class is a measure of the rate at which such particles lose their energy in travelling through that substance. As a first approximation the additive rule holds that the relative stopping power of a molecule is the sum of the relative stopping powers of the constituent atoms.<sup>3</sup> Too close an agreement should not be expected, since the nature of the excited and ion states should have a perceptible influence on the amount of interaction between the energetic particles and the molecules. Accordingly, it might be expected that any factors which would tend to change the energy levels of the various states involved would certainly change the stopping powers.

As a matter of fact, in the range of cases studied by Gibson and Eyring the additive rule was correct within about 4 per cent. An effect is obviously to be sought in the difference between the liquid and the gaseous states, but Philipp (16) found that the additive rule holds for all vapors and normal liquids (e.g., benzene and pyridine) studied, although values smaller than the true ones are found for associated liquids such as water and alcohol.

A conclusion from the results of Philipp together with those of Gibson and Eyring is that although more energy may be expended per unit of path length in associated liquids, the relative amounts of excitation and ionization certainly are not greatly affected by minor perturbations and displacements of energy levels, such as are produced in the molecular interactions characteristic even of



associated liquids. A corollary is that, although the energy required to produce an ion-pair in a liquid is different from that for the gaseous state of the same substance, it is never greatly different. It is interesting to note in the data of Gibson and Eyring that the relative amount of ionization increases with molecular complexity. It would be interesting to discover just how general this phenomenon is. It may indicate that factors which tend to increase the number of, or perturb, electronic energy levels serve likewise to increase, not to decrease, relative molecular ionization. If this conclusion is correct, molecular association characteristic of the liquid state would result in a slight lowering (never an increase) of the amount of energy required to produce an ion-pair.

A further conclusion from these results is that where substantial differences are existent in the radiation reactivity of substances in their gaseous and liquid states, the explanation is not to be sought in a substantial difference in the primary physical processes in the two states. The explanation must be in the considerably changed probabilities of processes following the primary processes of excitation and ionization. This conclusion is the obvious counterpart of the conclusion of Franck and Rabinowitch (6) anent the effect of the liquid state on photochemical reactions. The generally increased stability in that state is attributed to a cage effect by the surrounding molecules, so that the energy is tapped off before it becomes effective for decomposition or so that the decomposing fragments are made to recombine before they escape from each other's spheres of influence.

#### *Remarks on primary excitation*

Since roughly half of the energy expended in the irradiation of a compound causes excitation in a primary step, reactions must be expected in radiation chemistry which are somewhat analogous to those of photochemistry. There are, however, some differences.<sup>4</sup> In general, the conditions of excitation are such that almost any electronic orbital of the molecule may be involved. Thus, whereas in photochemistry only one upper electronic state is usually involved, in radiation chemistry there may be a great variety of such states. Furthermore, since more energy is available in high-energy radiation processes, it may be expected that higher states will also be excited. Thus, on two counts we may expect a much greater variety of primarily excited upper states in radiation chemistry and a possible increased complexity of ensuing reactions. To some extent this complexity may be offset by fluorescence, internal conversion, and energy-transfer processes so that in the end only a very few or even one electronic state may be involved in the chemical step. In general, however, in the case of compounds containing a variety of groupings, it may be expected that radiation-chemical excitation leads to greater complexity of reaction than does photochemical excitation; i.e., radiolysis through excitation alone should give a greater variety of products than does photolysis.

<sup>4</sup> In photochemistry, however, the excitation is usually specific. The same bond or group or excited state is initially involved in every activated molecule, provided the light is nearly monochromatic. In radiation chemistry a much broader range of excited states and of ensuing reactions is possible.

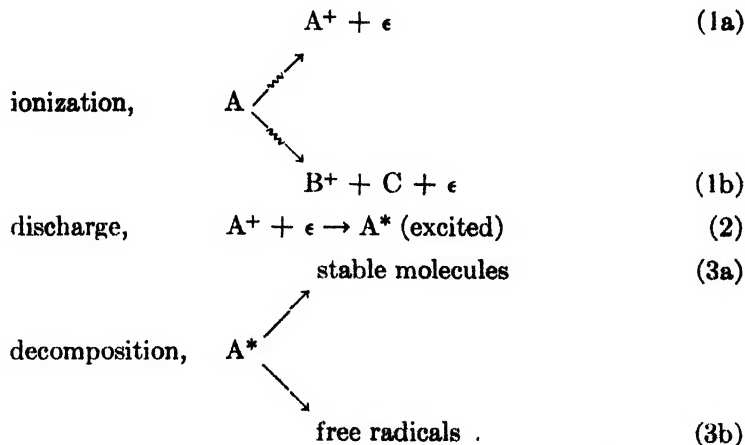
An exception in degree to a principle such as that just enunciated may be found in the case of highly symmetrical compounds, such as benzene. During radiation-chemical excitation almost any electronic orbital of the molecule may be involved but, since there are so many equivalent orbitals and electronic states, the result is that the number of different excited states is not greatly more than in photochemistry.

If the compound under irradiation is somewhat complicated (as are most organic compounds), there will be almost a continuum of excited states. In such a case the liquid state may permit the tapping-off of energy from upper excited levels before they make a chemical contribution. If there is a mechanism which requires some time between physical activation and chemical decomposition, tapping-off of energy and internal conversion both are almost certain to occur in the liquid state, so that radiolysis in that event may not lead to a greater variety of products than does photolysis.

#### SECONDARY PROCESSES

Secondary processes include ionic decomposition, reactions of ions or excited molecules with other ions or molecules, discharge of ions, transfer of energy from excited molecules (by fluorescence or by collisional deactivation), internal conversion of energy states, decomposition processes involving excited molecules and radicals, and addition processes involving also intermediate and final products.

Although ionization is the characteristic physical process of half of radiation chemistry (the other half is primary excitation), it is not the controlling process. The general mechanism<sup>5</sup> of such processes has been given by Eyring, Hirschfelder, and Taylor (5) and elaborated elsewhere (4, 18). In general, the features are:



<sup>5</sup> In the course of the discussion, Dr. F. S. Dainton suggested a grouping into primary and secondary physical processes and primary (etc.) chemical processes. The classification has obvious aspects of simplicity applicable to both radiation chemistry and photochemistry.

reactions similar to 2 and 3 involving the various ionic species  $B^+$  (which may be radical ions or molecular ions), reactions involving the fate of the various species C and any free radicals produced, and processes which may prevent decomposition reactions (reaction 3) of the excited molecules  $A^*$  and  $B^*$ .

We have already seen that we cannot account for large differences in radiation-chemical behavior merely on the basis of variations in relative amounts of ionization and excitation (*cf.* the ratio of relative molecular ionization to relative stopping power). Neither can we account for differences in the radiation resistance of different compounds merely on the basis of the possibly large variety of ions denoted by  $B^+$  in reaction 1b.

An excellent illustration of this latter fact is afforded in the comparison of benzene and cyclohexane. The ionic species produced by electron bombardment in the mass spectrometer are approximately equally varied in the two cases (*i.e.*, 44 reported in the case of benzene, 48 in the case of cyclohexane) (9).

TABLE 1

*Effect of fast-electron irradiation on liquid hydrocarbons, according to Flanagan, Hochanadel, and Penneman*

HYDROCARBON	$G_g$ (MOLECULES OF GAS PER 100 E.V.)	$G_p$ (MOLECULES REACTANT CONVERTED TO POLYMER PER 100 E.V.)
Benzene	0.04	0.5
<i>n</i> -Heptane	4.2	1.7
Cyclohexane	4.0	1.2
Cyclohexene	1.0	4.2
Methylcyclohexane	4.5	4.2
Toluene	0.09	0.7

Nevertheless, the chemical resistances of the two compounds to high-energy irradiation are quite dissimilar (4, 18). In the liquid state, benzene is very resistant whereas cyclohexane decomposes very readily. Some of the previously published results obtained by Flanagan, Hochanadel, and Penneman at the Metallurgical Laboratory are given in table 1. Liquid toluene is more like benzene in its reactivity than the mere presence of the methyl group might lead one to expect, but methylcyclohexane is considerably more reactive than cyclohexane.

#### *Effect of state*

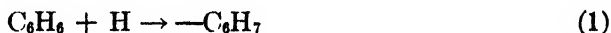
An indication that the results on benzene are in part the effect of state is afforded by the very limited studies on the vapors. Mund and Bogaert (15) found a pressure decrease in benzene exposed to alphas from radon contained in the same vessel. From this decrease they found that the ratio of number of molecules of gas disappearing to ions produced (calculated) was about unity. As the term is used in table 1, the corresponding value of  $G_p \simeq 4$  (9); *i.e.*, a change to the gaseous state causes an eightfold increase in polymerization. Unfor-

tunately, data on the radiolysis of benzene are rare. Linder and Davis (14) studied the amount of vapor non-condensable at  $-77^{\circ}\text{C}$ . produced by glow discharge acting on a variety of hydrocarbon vapors. The voltage of the bombarding particles was unknown and variable, but under the conditions of their experiments (not necessarily the same for the different compounds) the rate of gas production was about four times as great in either hexane or cyclohexene as in benzene. Although too much significance must not be attached to the value "four", the ratio is doubtless much lower than values found in the liquid state, as may be calculated from table 1.

The immediate question is why change of state affects aromatics like benzene and toluene so much more than it affects aliphatic compounds, which seem to be highly reactive both in gas and in liquid.

#### *Effect of type of compound*

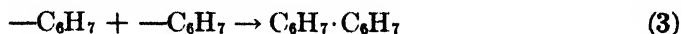
Table 1 illustrates a long-known fact that aliphatic hydrocarbons are much more resistant to the effects of high-energy radiation, measured in terms of gas production, than are aromatics and that the olefins lie in between (3, 4, 9, 14, 18). There is an immediate temptation, of course, to ascribe this fact to reaction of intermediate free atom or radical products with available unsaturated linkages and to resultant formation of non-gaseous products. For example, in the radiolysis of benzene the explanation of the low yield of hydrogen would be the reaction



followed by



or



Reaction 2 would be the first step in a polymerization series. The sequence of reactions 1 and 3 would consume the most atomic hydrogen per molecule of benzene converted to "polymer".

Let  $G_1$  be the number of molecules per 100 e.v. actually dissociated in the initial step of the radiolysis; i.e., in the case of benzene we shall assume primary decomposition to free phenyl and atomic hydrogen. The maximum value of  $G_1$  for benzene would be given by the assumption that reaction 2 and the ensuing series do not occur at all; i.e., that each molecule of benzene disappearing in polymer represents an atom of hydrogen produced by decomposition in reaction 1. Then

$$G_1 \leq 2G_p + G_p$$

where we neglect the fact that some contribution to  $G_p$  is from  $\text{C}_6\text{H}_5$  radicals. The minimum value would be given by the assumption that reaction 3 does not

occur at all and that the polymerization series is very long and involves many benzene molecules; i.e.,

$$G_1 \geq 2G_2$$

Similar remarks would apply to  $G_1$  defined generally as the primary 100 e.v. yield for radiolysis of any compound. Values calculated in this way are given for three significant cases in table 2.

The calculated maximum value of  $G_1$  in table 2 for the aromatics is considerably less than the calculated minimum for a corresponding aliphatic, cyclohexene. There are three "double bonds" in benzene and toluene compared with one in cyclohexene, and there may be an objection that the former correspondingly provide a threefold better chance for capture of free atoms or radicals. If we pay attention merely to the arithmetic, it is then not obvious why  $G_2$  in cyclohexene should exceed that in benzene and in toluene by factors of 25 and 11, respectively. However, the kinetics must not be ignored. Early work of Bonhoeffer and Hartek (2) indicates that atomic hydrogen has a destructive

TABLE 2  
*Some calculated values of primary 100 e.v. yield*

HYDROCARBON	$G_1$	
	Calculated minimum	Calculated maximum
Benzene	0.08	0.58
Toluene	0.18	0.88
Cyclohexene	2.0	3.1

effect on benzene vapor; methane, ethylene, and acetylene (all of which were found by Flanagan, Hochanadel, and Penneman in the products of the radiolysis) are produced. If liquid benzene behaves at all like the vapor, a part of the contribution to  $G_2$  may represent secondary action of free hydrogen atoms on otherwise inactivated benzene. The conclusion is that the maximum value for  $G_1$  for benzene given in table 2 is a real maximum and that the true value may be somewhat less.

A further conclusion from the limited information on the radiolysis of aromatics is that even in the gaseous state they appear to be far less reactive than paraffins or olefins (14) and that, in view of the fact that a presumptive intermediate product (atomic hydrogen) is known to attack benzene vapor destructively, it is likely that the low yields are not to be attributed to secondary reactions by which the intermediates are removed. We have already seen that the result cannot be attributed to any substantial differences in relative molecular ionization. The conclusion is that we must examine the behavior of the ions and excited molecules initially produced to see how their properties may be reflected in degree of reactivity of substances (in this case aromatic hydrocarbons) to irradiation.

*Behavior of excited molecules*

Since approximately half the energy in a radiation-chemical process is expended primarily in excitation (without ionization), it is desirable to examine the possible fate of excited molecules. Photochemistry teaches that not all molecules which are excited with sufficient energy necessarily decompose or react. Decomposition competes with other processes, including fluorescence and collisional deactivation.

Benzene furnishes an excellent example of a substance which photolyzes with low quantum yield. Its absorption spectrum begins with a sharp band structure at  $\lambda = 2667 \text{ \AA.}$  to  $\sim 2200 \text{ \AA.}$  From  $2200 \text{ \AA.}$  to  $1850 \text{ \AA.}$  the bands are diffuse on a continuous background. The continuum becomes prominent at  $1850 \text{ \AA.}$  and extends to the limit of observation, but there are a few bands at  $1789\text{--}1732 \text{ \AA.}$  discernible above the background (*cf.* 21). Bates and Taylor (1) found that the light of the full mercury arc gave only a very slight photolysis of the vapor when mercury vapor was excluded to avoid photosensitization. West (24) found no decomposition at  $2537 \text{ \AA.}$ , nor was he able to detect any para-ortho hydrogen conversion which might have been indicative of the transitory existence of atomic hydrogen. Krassina found evidence for hydrogen atoms in the regions  $2150\text{--}2000 \text{ \AA.}$  and  $2000\text{--}1850 \text{ \AA.}$ , using the Paneth mirror method and tungstic oxide and cupric sulfate indicators but not at longer wave lengths (12). Prileshajëwa (17) reported deposition of a polymer under the same conditions and made measurements of the hydrogen produced but gave no quantum-yield data. Wilson and Noyes (26) found evidence for formation of biphenyl at low wave length but were troubled by deposition of a polymer. They conclude that in the region  $2000\text{--}1850 \text{ \AA.}$  (6.2–6.7 e.v.) the quantum yield for production of hydrogen is of the order 0.01–0.001 and attribute its production to intermediate formation of acetylene.

In summary, photochemical studies of benzene give evidence for low quantum yield of decomposition of the vapor with evidence for the formation of a small but troublesome amount of polymer at low wave length. Evidently, the life of the excited state is sufficiently great so that even in the vapor the probability of deactivation by collision far exceeds the probability of decomposition. There is no information as to the amount of energy involved in the primary excitation process in radiation chemistry but it is reasonable to assume a value in the region of 6.2–6.7 e.v., since the appearance potential of  $\text{C}_6\text{H}_6^+$  is only 9.8 e.v. (9). Thus, the primary excitation contribution to  $G_r$  in the vapor state should be no greater than about 0.004 to 0.04.<sup>6</sup>

It is interesting to examine the reason for the photochemical stability of benzene. The most reasonable explanation involves the nature of the excitation process. Presumably a  $\pi$  orbital is involved. The initial electronic state cannot be considered localized in the vicinity of any carbon atom, nor can the final state

<sup>6</sup> Calculated on the following reasoning: One-half 100 e.v. gives about eight excited benzene molecules. Since the data of Wilson and Noyes indicate a quantum yield of hydrogen atom production of  $>0.00\text{--}0.01$ , the values given are obtained.

be so considered. Decomposition after the electronic excitation involves an internal conversion in which the energy is transferred to vibrational excitation. We have no information to teach us where this energy should appear. If the electronic excitation is originally localized (as in the aldehydes) the ensuing decomposition is also localized.<sup>7</sup> On the other hand, with the initial electronic excitation non-localized, it perhaps follows that the vibrational excitation will also be non-localized. Under such circumstances, although more than enough energy is available, flow of sufficient energy into a single bond is required for occurrence of decomposition. However, benzene and the aromatics generally are in just that class where such localized concentration of energy would occur with very low probability. Their high "resonance" stability implies a large number of equivalent energy states. Thus, the probability of production of an unstable state (involving concentration of energy in a particular bond) is relatively low in comparison with production of any one of a host of equivalent states.

The conclusion from this reasoning is that "resonance" in the thermodynamic sense tends to stabilize a substance to photochemical decomposition. A secondary conclusion is that complexity generally and complexity associated with symmetry, particularly, will also tend to produce photochemical stabilization.<sup>8</sup>

#### *Behavior of ions*

Ions primarily produced in radiation processes either are discharged and yield excited molecules (reaction 2) or decompose to yield a new ion and a radical or molecule product. If the latter occurs, we may conclude that, neglecting the rare possibility of a back-reaction, a chemical change will be detected. One important question therefore (discussed in a later paragraph) concerns the factors which favor or disfavor such a process.

If the ion survives without decomposition and is then discharged, the excited molecule produced will have energy roughly of the order of 10–15 e.v. (or 25–40 e.v. if a doubly charged ion was involved). The more the energy of the molecule exceeds a typical bond strength, the greater the probability that sufficient energy will flow into that bond to cause decomposition. In this connection it is interesting that the  $C_6H_6^+$  ion has an appearance potential of only 9.8 e.v. (9) and that its relative abundance in mass-spectrometric experiments on benzene is approximately equal to that of all the other ions combined (*cf.* 11). Thus, we may expect that excited  $C_6H_6$  produced from the discharge of  $C_6H_6^+$  ions may persist until deactivation, but perhaps with not so great likelihood as will the primarily excited  $C_6H_6$  molecules (presumably containing less energy). Approximately one-quarter of the energy absorbed goes to produce  $C_6H_6^+$ . If all the  $C_6H_6^+$

<sup>7</sup> *Cf.* the photochemistry of propionaldehyde. The electronic excitation is in the carbonyl group and the split of C—C links yields only free ethyl and formyl radicals; i.e., the energy is transferred preferentially during the internal conversion to an adjacent bond (see W. M. Garrison and M. Burton (7)).

<sup>8</sup> Neopentane is an interesting case in point. Steacie (private communication) says that neopentane is extremely stable to decomposition by mercury photosensitization.

ions survive until discharge and yield excited  $C_6H_6$ , we may conclude that the contribution of these highly excited entities to  $G_0$  for benzene vapor will perhaps also be of the order 0.004–0.04 for, although they are formed in less than half the number, they will be more likely to decompose than will the somewhat less excited (i.e., primarily excited) benzene molecules.

That the  $C_6H_6^+$  ions may survive until they are discharged is not unreasonable in the light of considerations entirely parallel to those in terms of which the photochemical stability of excited benzene has been interpreted. The point here is that any possible excited orbital, as well as the missing orbital, is not localized; it is spread over the whole molecule and there is insufficient local bond weakening to favor instantaneous rupture. In this connection it would be very helpful to have experiments similar to those of Hipple, Fox, and Condon (10) on the half-life of the  $C_6H_6^+$  and similar (e.g.,  $C_6H_5(CH_3^+)$ ) ions.

In general, any factor which tends to spread a missing (or excited) orbital over a large portion of a molecule (i.e., so that that orbital is not localized) will operate to favor stability of the ion. In molecules like the aromatics and substituted aromatics, the missing orbital may be in the ring or in the side chain. If it is in the ring, the ion may be quite stable. If it is in the side chain, internal conversion involving transfer of an electron from the ring may produce stability. Stability of a kind (i.e., prolongation of half-life) may be obtained also by a series of internal conversion processes in a straight-chain hydrocarbon, in which an empty orbital shifts rapidly from one bond to another and, in some cases, to a non-bonding position. Experimental data bearing on this point would also prove helpful.

We may conclude that in the case of benzene all ions in which the missing orbital may be presumed to be spread over the whole ion have a high probability of survival until discharge. Such ions not only include  $C_6H_6^+$  but may also include  $C_6H_5^+$ ,  $C_6H_4^+$ , and  $C_6H_3^+$  which, taken together, appear in abundance approximately one-quarter that of  $C_6H_6^+$  in some mass-spectrometer experiments (11). If the latter ions react favorably with H or  $H_2$ ,  $C_6H_6^+$  may be produced. Under such circumstances the yield might be kept low. However, in order for such a favorable reaction to occur means might have to be provided to remove the energy released in the reaction between H (or  $H_2$ ) and the hydrogen-deficient ion.

If we assume the same distribution of ion products in a radiation exposure as in the mass-spectrometer experiments related (11), we would conclude that approximately one-quarter of the energy goes to produce ions other than  $C_6H_6^+$ . If, further, we make the maximum assumption that in the vapor state all the ions other than  $C_6H_6^+$  inevitably lead to chemical change, their contribution to the total value of  $G_0$ , assuming an average appearance potential of  $\sim 20$  e.v. (9), would be  $\sim 1.2$ .

Noting the contributions from primarily excited  $C_6H_6$  and from  $C_6H_6^+$  already "calculated", it follows that a rough value of  $G_0 \sim 1.3$  for benzene vapor could reasonably be expected. There is no direct information on this value, although experiments by S. Gordon are now under way in this laboratory. However, it



is possible to get a rough notion from the results of Linder and Davis already cited (14). Their results indicate a value of  $G_0$  in benzene vapor approximately one-quarter that in aliphatic hydrocarbons. Early results cited by Lind (13) indicated an  $M/N$  value = 2 for disappearance of the hydrocarbon or a value of roughly  $G = 8$ . One-quarter of this value,  $G = 2$ , is not too far from our "calculated" value  $G_0 \sim 1.3$  for benzene vapor, particularly when we note in these early values some difficulty in establishment of the nature of the products.

*Superimposed effect of state*

We have already seen in connection with the various benzene ions that the  $C_6$  ions might revert to  $C_6H_6^+$  *via* reaction with H or  $H_2$ , provided means exist for picking off the energy. Such means always exist in the liquid state. Thus, there is a better possibility in the liquid than in the gas that those ions might not lead to a chemical change.

However, means for checking the chemical effects of such unfavorable ions would not be enough to account for the stabilizing influence of the liquid state on the radiation sensitivity of benzene. The explanation probably has to be sought in some failure of the unfavorable entities to form at all in liquid benzene. They include not only the various  $C_6$  ions but also  $C_6$ ,  $C_4$ ,  $C_3$ , and  $C_2$  ions as well. All these ions have appearance potentials higher than that of  $C_6H_6^+$ . If the mechanism of their formation is through excited  $C_6H_6^+$  ions, the benzene liquid may furnish excellent means to tap off the excess energy before those excited  $C_6H_6^+$  ions can decompose to yield the smaller ions. That benzene may be a specially favorable liquid for such collisional deactivation is indicated by some photochemical experiments of quite another type by West and Paul (25). They found that when alkyl halides are photolyzed in benzene solution the quantum yields are practically the same as in hexane solution, in spite of the fact that benzene absorbs in the same wave-length region as the alkyl halides studied. The explanation was that the benzene, which did not decompose of course, transferred its energy to the alkyl halide in a photosensitization process. The many available energy levels in liquid benzene should likewise make it a good acceptor of energy to remove energy from excited  $C_6H_6^+$  ions.

Thus, we might conclude that benzene because of its multiplicity of energy levels (since it has a complicated, symmetric, highly resonant structure) is an unusually favorable molecule for tapping off excess energy and thus decreasing not only its own decomposition by high-energy radiation but also that of any substance contained in it.

An interesting case in point (worthy of much more extensive study) was given by Schoepfle and Fellows (23). Some of their data on the effects of cathode rays are summarized in table 3. Under the conditions of their experiments, cyclohexane yielded 45.8 cc. of gas, benzene 2.2 cc. It might be expected, if there were no special effect, that a mixture of 90 per cent benzene and 10 per cent cyclohexane should yield  $\sim 6.5$  cc. of gas, whereas they found only 3.2 cc. One explanation could be that the "double bonds" in benzene absorb the free radicals or atoms intermediate to gas production. An objection to such an explanation

has already been reviewed in detail in the discussion of benzene itself. Another explanation is that just presented in the previous paragraph: namely, that benzene operates particularly favorably to pick off excess energy and thus to prevent reaction.

Table 3, however, underlines a couple of strange results. Phenylcyclohexane yields less gas than does the 90 per cent benzene + 10 per cent hexane solution. An explanation (other than possible uncertainty of the data) could be that the two rings are particularly favorably coupled for transfer of energy. Hexamethyl-

TABLE 3  
*Some effects of cathode rays on hydrocarbons, according to Schoepfle and Fellows*  
170 kv., 0.3 ma.

HYDROCARBON	TOTAL GAS PRODUCED IN 30 MIN.	HYDROCARBON	TOTAL GAS PRODUCED IN 30 MIN.
	<i>cc. at N.T.P.</i>		<i>cc. at N.T.P.</i>
<i>n</i> -Heptane	51.4	Benzene	2.2
Octylene	16.4	Toluene	2.7
Cyclohexane	45.8	Hexamethylbenzene	7.5
Methylcyclohexane	39.2	Naphthalene	<0.5
Cyclohexene	18.8	Anthracene	<0.5
		Biphenyl	<0.5
Diphenylmethane	0.8		
Triphenylmethane	0.9		
Tetrahydronaphthalene	2.6	90% benzene + 10% cyclohexane	3.2
Phenylcyclohexane	2.3		

benzene yields more gas. Evidently, a thorough study of these systems is in order.

#### SUGGESTED STUDIES

In the speculations of this paper it has frequently been necessary to cite experiments which have furnished only very limited data. More extensive experiments of many kinds are much required if the theory of action of high-energy radiation on organic compounds is to receive more definite form. Some suggested by this paper are:

(a) Studies of the amount of energy required to produce an ion-pair as a function of molecular size, complexity, bond type, etc.

(b) More accurate studies of the yields of a variety of hydrocarbons in which *G* values for each of the carefully determined products would be given.

(c) Studies of the radiation chemistry of solutions, particularly in benzene and in related hydrocarbons.

(d) Studies of the mechanism (perhaps using radioactive indicator techniques) of radiolysis.

(e) Lifetimes of various metastable ions (particularly  $C_6H_6^+$ ) as a function of their energy content.

(f) Comparison of effects of radiation particles of different mass in liquid-state radiolyses.

(g) Detailed comparison of liquid and gaseous radiolyses for a few typical cases.

#### SUMMARY

The processes occurrent in radiolysis of some organic compounds are reviewed. The size of the bombarding particle is not a significant factor in gases but may have a detectable effect in liquids. The state of the medium irradiated should have a minor effect on the primary process. If anything, a small increase in total relative molecular ionization should occur in the liquid. Where substantial differences in radiation reactivity of a compound are produced by change of state, the explanation does not lie in a possible change in the primary process. Primary excitation by high-energy radiation results in processes of the type occurrent in photochemistry. The variety of ions possibly produced in the primary process is not an indication of resultant reactivity. Benzene is compared with other hydrocarbons and it is concluded that its low reactivity is in part attributable to its photochemical stability and in part to the stability of the  $C_6H_6^+$  ion. The stabilities are explained in terms of the orbitals and internal conversion processes involved. The stabilizing effects of the liquid state in benzene and of benzene itself as a solvent are discussed. Some future experiments are suggested.

As Executive Secretary of this Symposium I wish to take this opportunity for a word of tribute to Dr. S. C. Lind and to Dr. James Franck. Dr. Lind, as Chairman of this Symposium, has the position which his pioneering efforts in this field have justly earned for him; radiation chemistry today prospers from his past and present endeavors. Dr. Franck was Chairman of the Chemistry Division of the Metallurgical Laboratory during much of my connection with it. He has been present at this meeting as an active participant in the discussions, and his criticisms and interpretations have clarified many problems. This paper and others by his former colleagues of the Metallurgical Project are some of the results of his generous advice and kindly guidance.

#### REFERENCES

- (1) BATES, J. R., AND TAYLOR, H. S.: J. Am. Chem. Soc. **49**, 2438 (1927).
- (2) BONHOEFFER, K. F., AND HARTECK, P.: Z. physik. Chem. **139** (Haber Band), 64 (1928).
- (3) BURTON, M.: J. Phys. Colloid Chem. **51**, 611 (1947).
- (4) BURTON, M.: J. Phys. Colloid Chem. **51**, 786 (1947).
- (5) EYRING, H., HIRSCHFELDER, J. O., AND TAYLOR, H. S.: J. Chem. Phys. **4**, 479, 570 (1936).
- (6) FRANCK, J., AND RABINOWITCH, E.: Trans. Faraday Soc. **30**, 120 (1934).
- (7) GARRISON, W. M., AND BURTON, M.: J. Chem. Phys. **10**, 730 (1942).
- (8) GIBSON, G. E., AND EYRING, H.: Phys. Rev. **30**, 553 (1927).
- (9) GLOCKLER, G., AND LIND, S. C.: *The Electrochemistry of Gases and Other Dielectrics*. John Wiley and Sons, Inc., New York (1939).
- (10) HIPPLE, J. A., FOX, R. F., AND CONDON, E. U.: Phys. Rev. **69**, 347 (1946).

- (11) HUSTRULID, A., KUSCH, P., AND TATE, J. T.: *Phys. Rev.* **54**, 1037 (1938).
- (12) KRASSINA, G. I.: *Acta Physicochim. U.R.S.S.* **10**, 189 (1939).
- (13) LIND, S. C.: *The Chemical Effects of Alpha Particles and Electrons*, 2nd edition. The Chemical Catalog Company, Inc., New York (1929).
- (14) LINDER, E. G., AND DAVIS, A. P.: *J. Phys. Chem.* **35**, 3649 (1931).
- (15) MUND, W., AND BOGAERT, E.: *Bull. soc. chim. Belg.* **34**, 410 (1925).
- (16) PHILIPP, K.: *Z. Physik* **17**, 23 (1923).
- (17) PILESHAJEWA, N. A.: *Acta Physicochim. U.R.S.S.* **10**, 193 (1939).
- (18) *Proceedings of Canadian Nuclear Chemistry Conference*, in press, 1947.
- (19) RABINOWITCH, E.: *Trans. Faraday Soc.* **33**, 1225 (1937).
- (20) RABINOWITCH, E., AND WOOD, W. C.: *Trans. Faraday Soc.* **32**, 1381 (1936).
- (21) ROLLEFSON, G. K., AND BURTON, M.: *Photochemistry and the Mechanism of Chemical Reactions*, p. 200. Prentice-Hall, New York (1938).
- (22) RUTHERFORD, E., CHADWICK, J., AND ELLIS, C. D.: *Radiations from Radioactive Substances*. Cambridge University Press, London (1930).
- (23) SCHOEFFLE, C. S., AND FELLOWS, C. H.: *Ind. Eng. Chem.* **23**, 1396 (1931).
- (24) WEST, W.: *J. Am. Chem. Soc.* **57**, 1931 (1935).
- (25) WEST, W., AND PAUL, B.: *Trans. Faraday Soc.* **28**, 688 (1932).
- (26) WILSON, J. E., AND NOYES, W. A., JR.: *J. Am. Chem. Soc.* **63**, 3025 (1941).

## RADIATION CHEMISTRY OF THE GEIGER-MUELLER COUNTER DISCHARGE<sup>1</sup>

PAUL B. WEISZ

*Research and Development Department, Socony-Vacuum Laboratories, Paulsboro, New Jersey*

*Received October 23, 1947*

### I. INTRODUCTION

The Geiger counter tube has by this time become a widely known instrument. Many investigators have used Geiger counter tubes as a tool in some research of nuclear, physical, chemical, or perhaps biological nature. It is safe to say that, whenever they have, their interest was concentrated on the experiment for which the counter served as a measuring instrument, and that they did not care about the various physical and chemical phenomena which took place inside the Geiger counter every time it produced an electrical impulse. This paper will not deal with the Geiger counter as the familiar research tool at all but will describe some of the phenomena occurring during the discharge process in the interior of the tube.

The mechanism of this particular type of self-sustaining corona discharge has been studied by many investigators, and much detailed knowledge has been accumulated, although this is not always apparent because of the scattered nature of the literature. This paper will review in a somewhat more integrated

<sup>1</sup> Presented at the Symposium on Radiation Chemistry and Photochemistry which was held at the University of Notre Dame, Notre Dame, Indiana, June 24-27, 1947.

form what might be called the present concept of that part of the discharge mechanism which is called "quenching" and is responsible for the self-extinguishing of each discharge pulse. It will try to indicate what radiation-chemical problems are involved, and furthermore try to show that the study of some aspects of the Geiger counter discharge may serve to investigate problems of ionics and radiation chemistry itself.

## II. THE QUENCHING MECHANISM

Some fundamental magnitudes will aid in introducing the subject: A typical Geiger counter tube consists of two concentric cylindrical electrodes (see figure 1): a cylindrical metal cathode of radius, say,  $b = 1$  cm.; axially suspended within this cathode an anode of much smaller diameter, such as a metal wire with a

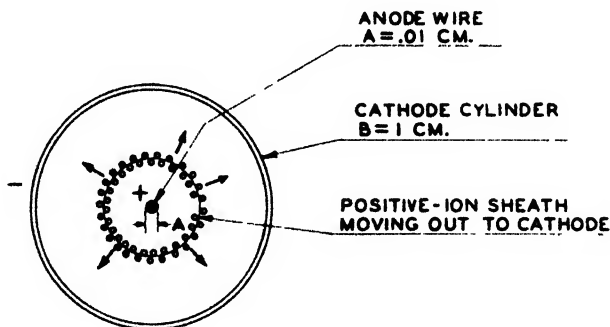


FIG. 1. Cross-section of counter tube approximately  $10^{-6}$  sec. after production of a discharge. The electrons produced simultaneously with the positive ions have all reached the anode wire.

radius  $a = 0.01$  cm. There is a gas or gas mixture present in such a self-quenching counter at a total pressure of around 10 cm. of mercury, about 90 per cent of this gas being an inert monatomic gas such as argon, and 10 per cent being a polyatomic molecule such as ethyl alcohol, ethyl ether, amyl acetate, butane, or others. A constant potential of about 1000 volts is applied between the two electrodes.

These typical figures give us additional basic information, such as the fact that the gradient of the electric field is highest near the wire, and high enough to produce electron multiplication (build-up of "avalanche") only within a distance of a few wire-diameters from the wire, that ions produced do not gain appreciable energies between collisions to produce secondary ionization in the gas, and that an ion traversing the tube radius must make about  $10^5$  collisions with gas molecules.

By way of introduction, it should be said that the condition for setting off a counter discharge is that of production of at least one free low-energy electron within the volume of the cathode cylinder. Only radiation which accomplishes this either directly or indirectly will initiate a measurable Geiger-counter pulse. On the other hand, the condition for the production of a short electrical

discharge rather than a continuous breakdown of the electrode interspace is that no more free electrons shall be liberated or exist in this interspace after a certain characteristic time interval from any source—other than radiation originally intended to be registered—has elapsed since initiation of the previous discharge pulse. This condition, involving a time interval of some 50 to 100 microsec., means that a thorough clean-up of all electrons and agents capable of producing electrons must have been accomplished within such a time interval.

In general the only two agents which have to be considered are (1) the positively charged, gaseous ions which are formed in the primary ionization and electron-multiplication process and (2) the photons which are emitted during the multiplication process as a by-product of the electron bombardment of molecules. This brings us to a discussion of the nature of the quenching mechanism, which must be one designed to suppress the production of any new electrons by the positive ions or by photons up to and including the time of the final collection of the ions by the electrodes.

Suppose that a single gas were present in the tube. Ions of this gas would be produced, having an ionization energy of  $I$  e.v. Furthermore, we can expect to find photons produced with energies ranging perhaps nearly as high in energy as the ionization energy  $I$ . Then the following process of detrimental electron-production may be possible: (1) Production of secondary electrons by the action of ions or excited molecules at the cathode surface; (2) production of photoelectrons on the cathode surface, since in general the work function,  $\Phi$ , of such surfaces is much smaller than the quantum energies available.

Quenching, therefore, requires that (1) no excited or ionized molecules capable of producing a secondary electron from the cathode surface shall reach the latter, and (2) a minimum of high-energy photons ( $E = h\nu \geq \Phi$ ) shall reach the cathode surface.

It is known that neutralization will take place by the act of drawing an electron from the metal (7, 8), when the positive ion approaches the cathode surface, at an expenditure of energy equal to, at least, the work function  $\Phi$ , leaving the neutralized molecule with a potential energy of  $I - \Phi$ , or less. It is now important that this neutral but excited molecule cannot eject another electron through further interaction with the metal, which is another well-known phenomenon (2, 6, 11). The probabilities of electron emission as a function of distance from the metal surface have been calculated for the case of the ion (neutralization process) (8) and for the case of excited molecules (5, 8) (electron ejection).

These calculations indicate that the critical distance for the neutralization process is appreciably greater (of the order of  $5$  to  $10 \times 10^{-8}$  cm. for  $\Phi = 4.5$  e.v.) than the critical distance for the electron emission due to an excited atom or molecule, the latter being of the order of  $2 \times 10^{-8}$  cm. The first process is one of field emission due to the strong local electrical field set up by the positive ionic charge when it approaches the metal. The latter process can be visualized as requiring a close and direct interaction between the excited molecule and the electron atmosphere of the metal,—classically speaking, a collision of the second

kind. Thus a certain average interval of time will elapse between the two processes, which for the nearly thermal ion velocities in the counter is of the order of  $10^{-13}$  to  $10^{-12}$  sec.

Thus one of the principal problems of discharge quenching becomes a problem of deëxciting a molecule during that time interval of  $10^{-13}$  to  $10^{-12}$  sec. to avoid electron emission subsequent to neutralization.

There are essentially three mechanisms that could be hoped for to obtain the loss of potential energy. Each has, if for a given species of molecule and excitation level it is at all possible, a certain order of magnitude of probability of occurrence in a  $10^{-12}$  sec. time interval. Table 1 summarizes these possibilities. Only the last mechanism provides deëxcitation fast enough to have value as a quenching mechanism. The absorption spectra of molecules, when available, yield the best available information on the behavior of the molecules with respect to dissociation, and continuous absorption in the band region where

TABLE 1

MECHANISM OF DEEXCITATION	ORDER OF MAGNITUDE OF TIME REQUIRED FOR PROCESS
Collision with other molecule	$10^{-9}$ sec. (average time between collisions)
Radiation of quanta*	$10^{-8}$ sec. (lifetime of quanta-emitting states)
Dissociation or predissociation	$10^{-11}$ to $10^{-13}$ sec. (lifetime of states leading to spontaneous dissociation)

\* Reference 12.

vibrational structure should be found indicates dissociable states having lifetimes near  $10^{-13}$  sec., which is about the time of a single interatomic vibration.

The probability for dissociation of electronically excited states generally rises so rapidly with atomic complexity of the molecule that it is almost a certainty that a polyatomic molecule having four or more atomic constituents will dissociate under the conditions here dealt with.

Starting out with the condition that no new electrons shall be liberated during the process of ion collection, a necessary requirement has been derived, namely, that the neutralized ion species must deëxcite within some  $10^{-12}$  sec. or less; ions of most polyatomic gases will satisfy this condition.

For a number of reasons (low operating voltage, favorable conditions for pulse-equalization, etc.) it is usually desirable to have an inert gas such as argon present as the major constituent in the gas phase. Ions of argon, if permitted to reach the wall, would not satisfy the above conditions. However, if a mixture of argon and a polyatomic gas is used, a transfer of ionization from the argon ions initially produced to ions of the polyatomic gas can be effected, since the number of collisions before reaching the wall is high. One requirement, however, is that the ionization potential of the quenching gas be lower than that of argon. This happens to be a condition which is easily satisfied, since as a rule the ionization potential decreases with increased complexity of the molecule and thus

is usually higher for the monatomic inert gases (with the possible exception of xenon). As was mentioned earlier, photons emitted during the initial electron multiplication process must be prevented from reaching the cathode surface also. Since photons of energy larger than the cathode-metal work functions are harmful, they involve the same order of magnitude as electronic excitation levels involved in the molecular deexcitation by dissociation. Since absorption bands in that energy region would be expected to exist to satisfy the deexcitation condition, it is usually safe to assume that the polyatomic constituent will also serve as an effective absorber of such photons as would otherwise reach the cathode and produce photoelectrons<sup>2</sup>.

### III. RADIATION-CHEMICAL CONSEQUENCES

The fact that dissociation of molecules is necessarily involved brings chemistry directly into the picture. The dissociation phenomena are naturally linked to the structure of the molecule, interatomic binding forces, and their electronic structure. There are three phases of interest, and in each, specific problems might be answered by studies on the discharge-quenching mechanism:

1. Phenomena regarding the neutralization mechanism at metal surfaces, such as lifetime against dissociation and critical distance of neutralization.
2. Phenomena concerned with the travel of polyatomic ions through a gas, such as ion mobility, change of mobility due to cluster formation, or possibly dissociation during collisions or spontaneous dissociation.
3. Phenomena concerning the kinetics of the dissociation products, such as studies on the new products formed by them.

#### *Kinetics of ion neutralization on metal surfaces*

The disappearance of initial polyatomic gas and the re-formation of new molecular material are closely related, of course, to the lifetime of the counter tubes. In connection with a few types of gases, the lifetime has been found to be limited to the number of discharges after which an appreciable percentage of the quenching gas has been dissociated. This was found to be true for ethyl alcohol (9) and for ethyl acetate (3). The lifetime of a methane-filled tube was reported much smaller (9), and more recent measurements (1) indicated that proper operation of the methane tube is not so much limited by the consumption of quenching gas as it is by formation of deposits on the cathode cylinder. The author has found this to be true for other hydrocarbons, such as propane

<sup>2</sup> Strictly speaking, the extent to which photoelectrons released at the cathode may be harmful must be tied in with the phenomenon of electron capture. Any photoelectron would arrive in the high-field region during the "dead-time" of the tube, because of the relatively high mobility of the electrons compared to that of the ion sheath. However, any electrons captured to form negative ions may reach that region after the "dead-time" period and release the discharge mechanism anew. With the product  $\alpha n N$  ( $\alpha$  = effective electron attachment coefficient,  $n$  = average number of electron-molecule collisions for a path equal to the tube radius,  $N$  = number of photoelectrons released from the cathode) sufficiently small—namely, much smaller than unity—such photons would actually be unable to interfere with the quenching mechanism.



and butane. It appears necessary to assume the deposition of dielectric polymers on small preferred areas of the cathode surface. Formation of such polymers is known to occur easily in electrical discharges (4) in the presence of even small quantities of hydrocarbon material. Watson has mentioned at this Symposium the observation of polymer deposits on metal surfaces in the electric fields of electron microscopes. It seems worth pointing out that the above-described surface mechanism provides an intense source of molecular radicals near metal surfaces, so that the metal surface acts as a catalyst to chemical action by providing radical production from whole molecules in excited states.

Neutralization mechanism and the life of the excited states are related to the ability for quenching. The critical distance of neutralization is dependent on the work function of the metal and somewhat on the ionization energy of the ion. Studies which concern these variables may lead to interesting conclusions. The probability of actual dissociation within the critical distance subsequently is related directly to the lifetime of the excited state, which would depend on the nature of the molecule and might be related by proper experiments to quenching action.<sup>3</sup>

#### *The mobility of polyatomic ions*

The motion of the ions and their final neutralization at the cathode are intimately related to the recovery of the counter tube after each individual discharge pulse. The cylindrical ion sheath produces a space-charge which lowers the electrical field near the anode wire. This field "recovers" slowly as the space-charge sheath moves out with a velocity characteristic of the electrical field in the particular geometry of the electrodes and the mobility of the ions under those conditions. Stever (10) has devised an experiment which essentially measures recovery of the electrical field due to the motion of the ion sheath as a function of time after an individual pulse has commenced. Figure 2 shows the type of characteristic obtained. This curve is obtained directly on a cathode-ray tube and reflects the position of the ion sheath at every instant, figured from the time of its formation.

Aside from the value of such an experiment for obtaining knowledge as to the practical recovery time of the counters, this type of measurement happens to yield the position of the ions on a continuous basis, and therefore upon recalculation will yield a continuous record of mobility along a path of travel some  $10^{-4}$  sec. in duration, or over some  $10^5$  molecular collisions. Since the present scope of knowledge on the mobilities of large ions is contradictory and somewhat chaotic, such measurements may be very valuable.

The shape of the "recovery time curve" can be calculated and an analytical expression obtained with the mobility as a variable. It is then possible to determine: (1) whether the mobility of the ions formed is essentially a constant over their entire path, i.e., during and after about  $10^5$  kinetic impacts; (2) what the mobility is under the particular pressure and field conditions.

<sup>3</sup> This was recently pointed out to me by S. C. Brown of the Massachusetts Institute of Technology.

A striking fact which such work has brought forth so far is that the observed mobilities,  $k$ , of the various organic gases do not necessarily relate to the molecular mass  $M$  of the parent molecule (e.g., by the relation  $k = \text{const. } (M)^{-1/2}$ ) as might be expected.

This conclusion is not surprising in view of mass-spectrometer research data which show very conclusively that, in the electron bombardment of a gas of complex molecular structure, ions are formed which are not necessarily the ions of the parent molecule, but that dissociation is taking place along with ionization, leading to the ions of smaller mass. The relative abundance is often definitely in favor of fragment ions; in fact in some molecules, such as tetramethyllead, no measurable parent ion intensity at all is found.

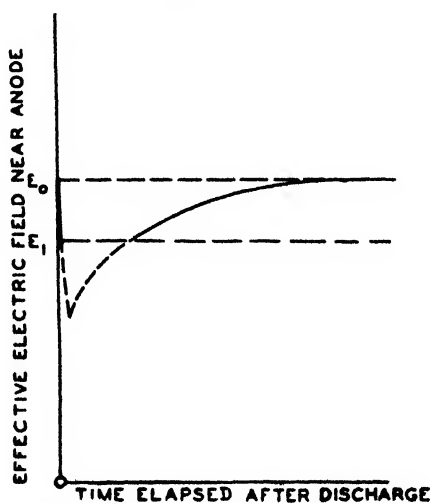


FIG. 2. The variation of the effective electrical field near the wire after a discharge was initiated.  $E_0$  = field when no discharge takes place.  $E_1$  = threshold field, or minimum field in which a full electron avalanche can be formed. Drawn-out curve is observed experimentally.

#### *Kinetics of dissociation products*

Molecular fragmentation not only into fragment ions, but also into electrically neutral radicals, takes place not only during the neutralization act at the cathode but also because of direct electron bombardment in the initial multiplication process.

As already mentioned, there is some evidence for the formation of polymers on the cathode when normal hydrocarbons supply the bulk of the effects. But aside from this effect there is considerable re-formation of gaseous products, and the modes of reaction and the type of products are of considerable interest. Conditions are similar to those which have been studied in connection with chemical effects in various gaseous electrical discharges (4). However, there is a difference in that there is not a continuous flow of bombarding electrons in the counter discharge, but only a short period of electron bombardment of less than

a microsecond duration, and also in that the size of this burst can be readily measured and controlled. Studies concerning the reaction product obtained under these conditions have been attempted (3, 9), and it is felt that they may help develop somewhat further the knowledge of the effects of slow-electron bombardment on molecules.

## REFERENCES

- (1) BROWN, S. C.: Private communication
- (2) COULLIETTE, J. H.: Proc. Roy. Soc. (London) **32**, 636 (1928)
- (3) FRIEDLAND, S. S.: Phys. Rev. **71**, 377 (1947).
- (4) GLOCKLER, G., AND LIND, S. C.: *The Electrochemistry of Gases and Other Dielectrics*. John Wiley and Sons, Inc., New York (1939)
- (5) MASSEY, H. S. W.: Proc. Cambridge Phil. Soc. **26**, 386 (1930); **27**, 460 (1931).
- (6) MESSENGER, H. A.: Phys. Rev. **28**, 962 (1926).
- (7) OLIPHANT, M. L. E.: Proc. Roy. Soc. (London) **A124**, 228 (1929).
- (8) OLIPHANT, M. L. E.: Proc. Roy. Soc. (London) **A127**, 388 (1930).
- (9) SPATZ, W. D. B.: Phys. Rev. **64**, 236 (1943).
- (10) KORFF, S. A., AND PRESENT, R. D.: Phys. Rev. **65**, 274 (1944).
- (11) STEVER, H. G.: Phys. Rev. **61**, 40 (1940).
- (12) WEBB, H. W.: Phys. Rev. **24**, 113 (1924).
- (13) WIEN, W.: Ann. Physik **60**, 597 (1919)

REACTIONS OF CARBON TETRACHLORIDE WITH BROMINE  
ACTIVATED BY ISOMERIC NUCLEAR TRANSITION AND  
BY THE NEUTRON-GAMMA REACTION<sup>1</sup>

JOHN E. WILLARD

*Department of Chemistry, University of Wisconsin, Madison, Wisconsin**Received October 23, 1947*

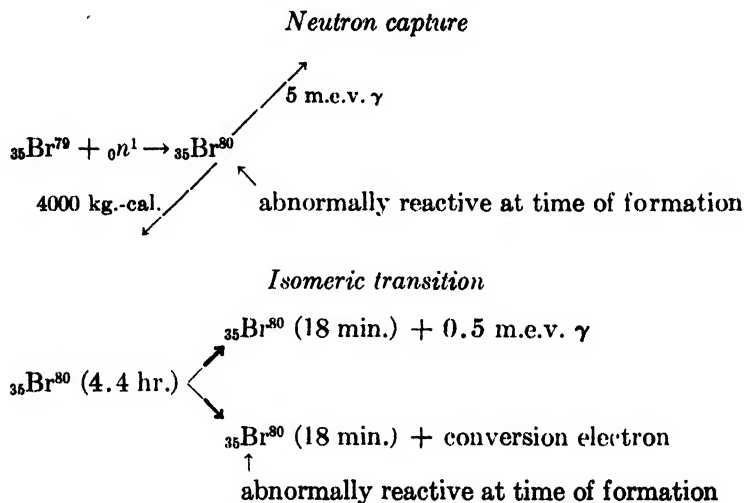
This paper will discuss investigations of the reaction of carbon tetrachloride with bromine activated by isomeric nuclear transition and by neutron capture (2, 14, 15). These studies have yielded evidence pertinent to the following topics: (1) the physical and chemical (Szilard-Chalmers process) phenomena associated with isomeric transition and neutron-gamma processes; (2) the possibility of multiple-bond rupture in a molecule which acts as a "third body" in the process of neutralization of an ion; (3) the Franck-Rabinowitch "cage" hypothesis. They are part of a more general program of investigation of reactions of halogens with halogenated methanes being carried on in our laboratories.

## TYPES OF ACTIVATION

Naturally occurring bromine consists of approximately equal amounts of two isotopes, Br<sup>79</sup> and Br<sup>81</sup>. Each of these isotopes is able to capture slow neutrons

<sup>1</sup> Presented at the Symposium on Radiation Chemistry and Photochemistry which was held at the University of Notre Dame, Notre Dame, Indiana, June 24-27, 1947.

to form a radioisotope one unit higher in atomic weight.  $\text{Br}^{82}$ , so formed, decays to  $\text{Kr}^{82}$  by beta emission with a half-life of 34 hr. The capture of neutrons by  $\text{Br}^{79}$  yields two energy states of the  $\text{Br}^{80}$  nucleus. The higher-energy state of  $\text{Br}^{80}$  decays to the lower with a half-life of 4.4 hr. by loss of energy as a gamma ray or, much more frequently, a conversion electron,<sup>2</sup> while the lower state decays to  $\text{Kr}^{80}$  by beta emission with a half-life of 18 min. Portions of these relationships of significance to the discussion of this paper are illustrated by the following equations:



The capture of a neutron by either of the natural bromine isotopes is an exoergic process accompanied by the emission of one or more high-energy gamma rays. For a typical case where a single gamma ray of 5 m.e.v. is emitted, it may be calculated, from considerations of conservation of momentum, that the bromine atom receives a recoil energy of about 4000 kg.-cal. per mole. Since this energy is far in excess of chemical-bond and activation energies, radio-bromine atoms formed by the neutron-gamma reaction are split out of their parent molecules (Szilard-Chalmers reaction) and may react with other molecules with which bromine does not normally react.

When the higher-energy state of the  $\text{Br}^{80}$  nucleus,  $\text{Br}^{80}$  (4.4 hr.), undergoes transition to the lower-energy state,  $\text{Br}^{80}$  (18 min.), the majority of the events lead to the ejection of a *K* electron. This in turn leads to the emission of an x-ray or to the ejection of an *L* electron (Auger electron). There is reason to believe that 90 per cent or more of the transitions produce a singly- or multiply-positively charged bromine atom. Such ions have been observed to undergo a variety of chemical reactions, some of which do not occur readily by other methods of activation. These reactions cannot be due to recoil energy of the bromine atom, since neither the conversion electron nor the occasional gamma ray emitted

<sup>2</sup> A conversion electron is an extranuclear electron ejected by the energy of the nuclear transition.

in the isomeric transition process is of sufficiently high energy to give a recoil energy equivalent to that required for the chemical reactions observed. The recoil energy from the 48.9 k.e.v. gamma ray characteristic of the isomeric transition is about 0.2 kg.-cal. per mole, and the recoil energy from the 47.2 k.e.v. conversion electron is about 3.7 kg.-cal. per mole. Therefore it seems necessary to assume that the chemical reactions which follow the isomeric transition are a result of the formation of a positive bromine ion by the loss of a conversion electron from a bromine atom.

## TYPICAL REACTIONS

Results of qualitative interest on a variety of reactions activated by the isomeric radioactive transition of bromine are given in table 1. In the case of the decomposition reactions, the "per cent efficiency" indicates the fraction of the transitions from  $\text{Br}^{80}$  (4.4 hr.) to  $\text{Br}^{80}$  (18 min.) which produced the  $\text{Br}^{80}$  (18 min.) in an inorganic form ( $\text{Br}_2$  or  $\text{HBr}$ ) which could be extracted from the organic par-

TABLE 1  
*Reactions activated by the isomeric radioactive transition of bromine*

DECOMPOSITION REACTIONS	PER CENT EFFI- CIENCY	REACTIONS OF FREE $\text{Br}_2^*$	PER CENT EFFI- CIENCY
$\text{C}_2\text{H}_5\text{Br}_2^*$ (liquid) (aniline present)	88	Mineral oil + $\text{Br}_2^*$	$\geq 41$
$\text{C}_2\text{H}_5\text{Br}_2^*$ (liquid) (no aniline)	69	$\text{CCl}_4$ (liquid) + $\text{Br}_2^*$	34
$\text{C}_2\text{H}_5\text{Br}_2^*$ (gas)	73	$\text{CCl}_4$ (gas) + $\text{Br}_2^*$	0
$\text{C}_2\text{H}_5\text{Br}_2^*$ (liquid) (aniline present)	65	Saturated $\text{CBr}_4$ in $\text{CCl}_4$ + $\text{Br}_2^*$	34
		$(\text{C}_2\text{H}_5)_2\text{O}$ (liquid) + $\text{Br}_2^*$	15
REACTION BETWEEN COMPOUNDS		$\text{H}_2$ + $\text{Br}_2^*$	0
$\text{C}_6\text{H}_5\text{CHBrCHBrCOOH}^* + \text{CCl}_4$	50		

$\text{Br}^*$  indicates  $\text{Br}^{80}$  (4.4 hr. half-life).

ent by aqueous reducing agent. In the case of the cinnamic acid dibromide reaction the "per cent efficiency" is the percentage of the isomeric transitions which produced organically bound  $\text{Br}^{80}$  (18 min.) which could be distilled away from the parent molecule (presumably as  $\text{CCl}_3\text{Br}$ ). For the reaction of elemental bromine with hydrogen gas the efficiency refers to the fraction of transitions which produced hydrogen bromide containing  $\text{Br}^{80}$  (18 min.). In the case of the other reactions of elemental bromine the efficiency indicates the fraction of the transitions which produced bromine not extractable with aqueous reducing agent.

It will be noted that the transition can lead to the splitting out of bromine from a parent molecule and to its subsequent reaction with other molecules, including such usually unreactive compounds as carbon tetrachloride. Since, as discussed above, an isomeric transition of  $\text{Br}^{80}$  in which the energy is lost by gamma emission cannot cause the breaking of a carbon-bromine bond, and since as much as 88 per cent of the transitions resulted in chemical separation in one

case cited in table 1, at least 88 per cent of the transitions must occur by the mechanism of conversion-electron emission. The conversion coefficient must be at least 88 per cent and may be higher, since some of the bromine atoms initially liberated may have reentered combination in the form of the parent molecule.

The fraction of nuclear events which lead to organically bound bromine when molecular bromine undergoing isomeric transition or neutron capture is dissolved in carbon tetrachloride is shown in figure 1 as a function of bromine concentration. This plot indicates that the efficiency of the two types of activation

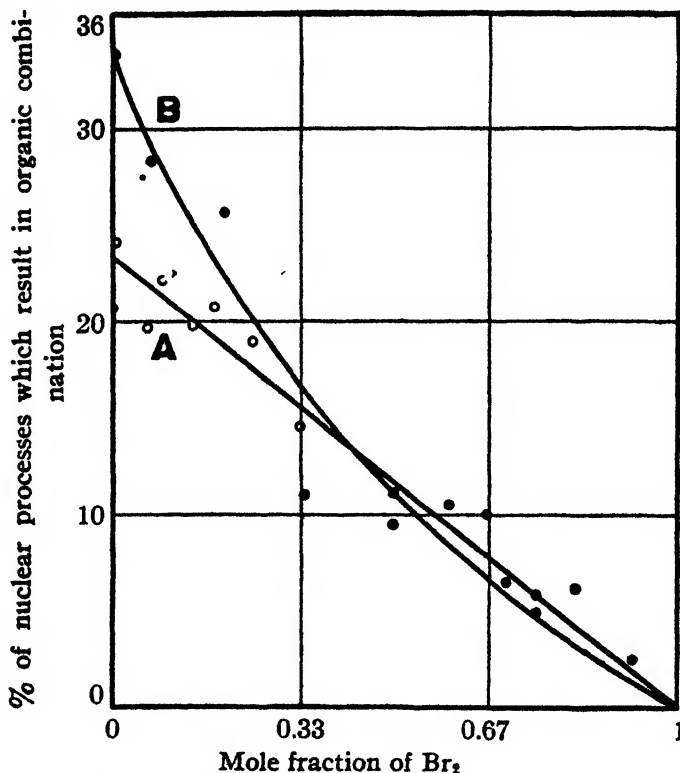


FIG. 1. Reaction of bromine with carbon tetrachloride. Curve A, reaction initiated by neutron capture; curve B, reaction initiated by isomeric transition.

for this particular reaction is similar, even though the initial activation in one case is in the form of high kinetic energy and in the other case in the form of ionization of the bromine atom. As would be expected, the fraction of the nuclear events which form organically bound bromine decreases with increasing bromine concentration and consequently increased opportunity for the tagged activated bromine atoms to lose their identity by exchange with inactive bromine in the system.

If the energy which is made available to a bromine atom by the transition from the 4.4-hr. to the 18-min. species is greatly in excess of the activation energy re-

quired for a given chemical reaction of the bromine, it is to be expected that the reaction will be independent of temperature. To test this point the maximum fraction of the activity which will enter organic combination by reaction with carbon tetrachloride has been determined at room temperature, at  $-10^{\circ}\text{C}$ . where the reaction mixture is a liquid, at  $-50^{\circ}\text{C}$ . where it is a solid, and at liquid-air temperatures. The results are given in table 2. The accuracy of the data is adequate to show qualitatively that temperature has little or no direct effect upon the reaction but that the reaction efficiency is reduced to about one-third of its liquid-phase value when the reaction system is frozen, since the system changed from liquid to solid in the change from  $-10^{\circ}$  to  $-50^{\circ}\text{C}$ .

Since the processes of nuclear activation "tag" those atoms, and only those atoms, which are chemically activated, one has the unique opportunity of observing the final chemical form of the initially activated atom. This is in contrast to photochemical activation, where the number of initially activated molecules is known but where it is impossible to tell whether these atoms or atoms

TABLE 2

*Effect of temperature and phase on the reaction of bromine with carbon tetrachloride as a result of isomeric transition*

<i>T</i>	TOTAL COUNTS PER MINUTE	Br IN ORGANIC COMBINATION	Br IN ORGANIC COMBINATION
$^{\circ}\text{C}$ .		<i>counts/min.</i>	<i>per cent</i>
25 (liquid)	1061	361	34
$-10$ (liquid)	518	155	30
$-50$ (solid)	566	45	8
$-190$ (solid)	1190	145	12

formed by secondary processes enter into the final products. However, the use of nuclear activation as a tool for the study of chemical kinetics suffers from the fact that the energy imparted to the atom is very much in excess of that necessary for the ordinary chemical reaction.

#### EXPERIMENTAL METHODS

The type of equipment which was used in one stage of the work on these processes is illustrated in figure 2.  $\text{Br}^{80}$  (4.4 hr.), available in the form of sodium bromide, was oxidized to free bromine in tube A, distilled and dried in tubes B and C, and admitted to pure dry carbon tetrachloride in ampules at F. Carefully purified carbon tetrachloride was stored in G after drying and degassing and was admitted to the ampules at F with the aid of all-glass taps opened by a magnetic hammer. This equipment was used in the early work on the nuclear activation to minimize the possibility of impurity effects such as those common to photochemical reactions of halogens. It was soon found, however, that the reactions resulting from nuclear activation were not sensitive to such impurities and much of the work was carried out without such rigorous purification.

After sealing the reaction mixtures in the ampules at F, they were allowed to

stand for several 18-min. half-lives, in the case of the isomeric transition reaction, and then were opened, extracted with an aqueous solution of reducing agent, and the extract and organic layer were counted separately in a solution-type Geiger-Mueller counter. These measurements gave information on the fraction of the transitions which had led to organic combination of the bromine which was originally present as the element. Similar techniques were used for the neutron-gamma study, except that the ampoules did not originally contain radioactive bromine but were exposed to neutron irradiation for an appropriate time before extraction and counting.

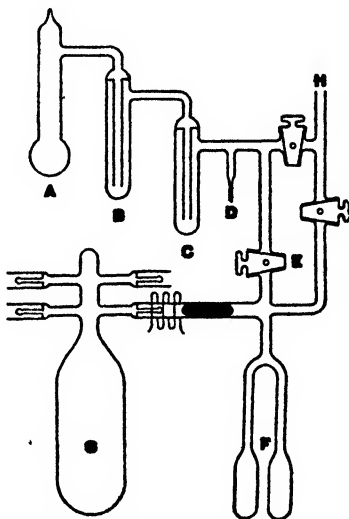


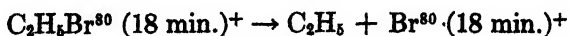
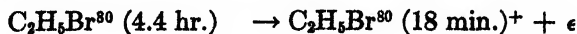
FIG. 2. Apparatus used in study of reactions resulting from isomeric transitions

#### MECHANISMS OF REACTIONS RESULTING FROM ISOMERIC TRANSITION

On the basis of the evidence now available, reactions accompanying the isomeric transition of  $\text{Br}^{80}$ , which lead to the separation of the daughter from the parent activity, may be classified tentatively according to three types as follows:

(1) Decomposition reactions which occur because a bromine-containing molecule is left in a repulsive (unstable) ionic state as the result of the loss of a conversion electron and Auger electrons by the bromine atom in the molecule. This may lead to the decomposition of the molecular ion into a radical and a  $\text{Br}^{80}$  (18 min.) ion. Included among the published examples of this type of reaction are the decompositions of bromate ion (3), ethylene dibromide (7), and other organic bromides (4). The loss of  $\text{Br}^{80}$  (18 min.) by *tert*-butyl bromide in water-alcohol solution (10) is probably also a result of this type of reaction.

The type may be illustrated by the case of ethyl bromide:





(2) Addition reactions in which a  $\text{Br}^{80}$  (18 min.) ion formed in a reaction of type 1 acquires an electron and then combines with a free radical. This free radical may be formed from a neighboring molecule by the energy released in the process of neutralization of the bromine ion. Reactions of type 2 will have a much greater probability of occurrence in solution than in the gas phase (table 3). The reaction of liquid and solid carbon tetrachloride with elemental radioactive bromine and the reaction of carbon tetrachloride with bromine incorporated in the cinnamic acid dibromide molecule are examples of this type of mechanism.

Steps such as those below may be involved:

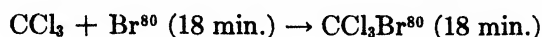
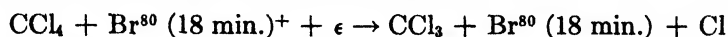


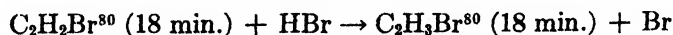
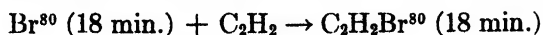
TABLE 3

*Percentage of bromine which enters organic combination following nuclear activation*

Concentrations: solutions for  $n-\gamma$  reactions, 0.7 mole per cent  $\text{Br}_2$ ; solutions for isomeric transition reactions, 0.1 mole per cent  $\text{Br}_2$ ; gas phase  $\text{Br}_2\text{-C}_2\text{Cl}_4$ ,  $n-\gamma$  reaction, 15 mm.  $\text{C}_2\text{Cl}_4$  to 30 mm.  $\text{Br}_2$ ; gas phase  $\text{Br}_2\text{-C}_2\text{Cl}_4$ , isomeric transition reaction, about 3 mm.  $\text{Br}_2$  to 3 mm  $\text{C}_2\text{Cl}_4$ ; gas phase  $\text{Br}_2\text{-CCl}_4$ ,  $n-\gamma$  reaction, 60 mm.  $\text{CCl}_4$  to 60 mm.  $\text{Br}_2$ ; gas phase  $\text{Br}_2\text{-CCl}_4$ , isomeric transition reaction, 700 mm.  $\text{CCl}_4$  to 100 mm.  $\text{Br}_2$

PHASE	ACTIVATION	WITH $\text{C}_2\text{Cl}_4$	WITH $\text{CCl}_4$
Solution	$n-\gamma$	37	24
Gas	$n-\gamma$	0	1.9
Solution	Isomeric transition	85	34
Gas	Isomeric transition	19	1.1

(3) Reactions in which a  $\text{Br}^{80}$  (18 min.) ion formed in a reaction of type 1 acquires an electron and then reacts with a normal molecule rather than with a radical as in type 2. This type of reaction is similar to reactions resulting from the photochemical production of bromine atoms. It occurs in the gas phase as well as in solution. It is illustrated by the reaction of  $\text{Br}^{80}$  (18 min.) from radioactive hydrogen bromide with acetylene (13).



#### MECHANISMS OF REACTIONS RESULTING FROM THE NEUTRON-GAMMA PROCESS

The very high kinetic energy of radiobromine atoms produced by the neutron-gamma reaction undoubtedly accounts for the splitting off of these atoms from the parent molecule. Since the kinetic energy is also probably sufficient to result in the stripping off of electrons from the atom as it moves through the surrounding medium, it is possible that the mechanism of subsequent reaction of such atoms with molecules of the medium is similar to the mechanism of reac-

tions produced by the isomeric transition. There is also the possibility that reaction results from the high kinetic energy of the atom. Reaction with different materials may depend on one or the other of these mechanisms in different degree. Reaction systems in which the probability of reaction following activation by the neutron-gamma reaction is not identical with that following the isomeric transition reaction are illustrated by the data of figure 1 and table 3.

PRODUCTS OF REACTION OF BROMINE WITH CARBON TETRACHLORIDE  
FOLLOWING NUCLEAR ACTIVATION

Table 4 shows the results of experiments in which some indication was obtained of the identity of the organic molecules formed by reaction of bromine with carbon tetrachloride following neutron capture and isomeric transition. These data were obtained by adding bromotrichloromethane and dibromodichloromethane to the organic fraction of reaction mixtures after extraction of the free bromine. The mixtures with these "carriers" were then distilled and the fraction of bromine in each species of organic compound was determined by taking counts on the appropriate fractions of the distillate. The fact that

TABLE 4  
*Identity of products of reaction of bromine with carbon tetrachloride resulting from  
nuclear activation*

	NEUTRON CAPTURE	ISOMERIC TRANSITION
	<i>per cent</i>	<i>per cent</i>
CCl <sub>3</sub> Br. . . . .	55	70
CBr <sub>2</sub> Cl <sub>2</sub> . . . . .	20	
Higher-boiling compounds	25	30

radiobromine appears in organic molecules containing more than one atom of bromine suggests the possibility that when a carbon tetrachloride molecule acts as a "third body" for the neutralization of a bromine cation the energy of neutralization can cause the rupture of more than one bond in the molecule. Multiple rupture must have occurred for more than one bromine atom per molecule to enter organic combination. The results do not exclude the possibility, however, that the bonds are broken in several steps as a result of the stepwise neutralization of a multiply charged bromine cation.

FRANCK AND RABINOWITCH HYPOTHESIS

Franck and Rabinowitch (5; see also 1, 8, 9) have discussed factors which might be expected to cause lower quantum yields in solution than in the gas phase in the case of photochemical reactions in which the primary process in the gas involves the production of atoms or radicals.

The reactions of bromine atoms following neutron capture and following isomeric transition appear to offer a definite experimental example of the effect of solvent in favoring the combination of atoms and radicals which are formed in

the same solvent envelope. If the mechanism which is pictured is correct, these bromine atoms split carbon tetrachloride molecules into radicals and atoms and then may react with the radicals formed. The atoms resulting from either neutron capture or isomeric transition are tagged with radioactivity, so it is possible to determine whether the *particular* atom which forms a radical reacts with it. The fact that little or no reaction between these atoms and the carbon tetrachloride occurs in the gas phase (table 3) in contrast to the liquid seems to indicate the ability of an envelope of carbon tetrachloride molecules to bring about the combination of carbon tetrachloride fragments and bromine atoms by decreasing the probability of their diffusing away from each other, and by removing their energy of combination before such diffusion occurs.

COMPARISON OF REACTIONS OF BROMINE WITH CARBON TETRACHLORIDE  
AND WITH TETRACHLOROETHYLENE FOLLOWING NUCLEAR ACTIVATION

For every bromine atom which enters organic combination with carbon tetrachloride following isomeric transition or neutron capture there are two or three which do not. What becomes of them? Suess (12) has shown that bromine atoms which have split out of hydrogen bromide following isomeric transition add to acetylene as photochemically produced atoms would.

We have chosen tetrachloroethylene as the compound most similar to carbon tetrachloride which would add bromine photochemically and have allowed bromine to react with it as a result of isomeric transition and of neutron capture in the dark.

Because of the presence of the tetrachloroethylene double bond those bromine atoms which are activated by neutron capture or isomeric transition but which become normal bromine atoms before entering organic combination might still be expected to react, just as photochemically produced atoms would. This should lead to a larger fraction of the captures or transitions resulting in the formation of organically bound radiobromine in tetrachloroethylene than in carbon tetrachloride. Such an increase might also result, however, from the formation of organically bound radiobromine in tetrachloroethylene by a free-radical mechanism similar to that of the carbon tetrachloride reaction but more efficient, owing to the different nature of tetrachloroethylene.

Table 3 shows that for the case of the isomeric transition the predicted increase occurs; the amount of reaction with tetrachloroethylene is much greater than with carbon tetrachloride. The fact that a reaction occurs in the gas phase with tetrachloroethylene suggests that the increased reaction is due to the reaction of normal atoms with the double bond, instead of an increased efficiency of the type of free-radical mechanism which is believed to account for the reaction with carbon tetrachloride. A free-radical combination would not be expected to occur in the gas (15), but a gas-phase photochemical bromination of tetrachloroethylene occurs at room temperature (11), indicating that bromine atoms can add to the double bond in the gas. In any case it is to be expected that the possibility for radioactive bromine atoms to exchange with non-radioactive bromine molecules will prevent some of the activity from appearing in organic com-

bination. This exchange may account for the difference between the percentages of organically bound bromine in the solution and gas-phase isomeric transition reactions with tetrachloroethylene. The ratio of bromine to tetrachloroethylene molecules in the gas was about 1 to 1, and in solution only 1 to 1000.

There remains the question as to why, as shown in table 3, isomeric transition is much more effective than neutron capture in causing reaction of bromine with tetrachloroethylene. One hypothesis will be suggested.

This assumes that a bromine atom with high recoil energy may collide with a chlorine atom of a tetrachloroethylene molecule with the formation of a bromine chloride molecule which has enough kinetic energy to escape from the trichloroethylene radical formed. If bromine chloride, like bromine (16) and chlorine (6), does not readily react with tetrachloroethylene in the dark, radioactive bromine would thus be prevented from entering organic combination. The bromine atom resulting from isomeric transition is activated by virtue of its charge rather than its kinetic energy and would not be expected to take part in a process such as that outlined. If it did not combine with a free radical formed in the process of its neutralization, it might then be expected to be free to add to the double bond.

#### REFERENCES

- (1) ATWOOD, K., AND ROLLEFSON, G. K.: *J. Chem. Phys.* **9**, 506 (1941).
- (2) BOHLMAN, E. G., AND WILLARD, J. E.: *J. Am. Chem. Soc.* **64**, 1342 (1942).
- (3) DEVAULT, D., AND LIBBY, W. F.: *Phys. Rev.* **55**, 322 (1939).
- (4) FAIRBROTHER, F.: *Nature* **145**, 307 (1940).
- (5) FRANCK, J., AND RABINOWITCH, E.: *Trans. Faraday Soc.* **30**, 120 (1934).
- (6) LEERMAKERS, J. A., AND DICKINSON, R. G.: *J. Am. Chem. Soc.* **54**, 4648 (1932).
- (7) LE ROUX, L. J., LU, C. S., AND SUGDEN, S.: *Nature* **143**, 518 (1939).
- (8) NOYES, W. A., JR., AND LEIGHTON, P. A.: *The Photochemistry of Gases*. Reinhold Publishing Corporation, New York (1941).
- (9) ROLLEFSON, G. K., AND BURTON, M.: *Photochemistry and the Mechanism of Chemical Reactions*. Prentice-Hall, Inc., New York (1939).
- (10) SEGRE, E., HALFORD, R. S., AND SEABORG, G. T.: *Phys. Rev.* **55**, 321 (1939).
- (11) SNELL, R. L.: Senior Thesis, University of Wisconsin, 1940.
- (12) SUESS, F.: *Z. physik. Chem.* **B45**, 297 (1940).
- (13) SUESS, F.: *Z. physik. Chem.* **B45**, 312 (1940).
- (14) WILLARD, J. E.: *J. Am. Chem. Soc.* **62**, 256 (1940).
- (15) WILLARD, J. E.: *J. Am. Chem. Soc.* **62**, 3161 (1940).
- (16) WILLARD, J. E., AND DANIELS, F.: *J. Am. Chem. Soc.* **57**, 2240 (1935).

CHEMICAL EFFECTS IN NUCLEAR ELECTRON EMISSION<sup>1,2</sup>

T. H. DAVIES

*Institute for Nuclear Studies, University of Chicago, Chicago, Illinois**Received October 23, 1947*

The chemical characteristics of atoms which have undergone nuclear disintegration have been studied at least since the appearance of induced radioactivity. The effects observed are usually attributed to either of two distinct processes. In one, the nuclear radiation interacts directly with orbital electrons to produce highly ionized and electronically excited atoms. If the radiating atom is a part of a molecular structure, the latter will ordinarily decompose. The liberated atom will then react with environmental species and reach a stable chemical state which may be quite different from its initial state. Dr. Willard (6) has presented an instructive discussion of the behavior of 18-min.  $\text{Br}^{80}$  by the decay of 4.4-hr.  $\text{Br}^{80}$ . The origin of the chemical reactivity observed has been shown to be the result of profound ionization following the loss of a  $K$  or  $L$  electron in the process of internal conversion.

In contrast, the very energetic  $\gamma$ -rays emitted immediately following neutron capture interact very rarely with the orbital electrons of the radiating atom. However, the  $\gamma$ -ray imposes a recoil of the order of several hundred electron volts on the radiating atom. The latter will nearly always break any chemical bonds of which it is a part and, furthermore, may by collision eject and replace atoms in surrounding species. These effects are exploited in the chemical separation of neutron-induced radiospecies from target substances of the same atomic number.

Whether the nuclear process of  $\beta^-$  decay will produce chemical effects by one of these two mechanisms is not clear in advance of test. Accurate calculation of the recoil associated with the radiation is difficult. The interaction of the  $\beta$ -rays with orbital electrons of the source atom has been discussed only briefly by theoretical physicists (1).

The usual chemical effect in  $\beta^-$  decay is properly attributed to the corresponding increase in atomic number. The new element is unstable in the same chemical state as its predecessor and an adjustment follows. Opportunity for a more interesting study, however, appears in the case of the rare earths and of the transition elements. Here, experimental conditions can be found such that similar compounds containing either parent or daughter are stable. If then the daughter element is found in a radically different chemical state from that of its precursor, direct perturbation by the nuclear process is suggested. Another area for experimentation is furnished by the electronegative elements in aqueous

<sup>1</sup> Presented at the Symposium on Radiation Chemistry and Photochemistry which was held at the University of Notre Dame, Notre Dame, Indiana, June 24-27, 1947.

<sup>2</sup> This presentation is based primarily on three papers of the Plutonium Project Record (awaiting publication): Volume 9B, Paper No. 3.3.4 by H. Gest, R. R. Edwards, and T. H. Davies; Volume 9B, Paper No. 3.3.5 by R. R. Edwards, H. Gest, and T. H. Davies; Volume 9B, Paper No. 3.3.2 by W. H. Burgus and T. H. Davies.

solution. These form oxygenated molecule-ions which for neighboring elements may differ only in total charge. The phosphate-sulfate and selenite-bromate pairs will illustrate.

Besides the considerations just discussed, several other factors must be favorable before an experimental study of  $\beta^-$  decay effects can be made. The product of the  $\beta^-$  decay must also be radioactive if the chemical characteristics of such small quantities of material are to be detected. This requirement confines study to the radiospecies which occur in fission or to the naturally radioactive heavy elements, since decay *chains* appear rarely elsewhere. Further, the half-life of the daughter must not be too much longer than that of the parent if distressingly high levels of radioactivity in the initial stage are to be avoided. Finally, the daughter element must exhibit at least several stable chemical states under the

TABLE 1  
*Radiations and genetics of nuclei used in tests*

19 min. La <sup>143</sup>	25 min. Se <sup>83</sup>	~2 min. Se <sup>84</sup>	77 hr. Te <sup>133</sup>
$\beta^-$ (?) m.e.v.	$\beta^-$ 1.5 m.e.v. $\gamma$ 0.2, 0.4, 1.1 m.e.v.	$\beta^-$ (?) m.e.v.	$\beta^-$ 0.28 m.e.v. $e^-$ (?) m.e.v. $\gamma$ 0.22 m.e.v. x rays
↓	↓	↓	↓
33 hr. Ce <sup>143</sup>	2.4 hr. Br <sup>83</sup>	30 min. Br <sup>84</sup>	2.4 hr. I <sup>133</sup>
$\beta^-$ 1.4 m.e.v. $\gamma$ 0.5 m.e.v.	$\beta^-$ 0.9 m.e.v.	$\beta^-$ 5.3 m.e.v. $\gamma$ (?) m.e.v.	$\beta^-$ 1.0 m.e.v. (50%) 2.1 m.e.v. (50%) $\gamma$ 0.6, 1.4 m.e.v.
↓	↓	↓	↓
13.8 d. Pr <sup>143</sup>	113 min. Kr <sup>83*</sup>	Kr <sup>84</sup> (stable)	Xe <sup>133</sup> (stable)

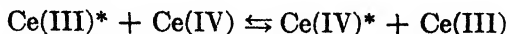
experimental conditions selected if the study is to have point. Despite these limitations, cases worth study may be found here and there in the isotope tables.

As a point of departure, we chose the fission product pair La<sup>143</sup>-Ce<sup>143</sup>, the decay characteristics for which appear in table 1. Our initial viewpoint was that tetravalent cerium ion should be expected from the decay of aqueous trivalent lanthanum ion provided the radiative process did not produce excitation:



To test this balanced nuclear and chemical equation, conditions had to be found under which *tracer* concentrations of both cerous and ceric ion were stable. Also required was a reagent which would distinguish the two valence states in such a solution. Success was finally obtained with a 5 *M* nitric acid solution, 0.3 *M* in iodic acid. When 10 mg. of *crystalline* zirconium iodate was suspended in 30 ml. of such a solution for 3 hr., 80-97 per cent of an authentic sample of

*ceric* tracer present was found with the solid after collection. In contrast, only 2 per cent on the average of a *cerous* tracer was found with the solid in a similar experiment. Early preparations of amorphous zirconium iodate were unsatisfactory because of high cerous-ion adsorption. Compounds of stable cerium could not be used for separation because of the rapid exchange between radioactive and stable species:



The experiments to determine the effect of  $\beta^-$  emission on the chemistry of the daughter  $\text{Ce}^{143}$  were carried out essentially as follows:

A partially purified fraction of rare earth fission products was prepared from pile-bombarded uranyl nitrate hexahydrate as rapidly as possible because of the short half-life of  $\text{La}^{143}$ . The preparation was added to the nitric acid-iodic acid solution and an aliquot taken for the determination of initial  $\text{Ce}^{143}$  by radiochemical analysis. A second aliquot was taken for the assay of total  $\text{Ce}^{143}$  at the end of the decay period. In a third aliquot, solid zirconium iodate was suspended by mechanical stirring for 3 hr., after which it was collected by centrifugation. Radiochemical analysis for  $\text{Ce}^{143}$  in the several aliquots, including the supernatant from the zirconium iodate slurry, permitted the distribution between the tri- and tetra-valent states of the cerium grown from lanthanum during the decay period to be estimated. In our best experiment 60 per cent of this cerium was found in the tetravalent state.

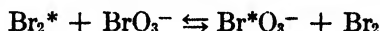
This result may represent the actual probability of  $\text{Ce(IV)}$  as the initial product of lanthanum decay. It is also possible, however, that the 40 per cent present as  $\text{Ce(III)}$  may represent the proportion of newly formed ceric ion which exchanges before adsorption can occur with the *stable* cerous ion unavoidably present in the system as contaminant. Because of this and other difficulties, experimentation was not carried further.

Later studies were made on the decay of aqueous selenium and tellurium ions to halogens. Here the variety of stable states known for both parent and daughter elements promised more opportunity for informative experimentation than was offered by the lanthanum-cerium chain. The characteristics of the decay chains used appear in table 1. The radiations of the nuclei in the first row are those for which accompanying chemical effects are sought. The radiations of the second-row members are the means by which the behavior of the daughter species in chemical fractionations can be determined. Note that the  $\beta^-$  radiations of the parent nuclei are "contaminated" with  $\gamma$ -rays and conversion electrons. In apology, we mention that these complexities were found only after the studies were begun.

A search was made for procedures by which the several aqueous stable states of bromine and iodine might be distinguished. Methods were found to fractionate the product bromine between a bromate and a reduced fraction and the product iodine among a periodate, an iodate, and a reduced fraction. Because of rapid exchange among the halide, halogen, and hypohalite states, no way to distinguish these species was found. The reduced fraction of the radiobromine

was separated from bromate ion by adsorption of the former with freshly prepared solid silver bromide. Reduced forms of radioiodine were precipitated directly with silver iodide, iodate was separated by precipitation of barium iodate at pH 3.0, and periodate by the precipitation of bismuth periodate in 1 *N* nitric acid.

Before the experiments on  $\beta^-$  decay could be made, a number of preliminary points required clarification. A few details from the selenium-bromine studies will illustrate. Since  $\text{SeO}_3^{--}$  is thermodynamically capable of reducing  $\text{BrO}_3^-$ , the rate of this reaction was tested. With carrier quantities of  $\text{SeO}_3^{--}$  and  $\text{BrO}_3^-$ , the oxidation-reduction proceeded with disturbing speed in all solutions acid to pH 7.0. An attempt was made to reduce the rate by use of tracer concentrations. In alkaline solutions no difficulty on this score was encountered. The reaction of  $\text{BrO}_3^-$  and  $\text{Br}^-$  to give  $\text{Br}_2$  had to be controlled also, since the original distribution of the radiobromine could be altered thereby before fractionation. This difficulty was entirely eliminated by the use of carrier bromate, but not bromide, in the decay solutions. Any chemically stable radiobromate ion produced by selenium decay should mix with the carrier and suffer reduction in the same proportion as the carrier. No more than a vanishing proportion of the carrier is reduced by bromide ion, however, since the only sources of the latter are from impurities in the reagents, from decay of selenium, and from the solubility of silver bromide. Of course, radiobromide ion from selenium decay may be oxidized to the elementary state, but as shown by test it will nevertheless coseparate with solid silver bromide as part of the reduced fraction. The exchange reaction:



was also a point of concern, since, if operative (3), all of the radiobromine resulting from the nuclear reaction could be transferred to the bromate state before fractionation. However, under the experimental conditions used, no exchange could be detected.

Finally, a number of problems of a more strictly radiochemical nature appeared in the preparation and counting of the radiospecies used, but we shall neglect these and close our discussion of procedure by outlining a typical run: Radioactive selenium was isolated from neutron-bombarded uranium trioxide, using a selenium carrier. The pure fission selenium in the selenite state was added to 30 ml. of dilute nitric acid containing 50 mg. of carrier selenium as  $\text{SeO}_3^{--}$ . Sufficient  $\text{BrO}_3^-$  was added to give 2 mg. Br per milliliter and the solution was adjusted to the desired pH value. Essentially complete decay of the 25 min.  $\text{Se}^{83}$  was then awaited (90 min. allowed). Aliquots (10 ml.) of the decay solution were taken for determination of (a) total  $\text{Br}^{83}$ , (b)  $\text{Br}^{83}$  in reduced states, and (c)  $\text{Br}^{83}$  as  $\text{BrO}_3^-$ . For (a) additional  $\text{BrO}_3^-$  carrier was added and hydrogen sulfide passed in at room temperature. The selenium precipitate was discarded, hydrogen sulfide was expelled by boiling after addition of perchloric acid, and the residual bromide ion precipitated with silver ion. For (b) freshly prepared silver bromide (235 mg.) was added and, after 10 min. mechanical stirring, collected. For (c) the supernatant from (b) containing the  $\text{Br}^{83}$  as  $\text{BrO}_3^-$  was



treated essentially as aliquot (a). The three samples were mounted and the 2.4 hr.  $\text{Br}^{83}$   $\beta^-$  activity compared in a conventional counting arrangement. Care was exercised throughout to examine equal weights of silver bromide at similar counting geometries.

In table 2 appears the observed distribution of  $\text{Br}^{83}$  from the decay of  $\text{Se}^{83}$  present as  $\text{SeO}^{--}$  or  $\text{SeO}_4^{--}$ . The scattering of values for experiments 1 to 4 is indicative of the reproducibility obtained. In experiment 4, the stock solution of fission selenium was prepared rapidly enough to include significant amounts

TABLE 2  
*Distribution of Br from the decay of radioselenite and radioselenate ions*

EXPERIMENT	CHAIN	SOURCE OF ACTIVITY	PARENT ION	pH	PER CENT OF TOTAL Br AS $\text{BrO}_3$
1	83	Se ( $n, \gamma$ )	$\text{SeO}_3^{--}$	7.0	38
2	83	U fission	$\text{SeO}_3^{--}$	7.2	30
3	83	U fission	$\text{SeO}_3^{--}$	7.0	42
4	83	U fission	$\text{SeO}_3^{--}$	7.2	56
	84	U fission	$\text{SeO}_3^{--}$	7.2	51
5	83	U fission	$\text{SeO}_4^{--}$	7.2	39

TABLE 3  
*Distribution of bromine from the decay of radioselenite at trace concentrations*

EXPERIMENT	pH	TIME FROM PREPARATION OF $\text{SeO}_3^{--}$ TO SEPARATION OF Br	PER CENT OF TOTAL $\text{Br}^{83}$ AS $\text{BrO}_3$
		min.	
1	3.1	80	20
2	6.6	80	26
3	6.9	80	39
4 (a)	7.0	80	32
(b)	7.0	160	30
(c)	7.0	340	26
5	7.0	80	40
6	7.0	80	54
7	10.6	80	24
8	11.1	80	27
9	11.2	80	30

of  $\sim 2$  min.  $\text{Se}^{84}$ . The distribution of the daughter 33 min.  $\text{Br}^{84}$  was distinguished from that of  $\text{Br}^{83}$  by a procedure utilizing the much harder  $\beta^-$  radiations and shorter half-life of the former. Since the distributions of the two radiobromine isotopes were obtained from the same samples after a single series of manipulations, the small "isotope effect" should be more significant than if observed in separate experiments. Note that in experiment 5 the decay of  $\text{Se}^{83}$  as  $\text{SeO}_4^{--}$  gave essentially the same distribution of radiobromine as in the decay of  $\text{SeO}_3^{--}$ .

The data of table 3 represent an attempt to detect an effect of acidity upon radiobromine distribution. In an effort to decrease the rate of interaction of

$\text{SeO}_3^{--}$  and  $\text{BrO}_3^-$ , the addition of carrier quantities of these was omitted. The decrease in radiobromate ion in experiment 4 with increased standing times after completion of selenium decay suggests that the device was not very successful. Reduction of  $\text{BrO}_3^-$  in experiment 1 was probably extensive. In experiment 7 a separate aliquot (10 ml.) of the neutral decay solution was taken at the beginning of the decay period in a test for reactive bromine species in the mixture. The aliquot was stirred for 90 min. with 10 ml. of ethylidene bromide,  $\text{CH}_3\text{CHBr}_2$ , which substitutes atomic bromine but not molecular bromine. Examination of the organic phase disclosed approximately 23 per cent of the  $\text{Br}^{83}$  produced during the decay period in the phase and not extractable with aqueous bisulfite solution. This interesting indication of high chemical reactivity of the daughter bromine has not yet been examined further.

Table 4 presents the results from a "best" set of experiments on the chemical distribution of 2.4 hr.  $\text{I}^{132}$  from the decay of 77 hr.  $\text{Te}^{132}$ .

Our determination of the distribution of radiohalogen among the several stable valence states leaves much to be desired in the way of precision,—despite much effort expended on the procedures. Nevertheless, the results are sufficiently

TABLE 4

*The chemical state of 2.4 hr.  $\text{I}^{132}$  from 77 hr.  $\text{Te}^{132}$  decay in 0.1 N nitric acid*

FRACTION	PER CENT OF TOTAL 2.4 HR. IODINE	
	From $\text{TeO}_3^{--}$	From $\text{TeO}_4^{--}$
$\text{I}^- + \text{I}^0 + \text{IO}^-$	75	60
$\text{IO}_3^-$	14	28
$\text{IO}_4^-$	11	12

consistent to show that the major fractions of both radiohalogens are in the more reduced states. Thus, the halate structure is usually destroyed when the parent is present as selenite or tellurite ion. We can further claim with some confidence, on the basis of tests and arguments already illustrated, that the decomposition of the halate structure is directly associated with the nuclear process. This focuses attention upon mechanisms by which  $\beta^-$  emission might produce the observed molecular disruption. Here we can only speculate for the present.

In discussing chemical effects from nuclear disintegration, first appeal is always to a recoil process. Unfortunately, calculation of the recoil accompanying  $\beta^-$  emission is complicated by the continuous spectrum of the  $\beta$ -particle and the unclear rôle of the companion neutrino. However, recent preliminary studies by Jacobsen (2), working with the  $\text{Kr}^{88}$ - $\text{Rb}^{88}$  pair at low gas pressures, indicate that the recoil atoms cover a relatively narrow energy range and have a value close to that expected from the emission of the most energetic  $\beta$ -particles observed. For our own problem, these observations are important in that they justify use of the maximum  $\beta^-$  energies in our calculations.<sup>3</sup>

<sup>3</sup> *Added in proof:* The Jacobsen observations are expected if neutrino and  $\beta$ -particle are emitted in the same direction. Since the presentation of this paper C. W. Sherwin (Bull.

For the energetic 1.5 m.e.v.  $\beta^-$  process of  $\text{Se}^{83}$ , relativistic expressions are required. By equating momenta of  $\beta$ -particle and radiating atom one obtains:

$$E_R = \frac{M_\beta + M_0}{2M_R} E_\beta$$

where  $E_R$  = kinetic energy of recoil atom

$M_0$  = rest mass of  $\beta^-$

$M_\beta$  = relativistic mass of  $\beta^-$

$M_R$  = mass of recoil atom

$E_\beta$  = energy of  $\beta^-$

Substitution for  $M_\beta$  from the familiar expression:

$$E_\beta = (M_\beta - M_0)C^2$$

gives:

$$E_R = 24 \text{ e.v.}$$

A recoil of this magnitude appears adequate to fracture bromide-oxygen bonds and give the observed decomposition. But several factors reduce the effective recoil energy.

The momentum of the system must be preserved throughout the process following escape of the  $\beta$ -particle. Momentum calculations for the aqueous phase actually used may be difficult, but a calculation for the bromate ion in collision-free space is straightforward and will illustrate the correction.

The final momentum of the bromate ion must equal that of the bromine atom immediately after loss of the  $\beta$ -particle,

$$p_R = M_R V_R = p_i = (M_R + 3M_{\text{ox}})V_i$$

where  $p_i$  = momentum of  $\text{BrO}_3^-$

$M_{\text{ox}}$  = mass of an oxygen atom

Since the process of momentum distribution is here an adiabatic one,

$$E_R = E_i + E_i$$

where  $E_i$  = final kinetic energy of  $\text{BrO}_3^-$

$E_i$  = internal energy (vibrational and rotational) of  $\text{BrO}_3^-$  after momentum distribution.

Combination of these expressions gives:<sup>4</sup>

$$E_i = E_R \times \frac{3M_{\text{ox}}}{M_R + 3M_{\text{ox}}} = 24 \times \frac{48}{131} = 8.8 \text{ e.v.}$$

Am. Phys. Soc. **22**, No. 6, 5 (1946)) has reported that neutrino and  $\beta$ -particle in  $\text{P}^{32}$  decay are emitted most frequently into different hemispheres, while R. F. Christy *et al.* (Phys. Rev. **72**, 698 (1947)) find no preferred angle between the two radiations when  $\text{Li}^8$  decays to  $\text{Be}^8$ . Thus, the calculation above, which assumes orientation of the neutrino *with* the  $\beta$ -particle, yields a maximum value for the  $E_R$  of  $\text{Br}^{83}$ . If the neutrino is oriented *against* the  $\beta$ -particle, as claimed for  $\text{P}^{32}$ , then  $E_R$  for the average  $\text{Br}^{83}$  recoil is about 5 e.v.

<sup>4</sup> See Suess (5) for a similar calculation.

The internal energy,  $E_i$ , rather than  $E_R$ , measures the strain placed upon the chemical bonds of the ion. At least one more consideration enters. The bromine atom is at the center of a tetrahedron of which the oxygen atoms form three apices. Accordingly, recoil of the bromine atom can hardly rupture any one bond without a considerable, perhaps equal, energy expenditure in shaking the other oxygen atoms. The recoil energy now appears as little more than sufficient to fracture a Br-O bond of about 2.5 e.v. energy. Our own attitude is that the estimates are too primitive to permit a decision.

Mention should be made at this juncture of the experiment with  $\text{Se}^{84}$ . The energies of the  $\beta$ -particles from  $\sim 2$  min.  $\text{Se}^{84}$  are not known, but they will of course not be the same as those of  $\text{Se}^{83}$ . If they differ markedly from those of  $\text{Se}^{83}$  and if a recoil process lies behind the observed chemical effects, then a new yield of  $\text{BrO}_3^-$  would be anticipated. Good agreement, however, was found for  $\text{Br}^{83}$  and  $\text{Br}^{84}$  (table 1).

We had hoped to introduce the findings on 2.4 hr. I as a clinching argument as to the rôle of recoil, since the 0.28 m.e.v.  $\beta$ -particles of  $\text{Te}^{132}$  should give only 3 per cent of the recoil calculated for  $\text{Se}^{83}$ . This approach too was frustrated. After the tellurium-iodine studies had been completed, a trusted colleague in a careful study of  $\text{Te}^{132}$  detected the presence of conversion electrons among the  $\beta$ - and  $\gamma$ -radiations (4). Since the internal conversion process is well known to produce profound chemical changes, our data on the tellurium-iodine pair can no longer be viewed as necessarily demonstrating the effects of  $\beta^-$  decay.

The intramolecular decomposition of the bromate ion to thermodynamically more stable products must also be considered. This is to say that a bromate ion with 9 e.v. of internal energy is a very excited species and may be sufficiently energetic to decompose by a path closed to normal bromate ion. In particular there is the process:



This reaction proceeds with a free-energy decrease of 13 kg.-cal. per mole. One is tempted to stress that aqueous  $\text{BrO}^-$  ions disproportionate to give  $\text{Br}^-$  and  $\text{BrO}_3^-$  in just the proportions in which we find them in our experiments:



However, the kinetics of this reaction are undoubtedly complicated and without more information than we have on the concentration of *total*  $\text{BrO}^-$  in the decay solutions, a choice among several possible disproportionation reactions cannot be made.

We shall indulge in just one further speculation. The readjustment of the orbital electrons to the increased nuclear charge following  $\beta^-$  decay may lead to excitation, ionization, and dissociation of the molecule containing the radiating atom. The total energies of the electrons of selenium and bromine differ by several kilovolts per mole. This difference should approximate the energy made available by the orbital shrinkage following decay. This is sufficient to eject many electrons and break several bonds. The immediate question is whether the readjustment is simultaneous with the loss of the  $\beta$ -particle and the energy is

to be found with the  $\beta$ -particle. If the readjustment occurs independently of the nuclear process, will the energy be dissipated as very soft x-radiation or by ionization? We have not yet received harmonious opinions on these points from colleagues more practiced in such considerations and prefer to delay discussion until more data on the chemical effects accumulate.

#### REFERENCES

- (1) FEINBERG, E. L.: J. Phys. (U.S.S.R.) **4**, 423 (1941).
- (2) JACOBSEN, J. C.: Phys. Rev. **70**, 789 (1946).
- (3) LIBBY, W. F.: J. Am. Chem. Soc. **62**, 1930 (1940).
- (4) NOVEY, T. B.: J. Am. Chem. Soc. **68**, 2411, reference (N115), (1946).
- (5) SUESS, F.: Z. physik. Chem. **B45**, 312 (1939).
- (6) WILLARD, J. E.: J. Phys. Colloid Chem. **52**, 585 (1948).

## THE SZILARD-CHALMERS REACTION IN THE CHAIN-REACTING PILE<sup>1, 2</sup>

R. R. WILLIAMS

*Department of Chemistry, University of Notre Dame, Notre Dame, Indiana*

*Received October 23, 1947*

### I. INTRODUCTION

The radiative capture of a neutron by a stable nucleus is an important nuclear reaction, which frequently gives rise to a useful radioisotope. The chemical identity of the active isotope with the unchanged target element frequently places serious limitations on the specific activities obtained by this reaction. The Szilard-Chalmers reaction, which effects separation of the activated atoms from the target material by virtue of the gamma-ray recoil, can be used to enhance the specific activity of the active material under favorable circumstances. This paper will discuss certain factors which govern the usefulness of this enrichment method, and in particular the effects of the intense radiation field of the chain-reacting pile.

### II. NECESSARY CONDITIONS FOR SZILARD-CHALMERS ENRICHMENT

Neutron capture by a nucleus is accompanied by the release of 8 or 9 m.e.v. of energy in the form of several energetic gamma quanta. The recoil energy

<sup>1</sup> Presented at the Symposium on Radiation Chemistry and Photochemistry which was held at the University of Notre Dame, Notre Dame, Indiana, June 24-27, 1947.

<sup>2</sup> This document is based on work performed by A. W. Adamson, G. E. Boyd, W. E. Cohn, G. Jenks, Q. V. Larson, W. B. Leslie, J. W. Richter, E. R. Tompkins, and R. R. Williams, under Contract No. W-7401-eng-37 for the Atomic Energy Project, and the information covered therein will appear in Division IV, Volume IX-B of the *National Nuclear Energy Series* (Manhattan Project Technical Section) as part of the contribution of the Argonne National Laboratory.

thus imparted to the capturing atom may be as much as one hundred times as great as the energies of the chemical bonds in which it participates, and we may expect the formation of an ionized, high-speed fragment. Such fragments can be physically separated from the bombarded material, but we shall be concerned only with chemical separations, for which the following conditions must hold: (1) The element must be capable of existence in at least two mutually stable and separable forms. (2) At least two of these forms must show lack of rapid isotopic exchange.

The reactions which the "hot" atom or fragment will undergo depend to some extent on the nature of its environment, and several workers are engaged in a study of these processes. For the present, however, the more fruitful approach, after choice of circumstances which fulfill conditions 1 and 2 above, is the trial and error method. Many Szilard-Chalmers reactions are known, several of which will be described below.

Attempts to enrich activities produced in the high flux of the chain-reacting pile have brought to light a third consideration governing the effectiveness of the proposed Szilard-Chalmers enrichment. The high radiation fields (principally  $\gamma$  and neutron) cause marked chemical changes in the bombarded compounds aside from the effects accompanying activation. That such reactions may yield products similar to those obtained in activation reactions is to be expected, since both types are essentially a decomposition by excitation. The radiation decomposition can yield microscopic amounts of the chemical form in which the activity is found, thus diluting the active isotope. It is also possible that the radiation field will cause further chemical reactions of the separable active isotope which may change it to a form which is no longer separable, although this effect is probably confined to rather limited circumstances.

Establishment of a successful Szilard-Chalmers enrichment reaction in experiments of low flux or short bombardment therefore does not ensure its success when longer or more intense bombardments are employed. Radiation decomposition may produce prohibitive amounts of inactive carrier and the fraction of activity separable may decrease. The next section of this paper will present a semiquantitative discussion of these two effects.

### III. SZILARD-CHALMERS ENRICHMENT IN HIGH RADIATION FIELDS

#### A. Definitions

The following discussion assumes that for the given case a Szilard-Chalmers reaction is known to take place, i.e., separation of an appreciable fraction of the active isotope from the inactive isotopes has been demonstrated. The enrichment factor,  $F$ , will be defined as the specific activity of the separated form divided by the specific activity of the pure element activated under the same conditions. Further nomenclature is as follows:

$E$  = element activated to give  $E^*$

$A$  = total amount of  $E$  present

$M$  = amount of  $E$  chemically identical with separable  $E^*$

- $N$  = total amount of  $E^*$   
 $N_M$  = amount of separable  $E^*$  (initially =  $N \cdot f$ )  
 $f$  = fraction of  $E^*$  atoms initially separable (a constant for a given element and a given environment)  
 $p$  = neutron flux or pile power  
 $\sigma$  = neutron cross-section for activation of  $E$  to give  $E^*$   
 $\lambda$  = decay constant of  $E^*$   
 $K_1$  = rate constant for radiation decomposition reaction giving  $M$   
 $K_2$  = rate constant for radiation reaction consuming  $N_M$  and  $M$

### B. Formulation

The reactions which govern the quantities  $M$  and  $N$  are all such that as a first approximation they will be assumed to follow a first-order rate law.

For  $M$ , the amount of inactive  $E$  which will be separated, we have:

$$\frac{dM}{dt} = pK_1(1 - M) - pK_2M \quad (1)$$

For  $N_M$ , the amount of active  $E^*$  which will be separated, we have:

$$\frac{dN_M}{dt} = p\sigma f \cdot 1 - \lambda N_M - pK_2 N_M \quad (2)$$

These rate equations, upon integration, yield:

$$M = 1 \left( \frac{K_1}{K_1 + K_2} \right) [1 - e^{-t(pK_1 + pK_2)}] \quad (3)$$

$$N_M = \frac{p\sigma f \cdot 1}{\lambda + pK_2} [1 - e^{-t(\lambda + pK_2)}] \quad (4)$$

The enrichment factor,  $F$ , is therefore given by

$$F = \frac{N_M/M}{N/A} = \frac{\lambda f(K_1 + K_2)}{K_1(\lambda + pK_2)} \times \frac{1 - e^{-t(\lambda + pK_2)}}{[1 - e^{-\lambda t}][1 - e^{-t(pK_1 + pK_2)}]} \quad (5)$$

and the specific activity of the separated radioisotope by

$$S = N_M/M = \frac{\sigma f(pK_1 + pK_2)}{K_1(\lambda + pK_2)} \times \frac{1 - e^{-t(\lambda + pK_2)}}{1 - e^{-t(pK_1 + pK_2)}} \quad (6)$$

Inspection of equation 5 shows that the enrichment factor obtainable for a given bombardment will depend on the values of the constants for the radiation reactions  $K_1$  and  $K_2$ . In dealing with a given Szilard-Chalmers reaction, i.e., given values of  $K_1$  and  $K_2$ , the enrichment will steadily decrease with increasing flux ( $p$ ) and increasing time of bombardment ( $t$ ), approaching  $\frac{\lambda f(K_1 + K_2)}{K_1(\lambda + pK_2)}$ .

The behavior of the specific activity,  $S$ , will depend on the relation of  $f$ ,  $\lambda$ ,  $p$ ,  $K_1$ , and  $K_2$  in a manner which will be considered below.

Two extreme cases of Szilard-Chalmers enrichment in high fluxes will now be considered. In the first case, we shall assume  $K_2 \ll K_1$ , or negligibly small loss

of separable activity due to further radiation effects, but appreciable formation of inactive atoms in separable form. The second case will assume  $K_1 \ll K_2$ , the opposite situation.

*C. Decomposition of bombarded form ( $K_2 \ll K_1$ ; also  $pK_2 \ll \lambda$ )*

In the case that  $K_2 \ll K_1$ , equation 5 takes the form

$$F = \frac{f}{[1 - e^{-pK_1 t}]} \quad (7)$$

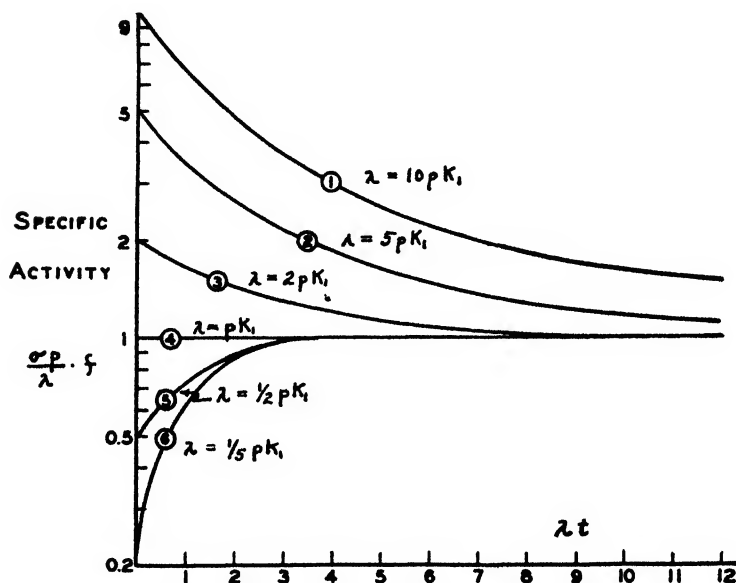


FIG. 1. Specific activity of enriched material as a function of time with varying rates of decomposition.

and equation 6 becomes

$$S = \frac{\sigma f p}{\lambda} \times \frac{1 - e^{-\lambda t}}{1 - e^{-pK_1 t}} \quad (8)$$

The dependence of the enrichment factor on  $p$  and  $t$  for a given Szilard-Chalmers reaction (constant  $f$  and  $K_1$ ) is quite clear. When the decomposition is not great,  $F$  will be approximately given by

$$F = \frac{f}{pK_1 t} \quad (9)$$

Figure 1 is a graphical representation of equation 8 for various values of  $\lambda/pK_1$ . To obtain increased generality, the quantity  $\lambda t$  is the abscissa and the specific activity (ordinate) is given in units of  $\frac{\sigma p}{\lambda} \cdot f$ , the value which all the curves



approach with increasing bombardment times. This limiting value should not be confused with the specific activity of the pure element at saturation, which is given by  $\sigma p/\lambda$ . The following generalizations can be made from the figure:

*Case 1:*  $\lambda > pK_1$  or the rate of decomposition is less than the rate of decay. Here the specific activity decreases steadily with the time of bombardment, approaching the saturation value (curves 1, 2, and 3, figure 1).

*Case 2:*  $\lambda = pK_1$ , or the rate of decomposition is equal to the rate of decay. The specific activity is independent of bombardment time (curve 4, figure 1).

*Case 3:*  $\lambda < pK_1$ , or the rate of decomposition is greater than the rate of decay. The specific activity increases with time, approaching the saturation value (curves 5 and 6, figure 1). Obviously a Szilard-Chalmers procedure is useless in this case.

Data from experiments on the enrichment of iron activity from bombarded ferrocyanides have been examined in the light of these equations and are discussed later.

#### D. Radiation loss of separable activity ( $K_1 \ll K_2$ )

In the case where  $K_1 \ll K_2$ , initially separated activity will be lost by a radiation-induced back-reaction. This situation is not expected to be as common as that of the radiation decomposition of the bombarded compound, since the separable form usually represents a less complicated breakdown product of the starting material. The Szilard-Chalmers enrichment experiments with antimony pentafluoride, however, show this loss of activity without apparent decomposition. Qualitative observations in the experiments with triphenylstibine indicate a similar loss, but here the picture is confused by accompanying decomposition of the bombarded form.

Imperfect chemical separation of the active material from the bombarded form places an upper limit on the specific activity obtainable. When radiation effects produce no appreciable amount of diluting carrier, the quantity  $M$  is essentially a small constant amount. Therefore the enrichment factor becomes,

$$F = \frac{N_M/M}{N/A} = \frac{Af\lambda}{M(\lambda + pK_2)} \times \frac{1 - e^{-(\lambda + pK_2)t}}{1 - e^{-\lambda t}} \quad (10)$$

and the specific activity of the separated activity is given by

$$S = \frac{N_M}{M} = \frac{p\sigma fA}{M(\lambda + pK_2)} \times 1 - e^{-(\lambda + pK_2)t} \quad (11)$$

Where  $M$  is constant, it is apparent that the enrichment factor will decrease with time approaching a limiting value,  $F_{\text{satd.}}$ , given by

$$F_{\text{satd.}} = \frac{Af\lambda}{M(\lambda + pK_2)} \quad (12)$$

or, if the fraction of extractable activity is measured, a limiting value  $f\lambda/(\lambda + pK_2)$  will be reached. The specific activity of the separated radioelement will show a growth parallel to that of the total activity, but the effective

decay constant will be  $\lambda + pK_2$  instead of  $\lambda$ . The saturation value,  $S_{\text{satd.}}$ , will be given by

$$S_{\text{satd.}} = \frac{p\sigma fA}{M(\lambda + pK_2)} \quad (13)$$

as compared to a specific activity of  $p\sigma/\lambda$  for the total activity. Since  $A/M$ , the chemical separation factor, will usually be quite large (say  $\sim 1000$ ) and since  $f$ , the radiochemical separation factor, will usually lie between 0.1 and 1.0, the relative magnitudes of  $\lambda$  and  $pK_2$  will determine the practical usability of a given Szilard-Chalmers reaction in this situation.

#### EXPERIMENTAL TESTS

##### A. *Enrichment of antimony activity*

A wide variety of antimony compounds were examined with particular interest in their behavior in intense fields. Several Szilard-Chalmers enrichment reactions were established in low-intensity experiments, but all showed excessive radiation effects in high fluxes.

Ammonium metafluoroantimonate ( $\text{NH}_4\text{SbF}_6$ ) was bombarded in the solid state, dissolved, and the activity was removed by precipitation of heavy metal sulfides. In short bombardments, no detectable amount of chemical antimony accompanied the active precipitate which constituted about one-third of the total antimony activity. Intense bombardments produced considerable amounts of inactive antimony in the sulfide precipitate (presumably  $\text{Sb}^{3+}$ ), and the activity yield dropped to around 1 per cent.

Triphenylstibine showed a very convenient Szilard-Chalmers reaction in short bombardments, in that the active antimony was ejected to a water-soluble state, while the target material was soluble in organic solvents. The extraction process used collected up to 60 per cent of the activity and very little inactive antimony. Long bombardments again produced large amounts of inactive antimony in the water-soluble form, and reduced the activity extraction below 10 per cent.

Bombardment of antimony pentafluoride produced antimony activity in a relatively non-volatile form, presumably antimony trifluoride. Volatilization of bombarded antimony pentafluoride left as much as 60 per cent of the activity behind, while less than 0.1 per cent of the total antimony remained. Long bombardments of this substance gave no greater chemical amounts of non-volatile antimony, but the activity in the non-volatile form decreased to 5 per cent of the total after several hours' bombardment at constant pile power (see figure 2).

Since the enrichment factor decreases with the length of bombardment, a back-reaction must return the activity to the original chemical state. The back-reaction was not observed outside the radiation field, and so must be attributed to it. A sample irradiated approximately 1 min. (60 per cent separation normally expected) was placed in a boron carbide shielded container and irradiated 1 hr. further. At the end of this time the activity separation had fallen to 25 per cent, indicating that the back-reaction must be due to some component of

the radiation field other than the slow neutrons, which would be cut off by the boron.

The data obtained in the bombardment of antimony pentafluoride may be compared with equation 10 of the section (III, D) which gave the enrichment factor  $F$ . The radiochemical separation factor, such as measured in the experiments with antimony pentafluoride, will be given by the same equation without the factor  $A/M$ , which is about 1000 in this case.

The form of the equation given indicates that a finite limiting value of the separation factor will be reached, and the data in figure 2 indicate that with antimony pentafluoride the value is about 0.05. This may be equated to the expression  $\frac{f\lambda}{\lambda + pK_2}$  and  $f$  may be taken as 0.60. Using the ratio of  $\lambda/(\lambda + pK_2)$

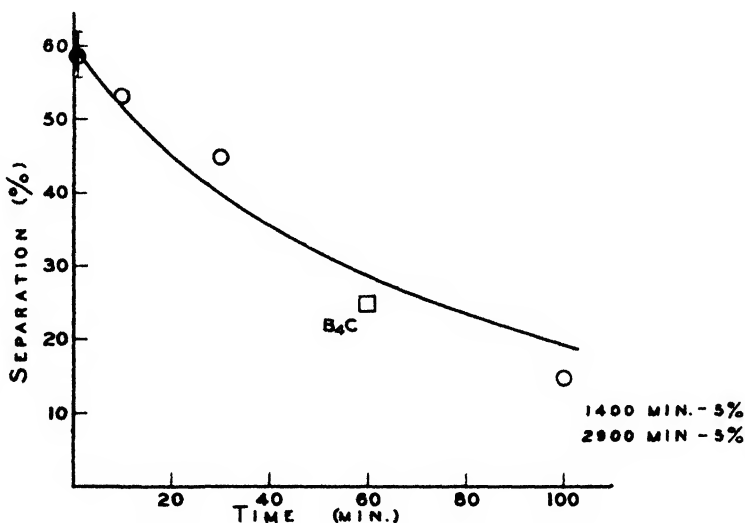


FIG. 2. Activity separation in antimony pentafluoride as a function of bombardment time

thus determined, a theoretical curve was constructed to fit most closely the observed values of the separation factor, treating  $\lambda$  as one of the parameters. The value of  $\lambda$  necessary to obtain the curve shown is  $2.9 \times 10^{-3} \text{ min.}^{-1}$ , as contrasted with the value of  $1.72 \times 10^{-4} \text{ min.}^{-1}$  describing the shorter period of  $\text{Sb}^{122}$ . This is a very serious discrepancy between theory and experiment, unless some shorter decay period is involved in the measurements. Apparently the separation factor approaches its limiting value more than ten times as rapidly as expected.

#### B. Enrichment of iron activity

A suitable enrichment reaction for iron activity was established by low-intensity neutron bombardment of potassium ferrocyanide. As much as one-third of the iron activity is freed from the complex and can be carried on alumi-

num hydroxide precipitates. Longer and more intense bombardments give rise to increasing amounts of non-activating decomposition of the complex and thus lower the specific activity, as shown in table 1. The fraction of activity separated by the hydroxide precipitate remains constant in spite of the increased radiation decomposition, which was less than 1 per cent in all cases.

TABLE 1  
*Szilard-Chalmers enrichment of Fe\* from potassium ferrocyanide*  
(All units arbitrary)

SAMPLE	SEPARATED ACTIVITY	INACTIVE Fe SEPARATED	SPECIFIC ACTIVITY OF SEPARATED Fe*
Blank*	0	0.017	0
2 . . . . .	31	0.106†	292
3 . . . . .	70	0.245†	286
4 . . . . .	106	0.409†	259
5 . . . . .	144	0.585†	246

\* Sample kept in oven at pile temperature.

† Corrected for blank.

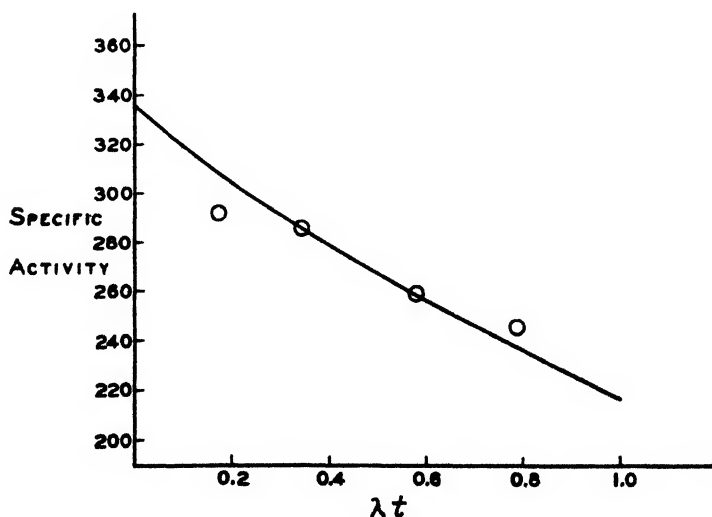


FIG. 3. Specific activity *versus* time in enrichment of Fe\*

Equation 8 of Section III,C is intended to describe the variation of specific activity,  $S$ , with intensity of bombardment and can be compared with the data obtained in these experiments. The equation is readily separable into two portions: one is the usual growth equation, and the remainder describes the radiation decomposition process. The value of  $\lambda$  in equation 8 can be evaluated from the data of these experiments or taken from the literature. The equation for decomposition (cf. equation 3 in Section III,B) can be written as follows

$$M = A(1 - e^{-pK_1t})$$

and compared with data of the type indicated in table 1, which represents a series of bombardments of increasing duration at approximately constant pile-power level. Relative bombardment times may be estimated by reference to figure 3. The four values of  $K_1$  calculated from these data show a small, but regular, increase with increasing  $\lambda t$ . The uncertain fluctuations in pile power which occurred during the experiments make it impossible to discuss the significance of this deviation. The specific activity at various times will be given to a good approximation by the equation

$$S = \frac{\sigma f}{K_1} \cdot \frac{(1 - e^{-\lambda t})}{\lambda t}$$

when decomposition is small. Using the values of  $\sigma$  and  $\lambda$  obtained from the data above, and taking a value of  $K_1$  to give best fit, the theoretical curve of specific activity *vs.*  $\lambda t$  was drawn (solid line in figure 3). The experimental points (circles) indicate, as expected from the variation of  $K_1$ , a less rapid decrease in  $S$  than was theoretically predicted.

As previously suggested, the rate of decomposition is undoubtedly related to different flux components from those responsible for activation. Variations among these components must be eliminated or measured before a quantitative test of the proposed equations will be possible. The present data furnish only a qualitative comparison with the rate equations.



# POLYMER FRACTIONATION OF HEAT-POLYMERIZED NON-CONJUGATED VEGETABLE OILS<sup>1</sup>

I. M. BERNSTEIN<sup>2</sup>

*H. D. Roosen Company, Brooklyn, New York*

*Received August 12, 1947*

## INTRODUCTION

In a previous paper of this series (6) mention was made of a method which had been devised for the quantitative fractionation of heat-polymerized non-conjugated vegetable oils. A few of the data abstracted from the present work were given in this previous paper, and were used for the purpose of testing the adequacy of the polymerization mechanism advanced by the author. It is the purpose of the present paper (1) to give a general account of the polymer-fractionation technique developed and to attempt the theoretical basis for its selectivity, (2) to give a detailed account of the specific procedure used in the fractionation of heat-polymerized linseed and soybean oils at various stages of the reaction, including that of the final stage of gelation, (3) to present the experimental data obtained, and (4) to interpret the data not only from the viewpoint of general polymerization theory and polymer distribution, but more specifically as a means of testing their correspondence to some of the postulates of the author's theory.

In contrast to the extensive work which has been done on polymer fractionation of other systems, very little has heretofore been attempted on the heat-polymerized drying oils. Morrell (26) in 1915 reported a fractionation on heat-bodied linseed oil using acetone. Only two fractions were obtained, an acetone-soluble one consisting essentially of the remaining monomers and an acetone-insoluble one consisting principally of a mixture of all the polymers which had formed. The acetone procedure has since been used by Elöd and Mach (16), Behar (4), McQuillen and Woodward (25), and more recently by Privett *et al.* (29). Their respective results are subject to the same inherent limitation, the reason for which will be indicated later in this paper. Solvent-mixture procedures have also been reported (15, 20, 30) but specific polymer fractionations have not been claimed, and their purpose is either to fractionate the unpolymerized oil or to separate the lower unsaturated monomers from the polymers as a group in the bodied oils. More recently there was announced a separation scheme involving liquid propane (21). The details of the process so far reported are concerned with the separation of the saturated and lower unsaturated monomers from the more highly unsaturated monomers in unbodied fish

<sup>1</sup> Presented in part before the Division of Paint, Varnish, and Plastics Chemistry at the 108th Meeting of the American Chemical Society, which was held in New York City, September, 1944.

<sup>2</sup> Present address: Gotham Ink & Color Company, Long Island City, New York.

and vegetable oils, rather than with the possibility of specific fractionation of polymers. The chromatographic adsorption technique has been successfully applied to the fractionation of unbodied vegetable oils by Walker (35), but no work has been reported on its applicability to the heat-polymerized oils. Mention must, of course, also be made of the molecular still procedure as developed by Hickman (19) and used by Morse (27), Bradley (9), and Waterman (36) in effecting the fractionation of polymers. This procedure has, however, two inherent difficulties: (1) that it is not applicable to the heat-polymerized glyceride vegetable drying oils except to remove the saturated and low unsaturated monomers remaining, and (2) that even with the methyl esters it is questionable, at the temperature of distillation, whether further polymerization of the residue does not occur after the dimers have been distilled off. As will be shown later in this paper, the higher polymers after being stripped from their adsorbed monomers and lower polymers are particularly sensitive to oxidation and/or polymerization and tend to form gels at room temperature even where precautions such as an inert atmosphere are observed in order to prevent access of air to the system.

#### I. FRACTIONATION BY SELECTIVE SOLUBILITY IN THE HOMOLOGOUS SERIES OF NORMAL MONOHYDRIC ALCOHOLS

##### *A. General discussion*

The fractionation method which is the basis of the present paper differs from those previously mentioned in that it enables one not only to separate the monomers from the polymers present in the heat-polymerized non-conjugated vegetable oils, but in addition to separate the polymer portion into a large number of fractions of varying polymeric sizes, the number of such fractions present depending on the extent of the polymerization (7).

This method is based on an observation by the author that linseed and soybean oils in the unpolymerized state, while completely soluble in *n*-propyl alcohol (although practically insoluble in methyl and ethyl alcohols), become progressively insoluble percentagewise in this solvent as the heat-polymerization progresses. Not only is this true for *n*-propyl alcohol, but it is likewise successively true for the other higher members of the homologous series of the liquid normal aliphatic saturated monohydric alcohols up to and including *n*-dodecyl alcohol, the highest liquid member of the series at room temperature. At any one stage in the polymerization of the above oils *complete* solubility can be obtained with some one of the ascending members of the homologous series of alcohols. As soon, however, as the polymerization exceeds the particular stage in question, partial insolubility in that alcohol occurs, and it is necessary to go to the next higher number of the series to achieve complete solubility again. The limiting point in the series is when the polymerization reaches the partial insolubility stage with *n*-dodecyl alcohol. Complete solubility at this critical point may, however, be achieved by the use of petroleum ether as the solvent. Petroleum ether, essentially hexane, continues as a complete solvent for all of the subsequent stages of polymerization up to but preceding that of gelation, where



partial insolubility again results through the formation of insoluble, infusible, cross-linked polymers. Tables 1 and 2 illustrate the relationship between the polymerization time of linseed and soybean oils and complete solubility in members of the above homologous series of normal monohydric alcohols.

As a corollary to these relationships, the members of the ascending series of normal monohydric alcohols are complete solvents for all of the heat-polymerized

TABLE 1

*Relationship between polymerization time and complete solubility in normal monohydric alcohols (at 26°C.) of heat-polymerized linseed oil\**

HOURS AT POLYMERIZATION TEMPERATURE (307°C.)	n-PROPYL ALCOHOL	n-BUTYL ALCOHOL	n-AMYL ALCOHOL	n-HEXYL ALCOHOL	n-OCTYL ALCOHOL	n-DECYL ALCOHOL	n-DODECYL ALCOHOL
0	X	-----	-----	-----	-----	-----	-----
1	.....	X	-----	-----	-----	-----	-----
2	.....	.....	X	-----	-----	-----	-----
4	.....	.....	.....	X	-----	-----	-----
6	.....	.....	.....	.....	X	-----	-----
7	.....	.....	.....	.....	.....	X	-----
8	.....	.....	.....	.....	.....	.....	-----
9	.....	.....	.....	.....	.....	.....	-----
10	.....	.....	.....	.....	.....	.....	-----

\* Dotted line = range of partial solubility.

Solid line = range of complete solubility.

TABLE 2

*Relationship between polymerization time and complete solubility in normal monohydric alcohols (at 26°C.) for heat-polymerized soybean oil\**

HOURS AT POLYMERIZATION TEMPERATURE (307°C.)	n-PROPYL ALCOHOL	n-BUTYL ALCOHOL	n-AMYL ALCOHOL	n-HEXYL ALCOHOL	n-OCTYL ALCOHOL	n-DECYL ALCOHOL	n-DODECYL ALCOHOL
0	X	-----	-----	-----	-----	-----	-----
1	.....	X	-----	-----	-----	-----	-----
5	.....	.....	X	-----	-----	-----	-----
8	.....	.....	.....	X	-----	-----	-----
12	.....	.....	.....	.....	X	-----	-----
14	.....	.....	.....	.....	.....	X	-----
16	.....	.....	.....	.....	.....	.....	X

\* Dotted line = range of partial solubility.

Solid line = range of complete solubility.

oil samples previous to the alcohol in which partial solubility occurs. Petroleum ether, on the other hand, is a complete solvent for all of the oil samples, from the unbodied stage to that immediately preceding gelation.

#### *B. Selective polymer solubility in homologous series of normal monohydric alcohols*

It may be inferred from tables 1 and 2 that the members of the homologous series possess a selective solvency for the oil polymers such that, as the polymers

grow in size, they exhibit progressively decreasing solubility in the successively lower members of the alcohol series. Thus, as will be shown later, the triglyceride linseed and soybean oil monomers are soluble in all of the normal alcohols from carbon atom chain length  $C_3$  to  $C_{12}$  but not below  $C_3$ , the dimers from  $C_4$  to  $C_{12}$ , the trimers from  $C_5$  to  $C_{12}$ , the tetramers from  $C_6$  to  $C_{12}$ , the pentamers from  $C_{10}$  to  $C_{12}$ , and the hexamers and heptamers not below  $C_{10}$ . This information is summarized in table 3.

There is a certain amount of overlapping in this solubility relationship, as will be shown later, but in general the correspondence is quite good. To account for this selective solubility there are three possible factors which may be considered: (1) the known decrease in polarity of the normal monohydric alcohols with increase in the length of the carbon atom chain; (2) the decrease in polarity of the oil polymers with growth; and (3) the relationship between the above two.

TABLE 3

*Solubility of monomers and specific polymers of linseed and soybean oils in the homologous series of normal monohydric alcohols\**

TYPE COMPOUND	HOMOLOGOUS SERIES OF NORMAL MONOHYDRIC ALCOHOLS						
	n-Propyl	n-Butyl	n-Amyl	n-Hexyl	n-Octyl	n-Decyl	n-Dodecyl
Monomer.....	<hr/>						
Dimer.....							
Trimer.....							
Tetramer.....							
Pentamer.....							
Hexamer.....							
Heptamer.....							

\* Solid line indicates range of complete solubility.

These three factors will subsequently be considered in turn, after some comment has first been made on the methods used for expressing polarity.

### *C. Methods of expressing polarity*

The simplest expressions of polarity are those of the experimentally determined values,—the dielectric constant and the refractive index. Other expressions include the dipole moment, a higher function of the dipole moment as in the expression  $\mu^2/\epsilon$  developed by Ostwald (28), molecular and specific polarization and refractivity, and cohesional energy density (13). Since these values, with the exception of the latter, are derived from the dielectric constant and the refractive index, it was considered sufficient for the purposes of the present paper to restrict, in the main, the expressions of polarity to these constants, and more particularly to that of the dielectric constant. One exception to this was made, however, in the use of a newly derived concept in which these values are related to the molecular weight of the particular substance under consideration.

These are designated as specific dielectric constants and specific refractive index and are defined as:

$$\text{Dielectric constant (specific)} = \frac{\text{dielectric constant}}{\text{molecular weight}}$$

$$\text{Refractive index (specific)} = \frac{\text{refractive index}}{\text{molecular weight}}$$

These derived expressions have proven useful in expressing the variation in solubility with respect to polarity of the members of a homologous series as well as for other related compounds. An analysis of the concept will be presented in a forthcoming paper.

#### *D. Polarities of solvents used in fractionating procedure*

Referring now to the first factor, that of the polarities of the members of the homologous series of normal monohydric alcohols, table 4 indicates a progressive

TABLE 4

*Comparative polarities of members of the homologous series of normal monohydric alcohols*

ALCOHOL	DIELECTRIC CONSTANT $\epsilon$	REFRACTIVE INDEX $n$	MOLECULAR WEIGHT MW	SPECIFIC DIELECTRIC CONSTANT $\frac{\epsilon}{\text{MW}}$	SPECIFIC REFRACTIVE INDEX $\frac{n}{\text{MW}}$	SPECIFIC POLAR- IZATION $\frac{\epsilon-1}{\epsilon+2} \cdot \frac{1}{\rho}$
Methyl . . . . .	33.7 (17°C.)	1.3294 ( $^{20}_{\text{D}}$ )	32	1.053	0.0415	1.151
Ethyl . . . . .	26.5 (20°C.)	1.36104 ( $^{20}_{\text{D}}$ )	46	0.576	0.0296	1.134
<i>n</i> -Propyl . . . . .	21.8 (20°C.)	1.38449 ( $^{20}_{\text{D}}$ )	60	0.363	0.0231	1.086
<i>n</i> -Butyl . . . . .	17.0 (20°C.)	1.39931 ( $^{20}_{\text{D}}$ )	74	0.230	0.0189	1.040
<i>n</i> -Amyl . . . . .	15.8 (20°C.)	1.4101 ( $^{20}_{\text{D}}$ )	88	0.179	0.0160	1.022
<i>n</i> -Hexyl . . . . .		1.41326 ( $^{20}_{\text{D}}$ )	102		0.0139	
<i>n</i> -Heptyl . . . . .	6.7 (21°C.)		116	0.058		0.797
<i>n</i> -Octyl . . . . .	3.4 (18°C.)	1.43035 ( $^{20}_{\text{D}}$ )	130	0.026	0.0110	0.539
<i>n</i> -Decyl . . . . .		1.43719 ( $^{20}_{\text{D}}$ )	158		0.0091	

decrease in polarity with increasing length of the carbon atom chain. In this table the specific polarization calculated on the basis of the Clausius-Mosotti equation was included for purposes of comparison with other expressions of polarity.

Since petroleum ether was successfully used in the fractionation of the heat-polymerized oil gels, to be discussed later, table 5 gives the polarity data for it as well as for cyclohexane, which proved ineffective for this separation. Cyclohexane was also later used as a cryoscopic solvent in the molecular-weight determinations and its limitations in this connection are directly attributable to its relatively high polarity. Of all the solvents used petroleum ether (hexane) possesses the lowest dielectric constant.

It will be noted in tables 4 and 5 that while the relation between polarity and

solubility is consistent in all of the polarity expressions given for the normal alcohols, it is not so evident for hexane in relation to those for the alcohols. For hexane the dielectric constant, specific dielectric constant, and the specific polarization all indicate a lowering of polarity consistent with its increased solvency property for the oil polymer systems under consideration, whereas the refractive index indicates an increase in polarity. The reason for this discrepancy is not apparent.

TABLE 5  
*Comparative polarities of hexane and cyclohexane*

SOLVENT	DIELECTRIC CONSTANT $\epsilon$	REFRACTIVE INDEX $n$	MOLECULAR WEIGHT MW	SPECIFIC DIELECTRIC CONSTANT $\frac{\epsilon}{\text{MW}}$	SPECIFIC REFRACTIVE INDEX $\frac{n}{\text{MW}}$	SPECIFIC POLAR- IZATION $\frac{\epsilon - 1}{\epsilon + 2} \cdot \frac{1}{\rho}$
Hexane....	1.87 (20°C.)	1.37506 ( $n_D^{20}$ )	86	0.0217	0.0160	0.341
Cyclohexane....	2.05 (20°C.)	1.4264 ( $n_D^{20}$ )	84	0.0244	0.0170	0.321

*E. Polarity of non-conjugated vegetable oils on heat-polymerization as a function of polymer growth in relation to the polarities of its constituent monomers*

With respect to the second factor, that of changes occurring in the polarity of the oil polymers on growth, both the initial polarity of the component fatty acids in the triglyceride oil monomers and the over-all net change in polarity on their progressive polymerization must be taken into account. It has been indicated by Langmuir (23) that the polarity of a fatty acid of the  $C_{18}$  group is dependent on its degree of unsaturation. Stepanenko, Agranat, and Novikova (34) have determined the dipole moments of three of the  $C_{18}$  fatty acids in dioxane and have shown that the dipole moment increases from 1.65 in stearic to 1.71 in linolic acid. These authors also reported the values for the dipole moments of tristearin and triolein as 2.95 and 3.06, respectively. Caldwell and Payne (12) investigated the dipole moments of unbodied linseed and perilla oils in the absence of solvents; while their values of 2.100 and 2.603, respectively, are generally of a somewhat lower order of magnitude than those of the previous authors, they likewise indicate an over-all higher polarity with increasing unsaturation.

A difficulty presents itself at this point with respect to the polarity-solubility relationships between the  $C_{18}$  fatty acids and their triglycerides, which merits some discussion. It is apparent from the above dipole-moment data that the fatty acids have an apparently lower polarity than do the corresponding triglycerides and yet, as is well known, the fatty acids are readily soluble even in methyl alcohol, whereas the triglyceride monomers require at least *n*-propyl alcohol for solubility. If one takes, however, the corresponding molecular weights of the fatty acids and their triglyceride monomers into account and calculates either the specific dielectric constant or the specific refractive index, the new

polarity values fall into the proper relation with respect to the solubility of these compounds. In this instance the Clausius-Mosotti specific polarization values are not in the proper sequence and hence do not correctly express the solubility-polarity relationship. This is summarized in table 6.

TABLE 6  
*Comparison of polarities of a  $C_{18}$  fatty acid and a mixed  $C_{18}$  fatty acid triglyceride*

$C_{18}$ COMPOUND	DIELECTRIC CONSTANT $\epsilon$	REFRACTIVE INDEX $n$	MOLECULAR WEIGHT MW	SPECIFIC DIELECTRIC CONSTANT $\frac{\epsilon}{MW}$	SPECIFIC REFRACTIVE INDEX $\frac{n}{MW}$	SPECIFIC POLAR- IZATION $\frac{\epsilon - 1}{\epsilon + 2} \cdot \frac{1}{\rho}$
Oleic acid. . .	2.45 (20°C.)	1.4582 ( $\frac{20}{D}$ )	282	0.0081	0.0052	0.3644
Linseed oil . .	2.725 (20°C.)	1.4792 ( $\frac{20}{D}$ )	878	0.0031	0.0016	0.3916

*F. Relationship of polarities of solvent and oil monomers and polymers with respect to solubility*

Having discussed the first two factors, that of the direction of change in polarity of the homologous series of normal monohydric alcohols, and of the oil polymers relative to their growth, we are now in a position to discuss the third factor, that of the relationship between the polarities of the normal alcohols (as well as of the other solvents mentioned) and those of the oil polymers with respect to their mutual solubilities.

If one considers methyl alcohol and petroleum ether as representing the extremes in polarity of the solvents discussed, with dielectric constants of 33.7 and 1.85, respectively, one finds that methyl alcohol has little or no solvency for the triglyceride monomers, let alone the polymers, whereas petroleum ether is an excellent solvent not only for the monomers but for all the polymers, up to the gelation stage. With respect to the lessened solubility of the higher polymers of lower polarity in the lower members of the normal alcohol series of higher polarity, one sees that for each stage of polymer growth corresponding to a given polarity, there is a normal alcohol of such polarity as will not exceed that required for solubility. Thus, for example, a low-polarity solvent such as dodecyl alcohol will dissolve the monomers and all the polymers up to the hexamer stages, whereas a solvent of relatively higher polarity, such as *n*-butyl alcohol, will dissolve only the monomers and dimers. The general rule may be summarized as follows: A low-polarity solvent will dissolve either a high- or a low-polarity oil polymer, but a high-polarity solvent will dissolve only a high-polarity oil polymer.

The degree of polarity of the solvent is therefore the variable factor, and its successive lowering in the ascending members of the homologous series of normal alcohols explains their stepwise selective solvency on the oil polymers of increasing size and progressively lowering polarity. The relation is further emphasized by the fact that the normal, secondary, and tertiary isomers of the monohydric alcohols with decreasing polarities in the order named exhibit inversely

increasing solubilities toward the higher oil polymers. A somewhat similar relationship was noted by Kunerth (22) in the increasing solubility of carbon dioxide, a highly polar compound, in a series of alcohols of increasing polarities.

The reason for the inability of acetone to effect fractionation of the oil polymers, previously referred to, can now be given. Acetone has a dielectric constant of 21.4, which is approximately that of *n*-propyl alcohol. Therefore it is capable of dissolving essentially only the monomers and not the polymers.

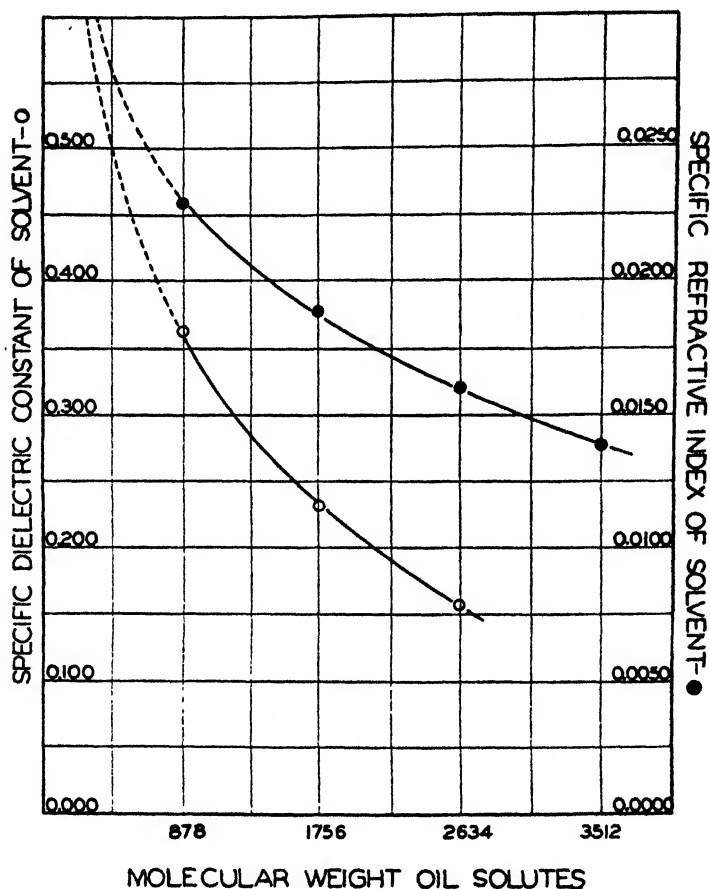


FIG. 1. Relationship between polarity expressions of solvents and molecular weight of oil solutes.

A graphical representation of the relationship between the solvent polarity and the molecular weights of the oil polymers is given in figure 1. The solvent polarity is expressed as ordinates by both the specific dielectric constant and the specific refractive index. All points for each relationship between solvent polarity and oil molecular weight fall on smooth curves. The following deductions may be made: (1) the curves are approximately exponential in form and apparently express a divergent series; (2) the extrapolations of the upper ends of

the curves intersect at a point the ordinate for which conforms approximately to polarity values between those for ethyl and methyl alcohols; and (3) the slope of the curves is greatest in the monomer region and least in that of the tetramer. This latter point conforms to the experimental fractionation data, since, as is evident from tables 1 and 2, the first few members of the normal alcohol series are more selective in polymer solubility than are the latter ones.

## II. EXPERIMENTAL

### *A. Fractionation of liquid heat-polymerized linseed and soybean oil samples*

A detailed account will now be given of the specific procedures used in the fractionation of heat-polymerized linseed and soybean oils. The preparation and general properties of the samples of heat-polymerized linseed and soybean oils used in this work will be described in a subsequent paper. The samples were represented by those taken immediately after each of the two oils had reached the polymerization temperature of 307°C. and by periodic samples taken thereafter up to the gelation point, as well as by those taken from the ensuing gelled oils. The fractionation of the latter represented a special case, since it necessitated the development of a technique for the separation of the gel-forming material before fractionation of the liquid part could be attempted. This will therefore be reserved for subsequent discussion. For the initial and periodic samples up to the gelation point, the following regular series fractionation procedure was developed and used. Special techniques were later developed to overcome specific difficulties which were encountered in the regular fractionated series; these will be referred to as the occasion presents itself.

### *B. Procedure for extraction of regular series of liquid polymers*

Seventy-five grams of the sample was accurately weighed into a 500-ml. glass-stoppered Erlenmeyer flask, to which 300 ml. of *n*-propyl alcohol was added. The free air space was swept out with nitrogen (oxygen free) to prevent oxidation and the contents shaken vigorously for 20 min. The extraction flask was then set aside and the contents allowed to settle overnight.

The clear extract was decanted into a glass-stoppered Erlenmeyer flask, covered with an atmosphere of nitrogen, and set aside for evaporation. This represented the first fraction. The volume of liquid in the extraction flask was made up to 350 ml. with additional *n*-propyl alcohol, and the second extraction repeated in the same manner as the first. After at least three such extractions with *n*-propyl alcohol, the remaining insoluble fraction was successively extracted an equal number of times with the other members of the homologous alcohol series, *n*-butyl, *n*-amyl, *n*-hexyl, *n*-octyl, *n*-decyl, and *n*-dodecyl alcohols, or as many of these as were required for the particular sample being fractionated. In spite of the care taken to keep an inert atmosphere of nitrogen over the liquids during the various extractions for the purpose of preventing oxidation and induced polymerization, considerable difficulty was nevertheless experienced during the latter part of the fractionations in that gelation occurred overnight in the

residue of the more highly polymerized samples. It was found later that the addition to each extraction of 0.1 per cent of solid hydroquinone acted as a polymerization retardant and solved this particular problem. This was not done, however, to the regular series of fractionations; consequently for this series it was not possible to extract beyond the *n*-hexyl or *n*-octyl alcohol stage. A few of the extractions were, however, repeated and treated with hydroquinone, and it was found possible to carry these fractionations through the *n*-dodecyl extraction stage without having gelation take place.

In addition to the regular series of fractionations which were all done at room temperature (approximately 26°C.), one sample of each of the two heat-polymerized oils was also fractionated at a lower and a higher temperature, 4°C. and 56°C., in order to study the temperature dependence. These will be referred to in Section IV.

After evaporation of the solvent from the various extractions the resulting fractions were set aside (properly stored in the dark and in an inert atmosphere) for subsequent determinations of acid value, molecular weight, viscosity, and iodine value. Before taking this up an account will be given of the technique developed for the quantitative fractionation of the samples of the gelled oils.

### *C. Fractionation of heat-polymerized gels formed from linseed and soybean oils*

The gel samples represented a considerable problem with respect to their fractionation. Three factors were involved: (1) the determination of the specific material causing gelation; (2) the quantitative separation of this material from its absorbed liquid phase; and (3) the fractionation of the liquid phase of the gel.

It has already been stated in Section I that since petroleum ether has the lowest dielectric constant and therefore the lowest polarity of the solvents studied, its solvency for the oil polymers of lowest possible polarity, i.e., those of greatest linear or branched-chain length, would be a maximum. Experimentally, this was borne out by the ready solubility in petroleum ether of all the polymerized-oil samples up to the gelation point, as has previously been pointed out. Because of this, it was reasonable to assume that long linear or branched oil polymers could not themselves constitute the primary adsorbate but rather that some specific insoluble cross-linked polymer was the primary cause of the gelation phenomena.

Some experimental work on the oil-gelation problem had previously been done by Bradley and Pfann (10), who showed that acetone-soluble material could be extracted from these gels, and by Long (24), who demonstrated the adsorptive properties of such gels. Neither, however, demonstrated except possibly by inference the existence of the cross-linked polymer matrix, nor was there sufficient known at the time of this previous work of the relationships between the polarities of solvent and the higher oil polymers to enable these investigators to achieve this experimental fractionation objective.

As a result of extensive experimentation it was discovered by the author: (1) that a material could be quantitatively separated from the oil gels by means



of petroleum ether, (2) that this separated material possessed the physical and chemical properties of an insoluble, infusible, cross-linked polymer, (3) that it was present in substantial amounts as postulated in the author's theory, and (4) that there was substantial basis for believing that it was formed from the cross-linking of relatively short chain polymers, those at or near the pentamer stage (8). The belief that this insoluble, infusible, cross-linked polymer was the specific cause of gelation was strengthened by the fact that the remaining liquid fraction or disperse phase of the gel exhibited normal fluidity, complete solubility in petroleum ether, and lastly that it could be fractionated, in the manner already given for the liquid oil-polymer samples, into monomers and an array of polymers of increasing stages of growth.

*D. Procedure for separation of insoluble, infusible, cross-linked polymer in heat-polymerized linseed and soybean oil gels*

The procedure by which the primary separation of the oil gel into its insoluble, infusible, cross-linked polymer phase and its adsorbed fluid monomer and polymer phase was effected is given in the following account: 600 g. of the heat-polymerized oil gel was weighed out into a 6-liter cylindrical jar to which was gradually added with continuous stirring 4000 ml. of petroleum ether (boiling range, 30-60°C.). Large masses of the gel remained undispersed during this preliminary stirring. The jar was then allowed to stand for 2 hr. The contents were then again stirred but without much effect on the dispersibility of the gel except that the petroleum ether layer had become slightly cloudy. After continued stirring for 6 hr., the gel masses had become partially dispersed in the petroleum ether layer and had consequently increased its viscosity to the point where the resulting extended gel was sufficiently rigid to support the glass stirring rod in an upright position. Additional petroleum ether (1000 ml.) was stirred in without having much effect on the gel rigidity except to thin it a little. However, after 96 hr. of standing with occasional stirring the contents of the jar became quite fluid, although still cloudy, and there had settled out on the bottom a white curdy material. After an additional 9 days of alternate standing and stirring and 1 day for final settling, the jar contents had separated into a perfectly clear fluid and dense curd layer at the bottom. The clear fluid was carefully decanted and reserved for evaporation. To the curdy residue, 4000 ml. of petroleum ether was added and allowed to extract for 24 hr. with continued stirring, after which it was allowed to settle for 24 hr. A test on the final extraction showed only 0.1 per cent of extractable material, which remained constant on further extraction. This was checked with two hot acetone extractions which likewise gave 0.1 per cent values. On this basis it was considered that the extraction of soluble material from the insoluble curds was complete. The curdy material was then dried to constant weight at room temperature in a nitrogen atmosphere, after which it was transferred to a glass-stoppered flask and stored in an inert atmosphere. For the linseed gel, the dried separated insoluble material represented 30 per cent by weight of the original gel sample, whereas for the soybean oil gel the weight was 17 per cent. Both gel curds were of similar properties: they were insol-

uble in a wide variety of solvents and infusible on heating. Hence they could be characterized as insoluble, infusible, cross-linked polymers. A detailed description of their specific chemical and physical properties confirming this characterization will be given in a subsequent paper. The collected petroleum ether washings were evaporated, the final stage being done in a nitrogen atmosphere under partial vacuum. The viscous oily residue after reaching constant weight was transferred to a glass-stoppered flask and stored in an inert atmosphere.

The mechanism by which petroleum ether dissolved the adsorbed fluid phase from the insoluble cross-linked polymers can be postulated to depend on two factors: (1) that the petroleum ether is a solvent for all the linear and branched liquid polymers up to the point of formation of the insoluble cross-linked polymers and (2) that the solution or diffusion forces between petroleum ether and these high liquid polymers are greater than the adsorptive or cohesive forces between them and the insoluble cross-linked polymer adsorbate. To demonstrate the point that the solubility factor is the major one, cyclohexane with a dielectric constant of 2.05 as compared to 1.85 for petroleum ether in a gel-fractionation experiment identical to the above gave only a uniformly extended gel with no desorption in evidence and no separation of the cross-linked polymers. The inference can therefore be drawn that cyclohexane is not a solvent for the highest linear or branched oil polymers present and therefore cannot desorb the gel. This inference was corroborated in the use of cyclohexane as a cryoscopic solvent in molecular-weight determinations, since for the high-polymer fractions anomalous molecular weights were obtained.

### III. DETERMINATION OF PHYSICAL CONSTANTS OF MONOMER AND POLYMER FRACTIONS

Because of the many samples fractionated, only a few of their more important constants were determined: namely, those which were considered to have a direct bearing on the general interpretation of the polymerization process as well as on the calculations directed toward arriving at the polymer distribution at various stages of the reaction. The following constants were selected for this study: free fatty acid value, number-average molecular weight (cryoscopic), absolute fluid viscosity, and iodine value. The following is a description of the analytical methods used.

#### *A. Free fatty acid value*

There are three distinct types of acidity present in varying percentages in heat-polymerized non-conjugated vegetable oils: free fatty acid, fatty acid-triglyceride copolymers, and polymerized fatty acid (11; and unpublished data of the author). The latter would normally be present in negligible amount and may be disregarded for our present purpose. The first two, however, are present in substantial quantities. Since the fatty acid-triglyceride copolymers are of a molecular size comparable to that of the triglyceride polymers, they can be assumed to cause not too great an interference in the polymer-distribution scheme to be discussed later. On the other hand the free fatty acids, particularly those which are pro-

gressively liberated during the polymerization process, are only one-third the molecular weight of a triglyceride monomer, and therefore a number-average molecular weight of a mixture of free fatty acid and triglyceride monomer would have to take this into account to arrive at the correct molecular weight of the triglyceride monomer component. Since these free fatty acids are readily soluble they are concentrated in the *n*-propyl alcohol extractions. The calculation for their correction will be discussed later in Section IV. The determination for free fatty acid was carried out in the usual manner on each of the fractions extracted with *n*-propyl alcohol and expressed as milligrams of potassium hydroxide required to neutralize the acids in 1 g. of sample.

### *B. Molecular weight*

Number-average molecular weights were determined cryoscopically using cyclohexane as the solvent, as recommended by Gay (18). Temperatures were read on a Beckman differential thermometer to 0.01°C. and estimated to 0.002°C. Duplicate determinations agreed to within 1.5 per cent. A control on each unbodied linseed and soybean oil gave average values of 875 and 890, respectively, which corresponded to the theoretical values of 878 and 880, respectively. It should be mentioned here in passing that benzene, which has in the past been extensively used as the solvent for these determinations, does not give reliable results, the values being consistently low. A critical study of the effect of solvents and solute concentration on the number-average molecular weight of oil monomers has since been made.<sup>3</sup>

### *C. Viscosity (absolute)*

Because of the relatively small amounts obtained for many of the fractions, it was not possible to use the Ostwald method for the determination of their viscosities. Instead comparison was made by the Gardner-Holdt Varnish Viscosity Tube Standards, either by the conventional bubble-rise procedure wherever possible or by a standardized paper-penetration method when the sample was too small. The latter technique enabled one to make a determination with a single drop.

### *D. Iodine value*

Iodine values were determined according to the usual 60-min. Wijs procedure. While no experimental difficulty was noted with the monomer and lower polymer fractions, considerable trouble was experienced with those of the higher polymers. This difficulty took the form of a dark brown precipitation or coagulation when the Wijs iodine solution was added to that of the sample in carbon tetrachloride. Apparently the higher polymers, while ostensibly dissolved in the carbon tetrachloride, were present only as a colloidal sol which flocculated in the presence of the iodine monochloride. The iodine values of the higher polymer fractions are

<sup>3</sup> I. M. Bernstein: Preprints of papers presented before the Division of Paint, Varnish, and Plastics Chemistry at the 112th meeting of the American Chemical Society, New York City, September, 1947, p. 160.

therefore of dubious value, as will be noted in the subsequent interpretation of the data given in Section IV.

#### IV. INTERPRETATION OF THE EXPERIMENTAL DATA AND CALCULATIONS RELATING THERETO

Because of the extensive experimental data assembled, not all are included in this paper for reasons of excessive length, but rather those fractionations were selected which indicated the trend of the polymerization. For linseed oil the samples reported represent the regular series fractionations after 1, 6, and 10 hr. at the polymerization temperature (tables 7, 8, and 9), while for soybean oil the 5-, 12-, and 17-hr. regular series fractionated samples are reported (tables 10, 11, and 12). Other data will be given in supplementary tables. Mention should be

TABLE 7

*Monomer-polymer fractionation (26°C.), with homologous series of normal monohydric alcohols, of linseed oil heat-polymerized for 1 hr. at 307°C.*

NORMAL ALCOHOL EXTRACTIONS	PR-1	PR-2	PR-3	BU-1	BU-2	UNFRACTIONATED REMAINDER	
						Weight per cent	Soluble in
Weight per cent extracted.....	39.8	27.6	14.5	9.5	8.6	0	
Molecular weight.....	900	966	1029	1318	1787		
Viscosity (poises).....	1.1	1.3	1.7	3.7	9.8		
Acid value.....	3.7	1.1	0.5				
Iodine value (Wijs).....	161.4	160.3	159.9	152.0	135.3		
Molecular species distribution (weight per cent).....	98-M 2-D	90-M 10-D	83-M 17-D	50-M 50-D	98-D 2-TR		

made here of the system of abbreviation used to describe the various extractions. The alcohols are abbreviated by their first letters, and the sequence of extraction by the number which follows: thus PR-1 is the first extraction with *n*-propyl alcohol, H-3 the third extraction with *n*-hexyl alcohol, DD-4 the fourth extraction with *n*-dodecyl alcohol, etc. In the tables the following abbreviations were used: M, monomer; D, dimer; TR, trimer; TE, tetramer; PE, pentamer; HEX, hexamer; HEP, heptamer.

On the basis of the experimental data it may in general be said that the heat-polymerization of the non-conjugated vegetable oils is essentially a stepwise addition reaction involving primary valence bonds, the resulting polymer growth being evidenced in the following four experimentally independent directions: (1) solubility, (2) molecular weight, (3) viscosity, and (4) iodine value. Comments on the data presented in these categories will now be made.

##### A. Solubility

The progressive insolubility of the various higher polymers as they appear in stepwise fashion during the heat-polymerization process is shown primarily by

TABLE 8  
*Monomer-polymer fractionation (26°C.), with homologous series of normal monohydric alcohols, of linseed oil heat-polymerized for 6 hr at 307°C.*

NORMAL ALCOHOL EXTRACTIONS	PR-1	PR-2	PR-3	BU-1	BU-2	BU-3	AM-1	AM-2	AM-3	H-1	UNFRACTIONATED REMAINDER	
											Weight per cent	Soluble in
Weight per cent extracted	25.7	24.4	5.3	7.2	3.2	2.7	6.6	4.6	3.2	7.8	9.3	n-Octyl alcohol
Molecular weight	1050	1146	1310	1600	2141	2917	2440	2580	2910	5925		
Viscosity (poises)	2.8	3.2	5.2	12.9	30.1	54.8	70.0	75.1	148	4200(c)		
Acid value	19.3	7.0	1.2				3.3			388		
Iodine value (Wijs)	125.3	124.6	121.3	121.2	121.2	121.7	121.0	118.0	115.3	93.8		
Molecular species distribution (weight per cent)	81-M	70-M	51-M	16-M	58-D	79-TR	22-D	6-D	69-TR	25-HEX		
	19-D	30-D	49-D	81-D	42-TR	21-TE	78-TR	94-TR	31-TE	75-HEP		

TABLE 9

*Monomer-polymer fractionation (86°C.), with homologous series of normal monohydric alcohols, of linseed oil heat-polymerized for 10 hr. at 307°C.*

NORMAL ALCOHOL EXTRACTIONS	PR-1	PR-2	PR-3	BU-1	BU-2	BU-3	AM-1	AM-2	AM-3
Weight per cent extracted.....	20.0	8.7	4.0	5.3	2.6	2.0	4.7	4.0	2.7
Molecular weight {	1115	1145	1283	1478	1705	1681	1596 2049(c)	1261 1800(c)	1667 2518(c)
Viscosity (poises) . .	3.0	4.5	8.1	15.3	29.5	63.1	46.2	36.3	109
Acid value . . . . .	24.5	3.5		2.3					
Iodine value . . . . .	119.2			121.2			113.9		
Molecular species distribution (weight per cent) {	70-M 30-D	73-M 27-D	55-M 45-D	31-M 69-D	6-M 94-D	9-M 91-D	67-D 33-TR	95-D 5-TR	12-D 88-TR

NORMAL ALCOHOL EXTRACTIONS	H-1	H-2	H-3	O-1	O-2	O-3	UNFRACTIONATED REMAINDER	
							Weight per cent	Soluble in
Weight per cent extracted.....	5.3	3.3	2.0	2.7	1.3	0.7	30.7	Petroleum ether
Molecular weight {	2280 3450(c)	1119 2415(c)	2821 2610(c)	3093 3240(c)	3720 3360(c)	3278 3840		
Viscosity (poises)...	393	98.8	139	309	368	588		
Acid value . . . . .								
Iodine value . . . . .	109.4							
Molecular species distribution (weight per cent) {	20-TR 80-TE	25-D 75-TR	2-D 98-TR	49-TR 51-TE	10-TR 90-TE	66-TE 34-PE		

TABLE 10

*Monomer-polymer fractionation (26°C.), with homologous series of normal monohydric alcohols, of soybean oil heat-polymerized for 5 hr. at 307°C.*

NORMAL ALCOHOL EXTRACTIONS	PR-1	PR-2	PR-3	PR-4	BU-1	BU-2	BU-3	AM-1	UNFRACTIONATED REMAINDER	
									Weight per cent	Soluble in
Weight per cent extracted...	53.4	22.7	8.7	3.3	6.7	2.6	1.3	1.3	0	
Molecular weight....	896	1015	1272	1720	1919	2220	2430	2634		
Viscosity (poises)....	1.3	1.4	4.4	8.8	17.6	33.1	41.2	63.4		
Acid value . . . . .	8.7	2.6	0.6							
Iodine value (Wijs) . . . .	120.3	120.0	116.0	113.2	110.3	109.1				
Molecular species distribution (weight per cent) {	98-M 2-D	85-M 15-D	56-M 44-D	4-M 96-D	82-D 18-TR	46-D 54-TR	23-D 77-TR	100-TR		

TABLE 11  
Monomer-polymer fractionation (26°C.), with homologous series of normal monohydric alcohols, of soybean oil heat-polymerized for 12 hr. at 307°C.

NORMAL ALCOHOL EXTRACTIONS	PR-1	PR-2	PR-3	BU-1	BU-2	BU-3	AM-1	AM-2	AM-3	H-1	H-2	H-3	UNFRACTIONATED REMAINDER	
													Weight per cent	Soluble in
Weight per cent extracted . . . . .	25.3	14.1	7.4	8.0	5.4	3.3	9.3	6.0	3.3	9.3	3.3	1.3	4.0	n-Octyl alcohol
Molecular weight . . . . .	953	1110	1260	1790	1732	2710	2875	3090	2260	4171	3951	4390		
Viscosity (poises) . . . . .	2.1	3.3	3.6	12.4	17.6	36.2	59.1	63.4	98.5	268	228	268		
Acid value . . . . .	18.7	7.8	4.6	2.5			3.5							
Iodine value (Wijs) . . . . .	103.5	101.0	100.1	100.9	99.5	100.5	98.1			96.1				
Molecular species distribution (weight per cent) . . . . .	92-M 8-D	72-M 28-D	58-M 42-D	3-M 97-D	68-D 32-TR	92-TR 8-TE	73-TR 27-TE	47-TR 53-TE	42-D 58-TR	25-TE 75-PE	50-TE 50-PE	100-PE		

TABLE 12  
Monomer-polymer fractionation (26°C.), with homologous series of normal monohydric alcohols, of soybean oil heat-polymerized for 17 hr. at 307°C.

NORMAL ALCOHOL EXTRACTIONS	PR-1	PR-2	PR-3	PR-4	BU-1	BU-2	BU-3	BU-4	AM-1	AM-2	AM-3	AM-4	UNFRACTIONATED REMAINDER	
													Weight per cent	Soluble in
Weight per cent extracted . . . . .	16.0	7.4	4.7	3.3	5.3	4.0	2.0	1.4	5.3	3.4	2.0	1.0	44.2	Petroleum ether
Molecular weight . . . . .	1010	1141	1270	1580	1914	2332	2420	3585	3940	2309	3185	2700		
Viscosity (poises) . . . . .	2.6	3.5	6.6	12.0	22.7	25.9	36.2	46.3	148	63.4	98.5	98.5		
Acid value . . . . .	23.1	6.0	2.7		2.6	2.6				3.4				
Iodine value (Wijs) . . . . .	95.5				98.8				90.2					
Molecular species distribution (weight per cent) . . . . .	85-M 15-D	70-M 30-D	57-M 43-D	20-M 80-D	82-D 18-TR	34-D 66-TR	25-D 75-TR	86-TE 14-PE	50-TE 50-PE	37-D 63-TR	36-TR 64-TE	92-TR 8-TE		

the necessity for using the successively higher members of the homologous series of normal monohydric alcohols and finally petroleum ether in order to effect solubility of the last remaining insoluble fraction. The magnitude of this solubility is dependent on the temperature, which is indicated in the study mentioned in Section II.

As previously stated, experiments in this study were made at extraction temperatures of 4°C., 26°C. and 56°C., on samples of linseed and soybean oils which had been heat-polymerized for 9 and 16 hr., respectively. The results show that the solubility is in some manner proportional to the temperature of extraction, as indicated in tables 13 and 14. From these data it is evident that some, although not too much, advantage is gained in performing the extractions at the lower

TABLE 13

*Weight percentage of combined extractions per member of normal alcohol series of linseed oil heat-polymerized for 9 hr. at 307°C.*

EXTRACTION TEMPERATURE	n-PROPYL ALCOHOL EXTRACTIONS	n-BUTYL ALCOHOL EXTRACTIONS	n-AMYL ALCOHOL EXTRACTIONS
°C.	weight per cent	weight per cent	weight per cent
4	32.9	7.8	10.4
26	33.8	8.9	11.8
56	44.4	14.0	18.9

TABLE 14

*Weight percentage of combined extractions per member of normal alcohol series of soybean oil heat-polymerized for 16 hr. at 307°C.*

EXTRACTION TEMPERATURE	n-PROPYL ALCOHOL EXTRACTIONS	n-BUTYL ALCOHOL EXTRACTIONS	n-AMYL ALCOHOL EXTRACTIONS
°C.	weight per cent	weight per cent	weight per cent
4	28.4	10.8	12.6
26	30.6	13.6	15.7
56	41.0	19.5	21.0

temperature. Consequently the results for the regular series of fractionations which were done at 26°C. are not at too great a disadvantage for the survey purposes of this paper. The extractions at 56°C., on the other hand, are not sufficiently selective in solubility.

#### 1. Dependence of extent of fractionation on occurrence of secondary gelation

Aside from the above, there is one definite advantage in the low-temperature fractionation: namely, that of minimizing the tendency to gel of the latter portion of the sample being fractionated. In the above examples, fractionation at 4°C. could be continued for both oil samples at least through the *n*-hexyl alcohol stage, whereas at 26°C. fractionation was often interrupted by the onset of gelation at the end of the *n*-amyl alcohol extractions. It is quite interesting that the more highly polymerized portion or fraction of a sample should be so sensitive to gela-



TABLE 15

*Monomer-polymer fractionation (4°C.), with homologous series of normal monohydric alcohols containing 0.1 per cent hydroquinone, of linseed oil heat-polymerized for 8 hr. at 307°C.*

NORMAL ALCOHOL EXTRACTIONS		PR-1	PR-2	PR-3	PR-4	BU-1	BU-2	BU-3	BU-4	AM-1	AM-2	AM-3	AM-4	H-1	H-2	H-3
Weight per cent extracted	...	16.7	6.6	3.9	3.0	3.6	2.3	2.0	1.6	3.6	2.3	3.0	1.3	3.0	2.6	2.0
Molecular weight	{	897	1018	1061	1108	1561	1450	1888	1642	1629	2165	2578	3140	4213	2711	2461
Viscosity (poises)	...	2.9	3.3	3.4	4.4	8.8	12.0	17.6	22.7	36.2	46.3	54.8	8.09	3219(c)	3219(c)	3219(c)
Acid value	...	28.0	9.5	5.6	2.3	4.3				3.6				123	123	123
Iodine value (Wijs)	...	119.4					122.6			119.6						
Molecular species distribution (weight per cent)	{	98-M	84-M	80-M	74-M	34-M	22-M	13-M	88-D	14-M	55-D	6-D	40-TR	33-TR	33-TR	33-TR
		2-D	16-D	20-D	26-D	66-D	78-D	87-D	14-TR	86-D	45-TR	94-TR	60-TE	67-TE	67-TE	67-TE

NORMAL ALCOHOL EXTRACTIONS		H-4	O-1	O-2	O-3	O-4	D-1	D-2	D-3	D-4	DD-1	DD-2	DD-3	DD-4	UNTRACTED REMAINDER	
Weight per cent extracted	...	1.6	3.3	1.6	1.0	1.0	3.6	3.0			6.6	4.3	2.0	2.0	Weight per cent	Soluble in
Molecular weight	{	3157	2330	3240		3650	2678	2105			4750	2722	6000	9860		Petro-leum ether
Viscosity (poises)	...	3805(c)	3331(c)	3090(c)	4110	4110(c)	4250(c)	4171(c)	5122(c)	5550	5048(c)	5048(c)	5048(c)	5443(c)		
Acid value	...	268	118	136	388	388	388	328	855	1066	766	789	855	1066		
Iodine value (Wijs)	...						103.2				3.9					
Molecular species distribution (weight per cent)	{	67-TE	20-TR	30-TR	33-TE	33-TE	17-TE	25-TE	17-PE	80-HEX	25-PE	25-PE	25-PE	80-HEX		
		33-PE	80-TE	70-TE	67-PE	67-PE	83-PE	76-PE	83-HEX	20-HEP	75-HEX	75-HEX	75-HEX	20-HEP		

TABLE 16

*Monomer-polymer fractionation (4°C.), with homologous series of normal monohydric alcohols containing 0.1 per cent hydroquinone, of soybean oil heat-bodied for 17 hr. at 307°C.*

NORMAL ALCOHOL EXTRACTS	PR-1	PR-2	PR-3	PR-4	BU-1	BU-2	BU-3	BU-4	AM-1	AM-2	AM-3	AM-4	H-1	H-2	H-3
	Weight per cent extracted	3.7	3.0	2.3	3.0	2.3	2.1	1.3	3.3	3.0	2.6	1.3	4.0	3.0	1.7
Molecular weight	927	1121	1155	1225	1229	1512	1665	1950	2275	2095	3505	3865	2172	3316	3132
Viscosity (poises)	2.7	3.7	4.9	5.6	8.8	29.0	17.6	25.9	36.2	36.2	80.9	80.9	98.5	148	148
Acid value	27.9	13.8	6.0	1.3					88.6						
Iodine value (Wijs)	97.2				93.5								92.8		
Molecular species distribution	95-M	73-M	69-M	62-M	61-M	27-M	25-M	78-D	39-D	60-D	5-TR	62-TE	66-TR	22-TR	37-TR
(weight per cent)	5-D	27-D	31-D	38-D	39-D	73-D	75-D	22-TR	61-TR	40-TR	95-TE	38-PE	34-TE	78-TE	63-TE

NORMAL ALCOHOL EXTRACTS	H-4	O-1	O-2	O-3	O-4	D-1	D-2	D-3	D-4	DD-1	DD-2	DD-3	DD-4	UNFRACTIONATED REMAINDER	
	Weight per cent extracted	4.3	3.0	2.1	1.3	5.3	3.3	1.0	1.3	8.0	5.0	3.3	2.1	Weight per cent	Soluble in
Molecular weight	2467	1021	2370	3344	1436	2180	1597	3383	4829(c)	2009	2225	2046	3815	9.0	Petro-leum ether
Viscosity (poises)	3331(c)	2719(c)	3805(c)	4171(c)	4171(c)	2927(c)	3805(c)	4829(c)	855	4171(c)	4171(c)	4683(c)	4683(c)		
Acid value	158	80.9	268	388	388	98.5	268	855		388	388	683	723		
Iodine value (Wijs)		80.4								85.4		82.2			
Molecular species distribution	66-TR	90-TR	67-TE	25-TE	25-TE	66-TR	67-TE	50-PE	50-HE	25-TE	25-TE	67-PE	67-PE		
(weight per cent)	34-TE	80-TE	33-PE	75-PE	75-PE	34-TE	33-PE	50-HE		75-PE	75-PE	33-HEX	33-HEX		

tion when present by itself. This points to the stabilizing effect of the monomers and the lower polymers on these higher polymers, since the unfractionated heat-polymerized oil samples, even at fairly high viscosities, show only slight viscosity changes on months of aging at room temperature. The secondary gelation in this case would appear to have been inhibited by the monomers and lower polymers being physically adsorbed onto the larger polymers and acting in a manner similar to that of a protective colloid. These adsorbed molecules, in the case under consideration, are however not too tightly held, since they are capable of being stripped during the fractionation procedure. Once stripped from their protective adsorbents, the large polymers are very sensitive to cross-linking, which can be activated by minute amounts of oxygen. Such oxygen might easily be present in spite of the precautions taken to prevent it.

In the study of the effect of the addition of 0.1 per cent hydroquinone on the retardation of secondary gelation, samples of the heat-polymerized linseed and soybean oils after 8 and 17 hr., respectively, at the reaction temperature of 307°C.

TABLE 17

HEAT-POLYMERIZED OIL (307°C.)	NUMBER OF FRACTIONS SEPARATED AFTER						
	0 hr.	1 hr.	4 hr.	5 hr.	8 hr.	12 hr.	17 hr.
Linseed . . . . .	2	—	10	—	29		
Soybean . . . . .	0	3	—	8	10	13	29

were used. Taken together, the presence of antioxidant plus the added experimental conditions of low temperature were excellent for the elimination of the oxygen polymerization gelation factor. The results given in tables 15 and 16 show that there was a total elimination of secondary gelation, and that for the first time it was possible to fractionate through the entire series of normal monohydric alcohols, including *n*-dodecyl alcohol. The still insoluble liquid residue after the last-named extraction was approximately only 9 per cent for each of the oil samples fractionated, and this was readily soluble in petroleum ether.

## 2. Number of fractions obtained as a function of time of polymerization

With respect to this it would of necessity follow that as the higher polymers successively appeared an increased number of alcohols of the series would be found necessary to effect their separation. Table 17 gives examples of this. These are selected from those in which the factor of secondary gelation was either absent, as during the early stages of polymerization, or prevented from occurring by the hydroquinone treatment. The number of fractions obviously has only qualitative significance.

### *B. Molecular weight*

Since new fractions are obtained as the reaction progresses, assumedly as the result of polymer growth, it should follow that the molecular weights of these successive fractions should also exhibit corresponding increases. The experi-

mental data in general confirm this, at least for all fractions up to and in most cases including those obtained from the *n*-amyl alcohol extractions. For the fractions obtained, however, from the members of the homologous series higher than *n*-amyl alcohol, anomalies in molecular weight are the rule. Most of the anomalies are exhibited as marked decreases rather than increases of the correct order of magnitude. In the few instances where increases in molecular weight for these higher fractions do occur, the increases are usually abnormally high ones. These anomalies are apparently due to the molecular insolubility and therefore non-ideality of the higher polymers in cyclohexane.

One might therefore postulate that a critical minimum value in polarity of the solvent in relation to that of the solute must not be exceeded in order that true or molecular solution be attained. This molecularity of solution is, of course, an essential requirement for the application of Raoult's law to the determination of molecular weights.

Current thought on the cryoscopic method for the determination of molecular weights stresses ideality of solution and infinite dilution as the prime requirements for accurate determinations (32). The first of these is of course essential, but it is the author's opinion, based on experimental data to be presented soon, that infinite dilution is not an essential requirement, at least not for the lower range of oil polymers. If ideality of solution is assured, the molecular weight appears to be experimentally independent of the concentration.<sup>4</sup>

Solvents are not known, however, of the required low polarity which also possess the requirement of having their freezing points within a temperature range experimentally desirable for cryoscopic measurement of the higher oil polymers. Therefore the osmotic-pressure method is indicated for the determination of the molecular weights of these higher polymers, since for them only the first of the two requirements need be met. Work on this is contemplated as well as on some other procedures which likewise appear feasible. These will be reported at a later date.

#### 1. Molecular-weight correction for free fatty acid content of fractions extracted with *n*-propyl alcohol

As was indicated in Section III, it is necessary to correct the experimentally determined values of the number-average molecular weights of the *n*-propyl alcohol extracted fractions for their free fatty acid content, in order to obtain the molecular weight of their contained triglyceride monomers and polymers. The number-average molecular weight is defined for a two-component system as:

$$MW_{\text{number average}} = \frac{n_A MW_A n_B MW_B}{n_A n_B}$$

where  $n_A$  = number of molecules of component A

$n_B$  = number of molecules of component B

$MW_A$  = molecular weight of component A

$MW_B$  = molecular weight of component B

<sup>4</sup> Unpublished data of the author.

If the percentages of components A and B are known, then

$$MW_{\text{number average}} = \frac{\frac{\text{per cent A}}{MW_A} \cdot MW_A + \frac{\text{per cent B}}{MW_B} \cdot MW_B}{\frac{\text{per cent A}}{MW_A} + \frac{\text{per cent B}}{MW_B}}$$

If  $MW_A$  is taken as the molecular weight of the contained triglyceride monomers and polymers,  $MW_B$  as the molecular weight of the free fatty acids, and  $MW_{\text{number average}}$  that of the experimental value of the mixture contained in the fraction, then solving for  $MW_A$ :

$$MW_A = \frac{(MW_B)(MW_{\text{number average}})(\text{per cent A})}{100(MW_B) - (MW_{\text{number average}})(\text{per cent B})}$$

Since per cent B, that of the free fatty acids, is known from the free fatty acid value, the percentage of triglyceride monomers and polymers, per cent A, is known by difference. For  $MW_B$ , the molecular weight of the free fatty acids, one might assume the use of the theoretical average value of 279 for a  $C_{18}$  acid but this is incorrect, as will be shown in a subsequent paper, and the dimer value of 558 is used instead. The final form of the equation is therefore:

$$MW_A = \frac{(558)(MW_{\text{number average}})(\text{per cent A})}{55800 - (MW_{\text{number average}})(\text{per cent B})}$$

As an example to indicate the magnitude of the correction: for a first *n*-propyl alcohol fraction of heat-polymerized linseed oil the acid value of which was 23.6 and the number-average molecular weight 955, the calculated value for the number-average molecular weight of the contained triglyceride monomers and polymers was found to be 1115. Both uncorrected and corrected values are given in the tables.

### C. Viscosity

As can be seen from the data the increase in absolute viscosity for the various fractions extracted from any of the heat-polymerized oil samples is a function of polymer growth, the values ranging from approximately 1 poise for a fraction extracted by *n*-propyl alcohol to over 1000 poises for one extracted by *n*-dodecyl alcohol. The much higher order of magnitude of viscosity of these higher polymer fractions as compared to the lower polymers is probably due to the effect of branching as well as to the formation of the previously postulated smaller soluble cross-linked polymers (6).

While current emphasis in high-polymer chemistry has been on solution viscosity and the concept of intrinsic viscosity, significant work has also been reported on fluid viscosity (17), which is the basis of the work reported in this paper. The application of the concept of intrinsic viscosity must be approached with caution, since it by no means is certain, as is sometimes tacitly assumed, that at infinite dilution a solute will be dispersed to the molecular state irrespective of

the solvent used. Intrinsic viscosity  $[\eta]$  is defined as the first coefficient,  $a$ , of a power series evaluating specific viscosity:

$$\eta_{sp} = a_1 c_1 + a_2 c_2^2 + \dots$$

The second coefficient,  $a_2$ , expresses the interaction between solute molecules. The magnitude of the forces constituting this interaction must be variable and must depend not only on the type of solute molecules but also on the relation of solute to solvent. For the oil polymers under discussion this interaction appears to be related to the postulated relationship of the polarities of solute and solvent. It does not of necessity follow that at infinite dilution the interaction constant is negligible, and indeed the work of Spurlin, Martin, and Tennent (33) shows that in the case of ethyl cellulose different solvents not only give different slopes when the concentration is plotted against the specific viscosity concentration, but also that when the curves are extrapolated to infinite dilution they do not meet at a common point. Alfrey (3) has recently reviewed the problem from the point of view of polymers sufficiently long as to coil. In such systems hydrodynamic interaction with respect to good and poor solvents comes into play. In the simpler oil polymer systems under consideration, of molecular weight in the range of 2000 to 6000 and constituting a maximum of five to six monomers, there would be relatively little likelihood of such mechanical interaction between solute and solvent.

Contrary to claims made by other workers in this field—Morrell (26), Powers (2), and Schwarzman (31)—there is according to the data presented no initial lag in viscosity increase during the early stages of the heat-polymerization. Since the order of magnitude of the viscosity is small, that of any increase in viscosity should likewise be correspondingly small,—as it is. The high order of magnitude of decrease in iodine value, on the other hand, in relation to the low order of magnitude of increase in viscosity was apparently either not discernible or not correctly interpreted by these investigators, who worked with unfractionated heat-polymerized oil samples. They ascribed the *apparent* failure of the viscosity to increase initially in a manner corresponding to the decrease in iodine value as due to intrapolymerization, a conclusion certainly not in conformity with the experimental data in this paper, and furthermore, one which has been shown untenable on theoretical grounds in a previous paper (6).

#### 1. Anomalous viscosity increase in the first *n*-propyl alcohol fractions as a function of time of polymerization

Contrary to the expectation that the viscosity of the first *n*-propyl alcohol extracted fractions should be the same irrespective of the extent of polymerization of the oil samples being fractionated, one finds that their viscosities are not constant but tend to increase with the time of polymerization. Thus, for example, whereas the viscosity of the unbodied linseed oil used was 0.50 poise and that of the first *n*-propyl alcohol extracted fraction after 0 hr. at the polymerization temperature 0.61 poise, the viscosity of the similarly extracted fraction after 4 hr. of polymerization rose to a value of 2.8 poises.

The reason for the anomalous viscosity increase has already been suggested in a previous paper (6),—namely, that as the polymerization progresses, more and more heat-stripping of the saturated and low unsaturated fatty acid components from the  $\beta$ -glyceryl positions occurs, leaving as products of this secondary reaction mono- and di-glycerides which are present as monomers and polymers. The data show, however, that having reached a maximum value of approximately 2.5, the viscosity of these first fractions extracted with *n*-propyl alcohol tends to become constant. This may be interpreted to mean that a diglyceride dimer may polymerize with a triglyceride monomer, and thus as a consequence of its lowered polarity become insoluble in *n*-propyl alcohol. An equilibrium may therefore be established between the constantly forming, soluble diglyceride dimers and the higher mixed di- and tri-glyceride polymers which are assumed to be insoluble in the *n*-propyl alcohol. A detailed quantitative study of this phenomenon is being made.

Having discussed both the molecular weight and viscosity aspects of the heat-polymerization process independently of each other, attention will now be directed to the relationship between them.

## 2. Absolute viscosity-molecular weight relationship

Dunstan (14) indicated that for a series of polymers, the members of which differ only in length of chain, the number-average molecular weight is an approximate first-power linear function of the  $\log$  of the absolute viscosity. This was subsequently shown to be incorrect, and Flory (17) in a subsequent paper showed that for linear polymers if the half-power of the weight-average molecular weight were used instead, the linearity was greatly improved.

In the present work the weight-average molecular weight was not convenient to calculate by the Flory equation (17), because of the heterogeneity of the oil polymer systems used; hence the more easily determined cryoscopic number-average value was used instead. In general, for the data presented here on the fractionated samples, it may be said that a considerable degree of linearity exists when the absolute viscosity is plotted against the half-power of the number-average molecular weight. This is particularly true for the lower region of polymer growth, where the molecular-weight determinations are experimentally significant. The statement of Adams and Powers (2) that they were unable to obtain a linear relationship between the logarithm of the viscosity and the half-power of the molecular weight may be attributed to the fact that they worked with unfractionated heat-polymerized oil samples.

Figures 2 to 13 give the relationship for the linseed and soybean heat-polymerized oil samples on the basis of the individual molecular weight and absolute viscosity values of the extracted fractions constituting the samples. These are divided into two groups: the first (figures 2, 3, 4, 5, 6, and 7) where the first power of the number-average molecular weight was used, and the second (figures 8, 9, 10, 11, 12, and 13) where the half-power was employed.

Since the  $\log$  of the highest viscosity encountered in any of the extracted fractions was approximately 3.30, the curves in the first group of figures were extra-

polated to this point. The molecular weights of fractions extracted above *n*-amyl alcohol were then read from the extrapolated curve.

It is of considerable interest that the slope of the line representing the absolute viscosity-(molecular weight)<sup>1</sup> relationship is, with one exception, practically identical for all of the fractionated samples, this being in the range of 1.570 to 1.601.

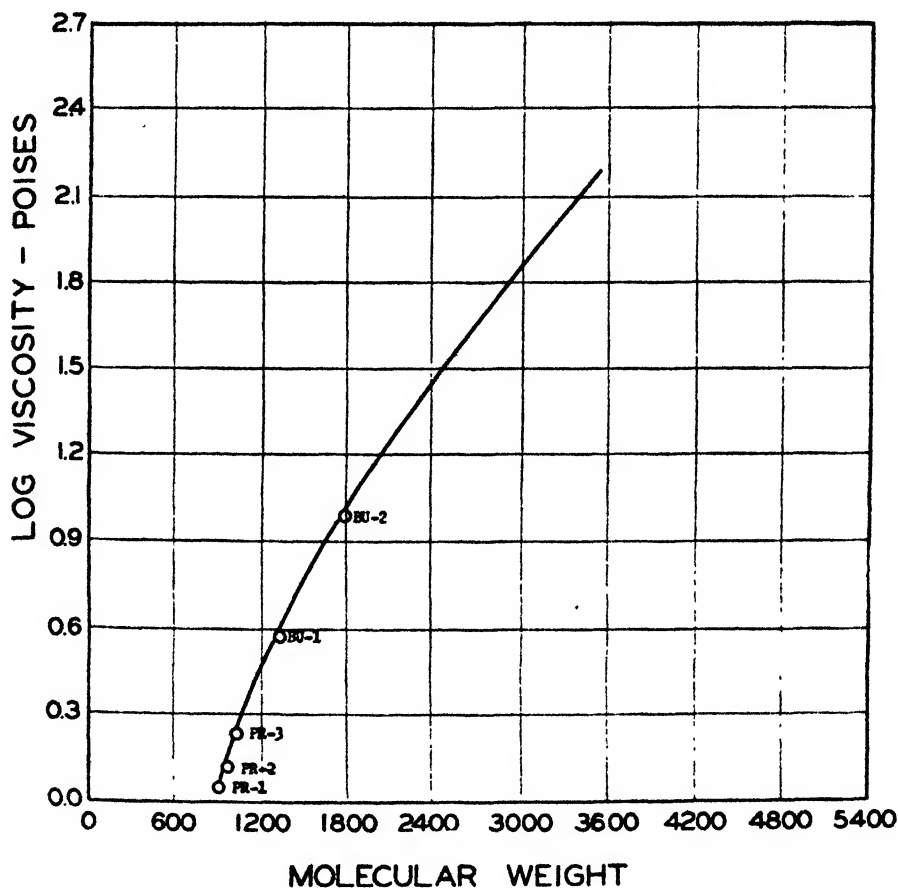


FIG. 2. Monomer-polymer fractionation. (26°C.), with homologous series of normal monohydric alcohols, of linseed oil heat-polymerized for 1 hr. at 307°C.

The single exception is the fractionated 10-hr. reacted linseed oil sample which has a slope of 2.904.

#### D. Iodine value

The heat-polymerization is much more difficult to follow from the viewpoint of decrease in iodine value of the various fractions removed from the oil samples. In the main, this difficulty is concerned with the heterogeneity of unsaturation which exists in the original unbodied oils, which means that both the reactants and the products of the reaction may have varying iodine values for the same molecular species. There is, moreover, another difficulty, that of colloidal floc-



ulation previously referred to, which renders the application of the Wijs method to the determination of the unsaturation in the higher polymers of dubious value. This phenomenon is indicative of the lack of molecularity in the solutions of these higher polymer fractions, and is the counterpart of the difficulty encountered with the determination of their molecular weights. The result of this situation

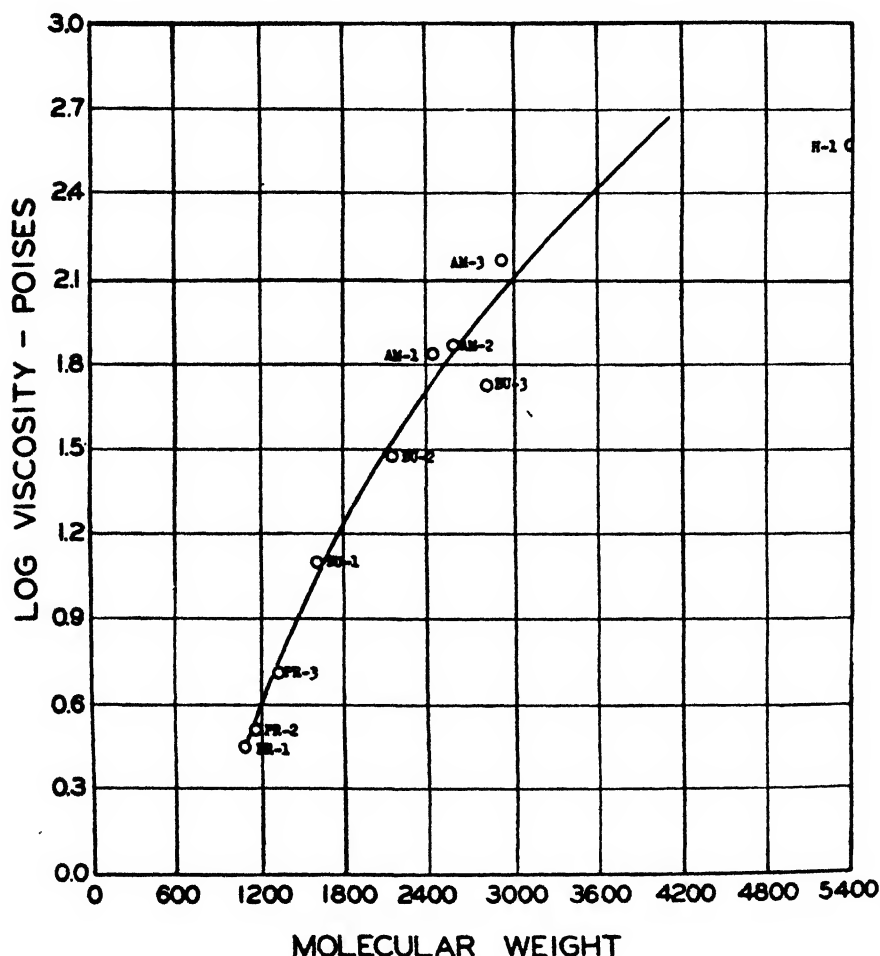


FIG. 3. Monomer-polymer fractionation (26°C.), with homologous series of normal monohydric alcohols, of linseed oil heat-polymerized for 6 hr. at 307°C.

is that the Wijs values for the later removed heat-polymerized oil samples containing these higher polymeric fractions are much too low, and that the magnitude of the attendant decrease is therefore entirely out of line with that for the earlier fractions in which the monomers and lower polymers predominate. Despite the obstacles it is nevertheless of exceeding interest to attempt the task of interpreting the data on iodine value because of the insight it affords in understanding the mechanism of the polymerization reaction.

1. Experimental evidence on the comparative polymerization reactivities of the various monomers present

It was stated in the previous paper in this series (6) that on the basis of the distribution analysis procedure described therein, the monomers present in the unbodied non-conjugated vegetable oils could be classified first, in accordance

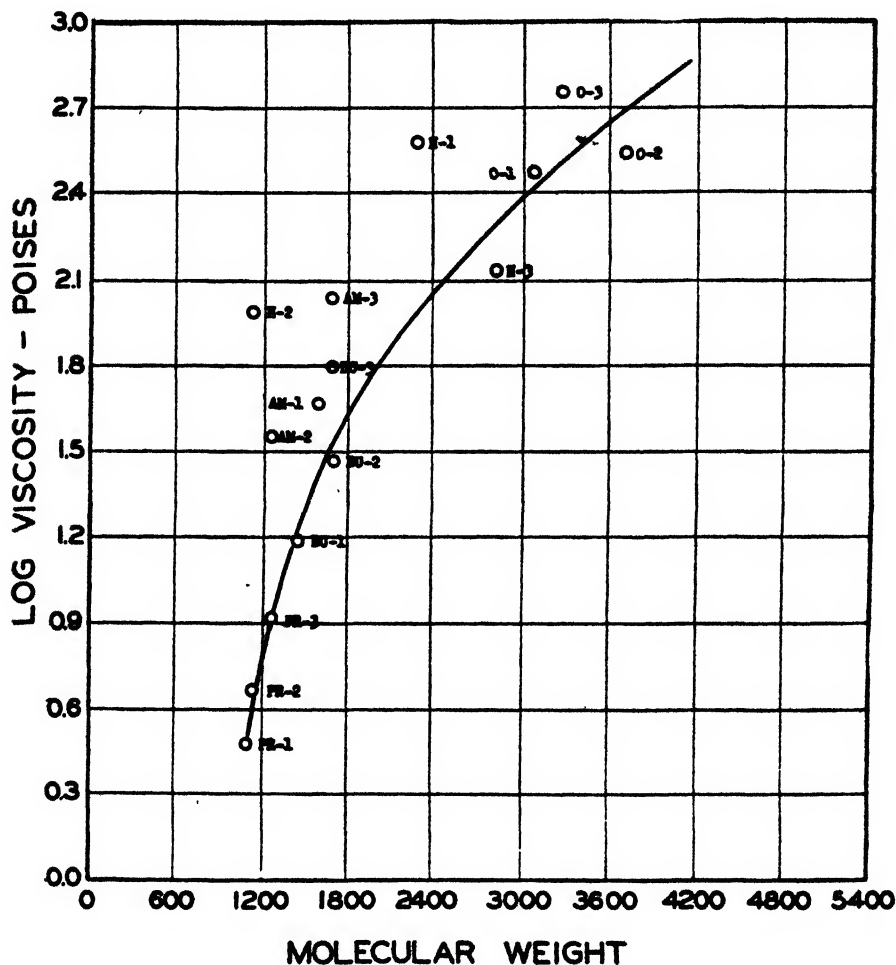


FIG. 4. Monomer-polymer fractionation (28°C.), with homologous series of normal monohydric alcohols, of linseed oil heat-polymerized for 10 hr. at 307°C.

with their *partial randomly constituted fatty acid component composition*, and secondly, with respect to their polymerization potentiality. According to this classification, the first of the monomers to polymerize would be the most highly unsaturated ones belonging to the first reactivity group. There are two theoretical consequences of these postulates: (1) that the iodine value of the remaining monomers at the latter stages of the polymerization should be at or near the

lower limit of the theoretically calculated unsaturation, and (2) that at the intermediate stages of the polymerization for the particular oil system in question, the iodine values of the remaining monomers should be between this lower limit and the upper one representing the average of the monomers initially present. For linseed and soybean oils the upper limits are obviously the initial iodine values of

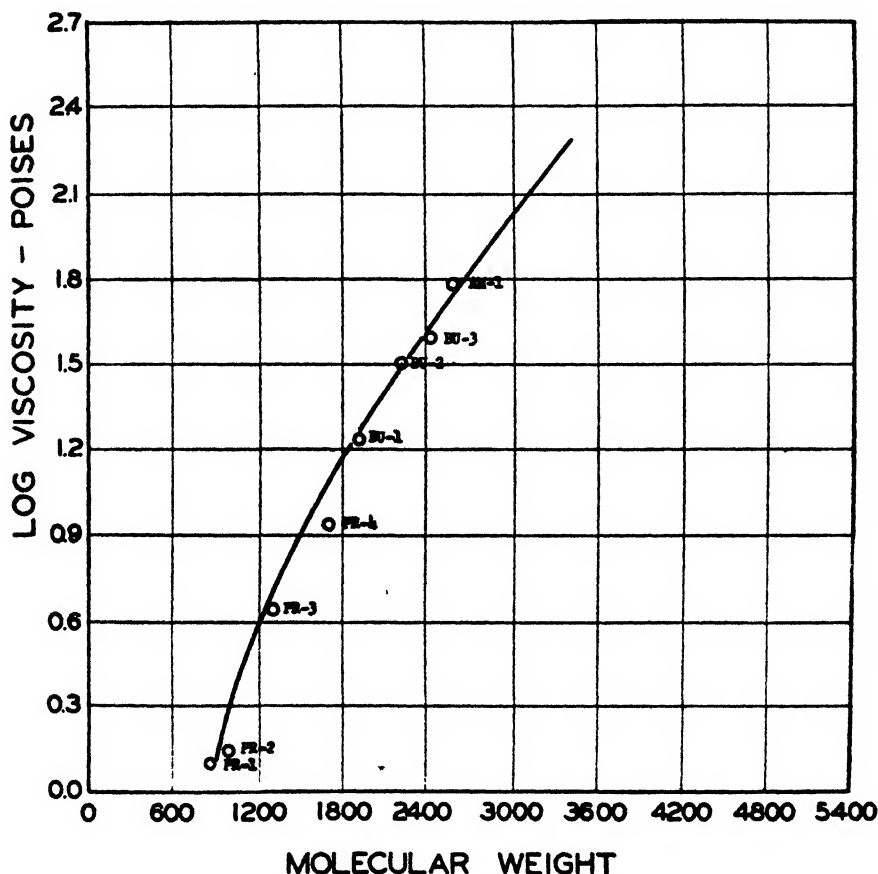


FIG. 5. Monomer-polymer fractionation (26°C.), with homologous series of normal monohydric alcohols, of soybean oil heat-polymerized for 5 hr. at 307°C.

the oils themselves,—namely, 180.1 and 140.7, respectively, whereas the lower limits of unsaturation should be theoretically represented by the base forms



respectively, for which the respective calculated iodine values are 115.8 and 68.8.

If the theory based on distribution analysis and polymerization potentiality is a satisfactory explanation of the experimental evidence, the data should conform to the following two requirements: first, that there shall be a qualitative decrease

in iodine value of the remaining monomers as a function of the time of polymerization, and second, that there shall be a quantitative correspondence of the iodine value of the monomers remaining after gelation with the theoretical values given above of 115.8 and 86.8, respectively, for the two oils.

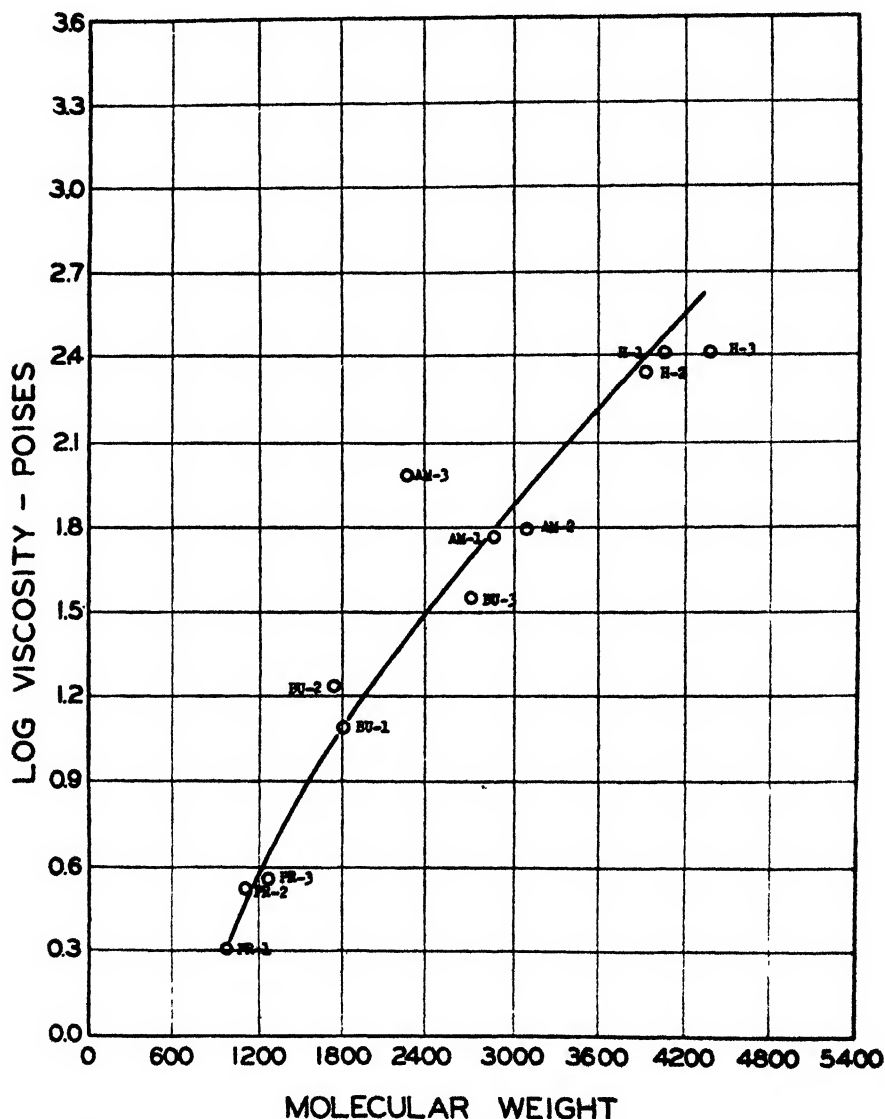


FIG. 6. Monomer-polymer fractionation (26°C.), with homologous series of normal monohydric alcohols, of soybean oil heat-polymerized for 12 hr. at 307°C.

If one assumes as a first approximation that the monomers are concentrated in the first *n*-propyl alcohol extracted fractions and that the iodine value of these fractions represents substantially the average of those of the monomers, the data

given in tables 18 and 19 for heat-polymerized linseed and soybean oils furnish the required evidence, both qualitative and quantitative.

The correspondence of the above data to the postulated requirements of the theory is, of course, evident; not only does the necessary qualitative relationship exist of progressively decreasing iodine value for the monomers remaining at the

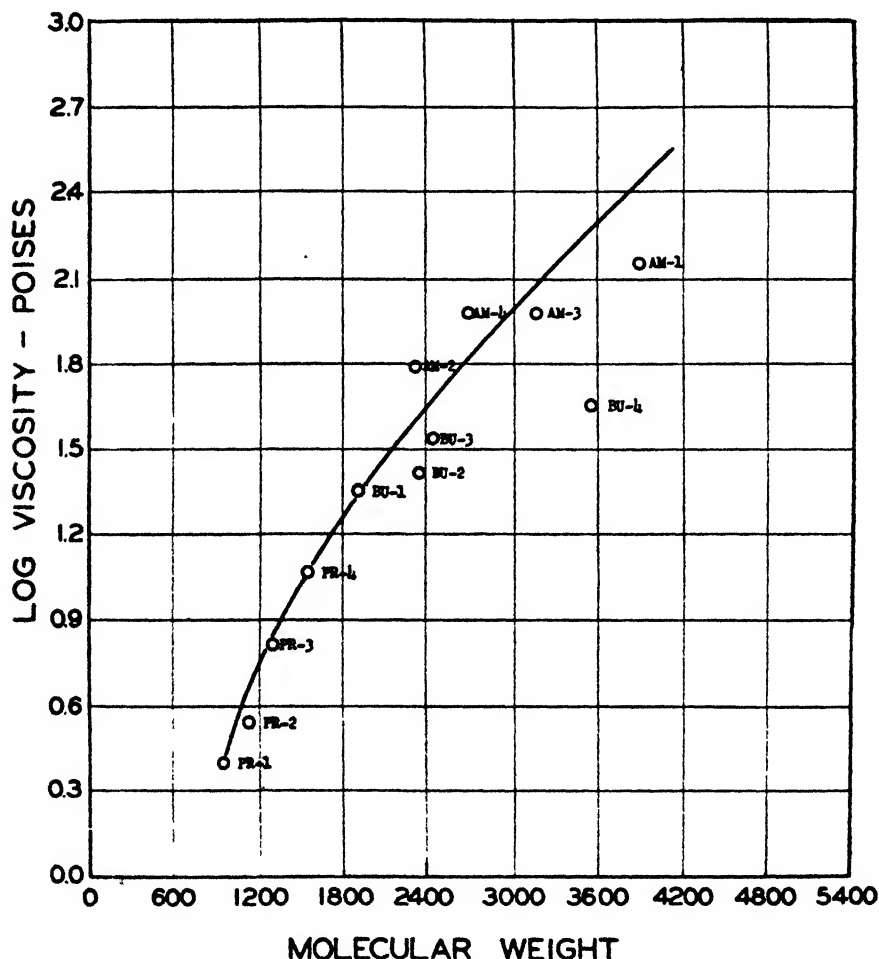


FIG. 7. Monomer-polymer fractionation (26°C.), with homologous series of normal monohydric alcohols, of soybean oil heat-polymerized for 17 hr. at 337°C.

successive stages of the polymerization, but even more important is the quantitative correspondence of the experimental iodine value lower limits of 113.3 and 88.7, respectively, for the monomers of linseed and soybean oils remaining in the gels with their theoretically calculated values of 115.8 and 86.8.

In contrast to the above excellent agreement, that for the polymers higher than the dimers is disappointing. An account will now be given of the interpretation of the data on iodine values for the polymers in general, which will be followed by that for dimers specifically.

## 2. Iodine value decrease as a function of the previous history of specific polymer size

As the polymerization reaction proceeds, utilizing more and more double bonds, one should find a progressive decrease in iodine value with increasing polymer size. This relationship for the non-conjugated vegetable oils is a complex one,

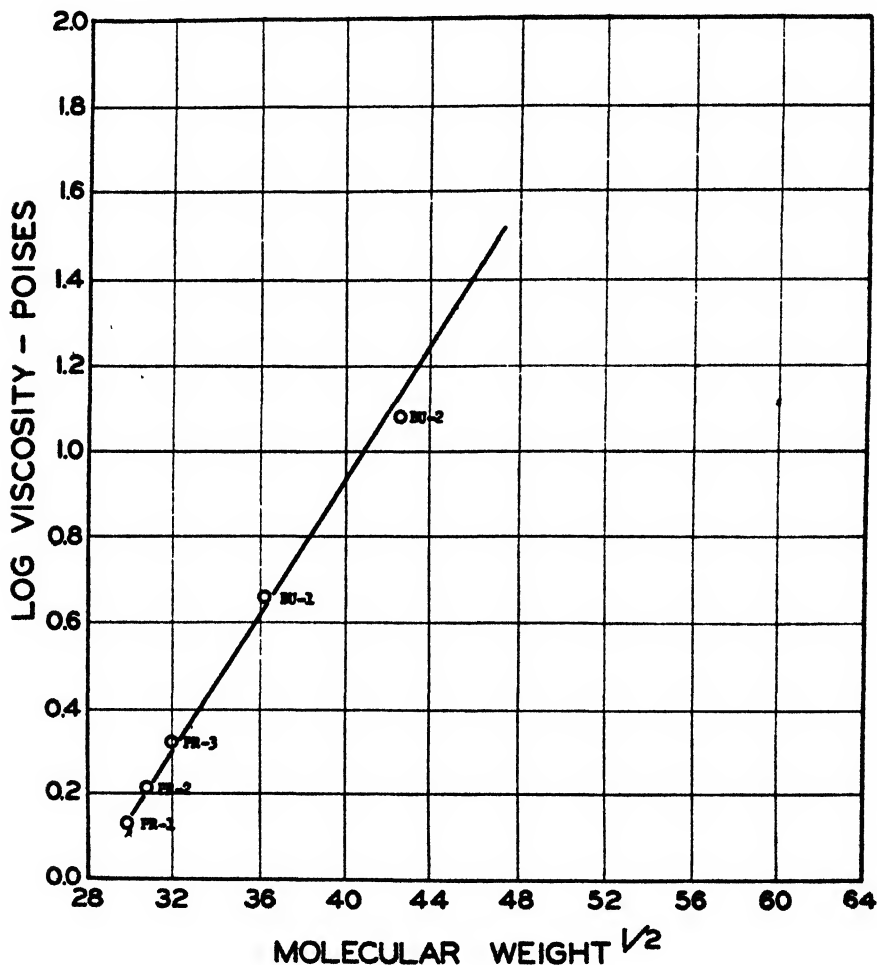


FIG. 8. Monomer-polymer fractionation (26°C.), with homologous series of normal monohydric alcohols, of linseed oil heat-polymerized for 1 hr. at 307°C.

two factors of which merit some discussion. The first has to do with the normal decrease in iodine value on polymerization for any particular level of unsaturation originally existing in the heterogeneous monomer oil system, while the second factor is concerned with the fact that as the level of unsaturation of the monomers decreases, the iodine value of the polymers ensuing from them should likewise be lower for any specific polymer size.

With regard to the first factor, this should evidence itself experimentally in a progressive decrease in iodine value of the polymers issuing from those monomers constituting the first reactivity group, which polymers are the first to attain the

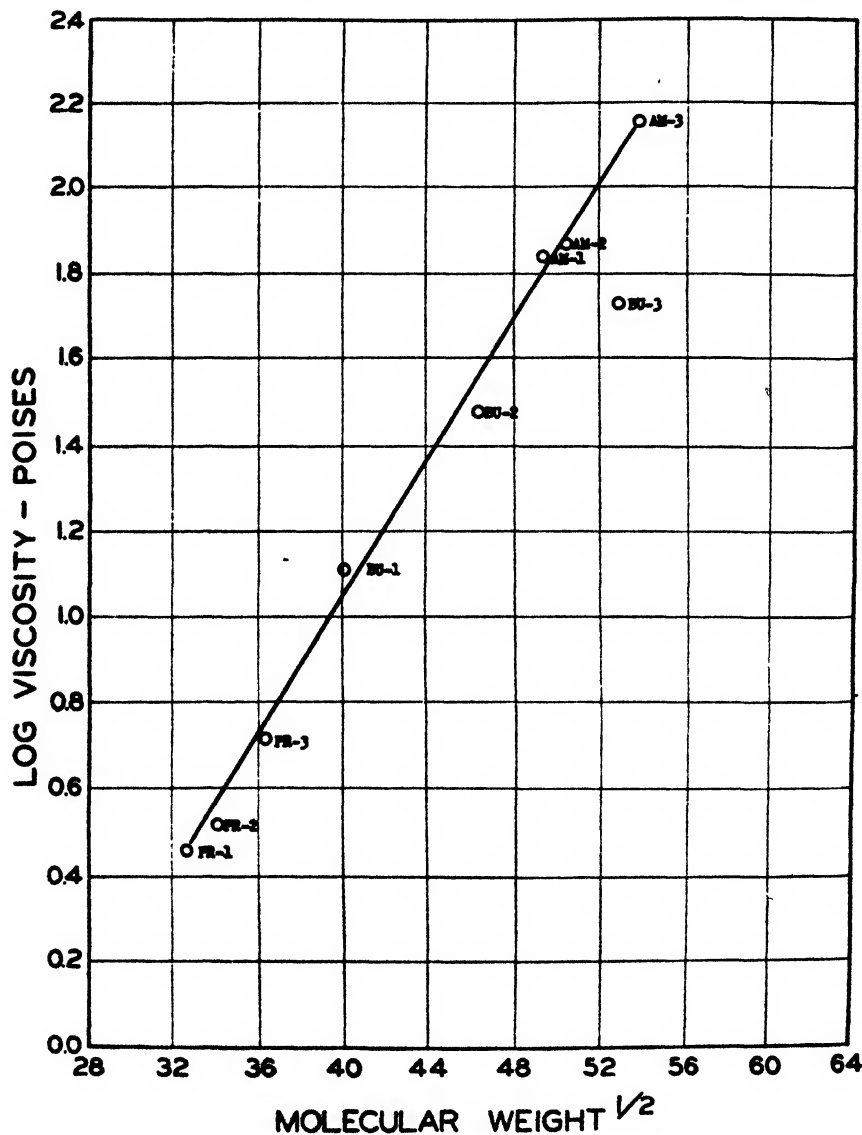


FIG. 9. Monomer-polymer fractionation (26°C.), with homologous series of normal monohydric alcohols, of linseed oil heat-polymerized for 6 hr. at 307°C.

extent of growth approaching that required for the formation of the insoluble cross-linked polymers and the onset of gelation. According to the method of theoretical calculations given in a previous paper (6) for an average linseed oil

sample, the average iodine value of all heat-polymerized linear and branched pentamers formed from the monomers of the first reactivity group is 141. This is considerably higher than the experimental iodine value of 83.3 for the fraction

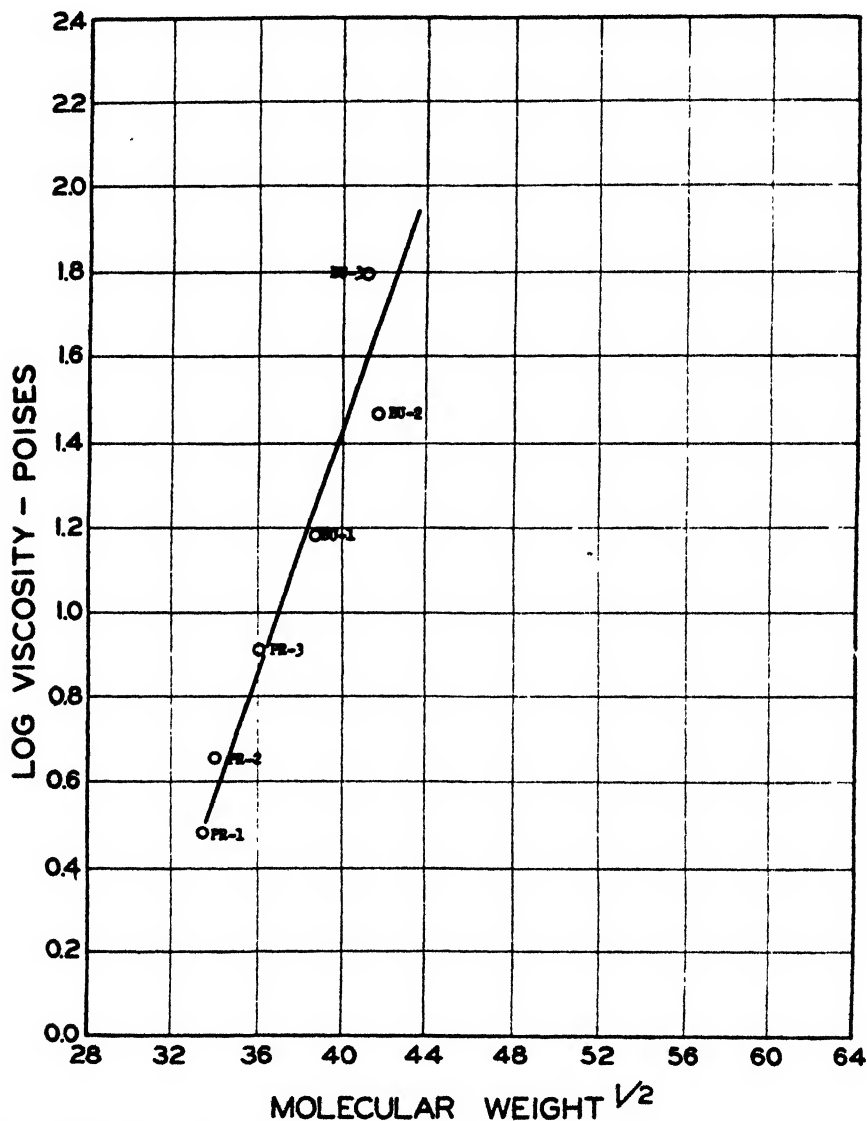


FIG. 10. Monomer-polymer fractionation (26°C.), with homologous series of normal monohydric alcohols, of linseed oil heat-polymerized for 10 hr. at 307°C.

extracted with *n*-dodecyl alcohol from an 8-hr. heat-polymerized linseed oil sample and is the consequence of the inapplicability of the Wijs method to the determination of unsaturation in these higher polymers. Since the experimental



iodine values of the higher polymeric fractions are without significance, one may inquire whether the correspondence between the theoretical and experimental iodine values is better at the lowest stage of polymer growth, that of dimerization. Because of the heterogeneity of monomers present, tending to form dimers from the various reactivity groups, it is impossible to do this for any single monomer.

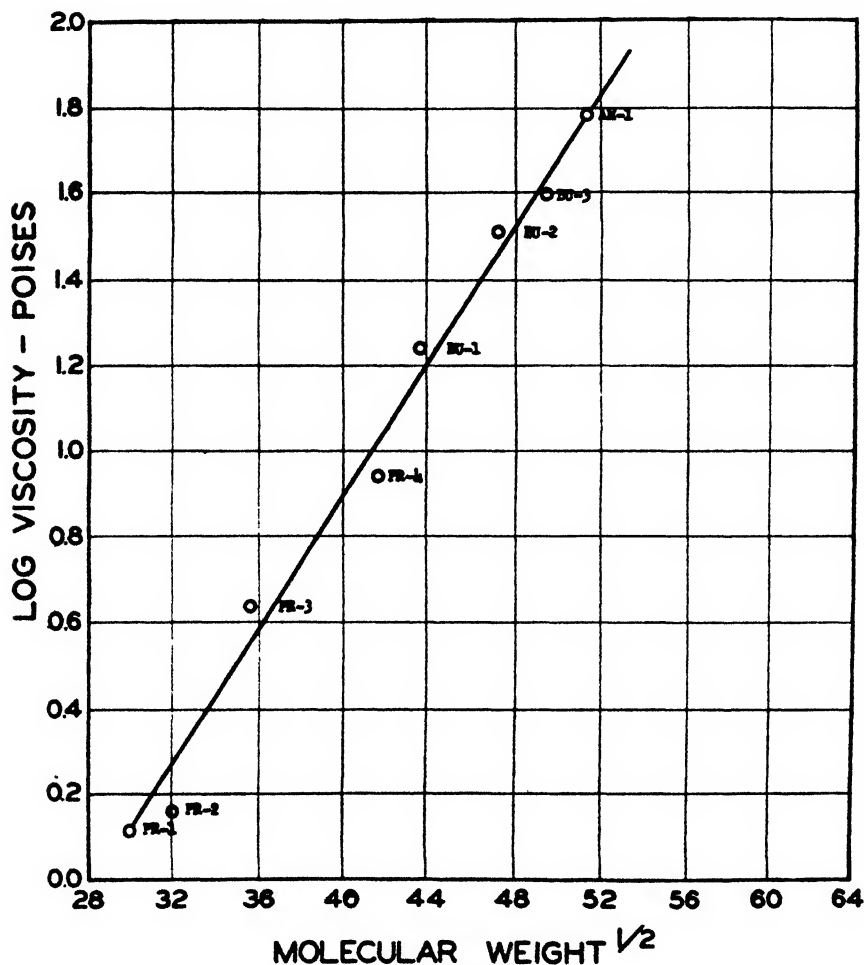


FIG. 11. Monomer-polymer fractionation (26°C.), with homologous series of normal monohydric alcohols, of soybean oil heat-polymerized for 5 hr. at 307°C.

This impasse leads to the possibility of interpreting the data on an averaging basis. This is related to the second factor mentioned,—the theoretical correspondence of the decrease in iodine value of the monomers to that of the dimers formed from them. As will subsequently be shown, the average of the experimentally determined iodine values on dimerization is in reasonable agreement with the theoretically calculated average.

This second factor is illustrated by the data in tables 20 and 21, and shows that at successive stages of the heat-polymerization of linseed and soybean oils the decreasing iodine value of the dimer fractions qualitatively follows that of the

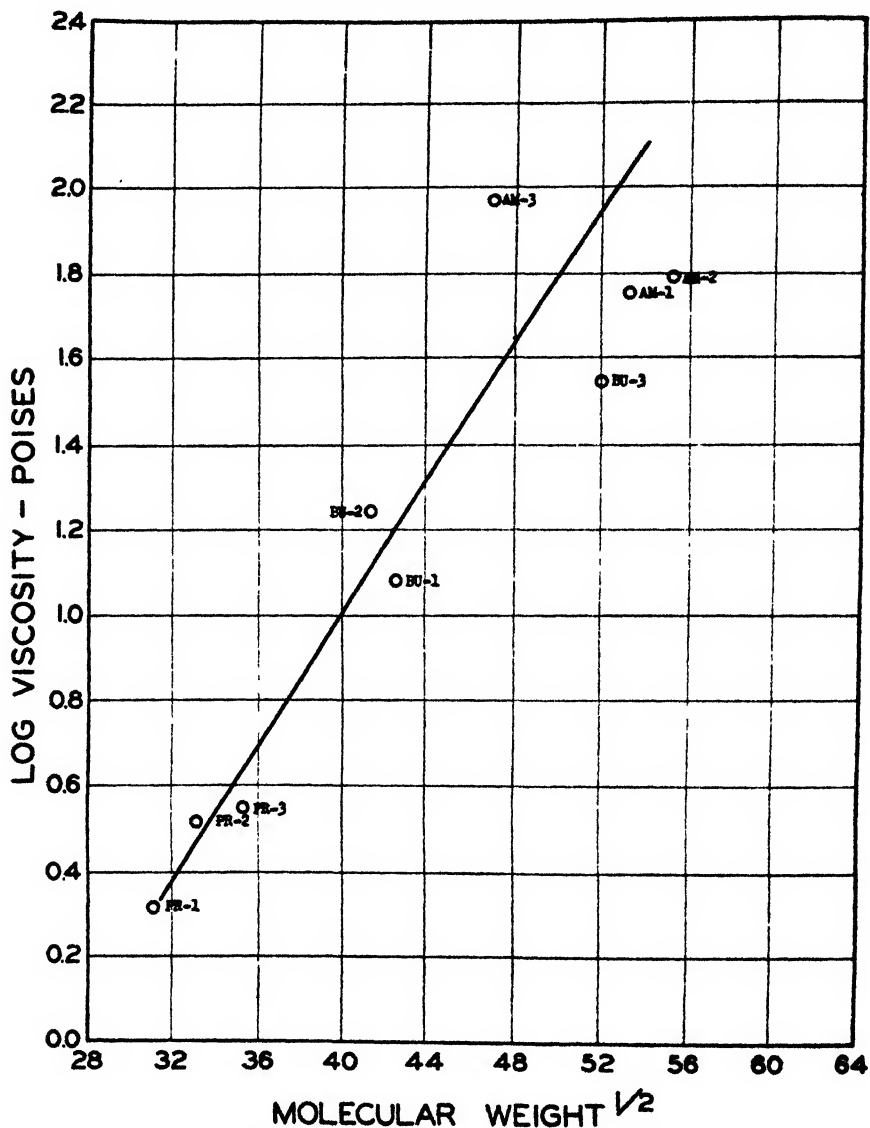


FIG. 12. Monomer-polymer fractionation (26°C.), with homologous series of normal monohydric alcohols, of soybean oil heat-polymerized for 12 hr. at 307°C.

monomers. It is, of course, obvious that the particular dimers for which the iodine values are given were not formed from the monomers listed but rather from the monomers immediately preceding them and possessing a slightly higher stage

of unsaturation. Nevertheless, even with this limitation, the qualitative correspondence is excellent.

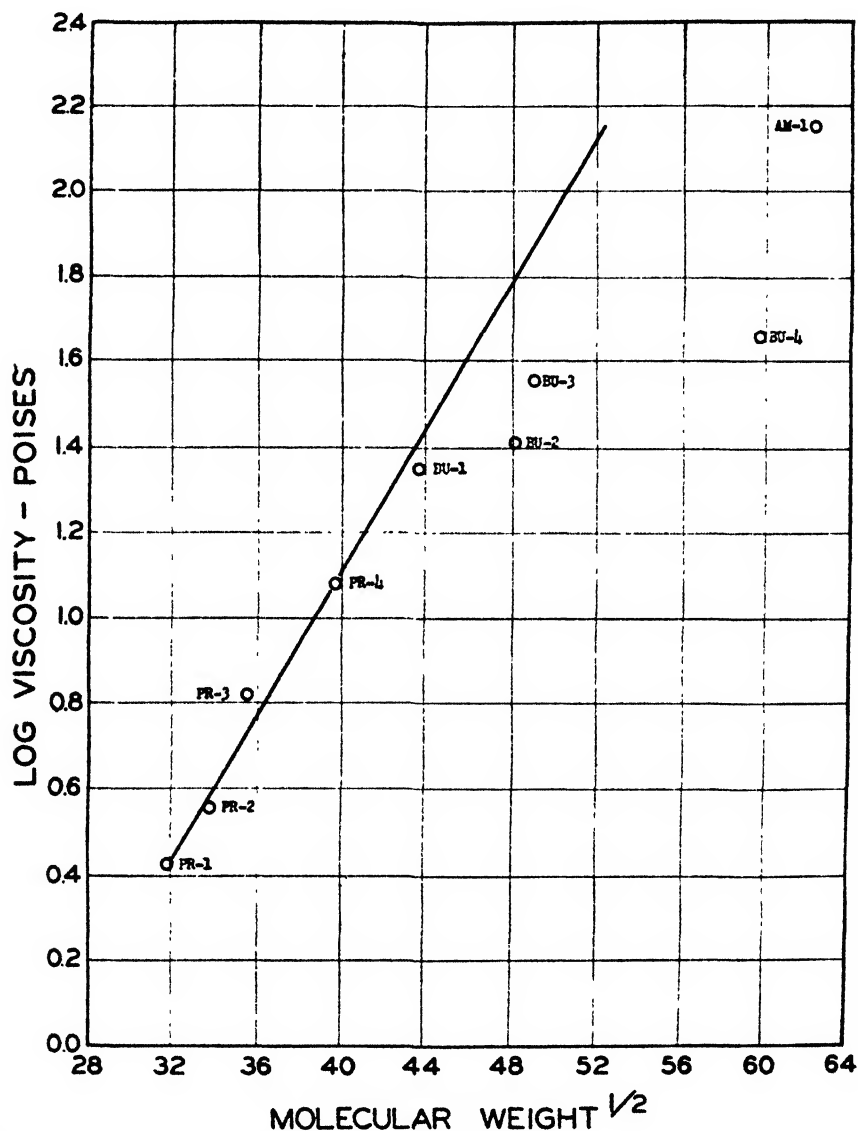


FIG. 13. Monomer-polymer fractionation (26°C.), with homologous series of normal monohydric alcohols, of soybean oil heat-polymerized for 17 hr. at 307°C.

The theoretically calculated possibilities of iodine value on dimerization for  
linseed oil range from a maximum of 188 for the reaction of two Le monomers  
Lo

of the first reactivity group to that of a minimum of 73 for the dimerization of  
Sa  
two Le monomers of the third reactivity group. Similarly for soybean oil the  
Ol

Lo  
range in iodine value on dimerization is from 159 for the reaction of two Le mono-  
Lo  
Lo  
mers of the first reactivity group to 87 for the dimerization of two Lo monomers  
Sa

TABLE 18

*Iodine value of the first n-propyl alcohol extracted fractions as a function of time  
of polymerization*

Heat-polymerized linseed oil (307°C.)

HOURS AT 307°C.	WIJS IODINE VALUE (60 MIN.)
(Original unbodied oil)	180.1
0 (on reaching 307°C.)	177.4
1	161.4
2	145.9
4	129.0
6	125.3
7	121.3
8	122.0
10	119.2
12	113.3

TABLE 19

*Iodine values of first n-propyl alcohol extracted fractions as a function of time of polymerization*

Heat-polymerized soybean oil (307°C.)

HOURS AT 307°C.	WIJS IODINE VALUE (60 MIN.)
(Original unbodied oil)	140.7
1	120.6
5	120.3
8	111.7
12	103.5
14	101.3
17	95.5
18 (liquid fraction of gel)	88.7

of the second reactivity group. It is clear that some weighted averages of these calculated values are in reasonable correspondence, in a qualitative sense, with the experimental iodine values on dimerization as given in the previous tables.

In addition to the above qualitative use of the experimental dimerization iodine value data, they may be further used from a quantitative point of view for the

express purpose of testing the correctness of the basic theoretical assumption proposed in a previous paper (5) as to the number of double bonds involved per oil molecule in any single addition-polymerization reaction between two monomer or polymer units. According to this theory it was postulated that two double bonds per oil molecule were consumed when the fatty acid component involved in the stepwise polymerization reaction was linolenic, and but one when the reacting fatty acid component was either linolic or oleic.

TABLE 20

*Decreasing iodine value of fractions of heat-polymerized linseed oil essentially dimeric at successive stages of their formation*

TIME AT 307°C.	SPECIFIC EXTRACTED FRACTION	APPROXIMATE MOLECULAR SPECIES DISTRIBUTION	WIJS IODINE VALUE (60 MIN.)	IODINE VALUE OF FIRST <i>n</i> -PROPYL ALCOHOL EXTRACTED FRACTION (ESSENTIALLY MONOMERIC)
<i>hours</i>		<i>weight per cent</i>		
1	BU-2	98% dimer-2% trimer	135.3	161.4
4	BU-1	90% dimer-10% monomer	124.0	129.0
6	BU-1	84% dimer-16% monomer	121.2	125.3
7	BU-1	88% dimer-12% monomer	120.4	121.3
8	BU-1	94% dimer-6% monomer	120.0	122.0

TABLE 21

*Decreasing iodine value of fractions of heat-polymerized soybean oil essentially dimeric at successive stages of their formation*

TIME AT 307°C.	SPECIFIC EXTRACTED FRACTION	APPROXIMATE MOLECULAR SPECIES DISTRIBUTION	WIJS IODINE VALUE (60 MIN.)	IODINE VALUE OF FIRST <i>n</i> -PROPYL ALCOHOL EXTRACTED FRACTION (ESSENTIALLY MONOMERIC)
<i>hours</i>		<i>weight per cent</i>		
5	PR-4	96% dimer-4% monomer	113.2	120.3
8	BU-1	95% dimer-5% monomer	106.8	111.7
12	BU-1	97% dimer-3% monomer	100.9	103.5
14	BU-1	90% dimer-10% monomer	98.9	101.3

### 3. Calculation of iodine value decrease on average dimerization for heat-polymerized linseed and soybean oils

This discussion will obviously be restricted to that of dimerization, but it will not, however, be restricted to a single species of monomer and dimer ensuing from it, since in this study this is not possible. The inquiry will rather be on the basis of the average decrease in iodine value on average dimerization. This is a particularly apt approach, since the iodine values of the unbody oils are themselves average values of all the monomers initially present and represent the various degrees of unsaturation. It would appear therefore, as a first approximation, that the difference in iodine values between the average of that of the monomers and of a representative group of the dimers should provide an adequate test of

the theoretical requirement for decrease in iodine value on dimerization for the two oils. This is predicated on an equal weighting of the iodine values of the essentially dimeric fractions, which is a fair assumption. Since in linseed oil the dominant fatty acid component is linolenic acid and in soybean oil linolic acid, these two oils should on dimerization give, if the theory is correct, a decrease in iodine value equivalent to slightly less than two double bonds per oil molecule for linseed oil, because its minor unsaturated fatty acid components are linolic and oleic, and somewhat more than one double bond per oil molecule for soybean oil, because its minor unsaturated fatty acid components are linolenic and oleic.

The average of the experimental dimerization iodine values given in tables 20 and 21 is 124.2 and 105.0, respectively, for linseed and soybean oils of the particular fatty acid component compositions specified in the previous paper (6). Since the average iodine value of the monomers of the two oils is that of the unbodied oils themselves—namely, 180.1 and 140.7—we can obtain by subtraction the average decreases in iodine value on dimerization, which are therefore 55.9 and 35.8 for linseed and soybean oils, respectively.

The above experimental average decreases in iodine value on dimerization for the two oils are related not only to their major fatty acid components with which we are primarily concerned, but to their minor fatty acid components as well, and it is therefore necessary to correct for the minor fatty acid components entering into the dimerization reaction. After these corrections are made, the experimental average decreases in iodine value on dimerization for the two oils, corresponding to the number of double bonds involved, will be ready for comparison with the theoretically postulated values.

#### 4. Correction for linolic and oleic reacting components in theoretical decrease in iodine value of linseed oil on dimerization

The minor fatty acid component correction for linseed oil was made on the basis of the percentage of possible reactions for a linolic and oleic component out of the total possible reactions for each of the five LC groups (6).

The results show that out of the 63 molecules constituting a distribution analysis 11 per cent will react on the basis of the minor linolic and oleic acid components, leaving 89 per cent of the monomers to react through linolenic acid components.

In a previous paper (5) theoretical calculations were made which indicated that on dimerization, or any other single step of heat-polymerization of the non-conjugated vegetable oils, there occurs a decrease in iodine value of 28.94 for each double bond per oil molecule involved in the reaction. This is contrary to the claim of Adams and Powers (1) that in the heat-polymerization of linseed oil the loss of one double bond is equivalent to a drop of 86.6 in iodine value. This would imply in a reacting triglyceride monomer the loss of three double bonds instead of one or two and hence can be ruled out. Therefore, for a linolenic reacting component involving, according to the present author's hypothesis, two double bonds per oil molecule, the decrease in iodine value would be  $2(28.94)$

or 57.88. Solving for the iodine value decrease on the basis of the relative percentages reacting through linolenic and (linolic and oleic) components we have

$$0.89(57.88) + 0.11(28.94) = 54.7$$

which is the theoretically calculated decrease in iodine value, based on the author's postulates, on dimerization of a specific linseed oil corrected for reactivity by its linolic and oleic acid components.

5. Correction for linolenic reacting component in theoretical decrease  
in iodine value of soybean oil on dimerization

The correction for soybean oil was made on the same basis as for linseed oil with the exception that the only reacting minor fatty acid component to be corrected for is the two-double-bond reacting linolenic acid component.

The results show that of the 64 molecules constituting a distribution analysis 9.5 per cent will react on the basis of the minor linolenic acid component, leaving 90.5 per cent of the monomers to react through linolic and oleic acid components. Solving for the iodine value decrease on the basis of the relative percentages involved:

$$0.905(28.94) + 0.095(57.88) = 31.7$$

which is the theoretically calculated decrease in the iodine value, based on the author's postulates, of a specific soybean oil upon dimerization, corrected for reactivity by its linolenic components.

The excellent correspondence between the above theoretically calculated decreases in iodine value, namely, 54.7 and 31.7 for dimerized linseed and soybean oil, respectively, and the respective average experimental values of 55.8 and 35.8 is of course of considerable interest. It represents a direct confirmation of the postulated requirements of two and one double bond per oil molecule for linolenic and linolic polymerization reactivity, respectively.

The above comparative experimental reaction rates of the more unsaturated monomers in the two oils through their various stages of heat-polymerization up to and including that of gelation may be accounted for, and in fact predicted, as a consequence of the postulate given in the previous paper in this series (6). This states that on the basis of the *cis-trans* geometric isomerism for the major fatty acid components of the two oils, the reactivity of a linolenic component of the most probably reactive *cis-cis-cis* form is twice that for the most probably reactive *cis-trans* or *trans-cis* forms of a linolic component.

The above agreement, while pointing quite clearly to the essential correctness of the theory presented, must nevertheless not be taken as proof. The fractional separations of dimers from heat-polymerized pure linolenic triglyceride and pure linolic triglyceride will provide the required rigorous proof. Work on this specific problem is contemplated.

## V. MOLECULAR SPECIES-WEIGHT PERCENTAGE DISTRIBUTION

As previously stated, one of the objectives of this paper was to arrive at some basis for quantitatively determining not only the various monomer weight percentage distributions as a means of following the course of the polymerization reaction, but the distribution of the specific polymers being formed as well. For the purposes of the present paper each of the above will to a certain extent be presented independently of the other, but where the general discussion necessitates their being considered together the term *molecular species-weight percentage distribution* will be used instead. As a first approximation it is necessary to make the assumption that for a given molecular weight only two species are present in any single extracted fraction,—namely, the immediate lower and upper stepwise limits. The exceptions to this, of course, are the *n*-propyl alcohol extracted fractions, since in these the free fatty acids constitute a third species. Since correction for these has already been made, all fractions will be treated on the basis of the assumption of two molecular species.

*A. Basis for computing total molecular species-weight percentage distribution of heat-polymerized linseed and soybean oil samples*

Since several extractions were made with each of the alcohols used, it was necessary to summarize the entire content of monomers, dimers, trimers, etc. from the results of the individual extracted fractions in order to arrive at the molecular species distribution present in the oil sample being fractionated. This was accomplished by multiplying the weight of each extracted fraction by its particular species percentage distribution, adding up all the individual species contributions, and specifying them as monomers, dimers, trimers, etc. This could not be done in the regular fractionation series for polymers higher than the dimer, because of the secondary gelation difficulty encountered, and it was therefore necessary to lump together the trimers and polymers higher than the trimers in evaluating the polymer growth for this series. It should be stated, however, that in the cases where the secondary gelation was eliminated, fairly complete molecular species-percentage weight distributions were worked out. These are given in detail in tables 22 and 23. For the regular series of fractionations, however, the total molecular species distributions are given in tables 24 and 25 on the basis already mentioned. From the quantitative information so obtained considerable insight was had as to the changes occurring during the polymerization process, from its initial stage to the end gel product.

It is interesting to note in general the main features of tables 24 and 25: the progressively decreasing weight percentages of monomers, the constancy of the weight percentages of dimers except for the marked decrease near the end of the reaction when gelation is imminent, and the progressive increase in weight percentages of trimers and polymers higher than trimers for the two oils with increasing time of polymerization. This latter point is indicated in the values of 16.3 and 5 per cent after 4 and 5 hr., respectively, at the reaction temperature for linseed and soybean oil in the order named, as against values of 43.7 per cent and 21.5 per cent after 8 hr. for each of the two oils.



TABLE 22

*Molecular species fractionation (4°C.), with homologous series of normal monohydric alcohols, of linseed oil (76-g. sample + 0.1 per cent hydroquinone) heat-polymerized for 8 hr. at 307°C.*

NORMAL ALCOHOL EXTRACTIONS	FREE FATTY ACIDS	MONO- MER	DIMERS	TRIMERS	TETRA- MERS	PENTA- MERS	HEXA- MERS	HEPTA- MERS	UNFRACTIONATED REMAINDER (BY DIFFERENCE)
	grams	grams	grams	grams	grams	grams	grams	grams	grams
PR-1.....	1.79	10.75	0.21						
PR-2.....	0.24	4.00	0.76						
PR-3.....	0.08	2.32	0.60						
PR-4.....	0.03	1.64	0.58						
BU-1.....		0.94	1.81						
BU-2..		0.38	1.37						
BU-3..		0.19	1.31						
BU-4..			1.07	0.18					
AM-1		0.39	2.36						
AM-2			0.96	0.79					
AM-3			0.13	2.12					
AM-4				0.40	0.60				
H-1				0.75	1.50				
H-2				0.68	1.32				
H-3				0.50	1.00				
H-4					0.83	0.42			
O-1				0.50	2.00				
O-2				0.38	0.87				
O-3					0.25	0.50			
O-4					0.18	0.57			
D-1					0.46	2.29			
D-2					0.56	1.69			
D-3						0.25	1.25		
D-4							1.00	0.25	
DD-1						1.25	3.75		
DD-2						0.81	2.44		
DD-3						0.37	1.13		
DD-4							1.20	0.30	6.75
Total weight (grams) . . .	2.14	20.61	11.16	6.30	9.57	8.15	10.77	0.55	6.75
Total weight (per cent) . . .	2.60	27.1	14.6	8.3	12.6	11.7	14.2	0.7	8.2

*B. Decreasing weight percentages of monomers as a function of time of polymerization*

At the start of the reaction one might expect the greatest decrease in monomers, since here there are present those units possessing the highest functionality and therefore the maximum reactivity. This is particularly noticeable in the case of linseed oil. For example, at the start of the reaction—that is, in the time interval of reaching the polymerization temperature of 307°C.—a decrease of 11.1 per cent by weight of monomers occurred in contrast to the average rate

of decrease of only 3 per cent per hour after 10 hr. at the polymerization temperature. Soybean oil does not conform to this pattern at the start of the reaction, since even after 1 hr. there is practically no apparent change in the monomer

TABLE 23

*Molecular species fractionation (4°C.), with homologous series of normal monohydric alcohols, of soybean oil (75-g. sample + 0.1 per cent hydroquinone) heat-polymerized for 17 hr. at 307°C.*

NORMAL ALCOHOL EXTRACTIONS	FREE FATTY ACIDS	MONOMER	DIMERS	TRIMERS	TETRAMERS	PENTAMERS	HEXAMERS	UNFRACTIONATED REMAINDER (BY DIFFERENCE)
	grams	grams	grams	grams	grams	grams	grams	grams
PR-1.....	1.33	7.75	0.42					
PR-2.....	0.19	1.86	0.70					
PR-3.....	0.07	1.50	0.68					
PR-4.....	0.03	1.07	0.65					
BU-1.....		1.39	0.86					
BU-2.....		0.48	1.27					
BU-3.....		0.37	1.13					
BU-4.....			0.78	0.22				
AM-1.....			0.98	1.52				
AM-2.....			1.34	0.91				
AM-3.....				0.09	1.91			
AM-4.....					0.62	0.38		
H-1.....				2.00	1.00			
H-2.....				0.50	1.75			
H-3.....				0.47	0.78			
H-4.....				0.82	0.43			
O-1.....				0.65	2.60			
O-2.....				2.02	0.23			
O-3.....					1.00	0.50		
O-4.....					0.25	0.75		
D-1.....					1.00	3.00		
D-2.....				1.65	0.85			
D-3.....					0.50	0.25		
D-4.....						0.50	0.50	
DD-1.....					1.50	4.50		
DD-2.....					0.94	2.81		
DD-3.....						1.68	0.82	
DD-4.....						1.00	0.50	6.75
Total weight (grams).....	1.62	14.42	8.81	10.85	15.36	15.37	1.82	6.75
Total weight (per cent)....	2.16	19.50	11.90	14.60	20.60	20.60	2.50	9.14

content. This is probably due to the presence of residual phosphatide which, as is well known, acts as a polymerization retardant. Since the next soybean oil sample taken was after 5 hr. had elapsed, nothing can be said as to the rate

TABLE 24

*Molecular species distribution of linseed oil heat-polymerized at 307°C.*  
 Fractionation at 26°C. with homologous series of normal monohydric alcohols

TIME AT 307°C.	FREE FATTY ACIDS	MONOMERS	DIMERS	TRIMERS AND POLYMERS OF TRIMERS	INSOLUBLE CROSS-LINKED POLYMERS	AVERAGE DECREASE OF MONOMERS PER HOUR	TOTAL DECREASE OF MONOMERS
hours	weight per cent	weight per cent	weight per cent	weight per cent	weight per cent	weight per cent	weight per cent
0 (to 307°C)...	0.5	88.9	10.6	0	0	11.1	11.1
1.....	1.6	79.0	19.2	0.2	0	9.9	21.0
2.....	2.1	72.9	25.0	0	0	6.1	27.1
4.....	2.4	54.9	26.4	16.3	0	9.0	45.1
6.....	3.4	38.8	23.8	34.0	0	8.1	61.2
7.....	2.8	29.6	19.8	47.8	0	4.0	70.4
8.....	2.7	28.2	25.4	43.7	0	1.4	71.8
9.....	3.0	25.8	19.9	51.3	0	2.4	74.2
10.....	2.6	22.8	25.4	49.2	0	3.0	77.2
11 (gel)*..	2.8	23.7	6.6	36.9	30.0	+0.9	23.7 (remaining monomer)
				66.9			
Total .....							95.9

\* The gel sample was fractionated at 4°C.

TABLE 25

*Molecular species distribution of soybean oil heat-polymerized at 307°C.*  
 Fractionation at 26°C. with homologous series of normal monohydric alcohols

TIME AT 307°C.	FREE FATTY ACIDS	MONOMERS	DIMERS	TRIMERS AND POLYMERS OF TRIMERS	INSOLUBLE CROSS-LINKED POLYMERS	AVERAGE DECREASE IN MONOMERS PER HOUR	TOTAL DECREASE IN MONOMERS
hours	weight per cent	weight per cent	weight per cent	weight per cent	weight per cent	weight per cent	weight per cent
0 (to 307°C.)..	0.5	99.5	0.0	0.0	0.0	0	0.5
1.....	1.3	98.0	0.7	0.0	0	1.5	1.5
5.....	2.6	73.9	18.5	5.0	0	6.0	24.1
8.....	3.1	52.0	23.5	21.5	0	7.3	48.0
12.....	3.1	35.0	21.7	40.0	0	4.3	65.0
14.....	2.9	27.7	21.6	47.8	0	3.7	72.3
16.....	2.5	21.6	17.9	58.0	0	3.0	78.4
17.....	2.1	20.3	16.4	61.2	0	1.3	79.7
18 (gel)*.....	2.2	23.3	12.0	45.5	17.0	+3.0	23.3 (remaining monomer)
				62.5			
Total.....							103.0

\* The gel sample was fractionated at 4°C. in the presence of 0.1 per cent hydroquinone.

of decrease in the intervening time. At the 5-hr. reaction stage, however, the average weight percentage decrease is 6 per cent per hour. This then rises, following the pattern observed for linseed oil, to a maximum of 7.3 per cent after 8 hr. of polymerization. From this point on the rate diminishes, reaching a

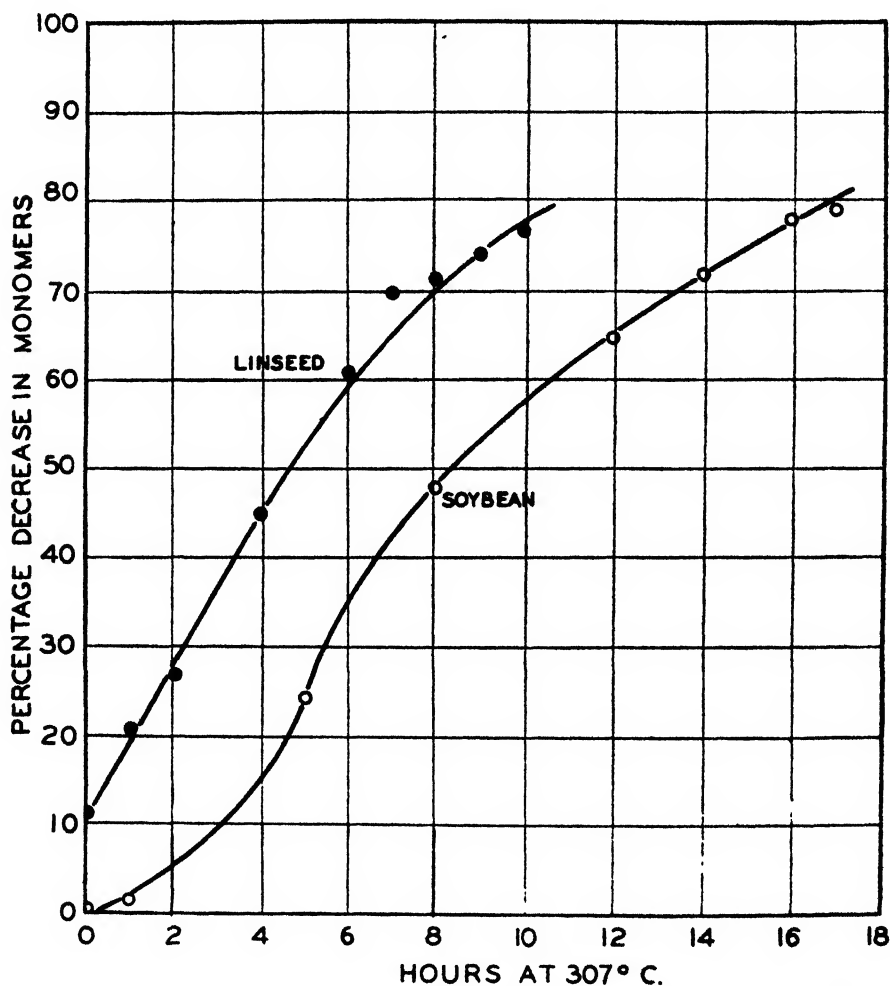


FIG. 14. Percentage decrease in monomers on heat-polymerization of linseed and soybean oils at 307°C.

minimum of 1.3 per cent after 17 hr., again conforming to the expected pattern. This information for the two oils is summarized in figure 14.

It will be noted that instead of there being a still further slight decrease in the monomer content of the liquid fraction of the separated gels of the two oils, there is, on the contrary, an unexpected slight increase. This may be interpreted to mean that the adsorption of the monomers onto the higher polymers during the polymerization had not been entirely desorbed by fractionation with the

various extractants of the homologous series of normal alcohols, but that these were desorbed by the more powerful (lower polarity) petroleum ether used in the gel separation.

One might be tempted in following the percentage decrease in monomers, to study the course of polymerization from a kinetic viewpoint and determine the order of the reaction. This has recently been done (2), but it is questionable whether the results are significant considering the heterogeneity of the system and the varying reaction rates of its component monomers.

*C. Rates of formation of dimers and higher polymers as a function of time of polymerization*

As has already been noted, the weight percentages of dimer for the two oils are fairly constant during the polymerization reaction. The rate of formation of the dimers is apparently equal to that of their disappearance. The disap-

TABLE 26  
*Decreasing rate of formation of trimers and polymers greater than trimers*

HEAT-POLYMERIZED LINSEED OIL (307°C.)		HEAT-POLYMERIZED SOYBEAN OIL (307°C.)	
Hours at 307°C.	Rate of formation in weight per cent per hour	Hours at 307°C.	Rate of formation in weight per cent per hour
6	8.9	8	5.5
8	4.9	12	4.9
10	2.8	14	3.9
		16	5.1
		17	3.2

pearance of the dimers results, of course, in the progressive appearance of trimers and polymers greater than trimers. Since the functionality of the entire system with respect to monomers, dimers, and trimers progressively decreases during the course of the polymerization reaction, one would expect not only a lowered rate of decrease in monomers, but also a lowered rate of increase for the dimers and the higher polymers. The tendency in the case of the dimers cannot be noted because of the equilibrium conditions prevailing, but if the above analysis is accurate, there should be an observable decrease in the rate of formation of polymers higher than the dimers. Table 26 presents data indicating this trend for the two oils.

*D. Molecular species-weight percentage distribution at gel stage*

From tables 24 and 25 it may be seen that at the gelation stage for the two heat-polymerized oils, the percentages of monomers remaining are approximately equal, 23.7 per cent for linseed oil and 23.3 per cent for soybean oil. The percentages of insoluble, infusible, cross-linked polymers are of course different for the two oils at their gel stage, these being 30 per cent and 17 per cent, respectively, or approximately in the ratio of two to one. This may be interpreted to mean

that the rate of formation of the highest linear or branched polymers just subsequent to the formation of the insoluble cross-linked polymer matrices is also different for the two oils. If it could therefore be established, as a first approximation, that this inequality were also in the ratio of two to one, then the reason for the formation of 30 per cent and 17 per cent of insoluble cross-linked polymers for linseed and soybean oils at the gel stage would be established.

If one takes from tables 24 and 25 the data for the percentages of trimers and polymers greater than trimers of the two oils at roughly comparable stages of polymerization, i.e., after 6 and 8 hr., respectively, the values for these are 34 per cent and 21.5 per cent. Since up to this stage of the reaction the formation of the linear and branched trimers and polymers greater than trimers originated from the more highly unsaturated monomers, they would, of course, be the first to reach the required stage of growth from which the insoluble cross-linked gel matrix polymers would be formed. The weight percentages given above of 34 per cent and 21.5 per cent, respectively, for the two oils are in fact approximately those for the subsequent formation of the insoluble cross-linked polymers. On the basis of this relationship, one may be permitted to use the corresponding rate of formation of these trimers and polymers greater than trimers at the 6- and 8-hr. reaction times for the two oils, which information is given in table 26. These values of 8.9 per cent and 5.5 per cent for linseed and soybean oils, respectively, are roughly in the ratio of two to one, if allowance is made for the linolenic component of the soybean oil.

It is also of considerable interest to note the fact, as given in table 26, that the percentages of trimers and polymers greater than trimers in the liquid fraction of the gels of the two oils drops markedly from the values just previous to the occurrence of gelation. This is, of course, good experimental evidence for the formation of the insoluble, infusible, cross-linked polymers from these higher linear or branched polymers.

#### SUMMARY AND CONCLUSIONS

1. An experimental solvent-extraction technique based on the selective solvency of the members of the homologous series of normal monohydric alcohols has been developed for the fractionation of the heat-polymerized non-conjugated vegetable oils.
2. An experimental solvent-extraction technique based on the desorbing action of hexane has been developed for the quantitative separation of the insoluble, infusible, cross-linked polymers present in heat-polymerized gels of the above oils. The liquid phase of these gels, after the above separation, can then be fractionated according to the technique referred to in 1.
3. The presence of the successively forming higher polymers in these heat-polymerized oil systems has been experimentally demonstrated at all stages of the reaction.
4. A theory to account for the operation of the above solvent-extraction technique has been presented. This is based on the relative polarities of the solvents and of the monomers and liquid polymers present.

5. The concepts of specific dielectric constant and specific refractive index have been introduced as a means of better characterizing the polarities of members of a homologous series.

6. The cause of the anomalies in the determinations of molecular weight by the cryoscopic method and of the iodine value by the Wijs method has been related to non-ideality of the solutions resulting from insufficiently low polarity of the solvents used.

7. The requirement of polymerization through two double bonds or one double bond for a reacting linolenic and linolic triglyceride component, respectively, per oil molecule, as previously postulated by the author, has been experimentally verified.

#### REFERENCES

- (1) ADAMS, H. E., AND POWERS, P. O.: *Ind. Eng. Chem.* **36**, 1124 (1944).
- (2) ADAMS, H. E., AND POWERS, P. O.: *J. Applied Phys.* **17**, 325 (1946).
- (3) ALFREY, T.: *J. Polymer Sci.* **2**, 99 (1947).
- (4) BEHAR, O. M.: U. S. patent 2,166,103.
- (5) BERNSTEIN, I. M.: *Am. Ink Maker* **21**, (July, August, and September, 1943).
- (6) BERNSTEIN, I. M.: *J. Polymer Sci.* **1**, 495 (1946).
- (7) BERNSTEIN, I. M.: U. S. patent 2,423,751.
- (8) BERNSTEIN, I. M.: U. S. patent application.
- (9) BRADLEY, T. F., AND JOHNSTON, W. B.: *Ind. Eng. Chem.* **33**, 86 (1941).
- (10) BRADLEY, T. F., AND PFANN, H. F.: *Ind. Eng. Chem.* **32**, 694 (1940).
- (11) CALDWELL, B. P., AND MATTIELLO, J. J.: *Ind. Eng. Chem., Anal. Ed.* **4**, 52 (1932).
- (12) CALDWELL, B. P., AND PAYNE, H. F.: *Ind. Eng. Chem.* **33**, 954 (1941).
- (13) DANIELS, H. E.: *Proc. Cambridge Phil. Soc.* **37**, 244 (1941).
- (14) DUNSTAN, A. E.: *Z. physik. Chem.* **56**, 370 (1906).
- (15) EIBNER, A.: U. S. patent 1,934,297.
- (16) ELÖD, E., AND MACH, U.: *Kolloid-Z.* **75**, 336 (1936).
- (17) FLORY, P. J.: *J. Am. Chem. Soc.* **62**, 1057 (1940).
- (18) GAY, P. J.: *Chemistry and Industry* **1933**, 703.
- (19) HICKMAN, K.: *Ind. Eng. Chem.* **29**, 968 (1937).
- (20) JENKINS, J. D.: U. S. patent 2,320,738.
- (21) KELLOGG CO., M.W.: U. S. patent 2,327,896.
- (22) KUNERTH, Y. M.: *Proc. Iowa Acad. Sci.* **8**, 150 (1923).
- (23) LANGMUIR, I.: *J. Am. Chem. Soc.* **39**, 1848 (1917).
- (24) LONG, J. S., ZIMMERMAN, E. K., AND NEVINS, C. S.: *Ind. Eng. Chem.* **20**, 806 (1928).
- (25) MCQUILLEN, T., AND WOODWARD, F. N.: *J. Oil & Colour Chem. Assoc.* **23**, 8 (1940).
- (26) MORRELL, R. S.: *J. Soc. Chem. Ind.* **34**, 105 (1915).
- (27) MORSE, R. S.: *Ind. Eng. Chem.* **32**, 1039 (1941).
- (28) OSTWALD, W.: *J. Oil & Colour Chem. Assoc.* **22**, 31 (1939).
- (29) PRIVETT, O. S., MCFARLANE, W. D., AND GASS, J. H.: *J. Am. Oil Chemists' Soc.* **24**, 204 (1947).
- (30) RANSOM, O. S., AND ZUCKER, M.: U. S. patent 2,403,457.
- (31) SCHWARCMAN, A.: *Oil & Soap* **21**, 204 (1944).
- (32) SKAU, E. L., AND WAKEHAM, H.: Chapter 1 in Weissberger's *Physical Methods of Organic Chemistry*. Interscience Publishers, Inc., New York (1945).
- (33) SPURLING, H. M., MARTIN, F., AND TENNENT, H. G.: *J. Polymer Sci.* **1**, 63 (1946).
- (34) STEPANENKO, N., AGRANAT, B., AND NOVIKOVA, T.: *Acta Physicochim. U.S.S.R.* **20**, 923 (1945).
- (35) WALKER, F. T.: *J. Oil & Colour Chem. Assoc.* **28**, 119 (1945).
- (36) WATERMAN, H. I., *et al.*: *Rec. trav. chim.* **52**, 895 (1933)..

REVERSIBLE PHOTBLEACHING OF CHLOROPHYLL<sup>1</sup>JOHN J. McBRADY<sup>2</sup> AND ROBERT LIVINGSTON*School of Chemistry, Institute of Technology, University of Minnesota, Minneapolis 14, Minnesota**Received August 12, 1947*

The reversible photobleaching of chlorophyll was discovered by Porret and Rabinowitch in 1937 (7). Its existence was confirmed and it was further studied by Livingston in 1941 (4). Since the experiments, both photometric and chemical, are difficult, both the earlier and the present researches are more or less exploratory in character. The present results, while confirming some of the earlier findings, necessitate some modification of the mechanism suggested previously (1, 4).

## EXPERIMENTAL METHODS AND MATERIAL

*The photometer*

The bleaching was measured with a differential photometer. It was so arranged that one of the absorption cells could be illuminated from the side, with a beam of intense light, without disturbing the photometric measurements. This apparatus is similar to but is an improvement on that described elsewhere by McBrady and Livingston (6). To attain the precision desired for the present work, it was found necessary to stabilize the mechanical system and to improve the amplifier.<sup>3</sup> Figure 1 is a circuit diagram of the amplifier. The apparatus is relatively free from drifts and fluctuations, and is capable of measuring relative changes of transmission of 0.01 per cent, reliably and reproducibly. The method of calibrating the photometer was similar to that described by Livingston (4).

The source of actinic light was a 1000-watt projection lamp, which was housed in a double-walled water-cooled cylindrical jacket (figure 2). The cooling water flowed between the glass walls of the window of the lamp house, and thereby removed much of the heat radiation from the light beam. A filter system, consisting of a cupric sulfate cell and a Corning glass filter No. 348, transmitted the red end of the spectrum but absorbed the blue and ultraviolet as well as the greater part of the infrared. A spherical condensing lens, followed by a cylindrical lens, served to concentrate the beam fairly uniformly over the length of the reaction cell. The lamp was run on d.c., hand controlled to 8 amp. Alternating current could not be used, since the response of the photocell and amplifier to the fluctuating fluorescent light is not negligible. The use of the reduced voltage increased the life of the lamp, without greatly reducing the intensity of the red light.

<sup>1</sup> This work was made possible by the support of the Office of Naval Research (Contract N6ori-212, Task Order 1). It was also supported in part by a grant-in-aid from the Graduate School of the University of Minnesota.

<sup>2</sup> Present address: Research Laboratories, Celanese Corporation of America, Summit, New Jersey.

<sup>3</sup> We are indebted to Mr. George DeWitt of the Department of Physics of the University of Minnesota for valuable assistance in redesigning and testing this circuit.



The filter combination used on the scanning light (4) isolated a narrow band with its maximum at approximately 6550 Å.

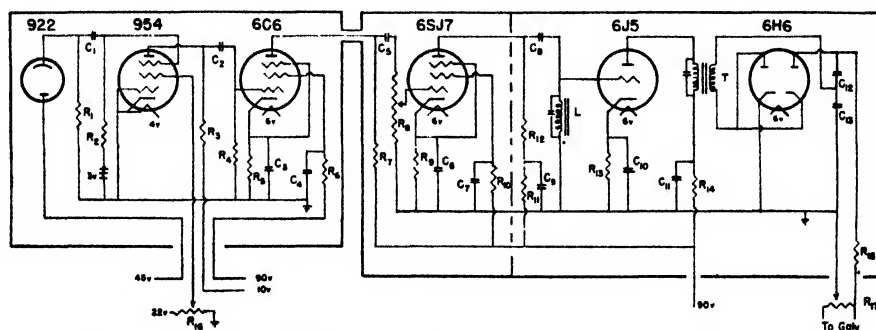


FIG. 1. Diagram of the amplifier. The indicated resistances have the following values in megohms:  $R_1$ , 100;  $R_2$ , 100;  $R_3$ , 0.24;  $R_4$ , 1.0;  $R_5$ , 0.005;  $R_6$ , 2.0;  $R_7$ , 0.5;  $R_8$ , 0.004;  $R_{10}$ , 1.6;  $R_{11}$ , 0.01;  $R_{12}$ , 0.5;  $R_{13}$ , 0.0015;  $R_{14}$ , 0.001;  $R_{16}$ , 2.0.  $R_9$  is the gain control potentiometer, constructed of several wire-wound resistors. Its total resistance is 1.5 megohms.  $R_{15}$  is a 0.01-megohm potentiometer, used to control the No. 2 grid of 954.  $R_{17}$  is a 0.003-megohm Ayrton shunt, which regulates the input to the galvanometer. The indicated condensers have the following capacities in microfarads:  $C_1$ , 0.0002;  $C_2$ , 0.002;  $C_3$ , 4.0;  $C_4$ , 0.05;  $C_5$ , 0.002;  $C_6$ , 4.0;  $C_7$ , 0.1;  $C_8$ , 0.002;  $C_9$ , 4.0;  $C_{10}$ , 5.0;  $C_{11}$ , 20;  $C_{12}$ , 1.0;  $C_{13}$ , 1.0.  $L$  is a filter choke tuned by a suitable condenser for the 150-cycle signal.  $T$  is a coupling transformer, tuned for 150 cycles. Positive potentials are as indicated,  $-B$  being grounded.

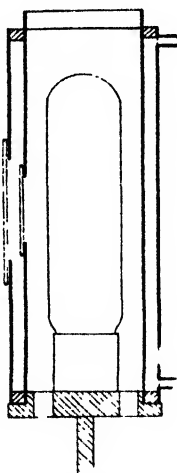


FIG. 2. Diagram of water-cooled lamp house for 1000-watt projection lamp

#### MATERIALS

The chlorophyll used in the majority of these experiments was isolated from market spinach by a modification (5) of Zscheile's method (11). Most of the experiments were performed with solutions of pure chlorophyll *a*, which were checked (11) for pheophytin and chlorophyll *b* content with the Beckmann

spectrophotometer.<sup>4</sup> A few experiments were performed with chlorophyll *b* solutions, which were prepared and checked by the same methods. For comparison with the earlier measurements (4) some measurements were made with an old solid sample (4) of a natural mixture of chlorophylls *a* and *b*.

The methanol was prepared by treating a sample of commercial synthetic methanol with a quantity of sodium which was estimated to be about three times as much as was required to react with the water present. It was then refluxed with dimethyl phthalate to remove the sodium hydroxide,<sup>5</sup> after which it was distilled through an efficient packed column. Two samples of carbon tetrachloride were used. One was of reagent grade and was used without further purification. The other, originally of U.S.P. grade, was saturated with chlorine and allowed to remain in the daylight laboratory for about 48 hr. It was then treated with an excess of potassium iodide solution. Finally, it was washed exhaustively, first with sodium thiosulfate solution and then with distilled water. It was dried over calcium chloride and distilled.

#### ENERGY MEASUREMENTS

To determine the intensity of the light absorbed by the chlorophyll, the chlorophyll-sensitized photooxidation of phenylhydrazine by methyl red (5) was used as an actinometer. The chief advantages of this actinometer are that it uses the same absorbing substance (chlorophyll) at the same concentrations as were used in the photobleaching experiments, and that no changes in the lens or filter system are necessary. It has the further advantage that the extent of the actinometric reaction can be readily measured with the Beckmann spectrophotometer. Measurements with this actinometer indicate that, when the full intensity of the actinic light was used and the solution was  $2 \times 10^{-6} M$  in chlorophyll *a*,  $2.3 \times 10^{16}$  quanta per cubic centimeter per second were absorbed. Under similar circumstances, chlorophyll *b* absorbed  $1.6 \times 10^{16}$  quanta per cubic centimeter per second.

#### EXPERIMENTAL RESULTS

Figures 3 to 9 summarize the principal experimental results. With the exception of figure 5, these plots illustrate the course of typical experiments. The duration of each experiment, in seconds, is plotted as abscissa, and the decrease in molarity of chlorophyll ( $\Delta C$ ) as ordinate. Except where otherwise indicated, the interval between measurements is 5 sec. The point at the end of each interval of illumination is indicated by an open circle; that following a dark interval, by a solid dot. In computing the decrease in molarity of chlorophyll, it was assumed (7) that the bleached form of chlorophyll does not absorb at all in the red end of the spectrum. If the bleaching reaction results only in a lowering of the average extinction coefficient,  $\bar{\epsilon}$ , for red light, the reported changes in the concentrations of chlorophyll are too small, but are directly proportional to the correct values.

<sup>4</sup> This instrument was the property of the Bureau of Ordnance of the United States Navy and was kindly put at our disposal by Dr. Bryce L. Crawford.

<sup>5</sup> We are indebted to Dr. R. Arnold of the Division of Organic Chemistry, who suggested this procedure and placed the distilling column at our disposal.

Figure 3 is a plot typical of the reversible bleaching which was observed in the present experiments when air-free methanol solutions of chlorophyll *a* or *b* were used. The outstanding characteristic of these results is the speed of the reverse process. In some experiments not shown in figure 3 it was observed that the steady-state bleaching was reached in less than 3 sec. (the period of the galvanometer) and that the solution returned to its original color too rapidly to be followed by our apparatus. By comparison with other results, it can be estimated that the half-life of the bleached chlorophyll in these methanol solutions

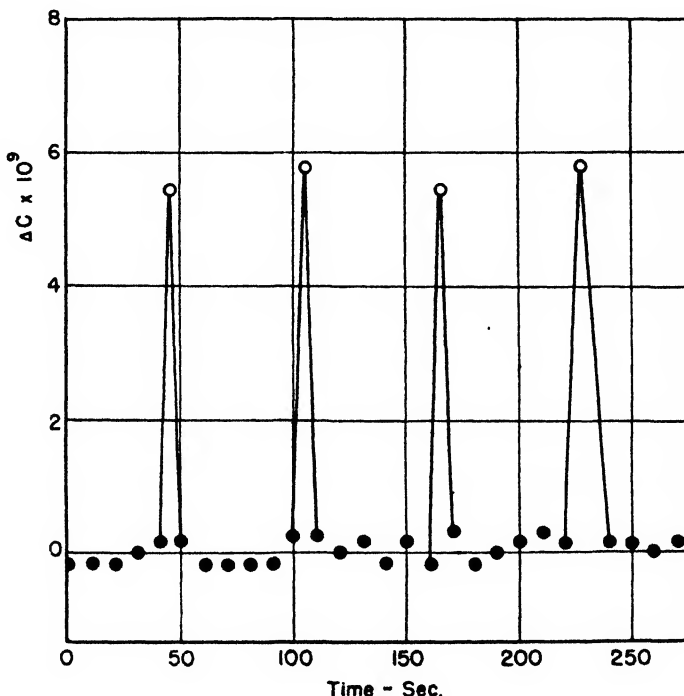


FIG. 3. Reversible photobleaching: chlorophyll *a* ( $2 \times 10^{-6} M$ ) in methanol

is less than 0.5 sec. Experiments in which the illumination was prolonged showed that the irreversible bleaching was less than 10 per cent of the reversible effect. The maximum bleaching obtained with these solutions varied with the samples of chlorophyll and of solvent used and with the previous treatment of the solution. Illumination of a solution, even in the absence of air, reduced its ability to undergo reversible bleaching, and this effect appeared to be greater than the concurrent irreversible bleaching. Using the full intensity of the actinic light and  $2 \times 10^{-6} M$  solutions, the following range of reversible bleaching, expressed as per cent reduction in the chlorophyll concentration, was obtained: chlorophyll *a*—0.6 to 0.2 per cent; chlorophyll *b*—1.5 to 0.4 per cent; solid chlorophyll (a natural mixture of *a* and *b* containing about 30 per cent of pheophytin)—0.2 per cent. Air-free solutions of chlorophyll *b* appear to be more resistant to irreversible photobleaching than corresponding solutions of chlorophyll *a*.

Dissolved oxygen completely suppresses the reversible bleaching and somewhat increases the irreversible bleaching. Figure 4 is a plot of the bleaching occurring in a methanol solution saturated with air. The rate of this irreversible bleaching is less than one-tenth of the rate of the reversible bleaching attained in the absence of oxygen but otherwise under the same conditions. It should be noted, however, that the rate of the irreversible bleaching is increased by five- or ten-fold by the addition of air.

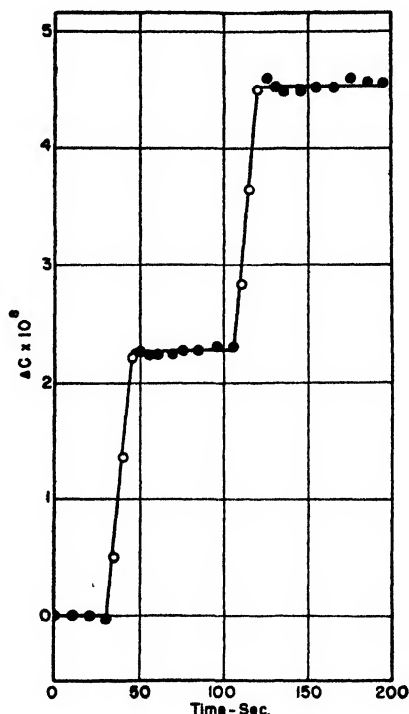


FIG. 4. Irreversible photobleaching. Experimental conditions similar to those represented by figure 6, except that the solution was saturated with air.

Figure 5 is a plot of the steady-state bleaching against the square root of the intensity of the actinic light. It is apparent that the steady-state (i.e., maximum) bleaching is a linear function of the square root of the intensity. The fact that the straight lines do not pass through the origin is due to the bleaching produced by the scanning (i.e., analytical) light, which cannot be neglected in comparison to the actinic light of reduced intensity. This correction is discussed quantitatively in the section on computations.

The short life of the bleached form in "pure" methanol solutions observed in the present experiments resembles the results obtained by Porret and Rabinowitch (7) rather than those obtained by Livingston (4). Since it was suspected that this short life might be caused by traces of peroxides present in

the ether which was used in the preparation of the chlorophyll, a sample of chlorophyll was prepared by a modification of Zscheile's (11) procedure, using carbon tetrachloride in place of the ether and the ether-ligroin mixture used in the standard procedure. The type of reversible bleaching obtained with a methanol solution of this sample of chlorophyll is illustrated by figure 6. The steady-state bleaching of this solution was about twice as great as that observed with the standard solution, and its back-reaction was much slower. While this experiment was consistent with the peroxide explanation of the short life observed in the other solutions, this hypothesis was ruled out by the following facts: If a

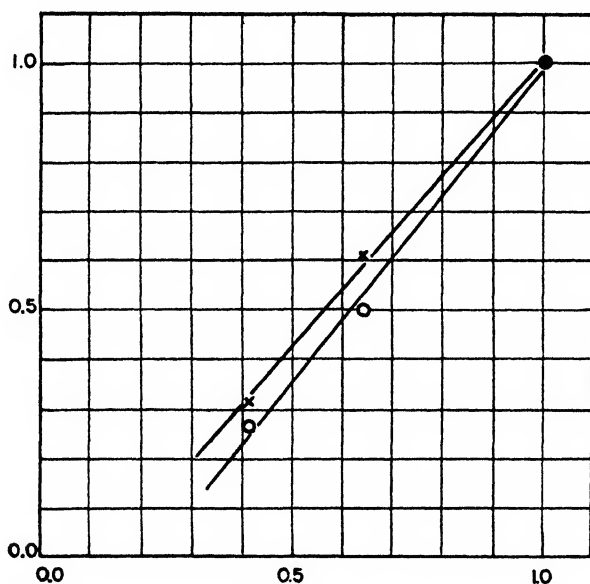


FIG. 5. The effect of the intensity of the absorbed light on the steady-state bleaching. Methanol solution. Abscissa: square root of the intensity in arbitrary units. Ordinate: decrease of chlorophyll concentration in arbitrary units. X, chlorophyll a; O, chlorophyll b.

quantity of ether was added to the solution which had been used for the experiment of figure 6, and then distilled off at low temperature, there was little or no change in the bleaching reaction, which still resembled that illustrated by figure 6. Any peroxides present in the ether would very probably have been left behind in the methanol solution. However, if a relatively small amount of carbon tetrachloride was added to a methanol solution of a standard preparation of chlorophyll, the bleaching of the resulting solution resembled that illustrated by figure 6, rather than that by figure 3. It must be concluded, therefore, that under the present experimental conditions the carbon tetrachloride or some impurity present in it is responsible for the increased life of the bleached form.

Experiments were performed to determine the effect of temperature and of chlorophyll concentration upon reversible bleaching. Chlorophyll prepared by

the modified (carbon tetrachloride) method was used in these experiments. The solvent used was methanol. Neither the extent of the steady-state bleaching nor the rate of the reverse reaction was detectably different at 7.5°C. from the results at 25°C.

To determine whether the steady-state bleaching ( $\Delta C$ ) varied with the initial concentration of chlorophyll, experiments were performed with  $1 \times 10^{-6} M$  and  $5 \times 10^{-6} M$  solutions. The ratio of the corresponding values of  $\Delta C$  is 3.0. Since

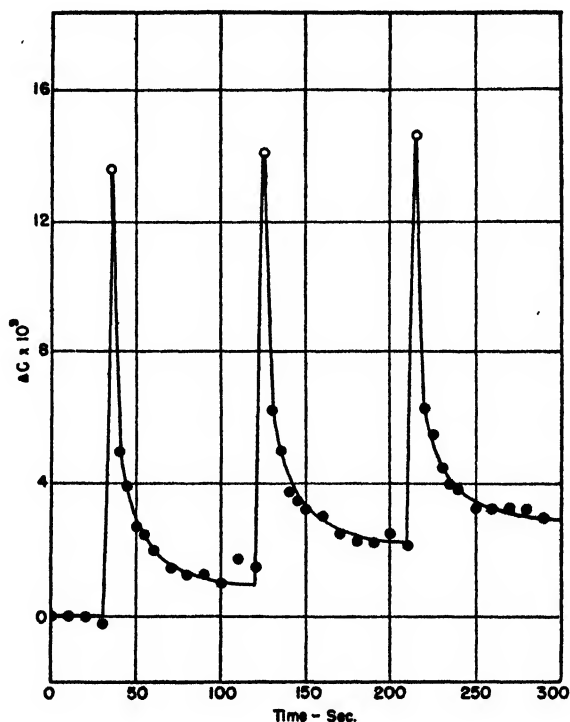


FIG. 6. Reversible photobleaching. Experimental conditions similar to those represented by figure 3, except that the sample of chlorophyll was prepared by a modified method in which carbon tetrachloride was substituted for ether as an extracting agent.

the path of the actinic light in the solution is short, the intensity of the absorbed light should be approximately proportional to the concentration of the chlorophyll. The observed increase in  $\Delta C$  can be attributed entirely to the increase in the intensity of the absorbed light. While no great precision can be claimed for the present measurements, they do show that the ratio,  $\Delta C/I_{ab}^{1/2}$ , does not increase appreciably with the concentration of chlorophyll.

A number of experiments were performed to determine if the presence of added substances changed the course of the bleaching. In methanol solutions, neither allylthiourea nor phenylhydrazine, at the relatively high concentration of 0.10  $M$ , had an appreciable effect upon the bleaching. It was previously

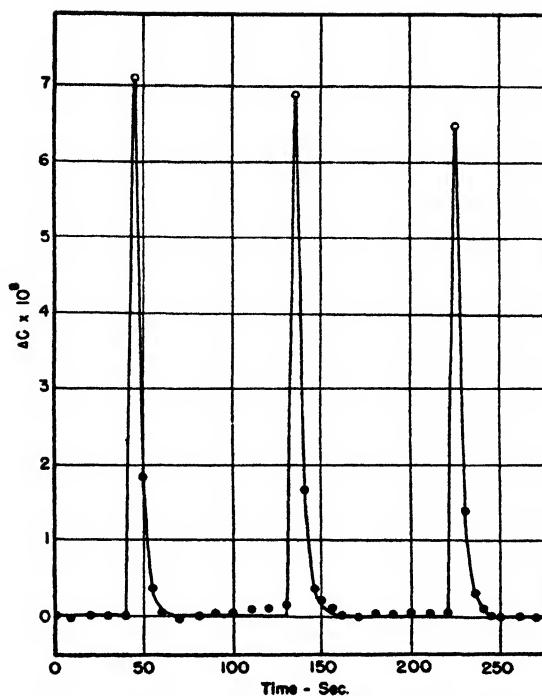


FIG. 7. Reversible bleaching. Chlorophyll *b* ( $2 \times 10^{-6} M$ ) in methanol to which oxalic acid ( $10^{-4} M$ ) had been added.

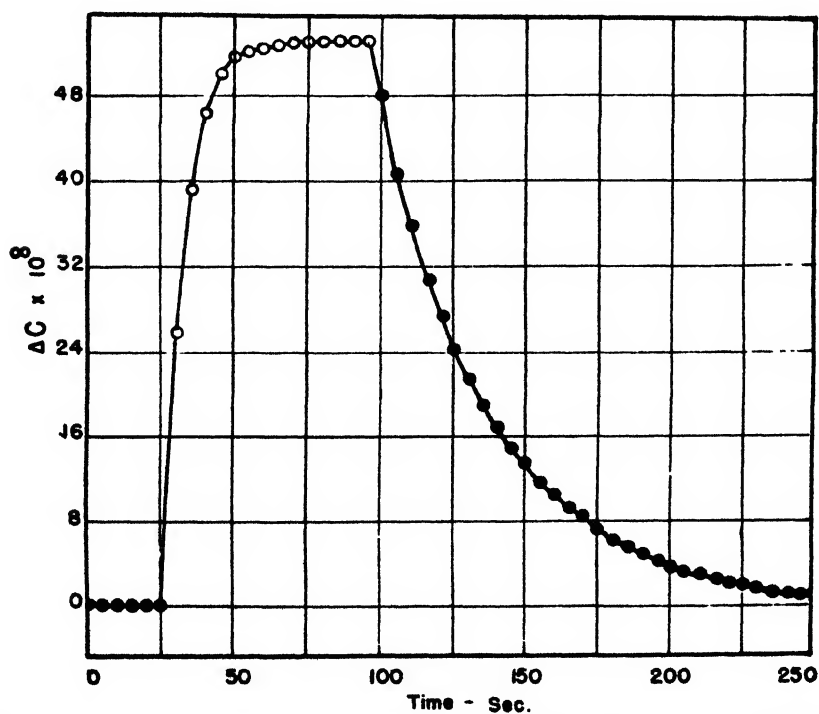


FIG. 8. Reversible bleaching. Chlorophyll *a* ( $2 \times 10^{-6} M$ ) in methanol to which iodine ( $10^{-3} M$ ) had been added.

shown (4) that hydroquinone and isoamylamine are equally without effect. Both Porret and Rabinowitch (7) and Livingston (4) reported that formic acid increases the bleaching. This result was not confirmed by the present experiments, in which it was found that  $10^{-4} M$  formic acid had only a slight effect upon the bleaching. This marked discrepancy suggests that the observed effect of formic acid was due to some impurity present in the samples used. In contrast, oxalic acid ( $10^{-4} M$ ) increased the steady-state bleaching by about threefold and

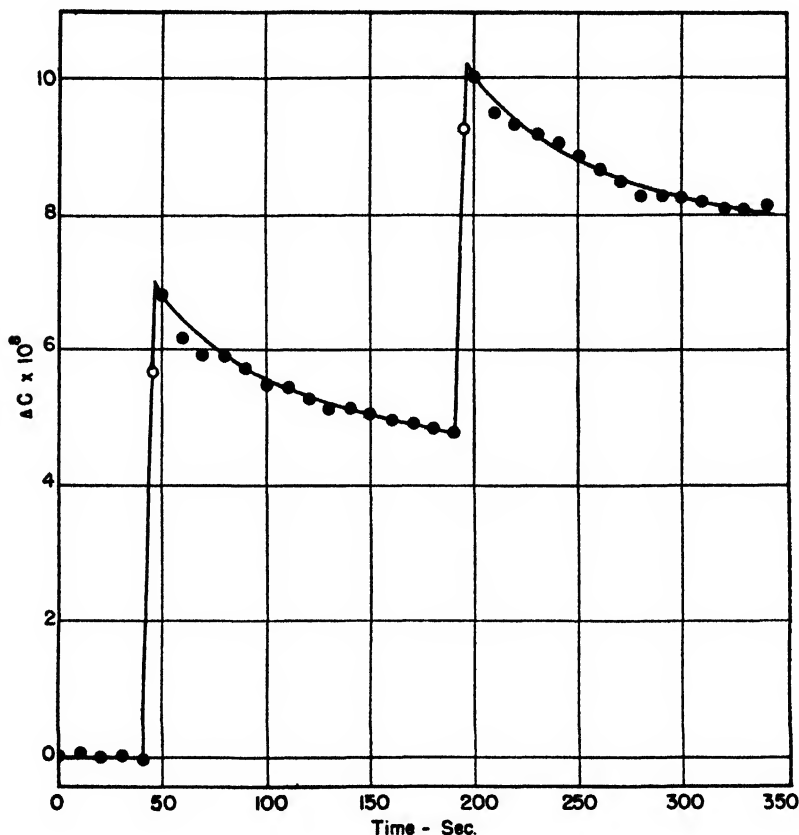


FIG. 9. Reversible bleaching: chlorophyll *a* ( $2 \times 10^{-6} M$ ) in carbon tetrachloride

the half-life of the bleached form by more than tenfold. Figure 7 shows the course of the bleaching in the presence of oxalic acid.

The addition of allylthiourea to methanol solutions containing carbon tetrachloride decreases the steady-state bleaching and shortens the half-life of the bleached form from 5 or 10 sec. to less than 0.5 sec.; in other words, the allylthiourea neutralizes the effect of the carbon tetrachloride upon the methanol solution. These results strongly suggest that the effect of carbon tetrachloride is due to the presence in it of an oxidizing impurity. Since iodine had been present during the purification of the carbon tetrachloride, it was suspected that



this might be the active impurity. This was quickly verified. A methanol solution to which iodine ( $10^{-6} M$ ) had been added exhibited the photobleaching illustrated by figure 8. The addition of the iodine increased the steady-state bleaching from about 0.2 to 26 per cent and the half-life of the bleached form from less than 0.5 sec. to about 20 sec. In addition, the irreversible bleaching was completely suppressed.

A number of experiments were performed with solutions in carbon tetrachloride. A typical experiment is illustrated by figure 9. These reactions exhibit two new effects. The irreversible reaction is considerably increased, and the bleaching continues in the dark for a short time after the light is cut off. This after-bleaching amounts to about 20 per cent of the photobleaching occurring in a 5-sec. interval. It was never observed in methanol solutions or in mixtures of methanol and carbon tetrachloride.

#### COMPUTATIONS

In attempting a quantitative analysis of the steady-state bleaching, it is necessary to allow for the effect of the scanning light. While the incident intensity of the scanning light is much less than that of the actinic light, this difference is partially offset by the difference in the lengths of the absorption paths. A direct actinometric determination, using the phenylhydrazine-methyl red reaction (5) sensitized by  $2 \times 10^{-6} M$  chlorophyll *a*, gave a value for the ratio of the intensity of the absorbed scanning light to that of the actinic light of about 0.012. When chlorophyll *b* was used, the ratio was about 0.017.

The observed bleaching,  $\Delta b$ , is the difference between the bleaching produced by the scanning and by the actinic lights. If the bleaching is proportional to the square root of the intensity of the absorbed light, we may write:<sup>6</sup>

$$\begin{aligned}\Delta b &= K(I_{sc} + I_{ac})^{1/2} - KI_{sc}^{1/2} \\ &= KI_{ac}^{1/2}(1 + I_{sc}/I_{ac})^{1/2} - KI_{ac}^{1/2}\end{aligned}$$

or to a first approximation:

$$\Delta b = K(I_{ac}^{1/2} - I_{sc}^{1/2})$$

This approximate equation has been fitted to the empirical values of the bleaching,  $\Delta b$ , produced by actinic light of intensities (in arbitrary units) of 1.00, 0.41, and 0.17.

$$\Delta b = 1.160(I_{ac}^{1/2} - 0.131) \text{ for chlorophyll } a$$

$$\Delta b = 1.273(I_{ac}^{1/2} - 0.222) \text{ for chlorophyll } b$$

The plots of these equations and the empirical points are shown in figure 5. The values for the ratios of the absorbed intensities of the scanning to those of the full actinic light, obtained from the preceding equations, are 0.017 for chloro-

<sup>6</sup> This equation is only approximate, since the intensity of the scanning light diminishes rapidly as it passes through the cell. However, the present data scarcely justify a more exact analysis.

phyll *a* and 0.049 for chlorophyll *b*. These values are in reasonable agreement with those obtained actinometrically,—0.012 and 0.017, respectively.

A determination of a quantum yield necessitates separate measurements of the number of molecules reacted and of the number of photons absorbed. For the present experiments, the number of photons absorbed can be obtained in each case from the actinometric measurements. When the rate of bleaching is constant (*cf.* figure 4) or when the initial rate of bleaching can be estimated approximately (as in figure 8), the number of chlorophyll molecules reacting per second can be obtained from the slope of the bleaching curve. The quantum yield,  $\phi$ , can also be computed for those cases where the rate of the (dark) reverse reaction can be measured. At the steady state, the following relation must hold if the back-reaction is second order:

$$\phi I_{\text{abs}} = k_2(\Delta C)^2$$

Similarly, when the reverse reaction is first order:

$$\phi I_{\text{abs}} = k_1 \Delta C$$

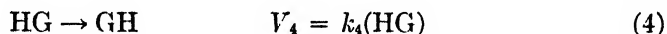
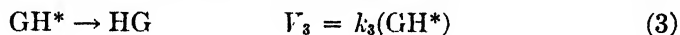
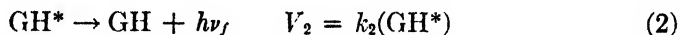
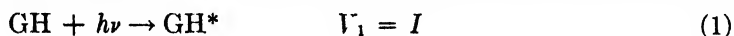
The measured value for  $I_{\text{abs}}$  (in quanta per cubic centimeter per second) was about  $2.3 \times 10^{16}$  for chlorophyll *a* and  $1.7 \times 10^{16}$  for chlorophyll *b*. The corresponding value for the quantum yield of the irreversible bleaching in the presence of oxygen (figure 4) is  $4 \times 10^{-5}$ . For the reversible bleaching, the yields corresponding to figures 6, 7, and 8 may be estimated with some confidence. The reverse reaction in a solution containing oxalic acid (figure 7) is first order and has a rate constant of  $0.28 \text{ sec.}^{-1}$ , which leads to a value  $\phi = 7 \times 10^{-4}$ . In the experiment represented by figure 6, the reverse reaction is second order with a rate constant of  $2.8 \times 10^7$  liters per moles  $\times$  seconds, corresponding to  $\phi = 1.3 \times 10^{-4}$ . The reverse reaction for the experiments shown in figure 3 must be at least twentyfold faster than in the preceding case (figure 6), and therefore  $\phi \geq 4 \times 10^{-4}$ . While the analysis of the data for the reaction occurring in the presence of iodine (figure 8) is not complete, an approximate value of  $\phi \simeq 1 \times 10^{-3}$  can be estimated from the initial slope of the bleaching curve. The initial slope of the bleaching curve for carbon tetrachloride solutions (figure 9) is due to simultaneous, comparable, reversible and irreversible reactions, the yield for the combined process being  $5 \times 10^{-4}$ .

The outstanding characteristic of these values of the yield is their relative constancy. The extreme values for the quantum yields are  $1.3 \times 10^{-4}$  and  $1 \times 10^{-3}$ , while for the same systems the absolute rates of the reverse reactions differ by at least 200-fold.

#### DISCUSSION

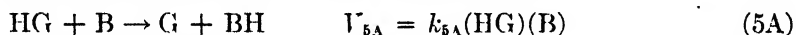
In general the present data support the mechanism proposed by Franck and Livingston (1); however, certain modifications and additions appear to be necessary. The following four steps presumably occur whenever dissolved

chlorophyll absorbs light. In concentrated solutions an additional step to account for the self-quenching (10) of chlorophyll fluorescence must be introduced.

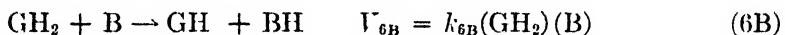
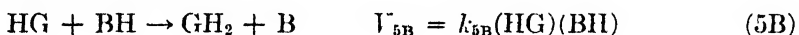


The special symbols used have the following significance: GH = normal chlorophyll; GH\* = electronically excited (singlet state) chlorophyll; HG = long-lived activated chlorophyll (probably in a tautomeric triplet state);  $I$  = the intensity of the absorbed light in appropriate units;  $V_i$  = the rate of the  $i^{\text{th}}$  reaction step; and  $k_i$  = the rate constant for the  $i^{\text{th}}$  reaction step.

The reversible bleaching in air-free solutions in "pure" solvents may be accounted for by either steps 5A and 6A or by 5B and 6B. The simple dismutation reaction between HG and GH (1) apparently is of negligible importance in the solutions which have been studied to date.<sup>7</sup> Mechanism A is based upon the postulate that the chlorophyll tautomer, HG, reacts with an oxidizing impurity, B (or a molecule of the solvent), to form the (bleached) radical, G:



If the reduced radical, GH<sub>2</sub>, is the bleached form of chlorophyll, the corresponding steps (mechanism B) are:

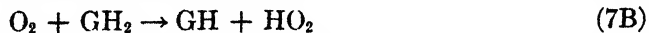


Steps 5A and 6A are supported by the fact that the presence of high concentrations of such reactive reducing agents as hydroquinone, allylthiourea, or phenylhydrazine does not increase the steady-state bleaching. Either pair of steps leads to an equation for the steady-state bleaching of the following form, which is consistent with the experimental results:

$$(\Delta C) = \left[ \frac{k_3}{k_2 + k_3} \times \frac{k_5(x)}{k_4 + k_5(x)} \frac{I}{k_6} \right]^{1/2}$$

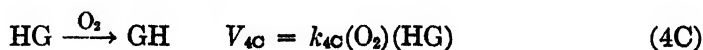
where  $k_5(x)$  represents  $k_{5A}(\text{B})$  for mechanism A and  $k_{5B}(\text{BH})$  for mechanism B.

The action of oxygen in inhibiting reversible bleaching requires that one or more steps be added to the mechanism. The reactions suggested by Franck and Livingston (1) can be modified slightly to be consistent with mechanism B.



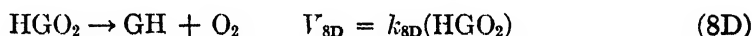
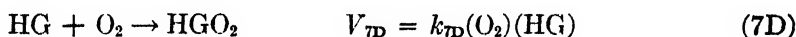
<sup>7</sup> Compare the discussions on page 1319 of reference 4 and pages 484-90 of reference 8.

This mechanism has the advantage of fitting directly into the  $\text{HO}_2$  mechanism (9) for chlorophyll-sensitized photochemical reactions. It appears to be energetically possible, but perhaps not too probable.



Another possible action of oxygen is to catalyze step 4. The experimental results on the oxygen-inhibition of bleaching would be fitted by this postulate if the rate of step 4 were increased by at least 100-fold. When it is remembered that HG is very probably a triplet state of the chlorophyll molecule and that oxygen is paramagnetic, an effect of this magnitude seems reasonable. This assumption is compatible with either mechanism A or mechanism B. It is also consistent with the reported (3) quenching of chlorophyll phosphorescence. The mechanism is somewhat difficult to reconcile with the results on chlorophyll-sensitized photochemical autoxidations, since it leads to the prediction that relatively high concentrations of oxygen should retard the chemical reaction. While the available data on autoxidation are not sufficient to justify the rejection of step 4C, they certainly reduce the confidence which one might otherwise place in it.<sup>8</sup>

A third possibility, which was suggested by Professor J. Franck,<sup>9</sup> is that oxygen stabilizes the tautomer (HG) by forming a short-lived, reactive mole-oxide,  $\text{HGO}_2$ .



This mole-oxide mechanism for the inhibition of reversible bleaching is obviously inconsistent with the  $\text{HO}_2$  mechanism for photooxidation. It faces the same difficulty in being reconciled to Gaffron's mechanism (2) of photosensitization as does the step 4C mechanism. There is the possibility, however, that the mole-oxide itself reacts directly with the reducing agent and so initiates the reaction. If this were true, it would be necessary for the mole-oxide to have a sufficiently short life to explain the inhibition of bleaching and a sufficiently long life to be consistent with the high quantum yield of photosensitized autoxidation. The first condition places the upper limit of the life at  $10^{-8}$  sec., which is probably too short to be comparable with Gaffron's (2) results, although this is not quite certain.<sup>10</sup>

<sup>8</sup> A further weakness of this postulate is that it necessitates the assumption of a separate explanation for the quenching of fluorescence by oxygen. A consistent assumption would be that the oxygen catalyzes step 3 as well as step 4.

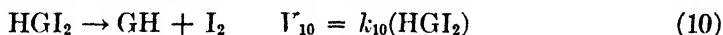
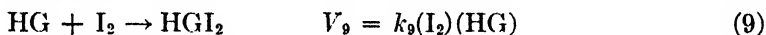
<sup>9</sup> Private communication.

<sup>10</sup> Gaffron's measurements (2) were made at relatively high concentrations of chlorophyll and exhibit a marked retardation of the oxidation by the sensitizer, which must be due to a competition between molecules of the substrate and of normal chlorophyll for some long-lived activated species.

The view expressed by Rabinowitch (8, p. 518), that Gaffron's data can be fitted by an

Of the several mechanisms for the effect of oxygen which are here discussed, the  $\text{HO}_2$  mechanism (steps 7B and 8B) appears to be the most probable. However, the evidence now available is not sufficient to permit the complete rejection of the other possibilities.

Regardless of whether the mole-oxide explanation is correct, the following mechanism for the effect of iodine appears very reasonable.<sup>11</sup>



These steps are consistent with the enhanced steady-state bleaching and with a first-order law for the reverse reaction. The necessary values  $k_9$  and  $k_{10}$  are entirely probable. It is an interesting consequence (as yet untested) of this mechanism that the iodine would be expected to increase the quantum yield of the bleaching as well as to reduce the rate of the reverse reaction. The magnitude of the expected increase of the quantum yield will depend upon the relative values of  $k_5(\text{B})$ ,  $k_9(\text{I}_2)$ , and  $k_4$ . A similar explanation for the effect upon the reversible bleaching of methyl red and of oxalic acid seems probable.

#### SUMMARY

Reversible photobleaching is observed in air-free solutions of chlorophyll in methanol and in several other organic solvents. The bleaching is completely inhibited by oxygen. The extent of the steady-state bleaching in "pure" solvents is proportional to the square root of the absorbed light. Both the extent of the bleaching and the rate of the reverse (dark) reaction are practically independent of the temperature in the range 5–25°C. The rate of the reverse reaction is very sensitive to the nature of the solvent and to traces of impurities. The bleaching is enhanced threefold by the addition of  $10^{-4}$  *M* oxalic acid to methanol, and 100-fold by the addition of  $10^{-5}$  *M* iodine. Reducing agents (such as allylthiourea, phenylhydrazine, hydroquinone, etc.) have little or no effect upon the reaction. The reverse reaction is second order in respect to the concentration of the bleached material in pure solvents, but is first order in solutions containing oxalic acid and (probably) in those containing iodine. The quantum yield for the bleaching reaction is approximately  $5 \times 10^{-4}$ . This yield appears to be much less sensitive to the nature of the solvent and to the presence of impurities than is the rate of the reverse reaction.

---

equation of the Stern-Volmer type with a correction for the chlorophyll effect, is incorrect. This view is apparently a consequence of his equation 18.32, in which the constants (0.004 and 0.023) are too small by a factor of  $10^6$  if the concentrations are expressed in moles per liter, or of  $10^3$  if in millimoles per liter. If the correct factors are used, it is apparent that the constant term in the denominator is completely negligible and there is no resemblance to the Stern-Volmer relation. It is, of course, possible that the quantum yield might follow a Stern-Volmer relation at much lower concentrations of chlorophyll.

<sup>11</sup> Suggested by Professor James Franck in a private communication.

## REFERENCES

- (1) FRANCK AND LIVINGSTON: *J. Chem. Phys.* **9**, 184 (1941).
- (2) GAFFRON: *Ber.* **68**, 1409 (1935).
- (3) KAUTSKY, HIRSCH, AND FLESCH: *Ber.* **68**, 152 (1935).
- (4) LIVINGSTON: *J. Phys. Chem.* **45**, 1312 (1941).
- (5) LIVINGSTON, SICKLE, AND UCHIYAMA: *J. Phys. Chem.* **51**, 774 (1947).
- (6) McBRADY AND LIVINGSTON: *J. Phys. Chem.* **50**, 177 (1946).
- (7) PORRET AND RABINOWITCH: *Nature* **140**, 321 (1937).
- (8) RABINOWITCH: *Photosynthesis*, Vol. I, Chap. 18. Interscience Publishers, Inc., New York (1945).
- (9) WEISS: *Naturwissenschaften* **35**, 610 (1935).
- (10) WEISS AND WEIL-MALHERBE: *J. Chem. Soc.* **1944**, 541, 544.
- (11) ZSCHEILE AND COMAR: *Botan. Gazz.* **102**, 463 (1941).

## THE DIFFUSION AND SEDIMENTATION OF SODIUM THYMONUCLEATE

HERBERT KAHLER

*National Institute of Health, Bethesda, Maryland**Received October 23, 1947*

## INTRODUCTION

Sodium desoxyribosenucleate (thymonucleate) is obtained from nucleoproteins found in the nuclei of cells. It has been the subject of several investigations by physicochemical methods, the results of which indicate that no two preparations are exactly alike. One of the first estimations of size was that of Signer, Caspersson, and Hammarsten (15), who assigned to the polymer a length of 6000 Å., a cross-sectional diameter of 20 Å., and a molecular weight of 1,000,000. This gave an axial ratio of 300:1, which was consistent with a rod-shaped structure. Later investigations have verified the conclusions of Signer, Caspersson, and Hammarsten as to the order of magnitude of dimensions.

Little attention has been given to the question of the polydispersity distribution of nucleate. From recent work (16) on tobacco mosaic virus it appears that a fresh monodisperse preparation in the course of a few days' standing becomes polydisperse. It seems clear that, if a choice has to be made between a monodisperse unstable polymer and a polydisperse substance which has reached a stable equilibrium under the conditions in which a given experiment is performed, the stable preparation would be preferable, particularly for diffusion studies in which the duration of the experiment is at least a week.

In the present investigation the diffusion and sedimentation constants were measured at different concentrations and extrapolated to infinite dilution; by combination of these values with the partial specific volume the molecular weight and shape factors were obtained.

## PARTIAL SPECIFIC VOLUME

The following values for partial specific volume have been reported: Schmidt, Pickels, and Levene (14), 0.465; Hammarsten (8), 0.52; Tennent and Vilbrandt (17), 0.55; Astbury and Bell (1), 0.61; Greenstein and Jenrette (7), 0.62; and Wissler (20), 0.66. It was decided to use the value of Tennent and Vilbrandt,  $V = 0.55$ , since a determination upon a sample of vacuum-dried material gave a value of 0.54. The large variation in these values may be caused by the difficulty in measuring the concentration, owing to different degrees of desiccation of the solid material used by the several investigators.

Tennent and Vilbrandt also found that the refractive index of a nucleate solution was proportional to the concentration, the refraction increment for a 1 per cent solution being 0.0016 at 25°C. The sodium thymonucleate used in the present study was the best of four preparations—as judged by viscosity, streaming birefringence, and absence of proteins—made by Greenstein and Jenrette (their preparation #2), by the method of Hammarsten-Bangs, and used in their study of structural viscosity and streaming birefringence (7).

## DIFFUSION

Prior to diffusion, the material was dialyzed at low temperatures for 5 days, using a motor-driven, slow-rocking device. Two days' dialysis under static conditions was found to be insufficient to attain complete equilibrium between nucleate solution and solvent. A long time of dialysis has the additional advantage of ensuring a more stable equilibrium of the polymer frequency distribution. The 20°C. runs were made with a drop of toluene added to 2 liters of the buffer to suppress bacterial growth. After dialysis, the material was centrifuged for  $\frac{1}{2}$  hr. at 20,000 g in order to remove fine air bubbles and to throw down any insoluble material. Nucleate is less soluble as the salt strength increases. The concentrations were obtained from the areas of the diffusion curves.

The diffusion cell was similar to that described by Neurath (12). The scale method of Lamm (10) and the scanning method of Longworth (11) were used interchangeably. The cell was mounted in a large water bath, the temperature regulation being constant to 0.01°C. Some diffusion runs were made at 5°C. and some at 20°C., the lowest concentrations being run at 5°C. The values were corrected to standard conditions, 20°C., by the usual reduction factors (19).

The diffusion curves of nucleate deviate from the normal curve which would be obtained for an ideally diffusing substance in two respects: (1) the deviation is characterized by a higher than normal peak, which indicates polydispersity of the nucleate (10); (2) skewness of the curves indicates that the diffusion is a function of the concentration. In figures 1 and 2 there are shown in normal coördinates curves for 0.9 per cent nucleate in neutral buffer, and for 0.2 per cent nucleate in 3 N potassium chloride solution, compared with the ideal normal distribution.

In such a situation the most reliable method of getting the diffusion constant is by the moment method of Lamm (10),  $D_{\text{Moment}} = \sigma^2/2T$ , where  $\sigma$  is the stand-

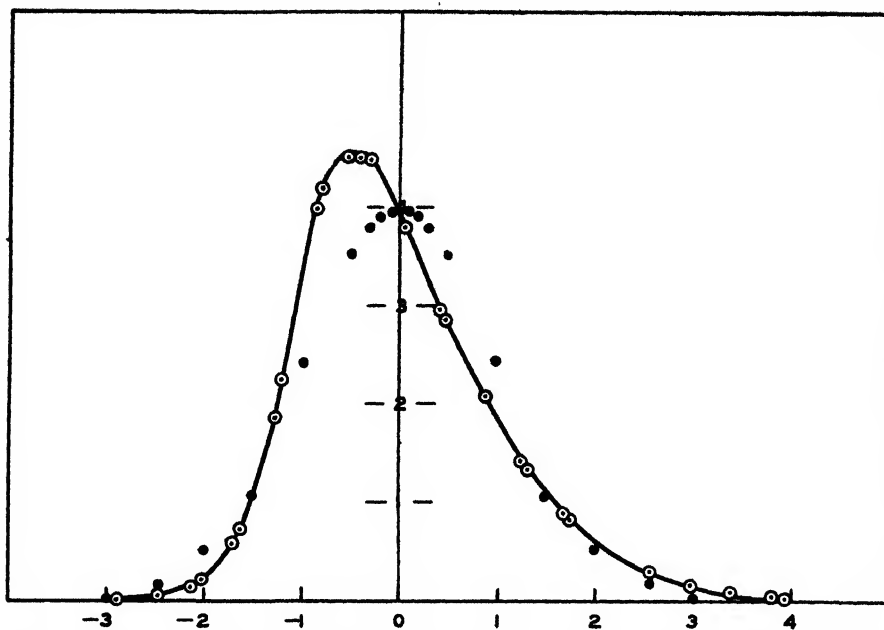


FIG. 1. Diffusion of 0.9 per cent nucleate in buffer ( $0.3 \mu$ ) at  $20^\circ\text{C}$ . in normal coördinates ( $\circ$ ). Ideal normal curve ( $\bullet$ ). Buffer composition:  $0.031 \text{ } m$  disodium hydrogen phosphate,  $0.006 \text{ } m$  potassium dihydrogen phosphate,  $0.2 \text{ } N$  sodium chloride; pH 7.4.

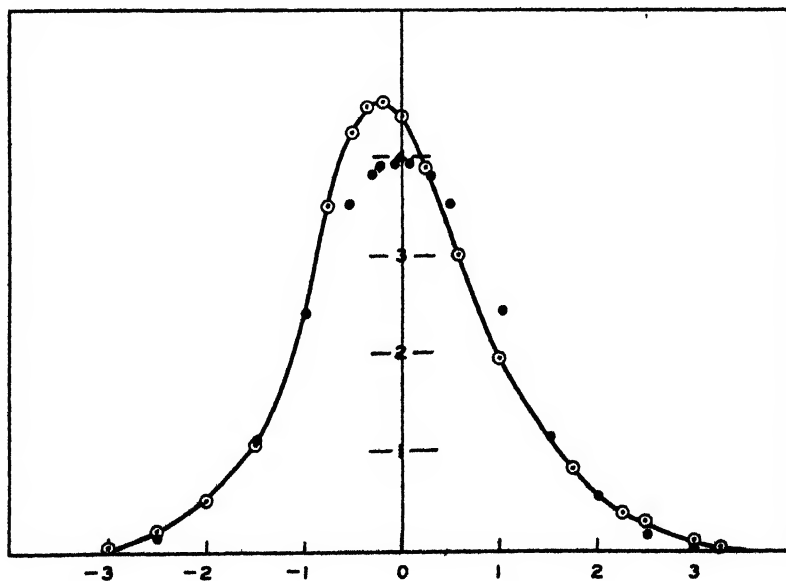


FIG. 2. Diffusion of 0.2 per cent nucleate in  $3 \text{ } N$  potassium chloride at  $5^\circ\text{C}$ . in normal coördinates ( $\circ$ ). Normal curve ( $\bullet$ ).



TABLE 1

Diffusion of nucleate in buffer  $0.1 \mu$  in phosphate,  $0.2 \mu$  in NaCl,  $pH = 7.4$ ,  $3 N$  KCl, and water. Composition of buffer:  $0.031 m$   $Na_2HPO_4$ ,  $0.006 m$   $KH_2PO_4$ . The  $D_M$  values correspond to concentrations,  $c_M$ .

SOLVENT	BATH TEMPERATURE	CONCENTRATION OF NUCLEATE ( $2 c_M$ )	$D_M \times 10^7$
	$^{\circ}C.$	per cent	
Buffer.....	20	0.90	1.10
	20	0.50	0.815
	20	0.38	0.75
	5	0.40	0.705
	5	0.16	0.52
	5	0.05	0.46
$3 N$ KCl.....	5	0.20	0.455
Water.....	5	0.20	(8.0)

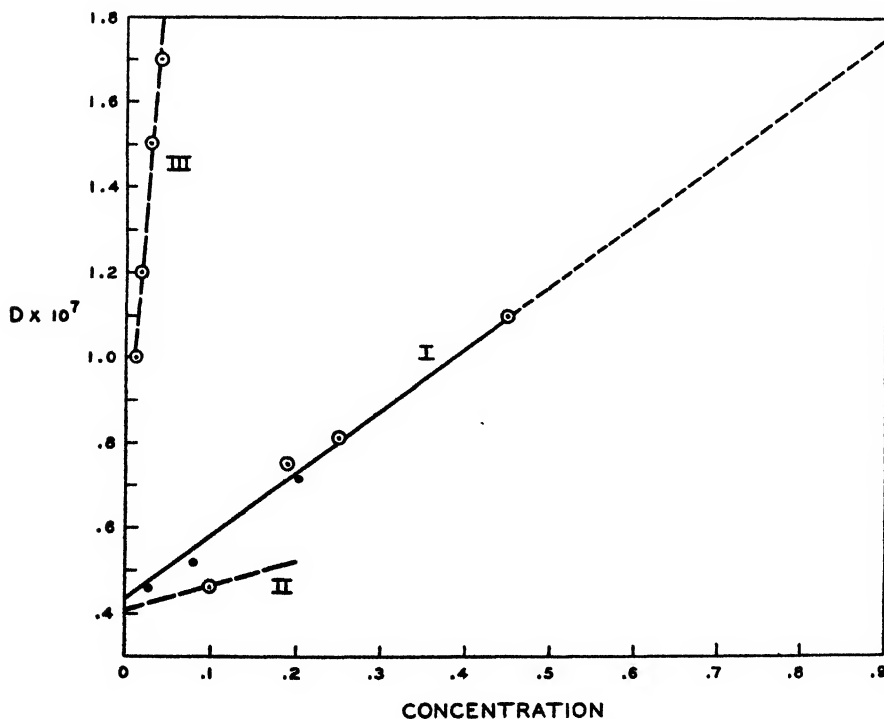


FIG. 3. Diffusion of nucleate in different solvents. Curve I: separate determinations of  $D_M$  for each concentration ( $c_M$ ) of nucleate in buffer-salt ( $0.3 \mu$ ). Experiments at  $20^{\circ}C.$  ( $\circ$ ); experiments at  $5^{\circ}C.$  ( $\bullet$ ). Curve II: estimated  $D_M$  line from Boltzmann's equation; 0.2 per cent nucleate in  $3 N$  potassium chloride (see figure 5). Curve III: estimated trend of  $D_M$  line from Boltzmann's equation; 0.2 per cent nucleate in water (see figure 6).

ard deviation of the curve and  $T$  is the time since diffusion started.  $D_{\text{Moment}}$  equals the weight-average diffusion constant,  $D_M$  (6). In our runs a plot of  $\sigma^2$  against  $2T$  gave a straight line passing through the origin, which indicates that there was not much change in the material during the experiment, since the slope of the line gives a constant  $D_M$ .

A series of diffusion experiments was run with different concentrations of nucleate in phosphate buffer of pH 7.4 plus sodium chloride, the ionic strength being 0.3 (table 1). A line through the points cuts the  $D$  axis at  $0.45 \times 10^{-7}$  (figure 3). The points for 5°C. fall slightly below the 20°C. points. The equation of this line is

$$D = D_0(1 + k_D c)$$

where  $c$  is the total concentration, or

$$D_M = D_0(1 + k_D c_M) = D_0(1 + k_D c/2) \quad (1)$$

where  $c_M = c/2$ , the mean concentration.

The relation between the slopes of the components in a polydisperse distribution and the slope of the weight-average diffusion from equation 1 has never been formulated. In the general case in which no restriction is put on variation in polydispersity with concentration, Jullander (9), in order to get a linear dependence of diffusion on total concentration, had to assume that polymers of different length all had the same  $k_D$ ; this is contrary to the experimental evidence, as he pointed out (*viz.*, longer particles have larger  $k_D$  values). This difficulty can be avoided in the following manner. For the  $i^{\text{th}}$  component where  $(D_M)_i$  is the mean diffusion coefficient taken at the concentration  $c_i/2$  and  $(D_0)_i$  is the extrapolated value at infinite dilution

$$(D_M)_i = (D_0)_i(1 + k_i c_i/2) = (D_0)_i(1 + k_i c r_i/2)$$

where  $c_i/c = r_i$ , the relative weight for constant polydispersity. When the  $i^{\text{th}}$  component is a member of the polydisperse system of  $n$  components, its independent diffusion is altered by the interaction with it of the remaining  $(n - 1)$  components. Its diffusion is now represented by

$$(D_M)_i = (D_0)_i(I + j_i k_i c r_i/2)$$

where  $j_i$  is the interaction coefficient, a constant for a fixed distribution of the  $r$ 's and having the value unity for independent diffusion. Multiplying by  $r_i$  and summing:

$$\Sigma(D_M)_i r_i = \Sigma(D_0)_i r_i (I + j_i k_i r_i c/2) \quad (2)$$

By definition

$$D_M = \Sigma(D_M)_i r_i \quad \text{and} \quad D_0 = \Sigma(D_0)_i r_i \quad (3)$$

Substituting equation 3 in equation 2 gives

$$D_M = D_0 + \Sigma(D_0)_i j_i k_i r_i^2 c/2 \quad (4)$$

which is a linear equation of the form:

$$D_M = D_0(I + k_D c/2) \quad (1)$$

Were there a change in polymer length with concentration, say  $L$  increases with  $c$ , a linear increasing relation between  $D$  and  $c$  no longer would exist. Here  $dD/dc = dD/dL \cdot dL/dc$ .  $dD/dL$  for low concentrations is negative, and in the assumed example  $dL/dc$  is positive, from which it follows that the diffusion would decrease with increasing concentration for low concentrations. Such a possibility is not confirmed by the data available.

To conserve material, in the case of diffusion in solvents of water and 3  $N$  potassium chloride, the method of Boltzmann (2) was used in order to determine

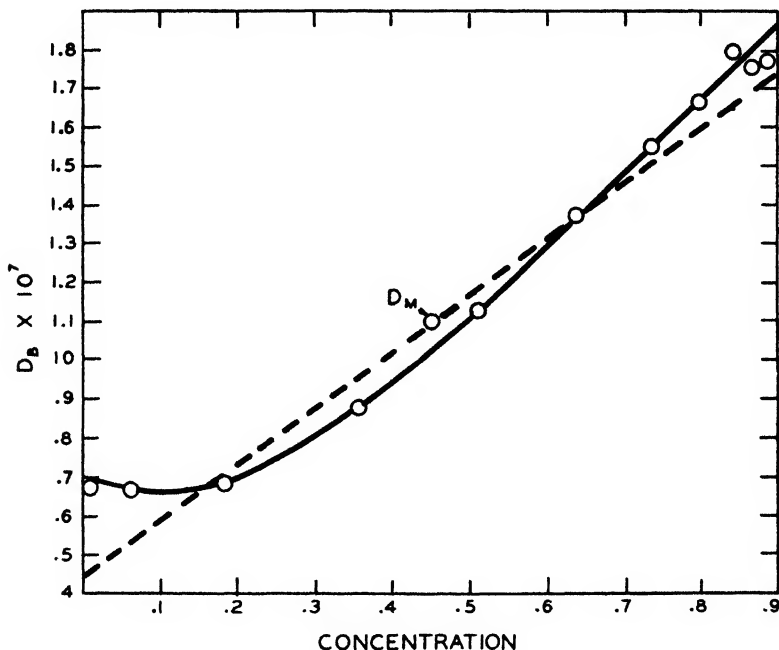


FIG. 4. Boltzmann's curve and estimated line for 0.9 per cent nucleate in buffer-salt (compare with figure 3).

the change of diffusion with concentration from a single experiment. Boltzmann's equation is

$$D_B = (1/2yt) \int_x^\infty yx dx \quad (5)$$

where  $D_B$  is the diffusion constant for any point of the curve corresponding to the concentration at that point,  $y$  is the ordinate,  $x$  the distance to the original starting position, and  $t$  is the time. Gralen (6) showed that the mean value of  $D_B = D_M$ . The shape of the Boltzmann curve is determined by both the polydispersity variation and the concentration dependence of diffusion. The values of  $D_B$  superpose upon the line of  $D_M$  values for a monodisperse material showing concentration dependence. In the cases where the material is also polydisperse, the Boltzmann curve has the form shown in figures 4, 5, and 6, which deviates

from the  $D_M$  line. The non-linear character of the  $D_B$  relation is an index of polydispersity variation in going from the bottom of the cell or high-concentration region to the top of the cell or low-concentration region. As the lowest concentrations are approached, the smallest or most rapidly moving particles separate from the larger particles. Hence the Boltzmann function, as the concentration approaches zero, will extrapolate to a value which is the diffusion

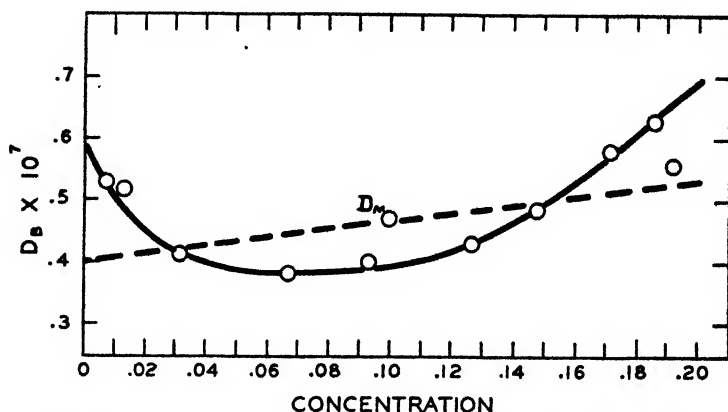


FIG. 5. Boltzmann's curve for 0.2 per cent nucleate in 3 *N* potassium chloride

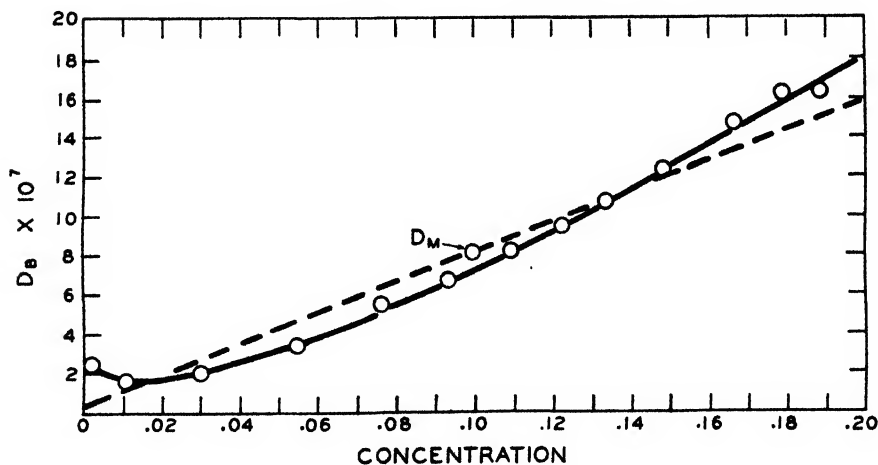


FIG. 6. Boltzmann's curve for 0.2 per cent nucleate in water

constant for the smallest particles. However, these extrapolated values are of low accuracy, since the experimental errors for concentrations below 0.02 per cent are very large.

At two positions in the boundary (where the  $D_B$  curve intersects the  $D_M$  line) the polydispersity distribution in the cell is the same as the distribution of the material before separation by diffusion has taken place (figures 4, 5, and 6).

The derivative at the maximum of Boltzmann's equation (5), where  $dy/dx = 0$  is

$$dD_B/dx = -\bar{X}/2t \text{ or } dD_B/dc = -\bar{X}/2t(dc/dx)_{\max.}$$

where  $\bar{X}$  is the distance from the starting boundary to the mode, usually a negative number, giving:

$$-\bar{X} = 2t(dc/dx)_{\max.} \cdot (dD_B/dc) \quad (6)$$

Gralen (6) made the assumption that  $dD_B/dc$  in the region of the maximum is equal to the slope of the weight-average line, and is therefore constant with re-

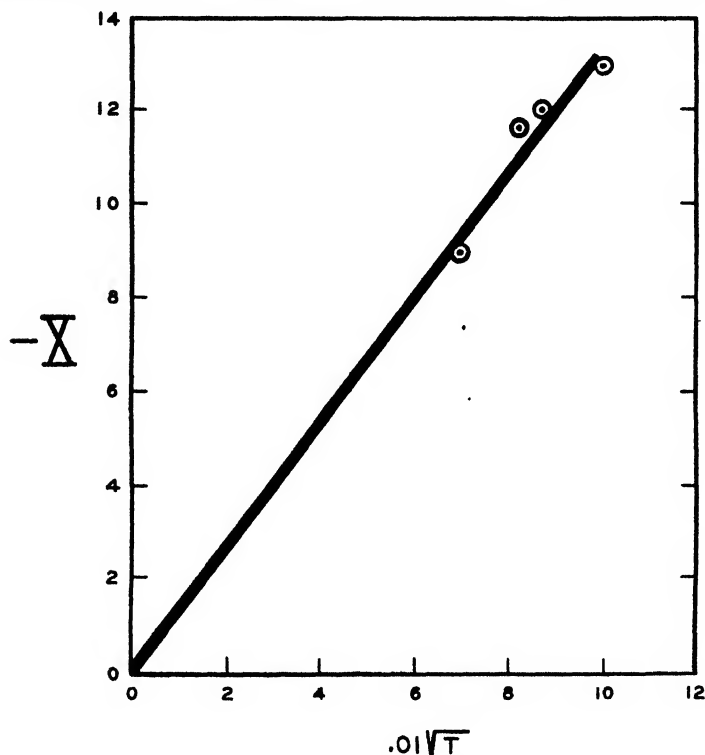


FIG. 7. Shift of the mode (in millimeters) of the diffusion curve for 0.9 per cent nucleate in buffer ( $0.3 \mu$ );  $t$  in seconds.

spect to both time and concentration.<sup>1</sup> For successive photographs of a normally diffusing material  $dc/dx = at^{-1/2}$  (10), which is a first approximation for concentration-dependent diffusion. Substituting in equation 6 gives  $-\bar{X} =$

<sup>1</sup> Gralen (6) assumed that  $(dD_B/dc)_{\max.}$  is equal to the slope of the weight-average line  $D_M$ , a constant. This gives

$$\frac{D_M - D_0}{c/2} = -\bar{X}/2t(dc/dx)$$

from which  $D_0 = D_M + (\bar{X}/4t)(c/dc/dx)$ , which is equivalent to  $D_0 = D_M + (\bar{X}/4t)A/H$ , where  $A$  is the area of the curve and  $H$  is the height. Gralen and Jullander used this equation to determine  $D_0$ .

$kt^{\frac{1}{2}}$ . This was tested in the experiment with 0.9 per cent nucleate in buffer-salt, with the result shown in figure 7.

For photographs taken at the same time interval or when reduced to normal coördinates, which eliminates the time,

$$-\bar{X} = K_1(dc/dx)$$

the shift of the mode increases with concentration gradient (cf. Gralen's figure 20. (6)).

In diffusion experiments with 3 *N* potassium chloride as solvent the concentration gradient diagram is still skewed, showing that high concentrations of monovalent salt do not entirely eliminate the concentration dependence of diffusion. However, the value of  $k_D$  is less than for the weaker buffer-salt solvents. The Boltzmann calculation of  $D_B$  as a function of  $c$  gave the result shown in figure 5 with an estimated extrapolated value of  $D_0 = 4.1 \times 10^{-8}$ . In this experiment, where the symmetry is higher than for the buffer solvents, the error in extrapolating to  $D_0$  by Gralen's equation<sup>1</sup> is probably not large.

When water was used as a solvent, the concentration dependence of diffusion rose sharply, with a great increase in skewness and sharpness of the peak of the experimental curve. The value of  $D_M$  increased to  $8.0 \times 10^{-7}$  (figure 6). The slope of the curve was so great that an accurate extrapolation to  $(D_M)_0$  could not be estimated. The high extrapolated  $(D_B)_0$  value,  $2 \times 10^{-7}$ , indicates that charge effects still operate at infinite dilution.

Polson (13) has recently published a theory of the concentration effect in diffusion. It is pertinent to note that the rotary diffusion constant decreases with increasing concentration (20), a result which would be expected from Polson's theory, since rotational motion of the colloid is converted into translational motion at collision.

#### SEDIMENTATION-VELOCITY MEASUREMENTS

Sedimentation-velocity determinations were made using an air-driven ultracentrifuge (Beams-Linke) and an optical rotor of the Svedberg-Bauer-Pickels type. The jacket of the ultracentrifuge was provided with a water coil through which water at a constant temperature, usually 20°C., from a thermostat was recirculated by a pump. The rotor was spun in a hydrogen atmosphere of 1 cm. pressure. Cells of thickness from 3 to 12 mm. were used. The optical system was of the Thovert-Svensson (18) type. After a few runs were made, it was evident that the bands were so sharp that high speeds were unnecessary, 600 r.p.s. being most satisfactory. The nucleate was made up in several solvents: (a) in distilled water; x-ray diffraction of the dry nucleate showed the presence of a small amount of sodium chloride so that the solution is to be considered as containing a trace of salt; (b) in neutral phosphate buffer plus sodium chloride, total ionic strength 0.3; (c) in 3.0 *N* potassium chloride; (d) in 0.09 *M* calcium chloride. The concentration ( $c_0$ ) of the nucleate was corrected for the dilution factor in the ultracentrifuge cell due to its sectorial shape. This factor is  $(x_0/x)^2$ , where  $x_0$  is the distance from rotor axis to the meniscus and  $x$  is the distance from

the axis to the boundary. The sedimentation constant was tabulated against the mean concentration in the cell when corrected in this manner. The determination of concentration by different workers may be expected to vary by the same amount as in the determination of partial specific volumes. This suggests that assumed concentrations are relative rather than absolute. Fortunately, in sedimentation and diffusion extrapolations to infinite dilution, the functions used are linear relations of the concentration. Under these circumstances the extrapolated value depends only on relative concentrations. On the other hand, the viscosity method for the determination of molecular shapes depends on absolute concentrations.

The shape of the sedimentation boundaries was essentially that of a sharp spike, with only slight asymmetry. Under these circumstances the only possibility in measuring sedimentation velocities was to measure the position of the maximum of the band. As shown by Gralen (6) and Jullander (9), this will give a sedimentation average value which does not differ much from the weight-average value. This procedure obviously could not be used in diffusion, where the asymmetry is relatively large.

No evidence of orientation of the particles during centrifugation could be found with polarized light, a result which agrees with conclusions from other investigations.

Despite the difference in frictional coefficient of a long asymmetric particle in moving with long axis parallel to and transverse to the rotor radius (5), single sharp bands result from the fact that every particle will have the same probability of going through all possible orientations; hence all the particles of similar size sediment alike.

The sedimentation-velocity measurements are shown in table 2, all corrections for viscosity of solvent, density, and temperature having been made according to Svedberg. The reciprocal velocity when plotted against corrected concentration gives a linear relation for concentrations below 0.5 per cent nucleate in the buffer-salt solvent (figure 8). The values of  $1/s$  for concentrations above 0.5 per cent show a marked deviation from the straight-line relationship, the change of sedimentation velocity with concentration leveling off. This seems to be a general characteristic of long polymers.

An alternative method of plotting, due to Burgers (3) and Gralen, is to plot  $s$  (the sedimentation velocity in Svedberg units) against  $sc$  on the assumption that the data fulfill the equation  $s = s_0/(1 + k'c)$ . When  $c \rightarrow 0$ ,  $s$  extrapolates linearly to  $s_0$ . The extrapolated velocity by both methods gives  $s_0 = 12.5$  S.

Three sedimentation runs were made with a 0.3 per cent solution of nucleate in 3 *N* potassium chloride, giving a corrected sedimentation velocity of 7.33 S, using the same partial volume of 0.55. The viscosities were taken from Taylor and Rankin (Landolt-Börnstein tables). These values are similar to those obtained with the phosphate buffer-salt solution for the same concentration of nucleate. This indicates that the sedimentation velocity is not greatly affected on increasing the salt strength above the value normally used to suppress the primary electrical charge effect. Signer (15) found a similar relation in viscosity

at very low velocity gradients. Nucleate in a 5 per cent salt solution gave the same viscosity as in a 1 per cent salt solution. This is in marked contrast to the results on viscosity at high velocity gradients (7).

TABLE 2

*Sedimentation (in Svedbergs) of nucleate in buffer (pH 7.4, 0.3  $\mu$ ), CaCl<sub>2</sub>, KCl, and water*  
Composition of buffer: 0.031 *m* Na<sub>2</sub>HPO<sub>4</sub>, 0.006 *m* KH<sub>2</sub>PO<sub>4</sub>, 0.2 *N* NaCl

SOLVENT	CONCENTRATION OF NUCLEATE	S	100/S
	<i>per cent</i>		
Buffer . . . . .	0.86	3.80	26.3
	0.455	5.06	19.8
	0.23	7.55	13.2
	0.18	7.60	13.16
	0.126	8.47	11.81
	0.108	8.80	11.36
	0.086	10.25	9.76
	0.041	10.80	9.26
	0.0233	12.61	7.93
	0.022	12.84	7.79
0.09 <i>M</i> CaCl <sub>2</sub> . . . . .	0.20	11.5	8.70
3 <i>N</i> KCl . . . . .	0.273	7.33	13.64
Water . . . . .	0.196	1.92	52.0

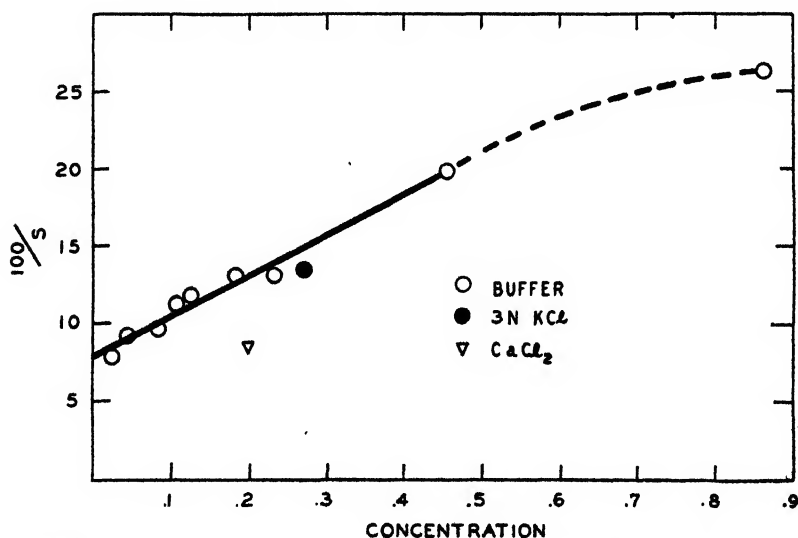


FIG. 8. 100  $\times$  reciprocal of sedimentation velocity (Svedberg units) against concentration in per cent.

The sedimentation of 0.25 per cent nucleate in a 0.09 *M* calcium chloride solution gave the high velocity of 11.5 *S*. This is similar to the finding of Carter (4)



on the sedimentation of nucleohistone in 2 per cent calcium chloride, in which the concentration dependence of sedimentation was nearly suppressed. In the presence of calcium chloride these materials sediment in a more nearly ideal manner. According to Hammarsten (8), nucleate viscosity determined at high gradients drops sharply in the presence of polyvalent cations.

The sedimentation velocity of nucleate 0.2 per cent in water was found to be 1.9 S. This is about one fourth the velocity in the neutral phosphate buffer-sodium chloride solution. A part of this retardation is brought about by the back electrical field  $dE/dx$ , caused by the slower sedimentation tendency of the positive sodium with respect to the negative nucleate ions.

The two forms of the sedimentation equation for independently sedimenting components

$$s_i = (s_0)_i / (1 + k'_i c_i) \quad \text{and} \quad 1/s_i - 1/(s_0)_i = k_i c_i \quad (8')$$

are equivalent, the constants for the two forms being related by  $k'_i = k_i (s_0)_i$ . The second form is convenient for showing the relation between the sedimentation for the  $i^{\text{th}}$  component and the sedimentation of the weight average taken over all components. In the case of a polydisperse system we again introduce the  $j$  factor to allow for the fact that the contribution of each component to the sedimentation of the whole system will be modified by interaction between components. Equation 8' then becomes

$$1/s_i - 1/(s_0)_i = j_i k_i c_i \quad (8'')$$

From equation 8''

$$r_i 1/s_i - r_i 1/(s_0)_i = j_i k_i r_i c_i = j_i k_i r_i^2 c$$

for constant polydispersity. Summing

$$\Sigma(r_i/s_i - r_i/(s_0)_i) = \Sigma j_i k_i r_i^2 c$$

where  $\Sigma r_i/s_i$  equals the weight average of reciprocal sedimentation velocity at concentration  $c$  and  $\Sigma r_i/(s_0)_i$  is the weight-average sedimentation constant at infinite dilution. From which

$$1/s - 1/s_0 = k_i c \quad (8)$$

The relation between  $1/s$  and  $c$  for a system of constant polydispersity will be linear, if the components  $i$  have a linear relationship between  $1/s_i$  and  $c_i$ .

#### *Molecular weight and shape*

Extrapolated values to infinite dilution having been obtained for  $s_0$  and  $D_0$ , the molecular weight may be obtained from the relation

$$M = RTs_0/D_0(1 - V\rho)$$

using the values  $D_0 = 0.45 \times 10^{-7}$ ;  $V = 0.55$ ;  $\rho = 1.015$ ; and  $s_0 = 12.5$  Svedbergs  $= 12.5 \times 10^{-13}$  c.g.s. This gives 1,500,000 for  $M$ . From these values the frictional ratio  $f/f_0$  is calculated as 6.82, from which  $a/b$  is 284,  $a$  is 5226 Å., and  $b = 18.4$  Å.

Wissler (20), by combining rotary diffusion with viscosity measurements, obtained a weight of 1,250,000 for nucleate. According to Jullander's (9) results with nitrocellulose, the molecular weights obtained by combining sedimentation and diffusion are higher than those obtained utilizing viscosity measurements.

### *Nucleohistone*

It appears likely that since nucleohistone (4) is a rod-shaped particle, its diffusion characteristics will have some features in common with nucleate and the cellulose derivatives. Before its size determination can be considered as satisfactory, it will be necessary to establish its diffusion-concentration relation. With a known chemical analysis of nucleohistone there should be agreement between the molecular weight of the nucleate determined directly and as determined from the molecular weight of nucleohistone, for a stable monodisperse material. However, exact agreement can hardly be expected between the chemically prepared highly disperse nucleate and the combined form in which nothing is known concerning the frequency with which histone combines with different size nucleates. From Carter's (4) investigation it may be concluded that the molecular weight of nucleate combined with histone is somewhat over 1,100,000.

### SUMMARY

The diffusion constant increases with concentration according to the relation

$$D = D_0(1 + k_D c)$$

In strong salt solution the value of  $k_D$  decreases. The Boltzmann equation is used to determine the trend of the diffusion constant with concentration and to estimate the diffusion for the smallest particles. It is shown that the distance of the mode from the starting point increases (negatively) approximately as  $t^{\frac{1}{2}}$ . It is shown that for a polydisperse system, if all components have a linear concentration dependence and the system has a constant polydispersity, the weight-average diffusion over all components is also linear.

The sedimentation is described by  $1/s - 1/s_0 = k_s c$ , the plot of  $1/s$  against  $c$  giving a straight line, extrapolating to  $1/s_0$ . Sedimentation in the presence of 3 *N* potassium chloride gives a slightly higher velocity, and 0.09 *M* calcium chloride gives a velocity approaching the velocity for infinite dilution. The sedimentation in water at 0.2 per cent nucleate concentration is about one-fourth the value in buffer.

It is shown that with constant polydispersity a linear relation between  $1/s_i$  and  $c_i$  leads to a linear relation for the weight-average reciprocal sedimentation constant. The molecular weight and shape factors were obtained. The relation between the molecular weights of nucleate and nucleohistone is discussed.

The writer is indebted to Dr. J. P. Greenstein for the sample of sodium nucleate used, and to Mr. J. Richey, Mr. H. Sipes, and Mrs. E. Wiley for assistance during the course of the work.

## REFERENCES

- (1) ASTBURY, W. T., AND BELL, F. O.: *Nature* **141**, 747 (1938); Cold Spring Harbor Symposium Quant. Biol. **6**, 109 (1938).
- (2) BOLTZMANN, L.: *Akad. Wiss. München Sitzungsber. math. phys. Klasse* **24**, 211 (1894); *Ann. Phys. Chem.* **53**, 959 (1894).
- (3) BURGERS, J. M.: *Proc. Nederl. Akad. Wetensch.* **44**, 1045, 1177 (1941); **45**, 9, 126 (1942).
- (4) CARTER, R. O.: *J. Am. Chem. Soc.* **63**, 1960 (1941).
- (5) GANS, R.: *Ann. Physik* **86**, 628 (1928).
- (6) GRALEN, N.: *Dissertation*, Uppsala, Sweden, 1944.
- (7) GREENSTEIN, J. P., AND JENNETTE, W. V.: *J. Natl. Cancer Inst.* **1**, 77 (1940).
- (8) HAMMARSTEN, E.: *Biochem. Z.* **144**, 383 (1924).
- (9) JULLANDER, I.: *Arkiv Kemi, Mineral. Geol.* **A21**, No. 8, p. 1 (1945).
- (10) LAMM, O.: *Nova Acta Regiae Soc. Sci. Upsaliensis* [4] **10**, No. 6 (1937).
- (11) LONGSWORTH, L. G.: *Ann. N. Y. Acad. Sci.* **41**, 267 (1941).
- (12) NEURATH, H.: *Science* **93**, 431 (1941).
- (13) POLSON, A.: *Nature* **157**, 406 (1947).
- (14) SCHMIDT, G., PICKELS, E. G., AND LEVENE, P. A.: *J. Biol. Chem.* **127**, 251 (1939).
- (15) SIGNER, R., CASPERSSON, T., AND HAMMARSTEN, E.: *Nature* **141**, 122 (1938).
- (16) SIGURGEIRSSON, T., AND STANLEY, W. M.: *Phytopathology* **37**, 26 (1947).
- (17) TENNENT, H. G., AND VILBRANDT, C. F.: *J. Am. Chem. Soc.* **65**, 424 (1943).
- (18) THOVERT, J.: *Ann. Phys.* [9] **2**, 369 (1914).
- (19) SVENNSON, H.: *Kolloid-Z.* **87**, 181 (1939).
- (19) TISELIUS, A., AND GROSS, D.: *Kolloid-Z.* **66**, 11 (1934).
- (20) WISSLER, A.: *Dissertation*, Bern, 1940.

## POLYAMIDE ANTIFOAMS. I

## RELATION BETWEEN CHEMICAL CONSTITUTION AND EFFECTIVENESS

ARTHUR L. JACOBY

*National Aluminate Corporation, Chicago, Illinois**Received July 24, 1947*

Recent research in the problem of foaming in steam boilers has resulted in the development of several types of new chemical compounds possessing unusual merit as antifoams. A large group of such compounds (2, 3, 4, 5) are broadly classed as polyamides. In testing a large number of polyamides as possible boiler antifoams, several interesting relationships were found to exist between chemical constitution and antifoam activity. These relationships are significant when examined in the light of a recently proposed theory of antifoam action (6), and tend further to support this theory.

## USE OF ANTIFOAMS

While proper water treatment for softening, clarification, coagulation, and scale-prevention will do much to improve foaming conditions in boiler waters, the benefits of such treatment can frequently be greatly extended by the addi-

tional use of an antifoam agent. In the past many substances have been claimed to exert an antifoaming effect in steam boilers and a few, notably castor oil, have been rather widely used. These earlier materials have suffered, however, from several disadvantages, the greatest being their instability under the conditions of alkalinity and temperature encountered in the boiler and their relatively low order of effectiveness. The use of certain polyamides as antifoams has resulted in the solution of many difficult foaming problems and has permitted the concentration of permissible dissolved solids in the boiler water to be increased two- to five-fold, and even more. Such results were unknown with castor oil. Moreover, these polyamide antifoams are effective in extremely low dosages, sometimes of only a few parts per million, or less, in the feed water.

#### LABORATORY TESTING

The studies reported here were undertaken as a part of a program of investigating the fundamental chemical and physical factors affecting the efficiency of boiler antifoams. The method employed for evaluating the compounds as antifoams has been described elsewhere (6). For the tests reported herein, a feed water was used having the following composition:

Calcium hardness (as $\text{CaCO}_3$ ).....	9.0 grains/gallon
Magnesium hardness (as $\text{CaCO}_3$ ).....	9.0 grains/gallon
Alkalinity (methyl orange) (as $\text{CaCO}_3$ ).....	42.5 grains/gallon
Sodium chloride (as $\text{NaCl}$ ).....	5.0 grains/gallon
Sodium sulfate (as $\text{Na}_2\text{SO}_4$ ).....	42.0 grains/gallon
Tannin extract, dry.....	2.0 grains/gallon

The material to be tested as an antifoam was added as a solution in dioxane of 1.0 mg. of the material per 1.0 ml. of solution. To each 5 gallons of the feed water was added 4.9 ml. of the dioxane solution, resulting in a concentration of antifoam in the feed water of 0.256 p.p.m. (0.015 grain/gallon).

Tests upon the same antifoam by the above procedure are reproducible within a range of approximately  $\pm 25$  grains/gallon dissolved solids in the boiler water at the time of carryover, when working in the range reported.

#### PREPARATION OF COMPOUNDS

Since most of the compounds tested and discussed have not previously been described in the literature, their preparation and properties are briefly given below (see table 1).

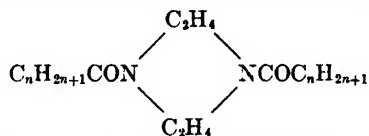
*Diacylated piperazines:* In each case, the diacylated piperazine was prepared by mixing together one molecular portion of piperazine or its hexahydrate and two molecular portions of the appropriate fatty acid in a 50-ml. flask. The flask was heated in an oil bath and the mixture stirred at a temperature slightly above  $100^\circ\text{C}$ . until any tendency for frothing had disappeared, after which it was stirred for 3 hr. at a bath temperature of  $150$ – $160^\circ\text{C}$ . The product, which was generally of the nature of a waxy substance, was then recrystallized, usually from methanol or acetone.

*N-Octadecylceramide:* This compound was made in an analogous manner

from theoretical proportions of erucic acid and *n*-octadecylamine and was recrystallized from a mixture of equal volumes of acetone and low-boiling petroleum ether. Melting point, 70°C. Calculated for  $C_{40}H_{78}ON$ : N = 2.38 per cent; found, N = 2.36 and 2.38 per cent.

*N,N'*-Dihexadecylsuccinamide: To 48.2 g. (0.20 mole) of stirred, molten *n*-hexadecylamine at 90–100°C. was added 7.75 g. (0.05 mole) of succinyl chloride fairly rapidly. The temperature was then brought up to 150°C. over a period of 30 min. The warm liquid reaction product was then poured into a mixture of about 400 ml. benzene and 200 ml. ether, treated with solid potassium hydroxide to remove hydrogen chloride, and the filtered solution freed of solvent by evaporation to leave a waxy solid. Recrystallization from a mixture of methanol and ethanol gave a colorless product, melting at 129–130.5°C. Calculated for  $C_{36}H_{72}O_2N_2$ : N = 4.97 per cent; found, N = 5.10 and 5.08 per cent.

TABLE 1  
*Melting points and analyses of the diacylated piperazines*



n	COMPOUND	FORMULA	MELTING POINT °C.	ANALYSIS FOR NITROGEN	
				Calculated per cent	Found per cent
7	Diocetanoylpiperazine	$C_{20}H_{38}O_2N_2$	166	7.73	7.79; 7.83
11	Didodecanoylpiperazine	$C_{28}H_{54}O_2N_2$	133–34	6.24	6.35; 6.19
13	Ditetradecanoylpiperazine	$C_{32}H_{62}O_2N_2$	75	5.53	5.55; 5.53
15	Dihexadecanoylpiperazine	$C_{36}H_{70}O_2N_2$	79.5–80	4.98	5.01; 5.05
17	Dioctadecanoylpiperazine	$C_{40}H_{78}O_2N_2$	83–83.5	4.53	4.42; 4.43

*N,N'*-Dioctadecylsebacamide: A mixture of 24.2 g. (0.09 mole) of *n*-octadecylamine and 8.1 g. (0.04 mole) of sebacic acid was placed in a 50-ml. flask immersed in an oil bath and stirred for 3 hr. at a bath temperature of 150–160°C. The product was recrystallized from 2-propanol, using decolorizing carbon. Melting point, 132–133°C. Calculated for  $C_{46}H_{92}O_2N_2$ : N = 3.97 per cent; found, N = 4.06 and 4.03 per cent.

#### TEST RESULTS

Laboratory boiler tests were carried out, as described above, on several materials, each employed at a dosage of 0.256 p.p.m. in the feed water entering the boiler. For purposes of comparison, runs were also made in which no material was added as an antifoam (but the usual amount of dioxane was included in the feed water), and in which castor oil was added. Results are shown in table 2. The higher the dissolved solids value shown, the more effective is the material as an antifoam.

## INTERPRETATION OF RESULTS

The results show, first, the remarkable superiority of certain of the polyamides as boiler antifoams over the previously used castor oil. The conditions of the test were purposely made rather severe so as not to prolong unduly a test in which one of the better antifoams was being evaluated. The substantial differences found between the action of castor oil and of several of the diamides are substantiated by field experience.

Secondly, the results tend to strengthen the theory of antifoam action recently suggested by Jacoby and Thompson (6). Briefly stated, the mechanism of the rupture of double-faced liquid films, e.g., of bubble films, consists of the gradual thinning of these films, due to drainage of liquid, until the film reaches a critical minimum thickness and is destroyed (7). In the presence of an adsorbed layer of surface-active insoluble material, the collapse of a foam bubble

TABLE 2  
*Test results on antifoams*

COMPOUND	BOILER WATER DISSOLVED SOLIDS AT CARRYOVER	MOLECULAR WEIGHT
	<i>grains/gallon</i>	
None (dioxane only).....	170	
Octadecanamide . . . . .	186	283
Diocetanoylpiperazine . . . . .	189	362
Didodecanoylpiperazine . . . . .	184	450
Ditetradecanoylpiperazine . . . . .	218	506
Dihexadecanoylpiperazine . . . . .	378	562
Diocadecanoylpiperazine . . . . .	475	618
<i>N</i> -Octadecylrucamide . . . . .	201	589
<i>N,N'</i> -Dihexadecylsuccinamide . . . . .	563	564
<i>N,N'</i> -Diocadecylsebacamide . . . . .	978	704
Castor oil . . . . .	186	

may be accompanied by a syneresis (8) or formation in the adsorption layers of dehydrated aggregates of the surface-active material. It has been observed that certain monolayers, although they may actually stabilize the bubble film while they are in the liquid state, lose this ability at once when the solid (brittle) state is attained (8). This indicates that one of the conditions for stabilization is the great mobility of the molecules of the adsorption layers, and if this mobility is lost by attainment of the solid state, the adsorption layers may contribute to the rupture of the bubble film. It is likely that the syneresis described above results essentially in the formation of patches of monolayer in the brittle state which are incapable of redispersion at a rate equal to or greater than the velocity of destruction of the bubble film.

Table 2 shows that the monoamide, octadecanamide, showed no antifoam action, and that a substantial increase in the molecular weight brought about by the introduction of a second long fatty chain, as in *N*-octadecylrucamide, im-

parted but slight antifoam action. However, the introduction into the molecule of a second amide group resulted in antifoam action if the molecular weight was sufficient. Thus, the diamide formed by the diacylation of piperazine with a fatty acid of fourteen or more carbon atoms showed pronounced antifoam action. The theory of antifoam action referred to above suggests that hydrogen bonding promotes antifoam action by enhancing the synergetic effect and creating a greater

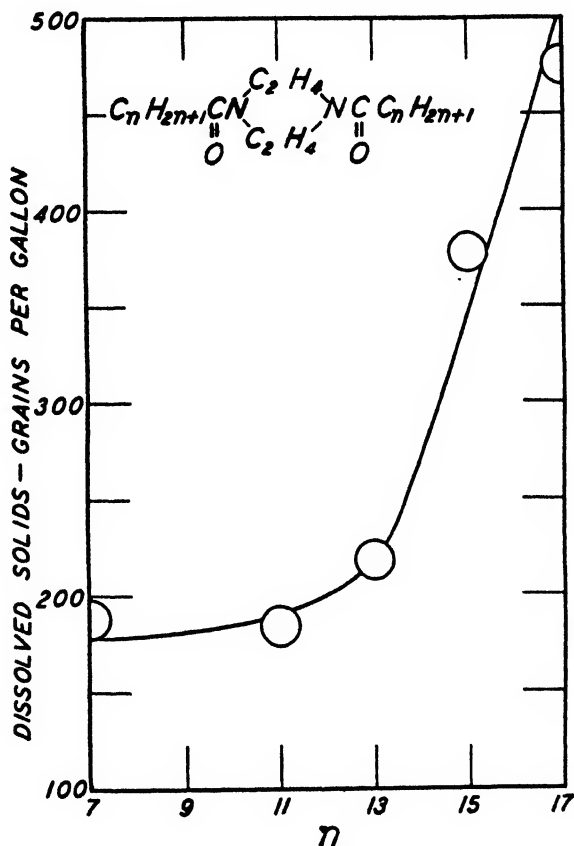


FIG. 1. Increasing antifoam effectiveness of diacylated piperazines with increasing molecular weight.

tendency for the monolayer to reach the solid or brittle state, as shown by Alexander (1). A consideration of the hydrogen bonding possible in the case of the monoamides as contrasted to that possible with the diamides will reveal that the extensive cross-linking of the latter should favor the effects believed responsible for antifoam action.

The superiority of the diamides over the monoamides cannot be ascribed merely to the fact that many of the better diamides are of relatively high molecular weight. While there appears to be a certain minimum requirement as to molecular weight in order that the diacylated piperazines act as antifoams in

a boiler, a comparison of the molecular weights given in table 2 will show that several of the diamides tested were of lower molecular weight than *N*-octadecylcerucamide, an almost ineffective, high-molecular-weight monoamide, yet they were effective antifoams. That an increase in molecular weight causes the diacylated piperazines to become increasingly effective is well shown by reference to figure 1. Table 2 will show that this same tendency holds in the case of *N,N'*-dihexadecylsuccinamide and *N,N'*-dioctadecylsebacamide, although in the case of these two compounds both the acid and the amine were increased in size in going from the former to the latter. The increase in effectiveness with increasing length of the fatty chains is probably due to an increase in the van der Waals cohesive forces whereby solidification is brought about more readily (1).

That chemical constitution, as well as molecular weight, is important is further demonstrated by a comparison of the effectiveness of dihexadecanoylpiperazine and *N,N'*-dihexadecylsuccinamide. The molecular weight of the latter is only two more than that of the former, yet the succinamide is considerably more effective as an antifoam. A possible explanation of this in the light of the theory under discussion is that the piperazine derivative can only be linked together by hydrogen bonding through the agency of another kind of molecule, such as water. In the case of the succinamide derivative, however, this is not the case. Each amide group in the succinamide bears a hydrogen whereby hydrogen bonding may be effected to the carbonyl oxygen of a neighboring molecule without the necessity for some intermediary.

#### SUMMARY

Antifoam tests were conducted in an experimental boiler on a series of piperazines diacylated by fatty acids, and on several other amides and castor oil. Of the diamides tested, those of sufficient molecular weight were more effective than castor oil or either of two monoamides. The effectiveness of the diacylated piperazines was shown to increase with increasing length of the fatty chains. Two diamides of almost identical molecular weight, one a diacylated piperazine and the other a succinamide derivative, differed widely in effectiveness. The results were interpreted in terms of a recently formulated theory of antifoam action.

#### REFERENCES

- (1) ALEXANDER: Proc. Roy. Soc. (London) **A179**, 470-85, 486-90 (1942).
- (2) BIRD AND JACOBY: Canadian patent 433,431 (March 5, 1946).
- (3) GUNDERSON: U. S. patent 2,328,551 (September 7, 1943).
- (4) IMPERIAL CHEMICAL INDUSTRIES, LTD.: British patent 568,318 (March 29, 1945).
- (5) IMPERIAL CHEMICAL INDUSTRIES, LTD.: British patent 568,510 (April 9, 1945).
- (6) JACOBY AND THOMPSON: Proceedings Seventh Annual Water Conference, Engineers, Society of Western Pennsylvania, January, 1947, pp. 31-41.
- (7) REHBINDER AND TRAPEZNIKOV: Acta Physicochim. U.R.S.S. **9**, 257-72 (1938).
- (8) TRAPEZNIKOV AND REHBINDER: Compt. rend. acad. sci. U.R.S.S. **18**, 427-30 (1938).



## FILTRATION OF AEROSOLS BY GRANULAR CHARCOAL

SIDNEY H. KATZ AND DUNCAN MACRAE

*Chemical Corps Technical Command, Army Chemical Center, Maryland**Received October 2, 1947*

It is generally known that it is not practicable to remove aerosols from air with gas mask charcoal. That is why toxic aerosols were introduced as war gases and why all combat gas masks must have a special filter to protect the wearer of the mask against aerosols. In some masks these filters consist of a number of plies and the performance of such filters has been represented (1) by the following equation:

$$Q = q^p \quad (1)$$

where  $Q$  = the fraction of the aerosol passing the filter,  $p$  = the number of plies (or other units of thickness), and  $q$  = the fraction passing a single-ply filter.

This equation may be written in the form

$$p = (1/\log q) \log C_e/C_0 \quad (2)$$

in which  $C_0$  = the concentration of aerosol entering the filter and  $C_e$  = the effluent concentration.

In equation 2  $p$  is the thickness of the filter in number of plies,  $1/\log q$  is a constant characteristic of the filter material, and  $\log C_e/C_0$  is a measure of the performance of the filter.

A somewhat similar equation is used by chemical engineers to define the height of a transfer unit and has been applied to the absorption of vapors by gas mask charcoal (2) under such conditions that the concentration of the vapor at the surface of the charcoal is negligible.

This equation may be written

$$I_t = 2.30H_t \log C_0/C_e \quad (3)$$

In equation 3  $I_t$  is the thickness of the filter,  $2.30H_t$  is a constant characteristic of the vapor and the bed of charcoal, and  $\log (C_e/C_0) = -\log (C_0/C_e)$  is the same, except for sign, as a term in equation 2. In fact, equations 2 and 3 become identical if  $-x/\log q = 2.30H_t$ , where  $x$  = the thickness of one ply. This is not surprising, for both relate to the process of removing substances from an air stream flowing through an irregular porous structure. It may, therefore, be that the principal difference in the filtration of aerosols and vapors by charcoal is the difference between the diffusion coefficients of the vapor molecules and of the small aerosol particles.

If this is so, it should be possible to calculate a value of  $H_t$  for a bed of charcoal and an aerosol with particles of known size by means of the equation

$$H_t = (1/a)(D_p G/\mu)^{0.41} (\mu/\rho D_v)^{0.67} \quad (4)$$

given in the article by Klotz cited above. In this equation:

- $a$  = the surface of the granules per unit volume of filter bed
- $D_p$  = the diameter of the granules
- $G = \rho V$  = the mass rate of flow
- $\mu$  = the viscosity of the air
- $\rho$  = the density of the air
- $V$  = the volume rate of air flow
- $D_v$  = the diffusion constant of the gas in air

If  $a = k_1/D_p$  and  $G = \rho V$ , equation 4 becomes:

$$H_t = (k_1/D_p)(D_p \rho V/\mu)^{0.41} (\mu/\rho D_v)^{0.67} \quad (5)$$

The diffusion constant of an aerosol is given by the relation (3):

$$D_v = \frac{kT}{6\pi\mu r} \left\{ 1 + (A + Be^{-c\mu/r}) \frac{\lambda}{r} \right\} \quad (6)$$

in which  $k$  = Boltzmann's constant,  $T$  = absolute temperature, and  $r$  = radius of aerosol particle. At 298°K.

$\lambda$  = mean free path of air molecules =  $5.9 \times 10^{-6}$  cm.

$\mu$  = viscosity of air =  $1.832 \times 10^{-4}$

$A = 0.874$

$B = 0.35$

$c = 1.7$

On the basis of these considerations arrangements were made to test equation 4 by measuring the penetration of charcoal beds by an aerosol in the laboratories of Division 10 of the National Defense Research Committee at Northwestern University in 1944. Mr. J. Fehrenbacher made a number of cylindrical, axial-flow canisters with charcoal beds 2.80 cm. deep and 10.64 cm. in diameter. Dr. Hugh B. Pickard measured the penetration of the canisters by an aerosol of dioctyl phthalate with particles of 0.151 micron radius at a flow rate of 85 liters per minute and a concentration of about 125 micrograms per liter. He obtained the results shown in table 1. In the last column the values of  $2.303H_t$  are obtained by dividing 2.80 by  $\log C_o/C_e$  and are the bed depths required for an aerosol penetration of 10 per cent.

If  $a$  is inversely proportional to the particle diameter and only the particle size is varied, equation 4 above reduces to

$$H_t = k_1 D_p^{1.41} \quad (7)$$

in which  $k_1$  is a constant. Plotting  $\log H_t$  against  $\log D_p$  from the data in the above table a value of 0.9 is obtained for the exponent instead of 1.41.

Similarly, equation 4 becomes

$$H_t = k_2(D_p)^{-0.67} \quad (8)$$

when only the diffusion coefficient is varied.

From some unpublished data reported by Dr. E. O. Wiig for ethyl chloride on 16-20 mesh charcoal, it was calculated that at a rate of air flow of 500 cm. per minute:

$$H_t = 0.095 \text{ cm.}$$

At an airflow of 955 cm. per minute, as used in the experiments of table 1, the value of  $H_t$  would have been

$$0.095(955/500)^{0.41} = 0.123 \text{ cm.}$$

So for ethyl chloride with a diffusion coefficient of 0.100

$$H_t = 0.123 \text{ cm.}$$

TABLE 1  
*Penetration of charcoal by dioctyl phthalate*

CANISTER NO.	CHARCOAL PARTICLE SIZE		PRESSURE DROP	PENETRATION		2.30 $H_t$
	Sieve	Diameter		$C_s/C_0$	$\log C_0/C_s$	
		cm.	mm. H <sub>2</sub> O			cm.
1	18-20	0.091	32	0.81	0.092	30.4
2	20-25	0.075	38	0.79	0.102	27.5
3	25-30	0.060	48	0.74	0.131	21.5
4	30-40	0.047	63	0.69	0.161	17.4

while for the dioctyl phthalate particles with a diffusion coefficient of  $1.08 \times 10^{-6}$ , and charcoal granules of very nearly the same size as those of Wiig:

$$2.303 \times H_t = 30.4$$

By means of this data a value of the exponent in equation 8 was calculated for comparison with the value of -0.67 there given as follows:

$$n = \frac{\log (30.4/0.123)/2.303}{\log (1.08 \times 10^{-6}/0.100)} = -0.41$$

The agreement, in the case of the two exponents, indicates that a layer of granular charcoal filters aerosol particles and vapor molecules by much the same mechanism over a 100,000-fold range of diffusion coefficients.

#### REFERENCES

- (1) KATZ, S. H., SMITH, G. W., AND MEITER, E. G.: U. S. Bureau of Mines Tech. Paper No. 394 (1926).
- (2) KLOTZ, IRVING M.: Chem. Rev. 39, 241-67 (1946).
- (3) MILLIKAN, R. A.: Phys. Rev. 22, 1 (1923). (Equation 6 above is obtained by combining Millikan's equation 3 with the equation  $D_s = kTv/F$ .)

## ANALYTICAL TREATMENT OF MULTICOMPONENT SYSTEMS

LOUIS A. DAHL

*National Bureau of Standards, Washington 25, D. C.**Received August 12, 1947*

## CONTENTS

I. Introduction .....	698
A. The intrinsic equation .....	698
B. Terminology .....	700
II. Secondary systems (conversion of compositions).....	702
A. Primary to secondary conversion equations. ....	702
B. Secondary to secondary conversion equations.....	705
III. Systems of $(N - 1)$ components .....	707
A. Properties of intrinsic equations .....	708
B. Classification of compositions.....	710
IV. Systems of less than $(N - 1)$ components .....	719
A. Limiting conditions for systems not passing through primary system.....	720
B. General method for multicomponent systems.....	721
V. Phase systems.....	723
A. Equilibria at a eutectic point (primary compositions) ....	724
B. Equilibria at a eutectic point (secondary compositions) .....	725
C. Equilibria at a peritectic point.....	726
VI. Summary .....	729
VII. References .....	729

## I. INTRODUCTION

## A. THE INTRINSIC EQUATION

The chief characteristic of a triangular diagram which is responsible for its usefulness in representing ternary systems is the opportunity it provides for representing three variables in a plane, with three axes of reference (the sides of the triangle). This is possible because in a ternary system only two of the composition variables are independent. When the methods of analytic geometry are employed in dealing with composition relations, the axes of reference refer only to independent variables, so that only two of the three components appear in equations. The procedure is equivalent to taking two of the sides of the triangular diagram as coordinate axes. Except in the case of binary systems represented by lines passing through the origin, the equation for a binary system possesses a constant term. The magnitude of this term depends upon the number of weight units taken as a total in the expression of composition. For example, if the equation  $x + 3y - 80 = 0$  represents a binary system when composition is expressed in percentages by weight, the equation  $x + 3y - 0.8 = 0$  represents the system when composition is expressed in weight fractions.

One of the significant properties of the triangular diagram is that each of the sides represents totality. If the total is 100 per cent, the side represents 100 per cent, and if the total is unity (weight fractions), the side represents unity. It is because of this property that triangular diagrams representing ternary

systems appear frequently without any indication of the units in which composition is expressed. Equations derived by analytic geometry do not possess this characteristic. Without a knowledge of the number of weight units representing totality the equations are meaningless.

Composition relations can be treated analytically by a method analogous to the use of the triangular diagram in geometric treatment. This is accomplished by eliminating the constant term which involves the number of weight units taken as a total in the expression of composition. To illustrate, let us consider a hypothetical ternary system X-Y-Z, in which percentages of the components are designated as  $x$ ,  $y$ , and  $z$ , respectively. Considering  $x$  and  $y$  as the independent variables, the equation for the binary system in which the components are  $x = 50$ ,  $y = 50$ ,  $z = 0$  and  $x = 80$ ,  $y = 0$ ,  $z = 20$  is:

$$5x + 3y - 400 = 0 \quad (1)$$

This equation is satisfied by all compositions in the binary system, provided that in each case  $x + y + z = 100$ , corresponding to a total of 100 per cent. The constant term may be eliminated by subtracting four times the latter equation from equation 1, obtaining:

$$x - y - 4z = 0 \quad (1b)$$

Since equation 1b does not possess a constant term, it represents the relation between the composition variables in any total quantity of material. The variables may refer to the number of grams in 100 g. (percentages), to the number of pounds in 1 pound (weight fractions), or even to the number of pounds in a long ton of 2240 pounds. As in the triangular diagram, the number of weight units representing totality does not need to be defined. Equations of this kind, in which the constant term is lacking, are not referred to coördinate axes or dimensions. Since they pertain only to composition, they will be referred to as *intrinsic equations*.

As will be shown presently, the intrinsic equation of an  $(N - 1)$ -component system within an  $N$ -component system may be derived directly, that is, without first deriving an equation with distances from coördinate axes in mind. This is an important consideration when dealing with systems of more than four components, since it eliminates the necessity of thinking in terms of hyperspace.

Intrinsic equations have other advantages which will appear as this study proceeds. However, the number of equations required to represent a system within an  $N$ -component system is not reduced by choosing the intrinsic form. For example, in a five-component system, a single equation represents a quaternary system, two equations are needed to represent a ternary system, and three to represent a binary system. In each case the number of equations is the same as with equations involving a constant term. In defining a system within any given system the number of equations increases as the number of components decreases in the system to be defined. Expression of very simple relations in a system of many components therefore may become quite complicated and awkward. To meet this difficulty another type of equation, involving pa-

rameters, may be employed. *Parametric equations* increase in complexity in the opposite direction, being easy to apply when the use of intrinsic equations becomes difficult, and *vice versa*. The properties and application of parametric equations will be considered in another paper which is in preparation.

## B. TERMINOLOGY

Some of the terms which will be used may be described with reference to figure 1, which is a diagram showing the final products of crystallization in the

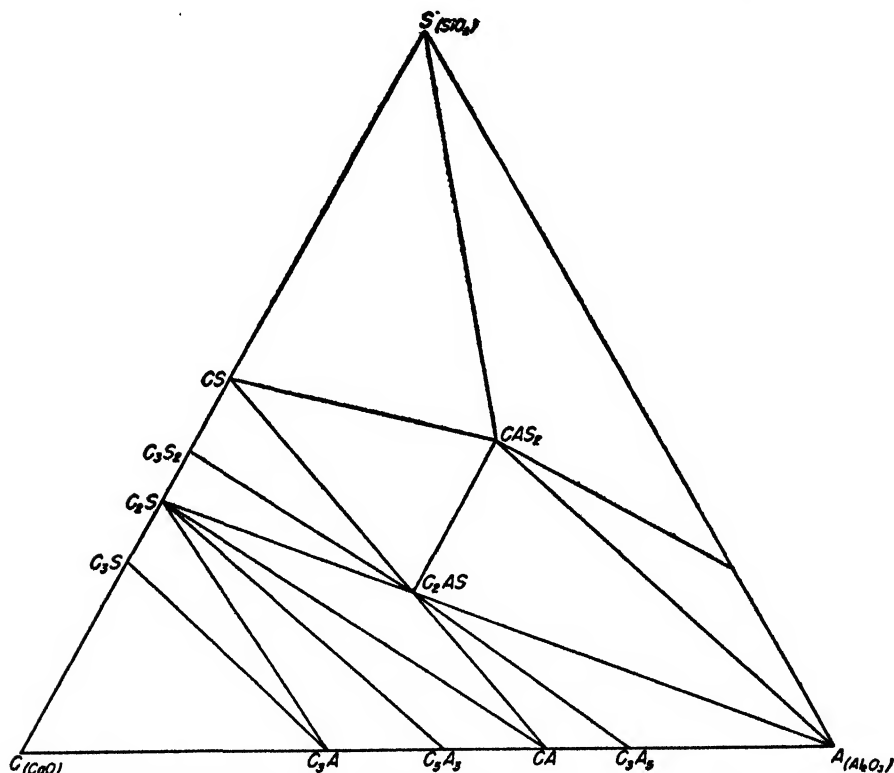


FIG. 1. Final products of crystallization in the system  $\text{CaO}-\text{Al}_2\text{O}_3-\text{SiO}_2$

system  $\text{CaO}-\text{Al}_2\text{O}_3-\text{SiO}_2$ , as determined by Rankin and Wright (3) and later investigators (1). In this figure the oxide components  $\text{CaO}$ ,  $\text{Al}_2\text{O}_3$  and  $\text{SiO}_2$  are represented by C, A, and S, respectively. The compounds are then designated as though C, A, and S were elements. For example, the compound  $2\text{CaO} \cdot \text{Al}_2\text{O}_3 \cdot \text{SiO}_2$  is given the formula  $\text{C}_2\text{AS}$ . This form of abbreviation is useful in the analytical treatment to be described.

Since the term *system* will be used frequently, the sense in which it is used in this paper should be clearly understood. The entire range of compositions which may be obtained by varying the proportions of a given set of components will be referred to as a system. Any substances, defined by their compositions, may be

selected as components of a system, provided that none of them can be formed from the others in any proportions, positive or negative. For example, two invariant points in a ternary system may be taken as components of a binary system, although they are neither elements nor compounds.

### 1. Primary and secondary systems

The system C-A-S (figure 1) is composed of fourteen individual ternary systems. It is convenient to refer to a system as a whole as a *primary system*, and to any system within it as a *secondary system*. The term "secondary system" is limited to systems of the same number of components as the primary system. The number of components is designated as  $N$ , which in this case is 3. Components of the primary system and secondary systems will be referred to as primary and secondary components, respectively. Similarly, compositions will be referred to as primary or secondary, depending upon the components in which they are expressed.

Because the secondary systems are each related to the primary system through the compositions of their components, there are mutual relations among the secondary systems, and these will prove to be useful. Any composition in the primary system may be formed from the components of any secondary system, if both positive and negative proportions are considered. For example, the composition  $CAS_2$  may be formed from the components of the system  $C_2S-C_6A_3-C_3A$ , if they are combined in the molar proportions indicated by the equation:



If interest is concentrated upon a particular secondary system and compositions are expressed in terms of the components of that system, the secondary system may be treated as the primary system. The original primary system and any other  $N$ -component systems within it are then treated as secondary systems.

### 2. Degrees of freedom

Considered with reference to composition only, the number of degrees of freedom of a system is the number of composition variables which must be fixed in order that any composition in the system may be defined. Each equation expressing a composition relation reduces the number of degrees of freedom by 1. An equation representing the condition that the total quantity of the components is constant is always understood. An  $N$ -component system therefore has  $N - 1$  degrees of freedom. If the equations are linear,  $N - n$  equations define an  $n$ -component system with  $n - 1$  degrees of freedom.<sup>1</sup>

When the number of degrees of freedom is 3 or less, the number may be defined

<sup>1</sup> Systems defined by one or more intrinsic equations extend to the boundaries of the primary system. When a system forming only a part of such a system is to be defined, limits must be imposed, in addition to the intrinsic equation or equations defining the complete system.

geometrically by reference to points, lines, surfaces or volumes, which have 0, 1, 2, or 3 degrees of freedom, respectively.

### 3. Notation

When the components of a primary system are designated by single letters, as in figure 1, it is convenient to use the same letters, in either italics or bold face, to denote quantities of these components. Other symbols may be employed in the same manner in algebraic expressions or equations to denote quantities of secondary components. If quantities of all the components, primary or secondary, are expressed in the same weight units, or in the same units relative to total weight (percentages or weight fractions), the quantities will be in italics. For example, *C*, *A*, and *S* represent quantities of components *C*, *A*, and *S* expressed in the same weight units. Although expressions involving such quantities, and lacking a constant term, refer to any total weight of material, they will be applied here to percentages and will therefore be referred to as being in percentage form. In the case of substances capable of being expressed by chemical formulas it is convenient to express composition in moles. In that case, the weight units for the different substances are not the same. Quantities expressed in moles will be in bold face. For example, **C**, **A**, and **S** refer to the number of moles of the components *C*, *A*, and *S*, respectively. Expressions involving such quantities will be referred to as being in molar form.

## II. SECONDARY SYSTEMS (CONVERSION OF COMPOSITIONS)

In dealing with composition relations it is frequently necessary to convert compositions from one system of components to another. For example, it may be necessary to convert compositions expressed in terms of *C*, *A*, and *S* to compositions in terms of *CS*, *C<sub>2</sub>AS*, and *CAS<sub>2</sub>*. Such conversions, from primary compositions to secondary compositions, will be referred to as primary to secondary conversions. Similarly, it may be necessary to perform a secondary to secondary conversion, as in converting compositions in terms of *C<sub>3</sub>S*, *C<sub>2</sub>S*, and *C<sub>3</sub>A* to compositions in terms of *C*, *C<sub>2</sub>S*, and *C<sub>3</sub>A<sub>3</sub>*.

### A. PRIMARY TO SECONDARY CONVERSION EQUATIONS

#### 1. Method of derivation

To illustrate the derivation of equations for primary to secondary conversion, let us consider the system *CS*–*C<sub>2</sub>AS*–*CAS<sub>2</sub>* (figure 1). The problem is to derive equations for converting compositions expressed in terms of the primary components, *C*, *A*, and *S*, into terms of the secondary components, *CS*, *C<sub>2</sub>AS*, and *CAS<sub>2</sub>*. Since the molar compositions of the secondary components are indicated in their formulas and involve small whole numbers, it is convenient to derive equations in molar form. In any quantity of mixture, let **C**, **A**, and **S** represent the number of moles of *C*, *A*, and *S*, respectively, and let **X**, **Y**, and **Z** represent the number of moles of *CS*, *C<sub>2</sub>AS*, and *CAS<sub>2</sub>*, respectively. Proceeding as though the primary components are actually combined in the form of the com-



pounds designated as secondary components, it can be seen from the chemical formulas that there are present  $X$  moles of C in the form of CS,  $2Y$  moles in the form of  $C_2AS$ , and  $Z$  moles in the form of  $CAS_2$ . This may be expressed in equation form as follows:

$$X + 2Y + Z = C \quad (2)$$

Considering the components A and S in the same manner,

$$Y + Z = A \quad (3)$$

$$X + Y + 2Z = S \quad (4)$$

Equations 2-4 may be solved for  $X$ ,  $Y$ , and  $Z$  by any of the usual methods. For our purpose, however, the determinant method is preferred. Let  $D$  denote the determinant of the coefficients in the equations.

$$D = \begin{vmatrix} 1 & 2 & 1 \\ 0 & 1 & 1 \\ 1 & 1 & 2 \end{vmatrix}$$

$$\text{Moles CS} = X = \frac{\begin{vmatrix} C & 2 & 1 \\ A & 1 & 1 \\ S & 1 & 2 \end{vmatrix}}{D} \quad (5)$$

$$\text{Moles } C_2AS = Y = \frac{\begin{vmatrix} 1 & C & 1 \\ 0 & A & 1 \\ 1 & S & 2 \end{vmatrix}}{D} \quad (6)$$

$$\text{Moles } CAS_2 = Z = \frac{\begin{vmatrix} 1 & 2 & C \\ 0 & 1 & A \\ 1 & 1 & S \end{vmatrix}}{D} \quad (7)$$

Evaluating the determinants:

$$\text{Moles CS} = X = (C + S - 3A)/2 \quad (5a)$$

$$\text{Moles } C_2AS = Y = (C + A - S)/2 \quad (6a)$$

$$\text{Moles } CAS_2 = Z = (A + S - C)/2 \quad (7a)$$

These equations in molar form can be converted to percentage form. The molecular weights of the primary components C, A, and S are 56.08, 101.94, and 60.06, respectively. The molecular weights of CS,  $C_2AS$ , and  $CAS_2$  are 116.14, 274.16, and 278.14, respectively. Then, in any quantity of mixture:

$$\begin{aligned} C &= \frac{C}{56.08} & A &= \frac{A}{101.94} & S &= \frac{S}{60.06} \\ X &= \frac{X}{116.14} & Y &= \frac{Y}{274.16} & Z &= \frac{Z}{278.14} \end{aligned}$$

Upon substituting in equations 5a-7a, the following equations are obtained:

$$\text{Weight of CS} = X = 1.0355C + 0.9669S - 1.7089A \quad (5b)$$

$$\text{Weight of C}_2\text{AS} = Y = 2.4444C + 1.3447A - 2.2824S \quad (6b)$$

$$\text{Weight of CAS}_2 = Z = 1.3642A + 2.3155S - 2.4799C \quad (7b)$$

Since these equations refer to any total quantity of material, they will apply to percentages, that is, the number of grams of each component in 100 g., or they may apply to weight fractions. They may also be applied to compositions in which the total percentage obtained in a chemical analysis is not exactly 100 per cent. In any case the total for the secondary components will be equal to the total for the primary components, since the sum of the equations is:

$$X + Y + Z = C + A + S$$

This provides a check on numerical computations. It should also be borne in mind when the percentage of one of the secondary components is obtained by difference. For example, if the total for the primary components is 99.5 per cent, this is also the total for the secondary components, and should be used instead of 100.0 in obtaining the percentage of one component by difference.

In the foregoing example, the primary to secondary conversion was performed with molar quantities, and the resulting equations were then converted to percentage form. This has certain advantages, particularly when  $N$  is greater than 3. The equations in molar form are simple and can be solved easily and exactly by any of the usual methods of solving simultaneous equations. Each of the coefficients in the equations in percentage form is found directly from the molecular weights of the substances involved in the conversion.

Equations lacking a constant term are particularly convenient when dealing with compositions in which the totals vary. If they are to be applied to primary compositions in which the total is always 100 per cent, the number of multiplications may be reduced by eliminating one of the primary components in the equations. For example, in equations 5b-7b, one of the primary components may be eliminated through the relation:

$$C + A + S = 100$$

To illustrate, we may eliminate  $A$  by substituting  $100 - C - S$  for  $A$  in each of the equations, obtaining

$$X = 2.7444C + 2.6758S - 170.89 \quad (5c)$$

$$Y = 1.0997C - 3.6271S + 134.47 \quad (6c)$$

$$Z = -3.8441C + 0.9513S + 136.42 \quad (7c)$$

Only two of these equations are needed, since the percentage of one of the secondary components may be obtained by difference.

## 2. The equation of an $(N - 1)$ -component system

The equations for primary to secondary conversion are positive for all compositions within the secondary system, while for all compositions outside of the

system at least one of the equations is negative. When substitution of a composition in one of the equations leads to a value of zero, the composition is in the boundary system represented by the remaining components, or on an extension of that system. Referring to equations 5a-7a, we find that a composition which gives a value of zero when substituted in equation 5a is in the binary system  $C_2AS-CAS_2$ . The equation  $C + S - 3A = 0$  is satisfied by all compositions in the system  $C_2AS-CAS_2$ , and is therefore the intrinsic equation of that system. The equations for the binary systems bounding the system  $CS-C_2AS-CAS_2$  may be found by equating each right-hand member of equations 5a-7a to zero, as follows:

<i>System</i>	<i>Equation</i>	
$C_2AS-CAS_2$	$C + S - 3A = 0$	(8)

$CS-CAS_2$	$C + A - S = 0$	(9)
------------	-----------------	-----

$CS-C_2AS$	$A + S - C = 0$	(10)
------------	-----------------	------

The solution of equations 2-4 by the determinant method, as in equations 5-7, suggests a direct method of deriving the equation of an  $(N - 1)$ -component system. The method may be illustrated by considering equation 5. According to the principle just discussed, the equation for the system  $C_2AS-CAS_2$  may be obtained by equating the determinant in equation 5 to zero, that is:

$$\begin{vmatrix} C & 2 & 1 \\ A & 1 & 1 \\ S & 1 & 2 \end{vmatrix} = 0$$

Upon examining the determinant it is seen that the elements of the second and third columns are the number of moles of C, A, and S in  $C_2AS$  and  $CAS_2$ , respectively, that is, the components of the binary system under consideration, as indicated in their chemical formulas. This illustrates the general method, which can be applied to systems of any number of components. To set up the equation of an  $(N - 1)$ -component system, the symbols representing molar quantities of the  $N$  primary components are indicated in one column, and the molar compositions of the  $N - 1$  secondary components are then indicated in the remaining columns of the determinant. The determinant is then equated to zero.

The same method may be applied in dealing with compositions expressed in percentage form. That is, the symbols representing percentages of the  $N$  primary components are indicated in one column, and the compositions of the  $N - 1$  secondary components, on a percentage or weight fraction basis, are indicated in the remaining columns.

Each secondary system is bounded by  $N$  systems of  $N - 1$  components. The equations for  $(N - 1)$ -component systems will therefore be referred to as *boundary equations*.

#### B. SECONDARY TO SECONDARY CONVERSION EQUATIONS

When it is necessary to convert compositions from one system of secondary components to another, the usual method is to perform the conversion in two

steps: (1) to convert the composition in the first system to a primary composition; (2) to convert the primary composition to the second system of components. Equations for direct secondary to secondary conversion are easily derived. The use of such equations eliminates one of the steps in the usual method. The equations are usually more simple than those for primary to secondary conversion, which is an additional advantage.

To illustrate the procedure, let us assume that compositions expressed in terms of  $C_2S$ ,  $C_3S$ , and  $C_4A$  are to be converted into terms of  $C$ ,  $C_2S$ , and  $C_3A$ . In any quantity of mixture, let:

SYSTEM 2		SYSTEM 1	
	Molecular weight		Molecular weight
$X = \text{moles } C$	56.08	$x = \text{moles } C_2S$	228.30
$Y = \text{moles } C_3S$	172.22	$y = \text{moles } C_2S$	172.22
$Z = \text{moles } C_4A$	586.22	$z = \text{moles } C_3A$	270.18

From the chemical formulas the total number of moles of  $C$  in system 2 is  $X + 2Y + 5Z$ , while in system 1 it is  $3x + 2y + 3z$ . These quantities are identical. Similarly, expressions for the number of moles of  $S$  and  $A$  in the two systems are identical, leading to the equations:

$$X + 2Y + 5Z = 3x + 2y + 3z \quad (11)$$

$$Y = x + y \quad (12)$$

$$3Z = z \quad (13)$$

Solving for  $X$ ,  $Y$ , and  $Z$ :

$$X = \frac{3x + 4z}{3} \quad (14)$$

$$Y = x + y \quad (15)$$

$$Z = \frac{z}{3} \quad (16)$$

Converting to percentage form by the method on page 702, we obtain the equations:

$$X = 0.2456x + 0.2768z \quad (14a)$$

$$Y = y + 0.7544x \quad (15a)$$

$$Z = 0.7232z \quad (16a)$$

For convenience, these equations may be written as shown below:

$$\begin{array}{ll} \text{System 2} & \text{System 1} \\ C & = 0.2456C_2S + 0.2768C_3A \end{array} \quad (14b)$$

$$C_2S = C_2S + 0.7544C_3S \quad (15b)$$

$$C_4A = 0.7232C_3A \quad (16b)$$

It will be shown later that in the analytical interpretation of phase equilibria data it is sometimes convenient to convert compositions from a secondary system to an adjacent system or a system further removed from it. In such cases, negative values appear in the expression of composition. For example, conversion between systems  $C_3S-C_2S-C_3A$  and  $C_2S-C_3A-C_5A_3$  may be expressed by either of the two sets of equations shown below, obtained by the foregoing method. The equations are in percentage form.

$$\begin{array}{ll} \text{System 1} & \text{System 2} \\ C_3S & = -1.5578C_5A_3 \end{array} \quad (17)$$

$$C_2S = C_2S + 1.1751C_5A_3 \quad (18)$$

$$C_3A = C_3A + 1.3827C_5A_3 \quad (19)$$

$$\begin{array}{ll} \text{System 2} & \text{System 1} \\ C_2S & = C_2S + 0.7544C_3S \end{array} \quad (20)$$

$$C_3A = C_3A + 0.8876C_3S \quad (21)$$

$$C_5A_3 = -0.6420C_3S \quad (22)$$

Referring to figure 1 we see that  $C_3S$  and  $C_5A_3$  are on opposite sides of the binary system  $C_2S-C_3A$ . This is reflected in the equations, since  $C_3S$  and  $C_5A_3$  are of unlike sign in equations 17 and 22.

### III. SYSTEMS OF $(N - 1)$ COMPONENTS

When an  $(N - 1)$ -component system is defined by designating its components, the relation between the primary components is indirectly defined, since all compositions in the system must be capable of being formed from the designated components. In addition, the range of compositions is limited to those which can be formed from the components in positive proportions. For example, the system  $C_2AS-CAS_2$  (figure 1) includes only the compositions on the line joining  $C_2AS$  and  $CAS_2$ , and does not include those on extensions of that line. An equation defines the relation between primary components directly, with no limitations other than the indicated relation. The equation derived for the system  $C_2AS-CAS_2$ , that is,  $C + S - 3A = 0$ , is satisfied not only by compositions in the system from which it is derived, but also by extensions of that system, such as  $C_3A$  and  $S_3A$ . Geometrically, the equation represents a line extending an infinite distance in either direction, so that it will include compositions outside of the primary system, involving negative quantities. This may be illustrated by the composition  $C_4AS_{-1}$ , which satisfies the equation, but is outside of the primary system.

Since the  $(N - 1)$ -component system represented by an intrinsic equation extends to the boundaries of the primary system, it always separates the primary system into two parts. The equation represents a boundary between the two parts, and may therefore be referred to as a *boundary equation*. It will be shown presently that the expression equated to zero in a boundary equation may be

used in the classification of compositions with reference to the secondary systems in which they lie. It is convenient, then, to refer to such expressions as *boundary expressions*. For example,  $C + S - 3A = 0$  is a boundary equation, and  $C + S - 3A$  is the corresponding boundary expression.

#### A. PROPERTIES OF INTRINSIC EQUATIONS

The binary systems which form the "edges" of a system may be found by taking its components in pairs. For example, the edges of the system A-B-C-D are the binary systems A-B, A-C, A-D, B-C, B-D, and C-D. The extension of a boundary system to the boundaries of the primary system may be traced by determining compositions on the edges which satisfy the equation of the system. This may be done by equating each pair of terms to zero. To illustrate, let us consider the following equation of a ternary system in the quaternary system A-B-C-D:

$$A - 2B - 3C - 4D = 0 \quad (8)$$

In this equation we have six pairs of terms, obtaining the following equations:

$$\begin{array}{ll} A - 2B = 0 & 2B + 3C = 0 \\ A - 3C = 0 & 2B + 4D = 0 \\ A - 4D = 0 & 3C + 4D = 0 \end{array}$$

The equations at the left, in which the terms are of opposite sign, are satisfied by compositions expressed in positive quantities:  $A_2B$ ,  $A_3C$ , and  $A_4D$ . Geometrically, these represent intersections of a plane with the edges of the tetrahedron A-B-C-D, and the equation therefore represents the ternary system  $A_2B-A_3C-A_4D$ . The equations at the right are satisfied by compositions in which both positive and negative quantities appear, that is,  $B_2C_{-2}$ ,  $B_2D_{-1}$ , and  $C_4D_{-3}$ . These are intersections of the plane with extensions of the remaining edges of the tetrahedron.

It should be noted that only pairs of terms of unlike sign lead to equations which are satisfied by compositions on the edges of the primary system. A boundary equation must therefore have at least one pair of terms of unlike sign to represent an  $(N - 1)$ -component system passing through the primary system. The boundaries of the primary system are represented by equations with only one term. For example, in the system C-A-S (figure 1) compositions on the C-S side satisfy the relation  $A = 0$ .

By determining compositions on the edges of the system A-B-C-D which satisfy equation 8, we found them to be components of a ternary system which includes all compositions in the primary system that satisfy the equation. This was possible because equation 8 has 3, that is,  $N - 1$ , terms of like sign. When there are less than  $N - 1$  terms of like sign, the number of compositions on the edges exceeds  $N - 1$ . This may be illustrated geometrically by considering a plane passing through the tetrahedron representing a quaternary system. Such a plane may intersect three edges, forming a triangle, or it may intersect four

edges, forming a quadrilateral. In the latter case, it is necessary to set up a ternary system with at least one component outside of the primary system if it is proposed to include all compositions in the primary system which satisfy the equation of the plane. To set up such a system is of no practical value. However, in dealing with multicomponent systems without reference to geometric relations it is well to understand that we can refer to any intrinsic equation as representing an  $(N - 1)$ -component system, rather than a line, plane, or hyperplane extending an infinite distance into space.

Let us consider the following equation representing a ternary system in the quaternary system A-B-C-D.

$$A - 2B + 3C - 4D = 0 \quad (8a)$$

This equation has four pairs of terms of unlike sign and two of like sign, leading to the following equations:

$$\begin{aligned} A - 2B &= 0 & A + 3C &= 0 \\ A - 4D &= 0 & B + 2D &= 0 \\ 2B - 3C &= 0 \\ 3C - 4D &= 0 \end{aligned}$$

The compositions on the edges of the system which satisfy equation 8a are  $A_2B$ ,  $A_4D$ ,  $B_3C_2$ , and  $C_4D_3$ . Those on the extensions of the edges are  $A_3C_{-1}$  and  $B_2D_{-1}$ . It can be seen that  $A_2B$  is in the system  $A_3C_{-1}-B_3C_2$ , since  $2A_3C_{-1} + B_3C_2 = 3A_2B$ . Similarly  $A_4D$  is in the system  $A_3C_{-1}-C_4D_3$ . The ternary system  $A_3C_{-1}-B_3C_2-C_4D_3$  therefore includes all compositions in the quadrilateral  $A_2B-A_4D-B_3C_2-C_4D_3$ .

Some of the properties of boundary equations may be illustrated by reference to figure 2. This figure represents the same primary system and secondary systems as figure 1. The intrinsic equation of each binary system, in molar form, is indicated. It will be noted that the boundary equations for the systems radiating from the vertex A are  $S = 0$ ,  $C - 2S = 0$ ,  $2C - S = 0$ , and  $C = 0$ . Each of these equations lacks an A term. This illustrates a condition which applies to systems of any number of components, that when a primary component is lacking in an expression, that primary component is one of the components of the  $(N - 1)$ -component system represented by the equation.

To illustrate the significance of boundary equations with reference to compositions on the corresponding boundaries, let us consider the expression  $C - A - S$  for the system CS-CA (figure 2). This expression is equal to zero for any composition in the system CS-CA. Now if C is added to any such mixture, the value obtained when the resulting mixture is substituted in the expression will be positive, since C is positive in the expression. Any composition in the area between the system CS-CA and the C vertex can be formed in this manner. Compositions in this area therefore give positive values when substituted in the boundary expression. Similarly, on the side of the system CS-CA toward the A

and S vertices the boundary expression has a negative value. In general, a boundary expression divides an  $N$ -component primary system into two parts, according to the sign obtained. If a positive sign is obtained when a composition is substituted in the boundary expression, the composition is on the side of the boundary system toward the primary components with positive signs in the expression; if negative, it will be on the side toward the components with negative terms in the expression.

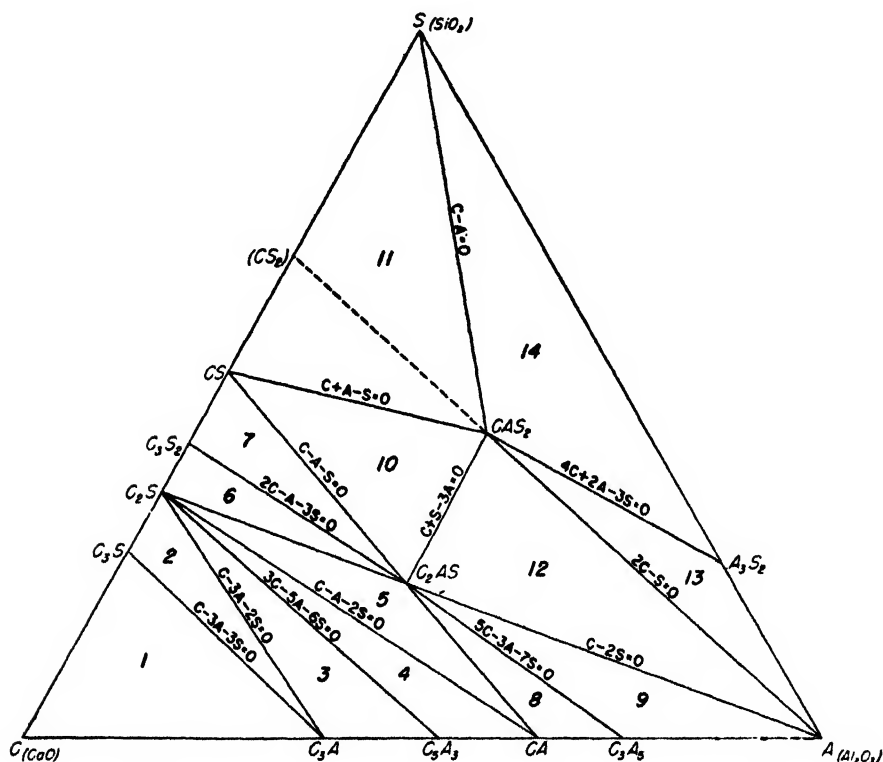


FIG. 2. Boundary systems and equations in the system  $\text{CaO}-\text{Al}_2\text{O}_3-\text{SiO}_2$

#### B. CLASSIFICATION OF COMPOSITIONS

In a ternary system the secondary system to which any given composition belongs may be determined graphically. In the case of systems of more than three components analytical methods must be employed. Boundary expressions may be used for the purpose. To illustrate a systematic method of classifying compositions with reference to the secondary systems in which they lie, the boundary equations for all binary systems in figure 1 are shown in figure 2. It will be seen from the equation of the system  $\text{CS}-\text{CA}$  that the boundary expression  $\text{C} - \text{A} - \text{S}$  divides the system into two groups of secondary systems: systems 1-7, which are positive to the expression; and systems 8-14, which are negative. The first group may be divided into two subgroups by the expression  $\text{C} - \text{A} - 2\text{S}$ : systems 1-4, which are positive to that expression, and systems



5-7, which are negative. By reference to the boundary expressions in figure 2, we may proceed in that manner to trace any composition in molar form to the particular secondary system in which it lies. To accomplish this without reference to a diagram, all that is necessary is to indicate the successive steps in a table arranged in a form similar to a botanical key, showing the groups and subgroups with reference to the signs of the boundary expressions. Table 1 is a classification key of this type for the system  $\text{CaO-Al}_2\text{O}_3\text{-SiO}_2$ , for an analytical classification of compositions in the system. Although such a key may be devised on a percentage basis, it is more convenient to set up the key in molar form.

To apply the key, each composition under consideration must be expressed in molar form. It may be expressed as the number of moles in any quantity of material. For example, the percentage of each primary component may be divided by the molecular weight to obtain the number of moles per 100 g. In this case:

$$C = \frac{\text{per cent CaO}}{56.08} = 0.01783 \text{ (per cent CaO)}$$

$$A = \frac{\text{per cent Al}_2\text{O}_3}{101.94} = 0.00981 \text{ (per cent Al}_2\text{O}_3\text{)}$$

$$S = \frac{\text{per cent SiO}_2}{60.06} = 0.01665 \text{ (per cent SiO}_2\text{)}$$

These quantities may be multiplied by a constant to obtain values to be substituted in the classification key. This provides a means of reducing the number of arithmetical operations required in converting percentage compositions to molar quantities. For example, we may multiply each quantity by 56.08, the molecular weight of CaO, obtaining:

$$C = \frac{56.08 \text{ (per cent CaO)}}{56.08} = \text{per cent CaO}$$

$$A = \frac{56.08 \text{ (per cent Al}_2\text{O}_3\text{)}}{101.94} = 0.5501 \text{ (per cent Al}_2\text{O}_3\text{)}$$

$$S = \frac{56.08 \text{ (per cent SiO}_2\text{)}}{60.06} = 0.9337 \text{ (per cent SiO}_2\text{)}$$

The values of *C*, *A*, and *S* obtained in this manner are the number of moles of CaO,  $\text{Al}_2\text{O}_3$ , and  $\text{SiO}_2$ , respectively, in 5608 g. This eliminates computation of *C*.

If substitution of a composition in one of the boundary expressions in the classification key leads to a value of zero, the composition is on the boundary between two secondary systems. One of these systems will be found by assuming the value to be positive, and the other by assuming the value to be negative. The secondary components common to the two systems are the components of the system of  $N - 1$  components (in this case a binary system) in which the composition lies. For example, if the composition is in the system  $\text{CS-C}_2\text{AS}$ ,

TABLE 1  
Classification key for system  $\text{CaO}-\text{Al}_2\text{O}_3-\text{SiO}_2$

C - A - S POSITIVE	System	C - A - S NEGATIVE	System
$(\text{C} - \text{A} - 2\text{S}) +$ $(\text{C} - 3\text{A} - 2\text{S}) +$ $(\text{C} - 3\text{A} - 3\text{S}) +$ $(\text{C} - 3\text{A} - 3\text{S}) -$ $(\text{C} - 3\text{A} - 2\text{S}) -$ $(3\text{C} - 5\text{A} - 6\text{S}) +$ $(3\text{C} - 5\text{A} - 6\text{S}) -$ $(\text{C} - \text{A} - 2\text{S}) -$ $(\text{C} - 2\text{S}) +$ $(\text{C} - 2\text{S}) -$ $(2\text{C} - \text{A} - 3\text{S}) +$ $(2\text{C} - \text{A} - 3\text{S}) -$	1. $\text{CaO}-\text{C}_2\text{S}-\text{C}_2\text{A}$ 2. $\text{C}_2\text{S}-\text{C}_2\text{S}-\text{C}_2\text{A}$ 3. $\text{C}_2\text{S}-\text{C}_2\text{A}-\text{C}_2\text{A}_2$ 4. $\text{C}_2\text{S}-\text{C}_2\text{A}_2-\text{CA}$ 5. $\text{C}_2\text{S}-\text{CA}-\text{C}_2\text{AS}$ 6. $\text{C}_2\text{S}-\text{C}_2\text{AS}-\text{C}_2\text{S}_2$ 7. $\text{C}_2\text{S}_2-\text{C}_2\text{AS}-\text{CS}$	$(\text{C} - 2\text{S}) +$ $(5\text{C} - 3\text{A} - 7\text{S}) +$ $(5\text{C} - 3\text{A} - 7\text{S}) -$ $(\text{C} - 2\text{S}) -$ $(2\text{C} - \text{S}) +$ $(\text{C} + \text{S} - 3\text{A}) +$ $(\text{C} + \text{A} - \text{S}) +$ $(\text{C} + \text{A} - \text{S}) -$ $(\text{C} + \text{S} - 3\text{A}) -$ $(2\text{C} - \text{S}) -$ $(\text{C} - \text{A}) +$ $(\text{C} - \text{A}) -$ $(4\text{C} + 2\text{A} - 3\text{S}) +$ $(4\text{C} + 2\text{A} - 3\text{S}) -$	8. $\text{CA}-\text{C}_2\text{AS}-\text{C}_2\text{A}_2$ 9. $\text{C}_2\text{A}_2-\text{C}_2\text{AS}-\text{Al}_2\text{O}_3$ 10. $\text{C}_2\text{AS}-\text{CAS}_2-\text{CS}$ 11. $\text{CS}-\text{CAS}_2-\text{SiO}_2$ 12. $\text{C}_2\text{AS}-\text{CAS}_2-\text{Al}_2\text{O}_3$ 11. $\text{CS}-\text{CAS}_2-\text{SiO}_2$ 13. $\text{CAS}_2-\text{A}_2\text{S}_2-\text{Al}_2\text{O}_3$ 14. $\text{CAS}_2-\text{A}_2\text{S}_2-\text{SiO}_2$

C, A, and S may represent the number of moles of the primary components in any total quantity of material, as in methods 1 and 2, below.  
Method 1 (total quantity 100 g.):

$$\text{C} = 0.01783 \text{ (per cent CaO)}, \text{A} = 0.00981 \text{ (per cent Al}_2\text{O}_3), \text{S} = 0.01665 \text{ (per cent SiO}_2)$$

Method 2 (total quantity 5608 g.):

$$\text{C} = \text{per cent CaO}, \text{A} = 0.5501 \text{ (per cent Al}_2\text{O}_3), \text{S} = 0.9337 \text{ (per cent SiO}_2)$$

Example (by method 2)

CaO	35 per cent	C =	35.00
Al <sub>2</sub> O <sub>3</sub>	25 per cent	A =	$25 \times 0.5501 = 13.75$
SiO <sub>2</sub>	40 per cent	S =	$40 \times 0.9337 = 37.35$

Since  $(\text{C} - \text{A} - \text{S})$  is negative, this composition is in the right-hand group of systems. It is then found to be in the subgroup in which  $(\text{C} - 2\text{S})$  is negative. Continuing in this manner, the composition is found to be in the system  $\text{C}_2\text{AS}-\text{CAS}_2-\text{CS}$  (system 10).

the expression  $C-A-S$  will be equal to zero. If the value is assumed to be positive, the composition will be traced to system 7,  $C_3S_2-C_2AS-CS$ . If the value is assumed to be negative, the composition will be traced to system 10,  $C_2AS-CAS_2-CS$ . The secondary components  $CS$  and  $C_2AS$  are common to systems 7 and 10. The composition is therefore in the binary system  $CS-C_2AS$ .

### 1. Relations between secondary systems and boundary expressions

In the development of a classification key for the ternary system  $CaO-Al_2O_3-SiO_2$  (table 1), boundary expressions for the successive division of the primary system into groups of secondary systems were selected by reference to figure 2, in which the relation of each secondary system to the boundary expressions can be readily seen. In developing a key for a system with a greater number of components, these relations must also be known, but they must be determined in other ways. The methods which will be employed in dealing with such systems may be found by a further study of figure 2.

It will be seen in figure 2 that binary systems on the boundaries of the primary system lack one of the primary components. For example, binary systems  $C_3S-C_2S$ ,  $C_2S-C_3S_2$ , etc., on the  $C-S$  side of the primary system, lack component  $A$ . These systems are boundaries of secondary systems, but they do not separate secondary systems from one another, and they are therefore of no significance in the development of a classification key. In forming a list of the  $(N-1)$ -component systems to be used in developing the key for an  $N$ -component system, all systems in which a primary component is lacking in the designation of the system are disregarded.

The relation between each secondary system and a boundary expression may be determined by the signs of the values obtained when their components are substituted in the expression. For example, the components of system 3,  $C_2S-C_3A-C_6A_3$ , give positive values when substituted in the expression  $2C-S$ , indicating that the system is entirely on the positive side of the system represented by the expression. When the components of system 12,  $C_2AS-CAS_2-A$ , are substituted in the expression  $2C-S$  the values obtained are +3, 0, and 0, indicating that system 3 is on the positive side of the binary system represented by the expression  $2C-S$ . For the purpose of developing the key, the fact that zeros are obtained in some instances is of no significance, and systems 3 and 10 are both classified as positive. By this procedure, it is found that systems 1-10 and system 12 are positive, while systems 13 and 14 are negative, with reference to the expression  $2C-S$ . When the components of system 11,  $CS-S-CAS_2$ , are substituted in the expression  $2C-S$ , a positive value is obtained for  $CS$  and a negative value for  $S$ . This indicates that the expression divides the system into two ternary systems, as indicated by the broken line extending the system  $CAS_2-A$  to the hypothetical compound  $CS_2$ . It is sometimes necessary to divide systems temporarily in developing a classification key. It will be observed that system 11 appears twice in table 1, indicating that this temporary division of system 11 was made in developing the key for the system  $CaO-Al_2O_3-SiO_2$ .

It appears from the foregoing discussion that it is possible to develop a classification key for a system of any number of components, since the relations between secondary systems and boundary expressions can be determined without reference to a diagram. In tabulating these relations it is convenient to use symbols. In listing secondary systems with reference to a particular boundary expression, those which are positive are designated by a plus sign, and those which are negative by a minus sign. When *one* plus and *one* minus sign are obtained in substituting the components of a secondary system in a boundary expression, the system is divided by the expression into two  $N$ -component systems, one positive and one negative. This is indicated in tables by a  $\pm$  sign. If unlike signs are obtained, but more than one is plus, or more than one is minus, the secondary system is divided into two parts, but at least one of these is not an  $N$ -component system. This is indicated by X. Such divisions are not useful in the classification of compositions.

## 2. Classification of compositions in multicomponent systems

To illustrate the general method of developing a classification key, we shall develop a key for the hypothetical system A-B-C-D, which will be assumed to be composed of the following secondary systems:

### *Secondary systems*

1.  $A_2BD-A-C-D$
2.  $A_2BD-A-B-C$
3.  $A_2BD-A_2BC_2D-B-D$
4.  $A_2BC_2D-B-C-D$

This group of systems has been designed to involve only a small number of secondary systems, and yet include all four types of relations between secondary systems and boundary expressions discussed in the previous section.

The four systems bounding each secondary system may be found by taking each combination of three secondary components. Eliminating those which are repeated, and those in which any primary component is lacking, we obtain eight boundary systems, with their boundary expressions, by the determinant method described on page 701.

BOUNDARY SYSTEMS AND EXPRESSIONS

Boundary systems	Boundary expressions
$A_2BD-A-C$	$B - D$
$A_2BD-C-D$	$A - 2B$
$A_2BD-B-C$	$A - 2D$
$A_2BD-A_2BC_2D-B$	$A - 2D$
$A_2BD-A_2BC_2D-D$	$A - 2B$
$A_2BC_2D-B-D$	$A - C$
$A_2BC_2D-B-C$	$A - 2D$
$A_2BC_2D-C-D$	$A - 2B$

Boundary systems with the same boundary expression are parts of a single  $(N - 1)$ -component system extending to the boundaries of the primary system. In this case, there are only four such systems, represented by the expressions  $A - C$ ,  $A - 2B$ ,  $A - 2D$ , and  $B - D$ .

The components of each secondary system are now substituted in each boundary expression, designating the relation between each system and expression by the appropriate designation indicated in the previous section. These designations are tabulated below:

SECONDARY SYSTEM	BOUNDARY EXPRESSION			
	$A - C$	$A - 2B$	$A - 2D$	$B - D$
1. $A_2BD-A-C-D$	X	+	$\pm$	-
2. $A_2BD-A-B-C$	X	$\pm$	+	+
3. $A_2BD-A_2BC_2D-B-D$	+	-	-	$\pm$
4. $A_2BC_2D-B-C-D$	-	-	-	$\pm$

A boundary expression will divide the secondary systems into two groups if there are only plus signs and minus signs in the column for that expression. Since this is not true in any column, the condition must be secured by dividing some system into two systems. For example, system 1 may be divided into two systems by the expression  $A - 2D$ , as indicated by the  $\pm$  sign in the column for that expression. One of these systems will be positive to  $A - 2D$ , and the other negative. Similarly system 2 may be divided into two systems by the expression  $A - 2B$ . Choosing the latter, system 2 is divided into systems, 2a and 2b, as shown in the following table:

SECONDARY SYSTEM	BOUNDARY EXPRESSION			
	$A - C$	$A - 2B$	$A - 2D$	$B - D$
1	X	+	$\pm$	-
2a	X	+	+	+
2b	X	-	+	+
3	+	-	-	$\pm$
4	-	-	-	$\pm$

In this table system 2a is the part of system 2 which is positive to the expression  $A - 2B$ , and system 2b is the part which is negative. The signs for systems 2a and 2b under the other expressions are the same as for system 2. Boundary expression  $A - 2B$  now divides the five systems into two groups: systems 1 and 2a, which are positive to this expression, and systems 2b, 3 and 4, which are negative. Systems 1 and 2a are separated by the expression  $B - D$ . Systems 3 and 4 may be separated from system 2b by the expression  $A - 2D$ , and then separated from one another by the expression  $A - C$ . The classification key may now be set up, as follows:

*Secondary system*

$$\begin{array}{ll}
 (\mathbf{A} - 2\mathbf{B}) + & \\
 (\mathbf{B} - \mathbf{D}) + & 2. \mathbf{A}_2\mathbf{BD}-\mathbf{A}-\mathbf{B}-\mathbf{C} \\
 (\mathbf{B} - \mathbf{D}) - & 1. \mathbf{A}_2\mathbf{BD}-\mathbf{A}-\mathbf{C}-\mathbf{D} \\
 (\mathbf{A} - 2\mathbf{B}) - & \\
 (\mathbf{A} - 2\mathbf{D}) + & 2. \mathbf{A}_2\mathbf{BD}-\mathbf{A}-\mathbf{B}-\mathbf{C} \\
 (\mathbf{A} - 2\mathbf{D}) - & \\
 (\mathbf{A} - \mathbf{C}) + & 3. \mathbf{A}_2\mathbf{BD}-\mathbf{A}_2\mathbf{BC}_2\mathbf{D}-\mathbf{B}-\mathbf{D} \\
 (\mathbf{A} - \mathbf{C}) - & 4. \mathbf{A}_2\mathbf{BC}_2\mathbf{D}-\mathbf{B}-\mathbf{C}-\mathbf{D}
 \end{array}$$

The method which has been described can be applied to systems of any number of components, involving any number of secondary systems. When dealing with a system involving a large number of secondary systems, the use of tables showing the relation of secondary systems to boundary expressions is not convenient, since they must be rearranged repeatedly as the work proceeds. In such cases, it is more satisfactory to use cards, one for each secondary system, indicating on each card the sign for each boundary expression. The cards can be rearranged when necessary, and separated into groups and subgroups. When a system is divided into two systems, the card for that system is replaced by two cards, each representing one of the two parts of the system.

*3. Primary to secondary conversion following use of classification key*

In some instances a classification key may be used to determine the secondary system in which a composition lies, but this may be merely a preliminary step in performing a primary to secondary conversion. In the course of applying the key, the expressions for the boundaries of the secondary system which is sought are always among those evaluated. It will be a convenience, then, if these expressions, in molar form, can be used directly in primary to secondary conversion, to obtain the secondary composition in percentage form. What we seek for this purpose is a series of equations in which the quantities of primary components are expressed in moles, and those of the secondary components in grams, in some specified total quantity. As an example, let us consider the system  $\text{CS}-\text{C}_2\text{AS}-\text{CAS}_2$  (system 10 in figure 2). For this system we found previously that:

$$\text{Moles CS} = \mathbf{X} = (\mathbf{C} + \mathbf{S} - 3\mathbf{A})/2 \quad (5a)$$

$$\text{Moles C}_2\text{AS} = \mathbf{Y} = (\mathbf{C} + \mathbf{A} - \mathbf{S})/2 \quad (6a)$$

$$\text{Moles CAS}_2 = \mathbf{Z} = (\mathbf{A} + \mathbf{S} - \mathbf{C})/2 \quad (7a)$$

In these equations the quantities of both primary and secondary components refer to the number of moles in any total weight of material, this total quantity of material being the same throughout. Let us specify that the total quantity is 100 g. Then, if  $X$ ,  $Y$ , and  $Z$  represent percentages of CS,  $\text{C}_2\text{AS}$ , and  $\text{CAS}_2$  (grams per 100 g.), respectively,

$$\mathbf{X} = \frac{X}{116.14} \quad \mathbf{Y} = \frac{Y}{274.16} \quad \mathbf{Z} = \frac{Z}{278.14}$$

Substituting in equations 5a-7a:

$$\text{Per cent CS} = X = 58.07(C + S - 3A)$$

$$\text{Per cent C}_2\text{AS} = Y = 137.08(C + A - S)$$

$$\text{Per cent CAS}_2 = Z = 139.07(A + S - C)$$

The expressions in parentheses are encountered and evaluated in the course of applying the classification key (table 1) to any composition in system 10. After locating compositions in this system, the values of these expressions may be multiplied by the indicated constants to obtain the percentages of CS, C<sub>2</sub>AS, and CAS<sub>2</sub>. In general, if the classification key is used to determine the secondary system in which a composition lies, expressions evaluated in that process may be used for a direct computation of secondary composition. It should be noted that the signs of some expressions used in this manner may be reversed. For example, the expression  $A + S - C$  in the third equation corresponds to the expression  $C - A - S$  in the table. After evaluating these expressions in applying the key, the secondary composition is easily computed.

It will be noted that in method 2 (table 1) the quantities C, A, and S represent the number of moles of C, A, and S in 5608 g. of material, not 100 g. If the above equations are applied to values of boundary expressions obtained by method 2, the values of X, Y, and Z will be 56.08 times the percentage sought. In that case, the coefficients of the boundary expressions in these equations are divided by 56.08, obtaining:

$$\text{Per cent CS} = X = 1.0355(C + S - 3A) \quad (7c)$$

$$\text{Per cent C}_2\text{AS} = Y = 2.4444(C + S - A) \quad (8c)$$

$$\text{Per cent CAS}_2 = Z = 2.4799(A + S - C) \quad (9c)$$

These equations are derived for the conversion of primary compositions to secondary compositions after determining by method 2 (table 1) that the compositions are in system CS-C<sub>2</sub>AS-CAS<sub>2</sub> (system 10 in figure 2). Similar equations for all of the secondary systems in the system CaO-Al<sub>2</sub>O<sub>3</sub>-SiO<sub>2</sub> are shown in table 2, to illustrate the manner in which a classification key may be supplemented by primary to secondary conversion equations of this type.

#### 4. Division of multicomponent systems into secondary systems

The division of a primary system into secondary systems may be based upon differences in characteristics of compositions in the various systems. The division of the system CaO-Al<sub>2</sub>O<sub>3</sub>-SiO<sub>2</sub> (figure 1) is an example of this kind, since the secondary systems differ from one another with reference to final products of crystallization of liquids in those systems. On the other hand, the division into secondary systems may be arbitrary, merely for the purpose of classification. In any case, the secondary systems must be mutually exclusive. This condition is easily met in the case of a ternary system, but the graphic methods suitable for a ternary system can not be employed in the division

of a system of many components into secondary systems. For such systems it is necessary to use other methods of determining whether secondary systems which are selected are mutually exclusive. Certain helpful principles will be discussed briefly.

When two secondary systems are adjacent, they will have  $N - 1$  components in common. For example, the adjacent systems  $AB-B_2C-A_3BD-C_2D$  and

TABLE 2  
Conversion equations for system  $CaO-Al_2O_3-SiO_2$   
 $C$  = per cent  $CaO$   
 $A$  = 0.5501 (per cent  $Al_2O_3$ )  
 $S$  = 0.9337 (per cent  $SiO_2$ ) } as in method 2 in table 1

SYSTEM	PER-CENT-AGE OF	EQUATIONS	SYSTEM	PER-CENT-AGE OF	EQUATIONS
1.....		$C_2S = 4.0710S$ $CaO = C - 3A - 3S$ $C_2A = 4.8178A$	8.....		$CA = 1.4089(5C - 3A - 7S)$ $C_2AS = 4.8888S$ $C_2A_3 = 6.0444(A + S - C)$
2.....		$C_2S = 4.0710(C - 3A - 2S)$ $C_2S = 3.0710(3A + 3S - C)$ $C_2A = 4.8178A$	9.....		$Al_2O_3 = 0.6059(3A + 7S - 5C)$ $C_2AS = 4.8888S$ $C_2A_3 = 4.0296(C - 2S)$
3.....		$C_2S = 3.0710S$ $C_2A = 5.8178(3C - 5A - 6S)$ $C_2A_3 = 10.4533(3A + 2S - C)$	10....		$CS = 1.0355(C + S - 3A)$ $C_2AS = 2.4444(C + A - S)$ $CAS_2 = 2.4799(A + S - C)$
4.....		$C_2S = 3.0710S$ $C_2A_3 = 5.2266(C - A - 2S)$ $CA = 1.4089(5A + 6S - 3C)$	11....		$CS = 2.0710(C - A)$ $SiO_2 = 1.0710(S - A - C)$ $CAS_2 = 4.9597A$
5.....		$C_2S = 3.0710(C - A - S)$ $CA = 2.8178(C - 2S)$ $C_2AS = 4.8888(A + 2S - C)$	12....		$Al_2O_3 = 0.6059(3A - C - S)$ $C_2AS = 1.6296(2C - S)$ $CAS_2 = 1.6532(2S - C)$
6.....		$C_2S = 3.0710(2C - A - 3S)$ $C_2S_2 = 5.1419(2S - C)$ $C_2AS = 4.8888A$	13.....		$CAS_2 = 4.9597C$ $A_2S_2 = 3.7976(S - 2C)$ $Al_2O_3 = 0.9089(4C + 2A - 3S)$
7.....		$C_2S_2 = 5.1419(C - A - S)$ $C_2AS = 4.8888A$ $CS = 2.0710(A + 3S - 2C)$	14.....		$CAS_2 = 4.9597C$ $A_2S_2 = 2.5317(A - C)$ $SiO_2 = 0.3570(3S - 2A - 4C)$

$B_2C-A_3BD-C_2D-AD$  have three components in common, forming the ternary system  $B_2C-A_3BD-C_2D$ , which is the common boundary. However, the fact that the two systems have  $N - 1$  components in common does not necessarily indicate that they are adjacent systems, and therefore mutually exclusive. The components not held in common, that is,  $AB$  and  $AD$ , must be on opposite sides of the ternary system  $B_2C-A_3BD-C_2D$ . To determine whether this is true, we



find the equation for the ternary system by the determinant method. The equation is:

$$5A - 3B + 6C - 12D = 0$$

Substituting the compositions AB and AD in the boundary expression, we obtain values of unlike sign, +2 and -7, respectively. This indicates that the systems are adjacent. When values of like sign are found, it is indicated that the systems have a common boundary, but are on the same side of that boundary, and consequently overlap.

By applying tests of this kind it is possible to develop a scheme of classification of compositions for a system of any number of components, with no overlapping systems.

#### IV. SYSTEMS OF LESS THAN $(N - 1)$ COMPONENTS

In dealing with systems of not more than four components, relations between quantities of the components may be represented geometrically by points, curves, surfaces, or volumes. Analytical expressions may be referred to such geometrical figures. For example, an equation involving components of a ternary system is called the equation of a particular line or curve. In formulating general relations, without reference to coordinate systems, it is preferable to refer to the number of degrees of freedom with respect to composition only.

An  $N$ -component system has  $(N - 1)$  degrees of freedom. A single equation defining a relation between components reduces the number of degrees of freedom by 1. Since the primary system has  $(N - 1)$  degrees of freedom, the equation defines an aggregate of compositions with  $(N - 2)$  degrees of freedom. If the equation is linear, the equation defines an  $(N - 1)$ -component system, with  $(N - 2)$  degrees of freedom.

Two equations may be introduced to define an aggregate of compositions which satisfy both. In geometrical terms we would say that the geometrical figure defined by the two equations is the intersection of the figures defined by each alone. The number of degrees of freedom is two less than that of the primary system, or  $(N - 3)$ . If the equations are linear, they define a system of  $(N - 2)$  components, with  $(N - 3)$  degrees of freedom.

Since we are concerned only with linear relations at present, we may state the general principle that to define an  $n$ -component system within a system of  $N$  components,  $(N - n)$  equations are required, and the number of degrees of freedom is  $(n - 1)$ . For example, a quaternary system has three degrees of freedom, and is therefore capable of being represented by a space model. In that system, a single linear equation defines a ternary system, with two degrees of freedom, that is, a plane. Two linear equations restrict compositions to those which are on both planes, and consequently on the intersection of the planes. The intersection is a line, which has one degree of freedom. Similarly, three equations restrict compositions to the intersection of three planes, and consequently define a single composition, which has zero degrees of freedom.

Since  $(N - n)$  linear equations are required to define a secondary system of  $n$  components, it is apparent that the number of equations required to define a system of a given number of components increases with  $N$ . For example, a binary system in a ternary system may be defined by a single equation, but a binary system in a quaternary system can not be defined by a single equation, two equations being required. Because this leads to difficulties in defining systems of a small number of components within a primary system of a considerably greater number of components, there is a temptation to try to simplify the situation by operating on the equations to reduce their number. For example, if two equations representing a system have been found, it may be supposed that if one of the variables common to the equations is eliminated, resulting in a single equation, this equation alone will define the system. To demonstrate the effect of such a procedure, we shall consider the boundary systems indicated below, in the hypothetical quaternary system A-B-C-D. Their equations, in molar forms, are shown at the right.

<i>System</i>	<i>Equation</i>	
$A_2BC-AC_3D_4-AB$	$2A - 2B - 2C + D = 0$	(23)

$A_2BC-AC_3D_4-CD$	$A - 3B + C - D = 0$	(24)
--------------------	----------------------	------

In the space model of the quaternary system these systems are planes. The binary system  $A_2BC-AC_3D_4$  is represented by the straight line formed by the intersection of these planes. It is defined by equations 23 and 24, taken as a pair, since any composition in the binary system will satisfy both equations. Now let us follow the procedure in question, adding equations 23 and 24 to eliminate  $D$ . The following equation is obtained:

$$3A - 5B - C = 0 \quad (25)$$

Equation 25 is the equation of the ternary system  $A_3B_3-AC_3-D$ , and is satisfied by any composition in that system. This system is a plane. It includes the binary system  $A_2BC-AC_3D_4$ , since  $A_2BC$  can be formed by combining 1 mole of  $A_3B_3$  with 1 mole of  $AC_3$ , and  $AC_3D_4$  by combining 1 mole of  $AC_3$  with 4 moles of  $D$ . All that has been accomplished by the procedure is to find another plane intersecting the first two planes on a single straight line,  $A_2BC-AC_3D_4$ . Equation 25 does not define the binary system, since there are an infinite number of compositions which satisfy the equation, but which are not in the binary system.

The  $N-n$  equations required to define an  $n$ -component system may include an equation indicating that the quantity of one of the primary components is zero, or it may include several equations of this kind. For example, an  $n$ -component system may be on the A-B-C face of the space model of the quaternary system A-B-C-D. In that case  $D = 0$  is one of the equations defining the  $n$ -component system.

#### A. LIMITING CONDITIONS FOR SYSTEMS NOT PASSING THROUGH PRIMARY SYSTEM

It was mentioned earlier (page 707) that the equation of an  $(N - 1)$ -component system represents a system extending to the boundaries of the primary

system. If the equation has been derived with reference to a given  $(N - 1)$ -component system not extending to the boundaries of the primary system, the equation is satisfied by all compositions within the given system, and also by all compositions in the extension of that system. For example, equation 8, representing the system  $C_2AS-CAS_2$  (figure 2), applies not only to that system, but also to its extensions to  $C_3A$  and  $S_3A$  on the boundaries of the primary system. That is, the equation does not completely define the system  $C_2AS-CAS_2$ . In general, the  $N - n$  equations for an  $n$ -component system do not completely define a system if the system does not extend to the boundaries of the primary system. To define the system completely it is necessary to indicate limiting conditions.

It is a simple matter to indicate the limits of a binary system in an  $N$ -component system. For example, the limits of the binary system  $C_2AS-CAS_2$  may be indicated by stating maximum and minimum percentages, or molar proportions, of one of the primary components. Another method will be described, however, since it suggests a general method which may be applied to systems of any number of components.

Referring to figure 2, let us consider system 10, the ternary system  $C_2AS-CAS_2-CS$ , with reference to the problem of indicating the limits of the system  $C_2AS-CAS_2$ . The boundary expression  $C + A - S$  is positive for all compositions in the system  $C_2AS-CAS_2$ , but is negative for compositions on the extension of that system toward the  $S-A$  side of the triangle. Similarly, the expression  $C - A - S$  is negative for compositions in the system  $C_2AS-CAS_2$ , but positive for compositions on its extension in the opposite direction. Thus, the system  $C_2AS-CAS_2$  may be completely defined by its equation,  $C + S - 3A = 0$ , and the limiting conditions that both  $C + A - S$  and  $A + S - C$  are positive or zero.

System 10 (figure 2) has been used to illustrate a method of using boundary expressions in defining the limits of a binary system within a ternary system. Any ternary system in which two of the components are  $C_2AS$  and  $CAS_2$  can be taken as a basis for the limiting conditions needed for completely defining the binary system  $C_2AS-CAS_2$ . For example, system 12 could have been selected. Or, if desired, any composition in the primary system may be selected to form a ternary system with  $C_2AS$  and  $CAS_2$ , provided that it is not in the system  $C_2AS-CAS_2$ . In the general method of completely defining  $n$ -component systems, which will now be described, an  $N$ -component system is formed by the addition of  $N - n$  components, selected arbitrarily. These added components are preferably primary components, since the limiting conditions are usually more simple. This may be seen in the case of the binary system  $C_2AS-CAS_2$  (figure 2). It will be noted that system 12, in which  $A$  is the component added, leads to more simple limiting conditions than system 10.

#### B. GENERAL METHOD FOR MULTICOMPONENT SYSTEMS

A method of completely defining any system of  $n$  components will be illustrated by the problem of defining the ternary system  $AB_2C_3D-A_2BCE-AC_2E$  in the

hypothetical system A-B-C-D-E. Here  $N - n = 2$ , so that it is known that two equations are required to define the system, including its extensions to the boundaries of the primary system. These equations and the limiting conditions are to be found.

The first step in the procedure is to set up a system of  $N$  components (in this case  $N = 5$ ) in which the components of the system to be defined are included as components, and the remaining components are selected arbitrarily. The latter are selected one by one, each time making sure that the substances selected as components can not be formed from any of the others in any proportions, positive or negative. Following this procedure, we have obtained the secondary system  $AB_2C_5D-A_2BCE-AC_2E-A-B$ . This system is bounded by the five quaternary systems listed below.

<i>System</i>	<i>Equation</i>
1. $AB_2C_5D-A_2BCE-AC_2E-A$	$B + C - 7D - 2E = 0$
2. $AB_2C_5D-A_2BCE-AC_2E-B$	$A + C - 6D - 3E = 0$
3. $AB_2C_5D-A_2BCE-A-B$	$C - 5D - E = 0$
4. $AB_2C_5D-AC_2E-A-B$	$C - 5D - 2E = 0$
5. $A_2BCE-AC_2E-A-B$	$D = 0$

All three of the components of the ternary system under consideration (the system  $AB_2C_5D-A_2BCE-AC_2E$ ) are components of systems 1 and 2. The equations of these systems are satisfied by the components of the ternary system. This pair of equations defines the ternary system, but includes its extensions to the boundaries of the primary system. The limiting conditions needed to exclude these extensions are supplied by the boundary expressions for the remaining systems. System 5 may be ignored, since its equation indicates that it is on one of the boundaries of the primary system. System 3 lacks the  $AC_2E$  component of the ternary system. Substituting this composition in the expression  $C - 5D - E$ , we obtain  $2 - 0 - 1$ , or  $+1$ . Since a positive value is obtained, the limiting condition in this case is that  $C - 5D - E$  must be zero or positive, or that  $E$  must not be greater than  $C - 5D$ . Similarly we find from the boundary expression for system 4 that  $E$  must not be less than  $1/2(C - 5D)$ . The ternary system is therefore completely defined by the following equations and inequalities. If any one of them is not satisfied by a particular composition, the composition is not in the ternary system  $AB_2C_5D-A_2BCE-AC_2E$ . If the equations are both satisfied, but either of the inequalities is not, the composition is in an extension of the ternary system:

$$B + C - 7D - 2E = 0$$

$$A + C - 6D - 3E = 0$$

$$E \geq (C - 5D)$$

$$E \leq 1/2(C - 5D)$$

A hypothetical system has been used to illustrate the general method. In the case of a real system, the equations and inequalities completely defining an  $n$ -component system may be converted to a percentage basis, by the method described on page 702.

The equations and inequalities necessary to define an  $n$ -component system completely are sometimes rather simple. As an example, let us consider the ternary system  $K_2O \cdot Al_2O_3 \cdot 2SiO_2 - CaO \cdot MgO \cdot 2SiO_2 - SiO_2$  in the five-component system  $K_2O - CaO - MgO - Al_2O_3 - SiO_2$ .<sup>2</sup> Following the plan of designating primary components by single letters, the problem may be stated as that of defining the system  $KAS_2 - CMS_2 - S$  in the system  $K - C - M - A - S$ . By the method just described, the ternary system may be completely defined in molar form as follows:

$$K - A = 0 \quad (26)$$

$$C - M = 0 \quad (27)$$

$$S \leq (2A + 2M) \quad (28)$$

These relations are expressed in percentage form below, as obtained by the method described on page 702.

$$K - 0.9240A = 0 \quad (26a)$$

$$C - 1.3909M = 0 \quad (27a)$$

$$S \leq (1.1783A + 2.9792M) \quad (28a)$$

Either set of equations and inequalities fully defines the system  $KAS_2 - CMS_2 - S$ . They are satisfied by all compositions in that system, while no compositions outside of that system will satisfy all three relations.

## V. PHASE SYSTEMS

In the sense in which the term "system" is used in this paper, any substances in a primary system may be taken as components in any system of  $N$  components or less, provided that none of these substances can be formed from the others in any proportions, positive or negative. It is therefore possible to treat phases as components of a system, for the purpose of estimating *phase composition*, that is, the proportions of phases at equilibrium under specific conditions. A system in which the components are phases will be referred to as a *phase system*. In the interpretation of data on phase equilibria the phases selected as components are those which are capable of coexisting at equilibrium at a specific temperature and pressure. Since we shall deal only with condensed systems in discussing phase systems, pressure and the presence of a vapor phase will be ignored. For problems involving  $N$ -component phase systems, such as those concerned with invariant points and univariant curves, intrinsic equations are useful. For phase systems of less than  $N$  components, it is usually more

<sup>2</sup> This problem has been selected because it has been previously treated from the standpoint of analytic geometry by Morey (2).

convenient to use parametric equations, considered in another paper. It will be sufficient at this time to confine our study to the peculiar problems encountered in dealing with equilibria at invariant points.

At an invariant point,  $N$  crystalline phases may exist in equilibrium with a liquid of invariant point composition, at a particular temperature. There are consequently  $N + 1$  phases capable of coexisting at equilibrium at that temperature. If it is possible to obtain the liquid composition by mixing the crystalline phases in positive proportions, the invariant point is a eutectic; otherwise it is a peritectic. In most instances, a peritectic composition may be obtained from the crystalline phases in proportions involving a negative quantity.

When the liquid arrives at an invariant point during the course of crystallization,  $N$  phases may be present. Changes in phase composition occur as heat is removed, but without change of temperature. During this interval,  $N + 1$  phases may be present. The quantity of one of these phases decreases as heat is removed, and that phase finally disappears. When this occurs, there are less than  $N + 1$  phases present, and further removal of heat results in a drop in temperature. It therefore appears that  $N + 1$  phases are present only in the interval between maximum and minimum heat content at the invariant temperature. Our interest is in the phase composition at maximum and minimum heat content at that temperature. In considering phase composition at an invariant point at maximum or minimum heat content, each combination of  $N$  phases which can be formed from the  $N + 1$  phases capable of coexisting at equilibrium at the invariant point temperature may be taken as components of a phase system. Examples will be selected from Rankin and Wright's (3) report of their investigation of the system  $\text{CaO-Al}_2\text{O}_3\text{-SiO}_2$ .

#### A. EQUILIBRIA AT A EUTECTIC POINT (PRIMARY COMPOSITIONS)

As an example of the application of analytical methods to equilibria at a eutectic point, we shall consider the invariant point 49.5 per cent  $\text{CaO}$ , 43.7 per cent  $\text{Al}_2\text{O}_3$ , 6.8 per cent  $\text{SiO}_2$ , which is the composition of a liquid capable of existing in equilibrium with the crystalline phases,  $\text{C}_2\text{S}$ ,  $\text{C}_3\text{A}$ , and  $\text{CA}$ , at  $1335^\circ\text{C}$ . Since these phases are essentially pure compounds, we have two possible methods of attack, that is, we may express compositions in percentages of either primary or secondary components. The latter form has advantages when dealing with pure crystalline compounds, but offers no advantages when solid solutions are involved. The method which will now be considered, in which compositions are expressed in percentages of primary components, is not limited to problems involving pure compounds as phases.

The primary compositions of the phases under consideration are shown in the following table, with the symbols which will be used to designate the phases:

		X $\text{C}_2\text{S}$	Y $\text{C}_3\text{A}$	Z $\text{CA}$	E Liquid
C.....	$\text{CaO}$	65.13	47.83	35.49	49.5
A.....	$\text{Al}_2\text{O}_3$		52.17	64.51	43.7
S.....	$\text{SiO}_2$	34.87			6.8

Taking the four phases in combinations of three, we may set up the following phase systems:

1.  $C_6A_3$ -CA-E
2.  $C_2S$ -CA-E
3.  $C_2S$ - $C_6A_3$ -E
4.  $C_2S$ - $C_6A_3$ -CA

Since the invariant point is a eutectic it can be recognized at once that systems 1-3 are systems of maximum heat content at  $1335^\circ\text{C}$ ., and that system 4 is a system of minimum heat content. Systems 1-3 are included in system 4. All compositions which are composed of  $C_6A_3$ , CA, and liquid E when the liquid arrives at E during the course of crystallization are in system 1. Similarly, systems 2 and 3 define the range of compositions which have the liquid phase and the indicated solid phases present when the liquid arrives at E during crystallization. The phase composition at maximum heat content at  $1335^\circ\text{C}$ . may be estimated by treating these phase systems as secondary systems, and deriving primary to secondary conversion equations. To illustrate the procedure, it will be sufficient to perform this operation for one of the three systems. Choosing system 2, the following equations may be set up from the table:

$$0.6513X + 0.3549Z + 0.495E = C$$

$$0.6451Z + 0.437E = A$$

$$0.3487X \qquad \qquad + 0.068E = S$$

Solving:

$$\text{Per cent } C_2S = X = -1.529C + 0.841A + 5.723S \quad (34)$$

$$\text{Per cent CA} = Z = -5.310C + 4.471A + 9.918S \quad (35)$$

$$\text{Per cent liquid} = E = 7.838C - 4.312A - 14.641S \quad (36)$$

Values of  $X$ ,  $Z$ , and  $E$  will be positive for all compositions which are composed of crystalline  $C_2S$ , CA, and liquid E when equilibrium is attained at  $1335^\circ\text{C}$ . with maximum heat content. The equations not only serve in estimating phase composition, but also define the limits of the phase system. Compositions in this system arrive at the invariant point from the univariant curve representing liquids capable of existing in equilibrium with  $C_2S$  and CA at definite temperatures above that of the invariant point.

#### B. EQUILIBRIUM AT A EUTECTIC POINT (SECONDARY COMPOSITIONS)

Although the method just described is applicable in any case, whether the crystalline phases are pure compounds or solid solutions, it was illustrated by an example in which these phases are pure compounds. This was done in order to provide a comparison by dealing with the same problem by the method now to be described, with compositions expressed in percentages of secondary components.

In this case the secondary components are  $C_2S$ ,  $C_6A_3$ , and  $CA$ . The first step in the procedure is to derive equations for primary to secondary conversion by the methods described on page 702. The equations so obtained are as follows:

$$\text{Per cent } C_2S = x = 2.8675S$$

$$\text{Per cent } C_6A_3 = y = 5.2266C - 2.8753A - 9.7606S$$

$$\text{Per cent } CA = z = 3.8753A + 7.8931S - 4.2266C$$

As noted previously, the liquid at the invariant point has the composition 49.5 per cent  $C$ , 43.7 per cent  $A$ , 6.8 per cent  $S$ . Substituting in the above equations, the secondary composition of the liquid is found to be 19.50 per cent  $C_2S$ , 66.69 per cent  $C_6A_3$ , 13.81 per cent  $CA$ . The secondary compositions of the four phases may now be tabulated in the same manner as in the previous table, as follows:

COMPONENTS	PHASES			
	X $C_2S$	Y $C_6A_3$	Z $CA$	E Liquid
$x C_2S$	100.0			19.50
$y C_6A_3$		100.0		66.69
$z CA$			100.0	13.81

It should be noted that  $x$ ,  $y$ , and  $z$  refer to percentages of three compounds as components of a secondary system, without reference to their actual presence as compounds or phases. On the other hand,  $X$ ,  $Y$ , and  $Z$  refer to these compounds as crystalline phases. When no liquid is present,  $X$ ,  $Y$ , and  $Z$  are identical with  $x$ ,  $y$  and  $z$ , respectively. Equations for system 2 can now be set up, as follows:

$$X + 0.1950E = x$$

$$0.6669E = y$$

$$Z + 0.1381E = z$$

Solving:

$$\text{Per cent } C_2S = X = x - 0.292y \quad (34a)$$

$$\text{Per cent } CA = Z = z - 0.207y \quad (35a)$$

$$\text{Per cent liquid} = E = 1.499y \quad (36a)$$

These equations may be applied directly to compositions expressed in percentages of  $C_2S$ ,  $C_6A_3$ , and  $CA$ , to determine the percentages of crystalline phases  $C_2S$  and  $CA$ , and liquid  $E$ , when equilibrium is attained at  $1335^\circ C$ . with maximum heat content. Similar equations may be obtained for systems 1 and 3.

#### C. EQUILIBRIA AT A PERITECTIC POINT

As noted previously, a peritectic liquid cannot be formed by positive proportions of the crystalline phases with which it is capable of existing in a state of



equilibrium. For example, a liquid of the composition 58.3 per cent  $\text{CaO}$ , 33.0 per cent  $\text{Al}_2\text{O}_3$ , 8.7 per cent  $\text{SiO}_2$  (an invariant point) may exist in equilibrium with the crystalline phases,  $\text{C}_3\text{S}$ ,  $\text{C}_2\text{S}$ , and  $\text{C}_3\text{A}$ , at  $1455^\circ\text{C}$ . However, conversion of this composition into terms of these phases leads to the composition -50.52 per cent  $\text{C}_3\text{S}$ , 63.06 per cent  $\text{C}_2\text{S}$ , 87.46 per cent  $\text{C}_3\text{A}$ . The fact that a negative value appears indicates that the point is outside of the system  $\text{C}_3\text{S}-\text{C}_2\text{S}-\text{C}_3\text{A}$ , and is therefore a peritectic. The point is located in a direction opposite the component which is negative. In this case, the point is outside of the system in a direction away from the  $\text{C}_3\text{S}$  vertex. This may be seen in figure 3, in which the peritectic composition is designated as P.

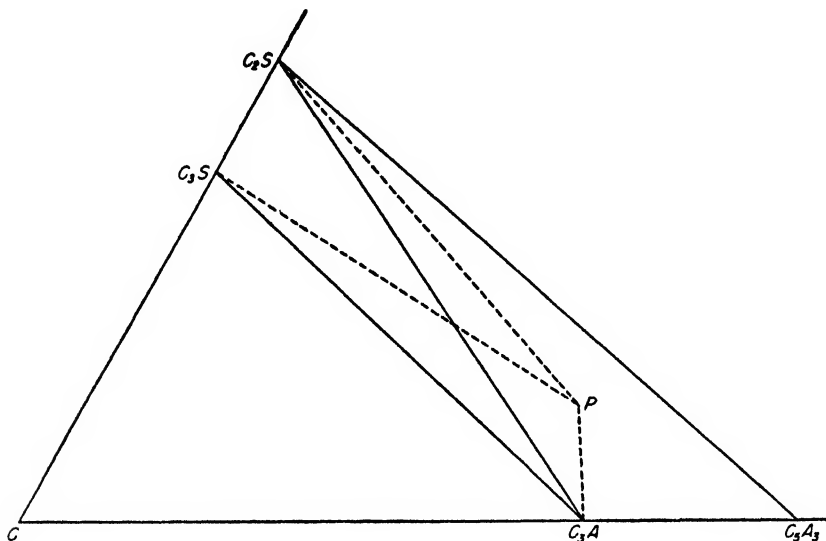


FIG. 3. Phase systems for equilibria at peritectic point

All mixtures which may be composed of the four phases  $\text{C}_3\text{S}$ ,  $\text{C}_2\text{S}$ ,  $\text{C}_3\text{A}$ , and liquid P at equilibrium at  $1455^\circ\text{C}$ . are located in the quadrilateral  $\text{C}_3\text{S}-\text{C}_2\text{S}-\text{C}_3\text{A}-\text{P}$  in figure 3. This area is divided into ternary phase systems of maximum heat content by the line  $\text{C}_3\text{S}-\text{P}$ , and into systems of minimum heat content by the line  $\text{C}_2\text{S}-\text{C}_3\text{A}$ . We thus have the following phase systems:

*Systems of maximum heat content*

1.  $\text{C}_3\text{S}-\text{C}_2\text{S}-\text{P}$
2.  $\text{C}_3\text{S}-\text{C}_3\text{A}-\text{P}$

*Systems of minimum heat content*

3.  $\text{C}_3\text{S}-\text{C}_2\text{S}-\text{C}_3\text{A}$
4.  $\text{C}_2\text{S}-\text{C}_3\text{A}-\text{P}$

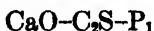
It will be observed that liquid P and the component which is negative, in this case  $\text{C}_3\text{S}$ , in the secondary composition of P are *both* represented in systems 1 and

2. This is a criterion by which phase systems of maximum heat content may be recognized without reference to a diagram. It may be applied to systems of any number of components. That is, after designating the various  $N$ -component systems which may be formed from the peritectic liquid, and the  $N$  crystalline phases with which it can exist in equilibrium, the criterion may be applied in distinguishing between phase systems of maximum and minimum heat content.

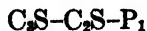
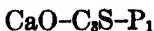
Equations for estimation of phase composition at maximum or minimum heat content are derived in the same manner as for equilibria at a eutectic point, whether compositions are expressed in terms of primary or of secondary components. It should be noted, however, that if compositions are expressed in terms of secondary components, these components should be the crystalline phases with which the liquid may exist at equilibrium. Although this principle should be followed in deriving equations for estimating phase composition, it is sometimes convenient to convert the equations into terms of other components. For example, phase system 4,  $C_2S-C_3A-P$ , is not in the system  $C_2S-C_3S-C_3A$ , but in the adjacent system  $C_2S-C_3A-C_3A_3$ . The equations for system 4 derived in terms of  $C_3S$ ,  $C_2S$ , and  $C_3A$ , may be converted into terms of  $C_2S$ ,  $C_3A$ , and  $C_3A_3$  if they are to be applied to compositions in the latter system.

The example just considered is typical of the usual condition, in which the crystalline phases which may exist in equilibrium with a peritectic liquid may be taken as components of a secondary system ( $N$  components). That is, none of these crystalline phases can be formed from the others, in any proportions. This is not the case when a crystalline phase decomposes at the invariant point temperature. As an example, a liquid  $P_1$ , of the composition 68.4 per cent  $CaO$ , 9.2 per cent  $Al_2O_3$ , 22.4 per cent  $SiO_2$ , may exist in equilibrium with  $CaO$ ,  $C_3S$ , and  $C_2S$  at  $1900^\circ C$ . At that temperature  $C_3S$  is in equilibrium with its decomposition products,  $CaO$  and  $C_2S$ , and with liquid  $P_1$ . Both  $CaO$  and  $C_2S$  may exist in equilibrium with liquid  $P_1$  at maximum heat content at  $1900^\circ C$ ., while at minimum heat content both can not be present. The phase systems are therefore as follows:

*Maximum heat content*



*Minimum heat content*



The fact that there are two phase systems of minimum heat content in which liquid  $P_1$  is a component indicates that on two univariant curves, (1) between the  $CaO$  and  $C_3S$  primary phase regions and (2) between the  $C_3S$  and  $C_2S$  primary phase regions, the direction of falling temperatures is away from  $P_1$ .

Upon determining the phase systems of minimum and maximum heat content, equations for estimating phase composition at  $1900^\circ C$ . under either of these conditions may be derived as previously described.

## VI. SUMMARY

Properties and applications of intrinsic equations, that is, equations derived without reference to coordinate axes, are described, with particular attention to their usefulness in the analytical treatment of multicomponent systems. Equations of this type may be derived directly in terms of composition without considering geometric relations, and may be applied to multicomponent systems without the necessity of thinking in terms of hyperspace. Specific applications discussed are conversion of compositions from one system of components to another, the classification of compositions with reference to the individual systems in which they lie, and the estimation of the proportions of phases at an invariant point.

A system of  $n$  components within an  $N$ -component system is defined by  $N - n$  intrinsic equations. It is suggested that when the necessary number of intrinsic equations is large, parametric equations may be employed more conveniently. The application of equations of the latter type will be considered in another paper (in preparation).

## REFERENCES

- (1) BOWEN, N. L., AND GREIG, J. W.: *J. Am. Ceram. Soc.* [4] 7, 238 (1924).
- (2) MOREY, GEORGE W.: *J. Phys. Chem.* 34, 1745-50 (1930).
- (3) RANKIN, G. A., AND WRIGHT, F. E.: *Am. J. Sci.* [4] 39, 1 (1915).

## BINARY SYSTEMS OF SOME CARBOXYLIC ACIDS. I

SYSTEMS CONTAINING BENZOIC ACID OR A SUBSTITUTED BENZOIC ACID  
AS ONE OF THE COMPONENTS<sup>1</sup>KURT MISLOW<sup>2</sup>

*Gates and Crellin Laboratories of Chemistry, California Institute of Technology,  
Pasadena 4, California*

*Received August 12, 1947*

The dependence of the specificity of a biologically active molecule upon its size and shape has been a generally recognized phenomenon in the field of immunology (12), as well as in other biological fields (21). Much work has been done in correlating isomorphism and physiological specificity (14), in order to test the idea that any two isosteric molecules which are isomorphous, as shown by the fact that they form solid solutions with one another, may also have similar biological activities.<sup>3</sup>

<sup>1</sup> Contribution No. 1133 from the Gates and Crellin Laboratories of Chemistry, California Institute of Technology.

<sup>2</sup> Present address: Department of Chemistry, New York University, University Heights, New York City, New York.

<sup>3</sup> For reviews of the concept of physiological isomorphism, see references 14, 18, 20.

The work reported in this and a subsequent paper represents part of a program begun in these laboratories to correlate isomorphism and serological cross-reactivity. The substances chosen for this research were simple and substituted aromatic carboxylic acids. These substances are soluble at serological pH, making possible their use as haptens, and their melting points lie in a range (100–300°C.) convenient for the ready determination of phase relationships. The results of the serological studies will be reported elsewhere.

#### MATERIALS

The following commercially available reagents were recrystallized from water to constant melting point: *p*-toluic acid, m.p. 177–178°C.; *o*-toluic acid, m.p. 104–105°C.; *p*-bromobenzoic acid, m.p. 252–253°C.; nicotinic acid, m.p. 233°C.; benzoic acid, m.p. 121–122°C.; pyrazinecarboxylic acid, m.p. 224–226°C. (dec.); picolinic acid, m.p. 136–137°C.; furoic acid, m.p. 132–133°C.; isonicotinic acid, m.p. 312–314°C. (dec.), reported: 317°C. (26); 315°C. (2).

The following acids were prepared by methods previously reported in the literature.

*5-Thiazolecarboxylic acid* was prepared as follows: Ethyl formate was condensed with ethyl chloroacetate, and the resulting formylchloroacetic acid ethyl ester (32) was reacted with thioformamide to give 5-carbethoxythiazole (6). Hydrolysis of this ester (6) gave 5-thiazolecarboxylic acid; after recrystallizations from water the acid melted at 218–220°C. (dec.) (reported, 218°C. (7)).

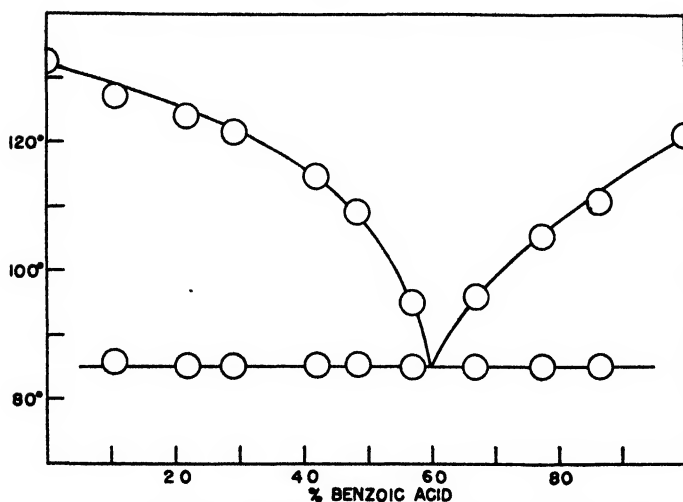
*2-Thiophenecarboxylic acid* was prepared by iodinating thiophene (16) and converting the resulting 2-iodothiophene into the desired acid by the Grignard synthesis (25). Successive recrystallizations from water and ligroin–benzene afforded needles, m.p. 127–128°C.

*3-Thiophenecarboxylic acid* was prepared by the following series of reactions: Ethyl crotonate (15) was reacted with potassium cyanide and barium hydroxide to give methylsuccinic acid (9). The sodium salt of the acid was heated with phosphorus trisulfide to give a 23 per cent yield of 3-methylthiophene (31). The procedure for the ring closure was based on the preparation of thiophene by Phillips (22). Oxidation of 3-methylthiophene (4, 17) gave a 4 per cent yield of 3-thiophenecarboxylic acid. Successive recrystallizations from water and ligroin–benzene and subsequent sublimation gave colorless platelets, m.p. 137–138°C.

*3-Methyl-2-thiophenecarboxylic acid* (23) was prepared by iodinating 3-methylthiophene (*cf.* 16), preparing the Grignard reagent of the resulting 2-iodo-3-methylthiophene, forming the carbon dioxide adduct, and hydrolyzing to give the desired acid (m.p. 146–147°C. after three recrystallizations from water).

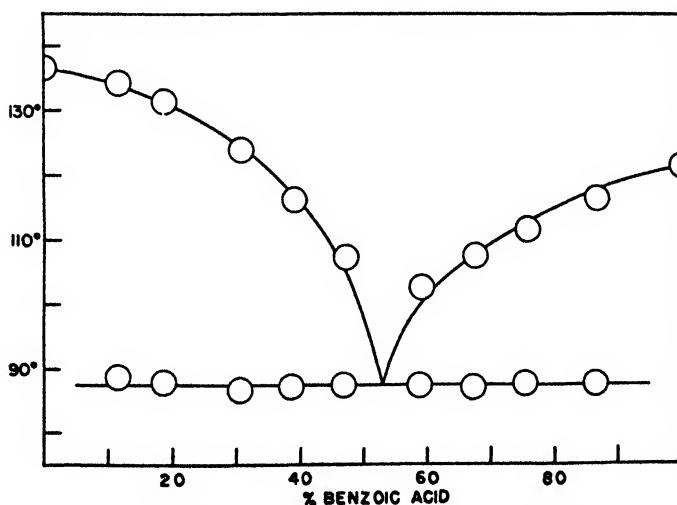
*5-Bromo-2-thiophenecarboxylic acid*, m.p. 140–141°C., was prepared by the direct bromination of 2-thiophenecarboxylic acid in glacial acetic acid (27).

*5-Methyl-2-thiophenecarboxylic acid* was prepared as follows: Levulinic acid was heated with phosphorus trisulfide to give a 9 per cent yield of 2-methylthiophene (11), the procedure of Phillips (22) being employed. Iodination (*cf.* 16) of that compound yielded 5-iodo-2-methylthiophene, which was con-

FIG. 1. Benzoic acid (A) *versus* furoic acid: O, point on phase boundary

Per cent A.....	0	10.4	21.7	28.9	42.0	48.6	57.0	66.9	77.5	86.5	100
Thawing point ....	132	85.6	85.1	85.0	85.3	85.5	85.0	85.0	85.1	85.1	121
Melting point.....	133	127.2	124.0	121.5	114.5	109.2	95.2	96.0	105.5	110.8	122

A eutectic is formed at 60 per cent A and 85°C. There is no indication of solid-solution formation.

FIG. 2. Benzoic acid (A) *versus* picolinic acid: O, point on phase boundary

Per cent A.....	0	11.6	18.6	30.3	38.3	46.5	58.8	67.2	75.5	86.6	100
Thawing point ....	136	88.4	87.6	86.4	87.0	87.2	87.4	87.0	87.6	87.6	21
Melting point.....	137	134.2	131.0	123.8	116.0	107.4	102.4	107.4	111.4	116.2	122

A eutectic is formed at 53 per cent A and 115°C. There is no indication of solid-solution formation.

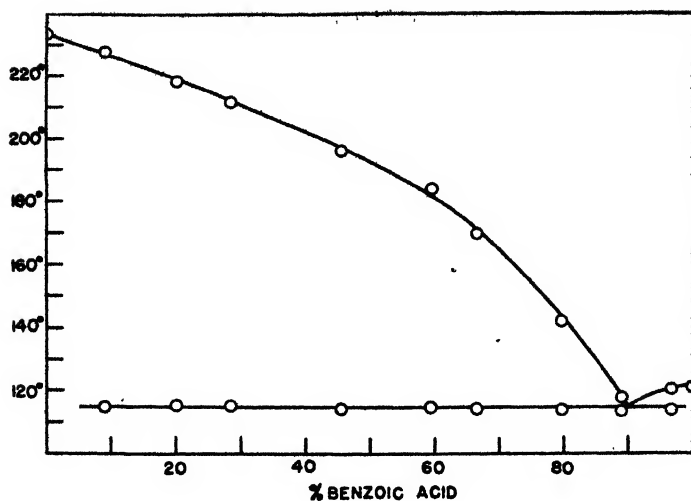


FIG. 3. Benzoic acid (A) *versus* nicotinic acid: O, point on phase boundary

Per cent A.....	0	9.0	20.0	28.6	45.4	59.5	66.6	79.8	89.0	96.8	100
Thawing point....	233	115.0	115.4	115.4	114.2	115.0	114.6	114.0	113.6	114.0	121
Melting point.....	233	227.6	217.6	211.2	195.8	184.0	169.8	142.2	117.8	120.4	122

A eutectic is formed at 90 per cent A and 115°C. There is no indication of solid-solution formation.

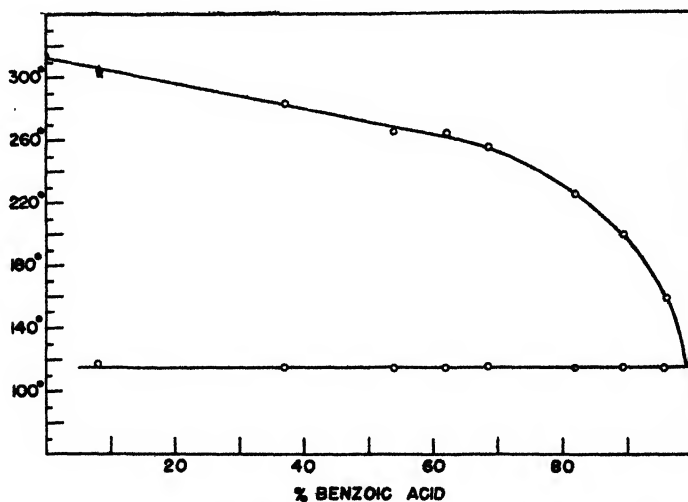


FIG. 4. Benzoic acid (A) *versus* isonicotinic acid. O, point on phase boundary; Δ, beginning of decomposition.

Per cent A.....	0	8.1	36.8	53.9	61.8	68.4	81.8	89.4	96.1	100
Thawing point....	312	118.6	115.4	115.0	115.0	115.0	114.8	115.4	115.4	121
Melting point.....	314*	304*	282.8	265.4	264.2	255.4	225.2	199.4	158.8	122

\* Decomposes.

A eutectic is formed at *ca.* 99 per cent A and 115°C. There is no indication of solid-solution formation.

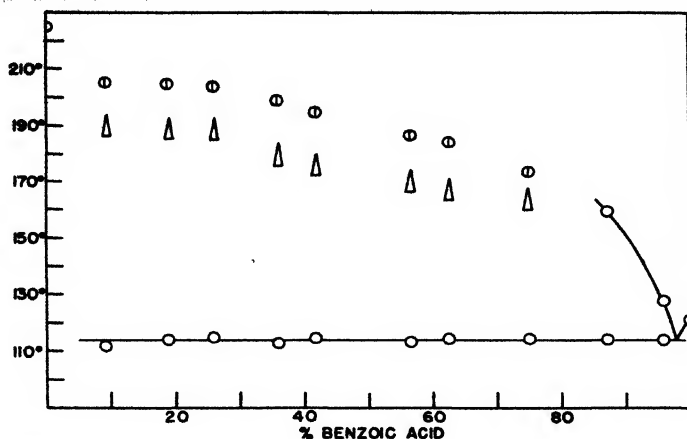


FIG. 5. Benzoic acid (A) versus pyrazinecarboxylic acid.  $\circ$ , point on phase boundary;  $\Delta$ , beginning of decomposition;  $\odot$ , point not representing an equilibrium condition (such as melting point after decomposition has set in).

Per cent A	0	9.1	18.8	25.8	35.8	41.8	56.6	62.6	75.0	87.2	95.8	100
Thawing point	224	111.8	114.0	115.0	113.0	114.6	113.6	114.4	114.6	114.4	114.0	121
Decomposition point	224	189.8	189.0	188.6	179.8	176.0	170.6	167.2	164.2			
Melting point	226	205.0	204.2	203.2	198.4	194.2	186.2	184.0	173.4	159.4	127.8	122

A eutectic is formed at *ca.* 98 per cent A and 114°C. Decomposition in the region 0-80 per cent A above 165°C. makes the liquidus indeterminate. There is no indication of solid-solution formation.

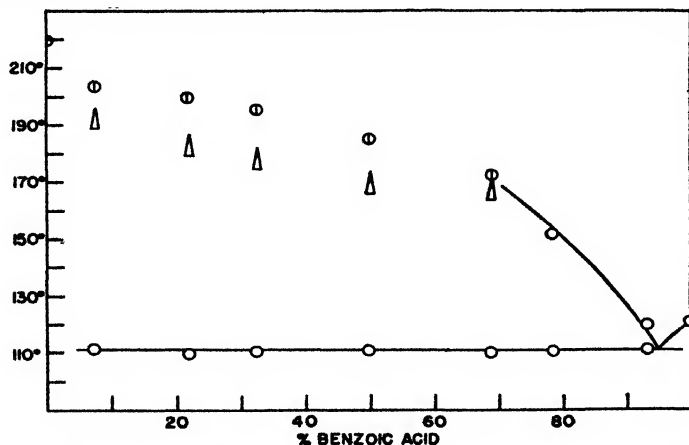


FIG. 6. Benzoic acid (A) versus 5-thiazolecarboxylic acid.  $\circ$ , point on phase boundary;  $\Delta$ , beginning of decomposition;  $\odot$ , point not representing an equilibrium condition (such as melting point after decomposition has set in).

Per cent A	0	7.6	22.0	32.7	50.0	69.0	78.5	93.3	100
Thawing point	218	111.4	109.6	111.0	111.2	110.6	111.0	111.6	121
Decomposition point	218	192.8	183.6	178.6	169.6	167.8			
Melting point	220	203.5	199.4	195.4	185.0	172.4	152.0	120.0	122

A eutectic is formed at 95 per cent A and 111°C. Decomposition in the region 0-70 per cent A above 170°C. makes the liquidus indeterminate. There is no indication of solid-solution formation.

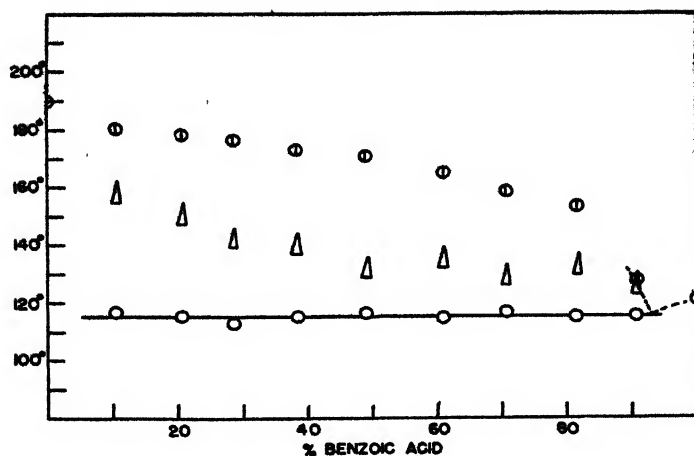


FIG. 7. Benzoic acid (A) versus 2-pyrrolecarboxylic acid.  $\circ$ , point on phase boundary;  $\Delta$ , beginning of decomposition;  $\odot$ , point not representing an equilibrium condition (such as melting point after decomposition has set in); ---, uncertain interpolation.

Per cent A.....	0	10.3	20.6	28.7	38.3	49.0	61.1	70.7	81.4	91.0	100
Thawing point....	190	116.8	115.6	113.2	115.6	116.4	115.0	116.8	115.4	115.6	121
Decomposition point.....	190	158.4	150.6	142.4	140.6	132.4	136.0	129.6	133.8	127.0	
Melting point....	190	180.4	178.4	176.2	172.8	171.2	165.0	158.2	153.2	127.6	122

A eutectic is formed at 93 per cent A and 115°C. Decomposition in the region 0-90 per cent A above 130°C. makes the liquidus indeterminate. There is no indication of solid-solution formation.

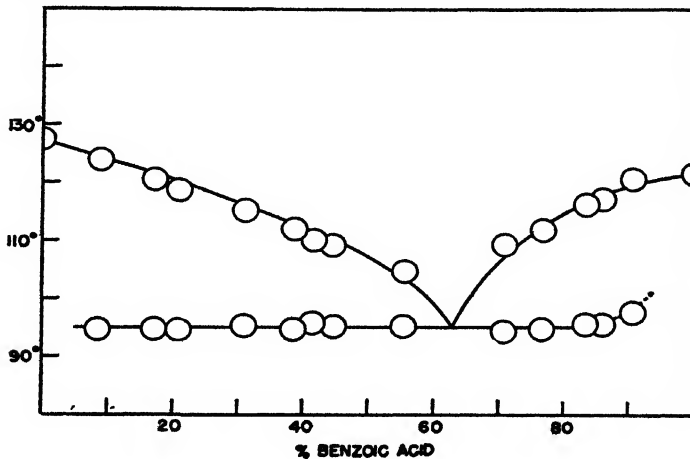


FIG. 8. Benzoic acid (A) versus 2-thiophenecarboxylic acid.  $\circ$ , point on phase boundary; ---, uncertain interpolation.

Per cent A.....	0	8.4	17.1	20.7	30.8	38.3	41.5	44.5	55.5	71.0	76.7	83.5	86.0	90.3	100
Thawing point....	127	94.6	94.8	94.8	95.4	94.8	95.8	95.2	95.4	94.4	94.8	95.6	95.6	97.6	121
Melting point....	128	123.8	120.4	118.6	115.2	112.0	110.2	109.2	104.8	109.2	111.6	116.2	117.0	120.6	122

A eutectic is formed at 63 per cent A and 95°C. There is an indication of solubility at ca. 90 per cent A.



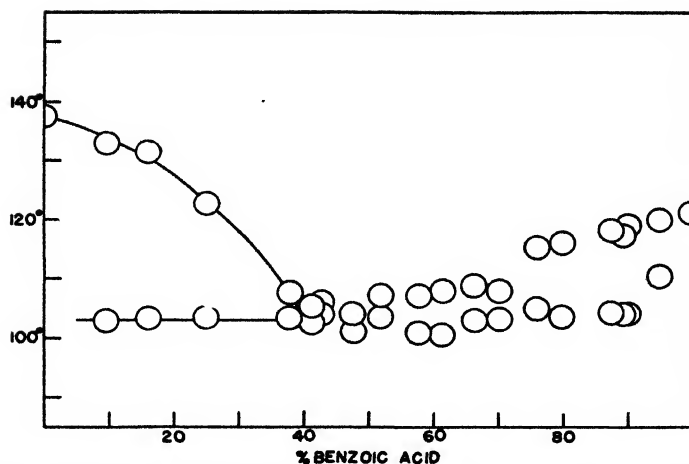


FIG. 9. Benzoic acid (A) versus 3-thiophenecarboxylic acid: O, point on phase boundary

Per cent A	0	9.5	15.9	25.0	37.8	41.4	42.8	47.7	52.0	57.8
Thawing point	137	102.9	103.2	103.5	103.3	102.6	104.0	101.0	103.6	101.0
Melting point	138	132.6	131.2	122.6	107.8	105.4	106.0	104.2	107.2	107.0
Per cent A	61.5	66.2	70.2	76.1	79.4	80.0	87.5	90.0	95.0	100
Thawing point	100.6	103.0	103.2	105.0	104.1	103.6	104.4	104.2	110.6	121
Melting point	108.0	108.8	108.0	115.4	117.2	116.0	118.2	119.0	120.0	122

A eutectic is formed at 40 per cent A and 103°C., and there is an indication of solubility at *ca.* 90 per cent A. The region 40-80 per cent A does not lend itself to ready interpretation. However, there might be another eutectic at *ca.* 64 per cent A and 103°C., and an addition compound at *ca.* 53 per cent A (m. p., 109°C.). A 1:1 compound would be at 49 per cent A

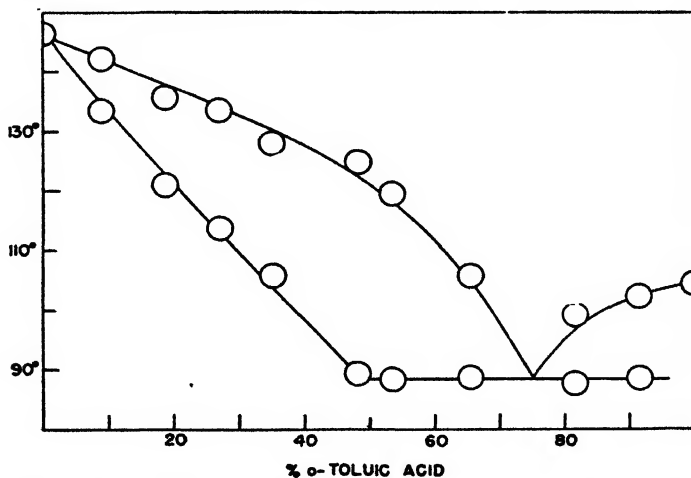


FIG. 10. *o*-Toluic acid (A) versus 3-methyl-2-thiophenecarboxylic acid: O, point on phase boundary

Per cent A	0	9.0	18.8	27.1	35.1	48.1	53.5	65.2	81.6	91.5	100
Thawing point	146	133.2	121.0	113.6	105.6	89.2	88.2	88.4	87.6	88.4	104
Melting point	147	142.0	135.6	133.4	127.8	124.8	119.6	105.6	99.0	102.2	105

Partial solid-solution formation exists, with a eutectic at 75 per cent A and 88°C., and a solubility gap over the range 48-100 per cent A.

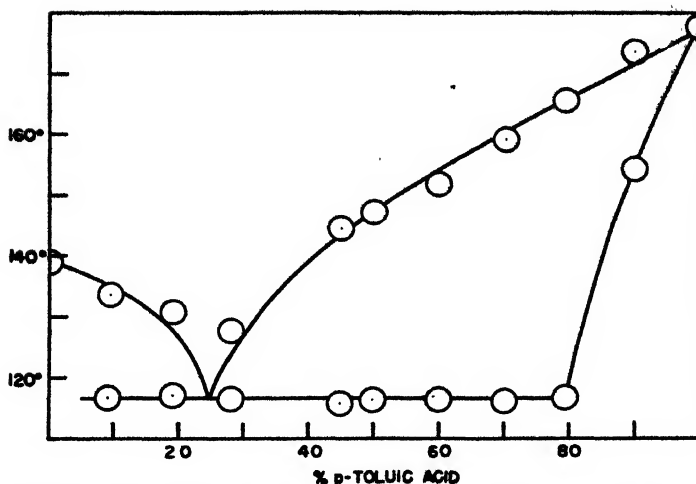


FIG. 11. *p*-Toluic acid (A) versus 5-methyl-2-thiophenecarboxylic acid: O, point on phase boundary

Per cent A.....	0	9.4	19.2	27.9	45.0	50.0	60.0	70.3	79.5	90.0	100
Thawing point....	138	116.6	117.0	116.2	115.6	116.2	116.4	116.2	116.8	154.2	177
Melting point....	139	133.2	130.4	127.4	144.4	147.0	151.8	159.0	165.4	173.4	178

A eutectic is formed at 25 per cent A and 116°C., with solid solution taking place at concentrations above 80 per cent A.

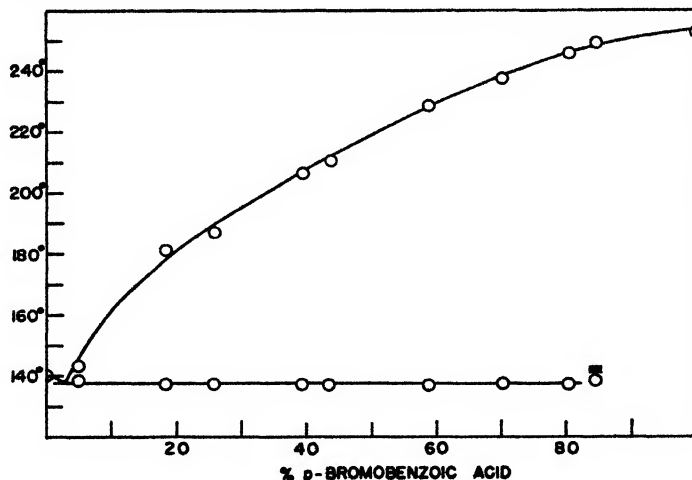


FIG. 12. *p*-Bromobenzoic acid (A) versus 5-bromo-2-thiophenecarboxylic acid. O, point on phase boundary; ■, initial melting with subsequent resolidification.

Per cent A.....	0	5.0	18.4	25.7	39.3	43.4	58.8	70.2	80.6	84.6	100
Thawing point....	140	139.0	137.6	137.6	137.8	137.6	137.4	137.8	137.8	137.8*	252
Melting point....	141	143.8	181.6	187.6	206.6	210.4	228.4	237.8	245.6	249.0	253

\* Resolidifies.

A eutectic is formed at 3 per cent A and 138°C. Above 80 per cent A solid-solution formation seems to take place, but the large range made the determination of resolidification and remelting highly uncertain.

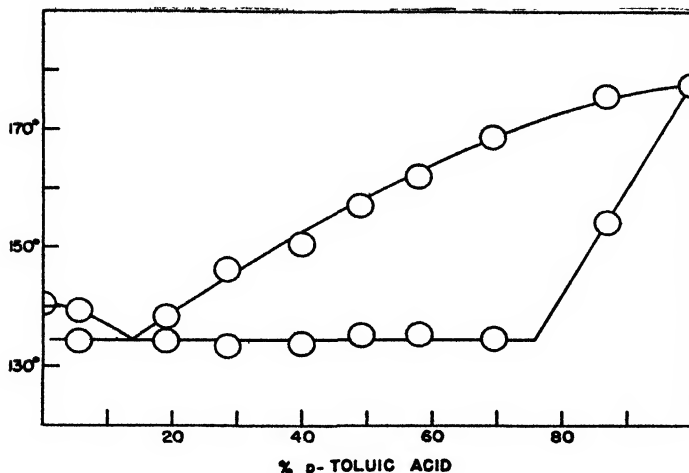


FIG. 13. *p*-Toluic acid (A) versus 5-bromo-2-thiophenecarboxylic acid: O, point on phase boundary

Per cent A . . .	0	6.6	19.0	28.5	39.8	49.1	58.0	69.6	86.9	100
Thawing point ..	140	134.2	134.2	133.6	133.8	135.2	135.4	134.6	154.2	177
Melting point ..	141	139.6	138.2	146.2	150.6	157.0	162.0	168.8	175.8	178

A eutectic is formed at 14 per cent A and 134°C., with solid-solution formation taking place at concentrations above 75 per cent A.

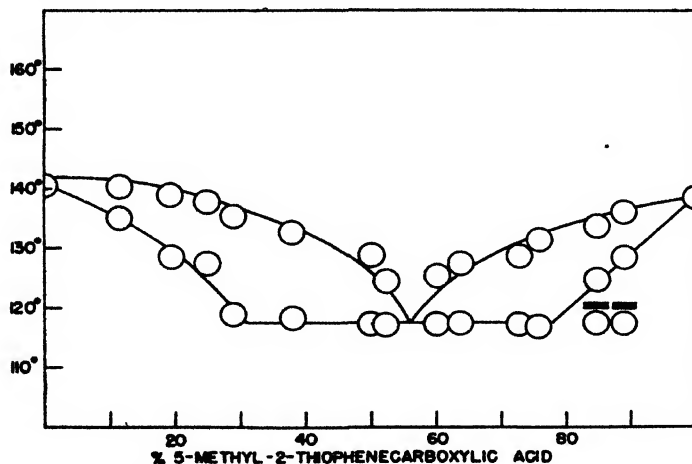


FIG. 14. 5-Methyl-2-thiophenecarboxylic acid (A) versus 5-bromo-2-thiophenecarboxylic acid.\* O, point on phase boundary;  $\bigcirc$ , initial melting with subsequent solidification.

Per cent A . . .	0	11.8	19.7	25.2	28.8	37.9	50.0	52.3	60.2	64.0	72.8	75.9	84.8	88.8	100
Thawing point.	140	135.0	128.6	127.4	119.0	118.2	117.1	117.2	117.2	117.4	117.2	117.0	124.8	128.6	138
Melting point.	141	140.2	139.0	137.8	135.4	133.0	129.0	124.8	125.2	127.6	128.8	131.4	133.6	136.0	139

\* This relationship was included because of its general interest with respect to figures 10 to 13, despite the fact that it is not included under the general title of this paper.

Partial solid solution takes place, with eutectic at 56 per cent A and 117°C. and a gap at 31-77 per cent A.

verted to 5-methyl-2-thiophenecarboxylic acid (24), m.p. 138–139°C., by the Grignard synthesis.

*2-Pyrrolicarboxylic acid* (8, 19) was obtained in a 24 per cent yield by treating pyrrole with methylmagnesium iodide, forming the carbon dioxide adduct, and hydrolyzing. The acid melted at 190°C. (dec.).

#### EXPERIMENTAL PROCEDURE

The procedure consisted in observing the thawing–melting behavior of mixtures of known composition. The mixtures were prepared by thoroughly mixing weighed amounts of the two components. Two capillaries were filled with the mixture and sealed at one end (the two samples gave a check on the homogeneity of the mixture). The capillaries rested next to the junction of a thermocouple in a hot stage (30) which was mounted on a polarizing microscope. Heating rates were kept at  $2^\circ \pm 1^\circ$  per minute. The thawing points (beginning of melting) were observed by reflected light, while the melting points were observed by transmitted light.

Decarboxylation often took place before all of the solid had melted. This has the effect of lowering the liquidus but does not affect the solidus. Decomposition points and the subsequent melting points, represented by suitably modified symbols, have been recorded. These points, which will be referred to as indeterminate, should not be taken as representing true phase boundaries, and no curve has been drawn through them.

The accuracy of the method, as judged by the reproducibility of the results, is  $\pm 2^\circ\text{C.}$  for the thawing and melting points and  $\pm 4^\circ\text{C.}$  for the decomposition points (beginning of decarboxylation as judged by the evolution of bubbles).

#### DATA

The data given on the following pages are represented by phase diagrams and tabulations. The coördinates are temperature ( $^\circ\text{C.}$ ) and composition (weight per cent); the compositions refer to the component indicated on the diagram. The diameter of the circles and the height of the triangles indicate the precision of the measurements.

#### DISCUSSION

The following conclusions can be reached from a study of the phase relationships investigated:

1. Benzoic acid is not isomorphous with any of the heterocyclic acids (Ciamician and Garelli (3) report solid-solution formation for the pairs benzoic acid: 2-thiophenecarboxylic acid and benzoic acid: 2-pyrrolicarboxylic acid. However their results, by the nature of their experiments, are of questionable value (for more detailed criticism, cf. 10)). In the case of 2- and 3-thiophenecarboxylic acids, there does exist an indication of solubility at about 90 per cent benzoic acid, due, probably, to the remarkable similarity in many of the physical properties of benzene and thiophene (5, 28). This insolubility of benzoic acid in heterocyclic acids would suggest that the specificity of hydrogen bonding (orien-

tation, strength) in crystals of these acids is sufficient to prevent mutual solubility in the solid state. In this connection it may be noted that 2- and 3-thiophenecarboxylic acids form with each other only partial solid solutions with a considerable solubility gap (29).

2. While 2-thiophenecarboxylic acid is only *ca.* 10 per cent soluble in benzoic acid, the 5-substituted (Br, CH<sub>3</sub>) 2-thiophenecarboxylic acids are about 20 per cent soluble in the corresponding para-substituted benzoic acids. In the case of an ortho substituent, the solubility becomes greater: *o*-toluic acid is about 50 per cent soluble in 3-methyl-2-thiophenecarboxylic acid. This increase in solubility, which is significant, is another manifestation of the "ortho effect" (1). Of interest in this connection is the observation (13) that of the three nitrobenzoic acids, only the *o*-isomer will form solid solutions (with *o*-toluic, *o*-chlorobenzoic, and *o*-bromobenzoic acids).

3. The isomorphogeny of Br and CH<sub>3</sub> is maintained: 5-bromo-2-thiophenecarboxylic acid is 18 per cent soluble in *p*-toluic acid. Furthermore, 5-methyl- and 5-bromo-2-thiophenecarboxylic acids are soluble in each other.

The results of this work made it of interest to investigate the solubility of the different heterocyclic acids in each other. This work is reported in a subsequent paper.

#### SUMMARY

In connection with a study of the relation between serological specificity and solid solubility, fourteen binary phase relationships have been investigated, the components being aromatic carboxylic acids.

The thiophenecarboxylic acids form very limited solid solutions with benzoic acid, which is not isomorphous with any of the other heterocyclic acids investigated. Isomorphism is noted with some methyl- and bromo-substituted benzoic and thiophenecarboxylic acids.

The author wishes to express his appreciation to Professor Linus Pauling for suggesting this problem.

#### REFERENCES

- (1) BRANCH AND CALVIN: *The Theory of Organic Chemistry*, pp. 257-65. Prentice-Hall, New York (1941).
- (2) CAMPS: *Archiv. Pharm.* **240**, 359 (1902).
- (3) CIAMICIAN AND GARELLI: *Z. physik. Chem.* **18**, 51 (1895).
- (4) DAMSKY: *Ber.* **19**, 3284 (1886).
- (5) ERLLENMEYER *et al.*: *Helv. Chim. Acta* **16**, 733, 1381 (1933).
- (6) ERLLENMEYER AND MEYENBURG: *Helv. Chim. Acta* **20**, 204 (1937).
- (7) ERLLENMEYER AND MOREL: *Helv. Chim. Acta* **25**, 1073 (1942).
- (8) FISCHER-ORTH: *Die Chemie des Pyrrols*, Vol. I, p. 237. Akademische Verlagsgesellschaft, Leipzig (1934).
- (9) HIGGINBOTHAM AND LAPWORTH: *J. Chem. Soc.* **1922**, 51.
- (10) JAEGER: *Z. Krist.* **42**, 236 (1906).
- (11) KUES AND PAAL: *Ber.* **19**, 556 (1886).
- (12) LANDSTEINER: *The Specificity of Serological Reactions*. Harvard University Press, Cambridge, Massachusetts (1945).

- (13) LETTRÉ: Ber. **73**, 386 (1940).
- (14) LETTRÉ: Ergeb. Enzymforsch. **9**, 1 (1943).
- (15) MICHAEL: Ber. **33**, 3766 (1900).
- (16) MINNIS: In *Organic Syntheses*, Collective Vol. II, p. 357. John Wiley and Sons, Inc., New York (1943).
- (17) MUHLERT: Ber. **18**, 3003 (1885).
- (18) NOWACKI: Mitt. Naturforsch. Ges. Bern (N.F.) **2**, 43 (1945).
- (19) ODDO *et al.*: Gazz. chim. ital. **39**, 656 (1909); **42**, 244 (1912).
- (20) PAULING: Chem. Eng. News **24**, 1064 (1946).
- (21) PAULING: Chem. Eng. News **24**, 1375 (1946).
- (22) PHILLIPS: In *Organic Syntheses*, Collective Vol. II, p. 578. John Wiley and Sons, Inc., New York (1943).
- (23) RINKES: Rec. trav. chim. **52**, 1052 (1933).
- (24) RINKES: Rec. trav. chim. **52**, 538 (1933).
- (25) SCHLENK AND OCHS: Ber. **48**, 679 (1915).
- (26) SKRAUP: Monatsh. **17**, 369 (1896).
- (27) STEINKOPF, JACOB, AND PENZ: Ann. **512**, 160 (1934).
- (28) STEINKOPF: *Die Chemie des Thiophens*. Verlag Th. Steinkopff, Dresden (1941).
- (29) VOERMAN: Rec. trav. chim. **26**, 295 (1907).
- (30) VOLD AND DOSCHER: Ind. Eng. Chem., Anal. Ed. **18**, 154 (1946).
- (31) VOLHARD AND ERDMANN: Ber. **18**, 455 (1885).
- (32) WISLICENUS: Ber. **43**, 3530 (1910).

## BINARY SYSTEMS OF SOME CARBOXYLIC ACIDS. II

### SYSTEMS CONTAINING HETEROCYCLIC ACIDS AS THE COMPONENTS<sup>1</sup>

KURT MISLOW<sup>2</sup>

*Gates and Crellin Laboratories of Chemistry, California Institute of Technology,  
Pasadena 4, California*

*Received August 12, 1947*

In connection with a study of the relation of isomorphism to serological cross-reactivity (8), the phase relationships of several unsubstituted heterocyclic aromatic carboxylic acids were investigated. The preparation of the materials and the experimental procedure have been previously described (8).

#### DATA

The data and results are presented in figures 1-11 and the corresponding tables.

<sup>1</sup> Contribution No. 1134 from the Gates and Crellin Laboratories of Chemistry, California Institute of Technology.

<sup>2</sup> Present address: Department of Chemistry, New York University, University Heights, New York City, New York.

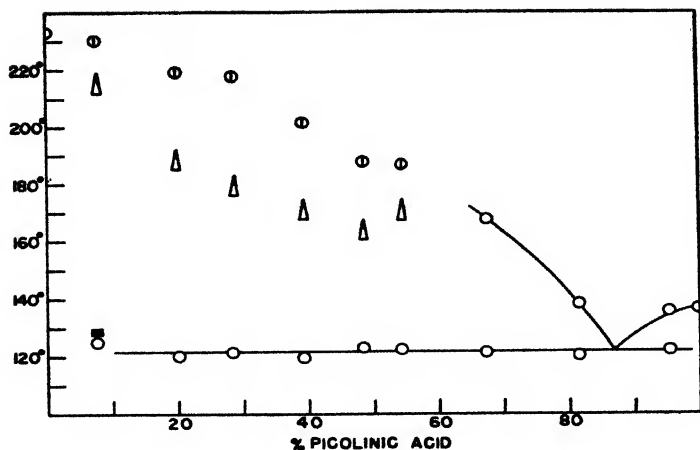


FIG. 1. Picolinic acid (A) *versus* nicotinic acid. O, point on phase boundary; Δ, beginning of decomposition; ⊙, point not representing an equilibrium condition (such as melting point after decomposition has set in); ⊞, initial melting with subsequent resolidification.

Per cent A.	0	7.5	20.0	28.4	39.3	48.6	54.2	67.3	81.6	95.5	100
Thawing point	233	125*	120.4	121.6	119.8	123.0	122.2	121.6	120.2	122.2	136
Decomposition point		215.8	189.0	180.0	171.6	164.2	170.8				
Melting point	233	230.2	219.2	217.4	201.2	188.0	186.8	167.8	138.2	136.0	137

\* Resolidifies

A eutectic is formed at 87 per cent A and 122°C. Decomposition in the region 0-60 per cent A above 165°C. makes the liquidus indeterminate. There is an indication that solid solution takes place at concentrations below 10 per cent A.

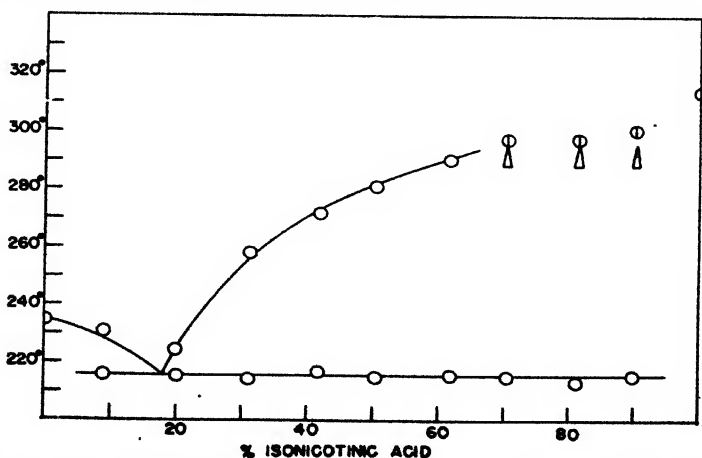


FIG. 2. Isonicotinic acid (A) *versus* nicotinic acid. O, point on phase boundary; Δ, beginning of decomposition; ⊙, point not representing an equilibrium condition (such as melting point after decomposition has set in).

Per cent A.	0	9.0	20.0	31.1	41.7	50.5	61.7	70.5	81.2	90.0	100
Thawing point	233	215.8	215.6	214.0	217.0	215.0	215.6	215.0	213.2	215.2	312
Melting point	233	231.0	224.6	258.4	271.0	280.2	290.0	297*	297*	300*	314*

\* Decomposes at 292°C.

A eutectic is formed at 18 per cent A and 215°C. Decomposition in the region 70-100 per cent A above 292°C. makes the liquidus indeterminate. There is no indication of

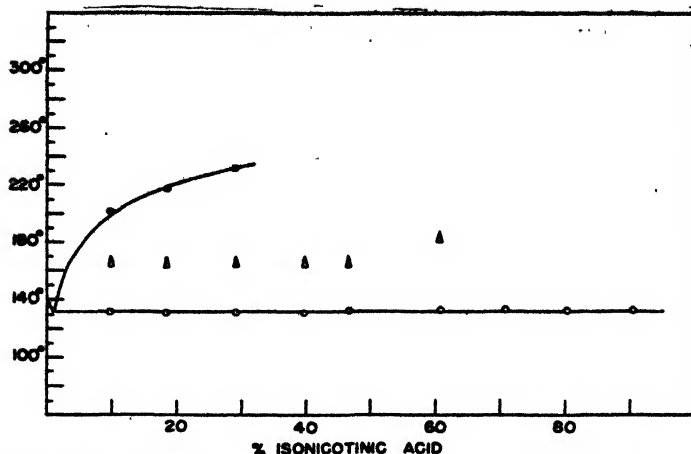


FIG. 3. Isonicotinic acid (A) *versus* picolinic acid. O, point on phase boundary; Δ, beginning of decomposition; ◊, point not representing an equilibrium condition (such as melting point after decomposition has set in).

Per cent A.....	0	9.5	18.4	29.3	39.8	46.7	60.8	70.8	80.5	90.5	100
Thawing point....	136	132.0	131.4	131.2	131.2	132.4	132.4	132.4	132.4	132.4	312
Decomposition point.....		166	166	166	166	166	184.0				
Melting point.....	137	200.8	216.8	231.2							314

A eutectic is formed at ca. 2 per cent A and 132°C. Decomposition above 165°C. makes the liquidus indeterminate. There is no indication of solid-solution formation.

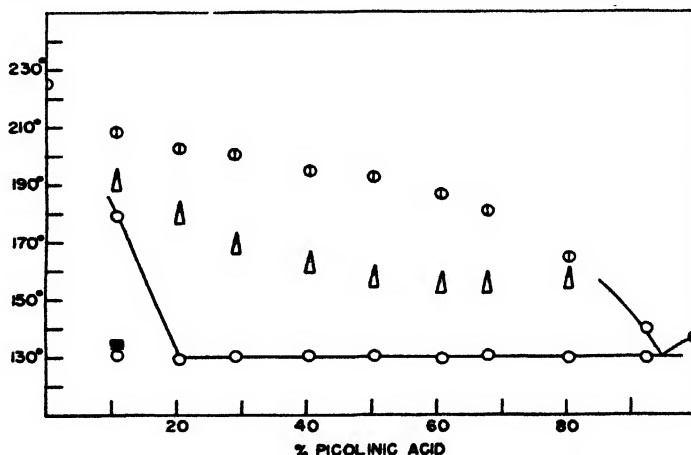


FIG. 4. Picolinic acid (A) *versus* pyrazinecarboxylic acid. O, point on phase boundary; Δ, beginning of decomposition; ◊, point not representing an equilibrium condition (such as melting point after decomposition has set in); ◻, initial melting with subsequent resolidification.

Per cent A.....	0	10.8	20.4	29.0	40.4	50.5	60.8	68.0	80.3	92.4	100
Thawing point....	224	179.4*	129.8	130.6	130.8	130.4	129.6	130.6	129.8	129.4	136
Decomposition	224	192.2	180.4	169.6	163.0	158.4	156.0	156.0	157.8		
Melting point....	226	208.8	202.6	200.2	194.8	192.4	186.6	180.8	164.2	139.6	137

\* Initially melted at 131.4°C., then resolidified.

A eutectic is formed at 95 per cent A and 130°C. Decomposition in the region 0-85 per cent A above 160°C. makes the liquidus indeterminate. Solid-solution formation is indicated at concentrations below 20 per cent A.



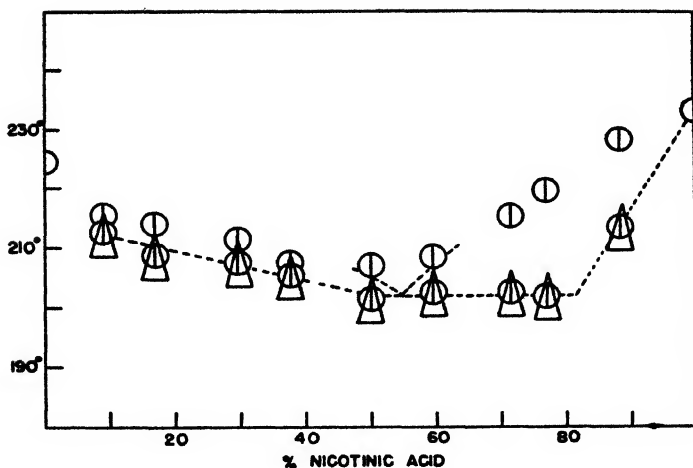


FIG. 5. Nicotinic acid (A) *versus* pyrazinecarboxylic acid. O, point on phase boundary; Δ, beginning of decomposition; ⊙, point not representing an equilibrium condition (such as melting point after decomposition has set in); ---, uncertain interpolation.

Per cent A.....	0	8.9	17.1	29.7	37.7	50.0	59.6	71.5	77.1	88.3	100
Thawing point* ..	224	212.8	208.8	207.8	205.2	201.2	202.6	202.6	202.0	213.8	233
Melting point ....	226	215.6	214.0	211.6	207.6	207.0	208.6	215.2	219.8	228.6	233

\* Identical with decomposition point (excepting the 100 per cent coördinate).

Partial solid-solution formation is shown, with a eutectic at 55 per cent A and 202°C., and a solubility gap over the range 50-82 per cent A. Decomposition at the solidus makes the phase boundaries indeterminate.

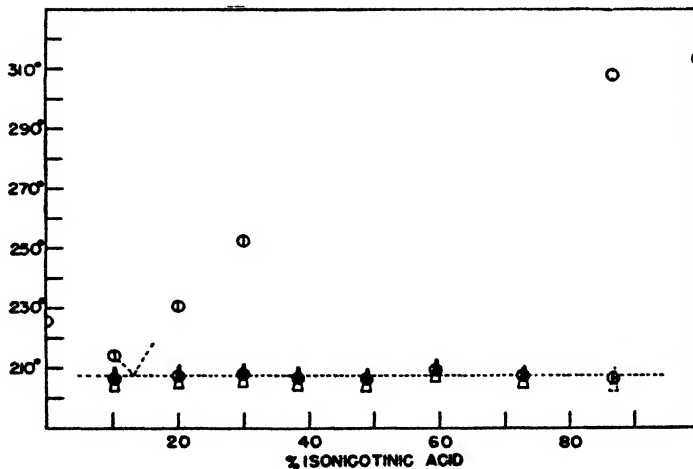


FIG. 6. Isonicotinic acid (A) *versus* pyrazinecarboxylic acid. O, point on phase boundary; Δ, beginning of decomposition; ⊙, point not representing an equilibrium condition (such as melting point after decomposition has set in); ---, uncertain interpolation.

Per cent A.....	0	10.3	20.2	30.0	38.5	49.0	59.5	72.8	86.8	100
Thawing point*...	224	206.8	207.4	208.2	207.0	206.8	209.4	207.6	206.8	312
Melting point....	226	214.2	230.8	252.2					308	314

\* Identical with decomposition point.

A eutectic is formed at 12 per cent A and 207°C. Decomposition at the solidus makes the phase boundaries indeterminate. There is no indication of solid-solution formation.

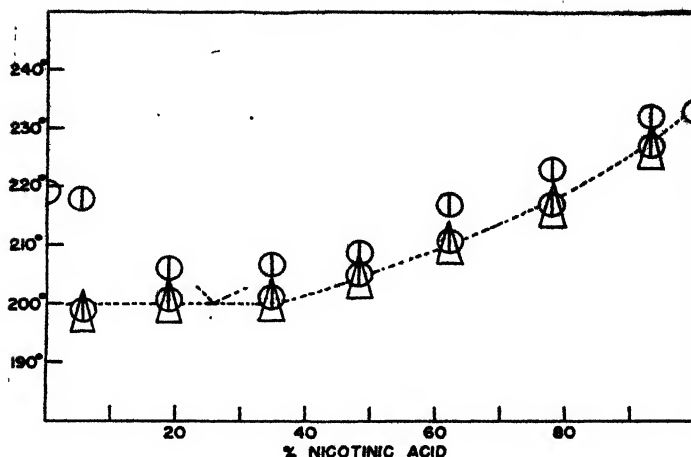


FIG. 7. Nicotinic acid (A) *versus* 5-thiazolecarboxylic acid. ○, point on phase boundary; △, beginning of decomposition; ⊙, point not representing an equilibrium condition (such as melting point after decomposition has set in); ---, uncertain interpolation.

Per cent A. . . . .	0	5.9	19.0	34.8	48.3	62.3	77.8	93.3	100
Thawing point* . . .	218	199.0	200.8	201.4	205.0	210.8	217.4	227.0	233
Melting point. . . .	220	209.8	206.0	206.6	208.8	217.0	223.0	232.4	233

\* Identical with decomposition point (except for 100 per cent coördinate).

Partial solid-solution formation is indicated, with a eutectic at 26 per cent A and 200°C. and a solubility gap over the range 0-35 per cent A. Decomposition at the solidus makes the phase boundaries indeterminate.

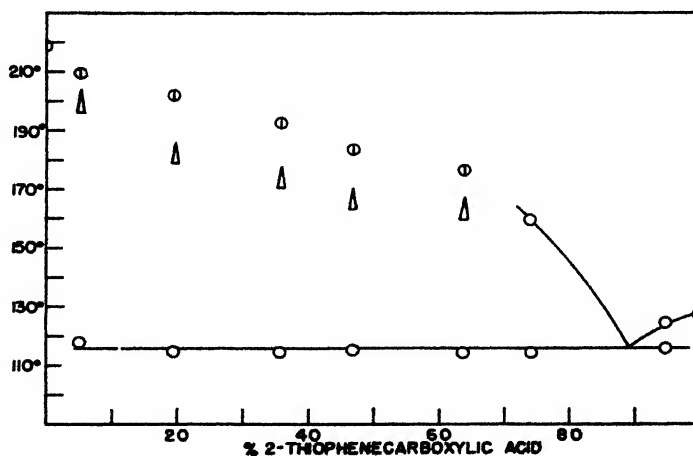


FIG. 8. 2-Thiophenecarboxylic acid (A) *versus* 5-thiazolecarboxylic acid. ○, point on phase boundary; △, beginning of decomposition; ⊙, point not representing an equilibrium condition (such as melting point after decomposition has set in).

Per cent A. . . . .	0	5.2	19.4	35.9	46.8	63.8	74.1	95.0	100
Thawing point. . . .	218	118.2	115.0	114.8	115.4	114.2	114.2	116.0	127
Decomposition point . . . . .	218	200.4	182.6	174.8	166.8	163.4			
Melting point. . . .	220	209.4	201.8	192.2	183.6	176.2	159.6	124.6	128

A eutectic is formed at 89 per cent A and 116°C. Decomposition in the region 0-70 per cent A above 165°C. makes the liquidus indeterminate. There is no indication of solid-solution formation.

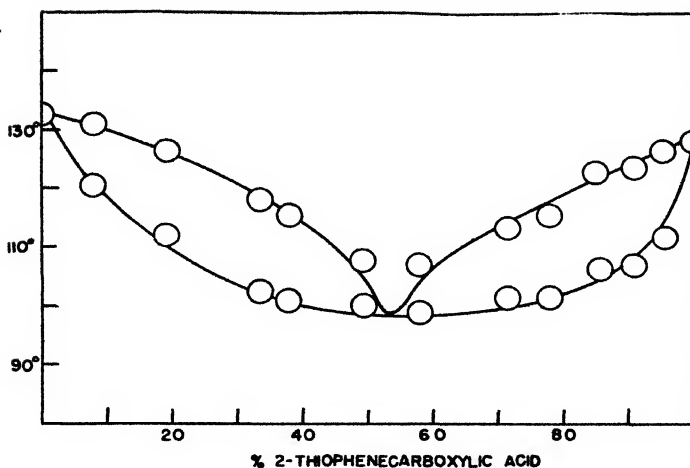


FIG. 9. 2-Thiophenecarboxylic acid (A) *versus* furoic acid: O, point on phase boundary

Per cent A	0	7.8	18.8	33.3	37.8	49.2	57.9	71.5	78.0	85.2	90.8	95.5	100
Thawing point	132	120.5	112.0	102.2	100.9	100.0	98.8	101.2	101.1	106.1	106.7	111.4	127
Melting point	133	131.0	127.2	118.0	115.2	107.6	106.8	113.0	115.2	122.6	123.4	126.3	128

The two compounds form solid solutions with a minimum at 54 per cent A and 100°C. Owing to the flatness of the minimum, the diagram might also be interpreted by assuming partial solid-solution formation, with a eutectic at 54 per cent A and 100°C. and a solubility gap over the range 38–77 per cent A.

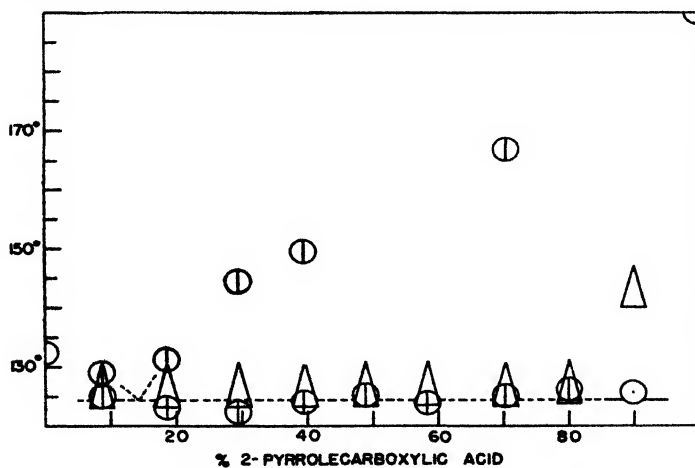


FIG. 10. 2-Pyrrolicarboxylic acid (A) *versus* furoic acid. O, point on phase boundary; Δ, beginning of decomposition; ⊙, point not representing an equilibrium condition (such as melting point after decomposition has set in); ---, uncertain interpolation.

Per cent A	0	8.7	18.6	29.6	39.8	49.0	58.5	70.5	80.2	90.0	100
Thawing point	132	125.2	123.2	122.6	124.0	125.4	124.0	125.2	126.4	125.6	190
Decomposition point		127	127	127	127	127	127	127	127	143.8	190
Melting point	133	129.2	131.4	144.6	149.6			166.8			190

A eutectic is formed at 15 per cent A and 124°C. Decomposition at the solidus makes the phase boundaries indeterminate. There is no indication of solid-solution formation.

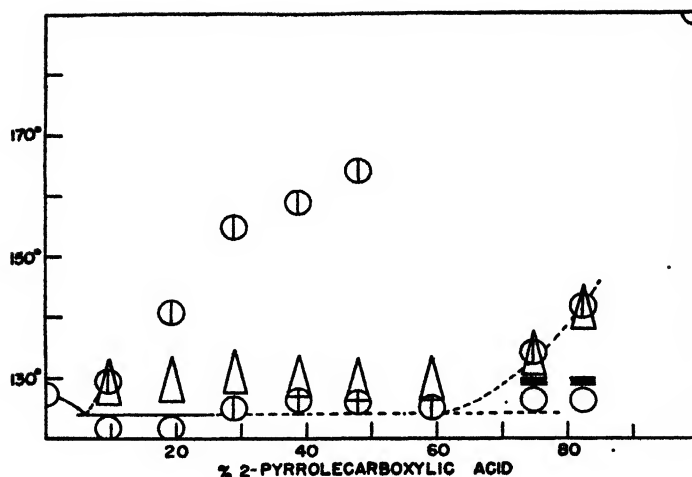


FIG. 11. 2-Pyrrolicarboxylic acid (A) *versus* 2-thiophenecarboxylic acid. ○, point on phase boundary; △, beginning of decomposition; ⊖, point not representing an equilibrium condition (such as melting point after decomposition has set in); ⊖, initial melting with subsequent resolidification; ---, uncertain interpolation.

Per cent A.....	0	9.7	19.4	29.0	38.7	48.2	59.4	75.5	82.6	100
Thawing point....	127	121.8	121.8	125.0	126.4	126.0	125.2	134.2*	141.6*	190
Decomposition point.....		129.4	130.0	131.2	130.6	129.8	130.0	134.2	141.6	190
Melting point....	128	129.4	140.6	154.6	158.4	164.0				190

\* Initially melted at 126.4°C., then resolidified.

A eutectic is formed at ca. 5 per cent A and 124°C. Decomposition at the solidus makes the phase boundaries indeterminate. Solid-solution formation is indicated at concentrations above 60-70 per cent A.

## DISCUSSION

In all but one of the binary systems reported in this paper, and in three of the systems reported in the previous communication (8), decomposition made either the liquidus or both liquidus and solidus indeterminate. It is, therefore, imperative to discuss the decarboxylation and its effect on the meaning of the phase boundaries, before proceeding to an interpretation of the phase relationships themselves.

The acids for which decomposition was observed are picolinic acid, pyrazine-carboxylic acid, 2-pyrrolicarboxylic acid, 5-thiazolecarboxylic acid, and isonicotinic acid. The following are the conclusions drawn from the decomposition behavior of these acids:

(a) Decarboxylation, as judged by the evolution of gas, takes place most readily when a liquid phase has been established. While it is not out of the question that a surface effect is involved when the two-phase system is established, it seems more likely that the acids simply decarboxylate most readily when they are in the liquid state, i.e., melted or in solution (*cf.* in this connection reference 5).

(b) At small concentrations of a given decarboxylating component, the beginning of decarboxylation (again judged by incipient bubble formation) appears to occur at a constant temperature. This temperature, which is constant within about 5°C.,<sup>3</sup> seems to be independent of the other acid component in the binary systems which were studied in this research, and it may be above or below the melting point of the decarboxylating component.

As the concentration of the decarboxylating component becomes appreciable, the decarboxylation temperature begins to rise. This may be interpreted to mean that at higher concentrations, the liquid decarboxylating component is able to retain to a larger degree the structure it has in the solid, corresponding to an apparent stabilizing effect.

It should be pointed out that the decarboxylation temperatures recorded in table 1 are not to be compared with other decarboxylating temperatures (4, 7, 9, 10), the term applying only to a given set of experimental conditions and procedures.

The two conclusions discussed above at once lead to the very interesting result that a solidus, even though it coincides with a decarboxylation curve, may be used in the interpretation of phase relationships. As an example, the decarboxylation temperature of 5-thiazolecarboxylic acid is *ca.* 170°C., to judge from the binary systems it forms with benzoic acid (8) and 2-thiophenecarboxylic acid (figure 8). In the system 5-thiazolecarboxylic acid-nicotinic acid (figure 7), the solidus lies above 170°C. over the whole range of compositions. At any point on the solidus, as soon as liquid begins to form, decomposition sets in.

<sup>3</sup> Below the immediate neighborhood of the "decarboxylation temperature" the rate of decarboxylation rapidly becomes small enough so that the fraction of acid which decarboxylated in the time of the experiment and up to the neighborhood of the decarboxylation temperature may safely be neglected.

In the particular case under discussion, the diagram may be interpreted to indicate solid-solution formation, since (*vide supra*) any point on this decarboxylation curve-solidus still signifies the point at which a liquid phase begins to be established.

Having justified the interpretation of our phase diagrams despite decarboxylation solidi, we may proceed to the discussion proper.

(1) The three pyridinecarboxylic acids are insoluble in each other (picolinic acid is very slightly soluble in nicotinic acid). The intermolecular bonding in crystals of these substances, no doubt involving complex hydrogen bonding of the amino acid type (1, 6), may differ considerably for the three isomeric acids, owing to the difference in the relative positions of the ring nitrogen and the carboxyl group. We can thus explain the low solubility of the pyridinecarboxylic acids in each other.

Of interest are the systems which the three pyridinecarboxylic acids form with pyrazinecarboxylic acid (figures 4, 5, 6). Isonicotinic acid and pyrazine-

TABLE 1  
*Decarboxylation temperatures for five heterocyclic acids*

CARBOXYLIC ACID	MELTING POINT	DECARBOXYLATION TEMPERATURE
	°C.	°C.
2-Pyridinecarboxylic acid.....	136-137	ca. 170*
Pyrazinecarboxylic acid. . . . .	224-226 (dec.)	ca. 170
2-Pyrrolecarboxylic acid. . . . .	190 (dec.)	ca. 130
5-Thiazolecarboxylic acid . . . . .	218-220 (dec.)	ca. 170
4-Pyridinecarboxylic acid . . . . .	312-314 (dec.)	ca. 300

\* Cf. in this connection Schenkel and Klein (11).

carboxylic acid are insoluble in each other; picolinic acid is about 20 per cent soluble in pyrazinecarboxylic acid; nicotinic acid forms solid solutions with pyrazinecarboxylic acid having but a relatively small solubility gap (50-82 per cent nicotinic acid). The first result is expected from the insolubility of isonicotinic acid in picolinic and nicotinic acids. The fact that pyrazinecarboxylic acid is a much better solvent for nicotinic acid than for picolinic acid suggests that its intermolecular bonding resembles more closely that of nicotinic acid than that of picolinic acid. Strength is lent to this argument by the fact that the melting points of pyrazinecarboxylic acid and nicotinic acid are very close.

(2) While 5-thiazolecarboxylic acid does not form solid solutions with 2-thiophenecarboxylic acid, it is soluble in nicotinic acid (figure 7). This result clearly indicates that interchanging a  $\text{—CH=CH—}$  and a  $\text{—S—}$  in a molecule already highly specifically bonded (such as nicotinic acid) has little effect on the intermolecular array, whereas it may be sufficient otherwise (as in benzoic acid (8)) to prevent isomorphism. It also shows that the interchange of a  $\text{—CH—}$  and an  $\text{=N—}$  under those circumstances will prevent isomorphism. The

results strongly suggest that the heteronitrogen is involved in intermolecular bonding and the heterosulfur is not.

In connection with the isomorphism of the thiazole and pyridine rings, it may be noted that 8-hydroxyquinoline and 4-hydroxybenzothiazole are isomorphous (2) but the pairs nicotinamide:5-thiazolecarboxamide, 2,2'-dithiazolyl:2,2'-dipyridyl, 4,4'-dithiazolyl:2,2'-dipyridyl, and 2,2'-dithiazolyl:4,4'-dithiazolyl (3) do not form solid solutions. An explanation of this fact is not obvious.

(3) The interpretation of the phase diagrams which involve as components the five-membered ring acids (pyrrole-, furan-, and thiophene-carboxylic acids) is not straightforward. 2-Pyrrolecarboxylic acid appears not to be isomorphous with the other two acids, although some solubility is indicated with 2-thiophene-carboxylic acid. However, 2-thiophenecarboxylic acid forms solid solutions with furoic acid. This result is unexpected (especially in view of the mutual insolubility of 2-thiophenecarboxylic acid and benzoic acid) and not readily interpretable.

#### SUMMARY

1. In connection with a study of the relation between serological specificity and solid solubility, eleven binary phase relationships have been investigated, the components being heterocyclic aromatic carboxylic acids.

2. The phase behavior of pairs involving picolinic, nicotinic, isonicotinic, and pyrazinecarboxylic acids may be explained on the basis of a difference in hydrogen bonding in crystals of these acids.

3. The isomorphism of thiazole and pyridine has been substantiated.

The author wishes to express his appreciation to Professor Linus Pauling for suggesting this problem and for many valuable discussions.

#### REFERENCES

- (1) ALBERT AND COREY: J. Am. Chem. Soc. **61**, 1087 (1939).
- (2) ERLÉNMEYER AND UEBERWASSER: Helv. Chim. Acta **21**, 1695 (1938).
- (3) ERLÉNMEYER *et al.*: Helv. Chim. Acta **22**, 698, 938 (1939); **25**, 375 (1942).
- (4) GILMAN, JANNEY, AND BRADLEY: Iowa State Coll. J. Sci. **7**, 429 (1933).
- (5) HINSHELWOOD: J. Chem. Soc. **1920**, 156.
- (6) LEVY AND COREY: J. Am. Chem. Soc. **63**, 2095 (1941).
- (7) MARSHALL: Rec. trav. Chim. **51**, 233 (1932).
- (8) MISLOW: J. Phys. Colloid Chem. **52**, 729 (1948).
- (9) NORRIS AND TUCKER: J. Am. Chem. Soc. **55**, 4697 (1933).
- (10) NORRIS AND YOUNG: J. Am. Chem. Soc. **52**, 5066 (1930).
- (11) SCHENKEL AND KLEIN: Helv. Chim. Acta **28**, 1211 (1945).

LIQUIDUS-SOLIDUS POINTS OF THE MANGANESE-NICKEL SYSTEM<sup>1</sup>

JACK M. PAUL AND G. V. BEARD

*Department of Chemistry, University of Utah, Salt Lake City, Utah**Received August 12, 1947*

This investigation was undertaken because of the currently enhanced interest in manganese, and because of the scarcity of reliable data concerning it and its alloys. Through the kindness of Dr. C. Travis Andersen of the U. S. Bureau of Mines, we were supplied with alloys made up from electrolytic manganese and other pure metals, in the present case manganese and nickel only. The alloys were melted in an electrical resistance furnace designed for the purpose.<sup>2</sup> The crucibles in which the melting and cooling of the alloys were carried out were made from granular alundum, the interior of the crucibles being 10 mm. wide by 45 mm. deep. Temperature measurements were made by means of a thermocouple of No. 22 B & S chromel and alumel wires.

The furnace was very carefully broken in by slowly increasing the current in small increments, and in all runs the temperature was gradually raised to the desired range over a period of several hours. The samples for the most part were prepared in rods  $\frac{1}{4}$  in. in diameter, and about 1 in. of such a rod was used as an individual sample. In order to prevent oxidation the samples were placed in the alundum sample container ( $\frac{3}{8}$  in. inside diameter and  $1\frac{3}{4}$  in. deep) only after the furnace temperature was considerably over the estimated melting point of the sample. As soon as the samples had been in the furnace long enough to reach furnace temperature, the alundum-covered thermocouple was pushed into the sample, and the current through the furnace was decreased to 2.5–3 amp. as a base which was held constant while the readings were being taken. This procedure was adopted to prevent too rapid cooling of the samples. As soon as the temperature started to fall, the voltage generated in the thermocouple was accurately measured and recorded every half-minute. The Bureau of Standards' conversion table for chromel-alumel thermocouples was used to find the temperature corresponding to each millivolt reading, and cooling curves were plotted with data so obtained. At the end of each run the standard cell was again used to check the Edison cell to be certain that it had remained constant. After each run the thermocouple was cut off and a new junction was prepared and covered with alundum as before.

## RESULTS

The cooling curve shown in figure 1 was obtained from a run on an alloy containing 70 per cent manganese and 30 per cent nickel, and was one of the better curves obtained.

<sup>1</sup> Contribution No. 75 from the Chemical Laboratories of the University of Utah. This investigation was carried out from October 1941 until April 1942.

<sup>2</sup> The details of this furnace will be supplied to anyone upon request.



Runs were made on several alloys with the results given in table 1. The temperature-composition diagram is shown in figure 2.

The manganese and nickel used in these results were of high purity; both were electrolytic and ran about 99.8 per cent by standard methods of analysis. Not

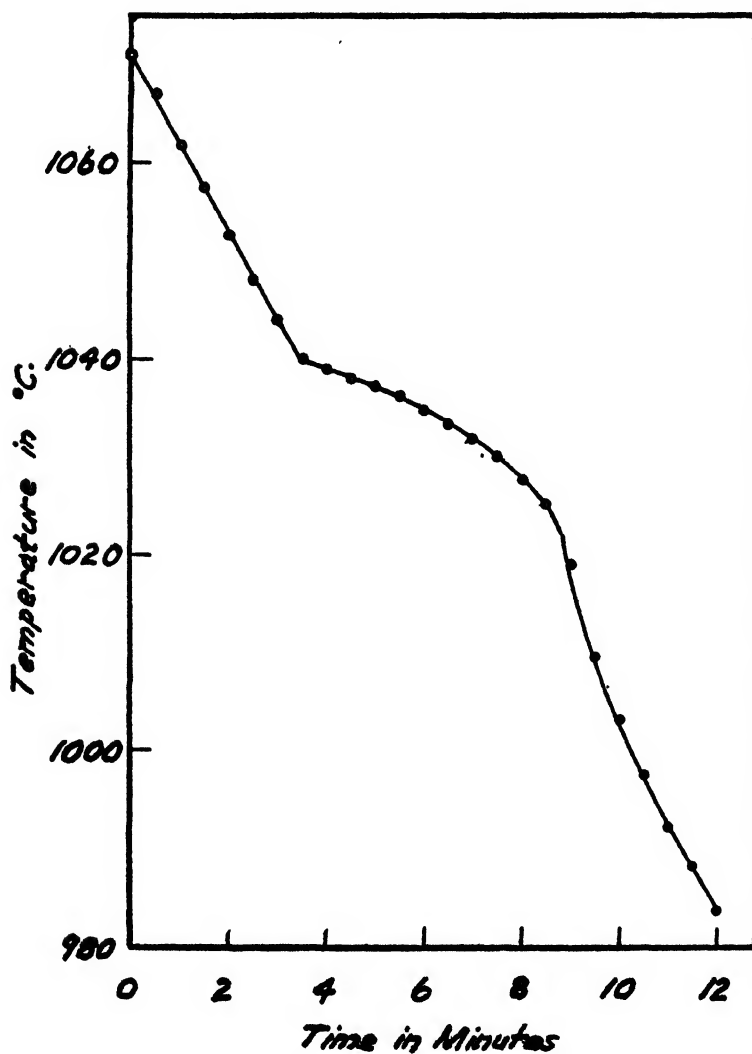


FIG. 1. Cooling curves for 70 per cent manganese-30 per cent nickel alloy

all samples were analyzed at the end of the experiment, but those analyzed indicated practically no contamination or oxide formation.

It is believed that our manganese samples are purer than those used by other investigators (1, 2, 3), although not all the articles referred to are available at this institution.

TABLE 1

Mn	Ni	LIQUIDUS POINT	SOLIDUS POINT
<i>per cent</i>	<i>per cent</i>	°C.	°C.
35	65	1123	1079
40	60	1089	1058
45	55	1046	1030
52.5	47.5	1011	1006
57.5	42.5	Melting point = 1006	
62.5	37.5	Melting point = 1005	
65	35	1012	1005
70	30	1040	1022
75	25	1066	1040
80	20	1105	1058

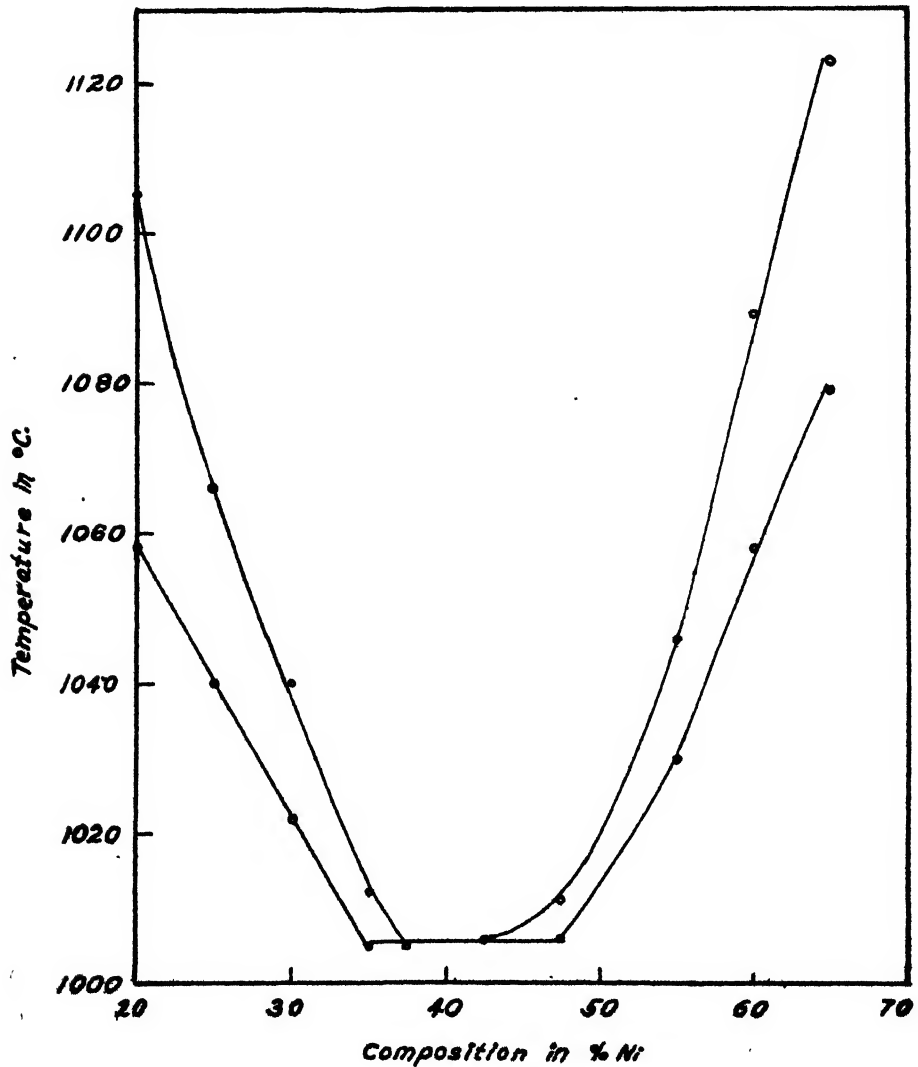


FIG. 2. Temperature-composition diagram for the manganese-nickel system

*Chemical Abstracts* does not give us this information. Our work is in fair agreement with the results published by M. Hansen (3).

## SUMMARY

The liquidus-solidus points of manganese-nickel alloys from 35 per cent manganese-65 per cent nickel to 80 per cent manganese-20 per cent nickel have been determined.

## REFERENCES

- (1) SHEMTSHUSKMY, S. F., URASOV, G. G., AND RYKOWSKOW, A. E.: *J. Russ. Phys. Chem. Soc.* **7**, 1051 (1906); **39**, 787-802 (1908).
- (2) DOURDINE, A. D.: *Rev. soc. russe de metall.* **1**, 11-23, 341-95 (1912); *Rev. mét.* **29**, 565-73 (1932).
- (3) HANSEN, M.: *Aufbau der Zweistofflegierungen*.

## THE VISCOSITY OF SOLUTIONS OF PRIMARY ALCOHOLS AND FATTY ACIDS IN BENZENE AND IN CARBON TETRACHLORIDE

W. J. JONES, S. T. BOWDEN, W. W. YARNOLD, AND W. H. JONES

*Tatem Laboratories, University College, Cardiff, Wales*

*Received May 28, 1947*

## INTRODUCTION

The viscosity of solutions of ethyl alcohol and acetic acid in benzene has been investigated by Dunstan (9) and by Muchin (21), of solutions of *n*-propyl alcohol in benzene by Dunstan and by Spells (24), and of solutions of certain butyl and amyl alcohols, other than *n*-butyl and *n*-amyl, in benzene by Muchin and by Spells. Dunstan found that at 25°C. in benzene ethyl alcohol gave a minimum viscosity at 6 per cent of the alcohol, *n*-propyl alcohol at 5 per cent of the alcohol, and acetic acid at 11 per cent of the acid. Findlay (10) determined the viscosity of solutions of methyl and ethyl alcohols in benzene, and of ethyl alcohol in carbon tetrachloride, at the boiling point of the solutions, and found maxima in the first and third systems, but not with ethyl alcohol in benzene. Staudinger and Ochiai (25) investigated the viscosity of dilute solutions of the fatty acids from *n*-caprylic acid to cerotic acid in carbon tetrachloride at 20°C. and observed that the viscosity increased proportionally to the chain length of the acid.

The present work was undertaken for the purpose of finding how viscosity varied with composition for the whole range of solutions from one pure component to the other at 25°C. in binary systems of alcohols and benzene, fatty acids and benzene, alcohols and carbon tetrachloride, and fatty acids and carbon tetrachloride; in particular, it was sought to ascertain how the positions of minima of viscosity shifted as the homologous series of alcohols and acids were ascended.

A limit was set to the investigation by the freezing point of the substances of higher molecular weight, by their availability commercially in a reasonably pure state, and by the work already accomplished by Dunstan and by Muchin.

#### PURIFICATION OF SUBSTANCES

The distilled water employed in standardizations of the viscometers was prepared with all the precautions usual in purifying water for electrical conductivity work. To remove dissolved air, it was heated to 100°C. immediately before use.

\* All the substances used in the measurements were the purest obtainable commercially, and were further purified by the following methods. Thiophene-free benzene was subjected to repeated processes of partial freezing and rejection of the liquid phase, and finally was dried by distillation from sodium wire; it froze at 5.5°C. and boiled at 80.1°C. Carbon tetrachloride of analytical grade was dried over calcium chloride and fractionated through an eight-pear column; its boiling point was 76.7°C. The alcohols were dried over lime and then distilled from calcium turnings or from sodium wire. The liquid fatty acids were purified by distillation. Acetic acid and *n*-caprylic acid were subjected to the fractional freezing process before distillation.

Each substance was purified in one large quantity, and not in separate batches, in order to ensure constancy of its viscosity and density throughout the series of measurements in which it was used.

#### VISCOSITY MEASUREMENTS

The measurements were made with Ostwald-type viscometers, each of which had been selected for the uniformity and circularity of the capillary bore, and in accordance with the recommendations and data given by Barr (2), and then had been tested that the times of flow of standard pure liquids of viscosities within the range for which it was used were, within 0.1 per cent, proportional to their kinematic viscosities. The viscometers had been designed to render drainage and surface-tension errors negligible. In order to prevent intrusion of dust and loss by evaporation, each instrument was provided with an inverted glass U-tube attachment connecting, through a glass tap of wide bore, the tops of the two limbs. Before use, the viscometer was cleaned with dichromate-sulfuric acid, thoroughly washed with dust-free conductivity water, and dried with a filtered current of air that had been passed over calcium chloride and phosphorus pentoxide. For the actual measurements the viscometer was clamped to a rigid brass holder, and set to the vertical by means of a plumb-line and levelling screws, in a thermostat maintained at 25.00°C.  $\pm$  0.01°. The times of flow were noted by means of a stop-watch, which was tested against a standard chronometer at frequent intervals.

The densities of the pure liquids and solutions, which were made up in stoppered bottles by weighing with standard weights, were determined by means of pycnometers of the Sprengel type, and all weighings were corrected for air displacement.

TABLE 1  
Viscosity of binary systems at 25°C.

PERCENTAGE COMPOSITION BY WEIGHT	DENSITY	VISCOSITY	DENSITY	VISCOSITY	DENSITY	VISCOSITY
	<i>n</i> -Butyl alcohol-benzene		<i>n</i> -Amyl alcohol-benzene		<i>n</i> -Hexyl alcohol-benzene	
0	0.8731	0.603	0.8731	0.603	0.8731	0.603
5	0.8689	0.604	0.8690	0.616	0.8693	0.615
10	0.8650	0.620	0.8651	0.641	0.8654	0.633
15	0.8610	0.640	0.8613	0.669	0.8620	0.663
20	0.8570	0.664	0.8574	0.709	0.8587	0.709
40	0.8433	0.842	0.8435	0.936	0.8456	0.980
50	0.8367	1.006	0.8377	1.132	0.8396	1.195
60	0.8304	1.178	0.8312	1.360	0.8338	1.505
80	0.8180	1.684	0.8194	1.963	0.8230	2.444
100	0.8064	2.587	0.8083	3.347	0.8124	4.329
	<i>n</i> -Butyric acid-benzene		<i>n</i> -Valeric acid-benzene		<i>n</i> -Caproic acid-benzene	
0	0.8731	0.603	0.8731	0.603	0.8731	0.603
5	0.8767	0.612	0.8753	0.620	0.8749	0.626
10	0.8797	0.624	0.8779	0.639	0.8769	0.653
15	0.8832	0.639	0.8802	0.662	0.8789	0.684
20	0.8864	0.656	0.8828	0.687	0.8809	0.718
40	0.9013	0.747	0.8943	0.825	0.8902	0.908
50	0.9094	0.808	0.9010	0.920	0.8950	1.058
60	0.9171	0.903	0.9072	1.062	0.9003	1.284
80	0.9345	1.100	0.9203	1.436	0.9116	1.844
100	0.9535	1.466	0.9344	1.970	0.9238	2.814
	<i>n</i> -Heptylic acid-benzene		<i>n</i> -Caprylic acid-benzene		Methyl alcohol-carbon tetrachloride	
0	0.8731	0.603	0.8731	0.603	1.5844	0.902
5	0.8746	0.631	0.8743	0.638	1.5085	0.858
10	0.8761	0.666	0.8754	0.680	1.4398	0.854
15	0.8777	0.705	0.8764	0.727	1.3771	0.846
20	0.8795	0.752	0.8776	0.781	1.3228	0.831
40	0.8869	0.990	0.8833	1.072	1.1320	0.746
50	0.8906	1.168	0.8867	1.295	1.0529	0.702
60	0.8942	1.490	0.8900	1.591	0.9887	0.665
80	0.9029	2.300	0.8981	2.505	0.8758	0.599
100	0.9130	3.784	0.9064	5.16	0.7865	0.552
	Ethyl alcohol-carbon tetrachloride		<i>n</i> -Propyl alcohol-carbon tetrachloride		<i>n</i> -Butyl alcohol-carbon tetrachloride	
0	1.5844	0.902	1.5844	0.902	1.5844	0.902
5	1.5069	0.872	1.5093	0.903	1.5101	0.918
10	1.4378	0.886	1.4437	0.946	1.4447	0.975
15	1.3752	0.915	1.3810	1.012	1.3827	1.046
20	1.3195	0.947	1.3271	1.089	1.3301	1.135
40	1.1313	1.037	1.1427	1.409	1.1462	1.560
50	1.0522	1.064	1.0654	1.554	1.0695	1.794
60	0.9877	1.079	1.0017	1.667	1.0023	1.979
80	0.8746	1.091	0.8902	1.880	0.8942	2.325
100	0.7851	1.093	0.8015	2.004	0.8064	2.587

TABLE 1—*Concluded*

	<i>n</i> -Hexyl alcohol-carbon tetrachloride		<i>n</i> -Heptyl alcohol-carbon tetrachloride		<i>n</i> -Octyl alcohol-carbon tetrachloride	
0	1.5844	0.902	1.5844	0.902	1.5844	0.902
5	1.5119	0.961	1.5123	0.982	1.5129	1.000
10	1.4467	1.058	1.4474	1.102	1.4480	1.139
15	1.3872	1.167	1.3877	1.237	1.3884	1.297
20	1.3341	1.299	1.3350	1.402	1.3360	1.470
40	1.1510	1.931	1.1536	2.175	1.1550	2.483
50	1.0741	2.317	1.0780	2.716	1.0821	3.124
60	1.0060	2.737	1.0151	3.302	1.0168	3.847
80	0.9007	3.570	0.9059	4.527	0.9089	5.58
100	0.8124	4.329	0.8188	5.71	0.8221	7.33
	<i>n</i> -Decyl alcohol-carbon tetrachloride		Acetic acid-carbon tetrachloride		<i>n</i> -Butyric acid-carbon tetrachloride	
0	1.5844	0.902	1.5844	0.902	1.5844	0.902
5	1.5141	1.031	1.5391	0.840	1.5293	0.911
10	1.4499	1.224	1.4983	0.822	1.4827	0.925
15	1.3903	1.441	1.4599	0.811	1.4404	0.945
20	1.3382	1.775	1.4241	0.808	1.3945	0.966
40	1.1586	3.091	1.2989	0.832	1.2493	1.079
50	1.0835	4.012	1.2468	0.863	1.1884	1.142
60	1.0218	5.08	1.1989	0.900	1.1372	1.201
80	0.9135	7.86	1.1154	1.007	1.0407	1.331
100	0.8263	11.35	1.0442	1.126	0.9535	1.466
	<i>n</i> -Caproic acid-carbon tetrachloride		<i>n</i> -Heptylic acid-carbon tetrachloride		<i>n</i> -Caprylic acid-carbon tetrachloride	
0	1.5844	0.902	1.5844	0.902	1.5844	0.902
5	1.5297	0.966	1.5298	0.990	1.5275	1.011
10	1.4767	1.033	1.4746	1.080	1.4727	1.124
15	1.4281	1.108	1.4252	1.175	1.4219	1.248
20	1.3834	1.188	1.3781	1.271	1.3763	1.380
40	1.2290	1.548	1.2220	1.767	1.2180	2.021
50	1.1638	1.743	1.1559	2.046	1.1517	2.406
60	1.1112	1.927	1.1009	2.362	1.0898	2.867
80	1.0133	2.343	1.0040	3.015	0.9936	3.905
100	0.9238	2.814	0.9130	3.784	0.9064	5.16

For each pair of components the viscosities and densities of about twelve different mixtures were measured, their values were plotted against the weight-percentage composition on a large-scale diagram, and the data given in table 1 were read off from the curves. Density is given in grams per cubic centimeter, viscosity in centipoises, and the percentage composition in parts of the alcohol or acid per hundred parts of the mixture by weight.

#### DISCUSSION OF RESULTS

For the carbon tetrachloride systems the displacement of the point of minimum viscosity with increasing molecular weight of the alcohol and the acid, respec-

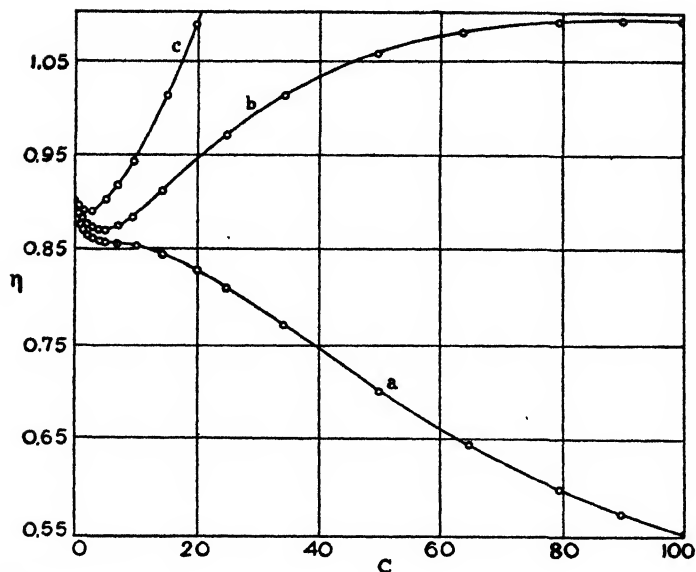


FIG. 1. Variation of viscosity ( $\eta$ ) with percentage ( $C$ ) of alcohol in carbon tetrachloride solution: curve a, methyl alcohol; curve b, ethyl alcohol; curve c, *n*-propyl alcohol.

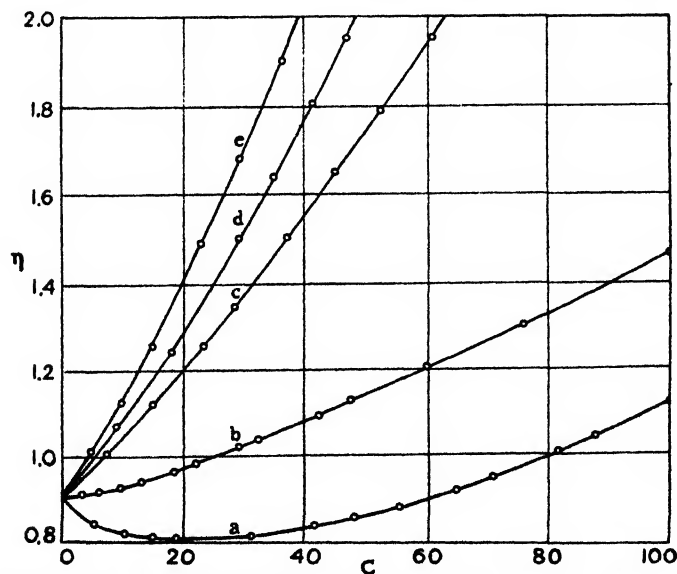


FIG. 2. Variation of viscosity ( $\eta$ ) with percentage ( $C$ ) of acid in carbon tetrachloride solution: curve a, acetic acid; curve b, *n*-butyric acid; curve c, *n*-caproic acid; curve d, *n*-heptylic acid; curve e, *n*-caprylic acid.

tively, is shown in figures 1 and 2. Minima of viscosity occur at the following values: 0.600 for 1.7 per cent by weight of *n*-butyl alcohol in benzene; 0.872 for 4.6 per cent of ethyl alcohol in carbon tetrachloride; 0.889 for 2.0 per cent of

*n*-propyl alcohol and 0.894 for 0.8 per cent of *n*-butyl alcohol in carbon tetrachloride; 0.808 for 19.0 per cent of acetic acid in carbon tetrachloride. In this connection it may be noted that the activity coefficients of methyl, ethyl, propyl, and butyl alcohols in benzene and in carbon tetrachloride are much higher than those of corresponding compounds which do not contain the hydroxyl group (6). Hitherto this association has been regarded as being due to a dipole effect, but it has been shown that the resulting complex has an electric moment and that the actual association must be referred to the formation of hydroxyl bonds (3). Furthermore, the fatty acids, up to *n*-valeric acid, exist almost completely as dimers even in dilute solution in benzene and in carbon tetrachloride (5, 19, 26). It would appear from the results of the present investigation that the effects of hydroxyl bonding in the alcohols and of dimerization in the acids are reduced the greater the length of the alkyl group.

TABLE 2  
*Acetic acid-carbon tetrachloride solutions at 25°C.*

PERCENTAGE OF ACID BY WEIGHT	VISCOSITY		
	Observed	Calculated	
		Spells	Macleod
0	0.902	0.902*	0.902*
5	0.840	0.853	0.848
10	0.822	0.831	0.827
15	0.811	0.815	0.812
20	0.808	0.808*	0.808*
40	0.832	0.808	0.821
50	0.863	0.844	0.860
60	0.900	0.881	0.900*
80	1.007	0.989	1.004
100	1.126	1.126*	1.126*

\* For significance of asterisks see page 759.

None of the relationships that have been proposed for the variation of the viscosity of a mixture of liquids with composition affords proper representations when applied to the binary systems of table 1. The equations of Arrhenius (1), Kendall (12), Lees (16), Bingham (4), Drucker and Kassel (8), and Meyer and Mylius (20) do not give curves with the minima required to delineate the change of viscosity with concentration in the mixtures containing the lower alcohols or fatty acids. Further, in unmodified form, the expressions of Kendall and Monroe (13), Dolezalek and Schulze (7), Sachanov and Rjachowsky (23), Van der Wyk (28), Lederer (15), Powell, Roseveare, and Eyring (22), Tuomikoski (27), Lutschinski (17), and Kottler (14) are inapplicable where a component is partly associated. Moreover, as table 2 shows for mixtures of acetic acid and carbon tetrachloride, even with the equations of Spells (24; the constant,  $\beta M = 5.7875$ ) and Macleod (18; the constants  $A_1 = 1.7715$ ,  $A_2 = 2.3841$ ), applied by the



authors themselves to mixtures containing associated components, the agreement given by the former is poor, and that given by the latter is necessarily better since it involves the use of an additional constant. Again, as table 3 indicates for mixtures of octyl alcohol and carbon tetrachloride, representation is often not close even where the viscosity-composition curves have no minima: in this table are given viscosities calculated by means of the equations of Arrhenius, Kendall and Monroe, Ishikawa (11; the constant,  $k_2a_2/k_1a_1 = 0.41404$ ), and of Sachanov and Rjachowsky (the constant,  $n = 1.2268$ ), taking the molecular weight of the alcohol as 130.24; the equations of Macleod and Spells are here inapplicable because of the great disparity between the viscosities of the pure components, and of the density of the mixtures being almost linearly related to the composition by volume. The viscosity values marked with asterisks in the tables denote those used in calculating the values of the constants of these

TABLE 3  
*n*-Octyl alcohol-carbon tetrachloride solutions at 25°C.

PERCENTAGE OF ALCOHOL BY WEIGHT	VISCOSITY				
	Observed	Calculated			
		Arrhenius	Kendall-Monroe	Ishikawa	Sachanov- Rjachowsky
0	0.902	0.902*	0.902*	0.902*	0.902*
5	1.000	1.094	1.072	1.063	0.998
10	1.139	1.305	1.258	1.233	1.127
15	1.297	1.533	1.461	1.413	1.286
20	1.470	1.783	1.680	1.603	1.474
40	2.483	2.928	2.723	2.483*	2.483*
50	3.124	3.584	3.341	3.014	3.123
60	3.847	4.272	4.023	3.623	3.841
80	5.58	5.76	5.57	5.16	5.48
100	7.33	7.33*	7.33*	7.33*	7.33*

\* For significance of asterisks see above.

equations. The limited applicability of the above equations, however, is not surprising in view of the molecular complexity of the alcohols and the acids in non-polar media.

The thanks of the authors are due to Messrs. V. A. Hewlett and W. T. Rees for assistance in the experimental work.

#### REFERENCES

- (1) ARRHENIUS, S.: Z. physik. Chem. **1**, 289 (1887).
- (2) BARR, G.: *A Monograph of Viscometry*, p. 130. University Press, Oxford (1931).
- (3) BERNAL, J. D., AND MEGAW, H. D.: Proc. Roy. Soc. (London) **A151**, 384 (1935).
- (4) BINGHAM, E. C.: Am. Chem. J. **35**, 195 (1906).
- (5) BRIEGLEB, G.: Z. physik. Chem. **B10**, 205 (1930).
- (6) BUTLER, J. A. V., AND HARROWER, P.: Trans. Faraday Soc. **33**, 171 (1937).

- (7) DOLEZALEK, F., AND SCHULEE, A.: *Z. physik. Chem.* **83**, 74 (1913).
- (8) DRUCKER, K., AND KASSEL, R.: *Z. physik. Chem.* **76**, 376 (1911).
- (9) DUNSTAN, A. E.: *J. Chem. Soc.* **85**, 817 (1904); **87**, 11 (1908).
- (10) FINDLAY, A.: *Z. physik. Chem.* **69**, 203 (1909).
- (11) ISHIKAWA, T.: *Bull. Chem. Soc. Japan* **4**, 7 (1929).
- (12) KENDALL, J.: *Medd. Vetenskapsakad. Nobelinst.* **2**, No. 25, 1 (1913).
- (13) KENDALL, J., AND MONROE, K. P.: *J. Am. Chem. Soc.* **39**, 1798 (1917).
- (14) KOTTLER, F.: *J. Phys. Chem.* **47**, 280 (1943); **48**, 76 (1944).
- (15) LEDERER, E. L.: *Nature* **139**, 27 (1937).
- (16) LEES, C. H.: *Phil. Mag.* **1**, 139 (1901).
- (17) LUTSCHINSKI, G. P.: *Symposium on the Viscosity of Liquids and Colloids*, Acad. Sci. U.S.S.R. **1**, 41 (1941).
- (18) MACLEOD, D. B.: *Trans. Faraday Soc.* **19**, 20 (1923).
- (19) MARTIN, A. E.: *Nature* **159**, 404 (1947).
- (20) MEYER, J., AND MYLIUS, B.: *Z. physik. Chem.* **95**, 374 (1920).
- (21) MUCHIN, G.: *Z. Elektrochem.* **19**, 819 (1913).
- (22) POWELL, R. E., ROSEVEARE, W. E., AND EYRING, H.: *Ind. Eng. Chem.* **33**, 432 (1941).
- (23) SACHANOV, A., AND RJACHOWSKY, N.: *Z. physik. Chem.* **86**, 532 (1914).
- (24) SPELLS, K. E.: *Trans. Faraday Soc.* **32**, 537 (1936).
- (25) STAUDINGER, H., AND OCHIAI, E.: *Z. physik. Chem.* **A158**, 45 (1931).
- (26) TRAUTZ, M., AND MOSCHEL, W.: *Z. anorg. Chem.* **155**, 13 (1926).
- (27) TUOMIKOSKI, P.: *Suomen. Kemistilehti* **15B**, 19 (1942).
- (28) VAN DER WYK, A. J. A.: *Nature* **138**, 846 (1936).

## COMMUNICATION TO THE EDITOR

## TEMPERATURE CONTROL FOR A CONSTANT-TEMPERATURE WATER BATH

Schwenk and Noble (J. Phys. Chem. **41**, 6 (1937)) have described a circuit incorporating a mercury-vapor triode as a temperature control for a constant-temperature water bath. Such a controlling device has been in constant use in our laboratories for the past ten years, with the occasional replacement of the tube as the only service necessary for the maintenance of the unit. This original circuit, however, called for the use of a thyatron using 110 volts on the heater; this made for simplicity in design of the circuit and yet limited its use somewhat, since tubes of this design are the product of one manufacturer.

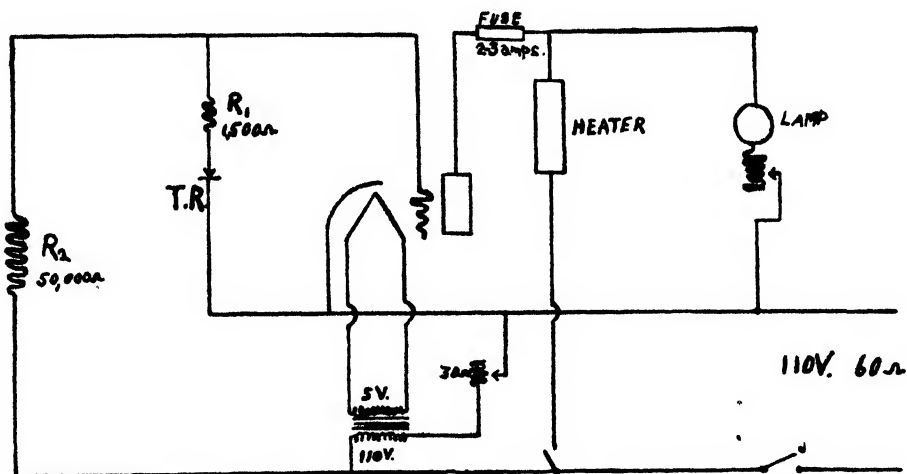


FIG. 1

Several other manufacturers are offering thyatrons with practically the same tube characteristics as the R.C.A.-91, the chief difference being in the use of a heater current of 5 volts instead of 110 volts. Such a tube may be used in this circuit with the inclusion of an inexpensive filament transformer to reduce the line voltage to the proper value. The General Electric thyatron FG-33 and the Westinghouse thyatron W.L.-33 have been found to work equally well in the modified circuit and may be obtained easily from their respective manufacturers.

The stability of this circuit, using tubes with low voltage on the heater, should be equal to and possibly better than that of the original circuit, although this point has not been demonstrated as yet.

University of Connecticut  
Storrs, Connecticut  
January 9, 1948

H. S. SCHWENK.

## NEW BOOKS

*Organic Chemistry.* By PAUL KARRER. Third English edition, translated by A. J. Mee. 7 x 10 in.; xx + 957 pp. New York: Elsevier Publishing Company, Inc., 1947. Price: \$8.50.

This is a new English edition of the well-known book by Professor Karrer. The previous edition (second English edition based on the eighth (1942) German edition) appeared about a year ago and was reviewed by Professor Koelsch (*J. Phys. Colloid Chem.* **51**, 627 (1947)). Little can be added to Professor Koelsch's review; what he had to say then applies also to the new edition. The title pages do not state the date of the "latest" German edition, upon which the translation is based, but the preface states that the edition is "new and revised".

In format, style, arrangement, and the like, the book follows the standards set by the previous editions. Karrer is an excellent book on general, descriptive organic chemistry—indeed, in the opinion of this reviewer, it is one of the two really good one-volume books on the subject today. There is a very good index.

The book-making is good, and it is a pleasure to record that the price, though a bit more than that of the previous edition, is still below the pre-war cost of \$11.00.

LEE IRVIN SMITH.

✓ *Encyclopedia of Chemical Technology.* Volume I, A to Anthrimerdes. Edited by RAYMOND E. KIRK and DONALD F. OTHMER. Assistant Editors: Janet D. Scott and Anthony Standen. 982 pp. New York: Interscience Encyclopedia, Inc., 1947. Price: \$20.00.

The present volume is the first of ten of about 960 pages each, planned to appear at the rate of two or three volumes per year. This comprehensive work is intended to present a critical survey of the knowledge of industrial materials, methods, processes, and equipment for chemists and chemical engineers. Ninety contributors have collaborated in writing for the first volume, though no authorship is assigned to any of the individual subjects. About one thousand subjects will be treated in the ten volumes, with suitable subdivision under each topic.

The treatment is modern, well illustrated, and apparently quite adequate to the purposes for which it is intended. Both domestic and foreign chemical processes are described. One can not inspect the contents of this impressive work without appreciating the tremendous strides that have been made in chemical technology, especially in the United States, since World War I. Naturally the full import of the work can not be grasped in the first volume. Many interesting subjects do not begin with A, though it is surprising how many do. But if the first volume is a fair sample of the ones to come, the editors and authors will have made a valuable contribution to chemical literature and are to be congratulated on the successful initiation of this large and worthwhile undertaking.

S. C. LIND.

*Psychrometric Tables and Charts.* By O. T. ZIMMERMAN and IRVIN LAVINE. 162 pp. Dover, N. H.: Industrial Research Service, 1945. Price: \$6.50.

In convenient form 32 tables and 22 charts present psychrometric data in English units for temperatures in degrees Fahrenheit over wide ranges.

S. C. LIND.

*Tables of Spherical Bessel Functions.* Vol. II. Prepared by Mathematical Tables Project, National Bureau of Standards. 330 pp. New York: Columbia University Press, 1947. Price: \$7.50.

The major part of the present volume is devoted to tables of the spherical Bessel functions  $\sqrt{\nu/2x} J_\nu(x)$  for  $\pm \nu$  ranging from 29/2 to 61/2. This set of tables complements those previously published in Vol. I for  $\pm \nu$  ranging from 1/2 to 27/2.

S. C. LIND.

# FOAMING OF MIXTURES OF HYDROCARBONS

J. V. ROBINSON<sup>1</sup> AND W. W. WOODS<sup>2</sup>

*Department of Chemistry, Stanford University, California*

*Received November 13, 1947*

The question of whether mixtures of pure hydrocarbons can foam is of both theoretical and practical significance. Specifically, if foaming in a lubricating oil were caused solely by stabilizing agents, they could possibly be removed. However, if the foaming is a property of the mixture of hydrocarbons themselves, an oil of petroleum source can be made non-foaming only by the use of anti-foaming additives.

## MATERIALS

The samples of hydrocarbons used were clear, colorless, and of low viscosity:

<i>Aromatic:</i>	
Benzene	Merck's "reagent" grade, thiophene free
Toluene	Baker's c.p. analyzed
Xylene	Merck's "reagent" grade
Cumene	Skelly Petroleum Company, "pure"
Butylbenzene	Eastman Kodak Company
<i>Aliphatic:</i>	
Isopentane	Phillips Petroleum Company, "pure grade 99% minimum"
Octene	Connecticut Hard Rubber Company
Octane	Connecticut Hard Rubber Company
Decane	Connecticut Hard Rubber Company

## TEST PROCEDURE

The foam-testing method used was to shake, by hand, the hydrocarbon mixture contained in a sealed glass tube, at room temperature, according to a carefully standardized routine, and to time the interval from cessation of shaking until all but two bubbles had disappeared. The last two bubbles in some cases were erratic in their behavior and much better reproducibility was obtained by not counting them. The values reported are the averages of at least ten determinations.

To prepare the sealed tubes, 15 x 1.8 cm. test tubes were drawn out to form a narrow neck, the hydrocarbons injected through the constriction from a syringe pipet, and the necks sealed off. The hydrocarbon pairs were mixed in the proportions 1:4, 2:3, 3:2, and 4:1, by volume, measured from the syringe pipet, the total volume of the mixture being approximately 10 cc. The liquid did not touch the constriction at the neck, and no evidence of burning was seen when the tubes were sealed. Most of the tubes were prepared in duplicate to reduce the possibility of accidental contamination.

<sup>1</sup> Present address: The Mead Corporation, Chillicothe, Ohio.

<sup>2</sup> Present address: Socony-Vacuum Corporation, Paulsboro, New Jersey.

## RESULTS

Cumene had the longest foam-life of the unmixed hydrocarbons (table 1), the foam lasting 1.0 sec., and xylene next with 0.8 sec. Three unmixed hydrocarbons had foam-lives of 0.6 sec., one 0.4 sec., and two 0.3 sec. A foam lifetime of 0.3 sec., as here measured, represents a minimal foaming tendency; redistilled water gives 0.3 sec.

TABLE 1

*Foaming of pure hydrocarbons; time in seconds for foam to collapse to last pair of bubbles*

ALIPHATIC HYDROCARBONS		ALKYL BENZENES	
TIME		TIME	
sec.		sec.	
Isopentane.....	0.4	Benzene.....	0.6
Octene.....	0.6	Toluene.....	0.3
Octane.....	0.3	Xylene.....	0.8
Decane.....	0.6	Cumene.....	1.0
		Butylbenzene.....	0.5

TABLE 2

*Foaming of mixtures of aliphatic hydrocarbons; time in seconds for foam to collapse to last pair of bubbles*

HYDROCARBON	PER CENT ISOPENTANE				PER CENT OCTANE				PER CENT OCTENE				PER CENT DECANE			
	20	40	60	80	20	40	60	80	20	40	60	80	20	40	60	80
	sec.	sec.	sec.	sec.	sec.	sec.	sec.	sec.	sec.	sec.	sec.	sec.	sec.	sec.	sec.	sec.
Isopentane....					0.8	0.7	0.6	0.5	0.8	0.6	0.4	0.4	1.1	0.9		0.6
Octane.....	0.5	0.6	0.7	0.8					0.6	0.6	0.6	0.6	0.7	0.7	0.6	0.7
Octene.....	0.4	0.4	0.6	0.8	0.6	0.6	0.6	0.6					0.6	0.6	0.5	0.7
Decane.....	0.6		0.9	1.1	0.7	0.6	0.7	0.7	0.7	0.5	0.6	0.6				

TABLE 3

*Foaming of mixtures of alkylbenzenes; time in seconds for foam to collapse to last pair of bubbles*

HYDROCARBON	PER CENT BENZENE				PER CENT TOLUENE				PER CENT XYLENE				PER CENT CUMENE				PER CENT BUTYL-BENZENE			
	20	40	60	80	20	40	60	80	20	40	60	80	20	40	60	80	20	40	60	80
	sec.	sec.	sec.	sec.	sec.	sec.	sec.	sec.	sec.	sec.	sec.	sec.	sec.	sec.	sec.	sec.	sec.	sec.	sec.	sec.
Benzene.....					0.7	0.7	0.7	0.7	0.8	0.8	0.9	1.0	0.8	0.9	1.0	1.0	0.8	0.7	0.7	0.7
Toluene.....	0.7	0.7	0.7	0.7					0.7	0.9	0.9	1.0	0.8	0.9	0.9	0.9	0.6	1.0	0.9	0.6
Xylene.....	1.0	0.9	0.8	0.8	1.0	0.9	0.9	0.7					1.0	1.0	1.0	0.9	0.8	0.8	0.7	0.8
Cumene.....	1.0	1.0	0.9	0.8	0.9	0.9	0.9	0.8	0.9	1.0	1.0	1.0					0.9	1.0	0.8	0.8
Butylbenzene...	0.7	0.7	0.7	0.8	0.6	0.9	1.0	0.6	0.8	0.7	0.8	0.8	0.8	1.0	0.9					

All combinations of the nine hydrocarbons in pairs were tested. It was found that the greatest foaming occurred when the aliphatic hydrocarbons were mixed with those containing a benzene ring in their molecules.

The mixtures of aliphatic hydrocarbons (table 2) and the mixtures of alkylbenzenes (table 3) had foam lifetimes of 1.1 sec. or less, or only slightly greater than the foam lifetimes of the unmixed hydrocarbons.

By contrast, fifty-one of the one hundred mixtures of aliphatic hydrocarbons with alkylbenzenes had foam lifetimes in excess of 1.0 sec., and twenty of the mixtures had foam lifetimes of from 2.0 to 6.1 sec.

The proportions in which the hydrocarbons were mixed greatly affected their foaming. The mixtures showing the greatest foaming were the alkylbenzenes containing 20 per cent aliphatic hydrocarbons, in twelve of twenty such mixtures (table 4). The effect of concentration was strikingly demonstrated by holding the six tubes of a series in one hand and shaking them simultaneously. For example, with a tube of pure toluene at one end of the series, a tube of pure octane at the other end, and the four tubes containing mixtures of these two in the order of the mixture proportion in between, the foam disappeared first from the end tubes, last in the tube containing 20 per cent octane, and at graduated intermediate times in the three remaining tubes. Although the whole demonstration lasts something less than 2 sec., the relative differences in foam lifetimes are large and reproducible.

TABLE 4

*Foaming of mixtures of aliphatic hydrocarbons with alkylbenzenes; time in seconds for foam to collapse to last pair of bubbles*

HYDROCARBON	PER CENT ISOPENTANE				PER CENT OCTENE				PER CENT OCTANE				PER CENT DECANTE			
	20	40	60	80	20	40	60	80	20	40	60	80	20	40	60	80
	sec.	sec.	sec.	sec.	sec.	sec.	sec.	sec.	sec.	sec.	sec.	sec.	sec.	sec.	sec.	sec.
Benzene	0.7	0.8	1.0	0.8	1.7	1.3	1.0	0.8	1.9	1.6	1.1	0.8	3.8	2.1	1.0	0.7
Toluene	0.7	0.6	0.6	0.6	1.4	1.6	1.1	0.9	1.9	1.8	0.8	1.0	4.0	2.4	1.3	0.7
Xylene	0.9	0.9	1.0	1.1	1.6	1.4	1.4	1.0	1.8	1.8	1.3	1.0	3.4	2.5	1.5	0.8
Cumene	0.7	0.8	1.0	1.3	1.4	1.5	1.3	1.0	2.0	2.0	1.8	1.1	3.2	3.0	2.1	1.2
Butylbenzene	0.9	1.3	1.4	1.8	1.7	2.3	2.2	1.9	1.9	2.9	2.6	2.0	6.1	6.0	4.6	2.6

## DISCUSSION

Foams can be formed on aeronautical lubricating oils containing no additives by bubbling air into them, or by shaking, beating, or other mechanical processes (5). Such a foam has a lifetime varying from about half an hour at room temperature to about 3 min. at 100°C. The foaming behavior of lubricating oils is in marked contrast to the behavior of pure liquids, such as glycerol, diethylene glycol, or dibutyl phthalate, which will not form a column of foam under any known conditions, even though they are of comparable viscosity. This is in accordance with the axiom, "Pure liquids do not foam" (*cf.* references 2 and 3).

By analogy with the stabilization by soaps and other surface-active materials of foams in aqueous solutions, it has frequently been assumed that foams of lubricating oils are similarly stabilized. It is known from experiments in this laboratory that certain additives in the oil may greatly increase the foam stability and the foam volume, and furthermore that these additives concentrate in the foam and may be partially segregated by collecting frothed-off liquid. (The frothing-off technique is well known for aqueous systems; see references 3 and 6.)

However, attempts made in this laboratory have been unsuccessful in segregat-

ing any material by frothing-off from a lubricating oil containing no additives. Apparently the hydrocarbon components of such a mixed oil are themselves solely responsible for its foaming ability.

The experiments of Foulk and Barkley (2) demonstrate a similar effect: mixtures of water with benzene, nitrobenzene, ether, acetone, and methanol show a tendency to form liquid films, while the carefully purified liquids alone do not.

These citations are intended to emphasize that considerations only of viscosity and the presence of surface-active agents appear unlikely to account for foaming ability (note the effect of adding water to diethylene glycol (5)). The systems chosen for analogy differ in both viscosity and volatility from lubricating oils. Because of the low viscosities the foam lifetimes must be of extremely short duration in the absence of surface-active agents. (Brady and Ross (1) show the dependence of foam lifetime upon viscosity.) Furthermore, the atmosphere in the sealed tubes is saturated with the vapor of the hydrocarbons, tending to decrease the film stability (Neville and Hazlehurst (4)). Since the system is nearly isothermal, the "pumping action" of evaporation is absent, a phenomenon said by Neville and Hazlehurst to be a primary stabilizing influence for films of volatile liquids.

In spite of these adverse influences, the differential stability of foams of the various series tested is clearly and reproducibly obvious when the tubes of a series are shaken and observed simultaneously, as described.

#### SUMMARY

A series of experiments is described which indicates that simple mixtures of hydrocarbons are capable of foaming, although the individual hydrocarbons taken separately do not foam. Likewise, mixtures of aliphatic hydrocarbons or mixtures of aromatic hydrocarbons scarcely foam, whereas mixtures of aliphatic hydrocarbons with aromatic hydrocarbons do foam.

The information contained in this paper was obtained in connection with an investigation sponsored and financed by the National Advisory Committee for Aeronautics and carried out under the supervision of Professor James W. McBain.

#### REFERENCES

- (1) BRADY, A. P., AND ROSS, SYDNEY: *J. Am. Chem. Soc.* **66**, 1348 (1944).
- (2) FOULK, C. W., AND BARKLEY, J. E.: *Ind. Eng. Chem.* **55**, 1013 (1943).
- (3) MCBAIN, J. W., AND DAVIES, G. P.: *J. Am. Chem. Soc.* **49**, 2230 (1926).
- (4) NEVILLE, H. A., AND HAZLEHURST, T. H.: *J. Phys. Chem.* **41**, 545 (1937).
- (5) ROSS, SYDNEY: *J. Phys. Chem.* **50**, 391 (1946).
- (6) SCHUTZ, F.: *Trans. Faraday Soc.* **42**, 437 (1946).



## HEREDITY AND ENVIRONMENT

WILDER D. BANCROFT

*Cornell University, Ithaca, New York**Received December 5, 1947*

One reason for the different ways in which the botanists and some chemists consider the colors of flowers, fruits, and leaves is that the botanists are interested in inheritance phenomena, whereas some chemists, including myself, think that we ought to study also the effects of environment in modifying the inheritance phenomena. Some cases are quite simple. Mendel's law is heredity. The action of light in determining the red color of the skins of apples and of pomegranates is environment. So is the effect of altitude and the alleged effects of the seashore. Royal Riviera pears, grown in Medford, Oregon, are red in color and probably require sunlight to develop the color, but I do not yet know this officially.<sup>1</sup> The red autumn color of the sumach is due to environment, while the corresponding colors of the autumn leaves of the sugar maple are due to heredity, though apparently modified to some extent in an unknown way by environment, meaning weather. The color of the flowers of lilacs is due predominantly to heredity at ordinary temperatures, and predominantly to environment at higher temperatures. Since some apples do not turn red, heredity must be a factor with them.

The Old Dirt Dobber, at Nashville, Tennessee, knows that alum causes hydrangeas to have blue flowers, because he wrote to me about it; but he does not consider that point worth mentioning in his garden book. He may be right and probably is; but it seems a pity to me. I recognize that he knows his public and that I do not; but still I am surprised.

The blue-grass country in Kentucky probably owes some of its characteristics to climate. We do not get similar effects in the marble regions of Vermont or on the chalk cliffs of England. The *Ithaca Journal* of September 29, 1947 says that the high phosphate content of the soil in Kentucky is the important factor. If this is the real answer, it should be possible to duplicate the blue-grass country in England.

Tobacco varies very much with the environment. The tobaccos grown in Connecticut and in Quebec are very different from those grown in Virginia and in Havana. Under suitable laboratory conditions it will be possible to grow Havana tobacco in Connecticut. This will not be profitable commercially; but it should be done at least once so as to be sure that no factor has been overlooked.

<sup>1</sup> Since the manuscript for this article was sent to the Editor I have received a letter from Professor James W. McBain of Stanford University in which he says that Royal Riviera pears that receive considerable direct sunshine usually have more or less red cheeks; none of them are red all over. Pears that grow in the heavily shaded parts of the tree seldom have much red color. He also says that Comice pears only get colored on the side exposed to direct sunlight. McBain believes that the Comice and the Royal Riviera pears are different trade names for the same pear. It is evident that, so far as studied, red pears are like red apples and owe their red color to environment. We do not yet know why most pears are not red. It is a matter of enzymes and of heredity.

I have never seen Sea Island cotton, but it must owe some of its properties to environment. We know that temperature conditions prevent the growing of good Indian corn in Prussia even if the Germans liked maize, which they do not. It must have been climatic conditions, though I do not know what they are, which made red leaves and twigs more common in North Sweden than in South Sweden. We might ascribe this to destabilization, except that there may be other factors. Originally it must have been environment that made so many autumn leaves turn red in the northeastern United States, though now the same trees will turn red through heredity when transplanted.

Acting on the suggestion of the Jackson and Perkins Company of New York City, I wrote in 1947 to the University of Maine at Orono, Maine, to learn what they could tell me about wild roses being redder near the seashore. Professor H. Steinmetz wrote to me about a local group of botanists and naturalists, some twenty-five in all, who met this year at Machias, Maine. "While driving through the blueberry barrens one observed a profusion of wild rose blossoms. At times and places one could have stopped and proved either contention. Later, when we arrived at the beach the same observations were made. With no over-all experiments using color charts for comparison of large numbers of blossoms I personally conclude that the variation in redness is the result of (1) the age of the petals, (2) individual plants. The latter probably should be called genetic variations." On this statement of facts we are not yet justified in saying that environment, meaning nearness to the sea, modifies the color, though it may be true. Evidently it was not of interest to Professor Steinmetz whether sea air does or does not have an effect on the colors of some flowers. This probably accounts for the botanists not having determined the facts.

I have been told that amaryllis, dahlias, and carnations are very brilliant near the sea in California; but I have not been able to get any confirmation or denial of this from a botanist or chemist.

As I remember the weigela bushes in Newport, Rhode Island, and they are common there, the flowers were dark red. The first weigela flowers that I saw in Ithaca, New York, were pale pink. This looked like a striking effect due to the sea; but I have since learned that there are two varieties of weigela, and that both grow in Ithaca. Mr. Pridham, professor of ornamental horticulture at Cornell University, tells me that the pink form is *Weigela floribunda* and that the dark red variety is *Eva Rathke*.

Sands, Milner, and Sherman (4) cite the snapdragon, *Antirrhinum majus*, as a case where the flavones and anthocyanins are abnormal, which is not surprising if the anthocyanin develops primarily from a leucoanthocyanin. Miss Rose Scott-Moncrieff (5) points out that the identification of antirrhinum as a cyanidin compound contradicts the theory of a simple relationship between this pigment and the ivory flavone. This simple relationship does not necessarily hold when the anthocyanin develops from a leucoanthocyanin. With an unspecified snapdragon, given me by a friend, the flowers came white or whitish at first, and then turned red. The red flowers undoubtedly develop from leucoanthocyanins; the change may be very slow or practically zero when the cut flowers are put in tap

water. They were not exposed to any appreciable amount of ultraviolet light. All these points should be confirmed as a tribute to Mr. Sorby and to Mrs. Onslow, who have not received the credit which I think is due them.

There should be plenty of data available in England to show whether salt air does or does not affect the colors of flowers. My guess is that it does, and I know no reason why the effects, if any, should be confined to anthocyanin pigments. If it is salt air that does the trick, the alleged effect should be noticeable further from the sea than people have assumed.

The development of marsupials in Australia must be due to the combined action of heredity and environment over a long time. That is also the case in Darwin's survival of the fittest. Such things cannot ordinarily be tested in the laboratory because the time available is not sufficient, but one can get interesting and satisfactory results with plants in reasonable times. Grafting flowers and fruits involves heredity, though protection against phylloxera seems a borderline case.

In a book called *Human Destiny*, and published in 1947, Lecomte du Noüy says that *Hatteria* or *Sphenodon punctata* is a big lizard about two feet long, which is found on several small islands off the coast of New Zealand. It is the last representation of the *fifth* order in the class of reptiles, otherwise totally extinct since the Jurassic period (about one hundred million years ago). By a prodigious chance it survives until our day and presents some very interesting archaic characters, such as the third eye in the top of the head. No suggestion is given as to the environments in which the third eye developed and then disappeared. One hundred million years could easily give time enough for these changes to occur; but I wish that the biochemists would give us some guesses as to the causes for the changes, or would present it as a problem to be solved.

Liberty Hyde Bailey published in 1896 a book called *The Survival of the Unlike*, in which he discussed many things about heredity and environment from the viewpoint of a horticulturist. Bailey looks upon heredity as an acquired character and not as an original endowment of matter. The hereditary power did not originate until, for some reason, it was necessary for a given character to reproduce itself. The longer any form was perpetuated, the stronger became the hereditary power. This does not seem right to me. We do not know what life is or when, or why, it originated. Consequently we do not know why it reproduces. I doubt whether we are justified in saying that heredity is an acquired habit, though some people claim that death is an acquired habit. Of course what Bailey published over fifty years ago does not necessarily mean what he believes now.

Bailey says (p. 82) that if he were a zoölogist, and particularly an entomologist, he would hold to the views of Lamarck; but, being a horticulturist, he accepts largely the principles of Darwin. He believes that both Lamarckism and Darwinism are true. He points out that Lamarck propounded his theory from studies of animals, while Darwin was led to his theory from observations on plants. Bailey also says (p. 99) that most northeastern varieties of apples tend to become elongated in the Pacific Northwest, to become heavy-grained and

coarse-striped in the Mississippi Valley and the Plains, and to take other characteristic forms in the higher lands of the South Atlantic states.

Bailey believes (p. 170) that change of climate is an important cause of variation in domestic plants. There is an increase in the intensity of colors of fruits and flowers in the north, but Bailey does not explain why. In 1859 Asa Gray stated that three general laws had been established: (1) that distribution of plants and animals is determined largely by climatic and other physical causes; (2) that species have a local or single origin; (3) that the origin of our present temperate flora is in the north.

These generalizations were written before Darwin's theories had appeared, and before Heer had published the histories of the fossils in the Arctic regions. Bailey says (p. 274) that this establishes Gray's place among philosophical naturalists.

Bailey (p. 276) considers that the most promising field for horticultural exploration and for the study of the ancestry of our fruits is now the interior of China and Japan.

The work of Burbank on the production of new fruits, which was so extraordinarily successful, involved a careful study of variations due to heredity. So far as I know, Burbank's work did not include any study of the effects due to environment.

Palladin (3) states that formalin is very helpful in killing the enzymes present in plants without damaging other very unstable substances which may be present in the plants. Treatment with formalin often gives better results than boiling, which destroys other substances in addition to enzymes. One gets in this way dead plants with killed enzymes, whereas in chloroform one gets killed plants with active enzymes. If this is what Palladin really means, he is stressing the wrong thing. One should have, and perhaps one does have, an antithesis between active plants with killed enzymes and killed plants with active enzymes. I hope that if one were to sponge a Northern Spy apple on the tree at suitable times with a suitable solution of formaldehyde one could kill or weaken the enzyme sufficiently to keep the apple from turning red without killing the apple. If formaldehyde will not do this, we must find something that will do it. I believe that the chemist can do this if Palladin has not already done it. Biochemistry without enzymes or with weakened enzymes would be an entirely new branch of science. I hope that we may some day point with pride to Palladin as the founder of this new science.

I have read in some circular that the pink-fleshed grapefruit grows only in limited, specific parts of Texas and does not retain its peculiarities when transplanted. This may be true, because I have not heard of a similar grapefruit from Florida. If this is true, the phenomenon must be connected with the presence of some element or group of elements in the soil of the region where the pink-fleshed grapefruit flourishes. That should be a relatively easy matter to clear up and would be a striking case of environment *versus* heredity.

In a book by Bailey called *The Evolution of Our Native Fruits* and published in 1898, he speaks (p. 54) of a book on the Catawba grape published in 1828 by

Adlum. Adlum says that the Catawba grapes which ripen in the sun are of a deep purple color; where they are partially shaded they are of a lilac color; and where they ripen wholly in the shade, and are perfectly ripe, they are white, rich, sweet, and vinous.

If this is true, one American grape differs from the European grapes described by Laurent (2) which did not require light to make the color develop. There is some question as to the facts.

Professor A. J. Heinicke, Director of the New York State Experiment Station at Geneva, wrote to me on August 13, 1947 as follows: "I have just called the experts on grape varieties to confirm my own information that, so far as we know, all grape varieties develop approximately normal color even in the shade. We have very positive evidence that the Catawba variety will develop its normal color when sunlight is excluded. As you probably know, we are engaged in fruit-breeding research at Geneva. One of the steps involved in the procedure is to enclose the developing bunch of grapes, while still green, in paper bags. Catawba grapes enclosed in such bags develop perfectly normal color. In the case of apples, similar paper bags prevent the formation of red color. I have further checked with the men who have observed literally thousands of different seedlings and none recalls any of these seedlings, which represent many varieties, that have failed to develop the normal color of the grape when the fruit is shaded. I am therefore inclined to think that Adlum in the reference you quoted was mistaken about Catawba requiring direct sunlight for color. Those of us who are engaged in biological research know that we cannot predict the behavior of all individuals of a species when it comes to such things as mutations, etc., and it is not impossible that some grape may show up which definitely requires sunlight for color. Certainly, however, that would be a very, very rare case."

This is conclusive that grapes do not require sunlight in Geneva. On the other hand, I find it difficult to believe that Adlum (1) did not observe what he said he did.<sup>2</sup> Professor Heinicke apparently did not take the question of temperature into account. The discrepancy between Adlum and Heinicke may be a question of environment, either climate or soil or both. I suspect that climate is the important thing. If the Catawba grape acts like the flowers of the lilac it might behave in one way in Washington, D. C., and in another way in Geneva, New York. It seems to me that we ought not to assume that Adlum was wrong until we have repeated his experiments as nearly as possible under his conditions, and that has not yet been done, so far as I can learn. It is conceivable that a century of cultivation may have modified the Catawba grape so fundamentally that we cannot repeat Adlum's experiments. That seems improbable to me, but I do not know that it is impossible. I should like very much to know about grapes grown on the Mediterranean coast of Africa. Bailey writes me that he does not consider random observations like Adlum's as scientific evidence. I should not have guessed that from Bailey's book, and I doubt whether Bailey felt that way fifty years ago.

<sup>2</sup> In the preface the author says, "I have not put down anything that I do not myself believe, and which I could not prove if necessary."

In a thesis called *Botanische Beobachtungen aus Spitzbergen*, published in Lund in 1902, Thorild Wulff says that botanists who have published books about the Arctic regions have been interested primarily in the botanical and geographical distribution, and not much in the colors of the flowers. That is similar to the comment which I am making in this article. Wulff cites, however, an article in which Middendorff in 1867 says that in the north, after the first autumn frosts, the foliage turns red to an extent quite unknown in most of Europe. Wulff points out that this is very striking with *Saxifraga hirculus* Linn., whereas in southern Sweden and in Denmark, the same plant shows no sign of red. In all of the plants studied, the red or violet appeared more strongly on the portions receiving the most light, except in some trailing plants which apparently utilize heat reflected from the ground. Since leucoanthocyanins had not been discovered in 1867 we cannot blame Wulff for not knowing about them.

The leaves and fruit of *Cardamine bellidiflora* Linn. are said to be a dark reddish-violet when grown by the sea (p. 45), but are not colored when the soil contains more nutrients. This should certainly be checked, because it is the only scientific statement of the sort that I have yet come across.

Wulff (p. 64) quotes Overton as saying that plants develop red color more easily when the water in the soil in which they grow is deficient in nutrients. Since salt damages vegetation, the presence of salt might be considered as equivalent to a deficiency of nutrients. If Overton's attention had been drawn to the problem he might have predicted the alleged action of sea air on flowers. It is certainly a legitimate subject for study, even though it does not interest the botanist.

I have never been in Spitzbergen and consequently do not know whether Wulff's standard of redness is what one would expect in Prussia or what would be standard in New York and New England. There are no trees in Spitzbergen, and Professor Hermannson, the Curator of the Fiske Icelandic Collection at Cornell, does not believe that there is anything in Spitzbergen to compare with the autumn color in the Ithaca gorges. He says that in Iceland they have only birch trees and mountain ash trees. The foliage of the birches turns yellow. Some heather turns red but not vividly.

Professor Pridham of Cornell University tells me that he thinks that autumn colors in Europe are not equivalent in any way to what they are in America, so far as the bright reds and yellows go. My own experience agrees with that, and I think that this is generally admitted. Professor Pridham says that the bright autumn colors do not continue much south of Virginia. Autumn color in the Carolinas and farther south is rather of a dull brown than the glowing reds and bright yellows which we have farther north. I have been told that maples do not grow in North Carolina.

The pink-flowered dogwoods grow native near Monticello in Virginia and presumably originated there, but I do not know why or when. It would be very interesting if they could be connected in some way with Thomas Jefferson; but I imagine that that connection would have been emphasized if it had existed. It might even have led to the pink dogwood becoming the flower of the Democratic party.

In Ithaca the leaves of the sugar maple, the sumach, and the Japanese creeper turn red in the late summer or early autumn. It seems a simple matter, but I have not yet been able to learn authoritatively whether these plants cease to turn red in the southernmost range of their growth.

Mr. James F. Couch writes to me from the Bureau of Agricultural and Industrial Chemistry in Philadelphia: "If you have not already considered it, I think you would be highly interested in the case of flowers of *Lupinus mutabilis* (this is probably identical with *Lupinus cruikshankii*). In blossoming the flowers first appear pure white and then gradually the standards turn reddish, passing through purple and finally appearing blue. There is a small area of yellow at the base of the keel. The lower petals turn from white to a final deep bluish red. Inasmuch as these changes are slow there seems to be a possibility here of collecting material from which the coloring matters and their precursors could be isolated for exact study. Seeds of this lupine are readily available in the market."

I do not know whether these flowers change with changing environment; but they certainly should be studied under the biochemistry of plant pigments.

When we shall have learned how to stabilize the blue form of anthocyanin it will be possible to grow blue roses, blue carnations, and blue hollyhocks. If I were not crippled and perhaps too old, I would start growing these flowers myself. If one starts on this kind of dreaming all sorts of possibilities open up. We have blue grapes and blueberries; why not blue apples and blue strawberries? White strawberries are known. The kind my father grew in Milton, Massachusetts, was Lennig's White, but there are others on the market. The white strawberry, as I knew it, was not as good a commercial strawberry as the red ones because it would not stand transportation, but it was a better tasting strawberry. Of course, I do not know what the blue strawberry, if grown, would be like as an eating strawberry. The white strawberry, like the Burbank fruits, was undoubtedly a product of heredity. The blue strawberry, if developed as I have suggested, would be the result of a changing environment. The white geranium is undoubtedly a product of heredity.

#### SUMMARY

1. In some cases, such as the reddening of apples, the effect of environment has been recognized officially.
2. At ordinary temperatures the colors of the lilac flowers do not depend on illumination, but they do at higher temperatures.
3. It is possible that with a suitable use of a suitable formaldehyde solution one can weaken or even kill enzymes without killing the plant or fruit.
4. It is not known to what extent salt in the air modifies the colors of flowers. The reports are scanty and contradictory.
5. In Geneva, New York, the development of color in Catawba grapes does not depend on exposure to light. Adlum claims that exposure to light is necessary in Washington, D. C., but this has not been confirmed independently. My guess is that Adlum was right. If and when this is proved true it will be

necessary to find out whether anything similar occurs with Concord, Niagara, Delaware, and Scuppernong grapes.

6. The pink-fleshed grapefruit apparently owes its characteristics to some element or group of elements in the soil, but I have never seen any scientific study of the subject.

7. Under suitable laboratory conditions one could grow Havana tobacco in Connecticut and perhaps in Canada. This has never been tried and perhaps never will be.

8. The grafting of flowers and fruits is usually a matter of heredity, but in the protection against phylloxera we seem to have a case where there is a transmission of characteristics through the graft. This may be a misunderstanding on my part.

9. The horticulturist ignores the question of environment when possible, even though the composition and structure of the soil are of tremendous importance to him.

10. It is startling to see how much is not yet known about the effect of environment on the colors of leaves, flowers, and fruits, and about the biochemistry of plants.

11. Some day it will be possible to grow blue apples, blue strawberries, blue roses, and blue hollyhocks; but nobody can say when.

#### REFERENCES

- (1) ADLUM: *A Memoir on the Cultivation of the Vine in America*, p. 173 (1828).
- (2) See BANCROFT: *J. Phys. Colloid Chem.* **51**, 1083 (1947).
- (3) PALLADIN: *Biochem. J.* **18**, 179 (1909).
- (4) SANDS, MILNER, AND SHERMAN: *J. Biol. Chem.* **109**, 204 (1905).
- (5) SCOTT-MONCRIEFF, ROSE: *Biochem. J.* **24**, 253 (1930).

## THE EFFECT OF ALKALINE ELECTROLYTES ON MICELLE FORMATION IN SOAP SOLUTIONS

REYNOLD C. MERRILL AND RAYMOND GETTY

*Philadelphia Quartz Company, Philadelphia, Pennsylvania*

*Received November 5, 1947*

Ever since micelles were shown to exist in soap solutions the concentration at which they first appear has been a subject of considerable interest and controversy. The difficulty of obtaining reproducible, accurate results in dilute soap solutions—due to hydrolysis, absorption of carbon dioxide, etc.—resulted in very few good experimental investigations at low soap concentrations. It was formerly believed that practically no micelles were formed in soap solutions at concentrations less than about 0.1 *N* or approximately 2 per cent for the most common soaps. This is above the soap concentration at which most practical



washing or detergent operations are done, so the assumption was made that the equilibrium between free ions and micelles was of little practical interest. However, recent studies of long-chain compounds, including the soaps, have shown that the formation of micelles begins at about 0.01 *N* or 0.2 per cent for detergents containing twelve carbon atoms and around 0.001 *N* for those containing sixteen carbon atoms. For example, the "critical" concentration at which micelle formation becomes readily apparent is around 0.023 *M* or 0.5 per cent for sodium laurate and less than 0.001 *M* or 0.029 per cent for potassium palmitate (11).

Micelle formation for most soaps, therefore, begins in the range of concentrations used for practical detergent operations. Data presented recently by Preston indicate that a great increase in detergent action occurs at about the concentration at which micelle formation becomes apparent (22). Any material which lowers the minimum concentration necessary for micelle formation in a soap solution may then likewise decrease the concentration necessary for good detergency. Several investigations have shown that various electrolytes decrease this critical concentration for micelle formation (4, 9, 14, 16, 24).

It was, therefore, of interest to study the effect of various silicates and other electrolytes commonly used as soap builders on the concentration at which micelle formation first becomes readily apparent in soap solutions. This paper reports such a study.

#### EXPERIMENTAL

The "critical" concentration for micelle formation in soap solutions was determined by both the dye-titration technique of Corrin and Harkins (4) and the solubilization method.

The first method depends on the fact that certain dyes, such as pinacyanol chloride, change color at the "critical" concentration. In this work a stock solution of soap above the "critical" concentration containing  $1 \times 10^{-5}$  moles of pinacyanol chloride per liter was titrated with the same concentration of dye in water. The "critical" concentration was determined as the point at which the blue soap-dye solution first acquired a purplish tinge. Comparison with an aliquot portion of the original soap-dye solution facilitated detection of the end point, which is otherwise rather difficult to determine accurately. All dye titrations were run in duplicate.

The solubilization method for determining critical concentrations depends on the fact that solutions containing soap or detergent micelles can solubilize water-insoluble materials, whereas soap or detergent solutions below the "critical" concentration do not (17, 20). The solubility of the water-insoluble dye, Orange OT (F. D. and C. Orange No. 2; 1-*o*-tolylazo-2-naphthol) was measured in varying concentrations of soap solutions at 60°C. The technique used was similar to those previously described (15, 17). Series of solutions of varying soap concentration but with constant salt content were made by diluting a definite volume of a stock soap solution with known amounts of a stock salt or silicate solution and water. These solutions were placed in 50-ml. glass bottles contain-

ing a slight excess of dye sealed with metal caps, and placed in an air oven at 60°C. At least several days were required for the solutions to dissolve the maximum amount of dye. After allowing excess dye crystals to settle, the dye concentration was measured by determining the percentage transmission of light from a blue filter in a photoelectric colorimeter. Special care was taken to avoid measuring suspended dye particles. From the transmission reading, the amount of dye dissolved is obtained by comparison with a calibration curve of known amounts of dye dissolved in acetone.

#### MATERIALS

The Orange OT (molecular weight, 262) was recrystallized from methyl alcohol and obtained in the form of small bright orange-red crystals. The pinacyanol chloride was a commercial product and was used without further purification. Sodium laurate was prepared from a lauric acid obtained by recrystallizing the Eastman Kodak Company's best product twice from acetonitrile. The recrystallized acid had a melting point of 43.7°C. The sodium soaps were made by neutralizing the acid in acetone solution with sodium methoxide to the phenolphthalein end point. The soap was washed with acetone and dried at 105°C. Potassium laurate was made similarly, using an acetone solution of potassium hydroxide, from a recrystallized lauric acid with a melting point of 42.2°C. and an equivalent weight of 200.8 (theory, 200.3). The palmitic acid from which the sodium palmitate was made was recrystallized from methyl alcohol and had a melting point of 62.6°C. and an equivalent weight of 256.2 (theory, 256.4). Analyses for three of the silicates used were given in a previous paper (19). The silicate with a silica-to-alkali ratio by weight of 1.6 was a standard commercial product ("BW") of the Philadelphia Quartz Company. The other salts were c.p., except for the polyphosphate ("unadjusted Calgon") and the carboxymethylcellulose, which were commercial products. The latter was the medium viscosity grade of the Hercules Powder Company. The moisture content of the Calgon was determined and its formula assumed to be  $(\text{NaPO}_3)_x$ . The sodium content of the carboxymethylcellulose was determined by ashing the material, acidifying the ash with hydrochloric acid, evaporating to dryness on a water bath, moistening twice with distilled water (evaporating to dryness each time), and titrating the dissolved residue with standard silver nitrate, using potassium chromate indicator.

#### EXPERIMENTAL DATA

The effects of various salts industrially important as soap builders on the "critical" concentration for micelle formation in sodium laurate solutions at room temperature ( $\sim 25^\circ\text{C}$ .) are given in table 1 and illustrated in figure 1. These data were obtained by the titration technique. The "critical" concentration is shown as a function of the equivalent concentration of added salt based on the sodium content. When sufficient salt is added to make the solution 0.065 *M*, the critical concentration for sodium laurate is reduced from 0.024 *M* or 0.53 per cent to 0.012 *M* or 0.26 per cent. The reduction in critical concentration is essentially

TABLE 1

The "critical" concentration for micelle formation of sodium laurate in the presence of added salts at 25°C.

MOLARITY OF SALT	"CRITICAL" CONCENTRATION	DECREASE OF "CRITICAL" CONCENTRATION	"CRIT." CONC. PURE SOAP "CRIT." CONC. WITH SALT
Sodium chloride			
<i>M</i>	<i>M</i>		
0	$2.37 \times 10^{-2}$		
$2.18 \times 10^{-2}$	$1.82 \times 10^{-2}$	23	1.29
$3.0 \times 10^{-2}$	$1.49 \times 10^{-2}$	37	1.58
$4.23 \times 10^{-2}$	1.41	40	1.67
6.9	1.15	51	2.04
Sodium hydroxide			
$7.29 \times 10^{-3}$	1.82	23	1.31
$1.07 \times 10^{-2}$	1.79	25	1.33
$3.17 \times 10^{-2}$	1.59	33	1.50
5.09	1.26	47	1.89
6.45	1.08	55	2.20
7.84	0.975	59	2.44
Sodium carbonate			
$7.57 \times 10^{-3}$	$1.91 \times 10^{-2}$	18	1.22
$1.03 \times 10^{-2}$	1.72	26	1.35
$1.24 \times 10^{-2}$	1.55	33	1.50
$2.64 \times 10^{-2}$	1.32	43	1.76
3.63	1.14	51	2.04
4.25	1.06	54	2.20
$4.66 \times 10^{-2}$	$0.932 \times 10^{-2}$	60	2.50
5.46	0.910	61	2.56
6.39	0.818	65	2.85
Trisodium phosphate			
$0.92 \times 10^{-2}$	$1.82 \times 10^{-2}$	23	1.30
1.54	1.54	35	1.54
2.39	1.19	50	1.99
2.44	1.22	48	1.94
4.0	1.0	58	2.37
Tetrasodium pyrophosphate			
$1.81 \times 10^{-3}$	$2.17 \times 10^{-2}$	8	1.09
$3.15 \times 10^{-3}$	1.88	21	1.26
4.3	1.73	27	1.37
5.4	1.62	32	1.46
$2.04 \times 10^{-2}$	1.22	48	1.94
2.59	1.04	56	2.28
3.15	0.942	60	2.52

TABLE 1—Continued

MOLARITY OF SALT	"CRITICAL" CONCENTRATION	DECREASE OF "CRITICAL" CONCENTRATION	"CRIT." CONCN. PURE SOAP "CRIT." CONCN. WITH SALT
Sodium tetraborate			
<i>M</i>	<i>M</i>		
$0.99 \times 10^{-2}$	$1.99 \times 10^{-2}$	16	1.19
$1.67 \times 10^{-2}$	1.67	29	1.42
$2.78 \times 10^{-2}$	1.39	41	1.70
$2.82 \times 10^{-2}$	1.41	37	1.68
4.40	1.10	54	2.15
Sodium metasilicate			
$6.51 \times 10^{-2}$	2.05	13	1.14
7.63	1.90	19	1.24
9.29	1.80	23	1.31
$1.04 \times 10^{-1}$	1.64	50	1.43
$1.21 \times 10^{-1}$	1.52	35	1.54
$2.55 \times 10^{-2}$	1.27	46	1.85
$4.04 \times 10^{-2}$	1.01	57	2.32
5.15	0.86	63	2.74
Sodium silicate: $\text{SiO}_2/\text{Na}_2\text{O}$ weight ratio = 1.60			
$0.89 \times 10^{-2}$	$1.72 \times 10^{-2}$	27	1.38
1.52	1.47	38	1.61
1.57	1.51	36	1.57
2.05	1.32	44	1.79
2.47	1.19	50	1.99
3.34	1.08	54	2.10
Sodium silicate: $\text{SiO}_2/\text{Na}_2\text{O}$ weight ratio = 2.46			
$0.98 \times 10^{-2}$	1.96	17	1.21
2.09	1.56	34	1.52
2.84	1.42	40	1.67
3.46	1.30	45	1.82
4.35	1.09	54	2.17
5.82	0.975	59	2.43
Sodium silicate: $\text{SiO}_2/\text{Na}_2\text{O}$ weight ratio = 3.93			
$0.43 \times 10^{-2}$	2.18	8	1.09
0.83	2.08	12	1.14
1.20	2.00	16	1.18
Calgon (unadjusted)			
$0.583 \times 10^{-2}$	$2.33 \times 10^{-2}$	2.	1.02
1.11	2.22	6.	1.07
2.18	2.18	8.	1.09
4.35	2.17	8.	1.10
Carboxymethylcellulose			
$0.96 \times 10^{-2}$	1.93	19.	1.23
1.96	1.88	21.	1.26

the same for all the salts tested when calculated to the same sodium concentration. Their effects on the critical concentration of sodium laurate are just slightly less than those found by Corrin and Harkins (4) for the influence of potassium chloride, potassium sulfate, and sodium pyrophosphate on the critical concentration of potassium laurate. The difference is not considered significant. The effect of the Calgon was not so great as that of the other salts up to a concentration of around 0.05 *M*, where it began to salt out the soap. This suggests that some of the sodium is "bound" to the colloidal phosphate ion.

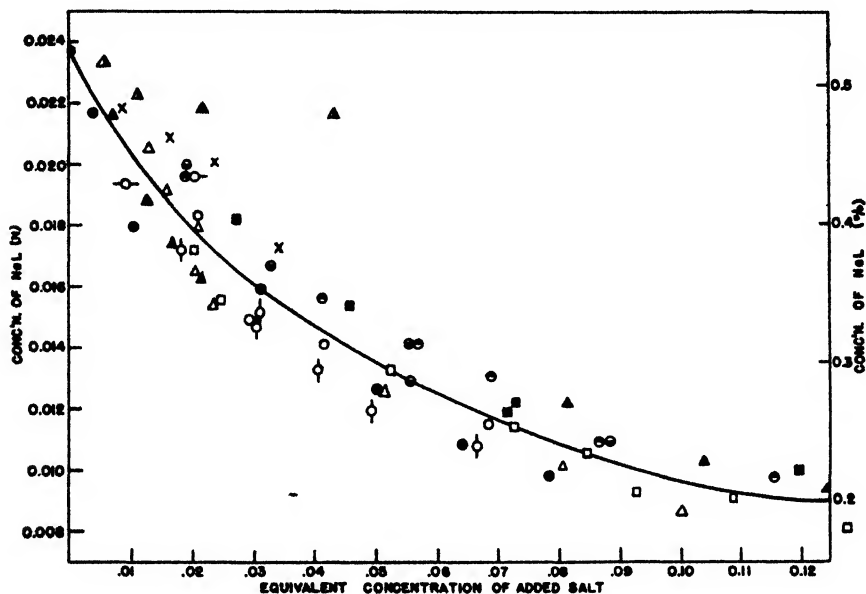


FIG. 1. Effect of alkaline electrolytes on the "critical" concentration for micelle formation in sodium laurate solutions at 25°C. ○, sodium chloride; ●, sodium hydroxide; □, sodium carbonate; ■, trisodium phosphate; △, sodium metasilicate; ▲, tetrasodium pyrophosphate; ●, tetrasodium borate; ○, sodium silicate with an  $\text{SiO}_2/\text{Na}_2\text{O}$  ratio of 1.60; ●, sodium silicate with an  $\text{SiO}_2/\text{Na}_2\text{O}$  ratio of 2.46; ×, sodium silicate with an  $\text{SiO}_2/\text{Na}_2\text{O}$  ratio of 3.93; ▲, sodium "hexametaphosphate" (Calgon); ○, carboxymethylcellulose.

The solubilities of the dye Orange OT at 60°C. in sodium and potassium laurates alone and in the presence of four sodium silicates are given in tables 2 and 3 and illustrated in figures 2 and 3.

The only comparable data in the literature are those of Green and McBain (8), who give 0.44 and 0.95 mg. per 100 cc. as the solubility of Orange OT in 0.025 *N* potassium and sodium laurate solutions, respectively, at 25°C. While solubilization is usually greater at higher temperatures, the reverse may be true in concentration regions where the proportion of micelles may decrease with temperature.

The most noteworthy feature of the data is the marked change in the amount of dye solubilized at around 0.023–0.024 *M* for the sodium and potassium laurates

TABLE 2

*Solubilization of Orange OT (M.W. = 262) in aqueous solutions of sodium laurate alone and in the presence of various sodium silicates at 60°C.*

MOLARITY OF SOAP	DYE PER 100 ML. OF SOLUTION	DYE PER MOLE OF SOAP	DYE PER MOLE OF SOAP $\times 10^3$
<i>M</i>	mg.	grams	moles
$2.0 \times 10^{-2}$	0.08	0.040	0.15
$2.10 \times 10^{-2}$	0.11	0.052	0.20
2.20	0.12	0.055	0.21
2.30	0.13	0.057	0.22
2.40	0.15	0.062	0.24
2.50	0.24	0.096	0.38
2.60	0.36	0.14	0.53
2.70	0.44	0.17	0.65
2.80	0.63	0.22	0.84

In 0.025 <i>M</i> (0.41 per cent) $\text{Na}_2\text{O} \cdot 1.7\text{SiO}_2$			
$1.0 \times 10^{-2}$	0.10	0.10	0.38
$1.2 \times 10^{-2}$	0.06	0.050	0.19
1.4	0.09	0.064	0.24
1.6	0.34	0.21	0.80
1.8	0.66	0.37	1.41
2.0	0.83	0.42	1.60

In 0.025 <i>M</i> (0.52 per cent) $\text{Na}_2\text{O} \cdot 5\text{SiO}_2$			
$1.0 \times 10^{-2}$	0.03	0.030	0.11
1.10	0.03	0.027	0.10
1.20	0.04	0.033	0.13
1.30	0.06	0.046	0.18
1.40	0.08	0.057	0.22
1.50	0.12	0.080	0.30
1.60	0.31	0.19	0.74
1.70	0.44	0.26	0.99
1.80	0.59	0.33	1.26
1.90	0.62	0.33	1.26
2.00	0.85	0.42	1.60

In 0.025 <i>M</i> (0.76 per cent) $\text{Na}_2\text{O} \cdot 4.0\text{SiO}_2$			
$1.0 \times 10^{-2}$	0.04	0.040	0.15
1.10	0.07	0.063	0.24
1.20	0.08	0.067	0.25
1.30	0.08	0.061	0.23
1.40	0.08	0.057	0.22
1.50	0.19	0.13	0.50
1.60	0.33	0.21	0.80
1.70	0.47	0.28	1.07
1.80	0.61	0.34	1.29
1.90	0.78	0.41	1.56
2.00	0.89	0.45	1.71

In 0.0125 <i>M</i> (0.20 per cent) $\text{Na}_2\text{O} \cdot 1.7\text{SiO}_2$			
$1.20 \times 10^{-2}$	0.05	0.040	0.15
1.40	0.12	0.086	0.33
1.60	0.14	0.088	0.34
1.80	0.18	0.10	0.38
2.00	0.33	0.16	0.61

TABLE 3

*Solubilization of Orange OT in aqueous solutions of potassium laurate and potassium laurate-sodium silicate mixtures at 60°C.*

MOLARITY OF SOAP	DYE PER 100 ML. OF SOLUTION	DYE PER MOLE OF SOAP	DYE PER MOLE OF SOAP $\times 10^4$
$M$	mg.	grams	moles
$2.00 \times 10^{-2}$	0.13	0.065	0.25
$2.10 \times 10^{-2}$	0.15	0.071	0.27
2.20	0.16	0.073	0.28
2.30	0.20	0.087	0.31
2.40	0.26	0.11	0.42
2.50	0.35	0.14	0.53
2.60	0.43	0.17	0.65
2.70	0.52	0.19	0.73
2.80	0.66	0.24	0.92

In 0.025 $M$ (0.33 per cent) $\text{Na}_2\text{SiO}_3$			
$1.00 \times 10^{-2}$	0.06	0.060	0.23
1.10	0.07	0.064	0.24
1.20	0.08	0.067	0.25
1.30	0.14	0.10	0.38
1.40	0.15	0.11	0.42
1.50	0.22	0.15	0.57
1.60	0.38	0.24	0.92
1.70	0.52	0.31	1.18
1.80	0.64	0.36	1.37
1.90	0.76	0.40	1.52
2.00	0.92	0.45	1.71

In 0.025 $M$ (0.41 per cent) $\text{Na}_2\text{O} \cdot 1.7\text{SiO}_2$			
$1.00 \times 10^{-2}$	0.10	0.100	0.38
$1.20 \times 10^{-2}$	0.06	0.050	0.19
1.40	0.13	0.093	0.35
1.60	0.33	0.21	0.80
1.80	0.60	0.33	1.26
2.00	0.85	0.43	1.64

In 0.0125 $M$ (0.20 per cent) $\text{Na}_2\text{O} \cdot 1.7\text{SiO}_2$			
$1.00 \times 10^{-2}$	0.03	0.030	0.11
$1.20 \times 10^{-2}$	0.06	0.050	0.19
1.40	0.06	0.043	0.16
1.60	0.10	0.062	0.24
1.80	0.11	0.061	0.23
2.00	0.38	0.19	0.73

in water, 0.018  $M$  in 0.0125  $M$  sodium silicate of  $\text{SiO}_2/\text{Na}_2\text{O}$  ratio 1.6, and 0.014  $M$  in 0.025  $M$  solutions of the sodium silicates. The concentration at which this occurs is taken as the "critical" concentration for micelle formation.

The value for the critical concentration of 0.024  $M$  for sodium laurate at 60°C.

thus obtained by the solubilization method agrees with our value of  $0.0237\text{ }M$  at  $25^{\circ}C$ . obtained by the dye-titration method. It also is in fair agreement with the value of  $0.028\text{ }M$  obtained by Ekwall (6) from electrical conductivity measurements at  $17$ – $70^{\circ}C$ ., and in good agreement with the figure of  $0.023\text{ }M$  obtained by measuring the solubilization of *p*-dimethylaminoazobenzene at  $50^{\circ}C$ . (11). Our value of  $0.023\text{ }M$  for the critical concentration of potassium laurate obtained from dye solubilization measurements at  $60^{\circ}C$ . agrees with the value of  $0.0235\text{ }M$  given by Corrin and Harkins (4) from their dye titrations at  $26^{\circ}C$ . The osmotic data of McBain and Bolduan at  $0^{\circ}C$ . (13) likewise indicate that micelle formation

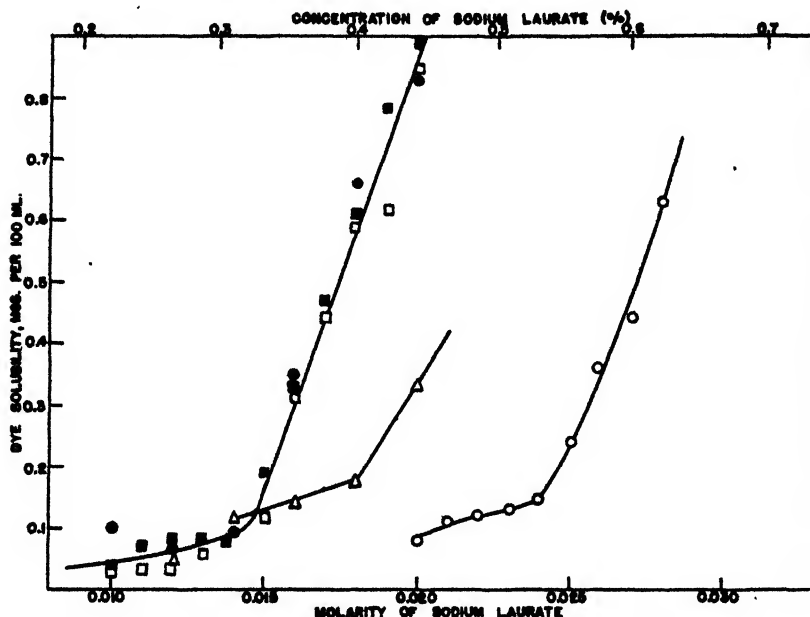


FIG. 2. Solubilization of Orange OT in sodium laurate solutions alone and with added sodium silicates at  $60^{\circ}C$ .  $\circ$ , sodium laurate in water;  $\bullet$ , sodium laurate in  $0.025\text{ }M$  sodium silicate with  $SiO_2/Na_2O$  ratio of 1.6;  $\square$ , in  $0.025\text{ }M$  sodium silicate with  $SiO_2/Na_2O$  ratio of 2.46;  $\blacksquare$ , in  $0.025\text{ }M$  sodium silicate with  $SiO_2/Na_2O$  ratio of 3.93;  $\triangle$ , in  $0.0125\text{ }M$  sodium silicate with  $SiO_2/Na_2O$  ratio of 1.6.

begins in this region, although their experimental points are not sufficiently numerous to show the "critical" concentration. However, Bury and Parry's data (2) on the density of potassium laurate solutions at  $25^{\circ}C$ . as a function of concentration show that an abrupt change of slope regarded as indicative of micelle formation occurs at 0.9 per cent or  $0.038\text{ }N$ .

It is also at a sodium laurate concentration of approximately  $0.024\text{ }M$  where solutions of this soap first show a minimum interfacial tension against heptane (5). However, changes in the surface-tension and interfacial-tension curves are not necessarily indications of micelle formation.

Our data on the solubilization of Orange OT by sodium palmitate solutions at



60°C. show that an increase in the dye solubilized per mole of soap, indicative of the "critical" concentration for micelle formation, occurs at  $4 \times 10^{-4} M$  or 0.011 per cent.

Figures 2 and 3 show that the four silicates varying in  $\text{SiO}_2/\text{Na}_2\text{O}$  ratio from 0.97 to 3.93 when compared at an equivalent  $\text{Na}_2\text{O}$  content increase the solubilization of Orange OT to about the same extent under our conditions. They lower the "critical" concentration similarly, and no variation in their effect on micelle formation of the soap at higher concentrations was detected in this work. McBain and Green (15) found that 1 *M* potassium hydroxide, potassium thiocyanate, and potassium chloride solutions and 0.5 *M* potassium sulfate solutions

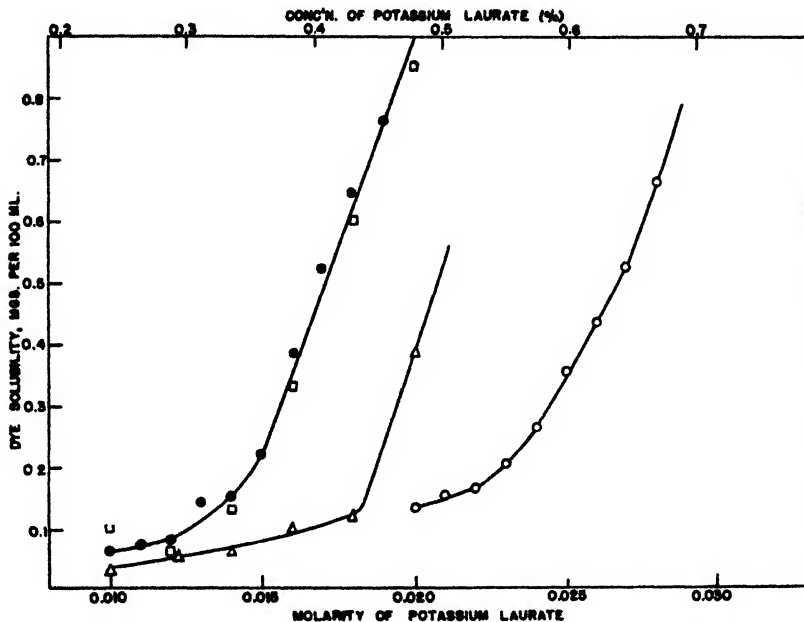


FIG. 3. Solubilization of Orange OT in potassium laurate solutions alone and in the presence of sodium silicates at 60°C. O, potassium laurate in water; ●, potassium laurate in 0.025 *M*  $\text{Na}_2\text{SiO}_3$ ; □, potassium laurate in 0.025 *M* sodium silicate with  $\text{SiO}_2/\text{Na}_2\text{O}$  ratio of 1.6; Δ, potassium laurate in 0.0125 *M* sodium silicate with  $\text{SiO}_2/\text{Na}_2\text{O}$  ratio of 1.6.

increased the solubilization of Orange OT by different amounts at higher soap concentrations. At the low soap concentrations ( $<0.028 M$ ) and elevated temperature (60°C.) studied here, potassium and sodium laurate solutions of equivalent concentrations are approximately equally effective as solubilizers for Orange OT. At higher concentrations and 25°C., Green and McBain (8) found the sodium soap to be definitely superior.

The turbidity of our dilute laurate solutions due to hydrolysis reached a maximum at about the concentration at which the dye solubility increased. Above this "critical" concentration the products of hydrolysis were apparently solubilized and clear solutions formed. No corrections were made for the absorption of

light due to turbidity as compared with our distilled water standard. Such a correction would make the true solubility of the dye somewhat less at the "critical" concentration and below, but would not appreciably change the values given at higher concentrations. Under our conditions the correction would be 0.08 mg. per 100 ml. or less. Applying this correction would make the change in slope even more than that shown in figures 2 and 3.

It is important that some dye was solubilized at concentrations below the "critical" concentration for micelle formation. The color due to this dye solubility was apparent to the eye. This slight solubilizing action may indicate the presence of a type of micelle or association product below the "critical" concentration for micelle formation. The existence of aggregates below this concentration is indicated by electrical conductivity (1, 12), by the effect of alcohol on electrical conductivity (7, 23), by interaction with dyes (10), and by surface anomalies (18).

TABLE 4  
*Solubilization of Orange OT in 0.6 per cent sodium laurate-sodium metasilicate mixtures at 60°C.*

SOAP IN MIXTURE	DYE PER 100 ML. OF SOLUTION
<i>per cent</i>	<i>milligrams</i>
100	0.48
95	0.42
90	0.45
85	0.46
75	0.42
60	0.26
50	0.29
35	0.26

Table 4 shows that in sodium laurate-sodium metasilicate mixtures containing 0.6 per cent solids, up to about 30 per cent of the soap can be replaced by metasilicate before its ability to dissolve water-insoluble dye changes very much, even though the metasilicate itself is not a solubilizer for the dye. Even when 65 per cent of the soap has been replaced, the solubility is still more than half that in the pure soap solution alone. The effect of the sodium metasilicate in increasing the proportion of soap micelles and their effectiveness as solubilizers is about sufficient to offset the lowered soap concentration.

#### DISCUSSION

Data obtained by the dye-titration method show that all sodium and potassium salts lower the critical concentration for micelle formation in soap solutions to the same extent when calculated on a cation-equivalents basis. Corrin and Harkins (4) first showed this to be true for potassium laurate solutions to which varying amounts of potassium chloride, potassium sulfate, and tetrasodium pyrophosphate had been added. They also found that the "critical" concentration of

sodium dodecyl sulfate was lowered to the same extent by the chloride and the sulfate. The "critical" concentrations of dodecylammonium chloride and decyltrimethylammonium bromide were lowered similarly by equal concentrations of sodium, barium, and lanthanum chlorides, calculated on an anion-equivalents basis. Our data show that the "critical" concentration for micelle formation in sodium laurate solutions of equivalent cation concentrations is lowered, within experimental error, to the same extent by sodium chloride, sodium hydroxide, sodium ortho- or pyro-phosphate, sodium tetraborate, and four sodium silicates with silica-to-soda ( $\text{Na}_2\text{O}$ ) ratios by weight of 0.97, 1.60, 2.46, and 3.93. The effect of the four sodium silicates on the "critical" concentration is confirmed by the solubilization method. In view of the well-known and thoroughly established fact that other physicochemical properties of soap solutions are affected very differently by various anions and cations and particularly by the pH, this at first seems a most surprising result. For example, Powney and Noad find that sodium chloride decreases the suspending power of soap solutions, whereas the various sodium silicates greatly increase it (21).

It is clear from the data and figures that the concentration at which micelle formation occurs is not dependent entirely on the amount of salt added or the total ionic strength of the solution. The variation of the "critical" concentration in the presence of added salts is not in accord with the Debye-Hückel equations. Probably this is because the high electrical charge on the micelle repels oppositely charged ions sufficiently so that variation of their charge has little or no effect on the electrical field around the micelle.

Since the average soap micelle contains neutral molecules, the equation governing the equilibrium between free ions and ions associated into micelles can be written, in accordance with the law of mass action, as:  $aA + bB = A_aB_b$ , where A represents the cation such as sodium or potassium, and B the anion such as the laurate. The small letters,  $a$  and  $b$ , are integers probably varying from 5 to 100 for soap solutions. The equilibrium constant will be given by

$$\frac{A^a \times B^b}{A_a B_b} = K$$

According to these equations any material furnishing an ion of the type A or B should increase micelle formation. In fact, any material which is incorporated into the micelle, such as solubilized organic dyes or liquids, might be expected to increase the formation of micelles. The action of various sodium salts in increasing micelle formation in soap solutions may then be regarded as a common-ion effect and in accordance with the law of mass action. Just as in the case of the analogous solubility-product relationship, this effect would be expected to be dependent mainly on the concentration of the common ion and relatively independent of the nature of the other ion associated with it. In the case of the effect on micelle formation, the "common ion" need not be the same as one of the soap ions or even ionic. Sodium and potassium salts behave identically in this respect. The "common ion" in this case need only be incorporated in the micelle. Possibly a modified equation would govern the interaction between ions, micelles, and

solubilized materials. Further evidence that added salts form micelles by a common-ion effect in accordance with the law of mass action is given by McBain and Brady (14), who show that potassium chloride and potassium sulfate lower the osmotic pressure of potassium laurate to approximately the same extent at equal potassium-ion concentrations.

Soap builders, such as the soluble silicates, may improve detergent action by lowering the concentration at which micelle formation begins, and increase the proportion of micelles at all soap concentrations. Probably they also increase sorption of soap by the fabric and dirt. However, their effect on micelle formation is not the main method by which builders improve detergent action, and certainly is not responsible for the wide variation in the effectiveness of the various alkaline electrolytes used as soap builders.

#### SUMMARY

At equal sodium-ion concentrations, solutions of sodium chloride, sodium hydroxide, sodium ortho- or pyro-phosphate, sodium tetraborate, sodium metasilicate, and three sodium silicates with silica-to-soda ( $\text{Na}_2\text{O}$ ) ratios of 1.60, 2.46, and 3.93 lower the "critical" concentration for micelle formation in sodium laurate solutions to the same extent. The data were obtained by the dye-titration method with pinacyanol chloride. Measurements of the solubilization of Orange OT in dilute sodium and potassium laurate solutions at 60°C. alone and with four sodium silicates confirm this result. The decrease in the "critical" concentration for micelle formation in soap solutions due to the salt is interpreted as a common-ion effect, in accordance with the law of mass action.

#### REFERENCES

- (1) BROWN, G. L., GRIEGER, P. F., EVERS, E. C., AND KRAUS, C. A.: *J. Am. Chem. Soc.* **69**, 1835 (1947).
- (2) BURY, C. R., AND PARRY, G. A.: *J. Chem. Soc.* **1935**, 626.
- (3) CORRIN, M. L., AND HARKINS, W. D.: *J. Am. Chem. Soc.* **69**, 679 (1947).
- (4) CORRIN, M. L., AND HARKINS, W. D.: *J. Am. Chem. Soc.* **69**, 683 (1947).
- (5) DAVIS, J. K., AND BARTELL, F. E.: *J. Phys. Chem.* **47**, 40 (1943).
- (6) EKWALL, P.: *Kolloid-Z.* **101**, 135 (1942).
- (7) EVERS, E. C., GRIEGER, P. F., AND KRAUS, C. A.: *J. Am. Chem. Soc.* **68**, 1137 (1946).
- (8) GREEN, SISTER AGNES ANN, AND MCBAIN, J. W.: *J. Phys. Colloid Chem.* **51**, 286 (1947).
- (9) HARTLEY, G. S.: *J. Chem. Soc.* **1938**, 1968.
- (10) KLEVEN, H. B.: *J. Phys. Colloid Chem.* **51**, 1143 (1947).
- (11) KOLTHOFF, I. M., AND JOHNSON, W. F.: *J. Phys. Chem.* **50**, 440 (1946).
- (12) MCBAIN, E. L., DYE, W. B., AND JOHNSTON, S. A.: *J. Am. Chem. Soc.* **61**, 3210 (1939).
- (13) MCBAIN, J. W., AND BOLDUAN, O. E. A.: *J. Phys. Chem.* **47**, 94 (1943).
- (14) MCBAIN, J. W., AND BRADY, A. P.: *J. Am. Chem. Soc.* **65**, 2072 (1943).
- (15) MCBAIN, J. W., AND GREEN, SISTER AGNES ANN: *J. Am. Chem. Soc.* **68**, 1731 (1946).
- (16) MCBAIN, J. W., AND MERRILL, R. C.: *Ind. Eng. Chem.* **34**, 915 (1942).
- (17) MCBAIN, J. W., MERRILL, R. C., AND VINOGRAD, J. R.: *J. Am. Chem. Soc.* **63**, 670 (1941).
- (18) MCBAIN, J. W.: In *Colloid Chemistry*, edited by J. Alexander, Vol. V, p. 102. Reinhold Publishing Corporation, New York (1944).
- (19) MERRILL, R. C.: *Ind. Eng. Chem.* **39**, 158 (1947).

- (20) MERRILL, R. C., AND McBAIN, J. W.: *J. Phys. Chem.* **46**, 10 (1942).
- (21) POWNEY, J., AND NOAD, R. W.: *J. Textile Inst.* **30**, T157 (1939).
- (22) PRESTON, W. C.: *J. Phys. Colloid Chem.* **52**, 84 (1948).
- (23) RALSTON, A. W., AND HOERR, C. W.: *J. Am. Chem. Soc.* **68**, 2460 (1946).
- (24) WRIGHT, K. A., ABBOTT, A. D., SIVERTZ, V., AND TARTAR, H. V.: *J. Am. Chem. Soc.* **61**, 549 (1939).

## COAGULATION OF HYDROUS FERRIC OXIDE SOLS BY ELECTROLYTES

ELIZABETH F. TULLER<sup>1</sup> AND E. I. FULMER

*Department of Chemistry, Iowa State College, Ames, Iowa*

*Received October 2, 1947*

### I. PHOTOMETRIC METHOD FOR THE DETERMINATION OF THE COAGULATION VALUE OF ELECTROLYTES

#### INTRODUCTION

The importance of coagulation phenomena in hydrophobic colloidal systems is attested by the large number of papers on the subject in the scientific literature. The "coagulation value" is generally expressed in terms of the millimoles of electrolyte, per liter of final volume of sol, required to produce coagulation. Since there are various definitions of the term "coagulation", the actual number assigned to the coagulation value depends on the purpose and method of the particular investigation.

The most basic method of determining complete coagulation is the direct observation of the phenomenon with the ultramicroscope. Since, however, this is a long tedious process usable only with dilute colloids and not easily adaptable to following the rate of coagulation, a number of other indirect methods have been employed. Of all the indirect methods, probably those involving some type of optical measurement are now the most frequently used. These measurements include turbidimetric, nephelometric, spectrophotometric, colorimetric, and photometric methods. The type of instrument used has gradually changed from the visual to the photoelectric type, so that the accuracy does not depend upon individual judgment.

Mukherjee and Papaconstantinou (5) were the first to use spectrophotometric and photometric methods. Since that time various types of these instruments have been employed. Sometimes the measurements were made only for the purpose of following the course of agglomeration as a means of studying such a phenomenon as the kinetics of coagulation. Where the methods were used to determine a coagulation value, the value was given in terms of the concentration

<sup>1</sup> Present address: Department of Chemistry, Wellesley College, Wellesley, Massachusetts.

of electrolyte necessary to produce a certain effect in a given time as determined by the methods mentioned above. That is, the limiting values of degrees of turbidity, angles of rotation, intensities of light, and other criteria are indicative of changes in the colloid. These methods are valid only for comparative purposes but not for absolute data, that is, curves may be drawn indicating trends.

In an attempt to improve upon the above methods, Wannow (10) described a procedure in which he first plotted the relative transmittancies against the time of coagulation for various concentrations of electrolytes. He then plotted the relative transmittancies for a specified time (such as 5 min.) against the activities of the coagulating (dominating) ion; the curve is S-shaped with a sharp inflection point. The concentration of electrolyte at the inflection point is taken to be the coagulating value. Wannow and Hoffmann (11) stated that this method gave absolute values, based on the fact that the curve obtained by plotting the number of particles in a given time against the activity coefficient of the coagulating ion showed about the same course, particularly the same inflection point, as did the corresponding curve of light transmission against activity coefficient. The work showing this correlation was reported on by Hoffmann and Wannow (2).

Troelstra and Kruyt (7) took exception to the above method of Wannow for determining the coagulation point. As they indicate, the inflection point for the curve based on transmission at 2 min. will not be the same as that taken at 5 min., and so forth. They, therefore, do not believe that it is characteristic of the coagulation capacity of the electrolyte used. They also question the standard method of investigating coagulation by determining sedimentation in a given length of time, because it indicates not only coagulation but a length of time for subsequent sedimentation. Differences in rates of coagulation will be associated with the formation of different kinds of aggregates which, in turn, settle at different rates. Therefore, from the point of view of kinetics, Troelstra and Kruyt suggest that it would be better to choose a certain degree of particle number obtained in a definite time as the criterion for the investigation of agglomeration. It is more important to know the point at which deformation of the double layer occurs, even though it might not lead to complete coagulation. But, at least, a method should be chosen, such as the color change of a gold sol, which indicates a certain aggregation degree independent of the occurrence of sedimentation.

In addition to the difficulties described above, the choice of definition of the coagulation also causes considerable confusion, since upon occasion it refers to an end point and at other times to a process. The authors, therefore, suggest the following terminology to clarify the issue. *Agglomeration* refers to the process of adhesion of the colloidal particles to form larger aggregates. *Coagulation* refers to the final stage of agglomeration which leads to separation into two obvious phases through sedimentation.

#### EXPERIMENTAL

The present paper deals with the development of a procedure to determine the coagulation value of hydrous ferric oxide sols, independent of the occurrence

of sedimentation. This procedure also permits the study of rate of agglomeration and the structure of the flocculate as evidenced by rate of subsequent sedimentation. The progress of the agglomeration was followed by determining the change in transmission of light by means of a KWSZ photometer purchased from the Wilkins-Anderson Company. This photometer consists essentially of a double-cell, balanced-bridge system using photoelectric cells and glass absorbent filters with a 100-watt lamp as a light source. The tubular cuvettes used were held in the instrument by adaptors placed on the carriage. The filter chosen was the #9 absorbing at 725 millimicrons; this filter gave the maximum light transmittancy for the hydrous ferric oxide sol used in the study. The standard employed was the colloid diluted to the appropriate concentration with distilled water. The per cent transmission of the agglomerating colloid was noted each minute for the first 5 min. and approximately every 5 min. thereafter until coagulation took place.

Since it is well known that a difference in the method of mixing the colloid and the coagulating electrolyte will cause a difference in the agglomeration behavior, a uniform method of mixing was employed. The procedure followed was to add to the colloid a sufficient quantity of electrolyte to make the total volume 5 ml. The mixture was immediately stirred and placed in the instrument. The first reading of transmission of light was taken 30 sec. after the addition of the electrolyte. The choice of the amount of colloid used was on the basis of the final concentration desired. The usual concentrations of colloid employed were 20, 20, 50, 20, and 80 per cent, although in some cases concentrations as low as 5 per cent were used.

The hydrous ferric oxide sol employed in the experiments was the so-called Sorum sol (6). The method of preparation was by the modification described by Tuller and Eblin (9). The procedure was further modified by using Visking cellophane sausage casing, which allowed maximum purification of the sol in 24-48 hr. of dialysis. Since the time of dialysis is only a qualitative indication of purity, the purity (designated as  $P$ ) is expressed as the ratio of iron to chloride in terms of gram-equivalents; the higher the value of  $P$ , the purer is the sol. Full details as to all of the above points have been given by Tuller (8).

When agglomeration takes place, absorption of light increases, causing a decrease in the intensity of light striking a photoelectric cell. This change of transmission was recorded as the per cent transmission at a given time. Thus the complete course of agglomeration could be followed as a function of transmission and time until coagulation, and finally sedimentation, resulted. The transmission for a given sol decreases with agglomeration until coagulation occurs, after which the transmission increases. The second phase of this change in transmission is related to the type of aggregate formed and the rate of sedimentation following coagulation. Although Wannow (10) and others have mentioned that the curves of opacity or per cent transmission plotted against time show an increase in transmission of light after the original decrease, none of these investigators have concerned themselves with the possibilities of using the change in slope. In fact, for the most part, they have failed even to indicate the full course of the agglomeration.

Graphs are presented in figure 1 showing the per cent light transmission as a function of time on addition of electrolyte to the sol. The letter A indicates the Sorum sol and the subscript the original batch chosen. However, different sols—for example, A<sub>4</sub> and A<sub>5</sub>—were found to give results in close agreement under otherwise identical conditions. The concentration of the sol is given in terms of volume of original sol per total volume; for example, 80 per cent refers to 80 ml. of the original sol diluted to 100 ml. with water. The symbol *P* refers to the purity of the sol and has been previously defined.

It will be noted that the transmittancy decreases as agglomeration progresses and then increases at the point of coagulation. It was found that the rate of increase of transmittancy is indicative of the subsequent rate of sedimentation. When cuvettes were removed from the instrument at the instant of change of slope, no sedimentation was observable. Sedimentation sufficient to show 2–3 mm. of clear supernatant liquid occurred from 15 sec. to several hours following the break in the curve. Floes (visible particles) were observed in every case just as the time of the change of slope, but not before. For convenience, the time at which the break occurs has been denoted as the *critical time* or *t<sub>c</sub>*. The critical time is therefore the coagulation time, i.e., the time when agglomeration is complete but sedimentation has not yet occurred.

The series of graphs in figure 1 illustrates the types of changes of light transmission that take place when an electrolyte is added to a colloid. Figures 1a through 1c show the changes in the transmission as the critical time or coagulation time is reached more rapidly. It should be noticed that as the critical time becomes smaller, the rate of change of transmission becomes greater. This indicates not only that agglomeration is more rapid but that sedimentation takes place more rapidly. This very general statement is most accurately applied to colloids differing only in concentration of the added electrolyte.

The concentration and purity of the sol affect the critical time and rate of sedimentation. The increase in transmittancy for the 80 per cent sol (figure 1d) does not increase as rapidly, following the critical time, as with the 50 per cent sols (figures 1a to 1c). Moreover, the more pure concentrated sol (figure 1e) shows a sharper change than does the less pure sol. These differences are associated with the types of coagulum formed and are indicated not only by changes in light transmittancy but also by the rate of sedimentation. In the case shown in figure 1d, the rate of change of light transmission during agglomeration is very rapid and the critical time has a small value; yet the increase in transmission is very slow. When examined, this colloid showed a granular, dense coagulum which settled very slowly. This is in contrast to the flocculent, massive, rapidly settling coagulum of the 50 per cent sols (figures 1a to 1c). The coagulum of the highly concentrated sol becomes more massive and flocculent as purification proceeds and hence settles more rapidly, as indicated in figure 1e.

If the colloid is of such nature that coagulation causes a tendency toward gelation, the critical time is frequently indicated by a sharp decrease in transmission before a rapid increase. This is illustrated by figure 1f, in which the sol was



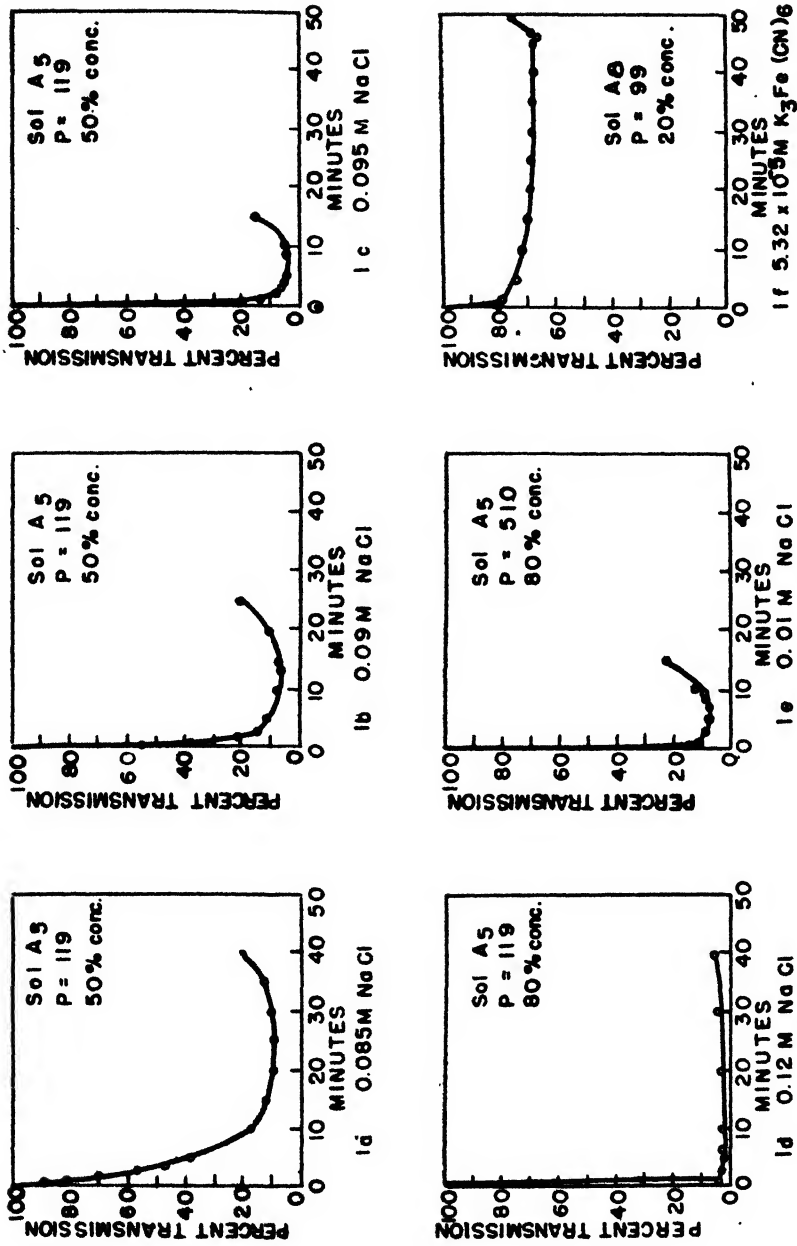


Fig. 1. Per cent transmission of agglomerating sols as a function of time

coagulated with potassium ferricyanide. The sharp decrease is due to a sudden packing effect occurring at the coagulation point and before sedimentation takes place. With some preparations of sols and high concentrations of polyvalent ions coagulation ultimately produced gelation such that there was just a steady decrease in transmission until sedimentation was nearly complete. The decrease in transmission was due to agglomeration and the packing following coagulation but gave no indication of the coagulation point. The critical time, therefore, can be determined only on colloids not showing gelation tendencies upon coagulation and is indicative only of the time needed for coagulation, not of the type of coagulum or the rate of sedimentation.

It was found that the transmission curves were exactly reproducible for 48 to 72 hr. following dialysis before the aging effects on the colloid were sufficient to produce a noticeable change in the properties of the system. For an additional 48 to 72 hr. the critical time was the same, but the total change in slope on either side of this point had started to vary. By this time the aging effects were producing a noticeable difference in the properties of the colloid. After this period of 5-6 days, the critical time had changed. Thus the transmission curves and the critical time may be used as an indication of the effects of aging on the colloid.

The critical time was also found to be related to the kinetics of coagulation. Coagulation phenomena are generally divided into two types, rapid and slow. Rapid coagulation is usually characterized by a rapid attainment of complete agglomeration followed by quick sedimentation and is produced by relatively high concentrations of a given electrolyte. Slow coagulation, on the other hand, is attained by relatively low concentrations of electrolytes, and slow sedimentation follows complete agglomeration. These, however, are merely qualitative indications of the rate of coagulation and, as has been emphasized in the earlier discussion, are not always adequate. That is, under certain circumstances, high concentrations of electrolytes may produce rapid and complete agglomeration but sedimentation may be relatively slow.

The use of the critical time in differentiating between rapid and slow coagulation is shown by the data in table 1 and figure 2, relating the critical times to concentrations of three electrolytes:—sodium chloride, sodium sulfate, and potassium ferricyanide. Figures 2b, 2d, and 2f show that, within the limits marked by asterisks, the critical time is a simple exponential function of the concentration of the electrolyte, that is, the logarithm of  $t_c$  is a linear function of the concentration of the electrolyte. The deviation from this linear function which occurs with very rapid coagulation, i.e., when the value of  $t_c$  is small, may be due to limitations of the method rather than to any difference in behavior of the colloid. The high-value times not falling within the exponential function, however, are due to slow coagulation. In other words, the extent of the rapid coagulation is indicated by the range of the exponential function, while the slow coagulation is indicated by critical times too long to be included in the linear relationship.

The range of critical times over which the exponential function was applicable varied with the electrolyte used. For example, the length of the straight-line function is shorter for the univalent electrolytes, as exemplified by sodium

TABLE 1

Critical time,  $t_c$ , as a function of the concentration of electrolyte for sols of 20 per cent concentration and purity ( $P$ ) as indicated

SOL	CONCENTRATION OF ELECTROLYTE	$t_c$	LOG $t_c$
	<i>M</i>	<i>min.</i>	
$A_5$ ( $P = 14.7$ ) . . . . .	0.27 NaCl	49	1.60
	*0.32	19	1.28
	0.40	14	1.15
	*0.48	10	1.00
$A_7$ ( $P = 475$ ) . . . . .	* $1.20 \times 10^{-4}$ $K_2SO_4$	35	1.54
	$1.25 \times 10^{-4}$	25	1.40
	$1.28 \times 10^{-4}$	18	1.25
	$1.31 \times 10^{-4}$	14	1.15
	* $1.36 \times 10^{-4}$	10	1.00
	$1.40 \times 10^{-4}$	9	0.95
$A_8$ ( $P = 99$ ) . . . . .	* $5.32 \times 10^{-5}$ $K_3Fe(CN)_6$	46	1.66
	$5.43 \times 10^{-5}$	25	1.40
	$5.60 \times 10^{-5}$	8	0.90
	* $5.80 \times 10^{-5}$	2	0.30
	$6.00 \times 10^{-5}$	2	0.30

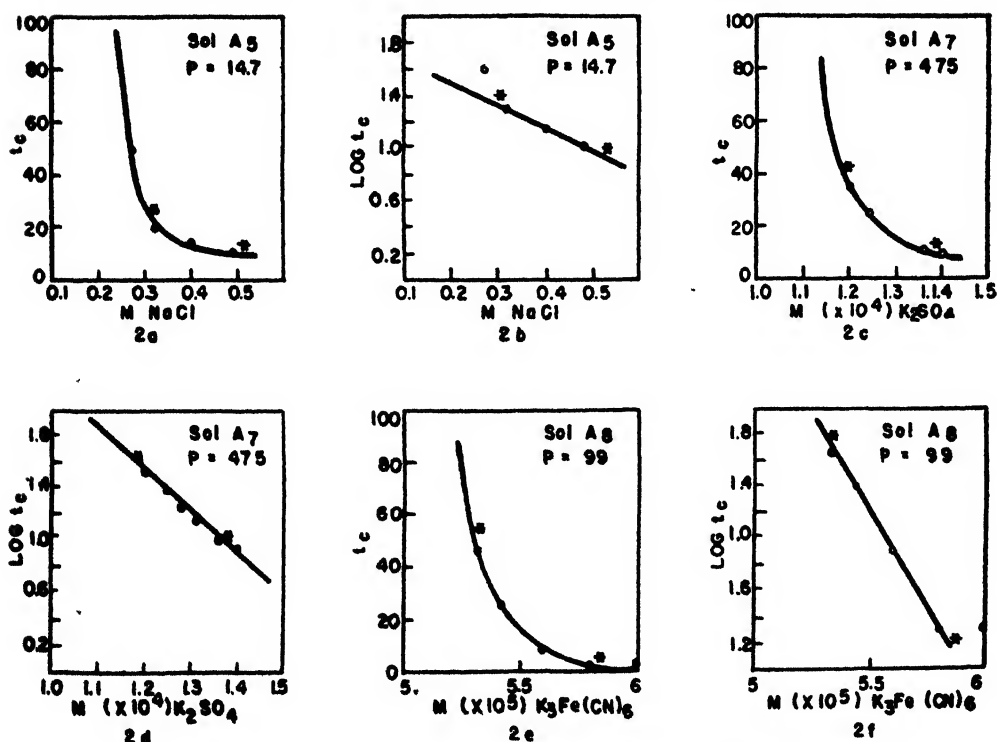


FIG. 2. Critical time ( $t_c$ ) as a function of the molarity of electrolyte for sols of 20 per cent concentration and purity ( $P$ ) as indicated.

chloride, than it is for potassium sulfate and potassium ferricyanide. In general, it was observed that the critical times for the univalent electrolytes extend at the most from 5 to 35 min., while those for potassium sulfate and potassium ferricyanide have ranged from 3 to 50 min. That is, the zone of rapid coagulation is greater for a polyvalent effective ion than for a monovalent ion.

Owing to the complexity of the colloidal system and the resultant hysteresis phenomena associated with it, at this time it is probably impossible to designate an absolute coagulation value. Since many concentrations of electrolytes may produce coagulation in a given colloidal system, it seems more logical to use for comparison purposes critical times and the concentrations of electrolytes corresponding to those times. Within the limitations imposed by hysteresis, probably the concentration of electrolyte needed to produce a given critical time for a colloid system defined in terms of method of preparation, purity, and concentration should be reasonably constant. It certainly is adequate as far as using critical times and the corresponding concentrations of electrolytes for comparison purposes. Caution must be observed to insure that any times taken for comparison are all from the same general type of coagulation, rapid or slow.

#### SUMMARY

In order to clarify confusion in the use of the term "coagulation" the following definitions have been proposed: *Agglomeration* refers to the process of adhesion of the colloidal particles to form larger aggregates; *coagulation* refers to the final stage of agglomeration which leads to separation into two obvious phases through sedimentation.

Agglomeration of hydrous ferric oxide sols was followed by a photometric procedure. The transmittancy of light decreases as agglomeration progresses and then increases at the point of coagulation. The rate of increase of transmittancy is indicative of the subsequent rate of sedimentation.

The time at which the direction of the transmittancy curve reverses direction is the time for coagulation and is designated  $t_c$ , the critical time. The value of  $t_c$  is, within limits, an exponential function of the concentration of electrolyte, that is,  $\log t_c$  is a linear function of the concentration of electrolyte. This linear relation holds only through the range of rapid coagulation. For values of  $t_c$  greater than the linear range, slow coagulation is indicated. Critical times within the range of rapid or slow coagulation may thus be chosen as a basis upon which to compare the concentrations of electrolytes required to produce coagulation of a given sol.

## II. RELATION OF THE PURITY OF THE SOLS TO THE BURTON-BISHOP RULE

#### INTRODUCTION

Burton and Bishop (1) in 1920 formulated a rule relating the concentration of hydrophobic colloids to the coagulation value of an added electrolyte. The so-called Burton-Bishop rule is as follows: (1) The coagulation values of univalent ions increase with decreasing sol concentration. (2) The coagulation values of bivalent ions remain almost constant regardless of sol concentration.

(3) The coagulation values of trivalent ions vary directly with sol concentration. Since the time of the formulation of this rule there has been considerable discussion as to the extent of its applicability, particularly in regard to the colloids known as the hydrous oxides.

Up until the time of the work of Judd and Sorum (3) it was generally believed that the hydrous oxides were an exception to the rule. Judd and Sorum, however, used a specially purified hydrous ferric oxide sol and showed that the Burton-Bishop rule held. They ascribed this correlation of concentration of the colloid and coagulation value of the electrolyte to the high purity of the colloid. Although Sorum's work was challenged several times, it was confirmed by Kauffmann (4) and Tuller and Eblin (9). Weiser and Milligan (12) pointed out that the Sorum effect is to be expected; the purer sol is more unstable to electrolytes and upon dilution becomes relatively more stable. Hence the sol formed by dilution of an unstable preparation would be relatively more stable to univalent coagulating ions than the sol formed by dilution of an impure highly stable preparation.

#### EXPERIMENTAL

##### (a) Sodium chloride as the electrolyte

The course of the agglomeration of hydrous ferric oxide sols was followed photometrically, using the techniques described in Section I of this paper. The critical time,  $t_c$ , was used as a criterion for coagulation of a hydrous ferric oxide sol, the purity of the sol with respect to the chloride-ion concentration, and the coagulation value of an added electrolyte. Most of the data were obtained in the region of rapid coagulation, i.e., the region in which the critical time is an exponential function of the concentration of electrolyte. The similarities and differences in slow and rapid coagulation were shown and will be discussed later. Several critical times were determined for each concentration of the sol, and data were obtained for three to six different concentrations for each sol purity.

Data are given in table 2 for the critical time,  $t_c$ , as a function of the concentration of sodium chloride and of the purity,  $P$ , and concentration of sol  $A_s$ . Values are given for  $m$  and  $b$ , through the range of application of the linear relation:

$$c = m \log t_c + b$$

in which  $c$  = concentration of electrolyte in millimoles per liter and  $t_c$  = critical time. The asterisks in the table indicate the demarcation between rapid and slow coagulation; in all cases at least one slow coagulation value and a limiting value is given. The limiting value is the concentration of electrolyte which will just produce agglomeration of the colloid, as indicated by a steadily decreasing transmittance. The value of the intercept,  $b$ , is the extrapolated coagulation value for a critical time of 1 min. While such values cannot be obtained experimentally at 1 min., they do serve a useful purpose in correlating the various results for rapid coagulation.

Data for  $P = 47, 119$ , and  $510$  are plotted in figures 3, 4, and 5. For values of  $P$  less than  $119$  the straight lines tend to intersect at a common point, as illus-

TABLE 2

Critical time,  $t_c$ , as a function of concentration of sodium chloride and of the purity,  $P$ , and concentration of sol  $A_1$

SOL		CONCENTRATION OF NaCl	$t_c$	LOG $t_c$	$m$	$b$
$P$	Concentration					
	<i>per cent</i>	<i>millimoles/liter</i>	<i>min.</i>			
14.7	20	240	Limiting value			
		272	45	1.65		
		*320	19	1.28		
		400	14	1.15		
		480	11	1.04	-781	1240
	40	240	Limiting value			
		276	39	1.59		
		*300	20	1.30		
		360	15	1.18		
		420	12	1.08	-500	955
		480	9	0.95		
	50	250	Limiting value			
		280	32	1.51		
		*300	19	1.28		
		350	13	1.11		
		400	10	1.00	-360	760
		450	7	0.84		
	60	250	Limiting value			
		270	32	1.51		
		*280	20	1.30		
		320	15	1.18		
		360	11	1.04	-348	730
		400	8	0.90		
	80	250	Limiting value			
		260	55	1.74		
		*280	20	1.30		
		300	14	1.15		
		320	10	1.00	-130	450
		360	5	0.70		
47.0	20	150	Limiting value			
		240	30	1.48		
		*272	22	1.32		
		304	15	1.18		
		320	13	1.11		
		400	6	0.77	-24.5	590

TABLE 2—Continued

SOL		CONCENTRATION OF NaCl	$t_0$	LOG $t_0$	$m$	$b$
$P$	Concentration					
	<i>per cent</i>	<i>millimoles/liter</i>	<i>min.</i>			
119	40	170	Limiting value			
		240	35	1.54		
		*288	17	1.23		
		300	15	1.18		
		336	10	1.00		
		360	8	0.90	-21.2	550
	50	190	Limiting value			
		200	40	1.85		
		*260	20	1.30		
		280	15	1.18		
		300	12	1.08		
		320	9	0.95	-16.2	475
	60	210	Limiting value			
		240	34	1.53		
		*254	24	1.38		
		280	15	1.18		
		300	10	1.00		
		320	7	0.84	-125	425
	80	230	Limiting value			
		240	50	1.70		
		*260	23	1.36		
		280	19	1.15		
		300	8	0.90	-88.0	380
	20	65.0	Limiting value			
		70.0	65	1.81		
		*76.8	33	1.52		
		78.4	26	1.41		
		85.0	11	1.04	-19.0	101
	40	60	Limiting value			
		70	60	1.78		
		*92	21	1.32		
		102	14	1.15		
		108	10	1.00		
		116	8	0.90	-48.5	165
	50	70	Limiting value			
		75	80	1.90		
		*85	25	1.40		
		90	14	1.15		
		95	9	0.95		
		100	5	0.70	-21.5	115

TABLE 2—Continued

SOL		CONCENTRATION OF NaCl	$t_0$	LOG $t_0$	$m$	$b$
P	Concentration					
	<i>per cent</i>	<i>millimoles/liter</i>	<i>min.</i>			
151	60	60	Limiting value			
		77	28	1.45		
		*92	13	1.11		
		96	11	1.04		
		112	7	0.84	-81.0	184
	80	70	Limiting value			
		78	51	1.71		
		*84	30	1.48		
		96	16	1.20		
		100	14	1.15		
		120	5	0.70	-43.5	150
	20	24.0	Limiting value			
		38.0	50	1.70		
		*40.0	23	1.36		
		43.2	13	1.11		
		44.8	10	1.00	-12.2	56.8
	40	30.0	Limiting value			
		35.0	80	1.90		
		*38.4	30	1.48		
		40.8	18	1.25		
		42.0	13	1.11		
		45.0	7	0.84	-10.5	53.8
	60	26.0	Limiting value			
		34.0	63	1.80		
		*36.0	36	1.56		
		38.4	27	1.42		
		40.0	21	1.32		
		42.0	15	1.18	-15.5	60.5
	80	28	Limiting value			
		35	63	1.80		
		*40	16	1.20		
		42	10	1.00		
		44	8	0.90	-11.5	54.2
262	20	14.0	Limiting value			
		18.0	40	1.60		
		*20.0	21	1.32		
		22.4	18	1.25		
		24.0	15	1.18	-28.8	58.0
	40	12.0	Limiting value			
		16.0	45	1.65		
		*18.0	22	1.34		
		21.6	14	1.15		
		24.0	11	1.04	-19.7	44.5



TABLE 2—Continued

SOL		CONCENTRATION OF NaCl	$t_c$	LOG $t_c$	$m$	$b$
$P$	Concentration					
	<i>per cent</i>	<i>millimoles/liter</i>	<i>min.</i>			
510	60	12.0	Limiting value			
		14.0	50 1.70			
		*16.0	26 1.41			
		18.0	17 1.23			
		20.0	12 1.08			
		21.6	9 0.95		-12.7	33.7
	80	10.0	Limiting value			
		14.0	55 1.74			
		*16.0	34 1.53			
		16.8	21 1.32			
		18.0	14 1.15			
		20.0	8 0.90		-7.2	26.5
	20	8.0	Limiting value			
		12.0	30 1.48			
		*14.4	17 1.23			
		16.0	12 1.08			
		17.6	9 0.95		-12.0	29.0
	40	4.5	Limiting value			
		6.0	44 1.64			
		*7.2	26 1.42			
		9.0	19 1.28			
		12.0	11 1.04		-12.9	25.5
	50	4.5	Limiting value			
		6.0	40 1.60			
		*9.0	16 1.20			
		10.0	13 1.11			
		11.0	11 1.04			
		12.0	9 0.95		-11.6	23.0
	60	4.0	Limiting value			
		6.0	32 1.51			
		*7.2	22 1.34			
		8.0	18 1.25			
		8.8	15 1.18			
		10.0	12 1.08		-11.2	22.0
	80	3.0	Limiting value			
		5.0	33 1.52			
		*7.2	15 1.18			
		8.0	13 1.11			
		9.0	10 1.00			
		10.0	8 0.90		-10.4	19.4

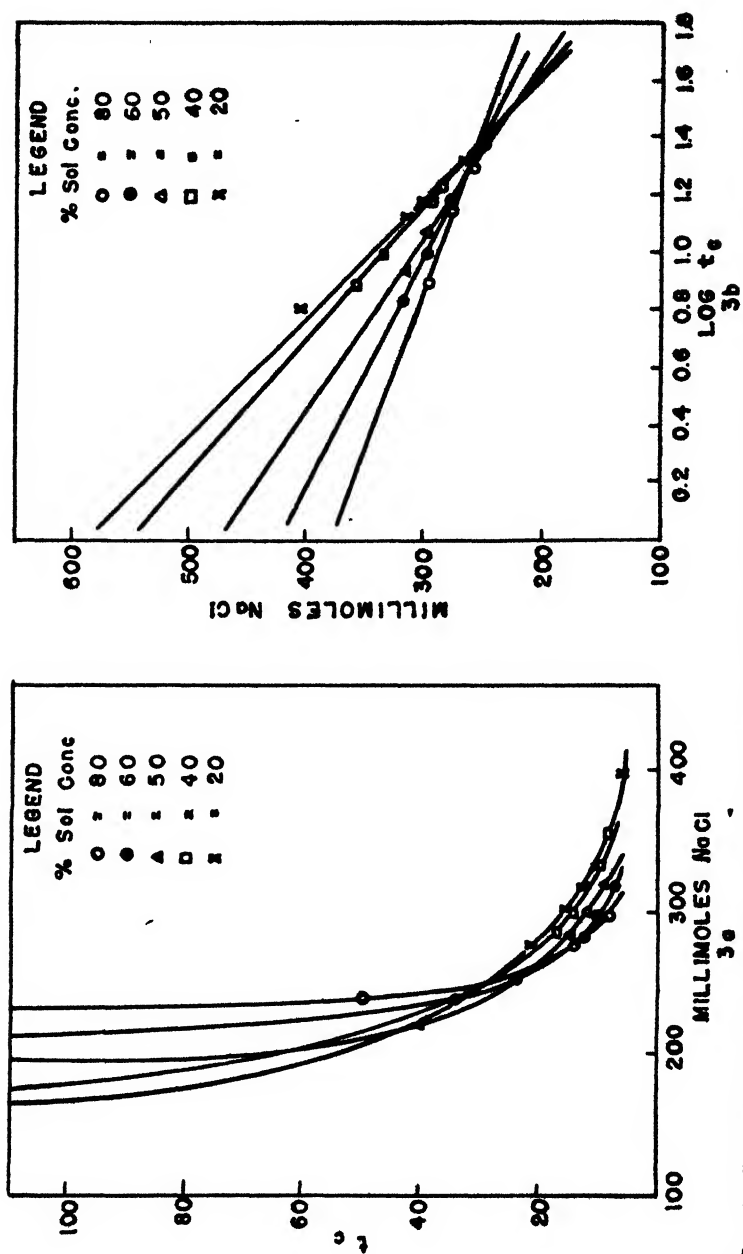


Fig. 3. Critical time as a function of the concentration of sodium chloride for sol A, ( $P = 47$ ) at several concentrations.

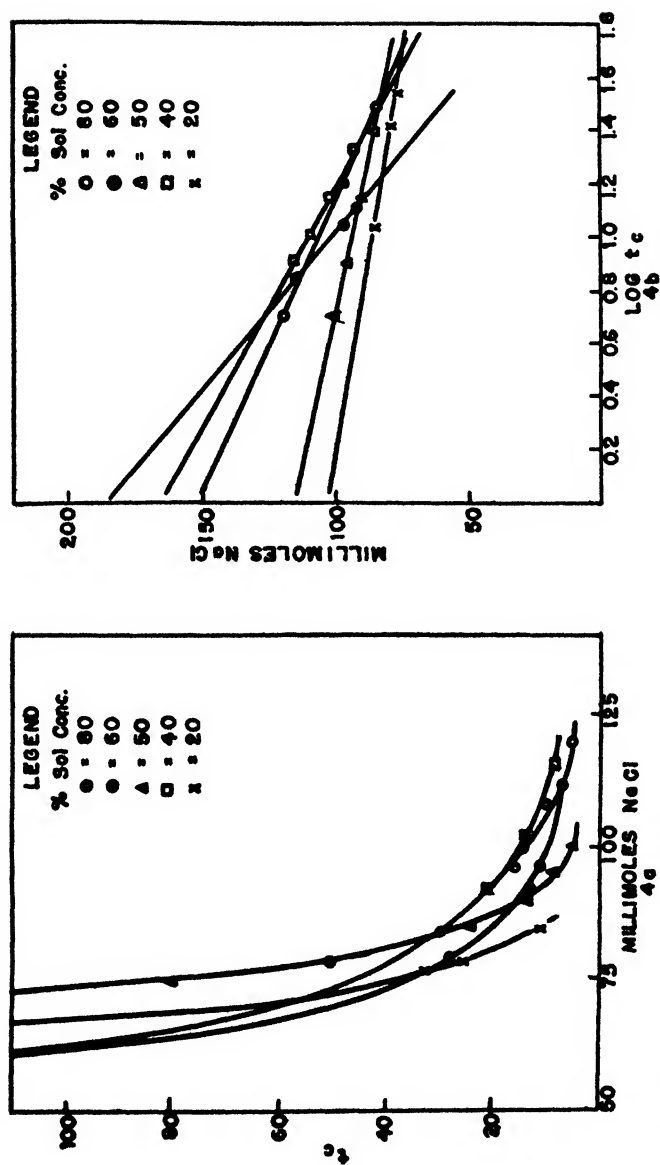


Fig. 4. Critical time as a function of the concentration of sodium chloride for sol  $A_3$  ( $P = 119$ ) at several concentrations.

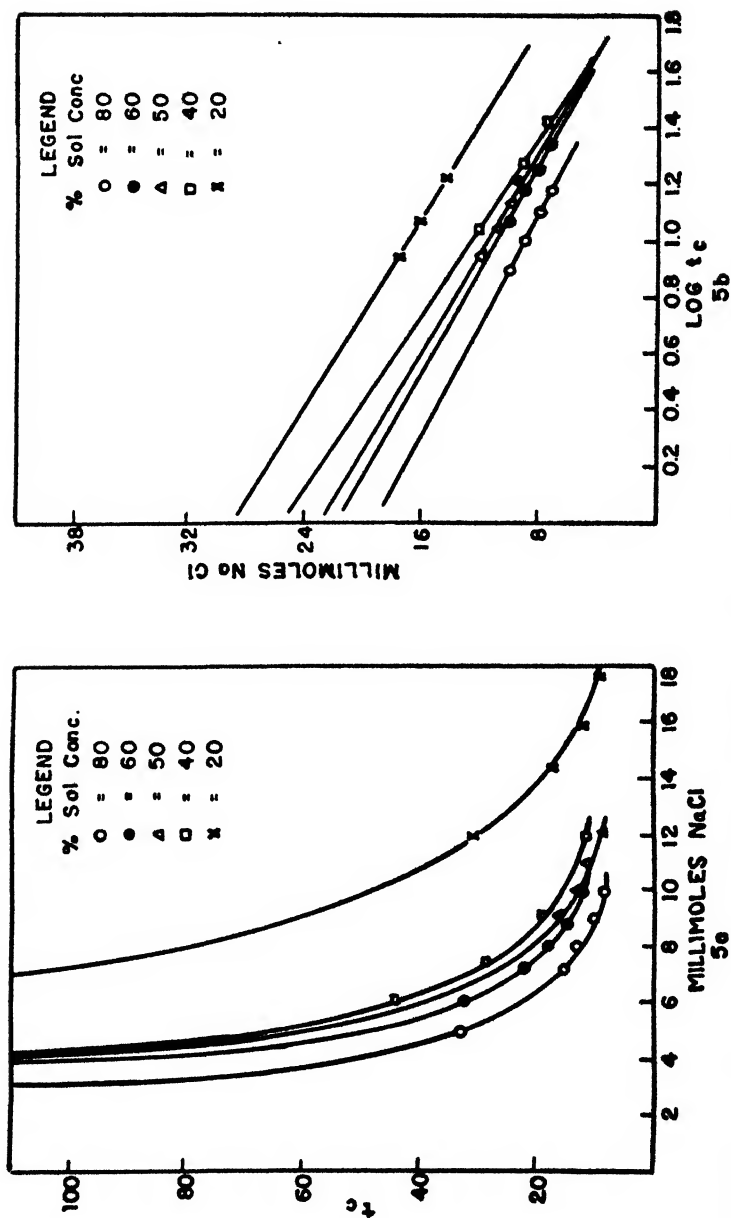


Fig. 5. Critical time as a function of the concentration of sodium chloride for sol A<sub>1</sub> ( $P = 510$ ) at several concentrations.

trated in figure 3b. The point of intersection may be within or just at the zone of rapid coagulation. If it lies within the zone of coagulation, the concentration of electrolyte for slow coagulation will be in the reverse order to that indicated by the intercept  $b$ . If the point of intersection is beyond the zone of rapid coagulation, the order of coagulation values may be, but are not necessarily, in the reverse order of that for rapid coagulation. Figure 3b illustrates a case in which slow coagulation values are the inverse of rapid coagulation.

For highly purified sols, that is,  $P$  is greater than 150, there is a tendency for the straight lines to become parallel as illustrated in figure 5b, and the curves of  $t_c$  against  $c$  also do not intersect as seen in figure 5a. This means that the order of coagulation values is the same for rapid as for slow coagulation.

For sols of intermediate purity, from 50 to 150, there is a scrambling effect as shown in figure 4. This case shows the relationship of coagulation values to concentration of the colloid when the coagulation values are not varying directly with or inversely to the concentration of the colloid. The decreasing order of the coagulation values in the most rapid coagulation is with concentrations of sol of 60, 40, 80, 50, and 20 per cent. The order of the coagulation values in the slow coagulation as indicated by the limiting values is not the exact inverse but decreases with the concentration in the order of 80, 50, 20, 40, and 60 per cent. In any case in which the scrambling takes place, the intersection of lines never occurs so nearly at a common point as in other cases in which the lines do intersect.

According to the Burton-Bishop rule, the coagulation value of the univalent ions increases with a decrease in the concentration of the colloid for any given sol. An examination of the intercept values in table 2 shows that the Burton-Bishop rule holds for all but two of the samples of the sol. In these two cases where the values of  $P$  are 119 and 151, there is a scrambling of the order of the coagulation values compared to the concentration of the colloid, but the tendency is toward a reversal of the Burton-Bishop rule. Examination of the limiting values as an indication of the order of the slow coagulation values shows that the Burton-Bishop rule is not obeyed until  $P$  for the sol is about 500. In summarizing the results for sodium chloride it can be stated that, in rapid coagulation, the Burton-Bishop rule is followed in all cases except in the range of purity of approximately 50 to 150 where there is the scrambling effect; in slow coagulation the Burton-Bishop rule is apparent only if the sol has a purity of 250 or higher.

#### (b) *Potassium sulfate as the electrolyte*

Potassium sulfate was employed as the source of the divalent ion. With this electrolyte, sol concentrations of 40 per cent or less must be used. With higher concentrations, either gelation occurs or the break between rapid and slow coagulation is so sharp as to preclude obtaining sufficient points. That is, coagulation was so rapid as to give a critical time of 1-3 min., or was so slow as to give no coagulation in 1-2 hr. With concentration of sol less than 40 per cent, no difficulty was met in determining sufficient critical times to determine a straight line.

TABLE 3

*Coagulation values of potassium sulfate as a function of the purity and concentration of sol A.*

SOL		CONCENTRATION OF $K_2SO_4$  millimoles/liter	$t_c$  min.	LOG $t_c$	$m$	$b$
P	Concentration  per cent					
28.9	5	0.171	31	1.49	-0.058	0.260
		0.190	16	1.20		
		0.208	8	0.90		
	10	0.180	20	1.30	-0.057	0.255
		0.189	14	1.15		
		0.197	11	1.04		
	20	0.176	19	1.28	-0.053	0.245
		0.184	14	1.15		
		0.192	10	1.00		
		0.208	5	0.70		
	30	0.168	32	1.50	-0.058	0.255
		0.181	19	1.28		
		0.183	18	1.25		
		0.189	14	1.15		
	40	0.312	14	1.15	-0.07	0.395
		0.318	12	1.08		
		0.324	10	1.00		
		0.360	3	0.40		
60.3	5	0.190	32	1.50	-0.040	0.250
		0.199	20	1.30		
		0.204	14	1.15		
		0.219	7	0.84		
	10	0.180	23	1.36	-0.033	0.225
		0.186	14	1.15		
		0.189	12	1.08		
		0.197	7	0.84		
	20	0.206	20	1.30	-0.041	0.260
		0.211	16	1.20		
		0.216	12	1.08		
		0.240	3	0.48		
	30	0.245	30	1.48	-0.038	0.300
		0.252	18	1.25		
		0.260	11	1.04		
		0.266	8	0.90		
	40	0.300	29	1.45	-0.023	0.335
		0.306	20	1.30		
		0.310	12	1.08		
		0.324	3	0.48		

TABLE 3—*Continued*

SOL		CONCENTRATION OF $K_2SO_4$	$t_c$	$\log t_c$	$m$	$b$
$P$	Concentration					
	<i>per cent</i>	<i>millimoles/liter</i>	<i>min.</i>			
114	5	0.190	38	1.58		
		0.208	16	1.20		
		0.214	12	1.08		
		0.219	10	1.00	-0.045	0.262
	10	0.173	17	1.23		
		0.180	13	1.11		
		0.189	8	0.90		
		0.198	5	0.70	-0.048	0.232
	20	0.168	17	1.23		
		0.175	12	1.08		
		0.185	7	0.84		
		0.192	5	0.70	-0.047	0.225
	30	0.210	25	1.40		
		0.224	12	1.08		
		0.238	5	0.70	-0.040	0.267
201	5	0.190	23	1.36		
		0.192	21	1.32		
		0.199	12	1.08		
		0.219	7	0.84	-0.035	0.237
	10	0.180	19	1.28		
		0.185	15	1.18		
		0.193	9	0.95	-0.034	0.225
	20	0.168	25	1.40		
		0.175	15	1.18		
		0.180	10	1.00		
		0.185	7	0.84	-0.028	0.208
	40	0.180	30	1.48		
		0.182	21	1.32		
		0.186	18	1.25		
		0.192	12	1.08	-0.035	0.230
300	5	0.146	28	1.45		
		0.150	21	1.32		
		0.152	17	1.23	-0.041	0.205
	10	0.144	31	1.49		
		0.148	22	1.34		
		0.151	18	1.25		
		0.153	16	1.20	-0.041	0.202

TABLE 3—Continued

SOL		CONCENTRATION OF $K_2SO_4$	$t_0$	LOG $t_0$	$m$	$b$
P	Concentration					
	per cent	millimoles/liter	min.			
	20	0.120	25	1.40		
		0.128	16	1.20		
		0.131	13	1.11		
		0.136	11	1.04	−0.043	0.180
	30	0.140	38	1.58		
		0.147	25	1.40		
		0.153	16	1.20	−0.041	0.205
	40	0.144	30	1.48		
		0.149	20	1.30		
		0.153	17	1.23		
		0.157	12	1.08	−0.041	0.205

TABLE 4

Coagulation values of potassium ferricyanide as a function of the purity and concentration of sol  $A_s$

SOL		CONCENTRATION OF $K_3Fe(CN)_6$	$t_0$	LOG $t_0$	$m$	$b$
P	Concentration					
	per cent	millimoles/liter	min.			
26.9	5	0.0219	25	1.40		
		0.0225	19	1.28		
		0.0228	15	1.18	−0.0034	0.0268
	10	0.0387	30	1.48		
		0.0396	15	1.18		
		0.0405	10	1.00	−0.0043	0.0448
	15	0.0555	16	1.20		
		0.0560	12	1.08		
		0.0565	9	0.95	−0.0040	0.0603
	20	0.0662	10	1.00		
		0.0669	6	0.78		
		0.0677	4.5	0.65	−0.0042	0.0704
52.2	5	0.0214	20	1.30		
		0.0220	14	1.15		
		0.0228	8	0.90	−0.0033	0.0258
	10	0.0335	28	1.45		
		0.0342	15	1.18		
		0.0349	10	1.00	−0.0031	0.0380
	15	0.0454	36	1.56		
		0.0460	14	1.15		
		0.0464	10	1.00	−0.0035	0.0500
	20	0.0595	35	1.54		
		0.0608	16	1.20		
		0.0614	11	1.04	−0.0038	0.0653



Data for the coagulation of sol A<sub>7</sub> at several purities by potassium sulfate are given in table 3. The slopes of exponential functions determined for various concentrations of a given purity of sol show that the lines tend to be parallel. This indicates that the order of coagulation values for both slow and rapid coagulation will be the same. The coagulation values, represented by  $b$ , were found to decrease slightly and then increase as the concentration of the sol increased. This slight minimum occurred at 10 or 20 per cent concentration of the sol. That is, the order of the intercept values indicated that potassium sulfate had a tendency to act like an electrolyte with a univalent dominating ion when coagulating low concentrations of the sol; at higher concentrations the electrolyte had a tendency to behave as though the dominating ion were trivalent. These tendencies were shown throughout the complete range of sol purities used and were at a minimum with highly purified sols. In conformity with the Burton-Bishop rule, the coagulation values of potassium sulfate show an intermediate position between the monovalent and trivalent ions.

(c) *Potassium ferricyanide as the electrolyte*

Investigation of potassium ferricyanide as the added electrolyte was hampered by two factors: inability to use high concentrations of the colloid due to the quick change from rapid to slow coagulation, and the gelation caused by agglomeration of the sol. Both of these changes have been discussed in previous sections of this paper. However, sufficient data were obtained, and are listed in table 4, to show that the exponential function of critical time against the concentration of the electrolyte gives a series of parallel lines from different concentrations of the same sample of sol. As with potassium sulfate, this indicates that the coagulation values of potassium ferricyanide will be in the same order for different sol concentrations in both rapid and slow coagulation. The data also show that the coagulation values of the electrolyte vary directly with the concentration of the colloid, a result which is in agreement with the Burton-Bishop rule.

SUMMARY

It has been found that critical times may be used in determining the relationship of the sol concentration to the coagulation values of an electrolyte. The order of the intercepts of the straight lines obtained by plotting the concentration of electrolyte against the logarithm of critical time indicates the order of the rapid coagulation values. If the straight lines are approximately parallel, the order of coagulation values in both rapid and slow coagulation are the same. However, if the lines intersect, the coagulation values in slow coagulation may be, but are not necessarily, in the inverse order to those of rapid coagulation. If the dominating ion is univalent, the order of the rapid coagulation values is in accord with the Burton-Bishop rule with all purities of the hydrous ferric oxide sol except between approximately 50 and 150. However, the order of slow coagulation values for univalent electrolytes agrees with the Burton-Bishop relation only if

the purity is 250 or higher. If the dominating ion is divalent, the behavior of the electrolyte is intermediate between the monovalent and trivalent ions, in accord with the Burton-Bishop rule. Although, for reasons previously noted, complete investigation could not be made of coagulation with a dominating trivalent ion, the data show that rapid coagulation values vary directly with the sol concentration, as has been expressed in the Burton-Bishop relation.

Further investigation is being made of the trend toward a minimum coagulation value found when potassium sulfate was the added electrolyte. The cause of the scrambling of the coagulation values in some sols when the dominating ion was univalent is being investigated.

#### REFERENCES

- (1) BURTON, E. F., AND BISHOP, E.: J. Phys. Chem. **24**, 701-15 (1920).
- (2) HOFFMAN, K., AND WANNOW, H. A.: Kolloid-Z. **83**, 258-62 (1938).
- (3) JUDD, R. C., AND SORUM, C. H.: J. Am. Chem. Soc. **52**, 2598-2602 (1930).
- (4) KAUFFMANN, V. H.: Kolloid-Z. **93**, 86-103 (1940).
- (5) MUKHERJEE, J. N., AND PAPAConstantinou, B. C.: J. Chem. Soc. **117**, 1563-8 (1920).
- (6) SORUM, C. H.: J. Am. Chem. Soc. **50**, 1263-8 (1928).
- (7) TROELSTRA, S. A., AND KRUYT, H. R.: Kolloid-Beihefte **54**, 225-6 (1943).
- (8) TULLER, E. F.: Doctoral thesis, Iowa State College, 1946.
- (9) TULLER, E. F., AND EBLIN, L. P.: J. Phys. Chem. **49**, 9 (1943).
- (10) WANNOW, H. A.: Kolloid-Z. **77**, 46-53 (1936).
- (11) WANNOW, H. A., AND HOFFMANN, K.: Kolloid-Z. **80**, 294-304 (1937).
- (12) WEISER, H. B., AND MILLIGAN, W. O.: J. Am. Chem. Soc. **62**, 1924-30 (1940).

## THE FIXING OF MOLECULAR ORIENTATION

JOHN F. DREYER

*General Polarizing Company, Cincinnati, Ohio*

*Received November 5, 1947*

#### INTRODUCTION

The liquid crystal phase, which is found to exist for certain rod-shaped or flat molecules surrounded by active groups, is characterized by fluidity and optical anisotropy. Orientation of liquid crystals of the nematic type can be influenced by contact with oriented surfaces (3), e.g., those oriented by shearing stresses (1).

It is the purpose of this paper to describe a method for the preparation of oriented films from certain dyes or dye-like substances which show the behavior of liquid crystals of the nematic type.

#### EXPERIMENTAL

A concentrated solution of the pure substance, usually a dye, in a polar liquid such as methanol or water is allowed to evaporate at a carefully controlled rate

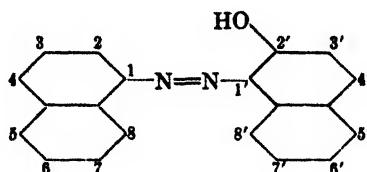
on a surface, such as that of glass, metal, or thermoplastic, previously rubbed well in one direction. By observation with polarized light dichroism can be seen before the film is dry. The resulting film is optically anisotropic, gives no cry-

TABLE 1  
*Compounds used in making oriented films*

DYE	CLASS	COLOR INDEX NO.
Naphthol yellow S. . . . .	Nitro	10
Amaranth . . . . .	Monoazo	184
Diamond black F. . . . .	Disazo	299
Tartrazine. . . . .	Pyrazonone	640
Xylene cyanol FF. . . . .	Triphenylmethane	715
Pinacyanol. . . . .	Quinoline	808
Methylene violet	Azine	842
New methylene blue	Oxazine	911
Methylene blue	Thiazine	922
Alizarin red S . . . . .	Anthraquinone	1034
Zapon fast blue HL* . . . . .	Metal organic	
Sodium amaranth-3,4,6'-trisulfonate† . . . .	Monoazo	
Sodium amaranth-4,6'-disulfonate† . . . .	Monoazo	
Sodium amaranth-5,3',6'-trisulfonate† . . . .	Monoazo	
Sodium amaranth-5,6'-disulfonate† . . . .	Monoazo	
Sodium amaranth-6,7'-disulfonate† . . . .	Monoazo	

\* Presumably a product of the reaction of laurylamine with a highly sulfonated copper phthalocyanine; molecular weight, about 1000.

† All of these compounds were crystallized from water. The numbering system is as follows:



It is interesting that the sodium amaranth-6',8'-disulfonate and the 5,6',8'-trisulfonate did not show the formation of liquid crystals or oriented films, presumably because the sulfonate group in the 8'-position prevents the two rings from being coplanar. The  $\beta$ -naphtholsulfonic acid series provides another series of this kind. Still another series may be obtained by substituting an amine aldehyde link in place of the azo link.

stalline x-ray diffraction pattern when examined by the Laue technique, and presumably consists of oriented molecules. Several precautions must be observed for successful preparation of these films: a low rate of drying results in crystalline formation; a high rate destroys the orientation of the film as a whole. Success sometimes depends on the choice of the correct polar solvent,<sup>1</sup> although methanol generally works best for the basic dyes and water for the acid dyes.

<sup>1</sup> For example, the dyestuff Color Index No. 159, which is water-soluble, shows orientation in the liquid crystal phase, but C. I. No. 69, which has the same structure except for the substitution of a methyl for a sulfonate group, is water-insoluble and does not form liquid crystals from dioxane, in which it is soluble.

Examples of some of the many classes of compounds which have been made into oriented films (2) are presented in table 1.

In addition, it may be remarked that a mixture of two or more similar dyes also shows the formation of a single oriented film, e.g., C.I. No. 184 plus C.I. No. 182. An investigation of the films by use of polarized light showed that the direction of light absorption for the basic dyes, such as methylene blue, was perpendicular to that for the azo dyes, such as amaranth.

#### REFERENCES

- (1) BEILBY, G.: *Aggregation and Flow of Solids*, p. 106. The MacMillan Company, New York (1921).
- (2) DREYER, J. F.: U. S. patent 2,400,877.
- (3) FRIEDEL, M. G.: In *Colloid Chemistry*, edited by J. Alexander, Vol. I, pp. 112-18. The Chemical Catalog Company, Inc., New York (1926).

### RADIATION CHEMISTRY. V

#### EFFECT OF MOLECULAR SIZE<sup>1, 2</sup>

MILTON BURTON

*Department of Chemistry, University of Notre Dame, Notre Dame, Indiana*

*Received November 13, 1947*

#### INTRODUCTION

All the electrons in a molecule are equally accessible to the high-energy particles and radiation characteristic of radiation chemistry. Potentially, all of them have approximately the same chance of being excited (or ionized) by such irradiation. These facts explain observations on the radiolysis of aliphatic hydrocarbons (25) and acids (17) which indicate that the relative yields of methane and hydrogen in the former and of hydrogen in the latter are almost linearly related to the frequency of occurrence of the parent groups in the molecule (2, 3).

However, it has also been shown that other features of the product yield in these cases are not readily explained on this basis (2, 3). The yields (for fixed energy input) of hydrogen, methane, and other gaseous products all decrease with increase in molecular weight of the hydrocarbons (3, 25). Sheppard and Whitehead (27) have studied a range of fatty acids (*cf.* Breger (1), Honig and Sheppard (18), Sheppard and V. L. Burton (26), Honig (17)). Hydrogen, carbon dioxide, carbon monoxide, and methane are produced in approximately equal yield in the radiolysis of acetic acid. In the radiolysis of palmitic acid only the first two are found among the gaseous products and *n*-pentadecane is

<sup>1</sup> Presented before the Division of Physical and Inorganic Chemistry of the American Chemical Society at the 112th Meeting, New York City, September 17, 1947.

<sup>2</sup> Work in radiation chemistry at the University of Notre Dame is assisted by the Office of Naval Research of the United States Navy Department under Contract N6ori 165 T.O.II.

the principal liquid product. The amount of *n*-pentadecane found far exceeds what would be expected on the mere statistical basis of number of parent groupings.

An explanation of these phenomena has been given by this author in a preliminary way (2, 3). However, since the existence of this apparent anomaly of the effect of molecular size has once again<sup>3</sup> been noted as a curious problem (1), the whole matter is reexamined in this paper with the result, as it appears below, that the explanation lies mainly in the Franck-Rabinowitch effect (11).

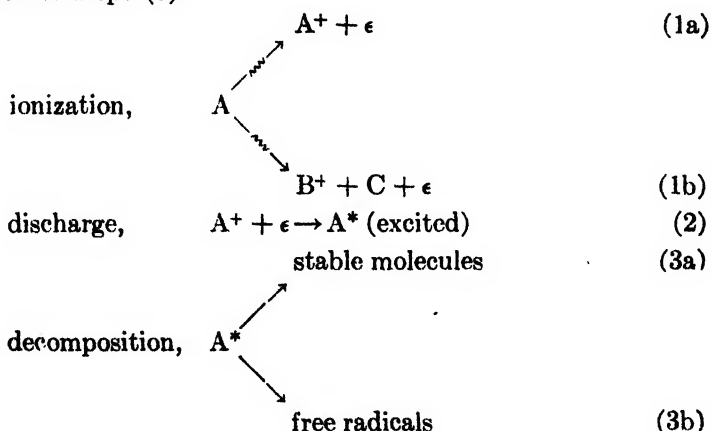
The general mechanism of radiation-chemical reactions was first put in satisfactory form by Eyring, Hirschfelder, and Taylor (8, 16). The theory has been reviewed in some detail, particularly in regard to the mechanism of radiolysis (2-5).

In the following sections the essentials of the theory particularly germane to this discussion are repeated and developed in greater detail.

#### PRIMARY PROCESSES

Initially, irradiation causes the molecules to become either excited or ionized. Presumably, any part of the molecule is equally susceptible to excitation or ionization and we may conclude from the existence of the phenomenon of multiple ionization (13) that multiple excitation also occurs to some extent. The excited electrons may be localized at bonds, may be non-bonding, or may even be non-localized (e.g., the  $\pi$  electrons in benzene). However, there is no requirement that the excitation should remain at the initial locale and there is a possibility, which should not be ignored, that the electronic excitation may proceed by an internal conversion process from its initial locale to a more favored region. Indeed, we see evidences of such a process of movement and of excitation in some of the phenomena of photographic sensitization by dyes (23) and in photosynthesis.

The processes starting with ionization and resultant in decomposition may be summarized in the three steps (5):



<sup>3</sup> That is, at the Symposium on Radiation Chemistry and Photochemistry, which was held at the University of Notre Dame, Notre Dame, Indiana, June 24-27, 1947.

where B and C may represent a variety of free-radical and molecular species, and where reactions analogous to 2 and 3 may be written for  $B^+$  and  $B^*$ . A full discussion requires also some analysis of the other fates of excited particles (fluorescence, collisional deactivation, and reaction) and of the fates of various radicals and any other chemically active species. Needless to say, any electron of the molecule may be involved in step 1.

Before proceeding any further, we should examine the possibility that the ionization (like the excitation) may shift from its initial, wholly accidental locale to some preferred region. As in excitation, we cannot neglect the possibility that such a shift may occur. However, we are confronted with the need of accounting for an unexpectedly high yield of particular products in the case of large molecules. If the explanation were a shift of excitation or ionization to a special region, we would have to conclude that the shift would be favored by increase in molecular size (3). Since there is apparently no *a priori* reason for such a relationship, we should look for some other simple explanation.

#### THE EFFECT OF STATE

It is convenient for a moment to omit details of the processes by which the molecule becomes first electronically and then vibrationally excited and to consider what can happen when it decomposes. We shall assume that the excited molecule is so constituted that sometime in its life a quite large amount of vibrational energy appears in one bond. This amount of energy may exceed the strength of that bond. In that event rupture will occur at that point within one vibration period. For appreciation of subsequent events we must consider the state of the substance.

The higher-molecular-weight substances are all liquid or solid under the conditions of radiolysis reported. Consequently, as Franck and Rabinowitch (11) pointed out (for photochemical processes), the effect of the cage of surrounding molecules on the excited state and on the products must be considered. In regard to the latter, it is apparent that the larger the molecules of the cage and the larger the radicals primarily produced, the less is the probability that they will escape the cage (3, 20). Thus, although hydrogen atoms might escape rather readily, larger radicals would be reflected from the cage and recombine with some loss of vibrational energy (11) before they have escaped each other's spheres of influence. Production of hydrogen in a reaction does not necessarily imply a free-radical process. The theory merely states that production of hydrogen in this way (as in the radiolysis of palmitic acid) is not precluded. On the other hand, the Franck-Rabinowitch effect does practically preclude decomposition by a free-radical mechanism when the radicals are large.

We continue to omit consideration of how the molecule became vibrationally excited and consider instead what happens to its energy. There is always the possibility that after any radical recombination act (cage effect) there may still be enough energy left to permit rupture at some other bond—if the energy should flow into that bond. As between possible ruptures at C—C and C—H bonds simple energetic considerations would suggest that, if any such effect does

occur, it would occur almost exclusively at the C—C bonds, which are in general weaker than the C—H bonds by about 14 kg.-cal. (27). Apparently, if rupture of a C—H bond is to occur at all, it is almost an absolute requirement that it occur initially in the process in which energy disappears as electronic excitation and appears as vibrational excitation of a single bond. Thus, we might expect that any rupture which occurs secondarily, so to speak, as a result of the flow of vibrational energy and accumulation into a single bond will involve a C—C bond. However, unless the free-radical product is sufficiently small, the cage effect continues to manifest itself and the net effect is that the amount of vibrational energy is gradually reduced in collision (about every  $10^{-13}$  sec.) with the surrounding molecules. Quickly, the energy is reduced to such a point (e.g.,  $< \sim 4$  e.v.) that decomposition by bond rupture is no longer possible. The only available mechanism is by rearrangement to ultimate molecules, which may require  $\sim 2$  e.v. or less. The effect of the liquid state in radiolysis is thus to prevent free-radical decompositions (except those which give small products like atoms or perhaps very small radicals) and to favor decompositions by rearrangement.

These remarks concerning the mechanism of decomposition are not intended to be restricted purely to internal conversion processes. Recently, Noyes has shown on the basis of fluorescence studies that in the photolysis of acetone the upper state is very long-lived and fluorescence emission occurs to a repulsive state (corresponding to molecular collision) at a point not more than 2 e.v. above the zero-point level of the ground state (21). While this mechanism is not the only conceivable one, it may not only be a possible mechanism for decomposition by rearrangement in radiolysis but may actually be much more common than is now appreciated.

Among a variety of possible rearrangement processes, that one will be favored which combines low energy requirement with maximum probability of attainment of the required configuration. The requirement is one of simplicity of execution and limits the number of possible products which may be produced. For a decomposition like



it is not too difficult to manipulate a configuration for the acid which resembles a close impact of RH and  $\text{CO}_2$ . The fact that the reaction is nearly thermo-neutral indicates the probability of low energy requirement.

Rearrangement of a hydrocarbon or fatty acid to yield molecular hydrogen and an unsaturated residue is configurationally simple. However, the activation energy for such a process is  $> 1$  e.v. higher than that of reaction 1 and thus, in comparison to that reaction, it practically does not occur.

The conclusion is that the Franck-Rabinowitch cage effect tends to prevent free-radical decomposition in the liquid state. This tendency increases with molecular size and manifests itself in an actual simplicity of products (and some decrease of lability) in radiolysis of very large molecules.

There is one point that should yet be made. We have considered thus far

only the vibrationally excited molecule  $A^*$  in step 3. However, the remarks that have been made concerning the effect of state and the effect of molecular size apply with equal force to any metastable ion  $A^+$  (containing excess energy) which might tend to decompose by rupture prior to the discharge step 2.

#### SECONDARY PHYSICAL PROCESSES

The theory, as so far outlined, does explain the simplicity of the products, as shown in the radiolysis of palmitic acid and other compounds.<sup>4</sup> It would likewise predict similar effects in thermal reactions in the liquid state.<sup>5</sup> For radiolytic data now existent it is unnecessary to develop any more involved theory in order to account for all the observed effects. Phenomena, for example, such as decrease of yield of hydrogen with increase of size of hydrocarbon molecule (3, 25) can be explained on the basis of the increased importance of competing processes, not the least of which is deactivation.<sup>6</sup> Until more is known of the facts, no more complicated explanation is necessary. However, it is worth while to explore further the details of the excitation and internal conversion processes by which electronic energy is converted to vibrational in order to discover any possibilities which might act conversely to the cage effect.

#### *Multiple excitation and its effects*

It is a mistake to think of a molecule as being ionized or excited initially. Indeed, both processes may occur in one molecule. We have clear evidence from the instability of ions such as  $A^+$  and  $B^+$  (15) that many ionized particles are themselves excited. Thus, the particle  $A^*$  formed by the discharge process (step 2) may have two or more positions of electronic excitation as the result of the primary process itself. The chances of such double excitation should increase with the size of the molecule. In general, the effect is to increase the average energy per excited molecule as the molecule increases in size. Thus,

<sup>4</sup> V. L. Burton, of the Massachusetts Institute of Technology group, pointed out at the September 1947 meeting of the American Chemical Society in New York City that the nature of the liquid products from the radiolysis of oleic acid indicates that the decomposition proceeds mainly by decarboxylation.

<sup>5</sup> Of course, simplicity of products in photochemical reactions is generally to be expected.

<sup>6</sup> The drop of hydrogen yield suggests the possibility that some of the decomposition actually does occur, as already mentioned, by flow of distributed vibrational energy into single bonds. The larger the molecule, the more widely is the vibrational energy distributed (after Franck-Rabinowitch stabilization). Thus, the time required for flow of sufficient energy into the C—H bond increases with molecular size. In that greater time, more deactivating collisions take place and the chance of C—H rupture is correspondingly decreased. Other effects, such as the relative time required for activation of the C—C bond may also be significant. However, it is not required that hydrogen be formed by bond rupture. Some may be formed by a rearrangement mechanism. In such a case also, the larger the molecule, the more time is necessary for approach to a proper configuration. In consequence, the deactivation process is favored and the product yield is decreased with increase in molecular size.



we might expect *a priori* that in this way size might tend to increase the lability of a molecule toward radiation. We will see later that because internal conversion (of electronic to vibrational energy) is, except when a repulsive level is involved, a necessary precedent to rupture, multiple electronic excitation does not, in fact, increase the lability of a molecule.

The Franck-Condon principle indicates that the ion  $A^+$  formed in step 1 has, at the instant of its formation, the same configuration as the parent molecule. However, since an electron has been removed, expansion to a more stable configuration occurs (8). The expansion may be more or less localized, depending on the nature of the empty orbital. If the empty orbital is spread over the whole molecule (as in benzene), the expansion may occur slightly in all bonds of the molecule (5). However, the over-all expansion of the molecule in such a case might be not greatly different from the total expansion if it had occurred all at one bond. In general, although expansion of a molecule may be large, local distortion may be small.

Expansion of the ion and the existence of an empty localized orbital imply a shift of all the other orbitals, much as if the electronic charge of the molecule shifts in the direction of excess positive charge. Up to a certain limiting point we may expect that the larger the molecule the more will such shifts be distributed. Since there is complete removal of an electron, the effect will be greater than that resultant from substitution of an atom of grossly unlike charge distribution (e.g., Cl for H); we may surmise that electron shifts will occur at least five atoms away in any direction. The net result is to distribute the excitation of the molecule, and the larger the molecule the greater will be the distribution of such excitation. Since in the process of stabilization of the ion  $A^+$  the electron orbitals have shifted, the positions of the atoms concerned relative to the configuration of the parent molecule will also have shifted. The whole molecule will be distorted, but the larger the molecule, the smaller will be any local distortion.

The distribution of excitation becomes manifest in step 2. The electron which discharges the ion  $A^+$  produces a molecule quite different in its configuration from its parent molecule. It is distended and therefore vibrationally excited. Also, it is electronically excited, perhaps in more than one orbital. The proof that excitation in  $A^*$  is widely distributed lies in the fact of discharge itself. It is the actuality of excitation in various modes that permits the existence of a molecule containing more than sufficient energy to become ionized. Before sufficient available energy flows into an orbital to reverse the process and again to give ionization (i.e., by internal conversion) sufficient collisional deactivation, or perhaps fluorescence, occurs to preclude such a possibility.

It is not to be expected that localized distortion resultant after step 1 will be very great. Moreover, even if, as a result of such distortion, vibrational energy produced in step 2 is, or becomes, sufficient in one bond to cause rupture, the possible ensuant processes are limited by the cage effect. However, although some of the excitation resident in  $A^*$  after step 2 may be vibrational, it is likely

that most of it may lie in one or more excited orbitals.<sup>7</sup> The more likely process for appearance of considerable vibrational energy in the molecule would then be an internal conversion in which one of the excited orbitals would lose its energy to give vibrational energy. Theoretically, there is a probability that the process may happen to two excited orbitals simultaneously, but the probability appears so small that it may be neglected. It is for this reason that possible increase in the number of excited orbitals with increase in the size of the molecule already noted is probably without effect on radiolytic lability. Nevertheless, internal conversion of the energy from even one excited orbital to give vibrational energy might be sufficient to cause rupture if it would all appear in one bond. The amount of energy associated with ionization is of the order of 15 e.v., while the strength of the usual bond is 4-6 e.v. Thus, only a part of the available energy (if it were properly concentrated) would be sufficient to cause rupture, with the results we have already considered.

We have surmised from a consideration of the excited molecule  $A^*$  that the electronic excitation may be distributed to some extent in the molecule. If the orbital distortion occurrent in stabilization of  $A^+$  is sufficiently great, there might even be several orbitals excited in step 2. The objection may be voiced that the electronic orbitals would return to their original state (i.e., of the original ion formed in step 1) in the discharge process, but this action is impossible. The states of the orbitals in the ion correspond to a distorted configuration of atoms which do not change their positions during the time required for discharge (Franck-Condon principle). Thus, electronic excitation may reside in other parts of the molecule as a result of the process of discharge. Actually, we do not have to speculate very far on this point.

It makes little difference whether the energy distributed in the molecule as a result of step 2 is electronic or vibrational. The point is that it may be widely distributed and that the larger the molecule the less the probability that a significantly large amount of energy (of the order of a bond strength) may be in any one excited orbital. In any event, whatever the effect is, it will not be opposite in its action to the cage effect already noted. As a matter of fact, this effect of distribution of excitation, and particularly the effect of lowering the amount of excitation in any one orbital, would serve to decrease the probability of rupture of the stronger bonds. Thus, we see another way in which increase of molecular size might serve to decrease both the probability of C-H rupture and the yield of hydrogen, already noted for the long-chain hydrocarbons.

The time required for an internal conversion process may be surmised from our knowledge of predissociation in photochemistry (7). It may be as little as

<sup>7</sup> The possibility exists that in the discharge process there results a repulsive or very weakly attractive state in which radicals are immediately formed. The factors governing their subsequent behavior are analogous to those already considered for products from molecules which are no longer electronically excited. Electronically excited molecules in attractive states produced by recombination of such radicals behave like molecules in similar states produced directly in discharge. Their properties are considered in the ensuing paragraphs.

$10^{-12}$  sec. or even much greater than  $10^{-8}$  sec. In the liquid state the molecule is practically constantly in a state of collision. Deactivation will occur with greater likelihood than the shift of the vibrational energy to a single locale necessary for rupture; that likelihood will increase with size of the molecule and with distribution of the vibrational energy. Apparently, the most favored circumstance for rupture of a bond is the initial creation of a repulsive or weakly attractive state or an internal conversion process in which the energy initially associated with electronic excitation is converted into vibrational energy at one point.

We have repeated, direct, free-radical evidence from photochemistry (*cf.* the cases of aliphatic acids (6, 14), ketones (9, 10), aldehydes (22), and particularly propionaldehyde (12, 19)) that a molecule electronically excited in one locale may be ruptured preferentially in a closely adjacent locale. For the rupture to occur, an internal conversion of electronic excitation to vibrational energy must occur; the phenomenon is known as predissociation (7). The evidence for propionaldehyde particularly indicates that *nearly all* the energy appears as vibrational energy in the C—C group adjacent to the electronically excited carbonyl. Also, the other evidence must not be neglected. The production of hydrogen atoms and the absence of alkyl radicals in the photolysis of acetic and propionic acids, and the production of alkyl radicals but no hydrogen atoms from aliphatic esters (24), aldehydes, and ketones, all indicate that the internal conversion is highly preferential and that the vibrational energy sufficient for bond rupture appears in a single bond closely adjacent to the locale of the initial electronic excitation.

On such evidence, we may expect that when internal conversion occurs subsequent to electronic excitation (however produced) in radiation chemistry, the resultant vibrational energy will appear in a single bond close to the site of the electronic excitation. If there are two (or more) electronically excited sites in a molecule, it is unlikely that both will internally convert to vibrational excitation at once. We may address our attention then to the single phenomenon. The existence of a second site of electronic excitation is largely without effect on the possible chemical processes.

#### *A possible effect of molecular size on probability of rupture*

What happens after the internal conversion of electronic energy to vibrational energy at a single bond would appear then to depend on the amount of energy converted. If enough energy is converted, the molecule should rupture. We have already seen why it might possibly be that with large molecules the amount of energy in any one electronic excitation may be low even prior to the internal conversion. If it is sufficiently low and if the amount of energy is sufficiently well distributed vibrationally, the internal conversion may simply not lead to rupture at all. We would expect then the total absence of products resultant from rupture. In particular, we might expect that radiolysis of large molecules would produce no free atoms or radicals. Such an extreme conclusion seems far-fetched and certainly in the present state of these speculations unnecessary.

## CONCLUSION

The evident conclusion is that the worst that can happen to an excited molecule—from the point of view of its survival—is an internal conversion process in which a significantly large amount of vibrational energy appears at one bond. Rupture at that point may then occur but the cage effect takes command. If the radicals thus produced are sufficiently large, they recombine while still within each other's spheres of influence. With large molecules the more probable path of decomposition becomes the slow rearrangement mechanism,<sup>8</sup> in which stable molecules are produced in the primary chemical act. Then, in spite of the cage, the reaction is complete. The precise decomposition which does occur will depend on steric and energetic considerations but evidently, of a variety of possible rearrangement processes, one alone may combine simplicity and small energetic requirements and thus, being most favored, yield only a small number of products.

## SUMMARY

In previous papers, it has been shown that the relative amounts of the various products of radiolysis are frequently determined by a matter of mere statistics, i.e., by the frequency of occurrence of the parent grouping in the original molecule. There are notable exceptions to this rule (for example, in the preferential decarboxylation of high-molecular-weight fatty acids). The explanation lies in the fact that most high-molecular-weight substances are liquid or solid. In the liquid state increased molecular size has two effects. It increases the size of the primary products of the decomposition (as well as of the molecules composing the cage) and thus favors conditions for primary recombination (Franck-Rabinowitch effect). Consequently, free-radical decompositions will be decreased in number relative to ultimate-molecule decompositions. With larger molecules the amount of a product of a particular type may exceed by far the amount to be expected on the purely statistical basis. The explanation is that in large molecules ultimate-molecule decompositions become more and more favored and occur preferentially over the lowest energy pass. Another possible effect of increased molecular size is to distribute the excitation energy (either electronic or vibrational) in a greater number of modes of excitation. Such an effect also would increase the probability of deactivation (before rupture or any high-activation-energy process) and thus tend to favor decomposition via a low-energy pass requiring a minimum of rearrangement. Thus, increased molecular size tends to favor one mode of decomposition over a variety of others.

## REFERENCES

- (1) BREGER, I. A.: *J. Phys. Colloid Chem.* **52**, 551 (1948).
- (2) BURTON, M.: *J. Phys. Colloid Chem.* **51**, 611 (1947).
- (3) BURTON, M.: *J. Phys. Colloid Chem.* **51**, 786 (1947).

---

<sup>8</sup> That is, slow in comparison with rupture, which occurs within one vibration period if sufficient vibrational energy is in one bond.

- (4) BURTON, M.: Proceedings of the Canadian Nuclear Chemistry Conference, in press.
- (5) BURTON, M.: J. Phys. Colloid Chem. **52**, 564 (1948).
- (6) BURTON, M.: J. Am. Chem. Soc. **58**, 1645 (1936).
- (7) BURTON, M., AND ROLLEFSON, G. K.: J. Chem. Phys. **6**, 416 (1938).
- (8) EYRING, H., HIRSCHFELDER, J. O., AND TAYLOR, H. S.: J. Chem. Phys. **4**, 479, 570 (1936).
- (9) FELDMAN, M., BURTON, M., RICCI, J. E., AND DAVIS, T. W.: J. Chem. Phys. **13**, 440 (1945).
- (10) FELDMAN, M., RICCI, J. E., AND BURTON, M.: J. Chem. Phys. **10**, 618 (1942).
- (11) FRANCK, J., AND RABINOWITCH, E.: Trans. Faraday Soc. **30**, 120 (1934).
- (12) GARRISON, W. M., AND BURTON, M.: J. Chem. Phys. **10**, 730 (1942).
- (13) Cf. GLOCKLER, G., AND LIND, S. C.: *The Electrochemistry of Gases and Other Dielectrics*, pp. 368 *et seq.* John Wiley and Sons, Inc., New York (1939).
- (14) HENKIN, H., AND BURTON, M.: J. Am. Chem. Soc. **60**, 831 (1938).
- (15) Cf. HIPPLE, J. A., FOX, R. E., AND CONDON, E. U.: Phys. Rev. **69**, 347 (1946).
- (16) HIRSCHFELDER, J. O.: J. Phys. Colloid Chem. **52**, 447 (1948).
- (17) HONIG, R. E.: Science **104**, 27 (1946).
- (18) HONIG, R. E., AND SHEPPARD, C. W.: J. Phys. Chem. **50**, 119 (1946).
- (19) MAY, L., TAYLOR, H. A., AND BURTON, M.: J. Am. Chem. Soc. **63**, 249 (1941).
- (20) NORRISH, R. G. W.: Trans. Faraday Soc. **33**, 1521 (1937).
- (21) NOYES, W. A. JR.: Private communication.
- (22) PEARSON, L. T. G., AND PURCELL, R. H.: J. Chem. Soc. **1935**, 1151.
- (23) ROLLEFSON, G. K., AND BURTON, M.: *Photochemistry and the Mechanism of Chemical Reactions*, pp. 395 *et seq.* Prentice-Hall, Inc., New York (1939).
- (24) ROYAL, J. K., AND ROLLEFSON, G. K.: J. Am. Chem. Soc. **63**, 1521 (1941).
- (25) SCHOEFFLE, C. S., AND FELLOWS, C. H.: Ind. Eng. Chem. **23**, 1396 (1931).
- (26) SHEPPARD, C. W., AND BURTON, V. L.: J. Am. Chem. Soc. **68**, 1636 (1946).
- (27) SHEPPARD, C. W., AND WHITEHEAD, W. L.: Bull. Am. Assoc. Petroleum Geol. **30**, 32 (1946).
- (28) SKINNER, H. A.: Nature **158**, 592 (1946).

## BERYLLIUM FLUORIDE IN WATER AND ETHANOL SOLUTIONS<sup>1</sup>

ROBERT H. LINNELL<sup>2</sup> AND HELMUT M. HAENDLER

*Department of Chemistry, University of New Hampshire, Durham, New Hampshire*

*Received October 28, 1947*

### INTRODUCTION

Early investigations on the preparation and properties of beryllium fluoride were carried out by Lebeau (4, 5). He found that basic residues of varying composition resulted on evaporation of aqueous beryllium fluoride solutions, but that anhydrous fluoride could be prepared by heating the double ammonium beryl-

<sup>1</sup> This work was part of a program of fluoride research supported by a Research Corporation Grant-in-Aid.

<sup>2</sup> Present address: Department of Chemistry, University of Rochester, Rochester, New York.

lithium fluoride. He reported that the fluoride was very soluble in water, only slightly soluble in absolute alcohol, but readily soluble in 90 per cent ethanol. It was also reported that cooling an ethanol solution to  $-23^{\circ}\text{C}$ . produced a white crystalline mass. A summary of this early work is given in Parsons (7).

However, little additional work has been reported. Biltz and Rahlfs (1) give the density of beryllium fluoride as 1.986 g./cc. at  $25^{\circ}\text{C}$ ., and report the formation of a monoamine with ammonia below  $-78.5^{\circ}\text{C}$ . Neumann and Richter (6) report that molten beryllium fluoride is a very poor conductor of electricity. Potentiometric and conductimetric titrations of aqueous solutions of beryllium fluoride and chloride were made by Pritz (9). It was found that the fluoride gave curves markedly different from those of other beryllium salts. There were no sharp breaks in these curves, and the equivalence point could not be detected. This behavior was explained in terms of decreased solubility of beryllium fluoride and the eventual precipitation of a double salt. The nature of this double salt was not made clear.

In connection with a program of research on inorganic fluorides, it seemed advisable to check some of the early work on beryllium fluoride and to obtain additional data on the nature of the compound and its solutions.

#### EQUIPMENT AND MATERIALS

Beryllium fluoride was obtained from the Brush Beryllium Company<sup>3</sup> as lot No. 838. The reported analysis for this sample was:  $\text{BeF}_2$ , about 99.9 per cent; Al, 0.02–0.06 per cent; Fe, 0.01–0.03 per cent; Si, 0.02 per cent. This fluoride was in the form of glassy lumps and was ground to a white powder. A specially constructed "dry-box" was used for handling the fluoride. Air within the box had a water content of less than 1 mg. per liter. Beryllium fluoride was not exposed to the atmosphere more than absolutely necessary and then only on days when the relative humidity was below 35 per cent.

The ethanol used was twice distilled in glass. The water used for the conductivity work had a specific conductance of about  $1 \times 10^{-6}$  mhos/cc.

Electrical conductance was measured in a conventional bridge arrangement, using the following equipment: Leeds and Northrup 441950 bridge and 4750 resistance box; General Radio 813 oscillator, 814-A amplifier, and 219-M capacitor box; Freas-type conductance cells with shiny platinum electrodes.

An oil thermostat at  $25.00^{\circ}\text{C} \pm 0.05^{\circ}$  was used for the conductance work and a similar water thermostat for the solubility work.

pH measurements were made with a glass electrode and a Leeds and Northrup 7661-A1 assembly.

Freezing-point depressions were determined in a cell equipped with a Beckmann thermometer, mechanical stirrer, air jacket, and salt-ice bath.

<sup>3</sup> Address: 3714 Chester Avenue, Cleveland 14, Ohio.

## EXPERIMENTAL

## 1. Analytical

The volumetric method for fluoride of Rowley and Churchill (10) was tried. The results for aqueous beryllium fluoride solutions were poor in precision and gave values much less than the theoretical on samples of the pure fluoride. The reason for this peculiar behavior is not known but may be connected with the formation of stable beryllium fluoro complexes.

A rapid method for the determination of beryllium was developed. This involved conversion of the fluoride to sulfate and weighing in this form. The sulfate has been suggested as a weighing form for beryllium by Taboury (13) and Kolthoff and Sandell (3). Samples of the solutions were weighed into platinum crucibles and slowly evaporated on an air-bath. Solutions containing ethanol were evaporated several times, distilled water being added. The evapo-

TABLE 1  
*Time-solubility data for BeF<sub>2</sub>-H<sub>2</sub>O solutions*

NO.	TIME	CONCENTRATION	$\text{LN} \frac{c_s}{c_s - c_t}$	$k$
	days	moles/liter		days <sup>-1</sup>
1	21	9.72	0.77	0.037
2	38	13.74	1.44	0.038
3	66	16.73	2.65	0.040
4	82	17.08	2.97	0.036

\*  $c_s$  = saturation concentration;  $c_t$  = concentration at time  $t$ .

rations were not carried to dryness, to prevent spattering. An excess of 1:1 sulfuric acid was added, and the samples taken to dryness. A few drops of water were added and the samples taken to dryness and to constant weight at 350°C.  $\text{BeF}_2 = 0.4475 \times \text{BeSO}_4$ . The beryllium fluoride used in these experiments analyzed as 99.7 per cent, 100.2 per cent, 100.3 per cent.

## 2. Beryllium fluoride-ethanol-water systems

A series of water-ethanol solutions was prepared from conductance water and absolute or 95 per cent ethanol. The composition ranged from absolute ethanol to water. Beryllium fluoride was added to these solutions, in Pyrex bottles, the stoppers sealed, and the bottles rotated in the thermostat at 25°C. It was found that the fluoride was very soluble in all the solutions of high water content, but that the solution process was extremely slow. Table 1 gives time-solubility data for beryllium fluoride in water and gives values for the application of the first-order rate equation. Figure 1 illustrates the data and the extrapolated saturation concentration of 18 moles per liter.

Table 2 gives density data for the water solutions, leading to a ratio of 2.17 moles of water per mole of beryllium fluoride at a concentration of 18 moles per liter.

Because of the extremely high solubility of beryllium fluoride in water, small changes in water content of the ethanol solutions would cause large solubility changes. Work on ethanol-water solubilities was discontinued. The solubility of beryllium fluoride in absolute ethanol is small, probably less than 1 g. per liter.

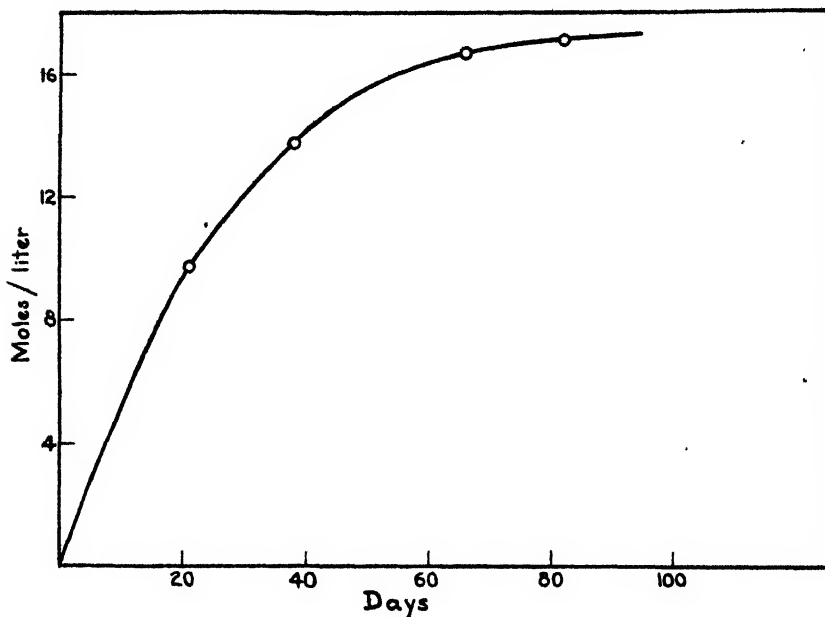


FIG. 1. Solubility of beryllium fluoride in water

TABLE 2  
Density data on  $\text{BeF}_2\text{-H}_2\text{O}$  solutions at  $25^\circ\text{C}$ .

CONCENTRATION	DENSITY	MOLES $\text{H}_2\text{O}$ /MOLE $\text{BeF}_2$
<i>moles/liter</i>	<i>g./ml.</i>	
2.08	1.070	25.9
4.73	1.155	10.9
9.72	1.298	4.80
13.7	1.406	3.08
17.1	1.545	2.41

All of the fluoride-water-ethanol solutions were cooled in a dry-ice bath to as low as  $-72^\circ\text{C}$ . and subjected to mechanical agitation. A beryllium fluoride-95 per cent ethanol solution was refluxed for several hours and cooled to  $-30^\circ\text{C}$ . In no case did crystallization occur.

### 3. Hygroscopicity studies

Beryllium fluoride was stored in platinum crucibles over aqueous solutions with partial pressure of water of 7.3 mm., 10.2 mm., 12.2 mm., and 18.2 mm., at  $25^\circ\text{C}$ .



TABLE 3

*Weight gain of beryllium fluoride at 10.2 mm. partial pressure of water*

TIME	TOTAL MOLES H <sub>2</sub> O/MOLE BeF <sub>2</sub> (1.1736 g. BeF <sub>2</sub> )	TOTAL MOLES H <sub>2</sub> O/MOLE BeF <sub>2</sub> (1.2392 g. BeF <sub>2</sub> )
days		
7.1	0.588	0.612
12.0	0.819	0.852
24.0	1.256	1.309
32.8	1.518	1.567
40.2	1.656	1.689
48.3	1.762	1.778

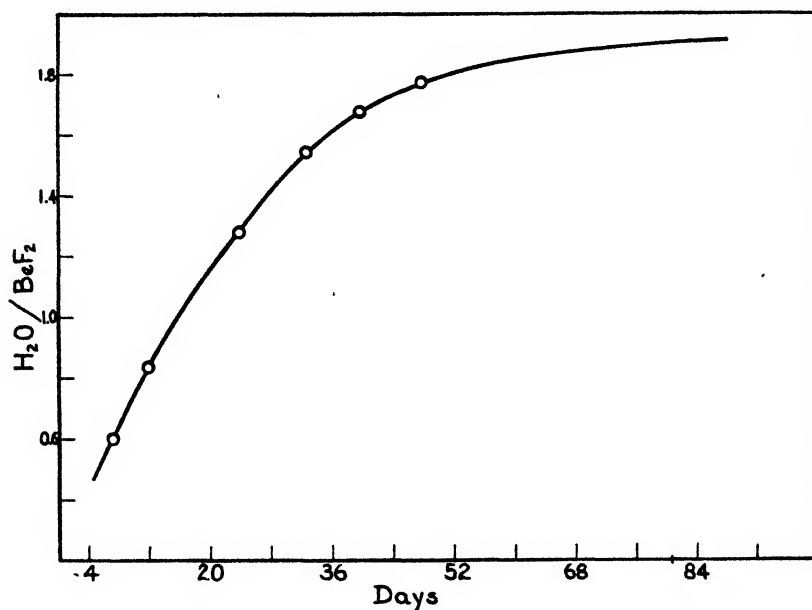


FIG. 2. Weight gain of beryllium fluoride at 10.2 mm. water pressure

TABLE 4

*Summarized hygroscopic data for beryllium fluoride at 25°C.*

PARTIAL PRESSURE OF WATER	LIMITING RATIO OF MOLES H <sub>2</sub> O/MOLE BeF <sub>2</sub>
mm.	
7.32	0.04
10.2	1.94
12.2	2.48
18.2	5.15

The change in weight of these samples was followed as a function of time. At 7.3 mm. there was no significant change in weight. Table 3 and figure 2 give the data for the gain in weight at 10.2 mm.

Data for weight gain over these solutions are summarized in table 4. In all cases the gain in weight was assumed to be due entirely to water.

TABLE 5  
*Conductance of BeF<sub>2</sub>-H<sub>2</sub>O solutions at 25°C.*

CONCENTRATION	(CONCENTRATION) <sup>1/2</sup>	EQUIVALENT CONDUCTANCE
<i>equiv./liter</i>		
1.9876	1.257	3.003
1.1088	1.035	3.206
0.3976	0.7353	4.014
0.2218	0.6053	3.970
0.07950	0.4300	4.486
0.04436	0.3540	4.645
0.01590	0.2515	5.615
0.008870	0.2070	6.260
0.006360	0.1853	7.215
0.003548	0.1527	8.945

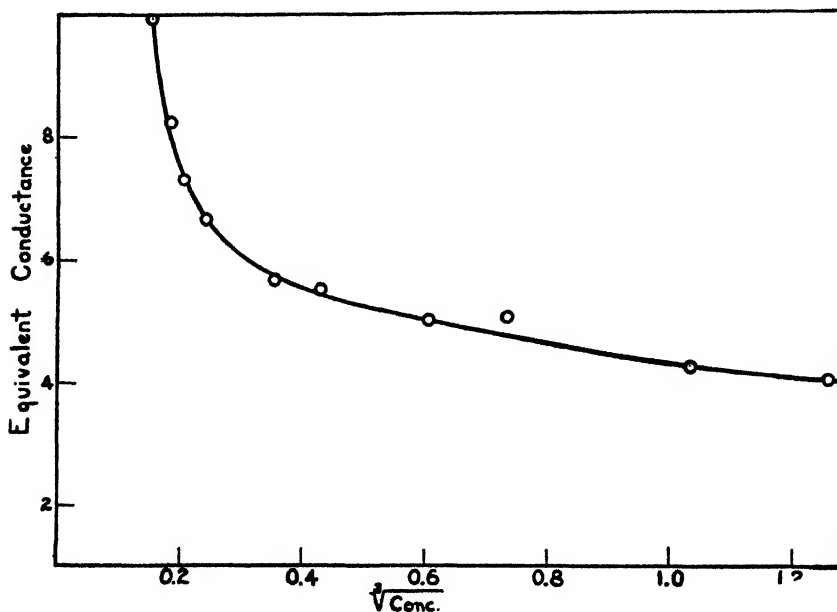


Fig. 3. Conductance of beryllium fluoride solutions

#### 4. Conductance of beryllium fluoride-water solutions

With the conductance equipment available it was found necessary to determine the cell constant as a function of resistance measured. The values of Shedlovsky (11) were used to compute cell constants from a series of potassium chloride solutions. Table 5 gives the conductance of aqueous beryllium fluoride solutions. These values have been corrected for the conductance of the water

used. Since hydrolysis was shown to be small, no hydrolysis correction was made. No viscosity correction was made. Figure 3 gives a graph of this data.

### 5. pH measurements

Table 6 gives pH data for beryllium fluoride–water solutions at 25°C.

### 6. Freezing-point depression

Table 7 lists the freezing-point depression data for aqueous beryllium fluoride solutions.

TABLE 6  
*pH of BeF<sub>2</sub>–H<sub>2</sub>O solutions*

MOLAR CONCENTRATION	pH	$a[\text{H}_2\text{O}^+]$	$\frac{a[\text{H}_2\text{O}^+]}{[\text{BeF}_2]} \times 100$	$\frac{a[\text{H}_2\text{O}^+]^{1/2}}{[\text{BeF}_2]^{1/2}} \times 100$
9.72	2.04	$9.12 \times 10^{-3}$	0.094	0.98
4.73	2.62	$2.40 \times 10^{-3}$	0.050	1.0
3.40	3.02	$9.55 \times 10^{-4}$	0.028	0.91
2.08	3.40	$3.98 \times 10^{-4}$	0.019	0.96
1.29	3.60	$2.51 \times 10^{-4}$	0.019	1.2
1.26	3.65	$2.24 \times 10^{-4}$	0.018	1.2
0.854	4.04	$9.20 \times 10^{-5}$	0.011	1.1
0.756	4.01	$9.77 \times 10^{-5}$	0.013	1.3
0.517	4.30	$5.01 \times 10^{-5}$	0.010	1.4
0.286	4.51	$3.01 \times 10^{-5}$	0.011	1.9
0.135	4.94	$1.15 \times 10^{-5}$	0.008	2.5

TABLE 7  
*Freezing-point depressions of BeF<sub>2</sub>–H<sub>2</sub>O solutions*

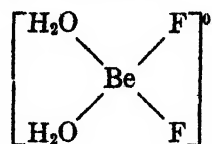
MOLAL CONCENTRATION	FREEZING-POINT DEPRESSION	
	°C.	MOLAL FREEZING-POINT DEPRESSION °C.
0.995	1.892	1.90
0.554	1.042	1.88
0.268	0.518	1.93
0.198	0.382	1.93
0.154	0.304	1.97

### DISCUSSION OF RESULTS

Beryllium has a strong tendency to assume a coördination number of four. Soluble beryllium salts usually have four molecules of water of hydration. The tendency of the beryllium atom to exist in the covalent state is shown by the stability and non-ionic behavior of such compounds as basic beryllium acetate and beryllium oxalate (12).

The experimental data indicate that the limiting solubility of beryllium fluoride in water at 25°C. is that corresponding to the ratio of 2 moles of water per mole

of fluoride. This would give the beryllium the stable covalency of four with the formation of the relatively stable complex:



In solutions more dilute than this saturation value there would be ionization, with the production of aquoberyllium and aquofluoroberyllium ions. The extremely low values for the equivalent conductance and the small molal freezing-point depressions indicate weak electrolyte behavior. Although literature values for the limiting conductance of fluoride and beryllium ions are not very consistent, a value of 144 can be estimated as the limiting conductance of beryllium fluoride. With this value, the ionization of the fluoride can be estimated, for various concentrations, as 2 per cent at 1 molar (in agreement with freezing-point estimates) and 6 per cent at 0.002 molar.

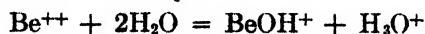
This concept can also explain the low solubility rate of beryllium fluoride in water. Experimentally, the solutions near saturation were clear, viscous, and almost jelly-like. It suggests that on dissolving in water a layer of  $[(\text{H}_2\text{O})_2\text{BeF}_2]$  forms on the surface of the solid. This concentrated layer diffuses into the solution at a slow rate because of its high viscosity. The constant value for the first-order rate equation is evidence that a diffusion process is involved.

Evaporation of beryllium fluoride-water solutions leads to formation of basic residues and elimination of hydrogen fluoride. Thomas and Miller (14) explain cationic basic beryllium hydrosols by applying Werner-Pfeiffer ideas of hydrolysis. Similarly, beryllium fluoride can be pictured as ionizing to form hydronium ions, fluoride ions, and basic aquofluoro complexes.

The hydrolysis data agree qualitatively with those of Pritz (8) and Bjerrum (2) obtained for other beryllium salts. The expression

$$\frac{a[\text{H}_3\text{O}^+]}{[\text{BeF}_2]} \times 100$$

is a measure of the extent of hydrolysis if this reaction can be represented as:



It is apparent from the data that the hydrolysis of the fluoride is not represented by such a simple expression. For the hydrolysis reaction



the expression

$$\frac{a[\text{H}_3\text{O}^+]^{1/2}}{[\text{BeF}_2]} \times 100$$

would be a measure of the hydrolysis. These values agree with the qualitative assumption that the hydrolysis increases with decreased concentration of fluoride.

## SUMMARY

Beryllium fluoride is very soluble in water, the limiting solubility at 25°C. being  $\text{BeF}_2 \cdot 2\text{H}_2\text{O}$ . The rate of solution is low and follows the first-order rate equation, for which  $k$  has a value of  $0.038 \text{ days}^{-1}$ . This indicates a diffusion process.

Beryllium fluoride acts as a weak electrolyte in aqueous solution. The ionization is about 2 per cent for a 1 molar solution and 6 per cent for a 0.002 molar solution. This concept is confirmed by both conductance and freezing-point data.

Aqueous solutions of beryllium fluoride are weakly hydrolyzed, of the order of 0.01–1 per cent. No simple hydrolysis expression will explain the observed pH values.

There is no evidence to suggest that a compound is formed between beryllium fluoride and ethanol. The solubility of beryllium fluoride in absolute ethanol is small but is very sensitive to traces of water present.

## REFERENCES

- (1) BILTZ AND RAHLFS: *Z. anorg. Chem.* **166**, 351 (1927).
- (2) BJERRUM: *Metal Ammine Formation in Aqueous Solution*, p. 176. P. Haase and Son, Copenhagen (1941).
- (3) KOLTHOFF AND SANDELL: *J. Am. Chem. Soc.* **50**, 1903 (1928).
- (4) LEBEAU: *Chem. News* **77**, 288 (1898).
- (5) LEBEAU: *Ann. chim. phys.* [7] **16**, 457 (1899).
- (6) NEUMANN AND RICHTER: *Z. Elektrochem.* **31**, 484 (1925).
- (7) PARSONS: *The Chemistry and Literature of Beryllium*, p. 18. The Chemical Publishing Co., Easton, Pennsylvania (1909).
- (8) PRITZ: *Z. anorg. Chem.* **180**, 355 (1929); **197**, 103 (1931).
- (9) PRITZ: *Z. anorg. Chem.* **231**, 238 (1937).
- (10) ROWLEY AND CHURCHILL: *Ind. Eng. Chem., Anal. Ed.* **9**, 551 (1937).
- (11) SHEDLOVSKY: *J. Am. Chem. Soc.* **54**, 1424 (1932).
- (12) SIDGWICK AND LEWIS: *J. Chem. Soc.* **1926**, 1297.
- (13) TABOURY: *Compt. rend.* **159**, 180 (1913).
- (14) THOMAS AND MILLER: *J. Am. Chem. Soc.* **58**, 2526 (1936).

THE EFFECT OF TEMPERATURE AND IMPURITIES ON CERTAIN  
PHOTOCHEMICAL REACTIONS IN SOLIDSC. F. GOODEVE AND M. R. TAYLOR<sup>1</sup>*University College, London**Received September 29, 1947*

## INTRODUCTION

Certain oxides of metals are affected by light; for example, when antimony oxide is exposed to light of a wave length less than its absorption threshold it darkens, with the production of what is believed to be antimony metal (3). Titanium dioxide, on the other hand, has been shown by Goodeve and Kitchener (5) to be stable itself to light but to sensitize the bleaching of an organic dye, Chlorazol Sky Blue FF, which had been deposited upon it, the reaction having a quantum efficiency of  $4 \times 10^{-3}$  when bleaching is brought about by light of a wave length in the absorption region of titanium dioxide. When exposed by itself, or on the surface of some non-absorbing material such as barium sulfate, the dye is stable to light.

Although Goodeve and Kitchener noted that temperature affected the rate of the reaction, neither in the case of the bleaching of the dye, nor in the decomposition of antimony oxide, has the effect of temperature been carefully studied. The work of Hilsch and Pohl on the photolysis of the alkali halides has included the effects of temperature on the decomposition of KH and KD in potassium bromide (6), and they found that the quantum yield dropped from unity at 500°C. to almost zero at -100°C.

The sensitivity of the photographic process is known to be considerably decreased at the temperature of liquid air (1), and some observations on some organic solids (7, 10) have shown that the photochemical reaction rate is increased as the temperature is raised. Apart from these exceptions, little is known of the effect of temperature on photochemical reactions of solids.

This report gives the methods and results of an investigation undertaken to determine the effect of temperature upon the darkening of antimony oxide and upon the bleaching of a dye deposited upon titanium dioxide. The results are put forward without discussion.<sup>2</sup>

## MATERIALS

One sample (H & W) of the antimony oxide used was a commercially pure, stock reagent as supplied by Messrs. Hopkins and Williams. It was of a slight brown tinge and its x-ray pattern showed it to be the orthorhombic form of antimony oxide, valentinite. Another sample (Pr) of valentinite was prepared by adding crushed crystals of antimony chloride to boiling aqueous ammonia, filter-

<sup>1</sup> Formerly at the Sir William Ramsay and Ralph Forster Laboratories of Chemistry, University College, London.

<sup>2</sup> This work is described in more detail in the Ph.D. thesis of M. R. Taylor, University of London, 1946.

ing, washing, and drying. This sample (Pr) was whiter, and much less sensitive to light, having a reflection of 97 per cent over the whole visible spectrum as against 79 per cent for the sample (H & W). The absorption and photochemical threshold of these two samples were determined and found to agree with those reported by Cohn and Goodeve (3).

The dyed titanium dioxide was prepared as follows: Pure titanium tetrachloride was dissolved in a large volume of water and boiled for half an hour, when titanium dioxide began to precipitate in a semicolloidal form. While still at 100°C. the solution was slowly neutralized with ammonia to cause coagulation. This titanium dioxide was washed, and the wet precipitate was dyed by adding a

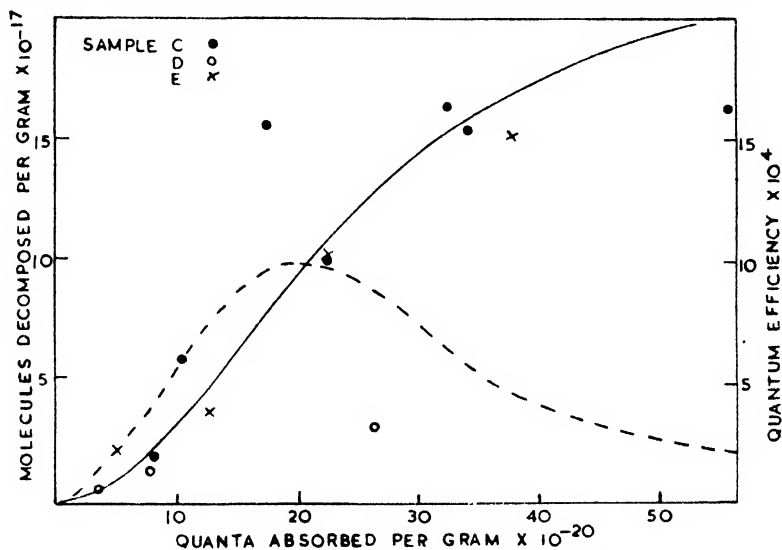


FIG. 1. The progress of the photodecomposition of a dye on titanium dioxide. Sample C, 1.87 per cent dye by weight, sample D, 0.38 per cent dye by weight; sample E, 0.57 per cent dye by weight. Broken line, the quantum efficiency deduced from the mean (solid) curve.

c solution of Chlorazol Sky Blue dissolved in alcohol, and then an excess of barium chloride. The dyed suspension was then washed, filtered, dried, ground, and sieved. One sample (E) was digested for 24 hr. at 80°C. prior to being washed etc. The dyed powders were light blue, were sensitive to light, and possessed a photochemical threshold and absorption corresponding to that determined by Goodeve and Kitchener for powders prepared in a similar manner.

An independent check of the determination of the quantum efficiency of bleaching was made using the previous procedure (5), but the concentration of the dye was varied over a wider range. The results of the quantum efficiency of bleaching are shown in figure 1. The quantum efficiency curve follows the same trend as found by Goodeve and Kitchener, falling off at long exposures to a constant value, although the maximum value obtained was  $1 \times 10^{-3}$  as against  $4 \times 10^{-3}$  obtained by them.

DETERMINATION OF THE EFFECT OF TEMPERATURE ON THE  
PHOTOCHEMICAL REACTION

The method used for the determination of quantum efficiencies was not suitable for studying the effect of temperature and two new comparative methods were devised. These are based on the bleaching or darkening of the surface of a simple static layer of the material as distinct from a change in a continuously mixed sample. It is not considered that the relation between the extent of the surface bleaching or darkening and the amount of photochemical change is a linear or even a known one; indeed, a comparison between the results given later in figure 5 and those in figure 1 shows that the relation is complex. It is, however, assumed that two static samples showing the same change in shade have undergone the same amount of chemical change. In other words, it is assumed that the penetration of photochemical activity is the same in two such samples.

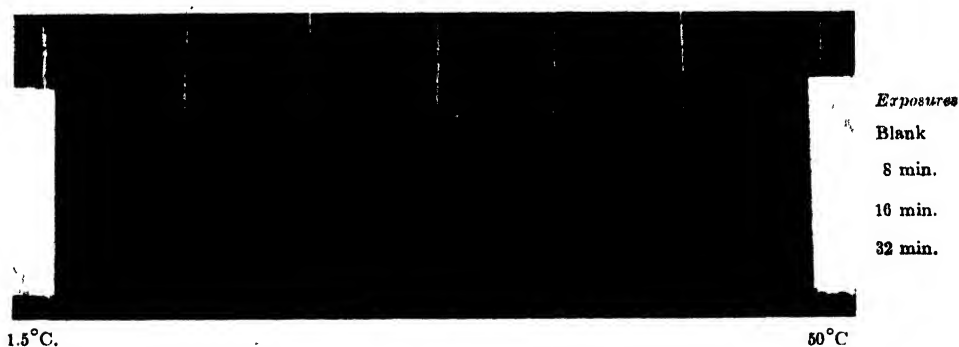


FIG. 2. The photochemical bleaching of a strip of titanium dioxide-dye powder over a range of temperatures.

In the first of the two methods the sample to be tested was deposited as a thin film of powder by allowing a water suspension to evaporate to dryness on to a metal bar 4 in. long and 1 in. wide. One end of the bar was cooled, and the other end heated, and the temperature was measured at intervals along the bar by means of thermocouples. It was found that when the powder was placed on a copper bar the bleaching was strongly inhibited by traces of metallic salts. By coating the bar with a thin layer of polymerized methyl methacrylate, known to be innocuous, this effect was avoided.

The film was exposed in three longitudinal strips which were given different exposures, together with a blank strip; the whole was then photographed. An example is shown in figure 2 for dyed titanium dioxide. The positions of the thermocouples are shown by the vertical white lines. Microphotometer tracings were made along each strip, and from these it was hoped to obtain quantitative comparisons. It was found, however, that although this method was capable of indicating immediately if the photochemical reaction rate was affected by temperature, the accuracy was too poor for quantitative measurements.

In the second method the powder was exposed in the apparatus as shown in



figure 3A. The powder was placed as a smooth film about 0.5 mm. thick on a glass disc D, 1 in. in diameter. The whole system was rigidly mounted in position. The tube T containing the sample was  $1\frac{1}{4}$  in. in diameter and 8 in. long. It could be sealed at the top by an optically plane quartz plate, and a side arm permitted its evacuation. The tube was so mounted that, when swung into position, it could be immersed in a cooling mixture, or in a thermostat at the desired temperature. A duplicate tube ( $T_1$ ), in which the position of the sample was occupied by a thermopile, could be swung into exactly the same position to check the constancy of incident light. The light source was a quartz mercury arc

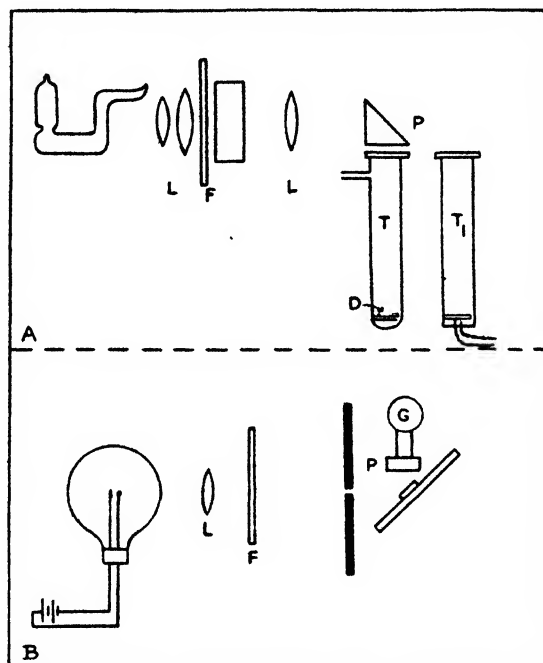


FIG. 3. Apparatus for exposure of samples and measurement of reflection

of the high-pressure type, run in a vertical position and fed from a constant D.C. source. The light from this was focussed by means of quartz lenses (L) on to a quartz  $45^\circ$  prism which reflected the light down the tube and on to the sample.

The inner walls of the tube were coated with dead-black paint to avoid reflection. A cell containing a 1 per cent solution of cupric sulfate (plus a Woods glass filter in the case where the titanium dioxide-dye system was being bleached) was placed at F. In the normal procedure the samples were lowered to the bottom of the tube in a fitted holder and allowed to stand for 1 hr. to come to equilibrium temperature before exposure was made. All the exposures of antimony oxide were carried out in vacuum to prevent condensation on the sample during long exposures at low temperatures. These conditions should not influence the experiment, it having been shown (3) that the darkening of antimony

oxide is not affected by drying in vacuum for at least 24 hr. With dyed titanium dioxide, however, the bleaching is dependent upon the immediate presence of moisture and all the exposures were made under atmospheric pressure. The majority of the exposures with dyed titanium dioxide were made above 0°C., but during a few exposures at -60°C. little condensation was apparent.

The arrangement for comparing the amount of bleaching is shown in figure 3B. The method is based on measurements of the diffuse reflecting power of the sample after exposure. The light source was a tungsten filament Point-O-Lite lamp, which was run from batteries and was focussed by a lens (L) to a parallel beam. A diaphragm allowed a small beam of light to fall on to the sample, which was placed at an angle of 45° to the light source. A copper oxide photocell (P) was placed close to the sample and at an angle of 45° to it and 90° to the light source. The photocell was screened from any direct light from the lamp. The samples were mounted by simply gluing the glass disc to a stiff section of cardboard, and they could be clipped into position without disturbing the rest of the apparatus, which was rigidly fixed. The photocell was connected directly to a sensitive galvanometer and its deflection read directly from a scale. The reflections of the various samples were referred to an absolute standard,—namely, smoked magnesium oxide, which has been found to have a constant reflecting power down to 254  $\mu$ . Its absolute reflecting power has been determined (8, 11) and has been taken as 97 per cent over the range measured in these experiments.

#### RESULTS

The effect of temperature on the photochemical darkening of antimony oxide and the bleaching of dyed titanium oxide was investigated, using the procedure described above. The percentage reflection changes of antimony oxide (H & W) for a series of exposures at temperatures of 50°, 0°, -20°, -50°, and -78°C. are shown graphically in figure 4, as well as a few observations on samples (Pr) at 50°C. The curve obtained with (Pr) is similar to that of (H & W), but the former is much less sensitive.

The results for the bleaching of the dyed titanium dioxide powder for a series of exposures at 50°, 30°, 10°, and 0°C. are shown in figure 5. Some exposures were made at -60°C. and showed no measurable bleaching after some hours. The preliminary experiments with the powder spread along a bar had shown that there was negligible thermal bleaching up to 50°C.

In both the bleaching of dyed titanium oxide and the darkening of antimony oxide the percentage reflection approaches a constant value at long exposures. The reaction rate,  $R$ , is taken as the slope of the curves in figures 4 and 5 in the units given, and the relation between  $\log R$  and  $1/T$  is plotted in figure 6. In the case of the dyed titanium dioxide system, the relation between bleaching and time was, except for the very long exposure, effectively linear (figure 5),  $R$  therefore being a constant for each temperature. With antimony oxide however, the relation was not linear; accordingly,  $R$  has been taken as the slope of the darkening curves at points corresponding to both 60 per cent and 70 per cent reflection, giving the other two curves shown in figure 6. It will be seen that all three curves

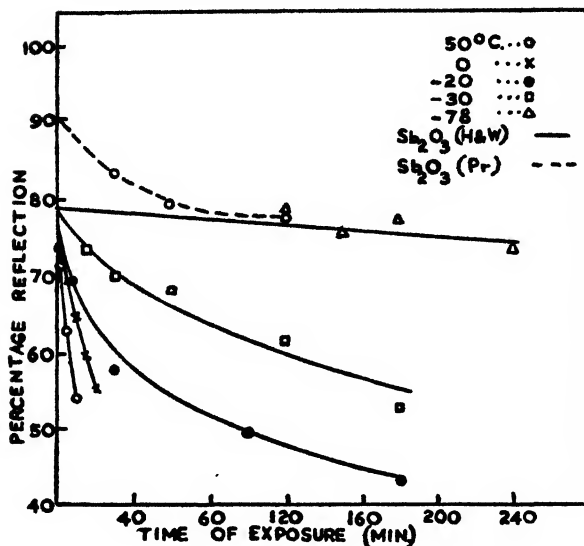


FIG. 4. The effect of exposure at different temperatures on the reflection of antimony oxide, referred to whiteness of smoked magnesium oxide.

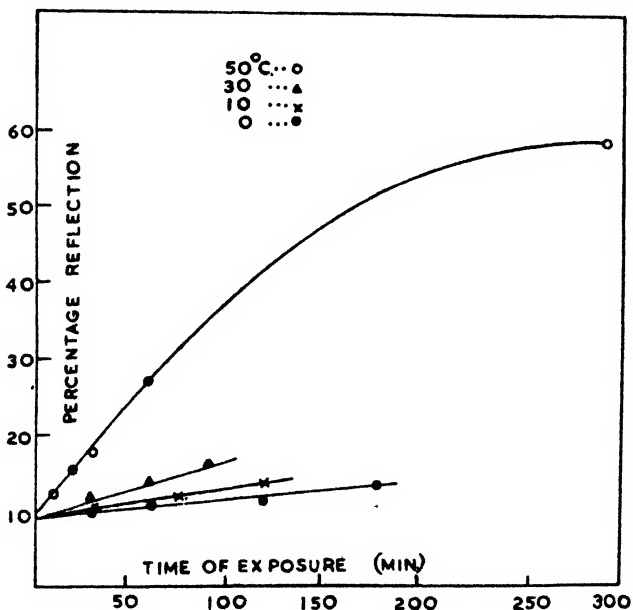


FIG. 5. The effect of exposure at different temperatures on the reflection of dyed titanium dioxide, referred to whiteness of smoked magnesium oxide.

are approximately linear, showing that the energy of activation is independent of the temperature. In the case of antimony oxide the parallelism of the two curves indicates that the energy of activation is independent of the percentage reaction

over the range measured. The numerical values of the energy of activation as calculated from the slopes of these curves are 5.5 kg.-cal. per mole for the darkening of antimony oxide and 8.2 kg.-cal. for the bleaching of dyed titanium dioxide. A calculation from the results of Hilsch and Pohl, and of Padoa, give values of about 2, and 1-10, kg.-cal. for the energies of activation for the decomposition of KH in potassium bromide and of certain organic reactions, respectively.

The temperature coefficients for the reactions studied here are higher than the coefficient for the photographic process. Results of various workers (1, 2, 9) are consistent and give a value of the energy of activation around 0.7 for the temperature interval from room temperature to the temperature of liquid air.

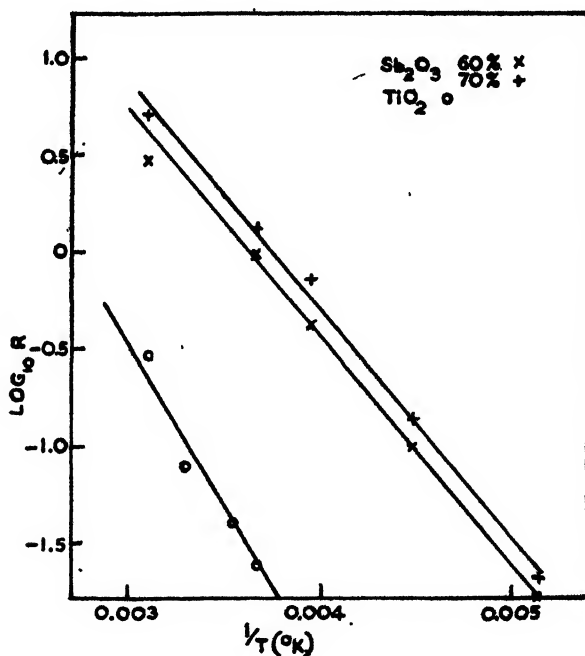


FIG. 6. The effect of temperature on the photochemical reaction rate of antimony oxide and dyed titanium dioxide.

The temperature-dependent reaction in this case is considered to be the ionic conduction, following the quantum absorption and photoconduction processes.

#### THE EFFECT OF THE ADDITION OF IMPURITIES UPON THE BLEACHING OF DYED TITANIUM DIOXIDE

During the exposure of dyed titanium dioxide on a metal bar it was noted that traces of metallic salts had a very strong inhibiting effect upon the photochemical bleaching. Cohn (4) has pointed out that in most photochemical reactions of solids it is apparently necessary to have moisture present and that certain other agents tend to increase the reaction rate. The necessity of moisture is known

for the photochemical reactions of zinc sulfide, silver salts, cadmium iodide, cadmium bromide, and antimony oxide, and these reactions are sensitive to the presence of impurities.

Some qualitative experiments were made to investigate this effect as applied to dyed titanium dioxide. To a water suspension of the powder a small amount of the reagent was added and, after being allowed to dry, the sample was exposed with a blank and comparisons made. It was found that:

- (a) Bleaching was increased by the presence of mercurous chloride, lead sulfate, antimony chloride, thorium hydroxide, and barium hydroxide in ascending order of effectiveness.
- (b) Bleaching was inhibited by cadmium chloride, copper sulfate, magnesium sulfate, aluminum chloride, and zinc sulfate, in ascending order of effectiveness.
- (c) The addition of potassium hydroxide and sodium hydroxide tended to remove the dye from the surface of the titanium dioxide, and appeared usually to increase the bleaching. The addition of sulfuric acid and hydrochloric acid inhibited the reaction slightly.
- (d) In general, acidic materials tend to decrease and basic materials increase the bleaching, although the maximum effect was shown by metallic salts rather than acids or bases.
- (e) The effectiveness of the impurity in inhibiting or increasing bleaching increases as the concentration of the impurity is increased, although it was found that a concentration as low as four molecules of copper to one of dye was sufficient to keep the powder stable to 15 min. exposure, while a pure sample was completely bleached in 2 min.
- (f) The effect of moisture on the bleaching was tested by exposing samples in a vacuum, in the presence of water vapor with air excluded, and in the presence of air and moisture. The sample exposed in a vacuum did not bleach but both of the other samples bleached readily.
- (g) Thermal bleaching, which takes place above 100°C., was found to be dependent upon the presence of moisture.

#### SUMMARY

It has been shown that the photochemical bleaching of a dye, Chlorazol Sky Blue FF, deposited upon the surface of titanium dioxide is greatly increased by an increase in temperature, the reaction having an activation energy of about 8.2 kg.-cal.

The darkening of antimony oxide when exposed to light is also affected by an increase in temperature, the activation energy being about 5.5 kg.-cal. The energy of activation for both these systems is independent of the temperature over the range measured.

The bleaching of the dye on titanium dioxide is considerably influenced by the presence of small quantities of metallic salts, and neither the photochemical nor the thermal bleaching will proceed in the absence of moisture.

The authors are indebted to Professor A. J. Allmand of King's College, London, for the use of laboratory facilities during the war-time evacuation of University College.

#### REFERENCES

- (1) BERG: *Trans. Faraday Soc.* **35**, 445 (1939).
- (2) BERG AND MENDELSON: *Proc. Roy. Soc. (London)* **168**, 168 (1938).
- (3) COHN AND GOODEVE: *Trans. Faraday Soc.* **36**, 433 (1940).
- (4) COHN AND HEDVAL: *J. Phys. Chem.* **47**, 603 (1943).
- (5) GOODEVE AND KITCHENER: *Trans. Faraday Soc.* **34**, 570 (1938).
- (6) HILSCH AND POHL: *Trans. Faraday Soc.* **34**, 883 (1938).
- (7) PADOA: *Atti accad. Lincei*, 1909-1916.
- (8) PRESTON: *J. Optical Soc. Am.* **31**, 15 (1930).
- (9) SHEPPARD, WIGHTMAN, AND QUIRK: *J. Phys. Chem.* **38**, 817 (1934).
- (10) STOBBE: *Ber.* **40**, 3372 (1907).
- (11) TAYLOR: *J. Optical Soc. Am.* **24**, 192 (1934).

## STUDIES ON THE AGING OF PRECIPITATES AND COPRECIPITATION. XL

### THE SOLUBILITY OF LEAD CHROMATE AS A FUNCTION OF THE PARTICLE SIZE<sup>1</sup>

D. R. MAY<sup>2</sup> AND I. M. KOLTHOFF

*School of Chemistry, University of Minnesota, Minneapolis 14, Minnesota*

*Received October 23, 1947*

#### INTRODUCTION

Willard Gibbs (10) in 1878 was the first to relate the particle size of a solid to its solubility. Ostwald (20) somewhat later derived an expression which was improved by Freundlich (8) and which is generally known as the Ostwald-Freundlich equation. According to this equation the solubility of a solid is a function of its particle size:

$$\frac{RT}{M} \ln \frac{S_r}{S} = \frac{2\sigma}{rd} \quad (1)$$

where  $R$  is the gas constant,  $T$  the absolute temperature,  $S$  and  $S_r$  the solubility of large solid particles and of particles having small radii  $r$ , and  $M$ ,  $\sigma$ , and  $d$  are the molecular weight, surface tension, and density of the solid.

The Ostwald-Freundlich equation does not take into account the possible ionic

<sup>1</sup> From a thesis submitted by D. R. May to the Graduate School of the University of Minnesota in partial fulfillment of the requirements for the degree of Doctor of Philosophy July, 1944.

<sup>2</sup> Present address: American Cyanamid Company, Stamford, Connecticut.

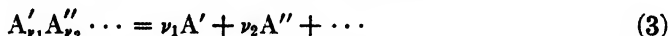
dissociation of the solid in solution. To correct this, Dundon (6) in 1923 introduced van't Hoff's number  $i$ .

$$i \frac{RT}{M} \ln \frac{S_r}{S} = \frac{2\sigma}{rd} \quad (2)$$

On the basis of thermodynamics a slightly different expression is derived.

In a heterogeneous system such as that of a slightly soluble solid suspended in water, the region between the solid and liquid phases has a different composition from either the solid or the liquid phase. This region, having a small but finite thickness of the order of several molecular diameters, is described as the surface phase. Thus three phases must be considered: the solid phase  $\alpha$ , the liquid phase  $\beta$ , and the surface phase  $s$ .

Consider a system made up of a solid substance in equilibrium with its saturated solution. If the dissolved substance is a strong electrolyte, then the dissolution of the solid may be represented by the equation



where  $A'_1, A''_2 \cdots$  represent the ionizing atoms or radicals of the substance and  $\nu_1, \nu_2 \cdots$  represent the number of atoms or radicals involved. At equilibrium

$$\sum \nu_i \mu_i = 0 \quad (4)$$

where  $\mu_i$  is the chemical potential of the  $i^{\text{th}}$  constituent. At equilibrium the chemical potentials of a given constituent in the solid, surface, and solution phases are all equal. Thus

$$\mu^s = \nu_1 \mu_1^s + \nu_2 \mu_2^s + \cdots \quad (5)$$

where  $\mu^s$  is the chemical potential assigned to the surface phase, and  $\mu_1^s, \mu_2^s \dots$  are the chemical potentials of the ionizing atoms or radicals in the solution phase.

The right-hand side of equation 5 is evaluated from the equation for a constituent ion in solution

$$\mu_i^s = \mu_{0,i}^s + RT \ln a_i \quad (6)$$

where  $\mu_i^s$  is the chemical potential of the  $i^{\text{th}}$  constituent ion,  $\mu_{0,i}^s$  is a constant depending upon the substance, the temperature, and the pressure,  $R$  is the gas constant,  $T$  is the absolute temperature, and  $a_i$  is the activity of the  $i^{\text{th}}$  constituent. Substituting equation 6 into equation 5:

$$\mu^s = \mu_0^s + RT \ln a_1 a_2 \cdots \quad (7)$$

Since the activity product,  $K$ , is represented by

$$K = a_1^{\nu_1} a_2^{\nu_2}$$

equation 7 may be written as:

$$\mu^s = \mu_0^s + RT \ln K \quad (8)$$

The chemical potential of the surface phase,  $\mu^s$ , in terms of surface tension is not so readily evaluated. Thermodynamically an expression may be derived

for the chemical potential based upon the surface work function. However, for the complete evaluation of  $\mu^s$  the treatment must be extended to include the energy supplied by the charges known to exist in the solid-liquid interface.

At constant temperature and composition of the surface phase when only the work function is considered,

$$dF^s = \sigma dA^s \quad (9)$$

where  $dF^s$  is an infinitesimal change in the free energy assigned to the surface phase,  $\sigma$  is the surface tension, and  $dA^s$  is an infinitesimal change in the surface area. The chemical potential of the surface phase at a given temperature and pressure is equal to a constant,  $\mu_0^s$ , characteristic of the constituent in the surface phase plus the partial derivative of  $dF^s$  with respect to the number of moles,  $n$ , keeping the other constituents constant.

$$\mu^s = \mu_0^s + \sigma \frac{\partial A^s}{\partial n} \quad (10)$$

The term  $\partial A^s / \partial n$  can be evaluated if the substance is considered to be divided into spherical particles of radius  $r$ . The surface area of a single particle is then:

$$A^s = 4\pi r^2 \quad (11)$$

Differentiating with respect to  $n$ :

$$\frac{dA^s}{dn} = 8\pi r \frac{dr}{dn} \quad (12)$$

The volume of the solid substance is equal to the number  $n$  of moles of the substance times the molar volume. Thus

$$n \frac{M}{d} = \frac{4}{3} \pi r^3 \quad (13)$$

where  $M$  is the molecular weight and  $d$  is the density of the substance. Differentiating equation 13

$$\frac{dr}{dn} = \frac{M}{4\pi r^2 d} \quad (14)$$

and substituting into equation 12

$$\frac{dA^s}{dn} = \frac{2M}{rd} \quad (15)$$

equation 10 becomes:

$$\mu^s = \mu_0^s + \frac{2\sigma M}{rd} \quad (16)$$

In view of equation 16, equation 8 becomes

$$\mu_0^s + \frac{2\sigma M}{rd} = \mu_0^b + RT \ln K \quad (17)$$



Consider two systems which differ in that the particles have different radii,  $r_1$  and  $r_2$ , and corresponding activity products,  $K_1$  and  $K_2$ . It follows from equation 17 that

$$RT \ln \frac{K_2}{K_1} = \frac{2\sigma M}{d} \left( \frac{1}{r_2} - \frac{1}{r_1} \right) \quad (18)$$

Equation 18 may be simplified by letting  $r_1$  be the radius of particles of macro size. Therefore,  $K_1$  would be the normal activity product  $K$ . Let  $K_2$  and  $r_2$  be the activity product and radius of a finely divided substance and represented by  $K_r$  and  $r$ . Thus  $1/r_1$  will be very small as compared to  $1/r_2$  and equation 18 may be written as:

$$\frac{RT}{M} \ln \frac{K_r}{K} = \frac{2\sigma}{rd} \quad (19)$$

Equation 19, derived above, does not take into consideration the surface energy derived from the electrical charge on the surface of the particles. W. C. M. Lewis (17) and Knapp (14) suggested that electrical charges would decrease the solubility, and Knapp extended the Ostwald-Freundlich equation to include an expression for the electrical charges. His general development can be adapted to the derivation above and an expression involving the activity products obtained (in place of solubilities as in Knapp's derivation).

According to Helmholtz's theory there is an electrical "double layer" at the solid-liquid interface. The surface of the particle is charged by an excess of either positive or negative ions and is surrounded by the oppositely charged ions which lie at a fixed distance from the surface. If each particle is regarded as a rigid double-layer condenser, its electrical energy, which is also the free energy due to the electrical forces, is given by the expression

$$F_e = \frac{q^2\delta}{2Dr(r+\delta)} \quad (20)$$

where  $q$  is the electrical charge on each layer,  $\delta$  is the distance between layers,  $D$  is the dielectric constant of the medium, and  $r$  is the radius of the particle. The distance between layers is small compared to the radius  $r$ . Thus equation 20 may be written as:

$$F_e = \frac{q^2\delta}{2Dr^2} \quad (21)$$

If the free energy due to electrical forces as well as the free energy due to the surface work function is included in the total free energy, in place of equation 10, the chemical potential of the surface phase is expressed as:

$$\mu^s = \mu_0^s + \sigma \frac{\partial A^s}{\partial n} + \frac{\partial F_e}{\partial n} \quad (22)$$

Differentiating equation 21 with respect to  $n$ :

$$\frac{\partial F_e}{\partial n} = - \frac{q^2\delta}{Dr^3} \frac{dr}{dn} \quad (23)$$

In view of equation 14

$$\frac{\partial F_e}{\partial n} = - \frac{q^2 \delta M}{4\pi D d r^5} \quad (24)$$

Combining equations 8, 15, 22, and 24

$$\mu_0^s + \frac{2\sigma M}{rd} - \frac{q^2 \delta M}{4\pi D d r^5} = \mu_0^s + RT \ln K \quad (25)$$

and

$$\frac{RT}{M} \ln \frac{K_2}{K_1} = \frac{2\sigma}{d} \left( \frac{1}{r_2} - \frac{1}{r_1} \right) - \frac{q^2 \delta}{4\pi D d} \left( \frac{1}{r_2^5} - \frac{1}{r_1^5} \right) \quad (26)$$

or, where  $r_2$  is much smaller than  $r_1$ ,

$$\frac{RT}{M} \ln \frac{K_r}{K} = \frac{2\sigma}{rd} - \frac{q^2 \delta}{4\pi D d r^5} \quad (27)$$

Equation 27 is essentially the equation developed by Knapp (14). It differs from Knapp's equation only in that the activity products  $K_r$  and  $K$  are used in place of the solubilities  $S_r$  and  $S$ .

On a purely theoretical basis, the solubility would increase exponentially with decreasing particle size on the basis of the Ostwald-Freundlich equation. But the Knapp equation predicts that the solubility increase with decreasing particle size would be lessened by the electrical charge and that for very small particles the solubility would approach zero.

The relation between particle size and solubility is undoubtedly influenced by factors other than the surface work function and the simple electrical picture developed above. Recently, Harbury (11) has suggested the substitution of  $\sigma'$  in equation 2 as a "catch-all" for all corrections. The theoretical soundness of this substitution of a variable  $\sigma$  is questioned, but empirically it has some advantages over the original equation.

A number of measurements of the relative solubilities of large and small particles has been made. The method used by investigators for the determination of the differences in solubility was generally that of conductimetric measurements. A pure crystalline substance ground to a fine powder showed a higher conductance than the coarse unground powder.

Ostwald (20) and Hulett (12) in 1901 were the first to make measurements of this kind. According to Hulett's findings, admittedly semiquantitative, the solubility of gypsum ( $\text{CaSO}_4 \cdot 2\text{H}_2\text{O}$ ) could be increased 20 per cent and of barium sulfate 80 per cent by grinding to particle size diameters of 0.1 micron. Mercuric oxide when ground also exhibited greater solubility. Later, Dundon and Mack (6) measured the increase in solubility due to particle size for a number of substances. Calculations of the surface tension were made from measurements of particle size and solubility, using equation 1. A qualitative correlation was found between the calculated surface tension and the hardness.

Hulett's and Dundon's results agreed closely in the case of barium sulfate, but not in that of gypsum. A plausible explanation was given by Dundon. In

the latter's experiments precautions were taken to prevent the dehydration of gypsum by grinding. The dehydrating effect of grinding had been known and was shown by Dundon to reduce the water content from 20.93 per cent (theoretical value) to 12 per cent or less, depending upon other conditions. Since it was well known (18) that anhydrous calcium sulfate is more soluble than the dihydrate, the presence of partially dehydrated gypsum was probably the reason for Hulett's higher solubility.

The results of Hulett and Dundon were more critically examined by Balarew (1). He also found a higher conductance with finely ground barium sulfate than with a coarse product. The conductance of ground powder, high at first, rapidly decreased to values approximating that of a coarse unground powder. The same results were observed when a drop of barium chloride solution was added to a solution saturated with coarse barium sulfate: the conductance, high immediately after adding the barium chloride, decreased rapidly to a value very nearly equal to the conductance before the addition. The implication of this observation is that grinding might expose impurities in the coarse powder (such as barium chloride) which would give rise to a higher conductance. After standing a while the barium sulfate would absorb most of the barium chloride. Thus the higher conductance of the ground product could be caused by impurities.

Cohen and Blekkingh (5) have pointed out another effect which interferes in the conductimetric method for determining solubilities,—that of conductance due to finely divided, suspended material. This was demonstrated by grinding salicylic acid with gold spheres. The conductance of such a salicylic acid solution is greater than the conductance of a solution saturated with coarse salicylic acid. After proper filtering, however, a conductance corresponding to normal solubility was found. As pointed out by Cohen and Blekkingh, this greater conductance may be caused by two factors: the conductance of charged particles (14) and the conductance of ions in the double layer which, according to Rutgers and Overbeek (21), conduct current as if they were free in solution. Using a chloride-free, pure barium sulfate prepared by precipitation from concentrated sulfuric acid, Cohen and Blekkingh *found no evidence of influence of particle size upon solubility*. Their results are based upon a critical examination of their conductimetric measurements and upon polarographic determination of the barium-ion concentration. A slightly higher conductance resulting when a ground powder was used could be practically eliminated by proper filtering. Cohen and Blekkingh do not give any particle-size measurements and their results are not conclusive for this reason. A paper by Balarew (2) appearing at the same time as that of Cohen and Blekkingh substantiates the conclusion that no increase in the solubility of barium sulfate is observed for particles 0.1 micron in diameter.

#### EXPERIMENTAL: EFFECT OF SPECIFIC SURFACE UPON THE SOLUBILITY OF LEAD CHROMATE IN 0.1 *M* PERCHLORIC ACID SOLUTION

As pointed out by Cohen and Blekkingh (5), the difficulty involved in using conductimetric measurements to determine the effect of particle size upon the solubility of a substance lies in the fact that an increase in the conductance does

not necessarily represent an increase in the solubility. A true determination of the increase in solubility can be obtained only if the concentrations, or activities, of the ions of the substance are measured.

In the present study lead chromate was used. It has been established by Kolthoff and Eggertson (15) that lead chromate can be precipitated as a fine powder which ages rapidly with a large increase in its specific surface. In the present study the concentrations of lead and chromate ions in solution were determined by voltametric measurements. Although the concentration of lead chromate in water is too small to be measured voltametrically, in 0.1 *M* perchloric acid the concentration is sufficiently large to be measured in this manner. In the experiments to follow, 0.1 *M* perchloric acid was used as solvent and solubility measurements were made at various stages of aging of lead chromate. Specific-surface measurements were also made and correlated with the solubility data.

#### *Analytical methods for chromate and lead*

Two separate methods were used for the determination of both lead and chromate in acid solution. Chromate concentration was determined by amperometric titration with ferrous ammonium sulfate, using a rotating microelectrode of platinum. The lead concentration was determined by diffusion-current measurements with a dropping mercury electrode after the chromate had been reduced to the chromic state with hydroxylamine hydrochloride. Chromate and lead were also determined together polarographically, by measuring the diffusion currents at potentials of 0 and -0.6 volt.

The amperometric determination of small concentrations of chromate has been described in a previous publication (16). Chromate (in acid solution) can be titrated rapidly by amperometric titration with ferrous iron, using the rotating platinum-wire microelectrode as the indicator electrode. The potential of the indicator electrode is maintained at +1.0 volt *vs.* the saturated calomel electrode, which is used as the reference electrode. The method is accurate and is precise to within 0.5 per cent at concentrations as small as 1 to  $2 \times 10^{-4}$  *M* chromate.

The half-wave potential of lead in acid solution is at approximately -0.4 volt *vs.* a saturated calomel electrode. If chromate is also present in an acid lead solution two waves are obtained, chromate at a positive potential and lead at -0.4 volt. The current-voltage measurements of such a solution are shown in figure 1, curve 1. This curve represents the current-voltage measurements after the removal of oxygen from a solution  $1.33 \times 10^{-4}$  *M* in lead nitrate and  $1.33 \times 10^{-4}$  *M* in potassium chromate in 0.1 *M* perchloric acid. The solution was made by mixing equal volumes of  $2.66 \times 10^{-4}$  *M* lead nitrate and  $2.66 \times 10^{-4}$  *M* potassium chromate, both in 0.1 *M* perchloric acid. The chromate wave may be eliminated by the addition of hydroxylamine hydrochloride. Curve 2 in figure 1 represents the current-voltage curve of the same lead chromate solution as curve 1 but after the addition of one drop of 20 per cent hydroxylamine hydrochloride to 20 ml. of solution. In curves 1 and 2 a wave is observed at about -0.8 volt. The probability that this wave represents the reduction

of chromic ion to chromous is demonstrated by current-voltage measurements using  $2 \times 10^{-4}$  M chromium chloride in 0.1 M perchloric acid, which are shown by curve 3. This wave does not interfere with the lead diffusion-current measurements at -0.6 volt. Curve 4 represents current-voltage measurements of 0.1 M perchloric acid and of 0.1 M perchloric acid containing one drop of hydroxylamine hydrochloride per 20 ml. The difference between the diffusion currents of curves

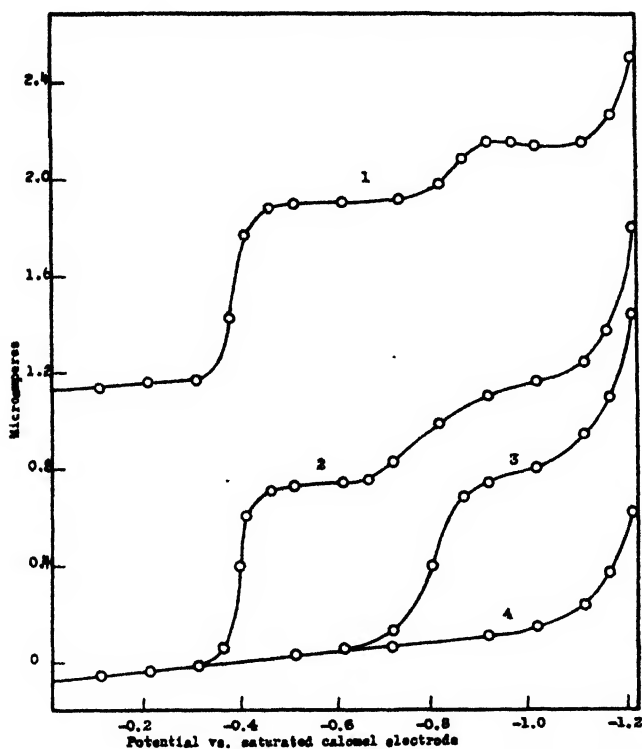


FIG. 1. Current-voltage measurements with a dropping mercury electrode of lead, chromate, and chromic solutions at 25°C. Curve 1:  $1.33 \times 10^{-4}$  M potassium chromate and  $1.33 \times 10^{-4}$  M lead nitrate in 0.1 M perchloric acid. Curve 2: As curve 1, but one drop of 20 per cent hydroxylamine hydrochloride added. Curve 3:  $2 \times 10^{-4}$  M chromium chloride in 0.1 M perchloric acid. Curve 4: 0.1 M perchloric acid containing 1 drop of 20 per cent hydroxylamine hydrochloride.

2 and 4 at -0.6 volt corresponds to the lead diffusion current. Using measurements of the current at -0.6 volt an accurate determination of lead in solutions of small concentrations was obtained. The accuracy of the lead-concentration measurements with known solutions of lead nitrate and potassium chromate in 0.1 M perchloric acid was 1-2 per cent for lead concentrations of 1 to  $2 \times 10^{-4}$  M.

The difference between the current at 0 volt of an acid lead chromate solution (curve 1) and the residual current at the same potential (curve 4) can be used to determine the diffusion current of chromate. The difference between the

current at  $-0.6$  volt (curve 1) and the residual current at that potential (curve 4) can be used to determine the sum of the diffusion currents for chromate and lead. By subtracting the diffusion current of chromate from the sum of the diffusion currents for chromate and lead a value can be obtained representing the lead diffusion current. Using such measurements accuracies of 2 per cent for both lead and chromate were obtained with known solutions of  $1$  to  $2 \times 10^{-4}$   $M$  concentrations of lead and chromate in  $0.1 M$  perchloric acid.

The acid solution of chromate formed a thin film on the mercury by chemical interaction of the chromate with mercury. This tended to corrupt the tip of the capillary when the dropping electrode was in contact with the solution for several minutes. The result was a decrease in the drop time. To eliminate this difficulty the electrode was placed in the solution after the air was removed and immediately before making diffusion-current measurements. After each set of measurements the tip of the capillary was cleaned by dipping in concentrated nitric acid and rinsing with distilled water. The formation of chromate film gave no measurable depletion in the chromate concentration of the solution even with a pool of mercury in the bottom of the cell for a period of an hour. By using a saturated calomel reference electrode as an outside electrode instead of a mercury pool and inserting the mercury electrode immediately before use, interference was eliminated. It should be mentioned at this point that no maximum suppressor was necessary for diffusion-current measurements of lead chromate solutions of low concentrations. Except at concentrations higher than those used in this work no maximum occurred. In concentrations of  $10^{-3} M$  or greater both chromate and lead give maxima. There was no appreciable difference in the diffusion currents of the freshly made colloidal solution and the completely coagulated solutions of lead chromate at potentials between  $0$  and  $-1.6$  volts. Thus measurements of lead and chromate at potentials of  $0$  and  $-0.6$  volt should be free of inaccuracies due to colloidal material.

#### *Particle-size measurements*

Methods for the determination of the specific surface of lead chromate have been described by Kolthoff and Eggertson (15). Two methods were found satisfactory: adsorption of wool violet dye and thorium B exchange. Determinations by these methods give specific-surface measurements in terms of amount of wool violet adsorbed or lead exchanged in the surface layer. From these values it is possible to calculate the actual surface areas per gram of substance and an average particle size.

Particle-size determinations from specific-surface measurements give approximate values only. Assuming that all of the particles are spherical in shape and of uniform size, an expression relating the surface-area measurements to the particle size may be simply derived. Kolthoff and Eggertson (15) found that  $1$  mg. of wool violet was adsorbed per  $0.54$  mg. of lead in the surface layer of precipitated lead chromate. It is readily determined that the specific surface area in square centimeters per gram is  $3040$  times the milligrams of wool violet adsorbed. The radius in centimeters is  $1.57$  divided by the milligrams of lead

adsorbed per gram of material, assuming the particles to be of uniform size and spherical.

### *Preparation of lead chromate samples*

Three separate lead chromate samples were prepared. These products, described below, will hereafter be referred to as *aged*, *fresh*, and *fresh acid-precipitated* samples.

The *aged* sample was prepared by Dr. F. T. Eggertson. The method used in the preparation (17) is as follows: With mechanical stirring a solution containing 500 g. of lead nitrate and 1 ml. of glacial acetic acid in 1.5 liter of distilled water was added to 293 g. of potassium chromate dissolved in 1.5 liter of distilled water. The temperature of the lead nitrate solution at the time of mixing was 55°C. and that of the chromate solution 60°C. The suspension was shaken for 2 hr. and allowed to stand overnight. Using a large Büchner funnel the lead chromate was filtered and washed with warm distilled water. Left with 5 liters of distilled water in a carboy the lead chromate was aged for two and a half months. During this time the water was decanted and fresh distilled water added a total of fifteen times. After standing an additional four months with water the preparation was collected on a Büchner funnel, washed with distilled water, ethanol, and ether, and suction-dried.

The *fresh* lead chromate sample was prepared by adding, with mechanical stirring at room temperature, 100 ml. of 0.5 *M* potassium chromate to 106 ml. of 0.5 *M* lead nitrate. Analytical reagents, recrystallized once from water, were used in preparing the solutions. Immediately after precipitation the suspension was filtered on a large Büchner funnel and the precipitate washed with five 50-ml. portions of distilled water. Washing was continued using alcohol and ether. The preparation was then air-dried for 2 hr. The resulting preparation was a fine powder. A similar preparation has been described by Kolthoff and Eggertson (15).

The *fresh acid-precipitated* sample was prepared exactly as the *fresh* sample, except that the potassium chromate and lead nitrate solutions were both 0.001 *M* in perchloric acid. The preparation was washed and dried exactly as was the *fresh* sample.

## EXPERIMENTAL RESULTS

### *Solubility of lead chromate in 0.1 M perchloric acid solution*

The solubility of lead chromate in 0.1 *M* perchloric acid solution was determined. All three preparations were used: *fresh*, *fresh acid-precipitated*, and *aged*. The results, given in tables 1 and 2, show the lead and chromate concentrations and the apparent solubility product of lead chromate in 0.1 *M* perchloric acid solution. The solubility data, also given, are calculated by taking the square root of the apparent solubility product. This solubility product corresponds to the product of the lead concentration and the total chromium concentration in 0.1 *M* perchloric acid. Since most of the chromium in 0.1 *M* perchloric

acid is present as  $\text{HCrO}_4^-$  and only a small fraction as  $\text{CrO}_4^{2-}$ , the "apparent solubility product" in 0.1 *M* perchloric acid is much greater than the true solubility product.

Solubility measurements using 0.01, 0.1, and 1 g. of lead chromate in 100 ml. of 0.1 *M* perchloric acid were made in the following manner: The lead chromate and perchloric acid were placed in a 125-ml. glass-stoppered bottle and the stopper of the bottle fastened firmly with the application of strips of Scotch tape. The bottle and contents were placed in a mechanical shaker and shaken for 24 hr. at a temperature of 25°C. At the end of that time the bottle was removed, the lead chromate allowed to settle, and the solution filtered through a sintered-glass filter of medium porosity. About 20 ml. of the filtered solution was placed in a polarographic cell, and the diffusion currents of lead and chro-

TABLE 1

*Solubility of lead chromate in 0.1 M perchloric acid after shaking for 24 hr., using 0.01, 0.1, and 1 g. of lead chromate in 100 ml. of 0.1 M perchloric acid solution at 25°C.*

LEAD CHROMATE PREPARATION	AMOUNT OF $\text{PbCrO}_4$	MOLAR CHROMATE CONCENTRATION $\times 10^4$	MOLAR LEAD CONCENTRATION $\times 10^4$	APPARENT SOLUBILITY PRODUCT $\times 10^8$	MOLAR SOLUBILITY $\times 10^4$
	GRAMS				
Aged.....	0.01	1.26	1.27	1.60	1.26
	0.1	1.15	1.47	1.69	1.30
	1	1.09	1.51	1.65	1.28
Fresh acid-precipitated.	0.01	1.28	1.27	1.62	1.27
	0.1	1.21	1.41	1.71	1.31
	1	1.13	1.49	1.68	1.29
Fresh.....	0.01	1.24	1.29	1.60	1.26
	0.1	0.90	1.81	1.64	1.28
	1	0.28	6.09	1.70	1.30

mate were measured by the procedure described previously. The results are given in table 1. The *aged*, *fresh acid-precipitated*, and *fresh* lead chromate preparations were used in these measurements.

The effect of repeated digestion and decantation operations upon the concentrations of lead and chromate found in the solution was investigated. The following procedure was used: One gram of lead chromate and 100 ml. of 0.1 *M* perchloric acid were placed in a 125-ml. glass-stoppered bottle, the stopper fastened, and the bottle and contents shaken for 24 hr. at 25°C., as in the experiments described above. At the end of that time the bottle was removed and the lead chromate allowed to settle by centrifuging. The supernatant liquid was decanted, and the lead and chromate concentrations determined by the procedure described previously. To the bottle containing the solid lead chromate remaining after decantation, 100 ml. of fresh perchloric acid was added. This was then shaken for 24 hr., centrifuged, and the supernatant liquid analyzed for lead and chromate as before. Third, fourth, and fifth similar operations of



digestion, decantation, and analysis of the supernatant liquid were made. The results are given in table 2 for the *aged* and *fresh* preparations.

It is apparent from tables 1 and 2 that the lead chromate preparations contain an excess of lead. The *aged* and *fresh acid-precipitated* preparations contain only a slight excess of lead but the *fresh* one contains somewhat more. The amount of excess lead can be estimated from table 2. From the experimental results it is estimated that the *fresh* preparation contains 1.4 per cent excess lead and the *aged* preparation contains 0.2 per cent excess.

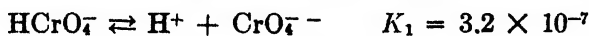
The average of all the values in tables 1 and 2 for the solubility of lead chromate in 0.1 *M* perchloric acid at 25°C. is  $1.27 \times 10^{-4}$  moles per liter. The maximum deviation from this value is 3 per cent.

TABLE 2

*Effect of repeated digestion and decantation operations upon the concentrations of lead and chromate, using 1 g. of lead chromate per 100 ml. of 0.1 M perchloric acid at 25°C.*

LEAD CHROMATE PREPARATION	MOLAR CHROMATE CONCENTRATION $\times 10^4$	MOLAR LEAD CONCENTRATION $\times 10^4$	APPARENT SOLUBILITY PRODUCT $\times 10^8$	MOLAR SOLUBILITY $\times 10^4$
<b>Aged:</b>				
1st 24 hr. . . . .	1.15	1.47	1.69	1.30
2nd 24 hr. . . . .	1.18	1.39	1.64	1.28
3rd 24 hr. . . . .	1.21	1.37	1.66	1.28
4th 24 hr. . . . .	1.26	1.35	1.70	1.30
5th 24 hr. . . . .	1.19	1.29	1.53	1.24
<b>Fresh:</b>				
1st 24 hr. . . . .	.27	6.09	1.65	1.28
2nd 24 hr. . . . .	.94	1.66	1.56	1.24
3rd 24 hr. . . . .	1.15	1.35	1.55	1.24
4th 24 hr. . . . .	1.20	1.33	1.60	1.26
5th 24 hr. . . . .	1.16	1.31	1.52	1.23

From the known equilibrium constants (19) at 25°C. and the estimated activity



coefficients it is calculated from our value in 0.1 *M* perchloric acid that in pure water at 25°C.

$$K = a_{\text{Pb}^{++}} a_{\text{CrO}_4^{2-}} = 1.6 \times 10^{-14}$$

Beck (29) reported a value of  $1.8 \times 10^{-14}$  at 18°C.

A recalculation of his data yields an activity product of  $1.5 \times 10^{-14}$  at 18°C.

*Changes in the solubility of the lead chromate preparations with the time of digestion in 0.1 M perchloric acid*

The lead and chromate concentrations were determined by using 0.1 g. of each of the lead chromate preparations and 100 ml. of 0.1 *M* perchloric acid after

shaking for periods ranging from 1 min. to 24 hr. Each determination was made in the following manner: The lead chromate and perchloric acid were placed in a 125-ml. glass-stoppered bottle, and shaken for a given period of time on a mechanical shaker. The bottle was removed and its contents immediately filtered, using a sintered-glass filter. In table 3 the lead and chromate concentrations were determined in the filtrate by measuring the diffusion currents with a dropping mercury electrode. The check determinations were made using the amperometric titration technique for chromate and determining the lead after the chromate had been reduced by hydroxylamine hydrochloride. The check determinations were, on the average, 1.9 per cent higher than those in table 3. The probable reason for the slightly higher results is the presence of a small amount of very finely divided lead chromate in the filtrate. In the amperometric

TABLE 3

*Change in the solubility with time of shaking in 0.1 M perchloric acid at 25°C., using 0.1 g. of lead chromate*

LEAD CHROMATE PREPARATION	TIME OF SHAKING	MOLAR CHROMATE CONCENTRATION $\times 10^4$	MOLAR LEAD CONCENTRATION $\times 10^4$	APPARENT SOLUBILITY PRODUCT $\times 10^8$	MOLAR SOLUBILITY $\times 10^4$
	<i>minutes</i>				
Aged.....	1	1.18	1.43	1.69	1.30
	6	1.14	1.43	1.63	1.28
	1440	1.14	1.45	1.65	1.28
Fresh acid-precipitated..	1	1.21	1.51	1.83	1.35
	6	1.15	1.33	1.53	1.24
	1440	1.12	1.41	1.58	1.26
Fresh.....	1	1.85	2.38	4.40	2.10
	5	1.60	2.14	3.42	1.85
	20	1.13	1.76	1.99	1.41
	1440	0.90	1.71	1.54	1.24

titration of chromate and the lead determination the chromate was completely reduced. Thus any finely divided suspended lead chromate would have dissolved. In the determinations given in table 3 lead and chromate were determined together without removal of either constituent.

The change in the solubility of lead chromate with the time of digestion in 0.1 M perchloric acid, using 0.05 and 1 g. of fresh lead chromate instead of 0.1 g., was determined. The results are given in table 4.

The *aged* lead chromate preparation does not show an appreciable change in solubility during digestion with 0.1 M perchloric acid and the *fresh acid-precipitated* lead chromate shows only a slight change. The *fresh* preparation shows a very marked change in solubility with the time of digestion. During the first 20 min. of digestion the solubility of the *fresh* lead chromate was considerably greater than the normal solubility of  $1.27 \times 10^{-4}$  M. The maximum solubility

TABLE 4

*Effect of amount of the fresh lead chromate upon the change in solubility with time of shaking in 0.1 M perchloric acid at 25°C.*

AMOUNT OF LEAD CHROMATE	TIME OF SHAKING	MOLAR CHROMATE CONCENTRATION $\times 10^4$	MOLAR LEAD CONCENTRATION $\times 10^4$	APPARENT SOLUBILITY PRODUCT $\times 10^8$	SOLUBILITY $\times 10^4$
grams	minutes				
0.05	1	1.86	2.24	4.16	2.04
	5	1.84	2.14	3.94	1.98
	20	1.43	1.74	2.49	1.58
	1440	1.18	1.41	1.66	1.29
0.1	1	1.85	2.38	4.40	2.10
	5	1.60	2.14	3.42	1.85
	20	1.13	1.76	1.99	1.41
	1440	0.90	1.71	1.54	1.24
1	1	0.94	5.37	5.04	2.24
	5	0.43	5.90	2.54	1.59
	20	0.29	6.06	1.76	1.33
	1440	0.27	6.09	1.64	1.28

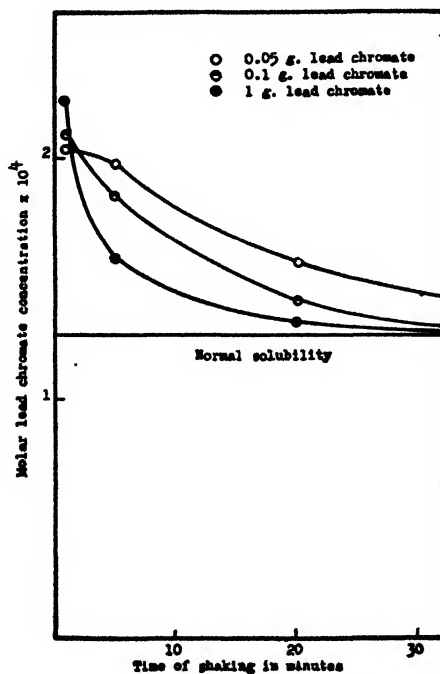


FIG. 2. Change in solubility with time of shaking of freshly precipitated lead chromate and 100 ml. of 0.1 M perchloric acid at 25°C.

obtained after 1 min. of digestion, was from 60 to 76 per cent higher than the normal solubility, depending upon the amount of lead chromate used.

The initial values of the solubility were affected only very slightly by the amount of lead chromate used. From the values in table 4, the solubility with 0.05 g. after 1 min. of shaking with 100 ml. of 0.1 *M* perchloric acid was  $2.04 \times 10^{-4}$  *M*, with 0.1 g. it was  $2.10 \times 10^{-4}$  *M*, and with 1 g. it was  $2.24 \times 10^{-4}$  *M*. This result indicates that the high solubility of the *fresh* preparation was not caused by an impurity in the lead chromate. If it were caused by an impurity an increasing effect should have been found with increasing amounts of lead chromate.

The solubility data given in table 4 are plotted in figure 2. The solubility, which is the square root of the apparent solubility product, is plotted against the time of shaking of the *fresh* lead chromate with 0.1 *M* perchloric acid at 25°C. The rate of aging is seen to increase with the amount of lead chromate used.

TABLE 5

*Rate of precipitation of a supersaturated lead chromate solution upon shaking with the aged lead chromate preparation at 25°C.*

TIME OF SHAKING	MOLAR CHROMATE CONCENTRATION $\times 10^4$	MOLAR LEAD CONCENTRATION $\times 10^4$	APPARENT SOLUBILITY PRODUCT $\times 10^8$	MOLAR SOLUBILITY $\times 10^4$
Before	1.97	2.48	4.88	2.21
20 sec.	1.10	1.52	1.67	1.29
20 sec.	1.06	1.48	1.57	1.25
1 min.	1.07	1.48	1.58	1.26
10 min.	1.09	1.50	1.63	1.28

*Rate of precipitation of a supersaturated lead chromate solution upon shaking with the aged lead chromate preparation*

It is seen from the previous experiments that the solubility of lead chromate when the *fresh* preparation was shaken with 0.1 *M* perchloric acid decreased from the maximum obtained in the first minute to normal solubility in about 20 min., using 1 g. of lead chromate. The possibility exists that the greater than normal solubility observed in the previous experiments might be caused by impurities in the lead chromate. It has been shown that the fresh product contains lead in excess to chromate. Thus upon shaking with perchloric acid the impurities (basic lead chromate) dissolve, causing the concentrations of lead and chromate in the solution to be greater than corresponds to the normal solubility. Experiments were made to determine the rate of precipitation of a supersaturated lead chromate solution, using the *aged* lead chromate as solid body. These measurements should give an indication as to whether or not impurities could contribute appreciably to the high solubility obtained using the *fresh* preparation.

The following procedure was used: A volume of 100 ml. of a supersaturated solution of lead chromate in 0.1 *M* perchloric acid and 0.1 g. of the *aged* preparation were shaken in 125-ml. bottle for a given period of time. The mixture was filtered

over a sintered-glass filter, and analyses were made of the filtrate for lead and chromate by the method employing measurements of the respective diffusion currents at the same time. The supersaturated solutions were made by mixing  $4 \times 10^{-4} M$  lead nitrate and  $5 \times 10^{-4} M$  potassium chromate, both in  $0.1 M$  perchloric acid. This solution was stable for 1 hr. or more.

The results are given in table 5 and show that supersaturation is overcome very rapidly. By inspection of the results, it is clearly seen that if the high solubility of the *fresh* preparation were a supersolubility due to impurities, rather than the result of a temporary equilibrium between the very small particles and solution, then a normal solubility could be attained within a few seconds. These results further substantiate the conclusion that the higher solubility of the *fresh* lead chromate is related to the size or structure or both of the fine imperfect particles and not to coprecipitated basic lead chromate.

TABLE 6

*Specific surface and average particle size from wool violet adsorption data on lead chromate preparations*

LEAD CHROMATE PREPARATION	SPECIFIC SURFACE IN MILLIGRAMS OF WOOL VIOLET PER GRAM OF LEAD CHROMATE	SPECIFIC SURFACE IN CM. <sup>2</sup> PER GRAM $\times 10^{-4}$	CALCULATED PARTICLE RADIUS IN MICRONS
Aged . . . . .	3.5	1.1	0.45
Fresh acid-precipitated . . . . .	6.0	1.8	0.26
Fresh . . . . .	18.3	5.6	0.086
After 20 min. aging in $0.1 M HClO_4$ . . . . .	5.7	1.7	0.28
After 24 hr. aging in $0.1 M HClO_4$ . . . . .	5.2	1.6	0.30

#### *Specific-surface measurements*

The specific surface of the three lead chromate preparations used in the previous experiments was determined by the wool violet adsorption method. In addition, the specific surface of the *fresh* preparation after given periods of digestion in  $0.1 M$  perchloric acid at  $25^\circ C$ . was determined. The procedure used was as follows: In a 30-ml. paraffined bottle 0.2 g. of the *fresh* lead chromate preparation and 20 ml. of  $0.1 M$  perchloric acid were shaken for a given period of time. The perchloric acid was removed, and the specific surface determined by the wool violet adsorption method. The perchloric acid was removed by three separate washings, decanting the supernatant liquid after centrifuging, and shaking with a fresh solution. After this treatment the lead chromate and bottle contained a small amount of water, the weight of which was determined by suitable weighings and was taken into consideration in the measurement of the adsorption of the wool violet concentration. The results are given in table 6. The specific-surface measurements are given and the specific surface in square centimeters per gram, and the particle sizes calculated from the data of Kolthoff and Eggertson (15).

From the data in table 6 it is seen that the specific surface varied from 1.1 sq. m.

per gram for the *aged* preparation to 5.6 for the *fresh* one. The estimated average particle radii varied from 0.45 to 0.086 micron. Upon digestion of the *fresh* preparation in 0.1 *M* perchloric acid the specific surface decreased in 20 min. to about one-third of its original value. It is at that point in the digestion that the solubility of the *fresh* preparation approaches the normal value.

#### DISCUSSION

The solubility measurements were performed in such a manner as to eliminate factors that have been pointed out as invalidating the work of previous investigators. The solubility of lead chromate was determined from concentration measurements of both chromate and lead. A difference in solubility was found between a fresh, finely divided preparation and that of an aged one consisting of larger particles. The solubility of the fresh lead chromate was considerably higher than normal the first few minutes after shaking with 0.1 *M* perchloric acid but decreased rapidly as the particle size increased as a result of aging. The greater solubility cannot be accounted for by the fact that the fresh preparation was not pure but contained an excess of lead, for the following reasons: (1) The apparent solubility product was calculated from the observed concentrations of both lead and chromate. Thus impurities other than lead and chromate do not affect solubility determinations. (2) If the greater than normal solubility were caused by impurities such as lead nitrate or potassium chromate, a supersaturated solution would exist. In the experimental part it has been shown that supersolubility was so rapidly overcome that the conclusion is justified that the greater than normal solubility could not have been caused by impurities. (3) The amount of solubility in excess of normal is affected only very little by the amount of solid used.

The greater solubility of the freshly precipitated lead chromate might be interpreted on a basis entirely different from that of an increase in the surface work function. Two interpretations may be considered to explain the greater than normal solubility.

(1) The explanation for the greater than normal solubility might lie in the existence of various crystalline modifications of lead chromate. It has been shown by Jager and Germs (13) and by Wagner, Haug, and Zipfel (22) that lead chromate has three crystalline forms: monoclinic, rhombic, and tetragonal. The monoclinic form is found in nature and is known as the mineral crocoite. It is stable below 707°C. The rhombic form, stable between 707° and 783°C., is unstable at lower temperatures, changing to monoclinic. The tetragonal modification is stable between 783°C. and the melting point. In attempting to interpret the solubility results the possible coexistence of two or all three of these modifications of lead chromate should be kept in mind. It is possible that the freshly precipitated product consists partly of one of the less stable modifications, the solubility of which would be greater than that of the stable monoclinic form. If this were the case, the solubility would be high at first, decreasing to normal as the solid lead chromate is converted to the monoclinic modification. Since the solubility became close to normal within 20 min., the above interpretation implies that the transformation of the metastable to the stable form would

be extremely rapid. This does not seem very plausible, although this interpretation cannot be dismissed without further study. Experiments of a preliminary nature made in this laboratory would tend to eliminate this interpretation. Dr. I. Shapiro made Debye-Scherrer powder photographs of lead chromate samples. Examination failed to show any difference between the photographs obtained using a freshly precipitated sample and an aged one. Thus it is tentatively concluded that the two samples had the same crystal modification.

(2) Lattice distortion might explain the greater than normal solubility. Fricke and coworkers (9) have investigated this kind of distortion in several papers since 1933. The distortion was determined roentgenographically. Distortions are "active spots", either corner atoms or gaps in the surface areas not completely occupied. The degree of distortion has been related to the heat content of the substance. It is not improbable that the existence of lattice distortions could give rise to a higher solubility and may have been responsible for the high solubility values obtained with the *fresh* lead chromate of large surface. Although a thorough investigation has not been made of the lattice distortion of the lead chromate samples, Dr. Shapiro's Debye-Scherrer powder photographs did not show evidence of distortion.

In view of the above discussion it is concluded that the greater solubility product of the fresh lead chromate prepared in the absence of acid is to be attributed to its very small particle size.

#### SUMMARY

1. The Ostwald-Freundlich equation (3) has been modified to relate the activity product on the one hand and particle size on the other. The expression of Knapp (14) extending the Ostwald-Freundlich equation to induce the surface electrical charge also was modified (see equations 19 and 27 in this paper).

2. Solubility determinations on *fresh* (very small particles) and *aged* lead chromate have been made in 0.1 *M* perchloric acid. Chromate was determined by amperometric titration and lead and chromate also polarographically. The *fresh* lead chromate has a considerably greater solubility (about 70 per cent) than the aged product. Aging of the fresh product in 0.1 *M* perchloric acid occurs very rapidly at 25°C., a normal solubility being found after a 20-min. period of contact between the fresh lead chromate and the acid.

3. The *fresh* lead chromate used in these studies had a specific surface of 5.6 sq.m. per gram, corresponding to an average radius of a particle of 0.086 micron. Upon aging for 20 min. at 25°C. in 0.1 *M* perchloric acid the surface decreased to 1.7 sq.m. per gram (radius 0.28 micron).

4. The normal solubility of lead chromate in 0.1 *M* perchloric acid was found to be  $1.27 \times 10^{-4}$  *M* at 25°C. This corresponds to an activity product  $a_{\text{Pb}^{++}} \times a_{\text{CrO}_4^{--}}$  of  $1.6 \times 10^{-14}$ .

#### REFERENCES

- (1) BALAREW, D.: Z. anorg. allgem. Chem. **145**, 122 (1925); **151**, 68 (1926); **154**, 170 (1926).
- (2) BALAREW, D.: Kolloid-Z. **96**, 19 (1941).
- (3) BECK, K.: Z. Elektrochem. **17**, 846 (1911).
- (4) BIKERMAN, J. J.: Z. physik. Chem. **A163**, 378 (1933).

- (5) COHEN, E., AND BLEKKINGH, J. J. A., JR.: *Z. physik. Chem.* **A186**, 257 (1940).
- (6) DUNDON, M. L., AND MACK, E.: *J. Am. Chem. Soc.* **45**, 2479 (1923); **45**, 2658 (1923).
- (7) EGGERTSON, F. T.: Ph.D. thesis, University of Minnesota.
- (8) FREUNDLICH, H.: *Colloid and Capillary Chemistry* (English translation), p. 155. Methuen and Co., Ltd., London (1926).
- (9) FRICKE, R., AND GWINNER, E.: *Z. physik. Chem.* **A183**, 165 (1938).  
FRICKE, R.: *Z. Elektrochem.* **46**, 491 (1940).  
FRICKE, R.: *Kolloid-Z.* **96**, 211 (1941).
- (10) GIBBS, W.: *Scientific Papers*, Vol. I. Longmans, Green and Company, New York (1906).
- (11) HARBURY, LAWRENCE: *J. Phys. Chem.* **50**, 190 (1946); *J. Phys. Colloid Chem.* **51**, 382 (1947).
- (12) HULETT, G. A.: *Z. physik. Chem.* **37**, 385 (1901); see also HULETT, G. A., AND DUSCHAK, L. H.: *Z. anorg. allgem. Chem.* **40**, 196 (1904).
- (13) JAGER, F. M., AND GERMS, H. C.: *Z. anorg. allgem. Chem.* **119**, 145 (1921).
- (14) KNAPP, L. F.: *Trans. Faraday Soc.* **17**, 457 (1922).
- (15) KOLTHOFF, I. M., AND EGGERTSON, F. T.: *J. Am. Chem. Soc.* **62**, 2125 (1940); **63**, 1412 (1941).
- (16) KOLTHOFF, I. M., AND MAY, D. R.: *Ind. Eng. Chem., Anal. Ed.* **18**, 208 (1946).
- (17) LEWIS, W. C. M.: *Kolloid-Z.* **5**, 71 (1909).
- (18) MARIIGNAC, C.: *Ann. chim. phys.* [5] **1**, 274 (1874).
- (19) NEUSS, J. D., AND RIEMANN, W., III: *J. Am. Chem. Soc.* **56**, 2238 (1934).
- (20) OSTWALD, W.: *Z. physik. Chem.* **34**, 503 (1900).
- (21) RUTGERS, A. J., AND OVERBEEK, J. Th. G.: *Z. physik. Chem.* **A177**, 29 (1936).
- (22) WAGNER, H., HAUG, R., AND ZIFFEL, M.: *Z. anorg. allgem. Chem.* **208**, 249 (1932).

## BEAKER-TYPE CENTRIFUGAL SEDIMENTATION OF SUBSIEVE SOLID-LIQUID DISPERSIONS. I

### THEORY<sup>1</sup>

HENRY E. ROBISON<sup>2</sup>

*Armour Research Foundation, Chicago, Illinois*

AND

S. W. MARTIN

*Portland Gas & Coke Co., Portland, Oregon*

*Received October 9, 1947*

### I. INTRODUCTION

The gravitational, beaker-type centrifugal, supercentrifugal, and ultracentrifugal types of sedimentation define a so-called sedimentation spectrum that includes practically the entire range of subsieve particle sizes of matter.

The gravitational sedimentation theory, first evolved by S. Oden (14), is now well established for both monodisperse and polydisperse solid-liquid systems,

<sup>1</sup> Contribution from the laboratory of the Institute of Gas Technology.

<sup>2</sup> This paper is based on the dissertation submitted by Henry E. Robison to the Graduate School of the Illinois Institute of Technology in partial fulfillment of the requirements for the degree of Doctor of Philosophy, June, 1946.



in which particles vary in size from a few microns to 45 microns and greater. A large variety of experimental techniques based on Oden's cumulative sedimentation method have been developed and have been adequately described in numerous publications.

The development of ultracentrifugal theory and practice for extremely fine colloidal particles is chiefly due to the efforts of T. Svedberg (19, 20, 21) and coworkers. Ultracentrifugal sedimentation is uniquely applicable to the determination of the molecular weights of large molecules and true colloidal particles varying from 100 millimicrons down to macromolecular sizes. An extensive literature exists on this subject.

Supercentrifugal sedimentation borders on the particle-size range of the ultracentrifugal and may be extended to approximately 1-micron sizes. Theory and experimental technique have been fully developed by E. A. Hauser (6, 7) and coworkers.

The beaker-type centrifuge, available in most laboratories, is readily and conveniently adapted to studies of colloidal polydisperse systems composed of particles from 0.1 to 1.0 micron in size. This intermediate portion of the sedimentation spectrum is not as well defined, theoretically and experimentally, as the sedimentation extremes previously considered.

Beaker-type centrifugal sedimentation theory and practice are now reviewed to develop some of the problems that existed at the time when this investigation was initiated.

## II. A REVIEW OF BEAKER-TYPE CENTRIFUGAL SEDIMENTATION

The principal forces acting on a particle in a centrifugal field are the centrifugal force, the viscous drag due to the motion of the particle relative to the fluid, and an accelerative force. Svedberg and Nichols (19) equated the viscous drag as given by Stokes's law and the centrifugal force. Integration yielded the formula

$$\ln \frac{X_2}{X_1} = \frac{d_1 - d_0}{18\eta} w^2 y^2 t \quad (1)$$

where  $X_2$  = the distance of the particle from the center of rotation at a time  $t$ ,

$X_1$  = the distance from the center of rotation at zero time,

$d_1$  = the density of the particle,

$d_0$  = the density of the fluid,

$\eta$  = the viscosity,

$w$  = the angular velocity,

$t$  = the time in the centrifugal field, and

$y$  = the diameter of the particle.

In deriving this equation, two accelerating effects were neglected: (1) Initially the particle is at rest and must be accelerated until the viscous and the centrifugal forces are equal. (2) Since the centrifugal field intensity varies along the particle's path, the particle must be constantly accelerating in order to approach a force equilibrium.

In appendix A, the differential equation that includes the accelerative term is solved and, for very small values of the Reynolds number, it is demonstrated that this solution can be reduced to equation 1.

Beaker-type centrifugal sedimentation is dependent on the following experimental conditions and assumptions:

- (1) An ordinary beaker-type laboratory centrifuge is used, such as that manufactured by the International Equipment Company (Size 2). Angle centrifuges are not amenable to the mathematical analysis to be presented. Moderate centrifugal forces are employed with this type of equipment.

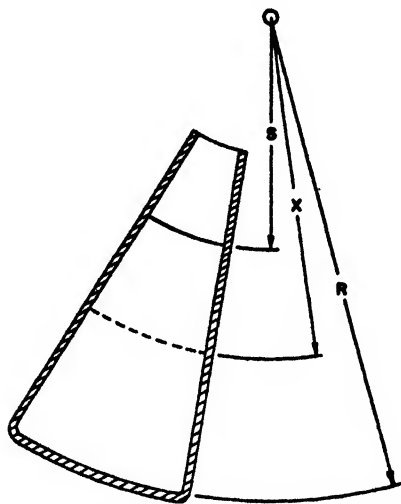


FIG. 1. Schematic diagram of a sector cell

- (2) A vibrationless sedimentation is postulated.
- (3) A sector cell (shown in figure 1) is assumed in the mathematical analysis.
- (4) The weight of sediment deposited after a certain time,  $t$ , is measured.
- (5) A polydisperse system is assumed.
- (6) Diffusion effects are negligible and are therefore omitted.
- (7) Equation 1 is assumed to describe the position of the particle along a radius with time.

A weight-distribution function  $F(y)$  is shown in figure 2. The per cent by weight of a certain particle diameter is plotted against the diameter. The fraction in an infinitesimal range of diameters is  $F(y) dy$ . It is assumed that this curve is continuous, possesses all derivatives, and is zero at  $y$  equal to zero and infinity. Moreover, it may be assumed that all derivatives are zero at zero and infinity.

Figure 1 shows the sector cell generally assumed in the mathematical formulation of centrifugal sedimentation. From the side view the cell is a sector of a

circle, and is designed to minimize collisions of the particles with the sides during sedimentation. The distance from the center of rotation to the meniscus of the dispersion in the cell is designated  $S$ ; that to the bottom of the cell,  $R$ .

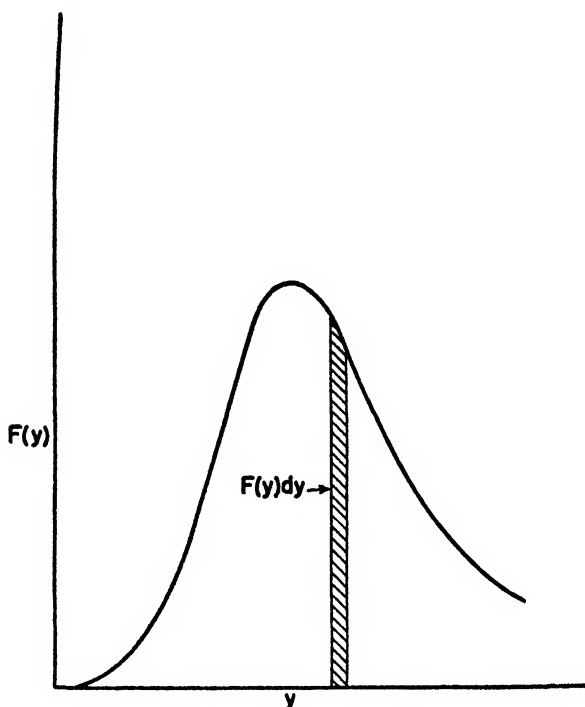


FIG. 2. The function  $F(y)$

A particle of diameter  $z$  is defined as that particle which will just travel from the meniscus to the bottom of the cell during the time of centrifuging. From equation 1

$$\ln \frac{R}{S} = \frac{d_1 - d_0}{18\eta} w^2 z^2 t = k z^2 t \quad (2)$$

where

$$k = \frac{d_1 - d_0}{18\eta} w^2$$

These particles and all larger particles will settle during the centrifuging, whereas only a certain fraction of the particles smaller than  $z$  will be deposited. The total fraction of the original material sedimented,  $p$ , is given by the equation:<sup>3</sup>

$$p = \int_s^\infty F(y) dy + \int_0^s \frac{R^2}{R^2 - S^2} [1 - \exp(-2ky^2 t)] F(y) dy \quad (3)$$

<sup>3</sup>  $e^x$  will be designated as  $\exp(x)$ .

By substituting values from equation 2:

$$p = \int_z^\infty F(y) dy + \int_0^z \frac{R^2}{R^2 - S^2} \left[ 1 - \exp\left(-\frac{y^2}{z^2} \ln \frac{R^2}{S^2}\right) \right] F(y) dy \quad (4)$$

This is the formulation of Brown (2), whose treatment is essentially that of Romwalter and Vendl (16).

Equation 3 is an integral equation involving a known function,  $p(z)$ , which is determined by experiment, and an unknown function  $F(y)$ .

Two methods are employed experimentally to evaluate particle-size distributions,  $F(y)$ : (1) The dispersions are sedimented for various time intervals and a curve  $p$  versus  $t$  is plotted. (2) Sedimentations are carried out at different heights and values of  $p$  versus  $R - S$  are obtained.

If  $k$  is constant in equations 2 and 3, the variables in the equations are  $z$ ,  $R/S$ , and  $t$ . Since both equations hold simultaneously, and if  $\ln R/S$  is held constant,  $p$  may be regarded as a function of  $z$  or  $t$  alone; whereas if  $t$  is held constant,  $p$  is a function of  $z$  or  $R/S$  alone.

Solutions to equation 3 are obtained by differentiating with respect to  $t$  or  $S$  according to the rule for differentiation under the integral sign.

To develop the mathematical basis for the time variation method, Romwalter and Vendl (16) differentiated equation 3 with respect to time and published the equation:

$$\frac{dp}{dt} = \int_0^z \frac{R^2}{R^2 - S^2} [2ky^2] \exp(-2ky^2t) F(y) dy \quad (5)$$

For the functions within the integral,  $\exp(-2ky^2t)$ , and  $2ky^2$ , Romwalter and Vendl substituted the particular values at the upper limit  $z$  with the following result:

$$\frac{dp}{dt} = \int_0^z \frac{S^2}{t(R^2 - S^2)} \ln \left( \frac{R^2}{S^2} \right) F(y) dy \quad (6)$$

From equation 6 they concluded that Oden's method of tangential intercepts could be used to evaluate particle-size distributions from a  $p$  versus  $t$  curve. The method of tangential intercepts that is shown in figure 3 is simply a graphical method of evaluating the integral<sup>4</sup> of the distribution function (for gravitational sedimentation) over the limits 0 to  $z$  from a  $p$  versus  $t$  curve.

Later, Brown (2) pointed out that the substitution of the values at the upper limit for functions inside an integral is an illegitimate mathematical procedure; therefore equation 6 must be regarded as false. He stated that equation 5 is the correct expression for the slope of the sediment-time curve, but an exact solution for the distribution function appeared difficult, if not impossible, to obtain.

Brown then developed a mathematical basis for determining the distribution function from a curve of sediment versus height of suspension at a constant time. He differentiated equation 3 with respect to  $S$ , and also with respect to both  $S$

<sup>4</sup> This integral may be designated the cumulative distribution function and is denoted by  $Q(x)$ .

and  $t$ , to derive three expressions by means of which the particle-size distribution function may be calculated.

$$\left(\frac{R^2 - S^2}{2S}\right) \frac{dp}{dS} + (1 - p) = \int_0^z F(y) dy = Q(z) \quad (7)$$

$$\frac{\ln R/S}{z} \left[ \left(\frac{R^2 - 2S^2}{S}\right) \frac{dp}{dS} - (R^2 - S^2) \frac{d^2p}{dS^2} \right] = F(z) \quad (8)$$

$$\frac{2t}{z} \left[ \frac{\partial p}{\partial t} - \left(\frac{R^2 - S^2}{2S}\right) \frac{\partial^2 p}{\partial S \partial t} \right] = F(z) \quad (9)$$

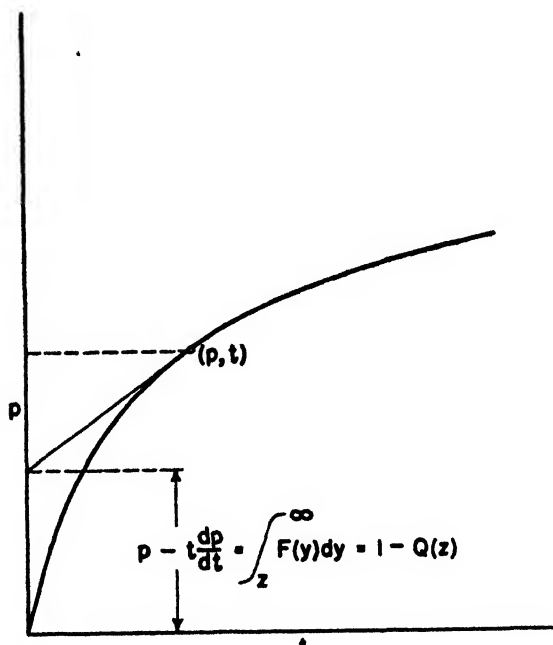


FIG. 3. Oden's method of tangential intercepts

Formula 9 has little utility, since a parametric system of curves is needed to evaluate the second derivative of  $p$  with respect to  $S$  and  $t$ . Generally, the fraction of the material between two diameters is of interest and not the actual distribution function itself, i.e., the integral of the distribution function between two limits.

Brown, using suspensions of barium and strontium carbonates in alcohol, determined the particle-size distribution by varying the height of the dispersion in the sedimentation tubes. Cylindrical tubes were employed and calculations were made with equation 7 suitably modified to account for the cylindrical shape. He did not feel justified in using equation 8 because the second derivative was subject to considerable error, inasmuch as many of the particles could strike the sides of the tube.

Furthermore, the range of variation of the height of the fluid in the sedimentation tubes is limited by the following: (1) The construction of the ordinary centrifuge usually permits a minimum  $S$  of about  $3\frac{1}{2}$  in. and a maximum  $R$  of  $10\frac{1}{2}$  in. (International No. 2). (2) As Brown stated, at high speeds and with tubes filled to a high level the effect of convection currents is rather marked.

Brown determined a threefold range of particle sizes, i.e., the maximum diameter was three times the smallest. By running the height variation method at different values of  $w^2t$ , it was possible to analyze over a wider range of particle sizes.

Dumanski, Zabolinski, and Ewsejew (4) were apparently the first investigators to attempt to use the ordinary centrifuge for accurate particle-size determinations of monodisperse silver sols. The amount sedimented was determined by ultramicroscopic counts before and after centrifuging. The values calculated agreed very poorly with those of the ultramicroscopic method. Svedberg (20) ascribed this discrepancy to the fact that serious deviations from ideal sedimentation were caused, chiefly by convection currents.

Schlesinger (17) determined the particle size of monodisperse gold sols in an ordinary laboratory centrifuge. Filter paper was fitted into the bottom of the tube to avoid disturbance of the sediment. The centrifuge was not vibrationless, and calculations of particle size were made with a formula derived on the assumptions that (1) the vibrations kept the main body of solution at a uniform concentration and (2) in a narrow layer adjacent to the bottom of the tube, sedimentation took place according to Stokes's law.

Schlesinger's work was not directly applicable to the sedimentation problem to be discussed in this paper; however, he suggested that polydisperse systems might be analyzed by the variation of the height of the dispersion in the tubes as a parameter.

Marshall (9) separated a clay dispersion into relatively clear-cut fractions by placing a thin layer of the dispersion over a column of a cane sugar or urea solution. By adjusting the specific gravities and viscosities of these media, and making the layer of dispersion thin, fractions within definite size limits were obtained. Adjustment of the viscosities and lengths so that the time of travel through the upper layer is small compared to that through the lower layer minimized the weight of fines, i.e., particles of diameter less than  $z$ , that settled out.

Martin (10) applied Romwalter and Vendl's mathematical analysis to the determination of the particle-size distribution of titanium dioxide pigments in various vehicles. He used Oden's method of tangential intercepts to calculate particle-size distributions of practical pigmentary dispersions. In a later paper Martin (11) independently checked the particle-size distribution so obtained with a microscopically determined distribution, and found good agreement. He covered the range 0.3 to 2.0 microns. In appendix B the mathematical basis of Oden's method of tangential intercepts is derived for gravitational sedimentation. In appendix C a similar formula is derived for centrifugal sedimentation, with the difference that there are extra terms whose magnitude

depends on  $\ln R/S$ . As  $R/S$  approaches 1, the extra terms approach 0. Therefore, the application of Oden's method of tangential intercepts to centrifugal sedimentation may be regarded as an approximate determination of particle-size distributions.

Parkinson (15) assumed that the variation of the centrifugal field was negligible and applied Oden's method as if it were a gravitational sedimentation. Dispersions of carbon black in water were investigated. He stated that a complete mathematical solution of the problem (size distribution by centrifugal sedimentation by the constant-height method) had not been achieved. However, he made no reference to the previous work of Martin and of Romwalter and Vendl. Parkinson's results were subject to the same approximations as Martin's.

Jacobsen and Sullivan (8), by employing a very low value of  $R/S$  (1.05), were able to use Oden's method with sufficient accuracy to check the results obtained by varying the height of suspension. A good agreement was achieved using a titanium dioxide paint pigment. The height of the dispersion was 1 cm. Such low heights are experimentally inconvenient because of the small amount of dispersion available for analysis.

Norton and Spiel (13) attempted to minimize the variation of the centrifugal force field by constructing a centrifuge with long arms for the determination of the particle-size distribution of clays. The amount sedimented was measured by specific gravity determinations with a hydrometer in accordance with the Casgrande method for gravitational sedimentation. Times of centrifugal sedimentation were converted into so-called equivalent times of gravitational sedimentation. Equation 4 shows that the variation of the centrifugal field for a given particle diameter that has completely settled is a function of  $R/S$ . Although Norton and Spiel give no accurate measurements, it may be calculated from their data that the over-all  $R/S$  was 1.46. If the hydrometer measured the gravity near the middle of the column, the effective  $R/S$  was over 1.20. Consequently, Norton and Spiel defeated their main purpose by using a high value of  $R/S$ , since a value of  $R/S$  of 1.20 is readily obtainable in an ordinary beaker-type laboratory centrifuge. The departure of centrifugal from gravitational sedimentation is a function of  $R/S$ , as demonstrated in appendix C.

Bray (1) determined the particle size of clays by a method recommended by Steele and Bradfield (18). According to their procedure, a 5-cc. sample was removed 2 cm. from the meniscus of a 25-cc. sample that had been centrifuged. The amount of sediment in the aliquot was determined by evaporation to dryness. From such determinations and the radius of the particles just sedimented, a particle-size distribution was calculated. Bray's mathematical procedure was not accurate and his results are only roughly approximate.

Dana (3) employed a method similar to Bray's. Furthermore, an inclined-tube centrifuge, which is not amenable to simple mathematical analysis, was used. Gurevich (5) determined the particle-size distribution for a titanium dioxide pigment by essentially the same method. Gurevich and Dana's determinations are subject to the same criticism as Bray's.

Among the investigators who have studied particle-size determinations by

means of an ordinary beaker-type centrifuge Brown, Marshall, and Schlesinger developed an adequate mathematical basis for treating their data. The studies of Marshall and of Schlesinger were limited to the simplest colloidal systems, i.e., essentially monodisperse. Brown solved the integral equations for the variable-height method for polydisperse systems. The experimental work, however, was not carried out in sector cells, which were assumed in the theory.

As a result of this critique of beaker-type centrifugation, the writers attempted solutions of integral equations (3) for the variable time-constant height method. Although only approximate mathematical solutions are at present obtainable, the fact remains that the error in the final approximate equations is reducible to well within the tolerances inherent in experimental techniques which may be employed to specify the degree of polydispersity of a subsieve solid-liquid system by its corresponding particle-size distribution.

### III. BEAKER-TYPE CENTRIFUGATION THEORY FOR THE VARIABLE TIME-CONSTANT HEIGHT METHOD

The quantities appearing in equations 3 and 4 that may be regarded as parameters are:

$$\frac{d_1 - d_0}{18\eta}, \frac{R}{S}, w, z, \text{ and } t$$

The ratio of the density difference of the solid and medium to the viscosity is treated as a single parameter, since the densities and viscosity are all dependent on the physical characteristics of the subsieve solid and the dispersion medium. In a mathematical sense the ratio  $R/S$  is unique. It appears as the coefficient of the quadrature to the right in equation 3 and as a logarithm in equation 2. Consequently, the use of this parameter involves a different type of solution of the integral equation than the solution for the other parameters. Since the other parameters occur in the exponent only, in equation 4 their mathematical treatment is essentially the same.

From an experimental point of view  $z$ , the particle diameter, is a derived parameter because it is not directly measured. It is the logical parameter to use in plotting experimental curves, since it occurs in the limits of integration and final results are expressed in terms of it. Furthermore, a curve,  $p$  versus  $z$ , is independent of the other experimental parameters utilized to vary  $z$ . Although it is customary to vary the time alone in the constant-height method, greater flexibility of operation is permitted by varying the quantity  $w^2t$ . A set of experiments to be described in a later paper will establish a remarkable check on the constancy of the fractional weight sedimented at a given value of  $w^2t$ , yet at different values of  $w$ , indicating that this is a permissible method of operation.

Wide variations of liquid viscosities might be selected, but to vary the ratio of the density difference to the viscosity is experimentally subject to difficulties, because changes in the degree of dispersion are likely to occur with the different media which would have to be chosen.



## A. First approximate solution

Weight data for particle-size distribution are expressed as the weight of the material between certain size limits. This corresponds to the integral of the function  $F(y)$  over the interval. Solutions of the integral equations will be derived in terms of this integral from zero to  $z$ , which is designated by the function  $Q(z)$ .

When equation 4 is differentiated repeatedly, the quadrature term of a given derivative will contain the function  $\exp\left(-\frac{y^2}{z^2} \ln \frac{R^2}{S^2}\right)$  multiplied by a polynomial of the form

$$\frac{1}{z^n} \left[ C_1 \left( \frac{y^2}{z^2} \ln \frac{R^2}{S^2} \right) + C_2 \left( \frac{y^2}{z^2} \ln \frac{R^2}{S^2} \right)^2 + \cdots + C_n \left( \frac{y^2}{z^2} \ln \frac{R^2}{S^2} \right)^n \right]$$

where  $C_1, C_2, C_n$  are constants and  $n$  is the order of the derivative. If each derivative is multiplied by  $z^n$  and a certain constant, the derivatives may be added to give a quadrature in which the polynomial forms the initial terms in the expansion of the function,  $\exp\left(\frac{y^2}{z^2} \ln \frac{R^2}{S^2}\right)$ , according to Maclaurin's theorem.

Then this polynomial times  $\exp\left(-\frac{y^2}{z^2} \ln \frac{R^2}{S^2}\right)$  will have values very close to 1.

This is the principle employed to develop approximate solutions to the integral equation. By utilizing higher and higher derivatives, terms farther out in the series may be included and the error involved in the approximation may be made arbitrarily small.

If the substitutions

$$\frac{R^2}{R^2 - S^2} = b \text{ and } \ln \frac{R^2}{S^2} = a$$

are made, and since

$$\int_0^\infty F(y) dy = 1$$

equation 4 with some rearrangement becomes

$$(1 - p) = \int_0^z F(y) dy + b \int_0^z \left[ \exp\left(-\frac{ay^2}{z^2}\right) - 1 \right] F(y) dy \quad (10)$$

By differentiating this expression successively and multiplying each derivative by  $z^n$ , where  $n$  is the order of the derivative, the following expressions are obtained:

$$-z \frac{dp}{dz} = b \int_0^z \frac{2ay^2}{z^2} \exp\left(-\frac{ay^2}{z^2}\right) F(y) dy \quad (11)$$

$$-z^2 \frac{d^2p}{dz^2} = b \int_0^z \left( -\frac{6ay^2}{z^2} + \frac{4a^2y^4}{z^4} \right) \exp\left(-\frac{ay^2}{z^2}\right) F(y) dy + 2(b-1)azF(z) \quad (12)$$

$$-z^3 \frac{d^3p}{dz^3} = b \int_0^z \left( \frac{24ay^2}{z^2} - \frac{36a^2y^4}{z^4} + \frac{8a^3y^6}{z^6} \right) \exp\left(-\frac{ay^2}{z^2}\right) F(y) dy + (b-1)(4a^2 - 8a)zF(z) + 2(b-1)az^2 \frac{dF}{dz} \quad (13)$$

and

$$\begin{aligned}
 -z^4 \frac{d^4 p}{dz^4} = & (b-1)(36a - 44a^2 - 8a^3)z^2 F(z) + (b-1)(4a^2 - 10a)z^3 \frac{dF}{dz} \\
 & + 2(b-1)az^3 \frac{d^2 F}{dz^2} + b \int_0^z \left( -\frac{120ay^2}{z^2} + \frac{300a^2 y^4}{z^4} \right. \\
 & \left. - \frac{144a^3 y^6}{z^6} + \frac{16a^4 y^8}{z^8} \right) \exp\left(-\frac{ay^2}{z^2}\right) F(y) dy \quad (14)
 \end{aligned}$$

Differentiation of

$$Q(z) = \int_0^z F(y) dy$$

yields the following relations:

$$\frac{dQ}{dz} = F(z), \quad \frac{d^2 Q}{dz^2} = \frac{dF}{dz}, \quad \text{and} \quad \frac{d^3 Q}{dz^3} = \frac{d^2 F}{dz^2} \quad (15)$$

If equations 10, 11, and 12 are multiplied by 1, 7/8, and 1/8, respectively, and the three resultant equations are added, and if relations 15 are substituted, the following equation results:

$$\begin{aligned}
 1 - \left( p + \frac{7z}{8} \frac{dp}{dz} + \frac{z^2}{8} \frac{d^2 p}{dz^2} \right) = & Q + \frac{(b-1)az}{4} \frac{dQ}{dz} \\
 & + b \int_0^z \left[ \left( 1 + \frac{ay^2}{z^2} + \frac{a^2 y^4}{2z^4} \right) \exp\left(-\frac{ay^2}{z^2}\right) - 1 \right] F(y) dy \quad (16)
 \end{aligned}$$

The ratio  $y/z$  is never greater than 1; consequently for small values of  $a$  the product of the polynomial and the exponential function will be close to 1, and the quadrature approaches zero in value. Therefore, if the quadrature is neglected:

$$z \frac{dQ}{dz} + \frac{4}{(b-1)a} Q = \frac{4}{(b-1)a} \left[ 1 - \left( p + \frac{7z}{8} \frac{dp}{dz} + \frac{z^2}{8} \frac{d^2 p}{dz^2} \right) \right] \quad (17)$$

By changing the variables according to the equation

$$\ln z = \phi$$

and substituting

$$M = \frac{4}{(b-1)a}, \quad \text{and} \quad S(z) = 1 - \left( p + \frac{7z}{8} \frac{dp}{dz} + \frac{z^2}{8} \frac{d^2 p}{dz^2} \right)$$

equation 16 is transformed into

$$\frac{dQ}{d\phi} + MQ = MS(z) \quad (18)$$

This is a linear differential equation with constant coefficients whose solution is well known and is presented in most standard texts on differential equations. The complete solution after the substitution of the variable  $z$  for  $\phi$  is

$$Q(z) = \frac{c}{z^M} + \frac{1}{z^M} \int_0^z MS(z)z^{M-1} dz \quad (19)$$

Because there are no particles in a small interval close to 0,  $Q(z)$  equals 0 and  $p$  is equal to 1 and is constant in this interval. Consequently all the derivatives of  $p$  are 0, and the function of  $S(z) = 0$ . Therefore,

$$Q(\delta) = \frac{c}{\delta^M} + \frac{1}{\delta^M} \int_0^\delta MS(z)z^{M-1} dz \quad (20)$$

Since the quadrature and  $Q(z)$  are both equal to 0, the arbitrary constant  $c$  must also equal 0.

The first approximate solution is, by substitution for  $S(z)$ :

$$Q(\cdot) = \frac{1}{z^M} \int_0^z M \left( 1 - \left[ p + \frac{7z}{8} \frac{dp}{dz} + \frac{z^2}{8} \frac{d^2p}{dz^2} \right] \right) z^{M-1} dz \quad (21)$$

By integration by parts this solution may be converted to the form:

$$Q(\cdot) = 1 - \left[ \frac{M(6-M)}{8} p + \frac{Mz}{8} \frac{dp}{dz} + \frac{M(M-2)(M-4)}{8} \int_0^z pz^{M-1} dz \right] \quad (22)$$

Because second derivatives of experimental curves may be rather inaccurate, equation 22 has the advantage that only first derivatives are required. Furthermore, the quadrature is rather simple and may be easily evaluated by Simpson's one-third rule. It is interesting to note that, as the ratio  $R/S$  approaches 1, the constant  $M$  approaches 4, the coefficient of the quadrature becomes 0, that of  $p$  1, and that of the derivative  $\frac{1}{2}$ . Thus this solution reduces to Oden's method of tangential intercepts which, if expressed in terms of  $z$ , is:

$$Q = 1 - \left( p + \frac{z}{2} \frac{dp}{dz} \right) \quad (23)$$

It will be shown that the error due to the mathematical approximation is not serious even at values of  $a$  as high as 0.7022 corresponding to a ratio,  $R/S$ , of 1.420 for sector cells or of 2.016 for cylindrical tubes.

### B. Second approximate solution

The fourth term in the expansion of  $\exp\left(\frac{ay^2}{z^2}\right)$  is obtainable by changing the constants and adding the next higher derivative. If equations 10, 11, 12, and 13 are multiplied by 1, 19/16, 5/16, and 1/48, respectively, and added, the resultant equation is:

$$\begin{aligned} 1 - \left( p + \frac{19z}{16} \frac{dp}{dz} + \frac{5z^2}{16} \frac{d^2p}{dz^2} + \frac{z^3}{48} \frac{d^3p}{dz^3} \right) \\ = b \int_0^z \left[ \left( 1 + \frac{ay^2}{z^2} + \frac{a^2y^4}{2z^4} + \frac{a^3y^6}{6z^6} \exp\left(-\frac{ay^2}{z^2}\right) - 1 \right) F(y) dy \right. \\ \left. + Q + (b-1) \left( \frac{a^2}{12} + \frac{22a}{48} \right) z \frac{dQ}{dz} + \frac{(b-1)a}{24} z^2 \frac{d^2Q}{dz^2} \right] \quad (24) \end{aligned}$$

By neglecting the quadrature and letting

$$V(z) = 1 - \left( p + \frac{19z}{16} \frac{dp}{dz} + \frac{5z^2}{16} \frac{d^2p}{dz^2} + \frac{z^3}{48} \frac{d^3p}{dz^3} \right)$$

equation 24 becomes

$$\frac{az^2(b-1)}{24} \frac{d^2Q}{dz^2} + (b-1) \left( \frac{a^2z}{12} + \frac{22az}{48} \right) \frac{dQ}{dz} + Q(z) = V(z) \quad (25)$$

This equation is converted to a linear equation with constant coefficients by the change in variables

$$\phi = \ln z$$

becoming, after division by the coefficient of the second derivative,

$$\frac{d^2Q}{d\phi^2} + g \frac{dQ}{d\phi} + BQ(z) = BV(z) \quad (26)$$

where

$$g = (2a + 10)$$

$$B = \frac{24}{(b-1)a}$$

In operational notation this equation may be rewritten

$$(D^2 + gD + B)Q = BV(z) \quad (27)$$

where

$$D = \frac{d}{d\phi}$$

The constants  $g$  and  $b$  depend on the ratio  $R/S$  alone. The roots of the operator may be different and real, equal and real, or conjugate complex. The range of possible experimental values of  $R/S$  permits all three situations.

The type of roots depends on the magnitude of the ratio  $g^2/4B$ . When it equals 1, the roots are equal and real; when greater than 1, different and real; when less than 1, conjugate complex. Table 1 shows the variation of this ratio for different values of the ratio  $R/S$ .

Experimental work with cylindrical tubes should be done at values of  $R/S$  below 1.383, because higher levels of liquid are more readily subject to convection currents due to vibrations. In the case of sector cells values of  $R/S$  below 1.176 are experimentally possible; therefore, the solution to equation 26 for all three pairs of roots will be presented.

The complete solution consists of a reduced solution plus the particular solution. The arbitrary constants are evaluated by the initial conditions that  $Q(\delta) = 0$ , where  $\delta$  is near 0 and all the derivatives of  $Q$  are 0 at  $\delta$ . Also the function  $V(z)$  is 0 in this region because all the derivatives of  $p$  are 0.

All the derivatives of the particular solutions in each case will equal 0 in the range  $0 \leq z \leq \delta$ , because  $V(z)$  is 0 and constant over that range. Therefore only the reduced solutions will be considered in the evaluation of the constants.

The solutions for these three cases are given by Murray (11). In considering the three cases the following notation will be used for the roots:

- (a) two real roots,  $-M$  and  $M'$
- (b) equal roots,  $-N$
- (c) conjugate complex roots,  $-\alpha + i\beta$  and  $-\alpha - i\beta$ , where  $i$  is the square root minus 1

TABLE 1  
Variation of  $g^2/4B$  with  $R/S$

$R/S$ (CYLINDRICAL TUBES)	$R/S$ (SECTOR CELLS)	$\frac{g^2}{4B}$
1.240	1.114	1.016
1.280	1.131	1.011
1.320	1.149	1.007
1.360	1.166	1.003
1.383	1.176	1.000
1.400	1.183	0.998
1.440	1.200	0.994

The reduced solutions follow:

- (a) two real roots

$$Q(z) = C_1 z^{-M} + C_2 z^{-M'}$$

- (b) equal roots

$$Q(z) = z^{-N}(C_1 + C_2 \ln z)$$

- (c) conjugate complex

$$Q(z) = z^{-\alpha}(C_1 \cos [\beta \ln z] + iC_2 \sin [\beta \ln z])$$

where  $C_1$  and  $C_2$  in each case are real arbitrary constants.

The arbitrary constants are evaluated in each case by setting  $Q$  and its first derivative equal to zero at  $\delta$ , which is finite but close to zero. The three cases follow:

- (a) two real roots:

$$0 = C_1 \delta^{-M} + C_2 \delta^{-M'}$$

$$0 = MC_1 \delta^{-M-1} - M'C_2 \delta^{-M'-1}$$

Since the determinant of the coefficients of  $C_1$  and  $C_2$  is not zero, these two equations can be simultaneously true only if  $C_1$  and  $C_2$  are zero.

- (b) equal roots:

$$0 = \delta^{-N}(C_1 + C_2 \ln \delta)$$

$$0 = -N\delta^{-N-1}C_1 + C_2\delta^{-N-1}(1 - N \ln \delta)$$

The quantity  $(1 - N \log \delta)$  will be negative and large; therefore, these equations can be satisfied simultaneously only if  $C_1$  and  $C_2$  are both zero.

(c) *conjugate complex roots:*

$$0 = C_1 \delta^{-\alpha} \cos(\beta \ln z) + i C_2 \delta^{-\alpha} \sin(\beta \ln z)$$

$$0 = C_1 \delta^{-\alpha} [\alpha \cos(\beta \ln z) + \sin(\beta \ln z)] - i C_2 \delta^{-\alpha} [\alpha \sin(\beta \ln z) - \cos(\beta \ln z)]$$

At small values of  $\delta$  near 0, the functions  $\sin(\beta \ln z)$  and  $\cos(\beta \ln z)$  will oscillate rapidly. If a value of  $\delta$  is chosen where  $\sin(\beta \ln z)$ ,  $\cos(\beta \ln z)$ , and  $\alpha \sin(\beta \ln z) - \cos(\beta \ln z)$  have finite values, the constants  $C_1$  and  $C_2$  will be 0 for the same reasons given in the previous cases. Because the sin and cos functions oscillate with greater and greater rapidity as 0 is approached, it is possible to choose this value of  $\delta$ .

The constants of the reduced solutions in each case are zero; therefore, the particular solutions alone satisfy the limiting conditions. The particular solution in the case of two real but different roots is

$$Q(z) = \frac{B}{M' - M} \left[ z^{-M} \int_0^z V(z) z^{M-1} dz - z^{-M'} \int_0^z V(z) z^{M'-1} dz \right] \quad (28)$$

where  $M' > M$ . In order to put the equations in a more convenient form, new constants are introduced, i.e.,

$$M = -n - m$$

$$M' = -n + m$$

By using these expressions, integrating by parts, and substituting for  $V(z)$  equation 28 may be expressed in the following form:

$$Q(z) = \frac{B}{48} \left[ 1 + (2n - 12)p - z \frac{dp}{dz} + \frac{(M - 2)(M - 4)(M - 6)}{48z^M} \int_0^z pz^{M-1} dz + \frac{(M' - 2)(M' - 4)(M' - 6)}{48z^{M'}} \int_0^z pz^{M'-1} dz \right] \quad (29)$$

This equation is very similar in form to the first approximate solution. When the ratio  $R/S$  becomes 1,  $B$  becomes 24,  $n$  5,  $M$  4, and  $M'$  6; the coefficients of the quadratures become 0 and the formula reduces to Oden's method of tangential intercepts.

If the roots are equal, i.e., at  $R/S$  for sector cells equal to 1.176, the particular solution is

$$Q = \frac{1}{z^N} \left[ \int_0^z z^{N-1} \ln z BV(z) dz - \ln z \int_0^z z^{N-1} BV(z) dz \right] \quad (30)$$

Numerical integrations will be somewhat tedious with this equation because of the function  $\ln z$ . This equation is applicable only at one particular value of the ratio  $R/S$ , i.e., 1.383 for cylindrical tubes or 1.176 for sector cells.

In the case of conjugate complex roots, the solution must be real to have any meaning in the interpretation of the physical system. The solution after conversion to a real form is

$$Q = \frac{Bz^{-\alpha}}{\beta} \left[ \sin(\beta \ln z) \int_0^z V(z) z^{\alpha-1} \cos(\beta \ln z) dz - \cos(\beta \ln z) \int_0^z V(z) z^{\alpha-1} \sin(\beta \ln z) dz \right] \quad (31)$$

Equation 31 may be used only when the value of  $R/S$  exceeds 1.176 for sector cells or 1.383 for cylindrical tubes. Because high liquid heights are more susceptible to convection currents, which interfere with sedimentation according to Stokes's law, it is desirable to minimize the ratio  $R/S$ . Moreover, at low values of  $R/S$  effects due to particles striking the walls of the tube will diminish in cylindrical tubes, and the sedimentation results will be equivalent to those obtained from sector cells. On the other hand, for convenience in analysis a certain minimum volume of dispersion is needed.

From these considerations it may be concluded that in the practical employment of the constant height-variable time method, cylindrical tubes should be used with a value of the ratio  $R/S$  at about 1.20. In this range, the simple formula 21 will be more accurate than the experimental curves (shown in error analysis later). To obtain a more accurate approximation, formula 29, which involves an extra numerical integration, should be used. Formulae 30 and 31 are very tedious to employ because of the nature of the functions that must be computed in the numerical integrations.

### C. Differential equation of third approximate solution

As an item of theoretical interest, the differential equation of a third approximate solution will be derived. The solution of the third approximate differential equation is much too complicated for practical and rapid application. It may be solved rapidly by the methods of operational calculus and the solutions will resemble those derived for the second approximation with, however, the addition of another quadrature. The case of two conjugate complex and one real root will arise.

If equations 10, 11, 12, 13, and 14 are multiplied by 1, 187/128, 69/128, 13/192, and 1/384, respectively, and the five resultant equations added, the sum is

$$\begin{aligned} 1 - \left( p + \frac{187z}{128} \frac{dp}{dz} + \frac{69z^2}{128} \frac{d^2p}{dz^2} + \frac{13z^3}{192} \frac{d^3p}{dz^3} + \frac{z^4}{384} \frac{d^4p}{dz^4} \right) = Q(z) \\ + (b-1) \left( \frac{147a}{288} + \frac{15a^2}{96} + \frac{a^3}{48} \right) zF(z) + (b-1) \left( \frac{21a}{192} + \frac{a^2}{96} \right) z^2 \frac{dF}{dz} + \frac{az^3}{192} \frac{d^2F}{dz^2} \\ + b \int_0^z \left[ \left( 1 + \frac{ay^2}{z^2} + \frac{a^2y^4}{2z^4} + \frac{a^3y^6}{6z^6} + \frac{a^4y^8}{24z^8} \right) \exp\left(-\frac{ay^2}{z^2}\right) - 1 \right] F(y) dy \quad (32) \end{aligned}$$

By substituting relations 15 and neglecting the quadrature, equation 32 becomes

$$\frac{az^3}{192} \frac{d^3Q}{dz^3} + (b-1) \left( \frac{21a}{192} + \frac{a^2}{96} z^2 \frac{d^2Q}{dz^2} \right) + (b-1) \left( \frac{147a}{288} + \frac{15a^2}{96} + \frac{a^3}{48} \right) z \frac{dQ}{dz} + Q(z) = W(z)$$

where

$$W(z) = 1 - \left( p + \frac{187z}{128} \frac{dp}{dz} + \frac{69z^2}{128} \frac{d^2p}{dz^2} + \frac{13z^3}{192} \frac{d^3p}{dz^3} + \frac{z^4}{384} \frac{d^4p}{dz^4} \right)$$

This equation may be readily transformed into a linear differential equation of the third order with constant coefficients by the change of variables used in the previous cases. Inasmuch as the first approximate solution is sufficiently accurate and the second approximate solutions are probably considerably more accurate than available experimental data, the third approximate differential equation will not be solved.

#### IV. AN ERROR ANALYSIS OF THE FIRST APPROXIMATE FORMULA

The first approximate formula is the most suitable of the formulas developed for practical routine calculations. It is of interest, therefore, to evaluate the mathematical accuracy at various values of  $R/S$ . An error analysis depends on the nature of the distribution function  $F(z)$ , and consequently the error can be computed only for specific types of this function. In general, particle-size distribution functions are of the same class, i.e., unimodal functions of a gaussian type with various degrees of skewness and kurtosis. For this reason and the fact that the function  $Q(z)$  varies only between 0 and 1, the magnitude of the error for the specific functions considered should be comparable to that of the ordinary distribution functions encountered with practical dispersions of sub-sieve materials.

A simple and yet exact calculation of the approximation is made by utilizing two simple algebraic functions which have the property of an easy integration in equation 3.

The first is a straight line:

$$F(z) = 0.5000z \quad 0 \leq z \leq 2 \quad (34)$$

Since the integral of  $F(z)$  over interval must be 1, the range of  $z$  is 0 to 2. Upon substitution for  $F(y)$  in equation 3 and integration, a theoretical or hypothetical sedimentation curve is derived:

$$(1-p) = 0.2500 \left[ \frac{1}{a} - (b-1) \right] z^2 \quad (35)$$

The function  $S(z)$  is

$$S(z) = 0.7500 \left[ \frac{1}{a} - (b-1) \right] z^2 \quad (36)$$



The function  $Q(z)$  is computed by substitution of this value of  $S(z)$  into equation 21 and by subsequent integration. The values of the computed  $Q$ , the theoretical  $Q$ , and that from Oden's method are listed in table 2 for various values of  $R/S$ .

An examination of the per cent theoretical  $Q$  column reveals that, even at the highest value of  $R/S$ , the  $Q$  calculated according to formula 21 is only 1.4 per cent too low, which is good agreement considering the inherent errors in the experimental determination of particle-size distribution. At lower values of  $R/S$ , the error definitely is negligible. The  $Q(z)$  calculated according to Oden's method of tangential intercepts shows a considerable departure from the theoretical  $Q$ . At the lowest value of  $R/S$ , the error is greater than the highest error calculated from formula 21. For high values of  $R/S$ , i.e., 1.42 (sector cells), the use of Oden's method involves an incremental deviation of about 12 per cent.

TABLE 2

*Comparison of results obtained from formula 21 and Oden's method with the theoretical  $Q(z)$  for the assumed distribution  $F(z) = 0.5000z$*

$R/S$		CALCULATED $Q(z)$	ODEN'S $Q(z)$	PER CENT THEORETICAL $Q^*$	
Sector cells	Cylindrical tubes			Calculated	Oden's
1.07	1.146	0.2499 $z^2$	0.2443 $z^2$	99.9	97.7
1.17	1.369	0.2493 $z^2$	0.2369 $z^2$	99.7	94.8
1.27	1.613	0.2484 $z^2$	0.2301 $z^2$	99.4	92.0
1.42	2.016	0.2465 $z^2$	0.2210 $z^2$	98.6	88.4

\* The theoretical  $Q$  equals  $0.2500z^2$ .

Another distribution function which is readily integrated and yet resembles actual particle-size distributions more closely than equation 34 is

$$F(z) = 2z - z^3 \quad 0 \leq z \leq 1.414 \quad (37)$$

Distribution functions 34 and 37 are shown graphically in figure 4.

By proceeding as in the case of the straight line the following expressions are calculated:

$$(1 - p) = \left[ \frac{1}{a} - (b + 1) \right] z^2 - \frac{1}{2a} \left[ \left( \frac{1}{a} + 1 \right) - b - \frac{a(b-1)}{2} \right] z^4 \quad (38)$$

$$S(z) = 3 \left[ \frac{1}{a} - (b - 1) \right] z^2 - \frac{3}{a} \left[ \left( \frac{1}{a} + 1 \right) - b - \frac{a(b-1)}{2} \right] z^4 \quad (39)$$

The values of  $Q$  calculated from formula 21 are listed in table 3. This table reveals the fact that the calculated  $Q$  agrees with the theoretical  $Q$  to approximately the degree that occurred in the case of the straight-line distribution function (see table 2).

Inasmuch as the two previously considered distribution functions differ in magnitude and range from the particle-size distribution in a forthcoming paper on the experimental aspects of this subject, the error involved in the application

of the first approximate formula to a distribution which closely approximates an actual particle-size distribution was also calculated.

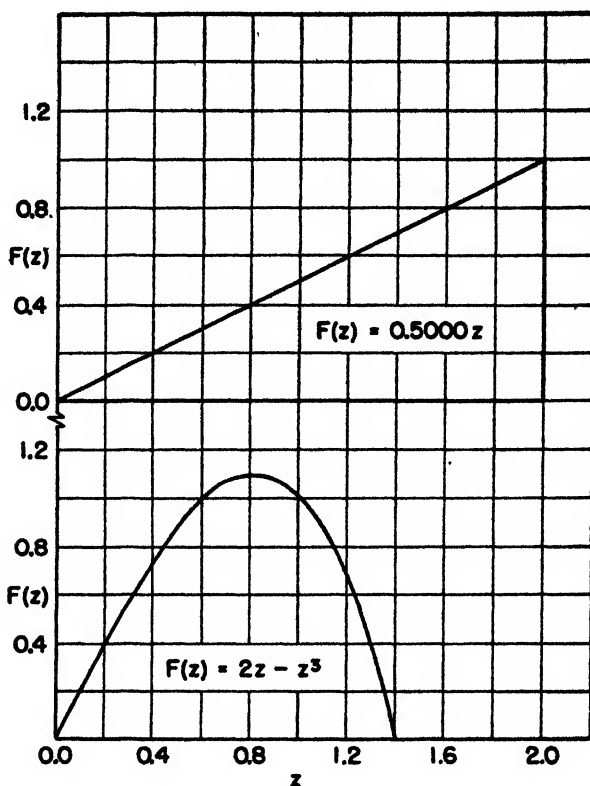


FIG. 4. The assumed algebraic distributions

TABLE 3

Comparison of the results from formula #1 with the theoretical  $Q(z)$  for the assumed distribution  $F(z) = 2z - z^3$

<i>R/S</i>		CALCULATED $Q$	APPROXIMATE PER CENT THEORETICAL $Q^*$
Sector cells	Cylindrical tubes		
1.07	1.146	$0.9996(z^3 - 0.2499z^4)$	100.0
1.17	1.369	$0.9973(z^3 - 0.2499z^4)$	99.7
1.27	1.613	$0.9936(z^3 - 0.2496z^4)$	99.4
1.42	2.016	$0.9859(z^3 - 0.2491z^4)$	98.6

\* The theoretical  $Q$  equals  $z^3 - 0.2500z^4$ .

The curve  $F(z)$  vs.  $z$  for a titanium dioxide pigment was determined by drawing tangents to the curve  $Q(z)$  vs.  $z$ , which was calculated from experimental data with  $R/S = 1.166$  (sector cells). A stepwise distribution was drawn which had about the same area in each interval as that of a smooth curve  $F(z)$  vs.  $z$ . The

stepwise curve is the assumed distribution and was selected in order to permit exact integrations in making an error analysis for the conditions specified. The smooth and the stepwise distribution curves are shown in figure 5.

In the derivation of the first approximate solution the quadrature in equation 15 was discarded as being negligible. The error in  $Q$  when this term is included will be evaluated for the assumed distribution. If

$$E(z) = b \int_0^z \left[ 1 - \left( 1 + \frac{ay^2}{z^2} + \frac{a^2 y^4}{2z^4} \right) \exp\left(-\frac{ay^2}{z^2}\right) \right] F(y) dy \quad (40)$$

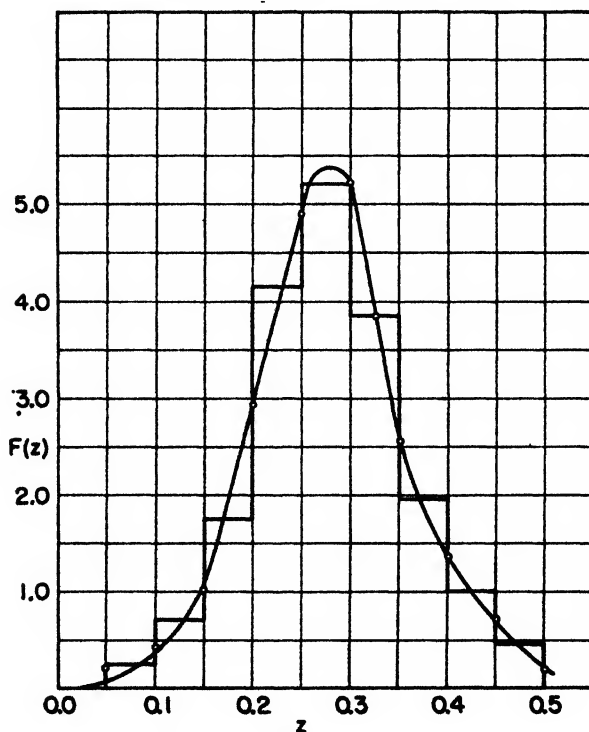


FIG. 5. Comparison of smooth with stepwise distribution

then

$$Q'(z) = \frac{1}{z^M} \int_0^z M z^{M-1} [S(z) + E(z)] dz \quad (41)$$

Since  $E(z)$  is always positive, equation 41 indicates that the  $Q(z)$  calculated according to formula 21 will always be too small because of the approximation.

If  $q$  is the error in  $Q(z)$ , then

$$Q'(z) = Q(z) + q$$

where  $q$  is given by the expression

$$q = \frac{bM}{z^M} \int_0^z z^{M-1} \int_0^z \left[ 1 - \left( 1 + \frac{ay^2}{z^2} + \frac{a^2y^4}{2z^4} \right) \exp\left(-\frac{ay^2}{z^2}\right) \right] F(y) dy dz \quad (42)$$

By integration by parts this double integral is converted into two single integrals. This expression after some simplification is

$$\begin{aligned} \frac{q}{b} &= \int_0^z \left[ 1 - \left( 1 + \frac{ay^2}{z^2} + \frac{a^2y^4}{2z^4} \right) \exp\left(-\frac{ay^2}{z^2}\right) \right] F(y) dy \\ &\quad - \frac{1}{z^M} \int_0^z y^{M-1} \left[ 1 - \left( 1 + \frac{ay^2}{z^2} + \frac{a^2y^4}{2z^4} \right) \exp\left(-\frac{ay^2}{z^2}\right) \right] F(y) dy \end{aligned} \quad (43)$$

Let

$$\frac{ay^2}{z^2} = H^2$$

then

$$\frac{a^{\frac{1}{2}}y}{z} = H \quad \text{and} \quad dy = \frac{z}{a^{\frac{1}{2}}} dH$$

Upon making these substitutions equation 43 becomes

$$\begin{aligned} \frac{q}{b} &= \frac{z}{a^{\frac{1}{2}}} \int_0^{a^{\frac{1}{2}}} \left[ 1 - \left( 1 + H^2 + \frac{H^4}{2} \right) \exp(-H^2) \right] F\left(\frac{zH}{a^{\frac{1}{2}}}\right) dH \\ &\quad - \frac{1}{a^{\frac{M}{2}}} \int_0^a H^M \left[ 1 - \left( 1 + H^2 + \frac{H^4}{2} \right) \exp(-H^2) \right] F\left(\frac{zH}{a^{\frac{1}{2}}}\right) dH \end{aligned} \quad (44)$$

By letting

$$\begin{aligned} N(H) &= \left[ 1 - \left( 1 + H^2 + \frac{H^4}{2} \right) \exp(-H^2) \right] \\ T(H) &= \frac{H^M}{a^{\frac{M}{2}}} \left[ 1 - \left( 1 + H^2 + \frac{H^4}{2} \right) \exp(-H^2) \right] \end{aligned} \quad (45)$$

equation 44 becomes

$$\frac{q}{b} = \frac{z}{a^{\frac{1}{2}}} \int_0^a [N(H) - T(H)] F\left(\frac{Hz}{a^{\frac{1}{2}}}\right) dH \quad (46)$$

Since

$$F\left(\frac{zH}{a^{\frac{1}{2}}}\right) = C_n = \text{constant}$$

over the interval  $j \leq \frac{Hz}{a^{\frac{1}{2}}} \leq k$ , equation 46 may be written (for this interval)

$$\frac{q(k) - q(j)}{b} = \frac{zC_n}{a^{\frac{1}{2}}} \int_0^k [N(H) - T(H)] dH - \int_0^j [N(H) - T(H)] dH \quad (47)$$

and

$$q = \sum q(k) - q(j) \quad (48)$$

over the range zero to  $a^{\frac{1}{2}}$ .

In order to calculate the values of the integrals of the functions  $N(H)$  and  $T(H)$ ,  $\exp(-H^2)$  is expanded in a series and the terms are integrated term by term. Since the series expansion of  $\exp(-H^2)$  alternates in sign and is uniformly convergent, the maximum error involved in discarding terms above a certain number is no greater than the first term discarded and has the same sign. In these calculations the sixth and all higher terms are neglected. Thus the maximum error in the series expansion of  $\exp(-H^2)$  is 0.021 per cent for the greatest value of  $a^\dagger$ , which is 0.85.

After performing these operations and integrating, the following expressions are obtained for the integrals of  $N(H)$  and  $T(H)$ :

$$\int_0^H N(H) dH = \frac{H^7}{42} - \frac{H^9}{72} + \frac{H^{11}}{220} - \frac{H^{13}}{2040} + \frac{H^{15}}{3600}$$

$$\int_0^H T(H) dH = \frac{H^M}{\alpha^{M/2}} \left[ \frac{H^7}{6(7+M)} - \frac{H^9}{8(9+M)} + \frac{H^{11}}{20(11+M)} - \frac{H^{13}}{80(13+M)} + \frac{H^{15}}{240(15+M)} \right] \quad (49)$$

Let

$$\int_0^H [N(H) - T(H)] dH = G(H) \quad (50)$$

With this notation values of the function  $G(H)$  are compiled in table 4 for various values of  $M$ .

This function  $G(H)$  may be used to calculate the error in any unusual particle-size distribution that may occur in practice.

These calculated values (table 4) were plotted and intermediate values were taken from the curve. Values of  $R/S$  and  $G(H)$  corresponding to the values of  $M$  selected are included in table 5. The values of  $R/S$  for sector cells are very close to those actually used in the experimental work to be presented in a forthcoming paper. These particular values were selected because  $H^M$  could be computed easily from tables.

The error  $q$  was calculated from the assumed distribution function shown in figure 5, and the plotted values of  $G(H)$  listed in table 5, according to formulas 47 and 48 for values of  $z$ , 0.3, 0.4, and 0.5 microns. The error  $q$  is compiled in table 6.

In everyday particle-size distribution analyses, the mathematical errors listed in table 6 would hardly be detected. Combined experimental errors will exceed by far the above mathematical errors attributable to the approximations made in the derivation of equation 21.

## V. SUMMARY

Beaker-type centrifugation of polydisperse colloidal system was first placed on a sound theoretical basis by C. Brown. However, his treatment of this subject was limited to a constant time-variable height method. On considering the variable time-constant height approach to beaker-type centrifugation,

Brown stated, "an exact solution for the distribution function seems to be extremely difficult if not impossible to obtain."

TABLE 4  
Values of the function  $G(H)$

$M = 4.70$		$M = 5.10$		$M = 5.70$	
$H$	$G(H)$	$H$	$G(H)$	$H$	$G(H)$
0.0000	0.000000	0.0000	0.000000	0.0000	0.000000
0.1000	0.000000	0.1000	0.000000	0.1000	0.000000
0.2000	0.000000	0.2000	0.000000	0.2000	0.000000
0.3000	0.000005	0.3000	0.000005	0.3000	0.000005
0.4000	0.000031	0.4000	0.000034	0.4000	0.000035
0.5000	0.000105	0.5000	0.000141	0.5000	0.000157
0.5604	0.000135	0.6000	0.000378	0.6000	0.000501
		0.6500	0.000502	0.6500	0.000805
		0.6839	0.000552	0.7000	0.001211
				0.7500	0.001679
				0.8000	0.002107
				0.8380	0.002213

TABLE 5  
Values of  $a^{1/2}$  and  $R/S$  corresponding to  $M$

$M$	$a^{1/2}$	$R/S$	
		Sector cells	Cylindrical tubes
4.70	0.5604	1.170	1.369
5.10	0.6839	1.263	1.595
5.70	0.8380	1.420	2.016

TABLE 6  
The error in formula 21 for a distribution approximating the experimental distribution

$z$	$Q$	$q^*$		
		$R/S = 1.17$	$R/S = 1.263$	$R/S = 1.420$
0.3	0.605	0.001	0.003	0.007
0.4	0.895	0.001	0.003	0.008
0.5	0.968	0.001	0.002	0.005

\* For values of  $R/S$  corresponding to sector cells.

In this paper, first, second, and third approximate solutions to the preceding problem were derived. The first approximate solution is given by:

$$Q(z) = 1 - \left[ \frac{M(6-M)}{8} p + \frac{Mz}{8} \frac{dp}{dz} + \frac{M(M-2)(M-4)}{8} \int_0^z p z^{M-1} dz \right]$$

As the ratio of  $R/S$  approaches unity, the above solution to the variable time-constant height method of beaker-type centrifugation reduces to Oden's method

of tangential intercepts for gravitational sedimentation which, if expressed in terms of  $z$ , is

$$Q(z) = 1 - \left( p + \frac{z}{2} \frac{dp}{dz} \right)$$

An error analysis was made of the theory presented in this paper. The calculations based on assumed distribution functions, one of which simulated a practical dispersion of a fine pigment, indicated that the first approximate solution equation is sufficiently accurate for ordinary particle-size distribution determinations. Actually, the errors attributable to the mathematical approximations inherent in the derivation of the final equation are well within the experimental inaccuracies of beaker-type centrifugation.

Second and third mathematical approximations were derived but these equations are of theoretical interest only, even though they permit a higher degree of mathematical accuracy. With Brown's theoretical treatment of the constant time-variable height method and the writers' development of approximate, yet mathematically accurate, equations for the variable time-constant height method, a complete theoretical basis is established for beaker-type centrifugal sedimentation of colloidal dispersions.

There is suggested, as a result of the theory now defining beaker-type centrifugal sedimentation, a great deal of experimental work to evaluate the advantages of the variable time-constant height *versus* the constant time-variable height methods for determining particle-size distributions. The results of such an investigation are the subject of a second paper on beaker-type centrifugation.

#### APPENDIX A

##### *The effect of the accelerative term on the motion of a particle in a centrifugal field*

According to Stokes's law, the force resisting movement of a spherical particle in a field is given by the equation

$$F_v = 3\pi\eta y \frac{dX}{dt}$$

The accelerative force is

$$\frac{\pi y^3 \Delta}{6} \frac{d^2 X}{dt^2}$$

and the centrifugal force

$$\frac{\pi y^3 \Delta w^2 X}{6}$$

From the laws of mechanics the centrifugal force minus the viscous force must equal the accelerative force; therefore with some simplification

$$\frac{d^2 X}{dt^2} - \frac{18 \eta}{y^2 \Delta} \frac{dX}{dt} - w^2 X = 0 \quad (50)$$

where

$$\Delta = d_1 - d_0$$

This is a differential equation of the second order with constant coefficients whose solution is presented in most elementary texts on differential equations. The solution to this equation, after imposing the limits that when  $t$  equals zero the velocity of the particle is zero and that the particle is at the point  $X$  equals  $X_0$  on the axis, is

$$X = X_0 \left[ \frac{1}{2\sqrt{1 - \left(\frac{y^2 \Delta w}{9\eta}\right)^2}} + \frac{1}{2} \right] \exp \left[ -\frac{9\eta t}{y^2 \Delta} \left( 1 - \sqrt{1 - \left(\frac{y^2 \eta w}{9\Delta}\right)^2} \right) \right] \quad (51)$$

If the functions under the square root sign are expanded by the binomial theorem, the following relations are obtained:

$$\sqrt{1 + \left(\frac{y^2 \Delta w}{9\eta}\right)^2} = 1 + \frac{1}{2} \left(\frac{y^2 \Delta w}{9\eta}\right)^2 - \frac{3}{8} \left(\frac{y^2 \Delta w}{9\eta}\right)^4 + \dots \quad (52)$$

$$\frac{1}{\sqrt{1 + \left(\frac{y^2 \Delta w}{9\eta}\right)^2}} = 1 - \frac{1}{2} \left(\frac{y^2 \Delta w}{9\eta}\right)^2 + \frac{3}{8} \left(\frac{y^2 \Delta w}{9\eta}\right)^4 + \dots \quad (53)$$

For the particular case of a spherical particle of titanium dioxide 2 microns in diameter immersed in water and being rotated at 1200 R.P.M., the following equation holds:

$$\left(\frac{y^2 \Delta w}{9\eta}\right)^2 = 0.65 \times 10^{-10}$$

Since this is an extremely small number, expansions 52 and 53 may be broken off at any term beyond the first without serious error. The exponent contains the expression 1 minus expansion 52, therefore the first two terms are retained. All terms beyond the first are neglected in expansion 53. With these substitutions equation 51 reduces to equation 54.

$$X = X_0 \exp \left( \frac{y^2 \Delta w^2 t}{18\eta} \right) \quad (54)$$

This is the same result as that obtained by equating the viscous and centrifugal forces, which is the method used to derive equation 1.

#### APPENDIX B

##### *Derivation of Oden's method of tangential intercepts*

The method of tangential intercepts was originally developed by Oden (13). In the notation used in this paper the formula for the weight sedimented in a cylindrical tube by gravitational force is

$$p = \int_z^\infty F(y) dy + \int_0^z \frac{y^2}{z^2} F(y) dy \quad (55)$$



By differentiation with respect to  $z$ :

$$\frac{dp}{dz} = - \int_0^z \frac{2y^2}{z^3} F(y) dy \quad (56)$$

If this equation is multiplied by  $z$ , and half of the result substituted in the first equation,

$$p = \int_z^\infty F(y) dy - \frac{1}{2} z \frac{dp}{dz} \quad (57)$$

or

$$p = 1 - \left[ Q + \frac{1}{2} z \frac{dp}{dz} \right] \quad (58)$$

since

$$\int_0^\infty F(y) dy = 1$$

By rearrangement of terms in equation 58

$$Q = 1 - \left[ p + \frac{1}{2} z \frac{dp}{dz} \right] \quad (59)$$

This equation is customarily expressed in the form

$$p = s + t \frac{dp}{dt} \quad (60)$$

where

$$s = \int_z^\infty F(y) dy \quad (61)$$

From equation 61 and Stokes's law for a particle settling in a gravitational field, i.e.,

$$z = \frac{K}{t^{\frac{1}{2}}}$$

where  $K$  is a constant and  $t$  is the time, equation 59 may be directly transformed into equation 60.

#### APPENDIX C.

*Reduction of the integral equation of centrifugal sedimentation to Oden's method as  $R/S$  approaches 1*

If the exponential term in equation 4 is expanded in a series, it becomes:

$$p = \int_z^\infty F(y) dy + b \int_0^z \left[ \frac{ay^2}{z^3} - \frac{a^2 y^4}{2z^4} + \frac{a^3 y^6}{6z^6} + \dots \right] F(y) dy \quad (62)$$

By differentiation of equation 4 with respect to  $t$

$$t \frac{dp}{dt} = b \int_0^z \frac{ay^2}{z^3} \exp\left(-\frac{ay^2}{z^2}\right) F(y) dy \quad (63)$$

Again by expanding the exponential function in a series, equation 63 becomes:

$$t \frac{dp}{dt} = b \int_0^s \left[ \frac{ay^2}{z^2} - \frac{a^2 y^4}{z^4} + \frac{a^3 y^6}{2z^6} + \dots \right] F(y) dy \quad (64)$$

The first terms in the quadratures containing the expansions are equal in equations 62 and 64. By the substitution of the value of this term in equation 64 into equation 62 and by the use of the notation in appendix B, equation 62 becomes:

$$p = s + t \frac{dp}{dt} + b \int_0^s \left[ \frac{a^2 y^4}{2z^4} - \frac{a^3 y^6}{3z^6} + \dots \right] F(y) dy \quad (66)$$

Since

$$\lim_{R/S \rightarrow 1} ba^n = 0 \quad n \geq 2$$

the quadrature in equation 66 approaches zero as  $R/S$  approaches 1 and the equation reduces to Oden's method. The elimination of the first terms in the quadratures of equations 62 and 64 is however, valid, as  $R/S$  approaches 1, because

$$\lim_{R/S \rightarrow 1} ba = 1$$

The senior author was the recipient of a fellowship in the Institute of Gas Technology while this problem was being investigated. The authors are indebted to Dr. H. S. Wall, formerly of the Mathematics Department of Illinois Institute of Technology, who reviewed the mathematical developments.

#### REFERENCES

- (1) BRAY, R. H.: J. Am. Ceram. Soc. **20**, 257-61 (1937).
- (2) BROWN, C.: J. Phys. Chem. **48**, 246 (1944).
- (3) DANA, S. W.: J. Sediment. Petrol. **13**, 21-7 (1943).
- (4) DUMANSKI, A., ZABOTINSKI, E., AND EWSEJEW, E.: Kolloid-Z. **12**, 6 (1913).
- (5) GUREVICH, Y. M.: Byull. Obmena Opyt. Lakokrasoch. Prom. **3**, 13-18 (1940).
- (6) HAUSER, E. A., AND LYNN, J. E.: Ind. Eng. Chem. **32**, 659 (1940).
- (7) HAUSER, E. A., AND SCHACKMAN, H. K.: J. Phys. Chem. **44**, 584 (1940).
- (8) JACOBSEN, A. E., AND SULLIVAN, W. F.: Ind. Eng. Chem. Anal. Ed. **18**, 360 (1946).
- (9) MARSHALL, C. E.: Proc. Roy. Soc. (London) **A126**, 427-39 (1930).
- (10) MARTIN, S. W.: Ind. Eng. Chem. Anal. Ed. **11**, 471-5 (1939).
- (11) MARTIN, S. W.: "Determination of Subsieve Particle Size Distributions by Sedimentation Methods", A.S.T.M. Symposium on New Methods for Particle Size Determination in the Subsieve Range, Philadelphia, 1941.
- (12) MURRAY, D. A.: *Introductory Course in Differential Equations*. Longmans, Green and Company, London (1938).
- (13) NORTON, F. H., AND SPIEL, S.: J. Am. Ceram. Soc. **21**, 89-98 (1937).
- (14) ODEN, S.: In *Alexander's Colloid Chemistry*, Vol. I. The Chemical Catalog Company, Inc., New York (1926).
- (15) PARKINSON, D.: Rubber Chem. Tech. **14**, 98-112 (1941).
- (16) ROMWALTER, A., AND VENDL, M.: Kolloid-Z. **72**, 1-3 (1935).

- (17) SCHLESINGER, M.: *Kolloid-Z.* **67**, 135-42 (1934).
- (18) STEELE, J. G., AND BRADFIELD, P.: *Am. Soil Survey Assoc., Rept. 14th Ann. Meeting Bull.* **15**, 88-9 (1934); *Chem. Abstracts* **28**, 4813 (1934).
- (19) SVEDBERG, THE, AND NICHOLS, J. B.: *J. Am. Chem. Soc.* **45**, 2910 (1923).
- (20) SVEDBERG, THE, AND PEDERSON, K. O.: *The Ultracentrifuge*. Clarendon Press, Oxford (1940).
- (21) SVEDBERG, THE, AND RINDE, H.: *J. Am. Chem. Soc.* **46**, 2677-93 (1924).

## THE OSMOTIC BEHAVIOR OF SOME COLLOIDAL ELECTROLYTES AS DETERMINED BY MEANS OF THE HILL-BALDES VAPOR-TENSION APPARATUS<sup>1</sup>

MANUEL N. FINEMAN<sup>2</sup> AND JAMES W. MCBAIN

*Department of Chemistry, Stanford University, California*

*Received October 23, 1947*

### INTRODUCTION

Colloidal electrolytes in aqueous solution are characterized by the aggregation of individual ions into colloidal particles or micelles. Hence the osmotic activity of colloidal electrolytes is correspondingly diminished while their conductivity may remain comparatively high, owing to the conductivity of the charged micelles as well as that of the free ions. Prior to 1939 only conductivity and transport numbers (12, 20) had been measured for very dilute solutions where the transition from an ordinary uni-univalent electrolyte to a colloidal electrolyte occurs. In more recent years methods for studying the colligative properties of colloidal electrolytes have included extensive investigations of the freezing-point depression (8, 15, 16, 17), with the more accurate Scatchard apparatus (27) superseding the original Beckmann procedure (5).

However, materials which are only slightly soluble in water even at room temperature cannot be studied by the usual cryoscopic methods at 0°C. For such materials some accurate method for measuring the lowering of the vapor pressure would seem to be desirable. Early in the history of colloidal electrolytes, McBain and Salmon (19) used the dew-point lowering method, which they found to be useful at high concentrations but of questionable accuracy in dilute solutions. For the present investigation, a thermoelectric measurement of vapor pressure has been used, based upon the Hill-Baldes vapor-tension apparatus, sometimes misleadingly called the "thermoelectric osmometer".

In 1939 Baldes and his collaborators (3, 4) described a modification of the Hill vapor-pressure thermopile (10) for measuring the difference in vapor pressure

<sup>1</sup> Presented before the Division of Colloid Chemistry of the American Chemical Society at the 112th Meeting, New York City, September 16, 1947.

<sup>2</sup> Bristol-Myers Company Postdoctorate Fellow in Chemistry. Present address: Resinous Products and Chemical Company, Philadelphia, Pennsylvania.

between two aqueous solutions or between a solution and its solvent. The principle of this method is essentially that of the wet-bulb thermometer. It involves the thermoelectric measurement of the rates of evaporation from and condensation on droplets of the sample and a reference solution when these are placed on opposite junctions of a thermocouple enclosed in a moist chamber. The deflection of the galvanometer to which the thermocouple is connected is proportional to the difference in temperature between the two junctions and this, in turn, depends upon the difference in vapor pressure between the two droplets.

The theory of the steady-state condition in the vapor-pressure apparatus has been given by Baldes. Further, the accuracy, sensitivity, sources of error, and general scope of the procedure have been analyzed in detail by Roepke (24). Moreover, in recent years experimental results have been reported (23, 25) in which this technique has been employed to study the formation of micelles in aqueous solutions of bile salts, and other similar phenomena principally in the field of biochemistry.

#### APPARATUS

The apparatus used in this work was similar to that described by Baldes and Johnson except for minor modifications. For example, the manganin which Baldes and Johnson used in their constantan-manganin thermocouples, with copper leads, tended to become brittle and fractured easily. Therefore these thermocouples were replaced by copper-constantan thermocouples in which the copper lead wires formed part of the thermocouple junction. This apparatus has been sketched schematically and to scale in figure 1. Thermocouples of copper and constantan wires, 5 and 2 mils in diameter, respectively, with the loops about 8 mm. apart, were mounted on glass rods and were suspended in the center of glass containers. These containers were lined with moistened filter paper and sealed with rubber stoppers. They were then mounted below the surface of a constant-temperature bath ( $25^{\circ}\text{C.} \pm 0.002^{\circ}$ ) as indicated in the sketch. For several of these determinations a brass container was also used but, generally, it was found that the glass containers were better for the purpose, since they made the thermocouples less sensitive to minor fluctuations in the temperature of the water bath. The copper thermocouple leads connected through a convenient reversing switch directly to a very sensitive galvanometer of the Leeds and Northrup Type HS, List Number 2284b.

To eliminate asymmetry of the thermocouple with respect to the surrounding wall, and parasitic electromotive forces, the galvanometer deflection was also observed with the solutions reversed on the thermocouple loops. The average of the two readings was taken as the final value. For new thermocouples, properly constructed and carefully suspended in the centers of the containers, the differences due to asymmetry were found to be small.

Using a series of potassium chloride solutions of known molality as standards and water as the reference solution, each of the thermocouples used was first calibrated at a given temperature. The results gave straight lines when the galvanometer deflection was plotted against the product of the molality of the

potassium chloride and its osmotic coefficient at that molality. For potassium chloride, the osmotic data reported by Harned and Owen (9) were used. Then droplets of solutions of colloidal electrolytes of known concentration were placed on the thermocouple loops with water again as the reference solution and, from

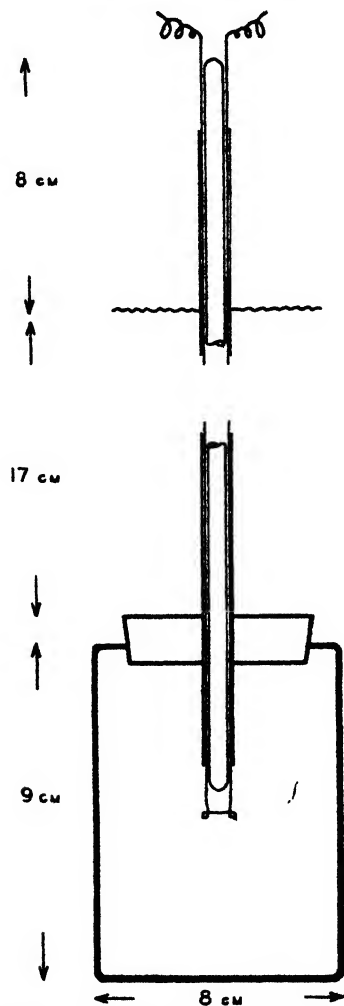


FIG. 1. Vapor-tension apparatus

the galvanometer deflection observed, the unknown osmotic coefficient of the colloidal solution could be calculated.

Each of the points represented on the graphs to follow, and obtained by the thermoelectric vapor-pressure method, represents the mean value of results using six or more systems at the same time. Although the sensitivity of the vapor-tension method is greater than that of the Beckmann freezing-point depression procedure, its reproducibility varies from 4 per cent to 8 per cent, the greater deviation being observed at the higher dilutions.

The colloidal electrolytes used in this work were the purest obtainable, as follows: potassium laurate and potassium myristate, special preparation by Kahlbaum; sodium oleate, Merck's best; sodium laurate, prepared from Eastman lauric acid. The cationic detergents were prepared by the Wm. S. Merrell Company. The anionic soaps were recrystallized from alcoholic solution, during which time any excess fatty acid present was neutralized by alkali so that the final product had a pH in the aqueous alcohol of about 7. On making up the aqueous solutions, however, 4 moles per cent excess of alkali was added to the soaps in order to suppress hydrolysis. In calculating the osmotic coefficient,  $g$ , of the colloidal solution, the galvanometer deflection due to this added alkali was subtracted from the total deflection observed. These solutions were stored in Jena-glass containers.

With some of the anionic detergents it was noticed that excessively prolonged exposure to carbon dioxide in the air inside the containers sometimes caused the soap droplets to turn cloudy. However, this did not seem to affect the galvanometer deflections during the first 2 hr. after droplet deposition. This cloudiness could be prevented by addition of a very small amount of alkali to the containers, which neutralizes the carbon dioxide in the air without affecting the magnitude of the galvanometer deflection.

#### RESULTS

Since the osmotic behavior of potassium laurate had already been investigated extensively at several temperatures, it was decided to apply the vapor-tension method first to this material as a standard. Therefore, potassium laurate was studied extensively at 25°C. and a few experiments were also attempted at 50°C. The results at both temperatures were found to be almost alike. In order to compare these data with the osmotic behavior of potassium laurate at 0°C., the freezing-point lowering curve was investigated at that temperature, using an apparatus similar to that of Scatchard and already described in detail by other investigators. The osmotic coefficients obtained confirm a previous determination at 0°C. reported from this laboratory by McBain and Brady (16), but appear to be about 30 per cent higher at 0°C. in the concentration range from 0.03 to 0.3 molal than the values obtained by the vapor-tension method at 25° and 50°C. These data are tabulated in table 1 and reported graphically in figure 2.

The straight lines of negative slope plotted at the tops of these graphs represent the Debye-Hückel behavior of ideal uni-univalent electrolytes. The curves then display the deviation from ideality observed for colloidal electrolytes.

In a recent paper (7) a simple method for determining the critical concentration for micelle formation has been described, based upon the spectral change of a dye. As a dilute aqueous solution of a dye is added to a soap solution, the color of the dye changes when the concentration of the soap decreases below the critical concentration. By noting the amount of dye solution required to bring about this color change, it is therefore possible to calculate the concentration of the soap at this point. For each of the materials investigated here, the critical concentration was determined by means of this dye method, using Rhodamine

6G for the anionic detergents and Niagara Sky Blue as well as Brom Cresol Purple for the cationic detergents. The values obtained are listed separately in the following tables and indicated on the graphs as falling on the idealized curve. The color change observed at the so-called "critical" concentration by this method was by no means sharply defined, there being a gradual transition from one color to the other through the spectrum over a fairly wide concentration range. Therefore, the results reported are only approximations within 10 per cent.

The critical concentration range in which the micelles of potassium laurate start to form was found to be about 0.025 molal by the vapor-tension method and

TABLE 1  
*Osmotic behavior of potassium laurate*

0°C.			25°C.			50°C.		
<i>m</i>	<i>m</i> <sup>1/2</sup>	<i>g</i>	<i>m</i>	<i>m</i> <sup>1/2</sup>	<i>g</i>	<i>m</i>	<i>m</i> <sup>1/2</sup>	<i>g</i>
0.248	0.498	0.218*	0.1877	0.433	0.188	0.1382	0.372	0.239
0.0978	0.313	0.413*	0.1577	0.397	0.182	0.0553	0.235	0.457
0.0449	0.212	0.752	0.1382	0.372	0.273	0.0272	0.165	0.769
0.0416	0.202	0.866*	0.0858	0.293	0.299			
0.031	0.176	0.899	0.0553	0.235	0.529			
0.0306	0.175	0.940*	0.0491	0.221	0.521			
0.0209	0.144	0.979	0.0332	0.182	0.765			
0.0147	0.121	0.979	0.0272	0.165	0.702			
0.0104	0.102	0.968	0.0214	0.146	0.821			
Dye method†.			0.017	0.13	(0.955)			

\* Data of McBain and Brady (16).

† *g* value arrived at by plotting critical concentration obtained by dye method as falling along the ideal *g* curve.

0.017 molal by the dye method. It has often been assumed that the critical concentration for micelle formation is reduced by the addition of a dye or other hydrocarbon which may be solubilized in the colloidal micelle. Thus, measurements by means of the solubilization of a dye usually yield lower values for the critical concentration than those obtained with the freezing-point depression technique. To investigate this phenomenon *n*-hexane was added to the potassium laurate solutions so that about 0.14 mole of hexane was solubilized per mole of soap, and the freezing-point determinations were repeated. The results of several such experiments showed that the solubilized hexane did indeed reduce the critical concentration of the soap by about 15 per cent. Further, this effect might have been magnified by the solubilization of a larger quantity of hexane. However, the general osmotic behavior observed was closely analogous to that of potassium laurate alone without hexane.

Potassium myristate and sodium laurate cannot be studied at 0°C. because of their low solubility. The results obtained at 25°C. are tabulated in table 2 and plotted in figure 3. The osmotic coefficient of potassium myristate is found to

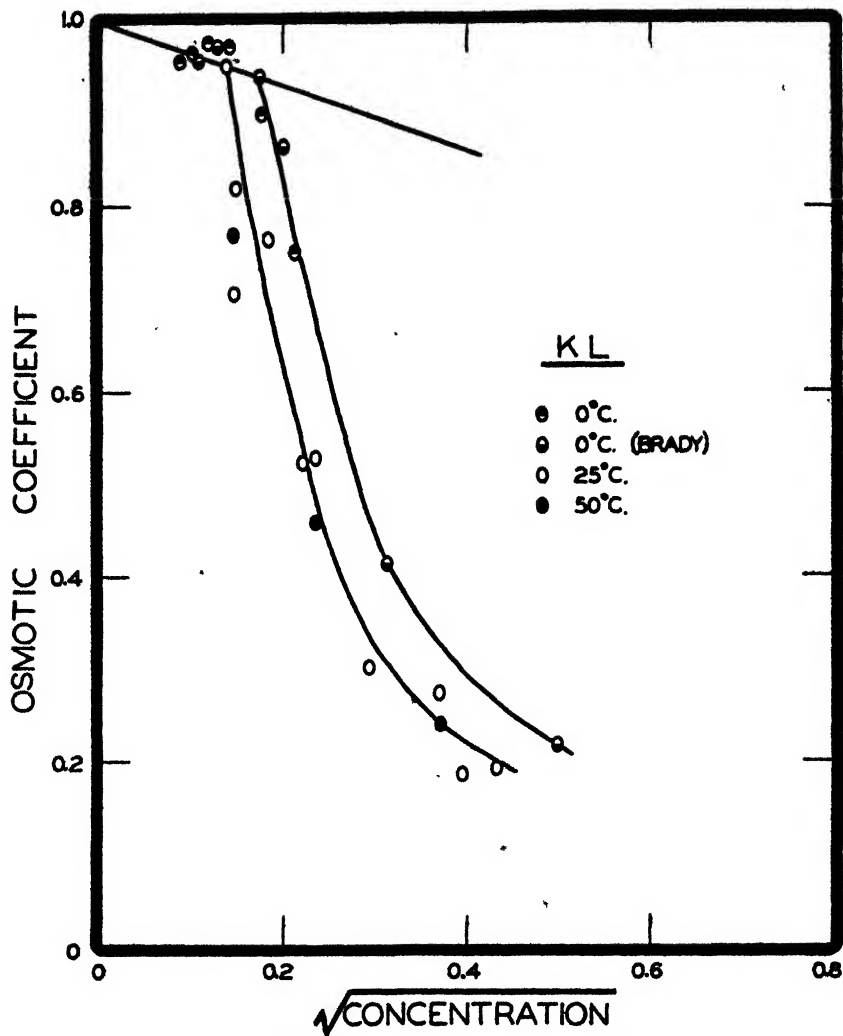


FIG. 2. Osmotic behavior of potassium laurate

TABLE 2

*Osmotic behavior of potassium myristate and sodium laurate at 25°C.*

POTASSIUM MYRISTATE			SODIUM LAURATE		
$m$	$m^{1/2}$	$\xi$	$m$	$m^{1/2}$	$\xi$
0.1966	0.443	0.127	0.0814 <sub>7</sub>	0.285	0.374
0.0616 <sub>8</sub>	0.248	0.193	0.0430 <sub>7</sub>	0.207	0.593
0.0210	0.144	0.453			
0.0119	0.109	0.660			
Dye method					
0.006	0.078	(0.975)	0.024	0.154	(0.945)



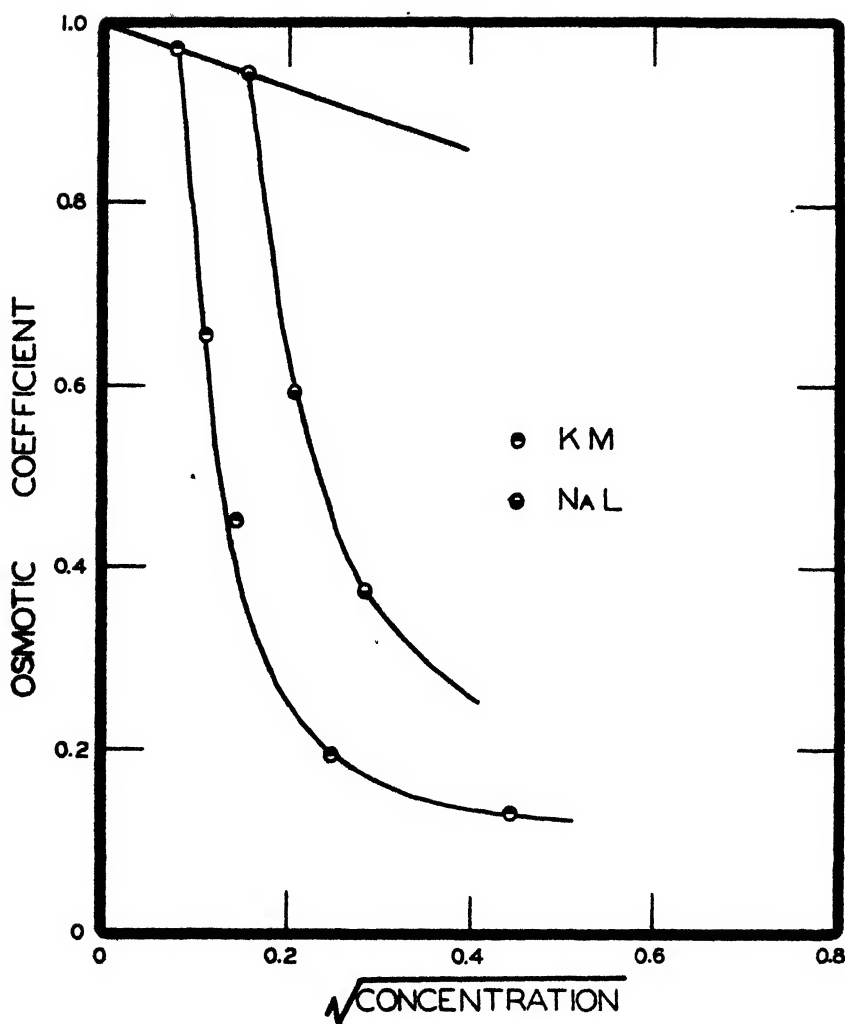


FIG. 3. Osmotic behavior of potassium myristate and sodium laurate

TABLE 3  
Osmotic behavior of sodium oleate

TEMPERATURE	METHODS	$m$	$m^{1/2}$	$\xi$	REFERENCE
25°C.	Vapor tension	0.0948 <sub>2</sub>	0.308	0.241	This work
		0.0419 <sub>1</sub>	0.204	0.244	This work
		0.0113 <sub>4</sub>	0.106	0.354	This work
	Dye	0.0015	0.039	(0.985)	This work
18°C.	Dew point	0.4	0.632	0.17	(13)
		0.6	0.774	0.17	(13)
0°C.	Beckmann	0.2	0.447	0.127	(18)
		0.4	0.632	0.098	(18)
		0.2	0.447	0.111	(15)

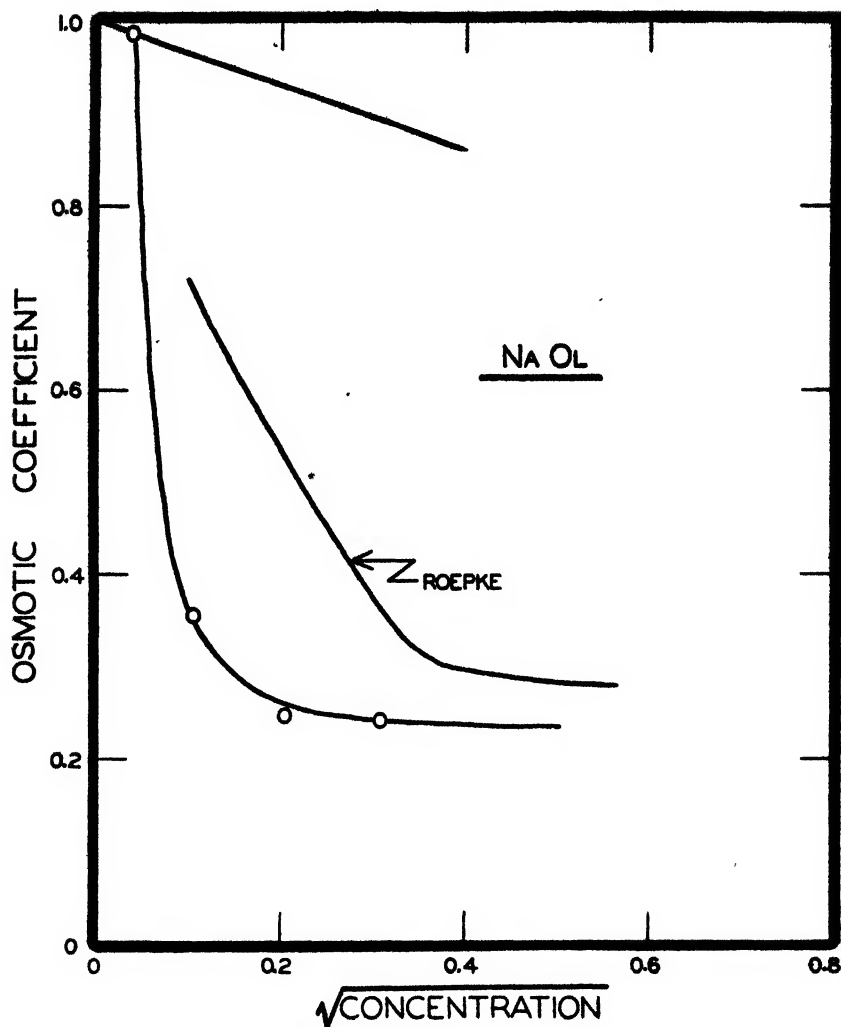


FIG. 4. Osmotic behavior of sodium oleate

TABLE 4

*Osmotic behavior of some cationic detergents at 25°C.*

CETYLPIRIDINIUM CHLORIDE			CETYLTRIMETHYLAMMONIUM BROMIDE			CETYLDIMETHYLBENZYLAMMONIUM CHLORIDE		
<i>m</i>	<i>m</i> <sup>1/2</sup>	<i>g</i>	<i>m</i>	<i>m</i> <sup>1/2</sup>	<i>g</i>	<i>m</i>	<i>m</i> <sup>1/2</sup>	<i>g</i>
0.0419	0.204	0.120	0.20	0.447	0.076 <sub>4</sub>	0.20	0.447	0.107
0.0096 <sub>8</sub>	0.098	0.412	0.10	0.316	0.087 <sub>8</sub>	0.10	0.316	0.105
0.0048 <sub>8</sub>	0.069	0.685	0.05	0.223	0.0573	0.05	0.223	0.101
			0.005	0.070 <sub>7</sub>	0.91	0.005	0.070 <sub>7</sub>	0.62
Dye method								
0.00003		(0.995)	0.0005		(0.990)	0.0002		(0.995)

drop sharply to a value less than 0.2 at a molality of about 0.06. The critical concentration for micelle formation is about 0.006 molal. For sodium laurate, a similar sharp drop in osmotic behavior is observed from a critical concentration value of about 0.024 molal. This value is very close to that observed for

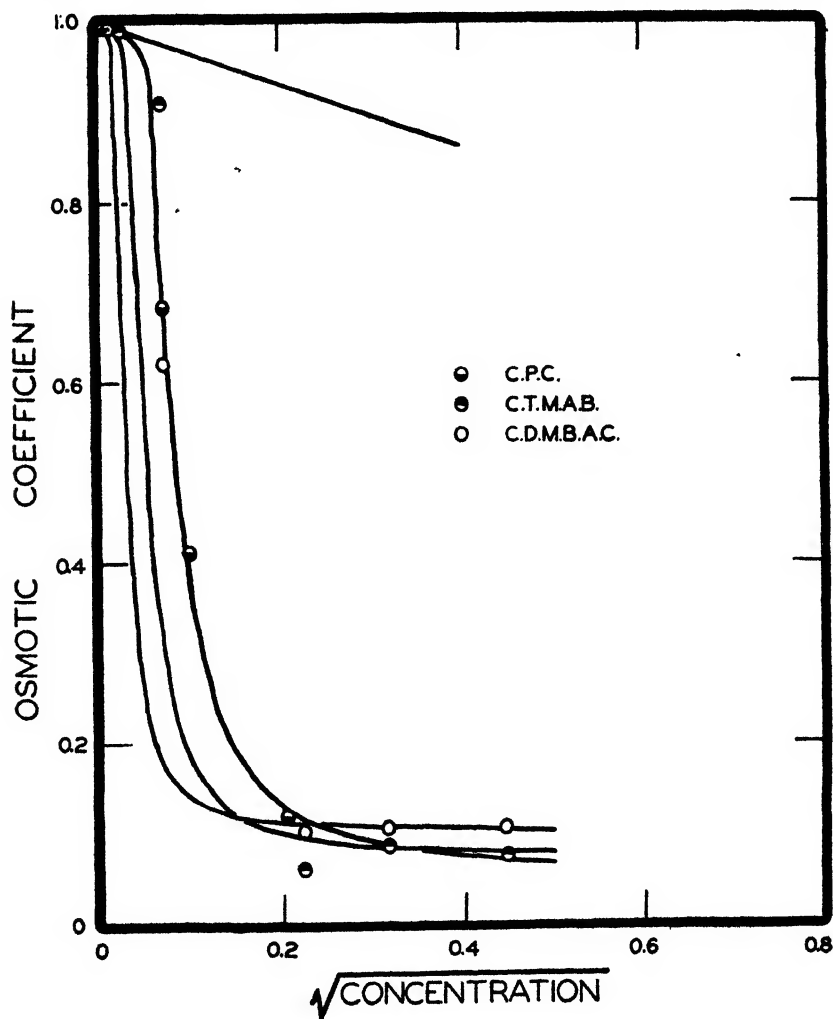


FIG. 5. Osmotic behavior of some cationic detergents

potassium laurate (i.e., 0.025). Data at higher concentrations of sodium laurate are not obtainable because of its poor solubility.

McBain and Johnston (17) showed that the few measurements of sodium oleate by the Beckmann and dew-point methods may be subject to some uncertainty. However, by comparison with potassium oleate, they concluded that the curve for sodium oleate reported by Roepke and Mason (26), who used the

thermoelectric method, was unaccountably high. Sodium oleate was therefore investigated at 25°C.; the results obtained are tabulated in table 3. For comparison, the available data at 0°C. and 18°C. are included. No numerical data or tables were given for the curve reported by Roepke and Mason. In figure 4 their curve is reproduced, together with our experimental observations.

Our results confirm the previous conclusion that the curve of Roepke and Mason for sodium oleate may be too high. These higher values may be due to hydrolysis of the soap in solution, since Roepke and Mason made no mention of precautions to suppress hydrolysis. The critical concentration for micelle formation in the case of sodium oleate is very close to that reported by McBain and Johnston for potassium oleate, i.e., 0.0015 molal.

Among the solutions of cationic detergents investigated at 25°C. in the vapor-tension apparatus were cetylpyridinium chloride (C.P.C.), cetyltrimethylammonium bromide, (C.T.M.A.B.), and cetyldimethylbenzylammonium chloride (C.D.M.B.A.C.). The data for these are listed in table 4 and presented graphically in figure 5.

For cetyltrimethylammonium bromide and cetyldimethylbenzylammonium chloride the solutions investigated at molalities less than 0.05 were subject to appreciable uncertainty; hence the portions of the curves plotted for these materials between  $g = 1.0$  and  $g = 0.2$  are only approximations. The method of arriving at the shapes of the curves in this region will be outlined below. Independent investigations in this laboratory, soon to be reported, on the equivalent conductivity and freezing-point depression of these materials yield results which may be correlated with the curves drawn here from the vapor-tension data.

#### DISCUSSION

The colligative properties of dilute solutions are those which deal with the number and not the nature of the particles present in solution. These are commonly called osmotic properties and include, in addition to the osmotic pressure, the lowering of the freezing point, rise of the boiling point, lowering of the dew point, etc. Since each of these properties depends upon the vapor pressure of the solution, it would seem reasonable to suppose that data obtained by any one of these methods could be replotted in terms of the lowering of the vapor pressure. More conveniently, the relative lowering of the vapor pressure would make these data independent of the temperature at which they were obtained. Such calculations have been made for the osmotic data obtained here by the thermoelectric vapor-tension method as well as by the freezing-point depression. Figures 6, 7, and 8 represent the osmotic data replotted in terms of relative vapor-pressure lowering.

The straight line which goes through the origin represents the relative vapor-pressure lowering for an ideal uni-univalent electrolyte such as potassium chloride. The other straight lines represent the deviation from ideality observed for the colloidal electrolytes and intersect the ideal curve at a concentration roughly equal to the critical concentration for micelle formation.

The fact that the osmotic behavior of these colloidal solutions may be charac-

terized by a straight-line relationship, first noted independently by Drs. Brady and Chandler of this laboratory, markedly simplifies investigations on these and like materials. In order to plot the complete osmotic-activity curve, it now merely becomes necessary to ascertain the critical concentration and the relative vapor-pressure lowering at one or two concentrations above the critical concentration. For this purpose any convenient colligative property of the material may be investigated. Then, from the straight line plotted between these points

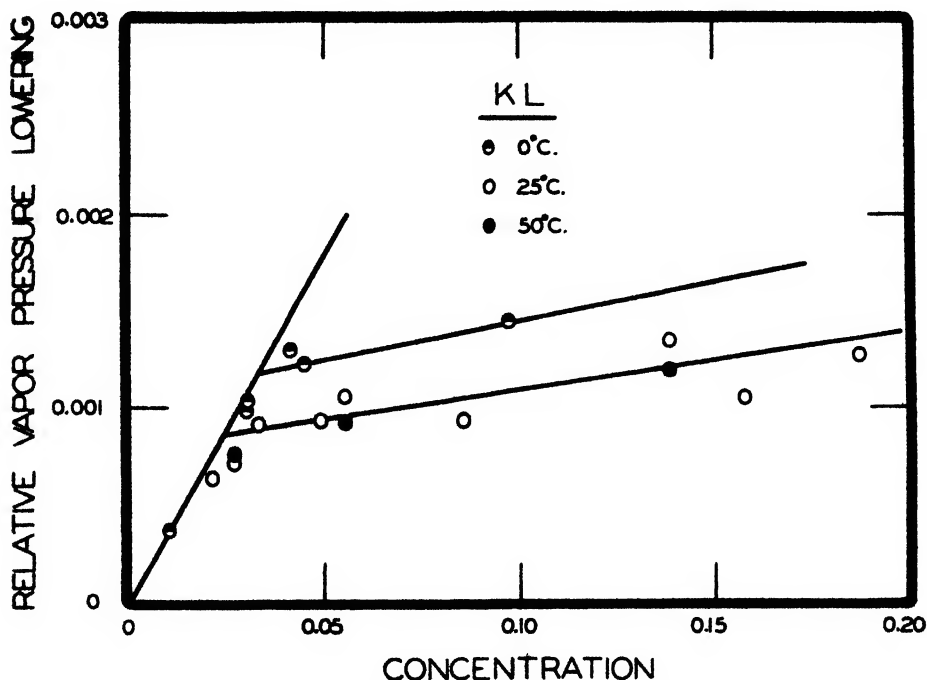


FIG. 6. Vapor-pressure lowering for ideal behavior in dilute solution and actual behavior of more concentrated solution, the intersection showing the influence of temperature on the so-called critical concentration for formation of micelles.

the osmotic activity at any other concentration above the critical concentration may now be calculated directly.

Other investigations in this laboratory show that the straight lines thus plotted for colloidal electrolytes fall off slightly in slope as they approach the ideal curve (6). However, these straight lines may be extrapolated to intersect the ideal curve. The concentration at this intersection is shown in figures 6 and 7 to coincide very closely with the value for the critical concentration for micelle formation obtained by the dye method. On the basis of the straight lines plotted in figure 8, it was possible to calculate the full curves shown in figure 5 for the cationic detergents even over the concentration range where no experimental points were obtained.

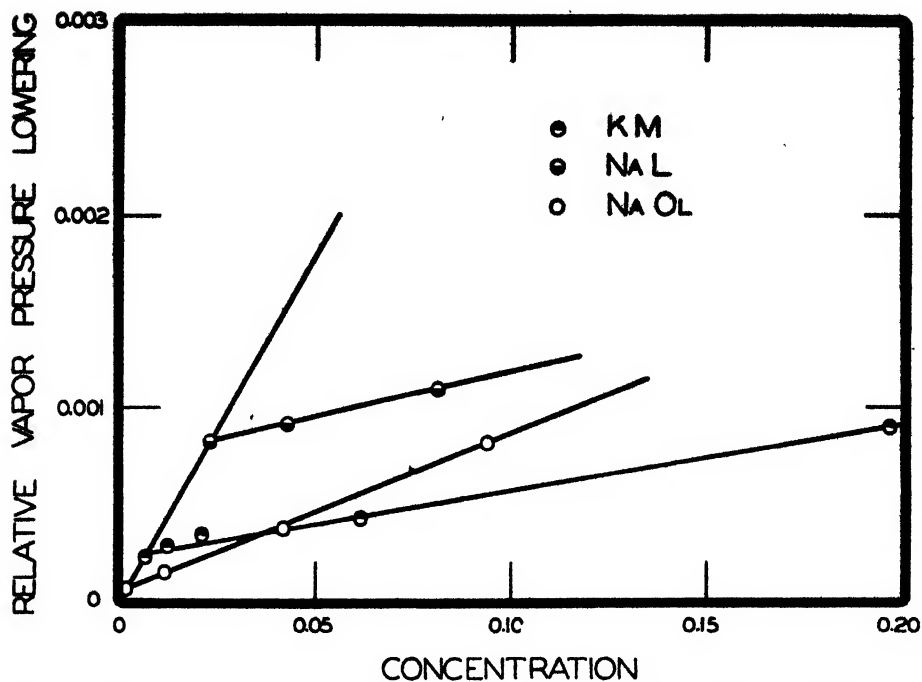


FIG. 7. The observed vapor-pressure lowerings terminating in very dilute solution in the straight-line curve for ideal behavior.

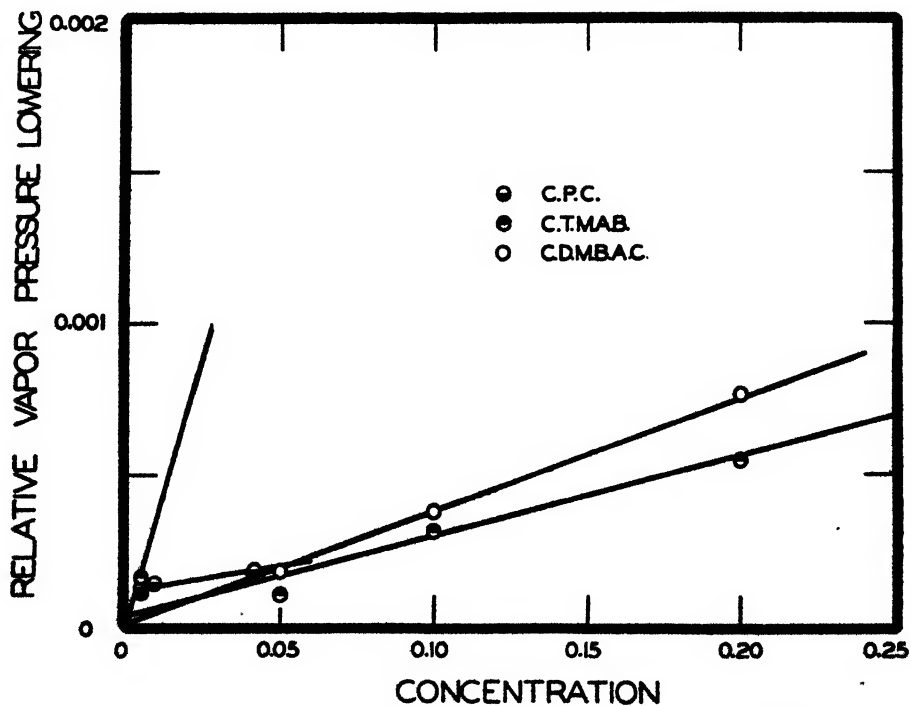


FIG. 8. The observed vapor-pressure lowerings terminating in very dilute solution in the straight-line curve for ideal behavior.

*Classification of detergents*

In describing generalized curves by which the osmotic behavior of different colloidal electrolytes may be related as to type, McBain and Brady (16) have demonstrated that all straight-chain detergents associate into micelles with equal readiness, branched-chain materials less readily than straight-chain, and polycyclic colloidal electrolytes least readily of all. By plotting the osmotic coefficient,  $g$ , against the logarithm of the concentration divided by the concentration at which  $g = 0.5$ , they were able to show that between  $g$  values of 0.2 and 0.9, a

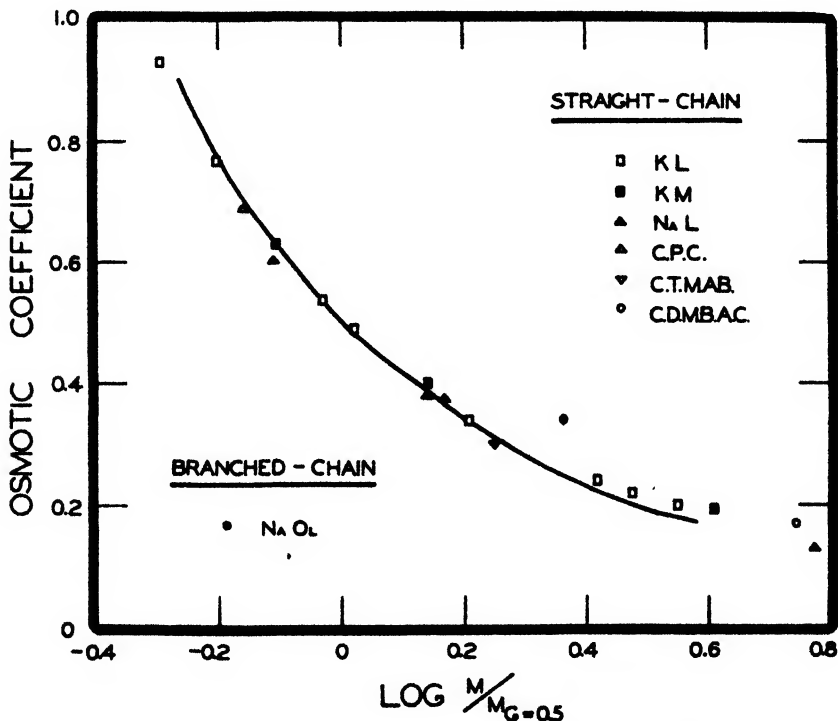


FIG. 9. Osmotic coefficients plotted on the Brady curve (16) characteristic of straight-chain colloidal electrolytes.

single curve may be drawn through the data for all straight-chain compounds, another for branched-chain materials, and still a third for those of polycyclic structure. Applying this method of plotting to the osmotic data obtained here and taking the best values for the osmotic coefficients from the curves in figures 2, 3, 4, and 5, figure 9 shows that all the compounds investigated seem to be of the straight-chain type. Sodium oleate, however, more closely approximates the branched-chain type of behavior, possibly because restricted rotation arising from the presence of a double bond prevents close packing of the chains in the micelles. This branched-chain type of behavior has also been reported for potassium oleate (16).

It is interesting to note here that the slopes of the straight lines plotted in figures 6, 7, and 8 for all the materials, except sodium oleate, seem to be constant about a mean value of 0.0031 (table 5). For sodium oleate, however, the slope is about 0.0082. From this one may infer that straight-chain, branched-chain, and polycyclic compounds may be readily identified by the slopes of the straight lines when the data are plotted as in figures 6, 7, and 8.

#### *Variation of osmotic behavior with temperature*

Because of the fact that the vapor-tension method may be used for solutions at any temperature below the boiling point of the solvent, it should be possible to determine the variation of the osmotic coefficient of colloidal electrolytes with temperature. For potassium laurate, figure 2 shows that the osmotic data at 25°C. and 50°C. coincide almost exactly. However, the data at these temperatures fall below those obtained by the method of the freezing-point depression at 0°C. There is still uncertainty as to whether this difference in osmotic behavior

TABLE 5  
*Classification of detergents*

MATERIAL	SLOPE OF STRAIGHT LINE	TYPE
Potassium laurate (0°C.)	0.0028	Straight-chain
Potassium laurate (25°C.)	0.0031	Straight-chain
Potassium myristate	0.0034	Straight-chain
Sodium laurate	0.0047	Straight-chain
Cetylpyridinium chloride	0.0020	Straight-chain
Cetyltrimethylammonium bromide	0.0023	Straight-chain
Cetyldimethylbenzylammonium chloride	0.0037	Straight-chain
Sodium oleate	0.0082	Branched-chain

is a true function of temperature, or only a methodic difference between the two procedures. The measurements at 0°C., using the Scatchard apparatus, are supposed to be the most accurate obtainable. Hence, assuming that the osmotic coefficient does not change very much with temperature between 0°C. and 25°C., it may be that the low results obtained with the vapor-tension method may be due to some error inherent in the apparatus or in the procedure.

The theory of the vapor-tension method as outlined by Baldes depends upon the rapid attainment of a condition of steady state between the droplets on the two junctions of the thermocouple. It has been assumed that this condition is reached very shortly after the droplets and their container reach the same temperature as the water bath. Very recently this assumption has been confirmed by Lifson and Lorber (14), who showed that the condition of steady state is reached within 40 sec. after deposition of the droplets on the thermocouple loops when the apparatus is immersed in the bath at a constant temperature. For the investigations reported in this work, galvanometer readings were taken over a period of 2 hr. from the time of deposition of the droplets.



In defining the scope of the vapor-tension apparatus, Roepke (24) suggested that the presence of a film on the surface of the droplets at the thermocouple junctions might retard the process of evaporation and give rise to low osmotic values. With some films it has been shown (28) that the rate of evaporation may be retarded by as much as 90 per cent.

To investigate what effect this phenomenon might have on the results obtained above with the vapor-tension apparatus, two solutions of 0.1 molal potassium chloride were made up. To one of these solutions a small amount of potassium laurate was added—sufficient to give the solution a surface pressure of about 35 dynes. This amount of potassium laurate was small enough to contribute nothing to the osmotic behavior of the potassium chloride, but the presence of the film might retard the evaporation as indicated above and show a reduced galvanometer deflection. To the other solution, nothing was added. Upon investigation, both these solutions of potassium chloride showed exactly the same galvanometer deflection. Therefore, it would appear that although the presence of a surface film may retard the rate of evaporation from a droplet, it does not seem to affect the equilibrium between solution and solvent once a steady state is attained; and it is this equilibrium which ultimately determines the magnitude of the galvanometer deflection in the vapor-tension apparatus.

Despite these checks on the precision of the vapor-tension apparatus, there are a number of other factors involved—such as loss of heat due to radiation between the junctions—which may tend to give values slightly lower than normal. Other possibilities of error include those which may arise whenever a method must be standardized against some so-called standard. Nevertheless, in spite of these difficulties, the method is obviously of merit for all comparative purposes. It is further useful and valuable in that it may be applied to solutions in solvents other than water at any temperature up to the boiling point of the solvent.

Other isopiestic vapor-pressure experiments in this laboratory (21), to be reported shortly, show that the osmotic coefficient of potassium laurate increases only very slightly with temperature from 35°C. to 105°C. Similar investigations of critical concentration by conductivity (29), surface tension (22), and refractive index (11) at varying temperatures, together with the coincidence of present data at 25°C. and 50°C., seem to support the view that the osmotic coefficient increases only slightly with temperature.

Several experiments have been attempted using thermistors (thermally sensitive resistors) in place of the thermocouples for determining the vapor-pressure lowering of these colloidal solutions. At a condition of steady state the droplets of solution and solvent deposited on the tips of the thermistors had a constant temperature difference which could be measured as a resistance differential on a Wheatstone bridge. From the results obtained it was apparent that the sensitivity of the particular type of thermistors used was not nearly as good as that of the thermocouples. However, thermistors having a high temperature coefficient of resistance are being manufactured at present, and these may find later use as a substitute for the thermocouple in the vapor-tension method. An added ad-

vantage in the use of the thermistors is that with these the temperature of each of the droplets can be measured separately, if desired, whereas the thermocouple only records the difference in temperature between them.

#### SUMMARY

The osmotic behavior of colloidal electrolytes, some of which are only slightly soluble in water at room temperature and hence cannot be studied by the usual cryoscopic methods at 0°C., has been investigated at 25°C. and at higher temperatures by means of a modification of the Hill-Baldes vapor-tension apparatus, sometimes called the "thermoelectric osmometer".

Data thus obtained are reported for some anionic detergents such as the sodium and potassium salts of lauric, myristic, and oleic acids as well as for cationic detergents of the substituted ammonium and pyridinium halide types. The results are in fair agreement with the generalized curves for colloidal electrolytes first described by McBain and Brady. Further, for potassium laurate, there does not seem to be any appreciable change in the value of the osmotic coefficient for changes in temperature from 0°C. to 50°C.

The usefulness of the vapor-tension apparatus for studying the behavior of colloidal electrolytes is demonstrated.

#### REFERENCES

- (1) BALDES, E. J.: *J. Sci. Instruments* **11**, 223 (1934).
- (2) BALDES, E. J.: Thesis, University of London, 1936.
- (3) BALDES, E. J.: *Biodynamica* No. **46** (1939).
- (4) BALDES, E. J., AND JOHNSON, A. F.: *Biodynamica* No. **47** (1939).
- (5) BECKMANN, E.: *Z. physik. Chem.* **2**, 638 (1888).
- (6) BRADY, A. P.: *J. Am. Chem. Soc.*, in press (March, 1948).
- (7) CORBIN, M. L., AND HARKINS, W. D.: *J. Am. Chem. Soc.* **69**, 673 (1947).
- (8) GONICK, E., AND MCBAIN, J. W.: *J. Colloid Sci.* **1**, 127 (1946).
- (9) HARNED, H. S., AND OWEN, B. B.: *Physical Chemistry of Electrolytic Solutions*, p. 289. Reinhold Publishing Corporation, New York (1943).
- (10) HILL, A. V.: *Proc. Roy. Soc. (London)* **A127**, 9 (1930).
- (11) KLEVEN, H. B.: *J. Colloid Sci.* **2**, 301 (1947).
- (12) LAING, M. E.: *J. Phys. Chem.* **28**, 673 (1924).
- (13) LAING, M. E., AND MCBAIN, J. W.: *J. Chem. Soc.* **117**, 1513 (1920).
- (14) LIFSON, N., AND LORBER, V.: *J. Biol. Chem.* **158**, 209 (1945).
- (15) MCBAIN, J. W., AND BOLDUAN, O. E. A.: *J. Phys. Chem.* **47**, 94 (1943).
- (16) MCBAIN, J. W., AND BRADY, A. P.: *J. Am. Chem. Soc.* **65**, 2072 (1943).
- (17) MCBAIN, J. W., AND JOHNSTON, S. A.: *Proc. Roy. Soc. (London)* **A181**, 119 (1942).
- (18) MCBAIN, J. W., LAING, M. E., AND TITLEY, A. F.: *J. Chem. Soc.* **115**, 1289 (1919).
- (19) MCBAIN, J. W., AND SALMON, C. S.: *J. Am. Chem. Soc.* **42**, 426 (1920).
- (20) MCBAIN, M. E. LAING: *Trans. Faraday Soc.* **31**, 153 (1935).
- (21) O'CONNOR, J. J.: Private communication.
- (22) POWNY, J., AND ADDISON, C. C.: *Trans. Faraday Soc.* **33**, 1243, 1253 (1937).
- (23) ROEPKE, R. R.: *J. Biol. Chem.* **126**, 349 (1938).
- (24) ROEPKE, R. R.: *J. Phys. Chem.* **46**, 359 (1942).
- (25) ROEPKE, R. R., AND BALDES, E. J.: *J. Cellular Comp. Physiol.* **20**, 71 (1942).
- (26) ROEPKE, R. R., AND MASON, H. L.: *J. Biol. Chem.* **133**, 103 (1940).
- (27) SCATCHARD, G., JONES, P. T., AND PRENTISS, S. S.: *J. Am. Chem. Soc.* **54**, 2676 (1932).
- (28) SEBBA, F., AND BRISCOE, H. V. A.: *J. Chem. Soc.* **1940**, 106.
- (29) WRIGHT, K. A., ABBOTT, A. D., SIVERTZ, V., AND TARTAR, H. V.: *J. Am. Chem. Soc.* **61**, 549 (1939).

DIFFUSION ACROSS OIL-WATER INTERFACES<sup>1</sup>ERIC HUTCHINSON<sup>2</sup>*Department of Chemistry, Stanford University, California**Received November 13, 1947*

The experiments described here form part of an investigation into the mechanism whereby molecules diffuse across an oil-water interface, and into the effect of monomolecular films on such diffusion processes.

Diffusion problems are of fundamental importance in the study of many physiological processes and have been the subject of very extensive research (9), but in many cases the systems investigated have been so complex that experimental proof of the various mechanisms proposed to explain the transfer of material, say through a cell membrane, has been difficult to obtain. These processes always involve the transfer of material across some kind of interface, be it oil-water or solid-water, and from the earliest days of the study of monomolecular films it has been recognized that such films must play an important rôle in physiology. However, no predictions as to the mode of action of these films are to be found in the literature, and direct experimental investigation seems desirable.

The structure of plasma membranes is generally considered to be a mosaic network of protein matter, in the interstices of which is retained lipid or oily material (12), and currently held theories on diffusion through such membranes are based on this conception. The original "lipoid" theory of diffusion postulated by Overton (11) (and in the special case of narcosis by Meyer (10)) suggested that there was a marked parallelism between the permeability of organic non-electrolytes in the membrane and the distribution coefficient of the diffusing molecule between the lipid material and water. Those compounds which are preferentially soluble in the lipid phase diffuse most rapidly. In an extensive study of the rates of penetration of a number of organic liquids into single cells of *Chara ceratophylla* Collander and Bärlund (5) found a good correlation between the rates of penetration and the respective distribution coefficients between olive oil and water. Discrepancies, particularly in the case of molecules of low molecular weight, in which greater rates are observed than theory predicts, have led to a modification of the Overton theory, and Collander and Bärlund propose a "lipoid-sieve" theory according to which the membrane is composed of islets of lipid held between sieve-like areas of protein mosaic, the sieve-like areas varying in degree of porosity. Thus, while all molecules are free to move by means of their lipid solubility, some may be prevented to some extent, owing to their size, from permeating by the sieve mechanism.

It seems extremely probable that, since the lipid contains surface-active ma-

<sup>1</sup> Presented in part at the Twenty-first National Colloid Symposium, which was held under the auspices of the Division of Colloid Chemistry of the American Chemical Society at Stanford University, June, 1947.

<sup>2</sup> Bristol-Myers Company Postdoctorate Fellow and Research Associate in Chemistry.

terials such as lecithin, the water-lipoid interface will be covered by a more or less oriented layer, and diffusion processes will involve penetration of these layers. On such a situation the experiments of Harkins (8) and Schulman (14) would have a direct bearing. It was decided, therefore, to restrict attention, in the first instance, to the lipoid portions of the membrane, and the following experiments were planned as a crude approximation to the system cell lipoid-water.

(1) Molecules were allowed to diffuse from aqueous solution across a benzene-water interface into benzene, and the rate of diffusion was studied as a function of distribution coefficient.

(2) The experiments were repeated under the same conditions, using now not simply a benzene-water interface, but a benzene-water interface at which a film of surface-active material was present.

#### EXPERIMENTAL

The materials used as the diffusing molecules were ethyl, *n*-propyl, *n*-butyl, and *n*-amyl alcohols. Ten milliliters of an aqueous solution of alcohol was placed in a graduate, thermostated at 25°C., and 20 ml. of benzene was carefully pipetted on top of the aqueous layer. Diffusion began immediately; the rate was followed by withdrawing 0.25-cc. samples of the benzene layer and determining the refractive index by means of a Zeiss interferometer. In earlier experiments the two layers were not stirred, as it was felt that stirring would disturb the interface unduly. All the compounds used yielded solutions, both in benzene and in water, with lower density than the pure solvents, so that for diffusion from the lower aqueous layer into the benzene, stirring by means of convection occurred. Later work in which stirring was used gave results identical with those in the absence of stirring, showing that uniformity of concentration in the two layers was obtained in either case. Stirring was achieved by means of two paddle wheels about 3 cm. in diameter soldered to a thin shaft about 2 mm. in diameter, so adjusted that one paddle was about 1 mm. above the interface and the other about 1 mm. below the interface. At the speeds of stirring used, 20-30 revolutions per minute, the interface was only slightly disturbed and it is estimated that the ripples induced by stirring changed the interfacial area by less than 5 per cent. Experiments with colored dyestuffs showed that the speeds of stirring used were sufficient to maintain bulk uniformity of concentration.

At first, attempts were made to *spread* films at the benzene-water interface, but none of the materials commonly used at air-water interfaces proved sufficiently stable over the several-hour periods required during these experiments. Accordingly, stable *adsorbed* films were obtained by using solutions of sodium cetyl sulfate and cetylpyridinium chloride. The concentrations of these surface agents were low, being less than 200 mg./liter, and their effect on diffusion in the aqueous layer may be neglected. By varying the concentration of surface agent the surface pressure of the film was readily varied. The water and benzene were mutually saturated at the beginning of each experiment to minimize side effects due to the diffusion of water.

As might be expected, the reproducibility of this type of experiment was not

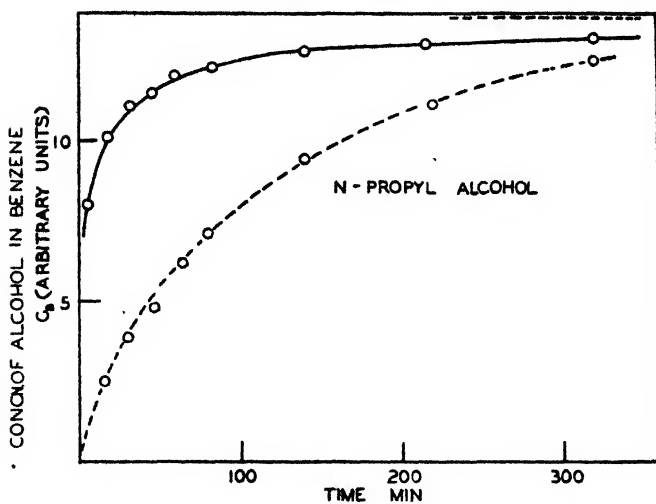


FIG. 1. Diffusion of *n*-propyl alcohol from water to benzene

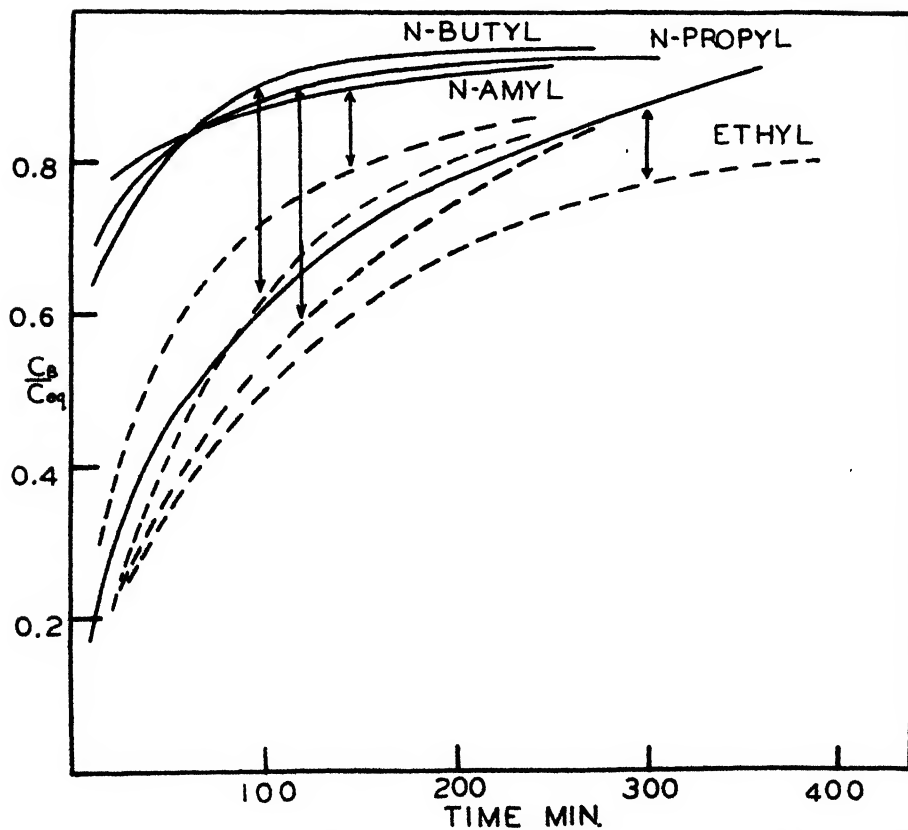


FIG. 2. Comparative rates of diffusion for homologous alcohols from water to benzene

very high. In the absence of films, variations of  $\pm 5$ –7 per cent were observed, but in the presence of films reproducibility was rather better. Accordingly it is emphasized that the results of these experiments are semiquantitative and that deductions therefrom are tentative.

### RESULTS

In figure 1 curves are given for the concentration,  $C_B$ , of *n*-propyl alcohol in the benzene layer as a function of time. The diffusion does not appear to fit the Fick law relating rate to concentration gradient (assuming any arbitrary thickness  $T$  for the interface) and no values of diffusion coefficients have so far been

TABLE 1  
*Distribution coefficients of normal alcohols between benzene and water*

ALCOHOL	CONCENTRATION IN WATER*	CONCENTRATION IN BENZENE†	DISTRIBUTION COEFFICIENT $K = \frac{MW}{MB}$	INITIAL RATE/ INITIAL CONCENTRATION DIFFERENCE
	<i>moles/liter</i>	<i>moles/liter</i>		<i>min.<sup>-1</sup></i>
Ethyl.....	6.17	0.643	9.61 $\pm$ 0.2	$1.6 \times 10^{-3}$
	4.72	0.336	14.05 $\pm$ 0.2	
	2.76	0.144	19.25 $\pm$ 0.2	
	1.51	0.060	25.14 $\pm$ 0.2	
<i>n</i> -Propyl .....	1.93	1.55	1.24 $\pm$ 0.1	$1.4 \times 10^{-3}$
	1.61	0.789	2.03 $\pm$ 0.1	
	1.00	0.256	3.90 $\pm$ 0.1	
	0.528	0.124	4.26 $\pm$ 0.1	
<i>n</i> -Butyl... ..	0.364	0.482	0.757 $\pm$ 0.1	$1.9 \times 10^{-3}$
	0.308	0.329	0.940 $\pm$ 0.1	
	0.225	0.204	1.10 $\pm$ 0.1	
	0.177	0.103	1.72 $\pm$ 0.1	
<i>n</i> -Amyl... ..	0.0511	0.132	0.388 $\pm$ 0.2	$2.5 \times 10^{-3}$
	0.0306	0.0618	0.49 $\pm$ 0.2	

\* Gram-formulae per liter = MW.

† Gram-formulae per liter = MB.

obtained. At low concentration of alcohol the initial slope of the  $C_B$ -time curves is proportional to the initial concentration but the proportionality disappears at higher concentrations. The initial concentrations varied for the different alcohols due to differences in solubility, distribution coefficient, and the need to have sufficient alcohol present to make measurement of the refractive index reasonably accurate, so that direct comparison of the rates is not easy.

In figure 2, values of a "saturation" function,  $C_B/C_{eq}$ , are plotted for the various alcohols to make a comparison possible.  $C_B$  is the concentration of alcohol in benzene at time  $t$ , and  $C_{eq}$  is the final equilibrium concentration in the benzene when distribution has been attained. Since  $C_{eq}$  is proportional to the

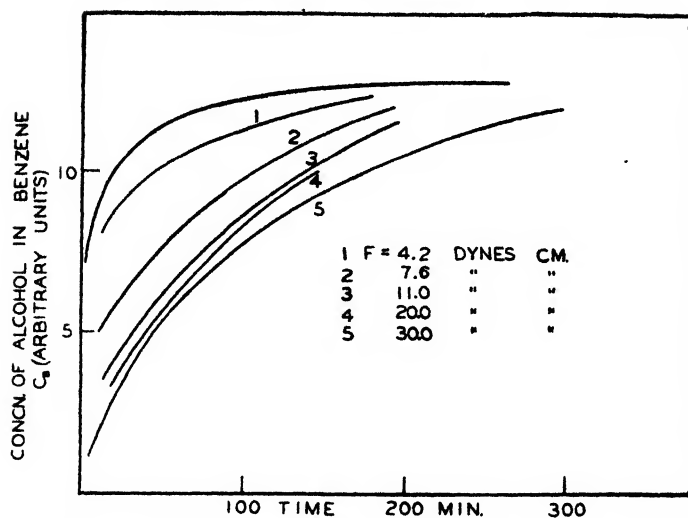
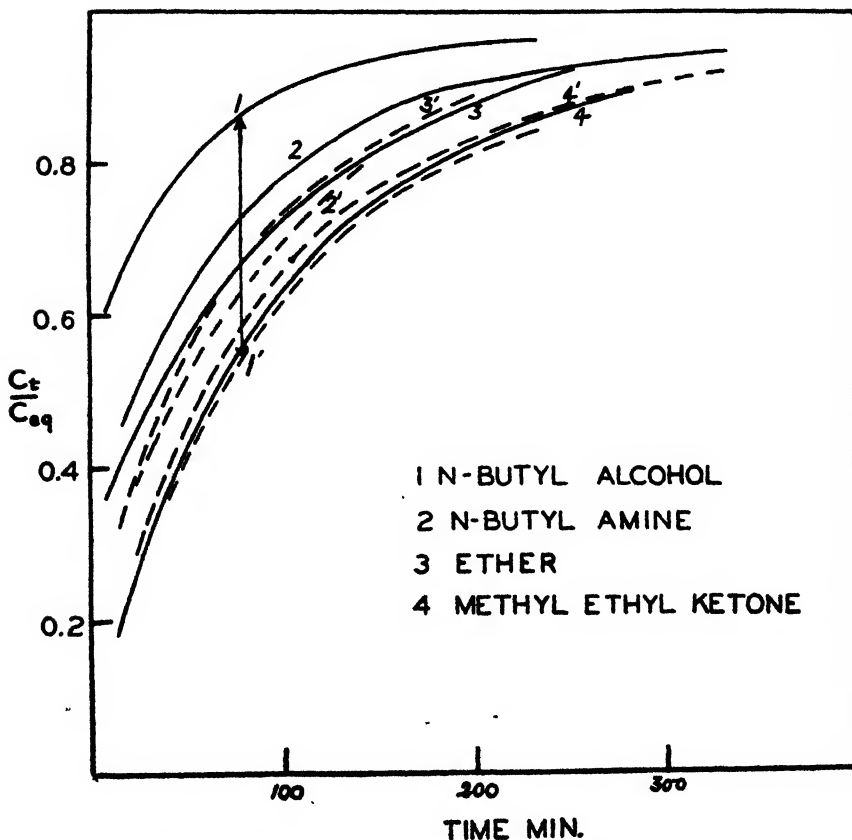

 FIG. 3. Effect of film pressure on the diffusion of *n*-propyl alcohol


FIG. 4. Comparative rates of diffusion for a number of four-carbon-atom compounds

initial concentration in the water, as are the initial values of  $C_2$  within limits, this "saturation" function may be used for a rough comparison of the series of alcohols.

In table 1 values are given for the initial rate/initial concentration, although as stated above this may not be an exact comparison owing to variation of this factor with concentration. The results show that, on this scale, the rates of diffusion are in the order *n*-amyl alcohol > *n*-butyl alcohol > *n*-propyl alcohol > ethyl alcohol. Qualitatively this is in accordance with the Overton-Meyer theory. The values obtained for the distribution coefficients of the various alcohols, however, show that the variation in distribution coefficients is much greater than that of the initial rates.

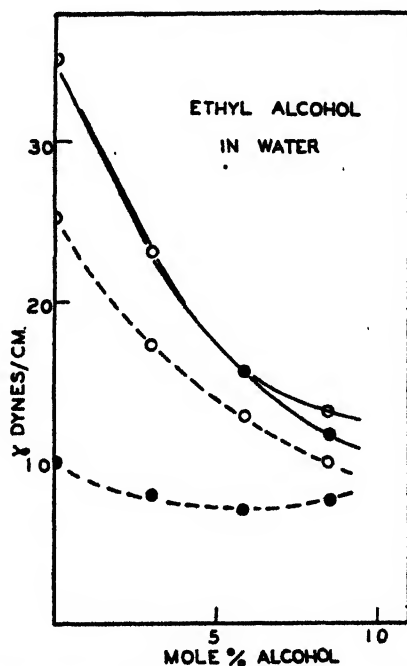


Fig. 5. Interfacial tension of the system aqueous ethyl alcohol-benzene

Turning now to the effect of films on the rate of diffusion, the dotted curves in figure 2 show the effect of a film of sodium cetyl sulfate at 30 dynes/cm. pressure. Clearly, under the same conditions of concentration gradient the rate of diffusion of a given alcohol is reduced considerably.

Materials other than sodium cetyl sulfate were used to give adsorbed films—e.g., cetylpyridinium chloride in water, cholesterol and palmitic acid in benzene—and in all cases similar retarding effects due to the interfacial film were observed.

The question now arises as to how the presence of the film can exert such a marked influence on the diffusion. A number of suggestions may be made *a priori*. (1) Distribution equilibrium is disturbed by the presence of surface agents in solution. (2) The molecules in the film occupy space in the interface



which would otherwise be available to the diffusing molecules, i.e., the film acts merely as a sieve. (3) The diffusing molecule may, on penetrating the film, interact with the film molecules and spend a greater time in the interface before passing into the benzene phase, i.e., the film would act as a potential barrier.

Experiment readily showed that the presence of sodium cetyl sulfate, at least in such concentrations as were used, had no measurable effect on distribution coefficients, so that hypothesis 1 could be abandoned.

Experiments were carried out with *n*-propyl alcohol at a number of film pressures, as shown in figure 3. Variation of the film pressure over a sevenfold range produced a much smaller change in the rate of diffusion. At first sight this might appear to indicate that the film does not act as a sieve, since a more critical de-

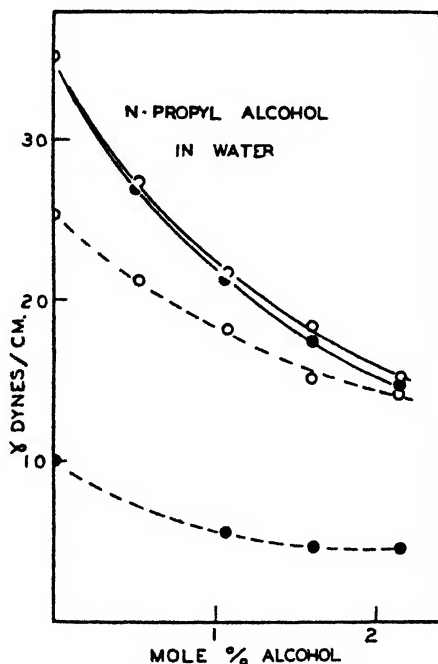


FIG. 6. Interfacial tension of the system aqueous *n*-propyl alcohol-benzene

pendence on pressure might be anticipated by analogy with experiments on the diffusion of water molecules through monolayers (15). However, it should be pointed out that (a) the final film pressure is slowly attained by surface aging over the first 30–40 min., during which a considerable fraction of the transfer has occurred, and (b) apart from one experiment by Alexander (2) no data are available for force-area curves for sodium cetyl sulfate, so that little is known about the packing of the film molecules at various pressures.

Rather more direct evidence was obtained by studying the rates of diffusion of a number of four-carbon-atom compounds, viz., *n*-butyl alcohol, *n*-butylamine, ether, and methyl ethyl ketone, as shown in figure 4. It will be seen that the retardation is very much less in the case of *n*-butylamine than for *n*-butyl alcohol,

while for ether and methyl ethyl ketone there is practically no retardation. Further, it was found that although *n*-amyl alcohol is strongly retarded, *tert*-amyl alcohol is scarcely retarded at all. This variation in the effect of the film with molecules differing in configuration, but not very greatly in size, suggests strongly that penetration and interaction in the film are of greater importance than mere mechanical obstruction.

Interfacial-tension experiments were carried out to see whether a study of the interfacial tensions would provide any evidence as to the mechanism. In order to make any possible effects of penetration of the film more clearly evident, solutions of sodium cetyl sulfate were used of such concentration as to give a film

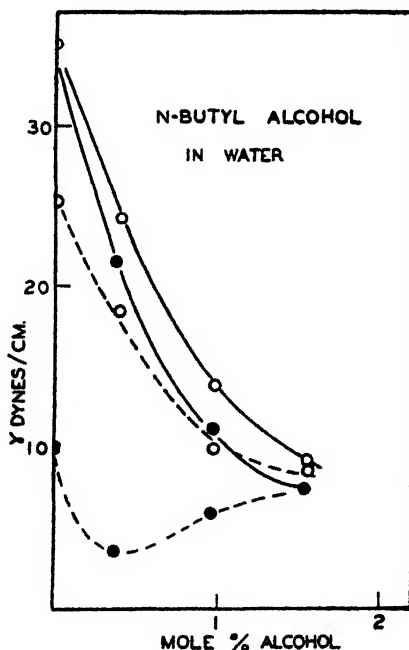


FIG. 7. Interfacial tension of the system aqueous *n*-butyl alcohol-benzene

pressure of 25 dynes/cm. instead of 30 dynes/cm. A variety of methods were used to measure the interfacial tension of the systems

- (1) aqueous alcohol-benzene
- (2) (aqueous alcohol + sodium cetyl sulfate)-benzene

both in the early stages of the diffusion and also at equilibrium. Four different methods were used, *viz.*, drop-volume, the ring method, pendant drop, and sessile bubble. Comparison of the methods will form the substance of a forthcoming paper, but it may be stated here that considerable disagreement between the various methods was observed and the values quoted here were obtained by means of the sessile-drop method. This method has been adequately described in the literature (1, 4, 7) and will not be described here. Correction factors

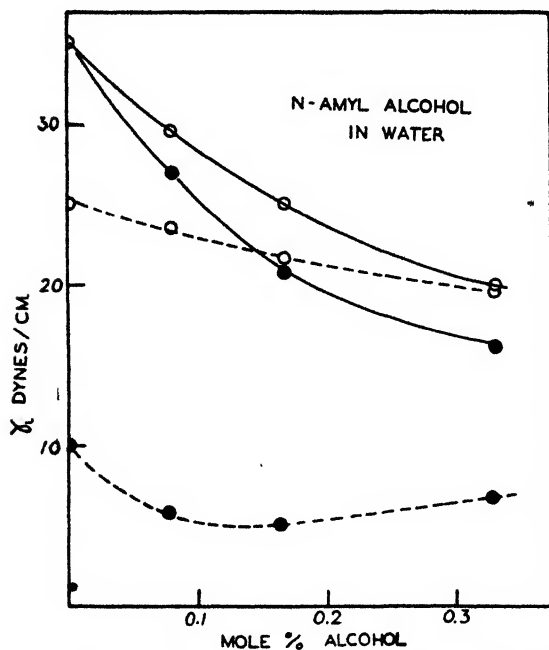


FIG. 8. Interfacial tension of the system aqueous *n*-amyl alcohol-benzene

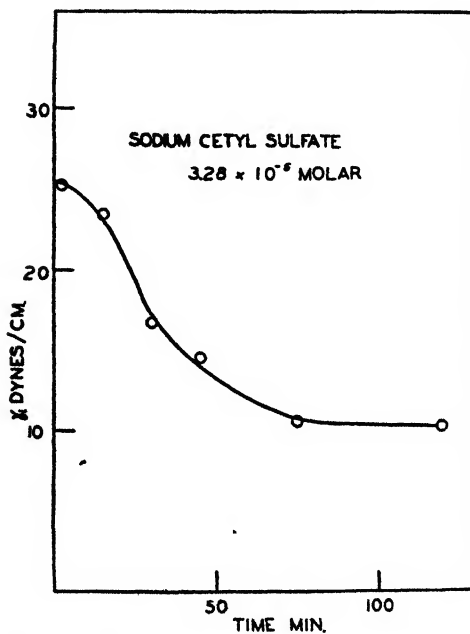


FIG. 9. Aging of the interface for the system aqueous sodium cetyl sulfate-benzene

derived directly from the tables of Bashforth and Adams (3) were obtained from a paper by Porter (13). Bubbles were used of such size that the correction factors were less than 10 per cent and were in the region where they may be calculated with considerable accuracy.

The bubble-forming tube was placed vertically in an optical cuvette containing 100 ml. of the solution of alcohol, and 10 ml. of benzene was carefully pipetted into the tube. Measurements of the interfacial tension were made from the time of formation of the interface until equilibrium was established, usually a period of 3-4 hr.

In figures 5-8 values are given for the interfacial tension of the various alcohol solutions over a range of concentrations, as measured 5 min. from the beginning

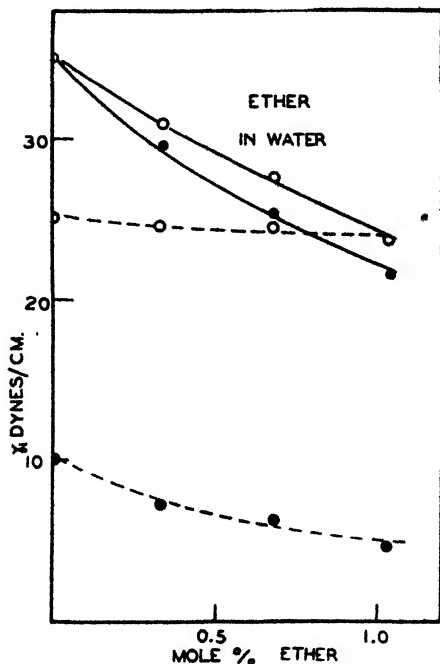


FIG. 10. Interfacial tension for the system aqueous ether-benzene

of the experiment. Values are also given for the same systems after distribution equilibrium had been established. The open circles refer to the 5-min. readings and the full circles to the equilibrium values; dotted curves show the effect of the presence of sodium cetyl sulfate on the system. (It will be observed that the values of interfacial tension corresponding to the system consisting of sodium cetyl sulfate + aqueous alcohol and benzene are not the same in both cases; this is due to the aging of such an interface, as shown in figure 9.)

#### DISCUSSION

It is clear that both in the initial stages of diffusion and at equilibrium considerable penetration of the sodium cetyl sulfate film occurs. Application of the

Gibbs adsorption equilibrium to such systems is not possible, owing to the number of variables involved, but if the strength of the interaction is measured as the increase of pressure, then at equal molar percentages the interaction increases in the order ethyl < propyl < butyl < amyl alcohol, as one might expect. This penetration of the film in both equilibrium and non-equilibrium states is taken as evidence that the interaction hypothesis is indeed correct, and this is borne out by the interfacial-tension curves of one of the materials for which retardation is almost negligible, *viz.*, ethyl ether in figure 10. Here there is a correspondingly poor penetration of the film during the early part of the diffusion process, and here is also a rough correlation between the lower rate of diffusion of ether, as compared with that of butyl alcohol, and its much lower surface activity. This again would be expected. Davson and Danielli (6) are at some pains, in describing the Overton-Meyer hypothesis, to minimize the importance of surface activity of the diffusing molecule, remarking that although with increasing chain length the surface activity of the molecule increases, yet so also does the distribution coefficient, and that the latter is the important factor. Now if any mechanism may be deduced from the Overton-Meyer theory it is simply that the driving force is that due to osmotic pressure. In these experiments, at the concentrations used, the initial lack of osmotic balance would be in the order butyl > propyl > ethyl > amyl, whereas the measured initial rates/concentration gradient are in fact amyl > butyl > propyl > ethyl, in agreement with the order of surface activities (at a given concentration). Indeed if, in biological processes, a molecule must pass through some kind of oil-water interface, then it is difficult to see how surface activity can be ignored in interpreting the phenomena.

Attempts were made to investigate any possible temperature effect of the diffusion process, but so far the results have been too erratic to enable any conclusion to be reached. Similarly, experiments were carried out to investigate diffusion from the benzene layer into water. Again the results were very erratic, and it is thought that greatly improved stirring is necessary to ensure uniformity of bulk concentration.

#### SUMMARY

The rates of diffusion of a number of alcohols from water into benzene across the benzene-water interface have been measured. Initial rates are in the order amyl > butyl > propyl > ethyl, in qualitative agreement with the Overton-Meyer theory. The retarding effect of films of surface-active materials on the diffusion has been investigated, and measurement of the interfacial tensions of the various systems supports the hypothesis that interaction in the film is responsible for the retardation. As yet no mathematical analysis of the diffusion curves has been possible, and the results quoted are semiquantitative.

The author wishes to acknowledge the helpful guidance of Professor James W. McBain throughout this investigation.

## REFERENCES

- (1) ADAM AND SHUTE: *Trans. Faraday Soc.* **34**, 758 (1938).
- (2) ALEXANDER AND TEORELL: *Trans. Faraday Soc.* **35**, 727 (1939).
- (3) BASHFORTH AND ADAMS: *An Attempt to Test the Theories of Capillary Action*. Cambridge (1883).
- (4) BURDON: *Trans. Faraday Soc.* **28**, 866 (1932).
- (5) COLLANDER AND BÄRLUND: *Acta Botan. Fennica* **11**, 1 (1933).
- (6) DAVSON AND DANIELLI: *The Permeability of Natural Membranes*. Cambridge University Press, London (1943).
- (7) GOUY: *Ann. phys.* **6**, 5 (1916).
- (8) HARKINS: *Colloid Science*, Vol. V. Reinhold Publishing Corporation, New York (1944).
- (9) HÖBER *et al.*: *The Physical Chemistry of Cells and Tissues*. The Blakiston Company, Philadelphia (1945).
- (10) MEYER: *Arch. exptl. Path. Pharmacol.* **42**, 109 (1899).
- (11) OVERTON: *Jshr. Naturf. Ges. Zurich* **40**, 159 (1895).
- (12) PARPART AND DZIEMIAN: *Cold Spring Harbor Symposia Quant. Biol.* **8**, 17 (1940).
- (13) PORTER: *Phil. Mag.* **15**, 163 (1933); **34**, 823 (1937).
- (14) SCHULMAN AND HUGHES: *Biochem. J.* **29**, 1243 (1935).
- (15) SEBBA AND BRISCOE: *J. Chem. Soc.* **108**, 128 (1940).

## ON THE EXPERIMENTAL BASES FOR THE CALCULATION OF THE SULFURIC ACID VAPOR PRESSURE ABOVE THE SULFURIC ACID-WATER SYSTEM

E. ABEL

*63 Hamilton Terrace, London N.W.8, England*

*Received May 27, 1947*

Recently a series of thermodynamic and thermal data have been determined which would have been applicable to the relationships developed in a previous paper (1) for the calculation of sulfuric acid vapor pressure, but which could not be fully used in that paper. They supply far more reliable numerical values for this calculation than could previously be obtained and it may therefore be desirable, in view of the importance of sulfuric acid, to examine the extent and the degree of accuracy to which the vapor pressure of sulfuric acid can now be calculated.

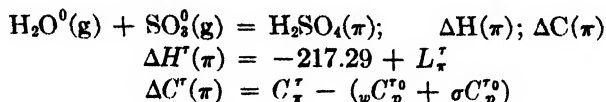
The calculation, as I have shown, is based on the reaction of the formation of sulfuric acid in its standard state ( $(\text{H}_2\text{SO}_4)^0$ ) from water vapor ( $(\text{H}_2\text{O}^0(\text{g}))$ ) and sulfur trioxide gas ( $(\text{SO}_3^0(\text{g}))$ ) in their standard states:



<sup>1</sup> With respect to notations see reference 1. As we are dealing with a binary liquid system, all thermodynamic quantities are, of course, partial molal quantities; for the sake of simplicity, the bar is omitted.

It is the thermodynamics of this reaction which has been submitted to a revision. Table 1 gives the best data at 25°C. at present available.<sup>2</sup>

More exact thermal data can now also be coordinated with the analogous reaction leading to  $\text{H}_2\text{SO}_4(\pi)$ :



insofar as the relative partial molal heat contents  $L_\pi^\tau$  and the partial molal heat capacities  $C_\pi^\tau$ , which so far could only be calculated indirectly, can now be replaced by experimental values (4). Even so, in view of the curious course of  $C_\pi^\tau$  as a function of  $\pi$ , much closer determinations could be desired.

TABLE 1\*  
Thermodynamic data  
 $T = \tau = 298^\circ$

$\text{H}_2\text{O}(\text{g})$			$\text{SO}_3(\text{g})$			$\text{H}_2\text{SO}_4$		
$-\Delta_w H^0$	$-\Delta_w G^0$	$-\Delta_w S^0$	$-\Delta_s H^0$	$-\Delta_s G^0$	$-\Delta_s S^0$	$-\Delta H^0$	$-\Delta G^0$	$-\Delta S^0$
57.8 (1a, 13)	54.5 (13)	11.08	$94.43 \pm 0.15$ (18)†	$88.48 \pm 0.20$ (18)†	$19.95 \pm 0.20$ (18)†	217.29‡	176.1 (10, 20) 176.5 (9, 13)§	138.22  136.88

$$\Delta G^\tau(0) = -33.52 \pm 0.20; \Delta H^\tau(0) = -65.06 \pm 0.15; \Delta S^\tau(0) = -105.85 \pm 0.20$$

\* Heats ( $\Delta H^0$ ) and free energies ( $\Delta G^0$ ) of formation in kilogram-calories; entropies ( $\Delta S^0$ ) in E.U. (calories per degree).

† See also references 6, 7, 15, 17.

‡ -193.75 (1a, 10, 11) - 23.54 (4).

§ The above-mentioned values seem to be preferable to the value -175.3 (11, 12); the following calculations are based on the value -176.5 (9, 13).

The heat capacities  ${}_wC_p^0$  and  ${}_sC_p^0$  of  $\text{H}_2\text{O}^0(\text{g})$  and  $\text{SO}_3^0(\text{g})$  can be shown to be in fair agreement with the data which have also in part been only recently calculated from the thermodynamic properties of these two gases (8, 18), using the equations

$$\begin{aligned}{}_wC_p^0 &= 4.33 + 3.101 \times 10^{-2}T - 1.67 \times 10^{-5}T^2 \text{ cal.} \\ {}_sC_p^0 &= 7.73 + 0.034 \times 10^{-2}T + 0.192 \times 10^{-5}T^2 \text{ cal.}\end{aligned}$$

so that

$$\begin{aligned}\Delta C^\tau(\pi) &= C_\pi^{\tau*} + \mu T + \nu T^2 \\ C_\pi^{\tau*} &= C_\pi^\tau - 12.06; \mu = +3.135 \times 10^{-2}; \nu = -1.478 \times 10^{-5}\end{aligned}$$

Thus a large part of the data applicable to the calculation of the vapor pressures of sulfuric acid appears to be on a far better basis than was previously the case.

<sup>2</sup> These data seem to be much more reliable than those published by Kapustinskiĭ (8a).

Some data, however, are still missing. *In the liquid phase:* Exact knowledge of the activities ( $a_{\pm}^r$ ) of the sulfuric acid component in the range of high concentrations—say from 85 per cent upwards—in which the water vapor pressures on which the calculation of the activities is based (1, p. 262) are known inadequately or not at all. Also, the exact dependence on temperature of the  $C_{\pm}^r$ -values is lacking.

*In the vapor phase:* Knowledge of the range of temperature within which the equilibrium constant,  $K_p$ , of the dissociation of sulfuric acid vapor (2) is represented with sufficient accuracy by the relationship:

$$\log K_p = k_1 + \frac{k_2}{T} + k_3 \log T + k_4 T^2$$

where

$$k_1 = 5.88, \quad k_2 = -5000, \quad k_3 = 1.75, \quad k_4 = -5.7 \times 10^{-4}$$

With regard to the activity, thanks to the increased accuracy of the thermal and thermodynamic data shown, it seems that it might be possible to calculate the activity of the sulfuric acid component in a special case of highly concentrated acids, and hence to make at least an approximate estimation of the course of the activities in the range of high concentrations. In view of the identity of the composition of liquid and vapor at the azeotropic boiling point ( $T_{\pm} = 599^\circ$ ), the sulfuric acid partial pressure ( $p_{\pm} = 356$  mm. Hg) can be calculated here (see 1, p. 270); with the aid of the numerical relationships which are given below and which may be regarded as fairly reliable at this high temperature,<sup>4</sup> this value enables us<sup>5</sup> to calculate the activity of the sulfuric acid component at the azeotropic concentration:  $\bar{\pi} = 98.3$ ;  $\log a_{\pm}^r = 8.74$ .

The level of this concentration and the course of the activity curve up to about 85 per cent further give us some indication of the probable course of the activity (figure 1; dotted curve) as it approaches highly concentrated and, finally, pure sulfuric acid. The activities and hence the partial molal free energies of formation of the sulfuric acid component seem—theoretically this is quite plausible—to be tending towards a limit ( $\log a_{\pm}^r = 8.76$ ) which seems to be very nearly reached at the azeotropic concentration.<sup>6</sup> For the free energy of formation of sulfuric acid, 100 per cent (25°C.), this limit would lead to  $\Delta G^r(\text{H}_2\text{SO}_4(l)) = -176.5 + R^* \bar{\pi} \times 8.76 \times 10^{-3} = -164.6$  Cal.

With regard to the dependence on temperature of the partial mola' heat capacities of the sulfuric acid component, I have tried (as shown in reference 1, p. 265; see also 5, 20) to calculate these from older measurements which were not partic-

<sup>3</sup> It should be noted that  $K_p$  is formulated on the tacit assumption that the gases follow the laws of ideal gases.

<sup>4</sup> See footnote 7.

<sup>5</sup> On the assumption that  $\alpha_{\pm}^r + \alpha_{\pi=100} = 0.037$ ;  $J^*(599) = -3.99$  (see page 911); the determinations in references 3, 16, and 17 are not as consistent as desirable. Partial and total quantities are practically identical at  $\pi = 100$ .

<sup>6</sup> It should be noted that the partial molal heat of formation of sulfuric acid also varies only by 0.44 Cal. (4) between  $\pi = 91.59$  and  $\pi = 100$  at an average value of  $-194$  Cal. (1a).



ularly well suited to this purpose; there are at present no direct determinations of these partial values. In these circumstances it may be desirable to summarize separately the terms of the vapor-pressure formula containing this dependence on temperature. Writing

$$C_{\tau} = C_{\tau}^{\tau} + \alpha_{\tau}(T - \tau)$$

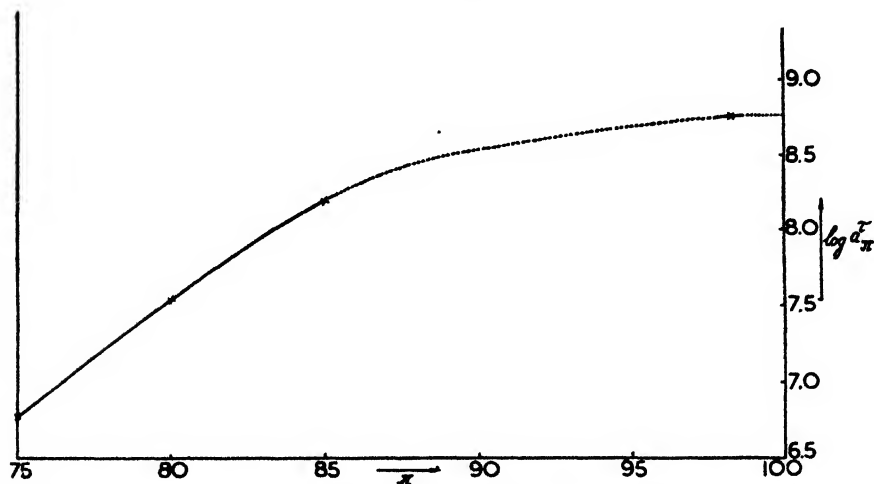


FIG. 1. Course of the activity curve for sulfuric acid of high concentration

TABLE 2  
Values for  $J^*(T)$

$T$	$-J^*(T)$	$T$	$-J^*(T)$
298	0	500	1.78
350	0.25	550	2.80
400	0.58	600	4.00
450	1.06	650	5.57

the term containing  $\alpha_{\tau}$  will be:

$$J_{\tau}(T) = -\alpha_{\tau} \int_{\tau}^T \frac{dT}{T^2} \int_{\tau}^T (T - \tau) dT = -\frac{\alpha_{\tau}}{2} \left[ \frac{T^2 - \tau^2}{T} - 2\tau \ln \frac{T}{\tau} \right] = \alpha_{\tau} \cdot 4.58 J^*(T)$$

Some values for  $J^*(T)$  are given in table 2.

Far more important than the last-named uncertainty, which is practically only a matter of a correction, is the above-mentioned doubt as to the range for which the  $K_p$  relationship (see page 910) is valid. The temperatures at which the equilibrium of the dissociation of the sulfuric acid vapor was studied years ago (2) lay between 483°C. and 325°C.;<sup>7</sup> the excellent way in which the above formula for  $K_p$  corresponds to these experiments seems to justify the assumption.

<sup>7</sup> The azeotropic boiling point (see page 910) therefore lies within the range for which the validity of  $K_p$  has been verified experimentally.

of its reliability also for a further, lower range of temperature. The extent of this range, however, cannot be determined for the time being. On the other hand, for highly concentrated sulfuric acid solutions, at temperatures close to their boiling points, i.e., in circumstances which command special interest, the dissociation constant defined by the above  $K_p$ -values can be taken to be at least very nearly valid. These  $K_p$ -values, therefore, may be included in the following numerical relationships, but it must be borne in mind that the data calculated necessarily become less reliable as the temperature is reduced.

If, by analogy with reference 1, we write, replacing the fugacity of the sulfuric acid vapor<sup>8</sup> by its partial pressure (in millimeters of mercury):

$$\log p_r = A_r + \frac{B_r}{T} + D_r \log T + E_r T + F_r T^2 + \alpha_r J^*(T)$$

we get

$$A_r = A + \log a_r^r + \frac{1}{R^*} \left[ -\frac{L_r^r}{\tau} + C_r^r (1 + 2.30 \log \tau) - (\mu + \nu^* \tau) \tau \right]$$

$$\left( R^* = 4.58; \nu^* = \frac{\nu}{2} \right)$$

$$A = - \left( \frac{\Delta S^r(0)}{R^*} + k_1 \right) + 5.76^9$$

$$B_r = \frac{1}{R^*} \left\{ \Delta H^r(\tau) - [C_r^r - (\mu' + \nu' \tau) \tau] \tau \right\} - k_2$$

$$\left( \mu' = \frac{\mu}{2}; \nu' = \frac{\nu}{3} \right)$$

$$D_r = - \frac{C_r^r}{R^*} - k_3$$

$$E_r = - \frac{\mu'}{R^*} - k_4$$

$$F_r = \frac{\nu''}{R^*}; \quad \nu'' = \frac{\nu}{6}$$

and when inserting<sup>10</sup> the numerical values (the thermal data in calories):

$$A = 23.00 \pm 0.04^{11}$$

<sup>8</sup> This substitution brings of course a further uncertainty into the calculation of the vapor pressures.

<sup>9</sup>  $5.76 = 2 \log 760$ .

<sup>10</sup> See the above remarks regarding the limits of validity.

<sup>11</sup> Worthy of note is the accuracy with which this constant can now be calculated; the uncertainty is now only about 5 per mille as against the previous 16 per cent. The alteration of the numerical value of  $A$  is largely compensated by opposite changes.—Taking  $-\Delta G^0 = 176.1$  (see table 1), this constant would be 23.3, and from this it can be seen, particularly in view of the logarithmic relationship between energy and pressure, that for the problem

$$A_{\tau} = 3.49 + \log a_{\tau}^{\tau} - \frac{L_{\tau}^{\tau}}{1365} + 1.46 C_{\tau}^{\tau}$$

$$B_{\tau} = \frac{\Delta H^{\tau}(\tau)}{4.58} - 65.07 C_{\tau}^{\tau} + 6060$$

$$D_{\tau} = -\frac{C_{\tau}^{\tau}}{1.988} + 4.31$$

$$E_{\tau} = 4.00 \times 10^{-3}$$

$$F_{\tau} = -5.37 \times 10^{-7}$$

TABLE 3

*Sulfuric acid pressure above pure sulfuric acid*

<i>t</i> (°C.)	250°	275°	300°	325°	350°	(380°)	(400°)
Sulfuric acid pressure (mm. Hg)	(60)	115	180	317	480	(760)	(980)

At  $T = \tau = 298^{\circ}$  we obtain immediately:

$$\log p_{\tau}^{\tau 12} = \frac{\Delta G^{\tau(0)}}{4.58 \times 298} - \log K_p^{\tau} + \log a_{\tau}^{\tau} + 2 \log 760 (\pm 0.15)$$

$$= -18.80 - \log K_p^{\tau} + \log a_{\tau}^{\tau} (\pm 0.15)^{13}$$

$$\begin{aligned} \Delta F_{298}^0(\text{H}_2\text{SO}_4(\text{g})) &= \Delta_w G^0 + \Delta_v G^0 + R^* \tau \log K_p^{\tau} \\ &= -142.98 + 1.365 \log K_p^{\tau} (\pm 0.20) \text{ Cal.}^{14} \end{aligned}$$

At temperatures within the range for which the validity of  $K_p$  has been proved experimentally, or at least not far beyond it, the sulfuric acid vapor pressure above pure sulfuric acid monohydrate can be calculated from the above formulae with the values ( $\tau = 100$ ):

$$\log a^{\tau} = 8.76$$

$$L^{\tau} = 23,540 \text{ (4)}$$

$$C^{\tau} = 32.9 \text{ (4)}$$

$$\Delta H_{(100)}^{\tau} = -41,520 \text{ (see table 1)}$$

$$\alpha = 0.037^{14}$$

as follows (table 3):

$$\begin{aligned} \log p_{\tau=100}^{\tau 12} &= 43.04 - \frac{5145}{T} - 12.24 \log T + 4.00 \times 10^{-3} T \\ &\quad - 5.37 \times 10^{-7} T^2 + 0.037 J^*(T) \end{aligned}$$

under discussion the thermodynamic data still need to be determined with even greater accuracy than that obtained or obtainable.

<sup>12</sup> Millimeters of mercury.

<sup>13</sup> The dissociation constant for  $25^{\circ}\text{C.}$  would be  $\log K_p^{\tau} = -6.74$ , calculated on the basis of the above  $K_p$  formula.

<sup>14</sup> See footnote 5.

At about 380°C. the pressure reaches 1 atm.; the boiling point, however, is naturally considerably lower, at a temperature where the sulfuric acid partial pressure plus the partial pressure of sulfur trioxide—which is necessarily very high, although ineffective—(plus the almost negligible partial pressure of water) arrives at 1 atm.; in the previous paper (1) I went into the consequences of this for the stability of pure sulfuric acid at temperatures where the latter still exists as a liquid.

#### SUMMARY

As a supplement to the preceding paper (1) relationships and data are shown which are derived from a series of thermodynamic and thermal values recently published. The results are critically discussed.

#### REFERENCES

- (1) ABEL, E.: J. Phys. Chem. **50**, 260 (1946).
- (1a) BICHOWSKY, F. R., AND ROSSINI, F. D.: *The Thermochemistry of the Chemical Substances*. Reinhold Publishing Corporation, New York (1936).
- (2) BODENSTEIN, M., AND KATAYAMA, M.: Z. Elektrochem. **15**, 244 (1909); Z. physik. Chem. **69**, 26 (1909).
- (3) CATTANEO, L.: Nuovo cimento [3] **26**, 50 (1889).
- (4) CRAIG, D. N., AND VINAL, G. W.: Bur. Standards J. Research **24**, 475 (1940).
- (5) DEE, T. P.: J. Soc. Chem. Ind. **64**, 40 (1945).
- (6) GERDING, H., AND LECOMTE, J.: Physica **6**, 737 (1939).
- (7) GERDING, H., NIJVELD, W. J., AND MULLER, G. J.: Z. physik. Chem. **B35**, 193 (1937).
- (8) GORDON, A. R.: J. Chem. Phys. **2**, 65 (1934); see also reference 14.
- (8a) KAPUSTINSKIĬ, A. F.: Compt. rend. acad. sci. U. R. S. S. **53**, 719 (1946).
- (9) KELLEY, K. K.: U. S. Bur. Mines Bull. No. **406**, (1937).
- (10) LATIMER, W. M.: *Oxidation States of the Elements and their Potentials in Aqueous Solutions*. Prentice-Hall, Inc., New York (1938).
- (11) LATIMER, W. M., HICKS, J. F. G., JR., AND SCHUTZ, P. W.: J. Chem. Phys. **1**, 620 (1933).
- (12) LATIMER, W. M., SCHUTZ, P. W., AND HICKS, J. F. G., JR.: J. Chem. Phys. **2**, 82 (1934).
- (13) LEWIS, G. N., AND RANDALL, M.: *Thermodynamics and the Free Energy of Chemical Substances*. McGraw-Hill Book Company, Inc., New York (1923).
- (14) MURPHY, G. M.: J. Chem. Phys. **5**, 637 (1937).
- (15) PALMER, K. J.: J. Am. Chem. Soc. **60**, 2360 (1938).
- (16) PICKERING, S. U.: Proc. Roy. Soc. (London) **49**, 11 (1891); J. Chem. Soc. **67**, 664 (1895).
- (17) SOKOLIK, A. (SOKOLIK, A. S.) (AND SAVARIZKY): Z. physik. Chem. **A159**, 305 (1932); Chem. J. Ser. A, J. Allgem. Chem. **2**, (64), 311 (1932).
- (18) STEVENSON, D. P.: See reference 21, p. 313.
- (19) STOCKMAYER, W. H., KAVANAGH, G. M., AND MICKLEY, H. S.: J. Chem. Phys. **12**, 408 (1944).
- (20) STOKES, R. H.: J. Am. Chem. Soc. **69**, 1291 (1947).
- (21) YOST, D. M., AND RUSSELL, H., JR.: *Systematic Inorganic Chemistry*. Prentice-Hall, Inc., New York (1944).

# SOLUBILIZATION OF DIMETHYLAMINOAZOBENZENE IN SOLUTIONS OF DETERGENTS. I

## THE EFFECT OF TEMPERATURE ON THE SOLUBILIZATION AND UPON THE CRITICAL CONCENTRATION<sup>1</sup>

I. M. KOLTHOFF AND W. STRICKS

*School of Chemistry, University of Minnesota, Minneapolis 14, Minnesota*

*Received November 13, 1947*

\*In a preliminary note (14) it has been shown that the critical concentration of various detergents is found easily from solubilization data of a water-insoluble dye like dimethylaminoazobenzene by plotting the amount of dye solubilized against the concentration of detergent. Graphs are obtained like those represented in figures 2 to 14.

In solubilization experiments with fatty acid soaps a type of graph is obtained as represented in figures 2 to 7. Starting with pure water the solubilization of the dye hardly increases with increasing concentration of the detergent until a "critical concentration" is reached, above which the solubilization of the dye increases markedly and becomes a linear function of the detergent concentration. When lines are drawn through the points giving the solubilization at various concentrations of the detergent, two straight lines are obtained which intersect at the *critical concentration*. It is of interest to note that even below the critical concentration a slight solubilization is found, indicating the presence of some micelles below the critical concentration (v.i.).

With several detergents like dodecylamine hydrochloride the solubilization of the dye above the critical concentration is not found to be a linear function of the concentration of the detergent. As seen in figure 8, a convex curve is found. In such instances the critical concentration is also found graphically by extrapolation of the solubilization line. Since the solubilization curve is almost straight near the critical concentration, the latter is found with about the same accuracy as of detergents of the type represented in figures 2 to 7.

Solubilization data do not yield only the critical concentration but they also give insight as to the solubilizing power of the micelles of various detergents. By carrying out the solubilization experiments at various temperatures the variation of the critical concentration and of the solubilizing power of the micelles with the temperature is found.

In the present paper we present data on the solubilization of dimethylaminoazobenzene, designated as DMAB, in aqueous solutions of various detergents at temperatures of 30°C. and 50°C. The dye used has the advantage of having a negligibly small solubility in water (less than 1 mg. per liter). Since some con-

<sup>1</sup> This investigation was started under the sponsorship of the Office of Rubber Reserve, Reconstruction Finance Corporation, in connection with the Synthetic Rubber Program of the United States Government.

clusions drawn from our experimental data are at variance with those reported by McBain and coworkers (10, 17) obtained with Orange OT as a solubilized dye, several experiments have been made by us using this dye.

#### MATERIALS

Dimethylaminoazobenzene (DMAB), an Eastman Kodak technical product, was recrystallized from hot petroleum ether solutions (about 20 g./l.). During the crystallization care was taken not to obtain too small sized crystals. The recrystallized dye was dried at 80°C. in a vacuum. The crystals were coarse enough to permit a ready separation of the dye from the detergent solution by filtration in the solubilization experiments.

Orange OT (F. D. and C., Orange No. 2; 1-*o*-tolylazo-2-naphthol), a Calco product, was purified according to directions received from Prof. J. W. McBain. The amorphous powder was recrystallized from alcohol and dried. The dye was found to be virtually insoluble in water at 30°C. and 50°C.

*Potassium and sodium laurates*: Solutions of these soaps were prepared by neutralization of Eastman Kodak white label lauric acid with standardized potassium hydroxide and sodium hydroxide solutions, respectively. The potassium and sodium hydroxides were Baker c.p. products. Solutions which were 1 *N* in alkali hydroxide were heated on the steam bath with the equivalent amount of lauric acid until the acid had dissolved. The stock solutions were 0.75 *M* (moles per liter) in potassium laurate and 0.375 *M* in sodium laurate, respectively. The more dilute solutions were obtained by proper dilution of the stock solutions.

*Potassium and sodium caprates, potassium and sodium oleates, potassium stearate, palmitate, and myristate*: Solutions of these soaps were prepared in the same way as given for the laurates. The fatty acids used were also Eastman Kodak white label products. A sample of pure oleic acid was obtained from Dr. W. C. Ault of the Eastern Regional Laboratories.

*Dodecylamine hydrochloride*: This detergent was prepared by neutralization of free dodecylamine (Armour product) dissolved in absolute ethanol with concentrated hydrochloric acid. After cooling to 0°C. the white mass of dodecylamine hydrochloride was filtered and finally purified by recrystallization from alcohol, washing with ether, and drying in a vacuum at 30°C. A 0.5 molar stock solution was prepared and the more dilute solutions were obtained by proper dilution.

*Potassium dehydroabietate*: A solution of this detergent was prepared by heating dehydroabietic acid (molecular weight = 301, 96.9 per cent pure, a product obtained from Prof. C. S. Marvel of the University of Illinois, Ill. No. 39) with the equivalent amount of sodium hydroxide solution on the steam bath.

*Sodium di-*sec*-butyl naphthalenesulfonate*: A commercial product obtained from the General Aniline and Film Corporation designated as SA-178. Molecular weight, 342. A 0.2 *M* solution was made up as stock solution. The 0.2 *M* solution remained clear at 50°C.; on standing at room temperature, it became turbid.

*Diamyl sodium sulfosuccinate*: Aerosol AY (molecular weight = 360), a product of the American Cyanamid and Chemical Corporation. Upon drying the material to constant weight at 30°C. in a vacuum it appeared to contain 7.8 per

cent water. A 0.92 *M* stock solution was prepared by dissolving 90 g. of the compound in 250 ml. of distilled water.

*Sodium rosinate*: A solution of this detergent was prepared by neutralizing a weighed amount of a Hercules 45-985 Rosin 731 (dehydrogenated rosin) with a standard sodium hydroxide solution. The equivalent weight of the rosin acid was found to be 340 by titration of an alcoholic solution with standard base. After the supply was exhausted another batch of Rosin 731 (No. 45-979) was used, the equivalent weight of which was found to be 325. After one recrystallization of this product from absolute alcohol a white product with an equivalent weight of 310 was obtained. The stock solutions were about 0.3 *M* and remained clear at room temperature.

*Daxad 11*: A product obtained from Dewey and Almy Chemical Co. It is reported to be a mixture of sodium sulfate and sodium salts of polymerized naphthalenesulfonic acids. The stock solution contained 200 g./l.

*Triton R-100*: A detergent of Rohm and Haas, sample No. 215, reported to be the neutral sodium salt of a complex condensed organic acid. The stock solution contained 200 g. of detergent per liter.

#### TECHNIQUE AND EXPERIMENTAL METHODS

Known volumes of solutions of varying concentrations of detergents were made up by proper dilution of the stock solutions of the detergents. The samples were placed in glass bottles sealed with metallic or plastic caps, lined with Buna-N or Koroseal. Sufficient dye was added to provide an excess of solid dye after attainment of solubilization equilibrium. The bottles containing the samples were rotated at 30°C. and 50°C. in thermostats kept constant within 0.1°C. It proved to be convenient to use only 10-ml. samples of detergent solutions, although originally most of the work was carried out with 50-ml. samples. The solubilization data were found to be independent of the volume of detergent solution used.

The time of attainment of solubilization equilibrium under the conditions of rotation depends on the kind and concentration of the detergent and also to some extent on the size and excess of the dye crystals. It was generally found that most detergent solutions required from 1 to 2 weeks to attain equilibrium. In most of the work the rotation was continued until upon further rotation the solubilization appeared to have become constant. In most of our experiments equilibrium was attained from the side of undersaturated solutions. However, some experiments were also carried out with supersaturated solutions in order to assure that the solubilization data found correspond to equilibrium values.

After a given period of rotation the bottles were placed in an upright position in the thermostat until the excess of dye had settled. This took from 3 to 5 hr. for dimethylaminoazobenzene, but from 12 to 24 hr. for Orange OT. Either a 5- or a 1-ml. portion of the clear colored detergent solutions was withdrawn and filtered with the aid of a pipet provided with a piece of rubber tubing about 2 in. long which contained a plug of glass wool as filter material. The samples so obtained were properly diluted in volumetric flasks with pure ethanol or 1:1 ethanol-water mixtures. After final dilution the extinction given by the dis-

TABLE 1

*Wave lengths of maximum absorption by DMAB in ethanol-water mixtures*  
 The concentration of DMAB is the same in all the solutions; slit width, 0.1 mm.

Volume per cent H <sub>2</sub> O. . . . .	0	10	20	50	80
Wave length of maximum absorption, m $\mu$ .	406	410	413	419	450

TABLE 2

*Extinction of DMAB in pure ethanol and ethanol-water mixtures*

DMAB in pure ethanol at 406 m $\mu$ ; 1-cm. cell; slit width = 0.1 mm.			DMAB in ethanol-water (1:1 by volume) at 419 m $\mu$ ; 1-cm. cell; slit width = 0.12 mm.		
CONCENTRATION (c) OF DMAB	EXTINCTION E	E/c	CONCENTRATION (c) OF DMAB	EXTINCTION E	E/c
mg./l.			mg./l.		
10.0	1.27	0.1270	10.09	1.09	0.1080
5.0	0.637	0.1274	5.045	0.546	0.1082
2.5	0.317	0.1268	2.522	0.272	0.1078

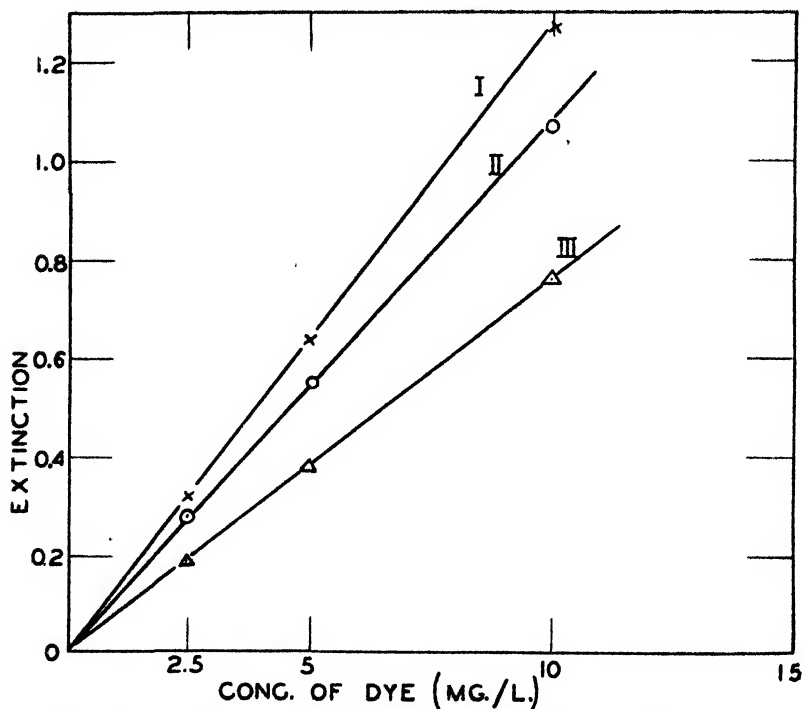


FIG. 1. Calibration curves of DMAB and Orange OT. Curve I: DMAB in pure ethanol, 406 m $\mu$ , slit = 0.1 mm., 1-cm. cell. Curve II: DMAB in alcohol-water (1:1 by volume), 419 m $\mu$ , slit = 0.12 mm., 1-cm. cell. Curve III: Orange OT in alcohol-water (1:1 by volume), 497 m $\mu$ , slit = 0.09 mm., 1-cm. cell.



TABLE 3

*Extinction of Orange OT in alcohol-water mixture (1:1 by volume)*1-cm. cell; wave length = 497 m $\mu$ ; slit width = 0.09 mm.

CONCENTRATION (c) OF ORANGE OT	EXTINCTION E	EXTINCTION COEFFICIENT E/c
mg./l.		
10.0	0.761	0.0761
5.0	0.381	0.0762
2.5	0.191	0.0764

TABLE 4

*Solubilization of DMAB in sodium and potassium laurate solutions at 30°C. and 50°C.*

CONCENTRATION OF SOAP	DMAB SOLUBILIZED PER LITER OF SOAP SOLUTION AT			
	30°C.		50°C.	
	Sodium laurate	Potassium laurate	Sodium laurate	Potassium laurate
moles/liter	mg	mg	mg	mg
0.75		981		1578
0.375	509	498	803	797
0.1875	242	249	398	393
0.0938	108	105	171	168
0.0469	33.1	31.8	55.3	55.0
0.0235	3.30	1.49	3.39	2.40
0.0118	2.54	1.19	3.05	2.04
0.0059	1.05		2.10	

TABLE 5

*Solubilization of Orange OT in sodium laurate at 30°C. and in potassium laurate at 30°C. and 50°C.*

SODIUM LAURATE AT 30°C.		POTASSIUM LAURATE		
Concentration of soap	Dye per liter of soap solution	Concentration of soap	Dye per liter of soap solution at 30°C.	Dye per liter of soap solution at 50°C.
moles/liter	mg.	moles/liter	mg	mg
		0.749	945	1379
		0.562	722	1000
0.281	342	0.374	462	637
0.1875	212.7	0.187	216.5	291.3
0.0938	88.0	0.0936	91.9	120.8
0.0468	27.25	0.0468	31.5	36.7
0.0235	3.02	0.0234	3.02	2.95
0.0118	0.815	0.0117	2.62	2.49
0.0059	0.682	0.0067	2.23	1.84

solved dye was measured in 1-cm. cells in the Beckman spectrophotometer. After having placed the cells into the apparatus it was necessary to wait for about 5-10 min. in order to let the solutions attain a constant temperature. It is important

to measure the extinctions in all the cells at the same temperature. We were led to this conclusion by the fact that the extinction values of the solutions in the cell farthest away from the spectrophotometer lamp usually increased by about 10

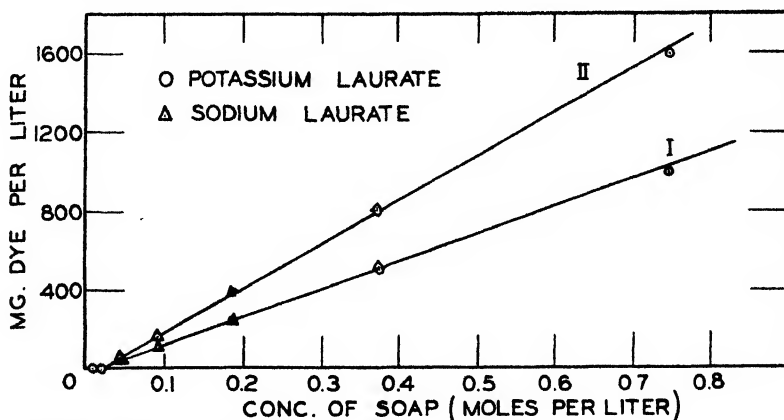


FIG. 2. Solubilization of DMAB in sodium and potassium laurate solutions at 30°C and 50°C. Curve I: sodium and potassium laurates at 30°C. Curve II: sodium and potassium laurates at 50°C.

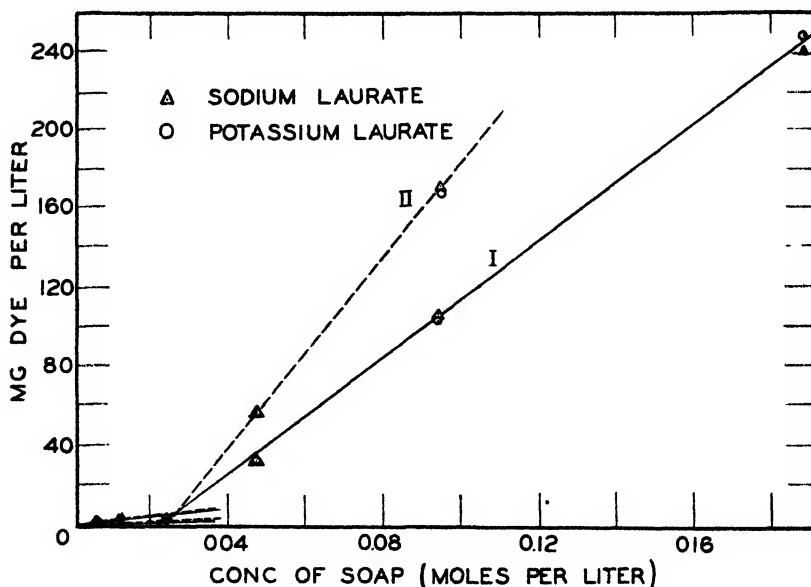


FIG. 3. Solubilization of DMAB in sodium and potassium laurate solutions at 30°C and 50°C. Curve I: sodium and potassium laurates at 30°C. Curve II: sodium and potassium laurates at 50°C.

per cent within the first 5-10 min. after the first reading. After this time the values remained constant. In one instance it was found that the extinction of a dye solution in pure ethanol in the cell farthest away from the lamp was 0.300

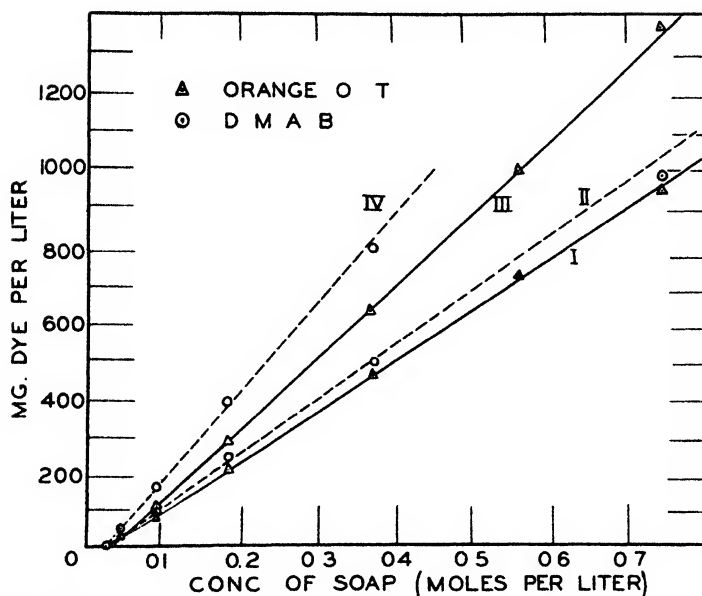


FIG. 4. Solubilization of Orange OT and DMAB in sodium and potassium laurate solutions at 30°C. and 50°C. Curve I: Orange OT in laurate at 30°C. Curve II: DMAB in laurate at 30°C. Curve III: Orange OT in laurate at 50°C. Curve IV: DMAB in laurate at 50°C.

TABLE 6

*Solubilization of DMAB in potassium and sodium caprates at 30°C. and 50°C.*

POTASSIUM CAPRATE.			SODIUM CAPRATE*		
Concentration of soap	DMAB solubilized per liter of soap solution		Concentration of soap	DMAB solubilized per liter of soap solution	
	At 30°C.	At 50°C.		At 30°C.	At 50°C.
<i>moles/liter</i>	<i>mg.</i>	<i>mg.</i>	<i>moles/liter</i>	<i>mg.</i>	<i>mg.</i>
0.75	412	736	0.20	63.2	149
0.563	300	542	0.18	48.5	124
0.375	185	328	0.16	36.2	87.0
0.281	119	219	0.14	22.9	
0.187	57.4	106	0.12		29.0
0.140	25.4	49.3	0.10	3.4	10.0
0.0938	1.48	6.76	0.04	1.1	3.9
0.0469	2.04	3.63			
0.0118	1.06	1.65			
0.0059	0.852	1.52			

\* Experiments reported in J. Phys. Chem. **50**, 440 (1946).

immediately after the cell with the solution had been placed into the cell compartment of the spectrophotometer. After 8 min. the extinction was 0.330, after 10 min. 0.331, and after 20 min. 0.332, after which time it remained constant for

several hours. The same solution was now put nearest to the spectrophotometer lamp. Now the first reading was 0.321, after 4 min. 0.325, and after 6 min. 0.331, and then it remained constant. The effect of temperature on the extinction of DMAB is more pronounced in pure ethanol solutions than in 1:1 ethanol-water mixtures. Therefore it is preferable to use the latter whenever possible.

The spectrum of DMAB in ethanol-water mixtures was found to be different from the spectrum in pure ethanol. The wave lengths of maximum absorption of DMAB in various ethanol-water mixtures are given in table 1.

The extinction of solutions of known concentrations of DMAB in pure ethanol

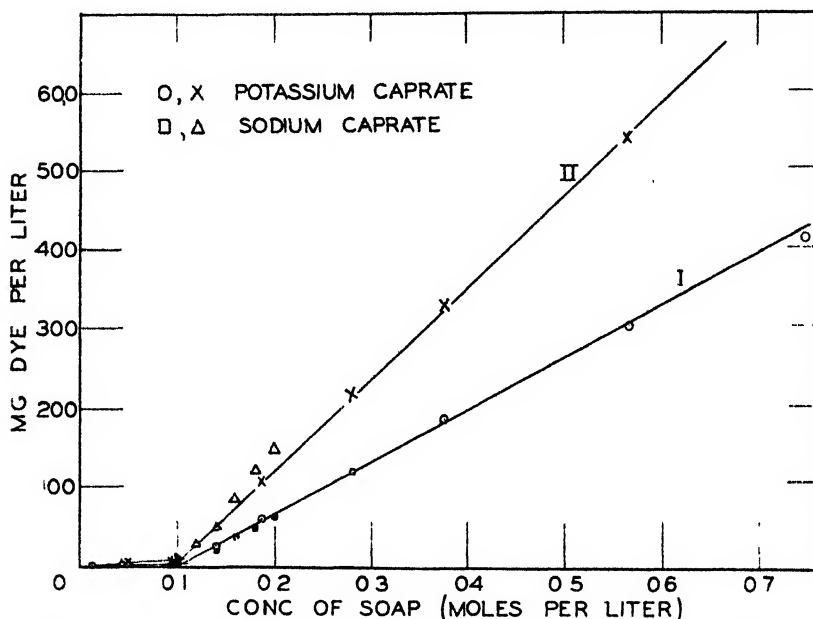


FIG. 5. Solubilization of DMAB in potassium and sodium caprate solutions at 30°C. and 50°C. Curve I: potassium and sodium caprates at 30°C. Curve II: potassium and sodium caprates at 50°C.

as well as in an ethanol-water mixture (1:1 by volume) was determined at the wave length of maximum absorption. The data are given in table 2.

The extinction of Orange OT was measured in the alcohol-water mixture (1:1 by volume) as a solvent. The wave length of maximum absorption was found to be 497  $\mu$  with a slit width of 0.09 mm. in a 1-cm. cell.

Beer's law was found to be obeyed by solutions of DMAB and Orange OT at the wave lengths of maximum absorption.

The extinction data of the two dyes are represented in figure 1. Under the experimental conditions the extinction of the dyes was not affected by the presence of the detergents. Several measurements were made at different dilutions of the same sample of the filtered solution saturated with dye in pure ethanol and in ethanol-water mixture (1:1 by volume). The results agreed to within 1 per cent.

It was found to be convenient to represent the experimental data on graphs in which the amount of dye solubilized is plotted against the concentration of the detergent.

In a few instances the experimental data of one set of experiments were reproduced in two graphs, one on a smaller concentration scale to show the change of

TABLE 7  
*Solubilization of DMAB in solutions of sodium and potassium oleates, potassium stearate, palmitate, and myristate*

CONCENTRA- TION OF SOAP	DMAB SOLUBILIZED PER LITER OF SOAP SOLUTION						
	Sodium oleate at 50°C.* (C <sub>18</sub> )	Potassium oleate		Potassium stearate at 50°C.* (C <sub>18</sub> )	Potassium palmitate at 50°C.* (C <sub>16</sub> )	Potassium myristate	
	At 50°C. (C <sub>18</sub> )	At 50°C. (C <sub>18</sub> )	At 30°C. (C <sub>18</sub> )	At 50°C.* (C <sub>18</sub> )	At 50°C.* (C <sub>16</sub> )	At 50°C. (C <sub>14</sub> )	At 30°C (C <sub>14</sub> )
moles/liter	mg	mg	mg.	mg	mg.	mg	mg
0.25							637
0.15		815	478				
0.125						494	320
0.10	575			782	582	375*	
0.090			291.5				
0.080	450					306*	
0.075		416		582	443		
0.060	335		189			224	152
0.050				375	302		
0.045			146				
0.040	241					142*	
0.030		162.5	99.1			90.3	69.0
0.025				193	154		
0.020	115					61.0*	
0.015		51.5	48.6			25.0	22.9
0.010	60.8						
0.009		44.0	29.2				
0.0075						1.85	3.52
0.006			20.2				
0.005						(15.82)	0.65
0.004	35.3						
0.003		7.87	9.07			(7.96)	0.925
0.0015		3.1	1.5			(17.1)	(7.68)
0.0006		(29.1)	(5.3)				
0.0003		3.2	1.3				

\* Experiments reported in J. Phys. Chem. **50**, 440 (1946).

solubilization at higher concentrations of the detergent, and one on a larger concentration scale to find the critical concentration.

#### EXPERIMENTAL RESULTS

##### *Sodium and potassium laurates*

In a preliminary note (14) the solubilization of DMAB was given in sodium laurate solutions up to a concentration of 0.1 *M* at temperatures of 40°C. and

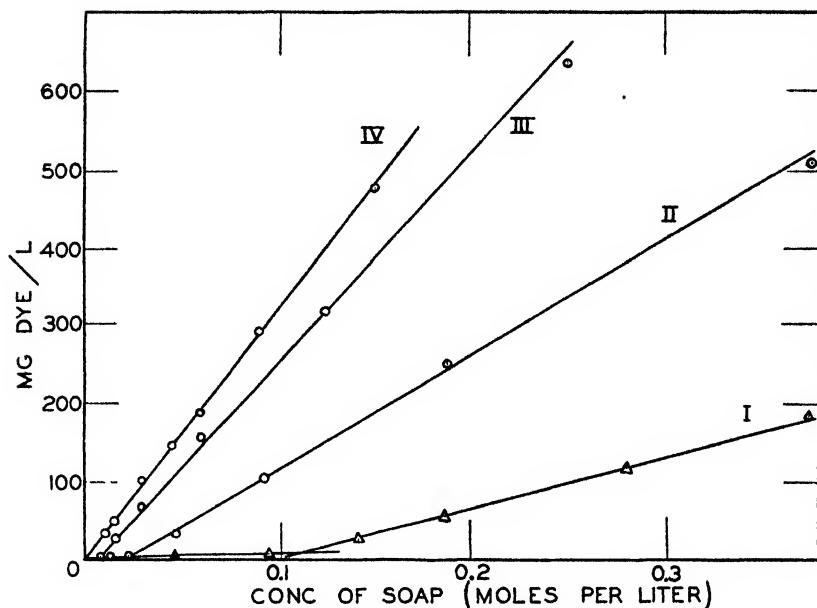


FIG. 6. Solubilization of DMAB in fatty acid soap solutions at 30°C. Curve I: potassium caprate. Curve II: potassium laurate. Curve III: potassium myristate. Curve IV: potassium oleate.

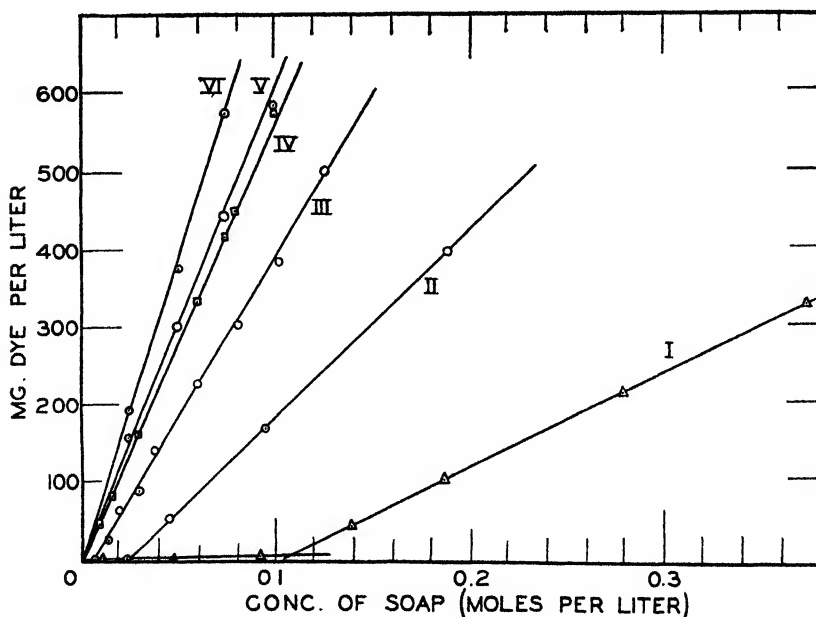


FIG. 7. Solubilization of DMAB in fatty acid soap solutions at 50°C. Curve I: potassium caprate. Curve II: potassium laurate. Curve III: potassium myristate. Curve IV: potassium oleate. Curve V: potassium palmitate. Curve VI: potassium stearate.

50°C. In the present work the measurements have been extended to a concentration of 0.375 *M* at temperatures of 30°C. and 50°C. Data are also presented on the solubilization of DMAB in potassium laurate solutions. Solubilization data are also given of Orange OT. The results are given in tables 4 and 5. The data of tables 4 and 5 are represented graphically in figures 2, 3, and 4.

TABLE 8

*Solubilization of DMAB in dodecylamine hydrochloride solutions at 30°C. and 50°C.*

CONCENTRATION OF SOAP	DMAB SOLUBILIZED PER LITER OF SOAP SOLUTION	
	At 30°C.	At 50°C.
<i>moles/liter</i>	<i>mg.</i>	<i>mg</i>
0.505	1848	2357
0.379	1272	1658
0.2525	757	949
0.126	293	406
0.0631	118	167
0.0316	41.2	59.7
0.0157	6.95	5.65
0.00787	0.832	1.90
0.00393	0.555	

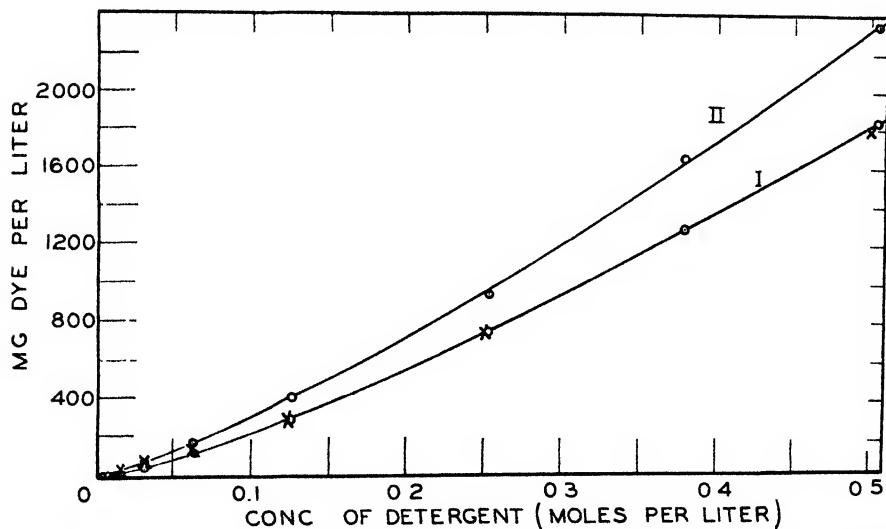


FIG. 8. Solubilization of DMAB in dodecylamine hydrochloride solutions at 30°C. and 50°C. (Curve I: at 30°C. Curve II: at 50°C.)

Because of the lower solubility of sodium laurate, the highest concentration investigated for this soap was 0.375 *M*.

*Sodium and potassium caprates*

The results are given in table 6 and represented graphically in figure 5.

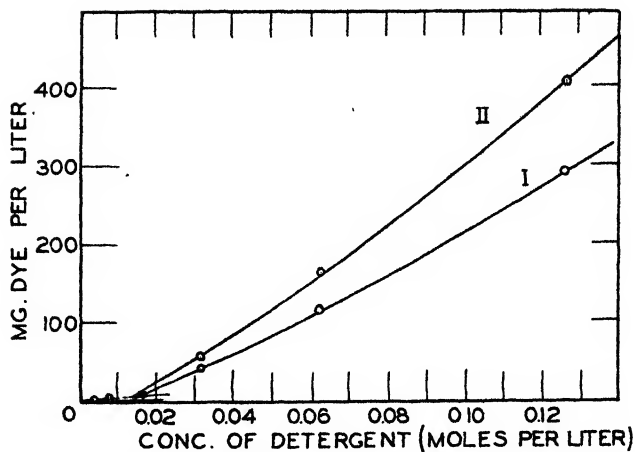


FIG. 9. Solubilization of DMAB in dodecylamine hydrochloride solutions at 30°C. and 50°C. Curve I: at 30°C. Curve II: at 50°C.

TABLE 9  
*Solubilization of DMAB in sodium di-sec-butyl naphthalenesulfonate (SA-178) at 30°C. and 50°C.*

CONCENTRATION OF DETERGENT	DMAB SOLUBILIZED PER LITER OF DETERGENT SOLUTION	
	At 30°C.	At 50°C.
<i>moles/liter</i>	<i>mg.</i>	<i>mg.</i>
0.2		900
0.125	276	487
0.1	211	313
0.0625	114	194
0.05	81	140
0.0313	42	71
0.025	31	50
0.0125	11	18

TABLE 10  
*Solubilization of DMAB in diamyl sodium sulfosuccinate (Aerosol AY) at 30°C. and 50°C.*

CONCENTRATION OF DETERGENT	DMAB SOLUBILIZED PER LITER OF DETERGENT SOLUTION	
	At 30°C.	At 50°C.
<i>moles/liter</i>	<i>mg.</i>	<i>mg.</i>
0.92	1936	3470
0.645	1236	2045
0.46	742	1200
0.323	435	739
0.23	185	288
0.161	84	191
0.115	23.4	36.8
0.058		6.18
0.029		1.94



*Potassium myristate, palmitate, oleate, and stearate*

Experiments were carried out with potassium myristate at temperatures of 30°C. and 50°C., and at 50°C. only with potassium palmitate and stearate.

TABLE 11  
*Solubilization of DMAB in Daxad 11 at 30°C. and 50°C.*

CONCENTRATION OF DAXAD 11*	DMAB SOLUBILIZED PER LITER OF DETERGENT SOLUTION	
	At 30°C.	At 50°C.
grams/liter	mg.	mg.
200	858	1148
150	599	828
100	354	545
75	262	392
50	164	265
25	84	138
12.5	44	73
6.25	27	36
3.13	15.6	21
1.5	8.9	13
0.75	5.9	10
0.38	4.5	4.3

\* Since the molecular weight of Daxad 11 and also its purity are unknown, the concentration is given in grams per liter. The same expression is used for Triton R-100 in table 12.

TABLE 12  
*Solubilization of DMAB in Triton R-100 at 30°C. and 50°C.*

CONCENTRATION OF TRITON R-100*	DMAB SOLUBILIZED PER LITER OF DETERGENT SOLUTION	
	At 30°C.	At 50°C.
grams/liter	mg.	mg.
200	1534	1703
100	645	740
50	270	335
25	130	152
12.5	68	81
6.25	36	43
3.125	24	24
1.563	16.5	17.9
0.781	11.5	12.1

\* The extinctions of Daxad 11 and Triton R-100 solutions containing no solubilized dye were measured to correct for the color of the detergents themselves.

Palmitate and stearate could not be used at 30°C. because of their low solubility. Experiments with sodium and potassium oleates were carried out at 50°C. and with potassium oleate also at 30°C. The results are given in table 7 and figures 6 and 7. These figures also give the data for laurate and caprate.

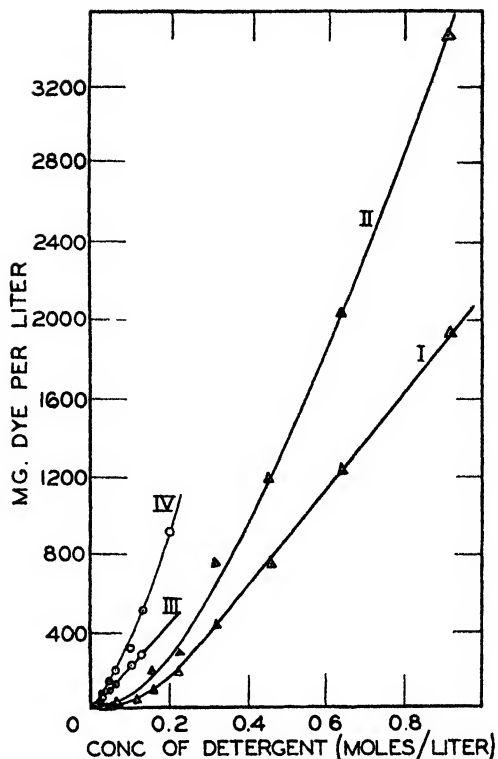


FIG. 10. Solubilization of DMAB in solutions of Aerosol AY and SA-178 at 30°C. and 50°C. Curve I: Aerosol AT at 30°C. Curve II: Aerosol AY at 50°C. Curve III: SA-178 at 30°C. Curve IV: SA-178 at 50°C.

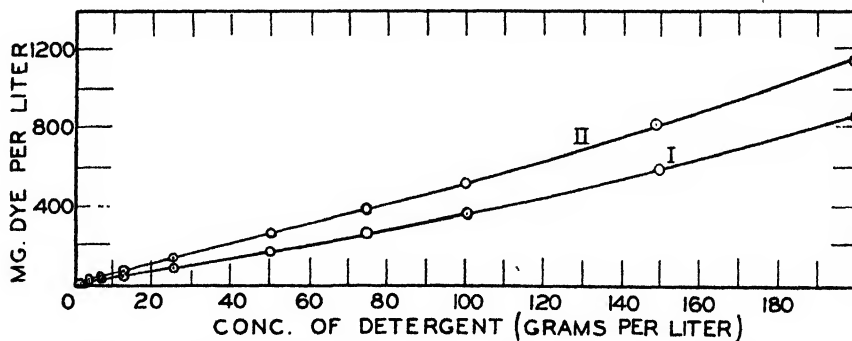


FIG. 11. Solubilization of DMAB in solutions of Daxad 11 at 30°C. and 50°C. Curve I: at 30°C. Curve II: at 50°C.

#### *Dodecylamine hydrochloride*

Solubilization experiments with dodecylamine hydrochloride as a typical cationic detergent were carried out at 30°C. and 50°C. Table 8 and figures 8 and 9 give the experimental data.

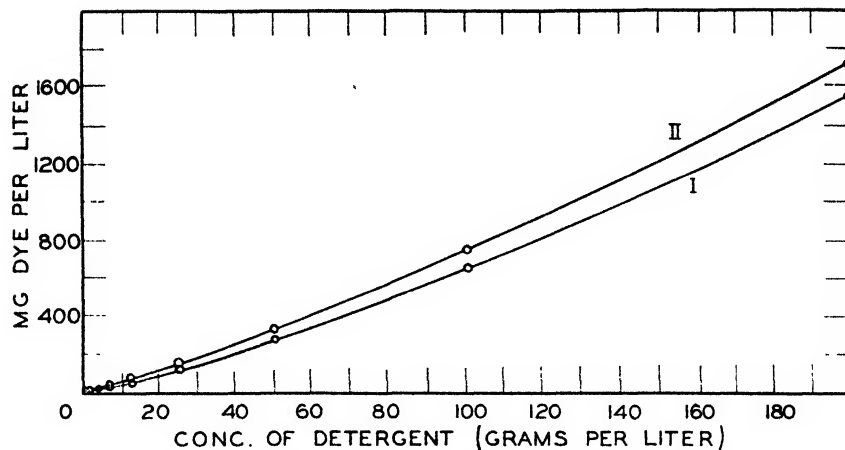


FIG. 12. Solubilization of DMAB in solutions of Triton R-100 at 30°C. and 50°C. Curve I: at 30°C. Curve II: at 50°C.

TABLE 13

*Solubilization of DMAB in potassium dehydroabietate at 50°C.*

CONCENTRATION OF DETERGENT	DMAB SOLUBILIZED PER LITER OF DETERGENT SOLUTION
<i>moles/liter</i>	<i>mg.</i>
0.2	448
0.1	128
0.05	31
0.025	3.5
0.0125	0.00

TABLE 14

*Solubilization of DMAB in sodium rosinate No. 45-985 (Rosin 731) at 30°C. and 50°C.*

CONCENTRATION OF DETERGENT	DMAB SOLUBILIZED PER LITER OF DETERGENT SOLUTION	
	At 30°C.	At 50°C.
<i>moles/liter</i>	<i>mg.</i>	<i>mg.</i>
0.294	764	1890
0.147	347	874
0.074	152	322
0.037	77	141
0.019	37	73
0.009	17	31

### *Commercial detergents*

The solubilization in solutions of a few technical detergents is shown in tables 9, 10, 11, 12 and in figures 10, 11, 12.

*Dehydroabietate and rosinate*

Solubilization experiments were carried out with potassium dehydroabietate and sodium rosinate solutions. It is of interest to compare the behavior of these two substances, since dehydroabietic acid is the main constituent of dehydrogenated rosin. Tables 13 and 14 give the solubilization data.

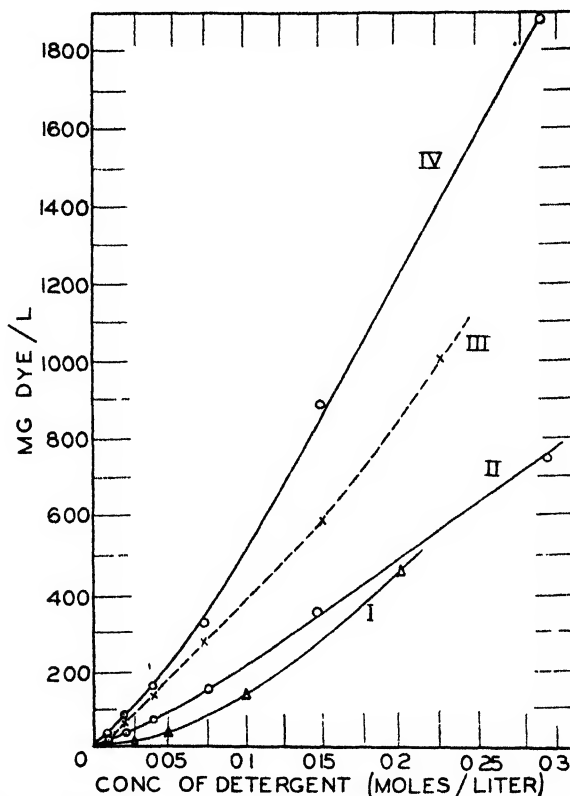


FIG. 13. Solubilization of DMAB in sodium rosinate solutions at 30°C. and 50°C. and in potassium dehydroabietate solutions at 50°C. Curve I: potassium dehydroabietate at 50°C. Curve II: sodium rosinate (No. 45-985) at 30°C. Curve III: sodium rosinate (No. 45-979) at 50°C. Curve IV: sodium rosinate (No. 45-985) at 50°C.

It was found that the extinction of the diluted rosin soap solutions which did not contain dye was negligible. The data in tables 13 and 14 are represented in figure 13. In figure 13 a few data are given on the solubilization of DMAB in sodium rosinate solutions prepared from a different sample of Hercules Rosin 731, the batch number of which was 45-979.

## DISCUSSION

## 1. Critical concentration

The critical concentration of various detergents as found from the solubilization graphs is given in table 15 and compared with values found by other methods

TABLE 15  
Critical concentrations

DETERGENT	TEMPERATURE	CRITICAL CONCENTRATION	METHOD OF DETERMINATION
	°C.	moles/liter	
Sodium caprate . . . . .	30	0.106	Solubilization with DMAB
	20	0.097	Hydrolysis (8)
	20	0.095-0.10	Conductivity (9)
	20	0.124	Viscosity (12)
	25	0.10	Na <sup>+</sup> activity (membrane electrode) (2)
	50	0.105	Solubilization with DMAB
Potassium caprate . . . . .	30	0.106	Solubilization with DMAB
	50	0.105	Solubilization with DMAB
	25.8	0.095	Spectral dye method (11)
		0.100	Spectral dye method (24)
Sodium laurate . . . . .	30	0.0255	Solubilization with DMAB
	30	0.0253	Solubilization with Orange OT
	50	0.0255	Solubilization with DMAB
	17-70	0.028	Conductivity (9)
	20	0.096	Viscosity (12)
	25	0.02	Na <sup>+</sup> activity (membrane electrode) (2)
	60	0.026	pH measurement (23)
Potassium laurate . . . . .	30	0.0235	Solubilization with DMAB
	30	0.0235	Solubilization with Orange OT
	50	0.0245	Solubilization with DMAB
	50	0.0285	Solubilization with Orange OT
	30	0.022	Laurate-ion activity (E.M.F.) (15)
	26±2	0.0231, 0.0235, 0.0230	Spectral dye method (3, 4, 5, 24)
	25.8	0.024	Spectral dye method (11)
	25	0.0215-0.0235	Spectral dye method (13)
	35	0.0205-0.0220	Spectral dye method (13)
	45	0.0200-0.0215	Spectral dye method (13)
	55	0.0200-0.0215	Spectral dye method (13)
	25	0.0255	Interferometric method (13)
	35	0.0270	Interferometric method (13)
	45	0.0305	Interferometric method (13)
	55	0.0350	Interferometric method (13)
	25	0.0380	Density (1)
Potassium myristate . . . . .	30	0.0070	Solubilization with DMAB
	50	0.0072	Solubilization with DMAB
	25.8	0.006	Spectral dye method (11)
		0.0059	Spectral dye method (24)
	25	0.0060-0.0067	Spectral dye method (13)
	35	0.0054-0.0060	Spectral dye method (13)

TABLE 15—*Continued*

DETERGENT	TEMPERATURE	CRITICAL CONCENTRATION	METHOD OF DETERMINATION
	°C.	moles/liter	
	45	0.0053–0.0057	Spectral dye method (13)
	55	0.0053–0.0057	Spectral dye method (13)
	25	0.0066	Interferometric method (13)
	35	0.0070	Interferometric method (13)
	45	0.0074	Interferometric method (13)
	55	0.0079	Interferometric method (13)
	25	0.003	Cation activity (membrane electrode) (2)
Sodium myristate . . . . .	17–80	0.007	Conductivity (9)
	60	0.01	pH measurement (23)
Potassium palmitate . . . . .	50	<0.001	Solubilization with DMAB
Sodium palmitate . . . . .	52–67	0.0032	Conductivity (9)
	60	0.003	pH measurement (23)
Potassium stearate . . . . .	50	<0.001	Solubilization with DMAB
Sodium stearate . . . . .	60	0.0008	pH measurement (23)
Potassium oleate . . . . .	30	0.0006	Solubilization with DMAB
	50	0.0011	Solubilization with DMAB
	25	0.0007–0.0012	Spectral dye method (11)
Sodium oleate . . . . .	50	<0.001	Solubilization with DMAB
	25	<0.001	Na <sup>+</sup> activity (2)
	20	0.23	Viscosity (12)
Dodecylamine hydrochloride . . . . .	30	0.0134	Solubilization with DMAB
	50	0.0134	Solubilization with DMAB
	30	0.0131, 0.0129	Conductivity (20, 21)
	50	0.0132	Conductivity (20)
	26±2	0.0124, 0.0127 0.0130, 0.0131, 0.0136	Spectral dye method (3, 4, 5, 11)
Sodium di- <i>sec</i> -butyl naphthalenesulfonate (SA-178) . . . . .	30	<0.01	Solubilization with DMAB
	50	<0.01	Solubilization with DMAB
Diamyl sodium sulfosuccinate (Aerosol AY) . . . . .	30	0.095±0.01	Solubilization with DMAB
	50	0.095±0.01	Solubilization with DMAB
Daxad 11 . . . . .	30	<1 g. per liter	Solubilization with DMAB
	50	<1 g. per liter	Solubilization with DMAB

TABLE 15—*Concluded*

DETERGENT	TEMPERATURE	CRITICAL CONCENTRATION	METHOD OF DETERMINATION
	°C.	moles/liter	
Triton R-100	30	<1 g. per liter	Solubilization with DMAB
	50	<1 g. per liter	Solubilization with DMAB
Potassium dehydroabi- tate	50	0.025–0.030	Solubilization with DMAB
	25–8	0.025–0.032	Spectral dye method (6)
Sodium rosinate (Hercu- les sample No. 45-985)	30	<0.01	Solubilization with DMAB
	50	<0.01	Solubilization with DMAB
Sodium rosinate (Hercu- les sample No. 45-979)	50	<0.01	Solubilization with DMAB

described in the literature. From table 15 it is seen that most of the values determined by the solubilization method agree well with those found by other methods. In a few instances it was not possible to find an accurate value of the critical concentration by means of solubilization experiments. When the critical concentration was found to be equal to or smaller than 0.001 *M* it could only be stated to be of that order. With some technical detergents an accurate value of the critical concentration could not be given because of the presence of impurities.

Not included in table 15 are values of the critical concentration based upon turbidity measurements. Referring to qualitative observations on the turbidity of soap solutions by Müller von Blumencron (19) and Lascaray (16), Ekwall (7) determined quantitatively the change of the turbidity with concentration in solutions of sodium stearate, palmitate, myristate, laurate, and oleate. Two distinct maxima of turbidity were observed, the first maximum occurring in all soap solutions at very small concentrations. This turbidity is attributed by Ekwall to suspended fatty acid formed by hydrolysis. Upon increase of the concentration the turbidity decreases as a result of the formation of acid soap,— $\text{NaFa} \cdot \text{HFa}$  (Fa denoting fatty acid radical). The acid soap being more soluble, all the soap solutions are practically clear in a certain concentration range. When the concentration is further increased, solutions become turbid as a result of the separation of acid soap which is kept in colloidal solution. A second maximum in the turbidity is observed at a certain concentration. The concentrations found by Ekwall at which the maxima appear are listed in table 16.

It is interesting to note that the first maximum appears at a concentration considerably below the critical one. On the other hand, the concentration at which the second maximum appears seems to correspond to the critical concentration. The agreement is especially good with myristate and laurate. On the basis of our present knowledge of soap solutions, the appearance of the second maximum of turbidity at the critical concentration is easily understood. The

insoluble acid soap is being solubilized in the micelles above the critical concentration when the soap solution becomes clear. It may be added that Stauff (23) showed by analysis that the insoluble substance at the first maximum turbidity is fatty acid and that at the second maximum is acid soap.

We found that the phenomena described by Ekwall are readily observed in solubilization experiments with DMAB visually with a naked eye. As a matter of fact, some of the dye is held tenaciously in colloidal solution at the concentration of maximum turbidity. This is the reason why solubilization data found for myristate and oleate at or slightly below the critical concentration are high and should be discarded.

TABLE 16  
*Concentration of maximum turbidities (moles per liter) for  
fatty acid soaps as found by Ekwall*

TEMPERATURE]	FIRST MAXIMUM	SOAP	SECOND MAXIMUM
°C.			
20-50	0.00070-0.00076	Sodium oleate	0.002-0.003
65	0.00019	Sodium stearate	
67	0.00020		0.0044-0.0068
20-50	0.0002	Sodium palmitate	
58			0.003
20-80	0.0009-0.0012	Sodium myristate	
43			0.007
48-80			0.007
		Sodium laurate	
13.5	0.0063		0.027
18-40	0.0063		0.023

Returning to the data of table 15 it may be concluded that within relatively wide limits the critical concentration is hardly affected by the temperature. For example, the critical concentrations of potassium caprate and myristate were found to be 0.106 *M* and 0.0070 *M* at 30°C. and 0.105 *M* and 0.0072 *M* at 50°C., respectively. The relatively large increase of the critical concentrations of potassium laurate and myristate with an increase of the temperature between 25°C. and 55°C., as found by Klevens (13) in his interferometric measurements, is not found in solubilization experiments with DMAB.

From table 15 it is seen that the critical concentration of fatty acid soaps decreases rapidly with increasing number of carbon atoms in the fatty acid. The critical concentration is 0.105 *M* for C<sub>10</sub>, 0.025 *M* for C<sub>12</sub>, 0.007 *M* for C<sub>14</sub>, and of the order of or smaller than 0.001 *M* for C<sub>16</sub> and C<sub>18</sub>.

By applying an equation derived by Schultz (22) on the solubility of compounds of high molecular weight Stauff (23) showed and confirmed experimentally that



the plot of the logarithm of the critical concentration *versus* the number of carbon atoms in fatty acid soaps with an even number of carbon atoms yields a straight line. Our data for soaps between  $C_{10}$  and  $C_{16}$  when plotted in this way also lie on a straight line.

The critical concentrations of sodium and potassium laurates (DMAB and Orange OT) were found to be the same within the experimental error.

In figure 14 we have plotted McBain's data obtained with Orange OT and our own data with the same dye. The agreement between the measurements in both laboratories is poor. From McBain's data it is derived that the critical concen-

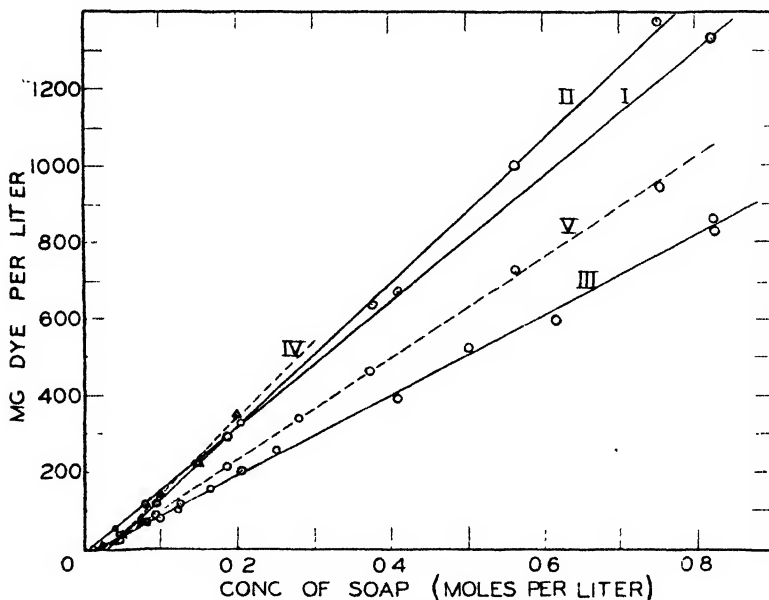


FIG. 14 Solubilization of Orange OT in potassium and sodium laurate solutions at 25°, 30°, and 50°C. Curve I, potassium laurate at 50°C. (McBain's curve). Curve II, potassium laurate at 50°C. (our data). Curve III, potassium laurate at 25°C. (McBain's curve). Curve IV, sodium laurate at 25°C. (McBain's curve). Curve V, potassium and sodium laurates at 30°C. (our data).

tration of potassium laurate at 50°C. is 0.01  $M$ , while it is 0.028  $M$  at 25°C. and 0.0195  $M$  for sodium laurate at 25°C. On the other hand, we found a critical concentration of 0.025  $M$  for both sodium and potassium laurate at temperatures between 30°C. and 50°C.

From McBain's data a critical concentration as found by extrapolation at 25°C. for sodium caprate is 0.07  $M$ , whereas we found a value of 0.105  $M$  between 30°C. and 50°C. for both sodium and potassium caprates (DMAB).

Sodium and potassium oleates also have the same critical concentration (0.0011  $M$ ), as found by our measurements with DMAB at 50°C.

It is of interest to note that the critical concentration of sodium laurate is 0.025  $M$ , while that of laurylamine hydrochloride is about half this value (0.013  $M$ ).

The two detergents are also quite different in regard to the solubilizing power of their micelles (v.i.).

It is not possible to determine the critical concentration of Aerosol AY accurately from solubilization data, since the solubilization line is fairly strongly curved near the critical concentration. By extrapolation it is concluded that the critical concentration is  $0.095 M \pm 0.01$ .

Although dehydroabiatic acid is the main constituent of dehydrogenated rosin (Hercules Powder Company), it is seen from figure 13 that the critical concentration of commercial sodium rosinate is considerably smaller than that of dehydroabietate (see also table 15).

## 2. Solubilizing power of micelles

The solubilizing power of a detergent in general is expressed as the amount of dye in grams per mole of micelles. In the case of a few commercial detergents, the molecular weights of which are unknown and which are of unknown purity, the solubilizing power is expressed in grams of dye per 100 g. of detergent (micelle).

The solubilizing power of the various detergents is given in table 17. When the solubilization line is straight above the critical concentration the solubilizing power of the micelles is constant at a given temperature. On the other hand, if the solubilization line is curved, the solubilizing power varies with the concentration. Its value is found at different concentrations from the tangent of the solubilization line.

The fact that the solubilizing power with regard to DMAB of micelles of fatty acid soaps and of some other detergents is constant above the critical concentration indicates that the solubilized DMAB does not affect the solubilizing power of the micelles. The constant molar solubilizing power of the micelles also indicates that the soap which is unmicellized at the critical concentration does not become micellized at higher concentrations. This conclusion is substantiated by E.M.F. measurements of Kolthoff and Johnson (15), who showed that the laurate-ion activity in sodium laurate solutions remains constant when the soap concentration is increased above the critical one. Finally, the constant value of the solubilization indicates that we are dealing only with one type of micelle above the critical concentration up to the highest concentration investigated. From the data of McBain and Green (10, 17) it is found that the solubilization line of Orange OT is straight (at 25°C. and 50°C.) when the amount of solubilized dye is plotted against the soap concentration. These experiments were done with potassium caprate up to a concentration of 0.84 *M*, with potassium laurate up to 1.4 *M*, potassium myristate up to 0.8 *M*, and sodium laurate up to 0.2 *M*.

We find that the solubilizing power with regard to DMAB and Orange OT of sodium laurate is the same as that of potassium laurate at both 30°C. and 50°C. Also, the solubilizing power of sodium caprate and of sodium oleate was found to be the same as that of the corresponding potassium soaps. These results do not agree with those reported by McBain and coworkers, who found that potassium laurate and oleate have a considerably smaller solubilizing power than the corresponding sodium soaps (figure 14). We find a solubilizing power of sodium and

TABLE 17  
*Solubilizing power of detergents*

DETERGENT	MAXIMUM CONCENTRATION AT WHICH SOLUBILIZATION WAS MEASURED	CONCENTRATION AT WHICH SOLUBILIZING POWER IS GIVEN	TEMPERATURE	SOLUBILIZING POWER GRAMS OF DYE PER MOLE OF MICELLIZED SOAP
	<i>moles/liter</i>		<i>°C.</i>	
Sodium caprate .. . . .	0.20	Constant	30	0.64 with DMAB
Potassium caprate.....	0.75	Constant	30	0.64 with DMAB
Sodium caprate .. . . .	0.20	Constant	50	1.19 with DMAB
Potassium caprate .. . . .	0.75	Constant	50	1.19 with DMAB
Potassium caprate (McBain's result (17))..	0.839	Constant	25	0.395 with Orange OT
Sodium laurate .. . . .	0.375	Constant	30	1.50 with DMAB
Sodium laurate .. . . .	0.375	Constant	30	1.31 with Orange OT
Sodium laurate (McBain's result (10)).. . . .	0.2	Constant	25	2.00 with Orange OT
Sodium laurate .. . . .	0.375	Constant	50	2.43 with DMAB
Potassium laurate .. . . .	0.75	Constant	30	1.50 with DMAB
Potassium laurate .. . . .	0.75	Constant	30	1.31 with Orange OT
Potassium laurate (McBain's result (17))	1.403	Constant	25	1.06 with Orange OT
Potassium laurate .. . . .	0.75	Constant	50	2.43 with DMAB
Potassium laurate .. . . .	0.75	Constant	50	1.88 with Orange OT
Potassium laurate (McBain's result (17))	0.819	Constant	50	1.65 with Orange OT
Potassium myristate .. . . .	0.25	Constant	30	2.71 with DMAB
Potassium myristate (McBain's result (17))	0.793	Constant	25	1.85 with Orange OT
Potassium myristate .. . . .	0.25	Constant	50	4.15 with DMAB
Potassium myristate (McBain's result (17))	0.793	Constant	50	2.96 with Orange OT
Potassium palmitate.. . . .	0.10	Constant	50	5.90 with DMAB
Potassium stearate .. . . .	0.10	Constant	50	7.86 with DMAB
Potassium oleate .. . . .	0.15	Constant	30	3.24 with DMAB
Sodium and potassium oleates .. . . .	0.15	Constant	50	5.72 with DMAB
Dodecylamine hydro- chloride {	0.505	0.4 M	30	4.32 with DMAB
	0.505	0.1 M	30	2.90 with DMAB
	0.505	0.06 M	30	2.23 with DMAB
Dodecylamine hydrochlo- ride (McBain's result (10)).	0.200	0.06 M	25	1.85 with Orange OT
Dodecylamine hydro- chloride {	0.505	0.4 M	50	5.63 with DMAB
	0.505	0.06 M	50	3.30 with DMAB
Sodium di- <i>sec</i> -butyl naph- thalenesulfonate (SA- 178) .	0.125	0.1 M	30	2.65 with DMAB
	0.20	0.1 M	50	4.80 with DMAB
Diamyl sodium sulfosuc- cinate (Aerosol AY) ...	0.92	0.8 M	30	2.60 with DMAB
	0.92	0.4 M	30	2.40 with DMAB
	0.92	0.2 M	30	1.86 with DMAB

TABLE 17—*Continued*

DETERGENT	MAXIMUM CONCENTRATION AT WHICH SOLUBILIZATION WAS MEASURED	CONCENTRATION AT WHICH SOLUBILIZING POWER IS GIVEN	TEMPERATURE	SOLUBILIZING POWER GRAMS OF DYE PER MOLE OF MICELLIZED SOAP
	<i>moles/liter</i>		<i>°C.</i>	
Diamyl sodium sulfosuccinate (Aerosol AY) (McBain's result (18)) . . .	0.80	0.8 <i>M</i>	25	1.13 with Orange OT
Diamyl sodium sulfosuccinate (Aerosol AY) (McBain's result (18)) . . .	0.80	0.4 <i>M</i>	25	0.65 with Orange OT
Aerosol AY . . . . .	0.92	0.8 <i>M</i>	50	5.30 with DMAB
	0.92	0.4 <i>M</i>	50	4.00 with DMAB
	0.92	0.1 <i>M</i>	50	0.65 with DMAB
	200 g. per liter	100 g. per liter	30	0.45 g. per 100 g. of detergent with DMAB
Daxad 11 . . . . .	200 g. per liter	100 g. per liter	50	0.52 g. per 100 g. of detergent with DMAB
Triton R-100 . . . . .	200 g. per liter	100 g. per liter	30	0.68 g. per 100 g. of detergent with DMAB
Triton R-100 . . . . .	200 g. per liter	100 g. per liter	50	0.83 g. per 100 g. of detergent with DMAB
Potassium dehydroabietate . . . . .	0.2	0.1 <i>M</i>	50	2.5 with DMAB
Sodium rosinate (Hercules sample No. 45-985) . . . . .	0.294	0.1 <i>M</i>	30	2.58 with DMAB
Sodium rosinate (Hercules sample No. 45-985) . . . . .	0.294	0.1 <i>M</i>	50	7.12 with DMAB
Sodium rosinate (Hercules sample No. 45-979) . . . . .	0.226	0.1 <i>M</i>	50	4.14 with DMAB

potassium laurates with regard to Orange OT at 30°C. of 1.31, whereas from McBain's data a value at 25°C. of 2.00 is found for sodium laurate and of 1.06 for potassium laurate. At 50°C. we find a solubilizing power of 1.88 for Orange OT and from McBain's data a value of 1.65. From our work we find that the solubilizing power of laurate increases from 1.50 at 30°C. to 2.43 at 50°C. for DMAB, but only from 1.30 at 30°C. to 1.82 at 50°C. for Orange OT. It is seen that the variation of the solubilizing power of a detergent with temperature depends upon the kind of substance which is solubilized.

Comparing the fatty acid soaps it is found that the solubilizing power increases markedly with increasing number of carbon atoms (see figures 6 and 7). For  $C_{10}$ - $C_{12}$ - $C_{14}$ - $C_{16}$ - $C_{18}$  (stearate) and  $C_{18}$  (oleate) fatty acid soaps the solubilizing power for DMAB is in the ratio of 1:2.04:3.49:4.95:6.60:4.8 at 50°C. At 30°C. the ratio for  $C_{10}$ - $C_{12}$ - $C_{14}$ - $C_{18}$  (oleate) is 1:2.34:4.23:5.05. It is seen that the

increase of the solubilizing power with the increase of the number of carbon atoms is greater at 30°C. than at 50°C. McBain and Green (17), who determined the solubilization of Orange OT in potassium caprylate, caprate, laurate, and myristate at 25°C. found a ratio of 1:2.14:6.48:11.61. Taking caprate as 1 this ratio would be 0.467:1:3.02:5.42. The ratio seems to depend on the kind of substance which is solubilized. For a given substance the ratio changes with the temperature.

It is of interest to note that the solubilizing power of oleate ( $C_{18}$ ) is found to be nearly the same as that of palmitate ( $C_{16}$ ), but considerably smaller than that of stearate ( $C_{18}$ ). Apparently the presence of the double bond in oleate decreases the solubilizing power of the micelles.

Figures 3 and 5 show that there is a small amount of solubilization in detergent solutions at concentrations below the critical one. Thus, a perfectly clear 0.06 *M* potassium caprate solution (critical concentration is 0.106) dissolves about 1.8 mg. of DMAB per liter at 30°C. and about 4 mg. of DMAB per liter at 50°C., while the solubility of DMAB in water is less than 1 mg. per liter at both temperatures. This indicates that there are micelles in detergent solutions below the critical concentration.

Dodecylamine hydrochloride provides a typical example of a detergent the solubilizing power of which increases markedly with the concentration above the critical one (see table 17). The effect is so large that it cannot be accounted for by a complete micellization above the critical concentration of all the detergent which is unmicellized at the critical concentration. Neither does it seem probable that it can be accounted for by an increase of the solubilizing power by the solubilized DMAB. Thus it seems that with dodecylamine hydrochloride and detergents behaving similarly there may be at least two different types of micelles with different solubilizing power and that with increasing concentration relatively more of the micelles are formed with the greater solubilizing power. It would be of importance to check this tentative conclusion by optical measurements in pure detergent solutions.

The solubilizing power of laurylamine hydrochloride (0.4 *M*) is considerably greater than that of laurate. This has already been found by McBain (10), who states that both dodecylamine hydrochloride and lauryl sulfonic acid have a greater solubilizing power than laurate.

The solubilizing power of the different detergents as found from the solubilization of DMAB and Orange OT (for laurate) increases with increasing temperature. The relative increase in the same temperature range is different for different detergents. The ratio of the solubilizing power (DMAB) at 30°C. and 50°C. is given for a few pure detergents in table 18.

McBain's experiments (10, 17) with Orange OT yield a ratio of 1.6 for potassium laurate between 50°C. and 25°C. The technical detergents also show a marked increase of their solubilizing power as the temperature is increased. The ratio of the solubilizing power at 50°C. and 30°C. for 0.1 *M* solution of SA-178 is 1.81. The corresponding ratio of Aerosol AY is 2.04 for a 0.8 *M* and 1.67 for a 0.4 *M* solution. The temperature effect on the solubilizing power of sodium

rosinate solutions is extremely great, the ratio being 2.76 for a 0.1 *M* solution of a commercial sample.

It is remarkable that the solubilizing power of sodium rosinate is much greater than that of potassium dehydroabietate, considering the fact that the rosinate contains about 60 per cent dehydroabietate. The solubilizing power of a given commercial sample of sodium rosinate was 7.12 and that of potassium dehydroabietate was 2.5 both at 50°C. and in 0.1 *M* solutions. Obviously other constituents in the dehydrogenated commercial rosin either have a very large solubilizing power as compared to dehydroabietate or these constituents affect the solubilization of DMAB in the dehydroabietate. It would be of interest to find out which constituents in the dehydrogenated rosin are responsible for the great solubilizing power of the commercial rosinate and the large temperature coefficient of solubilization as compared to dehydroabietate.

TABLE 18

*Change of solubilizing power (grams of DMAB per mole of soap) with temperature*

TEMPERATURE  °C.	DETERGENT						
	Caprate	Laurate		Myristate	Oleate	Dodecylamine hydrochloride	
		DMAB	Orange OT			At 0.4 <i>M</i>	At 0.06 <i>M</i>
50	1.19	2.43	1.82	4.15	5.72	5.63	3.30
30	0.64	1.50	1.30	2.71	3.24	4.32	2.23
Ratio: 50°C./30°C.	1.86	1.62	1.4	1.53	1.76	1.3	1.5

## SUMMARY

Solubilization of the water-insoluble dye dimethylaminoazobenzene has been measured at 30°C. and 50°C. in solutions of pure and technical detergents.

When plotting the solubilization against the concentration of the detergent, graphs were obtained from which the critical concentration was found. The solubilization line of fatty acid soaps above the critical concentration was straight (constant solubilizing power of the micelles), while that of many other detergents was convex (increase of solubilizing power of micelles with increasing detergent concentration).

The critical concentration of a large number of detergents is tabulated and compared with data obtained by other methods reported in the literature. The critical concentration is hardly affected by the temperature in a concentration range between 30°C. and 50°C.

The critical concentrations of sodium and potassium caprates and also of the corresponding laurates and oleates are the same. A quantitative expression is given of the solubilizing power of various detergents, and the data are tabulated.

At the same molar concentration sodium and potassium caprates and also the corresponding laurates and oleates have the same solubilizing power. This has

been found for the solubilization of DMAB and of Orange OT in laurate solutions, and of DMAB in caprate and oleate solutions.

The solubilizing power of a detergent increases with the temperature. The temperature coefficient of the solubilizing power varies for different detergents. It seems to depend also on the nature of the substance which is solubilized.

Very slight solubilization is observed below the critical concentration, indicating the presence of some micelles.

#### REFERENCES

- (1) BURY, C. R.: *J. Chem. Soc.* **1935**, 626
- (2) CARR, C. W., JOHNSON, W. F., AND KOLTHOFF, I. M.: *J. Phys. Colloid Chem.* **51**, 636 (1947).
- (3) CORRIN, M. L., AND HARKINS, W. D.: *J. Chem. Phys.* **14**, 640-1 (1946).
- (4) CORRIN, M. L., AND HARKINS, W. D.: *J. Am. Chem. Soc.* **69**, 679 (1947).
- (5) CORRIN, M. L., AND HARKINS, W. D.: *J. Am. Chem. Soc.* **69**, 683 (1947).
- (6) CORRIN, M. L., HARKINS, W. D., AND KLEVENS, H. B.: Private communication.
- (7) EKWALL, P.: *Kolloid-Z.* **77**, 320 (1936).
- (8) EKWALL, P.: *Kolloid-Z.* **97**, 71 (1941).
- (9) EKWALL, P.: *Kolloid-Z.* **101**, 135 (1942).
- (10) GREEN, A. A., AND MCBAIN, J. W.: *J. Phys. Colloid Chem.* **51**, 286 (1947).
- (11) HARKINS, W. D.: *J. Am. Chem. Soc.* **69**, 1428 (1947).
- (12) HESS, K., PHILIPPOFF, W., AND KIESSIG, H.: *Kolloid-Z.* **88**, 40 (1939).
- (13) KLEVENS, H. B.: *J. Colloid Sci.* **2**, 301 (1947).
- (14) KOLTHOFF, I. M., AND JOHNSON, W. F.: *J. Phys. Chem.* **50**, 440 (1946).
- (15) KOLTHOFF, I. M., AND JOHNSON, W. F.: *J. Phys. Colloid Chem.* **53**, 22 (1948).
- (16) LASCARAY, L.: *Kolloid-Z.* **34**, 73 (1924).
- (17) MCBAIN, J. W., AND GREEN, SISTER A. A.: *J. Am. Chem. Soc.* **68**, 1731 (1946).
- (18) MCBAIN, J. W., AND MERRILL, R. C., JR.: *Ind. Eng. Chem.* **34**, 915 (1942).
- (19) MÜLLER VON BLUMENCRON, C. F.: *Z. Deut. Öl-Fett-Ind.* **42**, 141 (1922).
- (20) RALSTON, A. W., HOERR, C. W., AND HOFFMAN, E. J.: *J. Am. Chem. Soc.* **64**, 97 (1942).
- (21) RALSTON, A. W., HOERR, C. W., AND HOFFMAN, E. J.: *J. Am. Chem. Soc.* **68**, 2460 (1946).
- (22) SCHULTZ, G. V.: *Z. physik. Chem.* **A179**, 321 (1937).
- (23) STAUFF, J.: *Z. physik. Chem.* **A183**, 55 (1938).
- (24) STEARNS, R. S., OPPENHEIMER, H., SIMON, E., AND HARKINS, W. D.: *J. Chem. Phys.* **15**, 496 (1947).

ZONES OF MUTUAL PROTECTION AGAINST CRYSTALLIZATION  
IN DUAL-OXIDE SYSTEMS<sup>1</sup>

HARRY B. WEISER AND W. O. MILLIGAN

*Department of Chemistry, The Rice Institute, Houston, Texas*

AND

G. A. MILLS

*Houdry Process Corporation of Pennsylvania, Marcus Hook, Pennsylvania**Received January 26, 1948*

The hydrous oxide of one metal in colloidal solution may act as a protecting colloid for the hydrous oxide of a second metal. To illustrate, hydrous chromic oxide is peptized readily by alkali hydroxide giving a clear green sol, whereas hydrous ferric oxide is peptized by alkali hydroxide only in very small amounts under special, carefully controlled conditions (8). Almost a century ago, Northcote and Church (7) reported that complete solution of mixed chromic and ferric oxides in alkali hydroxide takes place when chromic oxide is associated with not more than 40 per cent ferric oxide, whereas complete precipitation of both oxides results when chromic oxide is associated with not less than 80 per cent ferric oxide. The explanation of this behavior was given by Nagel (6) in Bancroft's laboratory: The green colloidal hydrous chromic oxide adsorbs to a limited degree and therefore carries into colloidal solution the hydrous oxide of iron; and conversely, the hydrous oxide of iron adsorbs hydrous chromic oxide to a limited degree so that, when the iron oxide is present in sufficient amount, it carries down and decolorizes practically completely the green colloidal solution of chromic oxide (*cf.* also 1, 2, 10, 11).

One oxide may also act as a protective colloid for another oxide in the solid state. In this case the protective action is not to prevent coalescence of the colloidal micelles in the dispersed phase, but to prevent growth in the solid phase into the ordered crystal state. It should follow that if oxide A is adsorbed by oxide B, it may inhibit the crystallization of B; and if oxide B is adsorbed by oxide A, it may inhibit the crystallization of A. This mutual protective action of the two oxides on each other may result in two composition zones of maximum protection against crystallization (one in which oxide A is in excess, and a second in which oxide B is in excess) and three zones of maximum crystallization (one in which B is in large excess, a second in which A is in large excess, and a third in which both A and B are present in proportionately large amounts). An indication of zones of mutual protection against crystallization has been observed within a specified temperature range with a number of dual-oxide systems, as shown by the experimental data reported in the next section.

<sup>1</sup> Presented before the Division of Colloid Chemistry at the 112th Meeting of the American Chemical Society, which was held in New York City, September, 1947.



TABLE 1  
*Dual-oxide gels*

SYSTEM	SALT SOLUTIONS USED
$\text{Al}_2\text{O}_3\text{-BeO}$	$\text{AlCl}_3$ and $\text{BeCl}_2$
$\text{Al}_2\text{O}_3\text{-BeO}$	$\text{Al}(\text{NO}_3)_3$ and $\text{Be}(\text{NO}_3)_2$
$\text{Al}_2\text{O}_3\text{-BeO}$	$\text{Al}_2(\text{SO}_4)_3$ and $\text{BeSO}_4$
$\text{Al}_2\text{O}_3\text{-ZrO}_2$	$\text{AlCl}_3$ and $\text{Zr}(\text{NO}_3)_4$
$\text{Al}_2\text{O}_3\text{-Bi}_2\text{O}_3$	$\text{AlCl}_3$ and $\text{BiCl}_3$ in excess $\text{HCl}$
$\text{Al}_2\text{O}_3\text{-SnO}_2$	$\text{AlCl}_3$ and $\text{SnCl}_4$ in excess $\text{HCl}$

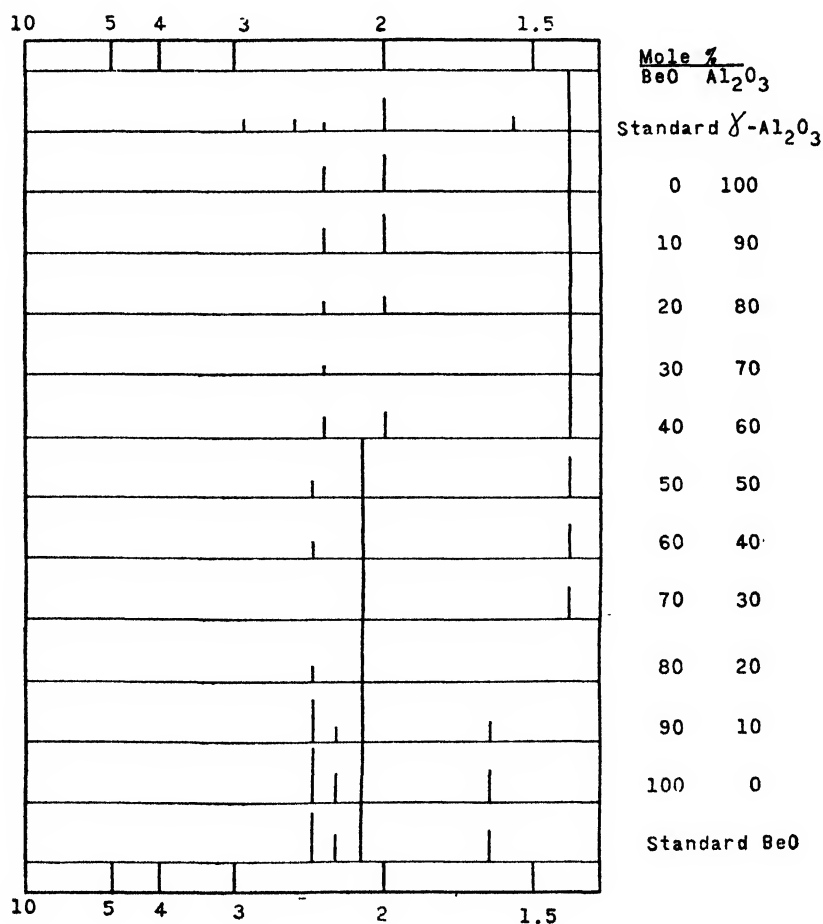


FIG. 1. Diagrams of x-ray diffraction patterns of alumina-beryllia gels heated 2 hr. at  $565^\circ\text{C}.$ ; precipitated from aluminum chloride and beryllium chloride.

## EXPERIMENTAL

*Preparation of samples*

Mixtures of varying volumes of metallic salt solutions (each 0.5 *M* with respect to the anhydrous oxide), as listed in table 1, were coprecipitated with a slight excess of ammonium hydroxide solution in a rapid-mixing device described else-

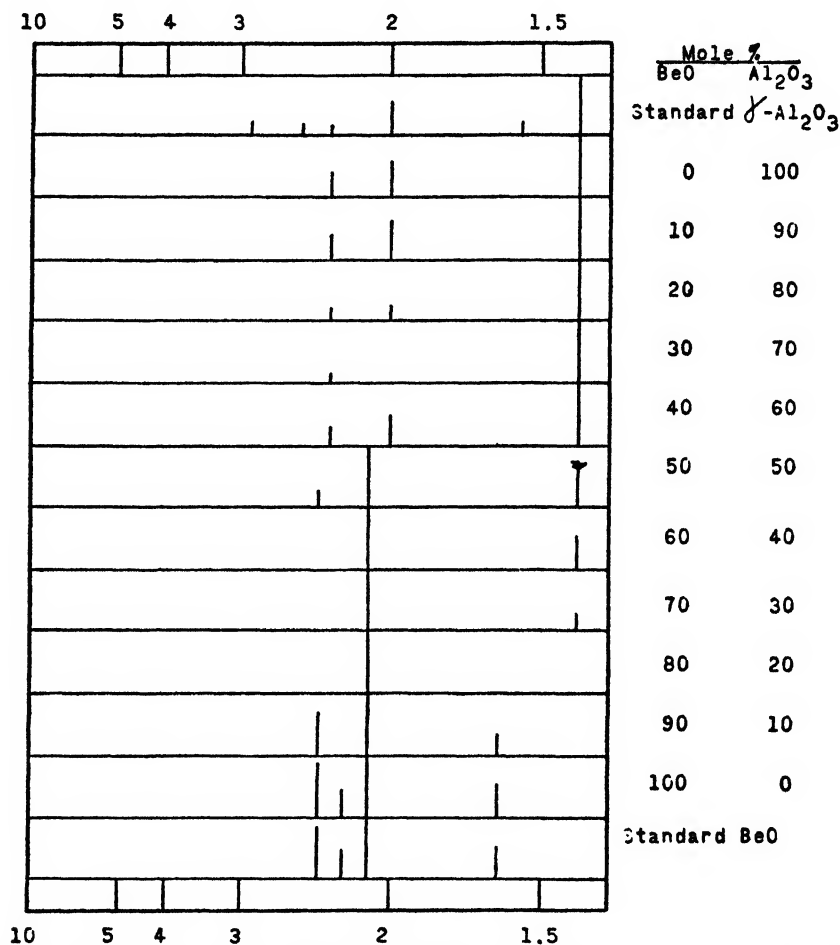


FIG. 2. Diagrams of x-ray diffraction patterns of alumina-beryllia gels heated 2 hr. at 565°C.; precipitated from aluminum nitrate and beryllium nitrate.

where (12). The compositions of the salt mixtures were adjusted so that for each system a series of eleven hydrous oxide mixtures was obtained, containing 0, 10, 20, 30, 40, 50, 60, 70, 80, 90, and 100 mole per cent (anhydrous basis) of aluminum oxide. The precipitated dual-oxide gels were washed with distilled water, using a centrifuge, until the supernatant liquid was essentially free of chloride or nitrate ions. The washed gels were dried at 105°C. for 12 hr., and then were heated for 2 hr. at 565°C. in an electric muffle furnace.

*X-ray diffraction analysis*

X-ray diffraction patterns were obtained from the samples described above, using copper  $K_\alpha$  x-radiation. The  $K_\beta$  x-radiation was removed by a nickel foil filter. The results obtained for the samples heated at 565°C. are given in figures 1-4 and tables 2-4.

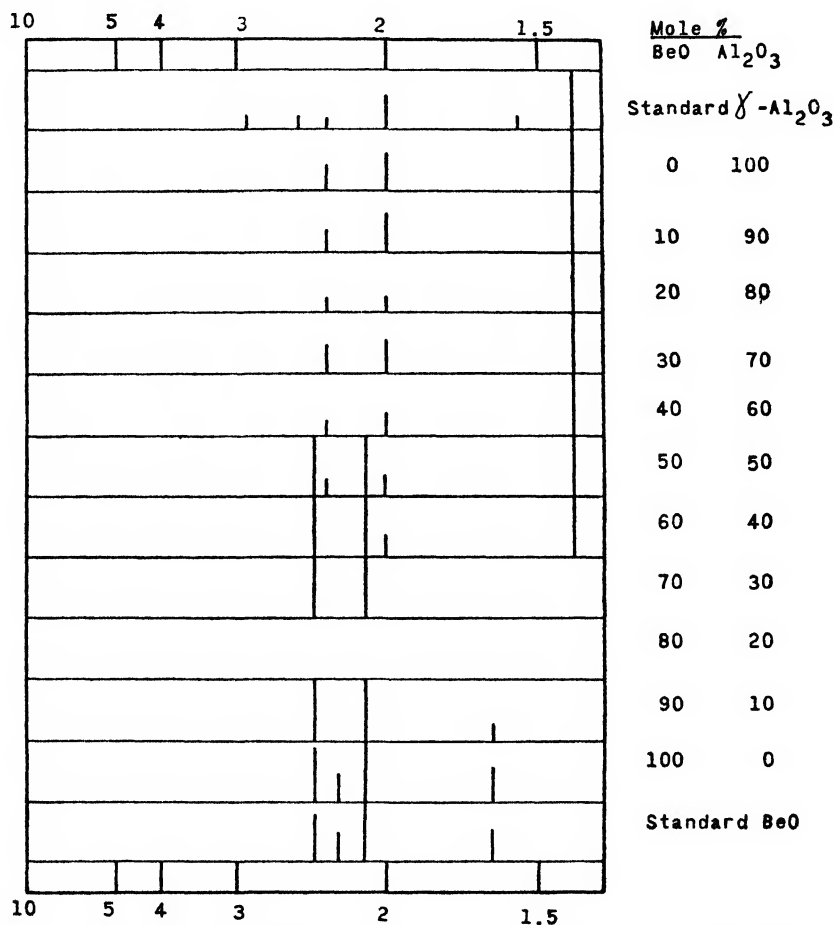


FIG. 3. Diagrams of x-ray diffraction patterns of alumina-beryllia gels heated 2 hr. at 565°C.; precipitated from aluminum sulfate and beryllium sulfate.

## DISCUSSION

*Mutual protective action*

The identification of phases present in the samples presents considerable difficulty, since most of the x-radiograms consist of extremely broad bands. It is difficult in many cases to distinguish between samples which are amorphous and samples which contain a relatively small amount of crystalline material in extremely finely divided form together with amorphous material. Microphotom-

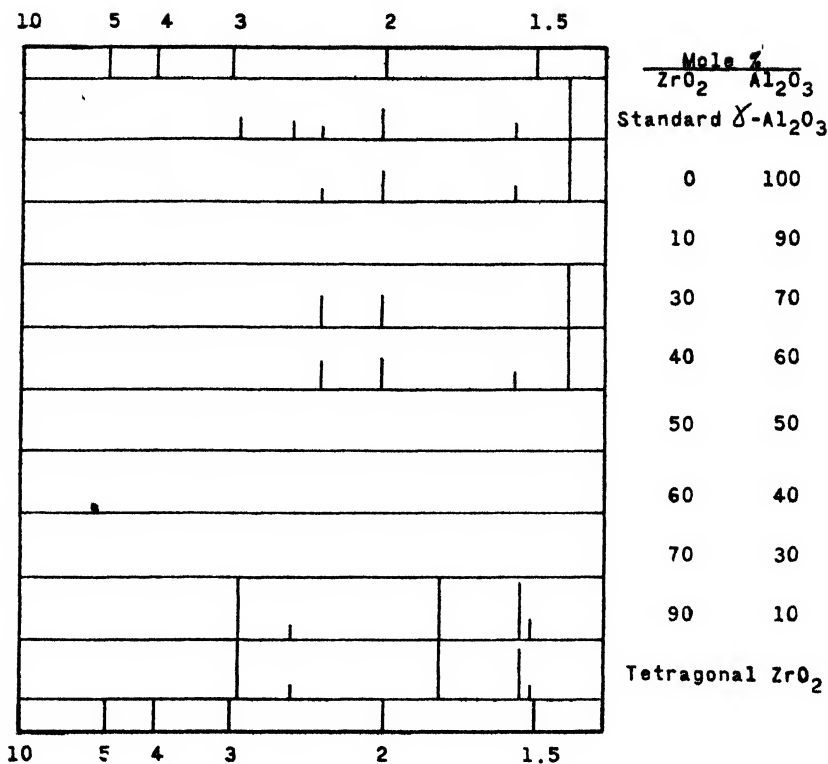


FIG. 4. Diagrams of x-ray diffraction patterns of alumina-zirconia gels heated 2 hr. at 565°C.; precipitated from aluminum chloride and zirconium nitrate.

TABLE 2  
*Alumina-zirconia gels*

COMPOSITION IN MOLE PER CENT		RESULTS OF X-RAY EXAMINATION (GELS HEATED 2 HRS. AT 565°C.)
ZrO <sub>2</sub>	Al <sub>2</sub> O <sub>3</sub>	
0	100	Standard $\gamma$ -Al <sub>2</sub> O <sub>3</sub> pattern
10	90	Amorphous
20	80	Not examined
30	70	$\gamma$ -Al <sub>2</sub> O <sub>3</sub> , faint bands
40	60	$\gamma$ -Al <sub>2</sub> O <sub>3</sub>
50	50	Amorphous
60	40	Amorphous
70	30	Amorphous
80	20	Not examined
90	10	Standard ZrO <sub>2</sub> , tetragonal
100	0	Standard ZrO <sub>2</sub> , monoclinic

eter traces of such negatives are usually of little value, and our interpretations are based on visual inspection of the negatives. However, the x-radiograms furnish conclusive evidence of mutual protection. As little as 10-30 mole per

cent of  $\text{BeO}$ ,  $\text{ZrO}_2$ ,  $\text{Bi}_2\text{O}_3$ , or  $\text{SnO}_2$  retards or prevents the crystallization of alumina. The protective action is mutual, since 10–40 mole per cent of alumina likewise retards or prevents the crystallization of the second component of each dual-oxide system. It will be noted that 10 mole per cent of alumina stabilizes the tetragonal form of zirconia, since the pure zirconia gel is essentially in the

TABLE 3  
*Alumina-bismuth trioxide gels*

COMPOSITION IN MOLE PER CENT		RESULTS OF X-RAY EXAMINATION (GELS HEATED 2 HR. AT 565°C.)
$\text{Bi}_2\text{O}_3$	$\text{Al}_2\text{O}_3$	
0	100	Standard $\gamma\text{-Al}_2\text{O}_3$ pattern
10	90	$\gamma\text{-Al}_2\text{O}_3$ , very faint bands, nearly amorphous
20	80	$\text{Bi}_2\text{O}_3$ , faint, but relatively sharp lines
30	70	$\text{Bi}_2\text{O}_3$ , relatively sharp lines
40	60	$\text{Bi}_2\text{O}_3$ , very broad bands, nearly amorphous
50	50	$\text{Bi}_2\text{O}_3$ , very broad bands, nearly amorphous
60	40	$\text{Bi}_2\text{O}_3$ , relatively sharp lines
70	30	$\text{Bi}_2\text{O}_3$ , relatively sharp lines
80	20	$\text{Bi}_2\text{O}_3$ , relatively sharp lines
90	10	$\text{Bi}_2\text{O}_3$ , relatively sharp lines
100	0	Standard $\text{Bi}_2\text{O}_3$

TABLE 4  
*Alumina-stannic oxide gels*

COMPOSITION IN MOLE PER CENT		RESULTS OF X-RAY EXAMINATION (GELS HEATED 2 HR. AT 565°C.)
$\text{SnO}_2$	$\text{Al}_2\text{O}_3$	
0	100	Standard $\gamma\text{-Al}_2\text{O}_3$
10	90	$\gamma\text{-Al}_2\text{O}_3$ , faint bands
20	80	$\gamma\text{-Al}_2\text{O}_3$ , faint bands
30	70	Essentially amorphous
40	60	Standard $\text{SnO}_2$ , relatively sharp lines
50	50	$\text{SnO}_2$ , relatively sharp lines
60	40	$\text{SnO}_2$ , faint broad bands
70	30	$\text{SnO}_2$ , faint broad bands
80	20	$\text{SnO}_2$ , sharper bands
90	10	$\text{SnO}_2$ , fairly sharp lines
100	0	Standard $\text{SnO}_2$

monoclinic crystalline form. Larger amounts of alumina render the zirconia amorphous. These observations on mutual protective action confirm similar results found in the systems  $\text{CuO-Fe}_2\text{O}_3$  (3),  $\text{NiO-Al}_2\text{O}_3$  (4), and  $\text{Cr}_2\text{O}_3\text{-Fe}_2\text{O}_3$  (5).

#### *Two zones of maximum protection*

In addition to the mutual protective action discussed above, the results clearly suggest the existence of two zones of composition wherein maximum protection

occurs. In the zones of protection, the gels are amorphous to x-rays or consist of extremely finely divided crystals which may correspond to regions of maximum surface, and which, therefore, may exhibit enhanced adsorptive and catalytic properties.

Two zones of maximum mutual protection are evident, especially in the system  $\text{Al}_2\text{O}_3\text{--ZrO}_2$ . The zones of mutual protection may be modified by the anions present. Indeed, in a series of samples prepared from aluminum sulfate and beryllium sulfate, the zones are wider than in a series prepared from the chlorides or nitrates. It is assumed that the more strongly adsorbed sulfate ion likewise contributes to the protective action (13).

#### CONCLUSIONS

1. Since one oxide A may act as a protecting colloid for a second oxide B, and since a protecting colloid will inhibit crystal growth, it follows that if oxide A is adsorbed by B, it may inhibit the crystallization of B, and that if oxide B is adsorbed by A, it may inhibit the crystallization of A.

2. Mutual protective action has been observed in the following dual-oxide systems heated for 2 hr. at  $565^\circ\text{C}$ .:  $\text{BeO--Al}_2\text{O}_3$ ,  $\text{ZrO--Al}_2\text{O}_3$ , and  $\text{SnO}_2\text{--Al}_2\text{O}_3$ . This confirms similar behavior described for the systems  $\text{NiO--Al}_2\text{O}_3$ ,  $\text{CuO--Fe}_2\text{O}_3$ , and  $\text{Cr}_2\text{O}_3\text{--Fe}_2\text{O}_3$ .

3. The mutual protective action of two oxides A and B on each other should result in two composition zones of maximum protection against crystallization (one in which A is in excess, and a second in which B is in excess) and three zones of maximum crystallization (one in which A is in relatively large excess, a second in which B is in relatively large excess, and a third in which A and B are present in proportionately large amounts). These conclusions have been confirmed for three dual-oxide systems referred to in paragraph 2 above.

4. Pure zirconia gel is usually monoclinic at a temperature level of  $500\text{--}600^\circ\text{C}$ ., but the tetragonal form is stabilized by 10 mole per cent of alumina. Larger amounts of alumina render the zirconia amorphous to x-rays.

5. The width of the zones of mutual protection against crystallization is modified by the anions in the solution from which the mixed gel is precipitated. The zones of mutual protection in the  $\text{BeO--Al}_2\text{O}_3$  system are wider when the gels are thrown down from sulfate solutions than from chloride or nitrate solutions, possibly because of stronger adsorption and protective action of divalent sulfate ions than of the univalent anions.

#### REFERENCES

- (1) KNOCHE: *Kolloid-Z.* **68**, 37 (1934).
- (2) LEPEZ AND STORCH: *Monatsh.* **10**, 283 (1889).
- (3) MILLIGAN AND HOLMES: *J. Am. Chem. Soc.* **63**, 149 (1941).
- (4) MILLIGAN AND MERTEN: *J. Phys. Chem.* **50**, 465 (1946).
- (5) MILLIGAN AND MERTEN: *J. Phys. Colloid. Chem.* **51**, 521 (1947).
- (6) NAGEL: *J. Phys. Chem.* **19**, 331 (1915).
- (7) NORTHCOTE AND CHURCH: *J. Chem. Soc.* **6**, 54 (1853).
- (8) POWIS: *J. Chem. Soc.* **107**, 818 (1915).

- (9) PRUDHOMME: Bull. soc. chim. [2] **17**, 253 (1872).
- (10) ROSE: Pogg. Ann. **112**, 164 (1861).
- (11) WEISER: J. Phys. Chem. **26**, 654 (1922).
- (12) WEISER AND MILLIGAN: J. Phys. Chem. **40**, 1075 (1936).
- (13) WEISER AND MILLIGAN: J. Phys. Chem. **44**, 1081 (1940).

## MELTING AND EVAPORATION AS RATE PROCESSES

S. S. PENNER

*Jet Propulsion Laboratory, California Institute of Technology, Pasadena, California*

*Received January 26, 1948*

### INTRODUCTION

Theories of melting (1, 6, 11, 17) and evaporation (7, 10, 13) for a number of models of the liquid and solid states have been reviewed by Lennard-Jones (12).

The kinetics of fusion has been discussed by Lindemann (15) and the rates of evaporation by Frenkel (3). However, neither melting nor evaporation appears to have been considered from the point of view of Eyring's rate theory (2, 5). It is the purpose of this paper to show that Eyring's rate theory leads to useful results for the rates of fusion and evaporation if reasonable assumptions are made concerning the nature of the activated complex formed during fusion and evaporation. The results obtained for the rates of evaporation are of the same order of magnitude as those predicted from the Knudsen equation (8, 11).

### THE KINETICS OF FUSION

According to the statistical theory of reaction rates (2, 5), the rate of fusion is given by the relation

$$j = \frac{kT}{h} \frac{F^*}{F} e^{-\epsilon_f/kT} \quad (1)$$

where  $F^*$  is the partition function of the activated complex formed during melting,  $F$  is the partition function of the original solid,  $\epsilon_f$  is the activation energy for fusion per molecule,  $k$  is the gas constant per molecule,  $T$  represents the absolute temperature, and  $h$  is Planck's constant. If the solid consists of Einstein oscillators with vibration frequency  $\nu$ , then, except for the factor corresponding to the internal partition function,

$$F = (1 - e^{-h\nu/kT})^{-3} \simeq (kT/h\nu)^3 \quad (2)$$

since

$$h\nu \ll kT$$

near the melting point. If the activated complex also consists of Einstein oscillators, then

$$F^* = (1 - e^{-h\nu^*/kT})^{-2} \simeq (kT/h\nu^*)^2 \quad (3)$$

where  $\nu^*$  is the vibration frequency of the Einstein solid in the activated state. In view of Lindemann's work (15) it is not unreasonable to expect that

$$\nu^* \simeq \nu \quad (4)$$

With this assumption the preceding expressions lead to the result

$$j = \nu e^{-\epsilon_f/kT} \quad (5)$$

If the solid at the melting point may be approximated by particles moving freely within a potential box, then  $F^*$  and  $F$  can be expressed in terms of liquid partition functions (12). In this case

$$F = (2\pi mkT)^{3/2} v_f / h^3 \quad (6)$$

and

$$F^* = (2\pi mkT) v_f^{2/3} / h^2 \quad (7)$$

where  $v_f$  represents the free volume per molecule and  $m$  is the mass per molecule. Equations 1, 6, and 7 lead to the relation:

$$j = v_f^{-1/3} (kT/2\pi m)^{1/2} e^{-\epsilon_f/kT} \quad (8)$$

Since equations 5 and 8 must lead to the same value for  $j$ , it follows that the free volume can be expressed as

$$v_f = (kT/2\pi m \nu^2)^{3/2} \quad (9)$$

Equation 9 is identical with a relation deduced previously by Lennard-Jones (12).

It is of interest to note that if the free volume is expressed in terms of the result obtained by Kincaid and Eyring (9), then equations 5 and 8 may be used to represent the vibration frequency of the solid in terms of the sound velocity. The resulting relation is

$$\nu = (\rho/m)^{1/3} u / (2\pi)^{1/2} \quad (10)$$

where  $u$  represents the sound velocity and  $\rho$  the density of the melting solid. Equation 10 leads to values for the Einstein frequency which are in good agreement with results obtained by other methods. Representative values are shown in table 1. The data shown in this table indicate that the Lennard-Jones and Kincaid and Eyring expressions for the free volume may be equated, at least for the solid elements considered in table 1.

#### THE RATE OF EVAPORATION

The rate of evaporation of liquids and solids into a vacuum is given by the Knudsen equation (8, 11). The maximum possible rate is obtained by equating the accommodation coefficient to unity. Under these conditions the rate of decrease of the radius of an evaporating spherical droplet with time can be shown to be given (16) according to the expression

$$- dr/dt = (M/2\pi RT)^{1/2} p_s / \rho_l \quad (11)$$

where  $- dr/dt$  is the rate of decrease of droplet radius with time,  $p_s$  is the sat-



urated vapor pressure of the evaporating compound at the temperature  $T$ ,  $\rho_l$  is the liquid density,  $R$  is the gas constant per mole, and  $M$  represents the molecular weight of the evaporating compound.

Application of Eyring's theory (2,5) should yield results similar to those predicted from equation 11, provided correct values are used for the partition functions. Corresponding to an accommodation coefficient of unity in the Knudsen equation, it is reasonable to set the transmission coefficient equal to unity in the rate process treatment, as was done in equation 1.

TABLE 1  
*Vibration frequencies of solid elements*

ELEMENT	$\nu \times 10^{12}^*$	$\nu \times 10^{12}^\dagger$
	sec. <sup>-1</sup>	sec. <sup>-1</sup>
Lead	1.6	1.8 to 2.2
Silver	4.2	4.1 to 4.5
Copper	6.6	5.7 to 6.8
Iron	8.7	6.5 to 9.4
Aluminum	8.0	6.6 to 8.3

\* Calculated from equation 10

† Determined by other methods, and summarized on page 414 of reference 4.

The partition function for an evaporating liquid is, as before.

$$F = (2\pi mkT)^{3/2} v_f / h^3 \quad (6)$$

If the partition function of the activated complex is similarly written as

$$F^* = (2\pi mkT) v_f^{2/3} / h^2 \quad (7)$$

in the rate expression for evaporation

$$j_e = (kT/h)(F^*/F)e^{-\Delta E_{act}/RT} \quad (12)$$

where  $\Delta E_{act}$  is the molar activation energy for evaporation, then the Frenkel equation (3) is obtained, i.e.,

$$j_e = v_f^{-1/3} (RT/2\pi M)^{1/2} e^{-\Delta E_{act}/RT} \quad (13)$$

The values of  $j_e$  calculated from equation 13 are much smaller than the values predicted by the Knudsen equation (3).

Since the activated complex for evaporation occurs during the formation of freely moving molecules, it is not unreasonable to equate  $F^*$  to the partition function of a gaseous molecule, allowing for the coördination of one degree of freedom with the reaction coördinate. Thus

$$F^* = (2\pi mkT) v^{2/3} / h^2 \quad (14)$$

where  $v$  is the volume per molecule. Introduction of equation 14 into equation 12 leads to the relation

$$j_e = (v^{2/3}/v_f)(RT/2\pi M)^{1/2} e^{-\Delta H_{vap}/RT} \quad (15)$$

where the molar activation energy for evaporation has been set equal to the heat of vaporization per mole,  $\Delta H_{\text{vap}}$ .

If the free volume in the liquid is replaced in terms of the result obtained by Kincaid and Eyring (9), then it is easy to show that equation 15 leads to the following expression for the rate of decrease of droplet radius with time (using equation 2 of reference 16 with  $j_e = k$ ):

$$-dr/dt = (u^3 M / RT \gamma) (2\pi \gamma)^{-1/2} e^{-\Delta H_{\text{vap}} / RT} \quad (16)$$

Here  $\gamma$  represents the ratio of the specific heat at constant pressure to the specific heat at constant volume. It should be noted that equation 16 applies to the sublimation of solids as well as to the vaporization of liquids as long as the Lennard-Jones and Kincaid and Eyring formulae for the free volume are identical.

Representative values of  $-dr/dt$  have been calculated for a number of liquids and solids from equations 11 and 16. Results are summarized in table 2.

Reference to the results shown in table 2 indicates that the values determined from equations 11 and 16 are generally of the same order of magnitude but that the temperature coefficients of the two theoretical equations are different. This result is similar to that obtained previously by application of a largely empirical relation for the evaporation of liquids into a vacuum (16). The agreement between the numerical values calculated from equations 11 and 16 is seen to be best for non-associated spherical molecules, where the formula used for the free volume is most likely to be valid. The data compiled for the sublimation of metals also show reasonably good agreement between results calculated from equations 11 and 16.

Some of the discrepancies observed between the calculated values may be the result of application of poor experimental data. This assumption seems to be borne out by the large differences observed where two sets of experimental data were used (*cf.* results for silver and copper). On the other hand, it is apparent that the present treatment represents an oversimplification of the evaporation process. It is possible that a more detailed consideration of the nature of the activated complex will remove the discrepancy existing with regard to the temperature coefficient of the calculated values of  $-dr/dt$ . A suitable correction may perhaps also be introduced by evaluating the transmission coefficient.

In view of the fact that treating the activated complex like a freely moving gas leads to relatively good agreement with the values calculated from the Knudsen equation, while the Frenkel formula leads to significantly different results, it is perhaps justifiable to conclude that the activated complex more nearly corresponds to a freely moving gaseous molecule than to a liquid or solid molecule.

It is possible to deduce a simple relation for the vibration frequency of the activated complex of a subliming solid by proceeding in a manner analogous to that used for the treatment of the kinetics of fusion. Thus, if the subliming solid is considered to be an Einstein oscillator, then

$$j_e = (\nu^3 / \nu^{*2}) e^{-\Delta H_{\text{vap}} / RT} \quad (17)$$

**TABLE 2\***  
*Evaporation of liquids*

COMPOUND	T	$-dr/dt$ †	$-dr/dt$ ‡	R§
	°C.	cm./sec.	cm./sec.	
Benzene.....	10	1.51	1.57	0.96
	30	4.42	4.03	1.1
	50	11.1	9.11	1.2
Carbon tetrachloride .....	0	1.09	0.883	1.2
	20	3.04	2.41	1.3
	40	7.61	5.67	1.3
Chloroform. . . . .	0	1.64	1.55	1.1
	20	4.79	3.96	1.2
	40	11.7	8.92	1.3
Carbon disulfide . . . . .	20	19.6	7.03	2.8
n-Pentane. . . . .	25	27.2	23.8	1.1
n-Hexane... . . . .	25	5.67	7.37	0.77
Cyclohexane . . . . .	18.4	2.94	2.92	1.0
n-Heptane . . . . .	25	0.926	2.29	0.40
n-Octane... . . . .	25	0.159	0.750	0.21
Ethyl ether . . . . .	20	13.6	18.2	0.75
Pyridine . . . . .	20	0.243	0.475	0.51
Water . . . . .	0	0.00231	0.0537	0.043
	20	0.0134	0.254	0.053
	40	0.0598	0.780	0.077
Ethyl alcohol . . . . .	0	0.0723	0.362	0.20
	20	0.305	1.28	0.24
	50	2.10	6.39	0.33
Methyl alcohol . . . . .	25	0.205	3.01	0.068
Acetone . . . . .	25	3.60	7.45	0.48
Mercury . . . . .	0	$8.32 \times 10^{-6}$	$6.80 \times 10^{-7}$	12
	20	$5.70 \times 10^{-5}$	$4.28 \times 10^{-5}$	13
	40	$3.19 \times 10^{-4}$	$2.10 \times 10^{-5}$	15

*Evaporation of solids*

ELEMENT	T	$-dr/dt$ †	$-dr/dt$ ‡	R§
	°K.	cm./sec.	cm./sec.	
Iron (α)	1200	$2.39 \times 10^{-10}$	$5.52 \times 10^{-10}$	0.43 *
	1300	$5.84 \times 10^{-9}$	$8.90 \times 10^{-9}$	0.66
	1400	$9.17 \times 10^{-8}$	$9.32 \times 10^{-8}$	0.98
	1500	$1.02 \times 10^{-6}$	$6.58 \times 10^{-7}$	1.6
Silver	1100	$1.68 \times 10^{-7}$	$3.88 \times 10^{-8}$	4.3
	1200	$2.25 \times 10^{-6}$	$5.34 \times 10^{-7}$	4.2
	1200	$2.25 \times 10^{-6}$	$1.33 \times 10^{-6}$	1.7
Zinc	617	$3.46 \times 10^{-4}$	$2.06 \times 10^{-5}$	17
Copper	1200	$3.32 \times 10^{-8}$	$6.21 \times 10^{-9}$	5.3
	1300	$4.45 \times 10^{-7}$	$7.87 \times 10^{-8}$	5.7
	1083	$8.69 \times 10^{-10}$	$8.54 \times 10^{-10}$	1.0
	1273	$2.29 \times 10^{-7}$	$1.26 \times 10^{-7}$	1.8
Nickel (α).	1500	$5.66 \times 10^{-7}$	$5.10 \times 10^{-7}$	1.1

\* Experimental data were taken from the Landolt-Bornstein tables.

† Calculated from equation 16.

‡ Calculated from equation 11.

§ R is the ratio of  $-dr/dt$  calculated from equation 16 to the value of  $-dr/dt$  calculated from equation 11.

where  $\nu^*$  is the vibration frequency of the activated complex. Comparison of equations 15 and 17 shows that

$$\nu^{*2} = \nu^3(2\pi M/RT)^{1/2}(\nu_f/\nu^{2/3})$$

or

$$\nu^* = \nu^{-1/3}(RT/2\pi M)^{1/2} \quad (18)$$

where  $\nu_f$  has been replaced by the Lennard-Jones formula for the free volume in terms of the vibration frequency  $\nu$ . Equation 18 shows that the vibration frequency of the activated complex during sublimation is equal to the collision frequency in the gas moving in a direction normal to the surface if equations 15 and 17 are to be identical.

In conclusion, the author wishes to express his appreciation to Professor J. G. Kirkwood for suggesting the statistical approach to the study of rates of evaporation and for continued advice during the work on this problem.

#### REFERENCES

- (1) BORN, M.: *J. Chem. Phys.* **7**, 591 (1939).
- (2) EYRING, H.: *J. Chem. Phys.* **3**, 107 (1935).
- (3) FRENKEL, J.: *Kinetic Theory of Liquids*, Chap. I, Clarendon Press, Oxford (1946); *Z. Physik* **26**, 117 (1924).
- (4) GLASSTONE, S.: *Textbook of Physical Chemistry*. D. Van Nostrand Company, Inc., New York (1940).
- (5) GLASSTONE, S., LAIDLER, K. J., AND EYRING, H.: *The Theory of Rate Processes*. McGraw-Hill Book Company, Inc., New York and London (1941).
- (6) HERZFELD, K. F., AND GOEPFERT-MAYER, M.: *Phys. Rev.* **46**, 995 (1934).
- (7) HIRSCHFELDER, J. O., STEVENSON, D. P., AND EYRING, H.: *J. Chem. Phys.* **5**, 896 (1937).
- (8) KENNARD, E. H.: *Kinetic Theory of Gases*. McGraw-Hill Book Company, Inc., New York (1938).
- (9) KINCAID, J. F., AND EYRING, H.: *J. Chem. Phys.* **6**, 620 (1938).
- (10) KIRKWOOD, J. G.: *J. Chem. Phys.* **7**, 908 (1939).
- (11) KNUDSEN, M.: *Ann. Physik* **47**, 697 (1915).
- (12) LENNARD-JONES, J. E.: *Proc. Roy. Soc. (London)* **52**, 729 (1940).
- (13) LENNARD-JONES, J. E., AND DEVONSHIRE, A. F.: *Proc. Roy. Soc. (London)* **A163**, 53 (1937); **A165**, 1 (1938); **A169**, 317 (1939); **A170**, 464 (1939).
- (14) LENNARD-JONES, J. E., AND DEVONSHIRE, A. F.: *Proc. Roy. Soc. (London)* **A169**, 317 (1939); **A170**, 464 (1939).
- (15) LINDEMANN, F. A.: *Physik. Z.* **11**, 609 (1910).
- (16) PENNER, S. S.: *J. Phys. Colloid Chem.* **52**, 367 (1948).
- (17) RICE, O. K.: *J. Chem. Phys.* **7**, 883 (1939).

A NEW AND EASILY CONSTRUCTED PRECISION COULOMETER<sup>1</sup>ELLIOTT L. ABERS<sup>2</sup> AND ROY F. NEWTON*Department of Chemistry, Purdue University, Lafayette, Indiana**Received December 29, 1947*

## INTRODUCTION

The need of a precision coulometer to measure currents of the order of 1 amp. was recently encountered in this laboratory. The instrument to be described here is the result of the search to find a suitable and easily constructed coulometer to fit the requirements.

Volume coulometers based on the electrolysis of a mercurous nitrate solution and a solution of mercuric iodide in an excess of potassium iodide are described in the literature (4, 6, 8); in these coulometers the mercury liberated at the cathode was allowed to fall into a graduated tube. Mercurous nitrate (3) and mercurous perchlorate (5) have been used for the electrolytes in weight coulometers, in which the loss or gain in weight of a mercury anode or cathode was measured. The maximum allowable current density permitted in these coulometers and the accuracy obtainable were too low.

The silver and iodine coulometers are accepted as being the most reliable; however, they present a serious limitation in that only low current densities may be measured. Special and expensive equipment, or recrystallized salts, are necessary and extreme care must be taken to insure that the results will be accurate.

It was decided to explore the use of the bivalent reduction of mercuric iodide in the complex with excess potassium iodide, with gravimetric determination of the weight changes at the anode and the cathode. It was found that the measurement of the weight decrement at the anode was highly reliable up to current densities of 0.75 amp. per square centimeter, and that errors due to side reaction become unimportant at fairly high current densities.

## • EXPERIMENTAL

The design of the coulometer is shown in figure 1. The anode cup is a 10-ml. beaker filled with 5-8 ml. of mercury, and the cathode consists of about 25 ml. of mercury on the bottom of a 400-ml. beaker. The iron rings are  $\frac{3}{4}$ -in. pieces of 4-in. pipe and are needed to overcome the stirrer vibration and to steady the coulometer. The electrodes are made from nickel welding rod, and all electrical connections are soldered. The stirrer, glass sleeves, anode support, and nitrogen inlet are held in place by corks inserted in the appropriate holes of a plywood cover.

The electrolyte is prepared by dissolving 180 g. of mercuric iodide and 600 g. of potassium iodide in enough water to make a liter of solution. At the end of

<sup>1</sup> Abstracted from the thesis submitted by Elliott L. Abers to the Faculty of the Graduate School of Purdue University in partial fulfillment of the requirements for the degree of Doctor of Philosophy, June, 1947.

<sup>2</sup> Present address: Massachusetts Institute of Technology, Cambridge, Massachusetts.

the run the anode cup is carefully removed and the mercury poured into a 30-ml. beaker for washing, the glass sleeve and metal electrode being carefully washed free of any adhering mercury. The mercury is then washed in the beaker by gently swirling the mercury, twice with 20 ml. of 25 per cent potassium iodide to prevent precipitation of mercurous iodide and four times with successive 20-ml. portions of distilled water. The mercury is then transferred to a glazed porcelain crucible and, after removing the excess moisture with filter paper, placed in a

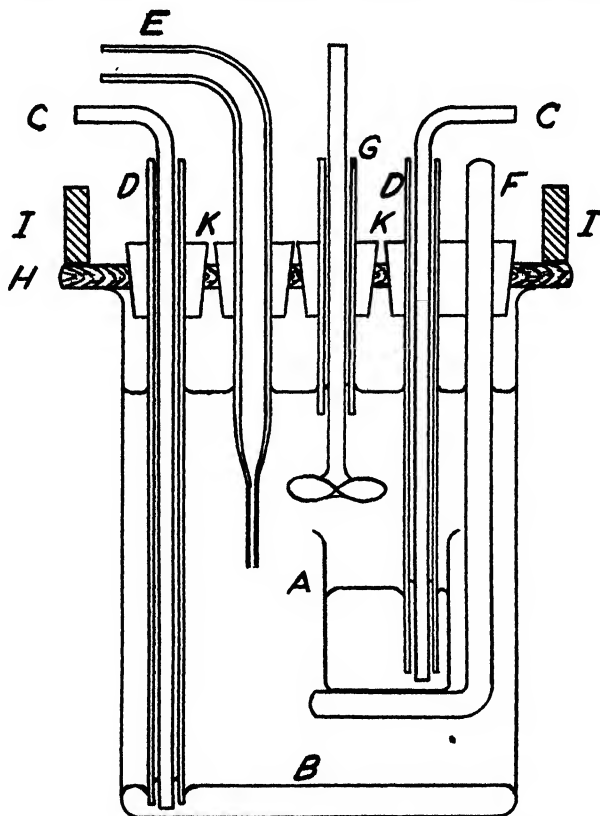


FIG. 1. Coulometer. A, anode cup, filled with mercury; B, cathode mercury; C, nickel electrodes, 1/8-in. welding rod; D, glass sleeve to protect nickel electrodes from electrolytes; E, nitrogen inlet; F, glass support for anode cup; G, glass stirrer with bushing; H, wooden support for corks; I, iron ring to weight and steady the wooden support; K, corks.

desiccator having calcium chloride as the drying agent. Mercury from the cathode may be used again after filtering through a pin hole in a dry filter paper. The mercury from the anode may be used again after washing with 10 per cent nitric acid. The electrolytic solution may be used repeatedly, and when not in use stored in a stoppered bottle.

The accuracy of the coulometer was determined by placing a standard 1-ohm resistance in series with several mercury coulometers also connected in series and measuring the potential drop across the standard resistance with a Rubicon type

K potentiometer. The potential drop was measured every minute for 3 hr., the variation of the current for each minute being smaller than the precision to which the potentiometer could be read. In these experiments the current was supplied by three new 6-volt storage batteries connected in parallel. The current for all other experiments was supplied by a d.c. generator.

## DISCUSSION

The results of the runs in which the current was accurately measured by means of the potentiometer are given in table 1 as a comparison between the observed anode decrement and that calculated from the current passed. The potential drop was plotted *versus* time, and the total number of coulombs was found from the area under the curve from zero time to 3 hr. The calculation of decrements from observed current is based on the Birge value (2) of  $96,501 \pm 10$  int. coul./g.-equiv. and the value of 200.610 (1) for the atomic weight of mercury. It

TABLE 1  
*Calculated vs. observed anode decrement*

RUN	I	II
Current density, amperes per square centimeter . . . . .	0.1	0.1
Coulombs (graphical) . . . . .	5018.1	4835.8
Faradays. . . . .	0.052001	0.050112
Calculated anode decrement, grams of mercury . . . . .	5.2160	5.0264
Observed anode decrement, grams of mercury:		
Cell 1. . . . .	5.217	5.0245
Cell 2 . . . . .	5.215	5.0261
Cell 3 . . . . .		5.0261
Per cent deviation . . . . .	0.00	-0.018

is seen that the deviation, allowing for the uncertainty of the value of the faraday, is within 0.03 per cent.

When the cathode increment was studied, connections were reversed and the cup was used for the cathode, with the same operations. The decrement in grams of mercury at the anode and the increment in grams of mercury at the cathode were measured when the same current passed through identical electrodes for the same length of time. The anode decrement was found to be greater than the cathode increment, by 0.15 per cent at 0.75 amp., and by 0.25 per cent at 0.3 amp.

Several coulometers differing only in anode area were connected in series in order that an identical current would pass through each one. The precision and the accuracy fell off at low current densities and for runs of long duration, 3-24 hr. The deviation of the anode decrement from the predicted value was found to be inversely proportional to the current density. The discrepancies at low current densities, attributed to air oxidation, were found to disappear when a stream of oxygen-free (7) nitrogen was bubbled continuously through the electrolyte to flush out all the dissolved oxygen. These were placed in series with other cells,

similar in all respects except for the absence of a nitrogen stream. A discrepancy of 12.4 mg. of mercury, the difference in anode decrements between cells flushed with nitrogen and those that were not flushed with nitrogen, was found during a 24-hr. run at a current of 0.11 amp. for an anode area of 4.5 cm.<sup>2</sup> When the same experiment was tried at a higher current density, this discrepancy was reduced to less than 1.5 mg., a value which is within experimental error. At a current density above 0.1 amp./cm.<sup>2</sup> (anode) the error due to oxidation was found to be within experimental error and it was not necessary to flush out the cell with nitrogen.

Having established that oxidation is important only at the lower densities, the upper limit of the current density was determined. This was accomplished by placing in series cells having different anode areas, always having in the series one current density that had previously been established as accurate. The currents up to 3.4 amp. (0.75 amp./cm.<sup>2</sup>) were found to give accurate results. At the higher current density the resistance of the cell is large enough to raise the temperature of the electrolyte considerably (to about 75°C.). When the current was raised above 3.4 amp., mercuric ion was formed faster than the iodide ion could be furnished, and precipitates of mercurous iodide and mercuric iodide were formed on the anode surface.

#### SUMMARY

A new type of mercury coulometer has been developed having an accuracy of better than 0.03 per cent. Liquid mercury is used for both anode and cathode (electrical contact being made with nickel electrodes). The electrolyte is a solution of mercuric iodide in excess potassium iodide. This coulometer is very easy to construct and all the materials are readily obtainable. Chemicals need be of only "reagent grade" and require no further purification. These conditions make this coulometer much more convenient than the silver or iodine coulometers, except when accuracy of the order of 0.002 per cent is required.

The maximum current measured was 3.4 amp., which corresponded to a current density of 0.75 amp./cm.<sup>2</sup> Below a current density of 0.024 amp./cm.<sup>2</sup> the accuracy fell off, but was better than 0.1 per cent.

The authors wish to acknowledge the valuable aid and assistance of Professor F. D. Martin.

#### REFERENCES

- (1) BAXTER: J. Am. Chem. Soc. **65**, 1446 (1943).
- (2) BIRGE: Rev. Modern Phys. **13**, 233-9 (1941).
- (3) BOLTON: Z. Elektrochem. **2**, 75 (1895).
- (4) HATFIELD: Z. Elektrochem. **15**, 728 (1907).
- (5) MATHESSE AND GERMAN: Ind. Univ. Stud. **1**, 41 (1910).
- (6) SCHULTE: Z. Elektrochem. **27**, 475 (1921).
- (7) STONE AND SKAVINSKI: Ind. Eng. Chem., Anal. Ed. **17**, 495 (1945).
- (8) WRIGHT: Electrician **60**, 279, 319 (1910).



X-RAY DIFFRACTION ANALYSIS OF INDIUM HYDROXIDE  
AND "INDIUM CHROMATE"

ANN PALM

*Department of Chemistry, New York University, New York, New York**Received October 2, 1947*

The transmission pattern of indium hydroxide has been studied with the object of gaining further information as to the nature of the yellow precipitate obtained upon the addition of potassium chromate to an indium chloride solution. The present investigation substantiates the contention previously held by the author, that the yellow precipitate long believed to be indium chromate is really the hydroxide of indium, with a variable amount of adsorbed chromate. Several studies of the diffraction patterns of indium hydroxide have been made, emphasizing the effect of change of temperature on the degree of hydration and in turn on the diffraction of x-rays. This factor was omitted completely in this paper, which was rather intended to be a comparative study of indium hydroxide as precipitated from indium chloride solution by means of ammonium hydroxide and of potassium chromate, under similar conditions, and to demonstrate the close identity of the two precipitates.

## EXPERIMENTAL

Crystals of indium hydroxide were prepared by the addition of ammonium hydroxide to an indium chloride solution which was brought to the boiling point and kept at approximately 100°C. for some time in order to assure precipitation of well-formed indium hydroxide crystals, which were afterwards dried at room temperature. The substance to be compared with it was prepared by the addition of potassium chromate to indium chloride, with subsequent similar treatment. These two precipitates will be referred to below as hydroxide A and hydroxide B, respectively.

The density of hydroxide A was determined to be  $4.4 \pm 0.15$ .

The transmission patterns were obtained from hydroxides A and B, as well as from hydroxide B after digesting it for 2, 4, and 6 days, in view of previous experiments tending to show the sorption of chromate by the hydroxide.

X-ray diffraction patterns were obtained by the usual powder method. The crystals were sprinkled on a collodion-coated fine glass rod which was mounted on the stage of the 71.62 mm. camera of the Picker x-ray machine. Radiation was obtained from an iron target filtered with manganese oxide foil. The  $\alpha_1\alpha_2$  doublet was not resolved in this case. The films were mounted in the ordinary manner. Lines were measured to  $\pm 0.02$  mm. at the darkest part of the line.

## RESULTS AND DISCUSSION

A comparison of the diffraction patterns of indium hydroxides A and B proved them to be alike in every detail. Both kinds show a simple pattern resembling the line system given by cubic materials.

On this assumption, then, the formula

$$d = \frac{a_0}{\sqrt{h^2 + k^2 + l^2}}$$

may be employed to calculate the lattice constant  $a_0$ . This value will depend on the values of  $\sqrt{h^2 + k^2 + l^2}$  assigned to the observed diffraction lines. If the

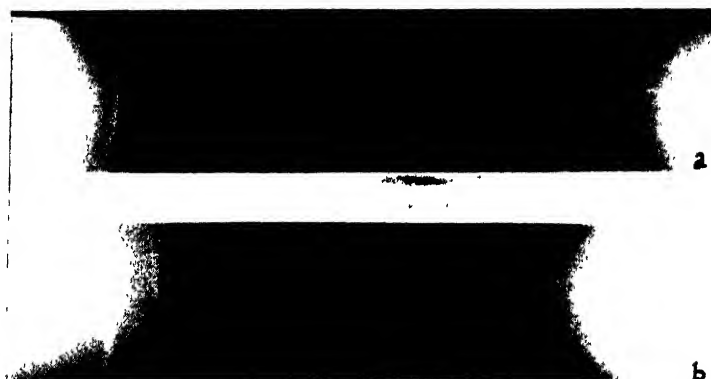


FIG. 1. X-ray diffraction patterns of indium hydroxide: (a) precipitated with ammonium hydroxide; (b) precipitated with potassium chromate.

TABLE 1

$hkl$	$d/n$ (CALCD.)	$d/n$ (OBSD.)	$I$
200	3.950	3.880	vs
210	3.533	3.506	vvw
211	3.224	3.190	vvw
220	2.793	2.767	s
310	2.498	2.498	vvw
222	2.280	2.266	m
400	1.985	1.970	m
420	1.765	1.773	s
422	1.613	1.613	s
440	1.397	1.399	w
600, 442	1.316	1.321	s
620	1.249	1.253	s
622	1.191	1.196	s
631	1.165	1.170	vvw
444	1.140	1.145	vw
640	1.096	1.101	m
642	1.056	1.061	vs

stronger lines visible in figure 1 are indexed as  $\sqrt{4}$ ,  $\sqrt{8}$ ,  $\sqrt{12}$  . . . , all lines can be accounted for, whereas the assignment of the values  $\sqrt{1}$ ,  $\sqrt{2}$ ,  $\sqrt{3}$  would exclude the faint lines indexed as 210, 211, 310, and 631 in table 1. The lattice constant is then found to be  $7.90 \pm 0.04$  Å.

The crystal structure of indium hydroxide may be assumed to be simple cubic, in view of the characteristic appearance of the diffraction pattern. The number

of molecules of  $\text{In}(\text{OH})_3$  per unit cell of lattice constant  $7.90 \text{ \AA}$ . would be eight. The values agree with those reported previously by W. O. Milligan.<sup>1</sup> Table 1 compares observed and calculated interplanar distances, on the basis of  $a_0 = 7.90 \text{ \AA}$ . and eight molecules per unit cell.

#### SUMMARY

X-ray diffraction data indicate that the yellow compound precipitated upon the addition of chromate to indium chloride has a crystalline structure identical with that of indium hydroxide, and furnish further evidence for the fact that no indium chromate is precipitated in this reaction.

The cubic crystal structure of  $\text{In}(\text{OH})_3$  has a lattice constant of  $7.90 \pm 0.04 \text{ \AA}$ .

The appreciation of the author is due to Professor W. F. Ehret and Harry Wiener for their constant interest and assistance and to Professor I. Fankuchen for some valuable discussions.

#### REFERENCES

- (1) MILLIGAN, W. O.: Paper No. 44 in abstracts of papers presented before the Division of Physical and Inorganic Chemistry at the 96th Meeting of the American Chemical Society, which was held in Milwaukee, Wisconsin, September 5-9, 1938.
- (2) MILLIGAN, W. O., AND WEISER, H. B.: *Trans. Faraday Soc.* **32**, 373 (1936).
- (3) MILLIGAN, W. O., AND WEISER, H. B.: *J. Am. Chem. Soc.* **59**, 1670 (1937).
- (4) MOELLER, TH., AND SCHNIZLEIN, J. G.: *J. Phys. Colloid Chem.* **51**, 771 (1947).
- (5) PALM, A.: *J. Am. Chem. Soc.* **69**, 224 (1947).

---

<sup>1</sup> The author is indebted to Dr. Milligan for calling her attention to this unpublished paper.

## INFRARED ABSORPTION SPECTRA OF SOME AMINO ACIDS AND THEIR COMPLEXES<sup>1</sup>

IRVING M. KLOTZ AND DIETER M. GRUEN

*Department of Chemistry, Northwestern University, Evanston, Illinois*

*Received January 16, 1948*

#### INTRODUCTION

Direct optical evidence of the dipolar nature of amino acids was furnished first by Edsall (3) in his studies of the Raman spectra of these substances. Raman frequencies of the carboxyl group of the amino acids definitely coincided with those observed for the alkali salts of aliphatic acids rather than with the values obtained with the non-ionized acids. Additional optical evidence of the dipolar

<sup>1</sup> Abstracted from a portion of the thesis of D. M. Gruen, which was presented to the Faculty of the Graduate School of Northwestern University in partial fulfillment of the requirements for the M.S. degree, March, 1947.

character of the amino acids has been obtained in infrared studies by Freymann, Freymann, and Rumpf (4). Their investigations of N—H frequencies, primarily in the region from 0.8 to 1.2  $\mu$ , showed the presence of quaternary nitrogen atoms in the neutral amino acids.

Though some measurements have been made of the absorption by amino acids of infrared radiation above 3  $\mu$  (5, 6, 9), no systematic attempt has been reported to complement the Raman work by corresponding investigations of the absorption frequencies of the carboxyl group in the 6  $\mu$  region of the infrared. The present studies show that the infrared bands parallel quite closely those found in Raman scattering. In addition, investigations have been made of spectra of complexes of the amino acids with sodium dodecyl sulfate as a prelude to the study of analogous complexes with proteins.

#### EXPERIMENTAL

Infrared absorption spectra were obtained with the Beckman Infrared Spectrophotometer, Model IR2. The wave-length scale was calibrated with methylcyclopentane, the infrared absorption spectrogram No. 510 of the American Petroleum Institute Research Project 44 of the National Bureau of Standards being used as the reference standard. The instrument was operated in a room near 21°C. and at a relative humidity below 45 per cent. Water from a thermostat at 25°C. was circulated through the spectrophotometer. All reported absorptions were recorded manually, though some data were obtained also with an automatic recorder.

Films of the amino acids were deposited on various supporting materials by evaporating 1 cc. of a 1 per cent aqueous solution in a vacuum desiccator containing phosphorus pentoxide. The most successful supports for the films were silver chloride plates made by the Harshaw Chemical Company. These slides of about 1-mm. thickness transmit over 80 per cent of the incident radiation, at least up to 10  $\mu$ . Satisfactory spectra were obtained also with polythene sheets of 0.005-mm. thickness, but this material was less convenient because it has steep absorption bands at 3.45 and 6.90  $\mu$  due to C—H vibrations.

Some samples were prepared also by grinding the amino acid in an agate mortar and dusting the powder on to the carrier slide.

Spectra of caproic acid, caproamide, and isohexylamine, respectively, were obtained in carbon tetrachloride solution at a concentration of approximately 0.01 molar. The thickness of the solution in the optical path was 0.1 mm.

All of the amino acids were of reagent grade. The sodium salts were obtained by adding an equimolar quantity of base, and the hydrochlorides by treatment with an excess of hydrochloric acid. Creatinine and creatine were kindly furnished by Professor Byron Riegel and were recrystallized from alcohol and water, respectively. A very pure sample of methylcyclopentane was kindly furnished by Professor H. Pines and Dr. B. M. Abraham. It had a refractive index of 1.4100. Isohexylamine was a reagent-grade sample with a boiling point of 122–123°C. Its hydrochloride was prepared by passing gaseous hydrogen chloride into an ether solution of the base, washing the precipitate with alcohol and water, and drying.

The sodium dodecyl sulfate was a specially purified sample generously supplied by the Fine Chemicals Division of the du Pont Company.

## RESULTS AND DISCUSSION

### 1. Amino acids and related compounds

In confirmation of previous work (2), the absorption of  $\text{C}=\text{O}$  in the unionized carboxyl group was established at  $5.8\ \mu$ , as is evident in figure 1. The other absorption bands of caproic acid, at  $7.00$  and  $7.80\ \mu$ , may be attributed to the  $-\text{CH}_2-$  and  $-\text{C}-\text{O}-$  groups, respectively. The spectrum of the ionized carboxylate group, on the other hand, lacks the  $5.8\ \mu$  band and absorbs instead at a frequency corresponding to  $6.45\ \mu$ . Similarly, the  $7.8\ \mu$  band, which generally

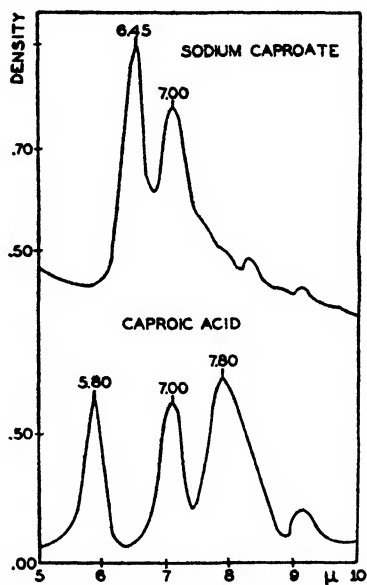


FIG. 1. Infrared spectra of caproic acid and sodium caproate

occurs with a  $-\text{C}-\text{O}-$  group in which the carbon has an additional double bond (1), is no longer present in sodium caproate. On the other hand, the  $7.0\ \mu$  band remains, as one would expect if it is due to the methylene groups.

In glycine, valine, and norleucine, a strong band appears at  $6.3\ \mu$  (figure 2). In each one, therefore, the carboxyl group exists in the ionized form. Furthermore, as one would expect, the formation of the sodium salt of each of these amino acids does not affect significantly the position of the  $6.3\ \mu$  band, for on the zwitterion model the removal of the hydrogen is from the ammonium group and not from the carboxyl. Similarly, the formation of the hydrochloride of the amino acid produces a band below  $6.3\ \mu$ , corresponding to the formation of an unionized carboxyl group. For glycine and valine hydrochlorides, respectively, the unionized carboxyl band appears near  $5.8\ \mu$ , as is found in caproic acid. For norleucine hydrochloride, however, the absorption peak occurs at  $6.05\ \mu$ . It seems likely

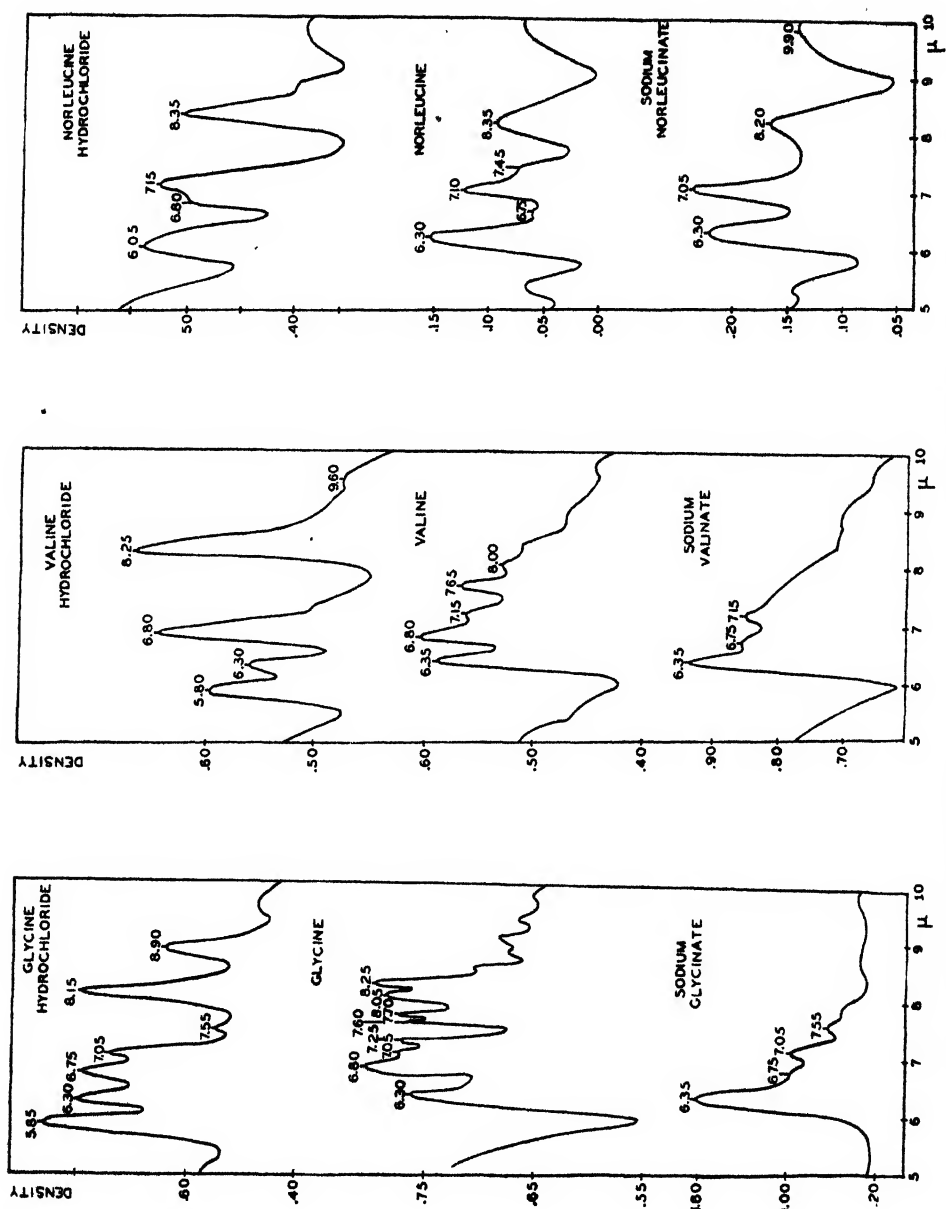


Fig. 2. Infrared spectra of some amino acids, their hydrochlorides, and their sodium salts

that this displacement from the normal position is due to an arrangement in the crystal which is particularly favorable toward the formation of hydrogen bonds, for a similar situation is encountered with caproamide (figure 3). In dilute solution a band appears at  $5.9\ \mu$ , near the expected position for a  $\text{C}=\text{O}$  group. In the solid, however, a decided displacement to  $6.05\ \mu$  is evident. In view of x-ray evidence (8) that amides are strongly hydrogen-bonded in the solid state, it seems likely that this factor is also responsible for the shift in frequency of the  $\text{C}=\text{O}$  vibration as one goes from dilute solution to the solid. A shift in the

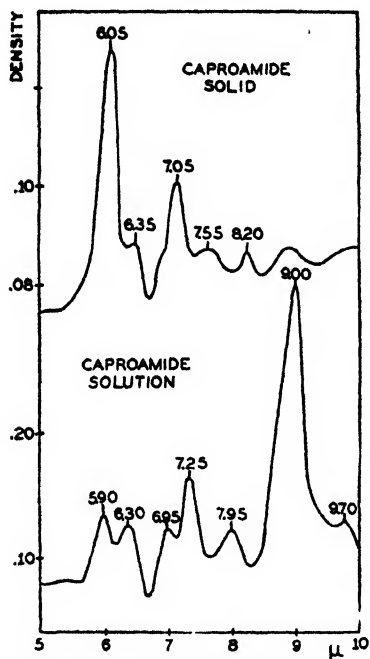


FIG. 3

FIG. 3. Effect of state on infrared spectrum of caproamide

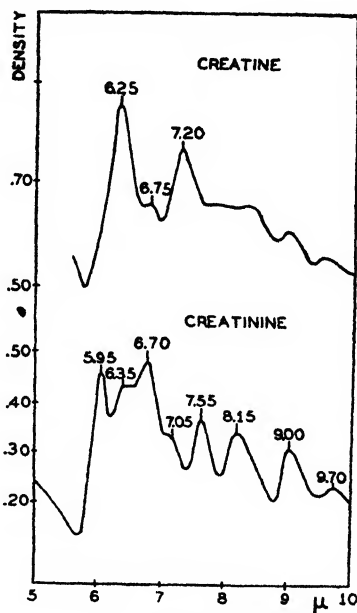


FIG. 4

FIG. 4. Infrared spectra of creatine and creatinine

same direction has been observed in acetic acid dimers (2), which are also held together by hydrogen bonds.

It is of interest to note (figure 2) that both glycine and valine hydrochlorides show bands at  $6.30\ \mu$ , and that norleucine hydrochloride shows a hump in that region. This absorption frequency is probably due to an  $\text{N}-\text{H}$  deformation vibration (7), for it is apparent also in caproamide (figure 3) and in creatinine (figure 4), neither of which has a free carboxylate anion. A distinct band in this region is also found in isohexylamine and its hydrochloride (figure 5).

An absorption band near  $7.55\ \mu$  also occurs in each of the amino acids, as well as in creatinine and caproamide, and it too may be related to an  $-\text{NH}$  vibration of some form.

All of the amino acids give some indication of a band near  $6.8 \mu$ , apparently due to the methylene group. Several also show absorption near  $7.1 \mu$ , corresponding to the Raman frequencies observed by Edsall (3).

The absorption spectrum of creatine,

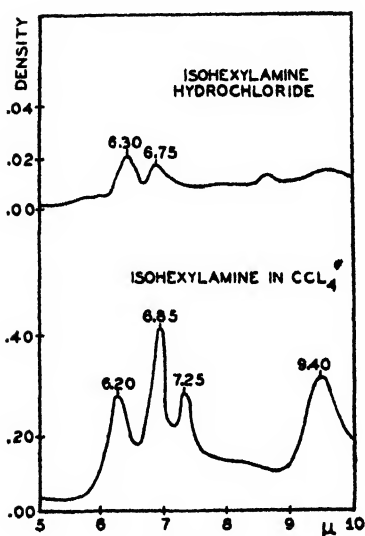
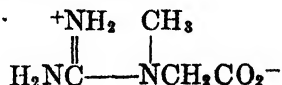


FIG. 5

FIG. 5. Infrared spectra of isohexylamine and its hydrochloride

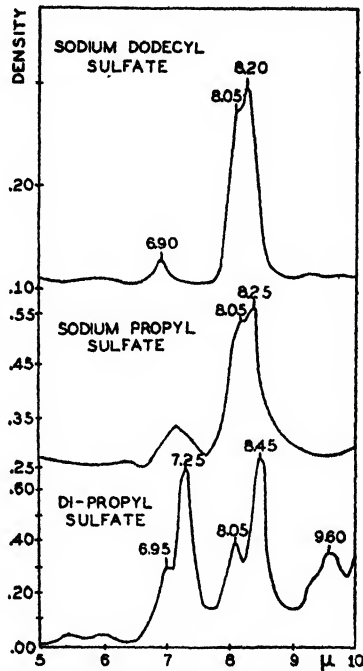
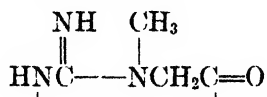


FIG. 6

FIG. 6. Infrared spectra of some alkyl sulfates

(figure 4) with its  $\text{C}=\text{O}$  band at  $6.25 \mu$ , is clear evidence for the dipolar nature of this molecule also. In contrast, creatinine,



has its  $\text{C}=\text{O}$  band at  $5.95 \mu$ , as one would expect from the accepted structure if due recognition is given to hydrogen bonding in the solid state.

## 2. Complexes with sodium dodecyl sulfate

The spectra of sodium dodecyl sulfate and two related compounds, sodium propyl sulfate and dipropyl sulfate, are recorded in figure 6 for reference in



connection with the discussion to follow. The large band at  $8.05\text{--}8.20\ \mu$ , due to the  $\text{—OSO}_3^-$  group, should be noticed in particular.

The interactions of some amino acids with sodium dodecyl sulfate are evident from phenomena as gross as precipitation reactions. Thus, arginine hydrochloride may be precipitated from an acidified aqueous solution by the addition of dodecyl sulfate. It seemed of interest, therefore, to examine the spectrum of this complex to obtain information on the nature of the binding forces. The relevant spectra are illustrated in figure 7. It is apparent that the relative absorption of the  $6.05\ \mu$  band is reduced in the complex, since a valley is now per-

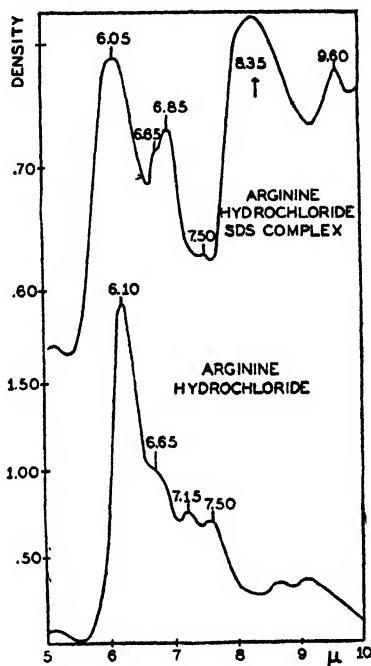


FIG. 7. Infrared spectra of arginine hydrochloride and its complex with sodium dodecyl sulfate.

ceptible between it and the shoulder at  $6.65\ \mu$ . This may indicate a disturbance of the  $\text{—NH}$  frequency in this region, but since the latter is strongly overshadowed by the carbonyl band, it is difficult to obtain direct evidence of any interaction involving the quaternary nitrogens of the amino acid. The sulfate band at  $8.35$ , however, seems much broadened and somewhat displaced toward higher wave lengths in the complex as compared with the free state. Such a displacement would be in general agreement with that mentioned previously for  $\text{C=O}$  groups when hydrogen-bonded. The appearance of a band at  $6.85\ \mu$  in the complex is presumably the result of the methylene group of the added dodecyl sulfate.

Other amino acids, such as glycine or valine, are not precipitated by sodium

dodecyl sulfate. Nevertheless, it is feasible to examine the possibility of interactions by obtaining spectra of evaporated aqueous solutions of the respective amino acid (or its salt) and sodium dodecyl sulfate in a 1:1 mole ratio. With the hydrochlorides or sodium salts of glycine or valine, no significant changes could be detected. The neutral amino acids, however, did show a small shift ( $0.1 \mu$ ) in the  $6.3 \mu$  region, the band in the complex being at a lower wave length. Such an increase in frequency of the C=O group may indicate its release from hydrogen bonding in the crystal, presumably owing to competition by the sulfate group.

In all these cases, however, the changes observed in the presence of the sodium dodecyl sulfate are small. It is thus evident that the bonds formed are primarily of electrostatic nature, though some accompanying disturbance of the CO—HN bond is also involved.

#### SUMMARY

Infrared spectra in the region of  $5$  to  $9 \mu$  are reported for glycine, valine, and norleucine, their sodium salts, and their hydrochlorides. By comparison with corresponding bands in caproic acid and caproamide, the dipolar nature of the amino acids is again evident. Similar conclusions may be reached for creatine. Creatinine, however, shows the spectrum to be expected for an amide.

The spectrum of arginine hydrochloride, as well as those of glycine and valine, undergoes small changes when complexes are formed with sodium dodecyl sulfate. Some disturbances in hydrogen bonding are indicated.

#### REFERENCES

- (1) BARNES, R. B., GORE, R. C., LIDDELL, U., AND WILLIAMS, V. Z.: *Infrared Spectroscopy*, p. 24. Reinhold Publishing Corporation, New York (1944).
- (2) DAVIES, M. M., AND SUTHERLAND, G. B. B. M.: *J. Chem. Phys.* **6**, 755 (1938).
- (3) EDSALL, J. T.: *J. Chem. Phys.* **4**, 1 (1936); **5**, 508 (1937).
- (4) FREYMAN, R., FREYMAN, M., AND RUMPF, P.: *J. phys. radium* [7] **7**, 30, 476, 506 (1936).
- (5) HEINTZ, E.: *Compt. rend.* **201**, 1478 (1935).
- (6) LENORMANT, H.: *Compt. rend.* **222**, 1432 (1946).
- (7) MANN, J., AND THOMPSON, H. W.: *Nature* **160**, 17 (1947).
- (8) SENTI, F., AND HARKER, D.: *J. Am. Chem. Soc.* **62**, 2008 (1940).
- (9) WRIGHT, N.: *J. Biol. Chem.* **120**, 641 (1937); **127**, 137 (1939).

SURFACE TENSION OF SOLIDS AND METHODS OF  
MEASURING THE SAME

GEORGE ANTONOFF

*Department of Chemistry, Fordham University, New York 58, New York**Received October 23, 1947*

## INTRODUCTION

The surface tension of solids has always been regarded as a metaphysical property and no real existence has been attributed to it. However, Pierre Curie over half a century ago gave a great deal of thought to this and emphasized its importance, as can be seen from his *Oeuvres* (collected papers published by the Société Française de Physique). Owing to his premature death and want of a method of measurement, no further progress could be made. Only after prolonged research by the author on surface tension relations between two phases has it been possible to devise a method and thus open up a new line of research.

The surface tension of solids can be easily measured if it is possible to find fluids whose surface tension is nearly equal to that of the solid in question and can be made larger and smaller by the addition of a third substance. If the surface tension is larger, the liquid does not wet the solid; but if it is smaller, the liquid adheres to it. By changing the concentration of the third substance in the liquid by small increments, one can reach a point where the liquid just begins to wet the solid. At this point, the surface tension of the solid is equal to that of the liquid, whose surface tension can be measured by known methods. Among transparent liquids water has the highest surface tension, about 75 dynes/cm. There is therefore no means of applying the above method to solids of higher surface tension.

It was found, however, that by mixing edible oils with some pigments, pastes could be obtained having enormous surface tensions. By varying the pigment concentration one can prepare pastes which will wet a given solid, or otherwise. This can serve for measuring the surface tension of such solids as glass, rock salt, etc., if a method of measuring the surface tension of these pastes can be found. Neither the capillary nor the drop method can be used, owing to the viscosity of the pastes.

It was found that this can be done by means of the breaking stress method. This is not obvious at first glance, because it has never been made clear whether or not the frictional forces responsible for viscosity add to the effects produced by molecular forces, which are the primary cause of surface tension.

## EXPERIMENTAL PROCEDURE

The problem of surface tension presents difficulty for two reasons. One is due to purely theoretical misrepresentation of the subject by many authors. The other is due to the limitations imposed upon us by nature in devising suitable experimental methods for measuring the same. I was confronted with these difficulties from the early days of my scientific activities. In those days there

was only one authority in this field, G. Quincke in Heidelberg, and I learned the experimental technique directly from him. One of the first experiments I performed in his laboratory was that with two rods, as shown in figure 1. Rod A is fixed in position. Rod B is carrying a tray. If the rods A and B are brought together and moistened with a liquid, they will adhere to each other. By placing small weights on the tray one can detach the two rods; the weight necessary and sufficient to produce separation of the rods by formation of the film of the liquid or by rupture of the same, divided by twice the length ( $l$ ) of the rods (because there are two surfaces) and multiplied by the acceleration due to gravity is the value in dynes per centimeter of the surface tension of the liquid.

The next experiment was done by the capillary method, which gave substantially the same figures as the above method for oils. It was found that for oils it is much better to use the apparatus shown in figure 1 than the capillary method.

The opinion is widely held that the breaking stress method does not yield a true measure of surface tension because of viscosity effects. To refute this view new experiments were carried out with olive oil by both methods. The capillary

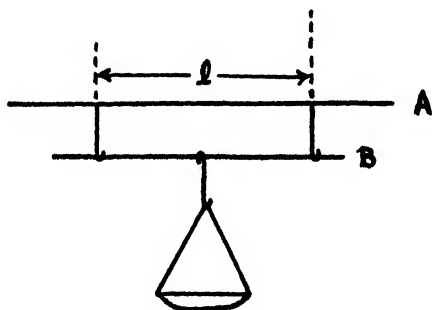


FIG. 1

method presented its own difficulties. Thus, using a capillary of 0.02-cm. radius no results at all could be obtained, because the liquid was too viscous and did not respond to changes in the position of the capillary when it was moved up and down. With a capillary of 0.056-cm. radius the capillary rise could be measured as a definite parameter, because the liquid immediately followed all changes in the position of the capillary. The best procedure was to tilt the capillary and then put it in an upright position. The liquid goes down a little and gives a meniscus, wetting the capillary bore with a contact angle equal to zero. Thus at about 25°C. the surface tension,  $\gamma$ , was found to be 36.31 dynes/cm. The capillary rise was 1.71 cm., large enough for accurate readings.

The breaking stress experiment was repeated five times; the average value producing the breakage of the film was found to be 0.173 g. The individual readings occasionally show large deviations, but the average of another five readings gave very nearly the same result. The mass of the rod B with the tray was 0.291 g. Thus  $0.291 + 0.173 = 0.469$  g. was necessary to detach the two rods from each other. The length of rod A was 6.50 cm.; whence

$$\gamma = \frac{0.469 \times 981}{13.00} = 35.38 \text{ dynes/cm.}$$

One would expect a much higher figure if viscosity had something to do with it, but instead this figure is 2.5 per cent lower than that obtained by the capillary rise.

The same sample of oil stood a week open to the air although protected from dust. After this a capillary experiment gave  $\gamma = 37.50$  dynes/cm., and the breaking stress method gave  $\gamma = 36.45$  dynes/cm. Both figures were higher than the previously described results. This is probably due to moisture, which increases the surface tension appreciably. As in the previous case, the breaking stress figure is about 2.7 per cent less than the capillary rise figure.

If one takes the figures obtained by the capillary method as a standard, one can increase the breaking stress value by 2.6 per cent and obtain values accurate to within 0.1 per cent. The agreement between the two methods is good, considering that different methods of measuring surface tension do not give agreement very much better than this (4). Thus the breaking stress method can yield accurate values, and it is sometimes the only method which can be used for measuring the surface tension of viscous fluids. In some cases a still better demonstration of the utility of this method can be given. If, for example, one takes soaps, the weights applied do not produce rupture of the film, but a film of large area of the liquid may be produced while the lower rod is separated from the upper one. By reducing the weights one can observe shrinkage of the film, and can demonstrate the reversibility of these effects by repeating the experiment several times. In the case of olive oil the breakage of the film takes place practically immediately when one rod separates from the other; therefore experiments as above are hardly possible, but comparative experiments supported by numerical data show that the method is good.

The question therefore arises as to whether or not the same method is still valid if the viscosity of the fluid increases very much. It was found that, by adding finely divided pigments to the oil, pastes could be formed having a greatly increased breaking stress (2). With increased concentration the viscosity also increases, but there is every reason to believe that the increase of breaking stress is exclusively due to molecular forces. Some of these reinforced pastes are capable of forming films which last some time after the separation of the two rods. They are so thin that they are translucent; they can shrink and have all the characteristics of a liquid film. They are so thin that their other properties, such as viscosity or rigidity, do not make themselves felt. They cannot be unimolecular in thickness, because the particles of the pigment are of much greater dimensions. Particles of the finest pigments have an estimated diameter of  $0.1 \mu$ , which is well above molecular dimensions.

There is another argument. Some powders do not reinforce oils at all, or very little. To this category belongs, for example, finely divided carbon. At high concentrations of the pigment the paste is very stiff, but the breaking stress determination gives figures characteristic of pure oils. Of course the experiment must be conducted very slowly. In this case the field of force causing the reinforcement is absent. Substances like carbon black do exhibit this field of force, which reinforces very highly, but this is not pure carbon. The reinforcement depends also on some ingredients in edible oils, not yet identified.

Generally speaking, any fluid system is suitable for these experiments. The temperature coefficient of viscosity is generally large, whereas that of surface tension is very small. Thus, very often it pays to raise the temperature during these experiments. For example, butter is quite stiff and even brittle at low temperatures, but with elevation of temperature it approaches a fluid in its characteristics.

But the most important evidence in favor of the view that the increase of breaking stress is due to molecular forces and not viscosity is this: When pastes with different predetermined breaking stresses are pressed through a capillary made of a given solid, up to a certain value of breaking stress they leave behind a visible film of paste on the capillary walls. This film is by no means unimolecular and can be compared with the case of water wetting clean glass; if the surface of the glass is inclined, the drops of water leave a visible layer which is not at all thin. When the breaking stress exceeds a certain value, the paste does not adhere to the material of the capillary wall. The transition point, which can be located fairly accurately with due patience, is characteristic of the solid. Thus, using ordinary glass, or lead glass, different constants are obtained, but the same figures have been obtained with different pastes. With ordinary glass the transition takes place when the breaking stress of the paste is 130 dynes/cm. One paste may be more fluid than another, but its breaking stress determines this phenomenon, not its viscosity. These experiments make it clear that 130 dynes/cm. is the value of the surface tension of glass, which is a constant characteristic for a given material independent of the nature of the paste.

At the time when these experiments of mine were published, there was no standard of comparison with which to determine whether or not pastes with high breaking stress owed this property to surface tension. Since then the work of Loman and Zwikker (7) has appeared, based upon an entirely different theory, which gave the value of 135 dynes/cm. for the surface tension of glass. This figure is a good confirmation of mine. Subsequently, a paper by Saal and Blott (8) criticized very sharply all work done on surface tension of solids, with the conclusion that nobody has ever succeeded in measuring the same.

Loman and Zwikker's work was criticized on the ground that the values of contact angles vary with time. This may be a factor affecting the result to a certain extent, but the fact that it so closely coincides with my value makes me believe that their method is substantially correct. Saal and Blott's criticism of my method is based upon a misunderstanding. They attribute to me the use of what they call "Antonoff's method of flat meniscus," which I have never used nor can I see how it could be used. I make mention of it in my writings only in connection with the critical region. The flat meniscus there is evidence that the vapor has a surface tension equal to that of the liquid. Loman and Zwikker also attribute to me the same error and thus think that my figure should be 60 dynes/cm. Neither of them understood my method.

My work originated as a result of experiments with beeswax and paraffin. They were done in two ways. Drops of solution of various concentrations were discharged on inclined surfaces of either paraffin or beeswax. Water does not

leave any trace. Only when the surface tension of a solution falls below a certain value does the solution begin to wet the solid. At this point the surface tension of the fluid is equal to that of the solid.

According to another method a capillary tube coated with paraffin was placed in solutions of isobutyric acid in water of various concentrations. Instead of rising water gave a capillary depression, just as mercury in glass. Solutions rich in acid did the reverse. At a certain concentration there was neither a capillary rise nor a depression. At this point the solution has a surface tension equal to that of paraffin. Both methods give the same results. In both cases the time factor does not affect the results appreciably, because the contact with the solids can be made of very short duration. On standing, water begins to wet paraffin. In both of these methods the problem of a flat meniscus does not arise at all. It is true that in the capillary at the transition point the meniscus is flat, but this is not easy to observe, and I based my conclusions on the absence of any capillary rise or fall. I therefore cannot understand at all why the Dutch authors gave such a wrong interpretation to my work.

To make sure that the above figures were good, capillary experiments were undertaken with molten paraffin at two temperatures. By extrapolation to the melting point a figure of the order of magnitude expected was obtained.

It is obvious that neither of the two methods described is applicable to pastes. But the method of forcing the paste through a broad capillary of the material in question joined to a narrow capillary, showed itself to be quite satisfactory. The proof that we are dealing here with a capillary phenomenon is given by the fact that if one uses a tube with a somewhat larger diameter the air makes its way through the paste. But when capillary forces make themselves felt, the suction causes a slow movement of the paste through the capillary. It should be mentioned that purity of the capillary is of no importance, because the paste rubs out all impurities present at the beginning of the experiment. Here again the question of the flat meniscus does not arise at all. In these experiments it is not easy to specify the diameter of the capillary to be used.

#### THEORETICAL CONSIDERATIONS

My work on surface tension of solids was criticized adversely by H. Freundlich (5). The theory was found "vorläufig unsicher," i.e., provisionally uncertain, but no explanation was given. When I asked about the reasons for such an opinion, the late H. Freundlich did not know anything about it, because the 1930 edition of his *Kapillarchemie* was edited by J. J. Bikerman.

My theory has originated as a result of my work on liquid-liquid systems, for which I formulated a definite law:

$$\gamma_1 - \gamma_2 = \gamma_{12} \quad (1)$$

where  $\gamma_1$  = the surface tension of one liquid layer,  $\gamma_2$  = the surface tension of the other liquid layer, and  $\gamma_{12}$  = the interfacial tension. This law is valid only when the system is in equilibrium. In the course of time it has been adversely criticized by many authors. This was, however, due to the fact that the concept of

equilibrium was not rightly understood. The whole subject was clarified as a result of an attack by W. D. Harkins. I had no difficulty in showing that the time factor has to be considered in establishing the equilibrium; it depends upon the formation of aggregates of high complexity, which takes time. Thus the large deviations from equation 1 observed by many authors are due to the fact that the systems were not in equilibrium (1).

As this is a law of equilibrium it is immaterial whether or not the substances used are chemically pure. The equilibrium is bound to establish itself, but with chemically pure substances the process is sometimes much slower, owing to the lack of such impurities which may accelerate the attainment of equilibrium catalytically.

There is no doubt that a relation of the same form is valid at the interface solid-liquid. In this case, however, there is no equilibrium and the same symbols mean surface tensions of pure substances at the moment of contact. The subject presents difficulties for investigation for want of methods; but important conclusions can be drawn from analogy with liquid-liquid systems which are best of

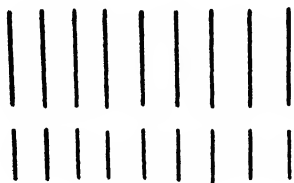


FIG. 2

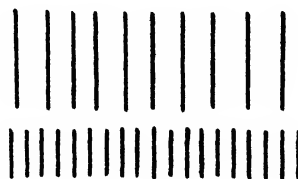


FIG. 3

all suited for experimentation. From a study of the critical region in liquid-liquid systems it becomes clear that there the two layers have the same surface tension, and that the interfacial tension is zero. Therefore

$$\gamma_1 - \gamma_2 = \gamma_{12} = 0 \quad (2)$$

which is a special form of relation 1. In liquid-solid systems a similar relation ought to be valid, but the difficulty is that of the three quantities we can measure experimentally only one, *viz.*, the surface tension of a liquid. We have no means of measuring  $\gamma_{12}$ . But if we can create conditions wherein  $\gamma_1 - \gamma_2 = 0$ , the problem becomes definite, because then the surface tension of the liquid is equal to that of the solid. Thus if we know the surface tension of the fluid, that of the solid will also be known. The work of Loman and Zwikker gives ample confirmation of the above theory. They were surprised by the fact that the relation works so well, whereas in liquid-liquid systems considerable deviations were observed. At the time these authors did not know to what these were due, and that they could easily be eliminated by bringing the system into equilibrium.

In considering the above results one must ascertain whether or not any changes of properties take place when the two media are placed in contact, and whether such changes are due to special orientation. When two liquid phases are in equilibrium, there is no room for any orientation. Langmuir (6) thought that



deviations from Antonoff's law could be explained in that manner. But I showed definitely that these deviations disappeared when the system was brought into equilibrium. The essential feature of equilibrium is the condition that the two phases contain an equal number of particles per unit volume (1). This means that some of them are aggregates of a very high degree of complexity. If these particles can be regarded as dipoles, they must be equidistant, as in figure 2; the dipoles in the two phases differ in length, but they are so situated that there is no reason why they should be distorted and deviated from their positions, as in figure 3.

In liquid-solid systems where there is no equilibrium, as in the case paraffin-water, the situation is different. The dipoles in the two media are not equidistant as a rule (although it may be so in some individual cases). Thus one can expect distortion and change of properties with time, as in figure 3.

Therefore, experiments with paraffin and water or aqueous solutions were performed dynamically.

In the case of pastes, no changes with time were observed, although it was found that if the breaking stress experiment was repeated many times in succession, there was a change in the properties of the system. This is possibly a thixotropic effect or is due to electrification in the case of highly insulating oils.

#### CONCLUSION

The above considerations show that this method of measuring the surface tension of solids is quite sound. The criticism raised by various authors does not deserve serious consideration. The Dutch authors should withdraw their objections, since they were based upon a crude misunderstanding. J. J. Bickerman expressed himself adversely about the theory in the last German edition of Freundlich's *Kapillarchemie* because he did not understand it correctly (5). And his tendency to minimize the importance of molecular forces and to overemphasize the effect of viscosity (3) is in contradiction to the elementary theory of surface tension. Moreover, all evidence herein before detailed shows that the effect of frictional forces does not come into question at all.

#### REFERENCES

- (1) ANTONOFF, G.: Arch. Biochem. **6**, 199 (1945).
- (2) ANTONOFF, G.: Rubber Age **60**, 2, 187 (1946).
- (3) BICKERMAN, J. J.: J. Colloid Sci. **2**, 163-75 (1947).
- (4) FREUNDLICH, H.: *Colloid and Capillary Chemistry*, p. 24. E. P. Dutton and Company, New York (1922).
- (5) FREUNDLICH, H.: *Kapillarchemie*, Vol. 1, p. 148. Hirschwaldsche Buchhandlung, Leipzig (1930).
- (6) LANGMUIR, I.: Colloid Symposium Monograph **5**, 48 (1925).
- (7) LOMAN, R., AND ZWIKKER, N. F.: Physica **1**, 1181 (1934).
- (8) SAAL, R. N. J., AND BLOTT, J. F. T.: Physica **3**, 1099 (1936).

# THE APPLICATION OF FLOW BIREFRINGENCE MEASUREMENTS TO HIGH-POLYMER SOLUTIONS

MICHAEL WALES

*Department of Chemistry, University of Wisconsin, Madison, Wisconsin*

*Received November 26, 1947*

The object of this paper is to review some experimental data on flow birefringence (4) with the purpose of exploring the possibilities of flow birefringence measurements as a secondary method of determining the molecular weights of high polymers. This method appears particularly attractive, since it gives two different types of average molecular weight, instead of one as with the intrinsic viscosity. One average is obtained from measurements of the extinction angle, the other from the birefringence. The types of average obtained will be later discussed.

It has been shown (16) that for polydisperse systems of any type, with no interaction between components

$$\tan 2\Psi = \frac{\sum_i \Delta_i \sin 2\Psi_i}{\sum_i \Delta_i \cos 2\Psi_i} \quad (1)$$

and

$$\Delta^2 = \left(\sum_i \Delta_i \cos 2\Psi_i\right)^2 + \left(\sum_i \Delta_i \sin 2\Psi_i\right)^2 \quad (2)$$

where  $\Psi$  is the extinction angle and  $\Delta$  is equal to  $n_e - n_o$ , the difference in principal refraction indices for the birefringent solution.

These equations have been experimentally tested (17), the agreement being excellent for a mixture of cellulose acetates in cyclohexanone, but only fair for mixtures of methyl cellulose and sodium thymonucleate in water, at finite concentrations.

The various quantities in equations 1 and 2 have been expressed in terms of molecular constants for the case of rigid ellipsoidal particles by Boeder (1), Peterlin (13), and Peterlin and Stuart (14). These equations have been used to interpret the data for various protein solutions (7). They will be modified for the case of threadlike polymers.

$$\tan 2\Psi_i = \frac{6}{\alpha_i} \quad (3)$$

$$\Delta_i = (n_e - n_o)_i = \frac{2\pi c_i}{15n} (g_1 - g_2)\alpha_i \quad (4)$$

These relationships hold for values of

$$\alpha_i = \frac{G}{\Theta_i} \quad (5)$$

which are not excessively large. Here  $\Theta_i = (\Theta_b)$  the rotary diffusion constant of species  $i$  with major axis  $a$ , and minor axis  $b$ .  $G$  is the velocity gradient.  $g_1 - g_2$  is a function of the particle shape and of the refractive indices of the particle and of the solution. For sufficiently long particles it is constant. For  $\Theta_i$  (12)

$$\Theta_i = \frac{3kT}{16\pi\eta a^3} \left\{ -1 + 2 \ln \frac{2a_i}{b_i} \right\} \quad \frac{a_i}{b_i} \geq 5 \quad (6)$$

The symbol  $\eta$  refers throughout to the viscosity of the solution.

For the case of rigid ellipsoidal molecules it then follows that for long molecules at low gradients and concentrations

$$a_\Psi = \left( \frac{\sum_i a_i^6 x_i}{\sum_i a_i^3 x_i} \right)^{1/3} \quad (7)$$

where  $x_i$  is a weight fraction. This equation is as accurate as equations 3-6 for particles having the same  $f = a/b$ ; for very long particles it is also true when all particles have the same minor axis but varying major axis. For the Lansing-Kraemer (10) and Schulz (18) distribution functions this expression is equal to

$$a_\Psi = \frac{\sum_i a_i^5 x_i}{\sum_i a_i^4 x_i} \quad (8)$$

By the use of the birefringence

$$a_\Delta = \left( \sum_i a_i^3 x_i \right)^{1/3} \quad (9)$$

For the equation of Schulz this is

$$a_\Delta = (a_w a_s a_{z+1})^{1/3} \quad (10)$$

where

$$a_w = \sum_i x_i a_i, \quad a_s = \frac{\sum_i x_i a_i^2}{\sum_i x_i a_i}, \quad \text{etc.}$$

For the equation of Lansing and Kraemer this becomes equal to  $a_s$ .

It can be now seen that flow birefringence results can be expected to give very high weighting of the molecular length. If  $f = a/b$  is constant, equations 7 and 9, yield  $M_s$  and  $M_w$ , respectively, for the average molecular *weight*. If  $b$  is constant while  $a$  varies, the averaging of the molecular weight and length is the same.

It is proposed that the quantities

$$\left( \frac{\Delta}{G\eta C} \right)_{C=0} \equiv [\Delta] \quad \text{and} \quad \left( \frac{\omega}{\eta G} \right)_{C=0} \equiv [\omega]$$

be defined in analogy to the intrinsic viscosity. Here  $\omega = \frac{\pi}{4} - \Psi$ . These quan-

tities have previously been discussed in terms of a theoretical model by W. Kuhn and H. Kuhn (9), although no extrapolations to zero concentration and gradient were made. The use of these quantities in characterizing colloidal materials would eliminate questions of the correctness of equations 1 and 2 at finite concentrations and the dependence of  $\omega$  on  $G$  at high rates of shear except as this affected the extrapolation to  $G = 0$ . For the rigid ellipsoidal model

$$[\Delta] = K_1 a^3 \quad (11)$$

$$[\omega] = K_2 a^3 \quad (12)$$

and for polydisperse systems equations 7 and 9 would apply.

For rigid randomly kinked polymers one would expect an effective value of  $a$  to be proportional to  $M^{1/2}$  (6) and

$$[\Delta] = K_1 M^{3/2} \quad (13)$$

$$[\omega] = K_2 M^{3/2} \quad (14)$$

For polystyrene, at least, calculations made from the intrinsic viscosity by Debye (2) show that the chain is more extended in solution than would be expected from proportionality to the square root of the molecular weight. Hence, the exponents would be expected to be larger than 3/2 for this material. However, as the molecular weight increases, a "shielding" effect occurs (2) which would increase the rotary diffusion constant for a given molecular weight, since we now have less effective chain length to contribute to the frictional factor. Therefore the exponents in expressions 13 and 14 will vary slightly with the molecular weight (2) and in addition will not be necessarily equal to 3/2. W. Kuhn and H. Kuhn (9) have deduced that the exponents in expressions 13 and 14 are equal to 1 and 2, respectively, for flexible chain molecules with restricted rotation. If the behavior of the intrinsic viscosity as a function of molecular weight is any criterion, probably the exponents will be unequal and range from 1 to 3, for various materials. Hence, for high polymers over not too wide a range of molecular weights:

$$[\Delta] = K_1 M^\beta \quad (15)$$

$$[\omega] = K_2 M^\gamma \quad (16)$$

For polydisperse systems:

$$M_{[\Delta]} = \left( \sum_i M_i^\beta x_i \right)^{1/\beta} \quad (17)$$

$$M_{[\omega]} = \left( \frac{\sum_i x_i M_i^{\beta+\gamma}}{\sum_i x_i M_i^\beta} \right)^{1/\gamma} \quad (18)$$

For polydisperse materials  $\omega/\eta G$  will not have the same relationship to  $G$  as for monodisperse materials, in contrast to the behavior of the quantity  $\eta_{sp}/C$  with respect to  $C$ . This is caused by the fact that at large velocity gradients all com-

ponents are somewhat oriented, while at low velocity gradients only the largest molecules are appreciably oriented (7). This introduces a very complex type of averaging at large velocity gradients, which is less heavily weighted than for the limiting case.

For fractionated nitrocelluloses in cyclohexanone (see figure 1), the author has found a function which represents  $\omega$  as a function of  $G$  with excellent agreement with experiment. For nitrocellulose fractions studied by Signer and Gross (19):<sup>1</sup>

$$\frac{G}{\omega} = \left( \frac{G}{\omega_0} \right) + \frac{G}{\omega_\infty} \quad (19)$$

This function serves to extrapolate the results to  $G = 0$ . The same equation also fitted some results for polystyrene fractions studied by the same authors (see figure 2). For polyisobutylene (22) and for polystyrene (19, 20) a discontinuity

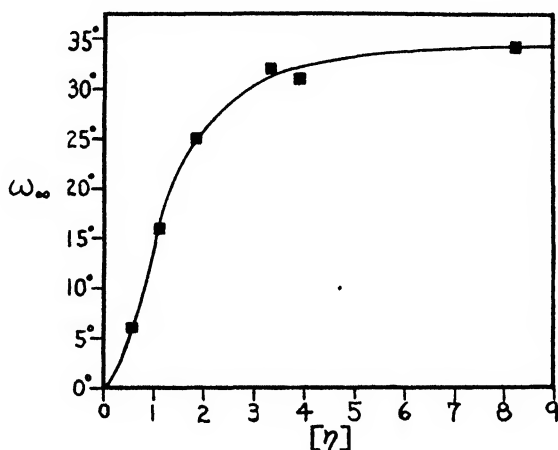


FIG. 1.  $\omega_\infty$  as a function of  $[\eta]$  for nitrocellulose fractions in cyclohexanone. Calculated from the data of Signer and Gross (19).

is observed in both  $\Delta$  and  $\omega$  as  $G$  becomes large. This did not occur for nitrocellulose in the range of  $G$  values investigated nor for polymethyl methacrylate (3). This phenomenon was considered to be caused by a deformation of the molecules (20). If the velocity gradient becomes large enough, the forces exerted on the molecules may become great enough to overcome the restrictions on rotation about bonds in the chain. This would result in some "straightening out" of the molecule and cause the sudden observed increase in  $\omega$  and  $\Delta$ .

The quantity  $\omega_\infty$  in equation 19 represents the value of  $\omega$  at infinite  $G$ .  $\omega_\infty$  is plotted as a function of  $[\eta]$  for the several nitrocellulose fractions of Signer and Gross. It can be seen that the theoretical limiting value of  $\omega$  of  $45^\circ$  is never attained.

It was observed by Signer and Gross (19) and De Rosset (3) that at low polymer concentrations  $\omega$  and  $\Delta/G\eta C$  are independent of concentration. Hence, th

<sup>1</sup> No correction was made for the birefringence of the solvent.

value  $\omega_\infty$  as obtained directly should be the same as that at infinite dilution. Extrapolation to infinite dilution is probably unnecessary provided measurements are carried out in this dilute range, although this question would have to be settled by experimental measurements in the polydisperse case. At higher concentrations there is a discontinuity in  $\omega$  and  $\Delta/G\eta C$  as functions of concentration, at which point they become concentration dependent. This point is known as the "interference limit" (19), and occurs at progressively lower concentrations at higher molecular weights. At this point the polymer molecules are far enough apart so that there is no mutual interference.

The quantities  $[\Delta]$  and  $[\omega]$  for the above-mentioned nitrocellulose fractions are plotted in figures 3 and 4 as functions of intrinsic viscosity. For low-molecular-weight polystyrene in cyclohexanone  $[\Delta]$  is plotted as a function of  $[\eta]$ . For this

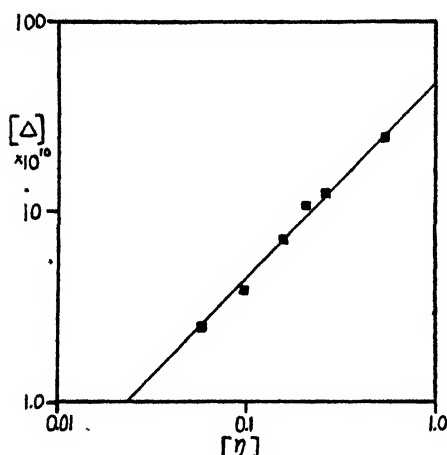


FIG. 2

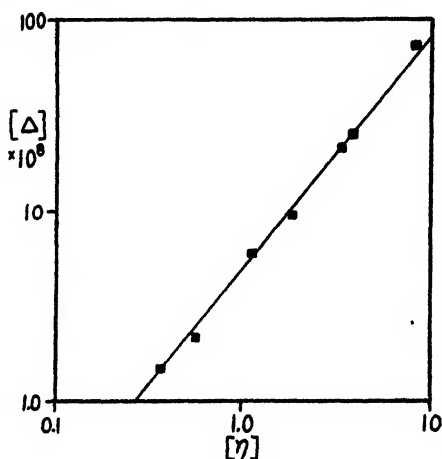


FIG. 3

FIG. 2.  $[\Delta]$  as a function of  $[\eta]$  for low-molecular-weight polystyrene in cyclohexanone. From Signer and Gross (19).

FIG. 3.  $[\Delta]$  as a function of  $[\eta]$  for nitrocellulose fractions in cyclohexanone. From Signer and Gross (19).

material  $\omega$  was zero except for the fraction of highest molecular weight. This is a shortcoming of this method as applied to polystyrene, which is not as strongly birefringent as other materials, such as polymethyl methacrylate (3) and nitrocellulose. This would be expected from structural considerations.

For these polystyrenes, since  $[\Delta]$  is proportional to  $[\eta]$ ,  $\beta \cong 0.8$ . Two isolated points obtained (19) with higher-molecular-weight fractions of polystyrene indicate that  $\gamma$  may be as high as 3. This looks like agreement with Kuhn's theory (9). Here  $\omega_\infty$  decreases with increasing molecular weight and is greater than  $45^\circ$ . More data for very thoroughly fractionated samples are needed before any definite conclusions can be drawn.

It can be seen that there is some scattering in the  $[\omega]$  vs.  $[\eta]$  curve for nitrocellulose. The  $[\Delta]$  vs.  $[\eta]$  curve shows much less scattering. Plotting either  $(\omega/\eta G)_0$  or  $(\omega/G)_0$  against  $[\eta]$  gives an equal amount of scattering, since the vis-

cosities of all the solutions used in the low concentration range did not differ greatly. To obtain the value of  $\omega/\eta G$  at  $C = 0$ , the  $[\omega]$  values for nitrocellulose should be multiplied by  $\eta_r$ . This erratic behavior is attributed to polydispersity of the fractions, since  $M_{[\omega]}$  is weighted higher than  $M_{[\Delta]}$ . For nitrocellulose in cyclohexanone  $\beta = 1.3$  and  $\gamma = 1.4-1.5$ , assuming Staudinger's rule for  $[\eta]$  as a function of  $M$  (11). This is quite close to the rough prediction of equations 13 and 14, for rigid randomly kinked molecules. This checks well with the fact that nitrocellulose gives no discontinuity in  $\omega$  and  $\Delta/G\eta C$  at high rates of shear.

In general, fractions used in investigating flow birefringence cannot be too carefully fractionated, because of the high weighting in both  $\Delta$  and  $\omega$ . It is recommended that such fractions should be first doubly precipitated; then two small cuts should be taken off the high and low ends of the fractions by careful adjustment of the temperature and amount of precipitant. The equilibrium

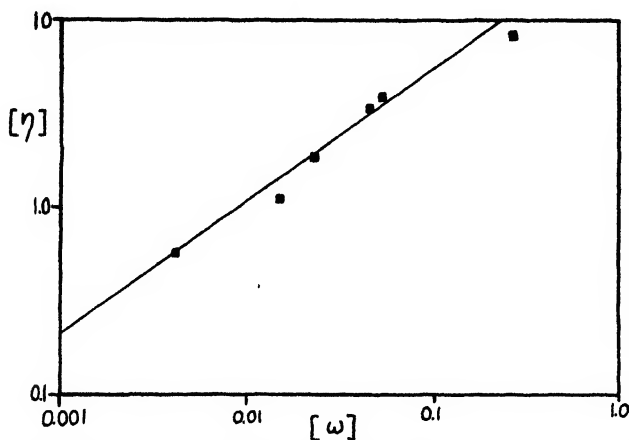


FIG. 4.  $[\omega]$  as a function of  $[\eta]$  for nitrocellulose fractions in cyclohexanone. Calculated from the data of Signer and Gross (19).

ultracentrifuge could be very useful here in determining the average molecular weights,  $M_w$ ,  $M_z$ , and  $M_{z+1}$  (21). An approximation procedure could then be used to estimate  $M_{[\Delta]}$  and  $M_{[\omega]}$ , as in estimating  $M_{visc}$  from  $M_w$  and  $M_n$  (21).

In conclusion it would be of interest to calculate  $M_{[\Delta]}$  and  $M_{[\omega]}$  for distributions (18) of the form

$$dW = KM^{b+1}e^{-(b+2)M_w M} dM \quad (20)$$

For  $M_{[\Delta]}$ ,

$$M_{[\Delta]} = \frac{M_w}{b+2} \left\{ \frac{\Gamma(b+2+\beta)}{\Gamma(b+2)} \right\}^{1/\beta} \quad (21)$$

$$M_{[\omega]} = \frac{M_w}{b+2} \left\{ \frac{\Gamma(b+2+\beta+\gamma)}{\Gamma(b+2+\beta)} \right\}^{1/\gamma} \quad (22)$$

For the case of the nitrocellulose used by Signer and Gross, for  $b = 0$ ,  $M_{[\omega]} =$

$1.75M_w$  and  $M_{[\Delta]} = 1.07M_w$ .  $M_{[\omega]} \cong \sqrt{M_z M_{z+1}}$  for this case. If  $\beta = 1$ ,  $\gamma = n$  ( $n$  integral),  $M_{[z]} = M_w$ :

$$M_{[\omega]} = (M_2 M_3 M_4 \cdots M_{n+1})^{1/n} \quad (23)$$

for Schulz' distribution, where  $M_2 = M_z$ ,  $M_3 = M_{z+1}$ , etc. (21).

If  $\gamma = 1$ ,  $\beta = n$  ( $n$  integral):

$$M_{[\Delta]} = (M_1 M_2 \cdots M_n)^{1/n} \quad (\text{For } n = 1 \text{ this is } M_w) \quad (24)$$

$$M_{[\omega]} = \frac{M_w}{b+2} (b+2+n)^{1/n} \quad (\text{For } n = 1 \text{ this is } M_z) \quad (25)$$

It can easily be seen that these measurements could be used as a test for polydispersity, after calibration with a good set of fractions. Unfortunately, the experimental difficulties are far greater than in measuring viscosity (5, 8, 15). Once the apparatus was set up, however, results could be obtained fairly rapidly. The method also could be made to serve as a standardized check of uniformity for process control, as viscosity is used at present.

#### SUMMARY

Flow birefringence data from the literature are briefly reviewed. It is shown that flow birefringence data can be used as a secondary method of molecular weight determination, in analogy to the intrinsic viscosity. Two different average molecular weights are obtained from flow birefringence, in contrast to the intrinsic viscosity. The type of average obtained is discussed.

The author wishes to thank Professor J. W. Williams for suggesting this problem. His continued interest and aid have been most valuable.

#### REFERENCES

- (1) BOEDER, P.: *Z. Physik* **75**, 258 (1938).
- (2) DEBYE, P.: Paper presented at the Chicago Meeting of the American Chemical Society, September, 1946; cf. also *J. Chem. Phys.* **14**, 636 (1946).
- (3) DE ROSSET, A. J.: *J. Chem. Phys.* **9**, 766 (1941).
- (4) (a) EDSALL, J. T.: In *Advances in Colloid Science*, Vol. I, p. 269. Interscience Publishers, Inc., New York (1943).  
(b) EDSALL, J.: In *Proteins, Amino Acids and Peptides*, p. 506, Reinhold Publishing Corporation, New York (1943). Reviews.
- (5) EDSALL, J. T., GORDON, C. G., MEHL, J. W., SCHEINBERG, H., AND MANN, D. W.: *Rev. Sci. Instruments* **15**, 243 (1944).
- (6) (a) EYRING, H.: *Phys. Rev.* **39**, 746 (1932).  
(b) Cf. LASKOWSKI, L., AND BURK, R. E.: *J. Chem. Phys.* **7**, 465 (1939).
- (7) FOSTER, J. F., AND EDSALL, J. T.: *J. Am. Chem. Soc.* **67**, 617 (1945).
- (8) FREY-WISSLING, A., AND WEBER, E.: *Helv. Chim. Acta* **24**, 278 (1941).
- (9) (a) KUHN, W., AND KUHN, H.: *Helv. Chim. Acta* **29**, 71 (1946).  
(b) KUHN, W., AND KUHN, H.: *Helv. Chim. Acta* **26**, 1394 (1943).
- (10) LANSING, W. D., AND KRAEMER, E. O.: *J. Am. Chem. Soc.* **57**, 1369 (1935).
- (11) MOSIMANN, H.: *Helv. Chim. Acta* **26**, 369 (1943).
- (12) PERRIN, F.: *J. phys. radium* [7] **5**, 497 (1934).



- (13) (a) PETERLIN, A.: *Z. Physik* **111**, 232 (1938).  
(b) PETERLIN, A.: *Kolloid-Z.* **86**, 230 (1939).
- (14) (a) PETERLIN, A., AND STUART, H. A.: *Z. Physik* **112**, 1 (1939).  
(b) PETERLIN, A., AND STUART, H. A.: *Z. Physik* **112**, 129 (1939).
- (15) (a) SADRON, C.: *J. phys. radium* [7] **7**, 263 (1936).  
(b) SADRON, C., BONOT, A., AND MOSIMANN, H.: *J. chim. phys.* **36**, 78 (1939).
- (16) SADRON, C., AND MOSIMANN, H.: *J. phys. radium* [7] **9**, 381 (1938).
- (17) SADRON, C., AND MOSIMANN, H.: *J. phys. radium* [7] **9**, 384 (1938).
- (18) (a) SCHULZ, G. V.: *Z. physik. Chem.* **B43**, 25 (1939).  
(b) BOYER, R. F.: *Ind. Eng. Chem., Anal. Ed.* **18**, 342 (1946).
- (19) SIGNER, R., AND GROSS, H.: *Z. physik. Chem.* **A165**, 161 (1933).
- (20) SIGNER, R., AND SADRON, C.: *Helv. Chim. Acta* **19**, 1324 (1936).
- (21) (a) WALES, M.: *J. Phys. Colloid Chem.* **52**, 235 (1948).  
(b) WALES, M., WILLIAMS, J. W., THOMPSON, J. O., AND EWART, R. H.: *J. Phys. Colloid Chem.* **52**, 983 (1948).
- (22) (a) ZVETKOV, W., AND FRISMAN, E.: *Acta Physicochim. U.R.S.S.* **20**, 61 (1945).  
(b) REHNER, J.: *J. Chem. Phys.* **13**, 450 (1945).

## SEDIMENTATION EQUILIBRIA OF POLYDISPERSE NON-IDEAL SOLUTIONS

### EXPERIMENT

MICHAEL WALES, J. W. WILLIAMS, J. O. THOMPSON, AND R. H. EWART

*Department of Chemistry, University of Wisconsin, Madison, Wisconsin, and the General Laboratories, United States Rubber Company, Passaic, New Jersey*

*Received November 26, 1947*

In a previous communication (14), a theory of the equilibrium behavior of high-polymer solutions in a centrifugal field was developed. In this article, results are presented which substantiate the theory and show that the sedimentation-equilibrium method offers a reliable means for the characterization of high polymers. Its great advantage over other methods lies in the fact that it is possible not only to determine an average molecular weight, but also a molecular-weight distribution curve, if the polymer is known to have a "continuous" distribution of molecular weights. In addition, only milligram quantities of material are required for an experiment.

Polystyrene was selected as the polymeric material to be studied in this investigation, since it is easily prepared under reproducible conditions and because some fractionated samples were available which had had weight-average molecular weights determined by the light-scattering technique. Butanone was selected as a solvent, since it forms solutions with polystyrene which deviate less from ideality than those with any other pure solvent known to the authors. The slope of the reduced osmotic pressure curve, which determines the value of this non-ideality correction factor, was also known to be independent of molecular

weight and concentration over the concentration range used (4). This is a necessary requirement for the rigorous application of our theory (14).

The experiments were carried out in a small Svedberg equilibrium ultracentrifuge with direct electric motor drive. The scale method was used to measure concentration gradients in the sedimentation cell (13). Here,

$$Z = Gab\alpha \frac{dc_z}{dz} \quad (1)$$

where  $Z$  = scale line displacement

$G$  = scale magnification factor

$a$  = cell thickness

$\alpha$  = refractive index increment =  $dn/dc_z$

As previously found by Svedberg and Pedersen (13), the optimum angular velocity is that which gives a concentration ratio of about three to one between the extremities of the sedimentation cell. All experiments were performed under these conditions.

Details of the apparatus and techniques used may be found elsewhere (13), so they will not be discussed at length here. Nevertheless, some modifications in procedure were employed which have not been fully described in the literature. It is felt that they will be of sufficient assistance to future investigators in this field to be worthy of mention.

Since the concentration, as well as its derivative, is needed to calculate weight-average molecular weights, it must be obtained by integrating  $dc/dz$  over the cell, using the known initial concentration as a constant of integration. Hence, the position of ends of the solution column, the limits of this integration, must be determined with considerable accuracy. This was done by taking a photograph of the cell during the course of an experiment. The meniscus appeared on the negative as a thin line, and the distances from the meniscus to the bottom of the cell and from the bottom of the cell to the center of the index hole could be measured on the photograph with great accuracy by means of a microcomparator. The actual distance from the bottom of the cell to the index hole was known by direct measurement with a precision cathetometer to  $\pm 0.01$  mm. Thus, by a comparison of the true distance with that measured on the photograph, the distances from the center of rotation to the extremities of the column of solution could be obtained to  $\pm 0.01$  mm.

Another improvement in technique made it possible to detect any shift of the scale image as a whole with respect to the cell. This could result from the departure from normal incidence of the light from the scale on the cell windows, or from the windows not being strictly parallel to each other. This behavior was noticed in the earlier experiments and required correction, but it disappeared when the optical system was readjusted. It was detected by comparing the actual distances from a reference scale line to the other scale lines, with the same distances on a photograph taken through the cell filled with solvent at very low rotor speed. Allowance was made for the scale magnification factor.

The rotor speed was measured with a stroboscope, which made it possible to estimate the speed to a few tenths of a revolution per second.

In addition, it is felt that the  $z$  vs.  $s$  curve (13) should be fitted to the data by the method of least squares, instead of visually as was done. However, this would add a prohibitive amount of labor to the calculations. The trapezoidal rule was found to be adequate to perform the integrations. Only negligible differences were found between this method and Simpson's three-point rule.

A constant source of difficulty during part of this work was the presence of some impurity in the butanone used as solvent. This impurity is apparently sorbed by the polymer and leads to an anomalous shape for the  $dc/dx$  vs.  $x$  curve near the meniscus. The curve in this region starts out with a fairly large slope which then decreases, after which the curve is concave upward, as required. This trouble was not encountered with freshly distilled butanone but occurred after the material had aged for several months. Redistillation eliminated this behavior to a very large extent. It is recommended that all solvents used in work of this sort be very carefully purified immediately before use. Any set of data for which  $dc/dx$  starts out to be convex upward should be suspect. The error caused by this behavior is not very great by former standards, about 5–10 per cent, but it is believed that in the complete absence of this phenomenon, it should be possible to obtain  $M_w$  to  $\pm 3$  per cent.

In this investigation, measurements were made with fractionated and unfractionated polystyrenes in solution, to determine weight-average molecular weights and to obtain information about the molecular-weight distribution. A fractionation of a sample of a peroxide-catalyzed polystyrene was performed, and the sedimentation-equilibrium molecular-weight distribution curve was compared with that obtained from the fractionation. Refractionation of a fraction was carried out with the same object in mind. An experiment was also done on a synthetic mixture of material which had been separately characterized, to check the reliability of the higher average molecular weights. These are designated as "moments", although strictly speaking they are ratios of moments.

The essential formulae used (14) in treating the data are summarized below:

$$M_{1x} \equiv M_{vx} = \frac{\frac{dc_x}{dx}}{c_x \left( 2Ax - B \frac{dc_x}{dx} \right)} \quad c_x \text{ in volume units (g./100 cc.)} \quad (2)$$

$$B = \frac{20gb'}{RT\rho} \quad (3)$$

$$A = \frac{(1 - \bar{V}\rho)\omega^2}{2RT} \quad (4)$$

$$M_{qx} = M_{(q-1)x} + M_{1x} \frac{d \ln M_{(q-1)x}}{d \ln c_x} \quad (5)$$

where

$$M_q = \frac{\sum_i M_i^q c_i}{\sum_i M_i^{q-1} c_i} \quad (6)$$

$$M_w \equiv M_1 = \frac{\int_a^b M_{wz} dW}{\int_a^b dW} \quad (7)$$

$$M_q = \frac{\int_a^b \prod_{p=1}^{p=q} M_{pz} dW}{\int_a^b \prod_{p=1}^{p=q-1} M_{pz} dW} \quad q > 1 \quad (8)$$

$$dW = (x \pm \delta) c_x dx \quad \text{for a sector-shaped cell} \quad (9)$$

Here  $x$  = distance from the center of rotation to the point in question

$c_x$  = concentration at distance  $x$ , in volume units (g./100 cc.)

$g$  = acceleration of gravity, cm./sec.<sup>2</sup>

$b' = \frac{d(\pi/c)}{dc} = \frac{\text{mm. solvent}}{(\text{g./100g.})^2}$

$\rho$  = density of solution (variation with  $x$  negligible)

$V$  = partial specific volume of polymer

$\omega$  = angular velocity

$b, a$  = distances from center of rotation

$\delta$  = correction factor for non-coincidence of the cell sector center with the center of rotation

The factor  $RT$  has the usual significance. In this report it is expressed in c.g.s. units. The quantity  $M_n = M_0$  cannot be determined from these equations alone, but an approximation can be made for its calculation (14) unless the integral equation of sedimentation equilibrium is to be solved to obtain the molecular-weight distribution function for the polymer, and through it,  $M_n$ .

The time required for the attainment of equilibrium in the experiments varied from less than a week to 2 weeks (for high-molecular-weight samples). The higher the molecular weight, the slower is the approach to equilibrium. This follows from the fact that the angular velocity must be lowered in order to obtain a favorable concentration ratio as the molecular weight increases.

#### RESULTS AND DISCUSSION

Results for some polystyrene fractions which had been characterized by osmotic pressure and light-scattering measurements at the General Laboratories, United States Rubber Company, Passaic, New Jersey (US), are presented in table 1. It can be seen that the agreement between  $M_w$ , as determined by light scattering and by sedimentation, is satisfactory. It should be mentioned that sedimentation equilibrium should in general give higher results for  $M_w$  than light scattering for polymers of appreciable molecular weight, unless a correction for the dissymmetry of scattering is applied. A detailed discussion of the polydispersity of the fractions will be postponed until the experimental material for a second set of fractions is presented.

This second set of fractions was obtained from a polystyrene prepared in this laboratory in the oil phase at 60°C. in the presence of 0.13 mole per cent benzoyl peroxide. The conversion was 18.5 per cent after 11½ hr. The polymerization was carried out in sealed tubes under nitrogen, using dried, vacuum-distilled styrene which had been freed of inhibitor by multiple washing with dilute sodium hydroxide. The fractionation was carried out in a thermostat by simultaneous variation of the amount of precipitant and the temperature. The solvent precipitant system was benzene-methanol. Each fraction was reprecipitated, care being taken not to precipitate all the material, and the supernatant added to the main batch of solution. Then another and another fraction was removed. The material remaining in solution at the end of this process was the final fraction. Data for the polymer fractions (*W*) so obtained are presented in table 2. In-

TABLE 1  
*Comparison of light-scattering and sedimentation-equilibrium molecular-weight data*

FRACTION	OSMOTIC $M_n \times 10^{-3}$	LIGHT SCAT- TERING* $M_w \times 10^{-3}$	SPEED OF CENTRIFUGE IN R.P.M.	CONCENTRA- TION AT 25°C.  g./100 cc.	SEDIMENTATION DATA $\times 10^{-3}$			
					$M_n = M_0$	$M_w = M_1$	$M_s = M_2$	$M_{s+1} = M_3$
5US	260	297	2950	0.3095	ca. 200	315	464	570
6US	160	190	3010	0.1618	170	190	210	†
7US†	110	120	4600	0.1592	120	132	181	†
9US	47§	62	6030	0.4066	39	53.1	88.1	220

\* Not corrected for dissymmetry of scattering. For butanone  $\alpha = dn/dc = 0.00219$  (3),  $B = 0.02966 \times 10^{-4}$ , in units of grams per 100 cc. (4).  $V = 0.906$  for polystyrene. As far as could be determined  $\bar{V}$  did not differ for two samples having  $M_w = 75,000$  and 500,000.

† Data obtained at the lower concentrations are not believed to be sufficiently precise to warrant the calculation of  $M_{s+1}$ .

‡ In carbon tetrachloride,  $\alpha = dn/dc = 0.00151$  (3),  $B = 0.1076 \times 10^{-4}$  in units of grams per 100 cc.

§ End-group method gives 39,000.

intrinsic viscosities were computed from data obtained in benzene at 30°C., in units of grams per 100 cc. Viscosity molecular weights were obtained for all fractions from a composite  $[\eta]$ - $M$  relationship. This relationship was derived by a combination of the data of Alfrey, Bartovics, and Mark (1), those of Ewart and Tingey (4), and those obtained in this investigation for polymers prepared at 60°C. Where  $M_n$  and  $M_w$  were both available, as was the case except for Alfrey's data,  $M_{visc.}$  was obtained by the relationship:

$$\frac{M_{visc.}}{M_w} = \frac{R-1}{R} \left[ \frac{\Gamma\left(\frac{R}{R-1} + \epsilon\right)}{\Gamma\left(\frac{R}{R-1}\right)} \right]^{1/\epsilon} \quad (10)$$

Here  $[\eta] = KM^*$  and  $R = M_w/M_n$ . This assumes a distribution function of the form  $M^n e^{-kM}$ , but the error is small if  $M_n$  and  $M_w$  are fairly close together. In

any event  $M_{visc.}$  is always rather close to  $M_w$ , with the ratio  $M_{visc.}/M_w$  varying from 0.95 to 0.99 for the data treated by equation 10. The constant  $\epsilon$  was taken as 0.78, although for the actual relationship it varied from 0.75 to 0.69 for a hundredfold variation in  $M$ . This relation is plotted in figure 1. The points marked with an arrow are known to be too low. It will not be discussed further here, since the primary concern of this work lies elsewhere.

TABLE 2  
Collected data for a fractionation of a polystyrene sample

FRACTION	WEIGHT  grams	[ $\eta$ ]	$k'^*$	$q(M)^\dagger$	VISCOSITY $M \times 10^{-4}$	OSMOTIC $M_n \times 10^{-3}$	ULTRACENTRIFUGE				SPEED IN R.P.M.	CONCENTRATION  g./100 cc.
							$M_n \times 10^{-3}$	$M_w \times 10^{-3}$	$M_z \times 10^{-3}$	$M_{z+1} \times 10^{-3}$		
1W§	1.86	1.442	0.286		471							
1A-W..	0.74	1.672	0.350	0.981	586							
1B-W...	1.12	1.268	0.292	0.839	390							
2W§	5.05	1.294	0.344		401							
2A-W..	1.92	1.512	0.304	0.915	507	400						
2B-W..	3.13	1.236	0.298	0.733	375	288						
3W	3.40	1.053	0.309	0.569	298	250						
4W..	1.86	0.972	0.316	0.438	263	210		290	370		2850	0.3009
5W...	3.89	0.746	0.317	0.294	185	155	168	186	230		3710	0.1611
6W..	2.13	0.544	0.324	0.144	122	90	113	125	139	193	4480	0.3172
7W..	1.59	0.354	0.375	0.051	67.3	44	57	66.6	78.1	88	5410	0.3998
8W	0.22	0.18		0.005	28.7							

Original polymer = 20 g.

Recovered = 20 g.

$[\eta] \times W$ , original = 19.36,  $[\eta] = 0.968$

$\sum [\eta]_i W_i$  = 19.27, for fractions

$$* k' = \frac{1}{[\eta]^2} \frac{d\left(\frac{\eta_{sp}}{c_v}\right)}{dc_v}$$

† Integral molecular-weight distribution function.

‡ From composite relationship between  $[\eta]$  and  $M$  obtained from data shown here, from data of Alfrey, Bartovics, and Mark (1), and from data of Ewart and Tingey (4).

§ Separated into two fractions by precipitation.

It can be seen that both the fractions prepared at the University of Wisconsin and those prepared at the United States Rubber Company are appreciably polydisperse. Some qualitative information about the shape of the distribution curves of these fractions may be obtained from the "moment ratios",  $M_w/M_n$ , etc. The osmotic number-average molecular weights are thought to be more dependable than the approximate number-average molecular weights determined with the ultracentrifuge (14) and will be used preferentially, when available.

If the ratio  $M_q/M_{q-1}$  is constant for all values of  $q$ , the distribution curve can be fitted (9) by the equation

$$dW = \frac{1}{M_n \beta \sqrt{\pi}} \cdot e^{-(1/\beta^2)(\ln M/m)^2} \cdot dM \quad (11)$$

where  $m = M_n e^{\beta^2/4}$  and  $M_q/M_{q-1} = e^{\beta^2/2}$ .

If the difference  $M_q - M_{q-1}$  is constant for all values of  $q$ , it is possible to fit the distribution curve by the following expression (10):

$$dW = \frac{\left(\frac{b+2}{M_w}\right)^{b+2}}{\Gamma(b+2)} \cdot M^{b+1} \cdot e^{-(b+2/M_w)M} \cdot dM \quad (12)$$

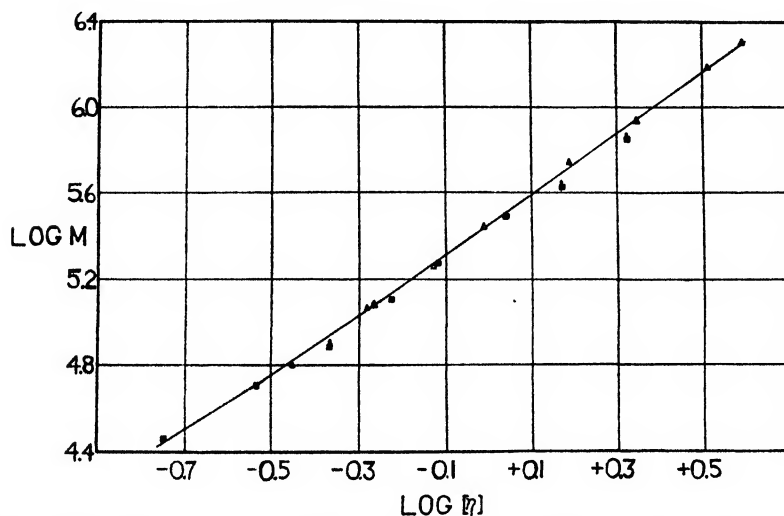


FIG. 1. Plot of  $\log [\eta]$  against  $\log M$ .  $\blacktriangle$ , Alfrey *et al.*;  $\blacksquare$ , Ewart *et al.*;  $\blacklozenge$ , Wales *et al.*

Here

$$\frac{M_q}{M_{q-1}} = \frac{b+q+1}{b+q}$$

and the ratio decreases with increasing  $q$ .

For more rapidly decreasing moment ratios, functions of the form of equation 13

$$dW = KM^n e^{-\alpha M^2} dM \quad (13)$$

may serve the purpose (14). The integrals of these functions are available in many mathematical tables.

All of these distributions have positive skewness, i.e., the peak in the size-frequency curve occurs at low molecular weights, while the tail stretches toward high molecular weights. A positively skewed curve with a very sharp peak and very long tail has been shown by graphical integration to give moment ratios  $M_q/M_{q-1}$  which increase with  $q$ . This behavior is more pronounced as the peak becomes sharper and the tail longer.

For negatively skewed distributions, the moment ratios would be expected to decrease rather rapidly as  $q$  increases. For a sharp cut-off at a certain value of  $M$ ,  $M_q$  should approach a limit as  $q \rightarrow \infty$ . This would be true for a positively skewed distribution, provided the function also became zero at a certain value of  $M$ . However, the limit would not be approached nearly as rapidly as in the former case.

TABLE 3  
Moment ratios of fractions,  $M_q/M_{q-1}$

FRACTION	$\frac{M_w}{M_n} \frac{M_1}{M_0}$	$\frac{M_z}{M_w} \frac{M_2}{M_1}$	$\frac{M_{z+1}}{M_z} \frac{M_3}{M_2}$	REMARKS
5US. . . .	1.21	1.47	1.23	Fairly broad distribution curve of uncertain shape
6US. . . .	1.19	1.11		Fitted approximately by $M^2 e^{-\alpha M^2} dM$
7US. . .	1.20	1.37	Increases	Narrow peak; long high-molecular-weight tail
9US. . .	1.36	1.66	2.50	Obviously contaminated with high-molecular-weight material
4W. . .	1.38	1.28		Fitted by equation 12, $b = 1.63$
5W. . .	1.20	1.24		Fitted by equation 11, $\beta = 0.6$
6W. . .	1.39	1.11	1.39	Similar to 5US
7W. . .	1.51	1.17	1.13	Cannot be fitted by any single simple curve given here; possibly negative skewness

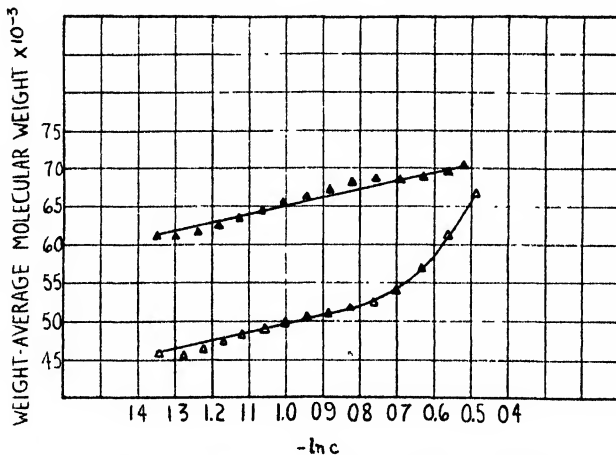


FIG. 2. Some typical curves of  $M_{wx}$  versus  $\ln c_x$ :  $\blacktriangle$ , fraction 7W;  $\triangle$ , fraction 9US

The moment ratios for all fractions are tabulated in table 3.

For these polymers,  $M_{wx}$  was first calculated by the use of equation 2 and the higher moments by equation 5, employing graphical differentiation. Some typical curves of  $M_{wx}$  vs.  $\ln c_x$  are shown in figure 2. For fraction 9US one observes the typical behavior of a fraction containing a small quantity of material which has a molecular weight a great deal higher than that of the fraction as a whole.

Nearly all fractions can be said to have positively skewed distributions. All



were reprecipitated to remove a low-molecular-weight "tail-fraction". Either through incomplete settling of the first (high-molecular-weight) fractions, or by some as yet unknown mechanism, all contain a small amount of material which is of considerably higher molecular weight than  $M_w$  for the fraction. Scott (12) has developed equations for the distribution curves of successive fractions in terms of the initial distribution of the whole polymer. Since our fractions were doubly precipitated, the second supernatant being recycled, his results are not strictly applicable. In no case does Scott's treatment predict the existence of a long "tail" stretching toward high molecular weights. However, the greater the positive skewness of the original distribution, the greater should be the positive skewness of the distribution curves for the fractions. Theoretically, the higher fractions should contain a considerable quantity of material of low molecular weight, also.

It is rather discouraging to note that in table 3 the only fractions for which the distribution may be approximated by a simple curve are those for which  $M_{z+1}$  is not available. In one case (4W) the points defining the curve of  $M_{wx}$  vs.  $\ln c_x$  are too scattered to permit the evaluation of  $M_{z+1}$ ; in the other cases the initial concentration was not as high as it should have been for the best results.

Some alternative methods of obtaining approximate distribution curves from the moments were attempted. The averaging over the cell for the over-all values of the moments (equations 7, 8) was split into two parts and the previous methods of analysis applied to each part. This led to no improvement in the interpretation of the results. A general method in which the observed  $M_q$ ,  $q = 0, 1, 2, 3$ , etc., were expressed as a function of  $q$  and the distribution function as a sum of exponentials in  $M$  failed because of mathematical complexity. The principle of this method was to make  $M_q$  as calculated from the generalized distribution curve as a function of  $q$  identical with the experimental  $M_q(q)$  and thus pick out the constants in the generalized distribution function.

The question of whether the higher moments as calculated here are to be relied upon was answered in the affirmative, at least for  $M_z$  and often for  $M_{z+1}$ . Among other results, which will be presented in due course, data for the whole polymer, from which the fractions in table 2 were obtained, led to this conclusion. These results are presented in table 4. The  $M_{wx}$  vs.  $\ln c_x$  curve for this polymer is shown in figure 3. The three points nearest to the meniscus are usually discarded. One of these points has not been included in this plot. It can be seen that  $M_{wx}$  becomes erratic in this region. This is believed to be caused by diffraction around the meniscus.

The values in the second column of table 4 were obtained by solving for the distribution function as outlined in the companion paper (14) and calculating the moments by integration. The distribution function is plotted to give figure 4. It can be seen that there is a remarkable similarity to some distribution functions which have been derived from a mathematical treatment of the kinetics of vinyl polymerization (5, 6, 7, 8, 10).

This distribution function, *per se*, could signify several things: (a) A constant rate of initiation, termination by collision with the monomer, or by disproportion-

tionation. This is limited to low extents of reaction (8). (b) Second-order initiation, with respect to the monomer, termination by disproportionation (5).

TABLE 4

*Ultracentrifugal analysis of a whole polymer*

Speed = 3130 R.P.M.; concentration = 0.2406 g./100 cc.;  $[\eta] = 0.968$

	GRAPHICAL, EQUATIONS 2, 5, ETC.*	FROM SOLUTION OF INTEGRAL EQUATION (REFERENCE 14)	RATIOS, $\frac{M_g}{M_{g-1}}$	EQUATION 11, $\frac{M_g}{M_{g-1}}, b = 0$
$M_n$ .....	150,000†	146,000‡	1.97	2.00
$M_w$ .....	287,000§	289,000	1.62	1.50
$M_z$ .....	495,000	464,000	1.50	1.33
$M_{z+1}$ .....	785,000	705,000		

\* The curve of  $M_{wx}$  vs.  $\ln c_x$  is shown in figure 3.

† Average of 126,000 and 172,000 from approximation procedure (14).

‡ This value is subject to no approximation whatsoever.

§  $M_w$  (light scattering) = 299,000.

$M_n$  (osmotic) = 144,000

$M_w$  (from fractionation) = 283,000. Here values of  $M_{visc.}$  were used when  $M_w$  was not available.

$M_{visc.} = 267,000$  (from curve).  $M_{visc.} = 271,000$ , from  $M_n$ ,  $M_w$ , and equation 10,  $\epsilon = 0.73$ .

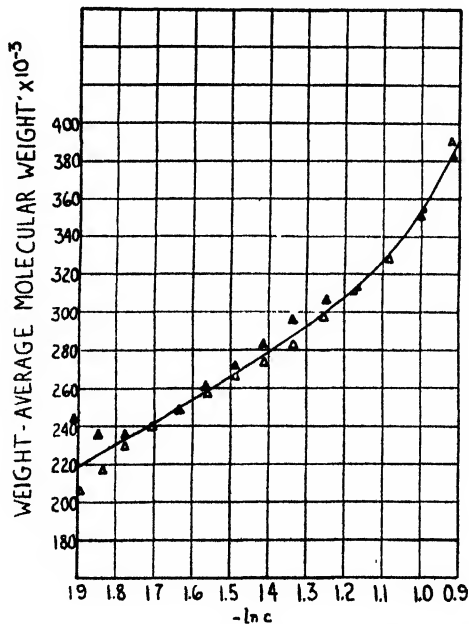


FIG. 3. Plot of  $M_{wx}$  versus  $\ln c_x$ : ▲, scale setting 60; △, scale setting 30

(c) Any initiation, termination by collision with the monomer (5, 6, 7). (d) First-order initiation, mutual combination (5).

Since the authors have obtained similar results with an uncatalyzed polystyrene (15), where the initiation is known to be second order, it is believed that cases (a) or (c) correspond to the present experimental conditions. From these results alone one cannot distinguish between collision with the monomer and disproportionation, but since evidence exists (11) for a second-order termination reaction with respect to free radicals, case (a) follows for our experimental conditions (60°C., 11½ hr., 0.13 mole per cent benzoyl peroxide, 18.5 per cent conversion). From the data of Barnett and Vaughan (2) it is estimated that only 10 per cent of the catalyst decomposed during the reaction. This is not too great a deviation from constant initiation, since the rate of decomposition of peroxide would vary by only 10 per cent from the beginning to the end of the reaction.

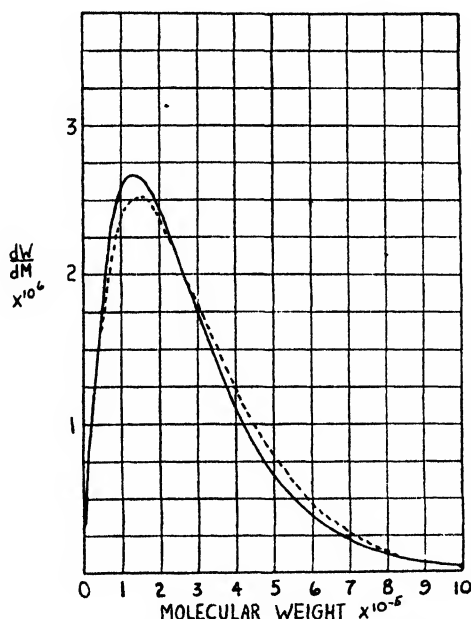


FIG. 4. Plot of distribution function *versus* molecular weight. The dashed curve is the theoretical distribution function for  $b = 0$  (equation 12)

In figure 5, the fraction of polymer of given molecular weight as obtained with the numerous fractions is compared directly with the ultracentrifugal integral molecular-weight distribution curve for the whole polymer from which the fractions were obtained. The integral distribution curve was obtained from the heavy curve in figure 4. The triangles represent the values of the integral distribution function as determined by fractionation. Number-average molecular weights were used when available, otherwise viscosity molecular weights were used. It can be seen that the highest fractions deviate somewhat from the ultracentrifugal analysis, although the agreement is good for the lower fractions. This could be explained by the presence of low-molecular-weight material in the higher fractions, in agreement with the conclusions of Scott (12), and in spite of the double precipitation. No ultracentrifugal data were obtained for them.

Because of the inordinately long time required for equilibrium, it was felt that more information would be obtained in running a greater number of experiments with material of lower molecular weight.

On comparison of the results for the fractionated samples with the ultracentrifugal analysis for the whole polymer, one is strongly tempted to conclude that the latter is the better method of obtaining a molecular-weight distribution curve. The great disadvantage of this method is that the calculations required are very time-consuming. In addition, difficulties are still being experienced in trying to determine distribution curves for some of the fractions. Apparently some higher terms in the polynomials used in solving the integral equation are important in determining the distribution function. However, whole polymers formed by chain polymerization usually have distributions such that this diffi-

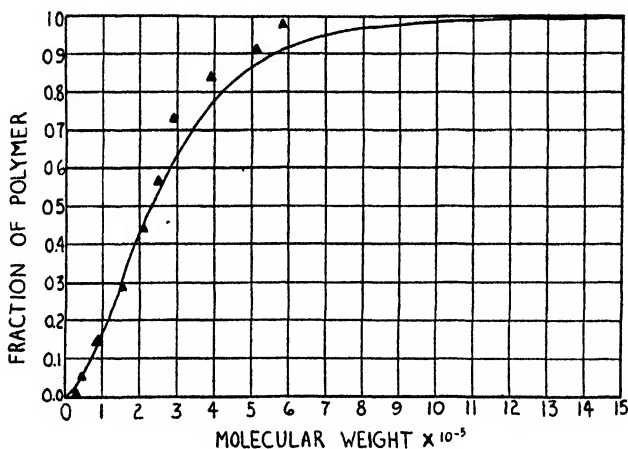


FIG. 5. Integral molecular-weight distribution function for whole polymer

culty will not be expected to occur. Thus, the application of the techniques of ultracentrifugal analysis to polymerization kinetics should be a very fruitful field for further investigation.

After obtaining the distribution curve, some measure of the "resolving power" of the instrument was desired. By this is meant a measure of the breadth of that distribution which just may be distinguished from an infinitely sharp distribution, under the present experimental conditions. For this purpose some calculations were made for an ideal system, the polymer having the distribution given by equation 12. It turns out that

$$M_{uz} = (\beta + 3) \frac{\sum_{j=1}^{\infty} \frac{1}{(K_j - Ax^2)^{\beta+4}}}{\sum_{j=1}^{\infty} \frac{1}{(K_j - Ax^2)^{\beta+3}}} \quad (14)$$

where

$$K_j = jAb^2 + (1 - j)Aa^2 + \frac{\beta + 2}{M_w}$$

The symbols have the meanings as defined above, except that  $\beta$  is used for  $b$  in equation 12 to avoid confusion with  $b$  as used for the outer end (bottom) of the sedimentation cell. From this expression it was found that  $M_{wx}$  varies by 7 per cent from one end of the cell to the other when  $\beta = 12$ ,  $M_w = 120,000$ , under the present experimental conditions (for an ideal system). The error in  $M_{wx}$  is estimated at  $\pm 3$  per cent on the basis of the uncertainty in the various quantities used in obtaining it, provided the point  $x$  is not too near the meniscus and provided the solvent is very pure. Therefore, it is estimated that it is theoretically possible to detect the degree of heterogeneity given by  $\beta = 12$ . The distribution assumed here has positive skewness. For distributions with negative skewness it will be later shown that the resolving power may be much less than this, assuming roughly equal measures of dispersion. Also, the greater the deviation of the solution from ideality, the less is the resolving power. For the whole

TABLE 5  
*Precipitation experiments with fraction 6W*

	I ORIGINAL	II SUPERNATANT 89.7 PER CENT	III PRECIPITATE 10.3 PER CENT	IV I AS CALCULATED FROM II AND III	V III REPRECIPITATED, 13 PER CENT REMOVED IN PRECIPITATE
$M_n$	90,000	90,000*	124,000†	Not justified	90,000
$M_w$	125,000	121,000	147,000	124,000	122,000
$M_z$	139,000	127,000	180,000	134,000	122,000
$M_{z+1}$	193,000	163,000	212,000	171,000	125,000
$[\eta]$	0.544				0.524

\* Osmotic pressures were actually measured for I and V; hence II should have the same value of  $M_n$ .

† Estimated from sedimentation-equilibrium data; true value is probably lower than one given.

polymer,  $M_w/M_n = 2$ , and for the fractions  $M_w/M_n = 1.2$  to 1.5. Thus, we are well within the limits of the method.

Some further experiments designed to test the reliability of the results were performed with solutions of fraction 6W. The data are tabulated in table 5. In the preparational work, the first precipitation was carried out by alternate addition of benzene and methanol to a 0.5 per cent solution until the solution was turbid at 25.0°C. and clear at 25.5°C. The precipitate was allowed to settle at 25.0°C. in a thermostat. In the second precipitation, a temperature differential of 0.2°C. was used.

The  $M_{wx}$  vs.  $\ln c_x$  curves are shown in figure 6. The three erratic points near the meniscus have been included in these curves. (cf. also figure 3). The value of  $M_w = 147,000$  is highly significant for the precipitated material (see table 5, column III), since the error in  $M_{wx}$  is estimated at  $\pm 2$  per cent. This can also be seen from the curves in figure 6. The combined value of  $M_{z+1}$  for the two portions does not agree very well with that for the original material.

For the moments of a polymer mixture in terms of its components,

$$M_n = \frac{1}{\frac{x_1}{M_{n1}} + \frac{x_2}{M_{n2}}} \quad (15)$$

$$M_w = M_{w1}x_1 + M_{w2}x_2 \quad (16)$$

$$M_z = \frac{M_{w1}M_{s1}x_1 + M_{w2}M_{s2}x_2}{M_{w1}x_1 + M_{w2}x_2} \quad (17)$$

$$M_{s+1} = \frac{M_{w1}M_{s1}M_{(s+1)1}x_1 + M_{w2}M_{s2}M_{(s+1)2}x_2}{M_{w1}M_{s1}x_1 + M_{w2}M_{s2}x_2} \quad (18)$$

where  $x$  is a weight fraction.

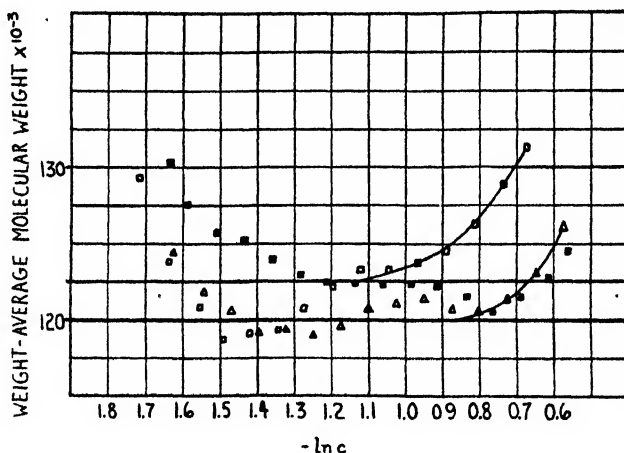


FIG. 6. Plot of  $M_{wx}$  versus  $\ln c_x$  for fraction 6W: ■, twice precipitated; □, original fraction; △, once precipitated.

One would also suspect the doubly precipitated polymer to be nearly monodisperse, judging from the ultracentrifugal data alone. But from the value of the osmotic molecular weight this is obviously not so. This anomaly may be caused by some hitherto undetected error in the sedimentation experiment, but it is believed it can be at least partially explained by the following discussion, since the data indicated perfectly normal behavior.

By inspection of the moment ratios for the original fraction, it can be seen that the size-frequency curve possesses what appears to be a positive skewness. However, for the doubly precipitated polymer, much of the portion of higher molecular weight has been removed without touching the lower portions. Very probably then, what we have here is a sample with a peak near the extreme upper end of the distribution curve. Hence the "polydisperse part" of the material (the portion of lower molecular weight) is preferentially distributed toward the meniscus, while the "monodisperse" (higher-molecular-weight) part will be

concentrated toward the bottom. This means that the moments should be closer together near the bottom of the cell than at the top. By a consideration of equation 5, together with the facts that  $M_{(q+1)z} > M_{qz}$  and all moments increase toward the bottom of the cell, this should give a curve of  $M_{wz}$  vs.  $\ln c_z$  which is convex upward. This curve should have a slope decreasing or approaching zero near the bottom of the cell. This is exactly the reverse of the behavior of a positively skewed distribution of molecular weights (*cf.* figure 3). As one goes to higher and higher moments, the change of the moment with concentration becomes less and less, and the higher moments become closer and closer together. In this experiment, also, the three points (at low  $c_z$ ) near the meniscus are known to be unreliable so that any sharp initial change here is undetectable. This sort of behavior with a negatively skewed distribution must be considered to be somewhat of a general weakness of the method. In a future article, it is planned to calculate the sort of  $M_{wz}$  vs.  $\ln c_z$  curves one obtains from polymers with various molecular-weight distribution curves, to investigate this point further, and to see

TABLE 6

*Sedimentation-equilibrium experiment with a mixture of fraction 6W and the whole polymer*

	CALCULATED	OBSERVED	DEVIATION
			<i>per cent</i>
$M_w$ . . . . .	174,000	163,000	-6
$M_z$ . . . . .	303,000	295,000	-3
$M_{z+1}$ . . . . .	575,000	370,000	-35

what can be done about relating the shape of the  $M_{wz}$  vs.  $\ln c_z$  curve to that of the molecular-weight distribution curve.

An experiment with a solution of a mixture of fraction 6W and the whole polymer was also performed. The results are tabulated in table 6.

Unfortunately, the anomalous behavior observed with impure solvent butanone was noticed to some extent here, and would account for the low values of the molecular weights for the mixture. The authors believe, however, that provided a very pure solvent can be obtained, this method should be capable of reproducing  $M_w$  values to  $\pm 3$  per cent. It can be seen that  $M_{z+1}$  is not very reliable. It is affected more than the other moments by any errors which may be present.

In conclusion, it should be stated that this method of characterization of polymers shows promise of considerable utility in polymerization and degradation studies.

#### SUMMARY

Data are presented which substantiate a theory of the equilibrium behavior of polymer solutions in a centrifugal field. It is shown that fractions obtained in the conventional manner are detectably polydisperse. A comparison is made between a molecular-weight distribution curve obtained by fractionation and

by ultracentrifugal analysis. It is suspected that the latter is the better approximation to the true distribution curve. Evidence for disproportionation as a termination mechanism in vinyl polymerizations is deduced from molecular-weight distribution data obtained here and elsewhere. Equilibrium ultracentrifuge experiments with mixed samples are in agreement with experiments on the separate components.

The authors desire to thank Dr. K. J. Arnold and Mrs. Marie Glissendorf of the Department of Mathematics, University of Wisconsin, for the performance of calculations to give the molecular-weight distribution function from the experimental data.

The assistance of Mr. Edwin M. Hanson in the construction of cells and in the maintenance of the apparatus contributed materially to the success of this investigation, and his aid is gratefully acknowledged.

This work was supported in substantial part by a grant from the Wisconsin Alumni Research Foundation.

#### REFERENCES

- (1) ALFREY, T., BARTOVICS, A., AND MARK, H.: *J. Am. Chem. Soc.* **65**, 2319 (1943).
- (2) BARNETT, B., AND VAUGHAN, W. E.: *J. Phys. Colloid Chem.* **51**, 942 (1947).
- (3) EWART, R. H., ROE, C. P., DEBYE, P., AND MCCARTNEY, J. R.: *J. Chem. Phys.* **14**, 686 (1946).
- (4) EWART, R. H., AND TINGEY, H. C.: Abstracts of papers presented at the 111th Meeting of the American Chemical Society, Atlantic City, New Jersey, April 14-18, 1947.
- (5) GEE, G., AND MELVILLE, H. W.: *Trans. Faraday Soc.* **40**, 240 (1944).
- (6) GINELL, R., AND SIMHA, R.: *J. Am. Chem. Soc.* **65**, 706 (1943).
- (7) GINELL, R., AND SIMHA, R.: *J. Am. Chem. Soc.* **65**, 715 (1943).
- (8) HERINGTON, E. F. G., AND ROBERTSON, A.: *Trans. Faraday Soc.* **38**, 490 (1942).
- (9) LANSING, W. D., AND KRAEMER, E. O.: *J. Am. Chem. Soc.* **57**, 1369 (1935).
- (10) SCHULZ, G. V.: *Z. physik. Chem.* **B43**, 25 (1939).
- (11) SCHULZ, G. V., AND HUSEMANN, E.: *Z. physik. Chem.* **B39**, 246 (1938).
- (12) SCOTT, R. L.: *J. Chem. Phys.* **13**, 178 (1945).
- (13) SVEDBERG, T., AND PEDERSON, K. O.: *The Ultracentrifuge*. University Press, Oxford (1940).
- (14) WALES, M.: *J. Phys. Colloid Chem.* **52**, 235 (1948).
- (15) WALES, M., BENDER, M. M., WILLIAMS, J. W., AND EWART, R. H.: *J. Chem. Phys.* **14** 353 (1946).



THE DENSITIES OF MAGNESIUM-CADMIUM SOLID SOLUTIONS<sup>1</sup>J. M. SINGER<sup>2</sup> AND W. E. WALLACE*Department of Chemistry, University of Pittsburgh, Pittsburgh, Pennsylvania**Received January 20, 1948*

Recently a thermochemical study of the magnesium-cadmium alloy system was begun in this Laboratory. It was evident from the outset that a considerable number of samples of alloy would be needed in the course of the investigation and that the establishment of the composition of the samples would require a substantial expenditure of time in routine chemical analysis. It occurred to us that, in view of the large difference in density of the two metals, a density-composition curve might well serve as a rapid analytical tool of sufficient precision for most of our needs.

Although it was not our original intent to make additional use of the densities reported in this communication, it became apparent later that they would be of some interest in connection with the nature and extent of the deviations of magnesium-cadmium solid solutions from ideal behavior. In view of the original intent of this study the data are neither as exhaustive nor as precise as might be desired for a really comprehensive study of these solutions. However, considering the scant information available in the literature pertaining to these solutions, it seems in order to present our results, which are in themselves fairly conclusive, for it is not our plan to extend the present experimental work.

## I. EXPERIMENTAL

The magnesium and cadmium used in preparing the alloys were obtained from the National Lead Company and the Anaconda Copper Mining Company, respectively, and were stated to be of the highest purity obtainable commercially. Spectrographic analysis of the material confirmed the absence of metallic impurities within 0.01–0.02 per cent, and gravimetric analysis of the pure materials indicated completely pure materials within the error of the determination.

The alloys were prepared in steel crucibles provided with a thin graphite lining machined from a graphite electrode of the type used in spectrographic analysis. The crucible was provided with a stirrer consisting of a steel rod tipped with graphite so that the only material coming in contact with the melt was spectroscopically pure graphite. The crucible was contained in a Pyrex tube which could be evacuated and refilled with an inert atmosphere,—in this case argon, which had been purified by condensing over activated charcoal at liquid-air temperatures. The stirrer could be operated externally by a bellows arrangement, and the melt was stirred vigorously to insure complete mixing. Melting was

<sup>1</sup> This work was supported by a basic research grant from the Office of Naval Research of the United States Navy Department, Contract N6ori 43, Task Order 2

<sup>2</sup> This paper is based upon a thesis submitted by J. M. Singer to the Faculty of the Graduate School of the University of Pittsburgh in partial fulfillment of the requirements for the degree of Master of Science, February, 1947.

accomplished by use of an induction furnace which surrounded the Pyrex tube. The samples so prepared were practically free of oxidation. Nevertheless, the surface was machined away prior to determining the densities.

After its density had been measured, the alloy was analyzed for its cadmium content by the electrodeposition method. The compositions are believed to be reliable to slightly better than 0.1 per cent.

Densities were measured using the method of Archimedes with redistilled c.p. grade carbon tetrachloride as the confining liquid. The density of the carbon tetrachloride used in these experiments was determined over the temperature range required. Differences between our results and published values were insignificant for the present purpose. The technique employed by Egerton and Lee (2) for eliminating surface tension effects on the supporting wire was used in these determinations. The precision with which duplicate determinations on the same specimen agreed was approximately 0.1 per cent. No attempt was made to measure the density at exactly 25°C. In all cases the actual temperatures were measured, and since they fell between 20°C. and 30°C., no correction was necessary.

## II. THE PHYSICAL STATE OF THE ALLOYS AND FACTORS LIMITING PRECISION OF THE DENSITIES

### *A. Cavitation*

The principal systematic error associated with measurements of density by the method of Archimedes arises from the existence of cavities within a sample which appears upon external examination to be sound. It is possible that our samples were imperfect in this respect, but it is felt that the error due to cavities is small and is probably overshadowed by possible effects of varying degrees of order in the alloys. The influence of the latter will be referred to below. The case against appreciable cavitation is based upon two lines of evidence.

First, we have compared our results with those calculated from the lattice parameters obtained from x-ray diffraction studies. Hume-Rothery and Raynor (4, 9) have made an extremely careful investigation of this system. Unfortunately, much of the work was at an elevated temperature (310°C.) and in the absence of reliable thermal expansion data is not suitable for comparison with the results of this study. However, some of the data are of use and the results, together with the value for pure cadmium calculated from the data of Jette and Foote (6), are shown in table 1. Since densities computed from lattice parameters are unaffected by the presence of cavities in the alloys subjected to diffraction study, the existence of cavities in our alloys should be revealed by consistently smaller densities.<sup>3</sup> The lack of such differences can be taken as evidence against cavitation.

<sup>3</sup> The pure metals as obtained from the source were unsound. Cavities were observed as the material was machined prior to preparing alloys. Also, the densities were low. Upon remelting, stirring, and in all ways handling the material as if it were an alloy, the density increased to the value given in table 1.

Second, Stockdale (12) has shown in a very careful study of the densities of alloys of silver and zinc that certain otherwise unexplained variations in density can be attributed to cavitation and the sample can be made sound and the densities reproducible by subjecting the specimens to pressure of the order of 10,000 atm. Although our densities were quite reproducible and gave a smooth curve when plotted against composition, we thought it advisable to test for possible cavitation by a procedure similar to that of Stockdale. After subjecting eight samples covering the entire composition range to approximately 10,000 atm. pressure, the densities were remeasured and found to have increased on the average 0.11 per cent. The maximum increase noted was 0.25 per cent. It may be concluded, therefore, that if the alloys were unsound, the extent must have been small, probably insufficient to affect the density by more than 0.2–0.3 per cent. Possibly, those density increments are due to ordering of the alloy rather than to a filling in of cavities, since ordered structures are more dense (3).

TABLE 1  
*Comparison of measured densities with densities computed from x-ray data*

COMPOSITION: ATOMIC PER CENT CADMIUM	DENSITY (MEASURED)	DENSITY (CALCULATED)
	<i>g./cc.</i>	<i>g./cc.</i>
0	1.737	1.7367
6.65	2.192	2.187
17.02	2.902	2.908
100	8.642	8.644

### *B. Non-homogeneity of the solid solutions*

The mutual solid solubility of magnesium and cadmium has been established to be very extensive, if not complete (3, 4, 5). It is well known that the cooling of melts of substances exhibiting appreciable solid solubility produces non-homogeneous solid phases because of the initial preferential crystallizing out of the higher melting component. Homogeneous solid solutions are obtained by subsequent annealing at temperatures close to the melting point. In connection with other phases of the work with this system we were interested in both homogeneous and non-homogeneous samples, so that we have measured densities of some of the alloys in the annealed and unannealed state. As we shall indicate below, the effect of annealing on the density is practically negligible.

### *C. Order-disorder transformation*

Perhaps the least satisfactory feature of this work was our ignorance of the extent to which the order-disorder transformation in the alloys had taken place. It is our opinion that the densities reported refer to the almost completely disordered alloy. We base this opinion upon the detailed studies of the order-disorder transformation made by Grube and Schiedt (3) at Stuttgart and by Stepanov and coworkers (7, 8, 10, 11) at Leningrad.

Transformations based upon the compositions  $\text{Mg}_3\text{Cd}$ ,  $\text{MgCd}$ , and  $\text{MgCd}_3$  occur at the approximate temperatures  $150^\circ$ ,  $250^\circ$ , and  $90^\circ\text{C}$ ., respectively. The rate studies of Stepanov indicate that, except for compositions in the region of  $\text{MgCd}_3$ , the ordered structure is formed rather slowly, if at all, at room temperature. Special low-temperature annealing ( $100$ – $200^\circ\text{C}$ .) was required to develop the superlattice. However, for compositions between 72 and 78 atomic per cent cadmium, ordering was observed to proceed with an appreciable rate at  $0^\circ\text{C}$ . (8).

The thermal treatment given our alloys was such as to suppress superlattice formation. They were brought immediately from the temperature of solidification or annealing to room temperature and the density determined within a few hours. The single alloy (72.37 atomic per cent cadmium) which might have become appreciably ordered fell on the smooth curve of density *versus* composition.<sup>4</sup>

TABLE 2  
*Densities of magnesium-cadmium alloys*

COMPOSITION: ATOMIC PER CENT CADMIUM	DENSITY	COMPOSITION: ATOMIC PER CENT CADMIUM	DENSITY
	<i>g./cc.</i>		<i>g./cc.</i>
0	1.737	66.57	6.485
6.65	2.192	69.19	6.591
17.02	2.902	72.37	6.800
35.38	4.248	87.80	7.727
39.43	4.511	90.67	7.905
52.87	5.518	96.32	8.300
60.36	6.048	100	8.642
63.24	6.270		

Calculations based upon the thermal expansion data determined by Grube and Schiedt (3) indicate that the order-disorder transformation may be accompanied by changes in the density amounting to as much as 0.5 per cent in some instances. The uncertainties in the densities due to an undetermined extent of ordering probably do not amount to more than 0.2–0.3 per cent. However, the actual effect is difficult to assess exactly and this factor would undoubtedly prevent one from ascertaining densities for this system to better than 0.1 per cent unless the degree of order were controlled.

### III. EXPERIMENTAL DATA AND DISCUSSION OF RESULTS

The measured densities are given in tables 2 and 3. The results given in table 2 are presented in graphical form in figure 1. Values at rounded concentrations taken from a large-scale plot of the data in table 2 are shown in table 4. In table 3 the effect of annealing is summarized. Annealing was carried out for periods of 3–4 weeks at temperatures within  $50^\circ$  of the melting point of the particular alloy

<sup>4</sup> It may be that the non-homogeneity of this sample retarded formation of the superlattice.

TABLE 3

*Effect of annealing on the densities*

COMPOSITION: ATOMIC PER CENT CADMIUM	DENSITY (UNANNEALED)	DENSITY (ANNEALED)	CHANGE
	<i>g./cc.</i>	<i>g./cc.</i>	<i>per cent</i>
21.7	3.251	3.245	-0.2
35.4	4.252	4.251	0.0
38.25	4.450	4.450	0.0
56.0	5.749	5.752	+0.1
57.1	5.840	5.827	-0.2
73.1	6.856	6.859	0.0
84.0	7.555	7.558	0.0

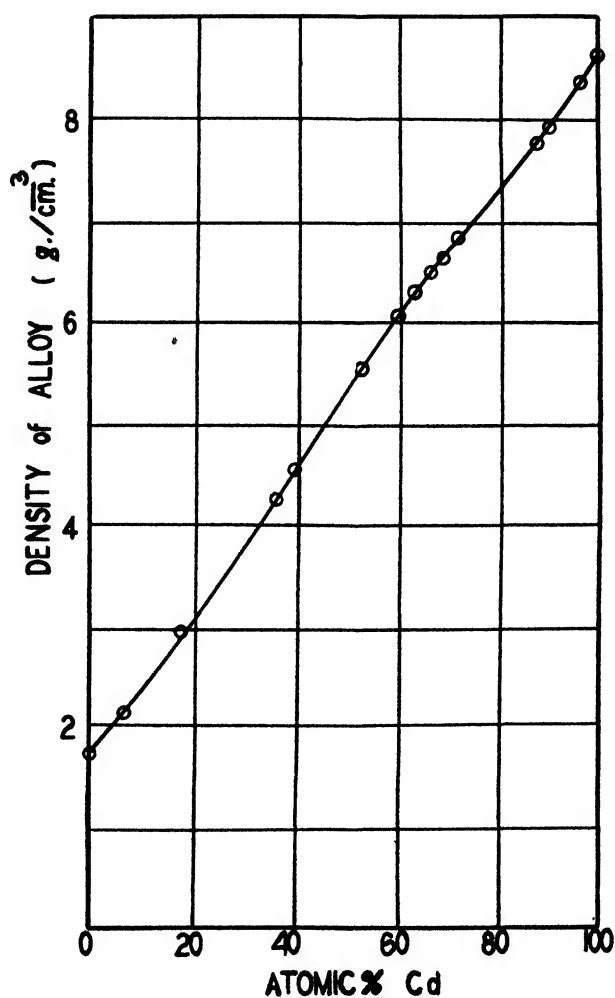


FIG. 1. Graph showing the variation of density with composition for magnesium-cadmium alloys (solid solutions).

after the samples had been sealed into evacuated Pyrex tubes. The effect of annealing on the densities is seen to be practically negligible.

TABLE 4  
*Densities of magnesium-cadmium alloys at rounded concentrations*

COMPOSITION: ATOMIC PER CENT CADMIUM	DENSITY	COMPOSITION: ATOMIC PER CENT CADMIUM	DENSITY
	<i>g./cc.</i>		<i>g./cc.</i>
0	1.737	60	6.035
10	2.418	70	6.670
20	3.127	80	7.250
30	3.856	90	7.850
40	4.577	100	8.642
50	5.312		

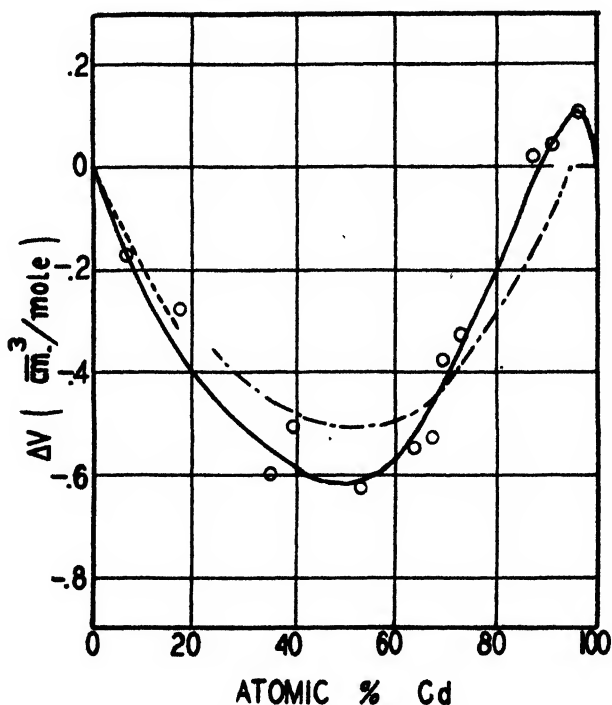


FIG. 2. Graph showing the volume change accompanying the formation of 1 mole of alloy (solid solution) as a function of composition. O, calculated from the data in table 2; ---, calculated from Raynor's x-ray data at 25°C.; - · -, calculated from Hume-Rothery and Raynor's x-ray data at 310°C.

The curvature in the density-composition curve apparent in figure 1 is probably real, since it is in general accord with other thermodynamic information available for this system. If the solutions were ideal, the density-composition curve would be concave upward for the entire composition range. Biltz and

Hohorst (1) determined the heat of formation of an alloy of composition MgCd and demonstrated that for this composition the solid solution exhibited a strong negative deviation from ideal behavior. Such deviations would modify the ideal density curve and, if sufficiently pronounced, lead to the two points of inflection apparent in figure 1.

Volume changes accompanying the formation of the alloy from its components are shown in figure 2. The negative values were more or less expected, as they are consistent with the general chemical tendencies which lead to the formation of ordered structures. The positive deviations at high cadmium concentrations were not anticipated and may possibly be attributed to unsuspected systematic errors in the densities of 0.4–0.6 per cent, although these errors are somewhat larger than had been assigned to the measurements. Included in figure 2 are values of the volume changes computed from the x-ray data of Raynor (9) at 25°C. and Hume-Rothery and Raynor (4) at 310°C. The general similarity of the three curves is evident.

There seems little doubt that alloys of compositions 0–80 atomic per cent cadmium are formed from their components with a decrease in volume. The increments in volume noted at high cadmium concentrations perhaps should not be regarded as definitely established. It is perhaps worth pointing out in this connection, however, that the x-ray data at 310°C. indicate a behavior at the cadmium end unlike that in solutions less rich in cadmium. Conceivably, the region of zero slope at 310°C. might be modified in the direction of positive deviations as the temperature is lowered.

Returning to the question of using the density–composition curve as an analytical tool, by examination of the slope of the curve one finds that a density precise to 0.3 per cent will establish composition to 0.36 unit on the atomic per cent scale in the region of pure cadmium and 0.09 unit at the magnesium end, if the curve is assumed to be exact. Allowing for lack of precision in both the curve and the density measurement, it seems that one could definitely establish composition within limits of 0.5 unit on the atomic per cent scale for all cases and within narrower limits, perhaps 0.1–0.2 unit, for magnesium-rich alloys. This method is obviously inferior in precision to conventional chemical analysis but has a distinct advantage in the time required for cases where high precision is not essential.

#### IV. SUMMARY

The densities of thirteen unannealed magnesium–cadmium alloys, ranging in composition from 6.65 to 96.32 atomic per cent cadmium, have been determined with an estimated precision of 0.1 per cent. The densities of seven additional alloys, ranging in composition from 21.7 to 84.0 atomic per cent cadmium, have been determined before and after annealing. The influence of annealing on the density is practically negligible in comparison with the stated precision of the measurements.

Computations of volume changes accompanying formation of the alloys show that between 0 and 85 atomic per cent cadmium there is an appreciable decrease in volume. Above 85 per cent slight increments in volume are observed.

The effectiveness of the density-composition curve as an analytical tool is sufficient to establish composition to about 0.5 unit or better on the atomic per cent scale.

#### REFERENCES

- (1) BILTZ, W., AND HOHORST, G.: *Z. anorg. allgem. Chem.* **127**, 1 (1923).
- (2) EGERTON, A. C., AND LEE, W. B.: *Proc. Roy. Soc. (London)* **A103**, 487 (1923).
- (3) GRUBE, G., AND SCHIEDT, E.: *Z. anorg. allgem. Chem.* **194**, 190 (1930).
- (4) HUME-ROTHERY, W., AND RAYNOR, G. V.: *Proc. Roy. Soc. (London)* **A174**, 471 (1940).
- (5) HUME-ROTHERY, W., AND ROWELL, S. W.: *J. Inst. Metals* **33**, 137 (1927).
- (6) JETTE, E. R., AND FOOTE, F.: *J. Chem. Phys.* **3**, 605 (1935).
- (7) KORNILOV, I. I.: *Bull. acad. sci. U.R.S.S., Classe sci. math. nat., Ser. chim.* **1937**, 313.
- (8) KORNILOV, I. I.: *Compt. rend. acad. sci. U.R.S.S.* **19**, 157 (1938).
- (9) RAYNOR, G. V.: *Proc. Roy. Soc. (London)* **A174**, 457 (1940).
- (10) STEPANOV, N. I., AND BULACH, S. A.: *Compt. rend. acad. sci. U.R.S.S. [N.S.]* **4**, 147 (1935).
- (11) STEPANOV, N. I., AND KORNILOV, I. I.: *Ann. secteur anal. phys.-chim., Inst. chim. gén. (U.S.S.R.)* **10**, 78, 97 (1938).
- (12) STOCKDALE, D.: *J. Inst. Metals* **66**, 287 (1940).

#### THE DISTRIBUTION OF THORIUM NITRATE BETWEEN WATER AND CERTAIN ALCOHOLS AND KETONES

B. F. ROTHSCILD, C. C. TEMPLETON, AND NORRIS F. HALL

*Department of Chemistry, University of Wisconsin, Madison, Wisconsin*

*Received January 26, 1948*

In continuation of studies on the solvent extraction of thorium started by two of us (6), we have determined the distribution of thorium nitrate at room temperature between water and each of the following solvents: isoamyl alcohol, *n*-hexyl alcohol, methyl isobutyl ketone, methyl *n*-amyl ketone, and methyl *n*-hexyl ketone. These five organic solvents appear to be the most promising for the liquid-liquid extraction of thorium nitrate from aqueous solutions also containing the nitrates of the rare earths and zirconium. The effect of added nitric acid has been ascertained on the systems containing *n*-hexyl alcohol and methyl *n*-hexyl ketone. Some preliminary extractions with methyl *n*-hexyl ketone have been described to show the applicability of the conclusions drawn from these distribution data.

#### DETERMINATION OF DISTRIBUTION DATA

The experimental technique was that used in the earlier solubility work (6). Each system was composed of 5 ml. of the organic solvent (Eastman Kodak Company, practical grade) and 5 ml. of an aqueous phase brought to the proper



concentration by the dilution of a saturated aqueous thorium nitrate solution. The test tube containing this system was agitated end over end at 30 R.P.M. for 24 hr. The phases were then separated, and each was analyzed by direct ignition to thorium dioxide. The primary data (the percentages of thorium dioxide in each of the phases) are recorded in table 1, with other quantities calculated therefrom. Two sets of experiments were made on methyl *n*-hexyl ketone, one at room temperature, the other thermostated at  $25^{\circ}\text{C.} \pm 0.05^{\circ}$ . Since the two sets of data were indistinguishable when plotted on the same graph (figure 1), thermostating was abandoned for later runs. That the change with temperature is negligible with respect to the analytical errors is consistent with other data. We have previously shown that the change of the solubility of  $\text{Th}(\text{NO}_3)_4 \cdot 4\text{H}_2\text{O}$  with temperature in these solvents is no greater than the experimental error (6). Seidell (4) quotes Misciattelli (3) to the effect that the solubility of thorium nitrate in water (from separate sets of data) is:

TEMPERATURE °C.	Th(NO <sub>3</sub> ) <sub>4</sub> PER 100 G. OF SOLUTION	
	grams	grams
0	65.0	65.2
20	65.0	65.6

The heat effect of the nitrate on passing from one solvent to the other is the difference between the two very small heats of solution corresponding to these two small temperature changes ( $d \ln K/dT = \Delta H/RT^2$ ). Consequently the change in composition of the system with temperature corresponding to the partition heat effect should be less than those shown by the simple solubilities.

Data on the effect of increased nitric acid concentration on these distribution equilibria were desired, inasmuch as nitric acid will probably be present in most aqueous nitrate solutions. The effect was correlated with the quantity of nitric acid added to the aqueous phase before mixing. Thus the aqueous phases, later mixed with methyl *n*-hexyl ketone, were made 0.5 *N*, 1.0 *N*, and 5.0 *N* in added nitric acid, respectively, for three sets of data, by the use of standardized acid solutions in mixing. Two runs were made with *n*-hexyl alcohol in which the aqueous phases were 1.0 *N* and 5.0 *N*, respectively, in added nitric acid. These systems were agitated and analyzed in the same manner as the unacidified systems. Mole fractions of thorium nitrate were calculated on the approximation that each phase contained besides thorium nitrate only its respective solvent. The results are listed in tables 2 and 3.

All the above analyses were made as quickly as possible to avoid the effects of chemical changes. Some measurements were made on the acidified systems after long periods of standing, and marked changes were noted. Coincident with these changes, gas evolution was observed similar to that noted in the previous solubility work (6). This probably resulted from oxidation of the organic solvents by the nitric acid.

TABLE 1

*The compositions of thorium nitrate-water-solvent systems*

SAMPLE NO.	PERCENTAGE OF ThO <sub>2</sub>		CALCULATED MOLE FRACTIONS		
	Solvent phase	Aqueous phase	$s^X_{\text{Th}(\text{NO}_3)_4}$ Solvent phase	$w^X_{\text{Th}(\text{NO}_3)_4}$ Aqueous phase	$s^X_{\text{Th}(\text{NO}_3)_4}$ Solvent phase

Methyl <i>n</i> -hexyl ketone (unthermostated)					
1.....	9.82	32.40	0.05497	0.05738	0.008217
2.....	6.39	31.25	0.03391	0.04948	0.005145 (a)
3.....	2.75	29.40	0.01372	0.04308	0.001998 (b)
4.....	1.67	28.80	0.00827	0.04125	0.001190
5.....	0.91	27.70	0.00516	0.03807	0.000643
6.....	0.65	26.95	0.00318	0.03605	0.000456
7.....	0.37	26.01	0.00197	0.03341	0.000282
8.....	0.18	24.38	0.00088	0.02987	0.000125 (c)
9.....	0.13	23.66	0.00062	0.02832	0.000089 (d)

Methyl <i>n</i> -hexyl ketone (25°C. $\pm 0.05^\circ$ )					
1T.....	9.40	32.50	0.05335	0.05417	
2T.....	6.18	31.31	0.03266	0.04958	
3T.....	2.54	29.41	0.01308	0.04342	
4T.....	1.70	28.68	0.00843	0.04089	
5T.....	0.83	27.54	0.00513	0.03763	
6T.....	0.53	26.74	0.00258	0.03550	
7T.....	0.34	25.87	0.00165	0.03332	
8T.....	0.17	24.78	0.00083	0.03077	
9T.....	0.08	23.61	0.00031	0.02826	

Methyl <i>n</i> -amyl ketone					
43.....	12.65	31.99	0.06632	0.05214	0.01005
44.....	8.85	30.59	0.04362	0.04701	0.006473 (a)
45.....	4.48	28.92	0.02062	0.04161	0.002999 (b)
46.....	2.31	27.58	0.01035	0.03772	0.001492
47.....	1.15	26.31	0.00507	0.03440	0.000728 (c)
48.....	0.58	24.77	0.00254	0.03074	0.000364 (d)

Methyl isobutyl ketone					
16.....	14.07	31.12	0.06688	0.04887	0.01013
17.....	10.21	29.70	0.04536	0.04403	0.006740 (a)
18.....	5.99	28.42	0.02487	0.04011	0.003630 (b)
19.....	2.98	27.14	0.01180	0.03655	0.001702
20.....	2.06	26.52	0.00806	0.03494	0.001159 (c)
21.....	1.15	25.55	0.00443	0.03254	0.000635 (d)

TABLE 1—Continued

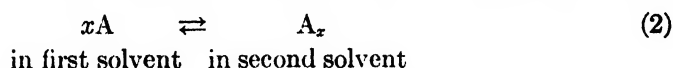
SAMPLE NO.	PERCENTAGE OF ThO <sub>2</sub>		CALCULATED MOLE FRACTIONS		
	Solvent phase	Aqueous phase	$s^X \text{Th}(\text{NO}_3)_4$ Solvent phase	$w^X \text{Th}(\text{NO}_3)_4$ Aqueous phase	$s^Y [\text{Th}(\text{NO}_3)_4]_2$ Solvent phase
Isoamyl alcohol					
28 . . . . .	13.97	31.21	0.05883	0.04922	
29 . . . . .	10.87	29.65	0.04328	0.04389	
30 . . . . .	7.46	27.83	0.02799	0.03841	
31 . . . . .	5.62	26.88	0.02049	0.03586	
32 . . . . .	3.60	25.54	0.01272	0.03253	
33 . . . . .	2.31	24.13	0.00799	0.02934	
<i>n</i> -Hexyl alcohol					
49 . . . . .	13.78	32.06	0.06640	0.05244	
50 . . . . .	11.17	30.04	0.05144	0.04649	
51 . . . . .	7.82	28.69	0.03405	0.04092	
52 . . . . .	4.53	26.95	0.01873	0.03604	
53 . . . . .	2.91	25.69	0.01172	0.03365	
54 . . . . .	1.69	24.16	0.00654	0.02940	

## DISCUSSION OF DISTRIBUTION DATA

If a solute A exists as A in one solvent and in another state of aggregation, A<sub>x</sub>, in a second solvent, thermodynamics (1) requires that the distribution of A between the two be governed by a relation of the type:

$$\frac{X_{A_x} \text{ in second solvent}}{X_A^x \text{ in first solvent}} = K \quad (1)$$

where X denotes mole fraction and K is the equilibrium constant for the reaction:



These relations apply exactly, of course, only to solutions which are dilute enough for the chemical potential to be expressible as a logarithmic function of the mole fraction.

Ignoring for the moment the ionization of the solute and setting A equal to Th(NO<sub>3</sub>)<sub>4</sub>, the first solvent to be water, and the second to be the organic solvent, we have

$$\frac{sX_{[\text{Th}(\text{NO}_3)_4]_2}}{aqX^x_{\text{Th}(\text{NO}_3)_4}} = K \quad (3)$$

where the subscripts "s" and "aq" denote the organic and aqueous phases, respectively. Since x is not initially known, this expression must be modified. However,

$$sX_{\text{Th}(\text{NO}_3)_4} \simeq x \cdot sX_{[\text{Th}(\text{NO}_3)_4]_2} \quad (4)$$

quite closely for dilute solutions.

TABLE 2

*Effect of the addition of nitric acid to water-thorium nitrate-methyl n-hexyl ketone systems*

SAMPLE NO.	PERCENTAGE OF ThO <sub>2</sub>		CALCULATED MOLE FRACTIONS	
	Ketone phase	Aqueous phase	$k X_{\text{Th}(\text{NO}_3)_4}$ Ketone phase	$w X_{\text{Th}(\text{NO}_3)_4}$ Aqueous phase
0.5 N in added nitric acid				
37.....	10.34	31.97	0.05820	0.05206
38.....	8.02	31.08	0.04357	0.04875
39.....	5.65	30.16	0.02967	0.04553
40.....	3.36	29.03	0.01710	0.04194
41.....	1.90	27.86	0.01066	0.03832
42.....	0.90	25.64	0.00430	0.03277
1.0 N in added nitric acid				
10.....	5.68	30.15	0.02984	0.04551
11.....	4.03	28.87	0.02069	0.04141
12.....	2.70	27.89	0.01359	0.03861
13.....	1.65	26.74	0.00818	0.03550
14.....	0.91	25.67	0.00446	0.03281
15.....	0.55	24.48	0.00269	0.03010
1.0 N after 28 days of standing				
11*.....	2.49	29.17	0.01252	0.04236
12*.....	1.51	28.15	0.00748	0.03933
13*.....	0.39	26.85	0.00192	0.03579
14*.....	0.93	25.40	0.00457	0.03218
5.0 N in added nitric acid				
36.....	7.88	30.23	0.04273	0.04579
34.....	3.51	29.44	0.01785	0.04321
22.....	2.34	28.10	0.01174	0.03827
23.....	1.80	27.14	0.00887	0.03654
24.....	0.38	26.18	0.00186	0.03432
24.....	4.82	25.95	0.02497	0.03352
25.....	1.16	25.86	0.00573	0.03329
26.....	0.63	23.73	0.00306	0.02847
27.....	0.34	22.53	0.00165	0.02602
5.0 N after 14 days of standing				
22*.....	0.12	30.65	0.00056	0.04722
23*.....	0.15	27.38	0.00074	0.03720
25*.....	0.04	25.68	0.00017	0.03286
26*.....	0.01	24.18	0.00006	0.02940

Substitution in equation 3 yields

$$\frac{X_{\text{Th}(\text{NO}_3)_4}}{X_{\text{Th}(\text{NO}_3)_4}^2} = xK = K' \quad (5)$$

since  $x$ , though unknown, is a constant. Thus the expression of the results on the basis of the simple thorium content does not appreciably change the value of the exponent  $x$ . Since

$$\log {}_sX_{\text{Th}(\text{NO}_3)_4} = \log K' + x \log {}_{\text{aq}}X_{\text{Th}(\text{NO}_3)_4} \quad (6)$$

the plotting of  $\log {}_sX_{\text{Th}(\text{NO}_3)_4}$  against  $\log {}_{\text{aq}}X_{\text{Th}(\text{NO}_3)_4}$  should yield a straight line of slope  $x$ . This was done for all the distribution data. Figure 1 is for the ketones, and figure 2 for the alcohols. The ketones are seen to show more family regularity than the alcohols, but all the curves are seen to be essentially linear save for the concentrated end.

TABLE 3

*Effect of the addition of nitric acid to water-thorium nitrate-*n*-hexyl alcohol systems*

SAMPLE NO.	PERCENTAGE OF $\text{ThO}_2$		CALCULATED MOLE FRACTIONS	
	Alcohol phase	Aqueous phase	${}_aX_{\text{Th}(\text{NO}_3)_4}$ Alcohol phase	${}_wX_{\text{Th}(\text{NO}_3)_4}$ Aqueous phase
1.0 N in added nitric acid				
55	10.37	29.87	0.04712	0.04468
56	8.58	28.77	0.03782	0.04116
57	6.79	27.68	0.02910	0.03802
58	5.48	26.76	0.02302	0.03553
59	4.40	26.05	0.01817	0.03376
60	3.29	25.16	0.01335	0.03163
5.0 N in added nitric acid				
61	8.20	27.53	0.03593	0.03759
62	6.76	26.74	0.02896	0.03550
63	6.65	25.97	0.02841	0.03341
64	4.74	25.07	0.01966	0.03215
65	2.36	23.95	0.00944	0.02894
66	1.81	22.53	0.00720	0.02603

Trial calculations showed that in this case more consistent values of  $x$  and  $K'$  could be obtained graphically from the curves than by averaging the values calculated from pairs of points of the original data. For each curve, two points from the extreme ends of the linear portion were read off, and the simultaneous solution of the two equations of type 6 yielded the values of  $x$  and  $K'$  given in table 4.

For the ketones an attempt was made to improve the expressions by recalculating the data as  ${}_sX_{[\text{Th}(\text{NO}_3)_4]_7}$ . These results are listed in the last column of table 1. Values of  $x$  were calculated directly from pairs of points with two equations of type 6. The points used are lettered in parentheses in table 1 and the pairs used are indicated in table 5. The data were also plotted on a log-log scale (not reproduced here), and the  $x$  values were also determined graphically.

The calculated values show a wide spread. The graphical values show a trend

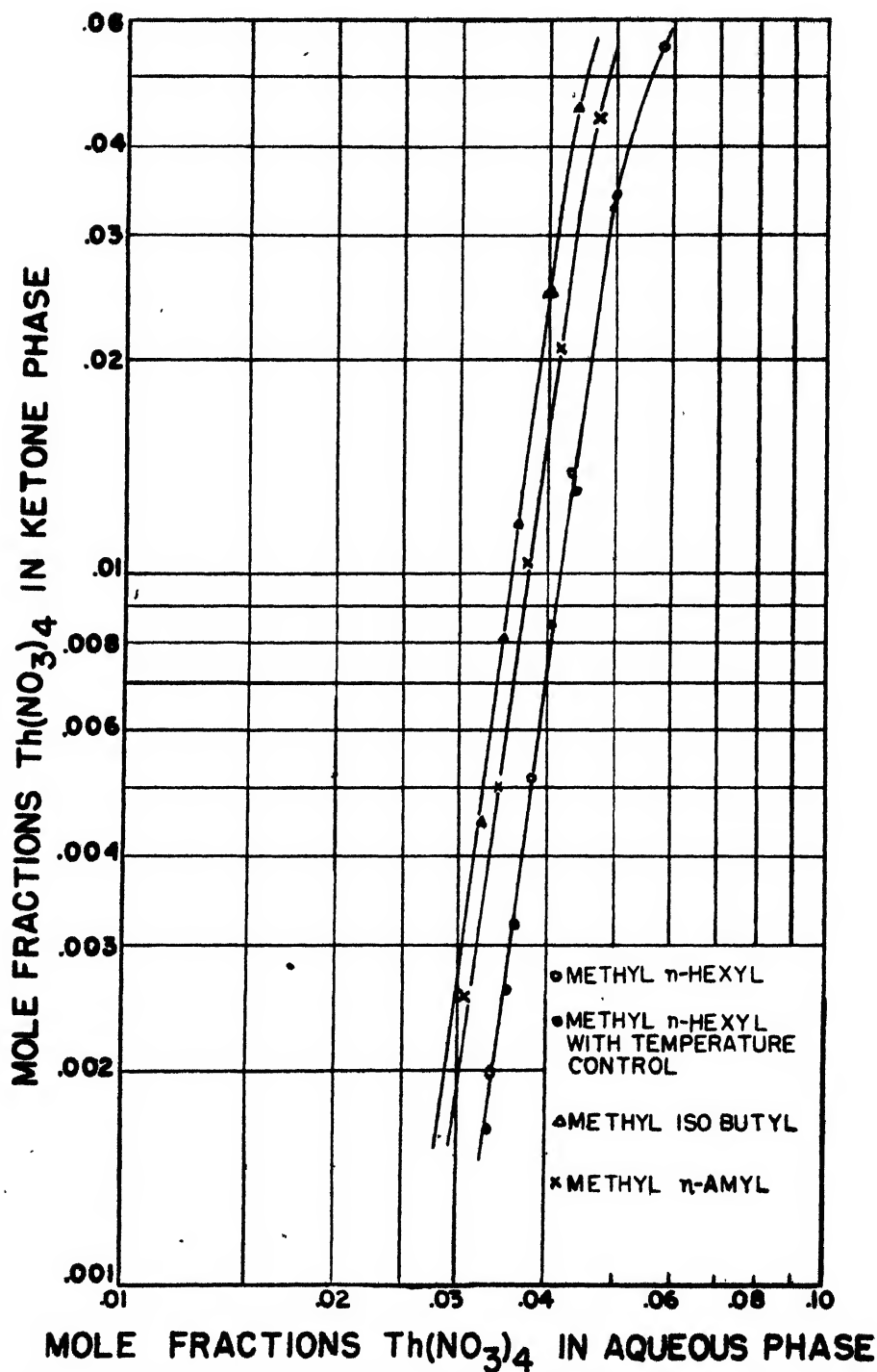


FIG. 1. Distribution of thorium nitrate between water and various methyl ketones

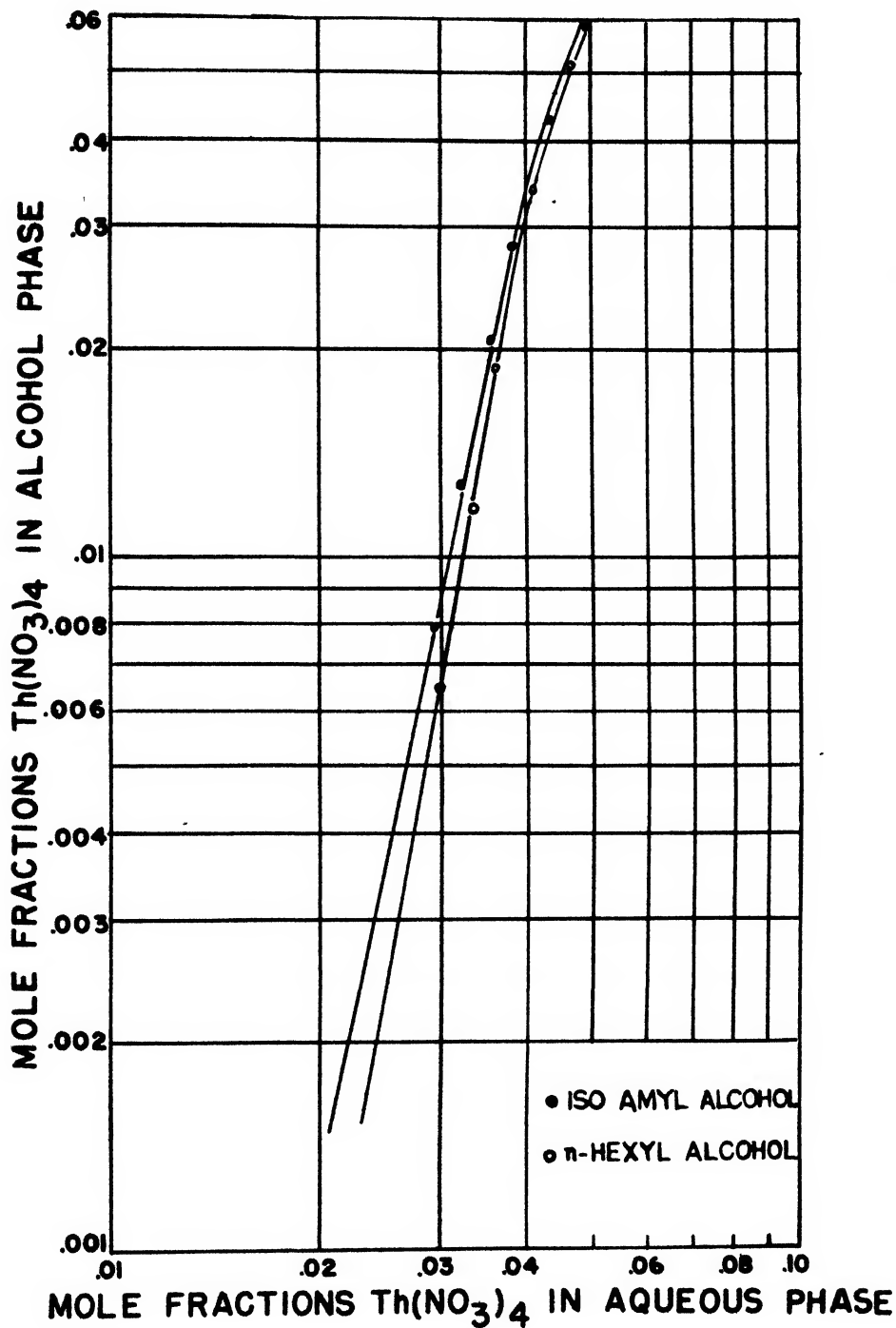


FIG. 2. Distribution of thorium nitrate between water and various alcohols

of  $x$  toward an integral value of 7, but the accuracy of the method is not great. These results persuaded us to present the expressions in their original empirical form for their practical value in predicting the behavior of experimental systems, and to defer further theoretical treatment of the data until more evidence is gathered on the state of aggregation of thorium nitrate in the ketone solutions. Our treatment so far has included no water or ketone components in the aggregation. That water might be so included seems plausible from the fact that while water is "insoluble" in methyl *n*-hexyl ketone, thorium nitrate tetrahydrate dissolves in this ketone to form a single phase containing about 4.7 per cent

TABLE 4  
*Values of  $x$  and  $K'$  for unacidified systems*

SOLVENT	$K'$	$x$
Methyl <i>n</i> -hexyl ketone	129 $\times 10^6$	7.34
Methyl <i>n</i> -amyl ketone	224 $\times 10^6$	7.28
Methyl isobutyl ketone	490 $\times 10^6$	7.40
<i>n</i> -Hexyl alcohol	2.08 $\times 10^8$	5.58
Isoamyl alcohol	0.162 $\times 10^8$	4.77

TABLE 5  
*Values of  $x$  for ketones from second calculation attempt*

	METHYL ISOBUTYL	METHYL <i>n</i> -AMYL	METHYL <i>n</i> -HEXYL
Calculated:			
Points a-d	7.60	6.76	7.40
Points a-c	7.80	7.00	7.26
Points b-d	8.30	6.96	7.36
Points b-c	8.35	7.43	7.41
Average	8.01	7.04	7.40
Graphical	7.0	7.1	7.3

water (6). Further,  $\text{Th}(\text{NO}_3)_4$  has been treated as a unit with no mention of ionization. It should be possible to get further information on the molecular weight of this complex by investigation of some colligative property of the solution, such as the freezing-point depression or electrical conductivity. In view of these complications, the present data are not evidence that thorium nitrate is actually polymerized in ketone solution, although we have used this idea to suggest the form of the empirical distribution expression.

In preliminary liquid-liquid extraction runs with methyl *n*-hexyl ketone it has sometimes been necessary to add nitric acid to prevent the formation of emulsions. The data of table 2 on the addition of nitric acid to methyl *n*-hexyl ketone systems are plotted in figure 3 for the 1.0 *N* and 5.0 *N* cases. The 0.5 *N*



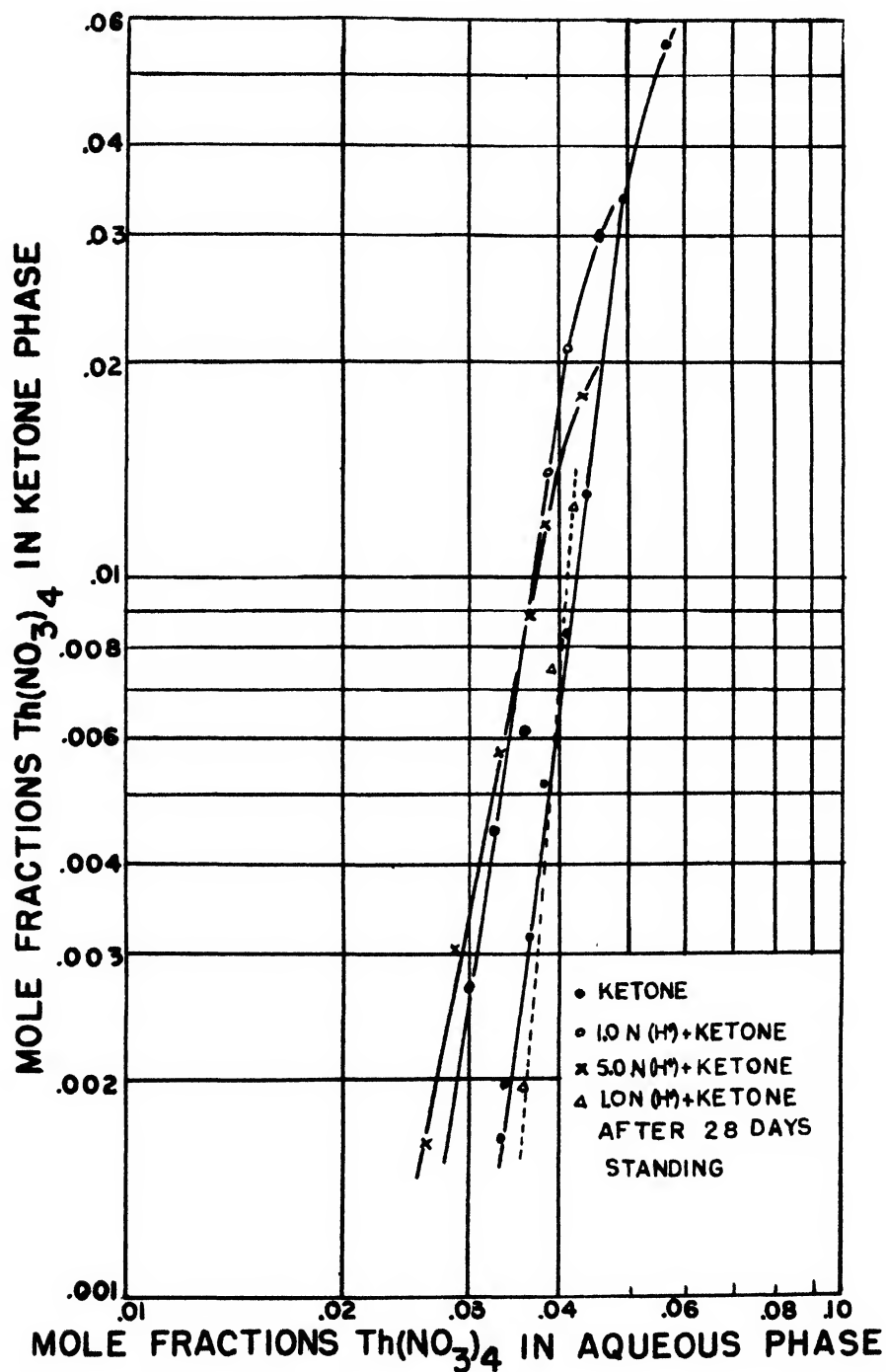


FIG. 3. Effect of acidity on the distribution of thorium nitrate between water and methyl *n*-hexyl ketone.

data, if plotted, would fall slightly below and parallel to the 1.0 *N* curve. In all these cases the acid has caused more thorium to enter the ketone phase. Also plotted are the 1.0 *N* data after 28 days of standing, in which case the trend has reversed. Thus the nitric acid aids in the ketone extraction of thorium nitrate from aqueous solution up to the point at which the acid begins to react with the ketone.

Figure 4 is the plot of the data of table 3 for acidified *n*-hexyl alcohol systems. Again, the addition of nitric acid has caused more thorium nitrate to pass into the organic solvent.

The distribution expressions themselves imply two considerations of fundamental importance in the extraction of thorium nitrate from aqueous solution with any of these solvents: (1) The concentration of thorium nitrate in the aqueous phase must be very near to saturation for any appreciable portion of the thorium to be extracted. (2) When even a concentrated ketone or alcohol solution of thorium nitrate is washed with pure water for a sufficient time for equilibrium to be reached, the thorium passes into the aqueous phase almost quantitatively.

Both of these statements may be verified by inspection of the data in table 1. The first presents a problem in that a means must be found to keep the aqueous phase very concentrated, without having solids present. The second, however, completely and easily solves the problem of the removal of the extracted thorium from the organic solvent. This is extremely fortunate, since distillation or other use of heat to accomplish this would destroy an appreciable portion of the solvent in each cycle. Leaching of solid nitrates with these solvents becomes a very simple process, because the extracted thorium may be washed out, and the solvent immediately recycled.

#### PRELIMINARY EXTRACTIONS

Although the thorough investigation of the usefulness of these solvents for the extraction of thorium is a project requiring extensive work, sufficient facts are presented here to demonstrate the applicability of the distribution data. Two types of extraction schemes are possible: leaching with an organic solvent, and liquid-liquid extraction of an aqueous solution with an organic solvent. Leaching is simpler, but attains its maximum enrichment in a single step. Thus it is particularly applicable to the initial enrichment of material low in thorium. Liquid-liquid extraction is capable of multistage fractionation, and therefore would seem to be of more value for the final purification of material fairly rich in thorium. However, liquid-liquid extraction with these solvents involves many more problems of manipulation than does leaching.

The separation of thorium from mixtures also containing the rare earths, zirconium, the alkalis, and the alkaline earths was chosen for the initial work because these metals often occur together in monazite (2). C.P. thorium, zirconyl, calcium, and potassium nitrates were used for the mixtures. The rare

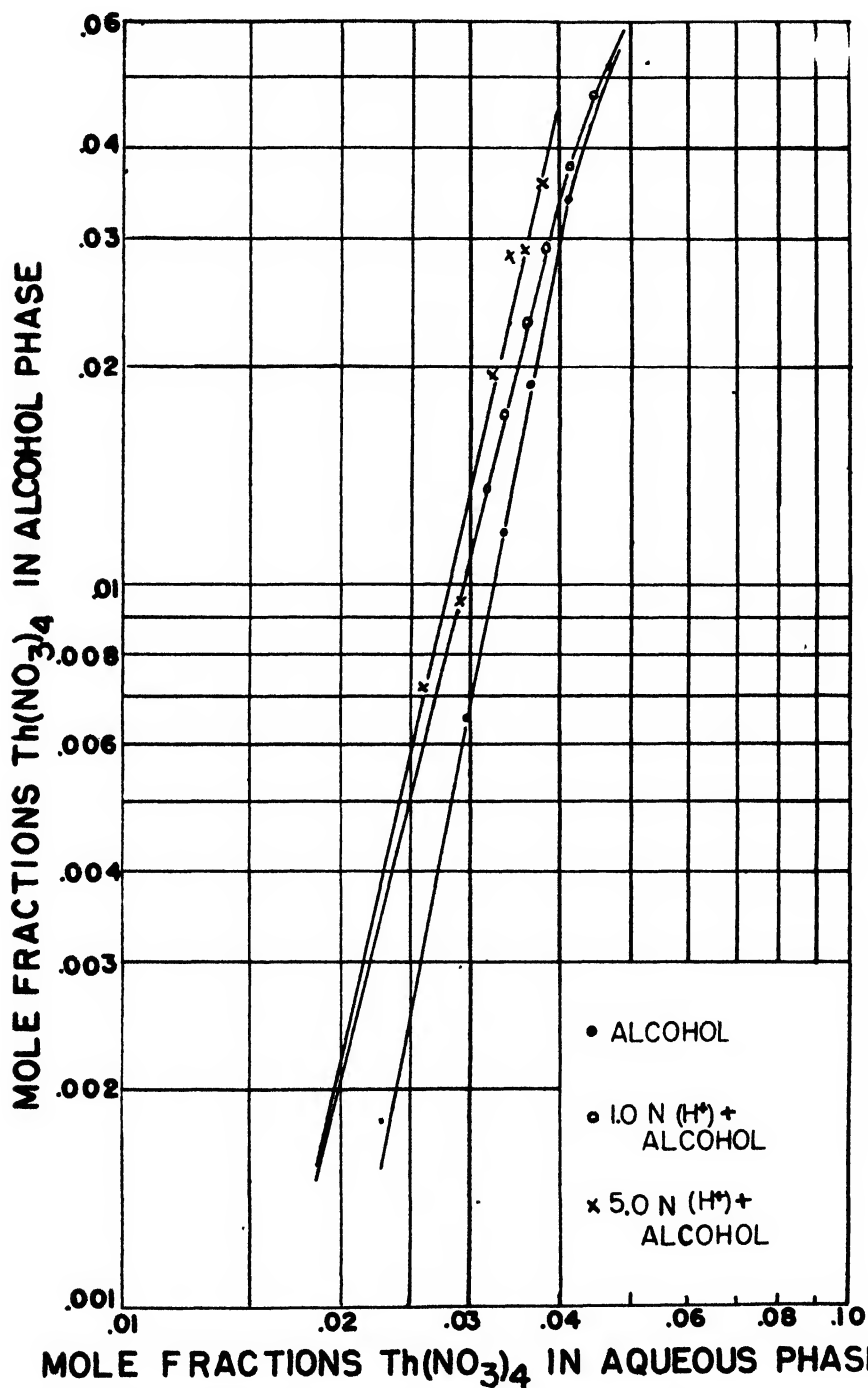


FIG. 4. Effect of acidity on the distribution of thorium nitrate between water and *n*-hexyl alcohol.

earth nitrates were prepared from a mixture (A) of the following composition (percentages as metal in an oxalate mixture):

La . . . . .	7.0	Sm. . . . .	3.0	Dy. . . . .	1.0	Yb. . . . .	0.5
Ce . . . . .	0.0	Eu. . . . .	0.05	Ho . . . . .	0.3	Y. . . . .	10.0
Pr . . . . .	5.7	Gd . . . . .	1.5	Er . . . . .	0.5		
Nd. . . . .	12.5	Tb . . . . .	0.2	Tm . . . . .	0.1		

Methyl *n*-hexyl ketone was chosen because it was the most water-immiscible of the ketones, and ketones have better solvent properties than the alcohols for this problem. In table 6 are given the solubilities of each nitrate in methyl

TABLE 6  
*Solubilities of various nitrates at room temperature*

NITRATE	ANHYDROUS NITRATES PER 100 G. OF SOLUTION	
	Methyl <i>n</i> -hexyl ketone	Isoamyl alcohol
	grams	grams
Th(NO <sub>3</sub> ) <sub>4</sub> ·4H <sub>2</sub> O . . . . .	31.06 (6)	37.82 (6)
ZrO(NO <sub>3</sub> ) <sub>2</sub> ·2H <sub>2</sub> O . . . . .	<0.1	0.37
Ca(NO <sub>3</sub> ) <sub>2</sub> ·4H <sub>2</sub> O . . . . .	<0.1*	3.73*
Rare earth nitrate (B) . . . . .	3.22	12.0

\* Susor (5).

*n*-hexyl ketone and isoamyl alcohol. The rare earth mixture (B) used in table 6 was of the following composition (percentage as metal in an oxalate mixture):

La. . . . .	0.1	Sm . . . . .	0.5	Dy . . . . .	2 0	Yb . . . . .	2.0
Ce . . . . .	0.5	Eu . . . . .	0 02	Ho . . . . .	0 6	Lu . . . . .	0.4
Pr . . . . .	0 1	Gd . . . . .	1.0	Er . . . . .	1 5	Y . . . . .	23 0
Nd. . . . .	0.5	Tb . . . . .	0 2	Tm . . . . .	0.3		

The "solubility" of this rare earth mixture is, of course, dependent on this arbitrary mixture and is valuable only as it predicts the order of magnitude. Potassium nitrate, not listed in table 6, has quite low solubility in acetone and ethanol (4) and therefore is probably insoluble in these higher solvents.

Spot measurements were made of the distribution of each of the nitrates between water and methyl *n*-hexyl ketone. In table 7 are given the ratios of the concentration of each metal in the ketone to that in the aqueous phase, for various arbitrary aqueous concentrations. It may be seen that all these data predict both successful leaching and liquid-liquid extraction under the conditions chosen.

### *Leaching*

Ten milliliters of methyl *n*-hexyl ketone was agitated for 4 days with Th(NO<sub>3</sub>)<sub>4</sub>·4H<sub>2</sub>O and rare earth nitrate mixture A until saturated in both. The presence of both phases among the remaining solids was assured, as there were

distinct white (Th) and pink (Nd) lumps. The solids settled quickly, and the solution was filtered. The total oxide content of the solution was 17.8 per cent. The nitrates were extracted with a water wash (complete in 2 hr.) and crystallized. Two analyses for thoria by the iodate method, referred to the total oxides precipitated by ammonia, gave 93.0 per cent and 93.24 per cent.

This is an indication of the extent to which thorium could be enriched in a single-step process, after the original material is converted to nitrates. Liquid-liquid extraction can then be applied mainly to materials already high in thorium.

#### *Liquid-liquid extraction*

A starting material was mixed from thorium, zirconyl, potassium, calcium, and rare earth (A) nitrates. By calculation and analysis, it contained 50.6 per cent thoria in the total oxides precipitated by ammonia (thorium, zirconium, rare earth). Sixty-five grams of this in a concentrated aqueous solution was extracted with 50 ml. of methyl *n*-hexyl ketone for 24 hr. The layers were sepa-

TABLE 7

*Distribution of various nitrates between water and methyl n hexyl ketone at room temperature*

NITRATE	RATIO OF CONCENTRATION IN KETONE TO CONCENTRATION IN AQUEOUS PHASE	ANHYDROUS NITRATE IN AQUEOUS PHASE
		<i>per cent</i>
Rare earth nitrate (A)	<0.0012	33.0
$\text{Ca}(\text{NO}_3)_2 \cdot 4\text{H}_2\text{O}$	0.012	31.9
$\text{KNO}_3$	0.0085	14.5
$\text{ZrO}(\text{NO}_3)_2 \cdot 2\text{H}_2\text{O}$	<0.0029	12.8

rated, the ketone washed with water, and the nitrates were crystallized. This 0.8-g. product analyzed 94.7 per cent thoria in the total heavy oxides. An attempt to concentrate the residual aqueous solution by heating caused the loss of about half of the material. The remainder was reagitated with the washed ketone; the yield of this second extraction was 1.5 g. of nitrate containing 89.0 per cent thoria in the total heavy oxides. That the potassium and calcium were not appreciably extracted was ascertained by other ignitions.

It is seen that the yields are very dependent upon the exact concentration of the initial aqueous solution. There are many problems of manipulation involved in liquid-liquid extraction with these solvents, which must be solved by further work. The iodate method used here for thorium tends to give results about 1 per cent low; therefore all enrichments given are conservative.

#### SUMMARY

1. Complete data have been obtained for the distribution of thorium nitrate between water and each of the following solvents: methyl *n*-hexyl ketone, methyl *n*-amyl ketone, methyl isobutyl ketone, isoamyl alcohol, and *n*-hexyl alcohol. Distribution expressions have been calculated, discussed, and plotted.

2. The effect of added nitric acid on the systems containing methyl *n*-hexyl ketone and *n*-hexyl alcohol has been investigated.

3. Preliminary leaching and liquid-liquid extraction runs with methyl *n*-hexyl ketone have been presented to show the use of these solvents in extracting thorium from the rare earths and zirconium.

This research was supported in part by the Research Committee of the University of Wisconsin Graduate School from funds supplied by the Wisconsin Alumni Research Foundation.

#### REFERENCES

- (1) MACDOUGALL, F. H.: *Thermodynamics and Chemistry*, pp. 245-7. John Wiley and Sons, Inc., New York (1939).
- (2) MELLOR, J. W.: *Comprehensive Treatise on Inorganic and Theoretical Chemistry*, Vol. VII. Longmans, Green and Company, London (1927).
- (3) MISCIATTELLI: *Gazz. chim. ital.* **60**, 833-42 (1930).
- (4) SEIDELL, A.: *Solubilities of Inorganic and Metal Organic Compounds*, Vol. I. D. Van Nostrand Company, New York (1940).
- (5) SUSOR, MARGARET J.: B.S. thesis, University of Wisconsin, January, 1947.
- (6) TEMPLETON AND HALL: *J. Phys. Colloid Chem.* **51**, 1441-9 (1947).

## STUDIES ON AGING OF PRECIPITATES AND COPRECIPITATION. XLI

### THE BULKINESS AND POROSITY OF SILICA POWDER

I. SHAPIRO<sup>1</sup> AND I. M. KOLTHOFF

*School of Chemistry, University of Minnesota, Minneapolis 14, Minnesota*

*Received November 13, 1947*

From the studies of Roller (15) on the bulkiness of various powders it follows that when the particle size of a powder decreases below a critical value, the bulkiness increases rapidly; and when the particle size becomes greater than the critical diameter, the bulkiness of the powder mass remains essentially constant. For the several powders investigated the relation of bulkiness to particle size can be expressed by the empirical equations:

$$V = k \left( \frac{1}{d} \right)^n \quad d \leq d_c \quad (1a)$$

and

$$V = K \quad d \geq d_c \quad (1b)$$

where  $V$  is the volume of voids per unit weight of material,  $d$  is an average (statis-

<sup>1</sup> Present address: United States Naval Ordnance Test Station, Pasadena, California.

tical) diameter of the powder with the subscript  $c$  denoting the critical diameter, and  $K$ ,  $k$ , and  $n$  are constants.

The bulkiness has been ascribed (15) to general electrostatic forces of repulsion and to surface irregularities and other specific properties of the powder grains such as shape and hardness. In addition, the bulkiness depends upon such factors as the method of packing the powder and the superincumbent weight of powder in the measuring container. The latter factors are a function of the experimental techniques employed and thus can be minimized or held constant.

In the experiments carried out by Roller the values of the density of the various powders were of the same order of magnitude but their shape characteristics were different. Hence differences in the values of the constants in equation 1 became attributes of the particle shape. By utilizing a powder composed of particles whose shape is fairly uniform and approaches spheres but whose density is of a different order of magnitude from the powders employed in Roller's experiments, one can ascertain the applicability of equation 1 over wide limits and get more insight into the phenomenon of increasing bulkiness with decreasing particle size. A powder which fulfills the necessary requirements for such a type of an experiment is silica gel. The highly porous nature of the gel structure decreases the effective density appreciably, yet the rigidity of the structure keeps the particles from collapsing. A "grain" of silica gel is actually an aggregate of minute primary particles.

From the experiments reported by Roller and in this paper it appears that the bulkiness of coarse grains (above a critical size) is determined entirely by the porosity of the grains and a constant packing factor. In other words, above the critical size the void between the grains becomes constant. Below the critical size the void is found to increase markedly with decreasing size. It becomes evident that in order to correlate the bulkiness of the powder with particle size, it is necessary first to differentiate between the interstitial or intraparticle voids, i.e., voids between individual primary particles, and the interparticle voids, i.e., voids between aggregate particles composed of primary particles. This distinction has been accomplished by determining the porosity of the grains prior to the bulkiness of the powder.

#### EXPERIMENTAL

*Material:* The silica gel used in these experiments was a product of the Mallinckrodt Chemical Works and was labeled "Acid Silicic, precipitated, analytical reagent". A gravimetric analysis (8) of the silica (volatility by hydrofluoric and sulfuric acids) showed 0.25 per cent non-volatile impurities. The particle size of the gel grains varied from less than  $1\ \mu$  to over  $200\ \mu$ . Hygroscopicity measurements indicated that the water content of the silica depends upon the relative humidity of the atmosphere.

*Water content:* The silica contained a small percentage of "bound water," i.e., water that is retained by the silica at  $110^{\circ}\text{C}$ ., and a variable amount of adsorbed water which is found from water-adsorption experiments. Essentially the hygroscopicity experiments consist of placing weighed samples of a definite

size fraction of silica powder in hygrometers at fixed relative humidities at room temperature. After equilibrium has been established, the samples are reweighed and then ignited at 1000°C. to obtain the dry weight of silica.

*Particle-size separation:* An air elutriation method was used for sizing the microscopic (subsieve) particles. The apparatus consisted of a Roller air separator (16) through which air of low relative humidity was maintained at certain velocities corresponding to definite size particles as calculated from Stokes's law.

*Particle-size measurement:* Each fraction of the powder was examined microscopically. The technique for mounting the powder on slides is to place a minute quantity of sample (the amount of powder required increases with the size of the particles) toward one edge of the slide and to add several drops of amyl acetate so that the liquid flows into the powder. Then the sample is "touched" with one end of a glass rod. This motion is sufficient to disperse the powder completely. By tilting the slide slightly to one side and then rotating it, one can spread the powder evenly over the entire slide. The amyl acetate is allowed to evaporate and the "dry mounting" is examined under suitable magnification (100 $\times$ , 200 $\times$ , and 500 $\times$ ) with a filar micrometer eyepiece. The success of this type of mounting is apparent from the photomicrographs of figure 1, which shows each specimen at a magnification of 100 $\times$  for comparison purposes.

Two hundred particles from each sized fraction of powder were measured according to the method of Martin (13). The frequency-size-distribution data were plotted on logarithm-probability paper (1, 12), so the statistical diameters could be calculated from the equations of Hatch and Choate (6).

*True density:* The true density of vitreous silica as reported by Sosman (18) is 2.20 g./cc. Identical values have been obtained on the silica used in these experiments by two different methods: (1) By measuring the density by the pycnometer-benzene liquid technique after the silica had been heated to a temperature of 1000°C., and (2) by compressing (ca. 4000 atm. pressure) the unheated silica of very high water content in a specially constructed die (whose dimensions are known accurately) until part of the water is squeezed out of the silica pellet. The water content remaining in the pellet after compression is determined by ignition. The apparent density of the water-soaked pellet was 1.178 g./cc. and the water content was 39.5 per cent based on dry silica. From these data the true density is calculated to be 2.20 g./cc., assuming that the water in the silica has its normal density.

*Apparent density:* The apparent density of the particles has been determined by several methods. The mercury pycnometer method (7, 11) utilizes a small glass bulb of 6-cc. capacity which is attached through a three-way stopcock to a vacuum pump and a small funnel, respectively. A known weight of powder is placed in the bulb and the system is evacuated; then mercury is introduced into the bulb through the funnel. Since the air has been removed by evacuation, the mercury may be expected to fill all of the space between the individual grains, but no mercury will penetrate the "submicroscopic pores and capillaries" (14) within the grains.



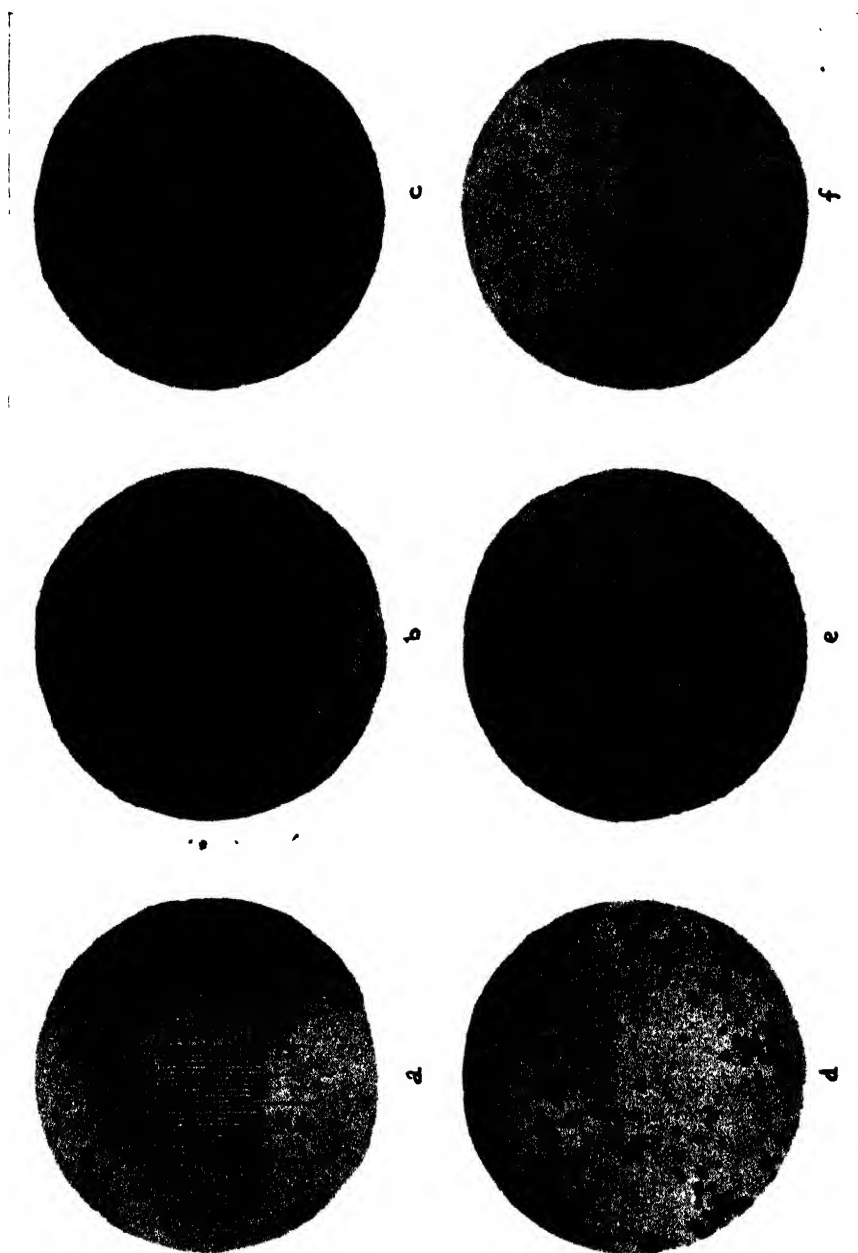


FIG. 1 Photomicrographs of silica powder

a 1 division =  $10\ \mu$ b.  $d_g = 2.3\ \mu$ c.  $d_g = 6.0\ \mu$ d.  $d_g = 15.8\ \mu$ e.  $d_g = 20.6\ \mu$ f.  $d_g = 30.4\ \mu$

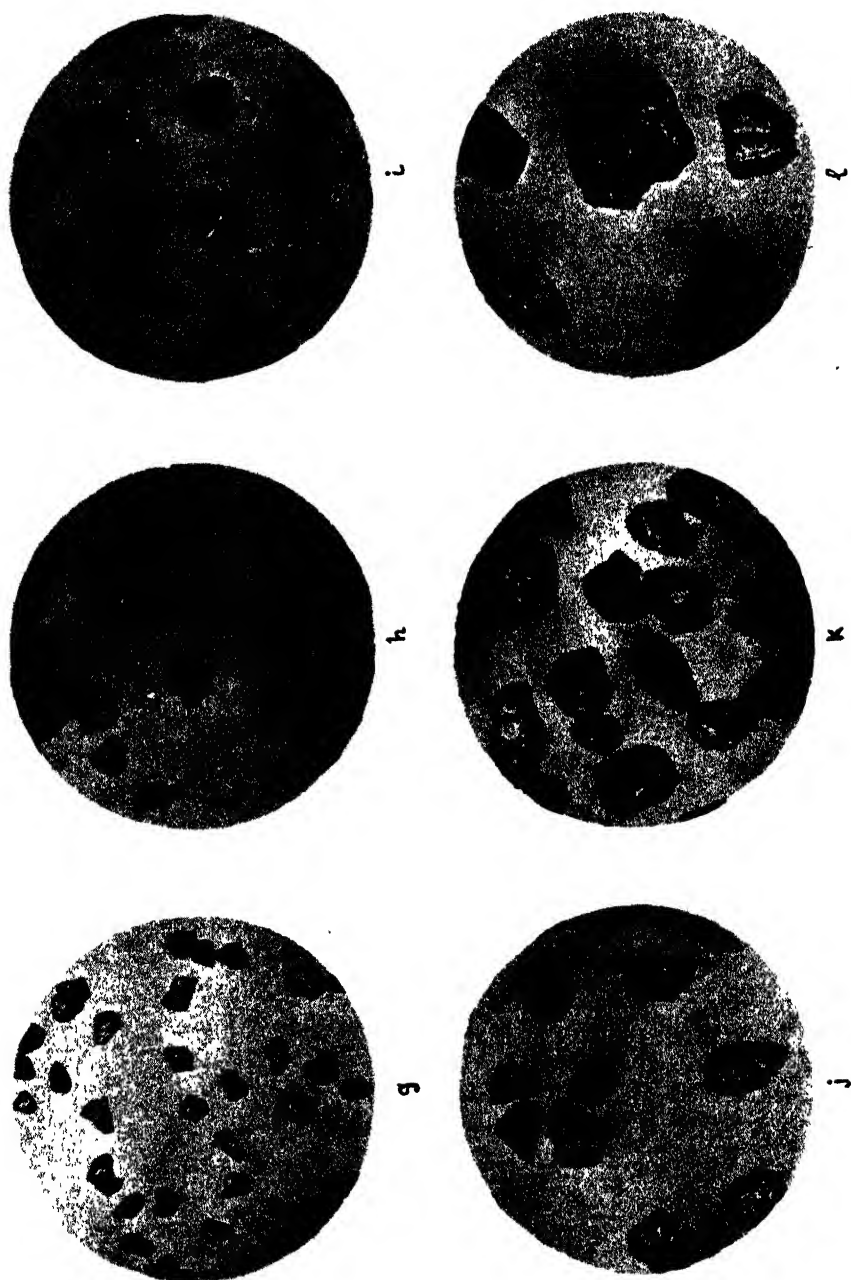


FIG 1. Photomicrographs of silica powder

g.  $d_g = 48.5 \mu$ h.  $d_g = 64.0 \mu$ i.  $d_g = 82.0 \mu$ j.  $d_g = 102.5 \mu$ k.  $d_g = 124.0 \mu$ l.  $d_g = 183.0 \mu$

In order to find the "true" apparent density by the mercury pycnometer method, it appeared necessary that the average particle (grain) size of the silica be greater than *ca.* 70  $\mu$ . Below this value the mercury does not surround completely the individual grains; large clumps of white powder remain visible in the pycnometer bulb after the addition of mercury. In these instances the volume of displaced mercury really represents the volume of the particles plus the volume of void space between some of the particles. Thus while it is possible to find an experimental value for the apparent density of the powder irrespective of the size of its grains, this value would not correspond to the "true" apparent density unless the average value of the grain size exceeds 70  $\mu$ . This value of 70  $\mu$  applies to the heated powder as well as the unheated powder.

Another method for determining apparent density is to measure the relative decrease in grain size (microscopic examination) of a sized sample (greater than 70  $\mu$ ) upon heating to high temperatures (1000°C.), and then measuring the apparent density of the heated powder. No perceptible sintering occurred at this elevated temperature, so no difficulty was encountered in dispersing the grains with amyl acetate for the microscopic examination. Studies on thermal aging of silica to be published at a later date show that at 1000°C. the silica loses all of its bound water and no longer has the capacity to absorb water. Also, heating the particles does not alter appreciably the shape of its size-distribution curve. While no intragrain sintering was found to occur between large particles or grains, some intersintering within the individual grains occurs because they shrink and become harder to crush.

As a third method the apparent density of the unheated powder can be calculated from the bulk density of the powder before and after heating and the apparent density of the heated powder.

*Bulking of silica:* The bulk density  $\rho_B$  is defined as the weight of dry powder, i.e., corrected for water content, that is required to fill a unit volume of a packing when no external pressure is applied to the powder. The measuring container was a covered weighing bottle (approximate dimensions 1.3 cm. diameter x 4 cm. length) whose volume up to a scratch mark was obtained by weighing the vial with mercury. In calibrating the vial, a plunger was inserted in the container in order to eliminate any correction in volume for the curvature of the mercury meniscus. The volume of the container to the level of the mark was 4.92 cc.

A uniform packing of the powder in the container was obtained by rotating and tapping the bottle simultaneously on a hard baseboard until the level of powder no longer settled. Sufficient powder was added so that the level of powder finally coincided with the scratch mark on the bottle. After weighing, the bulked powder was poured directly from the weighing bottle into a platinum crucible and ignited. For the finer fractions of the powder a reproducibility within several per cent was achieved, while for the coarser fractions the reproducibility was within 1 per cent.

## RESULTS AND DISCUSSION

*Particle size*

In figure 1 are photomicrographs of the various sized fractions of the silica powder. The actual size distribution of the silica particles in each fraction is

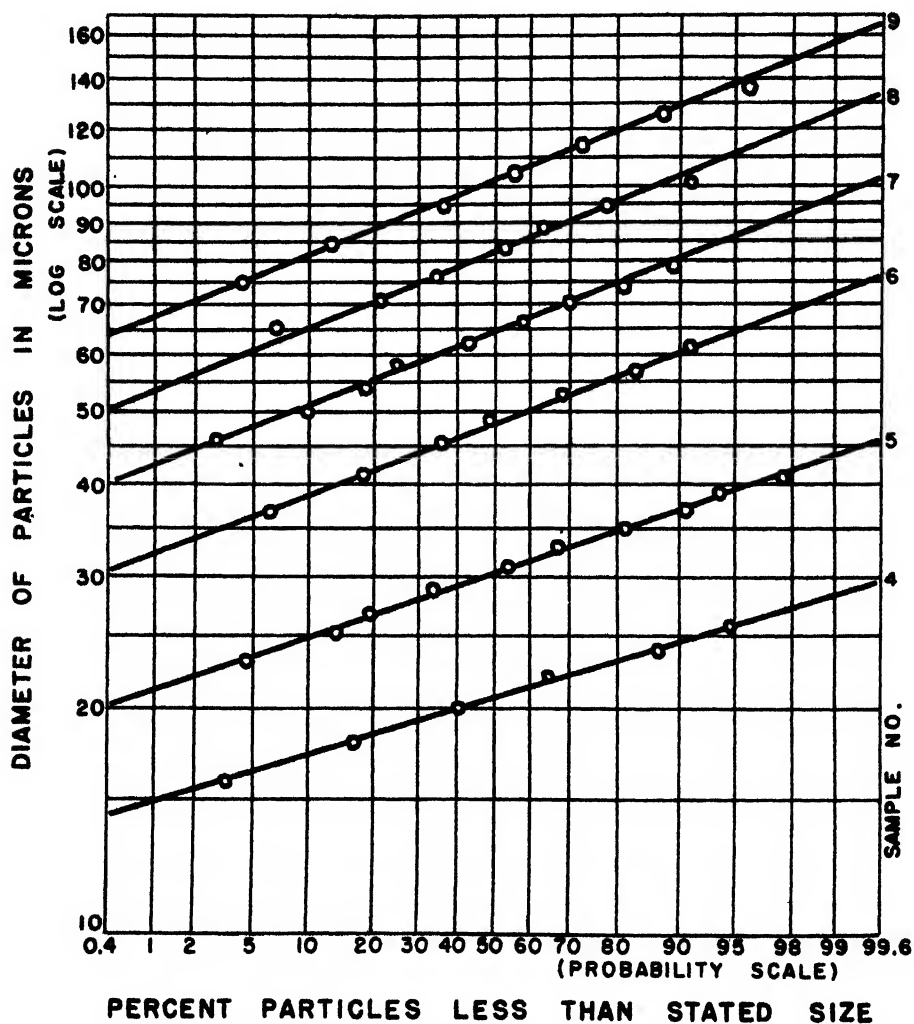


FIG. 2. Size distribution of silica particles

shown graphically by logarithm-probability curves in figure 2. The mean-volume diameter,  $d_v$ , is obtained from the following equation (6):

$$d_v = \sqrt[3]{\frac{\sum n d^3}{\sum n}} = \exp(\ln d_g + 1.5 \ln^2 \sigma) \quad (2)$$

where  $d_g$  is the log-geometric mean diameter which corresponds to the value of

50 per cent on the probability scale of figure 2, and  $\sigma_g$  is the log-geometric standard deviation which can be found by

$$\sigma_g = \frac{d_{84.13\% \text{ size}}}{d_{50\% \text{ size}}} = \frac{d_{50\% \text{ size}}}{d_{15.87\% \text{ size}}} \quad (3)$$

The geometric-mean diameters are tabulated in table 1.

The theoretical particle size for each size fraction listed in table 1 is the arithmetic mean of the limiting diameters of particles that correspond to certain air

TABLE 1  
*Size separation of silica powder*

SAMPLE NO.	AIR VELOCITY*	THEORETICAL LIMIT DIAMETER	H <sub>2</sub> O	ARITHMETIC AVERAGE DIAMETER $\bar{d}$	GEOMETRIC- MEAN DIAM- ETER $d_g$	RATIO $d_g/\bar{d}$
	<i>cm./second</i>	$\mu$	<i>per cent</i>	$\mu$	$\mu$	
1	0.0407	2.5	10.58	1.25	2.3	1.84
2	0.163	5.0	9.24	3.75	6.0	1.60
3	0.651	10	9.11	7.5	15.8	2.11
4	1.462	15	9.54	12.5	20.6	1.65
5	2.60	20	9.53	17.5	30.4	1.74
6	5.85	30	9.82	25.0	48.5	1.94
7	10.4	40	11.58	35.0	64.0	1.83
8	16.3	50	11.11	45.0	82.0	1.82
9	23.4	60	12.32	55.0	102.5	1.86
10. ....	36.5	75	9.37	67.5	124.0	1.84
11 ....		>75	9.36		183.0	

\* Relative humidity of air = *ca.* 10 per cent.

velocities as calculated from Stokes's law. Stokes's law can be expressed by the equation (16):

$$v = \frac{10^{-8} g \rho d^2}{18\eta} \quad (4)$$

where  $v$  is the terminal velocity of fall in centimeters per second in a stationary fluid,  $g$  is the constant of gravitation in c.g.s. units ( $= 980 \text{ cm./sec.}^2$ ),  $\rho$  is the density of the particle in grams per cubic centimeter,  $\eta$  is the viscosity of fluid in c.g.s. units ( $\eta = 1.82 \times 10^{-4}$  poises at  $20^\circ\text{C.}$  for air), and  $d$  is the diameter of the sphere in microns. By arbitrarily selecting convenient values for the diameter (column 3, table 1), one obtains the corresponding air velocity (from equation 4) which will remove all particles less than the stated size from the original mixture of the powder. The value of the density of the silica particle used in equation 4 for arriving at the theoretical particle sizes was taken as 2.20 g./cc. The large difference between actual particle size and theoretical particle size indicates that the effective density of the grains is considerably smaller than the assumed value of 2.20 g./cc.

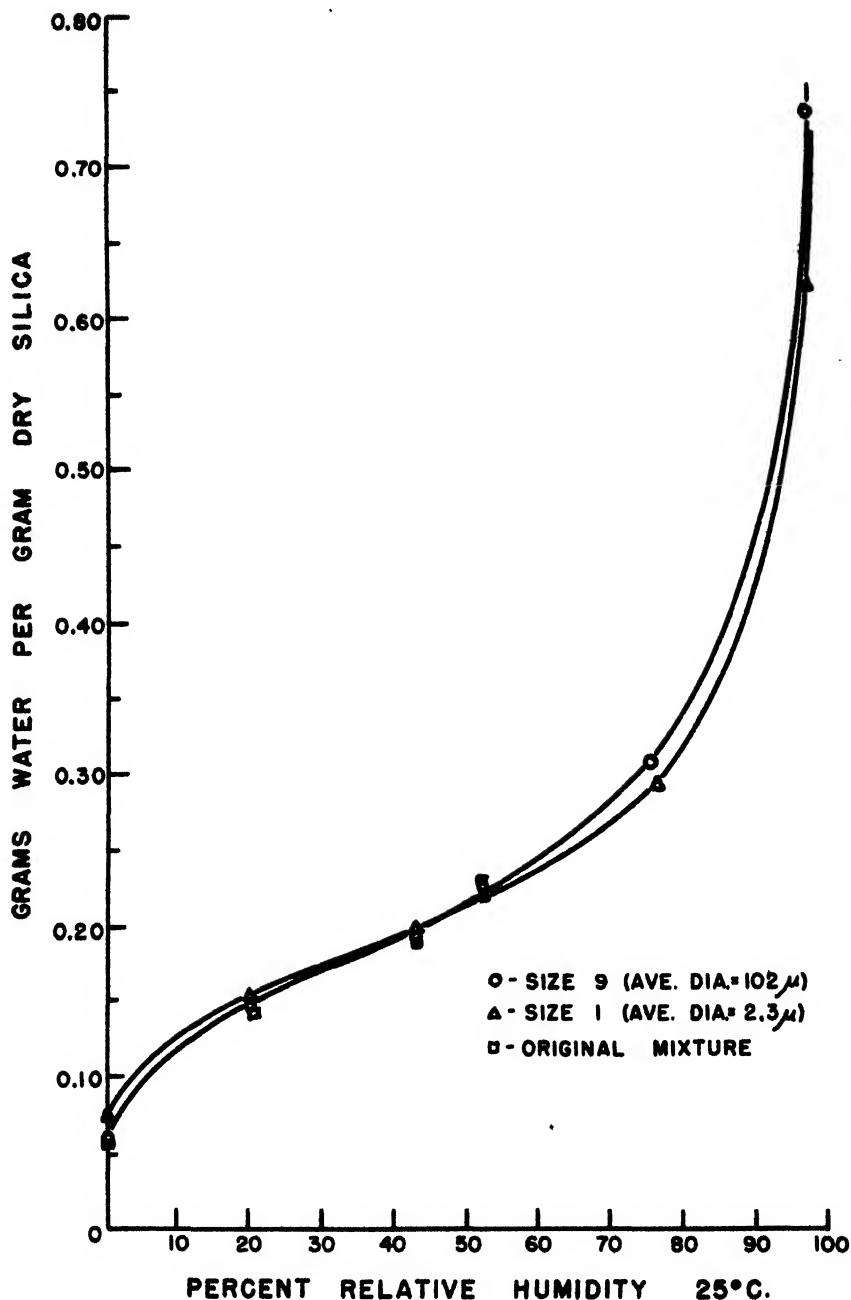


FIG. 3. Sorption isotherms of water on silica powder at 25°C.

*Water content*

The sorption isotherms of water on silica shown in figure 3 are sigmoidal in shape. Identical curves were obtained for a fine powder (sample No. 1), a coarse powder (sample No. 9), and a mixture of various-sized particles. The specific

surface calculated by the method of Brunauer, Emmett, and Teller (2), using  $10.6 \text{ \AA}^2$  as the cross-sectional area of a single water molecule (10), and by the method of Harkins and Jura (5) gives a value of 300 sq.m. per gram of dry silica. In calculating the specific surface only the reversibly held water was considered as being adsorbed. The 6 per cent water retained by the powder at zero humidity is not driven off at  $110^\circ\text{C}$ . and therefore is considered as "bound" water and does not represent "available surface" by adsorption.

A calculation of the external surface (from geometric considerations) for sample No. 9 gives approximately 0.1 sq.m. per gram of silica. Thus the enormous internal surface is indicative of the highly porous nature of the silica powder. As expected from figure 3, one finds from table 1 that the water content for the various size fractions of the powder is essentially constant when exposed to air of approximately 10 per cent relative humidity. Hence from surface considerations one can surmise that the gel structure (or porosity) of the particles is in

TABLE 2  
*Apparent density of silica powder*

SAMPLE	DENSITY BY MERCURY PYCNOMETER $\rho_h$	AVERAGE DIAMETER $d_g$		BULK DENSITY OF POWDER		CALCULATED APPARENT DENSITY, $\rho_f$	
		Un heated	Heated	Unheated ( $\rho_h$ ) <sub>f</sub>	Heated ( $\rho_h$ ) <sub>h</sub>	$\rho_h \left( \frac{d_h}{d_f} \right)^3$ (equation 5)	$\rho_h \left( \frac{(\rho_B)_f}{(\rho_B)_h} \right)$ (equation 6)
	grams/cc.	$\mu$	$\mu$	grams/cc	grams/cc	grams/cc	grams/cc
No. 9 (heated to $980^\circ\text{C}$ .)	1.530	102	80	0.498	1.002	0.738	0.760
No. 10 (heated to $980^\circ\text{C}$ .)	1.600	124	97	0.500	1.048	0.764	0.764
No. 9 (unheated; 6 per cent $\text{H}_2\text{O}$ on dry basis).	0.762	102					(0.762)

dependent of its grain size. The grains can be considered as agglomerates of minute primary particles to the surface of which water vapor has free access. This picture accounts for the large internal surface and uniformity in porosity regardless of grain size. In this respect attention is called to the fact that Elkin, Shull, and Roess (3) have estimated the average size of the primary particles (assumed spherical) in freshly prepared silica gel to be around 30–60  $\text{\AA}$ . from small-angle x-ray scattering measurements.

#### *Apparent density*

The data for calculating the apparent density by the several methods are tabulated in table 2. For two of the sized samples the particle sizes were measured before and after heating the powder to  $980^\circ\text{C}$ . At the elevated temperature the grain size decreased, owing to "thermal aging" of the primary particles, but no perceptible sintering of the grains occurred. The apparent densities of the heated powders were obtained by the mercury pycnometer method. The apparent density of the unheated powder was calculated from the relationship

$$\rho_f = \rho_h \left( \frac{d_h}{d_f} \right)^3 \quad (5)$$

where  $\rho$  and  $d$  are the apparent density and average diameter, respectively, with the subscripts  $f$  and  $h$  referring to "fresh" and "heated" samples.

The apparent density was calculated in another manner by determining the weight of (dry) silica that can be bulked for the heated and unheated samples under similar experimental conditions. Later it is shown that as long as the particles of a powder are fairly uniform in size and above a critical value, the packing fraction constant ( $C$ ) for the heated and unheated powders is essentially the same, so the ratio of the bulk density for the heated and unheated powder becomes equal to the ratio of the apparent density of the heated and unheated grains, *viz.*:

$$\frac{(\rho_B)_h}{(\rho_B)_f} = \frac{\rho_h(1 - C_h)}{\rho_f(1 - C_f)} \approx \frac{\rho_h}{\rho_f} \quad (6)$$

It is interesting to note that the apparent density calculated by the indirect methods agrees fairly well with the apparent density obtained from direct measurements on the unheated silica. The value of 0.762 g./cc. is based upon water-free silica. Taking the true density of the silica as 2.20 g./cc., the porosity of the individual grains or the intraparticle porosity is 65.4 per cent.

From table 1 it is observed that the ratio of measured particle size to theoretical particle size is approximately constant. By substituting the value for the apparent grain density for the solid density in equation 4, the ratio of the measured diameter to theoretical diameter becomes 1.1 instead of 1.8. This slight deviation of the ratio from unity can be attributed to the effect of the shape of the particles. In calculating the particle size from Stokes's equation, the value of the apparent density used in equation 4 was 0.84 instead of 0.762 g./cc. because of the *ca.* 10 per cent water content in the particles.

#### Bulkiness

The values of the bulk density (on the dry basis) of the various size fractions of silica powder are given in table 3. The bulk density is found to be independent of the amount of water adsorbed by the silica. The total air space in the bulked powder represents the void between the particles and the void within the aggregate particles, *i.e.*, the space between the primary colloidal particles of the gel which constitute the grains shown in figure 1. Since the packing of the primary particles within the grains has been shown to be unaffected by the size of the grains, the increase in bulkiness with decreasing particle size must be a measure of the increase in void between grains. The fraction of interparticle void space,  $C$  in cubic centimeters per 1 cc. of dry powder (column 6, table 3), can be calculated with the help of the following equation:

$$C = 1 - \frac{\rho_B}{\rho_f} \quad (7)$$

The volume of the void space,  $V$ , between grains expressed in cubic centimeters per gram of dry silica is obtained by

$$V = \frac{1}{\rho_B} - \frac{1}{\rho_f} = \frac{C}{\rho_h} \quad (8)$$



By plotting the data for  $V$  and  $d$  (mean-volume diameter) from table 3 on log-log paper, one obtains a curve (figure 4) which can be represented mathemati-

TABLE 3  
*Bulkiness of unheated silica powder*

SAMPLE NO.	MEAN-VOLUME DIAMETER	H <sub>2</sub> O	WEIGHT OF (DRY) POWDER IN 4.92 CC.	BULK DENSITY $\rho_B$	INTERPARTICLE VOID SPACE $C$	VOLUME INTER- PARTICLE VOID SPACE $V$
	$\mu$	per cent	grams	grams/cc.	per cent	cc./gram
1. ....	2.3	10.58	0.420	0.0855	88.8	10.40
2. ....	6.1	9.24	0.950	0.193	74.7	3.87
3. ....	16.1	9.11	2.121	0.431	43.4	1.005
4. ....	21.2	9.54	2.290	0.466	38.8	0.832
5. ....	31.6	9.53	2.396	0.487	36.1	0.741
6. ....	50.8	9.82	2.444	0.497	34.7	0.698
7. ....	67.2	11.58	2.432	0.494	35.1	0.711
8. ....	86.0	11.11	2.457	0.499	34.5	0.692
9. ....	107.0	12.32	2.450	0.498	34.5	0.693
10. ....	130.0	9.37	2.460	0.500	34.4	0.688
Original		12.63	2.447	0.498	34.5	0.693

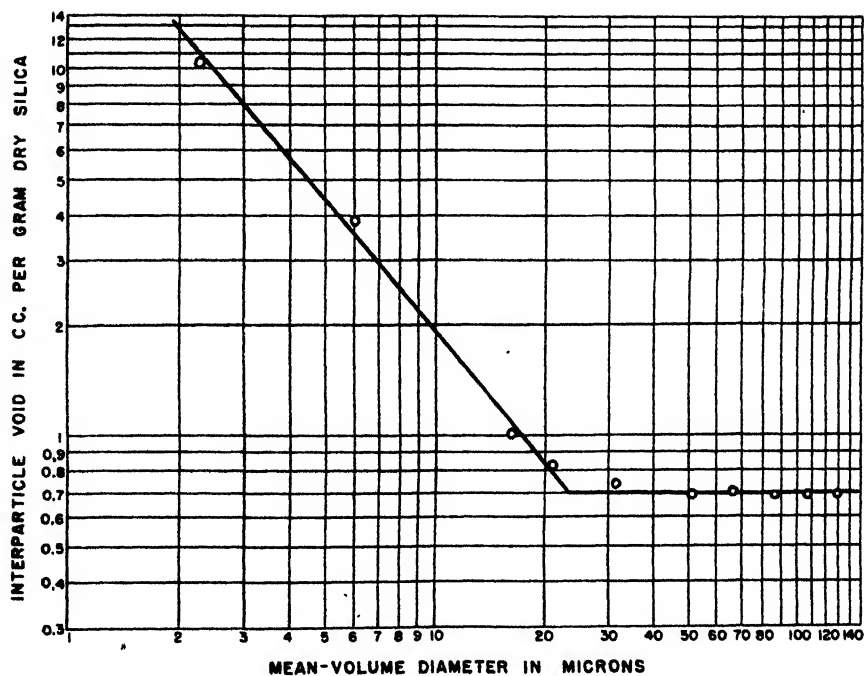


FIG. 4. Bulkiness of silica powder

cally by equation 1. The values of the constants are:  $k = 29.5$ ,  $n = 1.183$ , and  $K = 0.69$ . The critical diameter,  $d_c$ , from figure 4 is  $23 \mu$ , a value which is within

the range found by Roller for other powders. Since the apparent density of the silica powder is very small (0.762 g./cc.) as compared to powders such as anhydrite (2.91 g./cc.), it may well be that the critical diameter is independent of the chemical composition and shape of the particle but depends solely upon its size (and electrostatic charge).

The constancy of the value for per cent interparticle void space for particles greater than the critical diameter (table 3) is a good indication of the similarity in packing of the particles. In this connection, when data from table 2 of samples No. 9 and 10 which were preheated to 980°C. are placed in equation 7 (substituting  $\rho_h$  for  $\rho_f$ ), the calculated values of  $C$  become 34.6 per cent and 34.5 per cent, respectively. These values are in agreement with porosity values for unheated silica. From geometric considerations the packing of uniform-size spheres in a hexagonal close-packed arrangement gives a calculated porosity of 26 per cent, which represents a lower limit for the relative volume of pore space between particles. Since the volume of irregular shaped particles is smaller than the volume of spheres of the same mean diameter, the porosity for irregular particles will be somewhat greater than 26 per cent. Actually, the interparticle porosity of irregular particles varies mainly between 35 and 45 per cent (9). The over-all value of 34.5 per cent porosity found for silica powder is indicative of the low degree of irregularity in shape.

An examination of particles under 1  $\mu$  diameter at high magnification shows that their degree of irregularity is the same as that of particles of larger size. Thus the large values of interparticle void space for the small-size particles cannot possibly be attributed to mere surface irregularities. Studies on the electrification of particles show that dust particles are charged and that the charge is a function of the chemical composition and size of the particles (17, 19). Böning (1) has demonstrated that charges could be produced by friction and contact between particles themselves. In this connection it was found that in the size separation of the silica particles it became necessary to ground all metal parts of the apparatus, otherwise the small particles tended to adhere to the metal. Thus it appears that the electrostatic charges are the contributing factor for the increase in bulkiness with decreasing particle size.

#### SUMMARY

The porosity and bulking properties of silica powder as a function of particle size have been investigated. The "grains" of silica, which are believed to consist of aggregates of minute primary particles, had a total surface of 300 sq.m. per gram of dry silica, a value which is many-fold greater than that corresponding to the external surface of the grains. The porosity of the grains or intraparticle porosity is independent of the grain size and has been calculated to be 65.4 per cent.

The bulkiness or volume of interparticle void space  $V$  in cubic centimeters per gram (void between grains of powder) increases markedly as the grain size decreases below a critical diameter  $d_c$ , and can be expressed empirically by the Roller equation,

$$V = k \left( \frac{1}{d} \right)^n \quad d \leq d_c$$

where the values of the constants were  $k = 29.5$  and  $n = 1.183$ . Above the critical diameter ( $d_c = 23 \mu$ ) the volume of interparticle void space remained essentially constant at 0.69 cc./g. This value corresponds to an interparticle porosity of 34.5 per cent.

The increase in bulkiness with decreasing grain size is ascribed to general electrostatic forces of repulsion.

The authors are grateful to Mr. M. W. Welch of the W. M. Welch Scientific Company, Chicago, for the financial grant that made possible this research.

#### REFERENCES

- (1) BÖNING, P.: *Z. tech. Physik* **8**, 385 (1927).
- (2) BRUNAUER, S., EMMETT, P. H., AND TELLER, E.: *J. Am. Chem. Soc.* **60**, 309 (1938).
- (3) ELKIN, P. B., SKULL, C. G., AND ROESS, L. C.: *Ind. Eng. Chem.* **37**, 327 (1945).
- (4) HAZEN, A.: *Trans. Am. Soc. Civil Engrs.* **77**, 1539 (1914).
- (5) HARKINS, W. D., AND JURA, G.: *J. Am. Chem. Soc.* **66**, 1366 (1944).
- (6) HATCH, T., AND CHOATE, S. F.: *J. Franklin Inst.* **207**, 369 (1929).
- (7) HERBST, H.: *Kolloid Beihefte* **42**, 276 (1935).
- (8) KOLTHOFF, I. M., AND SANDELL, E. B.: *Quantitative Inorganic Analysis*, p. 388. The Macmillan Company, New York (1936).
- (9) KRAEMER, E. O.: *Advances in Colloid Science*, pp. 51-6. Interscience Publishers, Inc., New York (1942).
- (10) LIVINGSTON, H. K.: *J. Am. Chem. Soc.* **66**, 569 (1944).
- (11) LOTTERMOSER, A., AND TU, CHUN YEN: *Kolloid-Beihefte* **46**, 430 (1937).
- (12) LOVELAND, R. P., AND TRIVELLI, A. P. H.: *J. Franklin Inst.* **204**, 193 (1927).
- (13) MARTIN, G., BLYTH, C. E., AND TONGUE, H.: *Trans. Brit. Ceram. Soc.* **23**, 61 (1924).
- (14) RITTER, H. L., AND DRAKE, C. C.: *Ind. Eng. Chem., Anal. Ed.* **17**, 782 (1945).
- (15) ROLLER, PAUL S.: *Ind. Eng. Chem.* **22**, 1206 (1930).
- (16) ROLLER, PAUL S.: *U. S. Bur. Mines, Tech. Paper* **490** (1931); *Ind. Eng. Chem., Anal. Ed.* **4**, 341 (1932); *Proc. Am. Soc. Testing Materials* **59** (1932).
- (17) RUDGE, W. A. D.: *Phil. Mag.* **23**, 852 (1912).
- (18) SOSMAN, R. B.: *Properties of Silica*, p. 289. The Chemical Catalog Company, Inc. (Reinhold Publishing Corporation), New York (1927).
- (19) WHITMAN, V. E.: *Phys. Rev.* **28**, 1287 (1926).

DETERMINATION OF SEDIMENTATION CONSTANTS IN  
THE SHARPLES SUPERCENTRIFUGEH. K. SCHACHMAN<sup>1</sup>*Department of Animal and Plant Pathology, Rockefeller Institute for Medical Research,  
Princeton, New Jersey**Received November 13, 1947*

## INTRODUCTION

The high-speed centrifuge in recent years has become an invaluable tool in many branches of colloid and biochemical research. In addition to the technical improvements enabling the attainment of centrifugal fields as high as 500,000 times gravity, there have been developments in the optical methods used for study of the sedimenting material. The brilliant researches of The Svedberg and his collaborators (15) have culminated in the development of the ultracentrifuge. Centrifuges of another design have been developed by Beams and coworkers (2), Bauer and Pickels (1), and Wyckoff and Lagsdin (17) with the logical addition of a quantity-type rotor for centrifuging moderate quantities of liquids. The work of Stanley (12) has shown this quantity-type centrifuge to be of inestimable value in the isolation and purification of viruses. However, the need for a less expensive centrifuge capable of continuous flow operation and of sedimenting particles as small as the viruses resulted in investigations concerning the possibilities of the Sharples supercentrifuge.

Hauser *et al.* (4, 5) devised an efficient procedure for fractionating bentonite suspensions into several reasonably monodisperse fractions by utilizing the theory and equations derived for the Sharples supercentrifuge. It was also demonstrated (5) that, with very little effort, the size of a well-defined fraction of particles could be evaluated. Success in quite a different field was experienced by Stanley (13, 14), who sought a better method for the isolation of viruses on a large scale. In view of the practical value of the Sharples supercentrifuge in the purification of tobacco mosaic and influenza viruses, it seemed worthwhile to reexamine the theory of sedimentation in the supercentrifuge in an attempt to adapt it for the calculation of the sedimentation constants of those materials capable of being sedimented in fields of about 60,000 times gravity. An estimate of the reliability of the supercentrifuge method could then be made by comparing the results with those obtained by direct measurement in the ultracentrifuge.

## THEORETICAL

Hauser and Reed (4) assumed that every particle in the bowl of the Sharples centrifuge is subjected to two velocity components, one perpendicular and the other parallel to the axis of rotation of the bowl. The first, whose magnitude is dependent on the centrifugal field, can be expressed quantitatively by a modified Stokes law for falling bodies; the second is proportional to the rate of flow of

<sup>1</sup> Junior Research Fellow of the National Institute of Health.

material through the bowl and can be defined by Newton's law of viscous flow. Under given experimental conditions the point at which a particle hits the wall will be a function of the point of departure and the effective mass and shape of the particle. This can be expressed by

$$Y = F(X_0, m_e, f) \quad (1)$$

where  $Y$  is the distance in centimeters from the top of the straightening vanes to the point at which the particle settles,  $m_e$  is the effective mass of the particle,  $f$  is the frictional coefficient of the particle, and  $X_0$  is the distance from the axis of rotation at which sedimentation started (figure 1). The velocity component in the  $x$  direction can be expressed by

$$\frac{dx}{dt} = \frac{m_e \omega^2 x}{f} \quad (2)$$

where  $\omega$  is the angular velocity of the centrifuge bowl in radians per second. Reed (9), following the treatment of Lamb (6), found

$$\frac{dy}{dt} = \frac{Q_{\min.} K}{60\pi(R_2^2 - R_1^2)} \left[ R_1^2 \ln \frac{x}{R_2} + \frac{R_2^2 - x^2}{2} \right] \quad (3)$$

for the velocity component parallel to the axis of rotation.<sup>2</sup> In the present work the bowl has the dimensions  $R_1 = 0.734$  cm.,  $R_2 = 2.22$  cm., and  $K = 1.11$ , and  $Q_{\min.}$  is the rate of flow of solution through the bowl in milliliters per minute. Combining equations 2 and 3 and integrating between the limits  $x = X_0$ ,  $y = 0$  and  $x = R_2$ ,  $y = Y$  leads to equation 4:

$$Y = \frac{Q_{\min.}}{60\pi(R_2^2 - R_1^2)} \cdot \frac{f}{m_e} \cdot \frac{K}{\omega^2} \left[ \frac{R_2^2}{2} \ln \frac{R_2}{X_0} - \frac{R_1^2}{2} \left( \ln \frac{R_2}{X_0} \right)^2 + \frac{X_0^2 - R_2^2}{4} \right] \quad (4)$$

<sup>2</sup> Lamb (6) derived the equation

$$\frac{dy}{dt} = -\frac{p_1 - p_2}{4\eta l} x^2 + A \log x + B \quad (3a)$$

for the velocity of flow of liquid in a pipe of uniform circular section where  $l$  is the length of the section under consideration,  $(p_1 - p_2)$  is the pressure drop across that section,  $\eta$  is the viscosity of the medium, and  $A$  and  $B$  are constants of integration. In the case of flow in the centrifuge bowl the treatment differs from that of Lamb in that the boundary conditions for integration are those of a concentric shell of fluid rather than a solid tube of fluid. The constants  $A$  and  $B$  are evaluated by the use of the boundary conditions,  $dy/dt = 0$  at  $x = R_2$ , and  $\frac{d}{dx} \left( \frac{dy}{dt} \right) = 0$  at  $x = R_1$ . Combination of the resulting equation with the equation for the flux across any section,

$$Q = \int_{R_1}^{R_2} \frac{dy}{dt} 2\pi x \, dx$$

leads to equation 3.

Following the notation of Svedberg (15), the sedimentation constant,  $s$ , is defined as

$$s = \frac{1}{\omega^2 x} \cdot \frac{dx}{dt}$$

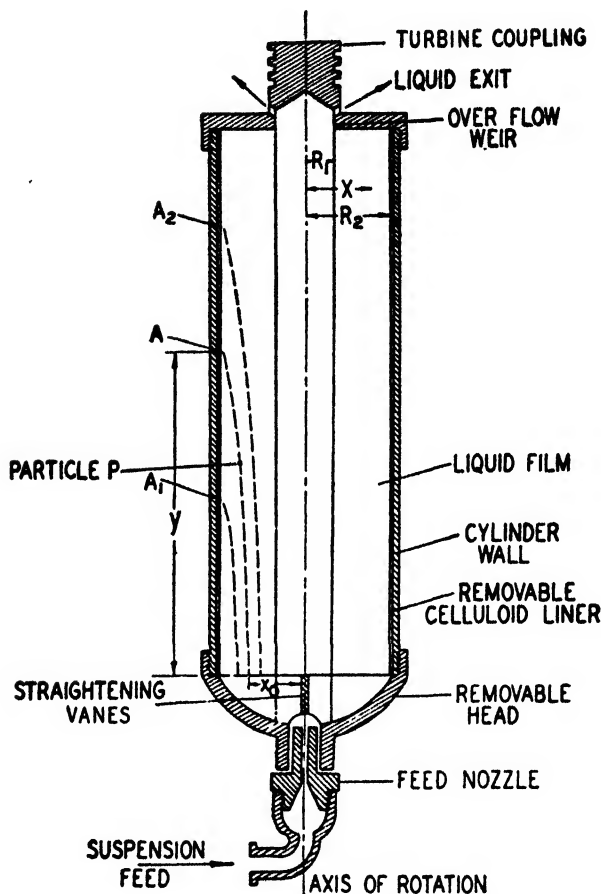


FIG. 1. Section through supercentrifuge bowl

which, according to equation 2, is equal to  $m_0/f$ . Substituting for the appropriate constants, correcting radians per second to R.P.M., and rearranging terms leads to equation 5

$$s = \frac{0.1097 Q_{\min.} \cdot C}{(\text{R.P.M.})^2 \cdot X_0} \quad (5)$$

where  $C = 0.6235 + 0.277X_0^2 - 5.19 \log X_0 - 1.58 (\log X_0)^2$ .

According to the treatment proposed by Hauser *et al.* (4, 5) it is expected that under a given set of experimental conditions the larger particles in the solution would settle out on the liner sooner than the smaller particles. Still smaller

particles would pass out of the bowl, because insufficient time is allowed for the centrifugal force to act. If the rate of input of solution is decreased or the centrifugal force increased, some of the smaller particles would also settle onto the wall of the centrifuge bowl. It thus would be possible to vary the yield of sedimentation and the distribution of particles along the centrifuge bowl by changing the experimental conditions. At very low rates of flow most of the particles would be found at the bottom of the bowl and a good yield would result. At higher rates of flow the distribution of sediment along the bowl would be approximately uniform but the yield poor, because many particles would pass out the overflow weir. It follows that there would exist an optimum set of operating conditions combining high yield and large capacity. In general, the distribution of particles along the bowl after a run under optimum conditions would be non-uniform, with more particles at the bottom than at the top. In the special case in which the solution under investigation contains particles covering but a small range of size and shape, the distribution of sediment obtained under optimum operating conditions would approach uniformity with only slightly more particles at the bottom of the bowl than at the top. This is to be contrasted with the case of solutions containing particles of many sizes. Under such circumstances the distribution of sediment obtained under optimum conditions would not approach uniformity. The rate of flow which gives a nearly uniform layer would be too fast for the settling of the small particles in the suspension and a poor yield would result. Similarly, at a rate of input slow enough to produce a good yield, the large particles would settle at the bottom of the bowl and the resulting layer would be decidedly non-uniform.

Equation 5 applies to solutions containing any distribution of particle sizes, and it can be simplified for the special case of solutions of homogeneous material. When such solutions are used there will be but one particle size at each point on the bowl; conversely, a particle at a given value of  $Y$  must have started from a unique value of  $X_0$ . It can thus be assumed that  $Y = f_1(X_0)$ . Figure 2, an empirical chart illustrating  $Y = f_1(X_0)$ , was obtained by means of a careful study of a fractionated bentonite suspension which was analyzed for particle size by measuring experimentally the weight distribution along the bowl and calculating the particle size distribution by the equations derived by Hauser and Reed (4). The calculations indicated that the values of  $X_0$  for a definite value of  $Y$  did not vary much for different particle sizes. This, of course, is true only if the size distribution curve is sharp and the sedimentation along the bowl is nearly uniform and in good yield. In this way, average values of  $X_0$  for the different  $Y$  values were obtained empirically. Since  $C$  is a function of  $X_0$ , it is possible to obtain  $C = f_2(Y)$ . In view of the approximations involved in this treatment an average sedimentation constant can be calculated by using the value  $C = 0.32$  for  $Y = 10$  (10). Substituting for  $C$  and  $Y$  into equation 5 leads to:

$$s = 0.0035 \frac{Q_{\min.}}{(\text{R.P.M.})^2} \quad (6)$$

It must be restated that equation 6 can be used for the calculation of sedimenta-

tion constants only if the experimental conditions are optimal so that an approximately uniform layer of sediment and good yield are obtained.

#### EXPERIMENTAL

In a detailed series of experiments, Stanley (13) found that yields of tobacco mosaic virus as high as 93 per cent were obtained by passing the virus solution through the laboratory-model Sharples supercentrifuge operating at 50,000 R.P.M. with the rate of input of solution about 15 ml. per minute. Using equation 6 and these data a value of 210 S for  $s$  is obtained. To test the sensitivity and

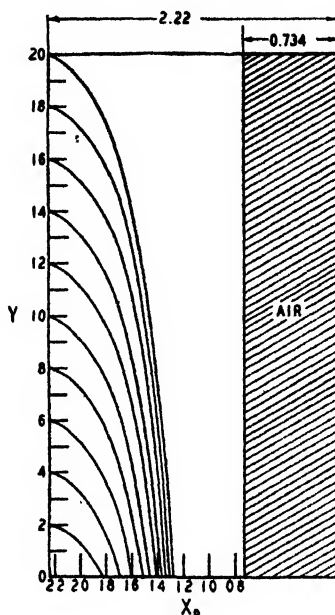


FIG. 2. Paths of the particles in the bowl

accuracy of the method, further experiments were conducted with tobacco mosaic virus.

A stock solution containing 60.2 mg. of tobacco mosaic virus per milliliter, which had been partially purified by precipitation with ammonium sulfate, was used. Three liters of a solution containing 3.23 mg. of protein per milliliter in distilled water were fed into the centrifuge bowl at 12.1 ml. per minute at a temperature of 21°C. The angular rotation of the bowl was 50,000 R.P.M. Upon inspection, approximate uniformity of sedimentation of the virus along the entire length of the liner was observed with a yield of about 91 per cent. Substitution of the appropriate quantities into equation 6 leads to a value of 170 S for the sedimentation constant of tobacco mosaic virus under the conditions of the run. A certain amount of ambiguity necessarily complicates a complete understanding of the true sedimentation rate, owing to the temperature gradients that were



present. It was found that the liquid which drained from the bowl on stopping was at a temperature of about 26°C., despite attempts at cooling by incorporating into the otherwise regular supercentrifuge a cooling coil, through which water at about 0°C. was passed. The temperature of the effluent unfortunately cannot be used to advantage because of the evaporation and accompanying cooling of the liquid as it leaves the bowl and passes through the exit spout through which air is constantly circulating. Until more accurate determinations of temperature conditions in the bowl itself are made, the value obtained from the drainings will be used. Correcting the value of  $s$  at 26°C. to the reference temperature of 20°C. yields 147 S (uncorrected for viscosity and density of the medium because of lack of knowledge of impurities). The value 159 S (also uncorrected for the medium) was obtained by a study in the analytical ultracentrifuge of the Bauer and Pickels type equipped with the Svensson optical system. The agreement of the value obtained with the Sharples supercentrifuge with that obtained with the reliable ultracentrifuge was good, for the discrepancy was only about 8 per cent.

In the second experiment two batches of virus solution were prepared containing 2.91 mg. of protein per milliliter. One solution was run through the machine at 14 ml. per minute at a temperature of 27°C. with the resultant yield of 84.5 per cent. The second solution was passed through the bowl at 12.5 ml. per minute. In this case the yield was 85.4 per cent, a value not significantly different from the previous run. More efficient cooling was obtained during the second run, with the result that the temperature was very nearly constant at 22.5°C. Values of  $s_{20}$  equal to 166 S and 165 S were obtained in these runs. The analytical ultracentrifuge gave a value of 169 S for  $s_{20}$ , in excellent agreement with the values obtained by the Sharples supercentrifuge.

A third experiment was conducted to determine the uniformity of the sediment along the centrifuge bowl. About 1600 ml. of a solution of purified tobacco mosaic virus in distilled water containing 3.06 mg. of protein per milliliter was passed through the centrifuge, rotating at 50,000 R.P.M., at 11.4 ml. per minute. The use of a brine-ice mixture to cool the centrifuge bowl served to reduce the operating temperature so that the bowl drainings were at 14.5°C. The yield in this run was 78 per cent and the plot of cumulative weight per cent *vs.* distance in centimeters along the bowl was approximately linear. A value of  $s_{20}$  of 183 S was calculated for this run by means of equation 6. The value  $s_{20} = 170$  S was obtained by a study of the same material in the ultracentrifuge.

#### DISCUSSION

Under controlled experimental conditions, as shown in the above experiments, the error in evaluating the sedimentation constant of tobacco mosaic virus by means of the Sharples supercentrifuge is small. In order that equation 6 be satisfied, the material under investigation must be in a reasonably homogeneous state, as in the cases of purified viruses or fractionated bentonite. Another precaution to be observed concerns the rate of input of solution. Optimum oper-

ating conditions must be adhered to, so that the material will sediment in yields of about 85 per cent and with approximate uniformity of sediment along the bowl. Obviously the supercentrifuge is incapable of efficiently sedimenting materials as small as egg albumin, but it is useful for materials, like the viruses, with sedimentation constants of about 100 S and larger.

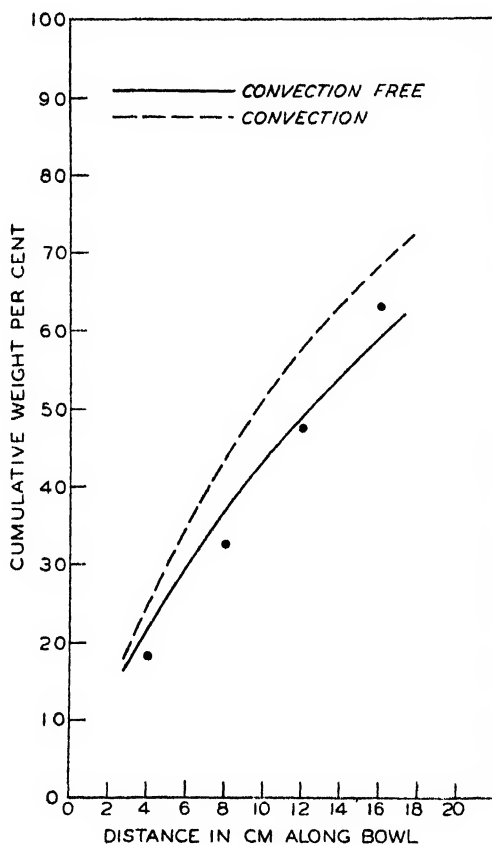


FIG. 3. Plot of calculated cumulative weight per cent *vs.* distance in centimeters along the bowl. ● represents experimental data.

Of interest is the fact that the data of figure 3, corresponding to the third experiment, can be used to calculate the sedimentation constant of the virus without assumptions regarding  $Y = f_1(X_0)$  and without the empirical calibration factor,  $C = 0.32$  at  $Y = 10$ .

Hauser and Reed (4) showed that the number of particles which have settled out on the wall before point A (figure 1) is reached is proportional to the ratio of the total volume of solution flowing across the area enclosed by the concentric circles of radii  $X_0$  and  $R_2$  to the total amount of suspension fed into the bowl. Since the weight of the particles is proportional to their number this relationship

can be expressed as

$$W_r = W \frac{\int_{x_0}^{R_2} \frac{dy}{dt} 2\pi x dx}{Q} \quad (7)$$

where  $W_r$  is the weight of particles which have settled out at a given point and  $W$  is the total weight of particles entering the bowl. The values of the cumulative weight per cent,  $(W_r/W) \times 100$ , are determined experimentally. Equation 3 gives  $dy/dt$  as a function of  $x$ , and thus the integral of equation 7 is in terms of  $X_0$  alone. However,  $X_0$  depends on  $S$  and  $Y$  in a complicated fashion, thereby presenting almost insuperable obstacles to an exact solution of equation 7. By a series of approximations it is possible to solve the equation. A table for each assumed value of  $S$  is set up containing the values of  $Y$  considered, the values of  $C$  calculated from equation 5 for the known experimental conditions, the values of  $X_0$  equivalent to the calculated  $C$ , and finally a column corresponding to

$$\frac{1}{Q} \int_{x_0}^{R_2} \frac{dy}{dt} 2\pi x dx$$

which is equal to the theoretically determined cumulative weight per cent. For the purposes of comparison a column is included which tabulates the experimental values of the cumulative weight per cent. The integral in equation 7 has been evaluated for the centrifuge bowl involved in these studies and can be expressed by equation 8 (10):

$$\frac{1}{Q} \int_{x_0}^{R_2} \frac{dy}{dt} 2\pi x dx = 1.2 - 0.3125X_0^2 \log X_0 - 0.445X_0^2 + 0.632X_0^4 \quad (8)$$

Table 1 represents a sample calculation for the assumed value  $s = 160$  S.

This calculation is repeated for several assumed values of the sedimentation constant and the assumed value which gives the best correlation between the experimental and theoretical values for the cumulative weight per cent is considered to be the most nearly correct. Table 2 shows the results of the calculations for several different assumed sedimentation constants. These results indicate clearly that  $s = 130$  S and  $s = 190$  S cannot be considered as solutions of equation 8. Similarly, it is clear from the results presented in the table that values corresponding to  $s = 150$  S to  $s = 170$  S represent the best solution. The table also shows that no single value of the sedimentation constant can completely account for the distribution of the virus sedimented on the walls of the centrifuge bowl. This is probably due to the limitations of the theory proposed in this treatment. Under the conditions of operation of the centrifuge it is likely that streamline flow is not realized completely and the end effects at the bottom and top of the bowl are not negligible, as was assumed in the theory. It is of interest that the value obtained by the approximate treatment as expressed by equation 6 is in very good agreement with the value obtained by the more tedious and complicated method involving the cumulative weight distribution curve.

Of additional interest is the fact that the calibration factor used in obtaining equation 6 was obtained from studies on a fractionated bentonite suspension and applied with considerable accuracy to the experiments on tobacco mosaic virus.

The studies conducted by Stanley on the sedimentation of influenza virus in the Sharples supercentrifuge prove of interest in a further evaluation of the theory presented for the sedimentation in the centrifuge. Stanley (14) concluded that the infectious allantoic fluid can be passed through the centrifuge at rates of flow between 40 and 50 ml. per minute with the recovery of approximately 80 per cent or more of the biological activity. His studies were conducted at 50,000 R.P.M. According to equation 6 the sedimentation constant of the influenza

TABLE 1  
Sample calculation for the assumed value  $s = 160 S$   
 $s = 160 S$ ;  $s_{20} = 184 S$

$r$	$C$	$X_0$	$[(W_Y/W) \times 100]$ (THEORY)	$[(W_Y/W) \times 100]$ (EXPERIMENT)
4	0.128	1.72	22	18
8	0.256	1.53	37	33
12	0.384	1.39	49	47
16	0.512	1.271	59	63

TABLE 2  
Results of calculations for several assumed sedimentation constants

$Y$	$[(W_Y/W) \times 100]$ (THEORY)					$[(W_Y/W) \times 100]$ (EXPERIMENT)
	$s = 130 S$ $s_{20} = 149 S$	$s = 150 S$ $s_{20} = 172 S$	$s = 160 S$ $s_{20} = 184 S$	$s = 170 S$ $s_{20} = 195 S$	$s = 190 S$ $s_{20} = 218 S$	
4	18	21	22	23	25	18
8	32	36	37	39	42	33
12	43	47	49	51	55	47
16	52	57	59	62	67	63

viruses would be about 630 S. The most frequently reported values of the sedimentation constants of the strains of influenza virus lie between 600 and 700 S. Again, the results with the Sharples supercentrifuge are in excellent agreement with the value obtained by the reliable ultracentrifuge technique.

It is of interest that Markham (8), following the approach of Bechhold and Schlesinger (3) and of Schlesinger (11), calculated the sedimentation constant of tobacco mosaic virus on the basis of completely stirred sedimentation. Making use of the formula for convective centrifuging,

$$\frac{C_t}{C_0} = e^{-(R_2 \omega^2 s A t / v)} \quad (9)$$

he calculated values for the sedimentation constant which were in satisfactory

agreement with those found by Lauffer (7) by means of the ultracentrifuge. In equation 9,  $C_t$  is the concentration of virus in the supernatant fluid at time  $t$ ,  $C_0$  is the initial concentration of virus,  $A$  is the area of the internal surface of the bowl (279 cm.<sup>2</sup>), and  $V$  is the volume of solution that has passed through the bowl in the time  $t$ . As Markham pointed out, equation 9 applies to the most unfavorable conditions for sedimentation, and the sedimentation constant values derived from it should be minimal. That they were, in fact, larger than the accepted value for tobacco mosaic virus could mean, as Markham indicated, that there was some concentration gradient formation in the supernatant. In that case sedimentation would occur more rapidly than expected and the values obtained by equation 9 should be high. Table 3 shows the results obtained from the present data for the sedimentation constants on the basis of convectionless sedimentation as expressed by equation 6 and under the conditions of convective centrifuging calculated by equation 9. In all experiments except the last the values obtained on the basis of stirred sedimentation are too high. The value, 840 S, for the sedimentation constant of influenza virus is obtained by the use of

TABLE 3

*Comparison of experimental results with values calculated from two theories*

$Q_{\min.}$  <i>ml./min.</i>	YIELD  <i>per cent</i>	SEDIMENTATION CONSTANTS, S		
		Equation 6	Equation 9	Ultracentrifuge
12.1	91	147	248	159
14	84.5	166	217	169
12.5	85.4	165	222	169
11.4	77	183	188	170

the data of Stanley (14) and equation 9. As in the case of most of the experiments with tobacco mosaic virus, the sedimentation constant for influenza virus calculated on the basis of convective centrifuging is too high.

In an attempt to evaluate further the two theories for sedimentation in the Sharples supercentrifuge the cumulative weight per cent curve was calculated in the following manner on the basis of convective centrifuging:

$$\frac{dC}{dt} = -\frac{R_2 \omega^2 s A}{V} C \quad (10)$$

and

$$\frac{dC}{dt} = \frac{dC}{dy} \cdot \frac{dy}{dt} \quad (11)$$

In equation 11,  $dy/dt$  is the velocity of flow through the bowl, which is  $Q/\pi(R_2^2 - R_1^2)$ . Substituting for  $dy/dt$  in equation 11, equating 10 and 11, and integrating the resulting equation leads to:

$$\frac{C_Y}{C_0} = e^{-R_2 \omega^2 s A \pi (R_2^2 - R_1^2) Y / V Q} \quad (12)$$

In equation 12,  $C_Y$  is the virus concentration of the supernatant at point  $Y$ ,  $V$  is now the volume of liquid contained in the bowl, and the other terms are the same as defined earlier. By the use of equation 12 it is possible to calculate the per cent of virus sedimented at any point along the centrifuge bowl. Figure 3 shows the results obtained by the two methods along with the experimental points. It can be seen that the results based on convectionless sedimentation are in closer agreement with experiment.

Of some interest is the attempt at increasing the efficiency of the Sharples supercentrifuge by decreasing the volume of the bowl through an increase in  $R_1$  (14, 16). Stanley (14), in studies on tobacco mosaic and influenza viruses, found that no significant increase in efficiency resulted from decreasing the liquid layer. Qualitatively, that is the result expected on the basis of convection-free sedimentation. Although the decrease in the distance,  $x$ , along which the particle sediments would tend to increase the efficiency, it is mainly compensated by the decrease in the time the particle is in the bowl. Favoring a slight increase in efficiency is the fact that the particles are subjected to higher average centrifugal fields because of the larger values of  $X_0$ . The use of  $V$  in equation 9 as the total amount of fluid passing through the bowl implies a rapid flow of solution. Under such conditions no significant increase in efficiency would be expected on the basis of stirred sedimentation if the liquid layer were decreased. It is of considerable interest that a decrease in the liquid layer by an increase in  $R_1$  would enable the sedimentation of particles which are too small to be centrifuged out in the conventional clarifier bowl. In this way the practical usefulness of the Sharples supercentrifuge could be greatly enlarged. A detailed analysis of the sediment along the bowl for different values of  $R_1$  would be necessary before a quantitative evaluation of the resolving power of the centrifuge could be made.

Complete accord with experiment cannot be expected, because of the simplifying assumptions and approximations made in the theoretical treatment. The existence of a density gradient in the bowl in a direction perpendicular to the intense centrifugal field would lead to instability, with a resultant tendency for the sedimenting particles to be distributed uniformly along the length of the bowl. The fact that non-uniform layers of sediment are obtained under some experimental conditions indicates that this cannot be a dominant factor. However, a true picture of conditions in the bowl must necessarily include the contribution of convection caused by the density gradient along the bowl.

#### SUMMARY

An extension and modification of earlier theoretical work on the Sharples supercentrifuge was performed. With the aid of a calibration factor obtained by a detailed study on a fractionated bentonite suspension, the sedimentation constant of many substances can be calculated from a simple equation derived on the basis of convection-free sedimentation. Experiments with tobacco mosaic virus designed to test the sensitivity and accuracy of the method were described. Excellent agreement was obtained by a comparison of the calculated results with those obtained in the more elaborate ultracentrifuge. A theory for

sedimentation in the Sharples supercentrifuge on the basis of complete convection was discussed and the results obtained by its use were presented. An attempt at evaluating the relative contribution of convection was made by an analysis of the weight distribution of sediment along the wall of the centrifuge bowl. The results indicated that the equations based on convection-free sedimentation yield values which are in closer agreement with experimental values.

The author is indebted to Dr. W. M. Stanley of the Rockefeller Institute for Medical Research, Dr. M. A. Lauffer of the University of Pittsburgh, Dr. W. Kauzmann of Princeton University, and Dr. E. A. Hauser of the Massachusetts Institute of Technology for suggestions and valuable discussions during the preparation of this paper.

#### REFERENCES

- (1) BAUER, J. H., AND PICKELS, E. G.: *J. Exptl. Med.* **64**, 503 (1936).
- (2) BEAMS, J. W.: *Rev. Modern Phys.* **10**, 245 (1938).
- (3) BECHHOLD, H., AND SCHLESINGER, M.: *Biochem. Z.* **236**, 386 (1931).
- (4) HAUSER, E. A., AND REED, C. E.: *J. Phys. Chem.* **40**, 1169 (1936).
- (5) HAUSER, E. A., AND SCHACHMAN, H. K.: *J. Phys. Chem.* **44**, 584 (1940).
- (6) LAMB, H.: *Hydrodynamics of Fluids*, 3rd edition. Cambridge University Press, London (1906).
- (7) LAUFFER, M. A.: *J. Phys. Chem.* **44**, 1137 (1940).
- (8) MARKHAM, R.: *Parasitology* **35**, 173 (1944).
- (9) REED, C. E.: Sc. D. thesis, Department of Chemical Engineering, Massachusetts Institute of Technology, 1937.
- (10) SCHACHMAN, H. K.: S. B. thesis, Department of Chemical Engineering, Massachusetts Institute of Technology, 1939.
- (11) SCHLESINGER, M.: *Kolloid-Z.* **67**, 135 (1934).
- (12) STANLEY, W. M.: *J. Biol. Chem.* **121**, 205 (1937).
- (13) STANLEY, W. M.: *J. Am. Chem. Soc.* **64**, 1804 (1942).
- (14) STANLEY, W. M.: *J. Immunol.* **53**, 179 (1946).
- (15) SVEDBERG, T., AND PEDERSEN, K. O.: *The Ultracentrifuge*. University Press, Oxford (1940).
- (16) TAYLOR, A. R., SHARP, D. G., MCLEAN, I. W., BEARD, DOROTHY, AND BEARD, J. W.: *J. Immunol.* **50**, 291 (1945).
- (17) WYCKOFF, R. W. G., AND LAGSDIN, J. B.: *Rev. Sci. Instruments* **8**, 427 (1937).

## METAL ELECTRONS AND ALLOY CATALYSIS

## THE SYSTEM GOLD-CADMIUM

GEORGE-MARIA SCHWAB AND SOTERIA PESMATJOGLOU<sup>1</sup>*Department of Inorganic, Physical, and Catalytic Chemistry, Institute of Chemistry and Agriculture Nicolaos Canellopoulos, Piraeus, Greece**Received March 13, 1947*

## INTRODUCTION

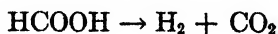
In a series of previous communications (7, 9, 10, 11) some new light was thrown upon the catalytic interaction of the components in catalytic alloys. For the gas-phase dehydrogenation of formic acid, catalyzed by Hume-Rothery alloys, the following rules have been found to hold: (1) Within the range of existence of a phase (the cubic face-centered  $\alpha$ - or the hexagonal  $\epsilon$ -phase), the activation energy increases with increasing concentration of the multivalent component, or, at variation of the component, with increasing valence. (2) On comparing different phases, the saturated  $\alpha$ -,  $\epsilon$ -, and  $\eta$ -phases roughly show the same activation energy, while the (deformed space-centered)  $\gamma$ -phase shows a sharp maximum.

Both findings can be expressed in common by the statement that the activation energy depends on the electron concentration being higher according as the  $k$ -space of the first Brillouin zone in the reciprocal lattice is filled up by the sphere of impulse of the Fermi distribution. For example, the Brillouin zone of the  $\gamma$ -phase, because of its nearly spherical shape, is nearly entirely filled by the Fermi sphere at the saturation concentration of electrons, whereas in the  $\alpha$ -,  $\epsilon$ -, and  $\eta$ -phases considerable regions of the  $k$ -space remain empty.

The bearing of these results on catalytic activation is that thermal activation is needed to force valence electrons of the substrate into free energy levels of the metal electron gas.

In another paper (6) it has been shown that the activation energies exhibit a striking parallelism not only, as is to be expected, with the electrical resistance of the respective alloys, but also with their mechanical strength, expressed for practical purposes as Brinell hardness. An explanation has been attempted on the assumption that a nearly full Brillouin zone exerts a strong resistance to lattice distortions or zone compressions.

The results described here have been obtained on different silver and copper alloy systems. In the present investigation they are extended to a system containing gold as a univalent component. We have measured the activation energy of the reaction



on gold-cadmium alloys of different compositions. The hardness of all but the very brittle specimens has been measured by the usual Brinell method of sphere indenting. The system gold-cadmium gives us for the first time an opportunity

<sup>1</sup> Present address: Western Reserve University, Cleveland, Ohio.



of examining the catalytic behavior of a space-centered cubic  $\beta$ -phase, which in the alloy systems hitherto examined is not stable in the temperature interval of the catalytic reaction. According to Mott and Jones (3), in the  $\beta$ -phase the Brillouin zone is far from being electronically saturated, and thus we must expect the activation energy and hardness to have the order of magnitude of the other phases except the  $\gamma$ -phase.

#### APPARATUS

The experimental procedure, differing somewhat from that used in the experiments cited above, has been described recently in this Journal (12). The method, based on reflux circulation of formic acid vapor over the catalyst and measurement of the rate of product formation with a flowmeter (see figure 1 in reference 12), has been improved in two respects: (1) the evaporation tube B has been filled with fine longitudinal glass capillaries, giving the same effect of smooth boiling; (2) the thermocouple tube M, instead of being sealed in, has been inserted with a ground-glass joint at the top of the dephlegmator chamber F. By this means the catalyst can be removed after use by holding the emptied and dried apparatus head down, and a new catalyst can be placed in E without cutting the apparatus. Vessel A contained liquid formic acid (98 per cent). In all other respects the work was carried out in the manner previously described.

#### CATALYSTS

The gold used was prepared from commercial gold by the modified method of Krüss (2), i.e., dissolution in aqua regia, evaporation, dilution, filtration, precipitation with oxalic acid, boiling with concentrated sulfuric and nitric acids, repeated fusion with potassium bisulfate, and then repetition of all of these operations. Finally, the precipitate was melted on charcoal in an alcohol-blowpipe flame, and rolled into foils of about 0.05 mm.

The cadmium used was Schering-Kahlbaum's *metallicum puriss.*

The alloys were prepared by melting weighed portions of both metals in porcelain crucibles under borax in a blowing furnace. Because of the considerable heat of formation, great care is needed lest the temperature exceed the low boiling point of the alloys and so cause losses. As in the case of silver alloys, the final concentration of the alloys was calculated from their weight on the assumption that only cadmium is oxidized and was controlled by x-ray analysis (see below).

On a flat side of the reguli two or three spherical indentations were made with a Brinell sclerometer, the reguli tempered for 24 hr. at about 400°C., and the hardness measurement repeated. Then the reguli were broken into small lumps of at most 1 mm. size. The surface of the catalyst samples was calculated approximately on the basis of the size statistics. Each sample weighed between 200 and 300 mg.

In figure 1 the phase diagram of the system gold-cadmium is given according to Hansen (1). The regions of homogeneous solids are shaded. From pure gold up to 24 per cent by weight of cadmium, the solid solution  $\alpha$  of cadmium

in the face-centered cubic lattice of gold is stable. We have measured the x-ray diagrams in alloys containing 3, 8, 18, and 24 per cent of cadmium. In the last two, in spite of tempering, certain amounts of a space-centered phase ( $\beta$ ) were found to be present. Between 33 and 41 per cent cadmium (AuCd) and above 267°C., and consequently in the interval of our catalytic observations, only the  $\beta$ -phase exists. This crystallizes, according to Oelander (4), in the body-centered cubic cesium chloride type. At lower temperatures the ordered rhombic  $\beta'$ -phase is formed, being approximately a tetragonally flattened intermediate between a face-centered and a body-centered type. According to Oelander (4), this transition is not supercooled. At room temperature we found this lattice in a 35 per cent alloy, but in a 40 per cent alloy after catalysis the  $\beta$ -lattice had remained as a metastable state at ordinary temperature. At about 50 per cent

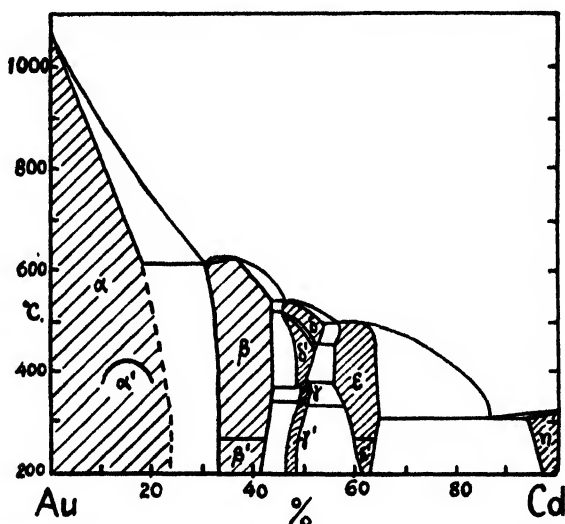


FIG. 1. Phase diagram of the system gold-cadmium according to Hansen (1)

cadmium ( $\text{Au}_3\text{Cd}_3$ ) and in the observed temperature interval the  $\gamma$ -phase occurs, having the large elementary cubic cell of  $\gamma\text{-Cu}_{31}\text{Sn}_8$  with 416 atoms. Below 340°C. this changes into a  $\gamma'$ -phase (5), which, *per exclusionem*, is probably hexagonal. At 47.5 per cent before and after catalysis, as well as at 53 per cent cadmium, our samples even at room temperature gave the diagram of the supercooled cubic  $\gamma$ -phase. Admixture of the  $\beta$ -phase, which is bound to exist at 47.5 per cent, cannot be discerned because of line coincidences. Around 60 per cent cadmium (*ca.*  $\text{Cd}_3\text{Au}$ ) and above 267°C. the hexagonal close-packed arrangement  $\epsilon$  is stable, which below that temperature changes into  $\epsilon'$ , a phase similar to the  $\gamma$ -phase with 32 atoms per unit cell. Our catalysts with 58 per cent cadmium give  $\epsilon'$ -phase diagrams at ordinary temperature.

Unfortunately, x-ray diagrams at elevated temperatures could not be taken, but the results obtained leave no doubt that at the temperatures of catalysis (around 300°C.), and in the  $\beta$ - and  $\gamma$ -phases even below these temperatures, our

catalysts represent the complete series of  $\alpha$ -,  $\beta$ -,  $\gamma$ -, and  $\epsilon$ -phases as well as some binary mixtures. Beyond the  $\epsilon$ -phase, catalytic observations are precluded by the low eutectic melting point of 309°C. between the  $\epsilon$ - and  $\eta$ -phases.

## RESULTS OF MEASUREMENTS

Two samples of most alloys were measured independently, and most samples were remeasured after remaining 24 hr. within the apparatus in an atmosphere of air saturated with formic acid vapor. With the exception of pure gold, where a

TABLE 1  
*Experimental results*

PERCENTAGE OF CADMIUM		ELECTRON CONCENTRATION	PHASE	SURFACE	NUMBER OF MEASUREMENTS	$v(1/T)$ CC. H <sub>2</sub> PER MINUTE	$\frac{10^3}{T}$	$q$	$B'$	$B$ (15 cm. <sup>2</sup> )	$q_m$	$B_m$	HARDNESS	
By weight	In atoms												Before tempering	After tempering
				cm. <sup>2</sup>		cc.		kcal.			kcal.			
0	0	1	$\alpha$	12.5	4	2.25	1.611.5	4.38	4.46		11.5	4.5	57	18
3	5.2	1.05	$\alpha$	18	4	3.4	1.613.5	5.26	5.18		13.5	5.2	63	25
8	13.2	1.13	$\alpha$	3.5	6	5.6	1.627	10.19	10.82					
After 24 hr					6	4.8	1.626.3	9.85	10.48					
8	13.2	1.13	$\alpha$	5.8	5	4.7	1.628	10.47	10.89		27	10.6	94	108
After 24 hr.					6	2.4	1.627	9.82	10.23					
18	27.8	1.28	$\alpha$ + trace of $\beta$	8	6	4.3	1.627	10.07	10.32		27	10.3	109	88
24	35.7	1.36	$\alpha$ + $\beta$	10	4	10	1.620	8.00	8.18		20	8.2	125	108
40	54	1.54	$\beta$	6.28	6	9.2	1.620.5	9.04	9.42		20.7	9.5	94	88
After 24 hr.					5	9.4	1.621	9.24	9.62					
47	61	1.61	$\beta$ + $\gamma$	5.2	6	4.5	1.823	9.71	10.42					
After 24 hr.					6	6.4	1.822	9.44	10.16					
47	61	1.61	$\beta$ + $\gamma$	6	6	4.3	1.824	10.07	10.47		24	10.7	Brittle	
After 24 hr.					4	9.1	1.826	11.21	11.60					
53	66.5	1.67	$\gamma$	5.3	4	8.2	1.935.5	15.89	16.52		35.5	16.1	Broke under the sphere	
58	70.9	1.71	$\epsilon$	6.5	4	5.6	1.821	9.02	9.38		20.5	9.2		
58	70.9	1.71	$\epsilon$	5	3	4.5	1.820	8.52	9.03				Brittle	

slight but reproducible decrease of activation energy by a few hundred calories occurred (*cf.* Schwab and Holz (9)), the repetitions gave nearly identical results. Every measurement was repeated at rising and falling temperatures, as previously described, until the curves coincided. This in most cases happened after the first rise and fall; otherwise the sample was discarded. The degree of accuracy may be seen from typical diagrams which have been published previously (7, 9, 12). It proved to be somewhat better with pure phases than with binary mixtures. The final accepted results are tabulated in table 1.

$v(1/T)$  indicates the velocity in cm.<sup>3</sup> of hydrogen per minute at a suitable com-

parison temperature, which is given in the next column. These numbers are given as a measure of the absolute position of the Arrhenius lines. From them and  $q$  the logarithm of the temperature-independent factor  $B'$  of the sample was calculated according to equation 1:

$$\log v = B' - q/2.3RT \quad (1)$$

For comparison with our former work,  $B$  refers to a 15 cm.<sup>2</sup> surface.  $q_m$  and  $B_m$  are mean values for each concentration of cadmium.

In the case of pure gold Schwab and Holz (7, 9) found  $q = 12.5$  kcal. and  $B = 5.03$ . The agreement, in view of the strong influence of impurities, is satisfactory.

## DISCUSSION OF RESULTS

### 1. The activity $B$

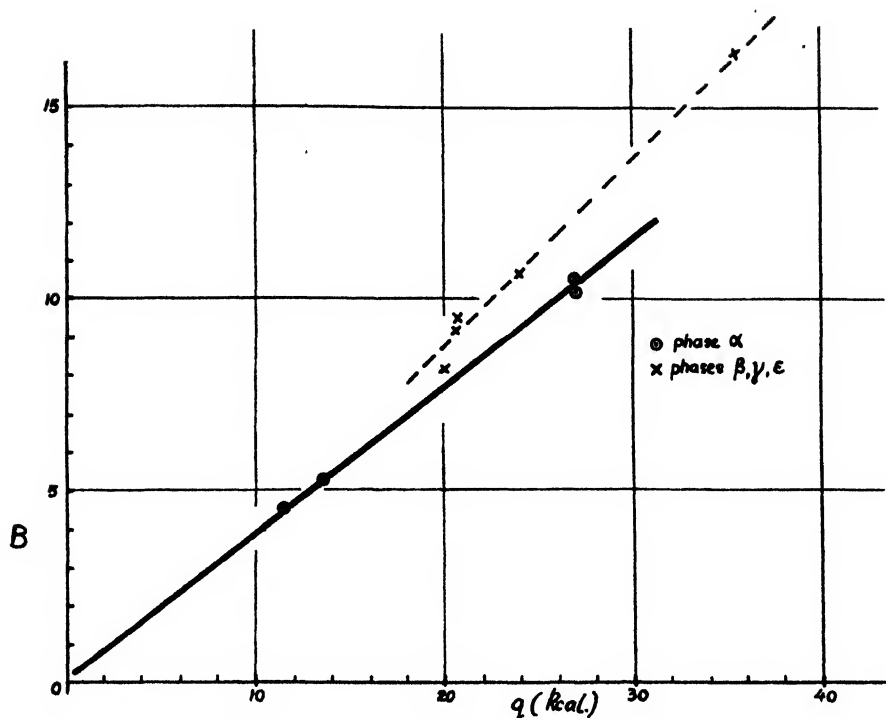
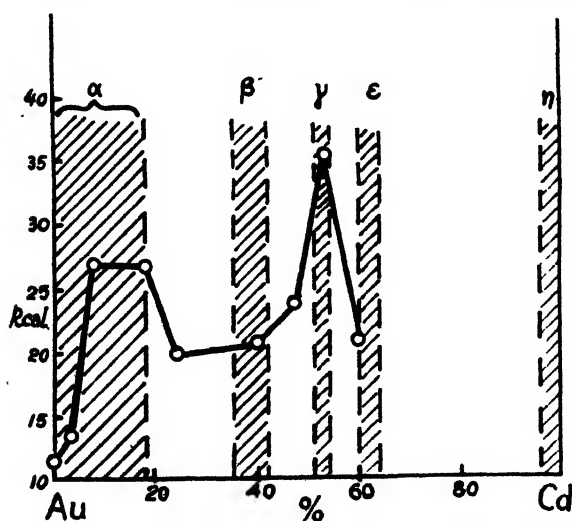
It is apparent that the "activity"  $B$  generally increases with increasing activation energy. This is known (see 7, 9, 12) to be a general phenomenon in heterogeneous catalysis. The increase may be expressed by an equation of the form (8):

$$B = B_0 + q/2.3R\theta \quad (2)$$

In figure 2 our  $B$ -values have been plotted against the respective  $q$ -values. It is seen that two straight lines, each of them corresponding to equation 2, represent the results, one for the  $\alpha$ -phases of different compositions, and another, steeper, one for the  $\beta$ -,  $\gamma$ -, and  $\epsilon$ -phases. A very similar diagram concerning the systems silver-antimony and copper-tin has been published by Schwab and Karatzas (10, figure 1). This general deviation of the intermetallic phases from the curve of the  $\alpha$ -solid solutions, hitherto unexplained, may be due to the fact that the hardness increases with increasing activation energy and therefore the breaking surfaces become increasingly rougher, while  $B$  refers to the geometrical minimum surface. Schwab and Theophilides (12) have calculated a theoretical value of  $B = 12$  for a smooth surface and showed that the highest value found for an  $\alpha$ -phase exceeds this by about 1 unit. In the catalyst with 53 per cent cadmium this value is seen to be exceeded by as much as 4 units. As this is the hardest of all the alloys, this fact may, at least in part, be due to the reason just mentioned. A slight error in  $q$  and some implicit simplifications in the derivation of the Arrhenius equation may also contribute. In any case, the existence of a defined relation between  $B$  and  $q$  enables us to restrict the comparison of different catalysts to their activation energy  $q$ .

### 2. The activation energy

The  $q$ -values of table 1 are plotted in figure 3 against the composition (in weight per cent) of the alloys. The regions of existence of the homogeneous phases at experimental temperatures have been shaded. In our x-ray measurements the  $\alpha$ -range was only extended to 18 per cent. It is clearly seen that in the

FIG. 2. Plot of  $B$ -values against the respective  $q$ -valuesFIG. 3. Plot of  $q$ -values against the composition of the alloys

$\alpha$ -domain, as has been found in all  $\alpha$ -phases, the activation energy is increased by adding cadmium; the initial "atomic inactivation", i.e., the increase in kilogram-calories per atomic per cent, is  $\alpha = 120 \times 10^{-2}$ . For the analogous system

silver-zinc it has been found (9) to be  $100 \times 10^{-2}$ . The convergence of the activation energy to a constant value at higher additions is also a common effect, found, for example, in the systems silver-thallium, silver-antimony, and copper-tin.

The space-centered  $\beta$ -phase has been examined catalytically for the first time. On theoretical grounds we expected a moderate value of the activation energy. In fact, the value of 20 kcal. is lower than that of the saturated  $\alpha$ -phase, and equal to that of the  $\epsilon$ -phase. In the system silver-antimony the  $\epsilon$ -phase, being there the only intermetallic compound, has an activation energy lower than that of the saturated  $\alpha$ -phase. Why, in the heterogeneous region  $\alpha + \beta$ , the value is lower than additivity would predict, is difficult to answer.

The  $\gamma$ -phase again shows the characteristic maximum mentioned previously.

Thus in this system the rules formerly found are fully confirmed and are extended to the  $\beta$ -phase, which falls in the same line with  $\epsilon$  and  $\eta$ .

### 3. The hardness

Unfortunately, the Brinell hardness for the  $\gamma$ - and  $\epsilon$ -phases could not be measured, as these specimens broke under the sclerometer sphere at a load as low as 35 kg. But from the manner of breaking it was obvious that the  $\gamma$ -phase is harder than either  $\epsilon$  or  $\beta + \gamma$ , as we would have expected. Within the  $\alpha$ -phase the hardening effect of added cadmium is clearly seen, although the maximum is not found at the saturation limit. Some anomaly seems to manifest itself in that at 8 per cent cadmium tempering does not, as usual, lower the hardness. Probably here an anomalous hardening, comparable to that of duralumin, takes place, due to the formation of the first traces of the (ordered)  $\alpha'$ -phase. In any case for the hardness, as for the activation energy, the  $\beta$ -phase shows a value lower than the highest of the  $\alpha$ -phase, and the  $\gamma$ -phase is the hardest.

### SUMMARY

The two constants of the Arrhenius equation have been measured for the dehydrogenation of gaseous formic acid with gold-cadmium alloys as catalysts.

A functional relationship between the two has been observed and discussed.

The true energy of activation increases within the  $\alpha$ -phase with increasing electron concentration up to a limiting value; in the  $\beta$ - and  $\epsilon$ -phases it is lower than this, while the  $\gamma$ -phase shows a sharp maximum.

As for the  $\alpha$ -,  $\gamma$ -, and  $\epsilon$ -phases the present results confirm our former results on Hume-Rothery catalysts and their explanation; as for the  $\beta$ -phase, they show for the first time that this case too fits in with the general rules.

In accordance with a former statement, the Brinell hardness of the alloys seems to run parallel to the activation energies.

### REFERENCES

- (1) HANSEN, M.: *Der Aufbau der Zweistofflegierungen*. J. Springer, Berlin (1936).
- (2) KRÜSS, G.: *Ann.* **233**, 30 (1887); cf. FUNK, H.: *Darstellung der Metalle in Laboratorium*, p. 113, F. Enke, Stuttgart (1938).
- (3) MOTT, N. F., AND JONES, H.: *The Theory of the Properties of Metals and Alloys*. University Press, Oxford (1936).

- (4) OELANDER, A.: Z. Krist. **83**, 145 (1932).
- (5) OELANDER A.: J. Am. Chem. Soc. **54**, 3819 (1932).
- (6) SCHWAB, G.-M.: Experientia **2**, 103 (1946).
- (7) SCHWAB, G.-M.: Trans. Faraday Soc. **42**, 689 (1946).
- (8) SCHWAB, G.-M., AND CREMER, E.: Z. physik. Chem. **A144**, 243 (1929); **B5**, 406 (1929).
- (9) SCHWAB, G.-M., AND HOLZ, G.: Z. anorg. Chem. **252**, 205 (1944); Naturwissenschaften **31**, 345 (1943).
- (10) SCHWAB, G.-M., AND KARATZAS, A.: Z. Elektrochem. **50**, 242 (1944); Chem. Abstracts **40**, 4942 (1946).
- (11) SCHWAB, G.-M., AND SCHWAB-AGALLIDIS, ELLY: Ber. **76**, 1228 (1943); Naturwissenschaften **31**, 322 (1943).
- (12) SCHWAB, G.-M., AND THEOPHILIDES, N.: J. Phys. Chem. **50**, 427 (1946).

## THE CATALYTIC ACTION OF SALT PAIRS

GEORGE-MARIA SCHWAB AND ALEXANDER KARATZAS

*Department of Inorganic, Physical, and Catalytic Chemistry, Institute of Chemistry  
and Agriculture Nicolaos Canellopoulos, Piraeus, Greece*

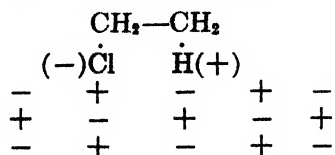
Received March 13, 1947

### INTRODUCTION

Those catalytic reactions which, on account of their technical importance, have been examined with respect to relation between catalytic action and phase composition are mainly hydrogenations, dehydrogenations, oxidations, ammonia synthesis, and petroleum synthesis. In most of them homopolar or interstitial (2) catalyst compounds are to be considered as intermediate states. The catalyst systems are seldom suitable for thermal analysis; thus usually the proper problem concerns the nature of the catalytically active phase. An exception is provided by dehydrogenation reactions on alloy systems, where recently distinct relations between the phase-determining electron concentration and the catalytic action were established (7). In order to gain more fundamental knowledge as to the relation between catalysis and the phase diagram, we have investigated another type of reaction, in which again the phases are well characterized by thermal analysis. This is the salt catalysis of the decomposition of ethyl chloride:



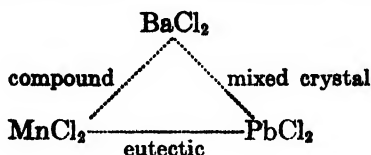
Here, probably, a more polar adsorption of the type



forms the intermediate state. The reaction has been studied kinetically by

Grimm and Schwamberger (3) with different simple chlorides as catalysts, and small, but characteristic, trends of activation energy with the lattice dimensions have been found. At the same time this work gave one of the first bases for the establishment of a relation between the two constants of the Arrhenius equation by Schwab and Cremer (8) which has since been amply confirmed.

In the present paper we propose to investigate the behavior of this reaction on *binary* catalysts belonging to the three principal Roozeboom types of binary systems: mixed crystals, chemical compounds, and eutectics. In order to have as few as possible comparative measurements with the pure components and to avoid a good deal of the uncertainties of comparing different substances, we sought a salt triad representing all three cases. We found the following:



Barium chloride and lead chloride form a continuous series of mixed crystals without a melting-point minimum (5); barium chloride and manganous chloride (in addition to a eutectic at 63 mole per cent manganous chloride) form a compound  $\text{BaMnCl}_4$ , incongruently melting at  $650^\circ\text{C}$ . (5); and lead chloride and manganous chloride form a eutectic at 70 mole per cent lead chloride and melting at  $408^\circ\text{C}$ . (6). We measured the activity and the apparent activation energy of the above reaction with the three pure salts, a mixed crystal, the eutectic, and the compound as catalysts.

#### APPARATUS

A constant stream of gaseous ethyl chloride of 18 cc. per minute was generated in the following way, as described by Schwab and Schultes (10): From a Mariotte bottle A (see figure 1) a saturated sodium chloride solution is dropped at a constant rate into a cylinder (B), whose level communicates with that of the gasometer C. From this the gas is forced at a constant rate through a drying system D and a flowmeter E. Within the electric furnace G it passes through the pre-heating coil F and the catalyst chamber H, containing the mercury vessel of the thermometer I in the middle of the catalyst pieces. The reaction gases were analyzed by the method of Grimm and Schwamberger, later described by Schwab and Drikos (9): The gas is bubbled through 10 cc. of  $N/2000$  sodium hydroxide in the analysis vessel L and the time needed for the color change of dissolved methyl red is measured with a stopwatch. Its reciprocal value is a measure of the reaction velocity. (At very low velocities  $N/10,000$  sodium hydroxide was used.) During the refilling of the analysis vessel the gas mixture was conducted through the wash bottle M of the same counterpressure by changing the threeway stopcock K; thus changes of pressure and flow rate over the catalyst were avoided. The temperature of the catalyst was changed in rising or falling direction without interruption of flow, and at each temperature the de-



scribed measurements were repeated until reproducible time values were obtained. Overnight interruptions did not influence the action of the catalysts used.

#### MATERIALS

(a) *The substrate* was ethyl chloride of the grade used for narcotic purposes, DAB VI, manufactured by Kringske, Speer & Co., Berlin, or Biopharm, Athens. Both preparations gave identical results. The gas was vaporized immediately from the glass bulb into the gasometer C.

(b) *The catalysts*: The pure salts, barium chloride, manganous chloride, and lead chloride, were Merck's *purissimum*. To bring them into a surface state comparable to that of the mixed catalysts, they were melted in porcelain crucibles and poured onto a porcelain plate. The solidified plates were broken into pieces of  $2 \div 0.2$  mm. About 2 cc. of these pieces was placed in H. In the same way the following mixtures were fused: The compound of equivalent amounts of barium chloride and manganous chloride, the eutectic of 30 mole per cent man-

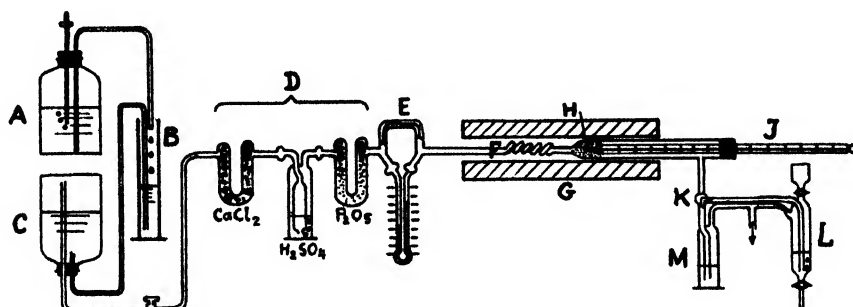


FIG. 1. Apparatus

ganous chloride and 70 mole per cent lead chloride, and a mixed crystal containing equimolecular amounts of barium chloride and lead chloride. A second specimen of manganous chloride was fused in a Rose crucible in a hydrogen chloride atmosphere. For comparison with previous measurements (3) silver chloride, potassium chloride, and sodium chloride were prepared in the same way. A sample of manganese dioxide was prepared by heating below liquid sodium chloride and extracting with water, to check an eventual influence of traces of manganese dioxide on the action of the air-molten manganese preparations; but it showed no catalytic action, apart from a slight formation of phosgene in the fresh (non-annealed) state. The binary catalysts were annealed for 15–48 hr. at 300–500°C.

(c) *Examination of the catalysts*: (1) Microscopically the eutectic lead chloride–manganous chloride showed needles of lead chloride perpendicular to the plate plane, and needles of darker manganous chloride irregularly dispersed between them. (2) With x-rays: The three single salts naturally showed their respective characteristic diagrams; those of barium chloride and lead chloride are entirely identical (isomorphy). In the eutectic both components are discernible, of

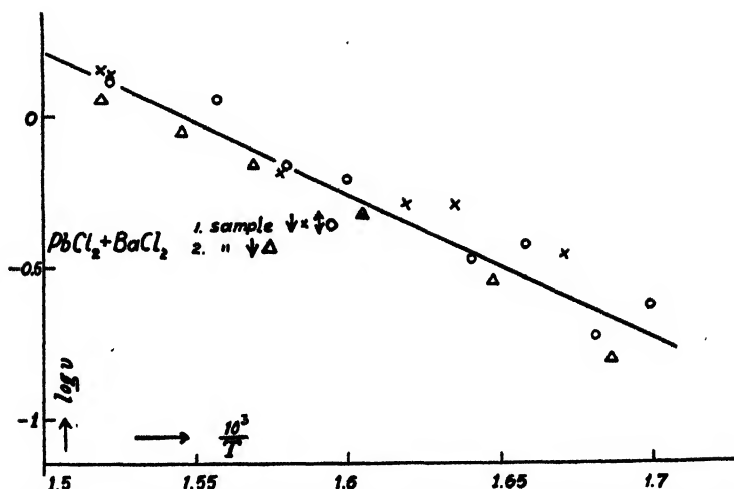


FIG. 2. Results obtained with the mixed catalyst barium chloride-lead chloride

TABLE 1  
Results of measurements

CATALYST	SAMPLE NO.	LOG $v_{1.6}$	$q$	$B$	$q_m$	$B_m$	$\Delta \text{ LOG } v$	REMARKS		
			kcal./mole		kcal./mole					
BaCl <sub>2</sub> .....	1	0.52-1	25	7.77	27	8.4	0.3	After stabilization Air-molten HCl-molten		
	2	0.26-1	28	9.06						
PbCl <sub>2</sub> .....	1	0.95-2	37	11.9	37	11.9	0.2			
MnCl <sub>2</sub> .....	1	0.38-1	39	13.04	39	13.0				
	2	0.5-1	28 <sub>5</sub>	9.48	28 <sub>5</sub>	9.5	0.1			
Mixed crystal BaCl <sub>2</sub> -MnCl <sub>2</sub> .....	1	0.77-1	21	6.69	22	7.0				
	2	0.68-1	23	7.26		0				
Eutectic MnCl <sub>2</sub> - PbCl <sub>2</sub> .....	1	0.5-1	39	13.16	38				12.8	
	2	0.53-1	37	12.48		0.3 (0.7)				
Compound BaMnCl <sub>4</sub> .....	1	0.93-1	13	4.41	13				4.2	
	2	0.88-1	14	4.50						
	3	0.48-1	13	3.96						
	4	0.15	12	4.10						
AgCl .....	1	0.72-2	29	8.87	29	8.9		Sample 2, six months in the apparatus Sample 2, six months in desiccator		

It is seen that after the described pretreatment the catalysts show a relatively reproducible action; different samples differ by about 0.3 in  $\log v$  (excluding the sample BaMnCl<sub>4</sub> No. 3, poisoned during a dead period of six months in the apparatus), a result which is good for this type of measurement.

course lead chloride much more distinctly. The mixed crystal barium chloride-lead chloride gave broad bands in the regions of the line groups of the com-

ponents; consequently it consists of very small crystallites. The compound  $\text{BaMnCl}_4$  does not show any lines of its components, but a number of new lines. Thus the predictions of the phase diagrams are confirmed in all our preparations.

#### RESULTS OF MEASUREMENTS

The reaction velocity is always extremely small; at temperatures about  $360^\circ\text{C}$ . the fraction decomposed is less than 1 per cent, as mentioned by Grimm and Schwamberger. It is therefore justifiable to use the measured velocity directly instead of the velocity constant, and to apply the Arrhenius equation directly to it. The results, represented by straight lines  $\log v$  against  $1/T$ , thus yield the constants  $B$  and  $q$  of the equation

$$\log_{10} v = B - q/2.3RT$$

$v$  being the velocity in 10 cc. of  $N/2000$  sodium hydroxide per minute, and  $q$  the apparent and possibly true activation energy in calories per mole. At least two samples were measured independently of each catalyst (except lead chloride). In figure 2 the results obtained with the mixed catalyst barium chloride-lead chloride are shown graphically. Owing to the nature of the reaction studied, these are not precision measurements like those obtained by our more recent methods (7). The activation energies can be determined within an uncertainty of a few kilogram-calories and the values of logarithm  $B$  to within  $\pm 1$ . In table 1 the results tabulated are the velocities at  $1/T = 1.6 \times 10^{-3}$  and the mean values of  $B$  and  $q$ . The range of temperature is  $330\text{--}380^\circ\text{C}$ .

The following additional measurements may be mentioned: A eutectic mixture of silver chloride and barium chloride showed a catalytic action ten times lower than that of barium chloride, because at the temperatures of observation it is liquid and has a very small surface. Sodium chloride and potassium chloride gave no reproducible results (see also 3). In comparing our results with those of Grimm and Schwamberger (3), the agreement found is reasonable in the case of barium chloride (27 kcal. against 21 kcal.), very bad in the case of lead chloride (37 kcal. against 25 kcal.), and acceptable for silver chloride (29 kcal. against about 35 kcal.). This shows the strong influence of pretreatment; Grimm and Schwamberger worked on catalysts crystallized from solution and stabilized in the reaction vessel, whereas we used fused samples. An influence of this sort is most evident in our measurements on manganous chloride; the air-molten specimen shows a considerably higher activation energy than the  $\text{HCl}$ -molten specimen. (It has been shown above that this is *not* due to traces of manganese dioxide.) Of course the air-molten product is to be considered as a component of the air-molten mixtures containing manganous chloride.

#### DISCUSSION OF RESULTS

##### 1. The activity

The logarithm  $B$  of the first term in the Arrhenius equation is found to be a definite function of the activation energies; large activation energies are accompanied

and compensated for by large activities. Graphically, we find that the relation

$$B = 0.343 q \text{ (kcal.)} - 0.25$$

holds exactly. According to Schwab and Cremer (8) we have:

$$B = A + q/R\Theta$$

$\Theta$  being the temperature of preparation or of the last stabilization of the catalyst; then  $\Theta$  is calculated to be 366°C., i.e., a temperature near the upper limit of the reaction interval used, where in fact the final stabilization of all the catalysts took place. The existence of a defined  $B$ - $q$  relation makes it sufficient to discuss the effect of the catalyst material on the characteristic activation energy only instead of both constants of the Arrhenius equation.

Before doing this, we must see whether the absolute values of  $B$  correspond to the requirements of a simple heterogeneous catalytic decomposition. In a previous paper (Schwab and Theophilides (11)) a formula has been derived for the logarithm of the temperature-independent factor, expressed in flow rate of one product, with the assumption of a fully active surface, completely covered by reactant, i.e., zero order:

$$B = \log \frac{60RT_z F \delta \nu}{pV_m}$$

$R$  being the gas constant, 62.300 cc. (mm.Hg) degrees<sup>-1</sup>;  $T_z$  the room temperature, 300°K.;  $F$  the geometrical surface of the catalyst (as a minimum 60 sq. cm. for 2 cc. of pieces of 2-mm. size);  $\delta$  the thickness of the adsorption space, 10<sup>-8</sup> cm.;  $\nu$  the frequency of the activating oscillation, 10<sup>13</sup> sec.<sup>-1</sup>;  $p$  the pressure of reactant, 760 (mm. Hg);  $V_m$  the molal volume of the reactant in the condensed state, here 70 cc. This formula gives  $B = 11.1$  (in cm.<sup>3</sup> sec.<sup>-1</sup> for  $\nu$ ). As a mole has 24.600 cc. and our velocity unity corresponds to  $5 \times 10^{-6}$  mole min.<sup>-1</sup>, in our units we find:

$$B_{\max} = 12.0$$

Table 1 shows that in fact this value is never exceeded by more than 1 unit (one power of ten in the velocity). This excess may easily be accounted for by slight modifications of the catalyst surface, the frequency, and the thickness of the adsorption space. The agreement is good enough to justify the conclusion that our reaction is a simple (non-chain) decomposition in the surface and is of zero order. The fact that the maximum value of  $B$  often is not attained, according to reference 8, simply means that active centers with small activation energies can occur in fractions of the total surface only.

Schwab and Theophilides showed further that a first-order reaction *ceteris paribus* is bound to have a temperature-independent factor smaller by the factor  $V_g/V_m$ ,  $V_g$  being the molal gas volume at the catalyst temperature. This, under our conditions, would give  $B_{1(\max)} = 9.1$ . This value is surpassed by so many catalysts that with certainty the first order is precluded.

## 2. The activation energies

In comparing the activation energies found with different catalysts, the following remarks may be made about the pure salts: Perhaps the smaller activation energy of barium chloride as compared with lead chloride may be explained by the more polar character of the bond, as the  $\text{Pb}^{++}$  ion, being smaller and not having an outer inert gas shell, has a much stronger deformation effect, and the lattice types are identical. As for the  $\text{Mn}^{++}$  ion, which is still smaller, nothing may be predicted with certainty, as the lattice type of the chloride is different. (Possibly the great difference between air-molten and  $\text{HCl}$ -molten manganous chloride is caused by the different surface properties of the "manganese body" and the "chlorine body".)

For the three different cases of mixed catalysts the following is found: The mixed crystal barium chloride-lead chloride has a somewhat smaller activation energy (and activity) than the more active one of its components, barium chloride. This is a "promoter effect" in a homogeneous mixture, although the difference is rather insignificant. The eutectic lead chloride-manganous chloride (to be compared with air-molten manganous chloride, see above) ranges between the values of its components; it is an exactly "additive" catalyst, and nothing like a "synergetical promotion" in the phase boundaries (10) is observed. On the other hand, a strong catalytic interaction of the components occurs in the system barium chloride-manganous chloride. The newly formed compound,  $\text{BaMnCl}_4$ , has an activation energy as low as 13 kcal. per mole, unusually much lower than those of both components. It is difficult to develop a distinct picture without a knowledge of the lattice of the compound; but it is plausible that the  $\text{Cl}^-$  ions, polarized and coordinated into the complex  $\text{MnCl}_4^{--}$ , will all have greater distances from the  $\text{Ba}^{++}$  ions than in barium chloride, and that thus the grouping  $\text{Ba}-\text{Cl}$ , probably acting as the active doublet (see introduction), has a higher dipole moment. Perhaps a tendency toward this effect is realized in the mixed crystal barium chloride-lead chloride.

It is to be emphasized that the decomposition of ethyl chloride, according to Rudkowski, Trifel, and Frost (4; see also Balandin and Limanova (1)), is endothermic with 13.4 kcal. At the surface of  $\text{BaMnCl}_4$  therefore, the necessary heat of activation is equal to the heat of reaction, and no additional activation energy is required. The back-reaction with this catalyst must go on without activation energy and independently of temperature; this gives a good impression of the optimal magnitude of the interaction of the components.

## SUMMARY

The catalytic decomposition of ethyl chloride has been studied kinetically at the surfaces of barium chloride, manganous chloride, lead chloride, and three binary systems of two of these components at atmospheric pressure and at temperatures between  $330^\circ$  and  $380^\circ\text{C}$ .

The logarithm of the first term of the Arrhenius equation has been found to be a linear function of the activation energy.

The maximal absolute velocity corresponds to that calculated for a zero-order reaction.

The eutectic lead chloride-manganous chloride appears to be an exactly additive mixed catalyst, but in the mixed crystal barium chloride-lead chloride slight promotion is detected. In the compound  $\text{BaMnCl}_4$  the activation energy is lowered to the value of the endothermic heat of reaction.

Two of these effects are tentatively explained as due to an increase of the dipole moment of the active doublet.

The authors wish to thank Dr. G. Drikos for construction of the apparatus and preliminary experiments, and especially Prof. G. Matthaopoulos and Dr. Makris, who for a year offered generous hospitality to our air-damaged laboratory and thus enabled us to finish this investigation.

#### REFERENCES

- (1) BALANDIN, A., AND LIVANOVA, O.: *Sci. Repts. State Univ. Moscow* **2**, 237 (1934); *Zentr.* **1935**, II, 1528.
- (2) CRAXFORD, S. R.: *Trans. Faraday Soc.* **42**, 576, 580 (1946).
- (3) GRIMM, H. G., AND SCHWAMBERGER, E.: *Réunion intern. phys. chim.*, Paris **1928**, 214.
- (4) RUDKOWSKI, D. M., TRIFEL, A. G., AND FROST, A. W.: *Ukrain. Khim. Zhur.* **10**, 277 (1935); *Zentr.* **1936**, I, 3667.
- (5) SANDONNINI, C.: *Atti accad. Lincei* **20**, II, 646 (1911); **21**, I, 208 (1912).
- (6) SANDONNINI, C., AND SCARPA, G.: *Atti accad. Lincei* **20**, II, 61 (1911).
- (7) SCHWAB, G.-M.: *Trans. Faraday Soc.* **42**, 689 (1946).
- (8) SCHWAB, G.-M., AND CREMER, E.: *Z. physik. Chem.* **A144**, 243 (1929); **B5**, 406 (1929).
- (9) SCHWAB, G.-M., AND DRIKOS, G.: *Z. physik. Chem.* **A185**, 405 (1940).
- (10) SCHWAB, G.-M., AND SCHULTES, H.: *Z. physik. Chem.* **B9**, 265 (1930).
- (11) SCHWAB, G.-M., AND THEOPHILIDES, N.: *J. Phys. Chem.* **50**, 427 (1946).

## CRITICAL DENSITIES AND RELATED PROPERTIES OF LIQUIDS

SIDNEY W. BENSON

*Department of Chemistry, University of Southern California, Los Angeles 7, California*

### I. REDUCED DENSITIES OF LIQUIDS

Since van der Waals first proposed the theory of corresponding states in the last century, the concept has become a convenient tool in dealing with the thermodynamic properties of both gases at high pressures and vapors. Because of the close relation between vapors and liquids and their identity above the critical temperature, most authors have tacitly assumed that both could be treated from the standpoint of corresponding states. The concept has thereby also gained wide usage in the field of liquids.

The first theoretical justifications for the application of the law of corresponding states to gases and liquids were made recently by DeBoer and Michels (2)

and Pitzer (6), respectively. The arguments presented by these authors indicate that the law of corresponding states may be used as a first approximation in dealing with gas imperfections and with liquid properties. Pitzer has shown that for liquids the sufficient conditions for such an approximation are the assumption of a universal intermolecular potential of the form  $AU(R/R_0)$  and a time-average spherically symmetrical force field for molecules in a liquid.  $A$  and  $R_0$  are specific parameters for a given liquid and  $R$  is the intermolecular distance of a pair of molecules. Since  $R$  in a liquid is simply related to the volume, we see that aside from the constant  $A$ , the volume of a liquid is a convenient parameter in computing its physical properties. Pitzer's development is such that  $T$  and  $V$  become the simplest choices for independent variables of the liquid.

This theoretical justification was a long time overdue, since there has been a great deal of experimental evidence for applying the law of corresponding states to liquids. In addition there are good grounds for considering that the boiling point,  $T_B$ , is approximately a corresponding point. Empirical relations supporting this view of  $T_B$  are:

1. Trouton's rule:  $\Delta S_{\text{vap}} = 21 \text{ cal./mole}^\circ\text{A. at } T_B$ .

2. Guye-Guldberg rule:  $T_B/T_c \equiv \Theta_B \sim 0.60$  ( $T_c$  = critical temperature). (As we can see in tables 1-4, with perhaps one or two exceptions  $\Theta_B$  lies within a range of values from 0.57 to 0.70 with a mean value at about 0.63.)

The additional fact that many approximate empirical expressions for liquids and vapors can be thrown into a reduced form lends additional support to a corresponding law. Typical are the van der Waals expression for vapor pressure:

$\text{Log } \pi = k \left(1 - \frac{1}{\Theta}\right)$  ( $k \sim 2.75$  for most liquids); the Mathias and Cailletat law of rectilinear diameters:

$$\Delta_m = \frac{\Delta_g + \Delta_l}{2} = 1 + a(1 - \Theta)$$

( $a \sim 1$  for most liquids); and the various equations of state such as those of van der Waals, Dieterici, and Berthelot.

The most recent work on reduced equations of state for liquids is the empirical representations of Bauer *et al.* (1). By redefining reduced variables  $\Theta$  and  $V$  to include the range from melting to critical, they get striking uniformity of representation for reduced volumes, compressibilities, and surface tensions for liquids through this range.

#### *Reduced densities at the boiling point*

In the light of this information it was therefore not completely surprising when a study of reduced densities of liquids at the boiling point showed fairly good constancy. The data plotted in figure 1 and presented in tables 1-5 represent the best available critical values for ninety-six liquids.

For normal liquids and even most liquids which are considered associated, it

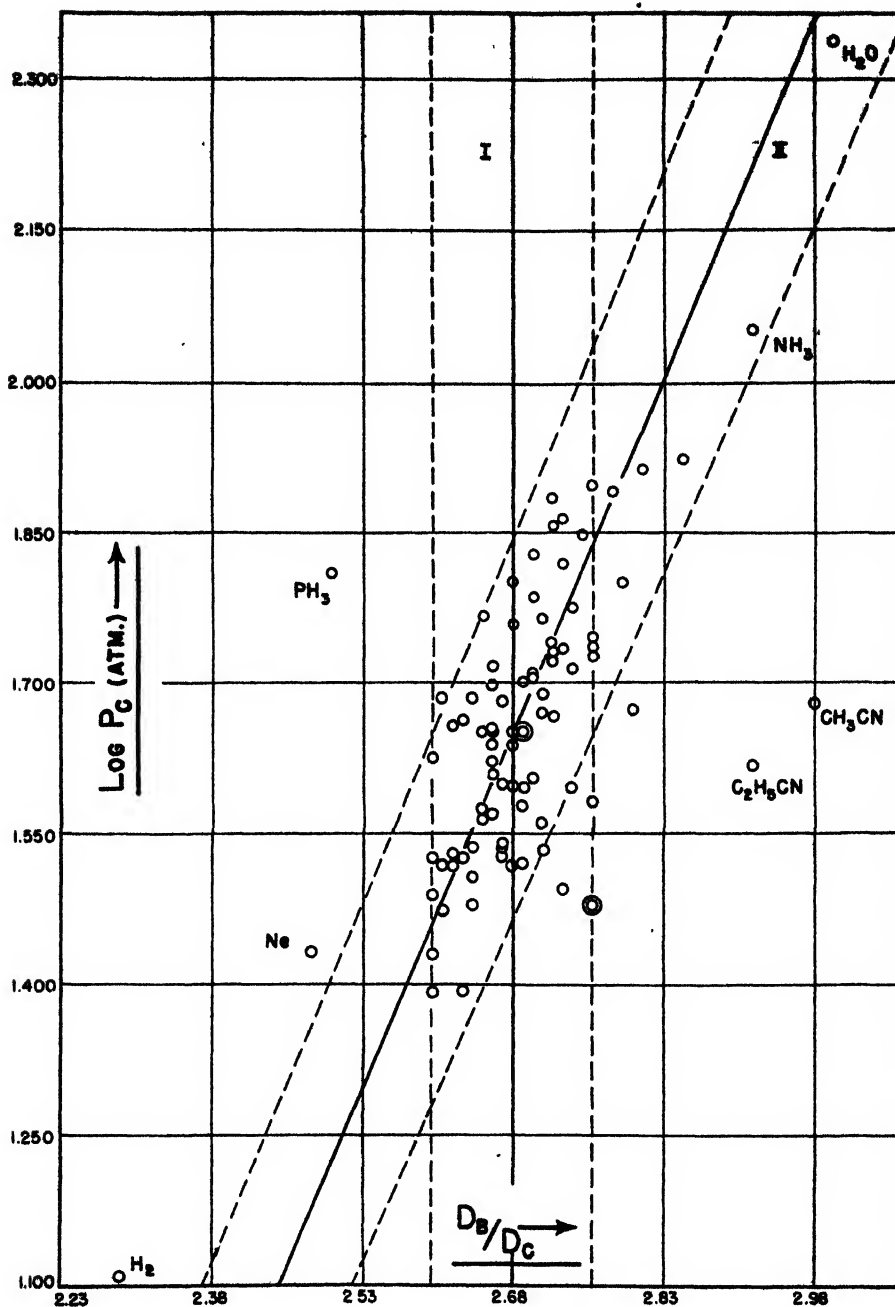


FIG. 1. Plot of reduced liquid densities at the boiling point against  $\log P_c$  (atmospheres). (The dotted lines which bound solid lines I and II represent the range of values,  $\pm 3$  per cent.)

was found that the reduced density at the boiling point,  $\Delta_B$ , is approximately constant with a mean value of 2.68. The vertical solid line labelled I in figure 1



represents this mean value. The two dashed lines parallel to this line represent a range of values of  $\pm 3$  per cent from 2.68.

TABLE 1  
Elements

SUBSTANCE	FOR- MULA	MOLEC- ULAR WEIGHT	$T_b^*$	$T_c$	$D_b$	$D_c$	$P_c$	$P_b/P_c$ $\times 100$	$T_b/T_c$	$D_b/D_c$
			$^{\circ}\text{A.}$	$^{\circ}\text{A.}$	moles/ liter	moles/ liter	atm.			
Hydrogen . . . . .	H <sub>2</sub>	2.00	20.4	33.2	35.5	15.5	12.8	7.80	0.615	2.29
Helium . . . . .	He	4.00	4.21	5.2	31.3	16.5	2.261	44.1	0.81	1.9
Neon . . . . .	Ne	20.2	27.3	44.4	59.6	23.9	26.9	3.72	0.615	2.48
Argon . . . . .	A	39.9	87.5	150.8	35.10	13.29	48.0	2.08	0.580	2.64
Krypton . . . . .	Kr	83.7	121.1	210.6	25.7	9.31	54.2	1.84	0.575	2.76
Xenon . . . . .	Xe	131.3	164.1	289.8	23.3	8.80	58.2	1.72	0.569	2.65
Nitrogen . . . . .	N <sub>2</sub>	28.0	77.4	126.0	28.8	11.10	33.5	2.98	0.614	2.60
Oxygen . . . . .	O <sub>2</sub>	32.0	90.2	154.5	35.8	13.42	49.7	2.01	0.585	2.66
Ozone . . . . .	O <sub>3</sub>	48.0	160.8	268.2	30.3	11.19	67	1.49	0.599	2.70
Chlorine . . . . .	Cl <sub>2</sub>	71.0	238.6	419.2	21.98	8.09	76.1	1.31	0.569	2.72
Mercury . . . . .	Hg	200.6	630.0	1830†	6.35	2.3†			0.34†	2.7†

\*  $T_b$ , boiling point;  $T_c$ , critical temperature;  $D_b$ , density of liquid at the boiling point;  $D_c$ , critical density;  $P_c$ , critical pressure;  $P_b/P_c$ , reduced pressure.

† Values estimated.

TABLE 2  
Inorganic compounds

SUBSTANCE	FORMULA	MOLEC- ULAR WEIGHT	$T_b$	$T_c$	$D_b$	$D_c$	$P_c$	$P_b/P_c$ $\times 100$	$T_b/T_c$	$D_b/D_c$
			$^{\circ}\text{A.}$	$^{\circ}\text{A.}$	moles/ liter	moles/ liter	atm			
Water . . . . .	H <sub>2</sub> O	18.0	373.2	647.3	55.4	17.72	217.7	0.460	0.577	3.00
Hydrogen chloride . . . . .	HCl	36.5	188.2	324.6	32.7	11.60	81.55	1.224	0.580	2.81
Sulfur dioxide . . . . .	SO <sub>2</sub>	64.0	263.2	430.4	22.78	8.18	77.7	1.288	0.611	2.78
Sulfur trioxide . . . . .	SO <sub>3</sub>	80.0	317.8	491.5	22.60	7.92	83.6	1.194	0.645	2.85
Carbon monoxide . . . . .	CO	28.0	81.2	134.2	28.7	10.75	34.53	2.896	0.610	2.67
Carbon dioxide . . . . .	CO <sub>2</sub>	44.0	194.7	304.3	28.8*	10.54	72.95	1.370	0.640	2.73
Carbon disulfide . . . . .	CS <sub>2</sub>	74.0	319.5	546.2	16.55	4.97	75	1.33	0.584	3.32
Phosgene . . . . .	COCl <sub>2</sub>	99.0	281.1	455	14.24	5.25	56	1.79	0.618	2.71
Tin tetrachloride . . . . .	SnCl <sub>4</sub>	260.5	387.3	591.9	7.59	2.84	37.0	2.70	0.654	2.66
Phosphine . . . . .	PH <sub>3</sub>	34	185.7	324.5	22.0	8.82	64.5	1.55	0.571	2.5
Ammonia . . . . .	NH <sub>3</sub>	17.0	239.8	406.1	40.12	13.73	112.3	0.890	0.590	2.92
Nitrous oxide . . . . .	N <sub>2</sub> O	44.0	183.7	309.7	27.8	10.50	71.7	1.393	0.593	2.72
Hydrogen cyanide . . . . .	HCN	27.0	298.8	456.7	25.2	7.4	50	2.0	0.654	3.4

\* Value extrapolated for supercooled liquid.

Attempts were made to correlate the deviations from this mean value with other properties. Interestingly enough it was found that there is no better correlation of these deviations with reduced temperature at the boiling point

$\Theta_B$ . However, a plot of  $\Delta_B$  against  $\log P_c$  (atm.) =  $\log 1/\pi_B$  showed a good correlation. The straight line labelled II in figure 1 stands for the best representation of this relation. It is given by the equation:

$$D_B/D_c = 0.422 \log P_c + 1.981 \quad (P_c \text{ in atmospheres})$$

or in reduced form:

$$\Delta_B = -0.422 \log \pi_B + 1.981 \quad (1)$$

TABLE 3  
Hydrocarbons

SUBSTANCE	FORMULA	MOLECULAR WEIGHT	$T_b$	$T_c$	$D_b$	$D_c$	$P_c$	$P_b/P_c \times 100$	$T_b/T_c$	$D_b/D_c$
			$^{\circ}\text{A.}$	$^{\circ}\text{A.}$	moles/liter	moles/liter	atm.			
Methane.....	$\text{CH}_4$	16	111.6	191.1	26.50	10.08	45.8	2.18	0.584	2.63
Ethane.....	$\text{C}_2\text{H}_6$	30	184.7	305.4	18.21	7.1	48.2	2.07	0.605	2.61
Propane.....	$\text{C}_3\text{H}_8$	44	231.0	370.0	13.24	5.10	42.1	2.37	0.624	2.60
<i>n</i> -Pentane.....	$\text{C}_5\text{H}_{12}$	72	809.3	470.4	8.47	3.23	33.03	3.02	0.656	2.62
Isopentane.....	$\text{C}_5\text{H}_{12}$	72	301.1	461.0	8.50	3.26	32.90	3.04	0.652	2.61
<i>n</i> -Hexane.....	$\text{C}_6\text{H}_{14}$	86	342.1	508.0	7.13	2.73	29.61	3.38	0.674	2.61
Diisopropyl.....	$\text{C}_6\text{H}_{14}$	86	331.3	500.5	7.29	2.80	30.7	3.26	0.662	2.60
<i>n</i> -Heptane.....	$\text{C}_7\text{H}_{16}$	100	371.7	540.0	6.14	2.34	26.84	3.72	0.689	2.62
<i>n</i> -Octane.....	$\text{C}_8\text{H}_{18}$	114	399	569.4	5.36	2.04	24.6	4.06	0.703	2.63
Diisobutyl.....	$\text{C}_8\text{H}_{18}$	114	382.4	550	5.40	2.08	24.6	4.06	0.696	2.60
Cyclopentane.....	$\text{C}_5\text{H}_{10}$	70	322.4	511.8	10.20	3.86	44.55	2.24	0.630	2.65
Methylcyclopentane.....	$\text{C}_6\text{H}_{12}$	84	345.0	532.8	6.32	3.14	37.36	2.68	0.647	2.65
Ethylcyclopentane.....	$\text{C}_7\text{H}_{14}$	98	376.7	569.5	7.01	2.68	33.53	2.98	0.661	2.63
Cyclohexane.....	$\text{C}_6\text{H}_{12}$	84.2	353.9	554.2	8.55	3.21	40.6	2.46	0.639	2.66
Methylcyclohexane.....	$\text{C}_7\text{H}_{14}$	98	374.1	572.3	7.12	2.71	34.32	2.917	0.654	2.64
Ethylene.....	$\text{C}_2\text{H}_4$	28	169.4	282.8	20.3	7.50	50.6	1.972	0.599	2.70
Acetylene.....	$\text{C}_2\text{H}_2$	26	189*	309.1	23.9	8.85	61.7	1.620	0.611	2.70
Propylene.....	$\text{C}_3\text{H}_6$	42	225.5	364.6	14.53	5.55	45.4	2.202	0.635	2.62
Isobutylene.....	$\text{C}_4\text{H}_8$	56	266.6	418	11.20	4.17	39.48	2.530	0.639	2.68
Benzene.....	$\text{C}_6\text{H}_6$	78	353.4	561.7	10.44	3.90	47.9	2.090	0.629	2.67
Toluene.....	$\text{C}_7\text{H}_8$	92	384.0	593.8	8.45	3.17	41.6	2.40	0.648	2.66

\* Extrapolated for supercooled liquid.

The two dashed lines parallel to II (figure 1) represent a range of  $\pm 3$  per cent. It will be seen that, but for a few exceptions which will be discussed, this is a much better general relation between reduced pressure and density at the boiling point. It includes most of the "associated" liquids such as water, ammonia, and hydrogen chloride, as well as the supposedly "normal" liquids such as the hydrocarbons and the heavier rare gases.

An empirical justification for the value of 2.68 for  $\Delta_B$  can be obtained from a consideration of equations of state. If we take van der Waals' equation in reduced form it is:

$$\left(\pi + \frac{3}{\phi^2}\right)\left(\phi - \frac{1}{3}\right) = \frac{8}{3}\Theta \quad (2)$$

in which  $\phi = V/V_c$ ,  $\pi = P/P_c$ , and  $\Theta = T/T_c$ .

TABLE 4  
Organic compounds (containing oxygen)

SUBSTANCE	FORMULA	MOLEC- ULAR WEIGHT	$T_b$	$T_c$	$D_b$	$D_c$	$P_c$	$P_b/P_c$ $\times 100$	$T_b/T_c$	$D_b/D_c$
			$^{\circ}\text{A.}$	$^{\circ}\text{A.}$	moles/ liter	moles/ liter	atm.			
Acetic acid	$\text{C}_2\text{H}_4\text{O}_2$	60	391.7	594.8	15.63	5.84	57.2	1.748	0.659	2.68
Propionic acid...	$\text{C}_3\text{H}_6\text{O}_2$	74	414.3	612.7	11.60	4.26	53	1.89	0.676	2.72
<i>n</i> -Butyric acid...	$\text{C}_4\text{H}_8\text{O}_2$	88	436.7	628	9.27	3.43			0.695	2.70
Isobutyric acid	$\text{C}_4\text{H}_8\text{O}_2$	88	427.7	609	9.18	3.45			0.702	2.66
Methyl formate	$\text{C}_2\text{H}_4\text{O}_2$	60	305.1	487.2	15.95	5.82	59.15	1.690	0.625	2.74
Ethyl formate	$\text{C}_3\text{H}_6\text{O}_2$	74	327.5	508.5	11.87	4.36	46.7	2.14	0.645	2.71
Propyl formate	$\text{C}_4\text{H}_8\text{O}_2$	88	354.1	538	9.47	3.51	40.13	2.485	0.659	2.70
Isobutyl formate	$\text{C}_4\text{H}_{10}\text{O}_2$	102.1	371.4	551	7.78	2.82	38	2.63	0.673	2.76
Isoamyl formate	$\text{C}_6\text{H}_{12}\text{O}_2$	116.2	396.7	576	6.55	2.42	34	2.94	0.688	2.71
Methyl acetate	$\text{C}_3\text{H}_6\text{O}_2$	74	330.3	506.9	11.94	4.40	46.31	2.160	0.650	2.72
Ethyl acetate	$\text{C}_4\text{H}_8\text{O}_2$	88	350.3	523.3	9.40	3.49	37.8	2.64	0.670	2.69
Propyl acetate	$\text{C}_5\text{H}_{10}\text{O}_2$	102	374.7	549.4	7.76	2.90	32.91	3.04	0.684	2.68
Isobutyl acetate	$\text{C}_6\text{H}_{12}\text{O}_2$	116.2	389.7	561	6.60	2.41	31	3.3	0.694	2.73
Methyl propionate	$\text{C}_4\text{H}_8\text{O}_2$	88	352.9	530.6	9.55	3.53	39.34	2.540	0.665	2.69
Ethyl propionate	$\text{C}_5\text{H}_{10}\text{O}_2$	102	372.2	546.1	7.81	2.91	33.0	3.03	0.681	2.69
Methyl <i>n</i> -butyrate	$\text{C}_6\text{H}_{10}\text{O}_2$	102	375.9	554.5	7.87	2.94	34.2	2.92	0.679	2.67
Methyl isobutyrate	$\text{C}_6\text{H}_{10}\text{O}_2$	102	365.5	540.7	7.87	2.95	33.7	2.97	0.675	2.67
Ethyl <i>n</i> -butyrate	$\text{C}_6\text{H}_{12}\text{O}_2$	116.2	394.5	566	6.55	2.37	30	3.3	0.696	2.76
Ethyl isobutyrate	$\text{C}_6\text{H}_{12}\text{O}_2$	116.2	384.9	553	6.55	2.37	30	3.3	0.696	2.76
Acetone	$\text{C}_3\text{H}_6\text{O}$	58	329.2	508.2	12.93	4.62	47.0	2.13	0.648	2.80
Methyl alcohol	$\text{CH}_4\text{O}$	32	337.9	513.2	23.43	8.51	78.67	1.270	0.659	2.76
Ethyl alcohol	$\text{C}_2\text{H}_6\text{O}$	46	351.4	516.3	16.00	5.97	63.1	1.583	0.680	2.68
<i>n</i> -Propyl alcohol	$\text{C}_3\text{H}_8\text{O}$	60	370.6	536.9	12.23	4.55	50.0	2.000	0.690	2.69
Dimethyl ether	$\text{C}_2\text{H}_6\text{O}$	46	249.5	400.1	15.70	5.90	52.0	1.922	0.624	2.66
Diethyl ether	$\text{C}_4\text{H}_{10}\text{O}$	74	307.8	467.0	9.41	3.55	36.5	2.74	0.658	2.65
Methyl ethyl ether	$\text{C}_3\text{H}_8\text{O}$	60	280.7	437.9	11.93	4.50	43.4	2.304	0.641	2.66
Ethyl propyl ether	$\text{C}_5\text{H}_{12}\text{O}$	88	334.6	500.6	7.75	2.93	32.1	3.11	0.669	2.64

Using the reduced density  $\Delta = 1/\phi$  and clearing terms this equation becomes:

$$\Delta^3 - 3\Delta^2 + \left(\frac{8\Theta + \pi}{3}\right)\Delta - \pi = 0 \quad (3)$$

This equation has in general three positive roots. One of them is small and corresponds to the gas density. The largest corresponds presumably to the liquid.

At the boiling point, the last term ( $\pi$ ) in equation 3 may be neglected compared to the other terms (its value ranges from 0.05 to 0.004). This gives us a quadratic equation which we can solve for  $\Delta$  as a function of  $\Theta$  and  $\pi$ . A good approximate

solution for the larger of the two values in the neighborhood of the boiling point is:

$$\Delta_B = 1.5 [1 + \sqrt{1 - 1.185\Theta}] \quad (4)$$

TABLE 5  
Organic compounds (sulfur, nitrogen, and halogens)

SUBSTANCE	FORMULA	MOLEC- ULAR WEIGHT	$T_b$	$T_c$	$D_b$	$D_c$	$P_c$	$P_b/P_c$ $\times 100$	$T_b/T_c$	$D_b/D_c$
			$^{\circ}\text{A.}$	$^{\circ}\text{A.}$	moles/ liter	moles/ liter	atm.			
Methyl mercaptan	$\text{CH}_3\text{S}$	48	279.2	470.0	18.49	6.72	71.4	1.400	0.594	2.75
Ethyl mercaptan...	$\text{C}_2\text{H}_5\text{S}$	62	307.6	498.7	13.27	4.85	54.2	1.842	0.616	2.73
Dimethyl sulfide...	$\text{C}_2\text{H}_6\text{S}$	62	309.0	503.1	13.40	4.94	54.6	1.830	0.615	2.72
Diethyl sulfide....	$\text{C}_4\text{H}_{10}\text{S}$	90	363.5	557.0	8.50	3.10	39.1	2.56	0.652	2.74
Acetonitrile . . . .	$\text{C}_2\text{H}_3\text{N}$	41	355	547.9	17.43	5.85	47.7	2.095	0.648	2.98
Propionitrile.....	$\text{C}_3\text{H}_5\text{N}$	55	370.3	565	12.78	4.39	41.3	2.42	0.655	2.92
Ethylamine....	$\text{C}_2\text{H}_7\text{N}$	45	289.8	456.6	15.28	5.53	55.5	1.80	0.635	2.76
Diethylamine...	$\text{C}_4\text{H}_{11}\text{N}$	73	328.6	496.7	9.14	3.35	36.2	2.76	0.661	2.71
Triethylamine . . .	$\text{C}_6\text{H}_{15}\text{N}$	101	362.2	535.2	6.55	2.48	30.0	3.3	0.678	2.64
Methyl chloride . .	$\text{CH}_3\text{Cl}$	50.5	249.2	416.3	19.73	7.23	65.8	1.520	0.597	2.73
Chloroform.	$\text{CHCl}_3$	119.4	334.3	536	11.79	4.32	53.8	1.860	0.624	2.72
Carbon tetra- chloride . . . .	$\text{CCl}_4$	154	349.9	556.3	9.63	3.62	45.0	2.22	0.629	2.66
Ethyl chloride.	$\text{C}_2\text{H}_5\text{Cl}$	64.5	283.4	460.4	14.05	5.13	51.6	1.935	0.615	2.74
Ethyl bromide..	$\text{C}_2\text{H}_5\text{Br}$	109	312	504	13.00	4.65	61.5	1.625	0.620	2.79
Ethylene dichlo- ride . . . . .	$\text{C}_2\text{H}_4\text{Cl}_2$	99.0	357	561	11.65	4.22	53	1.89	0.636	2.76
Difluorochloro- methane. . . .	$\text{CHClF}_2$	86.5	232.4	369.2	16.37	6.04	48.7	2.05	0.630	2.71
Dichlorofluoro- methane. . . .	$\text{CHCl}_2\text{F}$	103	282.1	451.7	13.66	5.06	51.0	1.960	0.624	2.70
Difluorodichloro- methane. . . .	$\text{CCl}_2\text{F}_2$	121	243.4	384.6	12.22	4.59	39.6	2.525	0.632	2.67
Trichlorofluoro- methane. . . .	$\text{CCl}_3\text{F}$	137.4	296.9	471.2	10.79	4.02	43.2	2.315	0.630	2.68
1,1,2-Trichloro- 1,2,2-trifluoro- methane. . . .	$\text{C}_2\text{Cl}_2\text{F}_3$	187.4	320.8	487.3	8.06	3.25	33.7	2.97	0.659	2.62
Fluorobenzene...	$\text{C}_6\text{H}_5\text{F}$	96	358.4	559.7	9.81	3.69	44.6	2.24	0.641	2.66
Chlorobenzene....	$\text{C}_6\text{H}_5\text{Cl}$	112.6	405.2	632	8.72	3.25	44.6	2.24	0.641	2.68
Bromobenzene...	$\text{C}_6\text{H}_5\text{Br}$	157.0	429.4	670	8.31	3.09	44.6	2.24	0.641	2.69
Iodobenzene.....	$\text{C}_6\text{H}_5\text{I}$	204	461.6	721	7.67	2.85	44.6	2.24	0.641	2.69

The same treatment when applied to the Berthellot equation, which is known to give a better representation for vapors than the van der Waals equation, yields:

$$\Delta^3 - 3\Delta^2 + \frac{\Theta}{3}(8\Theta + \pi)\Delta - \pi\Theta = 0 \quad (5)$$

and to the same degree of approximation:

$$\Delta_B = 1.5[1 + \sqrt{1 - 1.185\Theta_B^2}] \quad (6)$$

We see interestingly enough that in the vicinity of the boiling point  $\Delta_B$  is approximately independent of  $\pi$  and dependent only on  $\Theta$ . Values of  $\Delta_B$  computed for different values of  $\Theta_B$  from equations 4 and 6 are presented in table 6.

It can be seen that if  $\Theta_B$  is given the observed mean value of 0.63, then the Berthelot equation gives the value of 2.60 for  $\Delta_B$ . This can be considered as excellent agreement, in view of the general deficiencies of these equations when applied to the liquid state.

The form of equation 1 can be derived by combining van der Waals' equation for vapor pressures,  $\log \pi = 2.74(1 - 1/\Theta)$ , with his equation of state. The latter in the vicinity of the boiling point reduces to equation 4. If we expand equation 4 by the binomial theorem and neglect higher-order terms in  $\Theta_B$ , we find:

$$\Delta_B = 3.00 - 0.89\Theta_B \quad (7)$$

TABLE 6  
*Variation of  $\Delta_B$  with  $\Theta_B$*

$\Theta_B$	$\Delta_B$ CALCULATED FROM VAN DER WAALS EQUATION (EQUATION 4)	$\Delta_B$ CALCULATED FROM BERTHELLOT EQUATION (EQUATION 6)
0.57	2.35	2.68
0.60	2.30	2.64
0.63	2.25	2.60
0.65	2.22	2.56
0.70	2.11	2.47
Mean value $\Theta_B$ (obsd.) = 0.63		Mean value $\Delta_B$ (obsd.) = 2.68

Now, substituting the value of  $\Theta_B$  from the vapor pressure equation this becomes:

$$\Delta_B = 3.00 - \frac{0.89}{1 - 0.37 \log \pi}$$

or:

$$\Delta_B \cong 2.11 - 0.33 \log \pi \quad (8)$$

which compares well with equation 1.

#### *Deviations of liquid behavior from equation 1*

Pitzer (6) has defined a "normal" liquid as one which obeys the assumptions of time-average spherical symmetry and a universal potential function. Such a liquid could be represented by a reduced equation of state, and we see from curve I (figure 1) that to the first approximation  $\Delta_B = 2.68$  may be taken as a

point in such a representation. We may interpret the nature of this approximation as assuming that normal liquids will have a common reduced boiling point of  $\Theta_B = 0.63$ . From this point of view "associated" liquids will have lower reduced boiling temperatures and correspondingly higher reduced boiling densities.<sup>1</sup>

Equation 1 may then be looked upon as a better approximation which takes into account the fact that the boiling point is not quite a corresponding point. Thus it is not surprising to find an improved relation between  $\Delta_B$  and another of the reduced variables, in this case  $\pi_B$ . As is evident from figure 1, equation 1 may be taken empirically as representing an expected behavior for liquids. It is then a matter of interest to understand the reasons for deviations from this behavior for the few liquids that do deviate.

Direct visual observation of the critical volume is almost never reliable because of the rapid change of volume in the vicinity of the critical temperature. For most liquids, the density undergoes an exponential change of from 20 per cent to 60 per cent in the 1°C. temperature interval preceding  $T_c$ . This corresponds to a change of about 4–5 per cent in the 0.1°C. interval below  $T_c$ .

Because of this rapid change, reliable values of the critical volume are almost always made with the aid of the law of rectilinear diameters, extrapolating the mean density of liquid and vapor to the critical temperature. In most cases it has been shown necessary to modify the law by adding higher-order temperature terms to obtain agreement better than 1 per cent (5, 8).

For these reasons it was decided to use  $\pm 3$  per cent as a point of departure in discussing the deviation of  $\Delta_B$  from equation 1. Four liquids have values of  $\Delta_B$  lower than equation 1 predicts. They are helium (–11 per cent), hydrogen (–6.5 per cent), neon (–4 per cent), and phosphine (–10 per cent). (Helium was not included in figure 1 for reasons of space conservation.) The low values for the first three are not surprising, since they have very low critical and boiling temperatures which lie in a region in which they show quantum effects (6). The decreasing magnitude of the deviation with increasing  $T_c$  for these three liquids is in agreement with such a viewpoint. The low value for phosphine is surprising since its structure, relatively high critical pressure (64.5 atm.), and low reduced temperature (0.57) would seem to align it with associated compounds which tend to have high reduced densities. The orthobaric densities reported for it are of poor accuracy ( $\pm 5$  per cent or worse) and it is quite probable that the deviation is due to experimental error rather than a real physical effect.<sup>2</sup>

There are nine liquids which show positive deviations from equation 1. Three of these are acetone (+4 per cent), isobutyl formate (+4 per cent), and isobutyl acetate (+4.5 per cent), represented in figure 1 by the three circles just outside of the dashed line parallel to II. For all of these it seems very likely that the

<sup>1</sup> For Pitzer's "perfect liquid," at  $\Theta_B = 0.63$  he gives the values  $1/\pi_B = 23.1$ ,  $\Delta_B = 2.53$ , and  $\Delta S_{vap} = 15.6$  cal./mole-°A.

<sup>2</sup> Such predictions were made in the course of this study for many critical values taken from the *International Critical Tables* and *Landolt-Bornstein*. They were invariably confirmed when further research in the literature uncovered more recent (and more reliable) measurements of these same critical constants.

experimental values are in error. In the case of two additional liquids, ethyl *n*-butyrate and ethyl isobutyrate, both with deviations of +5 per cent (double circle figure 1), it is almost certain that the experimental values are in error by this amount.

The four remaining liquids showing positive deviations are carbon disulfide (+23 per cent), hydrogen cyanide (+25 per cent), acetonitrile (+11 per cent), and propionitrile (+8 per cent).

The high value for carbon disulfide may be understandable on the basis of a dense packing in the liquid structure which is compatible with its linear structure and the chain-forming tendency of the sulfur atoms due to the availability of 3*d* orbitals. This would be in agreement with similar observations which have been made on both this liquid and its analogue CSeS by Frank (3) and Hildebrand (4).

This is apparently a coöperative phenomenon for the liquid state, since the vapor densities at the boiling point seem to be almost "normal". The low reduced boiling temperature ( $\Theta_B = 0.58$ ) and the high critical pressure (75 atm.) are both characteristic of such association in the liquid. The extent of the deviation (+23 per cent), however, seems rather large and it would be worthwhile to repeat the experimental determinations of the orthobaric densities for this liquid.

The relatively large deviations of the nitriles and their regular change with decreasing molecular weight indicate that these deviations are not due to experimental error but are real effects. From the viewpoint of equation 1 they seem to form a special class of liquids.

Hydrogen cyanide is unquestionably unique among liquids. Quite aside from its chemical properties and instability (explosive), its physical properties are extreme in almost all respects. Its dielectric constant (95) is the largest known. It has an abnormally high boiling point (25.8°C.) for its molecular weight of 27. Its critical ratio ( $RT_c/P_cV_c$ ) is 5.56, again the highest known value for a liquid, indicating considerable association even at the critical temperature. (The expected value for "normal" liquids is 3.7.) Also significant is its vapor density at the boiling point (1.19 g./l.), which gives a "calculated" molecular weight for the vapor of 34. (This is a deviation of 26 per cent compared to expected deviations of 5 per cent for most liquids, and indicates a high degree of association in the vapor state.) Its entropy of vaporization at the boiling point is 22.2 cal./mole-°A., a value which is not high but in fact is almost normal. However, if this value is corrected for vapor association, the corrected entropy of 27 cal./mole-°A. compares with that of water.

Further evidence for the abnormality of the nitriles compared to other liquids is to be found in their high dipole moments. Table 7 shows the dipole moments of some associated compounds.

These values for the physical constants of hydrogen cyanide indicate a possible explanation for the unique position which its reduced boiling density occupies in figure 1 ( $\Delta_B = 3.4$ ). The value for  $\Delta_B$  is compatible with the simultaneous existence of association for hydrogen cyanide both in the liquid and in the vapor.

If we assume a high degree of association in both liquid and vapor even up to the critical point, these will tend to compensate each other and tend to make almost normal such constants as  $\Theta_b$  (0.654), the critical pressure (50 atm.), and the entropy of vaporization (22.2 cal./mole-°A.). The responsibility for the high reduced boiling density may then be placed upon the existence of long chains which pack closely in the liquid. The linear structure of hydrogen cyanide and its high dipole moment both favor such an explanation. The same explanation would also account for the behavior of the methyl and ethyl cyanides. The latter of course show much smaller discrepancies than the hydrogen cyanide.

## II. RELATED PHYSICAL PROPERTIES

Tables 1-5 show that with the exception of strongly associated liquids,  $\Delta_b = 2.68$ . For the larger number of "regular" liquids which fit this relation, the density at the boiling point may be used to compute their critical volumes with an accuracy of  $\pm 3$  per cent. These computed values of the critical volume can then in turn be used to calculate, with similar accuracy, other physical constants

TABLE 7  
*Dipole moments of some associated compounds (7)*

COMPOUND	DIPOLE MOMENT
H <sub>2</sub> O.....	1.87 (gas 25°C.)
NH <sub>3</sub> .....	1.53 (gas 0°C.)
HCl.....	1.03 (gas)
HCN.....	2.8 (gas 30°C.)
CH <sub>3</sub> CN.....	3.4 (benzene solution 20°C.)
C <sub>2</sub> H <sub>5</sub> CN.....	3.4 (benzene solution 20°C.)
Alcohols.....	~ 1.7
Alkali halides.....	~ 2.00 (gas)
Acetone.....	2.97 (gas) (27-180°C.)

such as the van der Waals'  $b$ . Further, if the critical temperature is known, then the constant  $\alpha$  in the law of rectilinear diameters and the coefficient of expansion of the liquid may be calculated. Conversely, if the critical temperature is not known but the coefficient of liquid expansion is known, then both the critical temperature and the constant  $\alpha$  may be calculated.

### *Van der Waals' constant $b$ and critical volumes*

The critical volumes of regular liquids may be computed from the density at the boiling point by means of the relation:

$$V_c = \frac{2.68}{D_b} \quad (9)$$

For regular liquids, the ratio of  $V_c$  to  $b$  is about 2.20 (see table 8). Substituting this into equation 9 we find for  $b$ :

$$b = \frac{1.22}{D_b} \quad (10)$$



In table 8 values of  $V_c$  and  $b$  computed from equations 9 and 10, respectively, are compared with observed values for representative liquids taken from the literature.

*Law of rectilinear diameters and coefficient of liquid expansion*

The equation for the law of rectilinear diameters,

$$D_l + D_g = 2D_c + \alpha(T_c - T) \quad (11)$$

may be solved for  $\alpha$  in terms of the other quantities. At the boiling point the

TABLE 8  
*Critical volumes and van der Waals' constant  $b$  for regular liquids*

COMPOUND	$V_c$ (OBSERVED)	$V_c$ (CALCULATED)	$b$ (OBSERVED)	$b$ (CALCULATED)	$V_c/b$ (OBSERVED)
	cc./mole		cc./mole		
Acetone.....	216	208	99.4	95	2.18
Argon.....	75.3	76.4	32.2	35	2.33
Benzene.....	256	256	115.4	116	2.22
Carbon tetrachloride	276	278	138	128	1.99
Chlorine.....	123.8	122	56.2	56	2.20
Cyclohexane.....	312	314	142.4	142	2.19
Diethylamine.....	298	293	139.2	133	2.14
Ethane.....	141	147	63.8	67	2.21
Ethyl acetate.....	286	285	141.2	130	2.02
Ethyl chloride.....	195	191	86.5	86	2.25
Ethyl ether.....	282	285	134.4	130	2.10
Ethylene.....	133.2	132	57.1	60	2.33
Hydrogen chloride.....	86.1	82	40.8	38	2.11
Isopentane.....	307	316	141.7	143	2.17
Nitrogen.....	90.0	92.8	39.1	42	2.30
Oxygen.....	74.4	75	31.8	33	2.33
Sulfur dioxide.....	122.2	118	56.4	54	2.17

gas density ( $D_g$ ) is negligible compared to the density of the liquid ( $D_l$ ) and the expression for  $\alpha$  reduces to:

$$\alpha = \frac{D_b(\text{liq.}) - 2D_c}{T_c - T_b} \simeq \frac{0.254D_b}{T_c - T_b} \quad (12)$$

Table 9 shows the values of  $\alpha$  calculated from equation 12 with values taken from the literature. The average absolute deviation is about 4 per cent.

By differentiating equation 11 with respect to  $T$  we obtain a relation between  $\alpha$  and the coefficients of expansion of the liquid and vapor:

$$-\alpha = \left( \frac{\partial D_l}{\partial T} \right)_{\text{sat.}} + \left( \frac{\partial D_g}{\partial T} \right)_{\text{sat.}} \quad (13)$$

Thermodynamically, it may be shown that:

$$\left( \frac{\partial D_g}{\partial T} \right)_{\text{sat.}} = -\frac{1}{V_g^2} \left[ \left( \frac{\partial V_g}{\partial T} \right)_P + \left( \frac{\partial V_g}{\partial P} \right)_T \frac{\Delta H}{T \Delta V} \right] \quad (14)$$

At the boiling point, we may assume the vapor to be nearly ideal and also neglect the volume of the liquid compared to the vapor. Equation 14 then becomes:

$$\left(\frac{\partial D_g}{\partial T}\right)_{\text{sat.}} \simeq \frac{P_b}{RT_b^2} \left(\frac{\Delta E_b}{RT_b}\right) \quad (15)$$

Applying Trouton's rule,  $(\Delta E/RT)_b \sim 9.5$ , also  $P_b = 1$  atm., and finally multiplying by 1.05 to take into account the average deviation of vapors from ideality at the boiling point, we have:

$$\left(\frac{\partial D_g}{\partial T}\right) \simeq \frac{0.122M}{T_b^2} \quad (16)$$

TABLE 9  
Parameters from the law of rectilinear diameters

COMPOUND	$\left(\frac{\partial D_l}{\partial T}\right)_{\text{sat.}}$ $\times 10^3$ (OBSERVED)	$\alpha \times 10^3$				$T_c$	
		Observed	Calculated from equation 12	Calculated from equation 17		Observed	Calculated
	g./cc.-°A.	g./cc.-°A.	g./cc.-°A.	g./cc.-°A.		°A.	°A.
Hydrogen chloride . . . . .	2.60	2.56	2.22	2.48		324.6	311
Nitrous oxide . . . . .	2.84	2.59	2.47	2.69		309.7	300
Methane . . . . .	1.50	1.30	1.35	1.35		191.1	191
Ethylene . . . . .	1.49	1.33	1.27	1.38		282.8	275
Methyl chloride . . . . .	1.70	1.61	1.52	1.60		416.3	407
Stannic chloride . . . . .	2.77	2.46	2.45	2.56		591.9	584
Phosgene . . . . .	2.40	2.20	2.06	2.24		455	442
Dimethyl sulfide . . . . .	1.20	1.14	1.09	1.13		503.1	497
Dimethyl ether . . . . .	1.34	1.208	1.22	1.25		400.1	396
Methyl ethyl ether . . . . .	1.25	1.14	1.16	1.16		437.9	437
Methyl formate . . . . .	1.51	1.441	1.33	1.43		487.2	476
Diethyl ether . . . . .	1.26	1.12	1.11	1.16		467.0	461
Diethylamine . . . . .	1.10	1.07	1.01	1.03		496.7	493
Isopentane . . . . .	1.04	0.96	0.97	0.96		461.0	463
Carbon tetrachloride . . . . .	2.05	2.016	1.87	1.91		556.3	547
Chlorobenzene . . . . .	1.24	1.108	1.10	1.15		632	622

$M$  is the molecular weight,  $T_b$  is the boiling point in °A., and  $(\partial D_g/\partial T)_{\text{sat.}}$  is in grams per cubic centimeter. Note also that it is positive in contrast to the negative coefficient obtained for liquids.

Substituting from equation 16 into equation 13, we find:

$$\alpha = -\left(\frac{\partial D_l}{\partial T}\right)_{\text{sat.}} - \frac{0.122M}{T_b^2} = \alpha_l D_l - \frac{0.122M}{T_b^2} \quad (17)$$

The partial  $\left(\frac{\partial D_l}{\partial T}\right)_{\text{sat.}}$  is always negative, so that  $\alpha$  is always greater than this quantity. ( $\alpha_l = -\frac{1}{D_l} \left(\frac{\partial D_l}{\partial T}\right)_{\text{sat.}}$  = coefficient of liquid expansion.)

Equation 17 thus provides a method of calculating  $\alpha$  from the coefficient of expansion of the liquid at the boiling point. In table 9 values of  $\alpha$  calculated from this relation are compared with observed values. The agreement is better than that obtained with equation 12. The average absolute deviation is about 2.5 per cent.

Equations 12 and 17 may be combined and solved for  $T_c$ :

$$T_c = T_b + \frac{0.254D_l}{\alpha} = T_b + \frac{0.254}{\alpha_l - \frac{0.122M}{T_b^2 D_l}} \quad (18)$$

$$\cong T_b + \frac{0.254}{\alpha_l} \left( 1 + \frac{0.122M}{T_b^2 \alpha_l D_l} \right) \quad (18')$$

Equation 18 makes it possible to calculate  $T_c$  from quantities measured at the boiling point, the density and the coefficient of expansion of the liquid. Values of  $T_c$  thus computed are shown in table 9. For these regular liquids, the average absolute deviation of  $T_c$  (calculated) is about 7°A. or about 2 per cent.

#### SUMMARY

1. For most liquids, the reduced density at the boiling point is equal to  $2.68 \pm 3$  per cent. Only hydrogen, helium, neon, and phosphine fall below this range of values.

2. The empirical relation  $\Delta_B = -0.422 \log \pi_B + 1.981$  represents  $\Delta_B$  to within  $\pm 3$  per cent for both associated and regular liquids and may be taken as a representative liquid behavior.

3. From the standpoint of (2) above, there are four very "abnormal" liquids,—carbon disulfide, hydrogen cyanide, methyl cyanide, and ethyl cyanide. It is suggested that their abnormality arises from their ability to form close-packed chains in the liquid.

4. For regular liquids, the relation in (1) above may be used to compute critical volumes from densities at the boiling point:  $V_c = 2.68/D_b$ .

5. Values for van der Waals' constant  $b$  may be computed from  $D_b$  by the equation:  $b = 1.22/D_b$ .

6. Values of the constant  $\alpha$  in the law of rectilinear diameters may be computed from  $D_b$ ,  $T_b$ , and  $T_c$  by means of:

$$\alpha = \frac{0.254D_b}{T_c - T_b}$$

7. Values of  $\alpha$  may also be computed from  $T_b$ ,  $D_b$ , and the coefficient of expansion of the liquid at the boiling point ( $\alpha_l$ ) from the relation:

$$\alpha = \alpha_l D_b - \frac{0.122M}{T_b^2}$$

8. Values of  $T_c$  may be computed from  $T_b$ ,  $D_b$ , and  $\alpha_l$ , using the equation:

$$T_c = T_b + \frac{0.254}{\alpha_l} \left[ 1 + \frac{0.122M}{T_b^2 D_b \alpha_l} \right]$$

## REFERENCES

- (1) BAUER, E., MAGAT, M., AND SURDIN, M.: *Trans. Faraday Soc.* **33**, 81 (1937).
- (2) DE BOER, J., AND MICHELS, A.: *Physica* **5**, 945 (1938).
- (3) FRANK, H. S.: *J. Chem. Phys.* **13**, 504 (1945).
- (4) HILDEBRAND, J. H.: *Solubility*, 2nd edition. Reinhold Publishing Corporation, New York (1936).
- (5) KEENAN, J. H., AND KEYES, F. G.: *Steam Tables*, John Wiley and Sons, Inc., New York (1936).
- (6) PITZER, K. S.: *J. Chem. Phys.* **7**, 583 (1939).
- (7) SIDGWICK, N. V.: *Dipole Moments*, Faraday Society Monograph (1933).
- (8) YOUNG, S.: *Proc. Roy. Soc. (Dublin)* **12**, 374 (1910).

MOLECULAR-WEIGHT DETERMINATIONS OF NON-VOLATILE  
SUBSTANCES BASED ON THE EVAPORATION VELOCITIES  
OF THEIR SOLUTIONS

ALEXANDER SCHÖNBERG AND MOHAMED ZAKI BARAKAT

*Chemistry Department, Faculty of Science, Fouad I University, Abbassia, Cairo, Egypt**Received November 4, 1947*

This paper deals with a method of ascertaining the molecular weight of an organic solute from the rate of evaporation of its solution in a vacuum in a desiccator over concentrated sulfuric acid, having in principle some similarity with Barger's (1) method and the Bousfield (2) method, improved by Sinclair (3) and Sinclair and Robinson (4).

## EXPERIMENTS WITH PURE SOLVENTS AND WITH EQUIMOLAL SOLUTIONS

Our experiment requires two petri dishes (A and B), which are as nearly as possible of the same size and form (twin dishes). When equal weights of ethylene dibromide are put in them and the dishes placed in a symmetrical position in a vacuum desiccator over concentrated sulfuric acid, they lose equal weights of the solvent, within the experimental error of the method (about 0.5 per cent in an equal time, e.g., 24 hr.), whatever the length of time may be. The experimental error is mainly due to the fact that there is practically always a small difference in the size of the dishes. Further experiments (listed in table 1) have shown that the same results are obtained when the experiments are carried out, not with pure solvents, but with two solutions each containing the same number of molecules of the same or different solutes in the same weight of ethylene dibromide. It is not necessary that the experiment should be carried out at a constant temperature; we may start at 15°C. and finish at 25°C. Also, it is not necessary that the pressure within the vacuum desiccator remain constant during the experiment.

## EXPERIMENTS WITH NON-EQUIMOLAL SOLUTIONS

When the number of molecules dissolved in the same weight of ethylene dibromide are not the same but are, for example, in the ratio 2:1 (compare table 2), considerable differences in the loss of the solvent are experienced, whatever the conditions of the experiment with regard to time, temperature, and pressure

within the vacuum desiccator. Great differences are even observed when the ratio is 1:2/3 or 1:1½ (compare table 3).

The results obtained with non-equimolal solutions do not allow us to calculate the molecular weight, as they depend on the conditions under which the experiments are carried out, but in all cases the solution which contains the smallest (greatest) number of molecules of the solute loses most (least), all other conditions being equal.

#### ADVANTAGES OF THE NEW METHOD

The new method can be carried out with a solvent of unknown molecular depression or elevation constant and the only manipulations necessary are weighing,

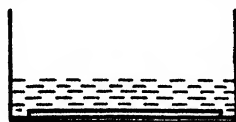


FIG. 1

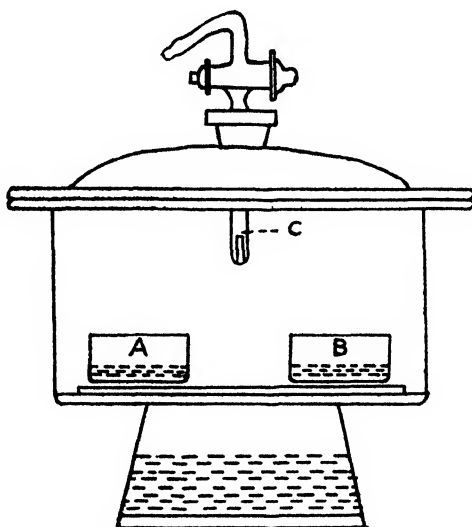


FIG. 2

the preparation of solutions, and the evacuation of the desiccator. The equipment needed is very simple, consisting only of a balance (if possible air-damped), a vacuum desiccator, two dishes, and two small glass stirrers. Whereas the methods ordinarily used in the laboratory for the estimation of the molecular weights of organic substances can only be employed at the freezing or the boiling point of the solution, the above method can be used at intermediate temperatures at will.

The possibility of using this method when working with small amounts of the substance under investigation should not be overlooked.

In the routine work of the organic chemist—provided he does not investigate high polymers—the value of the molecular weight of a substance can be limited

TABLE 1  
*Experiments with solutions of equimolar concentration*

EXPERIMENT NO.	SUBSTANCE	MOLECULAR WEIGHT	WEIGHT OF SOLUTE <i>grams</i>	WEIGHT OF SOLVENT <i>grams</i>	LOSS OF WEIGHT OF THE SOLUTION		
					In grams	In percent- age	Mean loss <i>per cent</i>
1a.....	Benzophenone Azobenzene	182.2	0.4000	19.9710	1.1180	100	$\frac{\text{Benzophenone solution}}{\text{Azobenzene solution}} = \frac{100}{99.95}$
		182.2	0.4000	19.9534	1.1268	100.78	
1b.....	Benzophenone Azobenzene	182.2	0.4000	19.9700	1.4922	100	$\frac{\text{Benzophenone solution}}{\text{Azobenzene solution}} = \frac{100}{99.95}$
		182.2	0.4000	19.9558	1.4792	99.12	
2a.....	Azobenzene Triphenylmethane	182.2	0.4549	19.9806	1.0566	100	$\frac{\text{Azobenzene solution}}{\text{Triphenylmethane solution}} = \frac{100}{100.96}$
		244.3	0.6100	19.9634	1.0460	99.0	
2b.....	Azobenzene Triphenylmethane	182.2	0.4549	19.9634	1.2544	100	$\frac{\text{Azobenzene solution}}{\text{Triphenylmethane solution}} = \frac{100}{100.96}$
		244.3	0.6100	19.9610	1.2760	101.7	
3a.....	Azoxybenzene Triphenylphosphine	198.2	0.4949	12.0008	1.2632	100	$\frac{\text{Azoxybenzene solution}}{\text{Triphenylphosphine solution}} = \frac{100}{99.80}$
		262.3	0.6550	12.0002	1.2800	101.3	
3b.....	Azoxybenzene Triphenylphosphine	198.2	0.4949	11.9944	0.8452	100	$\frac{\text{Azoxybenzene solution}}{\text{Triphenylphosphine solution}} = \frac{100}{99.80}$
		262.3	0.6550	12.0032	0.8310	98.3	
4a.....	Benzil Dibenzalacetone	210.2	0.4195	11.9984	0.8510	100	$\frac{\text{Benzil solution}}{\text{Dibenzalacetone solution}} = \frac{100}{99.89}$
		234.3	0.4680	12.0038	0.8520	100.1	
4b.....	Benzil Dibenzalacetone	210.2	0.4195	19.9748	1.5218	100	$\frac{\text{Benzil solution}}{\text{Dibenzalacetone solution}} = \frac{100}{99.89}$
		234.3	0.4680	19.9544	1.5172	99.69	
5.....	Azoxybenzene Benzylidenefluorene	198.2	0.3299	11.9776	1.5174	100	$\frac{\text{Azoxybenzene solution}}{\text{Benzylidenefluorene solution}} = \frac{100}{100.14}$
		254.3	0.4233	11.9789	1.5196	100.14	

6a.....	{ Azoxybenzene Desoxybenzoin	198.2 196.2	0.4947 0.4900	11.9808 11.9782	0.9420 0.9442	100 100.23	$\frac{\text{Azoxybenzene solution}}{\text{Desoxybenzoin solution}} = \frac{100}{99.55}$
6b.....	{ Azoxybenzene Desoxybenzoin	198.2 196.2	0.4947 0.4900	19.9182 19.8600	1.1402 1.1274	100 98.87	
7a.....	{ Azoxybenzene Benzalazine	198.2 208.3	0.3958 0.4160	19.9650 19.9462	1.9624 1.9748	100 100.63	$\frac{\text{Azoxybenzene solution}}{\text{Benzalazine solution}} = \frac{100}{100.32}$
7b.....	{ Azoxybenzene Benzalazine	198.2 208.3	0.3958 0.4160	14.9388 14.9390	1.2492 1.2492	100 100	
8a.....	{ Azoxybenzene Triphenylchloroethylene	198.2 230.5	0.2831 0.4150	11.9318 11.9190	1.9494 1.9410	100 99.56	$\frac{\text{Azoxybenzene solution}}{\text{Triphenylchloroethylene solution}} = \frac{100}{99.65}$
8b.....	{ Azoxybenzene Triphenylchloroethylene	198.2 230.5	0.2831 0.4150	19.8803 19.8575	1.3105 1.3070	100 99.74	

to two or, at most, three possibilities if the empirical formula and the physical and chemical properties of the compound are known. Therefore, as a rule, only two or three sets of experiments are necessary, and it is simple to decide what multiple of the empirical formula represents the molecular formula of the substance under investigation (cf. table 3).

#### GENERAL REMARKS

*Equipment:* The necessary equipment has been enumerated previously; the desiccator is filled with about 400 cc. of concentrated sulfuric acid, which is replaced after each experiment. The disc must be horizontal. The opening C (cf. figure 2) must be exactly in the middle between the two dishes. The stirrers should be cut from the same glass rod and should have approximately the same length. This length should be smaller than the diameter of the dishes in which they are placed horizontally in the course of the experiment; the two dishes employed were approximately 2.5 cm. high and 5 cm. in diameter. It is advisable to mark one set consisting of a standard dish, a watch glass used as its cover, and a glass rod serving as a stirrer by a special mark, e.g., A, and the other set by another mark, e.g., B.

*Solvent and solute:* The ethylene dibromide was freshly distilled and the same fraction used in both dishes. The substances investigated belonged to various chemical families: hydrocarbons, azo and azoxy compounds, azines, halogen compounds, ethers, esters, mono- and poly-ketones, and organic compounds containing phosphorus were used; all the solutes chosen were non-volatile and did not associate or dissociate in solution.

Ethylene dibromide was chosen on account of its good solvent power and because it does not wet glass. This is important, as no drops are formed on the walls of the petri dishes when they are moved, which would of course influence the area from which evaporation occurs and consequently the rate of evaporation. Care must be taken that at the end of the experiment the dishes do not contain solids or over-saturated solutions which are the result of too much concentration.

*Minimization of the experimental error:* Slight differences in the diameter of the twin dishes cause an error which can be minimized by doing two experiments in which the dishes are exchanged and by taking the mean value in calculating the results. Furthermore, to minimize any influence which the difference in position of the two solutions within the desiccator may cause, the position of the solutions is exchanged; for example, in experiment No. 1a benzophenone was dissolved in dish A standing east in the desiccator and azobenzene in dish B standing west; in experiment 1b, benzophenone was dissolved in dish B standing west and azobenzene in dish A standing east in the desiccator.

#### EXPERIMENTAL

The first step is to weigh each set *in toto*, consisting of the petri dish, its cover, and the stirrer; then by means of a pipet, approximately 20 g. of ethylene dibromide is added to each of the vessels. The weight of the ethylene dibromide added to each dish must be almost identical, and if one of the dishes contains more than the other, the weight is adjusted by removal of small quantities by dipping



TABLE 2  
Experiments with solutions of molar concentration 2:1

EXPERIMENT NO.	SUBSTANCE	MOLECULAR WEIGHT	WEIGHT OF SOLUTE grams	WEIGHT OF SOLVENT grams	LOSS OF SOLVENT	
					In grams	In percentage
9 . . .	{ Azoxybenzene (2 mols) Desoxybenzoin (1 mol)	198.22	0.4947	19.9413	1.1067	Azoxybenzene solution = 100
		196.24	0.2450	19.9357	1.1967	Desoxybenzoin solution = 108.14
10 . . . . .	{ Azoxybenzene (2 mols) Benzalazine (1 mol)	198.22	0.3958	19.9503	1.1266	Azoxybenzene solution = 100
		208.25	0.2080	19.9609	1.2327	Benzalazine solution = 109.41
11 . . . . .	{ Azoxybenzene (2 mols) Triphenylchloroethylene (1 mol)	198.22	0.5861	19.8815	1.0163	Azoxybenzene solution = 100
		290.56	0.4150	19.8875	1.1025	Triphenylchloroethylene solution = 108.48
12 . . . . .	{ Benzil (2 mols) Dibenzalacetone (1 mol)	210.22	0.4199	19.9409	1.2539	Benzil solution = 100
		234.28	0.2340	19.9465	1.3761	Dibenzalacetone solution = 109.74
13 . . . . .	{ Benzophenone (2 mols) Azobenzene (1 mol)	182.21	0.5000	10.0003	0.6216	Benzophenone solution = 100
		182.22	0.2500	9.9985	0.8210	Azobenzene solution = 132.08
14 . . . . .	{ Triphenylmethane (2 mols) Azobenzene (1 mol)	244.32	1.2200	20.0016	0.9342	Triphenylmethane solution = 100
		182.22	0.4550	19.9986	1.2865	Azobenzene solution = 137.71
15 . . . . .	{ Azoxybenzene (2 mols) Triphenylphosphine (1 mol)	198.22	0.9899	19.9707	1.3205	Azoxybenzene solution = 100
		262.28	0.6550	19.9653	1.6817	Triphenylphosphine solution = 127.35
16 . . . . .	{ Benzil (2 mols) Tribromoanisole (1 mol)	210.22	0.4206	19.9711	2.3515	Benzil solution = 100
		344.86	0.3450	19.9655	2.6394	Tribromoanisole solution = 112.24

TABLE 3

*Experiments with solutions of various molal concentrations*

In this case the experimentalist knew that the substance under investigation had the empirical formula  $(C_6H_5O_2)_n$ . The table shows how the value of  $n$  was deduced.  $n$  was correctly found to be 3, as the substance investigated was tribenzoylpyrogallol. The two solutions used in experiments 17, 18, 19, and 20 would be equimolar if  $n = 1, 2, 3$ , and 4, respectively.

EXPERIMENT NO.	SUBSTANCE	MOLECULAR WEIGHT	WEIGHT OF SOLUTE GRAMS	WEIGHT OF SOLVENT GRAMS	LOSS OF SOLVENT	
					In grams	In percentage
17.....	Tribromoanisole Unknown substance	344.86	0.3449 0.1461	19.9575 19.9640	1.2022	$\frac{\text{Tribromoanisole solution}}{\text{Unknown solution}} = \frac{100}{107.6}$
					1.2935	
18.....	Tribromoanisole Unknown substance	344.86	0.3449 0.2921	19.9666 19.9696	1.3445	$\frac{\text{Tribromoanisole solution}}{\text{Unknown solution}} = \frac{100}{104.2}$
					1.4016	
19.....	Tribromoanisole Unknown substance	344.86	0.3449 0.4382	19.9842 19.9780	1.4014	$\frac{\text{Tribromoanisole solution}}{\text{Unknown solution}} = \frac{100}{100.1}$
					1.4028	
20.....	Tribromoanisole Unknown substance	344.86	0.3449 0.5842	19.9653 19.9695	1.3900	$\frac{\text{Tribromoanisole solution}}{\text{Unknown solution}} = \frac{100}{96.1}$
					1.3353	

a small twisted filter paper in the center of the dish, just touching the surface of the liquid to absorb the slight excess. After each dish is filled with ethylene dibromide it is placed on the marble on which the balance stands and covered with its respective cover, with the stirrer in front. Dish A (B) is filled first (last) in this operation.

The substances to be investigated are previously powdered and dried *in vacuo* over concentrated sulfuric acid. The weighing is done on two equally balanced pieces of paper of such a kind that the powders do not adhere to the surface. The substance weighed first (last) is added to dish A (B) and after addition of the solute, each dish is covered again with its cover and both are left until solution is complete. Then each solution is stirred with its corresponding stirrer, in such a way that the stirrer is slowly moved within the solution in the same direction three times and is then cautiously placed full length at the bottom of the dish (compare figure 1), which is covered immediately.

After about 5 min. set A, and afterwards set B, is exactly weighed. The weight of solvent thus deduced is entered in the tables under the heading "Weight of solvent in grams."

Each set after weighing is introduced into the desiccator, set A being introduced first. The two sets are placed in a symmetrical position (compare figure 2), then the cover of each dish is placed in front of it within the desiccator. The desiccator, if possible without moving, is connected with the pump and evacuated for about 10 min. and left without being moved for 20–24 hr.

After this period, air is allowed to enter slowly into the desiccator, then it is opened, and each vessel is closed with the corresponding cover and transferred to the marble on which the balance stands. After 5 min. the sets are weighed (set A first) and from the results the loss of solvent of each set during the 20–24 hr. is calculated.

The experiment is then repeated in the way described under the heading "Minimization of the experimental error."

The mean loss of the solvent is then entered in the tables as a percentage (compare last columns in tables 1–3).

The results listed in tables 1–3 are typical and not the best results obtained from a great number of experiments.

#### SUMMARY

It is shown how the velocity of evaporation of solutions prepared from ethylene dibromide as a solvent in a vacuum desiccator may be used to determine the molecular weight of the solute. This determination may be carried out at temperatures between the boiling and the freezing points of the solvent; it is not necessary to know the molecular elevation or depression constant of the solvent. The method is a very simple one, the necessary manipulations being the preparation of solutions, weighing, and the evacuation of a desiccator.

#### REFERENCES

- (1) BARGER: J. Chem. Soc. **85**, 286 (1904).
- (2) BOUSFIELD: Proc. Roy. Soc. (London) **A103**, 429 (1923).
- (3) SINCLAIR: J. Phys. Chem. **37**, 495 (1933).
- (4) SINCLAIR AND ROBINSON: J. Am. Chem. Soc. **56**, 1830 (1934).

# RELATION OF THE PHYSICAL PROPERTIES OF THE ISOMERIC ALKANES TO MOLECULAR STRUCTURE

## SURFACE TENSION, SPECIFIC DISPERSION, AND CRITICAL SOLUTION TEMPERATURE IN ANILINE

HARRY WIENER

*Department of Chemistry, Brooklyn College, Brooklyn, New York*

*Received January 16, 1948*

A series of thermal properties of the branched-chain alkanes can be correlated with molecular structure by means of the equation:

$$\Delta G = \frac{k}{n^2} \Delta w + b \Delta p \quad (1)$$

These properties include the boiling point at atmospheric pressure (13), the heat of isomerization and the heat of vaporization (14), the boiling point at pressures other than 760 mm. of mercury (15), and the constants of the Antoine vapor-pressure equation (15).

It will be shown in this paper that the available data for surface tension are also well represented by an equation of this type, and that the specific dispersion and the critical solution temperature in aniline of the branched-chain paraffin isomers may be correlated with structure by equations employing the same structural variables. No other methods of correlation of these three properties have appeared in the literature.

### METHOD OF CALCULATION

The structural variables are identical with those used in the papers cited above. In equation 1, the path number  $w$  is calculated by multiplying the numbers of carbon atoms on either side of a carbon-carbon bond and adding these products for all bonds in the molecule; the polarity number  $p$  is defined as the number of pairs of carbon atoms separated by three carbon-carbon bonds;  $n$  is the number of carbon atoms in the paraffin molecule;  $\Delta G = G_n - G$  gives the difference in the value of the physical property for the branched-chain paraffin and its normal isomer; similarly,  $\Delta w = w_n - w$ ;  $\Delta p = p_n - p$ . Examples of calculation of these variables may be found in reference 13.

Within any group of alkane isomers, the variation of a physical property with isomeric structure may be expressed by the simple linear equation:

$$\Delta G = a \Delta w + b \Delta p \quad (2)$$

The majority of the properties of the alkanes obey this relation. To extend it from a single group of isomers to the entire series of alkanes,  $a$  and  $b$  must be expressed empirically as functions of  $n$ , these functions being different for the various properties.

The values of the surface tension ( $\gamma$ ) at 20°C., of the specific dispersion ( $\sigma$ ) at 20°C., of the critical solution temperature ( $cs$ ) in aniline, and of  $w$  and  $d$  for the normal paraffins from  $C_5H_{12}$  to  $C_{10}H_{20}$  are given in table 1.

## SURFACE TENSION OF THE NORMAL ALKANES

The surface tensions of the normal alkanes may be correlated with the number of carbon atoms in the compound by means of a logarithmic function similar in

TABLE 1  
*Reference values for the normal alkanes*

COMPOUND	$\gamma_n$	$\sigma_n$	$cs_n$	$w_n$	$d_n$
<i>n</i> -Pentane . . . . .	15.97	98.0	71.7	20	2
<i>n</i> -Hexane . . . . .	18.41	98.2	69.1	35	3
<i>n</i> -Heptane . . . . .	20.28	98.2	70.1	56	4
<i>n</i> -Octane . . . . .	21.75	98.2	72.1	84	5
<i>n</i> -Nonane . . . . .	22.91	98.1	74.9	120	6

TABLE 2  
*Surface tension of the normal alkanes*

COMPOUND	$n$	$\gamma_{\text{obsd.}}$	$\gamma_{\text{calcd}}$	DEVIATION
		<i>dynes/cm.</i>	<i>dynes/cm.</i>	
<i>n</i> -Pentane . . . . .	5	15.97	15.92	-0.05
<i>n</i> -Hexane . . . . .	6	18.41	18.49	+0.07
<i>n</i> -Heptane . . . . .	7	20.28	20.31	+0.03
<i>n</i> -Octane . . . . .	8	21.75	21.73	-0.02
<i>n</i> -Nonane . . . . .	9	22.91	22.88	-0.03
<i>n</i> -Decane . . . . .	10	23.92	23.86	-0.06
<i>n</i> -Undecane . . . . .	11	24.71	24.71	0.00
<i>n</i> -Dodecane.. . . .	12	25.40	25.45	+0.05

form to that employed by Egloff, Sherman, and Dull (3) to derive boiling-point relationships among aliphatic hydrocarbons. The equation proposed is:

$$\gamma_n = 14.6 \log (n - 3) + 11.52 \quad (3)$$

Values calculated from this equation are compared with the observed values in table 2. The average deviation is  $\pm 0.04$  dynes/cm., which corresponds to the probable experimental error of the data.

The observed values for the last three compounds are those given by Quayle, Day, and Brown (5). The surface tensions of the first five alkanes in table 2 are given by these authors as well as by Wibaut *et al.* (12). The close agreement between observed and calculated values indicates that the experimental values shown are fully self-consistent.

## SURFACE TENSION OF THE BRANCHED-CHAIN ALKANES

The variation of the surface tension of the alkanes with molecular structure can be calculated with good accuracy from the equation:

$$\Delta\gamma = \frac{12.3}{n^2} \Delta w + 1.1\Delta p \quad (4)$$

TABLE 3

*Calculated and observed values of the surface tension of C<sub>5</sub> to C<sub>8</sub> alkanes*

COMPOUND	$\Delta w$	$\Delta p$	$\Delta\gamma_{\text{calcd.}}$	$\gamma_{\text{calcd.}}$	$\gamma_{\text{obed.}}$	REFERENCES	DEVIATION
			dynes/cm.	dynes/cm.	dynes/cm.		
n-Pentane...	0	0	0.00	15.97	15.97	(5, 12)	0.00
2-Methylbutane. ....	2	0	0.98	14.99	14.97	(12)	+0.02
n-Hexane....	0	0	0.00	18.41	18.41	(4, 5, 12)	0.00
2-Methylpentane.....	3	0	1.03	17.38	17.31	(12)	+0.07
3-Methylpentane..	4	-1	0.27	18.14	18.11	(5, 12)	+0.03
2,2-Dimethylbutane.....	7	0	2.39	16.02	16.18	(12)	-0.16
2,3-Dimethylbutane.....	6	-1	0.95	17.46	17.43	(12)	+0.03
n-Heptane. ....	0	0	0.00	20.28	20.28	(2, 5, 12)	0.00
2-Methylhexane. ....	4	0	1.00	19.28	19.17	(12)	+0.11
3-Methylhexane. ....	6	-1	0.41	19.87	19.56	(2)	+0.31
3-Ethylpentane. ....	8	-2	-0.19	20.47	20.16	(2)	+0.31
2,2-Dimethylpentane. .	10	0	2.51	17.77	18.05	(12)	-0.28
2,3-Dimethylpentane. .	10	-2	0.31	19.97	19.82	(12)	+0.15
2,4-Dimethylpentane..	8	0	2.01	18.27	18.12	(12)	+0.15
3,3-Dimethylpentane..	12	-2	0.81	19.47	19.44	(12)	+0.03
2,2,3-Trimethylbutane..	14	-2	1.31	18.97	18.86	(12)	+0.11
n-Octane..	0	0	0.00	21.75	21.75	(4, 5, 6, 7, 12)	0.00
2-Methylheptane. ....	5	0	0.96	20.79	20.81	(5, 6, 7)	-0.02
3-Methylheptane. ....	8	-1	0.44	21.31	21.30	(5, 7, 9, 12)	+0.01
4-Methylheptane. ....	9	-1	0.63	21.12	21.15	(5, 7)	-0.03
3-Ethylhexane. ....	12	-2	0.11	21.64	21.62	(5)	+0.02
2,2-Dimethylhexane....	13	0	2.50	19.25			
2,3-Dimethylhexane....	14	-2	0.49	21.26	21.22	(12)	+0.04
2,4-Dimethylhexane. ....	13	-1	1.40	20.35	19.97	(9)	+0.38
2,5-Dimethylhexane....	10	0	1.92	19.83	19.80	(7, 9, 12)	+0.03
3,3-Dimethylhexane. .	17	-2	1.07	20.68			
3,4-Dimethylhexane. .	16	-3	-0.22	21.97	21.70	(12)	+0.27
2-Methyl-3-ethylpentane. .	17	-3	-0.03	21.78			
3-Methyl-3-ethylpentane. .	20	-4	-0.55	22.30	22.02	(12)	+0.28
2,2,3-Trimethylpentane. .	21	-3	0.74	21.01	20.80	(12)	+0.21
2,2,4-Trimethylpentane. .	18	0	3.46	18.29	18.85	(7, 12)	-0.56
2,3,3-Trimethylpentane. .	22	-4	-0.17	21.92			
2,3,4-Trimethylpentane. .	19	-3	0.35	21.40			

In table 3 calculated and observed values of the surface tension at 20°C. for the alkanes C<sub>5</sub> to C<sub>8</sub> are compared. The observed values are averages of the experimental data in the literature, obtained by assigning to each reported result a weight inversely proportional to the estimated experimental uncertainty of the

determination. The average deviation of calculated from observed values for twenty-eight alkanes, disregarding sign, is  $\pm 0.13$  dynes/cm.; this is of the order of magnitude of the average experimental error, which is estimated at  $\pm 0.10$  dynes/cm. Predicted values of the surface tension are given for five alkanes for which experimental data are not available; the estimated uncertainty of these values is  $\pm 0.2$  dynes/cm. The experimental data for 3-methylhexane and 3-ethylpentane are unreliable, and the calculated surface tensions for these compounds are believed to be closer to the correct values.

The surface tension is similar to thermal properties such as the boiling point and the heat of vaporization in that it, too, is a measure of the cohesive forces acting between molecules of the liquid. It is therefore not surprising that its relation to molecular structure is given by equation 1, which has previously been used to correlate various thermal properties. In view of this fact, the surface tension of the branched-chain alkanes may be related to any of their thermal properties by means of a simple linear equation. For example, the boiling point of the branched-chain paraffin isomers has been shown to follow the equation:

$$\Delta t = \frac{98}{n^2} \Delta w + 5.5 \Delta p \quad (5)$$

The  $\Delta w$ -term may be eliminated between equations 4 and 5, giving:

$$\Delta \gamma = 0.13 \Delta t + 0.4 \Delta p \quad (6)$$

The average absolute deviation between values calculated from this equation and the experimental data listed in table 4 is  $\pm 0.115$  dynes/cm. for twenty-eight alkanes. This equation is therefore both simpler and somewhat more accurate than equation 4; its disadvantage, however, lies in the fact that it can be used only to predict the surface tensions of compounds the boiling points of which have been measured.

#### SPECIFIC DISPERSION

The specific dispersion is defined as

$$\sigma = \frac{n_F - n_C}{d} 10^4 \quad (7)$$

where  $n_F$  and  $n_C$  are the refractive indices for the sodium D (5892.6 Å.), and the hydrogen C (6562.8 Å.) lines, and the units of  $\sigma$  are milliliters per gram.

Determination of the specific dispersion is a physical method of considerable value in analyzing hydrocarbon mixtures. Details of methods of determination of structure, based on the use of this property, are given by Ward and Fulweiler (10), Ward and Kurtz (11), and Thorpe and Larsen (8). The latter authors give methods of correlation for numerous types of hydrocarbon molecules, based on an extensive review of the literature. In their method, however, no account is taken of variation in structure of the various alkanes; the value of the specific dispersion is taken as 98.4 for all paraffin hydrocarbons.

The variation of the specific dispersion at 20°C. with molecular structure is given by the equation:

$$\Delta\sigma = -\Delta\rho - 0.09\Delta w \quad (8)$$

TABLE 4  
*Specific dispersion of alkanes*

COMPOUND	$\Delta w$	$\Delta\rho$	$\sigma_{\text{calcd.}}$	$\sigma_{\text{obsd.}}$	DEVIATION
			ml./g.	ml./g.	
n-Petane.....	0	0	98.0	98.0	0.0
2-Methylbutane.....	2	0	98.2	98.7	-0.5
n-Hexane.....	0	0	98.2	98.2	0.0
2-Methylpentane.....	3	0	98.5	98.7	-0.2
3-Methylpentane.....	4	-1	97.5	97.2	+0.3
2,2-Dimethylbutane.....	7	0	98.8	99.9	-1.1
2,3-Dimethylbutane.....	6	-1	97.7	98.4	-0.7
n-Heptane.....	0	0	98.2	98.2	0.0
2-Methylhexane.....	4	0	98.6	98.6	0.0
3-Methylhexane.....	6	-1	97.7	97.3	+0.4
3-Ethylpentane.....	8	-2	96.9	96.3	+0.6
2,2-Dimethylpentane.....	10	0	99.1	99.9	-0.8
2,3-Dimethylpentane.....	10	-2	97.1	96.9	+0.2
2,4-Dimethylpentane.....	8	0	98.9	98.7	+0.2
3,3-Dimethylpentane.....	12	-2	97.3	97.2	+0.1
2,2,3-Trimethylbutane.....	14	-2	97.5	98.2	-0.7
n-Octane.....	0	0	98.2	98.2	0.0
2-Methylheptane.....	5	0	98.6	98.6	0.0
3-Methylheptane.....	8	-1	97.9	97.6	+0.3
4-Methylheptane.....	9	-1	98.0	97.6	+0.4
3-Ethylhexane.....	12	-2	97.3	96.5	+0.8
2,2-Dimethylhexane.....	13	0	99.4	99.8	-0.4
2,3-Dimethylhexane.....	14	-2	97.5	97.1	+0.4
2,4-Dimethylhexane.....	13	-1	98.4	97.9	+0.5
2,5-Dimethylhexane.....	10	0	99.1	99.1	0.0
3,3-Dimethylhexane.....	17	-2	97.7	97.4	+0.3
3,4-Dimethylhexane.....	16	-3	96.6	96.7	-0.1
2-Methyl-3-ethylpentane.....	17	-3	96.7	96.2	+0.5
3-Methyl-3-ethylpentane.....	20	-4	96.0	95.9	+0.1
2,2,3-Trimethylpentane.....	21	-3	97.1	97.3	-0.2
2,2,4-Trimethylpentane.....	18	0	99.8	100.6	-0.8
2,3,3-Trimethylpentane.....	22	-4	96.2	96.2	0.0
2,3,4-Trimethylpentane.....	19	-3	96.9	97.0	-0.1

The simple form of this equation is due to the fact that the experimental data are not sufficiently precise to permit evaluation of the constants  $a$  and  $b$  in equation 2 as functions of  $n$ .

Observed and calculated values of the specific dispersion for the thirty-three alkanes liquid at 20°C. are compared in table 4. The observed values are those compiled in the tables of the American Petroleum Institute (1). The experimen-



tal uncertainty of these values is believed to vary between  $\pm 0.3$  and  $\pm 0.7$  ml./g. The average absolute deviation between calculated and observed values is  $\pm 0.32$  ml./g.

The theoretical significance of the possibility of correlating specific dispersion

TABLE 5  
*Critical solution temperature of alkanes in aniline*

COMPOUND	$\Delta w$	$\Delta p$	$\Delta c_{st}^{\text{calcd.}}$	$c_{st}^{\text{calcd.}}$	$c_{st}^{\text{obsd.}}$	DEVIATION
			°C.	°C	°C.	
<i>n</i> -Pentane.....	0	0	0.0	71.7	71.7	0.0
2-Methylbutane.....	2	0	-6.6	78.3	78.9	-0.6
<i>n</i> -Hexane.....	0	0	0.0	69.1	69.1	0.0
2-Methylpentane.....	3	0	-4.8	73.9	73.9	0.0
3-Methylpentane.....	4	-1	+0.3	68.8	69.3	-0.5
2,2-Dimethylbutane.....	7	0	-11.1	80.2	81.2	-1.0
2,3-Dimethylbutane.....	6	-1	-2.9	72.0	71.9	+0.1
<i>n</i> -Heptane.....	0	0	0.0	70.1	70.1	0.0
2-Methylhexane.....	4	0	-3.4	73.5	73.6	-0.1
3-Methylhexane.....	6	-1	+0.2	69.9	70.5	-0.6
3-Ethylpentane.....	8	-2	+3.8	66.3	66.3	0.0
2,2-Dimethylpentane.....	10	0	-8.6	78.7	78.3	+0.4
2,3-Dimethylpentane.....	10	-2	+2.0	68.1	68.0	+0.1
2,4-Dimethylpentane.....	8	0	-6.8	76.9	78.7	-1.8
3,3-Dimethylpentane.....	12	-2	+0.3	69.8	69.7	+0.1
2,2,3-Trimethylbutane.....	14	-2	-1.4	71.5	72.2	-0.7
<i>n</i> -Octane.....	0	0	0.0	72.1	72.1	0.0
2-Methylheptane.....	5	0	-2.5	74.6		
3-Methylheptane.....	8	-1	0.0	72.1	72.2	-0.1
4-Methylheptane.....	9	-1	-0.5	72.6		
3-Ethylhexane.....	12	-2	+2.0	70.1		
2,2-Dimethylhexane.....	13	0	-6.5	78.6		
2,3-Dimethylhexane.....	14	-2	+1.0	71.1	70.6	+0.5
2,4-Dimethylhexane.....	13	-1	-2.5	74.6		
2,5-Dimethylhexane.....	10	0	-5.0	77.1	78.0	-0.9
3,3-Dimethylhexane.....	17	-2	-0.5	72.6		
3,4-Dimethylhexane.....	16	-3	+4.0	68.1	68.0	+0.1
2-Methyl-3-ethylpentane.....	17	-3	+3.5	68.6		
3-Methyl-3-ethylpentane.....	20	-4	+6.0	66.1	65.9	+0.2
2,2,3-Trimethylbutane.....	21	-3	+1.5	70.6	70.8	-0.2
2,2,4-Trimethylbutane.....	18	0	-9.0	81.1	80.4	+0.7
2,3,3-Trimethylbutane.....	22	-4	+5.0	67.1		
2,3,4-Trimethylbutane.....	19	-3	+2.5	69.6		

with molecular structure by a method similar to that applicable to the thermal properties is not clear. The fact, however, that this can be done with good agreement between calculated and experimental values makes it likely that the differences between the values of other optical properties, taken at two different wave lengths, may also be correlated by this method. In particular, this pro-

cedure may prove to be useful in correlating absorption spectra and molecular structure of hydrocarbon isomers.

TABLE 6

*Predicted values of surface tension, specific dispersion, and critical solution temperature of nonanes*

COMPOUND	$\Delta w$	$\Delta \rho$	$\sigma_{\text{calcd.}}$ ml./g.	$\gamma_{\text{calcd.}}$ dynes/cm.	$t_{\text{calcd.}}$ °C.
n-Nonane.....	0	0	98.1	22.9	74.9
2-Methyloctane.....	6	0	98.6	22.0	76.8
3-Methyloctane.....	10	-1	98.0	22.5	75.3
4-Methyloctane.....	12	-1	98.2	22.2	76.0
3-Ethylheptane.....	16	-2	97.5	22.7	74.5
4-Ethylheptane.....	18	-2	97.7	22.4	75.1
2,2-Dimethylheptane.....	16	0	99.5	20.5	79.9
2,3-Dimethylheptane.....	18	-2	97.7	22.4	75.1
2,4-Dimethylheptane.....	18	-1	98.7	21.3	77.8
2,5-Dimethylheptane.....	16	-1	98.5	21.6	77.2
2,6-Dimethylheptane.....	12	0	99.2	21.1	78.7
3,3-Dimethylheptane.....	22	-2	98.1	21.8	76.4
3,4-Dimethylheptane.....	22	-3	97.1	22.9	73.7
3,5-Dimethylheptane.....	20	-2	97.9	22.1	75.8
4,4-Dimethylheptane.....	24	-2	98.3	21.5	77.0
2-Methyl-3-ethylhexane.....	24	-3	97.3	22.6	74.3
2-Methyl-4-ethylhexane.....	22	-2	98.1	21.8	76.4
3-Methyl-3-ethylhexane.....	28	-4	96.6	23.0	72.9
3-Methyl-4-ethylhexane.....	26	-4	96.4	23.3	72.2
2,2,3-Trimethylhexane.....	28	-3	97.6	21.9	75.6
2,2,4-Trimethylhexane.....	26	-1	99.4	20.0	80.3
2,2,5-Trimethylhexane.....	22	0	100.1	19.6	81.8
2,3,3-Trimethylhexane.....	30	-4	96.8	22.7	73.5
2,3,4-Trimethylhexane.....	28	-4	96.6	23.0	72.9
2,3,5-Trimethylhexane.....	24	-2	98.3	21.5	77.0
2,4,4-Trimethylhexane.....	28	-2	98.6	20.8	78.3
3,3,4-Trimethylhexane.....	32	-5	96.0	23.5	71.4
3,3-Diethylpentane.....	32	-6	95.0	24.6	68.7
2,2-Dimethyl-3-ethylpentane.....	32	-4	97.0	22.4	74.1
2,3-Dimethyl-3-ethylpentane.....	34	-6	95.2	24.3	69.3
2,4-Dimethyl-3-ethylpentane.....	30	-4	96.8	22.7	73.5
2,2,3,3-Tetramethylpentane.....	38	-6	95.5	23.7	70.6
2,2,3,4-Tetramethylpentane.....	34	-4	97.2	22.1	74.7
2,2,4,4-Tetramethylpentane.....	32	0	101.0	18.0	84.9
2,3,3,4-Tetramethylpentane.....	36	-6	95.3	24.0	70.0

#### CRITICAL SOLUTION TEMPERATURE IN ANILINE

The critical solution temperature in aniline has been used to a considerable extent as an indication of the composition of hydrocarbon mixtures. Within a single group of paraffin isomers, this property closely obeys equation 2. Extension to the entire series of alkanes leads to the somewhat more complicated equation:

$$\Delta c_{st} = -\frac{2050}{n^4} \Delta w - (14.4 - 1.3n)\Delta p \quad (9)$$

The observed values of the critical solution temperature in aniline, given in table 5, are those determined by Wibaut (12), except for two paraffins, 3-methylhexane and 3-ethylpentane, which were not prepared by Wibaut and for which the older values of Edgar and Calingaert are given (2). The average experimental uncertainty is estimated at  $\pm 0.25^\circ\text{C}$ . The average deviation between calculated and observed values is  $\pm 0.34^\circ\text{C}$ .

#### PHYSICAL PROPERTIES OF THE NONANES

In table 6 predicted values of the surface tension, specific dispersion, and critical solution temperature of the thirty-five nonanes, calculated from equations 4, 8, and 9 are listed. The average probable error of the predicted values may be estimated at  $\pm 0.3$  dynes/cm. in surface tension,  $\pm 0.6$  ml./g. in specific dispersion, and  $\pm 0.7^\circ\text{C}$ . in aniline point.

#### SUMMARY

Simple empirical equations, permitting the calculation of physical properties of the alkanes from their molecular structure, are proposed. The properties correlated are the surface tensions of the normal alkanes, the difference in surface tension between any branched-chain alkane and its normal isomer, and the difference in specific dispersion and aniline point between branched-chain and normal alkanes. Comparison with experimental data from the literature shows that the average deviations of the calculated from the observed values are of the order of the experimental uncertainties in all cases. Predicted values of these three physical properties for the nonanes are given.

#### REFERENCES

- (1) AMERICAN PETROLEUM INSTITUTE RESEARCH PROJECT 44 AT THE NATIONAL BUREAU OF STANDARDS. Selected Values of Physical and Thermodynamic Properties of Hydrocarbons. Tables 1b, 2b, 3b, 4b, dated June 30, 1945.
- (2) EDGAR, G., AND CALINGAERT, G.: J. Am. Chem. Soc. **51**, 1541 (1929).
- (3) EGLOFF, G., SHERMAN, J., AND DULL, R. B.: J. Phys. Chem. **44**, 730 (1940).
- (4) HARKINS, W. D., AND CHENG, Y. C.: J. Am. Chem. Soc. **43**, 35 (1921).
- (5) QUAYLE, O. R., DAY, R. A., AND BROWN, G. M.: J. Am. Chem. Soc. **66**, 938 (1944).
- (6) RICHARDS, T. W., SPEYERS, C. L., AND CARVER, E. K.: J. Am. Chem. Soc. **46**, 1196 (1924).
- (7) SMITH, G. W.: J. Phys. Chem. **48**, 170 (1944).
- (8) THORPE, R. F., AND LARSEN, R. G.: Ind. Eng. Chem. **34**, 853 (1942).
- (9) TUOT, M.: Compt. rend. **197**, 1434 (1933).
- (10) WARD, A. G., AND FULWEILER, W. H.: Ind. Eng. Chem., Anal. Ed. **6**, 396 (1934).
- (11) WARD, A. L., AND KURTZ, S. S., JR.: Ind. Eng. Chem., Anal. Ed. **10**, 559 (1938).
- (12) WIBAUT, J. P., WITH HOOGE, H., LANGEDIJK, S. L., OVERHOFF, J., AND SMITTEBERG, J.: Rec. trav. chim. **58**, 329 (1939).
- (13) WIENER, H.: J. Am. Chem. Soc. **69**, 17 (1947).
- (14) WIENER, H.: J. Am. Chem. Soc. **69**, 2636 (1947).
- (15) WIENER, H.: J. Phys. Colloid Chem. **52**, 425 (1948).

DESENSITIZATION BY SENSITIZING DYES<sup>1</sup>

JOHN SPENCE AND B. H. CARROLL

*Kodak Research Laboratories, Rochester 4, New York.**Received January 20, 1948*

## INTRODUCTION

Early investigations of optical sensitization disclosed an optimum concentration for any combination of dye and emulsion. It was further evident that dyed emulsions generally did not show an increase in white-light speed proportional to the increase in energy absorbed. The existence of desensitization by optically sensitizing dyes has been recognized, and more recently has been proved beyond dispute. However, its importance appears to have been generally underestimated, and its connection with the existence of an optimum concentration has never been established.

Eder (3) attributed the loss of sensitivity produced by excessive amounts of dye to filter action by dye which is not adsorbed by the grains. The effect would increase with the concentration of the dye, as is actually observed. This view, which was supported by another pioneer in the field, von Hübl (6), appears quite plausible, and has some basis in fact for emulsions containing weakly adsorbed dyes, such as the eosins. It has been widely accepted in textbooks. However, other early workers recognized the existence of true desensitization. König and Lüppo-Cramer (8, 10) realized that when optical sensitization fails to increase white-light speed, there must be a loss of sensitivity in the region of silver halide absorption, to compensate for the increase of sensitivity to the longer wave lengths. The first definite evidence was supplied by Heisenberg (5), who showed that pinacyanol reduced the sensitivity of silver halide to radiation which it did not absorb. Further data on desensitizing by a number of sensitizing dyes were obtained by Breido and Gorokhovski (1), who measured changes of sensitivity at a number of wave lengths in the ultraviolet region. However, Dieterle (2), in a short article on the effect of sensitizing dyes on natural sensitivity, expressed the opinion that desensitizing was no longer of practical importance. While admitting the possibility of true desensitization, he considered that impurities in the dye and filter action are the usual causes of loss in natural sensitivity. It is shown that desensitization can be readily measured in cases where these explanations are inadequate; it is even a factor to be considered when white-light speed is greatly increased by optical sensitization.

Earlier data from these Laboratories had indicated that desensitization by practically useful dyes was associated primarily with the use of excessive concentrations. Leermakers, Carroll, and Staud (9) have given examples of the change in sensitivity to light transmitted by the standard tricolor filters, corresponding to varying concentrations of dye. Sensitivity to exposure through the red and green filters passed through well-defined maxima as the concentration was increased; sensitivity to light transmitted by the blue filter remained practically

<sup>1</sup> Communication No. 1174 from the Kodak Research Laboratories.

constant for all concentrations up to the value corresponding to the red and green maxima, and then decreased rapidly. This implied that desensitization increased sharply when the optimum sensitizing concentration was exceeded. It is now demonstrated that, while the data are correct, the method of measurement included compensating effects which concealed the continuous variation of desensitization with concentration of sensitizing dye.

Optical sensitization may be expressed in a number of ways. A useful measure may be obtained by exposure to a continuous spectrum through a filter which absorbs only the radiation to which the silver halide is sensitive in the absence of dye; results measured in this way are called "total" sensitization. For the following comparison of dyes, sensitization is expressed in terms of  $1/E_{\max}$ , where  $E_{\max}$  is the energy of wave length corresponding to the maximum of spectral sensitivity required to produce a developed density of 1.0 (or in some cases, 0.5). It is shown that the selection of narrow spectral regions other than those of the absorption maxima does not affect the results.

Desensitization may be measured by the changes in  $E_{400}$ , which is the corresponding energy of incident light of wave length 400  $m\mu$  required to produce the same developed density. This wave length was chosen because it is not appreciably absorbed by any of the dyes used in these experiments. The ratio of  $E_{400}$  for the unsensitized emulsion to  $E_{400}$  of the sensitized is a direct measure of the desensitization which the dye has produced. Both  $E_{\max}$  and  $E_{400}$  were measured in the Physics Department of these Laboratories by exposure with a monochromatic sensitometer, using a slit width of 7.5  $m\mu$  (4).

The observed optical sensitization in any given emulsion is the resultant of three factors: (1) the radiant energy absorbed by the dye, (2) the efficiency of energy transfer from the dye to the silver halide grains, and (3) desensitization by the dye. The effectiveness of a dye may be analyzed readily in terms of  $E_{\max}$ ,  $E_{400}$ , and the corresponding absorptions. Total sensitization, while readily measured, may be computed only by a complicated integration of absorption and sensitivity over the whole region of optical sensitization.

Absorption,  $A$ , is expressed as the percentage of light of the selected wave length which is absorbed by the dyed emulsion layer. It is equal to  $100 - (R + T)$ , where  $R$  and  $T$  are diffuse reflectance and transmittance of the dyed emulsion layers. As in previous communications, these quantities were measured in the Physics Department of these Laboratories by means of the automatic photoelectric spectrophotometer. In regions where there is no absorption, the sum of reflectance and transmittance varies from 96 to 101 per cent, so the error in  $A$  is believed to be not more than a few per cent.

The efficiency of energy transfer from the excited dye to the silver halide grains cannot be measured in absolute terms by photographic measurements. However, by use of  $E_{\max}$ ,  $E_{400}$ , and the corresponding values of  $A$ , it is possible to calculate the desensitization and the relative quantum efficiency of the sensitized photographic process compared to the process in the region of natural absorption by the silver halide. The relative quantum efficiency is the best

available measure of the efficiency of transfer of energy from the dye to the silver halide grains. The quantum efficiency,  $\phi$ , is defined as (molecules reacting)/(quanta absorbed). In photographic measurements the density,  $D$ , is proportional to the amount of silver developed, with sufficient accuracy for our purposes. Therefore, for the total photographic process,

$$\phi = \frac{KD}{AE\lambda}$$

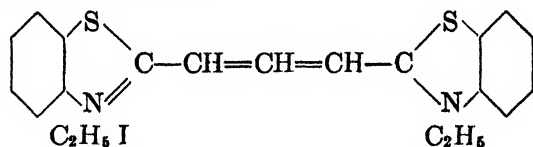
where  $K$  is a constant; and the relative quantum efficiency,

$$\phi_r = \frac{\phi_{(\lambda=\text{sens. max.})}}{\phi_{(\lambda=400\text{ m}\mu)}}$$

where  $\phi_{\text{max.}}$  and  $\phi_{400}$  are derived from  $E_{\text{max.}}$  and  $E_{400}$  and the corresponding values of absorption.  $\phi_r$  never exceeds 1.0. In all the following experiments,  $\phi_r$  was found to be independent of dye concentration. It is, therefore, not affected by the desensitization, which varies with the concentration. This simplifies the comparison of dyes.

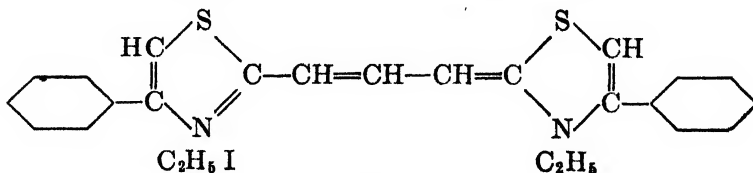
#### COMPARISON OF DYES FOR DESENSITIZATION AND RELATIVE QUANTUM EFFICIENCY

To illustrate the analysis of optical sensitization, two dyes of similar structure and similar distribution of optical sensitization have been compared. These are 3,3'-diethylthiacarbocyanine iodide



Dye 1

and 3,3'-diethyl-4,4'-diphenylthiazolocarbo-cyanine iodide.



Dye 2

Both dyes have their maximum sensitivity at 590 m $\mu$  and secondary maxima at about 540 m $\mu$ . Neither has appreciable absorption at 400 m $\mu$ . Sensitization by both dyes is measured by  $1/E_{590}$  and  $1/E_{540}$ . Desensitization is measurable by the ratio of  $E_{400}$  for the sensitized emulsion to  $E_{400}$  for the unsensitized; since the latter is a constant for each group of experiments,  $E_{400}$  may be used as a direct expression of desensitization. Table 1 gives the data for a series of concentra-

tions of both dyes in the same emulsion. The relations of  $1/E_{640}$ ,  $1/E_{590}$ ,  $A$ ,  $\phi_r$ , and  $E_{400}$  to dye concentrations are shown in figures 1, 2, 3, and 4.

TABLE 1  
*Comparison of sensitization by dyes 1 and 2*

CONCENTRATION OF DYE	$\lambda$	$1/E$	$A$	$\phi_r$
Dye 1				
<i>mg./liter</i>	<i>m<math>\mu</math></i>		<i>per cent</i>	
20	400	5.15	75.0	
	400	3.40	75.0	
	540	0.85	34.5	0.40
	590	1.12	34.0	0.49
30	400	3.40	75.0	
	540	1.26	46.5	0.44
	590	1.23	42.0	0.43
40	400	3.15	74.5	
	540	1.23	53.0	0.41
	590	1.38	47.5	0.47
60	400	2.70	74.5	
	540	1.26	61.5	0.42
	590	1.32	54.0	0.46
Dye 2				
20	400	5.15	75.0	
	400	0.535	74.5	
	540	0.245	27.5	0.92
	590	0.265	25.0	0.98
30	400	0.405	75.0	
	540	0.230	37.5	0.84
	590	0.230	33.0	0.87
40	400	0.345	74.5	
	540	0.265	43.5	0.95
	590	0.265	39.5	0.95
60	400	0.295	75.0	
	540	0.250	52.0	0.91
	590	0.230	47.0	0.85

In terms of total sensitization, dye 1 is about six times stronger than dye 2, but the spectral distribution of sensitivity which they produce is nearly the same.

Examination of the data in table 1 shows that these results may be explained in the following terms:

(1) The absorptions are quite similar; that of dye 1 is greater by 10 per cent, which is a small difference when compared to the difference in effective sensitivities.

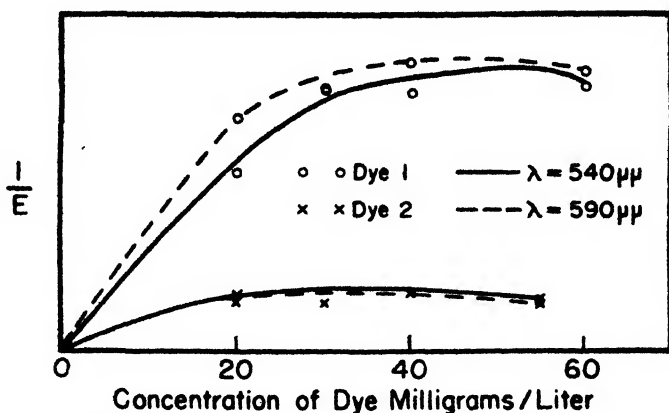


FIG. 1. Comparison of the optical sensitizations of dyes 1 and 2 at different concentrations

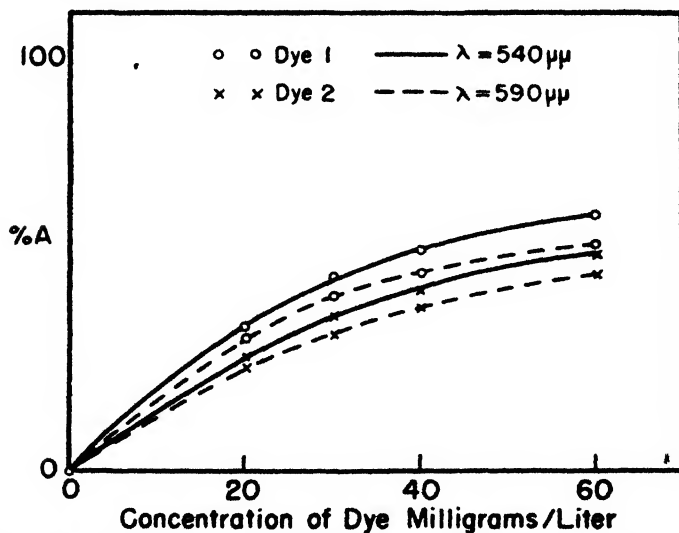


FIG. 2. Comparison of the absorptions of dyes 1 and 2 at 540  $m\mu$  and 590  $m\mu$  at different concentrations.

(2) The relative quantum efficiencies of both dyes are nearly constant over the range of concentrations which were used, and the efficiency of dye 2, the weaker sensitizer, is the higher. In each case, the efficiency of the dye is the same at 590  $m\mu$  and at 540  $m\mu$ .

(3) Desensitization by dye 2 is much the greater; it is actually of the same order as that of pinakryptol green. It is the desensitization which is responsible for the great difference between the dyes. It was not expected that a dye show-



ing strong desensitization should have a high efficiency of energy transfer, but the data available indicate that there is no inherent connection between these properties.<sup>2</sup>

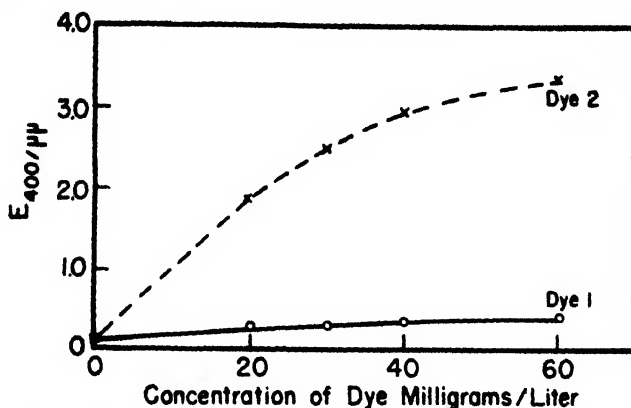


FIG. 3. Comparison of the desensitizing effects of dyes 1 and 2 at different concentrations

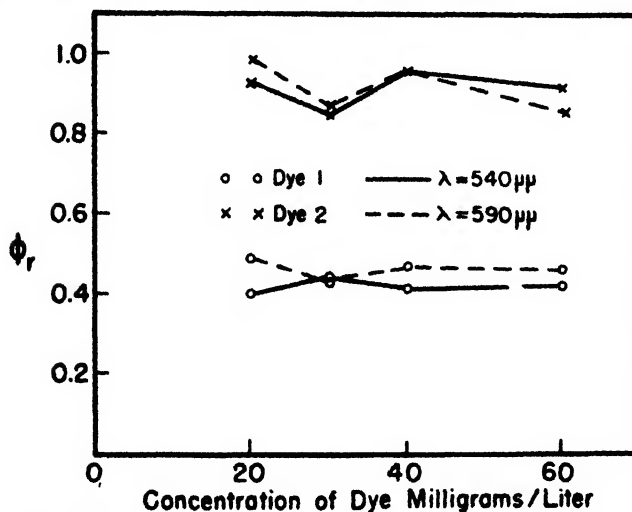


FIG. 4. Comparison of the relative quantum efficiencies of dyes 1 and 2 at different concentrations.

Dyes may be found with almost any combination of absorption, efficiency of transfer, and desensitization. The best sensitizers have high efficiency of energy

<sup>2</sup>This is particularly well shown by the photoconductivity of photographic emulsions containing dye-desensitizers (W. West and B. H. Carroll: *J. Chem. Phys.* **15**, 539 (1947)). In these experiments the primary act, involving the production of mobile electrons in the silver halide crystal, is isolated from the subsequent photographic phenomena involving the formation and stability of the latent image and its development to a visible image, and it has been shown that many strongly desensitizing dyes do not inhibit the primary production of electrons by light. Some, indeed, are excellent optical sensitizers for the photoconductive process.

transfer, high absorption, and little desensitization, but this is quite rare, and there is a considerable range of properties among commercially useful dyes. Illustrative values are given in table 2 for dyes at optimum concentrations.

#### EFFECT OF DESENSITIZATION ON THE OPTIMUM DYE CONCENTRATION

As the concentration of sensitizing dye added to an emulsion is increased, the optical sensitization (expressed either as  $1/E_{\max}$  or total sensitization) passes through a maximum. The concentration corresponding to this maximum is referred to as the sensitizing optimum. It is dependent on both emulsion type and dye.

Leermakers, Carroll, and Staud (9) found that, for a given dye, the amount adsorbed per unit area of silver halide surface at the maximum sensitization was reasonably constant in seven emulsions of different grain sizes. The optimum corresponded to coverage of the grain surface by a monomolecular layer of dye adsorbed flat on the surface; if the dye is adsorbed edge-on, as indicated by the

TABLE 2  
*Properties of representative dyes*

DYE NO.	ABSORPTION	DESENSITIZATION	RELATIVE QUANTUM EFFICIENCY	DESCRIPTION
	<i>per cent</i>	<i>per cent</i>		
7.....	64	40	0.77	Excellent sensitizer
8. ....	55	67	0.78	Good sensitizer; also used as supersensitizer
9.....	68	74	0.44	Selective sensitizer for red; used in color processes
10.....	37.5	80	0.18	Early type of dye; no longer in use
11.....	36	50	0.64	Only moderate sensitizer because of weak absorption

data of Sheppard, Lambert, and Walker (11), the grain surface is not completely covered. They concluded that the optimum was connected with the degree of saturation of the grain surface, a conclusion that was supported by the rapid increase in unadsorbed dye when the concentration was increased past a point near the optimum. However, the reduction in the sensitizing optimum on changing from carbocyanines to a dicarbocyanine was greater than that computed from the increase in surface coverage.

It has now been found that the optimum concentration is determined in the main by absorption and desensitization; the approximate agreement of sensitizing optimum and surface saturation for some cyanines and carbocyanines arises from a similar contribution of these factors.

Optical sensitization may be expressed by the following formula:

$$\frac{1}{E} = \frac{f(A) \cdot f(\phi_r)}{K + f(\text{De})}$$

in which  $A$  and  $\phi_r$  have the meanings already assigned,  $K$  is a constant, and  $\text{De}$  is the desensitization. Since the experimental evidence shows that  $\phi_r$  is substantially

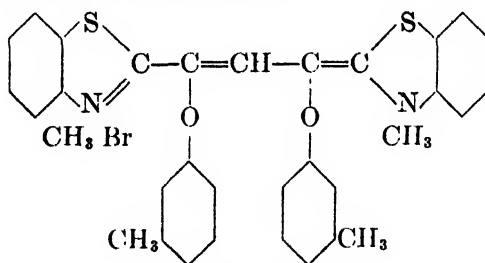
constant, the optimum sensitization corresponds to the maximum of  $f(A)/f(De)$ ;  $A$  varies exponentially with the amount of dye, the rate of change becoming less and less as the concentration increases. Since  $De$  increases with concentration at a more uniform rate,  $A/De$  passes through a maximum.

The effect of desensitization on the optimum concentration is clearly illustrated

TABLE 3  
*Comparison of sensitization by dyes 3 and 4*

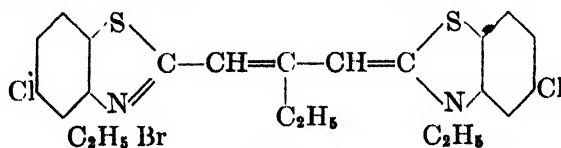
CONCENTRATION OF DYE	OPTICAL SENSITIVITY $1/E$ ( $\lambda = 640 \text{ m}\mu$ )	ABSORPTION $A$	$E \times 10^3$ ( $\lambda = 400 \text{ m}\mu$ )	RELATIVE QUANTUM EFFICIENCY $\phi_r$
Dye 3				
mg /liter		per cent		
0			4.55	
1	6.3	25.0	4.55	0.06
2	6.9	34.0	4.55	0.05
5	14.8	42.0	6.17	0.13
10	5.15	59.0	13.5	0.06
15	5.3	69.0	15.20	0.06
30	1.15	75.0	56.0	0.04
40	Too low to measure	79.0	220.0	
Dye 4				
10	31.0	56.5	7.95	0.24
15	37.0	67.5	7.40	0.23
30	34.0	72.0	12.3	0.29
40	30.0	76.0	14.8	0.32

by the following data for sensitization by two carbocyanine dyes: 3,3'-dimethyl-8,10-di-*m*-toloxythiacarbocyanine bromide,



Dye 3

and 3,3',9-triethyl-5,5'-dichlorothiacarbocyanine bromide:



Dye 4

Table 3 shows  $1/E_{\max}$ ,  $E_{400}$ , and absorption for a series of concentrations of each of the dyes in the same emulsion. Both of these dyes sensitise with sharp maxima at  $640\text{ m}\mu$ . The spectral absorptions of the silver halide plus dyes 3 and

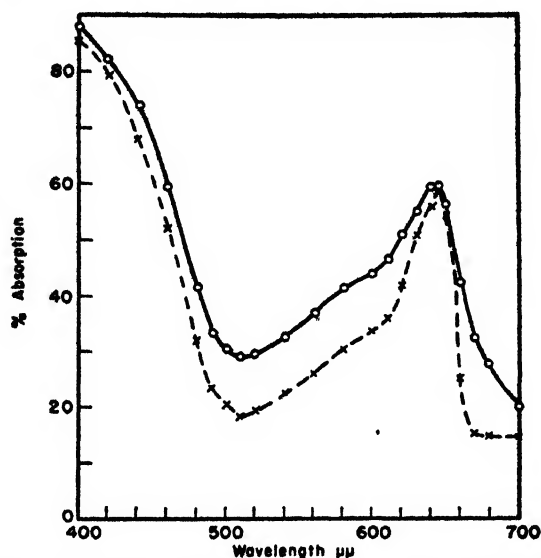


FIG. 5. Absorptions of dye 3 (o) and dye 4 (x) adsorbed to silver halide (silver halide absorption extends to  $510\text{ m}\mu$ ).

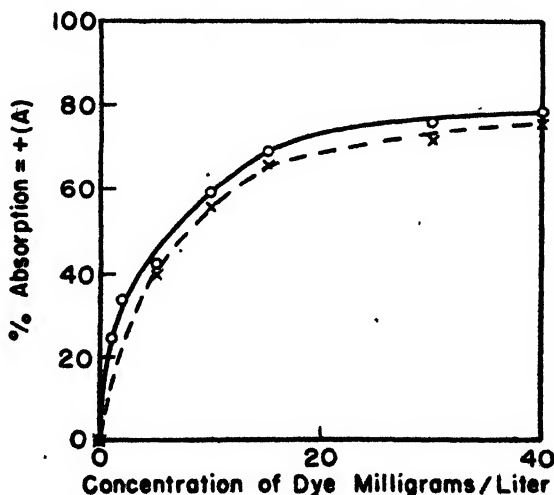


FIG. 6. Plots of absorption at  $640\text{ m}\mu$  against concentration of dye 3 (o) and of dye 4 (x)

4 are given in figure 5, and the relation between concentration and  $A_{\max}$  in figure 6. The similarity of the dyes in these characteristics is evident.

However, dye 3 has its optimum concentration at 5 mg. per liter of emulsion and dye 4 at 15 mg. per liter, so that the absorption of dye 3 at its optimum is less

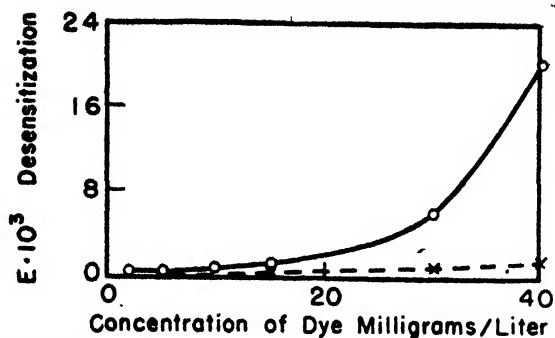


FIG. 7. Plots of desensitization— $E$  at  $400\text{ m}\mu$ —against concentration of dye 3 (o) and of dye 4 (x).

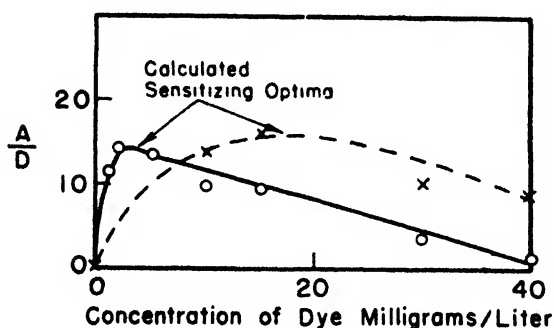


FIG. 8. Plots of absorption-desensitization ratios against concentration of dye 3 (o) and of dye 4 (x).

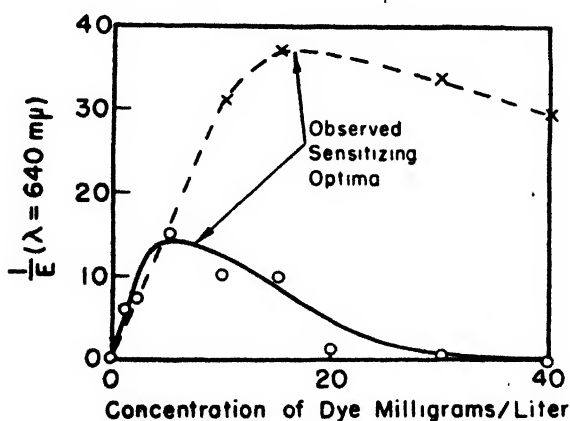


FIG. 9. Plots of observed optical sensitization against concentration of dye 3 (o) and of dye 4 (x).

than that of dye 4. In addition to this, the relative quantum efficiency of dye 3 is lower, so that its effective sensitivity is further limited. Neither of these factors, however, explains a ratio of three to one in the optimum concentrations

of dyes of similar structure and molecular size. The relative desensitizations by the two dyes which are plotted in figure 7 account for this difference. Using  $E_{400}$  as the measure of  $De$ , the ratios of  $A/De$  for the two dyes have been plotted in figure 8, against concentration as abscissas. In figure 9,  $1/E_{\max}$  has been plotted against concentration. It is evident that the maxima of the curves for each dye agree within the limits of error, and that the optimum concentrations are determined by the relation between absorption and desensitization.

It is well known in practice that the optimum concentration of infrared sensi-

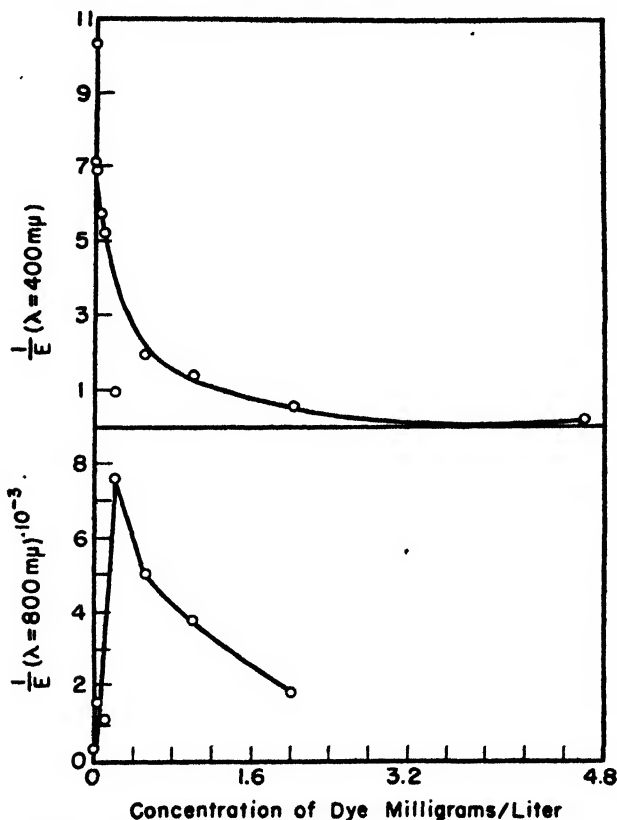
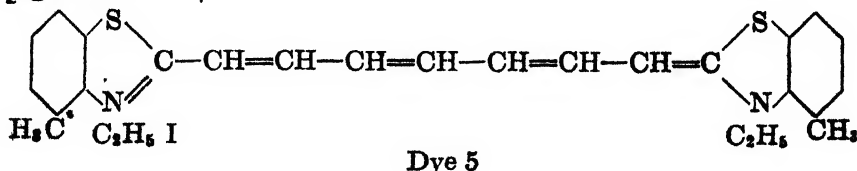


Fig. 10. Plots of  $1/E$  ( $\lambda = 400 \text{ m}\mu$ ) and  $1/E$  ( $\lambda = 800 \text{ m}\mu$ ) of dye 5

tizers is low. While the tendency to cause fog limits the useful concentration in some cases, it is normally the desensitization which is the controlling factor. This is illustrated by the data for dye 5, a tricarbo-cyanine, which are given in table 4 and figure 10:



Absorption could not be measured with sufficient accuracy to calculate  $\Delta/De$ , since it is less than 10 per cent at the optimum, but it is evident that the desensitization, measured by the change in  $1/E_{400}$ , explains the loss in sensitization past 0.10 mg. per liter. The molecular area of dye 5 is only one-fifth greater than that of a carbocyanine, so that the change in surface saturation has a relatively

TABLE 4  
*Characteristics of an infrared sensitizer*

CONCENTRATION mg./liter	$1/E_{400} \times 10^3$	$1/E_{400} \times 10^2$
0.00	0	10.50
0.01	4.5	7.25
0.02	16.0	6.91
0.05	12.0	5.75
0.10	76.0	5.36
0.20	50.0	0.91
0.50	38.0	1.95
1.00	18.0	1.38
2.00		0.54
5.00		0.19

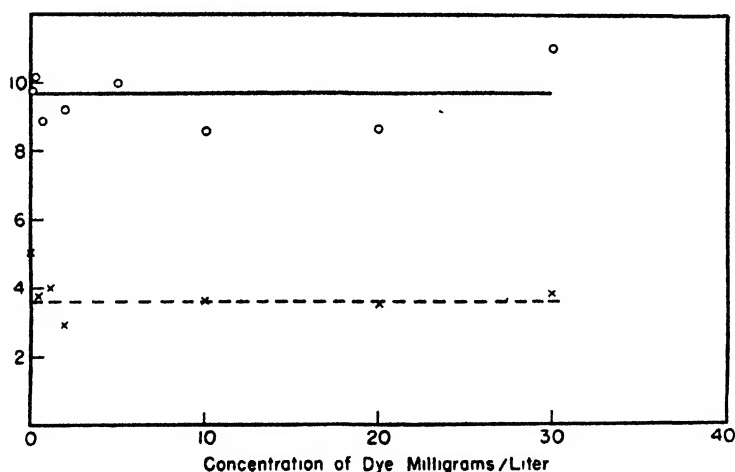


FIG. 11. Plots of inertia speeds exposure through blue (No. 47) Wratten filter against increasing concentration of dye 6. o, Leermakers, Carroll, and Staud; x, this paper.

small effect on the optimum. Computing areas in  $\text{\AA}^2$  by the methods of Huggins (7), the computed areas are as follows:

DYE	ORIENTATION		
	Flat	On edge	On end
Dye 5.....	161	72	26
Dye 1.....	137	57	26

The data already given make it evident that desensitization is a major factor in sensitization at concentrations of dyes well below optimum. It may not be detected by exposures through a blue filter because of compensating sensitization in the blue-green region transmitted by the filter. The published results of Leermakers, Carroll, and Staud (9) showed that the speed through a blue filter was practically unchanged until the sensitizing optimum was reached. These were repeated using the same dye, 3,3'-diethyl-9-methyl-4,5,4',5'-dibenzo-thiacarbocyanine chloride (dye 6) in another batch of the same emulsion. The results of exposure through a Wratten No. 47 filter are plotted in figure 11 on a linear scale, along with the data of Leermakers, Carroll, and Staud (9). In figure 12, values of  $1/E_{400}$  for the same coatings are plotted against concentration; these show that desensitization can be measured at the lowest concentrations of

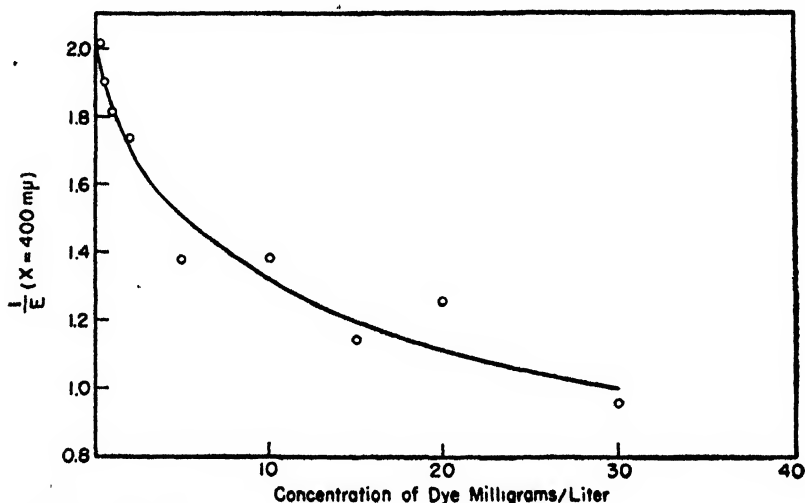


FIG. 12. Plot of  $1/E$  ( $\lambda = 400 \text{ m}\mu$ ) values against increasing concentration of dye 6

dye. Results in this system are therefore in agreement with the conclusions derived from the data described in this paper.

#### CONCLUSIONS

1. The effectiveness of a given sensitizing dye is the resultant of its spectral absorption, efficiency of transfer of adsorbed energy to the silver halide, and desensitization of the emulsion. Changes in the structure of the sensitizing dyes appear to vary these properties independently.
2. Efficiency of energy transfer is practically independent of dye concentration.
3. Desensitization is an important factor in sensitization even with the best sensitizing dyes. It is readily measured by the change in sensitivity at  $400 \text{ m}\mu$ . Because desensitization and absorption increase with concentration by different functions, the ratio absorption/desensitization passes through a maximum, and this has been shown to correspond with the maximum of sensitization. There is



no inherent connection between sensitizing optimum and saturation of the grain surface by dye.

#### REFERENCES

- (1) BREIDO, I. I., AND GOROKHOVSKI, YU. N.: J. Phys. Chem. U.S.S.R. **17**, 57 (1943).
- (2) DIETERLE, W.: In Eder's *Ausführliches Handbuch der Photographie*, 5th edition, Vol. III, p. 152, W. Knapp, Halle (1903).
- (3) EDER, J. M.: Sitzber. Akad. Wiss. Wien, math.-phys. Klasse **90**, 1097 (1884); *Ausführliches Handbuch der Photographie*, 5th edition, Vol. III, p. 152, W. Knapp, Halle (1903).
- (4) EVANS, C. H.: J. Optical Soc. Am. **12**, 401 (1926).
- (5) HEISENBERG, E.: Veröffentl. wiss. Zentral-Lab. phot. Abt. AGFA **3**, 115 (1933).
- (6) HÜBL, A. VON: In Eder's *Jahrbuch*, p. 289. W. Knapp, Halle (1896).
- (7) HUGGINS, M. L.: Private communication.
- (8) KÖNIG, E.: *Das Arbeiten mit farbenempfindlichen Platten*, p. 46. G. Schmidt, Berlin (1909).
- (9) LEERMAKERS, J. A., CARROLL, B. H., AND STAUD, C. J.: J. Chem. Phys. **5**, 893 (1937).
- (10) LÜPPO-CRAMER, H.: Phot. Korr. **63**, 332 (1927).
- (11) SHEPPARD, S. E., LAMBERT, R. H., AND WALKER, R. D.: J. Chem. Phys. **7**, 265 (1939).

## COMMUNICATIONS TO THE EDITOR

### THE OXIDATION OF FERROUS SULFITE IN AIR

Samples of ferrous sulfite were obtained by mixing ferrous sulfate and sodium sulfite solutions in a hydrogen atmosphere; they were creamy white precipitates and were washed with air-free water and alcohol and then dried in a vacuum desiccator over sulfuric acid. These precipitates became more or less dark on the surface, owing to unavoidable short contact with the air; when dry, they were cream to various shades of brown. Under the microscope they were seen to consist of colorless or pale greenish yellow crystals with a coat of yellow-brown oxidized material; this latter was sometimes of a cauliflower-like growth from the crystals. When dry, the samples were exposed to air in a large desiccator containing calcium chloride which was opened only occasionally; or they were exposed to the air in a balance case containing some sulfuric acid, but this case was opened more often to the air. These samples were analyzed from time to time over a period of years. The per cent of ferrous sulfite fell regularly and continuously, often slowly at the rate of about 0.4 per cent per year, but sometimes much more quickly, even up to 25 or 50 per cent per year. The purer and the drier the original sample, the slower is the subsequent oxidation. If the original sample is moist or contains much disseminated oxidation product (iron hydroxides?), then the subsequent oxidation is more rapid.

The analysis of the ferrous sulfite presents some difficulties. By placing a weighed sample in an excess of standard potassium dichromate solution plus hydrochloric acid, the oxidation is rapidly completed to ferric sulfate, and the

excess of dichromate is found by using an excess of standard ferrous chloride solution and finishing with dichromate titration. This method gives concordant results; duplicates differ by less than 0.5 per cent ferrous sulfite; it estimates, of course, the combined ferrous and sulfite radicals, which are calculated as  $\text{FeSO}_3$ . The use of potassium permanganate, instead of dichromate, gives low results for ferrous sulfite, the usual oxidation of sulfite to other than sulfate then occurring. Tests with sodium sulfite indicated that the above dichromate method gave higher results than the iodine method used in the same manner; e.g., 84.9 per cent sodium sulfite was found by the dichromate method and 83.8 per cent by the iodine method.

Of course the per cent of ferrous sulfite found in the ferrous sulfite samples by the dichromate method will be high if the samples contain ferrous hydroxide, etc. In the final solutions from these assays the sulfate was determined as barium sulfate. The sulfate due to the oxidation of the sulfite was calculated, and then by subtracting this from the total sulfate found, the original sulfate in the sample was found. In many cases during the oxidation of the ferrous sulfites the gain of sulfate was equivalent to the ferrous sulfite loss, but sometimes this was not observed or was obscured by the greater experimental error accumulating in the sulfate determination. The fresh samples of ferrous sulfite showed a sulfate value less than that equivalent to the ferrous sulfite content: the latter value therefore was high due to ferrous hydroxide, etc. This deficiency of sulfate value (up to 5 per cent at the start) cut out in about 70 days; any ferrous hydroxide in the samples is thus oxidized faster than the ferrous sulfite.

A set of four samples of ferrous sulfite was made by placing solid ferrous sulfate and sodium sulfite crystals and water in tubes which were then sealed. On solution and mixing, buff to brown precipitates appeared. After seven years the solutions were colorless or brownish over cream white powders; the latter were washed with water and alcohol and were dried over sulfuric acid *in vacuo* for from 1 to 7 days. In two of the tubes a crust of ferrous sulfite had separated; these were washed and dried as before, apart from the loose precipitates above; this bulked sample was the purest sample of ferrous sulfite obtained. This sample was kept in a small weighing bottle, generally closed, in the balance case; it contained 70.3 per cent ferrous sulfite at the start and 69.3 per cent ferrous sulfite a year later. Another of these samples decreased from 69.9 to 65.4 per cent ferrous sulfite in a year, this sample being open continuously in the balance case and occasionally stirred up: the two other samples were kept in the same manner, and the average loss of ferrous sulfite in a year was 7 per cent. The first sample in the weighing bottle was analyzed seven times over the year; the mean values of the last six analyses were: per cent  $\text{FeSO}_3 = 69.6$ , ( $= 49.1$  per cent  $\text{SO}_4$  and 28.6 per cent ferrous Fe); per cent  $\text{SO}_4$  (total) = 49.5; per cent  $\text{SO}_4$  (free) = 0.4; per cent ferrous Fe (direct) = 28.6; per cent total Fe (direct) = 29.0. It would therefore contain 97.3 per cent  $\text{FeSO}_3 \cdot 3\text{H}_2\text{O}$  plus 2.7 per cent (or probably less) of iron hydroxides. ( $\text{FeSO}_3 \cdot 3\text{H}_2\text{O}$  contains 71.6 per cent  $\text{FeSO}_3$ , 29.4 per cent ferrous Fe, and would give equivalent  $\text{SO}_4 = 50.5$  per cent.)

Of the samples of ferrous sulfite kept in the calcium chloride desiccator one

decreased regularly from 68.2 to 64.9 per cent ferrous sulfite in 91 months, i.e., underwent a loss of 0.36 per cent ferrous sulfite in a year; two other samples behaved similarly. Two samples were kept for some months in the desiccator, then were sealed in a tube for six years, then were exposed again to the air, in the balance case, when the oxidation (which had ceased in the sealed tube) again became very rapid; one of these samples showed the following *time* and *analysis* results: 0 (start), 60.3 per cent  $\text{FeSO}_3$ ; 6 months, 46.5 per cent  $\text{FeSO}_3$ ; then sealed until 86 months, 48.0 per cent  $\text{FeSO}_3$ ; thereafter open, at 91 months, 26 per cent  $\text{FeSO}_3$ ; at 97 months, 8.5 per cent  $\text{FeSO}_3$ . This sample had much red-brown iron hydroxide mixed with it from the start, and that oxide or that disseminated form of ferrous sulfite quickened the oxidation; this sample showed the most rapid oxidation of all the samples of ferrous sulfite. But pure dry crystals of  $\text{FeSO}_3 \cdot 3\text{H}_2\text{O}$  evidently oxidize very slowly (and dehydrate very slowly) under ordinary conditions.

JAMES R. POUND.

The School of Mines  
Ballarat  
Victoria, Australia  
November 29, 1947

## ANODIC BEHAVIOR OF ALUMINUM IN A MAGNETIC FIELD

It is well known that aluminum immersed in a solution of certain aluminum salts does not conduct anodically, or does so very poorly. This property is taken advantage of for rectifying the current, and the usual explanation given for this phenomenon is that the passage of the current is prevented by the formation of a film of oxide.

Certain facts have come to my attention which indicate that there are other factors which may be responsible for this peculiarity of aluminum and of other metals.

In electrolyzing an aluminum sulfate solution with a platinum anode, an aluminum strip was inserted into the anode compartment. The solution was hot, and the strip of aluminum dissolved with energetic evolution of gas. The strip of aluminum was then connected to the platinum anode and the evolution of gas stopped, or very nearly so. On breaking the connection with the platinum anode the evolution of gas reappeared instantaneously. The fact that these effects are observed at once does not seem to support the theory of an oxide film, because its formation and disappearance must take time. The film of oxide can be a contributing factor, but it cannot be solely responsible for the obstruction of the current.

The idea came to mind that it may be due to some special electronic structure, such that electrons under the electrical field can move only in one direction and not in the other.

If there is any justification for this view, a magnetic field should produce an effect; to test this the following experiments have been performed.

A test tube of such a size that it just fitted into the gap between the two poles of a powerful alnico magnet was filled with a solution of aluminum sulfate and

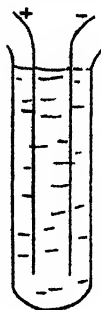


FIG. 1

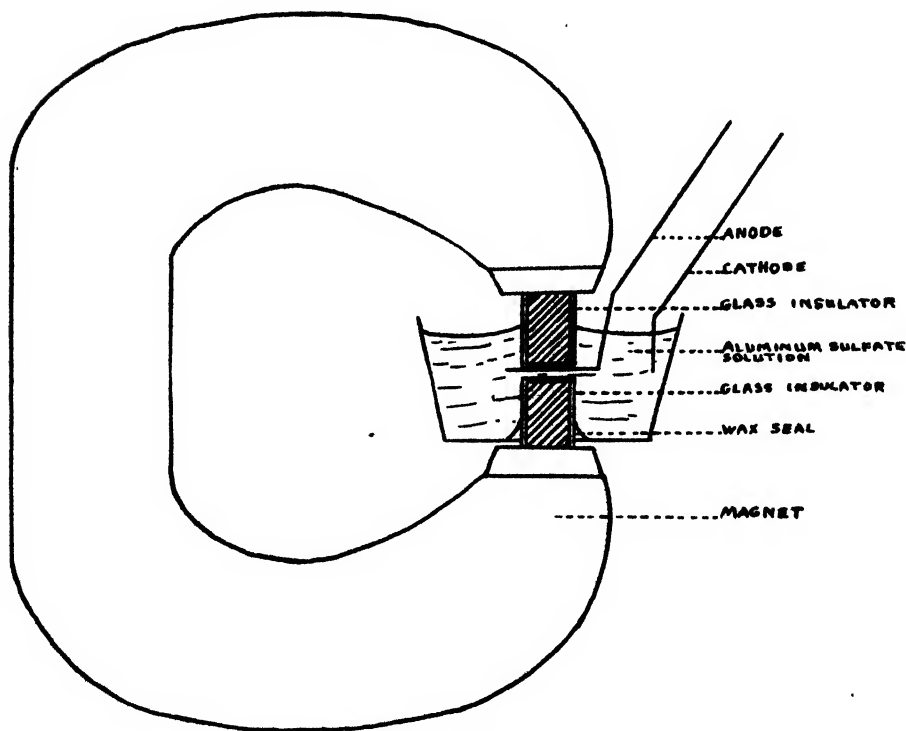


FIG. 2

two aluminum electrodes were inserted (figure 1). This cell was connected to a 45-volt battery, with no visible effects of the passage of current. But when it was placed between the poles of the magnet, the anode began to produce gas, a result which indicated some increase in conductivity of the solution.

Next an experiment was carried out with a powerful electromagnet of about 2000 Gauss. Two iron rods were screwed into its body as in figure 2. They

were insulated with thin glass caps having a wall thickness of 0.3 mm. These caps were 8 mm. in diameter and 3 mm. apart. On the lower rod a container capable of holding a solution of aluminum sulfate was fixed. It was thus possible



FIG. 3

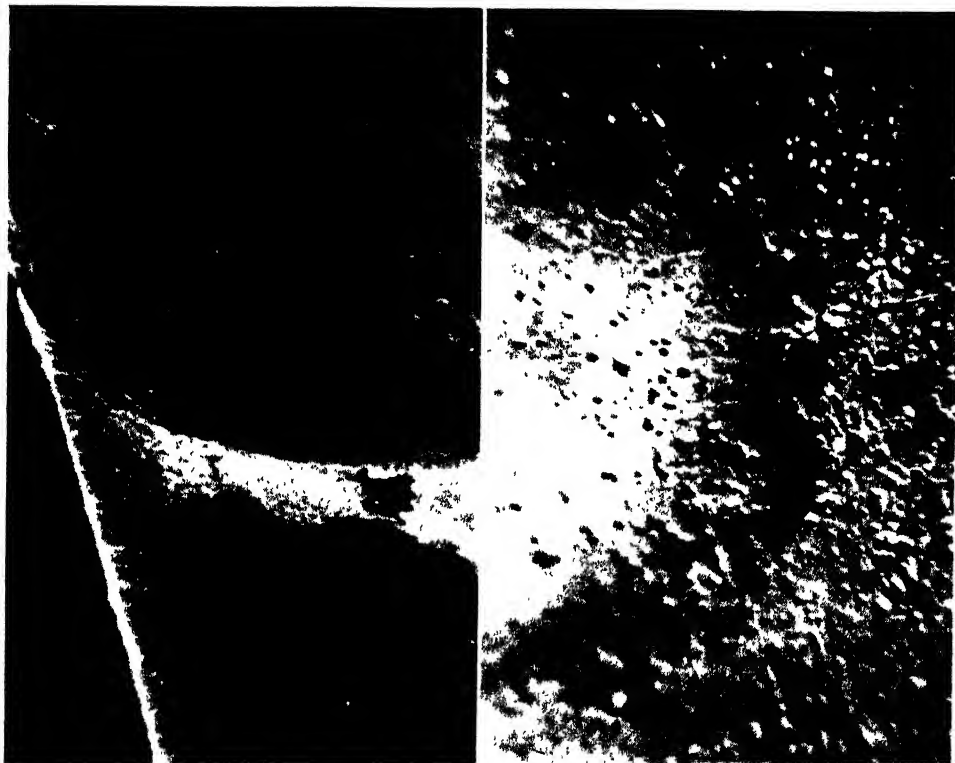


FIG. 4

to place a strip of aluminum anode between two poles of the magnet. A platinum wire served as cathode. With the 45-volt battery connected to the electrodes in a saturated solution of aluminum sulfate there was no drop of potential observed. However, when a magnetic field was established the potential fell to

10 volts and passage of the current became evident. At the same time it was observed that the aluminum strip was covered with a deposit having the appearance of a molten mass and the shape of a disc of the same diameter as the iron rod facing it (figure 3A). The disc appeared on the upper surface; on the other surface there could be observed small amounts of the same matter deposited here and there.

A similar experiment was performed with a permanent alnico magnet. In this case the two iron rods need not be screwed into the body of the magnet, because they are held by the magnetic force itself. The permanent magnet did not have the strength of the electromagnet, but the effect observed was of the same nature. The same substance was deposited in a circle which was, however, not completely covered with the deposit, as in the case with the electromagnet (figure 3B). It was found afterwards that even with a very weak magnetic field a deposit of the same kind is formed in a circle.

Without the magnetic field, especially if one uses pure aluminum, one observes deposits in small quantities of the same matter here and there, and not in a circle. This matter is not easily detachable from the metal itself, so that a way of collecting it for analysis has not yet been found.

A number of photographs were taken under a microscope. Figure 4 shows figures 3A and 3B magnified twenty times.

GEORGE ANTONOFF.  
ANNE ROWLEY.

Department of Chemistry  
Fordham University  
New York, New York  
January 26, 1948

## NEW BOOKS

*Small Wonder: The Story of Colloids.* By GESSNER G. HAWLEY. ix + 220 pp.; x and xxi plates. A Borzoi book. New York: Alfred A. Knopf, 1947. Price. \$3.50.

The author has written entertainingly about the science of particles too small to be seen in a microscope yet larger than molecules. As he points out, they hold the key to the secret of life—they pervade all matter, both living and non-living. Written for the intelligent layman, most of the material presented will be understood by those who have no more than a high school knowledge of physics and chemistry. In order to emphasize the place of colloidal systems in the physical universe, the author surveys the seven divisions or size ranges into which it falls. In this scheme the colloidal size realm comes above the atomic and molecular divisions but below the microscopic range. The description of these seven size divisions points up the importance of the colloidal state in the life process.

In discussing the purpose of the book the author points out that he is attempting "to acquaint those interested in what science is discovering with some of the more salient facts about it." He assures his readers that he is presenting one of the newer points of view with regard to the behavior of matter. In this he is quite successful. Furthermore, he should appeal to the lay reader because he illustrates his theme by discussing such everyday things as the purification of water, rubber, curds and whey, soaps, detergents, emulsifiers, blood,

and the chemistry of life. Here one has an array of subjects, one or more of which should interest almost everyone. There are a few errors of fact but they do not detract from the whole story. Residents of St. Louis, where the smoke problem has been solved better than in most other cities, will resent the statement that they are more begrimed than Pittsburgh. This little volume might well be used for assigned reading for a survey course in the physical sciences. It cannot be considered as a textbook in colloid chemistry.

L. H. REYERSON.

*Physikalische Chemie.* By WERNER KUHN. Third edition. 5 x 7½ in.; xi + 374 pp. Basel: Wepf and Co., 1947. Price: 15 fr. (Swiss).

In content this introductory text is in interesting contrast to a number of recent American books on elementary physical chemistry. The author of this textbook makes no attempt to survey the entire field of physical chemistry, nor to include superficial accounts of specialized or advanced subjects merely because they are at present attracting popular attention. Only the classical aspects of physical chemistry are discussed. The first nine chapters, comprising about 85 per cent of the text, are devoted to an orderly presentation of the properties of matter and of equilibria from the thermodynamic viewpoint. The material is arranged to clarify the basic principles, examples being chosen from the properties of solid, liquid, or gaseous systems as seems best fitted for the purpose. There are no complete chapters devoted exclusively to each of the three states of matter, as seems to be an almost universal custom in American texts. The last three chapters introduce, respectively, reaction kinetics, surface phenomena, and the properties of colloids.

The presentation is simple and relatively non-mathematical. The reader is apparently expected to have some acquaintance with elementary calculus, but no great proficiency in this subject is required. While occasional references to experimental methods or results are made in the text, the amount of such illustrative material is comparatively scanty.

ROBERT LIVINGSTON.

*Organic Syntheses.* Volume 27. Edited by R. L. SHRINER. vi + 121 pp. New York: John Wiley and Sons, Inc., 1947. Price: \$2.25.

In this volume the tradition of *Organic Syntheses* of providing the chemist with well-developed and thoroughly checked procedures for the preparation of organic compounds has been continued. The preparative procedures are about equally divided among aliphatic, aromatic, and heterocyclic compounds. Each procedure is complete with notes, explaining possible difficulties, and with pertinent references to the original literature. The subject index is cumulative, covering Volumes 20 through 27.

The following preparations are included in this volume:  $\beta$ -alanine,  $\beta$ -aminopropionitrile, and bis( $\beta$ -cyanoethyl)amine, benzalacetone dibromide, biallyl,  $\alpha$ -bromobenzalacetone, *tert*-butylamine, carboxymethoxylamine hemihydrochloride, decamethylenediamine, diethylaminoacetonitrile, dihydroresorcinol, 3,5-dimethyl-4-carbethoxy-2-cyclohexen-1-one and 3,5-dimethyl-2-cyclohexen-1-one, 1,5-dimethyl-2-pyrrolidone, 2,3-diphenylindone (2,3-diphenyl-1-indenone), 2,4-diphenylpyrrole, ethyl  $\alpha$ -isopropylacetoacetate, 4-ethylpyridine, glycolonitrile, 5-hydroxypentanal, isatoic anhydride, 6-methoxy-8-nitroquinoline, 1-methyl-2-imino- $\beta$ -naphthothiazoline, *N*-methyl-1-naphthylcyanamide, 1-methyl-1-(1-naphthyl)-2-thiourea, mucobromic acid, *m*-nitrodimethylaniline, 3-penten-2-ol,  $\gamma$ -*n*-propylbutyrolactone and  $\beta$ -(tetrahydrofuryl)propionic acid, pseudothiohydantoin, rhodanine, stearolic acid, tetraiodophthalic anhydride, *m*-thiocresol, *o*-toluic acid, *p*-toluic acid, *o*-toluidinesulfonic acid, and 1,3,5-triacetylbenzene.

R. M. DODSON.

*Colloid Science. A Symposium.* Contributors: E. K. Rideal, A. E. Alexander, D. D. Eley, P. Johnson, F. Eirich, R. F. Tuckett, J. H. Schulman, M. P. Perutz, G. S. Adair, G. B. B. M. Sutherland, and R. R. Smith. x + 188 pp. + index. Brooklyn, New York: Chemical Publishing Company, Inc., 1947. Price: \$6.00.

According to the "Foreword to the First American Edition," this book is made up from

a series of lectures given as a course in colloid science at Cambridge University, Cambridge, England, under the auspices of the Royal Institute of Chemistry. The topics appear to have been selected on the basis of the activities and interests of the staff members of the Department of Colloid Science at Cambridge rather than from the point of view of any integrated course in the subject. In all there are ten main topics which are considered: 1. Surface Chemistry and Colloids—Alexander. 2. Thermodynamics and Colloidal Systems—Eley. 3. The Study of Macromolecules by Ultracentrifuge, Electrophoresis and Diffusion Measurements—Johnson. 4. The Viscosity of Macromolecules in Solution—Eirich. 5. The Kinetic Theory of High Elasticity—Tuckett. 6. Emulsions *in vivo*—Schulman. 7. The Study of Colloidal Systems by X-ray Analysis—Perutz. 8. Membrane Equilibrium—Adair. 9. Infra-red Spectra and Colloids—Sutherland. 10. Vinyl Polymerization in the Liquid Phase—Smith.

In general, the present status of information in the several fields is reviewed in readily understandable form. By and large the emphasis lies where it must in a small book—namely, on the descriptive aspects—but in certain instances some mathematical attention is given to the subject. In some cases the connection with colloid science is not too apparent.

The reviewer was especially impressed with the sections by Drs. Eirich, Perutz, and Adair. The section by Dr. Johnson seemed to lack something in incisive treatment. For instance, discussion of the subject of electrophoresis is hardly representative of the advances of the past decade.

The printing, the paper, and the binding are excellent. So it is to be regretted that more attention was not given to proof-reading. The book contains too many errors of this kind.

J. W. WILLIAMS.

*Conversion Factors and Tables.* By O. T. ZIMMERMAN AND IRVIN LAVINE. 262 pp. Dover, N. H.: Industrial Research Service, 1945. Price: \$2.75.

In pocket-size form this little booklet contains conversion factors for all of the usual and many unusual units of scientific, industrial, and commercial use. The alphabetical arrangement presents all the factors in a most convenient form. The extent of the tables can be seen by consulting that for "cubic centimeter," under which thirty-five different units will be found, including British fluid drachms and U. S. fluid drams as well as British pottles and noggins. One could not want better evidence of the necessity of universal adoption of the c.g.s. system of weights and measures (indeed, adoption is world-wide except for England and the United States) than by looking through such a comprehensive set of conversion factors. And the convenience of having such tables should not for a moment lessen our desire to adopt and use more scientific units in the two great English-speaking countries.

S. C. LIND.

*Research. A Journal of Science and its Applications.* No. 2, November, 1947. London: Butterworth's Scientific Publications, Ltd. Price: \$10 per year.

In a foreword to this new journal, launched with a very imposing board of advisors, Sir Charles Darwin expresses the need for a new journal to cover the various fields of science in a more exact way than the popular periodicals and at the same time to present material in a more understandable and less rigid style than is usual in the records of the learned and the professional societies.

The present number contains papers on glass, whaling, British commercial high explosives, labile molecules, and research in rubber production. One of the papers has extensive references to the literature of its subject; the others do not have any references. Apparently the journal is not intended as a permanent contribution to scientific literature, which would be difficult without volume numbers. However, the paging is continuous from Number 1, so that volume numbers could be added if it seemed desirable to do so.

S. C. LIND.



# HEATS OF ADSORPTION. I<sup>1</sup>

CONWAY PIERCE AND R. NELSON SMITH

*Department of Chemistry, Pomona College, Claremont, California*

*Received February 6, 1948*

Although a considerable amount of work has been done on heats of adsorption (2), most of it is concerned with porous adsorbents for which the number of layers is limited by the filling of capillaries. Recently Harkins and Jura (7) have determined the heats of adsorption of polymolecular films of water on titanium dioxide by measurement of the heats of immersion of powders containing varying amounts of adsorbed water. They find that the heat of adsorption decreases as the thickness of the water film increases but that at the thickest films that could be measured the heat of adsorption is still greater than the heat of liquefaction of water. Beebe, Biscoe, Smith, and Wendell (1) have measured the heats of adsorption of gases on carbon blacks, which are non-porous, by direct calorimetry. These measurements show that the heat of adsorption falls off rapidly after the first layer is completed, but they were extended only to a value of  $V/V_m$  near 1.5. In later work (1a) it is found that the heats of adsorption of hydrocarbons tend to be, even in the second layer, considerably in excess of  $E_L$ .

The isosteric method, which has often been used for measurement of the heat of adsorption, provides a more sensitive tool than calorimetry for investigation of the heat effects associated with the formation of polymolecular films. In calorimetric measurements the relative error increases as the heat effects become smaller, whereas the isosteric method does not depend upon measurements of small heat effects but rather upon relative pressure measurements, which are quite accurate up to the regions of high adsorption. Any shift of the volume *vs.* relative pressure curve with temperature shows that the heat of adsorption is different from the heat of liquefaction, as pointed out by Coolidge (4), who has carefully examined the validity of applying the Clausius-Clapeyron equation to the equilibrium between vapor and an adsorbed phase.

## EXPERIMENTAL

A sample of graphite provided by the National Carbon Company<sup>2</sup> was used as adsorbent in this study. It has an ash content below 0.001 per cent and was prepared so as to be essentially free of oxygen complex. Before use it was heated at 900°C. for 3 hr. *in vacuo*. The surface area is 4 sq. m. per gram.<sup>3</sup> We believe that the sample is quite similar to the one used by Harkins, Jura, and Loeser (8), which was also provided by the National Carbon Company.

<sup>1</sup> This paper consists of a report of work done under contract with the Technical Command, Chemical Corps, United States Army.

<sup>2</sup> We wish to thank Dr. L. L. Winter of the National Carbon Company Research Laboratory for preparation of the sample and for the analytical data.

<sup>3</sup> The authors wish to thank Professor R. A. Beebe and Miss M. H. Polley of Amherst College for determination of the nitrogen isotherm and computation of the area.

Ethyl chloride was used as adsorbate because of its availability in high purity and its suitable vapor pressure range. Eastman "white label" grade was purified by treatment with sulfuric acid and repeated distillation in the vacuum line. The final product had vapor pressures of 471 mm. at 0°C. and 3.44 mm. at -78°C. The average heat of liquefaction, computed by the Clausius-Clapeyron equation from these vapor pressures, is 6700 cal. per mole in the temperature range 0°C. to -78°C.

Ice-water mixtures and dry ice were respectively used for the two constant-temperature baths. The dry ice gave some supercooling when first added to the Dewar flask but returned to a constant value within an hour. It was found

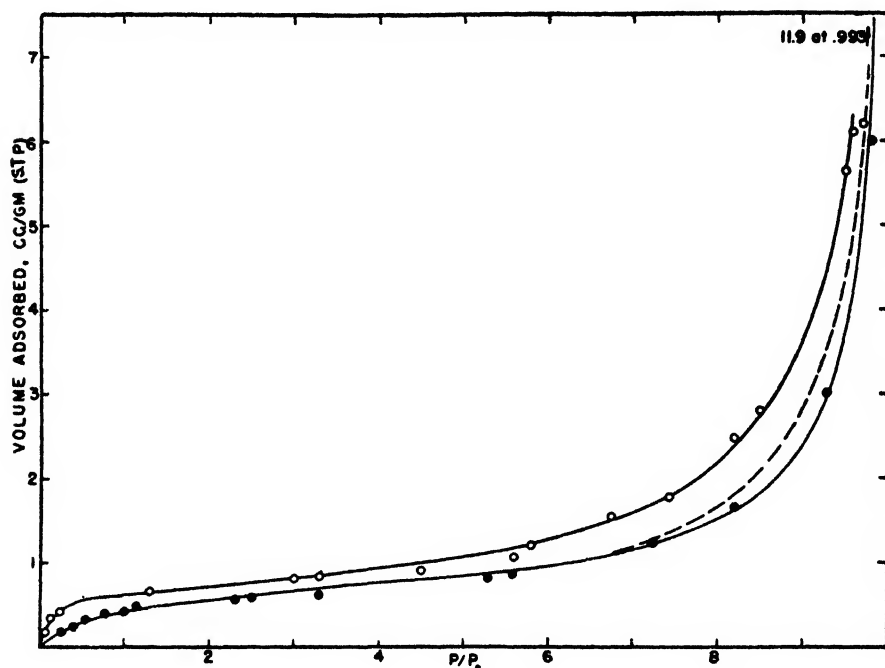


FIG. 1. Isotherms for ethyl chloride on graphite. Upper curve at -78°C., lower at 0°C. The dashed curve is for desorption at 0°C. The 0°C. curve gave an adsorption of 11.9 cc. at  $p/p_0 = 0.993$ .

best not to add acetone or other liquid to the dry ice bath. As used, the bath kept pure ethyl chloride within a vapor pressure range of  $\pm 2$  per cent. All the isotherm points were determined gravimetrically, except those at relative pressures below 0.05. The sample bulb was attached by a standard-taper joint, so that after each addition it could be removed and weighed. All pressures below 5 mm. were read from a McLeod gage. To minimize error due to unadsorbed gas in the sample tube we employed an 8-g. sample in a tube whose free volume (helium) at 0°C. was only 8.5 ml.

Isotherms for 0°C. and -78°C. are shown in figure 1. Each curve shows all experimental points for two or more separate determinations. The -78°C.

curve was not carried to higher relative pressures because of the  $\pm 2$  per cent uncertainty in the pressure measurement, due to temperature fluctuations in the dry ice bath. It is not possible to determine experimentally whether the curves come together at relative pressures below 1.0 or not, but there is no indication that this occurs.

Desorption points, determined for the isotherm at  $0^{\circ}\text{C}.$ , are indicated by the dashed curve of figure 1. Desorption was not determined for the  $-78^{\circ}\text{C}.$  isotherm because of the large temperature change each time the tube was removed from the bath for weighing. A hysteresis loop, such as shown in the  $0^{\circ}\text{C}.$  isotherm, is usually interpreted as due to capillaries which fill at the high relative pressures. Whether these are crevices in the graphite particles or voids between the particles cannot be determined, but in any event the small amount of capillarity does not affect the conclusion that most of the adsorption is in polymolecular films of considerable thickness; if capillaries are present, they are so wide that they do not fill until the film on each wall is several molecules in thickness.

#### DISCUSSION

The Clausius-Clapeyron equation

$$E = \frac{RT_1T_2}{T_1 - T_2} \ln \frac{p_1}{p_2}$$

has been used to compute the differential heat of adsorption. Computed values are shown in figure 2, plotted as a function of the amount adsorbed. The base line is  $E_L$ , the heat of liquefaction of ethyl chloride, computed from the  $p_0$  values at the two temperatures. At all measurable pressures the heat of adsorption exceeds the heat of liquefaction. (This is shown in the isotherms for the two temperatures. They would coincide if  $E = E_L$ .)

The upper scale of figure 2 shows heat of adsorption as a function of the number of statistical layers. The value of  $V_m$  was computed by B.E.T. plots for the two isotherms as 0.62 cc. per gram at  $-78^{\circ}\text{C}.$  and 0.57 cc. per gram at  $0^{\circ}\text{C}.$  In figure 2 we used an average value for  $V_m$  of 0.60 cc. per gram, since the isosteric heats represent the heat of adsorption at the mean temperature. In plotting  $E$  vs. number of layers we do not imply that a given value of  $E$  corresponds to covering the surface with a uniform layer  $n$  molecules in depth. Rather, we believe that for a given number of statistical layers part of the surface is covered by a greater number of layers and part by a lesser number, with some portions holding only a monolayer.

Our isosteric heats cannot be compared with the calorimetric values of Beebe and associates (1, 1a), since our method lacks precision in the region of small adsorption and the calorimetric method is not very exact beyond about 1.5 to 2  $V_m$ .

The falling off in  $E$  with volume is much like that observed by Harkins and Jura (7) for water on titanium dioxide. We have searched for other published isotherms of non-porous adsorbents, to see whether the effect is general, but find

only one other case where isotherms have been determined at two temperatures and extended to high relative pressures. This is for the adsorption of butane at  $0^{\circ}\text{C}$ . and  $-78^{\circ}\text{C}$ . by 200-mesh glass spheres, reported by Davis, DeWitt, and Emmett (6). Their results are much like ours; the isotherm at the lower temperature is shifted to the left of the one at the higher temperature, at all pressures. Thus it is shown that  $E > E_L$  at all measurable pressures. There are

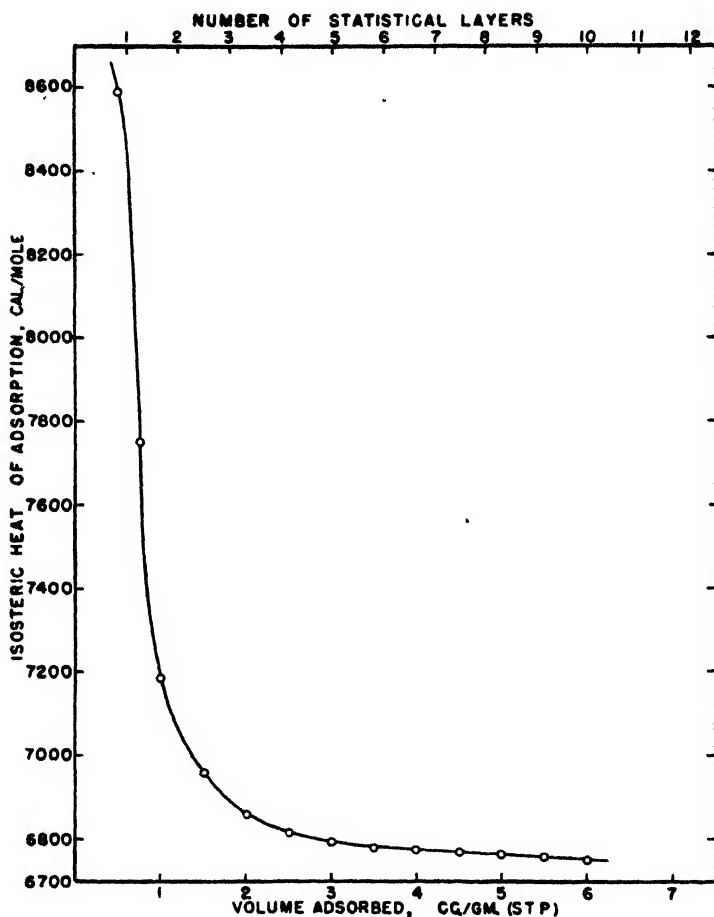


FIG. 2. Isosteric heat of adsorption for ethyl chloride on graphite. The base line at 6700 cal. per mole is the heat of liquefaction, computed from  $p_0$  values at the two temperatures.

a number of isotherms for porous adsorbents that show a shift to more adsorption as the temperature is decreased, thus indicating that  $E > E_L$ , but these usually reach saturation at low relative pressure, owing to filling of capillaries, and one cannot determine from them whether  $E$  becomes equal to  $E_L$  at high relative pressures.

The isotherms of Coolidge (6) for water on charcoal, and of Reyerson and Cameron (9) for iodine on silica gel, have been interpreted by Brunauer (2) as

evidence that  $E = E_L$  for these systems which give Type III isotherms. Aside from these we know of no case in which it has been proved that adsorption will occur when  $E = E_L$ . Even here there is some question as to whether the experimental precision is sufficient to detect the small shifts of isotherms with temperature that would result were the heat of adsorption only slightly greater than the heat of liquefaction.

In view of our data for a typical Type II isotherm and the observation that the butane isotherms of Davis, DeWitt, and Emmett (6) also show that  $E > E_L$  up to multilayers many molecules in thickness, we feel that the B.E.T. assumption (3) that  $E_2 = E_3 = \dots E_L$  is unsound. After perhaps the third layer it is a fair approximation, but for smaller adsorptions  $E$  may exceed  $E_L$  by as much as several hundred calories per mole.

#### SUMMARY

Isosteric measurements have been made of the heats of adsorption of ethyl chloride on graphite at temperatures of 0°C. and -78°C. It is found that the differential heat of adsorption is much higher than the heat of liquefaction during the adsorption of the first and second layers, that  $E_A$  drops to only slightly above the heat of liquefaction when the adsorbed film becomes several molecules in thickness, and that  $E_A$  never becomes equal to  $E_L$  within the measurable pressure range.

#### REFERENCES

- (1) BEEBE, BISCOE, SMITH, AND WENDELL: J. Am. Chem. Soc. **69**, 95 (1947).
- (1a) BEEBE, POLLEY, SMITH, AND WENDELL: J. Am. Chem. Soc. **69**, 2294 (1947).
- (2) BRUNAUER: *The Adsorption of Gases and Vapors*, Chap. VIII. Princeton University Press, Princeton, New Jersey (1943).
- (3) BRUNAUER, EMMETT, AND TELLER: J. Am. Chem. Soc. **60**, 309 (1938).
- (4) COOLIDGE: J. Am. Chem. Soc. **48**, 1795 (1926).
- (5) COOLIDGE: J. Am. Chem. Soc. **49**, 708 (1927).
- (6) DAVIS, DEWITT, AND EMMETT: J. Phys. Colloid. Chem. **51**, 1232 (1947).
- (7) HARKINS AND JURA: J. Am. Chem. Soc. **66**, 919 (1944).
- (8) HARKINS, JURA, AND LOESER: J. Am. Chem. Soc. **68**, 554 (1946).
- (9) REYERSON AND CAMERON: J. Phys. Chem. **39**, 181 (1935).

#### HEATS OF ADSORPTION. II<sup>1</sup>

R. NELSON SMITH AND CONWAY PIERCE

*Department of Chemistry, Pomona College, Claremont, California*

*Received April 27, 1948*

In the derivation of the Brunauer, Emmett, Teller (B.E.T.) equation for multilayer adsorption (4) it is necessary to make the assumption that the heats of

<sup>1</sup> This paper consists of a report of work done under contract with the Technical Command, Chemical Corps, United States Army.

adsorption for all layers beyond the first are equal to the heat of liquefaction. In a previous paper (14) we have shown experimentally that this assumption is not valid for a typical Type II isotherm, that of ethyl chloride on graphite. It was found, by application of the Clausius-Clapeyron equation to isotherms for two different temperatures, that  $E$  is large in the region where formation of the multilayer film begins and that  $E$  approaches  $E_L$  only when  $p$  approaches  $p_0$ . (The heat-volume curve is reproduced in figure 2.) We have now extended this study to a Type III isotherm, that of ammonia on graphite.

#### EXPERIMENTAL

The graphite was from the same lot<sup>2</sup> as that used for the ethyl chloride isotherm. We have designated it NC-1. The nitrogen surface area<sup>3</sup> is 4.0 sq. m. per gram.

Ammonia from a commercial cylinder was purified by distillation *in vacuo* until constant vapor pressure at dry ice temperature was obtained. Isotherms were determined by the conventional pressure-volume method, at temperatures of  $-78.5^\circ\text{C}$ . and  $-35.7^\circ\text{C}$ . Dry ice, without a solvent, was used for the former temperature and an ethylene chloride freezing bath for the latter. This bath was made by adding sticks of frozen ethylene chloride to the liquid as needed to maintain the temperature. Temperatures were measured by the vapor pressure of ammonia in a small tube next to the sample bulb. Temperature variation was less for the ethylene chloride bath than for the dry ice; both could be maintained quite constant for a period of 8-11 hr. without recharging.

Isotherms for the two temperatures are shown in figure 1. It will be noted that the experimental precision is not nearly so good as that found for ethyl chloride and that there is considerable spread of points in the middle pressure region. In this region the correction for unadsorbed gas is large, which contributes to experimental error. Despite the observed spread of points, it is clear from the data that the  $-78.5^\circ\text{C}$ . isotherm is shifted to the left of the  $-35.7^\circ\text{C}$ . isotherm, a result which shows conclusively that the heats of adsorption are greater than the heats of liquefaction. Isothermic heats of adsorption, computed from the smoothed curves of figure 1, are shown in figure 2. The plot of  $E$  vs.  $V$  shows that  $E$  approaches  $E_L$  only when  $p$  approaches  $p_0$ .

An isotherm was also determined for water on graphite NC-1. This is of interest because it represents an extreme case of a Type III isotherm, with exceedingly low adsorption at low relative pressures and very large adsorption at high relative pressures. For this isotherm we used a 28-g. sample of graphite. The amount of adsorption was determined gravimetrically, by the same procedure as used for the ethyl chloride isotherms. Our results for water are shown in figure 4, which gives for comparison a water isotherm determined by Harkins,

<sup>2</sup> Furnished through the courtesy of Dr. Lester L. Winter, National Carbon Company, Cleveland, Ohio.

<sup>3</sup> The authors wish to express their appreciation to Professor R. A. Beebe and Miss M. H. Polley of Amherst College for determination of the nitrogen isotherm and computation of the surface area. Their isotherm is shown in figure 1.

Jura, and Loeser (9) for a different sample of graphite. It will be noted that our isotherm shows much less adsorption in the low-pressure region than theirs. We do not know to what the difference can be attributed.

Our isotherms for ethyl chloride on graphite at 0°C. and -78.5°C. are reproduced in figure 4 so that comparisons may be made of the isotherms of water, nitrogen, ethyl chloride, and ammonia on the same adsorbent. B.E.T. plots give  $V_m$  values of 0.62 cc./g. at -78°C. and 0.57 cc./g. at 0°C. for ethyl chloride. The "point B" values (8) are slightly higher than the B.E.T. values for  $V_m$ . If the nitrogen area is taken as 4.0 sq. m. per gram, the  $V_m$  value of 0.57 cc./g.

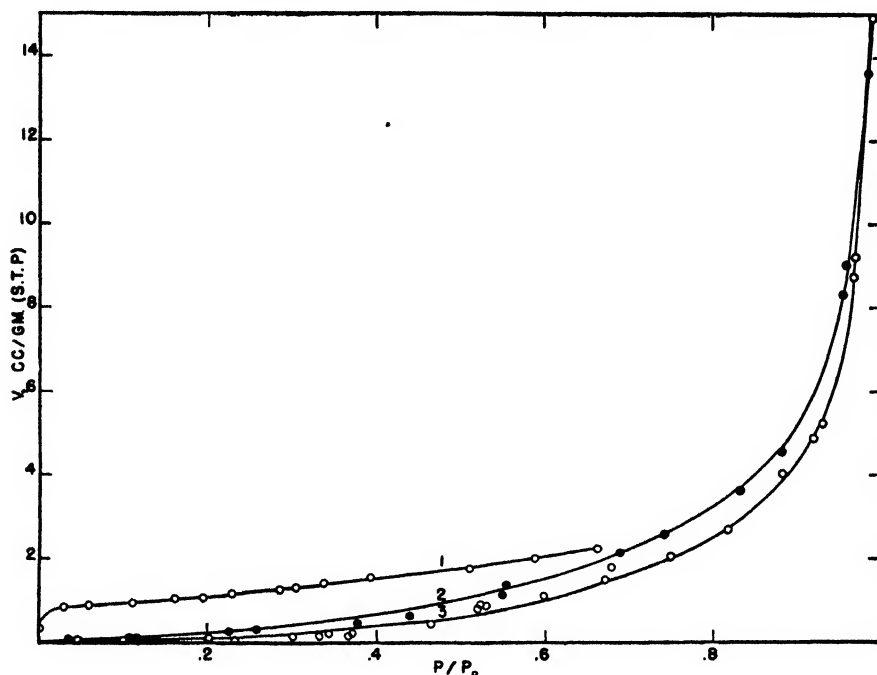


FIG. 1. Isotherms of graphite NC-1. (1) Nitrogen at -195.3°C. (Beebe and Polley). (2) Ammonia at -78.5°C. (3) Ammonia at -35.7°C.

at 0°C. gives an area of 26.1 sq. Å. per molecule for ethyl chloride. This is in good agreement with the value of 23.9 which is computed from the molecular volume.

#### DISCUSSION

The ammonia isotherms of figure 1 and ethyl chloride isotherms of figure 4 show conclusively that for both systems the heats of adsorption are greater than the heats of liquefaction, up to the highest relative pressures that can be accurately measured. A similar conclusion can be drawn from the isotherms of Davis, DeWitt, and Emmett (6) for butane on 200-mesh glass spheres at 0°C. and -78°C., shown in figure 6. These isotherms are not carried to as high relative pressures as ours, but they clearly show a shift to higher adsorption at

lower temperature. These three sets are the only isotherms we know of which give data for two temperatures and over a wide pressure range, for non-porous adsorbents. Since they include two typical Type II isotherms and one Type III, we believe it sound to conclude that in general the heat of adsorption is greater than the heat of liquefaction.<sup>4</sup> Further, we believe the evidence warrants the hypothesis that adsorption occurs only when  $E > E_L$  and that when the film

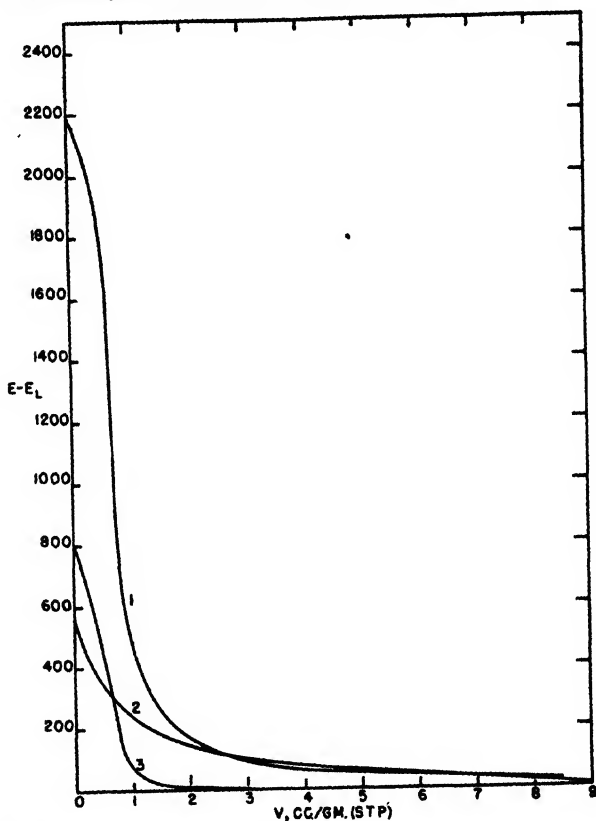


FIG. 2. Isosteric heats of adsorption. (1) Ethyl chloride on graphite. (2) Ammonia on graphite. (3) Butane on glass spheres. Equation 18 was used to extrapolate in the low-pressure region.

becomes of such thickness that the effect of the substrate vanishes,  $E = E_L$  and no further adsorption occurs. This, of course, suggests that adsorption at a

<sup>4</sup> Brunauer (2) cites the data of Coolidge for water on charcoal (5) and of Reyerson and Cameron (15) for iodine on silica gel as evidence that a Type III isotherm is obtained when  $E \leq E_L$ . We feel that this conclusion is questionable. Coolidge's data that show increased adsorption at increased temperature are for an isotherm for a porous adsorbent. Further, there is the possibility of chemisorption at his higher temperatures. The iodine isotherms, when replotted on a relative pressure basis, show that the one at 137.6°C. is shifted to the left of the ones at 158.3°C. and 178.4°C., a result which indicates that  $E > E_L$ .



relative pressure of unity is finite rather than infinite, as is usually assumed. A study of all known isotherms for non-porous adsorbents leads us to believe that there is a finite limit to adsorption. This point is discussed later.

Over a considerable range (1-8 cc./g.) the heat of adsorption of ammonia is related to the volume by the equation

$$E - E_L = Ae^{-\kappa v} \quad (1)$$

but this does not apply in the low-pressure region. There, the heat exceeds the value computed by equation 1.

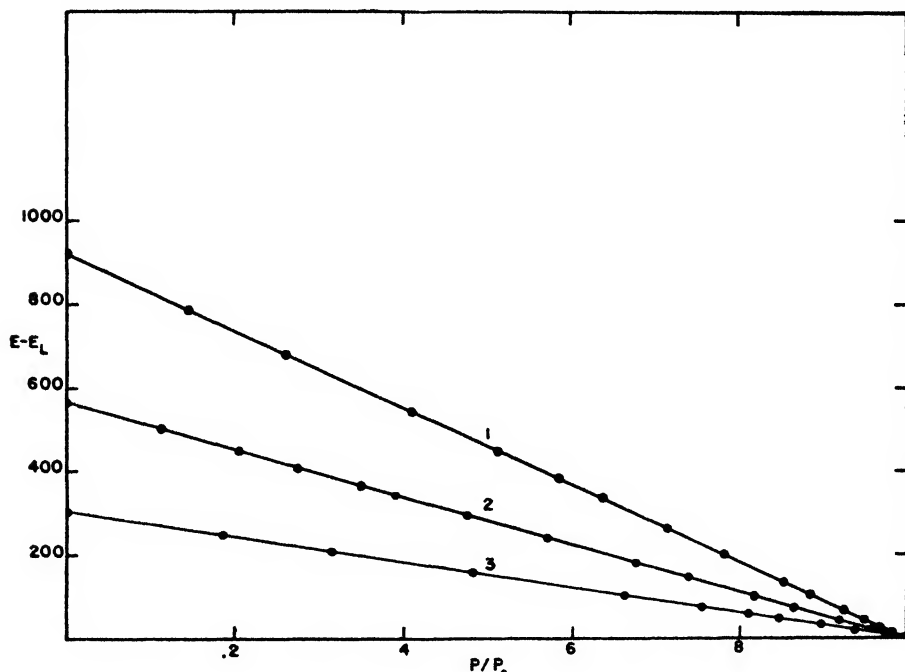


FIG. 3. Relation between net heat of adsorption and relative pressure. (1) Multilayer adsorption of ethyl chloride on graphite. (2) Ammonia on graphite. (3) Multilayer adsorption of butane on glass spheres.

The ammonia data reveal an exact relation between heat of adsorption and relative pressure. It is a linear equation of the form

$$E - E_L = K(1 - p/p_0) = K(p_0 - p)/p_0 \quad (2)$$

where  $K$  is the net heat at zero pressure. This relation holds for the entire measurable pressure range and can apparently be used to obtain extrapolated heat values near relative pressures of 0 and 1, where the isotherms are least exact. Figure 3 shows the  $E - E_L$  vs.  $p/p_0$  plot obtained for ammonia. This linear relation is our most direct proof of the statement that  $E$  approaches  $E_L$  when and only when  $p$  approaches  $p_0$ . To obtain the experimental relation of

equation 2 between heat and relative pressure, we needed an isotherm for the *mean* temperature, since the isosteric heats of adsorption are averages over the temperature range covered by the two isotherms. An isotherm for the mean temperature ( $-57^{\circ}\text{C}.$ ) can be constructed with sufficient accuracy by interpolation between the ammonia isotherms at  $-35.7^{\circ}\text{C}.$  and  $-78.5^{\circ}\text{C}.$ , since these lie quite close together. This interpolated isotherm was used to obtain  $p/p_0$  values for volumes whose heat values were then determined from figure 2.

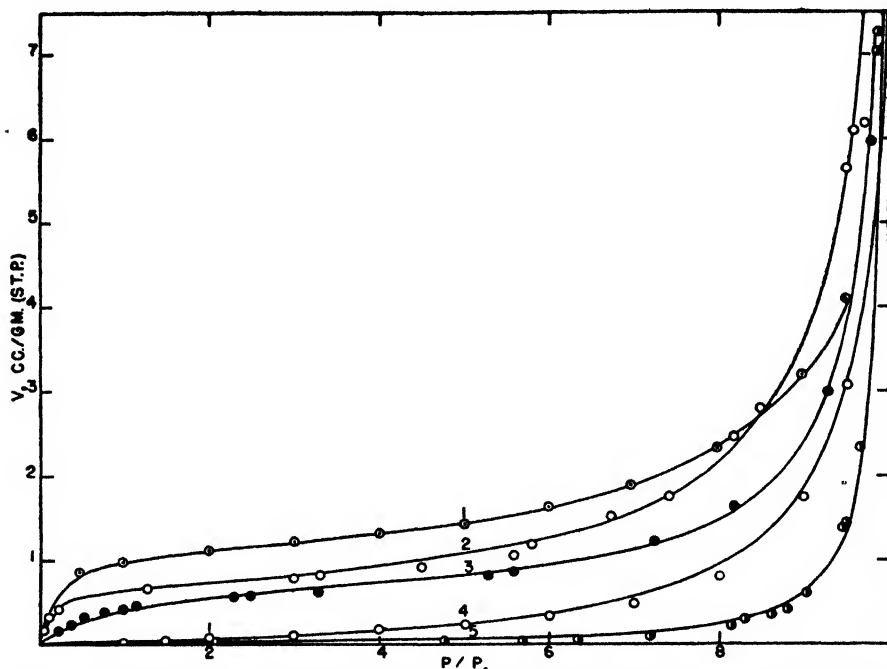


FIG. 4. Application of equation 18 to experimental isotherms. Solid lines computed. using constants of table 1. Points experimental. (1) Freon on zinc oxide at  $0^{\circ}\text{C}.$  (6), (2) Ethyl chloride on graphite NC-1 at  $-78^{\circ}\text{C}.$  (this laboratory). (3) Ethyl chloride on graphite NC-1 at  $0^{\circ}\text{C}.$  (this laboratory). (4) Water on graphite at  $25^{\circ}\text{C}.$  (9). (5) Water on graphite NC-1 at  $22.2^{\circ}\text{C}.$  (this laboratory).

Since all derivations of the B.E.T. equation are based upon the assumption that  $E = E_L$ , which is experimentally incorrect, we must conclude that the derivations are not strictly rigorous. This is probably the explanation of why the equation does not fit at relative pressures greater than about 0.35. At the time the equation was derived there were no published isotherms (for non-porous adsorbents) that extended to high relative pressures and this deficiency was not immediately apparent. As such isotherms have been determined, it has become generally recognized that the equation does not fit in the high relative pressure region.

Another deficiency of the B.E.T. equation is that it does not correctly account for a Type III isotherm. True, the general equation reduces to the form

$$V/V_m = \frac{p/p_0}{1 - p/p_0} \quad (3)$$

when constant  $C = 1$  and a plot of this equation gives a curve of the general shape of a Type III isotherm. It is not, however, correct to assume that  $C = 1$  since this means that  $E = E_L$ , which is not, according to our ammonia data, true. Further, equation 3 does not in general give a good fit to an experimental isotherm of Type III, since the equation gives only plots of the function  $x/(1 - x)$ , multiplied by various values for  $V_m$ . Finally, according to the B.E.T.

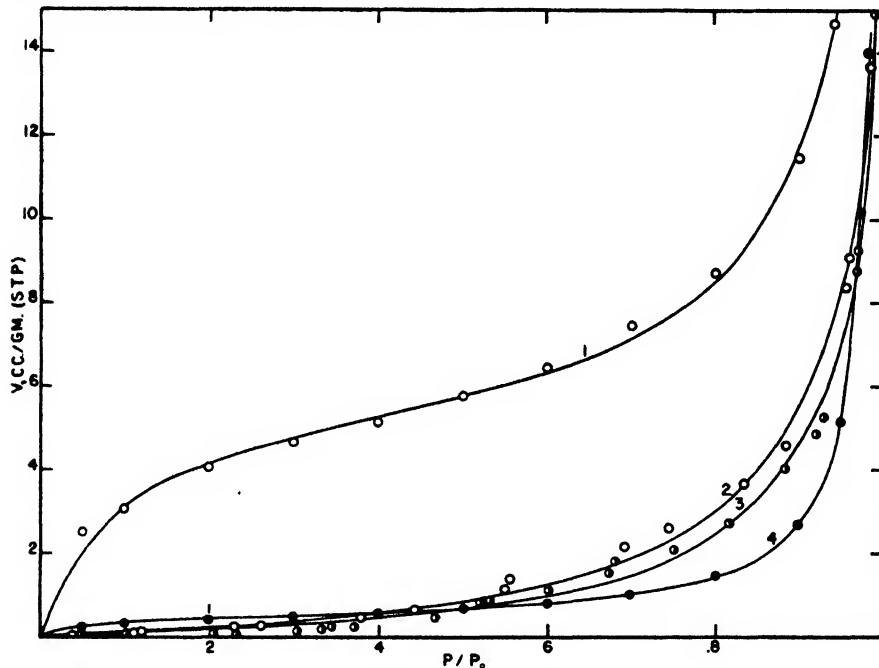


FIG. 5. Application of equation 18 to experimental isotherms. Solid lines computed, using constants of table 1. Points experimental. (1) Water on titanium dioxide at 25°C. (10). (2) Ammonia on graphite NC-1 at -78.5°C. (this laboratory). (3) Ammonia on graphite NC-1 at -35.7°C. (this laboratory). (4) *n*-Heptane on ferric oxide at 25°C. (11).

interpretation, the volume adsorbed at a relative pressure of 0.5 in a Type III isotherm is equal to  $V_m$ . This is not correct; it appears on comparison of the ammonia and water isotherms that the amount adsorbed in a Type III isotherm is in no way related to the value of  $V_m$ . At relative pressure 0.5, the volume of ammonia is about 0.85 cc./g. and the volume of water is 0.07 cc./g. Both of these cannot represent the volumes to form a monolayer, since the cross-section areas of ammonia and water molecules are of the same order of magnitude, as computed from molar volumes.

One of the tests which has been applied to the B.E.T. equation is to use it to compute isotherms for specified temperatures after first determining the constants by an experimental isotherm. A good approximation can be obtained in this

way, but the procedure is not at all exact for two reasons. First, it is necessary to know  $E_1$ , which is usually computed from the value of  $C$  obtained from a plot of the equation. In general, the computed value of  $E_1$  does not agree with experimental values. Second, it is assumed that beyond the first layer  $E = E_L$ . If this were true, a Type III isotherm would be the same for any temperature, when plotted on a relative pressure basis. Our data in figure 1 show that there is a displacement when the temperature is decreased. In order to be able to compute an isotherm accurately one must know  $E$  as a function of volume or

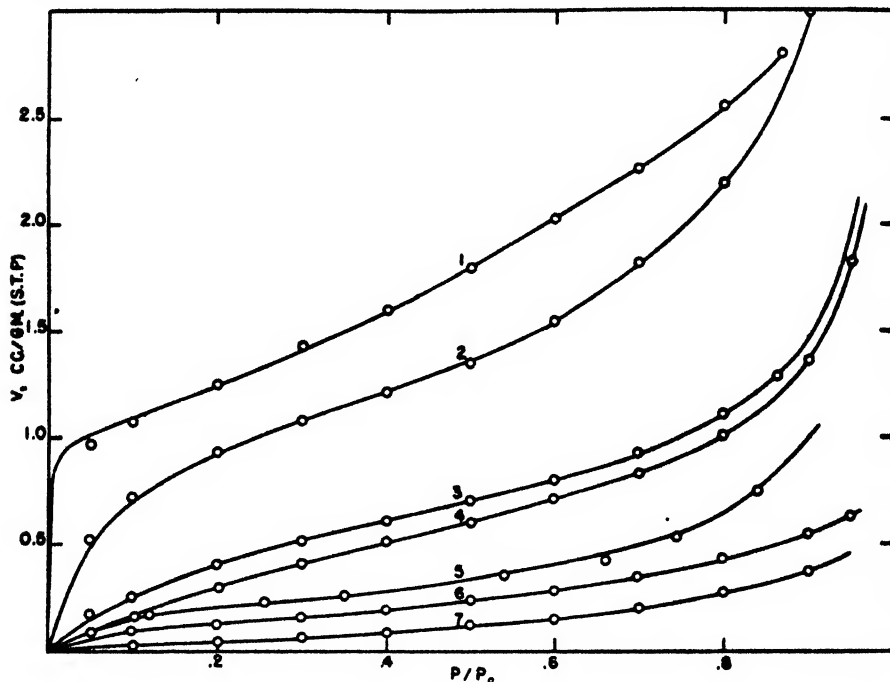


FIG. 6. Application of equation 18 to experimental isotherms for *n*-butane. Solid lines computed, using constants of table 1. Points experimental. (1) Copper at 0°C. (3). (2) Zinc oxide at 0°C. (6). (3) Glass spheres at -78°C. (6). (4) Glass spheres at 0°C. (6). (5) Tungsten powder at 0°C. (6). (6) Silver foil at -78°C. (6). (7) Monel ribbon at -78°C. (6).

relative pressure, so that the exact amount of the shift with temperature can be computed by means of the Clausius-Clapeyron equation.

Numerous attempts have been made to improve the fit of the B.E.T. equation, but all are based upon incorrect assumptions regarding the heats of adsorption. Consequently none of the proposed modifications gives an equation that fits all isotherms.

On the basis of our experimental heat-volume and heat-relative pressure relations, we believe that the basic model of the B.E.T. equation is incorrect. Instead of being essentially of uniform activity we believe that the surface is composed of regions of varying activity, which we shall designate as active sites.

Adsorption may occur at a given site only when the relative pressure attains the value which corresponds to the heat of adsorption for that site. A Type II isotherm is obtained when a large fraction of the surface has such high activity that it may adsorb at low relative pressure, but if only a small fraction of a surface will adsorb at low relative pressure, a Type III isotherm is obtained.

The idea of active sites is not confined to adsorption in the first layer. A site of high activity may hold a layer several molecules in thickness before the induced polarization from the substrate vanishes and  $E$  becomes equal to  $E_L$ . Thus, the heat of adsorption of the  $n^{\text{th}}$  layer on a very active site may be greater than that of the first layer on a relatively inactive site. In the case of a Type III isotherm, the surface may never be covered completely but instead there may be islands of multilayer adsorption.

The slope of an isotherm is a measure of the number of sites that have sufficiently high heats of adsorption to hold vapor in the given pressure range. We believe it to be significant that for a given surface the isotherms of various adsorbates have somewhat comparable slopes in the relative pressure range of 0.1 to 0.8, regardless of whether the isotherm is Type II or III. This is observed in numerous examples. It is shown by the isotherms for nitrogen, ethyl chloride, and ammonia on graphite. Harkins, Jura, and Loeser (9) find that the isotherms for *n*-heptane and water on a graphite sample have almost identical slopes for the entire pressure range, and Jura and Harkins (10) find that the Type II isotherms of nitrogen and water on titanium dioxide are almost identical.

The similarity in slopes of many Type II and Type III isotherms for a given surface suggests that after the low-pressure monolayer is formed in a Type II isotherm, the subsequent adsorption is determined by the distribution of active surface on which multilayer adsorption can occur. Further, the distribution of such activity is very much the same as the distribution on the same surface for a Type III isotherm.

We do not imply in the foregoing that heat of adsorption is a function solely of the surface; it depends also upon the adsorbate and the temperature. Graphite NC-1 has high heat of adsorption over the entire surface for the first layer of nitrogen at  $-196^{\circ}\text{C}$ . or for ethyl chloride at  $-78^{\circ}\text{C}$ ., but only a fraction of the surface will hold ammonia or water molecules in the region of low relative pressure.

Change in temperature may cause a marked change in the activity of a surface for a given adsorbate. This is shown in the ethyl chloride isotherms of figure 4. At  $0^{\circ}\text{C}$ . a much higher pressure is needed to make the first layer essentially complete than is needed at  $-78^{\circ}\text{C}$ . The iodine isotherms of Reyerson and Cameron (15) show that increase in temperature may even cause a Type II isotherm to change over into a Type III. This must mean that the fraction of highly active surface drops off rapidly as  $T$  is increased.

On the basis of this model we believe it possible to have a Type II isotherm without complete coverage of the surface by a monolayer. If, for example, only half of the surface atoms have high enough heat of adsorption to hold vapor at low pressure, then there might be obtained a Type II isotherm in which  $V_m$

represented the amount of adsorbate to cover only half the surface. When an isotherm has no sharply defined "point B," there may be some question regarding the identity of the computed  $V_m$  with the geometric surface.

We have developed an isotherm equation based on the model described above, which fits over the entire relative pressure range. In this equation we have treated the adsorption of the first layer separately from that of the multilayer, since the former generally corresponds to adsorption over the entire surface and the latter only at active sites. The monolayer adsorption is given by the Langmuir equation (12)

$$V = \frac{ax}{1 + bx} \quad (4)$$

and the multilayer adsorption by an equation which fits Type III isotherms:

$$V = \frac{\alpha x}{1 - \beta x} \quad (5)$$

In these equations  $x = p/p_0$ , and  $a$ ,  $b$ ,  $\alpha$ , and  $\beta$  are experimentally determined constants.

In developing equation 5 we have retained the basic B.E.T. idea of microscopic reversibility between the various layers and have used equations developed by Langmuir (13) for vapor pressure, evaporation, and condensation of liquids. The vapor pressure of a pure liquid is

$$p_0 = \Gamma T^{3/2} e^{-(E_L/RT)} \quad (6)$$

The rate at which gaseous molecules strike a unit area of surface is

$$\mu = (2\pi MRT)^{-1/2} p \quad (7)$$

If all portions of the surface are capable of holding adsorbate molecules at all relative pressures, the rate of condensation is

$$U_c = \beta \mu S_0 = \beta (2\pi MRT)^{-1/2} p S_0 \quad (8)$$

where  $\beta$  is the condensation efficiency or accommodation coefficient and  $S_0$  is the surface area available for condensation. The rate of evaporation is

$$U_e = \Gamma (2\pi MR)^{-1/2} T e^{-(E/RT)} S_1 \quad (9)$$

where  $E$  is related to the relative pressure by equation 2 and  $S_1$  is the surface area from which molecules may escape. If the solid involved has a surface of low, non-uniform activity toward the gas used, then not all of the gas-surface collisions will result in condensation. If one assumes that at a given pressure the fraction of the surface having sufficient net heat of adsorption for condensation to occur is given by  $e^{-(E-E_L)/RT}$ , then the rate of condensation will be

$$U_c = \beta (2\pi MRT)^{-1/2} p S_0 e^{-(E-E_L)/RT} \quad (10)$$

When  $p = p_0$ ,  $E = E_L$  and if all steric or special surface effects characterized by  $\beta$  are ignored ( $\beta = 1$ ), the rate of condensation is the same as that for the

pure liquid, as expected. At equilibrium  $U_s = U_s$  and

$$\beta(2\pi MRT)^{-1/2} p S_0 e^{-(s-s_L)/RT} = \Gamma(2\pi MR)^{-1/2} T e^{-(s/RT)} S_1 \quad (11)$$

$$\beta p S_0 = \Gamma T^{3/2} e^{-(s_L/RT)} S_1 = p_0 S_1 \quad (12)$$

If the adsorbing surface is divided into areas  $S_0, S_1, S_2 \dots$  (as done in the B.E.T. derivation) to correspond to areas holding 0, 1, 2  $\dots$  layers of adsorbate, and if the B.E.T. argument based on the principle of microscopic reversibility is followed, there results the general expression:

$$\beta p S_{i-1} = p_0 S_i \quad (13)$$

$$S_i = \beta(p/p_0) S_{i-1} = (\beta p/p_0)^2 S_{i-2} = \dots (\beta p/p_0)^i S_0 = y^i S_0 \quad (14)$$

The total adsorbing area (not necessarily the geometric surface of the adsorbent) is

$$A = \sum_{i=0}^{i=\infty} S_i \quad (15)$$

and the total volume adsorbed is

$$V = v_0 \sum_{i=0}^{i=\infty} i S_i \quad (16)$$

where  $v_0$  is the volume adsorbed per square centimeter if a complete monolayer is formed. By combining equations 15 and 16 and making the indicated summations, one obtains:<sup>5</sup>

$$\frac{V}{A v_0} = \frac{\sum_{i=0}^{i=\infty} i S_i}{\sum_{i=0}^{i=\infty} S_i} = \frac{\sum_{i=1}^{i=\infty} i y^i S_0}{S_0 + \sum_{i=1}^{i=\infty} y^i S_0} = \frac{\frac{y}{(1-y)^2}}{1 + \frac{y}{1-y}} = \frac{y}{1-y} = \frac{\beta x}{1-\beta x} \quad (17)$$

Equation 5 is obtained by solving for  $V$ :

$$V = \frac{A v_0 \beta x}{1 - \beta x} = \frac{\alpha x}{1 - \beta x} \quad (5)$$

The complete equation for a Type II isotherm is

$$V = \frac{\alpha x}{1 + b x} + \frac{\alpha x}{1 - \beta x} \quad (18)$$

This equation has been applied to twenty-five isotherms for surfaces that appear to be non-porous, giving a uniformly good fit. Constants for the fitted isotherms are given in table 1. Figures 4, 5, and 6 show the agreement obtained between experimental and computed isotherms. The solid lines are computed, using the constants of table 1, and the points are experimental. (For our own data, the points are those actually determined and for data of others, the points

<sup>5</sup> Dole (7) has developed an equation of this form for sorption by a gel, but his conditions do not fit the model that we have assumed.

TABLE I  
Isotherm data

GAS	ADSORBENT	T °C.	a	b	$\alpha$	$\beta$	$V_s$ (B.E.T.)	$V_m$ (SQUA- TION 18)	$V_{max.}$	C (B.E.T.)	REFER- ENCE
NH <sub>3</sub> . . . . .	Graphite NC-1	-78.5	0		0.91	0.945			16.6		†
	Graphite NC-1	-35.7	0		0.70	0.96			17.5		†
n-C <sub>4</sub> H <sub>10</sub> . . . .	Silver foil	-78	0.94	6.0	0.15	0.75	0.152	0.134	0.7	6.4	(6)
	Copper metal	0	151.8	145	1.15	0.50	1.000	1.040	3.34	*	(3)
	Glass 7 $\mu$	-78	0.218	2.52	0.012	0.90	0.042	0.062	0.18	6.7	(6)
	Glass, 200 mesh	-78	3.10	3.20	0.125	0.95	0.442	0.739	3.24	11.6	(6)
	Glass, 200 mesh	0	1.70	1.30	0.10	0.96	0.389	0.739	3.24	5.4	(6)
	Monel metal	-78	0.30	17.0	0.13	0.75	0.081	0.017	0.54	4.1	(6)
	TiO <sub>2</sub> , crystal- line	0	14.4	7.6	0.30	0.98	1.100	1.670	16.7	25	(10)
	Tungsten powder	0	3.7	15.5	0.13	0.95	0.192	0.224	2.82	26	(6)
	Zinc oxide powder	0	15.4	13.4	0.40	0.90	0.837	1.070	5.10	52	(6)
CCl <sub>4</sub> . . . . .	Carbon black	25	10.0	153	0.04	0.999	0.061	0.065	*	*	†
C <sub>2</sub> H <sub>5</sub> Cl . . . . .	Graphite NC-1	-78	41.4	59.0	0.41	0.97	0.615	0.690	14.4	107	†
	Graphite NC-1	0	8.3	11.0	0.21	0.985	0.573	0.690	14.7	16.6	†
CHCl <sub>3</sub> F . . . . .	Silver foil	-78	1.8	13.0	0.19	0.75	0.170	0.129	0.9	11	(6)
	Glass, 7 $\mu$	-78	1.29	18.3	0.01	0.90	0.047	0.067	0.17	106	(6)
	Glass, 200 mesh	-78	5.0	7.20	0.23	0.90	0.420	0.610	2.91	20	(6)
	Monel metal	-78	0.6	17.0	0.153	0.75	0.086	0.033	0.64	6.6	(6)
	Tungsten powder	0	3.82	10.8	0.11	0.95	0.242	0.324	2.52	21	(6)
	Zinc oxide powder	0	61.0	56.0	0.45	0.90	0.929	1.070	5.60	215	(6)
n-C <sub>7</sub> H <sub>16</sub> . . . .	Fe <sub>2</sub> O <sub>3</sub>	25	7.00	13.0	0.25	0.999	0.370	0.500	*	56	(11)
	Graphite	25	15.8	32.6	0.28	0.97	0.390	0.470	9.8	*	(9)
H <sub>2</sub> O . . . . .	Graphite	22.2	0		0.07	0.999			*		†
	Graphite NC-1	25	0		0.27	0.965			7.7		(9)
	TiO <sub>2</sub> , crystal- line	25	66.0	11.7	1.00	0.96	3.450	5.200	30.2	42	(10)

\* Very large number, of uncertain value.

† Results obtained in this laboratory.



are selected from the author's smoothed curve.) In almost all the isotherms of figures 4, 5, and 6 the computed curve represents the best smooth curve that can be drawn for the experimental points.

Equation 18 does not contain the constant  $V_m$ . In fact, if our model is correct the term  $V_m$  has no meaning as applied to adsorption beyond the first layer, since the second layer may never cover the entire surface which is covered by the first layer, but rather may cover only the active sites. One can, however, obtain from equation 18 a value for  $V_m$ , by setting  $x = 1$  and evaluating the first term. The value so computed is shown in table 1 for all the fitted Type II isotherms. For comparison the  $V_m$  values computed by means of B.E.T. plots are also shown. In general, the two  $V_m$  values agree fairly well and both are in accord with estimates based upon visual location of point  $B$ .

It is inherent in the form of equation 18 that the adsorption when  $p = p_0$ , designated as  $V_{max.}$ , is finite whenever constant  $\beta$  is less than unity, as it generally is. Values computed for the maximum adsorption of all the fitted isotherms are shown in table 1. In general, we believe these computed values to be fairly reliable, since they depend chiefly upon the value chosen for  $\beta$ . It happens that the fit of equation 18 to an experimental isotherm is quite sensitive to the value of this constant and a change of 0.01 to 0.03 in  $\beta$  may alter a curve markedly. In those cases where the curve is very steep as  $p$  approaches  $p_0$ , and  $\beta$  is greater than 0.99, there is of course much uncertainty in the computed value of  $V_{max.}$ , since now it depends upon knowing  $\beta$  to an accuracy of 0.001. When  $\beta$  is less than 0.99 the computed values agree well with extrapolations of the isotherm to  $p = p_0$ . Further, for the isotherms taken at two different temperatures, the computed values of  $V_{max.}$  for the two temperatures are in good agreement, even though the constants of equation 18 for the two may be quite different. We believe therefore that adsorption is finite when  $p = p_0$ . True, more may be taken on after this point, just as an infinitesimal increase in pressure will cause vapor to condense on a liquid surface, but we think that  $V_{max.}$  represents the amount of adsorption when  $p$  just becomes equal to  $p_0$ .

If we are correct in treating separately the adsorption in the first layer and that of other layers, it is then possible to evaluate separately the isosteric heats of adsorption in the mono- and multi-layers. This is done by fitting isotherms for two temperatures by equation 18, and then using the equations to compute relative pressures at the two temperatures which correspond to given volumes adsorbed in the mono- or multi-layer.

We have made such computations for the adsorption of ethyl chloride on graphite (figure 4) and butane on glass spheres (figure 6). The values so computed for heats of adsorption in the first layer are much less than calorimetric heats determined by Beebe and associates (1) for somewhat similar systems, in the very low-pressure region. This we anticipated, for in general the Langmuir equation, which is based upon the assumption that the surface is of uniform activity, does not fit exactly in the very low pressure region (some isotherms can be fitted better by a two-term Langmuir-type equation). The isosteric heats for the multilayer portion we believe to be more reliable, since this portion of the

computed isotherm is not highly dependent upon the constants chosen for the first term and at high relative pressure the adsorption of the first layer contributes only a small fraction of the total.

It was found that for the multilayer portions of the ethyl chloride and butane isotherms the heats of adsorption are exactly like those for the Type III ammonia isotherm, or linear with respect to relative pressure. This is shown in the plots of figure 3. This linear relation is, we believe, the best evidence that there is a distribution of surface activity which determines the amount adsorbed in multilayers and that the same type of distribution applies to both Type II and Type III isotherms. This strongly supports the view that monolayer and multilayer adsorption should be treated separately, as we have done in equation 18.

#### SUMMARY

Experimental isotherms are given for water, ammonia, and ethyl chloride on graphite of nitrogen area 4 sq. m. per gram. Isosteric heats of adsorption are computed for ammonia and ethyl chloride.

It is shown that for all relative pressures the heat of adsorption exceeds the heat of liquefaction. The heat of adsorption for all layers beyond the first is a linear function of relative pressure:

$$E - E_L = K \left( \frac{p_0 - p}{p_0} \right)$$

Certain limitations of the B.E.T. equation are discussed. An isotherm equation, based upon a new interpretation of multilayer adsorption, is proposed. This is applied to twenty-five isotherms for non-porous substances and fits well in all cases.

#### REFERENCES

- (1) BEEBE, POLLEY, SMITH, AND WENDELL: *J. Am. Chem. Soc.* **69**, 2294 (1947).
- (2) BRUNAUER: *The Adsorption of Gases and Vapors*, pp. 164-5, 175-7, 243. Princeton University Press, Princeton, New Jersey (1943).
- (3) BRUNAUER AND EMMETT: *J. Am. Chem. Soc.* **59**, 2682 (1937).
- (4) BRUNAUER, EMMETT, AND TELLER: *J. Am. Chem. Soc.* **60**, 309 (1938).
- (5) COOLIDGE: *J. Am. Chem. Soc.* **49**, 708 (1927).
- (6) DAVIS, DEWITT, AND EMMETT: *J. Phys. Colloid Chem.* **51**, 1232 (1947).
- (7) DOLE: *J. Chem. Phys.* **16**, 25 (1948).
- (8) EMMETT AND BRUNAUER: *J. Am. Chem. Soc.* **59**, 1553 (1937).
- (9) HARKINS, JURA, AND LOESER: *J. Am. Chem. Soc.* **68**, 554 (1946).
- (10) JURA AND HARKINS: *J. Am. Chem. Soc.* **66**, 919, 1356 (1944).
- (11) JURA, LOESER, BASFORD, AND HARKINS: *J. Chem. Phys.* **14**, 117 (1946).
- (12) LANGMUIR: *J. Am. Chem. Soc.* **40**, 1361 (1918).
- (13) LANGMUIR: *J. Am. Chem. Soc.* **54**, 2798 (1932).
- (14) PIERCE AND SMITH: *J. Phys. Colloid Chem.* **52**, 1111 (1948).
- (15) REYERSON AND CAMERON: *J. Phys. Chem.* **39**, 181 (1935).

## TEMPERATURE LAG AND CHEMICAL KINETICS

WILLIAM S. HORTON

*Department of Chemistry, University of Connecticut, Storrs, Connecticut**Received February 20, 1948*

Rates of chemical reactions in liquids are most often measured by determining changes in a property or the concentration of a sample enclosed in a glass vessel and kept in a constant-temperature bath. Ideally, of course, the constituents of the sample should be brought separately to the reaction temperature, mixed in the vessel in zero time, and the time counted from the instant of mixing. Ideally, also, the sample should be well mixed during reaction so as to dissipate or acquire any heat necessary to the reaction. Under certain circumstances these conditions cannot be attained. The nature of the reaction may prevent, for example, the possibility of bringing an essential constituent to the reaction temperature before mixing because of decomposition during the preheating. In view of this circumstance it would seem desirable to have a theoretical treatment of the effect of mixing the constituents at room temperature, pouring the mixture into the glass vessel kept in the constant-temperature bath, and counting time from this point. The following treatment of this situation is presented with the purpose of indicating a method for calculating the results that might be expected of a kinetic experiment run under non-isothermal conditions where these are due to lag in attaining bath temperature.

Probably most experimental arrangements provide for stirring the sample, although in small vessels this may be difficult and therefore omitted. The efficiency of the stirring procedure will profoundly affect the rate of heat transfer and is somewhat variable from one experiment to another. To treat the effect of stirring efficiency would be quite laborious and probably not very enlightening. However, the treatment of the two extreme cases between which the truth must lie should be of interest. If we discuss the case of perfect mixing we know that the thermal mixing error can be no less than that estimated by such a treatment. By treating the case of no mixing we obtain an upper limit to the error.

The following hypothetical system is set up for the purpose. A completely spherical glass shell is assumed as the vessel. The reacting material is assumed to be a liquid completely filling the vessel. The vessel is assumed to be in a constant-temperature bath above room temperature. At time  $t = 0$ , the vessel is immediately filled with the reacting liquid which is at room temperature. The rate of reaction is to be theoretically studied under two conditions: (A) perfect mixing and (B) no mixing. In the case of perfect mixing, resistance to the heat flow is mainly in the container. For no mixing this resistance is mainly in the reaction mixture.

## CASE A: PERFECT MIXING

Perfect mixing may be arbitrarily defined as existing for the purpose of this discussion when heat conducted through the container wall is instantaneously

distributed throughout the entire sample. The fact that such perfect mixing cannot be attained in practice does not affect the discussion adversely, for investigation of this case will yield results that represent the limit approachable with better and better mixing.

The fundamental difference introduced into the reaction kinetics is that the equation

$$-\frac{dx}{dt} = kf(x) \quad (1)$$

cannot be integrated assuming a constant value of  $k$ , the specific velocity constant. During our supposed experiment  $k$  changes because of the temperature change from the moment of sample introduction until essentially constant sample temperature has been attained. Thus instead of our usual solution to equation 1 we have

$$-\int_{x_0}^x \frac{dx}{f(x)} = \int_0^t k dt \quad (2a)$$

or

$$\ln \left( \frac{x_0}{x} \right) = \int_0^t k dt \quad (2b)$$

where equation 2b shows the result for a first-order reaction,  $f(x) = x$ . In the  $k$ -integral,  $k$  is given by the Arrhenius equation in which  $T$ , the absolute temperature of the sample, is determined by the heat-flow conditions.

The heat-flow problem, although comparatively simple, appears not to have been treated before. It involves heat flow through a spherical shell, of which the outer surface is at the constant temperature of the bath and the inner surface is at the temperature of the contained liquid which is constantly rising. The temperature of the liquid at any one instant is uniform throughout the sample.

The rate of heat flow, in calories per second, in spherical bodies is given by

$$\frac{dQ}{dt} = 4\pi r^2 \kappa \frac{dT}{dr} \quad (3)$$

By rearrangement we get

$$\frac{dQ}{dt} \int_{r_1}^{r_2} \frac{dr}{r^2} = 4\pi \kappa \int_T^{T_2} dT \quad (4)$$

where  $dQ/dt$  is considered constant during the integration from the inner surface of the glass shell to the outer surface. Actually, this is an approximation which is more closely approached the smaller the heat capacity of the vessel is in proportion to that of the contents. The solution of equation 4 is simple.

$$\frac{dQ}{dt} = \frac{4\pi \kappa r_1 r_2}{r_2 - r_1} (T_2 - T) \quad (5)$$

Thus at any instant of time the rate of heat flow into the vessel and into the

liquid is given by equation 5, where  $r_1$  and  $r_2$  are the inner and outer radii of the vessel,  $\kappa$  is the coefficient of thermal conductivity of the vessel,  $T_2$  is the constant bath temperature, and  $T$  is the instantaneous temperature of the inner vessel wall and of the liquid contents.  $T$  is determined by the rate of heat influx and the heat capacity of the contents. Thus

$$\frac{dT}{dt} = \frac{1}{c\rho v} \frac{dQ}{dt} \quad (6)$$

where  $c$  is the specific heat,  $\rho$  is the density, and  $v$  is the volume of the contained liquid. The desired solution is now easily obtained by introducing equation 5 into equation 6 and integrating. The result is equation 7:

$$T = T_2 - \Delta T \exp(-Bt) \quad (7)$$

where

$$B = \frac{3\kappa r_2}{c\rho r_1^2(r_2 - r_1)} \quad (8)$$

In this derivation, variations in the physical constants themselves are assumed negligible. If account of these variations is desired, mean values for the temperature range involved may be used.

Equation 7 gives the value of  $T$  to be used in the Arrhenius equation for  $k$ , and the result introduced into equation 2a is expressed in equation 9,

$$-\int_{x_0}^x \frac{dx}{f(x)} = \int_0^t s \exp[-A/T_2 - \Delta T \exp(-Bt)] dT \quad (9)$$

where  $s$  and  $A$  are constants from the Arrhenius equation,  $k = s \exp(-A/T)$ . For the first-order reaction  $\ln(x_0/x)$  may be substituted for the left-hand member, as was done previously in equation 2b. Integration of equation 9 for various upper limits will give the reactant concentration at various times during the hypothetical experiment. A treatment of integrals similar to the right-hand member of equation 9 has been given (1), but the methods presented are not well suited for the purpose desired here. A numerical approximation method based upon the trapezoidal formula is much more helpful. First, a list of values of  $k$  is made for various values of  $t$  from 0 to any desired time; in the case given below 5-sec. intervals were chosen. Then the value of the integral to a chosen time  $t_n$  is given by

$$\int_0^{t_n} k dt = \frac{h}{2} \left[ k_0 + \sum_{i=1}^{n-1} 2k_i + k_n \right] \quad (10)$$

The practical advantage of this numerical method is that it lends itself to quick computation on an electric calculator because of the additivity of the right-hand member of equation 10. Thus it is easy to show that

$$\int_0^{t_{n+1}} k dt = \int_0^{t_n} k dt + \frac{h}{2}(k_n + k_{n+1}) \quad (11)$$

In these relations  $k_n$  is the value of the specific velocity constant at  $t_n$  and  $h$  is the interval of time chosen in the numerical evaluation. Equation 11 indicates that any successive value of the integral can be obtained by adding to the previous value the term  $(h/2)(k_n + k_{n+1})$ .

#### CASE B: NO MIXING

Measurements of concentration as a function of time in this case actually are measurements of average concentration, since, in contrast to case A, the temperature, reaction velocity, and therefore concentration vary with position in the vessel. Thus if  $y$  is the average concentration, the quantity measured, instantaneously,

$$y = \bar{x} = \frac{1}{V} \int_V x \, dv \quad (12)$$

where  $V$  is the total volume and  $dv$  is a small volume element in which the concentration is  $x$ . The change in  $y$  with time is

$$\frac{dy}{dt} = \frac{1}{V} \int_V \frac{\partial x}{\partial t} \, dv \quad (13)$$

But

$$\frac{\partial x}{\partial t} = -kx$$

and therefore

$$\frac{dy}{dt} = -\frac{1}{V} \int_V kx \, dv = -\bar{kx} \quad (14)$$

where now  $k$  is the specific velocity constant for the temperature which exists in the small volume element  $dv$ , and  $\bar{kx}$  is the average value of the product of  $k$  and  $x$  over the entire volume at the instant of time under consideration. Note that here a first-order reaction has been assumed for simplicity. Modification is possible for other orders.

The observed concentration-time relationship should be given by

$$y - y_0 = - \int \bar{kx} \, dt \quad (15)$$

In principle this integral could be evaluated by an extension of the method used in case A. It would be necessary to divide the volume into small elements. Compute the average temperature in each element and the value of  $k$  corresponding to that temperature. Compute the average value of  $k$  during the small time interval since the last computation, and using this result compute the new concentration in the volume element. Multiply  $k$  by  $x$ , thus obtaining  $kx$  for the element. Do this for all elements and determine the average of  $kx$  over the sample. Having done this for one time, it is then done for the next time, only a small interval away. This procedure is obviously laborious, so the following

was adopted as an approximation that might yield results not too divergent from the more rigorous approximation. It is suggested by considering a case where either  $k$  or  $x$  does not vary too widely over the sample at any instant. In such a case, approximately

$$\overline{kx} = \bar{k} \bar{x}$$

Then equation 14 may be modified to

$$\frac{1}{y} \frac{dy}{dt} = -\frac{\bar{k} \bar{x}}{\bar{x}} = -\bar{k}$$

and

$$\ln \left( \frac{y}{y_0} \right) = -\int \bar{k} dt \quad (16)$$

A further approximation which simplifies calculation and probably does not introduce great error is to replace the average value of  $k$  by its value at the average temperature of the sample. These approximations reduce the problem to one of heat flow, i.e., to determination of the transient average temperature.

The solution to this heat-flow problem is well known (2).

$$T = \frac{2b}{\pi} \left( \frac{c}{r} \right) \sum_{m=1}^{\infty} \frac{(-1)^m}{m} \sin [m\pi r/c] \exp[-a^2 m^2 \pi^2 t/c^2] + T_2 \quad (17)$$

where  $b$  is the original temperature difference,  $c$  is the inner radius of the vessel,  $a$  is  $\sqrt{\kappa/c\rho}$  ( $\kappa$  is the coefficient of thermal conduction for the liquid and  $\rho$  is the liquid density), and  $T_2$  is the bath temperature.

The average temperature is seen to be

$$\bar{T} = \frac{-6b}{\pi^2} \sum \left( \frac{1}{m^2} \right) \exp[-\beta m^2 t^2] + T_2 \quad (18)$$

where  $\beta$  has been substituted for  $(a^2\pi^2/c^2)$ . The integral  $\int k dt$  may be determined in the same manner as the similar one for case A.

## RESULTS

To illustrate the results obtainable with this procedure, the methods described were used, assuming the following values of constants:  $T_2 = 308.1^\circ\text{K.}$ ,  $\Delta T = 10.0$ ,  $B = 0.02303$ ,  $s = 10^{12}$ ,  $A = 4371$ . This corresponds to using a spherical glass shell of about 4-cm. radius and 1-mm. thickness containing a liquid with physical constants close to those of water. The value of  $A$  corresponds to an activation energy of 20 kcal. A first-order reaction was chosen for illustrative purposes.

The numerical results are illustrated in the accompanying graphs and tables. Figure 1 shows the value of  $k$  as a function of time. For the case of perfect mixing this is the value throughout the sample at any given time. For no mixing the  $k$  is for the average temperature in the sample at that time. Although the curves are not shown, it is interesting to note that the temperature-time curves

for the two cases show a relation strikingly similar to that in figure 1 for  $k$ . Figure 2 shows the "observed" ratio of reactant concentration. Here also that expected for the ideal case (i.e., no temperature lag) has been shown. It is interesting to note that the case for perfect mixing starts out as if there were no mixing but tends later toward the ideal case. Figure 3 shows this also, where the logarithm of the concentration ratio has been plotted. This latter plot also shows another interesting point. During the latter part of the case of perfect

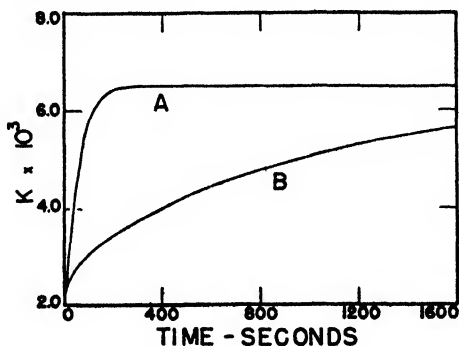


FIG. 1. Variation of rate constant during the hypothetical experiment. Curve A is for perfect mixing; curve B for no mixing. The ideal case, with no temperature lag, would be a straight horizontal line, the asymptote of A and B at  $k \times 10^3$  equal to 6.48 sec.<sup>-1</sup>

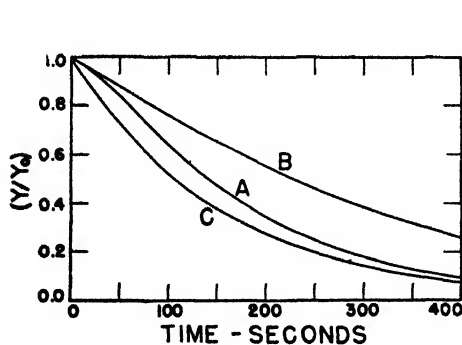


FIG. 2

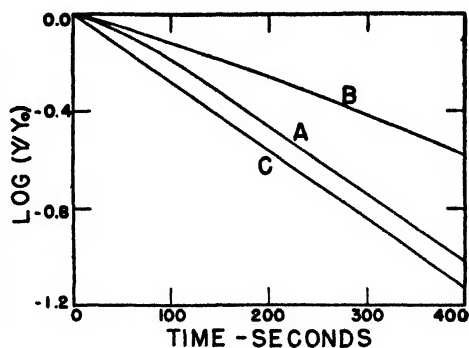


FIG. 3

FIG. 2. "Observed" concentration ratio for a hypothetical first-order reaction. Curves A and B are as in figure 1; curve C is the ideal case.

FIG. 3. Characteristic graph for the hypothetical first-order reaction. Curves A, B, and C are as in figures 1 and 2.

mixing it appears as if the slope were the same as the ideal slope, suggesting that in such a case ignoring the early part of the reaction and determining  $k$  by the slope method from the remainder may remove a good deal of the error due to temperature lag. The tables give some indication of this.

In table 1,  $f$  is the amount of reaction completed and  $t_f$  is the corresponding life time. In table 2, "per cent completion range" refers to the region over which the slope measurement was made in order to determine  $k$ . The regions were chosen so that with random errors included a reasonable straight line could be drawn.



Table 1 shows the expected error in a  $k$  determined from experiments in which the two types of mixing are used. In this table  $k$  is computed from observed values of various life times. The errors are quite high, and, as expected, higher for case B than case A. Table 2 shows corresponding results when the slope method is used. Here we see that for perfect mixing a good reduction in the

TABLE 1  
*Errors in  $k$  by life-time method*

$f$	$t_f$ (TRUE)	PERFECT MIXING		NO MIXING	
		$t_f$	Error	$t_f$	Error
	<i>seconds</i>	<i>seconds</i>	<i>per cent</i>	<i>seconds</i>	<i>per cent</i>
1/4	44.4	72.7	39	104.1	57
1/3	62.5	93.9	33	141.3	56
1/2	106.9	141.7	25	226.0	53
2/3	169.	206.	18	335.	49
3/4	214.	250.	14	408	48
4/5	248.	285.	13	462	46

TABLE 2  
*Errors in  $k$  by slope method*

	PERFECT MIXING	NO MIXING
Per cent completion range . . . . .	26-82	24-83
$k \times 10^3$ . . . . .	6.26	3.73
Per cent error . . . . .	3.4	42.

True value:  $k \times 10^3 = 6.48 \text{ sec.}^{-1}$

TABLE 3  
*Results for slower reactions with perfect mixing*

$f$	$s = 0.5 \times 10^{13}$		$s = 1 \times 10^{14}$	
	$t_f$	Error	$t_f$	Error
	<i>seconds</i>	<i>per cent</i>	<i>seconds</i>	<i>per cent</i>
1/4	123	28	481	8.3
1/3	161	22	625	5.9
1/2	250	14	1069	3.5
2/3	375	10	1694	2.2
3/4	464	8	2138	1.7
4/5	633	6	2482	1.5

error has been achieved, although not complete removal. For the other case a smaller improvement is noted. The result is still far from satisfactory here.

Table 3 shows the expected result for errors in  $k$  by the life-time method for slower reactions with other conditions the same. The slower the reaction as compared to rate of heat flow, the smaller the error.

## DISCUSSION

It appears that certain generalizations may be made from the results of the computations described above. Obviously, where conditions do not permit reactants to start at the desired temperature, as efficient a mixing procedure should be devised as possible. For without mixing the values of  $k$  and any activation energies determined from them may be extremely erroneous, even though straight lines seem to be obtained in the characteristic graphs. All possible ingenuity should be used to increase the rate of heat flow through the vessel, so that the ratio of reaction rate to heat-flow rate may be made as small as possible. The slope method rather than that of fractional life times should be used in order to determine the rate constants. Measurement of actual sample temperature, rather than trusting to bath temperature, is also advisable. It is not believed that the accuracy of the calculations given here warrants using this method as a means of correcting experimental results. Rather, it is suggested that much experimental caution be used to reduce these errors.

## SUMMARY

In this article is given a method of computing the concentration of reactant to be expected during a kinetic experiment where thermal equilibrium is not instantly attained. This is done for the two extremes of mixing, with the view that any actual case lies between these limits. In view of the results, suggestions are offered for *reducing* the errors in specific velocity constants determined in such experiments.

## REFERENCES

- (1) SHERMAN, J.: Ind. Eng. Chem. **28**, 1026 (1936).
- (2) WILLIAMS, E. D., AND ADAMS, L. H.: Phys. Rev. **14**, 99 (1919).

THE VAPOR PRESSURE OF BENZOTRIFLUORIDE MEASURED  
BY THE RODEBUSH MANOMETER<sup>1</sup>

G. W. SEARS AND E. R. HOPKE

*Department of Physics, Duke University, Durham, North Carolina**Received January 26, 1948*

## INTRODUCTION

In connection with the complete interpretation of the ultraviolet absorption spectra of organic molecules in the vapor state, it is desirable to have accurate data on vapor pressures of these compounds in the region of small pressures, i.e., 0.01 mm. to 1.0 mm. of mercury. Rodebush and Coons (7) have described an apparatus which bridged this pressure range. It operated by electromagnetically balancing the force exerted by the vapor pressure on a movable plate. Rodebush and Henry (8) measured the vapor pressure of sodium by using such a device. Variations of the method have been used by Dietz (3) and by Balson (1). The present investigation involves the application of the Rodebush gauge to the measurement of the vapor pressure of benzotrifluoride. A description of the factors which limit the accuracy and range of the gauge is given.

## APPARATUS

The Rodebush gauge used in this investigation was a modification described by Rodebush and Henry (8). Briefly, the gauge consists of a soft-iron armature and a quartz plate hung by a common suspension from a quartz cantilever. The vapor under investigation exerts an upward force on the plate by virtue of its pressure.

A solenoid is mounted coaxial to and slightly below the armature. In operation a current is passed through the solenoid and is increased until the electromagnetic force downward on the armature balances the upward force of the vapor on the plate. The balance is detected by the plate jumping away from its initial position. The calibration of the gauge is thus a curve of pressure *versus* the corresponding equilibrium solenoid current.

The gauge was calibrated against a McLeod gauge, whose calibration is described in some detail in the following paragraphs. The McLeod gauge was connected to the vapor enclosure of the Rodebush gauge *via* a dry ice trap and a 2-liter bulb. Two stopcocks in series led from the bulb to a supply of dry air at atmospheric pressure. When the air between the two stopcocks expanded into the 2-liter bulb, its pressure decreased to about 0.250 mm. of mercury. A sample of air introduced in this way was used to determine three or four additional points on the calibration curve at successively lower pressures.

The order of magnitude of the pumping speed past the plate in closed position was measured to be  $10^{-5}$  liter sec.<sup>-1</sup> In the time necessary to measure the

<sup>1</sup> This investigation was assisted by the Office of Naval Research under Contract N6ori-107, Task Order I, with Duke University and the Duke University Research Council.

McLeod pressure and to determine the equilibrium current the pressure decreased by only 0.03 per cent.

The uncompressed volume of air in the McLeod gauge was calibrated by weight of distilled water. This value was found to be  $218.17 \pm 0.02$  cm.<sup>3</sup> The compressed volume of gas in the gauge was calibrated by weight of mercury, and was found to be  $0.2101 \pm 0.0004$  cm.<sup>3</sup> The compression ratio was thus  $1,038 \pm 2$ . Temperature corrections were applied to the densities of water and mercury. A correction was made for the volume of the mercury meniscus. The change of volume of the Pyrex bulb with temperature was found to be negligible.

The pressure difference between the two arms of the McLeod gauge was measured with a Gärtner Student Type Cathetometer to an accuracy of 0.1 mm. The measured pressures were corrected to millimeters of mercury at 0°C., and an acceleration of gravity of 980.665 cm. sec.<sup>-2</sup> The acceleration of gravity in Durham was calculated by Helmert's equation to be 979.77 cm. sec.<sup>-2</sup> The difference in capillary depression in the two arms caused by a measured variation in capillary diameter of 1 per cent was calculated to be less than 0.01 mm. It was found that the mercury columns were slow to assume their final positions, because of their capillary interaction with the glass. The effect became important with small capillaries and slight pressure differences. In this experiment, using a 2-mm. capillary, the error from this effect was found to be about 0.2 mm. under the most unfavorable conditions.

The air in the McLeod gauge was assumed to obey the perfect gas law. From the data of Holborn and Otto (5) this was calculated to introduce an error of less than 0.01 per cent. The error caused by adsorption of gas on the capillary walls during compression was given an upper limit from the data of Moles and Crespi (6). The maximum error was placed at 0.2 mm. No correction was applied, since according to Hartley, Henry, and Whytlaw-Graves (4) the desorption process is very slow at room temperature. The calculated absolute error in the McLeod gauge pressure measurements ranged from 0.4 per cent at 250 microns to 0.8 per cent at 80 microns pressure.

A calibration curve of solenoid current *vs.* pressure is shown in figure 1. The curve is somewhat concave as seen from the pressure axis. The individual points on the curve were reproducible to within an average error of 1.0 per cent calculated as error in pressure. The maximum observed error was 2.5 per cent. The average error tended to increase at high pressures.

As has been previously stated, each point on the calibration curve represents a balancing of electromagnetic and pressure forces. Since the quartz cantilever arm is almost perfectly elastic, the upward force exerted by it on the plate in closed position was considered constant. The variation in weight of the plate and armature caused by pressure variation in the vessel was less than 0.01 per cent. The force exerted upwards on the plate by the pressure was known to within 0.4–0.8 per cent, dependent on the pressure region. Since the maximum error of 2.5 per cent was observed on the calibration curve of the Rodebush gauge, a part of this error was presumed to stem from the irreproducibility of the magnetic force on the iron armature as a function of solenoid current.

The force on an armature placed in a solenoid depends on the magnetic field of the solenoid, on the magnetic permeability of the armature, and on their relative positions. The magnetic field for a given solenoid is a function only of the current. The permeability is dependent not only on the field, and hence the solenoid current, but also on its own past magnetic history. Since the relative positions of the solenoid and armature were quite well defined, it seemed reasonable to assume that hysteresis of the iron armature was responsible for the observed error in the calibration curve.

Two experimental facts supported this surmise. First, the deviations of experimental points from the calibration curve increased with increasing pressure.

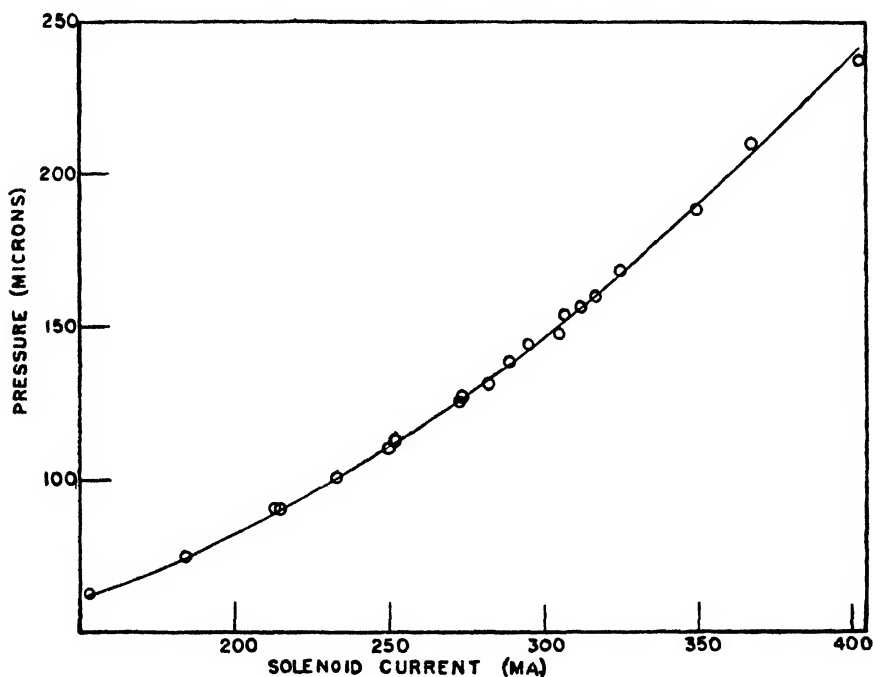


Fig. 1. Calibration curve of solenoid current *vs.* pressure

This is in contradiction to the observation that the pops were more sharply defined at high than at low pressures. The increase of deviations with pressure could be correlated with the increase of hysteresis with magnetic field. Secondly, when the Armco soft-iron armature was replaced by an iron sample with a much larger hysteresis loop, the calibration curve was much less reproducible.

Another factor which had a significant effect on the reproducibility of the calibration curve was the rate at which the solenoid current approached the equilibrium value. It was found that the reproducibility of the calibration curve improved with a decrease of  $dI/dt$ . Below approximately 20 milliamp.  $\text{min}^{-1}$ , no further improvement was noted.

The sensitivity of the gauge is represented by the slope of the calibration curve

in milliamperes per micron. The sensitivity can be increased by decreasing the number of turns in the solenoid, by increasing the axial distance from the solenoid to the armature, and by increasing the cover plate area.

The upper limit of usefulness of a given Rodebush gauge is set by one of two factors: First, a gauge can not be used above a pressure which exerts a force upwards on the cover plate equal to, or greater than, the force of gravity acting downward on the plate. The pop distance increases with increasing pressure. This limits the pressure to below that at which the jump of the plate would damage the gauge.

Satisfactory operation is dependent upon the pop distance exceeding some minimum value. The lower limit of the Rodebush gauge is thus dependent on two factors,—the cover plate area, and the stiffness of the quartz cantilever. For low pressures the plate area should be large, and the cantilever weak.

#### MEASUREMENTS AND RESULTS

The calibrated gauge was then applied to the measurement of the vapor pressure of benzotrifluoride. The substance was of interest because Saylor and Field (9) of the Chemistry Department had just completed measurements in the region 10–760 mm. of mercury, and also because a spectroscopic investigation of the substance in this laboratory made it desirable to supplement the data of Saylor and Field (9) and of Booth, Elsey, and Burchfield (2).

A pure sample of benzotrifluoride, which was obtained through the courtesy of the Chemistry Department, was used in this and the spectroscopic investigation.

A wide-mouthed pint Dewar flask, partially filled with acetone, served as a temperature bath. The acetone was cooled to  $-50^{\circ}\text{C}.$  with fragments of dry ice, and the bath temperature was allowed to rise to  $-40^{\circ}\text{C}.$  over a period of 90 min. The bath was stirred by hand. The temperature was measured to within  $0.1^{\circ}\text{C}.$  by an alcohol-in-glass thermometer, which had been calibrated against a Heraeus 25-ohm calibrated platinum resistance thermometer, using a Leeds and Northrup No. 4725 Wheatstone bridge. Since the temperature rose  $0.1^{\circ}\text{C}.$  per minute, and the bath temperature was read within 10 sec. after a pressure measurement, the error involved was negligible. A rough calculation indicated that the time lag between bath and sample temperatures was less than 10 sec. under the conditions of this experiment, which also introduced negligible error.

One milliliter of sample was sealed into the vapor enclosure. The apparatus was then evacuated to a pressure of  $10^{-6}$  mm. of mercury with the sample cooled by dry ice. The benzotrifluoride was melted with the vapor enclosure closed, and was refrozen with dry ice. The evolved gases were pumped out, and the process was repeated four or five times. It was also necessary to pump on the sample at dry ice temperatures for 4 days to remove a small amount of volatile impurity without simultaneously removing the sample.

The pressure measurements on an outgassed sample were carried on over a 4-day period. About 15 per cent of the sample was evaporated during the measurements. No shift of the vapor-pressure data was observed over this period.

It should be noted that a small amount of a volatile organic impurity might

change the order of magnitude of results at 0.1 mm. of mercury and be undetectable at 50 mm. of mercury.

The curve of  $\log P$  vs.  $1/T$  for the vapor pressure of benzotrifluoride is shown in figure 2. Fifty points from two separate experiments are plotted on the graph. The data were treated by the method of least squares to give the equation

$$\text{Log } P = -2839.5/T + 11.616$$

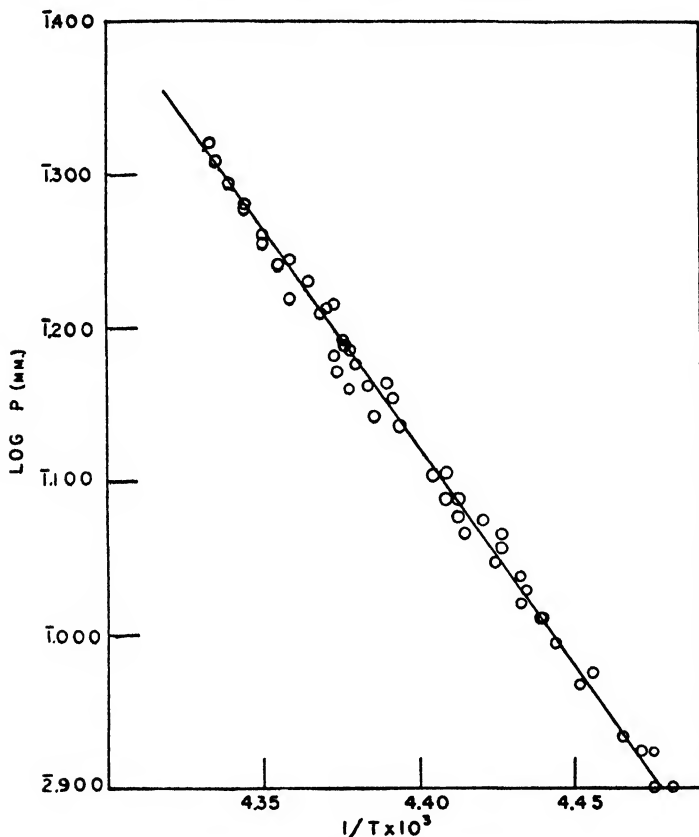


FIG. 2. Plot of  $\log P$  vs.  $1/T$  for the vapor pressure of benzotrifluoride

where  $P$  is given in millimeters of mercury and  $T$  is the absolute temperature. The ice point was taken as 273.2°K. A plot of equation 1 is shown in figure 2.

The maximum per cent deviation of an experimental pressure from the corresponding least squares value was 5.2 per cent. The maximum error estimated from the McLeod gauge calibration, the Rodebush gauge calibration, and the temperature uncertainty was 4.8 per cent. The average per cent deviation of experimental from least squares values was 1.5 per cent.

At the melting point the vapor pressures of the solid and liquid phase are equal. Hence, Saylor and Field's data on liquid benzotrifluoride were extrapolated

downward, and the present data on solid benzotrifluoride were extrapolated upward to the melting point ( $-29.3^{\circ}\text{C}.$ ). The corresponding values were (Saylor) 1.01 mm. and (this paper) 0.94 mm. of mercury. This is satisfactory agreement, considering the errors of the two determinations and the uncertainty involved in the extrapolation.

The heat of vaporization of solid benzotrifluoride was calculated from the vapor pressure (equation 1) to be  $12,990 \text{ cal. mole}^{-1}$ . A corresponding calculation on Saylor and Field's (9) data gave  $10,460 \text{ cal. mole}^{-1}$  as the heat of vaporization of liquid benzotrifluoride at its melting point. The heat of fusion was thus found to be  $2520 \text{ cal. mole}^{-1}$ . The entropy of fusion was  $10.3 \text{ E.U.}$

#### SUMMARY

1. Some salient factors limiting the operation of the Rodebush manometer were discussed.

2. The vapor pressure of solid benzotrifluoride was measured over the range  $-51^{\circ}\text{C.}$  to  $-40^{\circ}\text{C.}$  The vapor-pressure equation was calculated by the method of least squares.

3. In conjunction with the data of Saylor and Field (9) the heats of vaporization of solid and liquid benzotrifluoride, and the heat of fusion were calculated at the melting point.

The authors wish to express their appreciation to Dr. Hertha Spöner for her advice and interest.

#### REFERENCES

- (1) BALSON: *Trans. Faraday Soc.* **43**, 48 (1947).
- (2) BOOTH, ELSEY, AND BURCHFIELD: *J. Am. Chem. Soc.* **57**, 2067 (1935).
- (3) DIETZ: *J. Chem. Phys.* **4**, 575 (1936).
- (4) HARTLEY, HENRY, AND GRAVES: *Trans. Faraday Soc.* **35**, 1452 (1939).
- (5) HOLBORN AND OTTO: *Z. Physik* **33**, 1 (1925).
- (6) MOLES AND CRESPI: *Anales soc. españ. fís. y quím.* **27**, 529 (1929).
- (7) RODEBUSH AND COONS: *J. Am. Chem. Soc.* **49**, 1953 (1927).
- (8) RODEBUSH AND HENRY: *J. Am. Chem. Soc.* **52**, 3159 (1930).
- (9) SAYLOR AND FIELDS: *J. Am. Chem. Soc.* **68**, 2649 (1946).



## SOLUBILITY STUDY OF AN AQUEOUS POTASSIUM LAURATE-POTASSIUM SILICATE SYSTEM

REYNOLD C. MERRILL

*Philadelphia Quartz Company, Philadelphia, Pennsylvania**Received February 20, 1948*

Interest in the addition of a potassium silicate to liquid soap products to influence viscosity and to provide increased detergency at lower cost stimulated this study of the solubilities of potassium laurate in aqueous potassium silicate solutions. The particular potassium silicate used had a silica-to-potassium oxide ratio by weight of 2.04, corresponding to the molecular formula  $K_2O \cdot 3.21SiO_2$ . Potassium laurate concentrations to 56 per cent, potassium silicate concentrations to 34 per cent, and temperatures to 180°C. were studied. The binary system, potassium laurate-water, has been partially investigated in a phase study by McBain and Field (2). No phase study of the system  $K_2O-SiO_2-H_2O$  at concentrations and temperatures of interest in this work has appeared, although Morey (4) has studied the system  $K_2SiO_3-SiO_2-H_2O$  at temperatures from 200° to 1000°C. Ternary aqueous systems with potassium chloride have been reported for both potassium laurate (2) and potassium oleate (1) by McBain and collaborators.

## EXPERIMENTAL

The potassium laurate was made from a sample of Eastman's best quality lauric acid, which had been recrystallized from acetone to give a melting point of 43.9°C. and an equivalent weight by titration with sodium hydroxide agreeing with the theoretical (200.3) within experimental error. The soap was prepared from an alcoholic solution of the acid by neutralization to a phenolphthalein endpoint with potassium ethylate. It was dried to constant weight at 105°C.

The potassium silicate was identical with that used in a previous publication for which a complete analysis was given (3). It was a product of the Philadelphia Quartz Company used in this work as an aqueous solution containing 12.7 per cent  $K_2O$  and 25.99 per cent  $SiO_2$ . The water was freshly distilled.

The synthetic method was used in obtaining all data. Soap-potassium silicate-water systems of known composition in 13 x 50 mm. sealed glass tubes were heated until they became homogeneous and isotropic. The tubes were then cooled very slowly and the temperature,  $T_i$ , observed at which a birefringent phase first appeared. The  $T_i$  values were determined with calibrated thermometers and are precise and reproducible to  $\pm 2^\circ C$ .

For all data reported in this paper the phase separating when the solution is cooled is liquid crystalline. Experience has shown that supercooling does not occur in these cases when the system is agitated and cooled slowly (e.g., 1, 2, 3), although it often may when the phase separating is crystalline. The data, therefore, represent equilibrium solubility determinations, since the same values within  $\pm 2^\circ C$ . are obtained from supersaturation and undersaturation. Since the liquid

crystalline phase studied in this work was rather difficult to dissolve to its equilibrium solubility from undersaturation, most of the determinations were made only from supersaturation.

#### RESULTS AND DISCUSSION

The data are given in table 1 and illustrated in figure 1. The curves show the progressive decreases in solubility of potassium laurate in increasing concentrations of potassium silicate solutions at 0°, 50°, 100°, 150°, and 175°C. They were

TABLE 1

*T<sub>i</sub> values for potassium laurate-2.04 weight ratio potassium silicate-water systems*

POTASSIUM LAURATE	2.04 RATIO POTASSIUM SILICATE	T <sub>i</sub> *	POTASSIUM LAURATE	2.04 RATIO POTASSIUM SILICATE	T <sub>i</sub> *
<i>per cent</i>	<i>per cent</i>	<i>°C.</i>	<i>per cent</i>	<i>per cent</i>	<i>°C.</i>
33.4	0	<0	27.6	8.15	<0
36.1	0	79	33.1	7.50	104
37.5	0	110	32.6	11.0	134
40.0	0	139	21.3	18.1	<0
42.0	0	154	50.0	4.91	178
46.7	0	176	52.5	3.25	177
52.3	0	182	45.5	2.98	176
55.7	0	175	32.0	20.7	171
40.0	10.2	175	34.4	3.36	81
33.9	25.6	>180	34.3	1.46	46
39.8	3.24	150	31.3	5.12	51
40.0	10.0	176	26.0	12.1	<0
39.9	17.7	>180	26.4	28.5	>175
34.8	4.01	98	15.3	32.8	<20 >0
34.5	11.0	148	16.1	28.6	<0
29.8	10.6	67	22.3	20.6	<20 >0
28.0	14.4	94	24.7	28.5	165
40.0	5.10	158	29.6	18.7	138
35.5	7.80	137	17.3	32.0	75
32.6	3.20	<0			

\* Tubes marked <0 remained isotropic after contact with melting ice for more than a week. Their composition was sufficiently close to a phase boundary to be of assistance in locating it.

obtained by linear interpolation between the  $T_i$  values, or solution temperatures for systems of known composition. Solutions of known compositions which remained isotropic at 0°C. were used to determine the 0°C. isotherm. The  $T_i$  values for the binary soap-water system are in excellent agreement with those of McBain and Field (2).

The equilibrium solid phase for all  $T_i$  values in table 1 is apparently the liquid crystalline phase middle soap shown in the binary system (2), since the data show no indication of a discontinuity or "break" in the solubility curve indicative of a different equilibrium solid phase. The birefringence of the separating phase at different electrolyte concentrations does not vary as much as would be

expected if some neat soap were formed. This is in contrast to the corresponding system with potassium chloride, where on the addition of salt a definite "break" in the solubility curve occurs owing to the appearance of the new equilibrium phase, neat soap (2).

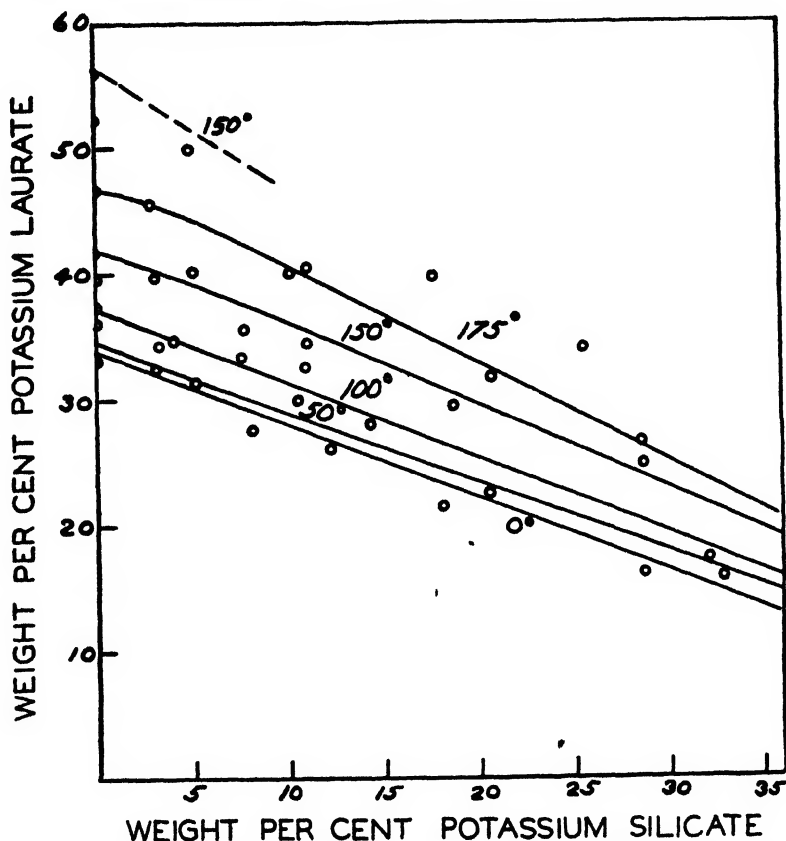


FIG. 1. Solubility curves for potassium laurate in potassium silicate ( $K_2O \cdot 3.21SiO_2$ ) solutions having an  $SiO_2/K_2O$  ratio by weight of 2.04 at  $0^\circ$ ,  $50^\circ$ ,  $100^\circ$ ,  $150^\circ$ , and  $175^\circ C$ . Boundaries outline limits of isotropic solution field at these temperatures. Isotherms (curves) obtained by linear interpolation of various solution temperatures (circles) of systems of known composition.

The upper dotted line represents compositions which dissolve at  $150^\circ C$ . At just slightly higher concentrations the solution temperature is less. At still greater concentrations, the liquid crystalline phase neat soap is formed (2) and the solution temperature is again increased. No separation into two immiscible isotropic phases such as occurs in the system with potassium chloride was observed with potassium silicate. However, this may occur at higher silicate concentrations.

The practical importance of this work is the demonstration that a liquid soap containing 33 per cent soap corresponding to potassium laurate can be mixed in

all proportions with a commercial potassium silicate containing 38.7 per cent solids with a silica-to-alkali ratio by weight of 2.04.

#### SUMMARY

A solubility study of the system potassium laurate-potassium silicate (with a molal ratio of silica to alkali of 3.2)-water has included soap concentrations to 56 per cent, silicate concentrations to 34 per cent, and temperatures to 180°C.

#### REFERENCES

- (1) MCBAIN, J. W., AND ELFORD, W. J.: *J. Chem. Soc.* **1926**, 421.
- (2) MCBAIN, J. W., AND FIELD, M. C.: *J. Phys. Chem.* **30**, 1545 (1926).
- (3) MERRILL, R. C.: *Ind. Eng. Chem.* **39**, 158 (1947).
- (4) MOREY, G. W.: *J. Am. Chem. Soc.* **39**, 1173 (1917); *cf.* W. PUKALL: *Ber.* **49**, 397 (1916).

## ABSOLUTE REACTION KINETICS OF TOBACCO MOSAIC VIRUS AND A PROPOSED THEORY OF DENATURATION

GEORGE A. BOYD

*Department of Radiation Biology, School of Medicine and Dentistry,  
University of Rochester, Rochester, New York*

AND

JAMES J. EBERL

*Johnson and Johnson Company, New Brunswick, New Jersey*

• Received February 6, 1948

Eyring and Stearn (3) have applied the theory of absolute reaction rates to the denaturation of several proteins, from which it was possible to draw certain conclusions regarding the mechanism of this general type of reaction. We thought it of interest to apply the absolute reaction rate theory to the denaturation of tobacco mosaic virus, the kinetics of which have been studied experimentally by Lauffer and Price (6).

The equation for absolute reaction rates is (2):

$$k' = \kappa \frac{kT}{h} e^{-(\Delta F^\ddagger/RT)} \quad (1)$$

Here  $k'$  is the specific reaction velocity constant in reciprocal seconds. The transmission coefficient,  $\kappa$ , is taken as unity;  $k$  is Boltzmann's constant,  $h$  is Planck's constant,  $T$  is the absolute temperature, and  $\Delta F^\ddagger$  is the free energy of activation.

From  $\Delta F^\ddagger$  calculated from equation 1 and the relations

$$2.303R \frac{d \left[ \log_{10} \left( \frac{k}{h} \right) \right]}{d \left( \frac{1}{T} \right)} = \Delta H^\ddagger \quad (2)$$

and

$$\Delta F^\ddagger = \Delta H^\ddagger - T\Delta S^\ddagger \quad (3)$$

the heats and entropies of activation are calculated.

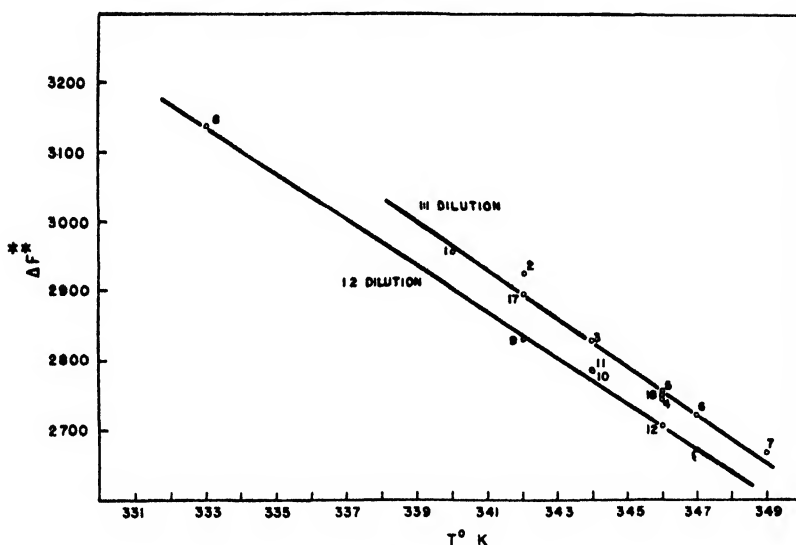


FIG. 1. Free energy of activation *versus* temperature

Sufficient rate data for analysis are given by Laufer and Price for two sets of conditions, precipitation being used as the criterion of denaturation. These conditions are (1) pH 7.05 and a dilution of 1:1, and (2) pH 7.05 and a dilution of 1:2. For a third set of conditions, pH 6.1 and a dilution of 1:1, three data are given but are inadequate for reliable calculations.

From equation 1,  $\Delta F^\ddagger$  for each condition given by Laufer and Price in Table 1 of their paper is calculated. The values for the two dilutions at pH 7.05 are plotted against temperature in figure 1. The energies of activation,  $\Delta H^\ddagger$ , for the two sets of conditions are obtained by multiplying the slope of the lines of figure 2 by  $2.303R$ .

As pointed out by Eyring and Stearn (3) for other protein denaturation reactions, with the exception of denaturation by urea,  $\Delta F^\ddagger$  for tobacco mosaic virus decreases slowly with increasing temperature. There are two  $\Delta H^\ddagger$  values,

146,000 cal. for the 1:1 dilution and 150,000 cal. for the 1:2 dilution. From equation 3 and the calculated values of  $\Delta F^\ddagger$  and  $\Delta H^\ddagger$  the entropies of activation,

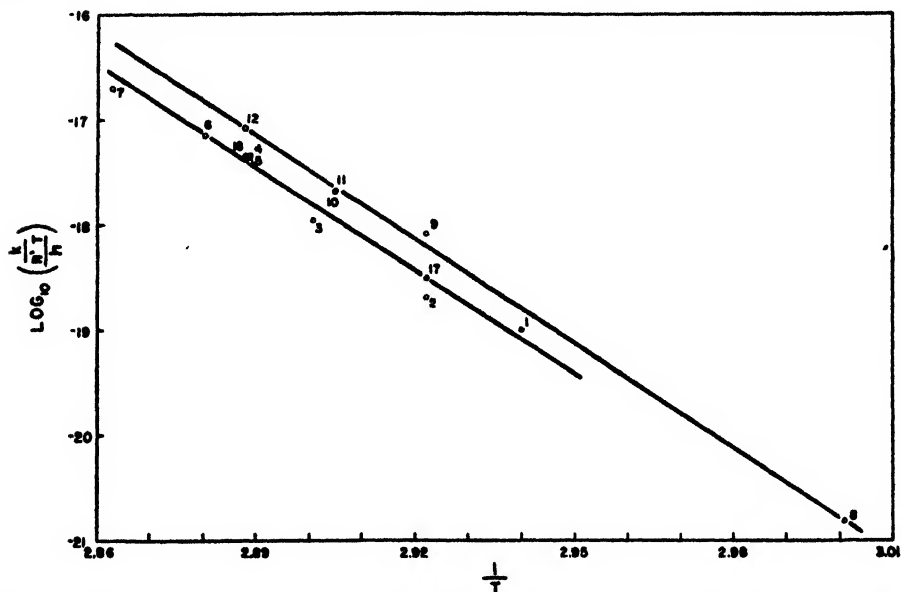


FIG. 2. Plot of the calculated value for the determination of activation energies by equation 2.

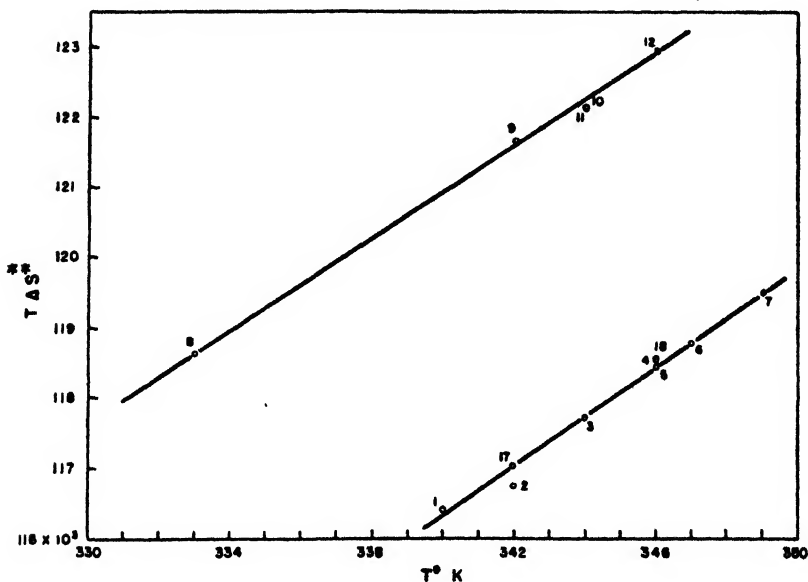


FIG. 3. Activation energy values as calculated from equation 3

$\Delta S^\ddagger$ , are calculated for all temperatures at each of the two sets of conditions.  $T\Delta S^\ddagger$  and  $\Delta S^\ddagger$  are plotted against temperature in figures 3 and 4, respectively.

Again, as pointed out by Eyring and Stearn for other protein denaturation reactions,  $T\Delta S^\ddagger$  for tobacco mosaic virus increases with temperature, while  $\Delta S^\ddagger$  decreases with temperature, as seen in figure 4.

Eyring and Stearn suggested that the increase of  $T\Delta S^\ddagger$  might be due to the temperature factor, and this is borne out for tobacco mosaic virus.

#### DISCUSSION

The above calculations and results for the three thermodynamic quantities in the denaturation reaction of tobacco mosaic virus give rise to certain interesting conclusions relative to possible molecular structure and reaction mechanism.

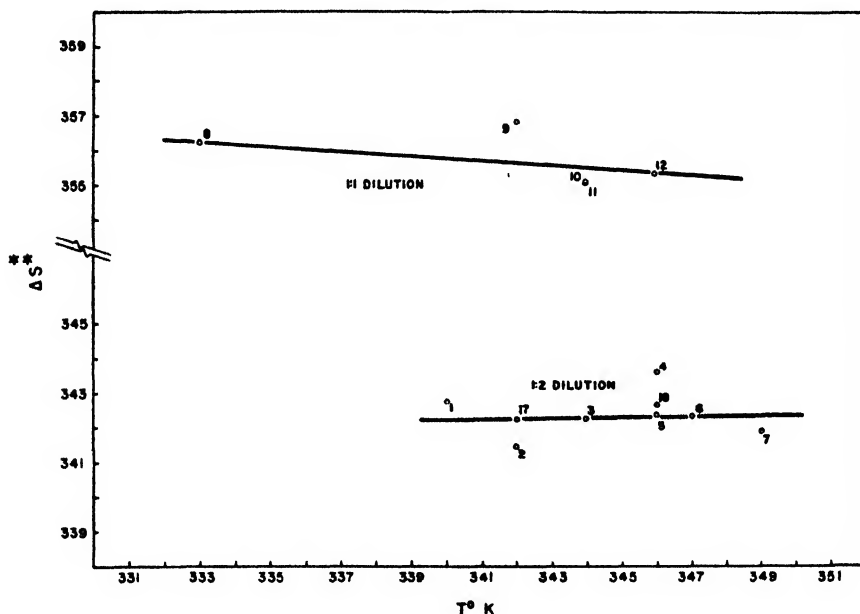


FIG. 4.  $T\Delta S^\ddagger$  as calculated from equation 3 versus temperature

The values of  $\Delta H^\ddagger$  and  $\Delta S^\ddagger$  as calculated from absolute reaction rate analysis provide for an interpretation of the increasing rate of reaction with dilution. The general symmetrically rod-shaped structure of tobacco mosaic virus with its active side chains suggests the possibility of molecular association. Such an association is suggested by Lauffer (5) to interpret the slower-moving sedimentation boundary in the ultracentrifuge. This view is also supported by electron-microscopic studies (1), where the micrographs show a considerable number of molecules in close contact.

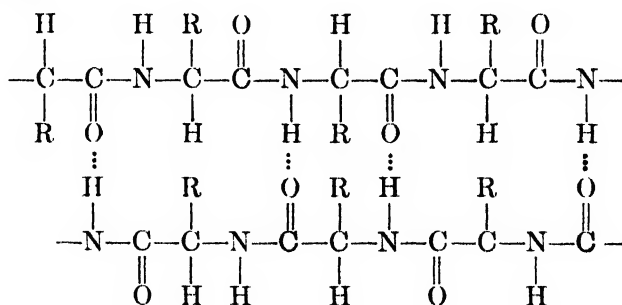
At the higher dilution, 1:2, where presumably less association occurs, the heat of activation is 4000 cal. less than at a lower dilution of 1:1, i.e., a higher concentration. It is also noticed from the entropy curve that there is a corresponding change in entropy where the  $\Delta S^\ddagger$  values for the more concentrated solution are consistently higher than those for the more dilute solution. It is, therefore,

indicated that the denaturation in the more concentrated solutions involves simultaneous unfolding and dissociation of the associated molecules where part of the heat of activation is involved in the latter process.

The heat of activation for the denaturation of tobacco mosaic virus is 150,000 cal. at pH 7.05 and at a dilution of 1:1. Following the general procedure of assigning 5000 cal. for the rupture of a hydrogen bond,<sup>1</sup> this would indicate that thirty bonds are broken during the denaturation step. This number of broken bonds is identical with the value obtained by Mirsky and Pauling (7) for the denaturation of trypsin. However, when we consider that the molecular weight of tobacco mosaic virus is 42,000,000, as compared to 36,500 for trypsin, the rupture of thirty hydrogen bonds in the large molecule is quite small in view of its size. In the calculation, it is to be mentioned that the hydrogen bonds broken upon the dissociation of associated molecules have been neglected. This factor appears to be small because of the relatively few associated molecules and has little effect upon the conclusion drawn.

In order to obtain a more fundamental picture of the effect caused by the rupture of thirty hydrogen bonds in tobacco mosaic virus, it appears logical to calculate the total number of hydrogen bonds in the virus. It is, of course, obvious that the result obtained from this calculation will depend upon the particular configuration assumed, but it is a simple matter to calculate the maximum and minimum number of hydrogen bonds from x-ray data.

The tobacco mosaic virus molecule is rod-shaped with the dimensions of the rod as 2800 Å. long and 150 Å. in diameter (1). Assuming average spacings of the protein (9) which agree fairly well with Wyckoff (11), the side-chain spacing is 10.5 Å. while the backbone spacing is 4.5 Å. and the repetition of the peptide group along the backbone is 3.5 Å. There will be two types of hydrogen bonds contributing to the total—namely, backbone-to-backbone bonds—as represented below



and the side-chain hydrogen bonds from the amino carboxylic side chains. In the most symmetrically folded structure for tobacco mosaic virus, the hydrogen bonds in the backbone-to-backbone interaction are predominant. A calculation

<sup>1</sup> The value of 5000 cal. neglects the energy contribution of the solvent and hence is not exact. However, the value does not prejudice the principle of the argument for the theory of the denaturation process.



shows 333,000 as the maximum number possible. The contribution from side-chain interaction is 58,000, assuming a cross bond at every 20 Å. This gives 391,000 as the approximate possible number of hydrogen bonds in tobacco mosaic virus, using the most symmetrical structure. The minimum number of hydrogen bonds is calculated by assuming that it would be necessary to have one hydrogen bond per fold; hence this number is 416. This figure is physically impossible for stability reasons alone and in addition is not likely on a structural basis of the molecule.

It seems reasonable to assume, then, that while the number of hydrogen bonds may not be the maximum figure of 391,000 for the most symmetrical structure, it is, nevertheless, a large number and must be well over 10,000. The rupture of thirty bonds, randomly distributed in 10,000, in the denaturation process is quite small for the profound physical effects observed.

For the theoretical analysis of protein denaturation, Neurath and his co-workers (8) suggest the method of Steinhardt (10) and La Mer (4) as giving more significant results in comparison to the method of Eyring. This is based on the fact that the former method corrects for that portion of the energy of activation which is consumed in the ionization of the protein. The mechanism of denaturation is considered as a two-step process.

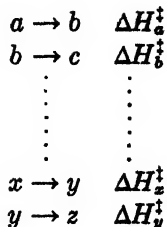


Here  $P_0$  is the initial protein molecule,  $P_n$  is the molecule after an  $n$ -fold ionization, and  $P_n^\ddagger$  is the activated ionized complex. Thus, the true heat of activation is the energy of activation involved in equation 5, while the experimental value is the sum of the energies of equations 4 and 5.

The thermal denaturation of tobacco mosaic virus varies inversely as the third power of the hydrogen-ion concentration (6). The pH dependence can be ascribed to the dissociation of a proton from each of three primary amino groups of the initial molecule, leading to an increase of three in the net charge. Since a value of 9000 cal. is required in the ionization of a proton, a total  $\Delta H$  of 27,000 cal. is represented by reaction 4. The experimentally observed energy of activation is 152,000 cal. (6), which upon correction for the heat of dissociation is reduced to a value of 125,000 cal.

The corrected value for the energy of activation leads to the conclusion that a total of twenty-five bonds are broken instead of the previously calculated thirty. This corrected value certainly does not improve the difficulty already pointed out, i.e., that there are an insufficient number of bonds broken in the activation process to account for the profound physical changes that take place. It serves to indicate the inadequacy of our present theories of protein denaturation.

It is possible to reconcile the paradox, however, if we assume that the initial step in the denaturation process is the first of a series of chain reactions which lead to the denatured state. The chain mechanism is illustrated below,



where  $a \rightarrow b$  is the first step in the denaturation process involving the simultaneous breaking of twenty-five to thirty bonds consuming a large heat of activation,  $\Delta H_a^\ddagger$ . The succeeding reactions,  $b \rightarrow c$  to  $y \rightarrow z$ , are successive and essentially spontaneous, involving the breaking of single bonds with small  $\Delta H^\ddagger$  values (*ca.* 5000 cal.). The final reaction,  $y \rightarrow z$ , produces the precipitable molecule, the criterion of denaturation and the measurement of which is the basis for energy calculation. The energy absorbed in the fast reactions would not show up in the kinetic calculations, since the  $a \rightarrow b$  reaction is the determining step.

If we consider a symmetrical virus molecule composed of orderly polypeptide chains, it is clear that a sufficient number of bonds must be broken before the freed ends are sufficiently separated so that re-formation is not more probable than further opening of the folded structure. The denaturation mechanism is analogous to the tearing of an oriented film, e.g., cellophane. If the direction of tear is in the direction of orientation, it is found that considerable force is needed to initiate the tear, but once the tear is started the film parts readily along a straight line. In this process, like the denaturation of a protein molecule, the initial step required the simultaneous rupture of many hydrogen bonds, but further separation was done easily by shearing one bond at a time.

This denaturation mechanism, then, gives a new interpretation for several facts. First, the number of bonds broken in the denaturation of a tobacco mosaic virus molecule must be much larger than indicated by kinetic calculation. The number indicated by the calculation, i.e., twenty-five bonds, is required to initiate the intramolecular process. These and only these show up in the calculations. Additional bonds are broken but the rapidity of their breaking precludes observation.

The profound physical changes, e.g., solubility, molecular shape, reactivity, and biological activity, which we feel must involve a number of bonds much greater than twenty-five can be accounted for by the intramolecular mechanism.

In the presence of certain denaturation catalysts such as acids, alkali, urea, etc., the heat of activation is lowered. This is consistent with the proposed intramolecular mechanism if we visualize the catalysts as assisting the initial simultaneous rupturing of bonds.

#### SUMMARY

From the absolute reaction rate theory applied to rate data of the denaturation of tobacco mosaic virus, the free energies, entropies, and heats of activation were

calculated. From the entropies, an explanation of the different rates at different dilutions is proposed. A chain mechanism of the denaturation of virus and other proteins is proposed which qualitatively accounts for much of the experimental data.

## REFERENCES

- (1) ANDERSON, THOMAS F.: *Advances in Colloid Science*, pp. 380-1. Interscience Publishers, Inc., New York (1942).
- (2) EYRING, HENRY: *J. Chem. Phys.* **3**, 107 (1935).
- (3) EYRING, HENRY, AND STEARN, A. E.: *Chem. Revs.* **24**, 253 (1939).
- (4) LA MER, V. K.: *Science* **86**, 614 (1937).
- (5) LAUFFER, MAX A.: *J. Biol. Chem.* **126**, 483 (1938).
- (6) LAUFFER, MAX A., AND PRICE, W. C.: *J. Biol. Chem.* **133**, 1 (1940).
- (7) MIRSKY, A. E., AND PAULING, L.: *Proc. Natl. Acad. Sci. U.S.* **22**, 439 (1936).
- (8) NEURATH, H., GREENSTEIN, J. P., PUTNAM, F. W., AND ERICKSON, J. O.: *Chem. Revs.* **34**, 157 (1944).
- (9) SPONSLER, O. L.: *The Cell and Protoplasm*, p. 171. The Science Press, Lancaster, Pennsylvania (1940).
- (10) STEINHARDT, J.: *Kgl. Danske Videnskab. Selskab Mat.-fys. Medd.* **14**, No. 11 (1937).
- (11) WYCKOFF, R. W. G., AND COREY, R. B.: *J. Biol. Chem.* **116**, 51 (1936).

## A NOTE ON THE MATHEMATICS OF ADSORPTION IN BEDS

NEAL R. AMUNDSON

*School of Chemistry, Division of Chemical Engineering, University of Minnesota,  
Minneapolis 14, Minnesota*

*Received March 10, 1948*

The mathematical solution of the adsorption of solutes from liquids and gases on solids in beds is complicated to the extent that of the many mechanisms which can be imagined, all have some basis in physical fact. The mathematical complications have their origins in our inability to cope with the non-linear partial differential equations which arise. Certain problems have been solved completely, while others in which more complex mechanisms are assumed have been solved only partially, by either linearizing approximations or numerical methods. Two recent review articles by Thiele (5) and Klotz (3) cover the literature carefully. It is the purpose of this note to supply a complete mathematical solution of one particular problem, i.e., that in which the adsorption occurs irreversibly at a local rate of removal described by equation 2 below.

If we assume that we have a bed of unit cross section where depths are measured as  $z$ , and if

- $c$  = concentration in moles per unit volume of adsorbate in the fluid stream,  
 $n$  = amount of adsorbate on bed in moles per unit volume of bed,  
 $V$  = velocity of fluid through the interstices of the bed in length per second,

$\alpha$  = fractional void volume of the bed, and

$t$  = time in seconds,

then on making a material balance over an elemental thickness of bed, we obtain the equation (see Klotz (3)):

$$V \frac{\partial c}{\partial z} + \frac{\partial c}{\partial t} + \frac{1}{\alpha} \frac{\partial n}{\partial t} = 0 \quad (1)$$

If the solute is adsorbed irreversibly, Bohart and Adams (1) and later Hinshelwood (2) assumed that the local rate of removal is governed by

$$\frac{1}{\alpha} \frac{\partial n}{\partial t} = kc(N_0 - n) \quad (2)$$

where  $N_0$  is the saturation capacity of a unit volume of bed. To equations 1 and 2 we must append certain auxiliary conditions. The first states that until the fluid has traversed a distance  $z$  in the bed, the bed at point  $z$  must contain the amount of adsorbate it had before adsorption began, i.e.,

$$n(z, t) = n_0(z), \quad \text{when } t \leq \frac{z}{V}, \quad t \geq 0 \quad (3)$$

If a fresh bed of adsorbent were present at the beginning, then  $n_0(z) = 0$ . The second condition states that at the bed entrance the concentration of adsorbate in the fluid may vary with time, i.e.,

$$c(z, t) = c_0(t), \quad \text{when } z = 0 \quad (4)$$

In order to obtain a solution of the problem two functions,  $n(z, t)$  and  $c(z, t)$ , must be found which will satisfy equations 1, 2, 3, and 4. Partial solutions have been obtained by the previously mentioned writers (1, 2).

In order to facilitate the solution we make the following changes of variable. Let

$$m = N_0 - n$$

$$x = z/V$$

$$y = \alpha(t - z/V)$$

then equations 1, 2, 3, and 4 become

$$\frac{\partial m}{\partial y} - \frac{\partial c}{\partial x} = 0 \quad (5)$$

$$\frac{\partial m}{\partial y} = -kcm \quad (6)$$

$$m(x, y) = N_0 - n_1(x), \quad \text{when } y = 0 \quad (7)$$

$$c(x, y) = c_1(y), \quad \text{when } x = 0 \quad (8)$$

where  $n_1(x) = n_0(Vx)$ ,  $c_1(y) = c_0(y/\alpha)$ . Note that equation 5 says

$$\frac{\partial m}{\partial y} = \frac{\partial c}{\partial x}$$

which implies that there exists a function  $f(x, y)$  such that

$$df = m dx + c dy$$

and

$$\frac{\partial f}{\partial x} = m, \quad \frac{\partial f}{\partial y} = c \quad (9)$$

Substituting in equation 6 we obtain

$$\frac{\partial^2 f}{\partial x \partial y} + k \frac{\partial f}{\partial x} \frac{\partial f}{\partial y} = 0 \quad (10)$$

which is a non-linear hyperbolic partial differential equation. In order to find solutions of this equation we make the substitution used by Thomas (6):

$$f(x, y) = \frac{1}{k} \log \phi(x, y)$$

Equation 10 becomes

$$\frac{\partial^2 \phi}{\partial x \partial y} = 0 \quad (11)$$

and equations 9 become

$$m = \frac{1}{k} \frac{\partial \log \phi}{\partial x}$$

$$c = \frac{1}{k} \frac{\partial \log \phi}{\partial y}$$

From these two equations, it is seen that the auxiliary conditions 7 and 8 are

$$N_0 - n_1(x) = \frac{1}{k} \frac{\partial \log \phi(x, 0)}{\partial x}$$

$$c_1(y) = \frac{1}{k} \frac{\partial \log \phi(0, y)}{\partial y}$$

Note that these are ordinary differential equations which can be integrated to

$$\log \phi(x, 0) = \int_0^x k[N_0 - n_1(\xi)] d\xi + C_1$$

$$\log \phi(0, y) = \int_0^y k c_1(\eta) d\eta + C_2$$

Since an arbitrary constant added to  $\log \phi$  is immaterial, we can define  $\phi(0, 0)$

= 1 so that

$$\phi(x, 0) = \exp \int_0^x k[N_0 - n_1(\xi)] d\xi \quad (12)$$

$$\phi(0, y) = \exp \int_0^y kc_1(\eta) d\eta \quad (13)$$

Now the general solution of equation 11 is

$$\phi(x, y) = f(x) + g(y)$$

where  $f(x)$  and  $g(y)$  are arbitrary functions. Therefore

$$\phi(x, 0) = f(x) + g(0)$$

$$\phi(0, y) = f(0) + g(y)$$

but since  $f(0) + g(0) = 1$ ,

$$\phi(x, y) = \phi(x, 0) + \phi(0, y) - 1$$

So, from equations 12 and 13

$$\phi(x, y) = \exp \int_0^x k[N_0 - n_1(\xi)] d\xi + \exp \int_0^y kc_1(\eta) d\eta - 1$$

Therefore

$$c = \frac{c_1(y) \exp \int_0^y kc_1(\eta) d\eta}{\exp \int_0^x k[N_0 - n_1(\xi)] d\xi + \exp \int_0^y kc_1(\eta) d\eta - 1}$$

$$m = \frac{[N_0 - n_1(x)] \exp \int_0^x k[N_0 - n_1(\xi)] d\xi}{\exp \int_0^x k[N_0 - n_1(\xi)] d\xi + \exp \int_0^y kc_1(\eta) d\eta - 1}$$

Changing back to the original variables, there results:

$$\begin{aligned} c(z, t) &= \frac{c_0(t - z/V) \exp \left[ k\alpha \int_0^{t-z/V} c_0(\eta) d\eta \right]}{\exp \left[ \frac{k}{V} \int_0^z [N_0 - n_0(\xi)] d\xi \right] + \exp \left[ k\alpha \int_0^{t-z/V} c_0(\eta) d\eta \right] - 1}, \quad t \geq \frac{z}{V} \quad (14) \end{aligned}$$

$$\begin{aligned} n(z, t) &= N_0 - \frac{[N_0 - n_0(z)] \exp \left[ \frac{k}{V} \int_0^z [N_0 - n_0(\xi)] d\xi \right]}{\exp \left[ \frac{k}{V} \int_0^z [N_0 - n_0(\xi)] d\xi \right] + \exp \left[ k\alpha \int_0^{t-z/V} c_0(\eta) d\eta \right] - 1}, \quad t \geq \frac{z}{V} \quad (15) \end{aligned}$$

$$= n_0(z), \quad t \leq \frac{z}{V}$$

For  $t < z/V$ ,  $c(z, t)$  is undefined since the fluid has not yet reached the point  $z$ . By letting  $t \rightarrow z/V$  we see that equation 15 reduces to  $n_0(z)$  and by letting  $z \rightarrow 0$ , equation 14 reduces to  $c_0(t)$ , as demanded by equations 3 and 4. Special cases of this solution have been obtained by Bohart and Adams and by Hinshelwood where  $n_0(z) = 0$  and  $c_0(t) = c_0$ , a constant. Previous solutions have neglected the term  $\partial c/\partial t$ . Marshall and Pigford (4) state that this is permissible for gases but not in general for liquids. In this case equations 14 and 15 reduce to:

$$\frac{c_0}{c} = 1 + \left[ \exp(-k t c_0 \alpha) \right] \left[ \exp\left(\frac{k N_0 z}{V}\right) - 1 \right]$$

$$\frac{N_0}{n} = 1 + \left[ \exp\left(\frac{k N_0 z}{V}\right) \right] \left[ \exp(k t c_0 \alpha) - 1 \right]^{-1}$$

## REFERENCES

- (1) BOHART, G. S., AND ADAMS, E. Q. J. Am. Chem. Soc. **42**, 543 (1920)
- (2) HINSHELWOOD, C. N., *et al*, 1941. This reference was not available to the author, see reference 3.
- (3) KLOTZ, I. M. Chem. Revs. **39**, 241 (1946).
- (4) MARSHALL, W. R., AND PIGFORD, R. L. *Application of Differential Equations to Chemical Engineering Problems*, p. 163. University of Delaware, Newark, Delaware (1947)
- (5) THIELE, E. W. Ind. Eng. Chem. **38**, 563 (1946)
- (6) THOMAS, H. C. J. Am. Chem. Soc. **66**, 1664 (1944)

## INTERFACIAL TENSION AT ELEVATED PRESSURES AND TEMPERATURES. I

## A NEW AND IMPROVED APPARATUS FOR BOUNDARY-TENSION MEASUREMENTS BY THE PENDENT-DROP METHOD

E. A. HAUSER AND A. S. MICHAELS

*Department of Chemical Engineering, Massachusetts Institute of Technology,  
Cambridge, Massachusetts*

*Received February 20, 1948*

Progress in several fields, notably petroleum production, has recently stimulated interest in the development of equipment for interfacial-tension measurements at high pressures and temperatures. At this time we wish only to report the completion of an apparatus for measurement of interfacial tension by the pendent-drop method of any liquid-liquid system in the temperature range 20–200°C. and the pressure range 0–10,000 pounds per square inch.

The pendent-drop method was developed and first employed by Andreas, Hauser, and Tucker (1) in 1938. The method, with various modifications of equipment, has since been used by Mack, Davis, and Bartell (6), Smith (8), Sorg (9), and others. The pendent-drop method is a highly refined and accurate

technique, and seemed to us particularly well adapted to situations involving boundary-tension measurements at high pressures.

#### OPTICAL SYSTEM

Although the basic principles of the pendent-drop technique remain unchanged, the optical system of the new pendent-drop tensiometer offers many unusual features. Firstly, the need for a telecentric lens system to insure true silhouette images of the pendent drops has been obviated through the use of a "concentrated-arc" lamp developed by the Electronics Division of Western Union

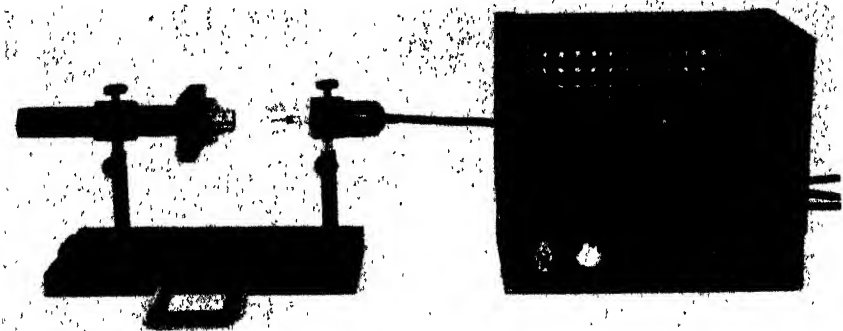


FIG. 1. Illuminating system



FIG. 2. Photomicrographic camera

Telegraph Company (3), coupled with a highly corrected parallelizing lens and a monochromatic filter (figure 1). This illuminating system produces an almost perfectly parallel beam of light, making the use of a telecentric stop unnecessary.

Secondly, a special photomicrographic camera has been built which is compact and simple to operate (figure 2). The instrument is equipped with a highly corrected lens (a 48-mm. Spencer Lens Company "Teleplat" objective), which is designed to be essentially free from distortion even at high magnification ratios. Drop silhouettes are recorded on  $3\frac{1}{4}$  in. by  $4\frac{1}{4}$  in. Wratten "M" or Wratten Metallographic plates. The magnification ratio is adjustable, the maximum magnification with the present lens being approximately  $16\times$ . The camera is



not equipped with a shutter; in order to eliminate the possibility of changing the temperature of the system under test owing to the heating effect of the light beam, a shutter is instead incorporated in the illuminating system. This shutter prevents light from entering the cell in which the drops are formed except when the camera is being focussed, or when plates are being exposed.

With the (25-watt) point light source, exposure times are 1 sec. with a green interference filter (wave length,  $5560 \text{ \AA.}$ ), and  $\frac{1}{50}$  sec. without the filter. Photographs taken in unfiltered light appear only slightly less sharply defined than those taken with the filter.

At present, measurements of the photographs are being made with an engraved rule and a hand magnifier, and are estimated to the nearest 0.1 mm. The magni-

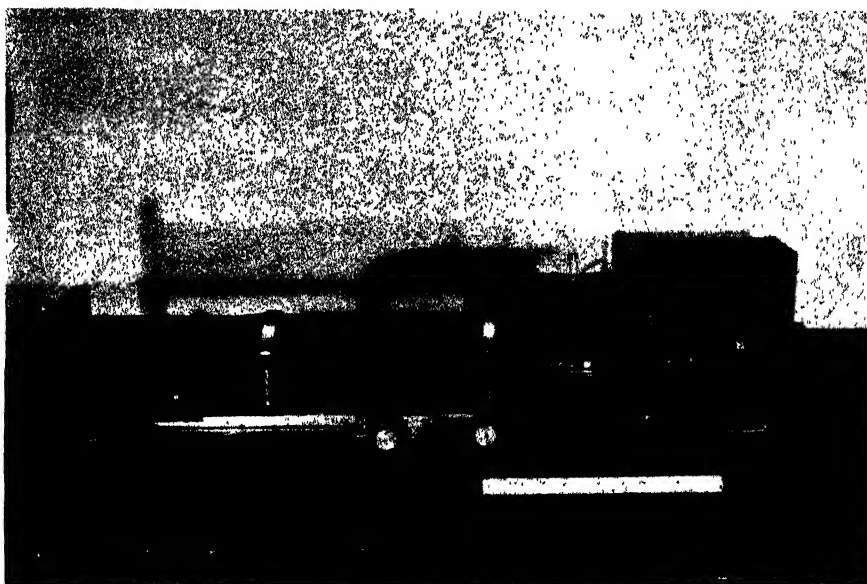


FIG. 2A. Atmospheric pressure set-up

fication of the camera is calculated from the known diameter of the tip from which the drop is suspended. With this measuring technique, results are reproducible to within 1 per cent. Provision will soon be made for direct measurement of drop dimensions on the ground-glass focussing screen of the camera. This will, of course, greatly decrease the time required to complete a given observation, and will increase the general utility of the method.

By virtue of its compactness and simplicity, we believe that this optical system possesses a decided advantage over those previously employed for this work. Although the apparatus is at present being used with the high-pressure equipment described below, it can readily be employed for pendent-drop measurements at atmospheric pressure. For such determinations, we have used a rectangular glass cell surrounded by a thermostatically controlled jacket, and a hypodermic syringe to which are fitted ground-off, stainless-steel hypodermic needles. This assembly is shown in figure 2A.

## HIGH-PRESSURE EQUIPMENT

The high-pressure equipment consists of three units: (1) the pendent-drop cell, (2) the drop-forming system, and (3) the pressure-generating system.

Details of the pendent-drop cell are shown in figure 3. The cell body was machined from a solid bar of 18-8 chrome-stainless steel, Type 303. It is  $5\frac{1}{2}$  in. in diameter and  $3\frac{7}{8}$  in. long. The cell windows (5) are standard optical flats approximately 0.6 in. thick and  $1\frac{3}{8}$  in. in diameter. According to the design suggested by Poulter (7) and Bridgman (2), the glass flats are in direct contact with optically flat stainless-steel seats (3). No gasket is necessary to effect a liquid-tight seal at these points.

The window seats are held in place by stainless-steel flanges (2) and sealed with gaskets (6) of appropriate composition (Garlock 210). This design employs the so-called "principle of the unsupported area," so that the window assemblies are selfsealing.

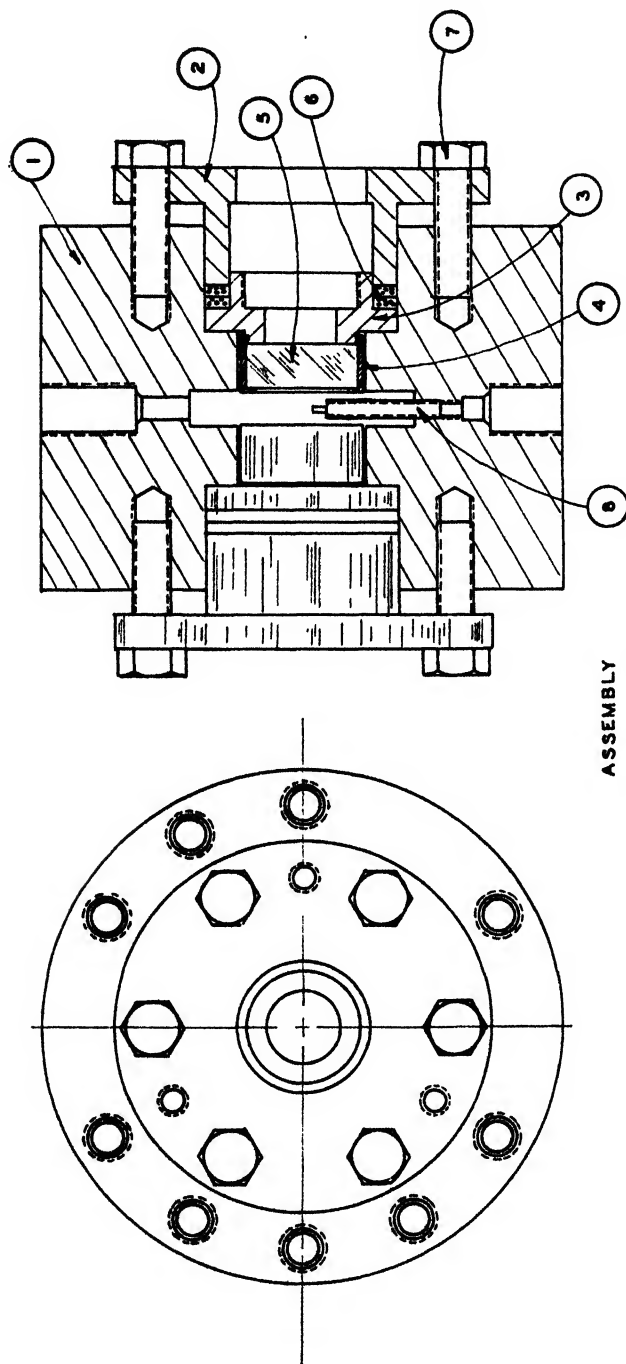
The general window design of this equipment parallels that employed in a windowed cell described by K. E. Eilerts *et al.* (4) of the U. S. Bureau of Mines, Bartlesville, Oklahoma, which has been in successful operation for several years. The authors are also indebted to the Carter Oil Company Laboratory, Tulsa, Oklahoma, for the suggestions and advice offered for the design of the cell, and for providing the glass flats described above.

The stainless-steel drop-forming tips (8) screw into the interior of the cell as indicated in the figure. This feature permits change of tips without disturbing the cell windows.

The cell is heated electrically by means of coils placed in the holes drilled longitudinally through the cell body. Very sensitive temperature control (within  $0.05^{\circ}\text{C}.$ ) is obtained by means of an electronic proportional temperature controller.

The mechanism for forming drops at elevated pressure is shown schematically in figure 4. The drop-forming system consists essentially of three thick-walled cylinders, two of which (number I and II in the diagram) are connected to coils of high-pressure tubing so that they can be raised or lowered. Cylinder I is connected to the pressure-generating system and to the body of the pendent-drop cell. Mercury is used to transfer the pressure from the generator to the liquid in the cell ("B"), and the mercury level is so adjusted that no pressure difference exists between the top of cylinder I and the interior of the cell. Cylinders II and III constitute a simple differential manometer. Pressure is transmitted from the generator to cylinder II, and from II to III *via* the mercury leg. The liquid ("A") from which drops are to be formed is placed above the mercury in cylinder III, and is led through stainless-steel capillary tubing to the drop-forming tip in the cell. Irrespective of the total pressure on the system, a differential pressure sufficient to force liquid into the drop-forming tip can be produced simply by raising cylinder II (or by lowering cylinder I, or both). Worm-gear mechanisms for changing the positions of the cylinders permit accurate and convenient control of drop size.

The entire drop-forming system, with the exception of the needle valves, is





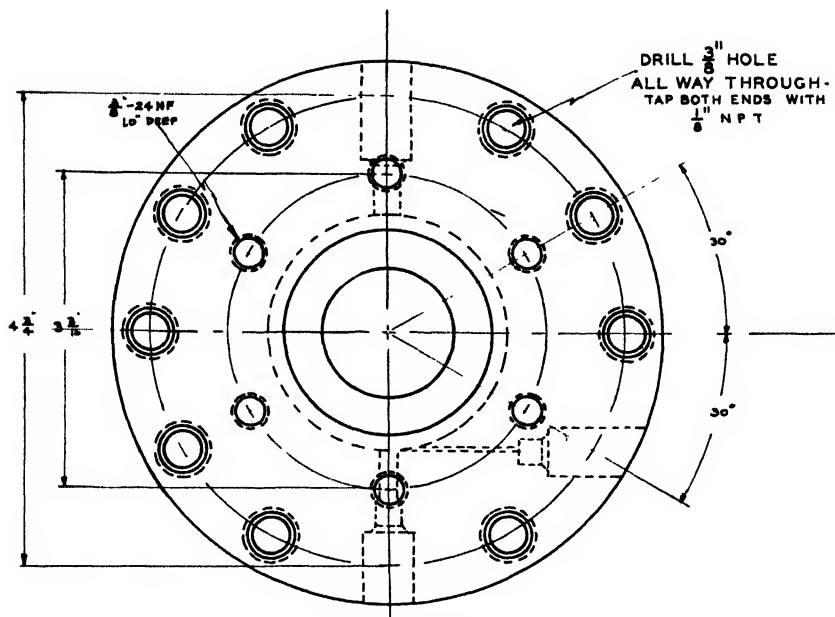
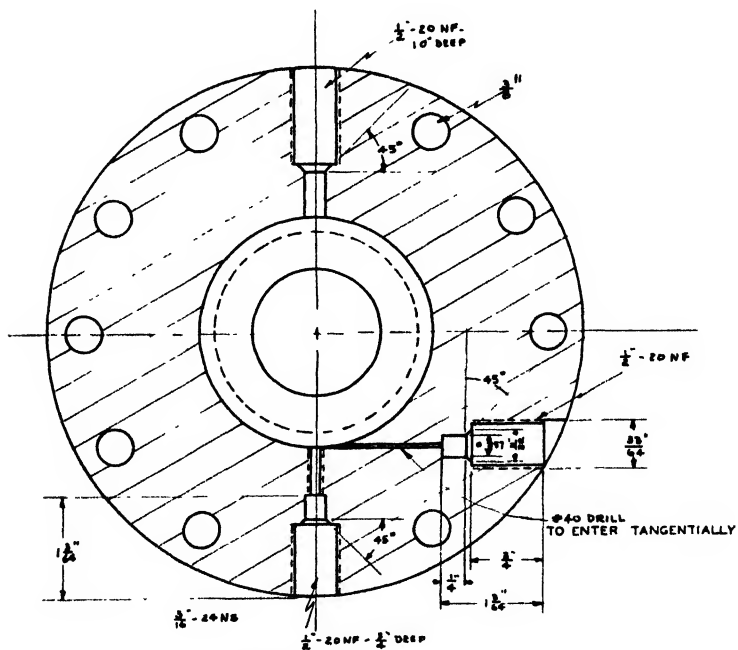


FIG. 3C



SECTION "AA"

FIG. 3D

The fluid used in this system is a mixture of U.S.P. mineral oil and petroleum ether. Although this liquid lacks certain qualities desirable in a hydraulic fluid

it is essentially non-capillary-active, and is thus well adapted for use in boundary-tension-measuring equipment where surface contamination is a frequent and serious problem.

#### LIMITATIONS AND APPLICATIONS OF THE APPARATUS

The fact that the Poulter-type high-pressure windows described above are not in general gas-tight except at exceedingly high pressures limits the use of this new apparatus to the extent that the cell chamber must always be filled with liquid. This does not, however, exclude the measurement of gas-liquid boundary tensions, because the "drop" can just as well be a gas bubble.

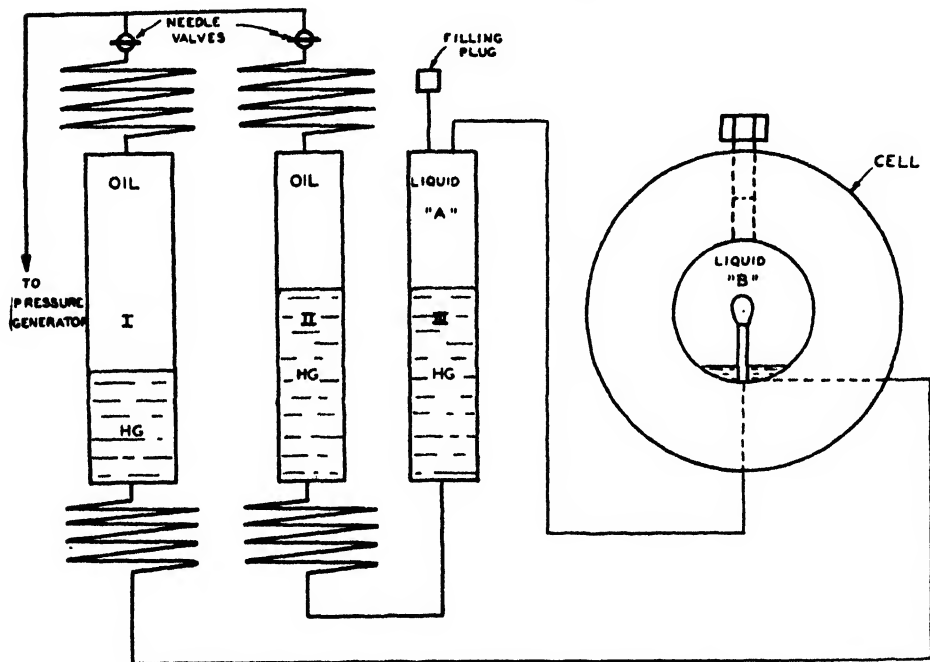


FIG. 4. Drop-forming system

The equipment is at present being used for the determination of the pressure and temperature coefficients of interfacial tension between pure hydrocarbons and water. When this fundamental research is completed, measurements will be made on the system *n*-decane-distilled water in the presence of dissolved methane. It is anticipated that this latter information will be of value in predicting and interpreting the interfacial behavior of systems of crude petroleum and natural brine under physical conditions comparable to those existing in subterranean oil reservoirs.

Succeeding articles in this series will be devoted to the presentation and interpretation of data obtained with this equipment, and, it is hoped, will suggest new problems to which the apparatus can be conveniently applied.

## REFERENCES

- (1) ANDREAS, J. M., HAUSER, E. A., AND TUCKER, W. B.: J. Phys. Chem. **42**, 1001 (1938).
- (2) BRIDGMAN, P.: *The Physics of High Pressure*, p. 58. The Macmillan Company, New York (1931).
- (3) BUCKINGHAM, W. D., AND DEIBERT, C. R.: J. Phot. Soc. Am. **12**, 610 (1946).
- (4) EILERTS, C. K., *et al.*: Am. Gas Assoc. Monthly **28**, 435 (1946).
- (5) KEYES, F. G.: Proc. Am. Acad. Arts Sci. **68**, 529 (1932-33).
- (6) MACK, G. L., DAVIS, J. K., AND BARTELL, F. E.: J. Phys. Chem. **45**, 846 (1941).
- (7) POULTER, T. C.: Phys. Rev. **35**, 297 (1930).
- (8) SMITH, G. W.: J. Phys. Chem. **48**, 168 (1944).
- (9) SMITH, G. W., AND SORG, L. V.: J. Phys. Chem. **45**, 671 (1941).

SILICIC CHEMISTRY<sup>1,2</sup>

## A NEW BRANCH OF COLLOID SCIENCE

ERNST A. HAUSER

*Department of Chemical Engineering, Massachusetts Institute of Technology,  
Cambridge, Massachusetts*

*Received February 20, 1948*

"In science the credit goes to the man who convinces the world, not to the man to whom the idea first occurs." These words were spoken by the British physician Sir William Osler in the last lecture he gave before the Royal Society of Medicine in 1918. One could hardly find a more striking example of their significance than by offering a brief historical review of the colloid chemistry of silicon.

In 1861, Thomas Graham read before the Royal Society in London a paper on "Liquid diffusion applied to analysis." He differentiated therein between matter which would and substances which would not diffuse through a membrane. References to this lecture (3), which must be regarded as the foundation of colloid science, are mostly limited to the following statement: "As gelatine also appears to be of the non-diffusing type, it is proposed to designate substances of the class as COLLOIDS, and to speak of their peculiar form of aggregation as the COLLOIDAL CONDITION OF MATTER."

What has dropped into oblivion, however, is the following sentence:

"The comparatively *fixed* class as regards diffusion, is represented by a different order of chemical substances, marked out by the absence of the power to crystallize. Among the

---

<sup>1</sup> Presented before the Symposium on Colloid Chemistry of the Silicates, which was held under the auspices of the Division of Colloid Chemistry at the 112th Meeting of the American Chemical Society, New York City, September 15-19, 1947.

<sup>2</sup> This paper is based on the book *Silicic Chemistry* by E. A. Hauser and D. S. le Beau, to be published by D. Van Nostrand Company, Inc., New York, and on notes for the newly inaugurated class on "Colloid Chemistry of Silicon" at the Massachusetts Institute of Technology, Cambridge, Massachusetts, starting with the fall term, 1947.

latter are hydrated silicic acid, when it exists in the soluble form. Soluble silicic acid forms a peculiar class of compounds, which are interesting by their analogy to organic substances."

Three years later Thomas Graham wrote another paper (4), from which the following excerpts have been taken:

"We have no degrees of solubility to speak of with respect to silicic acid, like the degrees of solubility of a salt. . . . The ultimate pectization of silicic acid is preceded by a gradual thickening in the liquid itself. The production of the compounds of silicic acid described, indicates the possession of a wider range of affinity by a colloid than could well be anticipated. The organic colloids are no doubt invested with similar wide powers of combination."

Thomas Graham unquestionably deserves credit for having been the first to convince the world that a colloidal condition of matter exists. That siliceous compounds exhibit properties characteristic of this state had already been mentioned eighty-two years prior to Graham's first disclosure, in the dissertation of the Swedish scientist Torbern Bergman, "*De Terra Silicea*," which a few years later was reprinted in one of his textbooks (1). The following is an excerpt of the most pertinent part therefrom:

"Finally I must still think of those incomplete phenomena, which depend on a seeming solubility. This silicious liquor [alkali silicate solution—E.A.H.] is precipitated by all acids, because the alkali prefers to hang on to them rather than to the gravel. This precipitated gravel has a very expanded and loose texture, is filled with water, so that it is twelve times as heavy when moist, than when dry. However if one first adds more water before adding acid, the solution remains clear, even if more acid is then added as would be needed to neutralize the alkali. THIS IS A PECULIAR PHENOMENON and the reason for it probably is the following: Through the dilution with water the silicious particles are very much separated from each other, or made finer and better distributed throughout the liquid. Although the particles, being heavier than the liquid, should settle out, they can in this case not overcome the resistance due to friction, because a greater force will be needed to accelerate sedimentation than the one resulting from the difference in specific gravity. The silica particles remain suspended in the liquid and at the same time invisible due to their fineness and transparency."

We colloid chemists must blame ourselves that it took so long, nearly a century, for it to dawn upon us that the colloidal properties of siliceous matter are just as important for the explanation of some phenomena it exhibits as they are with many high-molecular organic compounds. This is the more surprising if one takes into consideration the fact that silicon in combination with oxygen accounts for 76 per cent of the earth's crust. Structural chemistry, largely based on the results of chemical analysis combined with x-ray diffraction studies, has shown that silicon is tetravalent in its chemical behavior. This is in accord with its position in the fourth group of the Periodic System of elements. Silicon, however, differs from carbon, because its maximum covalency can be 6, as exemplified by  $\text{SiF}_6^{2-}$ . The two elements also differ in their reactivity toward hydration and hydrolysis of their halides and the ease of rupture of silicon-to-silicon bonds by water or hydroxyl ions. The most plausible explanation for these differences is based on the size of the atoms (silicon = 1.172 Å; carbon = 0.77 Å) and the



correspondingly greater screening of the nuclear charge of the silicon. It also should be noted that of all the single bonds between tetravalent silicon and other elements, the Si—O bond with an energy value of 89.3 kg.-cal. per mole is by far the strongest (11).

Another tool for structural research which is becoming more and more important is infrared spectroscopy. Vibrations involving the Si—O bond have shown that the intensity of the bonds is about five times stronger than that of the C—O bonds. As far as the ionic character of silicon bonds is concerned, measurements of relative intensities of absorption in the infrared permitted estimating the ratio of the ionic character of the Si—O bond to that of the C—O bond to be 2.3 (14). This is in line with the relationship between electronegativity difference and per cent ionic character. For the Si—O bond it amounts to 51 per cent, and for the C—O bond to 22 per cent. The ratio  $51/22 = 2.3$ . In the case of Si—F and C—F the ratio, although smaller, is still 1.6 (11).

These facts should suffice to point out how futile it would be to attempt to apply the laws of classical organic chemistry to the chemistry of silicon (12).

There are, however, also many similarities between the elements carbon and silicon and their compounds which are worth recording. To explain them in spite of the difference between the homeo- and hetero-polar bindings of these elements, the colloidal state must be taken more into consideration than has so far been the case. A silicon atom is known to share four electrons with neighboring atoms. But each oxygen atom needs two electrons for saturation. The silicon-oxygen tetrahedron (figure 1) is not saturated. If the oxygen atoms are replaced with hydroxyl groups, the tetrahedron then is saturated because each hydroxyl needs only one electron. Thus, by sharing the right number of electrons, two or more atoms are firmly held together; in this specific case, reference is generally made to a chemical bond or a covalent bond.

If several silicon-oxygen tetrahedra are combined so that two always share one oxygen, a chain-like structure results. In such a chain, two of the oxygen atoms belonging to one silicon atom remain unsaturated. This deficiency may be compensated by attaching a sodium atom to every unsaturated oxygen. A fibrillar aggregate is thus formed, which, if dispersed in water, represents the structure of sodium silicate or water glass (figure 2). The fact that the sodium ion hydrates appreciably and the presence of such long-chain aggregates offer a simple explanation for the solubility of sodium silicate and the high viscosity of its solutions. The entanglement of these fibrillar aggregates on desiccation also explains the formation of coherent sodium silicate films. Their structure is comparable to films obtained from long-chain high-molecular-weight organic compounds such as rubber or cellulose. If sodium silicate is reacted in solution with a solution of an acid, the sodium will exchange for the acid hydrogen, thus forming a silicic acid chain (figure 3). If two or more of these chains come close together or tangle up, condensation between neighboring hydroxyl groups occurs. Water is split off and the chains are now held together by shared oxygen atoms. A loose, unoriented, but nevertheless rigid tridimensional structure results, and a hydrous silica gel has been formed.

Just as it was possible to link two or more silicic acid chains together by condensation, two or more silicon-oxygen tetrahedra chains may be joined by having

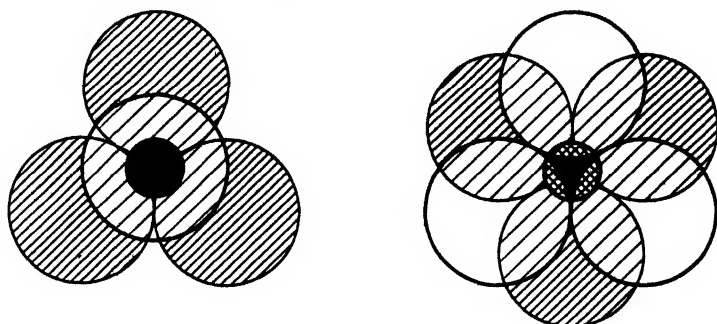


FIG. 1. Left: Silicon-oxygen tetrahedron (schematic), top view. The oxygen atom on top has been drawn transparent to show the location of the silicon atom in the cavity formed by the four oxygen atoms. Right: Aluminum (magnesium) octahedron (schematic).



FIG. 2. Model of a sodium silicate chain (theoretical): white balls represent oxygen atoms; smaller black balls, sodium atoms.

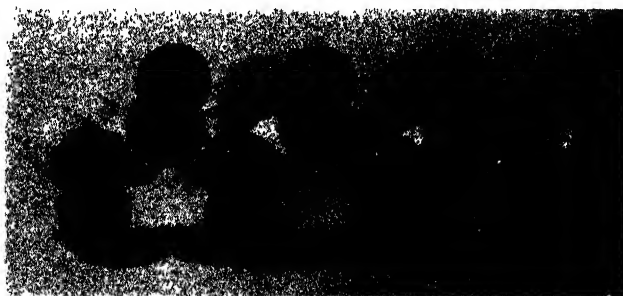


FIG. 3. Model of silicic acid chain (schematic), top view: white balls represent oxygen atoms; black balls, hydroxyl groups.

them share oxygen atoms (figure 4). A hexagonal network or silicon-oxygen sheet has been formed. If these hexagons thus formed are symmetrical, a sheet of crystalline structure results; if they are not symmetrically aligned, a silica

glass is obtained. The oxygen in the vertex position of every tetrahedron only remains unsaturated.

Similar sheets may be formed by joining magnesium or aluminum octahedra together (figure 1). If a sheet of aluminum octahedra is superimposed on a hydrated silica sheet, they are held together by secondary valence forces, but they can also condense. This is how the most abundant clay, kaolinite, was formed. When a sheet of aluminum hydroxide octahedra is sandwiched between two silica sheets and condensation follows, the clay mineral pyrophyllite is formed. If the aluminum hydroxide is replaced by magnesium or iron hydroxide, the minerals talc and nontronite, respectively, result by condensation. If some of the silicon is replaced by an ion of lower valency, we have built up the basic structure for mica. If we replace the aluminum with an ion of lower valency, the nucleus for the highly reactive clay mineral bentonite has been formed (5).

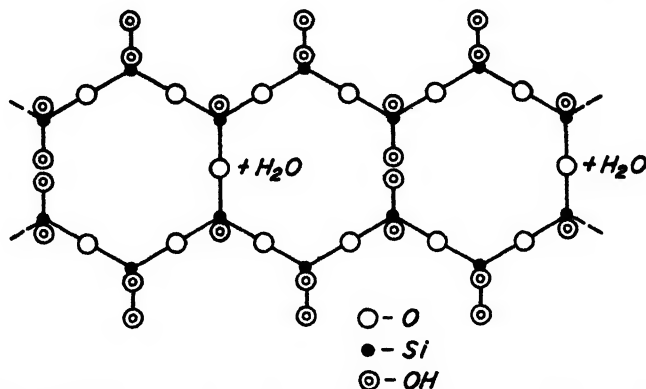


FIG. 4. Condensation of silicic acid chains to form silica sheet

We owe these deductions to the combination of results from chemical analysis and x-ray diffraction studies (2). The first visual proof for the assumed platy shape of these clay particles has only fairly recently been offered by electron-microscopic studies (5).

All this information, however, is still inadequate to offer a satisfactory explanation for many of the properties exhibited by siliceous matter, just as classical organic chemistry alone is unable to account for some properties exhibited by many organic colloids, as for example gelation, the high viscosity of their solutions, and elasticity.

It is here that the importance of colloid science becomes self-evident. It is the bridge which spans the gap in our knowledge of the properties exhibited by matter present in the range of dimensions we may no longer neglect.

To avoid coining new terms for this branch of colloid science, let us see if one cannot adopt some of the terminology already familiar to scientists specializing in the chemistry of high-molecular organic compounds. We shall classify the silicon hydroxide tetrahedra and the octahedra of magnesium, aluminum, and iron hydroxides as monomers (figure 5) comparable to isoprene or styrene. By

condensation of these monomers individually we produce a polymer comparable to natural rubber or to polystyrene (figure 5). If the silicon hydroxide polymer reacts with the aluminum or magnesium hydroxide polymer, or mixtures of these by further condensation, the result is an inorganic copolymer, comparable to the copolymers of butadiene and styrene, or of isobutylene and isoprene (figures 6 and 7). The resulting particle now represents the nucleus of a colloidal micelle. Its properties will depend on the distribution of electrical charges in its surface. The finer the particle, the more surface is exposed and the more pronounced will be the tendency to have its electric charge, caused by the unbalanced electron

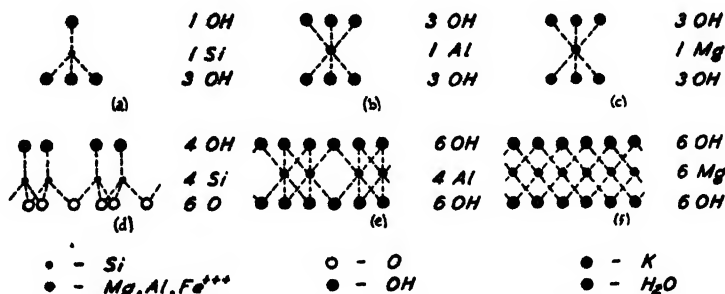


FIG. 5. Monomers: (a)  $\text{Si}(\text{OH})_4$ ; (b)  $\text{Al}(\text{OH})_3$ ; (c)  $\text{Mg}(\text{OH})_2$   
 Polymers: (d)  $[\text{Si}(\text{OH})_4]_x$ ; (e)  $[\text{Al}(\text{OH})_3]_x$ ; (f)  $[\text{Mg}(\text{OH})_2]_x$

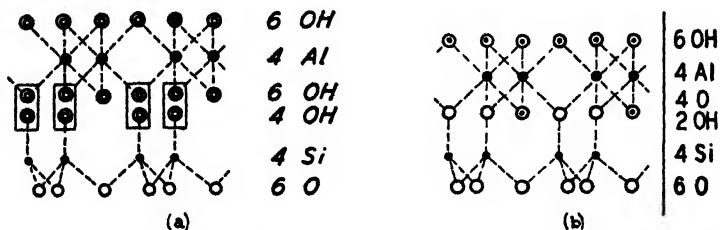


FIG. 6. Copolymers: (a) prior to condensation (halloysite); (b) after condensation (kaolinite).

distribution, neutralized. What this implies can best be explained by offering a few examples.

The question why solutions of alkali silicate polymers have such high viscosities and set to a gel like many high-molecular organic colloids has baffled chemists for a long time. Quite recent work proves that the comparatively high viscosity of water glass solutions and their gelation upon the addition of acids or electrolytes carrying cations of higher valency, or less hydratability, than sodium ion are based solely on the morphology of the alkali silicate particle. Sodium silicate, for example, owes the viscosity of its solutions to the water hulls, or lyospheres, carried by the sodium ions, which must be considered as ionizable counter ions and not as fixed components of the silicate structure. These lyospheres also prevent the colloidal particles from condensing and forming larger particles. Upon the addition of an acid or a multivalent cation, a base-exchange reaction

results, the zeta potential of the micelle drops and its lyosphere is decreased in size (figure 8). This is then followed by condensation and, as previously stated, by the formation of filamentitious polymers. Depending on the type of counter ions involved in this reaction and their concentration, a thixotropic or rheopectic gel with separated particles, or a permanent gel with a three-dimensional structure of interwoven filaments results. This is also the reason why these gels upon desiccation yield extremely porous, highly reactive solids, a result which accounts for their strong adsorbing property. It is nothing but the surface development

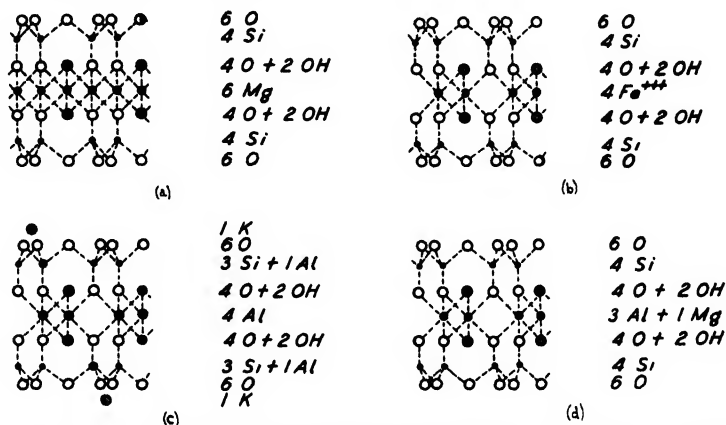


FIG. 7. Copolymers—continued: (a) talc; (b) nontronite. Copolymers (substituted): (c) mica; (d) bentonite.

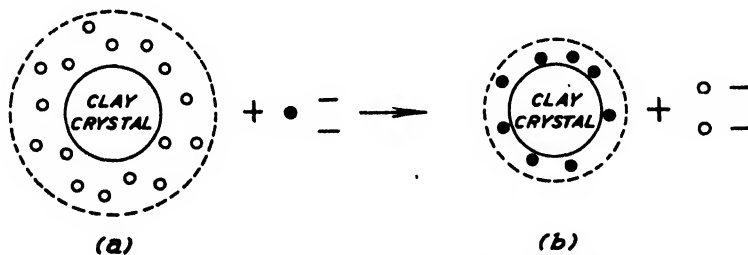


FIG. 8. Effect of ionic valency on dimension of lyosphere. O, monovalent counter ion; ●, polyvalent counter ion; —, monovalent anion.

and the chemical unsaturation and type of the ions located therein which are responsible for the increasing uses which colloidal silica is finding in such diversified applications as in mouthpiece filters of gas masks, in air- and water-purification units, or as bleaching and decolorizing agents and as catalysts.

Our increasing knowledge of the structure of the condensation copolymers of silicon hydroxide with aluminum or magnesium hydroxide has opened up some entirely new uses for these abundant natural products. When it was discovered that certain colloidal clays exhibit the phenomenon of thixotropy and how it could be controlled, they were put to use in the formulation of oil well drilling muds (10). Since most naturally occurring colloidal clays which give thixotropic gels

are sodium bentonites (5), they will not yield thixotropic gels in contact with a brine solution or oil. On the basis of our knowledge of their composition and their micelle structure, we can now change their reactive surface so that they become reactive even in such environments.

By spreading thixotropic gels of purified sodium bentonite and drying them, the platey particles are aggregated into fibers which interweave and form a coherent self-supporting film (figure 9) (7, 9). By exchanging the sodium ion with a less hydrophilic one, a water-resistant film of high dielectric properties results. If the exchanging ion is potassium, synthetic mica is formed. If the sodium ion is substituted, with a complex ion carrying an organic radical, the clay will now expose an organic surface. Such clay exhibits interesting properties as a compounding ingredient for organic matter like rubber and plastics (5, 7). If the organic radicals, like organic ammonium complexes or metal

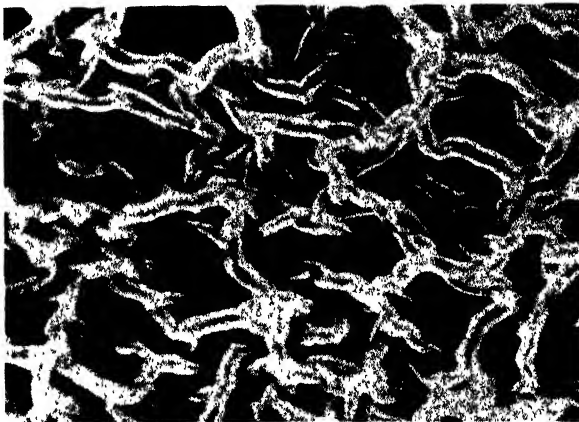


FIG. 9. Filamentitious structure of clay films

acrylates (5, 8), can be polymerized by condensation or addition, the result is a copolymer of organic and inorganic monomers and not just a heterogeneous mixture. This reaction is of course not limited to clay films, but permits the production of plastics for pressure or extrusion molding. Depending on the type of organic radicals involved, thermoplastic or thermosetting compounds can be produced (5, 8, 9).<sup>3</sup>

In recent years the silicon resins have been added to this branch of colloid science. They too are neither entirely organic nor inorganic in composition. They have opened up new vistas for coating, impregnation, lubrication, and even in the field of elastomers (12). In combination with clay films they yield insulating tapes of unsurpassed electrical properties.

<sup>3</sup> The 34th Annual Report of the Mellon Institute, which came to the author's attention only recently, carries on p. 26 a note under the heading "Clay as a Chemical." Science News Letter (Vol. 51, p. 333 (1947)) refers thereto in an article "Plastics from common clay." This work, in which the author takes an active part, is carried out under a fellowship sponsored by the National Lead Company and is based on the above-mentioned discoveries.

Other fields which would benefit by paying more attention to the colloid chemistry of siliceous matter are geology, petrography, the ceramic and the paper industries, agriculture, highway construction, soil solidification (13), and flood control, to mention only a few. They all depend on the surface composition of clays and the colloidal phenomena based thereupon. In ceramics it is plasticity and shrinkage (5) of the clay slips, in the paper industry dispersion and coating (6), in agriculture the fertility of the soil, in flood control the assurance that sufficient permeability is maintained (13). In geology and petrography it is the phenomenon of rheopexy which deserves special attention. This is particularly so, since it has been shown that its occurrence is most pronounced if colloidal clay is contaminated with colloidal iron oxide (5). This phenomenon is probably responsible for the layer-type deposits of clays and in petrography for the petrifaction of such delicate structures as jellyfish. The Solnhofen slates are famous for these and it has been proven that they are largely composed of colloidal particles of siliceous matter (5).

In closing this survey, I should like to refer to a statement made nearly thirty years ago by a famous Austrian chemist, Dr. Rudolf Wegscheider. He said: "I predict that the day will come when the chemistry of Silicon will be a serious competitor to organic chemistry." It is hoped that colloid chemists who have been active in research with compounds of siliceous compositions will realize that this day has come, and that it therefore is not presumptuous to coin a new name for this branch of colloid science,—namely, "silicic chemistry."

Silicic chemistry has been born and is growing fast, and as with the development of every child, we are in for many surprises!

#### SUMMARY

The history of the colloid chemistry of silicon is reviewed to prove that this branch of the science of colloids is even older than the term "colloid" itself.

The opinion that certain properties of matter, such as the formation of solutions of high viscosity and the ability to form gels, are limited to organic compounds is disproved. Attention is drawn to the similarity of the reactions responsible for the formation of organic and siliceous colloids and a uniform terminology for these reactions is suggested. Examples of siliceous compounds exhibiting the same properties as organic ones are offered.

Various colloidal phenomena characteristic of silicon compounds and their importance to science and industry are discussed. Attention is drawn to the versatility of this new field, and the suggestion is made to give it the name "silicic chemistry."

#### *Addendum*

Only a few days before the author presented this paper, he was visited by Professor Nils Hast of the Royal Technical University and the Nobel Institute for Physics, in Stockholm, Sweden. Professor Hast gave him a detailed description of his new technique for studying the structure of clays and diatomaceous shells with the electron microscope (*Nature* 159, 354, 370 (1947)). This new

method of sample preparation has enabled Professor Hast to increase the microscope's resolving power far beyond what has been possible so far and to make the changes which the original structure undergoes during hydration and subsequent dehydration actually visible. Besides this, it has enabled him even to make the individual layers of clay particles discernible and also the process by which they are stacked up.

## REFERENCES

- (1) BERGMAN, T.: *Kleine physische und chemische Werke*, Vol. 3, p. 391. Frankfurt a/Main (1785).
- (2) BRAGG, W. H., AND BRAGG, W. L.: *X-Rays and Crystal Structure*. A. Bell and Sons, Ltd., London (1925).
- (3) GRAHAM, TH.: *Phil. Trans.* **1861**, 183; *Proc. Roy. Soc. (London)* **11**, 243 (1861).
- (4) GRAHAM, TH.: *Proc. Roy. Soc. (London)* **13**, 335 (1864).
- (5) HAUSER, E. A.: *Chem. Revs.* **37**, 287 (1945).
- (6) HAUSER, E. A.: *Paper Trade J.* 8-12-1937; 8-24-1939.
- (7) HAUSER, E. A.: U. S. patents 2,266,636; 2,266,637; 2,266,638; 2,317,685.
- (8) HAUSER, E. A., AND DANNENBERG, E. M.: U. S. patent 2,401,348.
- (9) HAUSER, E. A., AND LE BEAU, D. S.: *J. Phys. Chem.* **42**, 961, 1038 (1938); **43**, 1037 (1939); **45**, 54 (1941); *J. Alexander's Colloid Chemistry*, Vol. VI, p. 191, Reinhold Publishing Corporation, New York (1946).
- (10) LARSEN, D. H.: In *J. Alexander's Colloid Chemistry*, Vol. VI, p. 509. Reinhold Publishing Corporation, New York (1946).
- (11) PAULING, L.: *The Nature of the Chemical Bond*. Cornell University Press, Ithaca, New York (1940).
- (12) ROCHOW, E. A.: *An Introduction to the Chemistry of the Silicones*. John Wiley and Sons, Inc., New York (1946).
- (13) WINTERKORN, H. F.: In *J. Alexander's Colloid Chemistry*, Vol. VI, p. 459. Reinhold Publishing Corporation, New York (1946).
- (14) WRIGHT, N., AND HUNTER, M. Y.: *J. Am. Chem. Soc.* **69**, 803 (1947).



## EMULSION POLYMERIZATION OF STYRENE\*

ERNST A. HAUSER

*Department of Chemical Engineering, Massachusetts Institute of Technology,  
Cambridge, Massachusetts*

AND

ELI PERRY

*Monsanto Chemical Company, Springfield, Massachusetts**Received February 20, 1948*

That emulsion polymerization should be considered a surface phenomenon has already been stated by several colloid chemists. The question, however, if polymerization is initiated by the use of oil-soluble or water-soluble catalysts, or starts at the oil-water interface, has never been answered satisfactorily. With this in mind, two series of polystyrene emulsions were prepared, one with an oil-soluble catalyst and the other with a water-soluble catalyst. The concentration of the emulsifying agent was the only variable factor. The data show that polymerization occurred simultaneously in the oil and water phases, but not at the oil-water interface. The value of the oil-phase polymerization was definitely established. This is in direct contrast to those theories of emulsion polymerization which assume that only aqueous-phase reactions are involved.

Further work showed that a change in the amount of emulsifier and type of catalyst causes the molecular weight distribution to vary over a wide range. The effect of molecular weight distribution on the physical properties of the polymer was recognized qualitatively, and confirmed by studying the morphology of mixed fractions ultramicroscopically with incident light.

These results are in line with what has already been demonstrated with other high-polymeric substances.

This paper is concerned with the emulsion polymerization of styrene.

On the basis of the investigations of Harkins and coworkers (1), Vinograd and coworkers (8), Mark and coworkers (3), and Price and Adams (4), it has been suggested that polymerization was initiated in the aqueous phase. X-ray data supposedly indicated that polymer particles were expelled from the soap micelles after they had reached a certain size and that they then continued to grow at the expense of monomer, diffusing from the monomer droplets which serve as a reservoir to supply monomer to the aqueous phase to initiate the growth of the small particles.

A survey of the literature revealed that these theories and deductions are based on work carried out with water-soluble catalysts. It was believed that this type of catalyst obscured the contribution of oil-phase polymerization which was also occurring. The present work was therefore undertaken in an attempt to resolve

<sup>1</sup> This paper is based on the M.S. thesis of Eli Perry in the Department of Chemical Engineering of the Massachusetts Institute of Technology, June, 1947. It was presented before the Division of Colloid Chemistry at the 112th Meeting of the American Chemical Society, which was held in New York City, September, 1947.

this problem. For this purpose two series of emulsions were prepared, one with an oil-soluble catalyst (benzoyl peroxide) and the other with a water-soluble catalyst (potassium persulfate). The systems used were extremely simple and consisted only of styrene monomer, emulsifying agent (sodium stearate), catalyst, and distilled water. The recognized variables, such as catalyst concentration, ratio of oil to water phase, temperature, agitation, and type of atmosphere, were held constant. The only variable factor for each series of polymerizations was the amount of emulsifying agent used. In order to avoid any difficulties which might occur due to variations in the raw materials, enough of each constituent was obtained so that the same lot could be used throughout the whole investigation. To this end the styrene monomer was used as received (i.e., with inhibitor) so as to avoid any purification which might give slightly different grades of monomer for the various runs.

Polymerization was conducted under a nitrogen atmosphere in a three-necked flask equipped with ground-glass joints and a mercury seal.

The procedure consisted in weighing the water into the flask and dissolving the emulsifying agent and catalyst (if water-soluble) in the water. The monomer was added (with the catalyst dissolved in it if oil-soluble) and the dispersion was agitated for 25 min. A sample was withdrawn, and the constituents of the flask were brought to temperature in 15–20 min. The temperature was maintained within  $\pm 0.5^\circ\text{C}$ . until the monomer was 93–95 per cent converted to polymer. The emulsion was then cooled to  $35^\circ\text{C}$ . and strained into jars for storage. Any lumps were air dried and weighed.

The course of the reaction was followed by pipetting samples out of the dispersion and analyzing them for unreacted monomer. The analytical procedure used in this work was a modification of the method of Uhrig and Levin (7).

A rough estimate of the degree of conversion to polymer was obtained as follows: 5 ml. of emulsion was mixed with 40 ml. of water. Ten milliliters of precipitating reagent (12.5 cc. of concentrated sulfuric acid, 50 g. of sodium chloride, and 1 l. of water) was added slowly to the diluted emulsion. If the conversion was less than 40 per cent no precipitate resulted, but an oily layer of monomer was salted out. At 50–60 per cent conversion small particles of polymer separated and formed a dispersion resembling shredded cotton rags in a liquid medium. At 70–80 per cent conversion the polymer lumped to form a single, solid, sticky ball. Above 90 per cent conversion a fine, hard precipitate formed, leaving a clear or almost clear supernatant liquid above it.

Nitrogen was bubbled through the dispersion from the time the water was charged to the very end of the run.

The following data were obtained for each polymer: (1) total time of reaction at the reaction temperature; (2) the per cent conversion as a function of time; (3) the approximate time of the induction period; (4) the amount of lumps formed; (5) the approximate particle size in the final product; (6) the "gross" molecular weight of the product polymer; (7) an approximate molecular weight distribution curve.

## PARTICLE-SIZE MEASUREMENT

The particle size was estimated ultramicroscopically and by means of light transmission measurements. Neither method allowed an absolute determination of particle size, but a comparison between the various emulsions was all that was wanted.

## FRACTIONATION PROCEDURE FOR MOLECULAR WEIGHT DISTRIBUTION

Fifty grams of polymer was purified by dissolution in 1000 cc. of methyl ethyl ketone and reprecipitation with 2500 cc. of methanol.

Thirty grams of reprecipitated polymer was dissolved in 1500 cc. of methyl ethyl ketone in a 2000-cc. Erlenmeyer flask. Methanol was added in small increments to precipitate the different molecular weight fractions of the polystyrene.

The recovery of polymers as a result of fractionation was always 97 per cent or better.

## MOLECULAR WEIGHT DETERMINATION

The molecular weight was determined viscometrically, giving a weight average.

The specific viscosity ( $N_{sp}$ ) was calculated and a plot of  $N_{sp}/C$  vs.  $C$  allowed the intrinsic viscosity, ( $N$ ), to be found. The molecular weight was calculated from the formula (5):

$$(N) = 4.94 \times 10^{-5} M^{0.78}$$

It is believed that emulsion polymerization is initiated simultaneously in the oil and water phases, and that the use of the oil-soluble catalyst has emphasized the contribution of the oil-phase polymerization to such a degree that it could be easily distinguished from the polymerization which was initiated in the aqueous phase.

Most of the polymerization occurs as a zero-order reaction for both types of catalyst.

Other investigators have demonstrated that the reaction rate should increase as the solubility of monomer is increased in the aqueous phase.

The length of the induction period decreased as the concentration of the emulsifying agent was increased. If one pictures the induction period as lasting until all of the inhibitor reacts with active nuclei, anything that promotes the rate of formation of nuclei (e.g., increased amount of emulsifying agent) shortens the induction period. The extra soap also solubilizes more of the inhibitor to increase its rate of consumption.

The particle size of the polymer decreased with an increased soap concentration, as indicated in figures 1 and 2 (3). The increased concentration of monomer results in more rapid formation of nuclei, each of which may become a new particle. Also, more soap is available for adsorption on the surface of new particles before the emulsifying agent disappears. This increase in the number of particles for a given charge implies that each individual particle is smaller.

The initial sample of dispersion from the flask separated into two layers immediately, showing that the emulsion polymer was not formed totally by mechanical means. The "two-layer sample" formed an emulsion polymer when allowed to stand unagitated on the shelf for 3 weeks at room temperature. This phenomenon is a consequence of the picture of polymerization occurring in the micelles and the molecules being expelled as particles when they reach a certain size (3).

The experimental facts which the theory of aqueous-phase polymerization does not explain but which the picture of dual-phase polymerization can explain is

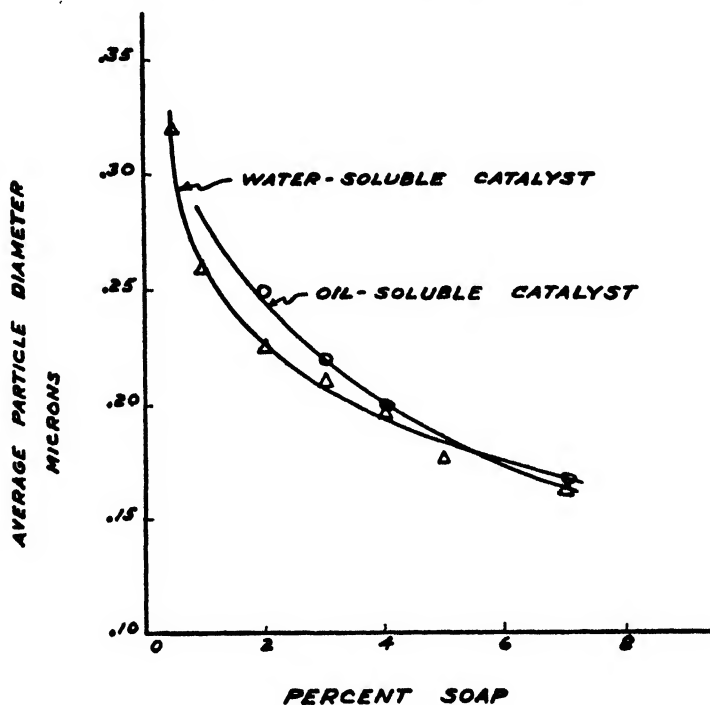


FIG. 1. Effect of soap concentration on particle size (estimated microscopically)

lump formation. Figure 3 shows that lump formation decreases with increasing soap concentration. Any satisfactory theory must be able to explain this decrease and also the great differences found when using oil-soluble and water-soluble catalysts. Lump formation was appreciable for resins made with an oil-soluble catalyst, but resins made with a water-soluble catalyst gave very little lump formation. In fact, with the latter actual lumps did not form, but instead an "oily" spot was seen on the surface at 75–85 per cent conversion. This "oily" spot disappeared as the reaction proceeded and was present in the final polymer as a lump  $\frac{1}{16}$  in. to  $\frac{1}{8}$  in. in diameter for the range of soap concentrations used. For this reason, the size of the "oily" spot was recorded qualitatively instead of weighing the lumps (*cf.* figure 3).

For an explanation of lump formation one must also take into consideration that polymerization occurs simultaneously in the oil and aqueous phases. The droplets which are "oil-phase initiated" differ in one important respect from particles which are initiated in the aqueous phase in that they must vary in solids content from 100 per cent to 0 per cent monomer during the course of the reaction. This variation in solids content is a consequence of simultaneous polymer

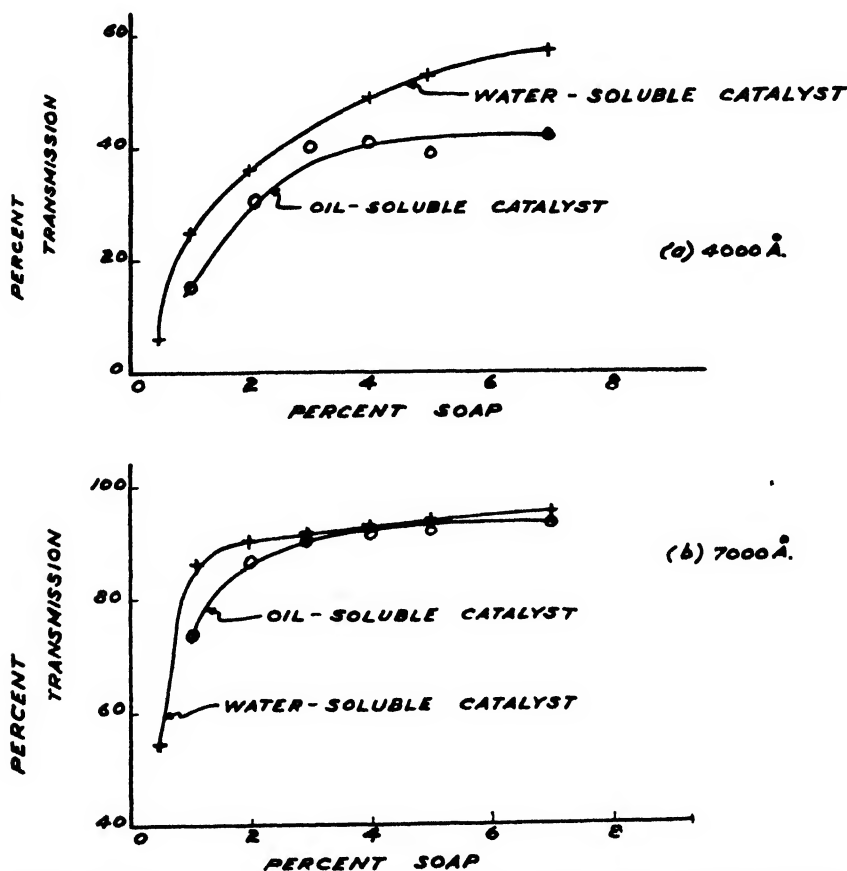


FIG. 2. Effect of soap concentration on the light transmission of the emulsions

formation and loss of monomer by diffusion. Therefore, at some stage in the reaction these latex-like particles must exist in a "sticky" state. If, at this stage, the particle size of the droplets is so large that the adsorbed soap film cannot stabilize them, the agitation will bring the droplets together and cause them to coalesce. Therefore, only certain particles in the emulsion coalesce and form lumps. Since an oil-soluble catalyst accentuates the contribution of oil-phase polymerization, the amount of lump formation will be greater than when using a water-soluble catalyst. With both an oil-soluble and a water-soluble catalyst the over-all time of reaction is controlled by the fastest rate, namely, that in the

aqueous phase. This implies a decrease in over-all reaction time when the soap concentration is increased, and less polymerization occurs in the oil phase with the resultant decrease in lump formation.

If this picture of lump formation is correct, agitation should be important in regard to the amount and nature of the lumps formed. The experimental data confirm this deduction.

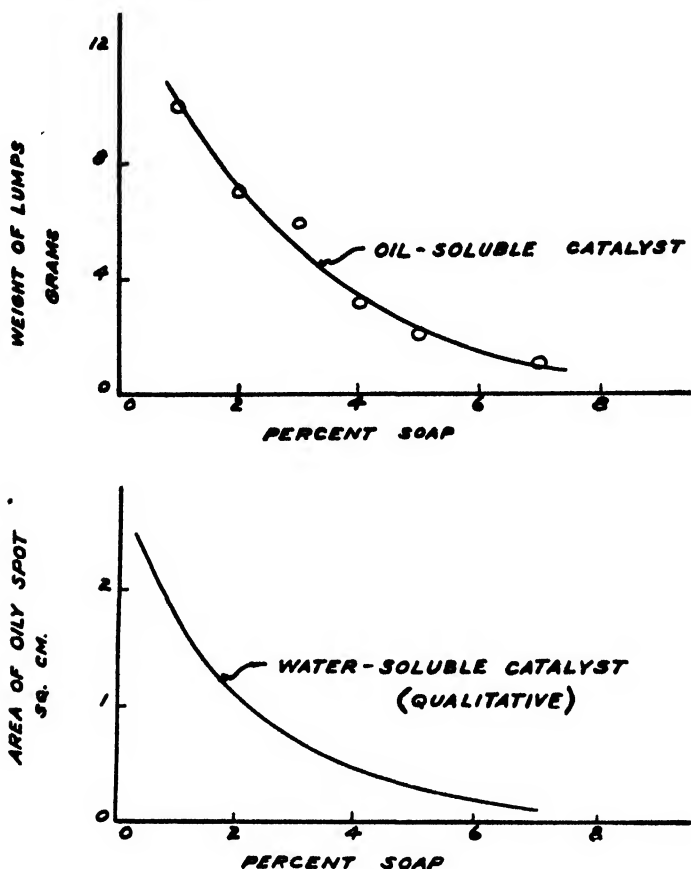


Fig. 3. Effect of soap concentration on lump formation

As shown in figure 4, the extrapolated value of the reaction rate constant is not zero at zero soap concentration for an oil-soluble catalyst. For the water-soluble catalyst, the extrapolated intercept was negligible. With a water-soluble catalyst at zero soap concentration one essentially separates the monomer and catalyst into different phases, so that very little oil-phase or aqueous-phase polymerization occurs. Therefore, the reaction rate constant must be very small. For the oil-soluble catalyst at zero soap concentration one excludes monomer and catalyst from the aqueous phase, but brings them into contact in the oil phase. The large reaction rate constant is due to the appreciable oil-phase polymerization, and demonstrates that it makes a significant contribution to the whole reaction.

More low-molecular-weight material was produced in the polymer as the soap concentration was decreased. This is seen in figures 5 and 6. The data of these figures are plotted in such a way that a curve tending away from the abscissa represents a preponderance of high-molecular-weight material, a straight line represents uniform molecular weight distribution, and a curve tending toward the abscissa represents a preponderance of low-molecular-weight material. The

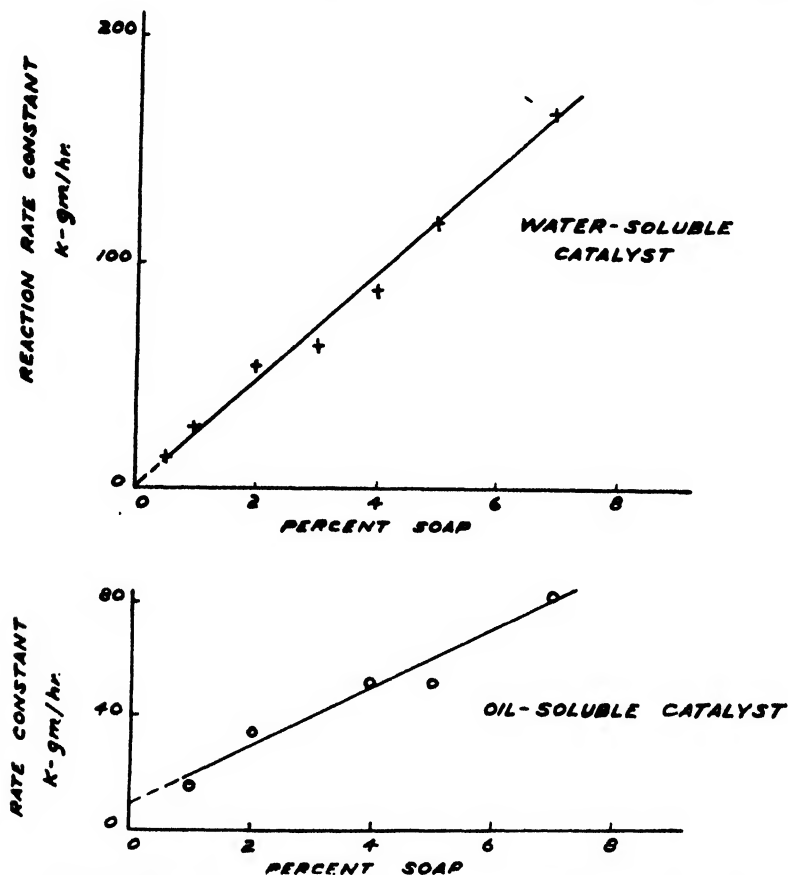


FIG. 4. Effect of soap concentration on the reaction rate constant

trend toward increased low-molecular-weight material with a decreased soap concentration is unmistakable for both the oil-soluble and water-soluble catalysts.

It must be emphasized that the molecular weights were estimated viscometrically by finding the intrinsic viscosity, ( $N$ ). The recorded molecular weights therefore represent a measure of the difference of degree of polymerization rather than absolute values.

A satisfactory picture of the variation of the molecular weight distribution curves with the soap concentration is presented by considering dual-phase polymerization. Less soap results in a longer reaction time, allows oil-phase polymerization to occur, and reduces the concentration of monomer and catalyst

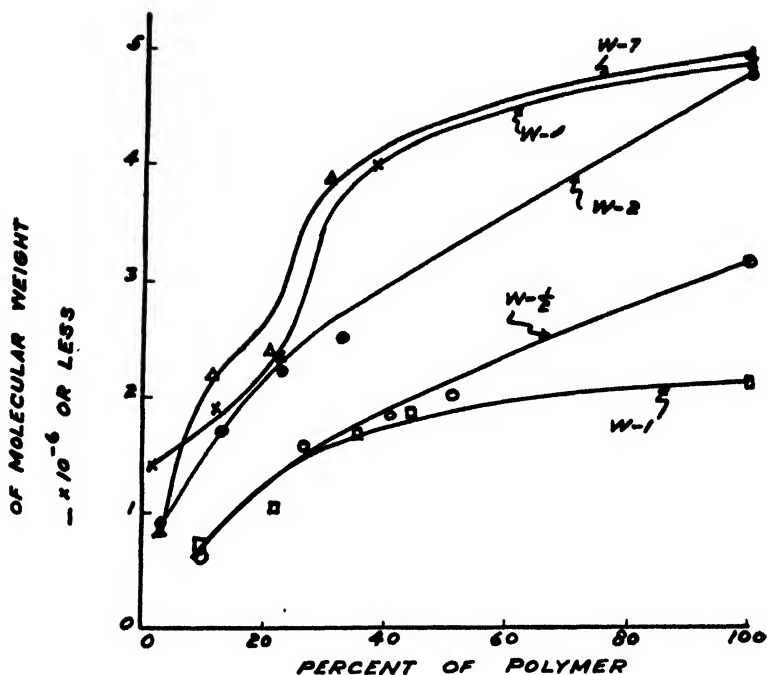


FIG. 5. Effect of soap concentration on the molecular weight distribution in the polymer (water-soluble catalyst).

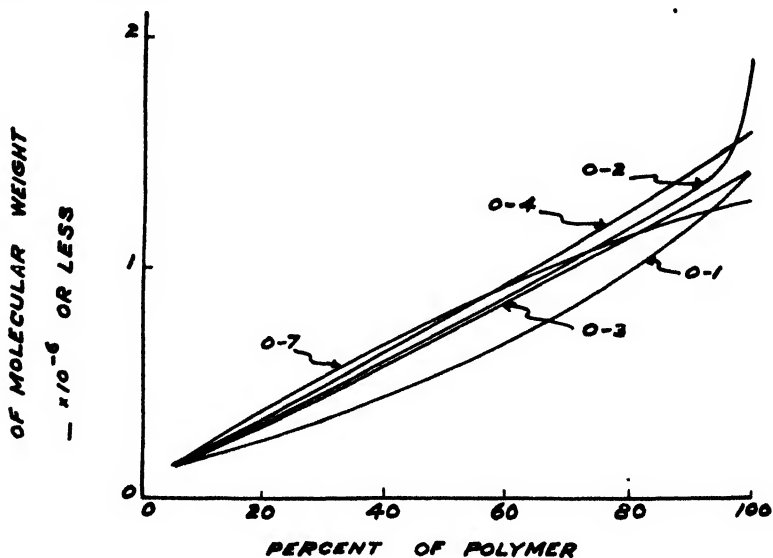


FIG. 6. Effect of soap concentration on the molecular weight distribution in the polymer (oil-soluble catalyst).

(if oil-soluble) in the aqueous phase (so that less aqueous-phase polymerization occurs). Therefore, less soap implies more low-molecular-weight material and



less high-molecular-weight material in the polymer (*cf.* figures 5 and 6). Although the shape of the curve changes for the polymers made with an oil-soluble catalyst as the soap concentration decreases from 7 to 1 per cent (figure 6), the trend is not as apparent as in figure 5 for two reasons: (a) With an oil-soluble catalyst, the amount of oil-phase polymerization is large for any soap concentration, so that one is trying to detect a small addition to a large quantity. (b) With increased oil-phase polymerization (*i.e.*, decreased soap concentration), the amount of lump formation increases greatly (figure 3). Since lump for-

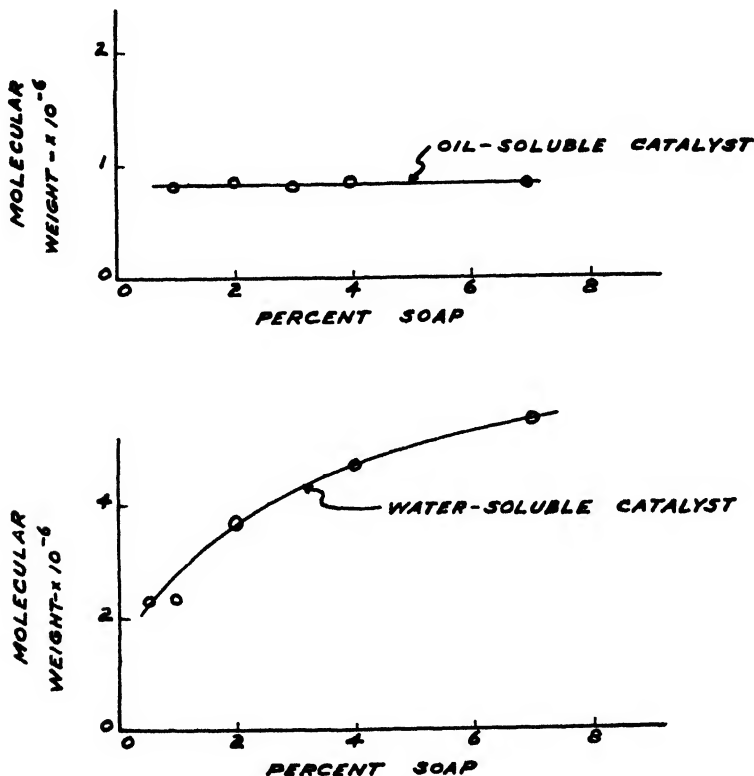


FIG. 7. Effect of soap concentration on the molecular weight of the unfractionated polymer  
Photomicrographs of polystyrene fractions

mation is due to oil-phase initiation, the more oil-phase polymerization which occurs, the more of that type of polymer is removed as lumps, which do not remain in the product.

A study of figure 5 indicates that the mechanism of aqueous-phase polymerization may change as the soap concentration is varied. This idea is suggested by the difference in the molecular weight fractions of the polymers, and variation in its gross molecular weight (*cf.* figure 7). In any case, the present report does not pretend to deal with the mechanism of polymerization, but only its loci. The mechanism is still unknown and requires much more research.

One must also consider the evidence against polymerization taking place at the oil-water interface.

(1) Using a water-soluble catalyst, the reaction rate constant was negligible at zero soap concentration. As explained above, the catalyst and monomer are in different phases, so that if interface polymerization were important the reaction rate constant would be significant under these conditions.

(2) With a water-soluble catalyst lump formation was small, and with an oil-soluble catalyst lump formation was large. If interface polymerization were important one would expect the same reaction mechanism and, hence, approximately the same amount of lump formation with both types of catalyst.

(3) Polymer particles of colloidal size were formed without agitation. Interface polymerization does not provide any mechanism for the formation of small particles.

It was therefore concluded that the experimental facts could be explained only by the theory of dual-phase polymerization.

The molecular weight distribution in the polymers is of special interest.

Qualitative tests on films made from mixtures of fractions of different molecular weight confirmed the idea that the toughness and elasticity were markedly influenced by the molecular weight distribution. Thus, films containing 50-75 per cent of low-molecular-weight fractions were much tougher than films of pure high or pure low molecular weight material. Much work remains to be done, but once the optimum molecular weight distributions for the various properties are known, it should be possible to produce any molecular weight distribution desired in any molecular weight range by controlling such variables as type and amount of catalyst, per cent emulsifier, temperature of the reaction, and concentration of the monomer (6). The variation in the molecular weight distribution obtained in the present work indicates a general method of attack.

Some ultramicroscopic observations were made on the fractions of polystyrene, using the technique described by Hauser and le Beau (2). Films of the polymer were deposited on fine-mesh wire screen and viewed under a Leitz Ultrapak under controlled conditions of time and temperature. Photomicrographs published previously (2) showed glob formation for many substances, due probably to syneresis (flow whereby the low-molecular-weight material was squeezed out from between the high-molecular-weight chains). Therefore, the formation of globs depends in part on the molecular weight distribution of the polymer. The freedom of movement of the chains and how that movement is affected by side groups are other facts to be considered.

Various fractions of high-molecular-weight and low-molecular-weight polystyrene were mixed in the proportions of 75 per cent low molecular weight and 25 per cent high molecular weight. The individual unmixed fractions rarely showed glob formation at either room or elevated temperatures. Occasionally, globs were observed but they were attributed to the fact that the fractions were not sharp. Often, fragments or particles were observed which were similar to globs in appearance but which had sharp corners instead of smooth rounded surfaces. The mixed fractions did not form globs at all times, especially at room

temperature. However, on heating the samples, globs appeared and their formation was attributed to the spreading of the chains and the subsequent greater

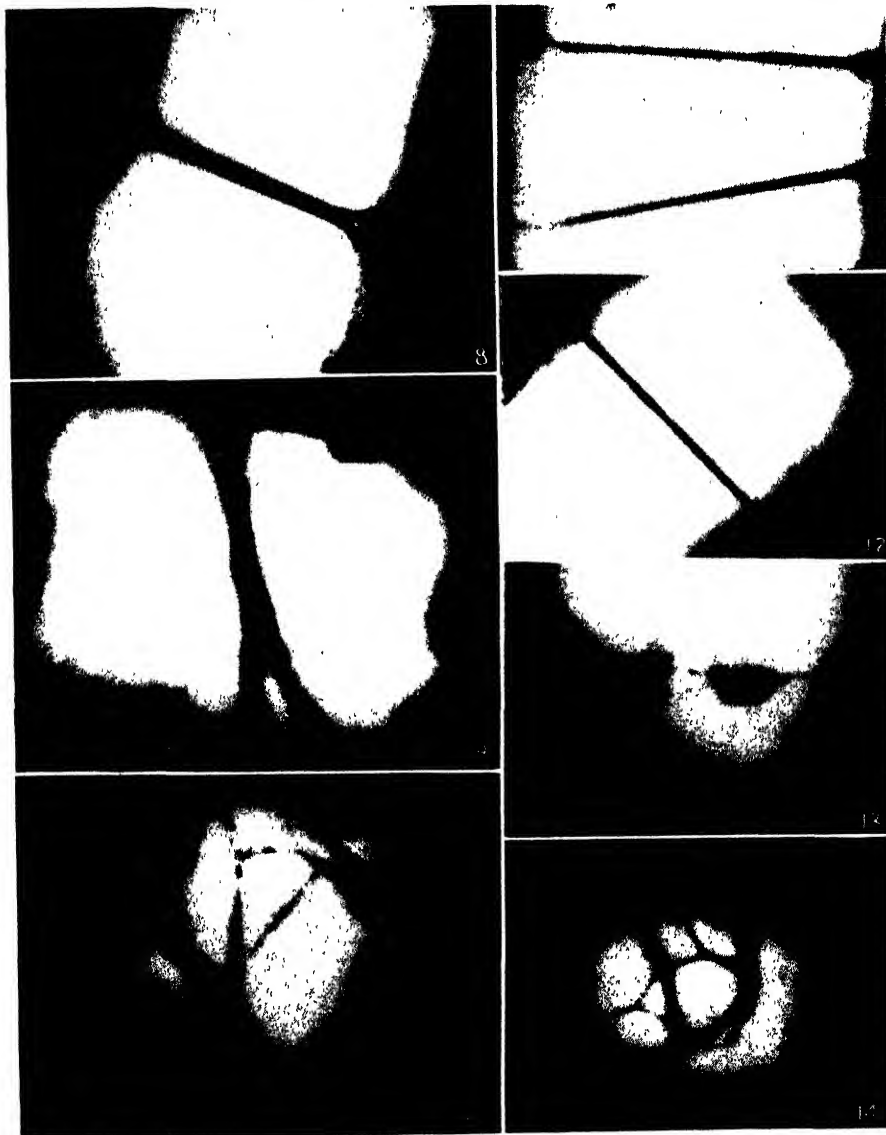


FIG. 8. 8000 MW at 25°C.

FIG. 9. 40,000 MW at 25°C.

FIG. 10. 250,000 MW at 25°C.

FIG. 11. Mixture of 8000 and 250,000 MW at 25°C.

FIG. 12. Mixture of 8000 and 250,000 MW heated to 90°C.

FIG. 13. Mixture of 40,000 and 1,000,000 MW at 25°C.

FIG. 14. Mixture of 40,000 and 1,000,000 MW heated to 90°C.

flow. The photomicrographs (figures 8-14) show some of the phenomena described above. This work is by no means complete but indicates that a more

exhaustive investigation of this type is necessary to help in solving some of the problems which still beg for answers.

We are greatly indebted to Dr. D. S. le Beau, Director of Research, Midwest Rubber Reclaiming Company, for making the preparations needed in the ultra-microscopic examination.

#### REFERENCES

- (1) HARKINS, W. D., *et al.*: J. Chem. Phys. **13**, 381 (1945); **14**, 47, 214, 215 (1946); J. Colloid Sci. **1**, 105 (1946).
- (2) HAUSER, E. A., AND LE BEAU, D. S.: Ind. Eng. Chem. **37**, 786 (1945); **38**, 335 (1946); J. Phys. Colloid Chem. **51**, 278 (1947); **52**, 27 (1948).
- (3) MARK, H., *et al.*: India Rubber World **111**, 173 (1944); **111**, 436 (1945); J. Polymer Sci. **1**, 549 (1946).
- (4) PRICE, C. C., AND ADAMS, C. E.: J. Am. Chem. Soc. **67**, 1674 (1945).
- (5) Private communication.
- (6) SAKUMA, N.: Kunststoffe ver. Kunststoff-Tech. u.-Anwend. **34**, 83 (1944).
- (7) UHRIG, K., AND LEVIN, H.: Ind. Eng. Chem., Anal. Ed. **13**, 90 (1941).
- (8) VINOGRAD, J. R., *et al.*: Abstracts of Papers Presented at the 108th Meeting of the American Chemical Society, New York City, September, 1944.

### AN ELECTRON DIFFRACTION STUDY OF OXIDE FILMS FORMED ON HASTELLOY ALLOYS A, B, C, AND D

J. W. HICKMAN AND E. A. GULBRANSEN

*Westinghouse Research Laboratories, East Pittsburgh, Pennsylvania*

*Received January 7, 1948*

#### INTRODUCTION

Metals or alloys which are to be used in high-temperature service must meet certain requirements of room-temperature properties, such as ductility, must have high-temperature strength, oxidation and corrosion resistance, and structural stability. Surface stability is as important as load-carrying ability, since it governs the length of time the material will be able to stand the stress. Failure at elevated temperatures may occur as the result of general, intragranular, or intergranular attack. Of the three, intergranular attack is generally considered to be the most serious.

The Hastelloy alloys are interesting because of their unusual compositions, high-temperature strengths, and resistance to corrosive media. In addition, the use of some of these alloys in high-temperature service makes the study of the oxides which form on them at various temperatures of interest to metallurgists and engineers.

Hastelloy alloys A, B, and D are resistant to progressive atmospheric oxidation and to oxidizing and reducing flue gases, carbon monoxide, carbon dioxide, and

hydrocarbons at temperatures up to 800°C. Hastelloy alloy C is resistant up to higher temperatures, the upper limit being about 1000°C. (5). Experimental work on superchargers, using alloys A, B, and C, showed that the stress rupture strengths of the cast alloys were definitely superior to those of the wrought alloys at 815°C. but that the high strength of alloy B in the wrought condition below 760°C. encouraged its use. Alloy B, which contains no chromium, cannot be used above 760°C., since it lacks surface stability under oxidizing conditions which result in loss of molybdenum from the surface (1). Considerable attention is being given to alloy C for use in high-temperature service, such as tail cone stacks of gas turbines and outlet nozzles of jet engines, since it is easier to form into the desired shapes than most of the other high-alloy materials (11).

#### LITERATURE SURVEY

The oxidation of some of the metals which comprise the Hastelloy alloys has been studied by the electron diffraction technique. In two earlier papers (4, 7) the authors have reported electron diffraction studies of the oxides occurring on the metals nickel, iron, chromium, molybdenum, and tungsten. These studies have shown that NiO and Cr<sub>2</sub>O<sub>3</sub> are found on nickel and chromium, respectively, over the temperature range 300–700°C. The oxidation of iron is much more complicated, since the oxide which occurs on the surface is dependent upon both the temperature and the time of oxidation. Four oxides,  $\gamma$ -Fe<sub>2</sub>O<sub>3</sub>, Fe<sub>3</sub>O<sub>4</sub>,  $\alpha$ -Fe<sub>2</sub>O<sub>3</sub>, and FeO, are found on iron in the temperature range 225–700°C. MoO<sub>2</sub> is the oxide stable in contact with molybdenum throughout the temperature range 300–700°C., while MoO<sub>3</sub> becomes predominant on the surface as the films get thicker in the low-temperature range. Above 400°C. MoO<sub>3</sub> is no longer observed; MoO<sub>2</sub> is the only oxide obtained. On tungsten WO<sub>3</sub> is the oxide stable in contact with the metal up to approximately 600°C., while WO<sub>2</sub> forms first at 700°C. In this respect tungsten differs from molybdenum, since the dioxide of molybdenum is in contact with the metal while the trioxide occupies the same position on tungsten.

To the best of our knowledge no electron diffraction studies of the elements manganese and silicon have been made, although alloys containing them have been investigated.

The oxides occurring on alloys containing two or more of the metals which make up the Hastelloy alloys have been investigated by electron diffraction. Alloys of nickel with molybdenum and tungsten (7) show only the presence of molybdenum and tungsten oxides, indicating that molybdenum and tungsten may have higher rates of formation and diffusion of ions than nickel. Alloys of nickel and chromium (10) show the presence of NiO in the low-temperature range, while above 400°C. either Cr<sub>2</sub>O<sub>3</sub> or NiO·Cr<sub>2</sub>O<sub>3</sub> or a mixture of these oxides occurs on the surface. This indicates that the rates of formation and diffusion of nickel and chromium ions may vary in a different manner with temperature. It is also significant that an increase in the concentration of silicon in alloys of nickel and chromium prevents the formation of NiO·Cr<sub>2</sub>O<sub>3</sub> and permits only Cr<sub>2</sub>O<sub>3</sub> to form.

No systematic study of the oxides occurring on the Hastelloy alloys has been made using the electron diffraction technique. Yamaguchi (12) has reported that an electron diffraction study of the corrosion products found on an alloy of iron with 5-10 per cent molybdenum and on Hastelloy alloy A shows only the presence of  $\text{MoO}_2$ . Unfortunately, the conditions under which the corrosion product formed are not available to us.

#### SAMPLE PREPARATION AND METHOD

A complete description of the apparatus used in this study has been reported by Gulbransen (2, 3). Samples, as received, in the form of rods of 0.375-in. diameter are cut to 0.375-in. lengths. These are given a surface finish, using the precision abrader (2) and ending up with 4/0 emery paper. Experiments have shown that a clean, flat, slightly matted surface, such as is obtained with 4/0 emery paper, gives sharp intense reflection patterns. Oxidations are carried out af-

TABLE 1  
*Analyses of the alloys\**

ELEMENT	ALLOY A	ALLOY B	ALLOY C	ALLOY D
Ni.....	55-60	60-65	55-60	85
Mo.....	15-20	25-35	15-20	
Fe.....	15-20	5	6	
Cr.....			12-16	
Mn.....	2			
Cu.....				3
Si.....				10
Al.....				2
C.....	0.13-0.20			
W.....			5	

\* Hoyt: *Metals and Alloys Data Book*, p. 265.

ter the abrading treatment without any other pretreatment such as annealing or etching. Purified oxygen under approximately 1 mm. pressure is used in all the oxidations. Electron diffraction photographs are taken in the vacuum of the camera before oxidation; after 1, 5, 30, and 60 min. oxidation; and after cooling to room temperature under approximately 0.05 atm. pressure of hydrogen.

Table 1 lists the samples investigated together with the approximate analyses available to us. All alloy samples were obtained through the courtesy of Haynes Stellite Company, Kokomo, Indiana.

#### METHOD OF INTERPRETATION

In order to identify the oxides which form on the surfaces of the alloys, it is necessary to compare the interplanar distances and intensities from the electron diffraction patterns with data obtained by other workers using x-ray diffraction. Some of the electron diffraction patterns show the presence of intense arcs or spots, indicating that the oxide has grown in a preferential manner on the

metallic substrate. In these cases no attempts are made to determine the orientations which the oxides assume. The data from the oxidations are presented in the form of existence diagrams of the oxides plotted on a time-temperature scale (figures 1-4). The terms "oriented," "sharp," "medium," and "diffuse" occurring on the existence diagrams and represented by the letters O, S, M, and D, respectively, refer to the types of diffraction patterns. Those patterns are termed "oriented" where intense arcs or spots occur as the result of preferential growth of the oxide crystals on the surface; the remaining three classifications are made on the basis of line widths.

TABLE 2  
*Oxides found on the alloys*

ALLOY	FIGURE	OXIDE STRUCTURE
Hastelloy A. . . . .	1	300-900°C.—spinel
Hastelloy B. . . . .	2	300-500°C.—NiO 600°C.—MoO <sub>3</sub> + tr. MoO <sub>3</sub> ; 700°C.—spinel 800°C.—1 min.—spinel; 5-60 min.—NiO 900°C.—1 min.—MoO <sub>3</sub> ; 5-60 min.—spinel
Hastelloy C. . . . .	3	300-500°C.—spinel 600-700°C.—Cr <sub>2</sub> O <sub>3</sub> ; 800°C., 1-5 min.—Cr <sub>2</sub> O <sub>3</sub> + MoO <sub>3</sub> ; 30-60 min.—spinel 900°C., 1 min.—Cr <sub>2</sub> O <sub>3</sub> + MoO <sub>3</sub> ; 5-60 min.—spinel
Hastelloy D. . . . .	4	300-600°C.—Cu <sub>2</sub> O 700-900°C.—NiO

#### RESULTS AND DISCUSSION

Table 2 gives a synopsis of the results, which are presented more completely in graphical form in the existence diagrams (figures 1-4). Each point on the existence diagrams represents the oxidation of a sample for the time and temperature indicated. In all cases the lattice parameters given for the cubic oxides are the average lattice parameters where the maximum deviations are not greater than  $\pm 0.03$  Å. In some cases it is not possible to give the chemical composition unequivocally by examination of the lattice parameter alone. In these cases the most probable formula is given, although the possibility of solid solution exists.

In the interpretation of the data the relative thermodynamic stabilities of the oxides which may form are important only if the several metallic ions form and diffuse to the surface. In most cases the oxides which are observed are probably dependent primarily upon the relative rates of formation and diffusion of the several metallic ions.

No attempts have been made to study the stratification of the oxides on the surfaces of the alloys. Since only the outer 50 or 100 Å. of the oxide films are sampled by the electron beam, it is possible that the bulk of the oxide films may

differ widely in composition from the results reported. In a later report it is our intent to present an x-ray diffraction study of the oxides formed in air by oxidation in an auxiliary furnace.

#### HASTELLOY A

Hastelloy A, which consists primarily of nickel, molybdenum, and iron with a small quantity of manganese, is a solid-solution alloy with a face-centered cubic structure (5) containing a small proportion of carbides even when cooled rapidly from a high temperature. An inspection of figure 1 shows that the oxide occurring over the complete time-temperature range has a cubic structure of the spinel type. There are two principal oxides having a spinel-type structure which may occur on this alloy: namely,  $\text{Fe}_3\text{O}_4$  ( $a = 8.42 \text{ \AA.}$ ) and  $\text{NiO} \cdot \text{Fe}_2\text{O}_3$  ( $a = 8.34 \text{ \AA.}$ ). The lattice parameter observed,  $8.43 \text{ \AA.}$ , indicates that the oxide occurring on the surface consists primarily of iron oxide, although nickel may be present in solid solution. Although no chemical differences in the oxides occur over the time-temperature range under investigation, there are physical differences present as evidenced by the facts that some of the patterns are medium and oriented, and some are diffuse, while others are sharp. These variations are probably the results of differences in growth of the oxides on the surfaces of the metallic substrates.

The fact that no oxides of molybdenum or nickel are observed may indicate that ions of iron have greater rates of formation and diffusion than do ions of these metals. Earlier work on Hipernik (6) (49 per cent iron, 49 per cent nickel, 2 per cent manganese) showed only the presence of oxides of iron while the oxidation of an alloy of molybdenum and nickel (7) (93 per cent molybdenum, 7 per cent nickel) showed only the presence of molybdenum oxides. These facts indicate that the rates of formation and diffusion of the ions of these three metals may be in the order iron, nickel, and molybdenum. On this basis one might expect to find oxides of iron primarily on Hastelloy A; this is in agreement with the results obtained, as shown in figure 1. Of course, it is possible that the concentration of iron may be reduced in a ternary alloy of iron, molybdenum, and nickel to the point where ions of molybdenum will reach the surface. If all of the ions had equal probability of reaching the surface, one would still expect to observe oxides of iron at equilibrium primarily as evidenced by the free energies of formation of the oxides which are given in an earlier paper (8). It is realized, of course, that the rates of the several reactions will to a great extent influence the oxides which form on the surface.

#### HASTELLOY B

Hastelloy B contains the same metals as Hastelloy A except that the percentage of molybdenum is higher while that of iron is lower, as shown in table 1. This alloy is also face-centered cubic and contains a small proportion of carbides (1). A comparison of figures 2 and 1 shows that the changes in the concentrations of iron and molybdenum have greatly affected the oxides which occur on the surface. The reduction in the percentage of iron to one-third the value present



in Hastelloy A results in the appearance of NiO up to 500°C. Since oxides of iron are favored thermodynamically over NiO in the temperature range 300–500°C., the absence of iron oxides on the surface may be due to the fact that an

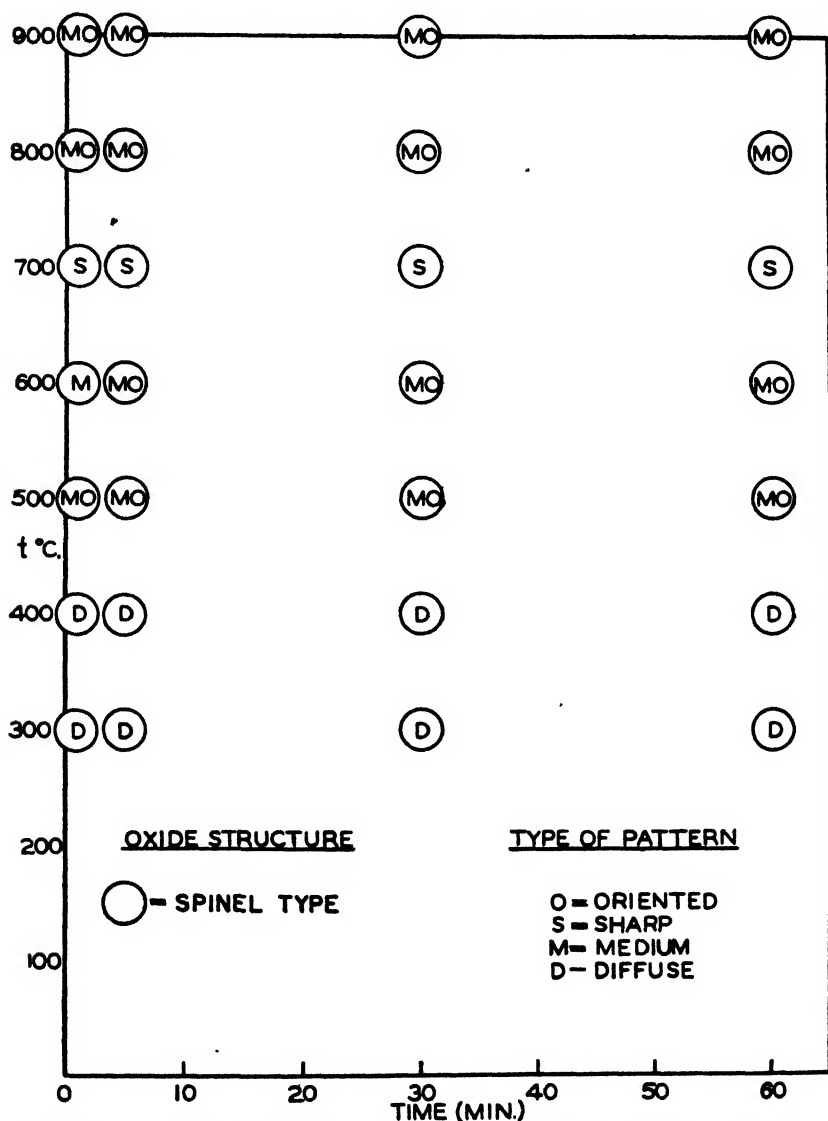
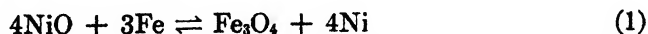


FIG. 1. Oxide films on Hastelloy A at 1 mm. oxygen for various times and temperatures

insufficient number of iron ions reach the surface to permit  $\text{Fe}_3\text{O}_4$  to form according to the following over-all equation:



At 600°C. oxides of molybdenum are observed, with  $\text{MoO}_2$  being the principal

oxide and  $\text{MoO}_3$  present only as a trace. This result is in agreement with a previous report on 93 per cent molybdenum, 7 per cent nickel (7), where a mixture of  $\text{MoO}_3$  and  $\text{MoO}_2$  was obtained at  $600^\circ\text{C}$ . At  $700^\circ\text{C}$ . a cubic oxide of

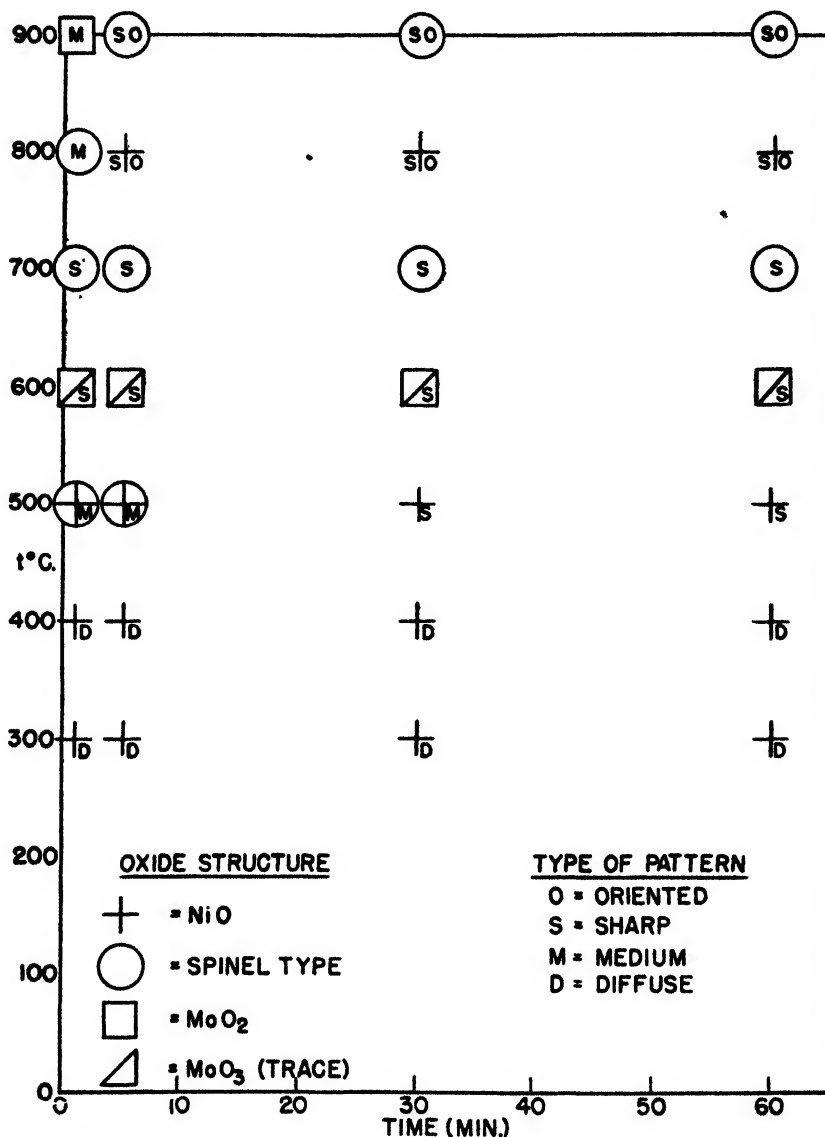


Fig. 2. Oxide films on Hastelloy B at 1 mm. oxygen for various times and temperatures

the spinel type is obtained. The composition of this oxide may not be determined from the electron diffraction data. At  $800^\circ\text{C}$ . NiO again becomes predominant on the surface, while at  $900^\circ\text{C}$ .  $\text{MoO}_2$  occurs for short oxidation times, followed by the appearance of an oxide with a cubic structure of the spinel type as the film becomes thicker.

Our interpretation of the data above 500°C. is as follows:

(1) The oxide occurring at 700°C. is probably primarily  $\text{Fe}_3\text{O}_4$ . This seems reasonable, since iron oxide is observed at 500°C. for short oxidation times, while at 600°C. molybdenum ions surpass iron in rates of formation and diffusion and reach the surface.

(2) At 800°C.  $\text{NiO}$  again appears on the surface, indicating that nickel ions are reaching the surface in greater numbers than iron ions.

(3) At 900°C. the spinel-type oxide probably consists of both iron and nickel with the formula  $\text{NiO} \cdot \text{Fe}_2\text{O}_3$ .

If molybdenum is reaching the surface and being oxidized above 600°C., the oxide formed probably is evaporating, since  $\text{MoO}_3$  melts at 795°C.

On the basis of our results on this alloy indications are that failure would occur rather quickly in an oxidizing atmosphere at temperatures much in excess of 600°C.

#### HASTELLOY C

Hastelloy C contains the same percentage of iron (5 per cent) as Hastelloy B, the same quantity of molybdenum (20 per cent) and nickel (60 per cent) as Hastelloy A, and additions of 12–16 per cent chromium and 5 per cent tungsten. The addition of chromium should reduce the oxidation rate and permit this alloy to be used in oxidizing atmospheres at temperatures in excess of those possible with alloys A and B.

Figure 3 shows that the oxides observed on the surface are dependent primarily upon the temperature and to a lesser extent upon the time of oxidation. In the temperature range 300–500°C. an oxide of the spinel type ( $a = 8.43 \text{ \AA.}$ ) is observed. Several spinel-type oxides are possible: namely,  $\text{Fe}_3\text{O}_4$  ( $a = 8.42 \text{ \AA.}$ ),  $\text{NiO} \cdot \text{Fe}_2\text{O}_3$  ( $a = 8.34 \text{ \AA.}$ ), and  $\text{NiO} \cdot \text{Cr}_2\text{O}_3$  ( $a = 8.31 \text{ \AA.}$ ). Earlier work on Hipernik (9) and Nichromes (10) indicates that this oxide is probably iron oxide, although nickel and chromium may be present in solid solution.

At 600°C. and 700°C.  $\text{Cr}_2\text{O}_3$  is the only oxide observed on the surface, while at 800°C. and 900°C. a mixture of  $\text{Cr}_2\text{O}_3$  and  $\text{MoO}_2$  is observed for short oxidation times, followed by the appearance of an oxide of the spinel type ( $a = 8.35 \text{ \AA.}$ ) as the films become thicker. From a study of the Nichromes (10) it seems reasonable to assume that this spinel oxide is mainly  $\text{NiO} \cdot \text{Cr}_2\text{O}_3$ , since the 80 per cent nickel and 20 per cent chromium series of Nichromes shows the presence of  $\text{NiO} \cdot \text{Cr}_2\text{O}_3$  ( $a = 8.31 \text{ \AA.}$ ) above 800°C. when the amount of silicon present is 0.30 per cent or less.

On the basis of the oxides which are obtained above 600°C., one would predict that this alloy would be much better in oxidation resistance than alloys A and B above this temperature. The investigation of the Nichromes (10) indicates that the presence of about 1 per cent of silicon and small quantities (0.10 per cent or less) of zirconium, calcium, and aluminum stabilizes the oxide structure such that  $\text{Cr}_2\text{O}_3$  is the only oxide observed up to 1050°C. Unfortunately we do not have complete analyses on Hastelloy C. We have no information concerning the presence of trace elements. If trace elements, such as silicon, zirconium,

calcium, and aluminum are absent, the addition of the above elements to the alloy might improve its oxidation resistance and increase its lifetime at elevated temperatures in oxidizing atmospheres. Of course, it is possible that such addi-

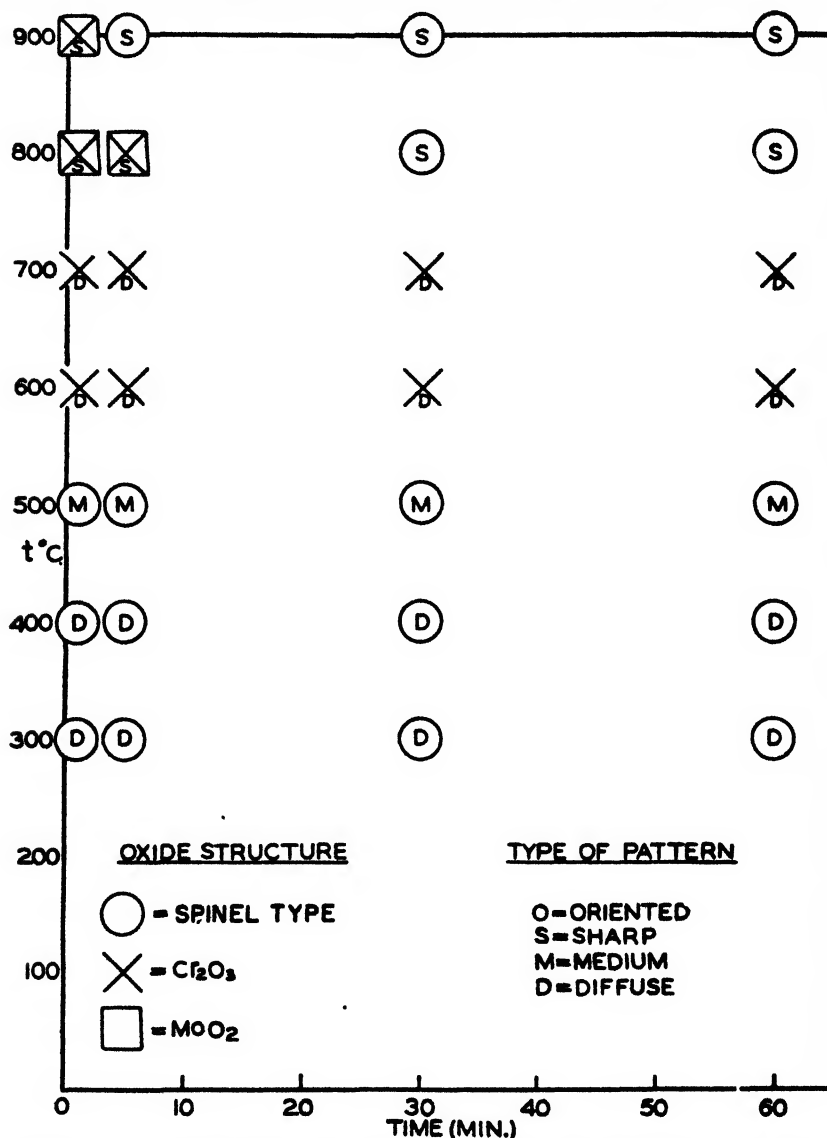


FIG. 3. Oxide films on Hastelloy C at 1 mm. oxygen for various times and temperatures. Oriented patterns would have deleterious effects on the high-temperature strength properties of the alloy.

#### HASTELLOY D

Hastelloy D consists primarily of nickel (85–90 per cent), silicon (10 per cent), and copper (3 per cent). An inspection of figure 4 shows that  $\text{Cu}_2\text{O}$  is observed

in the temperature range 300–600°C., while above 600°C. NiO occurs on the surface.

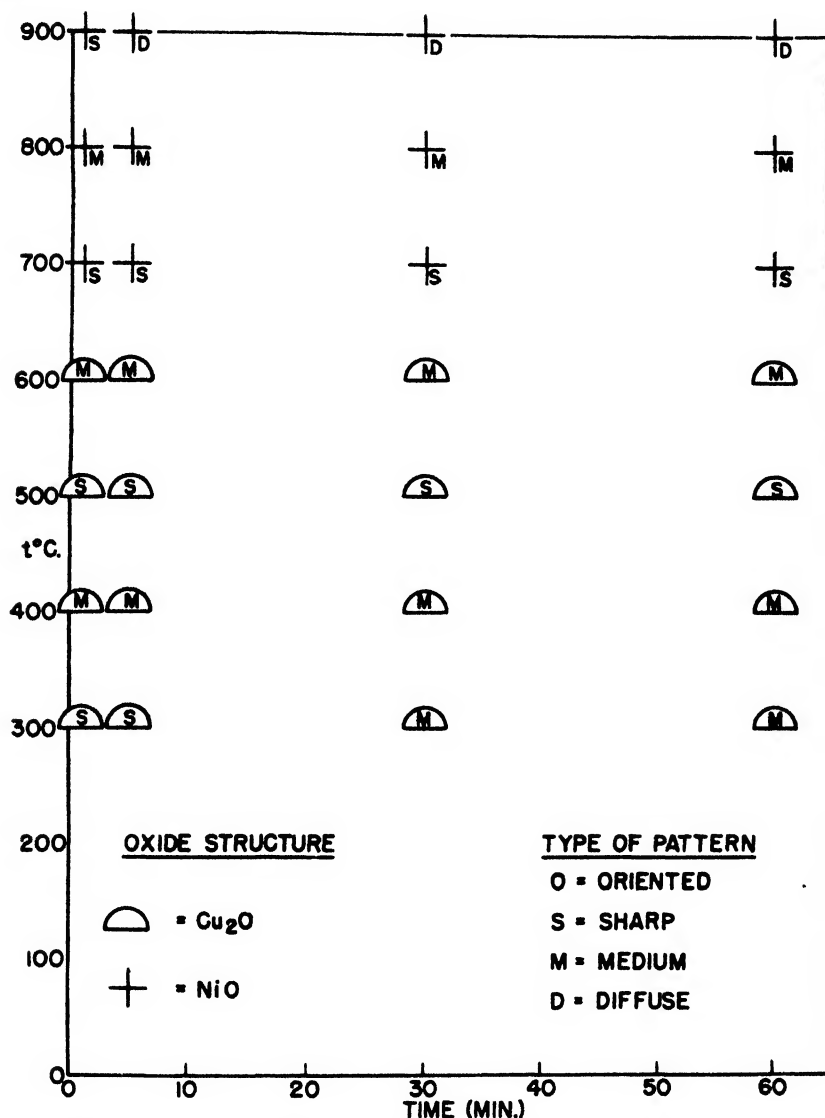


FIG. 4. Oxide films on Hastelloy D at 1 mm. oxygen for various times and temperatures

These results are in agreement with an earlier study (9) of alloys of copper and nickel. The rôle which silicon plays is not clear. It is evident, however, that no crystalline oxides of silicon are observed. If silicon does undergo oxidation, the oxide which forms is either amorphous and not identifiable by electron diffraction or it concentrates in contact with the metallic substrate and is not in diffracting position with the reflection technique. If the latter occurs, it is possible that

the presence of a silicon oxide film, either crystalline or amorphous, may hinder the passage of metallic ions to the surface and reduce the oxidation rate. This explanation has been given by the authors in a study of the Nichromes (10).

#### SUMMARY

The results of this investigation of thin oxide films formed on the Hastelloy alloys A, B, C, and D are presented as existence diagrams of the oxides on a time-temperature scale. The authors make no claims that the existence diagrams represent phase diagrams of the metal-oxygen systems. The diagrams, however, do represent graphically the results which should be obtained under identical experimental conditions.

Although Hastelloy A contains approximately 60 per cent nickel, NiO is not observed on its surface. This alloy is characterized by the presence of a spinel-type oxide which is probably  $\text{Fe}_3\text{O}_4$ . Hastelloy B, which contains approximately the same percentage of nickel, approximately twice the molybdenum, and one-fourth as much iron as Hastelloy A, oxidizes in a much more complicated manner. The reduction in the percentage of iron permits nickel ions to reach the surface and form NiO in the low-temperature region. Above  $500^\circ\text{C}$ . the oxidation pattern is quite complicated, with molybdenum and iron ions competing with each other to get to the surface. The appearance of NiO at  $800^\circ\text{C}$ . may be due to the fact that  $\text{MoO}_3$  may be evaporating from the surface, while at  $900^\circ\text{C}$ . the spinel oxide which forms probably contains both nickel and iron.

Even though Hastelloy C contains approximately the same quantities of nickel and molybdenum as Hastelloy A and roughly the same percentage of iron as Hastelloy B, it forms the same spinel oxide as Hastelloy A below  $500^\circ\text{C}$ . It would appear that the addition of chromium and the reduction in the quantity of molybdenum prevent the formation of NiO in the low-temperature region, as occurs on Hastelloy B. Above  $500^\circ\text{C}$ . chromium ions show great tendency to get to the surface, as evidenced by the appearance of  $\text{Cr}_2\text{O}_3$  at  $600^\circ\text{C}$ . and  $700^\circ\text{C}$ ., while at  $800^\circ\text{C}$ . and  $900^\circ\text{C}$ . the spinel oxide which forms is probably  $\text{NiO} \cdot \text{Cr}_2\text{O}_3$ . The oxidation resistance of this alloy may possibly be increased by the addition of a small quantity of silicon (1 per cent), which seems to have a tendency to stabilize  $\text{Cr}_2\text{O}_3$  on the surface.

Although Hastelloy D contains only a small percentage of copper,  $\text{Cu}_2\text{O}$  is dominant on the surface up to  $600^\circ\text{C}$ ., while above this temperature NiO is observed. No oxides of silicon are observed. It is possible, however, that silicon oxide may be in contact with the metallic substrate.

#### REFERENCES

- (1) BADGER, F. S., AND SWEENEY, W. O., JR.: Symposium on Materials for Gas Turbines, American Society for Testing Materials, 1946.
- (2) GULBRANSEN, E. A.: J. Applied Phys. **16**, 718 (1945).
- (3) GULBRANSEN, E. A.: Rev. Sci. Instruments **18**, 546 (1947).
- (4) GULBRANSEN, E. A., AND HICKMAN, J. W.: Metals Technol., A.I.M.E. (October, 1946, T.P. 2068).
- (5) *Hastelloy*, 6th edition. Haynes Stellite Company, Kokomo, Indiana.

- (6) HICKMAN, J. W., AND GULBRANSEN, E. A.: *Metals Technol.*, A.I.M.E. (October, 1946, T.P. 2069).
- (7) HICKMAN, J. W., AND GULBRANSEN, E. A.: *Metals Technol.*, A.I.M.E. (April, 1947, T.P. 2144).
- (8) HICKMAN, J. W., AND GULBRANSEN, E. A.: *The Electrochemical Society*, preprint 91-32 (April, 1947).
- (9) HICKMAN, J. W., AND GULBRANSEN, E. A.: In press.
- (10) HICKMAN, J. W., AND GULBRANSEN, E. A.: *Metals Technol.*, A.I.M.E. (June, 1948, T. P. 2372).
- (11) SWEENEY, W. O.: *Trans. Am. Soc. Mech. Engrs.* **69**, 569-80 (1947).
- (12) YAMAGUCHI, S.: *Chem. Abstracts* **41**, 5842 (1947).

## MOISTURE RELATIONSHIPS OF CELLULOSE. I

### THE HEAT OF WETTING IN WATER AND IN CERTAIN ORGANIC LIQUIDS

MAURICE WAHBA

*Department of Chemistry, Faculty of Science, Fouad I University, Cairo, Egypt*

*Received July 25, 1947*

#### I. INTRODUCTION

Few investigators have measured the heats of wetting of cellulosic materials in water and in other liquids.

Katz (8) measured the heat of imbibition of cellulose, woody fibres, and other gelatinous materials in water and found that the heat liberated depended on the degree of imbibition (the number of grams of water taken up by 1 g. of the swelling substance). He compared the results with the heat of mixing water with sulfuric acid, phosphoric acid, and glycerol. The similarity of the two kinds of systems led him to the conclusion that amorphous swelling substances differ from liquids only in viscosity.

Among his measurements of the heat of swelling (wetting) of some colloidal substances in water, Rosenbohm (17) obtained the following values (in calories per gram): 9.6 for fibre paper, 12.9 for pure cellulose, and 20.8 for cotton. Measurements of the heat of swelling of partially saturated gelatin led him to the conclusion that the swelling of gelatin takes place in two stages,—the first where a small amount of water is taken up and all the heat of wetting is liberated, and the second where a large amount of water is taken up with practically no heat evolved.

Measuring the heat of swelling of cellulose acetate in different mixtures of ethyl alcohol, benzene, and nitrobenzene, Knöevenagel (11) regarded his results as supporting a conception of definite (stoichiometric) solvate formation for the sorption of liquids by cellulose esters.

Sheppard and Newsome (18), on measuring the heats of wetting of an acetone-soluble cellulose acetate in some alcohols, benzene, and certain other liquids,

found no evidence of compound formation between solid and liquid. They observed that the time required to reach maximum temperature on immersing the solid in a liquid increased with the complexity of the molecules of the latter.

Argue and Maass (1) measured the heat of wetting of dry and partially saturated cellulose in water. They found that if the initial water content was left as a result of partial desorption, a higher value of the heat was obtained.

In all their determinations, these investigators measured the heat developed in a rather short time after immersion of the unevacuated solid in the wetting liquid. Since the rate of heat liberation varies with the cellulose-liquid system under investigation, the experimental results are rather dependent on the sensitivity of the calorimeter and upon the rate of heat liberation. Raw cotton, though it shows a sorption capacity for water nearly equal to that of "hydrophile" or medicated cotton, is very nearly unwettable. This is usually attributed to the presence of a film of wax on the exterior of the fibre cuticles. The angle of contact between water and the wax-covered fibres being large, air remains inside the cotton lump and on its surface, separating it from the water, a fact which leads to the "Masson effect." Masson (12) found that on immersing in water a lump of dry raw cotton wound round the bulb of a thermometer, the cotton rose in temperature several degrees in a few minutes and then cooled very slowly. Masson explained the large magnitude of this rise in temperature in terms of the heat of condensation of water distilled through the air film separating the cotton from the water.

In the present investigation, a device is therefore used in which the wetting liquid is allowed to rush into outgassed ampoules containing the dried cellulosic samples, whereby a quick contact between the solid and the liquid is assured without the interference of entrapped air. A main purpose of the investigation was to compare the heats of wetting so determined with the corresponding free-energy decrements at saturation, as computed by integration of the sorption isotherms.

## II. APPARATUS AND EXPERIMENTAL TECHNIQUE

The apparatus used in this investigation is similar to that of Razouk (15) for the determination of the heat of wetting of charcoal in some organic liquids. A diagram of the apparatus is shown in figure 1. Briefly, it is made up of a Dewar tube acting as a calorimeter. This is fitted with a cork through which pass a thermometer of the Beckmann type (graduated to  $0.002^{\circ}\text{C}.$ ), a heating manganin coil with a known resistance (about 4 ohms), and a shaft of a rotary paddle stirrer which acts also as a holder for the cellulose ampoule; the ampoule is fitted into the holder through a ground joint and is kept from falling by a light spring. A cylindrical glass jacket is fitted round the top of the Dewar tube in order to allow complete immersion of the calorimeter into a thermostat bath. The gearing wheel of the stirrer rests on a steel spring, so that the capillary tip of the cellulose ampoule may be broken to admit liquid by tapping the wheel.

On carrying out an experiment, about 1 g. of the cellulosic material (a new sample for each occasion) was introduced in the ampoule. The weight of dry



cellulose was obtained from a blank experiment.<sup>1</sup> The ampoule was then attached to an evacuation system through an S-shaped capillary, and outgassed at 65°C. for about 15 hr. After that time, when the pressure was less than  $10^{-6}$  mm., as shown by a McLeod gauge, the ampoule was sealed at its capillary

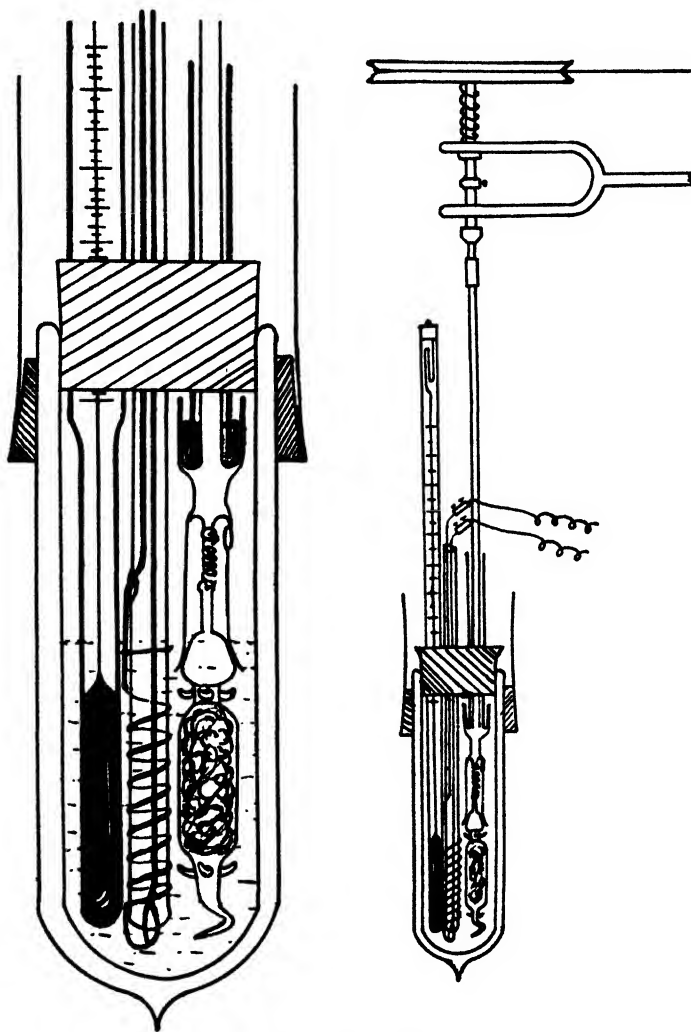


FIG. 1. The heat of wetting apparatus

end. The calorimeter was fitted up after introducing about 100 cc. of the wetting liquid, and then it was immersed in a thermostat regulated to within

<sup>1</sup> Several ampoules were filled at the same time with the same kind of cellulosic material and the weights of the samples determined. The cellulose in one of the ampoules was dried by outgassing for the usual time at the standard temperature. From the decrease in weight, the moisture content per gram of dry cellulose was known for all the samples.

0.01°C. When equilibrium was nearly attained the stirrer was pushed down slightly so as to break the capillary end of the cellulose ampoule under the wetting liquid. The rise in temperature was followed on the thermometer for at least 40 min. and then was corrected for cooling.

The heat capacity of the system was determined by measuring the temperature rise when a known quantity of electricity was passed through the heater coil, the potential difference across its ends being measured by the Poggendorff compensation method.

The heat of wetting was then calculated. A small correction (about 0.15 cal. as determined by a blank experiment) was applied owing to the dissipation, as heat, of the kinetic energy of the wetting liquid forced into the ampoule

### III. MATERIALS

*Raw cotton:* A sample of raw Egyptian cotton named "Giza 7" was kindly supplied by the Cotton Research Board, Cairo. This was immersed for 1 week in distilled water, renewed daily, in order to dissolve any soluble impurities. It was then dried in an air oven at about 70°C.

*Absorbent cotton:* A sample of that commonly sold under the name "Medicated Cotton" was used. This is believed to be raw Egyptian cotton that has been subjected to a bleaching process by means of soap solution and bleaching powder and then washed with water and dried. The commercial sample was again washed with distilled water for several days and then dried in the air oven at about 70°C.

*Standard cellulose:* A sample under that name, kindly supplied by the Shirley Institute, Didsbury, Manchester, was described as "cotton linters that had been submitted to a high pressure boil in caustic soda," and was stated to be a very pure cellulose.

*Viscose:* A sample of regenerated cellulose was also kindly supplied by the Shirley Institute. It was described as "Viscose rayon yarn, Courtauld's A quality, 150 denier." It was stated to contain a small quantity of oil and soap. It was therefore purified by steeping for 1 hr. in cold hydrochloric acid (about 0.1 *N*), washing with water, drying, and then extracting with ether.

*Water:* Conductivity water from a Hartley still was employed.

*Methyl alcohol, ethyl alcohol, acetone, and benzene:* These were samples of Kahlbaum's best quality. They were thoroughly dried and then fractionated several times.

### IV. RESULTS AND DISCUSSION

#### *A. The effect of drying temperature on the heat of wetting*

It has been shown by Urquhart and Williams (21) that the hygroscopicity of cotton decreases considerably on heating in a dry atmosphere, the effect being attributed (Urquhart (19)) to a rearrangement of the cellulose micelles with a consequent change in the availability of the hydroxyl groups. Knecht (10) has shown that when cotton is heated to about 80°C. for 336 hr. it gains distinct

reducing properties, and that when it is heated above 150°C. it suffers complete decomposition and the products are very complex. On evacuating either the standard cellulose or raw cotton used here at 100°C., a waxy material was found to be distilled; at 150°C. carbonization and distillation were rapid.

It was therefore necessary to measure the effect of drying temperature on the heat of wetting of cellulose. Experiments were carried out with raw cotton and with standard cellulose, samples of both of which were evacuated for 15 hr. at a series of temperatures ranging from 25°C. to 120°C. At and above 100°C. a waxy material was found to distil from both materials and condense in the cooler parts of the evacuation system. Since this product was obtained with standard cellulose as well as with raw cotton, and a side experiment showed that it was produced in very large quantity at 150°C., it cannot be identified as the cuticular material which renders the fibres of the natural cotton so nearly unwettable but must be regarded as a product of the thermal breakdown of cellulose itself.

TABLE 1

*Heats of wetting in water at 30°C. of raw cotton and standard cellulose dried at different temperatures for 15 hr.*

(Calories per gram of dry material\*)

CELLULOSIC MATERIAL	HEAT OF WETTING ON DRYING AT			
	25°C.	65°C.	100°C.	120°C.
Raw cotton....		12.3	12.2	12.1
Standard cellulose....	9.7	10.7	10.6	10.4

\* The weight of the dry material was obtained by drying at 65°C. on each occasion.

Table 1 shows the data for the heats of wetting in water of the samples dried *in vacuo* at four temperatures. As seen from this table, the heat of wetting did not vary appreciably with the drying temperature within the range 65–120°C., the time of outgassing being 15 hr. in every experiment. Although drying for 15 hr. at 25°C. resulted in the low value recorded in the table, more prolonged drying at this temperature was found to raise the heat of wetting to 10.5 cal. per gram, a value nearly equal to those obtained on drying at higher temperatures.

In the light of the above results it was made the practice to dry the samples for 15 hr. at 65°C., at which temperature good evacuation uncomplicated by thermal decomposition was ensured. Whilst evacuation for 8 hr. at this temperature gave a slightly reduced heat of wetting in water, prolonging evacuation to 20 hr. gave the same results as for 15 hr.

#### *B. The heats of wetting of some dried cellulosic materials in some common liquids*

The mean results of the experiments on the heats of wetting of raw cotton, absorbent cotton, standard cellulose, and viscose in water and some organic liquids are given in tables 2 and 3. The organic liquids chosen were those for which sorption data on cellulose were available.

## (1) The time required for complete wetting

The rate of the liberation of the heat of immersion (figure 2) seems to depend on the nature of the wetting liquid. Several investigators have found that for cellulose and charcoal the rate of heat liberation decreases with increasing complexity of the wetting molecules (7, 15, 18).

The time needed for the complete wetting of a solid in a liquid is also dependent on the nature of the solid as well as on the nature of the liquid; the chemical and the spacial structure of the two must be taken into consideration. For example, while methyl alcohol takes only 8 min. to evolve the apparent total heat of wetting

TABLE 2

*The heats of wetting of raw cotton, absorbent cotton, standard cellulose, and viscose in water at 30°C.*

CELLULOSIC MATERIAL	HEAT OF WETTING	TIME FOR APPARENT TOTAL HEAT
	<i>cal./gram</i>	<i>minutes</i>
Raw cotton. . . . .	12.3	Within 10
Absorbent cotton	10.0	Within 10
Standard cellulose. . . . .	10.7	Within 10
Viscose	20.3	Within 10

TABLE 3

*The heats of wetting of viscose and standard cellulose in certain liquids at 30°C.*

WETTING LIQUID	HEAT OF WETTING				$H_1/H_2$
	Viscose		Cellulose		
	$H_1$	Time	$H_2$	Time	
	<i>cal./gram</i>	<i>minutes</i>	<i>cal./gram</i>	<i>minutes</i>	
Water. . . . .	20.3	8	10.7	8	1.90
Methyl alcohol	(13.5)*	50	7.6	7	1.78
Acetone . . . . .	(2.6)	50	(1.5)	30	1.73
Benzene.....	1.5	10	0.8	6	1.88

\* Where the heat liberation was slow the values (in brackets) are less reliable on account of the difficulty of assessing the heat losses.

of cellulose or of charcoal, it takes over half an hour on the wetting of viscose. Again, whilst Razouk (15) found the heat of wetting of (non-activated) charcoal in benzene to take fully 30 min., the wetting of cellulose or viscose with the same liquid takes only 10 min. Water takes but a short while for the wetting of all three solids. There is clearly no close relation between the magnitude of the wetting energy and the rate at which it is liberated. The porosity of the solid and the volume of the molecules of the wetting liquid also have a deciding influence on the rate of energy release.

To sum up, three factors may be distinguished as controlling the rate of liberation of the heat of wetting: (1) the molecular volume of the wetting liquid,

(2) the pore restrictions of the adsorbent, and (3) the attractive forces between adsorbent and adsorbate.

It seems, moreover, that the factors which cause the vapors of different liquids to be sorbed in larger or smaller quantities affect in the same way the magnitude of the heat of wetting of the solid in the different liquids. Brimley (6) gives the percentage sorption values of some sorbates from the saturated vapors by

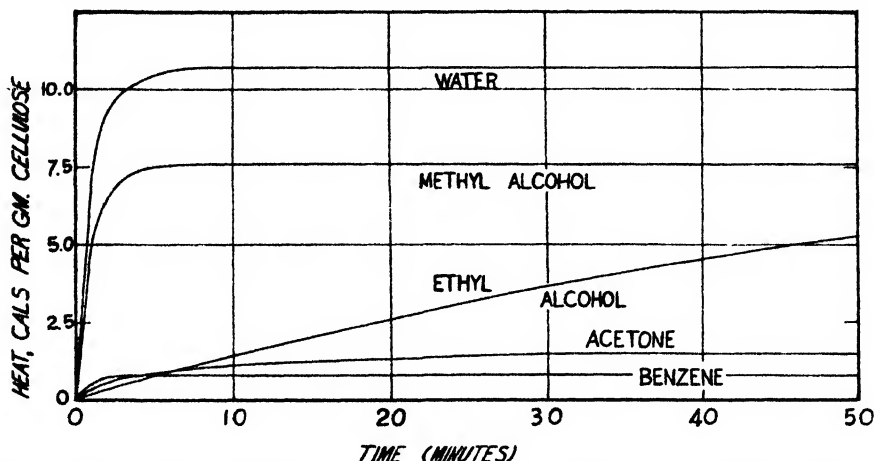


FIG. 2. The rate of evolution of the heat of wetting of cellulose in the different liquids

bleached cotton. For the sake of comparison some of these values are reproduced:

	per cent
Water	19 - 21
Ethyl alcohol	8.5 - 9
Acetone	6.4 - 7
Benzene	1 - 2

From table 3 and figure 2 it can be seen that the heat of wetting of standard cellulose in the above liquids decreases in the same order as the sorption values. One possibility to be borne in mind in this connection is that the wettable surface of cellulose is not constant with respect to the different wetting liquids. It is expected to be smaller the larger the molecules of the wetting liquid, and especially the smaller the tendency to penetrate into the cellulose pores. The higher values of the heat of wetting in certain cases may be partly due to a greater accessible surface and not only due to greater attractive forces between the solid and the liquid.

## (2) The ratio between the wettable surfaces of viscose and of cellulose

It has been noticed that the ratio of the heat of wetting of viscose to that of cellulose in water is 1.9, the same as the mean of the ratios between the sorption values of water vapor by the two adsorbents at different relative humidities.

(The sorption isotherms will be published elsewhere.) Table 3 shows that the ratio between the heats of wetting of viscose and of cellulose in the different liquids is practically constant. A similar result was previously found by Bartell and Almy (5) with different samples of silica gel. The results obtained here show that the wettable surface of viscose is nearly 1.9 times that of cellulose.

#### V. THE CALCULATION OF THE HEAT OF WETTING

The different theories put forward to explain the heat of wetting have been summarized by Razouk (15). The theory which is now well accepted is the one which explains the heat of wetting in terms of surface-energy changes. When 1 g. of a clean solid, with a surface area  $\Sigma$ , is immersed in a liquid, the solid-vacuum surface is replaced by an equal area of the interface solid-liquid (neglecting the small effect of swelling). This is accompanied by the evolution of a quantity of heat,  $(-\Delta H)_L$  calories per gram of solid, which represents the diminution of the heat content, or the total energy of wetting. That is given by the Gibbs-Helmholtz equation:

$$(-\Delta H)_L/\Sigma = F_L - T dF_L/dT \quad (1)$$

Bangham and Razouk (3) point out that  $F_L$  stands for the surface-energy lowering produced by immersion in the liquid, and is to be distinguished from  $F_v$ , the surface-energy lowering produced by exposure to the saturated vapor. The two are related to each other by the equation:

$$F_L = F_v + \gamma_{Lv} \cos \theta \quad (2)$$

where  $\gamma_{Lv}$  is the surface free energy of the liquid-vapor interface, and  $\theta$  is the wetting angle (angle of contact at equilibrium where the liquid-vapor interface meets the plane solid surface). Combining equations 1 and 2, Bangham and Razouk obtained:

$$(-\Delta H)_L = \Sigma \left( F_v - T \frac{dF_v}{dT} \right) + \Sigma \left( \gamma_{Lv} \cos \theta - T \frac{d\gamma_{Lv} \cos \theta}{dT} \right) \quad (3)$$

Now, supposing that we have a clean solid surface and a bulk liquid, there are two ways in which it can be imagined that the heat of immersional wetting can be developed: (1) by plunging the solid surface straight into the liquid, and (2) by allowing the vapor to distil from the liquid and be adsorbed on the solid surface until the latter becomes saturated, and then the solid with its saturated film is immersed into the liquid. According to the first law of thermodynamics, the energy released will be the same whichever way we proceed. In the second way, heat of evaporation will be absorbed at the liquid surface and a correspondingly greater amount released at the solid surface. When immersion afterwards takes place, the net effect is the algebraic sum of the two plus a heat term due to the immersional wetting of the saturated solid surface, a term which may be different from zero.

Equation 3 represents this equality of the energy released in the two paths. According to Bangham and Razouk, "the expression within the first bracket

represents the heat evolved by the formation *from the liquid* of an adsorbed film in equilibrium with the saturated vapor; it is less than the total heat of adsorption by an amount equal to the normal heat of condensation of just sufficient vapor to form the film." Let this expression be called  $(-\Delta H)_s$ . "The expression within the second bracket represents the heat generated when the surface, already saturated, is plunged into the liquid." It will be noted that equation 3, which was derived for a plane surface, would not be valid if the adsorbing surface were greater than the area of the film-vapor interface which the saturated solid presents to the wetting liquid, i.e., if the pores of the solid became largely filled up by adsorption from the vapor phase.

Bangham (2) has shown that the product  $(F_s \times \Sigma)$ , where  $\Sigma$  is the adsorbing surface per gram, can be evaluated by the integration of the Gibbs adsorption equation, if the adsorption in grams per gram is known as a function of the pressure  $p$ . Writing  $S$  for the adsorption in grams per gram of dry cellulose and  $M$  for the molecular weight of the adsorbate, we have:

$$F_s \Sigma = \frac{RT}{M} \int_{p=0}^{p=p_0} S \cdot d \ln p \quad (4)$$

$P_0$  being the saturation vapor pressure of the normal liquid at the temperature  $T$ .

Two *adsorption* isotherms at 25°C. and 35°C. have been determined for the taking up of water vapor by the raw cotton described above. The amount adsorbed,  $S$ , is plotted against  $\log p/P_0$  in figure 3.

The areas under the  $S$ - $\log p/P_0$  graphs were measured; the value of the integral being indefinite when  $p$  approached zero, Henry's law was assumed to be valid for the very early stages of adsorption. Such area measurements gave, for the free energy of saturation  $(F_s \Sigma)$ , the values: 5.47 cal. per gram of cotton at 25°C. and 5.23 cal. per gram of cotton at 35°C. Hence, between 25°C. and 35°C.,

$$d(F_s \Sigma)/dT = -0.024 \text{ cal. per degree}$$

The value of  $(F_s \Sigma)$  at 30°C. may be taken without a serious error as the mean of the values at 25°C. and 35°C.; it thus equals 5.35 cal. per gram of cotton. The heat of saturation of 1 g. of cotton at 30°C. will then equal

$$5.35 - (-303 \times 0.024) = 12.6 \text{ cal. per gram of cotton}$$

This value, whilst subject to an appreciable error arising from the evaluation of the integrals, is very nearly equal to the full heat of wetting of dry raw cotton in water as obtained calorimetrically, 12.3 cal. per gram (table 2).

The heat of the immersional wetting of the vapor-saturated standard cellulose was also measured calorimetrically. The outgassed cellulose was exposed to saturated water vapor at 30°C. (in a thermostat) for 3 days and then immersed in the liquid at the same temperature in the heat of wetting apparatus described above. Very little heat was liberated, only about 0.3 cal. per gram of cellulose.

Referring to equation 3, then, it appears that for the cellulose-water system the term  $\Sigma(\gamma_{Ls} \cos \theta - T d\gamma_{Ls} \cos \theta/dT)$  approximates to zero. The most probable explanation is that the area of film-water interface which the system

presents to the wetting liquid on immersion is relatively small, i.e., of a smaller order of magnitude than the adsorbing surface. This would be the case, for example, if much of the adsorption took place in cavities of molecular dimensions. On the other hand, that the adsorbing surface area per unit weight of cellulose has a definite meaning and significance is suggested by the nearly constant ratio of the heats of wetting of viscose and standard cellulose in the different liquids investigated.

The fact that very little heat is disengaged when an adsorbent, already exposed to saturated vapor, is plunged into the liquid has also been found by other investigators as with silica gel (Parks (13); Ray and Ganguli (14)), animal charcoal (Katz (9)), and unactivated wood charcoal (Razouk (16)). In this last case, however, with methyl alcohol as wetting liquid, Bangham and Razouk (4) found

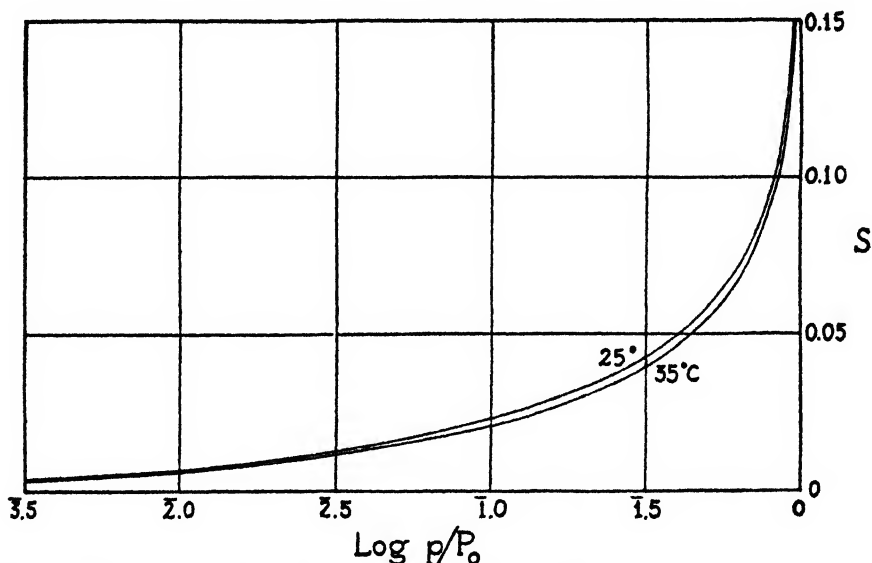


FIG. 3. The adsorption isotherms at 25°C. and 35°C. of water vapor by raw cotton

a disparity between  $(-\Delta H)_L$  and  $(-\Delta H)_I$ , which exceeded the experimental error. They attribute this to the wetting (on immersion) of an already saturated film of area equal (or nearly equal) to the adsorbing surface. Razouk (16) suggests that any heat developed by wetting the already saturated charcoal is liberated too slowly to be measured by the experimental technique used, the rate of penetration of the liquid even into the gross pores of the charcoal being but slow under these circumstances.

In reaching the tentative conclusion that for the cellulose-water system the heats of saturation and of immersional wetting are equal or nearly equal, certain limitations of the experimental methods used must be recognized. The integration of the isotherms from zero pressure up to saturation is attended by considerable difficulty, and there is the superimposed error of calculating the temperature coefficient of the saturation free-energy change. Further uncertainty



arises from the existence of two branches to the isotherms, one for adsorption and the other for desorption; from the data of Urquhart and Williams (20) for soda-boiled cotton at 20°C. ( $\Sigma F_s$ ) evaluated from the desorption isotherm is 5.58 cal. per gram of cotton as compared with 4.92 calculated from the adsorption branch ( $\Sigma F_s$ ) is evaluated here from the adsorption branch). The thermodynamic equations are of course strictly valid only when the same equilibrium is attained from either side. Finally, the liberation of the heat of wetting in the calorimetric experiment is sufficiently slow to render accurate calorimetry difficult.

One good reason, which would cause a difference between the calculated and measured values of the heat of wetting, is that the liberation of heat does not take place under thermodynamical equilibrium conditions. The actual wetting may involve, for the formation of a liquid layer in equilibrium with the solid surface, a process of orientation of the molecules of the liquid adjacent to the solid, a process which may be accompanied by energy changes that would be difficult to calculate theoretically from equilibrium sorption data.

The estimation of the angle of contact from such data unfortunately involves also too fine an issue on the experimental side, both in the accurate measurement of slow heat liberations and in the accurate determination (and interpretation) of the isotherm.

#### VI. SUMMARY

The heats of wetting of dried samples of raw cotton, medicated cotton, standard cellulose, and viscose in water were measured by a calorimeter in which the outgassed samples were directly immersed in the liquid without exposure to air. The effect of drying temperature on the heat of wetting was examined. The heats of wetting of viscose and of cellulose were also measured in each of the liquids methyl alcohol, acetone, and benzene. The rate of heat evolution seemed to depend on the pore size of the solid, the complexity of the molecules of the liquid, and the attractive forces between the solid and the liquid. The heats of wetting of cellulose in the different liquids changed in the same order as the adsorption values from the vapors of the liquids. The ratio between the heats of wetting of viscose and cellulose in any of the different liquids was nearly constant and equal to the ratio between the sorption values of water vapor by the two adsorbents. For the cellulose-water system the heat of immersionsal wetting is shown to be equal, within experimental error, to the heat of saturation as calculated from the free energy of saturation and its temperature coefficient.

The author wishes to express his gratitude to Dr. D. H. Bangham for his constant interest and advice during this investigation.

#### REFERENCES

- (1) ARGUE AND MAASS: *Can. J. Research* **12**, 564 (1935).
- (2) BANGHAM: *Trans. Faraday Soc.* **33**, 805 (1937).
- (3) BANGHAM AND RAZOUK: *Trans. Faraday Soc.* **33**, 1459 (1937).

- (4) BANGHAM AND RAZOUK: *Proc. Roy. Soc. (London)* **A166**, 572 (1938).
- (5) BARTELL AND ALMY: *J. Phys. Chem.* **36**, 985 (1932).
- (6) BRIMLEY: *Nature* **114**, 432 (1924).
- (7) ILIIN AND KISSELEW: *Kolloid-Z.* **66**, 28 (1934).
- (8) KATZ: *Proc. Acad. Sci. Amsterdam* **13**, 958, 975 (1911).
- (9) KATZ: *Proc. Acad. Sci. Amsterdam* **26**, 549 (1923).
- (10) KNECHT: *J. Soc. Dyers Colourists* **36**, 195 (1920).
- (11) KNÖEVENAGEL: *Kolloidchem. Beihefte* **16**, 180 (1922); **17**, 51 (1922).
- (12) MASSON: *Proc. Roy. Soc. (London)* **A74**, 230 (1904).
- (13) PARKS: *Phil. Mag.* **5**, 517 (1903).
- (14) RAY AND GANGULI: *Trans. Faraday Soc.* **30**, 2 (1934).
- (15) RAZOUK: *J. Phys. Chem.* **45**, 179 (1941).
- (16) RAZOUK: *J. Phys. Chem.* **45**, 190 (1941).
- (17) ROSENBOHM: *Kolloidchem. Beihefte* **6**, 177 (1914).
- (18) SHEPPARD AND NEWSOME: *J. Phys. Chem.* **37**, 389 (1933).
- (19) URQUHART: *J. Textile Inst.* **20**, 125 (1929).
- (20) URQUHART AND WILLIAMS: *J. Textile Inst.* **15**, 138T (1924).
- (21) URQUHART AND WILLIAMS: *J. Textile Inst.* **15**, 550T (1924).

## THE ADSORPTION OF WATER VAPOR ON GLASS SURFACES

RASHAD I. RAZOUK AND AHMED S. SALEM

*Department of Chemistry, Faculty of Science, Fouad I University, Cairo, Egypt*

*Received December 15, 1947*

### I. INTRODUCTION

The adsorption of water vapor on the surface of glass has been extensively studied. As early as 1830, Faraday (11) pointed out the large adsorptive capacity of glass and traced this to the presence of alkali, which would cause deposition of water owing to the lowering of its vapor pressure brought about by dissolution of the alkali. Warburg and Ihmori (1886) (35) confirmed this view and showed that if glass were coated with silica and freed from alkali by boiling with water, no appreciable adsorption occurred below 0.95 relative humidity.

Bunsen in 1885 (8) realized the importance of heating glass apparatus before using it in quantitative work with gases, in order to free it from adsorbed water. He estimated the thickness of the film on glass wool by passing through the latter a stream of highly desiccated air: it varied from 1052 Å. for a sample at 23°C. to 42 Å. for one heated to 468°C., whilst all water was removed by heating to 503°C. Uptakes of similar magnitudes were reported by Parks in 1903 (28). Thus, glass wool exposed to saturated water vapor adsorbed a film 1330 Å. thick; the appearance of the glass was unchanged, but it gave zero heat of wetting when dropped into liquid water. In 1920 Menzies (27) obtained films of the same order of thickness—varying between 400 and 4000 molecular layers—when he passed air saturated with water vapor through glass wool.

Trouton (1907) (34) found that when glass wool was dried in a vacuum at

160°C. for 70 hr. over phosphorus pentoxide, it adsorbed water vapor with greater difficulty than when it was less thoroughly dried, owing to the presence in the latter case of water nuclei which would initiate the adsorption process.

Langmuir in 1916 (25) noticed the slow rate at which relatively large quantities of water vapor were given off when glass was heated, and the length of time required for its readsorption. Thus an incandescent lamp bulb heated for several hours at 500°C., after being exhausted and dried at room temperature, gave up water vapor corresponding to 55 molecular layers. He concluded that the water had penetrated to a considerable depth into the glass, essentially by a process of solution. Later, he found that when glass was cleaned by heating it with chromic acid solution and washing with water, the water given up on heating to 300°C. corresponded to 4.5 molecular layers.

D'Huart (1925) (21) estimated the thickness of the film of water which remained adhering to glass after evacuation at room temperature in the presence of phosphorus pentoxide as three molecular layers. Similar results were obtained by Bent and Lesnick (1935) (5), using a rather different technique. The color change which resulted from the reaction of an ether solution of sodium triphenylmethyl with water was used to determine the water left adsorbed on acid-washed glass after evacuation; a thickness of five molecular layers was thus found on the glass at room temperature and of two molecular layers at 304°C.

McHaffie and Lenher (1925) (26) originated a method for measuring the thickness of adsorbed layers on plane glass surfaces in the neighborhood of saturation. They concluded that very slight adsorption of water vapor took place below 60 per cent relative vapor pressure (apart, probably, from a monomolecular layer) but that the thickness of the layer rapidly increased thereafter and reached about 200 molecular layers just below saturation.

The work was followed up by Frazer, Patrick, and Smith (1927) (13), using freshly blown surfaces of glass. Very small adsorption was observed, but the action of liquid water and cleaning agents was found to increase the uptake markedly. They showed that both water and cleaning agents had a corrosive action on glass, destroying its planeness and in fact conferring on it a gel-like structure.

Using a sensitive microbalance, Strömberg (1928) (33) obtained results similar to those of McHaffie and Lenher: very small adsorption at low pressures and a film of 250 molecular layers near saturation. He also recorded the presence of hysteresis effects.

Herzfeld and Frazer (1928) (20) investigated the problem by optical methods and came to the conclusion that no appreciable adsorption of water vapor took place with relative pressures less than 0.30, and that even near saturation the film was less than one molecule thick.

Using similar optical methods, Frazer (1929) (14) found that up to 0.30 relative vapor pressure, the adsorption of water vapor on freshly cracked glass was confined to a monomolecular layer which could be removed completely by evacuation. Beyond this pressure a cluster formation occurred and this resulted in gradual covering of the surface, until at about 0.70 relative pressure a second

molecular layer was completed. At higher pressures more extensive condensation took place, and at 0.90 relative pressure the adsorbed film was eight molecules thick.

Some workers have reported appreciable adsorption at quite low pressures, however; for example, Frank (1929) (12) found, using Pyrex glass tubes cleaned with boiling chromic acid solution, that the adsorption amounted to a film two molecules thick even at a relative pressure of only 0.005. Similar results were obtained by Barrett and Gauger (1933) (4): *viz.*, one molecule thick at 0.003 and four molecules thick at 0.03 relative pressures. In both cases the adsorption was found to obey approximately the Freundlich isotherm.

Recently, Iitterbeek and Vereycken (1941) (22) have shown that above 180°C. no adsorption of water on glass occurred. At lower temperatures the isotherm possessed an inflection point at a place corresponding to the formation of a second molecular layer; and the geometric surface of the glass plates used agreed satisfactorily with the area calculated from adsorption values of water and other vapors.

It is clear from this brief survey that there are wide differences of opinion as to the extent of the adsorption of water vapor on glass: estimates of the thickness of the adsorbed film near saturation vary from a few molecular layers to several hundreds. This disagreement is not surprising in view of certain facts. In the first place, the thickness of the adsorbed film was estimated in all cases, except where optical methods were used, on the basis of the apparent surface, and this may frequently have amounted to only a small fraction of the real surface,<sup>1</sup> for glass is highly sensitive to the attack of cleaning agents and even to water itself. In the second place, the use of different kinds of glass of unspecified composition renders comparison between the results of different workers very difficult. Finally, the experimental difficulties associated with the measurement of adsorption on small surfaces of few square meters in area have caused most investigations to be limited to one end or the other of the adsorption isotherm, and few have attempted to cover the whole pressure range from near zero to near saturation.

In the present work an attempt has been made to meet some of these deficiencies. The adsorption of water vapor has been measured over a wide range of relative pressure on glass samples of the same and known composition. The glass has been made into fibres, powder, and microspheres and treated in a number of different ways, some of which might be expected to change the surface area scarcely above the apparent surface, while others would give extensive increase.

## II. APPARATUS AND TECHNIQUE

The apparatus used in the present investigation resembles that of Bangham and Mosallam (2) and is shown in figure 1. The essential point in devising

<sup>1</sup> J. L. Shereshefsky and C. E. Wier (J. Am. Chem. Soc. **58**, 2022 (1936)) found that the surface of glass balls as determined from the adsorption of methylene blue was approximately 55 times the geometric surface.

this apparatus is to avoid the use of stopcocks (and tap grease) by replacing them with mercury cut-outs.

It comprised a supply system BAB', a calibrated gas buret C, a pressure gauge DD', an adsorption bulb E, three mercury cut-outs F<sub>1</sub> F<sub>2</sub> F<sub>3</sub>, a McLeod gauge reading to  $5 \times 10^{-6}$  mm. of mercury, and a train of phosphorus pentoxide tubes leading to a mercury diffusion pump coupled with a Cenco-Hyvac high-vacuum oil pump.

The gas buret, the manometer, the adsorption vessel, and the two cut-outs

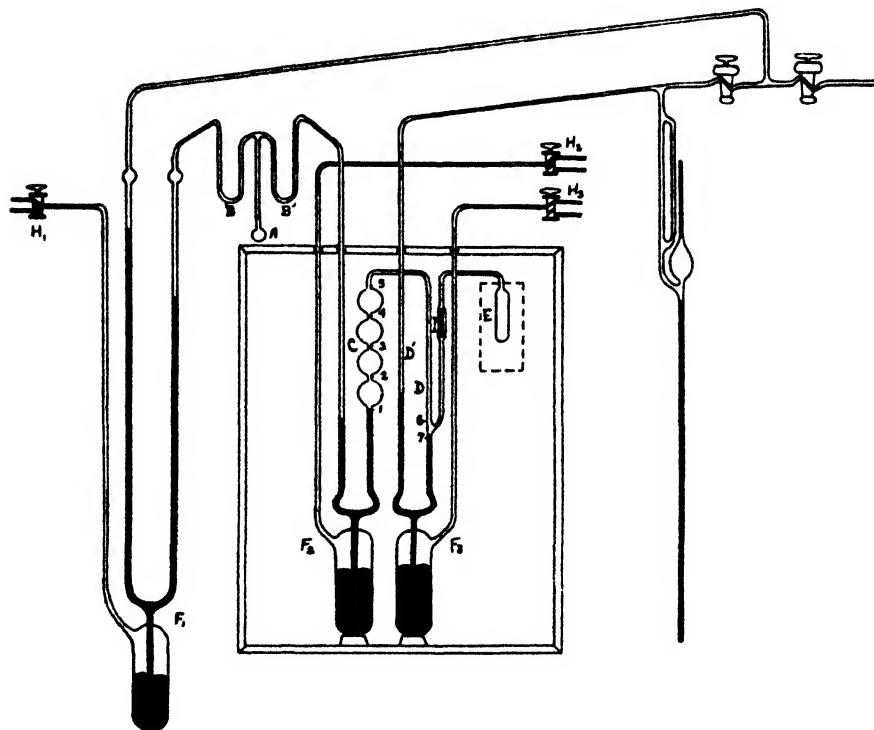


FIG. 1. The apparatus

F<sub>2</sub> and F<sub>3</sub> were all immersed in a thermostat kept at a temperature constant to within 0.01°C. The mercury in the three cut-outs was raised or lowered by means of pressure or vacuum applied to reservoirs through the three-way taps H<sub>1</sub> H<sub>2</sub> H<sub>3</sub>.

The dead space of the adsorption bulb and connecting tubes was determined by introducing a suitable volume of very dry purified nitrogen into the system and then setting the thermostat at the required temperature. By means of taps H<sub>2</sub> and H<sub>3</sub> the mercury was set at marks 1 and 7 on the buret and manometer, respectively, and the pressure of nitrogen taken while the limb D' of the manometer was under vacuum. The mercury in the gas buret was next raised to marks 2, 3, 4, and 5 and the corresponding pressures determined after readjust-

ing the mercury surface in the manometer to mark 7 each time. The volume of the dead space was calculated from these pressures and the known volumes of the four bulbs of the gas buret. The procedure was then repeated with the mercury in the manometer raised to mark 6, when the volume of connecting tubes between marks 5 and 6 could be determined in a similar way.

At the beginning of an experiment the adsorbent was evacuated *in situ* at the required temperature. For this purpose the thermostat was emptied of water and heat was applied to the adsorption bulb by means of a small, nichrome-wound, tubular electric heater, the temperature of which could be readily controlled.

In carrying out a run, the adsorbate was first freed from dissolved gases by its vacuum sublimation from one of the U-tubes BB' to the other, which was kept immersed in a mixture of carbon dioxide snow and acetone. A suitable volume of the vapor of the adsorbate was then introduced into the measuring system and imprisoned between marks 1 and 6 on the gas buret and manometer, respectively, and its pressure recorded. The vapor was next admitted to the adsorption bulb containing the pre-outgassed adsorbent by lowering the mercury in the manometer from mark 6 to mark 7. Any rush of mercury taking place was stopped by means of the float valve I from reaching the adsorption bulb. After the lapse of sufficient time (usually 24 hr.) the equilibrium pressure was recorded and the mercury in the buret raised to position 2. The procedure was repeated by raising the mercury to marks 3, 4, and 5, and finally the mercury in the manometer was raised to position 6 and the pressure of the residual vapor was determined before the introduction of a fresh supply of the adsorbate. The amount adsorbed was then calculated from the expression  $273\Delta pv/T \times 760 \times m$ , where  $\Delta pv$  is the change in the product of the pressure  $p$  (millimeters of mercury) and the volume of the system  $v$  (cubic centimeters),  $T$  is the temperature of the experiment ( $^{\circ}\text{K}.$ ), and  $m$  is the amount of adsorbent (grams). Table 1 illustrates the calculation of a typical run.

All pressure measurements were taken by means of a cathetometer reading to 0.02 mm. and were corrected for mercury depression and temperature.

A further correction was applied to the measured pressures in order to account for the deviation of water vapor from the laws of a perfect gas. From the data compiled by Dorsey (9) the best values for the relative departure of the specific volume of saturated water vapor from the ideal volume are 0.188 per cent, 0.236 per cent, and 0.306 per cent at 20°, 30°, and 40°C., respectively. On the basis that the deviation of  $pv$  from the theoretical value is proportional to the pressure (10), the correction which must be added to a measured pressure  $p$  (millimeters of mercury) is  $10.7 \times 10^{-5} p^2$ ,  $8.9 \times 10^{-5} p^2$ ,  $7.4 \times 10^{-5} p^2$ , and  $6.4 \times 10^{-5} p^2$  at 20°, 25°, 30°, and 35°C., respectively. Thus the correction at 35°C. is 0.11 mm. at saturation pressure (42.175 mm.) and 0.03 mm. at 0.50 relative pressure. Table 1 shows the experimental data of a run on glass microspheres and gives the amount adsorbed calculated with and without the latter correction. In most cases, however, this correction is very small.

No correction was made for the adsorption of water vapor on the walls of the

system, for blank experiments were not sensitive enough to estimate it, while experiments in which the amount of adsorbent was varied as much as fourfold showed the same degree of closeness as consecutive experiments on the same sample, so that the walls have no appreciable effect on the calculated adsorption. This is illustrated in table 2. In all cases the inner surface area of the adsorption bulb, which was heated with the adsorbent at 200°C., was always a small fraction of the area of the latter (1-2 per cent), while the whole surface of the system was kept at a minimum.

TABLE 1

*Adsorption of water vapor on glass microspheres at 35°C.*  
Mass of glass = 12.362; apparent surface area = 6329 cm.<sup>2</sup>  
(Figure 5, Curve I)

POSITION OF MERCURY IN BURET AND MANOMETER	VOLUME OF SYSTEM	PRESSURE (a, ADMITTANCE r, RESIDUAL)	PRESSURE (EQUILIBRIUM)	$\Delta p$ (UNCORRECTED)	$\Delta p$ (CORRECTED)	AMOUNT ADSORBED
	cc.	mm. Hg	mm. Hg			cc./gram
1, 6	128.8	a, 8.32				
1, 7	184.6		3.13	494	494	0.047
5, 7	61.1		5.72	723	723	0.068
5, 6	5.2	r, 6.53				
1, 6	128.8	a, 14.18				
1, 7	184.6		10.64	901	900	0.085
3, 7	117.9		15.27	1064	1064	0.100
4, 7	87.2		19.16	1195	1194	0.113
5, 7	61.1		24.33	1379	1378	0.130
5, 6	5.2	r, 27.65				
1, 6	128.8	a, 33.05				
1, 7	184.6		28.27	1760	1761	0.166
2, 7	152.3		31.02	2254	2255	0.213
3, 7	117.9		34.15	2951	2953	0.279
4, 7	87.2		36.79	3770	3772	0.356
5, 7	61.1		38.65	4617	4621	0.436

### III. MATERIALS

The glass wool used in the present work was from Schering-Kahlbaum (described as lead-free, purified by acid). Analysis gave the following composition:

	per cent		per cent		per cent		per cent
SiO <sub>2</sub> ...	70.9	Na <sub>2</sub> O...	12.9	MgO...	0.18	Al <sub>2</sub> O <sub>3</sub> ...	3.3
B <sub>2</sub> O <sub>3</sub> ...	8.0	K <sub>2</sub> O...	1.6	CaO...	0.5	Fe <sub>2</sub> O <sub>3</sub> ...	0.25
				BaO...	0.23		

The density of the gas-free glass wool was determined by a special pycnometric method permitting the outgassing of the glass in the pycnometer and filling the latter with gas-free water without exposing the glass to air. The density was

found to be 2.406 g./cc., in very good agreement with the calculated value 2.401 based on the density factors assigned by Winkelmann and Schott (36) to the different oxides composing the glass.

The geometric surface of the glass wool was determined by measuring the diameters of 100 fibres from their microphotographs (with magnification = 376). The distribution curve of these diameters is shown in figure 3a and the area was estimated to be 714 cm.<sup>2</sup>/g.

The glass wool was washed with water or with acid under specified conditions mentioned in the text.

The *glass powder* was prepared from the untreated glass wool by grinding it in an agate mortar. Only the fraction which passed twice through a sieve 325 meshes to the inch was used. It was washed a few times with distilled water.

The *glass microspheres* were prepared by a method similar to that first described by Sollner (32) and later by Bloomquist and Clark (6) and others.

Thoroughly dried glass powder, prepared as described above, was carried by a mixture of air and oxygen to a specially constructed Butagas burner. The powder melted in the flame and assumed a perfect spherical form free from strain. The glass microspheres were gathered in a big tray filled with water, against the surface of which the flame was directed. Great care was taken to ensure a steady, slow flow of the powder, as otherwise some balls tended to stick together. The process was repeated several times until microscopic investigation indicated almost complete conversion of the powder into spheres.

In order to get rid of the remaining very rare unspherical particles and also to obtain a fraction of glass balls having nearly the same diameter, the microspheres were subjected to repeated elutriation, using water. In this way it was possible to obtain a sample containing 100 per cent spheres, the diameter of 94 per cent of which varied between 0.042 and 0.058 mm. The distribution curve of the diameters of 300 microspheres measured from microphotographs is shown in figure 5a and the geometric surface was estimated as 512 cm.<sup>2</sup>/g.

The *water* used was conductivity water freshly prepared from a Hartley still.

The *methyl alcohol* was prepared from Schering-Kahlbaum's acetone-free methyl alcohol by refluxing it over freshly ignited quicklime for several hours. The fraction used boiled at 64.8°C. under 761 mm. of mercury.

#### IV. RESULTS AND DISCUSSION

##### *Outgassing temperature*

In order to choose an appropriate outgassing temperature, the adsorption isotherms of water vapor were determined on a sample of glass wool evacuated at 25°, 100°, 200°, and 300°C. for a period of 15 hr. in each case. The results of the experiments in the first three cases are shown in curves I, II, and III of figure 2, in which the abscissa represents the relative vapor pressure,  $p/p_0$ , and the ordinate the volume adsorbed,  $v$ , expressed in cubic centimeters (S.T.P.) per gram of glass wool.

It is evident that as the outgassing temperature is raised the glass surface



becomes cleaner, so that the adsorbed quantities increase for the same relative pressure. However, outgassing at 300°C. did not result in raising the adsorbed quantities, but rather led to values which did not show the close reproducibility met with in the other cases. It was also found that outgassing for a period longer than 15 hr. did not alter the isotherm. It was concluded, then, that outgassing at 200°C. for 15 hr. was most suitable.

This observation is in close agreement with the result of Iitterbeek and Verweycken (22) that no water is adsorbed on glass above 180°C. Sherwood (31) found also that for the removal of adsorbed gaseous products from the surface of glass, heating at 200°C. was practically as effective as at higher temperatures, especially in the case of soda glass. Above 200°C. there was a continual evolution of gases and vapors which were considered as decomposition products from

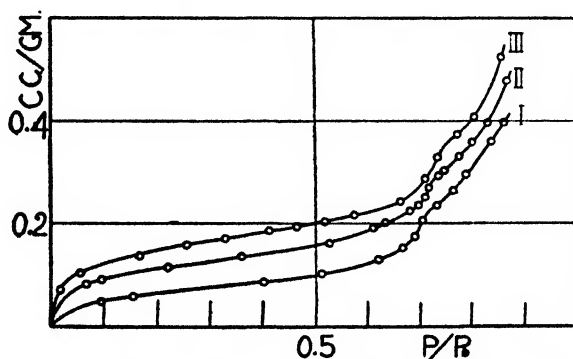


Fig. 2. Effect of outgassing temperature on adsorption isotherms of water vapor on glass wool at 25°C: Curve I, glass outgassed at 25°C.; curve II, glass outgassed at 100°C.; curve III, glass outgassed at 200°C.

the glass itself. Similar observations have been made by Harris and Schumacher (19) and others.

#### *Glass wool*

The results of experiments on glass wool treated in various ways are shown in figure 3. In general the isotherms are all of the usual sigmoid type, except for the fact that with water-washed samples there seems to be another point of inflection between 0.70 and 0.80 relative pressure (curves I, II, and III). It was also noticed that this range of sorption was a region of instability, for whereas it was possible to reproduce closely the isotherms before and after this region, the degree of reproducibility here was lower.

At low pressures the isotherm is concave to the pressure axis and, passing through an inflection point usually about 0.30 to 0.40 relative pressure, it becomes convex at higher pressures, rising rapidly in the neighborhood of 0.60 to 0.70 relative pressure. Then somewhere between 0.70 and 0.80 relative pressure the isotherm changes direction abruptly, becoming slightly less steep and finally rising again near saturation pressure.

The presence of a similar phenomenon was observed by Trouton (34), who found that the adsorption of water vapor on glass wool, dried in *vacuo* at 160°C. by exposing it to phosphorus pentoxide for 70 hr., appeared to pass through a

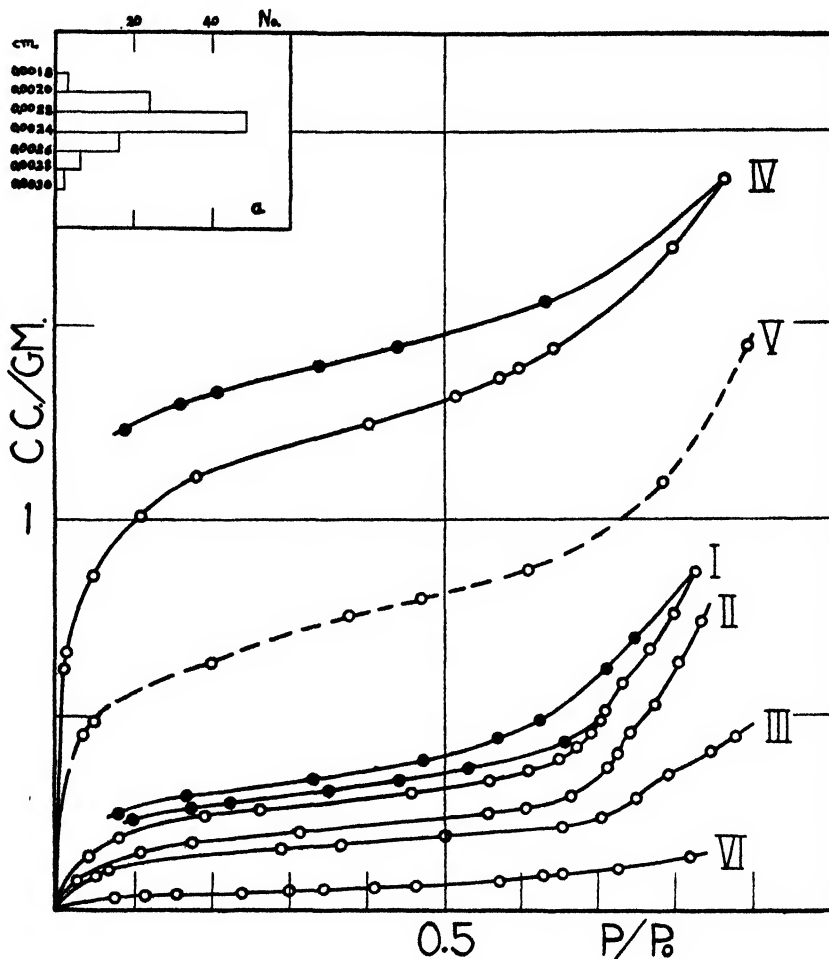


FIG. 3. Adsorption isotherms of water and methyl alcohol vapors on glass wool at 30°C. Solid symbols are desorption points. Curve I, water on glass washed with water for half an hour; curve II, water on glass washed for a few hours; curve III, water on glass washed for 6 days; curve IV, water on glass treated with a constant-boiling mixture of hydrochloric acid; curve V, water on acid-treated glass pre-outgassed at 30°C.; curve VI, methyl alcohol on water-washed glass.

FIG. 3a. Distribution of diameters of 100 fibres: abscissa, number of fibers; ordinate, diameters.

stage of supersaturation. Thus in the neighborhood of 0.50 relative pressure, a rapid adsorption took place with no change of pressure or even with a slight diminution; and then the adsorption proceeded with a curve convex to the pressure axis. Trouton explained this behavior by assuming two modes in which

molecules of water could arrange themselves in condensing on the surface of glass. In the first stage of adsorption, water vapor condensed as single molecules, while in the second stage, after the break, the molecules were associated. It was evident that in absence of nuclei, as after thorough drying, the latter mode of condensation could not happen readily and would result in the state of supersaturation. With less perfect drying, as with phosphorus pentoxide at room temperature, he found the same indication of supersaturation but to a less extent, owing to the presence of nuclei. It is interesting to note the similarity between Trouton's picture and the existence of phase changes in adsorbed films on water (1) and certain vapors on solids (15).

It is likely that the early stages correspond to the formation of an adsorbed phase (besides a firmly held monolayer, *vide infra*) differing from bulk liquid probably as a result of orientation. With film thickening the adsorbed phase changes and approaches bulk liquid after passing through the second inflection point.

This phenomenon was observed only with water-washed glass wool and not with the acid-treated sample, neither with glass powder nor glass microspheres. This is probably due to a particularly strained surface of glass wool produced by the process of drawing the fibres during their manufacture.

In figure 3 curves I, II, and III represent the isotherms on glass wool washed with water during half an hour, a few hours, and 6 days, respectively. It is to be noted that washing with water lowered the adsorptive capacity of glass wool. This may appear to disagree with the common belief that when glass is exposed to water, its surface remains no longer plane but becomes corroded and therefore its adsorptive capacity should increase. It must be remembered that while this is true for *freshly blown* glass surfaces, yet longer contact with water was found to decrease the adsorptive capacity. This is probably the result of a very slow penetration of water molecules into the glass, thus saturating some of the residual valencies which account for adsorption. Outgassing at 200°C. is efficient for removing the adsorbed molecules of water but may not be efficient for expelling the molecules that penetrated into the glass. Even outgassing at 300°C. for 15 hr. or at 200°C. for 45 hr. did not raise the adsorption isotherm.

On the other hand, acid treatment is found to increase greatly the adsorptive capacity of glass wool, as is well known. Sevenfold increase at intermediate pressures is obtained by boiling glass wool with a constant-boiling mixture of hydrochloric acid for 10 hr. and then thoroughly washing with water (curve IV, figure 3, and tables 2 and 3). The action of acid is to dissolve the alkali at the surface of the glass, rendering the latter very rough and full of cavities and small capillaries. The isotherm of acid-treated glass wool is very smooth and closely reproducible.

#### *Glass powder*

The results of experiments on the adsorption of water vapor by powdered glass wool are shown in figure 4. With water-washed powder the isotherms ran smoothly, but successive experiments on the same sample led to a persistent

shift of the isotherm towards the pressure axis, and even after several flushings with water vapor no concordant isotherms were obtained. Thus curves I, II and III of figure 4 represent the first, second, and fourth runs, respectively. A

TABLE 2

*Adsorption of water vapor at 30°C. on glass wool washed with water for 6 days*

MASS OF ADSORBENT = 4.939 g. SURFACE AREA = 3,526 cm. <sup>2</sup>		MASS OF ADSORBENT = 21.903 g. SURFACE AREA = 15,640 cm. <sup>2</sup>			
Run I (figure 3, curve III)		Run I		Run II	
$p/p_0$	Amount adsorbed	$p/p_0$	Amount adsorbed	$p/p_0$	Amount adsorbed
	cc./gram		cc./gram		cc./gram
0.0559	0.084	0.0240	0.077	0.0131	0.041
0.0679	0.102	0.1563	0.129	0.1904	0.134
0.2937	0.152	0.1854	0.141	0.2355	0.148
0.3673	0.168	0.3855	0.165	0.4762	0.176
0.5030	0.194	0.4275	0.177	0.6380	0.207
0.6558	0.208	0.5082	0.191	0.7087	0.234
0.7047	0.236	0.6473	0.209	0.7374	0.261
0.7516	0.282	0.7071	0.230		
0.7905	0.344	0.7415	0.260		
0.8487	0.398	0.7834	0.338		
0.8773	0.441				

TABLE 3

*Adsorption of water vapor at 30°C. on glass wool treated with boiling hydrochloric acid*

OUTGASSED AT 200°C. (FIGURE 3, CURVE IV)				OUTGASSED AT 30°C. (FIGURE 3, CURVE V)	
Adsorption		Desorption		Adsorption	
$p/p_0$	Amount adsorbed	$p/p_0$	Amount adsorbed	$p/p_0$	Amount adsorbed
	cc./gram		cc./gram		cc./gram
0.0091	0.617	0.6304	1.561	0.0352	0.446
0.0116	0.656	0.4427	1.434	0.0490	0.476
0.0521	0.848	0.3372	1.390	0.1152	0.570
0.1665	1.085	0.2077	1.325	0.1999	0.652
0.4025	1.237	0.1597	1.290	0.3742	0.744
0.5094	1.317	0.1087	1.250	0.4706	0.792
0.5707	1.361	0.0918	1.223	0.6099	0.866
0.5971	1.381			0.7036	0.955
0.6392	1.438			0.7820	1.090
0.7932	1.696			0.8923	1.444
0.8622	1.872				

similar behavior was observed by Lambert and Foster for the system water vapor-silica gel (24), by Harbard and King for chloroform-chromic oxide (18), and by Rao for water vapor-ferric oxide (30). These authors attributed the effect

to volume changes in the gel. to the destruction of small capillaries by the process of adsorption, and to the growth of particles, respectively.

The phenomenon was certainly not due to imperfect outgassing, for the same behavior was observed with powders outgassed for longer periods and at higher temperatures. Nor could it be attributed to the removal of impurities by repeated flushing, for the effect persisted even when the sample was flushed

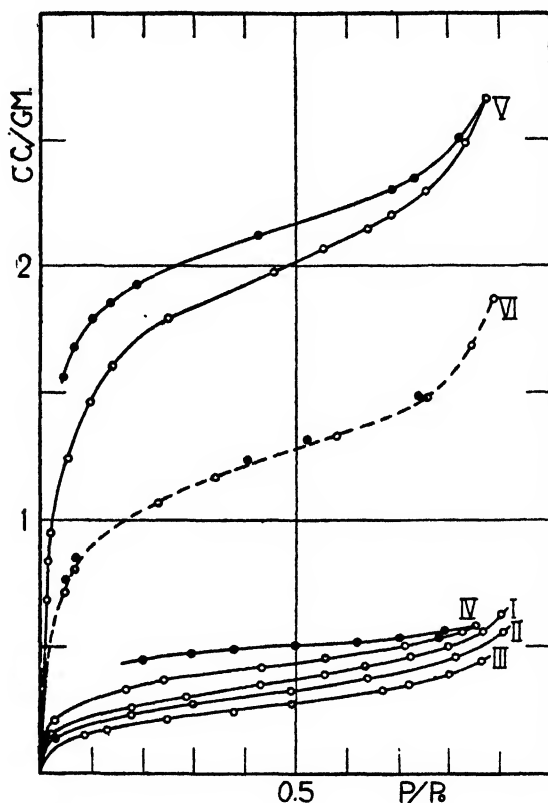


Fig. 4. Adsorption isotherms of water vapor on glass powder at 25°C. Solid symbols are desorption points. Curve I, first run on water-washed powder; curve II, second run; curve III, fourth run; curve IV, glass powder treated with cold 2 *N* hydrochloric acid for a week; curve V, glass powder treated with a constant-boiling mixture of hydrochloric acid and pre-outgassed at 200°C.; curve VI, same treatment but outgassed at 25°C.

several times. Besides, cleaning the surface would increase rather than decrease the adsorptive capacity.

However, when the powder was treated with cold 2 *N* hydrochloric acid for a week and then thoroughly washed with distilled water, the shift of the isotherms occurred to a much less extent. It disappeared completely when the powder was boiled with a constant-boiling mixture of hydrochloric acid for 10 hr. and then thoroughly washed with water. Meanwhile, it was found that treating the glass powder with cold or hot hydrochloric acid increased its adsorptive capacity at

intermediate pressures about two- or eight-fold, respectively (curves IV and V of figure 4 and tables 4 and 5).

As this drift occurred only in the case of powdered glass and not in the case of the original wool (described as washed with acid) or microspheres prepared by

TABLE 4  
*Adsorption of water vapor on glass powder at 25°C.*

UNTREATED POWDER (FIGURE 4, CURVE I)		POWDER WASHED WITH COLD 2 N HYDROCHLORIC ACID (FIGURE 4, CURVE IV)			
Adsorption		Adsorption		Desorption	
$p/p_0$	Amount adsorbed	$p/p_0$	Amount adsorbed	$p/p_0$	Amount adsorbed
	cc./gram		cc./gram		cc./gram
0.0204	0.150	0.0240	0.202	0.7898	0.563
0.1744	0.256	0.1646	0.328	0.7031	0.529
0.2857	0.302	0.2416	0.367	0.6215	0.510
0.4310	0.347	0.4327	0.415	0.3747	0.490
0.5552	0.392	0.5571	0.450	0.2939	0.465
0.6333	0.423	0.7164	0.504	0.2004	0.448
0.7216	0.458	0.8243	0.552		
0.7973	0.501	0.8502	0.581		
0.8660	0.558				
0.9055	0.624				

TABLE 5  
*Adsorption of water vapor at 25°C. on glass powder treated with boiling hydrochloric acid*

OUTGASSED AT 200°C. (FIGURE 4, CURVE V)				OUTGASSED AT 0°C. (FIGURE 4, CURVE VI)			
Run I		Run II		Adsorption		Desorption	
$p/p_0$	Amount adsorbed	$p/p_0$	Amount adsorbed	$p/p_0$	Amount adsorbed	$p/p_0$	Amount adsorbed
	cc./gram		cc./gram		cc./gram		cc./gram
0.0152	0.679	0.0170	0.835	0.0468	0.710	0.7396	1.484
0.0551	1.241	0.0202	0.945	0.0666	0.799	0.5199	1.320
0.1002	1.464	0.2534	1.793	0.1351	0.950	0.4017	1.240
0.1413	1.609	0.4612	1.965	0.2357	1.057	0.0685	0.851
0.5575	2.072	0.6424	2.144	0.3391	1.158	0.0495	0.762
0.6901	2.197	0.8712	2.165	0.5811	1.328		
0.7600	2.291			0.7546	1.462		
0.8383	2.484			0.8412	1.693		
				0.8876	1.867		

fusion, it is probably due to the exposure of certain constituents or structures of the glass in its interior as a result of the breaking down of glass fibres. The freshly formed surface might contain free alkali which took up water molecules slowly and irreversibly, the latter probably penetrating into the surface. Fire polishing, in the case of microspheres, and acid treatment in the case of powder

would lead to removing the alkali and coating the glass surface with a siliceous film, thus eliminating the cause of the drift.

### Glass microspheres

Two series of experiments were carried out on glass spheres and the results obtained are represented graphically in figure 5. Curve I gives the adsorption isotherm on water-washed spheres and curve II that obtained with the spheres after being boiled with a constant-boiling mixture of hydrochloric acid for 10 hr.

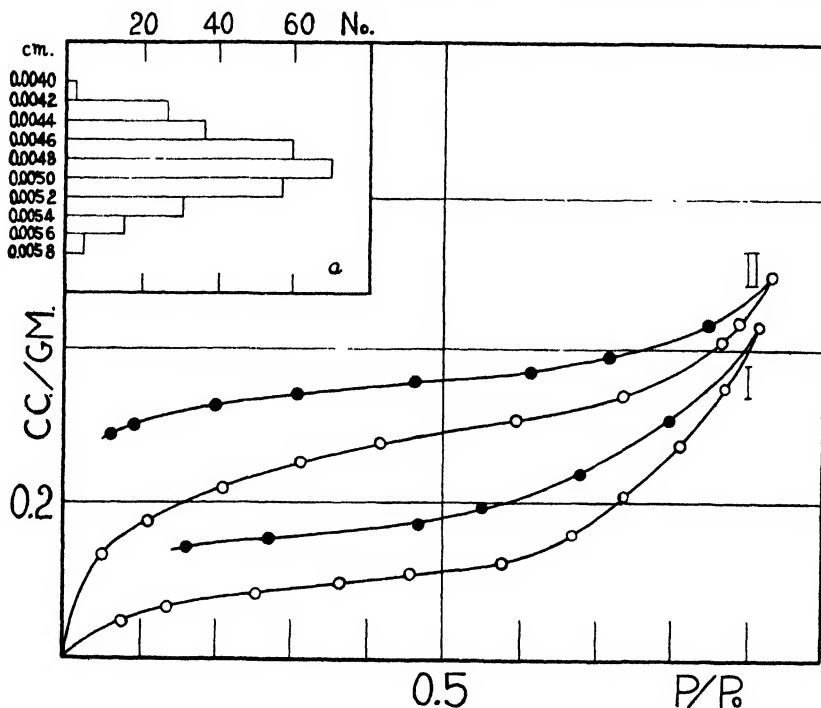


FIG. 5. Adsorption isotherms of water vapor on glass microspheres at 35°C. Solid symbols are desorption points. Curve I, spheres washed with water, curve II, spheres treated with a constant-boiling mixture of hydrochloric acid.

FIG. 5a. Distribution of diameters of 300 microspheres: abscissa, number of spheres, ordinate, diameters.

The curves differ slightly in shape from those of glass wool and glass powder, in being flatter at low and high relative pressures. They also do not show a second point of inflection corresponding to the case of glass wool, and are very closely reproducible, unlike the case of powdered glass. This is probably due to the existence of a predominantly siliceous coating on the surface of the spheres as a result of fire polishing and prolonged contact with water. This view is supported by the fact that acid treatment increased the adsorptive capacity of glass spheres by 150 per cent only, whereas in the case of glass wool and glass powder the increase was about 600 per cent.

*The thickness of adsorbed films*

The three forms of glass experimented with showed irreproducible hysteresis, which depended upon the point from which desorption proceeded (figures 3, 4, and 5). Moreover, the desorption curve did not join again the adsorption curve even at low pressures, unlike the case of silica gel (29) and other adsorbents. This is in agreement with the common belief that the water adsorbed by glass is made up of two parts: one part being readily removed by pumping and thus loosely held, the other part being held firmly and driven off only by heating at higher temperatures.

In order to determine the two parts separately, experiments were done in which

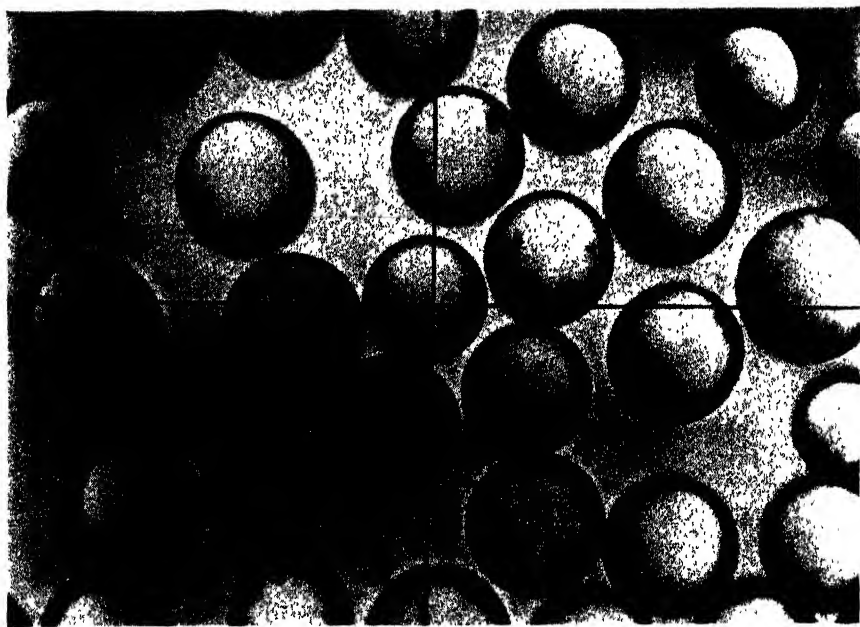


FIG. 5b. Microphotograph of glass spheres; magnification = 376

the glass, after being saturated with water vapor in an ordinary run, was evacuated for 15 hr. at room temperature to a pressure less than  $10^{-6}$  mm. of mercury, and then an adsorption isotherm was determined as usual. The results obtained on the acid-treated glass wool and glass powder are shown by the dotted curves in figures 3 and 4. These isotherms undoubtedly represent the physical adsorption of water vapor on glass, for desorption curves almost coincide with the adsorption curves with hardly any hysteresis, as is shown in figure 4. The difference between the values adsorbed in these runs and the corresponding values in the original runs when the glass was outgassed at  $200^{\circ}\text{C}$ . represents water held firmly probably through chemisorption or solution. Incidentally, this difference is found to be almost constant at intermediate pressures (see parallel curves IV and V in figure 3 and curves V and VI in figure 4) and to be equal to the



monolayer capacity, as determined by the method of Brunauer, Emmett, and Teller (7).

According to these authors, the isotherm equation of multimolecular physical adsorption on a free surface is given by the equation

$$\frac{p}{v(p_0 - p)} = \frac{1}{v_m c} + \frac{(c - 1)}{v_m c} \cdot \frac{p}{p_0} \quad (1)$$

where  $v_m$  is the monolayer capacity, i.e., the volume of gas adsorbed when the

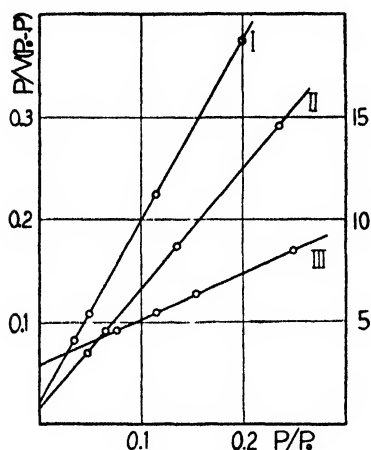


FIG. 6.

FIG. 6. Plots according to Brunauer, Emmett, and Teller. Curve I, water on acid-treated glass wool outgassed at room temperature; curve II, water on acid-treated glass powder outgassed at room temperature; curve III, methyl alcohol on water-washed glass wool outgassed at 200°C. (ordinate scale on right-hand side).

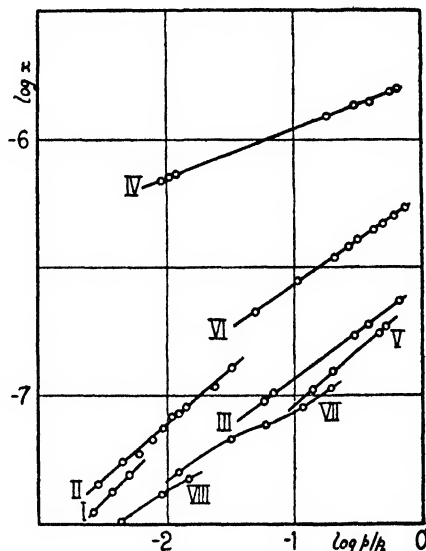


FIG. 7.

FIG. 7. Curve I, Frank's results, 20°C.; curve II, Barrett and Gauger's results, 29°C.; curve III, water-washed glass wool, 30°C.; curve IV, acid-treated glass wool, 30°C.; curve V, water-washed microspheres, 35°C.; curve VI, acid-treated microspheres, 35°C.; curve VII, Itterbeek and Vereycken's results, 0°C.; curve VIII, Itterbeek and Vereycken's results, 42°C.

entire surface of the adsorbent is covered with a complete unimolecular layer, and  $c = e^{(E_1 - E_L)/RT}$ ,  $E_1$  being the average heat of adsorption of the first layer, and  $E_L$  the latent heat of condensation of the vapor.  $R$  and  $T$  are the usual constants.

In figure 6 the values of  $p/v(p_0 - p)$  are plotted as a function of  $p/p_0$  for the adsorption of water vapor on acid-treated glass wool (curve I) and glass powder (curve II) pre-outgassed at room temperature. The experimental points fall well on straight lines up to about 0.30 relative pressure, as demanded by the Brunauer, Emmett, and Teller procedure. From the intercepts of the curves,

$1/v_{mc}$ , and the slopes,  $(c - 1)/v_{mc}$ , the monolayer capacities are found to be 0.544 and 0.825 cc. (S.T.P.) of water vapor per gram, respectively. The difference ( $E_1 - E_L$ ) between the average heat of adsorption of the first monolayer and the heat of liquefaction is estimated as 2710 and 2770 cal./gram-mole, respectively. The small difference between the net heats of adsorption obtained on two samples, one having approximately double the sorption capacity of the other, support the view of physical adsorption in this case.

Taking the area of one molecule of water as  $10.5 \text{ \AA}^2$ , the surface areas of acid-treated glass wool and glass powder become 15,450 and 23,430  $\text{cm}^2/\text{g.}$ , respectively, i.e., about twenty-one times as much as the geometric surface in the case of glass wool.

This estimate is substantiated by calculating the compressibility of the adsorbed film, a quantity which proved lately in the hands of several investigators to be of great value in studying the properties of films (17, 23). In particular, Gregg and Maggs (17) have shown that the compressibility of adsorbed films is largely a property of the adsorbate rather than the adsorbent; so that the minimum compressibilities of films of a certain adsorbate on different adsorbents including plane surfaces and porous solids are of the same order.

The compressibility of an adsorbed film is defined by analogy with the compressibility of matter in bulk as:

$$-\kappa = \frac{1}{A} \cdot \frac{dA}{dF} \quad (2)$$

where  $A$  is the area per molecule adsorbed and  $F$  the surface pressure of the film.  $dF$  can be calculated from the Gibbs isotherm applied to the adsorption of solids (3), viz.:

$$dF = \Gamma \cdot RT \, d \ln p \quad (3)$$

where  $\Gamma$  is the number of moles adsorbed per  $\text{cm}^2$ , and  $R$  and  $T$  have their usual meaning.

If  $v$  is the volume in cubic centimeters (S.T.P.) adsorbed by 1 g. of an adsorbent of specific area  $\Sigma$ , it can be easily shown that

$$-\kappa = \frac{22,400\Sigma}{RT} \cdot \frac{d(1/v)}{d \ln p} \quad (4)$$

Thus the compressibility of the film can be determined from the tangent to the curve obtained by plotting  $1/v$  against  $\ln p$ , if the specific area is known. In the case of glass wool, using the estimated area  $15,450 \text{ cm}^2/\text{g.}$ , the minimum value of  $\kappa$  is  $3.5 \times 10^{-3}$  c.g.s. units, a value which is in good agreement with the compressibilities of films of water on mercury, silica gel, and charcoal calculated by Gregg (16). On the other hand, if the geometric surface ( $714 \text{ cm}^2/\text{g.}$ ) is used in calculating  $\kappa$ , a value twenty-one times as small is obtained, but in no case has such a low value been found for films of water on other adsorbents.

In the case of water-washed glass wool the real surface is found to be two to three times its apparent surface, depending on the time of contact with water.

Experiments with methyl alcohol (curve VI, figure 3) confirmed this result, for the monolayer capacity according to the method of Brunauer, Emmett, and Teller is 0.04 cc./g. (curve III, figure 6), giving a surface factor of 2.7, on the assumption that a molecule of methyl alcohol occupies  $17.7 \text{ \AA}^2$ .

### *Comparison with published data*

The results obtained here are in good agreement with those found by some authors. Thus the difference between the amounts adsorbed on glass wool, washed with water for 6 days, when it is outgassed at  $200^\circ\text{C}$ . and at  $30^\circ\text{C}$ . is  $9 \times 10^{-5} \text{ mg./cm.}^2$  of the geometric surface, in surprisingly good agreement with the value obtained by d'Huart ( $9 \times 10^{-5} \text{ mg./cm.}^2$ ) for the amount of water retained by glass after outgassing at room temperature in the presence of phosphorus pentoxide (21).

It is found that for the different samples of glass the amounts adsorbed at 0.20 and 0.80 relative pressures correspond closely to one and two molecular layers (besides a firmly held monolayer). Frazer (14) obtained at 0.30 and 0.70 relative pressure a film thickness equal to one and two molecular layers, respectively.

The results are also in qualitative agreement with those of Frank (12) and Barrett and Gauger (4), who found that the adsorption isotherms obeyed approximately the Freundlich equation. In figure 7 are shown the double logarithm isotherms of Frank (curve I) and Barrett and Gauger (curve II), together with those on water-washed and acid-treated glass wool (curves III and IV) and glass microspheres (curves V and VI). The amount adsorbed is expressed as grams per square centimeter of the geometric surface. The points fall reasonably on a straight line up to about 0.50 relative pressure, and the curves of Frank and of Barrett and Gauger fall naturally between the curves of the water-washed and acid-treated glass, as is expected from the description of their glass. Comparison shows that the estimate of these authors for the thickness of the adsorbed film as two and four monolayers at very low pressures would fall to less than one molecular layer if the roughness of the surface were taken into consideration. The results of Itterbeek and Vereycken (22) are also included for comparison (curves VII and VIII). The double logarithm isotherms are not linear, since these authors found better agreement with the Langmuir equation, and the Brunauer, Emmett, and Teller equation, for experiments at  $42^\circ\text{C}$ . (curve VIII) and at  $0^\circ\text{C}$ . (curve VII), respectively.

### V. SUMMARY

1. The literature of the work on the adsorption of water vapor by glass surfaces has been reviewed.
2. Adsorption isotherms of water vapor have been determined on a glass of known composition in the form of fibres, powder, and microspheres.
3. The three surfaces show different adsorptive capacities per unit area of the geometric surface, and the amounts adsorbed are varied to different degrees by the same treatment of the glass.

4. It has been found that the adsorption of water vapor on glass surfaces is due partly to a firmly held (chemisorbed ?) monolayer which cannot be removed by pumping at room temperature, and partly to a physically adsorbed film, the thickness of which becomes one molecule at about 0.20 relative pressure, two molecules at 0.80 relative pressure, and several molecules at higher pressures.

5. The real surface is about two to three times greater than the geometric surface in the case of water-washed glass and about ten to twenty times in the case of acid-treated glass.

The authors wish to express their thanks to Dr. S. J. Gregg for kindly reading through this paper and for suggesting the calculation of the compressibility of the adsorbed films.

#### REFERENCES

- (1) ADAM, N. K., AND JESSOP, G.: *Proc. Roy. Soc. (London)* **A110**, 423 (1926).
- (2) BANGHAM, D. H., AND MOSSALLAM, S.: *Proc. Roy. Soc. (London)* **A165**, 552 (1938).
- (3) BANGHAM, D. H., AND RAZOUK, R. I.: *Trans. Faraday Soc.* **33**, 1463 (1937).
- (4) BARRETT, E. P., AND GAUGER, A. W.: *J. Phys. Chem.* **37**, 47 (1933).
- (5) BENT, H. E., AND LESNICK, G. J.: *J. Am. Chem. Soc.* **57**, 1246 (1935).
- (6) BLOOMQUIST, C. R., AND CLARK, A.: *Ind. Eng. Chem., Anal. Ed.* **12**, 61 (1940).
- (7) BRUNAUER, S., EMMETT, P. H., AND TELLER, E.: *J. Am. Chem. Soc.* **60**, 309 (1938).
- (8) BUNSEN, R. W.: *Wied. Ann. Physik* **24**, 321 (1885).
- (9) DORSEY, N. E.: *Properties of Ordinary Water Substance*, American Chemical Society Monograph, pp. 84, 576. Reinhold Publishing Corporation, New York (1940).
- (10) Reference 9, p. 78.
- (11) FARADAY, M.: *Phil. Trans. Roy. Soc.* **1**, 49 (1830).
- (12) FRANK, H. S.: *J. Phys. Chem.* **33**, 970 (1929).
- (13) FRAZER, J. C. W., PATRICK, W. A., AND SMITH, H. E.: *J. Phys. Chem.* **31**, 897 (1927).
- (14) FRAZER, J. H.: *Phys. Rev.* **33**, 97 (1929).
- (15) GREGG, S. J.: *J. Chem. Soc.* **1942**, 696.
- (16) GREGG, S. J.: Paper accepted for publication in *Trans. Faraday Soc.* (joint number with J. chim. phys.).
- (17) GREGG, S. J., AND MAGGS, F. A. P.: Paper accepted for publication in *Trans. Faraday Soc.*
- (18) HARBARD, E. H., AND KING, A.: *J. Chem. Soc.* **1940**, 19.
- (19) HARRIS, J. E., AND SCHUMACHER, E. E.: *Ind. Eng. Chem.* **15**, 176 (1923).
- (20) HERZFELD, K., AND FRAZER, J. H.: *Phys. Rev.* **31**, 1110 (1928).
- (21) D'HUART, M.: *Compt. rend.* **180**, 1594 (1925).
- (22) IJTERBEEK, A. VAN, AND VEREYCKEN, W.: *Z. physik. Chem.* **48B**, 131 (1941).
- (23) JURA, G., LOESEN, E. H., BASFORD, P. R., AND HARKINS, W. D.: *J. Chem. Phys.* **14**, 117 (1946).
- JURA, G., AND HARKINS, W. D.: *J. Am. Chem. Soc.* **68**, 1941 (1946).
- (24) LAMBERT, B., AND FOSTER, A. G.: *Proc. Roy. Soc. (London)* **A134**, 246 (1931).
- (25) LANGMUIR, I.: *J. Am. Chem. Soc.* **38**, 2284 (1916); **40**, 1361 (1918).
- (26) MCHAFFIE, I. R., AND LENHER, S.: *J. Chem. Soc.* **127**, 1559 (1925).
- (27) MENZIES, A. W. C.: *J. Am. Chem. Soc.* **42**, 978 (1920).
- (28) PARKS, G. J.: *Phil. Mag.* [6] **5**, 517 (1903).
- (29) RAO, K. S.: *J. Phys. Chem.* **45**, 513 (1941).
- (30) RAO, K. S.: *J. Phys. Chem.* **45**, 522 (1941).
- (31) SHERWOOD, R. G.: *Phys. Rev.* [2] **12**, 448 (1918).
- (32) SOLLNER, K.: *Ind. Eng. Chem., Anal. Ed.* **11**, 48 (1939).

- (33) STRÖMBERG, R.: Kgl. Svenska Vetenskapsakad. Handl. [2] **6**, 1 (1928).
- (34) TROUTON, F. T.: Proc. Roy. Soc. (London) **A79**, 383 (1907).
- (35) WARBURG, E., AND IHMORI, T.: Wied. Ann. Physik. **27**, 481 (1886).  
IHMORI, T.: Wied. Ann. Physik. **31**, 1014 (1887).
- (36) WINKELMANN, A., AND SCHOTT, O.: Ann. physik. Chem. **51**, 730 (1894). Cf. MOREY, G. W.: *Properties of Glass*, Reinhold Publishing Corporation, New York (1938).

## THE SURFACE TENSION AND VISCOSITY OF SOLUTIONS OF URANYL SALTS

W. E. GRANT, W. J. DARCH, S. T. BOWDEN, AND W. J. JONES

*Tatem Laboratories, University College, Cardiff, Wales*

*Received November 18, 1947*

The surface tension of water is increased by a dissolved salt, and Bugliginsky (4) and Quincke (28) have shown that the variation of the surface tension,  $\sigma_c$ , of a salt solution at constant temperature with its concentration,  $c$ , is well represented by the linear equation

$$\sigma_c = \sigma_0(1 + kc)$$

where  $\sigma_0$  denotes the surface tension of the solvent and  $k$  is a positive constant. To cover still wider ranges of concentration and other solutes besides salts, Freundlich (11) has put forward the exponential formula

$$\sigma_c = \sigma_0(1 + k'c^n)$$

where  $k'$  and  $n$  are constants dependent on temperature, solute, and solvent, but here  $k'$  is not necessarily positive. According to Heydweiller (15), however, the surface tension of very dilute solutions of salts does not vary simply linearly with concentration, and Jones and Ray (20) find a minimum capillary rise at about millinormal concentration. The effect of electrolyte on the surface tension of a solvent has been further discussed by several workers (26, 30). The depressions of surface tension observed by Jones and Ray amount only to 0.01 to 0.02 per cent of that of pure water, a difference too slight to be observable by the method of measurement adopted in the present work.

Dissolved salts generally increase the viscosity of water, but, as Wagner (31) found, the chlorides of potassium, rubidium, cesium, and ammonium, and thalious nitrate have the opposite effect. It was found by Grüneisen (13) that the function  $(\eta_c/\eta_0 - 1)/c$  passed through a minimum value at about seminormal concentration whether the salt increased or reduced the viscosity,  $\eta_0$ , of the solvent,  $\eta_c$  denoting the viscosity of a solution of concentration  $c$ . The existence of this effect was confirmed by Jones and Dole (17) and ascribed by them to interionic attraction. Jones and Talley (21) showed that for several salts in

aqueous solution the variation of viscosity over fairly wide ranges of concentration was given by the relation

$$\frac{\eta_c}{\eta_0} = 1 + A\sqrt{c} + Bc$$

where  $A$  is a positive constant and  $B$  is a constant, positive for a salt that increases the viscosity, but negative for a salt that decreases the viscosity of the solvent. The evaluation of the constant  $A$  in terms of the ionic conductances at zero concentration, the dielectric constant and viscosity of the solvent, and the temperature has been effected by Falkenhagen, Dole, and Vernon (9, 10), and the general correctness of this expression for  $A$  and the applicability of the above equation have been confirmed experimentally by a number of investigators (5, 16, 22, 23, 27), though  $A$  has been found to be negative for aluminum and nickel chlorides in ethanol by Dolian and Briscoe (7) and for ammonium sulfamate in water by Schmelzle and Westfall (29). Onsager and Fuoss (25) have also discussed the general theory of the interionic effect, and according to Jones and Fornwalt (18) their treatment simplifies to the relation:

$$\frac{\eta_c}{\eta_0} = 1 + A\sqrt{c} + Bc + Dc \log c + \dots$$

The object of the present investigation has been to examine the influence of uranyl salts on the surface tension and viscosity of water and methanol, and to ascertain whether the effects can be formulated in accordance with the above-mentioned equations.

#### EXPERIMENTAL

##### *Preparation of materials and solutions*

Uranyl nitrate hexahydrate of analytical grade was allowed to stand under sodium-dried benzene for 24 hr. in order to remove the film of moisture adhering to the crystals; the benzene was decanted and the crystals were freed from benzene by washing with dry petroleum ether; the hexahydrate thus treated had a purity of 99.92 per cent. Uranyl acetate dihydrate had a purity of 99.84 per cent after similar treatment. Anhydrous uranyl acetate was prepared from the dihydrate by entrainment distillation of the water with heptane, and the purity of the salt thus obtained was 99.60 per cent. Anhydrous uranyl nitrate could not be obtained by this method, owing to the occurrence of decomposition with evolution of nitrous fumes.

The liquids used in the investigation were subjected to the following purification processes: Water was distilled in an all-glass apparatus with the distillation, condensing, and receiving units sealed to one another to avoid contamination with grease. Benzene was dried over calcium chloride and then distilled from sodium wire. Methanol was obtained in the anhydrous condition by treatment of the liquid with magnesium methoxide prepared *in situ* (24).

Since anhydrous uranyl nitrate was not available, measurements were carried

out on the hexahydrate in methanol. The low solubility of anhydrous uranyl acetate in water and in methanol limited the investigation to dilute solution, but the solubility of the dihydrate in methanol permitted the examination of a series of these solutions. Each solution was freshly prepared at 20°C. in a 100-cc. flask, care being taken to avoid undue exposure to light; the solution was generally used for the measurement of density, surface tension, and viscosity over the entire temperature range of the experiments. Densities were determined by means of pycnometers with capacities of 10 cc. and 25 cc., respectively, using standardized weights and applying the usual buoyancy corrections.

*Surface tension and viscosity determinations*

The measurement of the surface tension of the pure liquids and solutions was carried out by the differential bubbling method, using the form of instrument described by Bowden and Butler (3). The apparatus was immersed in a thermostat (containing water or a solution of calcium chloride) provided with a bimetallic thermoregulator in circuit with a hot-wire vacuum switch which gave

TABLE 1  
*Density, surface tension, and viscosity of solvents*

	0°C.	20°C.	25°C.	30°C.	35°C.	40°C.	50°C.	60°C.	80°C.	100°C.
Water $\left\{ \begin{array}{l} d \\ \sigma \\ \eta \end{array} \right.$	0.9993	0.9983	0.9965	0.9954	0.9938	0.9924	0.9883	0.9833	0.9718	0.9584
	75.8	72.6	71.5	70.5	69.8	69.1	67.4	65.9	62.2	59.2
	1.793	1.006	0.893	0.800	0.724	0.657	0.550	0.469		
Methanol $\left\{ \begin{array}{l} d \\ \sigma \\ \eta \end{array} \right.$	0.8098	0.7916	0.7867	0.7823	0.7776	0.7727	0.7630	0.7537		
	24.7	22.7		21.8		20.9	20.1	19.0		
	0.801	0.589	0.551	0.512	0.477	0.445	0.391	0.346		

a maximum tolerance of 0.04°C. over the temperature range of the experiments. The instrument was calibrated with dry benzene, for which the surface tension at 20°C. was taken as 29.1 dynes per centimeter.

For the viscosity measurements an all-glass viscometer was constructed according to the specifications of the British Engineering Standards Association, and the design incorporated the recommendations made by Barr (1). The instrument was provided with a ground-glass stopper which had a by-pass to the capillary limb and also an orifice to bring the two limbs into communication so that the determination could be carried out in a dust-free atmosphere in a closed system. To avoid vapor losses the bulb of the viscometer was filled by applying pressure to the receiving limb. Times of flow were observed by means of a stopwatch which was periodically calibrated against a standard chronometer. The viscometer was set vertically in a thermostat whose temperature was controlled to 0.005°C. by a Sunvic electronic relay in conjunction with a toluene-mercury regulator provided with a bimetallic proportionating head.

In view of the differences of opinion (2, 8, 19) which still prevail concerning the form and magnitude of the correction to be applied to viscosity measurements

TABLE 2  
*Uranyl nitrate hexahydrate in water*

TEMPERATURE	<i>c</i>	<i>d</i>	<i>e</i>	<i>f</i>	<i>c</i>	<i>d</i>	<i>e</i>	<i>f</i>
°C.								
0	0.1529	1.0509		1.90	0.2291	1.0740	76.4	1.98
20					0.2286	1.0714	73.8	1.11
25	0.1523	1.0473		0.943	0.2283	1.0703	72.4	0.989
30	0.1521	1.0459		0.844	0.2280	1.0687	71.6	0.884
35					0.2277	1.0671	70.6	0.796
40	0.1515	1.0420		0.691	0.2273	1.0651	69.8	0.726
50	0.1507	1.0365		0.580	0.2262	1.0609	68.5	0.603
60	0.1501	1.0324		0.492	0.2253	1.0559	66.9	0.514
80					0.2230	1.0457	63.2	
100					0.2201	1.0315	59.9	
0	0.4127	1.1328	76.6	2.19	0.4842	1.1575		2.26
20	0.4112	1.1291	73.4	1.22	0.4828	1.1540		1.28
25	0.4107	1.1275	72.7	1.09	0.4821	1.1522		1.14
30	0.4102	1.1260	72.0	0.974	0.4815	1.1506		1.02
35	0.4094	1.1240	71.3	0.880	0.4804	1.1488		0.915
40	0.4088	1.1219	70.4	0.794	0.4800	1.1477		0.832
50	0.4071	1.1175	69.0	0.668	0.4777	1.1423		0.696
60	0.4053	1.1124	67.5	0.568	0.4755	1.1369		0.587
80	0.4019	1.1026	63.6					
100	0.3966	1.0889	60.6					
0	0.6250	1.1985	76.8	2.43	0.8316	1.2701	77.6	
20	0.6219	1.1920	73.7	1.33	0.8271	1.2634	74.6	
25	0.6210	1.1903	73.0	1.22	0.8260	1.2615	73.9	
30	0.6201	1.1886	72.2	1.09	0.8247	1.2596	73.4	
35	0.6191	1.1867	71.5	0.978	0.8231	1.2570	72.7	
40	0.6181	1.1847	70.6	0.892	0.8215	1.2546	71.8	
50	0.6158	1.1800	69.2	0.745	0.8181	1.2495	70.3	
60	0.6131	1.1748	67.8	0.632	0.8145	1.2440	69.0	
80	0.6074	1.1642	64.2		0.8063	1.2314	65.0	
100	0.5995	1.1492	61.0		0.7980	1.2187	61.9	

TABLE 3  
*Uranyl acetate dihydrate in water*

TEMPERATURE	<i>c</i>	<i>d</i>	<i>e</i>	<i>f</i>
°C.				
0	0.02391	1.0079	75.0	1.77
20	0.02383	1.0045	71.5	0.992
25	0.02380	1.0032	70.6	0.879
30	0.02377	1.0019	69.7	0.789
35	0.02374	1.0009	68.7	
40	0.02370	0.9987	68.2	0.663
50	0.02360	0.9947	66.7	0.542
60	0.02348	0.9900	65.0	0.463
80	0.02322	0.9788	61.4	
100	0.02288	0.9642	58.6	



TABLE 4  
*Uranyl nitrate hexahydrate and uranyl acetate dihydrate in water*

TEMPERATURE	<i>c</i> (NITRATE)	<i>c</i> (ACETATE)	<i>d</i>	$\sigma$
°C.				
20	0.1977	0.02324	1.0678	72.5
25	0.1974	0.02320	1.0664	71.6
30	0.1972	0.02318	1.0650	71.1
35	0.1969	0.02314	1.0633	70.2
40	0.1965	0.02310	1.0614	69.0
50	0.1958	0.02301	1.0573	67.2
60	0.1949	0.02291	1.0523	66.2
80	0.1929	0.02267	1.0411	62.9
100	0.1900	0.02232	1.0256	59.4

TABLE 5  
*Uranyl nitrate hexahydrate in methanol*

TEMPERATURE	<i>c</i>	<i>d</i>	$\sigma$	$\eta$	<i>c</i>	<i>d</i>	$\sigma$	$\eta$
°C.								
0	0.10050	0.8482	25.0	0.950	0.2043	0.8878	25.5	1.10
20	0.09826	0.8294	23.2	0.665	0.1999	0.8686	23.7	0.778
25	0.09770	0.8247	22.8	0.616	0.1987	0.8636	23.2	0.714
30	0.09718	0.8204	22.2	0.572	0.1976	0.8587	22.8	0.659
35	0.09658	0.8153	21.7	0.534	0.1965	0.8539	22.3	0.609
40	0.09603	0.8106	21.3	0.496	0.1954	0.8491	21.9	0.567
50	0.09493	0.8013	20.4	0.431	0.1932	0.8395	21.1	0.489
60	0.09378	0.7916	19.5	0.378	0.1911	0.8302	20.2	0.428
0	0.2974	0.9229	26.2	1.27	0.3947	0.9602	26.8	1.45
20	0.2931	0.9033	24.3	0.883	0.3865	0.9404	24.9	1.01
25	0.2916	0.8984	23.9	0.812	0.3845	0.9356	24.4	0.922
30	0.2899	0.8932	23.4	0.766	0.3824	0.9307	23.9	0.843
35	0.2886	0.8890	22.9	0.709	0.3805	0.9258	23.6	0.775
40	0.2870	0.8841	22.5	0.648	0.3784	0.9206	23.2	0.715
50	0.2837	0.8740	21.7	0.554	0.3743	0.9107	22.2	0.606
60	0.2806	0.8646	20.7	0.480	0.3701	0.9007	21.2	0.519
0	0.5128	1.0015	27.4	1.75				
20	0.5023	0.9811	25.6	1.19				
25	0.4997	0.9759	25.1	1.08				
30	0.4972	0.9709	24.7	0.981				
35	0.4945	0.9658	24.3	0.893				
40	0.4922	0.9614	23.9	0.817				
50	0.4868	0.9508	23.0	0.692				
60	0.4816	0.9408	22.1	0.586				

for the influence of surface tension, the values of the viscosity given in the present work have not been corrected for this effect.

The values found for the density, surface tension, and viscosity of the pure

solvents are contained in table 1, where  $d$  is the density in grams per cubic centimeter,  $\sigma$  is the surface tension in dynes per centimeter, and  $\eta$  is the viscosity in centipoises.

The results for the solutions are listed in tables 2 to 7, where  $c$  is the concentration of the dissolved compound in moles per liter of solution.

TABLE 6  
*Uranyl acetate dihydrate in methanol*

TEMPERATURE	$c$	$d$	$\sigma$	$\eta$	$c$	$d$	$\sigma$	$\eta$
°C.								
0	0.03248	0.8199	24.8		0.07194	0.8325	24.9	0.825
20	0.03178	0.8023	23.0		0.07036	0.8141	23.0	0.603
25	0.03161	0.7980	22.4		0.06995	0.8095	22.5	0.561
30	0.03142	0.7932	21.9		0.06956	0.8050	21.9	0.523
35	0.03124	0.7886	21.5		0.06915	0.8002	21.5	0.488
40	0.03105	0.7838	21.0		0.06876	0.7956	21.0	0.456
50	0.03067	0.7743	20.2		0.06792	0.7859	20.0	0.401
60	0.03028	0.7645	19.3		0.06708	0.7762	19.4	0.353
0	0.1446	0.8558	25.0	0.910	0.2147	0.8772	25.2	0.965
20	0.1406	0.8366	23.1	0.647	0.2100	0.8580	23.1	0.686
25	0.1398	0.8318	22.6	0.600	0.2088	0.8533	22.6	0.635
30	0.1390	0.8269	22.1	0.559	0.2077	0.8484	22.2	0.592
35	0.1382	0.8222	21.6	0.521	0.2065	0.8437	21.7	0.550
40	0.1374	0.8174	21.2	0.485	0.2053	0.8389	21.3	0.504
50	0.1358	0.8078	20.3	0.423	0.2031	0.8294	20.5	0.447
60	0.1342	0.7980	19.7	0.378	0.2005	0.8194	19.9	0.392

TABLE 7  
*Anhydrous uranyl acetate in methanol*

TEMPERATURE	$c$	$d$	$\sigma$	$\eta$
°C.				
0	0.02439	0.8226	24.8	0.815
20	0.02386	0.8050	22.9	0.581
25	0.02371	0.8000	22.5	0.539
30	0.02358	0.7954	22.0	0.503
35	0.02345	0.7911	21.5	0.470
40	0.02331	0.7863	21.0	0.441
50	0.02302	0.7766	20.2	0.386
60	0.02273	0.7667	19.3	0.342

#### DISCUSSION OF RESULTS

The present results show that while uranyl nitrate increases the surface tension of water, uranyl acetate has the opposite effect. That the relative magnitudes of these two opposing effects vary but little with change of temperature is proved by the data given in table 4 for a solution which was prepared at 20°C. to contain

TABLE 8

*Application of Bugliginsky and Freundlich equations*

$c$	$\Delta\sigma_B$	$\Delta\sigma_F$	$\Delta\sigma_{\text{obed.}}$	$c$	$\Delta\sigma_B$	$\Delta\sigma_F$	$\Delta\sigma_{\text{obed.}}$
Uranyl nitrate hexahydrate in water							
Temperature, 0°C.; $k = k' = 0.02429$ ; $n = 1.000$				Temperature, 20°C.; $k = 0.03098$ ; $k' = 0.03125$ ; $n = 1.019$			
0.2291	0.4	0.4	0.6	0.2286	0.5	0.5	0.7
0.4127	0.8	0.8	0.8	0.4112	0.9	0.9	0.8
0.6250	1.1	1.1	1.0	0.6219	1.4	1.4	1.1
0.8316	1.6	1.6	1.8	0.8271	1.9	1.9	1.9
Temperature, 40°C.; $k = 0.04200$ ; $k' = 0.04053$ ; $n = 0.9656$				Temperature, 60°C.; $k = k' = 0.05711$ ; $n = 1.000$			
0.2273	0.7	0.7	0.7	0.2253	0.9	0.9	1.0
0.4088	1.2	1.2	1.4	0.4053	1.5	1.5	1.7
0.6181	1.8	1.8	1.5	0.6131	2.3	2.3	1.9
0.8215	2.4	2.3	2.8	0.8145	3.1	3.1	3.1
Temperature, 80°C.; $k = k' = 0.05827$ ; $n = 1.000$				Temperature, 100°C.; $k = k' = 0.05603$ ; $n = 1.000$			
0.2230	0.8	0.8	1.0	0.2201	0.7	0.7	0.7
0.4019	1.4	1.4	1.4	0.3966	1.3	1.3	1.4
0.6074	2.2	2.2	2.0	0.5995	2.0	2.0	1.8
0.8063	2.9	2.9	2.9	0.7980	2.6	2.6	2.6
Uranyl nitrate hexahydrate in methanol							
Temperature, 0°C.; $k = 0.2087$ ; $k' = 0.2534$ ; $n = 1.171$				Temperature, 20°C.; $k = 0.2404$ ; $k' = 0.3028$ ; $n = 1.203$			
0.1005	0.5	0.4	0.3	0.09826	0.5	0.4	0.4
0.2043	1.1	1.0	0.8	0.1999	1.1	1.0	1.0
0.2974	1.5	1.5	1.5	0.2931	1.6	1.6	1.6
0.3947	2.0	2.1	2.1	0.3865	2.1	2.2	2.2
0.5128	2.6	2.9	2.7	0.5023	2.7	3.0	2.9
Temperature, 40°C.; $k = 0.2636$ ; $k' = 0.3422$ ; $n = 1.204$				Temperature, 60°C.; $k = 0.3225$ ; $k' = 0.3899$ ; $n = 1.203$			
0.09603	0.5	0.4	0.4	0.09378	0.6	0.4	0.4
0.1954	1.1	1.0	1.0	0.1911	1.2	1.0	1.2
0.2870	1.6	1.6	1.6	0.2806	1.7	1.6	1.6
0.3784	2.1	2.2	2.3	0.3701	2.3	2.2	2.2
0.4922	2.7	3.0	3.0	0.4816	3.0	3.1	3.1

TABLE 8—Continued

$c$	$\Delta\sigma_B$	$\Delta\sigma_F$	$\Delta\sigma_{\text{obsd.}}$	$c$	$\Delta\sigma_B$	$\Delta\sigma_F$	$\Delta\sigma_{\text{obsd.}}$
Uranyl acetate dihydrate in methanol							
Temperature, 0°C.; $k = 0.1014$ ; $k' = 0.1035$ ; $n = 1.005$				Temperature, 20°C.; $k = 0.07341$ ; $k' = 0.08095$ ; $n = 1.043$			
0.03248	0.1	0.1	0.1	0.03178	0.1	0.1	0.3
0.07194	0.2	0.2	0.2	0.07036	0.1	0.1	0.3
0.1446	0.4	0.4	0.3	0.1406	0.2	0.2	0.4
0.2147	0.5	0.5	0.5	0.2100	0.4	0.4	0.4
Temperature, 40°C.; $k = 0.08762$ ; $k' = 0.08517$ ; $n = 0.974$				Temperature, 60°C.; $k = 0.1820$ ; $k' = 0.1910$ ; $n = 1.023$			
0.03105	0.1	0.1	0.1	0.03028	0.1	0.1	0.3
0.06876	0.1	0.1	0.1	0.06708	0.2	0.2	0.4
0.1374	0.3	0.3	0.3	0.1342	0.5	0.5	0.7
0.2053	0.4	0.4	0.4	0.2005	0.7	0.7	0.8

99.33 g. of the nitrate hexahydrate and 9.858 g. of the acetate dihydrate per liter so that the surface activities of the two solutes should annul each other. Comparison of table 4 with table 1 shows that the surface tension of the solution containing the two solutes keeps close to that of pure water over the entire range of temperature. In methanol, however, the surface tension is raised by uranyl nitrate hexahydrate and by uranyl acetate dihydrate.

The applicability of the Bugliginsky and Freundlich equations is shown in table 8, where  $\Delta\sigma_B$  represents the difference between the surface tension of the solution and that of the solvent as calculated from the Bugliginsky equation,  $\Delta\sigma_F$  the difference given by the Freundlich relation, and  $\Delta\sigma_{\text{obsd.}}$  the experimentally observed value of  $\sigma_c - \sigma_0$ . Except for the system uranyl nitrate hexahydrate-methanol,  $n$  so closely approaches unity that the two equations are practically identical and each relation gives equally good correspondence between the observed and calculated values of  $\Delta\sigma$ . For the aforementioned system, however, where the value of  $n$  is about 1.2, the Freundlich equation is in better accord with the experimental results. It will be noticed that the constant  $k'$  of this equation for a given system is a non-linear function of temperature, and may attain a maximum or a minimum according to the nature of the solution.

The influence of uranyl salts on the viscosity of the liquids is seen by comparing the data in tables 2 to 7 with those in table 1. At the concentrations examined it is evident that uranyl nitrate hexahydrate increases the viscosity of water, and that uranyl acetate dihydrate has little effect. The viscosity of methanol is raised by the nitrate hexahydrate and the acetate dihydrate, but is only slightly influenced by the anhydrous acetate.

The constants obtained on applying the Jones-Talley equation to the results given in tables 2 to 6 are listed in table 9. In this table are also given, for three representative solutions, the values of the viscosity,  $\eta_{\text{calcd.}}$ , calculated using the

above constants, and the differences,  $\Delta\eta$ , between these values and the observed viscosities; these three solutions were those for which the molar concentrations at 0°C. were, respectively, 0.4127 of uranyl nitrate hexahydrate in water, 0.2043 of uranyl nitrate hexahydrate in methanol, and 0.1446 of uranyl acetate dihydrate in methanol.

For the range of concentration investigated the results accord satisfactorily with equations of the Jones-Talley type. The fact that the constant  $A$  is not positive for aqueous solutions of uranyl nitrate may be due to a variety of causes, for the ionization of uranyl salts in water is known to involve formation of complex ions which undergo change of constitution with dilution of the solution

TABLE 9  
*Constants and viscosities calculated from Jones-Talley equation*

	0°C.	20°C.	25°C.	30°C.	35°C.	40°C.	50°C.	60°C.
Uranyl nitrate hexahydrate in water								
$-A$ .....	0.141	0.142	0.180	0.172	0.200	0.180	0.180	0.155
$B$ ....	0.7515	0.7251	0.8266	0.8054	0.8379	0.8100	0.7938	0.7727
$\eta_{\text{calcd.}}$ ...	2.19	1.21	1.09	0.976	0.880	0.799	0.665	0.570
$\Delta\eta$ .....	0.00	0.01	0.00	0.002	0.000	0.005	0.003	0.002
Uranyl nitrate hexahydrate in methanol								
$-A$ .....	0.320	0.407	0.378	0.372	0.312	0.340	0.271	0.260
$B$ ....	2.486	2.509	2.397	2.346	2.203	2.183	1.893	1.812
$\eta_{\text{calcd.}}$ ...	1.09	0.778	0.720	0.665	0.618	0.568	0.487	0.427
$\Delta\eta$ ...	0.01	0.000	0.006	0.006	0.009	0.001	0.002	0.001
Uranyl acetate dihydrate in methanol								
$-A$ .....	0.330	0.294	0.300	0.252	0.262	0.195	0.220	0.150
$B$ ....	1.746	1.465	1.435	1.317	1.336	1.156	1.211	1.060
$\eta_{\text{calcd.}}$ ...	0.903	0.646	0.600	0.558	0.519	0.484	0.423	0.376
$\Delta\eta$ ....	0.007	0.001	0.000	0.001	0.002	0.001	0.000	0.002

(6, 12, 14); further, the negativity of this constant for solutions of the hydrates in methanol may be due partly to the effect of the water.

#### SUMMARY

The surface tension and viscosity of solutions of uranyl nitrate hexahydrate, uranyl acetate dihydrate, and anhydrous uranyl acetate in water and in methanol have been measured at a series of temperatures from 0°C. to the neighborhood of the boiling point of the solvent.

The surface tension of water is raised by uranyl nitrate but is lowered by uranyl acetate. The surface tension of methanol is raised by uranyl nitrate hexahydrate, by uranyl acetate dihydrate, and slightly by anhydrous uranyl acetate. The Bugliginsky equation applies to aqueous solutions of uranyl nitrate and

methanol solutions of uranyl acetate dihydrate, but the Freundlich relation is in better accord with the results for methanol solutions of uranyl nitrate hexahydrate.

The viscosity of water is increased by uranyl nitrate, but is little influenced by uranyl acetate. Uranyl nitrate hexahydrate and uranyl acetate dihydrate increase the viscosity of methanol, but the anhydrous acetate has only a slight effect. Equations of the Jones-Talley type are found to be applicable over the range of concentrations studied, but here the constants are purely empirical, calculation by means of the Falkenhagen-Dole-Vernon expressions not being possible even for the aqueous solutions, owing to the complexity of the ionization and the incidence of hydrolytic reactions.

#### REFERENCES

- (1) BARR, G.: *A Monograph of Viscometry*, p. 119. Oxford University Press, London (1931).
- (2) BARR, G.: *Proc. Phys. Soc. (London)* **58**, 575 (1946).
- (3) BOWDEN, S. T., AND BUTLER, E. T.: *J. Chem. Soc.* **1939**, 79.
- (4) BUGLIGINSKY: *Ann. Physik* **134**, 440 (1868).
- (5) COX, W. M., AND WOLFENDEN, J. H.: *Proc. Roy. Soc. (London)* **A145**, 475 (1934).
- (6) DITTRICH, C.: *Z. physik. Chem.* **29**, 465 (1899).
- (7) DOLIAN, F. E., AND BRISCOE, H. T.: *J. Phys. Chem.* **41**, 1129 (1937).
- (8) DRUCKER, C.: *Arkiv Kemi, Mineral. Geol.* **A22**, No. 20 (1946).
- (9) FALKENHAGEN, H., AND DOLE, M.: *Z. physik. Chem.* **B6**, 159 (1929).
- (10) FALKENHAGEN, H., AND VERNON, E. L.: *Phil. Mag.* [7] **14**, 537 (1932).
- (11) FREUNDLICH, H.: *Kapillarchemie*, p. 65. Akademische Verlagsgesellschaft, Leipzig (1909).
- (12) GOMEZ, L.: *Anales fis. y quím.* **17**, 24 (1919).
- (13) GRÜNEISEN, E.: *Wiss. Abhandl. physik.-tech. Reichsanstalt* **4**, 239 (1905).
- (14) GUITER, H.: *Bull. soc. chim. France* **1947**, 64.
- (15) HEYDWEILLER, A.: *Ann. Physik* [4] **33**, 145 (1910).
- (16) JONES, G., AND CHRISTIAN, S. M.: *J. Am. Chem. Soc.* **66**, 1017 (1944).
- (17) JONES, G., AND DOLE, M.: *J. Am. Chem. Soc.* **51**, 2950 (1929).
- (18) JONES, G., AND FORNWALT, H. J.: *J. Am. Chem. Soc.* **57**, 2041 (1935).
- (19) JONES, G., AND FORNWALT, H. J.: *J. Am. Chem. Soc.* **60**, 1683 (1938).
- (20) JONES, G., AND RAY, W. A.: *J. Am. Chem. Soc.* **57**, 957 (1935); **59**, 187 (1937); **63**, 288, 3262 (1941); **64**, 2744 (1942).
- (21) JONES, G., AND TALLEY, S. K.: *J. Am. Chem. Soc.* **55**, 624, 4124 (1933).
- (22) JOY, W. E., AND WOLFENDEN, J. H.: *Proc. Roy. Soc. (London)* **A134**, 413 (1931).
- (23) LAURENCE, V. D., AND WOLFENDEN, J. H.: *J. Chem. Soc.* **1934**, 1144.
- (24) LUND, H., AND BJERRUM, J.: *Ber.* **64A**, 210 (1931).
- (25) ONSAGER, L., AND FUOSS, R. M.: *J. Phys. Chem.* **36**, 2689 (1932).
- (26) ONSAGER, L., AND SAMARAS, N. N. T.: *J. Chem. Phys.* **2**, 528 (1934).
- (27) PATNAIK, T., AND PRASAD, B.: *J. Indian Chem. Soc.* **21**, 125 (1944).
- (28) QUINCKE, G.: *Ann. Physik* **160**, 337, 560 (1877).
- (29) SCHMELZLE, A. F., AND WESTFALL, J. E.: *J. Phys. Chem.* **48**, 165 (1944).
- (30) WAGNER, G.: *Physik. Z.* **25**, 474 (1924).
- (31) WAGNER, J.: *Z. physik. Chem.* **5**, 31 (1890).

WEATHERING SEQUENCE OF CLAY-SIZE MINERALS IN SOILS  
AND SEDIMENTS. IFUNDAMENTAL GENERALIZATIONS<sup>1</sup>M. L. JACKSON, S. A. TYLER, A. L. WILLIS, G. A. BOURBEAU,  
AND R. P. PENNINGTON*University of Wisconsin, Madison, Wisconsin**Received February 20, 1948*

Considerable progress has been made in the improvement of technics of preparation and identification of mineral species present in the colloidal fractions of soils and sediments, particularly of montmorillonite and the micas, through the x-ray diffraction method. As a result, considerable information has been accumulated on the relative abundance of the different specific minerals present in colloids of soils and sediments of diverse origins. Since the colloidal portions are the resultant products of weathering processes, they represent more or less stable end-products, which are more resistant to weathering than their parent materials.

It is the purpose of the present article to trace the course of weathering ("weathering sequence") of the finer mineral particles in soils and sediments, and to interpret the order of succession of minerals in the sequence on the basis of present concepts of crystal chemistry.

One view of weathering holds that the fundamental principle is embodied in the concept of direct weathering of a primary to a secondary mineral, each particle being a more or less closed system. Thus a primary mineral such as labradorite alters to a secondary mineral such as kaolinite (the "kaolinization" reaction), or "volcanic ash" alters to montmorillonite (the bentonite reaction), the calcium oxide, sodium oxide, and excess silica being carried away in solution. Accordingly, the source of each colloidal silicate clay mineral is sought as a specific parent mineral from which the colloidal mineral is a "primary weathering product." Observations of secondary colloidal products in pseudomorphic form of a parent crystal establish this binary transformation as a fundamentally sound view, in detail. The viewpoint herein developed recognizes this direct primary-secondary transformation, but seeks to extend the concept of weathering to include a summation, or integration, of a multiplicity of such binary transformations which may simultaneously be occurring in the soil or sediment, and responsible for its colloid composition.

In addition, the views are adopted that (a) one colloidal mineral may in some cases be a parent material of successive colloidal products as the weathering processes continue, (b) the weathering reactions are reversible, and (c) the entire mineral content of the clay-size fraction should be considered in the sequence,

<sup>1</sup> Joint contribution of the Wisconsin Agricultural Experiment Station and the Department of Geology, University of Wisconsin, Madison. Published by permission of the Director of the Agricultural Experiment Station. Supported in part by a grant from the Wisconsin Alumni Research Foundation.

without emphasis being placed on the older distinctions as to whether they are secondary or primary (unweathered) residuals. Interpretation of the mineralogy of youthful soils (important both to theoretical pedology and to agriculture), together with the recognition of the reversibility of the weathering reaction in both soils and sediments, requires this consideration of the entire mineral content of the clay-size fraction rather than merely the silicate "clay minerals." The unweathered residual minerals *truly enter the sequence* by virtue of their *relative resistance* to weathering, being residual *after more easily weathered minerals* of earlier stages have disappeared.

By "clay-size" is meant the finer portion of the soil or sediment, particularly the "fine clay" fraction of less than 0.2 micron equivalent spherical diameter, but also the "coarse clay" fraction, particles 0.2–2 microns in diameter, and to some extent the "fine silt" fraction, particles 2–5 microns in diameter. The inclusion of the coarser two fractions is justified partly because considerable of the clay minerals (illite and kaolinite particularly) occur in these fractions, but also because a functional consideration of the origin of clay-size particles requires *per se* a functional approach to the definition of clay size. Thus it is held that there is no definite "upper limit" of colloidal particle size of inorganic soil colloids, but rather a gradual change, depending in part on the mineral species being considered.<sup>2</sup>

#### THE MINERAL WEATHERING SEQUENCE: PRESENTATION

The minerals representing successive stages in the weathering sequence of clay-size minerals are listed in table 1. The more soluble or easily weathered substances appear in the first five stages. The first stages involving gypsum and other more or less freely soluble salts (stage 1) and calcite and related less soluble non-silicate minerals (stage 2) occur in well-developed soils only as secondary depositions in the lower horizons. When present, however, they usually dominate the important physical and chemical properties of the colloid, and are recognized therefore as a stage in the sequence for soils. They may constitute a small percentage of colloids of certain kinds of very young soils (e.g., reference 12, p. 43). Moreover, they are important constituents of the fine fractions of some sediments.

In stages 3 and 4, the silicates of the most easily weathered types (silicates groups I to V and certain members of VI) were first postulated on the basis of their occurrence in the fresh state in the finer sand and silt of young soils such as Rideau clay (16); later, amphibole (stage 3) and chlorite (stage 4) were actually found in the coarse clay of Abitibi soil, C horizon. This horizon is only slightly altered "rock flour," occurring as the subsoil of a soil developed from the glacial rock flour sediments of Lake Ojibway near James Bay in northern Quebec.<sup>3</sup>

<sup>2</sup> It is considered essential, however, that the clay-size minerals be studied in narrow particle-size ranges such as the three listed, for both theoretical and experimental reasons. Moreover, the limits of these arbitrary size ranges are also functional in character, rather than unique numerical limits.

<sup>3</sup> Collections obtained through the courtesy of Professor A. Scott, Laval University, St. Anne de la Pocatière, Quebec, Canada.



TABLE 1

*Weathering sequence of clay-size minerals in soils and sedimentary deposits*

WEATHERING STAGE AND SYMBOL	CLAY-SIZE MINERALS OCCURRING AT VARIOUS STAGES OF THE WEATHERING SEQUENCE	EXAMPLES OF OCCURRENCE OF MINERALS AT VARIOUS WEATHERING STAGES IN THE COLLOIDAL FRACTIONS	
		Of soils	Of sedimentary deposits
1 Gp	Gypsum (also halite, etc.)	Pierre clay, C horizon (South Dakota)	Polders clay (Holland)
2 Ct	Calcite (also dolomite, aragonite, etc.)	Minatare, B horizon (Nebraska)	Calcite limestones (Michigan)
3 Hr	Olivine-hornblende* (also diopside, etc.)	Abitibi, C horizon† (James Bay, Canada)	Fresh rock flour
4 Bt	Biotite‡ (also glauconite, chlorite, antigorite, nontronite, etc.)	Abitibi, C horizon§ (James Bay, Canada)	Glauconite in Cambrian sandstone (Wisconsin)
5 Ab	Albite (also anorthite, microcline, stilbite, etc.)	Rideau clay, C <sub>1</sub> horizon (Ontario)	Authigenic feldspars (10)
6 Qr	Quartz (also cristobalite, etc.)	Rideau clay, B horizon (Ontario)	Authigenic quartz
7 II	Illite (also muscovite, sericite, etc.)	Schomberg silt loam, B horizon (Ontario)	Pennsylvania underclays (Illinois)
8 X	Hydrous mica-intermediates ("X")	Dodgeville silt loam, A horizon¶ (Wisconsin)	Ordovician bentonite (Kentucky)
9 Mt	Montmorillonite (also beidelite, etc.)	Barnes silt loam, A horizon (South Dakota)	Bentonite (Wyoming)
10 Kl	Kaolinite (also halloysite, etc.)	Cecil clay, B horizon (Alabama)	China clay deposit (Georgia)
11 Gb	Gibbsite (also boehmite, etc.)	Fannin sandy loam, C horizon (North Carolina)	Bauxite (Arkansas)
12 Hm	Hematite (also goethite, limonite, etc.)	Nipe clay, B horizon (Puerto Rico)	Bog iron (Minnesota)
13 An	Anatase (also rutile, ilmenite, corundum, etc.)	Naiwa A <sub>2</sub> or B horizon (Kauai Island, Hawaii)	Metamorphosed bauxite

\* Silicate groups I to V, with structures ranging from independent tetrahedra (I) to the line hexagonal structure of the amphiboles (V).

† Silicate group VI containing Fe<sup>+++</sup> or Fe<sup>++</sup> and Mg<sup>++</sup> in the octahedral layer.

‡ Slightly altered "rock flour," bearing amphibole. Other members of stages 3 and 4 are postulated as occurring in soils on the basis of petrographic microscopic observations of occurrence in sand and silt of youthful soils.

§ Slightly altered "rock flour," bearing chlorite. Biotite may also occur in the clay of various young soils in association with illite, for example, in the mica of Rideau clay, C<sub>1</sub> horizon.

¶ In association with small amounts of illite (stage 7) and montmorillonite (stage 9).

This sediment has entered the weathering sequence, however, as evidenced, on the one hand, by extinction of the early stages 1 and 2 and near extinction of the early-intermediate stages 3 and 4, and on the other, by the occurrence of small amounts of illite and mica-intermediate and a slight amount of montmorillonite

(stages 7, 8, and 9) in the fine clay. This case illustrates the essential meaning (i.e., persistence) of stages 3 and 4 in the weathering sequence. The sequence view fits the observed mineralogical content, and is more fundamental than the oversimplified characterization of this rock flour as being "unweathered" or exhibiting "absence of weathering," which could not be true in a surface material exposed for 10,000–20,000 years.

The group I to group IV silicates would be expected to occur in dominant amounts only in the clay fraction of certain kinds of youthful soils, for example, from fresh glacial rock flour derived from basic rocks. It is singular that five of the seven silicate structural groups occur in these scarcely represented early five stages of weathering. These primary silicates are, in most soils, largely decomposed from the fractions of particle-size range below 5 microns. However, they occur more commonly in sedimentary deposits, where protected from leaching.

The occurrence of stages 5 to 10 in the clay-size range of soils is well established. In the young soil Rideau clay, albite (stage 5) constitutes nearly one-half of the fine colloid of the C<sub>1</sub> horizon ( $< 0.2 \mu$ ), and quartz (stage 6) the most of the remainder (16). Both albite and quartz occur in the coarse clay ( $0.2\text{--}2 \mu$ ) throughout the profile. Illite (clay mica with a  $10 \text{ \AA}$ . basal spacing line, stage 7) has been reported extensively in soil clays, most commonly in the coarse clay, but also to some extent in the fine. Stages 5 to 7 are recognized as being analogous to the familiar sericitization reaction of microcline, or of plagioclase through the introduction of potassium to quartz and sericite. Heavy sericitization of plagioclase to mica, possibly in part deuteric (late magmatic), was observed in the very fine sand of Rideau clay, B and C horizons. Thus sericite may be considered one of the earliest of the hydrous mica series in soils. The hydrous mica-intermediates ("X") or degraded micas (basal spacing line at  $12\text{--}13 \text{ \AA}$ . or absent) are recognized here as a separate and distinct stage (stage 8). The mica-intermediates occur very commonly in the fine clay of soils. Stages 3 to 7 correspond to the stability series of Goldich (cited in reference 14, p. 52) except that quartz and muscovite are reversed in the weathering sequence presented in accordance with their relative persistence in soil colloids.

The montmorillonite group appears at stage 9, and kaolinite at stage 10, representing advancements in weathering over the illites and mica-intermediates. Gibbsite appears in stage 11 as weathering (desilication) of kaolinite proceeds. Hematite occurs at stage 12 and anatase at stage 13 under conditions of extreme weathering, eluviation, and good oxidation. Anatase and, hypothetically, corundum should be more stable than hematite, especially since not affected by reduction, and therefore should conclude the series (stage 13). Corundum is not known to form in soils, but it may occur in metamorphosed sediments, and would be expected, for example, in metamorphosed gibbsite, boehmite, or diaspore deposits.

The application of the weathering sequence to colloids of soils and sediments may be summarized according to the following fundamental generalizations:

1. From three to five minerals of the weathering sequence are usually pre-

ent in the colloid of any one soil horizon. There is a tendency for the composition of the colloid to be in the form of a distribution curve, being dominated (40–60 per cent) by one or two minerals with other adjacent minerals of the sequence decreasing in amounts with remoteness in the sequence.

2. The percentage of minerals of the early stages of the weathering sequence present in a soil clay fraction decreases, and the percentage of the successive members increases, with increasing intensity of weathering.
3. One to three intermediate stages may occasionally be absent from the normal sequence, particularly those following quartz, giving, for example,

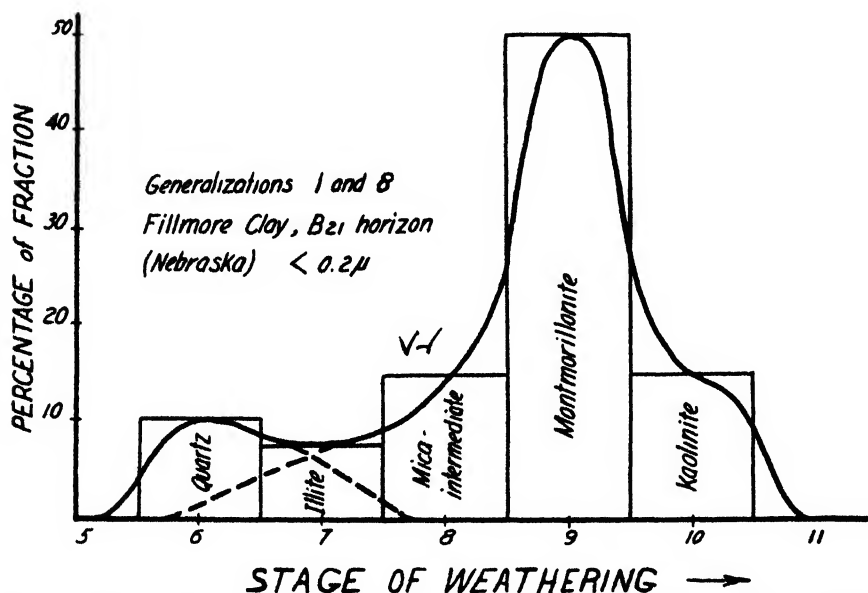


FIG. 1. Distribution curve of clay-size minerals in a Prairie planosol clay pan, showing asymmetry due to the quartz and illite being of a coarser fine-clay fraction.

a quartz-montmorillonite-kaolinite colloid, or a quartz-kaolinite-gibbsite colloid.

4. One or more stages may occasionally occur out of sequence as secondary depositions, particularly gypsum and calcite.

#### SOIL COLLOIDS AT VARIOUS STAGES OF WEATHERING: EXAMPLES

Application of the first generalization is illustrated in figure 1, wherein is illustrated the tendency for the occurrence of the minerals in the form of a distribution curve when plotted in order of their occurrence in the sequence. Important evidence<sup>4</sup> of the proper sequential order of quartz, illite, mica-intermediates, montmorillonite, and kaolinite is derived from the translation of this

<sup>4</sup> Confirmed by the particle-size function and soil-depth function, as discussed below.

distribution curve through the sequence. The almost continuous translation of the distribution curve is shown in figure 2, with a number of soil colloids, together with a summary of properties and implications.

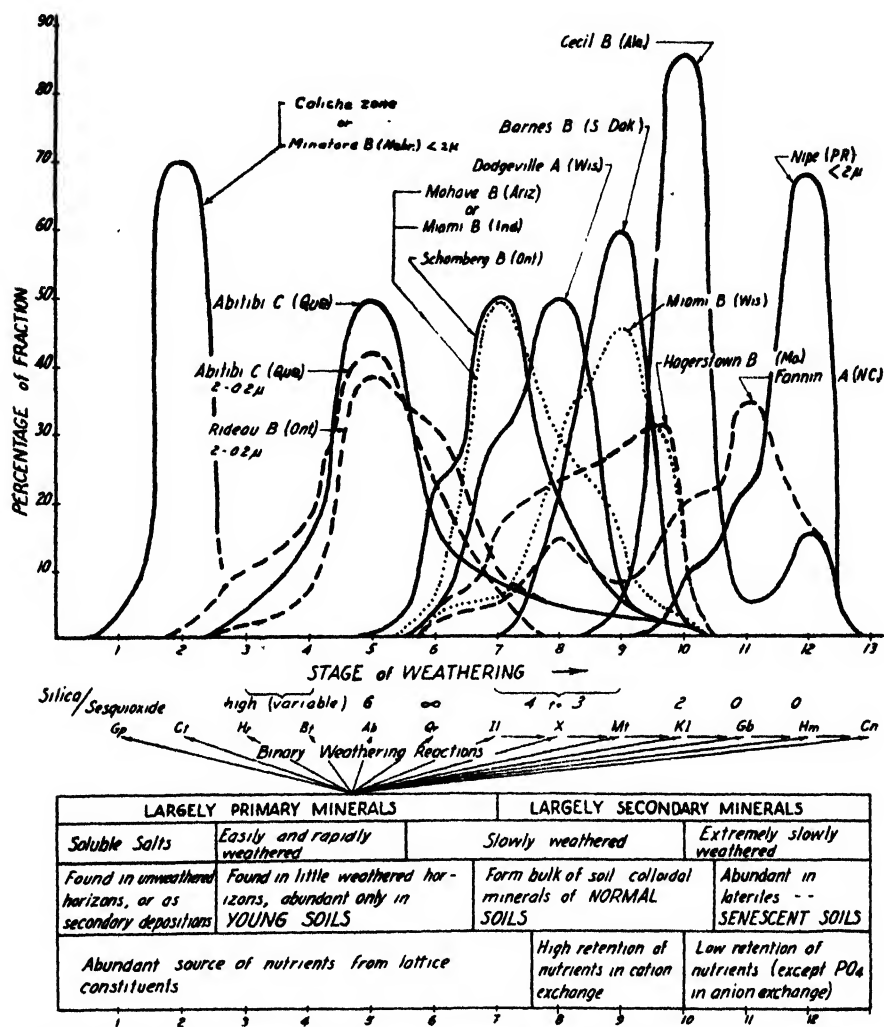


FIG. 2. Distribution curves for colloids of various stages of weathering and significance. (Particle sizes  $< 0.2 \mu$  unless otherwise stated.) "Cn" should read "An".

### Early stages -

Occurrence and disappearance of calcite (stage 2) in very young soils has been reviewed by Jenny (12, pp. 42-3). Under humid conditions, 5-10 per cent of calcium carbonate leached out of a dune sand during the course of 250 to 300 years of weathering, and of the Dutch polders reclaimed sea bottom in a similar period (12), i.e., during the embryonic stages of soil development.

The colloid of caliche zones (nearly pure calcite) or of Minatare silt loam B horizon (7), containing up to 75 per cent of calcite in the colloidal fraction, are examples taken from the semi-arid region (figure 2). Colloids high in calcite<sup>5</sup> also occur in the lower horizons of pedocals. The source of the calcite is generally secondary, through chemical precipitation, but in rare cases may involve sedimentation of colloids from eroded limestone.<sup>5a</sup> Preservation of calcite centers around the absence of sufficient leaching and the maintenance of high pH values. The dominating effect of such calcite on the properties of these colloids and of the soils themselves is well known.

In an analogous way, the presence of colloidal gypsum and other more soluble salts (stage 1) has a dominating influence on the nature of saline and solonized soils, particularly in the Pedocal region.<sup>5b</sup> These stage 1 and 2 colloids, representing secondary depositions, may occur out of sequence with respect to the silicate colloids present, as observed in the fourth generalization. It follows therefore, that the occurrence of these two early stages is not always associated with young soils, although it may be. Moreover, not all young soils contain minerals of the calcite or gypsum stages.

#### *Early intermediate stages*

The colloid from Abitibi silt loam, C horizon, is the youngest and least weathered soil material from the humid region which was studied (figure 2). The plagioclase of the albite-andesine end of the series is the dominant constituent, with lesser amounts of amphibole and chlorite of the two preceding stages, and quartz and mica of the two succeeding stages, thus further illustrating the distribution curve (first generalization). The colloid from Rideau clay, B horizon (16), is also centered on albite and quartz (stages 5 and 6) but lacks appreciable percentages of the earlier stages. Rideau clay is from southern Ontario and, while a young soil, is considerably advanced over the Abitibi sample of northern Quebec. The coarse clays of these two colloids are shown in figure 2 to illustrate the earlier stages of weathering. The fine clays also contained abundant feldspars and quartz (16), but were slightly further along in the weathering sequence, and only traces of minerals of stages 3 and 4 were present. The occurrence of amphibole and chlorite and of high amounts of feldspars in these colloids is believed to be the first instance reported for the fine fraction of soils. The occurrence of feldspars in the fine colloids of Rideau clay and other soils developed on the geologic Champlain sea was further verified by further collections from southern Quebec<sup>6</sup> of the St. Rosalie, A horizon, from two localities,

<sup>5</sup> The identity of the precipitated calcium carbonate of soils as being calcite has been amply verified by x-ray diffraction analyses in these and other laboratories.

<sup>5a</sup> Calcite and dolomite crystals of colloidal size have been observed in a podzol A<sub>2</sub> horizon, pedogenically formed within fragments of organic matter (Bourbeau, G. A.: Ph.D. Thesis, University of Wisconsin Library, Madison, 1948).

<sup>5b</sup> Since this manuscript was presented, Rodrigues and Hardy (Soil Sci. 64, 127-42 (1947)) have reported up to 30 per cent gypsum in the colloid in certain horizons (p. 140) of a tropical soil derived from shale.

<sup>6</sup> Collections obtained through the courtesy of Mr. Roger Baril, Chief of Soil Survey, Laval University, St. Anne de la Pocatière, Quebec, Canada.

and the St. Damase, A horizon, in which 20–35 per cent of the fine colloid ( $< 0.2 \mu$  diameter) was plagioclase of the albite-andesine end of the series. It is interesting to compare the age of these soils with ferromagnesian disappearing in the early intermediate stages of weathering (9,000 to 20,000 years) to the very young soils listed by Jenny (12, p. 32), ranging from 250 to 1000 years of age with calcite disappearing.

### *Intermediate stages*

The second generalization is exemplified in progressing through successive clays of figure 2. The fine colloids of Schomberg silt loam of Ontario (young soil of humid region), Miami silt loam of Indiana (retarded development for its region because of occurrence only on erosional slopes), and Mohave silt loam of Arizona (mature sierozem, desert region) are dominantly illite (stage 7). The colloid of Barnes silt loam of South Dakota (mature chernozem, subhumid region) is centered on montmorillonite (stage 9). The colloid of Miami silt loam of Wisconsin (mature gray-brown podzolic, cool humid region) is centered on montmorillonite with considerable kaolinite appearing. That of Hagerstown of Missouri (gray-brown podzolic, warmer humid region) is transitional, but with an increasing amount of kaolinite (stage 10) appearing. Both Miami and Hagerstown also contain appreciable mica (stages 7 and 8). A colloid of Hagerstown silt loam of Pennsylvania showed a similar composition. With the colloids from these gray-brown podzolic soils, the distribution curves are broader, extending from stage 7 (illite) to stage 10 (kaolinite), than in the chernozem (Barnes) centered on stage 9 (montmorillonite), with some mica-intermediate. The greater breadth of the curves for the gray-brown podzolic soils examined may be due to greater content of mica in the parent materials, coupled with greater intensity of weathering with some of the montmorillonite being carried on over to kaolinite. A postulate that the montmorillonite of the chernozem might represent an earlier stage of an alternative illite to mica-intermediate to kaolinite sequence is in conflict with the various lines of evidence to be presented. The illite percentage is higher in soils and horizons which have been subjected to less weathering. For example, the unweathered D horizon of the Miami soil (Wisconsin) is higher in illite than the A, B, or C horizons.

### *Advanced stages*

Proceeding to soils developed under further increased weathering intensity, the Susquehanna sandy loam, B horizon, of Alabama (red podzolic soil, warm humid region) is approximately equal in stage 9 (montmorillonite) and stage 10 (kaolinite), further linking the direct succession of montmorillonite to kaolinite (curve not shown). Only a little mica is present in the fine colloid of this soil. The colloid of Cecil clay of Alabama (red podzolic soil, warm humid region) is predominantly kaolinite (stage 10), but contains appreciable ferric oxide (hematite, stage 12). That of another Cecil clay of North Carolina contains considerable gibbsite (stage 11) along with the kaolinite (curve not shown).

The colloid of Fannin sandy loam, C horizon, of North Carolina is centered on kaolinite and gibbsite (stages 10 and 11) with appreciable quantities of hematite present (figure 2). The colloid of Nipe clay (figure 2) of Puerto Rico is dominantly hematite and goethite (stage 12) but contains about 20 per cent of gibbsite (stage 11) and a small quantity of kaolinite (stage 10). The A<sub>2</sub> or B<sub>21</sub> horizon of Naiwa soil of Kauai Island (the oldest Hawaiian island) consists of 25 per cent titanium dioxide, most of it anatase (stage 13), together with dominant amounts of hematite (stage 12).<sup>6a</sup> The translation of the distribution curves across the sequence of mineral weathering stages without a break in continuity emphasizes the procession of colloid composition as a continuous function of increasing weathering intensity (supporting evidence for generalization 2).

#### THE WEATHERING RATE FUNCTION: PROCESSION, ARREST, REVERSAL

##### *Components of weathering rate function*

The weathering rate may be viewed as a product of intensity and capacity factors. The intensity factors of weathering are temperature ( $T$ ) and its complementary relationship to accumulation of humus; rate of water movement, or leaching provided by internal drainage (water); acidity of the solution (proton intensity,  $H^+$ ) with particular reference to carbonic acid supply; and the degree of oxidation (electron intensity) and its fluctuation (oxidation-reduction,  $\Delta e^-$ ). The capacity factors of weathering are the specific surface of the particles ( $s$ ), and the specific nature of the mineral being weathered ( $k_m$ ). The weathering per unit time ( $t$ ) may be expressed in terms of these factors in the form of an equation:

$$\begin{aligned} \text{Weathering rate} &= \text{intensity factor} \times \text{capacity factor} \\ (\text{time rate}) &= f(\text{temperature, water, protons, electrons}) \times (\text{surface,} \\ &\quad \text{nature of mineral}) \end{aligned}$$

Then the weathering stage of the clay-size minerals may be represented as a summation:

$$\text{Weathering stage} = \Sigma f(T, H_2O, H^+, \Delta e^-, s, k_m, t)$$

The five cardinal factors of soil formation (climate, vegetation, relief, parent material, and time) may be recognized as being expressed in the various intensity and capacity factors.

For a given mineral species, and a given particle-size range (constant capacity factor), the weathering stage of the soil colloid is a product of the intensity functions multiplied by the time in which weathering has been occurring, or simply as "intensity  $\times$  time" product. Procession through various stages of the sequence follows increase of this product.

In general, increasing acidity and increasing oxidation must be considered as having a positive sense, favoring increased weathering intensity. Thus, pro-

<sup>6a</sup> From coöperative studies by Dr. G. D. Sherman, University of Hawaii, and the authors

longed leaching under reducing conditions would not lead through the sequence; laterite forms under oxidizing conditions. Byers (3) postulated that weathering is entirely expressible as a hydrolysis reaction, but noted the influence of temperature, water movement, particle size, and specific nature of the mineral on the rate.

#### *Arrest of weathering in the absence of leaching*

The normal weathering processes may be interrupted by lack of sufficient intensity of one of the functional factors. As an example, the occurrence of large amounts of montmorillonite in bentonites, in spite of their great age (time of weathering), is attributed to lack of leaching. Under normal weathering, in the absence of dissipation by erosion, a surface deposit would have weathered to the final stages (hematite). Absence of leaching has prevented weathering of the feldspars and other silicates of the volcanic ash from proceeding beyond stage 9. Frequently quartz or cristobalite (stage 6) is found occurring in association with montmorillonite in bentonites, residual because of little or no leaching; leaching under normal weathering would have removed the excess silica and allowed montmorillonite to undergo further weathering. The sodium bentonite (Upton, Wyoming) and the calcium bentonite (Monroe County, Mississippi) may well represent the product of weathering of albite-rich and anorthite-rich volcanic ash, respectively. The high montmorillonite content of Lufkin clay (Mississippi) and Alamance clay (North Carolina) similarly occurs as a resultant of poor drainage and partial arrest of weathering at stage 9, in localities where a more advanced weathering stage is normal. Arrest has not been complete in the Alamance, since appreciable kaolinite (stage 10) is also present.

#### *Reversal of weathering in sediments*

The interruption or shift of one or more of the weathering processes may serve to reverse the weathering equation, and lead to a reverse traverse of the mineral weathering sequence. Much support for the weathering sequence and its reversible character is found in the hydrothermal reactions of minerals, including the reactions occurring under pressure. A second major line of thought on the reversal sequence in sediments is embodied in the geologists' term "diagenesis," referring to reversion by metamorphic processes.

The sediments are thought to represent a certain amount of reversal of the weathering sequence, particularly because of little leaching and a lowered oxidation potential. Iron of hematite is reduced, for example, and is available for recrystallization, perhaps in glauconite. In some instances, slowly percolating waters may illuviate a new supply of soluble components to assist in the reversion. Thus, ordovician bentonite is thought possibly to be an ancient montmorillonite which has picked up potassium and reverted, to a certain extent, to mica-intermediate. Continuation of this process to a greater extent in the presence of a more adequate potassium supply would explain the conversion of vast sediments to shales rich in illite. Exclusion of water and further supplies of



solutes largely arrest the reversion at the illite stage.<sup>7</sup> To the extent that reversal is slowly continued either with or without influx of solutes from the outside of the sediment, authigenic quartz (stage 6), feldspars (stage 5) (10), zircon and tourmaline, etc. would be expected to occur *as found* in sedimentary deposits. Accessory chlorite and biotite of shales, glauconite of sandstones, and the calcite of limestones represent the ultimate reversal to stages 4 and 2 of the sequence. Or, in general:

5. The alteration sequence of the colloidal minerals of sedimentary deposits, under the impact of decreased or excluded leaching and oxidation, tends to be the reverse of that in the weathering of colloidal minerals of soils. Thus montmorillonitic sediments tend to revert by solution or metamorphic processes to micas and earlier stages. A gibbsitic (bauxite) sediment would be expected to resiliate to kaolinite or even to montmorillonite or illite to the extent that silica and potassium sources were available in the mixture of minerals in the sediment.<sup>8</sup>

To the extent that recent sediments (alluvium or aeolian) are left exposed to continued surface weathering and soil formation, the weathering sequence continues scarcely interrupted. Or, in general:

6. Colloids of soils being developed on fresh or recent alluvial or aeolian sediments continue from the weathering stage occupied by the soils from which the sediment was derived.

Thus, the colloid of a young soil from such source would usually represent the particular weathering stage of its source, which would not necessarily be an early stage.

#### THREE ANALOGOUS RECAPITULATIONS OF THE WEATHERING SEQUENCE OCCURRING IN NATURE

Three analogous recapitulations of the weathering sequence of clay-size minerals are found in nature: first, in accordance with the familiar geographic pattern of weathering; second, as a particle-size function; and third, as a depth function in soil or sediments. These trends may be set forth as generalizations 7 to 9.

7. *Soil geography*.—The mineralogical composition of soil colloids follows the weathering sequence geographically, in accordance with the variation in weathering intensity factors which are controlled by the geographic distribution of climate, together with time of weathering.

Sediments are influenced by the same geographic factors, to the extent that they are derived from soils so controlled. The mineral composition tends to vary in

<sup>7</sup> Evidence of reverse traverse of the weathering sequence from kaolinite (stage 10) back to illite (stage 7) in sediments formed in the Gulf of Lower California from suspended solids of the Colorado River has been noted by Dr. R. E. Grim (personal communication, September, 1947).

<sup>8</sup> Goldman and Tracey (Econ. Geol. 41, 567 (1946)) recently described resiliation to kaolinite occurring in Arkansas bauxites.

the various Great Soil groups, being far advanced (stages 11 and 12) in the laterites, intermediate (stages 8 and 9) in the chernozems, less advanced (stages 7 to 9) in the sierozems, and least advanced (stages 3 to 6) in certain types of young soils, for example, those developed on the sediments of the Champlain and Ojibway glacial seas (figure 2).

8. *Particle surface or size function.*—The rate of weathering of clay-size mineral particles of soils and sediments varies according to the surface of the particles, being more rapid with increasing fineness of the particles. Thus, in stages 1 to 9, the mineralogical composition of colloids from soils, and to some extent of sediments, advances in the weathering sequence with increasing fineness of the fraction separated for identification. Decreasing size is the "capacity factor equivalent" to translation through greater intensity of weathering. In stages 10 to 12, kaolinite, gibbsite, and hematite may show the

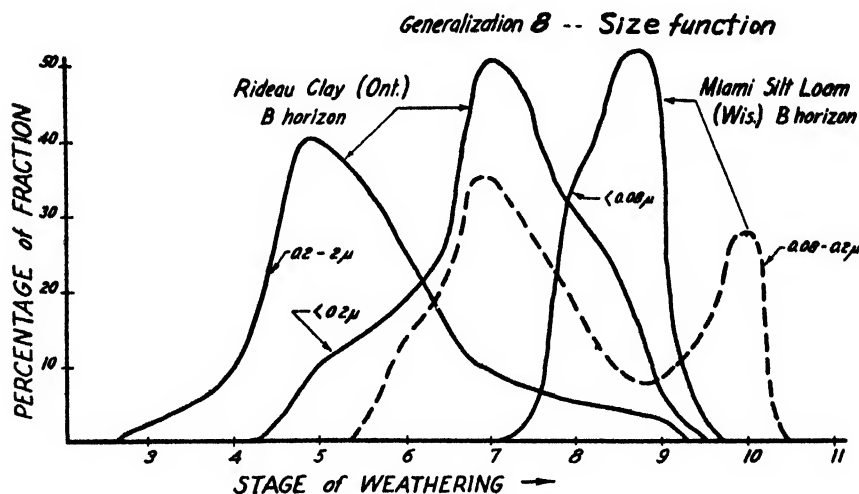


FIG. 3. Particle-size function in weathering stage of clay-size minerals

same trend; however, these minerals may undergo *crystal regrowth* and occur independently of the particle size.

With extreme fineness, weathering advances very rapidly with the result, for example, that hematite monolayers would be expected, and may be found, on almost any colloid developed under conditions of good oxidation. Likewise, the coarse clay fraction (0.2–2  $\mu$  diameter) almost invariably contains minerals of earlier stages of weathering than the fine clay (< 0.2  $\mu$  diameter). This is illustrated for these two fractions of Rideau clay, B horizon (Ontario), in figure 3. The coarser fraction is centered over feldspar (stage 5); the finer fraction over illite (stage 7). Both fractions contain quartz (stage 6); but the fine fraction contains small amounts of the more advanced stages (8 and 9), mica-intermediate and montmorillonite, while the coarser fraction contains small amounts of the earlier stages (3 and 4). One of the best lines of evidence that illite follows

quartz in the sequence is that mica persists in increasing ratio to quartz as the particle size of the fraction decreases. The minerals which are more resistant to chemical weathering persist in the greater quantities in the finer size fractions. The asymmetry of the distribution curve of figure 1 can be explained on the basis of particle-size function. The quartz occurs in the *coarser* sizes present in the fine clay fraction, and thus persists overly long, simply because its particles are larger than the average for the fraction. The colloid of Miami silt loam (Wisconsin) is centered over mica-intermediate and montmorillonite (stages 8 and 9) in the fine particle size range of  $< 0.08 \mu$  diameter (figure 3), but the coarser  $0.08-0.2 \mu$  fraction contains predominantly quartz and illite of earlier stages 6 and 7. A second peak occurs over kaolinite (stage 10), as an illustration of the process of crystal regrowth. If the generalization held perfectly, kaolinite would appear in a finer fraction than montmorillonite. The fact that its crystals can grow larger, however, may account in part for its increased stability to weathering. It is interesting that the distribution curve of the entire colloidal fraction ( $< 0.2 \mu$ ) of Miami silt loam (Wisconsin) is a symmetrical monodistribution (figure 2) in contrast to the bimodal nature of the coarser subfraction in figure 3.

9. *Horizon depth function.*—The weathering stage of the colloid of a soil horizon or of a sediment tends to advance with increasing proximity to the surface.

Thus, in soils, weathering stage *decreases* with depth down into the unweathered D horizon, but this change with depth usually is not great through the A, B, and C horizons, shifting only through one to three weathering stages. The change with depth is most pronounced in young soils in the humid region where weathering is in the early stages (Schomberg silt loam, Ontario, figure 4) (16). A strong line of evidence that montmorillonite follows illite and mica-intermediate in the sequence is the alteration of mica to montmorillonite in soils such as the Schomberg (figure 4). Bray (2) also noted a similar relationship for certain soils in Illinois. Weathering stages have been found to change little with depth through the A, B, and C horizons in many of the well-developed soils of the humid region. This is true of Miami silt loam (Wisconsin), although an analogous increase in illite with depth occurred in entering the D horizon of this soil.

In soils of the arid region, the weathering stage may increase with depth, in passing into horizons where the subsurface is kept more moist by protection from evaporation, while the surface mulch is dry over long periods. A somewhat analogous situation occurs in the planosol, wherein extra water supply and more sustained solution processes are provided by restricted rate of external drainage and consequent increased internal water supply. This situation of the accelerated weathering in the planosol, under restricted *rate* of drainage but ultimately *large total volume* of percolate, should not be confused with the arrest or reversal of weathering processes in sediments under conditions of virtually no internal drainage and percolation.

In sediments, the weathering stage would be expected in general also to advance with proximity to the surface, if the processes of change with time in the sediments are viewed as a reversal of the weathering equation. Thus the clay-

size minerals of a very recent sediment might be abundant in kaolinite or montmorillonite, while in deeper lithology the same parent sediment would have reverted (diagenesis) to the earlier stage illite, as already discussed.

These polyfunctional processes of weathering are illustrated in figure 5, wherein weathering stage is represented on the vertical axis. Weathering stage advances with increase of the product "intensity  $\times$  time" of weathering, and with decrease in particle diameter (or proportional increase of specific surface). Increments of weathering with decreased particle surface are indicated as  $\Delta w$  and  $\Delta s$  (figure 5). Weathering reaches completion in a short time with extreme fineness of particles, for example, the appearance of surface films of hematite early in weath-

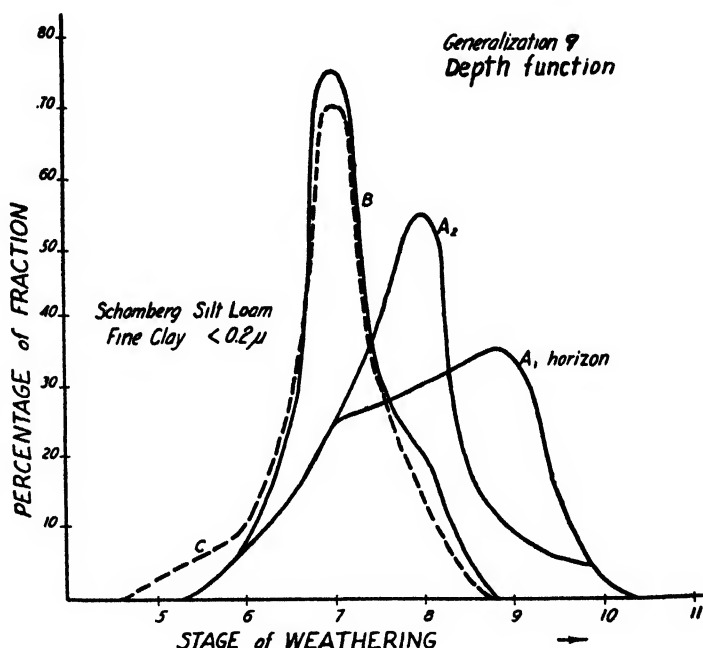


FIG. 4. Depth function in mineral weathering stage of colloids from a young soil

ering (figure 5). Specific properties of minerals ( $k_m$ ) favoring ease of weathering have an influence similar to decrease in diameter in hastening weathering.

Stages 1 to 4 are traversed in relatively short "time  $\times$  intensity" factors, while the sweep broadens (rate of change of weathering stage with "time  $\times$  intensity" decreases) in the intermediate stages of 5 to 9. This trend has led to the general statements that basic rocks form laterites (5, 9), whereas acid rocks yield kaolinite and free silica (5, 8, 11). These statements indirectly state that the acidic rocks require a much larger "time  $\times$  intensity" factor for complete weathering to stages 11 and 12, as compared to basic rocks.

The span of weathering stages found within the young Schomberg profile (figure 4) is represented by the increments A, B, C (figure 5) corresponding to these three horizons. This shortness of span with depth in the soil profile is considered typical—in fact, the span is usually much shorter in moderately well-

developed soils. The increment A', B' represents the span for a desert soil, with weathering being somewhat further advanced in the B horizon.

#### CRYSTAL CHEMISTRY OF THE WEATHERING SEQUENCE

The discussion thus far has been concerned with relative persistence of the colloidal minerals as a measure of their relative stability. Emphasis has been placed on minerals "found" rather than the mechanism of their formation. The crystal chemistry of the weathering sequence may be divided into the questions of (a) the underlying reason for the relative stability as an expression of factors

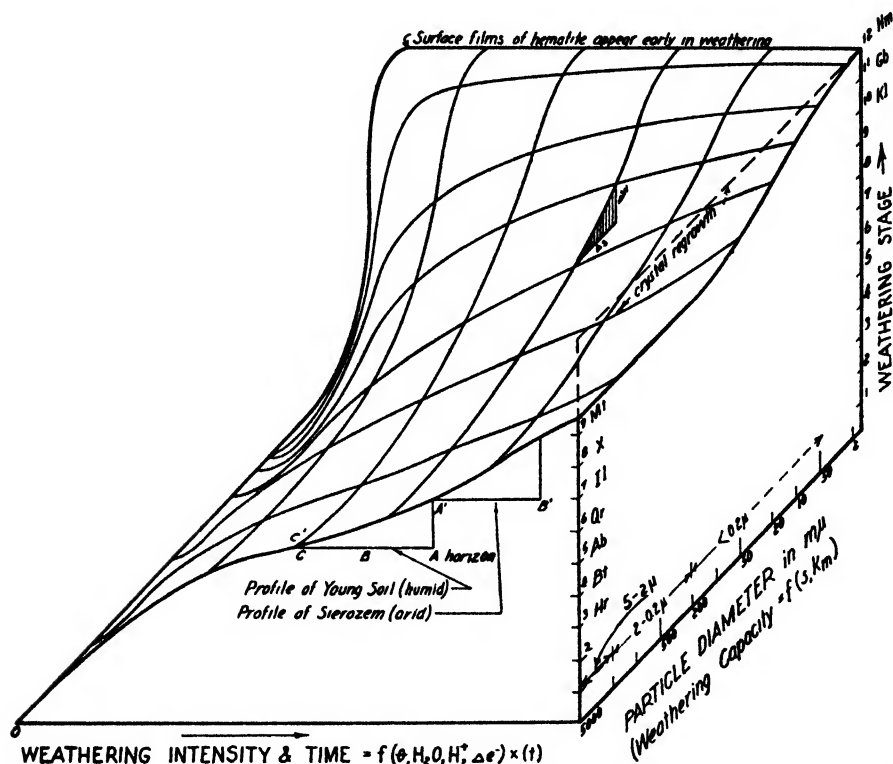


FIG. 5. Mineral weathering stage as a function of intensity  $\times$  time of weathering, and the capacity factors of weathering. (The symbol  $\theta$  should be  $T$ .)

of crystal structure, and (b) the chemical transformations involved in the formation of minerals of each stage. The second question resolves itself into an inquiry as to what extent each stage is the parent material for succeeding stages, or contrarily, to what extent each stage is a unique product of a primary parent material left either by eluviation of all else, or through a binary weathering reaction.

#### *Crystal chemistry of relative stability*

Chemical weathering takes place through simple solution, carbonation, hydrolysis, and oxidation and reduction. Simple solution and carbonation are the

reactions chiefly concerned in weathering loss in (embryonic) stages 1 and 2. Discontinuity of the silica portion of the lattice, coupled with activity of the basic cations, appears to be the dominating factor in stages 3, 4, and 5. Independent or incompletely linked silica tetrahedra (silica groups I to V) permit ready hydrolysis of the strong bases in stage 3. Weakness along the octahedral planes caused by the presence of  $\text{Fe}^{++}$  and  $\text{Fe}^{+++}$  gives rise to the relative instability of stage 4 (biotite, etc.). The continuous silica sheets are a factor for stability of the other group VI silicates, and account for the stage 4 minerals succeeding the other ferromagnesian minerals of stage 3. The fourfold silica linkage of albite (feldspars in general, stage 5) brings their stability one level higher, but the high content of active bases introduces ease of hydrolysis. This places the feldspars one stage less stable than quartz (stage 6), with fourfold silica linkage but without the bases present. Quartz solubility is a linear function of specific surface, and therefore quartz is expected, and is found, to decrease tenfold in quantity for each tenfold decrease in particle size of fraction considered. The occurrence of the micas at stage 7, more stable than quartz, is contrary to Goldich's series for coarse particles (cited on p. 52 of reference 14), but has abundant experimental verification in the observed mineral content of colloids of various stages of weathering and in the particle-size function as discussed. The basis for the occurrence of mica after quartz is explained on the principle that a layer of aluminum ions beneath a layer of silica ions in the silica sheet (oxygen lattice) increases the stability of the silica layer. This finds support in the great stability of the alumina sheet, which persists through five stages of weathering (7 to 11).

The mica-montmorillonite order is analogous to the albite-quartz order. Of the less stable mineral of each pair, for example, muscovite contains 350 milliequiv. of non-exchangeable but hydrolyzable potassium per 100 g., while orthoclase contains 550 milliequiv. of potassium per 100 g. Of the more stable mineral of each pair, each has silica surfaces, and little or no hydrolyzable lattice bases. Montmorillonite has more stable (more quartz-like) surfaces of its crystal plates than mica.

It is noteworthy that, whereas the octahedral alumina layer stabilizes the silica sheet (stage: quartz < mica), the substitution of  $\text{Al}^{+++}$  for  $\text{Si}^{++++}$  within the silica sheet has the opposite effect (albite < quartz, or mica < montmorillonite), perhaps because of distortion in the silica sheet and the accompaniment of the hydrolyzable basic cation to balance the charge. The 60-100 milliequiv. of exchangeable bases per 100 g. of montmorillonite may be exchanged without disturbance of the lattice. Mica apparently cannot release its potassium without alteration of its structure (i.e., weathering). With regard to crystal lattice factors:

10. The stability factor for silicates in the clay-size range is a resultant of the silicate structural groups in general, but is modified by considerable cross-over according to the ionic substitutions involved.

Beyond stage 7, the percentage occurrence no longer falls off with decreasing particle size, indicating that the lattice factors for stability ( $k_m$ ) have made the increase in specific surface relatively much less important in determining weathering rate.

The octahedral alumina sheet persists as desilication occurs in forming kaolinite (stage 10) and gibbsite (stage 11), illustrated diagrammatically in figure 6. Hematite and anatase are the final endpoints of weathering under conditions of good aeration and high temperature. Their insolubility under these conditions slightly exceeds that of gibbsite and boehmite, and these two minerals eventually dissolve and eluviate, leaving hematite and anatase. Corundum, the isomorphous analogue of hematite, hypothetically might end the series, but higher than soil temperatures would be required for such alteration of gibbsite and boehmite. The requirement of oxidizing conditions is mandatory if hematite is to persist as an end-product; otherwise it is subject to the instability factor of the ferromagnesian minerals of stages 3 and 4. Transitory periods of reduction may account for the loss of iron and relative enrichment in anatase (and ilmenite) noted in the Naiwa soil.

### *Chemical transformations*

Successive stages of the weathering sequence are invariably lacking in stoichiometric relationship to preceding stages. Thus, successive stages are not closed-system rearrangements of the chemical content of the parent material; in fact, some stages (e.g., stage 12) involve principally different chemical elements compared to preceding stages. In general:

11. Lack of stoichiometry between successive stages of the sequence arises through processes of eluviation and illuviation.

Thus a small residue of the parent material may constitute the bulk of a successive stage through eluviation of all else. This is analogous to the persistence of a few short threads as the "successive stage" after dissolution of a bag of sugar in which the threads had originally been a scarcely noticeable impurity. A great reduction in lithological volume accompanies such a transformation, a familiar example being the weathering away of several feet of limestone to produce a few inches of earthy material. This "simple residue" principle may be continued successively. In the analogy, the threads might consist of carbon pigment and cellulose, and the cellulose decompose leaving the trace of carbon pigment as the bulk of the next stage. Of the earthy residue of the limestone, for example, the antigorite (stage 4, iron-magnesium analogue of kaolinite) might decompose, leaving albite and illite present in the successive stage.

In addition to this "simple residue principle," the coarser minerals on the one hand, and the colloidal products of decomposition on the other, may not be entirely recovered in the residue, but in themselves give rise to (be the "successive parent materials" of) successive stages. In the analogy, the cellulose might give rise to a carbonaceous residue, almost as resistant as the carbon pigment, and might be considered as belonging to the same stage. In the earthy product of the limestone decomposition, some of the magnesium associated with the calcium carbonate might combine with a portion of the albite decomposition product and result in sericite-illite or montmorillonite. At the same time some of the original illite might weather into mica-intermediate and montmorillonite. The distribution curve of mineral composition of the colloid would thus advance through stages 5, 6, 7, 8, and 9. Under acid conditions, albite or illite may alter

in part directly to kaolinite, and some of the montmorillonite be desilicated to kaolinite. The colloid thus advances through stages 7, 8, 9, and 10.

By the time stages 10 and 11 are becoming prominent, wherein no isomorphous substitution of iron is possible, the goethite-hematite (stage 12) content will have begun to be built up appreciably, as iron is released from weathering of the minerals of earlier stages. Hematite and goethite thus build up in bauxites and laterites. The basis of the occurrence of three to five minerals as a distribution curve for a colloid at the later stages (first generalization) is thus apparent.

In addition to this "successive parent material principle," additional chemical sources are available through illuviation from other horizons. This is the complement of the "simple residue" process going on in the source horizon. The occurrence of gibbsite as a primary weathering product from feldspar and mica was noted by Alexander, Hendricks, and Faust (1), and they advance the principle that this gibbsite may normally be resilicated to kaolinite in the zone near the unweathered parent rock surface. This is an important observation bearing on the mechanism of clay formation. Harrison (11) postulated resilication of gibbsite through rise of silica through the ground water from freshly decomposing silicates.<sup>9</sup> It appears probable that resilication can proceed on to the montmorillonite and mica stages under some circumstances, particularly in sediments. That mineral weathering in soils is dominantly an open system rather than a closed system within individual mineral grains is apparent from these reactions brought about by illuviation.

### *Desilication*

Reversal of these silication equations, giving desilication (figure 6), in advancing stages of weathering is believed by the writers to be a dominant mechanism for the chemical transformations within the colloidal fraction between stages 7 to 11. In this range, minerals of each stage may be the parent material of those in successive stages. Simultaneously, the early-stage primary minerals of the silt and sand such as ferromagnesians and feldspars may, through binary weathering reactions, also form one or several of the minerals of stages 7 to 11, with accompaniment of eluviation of the excess iron and silica. In contrast, quartz undergoes gradual solution and eluviation in much the same way as gypsum and calcite, but more slowly (lower  $k_m$  factor).

Why desilication proceeds at an accelerated rate as acidity increases has been a much debated point, but the experimental fact is well established that kaolinite and gibbsite form under increased acidity associated with increased weathering intensity and time, at the expense of minerals of higher silica content. Chemically, the solubility of silica would be expected to decrease as the acidity increased. Various proposals have been advanced (cited in reference 14) that an isolated alkaline condition such as in the weathering shell of feldspar grains must intervene to remove the silica, but this proposed mechanism is inconsistent with the acidity of the soil systems actually existing, through which the silica must move. Moreover, ample basis exists for the assumption that desilication occurs

<sup>9</sup> See footnote 8.



in the acid regime of weathering. First, the increase of soil acidity to pH 4, though representing "extremely acid" soil conditions with reference to plant growth, represents only a *very slight* degree of acidity in the chemical system for insolubilizing silica. Marked insolubility of silica is brought about at negative pH values, which are 4 to 6 magnitudes more acid than pH 4. Second, from the viewpoint of relative stability, kaolinite, gibbsite, and boehmite, while structurally hydroxyl compounds, respond chemically more like insoluble weak acids or acid anhydrides, weaker than silicic acid. As such, they should tend to form in acid systems. In line with this property, the gibbsite and boehmite are solubilized more easily by treatment with alkali than with acid. The explanation of increasing depletion of silica ("laterization") associated with increasing acidity

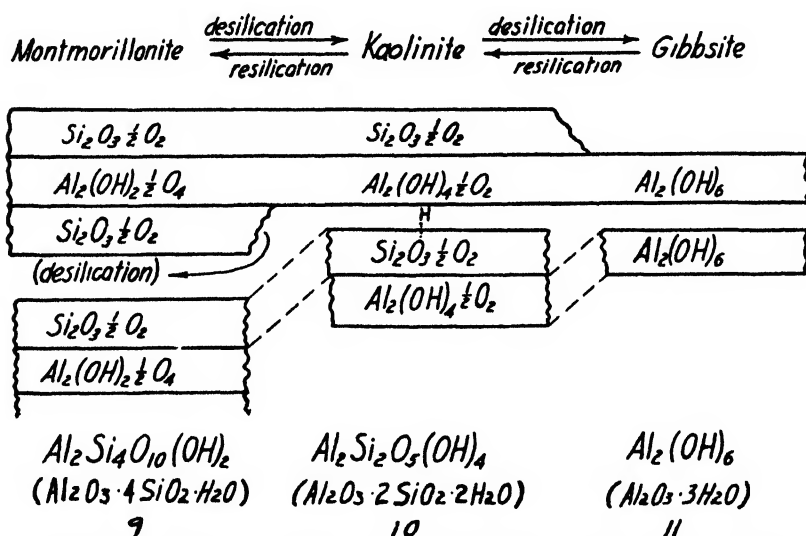


FIG. 6. Reversible silication reaction of the gibbsite layer of stages 9, 10, and 11. (Ionic substitution not shown in montmorillonite formula for the sake of simplicity.)

lies in the fact that both factors result *independently* from increased weathering (leaching, etc.).

The possibility of hydrogen bonding between crystal plates of minerals of stages 10 and 11 also tends toward more compact and more stable crystals, and this hydrogen bond is created in an acid regime by the desilication of one surface of montmorillonite to form kaolinite or of the second surface of kaolinite to form gibbsite. The fundamental basis for the continuously decreasing ratio of silica to sesquioxides and bases in colloids, with advance in weathering intensity, is apparent in the procession in the weathering sequence through ratios of infinity to zero, as shown in figure 2.

#### Podzolization

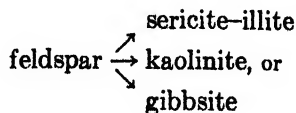
The dominant factor in the chemical transformations in podzolization is reduction, or deficiency of oxygen. Reducing conditions may be created by

accumulations of organic matter, either because of low average temperatures, or because of accumulation of excess water and exclusion of air. Reduction mobilizes the iron released by weathering by converting it to ferrous compounds and frequently to the form of organic complexes. The mobilized iron usually is deposited in deeper horizons where the oxidation potential is higher, owing to increased pH value and calcium saturation. In podzolization, therefore, one end-product of weathering (iron oxide) is removed from the site of weathering, and to this extent the  $A_2$  horizon represents a reversal of the normal weathering equation (oxidation considered positive). However, in other respects the mineral weathering sequence is followed, *viz.*, disappearance of feldspars and low content of quartz in the colloid, and the occurrence of a distribution curve of the illite, mica-intermediate, montmorillonite, and kaolinite in the colloid of podzols, even in the  $A_2$  horizon. Desilication of the lattices in the clay-size particles and succession through the sequence apparently takes place in the  $A_2$  horizon. The ashy appearance is considered to represent prominence of the gray silt and sand grains, resulting from removal of coloring agents and migration of some of the colloidal clay particles out of the  $A_2$  horizon. But it is not considered to represent precipitation of silica, or even an absence or retardation of the normal rate of dissolution and leaching of quartz and other forms of silica, particularly from the clay-size particles. Podzolic soils are frequently acid, but may be nearly neutral so far as the dominant chemical processes of podzolization are concerned. Podzolization has been reported at pH values of 6.5 or above, as might have been predicted.

#### *Laterization*

From the point of view of the weathering sequence, laterization represents the end-product of intensive desilication under conditions of intensive leaching, usually in the presence of slightly acidic solutions (e.g., pH 4), as discussed above. The process of laterization differs from that of podzolization in having good oxidation, which preserves the iron in the form of goethite and hematite (stage 12) and the aluminum in the form of gibbsite and boehmite (stage 11). Continuity and basic similarity of podzolic and lateritic weathering processes is intimated in the literature by recognition of previously formed "lateritic" soils as red and yellow "podzolic" soils.

The fundamental thesis of the concept of a mineral weathering sequence is an integration of the various binary weathering reactions (stoichiometric systems) such as ferromagnesium mineral  $\rightarrow$  hematite, volcanic ash  $\rightarrow$  montmorillonite, or



These processes may occur singly, simultaneously, or successively, according to circumstances. The integration occurs as a phenomenon of nature, but its defi-

dition in the weathering sequence presented could be achieved only through observation of a large body of data for colloids from diverse sources.

Thus, the integrated sequence function is considered to be continuous, and therefore the gradation from podzolization to laterization must be a continuous function, with all intermediate soil conditions to be expected (podzol-podzolic-lateritic-laterite sequence). One illustration of continuity will be presented centering around the extinction function of quartz in approaching the laterite (table 2). It will be noted that the quartz content of the soil decreases systematically with increasing weathering intensity, and that the percentage of quartz in the finer size fractions disappears more quickly than for the soil as whole, but continuously. In the Nipe clay soil, the quartz content is 10 or 15 per cent (as determined by x-ray diffraction analysis of the total soil ground to sufficient fineness by light crushing for a few minutes in an agate mortar). This establishes the fact that a considerable amount of silica in the upper 36 in. of soil has been available to be weathered into the finer sizes. However, weathering intensity

TABLE 2  
*Extinction of quartz in approaching the laterite*

SOIL AND SOURCE (B HORIZON IN ALL CASES)	PERCENTAGE OF QUARTZ IN VARIOUS SIZE FRACTIONS			PERCENTAGE OF STAGES 11 AND 12
	Fine clay <0.2 $\mu$	Coarse clay 0.2-2 $\mu$	Whole soil	Fine clay <0.2 $\mu$
Miami silt loam (Wisconsin) . . . . .	5-8	30-40	60-80	<2
Cecil clay (Alabama) . . . . .	<5	5-10	20-40	10
Catalina clay (Puerto Rico) . . . . .	<5	5-10		15
Fannin sandy loam (North Carolina). . . . .	<5	5-10	20-40	20
Nipe clay* (Puerto Rico) . . . . .	0	0	10-15	85
Laterite (Haiti) . . . . .	0	0	0	100

\* Sandy A horizon assumed lost by erosion.

(leaching in so far as quartz is concerned) has been great enough to prevent any appreciable accumulation of quartz in the size range below 2  $\mu$  diameter. According to the particle-size function (generalization 8), quartz cannot or scarcely can reach clay size under a weathering "intensity  $\times$  time" factor of sufficient magnitude to produce a laterite.

Later stages of the weathering sequence increase reciprocally with the quartz decline, particularly stages 11 and 12 (right-hand column of table 2). In the Fannin and Nipe soils, the gibbsite content of 10-20 per cent fitting between kaolinite and hematite in the distribution curve helps to establish the position of gibbsite in the sequence and substantiate the desilication reaction.

The necessity of eluviation and illuviation in building up the alumina and iron content at the close of the sequence has been stressed. Evaporation of illuviating ground waters (11) and oxidation of reduced iron contained undoubtedly has sometimes been a major contributing factor in the enrichment of laterites (5, 13, 14). Laterite in fact has been termed (5) a "fossil illuvial horizon of an an-

cient soil." To the extent to which illuviation has been a factor, the laterite is a counterpart (on a large scale) of the illuvial B horizon of the podzol. Moreover, a predominance of easily weathered minerals (high  $k_m$ , as in basic rocks) favors rapid progression through the weathering sequence, and from a practical standpoint may be a dominating factor (5, 9, 13, 14) in the development of some of the great laterite deposits.

The enrichment of the colloids in alumina and iron has been spoken of as a tropical weathering process (12, p. 36). The weathering sequence view emphasizes the depletion of silica and enrichment in alumina and iron as a trend in weathering generally. The accumulation of a quartz-rich A horizon on the surface of senescent laterites would appear to contradict the concept of hematite as the final weathering stage. Quartz is listed in weathering series for coarse particles as the most advanced (resistant) stage. However, this seeming paradox arises from the fact that quartz is perhaps the silicate mineral most resistant to *physical* weathering, being much more resistant than mica, for example. When it is in sufficiently fine grain size, chemical weathering takes precedence over physical weathering and the mica turns out to be more resistant. Sandy A horizons of senescent lateritic and laterite soils may develop through rather complete mechanical eluviation of the colloidal constituents.

#### *Weathering sequence in relation to the "normal" soil*

The concept of the "normal" soil advanced by Marbut implies that the soil profile is in equilibrium, being lost by erosion as fast as formed through weathering. The concept of weathering sequence operates to a considerable extent satisfactorily within this frame of reference. In agreement with Marbut's view, the sequence transcends the parent material as the key to trend of weathering of the colloid. In general:

12. The *course* of weathering (the sequence) is unaffected by the parent material, but the stage existing (the mineral content) at any time is influenced by the parent material to the extent that the "intensity  $\times$  time" product has been insufficient to complete transformation of the source material.

However, the concept of "normal" soil fails to describe the young soils which are common (*normal*) in Southern Ontario and so, according to Marbut's view, these are azonal soils. This terminology fails to fit these soils which, from a broad view, are truly both *normal* and *zonal*, but this discrepancy may be passed over as being only a fault in terminology. A more fundamental question is whether virgin profiles of the so-called "normal" soils are truly at equilibrium, i.e., at a steady state. To answer this requires conjecture as to what they would be like in another 20,000 to 100,000 years or more. It is important to note that the weathering sequence view as presented is *equally applicable* whether the soils are at equilibrium ("normal"), or whether they are continually moving into more advanced stages. The very old soils of the Southern Appalachian mountains and Piedmont plateau, with their high kaolinite, gibbsite, and hematite contents (6), probably should be classified as lateritic or early-stage laterites rather than as

red podzolic soils. Likewise, the old laterite soils on the peneplain of western Australia (4, 5, 15) are in still further advanced stages of weathering, as a result of a large "intensity  $\times$  time" factor. Comparison of these soils with younger soils in the same regions suggests that a true equilibrium, i.e., a steady state, has *not* been reached by soils generally, and that *most soils* are even now slowly *advancing further through the weathering sequence*.

#### SUMMARY

The stability series or weathering sequence of minerals present in the colloids of soils and sediments is considered both from the standpoint of the minerals found and from the standpoint of the basis in crystal chemistry for the sequence. The sequence of thirteen stages is represented by the type minerals: gypsum, calcite, hornblende, biotite, albite, quartz, illite, mica-intermediate, montmorillonite, kaolinite, gibbsite, hematite, and anatase (corundum). The weathering stage of a colloid is considered to be a resultant of intensity factors (temperature, moisture transfer, acidity, and oxidation-reduction) and capacity factors (particle size and specific nature of the minerals), together with time. The following generalizations are made on the basis of observed data:

1. From three to five minerals of the weathering sequence are usually present in the colloid of any one soil horizon, one or two minerals being dominant and other adjacent minerals in the sequence decreasing in amounts with remoteness in the sequence.

2. The percentage of minerals of the early stages of the weathering sequence decreases, and of the successive members increases, with increasing intensity of weathering.

3. Intermediate stages may occasionally be absent, giving a bimodal curve, and secondary deposits such as calcite or gypsum may occur out of sequence.

4. The weathering equations are considered reversible, moving largely to the right in soils, and to the left in sedimentary deposits. However, alluvial and aeolian sediments which remain exposed to continued weathering continue the sequence as of their parent soils.

5. The mineralogical composition of the soil colloids varies according to three analogous sequences: *viz.*, according to geographic (climatic) variations, particle surface function, and proximity to surface of the soil.

6. The stability factor of the minerals is a resultant both of crystal structure and of the specific isomorphous elements. Lack of stoichiometry between successive stages arises through processes of eluviation and illuviation. The course or direction of the sequence is unaffected by parent material, although the stage at hand may be.

Podzolization and laterization are considered to differ principally in the degree of oxidation and in summation of "weathering intensity  $\times$  time", but to be following through the sequence as otherwise fundamentally similar desilication processes in an acid regime. It is suggested that soils in general, instead of being at a steady state as embodied in the concept of the "normal" soil, may be even now slowly advancing in the weathering stage.

Helpful suggestions and criticisms of this manuscript offered by Professors P. D. Krynine and J. C. Griffiths of The Pennsylvania State College and by Professor R. J. Muckenhirn of the University of Wisconsin are acknowledged with gratitude.

## REFERENCES

- (1) ALEXANDER *et al.*: Soil Sci. Soc. Am. Proc. **6**, 52 (1942).
- (2) BRAY: Soil Sci. **43**, 1 (1937).
- (3) BYERS: Bull. Am. Soil Survey Assoc. **14**, 47 (1933).
- (4) CAMPBELL: Mining Mag. **17**, 67, 120, 171, 220 (1917).
- (5) CARROLL AND JONES: Soil Sci. **64**, 1 (1947).
- (6) COLEMAN, MEHLICH, AND JACKSON: Manuscript, University of Wisconsin, 1947.
- (7) FITTS: M. Sc. Thesis, University of Nebraska, 1937.
- (8) FOX: Records Geol. Survey India **69**, 389 (1936).
- (9) HANLON: J. Roy. Soc. N. S. Wales **78**, 94 (1945).
- (10) HONESS AND JEFFRIES: Sedimentary Petrol. **10**, 12 (1940).
- (11) HARRISON: Imp. Bur. Soil Sci. Harpenden, England (1933).
- (12) JENNY: *Factors of Soil Formation*. The McGraw-Hill Book Company, Inc., New York (1941).
- (13) MARTIN AND DOYNE: J. Agr. Sci. **17**, 530 (1927); **20**, 135 (1930).
- (14) REICHE: Univ. New Mex. Pubs. Geol. No. **1**, Albuquerque, 1945.
- (15) SIMPSON: Geol. Mag. **9**, 399 (1912).
- (16) WILLIS AND JACKSON: Manuscript, University of Wisconsin, 1947.

## COMMUNICATIONS TO THE EDITOR

A COMPARISON OF THE SENSITIVITY OF SPECTROGRAPHIC  
AND RADIOTRACER METHODS

A COMMENT ON THE PAPER "THE USE OF ION EXCHANGERS FOR THE DETERMINATION OF PHYSICAL-CHEMICAL PROPERTIES OF SUBSTANCES, PARTICULARLY RADIOTRACERS, IN SOLUTION. II. THE DISSOCIATION CONSTANTS OF STRONTIUM CITRATE AND STRONTIUM TARTRATE."

In the paper of the above title J. Schubert and J. W. Richter (*J. Phys. Colloid Chem.* **52**, 350 (1948)) state that the dissociation constant of an organometallic complex was measured when the metal component was present in radiochemical concentration, i.e., about  $10^{-11}$  mole per liter. Further they state that "spectrographic analysis of the solutions . . . revealed no detectable quantities of foreign cations or of carrier strontium."

No details are given on the spectrographic method used to establish the purity of their solutions. I. Noddack (*Angew. Chem.* **49**, 835 (1936)) has drawn attention to the probability that in any macroscopic sample of matter there are present appreciable numbers of atoms of all the chemical elements. It is of interest to ascertain whether the number of strontium atoms that could be present as a universal impurity would be comparable to the number of radioactive strontium atoms added.

In spite of the fact that no information is given as to the sensitivity of the spectrographic examination, an estimate can be made with the aid of the data on spectrographic sensitivity given in a recent publication (C.E. Harvey: *A Method of Semi-Quantitative Spectrographic Analysis*, Applied Research Laboratories, Glendale, California (1947)). If it is assumed that the residue from 100 ml. of solution is arced on graphite electrodes, then from the "sensitivity factor" of strontium, which is, for the most sensitive line, 0.003 per cent on a 10-mg. sample on the electrode, the concentration of strontium would be  $3 \times 10^{-8}$  mole per liter.

However, it will be fairer to consider calcium. The smallest amount of calcium that could be detected would be 0.00004 mg. The ratio of calcium to strontium in the earth's crust is 240 (V. M. Goldschmidt: *Skrifter Norske Videnskaps-Akad. Oslo. I. Mat. Naturv. Klasse* **1937**, No. 4), so that the concentration of strontium present would be about  $2 \times 10^{-11}$  mole per liter. This is still about the concentration of radiochemical strontium that was added ( $10^{-11}$  mole per liter).

Another way of arriving at the possible content of strontium is to consider the impurities of pure chemicals as stated by the makers. The writer has not available an analysis of ammonium tartrate, but tartaric acid may have 0.001 per cent of non-volatile matter of which 0.0001 per cent may be iron, and the purity of ammonium tartrate is taken to be the same. Assuming that calcium is present to the same extent as iron, and that the strontium content is 1/240th of that, the strontium in a 0.2 mole per liter solution of ammonium tartrate would be  $2 \times 10^{-9}$  mole per liter. With unavoidable contamination of the solutions in handling, the content of strontium in the solutions at the end of the reaction may well have been greater.

The spectrographic method used by Schubert and Richter was probably less sensitive than has been assumed, and it is likely that the statement they make can not be correct. The values they give for dissociation constants will not be affected, but it is thought that it will be of general interest to draw attention to the gap in sensitivity between radiotracer methods and the most sensitive of other methods.

STUART H. WILSON.

Dominion Laboratory  
Scientific and Industrial Research Department  
Wellington, New Zealand  
June, 1948

# ADDITIONS TO THE ARTICLE "MELTING AND EVAPORATION AS RATE PROCESSES"

(J. Phys. Colloid Chem. **52**, 949 (1948))

It has been shown in a recent discussion that the theory of absolute reaction rates leads to results for the isothermal rate of evaporation which are of the same order of magnitude as those obtained from the Knudsen equation (S. S. Penner: J. Phys. Colloid Chem. **52**, 949 (1948)). This conclusion can be made more explicit by use of a relation between free volume and vapor pressure obtained by H. Eyring and J. O. Hirschfelder (J. Phys. Chem. **41**, 249 (1937)).

The assumption that the activated state formed during evaporation is a gas-like molecule leads (S. S. Penner: *loc. cit.*)<sup>1</sup> to the following relation for the rate constant for evaporation,  $j_*$ :

$$j_* = e\kappa(kT/2\pi m)^{1/2}(v^{*2/3}/v_f) \exp(-\Delta H_v/RT) \quad (1)$$

where  $e$  is the base of the natural logarithms,  $\kappa$  is the transmission coefficient,  $k$  is the Boltzmann constant,  $T$  is the absolute temperature,  $m$  is the mass per molecule,  $v^* = v$  is the volume per molecule in the condensed state,  $v_f$  is the corresponding free volume per molecule,  $R$  is the molar gas constant, and  $\Delta H_v$  is the molar heat of evaporation. In the derivation of equation 1 it was assumed that the vibrational, rotational, and internal contributions to the partition functions remain unaltered during evaporation.

If the rate of loss of molecules from a given volume  $V$  is  $-dn_v/dt$  and is assumed to be proportional to the number of molecules  $n_s$  exposed at the surface with the proportionality constant given by the rate constant for evaporation (S. S. Penner: *loc. cit.*), then

$$-dn_v/dt = j_* n_s \quad (2)$$

But  $n_v = nV$  and  $n_s = n^{2/3}S$ , where  $n$  is the number of molecules per unit volume and  $S$  is the surface area. Therefore

$$G = -(1/S)(dV/dt)\rho = j_* \rho/n^{1/3} \quad (3)$$

where  $\rho$  is the density of the evaporating compound and  $G$  is the rate of loss of molecules by evaporation from a given volume per unit surface area per unit time. Combining equations 1 and 3 leads to the result

$$G = e\kappa(kT/2\pi m)^{1/2}(\rho v/\eta^{1/3}v^{1/3})(1/v_f) \exp(-\Delta H_v/RT) \quad (4)$$

But  $\rho v = m$  and

$$(1/v_f) = (p_s/kT) \exp(\Delta H_v/RT) \quad (5)$$

where  $p_s$  is the saturated vapor pressure of the evaporating compound whose vapor is assumed to behave as a perfect gas. Equation 5 was obtained by Eyring and Hirschfelder (*loc. cit.*), who noted that the Gibbs free energy of the evaporat-

<sup>1</sup> The factor  $e$  was omitted in the preceding discussion, since only order of magnitude calculations were carried out.



ing substance and of the gas with which it is in equilibrium must be equal to each other. From equations 4 and 5 it follows that

$$G = \epsilon \kappa p_s (m/2\pi kT)^{1/2} \quad (6)$$

since the product  $(nv)^{1/3} = 1$ .

Equation 6 is of the same form as the Knudsen equation with the accommodation coefficient of the Knudsen equation replaced by  $\epsilon \kappa$ . It may also be noted that if evaporation is a rate process in which equilibrium between normal and activated molecules is not established, and if the evaporating molecules move classically in the degree of freedom along which the molecules decompose with an average energy change of the order of  $kT$  between successive transfers of energy, then Hirschfelder's correction factor (J. O. Hirschfelder: J. Chem. Phys. **16**, 22 (1948)) of 0.387 should be introduced into equation 6, leading to the result:

$$G = 1.05 \epsilon \kappa p_s (m/2\pi kT)^{1/2} \quad (7)$$

It is evident that results calculated from equation 6 with  $\epsilon \kappa = 1$  should be identical with results calculated from the Knudsen equation with the accommodation coefficient set equal to unity. Therefore it appears likely that the discrepancies discussed previously (S. S. Penner: *loc. cit.*) were introduced by an incomplete description of the physical state through partition functions calculated on the basis of the free volume model.

The author wishes to express his appreciation to Professor J. G. Kirkwood for helpful discussions.

S. S. PENNER.

Jet Propulsion Laboratory  
California Institute of Technology  
Pasadena, California  
July 12, 1948

## PHASE EQUILIBRIUM DESCRIPTION

*Isosyst*, a new word of Greek etymology, is proposed to describe a condition, or family, or curve of constant composition. This word has utility in descriptions of vapor-liquid phase equilibria, joining therein two words, *isobar* and *isotherm*, which have long been used.

### DISCUSSION

In this laboratory's work in phase equilibrium, a concise, descriptive, unique word was needed to describe the condition of the same composition throughout a given experiment, or to label a curve of constant composition. The words "isobar" and "isotherm" have long been used to label conditions of constant

pressure and constant temperature, respectively, but no such apt or concise word exists to replace the cumbersome and verbose "state of constant composition."

Thus, for vapor-liquid equilibria, temperature may be plotted *versus* composition for various isobaric conditions and similarly pressure *versus* composition along isotherms. The third condition, pressure *versus* temperature, is plotted for "envelopes of constant or the same composition" as a parameter. Such wordiness in an era of abbreviation represented even by the extremes of governmental "alphabet soup" and bathing suits is unnecessary.

The word must be descriptive, easily pronounced, adaptable to international use, capable of easy recognition, and euphonious if possible. The prefix "iso" (*ισο*) seems logical for describing "the same" or "equal." Ready parallel is available for this choice and apparently automatically the remaining stem must be from the Greek to avoid mixed origin. "Element" or "compound" or "composition" is stoichiotesia (*στοιχειοθεσια*), which would give "isostoich" as a possibility. Its syllabilization is difficult and the adjective—"isostoichic"—a tongue twister. "Strength" is kratos (*κρατος*), but this is muscular in sense although the word "isocrat" does exist in political science to describe equal power. "Composition" or "compilation" is synthesis (*συνθεσις*), giving "iso-synth" as a possibility, but from many considerations systasis (*συστασις*)—composition, constitution, etc.—has much in its favor. The choice therefore inclines to the definitions: *isosyst*, noun (from Greek iso = equal, systasis = composition), a state of equal or the same composition; and *isosystic*, adjective, applied to an isosyst as, for example, an isosystic curve.

It is hoped that those in the physical and chemical sciences needing exactly descriptive words may find some use for this word.

Grateful acknowledgment is made to Clyde Murley and George Thodos (Northwestern University) and Duane Roller (Wabash College) for their multilingual inventiveness.

V. C. WILLIAMS.

Northwestern University  
Evanston, Illinois  
June 28, 1948

## NEW BOOKS

*Chemical Process Principles. Part II. Thermodynamics. Part III. Kinetics and Catalysis*  
By O. A. HOUGEN AND K. M. WATSON. New York: John Wiley and Sons, Inc., 1947.

Part II is a continuation of Part I by the same authors (reviewed in *J. Phys. Chem.* **48**, 232 (1944)) and is a revision of Chapters XI through XIX of *Industrial Chemical Calculations*. Chapter XI is a review of fundamental thermodynamics. Some may consider this too brief and want to expand it. However, this text should follow Part I and a good course in physical chemistry. At the bottom of p. 453 it should be pointed out that there are many systems in which three variables (two independent) are not sufficient to completely define

its state. The statement on p. 458 "By partial differentiation of the four differential energy functions Equations (27-30) . . ." is not mathematically correct. A similar criticism can be made about the sentence preceding Equation (114) on p. 467.

Chapters XII and XIII apply the fundamental principles to the thermodynamic properties and expansion and compression of fluids. In addition, generalized methods are used to predict properties of substances for which data are not available. So far as the reviewer is aware, this is the only single place in which such a collection of the generalized methods are brought together. Chapter XIV considers both gaseous and liquid solutions. Ideal solutions can be handled by previous generalized methods, but non-ideal solutions require experimental data. Chapters XV and XVI cover physical and chemical equilibrium. Although both of these subjects are covered in physical chemistry, the authors present the information with a practical rather than a theoretical viewpoint. Chapter XVII discusses available methods for the calculation of thermodynamic properties from molecular structure by both empirical and theoretical methods. Throughout the text the worked-out problems illustrate the principles discussed. In addition, there are a large number of unworked problems which are valuable when the book is used as a text. Most of the book is suitable for undergraduate classes; however, there are parts which should be given only to graduate students.

Part III is an addition to the original volume, *Industrial Chemical Calculations*. The object of this volume can best be given in the words of the authors as given in the preface: "All these principles are combined in the solution of the ultimate problem of the kinetics of industrial reactions. Quantitative treatment of these problems is difficult, and designs generally have been based on extensive pilot-plant operations carried out by a trial-and-error procedure on successively larger scales. However, recent developments of the theory of absolute reaction rates have led to a thermodynamic approach to kinetic problems which is of considerable value in clarifying the subject and reducing it to the point of practical applicability. These principles are developed and their application discussed for homogeneous, heterogeneous, and catalytic systems. Particular attention is given to the interpretation of pilot-plant data. Economic considerations are emphasized and problems are included in establishing optimum conditions of operation."

Chapter XVIII considers homogeneous reactions, making application of fundamental physical chemistry to the design of reactors. Chapter XIX discusses the theory of catalysts and applies the theory to practical problems. In some cases this involves empirical methods. Chapter XX brings up to date the correlations of mass and heat transfer in catalyst beds. The final results are mainly in the form of charts. Chapter XXI gives general methods for catalytic reactor design, including the calculation of pressure drops, optimum reaction temperatures, and temperature control. A completely worked out problem for the system sulfur dioxide-oxygen-nitrogen is given for the same composition used in an equilibrium calculation given in Part II. The last chapter deals with uncatalyzed heterogeneous reactions including liquid-liquid, liquid-solid, and gas-solid systems. There is a short section on systems involving unsteady state conditions. Part of the results are again given in the form of charts. This volume also has a number of illustrative problems worked out in detail. In general, Part III is suitable for graduate students only.

N. H. CEAGLSKE.

*Colorimetric Methods of Analysis*. Third edition. By F. D. SNELL AND C. T. SNELL. 239 pp. New York: D. Van Nostrand Company, Inc., 1948. Price: \$4.50.

The third edition of this well-known work is being published in three volumes, replacing the two of the second edition. The first volume covers the theory of colorimetry, instruments, and colorimetric determination of pH. In the previous edition these topics were treated in approximately 160 pages; now they are covered in about 200 pages. The expansion is largely due to the rise of photoelectric photometry in the twelve years which have elapsed since the second edition appeared. Many of the old references have been omitted. On the other hand, many photographs of more modern instruments have been added.

This compilation will be found more useful by the analyst than by the physical chemist.

From the academic and also from the practical viewpoint a more exact discussion of the terminology, including the names colorimetry and photometry, would be desirable. The use of the symbol  $\Sigma$  to designate the molar extinction coefficient is confusing.

The more practically minded analyst will welcome this book, which gives a reasonably complete discussion of the instruments and general methods and which contains many references to the literature.

I. M. KOLTHOFF.

E. B. SANDELL.

*The Water Soluble Gums.* By C. L. MANTELL. 279 pp. New York: Reinhold Publishing Corporation, 1947. Price: \$6.00.

Plant gums have been known and used in commerce for several hundred years and at the present time many millions of pounds are used each year in the United States alone. Such substances therefore merit attention. The term "gum" has been confusing; not infrequently the commercial gums are of questionable origin and many samples are undoubtedly mixtures. The reason for the wide use of soluble gums lies in their unique chemical and physical properties, and it will be apparent to those who read this book that an extension of the use of gums might well be brought about by fundamental studies.

The book has been written in an attempt to coordinate information relating to gums and to correlate the practice and art with the scientific knowledge of these substances. Some clarification of the gum field will result from a study of this book, but it appears to the reviewer that the work will be much more useful to the technologist than to the specialist for the reason that the present knowledge of the chemistry of gums and mucilages, by no means insignificant, was not included. Had this been done, the book would have had a much wider appeal.

FRED SMITH.

*The Systematic Identification of Organic Compounds.* Third edition. By RALPH L. SHRINER AND REYNOLD C. FUSON. 13.8 x 21.2 cm.; viii + 370 pp.; 23 fig.; 45 tables. New York: John Wiley and Sons, Inc., 1948. Price: \$4.00.

This revision of the widely accepted second edition embodies several improvements. The second chapter is now devoted to the presentation of the identification scheme, and the arrangement of subsequent chapters follows the same order. The chapter on classification reagents has been expanded and rewritten. Both the tables of compounds and the final problem section have also been expanded. The index now gives, for added convenience, the boiling points or melting points of the compounds listed. These improvements should assure the book of continued popularity in the field.

SCOTT MACKENZIE.

*Surface Chemistry for Industrial Research.* By J. J. BIKERMAN. 464 pp. New York: Academic Press, Inc., Publishers, 1947. Price: \$8.00.

The importance of knowledge of the physics and chemistry of surfaces as related to industrial research has but recently become generally appreciated. The author in this book has pointed out numerous applications of the principles of surface chemistry and has made a distinct contribution to industrial workers who encounter surface chemistry problems and wish to know how to solve them. The fundamental principles pertaining to the measurement of tensions and to free surface energy relations as well as to electrical properties at the different types of interfaces are given. Treatment of individual subjects is necessarily incomplete in a book of such limited size. This incompleteness of treatment is, however, compensated in part by the fairly extensive bibliography of 1026 references, appropriately arranged at the ends of the chapters. The over-all treatment makes interesting reading, and the author is to be commended for the timely presentation of this valuable book.

Chapters, in order, deal with the interfacial systems: I. Liquid-Gas, II. Liquid-Liquid,

III. Solid-Gas, IV. Solid-Liquid-Gas, V. Solid-Liquid-Liquid. A final chapter deals with electric surface phenomena.

Fuller and more detailed treatment of such topics as the pendent-drop method for surface-tension and for interfacial-tension measurements, the Gibbs adsorption theorem, monomolecular and expanded films, etc., would have been desirable, but these treatments were curtailed presumably by space limitation. The book is comparatively free of errors and misprints. One statement on p. 153 which reads "obtained W/O Emulsions for water 95 benzene 5" obviously should read "obtained W/O Emulsions for benzene 95 water 5."

The book would not be very satisfactory as a textbook; in fact, it was not intended that it should be so used. It is, however, an excellent reference book and should be at the disposal of all research workers in the field of surface chemistry.

F. E. BARTELL.

✓ *Research in Industry. Its Organization and Management.* C. C. FURNAS, *Editor*. xii + 574 pp. New York: D. Van Nostrand Company, Inc., 1948. Price: \$6.50.

The Industrial Research Institute, Inc., was established in 1938 under the auspices of the National Research Council:

1. To promote, through the coöperative efforts of its members, improved, more economical, and more effective techniques of organization, administration, and operation of industrial research.
2. To develop and disseminate information as to the organization, administration, and operation of industrial and social activity of the nation.
3. To stimulate and develop an understanding of research as a force in the economic, industrial, and social activity of the nation.
4. To promote high standards in the field of industrial research.

The publication of this book is a most valuable and most effective contribution towards these objectives.

Thirty-three successful executives of leading industrial research organizations have made available the best present-day thought on the proper management, organization, and operation of the research arm of modern American industry. Their contributions are recommended reading, not only for those engaged in industrial research, but also for those in the management, production, sales, patent, personnel, engineering, and public relations groups, all of whose activities border on company research organization. This volume also affords university graduate faculty members, who have had little recent occasion to be active in industrial research, an opportunity to gain a better understanding of a field for which they are training scientific personnel. Graduate students will profit from its study.

We hope that equally valuable contributions to the progress and understanding of American research will be made available with the preparation of similar books by experienced leaders in university and governmental research.

While most of the important phases of industrial research are treated from several viewpoints, and with surprisingly few major contradictions, more attention could profitably have been paid to the problems arising in the effective utilization of research teams or task forces. These, we know, played a very important rôle in war research. One wonders if this idea is being used today in industry as extensively as it might be.

Several chapters are clearly the result of extensive surveys of the opinions of the directors of many laboratories, and throughout the book an effort has obviously been made to present carefully the several viewpoints on difficult questions. Selected and representative references are also given.

A glance through the various chapters will quickly bring out the wide variety of technical, management, and personnel problems which the research director is apparently expected to handle. His training and experience need indeed be broad.

The Industrial Research Institute, the Editor, and the contributors are to be congratulated on their presentation of a book which is well organized and well thought out.

EDGAR L. PIRET.

*Proteins and Amino Acids in Nutrition.* MELVILLE SAHYUN, *Editor*. 566 pp. New York: Reinhold Publishing Corporation, 1948. Price: \$7.50.

For several years the concentration of nutritional interest, so long centered on vitamins, has been veering away toward proteins and amino acids, the break being conveniently bridged in part by such interrelationships as those of niacin and tryptophan in the etiology of pellagra. There is, indeed, danger that the enthusiasts who recently sought to cure all the world's ills by vitamin dosage, may now attempt a similar tour de force, more expensively, with amino acids. In any case there is obvious need of a scholarly review of the whole subject of proteins and amino acids in nutrition, and that is what Sahyun and his seventeen collaborators have attempted to provide in the present book.

In the introduction, H. B. Lewis points out the changes of opinion about the dietary intake of proteins proper for man. The high recommendations of the pioneer German workers gave way in the early years of this century to the low-protein school represented by Chittenden; recently, much pressure seems to be developing to complete the cycle and to return to levels which would have pleased Carl Voit and Justus von Liebig. But the present book, though showing many imprints of the new vogue, is largely a sober summary of evidence on protein utilization, deficiency, and protein nutrition in clinical states. There is little on the pure physics or chemistry of proteins or amino acids nor should one wish this in the present context.

The several chapters are of unequal interest and merit, nor do they together provide an integrated picture or develop a particular theme. While this, as well as the marked variations in style, may be regretted in the present book, it must be admitted that the day of the monumental treatise, planned and executed in detail by a single scholar, is over; the modern monograph by multiple authors seems to be the only solution to the growth of knowledge and the limitations of any single mind. We must be grateful for the historical chapter (of 45 pages) by Eliot Beach which, excellent in itself, serves to place the broad problems as a developmental frame for the whole book.

Several chapters, notably those on toxins and on filterable viruses, seem unrelated to the purpose of the book and, though good in themselves, might have been better omitted to provide for a more thorough treatment of protein utilization and requirements and the plasma proteins. The chapter on caloric, mineral, and vitamin requirements is disappointing in both organization and content. It is not clear why 78 pages should be devoted to reproducing a somewhat outmoded Department of Agriculture Circular on the proximate composition of foodstuffs.

By and large, the book is clearly and, in places, elegantly written. One must suspect that the editor did a labor of love in achieving a level of literary quality definitely superior to most compilations of this type. The documentation is fairly voluminous, but the absence of reference titles and author index will limit its use. The subject index is grossly inadequate. The book is well printed but one could wish for a stouter binding. Much of the book should be valuable for years and could be read with profit and more than a modicum of pleasure by chemists, physicians, and graduate students as well as by the nutritionists and physiologists who should certainly invest in personal copies.

ANCEL KEYS.

*Newer Methods of Preparative Organic Chemistry.* Translated and revised from the German, and published and distributed in the public interest with the consent of the Alien Property Custodian. xiii + 657 pp. New York: Interscience Publishers, Inc., 1948. Price: \$8.50.

This is a translation, with some extensions and revisions, of a series of review articles which appeared in *Die Chemie* beginning in 1940. The chapter headings, with the names of the authors and (in parentheses) translators, are: 1. Oxidations with Lead Tetraacetate and Periodic Acid, Criegee (Edens, Graham). 2. Dehydrogenations with Sulfur, Selenium, and Platinum Metals, Plattner (Armstrong). 3. Reductions with Raney Nickel Catalysts, Schröter (Salminen). 4. Hydrogenation with Copper Chromite Catalysts, Grundmann

(Burness). 5. Meerwein-Ponndorf Reduction and Oppenauer Oxidation, Bersin (Webster, Crawford). 6. Use of Biochemical Oxidations and Reductions for Preparative Purposes, Fischer (Crawford, Webster). 7. Substitution Reactions of Aliphatic Compounds, Nelles (Bachman). 8. Organic Fluorine Compounds, Bockemüller (Kibler). 9. Catalysis of Organic Reactions by Boron Trifluoride, Kästner (Jones). 10. Use of Hydrogen Fluoride in Organic Reactions, Wiechert (Jones). 11. Methods for Thiocyanation of Organic Compounds, Kaufmann (Tull). 12. The Diene Synthesis, Alder (Wilson, Van Allan). 13. Syntheses with Diazomethane, Eistert (Spangler). 14. Syntheses with Organolithium Compounds, Wittig (Thirtle).

The title of the book is somewhat of a misnomer, for most of the subject matter has been familiar to organic chemists in this country for several years; indeed, most of the subject matter has already been covered by adequate reviews published in *Organic Reactions*, *Chemical Reviews*, and elsewhere. Thus, the two chapters on reduction are covered by Adkins' book on the subject; Chapter 5 is covered by the excellent review of Wilds *Organic Reactions*, Vol. 2, p. 178 (1944); Chapter 8 by the review of Henne (*Organic Reactions*, Vol. 2, p. 49 (1944)) and by the printing of the recent symposium in *Industrial and Engineering Chemistry*, because of which the Translator has added a short supplement to the chapter; Chapter 11 by the review of Wood (*Organic Reactions*, Vol. 3, p. 240 (1946)); Chapter 12 by the review of Norton (*Chem. Revs.* **31**, 319 (1942)); Chapter 13 by the review of Bachmann and Struve (*Organic Reactions*, Vol. 1, p. 38 (1942)); and there are references to material in other chapters also.

Nevertheless, the book has value and it presumably does give a picture of the state of knowledge on these topics in Germany around 1940. The reviewer was particularly glad to see a translation of Plattner's excellent paper (Chapter 2), the papers by Alder (Chapter 12) and by Wittig (Chapter 14), and he found in Chapter 3 some material on the preparation of Raney alloys and the Raney catalysts—iron, copper, cobalt, in addition to nickel—which was new to him. The chapter by Nelles appeared sketchy and rather weak in comparison with the others, but that impression was caused, perhaps, by the rather large area which Nelles attempted to cover in thirty pages. On the whole, the reviews are very good and are well documented, particularly with reference to the patent literature; the authors are all men of prominence and of outstanding accomplishment in chemistry; and the book should serve as a useful supplement to the material already available in English.

The book-making is first rate, the paper and typography are excellent, and the binding is good. There are two indexes—one by subjects and the other by names of compounds.

LEE IRVIN SMITH.

*Volumetric Analysis. Vol. II. Titration Methods.* By I. M. KOLTHOFF AND V. A. STENGER. xiii + 374 pp. New York: Interscience Publishers, Inc., 1947. Price: \$6.00.

Kolthoff's *Volumetric Analysis* began life as *Die Praxis der Massanalyse* in 1928 and its various translations and new editions have had almost as many associate editors as Roosevelt had vice-presidents. H. Menzel of Dresden helped on the original manuscript, N. H. Furman of Princeton made the translation, and now with the aid of V. A. Stenger of the Dow Chemical Company, expansion of the work to three volumes is contemplated. The mechanics and ethics of shifting publishers from one edition to another would probably make an interesting story, but, of course, the true interest of a reviewer resides in the content of a book and not in the copyright or contract manipulations which attend its conception.

Volume I of this edition of *Volumetric Analysis* appeared in 1942 and dealt with the theory of volumetric analysis. Volume II deals with the practical aspects of titrimetric analysis as found in acid-base and in precipitation and complex-formation reactions. Volume III will treat with oxidation-reduction reactions.

The first thirty pages of Volume II deal with the calibration and use of volumetric apparatus. This is the usual material and the explanations are well written. The use of soda lime to protect standard alkali solutions as recommended on p. 14 is questionable; soda lime

is a fair drying agent, certainly good enough to take water away from 0.1 *N* or 1.0 *N* sodium hydroxide solutions. The weight buret shown in Fig. 11, page 18, was described four years earlier by G. F. Smith than by the workers to whom the credit is given.

Included in the next twenty pages under the heading of "Practical Principles" is a fine discussion of the properties which a primary standard should possess. It is hard to tell whether or not Kolthoff and Stenger really think a material is a primary standard only when it can be tested for its impurities (including occluded water); they present Sørensen's argument but apparently think the reader should decide for himself.

In the following section, some forty pages, is a detailed and thorough survey of the primary standards which have been proposed for acidimetry and alkalimetry. Sodium oxalate is given as the preferred primary standard for acid standardization, sodium carbonate being relegated to the section entitled "Other Standard Substances"; the six pages given to sodium oxalate will surprise industrial analysts, not one in five hundred of whom will work up a bath of sodium oxalate when he can pick sodium carbonate from the side shelf and with a simple heat treatment eliminate the bicarbonate. The off-hand disposal of sulfamic acid as "a possibly useful secondary standard" will come as a blow to those who have used it. While the absence of occluded water from sulfamic acid has probably not been adequately proved, sulfamic acid is considered by the reviewer to be the best of our present primary standard acids. In this connection commercial perchloric acid, which is a constant-boiling mixture of 73.60 per cent  $\text{HClO}_4/3.5\text{--}5\text{ mm.}$ , deserves more use by analysts (p. 68).

Chapters IV though VII deal with the various cases of acid-base titration. Although grouped under the usual headings: "The Titration of Strong Acid with Strong Base," "The Titration of Weak Acid with Strong Base," "Displacement Titrations," and so on, the information is highly detailed as to the analysis and behavior of specific materials. The side headings of a few pages, for example, run: "Arsenic Acid and Arsonic Acids," "Phosphorous Acid," "Hypophosphorous Acid," "The Determination of Ortho-, Meta-, Pyro-, and Polyphosphate in Mixtures." The discussions of these various methods are very complete. The Kjeldahl method occupies three pages, the titration of salts of heavy metals nine, the soap titration of calcium three, the titration of alkaloids three. A great number of tricky and even remarkable reactions involving the hydrogen or hydroxyl ion have been adapted as titrimetric methods, and Chapters VI and VII make good browsing material for the general reader. Going through this section the reviewer caught for a few precious minutes the same enchantment and breathless interest that awoke his enthusiasm for chemistry in his high school days.

Somewhat over a hundred pages of Volume II deal with precipitation and complex-formation reactions. As might be expected, most of this material is devoted to argentometric titrations, the methods indelibly associated with the names of Mohr, Volhard, and Fajans. A lot can be done, too, with standard solutions of ferrocyanide and of mercuric nitrate. (Kolthoff and Stenger prefer the term "mercurimetric" to "hydrargyrimetric" and for this future generations of chemists will call their names blessed.)

The principal discussions in this book are set in ten point type but much of the book is in eight point and a good bit in nine. Footnotes average three to a page. The book, though, is not simply another Beilstein or a mere compilation of literature references gleaned from the indexes of *Chemical Abstracts*. Kolthoff himself has published on a great many of these methods. The literature references reach from our Civil War era (and before, since the author index lists Liebig five times and Gay-Lussac six times) to the post-Hiroshima literature. Good reference lists are characterized by the items which have been culled as much as by those which have been included. Critical selection demands experience, the laboratory kind as well as the swivel chair variety, and is the hallmark of true scholarship. Volume II comes up to scratch on this point.

The publishers should have put this book on better paper. The reviewer has the feeling also that the cloth cover is not going to stand up too well to the hard use he expects to give his copy in the coming years.



Volume III of *Volumetric Analysis* is scheduled for the fall of 1948 and we bid its appearance on this date Godspeed. It too will be a fine book.

HARVEY DIEHL.

*Monograph on the Progress of Research in Holland during the War. Chemical and Physical Investigations on Dairy Products.* By H. EILERS, R. N. J. SAAL, AND M. VAN DER WAARDEN. 14.5 x 20.5 cm. xiii + 215 pp.; 51 fig.; 26 tables. New York: Elsevier Publishing Company, Inc., 1947. Price: \$4.00.

This is the twelfth of the series of monographs which Elsevier is publishing on various aspects of Dutch research during the war. It contains three treatises summarizing the results of investigations on the chemistry of dairy products which were carried out by the Amsterdam Laboratory of the N. V. de Bataafsche Petroleum Maatschappij at the instigation of the General Netherlands Dairy Union. These results had been published previously in greater detail in Dutch by the authors and their associates in *Verslagen Landbouwkundige Onderzoekingen*, Volumes 50 and 52. The three topics discussed are: (1) the colloid chemistry of skim milk (Eilers), (2) the oxidation-reduction potential of milk and of butter plasma (Saal), and (3) researches concerning the chemical processes underlying the deterioration of the flavor of butter in cold storage (van der Waarden).

Eilers devotes about half of his paper to the composition, state, properties, and behavior of the colloidal micelles, calcium caseinate-phosphate and milk serum protein present in skim milk. The composition of casein as reported in the literature is summarized, and a model molecule containing 1000 nitrogen atoms and having a molecular weight of 89,000 derived therefrom is used in explaining the properties of this protein. The titration curve of casein is shown to be consistent with the ionogenic groups of the model. Results from the literature as well as experiments by the author are used to support his contention that the caseinate-phosphate of milk is a double calcium salt of casein and phosphoric acid rather than a physical complex of calcium caseinate and calcium phosphate. The colloidal state of these micelles is described in terms of their size and light-scattering ability, voluminosity, and hydration. The discussion of milk serum proteins is largely taken from the literature. Experimental data are presented on the viscosity of skim milk and the effect of heat treatment thereon, which is shown to be related to changes in the caseinate micelles and to denaturation of the serum proteins. The second half of Eilers' paper deals with the behavior of skim milk on concentration both with and without addition of sugar. Viscosity and the distribution of phosphate among the phases are emphasized particularly.

Saal's paper on oxidation-reduction potential is a relatively short (36 pages) discussion of the components determining the potential, of factors affecting it, and of the relation of changes in the potential to the development of oxidized flavors in milk. Oxygen and ascorbic acid are the principal components determining the potential (average +0.27 v.) of fresh raw milk. Reducing substances formed on heat treatment lower the potential, while addition of copper or iron salts increases it with a concomitant development of oxidized flavors. Butter plasma has a high potential but there is no relation between the potential of the plasma and the flavor of the butter.

Van der Waarden discusses the development of storage flavors in butter, presenting evidence that, contrary to the generally accepted ideas, fishy flavors in storage butter arise from oxidative processes rather than from hydrolysis of lecithin to trimethylamine. The materials responsible for the off-flavor were prepared in a highly concentrated form but could not be isolated and identified. The relations of formation of peroxides and of partition of copper and iron among the phases of butter to the development of off-flavors were found to substantiate the hypothesis that the flavors are caused by oxidative processes.

In general, the book is well organized and fairly well written. Certainly it contains a large amount of information which is of interest to workers in the fields covered. The lack of access to foreign literature after 1940 is evident, particularly in regard to the discussion of milk serum proteins and oxidation-reduction potential. The book contains a consider-

able number of errors, particularly in orthography, and the translation is not always as smooth as possible, but these defects do not detract from the scientific value of the data which it contains.

ROBERT JENNESS.

*Organic Analytical Reagents*. Vol. 4. By FRANK J. WELCHER. xiii + 624 pp. New York: D. Van Nostrand Company, Inc., 1948. Price: \$8.00 per volume; \$7.00 per volume on series orders.

The author's purpose in this series of volumes is "to assemble in one place a description of all organic compounds used in the analysis of inorganic substances, and to present a discussion of the methods employing these reagents." The treatment is intended to be complete rather than critical, and the inclusion of many inferior reagents and methods is freely admitted. All of the literature on the subject available in the United States prior to January 1, 1946 is reviewed.

The analytical reagents are classified according to their structure rather than according to their function, and each compound is treated completely in one section. To facilitate their use, procedures for the preparation of many of the reagents are included. However, no yields are given for any of the preparations; so it is difficult to evaluate them. The analytical procedures are reasonably complete; references to the original literature are numerous. While structural formulas are given for most of the reagents, with the exception of the alkaloids, the structures for many of the metallic complexes are omitted.

In this volume the following general classes of organic analytical reagents are treated: acidic nitro compounds, arsonic acids, organic compounds containing sulfur, alkaloids, diazonium compounds, carbohydrates, and dyes. The index of organic reagents and the index of uses of these reagents for both the detection and the determination of inorganic substances appear to be complete. The paper and the binding of this volume are of excellent quality.

R. M. DODSON.

*Mechanical Behavior of High Polymers*. Vol. VI of *High Polymers*. By TURNER ALFREY, JR. 581 pp. New York: Interscience Publishers, Inc., 1948. Price: \$9.50.

The author states in the preface that "the attempt has been made to uncover the fundamental principles underlying the mechanical behaviour of high polymers, and to show how such behaviour is correlated with the molecular structures involved." Such an attempt may be expected to be fairly successful with regard to elastic properties, but is too ambitious (as the author points out) in dealing with properties so complex as ultimate strength.

An introduction of 90 pages gives a treatment along conventional lines of the geometry of stresses and strains, homogeneous and non-homogeneous stresses, Newtonian and non-Newtonian liquids, and thixotropy. The main contents of the book are found in the following chapters: "Plastoelastic Behaviour of Amorphous Linear High Polymers"; "Three-Dimensional Cross-Linked Polymers"; "Crystallization of High Polymers." The subjects of "Plasticization and Solution", and "Ultimate Strength and Related Properties" also are discussed.

An enormous amount of purely empirical work of practical utility has been done on various mechanical properties of high polymers. Quite correctly the author has not attempted to catalogue or describe such work, and has chosen instead to discuss those measurements which can be discussed qualitatively or quantitatively in terms of fundamental principles. The knowledge of the chemical and physical nature of many high polymers is increasing now at a considerable rate. For this reason, it is well worthwhile to have available a book which summarizes the recent developments in this field. The book as a whole is well written and interesting. The comments of the author regarding unsolved problems and the nature of the difficulties opposing their solution are illuminating. However, this reviewer personally is not in favor of the practice of giving verbatim quotations

of many pages in length direct from the original literature, as is done, for example, in pp. 243-287.

Binding and typography are excellent.

E. J. MEEHAN.

*Fatty Acids and their Derivatives.* By A. W. RALSTON. New York: John Wiley and Sons, Inc., London: Chapman and Hall, Ltd., 1948.

This book is a most valuable addition to the increasing American literature on fatty acids and oils. The organization is good, and coverage of the various subjects is quite complete, there being over 5000 well-chosen references in the twelve chapters composing the book. The numerous tables and graphs are well printed.

The first five chapters deal with the fatty acids, their synthesis, structure, physical properties, occurrence in nature, and methods of preparation from natural fats.

The remaining chapters are on the derivatives of fatty acids, their synthesis, properties, and uses. Reactions of the hydrocarbon chain (oxidation, addition, substitution, polymerization) are discussed according to the type of reaction. Reactions involving the carboxylic acid group are classified according to the structure of the derivatives (esters, amides, nitriles, amines, alcohols, ethers, mercaptans, sulfides, sulfonates, anhydrides, acid chlorides, aldehydes, ketones, hydrocarbons, and soaps). Chapter VIII on the amides, nitriles and amines is particularly complete and well-organized, as would be expected from the special interest and experience of the author in this field, evidenced by his statement, "Few, if any, series of derivatives of naturally occurring or synthetic substances possess the intrinsic academic and commercial interest which is to be found in the nitrogen-containing derivatives of the fatty acids."

The section on metallic soaps is rather short and makes bare mention of the considerable literature on physical and colloidal properties of aqueous soap solutions.

The inclusion of an author index would add greatly to the value of the book, as would the alphabetical listing of references, which are listed numerically at the ends of the chapters.

The duplications which exist between this book and Markley's recent *Fatty Acids* are inevitable, but the organization and emphasis of the two books are sufficiently different so that they complement one another very well.

The frequent mention of actual and suggested uses of the derivatives adds much to the usefulness of the book. This book should be owned by every person working in fields related to fatty acids and their derivatives.

DONALD H. WHEELER.

*Synthetic Methods of Organic Chemistry, A Thesaurus.* By W. THEILHEIMER, Vol. I, 1942-1944. With a foreword by T. REICHSTEIN. Translated by HANS WYNBERG. x + 254 pp. New York: Interscience Publishers, Inc., 1948. Price: \$5.00.

This, the first of a series of projected volumes, deals with the literature of 1942-1944. Reactions are classified according to an adaptation of the system devised by Weygand. The chief bases of the classification are (a) the elements linked together when a new bond is formed, (b) whether the reaction is addition, rearrangement, exchange, or elimination, and (c) the type of bond which is broken. This, combined with a definite order of the elements (H, O, N, S, Hal., etc.) and the "principle of latest position," borrowed from Beilstein, leads to a rigid order in which reactions will be considered—an index, so to speak, arranged on a different basis from the alphabetical. Not all of the possible permutations and combinations are represented, however.

The individual entries are sketchy, but complete enough to convey a pretty good idea of the method, and references to the original articles (and to *Chemical Abstracts* for this English edition) are included. The book is not primarily a book on laboratory methods, but, as the author states, "In this series of volumes there are going to be recorded regularly new methods for synthesis of organic compounds, improvements of known methods," etc.

Certainly there is a need for some sort of compendium of this kind, for the titles of published papers (on the basis of which such material usually becomes indexed) do not usually include references to improvements in techniques, etc. Whether or not this series of books will fill this need remains to be seen; this reviewer was not too impressed by this first volume. However, the author states that the first volume is to be considered as a trial of the plan and of the system of classification; perhaps the later volumes will be more useful.

To provide cross references, and for those who dislike learning new systems of classification, there is an alphabetical index which to this reviewer appears to be quite adequate. The paper and binding are good, and the typography is excellent.

LEE IRVIN SMITH.

*Encyclopedia of Chemical Reactions. Vol. II. Cadmium, Calcium, Carbon, Cerium, Cesium, Chlorine, Chromium.* Compiled and edited by C. A. JACOBSON. 917 pp. New York: Reinhold Publishing Corporation, 1948. Price: \$12.00.

The general setup of this encyclopedia has been presented in a review of Volume I (J. Phys. Colloid Chem. **51**, 626 (1947)). The same pattern is used in Volume II. This suffers from defects similar to those of Volume I, but it will be welcomed because of its wealth of information. The reviewer noticed several omissions: e.g., under cadmium one does not find this metal's reaction with mercury, and the reaction products of cadmium halides with pyridine are not mentioned. From the viewpoint of the analytical chemist it is to be regretted that the various reagents used for the detection of an element are not grouped together; this analytical part is incomplete and presented in an unsystematic way. Why should one look under cadmium sulfate for reactions of the aquo cadmium ion with inorganic and organic reagents, and why not under cadmium chloride or nitrate? If many reactions were referred to under the heading of the ion, duplication could be avoided. For example, under both cadmium chloride and cadmium sulfate the reaction with hydrogen sulfide is mentioned. Some more systematic treatment would make this encyclopedia much more valuable. The appearance and print of the book are excellent. An extensive index to reagents—formulas and an "index to substances obtained—formulas" greatly improve the usefulness of the book. An errata sheet to Volume I is added to Volume II.

I. M. KOLTHOFF.

*The Development of Theoretical Electrochemistry.* By R. M. FUOSS. Twenty-second Annual Priestley Lectures, April 12-16, 1948. 24 pp. The Pennsylvania State College, State College, Pennsylvania.

This series of five Priestley lectures presented by Professor Raymond M. Fuoss has been made available in printed form. The monograph contains the following five chapters: "Volts versus Amperes"; "Electrolyses: Puzzles and Progress"; "Precision enters Experiment"; "Precision enters Theory"; "The Ionic Atmosphere." The booklet offers a historical description of fundamental experiments and theories developed on the basis thereof in the field of electrolysis and of electrochemistry in general. It starts with William Henry's and Volta's classical papers in 1800 and ends with the development of the modern theory of electrolytes to the generally accepted theory of Debye and Hückel. The discussions are on a high scientific level and they are based on the knowledge at the time when the various discoveries were made. This series of lectures should be of great interest and importance to all scientists and especially to students of electrochemistry.

I. M. KOLTHOFF.

*Nuclear Forces. I.* By L. ROSENFELD. New York: Interscience Publishers, Inc., 1948. Price: \$5.00.

This work is the first extended survey of the theory of nuclear forces to appear since the end of the war; the volume under review is but the first instalment. The task which the author has set himself in reviewing critically both the experimental and the theoretical

literature is of herculean proportions, and his analysis earns him the sincere thanks of the many physicists and chemists who are interested in the subject.

The first three chapters of this volume are devoted to an elementary summary of the general properties of nuclear systems, about comparable in scope to that to be found in Bethe's well-known book *Elementary Nuclear Theory*. The remaining five chapters deal with the two-particle system on the basis of the hypothesis of central interaction forces. The general nature of the hamiltonian to be anticipated for a nucleon is obtained by the reduction of the Dirac equation following a method which has the merit of brevity if not of clarity, but as the type of analysis needed is standard in the literature the reader can have recourse to other sources if he finds the going too rough by the author's procedure. This is followed by a quite thorough summary of the various arguments and procedures used in studying the binding and scattering properties of the two-particle system. The treatment will be of most interest to the theoretically minded reader, who will welcome the summary of the work of some of the European theorists which perhaps is not widely known in this country. It could hardly have been anticipated that the author could arrive at any startling conclusions from his analysis, but the survey itself is of considerable value.

After reading this volume the reviewer is forced to wonder why this first part of the work was issued in advance of the remainder, and in any event why it was issued in its present incomplete form. There could have been real point in making this a self-contained work on nuclear systems up to the two-body configurations, but there seems to be little merit in any event in forcing the reader to turn to the later volumes for the index and for all literature references. For this reason alone the reader will find it a matter of practical necessity to have the complete work even to make this first volume of full value.

It is to be hoped that the remaining parts of the work covering the analysis of the systems of three or more particles, and of non-central forces, will be forthcoming soon.

EDWARD L. HILL.

*The Chemical Constitution of Natural Fats.* Second edition. By T. P. HILDITCH. New York: John Wiley and Sons, Inc., 1947. Price: \$9.00.

The constitution of triglyceride fats and oils is discussed in this volume in a manner designed to develop their interrelationships as a group of naturally occurring substances. After a brief survey of natural fats, the author proceeds in a logical manner with a thorough discussion of the component fatty acids of fats of aquatic, land animal, and vegetable origins, and follows with an extensive discussion of the composition of natural fats in terms of their component glycerides. A brief chapter dealing with some biochemical aspects of fats is followed by a chapter devoted to the chemical constitution of individual natural fatty acids. There is a miscellaneous chapter dealing with synthetic glycerides, naturally occurring fatty alcohols and related substances, and finally a very important chapter dealing with the techniques employed in the quantitative investigation of fats.

This second edition, published seven years after the first, has been lengthened by more than one hundred pages. Most of the increase is due to the inclusion of new data on the chemical composition of fats. The biggest addition has been made in the section dealing with the component acids of the fats of land animals, where a considerable amount of new information on the depot and milk fats of wild animals, domestic animals, and the human species is given.

Much new information is also given in the chapter on the component acids of vegetable fats and in the chapters on the component glycerides of animal and vegetable fats. Recently acquired knowledge about the constitution of the natural fatty acids, particularly the more unsaturated and some of the more rare fatty acids, is included.

The important chapter on biochemical aspects, dealing largely with the biosynthesis of fats, is understandably somewhat weak, largely because the progress of research in this field has been slow and difficult. The brief section on rancidity in this chapter appears not to have any important relationship to the rest of the material in the volume and, in view of the necessarily inadequate treatment, need not have been included.

The author has expanded the last chapter dealing with analytical techniques. This new material will be welcomed by many research workers. Since no one is better qualified than the author to discuss methods for making these very complex analyses, it is to be hoped that there will be a further expansion of this section in later editions to help others in understanding and overcoming the technical difficulties involved in the complete analysis of fats.

This work continues to be the outstanding source of information in its field. It is all the more remarkable since so much of the information on the composition of fats and so many of the ingenious analytical methods have been contributed by the author himself.

W. O. LUNDBERG.

*Isomerism and Isomerization of Organic Compounds.* By ERNST DAVID BERGMANN. xii + 138 pp. New York: Interscience Publishers, Inc., 1948. Price: \$3.50.

This book, based on a series of lectures presented at the Polytechnic Institute of Brooklyn, provides an extremely interesting introduction to isomerism and isomerization. Ernst Bergmann is an expert in this field and many of the examples cited are from his work. Chapters on resonance, *cis-trans* isomerism, isomerization of olefins, isomerization of paraffins, the mechanisms of substitution reactions, and the mechanisms of intramolecular rearrangements are included. Numerous references to the original literature are given.

The book, however, suffers from two serious defects. First, numerous errors occur in the formulas. For example, nitrogen atoms possessing five bonds  $\begin{array}{c} \diagup \\ \text{N} \\ \diagdown \end{array}$  are used throughout the book. The formula which is given on p. 83 as an example of a compound which is optically active because of steric effects possesses a plane of symmetry and could not possibly be resolved. On p. 59, the molecule used to illustrate the allylic rearrangement would form the same compound irrespective of the mechanism of the replacement reaction. Second, many of the theories presented are no longer generally accepted. For example, in the addition of bromine to a double bond, primary attack of the double bond by a positive bromide ion is now generally accepted, not attack by the negative bromide ion, as suggested on p. 57. Other serious differences with accepted theories could be noted.

In spite of these defects, the book is very stimulating if read critically. The paper is good and the binding excellent.

R. M. DODSON.

# THE THERMODYNAMIC PROPERTIES OF SODIUM SILICATE

NEWTON W. MCCREADY

*Philadelphia Quartz Company, Philadelphia, Pennsylvania*

*Received May 11, 1948*

## INTRODUCTION

Despite the importance of silicates, knowledge of their thermodynamic properties is quite unsatisfactory. This is particularly true of the sodium silicates. Published heats of formation of sodium metasilicate vary by as much as 40,000 cal. (3, 6) and in some cases are obviously erroneous. Only scattered data are available for the other forms of sodium silicate, and in some cases the reactions occurring appear to have been erroneously reported. Consequently it seems desirable to collect and examine critically the available data for the purpose of determining the best values.

It is important to use a consistent set of values for the basic compounds. Thus, quartz is involved in several of the reactions and reported heats of formation vary by 20,000 cal. (3). If the same value is used throughout, any error produced will cancel in many reactions involving quartz, or compounds derived from it, both as products and as reactants. This error is more likely to be made when the basic values used are not apparent in the final result.

The phase diagram of the system  $\text{Na}_2\text{O}-\text{SiO}_2$  (4, 9, 16) shows the presence of sodium orthosilicate ( $\text{Na}_4\text{SiO}_4$ ), sodium metasilicate ( $\text{Na}_2\text{SiO}_3$ ), and sodium disilicate ( $\text{Na}_2\text{Si}_2\text{O}_5$ ). The more alkaline region is still controversial; the presence of sodium pyrosilicate ( $\text{Na}_4\text{Si}_2\text{O}_7$ ) has been reported, but is still somewhat doubtful. However, there is independent evidence for its existence (11, 26), so it will be included here.

A sodium tetrasilicate (25) and crystalline hydrates of sodium metasilicate (2) and sodium sesquisilicate (1, 15) have been reported, but there are insufficient thermal data on them to warrant calculations. Melts of sodium silicate more siliceous than sodium metasilicate show a great tendency to vitrify on cooling, so that glasses of variable composition may be obtained. In such cases it is probable that the properties depend on their previous history. However, such glasses have sometimes erroneously been reported as normal compounds (11). Various solid silicic acids or hydrates of silica have also been reported, but these most probably consist only of water adsorbed on silica gel and are not definite, reproducible compounds.

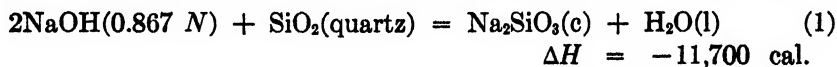
The values reported for heats of solution and of reaction, as well as for  $\Delta H$  and  $\Delta F$ , are in defined calories (= 4.1833 joules) absorbed in the process, in accordance with customary thermodynamic usage. These are based on 1 gram molecular weight of substance; sometimes this has required a revision of earlier data, owing to changes in accepted atomic weight values.

## SOURCES OF DATA

The most recent value for the heat of formation of quartz is that reported by Troitzsch (12, 23) from the combustion of silicon and a comparison of the heat of solution of the product in 20 per cent hydrofluoric acid with that of quartz. This yields for the formation of quartz from its elements  $\Delta H^0 = -208,300 \pm 350$  cal., a value which may be assumed to hold at 25°C., since the correction for temperature is much less than the probable error.

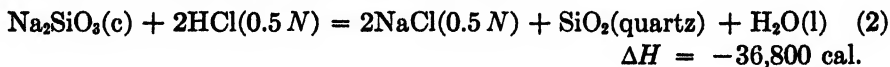
There are several sources of data for heats of formation of sodium silicates. Calorimetric measurements of various sorts have been made, but many of these are of questionable accuracy. Much of the work is quite old, and in some cases the products of the reaction are uncertain.

Mulert (18) lists for the heat of solution of sodium metasilicate in 20 per cent hydrofluoric acid, for the heat of solution of quartz in 20 per cent hydrofluoric acid, and for the heat of neutralization of hydrofluoric acid with sodium hydroxide the values  $-55,900$ ,  $-29,810$ , and  $-18,900$  cal., respectively. These yield:



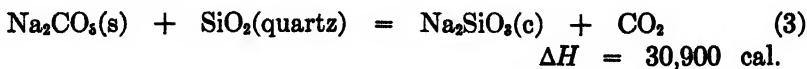
Using the heats of formation of quartz ( $-208,300$  cal.), of  $0.867\text{ }N$  sodium hydroxide ( $-112,150$  cal. (3)), and of water ( $-68,310$  cal. (3)) gives  $-376,000$  cal. for the formation of sodium metasilicate from the elements. These data were used by Bichowsky and Rossini, but with a different heat of formation of quartz, to obtain their listed heat of formation of sodium metasilicate,  $-371,200$  cal.

Matignon (13) found for the heat of neutralization of sodium metasilicate with hydrochloric acid, with silica gel as product, the value  $-32,800$  cal. Combining this with the heat of solution of silica gel and of quartz in hydrofluoric acid,  $-33,600$ , and  $-29,800$  cal., respectively, yields:



Together with the heats of formation of  $0.5\text{ }N$  hydrochloric acid ( $-39,400$  cal.) and  $0.5\text{ }N$  sodium chloride ( $-97,165$  cal. (3)), water, and quartz, this gives for the formation of sodium metasilicate from its elements,  $\Delta H = -355,300$  cal.

The direct heat of reaction of quartz and sodium carbonate was measured by Tschernobaef (24) in a bomb calorimeter.

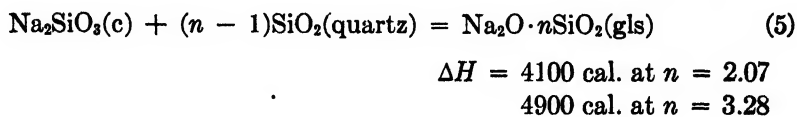
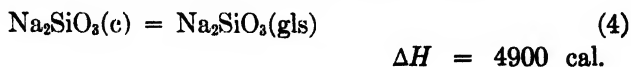


Using  $-270,830$  cal. as the heat of formation of sodium carbonate, from the value of  $-271,020$  cal. by Kelley and Anderson (8) corrected for the latest heat of formation of carbon dioxide ( $-94,052$  cal. (19)), gives  $-354,180$  cal. for the heat of formation of sodium metasilicate.

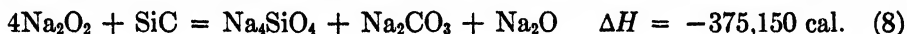
Troitzsch (23) measured the heats of solution of quartz, sodium carbonate, and sodium silicate in hydrofluoric acid, calculating for reaction 3,  $\Delta H = 20,380$  cal., or for the heat of formation of sodium metasilicate,  $-364,700$  cal.



The heats of solution of several vitreous silicates in hydrofluoric acid were also measured by Troitzsch (21, 23). These data may be expressed as:

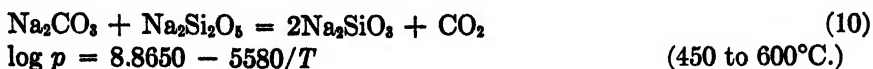
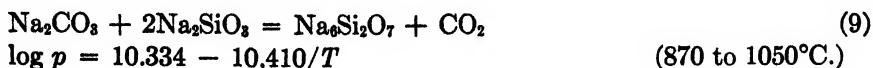
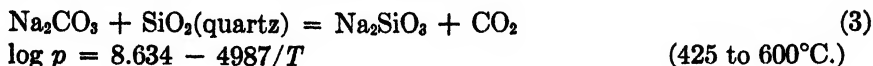


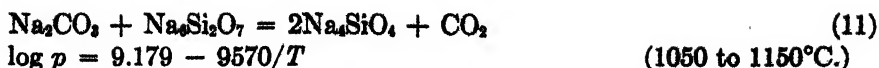
Mixer (14), and later Ruff and Grieger (22), measured the heats of reaction of sodium peroxide with silicon, with carbon black, and with silicon carbide. Their results are not in good agreement, but the latter investigators apparently took more care and made more careful corrections for side reactions. Both considered the products to include sodium metasilicate and sodium oxide, as did Bichowsky and Rossini. But sodium oxide has been shown to react with silica to form sodium orthosilicate (27), so the latter has been assumed to be the product, giving more reasonable results. From the results of Ruff and Grieger



Using equation 6 and the heat of formation of sodium peroxide ( $-119,200 \text{ cal.}$  (3)) yields for sodium orthosilicate the value  $-497,750 \text{ cal.}$  The difference between reactions 7 and 8, and the heat of formation of silicon carbide ( $-28,000 \text{ cal.}$  (3)), and correction for the heat of combustion of the carbon black used as compared with graphite give  $-498,900 \text{ cal.}$  for sodium orthosilicate. The latter value is less reliable, owing to the relatively large uncertainty in the heat of formation of silicon carbide.

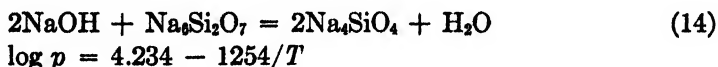
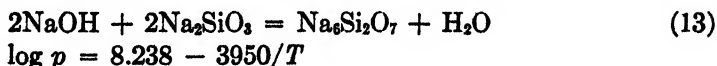
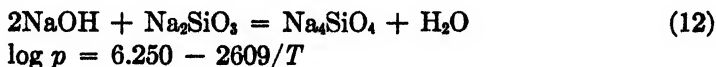
Equilibrium pressures of carbon dioxide in the reaction of sodium carbonate with quartz and with various forms of sodium silicate have been measured by Kröger and Fingas (11). The results are difficult to interpret, involving secondary reactions and sometimes apparently formation of solid solutions. A plot of  $\log p$  against  $1/T$  shows a series of points falling nearly on a straight line for each reaction, and also many points lying between. By a somewhat arbitrary choice of the points lying close to each straight line the following equations may be obtained by the method of least squares:





Two other lines are omitted, since vitreous silicates were used and the results cannot be interpreted. It is not certain that the other reactions are assigned correctly, as the products were not identified, but the above equations seem to be the most reasonable. However, the high-temperature heat capacity of sodium carbonate is unknown, as well as that of several of the silicates, so that an exact correction to room temperature is not possible. This is specially true of reactions 9 and 11, in which cases the sodium carbonate was fused and may have contained dissolved silicates.

The pressure of water vapor at equilibrium in the reaction of sodium hydroxide and sodium metasilicate has been measured by Zintl and Leverkus (26). The points fall very closely on three lines intersecting at  $400^\circ\text{C}$ . These may be interpreted as representing the following reactions:



Reactions 12 seems to occur mainly below  $400^\circ\text{C}$ ., and reactions 13 and 14 above  $400^\circ\text{C}$ ., indicating that  $\text{Na}_6\text{Si}_2\text{O}_7$  is stable only above this temperature, although it does occur occasionally as a metastable phase below  $400^\circ\text{C}$ . Since these reactions occur above the melting point of sodium hydroxide and its heat capacity is not known, correction to  $25^\circ\text{C}$ . cannot be made exactly.

Low-temperature heat capacities have been measured for sodium orthosilicate, metasilicate, and disilicate (6). These lead to the following entropies at  $25^\circ\text{C}$ .: 46.8, 27.2, and 39.4, respectively. High-temperature heat capacities have also been determined for sodium metasilicate and sodium disilicate (20). However, the transitions reported earlier in sodium disilicate (10) were not found. Possibly the quenching method did not allow time for the transitions to occur.

#### CALCULATIONS AND RESULTS

*Sodium metasilicate:* The heat of formation from the data of Mulert is far below that of the others, and is probably not of high accuracy. The neutralization with hydrochloric acid probably gave incomplete precipitation of silica, so that the result of Matignon would give too high a value. In the bomb calorimeter of Tschernobaef, the product probably fused and may not have crystallized completely on rapid cooling, yielding too high a result.

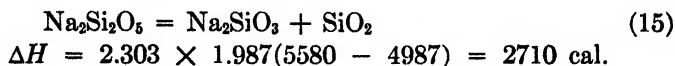
The equilibrium measurements of Kröger and Fingas yield for reaction 3,  $\Delta H = 22,800$  cal. at about  $500^\circ\text{C}$ . An estimated correction to  $25^\circ\text{C}$ . gives  $\Delta H = 23,900$  cal., from which the heat of formation of sodium metasilicate becomes

−361,200 cal. The value by Troitzsch, −364,700 cal., is probably the most reliable, and will be accepted.

From the entropies involved (6, 7), values for the formation of sodium metasilicate from its elements at 25°C. become

$$\Delta S^0 = -75.3 \text{ and } \Delta F^0 = -342,200 \text{ cal.}$$

*Sodium disilicate:* The only source of data on sodium disilicate is reaction 10. Subtracting equation 3 from equation 10 gives:



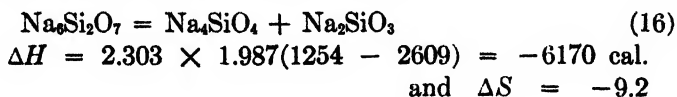
Correcting from 500°C. to 25°C. gives  $\Delta H = 3120$  cal. From the entropy values (6, 7) we find  $\Delta S^0 = -2.1$ . Therefore,  $\Delta F^0 = 3750$  cal. Consequently for the formation of sodium disilicate from its elements at 25°C.:

$$\Delta H = -576,100 \text{ cal.} \quad \Delta F^0 = -541,200 \text{ cal.}$$

*Sodium orthosilicate:* From equation 6 and the data of Ruff and Grieger the heat of formation of sodium orthosilicate becomes −497,750 cal., which is probably the most reliable value. This could also be calculated from equation 12 if an adequate correction for temperature were possible. A rough estimate yielded −492,500 cal. The use of equation 11 involves still greater uncertainty, owing to the very high temperatures; an estimated correction gave −488,000 cal. Both of the latter two may be neglected, and −497,800 cal. may be taken as the most probable value.

From the entropy of sodium orthosilicate, its free energy becomes −466,600 cal.

*Sodium pyrosilicate:* From the difference between equations 14 and 12:



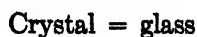
Since all the constituents are crystalline solids, assuming that heat capacities are additive, correction for temperature may be neglected. Thus for the formation of sodium pyrosilicate from its elements,  $\Delta H = -856,300$  cal. and  $\Delta F^0 = -812,200$  cal. at 25°C.

A rough estimate from equation 9 yields

$$\Delta H = -846,600 \text{ cal.}$$

*Vitreous sodium silicate:* Sodium silicate glasses of variable composition are readily formed by cooling a fused mixture and may be represented as  $\text{Na}_2\text{O} \cdot n\text{SiO}_2$ . Probably the thermodynamic properties vary with rate of cooling and other treatment, so that any values found would not hold in all cases. However, it is likely that such variations do not in general exceed a few hundred calories and that the major cause of the deviations found is experimental error, as similar differences have been obtained with crystalline compounds.

It is necessary that the heat of formation of a glass be greater than of the corresponding crystalline compound (if one exists), as is readily proven. For the reaction

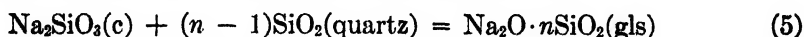


$\Delta S > 0$  owing to the greater randomness in the vitreous state, and below the melting point, where the crystalline form is more stable,  $\Delta F > 0$ . Therefore,  $\Delta H = \Delta F + T\Delta S > 0$ . This is not the case with the values reported by Bichowsky and Rossini (3) and in the *International Critical Tables* (5), so that at least one value is in error.

TABLE 1  
*Thermodynamic values at 25°C.*

COMPOUND	STATE	$\Delta H$	$\Delta F^\circ$	$S^\circ$
		<i>calories</i>	<i>calories</i>	
$\text{Na}_4\text{SiO}_4$ .....	Crystalline	-497,800	-466,600	46.8
$\text{Na}_6\text{Si}_2\text{O}_7$ .....	Crystalline	-856,300	-812,200	83.2
$\text{Na}_2\text{SiO}_3$ .....	Crystalline	-364,700	-342,200	27.2
$\text{Na}_2\text{SiO}_3$ .....	Vitreous	-359,800	(-338,000)	(29)
$\text{Na}_2\text{Si}_2\text{O}_5$ .....	Crystalline	-576,100	-541,200	39.4
$\text{Na}_2\text{O} \cdot n\text{SiO}_2$ .....	Vitreous	(-151,800 -208,300 <i>n</i> )	(-142,600 -195,600 <i>n</i> )	(18 + 11 <i>n</i> )
$\text{SiO}_2$ .....	Quartz	-208,300	-195,300	10.1
$\text{SiO}_2$ .....	Cristobalite	-208,000	-195,000	10.4
$\text{SiO}_2$ .....	Tridymite	-207,800	-195,000	10.2
$\text{SiO}_2$ .....	Vitreous	-206,000	-193,400	11.2
$\text{Na}_2\text{CO}_3$ .....	Crystalline	-270,830	-250,950	32.5
$\text{CO}_2$ .....	Gas	-94,052	-94,260	51.06
$\text{Na}_2\text{O}_3$ .....	Solid	-119,200		

The data of Richter and Roth (21) yield for the reaction



$\Delta H = 4900$  cal. at  $n = 1$ , 4100 cal. at  $n = 2.07$ , and 4900 cal. at  $n = 3.28$ . Within experimental error  $\Delta H$  may be taken as constant and equal to 4600 cal.

The entropy of silica glass is given as 11.2 (7), about one unit greater than for quartz. As there are no entropies known for vitreous sodium silicate, it may be assumed that there is one entropy unit for each mole of silica plus an entropy of mixing over that corresponding to the sum of the component oxides. For a perfect solution the entropy of mixing is given by  $-R(N_1 \ln N_1 + N_2 \ln N_2)$ , where  $R$  is the molar gas constant and  $N_1$  and  $N_2$  are mole fractions of the two constituents. For vitreous  $\text{Na}_2\text{O} \cdot n\text{SiO}_2$  (taken as a solution of  $\text{Na}_2\text{O}$  and  $\text{SiO}_2$ ) this varies from 1.39 to 1.00 as the value of  $n$  varies from 1 to 4. This may be put approximately equal to 1, so that as a rough estimate for reaction 5:

$$\Delta S = n + 1$$

**Silica:** The heat of formation of quartz, as already described, is taken as  $-208,300$  cal. Taking the entropy as  $10.1$  (7) gives a free energy of formation of  $-195,300$  cal. Corresponding values for other crystalline forms of silica may be obtained from heats of transition and entropies (17). The heat of formation of vitreous silica may be obtained from its difference in heat of formation from that of quartz (3).

For convenience the values obtained are summarized in table 1, together with those of several compounds used in obtaining them. Cases requiring the most approximations and assumptions are enclosed by parentheses.

#### SUMMARY

The thermal and equilibrium data on sodium silicates are reviewed and the most probable values for the heats and free energies of formation at  $25^{\circ}\text{C}$ . calculated for  $\text{Na}_4\text{SiO}_4$ ,  $\text{Na}_6\text{Si}_2\text{O}_7$ ,  $\text{Na}_2\text{SiO}_3$ , and  $\text{Na}_2\text{Si}_2\text{O}_5$ .

Estimated values are obtained for vitreous sodium silicate. Values for the various forms of silica consistent with these are also listed.

#### REFERENCES

- (1) BAKER, C. L.: U. S. patent 2,145,749 (1939).
- (2) BAKER, C. L., AND JUE, L. R.: J. Phys. Chem. **42**, 165 (1938).
- (3) BICHOWSKY, F. R., AND ROSSINI, F. D.: *The Thermochemistry of the Chemical Substances*. Reinhold Publishing Corporation, New York (1936).
- (4) D'ANS, J., AND LÖFFLER, J.: Z. anorg. allgem. Chem. **191**, 1 (1930).
- (5) *International Critical Tables*, Vol. V, p. 202. McGraw-Hill Book Co., Inc., New York (1929).
- (6) KELLEY, K. K.: J. Am. Chem. Soc. **61**, 471 (1939).
- (7) KELLEY, K. K.: U. S. Bur. Mines Bull. No. **434** (1941).
- (8) KELLEY, K. K., AND ANDERSON, C. T.: U. S. Bur. Mines Bull. No. **384** (1935).
- (9) KRACEK, F. C.: J. Phys. Chem. **34**, 1583 (1930).
- (10) KRACEK, F. C.: J. Am. Chem. Soc. **61**, 2863 (1939).
- (11) KRÖGER, C., AND FINGAS, E.: Z. anorg. allgem. Chem. **213**, 12 (1933); **225**, 1 (1935).
- (12) LANDOLT-BÖRNSTEIN: *Physikalisch-Chemische Tabellen*, Third Supplement, Vol. III, p. 2749. J. Springer, Berlin (1936).
- (13) MATIGNON, C.: Bull. soc. chim. **35**, 29 (1924).
- (14) MIXTER, W. G.: Am. J. Sci. [4] **24**, 130 (1907).
- (15) MOREY, G. W.: U. S. patent 1,948,730 (1934).
- (16) MOREY, G. W., AND BOWEN, N. L.: J. Phys. Chem. **28**, 1167 (1924).
- (17) MOSESSEN, M. A., AND PITZER, K. S.: J. Am. Chem. Soc. **63**, 2348 (1941).
- (18) MULERT, O.: Z. anorg. allgem. Chem. **75**, 198 (1912).
- (19) NATIONAL BUREAU OF STANDARDS: *Tables of Selected Values of Chemical Thermodynamic Properties* (1947).
- (20) NAYLER, B. F.: J. Am. Chem. Soc. **67**, 466 (1945).
- (21) RICHTER, H., AND ROTH, W. A.: Arch. Eisenhüttenw. **11**, 417 (1938).
- (22) RUFF, O., AND GRIEGER, P.: Z. anorg. allgem. Chem. **211**, 145 (1933).
- (23) TROITZSCH, H.: Dissertation, Braunschweig, 1936.
- (24) TSCHERNOBAEF, M. D.: Rev. mét. **2**, 729 (1905).
- (25) WEGST, W. F., AND WILLS, J. H.: U. S. patent 2,179,806 (1939).
- (26) ZINTL, E., AND LEVERKUS, H.: Z. anorg. allgem. Chem. **243**, 1 (1939).
- (27) ZINTL, E., AND MORAWIETZ, W.: Z. anorg. allgem. Chem. **236**, 372 (1938).

THE ELECTROCHEMICAL PROPERTIES OF MINERAL  
MEMBRANES. VIIITHE THEORY OF SELECTIVE MEMBRANE BEHAVIOR<sup>1</sup>

C. E. MARSHALL

*Department of Soils, University of Missouri, Columbia, Missouri**Received February 20, 1948*

Starting in 1939, the author and his associates have perfected methods for the determination of single mono- and divalent cations ( $K_1$ ,  $NH_4$ ,  $Na$ ,  $Ca$ ,  $Mg$ ) based on the use of mineral membranes (4, 5, 6, 7, 8). First, thin plates cut and ground from crystals of cation-exchange minerals were investigated (1). Chabazite and apophyllite were shown to act almost as though they were permeable to cations only, and their widespread use was precluded mainly by mechanical difficulties attendant on their preparation and the electrical limitations caused by very high resistance. Since 1941 the work has been concentrated upon membranes prepared from highly colloidal clays of the montmorillonite group. It was shown that heat treatments up to 400–600°C. improved both the mechanical and the electrochemical properties and rendered the clays very suitable for the determination of cationic activities. In all this work the comparison of different membranes was aided by a theory advanced independently by Teorell (12) and by Meyer and Sievers (9) for porous, electrically charged materials.

It was evident from the beginning that none of these membrane materials could properly be regarded as porous in the sense that water molecules could readily pass through them. Nevertheless, the Teorell–Meyer–Sievers theory predicted the behavior of all the mineral membranes studied in a qualitative and frequently in a semiquantitative way. This concordance in general behavior is undoubtedly due to the great practical importance of a quantity  $A$ , described as the selectivity constant. It is defined as the mean activity, within the membrane, of the mobile ion whose charge balances that of the membrane framework. The great advance which this concept represents stems from the clear recognition that membranes are electrochemical entities in their own right; they can therefore be treated formally as electrolytes.

The main features of the Teorell–Meyer–Sievers theory may be seen from figure 1. The effective charge  $A$  is responsible for the setting up of two Donnan potentials near the membrane surfaces. A liquid-junction potential arises within the membrane at the contact of the two salt solutions employed. The total potential measured when a single monovalent–monovalent salt is present on the two sides at two different concentrations is the sum of these three potentials. All involve  $A$ ; the liquid-junction potential is determined also by the ratio of mobility of cation to mobility of anion for the particular salt employed. Two limiting cases arise. When  $A$  is large compared with the salt concentrations, the liquid-junction potential disappears, that is, no salt penetrates to the interior.

<sup>1</sup> University of Missouri Agricultural Experiment Station Journal Series No. 1062.

At the same time the two Donnan potentials together simplify to  $\frac{RT}{F} \ln \frac{a_1}{a_2}$ , which is the Nernst equation. Secondly, when  $C_1$  and  $C_2$  are large compared with  $A$ , the two Donnan potentials become negligibly small and the liquid-junction potential, in the absence of a specific sieve effect, then has the normal value for free contact of the two solutions. For porous membranes, therefore, the measured potential should be between these two limiting values. When the ratio of cationic activities on the two sides has a fixed value, then the experimental curve obtained by plotting total potential against  $\log 1/a_2$  can, if it agrees with the theory, be used to determine two characteristics of the membrane: the thermodynamic charge  $A$ , or selectivity constant, and the ratio  $U_c/U_a$ , which may or may not be identical with the same ratio for the salt in water alone. If it is not

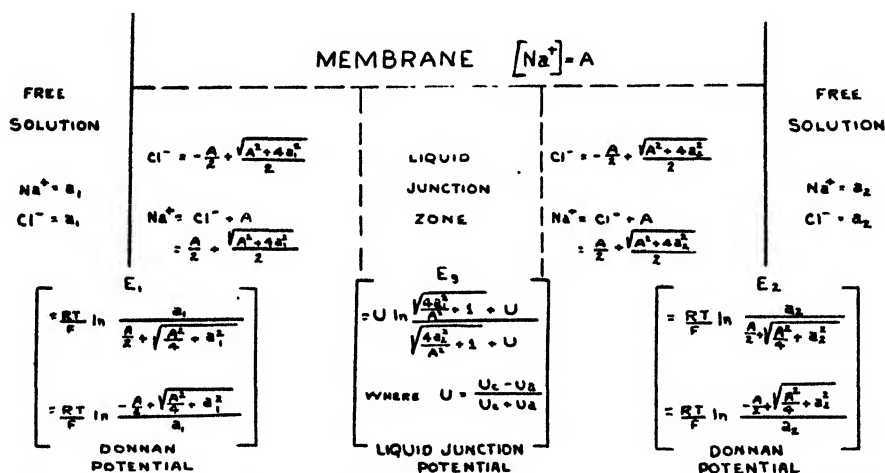


FIG. 1. A diagrammatic sketch indicating the main features of the Teorell-Meyer-Sievers theory of membrane potentials.

identical this means that the membrane itself exerts a mechanical sieve effect which can be measured by the ratio  $(U_c/U_a)_{\text{membrane}}/(U_c/U_a)_{\text{water}}$ . In practice the salt employed for such experiments is potassium chloride, for which  $(U_c/U_a)_{\text{water}}$  is approximately 1. Then  $(U_c/U_a)_{\text{membrane}}$  is a measure of the sieve effect.

The actual determinations of  $A$  and of  $(U_c/U_a)_{\text{membrane}}$  are effected graphically. Using a fixed ratio  $a_1/a_2$ , a family of curves is drawn for  $A = 1$  and assigned values of  $U_c/U_a$ . The experimental curve is then compared with these, as regards both shape and position. If the theory holds for the membrane under investigation, then it should match in shape one of the theoretical curves whose  $U_c/U_a$  value is known. The displacement of the experimental from the theoretical curve measures  $-\log A$ .

In actual fact, relatively few measurements even on porous membranes have extended over a sufficiently wide range of concentrations to afford a precise test of the theory. Our mineral membranes depart quite markedly from it in the

sense that  $U_c/U_a$  and  $A$  seem to decrease with increasing salt concentration. One of the primary assumptions, however, is that  $A$  is independent of the salt concentrations. This could only be strictly true if the membrane acted as a strong colloidal electrolyte, that is, if the activity coefficient of the dissociating ion were close to unity throughout. For many membrane materials this is unlikely to be the case. Certainly clay membranes, if they behave like clay suspensions, should dissociate only a small fraction of the total exchangeable cations. One could anticipate that this fraction would decrease considerably with increase in salt concentration. This departure from the theoretical behavior could arise with porous and non-porous membranes alike.

Several properties of clay membranes preheated to temperatures between 300° and 600°C. pointedly indicate that they are not porous in any ordinary sense of the term.

(a) The specific resistance of the membrane material in salt solutions is too high for any appreciable amount of salt to be present in internal pores.

(b) Osmosis experiments fail to show measurable water movement.

(c) Using hydrochloric acid solutions it is found that potentials lower than would arise with a free liquid junction may be obtained. To explain this fact using the Teorell-Meyer-Sievers theory one would have to assume the presence of a sieve effect which retards the hydrogen ion relative to chloride. In view of their relative sizes this seems impossible. On the other hand, this result would be a natural consequence of the absence of a liquid junction in the interior. The total potential would then be  $E_1 + E_2$  (figure 1), which diminishes continuously as  $a_1$  and  $a_2$  increase together in comparison with  $A$ . Instead of a family of theoretical curves for different values of  $U_c/U_a$  we should have the single curve for which  $U_c = U_a$ .

This situation is illustrated by figure 2, based on E. O. McLean's unpublished experiments with hydrochloric acid and hydrogen Putnam clay (beidellite) membranes preheated to 600°C. The membranes were first characterized by their curves with potassium chloride, then with hydrochloric acid, and finally were retested with potassium chloride to insure that their electrochemical properties had not been changed by the acid treatment. It was not possible to use very high acid concentrations. However, there is no doubt that potentials lower than for a free liquid junction are obtained.

(d) Studies of the moisture content of clay films heated to various temperatures have shown that more water is held than for the powdered clay. The bonding energy for interparticle water becomes indistinguishable from that of the intralayer water of the montmorillonite clays. The whole film thus acts more as a single phase than as a system of capillaries. As the temperature of pretreatment rises the film becomes more compact, its moisture content decreases, and its electrochemical properties become more favorable as shown by an apparent increase in  $A$ . The quantitative changes in these properties depend upon the exchange cation present.

On the other hand it is very evident from the decrease in potential with increase in salt concentration (the ratio of concentrations being held constant) that



these mineral electrodes cannot simply be treated like solid solutions or amalgams, which would give theoretical values at high concentrations. They evidently possess an intermediate character in which variation in  $A$  is still of great importance, whether caused by a change in total exchange capacity or by vari-

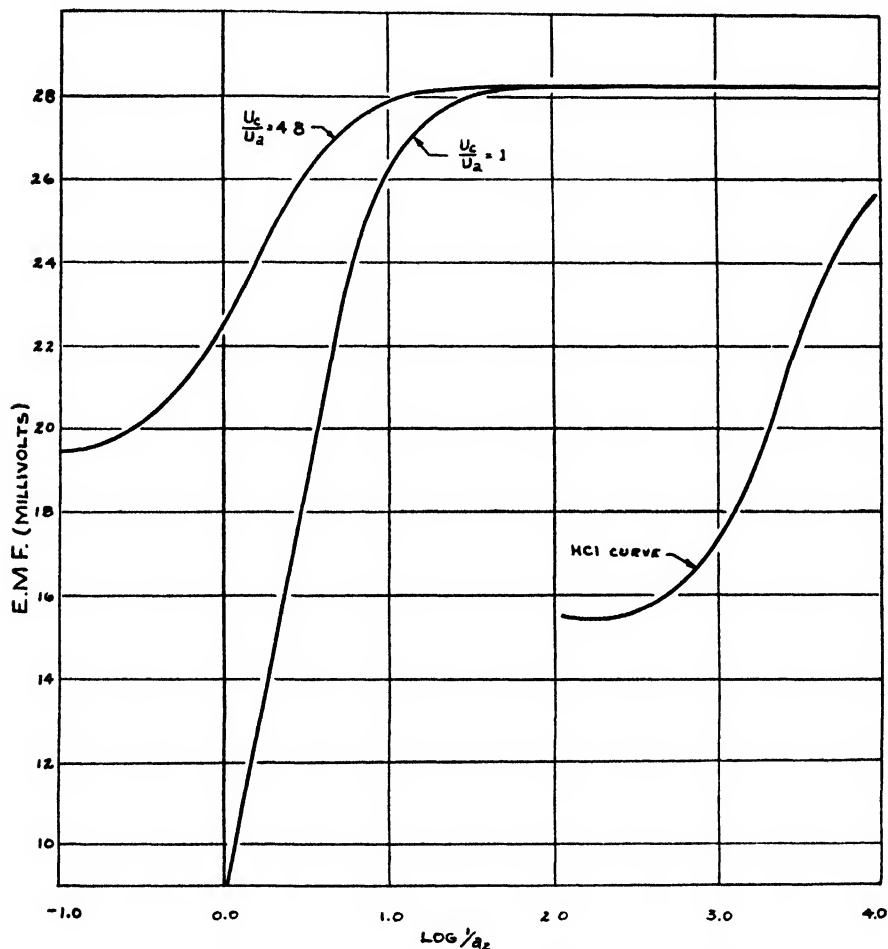


FIG. 2. The relationship of theoretical curves resulting from free liquid-junction potentials of hydrochloric acid in water,  $U_c/U_a = 4.8$ , and those arising only from Donnan effects,  $U_c/U_a = 1$ , to the experimental curve for hydrochloric acid using 600°C. Putnam membranes.  $a_1/a_2 = 3$  for all curves;  $A = 1$  for theoretical curves.

ation in the membrane ionization. They are essentially homoporous, to use Sollner's (11) term, as contrasted with the heteroporous nature of the oxidized collodion membranes studied by him.

#### MODIFICATION OF EXISTING THEORY

As far as experiments with the same salt on both sides of clay membranes go, it would seem that the Teorell-Meyer-Sievers theory needs simplifying in one

respect but amplifying in another. If the internal liquid junction is absent, then their equation involves only the two Donnan potentials and may be written in either of the forms:

$$E_{\text{membrane}} = \frac{RT}{F} \left\{ \ln \frac{a_1}{a_2} \cdot \frac{\left( \frac{A}{2} + \sqrt{\frac{A^2}{4} + a_1^2} \right)}{\left( \frac{A}{2} + \sqrt{\frac{A^2}{4} + a_2^2} \right)} \right\}$$

$$E_{\text{membrane}} = \frac{RT}{2F} \left\{ \ln \frac{\left( \sqrt{\frac{4a_2^2}{A^2} + 1} + 1 \right) \left( \sqrt{\frac{4a_1^2}{A^2} + 1} - 1 \right)}{\left( \sqrt{\frac{4a_2^2}{A^2} + 1} - 1 \right) \left( \sqrt{\frac{4a_1^2}{A^2} + 1} + 1 \right)} \right\}$$

A complete theory for this case should provide also for variation in  $A$  with variation in concentration of the external electrolyte. This does not seem to be at present feasible, owing to our imperfect theoretical knowledge of the behavior of colloidal electrolytes in general and to our practical ignorance of the dissociation of membrane materials in particular.

A concept which gives a qualitatively accurate picture of the behavior of these membranes, although probably oversimplified, represents the structure as essentially cellular on a molecular scale. Close to the outer surfaces are narrow zones accessible to the outer solution. Here the Donnan equilibria are set up. The actual depth of penetration will probably vary somewhat from place to place. Statistically we can imagine the Donnan effects to be operative within a certain mean volume close to the outer surfaces of the membrane. The interior can then be thought of as homogeneous, the exchange ions being held with specific bonding energies. This concept, as we shall now see, leads to a completely new interpretation of the potentials obtained when such a membrane separates different salt solutions.

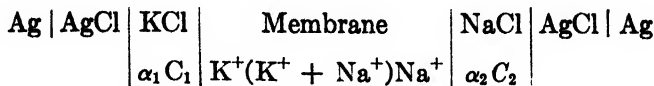
#### POTENTIAL THEORY FOR DIFFERENT SALTS

Considerable work was carried out by Michaelis and his collaborators on dried collodion membranes with different salt solutions on the two sides (10). They termed the potentials measured "biionic potentials" and showed how, for porous materials, these could be regarded as liquid-junction potentials in which the anion has zero mobility. From the measured potential it was possible to calculate the mobility ratio of cations within the membrane, provided the cationic activities were known. This treatment has also been used by us as a means of characterizing clay membranes for analytical applications involving mixtures of cations. The equations for the different cases are derived on the assumption that  $C_1$  and  $C_2$  are small compared with  $A$ ; that is, the determinations should lie within the range in which the membranes obey the Nernst equation for single salts. The Henderson or Planck equations for liquid junctions are then applied, zero mobility being assigned to all anions. The resulting equations are rela-

tively simple where cations of the same valency are used but become somewhat complex for mixtures of cations of different valencies (2).

#### A. Monovalent-monovalent case

Consider the energy changes involved in the operation of a reversible cell of the type:



The membrane is assumed to hold potassium ions only in contact with the potassium chloride solution and sodium ions only in contact with the sodium chloride solution; in the interior both sodium and potassium ions are held.  $\alpha_1$  and  $\alpha_2$  represent the activity coefficients, and  $C_1$  and  $C_2$  the concentrations of the potassium chloride and sodium chloride, respectively.

We consider the various changes which occur during the passage of  $dn$  faradays of electricity through the cell, the direction being such that potassium ions move from left to right.

(1) *Heat effects:* The potassium chloride solution loses  $dn$  equivalents of potassium ion to the membrane and  $dn$  equivalents of chloride ion to the silver. Simultaneously the sodium chloride solution gains  $dn$  equivalents of sodium ion from the membrane and  $dn$  equivalents of chloride ion from the silver chloride. The heat changes as regards the silver chloride balance. Let the differential heats of adsorption or combination of potassium and sodium ions on the membrane be respectively  $H_{\text{K}^+}$  and  $H_{\text{Na}^+}$ . The heat gain by the membrane is  $+dn H_{\text{K}^+}$  calories. The heat loss by the membrane is  $-dn H_{\text{Na}^+}$  calories. Thus the total heat effect  $= dn (H_{\text{K}^+} - H_{\text{Na}^+})$ .

(2) *Osmotic effects:*

Osmotic work gained in removal of  $\text{K}^+$  from  $\text{KCl} = dn RT \ln 2\alpha_1 C_1$

Osmotic work gained in removal of  $\text{Cl}^-$  from  $\text{KCl} = dn RT \ln 2\alpha_1 C_1$

Osmotic work lost in addition of  $\text{Na}^+$  to  $\text{NaCl} = -dn RT \ln 2\alpha_2 C_2$

Osmotic work lost in addition of  $\text{Cl}^-$  to  $\text{NaCl} = -dn RT \ln 2\alpha_2 C_2$

The total osmotic work  $= 2 dn RT \ln 2\alpha_1 C_1 - 2 dn RT \ln 2\alpha_2 C_2$

(3) *Electrical effects:* If  $E_{\text{total}}$  is the total potential of the above cell, then the electrical work in the passage of  $dn$  faradays of electricity is  $dn FE_{\text{total}}$  joules. This electrical work can now be equated to the sum of the heat effects and the osmotic work, the former being multiplied by 4.185 to convert calories to joules. We then have:

$$\begin{aligned} dn FE_{\text{total}} &= 4.185 dn (H_{\text{K}^+} - H_{\text{Na}^+}) + 2 dn RT \ln \frac{2\alpha_1 C_1}{2\alpha_2 C_2} \\ E_{\text{total}} &= \frac{4.185}{F} (H_{\text{K}^+} - H_{\text{Na}^+}) + \frac{2RT}{F} \ln \frac{\alpha_1 C_1}{\alpha_2 C_2} \end{aligned} \quad (1a)$$

The membrane potential is simply obtained by subtracting from  $E_{\text{total}}$  the sum

of the potentials at the silver-silver chloride electrodes—namely,  $\frac{RT}{F} \ln \frac{a'_{\text{Cl}}}{a''_{\text{Cl}}}$ —which for very dilute solutions can be set equal to  $\frac{RT}{F} \ln \frac{\alpha_1 C_1}{\alpha_2 C_2}$ . Thus we have

$$E_{\text{membrane}} = \frac{4.185}{F} (H_{\text{KCl}} - H_{\text{NaCl}}) + \frac{RT}{F} \ln \frac{\alpha_1 C_1}{\alpha_2 C_2} \quad (1b)$$

It is the membrane potential which is assumed to be measured when saturated calomel electrodes with saturated potassium chloride bridges are used in place of the silver-silver chloride electrodes. In either case, if the concentrations of salts are so chosen that  $\alpha_1 C_1 = \alpha_2 C_2$ , then the measured potential is a linear function of the difference in the differential heats of adsorption of the cations. Thus the potential measurement leads to the computation of  $H_{\text{K}^+} - H_{\text{Na}^+}$ .

Equation 1b may now be compared with the equation derived for the limiting case of a liquid junction in which the anions have zero mobility.

$$E_{\text{membrane}} = \frac{RT}{F} \ln \frac{a_{\text{K}^+}}{a_{\text{Na}^+}} \cdot \frac{U_{\text{K}^+}}{U_{\text{Na}^+}} \quad (1c)$$

Here  $a_{\text{K}^+}$  and  $a_{\text{Na}^+}$  are the individual cationic activities on the two sides of the membrane, and  $U_{\text{K}^+}/U_{\text{Na}^+}$  is the mobility ratio of these ions within the membrane. If the solutions concerned are sufficiently dilute that we can make the approximation

$$\frac{\alpha_1 C_1}{\alpha_2 C_2} = \frac{a'_{\text{K}}}{a''_{\text{Na}}}$$

then we shall have:

$$\frac{RT}{F} \ln \frac{U_{\text{K}^+}}{U_{\text{Na}^+}} = \frac{4.185}{F} (H_{\text{K}^+} - H_{\text{Na}^+}) \quad (1d)$$

In this way the apparent mobility ratio can be linked with a thermochemical property of the membrane: namely, the difference in the differential heats of adsorption (or combination) for the two monovalent cations.

The question must now be considered whether both these approaches can be justified for one and the same membrane. The mobility ratio equation is quasi-thermodynamic in the same sense as any liquid junction. Actually in deriving it we say nothing regarding porosity; and the assumption that the anions have zero mobility is simply another way of saying that they do not penetrate through, or that the Nernst equation is obeyed with respect to the cations alone. The same formal treatment thus can be applied to any membrane under this limitation.

Precisely the same is true of the thermochemical approach. The only limitation is that the Nernst equation should be obeyed, that is, that somewhere in the membrane there should be a layer of material which, when a small current is passed, merely loses one kind of cation and gains another, the anions having no part in the process. It would seem then that porous membranes will, under this limitation, follow the thermochemical equation derived above.

Hence there are two formal treatments applicable to all membranes showing complete selectivity towards cations. Under some circumstances the mobility ratio may be needed (for example, in certain analytical applications). Under other circumstances information on differences in differential heats of adsorption may be helpful. The use of the one or the other is a matter of choice, and does not imply that any special structure can be ascribed to the membrane itself.

Indeed it seems possible, although this has not yet been experimentally tested, to use equation 1a in order to learn something about differences in differential heats of adsorption or combination for various colloidal electrolytes in the gel form. A relatively thick immobile plug of the gel would take the place of the membrane. It would first be tested with different concentrations of a single salt in order to determine the range within which the Nernst equation is obeyed. Then within this range known concentrations of different salts could be used to determine  $(H_{K^+} - H_{Na^+})$ , or similar differences for other pairs of monovalent cations.

### B. Divalent-divalent case

Pursuing the same argument as in the previous example we first calculate the total potential of the cell.

$$\text{Ag} | \text{AgCl} | \text{CaCl}_2 \left| \begin{array}{c} \text{Membrane} \\ \alpha_1 C_1 \quad \text{Ca}^{++}(\text{Ca}^{++} + \text{Mg}^{++})\text{Mg}^{++} \end{array} \right| \text{MgCl}_2 | \text{AgCl} | \text{Ag}$$

$$E_{\text{total}} = \frac{4.185}{2F} (H_{\text{Ca}} - H_{\text{Mg}}) + \frac{3}{2} \frac{RT}{F} \ln \frac{3\alpha_1 C_1}{3\alpha_2 C_2} \quad (2a)$$

From this we subtract  $\frac{RT}{F} \ln \frac{a'_{\text{Cl}}}{a_{\text{Cl}}}$  or, to a first approximation for very dilute solutions,  $\frac{RT}{F} \ln \frac{\alpha_1 C_1}{\alpha_2 C_2}$ , which gives:

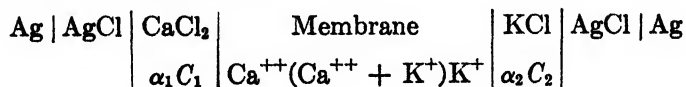
$$E_{\text{membrane}} = \frac{4.185}{2F} (H_{\text{Ca}} - H_{\text{Mg}}) + \frac{RT}{2F} \ln \frac{\alpha_1 C_1}{\alpha_2 C_2} \quad (2b)$$

The corresponding mobility ratio equation is

$$E_{\text{membrane}} = \frac{RT}{2F} \ln \frac{a'_{\text{Ca}}}{a'_{\text{Mg}}} \cdot \frac{U_{\text{Ca}}}{U_{\text{Mg}}} \quad (2c)$$

### C. Divalent-monovalent case

The cell under consideration is



The total potential is given by:

$$E_{\text{total}} = \frac{4.185}{F} (H_{\text{Ca}/2} - H_{\text{K}}) + \frac{RT}{F} \left\{ \frac{3}{2} \ln 3\alpha_1 C_1 - 2 \ln \alpha_2 C_2 \right\} \quad (3a)$$

The potential to be subtracted from this is  $\frac{RT}{F} \ln \frac{a_{Cl}'}{a_{Cl}''}$ , which, in view of the wide divergence in activity coefficients between salts of monovalent and divalent cations, cannot with accuracy be identified with  $\frac{RT}{F} \ln \frac{2a_1C_1}{a_2C_2}$ . However, since the relevant data are all known, particular cases can always be worked out.

The corresponding mobility ratio equation is also cumbersome.

$$E_{\text{membrane}} = \frac{RT}{F} \left\{ \frac{-a_K'' + \frac{U_{Ca}}{U_K} a_{Ca}'}{-a_K'' + 2\frac{U_{Ca}}{U_K} a_{Ca}'} \right\} \ln \frac{a_K''}{2a_{Ca}'} \cdot \frac{U_K}{U_{Ca}} \quad (3c)$$

To determine  $U_K/U_{Ca}$  it is necessary to set up an experiment such that  $a_K'$  is small compared with  $U_{Ca}/U_K \cdot a_{Ca}'$ . The simplified equation resulting can then be solved for  $U_K/U_{Ca}$  (2).

#### D. Cases of mixtures of salts

The thermochemical treatment does not lend itself to cases where a mixture of salts is present on one side of the membrane. The reason is that the proportions of the cations upon the membrane are not the same as in solution, and a separate series of adsorption isotherms would have to be obtained in order to find an empirical relationship between the two. The mobility ratio method here has the advantage that after this has been determined for a given pair of cations, results with mixtures can, in a number of cases, be interpreted (3).

#### CALCULATIONS FROM EXPERIMENTAL DATA ON CLAY MEMBRANES

In studying the properties of clay membranes for analytical use, extensive data on mobility ratios have already been obtained. It has been shown that, for cations of the same valency, reasonable constancy can be secured over a range of salt concentrations. Where the cations have different valencies, there is a strong tendency for the mobility ratio to vary with concentration (4). Certain membranes show this much more than others.

The influence of variation in mobility ratio upon the difference in differential heats of adsorption can best be appreciated by calculating particular cases under equation 1d for monovalent-monovalent cations. We can rewrite it

$$\frac{RT}{4.185} \cdot \ln \frac{U_K}{U_{Na}} = (H_{K^+} - H_{Na^+})$$

#### A. Monovalent-monovalent series

Table 1 gives potassium-sodium and hydrogen-potassium mobility ratio data for membranes prepared from hydrogen bentonite (montmorillonite from Wyoming). This stock of clay gave membranes showing different properties for high temperatures of pretreatment from those examined earlier. Instead of acquiring a high resistance and high selectivity towards monovalent cations around

490°C., the present series had a much lower resistance, and even after pretreatment at 550°C. the membranes were sensitive to divalent cations. The cause of this divergence in behavior is being investigated. The table illustrates the fact that the mobility ratios are relatively insensitive to change in concentration of the two solutions. There is sufficient difference between the 350°C. and 550°C.

TABLE 1  
*Mobility ratios and differences in differential heats of adsorption for potassium-sodium and potassium-hydrogen, using various clay membranes*

OBSERVER	CLAY	TEMPERATURE OF PRETREATMENT	ACTIVITIES OF CATIONS USED		MOBILITY RATIO $U_K/U_{Na}$	DIFFERENCE IN DIFFERENTIAL HEATS OF ADSORPTION $H_K - H_{Na}$
			K <sup>+</sup>	Na <sup>+</sup>		
E. O. McLean	Hydrogen bentonite . .	°C. 350	0.081	0.081	2.30	calories 496
			0.027	0.027	2.29	491
			0.009	0.009	2.18	461
			0.003	0.003	2.00	410
			0.001	0.001	1.58	271
		450	0.081	0.081	3.58	755
			0.027	0.027	4.07	831
			0.009	0.009	3.89	804
			0.003	0.003	3.77	786
			0.001	0.001	3.52	743
		550	0.081	0.081	4.14	841
			0.027	0.027	4.71	917
			0.009	0.009	5.14	969
			0.003	0.003	5.43	1002
C. A. Krinbill	Hydrogen Putnam . . . . .	600	0.027	0.026	2.68	
			0.009	0.009	2.53	
E. O. McLean	Hydrogen bentonite . . . .	350	H <sup>+</sup>	K <sup>+</sup>	$U_H/U_K$	$H_H - H_K$
			0.00021	0.003	3.40	724
		450	0.00021	0.001	2.84	618
			0.00021	0.003	2.69	585
		550	0.00021	0.001	2.62	570
			0.00018	0.003	2.85	620
			0.00018	0.001	2.94	638
			0.00018	0.00033	2.58	561

membranes to make it entirely feasible to estimate sodium and potassium in a mixture if other cations were absent. The most favorable concentration range for this is 0.03–0.003.

The hydrogen-potassium mobility ratios vary less with temperature of pretreatment than the potassium-sodium values.

The differences in differential heats of adsorption for potassium and sodium are seen to be very significant thermochemical quantities. One may compare them with the difference in differential heats of solution, which for potassium

and sodium chlorides amounts to 2790 cal. This quantity includes differences due to the two solids as well as differences in the heats of dilution.

*B. Divalent-divalent series*

Calcium-magnesium mobility ratios and the corresponding differences in differential heats of adsorption have been determined for a considerable range of pre-

TABLE 2  
*Mobility ratios and differences in differential heats of adsorption  
for calcium-magnesium using various clay membranes*

OBSERVER	CLAY	TEMPERATURE OF PRETREATMENT	ACTIVITIES		$U_{Ca}/U_{Mg}$	$H_{Ca} - H_{Mg}$
			Ca <sup>++</sup>	Mg <sup>++</sup>		
		°C.				calories
L. O. Eime	Hydrogen bentonite....	300	0.0081	0.0081	1.37	188
			0.0027	0.0027	1.26	139
		360	0.0081	0.0081	1.52	248
			0.0027	0.0027	1.36	182
		400	0.0081	0.0081	1.55	261
			0.0027	0.0027	1.59	275
	Calcium bentonite.....	405	0.0081	0.0081	1.41	206
			0.0027	0.0027	1.22	119
		455	0.0081	0.0081	1.44	215
			0.0027	0.0027	1.29	153
		500	0.0081	0.0081	1.45	220
			0.0027	0.0027	1.33	170
	Hydrogen Putnam.....	415	0.0081	0.0081	1.17	92
			0.0027	0.0027	1.27	142
		510	0.0081	0.0081	1.45	222
			0.0027	0.0027	1.42	209
		595	0.0081	0.0081	1.42	208
			0.0027	0.0027	1.51	245
	Calcium Putnam.....	405	0.0081	0.0081	1.21	116
			0.0027	0.0027	1.18	98
		500	0.0081	0.0081	1.46	224
			0.0027	0.0027	1.41	204
		550	0.0081	0.0081	1.55	261
			0.0027	0.0027	1.40	202

treatments (table 2). The values fall a little with concentration when both electrolytes are similar, but when the magnesium chloride solution decreases in concentration relative to the calcium chloride, distinct decreases in mobility ratio are observed. The values are seen to be lower than those for potassium-sodium. As in this latter case, the differences between calcium and magnesium become greater as the temperature of pretreatment of the membranes rises. However, the extremes found for  $U_{Ca}/U_{Mg}$  are not sufficiently far apart to provide an accurate means of determining both magnesium and calcium in a mixture.



## C. Divalent-monovalent series

In the papers dealing individually with the determination of calcium and magnesium, it has been shown that great variation of the mobility ratio with salt concentration is usually found, where divalent ions are used on one side of the membrane and monovalent on the other. This is not adequately accounted for by the somewhat unfavorable conditions imposed in utilizing a simplified equation. Reference to equation 3a shows that such variation may be expected. The activity term may be written:

$$\frac{RT}{F} \left\{ \frac{3}{2} \ln 3 + \ln \frac{(\alpha_1 C_1)^{3/2}}{(\alpha_2 C_2)^2} \right\}$$

Thus a fixed ratio  $\alpha_1 C_1 / \alpha_2 C_2$  will no longer be sufficient to define  $E_{\text{total}}$  when  $(H_{Ca/2} - H_K)$  is constant. The calculated value of  $(H_{Ca/2} - H_K)$  will include this variability with concentration, whereas the mobility ratio equation in the simplified form derived from equation 3c contains only the simple ratio  $a'_K / a'_{Ca}$ . Thus the mobility ratio itself will be variable with respect to concentration even when  $(H_{Ca/2} - H_K)$  is constant and *vice versa*. Under these circumstances a few comments may well replace a detailed tabulation of the values obtained for calcium-potassium, calcium-hydrogen, magnesium-potassium, and magnesium-hydrogen.

The thermochemical quantities,  $(H_{Ca/2} - H_K)$  etc., are found to be much larger than in the monovalent-monovalent and divalent-divalent cases. This is due largely to the unbalanced osmotic term discussed above. This in itself throws doubt on the validity of strict thermochemical comparisons between the divalent-monovalent cases and those in which both cations have the same valency. Furthermore, the variation with concentration represents the thermochemical aspect of the now well-established fact that for systems of differing relevant valencies, base-exchange equilibria vary with the dilution of the whole system. The relationship of these thermochemical quantities to the equations proposed for exchange equilibria now needs both theoretical and experimental clarification.

## REFERENCES

- (1) MARSHALL, C. E.: J. Phys. Chem. **43**, 1155 (1939).
- (2) MARSHALL, C. E.: J. Phys. Chem. **48**, 67 (1944).
- (3) MARSHALL, C. E., AND AYERS, A. D.: Soil Sci. Soc. Am. Proc. **11**, 171 (1946).
- (4) MARSHALL, C. E., AND AYERS, A. D.: J. Am. Chem. Soc., in press.
- (5) MARSHALL, C. E., AND BERGMAN, W. E.: J. Am. Chem. Soc. **63**, 1911 (1941).
- (6) MARSHALL, C. E., AND BERGMAN, W. E.: J. Phys. Chem. **46**, 325 (1942).
- (7) MARSHALL, C. E., AND EIME, L. O.: J. Am. Chem. Soc., in press.
- (8) MARSHALL, C. E., AND KRINBILL, C. A.: J. Am. Chem. Soc. **64**, 1814 (1942).
- (9) MEYER, K. H., AND SIEVERS, J. F.: Helv. Chim. Acta **19**, 649, 665, 987 (1936).
- (10) MICHAELIS, L.: Colloid Symposium Monograph **5**, 135 (1927).
- (11) SOLLNER, K.: J. Phys. Chem. **49**, 47 (1945).
- (12) THEORELL, T.: Proc. Soc. Exptl. Biol. Med. **33**, 282 (1935); Trans. Faraday Soc. **33**, 1054 (1937).

THE PORE SIZE-SURFACE AREA DISTRIBUTION OF A  
CRACKING CATALYST

T. D. OULTON

*Filtrol Corporation, 3250 E. Washington Boulevard, Los Angeles 23, California**Received February 20, 1948*

## I. INTRODUCTION

Certain problems involving the physical structure and the activity of porous solid catalysts require a knowledge not only of the total surface area, but also of the way in which this total area is distributed in capillaries of various sizes—that is, the pore size-surface area distribution.

The simple capillary condensation theory, which postulates that all adsorption in excess of that required for formation of the first monolayer is due to capillary condensation, has provided the basis for a number of efforts to find a solution to the problem by means of the direct application of the Kelvin (16) equation. By this equation the pressure axis of the conventional adsorption isotherm can be expressed in terms of the equivalent pore radius and a graphical or analytical differentiation of the isotherm gives a volume-pore size distribution directly. With the assumption of some definite pore geometry by which pore volume can be expressed in terms of surface area, a surface area-pore size distribution can be easily obtained.

E. N. Harvey (11) and also Kistler, Fisher, and Freeman (12) as recently as 1943 suggested interesting methods for estimating total surface area and indirectly a surface area distribution based on the Kelvin equation and the assumption that capillary condensation accounts for all sorption in excess of a monolayer. But the more recent work of Harkins and Jura (8) on the nature and the equations of state of adsorbed films on solid surfaces clearly demonstrates the existence of polymolecular films, and that in the majority of cases, true capillary condensation superimposed on a polylayered film does not begin until fairly high relative pressures are reached. Since any application of the Kelvin equation presupposes the existence of the adsorbate in the condensed liquid state, it is doubtful that any pore size distribution based on an analysis of the adsorption branch of the isotherm can be accepted.

It seems probable, however, that the desorption branch of the hysteresis loop which is characteristic of many adsorbents does represent (at least in part) evaporation of condensed liquid, and that the shape of the desorption branch does indeed depend on the pore size distribution of the adsorbent.

Harkins and Jura (9) have recently reviewed the uncertainties which accompany the application of the Kelvin equation to the determination of a pore size distribution. These may be restated briefly: (1) The use of the equation in any of its forms requires the assumption of a geometry for the pore which is necessarily idealized. (2) The values of the surface tension and the molal volume of the liquid condensed in very small pores are not necessarily the same as for the bulk liquid. (3) The thickness of the adsorbed film is not known. Harkins and

Jura (8) have shown, for instance, that in the case of water adsorbed on anatase, the attractive field of the solid may extend as far as five or six molecular diameters away from the solid surface. The gas held within the field of the solid is not liquid in the ordinary sense. The density is greater, the molal volume is less, and the surface tension of the film is greater than would be observed for the bulk liquid. However, there is no doubt that these values approach those of the bulk liquid as the film thickens.

As a result of the work described in this report, it has been found possible, subject to the acceptance of certain assumptions and approximations, to determine a surface area-pore size distribution by a method which largely evades the questions raised by Harkins and Jura. While the method cannot yet be said to be generally applicable, in the case of the adsorbents studied it appears to have a definite advantage over any of the methods which the author has seen reported in the literature.

A number of explanations have been advanced to account for hysteresis. Perhaps the most important of these are: (a) the incomplete wetting theory (17), (b) non-rigidity of the adsorbent, with consequent swelling and shrinkage, (c) the bottleneck theory (13), and (d) Cohan's theory of delayed meniscus formation (3, 4). In the case of the adsorbents studied, neither of the first two theories can apply, and it will be shown that neither the third nor the fourth theory is adequate to explain the type and the amount of hysteresis observed. As a second development from the current work, an alternate explanation can be offered which appears to comply more nearly with the experimental data in the specific case and which may be found to be generally valid.

## II. EXPERIMENTAL

### A. Materials

The adsorbent which was made the subject of this study was an acid-processed natural-clay cracking catalyst manufactured by the Filtrol Corporation in their research laboratories. Processing of certain bentonitic clays with acid results in the removal of aluminum and magnesium ions from the crystal lattice, in the development of a very porous structure with a large surface area, and in a decrease in the size of the individual montmorillonite crystallites. After thorough washing, there remains substantially a hydrogen base-exchanged clay, together with a certain amount of silica which is soluble in sodium carbonate solution and which is termed (for want of a better name) hydrated silica.

Preparation for use as a cracking catalyst consists of calcination at elevated temperatures for several hours. As a result of this treatment, the material is dehydrated and a portion of the lattice water is expelled; this results in an irreversible change in the montmorillonite crystal layers and loss of the ability to swell which is characteristic of the uncalcined clay. Thus, there is formed a rigid non-swelling adsorbent with a highly porous but stable structure.

### B. Methods

A conventional adsorption apparatus similar to that described by Emmett (6) was used. The experimental procedure for obtaining the complete adsorp-

tion-desorption isotherm has become standardized and has been adequately described by Emmett as well as by Reis, Van Nordstrand, and Teter (14) and many others.

### C. Results

Figure 1 is a nitrogen adsorption isotherm which is typical of Filtrol catalysts. The adsorption branch corresponds to Type II according to the Brunauer, Emmett, Teller (B.E.T.) classification, and hysteresis is pronounced.

The total surface area of this sample calculated by the B.E.T. method (1) was found to be  $339 \text{ m}^2/\text{g.}$ , and  $325 \text{ m}^2/\text{g.}$  by the Harkins-Jura (9) method. The B.E.T. surface area will be used for the computations which follow. It was found that the total surface area was substantially the same whether the catalyst was pelleted or powdered; also, a 0-40 micron fraction had the same surface area as a 40-100 micron fraction. This indicates that the fraction of the total surface area contributed by the gross particle surface is negligible compared to the internal capillary surface area, and is in agreement with results reported by Reis, Van Nordstrand, and Teter (14) for their H-G catalyst.

The experimental data represented by figure 1 will be used to demonstrate a proposed method for calculating the pore size-surface area distribution.

## III. THE PORE SIZE-SURFACE AREA DISTRIBUTION

### A. Assumptions

The following six assumptions are made:

- (a) The desorption branch of the isotherm represents the equilibrium state of lowest free energy.
- (b) The shape of the desorption isotherm is determined by the pore size distribution.
- (c) The entire pore structure is composed of cylindrical open-end capillaries.
- (d) At saturation, the liquid condensed in the capillaries can be divided into two distinct zones:
  - (1) The portion of the adsorbate next to the solid wall which is within the attractive field of the solid. The molecules of adsorbate in this zone are attracted toward the solid surface by forces greater than the intermolecular attractive forces of the bulk liquid. This zone will be defined as a "fixed film," and may extend several molecular layers away from the solid surface.
  - (2) The portion of the adsorbate which possesses the properties of the bulk liquid, that is, which is uninfluenced by the attractive forces of the solid. This zone is defined as an "inner capillary volume," abbreviated to ICV.

During desorption, as the equilibrium pressure is reduced, only the ICV is desorbed or evaporated, leaving the adsorbed film next to the solid wall substantially undisturbed. The ICV leaves the capillaries according to the Kelvin equation, and at any equilibrium pressure the

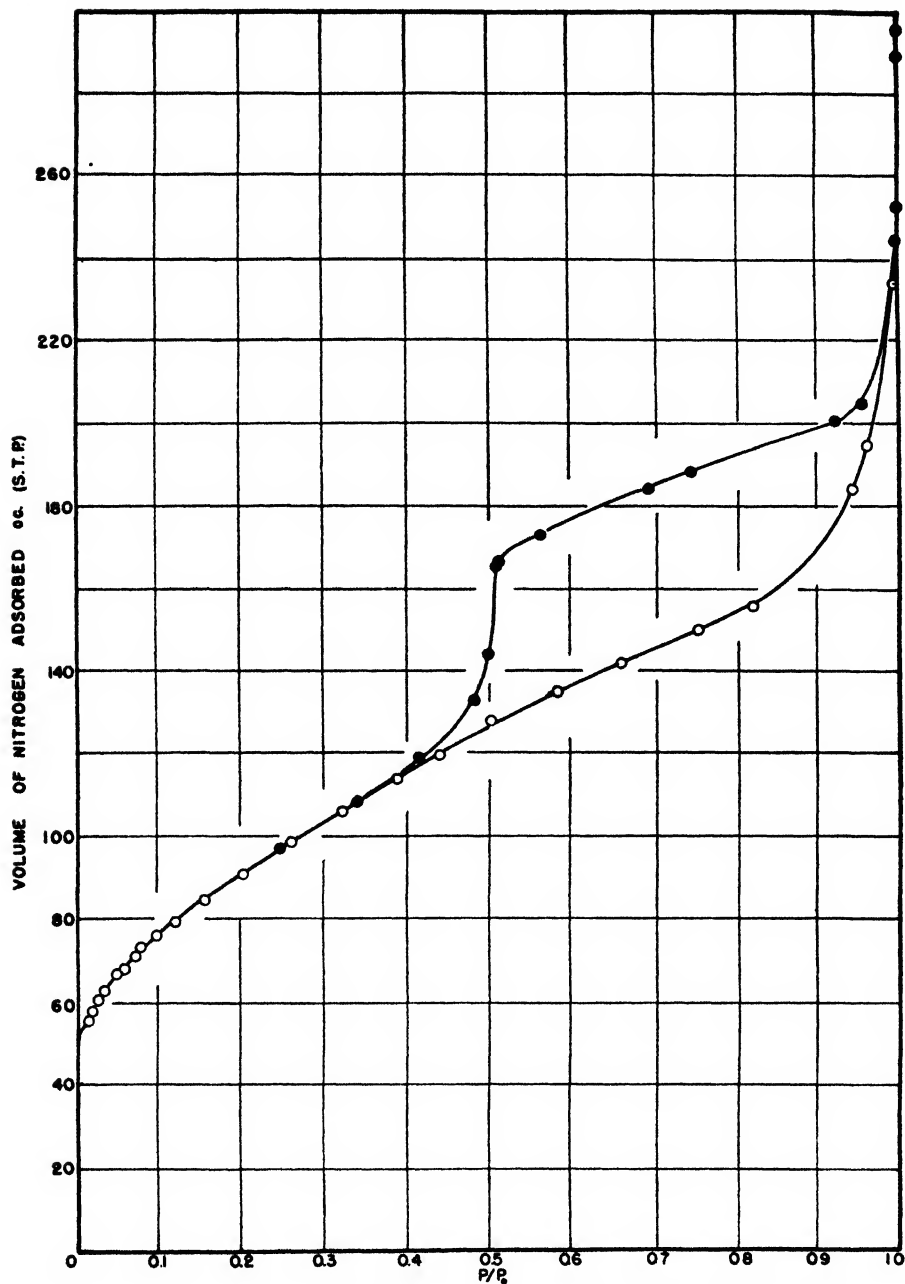


FIG. 1. Adsorption of nitrogen at 78.1°K. on activated clay catalyst sample A. Open circles indicate adsorption; solid circles, desorption.

pore radius calculated from the Kelvin equation is the radius of the ICV only and not the entire radius of the bare-walled pore.

The point where the desorption branch meets the adsorption branch

of the isotherm, i.e., where hysteresis starts, is also the point where the ICV has completely emptied. Continued desorption below this point represents evaporation from the fixed film. Substantially all of the volume desorbed above the hysteresis point is therefore ICV, subject to certain corrections which will be more completely discussed later in relating this concept to minimum pore size.

As the pressure in equilibrium with filled pores whose ICV radius is  $r_{K_2}$  is reduced to a pressure in equilibrium with smaller pores whose ICV radius is  $r_{K_1}$ , an amount of liquid ( $V_{a_2} - V_{a_1}$ ) is released which is equal to  $\Delta ICV$ . The Kelvin equation can be used to relate the pressures to corresponding ICV radii by the expressions:

$$\ln P_2/P_0 = -2\sigma V/r_{K_2}RT$$

and

$$\ln P_1/P_0 = -2\sigma V/r_{K_1}RT \quad (1)$$

where  $\sigma$  is the surface tension of liquid nitrogen at the isothermal temperature,  $V$  is the molal volume,  $P_2$  and  $P_1$  are equilibrium pressures,  $P_0$  is the condensation pressure, and  $r_{K_2}$  and  $r_{K_1}$  refer to the radii of the internal capillary volumes.

Thus for a category of capillaries whose ICV radii lie between  $r_{K_2}$  and  $r_{K_1}$ , a  $\Delta ICV$  can be taken from the desorption branch of the isotherm.

- (e) The radius of the bare-walled pore,  $r_c$ , is greater than the radius of the ICV by an amount equal to the thickness of the "fixed film" immediately before capillary condensation starts. The thickness of this film is  $Nd$ , where  $N$  is the number of molecular layers in the film and  $d$  is the diameter of a single molecule or the thickness of a monolayer.

$$r_c = r_K + Nd \quad (2)$$

- (f) There are few, if any, pores present whose radius is less than  $Nd$ . The entire surface area as measured by the B.E.T. method is distributed in pores equal to or greater than  $2Nd$  in diameter. The closing of the hysteresis loop determines the radius of the smallest pore present.

The first two assumptions require no further discussion. The evidence leading to the adoption of the remaining four will be developed in the course of the discussion of the distribution curve which follows.

### B. Equations

An element of surface area can be assigned to each  $\Delta ICV$  (assumption c) in the following way:

For cylindrical capillaries with open ends, the surface area,  $S_c$ , of a bare-walled capillary is given by

$$S_c = 2\pi r_c l \quad (3)$$

where  $r_c$  is the radius of the capillary and  $l$  its length.

The geometrical volume of the ICV of the same capillary is given by:

$$\text{ICV} = \pi(r_K)^2 l \quad (4)$$

$r_K$  is the radius of the ICV which is determined by the Kelvin equation relating  $r_K$  to the pressure at which the ICV is released. Combining equations 3 and 4,

$$S_c = 2\text{ICV}r_c/(r_K)^2 = 2\text{ICV}(r_K + Nd)/(r_K)^2 \quad (5)$$

In order to use this relation,  $r_K$  must be taken as the average radius of a category of pores, the limiting size of which is defined by  $P_2$  and  $P_1$ , whereupon ICV becomes  $\Delta\text{ICV}$  or the volume released as the equilibrium pressure is decreased from  $P_2$  to  $P_1$ , then

$$\Delta S = 2\Delta\text{ICV} \left[ \frac{\frac{r_{K_2} + r_{K_1}}{2} + Nd}{\left( \frac{r_{K_2} + r_{K_1}}{2} \right)} \right] \quad (6)$$

$$\text{Total B.E.T. area} = \Sigma \Delta S \quad (7)$$

$\Delta S$  is understood to mean the surface area to be found in all pores whose radii are larger than  $r_{c_1}$  and smaller than  $r_{c_2}$ . It will also be noted that equation 6 implies an approximation in that the arithmetical rather than the geometrical average of the pore radii is used. For convenience in computation a further approximation allows the larger radius of each category of pores to be taken rather than the average radius. However, as will be seen, the region of the isotherm where  $\Delta S$  is large corresponds ordinarily to an  $r_K$  value of about 15 Å. In this region the categories of radii are selected at intervals of 1 Å., and it can be shown that the choice between the geometrical average, the arithmetical average, or the larger radius has but little effect on the value of  $\Delta S$ . At larger values of  $r$ , where wider radii intervals are chosen, the values of  $\Delta S$  fall so low that a larger error introduced by the approximation has negligible effect on the value of  $\Sigma \Delta S$ .

Finally,

$$\text{Total area} = \Sigma \Delta S = \Sigma 2\Delta\text{ICV}(r_K + Nd)/(r_K)^2 \quad (8)$$

$$S = \Sigma 2\Delta\text{ICV}/r_K + Nd\Sigma 2\Delta\text{ICV}/(r_K)^2 \quad (9)$$

where  $r_K$  is defined by the higher of the pressures limiting each  $\Delta\text{ICV}$ .

All the terms of equation 9 except  $Nd$  can be evaluated if the assumptions outlined above are accepted.

### C. Application of the equations to a specific example

The calculation of the surface area-pore size distribution divides itself into two parts: (a) an estimation of  $Nd$ , the thickness of the fixed layer, and (b) with the use of this value, a final calculation in terms of  $r_c$ , the radius of the bare-walled capillary. The computation of  $Nd$  is summarized in table 1.

According to the B.E.T. convention, the projected area of the nitrogen mole-

cule (close packed in the liquid state at  $-198.2^{\circ}\text{C}.$ ) is  $16.2 \text{ \AA.}^2$   $d$ , the thickness of the monolayer, should be approximately  $\sqrt{16.2}$  or  $4.02 \text{ \AA.}$

Substitution of the appropriate constants for nitrogen at  $-198.2^{\circ}\text{C}.$  into the Kelvin equation gives

$$\ln P/P_0 = 4.1/r_K$$

From the experimental data represented by figure 1 (but plotted on

TABLE 1

Computation of  $Nd$

Catalyst A, calcined at  $454^{\circ}\text{C}.$ ;  $\Sigma\Delta S = \Sigma 2\Delta\text{ICV}/r_K + Nd\Sigma 2\Delta\text{ICV}/(r_K)^2$

(1) $P/P_0$	(2) $V_a$	(3) $\Delta\text{ICV}$	(4) $2\Delta\text{ICV}$	(5) $r_K$	(6) $r_K^2$	(7) $\frac{2\Delta\text{ICV}}{(r_K)^2}$	(8) $\frac{2\Delta\text{ICV}}{(r_K)}$
	cc. S.T.P.	cc. S.T.P.	cc. $\times 10^{-3}$	cm. $\times 10^{-8}$	cm. <sup>2</sup> $\times 10^{-14}$		
0.350	110.3			9.00	0.81		
0.385	114.4	4.1	1.27	9.89	0.98	1.30	12.81
0.42	120.1	5.7	1.76	10.88	1.18	1.49	16.19
0.46	127.0	6.9	2.13	12.16	1.48	1.44	17.53
0.48	133.2	6.2	1.92	12.86	1.65	1.16	14.90
0.51	167.0	33.8	10.44	14.02	1.97	5.31	74.49
0.56	173.6	6.3	1.95	16.28	2.65	0.74	11.96
0.59	176.5	3.2	0.99	17.89	3.20	0.31	5.53
0.62	179.3	2.8	0.87	19.75	3.90	0.22	4.38
0.65	181.9	2.6	0.80	20.80	4.33	0.19	3.86
0.68	184.2	2.3	0.71	24.48	5.99	0.12	2.90
0.71	186.2	2.0	0.62	27.56	7.60	0.08	2.24
0.745	188.8	2.6	0.80	32.07	10.28	0.08	2.50
0.77	190.5	1.7	0.53	36.12	13.05	0.04	1.45
0.81	193.5	3.0	0.93	44.80	20.07	0.05	2.07
0.85	196.2	2.7	0.83	58.09	33.74	0.03	1.44
0.90	199.7	3.5	1.08	89.60	80.28	0.01	1.21
0.95	205.3	5.6	1.73	184.02	338.60	0.005	0.94
						12.56	176.4

Total (B.E.T.) area =  $\Sigma\Delta S = 339 \text{ m.}^2/\text{g}.$

$Nd = 12.95 \text{ \AA.}$

$d = 4.02 \text{ \AA.}; N = 3.22 \text{ layers}.$

an expanded scale), hysteresis begins, as closely as one may estimate, at  $P/P_0 = 0.350$ , and the volume of gas adsorbed at this point is 110.3 cc. (S.T.P.).

In column 1 of table 1, values of  $P/P_0$ , starting with 0.350, are selected which, when converted by the Kelvin equation to corresponding values of the radii of "inner capillary volumes," provide increments which are sensitive to, and sufficiently reflect, changes in slope of the desorption branch of the isotherm.

In column 2 are listed the values of  $V_a$  (cc. at S.T.P.) taken from the desorption branch at points corresponding to the selected values of  $P/P_0$ . Column 3 lists the change in the volume of gas adsorbed between each set of radius



limits, and, according to the assumption that only ICV is released, leaving the "fixed film" virtually intact, these differences are equivalent to the  $\Delta\text{ICV}$  defined above. In column 4 the values of  $\Delta\text{ICV}$  are converted from gaseous volume (cc. at S.T.P.) to the corresponding liquid volume<sup>1</sup> of nitrogen at  $-198.2^\circ\text{C}$ . Columns 5 and 6 list the values of  $r_K$  and  $(r_K)^2$  which are calculated from the  $P/P_0$  values by the Kelvin equation.

TABLE 2  
Surface area distribution  
Catalyst A, calcined at  $454^\circ\text{C}$ .;  $\Sigma\Delta S = \Sigma 2\Delta\text{ICV}(r_K + Nd)/(r_K)^2$

(1) $r_0$	(2) $r_K$	(3) $P/P_0$	(4) $V_0$	(5) $\Delta\text{ICV}$	(6) $2\Delta\text{ICV}$	(7) $(r_K)^2$	(8) $\Delta S$
cm. $\times 10^{-8}$	cm. $\times 10^{-8}$		cc. S.T.P.	cc. S.T.P.	cc. $\times 10^{-3}$	cm. $\times 10^{-14}$	m. <sup>2</sup> /g.
21.95	9.0	0.350	110.3				
23.0	10.05	0.39	115.3	5.0	1.54	1.01	35.2
24.0	11.05	0.43	120.8	5.5	1.70	1.22	33.4
25.0	12.05	0.46	126.0	5.2	1.61	1.45	27.7
26.0	13.05	0.49	135.0	9.0	2.78	1.70	42.5
27.0	14.05	0.51	166.5	30.5	9.43	1.97	128.9
28.0	15.05	0.53	170.2	3.7	1.14	2.27	14.1
29.0	16.05	0.56	172.8	2.6	0.80	2.58	9.0
30.0	17.05	0.58	174.8	2.0	0.62	2.91	6.4
32.0	19.05	0.61	178.2	3.4	1.05	3.63	9.3
34.0	21.05	0.64	180.9	2.7	0.83	4.43	6.4
36.0	23.05	0.66	182.8	1.9	0.59	5.31	4.0
40.0	27.05	0.71	186.0	3.2	0.99	7.32	5.4
50.0	37.05	0.73	190.9	4.9	1.51	13.73	5.5
60.0	47.05	0.82	193.9	3.0	0.93	22.14	2.5
80.0	67.05	0.87	197.5	3.6	1.11	44.96	2.0
100.0	87.05	0.91	200.5	3.0	0.93	75.78	1.2
150.0	137.05	0.93	202.7	1.8	0.56	187.83	0.4
200.0	187.05	0.95	205.0	2.3	0.71	349.88	0.4
$\Sigma\Delta S$ .....							334.3
B.E.T. area.....							339 m. <sup>2</sup> /g.

Columns 7 and 8 give the respective values of  $2\Delta\text{ICV}/(r_K)^2$  and of  $2\Delta\text{ICV}/(r_K)$ ; the summation of columns 7 and 8 is then used to calculate the value of  $Nd$  from equation 9.

$Nd$  is found to be  $12.95 \text{ \AA}$ ., and since  $d = 4.02$ , the thickness of the film at the instant before condensation occurs is 3.22 molecular layers.

The final calculation of the pore size-area distribution is shown in table 2.

In column 1 are listed selected values of  $r_0$ , the radius of a bare-walled capillary. In the critical regions of the isotherm, radii are selected at intervals of only  $1 \text{ \AA}$ .; as the pore size increases, however, the area contributed becomes very small so

<sup>1</sup> Liquid volume = cc. (S.T.P.)  $\times M/V \times \rho$  = cc. (S.T.P.)  $\times 1.545 \times 10^{-3}$ , where  $M$  = molecular weight of nitrogen,  $\rho$  = density of liquid nitrogen at  $78.1^\circ\text{K}$ , and  $V$  = molar volume of perfect gas (S.T.P.) = 22,400 cc.

that the radius limits of succeeding categories of pores are widened roughly logarithmically.

In column 2 are listed the corresponding values of  $r_K$ . But since the critical point must correspond to  $P/P_0 = 0.35$ , the first  $r_K$  must be set at 9.0 Å., and  $r_c = r_K + Nd = 21.95$  Å.; thereafter, integral values of  $r_c$  are chosen and the corresponding values of  $r_K$  computed.

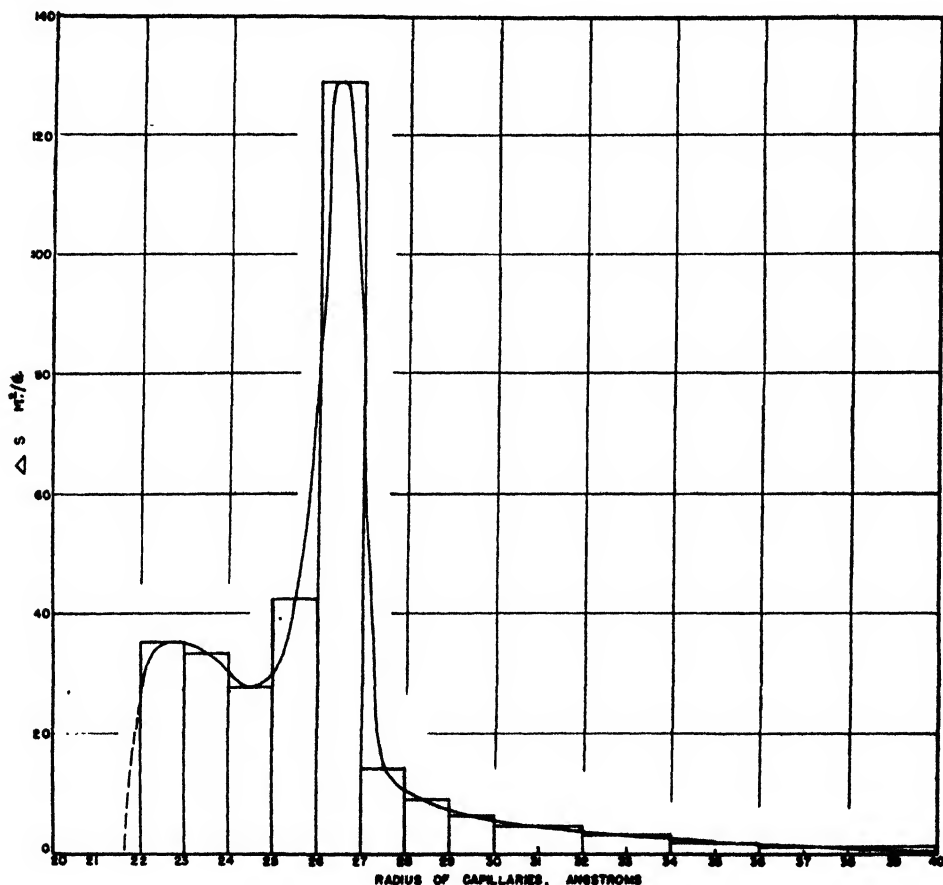


FIG. 2. Surface area-pore size distribution for catalyst A (calcined at 454°C.)

Column 3 gives the calculated values of  $P/P_0$  corresponding to each value of  $r_K$ . Column 4 shows the volume of gas adsorbed at each  $P/P_0$  point in column 3. Columns 5, 6, and 7 have the same significance as in table 1. Column 8 gives the final value of  $\Delta S$  for each category of pores.

Finally, the total B.E.T. surface area should equal  $\Sigma \Delta S$  as a check on the computation.

#### *D. The pore size-surface area distribution curve*

The values of  $\Delta S$  for each category of radii are plotted in figure 2. The data are plotted as a bar graph; the height of each bar represents the area to be found

in all the capillaries whose radii lie within the limits of the bar. Thus, 128.9 m.<sup>2</sup>/g. is to be found in pores larger than 26 Å. but smaller than 27 Å. in radius. In order to facilitate comparison with other data it is more convenient to draw a smoothed curve using the average radius of each pore group. An analysis of the curve and of the data from table 2 shows that (a) about 87 per cent of the total surface area is located in capillaries which range from 22 to 30 Å. in radius; (b) about 38 per cent of the total is located in pores between 26 and 27 Å. radius; (c) only 13 per cent of the surface is located in pores larger than 30 Å. radius; (d) there are few, if any, pores with radii less than 22 Å.

It will be noted that the analysis of the isotherm is discontinued at  $P/P_0 = 0.95$ , where the equivalent  $r_c$  is 200 Å. Although there certainly are larger pores present which contribute materially to the volume space available for condensation at saturation pressure, the surface area contributed by such pores is negligible. The pores in the 100–200 Å. radius range contribute only 0.8 m.<sup>2</sup>/g., about 0.3 per cent of the total.

The assumption that only ICV is released, leaving the "fixed film" completely intact, is not entirely correct. The gas desorbed from a region corresponding to one category of pores will include not only the ICV of that category, but also some small portion of the fixed film which has been exposed by previous ICV escape from larger capillaries. Since the exposed film must be in vapor-pressure equilibrium with the rest of the system, its thickness must gradually decrease as the pressure is lowered. Whatever portion of the fixed film still underlies condensed liquid still retains its maximum thickness. The pore distribution is seen to be such that succeeding fractions of ICV desorbed contain increasing relative amounts of fixed film.

Use of the approximation of constant fixed film thickness in the hysteresis pressure range results in an increased height of the first portion of the distribution curve and neglect of some surface area in smaller pores than are indicated by the curve. However, it is found that when the total surface area is fairly large (150 m.<sup>2</sup>/g.) and the value of  $N$  is less than about 3.5, the error arising therefrom is reasonably small. This is indirectly evidenced by agreement between  $\Sigma\Delta S$  and the total B.E.T. area. But if the total surface area is small, and  $N$  large, the approximation is no longer valid. In this case unlikely or unreasonable values of  $N$  are obtained and agreement between  $\Sigma\Delta S$  and the B.E.T. area is no longer found.

#### IV. DISCUSSION

##### *A. Catalytic evidence for minimum pore size*

A completely linear correlation between catalytic activity and the total surface area of a number of synthetic catalysts was recently shown by Conn and Connelly (5). A linear dependence has often been observed at the Filtrol Laboratories for groups of clay catalysts similarly processed but whose surface areas extended over an appreciable range as a result of various types of heat treatment and other processing variables. Such a linear correlation is possible only if (a) the entire surface area is available to the molecules of the charge stock being

cracked, or (b) every sample possesses exactly the same fraction of unavailable surface area. In view of the certainty that the pore size-surface area distribution of different preparations varies significantly, it is difficult to accept the second alternative.

The work of Greensfelder and Voge (7) on the catalytic cracking of hydrocarbons indicates that a  $C_6$  residue is the smallest fragment likely to undergo any appreciable amount of further degradation. Since the entire surface area is apparently "useful," the minimum pore opening must allow unhindered entrance to at least a  $C_6$  fragment and must have a radius at least as large as  $6 \times 1.4$  or about 8.5 Å.

### B. Hysteresis and pore structure

The current theories which have been advanced to account for hysteresis depend largely on presumed differences in the mechanism of capillary condensation and evaporation due to the shape or type of the pore. L. H. Cohan (3) has suggested that hysteresis may be due to a "delay in meniscus formation" during adsorption. Using a derivation similar to that of the Kelvin equation, Cohan obtains an expression for the vapor pressure of a cylindrical annular film

$$\ln P_r/P_0 = -\sigma V/(r_c - d)RT \quad (11)$$

where  $d$  is the thickness of an adsorbed monolayer, and the remaining terms have the same significance as previously defined. According to this equation, no condensation can occur in a pore of radius  $r$  until the pressure  $P_r$  is reached, whereupon the pore will fill completely, since the vapor pressure of any inner annular cylinder is less than that of the outermost layer. Once the pore is filled, a spherical meniscus is formed and desorption must then follow the Kelvin equation. At the hysteresis point ( $V_H$ ),  $P_a = P_d$ . This can only be true if

$$r_c = 2d \quad (12)$$

But Cohan's equation is subject to the same objections regarding  $\sigma$  and  $V$  as was raised for the Kelvin equation. If the same type of "fixed film" of width  $Nd$  is assumed, then the equations become:

$$\ln P_r/P_0 = -\sigma V/[r - (d + Nd)]RT \quad (13)$$

$$\text{and } P_a = P_d \text{ when } r_c = 2d + Nd. \quad (14)$$

Cohan, neglecting  $Nd$ , suggests that hysteresis can occur only in capillaries at least four molecular diameters wide. Including the  $Nd$  term, the pore must be six, eight, or more molecular widths in diameter (depending on the value of  $N$ ) before hysteresis could be observed.

Solution of either pairs of equations shows that the minimum pressure at which hysteresis can occur is given by

$$\ln P/P_0 = -2\sigma V/2dRT = -4.1/2d \quad (15)$$

Since  $d$  for nitrogen is 4.02 Å.,  $P/P_0 = 0.31$ .

Thus, if there were substantially any cylindrical capillaries present with radius as small or smaller than  $8.04 \text{ \AA}$ ., hysteresis should be observed at  $P/P_0 = 0.31$ . Experimentally, hysteresis is not observed at a pressure less than  $P/P_0 = 0.35$ .

Cohan points out that if pores so small are absent, hysteresis could not begin until pressures are reached corresponding to the open pores which are present. Past the hysteresis point, at any constant volume adsorbed,  $P_d$  and  $P_a$  are both, according to Cohan, in equilibrium with capillaries of the same radius. Having once established a pore size distribution from the desorption branch, one should be able to calculate an adsorption isotherm using Cohan's equation. This can be done by use of a volume-surface-radius relationship similar to that given previously for the desorption branch. It can be shown that the cylindrical capillary whose Kelvin radius,  $r_K$ , is in desorption equilibrium with some pressure according to the relation  $\ln(P_d/P_0) = -4.1/r_K$  should also during adsorption be in adsorption equilibrium with another larger pressure according to the relation  $\ln(P_a/P_0) = -4.1/2(r_K - d)$ . This calculation has been made from the data shown by figure 1 and is plotted in figure 3.

According to the generally accepted concepts, adsorption in a tapered closed-end pore is considered to be completely reversible (2, 4). A critical analysis of the bottleneck theory (13) leads to the conviction that any hysteresis arising therefrom would be less than that predicted by Cohan's theory of condensation in open-end cylindrical capillaries, since at least the lower portion of the bottleneck must be a closed-end cavity. If Cohan's concept of "delayed meniscus formation" is valid, then the assumption of 100 per cent cylindrical capillaries gives the theoretical extreme of hysteresis that should be observed. Condensation in any other assumed type or combination of types of pores should result in less hysteresis.

Actually, the Type II adsorption isotherm does not resemble in any way the type of curve to be expected if capillary condensation occurred according to either the Cohan or the McBain hypothesis. It seems likely that if there were any appreciable number of closed-end tapered pores, or any pores whose diameter was so small that condensation was thermodynamically possible at pressures near the closing of the hysteresis loop, their presence would be reflected by some evidence of condensation. Instead, it appears that no condensation whatever occurs until relatively much higher pressures are reached.

The preceding, combined with the evidence from catalytic activity, is the basis for the assumption that there are very few if any closed-end pores or cul-de-sacs and that the minimum pore size is determined by the position of the fork of the hysteresis loop (within the limits of uncertainty arising from the approximation discussed previously).

### *C. Hysteresis and the state of the adsorbate*

Although the conventional theories have been found inadequate to explain the type and the amount of hysteresis observed in this case, it is possible to offer an alternate explanation which also allows a partial confirmation of the calculated surface area distribution.

At constant volume adsorbed,  $V_a$ , the point  $A$  on the adsorption branch of the hysteresis loop (see figure 4) represents a state of higher free energy than

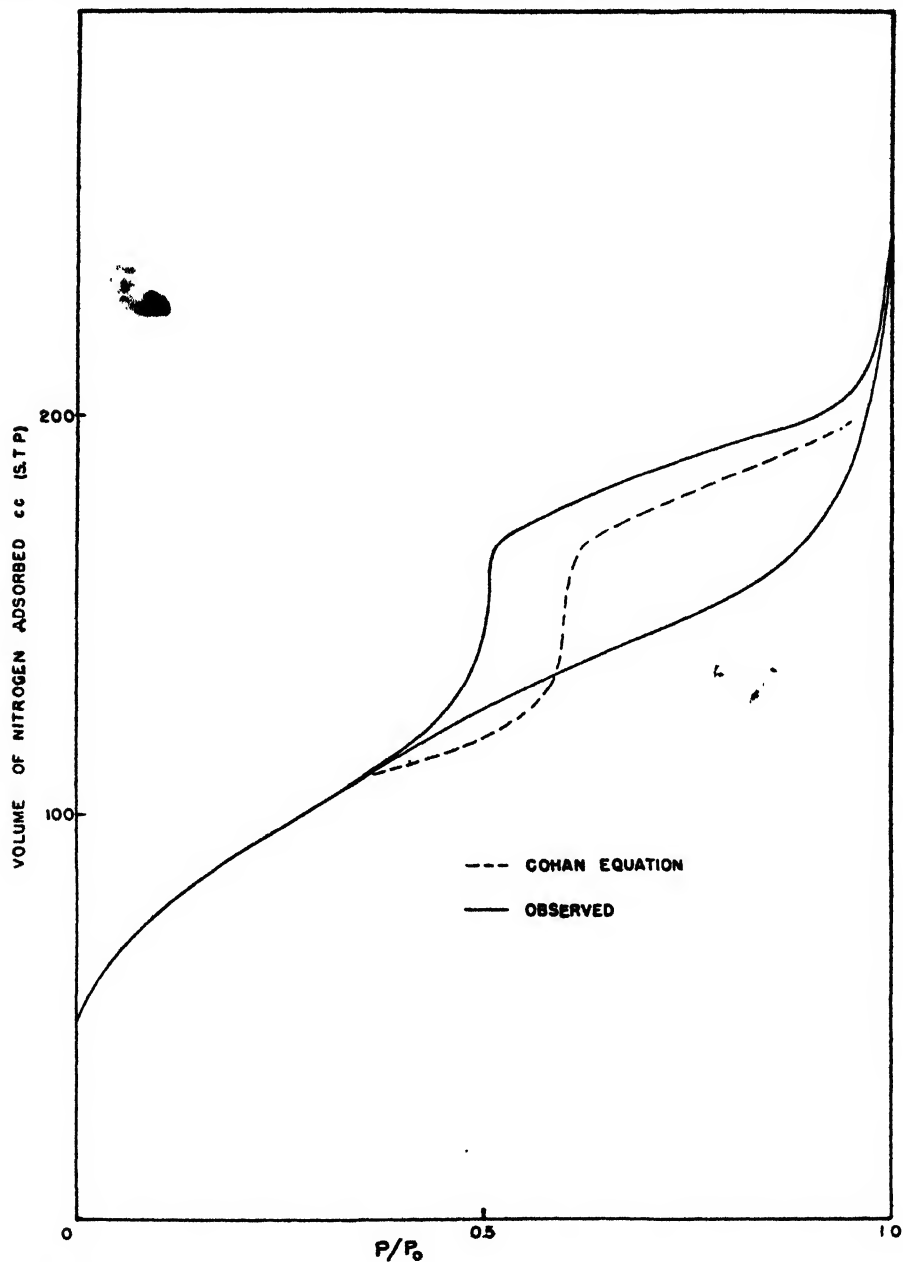


FIG. 3. Adsorption predicted by Cohan equation assuming capillary condensation in 100 per cent cylindrical open-end capillaries.

the point  $B$  on the desorption branch of the loop. The difference in the free energy of the two states is given by:

$$\Delta F = -nRT \ln (P_d/P_a) \quad (16)$$

It is suggested that this difference in free energy arises from the difference in the

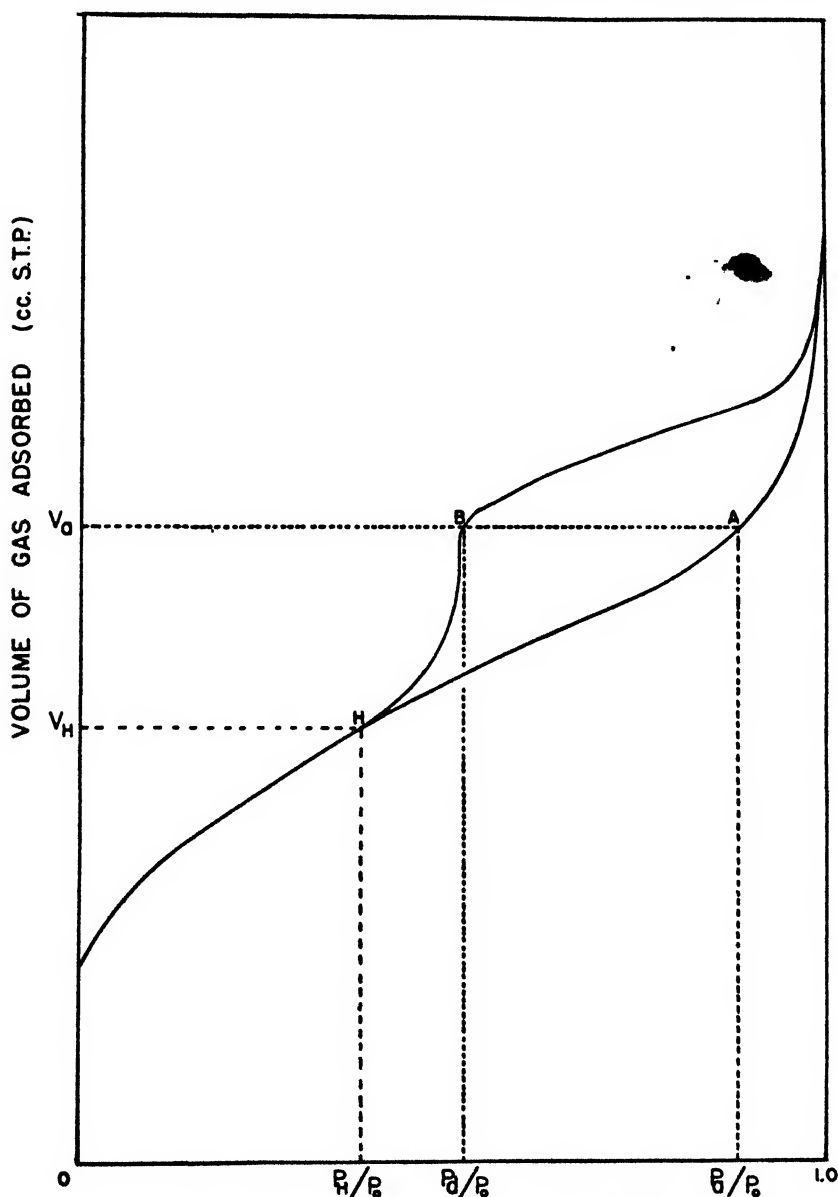


FIG. 4. The free energy difference between the adsorption and desorption branches at constant volume adsorbed.

state of the adsorbate when it is spread out over the entire surface in a multi-layered film (state A), and when some portion of the adsorbate is condensed as a liquid in the smaller capillaries (state B). Since the two states represent equal

adsorbed volumes, condensation to the liquid state in the smaller capillaries must be at the expense of the thickness of the film.

At point  $H$  the system has returned, after desorption, to exactly the same state that existed previous to adsorption past  $H$ . At this point, the total amount of gas adsorbed ( $V_H$ ) is spread over the entire surface in a film whose surface area is substantially equal to that of the solid surface. As adsorption proceeds (by increasing the pressure), the film thickens somewhat, but until actual capillary condensation starts the film area remains approximately the same. The free surface energy of the film-gas interface is given by

$$F_a = S_1 \sigma_f \quad (17)$$

where  $S_1$  is approximately equal to the total solid surface area and  $\sigma_f$  is the surface tension of the film. At the instant before capillary condensation starts, the molecular properties of the uppermost layer of the film have become nearly identical with those of the bulk liquid and  $\sigma_f$  must be very nearly equal to the surface tension of the bulk liquid.

Past this point, as the pressure is increased, capillary condensation starts, and as each capillary becomes completely filled, the film area which is very nearly equal to the total capillary wall area is replaced by the very much smaller condensed liquid-gas interfacial area. At complete saturation when all the pores are full, the area of the liquid-gas interface is equal to only the outer geometrical surface area of the catalyst particle, an area which is completely negligible when compared to the internal capillary area.

On desorption, evaporation of the ICV leaves bare a portion of the underlying film area, but the liquid-gas interfacial area contributed by those pores which are still full of condensed liquid is very small compared to the film area which still remains unexposed. The surface tension of the exposed film must still be equal to the surface tension of the condensed liquid in such pores as still remain full. The free surface energy of a point on the desorption branch is given by:

$$F_a = S_2 \sigma_f \quad (18)$$

where  $S_2$  is the sum of the exposed film area plus the area contributed by the condensed liquid surface.

When only a very small amount of adsorbate remains as ICV, then only a small fraction of the film surface is covered by condensed liquid and replaced by substitution of the relatively much smaller liquid surface. As the amount of adsorbate retained as ICV (on desorption) becomes larger, i.e., more capillaries filled with liquid, it is clear that proportionately larger fractions of film area are blocked off. The  $\Delta F$  between adsorption and desorption also increases, as is shown by the hysteresis loop. But the width of the hysteresis loop passes through a maximum, indicating that at some  $V_a$  there is a maximum  $\Delta F$  between the adsorption and desorption states. At still larger values of  $V_a$ , the  $\Delta F$  decreases. This may be due to the beginning of capillary condensation in the adsorption branch by which, just as during desorption, the total film surface area is reduced by condensation of liquid in the ICV space.



In the case of the sample studied, there is reason to believe that the maximum width of the hysteresis loop also very closely marks the point at which capillary condensation starts on the adsorption branch. At this point, the free energy difference between the adsorption and desorption branches is given by

$$\Delta F = \sigma_f[S_1 - (S_e + S_s)] = nRT \ln P_a/P_d \quad (19)$$

where  $S_1$  is the total fixed-film area and is approximately equal to the B.E.T. area,  $S_e$  is the film area exposed by desorption of ICV to the equivalent volume adsorbed on the desorption branch, and  $S_s$  is the area of the remaining condensed liquid surface.  $S_e$  can be taken from the surface area distribution curve, and  $S_s$  will be very small compared to  $S_1$  and can be neglected.

Careful measurement of the hysteresis loop of figure 1 shows a maximum width, and therefore a maximum  $\Delta F$  when the volume adsorbed equals 166 cm.<sup>3</sup> (S.T.P.) and the corresponding adsorption and desorption pressures ( $P/P_0$ ) are 0.86 and 0.51, respectively. The total B.E.T. surface area is 339 m.<sup>2</sup>/g. Reference to table 2 shows that when the equilibrium pressure has been reduced to 0.51, 66.6 m.<sup>2</sup>/g. of the fixed film has been exposed. Substitution of these values into equation 19 gives:

$$\sigma_f = 166/22400 \times 8.314 \times 10^7 \times 78/(399 - 66.6) \ln 0.86/0.51 = 8.3 \text{ dynes/cm.}$$

The surface tension of liquid nitrogen at 78°K. is 8.4 dynes/cm.

The excellent agreement between the calculated and measured values of  $\sigma$  indicates that this proposed explanation of hysteresis may be valid, and also that the surface area distribution is substantially correct.

#### *D. A possible model of the physical structure*

By rejecting the existence of any appreciable number of closed or dead-end pores, it is necessary to visualize a complete continuity of the pore spaces, each pore of probably continuously varying width, each interconnected with several others, with larger spaces and with constrictions alternating.

Each separate granule of the powdered catalyst might be visualized as consisting of an immense number of tiny crystallites, all attached to one another in some way, but each an individual. These microcrystallites may be of various irregular shapes and sizes, but in order to develop a model that can be analyzed mathematically, assume an idealized array of microparticles, all spherical, all of the same radius, and packed together in some systematic manner.

From the adsorption isotherm (figure 1) it is found that 0.379 cm.<sup>3</sup> of liquid nitrogen is condensed (as nearly as can be estimated) at complete saturation. This is the void volume per gram of catalyst. The true density of the material is about 2.6, so the volume occupied by the solid extension of 1 g. is 0.385 cc. The total volume of 1 g. of the sample is then 0.764 cc., of which 49.6 per cent by volume is void space or pores.

The theoretical porosity of cubic-packed spheres is 47.6 per cent and is independent of the radius of the sphere. Because of the remarkable agreement in the porosity factor, the close-packed cubic array is chosen as a model.

By inspection of the model (figure 5) it can be seen that the most frequent distance of separation of surfaces is along the body diagonals of the cube. This most frequent distance is assumed to correspond to the most frequent distance of separation, as located analytically by the peak of the distribution curve. This was previously noted to be twice  $26.5 \text{ \AA}$ , or  $53 \text{ \AA}$ .

The length of the body diagonal is given by  $L = 2r_s\sqrt{3}$ , where  $r_s$  is the radius of the spheres. The distance between the surface of the spheres on opposite corners of the cube is then  $(L - 2r_s)$ , so that

$$\begin{aligned} 2r_s(\sqrt{3} - 1) &= 53 \text{ \AA}. \\ r_s &= 36.2 \text{ \AA}. \end{aligned}$$

Each of the spheres, then, has a diameter of about  $72 \text{ \AA}$ .

Short-angle x-ray diffraction measurements have shown an average particle size for some similar Filtrol catalysts ranging from  $40$  to  $80 \text{ \AA}$ . Thus the crystal-

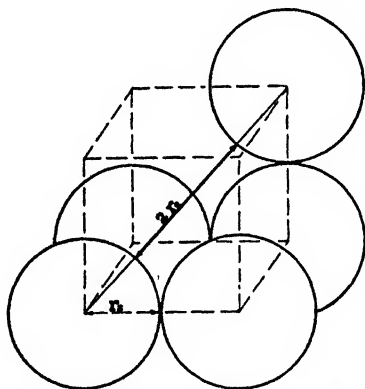


FIG. 5. Model of cubic close packing.  $r_s = 26.5 \text{ \AA}$ ;  $r_s = 36.2 \text{ \AA}$ ; area =  $319 \text{ m}^2/\text{g}$ .

lite diameter calculated for the model would appear to be of the correct order of magnitude.

The surface area of the model (per gram) can be calculated by the relation

$$S = 3.005/\rho r_s \times 10^4 \text{ m}^2/\text{g}. \quad (20)$$

where  $r_s$  is the radius (in centimeters) of the sphere and  $\rho$  is the density ( $= 2.6$ ). Substitution of the values gives

$$S_m = 319 \text{ m}^2/\text{g}.$$

The B.E.T. surface area of the sample is  $339 \text{ m}^2/\text{g}$ .

This model has many of the requisite properties. It possesses the continuous interlocking pore structure with no dead-end pores and with the observed void volume. With only the use of the "most frequent pore diameter" from the surface area distribution curve, the average crystallite size can be calculated to the correct order of magnitude and the calculated surface area of the model is in good agreement with the true surface area. This is not to say that the phys-

ical structure of the natural catalyst particle even approaches that of the highly idealized model but only that such a model helps to visualize the kind of crystallite aggregation which may very likely be typical of the natural material.

As a consequence of the preceding discussion it seems necessary to change the concept of the distribution of surface area in categories of pores of a certain size to the idea of a distribution of surface area separated from an opposite wall by a certain distance. This change does not modify the analysis by which the distribution curve is obtained, since it may still be assumed that the cross-sectional area of pores, even though irregular, can be treated as if they were statistically circular (15), and that even though the pores are continually changing the "distance of separation to an opposite wall," a differential length along the pore can be treated as a cylinder.

#### VI. SUMMARY

The complete nitrogen adsorption-desorption isotherm for an activated natural-clay cracking catalyst was obtained. The adsorption isotherm may be classified as Type II and marked hysteresis in the desorption branch is observed.

A method for determining the pore size-surface area distribution from the desorption branch is proposed which, unlike earlier methods, takes into account the thickness of the adsorbed film which is attracted to the solid surface by forces greater than the interaction forces of the liquid itself. A constant,  $N$ , can be calculated which appears to be approximately equal to the number of molecular layers in the film at the pressure at which capillary condensation starts.  $N$  is identified with the average number of molecular layers for which the heat of adsorption is greater than the heat of liquefaction, and so measures the average distance to which the attractive forces of the solid extend away from the surface.

The maximum width of the hysteresis loop corresponds to a maximum difference in free energy (at constant volume adsorbed) between the adsorption and desorption states. This  $\Delta F$  can be assigned to a difference in the area of the film-gas interface; on adsorption, the volume of gas adsorbed appears to be distributed in a film of (nearly) uniform thickness over the entire surface of the solid; on desorption, some fraction of the volume of gas adsorbed exists as a liquid condensed in smaller capillaries, thus reducing the total film area. In the case of the adsorbents studied, the adsorption point at the maximum width of the hysteresis loop also corresponds very nearly to the point at which condensation begins. At this point, the surface area of the film is substantially that of the solid surface; at the corresponding point on the desorption branch, the film area may be estimated from the pore size-surface area distribution curve. From the relations thus established the surface tension of the adsorbed film at its maximum thickness can be calculated and is found to agree closely with the surface tension of liquid nitrogen at 78.1°K.

The surface area distribution and the type of pore structure can be interpreted in terms of an idealized structure model, and information regarding the average particle size can be derived therefrom.

## REFERENCES

- (1) BRUNAUER, EMMETT, AND TELLER: J. Am. Chem. Soc. **60**, 309 (1938).
- (2) BRUNAUER: *Adsorption of Gases and Vapors*, Vol. I, p. 399. Princeton University Press, Princeton, New Jersey (1943).
- (3) COHAN: J. Am. Chem. Soc. **60**, 433 (1938).
- (4) COHAN: J. Am. Chem. Soc. **66**, 98 (1944).
- (5) CONN AND CONNELLY: Division of Petroleum Chemistry, 110th Meeting of the American Chemical Society, Chicago, Illinois, September, 1946, Preprint, p. 73.
- (6) EMMETT: *Advances in Colloid Science*, Vol. I, p. 1. Interscience Publishers, Inc., New York (1942).
- (7) GREENSFELDER AND VOGEL: Ind. Eng. Chem. **37**, 514 (1945).
- (8) HARKINS AND JURA: J. Am. Chem. Soc. **66**, 919 (1944).
- (9) HARKINS AND JURA: Division of Petroleum Chemistry, September 1945 Meeting in Print, p. 115.
- (10) HARKINS AND JURA: J. Am. Chem. Soc. **66**, 1366 (1944).
- (11) HARVEY: J. Am. Chem. Soc. **65**, 2343 (1943).
- (12) KISTLER, FISHER, AND FREEMAN: J. Am. Chem. Soc. **65**, 1909 (1943).
- (13) MCBAIN: J. Am. Chem. Soc. **57**, 699, (1935).
- (14) RIES, VAN NORDSTRAND, JOHNSON, AND BAUERMEISTER: J. Am. Chem. Soc. **67**, 1242 (1945).
- (15) SULLIVAN AND HERTEL: *Advances in Colloid Science*, Vol. I, p. 37. Interscience Publishers, Inc., New York (1942).
- (16) THOMPSON: Phil. Mag. [4] **42**, 448 (1871).
- (17) ZSIGMONDY: Z. anorg. Chem. **71**, 356 (1911).

THE KINETICS OF THE THERMAL DECOMPOSITION  
OF *tert*-BUTYL PROPIONATE<sup>1</sup>

EARL WARRICK AND PAUL FUGASSI

*Department of Chemistry, Carnegie Institute of Technology, Pittsburgh, Pennsylvania**Received March 10, 1948*

The gaseous decomposition of *tert*-butyl acetate (6), previously studied in this laboratory, proved to be a simple reaction which, on the basis of all known evidence, is a unimolecular process. As such a process represents the decomposition of isolated molecules similar studies on related molecules, if their decomposition proves to be unimolecular, offers an empirical method for the evaluation of the effects of substituent groups. It was planned originally to study the effects of substituting a chlorine atom for a hydrogen atom and a methyl radical for a hydrogen atom in the acetate portion of the molecule. However, the effect of chlorine substitution as exemplified in *tert*-butyl monochloroacetate is quite

<sup>1</sup> Presented before the Division of Physical and Inorganic Chemistry at the 105th Meeting of the American Chemical Society, Detroit, Michigan, April 12, 1943.

This paper is abstracted from the thesis submitted by Earl Warrick to the Faculty of the Graduate School of the Carnegie Institute of Technology in partial fulfillment of the requirements for the degree of Doctor of Science in Chemistry, March 22, 1943.

large, and the particular static method being used for rate measurements did not yield satisfactory results. Accordingly the gaseous decomposition of *tert*-butyl propionate was investigated, and the kinetics of this reaction will be described.

#### PREPARATION OF ESTER

The sample of ester used in this investigation had been prepared by Mr. Paul Cohen, using the method of Norris and Rigby (4). The propionic anhydride was obtained from the Eastman Kokak Company and was redistilled. Eastman *tert*-butyl alcohol was purified by fractional crystallization and distillation. After preparation and stripping, the crude ester fraction was distilled through a 5-ft. vacuum-jacketed column with wire-spiral packing. The purified ester boils at 116.4–116.5°C. at 738 mm., has a specific gravity,  $d_4^{25} = 0.8517$ , and a refractive index,  $n_D^{20} = 1.39320$ . The refractive index of the sample was identical with the value reported by Palomaa (5) for the same compound.

#### EXPERIMENTAL PROCEDURE

The apparatus used for the experimental rate measurements was similar to that employed by Rudy and Fugassi (6). Monoamlynapthalene was employed in place of mercury as the liquid in the vapor thermostat, and the stopcock previously used to seal the reaction cell from the vacuum line was replaced by a porous glass disk mercury cut-off (3). The null-point gauge was of the spoon type and was equipped with electrical contacts. A description of this gauge will be published later.

The reaction cell, which had a volume of about 60 cc., was located in the previously determined constant-temperature zone of the thermostat. A two-junction copper–constantan thermocouple was located alongside the cell and was used for determining the temperature. The thermocouple was constructed from calibrated wire, and its calibration was checked against the boiling points of naphthalene, biphenyl, and benzophenone.

#### HOMOGENEITY OF THE REACTION

As with the decomposition of *tert*-butyl acetate (6) and other *tert*-butyl compounds (7), the decomposition of *tert*-butyl propionate is heterogeneous and not reproducible in clean glass vessels. However, if the reaction products are allowed to remain in the flask overnight, the catalytic activity of the surface is decreased. At 300°C. the period of time necessary to deactivate the surface is quite long, but at 360°C. complete deactivation is obtained in a few hours. The following cycle of experiments was used to demonstrate that the measurements were reproducible. After deactivation of the surface overnight at 360°C. a series of experiments were made on successive days at some lower temperature such as 280°C. and it was observed that consistent results were obtained, although after each experiment the reaction products were allowed to remain in the flask at the temperature of the experiment until the next experiment was carried out. After the last experiment of the series, the cell containing the reaction products was raised to 360°C. and kept at that temperature for a day. The temperature

of the thermostat was then lowered to 260°C. and additional experiments made. The velocity constants obtained after the second treatment at 360°C. checked those obtained before, and it was concluded on the basis of this reproducibility that the reaction in the presence of treated surfaces was homogeneous. The fact that the usual  $\log k$  vs.  $1/T$  plot is a straight line over a temperature range of 55°C. also indicates the homogeneity of the reaction.

#### ORDER OF THE REACTION

Experimentally the final pressure,  $p_\infty$ , is twice the initial pressure,  $p_0$ . The initial pressure is obtained by extrapolating pressure readings back to zero time. The ester decomposition is first order, as a plot of  $\log p_0/(p_\infty - p_t)$  against time gives straight lines out to 90 per cent decomposition. In addition, as listed in table 1, the time of half-life is independent of the initial pressure and the ratio of the time of three-quarters life to the time of half-life is 2, as required by a first-order reaction.

TABLE 1  
Times of fractional life at 250°C.

$p_0$	$t_{1/2}$	$t_{3/4}$	$t_{3/4}/t_{1/2}$
mm. Hg	min.	min.	
18	52	108	2.08
45	43	84	1.95
75	42	88	2.10
90	40	81	2.02
120	42	84	2.00

#### VELOCITY CONSTANTS AND ENERGY OF ACTIVATION

Velocity constants were calculated graphically by preparing plots of  $\log p_0/(p_\infty - p_t)$  against time and measuring the slope of the best straight line through the experimental points. The values of  $k$  are listed in table 2. A plot of the logarithms of these constants against the reciprocal of the absolute temperature gives a straight line whose equation is

$$\log k (\text{sec.}^{-1}) = 12.794 - \frac{39,160}{2.3RT}$$

The energy of activation for the decomposition of *tert*-butyl propionate is 39,160 cal.

#### ANALYSIS OF PRODUCTS

The kinetic experiments on the decomposition of *tert*-butyl propionate showed that the final pressure,  $p_\infty$ , was twice the initial pressure,  $p_0$ , of the ester. By analogy with the decomposition of *tert*-butyl acetate one would expect isobutylene and propionic acid to be formed in equimolecular quantities. To determine whether these products were present in these amounts, a special reaction cell was employed. This consisted of a cylindrical cell of about 200-cc. capacity fur-

nished with two connections at the top and one at the bottom. One of the top connections was sealed through a mercury cut-off to the vacuum line. The other top connection was made of capillary tubing sufficiently long so that when the end of the tubing was immersed in a beaker of mercury and the cell evacuated, a barometric height of liquid mercury was present in the capillary tube. The bottom connection went to a mercury reservoir and by use of pressure or vacuum gas could be drawn into the reaction cell or expelled. Over the reaction cell a small furnace was fitted and the temperature of the cell was controlled manually.

In operation, with the cell evacuated, ester was admitted to the cell and the cell heated for a definite time interval at 315°C. Following the decomposition

TABLE 2  
*Velocity constants*

TEMPERATURE	$p_0$	$k \times 10^3$	TEMPERATURE	$p_0$	$k \times 10^3$
°C.	mm. Hg	sec. <sup>-1</sup>	°C.	mm. Hg	sec. <sup>-1</sup>
296	74.25	5.933	270.35	46.5	1.113
295.8	45.25	5.182	269.62	65.5	1.051
294.0	59.5	4.088	260.82	66.0	0.5803
293.7	58.8	3.858	260.4	31.0	0.5596
283.9	75.5	2.821	260.35	24.0	0.4836
282.35	30.5	2.114	260.28	55.0	0.5389
281.45	59.0	1.996	260.2	84.0	0.5297
281.45	76.0	2.386	260.05	111.0	0.4905
281.2	76.0	2.245	260.0	17.0	0.5527
281.1	80.0	2.234	250.5	90.0	0.2731
281.0	71.0	2.201	250.3	18.0	0.2264
280.95	125.0	2.280	250.3	45.0	0.2557
280.9	36.5	1.911	250.3	165.0	0.2570
280.7	71.5	2.057	250.1	120.0	0.2685
280.65	76.0	1.958	250.0	75.0	0.2464
280.0	59.8	2.245	240.75	65.0	0.1289
270.9	23.0	1.363	240.2	78.0	0.1357
270.9	88.0	1.350	240.1	43.0	0.1444
270.85	84.5	1.232	240.0	72.0	0.1458
270.45	73.5	1.076	239.9	45.0	0.1289

the cell was allowed to cool to room temperature and by suitable manipulation of the mercury a sample of boiled distilled water was drawn into the cell. The gas sample was next expelled into a eudiometer tube and the volume of gas subsequently measured. The water sample was next expelled and the cell flushed several times with distilled water. The washes were added to the original sample and titrated with standard base. In one experiment gas was expelled into a eudiometer tube using only mercury as the confining liquid. After the volume of gas had been measured, it was transferred to another eudiometer tube, using water as the confining liquid. Measurement of the volume of the gas over water gave the same number of moles present as when the gas was confined over mercury. This indicates that no appreciable portion of the gas was water soluble.

All samples of gas dissolved completely (better than 99 per cent) in Denigès' reagent, causing a yellow turbidity in the reagent. When the yellow Denigès reagent was boiled, a heavy orange precipitate was obtained. This specific test indicates that the gas was isobutylene. The sodium salt solutions obtained by basic titration of the water washes were pooled and concentrated. From the concentrated solution a derivative of bromophenacyl bromide was prepared. The melting point of the derivative was exactly the same as that obtained from a preparation made from pure propionic acid and bromophenacyl bromide.

Some of the analytical results obtained are tabulated in table 3. From these results it can be seen that for a 30-min. reaction time the ratio of propionic acid to isobutylene is unity. For longer reaction times isobutylene seems to be disappearing, as the ratio is greater than unity. It is believed that polymerization of isobutylene is occurring, and under conditions of our experiments where the surface is exposed to liquid water and liquid mercury, it does not seem possible to eliminate the polymerization reaction completely.

TABLE 3  
*Analytical results*

TIME OF HEATING	ESTIMATED DECOMPOSITION	ACID	GAS	MOLES ACID MOLES GAS
<i>min.</i>	<i>per cent</i>	<i>moles × 10<sup>4</sup></i>	<i>moles × 10<sup>4</sup></i>	
5	50	0.56	0.519	1.078
30	100	1.44	1.413	1.019
30	100	1.12	1.083	1.033
30	100	1.36	1.33	1.017
45	100	1.43	1.27	1.12
45	100	1.35	1.19	1.12
60	100	1.50	1.23	1.21
120	100	1.80	1.40	1.29

#### DISCUSSION

The analytical and kinetic data indicate that *tert*-butyl propionate decomposes according to the reaction:



Using the empirical standard free-energy equations of Bruins and Czarnecki (1) and the data of Essex and Clarke (2) for ethyl acetate, it is estimated that  $K_p$  for the above reaction at 513°K., the lowest temperature used in our experiments, is about  $3 \times 10^5$ . This indicates that the reaction is essentially complete in the direction indicated. Interpolation of the data of Trautz and Moeschel (8) for the dissociation of propionic acid dimer shows that at 510°K. and 200 mm. pressure practically all the propionic acid is present as the monomer.

The mechanism for the decomposition of *tert*-butyl acetate has been previously discussed (6) and the conclusions drawn there apply also to the decomposition of *tert*-butyl propionate because of the close similarity of the two reactions.

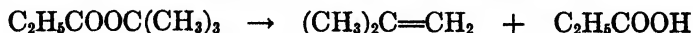
The effect of replacing a hydrogen atom by a methyl group in the acetate por-



tion of *tert*-butyl acetate is small, as would be expected from the known small inductive effect of the methyl group. The frequency factor is lowered slightly and the energy of activation decreases by only about 1300 cal., from 40,500 cal. to 39,160 cal.

## SUMMARY

1. The thermal decomposition of *tert*-butyl propionate follows the reaction:



2. The kinetics of the decomposition have been studied in the temperature range from 239.9° to 296°C. and at pressures from 17 to 125 mm. of mercury.

3. The reaction is first order. The relationship between velocity constant (*k*) and absolute temperature (*T*) is given by the equation:

$$\log k = 12.794 - \frac{39,160}{2.303RT}$$

4. Like the thermal decomposition of *tert*-butyl acetate, the decomposition of *tert*-butyl propionate appears to be a unimolecular process.

## REFERENCES

- (1) BRUINS AND CZARNECKI: *Ind. Eng. Chem.* **33**, 201 (1941).
- (2) ESSEX AND CLARK: *J. Am. Chem. Soc.* **54**, 1290 (1932).
- (3) FUGASSI AND WARRICK: *Ind. Eng. Chem., Anal. Ed.* **15**, 713 (1943).
- (4) NORRIS AND RIGBY: *J. Am. Chem. Soc.* **54**, 2088 (1932).
- (5) PALOMAA: *Ber.* **68B**, 303 (1935).
- (6) RUDY AND FUGASSI: *J. Phys. Colloid Chem.* **52**, 357 (1948).
- (7) SCHULTZ AND KISTIAKOWSKY: *J. Am. Chem. Soc.* **56**, 395 (1934).
- (8) TRAUTZ AND MOESCHEL: *Z. anorg. Chem.* **155**, 13 (1926).

STUDIES ON AGING OF PRECIPITATES AND  
COPRECIPITATION. XLIIAGING OF SILVER BROMIDE IN THE DRY STATE<sup>1</sup>I. SHAPIRO<sup>2</sup> AND I. M. KOLTHOFF*School of Chemistry, University of Minnesota, Minneapolis, Minnesota**Received March 10, 1948*

From previous work carried out in this laboratory it appeared that freshly precipitated silver bromide has a large surface development and is subject to thermal aging at room temperature in the air-dried state (2). The degree of

<sup>1</sup> This paper is based on a thesis submitted by Isadore Shapiro to the Graduate Faculty of the University of Minnesota in partial fulfillment of the requirements for the degree of Doctor of Philosophy, August, 1944.

<sup>2</sup> Present address: U. S. Naval Ordnance Test Station, Pasadena, California.

aging had been followed by measuring the decrease of the specific surface, as indicated by the amount of wool violet adsorbed on the surface saturated with the dye, and by determining the speed of penetration of radioactive bromide ions into the inactive precipitate when the latter was shaken with a solution of the former. In the present work the degree of aging was followed in a unique manner by determining the change in the electrical conductivity of the dry powder as a function of the "heat-treatment" of the powder.

It has already been shown that the electrical conductivity of silver bromide pellets at low (*viz.* room) temperatures is essentially a "surface conductivity" and can be expressed (5) by

$$\chi = BSe^{-U/kT} \quad (1)$$

where  $\chi$  is the specific electrical conductivity,  $U$  is an energy term showing the magnitude of the potential barrier which an ion must surmount in order to migrate to another position,  $T$  is the absolute temperature,  $S$  is the magnitude of the active surface,  $k$  is the Boltzmann factor, and  $B$  is a constant. Thus, by determining at a constant (room) temperature the electrical conductivity of silver bromide samples which had been subjected to various heat-treatments, it is possible to relate the active surface directly to the electrical conductivity of the pellets.

Since the aging of freshly precipitated silver bromide is very pronounced even at room temperature, it is expected that compression of the silver bromide powder under high pressures will accelerate the rate of aging. Thus the active surface of the loose powder will be greater than the active surface obtained from the electrical conductivity data of the compressed pellet. Since it is practically impossible to measure directly the electrical conductivity of a loose powder, a method has been devised to extrapolate this value from conductivity-pressure measurements.

The method for calculating the specific conductivity of compressed pellets is to measure the current flowing through a pellet of a certain size under the influence of a definite potential difference, and to apply the formula

$$\chi = \frac{I}{E} \times \frac{l}{A} \quad (2)$$

where  $\chi$  is the specific conductivity in  $\Omega^{-1}\text{cm.}^{-1}$ ,  $I$  is the current in amperes,  $E$  is the applied voltage,  $l$  is the length of the pellet (i.e., the distance between the electrodes) in centimeters, and  $A$  is the cross-sectional area of the pellet in square centimeters. In the case of the compressed pellets the values for  $l$  and  $A$  essentially do not change much with pressure and can be taken as equal to the experimentally measured dimensions of the pellets without serious error, because the apparent densities of the pellets are approximately the same as the density of a fused mass (6). However, the application of equation 2 for loosely formed pellets is complicated by the fact that both  $l$  and  $A$  are varying with the applied pressure. As a first approximation the value of  $l$  will be taken as the experimentally measured length, designated by  $l_0$ , of the pellet and the value of  $A$

will be calculated always by the following relation:

$$A_a = \frac{W}{l_a \rho_a} \quad (3)$$

where  $W$  is the weight in grams of the silver bromide sample, and  $\rho_a$  is the density of a fused mass of silver bromide ( $\rho_s = 6.478$  g./cc. (1)). By plotting  $\log \chi$  (using values of  $l_a$  and  $A_a$  in equation 2) against pressure for a powder mass of well-aged or fused silver bromide, one obtains a characteristic curve, represented by curve A in figure 1a. The experimental points at the higher pressures fall nearly on a straight line, which can be represented by line B in figure 1a. It is quite probable that the function of  $\log \chi$  with pressure in this case is analogous to that for compressed pellets (6). The increase in conductivity (curve A, figure 1a) at the lower pressures can be attributed to the better contact between individual particles with increasing pressure, while the decrease in conductivity at the higher pressures is caused by a decrease in active surface. Actually both phenomena

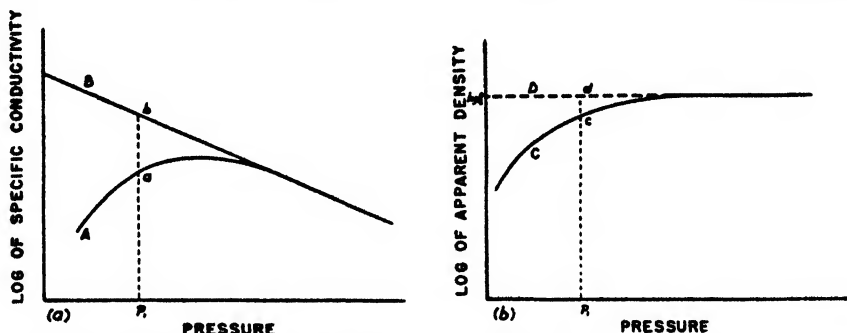


FIG. 1. Conductivity and compressibility of a powder mass as function of pressure

take place simultaneously; however, their relative influence varies with the pressure.

From a previous article (6) it is inferred that plots of the logarithm of the apparent density ( $\log \rho_a$ ) against pressure will give a characteristic curve, as illustrated by curve C in figure 1b. The curve approaches the logarithm of the true density asymptotically (line D). From a comparison of figures 1a and 1b it seems plausible that the deviation of curve A from line B is caused primarily by using the experimentally measured value of  $l$  in equation 2 instead of a corrected value for the length of the pellet. Thus from figure 1a at some pressure  $p_1$  the difference between the logarithms of the specific conductivity calculated from equation 2 by using<sup>3</sup>  $l_e$  and  $l_a$ , respectively, will be given by  $\bar{a}\bar{b}$ , where the value of  $\bar{a}\bar{b}$  is

$$\bar{a}\bar{b} = \log \chi_e - \log \chi_a = \log \left( \frac{l}{\bar{A}} \right)_e - \log \left( \frac{l}{\bar{A}} \right)_a = \log \frac{(l/A)_e}{(l/A)_a} \quad (4)$$

<sup>3</sup> In this article the subscript  $e$  refers to an effective or corrected value, and the subscript  $a$  to an apparent or measured value.

At the same pressure  $p_1$  the deviation of the logarithm of the apparent density from that of the true density is given by  $\overline{cd}$  (figure 1b), where

$$\overline{cd} = \log \rho_s - \log \rho_a = \log \frac{\rho_s}{\rho_a} \quad (5)$$

If the deviation of curve A from line B in figure 1a is attributed to the use of the apparent value of  $(l/A)$  instead of its effective value (which corrects for the porosity of the pellet), then one would expect a plot of  $\log \frac{(l/A)_s}{(l/A)_a}$  (from equation

4) against  $\log \frac{\rho_s}{\rho_a}$  (from equation 5) to be linear, with the line passing through the origin. Such relationships have been found in which the slope of the lines is constant for powders of silver bromide of widely different values of electrical conductivity and "age." Hence by this method of extrapolation it has been possible to differentiate between "pressure aging" and "thermal aging."

#### EXPERIMENTAL

The preparation of silver bromide powders aged in different ways and the subsequent measurement of their electrical conductivities and compressibilities are described in previous publications (5, 6) and in greater detail in the thesis of the junior author upon which this paper is based.

The silver bromide was prepared by a precipitation method (carried out in photographically inactive red light) and washed successively with copious volumes of water, acetone, and benzene and then air dried with dry air. Portions of the silver bromide powder were "thermally aged" by heating to various temperatures for different periods of time. A brief description of the thermal treatment of the various samples of silver bromide used in these experiments is given in table 3.

The compressibility and electrical conductivity measurements on the powders were carried out in a specially constructed die (5). Weighed portions of the fresh and "aged" silver bromide powders were compressed between two silver-plated plungers which also served as electrodes, and the electrical resistance of the powder mass between the electrodes was measured as a function of the applied pressure. The thickness of each pellet as a function of pressure was measured with a cathetometer to  $\pm 0.02$  mm. and then checked with a micrometer after the pellet had been removed from the die. All powders were compressed to a maximum pressure of 3000 atm. The electrical conductivity was measured at a constant temperature of 25°C.

#### TRANSFERENCE MEASUREMENTS

Since preliminary experiments had shown that the electrical conductivity of fresh silver bromide may be as much as  $10^4$  times as great as the values reported by Lehfelddt (4) on fused silver bromide, the possibility of electronic conductance was considered. Several grams of freshly prepared dry silver bromide powder were slightly compressed between two silver electrodes and connected in series

with a silver coulometer to several dry cells. The silver bromide between the electrodes was replaced each hour with freshly prepared powder, because the silver bromide ages even at room temperature (2). The replacement of the powder in this manner had the further purpose of preventing the formation of dendritic silver bridges in the silver bromide between the two silver electrodes. At the conclusion of such an experiment it was found that the loss in weight of the silver anode equalled the increase in weight of the silver in the coulometer; hence it is concluded that fresh silver bromide is essentially an ionic conductor similarly to fused silver bromide (7).

Next, experiments were carried out to measure the transference number of silver and bromide ions by utilizing the method of weighed pellets. In this procedure a series of three pellets and the two electrodes are weighed individually before and after a quantity of electricity (as measured by a coulometer) is passed through the system. The migration of ions across the middle pellet will be reflected in changes in weight of the electrodes and the two outer pellets, depend-

TABLE 1

*Weights of pellets and electrodes in transference number experiment*

ELEMENT	WEIGHT BEFORE	WEIGHT AFTER	DIFFERENCE IN WEIGHT
	<i>grams</i>	<i>grams</i>	<i>mg.</i>
Silver + silver iodide cathode . . . . .	1.42592	1.43248	+6.56
Silver bromide pellet No. 1 . . . . .	2.30195	2.30195	±0
Silver bromide pellet No. 2 . . . . .	2.05457	2.05456	-0.01
Silver bromide pellet No. 3 . . . . .	1.94550	1.94547	-0.03
Silver anode . . . . .	0.32303	0.31643	-6.60
Silver coulometer . . . . .	8.55448	8.56105	+6.57

ing upon the transference numbers of the cations and anions. In order to measure the true changes in weight of the outer pellets, the weight of the middle pellet must remain unchanged throughout the experiment. First attempts at this type of experiment proved unsuccessful, because it was found impossible to separate the pellets once they had been pressed together. Later this difficulty was overcome by using high pressures (3000 atm.) to form the pellets but low pressures (ca. 10 atm.) to hold them together during the course of the experiment. In order to prevent the formation of dendritic silver bridges, a pellet of silver iodide in conjunction with a silver plate was used as the cathode. All weighings were made on a Kuhlmann microbalance. The weights of the pellets and electrodes before and after a transference experiment are given in table 1. The data indicate that only silver ions are migrating through the silver bromide pellets.

That the bromide ions essentially do not migrate through the silver bromide pellet can be demonstrated further by radioactivity experiments. Radioactive silver bromide was prepared by adding a silver nitrate solution to a sodium bromide solution which had been shaken previously with ethyl bromide containing radioactive bromine. (The ethyl bromide had been exposed to a radon-beryllium

bulb for 16 hr.) A pellet of radioactive silver bromide was placed in contact with an inactive pellet, and a direct current was passed through the pellets until the silver bridges which formed caused a short circuit (approximate time of contact of pellets was 8 hr.). The radioactive pellet had been placed at the cathode end, so that the electric field would favor a movement of radioactive bromide ions into the inactive pellet. The radioactivity was measured with a Geiger-Müller counter. Experiments were performed in which the pellets were prepared under different pressures; in no case was there any evidence of the radio-

TABLE 2  
Conductivity correction for effective length of silver bromide pellet

PRESSURE, $\phi$	NO. 1 FUSED, COOLED SLOWLY, POWDERED				NO. 10 POWDER AGED ONE MONTH IN CONCENTRATED AMMONIUM HYDROXIDE			
	$\rho_a$	$\chi_a \times 10^7$	$\log \frac{\chi_e}{\chi_a}$	$\log \frac{\rho_e}{\rho_a}$	$\rho_a$	$\chi \times 10^6$	$\log \frac{\chi_e}{\chi_a}$	$\log \frac{\rho_e}{\rho_a}$
atm.	grams/cc.	$\Omega^{-1}\text{cm.}^{-1}$			grams/cc.	$\Omega^{-1}\text{cm.}^{-1}$		
205	4.76	1.76	0.395	0.133	4.24	2.24	0.571	0.183
304	5.04	2.00	0.327	0.109	4.53	2.68	0.482	0.155
465	5.47	2.31	0.242	0.073	4.97	3.53	0.345	0.114
616	5.75	2.56	0.178	0.051	5.27	4.05	0.266	0.089
770	5.92	2.76	0.124	0.038	5.51	4.48	0.206	0.069
925	6.04	2.88	0.086	0.030	5.70	4.90	0.149	0.055
1085	6.16	2.93	0.057	0.021	5.88	5.21	0.103	0.041
1245	6.24	2.93	0.035	0.016	5.98	5.40	0.069	0.034
1400	6.26	2.88	0.021	0.014	6.07	5.48	0.046	0.027
1555	6.32	2.83	*	*	6.13	5.55	*	*
1715	6.35	2.71			6.22	5.45		
1870	6.36	2.62			6.26	5.30		
2045	6.37	2.49			6.26	5.13		
2216	6.37	2.36			6.28	4.96		
2380	6.38	2.25			6.32	4.70		
2550	6.39	2.13			6.33	4.52		
2710	6.40	2.02			6.34	4.33		
2873	6.41	1.94			6.35	4.13		

\* Values no longer significant at higher pressures.

active bromide ions migrating into the inactive pellet. It is pointed out here that the above evidence of the immobility of bromide ions does not exclude the possibility that bromide ions in freshly prepared silver bromide can move on the surface from one position to a neighboring position in an irreversible manner.

#### CORRECTION FOR EFFECTIVE DIMENSIONS OF PELLETS

Plots of the logarithm of the specific conductivity ( $\log \chi_a$ ) against pressure for fused and well-aged samples of silver bromide powders as the powders are compressed give curves similar to the characteristic curve A of figure 1. In order to show that these curves actually correspond to straight lines when the data are corrected for the porosity of the pellets, the data for two samples of silver

bromide which show the characteristic curve but differ most widely in their values for conductivity are tabulated in table 2.

The characteristic conductivity curves with the extrapolated straight lines for these two samples are shown in figure 2. The values for  $\log \frac{(l/A)_s}{(l/A)_a}$  and  $\log \frac{\rho_s}{\rho_a}$  from table 2 are plotted in figure 3. At the very high pressures the ratios of  $(l/A)_s/(l/A)_a$  and  $\rho_s/\rho_a$  are practically unity, so that these values at the very high pressures are without significance in figure 3. As is to be expected from the

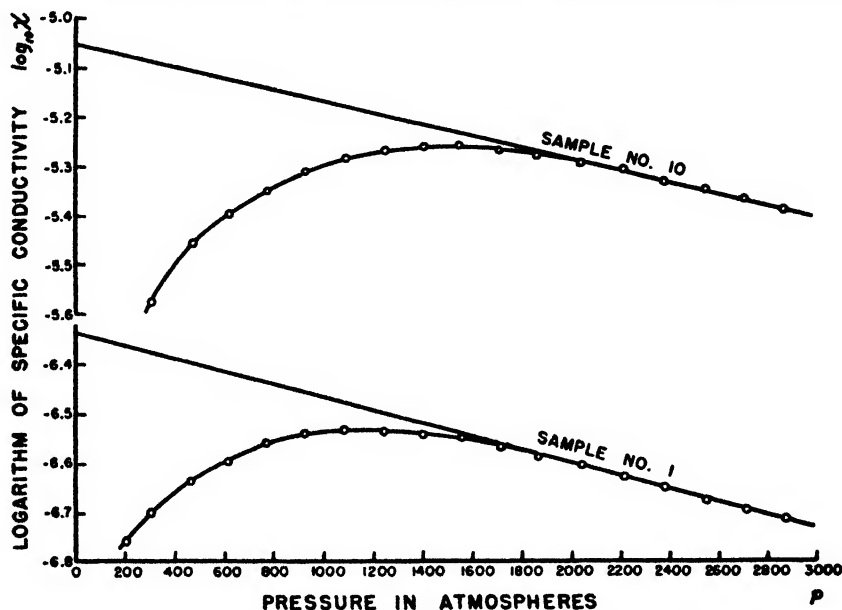


FIG. 2. Apparent and corrected conductivities of silver bromide powders during compression.

previous discussion, the data in figure 3 fall nearly on a straight line which passes through the origin. The empirical relation between  $(l/A)_s/(l/A)_a$  and  $\rho_s/\rho_a$  can be expressed as:

$$\left( \frac{l}{A} \right)_s = \left( \frac{\rho_s}{\rho_a} \right)^3 \left( \frac{l}{A} \right)_a \quad (6)$$

By applying the correction (equation 6) to the conductivity values for the fused and well-aged samples of silver bromide<sup>4</sup> and by plotting the resulting data, one obtains curves (figure 4) that can be represented by straight lines. It is pointed out here that the identical relationship as given by equation 6 or figure 3 could

<sup>4</sup> For the sake of brevity the tabulation of data of the conductivity values for the variously aged samples of silver bromide have been omitted here, but they can be found in the thesis upon which this paper is based.

have been obtained from the data of any curve given in figure 4 instead of the data given in table 2. This agreement with the theoretical aspects of the problem gives credence to the conception of conductivity taking place by way of "paths of surface."

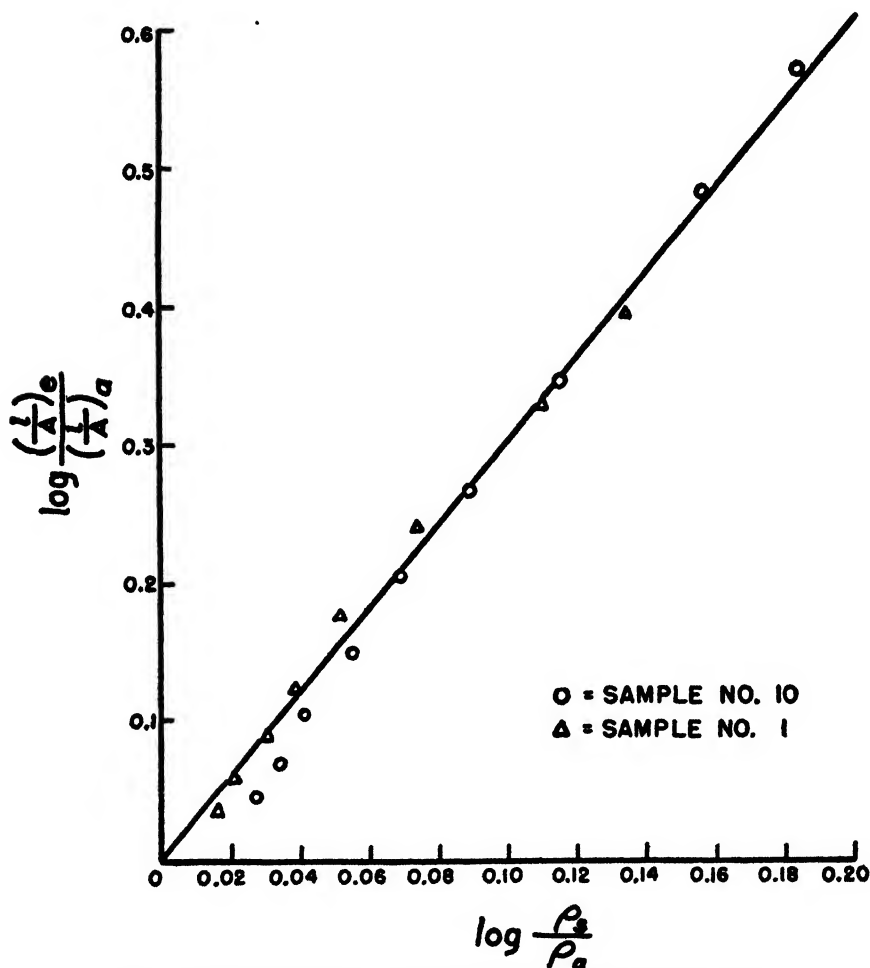


FIG. 3. Conductivity correction for effective length of pellets

#### CONDUCTIVITY OF FRESH SILVER BROMIDE

Plots of the logarithm of the specific conductivity (uncorrected) against pressure for pellets prepared from fresh silver bromide powders exhibit the general shape of the characteristic curve found in the case of the well-aged and fused silver bromide, but the maximum in the curves appears at lower pressures for the fresher samples. By applying the same correction (equation 6) to the data for the fresher products of silver bromide, one observes that the resulting curves



(figure 5) deviate considerably from a straight line. These deviations are attributed to the rapid aging which takes place when fresh powders with a high surface development are subjected to pressure. Under the conditions of the experiments as carried out here the derivative of the slope of the curves with pressure ( $d^2 \ln \chi / dp^2$ ) at a given pressure can be considered as representing the rate of aging. The conductivity-pressure-time sequence followed a rhythmic pattern. An increment of pressure, say 150 atm., was applied to the powder-pellet and the conductivity, i.e., current flowing under a definite potential difference, was noted as a function of time. The major portion of the change in conductivity (the increase or decrease in conductivity depends upon the value of the pressure)

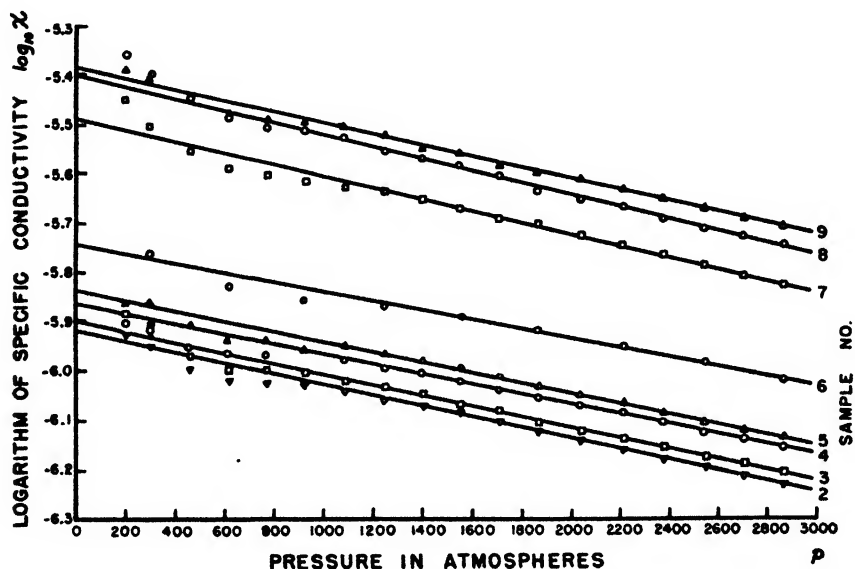


FIG. 4. Conductivity corrected for length of pellet as function of pressure (well-aged silver bromide samples).

took place within a matter of seconds after the increase in pressure and before the current values could be read on the micromilliammeter.<sup>5</sup> The conductivity-time function at each pressure reading approached a fairly constant value in the course of half a minute, though there was a slight drift in current values with time for the fresh samples. Evidently the fresh silver bromide continues to age regardless of the experimental conditions. From figure 5 it is noted that the slopes of the curves have the greatest numerical values at low pressures and tend to approach values which are comparable to the values for the well-aged products at high pressures.

<sup>5</sup> A continuous current could not be maintained on the silver bromide sample during the compression because of the tendency of the migrating silver ions to form dendritic bridges through the pellet.

## DISCUSSION OF RESULTS

The values of the slopes of the curves for the various well-aged samples of silver bromide (figure 4) cannot be compared directly with one another, since it

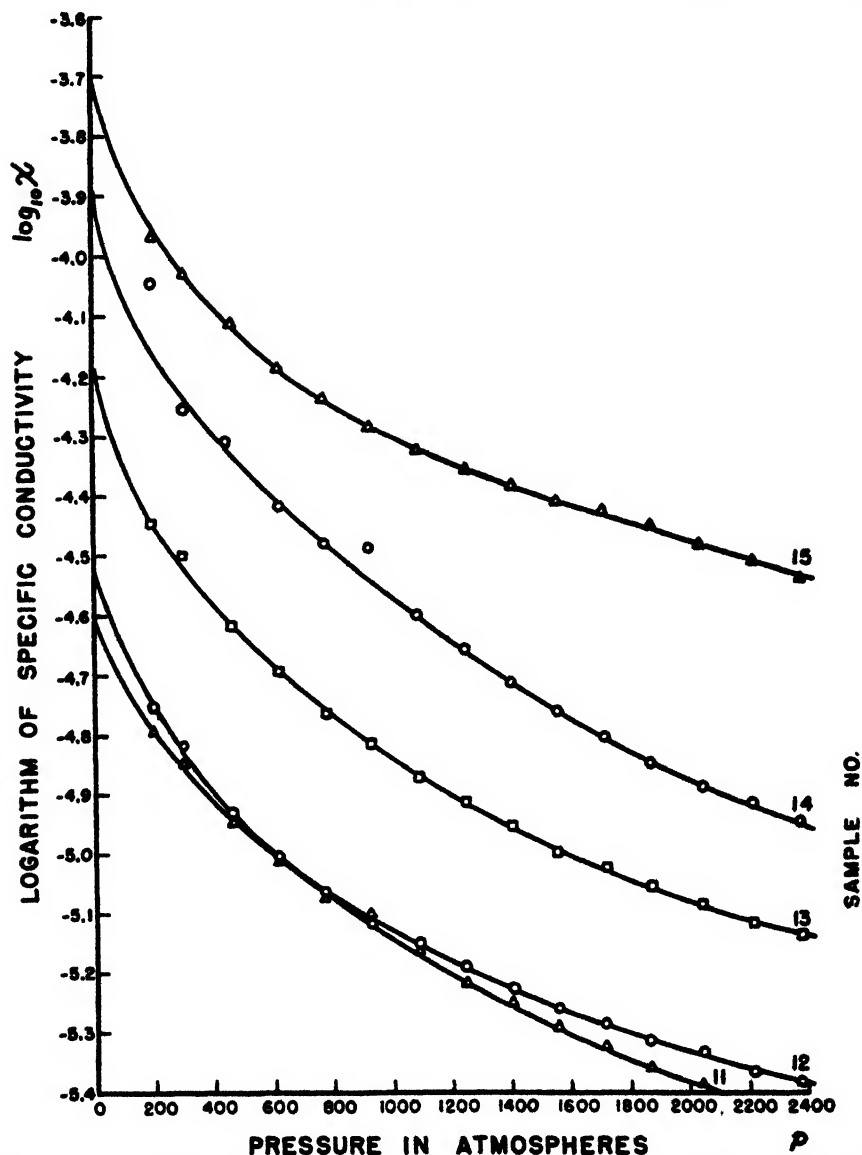


FIG. 5. Conductivity corrected for length of pellet as function of pressure (fresh silver bromide samples).

is known that the slopes in compressed pellets vary with the conductivity (5). However, by taking the difference in the slopes of the curves on pellets obtained on compression of the powder and on recompression of the pellets, one can

calculate the ratio of the conductivity in the loose powder to the conductivity in the compressed pellet by the following equation:

$$\ln \frac{\chi_0}{\chi_p} = -(k_2 - k_1) \cdot p_m = -\Delta k \cdot p_m \quad (7)$$

where  $\chi_0$  is the conductivity of the loose powder at zero applied pressure (extrapolated),  $\chi_p$  is the conductivity of the compressed pellet at zero pressure (extrapolated),  $k_1$  is the slope  $d \ln \chi / dp$  for the compressed pellet (5),  $k_2$  is the slope  $d \ln \chi / dp$  for the compression of the powder, and  $p_m$  is the maximum pressure applied to the pellet (i.e., 3000 atm.). The value of  $k_2$  is independent of the magnitude of the applied pressure, but the value of  $k_1$  will be a function of the maximum pressure applied to the pellet. The significance of the value for  $\chi_0/\chi_p$  is that it represents the relative decrease in surface when a loose powder is compressed under an external pressure.

The values for the relative decrease in conductivity from a loose powder to a compressed pellet (considered over a pressure range of 3000 atm.) for the various samples are given in table 3. In the case of the fresh samples the values for  $\chi_0$  were estimated from the curves in figure 5. Since the slopes of these curves at zero pressure probably are greater than the values indicated in figure 5, the values for  $\chi_0$  for the fresh powders may be considered as minimum values, so the ratio of  $\chi_0$  to  $\chi_p$  may be greater than listed. In table 3 the values for  $\chi_0/\chi_p$  for the more aged samples vary from 1.1 to 1.5, whereas the ratio for the fresh powders may be higher than 10. Thus, pressure has a large effect on decreasing the surface of fresh powders but very little effect on the well-aged powders. Since the latter had been aged drastically previous to the application of pressure, one would not have expected any further aging by pressure to take place for these powders.

The decrease in surface brought about by pressure for the fused and well-aged silver bromide powders can be termed a "mechanical aging" or "mechanical sintering" process. Consider a fused powder. As pressure is applied to the powder, the conductivity decreases according to the value of  $k_2$  (table 3). When pressure is released, the silver bromide is in the form of a pellet and the slope of conductivity curve with pressure is given by  $k_1$  (5). As long as the silver bromide remains compressed in a pellet, the conductivity will follow reversibly the slope given by  $k_1$ , providing the pressure does not exceed the maximum pressure applied previously, but if the pellet is crushed and powdered again, the conductivity will follow the slope given by  $k_2$  until the maximum pressure has been reached, and then it will follow the slope given by  $k_1$ . Since this cycle can be considered as reversible, the decrease in surface from powder to pellet in this case is purely a mechanical one. In contrast to this process the cycle described above is not reversible for the fresh samples, because they had undergone a true aging process with pressure. The aging process in these instances can be called "pressure aging."

It is pointed out here that the values for  $\chi_0/\chi_p$  (table 3) show only the relative decrease in surface of a powder by pressure. In order to compare relative sur-

TABLE 3

Surface conductivity and decrease in surface with pressure for silver bromide powders at room temperature

SAMPLE NO. (CORRESPONDS TO CURVE NUMBER IN FIGURES 4 AND 5)	"AGE" HEAT-TREATMENT OF SILVER BROMIDE	SURFACE CON- DUCTIVITY, $\chi_0$	$h_2$	$h_1$	$\Delta h$	$\frac{S_{\text{powder}}}{S_{\text{pellet}}} = \frac{\chi_0}{\chi_p}$
		$\Omega^{-1} \text{ cm.}^{-1}$	$\text{atm.} \times 10^4$	$\text{atm.} \times 10^4$	$\text{atm.} \times 10^4$	
1.....	Fused, cooled slowly, powdered	$4.84 \times 10^{-7}$	3.06	2.11	0.95	1.15-1.50
2.....	Fused, powdered, screened	8-10 mesh $1.21 \times 10^{-6}$	2.42	1.64	0.78	
3.....		10-14 mesh $1.27 \times 10^{-6}$	2.40	1.68	0.72	
4.....		mixed size $1.36 \times 10^{-6}$	2.22	1.73	0.49	
5.....		14-20 mesh $1.46 \times 10^{-6}$	2.35	1.65	0.70	
6.....	Fused, quenched, powdered	$1.81 \times 10^{-6}$	2.13	1.45	0.68	
7.....	Heated 2 hr. at 20-28 mesh	$3.25 \times 10^{-6}$	2.52	1.53	0.99	
8.....	375°C., powdered, 14-20 mesh	$4.00 \times 10^{-6}$	2.70	1.49	1.21	
9.....	screened, and 10-14 mesh	$4.16 \times 10^{-6}$	2.50	1.59	0.91	
10.....	Aged 1 month in concentrated $\text{NH}_4\text{OH}$	$9.34 \times 10^{-6}$	2.51	1.57	0.94	
11.....	Heated 4 hr. at 110°C.	$2.5 \times 10^{-5}$		1.63		6.3
12.....	Aged at room temperature for 3 yr. over $\text{P}_2\text{O}_5$	$2.8 \times 10^{-5}$		1.56		6.0
13.....	Aged at room temperature for 3 weeks	$6.3 \times 10^{-5}$		1.27		8.0
14.....	Fresh (1 day old)	$1.3 \times 10^{-4}$		1.25		12.5
15.....	Fresh (less than 1 day old)	$2.1 \times 10^{-4}$		0.64		10.0

TABLE 4

Correlation of specific conductivity with surface area measurements of silver bromide powders

SAMPLE NO.	SPECIFIC CONDUCTIVITY, $\chi_0$	SPECIFIC SURFACE AREA: WOOL VIOLET PER GRAM OF SILVER BROMIDE	$\left( \frac{\text{SPECIFIC CONDUCTIVITY}}{\text{SURFACE AREA}} \right) \times 10^6$
	$\Omega^{-1} \text{ cm.}^{-1}$	mg.	
1.....	$4.84 \times 10^{-7}$	$\sim 0$	
7.....	$3.25 \times 10^{-6}$	0.027	12.0
11.....	$2.5 \times 10^{-5}$	0.38	6.6
12.....	$2.8 \times 10^{-5}$	0.32	8.7
13.....	$6.3 \times 10^{-5}$	0.71	8.9
15.....	$2.1 \times 10^{-4}$	2.50	8.4

faces between variously aged powders, one must use only the  $\chi_0$  values. For example, the ratio of the surfaces for the freshest powder to the fused powder

listed in table 3 is

$$\frac{2.1 \times 10^{-4}}{4.84 \times 10^{-7}} \text{ or } 435$$

The specific surface (expressed in milligrams of wool violet dye per gram of silver bromide) of several of the variously aged powders of silver bromide has been measured by the dye-adsorption method (3), using wool violet dye and a Cenco Photelometer, and are tabulated in table 4. The specific conductivities, i.e., extrapolated conductivities of the powders at zero applied pressure, for those samples whose surface areas have been measured also are given in table 4. It is observed that the ratio of the specific conductivity to the specific surface area is essentially constant over a wide range of surface areas. These data tend to substantiate the validity of equation 1 that the low-temperature conductivity is predominantly a surface conductivity.

#### SUMMARY

Freshly precipitated silver bromide has been found to be an ionic conductor in which only silver ions are migrating through the powder.

A method of determining the electrical conductivity of a loose powder of silver bromide has been devised by extrapolation of measured conductivity-pressure data. An empirical correction for the ratio of the length to the cross-sectional area of a compacted powder as the powder mass is compressed has been found to be associated with the apparent bulk density according to the relation:

$$\frac{\left(\frac{l}{A}\right)_{\text{corrected}}}{\left(\frac{l}{A}\right)_{\text{measured}}} = \left(\frac{\rho_{\text{solid}}}{\rho_{\text{apparent}}}\right)^3$$

The decrease in surface upon compression of a powder as a function of the "age" of the powder has been followed by electrical conductivity measurements. Fresh silver bromide powders undergo considerable "pressure aging," whereas drastically aged powders suffer only a mechanical decrease in surface with pressure.

The specific conductance of silver bromide powders at low (*viz.* room) temperatures has been shown to be directly proportional to the surface areas of the powders, as measured by the dye-adsorption method in accordance with the proposed relation:

$$\chi = BSe^{-v/kt}$$

#### REFERENCES

- (1) BAXTER, G., AND HINES, M.: *Am. Chem. J.* **31**, 220 (1904).
- (2) KOLTHOFF, I. M., AND O'BRIEN, A. S.: *J. Chem. Phys.* **7**, 401 (1939).
- (3) KOLTHOFF, I. M., AND O'BRIEN, A. S.: *J. Am. Chem. Soc.* **61**, 3409 (1939).
- (4) LEHFELDT, W.: *Z. Physik* **85**, 717 (1933).
- (5) SHAPIRO, I., AND KOLTHOFF, I. M.: *J. Chem. Phys.* **15**, 41 (1947).
- (6) SHAPIRO, I., AND KOLTHOFF, I. M.: *J. Phys. Colloid Chem.* **51**, 483 (1947).
- (7) TUBANDT, C.: *Handbuch der experimental Physik*, Vol. XII, p. 402. Leipzig (1932).

## EFFUSION OF GASES AT CRITICAL VELOCITIES

A MICROMETHOD FOR MOLECULAR WEIGHTS OF GASES AND VAPORS<sup>1</sup>

SIDNEY W. BENSON AND RICHARD COSWELL

*Department of Chemistry, University of Southern California, Los Angeles 7, California**Received March 10, 1948*

Ever since Graham's discovery of the relation between the rate of diffusion of gases through fine porous diaphragms and the density of the gases, the method of gas diffusion has been variously employed both for molecular weight measurements and for isotope separation. However, the kinetic theory shows that the physical requirements for true diffusive flow are rather strict,—so strict, in fact, that true diffusive processes are rarely encountered in the laboratory. The mean free paths of most gases and vapors at atmospheric pressure and room temperature lie in the range  $10^{-6}$  to  $10^{-5}$  cm. To measure diffusion through membranes at atmospheric pressures would require that the membranes have pores with diameters less than the mean free path of the gas (i.e., 100–1000 Å.). This situation can be improved by working at lower pressures, but in the change, additional problems are introduced such as accurate, low-pressure measurement and surface adsorption. Outside of the very careful work of Knudsen (5), who did measure diffusion in the low-pressure range, using thin platinum diaphragms having extremely small holes, there have been very few reports in the literature on diffusion through diaphragms. Indeed, there has actually been some misunderstanding and confusion caused by the application of the term "diffusion" to what are not really true diffusion processes.

More common practice has been to measure the effusive flow of gases through thin orifices. There are many commercial models of effusimeters, which are supposed to measure gas density or molecular weight through dependence on flow rate. The hydrodynamic equations for effusive flow through thin orifices under adiabatic conditions are well known (6). The mass flow in grams per second,  $Q$ , under such conditions is given by:

$$Q = AP_0 \left( \frac{M}{RT} \right)^{1/2} \left( \frac{2\gamma}{\gamma - 1} \right)^{1/2} \left[ \left( \frac{P}{P_0} \right)^{2/\gamma} - \left( \frac{P}{P_0} \right)^{(\gamma+1)/\gamma} \right]^{1/2} \quad (1)$$

In this equation  $A$  represents the area of a circular hole in a thin diaphragm,  $\gamma$  the ratio of specific heats  $C_p/C_v$ ,  $R$  the gas constant,  $M$  the molecular weight,  $T$  the absolute temperature,  $P_0$  the high pressure and  $P$  the low pressure of the effusing gas. For very small pressure gradients ( $P/P_0 \cong 1$ ), the equation reduces to:

$$Q = A \left( \frac{M}{RT} \right)^{1/2} P_0^{1/2} (\Delta P)^{1/2} \quad (2)$$

<sup>1</sup> Presented before the Division of Physical and Inorganic Chemistry at the 113th Meeting of the American Chemical Society, which was held in Chicago, Illinois, April, 1948.

In this form it is suitable for use in relating molecular weights to flow velocities. It is, however, worthwhile pointing out that for regular laboratory practice, in addition to having  $\Delta P$  small, the experiment should be carried out when comparing different gases at constant  $\Delta P$ , for otherwise the interpretation and use become very difficult. On the other hand, at small  $\Delta P$  the flow becomes so slow as to change from adiabatic to isothermal for any finite orifice thicknesses.

Buckingham and Edwards (1) have made a rather extensive investigation of effusive flow under these conditions and have found that corrections of quite complicated form had to be introduced, which included both viscous effects and corrections for non-adiabaticity. The conclusion to be reached from a study of their work is that the effusimeter is not a trustworthy instrument for measuring gas densities and should be applied with considerable reservation to the analysis of unknown gases.

Equation 1 does, however, offer another possible avenue of approach. As the ratio  $P/P_0$  is decreased from unity, the flow reaches a maximum value for the ratio:

$$P/P_0 = \left( \frac{2}{\gamma + 1} \right)^{\gamma/(\gamma-1)}$$

Since this is a maximum, further reduction of the back pressure cannot increase the flow and certainly cannot decrease the flow as the equation paradoxically implies. The conclusion must be drawn that once the critical pressure ratio  $(P/P_0)_c$  is reached, the flow becomes independent of back pressure (6). Under these conditions, equation 1 reduces to:

$$Q_c = P_0 A (M/RT)^{1/2} f(\gamma) \quad (3)$$

in which  $f(\gamma)$  is given by:

$$f(\gamma) = \left[ \gamma \left( \frac{2}{\gamma + 1} \right)^{(\gamma+1)/(\gamma-1)} \right]^{1/2} \quad (4)$$

This equation shows that  $Q_c$  is well adapted for measurements of molecular weights of gases if  $\gamma$  is known. However, as can be seen in table 1, in which  $f(\gamma)$  is shown as a function of  $\gamma$ , for the values of  $\gamma$  which occur commonly (from 1.2 to 1.4), the maximum change in  $f(\gamma)$  is only 5 per cent. Only the monatomic gases fall outside of this range ( $\gamma = 1.67$ ) and even for these the change in  $f(\gamma)$  is only an additional 5 per cent.

Using some intermediate values of  $f(\gamma)$  such as 0.670, equation 3 reduces to a form in which the flow,  $Q_c$ , is simply related to  $P$ ,  $T$ , and  $M$ . For a given apparatus only  $M$  will vary from gas to gas and so the relation can be employed in molecular weight determinations. Table 2 shows how the values of the critical pressure ratio  $(P/P_0)_c$  will vary with different values of  $\gamma$ .

$(P/P_0)_c$  is a smooth, monotonic function of  $\gamma$  with very small variation in the region of commonly occurring values of  $\gamma$ . Thus for most gases, a ratio of forward to back pressure of about 2 is sufficient to ensure critical flow.

The following portion of this paper is a report on an experimental method for determining molecular weights of gases by measurements of their mass flow through an orifice at critical flow velocities.

TABLE 1  
*Variation of  $f(\gamma)$  with  $\gamma$  (equation 4)*

$\gamma$	$f(\gamma)$
1.670	0.712
1.500	0.701
1.400	0.685
1.300	0.670
1.200	0.652

TABLE 2  
*Variation of critical pressure ratio with  $\gamma$*

$\gamma$	$(P/P_0)_c$
1.670	0.496
1.500	0.512
1.400	0.525
1.250	0.555
1.100	0.580

#### EXPERIMENTAL

The effusimeter which was used in the present work is shown in figure 1. It consists of a mercury manometer, an orifice with by-pass (B, figure 1), and a vacuum-operated Toepler pump. The entire system could be evacuated to a pressure of 2 microns by means of a Welch Duo-Seal vacuum pump. A gas manifold, not shown in figure 1, had Pyrex bulbs in which gases could be stored and from which small samples of gas could be transferred to the manometer through the by-pass, using the Toepler pump.

By keeping the volume of all parts of the apparatus small and using a Toepler pump with a volume of 300 cc., all transfers within the system could be made with two or three strokes of the pump. Three strokes were sufficient to evacuate the manometer and orifice to a pressure of less than 0.1 mm. of mercury, starting at atmospheric pressure.

The orifice was a specially constructed platinum disc built to order by the American Meter Company. The disc was 0.0125 cm. thick and had a very fine circular hole 0.00493 cm. in diameter. The diameter of the opening was measured with an optical micrometer. The small hole was extremely regular, despite its size. The orifice was sealed to Corning glass No. 705AJ and then by graded seals to the apparatus.

The manometer was constructed of specially selected, 12-mm. O.D. Pyrex tubing. Tungsten wires, to the ends of which fine platinum wires had been



spot-welded through nickel, were sealed into the evacuated arm of the manometer and served as electrical contacts to indicate different gas pressures. After the manometer had been filled with mercury, the pressures corresponding to the different contacts were measured with a cathetometer to 0.01 cm. These pressures were: 27.13, 11.03, 7.02, 4.65, 2.19, and 1.00 cm., respectively. These differences were rechecked during the course of the work and found to be constant. Variations with room temperatures were checked and found to be less than 1 part in a thousand. This is consistent with the coefficients of expansion of mercury and glass.

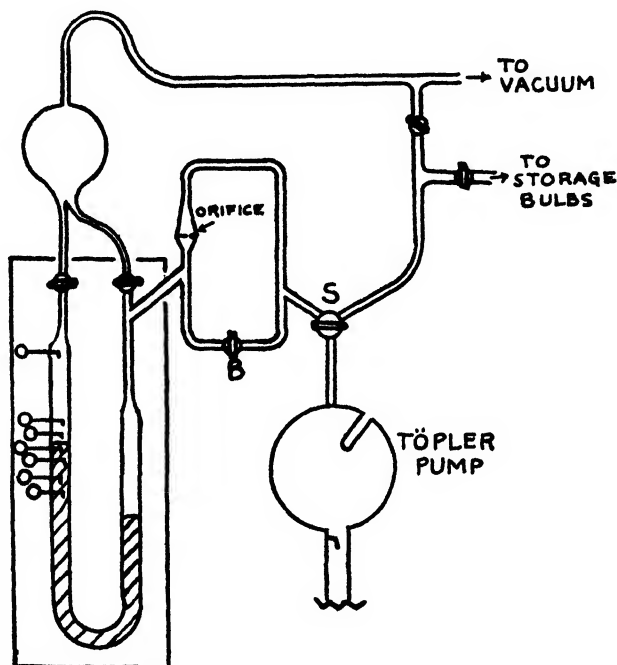


FIG. 1. Vacuum system

Flow rates were measured by observing the time for the pressure to fall through the values represented by the different contact points. The timing circuit is shown in figure 2, in which the bottom four contacts are shown operating. It is a further modification of a system originally described by Feskov (4) and later modified by Drake (2). In operation, the lowest contact shown in figure 1 and figure 2 is always below the mercury surface and serves as a common ground for the electric timers used. The runs were started at high pressures with all contacts under mercury. The top contact, on opening, tripped the relay and started all the timers. Then as each subsequent contact was passed, its timer would stop. In this way, using three electric timers simultaneously, three experimental points could be obtained at once.

There was no difficulty with mercury sticking at the contacts. The times were

measured to 0.1 sec., and time measurements were reproducible to within 1 part in a thousand for a given gas. The timers were checked against each other and found to be consistent to within 1 part in 10,000.

Runs were made by first evacuating the system to 1 micron. A sample of gas was then pumped from the gas manifold to the manometer, using the Toepler pump. The starting pressure was adjusted, again with the Toepler pump, and residual gas was displaced into the manifold. The by-pass stopcock S (figure 1) was opened, starting the run. Runs were made under three different sets of conditions: first with S (figure 1) turned to vacuum; then with S turned to the

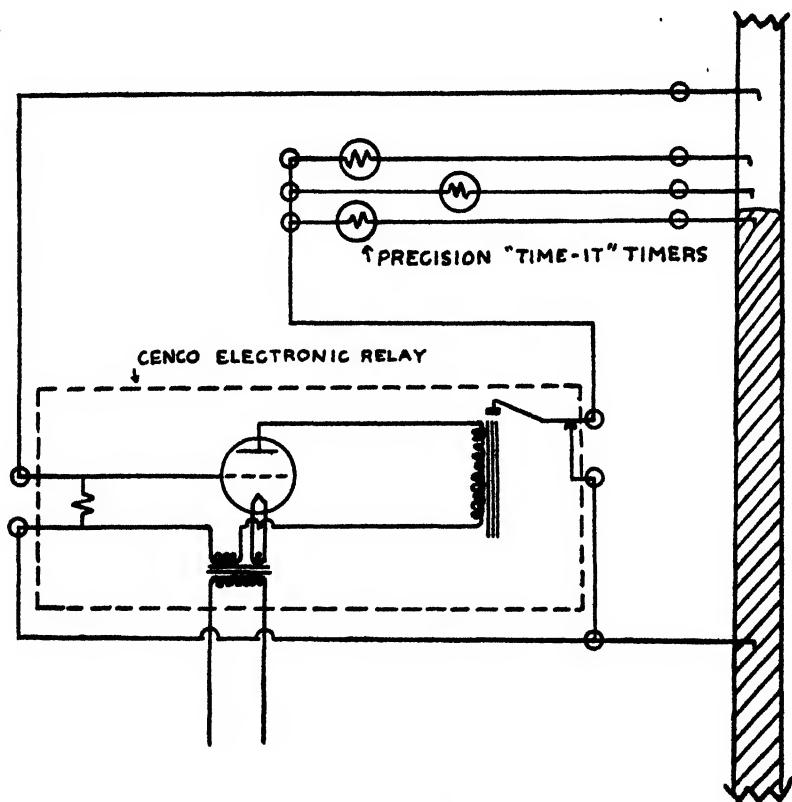


FIG. 2. Timing circuit

evacuated Toepler pump; and finally, in the case of condensible gases, with S turned to the Toepler pump with its well (figure 1) filled with liquid air. When runs were made with the gas passing into the Toepler pump, the samples were conserved and could be re-run. The entire time for a run was less than 10 min.

The gases used in the present work were chosen to cover a wide range of molecular weights. They were hydrogen, ammonia, oxygen, carbon dioxide, sulfur dioxide, and dichlorodifluoromethane (Freon 12). They were research-grade gases, taken directly from tanks and passed into the system through indicating Drierite. Both system and storage bulb were flushed and evacuated

twice with the gas to be stored before being allowed to fill to atmospheric pressure. Both hydrogen and oxygen were allowed to pass through a trap immersed in liquid nitrogen to remove condensibles. The other gases were put through two isothermal distillations to remove non-condensibles.

The system as described, although slightly more complicated, has many distinct advantages over the conventional type of effusimeter. It is a micro-effusimeter capable of operating on as little as 1 cc. (S.T.P.) of a gas. By operating at low pressures, corrections for the non-ideality of gases are avoided. Gas samples are not lost in measurement but may be recovered after runs and re-run or used for further tests. The trying difficulties due to dust particles settling on the orifice, which are described by Buckingham and Edwards (1), are completely avoided in this closed system. Finally, it is the belief of the authors that the method of gas effusion at critical pressure ratios is a theoretically more sound procedure than effusion at small pressure gradients.

#### EXPERIMENTAL RESULTS

All gases were run under as wide a variety of conditions as possible. Typical data are shown in figure 3 in which the time,  $t$ , is shown plotted against  $P$ , the pressure of the effusing gas. The data in figure 3 are for ammonia flowing into both vacuum (dotted line) and the Toepler pump (solid line) for two different starting pressures.

Because, in the present system, both the volume and the pressure of the effusing gas are changing, there is no simple analytical expression relating molecular weight to the time for given pressure drops. Nor can the flow rates be obtained directly from the efflux times. The mass flow  $Q$ , in grams per second, however, can be related to the pressure and its time derivative by the following equation:

$$Q = M \frac{dn}{dt} = \frac{MV_0}{RT} \left( 1 + \frac{\alpha P}{V_0} \right) \frac{dP}{dt} \quad (5)$$

In equation 5  $M$  represents molecular weight,  $T$  the absolute temperature,  $P$  the pressure,  $t$  the time,  $\alpha$  the cross-sectional area of the manometer (0.795 cm.<sup>2</sup>), and  $V_0$  the volume of the system behind the orifice at zero pressure.

All quantities in equation 5 are known except  $dP/dt$ , which is obtained from the experimental measurements. Instead of attempting to obtain  $dP/dt$  from the  $P$ - $t$  plot of figure 3, it was found simpler to plot  $\log P$  against  $t$  and obtain  $dP/dt$  from the slope of the resulting curve. The data of figure 3 are shown plotted in this manner in figure 4. This curve is very close to a straight line and the slopes are easily determined. In terms of such a plot, equation 5 transforms to:

$$Q = 2.303 \frac{MV_0 P}{RT} \left( 1 + \frac{\alpha P}{V_0} \right) \frac{d \log P}{dt} \quad (6)$$

Following the determination of  $Q$  at various pressures,  $\log Q$  was plotted against  $\log P$  for all gases in order to determine the pressure dependence of  $Q$ . The results for the different gases are shown in figures 5 to 10. As can be seen,

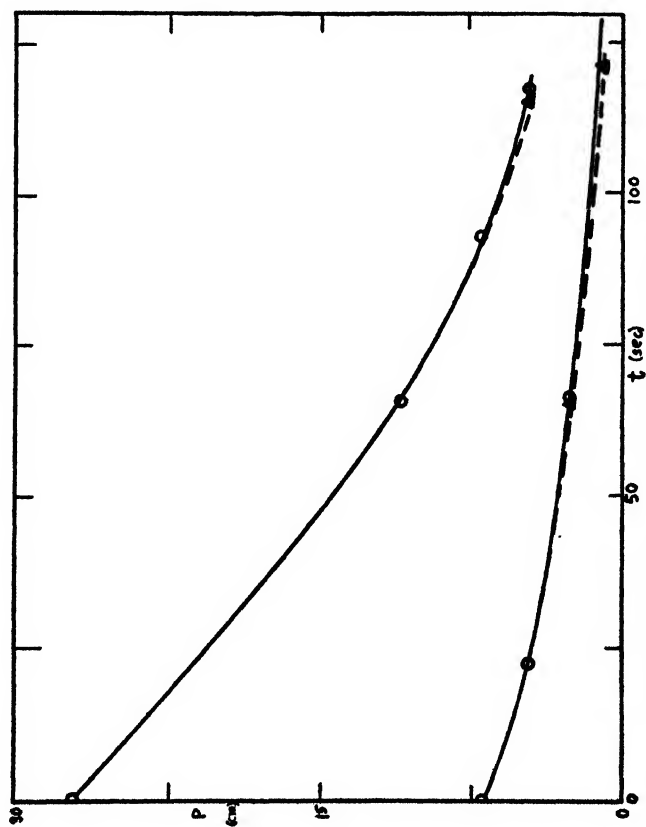


Fig. 3. Gas—ammonia. Plot of  $P$  (in centimeters of mercury) against  $t$  (in seconds) for different starting pressures. —, efflux with back pressure; ---, efflux into vacuum.

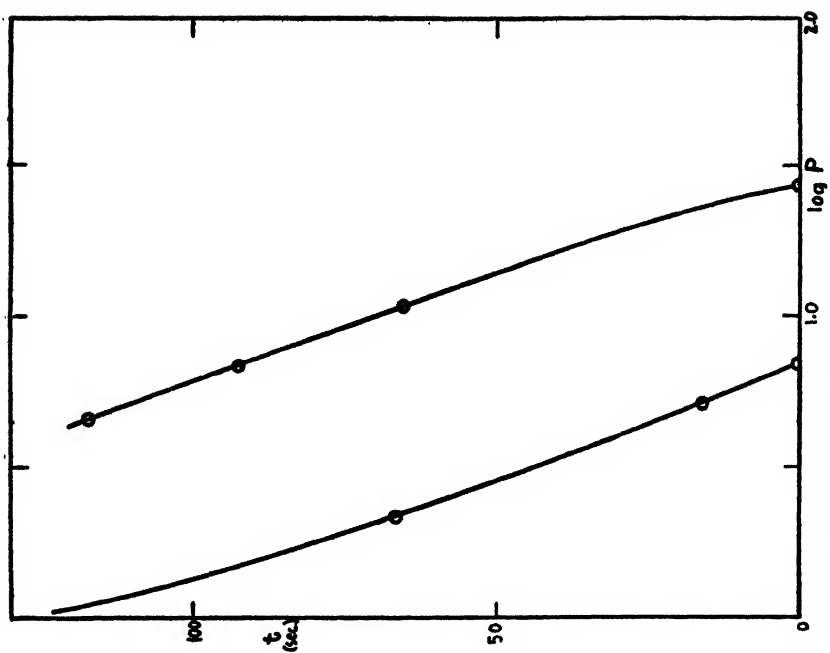


Fig. 4. Gas—ammonia. Plot of  $\log P$  (in centimeters of mercury) against  $t$  (in seconds).

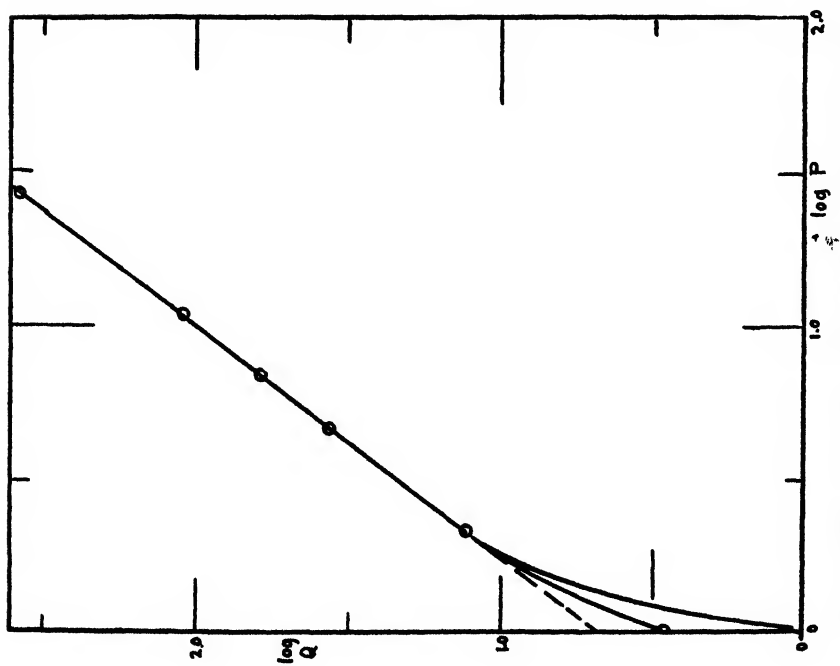


FIG. 5. Gas—hydrogen. Plot of  $\log Q$  against  $\log P$  (in centimeters of mercury).  $Q$  is the mass flow rate.

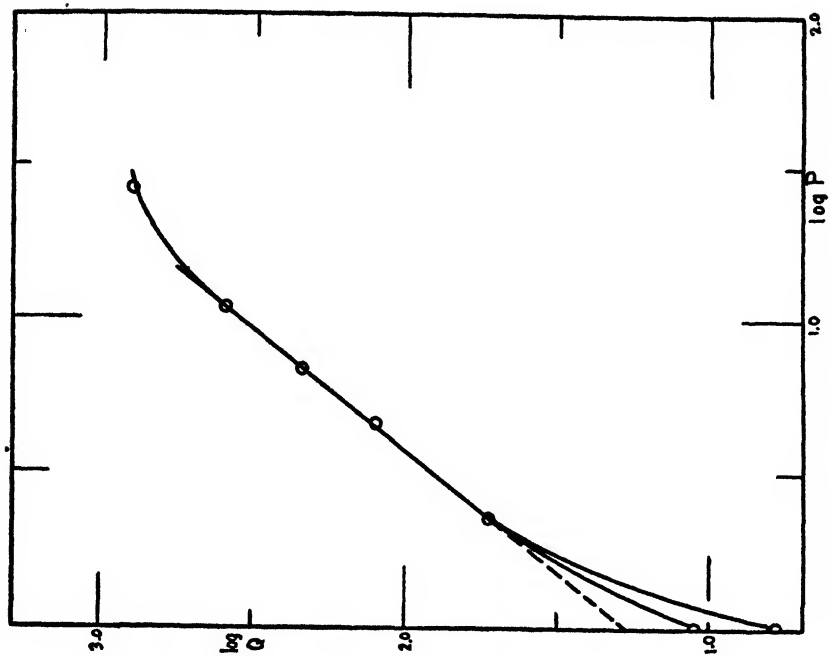


FIG. 6. Gas—ammonia: plot of  $\log Q$  against  $\log P$

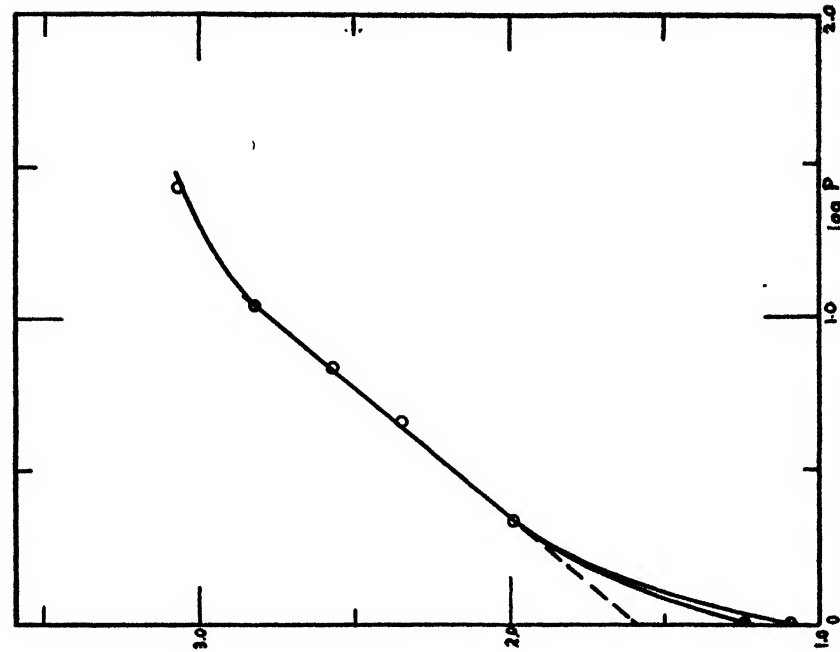


FIG. 8. Gas—carbon dioxide: plot of  $\log Q$  against  $\log P$

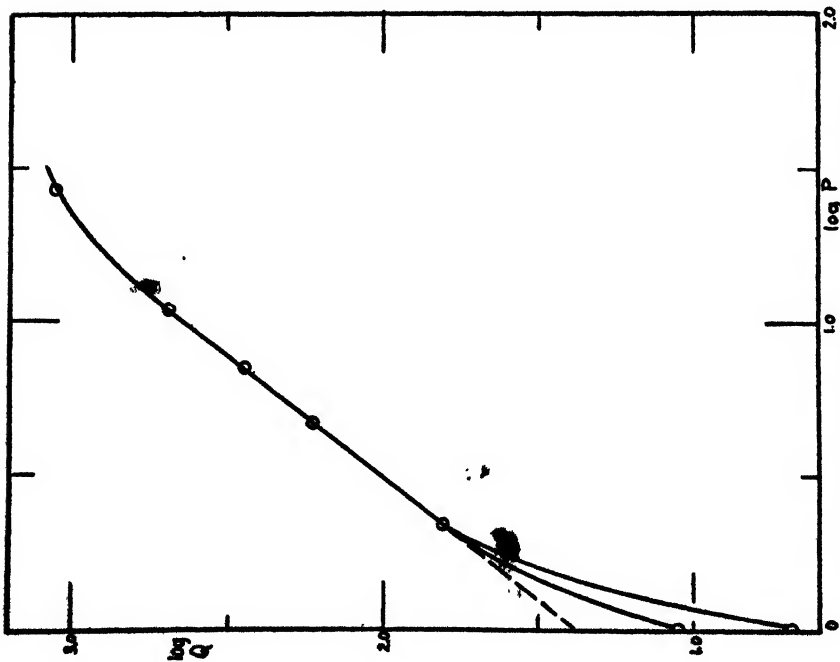


FIG. 7. Gas—oxygen: plot of  $\log Q$  against  $\log P$

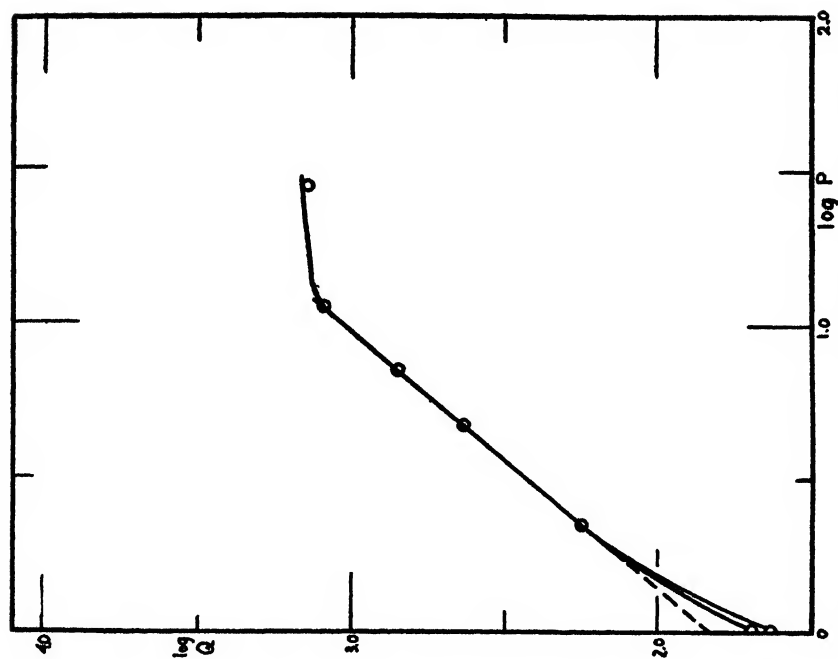


FIG. 10. Gas—Freon 12: plot of  $\log Q$  against  $\log P$

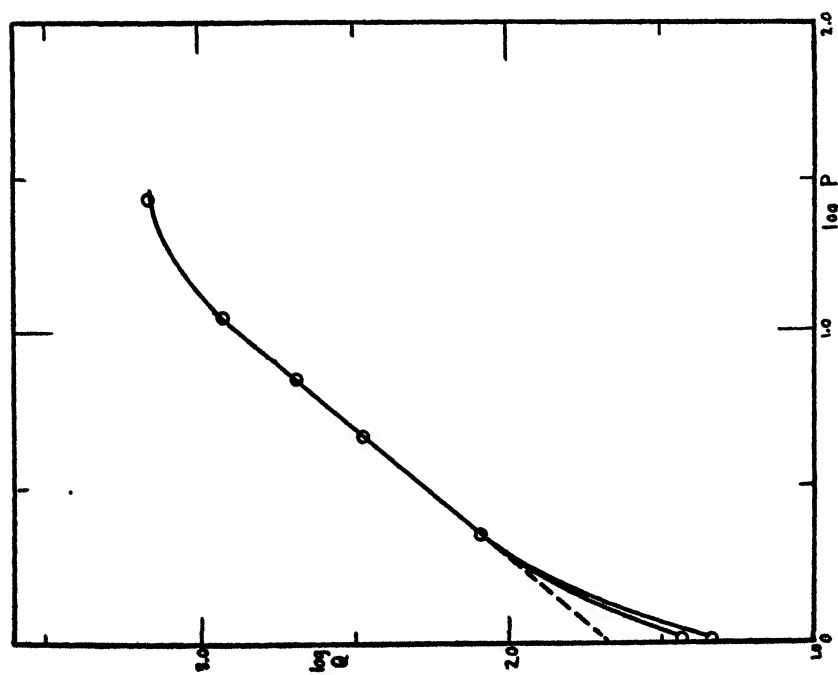


FIG. 9. Gas—sulfur dioxide: plot of  $\log Q$  against  $\log P$

for the intermediate pressure region,  $\log Q$  is a linear function of  $\log P$ . The slope of these portions of the curves is 1.20 for all of the gases with a deviation which is less than 2 per cent and certainly within the experimental error. Thus  $Q$  in this region varies directly as  $P^{1.20}$ . From the intercepts of these linear portions of  $M$ , dependence of  $Q$  can be obtained by comparing the different gases. In figure 11 these intercepts,  $\log Q$  (at unit pressure), are shown plotted against

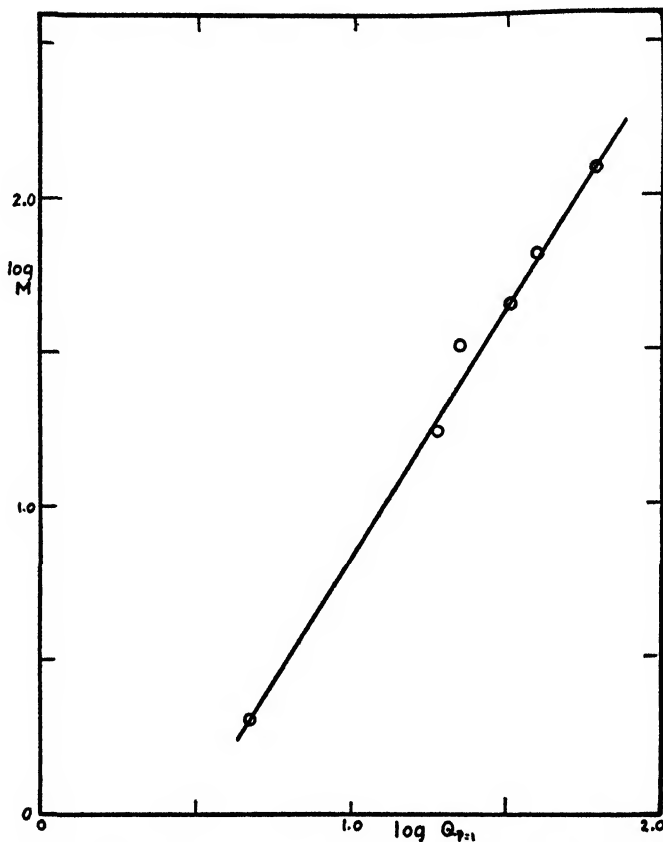


FIG. 11. Plot of  $\log M$  (molecular weight) against  $\log Q$  (at unit pressure)

$\log M$ . With the exception of oxygen, the points fall on a very good straight line. The two results indicate that the relation between  $Q$ ,  $P$ , and  $M$  is given by:

$$Q = kP^{1.20}M^{0.68} \quad (7)$$

#### DISCUSSION

For purposes of discussion, the relevant physical data for the gases used are presented in table 3 (values taken from *International Critical Tables*). From the values listed for the mean free paths it can be seen that even at the lowest pressures used (1 cm. of mercury) the orifice diameter was still about ten times the



longest mean free path. Under these conditions, the flow may be considered as effusive.

Inspection of figure 3 shows that back pressure has negligible effect on the flow rates down to very low forward pressures. This may be taken as very direct, experimental evidence for the fact that in this pressure region we are indeed beyond the limit of critical flow. Calculations of the expected back pressures in the Toepler pump system further confirm this. Except at the lowest points, for the higher starting pressures, the ratio  $P/P_0$  is always less than 0.5.

Another striking experimental fact which seems to justify further the reduction of equation 3 is the conformity of the  $Q$ - $P$  dependence for the different gases. Effusion that is not critical would be expected to show a  $Q$ - $P$  relation that would be a function of the  $\gamma$  for the specific gas. However, whereas equation 3 for ideal effusive flow predicts a linear relation between  $Q$  and  $P$ , the empirical equation 7 indicates that  $Q$  is proportional to  $P^{1.20}$ . Similarly, whereas equation 3 predicts that  $Q$  should vary as  $M^{1/2}$  for different gases, equation 7 shows that under our

TABLE 3  
*Physical data for gases studied*

GAS	MOLECULAR WEIGHT, $M$	VISCOSITY (20°C.) $\times 10^6$	MEAN FREE PATH, $L \times 10^6$	$C_p/C_v$ (20°C.)
		<i>poises</i>	<i>cm. (S.T.P.)</i>	
Hydrogen . . . . .	2.02	89	18.3	1.410
Ammonia . . . . .	17.0	100	7.0	1.310
Oxygen . . . . .	32.0	201	10.0	1.401
Carbon dioxide . . . . .	44.0	148	6.3	1.304
Sulfur dioxide . . . . .	64.0	125	4.6	1.28
Freon 12 . . . . .	121.0	100 (est.)	2.6 (est.)	1.19 (est.)

experimental conditions  $Q$  varies as  $M^{0.63}$ , with a large deviation shown by oxygen (figure 11). This deviation of oxygen cannot be accounted for by differences in  $\gamma$ , since  $f(\gamma)$  for oxygen is not significantly different from the values of  $f(\gamma)$  for the other gases.

A reasonable explanation for the discrepancy between equations 3 and 7 may be found from a consideration of the orifice dimensions. The orifice used was not an infinitely thin wall, but actually a short tube with a radius-to-length ratio of 1/5. The effect of this finite length is to introduce viscosity as one of the flow factors. For isothermal, viscous flow of an ideal gas through a long tube, the mass flow  $Q$  is given by:

$$Q = \left( \frac{\pi r^4}{16\eta l} \right) \left( \frac{M}{RT} \right) (P_0^2 - P^2) \quad (8)$$

For small back pressures,  $Q$  would be expected to vary as  $MP^2\eta^{-1}$ . For larger back pressures the apparent  $P$  dependence would be somewhat less than a power of 2. If we were to add a correction term of the form  $MP^2\eta^{-1}$  to equation 3, we might expect a net result to be similar in form to the odd powers found

in equation 7. In the case of oxygen, with a viscosity that is relatively high, the effect would be exactly in the direction observed. It was found that a small empirical correction of the form mentioned was partially successful in bringing all of the data into reasonable concordance.

It is likely that a much thinner orifice, which can easily be manufactured, would reduce the viscosity effect to negligible proportions. Further experiments should be made to verify this.

Despite the limitations imposed by high viscosities, the present system can be used to measure molecular weights for most gases, since most gases will have comparable viscosities. Eyring (3) has reported using a flow system for measuring molecular weights. A study of the dimensions of his system under the pressures used shows that the flow was effusive and in the region of critical velocities. The good agreement which he obtained using a diffusion-type equation is due in part to a fortuitous choice of gases and mainly to the remarkable coincidence that the equation for diffusion through an orifice into a vacuum is identical with equation 3, except for a numerical constant. The ratio of the constants for the two different equations is 1.6, the effusive flow being faster.

The present system should be very useful in measuring the composition of isotopic mixtures such as  $H_2$ - $D_2$  or  $NH_3$ - $ND_3$ . In such mixtures, the viscosity and  $\gamma$  effects will entirely cancel and the accuracy will depend only on the accuracy of timing, which is about 0.2 per cent.

#### SUMMARY

1. It is shown that when the ratio of forward to back pressure for a gas effusing through an orifice exceeds 2, a region of critical flow velocity is reached. In this region the flow  $Q$  is directly proportional to  $M^{1/2}Pf(\gamma)$ ,  $f(\gamma)$  varying very little for most gases.

2. A microeffusimeter is described having a small platinum orifice and equipped with automatic electric timers. It is shown that this instrument can be used in most cases to measure molecular weights to within 4 per cent. It is expected that the use of a thinner orifice would improve the absolute accuracy and extend the range through the elimination of viscosity effects.

3. The apparatus has the advantages of using small gas samples (1-2 cc. at S.T.P. minimum) and preserving the sample for further work. It should also be capable in its present form of measuring the relative densities of isotopic gases to within 0.2 per cent, since in these cases the effects of viscosity may be expected to cancel.

#### REFERENCES

- (1) BUCKINGHAM AND EDWARDS: Scientific Papers, U. S. Bureau of Standards, No. 359.
- (2) DRAKE: Ind. Eng. Chem., Anal. Ed. 15, 647 (1943).
- (3) EYRING: J. Am. Chem. Soc. 50, 2398 (1928).
- (4) FESKOV: Ind. Eng. Chem., Anal. Ed. 11, 653 (1939).
- (5) KNUDSEN: Ann. Physik 28, 75 (1909).
- (6) LAMB: *Hydrodynamics*, pp. 23-7. Cambridge University Press, London (1932).

HOMOGENEITY AND THE ELECTROPHORETIC BEHAVIOR  
OF SOME PROTEINS. II<sup>1,2</sup>

## REVERSIBLE SPREADING AND STEADY-STATE BOUNDARY CRITERIA

ELMER A. ANDERSON AND ROBERT A. ALBERTY

*Department of Chemistry, University of Wisconsin, Madison, Wisconsin**Received April 28, 1948*

## INTRODUCTION

In electrophoretic experiments carried out at the average isoelectric point of the protein and at a low protein concentration so that the electric field and pH are essentially constant through the protein boundary, reversible spreading indicates electrophoretic heterogeneity. Under these conditions, Alberty (1) has shown that in the case of a Gaussian mobility distribution, the standard deviation of the mobility distribution may be determined from the schlieren photographs of the protein boundary. In the case where there is measurable diffusion of the protein during the experiment and the mobility distribution may be represented by the Gaussian probability function, the experimental refractive-index gradient will have Gaussian form, and the standard deviation of the mobility distribution,  $h$  (heterogeneity constant), may be calculated by using equation 1.

$$D^* = \frac{\sigma^2 - \sigma_0^2}{2t_E} = D + \frac{E^2 h^2}{2} t_E \quad (1)$$

In this equation  $\sigma_0$  is the standard deviation of the gradient curve at the moment the field is applied,  $\sigma$  is the standard deviation after electrophoresis for  $t_E$  seconds,  $E$  is the electric field strength, and  $t_E$  is the time of electrophoresis in seconds. The determination of  $\sigma$  with the schlieren optical system is subject to several errors, which are discussed in the experimental section. The heterogeneity constant,  $h$ , is calculated from the slope of the plot of  $D^*$  vs.  $t_E$ .

In the following report the isoelectric points and heterogeneity constants of eleven purified protein preparations and of gelatin have been determined. It should be emphasized that the protein preparations used were not recrystallized for these tests, and except for urease, which was a suspension, were obtained as dry solids.

## STEADY-STATE BOUNDARY CRITERION

A disadvantage of the electrophoretic spreading test for homogeneity is that it cannot be applied to a number of proteins which are either unstable or insoluble at their isoelectric points. An additional criterion for the electrophoretic homogeneity of a protein which may be applied at pH levels away from the isoelectric

<sup>1</sup> The first paper of this series is referred to in reference 2.

<sup>2</sup> This work was also supported in part by grants from the U. S. Public Health Service and the Wisconsin Alumni Research Foundation.

point is obtained from the study of moving-boundary systems of inorganic electrolytes. The usual ascending protein boundary is of the type (15)



or



where A and R represent the buffer cation and anion, respectively, S represents a protein anion, and B represents a protein cation. The symbols  $\alpha$ ,  $\beta$ , and  $\gamma$

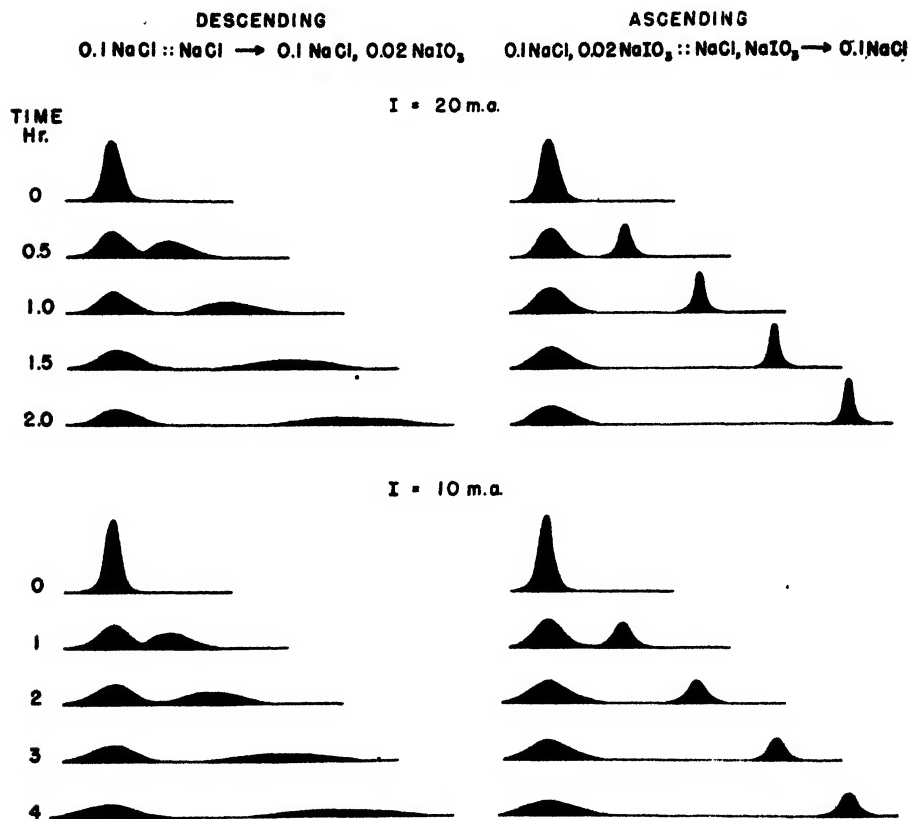


FIG. 1. Refractive-index gradient curves for iodate boundaries, showing steady-state ascending patterns.

designate the different homogeneous phase regions in order of decreasing density. The :: represents the protein concentration (or  $\delta$ ) boundary and  $\rightarrow$  the moving boundary. Following Longworth's convention, the system is written so that the current flows from left to right. Such moving-boundary systems in which S or B are ions of low equivalent weight rather than proteins are analogous to ascending protein boundaries and indicate the behavior to be expected from pure proteins. Longworth (15) has studied some systems of this type and has found that if  $|u_S| < |u_R|$  (for example, A = K<sup>+</sup>, R = Cl<sup>-</sup>, S = IO<sub>3</sub><sup>-</sup>), the boundary

moves with constant height and shape.<sup>3</sup> This is further illustrated by figure 1, which shows the moving-boundary systems:

Descending:  $\text{NaIO}_3 (0.02 N), \text{NaCl} (0.1 N) \leftarrow \text{NaCl} (\beta) :: \text{NaCl} (0.1 N)$

Ascending:  $\text{NaCl} (0.1 N) \leftarrow \text{NaIO}_3, \text{NaCl} (\beta) :: \text{NaIO}_3 (0.02 N), \text{NaCl} (0.1 N)$

In this experiment the iodate ion is analogous to a protein ion.

Photographs taken at regular time intervals indicate that while the descending boundary spreads with time, as is also observed in the electrophoresis of proteins, the ascending boundary moves with constant height and shape. The stationary boundaries are larger than in the protein case, because the equivalent weight of the iodate ion is much less than that of proteins, so the adjustment of salt concentration at the position of the initial boundary is relatively greater. Experiments at two current densities show another important characteristic of this type of steady-state boundary, which is that the height of the gradient curve is directly proportional to the current density. Longworth (14) has shown this to be true for boundaries of the type  $\text{AR}(\alpha) \leftarrow \text{AS}(\beta) :: \text{AS}(\gamma)$ .

It might be expected, therefore, that electrophoretically homogeneous proteins or other colloidal electrolytes would show steady-state ascending boundaries and that the value of the maximum gradient would be directly proportional to the current density. There are two limitations to the application of this proposed test to proteins which should be mentioned. First, at sufficiently high protein concentrations the conductivity effect which is responsible for the sharpening of the ascending boundary may be so great that the boundary of a somewhat heterogeneous protein would move as a steady state. However, at lower protein concentrations and electric field strengths, the ascending boundary for such a protein would spread with time. Second, the pH effect (16) which is present in electrophoretic experiments with proteins tends to cause broadening of the ascending protein boundary if the protein is negatively charged and sharpening if the protein is positively charged (provided the buffer is of the uncharged-acid type). If the buffer is of the uncharged-basic type, the situation will be reversed.

Formation of a steady-state ascending protein would, within limits, establish the protein as being electrophoretically homogeneous. None of the proteins which we have tested satisfy this test. In the experimental section, three proteins have been tested in this manner.

#### EXPERIMENTAL

The experimental procedure for the reversible spreading determination has been described previously (1, 2). The apparent diffusion constants,  $D^*$ , were calculated from the enlarged gradient curves by using the half-width at the inflection point,  $x_i$ , or the maximum height,  $H$ , and area,  $A$

$$D^* = \frac{(x_i)^2 - (x_i)_0^2}{2t_g G^2} \quad (2)$$

\* If  $|u_s| > |u_n|$  or  $|u_n| > |u_a|$  the boundary will spread with time. However, this latter case is seldom encountered with proteins.

$$D_A^* = \frac{\left(\frac{A}{H}\right)^2 - \left(\frac{A}{H}\right)_0^2}{4\pi t_x G^2} \quad (3)$$

Here  $G$  is the total magnification from cell to enlarged tracing, and the subscript zero indicates the value at the time  $t_x = 0$ . The heat dissipation in the electrophoresis cell was always kept below 0.015 watt/cc.

The determination of diffusion constants with the cylindrical-lens schlieren optical system requires attention to details which are generally ignored in the application of this optical method to electrophoretic analysis. Photographs may be taken by using diagonal knife edges, rectangular slits, spindle-shaped slits, and diagonal fine wires. In general, adjustable slits (5) and special-shaped slits (23) are not practical for diffusion measurements, because a different slit or adjustment is required for each photograph. For this reason diagonal knife edges and diagonal rectangular slits have been most used. Although it might be expected that identical results would be obtained by these two methods, this has been found experimentally not to be true because of the nature of the diffraction pattern of the diagonal slit or knife edge at the photographic plate. Photographs taken with a diagonal knife edge brought in from above the optic axis do not have the same appearance and do not give the same values for the maximum ordinate and area as photographs taken with a diagonal knife edge brought in from below the optic axis because of the diffraction pattern. In addition, the peak height and area vary with exposure time even when contrast plates are used, since the first diffraction band on either side of the peak is broad and diffuse. With a narrow rectangular slit, on the other hand, the value of the area and the maximum ordinates are independent of exposure time within the range in which satisfactory photographs are obtained. Data illustrating these points are given in tables 1 and 2. These data were obtained from a 0.7 per cent solution of crystallized bovine albumin at pH 4.7,  $\Gamma/2 = 0.10$ , at  $1^\circ\text{C}$ . The photographs were taken on Eastman Kodagraph C.T.C. plates between 30,240 and 31,860 sec. after the boundary had been sharpened and were developed in Eastman D-19. The photographs were enlarged 6.40 times and traced by hand. All measurements were made on these tracings. In the case of diffuse edges the line was drawn at a level at which the density was approximately one-fourth that of the first maximum, because this corresponds to the geometrical edge in the case of diffraction from a straight edge. Since the peak heights and widths changed during this period, owing to diffusion, it is better to compare the diffusion constants than the actual dimensions of the schlieren curves. The values given in the tables are means of the results obtained by two individuals. The average difference between the diffusion constants determined by these two individuals was  $0.2 \times 10^{-7}$  or about 7 per cent. It can be seen that with a diagonal knife edge the diffusion constant changes considerably with exposure time and the diffusion constants with upper and lower jaws agree better for long exposure times. It is to be emphasized that these exposure times are not extremes but all represent traceable photographs. Because of the wave nature of light, the maximum in the intensity of the lowest fringe in the interference pattern at

the knife edge does not coincide with the position determined by geometrical optics (9). Also, some light is found below the lowest position predicted by geometrical optics, and because of this diffuseness of the lowest fringe, the apparent height of the peak measured on the photographic plate varies with exposure time. This variation in height is important both in the height-area and the standard deviation methods for calculating diffusion constants. It is

TABLE 1

*Comparison of methods for determining diffusion constants from schlieren photographs (cylindrical-lens method)*

KNIFE EDGE OR SLIT ANGLE	EXPOSURE TIME	$D_A \times 10^7$						$D_\sigma \times 10^7$					
		Knife edge U = upper jaw L = lower jaw			Slit (0.5 mm.)			Knife edge U = upper jaw L = lower jaw			Slit (0.5 mm.)		
		45 sec.	90 sec.	180 sec.	90 sec.	180 sec.		45 sec.	90 sec.	180 sec.	90 sec.	180 sec.	
15° U.....		2.65	2.77	3.17	3.25	3.11		2.48	2.64	3.06	3.06	3.06	
L.....		4.22	3.75	3.41				4.01	3.76	3.36			
30° U.....		2.54	2.85	3.04	3.29	3.35		2.46	2.64	3.01	3.10	3.05	
L.....		4.05	3.90	3.48				3.79	3.70	3.35			

TABLE 2

*Comparison of areas (in.<sup>2</sup>) used in calculating  $D_A$  values in table 1*

KNIFE EDGE OR SLIT ANGLE	EXPOSURE TIME	Knife edge U = upper jaw L = lower jaw			Slit (0.5 mm.)	
		45 sec.	90 sec.	180 sec.	90 sec.	180 sec.
15° U.....		2.33	2.42	2.63	2.74	2.79
L.....		3.11	2.87	2.74		
30° U.....		5.00	5.41	5.63	5.85	5.90
L.....		6.80	6.51	6.08		

important in the determination of the standard deviation,  $\sigma$ , by the inflection point method because the half-width of the curve is measured at a height equal to  $1/\sqrt{e}$  of the maximum ordinate. By using a diagonal slit, the dependence of diffusion constant upon exposure time is largely avoided. The areas of the schlieren patterns are given in table 2. It can be seen that the areas obtained by using a diagonal knife edge brought in from above the optic axis (U) and below the optic axis (L) are considerably different. This effect should be considered in calculating refractive-index differences or protein concentrations from the

area of schlieren patterns. By using a diagonal slit, the dependence of area upon exposure time is avoided.

In addition to the effects noted above, Kegeles and Gosting (9) have pointed out that equations 2 and 3, which are based upon geometrical optical considerations, are not exactly true. This error is greatest for the most downward deflected light, and this has the effect of compressing the height of the peak and leading to high values for the diffusion constant. This error, which makes all determinations of diffusion constants with the schlieren optical systems somewhat high,<sup>4</sup> does not have a significant effect upon the heterogeneity constants calculated from equation 1.

The pH values recorded were measured with a glass electrode at 25°C., and sodium-ion corrections were applied above pH 9.5. Protein concentrations of 0.5–0.75 per cent were used for the electrophoresis samples except where otherwise noted. Where the protein stability was in question, the dialysis time was shortened by using continuous agitation, a large membrane area, and, in some cases, initial pH adjustment to bring the two phases closer to their equilibrium values.

#### CHYMOTRYPSIN<sup>5</sup>

The electrophoretic mobility of chymotrypsin has been determined from pH 6 to pH 9.5 at 0.01 ionic strength, and the mobilities are plotted against pH in figure 2. In these experiments a single symmetrical peak was obtained, and there was no indication of the presence of other proteins. The isoelectric point of chymotrypsin in diethylbarbiturate buffer of 0.01 ionic strength was found to be pH 8.6, and a heterogeneity constant of  $0.12 \times 10^{-6} \text{ cm.}^2 \text{ volt}^{-1} \text{ sec.}^{-1}$  was obtained in a spreading experiment under these conditions. At 0.10 ionic strength in sodium chloride–sodium diethylbarbiturate buffer the isoelectric point is pH 8.1. Here, as in all experiments involving labile proteins, the question of the stability of the protein must be considered. Kunitz (11) has found that at pH 9.0 and 35°C. the half-life of native ( $\alpha$ ) chymotrypsin is about 6 hr. Protein reactions often have high temperature coefficients, so that the denaturation rate at 1°C., where these experiments were carried out, cannot be reliably estimated from these data. However, some denaturation would be expected, and since the heterogeneity constant is low, it is possible that the original crystalline material was more homogeneous electrophoretically than the heterogeneity constant obtained would indicate.

The isoelectric points at 0.10 and 0.01 ionic strengths obtained by the moving-boundary method are considerably higher than the values determined by microscopic electrophoresis using coated collodion particles. Using the latter method,

<sup>4</sup> The magnitude of this error depends upon the concentration of the protein solution, the thickness of the electrophoresis cell, and the wave length of the light used. For the systems studied the error in the diffusion constant from this source is approximately 4 per cent (private communication from Dr. L. J. Gosting).

<sup>5</sup> The authors are indebted to Dr. M. Kunitz for the four times recrystallized sample of this protein. Some of the experiments were repeated with crystalline chymotrypsin obtained from Armour Laboratories, Chicago, Illinois, and the same results were obtained.



Kunitz (11) found the isoelectric point to be about pH 6 in 0.01 *M* buffer. One explanation for this discrepancy might be that the character of the protein is changed by adsorption on collodion. In general, proteins cannot be recovered after adsorption on a solid without extensive denaturation. It is usually

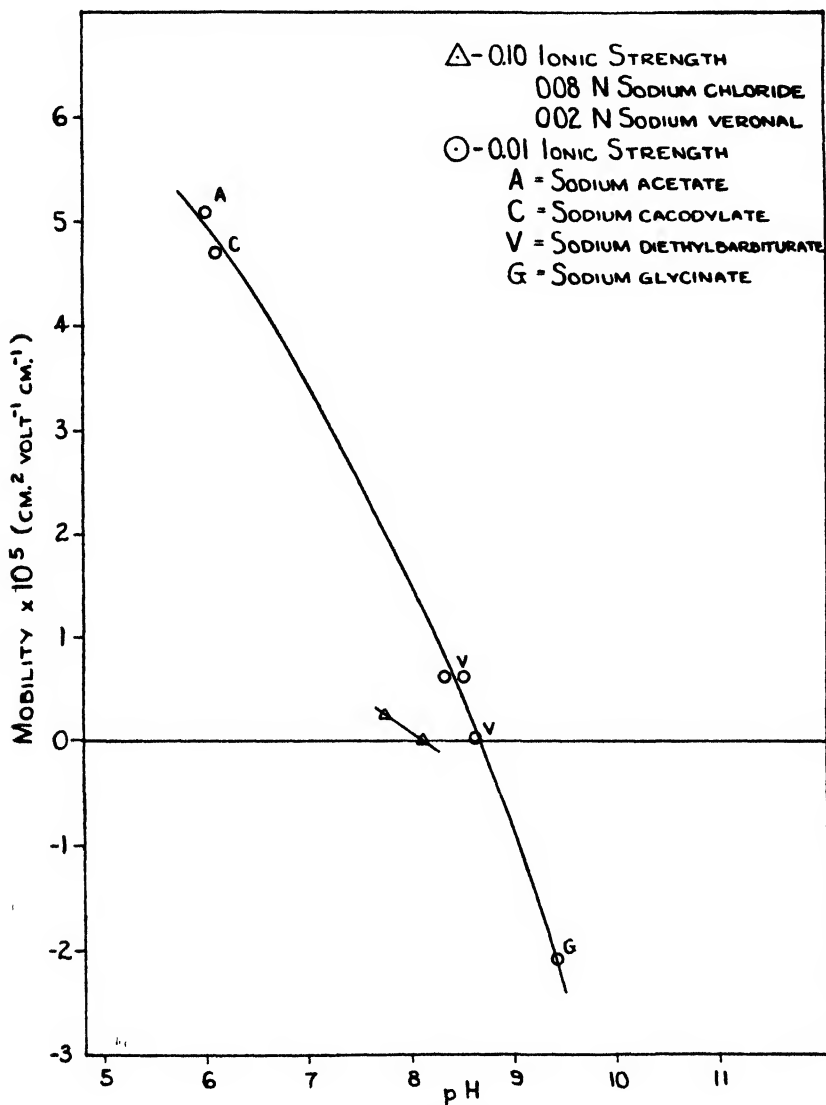


FIG. 2. pH-mobility curve for chymotrypsin

assumed that any protein will cover completely a collodion particle and hence give it the electrophoretic properties of the protein. However, this assumption may not always be justified. In any event, the high mobility obtained in electrophoresis at pH 6 and comparable ionic strengths makes the microscopic electro-

phoretic result untenable. Specific ion effects from the buffer have been ruled out, since a smooth curve was obtained even though four different buffers were used in covering the pH range studied.

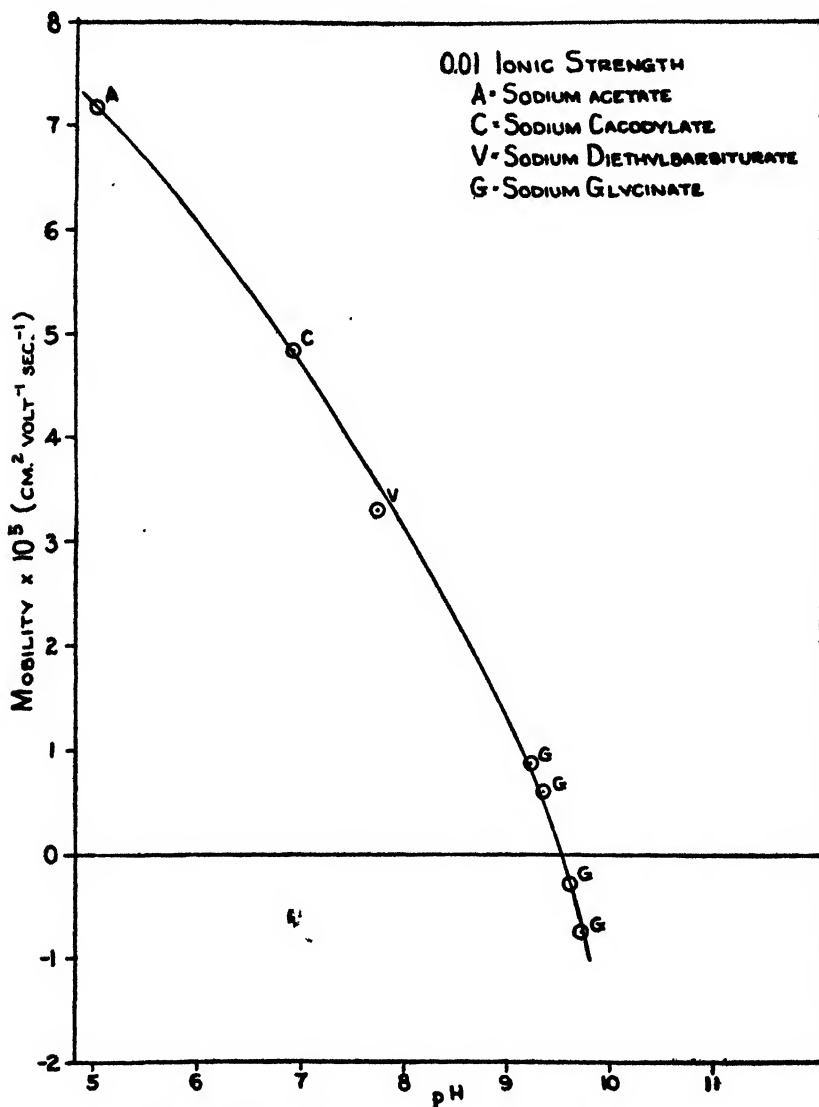


FIG. 3. pH-mobility curve for chymotrypsinogen

#### CHYMOTRYPSINOGEN\*

A pH-mobility curve for chymotrypsinogen at 0.01 ionic strength is given in figure 3. The isoelectric point in 0.01 *N* sodium glycinate buffers is pH 9.5. At the isoelectric point the protein showed reversible spreading, giving a hetero-

\* The authors are indebted to Dr. M. Kunitz for the crystalline sample of this protein.

**TABLE 3**  
*Summary of electrophoretic spreading experiments*

PROTEIN	$\frac{r}{2}$	pH	I.P.	BUFFER SALT*	$E$ <small>vols cm.<sup>-1</sup></small>	$u \times 10^4$ <small>cm.<sup>2</sup> sec.<sup>-1</sup> volt<sup>-1</sup></small>	$h \times 10^4$ <small>cm.<sup>2</sup> sec.<sup>-1</sup> volt<sup>-1</sup></small>
Chymotrypsin..	0.01	8.6	8.6	NaV	6.84	+0.03	0.12
	0.10	7.73		0.08 NaCl			
				0.02 NaV	1.56	+0.25	0.2
	0.10	8.1	8.1	0.08 NaCl			
				0.02 NaV	1.65	0	0.25
Chymotrypsin- ogen.....	0.01	9.55		G	5.49		0.5
1 week dialy- sis.....	0.01	9.35		G	4.84	-0.22	0.7
	0.01	9.71	9.5	G	5.65	-0.74	0.5
16 hr. dialysis	0.01	9.35		G	5.5	+0.6	0.3
	0.01	9.6		G	5.65	-0.3	0.6
Lysozyme							
Lot 1C2R73..	0.05	11.27	11.2	NaG	2.58	Major -0.21 Minor (6%) -7.0	0.32
Lot 801L1...	0.01	11.42	11.0	NaG	3.32	-1.3	0.5
Conalbumin ...	0.01	6.3		NaCac	6.96	Major 2.2	
Conalbumin minus flavin.	0.01	6.8	7.1	NaCac	5.93	0.54	
Hemocyanin ( <i>Limulus poly- phemus</i> ) .....	0.10	6.0		0.08 NaCl	2.5		0.29
				0.02 NaCac			
	0.05	6.11	5.6±0.1	0.03 NaCl	2.38		0.32
				0.02 NaCac		Major -6.6	
	0.10	8.5		NaV	6.0	Minor -5.1	
Horse $\gamma_2$ -glob- ulin (hyper- immune).....	0.10	8.02	7.5	0.08 NaCl	1.61	-0.87	0.56
	0.01	8.5	7.9	0.02 NaV	5.86	-1.0	1.3
Sample 2.....	0.01	8.05		NaV	6.24	-1.38	1.1
Horse $\gamma_2$ -glob- ulin (normal).	0.01	7.95	8.0	NaV	6.23	+0.14	0.8
	0.001	8.2		NaV	18.9		
Human $\gamma_2$ - globulin.....	0.001	8.35		NaV	18		
	0.003	8.2		NaV	6.55		1.0
Human $\gamma_1$ - globulin.....	0.10	5.84	5.4±.2	0.08 NaCl	1.55	-0.47	0.26
				0.02 NaCac			
	0.01	6.6	6.45	NaCac	5.9	-0.46	0.95

TABLE 3—*Concluded*

PROTEIN	$\frac{r}{2}$	pH	I.P.	BUFFER SALT*	$E$	$u \times 10^4 \dagger$	$h \times 10^4$
					<i>volts</i> <i>cm.<sup>-1</sup></i>	<i>cm.<sup>2</sup> sec.<sup>-1</sup> volt<sup>-1</sup></i>	<i>cm.<sup>2</sup> sec.<sup>-1</sup></i> <i>volt<sup>-1</sup></i>
Ribonuclease...	0.01	8.07	9.45	NaV	6.06	4.0	
	0.01	9.75		NaG	5.84	-0.96	
Gelatin.....	0.01	4.76	4.9	NaA	5.12	Major +0.24 Minor +1.9 (12%) (descending only)	From sym- metrical ascend- ing peak 0.51
Urease .....	0.01	7.4		NaV	6.28	+9.5	0.32-0.53
	0.01	6.43		NaCac	5.9	5.73	

\* G = glycinate; A = acetate; Cac = cacodylate; V = diethylbarbiturate.

† Descending mobilities are given.

geneity constant of  $0.3 \times 10^{-5}$  after dialysis for 16 hr. and  $0.7 \times 10^{-5}$  after dialysis for more than a week. This indicates that the protein is altered upon standing at this alkaline pH, and therefore the heterogeneity constant is a measure of the upper limit of electrophoretic heterogeneity. It would be necessary to compare these values with determinations of biological stability under the same conditions before any final statement could be made as to the electrophoretic homogeneity of the original crystalline material.

As in the case of chymotrypsin the isoelectric point determined by the moving-boundary method is much higher than the value (pH 5.0) determined by microscopic electrophoresis and reported by Kunitz and Northrop (13) for comparable ionic strengths. Determinations in which acetate and cacodylate buffers were used in the range pH 5-7 where the protein is reasonably stable yield high positive mobilities, indicating a much higher isoelectric point.

#### LYSOZYME<sup>7</sup>

The electrophoretic mobilities of this protein determined at ionic strengths of 0.01, 0.02, and 0.05 are plotted in figure 4. The isoelectric point of lysozyme in sodium glycinate buffer is about pH 11.0 at 0.01 ionic strength and pH 11.2 at 0.05 ionic strength. In several experiments a second component was observed to move with a high negative mobility. As estimated from the electrophoretic diagram the second component comprised 6-20 per cent of the total protein. In other experiments the second component did not appear at all. The heterogeneity constants of lysozyme were  $0.35 \times 10^{-5}$  at 0.05 ionic strength and about  $0.5 \times 10^{-5}$  at 0.01 ionic strength. Since lysozyme is only soluble to the extent of about 0.3 per cent at its isoelectric point, it is difficult to maintain a stable bound-

<sup>7</sup> Crystalline lysozyme, Lot 1C2R73 and Lot 801L1, was obtained from Armour Laboratories, Chicago, Illinois.

ary density gradient during electrophoresis. It was found particularly important here to use short efficient dialyses and to check roughly on the degree of completion of dialysis by pH and conductivity measurements on the protein and buffer phases.

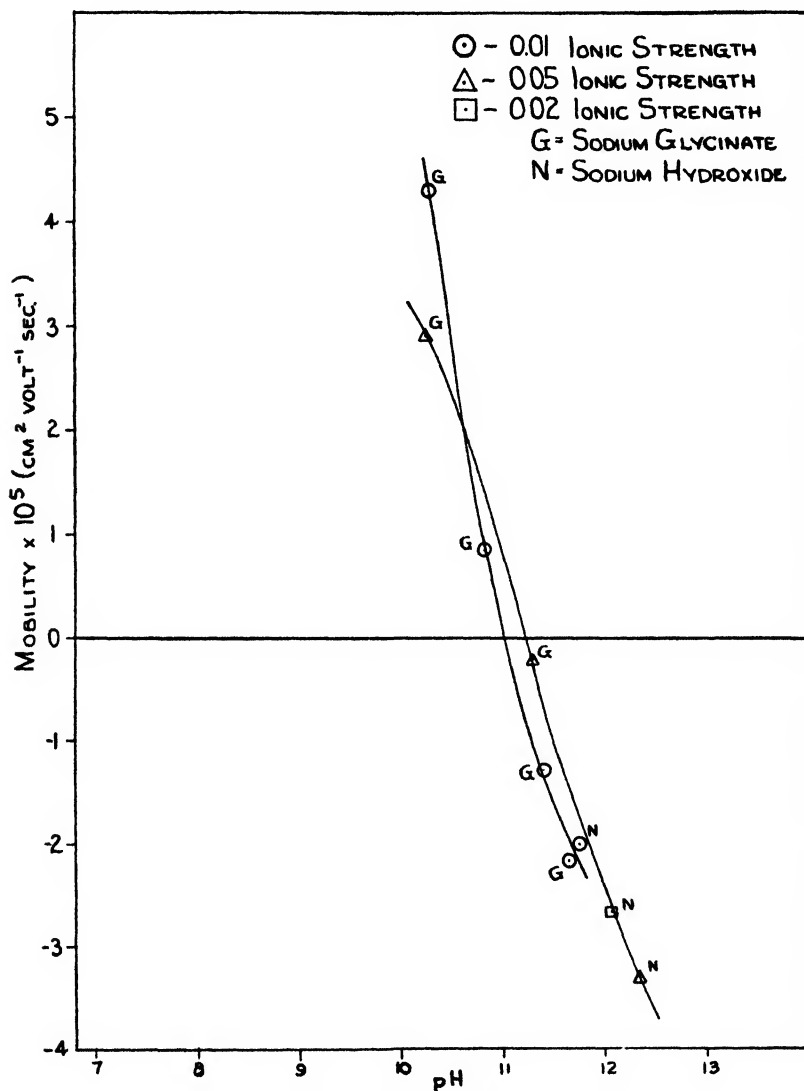


FIG. 4. pH-mobility curves for lysozyme

The unusually steep slope of the pH-mobility curve suggests that a large number of the groups ionizing in this range have approximately the same ionization constant. Binding of glycine has been suggested by Alderton *et al.* (3), who obtained mobilities more positive than expected with glycine. Glycine, however,

is negatively charged at these pH levels and any complex formation should make the mobility more negative.

#### CONALBUMIN<sup>8</sup>

The purified sample of conalbumin from hen's eggs appeared homogeneous in electrophoresis in diethylbarbiturate buffer of pH 8.6 and 0.10 ionic strength. However, at pH 6.3 and 0.01 ionic strength this protein was resolved into two or three components. Electrophoretic mobilities are greater at lower ionic strengths because of the decrease in the shielding effect of the ionic atmosphere, and higher electric field strengths may be used without convection. For this reason electrophoresis at low ionic strengths frequently makes possible better resolution of mixtures containing closely related proteins. Since conalbumin is highly fluorescent under ultraviolet light and is known to contain flavin, it was suspected that the various components observed at pH 6.3 represented protein molecules containing various amounts of flavin. Flavin is apparently bound on a basic group of the protein (10, 24); hence dissociation raises the isoelectric point. The flavin moiety was removed by dialysis at pH 4 for 1 week with a number of buffer changes, the dialyzable flavin being reversibly dissociated from the protein in acid solution. Electrophoresis on the remaining protein at 0.01 ionic strength indicated that two components were still present. The major component had a mobility of  $+0.54 \times 10^{-5}$  and the minor component, comprising about 15 per cent of the total, had a mobility of  $-0.26 \times 10^{-5}$  at pH 6.8.

#### HEMOCYANIN OF *Limulus polyphemus*<sup>9</sup>

Pedersen has reported (22) that the hemocyanin of *Limulus polyphemus* gave quite uniform electrophoretic migration inside the stability range (pH 5.0–10.5), and suggested that the components which are resolved in the ultracentrifuge have the same electrochemical properties. However, reversible electrophoretic spreading experiments indicate that this protein is electrically heterogeneous at both 0.1 and 0.05 ionic strengths at the corresponding isoelectric points, approximately pH 6.0 and pH 6.1. The heterogeneity constants are  $0.29 \times 10^{-5}$  and  $0.32 \times 10^{-5}$  at 0.1 and 0.05 ionic strengths, respectively. The diffusion constant determined after reversal of the current for an equal period of time was  $0.87 \times 10^{-7}$  cm.<sup>2</sup> sec.<sup>-1</sup> at 1°C., in substantial agreement with other hemocyanins having about the same molecular weight and sedimentation constant (no diffusion data on this particular species were available in the literature). Electrophoresis at pH 8.6 in 0.1 ionic strength diethylbarbiturate buffer indicated the presence of two components. The main component, corresponding to 75 per cent of the total material, had a mobility of  $-6.6 \times 10^{-5}$  and the smaller component, comprising 25 per cent of the total, had a mobility of  $-5.1 \times 10^{-5}$ .

<sup>8</sup> The authors are indebted to Dr. H. F. Deutsch for the sample of this protein, which was prepared by alcohol fractionation methods (4).

<sup>9</sup> Freshly drawn blood of *Limulus polyphemus* obtained from Dr. H. C. Bradley was allowed to clot while exposed to air and the clot was removed by filtration.

HORSE  $\gamma_2$ -GLOBULIN (HYPERIMMUNE)<sup>10</sup>

This protein contained antibody to diphtheria, tetanus, perfringens, vibron toxoids, and pertussis culture. It is responsible for part of the antibody activity of hyperimmune horse plasma. A single moving boundary was obtained in analytical electrophoresis at pH 8.6, showing less than 1 per cent  $\gamma_1$ -globulin. Spreading experiments at the isoelectric point at 0.1 and 0.01 ionic strengths yielded symmetrical Gaussian gradients, indicating that the mobility distribution may be represented by the Gaussian function. The material showed marked reversible electrophoretic spreading, and heterogeneity constants of  $0.56 \times 10^{-5}$  and  $1.3 \times 10^{-5}$  were obtained at 0.10 and 0.01 ionic strengths; respectively. The

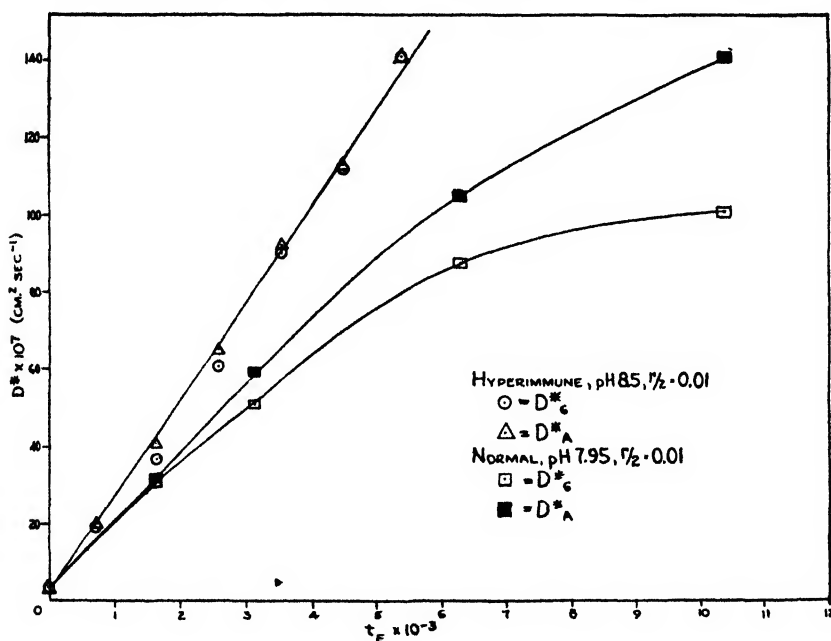


FIG. 5. Apparent diffusion constants during electrophoresis for horse  $\gamma_2$ -globulins

graph of apparent diffusion constant against time, which was used to calculate the heterogeneity constant at 0.01 ionic strength, is given in figure 5. The average isoelectric point is about pH 7.5 at the higher salt concentration and pH 7.9 at the lower concentration. For this protein, as well as for the corresponding normal horse  $\gamma_2$ -globulin, the broad mobility distribution suggests that the average properties observed would depend on the conditions of fractionation. Other

<sup>10</sup> The authors are indebted to Dr. H. F. Deutsch and Dr. J. C. Nichol for this protein sample, as well as for the normal horse  $\gamma_2$ -globulin reported in the following section. Both preparations were obtained by alcohol fractionation methods to be described in a future publication.

preparations<sup>11</sup> from the same serum have indeed shown shifts in these average properties but still have a Gaussian distribution of mobilities.

#### HORSE $\gamma_2$ -GLOBULIN (NORMAL)

At pH 8.6, 0.10 ionic strength, this protein showed less than 1 per cent of  $\gamma_1$ -globulin and no albumin. The electrophoretic spreading curves for this protein at pH 7.95 were not as nearly Gaussian in form as those of the hyperimmune  $\gamma_2$ -globulin. For this reason the apparent diffusion constant calculated from the half-width at the inflection point and from the height and area are not in good agreement, as shown in figure 5. Also as expected, the plot of  $D_e^*$  vs.  $t_E$  is not linear but tends to level off with time. In the case of the hyperimmune  $\gamma_2$ -globulin,  $D_e^*$  and  $D_A^*$  are in good agreement and plot linearly against  $t_E$ , indicating that the mobility distribution may be adequately represented by the Gaussian function. As a result of the fact that non-Gaussian spreading curves are obtained in the case of normal  $\gamma_2$ -globulin, it is possible to determine only an approximate value for the heterogeneity constant. The average heterogeneity constant calculated from the initial slope of the two curves was  $1.02 \times 10^{-5}$ . An experiment at 0.001 ionic strength gave a very asymmetric pattern with partially resolved peaks.

#### HUMAN $\gamma_2$ -GLOBULIN<sup>12</sup>

Human  $\gamma_2$ -globulin shows a nearly Gaussian distribution of mobilities in electrophoresis at 0.1 and 0.01 ionic strengths at its isoelectric point. In order to use high electric field strengths so as to minimize the importance of the spreading caused by diffusion, several experiments have been performed at even lower ionic strengths. Low ionic strength coupled with high field strength not only allows higher rate of boundary movement but also increases the value of the heterogeneity constant,  $h$ , as described previously (1, 2).

Experiments at ionic strengths of 0.003 and 0.001 indicated a broad mobility distribution which was non-Gaussian, as indicated by figure 6. Deviations from ideality due to the high ratio of protein to buffer salt make quantitative evaluation of these low ionic strength experiments more difficult; however, they are a very sensitive test of heterogeneity. If a protein is perfectly homogeneous and exactly at its isoelectric point, there will be no migration and so no electrical anomalies to interfere with the test. In the low ionic strength experiments reported a reasonable diffusion constant was obtained upon reversal of the current for an equal period. A rough calculation of the heterogeneity constant,  $h$ , at 0.003 ionic strength gives  $0.9\text{--}1.2 \times 10^{-5}$ , which is about the same as the value

<sup>11</sup> Sample 2 in table 3 is one of several fractions studied. Another sharper fraction prepared and studied by Dr. J. C. Nichol showed a heterogeneity constant of  $0.7 \times 10^{-4}$  at 0.01 ionic strength (personal communication).

<sup>12</sup> The sample of this protein which was prepared by method 4W (6) contained less than 2 per cent of  $\beta$ -globulin and  $\gamma_1$ -globulin and albumin, as judged by electrophoresis at pH 8.6 and  $r/2 = 0.10$ .



of  $h$  at 0.01 ionic strength. It can be shown from the Debye-Hückel-Henry theory that the value of  $h$  should be higher at lower ionic strengths (1). However, only a part of the protein was soluble at 0.003 ionic strength, the euglobulin being precipitated, so that this constant is more characteristic of the pseudoglobulin. Although the sharp part of the peak in figure 6 was first believed to represent a homogeneous component in human  $\gamma_2$ -globulin, it is probably a stationary concentration boundary, which, according to Dole's theory (7), represents a dilution of the protein and buffer solution at the site of the initial boundary

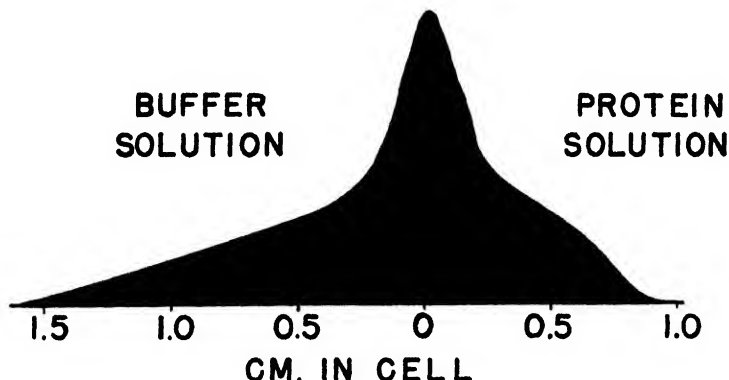


FIG. 6. Electrophoresis pattern for human  $\gamma_2$ -globulin at low ionic strength. The initial boundary position was at 0.0 cm. Ionic strength = 0.001; pH = 8.35;  $E$  = 18 volts/cm.;  $T$  = 34 min.

by the ratio of the Kohlrausch regulating functions for the buffer and the dialyzed protein solution. Since the regulating function,  $\omega$ , is

$$\omega = \sum_i \frac{c_i}{r_i}$$

where  $c$  is equivalent concentration and  $r$  is relative mobility, the contribution by the protein is large compared to the contribution by the buffer ions at low ionic strength.

Since this electrophoretic anomaly cannot be eliminated even by performing the electrophoresis experiment at the *average* isoelectric point of a heterogeneous protein such as human  $\gamma_2$ -globulin, it was thought that electrophoresis far enough away from the isoelectric point so that the protein peak could be completely separated from the  $\delta$ - and  $\epsilon$ -boundaries might yield further information on the mobility distribution. On the acid side of the isoelectric point the conductivity and pH effects add to each other, causing spreading on the descending side and sharpening on the ascending side. This makes it possible to obtain good resolution on the descending side, and an experiment at pH 5.5, 14.7 volts cm.<sup>-1</sup> indicated a mobility range of approximately  $2-8 \times 10^{-5}$  cm.<sup>2</sup> volt<sup>-1</sup> sec.<sup>-1</sup> at 0.01 ionic strength for human  $\gamma_2$ -globulin.

HUMAN  $\gamma_1$ -GLOBULIN<sup>13</sup>

At 0.10 ionic strength reversible electrophoretic spreading was observed, which yielded a heterogeneity constant of  $0.26 \times 10^{-5}$ . This protein contains a large amount of euglobulin, which is not soluble at lower ionic strengths. At 0.01 ionic strength, where only about one-third of the material was soluble, the heterogeneity constant was  $0.9 \times 10^{-5}$ . This would indicate that the pseudoglobulin component was considerably more heterogeneous and may have been responsible for much of the reversible spreading observed in the experiment at 0.10 ionic strength.

RIBONUCLEASE<sup>14</sup>

It has been previously noted that this crystalline enzyme exhibits some reversible spreading in electrophoresis (2, 19) at 0.055 ionic strength. The schlieren photographs become skewed at the isoelectric point and then become symmetrical again upon reversal of the current during electrophoresis. However, the apparent diffusion constants calculated by equation 2 are nearly independent of time of electrophoresis and equal to the diffusion constant, indicating that ribonuclease is essentially homogeneous. An experiment at 0.01 ionic strength, where higher electric field strengths may be used, also showed reversible skewing of the boundary, so that a heterogeneity constant could not be calculated. The isoelectric point shifted to pH 9.45 at this ionic strength, compared to pH 7.8 at 0.055 ionic strength (19). The former value is about the same as that found for the isoelectric point in 0.03 ionic strength borate buffer (19).

GELATIN<sup>15</sup>

Electrophoresis at pH 4.75 and 0.01 ionic strength was performed on a sample of degraded gelatin (20) having a number-average molecular weight of 17,000 (from osmotic pressure). Studies on this material have shown the presence of a wide range of molecular weights (20). The corresponding range in diffusion constants of the components introduces some error (less than 5 per cent for this determination) in using equation 1, which is derived assuming the same diffusion characteristics for all components. The protein was slightly below its isoelectric point but gave a symmetrical ascending boundary yielding a heterogeneity constant of  $0.5 \times 10^{-5}$ . The descending boundary partially resolved into two components. The major component, comprising 88 per cent of the whole, had a mobility of  $+0.24 \times 10^{-5}$ ; the minor component had a mobility of  $+1.86 \times 10^{-5}$  and merged with the major component upon reversal of the current for an equal period of time. Since the native collagen molecule had been split into many fragments in the autoclaving process, it is surprising that the protein is not even more heterogeneous. By this test of electrochemical nature the gelatin compares favorably with the purified protein fractions similarly tested (2).

<sup>13</sup> The sample of this protein contained approximately 5 per cent of  $\gamma_2$ - and  $\beta$ -globulins, as judged by electrophoresis at pH 8.6 in  $r/2 = 0.088$  diethylbarbiturate-citrate buffer.

<sup>14</sup> The authors are indebted to Dr. M. Kunitz for the crystalline sample of this protein.

<sup>15</sup> This sample of partially hydrolyzed gelatin was obtained through the courtesy of Dr. J. D. Ferry.

PROTEINS WHICH CANNOT BE STUDIED BY ELECTROPHORESIS AT THEIR  
ISOELECTRIC POINTS

Urease<sup>16</sup> is quite insoluble in 0.01 ionic strength buffer at pH 5.0, its isoelectric point (21). At pH 7.4, however, it was soluble and the electrophoretic behavior was studied in 0.01 ionic strength buffer. The ascending boundary moved as a sharp peak with a mobility of  $-10.2 \times 10^{-5}$  (calculated on the basis of the buffer conductivity). No steady state for the ascending peak was reached in 100 min. However, this could have been due to the fact that the equilibrium between electrical sharpening and diffusion is very slow, since urease has a low diffusion constant. The system did show reversible spreading in both the ascending and the descending limbs of the U-tube. This result could obtain only if the material were heterogeneous. The conductivity effect (18) would tend to give a low heterogeneity constant from the ascending boundary and a high constant from the descending boundary. The true value would probably lie between the two extreme results obtained. The heterogeneity constants calculated from the two boundaries were 0.32 and  $0.53 \times 10^{-5}$ , respectively. At the present time the conductivity and pH effects (16) are not well enough understood quantitatively, and therefore spreading at pH levels away from the isoelectric point (where these effects are minimized) cannot be used to obtain a quantitative measurement of the electrophoretic heterogeneity. Here again, the unusual instability of the protein makes the results subject to qualification. Special effort was made (stirring and large membrane area) to obtain efficient dialysis in order to shorten the time the protein was in the dissolved state.

Pepsin and trypsin undergo autodigestion at their isoelectric points and so cannot be tested for reversible electrophoretic spreading. It was thought, however, that a qualitative test of their homogeneity could be made by observing whether or not steady-state ascending boundaries were obtained in electrophoresis at the pH of their maximum stability.

The behavior of trypsin<sup>17</sup> was observed at pH 5.08 and ionic strength 0.01. The area of the ascending gradient peak became progressively smaller, and after 6.5 hr. another component comprising about 7 per cent of the total area was resolved. The mobility<sup>18</sup> of the minor component was  $+10.6 \times 10^{-5}$ , compared to  $11.3 \times 10^{-5}$  for the major component.

Preliminary experiments indicated that crystalline pepsin might be pure enough to give a steady-state moving boundary. A long experiment at pH 5.0, using a mechanically driven syringe to hold the boundary stationary in the cell, showed resolution of a minor component after about 10 hr., during which time the boundary moved with a mobility of  $13.9 \times 10^{-5}$  through about 54 cm. of buffer. The total area of the schlieren diagram decreased continuously and after 20 hr. only 72 per cent of the original moving gradient remained. This indicates that small amounts of components with widely separated mobilities were leaving the boundary continuously, giving no measurable peak height on the base line. The major

<sup>16</sup> The authors are indebted to Dr. J. B. Sumner for this crystalline enzyme.

<sup>17</sup> Crystalline pepsin and trypsin were obtained from Armour Laboratories, Chicago, Illinois.

<sup>18</sup> Calculated on the basis of the buffer conductivity.

peak moved with a mobility of about  $-13.9 \times 10^{-5}$  and the minor peak moved  $0.23 \times 10^{-5}$  mobility units more slowly.

The steady-state boundary test, while not quantitative, may be useful in many cases where solubility or instability at the isoelectric point would make reversible spreading results questionable. Also, no dialysis is necessary provided the protein is salt free. Continued decrease in height of an ascending peak with constant area would not show conclusively that the material was heterogeneous, since the boundary may be approaching a steady state very slowly. However, if a boundary is allowed to diffuse enough so that sharpening is evident after the current is applied, and then the peak again broadens and becomes shorter with further electrophoresis, the protein must be heterogeneous. The progressive decrease in area of the gradient peak noted with pepsin and trypsin experiments is another qualitative mark of heterogeneity. Considerably more work, both theoretical and experimental, is needed for further evaluation of steady-state boundaries used for this purpose. However, the method may give a provisional answer where no other procedure is applicable.

#### DISCUSSION

None of the samples of purified proteins which have been tested satisfy the electrophoretic criteria for homogeneity. It is possible that these proteins may have been damaged somewhat by the drying process since all, except urease, were in the dry form. If this is true, refractionation or recrystallization should yield proteins of lower heterogeneity constant.

Several limitations of the reversible spreading test for electrophoretic homogeneity have been pointed out. This test is limited to proteins which have a solubility of at least 0.3 g. per 100 cc. at their isoelectric points in buffers of 0.01–0.10 ionic strength. Use of buffers of very low ionic strength increases the sensitivity of the test greatly, but the so-called electrophoretic anomalies become important. No quantitative calculation of the degree of heterogeneity may be made by the method given, as the electrical effects result in abnormally large salt boundaries and badly skewed schlieren patterns if any electrophoretic migration occurs. If a schlieren pattern deviates from true Gaussian form, the heterogeneity constant calculated by using equation 1 is only an approximate measure of the degree of homogeneity. More complete knowledge of the laws governing electrophoretic migration might make quantitative calculation possible even in these non-ideal experiments. A quantitative relation for the rate of spreading of a homogeneous protein in the descending electrophoretic pattern cannot be readily obtained because of mathematical difficulties, although the basic theory is available (14, 17).

The more generally applicable steady-state boundary method seems to warrant further development. Quantitative interpretation of these boundaries in terms of degree of heterogeneity may prove too laborious mathematically to make this phase of application worthwhile. As a qualitative test of purity, the method is simple and easily interpreted. Either the protein can be made to move as a steady-state boundary or it cannot be made to do so. Assuming constant cur-

rent during an experiment the following qualitative conclusions can be drawn: (1) If a steady-state boundary is established the material is electrophoretically homogeneous within certain mobility limits.<sup>19</sup> (2) If the ascending boundary spreads continuously under all conditions, it must be heterogeneous. (3) If after resolution from the salt boundary, the moving protein boundary first sharpens, then after reaching a maximum becomes more diffuse again, the protein is heterogeneous. (The main conalbumin peak showed this behavior.) (4) If the boundary does not resolve but the total refractive-index difference (schlieren peak area) diminishes continuously, as shown by the behavior of trypsin, the protein must be heterogeneous. The case of diminution of area suggests the possibility of formulating a semiquantitative description of heterogeneity in terms of the fraction of the gradient pattern area disappearing after passing a definite amount of current under specified conditions of ionic strength, field strength, and protein mobility. Further work will be required to determine the optimum conditions of electrophoresis to obtain maximum sensitivity and to obtain a steady-state boundary in the minimum time.

#### SUMMARY

Fourteen purified proteins, including seven crystalline proteins, have been tested for electrophoretic homogeneity by the reversible spreading or by the steady-state moving-boundary methods. None of the preparations used satisfy the above criteria, and the heterogeneity constants range from  $0.12 \times 10^{-5}$  to  $1.3 \times 10^{-5} \text{ cm.}^2 \text{ sec.}^{-1} \text{ volt.}^{-1}$ . Isoelectric points for a number of the proteins have been determined. The isoelectric points of chymotrypsin and chymotrypsinogen determined by the moving-boundary method are 2.6 to 4.5 pH units higher than those reported by using the microscopic electrophoresis method.

#### REFERENCES

- (1) ALBERTY, R. A.: *J. Am. Chem. Soc.* **70**, 1675 (1948).
- (2) ALBERTY, R. A., ANDERSON, E. A., AND WILLIAMS, J. W.: *J. Phys. Colloid Chem.* **52**, 217 (1948).
- (3) ALDERTON, G., WARD, W. H., AND FEVOLD, H. L.: *J. Biol. Chem.* **157**, 43 (1945).
- (4) BAIN, J. A., AND DEUTSCH, H. F.: *J. Biol. Chem.* **172**, 547 (1948).
- (5) BURNS, J. W., AND HENKE, L. K.: *Rev. Sci. Instruments* **12**, 401 (1941).
- (6) DEUTSCH, H. F., GOSTING, L. J., ALBERTY, R. A., AND WILLIAMS, J. W.: *J. Biol. Chem.* **164**, 109 (1946).
- (7) DOLE, V. P.: *J. Am. Chem. Soc.* **67**, 1119 (1945).
- (8) FERRY, J. D., AND ELDRIDGE, J. E.: Paper presented at the Symposium of the American Physical Society, Chicago, Illinois, December, 1947.
- (9) KEGELES, G., AND GOSTING, L. J.: *J. Am. Chem. Soc.* **69**, 2519 (1947).
- (10) KEKWICK, R. A., AND PEDERSEN, K. O.: *Biochem. J.* **30**, 2201 (1936).
- (11) KUNITZ, M.: *J. Gen. Physiol.* **22**, 207 (1938).
- (12) KUNITZ, M.: *J. Gen. Physiol.* **24**, 15 (1940).
- (13) KUNITZ, M., AND NORTHROP, J. H.: *J. Gen. Physiol.* **18**, 455 (1935).

<sup>19</sup> The exact limits have not been mathematically defined; however, obviously in the limiting case no ion in the higher electrical field with a lower velocity than the boundary, and no ion in the lower electrical field with a higher velocity than the boundary can move along with that boundary.

- (14) LONGSWORTH, L. G.: J. Am. Chem. Soc. **66**, 449 (1944).
- (15) LONGSWORTH, L. G.: J. Am. Chem. Soc. **67**, 1109 (1945).
- (16) LONGSWORTH, L. G.: J. Phys. Colloid Chem. **51**, 171 (1947).
- (17) LONGSWORTH, L. G., AND MACINNES, D. A.: Chem. Revs. **11**, 171 (1932).
- (18) LONGSWORTH, L. G., AND MACINNES, D. A.: J. Am. Chem. Soc. **62**, 705 (1940).
- (19) ROTHEN, A.: J. Gen. Physiol. **24**, 203 (1940-41).
- (20) SCATCHARD, G., ONCLEY, J. L., WILLIAMS, J. W., AND BROWN, A.: J. Am. Chem. Soc. **66**, 1980 (1944).
- (21) SUMNER, J. B., AND HAND, D. B.: J. Am. Chem. Soc. **51**, 1255 (1929).
- (22) SVEDBERG, T., AND PEDERSEN, K. O.: *The Ultracentrifuge*. University Press, Oxford (1940).
- (23) SVENSSON, H.: Arkiv. Kemi Mineral. Geol. **22A**, No. 10 (1946).
- (24) THEORELL, H.: Biochem. J. **220**, 293 (1937).

## A CONTRIBUTION TO THE KNOWLEDGE OF SODIUM CONTAMINATION ON CRACKING CATALYSTS

MAURICE O. BAKER, S. D. CHESNUTT, AND THOMAS P. WIER, JR.

*Research Laboratories, Houston Refinery, Shell Oil Company, Incorporated, Houston, Texas*

*Received April 9, 1948*

### INTRODUCTION

Small amounts of sodium present in commercial silica-alumina catalysts used for the cracking of petroleum hydrocarbons have been considered to have an adverse effect on the cracking activity of the catalyst. In attempting to obtain a quantitative relationship for this effect, it has been customary to determine the total sodium content of the catalyst irrespective of whether the sodium might be distributed over the internal surface of the catalyst pores or buried in the solid phase. Since catalyst activity is a surface phenomenon, it seems reasonable that only that portion of the sodium which is on the surface should appreciably affect the activity.

Surface concentrations of sodium have been measured for several silica-alumina catalyst samples in order to determine what proportion of the total sodium content was on the surface and to learn the changes which may take place in the surface concentration during use of the catalyst for the cracking of hydrocarbons. Further, since carbon is deposited on the catalyst during the cracking process, thereby possibly covering some of the sodium, a brief study of surface sodium with respect to carbon deposition has been made. No attempt is made within this paper to examine the relationship between catalytic activity and the presence of sodium in the catalyst.

### EXPERIMENTAL

Experimentally, the study was quite simple. The amounts of carbon and extractable sodium were determined on samples of spent catalyst, regenerated

catalyst, and catalyst from which all of the carbon had been removed by careful combustion. Surface areas and total sodium contents were also measured, giving the following pattern:

Spent catalyst

- (a) Per cent extractable sodium
- (b) Per cent carbon

Partially regenerated catalyst (from unit)

- (a) Per cent extractable sodium
- (b) Per cent carbon
- (c) Surface area

Completely regenerated catalyst (from laboratory furnace)

- (a) Per cent extractable sodium
- (b) Per cent total sodium

This was repeated for samples taken at intervals during deactivation by use in a fluid-bed type pilot plant. The samples and analytical methods are more fully described below. No data on run conditions have been included, since no attempt to relate these to catalyst changes is made herein. It is sufficient to say that the catalysts were subjected to operating conditions in ranges ordinarily encountered in commercial application.

#### CATALYST SAMPLES

Two forms of silica-alumina (3-A) cracking catalysts for fluid-bed operation were studied. One of these was the commercial ground product of American Cyanamid and Chemical Corporation (referred to hereafter as "low sodium" catalyst), in which the only sodium present was that remaining after washing of the hydrogel with distilled water. The other was from an experimental batch of microspheroidal catalyst prepared by spray drying of a hydrogel furnished by the same company, which is of interest in this study not because of its microspheroidal character but because in this particular batch the greater part of the sodium present was introduced by the use of tap water in reslurrying the hydrogel for spray drying. This material is referred to hereafter as "high sodium" catalyst. Samples of each were taken before use and from both the reactor and the regenerator at intervals during fluid-bed pilot plant runs made to study rates of activity decline. An important point which must be emphasized is the fact that no fresh catalyst was added during the runs; thus catalyst samples are relatively homogeneous, rather than mixtures of new and old catalyst.

#### ANALYTICAL METHODS

The amount of sodium which could be extracted from the catalyst by strong acid in the presence of the existing carbon was quantitatively determined. This was accomplished, without removing the carbon, by shaking 5 g. of catalyst with 50 ml. of concentrated hydrochloric acid for 1 hr., centrifuging, removing exactly 25 ml. of solution for sodium analysis, adding 25 ml. of fresh acid, and repeating the extraction process. Even low concentrations of hydrogen ions are known to have a strong displacing effect for surface cations on silica gel (3), zeolites (1),

clays (2), and similar materials. Thus this extraction technique allowed the calculation of a value closely approximating the desired quantity, and in the case of the carbon-free samples the leachable sodium is considered to be equal to the entire amount of sodium on the surface of the catalyst. The probable leaching of a portion of the surface alumina has been assumed not to affect the results. The total sodium which the catalyst contained both on the surface and in the mass was determined by dissolving the catalyst sample in hydrofluoric acid and sulfuric acid.

Sodium in the extracts and solutions was determined gravimetrically as sodium uranyl zinc acetate hexahydrate, using blank determinations with careful duplication of technique to eliminate errors involved in determining the small quantities of sodium encountered. For catalysts containing of the order of 0.01 per cent by weight of sodium oxide, analyses were reproducible to  $\pm 4$  per cent of the mean, while for catalysts containing of the order of 0.1 per cent by weight of sodium oxide, the values were reproducible to  $\pm 1$  per cent of the mean. In order to give a standard basis for interpretation of the sodium contents, all sample weights have been corrected to the basis of no carbon and only that moisture retained on heating at 600°C. for 1 hr. The use of the term "per cent by weight of sodium oxide" to express the sodium concentration is merely to conform to practice and should not be construed as indicating the form in which the sodium is actually present.

Surface areas were determined by low-temperature nitrogen adsorption, the regenerated catalyst being used for reasons not pertinent to this study. The effect of carbon on surface area measurements (other than the effect on the weight of sample) has not been taken into account, since this is usually quite small.

High-temperature combustion analyses accurate to  $\pm 0.01$  per cent by weight on an absolute basis were used to determine the carbon contents of spent and regenerated catalyst. In producing the completely regenerated catalyst, the carbon was carefully and completely burned off in dry air at 600°C. This technique was known (4) not to affect the gel structure or extractability of sodium from silica gel, so that it is reasonable to assume no deleterious effect in this case.

#### RESULTS AND DISCUSSION

The results of the determinations described in the previous section are arranged in tables 1 and 2, the samples being listed in the order of increasing extent of pilot-plant use. Upon examining these tables it is seen immediately that the total sodium content of the "high sodium" catalyst is approximately six times that of the "low sodium" catalyst, so that the use of tap water in reslurrying the hydrogel introduces an appreciable amount of sodium into the catalyst. The percentage of the total sodium in each case which is on the catalyst surface is approximately 90 per cent for the "high sodium" catalyst and 65 per cent for the "low sodium" catalyst. These figures are based on the percentage of the total sodium which is extractable from the fresh sample. Thus, in both cases, the greater part of the sodium is located on the available interior surface rather than buried within the solid phase of the catalyst.



The use of these catalysts over an extended period in the pilot plant did not result in any appreciable change in the total sodium content; notably, there was no increase from sodium which is sometimes present in hydrocarbon feed stocks. During this period of use, however, there was a definite decline in both the surface area and the proportion of the sodium which is on the surface. Comparing the decline of these quantities graphically, using the original values as 100 per cent as is done in figures 1 and 2, it is seen that for both catalysts the surface area decreases somewhat more rapidly than does the amount of sodium on the surface.

TABLE 1  
*Tabulation of results\* for "low sodium" catalyst*

SAMPLE DESIGNATION	TOTAL Na <sub>2</sub> O	EXTRACTABLE Na <sub>2</sub> O	SURFACE AREA	CARBON
	<i>per cent by weight</i>	<i>per cent by weight</i>	<i>m.<sup>2</sup>/gram</i>	<i>per cent by weight</i>
Fresh. . . . .	0.026	0.0169	554	0
A—Spent . . . . .		0.0140		1.82
A—Regenerated . . . . .		0.0137	435	1.08
A—Carbon-free . . . . .		0.0159		0
B—Spent . . . . .		0.0114		1.00
B—Regenerated . . . . .		0.0145	400	0.25
B—Carbon-free . . . . .		0.0154		0
C—Spent . . . . .		0.0074		0.85
C—Regenerated . . . . .		0.0109	365	0.24
C—Carbon-free . . . . .		0.0131		0
D—Spent . . . . .		0.0080		0.83
D—Regenerated . . . . .		0.0115	341	0.33
D—Carbon-free . . . . .		0.0138		0
E—Spent . . . . .		0.0105		0.58
E—Regenerated . . . . .		0.0118	327	0.26
E—Carbon-free . . . . .		0.0132		0

\* In calculating each of these results, sample weights were corrected for volatile matter, using the loss in weight on heating in air at 600°C. for 1 hr., to give a standard basis for comparison.

This leads to a slight increase in the concentration of sodium per square meter of surface area as the catalyst is used, a factor which must be taken into account if there is to be any quantitative study of sodium as a contaminant in cracking reactions. Other surface chemical changes, such as a change in the surface alumina concentration, etc., may also take place.

The extent to which the presence of a carbon deposit interferes with the extraction of surface sodium may be learned by examining the data presented in figures 3 and 4 for the extractable sodium on samples of spent, regenerated, and carbon-free catalyst. The effect is most pronounced for the "low sodium" samples, for

TABLE 2<sup>a</sup>  
*Tabulation of results\* for "high sodium" catalyst*

SAMPLE DESIGNATION	TOTAL Na <sub>2</sub> O	EXTRACTABLE Na <sub>2</sub> O	SURFACE AREA	CARBON
	<i>per cent by weight</i>	<i>per cent by weight</i>	<i>m.<sup>2</sup>/gram</i>	<i>per cent by weight</i>
Fresh.....	0.145	0.1291	657	0
A—Spent.....		0.1029		1.48
A—Regenerated.....		0.1068	383	0.59
A—Carbon-free.....		0.1146		0
B—Spent.....		0.0889		1.35
B—Regenerated.....		0.0896	364	0.46
B—Carbon-free.....		0.1123		0
C—Spent.....		0.0984		1.99
C—Regenerated.....		0.1001	349	1.03
C—Carbon-free.....		0.1132		0
D—Spent.....		0.0944		0.93
D—Regenerated.....		0.0971	334	0.35
D—Carbon-free.....		0.1108		0
E—Spent.....		0.0856		1.09
E—Regenerated.....		0.0942	323	0.42
E—Carbon-free.....		0.1078		0
F—Spent.....		0.0912		1.70
F—Regenerated.....		0.0967	278	0.96
F—Carbon-free.....	0.147	0.1059		0

\* In calculating each of these results, sample weights were corrected for volatile matter, using the loss in weight on heating in air at 600°C. for 1 hr., to give a standard basis for comparison.

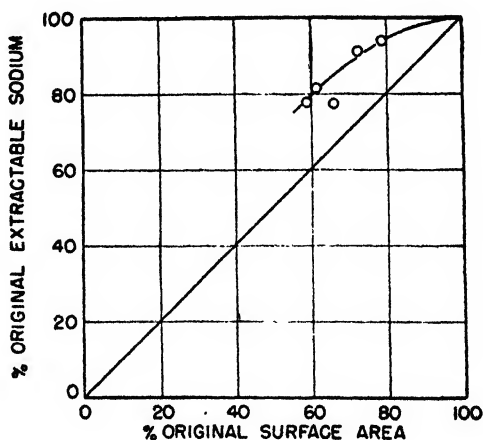


FIG. 1. "Low sodium" catalyst

which linear relationships were observed. It is interesting to calculate the percentage of the surface which is covered by a given amount of carbon (assuming

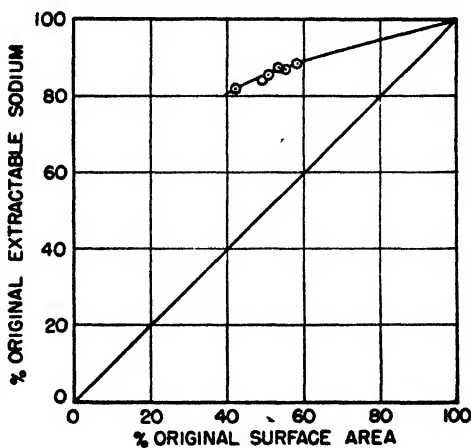


FIG. 2. "High sodium" catalyst

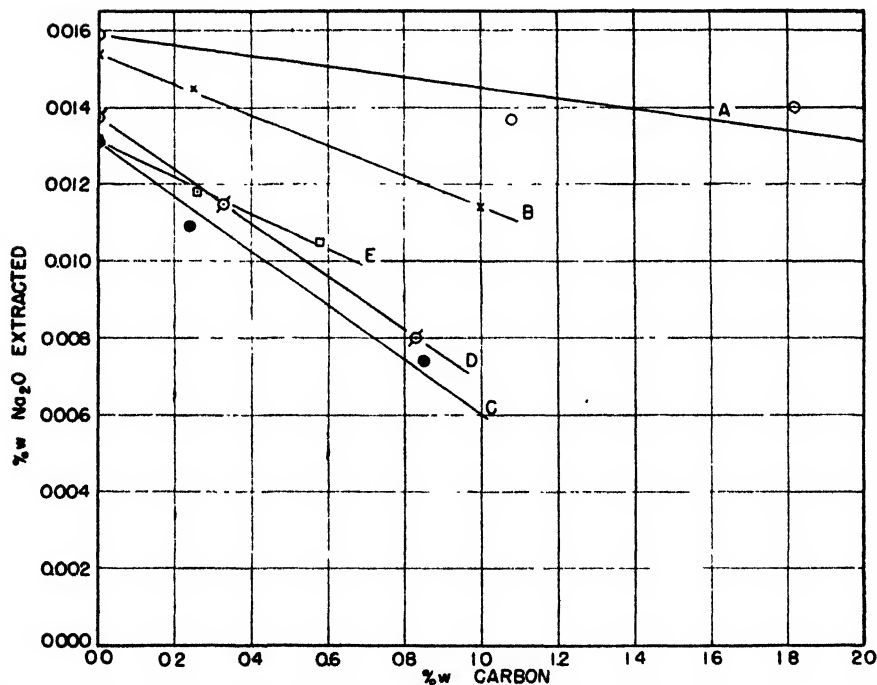


FIG. 3. Decrease in extractability of sodium by carbon deposition: "low sodium" catalyst.

a close-packed monolayer of carbon atoms) and compare this figure with the percentage of surface sodium which is rendered non-extractable by the same

amount of carbon. The following equation is used to calculate the surface covering power of the carbon:

Per cent of surface covered by assumed carbon-atom monolayer

$$= 4(0.866) \left[ \frac{M}{4\sqrt{2}Nd} \right]^{2/3} \frac{N}{M} \times 10^{-4} \times \frac{C_c}{S_c}$$

where  $M$  is the molecular weight (12.01 for carbon),  $N$  is Avogadro's number,  $C_c$  is the concentration of carbon in grams of carbon per 100 g. of catalyst,  $S_c$  is the specific surface area in square meters per gram of catalyst, and  $d$  is the density

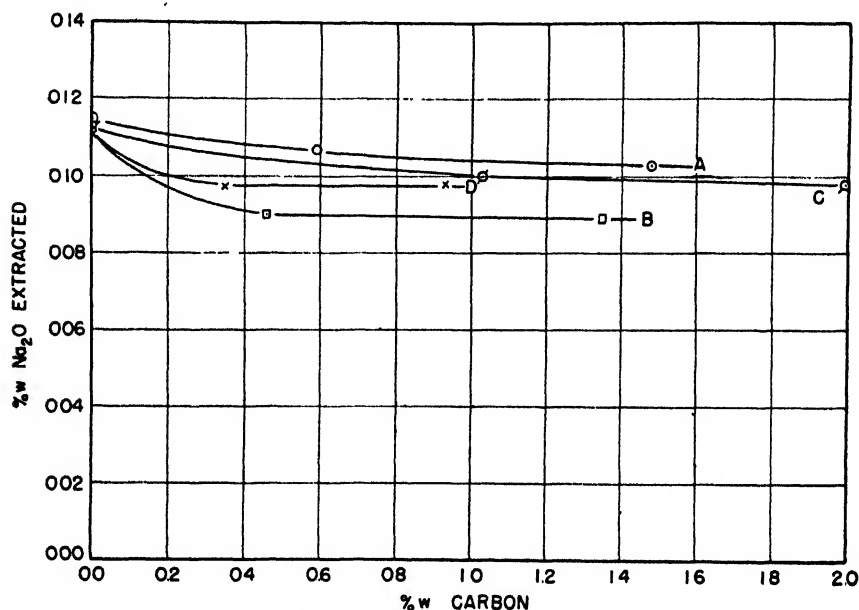


FIG. 4. Decrease in extractability of sodium by carbon deposition: "high sodium" catalyst.

(2.25 g./ml. for graphite). Insertion of the proper values in this equation reduces it to the form:

$$\text{Per cent of surface covered} = 2.35 \times 10^3 \frac{C_c}{S_c}$$

The given percentage of carbon at which the comparison is made is taken here to be 1.00 per cent, the results of the calculation being given in table 3.

There appears to be sufficient difference in the behavior of the "low sodium" and "high sodium" catalysts with respect to carbon deposition to warrant their separate discussion. For the "low sodium" catalyst, the deposition of 1 per cent by weight of carbon renders a much larger percentage of the sodium non-extractable than could be accounted for by simple uniform covering of the catalyst surface with a monolayer. Assuming that the sodium atoms are rather uniformly

distributed over the catalyst surface, the above behavior suggests that either (1) carbon has been selectively deposited on sodium sites, or (2) carbon is able to block off much more surface (and the sodium present on that surface) than if it were in the form of a monolayer of close-packed carbon atoms. This may be done by (a) closing of pore mouths with a small deposit or (b) non-penetration by the aqueous solution due to non-wetting of the surface, though there is not an actual sealing off of the pore or even complete covering of the surface by carbon.

Assuming the sodium to be distributed non-uniformly leads to a third possible explanation: namely, (3) surface sodium may be concentrated on the surface of the smaller (or larger) pores of the catalyst and during the cracking reaction carbon may be selectively deposited in these pores merely because of their size.

The selective deposition of carbon on sodium sites would involve a rather large

TABLE 3

*Comparison of the surface area covered by carbon monolayer and the sodium rendered non-extractable by the same amount of carbon*

CATALYST	AT 1.00 PER CENT BY WEIGHT CARBON	
	Surface covered by monolayer	Sodium on surface rendered non- extractable
	per cent	per cent
<i>"Low sodium" catalyst:</i>		
Sample A . . . . .	5.4	8.8
Sample B. . . . .	5.9	26.0
Sample C.. . . .	6.4	54.2
Sample D. . . . .	6.9	50.8
Sample E. . . . .	7.2	35.6
<i>"High sodium" catalyst:</i>		
Sample A . . . . .	6.1	12.2
Sample B . . . . .	6.5	20.6
Sample C. . . . .	6.7	11.7
Sample D . . . . .	7.0	12.6
Sample E. . . . .	7.3	20.4
Sample F. . . . .	8.5	8.5

number of carbon atoms being deposited in the vicinity of each sodium atom. Considering the data for sample B, which exhibits an intermediate slope in figure 3, it would be necessary to assume approximately 640 carbon atoms deposited in the vicinity of each sodium atom. There is probably sufficient space between sodium atoms for this to occur (there being an average of only one sodium atom for each 10,000 Å.<sup>2</sup> of surface). In this case sodium must exert its influence directly on the deposition of carbon at the great distances involved for most of the carbon atoms. However, it is still possible that sodium atoms may merely initiate carbon deposition, these carbon atoms in turn causing further deposition.

Considering the second explanation, the closing of pore entrances by a small deposit of carbon does not seem reasonable, in view of the extremely pronounced

effect which 1 per cent of carbon would thus be expected to produce in the cracking reaction, an effect of the necessary magnitude never being observed. Furthermore, non-wetting is not a satisfactory explanation, because the extractability of the sodium on the "high sodium" catalyst was not greatly decreased by carbon contents as high as 2.0 per cent by weight.

A positive evaluation of the explanations given above cannot be made at the present time. Because the covering of sodium by carbon may be very extensive in some practical cases, any study of the effect of sodium on cracking activity must take into account the amount of carbon deposit present during reaction.

Inspection of the data for the "high sodium" catalyst in figure 4 and table 3 leads to the conclusion that the sodium introduced by adding tap water to the hydrogel must have assumed a different position on the catalyst surface or a different mode of attachment to the surface so that carbon is not selectively deposited on the sodium to any marked degree. At low carbon concentrations there does appear to be selectivity, which might be explained by the postulation of two kinds of sodium: (1) that originally present in the hydrogel and (2) that introduced from the tap water.

#### SUMMARY

Sodium contaminant on commercial silica-alumina cracking catalyst is considered to be effective only when present on the surface, the surface sodium concentration being measured by extraction with strong acid. An increase in the concentration of sodium per square meter of surface is shown to occur, without any increase in total sodium, as the structure changes to one of lower area during use. The effect of carbon deposition on the extractability of the surface sodium is determined and interpreted in terms of the surface distribution and mode of attachment of the sodium to the surface. Both of these effects must be taken into account in any quantitative study of sodium as a contaminant.

#### REFERENCES

- (1) AUSTERWEIL, G.: *J. Soc. Chem. Ind.* **53**, 185-9T (1934).
- (2) JENNY, HANS: *J. Phys. Chem.* **36**, 217-58 (1932); WILLIAMS, RICE: *J. Agr. Sci.* **22**, 838-44 (1932); and others.
- (3) TAMELE, M. W. (Shell Development Company): Unpublished data.
- (4) TAMELE, M. W., AND WIER, T. P., JR. (Shell Development Company): Unpublished data.

## COLLOID PROPERTIES OF SOME WESTERN CLAYS

E. R. HARRINGTON

*223 North Cedar Street, Albuquerque, New Mexico**Received April 27, 1948*

As a substance containing colloidal matter, clay has been studied for more than fifty years. At first the studies followed the Thomas Graham supposition that colloidal particles must, necessarily, be of an amorphous nature. Up until the last twenty years this was generally thought to be correct, and experimenters sought to explain all properties of clay on the basis of variations in chemical composition and states of aggregation.

Early in the 1920's, however, it was shown that the clay particle was crystalline (6, 27). Since that time the crystalline nature of the clay minerals has been demonstrated by many investigators (3, 5, 7, 8, 9, 12, 13, 14, 19, 20, 21). The x-ray studies were followed by those made with the electron microscope (1, 7, 8, 17, 21, 22) and the shapes of the clay minerals were also ascertained. Differential thermal analysis techniques (23, 28) produced distinctive curves for individual clay minerals and the use of the supercentrifuge (10, 11) provided better samplings of material for study.

The study presented in this paper began with twelve California clays tested for dye adsorption in an effort to check colloid content. It was found that results obtained by the dye-adsorption method did not check the colloid content as determined by other means. Experimentation was continued in an effort to ascertain what correlation did exist between colloid content and the various properties attributed to its presence. The literature of the time abounded in claims that the colloid content of clays could be measured by the adsorption of dyes, water, or ammonia; also by studies of base exchange, shrinkage, heat of wetting, plasticity, Brownian movement, and by use of the hydrometer. Generally the conclusions had been reached after studies on similar clays and after relatively few tests. This investigation was made over a period of some ten years, using several different types of clay and a number of tests.

## SELECTION AND PREPARATION OF SAMPLES

Three California pottery and stoneware clays and twelve New Mexico clays of various types were used. The samples included kaolins, pottery clay, ball clay, and adobe of several types. Clays were soaked in water and pugged by hand. The thin slips obtained were poured through a 100-mesh sieve to remove larger fragments. The slips were settled out with small additions of hydrochloric acid. The settled clays were dried and ground for use. Since these fifteen samples will be referred to a number of times in the following pages they will be described briefly. An identification letter will also be given each sample.

(A) *San Ildefonso*: Chocolate-colored adobe from the Indian village of San Ildefonso 30 miles north of Santa Fe, New Mexico; clay much used in native pottery making; contains considerable calcium carbonate.

(B) *Kinney brick*: Gray-brown adobe from flood plain of the Rio Grande a few miles south of Albuquerque, New Mexico; contains considerable sand and calcium carbonate.

(C) *Tonque red adobe*: Rapidly settling red adobe formed from upland disintegration rather than stream deposition; location 35 miles north of Albuquerque; sample contains some calcium carbonate.

(D) *Tonque green shale*: Shale of Cretaceous age found near sample C; considerable sand and some selenite crystals.

(E) *Carthage-1*: Dark blue clay taken from above coal beds at the mining camp of Carthage 20 miles southeast of Socorro, New Mexico; dense, fine, plastic ball clay; no calcium carbonate.

(F) *Las Vegas brick*: Gray-green brittle shale 2 miles south of Las Vegas, New Mexico; some sand and calcium carbonate; used for making fine, dark red face brick.

(G) *Gallup fire clay*: Dark gray clay found adjacent to coal beds near Gallup, New Mexico; no calcium carbonate; the State's most important source of fire brick.

(H) *Organ Mountain Kaolin*: From the Torpedo mine 15 miles east of Las Cruces, New Mexico; derived from acid sulfate action on feldspar and sericite; white kaolin is stained in places by specks of stubelite, a copper-manganese silicate.

(I) *Carthage-2*: A variegated purple clay from a thick stratum above the coal beds at Carthage, New Mexico; a plastic, sticky, fine-grained ball clay; no calcium carbonate.

(J) *San Antonio tile*: Bright red, sticky clay used in making roofing tile 10 miles south of Socorro, New Mexico; a valley adobe, but very fine and plastic for such a clay; contains about 8 per cent calcium carbonate.

(K) *Santa Clara pottery*: Near Indian village of Santa Clara, 8 miles east of Los Alamos, New Mexico; dense brown ball clay, sticky and plastic; no calcium carbonate; State's most famous Indian pottery made of this clay.

(L) *Alberhill*: Very fine gray stoneware clay from near Riverside, California; no calcium carbonate.

(M) *Cala or Lincoln*: From near Lake Tahoe, California; light cream colored with pronounced soapy feeling; plastic and sticky; made into high-grade refractory stoneware.

(N) *S. H. 4*: Sample from near Riverside, California, where it is associated with a bed of lignite coal; dense, fine-grained blue clay streaked with organic matter; classed as a ball clay.

(O) *La Bajada*: Bright red plastic clay found in pockets beneath beds of volcanic ash 20 miles southwest of Santa Fe; used for pottery by Santo Domingo Indians; no calcium carbonate.

#### EXPERIMENTAL

The fifteen clays were subjected to a number of tests which were most unproductive of correlation with their colloid content. Such determinations were:

(1) pH determination, (2) chemical analysis, (3) thixotropy, (4) Liesegang phe-



nomenon, (5) plasticity, (6) base exchange, (7) electrophoresis, (8) Brownian movement, (9) sedimentation, and (10) physical properties before and after firing. Since these tests showed only the most general qualitative correlations, they will be omitted from consideration here. The tests included in this paper will be: (11) colloid content determination by extraction of total solids, (12) adsorption of dyes, water, and ammonia, and (13) heat of wetting.

#### *Colloid content by extraction of solids*

As a check on colloid content it is desirable to have a standard in which all the colloid matter is extracted and weighed. In indirect methods the experimenter is always faced with the possibility that he may have overlooked some of the colloid material. Even if he employs a method in which all the material is extracted and weighed he may still be in doubt, as some of the material left by the extraction may contain material showing colloid properties by virtue of its cellular lattice structure if not by its particle size. Even so, some start must be made for a standard and an arbitrary method had to be used.

Some twenty years ago Hilgard (15) arbitrarily classified as colloidal those particles which failed to settle out from an 8-in. water column in 24 hr. In somewhat modified form this classification has been used in more recent times (1, 3, 20). To secure possible standards for comparison four separate types of determinations were made as follows: (1) Determination of matter in suspension 24 hr. by means of the pipet method; (2) material in suspension 3 hr. by the pipet method; (3) material in suspension after 24 hr. by the percolator method; and (4) a 15-day extraction of colloid material.

In the pipet methods the clay was churned with water containing a few drops of ammonium hydroxide as a dispersing agent (1, 20). The sols were allowed to settle for the desired times, a sample was withdrawn by pipet, and the colloid content was determined by evaporation and weighing. In the percolator method the sols were allowed to settle for 24 hr.; then the entire supernatant liquid was drawn off and evaporated to dryness, and the residue was weighed. In the 15-day extraction the supernatant liquids were decanted from the residues fifteen successive times after as many churnings and settlings. The 15-day residue was then dried and weighed and the colloid content was determined by the difference from the original weight of the sample.

Samples of clays were churned with weighed amounts of dye and centrifuged samples were determined colorimetrically. Tests were made on raw clay, on clay treated with sodium oxalate, and on the non-colloid residue left from the 15-day extractions. Clay samples were exposed to saturated water vapor for 7 days and the adsorption was determined by weighing. Similar samples were exposed to anhydrous ammonia vapor for 24 hr., and the adsorbed ammonia was then driven off by heat and determined by titration.

The heat of wetting was determined in a Dewar-flask calorimeter and calculated in calories per gram of clay used.

#### RESULTS AND THEIR INTERPRETATION

In table 1 there is a presentation of data showing the per cent of material remaining in suspension as determined by the pipet methods, the percolator ex-

traction, and the 15-day extraction methods. Owing to stratification in the sols the pipet extractions are not judged to be accurate determinations of the material remaining in suspension. The percolator method, while superior to the pipet method, is also open to errors owing to the fact that larger particles settle

TABLE 1  
*Data on extractions by the total solids method*

NAME OF CLAY	LETTER	1*	2	3	4
		<i>per cent</i>	<i>per cent</i>	<i>per cent</i>	<i>per cent</i>
San Ildefonso.....	A	0.9	6.4	2.0	0.5
Kinney brick.....	B	2.1	6.5	5.6	1.5
Tonque red adobe.....	C	3.9	8.2	7.0	2.2
Carthage-1.....	D	4.3	9.1	10.7	2.7
Tonque green shale.....	E	4.6	12.0	7.7	2.4
Las Vegas brick.....	F	4.8	13.3	13.4	2.2
Gallup fire clay.....	G	5.8	15.1	26.7	4.4
Organ Mountain kaolin..	H	7.0	17.3	15.3	6.1
Carthage-2.....	I	11.1	23.0	18.0	7.9
San Antonio tile.....	J	2.7	23.3	6.7	3.3
Santa Clara pottery.....	K	6.9	24.9	6.3	3.5
Alberhill.....	L	20.1	27.7	30.6	18.2
Cala.....	M	16.5	28.1	31.7	11.8
S.H. 4.....	N	14.2	29.5	30.0	13.1
La Bajada.....	O	7.9	35.5	35.8	7.7

- \* 1. Twenty-four-hour extraction by the percolator.
- 2. Fifteen-day extraction, to be taken as standard.
- 3. Three-hour suspension by pipet method.
- 4. Twenty-four-hour suspension by pipet method.

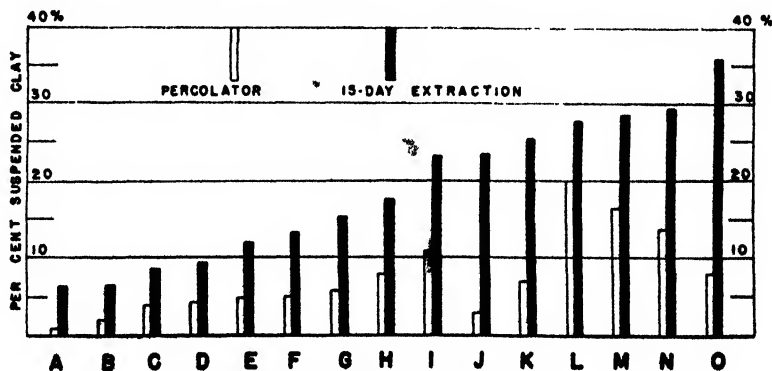


FIG. 1. Standards by extraction

out and carry down considerable adsorbed colloidal material. The 15-day extractions seem to be the most accurate as a real determination of colloidal material, in so far as this can be done by a sedimentation means. In the graphical representations which are to follow, this 15-day extraction is always presented as a

heavy black line on the graphs. It is considered the standard and all other findings are compared with it.

Figure 1 presents data on 15-day extractions, the standard, and the percolator method. Figure 2 shows the 24-hr. and the 3-hr. pipet extractions compared with the standards of figure 1. In all cases the clays are arranged in ascending order of colloid content, as determined by the standard 15-day extractions.

In figure 1 we note that the colloid matter extracted by the percolator method does not rise in the same ascending order as does the standard,—the 15-day extraction. Clay J in particular shows a big lag, while the highly colloidal clay O shows a lower percolator value than four other clays, all of lower colloid content. Actually these two clays offer the key to the situation. Most of the clays after 5 days of extraction furnished very little additional suspended material for a new extraction. In clays J and O, however, turbidity was not lost until after ten or more successive extractions. Evidently these two clays contain many

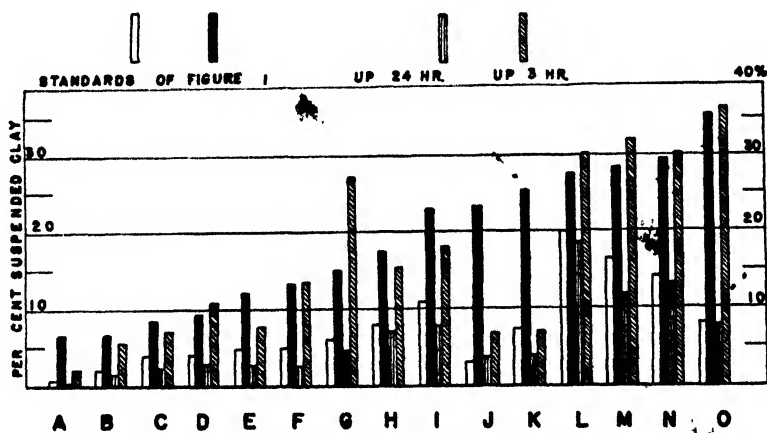


FIG. 2. Results of pipet method

mineral grains which can be readily broken up by water molecules. Also it is evident that these two clays did have considerable colloid material which was adsorbed to larger particles and taken to the bottom on the first few extractions.

In figure 2 we find cases where the conflicts are even more apparent. The 24-hr. pipet extraction—a method still in use in some laboratories—does not parallel the standard. Clay K, a highly colloidal and very plastic clay, joins O and J as extreme exceptions. The 3-hr. extraction started out to conform in a better way, but again J and K are excessive lows and clay G comes in with an excessively high value, clearly out of place on the graph.

The inference is of course clear. The pipet method does not show up as an accurate method of determining the colloid content of these clays. Stratification, currents caused by withdrawal of liquid, adsorption of colloid particles against particles too heavy for them to float, and the fact that certain clay minerals can be more easily broken up by water, all cause this method to produce large errors. If a carefully selected group of clays were used, the pipet method would probably

give results which were acceptable. For instance, if the J, K, L, and O samples were left out, the 24-hr. pipet extraction would be roughly in accord with our standard.

TABLE 2  
*Data on adsorption of dyes, water, and ammonia*

CLAY	1*	2	3	4	5	6
A.....	60	6.7	198	92	5.5	9.7
B.....	88	1.0	240	280	8.4	6.2
C.....	62	2.7	122	225	5.8	9.0
D.....	76	1.0	140	142	7.7	4.4
E.....	53	4.1	272	230	4.5	6.6
F.....	74	1.7	295	307	6.8	7.4
G.....	48	3.8	96	99	5.6	6.3
H.....	90	1.5	168	112	10.6	5.9
I.....	98	2.6	168	123	9.3	7.7
J.....	86	1.2	290	292	9.3	4.9
K.....	145	1.1	338	183	16.1	18.9
L.....	45	2.8	81	143	7.4	2.9
M.....	46	2.9	92	107	7.6	2.1
N.....	56	2.3	176	135	7.9	4.6
O.....	117	3.8	250	166	11.9	9.8

\* 1. Methylene blue in milligrams per gram of clay.

2. Colloid ratio for methylene blue.

3. Malachite green per gram of clay first treated with sodium oxalate to precipitate calcium.

4. Malachite green in milligrams per gram of raw clay.

5. Water vapor in per cent of weight of the clay sample.

6. Ammonia in milligrams per gram of clay.

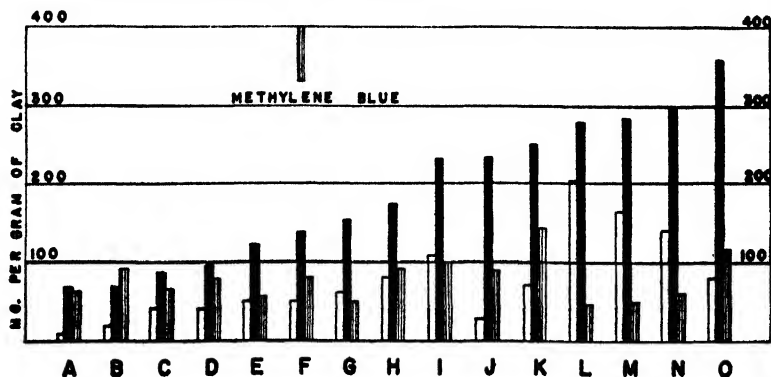


FIG. 3. Adsorption of methylene blue

The data for the adsorption of dyes, water, and ammonia appear in table 2, together with the colloid ratio worked out from the tests with methylene blue.

The adsorption of methylene blue is listed in column 1 of table 2 and presented graphically in figure 3. Originally Paneth (25) concluded that the amount of

adsorbed dye was never more than enough to form a monomolecular layer on the colloid surfaces. Some elaborate rules were worked out on this basis. According to such calculations no clay used in this study should adsorb more than 6 mg. of dye per gram of clay. However, it was found that even the clay with the least colloid matter adsorbed more than ten times this amount. Pallman (24) has presented diagrams to explain how clays can adsorb more than one layer of molecules, while Jewett (18) has suggested layers to the extent of sixteen molecules thick. It is also known that certain clay minerals readily act in base-exchange fashion to take up suitable ions. Since water-soluble dyes are electrolytes in water solution, it is not surprising that there should be variations due to factors other than the state of aggregation of the clay particles (2).

In figure 3 it is noted that there is no constant increase in dye adsorption from left to right. Clays L, M, and N are low in adsorption though high in colloid matter. Low-colloid clay B is a high dye adsorber, and sample K has a dye

TABLE 3  
*Data for methylene blue colloid ratio*

CLAY	1*	2	3	CLAY	1*	2	3
A.....	278	42	6.7	I.....	154	59	2.6
B.....	89	88	1.0	J.....	97	83	1.2
C.....	154	57	2.7	K.....	158	143	1.1
D.....	76	76	1.0	L.....	85	30	2.8
E.....	139	34	4.1	M.....	89	30	2.9
F.....	116	67	1.7	N.....	95	40	2.3
G.....	128	34	3.8	O.....	369	97	3.8
H.....	134	82	1.5				

\* 1. Methylene blue in milligrams adsorbed per gram of colloid material.

2. Methylene blue in milligrams adsorbed per gram of residue left after 15 days' extraction of colloid material.

3. Colloid ratio=column 1/column 2.

adsorption roughly equal to the sum of the adsorptions by the next three clays which follow it.

The colloid ratio as shown in tables 2 and 3 is also of interest. Here we have ratios varying from 1.0 to 6.7. For instance, in clay A the colloid matter is credited with adsorbing 6.7 times as much dye, gram for gram, as did the residue after the 15-day extraction. In clays B, D, H, J, and K the residues left after the 15-day extractions proved themselves to be practically as good adsorbers as the colloid material which had been removed. In the light of present information on the lattice structure of clay minerals it can be assumed that many particles heavy enough to settle out quickly have a cellular structure capable of adsorbing dye readily. It is also reasonable to conclude that certain extracted colloid fractions may be more potent as adsorbers than some other fraction extracted in the same manner from some other clay. The writer has obtained colloidal material from clay with as low an adsorption as 64 mg. of dye per gram

of extracted material. With colloidal material from other clays he has obtained results almost sixty times as high.

The adsorption of malachite green confirms the conclusions reached in the experiments with methylene blue. Figure 4 shows the malachite green adsorption compared with the standard. Once more we find clays K, L, and M as lows in the adsorption column though high in colloid material. Samples B, C, E, and

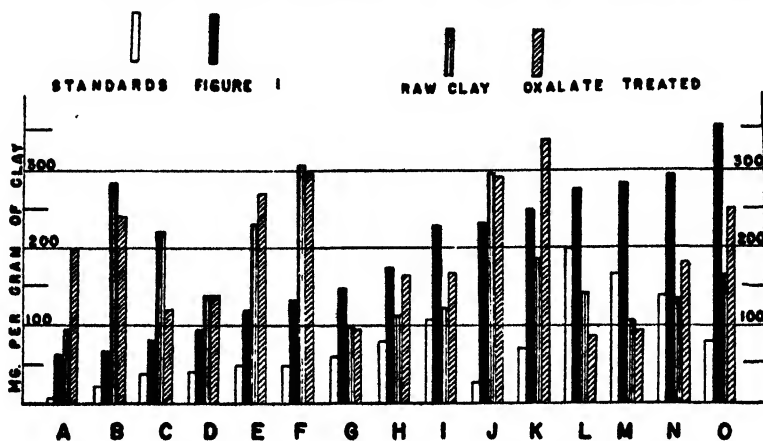


FIG. 4. Adsorption of malachite green

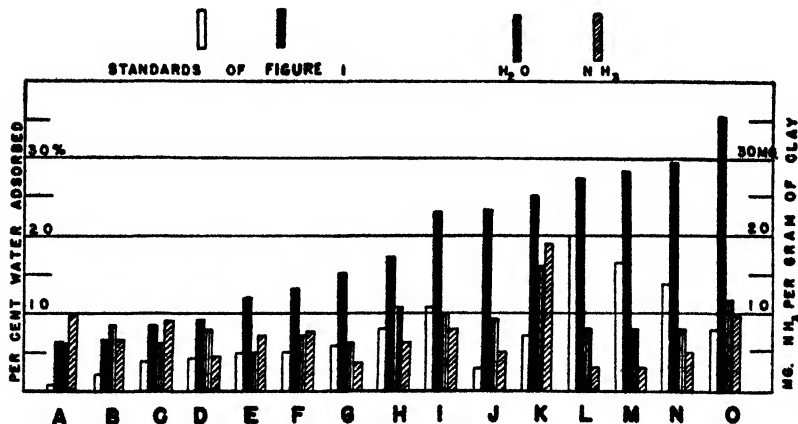


FIG. 5. Adsorption of water and ammonia

F also are far out of position. Actually the graph would be slightly more in keeping with the extraction standards if it were placed in complete reverse.

Knowing that clays B, C, E, and J were high in calcium salts, the experimenter might conclude that these salts were in part responsible for the high dye adsorption. To test this the samples were re-run after being treated with sodium oxalate to precipitate calcium. In seven cases (B, C, F, G, J, L, and M) it was found that the oxalate treatment did lessen the dye adsorption, yet only three of these clays had any appreciable calcium content. In sample J, which was

highest in calcium content, the treated and untreated samples showed almost exactly the same dye adsorption. In seven of the samples the addition of sodium oxalate produced a greater dye adsorption rather than a lesser one. The conclusions must necessarily be that the clays are highly selective in their adsorption and that this selectivity is not especially related to their calcium content and not even greatly related to their colloid content.

The adsorption of water and ammonia appears in table 2 and in figure 5. Anomalies are the rule rather than the exception, and we must conclude that the adsorption of these materials is at best only a qualitative measure of any colloid content. Heat of wetting has been listed as a property related to the colloid content of a clay and numerous experiments have been made on it (26). Figure 6 gives the results obtained here, indicating that this is no more satisfactory as a measure than the adsorptions previously tried.

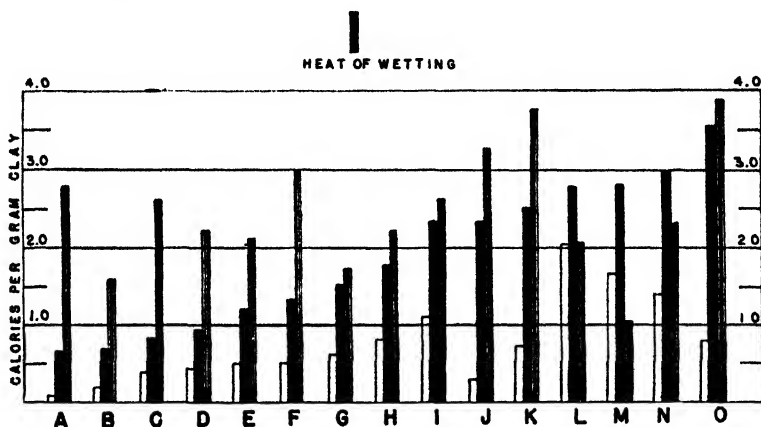


FIG. 6. Heat of wetting

#### CONCLUSIONS

An evaluation of methods of determining colloid content—such as the use of hydrometers, viscosimeters, the adsorption of various substances, base exchange, heat of wetting, plasticity, sedimentation, ion migration, and so forth—lead to the inevitable conclusion that such methods are qualitative rather than quantitative. The clay particles are evidently highly selective in their nature, and each clay must be studied individually. The properties of adsorption are more dependent on molecular arrangement in crystalline particles than on size of aggregation. Some clay minerals are easily broken up by water, going into a state of aggregation in which a large per cent of the particles can be recovered by various sedimentation and extraction means. Other clay minerals cannot be easily broken down into small particles which can be so recovered. Sedimentation and extraction methods will all list these clays as low in colloid content and yet, owing to their cellular structure, the material judged as non-colloidal may exhibit many of the properties usually assigned to a colloidal material. Multiple

extractions of colloid material, such as the 15-day method used here as a standard, are judged to be superior to shorter methods for determining standards for comparison, though still leaving behind material which exhibits colloidal properties.

## REFERENCES

- (1) ALEXANDER, L. T., FAUST, G. T., AND HENDRICKS, S. B.: *Am. Mineral.* **28**, 1-18 (1943).
- (2) BOSAZZA, V. L.: *Am. Mineral.* **29**, 235-41 (1944).
- (3) COLE, W. F.: *Soil Sci.* **56**, 153-71 (1943).
- (4) GILE, P. L.: *Soil Sci.* **25**, 361 (1928).
- (5) GRIM, RALPH E.: *J. Geol.* **50**, 225-75 (1942).
- (6) HADDING, A.: *Z. Krist.* **58**, 108 (1923).
- (7) HAUSER, E. A.: *Chem. Revs.* **37**, 287-321 (1945).
- (8) HAUSER, E. A., AND LE BEAU, D. S.: "Colloid Chemistry of Clay Minerals and Clay Films," in Jerome Alexander's *Colloid Chemistry*, Vol. VI, pp. 191-213. D. Van Nostrand Company, Inc., New York (1946).
- (9) HAUSER, E. A., AND LE BEAU, D. S.: *J. Phys. Chem.* **42**, 961-9 (1938).
- (10) HAUSER, E. A., AND LYNN, J. E.: *Ind. Eng. Chem.* **32**, 659-62 (1940).
- (11) HAUSER, E. A., AND SCHACHMAN, H. K.: *J. Phys. Chem.* **44**, 584-91 (1940).
- (12) HENDRICKS, S. B.: *J. Geol.* **50**, 276-89 (1942).
- (13) HENDRICKS, S. B. AND ALEXANDER, L. T.: *Soil Sci.* **48**, 257-79 (1939).
- (14) HENDRICKS, S. B., AND FRY, W. H.: *Bull. Am. Soil Survey Assoc.* **XI**, 194-5 (1930).
- (15) HILGARD, A.: *U. S. Dept. Agr. Bull. No. 1193*, p. 4 (1924).
- (16) HOLMES, HARRY N.: *Laboratory Manual of Colloidal Chemistry*, p. 207. John Wiley and Sons, Inc., New York (1934).
- (17) HUMBERT, R. P., AND SHAW, BYRON: *Soil Sci.* **52**, 481-7 (1941).
- (18) JEWETT, T. N.: *Soil Sci.* **50**, 163-73 (1940).
- (19) KELLEY, W. P.: *J. Geol.* **50**, 276-90 (1942).
- (20) KELLEY, W. P., AND DORE, W. H.: *Soil Sci.* **48**, 201-55 (1939).
- (21) MARSHALL, C. E., AND CALDWELL, O. G.: *J. Phys. Colloid Chem.* **51**, 311-20 (1947).
- (22) MARSHALL, C. E., HUMBERT, R. P., SHAW, B. T., AND CALDWELL, O. G.: *Soil Sci.* **54**, 149-58 (1942).
- (23) PAGE, J. B.: *Soil Sci.* **56**, 273-83 (1943).
- (24) PALLMAN, N. H.: *Ernäh. Pflanze* **30**, 225-34 (1934).
- (25) PANETH, FRITZ, AND THURMAN, WILHELM: *Ber.* **57B**, 1221 (1924).
- (26) PARMALEE, C. W., AND FRECHETTE, V. D.: *J. Am. Ceram. Soc.* **25**, 108-12 (1942).
- (27) RINNE, F.: *Z. Krist.* **60**, 55 (1924).
- (28) SCHAEFER, G. M.: *Soil Sci.* **53**, 353-64 (1942).
- (29) VALKO, E. I.: "Physical Chemistry of Dyeing," in Jerome Alexander's *Colloid Chemistry*, Vol. VI, pp. 594-619. D. Van Nostrand Company, Inc., New York (1946).



## THIXOTROPIC QUALITIES OF SOAP-HYDROCARBON SYSTEMS

C. J. BONER

*Battenfeld Grease & Oil Corporation, Kansas City 8, Missouri**Received June 23, 1948*

## INTRODUCTION

Thixotropy in lubricating greases is of importance to industry from several standpoints; hence, any explanation of the phenomenon should permit the production of more satisfactory commercial products. Thus if, after packaging, a lubricating grease increases in consistency the point may be reached where it will not flow to pumping equipment even under suction. This may be a nuisance, and therefore too great a degree of thixotropy is detrimental. On the other hand, a slight softening may aid in lubrication in some cases and if, after the lubricating grease is forced from the area of service it regains part of its body, it will act as a seal and prevent entrance of dirt or discharge of excessive lubricant.

If the definition "change by touch" is accepted for the term "thixotropy," there should be no question that lubricating greases possess this property, since most of them have a structure which when partially broken down rebuilds itself to some extent. Klemgard (6) states that all lubricating greases are more or less thixotropic.

## EXPERIMENTAL PROCEDURE

Since most of these systems are plastic products of relatively high soap content, rather violent shearing action is required to produce a change in consistency. Lutz and coworkers (8) demonstrated this quality on a rotary viscosimeter. In the present work some trials were made with this method, but in the products examined too much channeling was encountered to permit its use. Consideration was also given to the method used by Pigott (9), where viscosity was measured after repeated shearing. Ease of manipulation led to the use of the A.S.T.M. standard apparatus and procedure called for in determining the penetration of lubricating greases according to A.S.T.M. Method D217-47 T. Penetrations taken at intervals after shearing has ceased were then plotted against time intervals.

## PRODUCTS EXAMINED

The samples tested were all commercial products representing those manufactured by several firms. Notation of the general composition is shown on the curve sheets. Lubricating greases made from as great a variety of metal soaps as possible were tested in order to arrive at some conclusion as to the effect of soap cations. The products were then grouped so that a comparison of lubricating greases made from different soaps could be observed. The soap percentages and oil viscosities were similar in value in each group. Furthermore, it was usually possible to include lubricating greases with soaps of the same cation, made in one case from fat so that glycerol was present, and in another case from fatty acids.

## EXPERIMENTAL RESULTS

Figure 1 shows the change in penetration after shearing ceased for a series of soaps dispersed in mineral oil of comparatively low viscosity. The elapsed time in all cases was 70 min. The lubricating grease containing lithium soap, as well as a smooth type of sodium soap lubricating grease, changed little in consistency during this period. A fibrous type of sodium soap lubricating grease showed some increase in penetration, but not as much as the calcium and aluminum

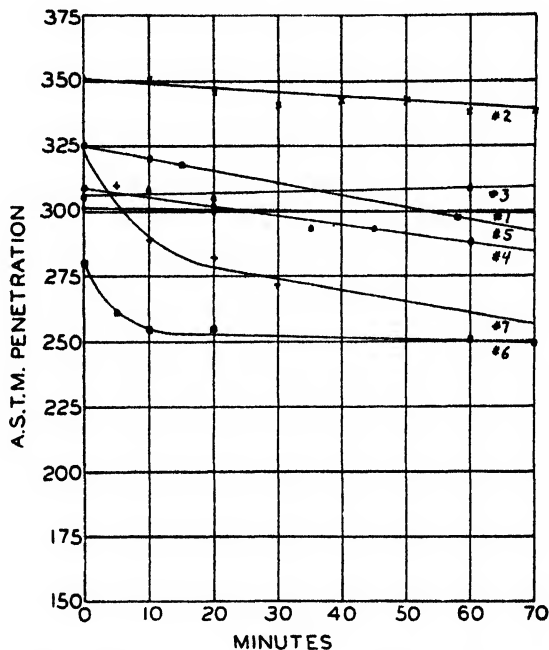


FIG. 1. Change in penetration after shearing ceased for soaps dispersed in mineral oil

Curve 1: 10 per cent lithium soap of fatty acids-oil 50 vis at 100°C.

Curve 2: 9 per cent sodium soap of glycerides-oil 300 vis at 100°C.

Curve 3: 6 per cent sodium soap of fatty acids-oil 300 vis at 100°C.

Curve 4: 10 per cent calcium soap of glycerides-oil 300 vis at 100°C.

Curve 5: 11 per cent aluminum soap of fatty acids-oil 300 vis at 100°C.

Curve 6: 18 per cent strontium soap complex-oil 100 vis at 100°C.

Curve 7: 18 per cent barium soap basic-oil 500 vis at 100°C.

soap lubricating greases. The lubricating greases made from barium and strontium soaps showed a very abrupt increase in consistency during the first 10 min., after which the change was in line with the performance of calcium and aluminum base lubricating greases.

In figure 2 a series of lubricating greases containing oils of somewhat higher viscosity showed much the same results. That is, the lithium and sodium soap products showed little increase in penetration over a period of 70 min., whereas the calcium and aluminum base products showed somewhat greater increases. Basic barium and strontium lubricating greases became much lower in pene-

tration, particularly the latter. On the other hand, a complex barium soap lubricating grease showed practically no change in penetration.

In figure 3 some of the same characteristics are confirmed and a couple of special products are included. Two calcium soap lubricating greases, one with less than a third as much soap as the other and with no glycerol, the other of a lower penetration than any product so far tested, showed about the same general increase in penetration.

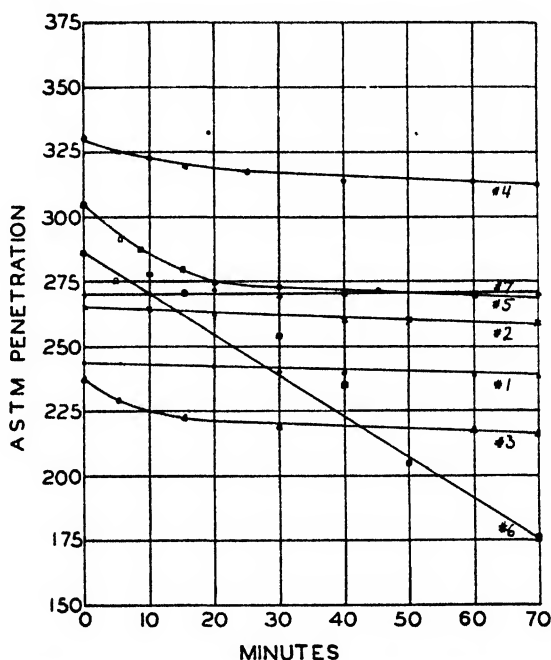


FIG. 2. Change in penetration after shearing for soaps dispersed in oils of higher viscosity than in figure 1.

- Curve 1: 14 per cent lithium soap of fatty acids-oil 650 vis at 100°C.
- Curve 2: 16 per cent sodium soap of glycerides-oil 500 vis at 100°C.
- Curve 3: 14 per cent calcium soap of glycerides-oil 500 vis at 100°C.
- Curve 4: 10 per cent aluminum soap of fatty acids-oil 100 vis at 210°C.
- Curve 5: 25 per cent barium soap basic-oil 500 vis at 100°C.
- Curve 6: 20 per cent strontium soap basic-oil 150 vis at 210°C.
- Curve 7: 20 per cent barium soap complex-oil 500 vis at 100°C.

Another calcium base lubricating grease is of particular interest. This is what is known as axle grease, and is made by the saponification of rosin oil with a large excess of hydrated lime. In this lubricating grease the change in penetration was more abrupt after working ceased than in any other product tested. Further comment will be made relative to this later.

One soap-mineral oil mixture is also included which does not strictly fall in a lubricating grease classification. Lead stearate and mineral oil were mixed and heated, and then left undisturbed to cool. A definite mixture of crystals in oil

resulted which was firm enough so that it would not move if tilted. After this mixture had been worked to a slurry which would pour readily, it did not return to a semisolid state within 70 min.; in 24 hr., however, it showed a definite gain in consistency.

In addition to rapid change in penetration, as shown above, one must consider what recovery in penetration occurs over a prolonged period. Therefore, this change has been tabulated over a period of 15 days (table 1). Some checks were

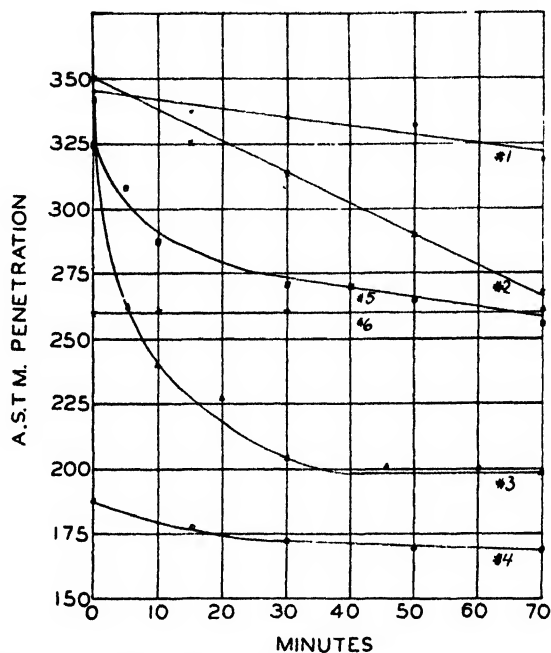


Fig. 3. Change in penetration after shearing for special soap-oil dispersions

Curve 1: 6 per cent calcium soap of fatty acids-oil 110 vis at 210°C.

Curve 2: 6 per cent aluminum soap of fatty acids-oil 70 vis at 210°C.

Curve 3: 11 per cent calcium soap of rosin oil-oil 50 vis at 210°C.

Curve 4: 20 per cent calcium soap of glycerides-oil 300 vis at 100°C.

Curve 5: 18 per cent barium soap basic-oil 500 vis at 100°C

Curve 6: 12.5 per cent lead stearate-oil 100 vis at 100°C.

made after longer standing, but no further change was noted in these particular samples.

#### STRUCTURE SPECULATIONS

Any conclusions or speculations as to what happens when lubricating greases are subjected to shear and then left undisturbed hinges upon what gives structural stability to the systems. Viscosity changes in colloidal systems can generally be attributed to (a) a change in the shape of the micelles, (b) a change in the relative volume of the disperse phase with respect to the dispersion medium, (c) a change in absorbed layers on the micelles, or (d) a change in the forces or bonds which contribute to structure.

Since most lubricating greases soften without violent shearing action, it does not seem reasonable that the shapes of the micelles have been changed by such action; nor do we have any evidence that the relative volume of the disperse phase has changed or that the absorbed layer has changed, since the systems revert to about the same consistency with time. Perhaps the most simple explanation is that the soap micelles are longer than they are broad, and that they can be oriented, owing to shear, giving a less firm body to the system. Recovery of body then would be due to return to random arrangement with time. Ex-

TABLE 1

SOAP		PENETRATIONS		
Type	Per cent	Initial worked	15 days later undisturbed	Change
				<i>per cent</i>
Sodium glycerides . . . . .	16	265	243	7.8
Sodium glycerides . . . . .	9	351	325	7.8
Sodium fatty acids . . . . .	6	307	275	10.4
Lithium fatty acids . . . . .	14	238	202	15.1
Lithium fatty acids . . . . .	10	302	247	18.2
Calcium glycerides . . . . .	20	188	160	14.9
Calcium glycerides . . . . .	14	238	200	15.9
Calcium glycerides . . . . .	10	309	260	15.8
Calcium fatty acids . . . . .	6	343	317	7.6
Barium glycerides (basic soap) . . . . .	25	309	231	25.2
Barium glycerides (basic soap) . . . . .	18	320	250	21.9
Barium fatty acids (complex soap) . . . . .	20	270	262	3.0
Strontium basic . . . . .	20	282	152	46.1
Strontium complex . . . . .	18	280	235	16.1
Aluminum fatty acids . . . . .	11	325	255	21.5
Aluminum fatty acids . . . . .	10	330	243	26.4
Aluminum fatty acids . . . . .	6	350	260	27.1

amination of worked and unworked lubricating greases with polarized light showed a change in the intensity of light transmitted and therefore gave some basis for the above explanation.

Gallay and coworkers (4) showed that a shearing force brings about parallelization of fibers in a lubricating grease system. Arveson (1) suggested that lime soap lubricating greases consist of "interlacing flexible solid members which may be themselves deformed or merely separated by the shearing action." He explained the immediate return to consistency from the highly sheared state by elastic recoil.

Lawrence (7) does not consider this explanation complete. He states that "interlacing confers no rigidity on the system unless there is adhesion at the points of contact. Working consists of breaking lumps of gel into a homogeneous mixture. Shearing then progressively breaks down the adhesion of the crystallites. On removal of the shearing force, adhesion occurs immediately at the points of contact by van der Waals forces." This agrees with the idea which Smith (11) has recently advanced that the thickening agent in a stable lubricating grease is not so much the fibers as the colloidal jelly or liquid crystal structures.

A further observation of Gallay and coworkers (4) is of interest here. They concluded that fibers in a lubricating grease structure are more plastic than elastic and that the apparent elasticity may be due to the surface tension of oil. They continue: "Flexibility, as contrasted with elasticity, is easily attained in a system of this kind as a result of the freedom of motion of the oriented fibrils with respect to one another."

Puddington (10) states that exposing soap-oil dispersions to conditions of shear at ordinary temperatures causes a breakdown in the crystals with a consequent shortening in the microfiber length.

While we are considering the possible effect of fiber structure on the thixotropic characteristics of lubricating greases, we must consider the electron micrograph of soap fibers from calcium base lubricating grease obtained by Ellis (2). Such a micrograph shows the fibers to be in the form of a two-stranded rope, which may twist on working and later spring back.

The length of fibers in lubricating greases might be considered in comparison with the relative thixotropy. Farrington and Davis (3) found that soda base lubricating greases had the longest fibers of those examined and that calcium and aluminum base lubricating greases had microfibers. The results of our work show that the former is less thixotropic than the latter and also that a smooth type of soda base lubricating grease has approximately the same thixotropic qualities as the fibrous type. Thus, it seems reasonable that the fibers present in soap-mineral oil systems are not the primary cause for thixotropy.

Gallay and Puddington (5), in considering the state of dispersion of calcium stearate in mineral oils, state that since this compound is heteropolar the forces holding the molecule in the lattice must consist of two types: *viz.*, (1) strong polar bonds between calcium carboxylic groupings and (2) weaker van der Waals forces along the length of the hydrocarbon chains. Van Wazer and Carver (12) made an extended study of an aluminum soap dissolved in gasoline and concluded that there was a cross-bonded structure which was partially destroyed under shear.

It may be that this bonding is due to the attraction of the unshared electrons from the oxygen, chiefly the carbonyl oxygen, by the metal of other molecules. This thought is illustrated in the case of a calcium soap lubricating grease in figure 4, which shows how a lattice structure might be built up. The results obtained over an extended period (see table 1) confirm what might be expected from the attraction of electrons. Thus, the elements in which the valence shell

is least removed from the positive nucleus should, mole for mole, be the most thixotropic in a particular group of the Periodic Table. It is seen that the lighter lithium soap does show a greater degree of thixotropy than sodium soaps. Since the basic barium and strontium soaps contain about twice the proportion of base as normal soap does, the calcium soap shows a greater degree of thixotropy per mole of metal than the barium soap, a result which would be expected. Why strontium does not conform to this behavior is not evident.

The case of calcium base grease made from rosin oil requires comment. The predominant acids in this material are isomerized abietic. Such an acid has four rings, and the spatial arrangement may be such that these rings are not all in the same plane. Shear may place more rings in one plane than before such treatment, but the rings may spring back quite rapidly and hence give an abrupt change in penetration after working.

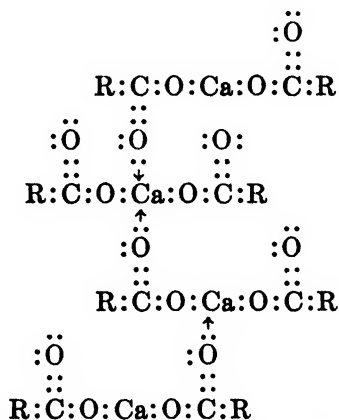


**FIG. 4. Possible lattice structure of a calcium soap lubricating grease**

## CONCLUSIONS

Soap-mineral oil systems containing soaps of monovalent metals are less thixotropic over a period of 70 min. than are such systems containing soaps of di- and tri-valent metals, the latter showing the greatest degree of thixotropy for short periods. Systems containing soaps of the metal of lowest atomic weight in a series are more thixotropic over an extended period than are systems containing heavier metals of the same series.

## REFERENCES

- (1) ARVESON, M. H.: Ind. Eng. Chem. **24**, 75 (1932).
- (2) ELLIS, S. G.: Can. J. Research **25A**, 119-23 (1947).
- (3) FARRINGTON, B. B., AND DAVIS, W. N.: Ind. Eng. Chem. **28**, 414-16 (1936).
- (4) GALLAY, W., PUDDINGTON, I. E., AND TAPP, J. S.: Can. J. Research **22B**, 66-75 (1944).
- (5) GALLAY, W., AND PUDDINGTON, I. E.: Can. J. Research **22B**, 161 (1944).
- (6) KLENGARD, E. N.: *Lubricating Greases: Their Manufacture and Use*. Reinhold Publishing Corporation, New York (1937).
- (7) LAWRENCE, A. S. C.: J. Inst. Petroleum Tech. **24**, 207-20 (1938).

- (8) LUTZ, W. A., AMBROSE, H. A., AND GRUSE, W. A.: *Oil Gas J.* **37**, No. 39, 62, 64, 65, 67; No. 40, 49, 50, 75 (1939).
- (9) PIGOTT, R. J. S.: *Inst. Spokesman* **11**, No. 9, 4-10 (1947).
- (10) PUDDINGTON, I. E.: *Inst. Spokesman* **9**, No. 9, 1-4 (1945).
- (11) SMITH, G. H.: *J. Am. Oil Chemists' Soc.* **24**, 353-9 (1947).
- (12) VAN WAZER, J. R., AND CARVER, E. K.: *J. Colloid Sci.* **2**, 223-36 (1947).

## A SEMIMICRO DIFFUSION METHOD FOR THE CHARACTERIZATION OF HIGH-POLYMER FRACTIONS<sup>1</sup>

MARVIN C. BROOKS AND RICHARD M. BADGER

*Gates and Crellin Laboratories of Chemistry, California Institute of Technology, Pasadena,  
California*

*Received May 11, 1948*

### INTRODUCTION

The studies here described were carried out in connection with a program which required the characterization with respect to molecular weight of nitrocellulose fractions available only in small quantities. A diffusion method has been developed which offers the advantages of simplicity of construction and operation of the apparatus and interpretation of results. Although diffusion is less sensitive to molecular weight than viscosity, the method submitted appears to be simpler for use on a milligram scale and to afford sufficient precision for many requirements.

The diffusion method reported herein differs from other diffusion methods in that the liquid medium is held fixed in position by a matrix of fine-grained filamentous material; more specifically, in these experiments the matrix was composed of a pad of filter papers. This feature effectively dampens out convection currents in the liquid medium; yet the matrix is not sufficiently dense to interfere appreciably with the diffusion process.

Experimental and theoretical diffusion studies have been extensively reviewed by Longsworth (6) and by Williams and Cady (8). The latter authors have given solutions of the diffusion equation for several sets of initial and/or boundary values. In principle, the diffusion constant can be calculated from an accurate knowledge of these initial and boundary values and one set of concentration, position, and time measurements at some time after diffusion has been allowed to commence. In practice, a number of sets of measurements are made and the diffusion constant is reported after some averaging process has been

<sup>1</sup> Contribution No. 1205 from the Gates and Crellin Laboratories of Chemistry, California Institute of Technology.

This paper is based on work supported by the Bureau of Ordnance, United States Navy, and done under contract with the Office of Naval Research, Contract N6ori-102, Task Order VI.



applied in interpreting the data. The procedure here outlined provides time and position data at one concentration only. Experimentally, these data are obtained by determining the distance through which the polymer diffuses in a saturated filter pad during arbitrary times, in just sufficient concentration to react positively to a color spot test. Somewhat less information is thus provided than by other methods. Computation is, however, greatly simplified.

From the point of view of the worker interested in estimates of molecular weight, as we have been, the advantage may be appreciated that the accuracy of the result is not limited by a determination of concentration.

#### APPARATUS AND EXPERIMENTAL PROCEDURE

The method here described was specifically designed for the characterization of nitrocellulose fractions dissolved in acetone. It should, however, be applicable to other polymers for which a sensitive spot test is available, and to other solvents.

The procedure employed is briefly as follows: Aliquot portions of the fraction to be characterized are deposited at intervals of about half an hour at suitably separated points upon the surface of a pad saturated with solvent. After about 4 hr. from the start, diffusion is frozen by rapidly separating the leaves of the pad. The maximum depth below each deposit at which nitrocellulose can be detected with a sensitive spot test is then determined. From the relation between time and depth of penetration, the diffusion constant is calculated.

The diffusion pad is composed of a stack of approximately 100 thin filter papers. Filters sold commercially as coffee filters have been found satisfactory. Those used in these experiments were obtained from the Acme Sales Company, Los Angeles, California. The papers are packed in units of 100. The diameter is approximately 8.5 cm., and the thickness of paper sheets averages about  $3.5 \times 10^{-3}$  cm. Since diffusion distances are measured in terms of the number of filter papers, it is important that variation in thickness be small. Our practice is to measure the thickness of the saturated pad with a micrometer immediately before diffusion is started and to count the number of sheets after diffusion is finished. An average value of the thickness of the sheets in the pad can then be calculated.

The diffusion pad is placed on another pad of heavier filters. Any porous filter paper reasonably free of nitrates will do for this purpose. A pad of approximately 25 of Eaton-Dikeman filter papers No. 613, 9 cm. size, is satisfactory. Both pads are placed in a petri dish upon a flat support, which may be a disc of plate glass or of brass, and sufficient solvent is added to wet the paper completely and provide a small excess. It has been found desirable to press the saturated paper pad for several days before use. This is conveniently done by placing a brass disc, approximately 9 cm. in diameter and weighing several pounds, on the saturated pad and allowing the whole setup to stand in an atmosphere saturated with solvent vapor. A laboratory desiccator with the desiccant replaced with solvent may be used to provide the necessary atmosphere of solvent vapor.

After standing approximately 48 hr. or longer, the weight is removed and the thickness of the diffusion pad determined with a micrometer. Checks should be made to ascertain that the variation in the thickness of the pad is not greater than about  $3 \times 10^{-3}$  cm. The pad is rinsed several times with fresh solvent to remove extractables which might change the character of the solvent medium. Sufficient solvent is again provided to allow a small excess at the bottom of the petri dish, and the setup consisting of the pad of thin filters and the pad of heavier filters in the petri dish is again put under a blanket of solvent vapor and is then ready for use.

Diffusion is started by placing a small disc of filter paper wetted with an acetone solution of the polymer under investigation on the top of the pad. It is desirable to use a thin piece of paper for the disc to satisfy more nearly an approximation which we shall introduce in the solution of the diffusion equation. However, it is also necessary that the paper disc have a certain amount of mechanical rigidity. Eaton-Dikeman No. 613 and Whatman No. 1 papers have been used by us. Discs about 1.8 cm. in diameter are satisfactory. A disc is held with tweezers, for instance, in a small vise, so that the surface is horizontal and 0.10 cc. of approximately 0.5 per cent solution of polymer is allowed to flow onto the surface. An attempt should be made to have the solution spread out as evenly as possible. Evaporation may be allowed to proceed until the volume of liquid on the filter disc is approximately the same as that which the disc will hold when placed in contact with the saturated filter pad. This operation is not critical; however, it has been found that much more reproducible results can be obtained than if the solution on the disc is allowed to evaporate to dryness.

In the determination of the diffusion constant of a given nitrocellulose fraction it is desirable to make determinations of penetration depth at five or six different diffusion times. It is therefore necessary to prepare five or six discs; it is essential that the amount of polymer on each disc be the same, although the absolute amount is not critical and need not be known. To secure adequate reproducibility it is also important that all of the discs should be placed on the same diffusion pad, a procedure which is possible with the pad described. The times at which the discs are placed on the pad, as is indicated in the section discussing the interpretation of the data, are conveniently chosen so that equal intervals between points on a log time plot will be obtained.

After diffusion has proceeded for the appropriate length of time, which may be about 4 hr., the process is stopped and the diffusion effectively frozen by removing the saturated pad from the desiccator and rapidly separating the filter sheets. The procedure used by us, which we believe to cause relatively little harmful convection, is to turn the diffusion pad over and place it again on the base pad of heavy filters and then proceed to separate the sheets of the diffusion pad as rapidly as possible. The sheets are marked as they are separated so that they can be oriented for analysis. It is important that not more than two or three sheets, preferably one, be removed at a time in that portion of the pad where the spot test end points are anticipated. The separated filter sheets are placed on an ordered set of heavy filters and are numbered consecutively prior to analysis. The actual separation of the sheets of the diffusion pad can be accomplished

in less than 2 min. The numbering may be carried out leisurely after the solvent has evaporated. When several sheets are allowed to adhere, it is noted that the polymer is found in greater concentration on the bottom sheet.

The analysis is carried out by using a color spot test. The extent of penetration is measured by the end point of color sensitivity. Hence, if five diffusions are started on a given pad at different times, color will be detected at five spots on the uppermost papers, corresponding to the positions under the discs from which the diffusions commenced. The penetration depths are detected sequentially. The last color-sensitive portion which remains corresponds to that diffusion which was started first. The penetration end points are recorded as the serial number of the last filter paper on which color is observed.

The color test used in these studies is that resulting from the reaction of a 0.25 per cent solution of diphenylamine in concentrated sulfuric acid, with nitrates. The filter sheets being tested are placed on a heavy white background paper, e.g., Eaton-Dikeman No. 613 filter paper, and the spot test is made by adding the reagent from an eye dropper. It is important that the background paper be insensitive to the color reagent. A blue color appears almost instantaneously if nitrates are present and persists for about 3 min., until it is overcome by a brown color resulting from the action of the sulfuric acid on the filter paper.

After the final end point has been determined, the remaining sheets are counted so that the average thickness of each sheet can be determined. The data recorded in these experiments are the times, and distances, in terms of number of papers, to the end point. Representative experiments are described below.

#### INTERPRETATION OF DATA

The data obtained by the experimental methods described in this report are adequately accounted for by Fick's second law of diffusion:

$$\frac{\partial c}{\partial t} = D \frac{\partial^2 c}{\partial x^2} \quad (1)$$

where  $D$  = diffusion constant,  $t$  = time,  $c$  = concentration, and  $x$  = distance in direction normal to the surface from which diffusion commences.

The diameter of the paper disc from which diffusion begins is large compared with the total distance normal to the surface, through which diffusion proceeds during the period of the experiment; hence, concentration losses through lateral diffusion will have negligible effect on the concentration gradient normal to the surface of the starting disc. Further, the sensitivity of the method does not warrant an analysis in which the dependence of the diffusion "constant,"  $D$ , on concentration is considered. Equation 1 integrated under appropriate initial values may therefore be applied.

The integration may be carried out by procedures such as those described in detail by Furth (3) and the following result is obtained:

$$C(x, t) = \frac{1}{2\sqrt{\pi Dt}} \int_{-\infty}^{+\infty} \Phi(\alpha) e^{-(x-\alpha)^2/4Dt} d\alpha \quad (2)$$

The parameter  $\alpha$  is to be interpreted as a distance used to describe the distribution of the diffusing substance at time  $t = 0$ . The origin for the measurement of  $\alpha$  is the same as that for  $x$ , and in the actual experiments lies in the upper surface of the disc initially containing the solute. The initial distribution is given by:

$$C(\alpha, 0) = \Phi(\alpha) \quad (3)$$

In the actual experiments the solute is initially contained in a layer of thickness  $\Delta$  in which its distribution is regarded as uniform. For diffusion processes the upper surface of this layer presumably acts as a reflecting plane. The situation is consequently mathematically equivalent to one in which a layer of thickness  $2\Delta$  is sandwiched between two filter pads. The initial distribution of diffusing substance which may be applied in these experiments is:

$$\begin{aligned} \Phi(\alpha) &= C_0 & -\Delta \leq \alpha \leq +\Delta \\ &= 0 & \begin{cases} \alpha < -\Delta \\ \alpha > +\Delta \end{cases} \end{aligned} \quad (4)$$

where  $C_0$  = concentration in the paper disc from which diffusion begins and  $\Delta$  = thickness of paper disc.

Expression 2 under condition 4 cannot be integrated directly, though computations may be made from probability integral tables. However, for values of  $\Delta$  sufficiently small the application of the mean value theorem gives a result (equation 5) which provides a method of approximation, concise and sufficiently precise to handle the experimental data.

$$C(x, t) = \frac{C_0\Delta}{\sqrt{\pi Dt}} e^{-(\bar{\alpha}-x)^2/4Dt} \quad (5)$$

In equation 5 the value of  $\bar{\alpha}$  is restricted by the mean value theorem to values between  $-\Delta$  and  $+\Delta$ , and more specifically for positive values of  $x$ , in the particular function considered, to values:  $0 < \bar{\alpha} < \Delta$ .  $\bar{\alpha}$  will depend upon  $x$ , but not strongly in the range of  $x$  for which the experiments are carried out. This weak dependence permits a choice of  $\bar{\alpha}$  which gives an approximation of  $C(x, t)$  certainly consistent with the precision of the diffusion distance determination.

It is appropriate for experimental application to make the change in variables:

$$\begin{aligned} d &= x - \Delta \\ \delta &= \Delta - \bar{\alpha} \end{aligned}$$

Further let:

$$\bar{d} = d + \delta = x - \bar{\alpha}$$

The parameter  $d$  is the experimentally determined distance from the top of the diffusion pad to the position where the spot color test last detects polymer;  $\bar{d}$  is the corrected distance which we may substitute in equation 5 to get:

$$C(\bar{d}, t) = \frac{C_0\Delta}{\sqrt{\pi Dt}} e^{-\bar{d}^2/4Dt} \quad (6)$$

If time-distance measurements are made for a given polymer and  $C$  and  $C_0$  are held constant, then convenient transformations of equation 6 for graphical representation of the data are:

$$\ln C + \frac{1}{2} \ln t = \ln \frac{C_0 \Delta}{\sqrt{\pi D}} - \frac{\bar{d}^2}{4Dt} \quad (7)$$

$$\log_{10} t = A(C, C_0, D) - \frac{\bar{d}^2}{4.6Dt} \quad (8)$$

The statement that  $C$  is held constant corresponds to the assumption that the respective concentrations of polymer at each color end point are equal. According to equation 8  $\log t$  varies linearly with  $\bar{d}^2/t$  and the slope of the straight line obtained by plotting  $\log t$  against  $\bar{d}^2/t$  is inversely proportional to the diffusion constant,  $D$ . The plot consequently affords a simple and direct method of determining  $D$  from the time and distance measurements.

If several diffusions of materials of varying molecular weight (diffusion constant) are started simultaneously and at equal concentration, data will be available under conditions of constant  $C$ ,  $C_0$ ,  $t$  but variable  $\bar{d}$  and  $D$ . Equation 6 can be transformed to the following form:

$$\log_{10} D = B(C, C_0, t) + F(t) \frac{\bar{d}^2}{D} \quad (9)$$

Hence, a plot of  $\log D$  against  $\bar{d}^2/D$  should give a straight line. Equation 9 is useful for checking the consistency of the diffusion constants obtained from the experiments suggested above. This use is demonstrated in the section below. Equation 9 may also be applied to determine the diffusion constant of a substance of unknown diffusion constant run in conjunction with several polymers of known diffusion constant. Although equation 9 is not a pleasant relation from which to make calculations of  $D$ , results can be obtained without too much effort by successive approximation based on slide rule computations.

#### EXPERIMENTAL DATA AND DISCUSSION

In order to calibrate the method described above and to test its reliability, diffusion experiments were conducted on five nitrocellulose fractions covering a rather wide range of molecular weight. These were prepared by an elaborate fractionation procedure (9) carried out under the direction of Professor J. W. Williams of the University of Wisconsin, who kindly provided them for our use. The fractions have been the subject of several investigations at this Institute. They have been found to be quite stable and in only one case has the intrinsic viscosity decreased appreciably since preparation. The molecular weights have been determined by measurement of osmotic pressure (1) and more recently by light-scattering methods which will shortly be reported (2). A summary of molecular weight data is given in table 2.

In the determination of the diffusion constant of a given fraction, the practice has been followed in this work of running five or six diffusions simultaneously,

although, in principle, two diffusions furnish sufficient data from which to calculate the constant. The diffusion pads were prepared according to the direc-

TABLE 1  
*Diffusion of nitrocellulose fractions in an acetone-saturated paper pad*

NITROCEL- LULOSE FRACTION NO.	EXPERI- MENT NO.	CONCEN- TRATION OF POLYMER SOLUTION	<i>t</i> DIFFUSION TIME	$\bar{x}$ DIFFUSION DIS- TANCE $\times 10^{-3}$ CM.	$\bar{x}^2/t$	<i>D</i> DIFFUSION CONSTANT (CALCULATED)
		g./100 ml.	sec.	cm. $\times 10^3$	cm. <sup>2</sup> sec. <sup>-1</sup> $\times 10^7$	cm. <sup>2</sup> sec. <sup>-1</sup> $\times 10^7$
S4,3.....	66A	0.59	7150	221 $\pm$ 3	62	24.5
			4200	194	89	
			2640	173	114	
			1800	152	128	
			1200	135	152	
S4,3.....	66D	0.59	7260	264 $\pm$ 3	96	24.0
			5100	228	102	
			2880	200	148	
			1860	175	164	
			1200	146	178	
S3,4.....	65A	0.60	14590	208 $\pm$ 3	30	10.4
			7980	173	38	
			4440	149	50	
			2340	121	63	
			1380	104	78	
S3,4.....	65B	0.60	14510	201 $\pm$ 3	28	10.7
			7680	170	38	
			4440	146	48	
			2400	121	61	
			1320	101	76	
S1,1-4.....	68A	0.58	15100	176 $\pm$ 3	20	6.8
			8350	148	26	
			4620	121	32	
			2460	100	41	
			1320	83	52	
S1,1-4.....	68C	0.58	16400	183 $\pm$ 3	20	7.1
			8350	141	24	
			4560	124	34	
			2820	107	41	
			1620	90	50	
P3,2. ....	59A	0.73	14700	120 $\pm$ 3	10	4.4
			8400	110	14	
			5450	96	17	
			3300	83	21	
			2280	73	23	
			1320	63	30	

TABLE 1—Continued

NITROCELLULOSE FRACTION NO.	EXPERIMENT NO.	CONCENTRATION OF POLYMER SOLUTION	$t$	$\bar{d}$	$\bar{d}^2/t$	$D$
			DIFFUSION TIME	DIFFUSION DISTANCE $\times 10^{-2}$ CM.		DIFFUSION CONSTANT (CALCULATED)
		g./100 ml.	sec.	cm. $\times 10^2$	cm. <sup>2</sup> sec. <sup>-1</sup> $\times 10^7$	cm. <sup>2</sup> sec. <sup>-1</sup> $\times 10^7$
P3,2..	59C	1.87	14700	121 $\pm$ 3	10	4.6
			9650	107	12	
			5750	97	16	
			4020	90	20	
			2520			
			1560	69	30	
P4,2 .	63A	0.65	21820	157 $\pm$ 3	11	3.6
			10550	126	15	
			4920	98	20	
			2820	84	25	
			1380	66	32	
P4,2 .....	63B	0.65	22000	162 $\pm$ 3	12	3.8
			9850	124	16	
			4680	100	21	
			2520	86	29	
			1380	69	35	

TABLE 2

Molecular weights, intrinsic viscosities, and diffusion constants of nitrocellulose fractions

NITROCELLULOSE FRACTION NO.	NITROGEN CONTENT	$\bar{M}_w^*$ WEIGHT-AVERAGE MOLECULAR WEIGHT (LIGHT-SCATTERING VALUE)	[ $\eta$ ] <sup>*</sup> INTRINSIC VISCOSITY	$D$
				DIFFUSION CONSTANT (CALCULATED, TABLE 1)
	per cent			cm. <sup>2</sup> sec. <sup>-1</sup> $\times 10^7$
S4,3 .....	13.18	9,400	0.30	24
S3,4 .....	13.36	35,000	1.33	10.6
S1,1-4 .....	13.44	50,000	2.26	6.9
P3,2. ....	13.41	93,000	4.4†	4.5
P4,2 .....	13.42	319,000	6.86	3.7

\* Reference 2.

† This value may be slightly high; a recent determination gave a somewhat lower value which could not be rechecked because of insufficiency of sample.

tions outlined above; acetone was used as the solvent. Paper discs, saturated with an acetone solution of one of the nitrocellulose fractions, were placed on the diffusion pad at scheduled times, the schedule being designed so that points would be separated by approximately equal intervals on a log time plot. Every effort was made to prepare the discs used on any one pad in the same manner. A summary of the diffusion data obtained in duplicate experiments on the five fractions is given in table 1.

The value of  $\delta$ , discussed in the section on the interpretation of data, applied as a correction on the diffusion distance,  $\bar{d}$  ( $\bar{d} = d + \delta$ ), has been taken as  $10 \times 10^{-3}$  cm. For very large values of  $x$  the proper theoretical value of  $\delta$  is the thickness of the filter disc from which diffusion starts. The average thickness of the discs used was about  $13 \times 10^{-3}$  cm. For smaller values of  $x$  the appropriate theoretical value of  $\delta$  is smaller; the value chosen for  $\delta$  is appropriate for values of  $x$  in the ranges measured, and the assumption that  $\delta$  is constant is consistent with the precision of the color end point measurement.

The values of the diffusion constants,  $D$ , given in the last column of table 1 are obtained from plots of the values of  $\log t$  against  $\bar{d}^2/t$ . The value obtained by dividing by 4.60 the reciprocal of the slope of the best straight line through the points is taken as the diffusion constant. The calculation follows from equation 8.

TABLE 3  
*Simultaneous diffusion measurements of nitrocelluloses of differing diffusion constants*

NITROCELLULOSE FRACTION NO.	EXPERIMENT NO.	$t$ DIFFUSION TIME	$\bar{d}$ DIFFUSION DISTANCE + $10^{-3}$ CM.	$D$ DIFFUSION CONSTANT (CALCULATED, TABLE 1)	$\bar{d}^2/D$
		sec.	cm. $\times 10^3$	cm. <sup>2</sup> sec. <sup>-1</sup> $\times 10^7$	sec. $\times 10^{-3}$
S4,3 .....	90B	8050	232 $\pm$ 3	24.2	22
S3,4 .....		8200	178	10.6	30
S1,1-4 .....		7800	157	6.9	36
P3,2 .....		7900	132	4.5	39
P4,2 .....		8100	117	3.7	37.5
S4,3 .....	90C	7800	217	24.2	19.5
S3,4 .....		7900	169	10.6	27
S1,1-4 .....		7700	155	6.9	34.5
P3,2 .....		7750	127	4.5	36
P4,2 .....		7850	110	3.7	32.5

In figure 1 representative data are plotted to demonstrate the graphical determination of  $D$ . No attempt was made to weight the points in determining the best straight line. Several factors should be mentioned, however. The average deviation in  $\bar{d}^2/t$  becomes smaller as  $\bar{d}$  increases. An example, *viz.*, experiment 65A, is given in figure 2 which shows the deviation in  $\bar{d}^2/t$  resulting from a deviation of  $\pm 1$  filter sheet ( $= \pm 3.5 \times 10^{-3}$  cm.) in  $\bar{d}$ ; the deviation in the measurement of  $t$  is considered inconsequential as compared with that of  $\bar{d}$ .

An observation of the experimental points from table 1 on a plot of  $\log t$  versus  $\bar{d}^2/t$  on an expanded scale shows that in a number of cases a concave curve could be drawn which would more nearly fit the data than the straight lines drawn in figure 1. For a polymer of heterogeneous molecular weight, a concave curve would be anticipated. Certainly no conclusion can be drawn with respect to heterogeneity of molecular weight from the data presented. However, at long diffusion times, the effect on the shape of the curve of small amounts of high-



molecular-weight polymer will be appreciable and it is advisable, therefore, to carry on diffusion experiments of this type over a relatively short period.

In order to check the consistency of the diffusion constants obtained from the data in table 1, simultaneous diffusions of all five fractions have been carried out. To perform this experiment, it is necessary to prepare solutions of equal concentration of each of the polymers; the concentration chosen was 0.50 g. per 100 cc. of acetone. The diffusions were started at as near the same time as possible

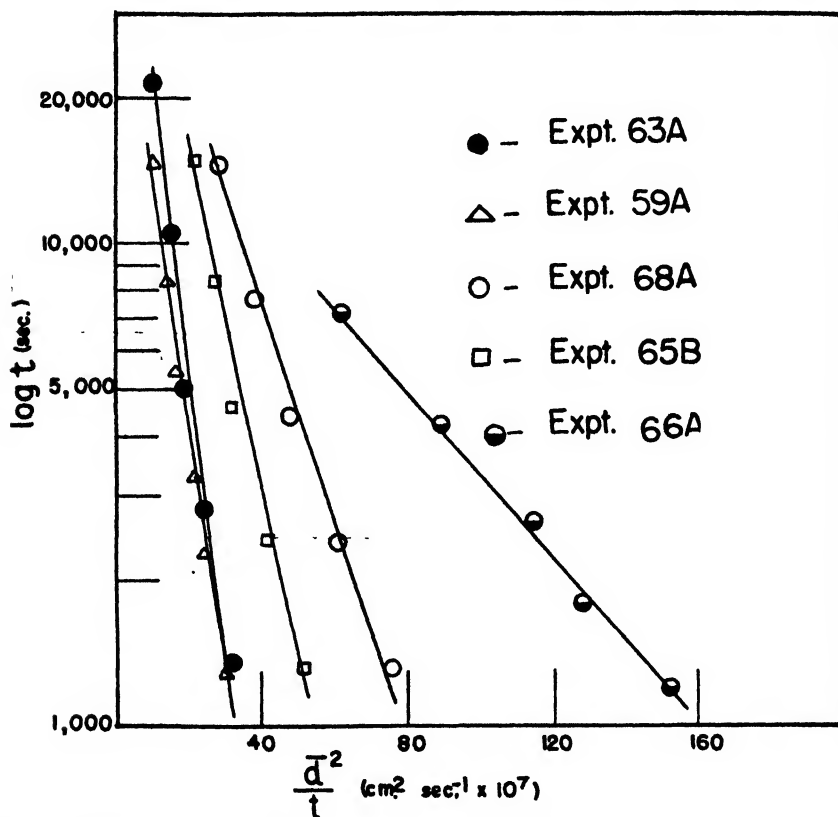


Fig. 1. Diffusion data for five nitrocellulose fractions in acetone: experiment 63A,  $D = 3.6$ ; experiment 59A,  $D = 4.4$ ; experiment 68A,  $D = 6.8$ ; experiment 65B,  $D = 10.7$ ; experiment 66A,  $D = 24$ .

and allowed to run for approximately 2 hr. A relatively long diffusion period, 2–4 hr., for instance, is preferable to a shorter period, since the relative precision of the  $\bar{d}$  measurement is greater for large values. The data obtained in duplicate runs are tabulated in table 3 and a plot of  $\log D$  against  $\bar{d}^2/D$  is shown in figure 3. According to equation 9,  $\bar{d}^2/D$  should vary linearly with  $\log D$ . Figure 3 shows this relation to be satisfied except for the diffusion constant of the fraction of highest molecular weight, P4,2. It is indicated by experiments 90B and 90C that the values for the diffusion constant obtained for fraction P4,2 in experi-

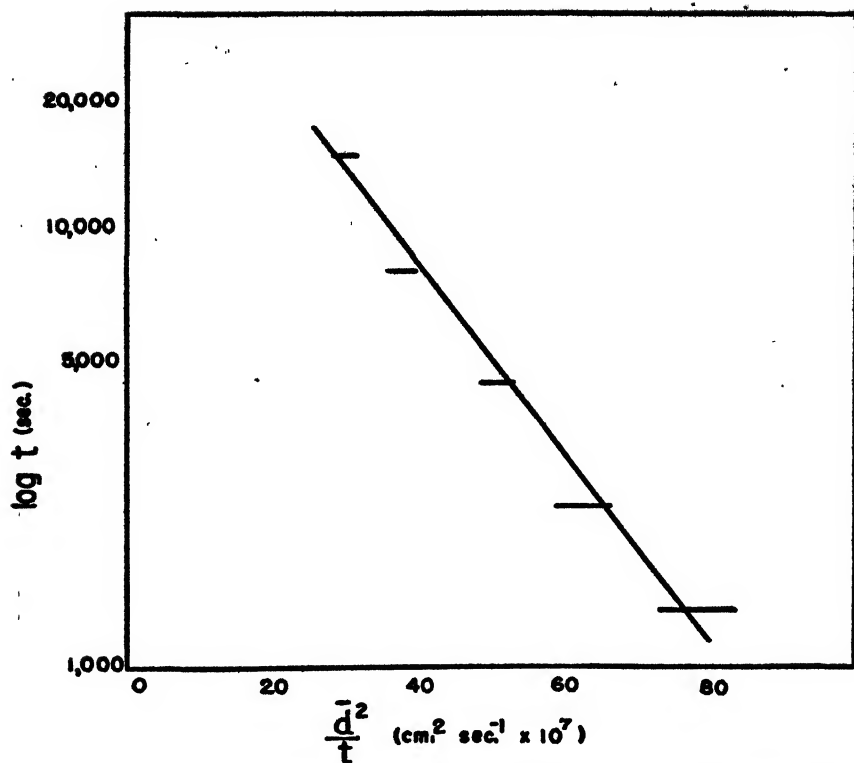


FIG. 2. Diffusion data for experiment 65A, showing deviation in  $\bar{d}^2/t$  resulting from a deviation in  $\bar{d}$  of  $\pm 3.5 \times 10^{-3}$  cm.

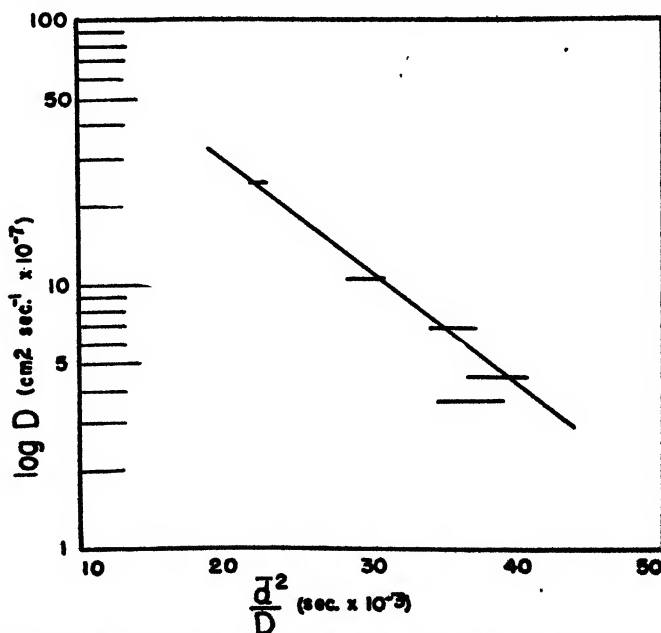


FIG. 3. Diffusion data from experiment 90B, showing linear dependence of  $\log D$  and  $\bar{d}^2/D$ . The lengths of the lines representing the data correspond to a precision in the  $\bar{d}$  measurements of  $\pm 3.5 \times 10^{-3}$  cm.

ments 63A and 63B were too high and that a value of  $D = 3.1$  for fraction P4,2 would be consistent with the other diffusion constants obtained.

#### CONCLUSION

In figure 4 is shown a log-log plot of intrinsic viscosity (see table 2) *versus* diffusion constants determined by the pad method. It is evident that, within the range investigated, viscosity and diffusion methods give equivalent information regarding molecular weights. When large amounts of material are available the

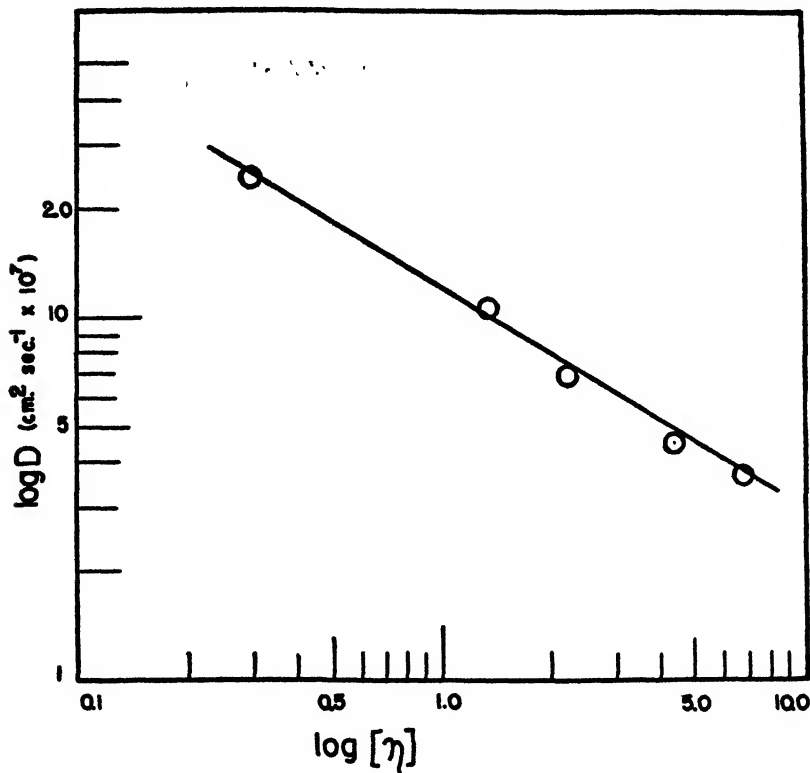


Fig. 4. The log of the diffusion constant, determined by the pad method, *versus* the log of the intrinsic viscosity for five nitrocellulose fractions.

viscosity method will be preferred because of its greater precision. However, when amounts only of the order of 5–25 mg. are available, the determination of intrinsic viscosity with good precision is both difficult and laborious and we believe that the precision of the diffusion method will be sufficient in many cases for preliminary characterization. In particular, we regard it as a useful tool in the development and testing of new fractionation methods where, in preliminary experiments, it is convenient to work on a very moderate scale.

It would be interesting to compare the "diffusion constants" obtained by the pad method with those obtained by conventional methods. They need not necessarily agree, since diffusion in the pad may conceivably be complicated by

adsorption and other phenomena, and the constant obtained might differ somewhat from the true diffusion constant. Unfortunately there appear to be no really suitable data for testing this point. Gralen (4) and Jullander (5) have recently examined a large number of nitrocelluloses which show a trend of diffusion constant with molecular weight which is identical with that found in our measurements. The absolute values of the diffusion constants are, however, about 25 per cent larger at any given molecular weight than we have found. Closer agreement could scarcely be expected, since the materials investigated in the laboratory at Uppsala were unfractionated, were not all of the same nitrogen

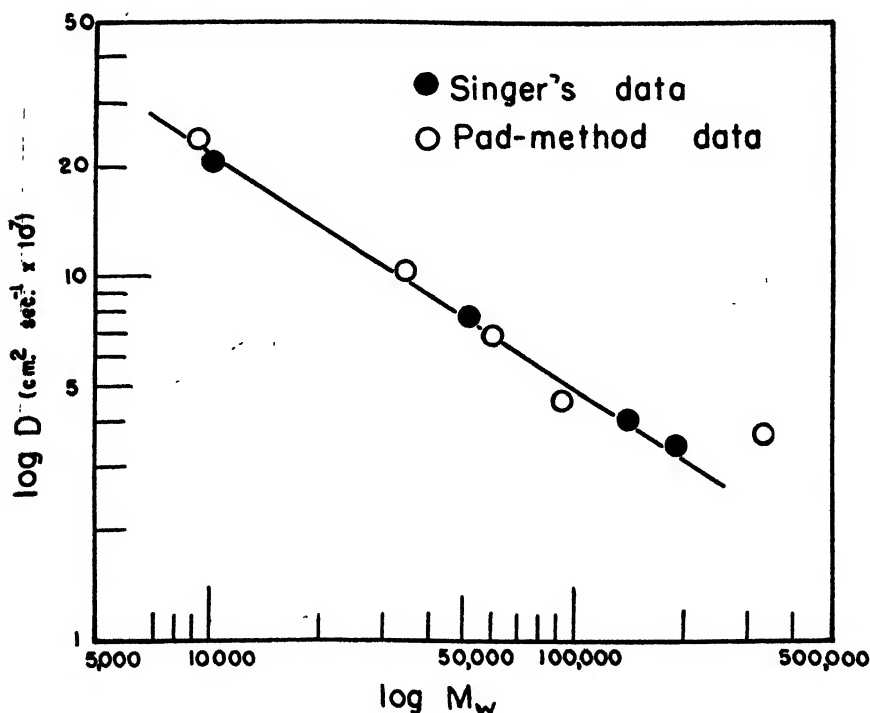


FIG. 5 The log of the diffusion constant plotted *versus* log weight-average molecular weight for some nitrocellulose (○) and cellulose acetate (●) fractions. Singer's data on the acetate were obtained by use of the Lamm cell and ultracentrifuge.

content, and the molecular weights were determined by sedimentation rather than by light scattering.

Well-fractionated specimens of cellulose acetate have been investigated recently by Singer (7), who obtained sedimentation and diffusion data. His data are shown together with ours (figure 5) on a log-log plot of diffusion constant *versus* molecular weight. The agreement of the absolute values is interesting but not necessarily to be expected, since two different polymers are being compared and the method of molecular weight determination is different.

On the plot of  $D$  *versus*  $M$ , our fraction of highest molecular weight shows anomalous behavior which does not appear in the  $D$  *versus*  $[\eta]$  plot. This is not en-

tirely unexpected, since the first fractions precipitated in a fractionation procedure sometimes show abnormal behavior. It is interesting that whatever peculiarity this specimen may possess, it appears to affect the viscosity and diffusion constant in similar fashion, as may be seen from the plot of  $D$  versus  $[\eta]$ .

#### SUMMARY

A semimicro diffusion method for the characterization with respect to molecular weight of high-polymer fractions has been described, and examples have been given of its application in the study of nitrocellulose fractions. The essential feature of the method is the use of a pad of filter papers as a matrix to reduce convection in the solvent. As is predicted by theory, the maximum depth,  $d$ , at which nitrocellulose is detectable by a sensitive spot test is found to be related to the diffusion time,  $t$ , by an equation of the form:

$$\log t = A - \frac{d^2}{4.6Dt}$$

where  $D$  is the diffusion constant.

The determination of a single diffusion constant requires about 15 mg. of nitrocellulose and an over-all time of about 5 hr. A precision of  $\pm 10$  per cent or better in the diffusion constant may be anticipated for well-fractionated samples.

#### REFERENCES

- (1) BLAKER, R. H., BADGER, R. M., AND NOYES, R. M.: *J. Phys. Colloid Chem.* **51**, 574 (1947)
- (2) BLAKER, R. H.: Private communication of unpublished results.
- (3) FURTH, R.: *In Differentialgleichungen der Physik*, P. Frank and R. v. Mises, *Editors*, Vol. II, p. 532. Rosenberg, New York (1943).
- (4) GRALEN, N.: Dissertation, Uppsala, 1944.
- (5) JULLANDER, I.: *Arkiv. Kemi, Mineral. Geol.* **21A**, 1 (1945).
- (6) LONGSWORTH, L. G.: *Ann. N. Y. Acad. Sci.* **46**, 211 (1945).
- (7) SINGER, S. J.: *J. Chem. Phys.* **15**, 341 (1947).
- (8) WILLIAMS, J. W., AND CADY, L. C.: *Chem. Revs.* **14**, 171 (1934).
- (9) WILLIAMS, J. W., CARTER, R. O., JR., SHUEY, H. M., AND GOSTING, L. J.: O.S.R.D. Report No. 4123, declassified April 3, 1946.

COLLOID PROPERTIES OF LAYER SILICATES<sup>1</sup>

W. F. BRADLEY AND R. E. GRIM

*State Geological Survey Division, State of Illinois, Urbana, Illinois**Received February 20, 1948*

From the viewpoint of one interested in the structural aspects of colloids, a fortunate condition is encountered in the case of the common clay and soil minerals. It is inherent in the colloidal condition that dispersed or dispersible phases be of such low degree of crystalline perfection that x-ray (or electron) diffraction diagrams are at best less intense and less complete than those obtainable from macrocrystalline solids.

X-ray diffraction studies, first of the micas, and successively of an extended series of related layer silicates such as the brittle micas, the chlorites, talc, and pyrophyllite, have established that a highly stable complex structural unit exists which controls the varied physical properties of these related minerals. It has further developed that this same unit is the assemblage on which the crystallization of the two large groups of clay minerals, the illite group and the montmorillonite group, are based. The configuration of such a layer is illustrated in figure 1. The wide latitude of cation substitutions within this framework has recently been reviewed by Ross and Hendricks (11). For present purposes it is sufficient to observe that, whereas some certain regularity of ion distribution characterizes the macrocrystalline members, there is a range through which the magnitude of residual charge resulting from presence of lesser valent cations or from cation deficiencies gives rise to two major groups of characteristically microcrystalline clay minerals. In the one group charge deficiencies in a layer are balanced mainly by interlayer potassium ions, and the minerals are dimensionally stable and are actually varieties of micas. These are the illite group. The over-all charge deficiencies are about half as frequent as those of the crystalline micas and are considered to arise mainly from the presence of trivalent aluminum ions in tetrahedral coordination. In the other group about equally frequent charge deficiencies arise mainly from substitutions or defects in the octahedrally coordinated portion of the layer and are commonly balanced by sodium and/or calcium ions. These are the montmorillonite group of minerals, and in this group the interlayer ions are readily exchangeable and, in addition, the individual layers are subject to separation from each other by water and are readily dispersible. In nature these minerals are commonly observed to occur with one or two layers of water already interleaved between the characteristic silicate skeleton.

Base exchange is of course commonly thought of as an inorganic phenomenon, but the activity of organic bases in exchange has become a subject of proven interest, following a study by Giesecking (5), and has been utilized by Hendricks (7) to measure the van der Waals thickness of a number of large organic bases.

The water associated with montmorillonite in nature disposes itself regularly in layers between the silicate skeletons, affording characteristic interlayer spac-

<sup>1</sup> Published by permission of the Chief, Illinois State Geological Survey, Urbana, Illinois.

ings which are measurable by x-ray diffraction methods; in addition to the simple interlayer diffraction, some of the better specimens afford a series of integral higher orders of diffraction from the fundamental spacing which establish the fact that the alternating sequence of silicate and water layers is repeated a large number of times without irregularity. In the presence of added water additional layers penetrate between each individual silicate unit, with swelling of the specimen, and regularly constituted "hydrates" have been observed in which as many as four water layers separate successive silicate layers (3). The configuration of such layers and the likelihood of indefinite extension of the mechanism into com-

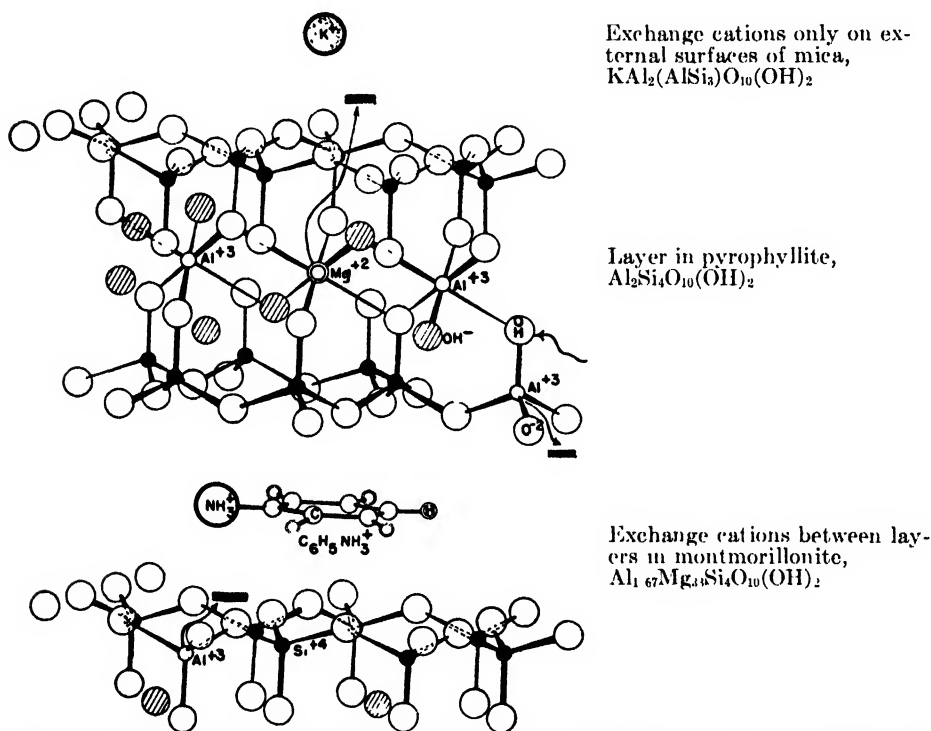


FIG. 1. The structural relationships of the montmorillonite type mineral with mica and pyrophyllite (after Hendricks).

plete dispersion is apparent from Hendricks' model of the association of such water (figure 2), which is based upon the known hydrogen-bonding properties (8). The concept of what constitutes bound water in this colloid system is thus particularly graphic.

One important commercial utilization of montmorillonite is in the preparation of drilling muds. Figure 3 illustrates the contrasting properties of suspensions of montmorillonite with those of a conventional clay mineral, kaolinite, whose crystalline particles disperse as entities. These diagrams represent the diffraction effects observed upon irradiation of a flowing stream of suspension as discharged through a capillary nozzle. The diagram of the kaolinite suspension

includes all the lines normally observed in solid specimens superposed over the characteristic water halos. The diagrams of the Wyoming bentonite suspension and of the montmorillonite base shale include the normal diagrams for the non-clay mineral accessories in each case, and the normal diffraction effects related to the prism zone—that is, to the lateral extension of the individual silicate sheets.

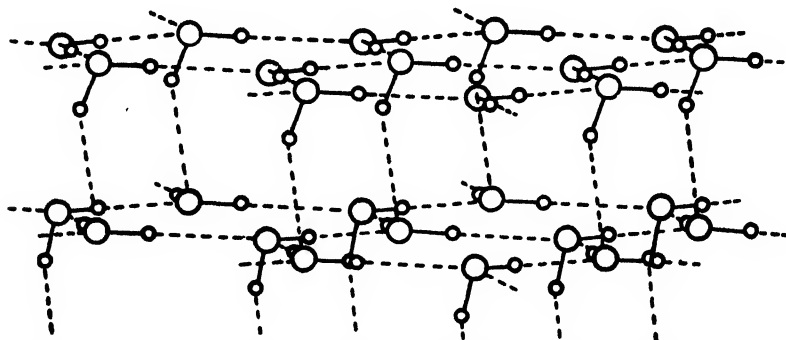


FIG. 2. Probable structural arrangement of multiple water layers (after Hendricks and Jefferson).

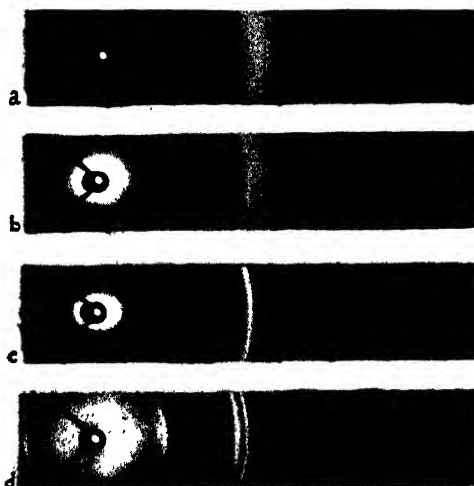


FIG. 3. X-ray diffraction diagrams of streaming clay suspensions issuing from a nozzle: (a) water; (b) suspension of 5 per cent of Wyoming bentonite in water; (c) suspension of 20 per cent of a montmorillonite containing oligocene shale in water; (d) suspension of 30 per cent of a kaolinitic clay in water. In suspensions (c) and (d) a phosphate dispersing agent was added.

No normal reflections or higher orders of reflection related to any basal spacing are observed. Except for the water halos, there is observed only a remarkably prominent low-angle scattering feature which arises from the dissemination of solid particles in the liquid medium. It is to be noted that of the two examples illustrated the low-angle feature is somewhat more pronounced for the Wyoming



bentonite, a natural sodium bentonite, than for the shale, which is mainly calcium saturated. The sodium bentonite is considered to be rather strictly dispersed down to individual silicate layers, whereas the calcium montmorillonite apparently retains a low degree of order between small groups of a few adjacent layers. One gram of the sodium bentonite appears to furnish as many dispersed particles as 3 or 4 g. of this particular shale.

In a system in which the condition of the dispersed phase is so clearly defined, and in which the nature of the water association upon particle surfaces has been subject to demonstration, a simple graphic mechanism for the striking thixotropic properties of such suspensions is easily visualized. In a set gel most if not all of the water molecules in the system are under the influence of one or more of the silicate lamellae, which are thus both isolated from each other, and at the same time bound together, by their associated water. Under mechanical deformation, moderate disruption of the water coordination permits ready yield, and the entire system may be worked into a suspension of only moderate viscosity by simple attrition of water molecules.

In this same vein it is also clearly true that in a given suspension the partition of water molecules between the "free" and the "bound" condition would be subject to influence by heat or by chemical agents. There is a highly developed art of controlling the viscosity of drilling muds by addition agents which suitably adjust the hydration state.

The flexibility of the above water relationships and the extensive activity of organic bases in exchange suggested promise in investigating the possible relationships with various organic liquids. The nature of the stable complexes resulting from the treatment of montmorillonite with two rather highly specialized types of organic compounds, the polyamines and the polyglycols, etc., has already received some study (1) and the value of this type of reaction in mineralogy is recognized (2, 10).

It seems to be rather generally true that simple polar organic solvents also "solvate" the montmorillonite surface, some of them affording clear instances of double layer complex formation comparable in configuration to those obtained with glycol or with the polyglycols. Such double-layer complexes are probably the general case. Among the amines, which are also active in base exchange, single-layer complexes are obtained with those molecules whose flat cross-section is less than the average area per exchange position for the montmorillonite, but the larger simple amines also exhibit the double-layer configuration. Figure 4 illustrates the nature of the clear sequences of orders of diffraction from the basal spacing which are observed in those cases where a definite characteristic complex formation is realized. In general, this type of complex does not swell in the presence of an excess of the same agent. Their stability is considered to be occasioned by a quite specialized interaction between the actual aliphatic chains and the oxygen-populated clay surface, amounting to something like a  $C-H \cdots O$  bond. Multiple layers such as those built successively by water would thus not be anticipated.

The recently reestablished method of thermal analysis has been used effec-

tively in qualitative estimation of the energy of association of water with montmorillonite under various circumstances (9). For complexes with the more vola-

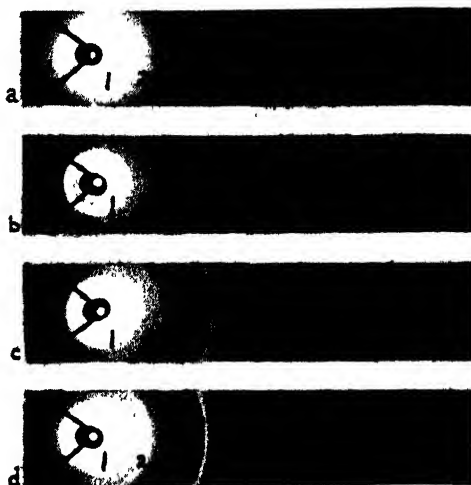


FIG. 4. Typical diffraction diagrams of montmorillonite-organic liquid complexes. (a) with ethanol; (b) with acetone; (c) with the monoethyl ether of propylene glycol; (d) with the dimethyl ether of tetraethylene glycol. The more prominent higher orders of diffraction from the base are indicated.

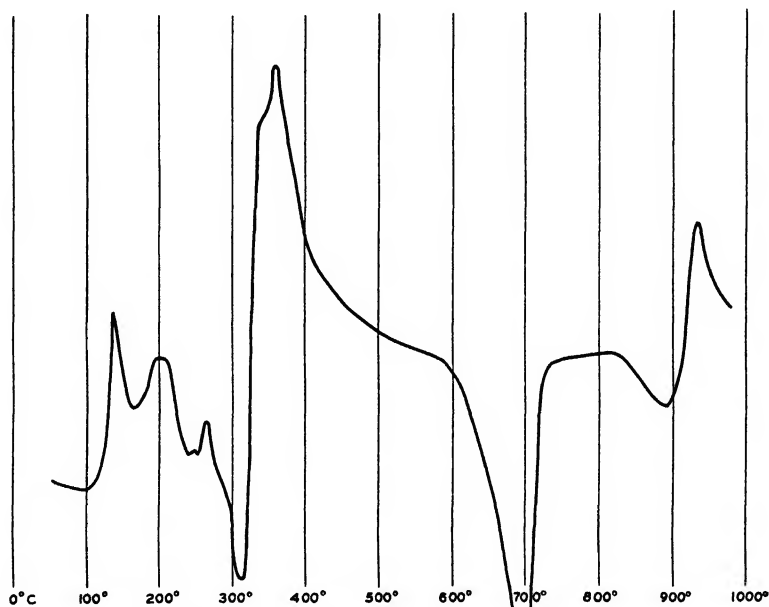


FIG. 5. Differential thermal analysis curve for complex of Wyoming bentonite with the dimethyl ether of tetraethylene glycol.

tile liquids, evaporation is far too ready at room temperatures to permit the application of such a method, but more stable complexes (as illustrated in figure

5 by that with the dimethyl ether of tetraethylene glycol) exhibit distinct, although not interpreted, effects. A series of amine complexes, stabilized by their activity in exchange, afford greater promise. In figure 6 are reproduced the differential curves for complexes with three normal primary amines, in the order of increasing chain lengths, and for an example of a quaternary ammonium base.

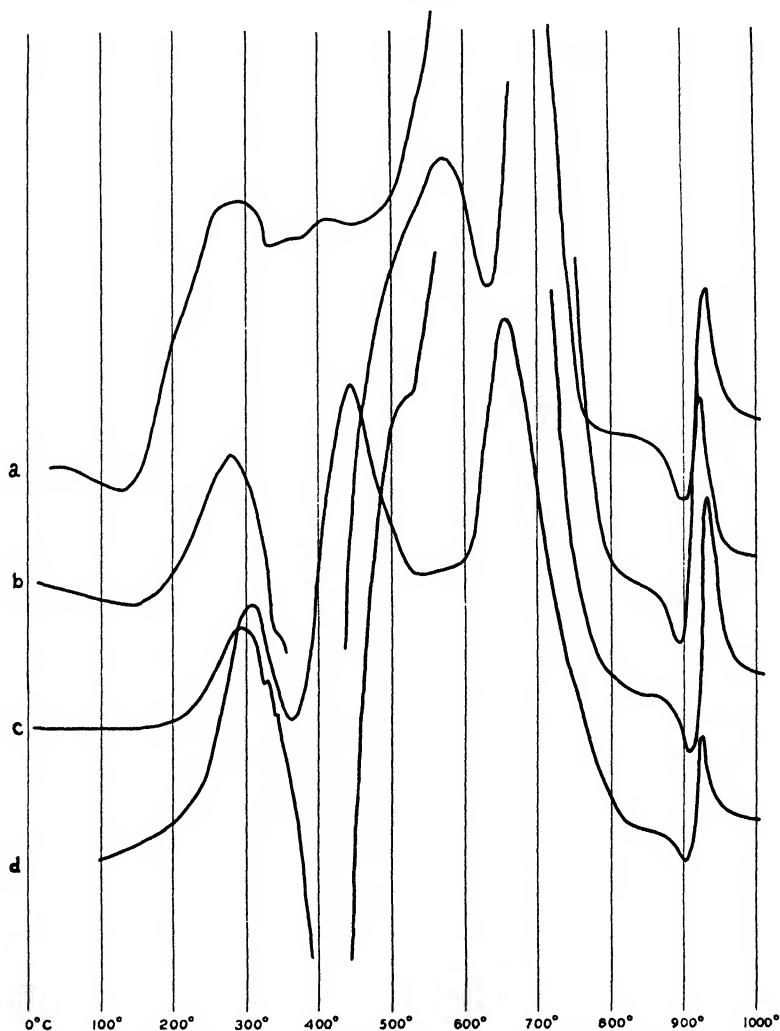


FIG. 6. Differential thermal analysis curves for dry complexes of Wyoming bentonite with amines: (a) butylamine; (b) dodecylamine; (c) octadecylamine; (d) dimethylcetyl-laurylammonium bromide.

The common feature of these curves is the shoulder indicating initiation of an endothermal reaction at around 300°C. In the registration of these thermal curves, it is also common practice to register simultaneously a record of the furnace temperature itself, such record being normally a smooth line of uniform gradient. Figure 7 is a reproduction of the composite record for the complex

with octadecylamine. On this curve it is noted that at about  $400^{\circ}\text{C}$ ., where the specimen temperature is still markedly below the reference temperature, a sudden combustion has heated up the whole furnace. The same effect, but less intense, is observed with the dodecylamine complex.

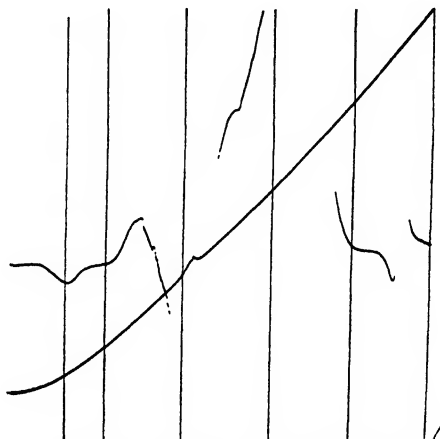


FIG. 7. Differential thermal analysis trace as in figure 6a (but not dry), showing the furnace temperature trace.

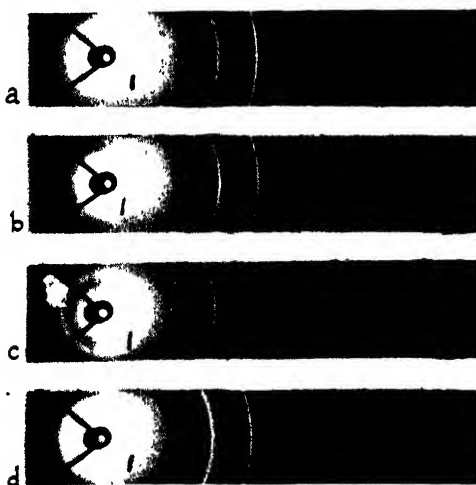


FIG. 8. X-ray diffraction diagrams of amine complexes with Wyoming bentonite: (a) complex with butylamine; (b) complex with dodecylamine; (c) butylamine complex heated to  $280^{\circ}\text{C}$ .; (d) octadecylamine complex heated to  $400^{\circ}\text{C}$ . Essentially equivalent diagrams result from heating of each complex within equivalent temperature range.

Materials being subjected to thermal analysis can, of course, be withdrawn at any chosen point and are available for examination. In figure 8 are reproduced x-ray diffraction diagrams for two amine complexes and for specimens withdrawn at about  $280^{\circ}\text{C}$ . and about  $400^{\circ}\text{C}$ . The complex cell heights have been altered

from those characteristic of the respective amines to a stable configuration of height about 12.8 Å, a figure below that which would accommodate one aliphatic chain but compatible with an alternation of montmorillonite layers with graphite. The endothermal feature remarked above can now be identified as the dehydrogenation of entire aliphatic chains; the released hydrogen ignites in the furnace atmosphere to overheat the whole specimen block sharply, and the coked carbon is left between the silicate layers, eventually burning off at higher temperatures. In table 1 are analyses of prepared coked specimens heated in an open oven to the indicated temperatures.

The carbon layers are not truly graphite. An ideal graphite layer would provide about 28 g. of carbon per 100 g. of ash. The deposit is more comparable to a single layer of petroleum coke, although it may well be partially graphitized. The hydrogen contents cited in table 1 are not subject to the degree of accuracy normally realized in hydrogen determinations because of the necessity of correction for water expelled from the silicate framework under the ignition conditions,

TABLE 1.  
*Analyses of prepared coked specimens*

SPECIMEN	GRAMS PER 100 G. OF ASH		
	N	C	H
Octadecylamine-bentonite .....	1.7	26.2*	4.8*
Same heated to 275°C. ....	Not determined	14	0.6
Same heated to 400°C. ....	1.0	8.5	0.23

\* Calculated from per cent nitrogen.

but are rather to be looked upon as maximum figures. The coke composition is clearly no more than one hydrogen atom to two carbon atoms.

The degradation of hydrocarbon chains of this sort to coke is presumably the ultimate in catalytic cracking. The activation treatment of natural montmorillonite clays for cracking seems only to be a suitable preparation of the oxygen-populated clay mineral surface to afford this dehydrogenation to only a useful degree.

The aspects of the colloid chemistry of this type of silicate layer which are outlined above are consequences of the phenomenon of "bound water" and the analogous concept "bound solvent." The same silicate skeleton exhibits another separate degree of water association in that part of the skeleton which includes hydroxyl ions. Far less is understood about these hydroxyl water relationships, and there is apparently less latitude of possible variation, but it is at least readily apparent that the dehydroxylated silicate skeleton is capable of reassociating with itself hydroxyl water of markedly lesser association energy than that of the natural structure. Figure 9 is a series of thermal analysis curves taken from a recent study of this feature (6). Illustrated are the thermal curves of a Wyoming bentonite and curves of the same bentonite after firing to various temperatures

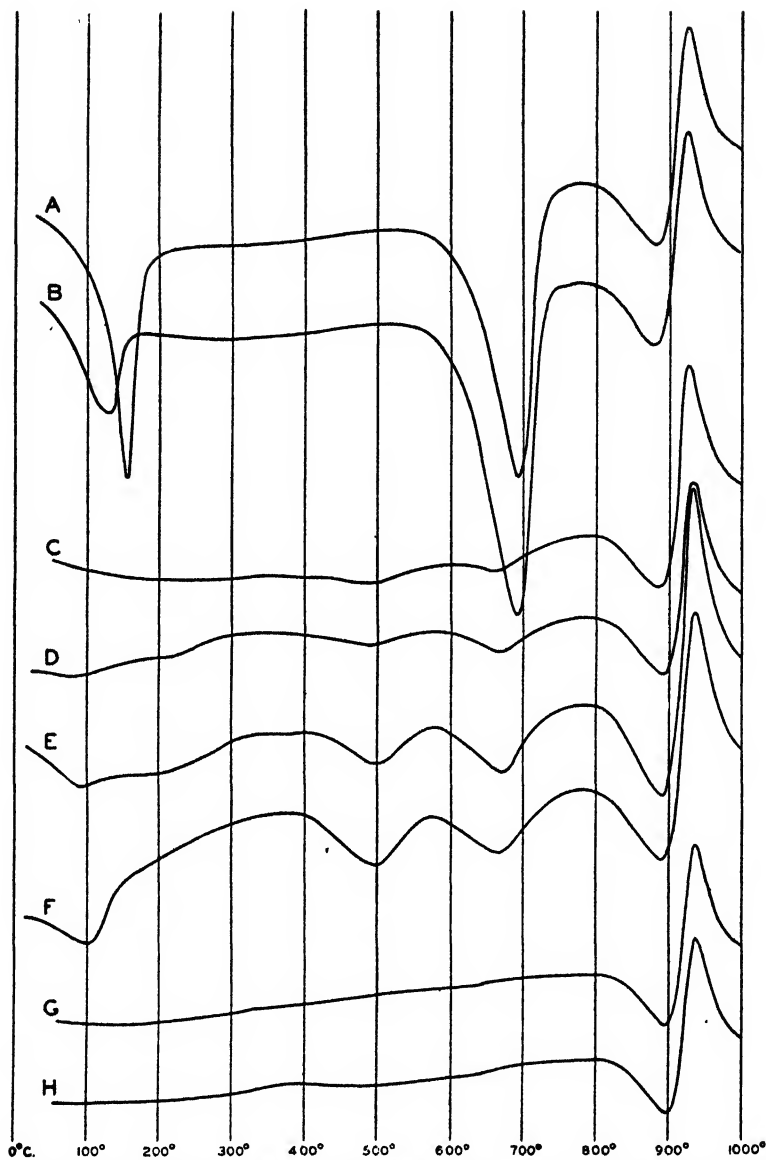


FIG. 9. Differential thermal analysis curves of dehydrated and rehydrated Wyoming bentonite.

A. Mill-run Wyoming bentonite

B. Heated to 500°C. for 1 hr.; curve run after standing 13 days

C. Heated to 600°C. for 1 hr.; curve run after standing 11 days

D. Heated to 600°C. for 1 hr.; curve run after standing 68 days

E. Heated to 600°C. for 1 hr.; curve run after standing 146 days

F. Heated to 600°C. for 1 hr.; curve run after standing 268 days

G. Heated to 800°C. for 1 hr.; curve run after standing 76 days

H. Heated to 800°C. for 1 hr.; curve run after standing 268 days

with rehydration under laboratory conditions. It is perhaps significant that it has been found in catalyst activation and regeneration that the use of steam to maintain a hydroxylated active product is effective in preventing the susceptibility of catalysts to sulfur poisoning (4).

## REFERENCES

- (1) BRADLEY, W. F.: J. Am. Chem. Soc. **67**, 975-81 (1945).
- (2) BRADLEY, W. F.: Am. Mineral. **30**, 704-13 (1945).
- (3) BRADLEY, W. F., GRIM, R. E., AND CLARK, G. L.: Z. Krist. **97**, 216-22 (1937).
- (4) DAVIDSON, R. C.: Petroleum Refiner, Sept. 1947, 3-12.
- (5) GIESEKING, J. E.: Soil Sci. **47**, 1-13 (1939).
- (6) GRIM, R. E., AND BRADLEY, W. F.: Am. Mineral., in press.
- (7) HENDRICKS, S. B.: J. Phys. Chem. **45**, 65-81 (1941).
- (8) HENDRICKS, S. B., AND JEFFERSON, M. E.: Am. Mineral. **23**, 863-75 (1938).
- (9) HENDRICKS, S. B., NELSON, R. A., AND ALEXANDER, L. T.: J. Am. Chem. Soc. **62**, 1457-64 (1940).
- (10) MACEWAN, D. M. C.: Nature **154**, 577-8 (1944).
- (11) ROSS, C. S., AND HENDRICKS, S. B.: U. S. Geol. Survey, Profess. Paper No. 205-B, 79 pp. (1945).





# THE EFFECT OF WATER AND OTHER ADDITIVES ON THE FIBER STRUCTURE OF CALCIUM SOAP GREASES<sup>1</sup>

D. H. BIRDSALL AND B. B. FARRINGTON

*California Research Corporation, Richmond, California*

*Received June 23, 1948*

## I. INTRODUCTION

The theory is now generally accepted that most lubricating greases are two-phase systems consisting of a continuous phase of lubricating oil and a dispersed phase of crystalline or fibrous soap. The physical and chemical properties of the dispersed soap phase largely determine the properties of the grease and dictate the conditions under which the grease will lubricate satisfactorily. Previous work by the authors (2, 3) has consisted of a general study of the fiber structure of greases of various soap types. Since calcium soap greases represent a large proportion of greases now marketed, a detailed study has been undertaken of this specific soap type.

In calcium soap greases the soap phase will readily agglomerate and separate from the oil phase unless a stabilizer is added to prevent this action. Several additives are effective in producing the desired stabilization effect, the most commonly used being water. This paper is concerned with stabilization by hydration as well as with anhydrous systems stabilized with calcium acetate and with stearic acid.

## II. EXPERIMENTAL

All micrographs presented in this paper were obtained with the RCA Model B electron microscope. They were taken at direct magnifications of 4000 $\times$  and 8200 $\times$ .

The particle size was relatively large in the materials studied, but it was found advisable, in order to improve surface detail, to use the shadow-casting technique as described by Williams and Wyckoff (7). Specimens were shadowed with gold at a ratio of filament height to specimen distance of 1 to 4 and at a pressure of  $10^{-4}$  mm.

All specimens were mounted on Parlodion substrates after having been diluted with small amounts of medicinal white oil to soften them. A few drops of a light petroleum naphtha were placed on each specimen after mounting on the individual specimen screens. This removed most of the mineral oil phase and thereby increased detail in the soap structure which would ordinarily have been masked by adsorbed oil.

<sup>1</sup> Presented at the Symposium on Gel Formation, Detergency, Emulsification and Film Formation in Non-Aqueous Colloidal Systems which was held under the auspices of the Division of Colloid Chemistry and the Division of Petroleum Chemistry at the 113th Meeting of the American Chemical Society, Chicago, Illinois, April, 1948.

*Sample preparation*

The grease used for the initial phase of the program (grease No. 1, table 1) was a commercial product prepared as follows: The soap concentrate was prepared by the saponification in a pressure autoclave of a high-grade tallow with calcium hydroxide in the presence of a small amount of mineral oil. After saponification was complete the soap concentrate was completely dehydrated by heating in an open vessel and was then gradually hydrated by adding water as the soap concentrate was cooled from 235°F. to 210°F. Part of the water was evaporated during this hydration process, but a substantial amount remained in the grease intimately associated with soap. The resultant hydrated soap concentrate was mixed with a mineral oil having characteristics as outlined in the

TABLE 1  
*Composition of greases*

GREASE NO.	SOAP		STABILIZER		MINERAL OIL			
	Type	Weight	Type	Weight*	Viscosity 100°F. SSU	Viscosity 210°F. SSU	Viscosity index	Weight
		<i>per cent</i>		<i>per cent</i>				<i>per cent</i>
1	Calcium tallow	17.7	Water	1.3	200	40	15	81
2	Calcium tallow	12.9	Water	1.1	2600	120	60	86
3	Calcium tallow	6.4	Water	0.6	4000	160	70	93
4	Calcium stearate	15	Calcium acetate	2.0	460	50	0	83
5	Calcium stearate	15	Calcium acetate	3.0	460	50	0	82
6	Calcium stearate	15	Calcium acetate	4.0	460	50	0	81
7	Calcium stearate	20	Stearic acid	0.2	460	50	0	79.8
8	Calcium stearate	20	Stearic acid	1.0	460	50	0	79
9	Calcium stearate	20	Stearic acid	2.0	460	50	0	78
10	Calcium stearate	20	Stearic acid	3.0	460	50	0	77

\* Indicates amount of stabilizer in completed grease.

table. The final grease had a water content of 1.3 per cent and a soap content of 17.7 per cent.

The above product was placed in an oven at 230°F. and was stirred frequently to insure even dehydration. Samples were taken from the bulk of the grease at hourly intervals until essentially all of the water had been removed. The water content of each sample was determined by the conventional "water by distillation" test (A.S.T.M. D95-46).

Samples for the second phase of the program were obtained during the commercial manufacture of a grease with a soap component similar to that of grease No. 1 but prepared with a mineral oil of higher viscosity. Samples were taken of the soap concentrate as it was being hydrated and of the finished grease after the constituent mineral oil had been mixed in. This grease is referred to as grease No. 2 in the table.

Grease No. 3 was a semifluid commercial product having a high-viscosity mineral oil. Samples of this grease were taken at only two stages of manufacture, as indicated, merely as a check on results obtained on the other two greases.

Greases Nos. 4, 5, and 6 were prepared in the laboratory from commercial, neutral, preformed calcium stearate<sup>2</sup> and were stabilized with varying concentrations of calcium acetate, as outlined in table 1. The greases were essentially anhydrous, since each grease was heated to 400°F. during preparation and no water was added as the greases were cooled.

Greases Nos. 7, 8, 9, and 10 were also anhydrous laboratory preparations of calcium stearate in oil which were stabilized with free stearic acid.

### III. HYDRATED CALCIUM SOAP GREASES

#### *Progressive dehydration of grease*

Micrographs in figure 1 are those taken of grease No. 1 as it was progressively dehydrated. Figure 1a represents the original grease before any of the water was removed. The twisted fibers characteristic of hydrated calcium soap greases, which probably consist mainly of the calcium soap-water complex (4), are clearly visible. This sample has a water content of 1.3 per cent.

In figure 1b the water content was reduced to 1.1 per cent. It can be seen that the fibers have softened and started to untwist, although the fiber dimensions have not changed appreciably. There is also an indication in this picture, as in previous micrographs, that the structure is actually made up of two or more individual fibers twisted about one another.

The water content of the sample in figure 1c is 0.7 per cent. Here a trace of fiber structure still remains, but most of the soap has agglomerated and is scattered throughout the field.

In figure 1d at a water content of 0.4 per cent all fibrous structure has disappeared and the soap has become essentially amorphous. At this stage of dehydration the grease was unstable and the soap readily separated from the oil when the mixture was agitated. Figure 1e, taken at a water content of 0.1 per cent, exhibits little or no change from figure 1d and no structural change was observed in further dehydrated samples.

#### *Hydration of calcium soap*

The samples for this phase of the program were taken from a calcium soap concentrate after saponification was complete and the soap concentrate had been dehydrated. This first sample, the dehydrated soap concentrate, is shown in figure 2a; no structure is visible and the amorphous mass is similar in appearance to the dehydrated soaps in figure 1.

Micrograph 2b is of a sample which was obtained after the first increment of water had been added to the soap concentrate during the hydration process. The water was added when the soap concentrate temperature was about 230°F. and, although a portion of the water evaporated, the actual water content of the sample is 1.3 per cent. The fibers or soap crystals form at this early stage of hydration but they are not so uniform in size or shape as are the final hydrated

<sup>2</sup> Mallinckrodt calcium stearate, impalpable powder.

soap fibers. These are apparently the seed crystals which form the basic structure for the final soap fibers as postulated by Hoepler (4).

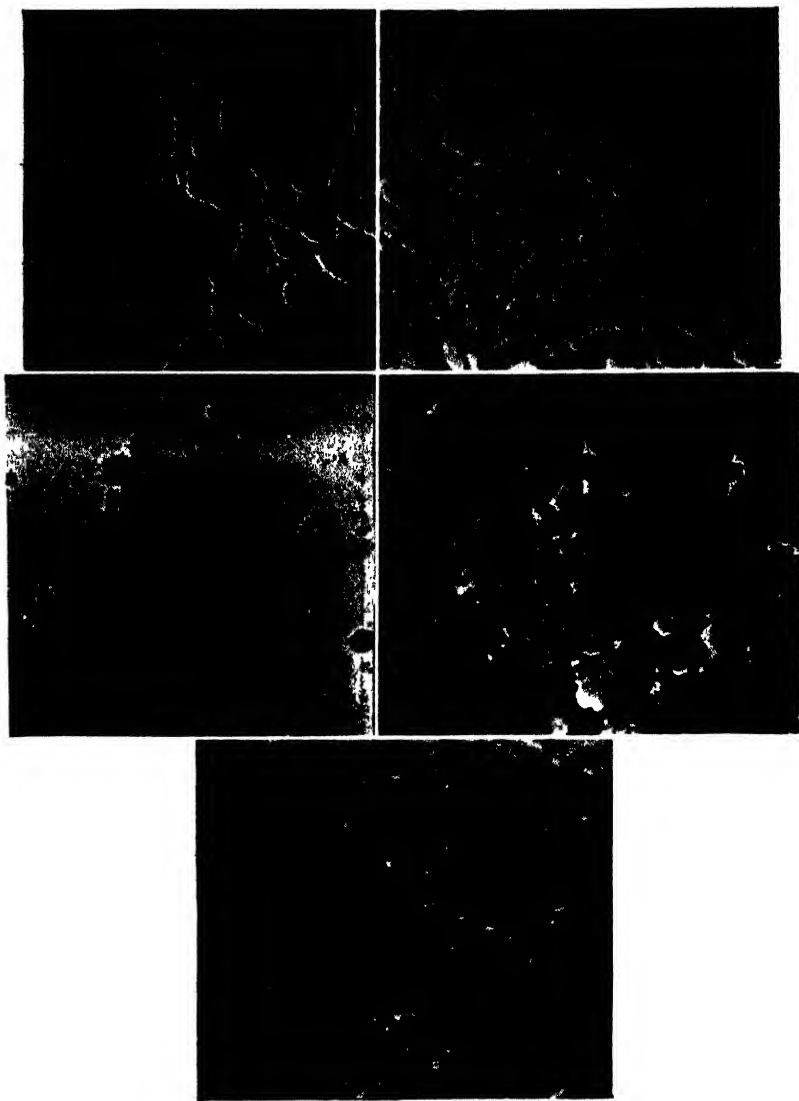


FIG. 1. Progressive dehydration of a calcium soap grease at 230°F. (grease No. 1). 8200  $\times$ . (a) original grease (1.30 per cent water); (b) 15 per cent dehydrated (1.1 per cent water); (c) 50 per cent dehydrated (0.7 per cent water); (d) 70 per cent dehydrated (0.4 per cent water); (e) 90 per cent dehydrated (0.1 per cent water).

In figure 2c the second increment of water has been added to the soap concentrate, the actual water content being 1.8 per cent. In this case the fibers have lengthened considerably and one fiber, to the lower left of the picture, appears to be nearly 3  $\mu$  in length. The heterogeneity of the structure in this picture indicates that the fibers tend to grow to considerable lengths but do not

change in width. The sample in figure 2d was taken after the total amount of water had been added to the soap concentrate. The soap concentrate tem-

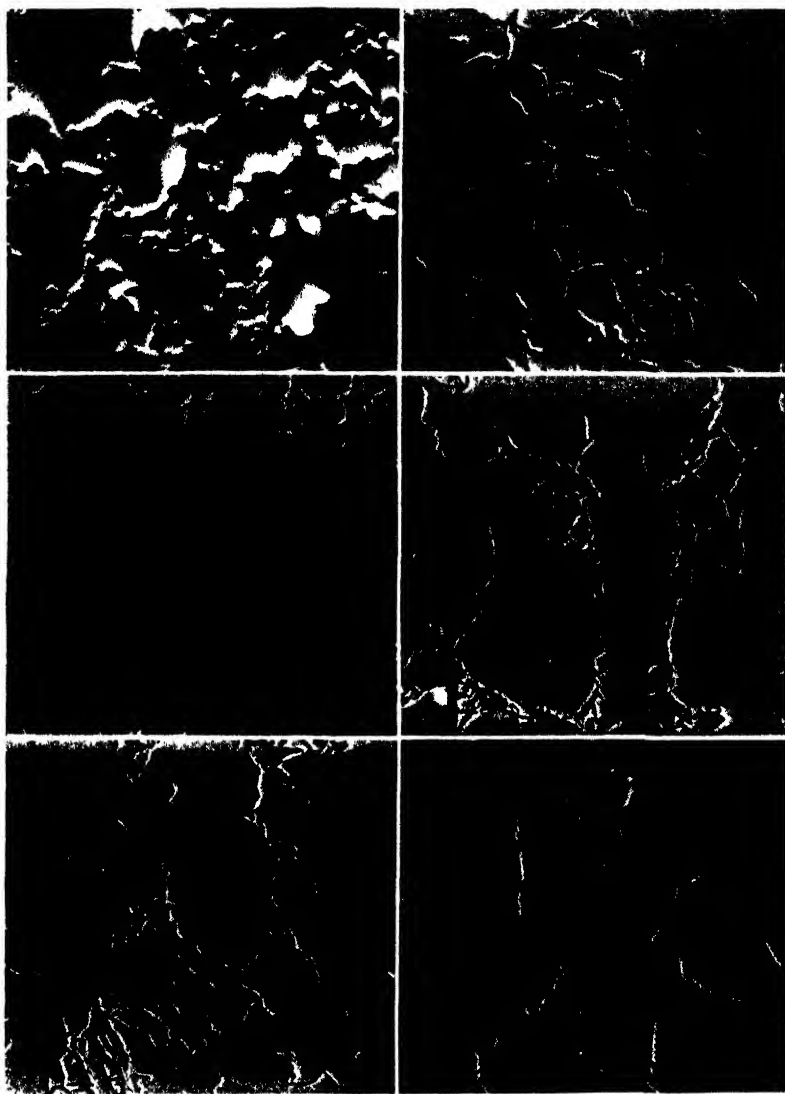


FIG. 2. Progressive hydration of calcium soap concentrate (grease No. 2). 8200  $\times$ . (a) dehydrated soap concentrate; (b) soap concentrate plus 1.3 per cent water; (c) soap concentrate plus 1.8 per cent water; (d) soap concentrate plus 2.4 per cent water; (e) finished soap concentrate, 1.9 per cent water; (f) finished grease, 1.1 per cent water.

perature at this point was about 210°F., and the actual water content of the sample is 2.4 per cent. Here the long fibers have been torn apart by the mechanical action of the mixer and are more uniform in length.

In figure 2e the hydrated soap concentrate had been mixed for 1 hr. at about

210°F. Some water was lost during this process, since the water content at this point is 1.9 per cent. Here a few of the fibers have assumed the tightly twisted formation typical of the final grease.

In figure 2f the entire mineral oil constituent had been added to the soap concentrate. The water content of this sample is 1.1 per cent. Since saponification and hydration were complete before the soap concentrate was mixed with the additional mineral oil, it is reasonable to assume that the tightly twisted structure is the result of mixing action rather than of chemical changes in the soap.

The above theory is supported by the micrographs in figure 3 of grease No. 3. Figure 3a is of a soap concentrate obtained immediately after the soap was



FIG. 3. Modification of fiber structure during "mixing off" of calcium soap concentrate for grease No. 3. 8200  $\times$ . (a) hydrated soap concentrate (contains about 75 per cent oil); (b) finished grease (94 per cent oil).

hydrated. Figure 3b is of the final grease made from this soap concentrate. Here again the twisted structure appears to be a result of prolonged stirring during the mixing process.

#### IV. ANHYDROUS CALCIUM SOAP GREASES

##### *Calcium acetate stabilization*

In the study of the effect of stabilizers other than water on calcium soap structure, it has been found that the fiber characteristics are almost entirely dependent upon the type of stabilizer or dispersant and its concentration. Calcium acetate has been used as a stabilizer, and figure 4 shows the effect of various concentrations of this salt on a grease prepared from preformed commercial calcium stearate and a mineral oil of medium viscosity. All greases were prepared with 15 per cent calcium stearate, the mineral oil content being varied to allow for differences in the concentration of calcium acetate. An attempt was made to prepare a grease with 1 per cent calcium acetate, but the resultant product was synergetic and did not form a grease. Figure 4a is of a grease containing 2 per cent calcium acetate. There is a faint trace of fiber

structure in this micrograph, although the greater percentage of the soap is amorphous and has not "fibred out."

In figure 4b the calcium acetate is present in a 3 per cent concentration. The fiber structure is more extensive than in figure 4a, and the grease is considerably more stable.

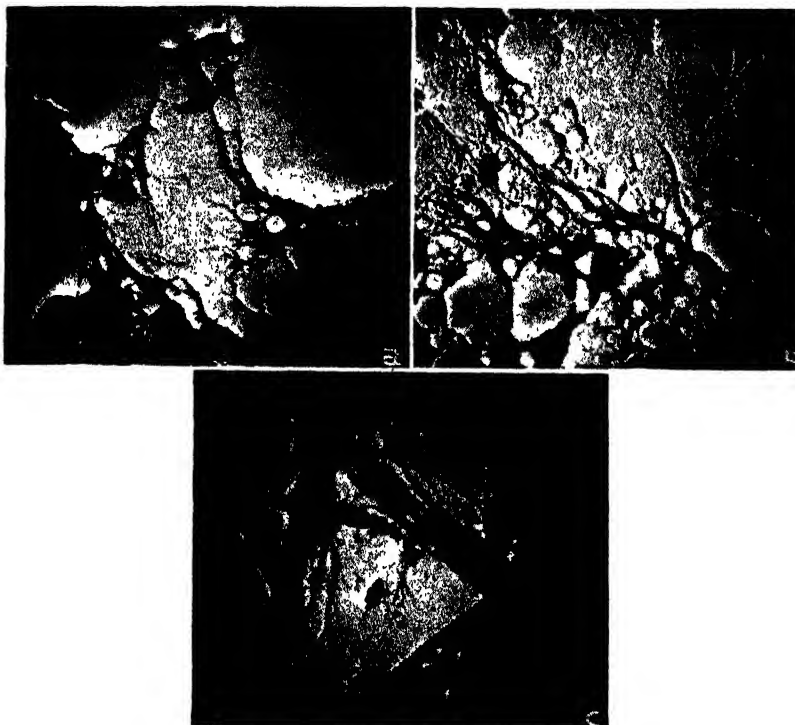


FIG. 4. Calcium acetate stabilization of calcium stearate grease (greases Nos. 4, 5, and 6). 4000 $\times$ . (a) 2 per cent calcium acetate; (b) 3 per cent calcium acetate; (c) 4 per cent calcium acetate.

Figure 4c portrays a grease with a calcium acetate concentration of 4 per cent. The fiber development here seems to be at a maximum, since there is little or no amorphous soap visible.

#### *Free fatty acid stabilization*

Small amounts of free fatty acids have long been known to improve the texture of greases as well as reduce synergetic tendencies. The electron micrographs of greases containing identical amounts of calcium stearate and varied concentrations of free stearic acid are shown in figure 5.

A mixture of calcium stearate, oil, and 0.2 per cent free stearic acid is shown in figure 5a. This quantity of free acid is insufficient to stabilize the granular soap structure, and the sample readily separates into two phases.

The sample shown in figure 5b contains 1 per cent free stearic acid. The mixture is synergetic but of slightly improved texture over the sample containing 0.2 per cent stearic acid.

A grease containing 2 per cent free stearic acid is shown in figure 5c. A crystalline or fibrous structure is readily visible in this micrograph, and the grease is smooth and exhibits no syneresis. It was semifluid when prepared but hardened in about 12 hr. to a buttery texture. This change in consistency or hardness upon aging is characteristic of greases containing an appreciable amount of free fatty acid. The phenomenon is probably indicative of a crystalline growth or a transformation from a gel to a pseudo-gel as the grease ages.

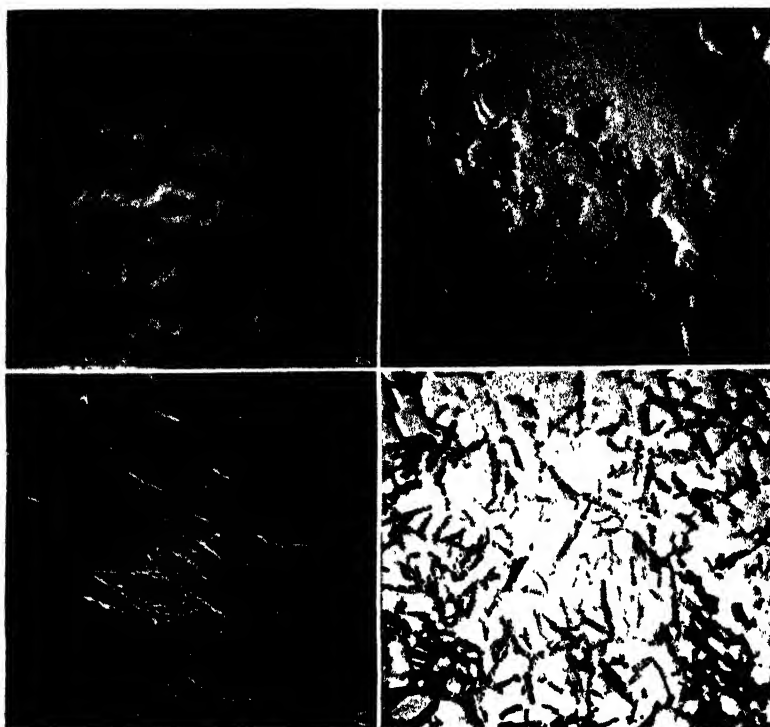


FIG. 5. Free fatty acid stabilization of calcium stearate grease (greases Nos. 7, 8, 9, and 10). 4000  $\times$ . (a) 0.2 per cent stearic acid; (b) 1 per cent stearic acid; (c) 2 per cent stearic acid; (d) 3 per cent stearic acid.

There appears to be a tendency for these greases to become more opaque as they harden, a fact which also indicates an enlargement of the particle size.

The grease in figure 5d contains 3 per cent free stearic acid. This product was stable immediately after preparation and remained stable, although it also hardened rapidly upon aging.

#### V. DISCUSSION

In comparing the micrographs of hydrated calcium soap greases at various stages of hydration with their physical appearance, it is evident that a fiber structure must be present before a stable product is formed, and that this structure is present only when a sufficient amount of water has been incorporated into the grease. While in anhydrous calcium soap greases stabilizers have a



radically different effect on the fiber shape and size, in the two cases studied the grease is stable only when a fibrous structure is visible under the electron microscope.

It is interesting to note that in both the calcium acetate-stabilized and the water-stabilized greases, the minimum concentration for a stable product is in the vicinity of equimolar concentrations of stabilizer and soap. The molecular configuration in the hydrated calcium soaps is probably of a type suggested by Doscher and Vold (1) in their study of sodium soaps; that is, soap anions bound together by molecules of water with the calcium ions distributed in the interstices. The molecular orientation in the case of calcium acetate stabilization and stearic acid stabilization is undoubtedly more complex; however, greases of this type may possibly be studied by x-ray diffraction or electron diffraction techniques.

The hydrated calcium stearate fibers have a reasonably uniform width of 400–500 Å. If the soap molecules are oriented perpendicularly to the long axis of the fibers, this fiber width would represent approximately the length of ten stearic acid unit cells or twenty stearic acid molecules (5). The hydrated calcium stearate fibers evidently have no tendency to split axially into smaller components, as do the fibers of sodium laurate reported by Marton *et al.* (6).

The calcium acetate-stabilized greases have a tendency to form fibrous bundles more typical of sodium soap fibers. However, the minimum fiber width noted in these micrographs is of the order of 250 Å, a value which would again indicate a fiber width of several molecules.

#### VI. SUMMARY

The micrographs presented indicate that the fiber or crystalline structure in hydrated calcium soap greases disintegrates concurrently with the removal of water. The fiber disintegration leads in turn to the separation of soap and oil.

Stearic acid and calcium acetate act as fiber builders in calcium soap greases but the fibers are radically different in size and shape from those in the hydrated grease.

For effective structural stabilization calcium acetate or water must be present in molar concentrations approximately equal to or greater than that of the soap.

The authors wish to express their gratitude to Dr. R. T. Macdonald and Dr. B. W. Hotten of the California Research Corporation, Richmond, California, for their helpful suggestions in the preparation of this paper and to the University of California, Berkeley, for the use of its electron microscope.

#### REFERENCES

- (1) DOSCHER, T. M., AND VOLD, R. D.: *J. Phys. Colloid Chem.* **52**, 148 (1948).
- (2) FARRINGTON, B. B., AND BIRDSALL, D. H.: *Inst. Spokesman (Natl. Lubricating Grease Inst.)* **11**, No. 1, 4 (1947); *Oil Gas J.* **45**, 268 (1947).
- (3) FARRINGTON, B. B., AND DAVIS, W. N.: *Ind. Eng. Chem.* **28**, 414 (1936).
- (4) HOEPLER, F.: *Fette u. Seifen* **49**, 700 (1942).
- (5) MARKLEY, K. D.: *Fatty Acids*, p. 84. Interscience Publishers, Inc., New York (1947).
- (6) MARTON, L., MCBAIN, J. W., AND VOLD, R. D.: *J. Am. Chem. Soc.* **63**, 1990 (1941).
- (7) WILLIAMS, R. C. AND WYCKOFF, R. W. G.: *J. Applied Phys.* **17**, 23 (1946).

PROPERTIES OF SYSTEMS OF CALCIUM STEARATE AND CETANE  
AS DEDUCED FROM X-RAY DIFFRACTION PATTERNS<sup>1, 2</sup>

ROBERT D. VOLD AND MARJORIE J. VOLD

*Department of Chemistry, University of Southern California, Los Angeles 7, California**Received June 23, 1948*

This paper presents the results of x-ray examination at room temperature of systems of anhydrous calcium stearate in cetane which had been equilibrated at various elevated temperatures and then quenched. A series of nineteen samples at closely spaced compositions from 17 to 100 per cent calcium stearate were quenched from 130°C. Four additional series, at 20, 38, 67, and 87 per cent calcium stearate, were quenched from a succession of temperatures between 100° and 220°C. Finally, the effects of other thermal and mechanical treatment, and the effect of water were investigated in a few instances. The x-ray work was supplemented by visual and microscopic examination of the samples.

The work is part of a broad general program which has for its object determination of the phases present in grease systems, the extent to which these represent an equilibrium condition, and the relationship between phase state and physical characteristics of the grease. The phase behavior of oil-free calcium stearate has already been reported (11). The next step is investigation of the behavior of calcium stearate with a number of pure hydrocarbons of varying structure, of which cetane is one example.

## EXPERIMENTAL

*Materials*

The calcium stearate used was preparation I, which has already been described (11). It was always freshly dried to constant weight at 110°C. immediately before use. Pure cetane was obtained from the du Pont Company. It was freed of dissolved oxygen by prolonged sweeping with nitrogen and dried over calcium chloride; it had  $n_D^{20} = 1.4345$  compared to  $n_D^{20} = 1.43449$  reported by Deanesly and Carleton (2).

*Preparation of samples*

Dry calcium stearate and cetane were weighed into Pyrex glass tubes, mixed intimately at room temperature, sealed, maintained for 1 hr. at the elevated temperature from which final quenching was to be made (except that 130°C. was used for systems ultimately quenched from still higher temperatures), cooled, re-mixed at room temperature, maintained for 1 hr. at the chosen elevated

<sup>1</sup> Presented at the Symposium on Gel Formation, Detergency, Emulsification and Film Formation in Non-Aqueous Colloidal Systems which was held under the auspices of the Division of Colloid Chemistry and the Division of Petroleum Chemistry at the 113th Meeting of the American Chemical Society, Chicago, Illinois, April, 1948.

<sup>2</sup> This work was undertaken as part of a project, "Phase Studies of Greases," sponsored by the Office of Naval Research.

temperature, and finally quenched in a freezing mixture of solid carbon dioxide and ethyl alcohol. This elaborate mixing technique is required to insure uniform distribution of the components, since all the anhydrous samples are extremely viscous even at high temperatures and are also subject to decomposition.

Diffraction patterns were obtained with the North American Philips Company x-ray spectrometer as previously described (11). Almost all patterns were obtained in duplicate, primarily to check the reality of faint lines almost lost in the background fluctuation. Samples for x-ray examination were made by pressing about 0.3 g. of the prepared mixture described above into a 15-mm. hole in a glass microscope slide, and smoothing the surface by passing a second microscope slide over the surface under gentle pressure. In dilute systems cetane is exuded in this process. Since this is cetane held loosely in large capillary spaces, its loss would not be expected to affect the diffraction pattern except in the intensity of the cetane halo relative to other lines in the pattern. That the pattern is substantially independent of the amount of cetane lost, provided the soap is not subjected to sufficient pressure to deform the soap lattice, has been directly verified by experiment. In the most dilute systems (10 per cent soap), and also for liquid cetane, the slide was covered with a film of polystyrene 0.0015 in. thick. This was sealed to the slide with a drop of acetone before filling so that covered samples were not smoothed off on the surface but merely pressed smooth against the polystyrene film.

Visual examination of the samples in the glass tubes in which they were prepared was conducted during heating, at dry ice temperature, and after warming to room temperature, supplemented at the latter temperature by observations of consistency and texture during preparation of the samples for x-ray analysis. Microscopic examination was made between crossed polaroid pieces at a magnification of 120 diameters. All samples were examined microscopically after 45 days' aging at room temperature as well as shortly after preparation.

## RESULTS

### *Visual observations*

Room temperature mixes of calcium stearate with cetane change gradually from fluid dispersions of soap in the solvent (which wets it), from which the soap readily sediments, to uniform pastes to "dry" powders in which the solvent has fully disappeared into interparticle spaces. There is no tendency for the soap to swell in the solvent nor, although no quantitative measures of sedimentation volume were made, is there any marked tendency to form a gel structure. The same is true of samples which have been equilibrated at 100°C.

As the samples are heated, transformation begins to occur, yielding an extremely viscous, translucent material. This change begins at about 105–113°C., depending on the soap content; little further decrease in opacity occurs above 130°C. in all samples up to and including 78.8 per cent soap. Samples containing from 63.6 to 78.8 per cent soap are markedly clearer at 130°C. than either more dilute or more concentrated systems. On continued heating the only detectable

change is a gradual increase in fluidity, up to even 300°C., except that the very concentrated systems (87 per cent) become somewhat less opaque, reaching a static condition at least by 160°C.

The samples heated to 130°C. or higher have all undergone conversion to a "solution" phase in which the crystalline soap lattice is altered or destroyed, with the incorporation of cetane into or between soap "micelles" to form a gel. The object of the visual examination of the quenched samples was to ascertain whether any differences in the reversibility of this transformation could be seen as a function of soap composition or the temperature from which the samples were quenched.

At dry ice temperatures the more dilute systems (up to and including 24 per cent) are white and opaque, but clear to translucent gels on warming to room temperature. This change is undoubtedly due to the freezing and re-melting of free cetane. Between 28 and 41 per cent the samples are only slightly more opaque at dry ice temperatures than at room temperature. This can be correlated with their smaller content of free cetane. Between 49 and 79 per cent the samples are very translucent even at dry ice temperatures, while above 79 per cent they are again considerably whiter and more opaque.

At room temperature all samples containing up to and including 57.5 per cent soap are translucent gels from which more or less free cetane exudes spontaneously or on slight pressure, the amount of this decreasing with increasing soap content. None could be detected in the 49 per cent sample, but a trace was noted in the 52.6 and 57.5 per cent samples during preparation of the x-ray sample. Although homogeneous in appearance these systems were soft and non-coherent and spread easily under the slide to give a smooth, slightly whitish surface. In addition to the absence of free cetane, samples between 63 and 79 per cent soap were very much clearer than the less concentrated group and formed discrete lumps of plastic gel which pressed into a translucent waxy surface. The two most concentrated, at 73.2 per cent and 79 per cent, disintegrate on slight working to a highly electrically charged powder; particles have been observed to fly apart a distance of several inches in air. This effect is striking and in its acute form confined to this narrow composition range, although some tendency to produce charged particles by rubbing was found also in all samples above 79 per cent soap. The two samples at 84.2 and 87 per cent were turbid in appearance and glassy in texture at room temperature. The most concentrated sample, 94.9 per cent soap, was a white granular solid.

Summarizing these results, it is seen that at room temperature the samples prepared by quenching from 100°C. are not distinguishable from room temperature mixes. Samples quenched from 130°C. or above fall into groups of somewhat different appearance as follows: 10-24 per cent; 28-57.5 per cent; 63.6-70 per cent; 73-79 per cent; 84-87 per cent; 95 per cent. In all except the most concentrated, the appearance at room temperature after quenching is similar to the appearance at elevated temperatures, indicating that if recrystallization has occurred, the individual particles are sufficiently small to yield a translucent gel or glass.

*Microscopic observations*

Samples for microscopic observation were made by transferring a bit of gel to a microscope slide, covering it with a cover glass, and pressing the latter down firmly. That this technique induces some orientation of the soap particles in dilute systems is made evident by concurrent examination of the blob before

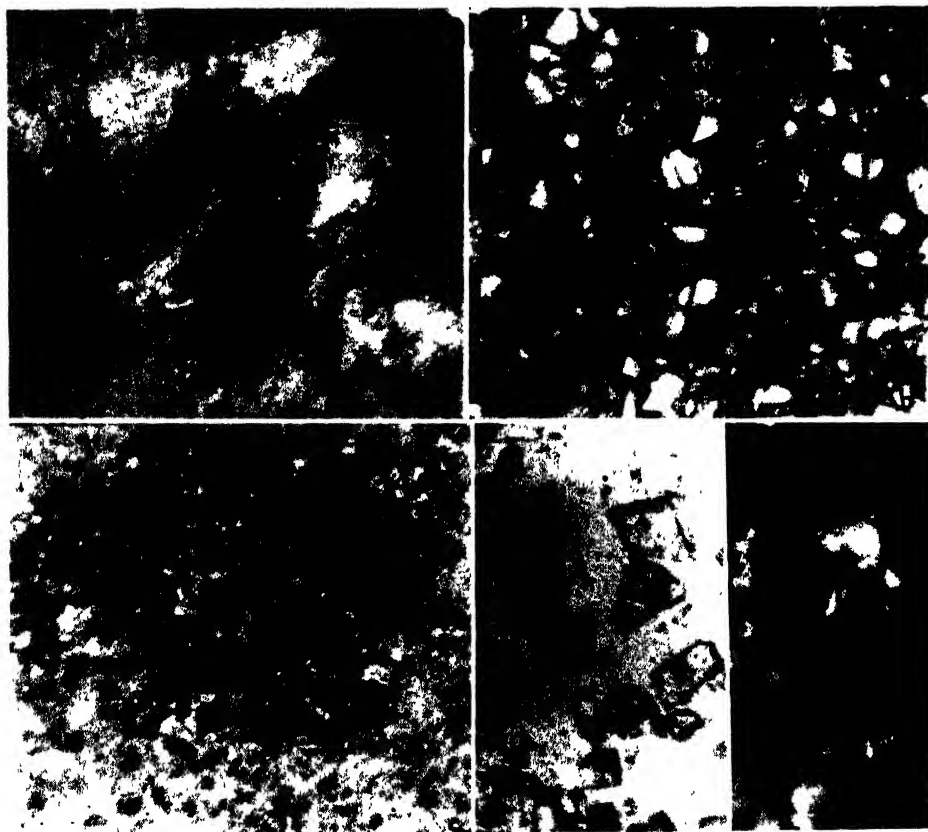


FIG. 1 Typical microscopic appearances of samples of calcium stearate in cetane quenched from various temperatures (crossed polaroids,  $120\times$ ): (a) from  $100^{\circ}\text{C}$ .; 69 per cent calcium stearate; anisotropic, partly oriented fibers; (b) from  $160^{\circ}\text{C}$ .; 38 per cent calcium stearate; optically homogeneous, variously oriented, anisotropic gel fragments; (c) from  $130^{\circ}\text{C}$ .; 49 per cent calcium stearate; spongy soap network with a few gel fragments; (d) from  $130^{\circ}\text{C}$ .; 87 per cent calcium stearate; optically inhomogeneous anisotropic glass; the left-hand field was photographed with the polaroids not quite crossed.

covering. These observations had for their purpose confirmation of the composition groups observed visually and further characterization of the differences between groups.

Typical appearances are shown in figure 1. All the room temperature mixes and the samples quenched from  $100^{\circ}\text{C}$ . resemble figure 1a. They show a uniform dispersion of fine, fibrous particles in an isotropic medium. In dilute systems,

particularly those quenched from 100°C., the individual fibers can be seen to extinguish at intervals of 90° as the sample is rotated between crossed polaroids.

All samples between 17 and 57.5 per cent soap quenched from 130°C. or above resemble figure 1b. They consist of gel fragments which are doubly refracting and variously oriented so that some are bright and some are extinguished at each setting of the rotating stage between polarizer and analyzer. Rotating the sample changes bright areas to dark and *vice versa*. Samples quenched from 130°C. and containing between 28 and 57.5 per cent show in addition a superposed network of dull white or yellow soap (exemplified in figure 1c); moreover, the gel fragments show striations indicative of optical inhomogeneity or internal strain. In the samples in this range quenched from 160° and 220°C. this appearance is absent. The amount of bright gel fragments decreases and the amount of the duller material increases as the soap concentration increases. In the 63.6 per cent sample almost all the bright fragments have disappeared.

Samples between 69.7 and 87.0 per cent soap quenched from 130°C. or above resemble figure 1d. They are composed of glassy fragments which contain within each individual variously oriented portions of doubly refracting material, so that the areas of light and dark in each particle change as the sample is rotated. The fragments also differ characteristically in shape from the gel fragments in more dilute systems, as can be seen in figures 1b and 1d, and are usually much larger in size. The 69.7 per cent system still contains a considerable amount of dull material as in figure 1c, but the more concentrated ones consist exclusively of the bright glassy fragments.

The most concentrated sample (94.9 per cent soap) quenched from 130°C. is a mixture of the glassy fragments and fibrous particles similar to those seen in the room temperature mixes.

The composition groups identified in the samples directly after quenching from 130°C. are thus 17-24 per cent, 28-57.5 per cent, 63.6-70 per cent, 73-87 per cent, and 95 per cent. In the first group are the gel fragments of figure 1b. The second group contains mixtures of soap in two forms, one being the gel fragments and the other the dull whitish material. The two samples in the third group both contain considerable amounts of soap in this latter form, and also a smaller amount of bright fragments which are not clearly like either "gel" or "glass." The fourth group is composed principally of glassy fragments, while the last contains these plus soap in its fibrous crystalline state.

#### *Effect of aging on the microscopic appearance*

On standing at room temperature for 6 weeks both the samples containing homogeneous gel fragments and glassy fragments had begun to form more opaque solid soap. In the former, the particles had shrunk and exuded cetane leaving a spongy net of soap particles, while in the latter individual particles retained their original outlines. The extent of the crystallization process was greater in the dilute systems (17-24 per cent) than in more concentrated ones, and greater in systems quenched from 130°C. than in those quenched from higher temperatures.

*Interpretation of the x-ray diffraction patterns*

Diffraction patterns for three representative sets of samples are given in figures 2-4. In these curves the intensity of the diffracted x-rays is given as a function of diffraction angle (twice the Bragg angle). The abscissa, however, is marked in Ångström units for ready reference.

These patterns are used qualitatively to determine if the presence of the solvent has effected any modification in the behavior established for the solvent-free soap quenched from the same temperature, and whether or not binding of the cetane in the soap gels affects its diffraction pattern. Differences in the soap pattern are to be related to varying degrees of undercooling or to varying degrees

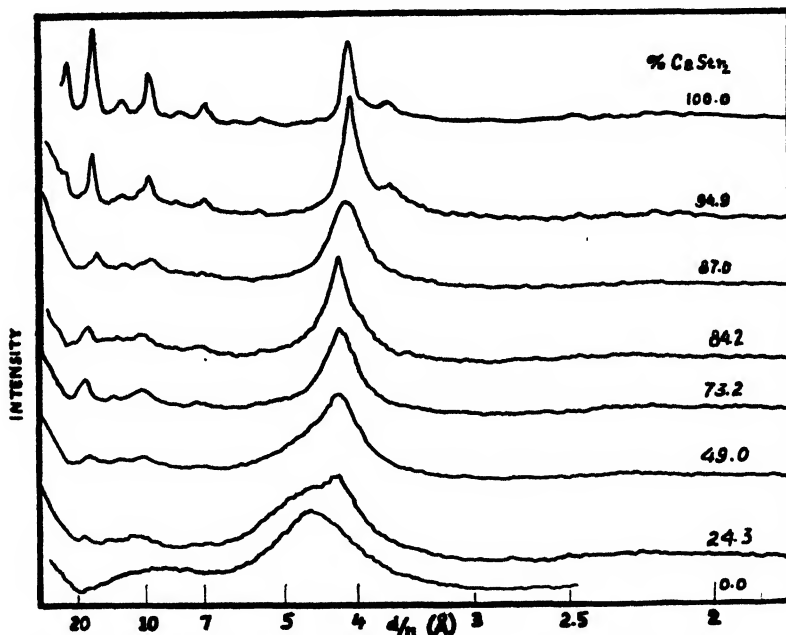


FIG. 2. X-ray diffraction patterns of samples of calcium stearate in cetane quenched from 130°C.

of lattice imperfection in the recrystallized soap. It is desired to determine whether these differences fall into composition groups that can be correlated with the visual and microscopic observations and used to derive information about the state of the systems either at room temperature or at the temperatures from which the samples were quenched.

On all the curves a series of peaks occur at small diffraction angles corresponding to successive orders of a single "long spacing," roughly twice the length of the stearate ion. In highly crystalline samples these peaks are sharp and intense. The long spacing can be determined with a mean deviation of  $\pm 0.3$  Å. from successive orders on any one pattern and  $\pm 0.05$  Å. between average values on

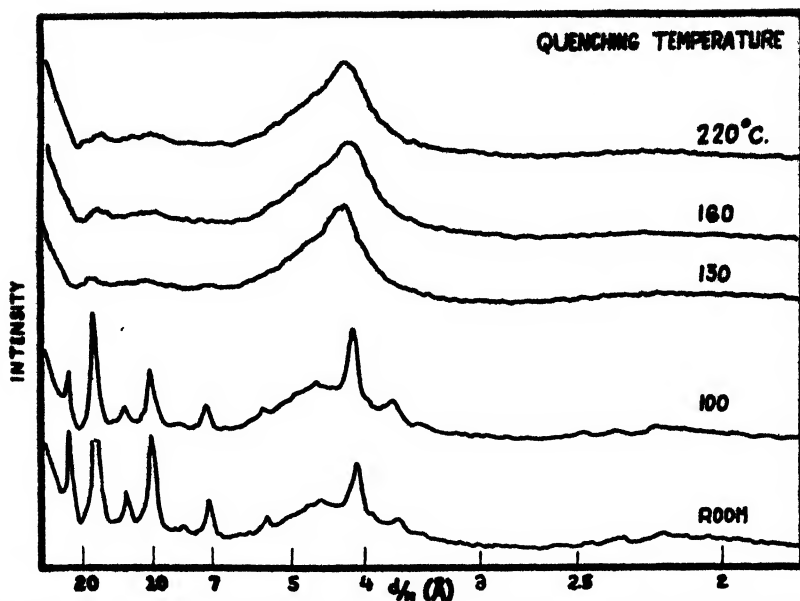


FIG. 3. X-ray diffraction patterns of samples of calcium stearate in cetane containing 40 per cent calcium stearate, quenched from various temperatures.

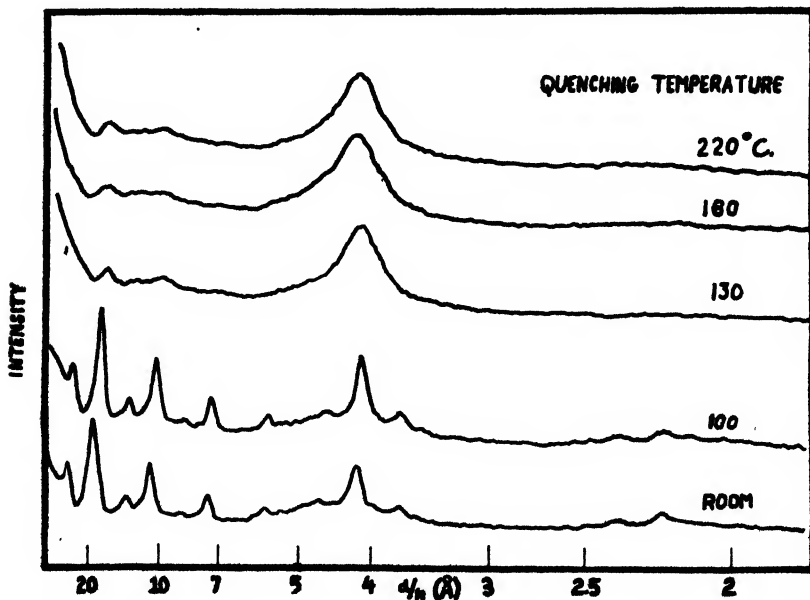


FIG. 4. X-ray diffraction patterns of samples of calcium stearate in cetane containing 60 per cent calcium stearate, quenched from various temperatures.

duplicate runs. In samples quenched from elevated temperatures, where the peaks are less intense and only two or three orders are available, the precision is



naturally lower, averaging  $\pm 0.4$  Å. from successive orders on any one pattern and  $\pm 0.15$  Å. on duplicate runs. Variations in the magnitude of this spacing between 48.5 and 51.2 Å. are observed. The variations are to be interpreted as due to differences in the angle at which the axis of the hydrocarbon chain is tilted relative to the planes containing the terminal polar groups which, in turn, may be due to the presence of the soap in varying phase states or to different degrees of distortion of the crystal lattice produced by quenching samples from different phase states. The intensity and sharpness (half-width; i.e., angular width of the peak at half its maximum intensity) of the peaks are also reproducible and are a measure of the degree of crystallinity of the samples.

All the curves also show an intense peak at a Bragg spacing of 4.1–4.2 Å. which is associated with the separation of parallel hydrocarbon chains in the calcium stearate lattice. This is reproducible in duplicate runs to well within  $\pm 0.01$  Å., even in samples where the peak is broad and partly overlapped by the halo due to liquid cetane. Variations in its magnitude of up to 0.15 Å. are observed. Very great variations in its sharpness provide a major criterion for degree of crystallinity of the sample.

Many of the curves also show a broad halo centering at 4.66 Å. due to liquid cetane. The position is not affected by the amount of cetane in the system, showing that the liquid must be regarded as essentially free. The intensity of the halo decreases with decreasing cetane content, but its exact point of disappearance is difficult to determine, since it overlaps the 4.1 Å. soap peak when the latter is broad and also the eleventh order of the long spacing.

Highly crystalline samples show two groups of weaker diffraction bands at Bragg spacings of 3.7–3.9 Å. and 2.1–2.2 Å. When the pattern is sharp these can be determined with considerable precision. When it is diffuse, they are difficult to locate. The first group appears as barely resolvable shoulders on the side of the peak at 4.1 Å., and the second as a single faint irregular halo. No weight has been attached to their exact position but their presence or absence is a valuable index of the crystallinity of the sample.

*X-ray results on room temperature mixes and samples quenched from 100°C.*

Table 1 presents the diffraction data for room temperature mixes of calcium stearate with cetane and also for pure anhydrous calcium stearate (dried to constant weight at 110°C.). The patterns all closely resemble the lower two curves of figures 3 and 4. The results with samples quenched from 100°C. are identical with those of room temperature mixes, except for a slight increase in the sharpness of the patterns. It is evident that the pattern is that of unaltered calcium stearate on which the pattern of liquid cetane is superposed with diminishing intensity as its amount decreases until it becomes undetectable (in the 87 per cent system). The long spacings are identical within  $\pm 0.16$  Å. (mean) and the short spacings within at most  $\pm 0.01$  Å. at room temperature and also at 100°C.; therefore solvent and soap are completely inert towards each other.

It is interesting that the absolute intensity of the pattern is greatest when the soap is mixed with a substantial amount of cetane (about 60 per cent), this

presumably leading to favorable conditions for orienting the soap in the sample mount. It is this increased intensity which leads to positive identification of a larger number of weak short spacings in the cetane-containing systems than in the dry soap. Since these spacings are here so readily apparent in dilute systems it is reasonable to conclude that when they are absent the soap must have undergone a change rather than to attribute their loss to diminished intensity resulting from low soap content in the system.

TABLE 1

*X-ray diffraction data for room temperature mixes of calcium stearate in cetane*

PER CENT CALCIUM STEARATE . . .	20.0	38.5	68.5	86.6	100*
Long spacing, Å . . .	50.15	50.24	50.59	50.35	50.0
Number of orders visible	5	7	6	7	6
Intensity, 3rd order† . . .	35	98	53	65	50
Relative intensity, 3rd order . . . . .	1.00	1.00	1.00	1.00	1.00
Principal side spacing, Å	4.101	4.112	4.110	4.108	4.14
Relative intensity . . .	0.40	0.37	0.49	0.43	0.94
Cetane halo—spacing, Å	4.66	4.66	4.66	Absent	Absent
Relative intensity . . .	0.46	0.15	0.09		
Other side spacings, ‡ Å	3.979(0.05) 3.669(0.11)	3.971(0.03) 3.679(0.07) 3.490(0.02)	3.958(0.06) 3.680(0.11) 3.517(0.06) 2.486(0.04)	3.965(0.05) 3.673(0.09) 3.500(0.05) 2.480(0.03)	3.96(0.10) 3.70(0.24) 3.58(0.08)
	2.199(0.06)	2.355(0.03) 2.199(0.03) 2.124(0.02) 2.062(0.12)	2.363(0.06) 2.202(0.11) 2.123(0.04)	2.357(0.06) 2.202(0.09) 2.124(0.03)	2.22(0.06)

\* Values from reference 11.

† In this and subsequent tables "intensity" is reported as the height of the given peak above the background in arbitrary units which, however, are roughly comparable from run to run. Relative intensity is the height of the given peak relative to that of the most intense peak in the given pattern.

‡ Number in parentheses gives relative intensity.

#### *X-ray results on samples quenched from 130°C.*

Table 2 presents the diffraction data for samples quenched from 130°C., while figure 2 contains representative members of the original set of nineteen curves. It has already been pointed out that these samples all undergo phase transformations between 100° and 130°C. and are, after quenching, in unstable states which can be divided into groups by composition on the basis of visual and microscopic observations. In the x-ray data, confirmation of the reality of these groups is sought and also some insight into the nature of the room temperature states produced in each.

The solvent-free soap is itself imperfectly crystallized on quenching from 130°C. Its long spacing is increased in value (by almost 1 Å.) and diminished in in-

TABLE 2  
X-ray diffraction data for samples of calcium stearate in cetane quenched from 190°C.

PER CENT CALCIUM STEARATE	17.2	20.5	22.9	24.4	28.3	33.5	37.8	40.6	49.0	52.6
Long spacing, Å. . . . .	50.55	51.38	50.07	51.22	49.79	49.70	49.96	50.24	50.40	49.71
Number of orders visible	2	3	3	3	3	2	3	3	3	3
Intensity, 3rd order . .	5	5	5	6	5	5	4	4	5	3
Relative intensity, 3rd order . .	0.12	0.11	0.16	0.19	0.16	0.14	0.11	0.12	0.13	0.09
Principal side spacing, Å . . . .	4.208	4.228	4.185	4.208	4.177	4.173	4.171	4.160	4.173	4.177
Relative intensity . . . . .	0.67	0.52	0.81	0.91	1.00	1.00	1.00	1.00	1.00	1.00
Cetane halo, relative intensity	1.00	1.00	1.00	1.00	0.84	0.80	0.46	0.49	0.40	0.61
Additional } 3.7-3.9 Å . .	Present	Present	Present	Present	Present	Present	Present	Present	Absent	Present
side spacings } 2.2 Å . . . .	Absent	Absent	Absent	Absent	Absent	Absent	Absent	Absent	Absent	Absent
PER CENT CALCIUM STEARATE	57.5	63.6	69.7	73.2	78.8	84.2	87.0	94.9	100	
Long spacing, Å. . . . .	50.29	50.59	49.58	50.34	50.18	49.41	49.27	50.55	51.1	
Number of orders visible	4	3	4	5	3	4	3	6	5	
Intensity, 3rd order . . . . .	5	8	7	13	10	10	11	29	27	
Relative intensity, 3rd order . .	0.14	0.22	0.18	0.28	0.21	0.18	0.24	0.43	0.56	
Principal side spacing, Å . . . .	4.168	4.171	4.158	4.150	4.176	4.150	4.156	4.120	4.14	
Relative intensity . . . . .	1.00	1.00	1.00	1.00	1.00	1.00	1.00	1.00	1.00	
Cetane halo, relative intensity.	0.36	0.19	0.13	0.07	0.07	0.05	0.04	1.00	1.00	
Additional } 3.7-3.9 Å . .	Present	Absent	Absent	Present	Present	Present	Present	Marked	Marked	
side spacings } 2.2 Å . . . . .	Absent	Absent	Absent	Absent	Present	Present	Absent	Marked	Marked	

tensity. The side spacing of greatest intensity is slightly increased but is still sharp and intense and several weaker short spacings are conspicuous. Substantially the same behavior is found for the system with 95 per cent soap.

The group of samples between 17 and 24 per cent calcium stearate, which resemble each other in visual appearance, also have similar x-ray patterns. The long spacing is significantly larger in magnitude than for the room temperature mixes (50.8 compared to 50.3). In this respect it resembles the solvent-free soap quenched from temperatures between 125° and 150°C., but the intensity is much lower. The principal side spacing is a wide intense halo and additional side spacings appear as faint shoulders on this peak, as in solvent-free calcium stearate quenched from temperatures above 150°C. The magnitude of the principal side spacing (4.21) is much larger than in room temperature mixes (4.11). The cetane halo is very conspicuous.

The group of samples between 28 and 57.5 per cent calcium stearate is sharply set off from the more dilute group by the fact that the long spacing is shorter on the average (50.0 Å.). The principal side spacing is also 0.03 Å. shorter. The effect of diminished cetane content in the diminishing intensity of its diffraction pattern is also evident, though it is still conspicuous. The intensity of the long spacing peaks is still low, and the peak at 4.18 Å. wide, although additional side spacings are visible as shoulders on it.

The two samples at 63.6 and 69.7 per cent have more intense long spacings out of all proportion to their increased soap content, while the relative intensity of the cetane halo is sharply decreased. In these samples also, alone among all those quenched from 130°C., there is no discernible trace of additional side spacings.

The remaining four samples, varying from 73 to 87 per cent soap, are similar to each other in that the long spacing is quite conspicuous, with up to five orders being measurable. Likewise, they are similar in that the cetane halo is barely discernible and in that the principal side spacing, with a value of 4.16 Å., has distinct shoulders corresponding to additional side spacings in the region of 3.5–3.9 Å. At 79 and 84 per cent traces of bands in the vicinity of 2 Å. are also apparent. However, both the 84 and the 87 per cent systems have patterns sufficiently different from the group as a whole to warrant setting them apart from it. Both have a very short long spacing (49.3–49.4 Å.). Also the pattern of the 84 per cent system is exceedingly sharp compared to either the 79 or the 87 per cent system. This is evident even in the reductions in figure 2.

*X-ray diffraction patterns of systems quenched from 160°, 220°, and higher temperatures*

Data for these systems are presented in table 3. Selected representative curves are given in figures 3 and 4. Solvent-free calcium stearate, quenched from any temperature above 150°C., shows only a single broad peak (at about 4.13–4.14 Å.) plus traces of additional side spacings and very weak and diffuse long spacings which decrease somewhat as the quenching temperature is raised above 220°C., being 50.3 Å. at 225°C. and 48.2 Å. at 320°C. (11). All of the systems

containing cetane resemble the solvent-free soap qualitatively, with the cetane halo superposed and distinctly visible up to about 70 per cent. The long spacing is nowhere elongated as in dilute systems at 130°C.; in the few systems quenched from 260°C. its shortening is evident. The principal side spacing tends to be larger with both increasing temperature and increasing cetane content. It is noteworthy that residual traces of side spacings could be found in all these samples, even though at 130°C. in 69 and 73 per cent systems none were discernible.

TABLE 3

*X-ray diffraction patterns of samples quenched from 160°C. and higher temperatures*

CALCIUM STEARATE	QUENCHING TEMPERA- TURE	LONG SPACING				PRINCIPAL SIDE SPACING		CETANE HALO
		Å.	Number of orders	Intensity 3rd order	Relative intensity	Å.	Relative intensity	Relative intensity
<i>per cent</i>	°C.							
10*	260	49.2	4	6	0.14	4.187	1.00	0.95
20.15	160	50.0	3	7	0.18	4.195	0.72	1.00
17.4	200	49.8	3	4	0.14	4.256	0.97	1.00
20.15	220	49.5	3	6	0.21	4.210	1.00	0.90
25*	260	48.9	3	6	0.19	4.256	1.00	0.71
37.6	160	49.5	2	7	0.20	4.183	1.00	0.83
38.0	220	50.2	2	6	0.19	4.222	1.00	0.90
67.6	160	49.4	3	6	0.14	4.191	1.00	0.12
69.0	220	49.6	3	6	0.15	4.193	1.00	0.15
86.4	160	49.9	3	10	0.23	4.188	1.00	0.02
86.4	220	49.9	2	8	0.18	4.185	1.00	
91.6	225	49.6	2	6	0.25	4.185	1.00	

\* These samples were made from a technical calcium stearate (Preparation IV of reference 11) which, however, had substantially the same diffraction pattern as the pure soap.

#### *Composition groups from x-ray diffraction data*

For the samples quenched from 130°C., composition groups 17–24 per cent, 28–57.5 per cent, 63–87 per cent, and 95 per cent can be clearly identified. The first group is characterized by an elongated long spacing, enlarged principal short spacing, and very prominent cetane halo. The second group is differentiated from the first by the lesser value of the long spacing and the principal side spacing, and by the lesser intensity of the cetane halo. The third group is not entirely homogeneous nor so sharply set off from its predecessor. There is a drop in the intensity of the cetane halo, and an increase in long spacing intensity, and also a loss in definition of the side spacings on passing from 57.5 per cent soap to 63.6 per cent soap. The 69.7 per cent sample is not greatly different from the 63.6 per cent. The 73 and 79 per cent samples are similar to each other but are a

little bit sharper than the 63–69.7 per cent group. The 84 per cent sample gives a much sharper pattern, differentiated from its predecessors also by a shortened long spacing. The shortened long spacing persists in the 87 per cent system but the sharpness of pattern has disappeared. The 87 per cent and 95 per cent systems are sharply differentiated, the latter giving substantially the same pattern as solvent-free soap.

*X-ray diffraction patterns of slowly cooled samples*

The pertinent features of the diffraction patterns of a few samples which were cooled from elevated temperatures at a mean rate of  $0.5^{\circ}/\text{min.}$  are assembled in table 4. It would be expected that slow cooling would result in a greater degree of recrystallization. That this occurs can be seen easily by inspection of

TABLE 4  
*X-ray diffraction patterns of systems of calcium stearate and cetane  
cooled slowly\* from various elevated temperatures*

PER CENT CALCIUM STEARATE.....	47.6	57.3	86.5
Temperature, $^{\circ}\text{C.}$ .....	170	200	207
Long spacing, $\text{\AA.}$ .....	49.37	48.48	49.88
Intensity, 3rd order.....	11	15	18
Relative intensity, 3rd order ..	0.27	0.41	0.35
Number of orders visible. ..	4	5	5
Principal side spacing, $\text{\AA.}$ ..	4.152	4.120	4.125
Relative intensity ..	1.00	1.00	1.00
Cetane halo, relative intensity ..	0.25	0.15	
Additional side spacings, $\dagger\text{\AA.}$ ....	3.94(0.37)	3.909(0.32) 3.700(0.16)	3.957(0.22) 3.684(0.15) 3.497(0.07) 2.459(0.04) 2.330(0.06)

\* Mean cooling rate  $0.5^{\circ}/\text{min.}$

$\dagger$  Numbers in parentheses give relative intensities.

figure 5, which shows two pairs of samples, cooled slowly and quenched from nearly the same temperatures. Except in the most dilute system (which had to be covered and whose pattern is therefore not directly comparable), short spacings in addition to the major one at  $4.1\text{ \AA.}$  are quite evident. The principal side spacing remains somewhat wider than in fully crystalline samples, and has a very slightly enlarged value.

The long spacing tends to be shorter than for the solvent-free soap. This is scarcely true at 86.5 per cent, but cannot be ignored at 47.6 per cent ( $49.4\text{ \AA.}$ ) and 57.3 per cent ( $48.5\text{ \AA.}$ ).

*Effect of water*

Figure 6 shows the diffraction pattern of two samples of calcium stearate-cetane systems of 15–17 per cent soap content quenched from  $200^{\circ}\text{C.}$ , to one of

which sufficient water was added (before heating) to just convert all the soap to calcium stearate monohydrate. In addition to showing values of the spacings characteristic of the hydrate, the pattern of the hydrous system is markedly sharper. The halo due to liquid cetane, on the other hand, is equally intense and in the same position for both samples, showing that the cetane in the hydrous

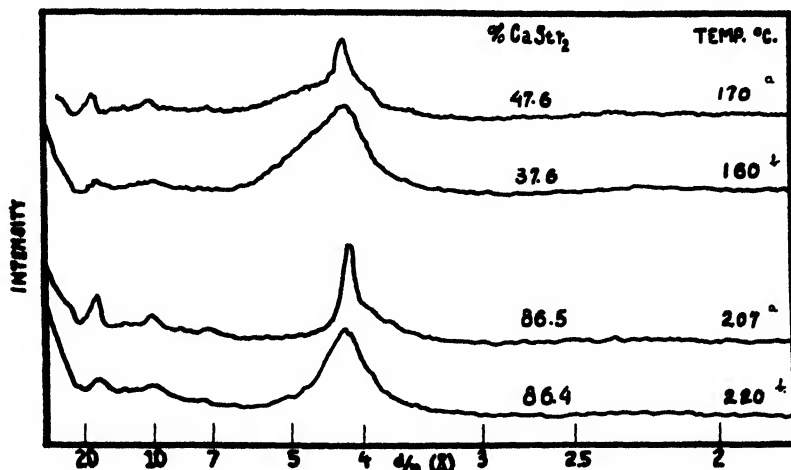


FIG. 5. Effect of rate of cooling on the diffraction pattern of samples of calcium stearate in cetane: a, cooled at a mean rate of 0.5°/min.; b, quenched (> 100°C./min.).

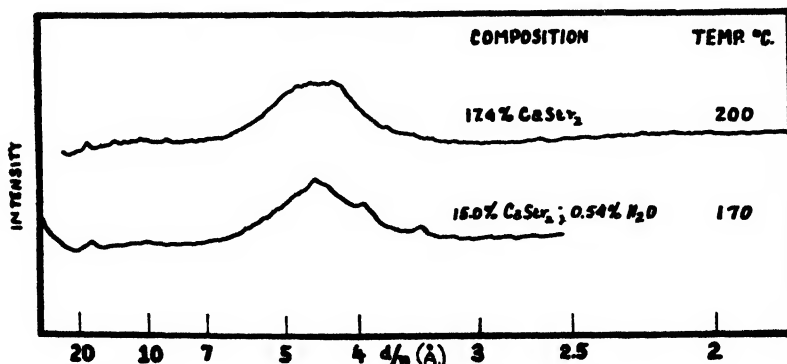


FIG. 6. Effect of water on the diffraction patterns of quenched systems of calcium stearate in cetane.

system is still free, despite the fact that the opaque gel formed is substantially non-syncretic.

#### *Effect of pressure on the diffraction pattern*

Table 5 shows the results obtained on a system containing initially 16.5 per cent of calcium stearate in cetane, quenched from 130°C., from which cetane had been expressed by nitrogen gas pressure leaving a residue containing 32.6 per cent

calcium stearate. It is apparent that even the 10 p.s.i. employed has had a pronounced effect on the structure of the gel, since the long spacing and principal side spacing are both decreased substantially. The increased intensity of the long spacing and the fact that a weak side spacing at 3.48 Å. is found instead of one at 3.8 Å. may be due to effecting some sort of preferred orientation in the pressed cake. The line at 3.48 Å. is close to a line of calcium stearate monohydrate. This latter would not be expected to form under the conditions of the experiment from crystalline calcium stearate, since its formation is slow even with soap suspended in warm water (60°C.) (11). The pure glassy soap hydrates more readily, but if the hydrate had formed one would expect also conspicuous lines at 3.9 and 4.4 Å., even though the latter might be hard to resolve from the cetane halo. Consequently the observed changes are attributed directly to mechanical deformation of the soap lattice.

TABLE 5

*Effect of expressing cetane under 10 p.s.i. from a sample quenched from 130°C.*

PER CENT CALCIUM STEARATE.....	32.6	17.2	33.5
Treatment.....	Pressed from 16.5 per cent	Unpressed	Unpressed
Long spacing, Å.....	49.53	50.55	49.70
Number of orders visible. ....	4	2	2
Intensity, 3rd order . ....	10	5	4
Relative intensity, 3rd order..	0.21	0.12	0.14
Principal side spacing, Å.....	4.162	4.208	4.173
Relative intensity.....	1.00	0.67	1.00
Cetane halo, relative intensity..	0.68	1.00	0.80
Additional side spacings, Å. ...	3.480	3.839	3.795
	2.7 (wide halo)		

## DISCUSSION

The preceding data permit deduction and evaluation of some hypotheses about the nature of the interaction of calcium stearate and cetane both at room temperature and at higher temperatures.

Smith and McBain (10) have presented phase diagrams for sodium stearate in a number of light hydrocarbons, while Vold, Philipson, and Doscher (3, 12) have studied sodium stearate and cetane. Both groups recognize the existence of a complex series of phases occurring as solvent-free sodium stearate is heated, many of which cannot dissolve much hydrocarbon without transformation, and above 100°C. of two liquid crystalline phases containing both soap and solvent and stable over wide ranges of temperature and composition. Doscher and Vold find that one of these is the solvent-free superwaxy phase of sodium stearate, which can incorporate large amounts of cetane, whereas neither of the binary liquid crystalline phases of Smith and McBain is continuous with any form of solvent-free sodium stearate.



A very different picture is presented by Lawrence (7), who postulates that there exists in the solvent-free soap a single "plastic" phase intermediate between crystal and liquid, and a single "gel phase" in soap-oil systems. In the absence of "peptizing agents" the gel phase is said to form, independent of composition, at the same temperature,  $T_2$ , at which the pure soap becomes plastic, and to melt at the melting point of the pure soap,  $T_1$ . Gels and greases can then be formed in soap-oil systems only under conditions such that the soap is in the "plastic" form. That this picture is oversimplified is clearly shown by the present data.

*Phase state of calcium stearate in cetane at room temperature*

Systems prepared by mixing at temperatures up to 100°C. show merely the unaltered diffraction patterns of crystalline calcium stearate and liquid cetane. Hence, the soap and oil must be completely inert to one another under these conditions, in accord with the physical appearance, and also with Lawrence's view that gels do not form if the soap is in the crystalline state. Since solvent-free calcium stearate undergoes transitions at 65° and 86°C. (11), it must be concluded that these do not permit sufficient loosening of the lattice to result in its penetration by cetane.

Systems prepared by quenching from 130°C. exhibit different appearances and diffraction patterns depending on the composition. The more dilute systems are clear or turbid gels, while the more concentrated are white and wax-like except the most concentrated, which are granular solids like the solvent-free soap, the changes in both visual and microscopic appearance agreeing quantitatively with the compositions at which changes occur in the diffraction pattern. Samples containing 24 per cent soap or less (17 per cent was the most dilute examined) show a long spacing nearly 1 Å. larger, and a principal side spacing about 0.1 Å. larger, than those of solvent-free crystalline soap. Samples containing 28–57.5 per cent soap show, on the average, a shorter long spacing, nearly equal to that of the pure soap and a principal side spacing shorter than for more dilute samples but still about 0.05–0.06 Å. greater than for the pure soap. Samples containing 63–87 per cent soap show patterns somewhat different from one another (particularly between 79 and 84 per cent) and from those from more dilute and more concentrated systems. The pattern for a sample containing 95 per cent soap is identical with that of the pure soap quenched from the same temperature. In addition to differences in spacing, the diffraction patterns show, to varying degrees, reduction of intensity and sharpness of the long spacings, and broadening or disappearance of the side spacings. In all but the 95 per cent system (and possibly the 87 per cent one) an unaltered halo like that of liquid cetane is present.

These observed differences in diffraction pattern may result from different soap phases at room temperature. The precise nature of the ultimate structural differences, and whether these should, in fact, be classified as differences of phase in the Gibbsian sense, is a matter of speculation. Variations in the long spacing may be brought about by change in the mean angle at which the hydrocarbon chains are tilted with respect to planes containing the calcium ions and carbox-

ylate groups. Variations in the principal short spacing may be brought about by changes in the way in which the parallel chains are packed.

The differences in intensity and sharpness are due to differences in regularity of the packing. Broadening of the lines may be due to intrinsic lack of order in the arrangement characteristic of the given phase, to crystal imperfection consequent on the quenching technique, or to very small crystal size. Differences in spacing may be due to retention of cetane within the soap lattice. Cetane molecules lying roughly parallel to stearate ions would be expected to alter the mode of packing of the chains, probably increasing the principal side spacing. It is also possible that the decreased intensity and sharpness of the long spacings result in part from irregular displacements of the stearate chains in an axial direction to make holes in which cetane molecules could be accommodated cross-wise to the axis of the stearate ions between terminal methyl groups. Whether the mean spacing is increased or decreased as a result would depend on how the angle of tilt is affected.

The phases found at room temperature in quenched samples are metastable; changes in microscopic appearance occur over periods of a few days to several weeks. However, it is to be expected that they could be stabilized through appropriate additives.

Samples which were cooled slowly rather than being quenched from elevated temperatures showed sharper lines, more intense long spacings but without change in value, and smaller values of the principal short spacing than the quenched samples. These differences are probably due partly to increased perfection of the crystallites, and partly to a greater extent of recrystallization of the high-temperature phases.

The few samples quenched from temperatures of 160°C. or above showed diffraction patterns all alike with very weak long spacings, broad intense principal short spacing, unaltered cetane halo of varying intensity, and traces of additional side spacings. This may mean that the phase differences in the soap at 130°C. responsible for the differences observed at room temperature in quenched samples do not persist at 160°C. However, the number of samples examined after quenching from temperatures above 130°C. is not adequate to warrant this conclusion. It seems more likely that at least some of them do persist but in unexplored composition ranges.

#### *Phase state of calcium stearate in cetane at elevated temperatures*

Inference of the phase state of these systems at the temperatures from which quenching occurred based on observations at room temperature depends on assuming that phase changes at intermediate temperatures are either slow or non-existent. For example, if two systems are different at room temperature after quenching from 130°C., they may have been (a) different at 130°C. and both undercooled; (b) the same at 130°C. but one underwent transformation at an intermediate temperature after which undercooling occurred; or (c) the same at 130°C. but both underwent transformations at intermediate temperatures on cooling. However, phase changes in soap systems hardly seem likely to be rapid compared to cooling rates of 100°C./min. such as were employed in the quench-

ing. Consequently, it seems reasonable to assume that a phase difference at room temperature between two samples quenched from a particular temperature is to be associated with a phase difference existing at that temperature.

It has already been pointed out that calcium stearate and cetane are mutually inert up to 100°C. despite transformations in the solvent-free soap occurring at 65° and 86°C.

The next transformation of the pure soap (11) occurs at 125°C., leading to a form (calcium stearate III) stable between 125° and 150°C. This form has a characteristic diffraction pattern at room temperature consisting of sharp lines, with a long spacing larger than that of calcium stearate VI (stable at room temperature). This pattern is found also for a sample containing 95 per cent soap quenched from 130°C. but not for the 87 per cent system. Therefore it can be inferred that at 130°C. calcium stearate III can dissolve 5 per cent cetane but not 13 per cent.

Although the phase of calcium stearate (II) stable between 150° and 195°C. can probably likewise dissolve some cetane, it does not seem likely that it occupies a very wide field in the phase diagram. Instead, the number of composition groups between which differences in visual and microscopic appearances and in diffraction pattern have been detected points to the existence of a liquid crystalline phase not continuous with calcium stearate II and containing 28–57.5 per cent soap at 130°C.

The sequence of phases postulated to exist at 130°C. as cetane is added to calcium stearate is, in summary: 100–95 per cent, calcium stearate III; 87–84 per cent, mixture of calcium stearates II and III; 79–73 per cent, calcium stearate II; 70–63.6 per cent, mixture of calcium stearate II and a new liquid crystalline phase; 57.5–28 per cent, liquid crystalline phase; 24–17 per cent, mixture of liquid crystalline phase and isotropic solution.

Solvent-free calcium stearate forms yet another mesomorphic phase (I) stable above 195°C., with which the liquid crystalline phase postulated at 28–57 per cent soap at 130°C. might be continuous. However, there is no observed difference in diffraction pattern between solvent-free samples quenched from just above and just below 195°C., so that x-ray patterns of quenched samples cannot be used to shed light on this question.

In the few samples quenched from 160° and 220°C. the very marked differences between the various composition groups identified at 130°C. have disappeared. Particularly striking is the absence of a long long spacing in the 20 per cent system and a short long spacing in the 87 per cent system, as found in samples quenched from 130°C. Consistently interpreted, this would mean that the phase state of the system was the same between 160° and 220°C. over this composition range, a condition which is not impossible. However, it is also possible that different phase states exist under these conditions of temperature and composition which do not yield different diffraction patterns after quenching.

#### *Disposition of the cetane in calcium stearate-cetane gels at room temperature*

It can be inferred from the given data that the cetane in gels of calcium stearate-cetane prepared by cooling from temperatures of 130°C. or above is

held in at least three different ways. Some is present as free liquid in large capillary spaces, as proven by the fact that it can be expressed under slight pressure and, in fact, exudes spontaneously as the samples age. The diffraction patterns of such systems show the pattern due to liquid cetane, a single halo centering at about 4.66 Å. superposed on that of the soap. Some must still exist as liquid but immobilized in small capillary spaces or otherwise bound, since the halo characteristic of liquid cetane persists even in samples from which no liquid can be expressed by considerable pressure. Finally, the increase in magnitude of the principal side spacing with increasing cetane content in systems quenched from 130°C. leads to the presumption that some cetane actually penetrates into the soap lattice.

#### *The stability of gels of calcium stearate and cetane*

On the basis of the above discussion it seems likely that gels of calcium stearate and cetane at room temperature comprise a network of soap particles which are crystallized only imperfectly, or may even retain configurations characteristic of phases stable at higher temperatures, and which may still contain some cetane. The bulk of the cetane, however, has been exuded and lies in capillary spaces from which it can be withdrawn more or less easily depending on the coarseness and rigidity of the soap network. These properties of the network change with time but it is not unlikely that such changes can be controlled by additives.

The rigidity of the network is likely to be determined by several factors, including the size and shape of the soap particles, their intrinsic strength, their number (i.e., soap concentration), and whether the net is formed by interlacing of separate fibers or by their growing together after the manner of crystal twins, as found for sodium laurate fibers by Marton, McBain, and Vold (8). Electron microscope photographs of Farrington and Birdsall (4) show separate fibers or at most intertwined individuals. However, it is not impossible that branched fibers may have been present in the grease and destroyed in preparing the sample for observation in the electron microscope.

It was observed that of gels prepared by quenching calcium stearate and cetane from elevated temperatures those giving the sharper diffraction patterns exuded liquid less readily (1). Although only tentative for anhydrous systems, this phenomenon is quite striking in systems containing small amounts of water. This suggests that individual fibers may be partly fused or grown together and that the network is stronger the more crystalline its nature.

#### *Rôle of water in stabilizing soap gels in oil*

Although the fact that small amounts of water are very effective in stabilizing greases, particularly calcium greases, against "bleeding" or liquid loss is well known, the mechanism of the effect has remained obscure. Recently the stable existence of stoichiometric hydrates of three different calcium soaps has been established: i.e., calcium palmitate monohydrate (5), calcium oleate dihydrate (6), and calcium stearate monohydrate (11). The results in figure 6 of this paper show that the calcium stearate monohydrate does actually form in the cetane-soap gel quenched from 160°C.

If the gel structure derives its strength only from mechanical entanglement of fibrils it is not apparent why hydrated soap should form a more oil-retentive structure than anhydrous soap, but if the particles are held together by associative forces at various points, the strength of the net can readily be imagined to depend both on whether the particles are hydrates or anhydrous soap, and on the degree of perfection of the crystal lattice. It seems possible that one mechanism by which hydrate formation stabilizes grease structure is by permitting or fostering the development of more nearly perfect strain-free crystallites which may be able to form a stronger gel net.

#### CONCLUSION

It seems likely that the phase diagram approach offers one of the most promising possibilities for achieving a genuine understanding of the complicated phenomena found with soap-oil systems. The stability and consistency of the grease appear to be functions primarily of the structure of the colloidal gel which enmeshes the oil but the possibility of developing such a structure, and its strength when formed, depend primarily on the phase state of the soap during processing and its rate of change with changing temperature, working, soap content, and number and kind of additives present.

#### SUMMARY

Calcium stearate is inert towards cetane at room temperature and at 100°C. Gels of calcium stearate in cetane prepared by quenching from more elevated temperatures differ from one another in the degree of perfection of molecular orientation in crystallites and in crystallite size, or alternatively in degree of undercooling of high-temperature phases. The observed differences fall into groups according to the composition of the samples and can be used to infer the phase state of the system at the elevated temperature from which quenching occurred. At 130°C. at least one anisotropic liquid crystalline phase is formed which has no counterpart in the solvent-free system.

The crystal lattice of calcium stearate in gels of the soap in cetane is highly imperfect, the extent of the imperfection or, conversely, degree of crystallinity, depending on the manner of preparation of the gel. It is suggested that greater stability is to be associated with a higher degree of perfection of individual crystallites in this particular system.

It has been established that small amounts of water in gels of calcium stearate and cetane act to form calcium stearate monohydrate. The enhanced stability of the hydrous gels may be associated with the greater degree of crystallinity of the hydrate.

The authors wish to express their appreciation to Mrs. Eleanor Lock, who assisted in the computation and derivation of the x-ray data from the original spectrometer curves.

#### REFERENCES

- (1) COSWELL, R. J.: Unpublished work in this laboratory.
- (2) DEANESLY, R. M., AND CARLETON, L. T.: *J. Phys. Chem.* **45**, 1104 (1941).

- (3) DOSCHER, T. M., AND VOLD, R. D.: J. Colloid Sci. **1**, 299 (1946).
- (4) FARRINGTON, B. B., AND BIRDSALL, D. H.: Inst. Spokesman (Natl. Lubricating Grease Inst.) **11**, 4 (1947); Oil Gas J. **45**, 268 (1947).
- (5) GARDINER, K. W., BUERGER, M. J., AND SMITH, L. B.: J. Phys. Chem. **49**, 417 (1945).
- (6) HÖPPLER, F.: Fette u. Seifen **49**, 700 (1942).
- (7) LAWRENCE, A. S. C.: J. Inst. Petroleum Technol. **24**, 207 (1938).
- (8) MARTON, L., MCBAIN, J. W., AND VOLD, R. D.: J. Am. Chem. Soc. **63**, 1990 (1941).
- (9) SMITH, G. H.: J. Am. Oil Chemists' Soc. **24**, 353 (1947).
- (10) SMITH, G. H., AND MCBAIN, J. W.: J. Phys. Colloid Chem. **51**, 1189 (1947).
- (11) VOLD, R. D., GRANDINE, J. D., 2nd, AND VOLD, M. J.: J. Colloid Sci. **3**, 339 (1948).
- (12) VOLD, R. D., AND PHILIPSON, J. M.: J. Phys. Chem. **50**, 39 (1946).

## USE OF ALUMINUM SOAPS AND OTHER FUEL THICKENERS IN GELLING GASOLINES<sup>1</sup>

WALTER H. C. RUEGGERBERG

*Technical Command, Army Chemical Center, Maryland*

*Received June 23, 1948*

### INTRODUCTION

Liquid incendiaries such as petroleum oils, carbon disulfide, wood-distillation products, and other inflammable liquids were tested during World War I. These materials all had the same drawback of excessive dispersion. To overcome this, the inflammable liquids were absorbed in some material such as cotton waste, but this method was only fairly satisfactory (26). During World War II this idea was revived and, based on development work, 14 per cent cotton waste saturated with 86 per cent of a 50/50 mixture of gasoline and fuel oil was suggested as a possible filling for the M69 incendiary bomb. Subsequently, it was suggested that cellocotton be employed because of its greater absorptive capacity and its availability in sheets, which permitted better packing and negligible scattering on ejection from the bomb (33). This type of filling appeared to be equal to gelled gasoline with the exception of lack of adhesion (9). The main advantage claimed for it was that commercial gasolines could be used and specifications would not need to be closely drawn with respect to Reid vapor pressure and aniline point as required for gelled gasoline (23).

### METHODS OF SOLIDIFYING LIQUID INCENDIARIES

Owing to the high degree of dispersion and consequent flash burn of liquid incendiaries, many materials have been proposed for use in solidifying liquid incendiaries. These are (17):

<sup>1</sup> Presented at the Symposium on Gel Formation, Detergency, Emulsification and Film Formation in Non-Aqueous Colloidal Systems which was held under the auspices of the Division of Colloid Chemistry and the Division of Petroleum Chemistry at the 113th Meeting of the American Chemical Society, Chicago, Illinois, April, 1948.

- (1) Fatty acid derivatives:
  - (a) Aluminum, sodium, zinc, and ammonium salts
  - (b) Lead salts of hydroxy acids
  - (c) Sulfonated products
  - (d) Amides
  - (e) Fatty acids *per se*
  - (f) Natural waxes
    - (1) Nitrated waxes
    - (2) Sulfonated waxes
    - (3) Waxes *per se*
  - (g) Anilides
- (2) Polyhydroxy derivatives:
  - (a) Glycol compounds
    - (1) Esters of fatty acids
  - (b) Ethanolamine compounds
    - (1) Esters of fatty acids
    - (2) Compounds of mono-, di-, and tri-ethanolamine
  - (c) Glycerol compounds
    - (1) Saponified vegetable oil mixes
    - (2) Nitrated vegetable oils
    - (3) Vegetable oils *per se*
  - (d) Polysaccharide compounds
    - (1) Lactose anhydride
    - (2) Dextrins
    - (3) Pectins
  - (e) Cellulose esters
    - (1) Ethyl cellulose (7-10 per cent)
    - (2) Pulp
- (3) Resinous derivatives:
  - (a) Natural
    - (1) Alkali-treated resin
    - (2) Shellac
    - (3) Damar
    - (4) East India fossil
    - (5) African fossil
    - (6) New Zealand fossil
  - (b) Synthetic
    - (1) Saponified polyacrylates
- (4) Hydrocarbon derivatives:
  - (a) Paraffin
  - (b) Synthetic rubber
  - (c) Natural rubber
  - (d) Salts of sulfonated petroleum fractions
  - (e) Salts of naphthenic acid

## (5) Inorganic derivatives:

## (a) Organosilicon compounds

## (1) Esters

## (b) Bentonite

## (c) Oil shale

Of all the materials listed above only a few were ever found practical for use in thickening incendiary liquids. These were:

## (1) Sodium stearate

## (2) Aluminum salts of mixed fatty acids and naphthenic acid

## (3) Polyacrylates

## (4) Rubber (natural and synthetic)

This paper presents a review of the use of aluminum soaps of fatty acids as fuel thickeners.

## SOAP-THICKENED GASOLINES

The first soaps considered for use as thickeners were the stringy aluminum ones. Aluminum naphthenate, oleate, and stearate were tested, but proved difficult to manufacture. All required compounding at about 250°F. However, when the soap content was reduced to about 20 per cent these soaps could be mixed at about 150°F. This mixing required the use of pressure equipment, or the addition of considerable heavy oil. The alternative method of cold ball-milling would be very cumbersome. The soap had to be made by double decomposition and had to be washed for satisfactory results. All of these soaps were found unreliable and difficult to use in grease making. In addition, the temperature susceptibility proved worse than that of rubber blends, causing the gum to melt and flash on ignition and to become very hard at -40°F. Calcium soaps were also considered, though the product was not at all like a rubber blend. It was an old process to gel oils with a mixture of lime and rosin oil to produce "Sett" greases, and this could be done with gasoline. However, this type of soap was very thixotropic, and the gel atomized completely on explosion. About 25 per cent of non-fuel material was required.

Tests were also made on batches prepared by cutting back ordinary cup greases (made from the cooked soap of pork fat) to the consistency of a heavy oil. These products were found to be too fluid and gave a flash burn on explosion. A process was developed for making a Sett type of grease from fatty acids. This type was much less thixotropic than the rosin-oil mixtures, but more difficult to compound. A gel was made with 15 per cent preformed soap present, and the necessary lime was dispersed in it. This grease was then dispersed in gasoline by stirring, after which the fatty acid was added. Setting took place in about 2 hr. The non-fuel content was about 20 per cent. The tar-lime gels used by the British were not investigated, because the vertical gas retort coal tar required was not produced in sufficient quantities in this country (27).



*Sodium stearate-gelled incendiaries*

Among the first materials tried in an attempt to thicken the liquid incendiary material sufficiently to improve dispersion was sodium stearate. This soap would not give a satisfactory product except with turpentine. Neither was it possible to solidify the incendiary liquid with oleic acid and sodium hydroxide, but when stearic acid dissolved in the incendiary liquid was saponified by the addition of sodium hydroxide dissolved in 85 per cent or purer alcohol, excellent gels were prepared. Two or three grams of stearic acid per 100 g. of liquid incendiary was required to solidify the material satisfactorily (26). This method was also found satisfactory in the development of solid incendiary oils carried out in World War II, but the use of solid sodium hydroxide was unsatisfactory (12).

The melted type of sodium soap gel was studied by several investigators and showed a number of advantages: It was easy to prepare, was of low non-fuel content, and melted sharply to a thin fluid so that it could be poured into cases.

TABLE 1  
*SOD formula 122*

INGREDIENT	WEIGHT
	<i>per cent</i>
Stearic acid (or hydrofoil) . . . . .	3.4
Rosin . . . . .	1.8
Cottonseed oil (castor oil) . . . . .	3.0
Caustic soda . . . . .	1.1
Water . . . . .	2.2
Motor gasoline . . . . .	88.4

Such a material, however, was a brittle gel which tended to bleed gasoline and required heating to about 130°F. during compounding. This required either pressure equipment or the use of a high-flash, low-vapor-pressure fuel. Large amounts of alcohol were also required to lower the melting point, and no readily available substitute was found. This gel was also found to shatter badly on explosion and gave a flash burn unless a binder was added (27).

The most satisfactory sodium stearate-thickened gasoline, designated as SOD Formula 122, had the composition shown in table 1 (31).

Gasoline, No. 2 kerosene, fuel oil, or combinations of these could be simply and satisfactorily solidified in bombs without the use of heat by dividing the oil to be solidified into two equal portions. In one portion, 6 per cent stearic acid was dissolved; in the other portion was an equivalent amount of sodium hydroxide dissolved in 95 per cent ethyl alcohol. These two mixtures were poured simultaneously into the bomb, and solidification took place immediately upon contact between the two streams (17).

*Aluminum soap thickeners*

These thickeners are aluminum salts of the saturated soap-forming fatty acids having eight to fourteen carbon atoms, an unsaturated soap-forming fatty acid, or a carboxylic acid containing a carbocyclic ring (e.g., naphthenic acid), or mixtures of these.

Aluminum stearate has certain disadvantages as a gelling agent because heat treatment is required for incorporation into the fuel and because the gels are hard and friable and lack the cohesive and adhesive character desired in an incendiary fuel. Soaps of acids of lower molecular weight (e.g., aluminum laurate or myristate) may solvate fairly rapidly at ordinary temperatures but give gels which lack body, which tend to undergo syneresis at low temperatures, and which are of generally inferior quality.

As regards aluminum oleate, gelation cannot be accomplished in a simple manner without heating. Furthermore, oleate soaps tend to be rather weak, and excessive amounts are required to produce a given viscosity.

The aluminum naphthenates are either resinous gums or low-melting solids. As thickening agents for hydrocarbon solvents these soaps have the disadvantage that the gelation of the fuel is not easily accomplished. Thus, although a resinous aluminum naphthenate can be processed by alcohol washing to give a product which will solvate at ordinary temperatures, the process is costly and the yield poor. Another method of processing a naphthenate to secure low-temperature gelation is by precipitation as the solid hydroxyaluminum soap. However, the melting point of the resulting product is so low that it may be difficult to avoid agglomeration of the material (8).

From tests covering a wide range of aluminum soap gels, made from saturated and unsaturated fatty acids and naphthenic acids, it was concluded that (1):

- (1) No class of aluminum gels was found to be free from instability. The results indicated both stable and unstable gels on every formula.
- (2) A gel of high concentration appeared to be more stable than one of lower concentration of the same formula.
- (3) There was some indication that an easily oxidized fatty acid led to an unstable gel. This, obviously, was not the whole explanation, as naphthenates also showed instability. However, the tendency to return to unthickened gasoline was more marked in oleate, cottonseed, and soya bean soaps, except crude cottonseed which contained lecithin. It appeared that oxidation might be a factor in instability.

Mixtures of aluminum soaps have been the most successful in producing incendiary gels. Among the most studied have been the "Napalm," "Steolate," and "W" soaps.

**NAPALM THICKENER**

The original Napalm polymer consisted of aluminum naphthenate which was heated to a maximum of 212°F., and then milled with a slurry of 50 parts by weight of aluminum palmitate and 100 parts of kerosene until homogeneous.

The resulting gum was then forced through a perforated iron plate with holes about  $\frac{1}{8}$  in. in diameter. The extruded strands issued into a tank containing the gasoline. The mixture was then circulated in the tank for 10 to 15 min. after the addition was complete. The thickened but still fluid material set into a gel in 5-6 hr. (16).

The Napalm thickener finally adopted for incendiary use consisted of a granular base aluminum soap of naphthenic, oleic, and coconut fatty acids. The sodium soap used for the precipitation of the aluminum soap contained 0.10-0.15 per cent  $\alpha$ -naphthol. The recommended formula for the organic acids used in making the Napalm thickener was as follows:

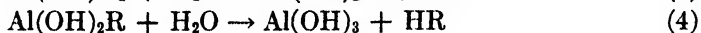
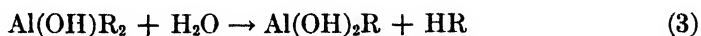
	<i>parts by weight</i>
Coconut fatty acids .. . . .	50
Naphthenic acid . . . . .	25
Oleic acid . . . . .	25

The aluminum content of the finished thickener should be from 5.4 to 5.8 per cent, and the moisture content not more than 0.8 nor less than 0.4 per cent (19).

A study of the effect of raw materials led to the following conclusions: Varying the composition of Napalm from the standard to a 2:1:1 ratio of coconut fatty acids to oleic acid to naphthenic acid indicated that the viscosity of the gel increased primarily with increase in oleic acid and, to a lesser extent, with increase in coconut fatty acids above the normal composition. The acid number of the coconut fatty acids was found important. Iron was an undesirable impurity when found in the alum but not in the acid (7). Impurities in Napalm thickener which may cause partial or complete breakdown of gels formed with gasoline, or oxidation of the thickener, include: excess water, lime, or caustic soda; soaps of sodium, copper, lead, iron, manganese, and cobalt; powdered or sheet zinc and lead; lead nitrate; rust preventives containing amines, alcohols, and all acids. Tetraethyllead, on the other hand, has no injurious effects (19). The fundamental reactions may be expressed as follows:



The soaps may hydrolyze:



Because of hydrolysis,  $\text{AlR}_3$  does not form and fatty acid in excess of that required remains as such:



In the above equations HR denotes the mixture of fatty and naphthenic acids (11).

The possible formulas for aluminum soaps are complex. There is definite evidence of three chemical compounds:

- (1) The disoaps  $—Al(OH)R_2$
- (2) The monosoaps  $—Al(OH)_2R$
- (3) The acid disoap  $—Al(OH)R_2HR$

There appears to be no evidence for the existence of the simple normal soap  $AlR_3$ . There may possibly be other soaps, and likewise there may be basic compounds, derived from aluminum hydroxide or mixed with fatty acid in colloidal form (22).

#### NAPALM MANUFACTURE

Three processes have been used successfully for the manufacture of Napalm. All are based on the aforementioned equations, but the mechanical details differ. In each process sodium hydroxide was added to the mixed fatty and naphthenic acids to form  $NaR$ . In the "tempered-alum" method no more sodium hydroxide was added than was required for the formation of  $NaR$ . The excess was added to the alum solution, as its equivalent in sodium carbonate. The alum solution containing the sodium carbonate was added to the alum solution. In the "one-stream" and "two-stream" methods all of the sodium hydroxide was added to the mixed fatty and naphthenic acids. In the "one-stream" method the alum solution was then added to the  $(NaOH + NaR)$  mixture. In the "two-stream" method both the alum solution and the  $(NaOH + NaR)$  mixture were run simultaneously into water. The "one-stream" method was the one most widely used.

If the mixture of coconut, oleic, and naphthenic acids has an acid number of 240, the average molecular weight of  $HR$  is 233. The monohydroxy soap of equation 1 then contains 5.31 per cent of aluminum, while the dihydroxy soap of equation 2 contains 9.22 per cent. The mixture of free acid and monohydroxy soap of equation 5 contains 3.64 per cent aluminum.

Napalm was specified in terms of the consistency of an 8 per cent gel in gasoline. Aluminum and the hydroxide parts of the soap are gasoline-insoluble, while  $R$  and  $HR$  are gasoline-soluble. The lower the aluminum content, the lower the  $OH$  content, and the higher the  $R$  and  $HR$  content. Hence, the lower the aluminum content, the weaker the gel.

Many other variables besides aluminum content affected gel strength. For instance, if some of the coconut acids were replaced by naphthenic acids, the acid number could be held at 240 and the aluminum content would remain unchanged, yet the gel would be weaker. Moisture also affected gel strength markedly, without measurably changing the aluminum content.

Hydrolysis also affected consistency more than it did aluminum content. Equations 3 and 4 illustrate this. The per cent aluminum of the monohydroxy soap of equation 3 is 5.31, while that of the mixture of dihydroxy soap and free acid is 5.13. Even more marked is the result of equation 4, since the  $Al(OH)_3$  would not gel at all, yet would analyze the same as aluminum soap.

The  $HR$  was always converted to the sodium soap before the alum was added.

In equation 1, for instance, 4 moles of sodium hydroxide are used to form NaR, while 2 moles remain free. In equation 2, 2 moles of sodium hydroxide are combined, while 4 moles are free. Excess caustic is defined as follows:

$$\text{Excess caustic} = \frac{\text{free NaOH}}{\text{combined NaOH}} \times 100$$

The excess caustic is zero per cent in equation 5, 50 per cent in equation 1, and 200 per cent in equation 2. It is seen that the aluminum content of the soap was controlled by the excess caustic used in the preparation of the soap and that it may be calculated, since the two are related by the expressions:

$$\text{Per cent Al} = 3.74 + 0.031x, \text{ where } x \text{ is less than 50 per cent}^2$$

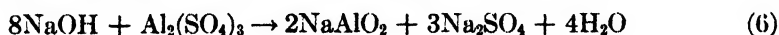
$$\text{Per cent Al} = 4.00 + 0.026x, \text{ where } x \text{ is greater than 50 per cent}$$

Since excess caustic could be controlled by the formulation of the soda-soap solution, it was more useful than the aluminum content. This was especially true when the alum contained silicates, giving high aluminum content in the soaps which did not contribute to the gel strength.

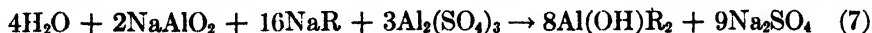
To manufacture Napalm with a gel strength between 500 and 800 g., the midpoint, or 650 g., was aimed for.

Equations 1, 2, and 5 require 1 mole of alum for 6 moles of sodium hydroxide, regardless of the HR used. That is, the alum required is independent of the excess caustic used, and hence has no connection with the gel strength of the resultant Napalm.

The per cent of alum added was calculated on the basis of 1 mole of alum for 6 moles of sodium hydroxide, correcting for the  $\text{Al}(\text{OH})\text{SO}_4$  in the alum. The curve (figure 1) shown was based on a plant run in which the excess caustic was 56 per cent. Because of the free caustic present, the first addition of alum to the sodium soap solution formed only soluble sodium aluminate:



When all of the free sodium hydroxide had reacted in this manner, additional alum decomposed the aluminate, and precipitated Napalm:



It will be noted that equations 6 and 7, combined, are equivalent to equation 1.

An excess caustic of 56 per cent means that 35.9 per cent of the total sodium hydroxide is free. While 6 moles of sodium hydroxide react completely with 1 mole of alum, 8 moles of sodium hydroxide, if free, react with 1 mole of alum to form aluminate. The break eventually occurred at this point. The first break also is found at a pH of about 10.6. This also is the pH at which sodium aluminate is decomposed by acid.

In the aluminate section of the curve, no Napalm should form. The precipitation of Napalm should commence after the pH drops below 10.6. This also agreed with observed behavior in plant production. However, when the

<sup>2</sup>  $x$  = excess caustic.

agitation was inferior, or the alum was added rapidly or at the wrong point, a local region of low pH might exist at the point of contact of alum solution and sodium soap solution, even when the over-all pH was above 10.6. Napalm then precipitated in this local region and did not redissolve in the available time when it was swept into the high-pH region. The Napalm so formed was usually a spherical shell containing mother liquor. These shells, or puff balls, tended to be so high in aluminum that they gave weak gels. They tended to smear on the screen or in the grinder, and, by occlusion of mother liquor, made satisfactory washing difficult. The presence of puff balls was avoided for these reasons. Their formation could be minimized by improvement of the agitation and method of addition of the alum solution.

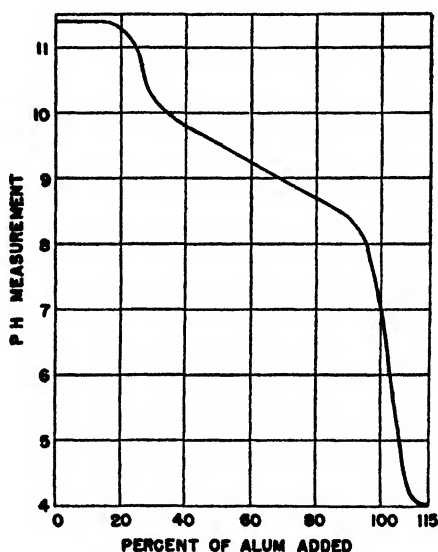


FIG. 1. Dependence of Napalm precipitation on per cent of alum added in the presence of 56 per cent excess sodium hydroxide.

Between pH 10.6 and about 7.5, the Napalm should precipitate in fine particles well dispersed in the mother liquor. With proper agitation and addition of alum, the appearance of the charge in this region should be that of latex. Foaming was most serious in the first part of this region. As the pH dropped rapidly, however, the latex coagulated suddenly and tended to float and cake on the surface. This coagulation was known as the strike. The rapidity with which it occurred could be controlled by the rate of addition of the alum solution.

Unless the agitation was excellent, and the rate of addition of alum ideal, occlusion of mother liquor occurred during the strike. This was evidenced by slight foam around the coagulated Napalm. To insure complete reaction with the sodium soap, excess alum was added (11).

Napalm thickener had been manufactured generally from two parts coconut

fatty acids, one part naphthenic acid, and one part oleic acid. A threatened shortage of naphthenic acid made it desirable to find a formula using minimum quantities of naphthenic acid. The Napalm thickener formula was somewhat flexible and changes could be made in the acid ratio provided the average effects of each acid were maintained. Coconut oil acid soaps had strength but, at the same time, had very fine particle size and required heat for aging to maximum strength. Oleic acid soaps were soft and required oxidation inhibitors, but the aging properties were good. Naphthenic acid soaps were gummy and had large particle size. They also contained natural inhibitors which made them very stable to oxidation.

With as little as 5 per cent naphthenic acid in the formula the coconut oil acid could not exceed 30 per cent, else the particle size would be too small and adversely affect the gelation rate. The reduction in naphthenic acid content could be made up by increasing the oleic acid content to 65 per cent and increasing the amount of inhibitor used. If less than 30 per cent coconut oil acid was used, the strength of the gel suffered. If more than 5 per cent naphthenic acid was used the particle size was increased, thus permitting the use of more coconut oil acids and resulting in an increase of strength. The new formula developed used 30 parts of coconut fatty acids, 65 parts of oleic acid, and 5 parts of naphthenic acid.

The new-formula Napalm thickener had a finer particle size and a higher iodine number than the standard-formula thickener. In other respects the chemical properties were very similar. The thickening power of the soap and the stability of the gels made therefrom were similar for both formulations. Added water affected both Napalms similarly. It was concluded from tests that the Napalm obtained from the new-formula thickener was similar to that made from the standard-formula thickener with respect to thickening power, stability of gel, stability of dry soap, oxidation stability, and water peptization. Gels made with the new formula were faster setting than gels made with the standard formula. It was recommended that the new formula for Napalm thickener be used in case of need for a formula with decreased naphthenic acid content (24).

#### OXIDATION STABILITY OF NAPALM

The unsaturated fatty acids and soaps of these acids present in Napalm account for its oxidation susceptibility. The oxidation of these unsaturated substances is supposed to take place through the intermediate formation of organic peroxides. The general character of the reaction is autocatalytic, presumably of a chain-mechanism type. Such reactions exhibit an induction period during which the reaction proceeds very slowly. The end of the induction period is characterized by a very rapid rise in the reaction rate. Since the organic peroxides that are formed react with potassium iodide to liberate iodine, the course of the reaction can be followed by measuring the quantity of iodine liberated by a given weight of sample. The number of milligrams of iodine liberated by 1 g. of the material under rigidly controlled conditions is defined as the peroxide number.

By following the change in the peroxide number of a soap stored in an oxidizing atmosphere it is possible to obtain considerable information about the course of the oxidation reaction. Thus, it is found that for a length of time the peroxide number is very low, indicating an extremely low rate of oxidation. This is followed by a sudden increase in the peroxide number, signaling the end of the induction period and the comparatively rapid rise in the rate of oxidation of the soap. The peroxide number finally reaches a maximum and then declines. This is a result of the further decomposition of the organic peroxide. The maximum peroxide value attained varies according to the amount of oxidizable material in the soap. The length of the induction period is a guide to the oxidation stability of the soap.

It is also possible to follow the oxidation of a soap by measuring its degree of unsaturation by treatment with iodine solution and back-titration of the unused iodine with thiosulfate. The quantity of iodine consumed by a given weight of soap (iodine number) decreases as oxidation proceeds, and the end of the induction period is indicated by a more rapid drop in the iodine number. The initial value of the iodine number depends upon the proportion of unsaturated acids in the soap.

The crucial test for oxidation susceptibility of a soap is the length of the induction period. Until a soap has passed through this period, there is little change. After exposure to the oxidizing action of the atmosphere, a portion of this induction period is consumed and this affects the time the soap can be stored or subjected to further oxidation before extensive breakdown sets in. A low peroxide number or high iodine number, therefore, does not necessarily mean that the soap will be satisfactory for long storage.

The length of the induction period depends chiefly on the amount and kind of inhibitors that are present in the soap. This is shown most clearly by acetone extraction of the soap. Thus, after such extraction the induction period even for the most stable soaps is reduced to a small fraction of its original value. Furthermore, the induction period of a readily oxidizable soap can be extended considerably by treatment with a small amount of certain well-recognized oxidation inhibitors (5). Among those recommended have been U.O.P. No. 5 or its more satisfactory homolog, dilauryl-*p*-phenylenediamine,  $\alpha$ -*o*-toluidinostearic acid (35), and  $\alpha$ -naphthol (19, 28).

Using the same fatty acids, the length of the induction period appeared to be dependent upon the soluble iron content of the alum used in the precipitation. Soaps with a high iron content usually, but not invariably, had a low induction period (6). The presence of manganese in amounts greater than 0.01 per cent by weight of aluminum sulfate resulted in extensive oxidation, as measured by the oxidation susceptibility test. The presence of ferric iron in amounts greater than 0.03 per cent by weight of aluminum sulfate was likewise harmful. Ferrous iron, on the other hand, did not show a marked effect. The presence of iron and lead in the sodium soap solution showed no marked effect on oxidation susceptibility; copper and chromium salts in the aluminum sulfate solution likewise showed no effect (30). Cobalt in moderate amounts as an impurity was sufficiently active to cause a temperature rise in the heat test (13).



## EFFECT OF MOISTURE ON NAPALM

Napalm is essentially a hygroscopic material analogous to gelatin or paper in its affinity for moisture, and thus gains or loses moisture when exposed to the atmosphere, except at the one humidity with which it is in equilibrium (inert point). Equilibrium at any given relative humidity appears to be attained fairly rapidly, being practically complete in 8 hr. in  $\frac{1}{8}$ -in. or  $\frac{1}{4}$ -in. layers under normal convection. The water absorbed greatly affects the consistency of the gel formed when the solid soap is dissolved in gasoline. The average of a large number of tests indicated that the absorption of 0.1 per cent moisture measured by the vacuum-oven method caused the consistency in the 24-hr. 150°C. test to drop approximately 40–50 g. (4, 18).

The cause of the moisture effect probably lies in the prevention of the formation or possibly the breaking of the soap chains by preferential coordination of water molecules at the points of attachment between the individual units. Osmotic pressure measurements indicated that the normal Napalm in solution in gasoline had a molecular weight of 160,000–200,000. It seems probable that these large molecules were built up largely by the coordination of the aluminum atom of each soap unit with one of the carboxyl oxygens of the next unit. Such chains can obviously be broken if a molecule to which aluminum coordinates more strongly than the carboxyl oxygen is introduced. This seems to be the case when water, amines, or free fatty acids of low molecular weight are added. The aluminum atoms coordinate preferentially with the amine or hydroxyl groups, the aluminum chains are broken, and there is a resultant drop in molecular weight and consistency (18).

## EFFECT OF GASOLINE QUALITY ON THE PROPERTIES OF NAPALM FUELS

The properties of Napalm fuels were found to be affected by the type of hydrocarbon employed. Cyclic hydrocarbons tended to give high consistencies, while the paraffin (*n*-heptane) gave the lowest consistency values. Eleven gasolines meeting the requirements for 80-octane, general-purpose motor fuels all gave thickened fuels having consistencies within relatively narrow limits. Based on a wide variety of automotive fuels exclusive of those meeting the requirements of 80-octane gasoline, highly naphthenic or aromatic gasolines may be encountered which would markedly increase fuel consistency. Oxidized gasolines may greatly decrease the consistency of Napalm fuels. However, oxidation-susceptible gasoline can be inhibited at the source with suitable commercial inhibitors as specified for U. S. Army 80-octane, general-purpose gasoline and should then be suitable for use, unless stored for unusually long periods with excessive exposure (32). The minimum oxidation stability had to be 5 hr. To obtain this stability, an approved inhibitor such as U.O.P. No. 4, U.O.P. No. 5, du Pont Anti-Oxidant No. 5, or du Pont Anti-Oxidant No. 6 could be used, in which case concentration of the active ingredient had to be  $20 \pm 15$  pounds per thousand 40-gallon barrels of gasoline (34).

Consistency studies of gels prepared with Napalm soap in various trade gasolines having aniline points from 75° to 140°F. indicated that apparent

viscosity and extensibility were substantially independent of the gasoline. However, the rate of solvation was markedly affected, but with most of the gasolines likely to be encountered in practice the variation in setting time could be tolerated in field computing (25). The CWS specification stated that the aniline point of the gasoline should not be greater than 46°C. (115°F.) (34).

The physical properties of gasolines which were studied did not adequately predict the gelation behavior of the hydrocarbon, but if consideration is limited to the common motor gasolines, the aniline point correlated fairly well with solvation rate and low-temperature stability. It appeared advisable to limit the aniline point to 120°F. maximum in order to insure that the setting time of Napalm would not exceed 45 min. and that the thickened incendiary fuels would withstand approximately three months' storage at 0-20°F. without excessive syneresis. Tests of Napalm fuels in the M69 incendiary bomb, made with the quantity of thickener employed in production (approximately 9 per cent soap), indicated that the ignitability of the gel was dependent on the vapor pressure. With fuels containing 11 per cent or more of Napalm soap, variation in gel Reid vapor pressure from 4.4 to 11.2 p.s.i. did not appear to affect ignition performance in the M69, although the evidence pointed to lower over-all ignitability than for the thinner, 9 per cent Napalm fuel (2). Specifications indicated that the vapor pressure of the gasoline (Class A60 or A70) should be not less than 9.0 p.s.i. or more than 10.5 p.s.i. (34).

It was possible to add a heavier oil to Napalm-gasoline gels, in amounts up to 50 per cent of the solvent, without significantly altering the apparent viscosity of the fuel. In addition to the possibility of increasing the burning temperature and the thermal yield of the fuel, the addition of the heavier oil produced an increase in the burning rate and a decrease in the amount of unburned material remaining. In the case of gels containing greater than 50 per cent oil in the solvent, the ignition of the gel was slower. Once burning had begun, however, the burning characteristics were equally as good as those of the gels of lower oil content (21).

Preliminary tests indicated that gasolines containing 20 per cent of alcohol would not yield gels of adequate viscosity (3).

#### PALMENE GUM

This incendiary gel was composed of seven parts of aluminum palmitate (mono salt; Metasap Chemical Company) and four parts of Neo-Fat 3-R (mixture of 40 per cent oleic acid and 60 per cent linoleic acid; Armour and Company) in 89 parts of gasoline. The gum was prepared by simply adding the palmitate powder to the gasoline, mixing by momentary shaking or paddling, adding the Neo-fat, mixing briefly, and allowing the mix to stand at 25°C. In 45 min. to an hour it set to a stiff jelly, but after standing for 12 to 24 hr. at 25°C. this changed to a stringy gum. The burning characteristics were improved by the addition of 0.5-1 per cent lamp black; the filler was merely added to the gasoline before adding the other ingredients (15).

## STEOLATE SOAPS

Early work on aluminum soaps revealed the fact that when prepared by usual precipitation methods, some free fatty acids remained in the soap. Thus, commercial aluminum stearate contained free acids, stearic acid among them. It was recognized that tallow-base, double-pressed stearic acid, from which aluminum stearate was made, was chiefly palmitic and stearic acid, the former 50–55 per cent, the latter 40–45 per cent, with other higher fatty acids present in small quantities. It has been shown that free stearic acid has deleterious effects on gels made from aluminum soaps. Soaps containing free stearic acid produced gels with gasoline but these gels were unstable at  $-40^{\circ}\text{F.}$  and broke down at room temperature after several days' standing. The effect of free oleic acid was quite different from that of free stearic acid. When free oleic acid was added to extracted aluminum stearate, the gel produced was more stable and had greater string than that produced from aluminum stearate containing free stearic acid. Aluminum oleate coprecipitated with aluminum stearate had a stabilizing influence. The effect was more evident if this coprecipitated aluminum stearate–aluminum oleate was extracted with acetone to rid it of free stearic and oleic acids, and then a gel was made with the extracted material and free oleic acid. Such a gel was stable at  $-40^{\circ}\text{F.}$  and at  $150^{\circ}\text{F.}$  and had considerable string.

An improved technique was developed for producing an intimate mixture of aluminum stearate and aluminum oleate, without the undesirable free stearic acid but containing free oleic acid. It involved extracting the free acids from aluminum stearate, suspending this extracted material in water, after wetting it with alcohol, and precipitating aluminum oleate and free oleic acid on the surface. Soaps made by this technique were called steolates. By this procedure it was possible to coat different soaps, thereby obtaining soaps with different gelling and aging rates. The preparation of gels from the steolates involved mixing the soap with gasoline, shaking or stirring for a few minutes (usually two or three), allowing to stand for approximately 15 hr., then aging for another 15 hr. at  $150^{\circ}\text{F.}$  in an air oven. The gel became transparent in 3–5 hr. at the aging temperature. The apparent viscosity of steolate gels changed with the oleic acid content. The effect was that the addition of free oleic acid gave less viscous gels (20). Steolate soaps which could be aged at room temperatures were produced by careful control of manufacture (29).

## W GUMS

Aluminum soaps of the "W" fatty acid (tallow fatty acid by-products of the meat-packing industry) were prepared and investigated for their suitability as thickening agents for incendiary gels. Preliminary attempts to form an aluminum soap of the "W" fatty acids in gasoline directly resulted in failure. Likewise, the heating of the fatty acids directly with potassium hydroxide solution, followed by the addition of aqueous alum, resulted in a gum which was unsatis-

factory. A successful soap was made by dispersing the fatty acids in water and heating to 125°F. The potassium hydroxide solution was then added, followed by stirring in an aqueous solution of alum. To prepare the gel, the soap had to be stirred in the gasoline and the temperature raised to 125°F., or the soap and gasoline were stirred in the cold until an even dispersion (paste) resulted. The mixture was then heated at 50°C. for  $\frac{1}{2}$ –1 hr. It was concluded that a satisfactory, stable, thickened gasoline for use in the M47 and M69 incendiary bombs could be prepared from the "W" thickener (14).

#### STEARATE-CAPRYLATE AND STEARATE-PELARGONATE SOAPS

Stearate and Napalm soaps are susceptible to oxidation; both of them contain at least 20 per cent of the oleate radical in the soap. It was felt advisable to find a suitable substitute for the oleic acid. The gelling effect of the oleic acid was expected to be due either to the fact that it was unsaturated or to the fact that it was a liquid, since stearic acid acted so differently. Liquid fatty acids of eight or nine carbon atoms could be used to test part of this hypothesis. A 50/50 stearate-caprylate or 50/50 stearate-pelargonate soap should have approximately the desired gelling properties if the double bond was not involved in gel formation. The 50/50 stearate-caprylate soap would withstand oxidation longer than Napalm and, in gel tests, it was comparable to Napalm. The difficulty in using this soap as an alternate for Napalm was that the source of caprylic acid was coconut oil fatty acids. The stearate-pelargonate soaps were made from raw materials which were available in limited quantities. No stearate-pelargonate soap was made that would give a gel aging at room temperature without the use of a peptizer. Among the peptizers tested, *p*-cresol and diethylene glycol monobutyl ether gave the most desirable results. A peptizer increased the string of a gel as well as the rate of gelation. Tests showed that the stearate-caprylate soap was more resistant to oxidation than Napalm. It contained no unsaturated linkages but would form a gel, aging at room temperature, with very desirable properties. It appeared that a stearate-pelargonate soap should have susceptibilities comparable to those of a stearate-caprylate soap (10).

#### SUMMARY

The liquid incendiaries tested during World War I possessed the drawback of excessive dispersion, which was, however, moderately well corrected by the absorption of the liquids in some materials such as cotton waste. During World War II this general idea was revived, resulting ultimately in the incendiary gels. Of the various substances tried for solidifying incendiary fuels, the following were found to be generally applicable: (1) sodium stearate; (2) aluminum salts of mixed fatty acids and naphthenic acid; (3) polyacrylates; and (4) rubber (natural and synthetic).

Sodium stearate would not give a satisfactory product with incendiary fuels. Stearic acid, however, when dissolved in the incendiary liquid, produced excellent gels after the addition of sodium hydroxide dissolved in 85 per cent (or purer)

alcohol. SOD 122, a product of the Standard Oil Company of New Jersey, was the most promising gel of this type.

Aluminum soap thickeners consist of either aluminum salts of the saturated soap-forming fatty acids having eight to fourteen carbon atoms, an unsaturated soap-forming fatty acid, or a carboxylic acid containing a carbocyclic ring (e.g., naphthenic acid), or a mixture of these. Napalm, the aluminum soap of an oleic, naphthenic, and coconut fatty acid mixture, falls into this class of thickeners. A review of this substance, from the standpoints of chemistry, manufacture, stability, effect of moisture, gasoline quality, etc., is presented.

In lieu of soaps, natural and synthetic rubber as well as resins such as the polyacrylates can be used as thickeners, yielding, however, gel-products possessing properties somewhat different in their characteristics from those of the soap-thickened fuels.

The author desires to express his appreciation to Drs. Vera Smalley and Leo Finkelstein of the Chemical Corps Technical Command for their assistance in the compilation of the bibliography and their interest in the preparation of this paper.

#### REFERENCES<sup>\*</sup>

- (1) BEERBOWER, A.: 1943.\*
- (2) BETTS, R. L.: 1943.\*
- (3) BETTS, R. L., AND MYERS, N. F.: OSRD Report No. 1345, April 15, 1943.
- (4) BIRNBAUM, N., AND EDMONDS, S. M.: CUMR 36, September 25, 1943.
- (5) BIRNBAUM, N., AND EDMONDS, S. M.: 1943.\*
- (6) BROUGHTON, J., AND BYFIELD, A.: OSRD Report No. 2036, November 17, 1943.
- (7) BROUGHTON, J., AND BYFIELD, A.: OSRD Report No. 2036a, March 7, 1944.
- (8) BULL, B. A.: 1943.\*
- (9) CARVER, E. K.: "The Use of Cellocotton in the M69 Bomb," Eastman Kodak Company, February 15, 1943.
- (10) CROMEANS, J. S.: CUMR 49, December 16, 1943.
- (11) DEGRAY, R. J. (CWS): "Napalm Manufacture," Edgewood Technical File No. 180-7, November 14, 1943.
- (12) DUNBAR, A.: TDMR 309, August 19, 1941.
- (13) EASTMAN KODAK COMPANY: 1943.\*
- (14) FAUPEL, J. H.: 1943.\*
- (15) FIESER, L. F.: 1942.\*
- (16) FIESER, L. F., *et al.*: Ind. Eng. Chem. **38**, 768-73 (1946).
- (17) FIESER, L. F.: "Recommendation for the Filling and Firing of the 100-lb. Oil Incendiary Bomb (M47 and M47A1)," NDRC B-7-D, April 17, 1942.
- (18) GUNDERSON, C. H.: 1941.\*
- (19) HOTEL, H. C.: "Joint CWS-NDRC Report on Napalm Manufacture and Properties," NDRC Section 11.3, October 8, 1943.
- (20) JAN Specifications, N-589, April 30, 1948.
- (21) KOKATNUR, V. R., SOUTHERN, J. A., AND ROTH, L. J.: 1943.\*
- (22) LITTLE, R. W.: 1943.\*
- (23) MCBAIN, J. W.: OSRD Report No. 4205, October 3, 1944.
- (24) MATHESON, G. L., AND MILLER, P.: "The Use of Cellocotton in the M69 Bomb," Standard Oil Development Company, February 15, 1943.

\* References marked with an asterisk are not currently available in the open literature.

- (24) MICHAEL, M. W.: TDMR 1209, January 2, 1946.
- (25) MYERS, N. F.: 1943.\*
- (26) RAY, A. B.: CWM XLIII, Part I, (1), pp. 36-46 (1918).
- (27) RUSSELL, R. P.: OSRD Report No. 382, February 7, 1942.
- (28) SOUTHERN, J. A.: 1943.\*
- (29) SOUTHERN, J. A., AND ROTH, L. J.: 1943.\*
- (30) SOUTHERN, J. A., AND ROTH, L. J.: 1943.\*
- (31) STANDARD OIL DEVELOPMENT COMPANY: "The Development of Oil Incendiary Bombs," NDRC Division 11, January 20, 1942.
- (32) STANDARD OIL DEVELOPMENT COMPANY: "Effects of Thickener and Gasoline Quality on the Properties of Napalm Fuels," NDRC Division 11, July 6, 1944.
- (33) THOMPSON, N. J.: OSRD Report No. 1702, August 11, 1943.
- (34) U. S. Army Specification 96-131-378, August 24, 1945.
- (35) WHITE, E. R.: "The Inhibition of the Oxidation of Napalm Soap," NDRC Division 11, August 30, 1943.

## RHEOLOGICAL PROPERTIES OF INCENDIARY GELS<sup>1</sup>

LEO FINKELSTEIN

*Technical Command, Army Chemical Center, Maryland*

*Received June 23, 1948*

Incendiary gels are essentially non-Newtonian liquids, whose viscosity varies with the stress. Three particular features are observed with such systems: a variable ratio of shearing stress to rate of shear; a finite relaxation procedure for suddenly applied stress or deformations; and a frequency-dependent dynamic viscosity in the case of alternating processes (8).

### MECHANICAL ANALOGIES

Carver and Van Wazer (5) consider the Maxwellian model, which separates elasticity and viscosity according to the thermodynamic definition, perhaps the most successful expedient for disentangling the combined elastic and viscous properties of a viscoelastic fluid. The theory of Maxwell on elastoviscosity approximates the structure of an elastoviscous liquid by means of a mechanical model. Such a model consists of series and parallel combinations of dashpots and springs. The dashpots contain Newtonian liquids and the springs obey Hooke's law. The first element represents a purely viscous resistance, while the second element is a purely elastic resistance representing a model for an ideal solid. Both elements are connected in the model, since in a structurally viscous liquid both elements are present. When the springs and dashpots are connected in series, the total extension is the sum of the extensions across individual com-

<sup>1</sup> Presented at the Symposium on Gel Formation, Detergency, Emulsification and Film Formation in Non-Aqueous Colloidal Systems which was held under the Auspices of the Division of Colloid Chemistry and the Division of Petroleum Chemistry at the 113th Meeting of the American Chemical Society, Chicago, Illinois, April, 1948.

ponents; when they are connected in parallel, the total force is the sum of the forces across the components. Most rheological instruments run under constant force or at constant rate of extension. Carver and Van Wazer (5) considered that the mechanical model of a spring with series and parallel dashpots offered a convenient qualitative approximation of the rheological properties of most incendiary gels, but that three-dimensional cross-bonded structures could not be treated by means of these analogies if the cross-bonds had elastic-viscous properties. Such a model is best studied according to the methods of statistical mechanics.

#### QUALITATIVE EVALUATION OF A GEL

The physical measurements described below were designed to characterize qualitatively the specific properties of incendiary gels. To test for *homogeneity*, the sample was cut in half and separated so as to expose a fresh surface, and examined visually and tactually.

To determine *friability* and the *rate of heal*, the gel was cut with a spatula and a sample withdrawn. If the sample and the area from which it was withdrawn retained their shape and sharp outline, the gel was hard and friable. In the most undesirable cases, gel shavings could be produced by scraping the surface with a spatula. If a cut healed immediately or a smooth surface re-formed as soon as a sample was withdrawn, the sample was soft and had insufficient body. The best gels were intermediate between these two extremes. The sharp edges of a cut or of a sample should become blurred almost immediately, and a cut should be completely healed in approximately 5 min. The *body* of the gel could be evaluated by placing a sample on a plane surface; a soft gel spread and lost its shape rapidly.

The *strength* and *resilience* of a gel were determined by forcing the flat surface of a spatula through the gel. The resistance offered to its passage was dependent on the strength of the gel. A friable gel might offer considerable initial resistance and then break away. This was considered a rigid, weak gel. When motion of the spatula was stopped, a resilient or elastic gel would tend to force the spatula back out of the "compressed" area.

When a gel sample was withdrawn on the end of a spatula, the *length* was qualitatively observed. The connection between the sample and the main body of the gel was maintained over a considerable distance with a long gel. If the gel was friable, it would be very short. A long gel was either excessively fluid or very elastic. These properties led to inferior firing characteristics.

A gel that was *adhesive* was difficult to remove from a spatula completely. A test of adhesion to wood could be conducted by using a physician's tongue-depressor as a standard wood strip. The strip in a vertical position was forced down into the gel, the gel allowed to heal around it for about 30 sec., and the strip then withdrawn vertically. With a good gel, at least 50 per cent of the submerged surface of the strip would be coated with the gel. A long elastic gel could be drawn part way out and would then snap back, leaving the wood clean.

If one dips his hand into a mass of thickened fluid and withdraws it rapidly,

the gel may string out, showing considerable extensibility, or it may break off, in which case it is said to be short. This property is variously known as *stringiness*, *shortness*, or *extensibility*. Short gels shatter, do not carry well, and show lack of adhesion.

#### DETERMINATION OF RHEOLOGICAL PROPERTIES

Attempts to characterize gels accurately by measurement of specific rheological properties were undertaken to correlate gel formulation work, to establish specification tests, and to obtain an insight into the factors influencing gel performance in incendiary munitions. Obviously, no test would fulfill all these functions. Plastic materials such as incendiary gels resist deformation by low shearing forces and tend to yield more easily to higher shearing forces. Since the over-all performance of a gel was dependent on its behavior under both conditions, it was important to characterize a gel at both high and low shearing forces.

#### THE PARALLEL PLATE TEST

This test was used to determine the consistency of incendiary oils containing isobutyl methacrylate polymers. It consisted of measuring the diameter, in centimeters, to which 5 cc. of gel spread in 1 min. between parallel plates of glass under a 2-kg. load. In the CWS tests the plates of glass were 9 in. square. Other tests were conducted with the plate-glass squares measuring 12 in. square. The test was a modification of a consistency test for putty (6). A plug syringe was used to measure the 5 cc. of incendiary oil to be tested. This syringe was composed of two concentric pieces of glass tubing, a seal between the two being made by an annulus of Neoprene tubing. The tubing of larger diameter served as a cylinder, calibrated to deliver the required amount of filling. The tubing of smaller diameter, to which a section of Neoprene tubing was held by friction, served as a piston to remove the incendiary filling from the syringe. A study of the various loads indicated that values in the most sensitive ranges were obtained with the recommended 2-kg. load. The majority of the gels would nearly reach an equilibrium spread in the 1-min. period of stress. When the load was applied for 5 min. to a typical isobutyl methacrylate, the parallel plate value was increased from 10.4 to 11.6 cm. Straight lines were obtained by plotting the diameter against the logarithm of the time for which the load was applied. The original technique involved increasing the applied load by 2-kg. increments every minute until a total load of 10 kg. resulted. When the diameters observed by this method were plotted against the logarithm of the applied load, parallel straight lines were obtained for gels of quite diverse composition. The simpler technique involving a single measurement was therefore recommended (9).

#### IMPACT STRENGTH

To determine consistency at a high rate of shear, a Schopper-Dynstat plastics impact tester was modified to handle gels (9). A  $\frac{1}{4}$ -in. wide blade was mounted on a pendulum with a total length of 15 in. A trough to retain the gel sample was placed horizontally at the bottom of the swing of the pendulum. The



horizontal length of the path of the blade through the gel was 26 cm. Various loads were placed on the pendulum arm. The pendulum was released from a horizontal position, allowed to swing down through the gel, and the vertical height of the upward swing was determined. When the gel trough was empty, the pendulum, being nearly frictionless, rose to the horizontal position. When the gel was present, the energy consumed in forcing the blade through the gel caused the pendulum to swing through to a maximum height somewhat short of the horizontal (or zero) point. The decrease in the height of the maximum swing from the zero point was proportional to the work done and, therefore, to the strength of the gel. To cover all types of gels, it was necessary to use three different loadings on the pendulum. These were referred to in increasing order of gel strength as B, C, and D scales. The B scale readings for the weakest gels ranged from one to ten units. (The units are empirical but in a rough way correspond to kilogram centimeters.) The C scale covered a range of one to 20 units. In the lower half of this range, the B and C scale readings were nearly equivalent. A few tough gels had values exceeding the C scale. These were measured by placing a small additional weight on the impact by raising the release point from  $90^\circ$  to  $120^\circ$  from the vertical. This increased angle of fall altered the zero point of the instrument. The D scale values, therefore, were not directly comparable to those of the B and C scales.

#### MODIFIED STORMER VISCOSIMETER

Because of its simplicity of operation and ease of cleaning, the Stormer viscosimeter had long been used for consistency measurements of paints and allied products. A modified Stormer viscosimeter, as described by Geddes and Dawson (7), consisted of a sample cup containing a paddle which was driven by the gravitational pull of a falling weight. For a given load, the speed with which the paddle would rotate was inversely proportional to the viscosity of the material in the sample cup. A true determination required that stirring be continued until a constant rate was obtained. At low shearing forces (low applied load) the rate of rotation was extremely slow, while under a somewhat higher load the increase in R.P.M. with an increase in the applied load was rapid. For the isobutyl methacrylate gels, the most satisfactory but time-consuming criterion of consistency was the load required to produce 10 R.P.M. With many gels, especially those containing methacrylate interpolymers, the viscosity of the gel increased during the measurement, and results could be duplicated only when fresh sample was used for each measurement. It was therefore not possible to obtain a constant rate. As a rapid generalized technique, a procedure was adopted which consisted in measuring the average rate of rotation during 100 revolutions of the paddle after an acceleration period of 10 revolutions under a standard load that appeared suitable for the particular type of gel (9).

#### GARDNER MOBILOMETER

This instrument was used to determine the consistency of incendiary gels of the Napalm type. It is an extrusion-type viscosimeter in which the rate of fall

of a loaded piston through the sample (contained in a tight-fitting cylinder) is determined (6). The mobilometer consisted of a tube, four-hole disk, plunger rod assembly, and bearing mounted on a suitable base and support. The pertinent dimensions of the standard instrument as used for incendiary gels are shown in table 1.

Owing to work-hardening phenomena, the value observed with methacrylate gels was markedly dependent upon the treatment of the sample. Reproducible values were obtained only when freshly prepared gels were allowed to age 24 hr. in the Gardner cylinder, and a single measurement was made subsequently on the unworked sample. W. H. Bauer (2) recommended that the consistency of incendiary gels be measured at one rate of shear by means of the Gardner mobilometer to specify a given gel for test purposes. Each type of Napalm gel has a specified consistency range expressed in grams. In reporting results two successive loads, in grams, for more than and less than 100 sec. are noted. The load required to give a time of fall of 100 sec. is obtained by linear interpolation from the two loads.

TABLE 1

*Dimensions of standard Gardner mobilometer for use with incendiary gels*

	in.
Internal diameter of tube. . . . .	1.538
Diameter of disk. . . . .	1.500
Thickness of disk. . . . .	$\frac{1}{16}$
Diameter of holes in disk. . . . .	0.250
Diameter of plunger rod. . . . .	0.250

#### TORSIOMETER METHOD

Barnard (1) developed a method which was used for determining the elasticity and consistency of incendiary oils of high consistency. The torsionmeter is shown in figure 1 assembled for use in the consistency test. The principal components of the torsionmeter include a disk calibrated in thirty-six ten-degree divisions, a combination pulley-indicator, a pulley mounted on the edge of the disk to carry a pulley cord from the center pulley over the edge of the disk to a weight (two weights are used, one after the other), which serves as the actuating force for the test, a testing paddle, and a trigger mechanism to release the pointer-indicator when making tests.

In making an elasticity test, the following procedure was used: When the pointer was released, the weight actuated the paddle, twisting it through one revolution. On completing 360°, the loop of the cord slipped off the peg (set in the groove of the pulley-pointer), permitting the paddle to return in a clockwise direction toward the original zero position. The extent of return, or recovery of original condition, was indicated in degrees, marked on the disk. The elasticity was reported as the average of two consecutive readings which agreed within 10°.

In determining the consistency of the incendiary oil being tested, the pointer

was released. The weight actuated the paddle, causing the pointer to rotate counter-clockwise. The average time, in minutes, that was required for the pointer to rotate through exactly  $360^\circ$  at the average rate of revolution observed in the test was computed. This time, expressed to the nearest 0.1 min., was the consistency.



FIG. 1. Torsionmeter

#### CLARK-HODSMAN VISCOSIMETER

In a fundamental investigation of gel rheology the Eastman Kodak Company (4) studied the use of the Clark-Hodsmen viscosimeter to determine the elasticity and viscosity and relaxation of gels. The instrument is a torsion viscosimeter used to determine the viscosities at low rates of shear (of the order of  $0.01$  to  $1.0 \text{ sec.}^{-1}$ ). By trial and error, it was necessary to determine the proper diameter of wire and angle of torque for each gel, to obtain a valid measurement. Many gels did not exhibit sufficient adhesion to the plumb to prevent slippage. The measurement did not, therefore, appear convenient as a method of characterizing new gels. The values observed on different preparations of the same gel formula

did not show sufficient variation for this technique to serve as a control method. For fundamental study of a particular gel, the device had the advantage over the parallel-plate method in that it gave the viscosity at low shearing forces directly in poises rather than in empirical units.

#### SOD PRESSURE VISCOSIMETER

This measuring instrument was developed by the Esso Laboratories of the Standard Oil Development Company (3). It was a capillary viscosimeter and consisted of an electric motor, gear-reducer unit, pump, gages, thermocouple and accessories, grease cylinders, and sundry fittings. Temperature control was obtained with the use of an air bath so that capillaries could be changed without removing the grease cylinder from the bath.

The flow rate which was found most useful at room temperature was about 0.083 cc. per second. With the thermocouple, the desired capillary, and the proper gage in place the determination of pressure was easy to estimate. The motor was turned on and the system was allowed to come to equilibrium pressure. The pressure was observed and pump speed was noted in revolutions per second. The flow rate in cubic centimeters per second was determined from the output of the pump in cubic centimeters per revolution and the pump speed in R.P.M. Each of the capillaries had to be calibrated and their effective radii determined by viscometric means. With the eight capillaries ranging in radii from 0.19 to 0.023 cm., the rate of shear for a flow rate of 0.083 cc. per second extended from about 15 to 8500 sec.<sup>-1</sup>

#### CAPILLARY VISCOSIMETER

To obtain velocity gradients ranging from 1,000 to 1,000,000 sec.<sup>-1</sup> a high-pressure capillary viscosimeter was used by Carver and Broughton (4). The liquid under test was charged into a cylinder, at the bottom of which was inserted a capillary of known length and radius. The liquid was forced out through this capillary by a constant, known nitrogen pressure. The constants of the instrument could again be determined by calibrating with a liquid of known viscosity or calculated from the dimensions of the apparatus.

#### JEWELER'S LATHE VISCOSIMETER

An attempt to obtain data on viscosity changes under sudden stress was made by Carver and Broughton (4) with the so-called jeweler's lathe viscosimeter. The instrument is a rotating cylinder-type viscosimeter with an outer cup that can be made to rotate instantaneously at 20-1080 R.P.M. by means of a gear train and clutch and synchronous electric motor, and an inner cylinder suspended from the tailstock of a jeweler's lathe by a torsion rod, 0.26 cm. in diameter, so that the movement of the inner cylinder, even with the most viscous materials, is almost negligible. The necessary accuracy in reading the deflection is obtained by attaching a mirror to the torsion rod and recording the trace on 35-mm. film, driven by a synchronous motor at 18.7 cm. per second. To obtain quick response the inner cylinder is hollow (filled with chloroform to avoid buoyancy)

and the torsion rod system has a period of vibration of only 0.011 sec. Minor features are the lower bearing which was found essential to prevent the inner cylinder from being dragged from its central position, a cover on top of the outer cylinder which was necessary to keep the material from crawling up the torsion rod, and a thermostatic cup placed around the outer cylinder. The material under investigation was placed in the cup and allowed to stand for several hours to remove any air bubbles. Rotation was then started and the deflection of the inner cylinder followed visually on a scale or photographically. The traces for a Newtonian fluid show a sudden, sharp rise at the moment the outer cylinder starts to rotate, followed by a constant deflection proportional to the viscosity of the fluid. Very different traces are given by Napalm and methacrylate gels, a pronounced rise which is a function of the time the gel is allowed to remain undisturbed in the cup between runs being obtained. The trace obtained with the jeweler's lathe viscosimeter is in essence a graph of force at constant rate of extension.

#### MACMICHAEL VISCOSIMETER

This instrument has a disk of 3-cm. radius suspended about 5 mm. from the bottom of a cylindrical cup which is fixed in a bath on a turntable driven at constant speed (normally 20 R.P.M.) by an electric motor and suitable gears. The suspension wire (about 25 cm.) is inclosed in and fixed near the bottom of a tube or spindle to which the disk is fastened by a bayonet catch; the top of the spindle carries a graduated dial, the deflection of which below a pointer indicates the twist produced in the wire when the cup (containing the liquid under test) is rotated. The circumference of the dial is divided into 300 equal parts (MacMichael degrees). The temperature is controlled by electric heating. A table is supplied so that errors due to permanent set may not occur. Measurements are made of the torque and the R.P.M. from these, and from these a curve of apparent viscosity *versus* rate of shear can be obtained, calibration being made with the aid of standard oil. This viscosimeter covers a rate-of-shear range of approximately 3-100 sec.<sup>-1</sup>

#### EXTENSIMETER (EASTMAN KODAK METHOD)

This method was developed to evaluate shortness (4). Two 2½-in. long glass tubes of 4-mm. inside diameter and having smooth flat ends were filled with the incendiary gel by gentle suction. The tubes were joined, by a short section of rubber tubing, as close to each other as possible to prevent inclusion of air in the gel column. The filled assembled tubes were placed vertically in a suitable support and the upper tube was secured to a line which ran over a pulley and was connected to a constant-speed motor arranged to pull the string at a rate of ½ in. per second. The string had to be carefully adjusted for tautness so that it would just hold the top tube upright when the rubber tube had been removed. The assembly was allowed to stand untouched for 1 min. while gel healing occurred. The rubber tube was then carefully slipped down below the division point and the motor started. The distance the upper tube had to be

raised to cause the gel string to break was reported in inches as the "extensibility" of the fuel.

#### STANDARD OIL DEVELOPMENT MODIFIED EXTENSIOMETER

Since some difficulty was experienced in obtaining reproducible results, a modified method was developed by Betts and Myers (3). The mechanical features of the modified extensiometer comprised a motor and gear-reduction system which pulled a string over a pulley at a rate of  $\frac{1}{2}$  in. per second. The other end of the string was attached to a glass tube of approximately 25 mm. inside diameter. The lower end of the glass tube had a sintered glass disk to which a piece of blotting paper was held by suction applied at the other end of the tube. Other variations were permissible in that a perforated disk could be substituted for the sintered glass. In operation, suction was applied to the tube to hold the paper in place and the tube was lowered until the blotting paper made complete contact with the gel surface. After the contact had been made for 1 min., the motor was started and the tube raised at a constant rate until the string of gel broke. The distance traversed was recorded as the "extensibility" of the gel. The size of the gel container markedly affected the result, but it was found that a 1-quart Mason-jar container was satisfactory provided the gel surface was smooth and not above the shoulder of the jar, and the sample was substantially free of air bubbles.

#### MEASUREMENT OF ELASTICITY AT HIGH FREQUENCIES

Early in the investigation of the rheological properties of thickened fuels, it was thought that it might be not the static rigidity and relaxation time which would be of importance, but their values at high frequencies. The Ferry method is optical in nature and depends upon the solution under investigation being optically clear and becoming birefringent under strain. Hence, it was possible to make measurements only upon the isobutyl methacrylate interpolymer gels (4).

#### BALL VISCOSIMETER METHOD

This test was developed to determine the consistency of thickened flame thrower fuels in the field. The viscosimeter consisted of a graduated transparent plastic tube (Tenite or similar), 10 in. in length and 2 in. in diameter, and a series of commercial steel ball-bearings, from  $\frac{4}{32}$  to  $\frac{8}{32}$  in. in diameter, graded in thirty-seconds of an inch. The consistency was measured by timing the fall, through the gel, of the series of balls past two successive graduations. The "ball consistency" was reported as a number equal to the number of thirty-seconds of an inch corresponding to the diameter of the ball whose time of fall was nearest 30 sec.

#### A.S.T.M. GREASE PENETROMETER

This instrument determined the depth of penetration in hundredths of centimeters of a cone into the gel in 5 sec. The standard A.S.T.M. procedure used a

load of 150 g. To obtain penetrometer values in the most sensitive region of the instrument, the load was reduced by a counter-balance to 50 and 25 g. Even under these conditions, the correlation between penetrometer values and apparent stiffness was still not good. The roughness of the gel surfaces and the presence of air bubbles in the gels seemed to introduce errors which exceeded the normal differences between gels (9).

#### SUMMARY

Rapid and reliable evaluation of incendiary gels has been the ever-present problem since adoption of this type of filling for incendiary bombs and flame thrower fuel. Various instruments have been tried, but only in a limited number of cases have satisfactory correlations with test firing data been obtained. The Gardner mobilometer was the only instrument found generally satisfactory for testing and evaluating Napalm-gasoline gels, but it did not prove applicable to other incendiary fillings.

Very good correlation has been found between the Gardner and Stormer instruments when used in testing gels prepared from a given soap. Either instrument may be used for evaluation of gel consistency, but for reasons of availability and simplicity the Gardner instrument is preferred. The correlation between the Gardner and falling-ball consistencies is sufficiently precise to justify use of the latter method for control of the viscosities of flame thrower fuels in the field.

Incendiary fuels are ejected from the flame thrower at rates of shear far in excess of that obtained in the instruments used for the evaluation of gel consistency. A comparison of the Gardner mobilometer with the capillary viscosimeter at shear rates obtained in the portable flame thrower indicates that the Gardner instrument appears adequate for predicting the performance of flame thrower fuels (3).

The parallel plate method, which has been useful in specifying methacrylate gels, could not be correlated with field tests.

Although the Stormer viscosimeter was considered as a test instrument for methacrylate gels, it proved unsatisfactory because the stiffness (rigidity) of the mixture required the use of greater weights for starting rotation of the test paddle than the instrument was designed to carry; when rotation was initiated the paddle quickly sheared through the material being tested and started racing. W. H. Bauer (2) determined that at very low rates of shear the Stormer instrument was satisfactory for methacrylate and Napalm gels. For consistencies exhibited by 10-14 per cent Napalm gels, the Stormer instrument was of no use, since the rotating paddle cut through the gel and spun in the space created.

The penetrometer designed for grease testing was applied to methacrylate gels with limited success. Extremely soft gels, while distinguishable from medium or stiff gels, were outside the range of the instrument. In the medium range the penetrometer could not differentiate with sufficient precision between satisfactory and unsatisfactory gels. The only instrument that has been found satisfactory for the evaluation, characterization, and specification for methacrylate incen-

diary gels has been the torsionmeter. The method developed for using the torsionmeter appears adequate for characterizing quantitatively the elasticity and consistency of such incendiary gels. The elasticity test as conducted on the torsionmeter appears to be in some respects and within certain limits also a measure of the fluidity and cohesiveness of the gel. The degree of flow is a function of time, and as yet no means of measuring the time required for the initial 360° rotation has been devised. When elasticity values are low, the cause may be other than high fluidity. Frequently a gel may be so brittle or short that a rupture occurs during the course of the 360° rotation. When this happens the elasticity will be markedly less. Gels which have low cohesive strength, low tensile strength, or shortness usually reflect these characteristics in terms of low elasticity (4).

The apparent viscosity coefficient determined with the capillary tube, MacMichael, and Clark-Hodsman viscosimeters has been found to be the same as the equilibrium apparent viscosity coefficient as determined on the jeweler's lathe viscosimeter (4).

#### REFERENCES\*

- (1) BARNARD, H.: TDMR 1260, August 15, 1946.
- (2) BAUER, W. H.: March 20, 1943.
- (3) BETTS, R. L., AND MYERS, N. F.: April 15, 1943.
- (4) CARVER, E. K., AND BROUGHTON, G.: December 7, 1942.
- (5) CARVER, E. K., AND VAN WAZER, J. R., JR.: May 7, 1943.
- (6) GARDNER, HENRY A.: *Physical and Chemical Examination of Paints, Varnishes and Lacquers, and Colors*, 8th edition. Institute of Paint and Varnish Research, Washington, D. C. (January 1, 1937).
- (7) GEDDES, J. A., AND DAWSON, D. H.: Ind. Eng. Chem. **34**, 163 (1942).
- (8) GEMANT, A.: J. Applied Phys. **13**, 210 (1942).
- (9) KIRKPATRICK, E. C.: October 2, 1944.

---

\* Since many of the references cited are still classified documents, only the authors' names and the dates of the reports are listed.



VARIABILITY AND INHOMOGENEITY OF ALUMINUM DILAURATE<sup>1,2</sup>KAROL J. MYSELS<sup>3</sup> AND JAMES W. MCBAIN*Department of Chemistry, Stanford University, California**Received June 23, 1948*

Technical aluminum soaps prepared from mixed fatty acids behave like complex mixtures whose properties depend greatly on minor variations in the method of preparation. An obvious explanation is that this is due to changes in composition brought about by reactions between basic aluminum soaps and fatty acids or by the formation of aluminum soaps of different acid combinations.

In the present paper an alternative possibility is pointed out through the study of pure aluminum dilaurate, whose properties may be changed drastically by mild physical treatment. This pure soap shows also complex inhomogeneous behavior, despite its apparent simplicity, and in many respects closely resembles technical aluminum soaps (7).

VARIABILITY OF  $\text{AlOHL}_2$ *The "original modification"*<sup>4</sup>

Aluminum dilaurate may be obtained as a fine white powder by addition of a sodium laurate solution to excess aqueous aluminum chloride and extraction of the washed precipitate with acetone (8, 10). It has ash values of 11.56–11.62 per cent and the lauric acid content of one of the samples was 89.3 per cent. The composition corresponding to  $\text{AlOHL}_2$ <sup>5</sup> is 11.49 per cent  $\text{Al}_2\text{O}_3$  ash and 90.5 per cent acid. The ash was determined by direct ignition at 900–1000°C. The lauric acid content was determined by Mr. R. H. Coe by displacement with aqueous hydrochloric acid, extraction with cyclohexane, and titration with

<sup>1</sup> Presented at the Symposium on Gel Formation, Detergency, Emulsification and Film Formation in Non-Aqueous Colloidal Systems, which was held under the auspices of the Division of Chemistry and the Division of Petroleum Chemistry at the 113th Meeting of the American Chemical Society, Chicago, Illinois, April, 1948.

<sup>2</sup> Study conducted under a contract between Stanford University and the Office of Emergency Management, recommended by Division 11.3 of the National Defense Research Committee and supervised by Professor J. W. McBain.

<sup>3</sup> Present address: Department of Chemistry, University of Southern California, Los Angeles 7, California.

<sup>4</sup> The term "modification" is used here in a purely empirical sense to denote materials having clearly different properties and the same composition without assuming anything about their structure or stability.

<sup>5</sup> The calculated compositions are based not on the theoretical molecular weights of lauric acid,  $\text{C}_{12}\text{H}_{24}\text{O}_2$ , but on that of the "lauric acid" used in the preparation and which was within 0.25 per cent of the theoretical. This procedure seems justified by the great difficulty of obtaining completely pure fatty acids and by our essential concern to differentiate, not between disoaps of various fatty acids, but between the various soaps (mono-, di-, tri-, etc.) of any given acid. Experience with sodium soaps suggested that small amounts of other fatty acids have, in general, negligible effects on the properties of a soap.

alkali in the presence of water. This soap is slightly hygroscopic and may be completely dried by evacuation or storage over phosphorus pentoxide at room temperature (9). It cakes readily. It shows no distinctive features under the microscope and even under the electron microscope only irregular agglomerates were found, too thick to be translucent to electrons. The x-ray diffraction pattern

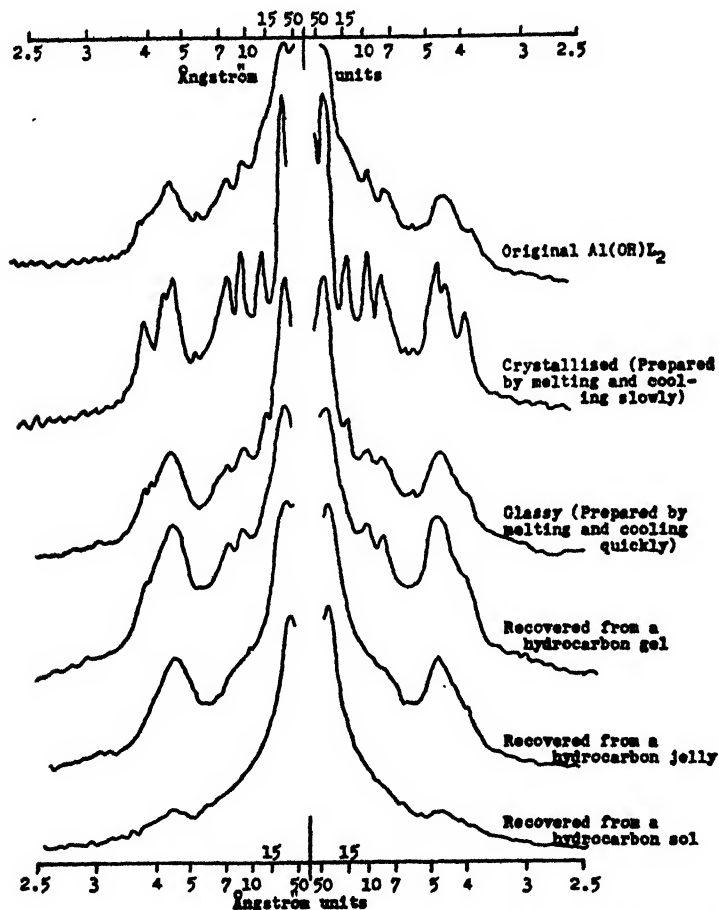


FIG. 1. Microphotometer tracings of x-ray diffraction patterns of six typical modifications of aluminum dilaurate,  $\text{Al(OH)L}_2$ , showing the same Bragg spacings but greatly differing sharpness (courtesy of Dr. Sydney Ross).

consists of a series of relatively sharp lines and a halo, as shown by the top tracings in figure 1. This and the other patterns here presented were obtained by Dr. Sydney Ross.

Reproducible behavior upon heating was obtained if the soap was sealed after drying in an evacuated tube by a technique essentially as described by Marsden (2). Gradual heating was effected either in a forced-draft air oven or with much better control in a Hershberg melting-point apparatus (1). Under these condi-

tions the powder sintered to a white opaque mass at 150–170°C., and became transparent rather sharply over less than 1°C. at a temperature between 190° and 193°C.; this is taken as the melting point because the resulting mass is homogeneous and isotropic although of exceedingly high viscosity. It withstands heating for short periods to 300°C. and flows slowly at this temperature. Prolonged heating at 300°C. in a sealed tube or even at much lower temperatures with drastic temperature gradients results in decomposition. The soap decomposes readily before melting unless the tube containing it is evacuated and sealed.

#### *The "crystallized" modification*

The original appearance of the soap is not restored when cooled from the molten state; instead, a hard brittle mass is formed whose properties depend on how it is cooled.

The mass becomes strongly birefringent and markedly opalescent when the soap is cooled slowly and kept for 15 min. to an hour between 160° and 170°C. It melts sharply upon heating again, losing its opalescence and birefringence over a range of less than 1°C. between 193° and 196°C., i.e., about 3° higher than the "original," the exact range of temperature depending on the sample of soap and on the way it was crystallized. The cycle of melting and crystallization may be repeated many times with a single sample.

This modification, upon cooling, yields a bluish white, slightly translucent, brittle solid. The x-ray diffraction pattern, when compared with that of the "original" modification, shows the same but much sharper lines and the halo is resolved into distinct lines (figure 1).

#### *The "glassy" modification*

On cooling rapidly the melt obtained by heating either the "original" or the "crystallized" modification, a clear, slightly brownish, transparent, brittle glass is produced. Its x-ray diffraction pattern is comparable in sharpness to that of the "original" modification (figure 1).

#### *The "recovered-from-gel" modification*

The "original" modification imbibes large amounts of cyclohexane at room temperature, forming a turbid gel (3) from which the soap may be recovered quantitatively by vigorous evacuation, yielding an almost transparent brittle glass having a less sharp x-ray pattern.

#### *The "recovered-from-jelly" modification*

The turbid gel formed by either the "original" or "crystallized" or "recovered-from-gel" modifications in cyclohexane changes upon heating to a clear jelly (3). This jelly generally remains clear for some time after cooling and the soap may be recovered therefrom by evacuation, whereupon it becomes transparent and brittle, and its x-ray diffraction pattern shows but faint lines. The position of the lines is, however, still the same as in the other modifications.

### *The "lyophilized" modification*

A dilute sol of the soap in cyclohexane may also be prepared, and after freezing and evacuation, the soap is recovered in the "lyophilized" modification, which is a white fluffy powder composed of extremely fine films and fibres as shown by the electron microscope (5). It gives an x-ray diffraction pattern which is only faint but still indicates the same spacing.

### *Comparison of these modifications*

There is no change in composition during all the above transformations, as they occur either in sealed tubes or with quantitative recovery. All of them, by proper heating and cooling, give the same either "crystallized" or "glassy" modification, or may be recovered from a sol in the "lyophilized" modification.

Thus these are all different modifications of the same material, corresponding to the composition  $\text{Al}(\text{OH})\text{L}_2$ .

The sharp x-ray diffraction pattern and the melting over less than  $1^\circ\text{C}$ . of the "crystallized" modification suggest that a single definite compound is present. The unchanging composition upon fractionation by cyclohexane, described below, confirms this point of view.

The differences between the above modifications are summarized in table 1. Besides their appearance, melting point, and sharpness of diffraction pattern, they also differ markedly in their behavior in cyclohexane at room temperature and upon heating. At room temperature, when placed in an excess of cyclohexane, the "crystallized" modification shows little perceptible interaction even after several months; the "lyophilized" modification, on the other hand, dissolved rapidly to a sol. Other modifications show an intermediate behavior; the "recovered-from-jelly" swells slowly but without apparent limit, forming a jelly. The "original" swells to 25–50 cc. per gram; the "recovered-from-gel" to only about one-third that much. The "glassy" swells markedly but is obviously inhomogeneous in its behavior, some parts swelling much more than others and most of them appearing as a jelly.

Upon heating, the viscosity of jellies decreases (6) and the degree of swelling of all gels increases (3), followed by a rather sharp transition from gel to jelly. The temperature of this transition is  $40^\circ\text{C}$ . for the "original" soap and  $48^\circ\text{C}$ . for the "crystallized." For the "recovered-from-jelly" and "lyophilized" ones it is presumably below room temperature (3).

Thus these modifications differ markedly in their properties and seem to fall between the two extremes of "crystallized" and "lyophilized." However, the order is not very well defined; for example, the "recovered-from-gel" swells distinctly less than the "original," despite a more amorphous x-ray diffraction pattern.

The identity of perceptible x-ray diffraction lines shows that no more than one crystalline form is present. The variation of sharpness of these lines shows great differences in the degree of orderliness; whether this is due to particle size, crystallite size, or actual variation in regularity within a crystal cannot be stated at present.

TABLE 1  
*Properties and preparation of five modifications of aluminum dilaurate*

FORM	CRYSTALLINE	FROM GEL	ORIGINAL	GLASSY	FROM JELLY	LYOPHILIZED
Appearance.....	Bluish white, slightly translucent, brittle Sharp 193-196	Translucent or transparent, brittle ?	White, caking powder Sharp 190-193	Slightly brownish, transparent glass ?	Transparent, brittle ?	Extremely fluffy, white 189 (?)
Melting point, °C.....						
One gram swells in cyclohexane at room temperature to.....	<2 cc. 48°C.	8-15 cc.	25-50 cc. 40°C.	Large, indefinite ?	∞ < room temperature	∞ < room temperature
Gel-jelly transition in cyclohexane.....						
X-ray pattern	Sharpness increasing ←					
Preparation	Any other form melted and kept at 160-170°C.	15-20% in cyclohexane; after 24 hr. evaporated	Aqueous anhydrous extraction	Any form melted and quenched	15-10% in cyclohexane heated to 60-85°C. until clear, cooled, and evaporated	Dilute (0.5%) sol frozen and evaporated

It seems apparent that by modifying the physical treatments many other modifications of this soap intermediate between or deviating slightly from the typical ones described above might be prepared. For example, "original" modifications prepared at different temperatures differ markedly in their resistance to hydrolysis by moist acetone (8).

#### INHOMOGENEITY OF ALUMINUM DILAURATE, $\text{AlOHL}_2$

Three hypotheses present themselves to account for the behavior of these modifications:

(1) The simplest is probably that the modifications actually observed are secondary mixtures or solutions of two primary modifications, one completely crystalline, the other completely amorphous, somewhat analogous to the Smith concept of the  $\lambda$  and  $\mu$  forms of sulfur.

(2) A more complicated hypothesis assumes that between the amorphous and the fully crystalline there is a continuous (or almost continuous) series of primary modifications, each with a definite degree of orderliness, and that the several modifications we have described are homogeneous, typical, primary modifications.

(3) A still higher degree of complexity may be assumed in which the primary modifications of hypothesis 2 exist but their mixtures or solutions give the actually observed secondary modifications. This type of complexity is well known in the case of high polymers, where molecules of definite size exist but any actual preparation is polydisperse, and widely differing properties may be obtained by varying the molecular weight distribution. It is also analogous to powders which cannot be prepared with exactly uniform particle size and which show different properties depending on size. (In these two examples, however, the ease of interconvertibility of the different modifications is much smaller.)

Some indication as to which of these three hypotheses is correct is given by the behavior of the "original" soap in cyclohexane (in which the most ordered "crystalline" modification is practically inert at room temperature and the most amorphous "lyophilized" modification dissolves completely).

If the modifications were all stable and reversibly soluble (like polymers), then according to the *first* hypothesis cyclohexane would fractionate any intermediate into varying proportions of two fractions, according to the *second* each modification would be homogeneous and have a definite solubility, and according to the *third* the solvent could fractionate each modification into a large number of different fractions.

The modifications of aluminum dilaurate are, however, certainly not truly stable nor reversibly soluble in cyclohexane. In the dry state, we have never noticed any change over a period of 18 months. Visual observations of the soap in the presence of cyclohexane in sealed tubes showed that, upon raising the temperature, the interaction between soap and solvent came apparently to a stable state within 20 min. or less once the soap was well swollen, and within 1 or 2 days if it was not yet swollen. Upon cooling, however, the interaction between soap and solvent seemed to be much slower with frequent marked supersatura-

tion. Furthermore, upon precipitation, more stable, more crystalline modifications might be formed (3). Thus any equilibrium between solute and solution is not too well defined and is probably an unstable one.

The appearance and volume of the swollen soap depend, however, on the modification considered and even after months of contact with the solvent at room temperature there is little indication of any change from one modification to another. Thus the rate of transformation between them is at least very slow at room temperature, compared with the rate at which cyclohexane interacts with each.

Nevertheless it seems that a definite amount of soap dissolves under reproducible conditions, such as gentle tumbling of the dried soap (9) with cyclohexane in 25-cc. graduates, maintained within  $0.1^{\circ}\text{C}$ . in an air thermostat. The amount dissolved was determined by weighing the residue of a known weight of filtered supernatant liquid after freezing and evacuation.

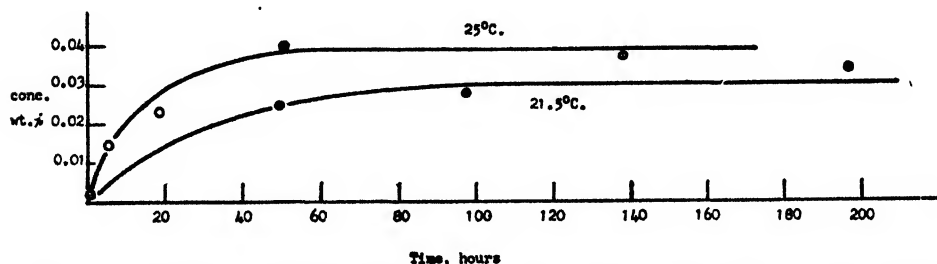


FIG. 2. "Original" aluminum dilaurate-cyclohexane. Variation of soap content of supernatant liquid with time.

#### EFFECT OF TIME

Figure 2 shows the effect of time over several days at two temperatures on systems containing "original" soap and cyclohexane. After about 2 days there is little further change. That there is a limit to the amount of soap which dissolves is definitely indicated by qualitative observations in sealed tubes, which show that even in systems containing only 0.3 per cent of soap the solution is only partial at room temperature even after many months. Therefore the terminal value after 2-4 days is quite definite for a given soap under specified conditions.

#### EFFECT OF VARYING SOAP TO SOLVENT RATIO

Figure 3 shows the change in concentration of the supernatant liquid as the proportion of soap to cyclohexane was changed, other conditions remaining the same. In one series the temperature was  $25^{\circ}\text{C}$ . and the time 2 days, in the other  $21.5^{\circ}\text{C}$ . and 4 days. Each series shows that the amount dissolved is proportional to the amount present within the range and precision of the experiment. This is shown in figure 4, where the proportion of soap dissolved is plotted and appears constant when the ratio of cyclohexane to soap varies.

In all the above experiments each point corresponds to a separate system opened only for analysis. In another experiment 25 cc. of cyclohexane was

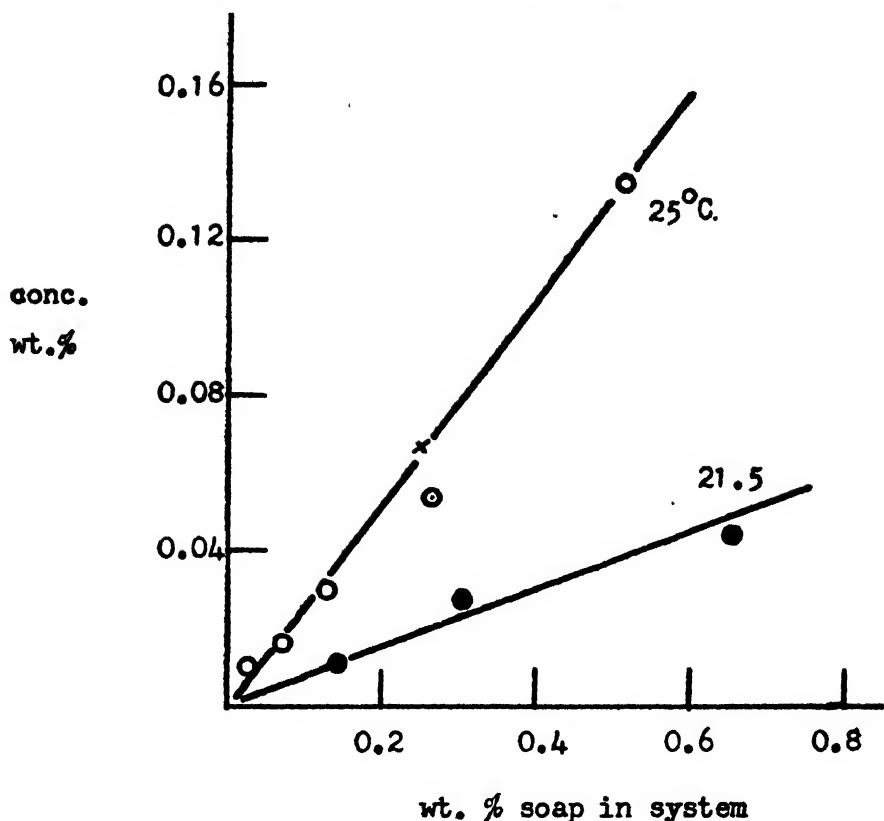


FIG. 3. "Original" aluminum dilaurate-cyclohexane. Variation of soap content of supernatant liquid with amount of soap present and with temperature.

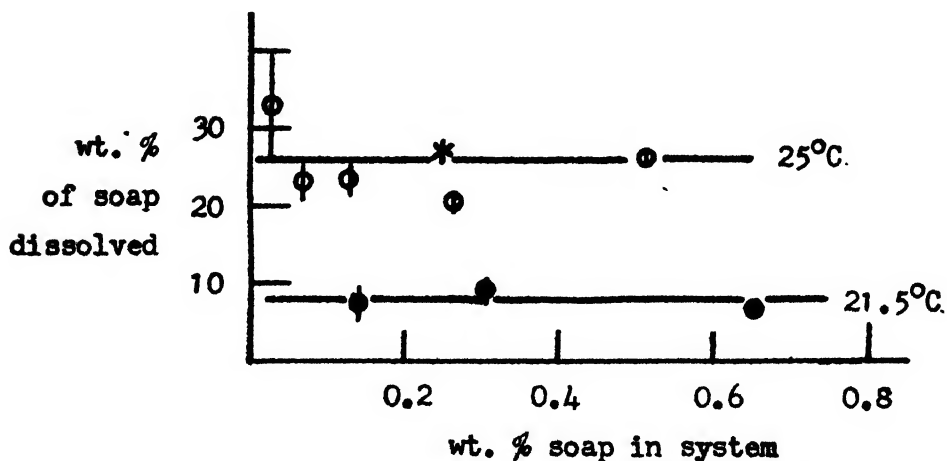


FIG. 4. "Original" aluminum dilaurate-cyclohexane. Variation of weight fraction of soap dissolved with amount of soap present and with temperature.



agitated with 99 mg. (0.51 weight per cent) of soap at 25°C. After 24 hr. as much as possible (19.5 cc.) of the supernatant liquid was withdrawn (and analyzed) and replaced by fresh solvent. This was repeated every day and the amount dissolved computed. Again 27 per cent of soap dissolved in the first 2 days and not more than 9 per cent in the following two, although the concentration of the supernatant liquid fell from 0.115 per cent after the first day to 0.03 per cent after the fourth day. Thus again a fraction of the soap dissolves readily while the remainder does not.

An obvious question is whether the dissolved and undissolved materials have the same composition as the initial soap, or if they are different. To answer this a fraction soluble at 25°C., recovered in "lyophilized" modification after the evaporation of the solvent, was heated in a sealed evacuated tube. It seemed to melt at 189–190°C. After being cooled and kept at 160°C. until completely birefringent, it melted at 194–195°C. A sample of the original soap melted (after crystallization at 160°C.) at 194.5–195.5°C. The x-ray diffraction pattern of the crystallized soap obtained from the dissolved portion was sharp and indistinguishable from that obtained from the original soap.

Thus the dissolved portion is identical in composition with the original soap, a result which confirms the view that the material studied is  $\text{AlOHL}_2$ .

Since the most likely impurity in the soap was lauric acid, a small amount of it was added to one of the systems but had no noticeable effect, as shown by the cross in figures 3 and 4.

#### EFFECT OF TEMPERATURE

As the temperature increases from 21.5° to 25°C. the proportion of soap dissolved increases from about 8 to 26 per cent, as shown by figures 3 and 4.

In this connection it may be noted that visual observation of the soap as the temperature is raised shows no abrupt changes in the system (the gel-jelly transition temperature, while sharp and easily observed, may correspond to the disappearance of only a minute quantity of soap, of the order of 0.05 per cent) (3). It seems therefore that 8 and 26 per cent are simply characteristic of these particular temperatures and that the proportion dissolved would vary continuously with temperature. Experiments at lower temperatures become difficult, however, owing to the extremely low concentration of the solution, and at higher temperatures the soap swells so much as to make the separation of supernatant liquid very difficult.

#### INTERPRETATION

These facts lead to definite conclusions with respect to the structure of the soap. Were the soap homogeneous, consisting of one primary modification (hypothesis 2), it should tend to saturate the cyclohexane always to the same extent, i.e., give a constant concentration in the solvent and varying proportions dissolved as the ratio of soap to cyclohexane is varied. This is exactly contrary to experiment.

If the soap is a mixture of two (or more) primary modifications (hypothesis 1 or 2) and if one (or more) is very soluble and the other one (or more) relatively insoluble in cyclohexane at a given temperature, then the proportion of soap dissolved should reflect the ratio of these primary modifications and the concentration in the solvent should vary as the supply of the soluble material varies. This is in agreement with each series of experiments.

If only two primary modifications are present (hypothesis 1), the proportion dissolved should be the same at both temperatures as long as the soluble one dissolves completely and the insoluble does not dissolve. (If the insoluble dissolves somewhat, the proportion dissolved should vary.) This is again contrary to experiment.

Thus only the third hypothesis remains: namely, that more than two primary modifications make up the soap. The experiments might agree with the existence of three such modifications: (a) not dissolving at 25°C. and forming 74 per cent of the soap; (b) dissolving at 21.5°C. (8 per cent); (c) not dissolving at 21.5°C. and dissolving at 25°C. (18 per cent). It seems more reasonable to assume, in agreement with qualitative observations, that there is a continuous series of degree and uniformity of organization.

#### SUMMARY

Aluminum dilaurate, in its "original" modification as prepared, is a fine white powder of formula  $\text{AlOHL}_2$ . This may be changed by physical treatments into other modifications differing definitely in their properties, such as melting point, solution and swelling in hydrocarbons, and sharpness of x-ray diffraction pattern, yet having the same composition and the same Bragg spacings and being transformable into identical modifications.

When placed in cyclohexane the original soap dissolves only partially, the proportion dissolved being independent of the amount of solvent but varying with temperature. This indicates that these modifications are not themselves homogeneous but are products covering a continuous range of degrees and uniformity of organization and therefore having different degrees of crystallinity, different stability, and different activity. These are presumably not allotropic modifications, but although thermodynamically unstable are of extremely long life in the dry state. They are not phases in the true Gibbsian sense. Their differences, due to varying orderliness of crystal arrangement or of crystallite size, have an effect analogous to that of particle size or degree of polymerization and give a continuous transition between a completely crystalline and an amorphous extreme.

#### REFERENCES

- (1) HERSHBERG, E. B.: *Ind. Eng. Chem., Anal. Ed.* **8**, 312 (1936).
- (2) MARSDEN, S. S.: *Rev. Sci. Instruments* **16**, 192 (1945).
- (3) MCBAIN, J. W., MYSELS, K. J., AND SMITH, G. H.: *Trans. Faraday Soc.* **42B**, 173-80 (1946).
- (4) MCBAIN, J. W., AND WORKING, E.: *J. Phys. Colloid Chem.* **51**, 974 (1947).
- (5) MYSELS, K. J.: *J. Gen. Physiol.* **30**, 153 (1946).

- (6) MYSELS, K. J.: *J. Colloid Sci.* **2**, 375 (1947).
- (7) MYSELS, K. J.: *Ind. Eng. Chem.*, in press.
- (8) MYSELS, K. J., POMEROY, H. H., AND SMITH, G. H.: *Anal. Chem.* **20**, 878 (1948); PB 31898 (issued by OSRD).
- (9) SHREVE, G. W., POMEROY, H. H., AND MYSELS, K. J.: *J. Phys. Colloid Chem.* **51**, 913 (1947).
- (10) SMITH, G. H., POMEROY, H. H., MCGEE, C. G., AND MYSELS, K. J.: *J. Am. Chem. Soc.* **70**, 1053 (1948).

## THE EFFECT OF ADDITIVES ON THE PHYSICAL-CHEMICAL PROPERTIES OF SOAP GELS IN ORGANIC SOLVENTS<sup>1</sup>

G. S. HATTIANGDI,<sup>2</sup> S. P. ADARKAR, J. P. JASSAWALLA, AND M. PRASAD

*Royal Institute of Science, Bombay, India*

*Received June 23, 1948*

The earliest greases were simple greases of lime soaps and oil (6) and did not prove to be satisfactory from the point of view of stability, texture, consistency, etc. Modern grease technology has overcome these drawbacks and has yielded very superior products, but the processes involved in the manufacture of these special greases are as a rule safely guarded, with the result that very little pertinent data is available in the literature. Additives doubtless play a major rôle in modifying the properties of these soap-oil systems, and it is on this aspect that the present paper is based.

Holmes and Maxson (5) found that small traces of water, fatty acids, etc., aid or hamper the dispersion of soaps in turpentine, paraffin oil, and benzene, and increase or decrease the solvent-holding capacity of the soaps considerably. Da Fano (1) and Lawrence (8) found that the gels of alkali and alkaline earth metal soaps in Nujol and other organic media are sensitive to the addition of small amounts of certain polar compounds with which they apparently form complexes. Lawrence (9) reports in a subsequent paper that the gelation temperature of gels of sodium stearate and calcium stearate in Nujol is lowered by the addition of free fatty acids, alcohols, and cresols, and attributes this phenomenon to the peptization of the soap and the formation of complexes of the type  $\text{NaStr}:\text{HF}_a$  and  $\text{CaStr}_2:\text{HF}_a$ , where  $\text{HF}_a$  is the fatty acid. More recently, Smith (14) has found that the addition of small amounts of water to systems of undried and anhydrous sodium stearate in toluene lowers the temperature of

<sup>1</sup> Presented at the Symposium on Gel Formation, Detergency, Emulsification and Film Formation in Non-Aqueous Colloidal Systems which was held under the auspices of the Division of Colloid Chemistry and the Division of Petroleum Chemistry at the 113th Meeting of the American Chemical Society, Chicago, Illinois, April, 1948.

<sup>2</sup> Present address: Department of Chemistry, University of Southern California, Los Angeles 7, California.

transformation to the isotropic phase (the temperature at which anisotropic material separates from an isotropic solution on cooling), and accelerates the transformation from the liquid crystalline state to the gel form. Similar modifications are observed on the addition of water, lauric acid, and methyl alcohol to systems of sodium stearate in cyclohexane, but the addition of nitrobenzene had no such effect.

Hattiangdi (2) and Prasad, Hattiangdi, and Adarkar (11) have investigated the effects of numerous additives, such as fatty acids, alkali soaps, and aromatic hydrocarbons, on the syneresis of sodium oleate gels in pinene. The soaps retard and tend to stop the syneretic phenomenon, the retardation decreasing in the order  $\text{NaP} > \text{KStr} > \text{NaStr}$ . The effects of the addition of three closely related fatty acids (palmitic, stearic, and oleic) are, however, very different. Benzene and toluene retard syneresis, while xylene and mesitylene accelerate it. The retarding effect of Nujol is analogous to that of the soaps, inasmuch as there is a tendency to stop syneresis on the addition of a small optimum amount of this heavy paraffin oil.

The present paper embodies the results of investigations on the effects of numerous other additives on the syneresis and setting time of soap gels in pinene, and on the opacity changes taking place during the gelation of soap-alcohol-water systems. These three properties were selected for observation since they permit direct comparison with the results of measurements made on the same soap-oil systems without any additives (11, 12, 13).

#### MATERIALS

The sodium palmitate and sodium oleate were products of the British Drug Houses, and the sodium stearate of E. Merck. Their melting points, as determined visually on a capillary-type melting-point apparatus, were  $270^\circ$ ,  $232^\circ$ , and  $260^\circ\text{C.}$ , respectively.

The pinene and ethyl alcohol were products of the Eastman Kodak Company, and the Government Distillery, Nasik (India), respectively, and were the fractions distilling at  $156^\circ\text{C.}$  (pinene) and  $79^\circ\text{C.}$  (alcohol). The refractive index and specific gravity of pinene, determined at  $30^\circ\text{C.}$ , were 1.4658 and 0.858, and of ethyl alcohol were 1.3624 and 0.785.

The organic solvents used as additives were pure products of either E. Merck, Schering-Kahlbaum, Reidel-Haen, or British Drug Houses, and were used after their purity was confirmed by means of standard methods. The palmitates and stearates of magnesium, calcium, strontium, barium, zinc, cadmium, and mercury were prepared by metathetic reaction of the sodium soaps with the heavy metal chlorides in 50:50 alcohol-water. Their specifications are given in detail elsewhere (15).

#### EXPERIMENTAL TECHNIQUE

##### *Syneresis*

Gel-forming solutions containing 0.09 g. of sodium oleate and small known amounts of the additive in 7 ml. of pinene were prepared in test tubes of the same diameter ( $2r = 1.45\text{ cm.}$ ) by heating the system to about  $140\text{--}145^\circ\text{C.}$  in an oil

bath. The hot homogeneous solutions were allowed to cool, gelate, and synerize in a water thermostat maintained at 30°C. The amount of synereticum exuded after 2 hr. was determined by the method employed by Prasad, Hattiangdi, *et al.* (12, 13), which involves weighing the gel system before and after the careful removal of syneretic liquid by small rolls of filter paper. The probable error is of the order of  $\pm 5$  per cent. The results obtained are presented on a percentage basis in table 1, the amount of synereticum exuded by the sodium oleate gel in pinene without any additive being taken as a standard for determining the increase or decrease in the extent of syneresis.

#### *Opacity*

Gel-forming solutions containing 0.6 g. of sodium oleate and 0.5 ml. of the additive in a mixture of 7.5 ml. of ethyl alcohol and 0.5 ml. of distilled water were prepared at about 60°C. The changes in the intensity of transmitted light during the sol-gel transformation of these systems were measured by means of a Klett-Summerson glass-cell photoelectric colorimeter. A projection-type electric lamp (100 watts; 230 volts) fitted with a blue filter (400–465 millimicrons) was used as the source of light, and the current produced by the photocells was measured by means of a galvanometer of the suspension wire type. The opacity of the system (that is, the reciprocal of the intensity of transmitted light) was measured in terms of the divisions on the potentiometer slide-wire which are necessary to nullify the potential applied to the galvanometer. The instrument yields very accurate results (within  $\pm 0.3$  per cent) and can be manipulated easily for rapid measurements. The experimental procedure was the same as that adopted by Hattiangdi (3). The results obtained are shown graphically in figure 2, in which the values of opacity, in terms of the scale divisions of the instrument, are plotted as a function of time.

#### *Setting time*

Gel-forming solutions containing 0.07 g. of either sodium palmitate, stearate, or oleate in 10 ml. of pinene were prepared as described earlier in test tubes of the same diameter ( $2r = 1.45$  cm.). Small amounts of any one of the heavy metal soaps were added and dissolved. The hot homogeneous solutions were then allowed to cool and gelate in a water thermostat maintained at 30°C. The system was considered to have set to a gel when it did not flow out of the container when inverted (4); the exact setting time was determined by repeating the experiment, each time disturbing the gel-forming system as little as possible. The results obtained are presented on a percentage basis in table 2, the setting time of a gel without any additive being taken as a standard for determining the extent of increase or decrease.

### RESULTS AND DISCUSSION

#### SYNERESIS

##### *Effect of alcohols*

The per cent increase or decrease in the extent of syneresis of sodium oleate gels in pinene in the presence of various additives is shown in table 1, from which

it will be seen that the enhanced syneresis caused by the addition of equal amounts of the normal aliphatic alcohols decreases in the order



Methyl alcohol is immiscible with pinene, and measurements could not therefore be made with this alcohol as an additive.

Contrary to the behavior of the normal alcohols, the isoalcohols decrease the

TABLE 1

*Effect of additives on the per cent increase (+) or decrease (-) in the syneresis of sodium oleate gels in pinene*

ADDITIVE	EFFECT	AMOUNT OF ADDITIVE PRESENT (IN MILLILITERS)							
		0.1	0.2	0.3	0.4	0.5	1.0	2.0	3.0
$\text{C}_2\text{H}_5\text{OH}$ .....	+	228.0		275.1		263.5	241.9		
$n\text{-C}_3\text{H}_7\text{OH}$ .....	+	160.0		201.4		208.1			
$i\text{-C}_3\text{H}_7\text{OH}$ .....	-	+46.6		+24.6		18.7	64.8	76.3	89.1
$n\text{-C}_4\text{H}_9\text{OH}$ .....	+	90.1	118.7	130.5					
$i\text{-C}_4\text{H}_9\text{OH}$ .....	-	24.4		53.5		63.2	82.2	88.1	96.1
$n\text{-C}_5\text{H}_{11}\text{OH}$ .....	+	23.8	45.4	52.2		44.0			
$\text{CHCl}_3$ .....	-	14.2		15.0		26.4	29.5	36.2	
$\text{CCl}_4$ .....	-	3.4		3.7		4.1	5.1	6.3	7.7
$\text{C}_6\text{H}_5\text{Cl}$ .....	+	56.3		73.7		65.4	55.5	54.1	59.7
$\text{C}_6\text{H}_5\text{Br}$ .....	+	103.3		120.8		111.8	88.5	85.1	81.7
$p\text{-CH}_3\text{C}_6\text{H}_4\text{Cl}$ .....	-	8.2		15.0		20.7	23.4	18.7	10.9
Methyl ethyl ether .....	+	88.1	134.2	125.1	145.4	172.4			
Anisole .....	+	73.3		59.6		47.1	28.5	19.7	29.3
Phenetole .....	+	144.4		131.4		111.4	71.0	52.5	51.6
Phenol .....	+	36.3							
<i>o</i> -Cresol .....	+	49.6	107.5	391.1	438.8				
<i>m</i> -Cresol .....	-	1.1	2.8	4.7	4.2	4.0			
<i>p</i> -Cresol .....	+	31.9	49.9	101.2	126.6				
Methyl ethyl ketone .....	+	91.3	141.2	148.9	188.8	198.2			
Benzyl alcohol .....	+	72.3		171.2		365.6			

extent of syneresis, the effect due to isobutyl alcohol being greater than that with isopropyl alcohol.

Curves obtained on plotting the per cent increase or decrease of syneresis against the amounts of the additives present are shown in figure 1, from which it will be seen that the presence of small amounts of the additives exerts a pronounced influence. With the addition of increasing amounts of the normal alcohols, the per cent increase is rapid initially, reaches a maximum, and then decreases slightly to an almost constant value. The behavior in the presence of isopropyl alcohol is rather anomalous, in that the initial accelerating effect

diminishes till it actually retards the syneretic process. The addition of increasing amounts of isobutyl alcohol diminishes syneresis rapidly initially and

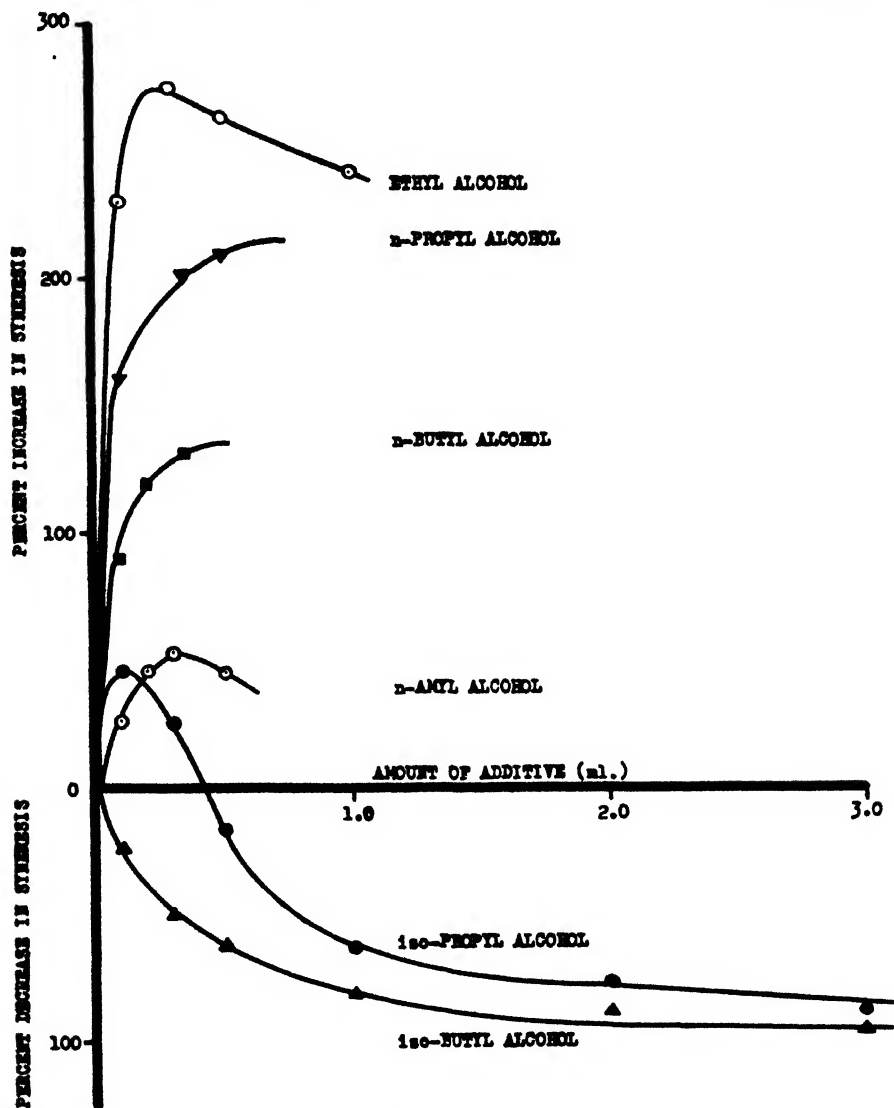


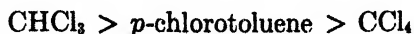
FIG. 1. Effect of the addition of aliphatic alcohols on the syneresis of sodium oleate gels in pinene.

fairly slowly as amounts larger than 1.0 ml. are added; no maximum point of inflection is shown.

#### *Effect of halogenated hydrocarbons*

Chlorobenzene and bromobenzene increase the extent of syneresis of sodium oleate gels in pinene, whereas carbon tetrachloride, chloroform, and *p*-chloro-

toluene diminish it. The increased effect due to bromobenzene is greater than that with chlorobenzene, while the diminution due to the other substances decreases in the order:



The curves obtained on plotting the per cent increase or decrease of syneresis against the amounts of the additives present show that the behavior in the presence of small increasing amounts of chlorobenzene and bromobenzene is similar to that with the normal aliphatic alcohols. The per cent decrease in the case of chloroform, carbon tetrachloride, and *p*-chlorotoluene increases rapidly initially and then rather slowly with increasing amounts of the additives; this behavior is similar to that with isobutyl alcohol.

#### *Effect of ethers*

All the three ethers used—namely, methyl ethyl ether, anisole, and phenetole—increase the extent of syneresis of sodium oleate gels in pinene. The per cent increase is very pronounced in the presence of small amounts of methyl ethyl ether but not so marked with larger additions. The behavior of anisole and phenetole is different inasmuch as the acceleration, which is profound with small additions, drops off considerably as increasing amounts of the additive are present. Also, for a given amount of the additive present, the per cent increase due to phenetole is greater than that with anisole.

#### *Effect of phenol and cresols*

The results presented in table 1 show that *o*- and *p*-cresols favor the syneresis of sodium oleate gels in pinene, whereas *m*-cresol hampers it. The amount of synereticum exuded in the presence of *o*- and *p*-cresols increases rapidly as the amount of the additive is increased. The retardation due to *m*-cresol, which is not very significant with small additions, increases slowly as the amount of this additive is increased.

The effect of the addition of phenol could be examined at only one concentration, since the system does not set to a gel even on long standing if larger amounts of this additive are present.

#### *Effect of other compounds*

The addition of esters yielded negative but interesting results. Methyl acetate is not miscible in pinene, and although butyl acetate is miscible, the soap crystallizes out on cooling the soap-pinene-butyl acetate system. Pseudo-gels are obtained in the presence of varying amounts of ethyl and amyl acetates, those with the former being weaker and more susceptible to breakdown than the pseudo-gels obtained with the addition of the latter ester.

The dihydroxy alcohols methylene glycol and ethylene glycol and the trihydroxy alcohol glycerol are not readily miscible in pinene, and gels are not obtained in their presence. Psuedo-gels are obtained in the presence of small



amounts of nitrobenzene, but the soap refuses to dissolve if the amount of this additive is increased.

Methyl ethyl ketone and benzyl alcohol accelerate the synergetic process of sodium oleate gels in pinene (*cf.* table 1), increasing rapidly as the amount of these additives is increased.

Quantitative measurements with carbon disulfide could not be made, as the system bumps vigorously on heating even when very small amounts of this additive are present. Qualitative measurements indicate, however, that it tends to increase syneresis to a marked degree.

### *Discussion*

Hattiangdi (2) has pictured the gelation of soap systems in organic solvents as composed of the following main steps: (a) the synthesis of primary colloidal particles from a molecular solution; (b) the gradual increase in size and number of the secondary aggregates; (c) the aggregation of these particles into fibrous threads; (d) the formation of a gel structure and the immobilization of the dispersion medium. The colloidal aggregates are held together by forces of residual valencies; hence they are not very stable units. In trying to go over to a stable state, such as that of coarse particles, the colloidal aggregates in a set gel approach one another and readjust the gel structure, thereby causing a shrinkage of the gel and the exudation of the synergetic liquid. The data presented in table 1 show that the orientation of gel structures, as manifested by syneresis, can be modified by suitable additives. In achieving this, the additives presumably affect the solubility of the soap-pinene system and/or favor peptization and complex formation.

Palit and McBain (10) have shown that the solubility of alkali and heavy metal soaps, which is comparatively low in pure hydrocarbons or alcohols or glycols, is very much enhanced in mixtures of the three types of solvents. By analogy, the presence of small amounts of the different additives either increases or decreases the solubility of sodium oleate in pinene. The extent of syneresis would presumably be more in the former case, and less in the latter. The maxima obtained in the various curves at about 0.5 to 1.0 ml. of the additives suggest that the effect on solubility is most pronounced in this range.

Another plausible explanation of the effect of additives seems to be the peptization of colloidal entities and the formation of colloidal complexes. The presence of the additives in the gel-forming solution would modify most of the steps involved in the process of gelation. When the binding forces of residual valencies are weak, the tendency to form adsorption complexes is attenuated and syneresis is pronounced. The factors which contribute towards the polarity of the added molecules, and which influence the forces by which the colloidal aggregates are held, are the number and positions of specific active groups, the length of the hydrocarbon chain, the molar polarization, and the molar density. It is interesting to examine the data on the behavior of the various additives in terms of the possible existence of a relation between the physical-chemical characteristics of the additives and their effects on the synergetic process.

It was observed in the case of the normal aliphatic alcohols that the per cent increase in syneresis diminishes in the order:



On plotting the per cent increase caused by the addition of an equivalent amount of the various alcohols against the number of  $\text{CH}_2$  groups contained in them, a straight line is obtained, indicating that the per cent increase in syneresis is proportional to the length of the alcohol molecules, decreasing as the chain length increases.

Among the aliphatic halogenated hydrocarbons, chloroform and chlorobenzene exert greater retarding effects than carbon tetrachloride and bromobenzene, respectively. This suggests that the increased density of the added molecule contributes towards the greater instability of the gel which is evidenced by more pronounced syneresis. The retarding effect of *p*-chlorotoluene suggests that the presence of a methyl group in the para position with reference to chlorine increases the length of the molecule and decreases the activity of the chlorine atom (*cf.*: a similar increase in the hydrocarbon chain of the alcohol molecules resulted in a diminishing influence of the hydroxyl group and the greater stability of the gel system).

The order in which the cresols affect syneresis is rather surprising, since a methyl group in the para position with respect to the active hydroxyl would be expected, on the above reasoning, to affect syneresis least. This anomalous behavior may be due to the fact that the peptizing efficiencies of isomers are, as pointed out by Lawrence (9), sometimes markedly different.

Thus, in general, the increase or decrease in the extent of syneresis in the presence of additives belonging to a homologous series varies in a regular manner, and appears to be related to (a) the length of the hydrocarbon chain attached to any active group (such as hydroxyl, halogen, etc.) in the molecule, and (b) the density of the molecule.

#### OPACITY

##### *Results*

The effect of the addition of various normal alcohols on the opacity changes with time taking place during the sol-gel transformation of sodium oleate systems in ethyl alcohol-water mixtures is shown graphically in figure 2, from which it will be seen that the opacity values, which are low and constant initially, rise very slowly at first and then very rapidly and once again rather slowly, tending to attain a constant value. After this stage, the curves rise very rapidly once again and later tend to run parallel to the time axis. The general nature of these opacity-time curves is very similar to those reported by Hattiangdi (3) for soap-pinene systems.

##### *Discussion*

Laing and McBain (7) have shown from conductivity and ebullioscopic data that alkali soaps behave like normal electrolytes at the boiling point of both

anhydrous and moist alcohol, and that the solutions are true molecular solutions. The soaps crystallize out like a normal substance on cooling the solutions in

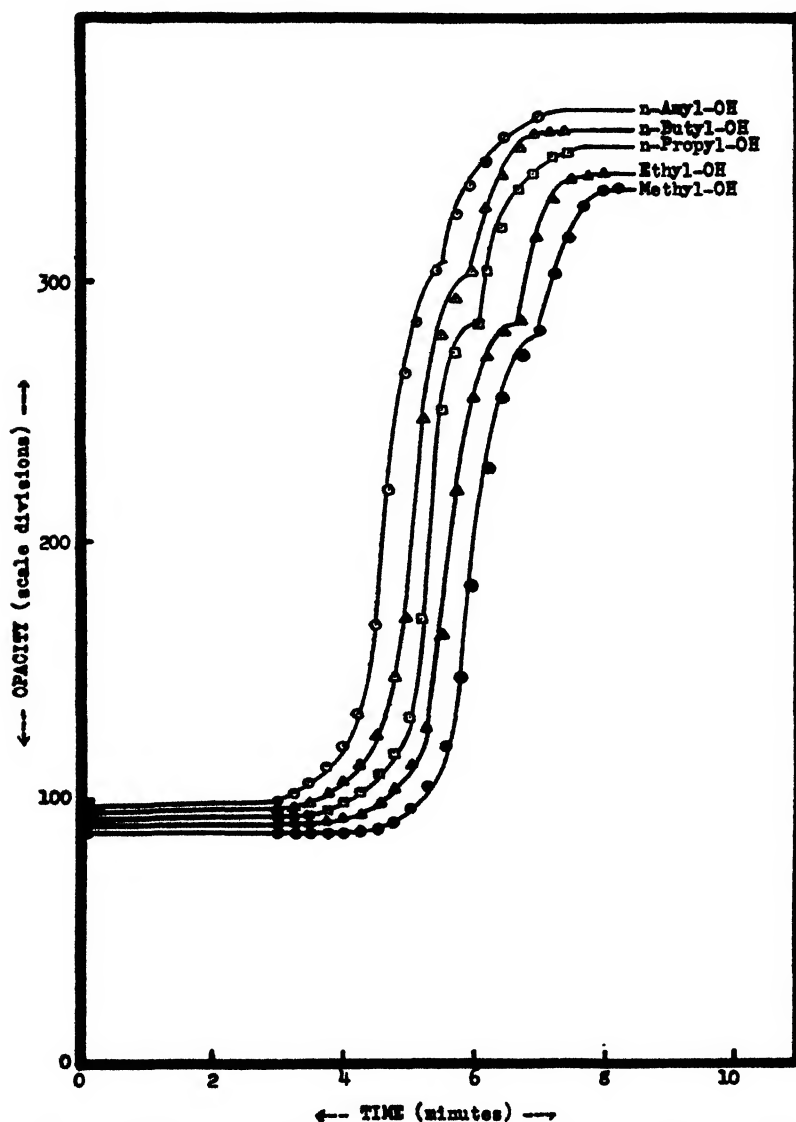


FIG. 2. Effect of the addition of normal aliphatic alcohols on the opacity of sodium oleate-ethyl alcohol-water systems.

anhydrous alcohol, but colloidal complexes are formed in the presence of small amounts of water.

The approximate constancy in the initial values of opacity of the gel-forming systems of sodium oleate in alcohol-water is due to the fact that the absorption of light by a true molecular solution does not change appreciably unless aggrega-

tion takes place and suspended particles interfere. Even if primary colloidal particles are formed in this period of initial cooling, their size and number is evidently extremely small such as would not affect the values of opacity appreciably.

Further cooling of the solutions increases their degree of saturation and causes the formation of a larger number of primary particles. This is evidenced by the slow increase in opacity values with time. The subsequent rapid rise suggests the formation of secondary aggregates and a general increase in both their size and number. As this process nears completion, the secondary aggregates become heavily solvated, greatly reducing the amount of free dispersion medium. The changes in the intensity of scattered light are not large during this period of solvation, owing to the changing refractive index of the micelles. Hence, the opacity increases rather slowly, tending to reach an almost constant value. It is interesting to note that this period coincides approximately with the setting time of the gels as observed by other methods.

The sudden change in the direction of the opacity-time curves at this stage is caused probably by structural changes which continue to take place in the set gels on further cooling and standing. In view of the fact that these gels set at a temperature much higher than the room temperature, it seems reasonable to assume that the structural changes are brought about by the separation of the soap from a state of solution or suspension in which it exists either in the intermicellary or in the interfibrillary liquid.

It will be seen from figure 2 that the general characteristics of the opacity-time curves are maintained in the presence of the different added alcohols. The additives increase the opacity of the original gel-forming system in the order:



It is interesting to note that this order is in accord with the position of the various alcohols in the homologous series, and suggests that the opacity of the system is a function of the refractive index of the added alcohol.

The decreased opacity in the presence of the lower alcohols may also be due to the fact that their peptizing action is proportionately larger, inasmuch as fewer number of small particles would on an average permit more light to be transmitted than a greater number of larger particles.

#### SETTING TIME

##### *Results*

It was found during experimentation that stable gels are obtained when small increasing amounts of the palmitates and stearates of calcium, strontium, and barium are added to the gel-forming systems of sodium palmitate, stearate, and oleate in pinene. However, typical gels are obtained in the presence of only 0.01 g. of the palmitates and stearates of magnesium, zinc, cadmium, and mercury, the addition of larger amounts of these additives yielding loose pseudo-gels. The effect of the addition of calcium, strontium, and barium soaps is thus very

different from that produced in the presence of magnesium, zinc, cadmium, and mercury soaps.

The per cent increase or decrease in setting time due to the addition of equal amounts of the several heavy metal soaps is shown in table 2, from which it will be seen that the addition of the heavy metal soaps to the gel-forming solutions of sodium palmitate, stearate, or oleate in pinene usually causes a decrease in the setting time, and this acceleration of the setting process increases with increasing

TABLE 2

*Per cent increase or decrease in setting time due to the addition of heavy metal soaps*  
(All values are (+) except where indicated otherwise)

ADDITIVE	PER CENT DECREASE (+) OR INCREASE (—) IN SETTING TIME OF SOAP GELS IN PINENE								
	Amount of additive in sodium palmitate gel			Amount of additive in sodium stearate gel			Amount of additive in sodium oleate gel		
	0.01 g.	0.02 g.	0.03 g.	0.01 g.	0.02 g.	0.03 g.	0.01 g.	0.02 g.	0.03 g.
CaP <sub>2</sub> . . . . .	4.49	11.91	18.75	12.62	14.29	21.27	28.68	29.36	34.19
CaStr <sub>2</sub> . . . . .	7.87	11.91	17.50	16.50	18.36	25.53	33.83	34.13	38.46
SrP <sub>2</sub> . . . . .	1.12	7.14	13.75	8.73	10.20	17.02	25.00	25.39	29.98
SrStr <sub>2</sub> . . . . .	3.37	7.14	12.50	11.65	14.29	21.27	30.15	30.95	35.04
BaP <sub>2</sub> . . . . .	—2.25	4.76	8.76	4.85	6.12	11.72	21.32	22.22	26.50
BaStr <sub>2</sub> . . . . .	0.00	3.57	7.50	7.76	10.20	17.02	26.47	26.99	31.62
MgP <sub>2</sub> . . . . .	7.76	*	*	21.39	*	*	32.36	*	*
MgStr <sub>2</sub> . . . . .	11.65	*	*	22.47	*	*	36.77	*	*
ZnP <sub>2</sub> . . . . .	4.85	*	*	19.10	*	*	29.42	*	*
ZnStr <sub>2</sub> . . . . .	8.74	*	*	20.22	*	*	33.09	*	*
CdP <sub>2</sub> . . . . .	0.00	*	*	16.86	*	*	24.95	*	*
CdStr <sub>2</sub> . . . . .	4.86	*	*	17.98	*	*	29.42	*	*
HgP <sub>2</sub> . . . . .	—6.79	*	*	12.36	*	*	18.39	*	*
HgStr <sub>2</sub> . . . . .	—1.94	*	*	13.48	*	*	22.80	*	*

\* Loose pseudo-gel; no measurements made.

amounts of the additives present. The only exceptions to this behavior are the effects of the addition of 0.01 g. of barium palmitate and stearate, cadmium palmitate, and mercuric palmitate and stearate to the gel system of sodium palmitate in pinene, these systems exhibiting a retarded setting process.

It will also be seen from table 2 that the heavy metal stearates accelerate the setting process to a greater extent than the corresponding palmitates. Further, the per cent acceleration of the setting process decreases in the order:



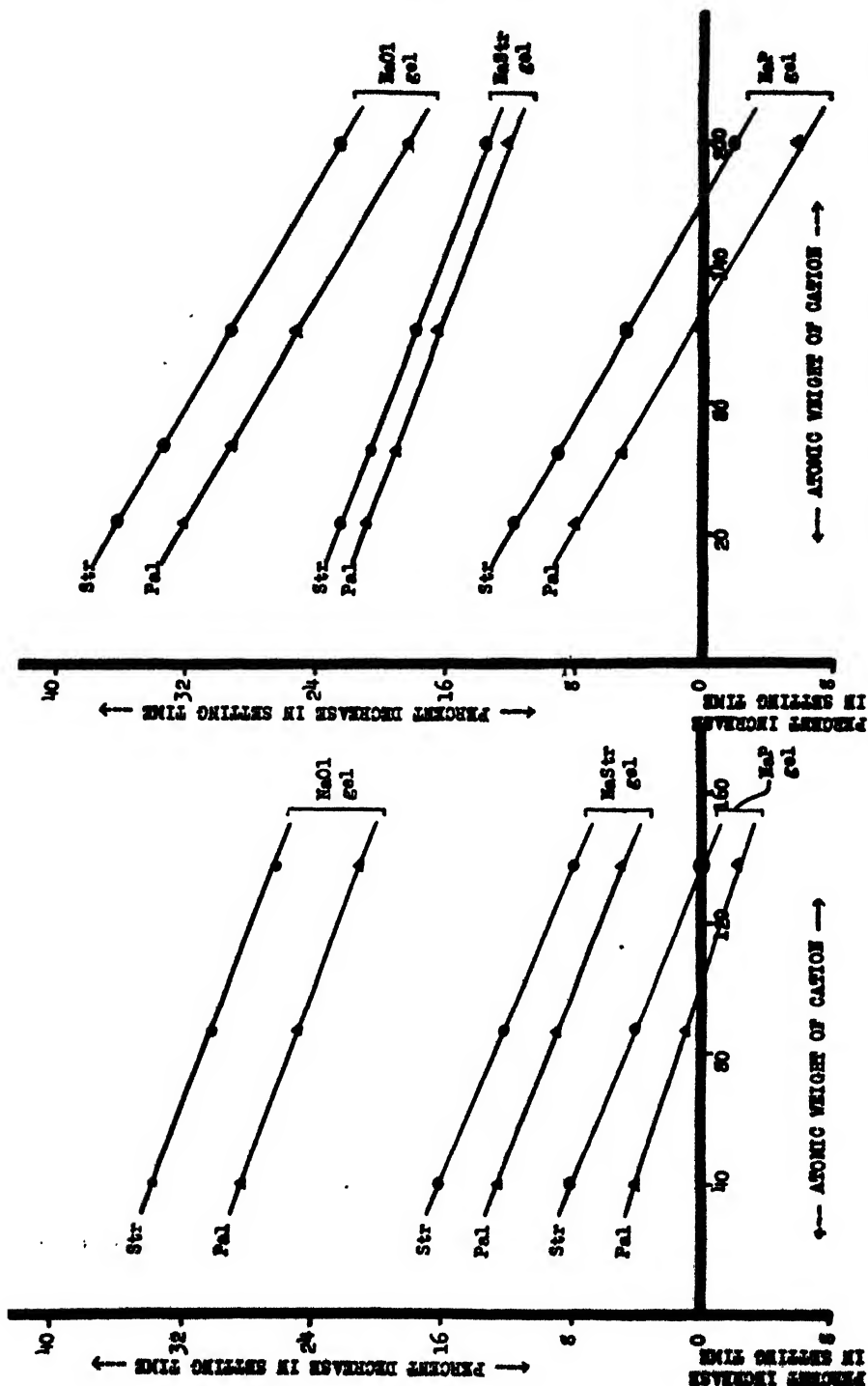


FIG. 3. Effect of the addition of calcium, strontium, and barium soaps on the setting time of some alkali soap gels in pinene.

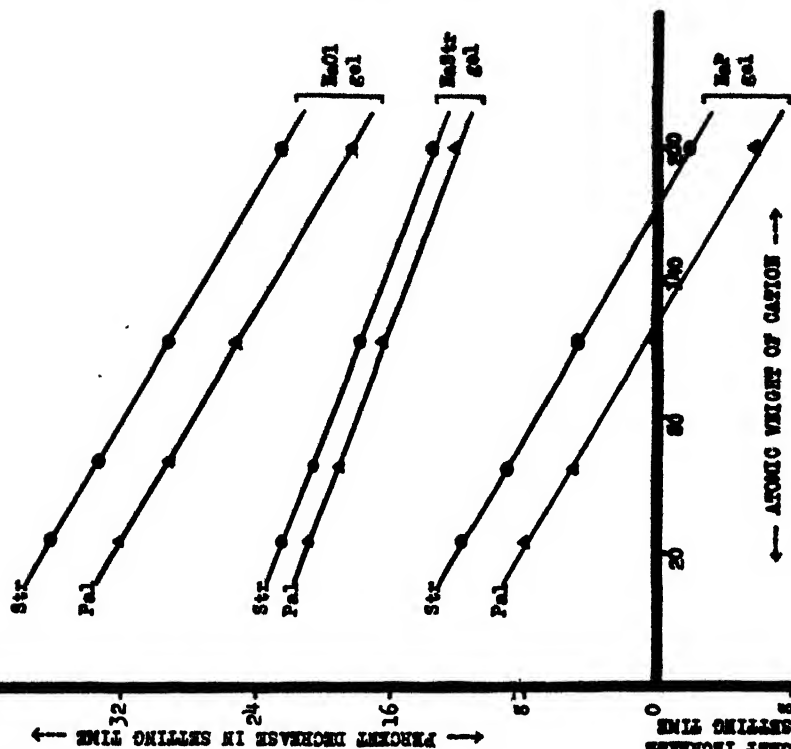


FIG. 4. Effect of the addition of magnesium, zinc, cadmium, and mercury soaps on the setting time of some alkali soap gels in pinene.

An attempt was made to see whether the per cent increase or decrease in setting time is related to the atomic weight of the cations in the added soaps. The various curves in figures 3 and 4 show that straight lines are obtained for both the palmitates and the stearates, and further that these are almost parallel to each other. Also, the points for calcium, strontium, and barium soaps lie on one straight line, whereas those for magnesium, zinc, cadmium, and mercury soaps lie on another. It is interesting to note that the effect of the addition of these heavy metal soaps is in keeping with the positions of the cations in the sub-groups, the effect of the magnesium soaps being aligned with those of the zinc, cadmium, and mercury soaps rather than with the calcium, strontium, and barium soaps.

### Discussion

As pointed out in a previous paragraph, the setting process of soap gels in organic solvents is a function of (i) the amount of supersaturation, (ii) the number and size of the secondary aggregates, and (iii) the forces of residual valencies by which the colloidal particles are held together at random in a sort of brush-heap structure. The presence of small amounts of the heavy metal soaps presumably favors the formation of certain complex compounds which facilitate a rapid increase in the three factors mentioned above, thus accelerating the setting process of the gel system. The exact nature of this influence is evidently dependent on the constitutive properties of the added soaps and, for a series of soaps in which the fatty acid part remains the same, the degree of acceleration is related to the atomic weight of the cation in the added soap.

### SUMMARY

The effect of numerous additives on the syneresis, opacity, and setting time of alkali soap gels in pinene and alcohol-water has been investigated.

The addition of normal aliphatic alcohols accelerates the syneretic process of sodium oleate gels in pinene, whereas isoalcohols retard it. The halogenated hydrocarbons bromobenzene and chlorobenzene accelerate syneresis, while *p*-chlorotoluene, carbon tetrachloride, and chloroform retard it. The addition of phenol and *o*- and *p*-cresols accelerates syneresis, but *m*-cresol has a retarding effect. All the other additives employed—namely, methyl ethyl ether, anisole, phenetole, methyl ethyl ketone, and benzyl alcohol—accelerate syneresis. The acceleration or retardation of syneresis appears to be dependent, in some cases, on the physical-chemical characteristics of the additives.

The effect of the addition of various normal aliphatic alcohols on the opacity changes taking place during the sol-gel transformation of sodium oleate-ethyl alcohol-water systems has been investigated. The additives increase the opacity in the order:



The addition of the palmitates and stearates of calcium, strontium, barium, magnesium, zinc, cadmium, and mercury accelerates the setting process of

alkali soap gels in pinene. The per cent acceleration is greater with a stearate than a palmitate, and decreases in the following order for the cations:



The per cent increase or decrease in setting time is related linearly to the atomic weights of the cations in the added soaps, and decreases with increasing atomic weights.

#### REFERENCES

- (1) DA FANO, E.: *Giorn. chim. ind. applicata* **11**, 199 (1929); *Ind. olii minerali e grassi* **9**, 105 (1929).
- (2) HATTIANGDI, G. S.: *J. Sci. Ind. Research (India)* **4**, 489 (1946).
- (3) HATTIANGDI, G. S.: *Proc. Indian Acad. Sci.* **27**, 23 (1947).
- (4) HOLMES, H. N.: *J. Phys. Chem.* **22**, 510 (1918).
- (5) HOLMES, H. N., AND MAXSON, R. N.: *Colloid Symposium Monograph* **5**, 287 (1928).
- (6) KLEMGARD, E. N.: *Lubricating Greases: Their Manufacture and Use*. Reinhold Publishing Corporation, New York (1937).
- (7) LAING, M. E., AND MCBAIN, J. W.: *Kolloid-Z.* **35**, 19 (1924).
- (8) LAWRENCE, A. S. C.: *Trans. Faraday Soc.* **34**, 660 (1938).
- (9) LAWRENCE, A. S. C.: *Trans. Faraday Soc.* **35**, 702 (1939).
- (10) PALIT, S. R., AND MCBAIN, J. W.: *Oil & Soap* **23**, 58, 72 (1946); **24**, 190 (1947); *Ind. Eng. Chem.* **18**, 246, 741 (1946).
- (11) PRASAD, M., HATTIANGDI, G. S., AND ADARKAR, S. P.: *Proc. Indian Acad. Sci.* **23**, 320 (1945).
- (12) PRASAD, M., HATTIANGDI, G. S., AND MATHUR, K. N.: *Proc. Indian Acad. Sci.* **21**, 105 (1945).
- (13) PRASAD, M., HATTIANGDI, G. S., AND VISHVANATH, C. V.: *Proc. Indian Acad. Sci.*, **21**, 56 (1945).
- (14) SMITH, G. H.: *J. Am. Oil Chemists' Soc.* **24**, 353 (1947).
- (15) VOLD, R. D., AND HATTIANGDI, G. S.: Communicated for publication.

### THE ELECTRICAL BEHAVIOR OF DODECYLAMMONIUM CHLORIDE IN WATER-ORGANIC SOLVENT SYSTEMS<sup>1</sup>

A. W. RALSTON AND D. N. EGGENBERGER

*Research Laboratory, Armour and Company, Chicago, Illinois*

*Received June 23, 1948*

Dodecylammonium chloride is a typical cationic colloidal electrolyte and the electrical behavior of its aqueous solutions has been the subject of several recent studies (9, 10, 13). Its critical concentration has been determined (2) by the dye method to be  $1.27 \times 10^{-2}$  molar, which value is in substantial agreement with

<sup>1</sup> Presented at the Symposium on Gel Formation, Detergency, Emulsification and Film Formation in Non-Aqueous Colloidal Systems which was held under the auspices of the Division of Colloid Chemistry and the Division of Petroleum Chemistry at the 113th Meeting of the American Chemical Society, Chicago, Illinois, April, 1948.



that of  $1.30 \times 10^{-2}$  which had been previously obtained by the conductivity method (14). A value of  $1.44 \times 10^{-2}$  molar has been recently reported (11). It has been observed (15) that solutions of dodecylammonium chloride in pure ethanol do not exhibit evidences of micelle formation when investigated by the conductivity method. Additions of small amounts of ethanol to dilute aqueous solutions of dodecylammonium chloride are attended by an irregular decrease in equivalent conductance, whereas similar additions to more concentrated solutions bring about a significant rise. The critical concentration is slightly lowered upon adding a small amount of ethanol; however, larger additions materially increase the concentration of colloidal electrolyte at the critical point. The solubility (16) of dodecylammonium chloride is much greater in mixtures of

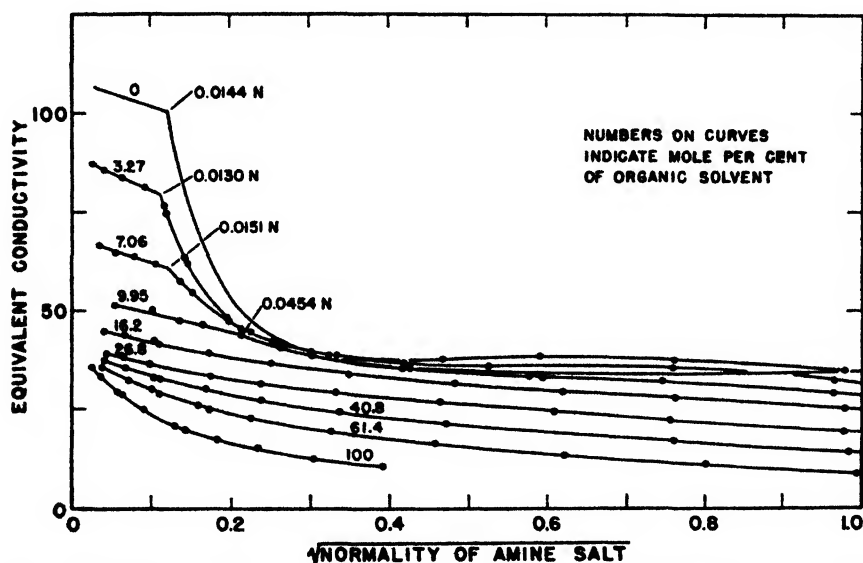


Fig. 1. The equivalent conductivity of dodecylammonium chloride in acetone-water solution.

water and ethanol than in either of the components of such mixtures. The addition of alcohols such as butanol and pentanol greatly lowers the critical concentration. That many of these effects can be attributed to the colloidal nature of dodecylammonium chloride has been shown by the facts that the solubility of hexylammonium chloride, which does not function as a colloidal electrolyte, is regularly reduced by the addition of ethanol to its aqueous solutions (16) and that the conductivity is uniformly lowered (15). In view of the previously observed behavior of dodecylammonium chloride in mixtures of water and ethanol it was decided to extend this work to include other water-organic solvent systems and also to repeat the conductometric work with ethanol-water mixtures. This present paper is, therefore, concerned with the conductivity behavior of dodecylammonium chloride in acetone, acetonitrile, methanol, and ethanol, and in aqueous mixtures of these solvents.

## EXPERIMENTAL

The preparation and properties of the dodecylammonium chloride used in this investigation have been previously described (16). Conductance measurements showed none of the organic solvents employed to contain appreciable amounts of electrolytes. Density determinations were made upon the absolute ethanol and methanol and corrections were made for their water contents. The acetone used was Baker's c.p. quality. Some difficulty was experienced in obtaining acetonitrile with a sufficiently low conductance. c.p. acetonitrile was shaken with phosphorus pentoxide and filtered. The filtrate was then shaken with anhydrous potassium carbonate and distilled through a glass-helices-packed fractionating column. It was necessary to repeat the latter operation before the conductivity was satisfactory. The water employed had a conductance of about  $1 \times 10^{-6}$  mhos.

The solutions were prepared by dissolving the amine salt in the water-organic solvent mixture. Dilute solutions were obtained by adding the appropriate solvent mixture to more concentrated solutions. The electrical conductivities were determined in the manner and with the equipment previously described (17).

## RESULTS AND DISCUSSION

*Acetone-water solutions*

Figure 1 shows the equivalent conductance of dodecylammonium chloride plotted against  $\sqrt{N}$ , in pure water and in various mixtures of acetone and water. The solubility of this salt in pure acetone is so small that a conductivity curve could not be obtained. It is apparent that when the solvent contains more than 9.5 mole per cent acetone the curves are no longer typical of those of colloidal electrolytes. In dilute solutions, below the critical concentration, progressive additions of acetone result in lowered conductivities. The curve obtained for the amine salt in 49.5 mole per cent acetone appears to be an exception to this statement at very low concentrations of the amine salt.

The addition of acetone increases the concentration of dodecylammonium chloride at the critical point. Thus, the value of 0.0144  $N$  in pure water increases to 0.0177  $N$  in 2.65 mole per cent acetone and to 0.0300  $N$  in 5.77 mole per cent acetone. This increase in the critical concentration may be attributed to two causes: the decreased number of free ions occasioned by the weaker ionizing properties of the solvent and a lessened tendency of the free ions to associate in the mixed solvent. This lessened tendency towards association may result from the decreased dielectric properties of the solvent, which decrease magnifies the effectiveness of the repulsion of similarly charged ions. The effect of acetone upon the critical concentration is the opposite of that produced by the addition of salts, since the presence of salts materially lowers the critical concentration (6, 7, 19, 20). It has been stated (4) that the position of the critical point is affected by the concentration of the salt ion opposite in charge to that on the colloidal aggregate and is independent of the nature and concentration of the other ion. The effect of various salts and acids upon the electrical conductance

of aqueous solutions of dodecylammonium chloride has been recently investigated, and it has been shown that whereas metallic ions have a decided effect, hydrogen ions are essentially without influence upon the position of the critical point. Such results are explainable on the basis of the decreased solubility of the hydrocarbon portion of the long-chain ions in the presence of salts. It has been shown (18) that the salting-out properties of salts have little connection with the valences of the salt ions. Since acetone increases the critical concentration, it is quite probable that its presence must increase the ability of the solvent to hold long-chain ions in solution and thus decreases their tendency towards association.

It will be noted that the conductivities of solutions of dodecylammonium chloride in 2.65, 5.77, 9.50, and 14.04 mole per cent acetone, beyond the critica

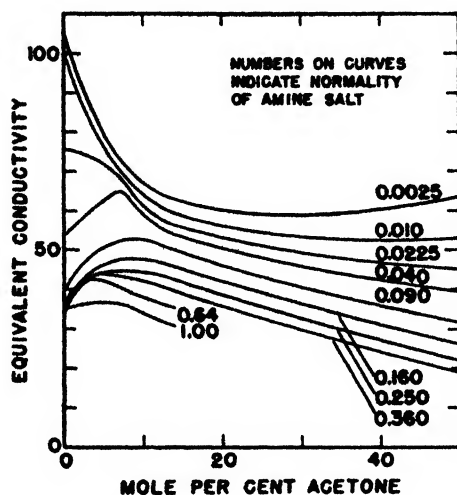


FIG. 2. The effect of acetone upon equivalent conductivity of dodecylammonium chloride

point, are higher than those in pure water. Solutions in 26.9 mole per cent acetone show a higher conductivity only over a limited concentration range, whereas those in 49.5 mole per cent acetone have a lower conductivity over the entire concentration range. It is, therefore, apparent that the effect of the addition of acetone upon the conductance of aqueous solutions of dodecylammonium chloride varies with the concentration of the amine salt.

Figure 2 shows the equivalent conductance of various concentrations of dodecylammonium chloride plotted against the mole per cent of acetone in the solvent. The addition of acetone to dilute solutions of dodecylammonium chloride produces a significant reduction in the conductivity. This effect is reversed with concentration of amine salt higher than the critical point, since increase in the percentage of acetone produces a decided increase in the conductance values. This increase is such that the conductance reaches a maximum at from 3 to 10 mole per cent of acetone. The occurrence of these maxima is undoubtedly dependent upon the colloidal properties of the colloidal electrolytes,

since they do not occur with non-colloids. At concentrations beyond the critical point it has been postulated (10) that the colloidal particle consists of associated ions which have solubilized the undissociated molecules of the colloidal electrolytes. The solubilized molecules greatly reduce the mobility of the colloidal aggregate and impart to it an abnormal transference number. A reduction in either the size or the number of the micelles will reduce the solubilization of the undissociated molecules. If this results in an increased number of free ions or an enhanced mobility of the micelles, the conductance of the system will rise. The maxima in the conductivity curves represent those points at which reduced association combined with the ionizing properties of the solvent gives maximum values. On the water side of these maxima the conductivity drops because of

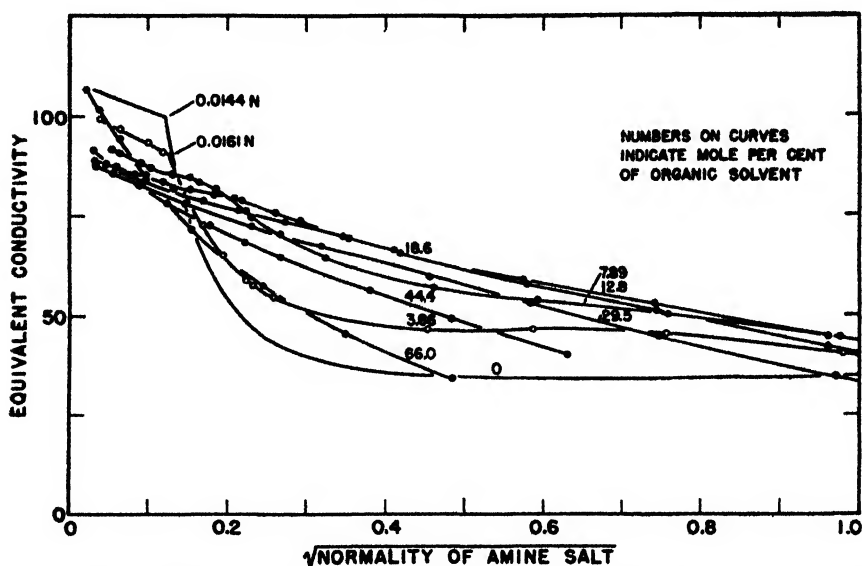


FIG. 3. The equivalent conductivity of dodecylammonium chloride in acetonitrile-water solution.

association attended by solubilization, whereas on the acetone side it drops because of the weaker ionizing properties of the solvent media.

#### *Acetonitrile-water solutions*

The equivalent conductances of dodecylammonium chloride plotted against  $\sqrt{N}$ , in pure water and in mixtures of water and acetonitrile up to and including 66.0 mole per cent of acetonitrile are shown in figure 3. Solutions containing more than 66.0 mole per cent of acetonitrile were not investigated because of the limited solubility of the amine salt in such solvents. The curve for this salt in 3.66 mole per cent acetonitrile is characteristic of a colloidal electrolyte, the conductance decreasing linearly until the critical point and then dropping abruptly. The critical concentration is slightly increased. The presence of 7.89 mole per cent or more of acetonitrile in the solvent brings about a profound

change in the shape of the curves. Instead of an abrupt drop at the critical point the curves for 7.89 and also 12.8 mole per cent acetonitrile actually show a slight rise followed by a gradual drop. A similar phenomenon has been recently reported (5) in the equivalent conductance curves of octadecylpyridinium chloride in methanol-water mixtures, the conductances showing maximum values at concentrations materially remote from infinite dilution. Maxima in equivalent conductance curves are not confined to solutions in mixed solvents, since they have been observed in aqueous solutions of methylene blue (8), hexadecyl- and octadecylpyridinium iodides (1), and in certain quaternary ammonium compounds which contain two long-chain alkyl groups, such as didodecylmethyl-

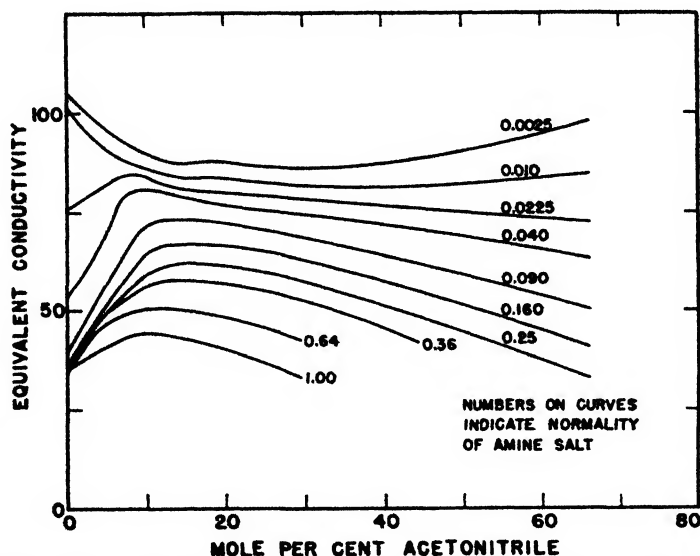


FIG. 4. The effect of acetonitrile upon equivalent conductivity of dodecylammonium chloride.

ammonium chloride (12). In the latter instance the presence of the maxima was attributed to a retarded solubilization of the undissociated molecules of the quaternary ammonium salts.

When the solvent contains more than 12.8 mole per cent acetonitrile the conductance curves fall linearly with concentration. At high dilutions the conductance of dodecylammonium chloride in 66.0 mole per cent acetonitrile is higher than in the other acetonitrile-water mixtures investigated.

The effect of the addition of acetonitrile upon the equivalent conductance of various concentrations of dodecylammonium chloride is shown in figure 4. The similarity of these curves to those obtained for the acetone-water mixtures is apparent. Beyond the critical concentration, the addition of small amounts of acetonitrile is attended by an abrupt rise in the conductance values. Unpublished observations indicate that the cationic transference numbers of dodecylammonium chloride at concentrations higher than the critical point are

materially lowered by the addition of acetonitrile. These results are explainable on the basis of a decreased association tendency attended by an increased number of free ions. It is of interest to note that these maxima occur at approximately that mole per cent of acetonitrile which represents a transition of the amine salt from a colloidal to an ordinary electrolyte.

#### *Methanol-water solutions*

Figure 5 shows the equivalent conductances of dodecylammonium chloride in pure water, pure methanol, and in various mixtures of water and methanol. The critical concentration of this salt increases from 0.0144 *N* in pure water to 0.0164 *N* in 4.82 mole per cent methanol and 0.0250 *N* in 12.71 mole per cent

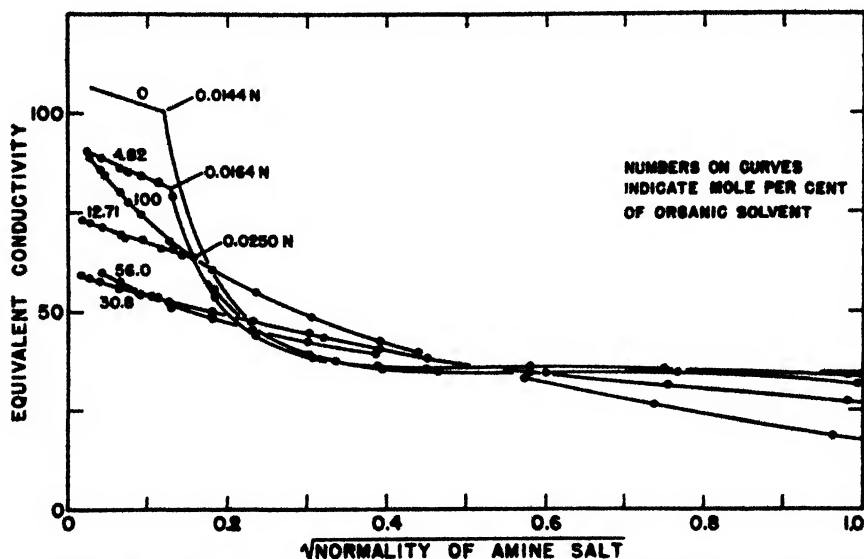


FIG. 5. The equivalent conductivity of dodecylammonium chloride in methanol-water solution.

methanol. Those solutions which contain 30.8 mole per cent or more of methanol show no discontinuities in their conductance curves. The high conductances of dilute solutions of this salt in pure methanol are noteworthy.

The equivalent conductances of various concentrations of dodecylammonium chloride plotted against the mole percentage of methanol in the solvent are shown in figure 6. At concentrations lower than the critical point the equivalent conductance is at a minimum at approximately 40 mole per cent methanol, the values then rising smoothly as the composition of the solvent mixture approaches either pure component. At concentrations somewhat beyond the critical point the addition of methanol is attended by a slight drop in equivalent conductance values. This drop is then followed by an appreciable rise. These curves differ from those obtained for acetone-water and acetonitrile-water mixtures in that the maxima occur at higher concentrations of the organic addend. The ability

of methanol to reduce association is, therefore, less than that of acetone or acetonitrile, as evidenced by the initial drop in conductance and also by the larger amounts required to produce a maximum value. The conductance of certain concentrations of this amine salt, beyond the critical point, is actually somewhat greater in pure methanol than in pure water. This accounts for the relative flatness of the curves.

#### *Ethanol-water solutions*

The electrical conductance of solutions of dodecylammonium chloride in aqueous ethanol has been previously investigated (16); however, because of a later correction (11) of the equivalent conductance curve for this amine salt in pure water, it appeared advisable to repeat this work. The equivalent con-

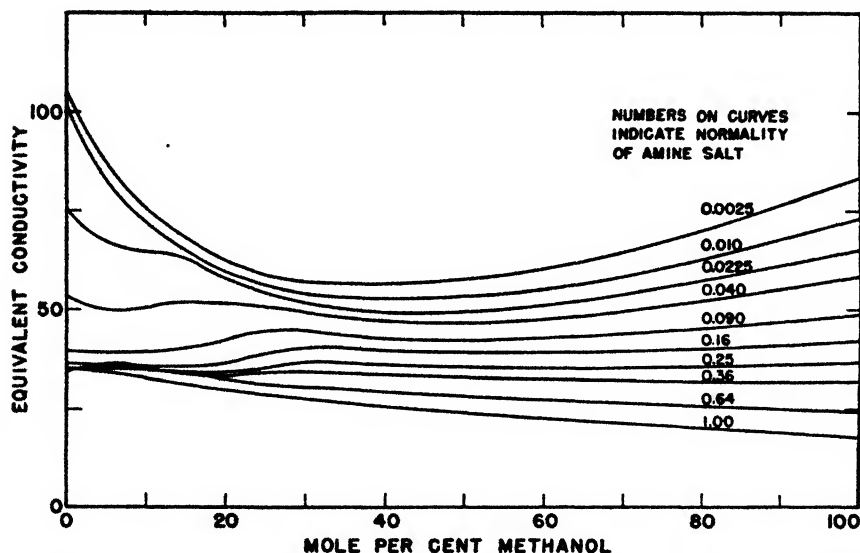


FIG. 6. The effect of methanol upon equivalent conductivity of dodecylammonium chloride

ductances of solutions of dodecylammonium chloride in pure water, pure ethanol, and in mixtures of ethanol and water are shown in figure 7. The presence of 3.27 mole per cent of ethanol in the solvent lowers the critical point slightly, the value of 0.0144 *N* in pure water being reduced to 0.0130 *N* in this solvent. Corrin and Harkins (3) have studied the effect of ethanol addition upon the critical concentration of dodecylammonium chloride, using dichlorofluorescein as the indicator. Their results showed an abrupt drop in the critical concentration of this amine salt attending successive additions of ethanol up to 15 per cent ethanol. Our results indicate a reversal of this effect, since 7.06 mole per cent ethanol gives a slightly higher critical point than that obtained in pure water. The addition of 9.95 mole per cent ethanol increases the critical concentration to 0.0454 *N*, whereas 16.2 or higher mole per cent shows smooth curves for this salt. The equivalent conductance of dilute solutions of dodecyl-

ammonium chloride regularly decreases upon the addition of ethanol; however, the conductance of more concentrated solutions is perceptibly increased.

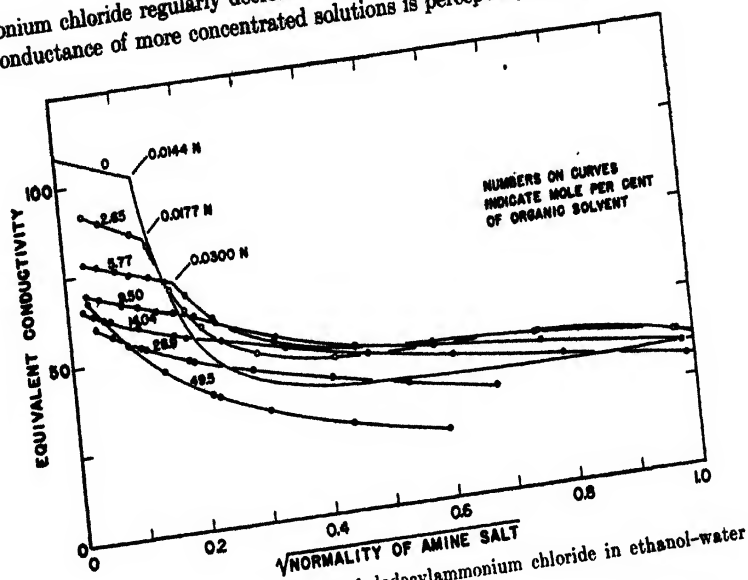


FIG. 7. The equivalent conductivity of dodecylammonium chloride in ethanol-water solution.

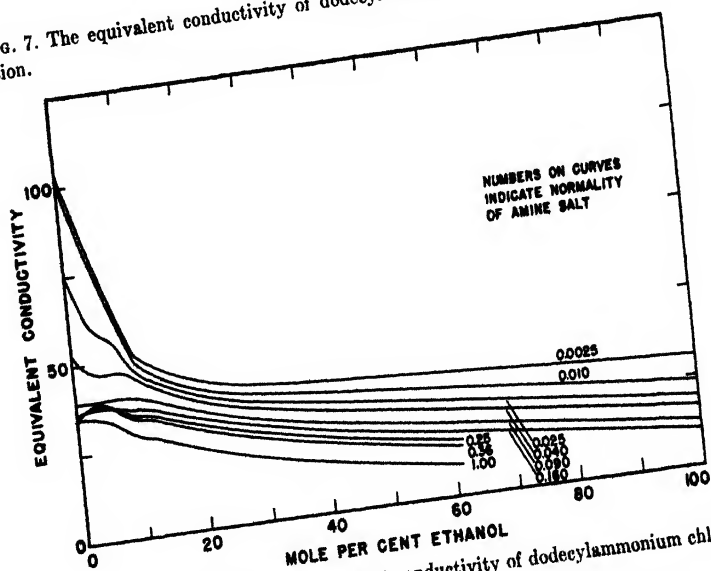


FIG. 8. The effect of ethanol upon equivalent conductivity of dodecylammonium chloride

Figure 8 shows the effect of ethanol upon the equivalent conductances of various concentrations of dodecylammonium chloride. The effect of ethanol is qualitatively similar to those of the other three addends investigated. These



results, combined with the previously observed lowering of the cationic transference number (15) in the presence of ethanol, indicate a decreased tendency towards association of dodecylammonium chloride in the solvent mixture as compared to pure water.

The addition of organic addends to aqueous solutions of dodecylammonium chloride brings about a progressive decrease in colloidal properties. This results in a transition of the amine salt from a colloidal to an ordinary electrolyte and maximum values in the equivalent conductances occur in the neighborhood of this transition point. Further experiments upon the effect of organic addends upon the electrical conductances of cationic colloidal electrolytes are now in progress.

#### SUMMARY

The equivalent conductance of dodecylammonium chloride has been determined in aqueous solutions of acetone, acetonitrile, methanol, and ethanol.

The concentration of dodecylammonium chloride at the critical point is materially increased by the addition of acetone, acetonitrile, or methanol. Small additions of ethanol decrease the critical concentration; however, larger additions bring about a substantial increase.

The addition of these solvents to aqueous solutions of dodecylammonium chloride at concentrations below the critical point of the amine salt lowers the critical conductance. Additions to concentrations beyond the critical point materially raise the equivalent conductance, maximum values being attained. The positions of these maxima are dependent on the concentration of amine salt and the nature of the organic addend.

These results have been interpreted as evidencing a transition of the dodecylammonium chloride from a colloidal to an ordinary electrolyte.

#### REFERENCES

- (1) BROWN, GRIEGER, EVERS, AND KRAUS: *J. Am. Chem. Soc.* **69**, 1835 (1947).
- (2) CORRIN AND HARKINS: *J. Am. Chem. Soc.* **69**, 679 (1947); *J. Chem. Phys.* **14**, 641 (1946).
- (3) CORRIN AND HARKINS: *J. Chem. Phys.* **14**, 640 (1946).
- (4) CORRIN AND HARKINS: *J. Am. Chem. Soc.* **69**, 683 (1947).
- (5) EVERS, GRIEGER, AND KRAUS: *J. Am. Chem. Soc.* **68**, 1137 (1946).
- (6) HARTLEY: *J. Chem. Soc.* **1938**, 1968.
- (7) MCBAIN AND BRADY: *J. Am. Chem. Soc.* **65**, 2072 (1943).
- (8) MOILLIET, COLLIE, ROBINSON, AND HARTLEY: *Trans. Faraday Soc.* **31**, 120 (1935).
- (9) RALSTON AND EGGENBERGER: *J. Am. Chem. Soc.* **70**, 980 (1948).
- (10) RALSTON AND EGGENBERGER: *J. Am. Chem. Soc.* **70**, 983 (1948).
- (11) RALSTON AND EGGENBERGER: *J. Am. Chem. Soc.* **70**, 436 (1948).
- (12) RALSTON AND EGGENBERGER: *J. Am. Chem. Soc.* **70**, 977 (1948).
- (13) RALSTON AND HOERR: *J. Am. Chem. Soc.* **69**, 883 (1947).
- (14) RALSTON AND HOERR: *J. Am. Chem. Soc.* **64**, 772 (1942).
- (15) RALSTON AND HOERR: *J. Am. Chem. Soc.* **68**, 2460 (1946).
- (16) RALSTON AND HOERR: *J. Am. Chem. Soc.* **68**, 851 (1946).
- (17) RALSTON, HOERR, AND HOFFMAN: *J. Am. Chem. Soc.* **64**, 97 (1942).
- (18) RANDALL AND FAILEY: *Chem. Revs.* **4**, 285 (1927).
- (19) TARTAR AND CADLE: *J. Phys. Chem.* **43**, 1173 (1939).
- (20) WRIGHT, ABBOTT, SIVERTZ, AND TARTAR: *J. Am. Chem. Soc.* **61**, 553 (1939).

SOAP-IN-OIL SYSTEMS<sup>1</sup>

A. S. G. LAWRENCE

*The University, Sheffield, England**Received June 23, 1948*

It is well known that many metal soaps, including those of the alkali and alkaline earth elements, form gels in hydrocarbon oils and some other organic solvents (1, 2, 4, 5, 6, 8, 10, 11, 13, 14, 15, 21, 22). The author has suggested that there is in oil a definite gel temperature range limited by the setting point,  $T_1$ , and  $T_2$ , the temperature at which the system is transformed into a two-phase system of solid soap and oil which is either a paste or a suspension of micro-crystals (11, 12). It will be seen that the dispersion of soaps in oil was attributed to phase changes in the soap lattice. Confirmation of this idea was provided by the observation that the gel-forming soaps when heated in the absence of a solvent passed through a plastic phase intermediate between crystalline solid and liquid; and it was found that  $T_1$  and  $T_2$ —in this case, the melting point and the temperature at which the crystal-plastic transition occurred—were only slightly above the corresponding values for the soap-oil systems. The choice of the name "plastic" was deliberate, insofar as this phase was regarded as similar to the long-chain macromolecules. Sodium soaps were an exception in that they exhibited signs of crystallinity in their intermediate phases. The numerous changes of texture when the soaps were heated between crossed Nicols were observed, but they were regarded as exceptional and some suspicion was felt that too much reliance should not be placed on changes of texture. The reality of these changes has, however, been demonstrated by Vold in a series of papers (19), but the possibility of complications due to small amounts of water and transitions from one fractional hydrate to another cannot yet be ruled out entirely. The meaning of results of x-ray examinations of sodium soap hydrates and soaps alleged to be anhydrous is difficult to assess, owing to the entire lack of any analytical information in the published work. Personally, I doubt whether a truly anhydrous sodium soap has yet been prepared. Whatever may be the true position, it seems certain that the sodium soaps are distinguished by a greater degree of crystallinity in their mesophases than are the soaps of the heavy metals.

Grease makers have ignored the question of these phase changes and claim that they can make fibrous or non-fibrous greases as they desire from a given soap by suitable "finishing." As will be shown later, the "finishing" may involve basic changes in the soap. All that this claim shows is the importance of the additional and difficult factor of crystal habit in addition to phase changes. Grease makers claim also that the effect of the chemical nature of the oil is of

<sup>1</sup> Presented at the Symposium on Gel Formation, Detergency, Emulsification and Film Formation in Non-Aqueous Colloidal Systems which was held under the auspices of the Division of Colloid Chemistry and the Division of Petroleum Chemistry at the 113th Meeting of the American Chemical Society, Chicago, Illinois, April, 1948.

much more importance for their greases than is the nature of the soap. This claim is entirely untrue and is made only because they have never made greases from pure soaps.

The assumption that the temperature  $T_1$  is a phase change in the soap is based on evidence which is far from complete. It is notable, however, that  $T_1$  in a given soap in a given oil is remarkably constant over a very wide concentration range; e.g., for sodium stearate:

SOAP	$T_1$
per cent	°C.
25	244
15	244
8	238
5	240

#### FACTORS DETERMINING THE GEL RANGE, $T_1 - T_2$

The setting point and consistency of a gel vary with the oil, being highest with least polar oils. It can be said roughly that the consistency at room temperature falls with fall of  $T_1$ , because at that temperature its value depends upon the temperature difference between room temperature and setting temperature; and that consistency will be the same for the same lowering of temperature below the setting point, whatever these temperatures may be, so long as the system remains in the gel temperature range. The difference in the behavior of pure soaps in any oil is very much greater than any difference due to change of oil. The effect of the cation is considerable. Calcium, barium, and strontium have very high values for  $T_1$ ; the alkali metals have moderately high values for  $T_1$  and  $T_2$ ; magnesium and aluminum also have moderately high values but copper and cobalt have much lower ones. The differences between the members of any group, e.g., the alkali metals, do not seem to be considerable nor to hold out any likelihood of making better grease by using, say, strontium or barium in place of calcium. The effect of mixing cations with a common fatty acid is most marked and will be discussed in another section.

The effect of the anion, that is, of the chain length of fatty acid, is very marked also, although this is masked in mixtures which obey an additive relation. Using pure soaps, no solubility can be expected below laurates. Even with this chain length, very high temperatures are required to get the soap into true solution and some, e.g., thorium and calcium soaps, do not dissolve in Nujol even at 350°C. Sodium laurate dissolves in Nujol at 344°C. and separates as a liquid which solidifies at a slightly lower temperature. The myristates, palmittates, and stearates show the full range of gelation phenomena. Higher soaps have not been examined, with the exception of the alkali cerotates. My observations show that they still gel but show a lowering of  $T_1$  from the values of stearates, presumably owing to the greater solvent action of the much longer hydrocarbon chain. Equimolecular mixtures of lithium soaps showed values of  $T_1$  inter-

mediate between those of the two components. Laurates insoluble in the oil can be incorporated into solution in more soluble soaps. Oleates give values for  $T_2$  considerably below those for the stearates but the values for  $T_1$  are erratic. Sufficient oleates have not been studied to make any more definite statements.

The assumption that a phase change occurs in the soap at  $T_1$  is not supported by conclusive evidence except in the case of the sodium soaps where birefringence appears. It is possible that this is not an abrupt change at all, but one occurring as a very great increase of viscosity over a few degrees, similar to the mass action equilibrium suggested by Hartley to explain the Krafft point in aqueous systems of the soda soaps (7). In most cases, however, the soap has no molecular solubility except above  $T_2$  and the gels cannot therefore be regarded as equilibrium mixtures of colloid and crystalloid. I have observed that pure calcium stearate dispersed in Nujol shows curious features. On heating from room temperature, segregation of the soap occurs to a lump swollen by oil with the remainder of the oil free from soap; just below its  $T_1$  the soap expands again until a homogeneous solution is obtained. This swelling appears to proceed over a temperature range of some  $5^\circ$ , but the very poor thermal conductivity of soaps requires that the experiment be carried out with much more adequate temperature control. Even better, measurements of the viscosity changes over this temperature range would show whether or not the change is discontinuous.

That  $T_2$  is a phase change is demonstrated in a number of ways. The soaps below it are, as one would expect from the very high viscosity of the plastic form in which they grow, micro- or crypto-crystalline. My original method of determining the temperature of the transition is very satisfactory. This depends upon the fact that the soap above  $T_2$  is sticky and adheres to glass, whereas below  $T_2$  it becomes brittle and does not adhere, but crumbles when rubbed. X-ray examination of the stearate and oleate of cobalt showed that the former, below  $T_2$  at room temperature, gave long and side spacings whereas the oleate above  $T_2$  gave only side spacings. Moreover, the crystalline form of soaps below  $T_2$  can be shown in a most elegant manner by drawing out a fiber on the end of a glass rod from a plastic melt slightly above its  $T_2$ . Under these conditions, a specimen is obtained which has a high birefringence and which shows parallel extinction. Soaps in the fully crystalline state are oil-repellent but the plastic phase is wetted.

In oil, it appears that a pseudo-gel can occur below  $T_2$ . The system is metastable and cryptocrystalline. A 1 per cent solution of aluminum monostearate required some 3 weeks to revert to suspension of soap in oil and then, on warming, suddenly cleared to gel with large increase of consistency at  $T_1$ . This was repeatable at will. When the soap content is increased, the metastability is also greatly increased, but I think that at concentrations of 15 per cent or so the crumbling which is observed is due to the system being in the two-phase state. It crumbles because the soap is present as hard fully crystalline lattice and not in flexible threads as in the plastic state. The excellent low-temperature performance of lithium soap greases is due, I think, to the habit of the solid soap. On cooling a hot solution of a lithium soap, a perfectly clear gel is formed first

but, on further cooling, bluish opalescence is seen. I suggest that this is the phase change at  $T_2$  which is peculiar to the lithium soaps only in that the solid soap remains with a crystal habit which still gives good gels. I suggest further that breakdown of gels on working is due to the soap being in its fully crystalline state and that any grease in which the soap is below its  $T_2$  will always show breakdown on working sufficiently. Measurement of streaming birefringence would be the best method of establishing this point. The failure of large-scale batches of aluminum soap greases is, I suggest, due to crystallization owing to the slow rate of cooling. That they gel on re-heating and sudden chilling supports this view. This must not be taken as suggesting that all greases below their  $T_2$  are metastable, since it is obvious that crystallization at  $T_2$  need necessitate no particle growth—only a change of the physical properties of the soap particles.

#### PEPTIZATION

Soaps dispersed in oil are readily peptized by small amounts of polar substances just as they are in aqueous systems and by the same sort of substances for the most part. In oil systems, water is most active. This property has been made use of by grease makers to stabilize lime soap greases. These, from the properties of the pure calcium soaps, should have high melting points. Addition of water, however, is necessary to stabilize them from syneresis at normal temperatures and this has the effect of lowering  $T_1$  to such an extent that the high-melting-point properties are lost in these greases. It has been stated frequently that this water is emulsified, and the statement often followed by the remark that the emulsified water cannot be seen under the microscope. The writer pointed out that the action of water is similar here to that of other peptizers and that some hydrolysis occurs (12). Figure 1 shows a general picture of peptization and, from it, we can see that the effect upon  $T_1$  is greater than upon  $T_2$ , so that the gel temperature range is reduced until it is eliminated and solid soap separates direct from *liquid* solution. It is consequently in larger crystals. It would seem from such experiments as I have carried out that there is a lower temperature limit beyond which it is impossible to peptize further. I have marked this  $T_3$ , and it is the temperature at which solid soap separates from the peptized solutions in oil. It would be surprising if it really were always the same nor would its physical significance be clear, but remarkable uniformity was found with peptizers such as cresylic acid plus oleic acid and amyl alcohol plus oleic or caprylic acid.

Sodium stearate, both in the dry state and in Nujol, appears to form a complex with 1 molecule of stearic acid. Calcium stearate is fully peptized by 1 molecule but adds on two before a transition occurs in the melting point-concentration diagram. Ferric stearate crystallizes from alcohol with 3 molecules of stearic acid.

There is a distribution of peptizer between soap and oil or water. Substances most soluble in the solvent, such as the lower alcohols, glycol, and glycerol in water, are poor peptizers in aqueous systems compared with their higher homologues. When, however, the peptizer molecule becomes too large, e.g., oleyl

alcohol or xyleneol (17), complex formation can still occur but the complex is not peptized as it is less soluble than the soap alone. Hence the best peptizers are substances of intermediate molecular weight, such as amyl alcohol, benzyl alcohol, cresol, aniline, and nicotine. In oil the reverse holds good, since the larger molecules tend to become distributed in favor of the solvent oil and less is attached to the soap. Cresol is still one of the best; glycol, lactic acid, and the intermediate alcohols are all good. The acids such as lactic and acetic can be used only up to one molecule per molecule of soap, after which further addition causes decomposition.

I have used the word "peptize" to describe this action deliberately in its proper sense, meaning to increase the dispersion, and to make clear the difference

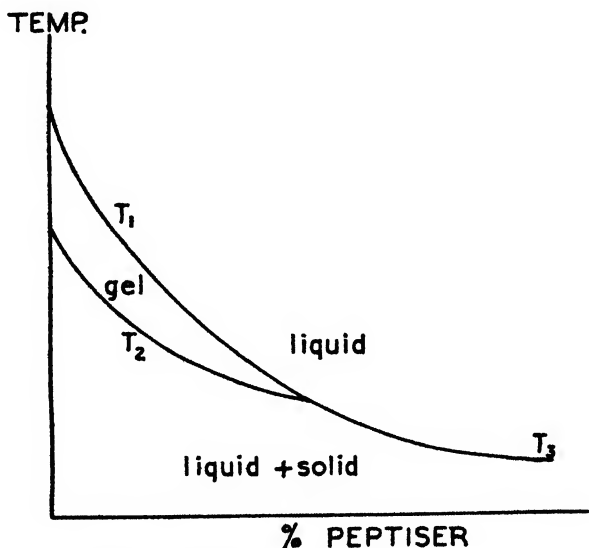


FIG. 1. A general picture of peptization

between this method of increasing the solubility of the added substance and that which I called "internal solubility" (9). The name "solubilization" is a good one so long as it is realized that it covers three distinct cases: true internal solubilization of inert substances insoluble in water; solubilization of substances insoluble in water but containing polar groups, e.g., dyes; and those cases where the soap is peptized by the substance solubilized.

I would suggest that the essential condition for all solubilization is that the soap should be in a mesomorphic state, such as the "soft" potassium soaps and sodium oleate. The case is less clear in solubilized substances in the synthetic wetting agents where these mesomorphic states are rarer, but the effect of the polar groups in substances solubilized must alter the soap lattice in some way. A number of lines of evidence point in the same direction, namely, that substances containing polar groups associate very readily with soaps and soap-like

substances: Speakman's results for the effect of oleyl alcohol upon the interfacial tension of solutions of soaps against oil (2); penetration of monolayers by long-chain alcohols; and Dervician's complexes of long-chain sulfates which show so beautifully the whole range of classical mesomorphs (3). It may be recalled too that an adsorbed film is physically a very concentrated solution however dilute the solution from which it is adsorbed. There seems to be a tendency in recent publications to describe the swelling of a lattice of soap by solubilized oil as an expansion of a fully crystalline lattice, an explanation which ignores entirely the fact that most of this work has been carried out in solutions of potassium soaps which are in the "soft" soap phase, whatever that may be

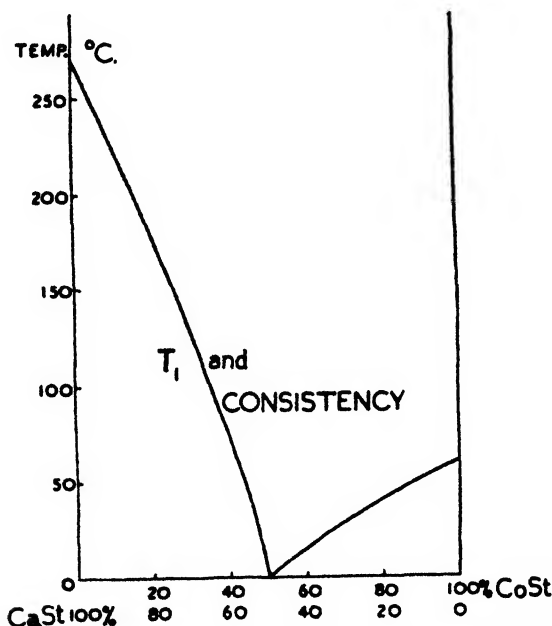


FIG. 2. Mutual peptization of soaps containing the same fatty acid but different cations.

physically. I consider it most unfortunate that these x-ray studies have not been accompanied by optical examination of the solutions in polarized light either in the stationary or the flowing condition.<sup>2</sup> This criticism also applies to the beautiful electron microscope photographs of lubricating greases which have been published recently.

<sup>2</sup> Vold has commented recently upon the golden yellow color of certain phases of sodium soaps when heated. I have observed the same phenomenon but have had no opportunity to examine it further. Why always yellow? It seems that it cannot be a normal interference color, otherwise it would vary with the thickness of the specimen and other colors would be seen. It would appear to be caused by some second-order interference effect due to regularity of layer spacing of some 3400 Å. and perhaps similar to the cholesteric colors shown by the fatty acid esters of cholesterol in the mesomorphic state.

## MUTUAL PEPTIZATION BY CATIONS

The writer tried to prevent the syneresis of pure dry calcium stearate in Nujol by adding a small amount of silver stearate, which is in the gel state at the temperature of syneresis. The experiment succeeded, but it was then found that further addition of silver stearate peptized the calcium stearate markedly until much consistency was lost and the setting point of the system fell. It was then found that mutual peptization of soaps containing the same fatty acid but different cations is quite general. Figure 2 shows the type of effect. Not only are the consistency and setting point of the gel greatly reduced but at the 1:1 molecular ratio eutectic point, the color of colored ions, such as cobalt, copper, nickel, and ferric,<sup>3</sup> is almost completely bleached. The peptization is so great at the eutectic composition that the gelation is eliminated and the setting point is the temperature at which crystalline soap separates. This bleaching of the above colored stearates has been achieved with stearates of sodium, lithium, aluminum, magnesium, and by the non-gelling zinc and thallous soaps. Mutual decolorization of ferric and cobalt soaps and of ferric and copper soaps has also been observed. The bleaching is never quite complete. It is a phenomenon, like other peptization, of the liquid state. When cooled sufficiently for solid soap to separate, the soaps crystallize out separately. This effect shows what care needs to be taken in ensuring that soaps of heavy metals, prepared by metathesis from sodium soaps and a salt of the metal, are freed from sodium soap. Analytical control should include determination of water-soluble ash.

This paper contains speculations and generalizations which are put forward not as proven conclusions so much as to stimulate discussion and further work and in the belief that the methods of physical chemistry can be applied successfully to systems apparently so complex as those of soap and oil. If the work carried out so far has done no more than indicate the fundamental experimental difficulties and the pitfalls to be avoided, it will have served a useful purpose. It is obvious that there is scope for important academic investigations as well as useful applications. We have seen that the properties of soaps are modified profoundly by just those impurities which are most likely to be present—water, fatty acid, and foreign cations. No work which is not carried out with a profound respect for chemical purity can do anything but increase confusion. Further increase of our knowledge of the metal soaps cannot fail one day to enrich our present meagre fundamental knowledge of emulsions. Professor McBain once remarked that the more colloidal soap systems were examined, the more crystalloidal they were found to be. Those were brave words; and they have been justified not only by his own work on soaps but by the great increase of

<sup>3</sup> Commercial ferric stearates are very impure. The tristearate was made by metathesis of anhydrous ferric chloride in warm benzene with triethylamine stearate also in benzene. Triethylamine hydrochloride separates out on cooling to about 30°C. and is filtered off; the ferric stearate separates on standing at room temperature. It is filtered off and purified by re-dissolving in petroleum ether (b.p. 80–100°C.), filtering the hot solution from the remaining triethylamine hydrochloride, and allowing the soap to separate on standing. It is extremely readily hydrolyzed and shows no signs of forming intermediate stoichiometric basic soaps like those of aluminum. It does not form gels in oil, m.p. 83°C.



our knowledge of the whole domain of colloids. The metal soaps must not be regarded as exceptions to that rule.

## REFERENCES

- (1) ARVISON, M. H.: *Ind. Eng. Chem.* **24**, 71 (1932).
- (2) BONER, C. J.: *Ind. Eng. Chem.* **29**, 58 (1937).
- (3) DERVICIAN, J.: *Bull. soc. chim. biol.* **28**, 419 (1946); *Trans. Faraday Soc.* **42**, (1946).
- (4) DOSCHER, T. M., AND VOLD, R. D.: *J. Colloid Sci.* **1**, 299 (1946).
- (5) GALLAY, W., AND PUDDINGTON, I. E.: *Can. J. Research* **24B**, 73 (1946) and other papers.
- (6) GARLICK, H. S.: *J. Inst. Petroleum Technol.* **20**, 829 (1934).
- (7) HARTLEY, G. S.: *Trans. Faraday Soc.* **31**, 183 (1935).
- (8) KOENIG, A. E.: *J. Am. Chem. Soc.* **36**, 951 (1914).
- (9) LAWRENCE, A. S. C.: *Trans. Faraday Soc.* **33**, 815 (1937); *Ann. Repts. on Progress Chem.* (Chem. Soc. London) **37**, 108 (1940).
- (10) LAWRENCE, A. S. C.: *J. Inst. Petroleum Technol.* **24**, 207 (1938).
- (11) LAWRENCE, A. S. C.: *Trans. Faraday Soc.* **34**, 325 (1938).
- (12) LAWRENCE, A. S. C.: *Trans. Faraday Soc.* **35**, 702 (1939).
- (13) LAWRENCE, A. S. C.: *J. Inst. Petroleum Technol.* **31**, 303 (1945).
- (14) MARSDEN, S. S., MYSELS, K. J., AND SMITH, G. H.: *J. Colloid Sci.* **2**, 265 (1947).
- (15) MCBAIN, J. W., AND MCCLATCHIE, W. L.: *J. Phys. Chem.* **36**, 2567 (1932).
- (16) OSTWALD, W., AND RIEDEL, R.: *Kolloid-Z.* **70**, 67 (1935).
- (17) REICHENBERG, D.: *Trans. Faraday Soc.* **43**, 815 (1947).
- (18) SPEAKMAN, J. B.: *Trans. Faraday Soc.* **29**, 358 (1933).
- (19) VOLD, R. D.: *J. Am. Chem. Soc.* **61**, 808 (1939).
- (20) VOLD, R. D., AND PHILIPSON, J. M.: *J. Phys. Chem.* **50**, 39 (1946).
- (21) WHITBY, G. S.: *Colloid Symposium Monograph* **4**, 213 (1926).
- (22) WHITMORE, W. F., AND LAURO, M.: *J. Ind. Eng. Chem.* **22**, 646 (1930).

## NEW BOOKS

*Weiss Magnetons as Components of Nuclear and Subnuclear Structures.* By THEODORE VAN SCHELVEN. 24 x 16 cm.; 34 pp.; 4 fig. Amsterdam: Kosmos Publishing Company, 1945. Price: \$3.00.

In the opening page the author correctly takes the ratio of the masses of the proton and electron to be 1840 and the ratio of the magnetic moments of the Bohr and Weiss magnetons to be very nearly 5. He then proceeds to say, "... the ratio of the mass of the protonic nuclear structure to the mass of the Weiss magneton is then  $5 \times 1840 = 9200$ ." Thus mass and magnetic moment are incorrectly treated as the same kind of quantity. The assumption is then made that 9200 Weiss magnetons are present in the proton, and 5 in the electron.

"The next problem is to find the structure in which these 9200 units can be arranged, probably in a regular manner in a space lattice, assuming that the Weiss magneton unit is approximately spherical and that the nucleus is not a gas or a liquid drop." The remainder of the volume is taken up by the author's speculations on the structures of various kinds of atoms based on this hypothesis. It does not appear to add anything of value to nuclear physics and is clearly basically opposed to current views on this topic.

S. SUGDEN.

*Inorganic Process Industries.* By KENNETH A. KOBE. 371 pp. New York: The Macmillan Company, 1948.

This excellent little book on the inorganic process industries considers the fundamental chemistry involved, applies physical chemistry, and represents the economics as well as the

unit operations that are used for any of the processes given. Alternate methods of production are not only presented but compared as to the economics as well as the equipment used. Statistics are numerous. All drawings of diagrams as well as of equipment are clear and understandable. The subject of water treatment, however, has been omitted. Though this might not be considered as a process industry, it is of such importance to industry that a chapter should have been included.

The first chapter on the chemical literature is desirable for the surveys that are recommended for the students to make. Few libraries are equipped with enough copies of this literature to accommodate a large class. The same criticism holds for the literature references at the end of each chapter which the students are supposed to use.

The material in this book is well selected and the arrangement in each chapter is good, but it requires an experienced instructor to supplement much of this material. It is an excellent and usable book on inorganic process industries and is limited in content to the work of about one semester. It should be a welcome volume to those teaching such courses as industrial chemistry or inorganic technology.

CHARLES A. MANN.

*Molybdenum: Steels, Irons, Alloys.* By R. S. ARCHER, J. Z. BRIGGS, AND C. M. LOEB, JR. 391 pp.; 188 fig.; 91 tables + appendices. 500 Fifth Avenue, New York, 18: Climax Molybdenum Company, 1948.

This treatise consists of ten main divisions: Technical Effects, Fundamental Effects of Heat Treatment on Microstructure, Additions, Wrought Alloy Engineering Steels, Wrought Corrosion Resistant Steels, Wrought Steels for Elevated Temperature Service, Tool Steels, Steel Castings, Cast Iron, Special Purpose and Non-ferrous Alloys. About 23 pages are appendices dealing with specifications of steels, conversion tables, etc.

The book is primarily for metallurgists rather than for chemists as it deals mostly with metallurgical data. It is well written and gives many references for each separate division. Most of the references are quite recent and have been carefully selected for the purpose intended.

The text is, in a way, a correlation of recent research information on the subject of molybdenum as applied to alloys. It is well indexed and is recommended to those interested in molybdenum alloys.

R. L. DOWDELL.

## SUBJECT INDEX

- Absorption spectra, infrared, of some amino acids and their complexes, 961
- Acetylene, polymerization by radiation, formation of benzene in, 474
- Acids, fatty, solutions in benzene and in carbon tetrachloride, viscosity of, 753
- Adsorption, heats of, 1111, 1115
  - in beds of charcoal, 1153
  - from solutions, thermodynamics of, 374
  - of water vapor on glass surfaces, 1208
  - theory, dual-surface, 47, 58
- Aerosols, filtration by granular charcoal, 695
- Affinity and reaction rate, 321
- Agents, surface-active, effect upon dispersions of lead monoxide in xylene, 363
- Alcohols, solutions in benzene and in carbon tetrachloride, viscosity of, 753
- Aldehydes, photochemistry of, 534
- Alkanes, structure of, relation to physical properties, 1082
- Alloys, cadmium-gold, catalysis by, 1046
  - cadmium-magnesium, densities of, 999
  - catalysis by, 1046
  - Hastelloy, oxide films on, 1186
- Alpha particles, transformation of organic substances by, 551
- Aluminum, anodic behavior in a magnetic field, 1105
- Aluminum dilaurate, variability and inhomogeneity of, 1471
- Amino acids, infrared absorption spectra of, 961
- Antifoams, polyamides as, 689
- Argon, liquid, surface energy of, 40
- Benzene, formation in radiochemical polymerization of acetylene, 474
- Benzoic acid, binary systems containing, 729
- Benzotrifluoride, vapor pressure of, 1137
- Beryllium fluoride, 819
- Boundary tension, measurement by pendant-drop method, 1157
- Bromine, reaction with carbon tetrachloride, activation by isomeric nuclear transition and by neutron capture, 585
- Butyl acetate (tertiary), thermal decomposition of, 357
- Butyl propionate (tertiary), decomposition by heat, kinetics of, 1314
- Cadmium-magnesium, solid solutions of, densities of, 999
- Calcium stearate-cetane system, properties of, 1424
- Carbon tetrachloride, cryoscopic behavior of, 332
  - tetrachloride, reaction with bromine, activation by isomeric nuclear transition and by neutron capture, 585
- Catalyst, cracking, pore size-surface area distribution of, 1296
- Catalysts, cracking, contamination with sodium, 1364
  - salt pairs as, 1053
- Cellulose, heat of wetting of, 1197
- Charcoal, granular, filtration of aerosols by, 695
- Chlorophyll, photobleaching of, 662
- Clays, western, colloid properties of, 1373
- Coagulation of sols by electrolytes, 787
- Colloidal solutions, properties of, effect of size, shape, and flexibility of the solute molecules on, 248
- Colloids, monodisperse, 65
- Colloid systems, mutual protection in, 942
- Coprecipitation, 836, 1020, 1319
- Coulometer, precision, 955
- Cryoscopy of carbon tetrachloride, 332
- Crystals, orientation of, fixing of, 808
- Decomposition, thermal, of tertiary butyl acetate, 357
  - thermal, of butyl propionate, 1314
- Denaturation, theory of, 1146
- Desensitization by dyes, 1090
- Detergent action, principles of, 84
- Detergents, critical micelle concentration of, 130
  - non-ionic, study by x-ray diffraction, 110
  - solubilization of dyes by, 915
  - solubilization of water-insoluble dye by, 12
- Deuterons, transformation of organic substances by, 551
- Diffusion across oil-water interfaces, 897
  - of sodium thymonucleate, 676
- Dimethylaminoazobenzene, solubilization by detergents, 915
- Dispersions, solid-liquid, sedimentation in beaker-type centrifuge, 854

- Dodecylammonium chloride, electrical behavior in water-organic solvent systems, 1494
- Drops, falling, potentials of, 1
- Dyes, photobleaching of, reversible, 527  
sensitizing, desensitization by, 1090  
solubilization by colloidal electrolytes and non-ionizing detergents, 12  
solubilization by detergents, 915
- Electrolytes, colloidal, osmotic behavior of, 881
- Electron, nuclear, chemical effects produced by emission of, 595
- Electron microscope, in study of radiation polymers, 470
- Electrons, controlled, production of reactions by, 451
- Evaporation of liquids, maximum possible rate of, 367  
as a rate process, 949, 1262
- Ferric oxide, sols of, coagulation by electrolytes, 787
- Ferrous sulfite, oxidation in air, 1103
- Flotation, physical chemistry of, 394  
process, kinetics of, 394
- Flow birefringence, for determination of molecular weights of high polymers, 976
- Fluorescence, quenching of, 518
- Foaming, polyamides in prevention of, 689
- Foaming of hydrocarbon mixtures, 763
- Fractionation, polymer, of heat-polymerized non-conjugated vegetable oils, 613
- Gases, effusion at critical velocities, 1332
- Gasoline, thickening with soaps, 1444
- Geiger-Mueller counter discharge, radiation chemistry of, 578
- Gels, incendiary, 1460  
incendiary, rheological properties of, 1460  
soap, in organic solvents, 1481
- Greases, calcium soap, fiber structure of, 1415
- Gum arabic, salts of, electrophoretic mobilities of, 76
- Hastelloy alloys, oxide films on, 1186
- Heredity, significance in colors of flowers and fruits, 767
- Hydrocarbons, mixtures of, foaming of, 763  
paraffin (branched-chain), vapor pressure-temperature relationships among, 425  
physical constants data for, gaps in, 387
- Hydrocarbon-soap systems, thixotropic qualities of, 1383
- "Indium chromate," x-ray diffraction analysis of, 959  
hydroxide, x-ray diffraction analysis of, 959
- Interfaces, oil-water, diffusion across, 897
- Ion exchangers, use for determination of physical-chemical properties of radio-tracers in solution, 340, 350
- Ionization processes, chemical reactions produced by, 447
- Ions, dissociation of, 456
- Keratin, feather, solubilization of, 180
- Keratin fibers, synthetic, 180
- Ketones, photochemistry of, 546
- Laurate ion, activity of, 22
- Lead chromate, solubility of, effect of particle size upon, 836
- Lead monoxide, dispersions in xylene, effect of surface-active agents on, 363
- Lignosulfonates, dissociation of, 267
- Lignosulfonic acid, properties of, 267
- Liquids, critical densities of, 1060
- Magnesia, active, 58
- Manganese-nickel system, liquidus-solidus points of, 750
- Manometer, Rodebuch, measurement of vapor pressure of benzotrifluoride with, 1137
- Mass spectrometer, detection of free radicals with, 463
- Melting as a rate process, 949, 1262
- Membranes, mineral, electrochemical properties of, 1284
- Mercury, surface energy of, 40
- Micelles, critical concentrations of, 130  
formation in soap solutions, effect of alkaline electrolytes on, 774
- Minerals, clay size, weathering sequence of, 1237
- Molecular weights, determination by measurement of flow birefringence, 976  
weights, determination by rate of evaporation of solutions, 1074  
weights, determination by sedimentation equilibrium method, 963  
weights of gases and vapors, determination by effusion, 1332

- Nucleoprotein, rabbit liver, 207
- Oils, vegetable, polymer fractionation of heat-polymerized non-conjugated, 613
- Organic compounds, transformation by radioactivity, 551
- Orientation of crystals, fixing of, 808
- Oxide systems, mutual protection in, 942
- Phase equilibrium description, 1263
- Photobleaching, reversible, of chlorophyll, 662  
reversible, of dyes and pigments, 527
- Photochemistry, relation to radiation chemistry, 441  
symposium on, 437
- Photochemistry of aldehydes, 534  
of ketones, 546
- Pigments, photobleaching of, reversible, 527
- Pile, chain-reacting, Szilard-Chalmers reaction in, 603
- Polymerization of acetylene by radiation, formation of benzene in, 474  
(emulsion) of styrene, 1175
- Polymers (high), fractions of, method for characterization of, 1390  
(high), molecular weights of, determination by measurement of flow birefringence, 976  
(high), molecular weights of, determination by sedimentation equilibrium method, 983  
(high), morphology of, 27  
radiation, electron microscopy of, 470  
(linear), scattering of light from solutions of, 260
- Potassium laurate-potassium silicate system, solubility study of, 1143
- Precipitates, aging of, 836, 1020, 1319
- Protection (mutual) in oxide systems, 942
- Proteins, homogeneity and electrophoretic behavior of, 217, 1345
- Rabbit liver nucleoprotein, 207
- Radiation, changes produced in aqueous solutions by, 479  
chemistry of, 564, 810  
effect on organic substances, 564  
effect on reaction between bromine and carbon tetrachloride, 585  
ionizing, effect on water and aqueous solutions, 490  
nuclear, chemical effects of, 595  
transformation of organic substances by, 551
- Radiation chemistry, relation to photochemistry, 441  
chemistry, symposium on, 437  
chemistry of Geiger-Mueller counter discharge, 578
- Radicals, free, detection with mass spectrometer, 463  
free, in solutions subjected to ionizing radiation, 490
- Radioactivity, chemical reactions produced by, 447
- Radiotracer methods, sensitivity as compared with spectrographic methods, 1260
- Radiotracers, properties (physical-chemical) in solution, determination with ion exchangers, 340, 350
- Reaction, Szilard-Chalmers, in the chain-reacting pile, 603
- Reaction rate close to equilibrium, affinity and, 321
- Reactions, chemical, production by controlled electrons, 451  
chemical, production by ionization, 447  
photochemical, in solids, 828
- Rosin soap-sodium chloride-water system, phase study of, 167  
soap-sodium silicate-water system, phase study of, 167
- Salt pairs, catalytic action of, 1053
- Sedimentation in beaker-type centrifuge, 854  
constants, determination in Sharples supercentrifuge, 1034  
equilibria of polydisperse non-ideal solutes, 235  
of sodium thymonucleate, 676
- Silica powder, bulkiness of, 1020  
powder, porosity of, 1020
- Silicates, layer, colloid properties of, 1404
- Silicic chemistry, 1165
- Silver bromide, aging of, 1319
- Soap gels in organic solvents, 1481  
-hydrocarbon systems, thixotropic qualities of, 1383  
-in-oil systems, 1504  
solutions, micelle formation in, effect of alkaline electrolytes on, 774  
systems, colloidal structures in, 97  
-water systems, electrical conductivity of, 148

- Soaps, critical micelle concentration of, 130  
Sodium silicate, thermodynamic properties of, 1277  
Sodium thymonucleate, diffusion and sedimentation of, 676  
Solids, photochemical reactions in, effect of temperature and impurities on, 828  
surface tension of, measurement of, 969  
Solid solutions, magnesium-cadmium, densities of, 999  
Sols, hydrous ferric oxide, coagulation by electrolytes, 787  
Solubilization of dye by colloidal electrolytes and non-ionizing detergents, 12  
of dyes by detergents, 915  
Solutions, aqueous, effect of ionizing radiation on, 490  
aqueous, radiation chemistry of, 479  
Spectrographic methods, sensitivity as compared with radiotracer methods, 1260  
Strontium salts, dissociation constants of, 350  
salts, radioactive, determination of dissociation constants of, 350  
Styrene, emulsion polymerization of, 1175  
Sucrose, solutions of, viscosity of, 314  
Sulfuric acid, vapor pressure above sulfuric acid-water system, calculation of, 908  
Supercentrifuge, Sharples, determination of sedimentation constants in, 1034  
Surface tension of solids, measurement of, 969  
Suspensions, spherical, viscosity-concentration relations in, 300  
Symposium, Colloid, Twenty-first National, 1  
Symposium on Gel Formation, Detergency, Emulsification and Film Formation in Non-Aqueous Colloidal Systems, 1415  
Symposium on Radiation Chemistry and Photochemistry, 437  
System calcium stearate-cetane, properties of, 1424  
chromic oxide-nickelic oxide-zirconium dioxide, 230  
manganese-nickel, liquidus-solidus points of, 750  
potassium laurate-potassium silicate, solubility study of, 1143  
sulfuric acid-water, vapor pressure of sulfuric acid above, calculation of, 908  
Systems, benzoic acid, 729  
binary, of carboxylic acids, 729, 740  
heterocyclic acid, 740  
hydrocarbon-soap, thixotropic qualities of, 1303  
multicomponent, analytical treatment of, 698  
of soaps in oil, 1504  
soap-water, electrical conductivity of, 148  
Temperature control for constant-temperature water bath, 761  
lag and chemical kinetics, 1129  
Theory of adsorption, dual-surface, 47, 58  
of selective membrane behavior, 1284  
Thermodynamics of adsorption from solutions, 374  
Thorium, solvent extraction of, 1006  
Thorium nitrate, distribution between water and five organic solvents, 1006  
Tobacco mosaic virus, absolute reaction kinetics of, 1146  
Uranyl salts, solutions of, surface tension of, 1227  
salts, solutions of, viscosity of, 1227  
Vapor pressure, measurement with Rodebush manometer, 1137  
pressure-temperature relationships among branched-chain paraffin hydrocarbons, 425  
tension apparatus, Hill-Baldes, in determination of osmotic behavior of some colloidal electrolytes, 881  
Viscosity of solutions, 300, 314  
of solutions, theory of, 277  
of solutions of alcohols and fatty acids in benzene and in carbon tetrachloride, 753  
of suspensions, 300, 314  
of suspensions, theory of, 277  
Water bath, constant-temperature, temperature control for, 761  
Water vapor, adsorption on glass surfaces, 1208  
Weathering sequence of minerals, 1237

## AUTHOR INDEX

- ABEL, E. On the experimental bases for the calculation of the sulfuric acid vapor pressure above the sulfuric acid-water system, 908
- ABERS, ELLIOTT L., AND NEWTON, ROY F. A new and easily constructed precision coulometer, 955
- ADARKAR, S. P. *See* Hattiangdi, G. S.
- ALBERTY, ROBERT A., ANDERSON, ELMER A., AND WILLIAMS, J. W. Homogeneity and the electrophoretic behavior of some proteins, 217  
*See* Anderson, E. A.
- ALEXANDER, MARY. *See* Corbin, Nancy
- ALLEN, A. O. Radiation chemistry of aqueous solutions, 479
- AMUNDSON, NEAL R. A note on the mathematics of adsorption in beds, 1153
- ANDERSON, E. A., AND ALBERTY, R. A. Homogeneity and the electrophoretic behavior of some proteins. II. Reversible spreading and steady-state boundary criteria, 1345  
*See* Alberty, Robert A.
- ANTONOFF, GEORGE. Surface tension of solids and methods of measuring the same, 969
- AND ROWLEY, ANNE. Anodic behavior of aluminum in a magnetic field, 1105
- ARGERSINGER, W. J., JR. *See* Davidson, Arthur W.
- BADGER, R. M. *See* Brooks, M. C.
- BAGOTSKAJA, J. *See* Frumkin, A.
- BAKER, M. O., CHESNUTT, S. D., AND WIER, T. P., JR. A contribution to the knowledge of sodium contamination on cracking catalysts, 1364
- BANCROFT, WILDER D. Heredity and environment, 767
- BARAKAT, MOHAMED ZAKI. *See* Schönberg, Alexander
- BARTELL, F. E. *See* Fu, Ying
- BEARD, G. V. *See* Paul, Jack M.
- BENSON, SIDNEY W. Critical densities and related properties of liquids, 1060  
AND COSWELL, R. Effusion of gases at critical velocities. A micromethod for molecular weights of gases and vapors, 1332
- BERNSTEIN, I. M. Polymer fractionation of heat-polymerized non-conjugated vegetable oils, 613
- BIRDSALL, D. H., AND FARRINGTON, B. B. The effect of water and other additives on the fiber structure of calcium soap greases, 1415
- BLACET, F. E. The photochemistry of the aldehydes, 534
- BOAZ, H. *See* Rollefson, G. K.
- BONER, C. J. Thixotropic qualities of soap-hydrocarbon systems, 1383
- BOURBEAU, G. A. *See* Jackson, M. L.
- BOWDEN, S. T. *See* Grant, W. E.  
*See* Jones, W. J.
- BOYD, GEORGE A., AND EBERL, JAMES J. Absolute reaction kinetics of tobacco mosaic virus and a proposed theory of denaturation, 1146
- BRADLEY, W. F., AND GRIM, R. E. Colloid properties of layer silicates, 1404
- BRAGER, IRVING A. Transformation of organic substances by alpha particles and deuterons, 551
- BRIGGS, D. R. Electrophoretic mobilities and conductometric activities of potassium, sodium, and lithium salts of gum arabic, 76
- BROOKS, M. C., AND BADGER, R. M. A semimicro diffusion method for the characterization of high-polymer fractions, 1390
- BURTON, MILTON. Radiation chemistry. IV. An interpretation of the effect of state on the behavior of some organic compounds and solutions, 564  
Radiation chemistry. V. Effect of molecular size, 810
- CARROLL, B. H. *See* Spence, John
- CHESNUTT, S. D. *See* Baker, M. O.
- CORBIN, NANCY, ALEXANDER, MARY, AND EGLOFF, GUSTAV. Gaps in physical constants data for hydrocarbons, 387
- COSWELL, R. *See* Benson, S. W.
- DAHL, LOUIS A. Analytical treatment of multicomponent systems, 698
- DAINTON, F. S. On the existence of free atoms and radicals in water and aqueous

- solutions subjected to ionizing radiation, 490
- DAMERELL, V. R., AND VOGT, M. J. The effect of surface-active agents upon dispersions of lead monoxide in xylene, 363
- DARCH, W. J. *See* GRANT, W. E.
- DAVIDSON, ARTHUR W., ARGERSINGER, W. J., JR., AND MICHAELIS, CARL I. The cryoscopic behavior of carbon tetrachloride, 332
- DAVIES, T. H. Chemical effects in nuclear electron emission, 595
- DOSCHER, TODD M., AND VOLD, ROBERT D. Colloidal structures in binary soap systems, 97
- DREYER, JOHN F. The fixing of molecular orientation, 808
- EBERL, JAMES J. *See* Boyd, George A.
- EGGENBERGER, D. N. *See* Ralston, A. W.
- EGLOFF, GUSTAV. *See* Corbin, Nancy
- ELTENTON, G. C. The mass-spectrometric detection of free radicals, 463
- ERNSBERGER, F. M., AND FRANCE, WESLEY G. Some physical and chemical properties of weight-fractionated lignosulfonic acid, including the dissociation of lignosulfonates, 267
- EWART, R. H. *See* Wales, Michael
- FARRINGTON, B. B. *See* Birdsall, D. H.
- FINEMAN, MANUEL N., AND MCBAIN, JAMES W. The osmotic behavior of some colloidal electrolytes as determined by means of the Hill-Baldes vapor-tension apparatus, 881
- FINKELSTEIN, LEO. Rheological properties of incendiary gels, 1460
- FRANCE, WESLEY G. *See* Ernsberger, F. M. *See* Van Winkle, Q.
- FRUMKIN, A., AND BAGOTSKAJA, J. The potentials of falling drops, 1
- FU, YING, HANSEN, ROBERT S., AND BARTLELL, F. E. Thermodynamics of adsorption from solutions. I. The molality and activity coefficient of adsorbed layers, 374
- FUGASSI, PAUL. *See* Rudy, Charles E., Jr. *See* Warrick, Earl
- FULMER, E. I. *See* Tuller, Elizabeth F.
- GETTY, RAYMOND. *See* Merrill, Reynold C.
- GLOCKLER, GEORGE. Controlled-electron reactions, 451
- GOODEVE, C. F., AND TAYLOR, M. R. The effect of temperature and impurities on certain photochemical reactions in solids, 828
- GRANT, W. E., DARCH, W. J., BOWDEN, S. T., AND JONES, W. J. The surface tension and viscosity of solutions of uranyl salts, 1227
- GRIM, R. E. *See* Bradley, W. F.
- GREEN, DIETER M. *See* Klotz, Irving M.
- GULBRANSEN, E. A. *See* Hickman, J. W.
- HAENDLER, HELMUT M. *See* Linnell, Robert H.
- HALL, NORRIS F. *See* Rothschild, B. F.
- HANSEN, ROBERT S. *See* Fu, Ying
- HARRINGTON, E. R. Colloid properties of some western clays, 1373
- HATTIANGDI, G. S., ADARKAR, S. P., JASAWALLA, J. P., AND PRASAD, M. The effect of additives on the physical-chemical properties of soap gels in organic solvents, 1481
- HAUSER, ERNST A. Silicic chemistry. A new branch of colloid science, 1165
- AND LE BEAU, D. S. The effect of temperature and molecular weight distribution on the morphology of natural and synthetic high polymers, 27
- AND MICHAELS, A. S. Interfacial tension at elevated pressures and temperatures. I. A new and improved apparatus for boundary-tension measurements by the pendent-drop method, 1157
- AND PERRY, ELL. Emulsion polymerization of styrene, 1175
- HELDMAN, M. J. *See* Vold, Robert D.
- HERBO, CL. *See* Prigogine, I.
- HICKMAN, J. W., AND GULBRANSEN, E. A. An electron diffraction study of oxide films formed on Hastelloy alloys A, B, C, and D, 1186
- HIPPLE, J. A. Spontaneous dissociation of ions, 456
- HIRSCHFELDER, JOSEPH O. Chemical reactions produced by ionization processes, 447
- HOPKE, E. R. *See* Sears, G. W.
- HORTON, WILLIAM S. Temperature lag and chemical kinetics, 1129
- HUGGINS, MAURICE L. The effect of size, shape, and flexibility of the solute molecules on the properties of colloidal solutions, 248



- HUTCHINSON, ERIC. Diffusion across oil-water interfaces, 897
- JACKSON, M. L., TYLER, S. A., WILLIS, A. L., BOURBEAU, G. A., AND PENNINGTON, R. P. Weathering sequence of clay-size minerals in soils and sediments. I. Fundamental generalizations, 1237
- JACOBY, ARTHUR L. Polyamide antifoams. I. Relation between chemical constitution and effectiveness, 689
- JASSAWALLA, J. P. *See* Hattiangdi, G. S.
- JOHNSON, WARREN F. *See* Kolthoff, I. M.
- JONES, W. H. *See* Jones, W. J.
- JONES, W. J., BOWDEN, S. T., YARNOLD, W. W., AND JONES, W. H. The viscosity of solutions of primary alcohols and fatty acids in benzene and in carbon tetrachloride, 753  
*See* Grant, W. E.
- JURA, GEORGE. Calculation of the surface energy of liquid argon and mercury, 40
- KAHLER, HERBERT. The diffusion and sedimentation of sodium thymonucleate, 676
- KARATZAS, ALEXANDER. *See* Schwab, George-Maria
- KATZ, SIDNEY H., AND MACRAE, DUNCAN. Filtration of aerosols by granular charcoal, 695
- KLEVENS, H. B. Critical micelle concentrations as determined by refraction, 130
- KLOTZ, IRVING M., AND GRUEN, DIETER M. Infrared absorption spectra of some amino acids and their complexes, 961
- KOLTHOFF, I. M., AND JOHNSON, WARREN F. Laurate-ion activity in solutions of potassium laurate in the absence and presence of neutral salts, 22  
AND STRICKS, W. Solubilization of dimethylaminoazobenzene in solutions of detergents. I. The effect of temperature on the solubilization and upon the critical concentration, 915  
*See* May, D. R.  
*See* Shapiro, I.
- KOORN, VIRGINIA M. *See* Lundgren, Harold P.
- LAWRENCE, A. S. C. Soap-in-oil systems, 1504
- LE BEAU, D. S. *See* Hauser, Ernst A.
- LIND, S. C. Introduction to Symposium on Radiation Chemistry and Photochemistry, 437
- LINNELL, ROBERT H., AND HAENDLER, HELMUT M. Beryllium fluoride in water and ethanol solutions, 819
- LIVINGSTON, ROBERT. The reversible photobleaching of dyes and pigments, 527  
*See* McBrady, John J.
- LUNDGREN, HAROLD P., STEIN, ANDREW M., KOORN, VIRGINIA M., AND O'CONNELL, RICHARD A. Stability of synthetic keratin fibers in alcohol-water mixtures. Theoretical basis for a new method for solubilizing feather keratin, 180
- MCBAIN, JAMES W., WILDER, ARTHUR G., AND MERRILL, R. C., JR. Solubilization of water-insoluble dye by colloidal electrolytes and non-ionizing detergents, 12  
*See* Fineman, Manuel N.  
*See* Marsden, Sullivan S., Jr.  
*See* Mysels, Karol J.
- MCBRADY, JOHN J., AND LIVINGSTON, ROBERT. Reversible photobleaching of chlorophyll, 662
- MCCREADY, N. W. The thermodynamic properties of sodium silicate, 1277
- MACRAE, DUNCAN. *See* Katz, Sidney H.
- MARSDEN, SULLIVAN S., JR., AND MCBAIN, JAMES W. Aqueous systems of non-ionic detergents as studied by x-ray diffraction, 110
- MARSHALL, C. E. The electrochemical properties of mineral membranes. VIII. The theory of selective membrane behavior, 1289
- MARTIN, S. W. *See* Robison, Henry E.
- MAY, D. R., AND KOLTHOFF, I. M. Studies on the aging of precipitates and coprecipitation. XL. The solubility of lead chromate as a function of the particle size, 836.
- MERRILL, REYNOLD C. Solubility study of an aqueous potassium laurate-potassium silicate system, 1143  
AND GETTY, RAYMOND. The effect of alkaline electrolytes on micelle formation in soap solutions, 774
- LA MER, VICTOR K. Monodisperse colloids and higher-order Tyndall spectra, 65

- AND GETTY, RAYMOND. Phase study of rosin soap-sodium chloride-water and rosin soap-sodium silicate-water systems, 167
- MERRILL, R. C., JR. *See* McBain, James W.
- MICHAELIS, CARL I. *See* Davidson, Arthur W.
- MICHAELS, A. S. *See* Hauser, E. A.
- MILLIGAN, W. O., AND WATT, L. MERTEN. X-ray diffraction studies in the system  $\text{NiO-Cr}_2\text{O}_3\text{-ZrO}_2$ , 230  
*See* Weiser, Harry B.
- MILLS, G. A. *See* Weiser, Harry B.
- MISLOW, KURT. Binary systems of some carboxylic acids. I. Systems containing benzoic acid or a substituted benzoic acid as one of the components, 729  
Binary systems of some carboxylic acids. II. Systems containing heterocyclic acids as the components, 740
- MYSELS, KAROL J., AND MCBAIN, JAMES W. Variability and inhomogeneity of aluminum dilaurate, 1471
- NEWTON, ROY F. *See* Abers, Elliott L.
- NOYES, W. ALBERT, JR. Some aspects of the photochemistry of ketones, 546
- O'CONNELL, RICHARD A. *See* Lundgren, Harold P.
- OUTLON, T. D. The pore size-surface area distribution of a cracking catalyst, 1296
- OUTER, P. *See* Prigogine, I.
- PALM, ANN. X-ray diffraction analysis of indium hydroxide and "indium chromate," 959
- PAUL, JACK M., AND BEARD, G. V. Liquidus-solidus points of the manganese-nickel system, 750
- PENNER, S. The maximum possible rate of evaporation of liquids, 367  
Melting and evaporation as rate processes, 949  
Additions to the article "Melting and evaporation as rate processes," 1262
- PENNINGTON, R. P. *See* Jackson, M. L.
- PERRY, ELI. *See* Hauser, Ernst A.
- PESMATJOGLOU, SOTERIA. *See* Schwab, George-Maria
- PIERCE, CONWAY, AND SMITH, R. NELSON. Heats of adsorption. I, 1111  
*See* Smith, R. Nelson
- POUND, JAMES R. The oxidation of ferrous sulfide in air, 1103
- PRASAD, M. *See* Hattiangdi, G. S.
- PRESTON, WALTER C. Some correlating principles of detergent action, 84
- PRIGOGINE, I., OUTER, P., AND HERBO, CL. Affinity and reaction rate close to equilibrium, 321
- RALSTON, A. W., AND EGGENBERGER, D. N. The electrical behavior of dodecylammonium chloride in water-organic solvent systems, 1494
- RAZOUK, RASHAD I., AND SALEM, AHMED S. The adsorption of water vapor on glass surfaces, 1208
- RICHTER, J. W. *See* Schubert, Jack
- ROBINSON, J. V., AND WOODS, W. W. Foaming of mixtures of hydrocarbons, 763
- ROBISON, HENRY E., AND MARTIN, S. W. Beaker-type centrifugal sedimentation of subsieve solid-liquid dispersions. I. Theory, 854
- ROLLEFSON, G. K., AND BOAZ, H. Quenching of fluorescence in solution, 518
- ROSENBLUM, CHARLES. Benzene formation in the radiochemical polymerization of acetylene, 474
- ROTHSCHILD, B. F., TEMPLETON, C. C., AND HALL, NORRIS F. The distribution of thorium nitrate between water and certain alcohols and ketones, 1006
- ROWLEY, ANNE. *See* Antonoff, George
- RUDY, CHARLES E., JR., AND FUGASSI, PAUL. The thermal dissociation of tertiary butyl acetate, 357
- RUEGGERBERG, W. H. C. Use of aluminum soaps and other fuel thickeners in gelling gasolines, 1444
- SALEM, AHMED S. *See* Razouk, Rashad I.
- SCHACHMAN, H. K. Determination of sedimentation constants in the Sharples "supercentrifuge, 1034
- SCHÖNBERG, ALEXANDER, AND BARAKAT, MOHAMED ZAKI. Molecular-weight determinations of non-volatile substances based on the evaporation velocities of their solutions, 1074
- SCHUBERT, JACK. The use of ion exchangers for the determination of physicochemical properties of substances, par-

- ticularly radiotracers, in solution. I. Theoretical, 341
- AND RICHTER, J. W. The use of ion exchangers for the determination of physical-chemical properties of substances, particularly radiotracers, in solution. II. The dissociation constants of strontium citrate and strontium tartrate, 350
- SCHWAB, GEORGE-MARIA, AND KARATZAS, ALEXANDER. The catalytic action of salt pairs, 1053
- AND PESMATJOGLU, SOTERIA. Metal electrons and alloy catalysis. The system gold-cadmium, 1046
- SCHWENK, H. S. Temperature control for a constant-temperature water bath, 761
- SEARS, G. W., AND HOPKE, E. R. The vapor pressure of benzotrifluoride measured by the Rodebush manometer, 1137
- SHAPIRO, I., AND KOLTHOFF, I. M. Studies on aging of precipitates and coprecipitation. XLI. The bulkiness and porosity of silica powder, 1020
- AND KOLTHOFF, I. M., Studies on aging and coprecipitation. XLII. Aging of silver bromide in the dry state, 1319
- SINGER, J. M., AND WALLACE, W. E. The densities of magnesium-cadmium solid solutions, 999
- SMITH, R. NELSON, AND PIERCE, CONWAY. Heats of adsorption. II, 1115
- See Pierce, Conway
- SPENCE, JOHN, AND CARROLI, B. H. Desensitization by sensitizing dyes, 1090
- STEACIE, E. W. R. The relation of radiation chemistry to photochemistry, 441
- STEIN, ANDREW M. See Lundgren, Harold P.
- STRICKS, W. See Kolthoff, I. M.
- SUTHERLAND, K. L. Physical chemistry of flotation. XI. Kinetics of the flotation process, 394
- TAYLOR, M. R. See Goodeve, C. F.
- TEMPLETON, C. C. See Rothschild, B. F.
- THOMPSON, J. O. See Wales, Michael
- TULLER, ELIZABETH F., AND FULMER, E. I. Coagulation of hydrous ferric oxide sols by electrolytes, 787
- TYLER, S. A. See Jackson, M. L.
- VAND, VLADIMIR. Viscosity of solutions and suspensions. I. Theory, 277
- Viscosity of solutions and suspensions. II. Experimental determination of the viscosity-concentration function of spherical suspensions, 300
- Viscosity of solutions and suspensions. III. Theoretical interpretation of viscosity of sucrose solutions, 314
- VAN WINKLE, Q., AND FRANCE, WESLEY G. Electrophoretic and ultracentrifugal investigation of rabbit liver nucleoprotein, 207
- VOGT, M. J. See Damerell, V. R.
- VOLD, MARJORIE J. See Vold, R. D.
- VOLD, R. D., AND HELDMAN, M. J. Electrical conductivity of crystalline and liquid-crystalline soap-water systems, 148
- AND VOLD, MARJORIE J. Properties of systems of calcium stearate and cetane as deduced from x-ray diffraction patterns, 1424
- See Doscher, Todd M.
- WAHBA, MAURICE. Moisture relationships of cellulose. I. The heat of wetting in water and in certain organic liquids, 1197
- WALES, MICHAEL. The application of flow birefringence measurement to high-polymer solutions, 976
- Sedimentation equilibria of polydisperse non-ideal solutes. I. Theory, 235
- WILLIAMS, J. W., THOMPSON, J. O., AND EWART, R. H. Sedimentation equilibria of polydisperse non-ideal solutes. Experiment, 983
- WALKER, WILLIAM C., AND ZETTMEOYER, ALBERT C. A dual-surface B.E.T. adsorption theory, 47
- See Zettlemoyer, Albert C.
- WALLACE, W. E. See Singer, J. M.
- WARRICK, EARL, AND FUGASSI, PAUL. The kinetics of the thermal decomposition of *tert*-butyl propionate, 1314
- WATSON, JOHN H. L. Electron microscopy of radiation polymerization products, 470
- WATT, L. MERTEN. See Milligan, W. O.
- WEISER, HARRY B., MILLIGAN, W. O., AND MILLS, G. A. Zones of mutual protection against crystallization in dual-oxide systems, 942

- WEISZ, PAUL B. Radiation chemistry of the Geiger-Mueller counter discharge, 578
- WIENER, HARRY. Relation of the physical properties of the isomeric alkanes to molecular structure. Surface tension, specific dispersion, and critical solution temperature in aniline, 1082
- Vapor pressure-temperature relationships among the branched paraffin hydrocarbons, 425
- WIER, T. P., JR. *See* Baker, M. O.
- WILDER, ARTHUR G. *See* McBain, James W.
- WILLARD, JOHN E. Reactions of carbon tetrachloride with bromine activated by isomeric nuclear transition and by the neutron-gamma reaction, 585
- WILLIAMS, J. W. *See* Alberty, Robert A.  
*See* Wales, Michael
- WILLIAMS, R. R. The Szilard-Chalmers reaction in the chain-reacting pile, 603
- WILLIAMS, V. C. Phase equilibrium description, 1263
- WILLIS, A. L. *See* Jackson, M. L.
- WILSON, STUART H. A comparison of the sensitivity of spectrographic and radio-tracer methods, 1260
- WOODS, W. W. *See* Robinson, J. V.
- YARNOLD, W. W. *See* Jones, W. J.
- ZETTLEMAYER, ALBERT C., AND WALKER, WILLIAM C. Active magnesia. IV. Application of dual-surface theory, 58  
*See* Walker, William C.
- ZIMM, BRUNO H. The dependence of the scattering of light on angle and concentration in linear polymer solutions, 260

## INDEX TO NEW BOOKS

- ALFREY, TURNER, JR. *Mechanical Behavior of High Polymers*, 1272
- ARCHER, R. S., BRIGGS, J. Z., AND LOEB, C. M., JR. *Molybdenum: Steels, Irons, Alloys*, 1512
- BERGMANN, ERNST DAVID. *Isomerism and Isomerization of Organic Compounds*, 1276
- BIKERMAN, J. J. *Surface Chemistry for Industrial Research*, 1266
- BOGUE, ROBERT HERMAN. *The Chemistry of Portland Cement*, 434
- BRIGGS, J. Z. *See Archer, R. S.*
- Colloid Science. *A Symposium*, 1109
- EASTMAN, E. D., AND ROLLEFSON, G. K. *Physical Chemistry*, 431
- EILERS, H., SAAL, R. N. J., AND VAN DER WAARDEN, M. *Monograph on the Progress of Research in Holland during the War. Chemical and Physical Investigations on Dairy Products*, 1271
- FUOSS, R. M. *The Development of Theoretical Electrochemistry*, 1274
- FURNAS, C. C. (*Editor*). *Research in Industry. Its Organization and Management*, 1267
- FUSON, REYNOLD C. *See Shriner, Ralph L.*
- HAWLEY, GESSNER G. *Small Wonder: The Story of Colloids*, 1103
- HILDITCH, T. D. *The Chemical Constitution of Natural Fats*, 1275
- HOUGEN, O. A., AND WATSON, K. M. *Chemical Process Principles. Part II. Thermodynamics. Part III. Kinetics and Catalysis*, 1264
- JACOBSON, C. A. (*Editor*). *Encyclopedia of Chemical Reactions. Vol. II. Cadmium, Calcium, Carbon, Cerium, Cesium, Chlorine, Chromium*, 1274
- KARRER, PAUL. *Organic Chemistry*, 762
- KIRK, RAYMOND E., AND OTHMER, DONALD F. (*Editors*). *Encyclopedia of Chemical Technology. Vol. I, A to Anthrimerdes*, 761
- KOBE, KENNETH A. *Inorganic Process Industries*, 1511
- KOLTHOFF, I. M., AND STENGER, V. A. *Volumetric Analysis. Vol. II. Titration Methods*, 1269
- KUHN, WERNER. *Physikalische Chemie*, 1109
- LAVINE, IRVIN. *See Zimmerman, O. T.*
- LOEB, C. M., JR. *See Archer, R. S.*
- MANTELL, C. L. *The Water Soluble Gums*, 1266
- Newer Methods of Preparative Organic Chemistry, 1268
- NORD, F. F. (*Editor*). *Advances in Enzymology. Vol. 7*, 433
- OTHMER, DONALD F. *See Kirk, Raymond E.*
- RALSTON, A. W. *Fatty Acids and their Derivatives*, 1273
- Research. *A Journal of Science and its Applications*, No. 2, November, 1947, 1110.
- RICHTER-ANSCHUTZ. *The Chemistry of the Carbon Compounds. Vol. IV. The Heterocyclic Compounds and Organic Free Radicals*, 432
- ROLLEFSON, G. K. *See Eastman, E. D.*
- ROSENFELD, L. *Nuclear Forces. I*, 1274
- SAAL, R. N. J. *See Eilers, H.*
- SAHYUN, MELVILLE (*Editor*). *Proteins and Amino Acids in Nutrition*, 1268
- SHRINER, R. L. (*Editor*). *Organic Syntheses, Vol. 27*, 1109
- AND FUSON, REYNOLD C. *The Systematic Identification of Organic Compounds*, 1266
- SNELL, C. T. *See Snell, F. D.*
- SNELL, F. D., AND SNELL, C. T. *Colorimetric Methods of Analysis*, 1265
- STENGER, V. A. *See Kolthoff, I. M.*

- Symposium on Plasticizers, 431
- Table of the Bessel Functions  $J_0(z)$  and  $J_1(z)$  for Complex Arguments, 434
- Tables of Spherical Bessel Functions. Vol. II, 762
- THEILHEIMER, A. Synthetic Methods of Organic Chemistry, A Thesaurus. Vol. I, 1942-44, 1273
- VAN SCHELVEN, THEODORE. Weiss Magneton as Components of Nuclear and Subnuclear Structures, 1511
- VAN DER WAARDEN, M. See Eilers, H.
- WALD, A. G. Colloids. Their Properties and Applications, 433
- WATSON, K. M. See Hougen, O. A.
- VELCHER, FRANK J. Organic Analytical Reagents. Vol. II, 431; Vol. III, 435; Vol. IV, 1272
- WILSCHUT, A. J. Monograph on the Progress of Research in Holland during the War. Technological and Physical Investigations on Natural and Synthetic Rubbers, 435
- ZERNERMAN, O. T., AND LAVINE, IRVIN. Conversion Factors and Tables, 1110
- LAVINE, IRVIN. Psychrometric Tables and Charts, 762







**Indian Agricultural Research Institute (Pusa)**  
**LIBRARY, NEW DELHI-110012**

**This book can be issued on or before.....**

<b>Return Date</b>	<b>Return Date</b>